McGRAW-HILL ENCYCLOPEDIA OF SCIENCE & TECHNOLOGY

10 LIB-META

www.MHEST.com

Libra

The Scales, a southern zodiacal constellation (see **illustration**). It has no bright stars. Traditional pictures show a set of scales (a balance) with pans held by chains. Perhaps its name comes from the nearby constellation Virgo, who was the goddess of justice and who would have used scales to balance good and evil deeds. Also, the autumnal equinox, with daytime and nighttime of equal length, used to occur in Libra, though the precession of the equinoxes has moved that point to Virgo. *See* EQUINOX; PRECESSION OF EQUINOXES; VIRGO; ZODIAC.

Libra's brightest stars have the Arabic names Zubenelschamali and Zubenelgenubi—meaning northern and southern claws—that show that they once belonged to Scorpius. *See* SCORPIUS.

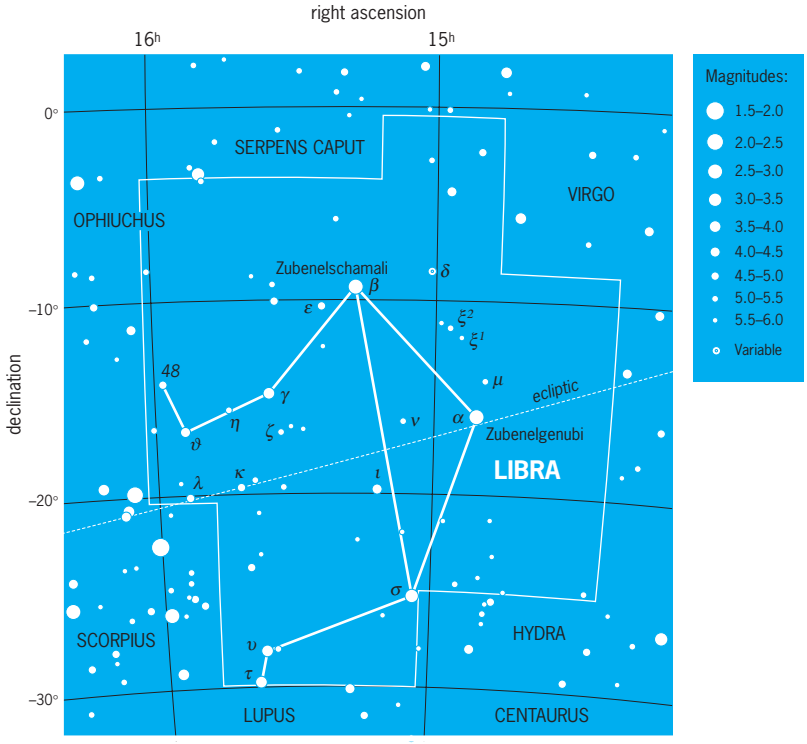

Modern boundaries of the constellation Libra, the scales. The celestial equator is 0° of declination, which corresponds to celestial latitude. Right ascension corresponds to celestial longitude, with each hour of right ascension representing 15° of arc. Apparent brightness of stars is shown with dot sizes to illustrate the magnitude scale, where the brightest stars in the sky are 0th magnitude or brighter and the faintest stars that can be seen with the unaided eye at a dark site are 6th magnitude. (*Wil Tirion*)

The modern boundaries of the 88 constellations, including this one, were defined by the International Astronomical Union in 1928. *See* CONSTELLATION.

Jay M. Pasachoff

Lichens

Symbiotic associations of fungi (mycobionts) and photosynthetic partners (photobionts). These associations always result in a distinct morphological body termed a thallus that may adhere tightly to the substrate or be leafy, stalked, or hanging. A thallus consists of layers, that is, a cortex and medulla made up of the fungus, and a photosynthetic layer of algal or cyanobacterial cells that are closely associated with fungal hyphae. Rhizoids anchor thalli to their substrates. Some lichens (*Stereocaulon*) with green photobionts have gall-like structures called cephalodia that contain cyanobacteria. *See* CYANOBACTERIA.

Lichens are formed from specialized groups of parasitic fungi; this association is one of a controlled parasitism rather than mutualism. Thus, the photobionts that lichen fungi slowly parasitize should be considered victims and not partners. Lichen-forming fungi share two characteristics with fungi that parasitize plants: concentric bodies and specialized branches of hyphae (haustoria) that penetrate host cells and absorb nutrients from them.

Distribution. Lichens have a worldwide distribution and grow on almost any inanimate object, such as bark, soil, roof tiles, or stone. Some also grow on living leaves of tropical plants and ferns, while a few grow inside sandstone rocks in the dry valleys of Antarctica. Lichens dominate about 8% of the Earth's surface, especially in the northern boreal forests of Canada and Siberia, where reindeer lichens form vast uninterrupted carpets of growth. They are among the hardiest of organisms and thrive in some of the Earth's harshest environments, such as polar regions, deserts, and high mountains.

Classification. The name given to a lichen applies only to the mycobiont, while the photobiont has a separate name. Most of the 15,000 lichen-forming fungi are in the fungal class Ascomycotina (ascolichens); common genera of lichens include *Cladonia, Parmelia, Lecanora, Lecidea*, and *Usnea*. Approximately a dozen species of basidiomycetes form lichens. *Dictyonema pavonium* is a common, tropical basidiolichen with lobed thalli and the blue-green *Scytonema* as photobiont. *Omphalina* forms gilled basidiocarps and two types of associations with the green alga *Coccomyxa* in the form of globular clusters (*Botrydina*-type thallus) or small lobes (*Coriscium*-type thallus). Lichens that do not have sexual reproduction (*Lepraria*) are placed in the Lichenes Imperfecti. *See* ASCOMYCOTA; BASIDIOMYCOTA.

Photobionts of lichens are either green algae (*Trebouxia, Trentepohlia*) or cyanobacteria (*Nostoc, Scytonema*). The most common photobiont is *Trebouxia*. This unicellular green algae has never been found in the free-living state. It is believed that *Trebouxia* is a lichenized and highly modified form of the filamentous alga *Pleurastrum terrestre*.

Growth and reproduction. Lichens grow very slowly. Indeed, the fastest-growing lichen from a temperate zone is *Ramalina menziesii*, which has a maximum annual radial growth of 1 in. (28 mm). Most temperate-zone lichens grow only 0.1–0.2 in. (2–6 mm) per year or less. Lichen growth can be measured in terms of an increase in linear dimension or biomass of thallus. Growth rates of thalli vary greatly according to season, habitat conditions, latitude, and age of the thallus, and even between the lobes of a single thallus. Individual lichens may live for hundreds and even thousands of years.

Fragmentation of thalli is a common way that lichens reproduce. Other asexual reproduction is by means of propagules that are simply outgrowths of the thallus and contain a few photobiont cells closely enclosed by fungal hyphae. Sexual reproduction is presumed to be common among lichen fungi because of their genetic variability and the presence of fungal sexual structures such as spermatia and ascogonial filaments. Ascospores, which are products of sexual recombination, are produced and discharged commonly by many lichens. What happens to the mycobionts after the spores germinate is not clear. Developing hyphae from spores may even steal photobiont cells from other lichens and use them to form their own thalli. *See* REPRODUCTION (PLANT).

Physiology. The basic metabolic processes of lichens are photosynthesis, respiration, and nitrogen fixation. Lichens have adapted these processes to different conditions of light, temperature, day length, and water. The mycobiont causes the photobiont to excrete most of the carbon that it fixes during photosynthesis. Only a single type of compound is excreted. The mycobiont absorbs these compounds and converts them to mannitol, its own storage compound. When dry lichens absorb water, they respire at levels much higher than normal for several hours. The mycobiont respires stored polyols, in the case of chlorolichens, instead of depleting valuable proteins and other structural compounds. *See* PLANT RESPIRATION.

Nitrogen-fixing lichens are common and contribute nitrogen to different ecosystems when they decay. In cyanolichens the mycobiont inhibits the nitrogen-assimilating enzymes of the cyanobiont, causing it to release most of the ammonia it produces. The ammonia is absorbed by the mycobiont and used to make proteins and nucleic acids. *See* NITROGEN FIXATION.

Chemistry. Lichens produce several hundred secondary compounds that accumulate as crystals in the thalli, often at high concentrations. These compounds may protect the slow-growing thalli from harmful bacteria, fungi, and insects and may play a regulatory role in the interactions between bionts. Lichen compounds have been produced by free-living fungi, especially species of *Aspergillus*, and by mycobionts growing alone in culture. Lichen

secondary compounds represent a new class of antibiotics in an age where standard antibiotics such as penicillin are becoming ineffective against antibiotic-resistant microbes. Secondary compounds are used extensively by taxonomists to characterize new taxa of lichens (chemotaxonomy).

Pollution indicators. Lichens have become useful bioindicators of air pollution because of their sensitivity to pollutants such as sulfur dioxide, hydrogen fluoride, ozone, and peroxyacetyl nitrate (PAN) and particulate pollutants such as lead, copper, and zinc. The most widespread and damaging pollutant for lichens is sulfur dioxide, which is most toxic when the pH of the substrate is acidic and the thallus is wet. Nitrogen fixation is the most sensitive to sulfur dioxide, followed by photosynthesis and respiration. Acid rain adversely affects lichen communities but also opens up new niches for acid-loving species. Pollution zones around many major cities have been mapped by using lichens. Lichens have also been useful in measuring radioactive fallout from explosions of nuclear bombs and nuclear reactors. *See* AIR POLLUTION.

Vernon Ahmadjian

Bibliography. V. Ahmadjian, *The Lichen Symbiosis*, 1993; V. Ahmadjian and M. E. Hale (eds.), *The Lichens*, 1973; C. F. Culberson, *Chemical and Botanical Guide to Lichen Products*, 1969; M. Galun (ed.), *CRC Handbook of Lichenology*, 3 vols., 1988; M. E. Hale, *The Biology of Lichens*, 1983; T. H. Nash and V. Wirth (eds.), *Lichens, Bryophytes, and Air Quality*, 1988.

Licorice

A product obtained from the licorice plant (*Glycyrrhiza glabra*) of the legume family (Leguminosae). It is a perennial herb which grows wild and is cultivated in southern Europe and in western and central Asia. The roots are dried for several months and then packaged for shipment. Spain leads in the production of cultivated licorice roots. Licorice is used in medicine to mask objectionable taste and as a laxative; as a flavoring material in the brewing, tobacco, and candy industries; and in the manufacture of shoe polish. *See* ROSALES; SPICE AND FLAVORING.

Perry D. Strausbaugh; Earl L. Core

Lidar

The optical analog of radar. The term lidar is an acronym for light detection and ranging. Lidar systems employ intense pulses of light, typically generated by lasers, and large telescopes and sensitive optical detectors to receive the reflected pulses. They are most commonly used to measure the composition and structure of the atmosphere. The very narrow beamwidth, narrow linewidth, and ultrashort pulses of the laser make it possible to optically probe the atmosphere with exceptional sensitivity and resolution. When used to measure the range and velocity of hard targets, lidars are usually called laser ranging systems or laser radars. *See* LASER; OPTICAL DETECTORS; RADAR.

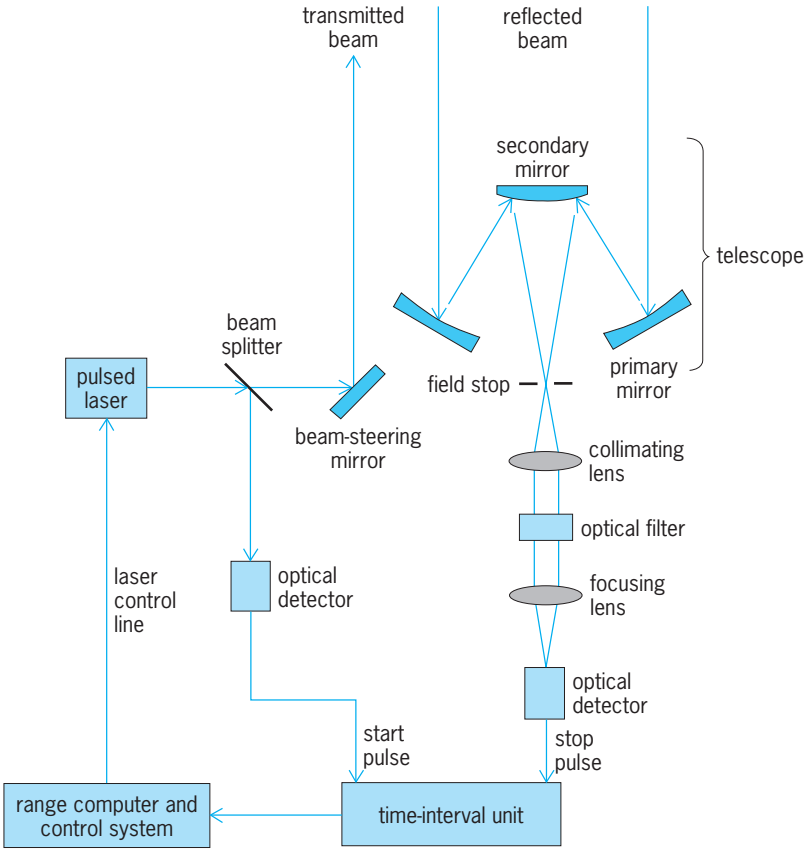

Fig. 1. Block diagram of a typical monostatic system used for ranging or altimetry applications.

Ranging and altimeter systems. The most common lidar configuration is the monostatic system (**Fig. 1**). The laser beam is either projected through the receiving telescope or propagates parallel to the optical axis of the telescope. If the system is designed for ranging or altimetry, the receiver measures the roundtrip propagation time of the laser pulse between the lidar and the target. The distance d to the target is given by the range equation below, where

$$d = \frac{c\tau}{2}$$

c is the speed of light and τ is the roundtrip propagation time of the laser pulse. Precision timing is accomplished electronically by a device called the time interval unit. A beam splitter directs a small fraction (<1%) of the transmitted laser beam to a photodetector. When illuminated by the laser, the photodetector generates an electrical pulse which triggers (starts) a precision clock in the time interval unit. The reflected laser pulse is collected by the receiving telescope and focused onto another, more sensitive photodetector, generating an electrical pulse that stops the clock. The elapsed time is then transmitted to the range computer, which calculates the target distance according to the range equation. The optical filter and field stop in the telescope are

designed to reduce interference and noise caused by other sources of light. The optical filter limits light transmission to the narrow wavelength range (color) of the laser, and the field stop limits the field of view of the telescope to the region illuminated by the laser beam. *See* INTERFERENCE FILTER.

The ranging accuracy depends upon many factors, including the laser pulse length, the received signal strength, and the timing accuracy of the time interval unit. The most sophisticated systems are used for ranging to retroreflector-equipped satellites and to the retroreflector arrays placed on the Moon by the Apollo astronauts. Accuracies of a few centimeters are achieved routinely. Data from these measurements are used to monitor geophysical phenomena such as continental drift, crustal dynamics, and the Earth's rotation rate. Because of the extremely high accuracy required, a more sophisticated version of the range equation must be used which includes the effects of the additional propagation delay introduced by the Earth's atmosphere.

The first successful laser ranging measurements to satellites were conducted in 1964. In the early 1970s, the first space-based laser altimeter was operated in lunar orbit from the *Apollo 15, 16,* and *17* command and service modules. Airborne laser altimeters provide maps of surface topography, coastal water depth, forest canopies, sea ice distribution, volcanic landforms, impact craters, and ocean wave heights. *See* REMOTE SENSING.

Atmospheric lidars. The targets of atmospheric lidars are either suspended dust and aerosols or gas molecules which are continuously distributed in the atmosphere along the propagation path of the laser beam. Atmospheric lidar systems are used to measure density profiles of the scatterers. Profile measurements are accomplished by pulsing the laser and then periodically sampling the detector output (**Fig. 2**). The sampling process is called range gating. The signal level is proportional to the density of scatterers and inversely proportional to the square of the distance to the scattering volume. Because reflected signals from atmospheric aerosols and gas molecules are usually very weak, most atmospheric lidars employ very sensitive photomultiplier tube detectors that operate in the photon-counting mode. The photomultiplier tube signal is processed by a pulse discriminator and range-gated counter. The pulse discriminator converts the low-level (few tenths of a volt) photomultiplier tube pulses generated by the individual detected photons to pulses that can be counted by conventional high-speed digital circuitry. The raw lidar data consists of a series of photon counts corresponding to consecutive range bins. The count in a given range bin is related to the number of scatterers in the corresponding volume illuminated by the laser pulse. *See* ATMOSPHERIC CHEMISTRY; PHOTOMULTIPLIER.

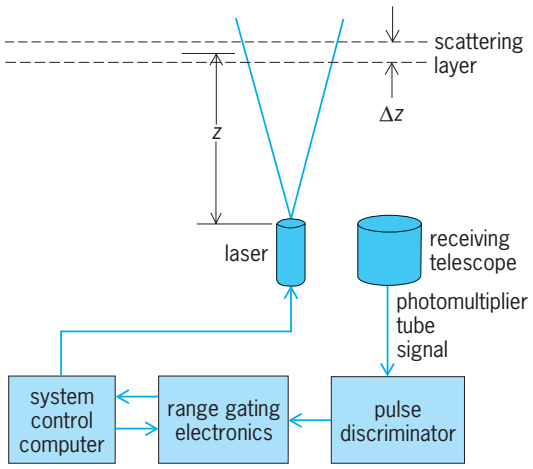

Fig. 2. Block diagram of a typical atmospheric lidar system. Range to scattering volume = *z;* thickness of scattering volume = Δ*z*.

In order to process the photon count profile to yield the density profile of scatterers, other factors, such as the thickness of the scattering volume and the backscatter cross section, must also be taken into account. The thickness of the scattering volume is related to the laser pulse length and the receiver range gate length. The backscatter cross section is the effective cross-sectional area of the scatterer, and depends upon many factors including scattering mechanism, optical wavelength, and optical properties of the scatterer. Only when the scatterer is large compared to the wavelength, which may be the case for aerosol scattering, does the physical size of the scatterer influence the value of the optical backscatter cross section. *See* SCATTERING OF ELECTROMAGNETIC RADIATION.

Atmospheric lidars are classified according to the type of scattering mechanism exploited to make the measurement.

Aerosol lidars. These measure scattering from atmospheric dust and aerosols. Observations with ground-based and airborne aerosol lidars have provided much of the data about the dispersion and global distribution of volcanic aerosols and about the life cycle and distribution of polar stratospheric clouds. Both phenomena occur in the altitude range between 10 and 35 km (6 and 22 mi). Volcanic aerosols can have a significant influence on climate, while polar stratospheric clouds play a major role in the springtime depletion of ozone over both polar caps.

Rayleigh lidars. These are designed to measure the molecular scattered signal, which is proportional to atmospheric density. The atmospheric temperature profile can be calculated from the density profile by using the ideal gas law and the hydrostatic equation. Density and temperature profiles at altitudes up to 100 km (60 mi) have been obtained with powerful ground-based systems. *See* ATMOSPHERE.

Resonance fluorescence lidars. These are used to measure the density profiles of specific molecular species such as sodium in the upper atmosphere. The laser wavelength must be tuned to the resonance absorption wavelength of the species of interest. When illuminated at the resonance wavelength by the lidar beam, the atoms fluoresce because some of the photons are resonantly absorbed and then reradiated. The resonant backscatter cross section is typically

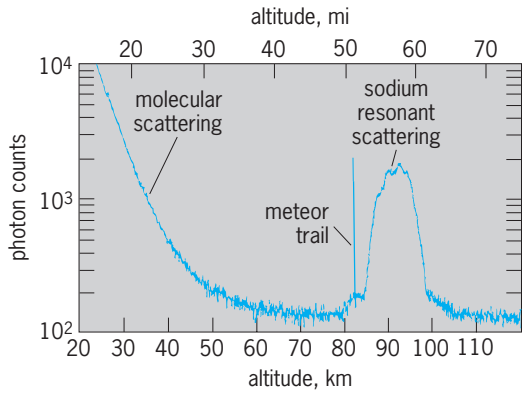

Fig. 3. Photon count profile measured with a sodium resonance fluorescence lidar.

many orders of magnitude larger than the molecular backscatter cross section of the species. **Figure 3** is a photon count profile measured with a sodium resonance fluorescence lidar. The high counts at altitudes below 70 km (45 mi) represent molecular scattering. Sodium resonant scattering is quite strong between 80 and 105 km (50 and 65 mi). The very thin scattering layer at 82 km (51 mi) is a meteor trail. Meteoric ablation is the major source of sodium and other metal layers in the upper atmosphere. By studying the density perturbations of these layers, the characteristics of the background wind perturbations and turbulence can be deduced. *See* METEOR.

Differential absorption lidar (DIAL). This technique is used to measure species concentrations in the lower atmosphere. DIAL systems employ two lasers, one tuned to an absorption line of the species of interest and the other tuned just off the absorption line. The received signal at the more strongly absorbed wavelength is weaker. By comparing the signal levels at the two wavelengths, a density profile of the species can be calculated. A wide variety of important minor constituents in the lower atmosphere, including ozone, are being studied by using DIAL systems.

Raman lidars. These measure the scattered signal at the Raman shifted wavelength. Because the Raman signal is very weak, measurements are usually restricted to the troposphere at altitudes below 10 km (6 mi). However, at these lower altitudes, Raman lidars have provided excellent measurements of atmospheric density, temperature, and water vapor concentration. *See* RAMAN EFFECT.

Doppler lidars. These are used to measure tropospheric winds. The scattered laser pulse is Doppler-shifted in frequency in proportion to the velocity of the scatterer along the propagation path. The frequency shift is measured by combining the reflected signal with the transmitted laser beam, so that the electrical signal generated by the detector is at a frequency equal to the difference between the frequencies of the transmitted and reflected beams. The signal-processing electronics following the photodetector are very similar to those used in Doppler radars. By scanning the lidar beam, the three-dimensional wind vector can be measured. Mobile Doppler lidars have been used to map wind fields associated with a variety of atmospheric phenomena such as frontal passages, downslope flows and gusts, canyon drainage flows, and down bursts caused by severe thunderstorms. *See* DOPPLER EFFECT; DOPPLER RADAR.

Chester S. Gardner

Bibliography. V. A. Banakh and V. L. Mironov, *LIDAR in a Turbulent Atmosphere*, 1988; J. W. Bilbro et al., Airborne Doppler lidar measurements, *Appl. Opt.,* 25:3952–3960, 1986; S. C. Cohen et al., The geoscience laser altimetry/ranging system, *IEEE Trans. Geosci. Remote Sens.,* GE-25:581–592, 1987; C. S. Gardner and J. A. Reagan (eds.), Special section on lidar applications, *Proc. IEEE,* 77(3):408–478, 1989.

Lie detector

A device intended to detect an involuntary physiological response that all persons exhibit when lying but never when telling the truth. Because there is no such specific lie response, the lie detector of popular fancy is mythological. In actual "lie protector" tests, widely used in the United States, breathing movements, blood pressure changes, and electrodermal responses are recorded on a polygraph while the respondent answers "yes" or "no" to a series of 8 to 12 questions. From the polygraph recordings, one can determine whether "relevant" questions had a greater impact on the respondent than did the interpolated "control" questions. In the standard lie test used in specific issue investigations, the relevant questions ask whether the respondent committed the act in question; for example, "On April 12, did you take $2000 from the office safe?" A typical control question might be, "In the first 20 years of your life, did you ever steal anything?" If the examinee reacts more strongly to the relevant than to the control questions, it is inferred that his or her answers to the relevant questions are deceptive. Because an innocent accused also may be disturbed by the relevant questions and react more strongly to them than to the controls, the lie test is biased against the truthful respondent. Research has shown that as many as 50% of innocent criminal suspects may "fail" control-question polygraph tests.

Polygraph tests are also widely used in the United States for preemployment screening. Screening tests normally do not use control questions, but include instead a series of relevant questions that are of interest to the prospective employer: "Have you ever stolen from a previous employer?"; "Have you ever used street drugs?" Strong physiological reactions to any of these questions are interpreted as indicating a deceptive reply. There has been no scientific study to prove the validity of this type of polygraph test, however.

Several devices have been marketed for use in lie detection which are alleged to measure "stress" in the respondent's voice. Because they do not require attachments to the body, such devices can be used covertly and can even be applied to broadcasts or to recordings of the voices of dead people. It has not

yet been shown that these devices can reliably distinguish between different degrees of voice stress. When voice analyzers have been used for lie detection, in parallel with a conventional polygraph, they have done no better than chance in distinguishing truth from deception.

In another type of polygraphic interrogation, the "guilty knowledge" test, the relevant questions name some fact that should be known only by someone who had been present at the crime; the control questions name alternatives that should seem equally plausible to innocent suspects. A differential physiological response to the relevant question suggests that the suspect recognizes its relevance and therefore that he or she possesses guilty knowledge. Although it would seem to hold promise as a tool of criminal investigation, the guilty knowledge test has not yet been adequately studied in real-life applications. *See* ELECTRODERMAL RESPONSE; EMOTION.

David T. Lykken

Bibliography. S. Abrams, *The Complete Polygraph Handbook,* 1989; G. Ben-Shakhar and J. J. Furedy, *Theories and Applications in the Detection of Deception*, 1989.

Lie group

A topological group with only countably many connected components whose identity component is open and is an analytic group. An analytic group or connected Lie group is a topological group with the additional structure of a smooth manifold such that multiplication and inversion are smooth. Many groups that arise naturally as groups of symmetries of physical or mathematical systems are Lie groups. The study of Lie groups has applications to analytic function theory, differential equations, differential geometry, Fourier analysis, algebraic number theory, algebraic geometry, quantum mechanics, relativity, and elementary particle theory. *See* GROUP THEORY; MANIFOLD (MATHEMATICS); TOPOLOGY.

Examples of Lie groups. Euclidean n-dimensional space with the standard differentiable structure and with vector addition as the group operation is an analytic group $\mathbf{R}^n$ of dimension n.

The nonsingular n-by-n real matrices form a Lie group $GL(n,\mathbf{R})$ with the differentiable structure obtained as an open set of n^2-dimensional space and with the group operation given by matrix multiplication. Similarly $GL(n,\mathbf{C})$, the group of nonsingular n-by-n complex matrices under matrix multiplication, forms a Lie group. The latter group is connected.

Each closed subgroup of a Lie group, in its relative topology, admits one differentiable structure on its identity component that makes it a Lie group. With $GL(n,\mathbf{R})$ and $GL(n,\mathbf{C})$, the subgroups of upper triangular matrices, matrices of determinant 1, rotation matrices, orthogonal matrices, and unitary matrices are all examples. *See* MATRIX THEORY.

Lie algebra. Let G be a Lie group. The identity component of G is an open subset of G and is a smooth manifold. Thus it makes sense to speak of tangent spaces. Let $\mathfrak{g}$ be the tangent space to G at the identity element. A multiplication $[X,Y]$ within $\mathfrak{g}$ is defined as follows.

By means of the differential of left translation by p, one can associate a tangent vector X_p to the point p of G. If f is a smooth real-valued function on G, let $\tilde{X}f$ be the function on G with $\tilde{X}f(p) = X_p f$. Then $\tilde{X}f$ is smooth. The tangent vector $[X,Y]$ is defined on the function f by Eq. (1).

$$[X, Y]f = X\left(\tilde{Y}f\right) - Y\tilde{X}f \tag{1}$$

The resulting multiplication satisfies the following properties:

i. $[X,Y]$ is linear in X and in Y.
ii. $[X,X] = 0$.
iii. $[X,[Y,Z]] + [Y,[Z,X]] + [Z,[X,Y]] = 0$.

The vector space $\mathfrak{g}$ equipped with this multiplication is called the Lie algebra of the Lie group G.

The Lie algebra $\mathfrak{g}$ determines the multiplication in G near the group identity by a result known as the Campbell-Hausdorff formula. Consequently, many properties of the identity component of G can be deduced from the simpler object $\mathfrak{g}$.

Homomorphisms. If φ is a smooth homomorphism from an analytic group G to an analytic group G', the differential $d\varphi$ of φ at the identity is a Lie algebra homomorphism in the sense that it is linear and satisfies $d\varphi([X,Y]) = [d\varphi(X),d\varphi(Y)]$. If φ is one-to-one or onto, so is $d\varphi$. Conversely, if G is simply-connected, each homomorphism of Lie algebras arises as the differential of some unique smooth group homomorphism.

Abstract Lie algebras. An abstract real Lie algebra is a finite-dimensional real vector space with a multiplication satisfying (i), (ii), and (iii). Each abstract real Lie algebra can be identified with the Lie algebra of some analytic group.

Examples. The Lie algebra of $\mathbf{R}^n$ is an n-dimensional vector space with all $[X,Y]$ equal to 0.

For $GL(n,\mathbf{R})$, the Lie algebra can be identified with the vector space of all n-by-n real matrices with multiplication given in terms of matrix multiplication as $[X,Y] = XY - YX$. The identification of a member L of the Lie algebra with a matrix X is done entry by entry. Namely, the i-jth entry of X is the result of applying L to the i-jth entry function, which is a smooth real-valued function on the group.

For $GL(n,\mathbf{C})$, the Lie algebra can be identified with all n-by-n complex matrices with multiplication $[X,Y] = XY - YX$.

For a closed subgroup G of $GL(n,\mathbf{R})$ or $GL(n,\mathbf{C})$, inclusion is a smooth one-to-one homomorphism and allows one to identify the Lie algebra of G with a Lie subalgebra of matrices. The matrices of the Lie subalgebra can be computed conveniently as all entry-by-entry derivatives $c'(0)$ of smooth curves $c(t)$ that lie completely within the subgroup and have $c(0)$ equal to the identity matrix. For unitary matrices, for example, the result is skew-hermitian matrices. (A skew-hermitian matrix is equal to the negative of the transpose of its complex conjugate).

Analytic subgroups. Let G be a Lie group. An analytic subgroup H of G is a subgroup of G that admits the structure of an analytic group in such a way that the inclusion mapping of H into G is smooth. The topology of H as a manifold need not be the relative topology inherited from G.

If H is an analytic subgroup of G, the differential of the inclusion mapping identifies the Lie algebra of H with a Lie subalgebra of the Lie algebra of G. Distinct analytic subgroups give rise to distinct Lie subalgebras. Every Lie subalgebra arises from some analytic subgroup by this construction.

Exponential map. Let G be a Lie group with Lie algebra $\mathfrak{g}$. Let $c(t)$ be a curve in G, that is, a smooth mapping from the real line into G, and suppose that $c(0)$ is the group identity. The image of d/dt under the differential dc of $c(t)$ at 0 is a member of $\mathfrak{g}$. For each X in $\mathfrak{g}$ there is one and only one such curve c_X such that $dc_X(d/dt) = X$ and $c_X(s + t) = c_X(s)c_X(t)$ for all s and t. The exponential mapping is the function from $\mathfrak{g}$ to G defined by $\exp X = c_X(1)$. It is smooth and, in a small open neighborhood of the group identity, has a smooth inverse function that provides local coordinates for G near the identity.

For $GL(n,\mathbf{R})$ or $GL(n,\mathbf{C})$ the exponential mapping is given by the series expansion for the ordinary exponential function e^X if the Lie algebra is identified with the Lie algebra of all matrices. *See* SERIES.

Fourier analysis. In many applications of Lie groups the notion of group representation is a basic tool. A unitary representation of the Lie group G on a Hilbert space H is a function R from G to the set of unitary operators on H such that $R(g_1g_2) = R(g_1)R(g_2)$ for all g_1 and g_2 in G and such that the mapping $g \to R(g)x$ is continuous from G into H for each x in H. [A unitary operator U on H is a linear operator from H onto H that preserves inner products; that is, $(Ux, Uy) = (x,y)$ for each x and y in H.] The representation R is irreducible if there is no proper nonzero closed subspace S such that $R(g)$ maps S into itself for all g in G.

Because of the applications, it is an important mathematical problem to classify the irreducible unitary representations of a given Lie group G and to investigate properties of decompositions of general unitary representations into irreducible ones.

In the analysis of the unitary representations, use of the Lie algebra plays an important role. If X is in the Lie algebra, it is possible to define $R(X)$ as a skew-hermitian operator on a dense subspace by differentiating $R(\exp tX)$ appropriately. Then $iR(X)$ extends to a self-adjoint operator that is easier to deal with than $R(\exp tX)$.

In many applications, H is a space of functions, and some linear operator or set of linear operators is acting in H. Typically, the representation of G is given by a group of transformations that commute with these linear operators. When the representation of G on H is decomposed suitably, one can expect the linear operators to act separately in each of the constituent spaces of H and to be easier to understand on each constituent space than on H.

The prototype for this analysis is the case of classical Fourier series of periodic functions on the line with period 2π. Here G is the circle group (the compact Lie group of real numbers modulo 2π, with addition modulo 2π as group operation), and H is the space $L^2(G)$ of square integrable functions on the interval $-\pi \le x \le \pi$. The unitary representation R is given by $[R(x_0)f](x) = f(x_0 + x)$, with addition taken modulo 2π. For this G, the irreducible unitary representations are all one-dimensional and are parametrized by the integers, the nth one being $R_n(x_0) = e^{inx_0}v$ for v in $\mathbf{C}$. The classical Fourier series expansion given in Eq. (2) corresponds to a de-

$$f(x) \sim \sum_{n=-\infty}^{\infty} c_n e^{inx} \tag{2}$$

composition of R into an infinite orthogonal sum of all R_n, since a single R_n can be realized in the one-dimensional space of multiples of e^{inx} and since Eq. (3) holds. In this context, let L be a bounded

$$R(x_0)f(x) = f(x_0 + x) \sim \sum c_n e^{inx_0} e^{inx}$$

$$= \sum R_n(x_0)\left(c_n e^{inx}\right) \tag{3}$$

linear operator on H that commutes with translations, that is, with all $R(x_0)$. An easy computation shows that L must carry e^{inx} into a multiple of itself. If that multiple is b_n, then L is operating in the space of R_n by multiplication by b_n. Equation (4) is then useful in studying L.

$$Lf(x) \sim \sum_{n=-\infty}^{\infty} b_n c_n e^{inx} \tag{4}$$

See OPERATOR THEORY.

Sample applications. Three examples will illustrate the principle of analyzing a linear operator by decomposing it with respect to a group of operators that commute with it.

Rotations and the Fourier transform. Let H be the Hilbert space of square-integrable functions on $\mathbf{R}^n$, let G be the rotation group, and let the representation of G on H be given by rotation of the coordinates. The Fourier transform is a linear operator on H that commutes with each member of G. The space H decomposes under the representation of G into a sequence of simpler spaces, the kth space being all sums of products of a radial function and a harmonic polynomial homogeneous of degree k. The Fourier transform has a simple form on the kth space, given as a one-dimensional integral involving a Bessel function. *See* BESSEL FUNCTIONS; FOURIER SERIES AND TRANSFORMS.

Solutions of differential equations. Some information about solutions in $\mathbf{R}^n$ to elliptic partial differential equations with constant coefficients can be obtained by using the Fourier transform. Here the differential operator commutes with the representation of $G = \mathbf{R}^n$ given by translation in the space of square-integrable functions on $\mathbf{R}^n$, and the Fourier transform is the device for decomposing the representation. For an operator with nonconstant coefficients, one can apply a freezing principle, replacing a

given equation by one with constant coefficients and obtaining an approximate solution near a point.

For many equations of subelliptic type, which are elliptic except for certain degeneracies, a similar analysis is possible by means of representations of a more complicated Lie group. In the simplest new case, the Lie group is the (non-abelian) group of 3-by-3 real upper-triangle matrices with ones on the diagonal, and the differential equation is Eq. (5) in $\mathbf{R}^3$. Other equations can be analyzed

$$\left(\frac{\partial^2 f}{\partial x^2}+\frac{\partial^2 f}{\partial y^2}\right)+\left(x\frac{\partial^2 f}{\partial y\partial z}-y\frac{\partial^2 f}{\partial x\partial z}\right)+\frac{1}{4}\left(x^2+y^2\right)\frac{\partial^2 f}{\partial z^2}=0 \qquad (5)$$

by a combination of this method and a freezing principle.

The laplacian $\Delta=\Sigma\partial^2/\partial x_j{}^2$ in R^n has constant coefficients and can be analyzed by the Fourier transform. But also it commutes with rotations and can be decomposed accordingly. In a ball, for example, the resulting decomposition of solutions of $\Delta u=0$ corresponds to solving the equation by separation of variables. If the solutions are restricted to a sphere, the analysis amounts to a decomposition of the space of square integrable functions on the sphere into (finite-dimensional) eigenspaces of the spherical laplacian, each of which is the Hilbert space for an irreducible representation of the rotation group. More generally, information about the generalized wave operator given in Eq. (6) can be

$$L=\frac{\partial^2}{\partial x_1^2}+\cdots+\frac{\partial^2}{\partial_{x_m}^2}-\frac{\partial^2}{\partial x_{m+1}^2}-\cdots-\frac{\partial^2}{\partial x_{m+n}^2} \qquad (6)$$

obtained by doing a Fourier analysis of functions on an orbit in R^{m+n} under the action of the noncompact group of linear isometries of a real quadratic form with m plus signs and n minus signs. *See* DIFFERENTIAL EQUATION.

Quantum mechanics. In quantum theory the things one observes from experiments are eigenvalues (or the spectrum, if there are not discrete eigenvalues) of certain self-adjoint operators on Hilbert spaces of wave functions. Conservation laws come from self-adjoint operators whose associated one-parameter groups of unitary operators commute with the hamiltonian. In this way a system of conservation laws leads to a group of symmetries, namely, a group of unitary operators commuting with the hamiltonian. Frequently this group is a Lie group. Analysis of the representation of the Lie group by the unitary operators gives information about the physical system. *See* ELEMENTARY PARTICLE; LORENTZ TRANSFORMATIONS; NONRELATIVISTIC QUANTUM THEORY; RELATIVISTIC QUANTUM THEORY; SYMMETRY LAWS (PHYSICS).

Anthony W. Knapp

Bibliography. M. F. Atiyah et al., *Representation Theory of Lie Groups*, 1980; T. Kawazoe, T. Oshima, and S. Sano, *Representation Theory of Lie Groups and Lie Algebras*, 1992; P. J. Oliver, *Applications of Lie Groups to Differential Equations*, 2d ed., 2000; A. L. Onishchik and E. B. Vinberg, *Lie Groups and Algebraic Groups*, 1990; D. H. Sattinger and O. L. Weaver, *Lie Groups and Lie Algebras with Applications to Physics, Geometry, and Mechanics*, 1993; V. S. Varadarajan, *Lie Groups, Lie Algebras, and Their Representations*, 1974, reprint 1988; N. T. Varopouos, L. Saloff-Coste, and T. Coulhon, *Analysis on Lie Groups*, 1993.

Life zones

Large portions of the Earth's land area which have generally uniform climate and soil and, consequently, a biota showing a high degree of uniformity in species composition and adaptations to environment. Related terms are vegetational formation and biome.

Merriam's zones. Life zones were proposed by A. Humboldt, A. P. DeCandolle, and others who emphasized plants. Around 1900 C. Hart Merriam, then chief of the U.S. Biological Survey, related life zones, as observed in the field, with broad climatic belts across the North American continent designed mainly to order the habitats of America's important animal groups. The first-order differences between the zones, as reflected by their characteristic plants and animals, were related to temperature; moisture and other variables were considered secondary.

Each life zone correlated reasonably well with major crop regions and to some extent with general vegetation types (see **table**). Although later studies led to the development of other, more realistic or detailed systems, Merriam's work provided an important initial stimulus to bioclimatologic work in North America. *See* DENDROLOGY; VEGETATION AND ECOSYSTEM MAPPING.

Work on San Francisco Mountain in Arizona impressed Merriam with the importance of temperature as a cause of biotic zonation in mountains. Isotherms based on sums of effective temperatures correlated with observed distributions of certain animals and plants led to Merriam's first law, that animals and plants are restricted in northward distribution by the sum of the positive temperatures (above 109.4°F or 43°C) during the season of growth and reproduction. The mean temperature for the six hottest weeks of the summer formed the basis for the second law, that plants and animals are restricted in southward distribution by the mean temperature of a brief period covering the hottest part of the year. Merriam's system emphasizes the similarity in biota between arctic and alpine areas and between boreal and montane regions. It was already recognized that latitudinal climatic zones have parallels in altitudinal belts on mountain slopes and that there is some biotic similarity between such areas of similar temperature regime.

In northern North America Merriam's life zones, the Arctic-Alpine, the Hudsonian, and the Canadian,

Characteristics of Merriam's life zones

Zone name	Example	Vegetation	Typical and important plants	Typical and important animals	Typical and important crops
Arctic-alpine	Northern Alaska, Baffin Island	Tundra	Dwarf willow, lichens, heathers	Arctic fox, musk-ox, ptarmigan	None
Hudsonian	Labrador, southern Alaska	Taiga, coniferous forest	Spruce, lichens	Moose, woodland caribou, mountain goat	None
Canadian	Northern Maine, northern Michigan	Coniferous forest	Spruce, fir, aspen, red and jack pine	Lynx, porcupine, Canada jay	Blueberries
Western division					
Humid transition	Northern California coast	Mixed coniferous forest	Redwood, sugar pine, maples	Blacktail deer, Townsend chipmunk, Oregon ruffed grouse	Wheat, oats, apples, pears, Irish potatoes
Arid transition	North Dakota	Conifer, woodland sagebrush	Douglas fir, lodgepole, yellow pine, sage	Mule deer, whitetail, jackrabbit, Columbia ground squirrel	Wheat, oats, corn
Upper Sonoran	Nebraska, southern Idaho	Piñon, savanna, prairie	Junipers, piñons, grama grass, bluestem	Prairie dog, blacktail jackrabbit, sage hen	Wheat, corn, alfalfa, sweet potatoes
Lower Sonoran	Southern Arizona	Desert	Cactus, agave, creosote bush, mesquite	Desert fox, four-toed kangaroo rats, roadrunner	Dates, figs, almonds
Eastern division					
Alleghenian	New England	Mixed conifer and hardwoods	Hemlock, white pine, paper birch	New England cottontail rabbit, wood thrush, bobwhite	Wheat, oats, corn, apples, Irish potatoes
Carolinian	Delaware, Indiana	Deciduous forest	Oaks, hickory, tulip tree, redbud	Opossum, fox, squirrel, cardinal	Corn, grapes, cherries, tobacco, sweet potatoes
Austroriparian	Carolina piedmont, Mississippi	Long-needle conifer forest	Loblolly, slash pine, live oak	Rice rat, woodrat, mocking bird	Tobacco, cotton, peaches, corn
Tropical	Southern Florida	Broadleaf evergreen forest	Palms, mangrove	Armadillo, alligator, roseate spoonbill	Citrus fruit, avocado, banana

are entirely transcontinental (**Fig. 1** and table). Because of climatic and faunistic differences, the eastern and western parts of most life zones in the United States (the Transition, upper Austral, and lower Austral) had to be recognized separately. The western zones had to be further subdivided into humid coastal subzones and arid inland subzones. The Tropical life zone includes the extreme southern edge of the United States, the Mexican lowlands, and Central America.

Although once widely accepted, Merriam's life zones are little used today because they include too much biotic variation and oversimplify the situation. However, much of the terminology he proposed persists, especially in North American zoogeographic literature.

Dice's zones. Another approach to life zones in North America is the biotic province concept of L. R. Dice. Each biotic province covers a large and continuous geographic area and is characterized by the occurrence of at least one important ecological association distinct from those of adjacent provinces. Each biotic province is subdivided into biotic districts which are also continuous, but smaller, areas distinguished by ecological differences of lesser extent or importance than those delimiting provinces. Life belts, or vertical subdivisions, also occur within biotic provinces. These are not necessarily continuous but often recur on widely separated mountains within a province where ecological conditions are appropriate.

Boundaries between biotic provinces were largely subjective, supposedly drawn where the dominant associations of the provinces covered approximately equal areas. In practice, however, too few association data including both plants and animals were available, and vegetation generally offered the most satisfactory guide to boundaries. The Dice system recognizes 29 biotic provinces in North America (**Fig. 2**). The two northernmost

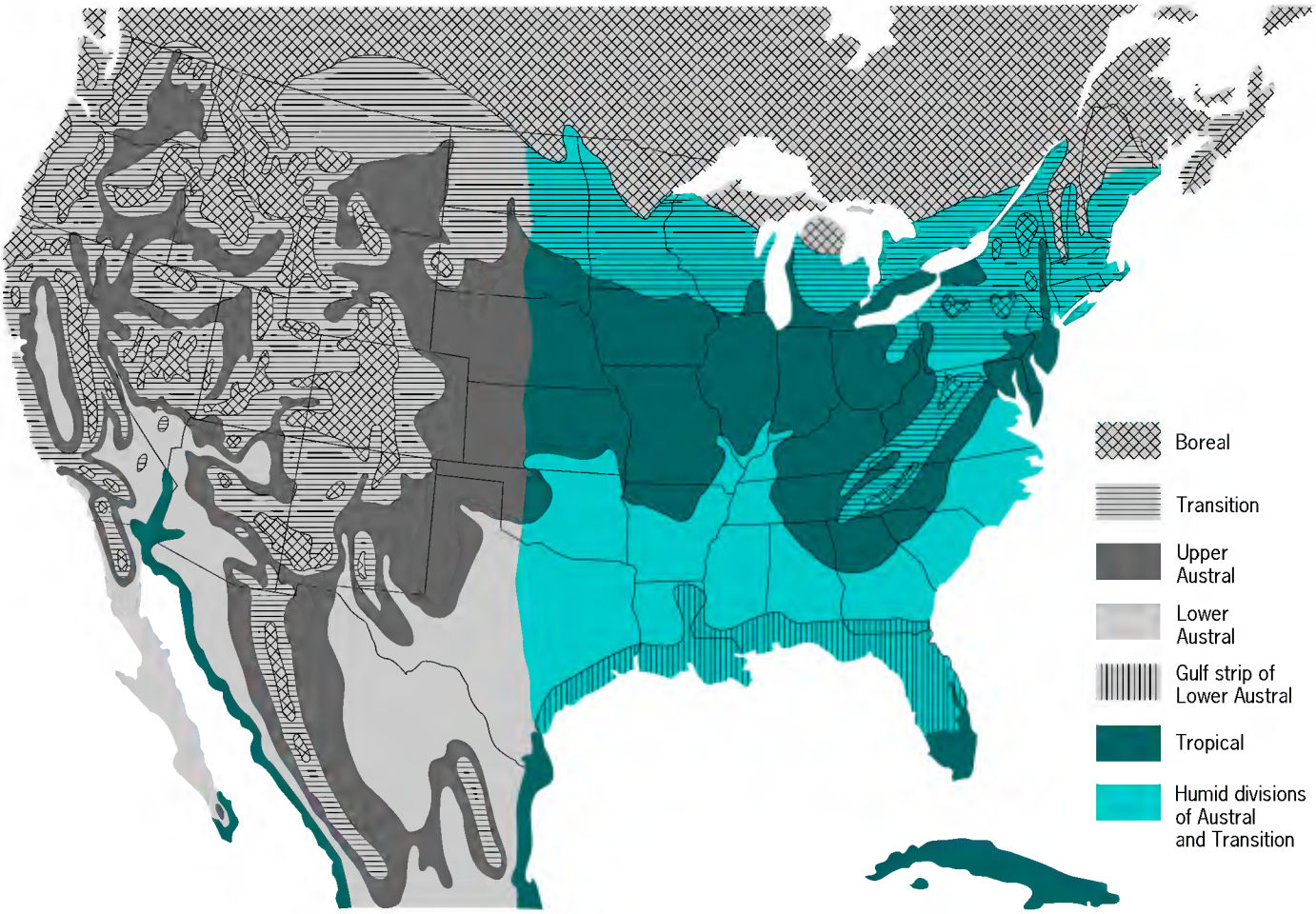

Fig. 1. Life zones of the United States. (*After C. H. Merriam, Life Zones and Crop Zones of the United States, USDA Bull. 10, 1898*)

Fig. 2. Biotic provinces of North America (Veracruzian not shown). 1 mi = 0.6 km. (*After L. R. Dice, The Biotic Provinces of North America, University of Michigan Press, 1943*)

(Eskimoan and Hudsonian) are transcontinental, reflecting broad, high-latitude climatic belts. Those in the eastern United States (Canadian, Carolinian, and Austroriparian) reflect both latitudinal temperature change and physiography, whereas province boundaries in the remainder of North America are strongly influenced by physiography.

Holdridge's zones. A life-zone system with boundaries more explicitly defined is that of L. R. Holdridge. These life zones are defined through the effects of the three weighted climatic indexes: mean annual heat, precipitation, and atmospheric moisture. Each axis of the triangle (**Fig. 3**) represents one climatic component, and the three sets of lines parallel to the axes define the life-zone framework. Climatic values which the lines represent progress geometrically. Mean annual biotemperature is computed by summing the monthly mean temperatures from 32°F or 0°C (setting negative winter months equal to 32°F or 0°C when they occur) to about 86°F or 30°C and dividing by 12. Values increase from top to bottom in Fig. 3 and, by extension to either margin, establish equivalent latitudinal regions and altitudinal belts. Precipitation is computed as mean annual precipitation in millimeters and increases from the apex toward the lower right margin of the diagram. The

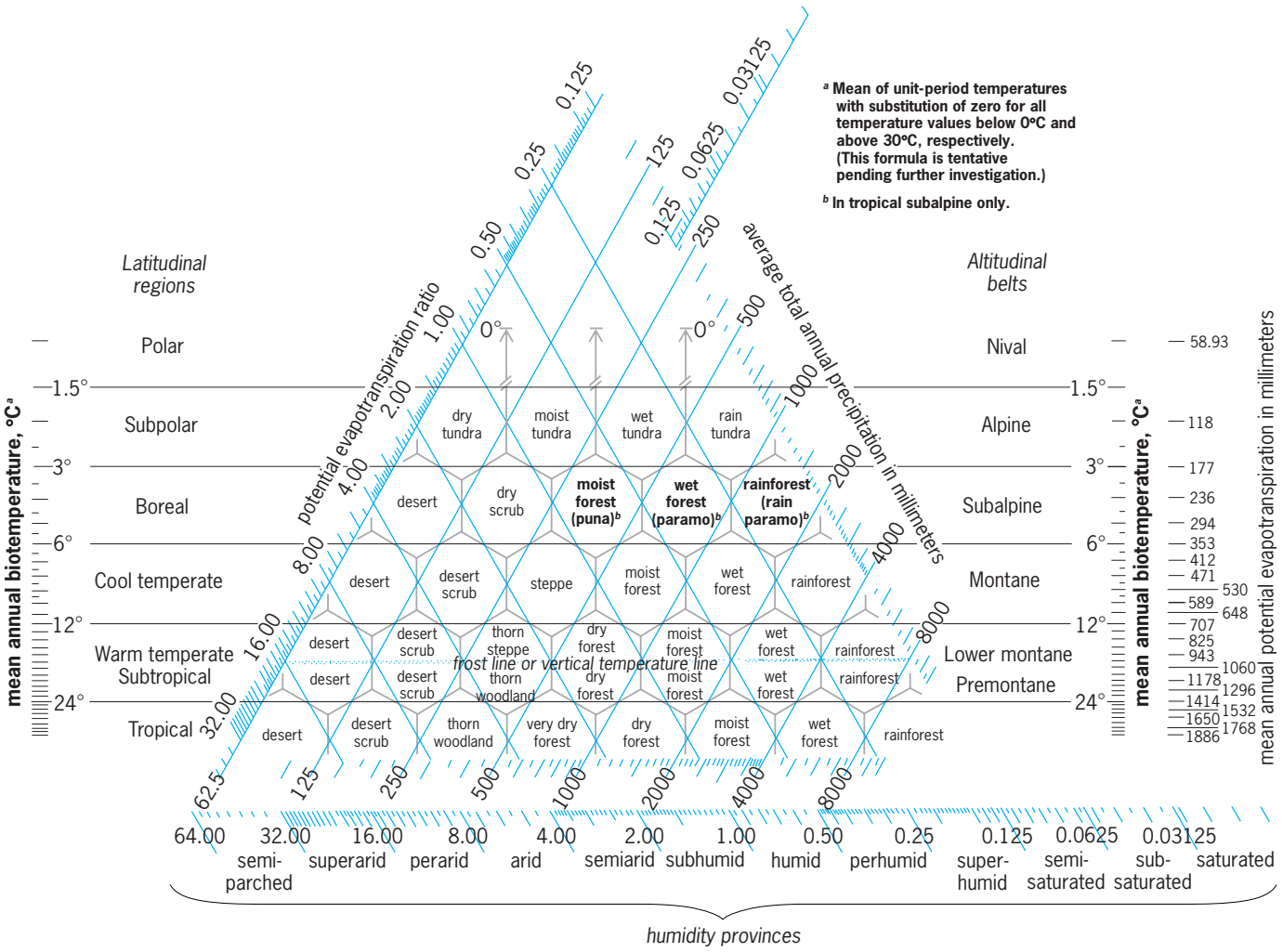

Fig. 3. World life zones. °F = (°C × 1.8) + 32. (*After L. R. Holdridge, Life Zone Ecology, rev. ed., Tropical Science Center, 1967*)

humidity factor is calculated by dividing the value of the mean annual potential evapotranspiration by the mean annual precipitation in millimeters. Values of this ratio increase toward the lower left side of the diagram, signifying a decrease in effective humidity.

Associations of vegetation, animals, climate, physiography, geology, and soils are interrelated in unique combinations, mostly having distinct physiognomy, in Holdridge's climatic grid. Local investigation should show how well the framework represents the most common life zones of Earth, both north and south of the Equator. The system has been applied with considerable success to the mapping of life zones, primarily in the American tropics. Names of Holdridge's life zones are based on the dominant vegetation of each climatic type; animal life of the zone is supposedly distinctive. *See* ALTITUDINAL VEGETATION ZONES; BIOME; ZOOGEOGRAPHY.

Arthur W. Cooper

Bibliography. W. H. Lewis, *Ecology Field Glossary: A Naturalist's Vocabulary*, 1977; C. H. Merriam, *Life Zones and Crop Zones of the United States*, USDA Bull. 10, 1898; H. Walter, *Vegetation of the Earth and Ecological System of the Geobiosphere*, 3d rev. ed., 1994; J. E. Weaver and F. E. Clements, *Plant Ecology*, 2d ed., 1938.

Ligament

A strong, flexible connective tissue band usually found between two bony prominences. Most ligaments are composed of dense fibrous tissue formed by parallel bundles of collagen fibers. They have a shining white appearance and are pliable, strong, and noncompliant. These ligaments are closely associated with all articulations and are largely responsible for the exact movement of the bones. Other ligaments may span larger gaps between bones and may serve as important controlling elements in complex bone-linkage systems.

A second kind of ligament, composed either partly or almost entirely of yellow elastic fibers, is extensible or compliant, thereby allowing the connected bones to move apart. The large ligamenta nuchae between the neural spines of cervical vertebrae and the skull in large ungulates are of this type, and permit lowering and raising the head with less muscular effort. *See* BIOMECHANICS; COLLAGEN; CONNECTIVE TISSUE; JOINT (ANATOMY).

Walter Bock

Ligand

A molecule with an affinity to bind to a second atom or molecule. This affinity can be described in terms of noncovalent interactions, such as the type of binding that occurs in enzymes that are specific for certain substrates; or of a mode of binding where an atom or groups of atoms are covalently bound to a central atom, as in the case of coordination complexes and organometallic compounds. Ligands of the latter type can be further distinguished by the nature of the orbitals used in bond formation. *See* ENZYME.

When a protein binds to another molecule, that molecule may be referred to as a ligand. The site where the ligand is bound is known as the binding or active site of the protein. In order for a molecule to be classified as a ligand for a protein, several weak interactions such as hydrophobic, van der Waals, and hydrogen bonds must take place simultaneously. Therefore, the binding of a ligand by a protein is generally quite specific. For example, the active site of copper-zinc superoxide dismutase (CuZnSOD) has been engineered so that only very small ligands such as superoxide, water, and other small anions are accepted.

Coordination complexes and organometallic compounds have ligands that are a class of ions or neutral molecules that donate an electron pair to a metal atom or ion. Molecules or ions that function as ligands behave as Lewis bases, while a central metal acts as a Lewis acid. The entire molecule, which includes the metal or metal atoms and the attached ligands, is generally known as a coordination complex. An example of a coordination complex having six ligands is hexaammineruthenium (III) (**Fig. 1**). The single pair

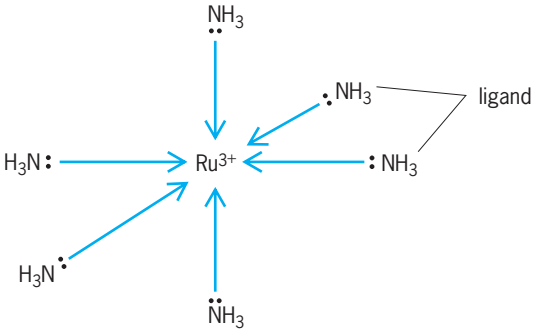

Fig. 1. The complex hexaammineruthenium(III); the six ammine groups (:NH_3) are the ligands.

of electrons present on the ammine (or ammonia) group is donated to a vacant orbital of the ruthenium tripositive ion (Ru^{3+} or Ru^{III}). *See* ACID AND BASE; COORDINATION COMPLEXES; ORGANOMETALLIC COMPOUND.

Mono-, bi-, and multidentate ligands. A monodentate ligand possesses one "tooth" or one pair of electrons available for binding to a metal center. In other words, there is only one site on the ligand where coordination to a metal may occur. Examples of monodentate ligands include the halides, [fluoride (F^-), chloride (Cl^-), bromide (Br^-), and iodide (I^-)] and neutral molecules such as water H_2O and ammonia

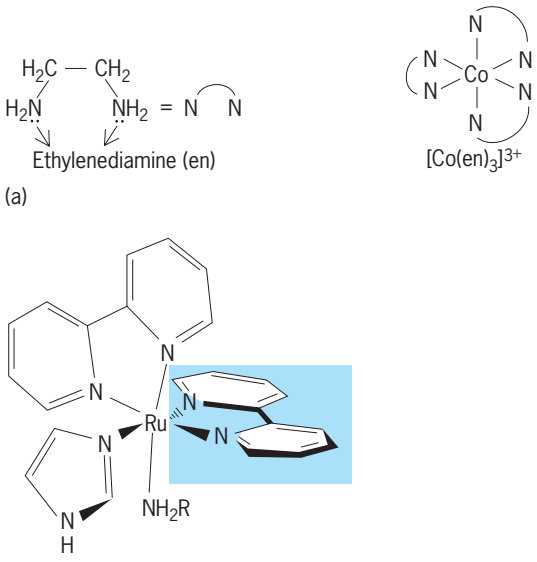

Fig. 2. Bidentate ligands. (*a*) Ethylenediamine (en) and the cobalt coordination complex $[Co(en)_3]^{3+}$ with three en ligands. (*b*) The bidentate aromatic imine 2,2′-bipyridine (bpy) ligand (highlighted) in the complex $Ru(bpy)_2imNH_2R$.

NH_3. Each of these ligands donates a single pair of electrons to the central metal atom.

Bidentate ligands possess two atoms (each with at least one pair of electrons), termed donor atoms, that may coordinate to a metal atom or ion. A well-known example of a bidentate ligand is ethylenediamine (en), and an example of a complex with three en ligands is $[Co(en)_3]^{3+}$ (**Fig. 2***a*). Another example of a bidentate ligand is 2,2′-bipyridine (bpy), an aromatic imine. The single pair of electrons on each of the bipyridine nitrogen (N) atoms is capable of donating to the metal center, as in the coordination complex with two bidentate bpy ligands, the ruthenium complex $Ru(bpy)_2imNH_2R$ (Fig. 2*b*), where R represents an organic group and im = imidazole.

Multidentate ligands possess three or more donor atoms; they are called chelating agents or chelating ligands. An example is diethylenetriamine (**1**) which has three nitrogen donor atoms. Triethylenetetramine derivatives are multidentate ligands that form a species known as tripod complexes (**2**). Ethylenediamine-tetraacetic acid (EDTA, **3**),

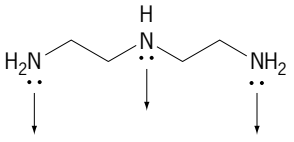

(1)

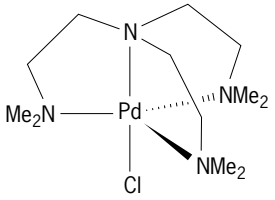

(2)

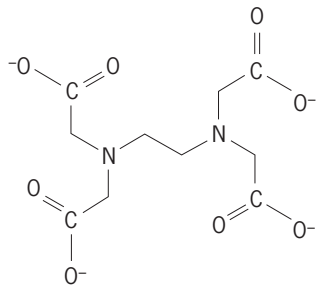

(3)

which has two nitrogen and four oxygen donor atoms, is another example of a multidentate ligand. Chelating ligands like EDTA (six donor atoms per molecule) and diethylenetriamine-pentaacetic acid (DTPA; eight donor atoms per molecule) bind metal ions very tightly because the formation constants of these complexes are very large. Therefore, multidentate ligands are commonly used as scavengers for metal atoms and ions. A Schiff base complex possesses monodentate and multidentate ligands such as the complex in structure (**4**), where the metal is

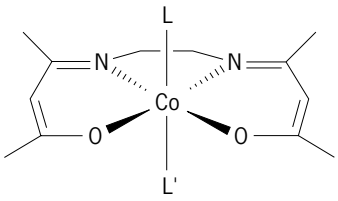

(4)

cobalt (Co); the complex has two nitrogen and two oxygen donor atoms and two monodentate ligands, L and L′. *See* CHELATION.

Bridging ligands. A ligand that is bound to more than one metal center is known as a bridging ligand. These ligands may form two, and in some instances three, bonds to different metal atoms. An example of a unidentate bridging ligand is structure (**5**). Bidentate ligands such as the acetate ion (CH_3COO) may behave as both a chelating ligand, where both donor atoms are bound to the same metal, and a bidentate bridging ligand, where binding takes place at more than one metal center as in structure (**6**), where

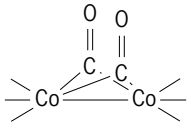

(5)

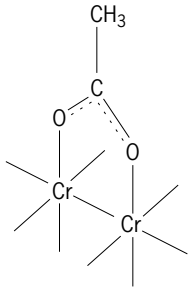

(6)

Cr = chromium and the broken-line bonds indicate that the structure is a resonance hybrid, a configuration in which an electron is delocalized between each carbon-oxygen bond. *See* DELOCALIZATION.

Backbonding ligands. Some ligands can form two or more bonds with a metal atom. These ligands have the capacity to serve as donors and acceptors of electron density that compose the ligand-metal bond. A sigma (σ) bond is formed by donation of a single pair of electrons from the ligand to the metal (M), as in structure (**7**), where the backbonding ligand is carbon monoxide (CO). The metal atom, in an effort to reduce the electron density, behaves as a π donor by transferring electrons back to the ligand to form a π bond. The backbonding ligand in this case acts as a π acid; that is, it is able to accept electron density into an empty π orbital. As a result of this type of interaction, complexes are produced with metals that have low oxidation states.

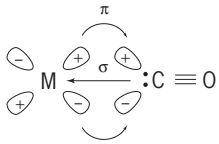

(7)

The backbonding ligand carbon monoxide (CO) forms complexes known as metal carbonyls. Finally, a prototypic example of metal binding to a π-donor ligand is the complex ferrocene (**8**), with a metal

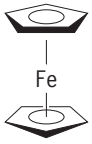

(8)

[in this case iron (Fe)], binding to a π-donor cyclopentadienyl ligand. Each of the cyclopentadienyl rings in this complex donate six electrons to the iron atom. *See* CHEMICAL BONDING; COORDINATION CHEMISTRY; METAL CARBONYL.

Thomas J. Meade

Ligand field theory

An essentially ionic approach to chemical bonding which is often used with coordination compounds. These compounds consist of a central transition-metal ion that is surrounded by a regular array of coordinated atoms or ligands. Accordingly, the ligands are assumed to be sources of negative charge which perturb the energy levels of the central metal ion. In this respect the ligands subject the metal ion to an electric field which is analogous to the electric or crystal field produced by the regular distribution of nearest neighbors within an ionic crystalline lattice. For example, the crystal field produced by the Cl ion ligand in octahedral $TiCl_6^{3-}$ is considered to be similar to that produced by the octahedral array of the six Cl ions about each Na ion in NaCl. The Na ion with its rare-gas configuration has an electronic charge distribution which is spherically symmetric

both within and without the crystal field. The paramagnetic Ti(III) ion, which possesses one 3*d* electron (d^1), has a spherically symmetric charge distribution only in the absence of the crystal field produced by the ligands. The presence of the ligands destroys the spherical symmetry and produces a more complex set of energy levels within the central metal ion. The crystal field theory allows the energy levels to be calculated and related to experimental observation. *See* COORDINATION CHEMISTRY.

To illustrate the results of a typical crystal field calculation, assume that the single *d* electron in the Ti(III) ion will experience a coulombic repulsion with each of the six nearest neighbor Cl ions which are taken as point negative charges. This model for coulombic repulsion may be described mathematically as the summation $eq\Sigma r^{-1}$, where *e* and *q* are the electronic and ligand charges, respectively, and *r* is the distance between the electron and the ligand. The summation extends over all the ligands. A detailed quantum mechanical calculation can then be made. Fortunately, it is possible to arrive at identical results by a very qualitative procedure. This method considers the spatial orientation of *d* orbitals with relation to the ligands when both are viewed within the same coordinate system (**Fig. 1**).

The d_{z^2} orbital is oriented along the *z* axis with a ring in the *xy* plane, while the $d_{x^2-y^2}$ orbital is oriented only along the *x* and *y* axes. Although it is not visually obvious, both are equivalent. The d_{xy}, d_{xz}, and d_{yz} orbitals are oriented between the *x*, *y*, and *z* axes and are geometrically equivalent. The ligands are placed along the coordinate *x*, *y*, and *z* axes. An electron in any of the five orbitals will experience a coulombic repulsion due to the crystal field of the ligands. However, since the d_{z^2} and $d_{x^2-y^2}$ orbitals are directed toward the ligands, an electron in these orbitals will undergo far more repulsion than one in any of the three other orbitals. The imposition of six point negative charges, then, will not allow the five *d* orbitals to be equally energetic (degenerate) as they are in the bare Ti(III) ion, but causes three of these orbitals to be more stable than the remaining two. The difference in energy is termed 10*Dq*. Thus, in the ground state of $TiCl_6^{3-}$, the single *d* electron will be found in the lower set of orbitals, whose energy is $-4Dq$. The crystal field stabilization energy (CFSE) is then said to be $4Dq$ (**Fig. 2**).

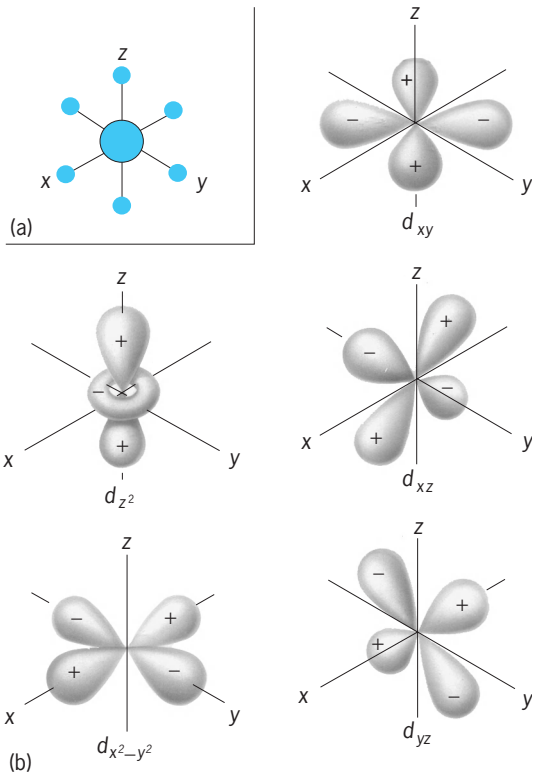

Fig. 1. Spatial orientation of *d* orbitals with relation to ligands in $TiCl_6^{3-}$. (*a*) The coordinate system for the octahedral $TiCl_6^{3-}$ ion. (*b*) The five *d* orbitals. The d_{z^2} orbital is symmetric with respect to the *z* axis.

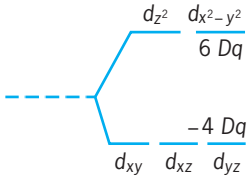

Fig. 2. The splitting of the five *d* orbitals because of an octahedral crystal field.

Coordination compounds are often colored. Crystal field theory suggests that in the case of $TiCl_6^{3-}$ its color is a result of an electronic excitation of the electron from the threefold set of orbitals into the twofold set. In the spectrum of $TiCl_6^{3-}$, an absorption band maximum is found at 13,000 cm^{-1}, which is then the energy associated with the transition, or 10*Dq*. *See* MOLECULAR STRUCTURE AND SPECTRA.

Several electrons. When more than one *d* electron is present, the spectroscopic evaluation of *Dq* is not as simple, but can generally be accomplished. Nevertheless, the CFSE may be easily and formally obtained for these cases, (see **table**), since this energy is simply the number of electrons occupying the orbital multiplied by the orbital energy. Thus, the CFSE amounts to 8*Dq* in an octahedral d^2 complex, and $(6 \times 4) - (2 \times 6) = 12Dq$ in a similar d^8 complex. With d^4, d^5, d^6, and d^7, however, two possibilities exist. If the crystal field is sufficiently strong to overcome the repulsion energy which will result from pairing the electrons in the lower set of orbitals, the

Crystal field stabilization energy

	Octahedral CFSE (*Dq*)	
d^n	Weak	Strong
1	4	4
2	8	8
3	12	12
4	6	16
5	0	20
6	4	24
7	8	18
8	12	12
9	6	6

maximum number of electrons will be found in the lower set. This situation is termed the strong-field case. In the weak-field case, the electron-pairing (repulsive) energy is greater than the crystal field (attractive) energy and the maximum number of unpaired electrons will result. Thus, in a strong crystal field a d^5 ion should have only one unpaired electron and a CFSE of $20Dq$. This is found in the $Mn(CN)_6^{4-}$ ion, which has been shown experimentally to possess only one unpaired electron. In most complexes of Mn(II), such as $Mn(H_2O)_6^{2+}$, the crystal field is weak so that five unpaired electrons result and the CFSE is zero.

Simple considerations such as these have enabled inorganic chemists to understand why certain coordination compounds containing a given metal ion may exhibit full paramagnetism, while others containing the metal in exactly the same formal oxidation state may show either a much weaker paramagnetism or none at all. A striking example of this is provided by paramagnetic CoF_6^{3-}, which possesses six unpaired d electrons and the diamagnetic $Co(NH_3)_6^{3+}$, in which none of the d electrons are unpaired. Both contain Co(III).

Tetrahedral array. Tetrahedral complexes may be treated in a similar fashion. The results indicate that the only difference, when compared to the octahedral complex, is in the orbital splitting pattern and the relative magnitude of Dq. The tetrahedral array of ligands causes an inversion of the pattern such that the d_{z^2} and $d_{x^2-y^2}$ orbitals lie lowest. The difference in energy between the two sets of orbitals is now found to be $^4/_9$ of that in an octahedral complex, or Dq (tetrahedral) = ($^4/_9$)Dq (octahedral). This particularly simple result has led to the understanding of many stereochemical phenomena. An important early example was found in the cation distribution of normal and inverse spinels. The former are double oxides having the general formula $M(II)[M'(III)]_2O_4$ in which the oxygens lie in a close-packed system. The divalent metal ions, M(II), occupy one-eighth of the tetrahedral holes. In the inverse spinel $M'(III)[M(II)M'(III)]O_4$ the divalent metal ions have changed places with one-half of the trivalent ions.

Experimentally, it has been found that $MnCr_2O_4$ [containing Mn(II) with five unpaired electrons] and $NiFe_2O_4$ [containing Fe(III) with five unpaired electrons] have the normal and inverse structures, respectively. A simple application of crystal field theory results in exact agreement with experiment. In $MnCr_2O_4$ the ion at each octahedral site has a stability of $12Dq$, while the tetrahedral site has no CFSE. The total CFSE is then $24Dq$. If the structure were inverse, the total CFSE would be only $^4/_9 \times 12 + 12 = 17.3Dq$. With $NiFe_2O_4$ the CFSE of the normal spinel is only $5.3Dq$, but in the inverse structure the CFSE increases to $12Dq$. In general, agreement between predicted cation distribution and that experimentally observed is good.

The application of these methods to conventional coordination compounds also meets with a fair amount of success. For example, with only one or two exceptions octahedral coordination of Cr(III) and diamagnetic Co(III) prevails in all compounds, as one would predict from crystal field theory. Important exceptions to these rules do exist and point out that other factors, such as ligand-ligand repulsions, sometimes outweigh the CFSE. Octahedral coordination of Ni(II) is favored over the tetrahedral arrangement insofar as CFSE is concerned, yet the tetrahedral $NiCl_4^{2-}$, $NiBr_4^{2-}$, and NiI_4^{2-} ions are well known.

Anomalous effects. Heats of hydration, lattice energies, crystal radii, and oxidation potentials of transition-metal ions and their complexes contain apparent anomalies which are best explained in terms of an effect due to the crystal field. As an example, when the heats of hydration of the ions of the first transition series are plotted with respect to atomic number, a peculiar double-humped curve is obtained (**Fig. 3**). The results for those ions not possessing any CFSE, that is, Ca, Mn, and Zn, lie nearly on a straight line. In the absence of any other effect, it might be expected that with the successive addition of each nuclear charge, a monotonic increase in the heat of hydration would occur. Instead, it was found that the heat of hydration of those metal ions possessing CFSE is far more exothermic than would be predicted by arguments pertaining only to the successive increase in atomic number. In fact, the excess heat is best accounted for in terms of the CFSE. The total heat of hydration may be written as $\Delta H = \Delta H^\circ + \text{CFSE}$, where ΔH° is the heat of hydration that would be expected for a hypothetical metal ion which ignored the crystal field. The change in ΔH° with atomic number would then be expected to be monotonic. When the observed heats of hydration are corrected for the CFSE obtained from spectroscopic data for the resulting $M(H_2O)_6^{2+}$ complexes, the expected monotonic

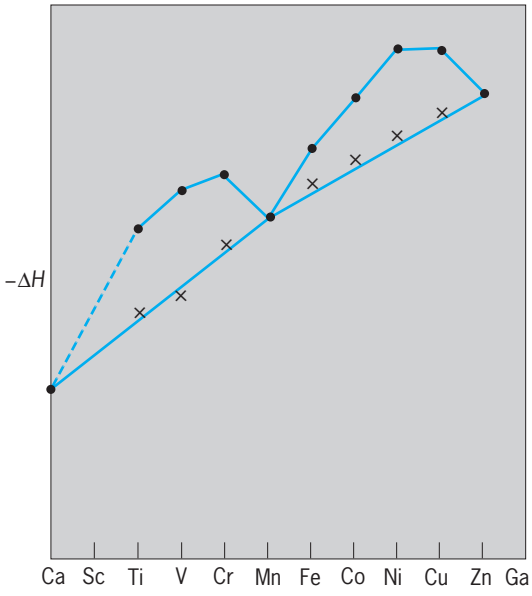

Fig. 3. Variation of heat of hydration $-\Delta H$ of divalent ions of first transition series. Experimental values are given by the dots, and the corresponding values, after correction for CFSE, are given by the x's.

increase is observed. Similar double-humped curves occur with the lattice energies and crystal radii and can be explained by including the effects due to the crystal field.

Stereochemical anomalies can also often be explained through the judicious use of simple arguments. A particularly important example is found in complexes of Cu(II). X-ray crystallography has established that most "octahedral" complexes containing that ion are in fact elongated along one axis. According to a theorem due to H. A. Jahn and E. Teller, this behavior is not unexpected. The theorem states that a system possessing a degenerate ground state will distort in some unspecified manner to remove the degeneracy.

The degeneracy in a regular octahedral complex of Cu(II) is easily illustrated by the possibility of writing the electronic configuration in two distinct, but equally energetic, ways: $(d_{xy})^2(d_{xy})^2(d_{yz})^2(d_{z^2})^2 \times (d_{x^2-y^2})^1$ or $(d_{xy})^2(d_{xz})^2(d_{yz})^2(d_{x^2-y^2})^2(d_{z^2})^1$. For each, the CFSE is $6Dq$. In addition to the twofold degeneracy, there are two separate means by which the degeneracy may be removed. If the ligands along the z axis of the octahedron move away from the metal ion while those in the xy plane move toward the center of the octahedron, then according to simple crystal field arguments, this movement will result in stabilizing the d_{z^2} orbital with respect to the $d_{x^2-y^2}$ orbital. Alternatively, the completely opposite movement will stabilize the $d_{x^2-y^2}$ orbital with respect to the d_{z^2} orbital (**Fig. 4**). In either case, an additional increment of energy is added to the CFSE of the Cu(II) complex: $6Dq + \Delta E$. Thus, the driving force for the distortion is the additional stabilization energy ΔE. Crystal field theory is unable to predict which mode of distortion will occur, but it clearly predicts that a distortion should occur. From structure determinations through the use of x-rays, it is found that elongation along one axis is by far the most predominant mode.

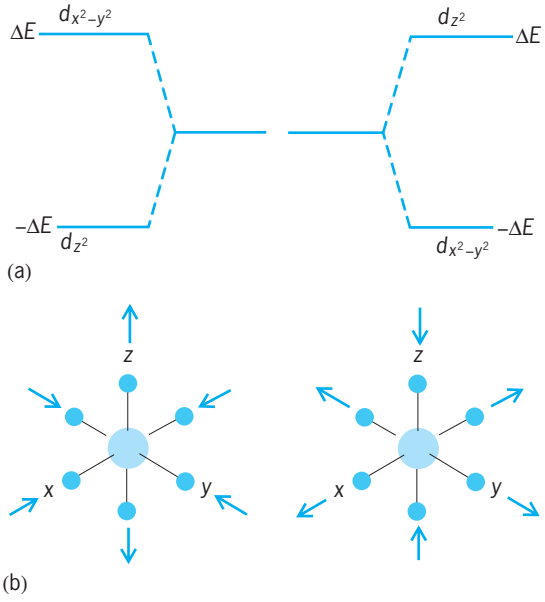

Fig. 4. The splitting of the $d_{x^2-y^2}$ and d_{z^2} orbitals by an axial distortion of the octahedron. (*a*) Alternate possiblities for writing the electronic configuration. (*b*) The two modes of distortion.

Complete theory. The many successes of crystal field theory in the interpretation of the natural phenomena associated with transition-metal compounds should not lead one to the conclusion that the bonding within these compounds can be truthfully represented by a strictly ionic model. Crystal field theory is essentially a very specialized form of the more complete molecular orbital theory. The need for the more complete theory becomes obvious when an attempt is made to rationalize the absolute value of Dq, the observation of ligand-to-metal electronic transitions, and certain observations in both nuclear magnetic resonance and electron spin resonance experiments, which can only be interpreted in terms of some covalent bonding. *See* MOLECULAR ORBITAL THEORY.

R. A. D. Wentworth

Bibliography. R. L. DeKock and H. B. Gray, *Chemical Structure and Bonding*, 2d ed., 1980, reprint 1989; M. Gerloch, *Orbitals, Terms, and States*, 1986; Y. Jean and F. Volatron, *Introduction to Molecular Orbitals*, 1993; A. Rauk, *Orbital Interaction Theory of Organic Chemistry*, 2d ed., 2000.

Light

The term light, as commonly used, refers to the kind of radiant electromagnetic energy that is associated with vision. In a broader sense, light includes the entire range of radiation known as the electromagnetic spectrum. The branch of science dealing with light, its origin and propagation, its effects, and other phenomena associated with it is called optics. Spectroscopy is the branch of optics that pertains to the production and investigation of spectra. *See* OPTICS; SPECTROSCOPY.

Any acceptable theory of the nature of light must stem from observations regarding its behavior under various circumstances. Therefore, this article begins with a brief account of the principal facts known about visible light, including the relation of visible light to the electromagnetic spectrum as a whole, and then describes the apparent dual nature of light. The remainder of the article discusses various experimental and theoretical considerations pertinent to the study of this problem.

Principal Effects

The electromagnetic spectrum is a broad band of radiant energy that extends over a range of wavelengths running from trillionths of inches to hundreds of miles; wavelengths of visible light are measured in hundreds of thousandths of an inch. Arranged in order of increasing wavelength, the radiation making up the electromagnetic spectrum is termed gamma rays, x-rays, ultraviolet rays, visible light, infrared waves, microwaves, radio waves, and very long electromagnetic waves. *See* ELECTROMAGNETIC RADIATION.

Speed of light. The fact that light travels at a finite speed or velocity is well established. In round numbers, the speed of light in vacuum or air may be said to be 186,000 mi/s or 300,000 km/s.

Measurements of the speed of light, c, which had attracted physicists for 308 years, came to an end in 1983 when the new definition of the meter fixed the value of the speed of light. The speed of light is one of the most interesting and important of the fundamental physical constants. It is used to convert light travel times to distance, as in laser and radio measurements of the distance to the Moon and planets. It relates mass m to energy E in Einstein's equation, $E = mc^2$. To fix the value of c in the new definition, highly precise values of c were obtained by extending absolute frequency measurements into a region of the electromagnetic spectrum where wavelengths can be most accurately measured. These advances were facilitated by the use of stabilized lasers and high-speed tungsten-nickel diodes which were used to measure the lasers' frequencies. The measurements of the speed of light and of the frequency of lasers yielded a value of the speed of light limited only by the standard of length which was then in use. This permitted a redefinition of the meter in which the value of the speed of light assumed an exact value, 299,792,458 m/s. The meter is defined as the length of the path traveled by light in vacuum during a time interval of 1/299 792 458 of a second. *See* ASTRONOMICAL UNIT; FUNDAMENTAL CONSTANTS; LASER.

Prior to the observations of O. Roemer in 1675, the speed of light was thought to be infinite. Roemer noted a variation of the orbiting periods of the moons of Jupiter that depended on the annual variation in the distance between Earth and Jupiter. He correctly ascribed the variation to the time it takes light to travel the varying distance between the two planets. The accuracy of Roemer's value of c was limited by a 30% error in the knowledge of the size of the planetary orbits at that time.

The first terrestrial measurement of c was performed by H. L. Fizeau in 1849. His measurement of the time it took light to travel to a distant mirror and return resulted in a value accurate to 15%.

J. C. Maxwell's theory of electromagnetic radiation showed that both light and radio waves were electromagnetic and hence traveled at the same speed in vacuum. This discovery soon led to another method of measuring c: it was the product of the frequency and wavelength of an electromagnetic wave. In 1891 R. Blondlot first used this method to determine a value of c by measuring both the wavelength and the frequency of an electromagnetic, radio-frequency wave. His measurement demonstrated that c was the same for radio and light waves. It is this method which now exhibits the greatest accuracy, and it is used in the most accurate measurements of c using a laser's frequency and wavelength.

In 1958 K. D. Froome reported the speed of light c to be 299,792,500 m/s, with an uncertainty of plus or minus 100 m/s. He measured both the frequency and the wavelength of millimeter waves from klystron oscillators to obtain this result. The major uncertainty lay in measuring the wavelength of the radiation. Since short wavelengths can be measured much more accurately than long wavelengths, a shorter-wavelength source was needed to improve the accuracy further; the stabilized laser soon provided such a source. However, a means of measuring its incredibly high frequency was needed. This problem, too, was soon overcome with the discovery of the tungsten-nickel point-contact diode.

Stabilized lasers. Before the advent of the laser, the most spectrally pure light came from the emission of radiation by atoms in electric discharges. The spectral purity of such radiation was about 1 part per million. Lasers, in contrast, have exhibited short-period spectral purities some 10^8 times greater than this. However, the frequency of this laser radiation was free to wander over the entire emission line, and a means of stabilizing and measuring the frequency was necessary before it could be used in a measurement of c. The technique of sub-Doppler saturated absorption spectroscopy permitted the "locking" of the frequency of the radiation to very narrow spectral features so that the frequency (and, of course, the wavelength) remained fixed. Several different lasers at different wavelengths have been stabilized, and they serve as precise frequency and wavelength sources. Three of the most common are: the helium-neon laser at a wavelength of 3.39 micrometers stabilized with a saturated absorption in methane, the 10-μm carbon dioxide (CO_2) laser stabilized to a saturated fluorescence in carbon dioxide, and the common red helium-neon laser stabilized to an iodine-saturated absorption. The frequencies and wavelengths of these three lasers have been measured to yield values of c. *See* LASER SPECTROSCOPY.

Measurement of wavelength. Precise measurements of wavelengths are commonly made in Fabry-Perot interferometers, in which two wavelengths are compared by the observation of interference fringes of waves reflecting between two mirrors. A bright fringe occurs when the optical path length between the high-reflectivity mirrors is a multiple of a half-wavelength.

With the use of special Fabry-Perot interferometers, wavelength measurements of stabilized lasers were made with accuracies limited by the length standard then in use, the 605.8-nanometer orange radiation from the krypton atom. This limitation affected all speed-of-light measurements, with a resulting uncertainty of about 4 parts in 10^9. *See* INTERFEROMETRY.

Frequency measurement. The measurement of the frequency of an electromagnetic wave in the laser region is performed by a heterodyne technique in which harmonics are generated in high-speed nonlinear devices. For the most accurate measurements of c, the accuracy of the frequency measurements were 10 times more accurate than the wavelength measurements; hence, the uncertainties were dominated by the wavelength measurements. *See* FREQUENCY MEASUREMENT.

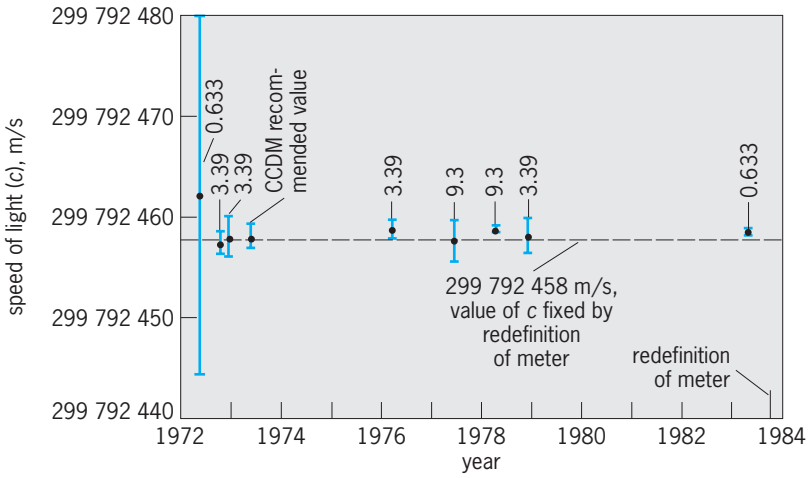

Fig. 1. Laser speed-of-light measurement made from 1972 to 1984. Separate frequency and wavelength measurements were combined to obtain the 1976, 1977, and 1983 measurements. Numbers accompanying data bars indicate the wavelengths in micrometers at which the measurements were carried out.

Results. The values of c obtained from the frequency and wavelength measurements of various lasers are shown in **Fig. 1**. Because of the stability and reproducibility of the stabilized lasers, separate frequency and wavelength measurements were sometimes combined to give independent values of c. The first 1972 measurement did not involve an absolute counting of the laser frequency and was somewhat less accurate. For the first time in history, the various values of the speed of light were in agreement. Prior to 1958, the measured values of c often varied outside the limits of error quoted by the experimenters, and even prompted some observers to think that c might be changing with time. The 1974 meeting of the Consultative Committee for the Definition of the Meter (CCDM) recommended that 299,792,458 m/s be the value of c to be used for converting wavelength to frequency and vice versa, and in all other precise applications involving c. This number was arrived at by the consideration of the first four values of c in Fig. 1. The subsequent measurements of c have shown that this was a good choice, and it is the value used in the redefinition of the meter. The 1983 measurement is the only entry for visible light, and is in excellent agreement with the others. In 1983 the General Conference on Weights and Measures (CCPM) used exactly 299,792,458 m/s in the redefinition of the meter. With this new definition, fixing the value of the speed of light, the era of speed-of-light measurements was at an end. *See* LENGTH.

Kenneth M. Evenson

Diffraction and reflection. One of the most easily observed facts about light is its tendency to travel in straight lines. Careful observation shows, however, that a light ray spreads slightly when passing the edges of an obstacle. This phenomenon is called diffraction. The reflection of light is also well known. The Moon, as well as all other satellites and planets in the solar system, are visible only by reflected light; they are not self-luminous like the Sun. Reflection of light from smooth optical surfaces occurs so that the angle of reflection equals the angle of incidence, a fact that is most readily observed with a plane mirror. When light is reflected irregularly and diffusely, the phenomenon is termed scattering. The scattering of light by gas particles in the atmosphere causes the blue color of the sky. When a change in frequency (or wavelength) of the light occurs during scattering, the scattering is referred to as the Raman effect. *See* DIFFRACTION; RAMAN EFFECT; REFLECTION OF ELECTROMAGNETIC RADIATION; SCATTERING OF ELECTROMAGNETIC RADIATION.

Refraction. The type of bending of light rays called refraction is caused by the fact that light travels at different speeds in different media—faster, for example, in air than in either glass or water. Refraction occurs when light passes from one medium to another in which it moves at a different speed. Familiar examples include the change in direction of light rays in going through a prism, and the bent appearance of a stick partially immersed in water. *See* REFRACTION OF WAVES.

Interference and polarization. In the phenomenon called interference, rays of light emerging from two parallel slits combine on a screen to produce alternating light and dark bands. This effect can be obtained quite easily in the laboratory, and is observed in the colors produced by a thin film of oil on the surface of a pool of water. *See* INTERFERENCE OF WAVES.

Polarization of light is usually shown with Polaroid disks. Such disks are quite transparent individually. When two of them are placed together, however, the degree of transparency of the combination depends upon the relative orientation of the disks. It can be varied from ready transmission of light to almost total opacity, simply by rotating one disk with respect to the other. *See* POLARIZED LIGHT.

Chemical effects. When light is absorbed by certain substances, chemical changes take place. This fact forms the basis for the science of photochemistry. Rapid progress has been made toward an understanding of photosynthesis, the process by which plants produce relatively complex substances such as sugars in the presence of sunlight. This is but one example of the all-important response of plant and animal life to light. *See* PHOTOCHEMISTRY; PHOTOSYNTHESIS.

Historical Approach

Early in the eighteenth century, light was generally believed to consist of tiny particles. Of the phenomena mentioned above, reflection, refraction, and the sharp shadows caused by the straight path of light were well known, and the characteristic of finite velocity was suspected. All of these phenomena except refraction clearly could be expected of streams of particles, and Isaac Newton showed that refraction would occur if the velocity of light increased with the density of the medium through which it traveled.

This theory of the nature of light seemed to be completely upset, however, in the first half of the nineteenth century. During that time, Thomas Young

studied the phenomena of interference, and could see no way to account for them unless light were a wave motion. Diffraction and polarization had also been investigated by that time. Both were easily understandable on the basis of a wave theory of light, and diffraction eliminated the "sharp-shadow" argument for particles. Reflection and finite velocity were consistent with either picture. The final blow to the particle theory seemed to have been struck in 1849, when the speed of light was measured in different media and found to vary in just the opposite manner to that assumed by Newton. Therefore, in 1850, it seemed finally to be settled that light consisted of waves.

Even then, however, there was the problem of the medium in which light waves traveled. All other kinds of waves required a physical medium, but light traveled through a vacuum—faster, in fact, than through air or water. The term ether was proposed by James Clerk Maxwell and his contemporaries as a name for the unknown medium, but this scarcely solved the problem because no ether was ever actually found. Then, near the beginning of the twentieth century, came certain work on the emission and absorption of energy that seemed to be understandable only if light were assumed to have a particle or corpuscular nature. The external photoelectric effect, the emission of electrons from the surfaces of solids when light is incident on the surfaces, was one of these. At that time, then, science found itself in the uncomfortable position of knowing a considerable number of experimental facts about light, of which some were understandable regardless of whether light consisted of waves or particles, others appeared to make sense only if light were wavelike, and still others seemed to require it to have a particle nature. *See* ETHER HYPOTHESIS.

Theory

The study of light deals with some of the most fundamental properties of the physical world and is intimately linked with the study of the properties of submicroscopic particles on the one hand and with the properties of the entire universe on the other. The creation of electromagnetic radiation from matter and the creation of matter from radiation, both of which have been achieved, provide a fascinating insight into the unity of physics. The same is true of the deflection of light beams by strong gravitational fields, such as the bending of starlight passing near the Sun.

A classification of phenomena involving light according to their theoretical interpretation provides the clearest insight into the nature of light. When a detailed accounting of experimental facts is required, two groups of theories appear which, in the majority of cases, account separately for the wave and the corpuscular character of light. The quantum theories seem to obviate questions concerning this dual character of light, and make the classical wave theory and the simple corpuscular theory appear as two very useful limiting theories. It happens that the wave theories of light can cope with a considerable part of the phenomena involving electromagnetic radiation. Geometrical optics, based on the wave theory of light, can solve many of the more common problems of the propagation of light, such as refraction, provided that the limitations of the underlying theory are not disregarded. *See* GEOMETRICAL OPTICS.

Phenomena involving light may be classed into three groups: electromagnetic wave phenomena, corpuscular or quantum phenomena, and relativistic effects. The relativistic effects appear to influence similarly the observation of both corpuscular and wave phenomena. The major developments in the theory of light closely parallel the rise of modern physics. These developments are charted in **Fig. 2**, and are discussed in the remainder of this article.

Wave phenomena. Interference and diffraction, mentioned earlier, are the most striking manifestations of the wave character of light. Their fundamental similarity can be demonstrated in a number of experiments. The wave aspect of the entire spectrum of electromagnetic radiation is most convincingly shown by the similarity of diffraction pictures produced on a photographic plate, placed at some distance behind a diffraction grating, by radiations of different frequencies, such as x-rays and visible light. The interference phenomena of light are, moreover, very similar to interference of electronically produced microwaves and radio waves.

Polarization demonstrates the transverse character of light waves. Further proof of the electromagnetic character of light is found in the possibility of inducing, in a transparent body that is being traversed by a beam of plane-polarized light, the property of rotating the plane of polarization of the beam when the body is placed in a magnetic field. *See* FARADAY EFFECT.

The fact that the velocity of light had been calculated from electric and magnetic parameters (permittivity and permeability) was at the root of Maxwell's conclusion in 1865 that "light, including heat and other radiations if any, is a disturbance in the form of waves propagated . . . according to electromagnetic laws." Finally, the observation that electrons and neutrons can give rise to diffraction patterns quite similar to those produced by visible light has made it necessary to ascribe a wave character to particles. *See* ELECTRON DIFFRACTION; NEUTRON DIFFRACTION.

Electromagnetic-wave propagation. Electromagnetic waves can be propagated through free space, devoid of matter and fields, and with a constant gravitational potential; through space with a varying gravitational potential; and through more or less absorbing material media which may be solids, liquids, or gases. Radiation can be transmitted through waveguides with cylindrical, rectangular, or other boundaries, the insides of which can be either evacuated or filled with a dielectric medium. *See* WAVEGUIDE.

From electromagnetic theory, and especially from the well-known equations formulated by Maxwell, a plane wave disturbance of a single frequency

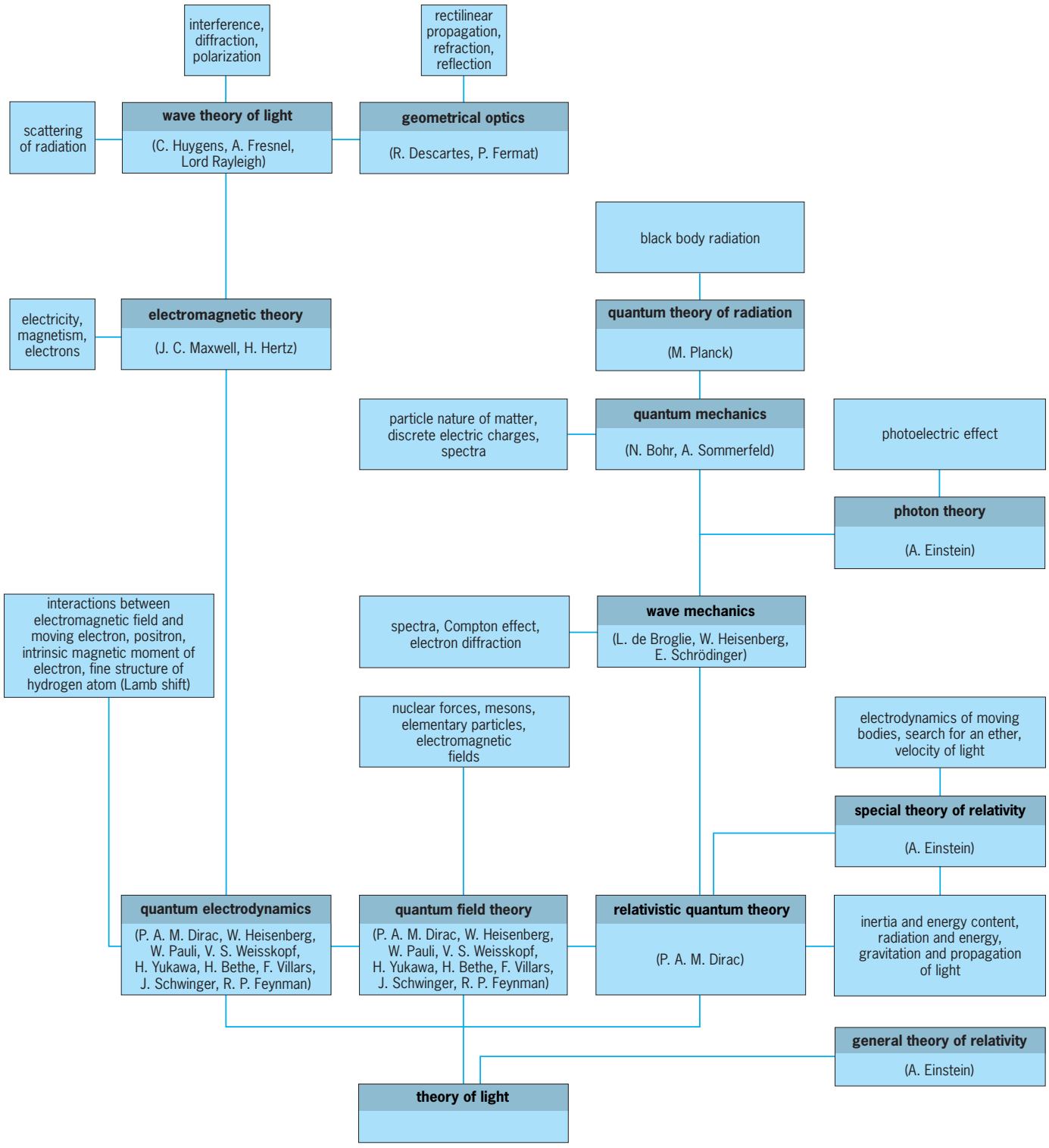

Fig. 2. Chart of important developments in the theory of light.

f is propagated in the x direction with a phase velocity $v = \lambda f = \lambda\omega/2\pi$, where λ is the free-space wavelength and $\omega = 2\pi f$. The wave can be described by the equation $y = A \cos \omega(t - x/v)$. Two disturbances of same amplitude A, of respective angular frequencies ω_1 and ω_2 and of velocities v_1 and v_2, propagated in the same direction, yield the resulting disturbance y', defined in Eq. (1). Here $\Delta\omega = \omega_1 - \omega_2$

$$y' = y_1 + y_2 = 2A \cos {}^1/_2 \left[(\Delta\omega)\, t - x\Delta\frac{\omega}{v}\right] \times \cos\left(\omega t - \frac{\omega x}{v}\right) \quad (1)$$

and $\omega = {}^1/_2(\omega_1 + \omega_2)$. The ratio $u = \Delta\omega/\Delta(\omega/v)$ is

defined as the group velocity, which is the speed of a light signal, just as the ratio $\omega/(\omega/\upsilon)$ is identical with the phase velocity, which is the speed of a wavefront. In the limit for small $\Delta\omega$, $u = d\omega/d(\omega/\upsilon)$. Noting that $\omega = 2\pi\upsilon/\lambda$, $d\omega = 2\pi(\lambda\, d\upsilon - \upsilon\, d\lambda)/\lambda^2$, and $d(\omega/\upsilon) = -2\pi\ d\lambda/\lambda^2$, an important relation, Eq. (2), between group and phase velocity is obtained. This shows that the group velocity u is different from the phase velocity υ in a medium with dispersion $d\upsilon/d\lambda$. In a vacuum, $u = \upsilon = c$. With the help of Fourier theorems, the preceding expression for u can be shown to apply to the propagation of a wave group of infinite length, but with frequencies extending over a finite small domain. Furthermore, even if the wave train were emitted with an infinite length, modulation or "chopping" would result in a degrading of the monochromaticity by introduction of new frequencies, and hence in the appearance of a group velocity. Such considerations of this nature were not trivial in earlier measurements of the velocity of light, but were quite fundamental to the conversion of instrumental readings to a value of c. Similar considerations apply to the incorporation of the effects of the medium and the boundaries involved in the experiments. Complications arise in the regions of anomalous dispersion (absorption regions), where the phase velocity can exceed c and $d\upsilon/d\lambda$ is positive. *See* DISPERSION (RADIATION); FOURIER SERIES AND TRANSFORMS; GROUP VELOCITY; MAXWELL'S EQUATIONS; PHASE VELOCITY; WAVE EQUATION; WAVE MOTION.

$$u = v - \lambda\frac{dv}{d\lambda} \tag{2}$$

Refractive index. A plane wavefront, in going from a medium in which its phase velocity is υ into a second medium where the velocity is υ', changes direction at the interface. By geometry, it can be shown that $\sin i/\sin i' = \upsilon/\upsilon'$, where i and i' are the angles which the light path forms with a normal to the interface in the two media. It can also be shown that the path between any two points in this system is that which minimizes the time for the light to travel between the points (Fermat's principle). This path would not be a straight line unless $i = 90^\circ$ or $\upsilon = \upsilon'$. Snell's law states that $n \sin i = n' \sin i'$, where n is the index of refraction of the medium. It follows that the refractive index of a medium is $n = c/\upsilon'$, because the refractive index of a vacuum, where $\upsilon = c$, has the value 1.

Dispersion. The dispersion $d\upsilon/d\lambda$ of a medium can easily be obtained from measurements of the refractive index for different wavelengths of light. The weight of experimental evidence, based on astronomical observations, is against a dispersion in a vacuum. Observation of the light reaching the Earth from the eclipsing binary star Algol, 120 light-years distant (1 light-year $\cong 6 \times 10^{12}$ mi or 9.5×10^{12} km is the distance traversed in vacuum by a beam of light in 1 year), shows that the light for all colors is received simultaneously. The eclipsing occurs every 68 h 49 min. Were there a difference of velocity for red light and for blue light in interstellar space as great as 1 part in 10^6, this star would show a measurable time difference in the occurrence of the eclipses in these two colors. *See* BINARY STAR.

Corpuscular phenomena. In its interactions with matter, light exchanges energy only in discrete amounts, called quanta. This fact is difficult to reconcile with the idea that light energy is spread out in a wave, but is easily visualized in terms of corpuscles, or photons, of light. *See* PHOTON.

Blackbody (heat) radiation. The radiation from theoretically perfect heat radiators, called blackbodies, involves the exchange of energy between radiation and matter in an enclosed cavity. The observed frequency distribution of the radiation emitted by the enclosure at a given temperature of the cavity can be correctly described by theory only if it is assumed that light of frequency ν is absorbed in integral multiples of a quantum of energy equal to $h\nu$, where h is a fundamental physical constant called Planck's constant. This startling departure from classical physics was made by Max Planck early in the twentieth century. *See* HEAT RADIATION.

Photoelectric effect. When a monochromatic beam of electromagnetic radiation illuminates the surface of a solid (or less commonly, a liquid), electrons are ejected from the surface in the phenomenon known as photoemission, or the external photoelectric effect. The kinetic energies of the electrons can be measured electronically by means of a collector which is negatively charged with respect to the emitting surface. It is found that the emission of these photoelectrons, as they are called, is immediate, and independent of the intensity of the light beam, even at very low light intensities. This fact excludes the possibility of accumulation of energy from the light beam until an amount corresponding to the kinetic energy of the ejected electron has been reached. The number of electrons is proportional to the intensity of the incident beam. The velocities of the electrons ejected by light at varying frequencies agree with Eq. (3), where m is the mass of the electron, υ_{max} the maximum observed velocity, ν the frequency of the illuminating light beam, and ν_0 a threshold frequency characteristic of the emitting solid.

$$^1/_2 m v_{max}^2 = h(\nu - \nu_0) \tag{3}$$

In 1905 Albert Einstein showed that the photoelectric effect could be accounted for by assuming that, if the incident light is composed of photons of energy $h\nu$, part of this energy, $h\nu_0$, is used to overcome the forces binding the electron to the surface. The rest of the energy appears as kinetic energy of the ejected electron.

Compton effect. The scattering of x-rays of frequency ν_0 by the lighter elements is caused by the collision of x-ray photons with electrons. Under such circumstances, both a scattered x-ray photon and a scattered electron are observed, and the scattered x-ray has a lower frequency than the impinging x-ray. The kinetic energy of the impinging x-ray, the scattered

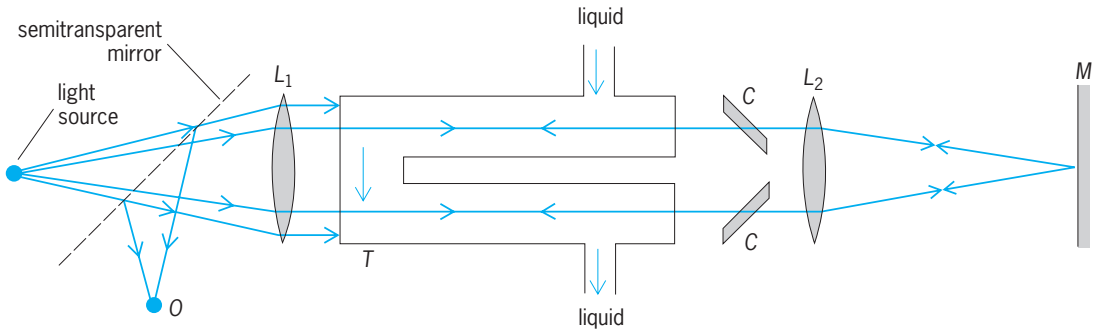

Fig. 3. Fizeau's experiment. *C*, compensator plates; *M*, mirror; L_1, L_2, lenses; *T*, tube; *O*, interference fringes.

x-ray, and the scattered electron, as well as their relative directions, are in agreement with calculations involving the conservation of energy and momentum. *See* COMPTON EFFECT.

Quantum theories. The need for reconciling Maxwell's theory of the electromagnetic field, which describes the electromagnetic wave character of light, with the particle nature of photons, which demonstrates the equally important corpuscular character of light, has resulted in the formulation of several theories which go a long way toward giving a satisfactory unified treatment of the wave and the corpuscular picture. These theories incorporate, on one hand, the theory of quantum electrodynamics, first set forth by P. A. M. Dirac, P. Jordan, W. Heisenberg, and W. Pauli, and on the other, the earlier quantum mechanics of L. de Broglie, Heisenberg, and E. Schrödinger. Unresolved theoretical difficulties persist, however, in the higher-than-first approximations of the interactions between light and elementary particles. The incorporation of a theory of the nucleus into a theory of light is bound to call for additional formulation.

Dirac's synthesis of the wave and corpuscular theories of light is based on rewriting Maxwell's equations in a hamiltonian form resembling the hamiltonian equations of classical mechanics. Using the same formalism involved in the transformation of classical into wave-mechanical equations by the introduction of the quantum of action $h\nu$, Dirac obtained a new equation of the electromagnetic field. The solutions of this equation require quantized waves, corresponding to photons. The superposition of these solutions represents the electromagnetic field. The quantized waves are subject to Heisenberg's uncertainty principle. The quantized description of radiation cannot be taken literally in terms of either photons or waves, but rather is a description of the probability of occurrence in a given region of a given interaction or observation. *See* HAMILTON'S EQUATIONS OF MOTION; NONRELATIVISTIC QUANTUM THEORY; QUANTUM ELECTRODYNAMICS; QUANTUM FIELD THEORY; QUANTUM MECHANICS; RELATIVISTIC QUANTUM THEORY; UNCERTAINTY PRINCIPLE.

Relativistic effects. The measured magnitudes of such characteristics as wavelength and frequency, velocity, and the direction of the radiation in a light beam are affected by a relative motion of the source with respect to the observer, occurring during the emission of the signal-carrying electromagnetic wave trains. *See* DOPPLER EFFECT.

A difference in gravitational potential also affects these quantities. Several important observations of this nature are listed in this section, followed by a discussion of several important results of general relativity theory involving light. For extended discussions of both the special theory of relativity and the general theory of relativity *see* RELATIVITY.

Velocity in moving media. In 1818 A. Fresnel suggested that it should be possible to determine the velocity of light in a moving medium, for example, to determine the velocity of a beam of light traversing a column of liquid of length d and of refractive index n, flowing with a velocity v relative to the observer, by measuring the optical thickness nd. The experiment was carried out by Fizeau in a modified Rayleigh interferometer, shown in **Fig. 3**, by measuring the fringe displacement in O corresponding to the reversing of the direction of flow. If v' is the phase velocity of light in the medium (deduced from the refractive index by the relation $v = c/n$), it is found that the measured velocity v_m in the moving medium can be expressed as $v_m = v' + v(1 - 1/n^2)$ rather than $v_m = v' + v$, as would be the case with a newtonian velocity addition.

Aberration. J. Bradley discovered in 1725 a yearly variation in the angular position of stars, the total variation being 41 seconds of arc. This effect is in addition to the well-known parallax effect, and was properly ascribed to the combination of the velocity of the Earth in its orbit and the speed of light. Bradley used the amplitude of the variation to arrive at a value of the velocity of light. George Airy compared the angle of aberration in a telescope before and after filling it with water, and discovered, contrary to his expectation, that there was no difference in angle. *See* ABERRATION (ASTRONOMY).

Michelson-Morley experiment. The famous Michelson-Morley experiment, one of the most significant experiments of all time, was performed in 1887 to measure the relative velocity of the Earth through inertial space. Inertial space is space in which Newton's laws of motion hold. Dynamically, an inertial frame of reference is one in which the observed accelerations are zero if no forces act. A point in an orbit is the

center of such a frame. *See* FRAME OF REFERENCE.

The rotation of the Earth about its axis, with tangential velocities never exceeding 0.3 mi/s (0.5 km/s) is easily demonstrated mechanically (Foucault's pendulum, precession of gyroscopes) and optically (Michelson's rectangular interferometer). The surface of the Earth is not an inertial frame. In its orbit around the Sun, on the other hand, the Earth has translational velocities of the order of 18 mi/s (30 km/s), but this motion cannot be detected by mechanical experiments because of its orbital nature. The hope existed, however, that optical experiments would permit the detection (and measurement) of the relative motion of the Earth through inertial space by comparing the times of travel of two light beams, one traveling in the direction of the translation through inertial space, and the other at right angles to it. The hope was based on the now disproven notion that the velocity of a light would be equal to the constant c only when measured with respect to the inertial space, but would be measured as smaller $(c - v)$ or greater $(c + v)$ with respect to a reference frame, such as the Earth, moving with a velocity v in inertial space if a light beam were projected respectively in the direction and in the opposite direction of translation of this frame. According to classical velocity addition theorems (which, as is now known, do not apply to light), a velocity difference of $2v$ would be detected under such circumstances. *See* EARTH ROTATION AND ORBITAL MOTION.

Not only does the Earth move in an orbit around the Sun, but it is carried with the Sun in the galactic rotation toward Cygnus with a velocity of several hundreds of miles per second, and the Galaxy itself is moving with a high speed in its local spiral group. Speeds of hundreds and possibly thousands of miles per second should be detectable by measurements on Earth in two orthogonal directions, assuming of course that the Earth motion is itself with respect to inertial space, or indeed that such a space has the physical meaning ascribed to it. The unexpected result of the experiment was that no such velocity difference could be detected, that is, no relative motion could be detected by optical means.

The Michelson-Morley apparatus (**Fig. 4**) consists of a horizontal Michelson interferometer with its two arms at right angles. The mirrors are adjusted so that the central white-light fringe falls on the cross hair of the observing telescope. This indicates equality of optical phase, and therefore an equality of the times taken by the light beams to travel from the beam-splitting surface to each of the two mirrors and back. Rotation of the entire system by 90°, or indeed by any angle, as well as repetition of the experiment at various times of the year all are found to leave the central white-light fringe and associated fringe system undisplaced, indicating no change in the time required by the light to traverse the two arms of the interferometer when their directions relative to the direction of the Earth's motion are varied. Had there been a difference in the velocity of light in the two directions *OM* and *ON*, the two arms would be of unequal length in the initial adjustment. For example, if the

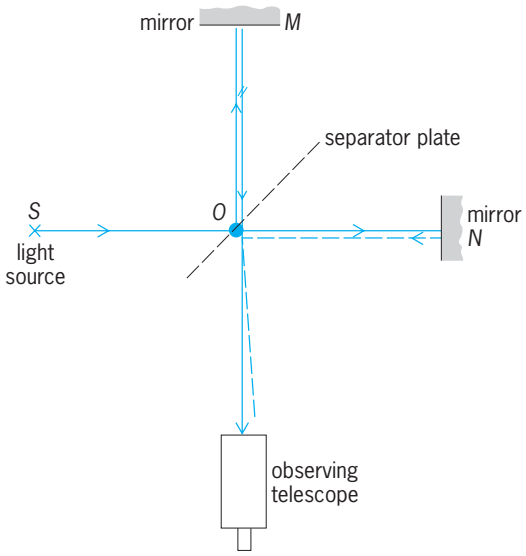

Fig. 4. Michelson-Morley experiment.

light traveled faster in the direction *OM* (on the average, going back and forth), then the corresponding arm would have to be longer so as to make the time of travel equal in both arms. If the apparatus were turned through 90°, the shorter arm would take the place of the longer arm, and the "faster" light would now travel in the shorter arm, and the "slower" light in the longer arm; a noticeable fringe displacement would, but actually does not, take place.

Einstein's theory accounts for the null result by the simple explanation that no relative motion between the apparatus and the observer exists in the experiment. No change in measured length has occurred in either direction, and because the propagation of light is isotropic, no velocity difference or detection of relative motion should be expected.

Gravitational and cosmological redshifts. Two different kinds of shifts, or displacements of spectral lines toward the red end of the spectrum, are observed in spectrograms taken with starlight or light from nebulae. One is the rare, but extremely significant, gravitational redshift or Einstein shift, which has been measured in some spectra from white dwarf stars. The other, much more widely encountered, is the redshift in spectra from external galaxies usually described as being caused by a radial Doppler effect characterizing an "expansion of the universe."

The most famous example of the gravitational redshift is that observed in the spectrum of the so-called dark companion of Sirius. The existence of this companion was predicted by F. W. Bessel in 1844 on the basis of a perturbation in the motion of Sirius, but because of its weak luminosity (1/360 that of the Sun, 1/11,000 that of Sirius), it was not observed until 1861. This companion is a white dwarf of a mass comparable to that of the Sun (0.95), but having a relatively small radius of 11,000 mi (18,000 km) and the fantastically high density of 61,000 times that of water. This companion shows a shift in its spectral lines relative to the ones emitted by Sirius itself; the shift of 0.03 nm for the Balmer β-line of hydrogen

was reliably determined by W. S. Adams. In 1960, R. V. Pound and G. A. Rebka, Jr., measured the gravitational redshift in a laboratory experiment involving the Mössbauer effect. *See* GRAVITATIONAL REDSHIFT.

The cosmological redshift is a systematic shift observed in the spectra of all galaxies, best measured with the calcium H and K absorption lines. Distances of galaxies are determined photometrically by measurements of their intensities, and it is found that the wavelength shift toward the red increases with the distance of the galaxies from the Earth. (The Earth does not have a privileged position if expansion of the universe is indeed involved. Rather its position is somewhat like that of a person in a crowd which is dispersing—each individual experiencing an ever-increasing distance from every other one.) The change of wavelength with distance d is given by Eq. (4), where $1/H$ is $1–2 \times 10^{10}$ light-years.

$$\frac{\Delta\lambda}{\lambda} = Hd \tag{4}$$

See REDSHIFT.

Results of general relativity. The propagation of light is influenced by gravitation. This is one of the fundamental results of Einstein's general theory of relativity which has been subjected to experimental tests and found to be verified. Three important results involving light need to be singled out.

1. The velocity of light, measured by the same magnitude c independently of the state of motion of the frame in which the measurement is being carried out, depends on the gravitational potential Φ of the field in which it is being measured according to Eq. (5). Here $\Phi = -GM/R$, where G is the universal

$$c = c_0\left(1 + \frac{\Phi}{c^2}\right) \tag{5}$$

constant of gravitation (6.670×10^{-11} in SI units), M the mass of the celestial body, R the radius of the body, and c_0 the velocity of light in a vacuum devoid of fields.

For example, the absolute value of the term Φ/c^2 is about 3000 times greater on the Sun than on Earth, making the measurements of c smaller by two parts in 10^6 on the Sun as compared to those on Earth.

2. The frequency ν of light emitted from a source in a gravitational field with the gravitational potential Φ is different from the frequency ν_0 emitted by an identical source (atomic, nuclear, molecular) in a field-free region, according to Eq. (6). Spectral lines

$$\nu = \nu_0\left(1 + \frac{\Phi}{c^2}\right) \tag{6}$$

in sunlight should be displaced toward the red by two parts in 10^6 when compared to light from terrestrial sources.

3. Light rays are deflected when passing near a heavenly body according to Eq. (7), where α is the

$$\alpha = \frac{4GM}{c^2R} \tag{7}$$

angular deflection in radians, and R the distance of the beam from the center of the heavenly body of mass M. The deflection is directed so as to increase the apparent angular distance of a star from the center of the Sun when starlight is passing near the edge of the Sun. The deflection according to this equation should be 1.75 seconds of arc, a value which compares favorably with eclipse measurements of the star field around the Sun in 1931. These measurements indicated values up to 2.2 seconds of arc when compared with photographs of the same field 6 months earlier. Measurements of the deflection of radio waves from extremely small diameter celestial radio sources in 1974–1975 agreed with Einstein's theory to within 1%. This prediction of Einstein's theory might seem less surprising today when the corpuscular-photon character of light is widely known, and when a newtonian M/R^2 attraction might be considered to be involved in the motion of a corpuscle with the velocity c past the Sun. However, application of Newton's law predicts a deviation only half as great as the well verified relativistic prediction.

Matter and radiation. The possibility of creating a pair of electrons—a positively charged one (positron) and a negatively charged one (negatron)—by a rapidly varying electromagnetic field (gamma rays of high frequency) was predicted as a consequence of Dirac's wave equation for a free electron and has been experimentally verified. I. Curie and F. Joliot, as well as J. Chadwick, P. M. S. Blackett, G. P. Occhialini, and others have compared the number of positrons and negatrons ejected by gamma rays passing through a thin sheet of lead (and other materials) and have found them to be the same, after accounting for two other groups of electrons also appearing in the experiment (photoelectrons and recoil electrons). Other examples of negatron-positron pair production include the collision of two heavy particles, a fast electron passing through the field of a nucleus, the direct collision of two electrons, the collision of two light quanta in a vacuum, and the action of a nuclear field on a gamma ray emitted by the nucleus involved in the action.

Evidence of the creation of matter from radiation, as well as that of radiation from matter, substantiates Einstein's equation (8), which was first expressed in

$$E = mc^2 \tag{8}$$

the following words: "If a body [of mass m] gives off the energy E in the form of radiation, its mass diminishes by E/c^2."

In regard to exchanges of energy and momentum, electromagnetic waves behave like a group of particles with energy as in Eq. (9) and momentum as in Eq. (10).

$$E = mc^2 = h\nu \tag{9}$$

$$p = \frac{h\nu}{c} = \frac{h}{\lambda} \tag{10}$$

Finally, many experiments with photons show that they also possess an intrinsic angular momentum, as

do particles. Circularly polarized light, for example, carries an experimentally observable angular momentum, and it can be shown that, under certain circumstances, an angular momentum can be imparted to unpolarized or plane-polarized light (plane wave passing through a finite circular aperture). In any case, the angular momentum will be quantized in units of $h/2\pi$.

The inverse process to the creation of electron pairs is the annihilation of a positron and a negatron, resulting in the production of two gamma-ray quanta (two-quantum annihilation). Nuclear chain reactions are known to involve similar processes. *See* CHAIN REACTION (PHYSICS); ELECTRON-POSITRON PAIR PRODUCTION; ELEMENTARY PARTICLE. George W. Stroke

Bibliography. M. Born and E. Wolf, *Principles of Optics*, 7th ed., 1999; W. Demtröoder, *Laser Spectroscopy: Basic Concepts and Instrumentation*, 2d ed., 1994; E. Hecht and A. Zajac, *Optics*, 3d ed., 1997; J. M. Jauch and F. Rohrlich, *The Theory of Photons and Electrons*, 2d ed., 1985; F. A. Jenkins and H. E. White, *Fundamentals of Optics*, 4th ed., 1976; R. Loudon, *The Quantum Theory of Light*, 3d ed., 2000; J. Meyer-Arendt, *Introduction to Classical and Modern Optics*, 4th ed., 1995; W. Rindler, *Essential Relativity*, rev. ed., 1986, paper 1993; F. G. Smith and J. H. Thomson, *Optics*, 2d ed., 1988.

Light amplifier

In the broadest sense, a device which produces an enhanced light output when actuated by incident light. A simple photocell relay–light source combination would satisfy this definition. To make the term more meaningful, common usage has introduced two restrictions: (1) a light amplifier must be a device which, when actuated by a light image, reproduces a similar image of enhanced brightness; and (2) the device must be capable of operating at very low light levels without introducing spurious brightness variations (noise) into the reproduced image. The term is used synonymously with image intensifier. The light amplifier increases the brightness of an image which is below the visual threshold to a level where it can be readily seen with the unaided eye. It is, of course, impossible to see under conditions of complete darkness. Indeed, there is a fundamental lower limit of illumination under which an image of a given quality can be recognized. This limitation arises because of the corpuscular nature of light. *See* PHOTON.

Photons arriving through a lens, or other optical system, onto an image area are random in time. If the number of photons per unit area arriving during the time allotted for image formation (for example, the period of the persistence of vision) is too low, the statistical fluctuation will be greater than the variation in number due to true differences in image brightness. Under these circumstances, image recognition is impossible.

Image-intensifier tubes. Intensifier tubes may consist of a semitransparent photocathode which emits electrons with a density distribution proportional to the distribution of light intensity incident on it. Thus, when a light image falls on one side of the cathode, an electron-current image is emitted from the other side. An electron optical system, which acts on electrons in much the same way as does a glass lens system on light, focuses the electron image onto an intensifier element. This electron optical system may be purely electrostatic or may utilize magnetic focusing. The intensified electron image from the other side of the intensifier element is again focused, by a second electron lens, onto a second intensifier element (if additional amplification is required) or onto a fluorescent viewing screen, where the electron energy is converted to visible light.

Proximity tubes are a class of intensifiers in which the photocathode and the fluorescent viewing screen are parallel and separated by only a short distance. No focusing is required for a proximity tube, since the electrons generated at the photocathode are accelerated along the tube axis by the high electric fields.

The spectral response of the image-intensifier tube depends on the type of photocathode employed, and the tube may serve as a wavelength converter as well as an intensifer. *See* CHARGED PARTICLE OPTICS.

Intensifier elements. Two types of intensifier elements are ordinarily employed. One consists of a transparent support (either a thin film or a fiber optics plate) with a phosphor screen on the side on which the electron image is incident, and a photocathode on the other. An electron striking the phosphor produces a flash of light which causes a release of 50 or more electrons from the photoemitter directly opposite the point of impact. Thus, the intensifier element increases the electron-image current density by a factor of 50. Two such intensifier elements in cascade give a gain of 2500. The **illustration** shows a three-stage electrostatic image-intensifier tube.

A second type of high-gain intensifier element is a thin secondary-emission current amplifier called a microchannel plate, which is placed between the photocathode and screen. It consists of a parallel bundle of small, hollow glass cylinders, where the inside walls of the cylinders are coated with a secondary emitting material. Electrons that are emitted from the photocathode strike the inside walls of the cylinders, causing secondary electron generation. These secondary electrons in turn continue to cascade down the inside walls of the cylinders, resulting in a high total current gain.

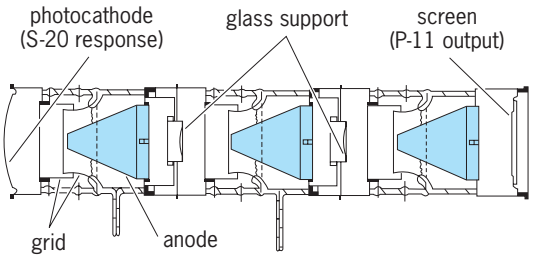

Three-stage eloctrostatically focused image tube.

Television camera tube. The intensifier image device can be combined with television pickup tubes to make a television camera whose sensitivity is very close to the threshold determined by the photon "shot noise" from the scene being televised. A silicon intensifier target (SIT) camera tube has a wide dynamic range and operates at very low light levels. In the SIT tube, the photoelectrons accelerated from the photocathode are focused onto a thin silicon target consisting of an array of *pn* junctions. The high-energy photoelectrons generate multiple hole-electron pairs in the silicon target, resulting in gain. The signal is read out by scanning the reverse side of the silicon target with an electron beam, similar to the method used in vidicon camera tubes. In other types of electron-bombarded silicon (EBS) tubes, the silicon *pn* junction target is replaced with scanned photodiode arrays or with charge-coupled device (CCD) imagers. In these cases, the electronic readout of the silicon targets is accomplished without the use of a scanned electron beam, and this results in even lower light-level performance. *See* TELEVISION CAMERA TUBE.

Solid-state image intensifiers. A greal deal of exploratory work has been done on solid-state light amplifiers. The form which has been extensively investigated consists of a photoconductive film in contact with an electroluminescent screen. Current flows through the photoconductor at illuminated areas, causing light to be generated in the electroluminescent layer. This type of intensifier gives considerable image enhancement at intermediate light levels, but fails at very low light levels because of extreme time lag. *See* ELECTROLUMINESCENCE.

Another type of solid-state light amplifier which works at intermediate light levels is the liquid-crystal light valve. The light valve consists of an electrically biased multilayer sandwich which has a liquid-crystal layer on the front face and a photoconductive layer on the rear face. In this system, the incident light is focused on the photoconductive side, while a bright, polarized light is projected onto the liquid-crystal side. The incident light from the photoconductive side causes an increase in voltage drop across the liquid crystal. This increased voltage causes a rotation in the orientation of the liquid-crystal molecules, which in turn modulates the polarization of the reflected projection light. Only the modulated reflected light is allowed to be viewed.

Applications. In addition to their application for night vision, light amplifiers have been useful in many fields of science, such as astronomy, nuclear physics, and microbiology. Dean R. Collins

Bibliography. G. Kychakoff (ed.), *Electro-Optic Sensing and Measurement*, 1988; K. Seyrafi and S. A. Hovanessian, *Introduction to Electro-Optical Imaging and Tracking Systems*, 1993.

Light curves

Graphs of the intensity of radiation from astronomical objects as they change with time. Variations may be caused by the changing perspective from the Earth of two stars in orbit around each other, by pulsations that change an individual star's size and surface temperature, by mass ejection or accretion, by explosions, by beams of radiation sweeping across the line of sight from the Earth, or by clouds of very high-energy electrons in powerful magnetic fields. The information contained in the light curve includes the timing of events, such as eclipses or pulses, and the amplitude of changes in the radiation received at Earth.

Each data point in a light curve is a photometric measurement, recorded at a particular time. These points represent measurements of the amount of radiation from the source received at Earth per second per area in a particular bandpass, for example, through a blue filter. In optical light, photometry is affected by the varying transparency of the atmosphere, so that light curves are often obtained as ratios to the intensities of nearby comparison stars. Simultaneous measurements can be made visually, with photometers that have two channels, or with imagers such as charge-coupled devices (CCDs) or photographic emulsions. These relative light curves are put on an absolute scale by means of calibrating measures of the comparison stars taken on clear nights. *See* ASTRONOMICAL PHOTOGRAPHY; CHARGE-COUPLED DEVICES; MAGNITUDE (ASTRONOMY); PHOTOMETRY.

Binary stars. If the orbital plane of a binary star system lies nearly along the line of sight from the Earth, the stars appear to eclipse each other periodically, either partially or totally, depending on the tilt of the orbit (**Fig. 1**). The larger drop in intensity represents the primary eclipse, when the dimmer star passes in front of the brighter; the secondary eclipse is shallower, produced when the light from the dimmer star is blocked. If one face of the cooler star is strongly irradiated by a hot primary or gravity distorts the star into a nonspherical shape, the light curve also shows a hump centered on the secondary eclipse. The timing of the eclipses yields the ratio of the radii of the two stars and the period and tilt of the orbit. Temperature differences between the two stars make the drop in intensity during eclipse differ among color bands. *See* BINARY STAR; ECLIPSING VARIABLE STARS.

Variable stars. Intrinsically variable single stars have distinct signatures in their light curves. Some giant stars have an instability in their outer layers that acts as a heat engine driving radial pulsations of the star's surface. A light curve (**Fig. 2**) reveals the amount of extra flux received at Earth during each pulsation. Spectroscopy gives the temperature and change in radius of the star during the same cycle. When combined, this information yields the distance to the variable star and its intrinsic power output. For example, Cepheid variables can be identified by their light curve signatures and used as distance indicators for nearby galaxies. *See* CEPHEIDS.

Other types of stars also show surface pulsations that appear as variations in their light curves. These types include early B stars on the main sequence, and stellar remnants such as planetary nebula nuclei and white dwarfs. The amplitudes of these

pulsations can be very low (<1% of the white light intensity) and can consist of a complicated blend of many frequencies. These variations are interpreted as nonradial pulsations that act like waves near the star's surface. The central stars of planetary nebulae are evolving so fast that the frequencies of the pulsations show tiny but measurable shifts over the course of 5 to 10 years that are produced by the collapsing cores as they become white dwarf stars. *See* PLANETARY NEBULA; WHITE DWARF STAR.

Many single stars show irregular variations brought about by mass loss. Illuminated ejecta add to the brightness until the material disperses. Newly formed stars may be accreting new gas from disks at their equators and ejecting material in jets at the poles. These T Tauri stars show strong variability. Hot stars of type B with emission lines (Be stars) on the main sequence also have disks or shells that vary in light with irregular mass-loss episodes. Red supergiant stars eject tremendous amounts of matter from their outer envelopes; long-period variables, Miras, and nebular variables all fall in this class. Light curves for these objects in both the optical and infrared provide the time history of mass ejection. *See* STAR; STELLAR EVOLUTION; T TAURI STAR; VARIABLE STAR.

Interacting binaries. The stars in some binary systems are so close together that gas flows between the components. If the primary is a high-density stellar remnant, the gas may spiral in, forming an accretion disk. The accretion flow itself may radiate much of the power from the system, especially in the ultraviolet and x-rays. These high-energy light curves show evidence for flickering and for a hot spot where the stream of material impacts the disk. If the compact star is a white dwarf, the buildup of gas on its surface can cause a nuclear explosion, which is a nova outburst. The light curve shows the object brightening by 10 to 100,000 times its quiescent level. X-ray light curves have shown that some unseen compact companions must be neutron stars or black holes. *See* BLACK HOLE; CATACLYSMIC VARIABLE; NEUTRON STAR; NOVA; X-RAY ASTRONOMY.

Supernovae. The ultimate explosion is when an entire star (or pair of stars) detonates; this explosion is a supernova, which can be brighter than a whole galaxy of stars combined. The shape of the light curves of supernovae demonstrates that after the initial explosion the energy input is dominated by the decay of radioactive elements such as cobalt and nickel isotopes produced by the thermonuclear runaway. The uniformity in the shapes of the light curves of one subgroup of supernovae (type Ia) has suggested that those objects achieve a similar maximum power output and can be used as so-called standard candles for extragalactic distance determinations (**Fig. 3**). The steepness of the light curve immediately after maximum light provides a fine tuning for determining the intrinsic brightness that has an important impact on the distances derived from such explosions. The comparison of the maximum brightness of distant supernovae with that of their local counterparts led to the discovery that the expansion of the universe is accelerating. *See* ACCELERATING UNIVERSE; SUPERNOVA.

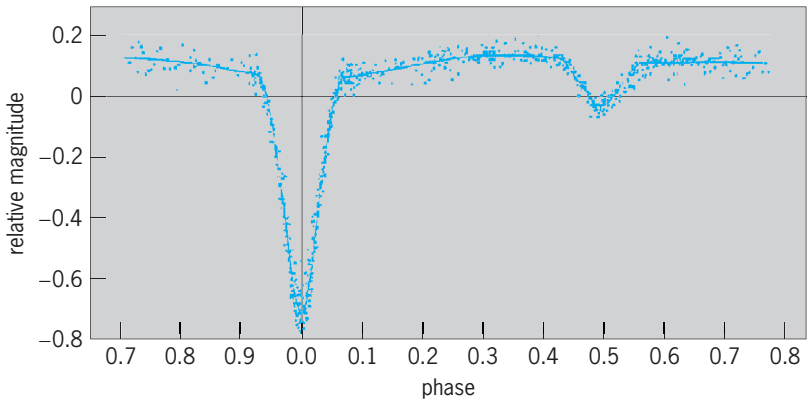

Fig. 1. Light curve of the eclipsing binary Algol. The measured infrared intensity on the vertical axis is given in magnitudes relative to the nearby star κ Persei. The phase is the fraction of the 2.9-day period elapsed relative to the deep primary minimum. Also apparent are the secondary minimum, when the K giant is eclipsed by the B star, and the brightening around secondary minimum caused primarily by heating of one face of the cooler star. (*After K.-Y. Chen and G. Reuning, Astron. J., 71:283–296, 1966*)

Exotic objects. Variable radiation can be emitted by clouds of very high-energy electrons moving in powerful magnetic fields. Beams and jets of radiated energy may result. Pulsars are an example, rapidly rotating neutron stars that sweep the Earth with such beams up to a thousand times per second. Their light curves are commonly observed at radio frequencies, but young pulsars also show pulses in optical light. The timing of the radio pulses for binary pulsars provides a general relativity laboratory for gravitational radiation. The frequency of the pulses from single pulsars can be determined with such accuracy that very small variations have been interpreted as

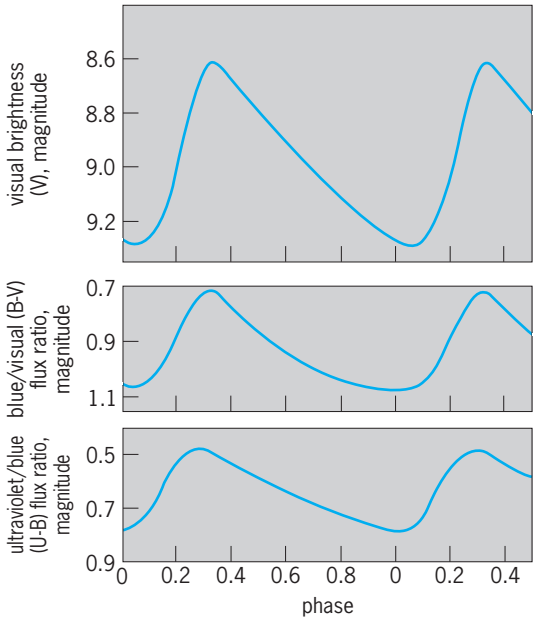

Fig. 2. Light curves of a Cepheid variable star. For the lower two curves, bluer colors are plotted toward the top. The phase is the fraction of the 4.9-day pulsation period, relative to the time of minimum brightness in the cycle. (*After R. I. Mitchell et al., Boletin de los Observatorios Tonantzintla y Tacubaya, 3:153–304, 1964*)

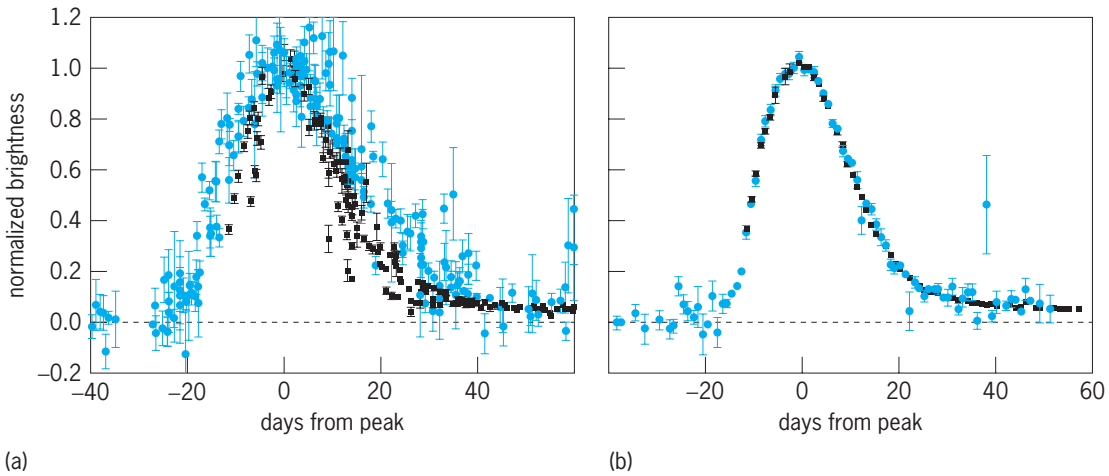

Fig. 3. Light curves for supernovae. (*a*) Composite of blue photoelectric measurements for 18 lower-redshift supernovae (black data points) and red measurements for 35 higher-redshift objects (color data points) normalized to maximum = 1 at time = 0. (*b*) Same data corrected for time dilation and light-curve shape. (*After G. Goldhaber et al., Timescale stretch parameterization of type Ia supernova B-band light curves, Astrophys. J., 558:359–368, 2001*)

arising from the perturbations of orbiting planets. *See* GRAVITATIONAL RADIATION; PULSAR.

Gamma-ray bursts are brief outbursts of high-energy radiation that are random in time and are distributed nearly uniformly over the sky. Most of the energy in a burst is higher than 100,000 eV (more than 7000 times the energy required to strip the electron off a hydrogen atom). Bursts can range in duration from 30 ms to over 1000 s. The shapes of the light curves range from single pulses or spikes through multiple peaks to chaotic or erratic episodes. Observational characterization of bursts has come from the National Aeronautics and Space Administration's (NASA's) *Compton Gamma-Ray Observatory* and more recently NASA's *SWIFT* satellite. Gamma-ray bursts are sometimes followed by afterglows in x-rays and optical light, allowing determination of redshifts for some sources. At least one gamma-ray burst has been unambiguously associated with a supernova. In general, models interpreting gamma-ray bursts are based on mergers of neutron stars or of a neutron star with a black hole, or the core collapse of a massive star in the midst of a merger. *See* GAMMA-RAY BURSTS.

Blazars are actively varying powerful nuclei of galaxies. They may have giant beams and jets produced by supermassive black holes, and present strongly variable light curves in radio, optical, ultraviolet, and x-rays. The time lag of variations in the light curve between the ultraviolet and high-energy x-rays suggests that relativistic beaming enhances the intensity of radiation in the direction of the Earth. The lag also suggests that the mechanism of relativistic electrons giving a boost in energy to optical photons to produce x-rays is not operative in these blazars. Quasars are modeled as having both accretion disks and jets from supermassive black holes. Their light curves show more modest variability than those of blazars. The time delays between variations in the continuous radiation from the central engine and the spectral lines emitted by the surrounding clouds of gas are interpreted to yield the physical size of these active galactic cores. *See* GALAXY, EXTERNAL; QUASAR.

Gravitational microlensing. Einstein's theory of general relativity is based on the underlying principle that the presence of matter determines the local curvature of space-time. A large, concentrated mass can therefore act as a lens and bend the path of light. Radiation from a distant source behind the lensing mass can be focused, thus amplifying the observed intensity. That amplification will vary if the relative position of the lens and background object changes with time. A characteristic gravitational microlensing light curve (roughly symmetrical in time and independent of color) is produced when the lensing object is a star with proper motion that carries it across our line of sight through a critical alignment with a background star. The detailed shape of the light curve can show whether the lensing object is a binary star or if it has an associated planetary system; one such planet was reported in 2006 based on a 1-day microlensing peak superimposed on a year-long microlensing stellar curve. The technique of searching for microlensing signatures in repeated exposures of dense star fields was used to search for the objects in our Galaxy's halo that stabilize its rotation and could comprise the local dark matter, termed massive compact halo objects (MACHOs). The low incidence of microlensing events towards the Large Magellanic Cloud puts stringent limits on the total masses of MACHOs. *See* DARK MATTER; GRAVITATIONAL LENS; MAGELLANIC CLOUDS; MILKY WAY GALAXY.

Richard F. Green

Bibliography. P. Mészáros, Theories of gamma-ray bursts, *Annu. Rev. Astron. Astrophys.*, 40:137–169, 2002; H. R. Miller and P. J. Wiita (eds.), *Variability of Active Galactic Nuclei*, 1991; B. Paczyński, Gravitational microlensing, *Annu. Rev. Astron. Astrophys.*, 34:419–459, 1996; J. R. Percy (ed.), *The Study of Variable Stars Using Small Telescopes*, 1986; E. Valtaoja and M. Valtonen (eds.), *Variability of Blazars*, 1992; S. E. Woosley (ed.), *Supernovae*, 1991.

Light-emitting diode

A rectifying semiconductor device which converts electrical energy into electromagnetic radiation. The wavelength of the emitted radiation ranges from the near-ultraviolet to the near-infrared, that is, from about 400 to over 1500 nanometers.

General considerations. Most commercial light-emitting diodes (LEDs), both visible and infrared, are fabricated from III–V semiconductors. These compounds contain elements such as gallium, indium, and aluminum from column III (or group 13) of the periodic table, as well as arsenic, phosphorus, and nitrogen from column V (or group 15) of the periodic table. There are also LED products made of II–VI (or group 12–16) semiconductors, for example ZnSe and related compounds. Taken together, these semiconductors possess the proper band-gap energies to produce radiation at all wavelengths of interest. Most of these compounds have direct band gaps and, as a consequence, are efficient in the conversion of electrical energy into radiation. With the addition of appropriate chemical impurities, called dopants, both III–V and II–VI compounds can be made *p*- or *n*-type, for the purpose of forming *pn* junctions. All modern-day LEDs contain *pn* junctions. Most of them also have heterostructures, in which the *pn* junctions are surrounded by semiconductor materials with larger band-gap energies. *See* ACCEPTOR ATOM; DONOR ATOM; ELECTROLUMINESCENCE; ELECTRON-HOLE RECOMBINATION; JUNCTION DIODE; JUNCTION TRANSISTOR; LASER; SEMICONDUCTOR; SEMICONDUCTOR DIODE.

Material synthesis. The fabrication of LEDs begins with the preparation of single-crystal substrates, typically 250 to 350 micrometers in thickness, which serve as templates for epitaxial growth and add mechanical strength to the completed device structure. The *p*- and *n*-type minority-carrier injection layers and the photon-generating active regions are formed on top of these substrates by depositing additional material from the liquid or vapor phase (**Fig. 1**). Infrared diodes are made of either gallium indium arsenide layers grown on gallium arsenide substrates or indium gallium arsenide phosphide deposited on indium phosphide. Red-emitting diodes are made of either aluminum gallium arsenide or gallium indium phosphide layers grown on gallium arsenide substrates. Orange- and yellow-emitting diodes are made of aluminum gallium indium phosphide layers deposited on gallium arsenide substrates. Green- and blue-emitting diodes are made of either gallium indium nitride layers grown on sapphire or silicon carbide substrates, or zinc cadmium selenide or zinc tellurium selenide deposited on zinc selenide. LEDs containing aluminum gallium arsenide are made using a process known as liquid-phase epitaxy. All the rest are made using one of three different vapor-based processes; namely, vapor-phase epitaxy, metallorganic chemical vapor deposition, or molecular-beam epitaxy. In the more common III–V LEDs, the *n*-type dopant of choice is either the column IV (or group 14) element silicon, or one of two column VI elements selenium or tellurium. The *p*-type dopant is usually a column II element, for example, zinc or magnesium; however, the column IV element carbon is now a viable alternative. For II–VI LEDs, the *n*-type dopant is the column VII (or group 17) element chlorine, and the *p*-type dopant is the column V element nitrogen. To facilitate electrical access, ohmic contacts are made by evaporating thin metallic films onto both *n*- and *p*-type layers. *See* BAND THEORY OF SOLIDS; CRYSTAL GROWTH; CRYSTAL STRUCTURE; MOLECULAR BEAMS; SEMICONDUCTOR HETEROSTRUCTURES.

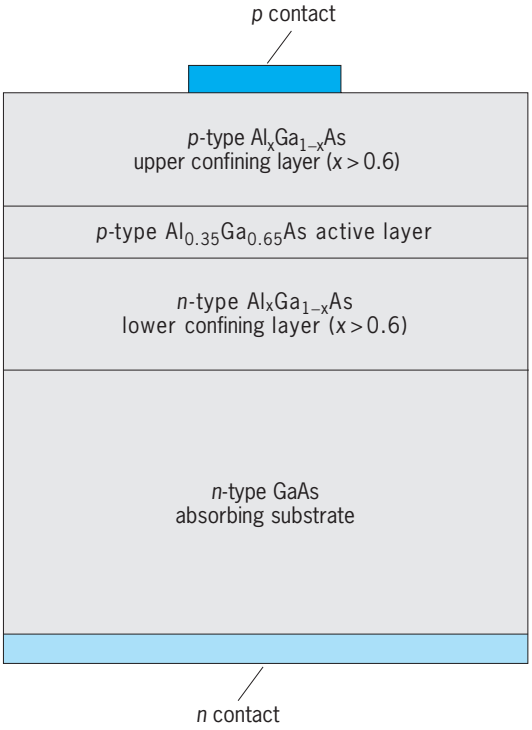

Fig. 1. Cross-sectional view of a typical light-emitting diode structure. The 250–350-μm-thick GaAs substrate serves as a template for epitaxial growth of the active layers and provides mechanical strength to the completed device. The *p*-type and *n*-type $Al_xGa_{1-x}As$ upper and lower confining layers form the *pn* junction that provides the means to inject excess electrons and holes into the active region. These layers are usually 1–2 μm thick. The $Al_{0.35}Ga_{0.65}As$ active region is where the excess electrons and holes recombine to generate photons. This layer is usually 0.1–0.5 μm thick. The *p* and *n* contacts are metal alloys or multilayer composites that are chosen specifically to make low-resistance electrical contacts to the adjacent semiconductor materials. (*Copyright 1993 Hewlett-Packard Company; reproduced with permission*)

Device design. One of the primary objectives of LED design is to maximize external quantum efficiency, defined as the radiant flux (in watts) emitted from the device divided by the product of the photon energy (in electronvolts) of the peak emission and the current (in amperes) flowing through the device. For discussion purposes, it is useful to separate this quantity into two distinct parameters: the internal quantum efficiency and the light extraction coefficient. The internal quantum efficiency (the number of useful photons created per electron-hole pair injected) is limited by the transfer of excess carriers to indirect energy band minima, their leakage

outside the active region, and the trapping of carriers at heterointerfaces—all of which eventually lead to either nonradiative recombination or radiative recombination at undesirable wavelengths. The influence of these excess carrier loss mechanisms can be mitigated by the proper choice of active region materials and layer thicknesses. In the ideal case of a well-developed semiconductor material, combined with an optimized structure, the internal quantum efficiency may approach unity. The light extraction coefficient (or the fraction of photons that escape from the device) is constrained by total internal reflection at the semiconductor/air interface. Light generated by spontaneous emission at any point within the active region is uniformly distributed in all directions. Given the large difference in the refractive indices between semiconductor and air, only a small fraction of light impinges upon the interface at angles less than the angle for total internal reflection. This component, which escapes by simple refraction on its first pass through the device, is of the order of 4% for each of the six escape cones inscribed within the semiconductor parallelepiped (**Fig. 2**). Hence, even without any additional obstructions, the light extraction coefficient has a maximum value of only 24%. With normal epitaxial layer thicknesses and device cross-sectional area, however, almost all of the light emitted toward the four side walls is reflected off the top surface or absorbed in the substrate. Most of the light emitted directly upward toward the top surface is reflected back into the substrate or absorbed within the opaque metal contact pad. All of the light emitted downward toward the substrate is lost to absorption before reaching the back surface. Thus, in practice, a typical red-light-emitting diode with near-unity internal quantum efficiency has an external quantum efficiency of less than 5%. *See* LUMINESCENCE; REFLECTION OF ELECTROMAGNETIC RADIATION; REFRACTION OF WAVES.

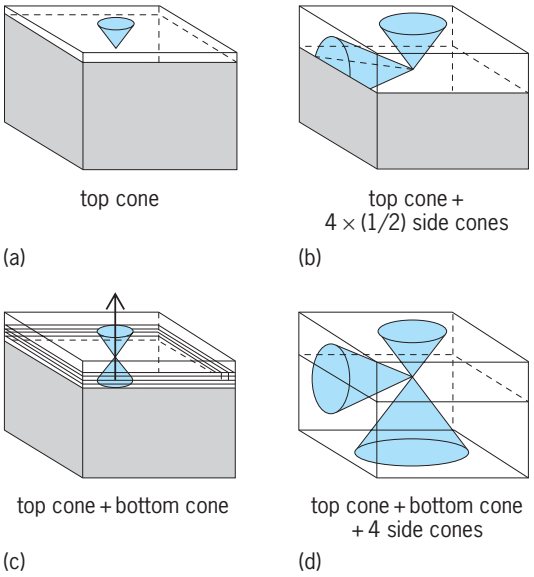

Fig. 2. Schematic diagram showing the means by which photons created at a point source inside a semiconductor parallelepiped escape to the outside environment. Photons incident on the semiconductor/air interface at angles larger than the critical angle are trapped by total internal reflection. The cones represent the solid angles over which photons can escape from the semiconductor after suffering only small Fresnel reflection losses. (*a*) Light escapes only from the top surface because the substrate is highly absorbing at the photon wavelength and the active region is too thin to allow escape from the sample edges. (*b*) Light escapes from both the top and bottom cones. A distributed Bragg mirror was inserted between the active region and the absorbing substrate so that photons emitted into the bottom cone would be reflected back toward the top surface. (c) Light escapes from the top surface and the upper halves of the four side cones because the active region was made thick enough that photons could reach the side walls of the parallelepiped before being trapped by total internal reflection off the top surface. (*d*) Light escapes from all six cones. The absorbing substrate was replaced by a transparent material, and thus photons emitted into the bottom cone and into the bottom halves of the four side cones can escape.

Applications. Conventional low-power, visible LEDs are used as solid-state indicator lights in instrument panels, telephone dials, cameras, appliances, dashboards, and computer terminals, and as light sources for numeric and alphanumeric displays. Modern high-brightness, visible LED lamps are used in outdoor applications such as traffic signals, changeable message signs, large-area video displays, and automotive exterior lighting. General-purpose white lighting and multielement array printers are applications in which high-power visible LEDs may soon displace present-day technology. Infrared LEDs, when combined in a hybrid package with solid-state photodetectors, provide a unique electrically isolated optical interface in electronic circuits. Infrared LEDs are also used in optical-fiber communication systems as a low-cost, high-reliability alternative to semiconductor lasers.

Indicators and displays. The advantages of using LEDs to produce visible electromagnetic radiation are their high efficiency, small size, ruggedness, long life, and compatibility with silicon integrated circuits. The most appropriate measure of electrical-to-optical power conversion for display applications is luminous efficiency, defined as the luminous flux (in lumens) divided by the product of applied voltage and drive current (in watts). The luminous flux emitted from an LED is determined by measuring its corresponding radiometric quantity, that is, the radiant flux, and correcting it to account for the wavelength-dependent response of the eye. LEDs with power conversion efficiencies greater than 10 lumens per watt are now commercially available at discrete wavelengths covering the entire visible spectrum. Individual red-, green-, and blue-light-emitting diodes can be combined to produce an enormous variety of intermediate hues, and specially designed ultraviolet diodes can be used to excite an inorganic fluorescent coating for the purpose of generating white light (**Fig. 3**). Within the spectral window from 600 to 640 nm, the luminous efficiency of LEDs exceeds that of tungsten and halogen lamps and, in some laboratory demonstrations, approaches that of fluorescent lighting. This high level of performance is the consequence of many improvements in material quality and device design, particularly in the area of light extraction. Special current spreading layers, distributed

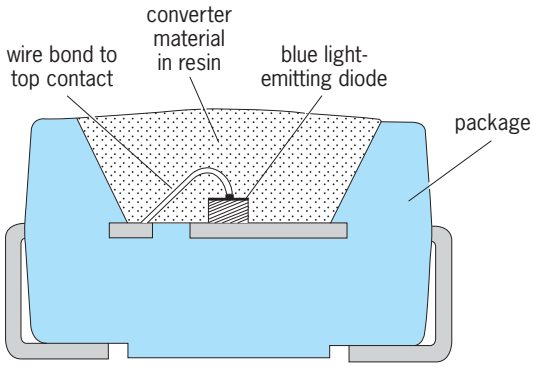

Fig. 3. Cross-sectional view of a light-emitting diode package designed to emit white light by combining blue, green, and red photons. The source of blue photons is the direct light emission from a AlGaN-GaInN double heterostructure LED chip. The sources of green and red photons are two distinct inorganic fluorescent materials embedded in the epoxy resin that encapsulates the LED chip. The green and red photons are generated by an energy down-conversion process; that is, blue photons emitted by the semiconductor LED are absorbed by the fluorescent materials, the excited electronic carriers lose energy through various internal mechanisms and drop down to an intermediate energy state, and then their electronic energy is converted back into photons by the process of flourescence. The intensity of the blue photon source is controlled by the choice of drive current passing through the semiconductor LED chip. The intensity of the green and red photon sources is set by adjusting the composition of the fluorescent materials in the epoxy resin.

Bragg reflectors, and wafer-bonded transparent substrates have been developed to move the light extraction coefficient closer to its theoretical limit (**Fig. 4**). Another important operating parameter is maximum light output power. The simplest way to increase the luminous flux from an LED is to raise its drive current. However, this is accompanied by an increase in Joule heating in the passive regions of the device, leading to a higher *pn* junction operating temperature. Thus, the output power of an LED lamp is limited by heat dissipation within the semiconductor chip, since an increase in junction temperature causes a reduction in internal quantum efficiency and shifts the emitted radiation to longer wavelengths. A luminous output as high as 20 lumens at 619 nm is sustainable by using a special high-power lamp package to improve thermal management. *See* ILLUMINATION; LUMINOUS EFFICIENCY; LUMINOUS FLUX; PHOTOMETRY.

Optoisolators. In the simplest optical interface, the optoisolator, an LED, and a photodetector are optically coupled, but electrically isolated, in a small package. This device can be used, for example, at the interface between two different circuits, such as the switching equipment in a telephone central office and the connecting loop circuit which carries the signals to the telephone sets. The electric signal from the central office is converted to radiation by the LED, which in turn is converted back into an electric signal by the photodetector before it enters the loop circuit. This type of interface is traditionally provided by electromechanical relays or isolation transformers. The electrical isolation resulting from the optical path protects the central office from electromagnetic interferences such as lightning which hits telephone wires or surge currents from electromechanical relays. LEDs are ideal for this application because they are very reliable and can be modulated to carry high-frequency signals. In a typical optoisolator structure, the LED and the phototransistor are mounted on separate metal lead frames, and the two components are coupled optically through a transparent plastic encapsulant (**Fig. 5**). This plastic is also the source of electrical isolation, typically on the order of 2500 V. Final encapsulation is completed with a black, opaque overmold which also provides mechanical stability. Optoisolators are compatible with silicon integrated circuits in size, reliability, and

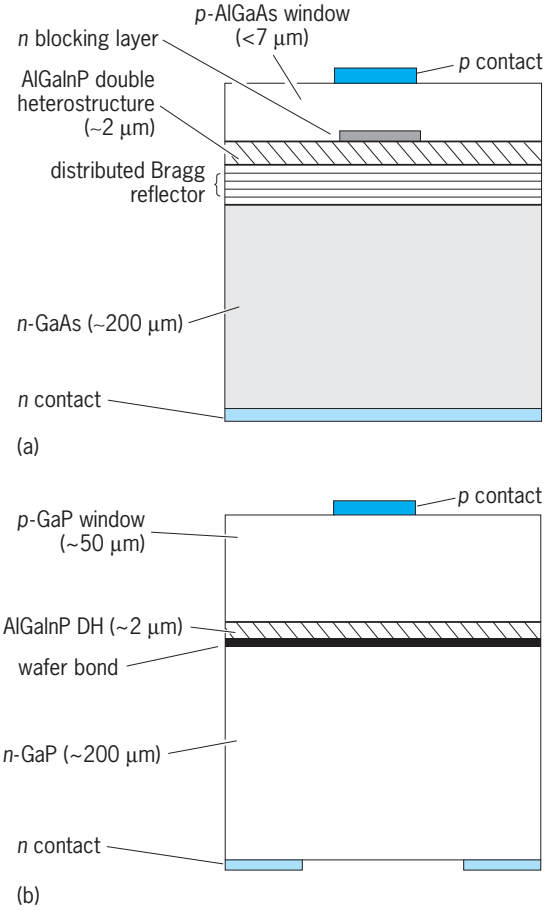

Fig. 4. Cross-sectional view of two different designs for maximizing the luminous efficiency of AlGaInP light-emitting diode structures. (*a*) A thick *p*-type AlGaAs layer between the AlGaInP active region and the top-side *p*-contact serves to spread the current out well beyond the cross-sectional area of the metal pad, combined with an *n*-type semiconductor blocking layer located directly adjacent to the active region that prevents the flow of current through the cross-sectional area directly shadowed by the opaque metal pad. A distributed Bragg mirror was inserted between the AlGaInP active region and the absorbing GaAs substrate to reflect light back up toward the top surface. (*b*) An extremely thick GaP window serves as both a current-spreading layer and a light extraction layer. The GaP window is thick enough that photons emitted within the four side cones can escape before reaching the top surface and being trapped by total internal reflection. The absorbing GaAs substrate that served as the original growth template for the AlGaInP active region was removed, and a transparent GaP substrate was attached to the bottom side of the active region using a wafer-bonding method.

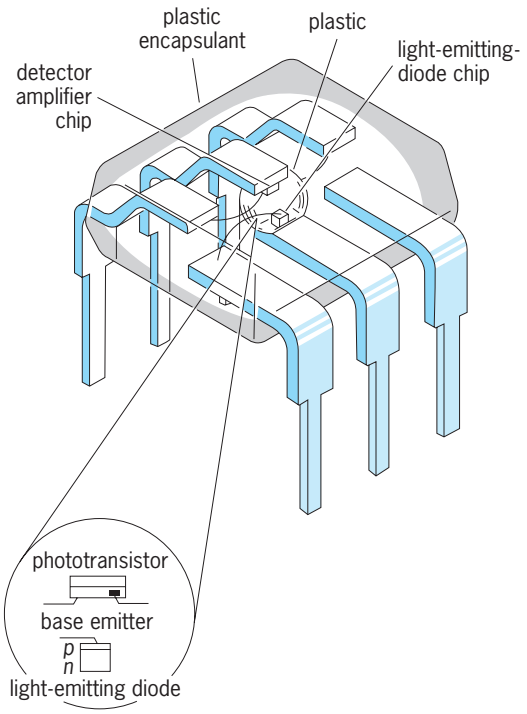

Fig. 5. Typical opto-isolator in a plastic-encapsulated dual in-line package.

performance parameters, giving them a prominent role in modern solid-state circuits. *See* OPTICAL ISOLATOR.

Optical fiber transmission. Another rapidly evolving application of infrared LEDs is in optical fiber communication. An optical signal is fed into a 50–100-μm-diameter glass fiber and transmitted over long distances without the need for regeneration. At the other end of the fiber, a photodetector converts the optical signal back to an electrical signal. This silica-glass fiber, which replaces coaxial cable, is smaller in volume, less expensive, and immune to electromagnetic interference. It also transmits higher data rates and provides longer repeater spacings than metal conductors. Since doped silica fibers exhibit both low loss and minimum material dispersion near 1.3 μm, LED sources at this wavelength can achieve a repeater spacing of 10 km (6 mi) at a data rate of 250 megabits per second. The key operating parameters for this application are fiber-coupled power and response time. Coupling infrared radiation into an optical fiber is difficult because the fiber has a very narrow acceptance angle (10–150°). This task is accomplished by extracting light through a well etched into the bottom side of the substrate with the fiber held in place by a special epoxy resin. A dielectric layer is deposited onto the top side of the structure to provide electrical isolation between the ohmic contact metal and the heavily doped semiconductor surface, thereby limiting the active area of the junction to the size of the optical fiber. It is also necessary to shorten the response time of the LED for high data-rate transmission. This goal can be realized by increasing the doping level in the active region with the intention of decreasing the radiative recombination lifetime. The challenge is to achieve the highest doping level possible without inadvertently introducing nonradiative recombination centers that act to reduce the internal quantum efficiency of the device. *See* OPTICAL COMMUNICATIONS; OPTICAL FIBERS.

Jerry M. Woodall; Louis J. Guido

Bibliography. A. A. Bergh and P. J. Dean, *Light Emitting Diodes*, 1976; G. Bogner et al., *Compound Semiconductor*, 5(4):28, 1999; S. E. Miller and I. P. Kaminow (eds.), *Optical Fiber Telecommunications*, vol. 2, 1988; G. B. Stringfellow and M. George Craford (eds.), *Semiconductors and Semimetals*, vol. 48: *High Brightness Light Emitting Diodes*, 1997.

Light panel

A surface-area light source that employs the principle of electroluminescence to produce light. Light panels are composed of two sheets of electrically conductive material, one a thin conducting backing and the other a transparent conductive film, placed on opposite sides of a plastic or ceramic sheet impregnated with a phosphor, such as zinc sulfide, and small amounts of compounds of copper or manganese. When an alternating voltage is applied to the conductive sheets, an electric field is applied to the phosphor. Each time the electric field changes, it dislodges electrons from the edges of the phosphor crystals. As these electrons fall back to their normal atomic state, they affect the atoms of the slight "impurities" of copper or manganese, and radiation of the wavelength of light is emitted. *See* ELECTROLUMINESCENCE.

In contrast to incandescent, vapor-discharge, and fluorescent lamps, which are essentially point or line sources of light, the electroluminescent light panel is essentially a surface source of light. Complete freedom of size and shape is a fascinating aspect of luminescent cells (see **illus.**).

Brightness of the panel depends upon the voltage applied to the phosphor layer and upon the electrical frequency. In general, higher voltage and higher frequency both result in a brighter panel. Blue, green, red, or yellow light can be produced by the choice of phosphors, and the proper blend of these colors

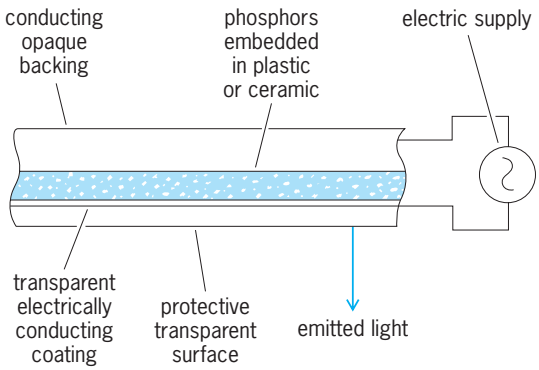

Simplified diagram of an electroluminescent cell; the sketch is not drawn to scale.

produces white light. Color can be varied for a particular phosphor by changing the frequency of the applied voltage. Increasing the frequency shifts the color toward the blue end of the spectrum.

The efficiency of these light panels is only a fraction of that of the most efficient fluorescent lamps. Theoretical limits indicate, however, that the efficiency can be further improved, probably to exceed that for fluorescent lamps. Because panel lights employ no filaments and no evacuated or gas-filled bulbs, replacement of units is virtually eliminated. Glareless uniform distribution of light from large-area sources is possible without shades, louvers, or other control devices. *See* FLUORESCENT LAMP; ILLUMINATION.

Warren B. Boast

Light-scattering techniques

A wide variety of analytic techniques in which the distribution and precise nature of the scattered light carry information about the object from which it was scattered. Light-scattering techniques are used for studying and characterizing particles ranging from nanometer to millimeter sizes.

Whenever light traveling through a medium encounters a change in optical properties (for example, meeting a particle suspended in air), some of the incident light energy is redirected from its original path. This is light scattering. If the wavelength (color) of the scattered light is the same as that of the incident light, the phenomenon is referred to as elastic light scattering; if there is a change in wavelength caused by the particle's motion relative to the incident light or its material properties, so-called quasi-elastic or inelastic light scattering may result. Light-scattering techniques are now found in virtually every branch of science and engineering, from polymer chemistry, pharmaceutical biochemistry, and clinical science to food processing, meteorology, and environmental pollution monitoring. Some of the principal light-scattering techniques used are described below.

Light is that part of the electromagnetic spectrum to which our eyes are sensitive, approximately 400–700 nm (blue to deep red) in wavelength (λ). Light-scattering techniques normally use wavelengths within this range, although the term is often loosely applied when shorter (ultraviolet) or longer (infrared) wavelengths are used. In such cases, the principles of the underlying science remain essentially the same. *See* ELECTROMAGNETIC RADIATION; LIGHT.

Scattering. Classically, the interaction of light with a particle may be considered in terms of the electromagnetic wave nature of light and the electrical charges bound within the particle. The oscillating electric field of the light wave (in the plane perpendicular to the wave's direction) causes the bound electrical charges to oscillate too, and so reradiate secondary electromagnetic waves in all directions (**Fig. 1**). Two arbitrary bound charges at positions A and B within the particle will radiate secondary waves as shown. In certain directions, these waves will be in phase and will constructively interfere, producing a higher intensity; in other directions, they will be out of phase and will tend to cancel out each other (destructive interference). The directions of constructive and destructive interference depend on both the relative positions of the charges and how they are bound within the molecules of the particle. When all bound charges are considered, the unique pattern of scattered light around the particle will depend on the size, shape, and material nature of the particle, as well as the wavelength and polarization state of the incident light (that is, how the electric field oscillations vary in time). It is this unique optical "signature" that is exploited in particle light-scattering techniques. In some cases, light energy may be absorbed by the particle and reemitted at a different wavelength some time later. These processes give rise to phenomena such as fluorescence and phosphorescence, and a more complex quantum-mechanical description is required for full understanding. *See* INTERFERENCE OF WAVES.

If the particle is much smaller than the incident wavelength, all of the bound charges will oscillate essentially in phase and the scattered energy will be virtually the same in forward and backward directions. This is referred to as Rayleigh scattering. When the particle size is the same order as the wavelength of the light, the pattern of scattered light becomes more complex and the energy scattered in the forward direction dominates. This is referred to as Mie scattering. *See* SCATTERING OF ELECTROMAGNETIC RADIATION.

Light-scattering techniques can be broadly divided into two categories: those that investigate individual particles in an attempt to characterize or classify them, and those that examine a large number of particles simultaneously in order to determine properties of the whole population. There are variants of both techniques, each of which fulfils an important analytic role. In the majority of cases, the preferred light source is a laser since this provides intense, monochromatic, and coherent (required in some applications) radiation. *See* LASER.

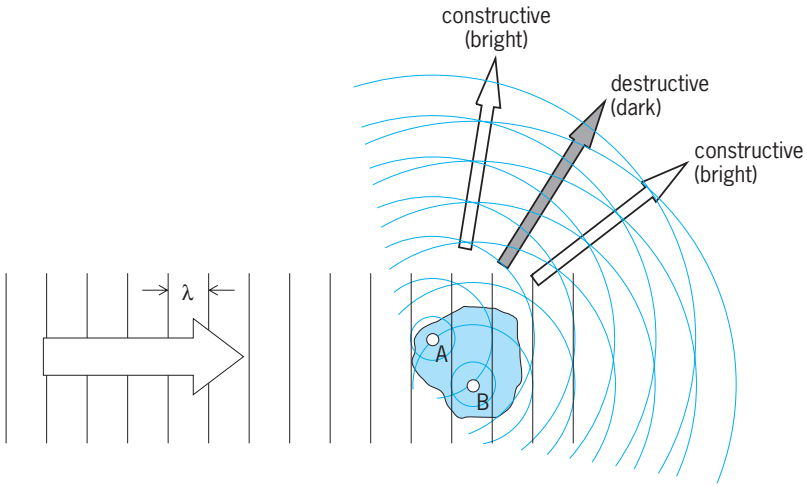

Fig. 1. Simplified interpretation of light scattering by a particle.

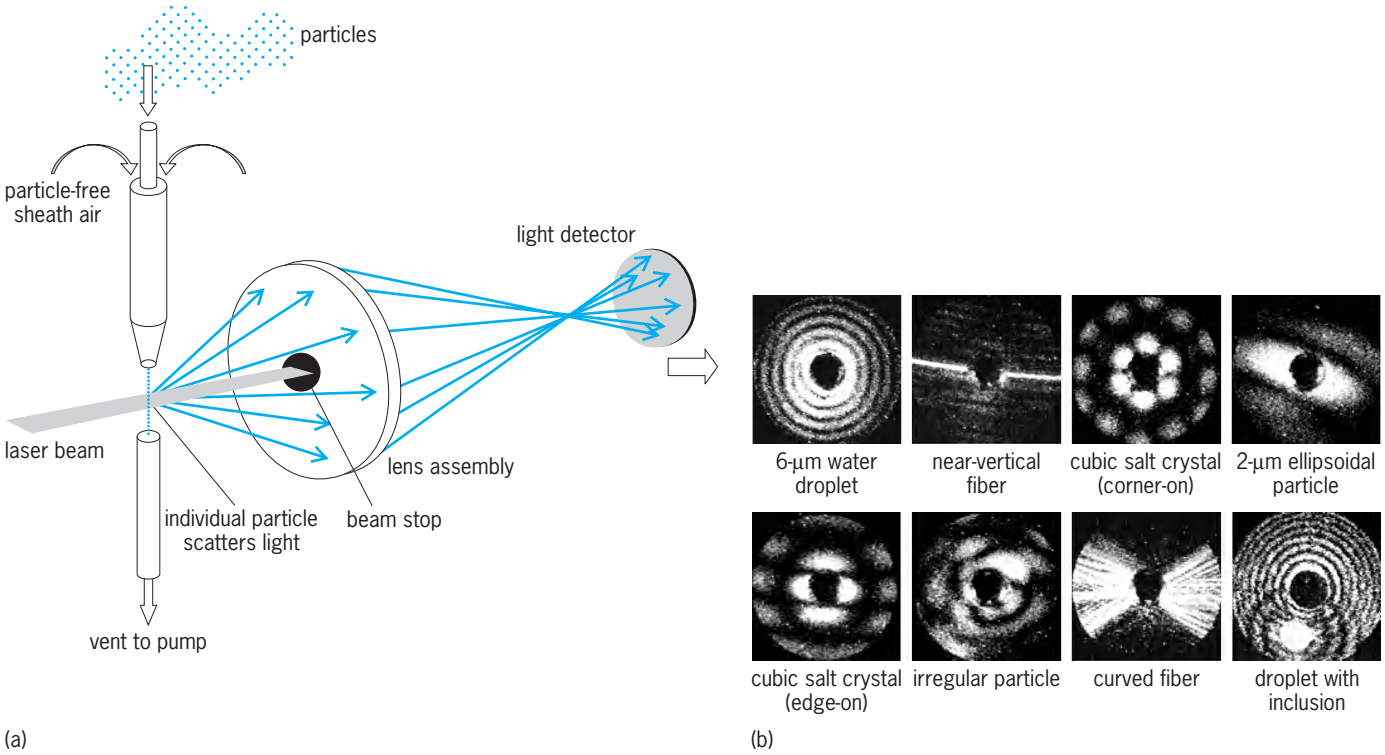

Fig. 2. Single-particle light scattering. (*a*) Apparatus. (*b*) Typical scattering patterns from various particle types.

Single-particle scattering. To achieve single-particle scattering from particles in air or liquid suspension, it is necessary to control the movement of the particles so that they pass rapidly through the illuminating light beam in single file and produce pulses of scattered light that can be detected and recorded. Often, an arrangement is used in which particles are constrained to flow through a laser beam by ensheathing the particle-laden air column with a layer of particle-free air (**Fig. 2***a*).

Optical particle counting. In the simplest case, light scattered by each particle may be recorded by a single optical detector that integrates the light signal across a large, solid angle of scattering. Such optical particle counters (OPCs) are an important class of instrument used in areas such as environmental or industrial monitoring, where knowledge of the number concentration and size distribution of airborne particles is important from a health or process-control point of view. Particles from ~0.3 to 100 μm may be measured, although sizing data must be treated with caution since the magnitude of scattered light falling on the detector will be a function of particle shape and material (refractive index) as well as absolute size. *See* OPTICAL DETECTORS.

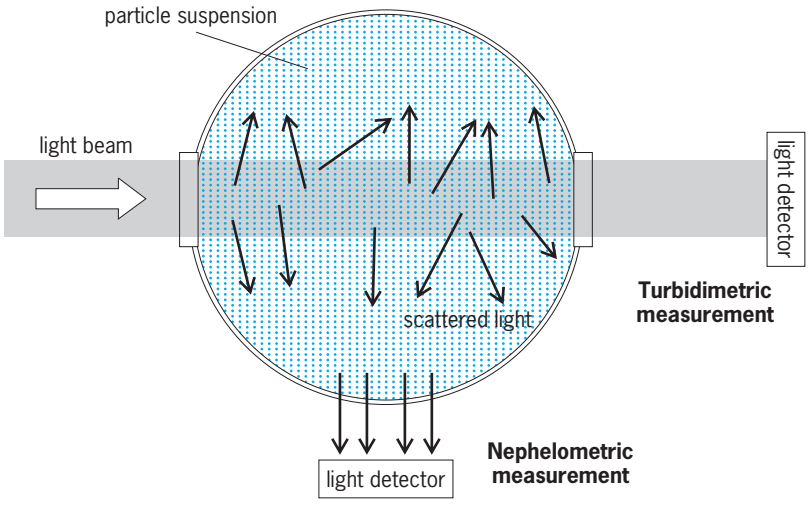

Fig. 3. Light-scatter measurement from particle suspensions.

Spatial light scattering. In more sophisticated instruments, the single detector is replaced by a detector array to record more detail of the complex pattern of scattered light (Fig. 2*b*). Such spatial light-scattering techniques can allow assessment of individual particle shape and structure as well as size, and are especially useful in areas where the classification of particles into different categories is required. For example, aircraft-borne instruments allow the classification of cloud ice crystals and water droplets (data important for meteorological climate-change research), while in clinical fields instruments can be used to sort various types of liquid-borne cells. Spatial light-scattering techniques are also of importance in monitoring applications where the detection of potentially low concentrations of hazardous particles is required in an ambient atmosphere. Examples include the detection of airborne asbestos fibers around demolition sites and the detection of airborne biological particles in environments susceptible to

terrorist attacks. In the latter case, measurements of other optical phenomena, such as particle fluorescence, are often used in parallel with light scattering to improve the confidence of particle classification.

Ensemble particle scattering. The most widely used light-scattering techniques, primarily for reasons of simplicity of implementation and ease of use, are those based on measurement of the scattering properties of large collections or ensembles of particles. In such methods, one or more detectors record the light intensity scattered simultaneously from possibly millions of individual particles, giving rise to average properties of the particle suspension (**Fig. 3**). While such techniques are used in fields such as meteorology and pollution monitoring for visibility assessment, they are most frequently applied to the quantitative measurement of powders, particle-liquid suspensions, and macromolecular suspensions associated with numerous industrial, chemical, or biochemical processes.

Turbidimetry and nephelometry. Measurement of the decrease in intensity of a beam of light resulting from its passage through a suspension of particles is referred to as turbidimetry. This simple technique provides a measure of the size and concentration of the particles, and is widely used in clinical chemistry and polymer science. In a related technique, nephelometry, the detector is placed at an angle, usually 90°, to the beam axis to measure the scattered light from the suspension. For very dilute suspensions or those containing particles much smaller than the wavelength of the light, even down to macromolecular sizes, the relative ease of measuring low scattered-light intensities against a dark background makes nephelometry an extremely sensitive technique. Measuring the change of light-scatter intensity over time, so-called rate nephelometry, allows chemical or biochemical reactions to be followed through changes in particle concentration or size. *See* IMMUNONEPHELOMETRY; POLYMER.

Laser diffraction. In the technique of laser diffraction, the forward-scattered light from a suspension of airborne or liquid-borne particles is measured using a multielement detector, usually comprising concentric annular detector rings. Since proportionally more of the scattered light from the smallest particles is scattered at higher angles while larger particles scatter predominantly at lower forward angles, such a detector arrangement can be used to assess the distribution of particle sizes within the suspension. The technique is applicable to particles from below ~100 nm up to several millimeters in size, depending on the range of scattering angles covered by the instrument and the optical geometry used. Being a noninvasive and essentially real-time technique, it has found application in powder and liquid-particle suspension measuring/monitoring applications in the production of foodstuffs, paints, ceramics, and pharmaceuticals.

Dynamic light scattering. The techniques described above measure the time-averaged intensity of scattered light and are often referred to as total-intensity scattering or static light scattering. For suspensions of particles or macromolecules that are extremely small compared with the wavelength of the light, the time-dependent fluctuations in the scattered light arising from the random Brownian motion of the particles can be exploited to assess particle size. This technique of dynamic light scattering (also known as quasi-elastic light scattering or photon correlation spectroscopy) requires the incident light to be coherent and monochromatic, and has benefited hugely from the development of lasers as well as from advances in computer power. By measuring their diffusion behavior, it allows routine sizing of the particles or macromolecules down to a few nanometers in size, and is a valued technique in numerous research fields and manufacturing processes.

Paul Kaye

Bibliography. B. J. Berne and R. Pecora, *Dynamic Light Scattering with Applications to Chemistry, Biology, and Physics*, Courier Dover Publications, Toronto, 2000; C. F. Bohren and D. R. Huffman, *Absorption and Scattering of Light by Small Particles*, Wiley Interscience, 1998; W. Brown, *Light Scattering: Principles and Development*, Oxford University Press, 1996; R. Xu, *Particle Characterization: Light Scattering Methods*, Kluwer Academic, 2000.

Light-year

A unit of measurement of astronomical distance. A light-year is the distance light travels in 1 sidereal year. One light-year is equivalent to 9.461×10^{12} km, or 5.879×10^{12} mi. Distances to some of the nearer celestial objects, measured in units of light time, are shown in the **table**.

Distances from the Earth to some celestial objects

Object	Distance from Earth (in light time)
Moon (mean)	1.3 s
Sun (mean)	8.3 min
Mars (closest)	3.1 min
Jupiter (closest)	33 min
Pluto (closest)	5.3 h
Nearest star (Proxima Centauri)	4.3 years
Andromeda Galaxy (M31)	2.3×10^6 years
Typical quasar	3×10^9 years
Epoch of recombination	13.7×10^9 years

This unit, while useful for its graphic presentation of the enormous scale of stellar distances, is seldom used technically except in cosmology. *See* ASTRONOMICAL UNIT; COSMOLOGY; PARALLAX (ASTRONOMY); PARSEC.

Jesse L. Greenstein; Jay M. Pasachoff

Bibliography. K. Ferguson, *Measuring the Universe*, Walker, New York, 1999; M. Rowan-Robinson, *Cosmology*, 4th ed., Oxford University Press, 2004.

Lighthouse

A distinctive structure, built on or near a shore, which exhibits a light of distinctive characteristics to serve as an aid to navigation (see **illus.**). Lesser lights may be displayed from fixed structures called beacons or from floating buoys or lightships.

Lighthouse overlooking sea from a coastal headland. (*U.S. Coast Guard*)

The characteristics of the lights displayed by lighthouses are given in light lists available to mariners and, in abbreviated form, on charts. Some lights have one or more sectors in which the light appears red, usually to warn of some danger in this sector. In other sectors most lights are white.

Lighthouses have been diverse in structure and type of light. Towers up to 200 ft (60 m) were constructed along the Mediterranean coast of Egypt many centuries before Christ, with beacon fires maintained by priests. Logs, coal, oil, gas, and electricity have been used to provide lights. An attendant is continuously on duty at many lighthouses, but some are unattended, and some modern installations are controlled remotely from a convenient location. *See* PILOTING. Alton B Moody

Bibliography. N. Bowditch, *American Practical Navigator, An Epitome of Navigation, 1995 edition,*, 1995; U.S. Coast Guard, *Aids to Navigation Manual*, CG-222, 1982.

Lightning

An abrupt, high-current electric discharge that occurs in the atmospheres of the Earth and other planets and that has a path length ranging from hundreds of feet to tens of miles. Lightning occurs in thunderstorms because vertical air motions and interactions between cloud particles cause a separation of positive and negative charges. *See* ATMOSPHERIC ELECTRICITY.

Lightning is both a fascinating weather phenomenon and a severe hazard. The vast majority of flashes are produced by thunderclouds, and most discharges remain within the cloud or are from cloud to air or from cloud to cloud. About one-third of all discharges are from cloud to ground, and this type of lightning is the primary hazard to people or objects on the ground. Lightning can also be initiated artificially (triggered) by tall structures when a thunderstorm is nearby, or by aircraft or rockets when they fly into a highly electrified environment. Triggered lightning can occur in clouds that otherwise do not produce natural lightning; hence this type of discharge is frequently unexpected.

Lightning between cloud and ground. The vast majority of lightning flashes between cloud and ground begin in the cloud with a process known as the preliminary breakdown. After perhaps a tenth of a second, a highly branched discharge, the stepped leader, appears below the cloud base and propagates downward in a succession of intermittent steps. The leader channel is usually negatively charged, and when the tip of a branch of the leader gets to within about 30 m (100 ft) of the ground, the electric field becomes large enough to initiate one or more upward connecting discharges, usually from the tallest objects in the local vicinity of the leader. When contact occurs between an upward discharge and the stepped leader, the first return stroke begins. The return stroke is basically a very intense, positive wave of ionization that propagates up the partially ionized leader channel into the cloud at a speed close to the speed of light. After a pause of 40–80 milliseconds, another leader, the dart leader, forms in the cloud and propagates down the previous return-stroke channel without stepping. When the dart leader makes contact with the ground, a subsequent return stroke propagates back to the cloud. A typical cloud-to-ground flash lasts 0.2–0.3 s and contains about four return strokes; lightning often appears to flicker because the human eye is capable of just resolving the interval between these strokes. In roughly one-third of all flashes to ground, the dart leader propagates down just a portion of the previous return-stroke channel and then forges a different path to ground. In these cases, the discharge actually strikes the ground in two places, and the channel has a characteristic forked appearance that has been frequently photographed (**Fig. 1**).

Lightning between cloud and ground is usually classified according to the direction of propagation and polarity of the initial leader. For example, in the most frequent type of cloud-to-ground lightning a negative discharge is initiated by a downward propagating leader as described above (**Fig. 2***a*). In this case, the total discharge will effectively lower negative charge to ground or, equivalently, will deposit positive charge in the cloud. In a photograph, the direction of the branches is the same as the direction of leader propagation.

A discharge can be initiated by a downward-propagating positive leader (Fig. 2*b*). Positive discharges occur less frequently than negative ones, usually just a few percent of the total number of

Fig. 1. Natural cloud-to-ground lightning near Tucson, Arizona. Note that each discharge strikes the ground in more than one place. (*Courtesy of Michael J. Leuthold*)

flashes, but positive discharges are often quite deleterious. Another type of lightning is a ground-to-cloud discharge that begins with a positive leader propagating upward (Fig. 2*c*); this type is relatively rare and is usually initiated by a tall structure or a mountain peak. The rarest form of lightning is a discharge that begins with a negative leader propagating upward (Fig. 2*d*).

The electric currents that flow in return strokes

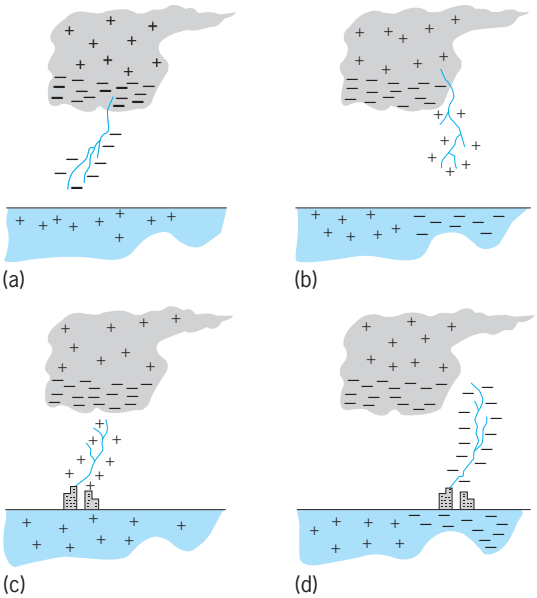

Fig. 2. Sketches of the different types of lightning between an idealized cloud and the ground: (*a*) type 1, (*b*) type 2, (*c*) type 3, and (*d*) type 4. Channel development within the cloud is not shown. Type 1 is the most common form of cloud-to-ground lightning, and type 4 is very rare. (*After M. A. Uman, The Lightning Discharge, Academic Press, 1987*)

have been measured during direct strikes to instrumented towers. The peak current in a negative first stroke (Fig. 2*a*) is typically 30 kiloamperes, with a zero-to-peak rise time of just a few microseconds. This current decreases to half-peak value in about 50 microseconds, and then low-level currents of hundreds of amperes may flow for a few to hundreds of milliseconds. The long-continuing currents produce charge transfers on the order of tens of coulombs and are frequently the cause of fires. Subsequent return strokes have peak currents that are typically 10–15 kA, and somewhat faster current rise times. The maximum rate of change of current during the initial rise of both first and subsequent return strokes is on the order of 100 kA/μs (10^{11} A/s). Five percent of the negative discharges to ground generate peak currents that exceed 80 kA, and 5% of the positive discharges (Fig. 2*b*) exceed 250 kA. Positive flashes frequently produce very large charge transfers, with 50% exceeding 80 coulombs and 5% exceeding 350 coulombs.

The rapidly rising return-stroke current heats the channel to a peak temperature near 55,000°F (30,000°C). This rapid heating produces high pressures that cause sections of the channel to expand behind shock waves that eventually become thunder. The peak light output from a 1-m (3.3-ft) vertical section of channel is over 10^6 W, and the peak light output from the entire stroke is typically 10^9 W or more. Occasionally, flashes produce a light output that exceeds 10^{11} W, and these are sometimes known as superbolts. *See* CLOUD PHYSICS; SHOCK WAVE.

Electromagnetic fields. Electric and magnetic fields that are radiated by different lightning processes have different but characteristic signatures that are reproduced from flash to flash. A typical cloud-to-ground flash at a distance of about 60 km (37 mi) can be characterized by a cloud pulse that was radiated during the preliminary breakdown, the waveform that was produced by the first return stroke, and the signature from a subsequent return stroke.

A peak field of 8 V/m at 100 km (60 mi) means that the peak electromagnetic power that is radiated by the stroke exceeds 10^{10} W; therefore, lightning is easily detected at very large distances. It also means that if such a pulse propagates upward into the middle atmosphere, it will be large enough to heat the electrons and cause regions of enhanced ionization in the lower ionosphere. Such phenomena have occurred in the United States and New Zealand. *See* ELECTROMAGNETIC RADIATION; GEOELECTRICITY; IONOSPHERE.

Triggered lightning. Mountains and tall buildings can sometimes initiate upward, ground-to-cloud lightning. Aircraft experiments have also shown that the majority of lightning strikes to airborne vehicles actually begin at, and hence are triggered by, the airframe.

When a thunderstorm is overhead and the electrical conditions are favorable, lightning can be triggered artificially by using small rockets to carry a grounded wire aloft. If the rocket is fired when the surface electric field is high (3–5 kV/m), about 70%

of all launches will trigger a discharge. Most triggers occur when the rocket is at an altitude of only 100–300 m (330–990 ft), and usually the first stroke in the flash propagates upward into the cloud and is not like natural lightning. The majority of the subsequent strokes, however, follow the first stroke to ground and are almost identical to their natural counterparts.

Triggered lightning is important for research because it provides the capability of studying both the physics of the discharge and its interactions with structures in a partially controlled environment. It is being used to investigate the luminous development of lightning channels, the waveforms of lightning currents, the velocities of return strokes, the relation between currents and fields, the mechanisms of lightning damage, the performance of lightning protection systems, and many other problems. Among the more important findings have been the discovery of submicrosecond fields and currents during return strokes and the general validity of the transmission line model equation. Submicrosecond current variations produce large voltages when lightning strikes an inductive load or a complex system, such as an airplane, that is sensitive to high-frequency disturbances. Submicrosecond currents also place more stringent requirements on the performance of surge arresters and other devices that are used in lightning protection, and also on the engineering tests and test standards that are used to verify that performance. *See* STORM ELECTRICITY; THUNDERSTORM.

E. Philip Krider

Detection. There are several techniques for detecting lightning: electric field amplitude, magnetic radiation field direction finding, electric and magnetic radiation field time of arrival and interferometers, radar, visible light detection, and thunder time of arrival. The electric field amplitude (flash counter) techniques are limited to a range of a few tens of kilometers; they are used primarily in lightning research for studies in small geographical regions. Magnetic field direction finding is the basis for one of two methods of detecting lightning flashes to ground. If two azimuths or directions are known to a lightning flash, the location of the flash to ground is determined by triangulation.

Radiation field time-of-arrival systems are operating over the United States and are effective in locating lightning when the precise relative time is known at four or more stations. The combination of magnetic direction finding and radiation time-of-arrival systems makes up the National Lightning Detection Network. Radar techniques depend on detecting the reflected energy from a lightning channel at wavelengths of 10 cm or longer, and the resulting pattern can produce a pattern of the channel in a cloud. Techniques using visible light for lightning location depend on instruments such as video cameras to record the image of lightning. The thunder time-of-arrival technique depends on the accurate recording of the arrival time of thunder following the time of the visible channel. Since the average speed of sound in the atmosphere is known, the distance to the channel is estimated by allowing 3 s for every kilometer (5 s for every mile) between the observer and the lightning. Of the various lightning-detection methods, the combined use of the magnetic direction finding and time-of-arrival methods provides the most effective technique for locating flashes to ground.

The U.S. National Lightning Detection Network is composed of over one hundred sensors strategically placed throughout the contiguous United States; it provides lightning locations to over 400 users, including universities, electrical power companies, telephone corporations, airlines, and federal agencies including the National Weather Service and Defense Agencies. The National Network was originally established as a large regional lightning detection network in the west to provide early warning of forest fires. The sensors record only lightning flashes to ground, and exclude the more frequent and usually harmless (for ground-based objects) intracloud lightning. Subsequent regional lightning detection networks were established in the Midwest and the East to study the meteorological and physical characteristics of lightning to ground.

A satellite detector launched in April 1995 is in a nearly circular orbit of 740 km (460 mi) with an inclination of 70°. From this altitude, the satellite has a field of view of 1300 by 1300 km (780 × 780 mi). Results from summer observations indicate that the lightning flash rate on Earth is approximately 40 flashes per second. A second satellite with a lightning sensor was launched in November 1997; it also contains a radar to measure rainfall from space. The lightning sensor is a small solid-state camera with special filters that transmit only the peak optical radiation emitted by lightning at 777.4 nanometers. The camera view is 600 km (370 mi) on a side, and each pixel in the focal plane covers 5–10 km (3–6 mi) on the ground, matching the smallest storm cells that might be producing lightning. Researchers are now overlaying these lightning locations onto visible, thermal, and radar images to learn more about storms around the globe. *See* METEOROLOGICAL SATELLITES.

National Lightning Detection Network operation. The National Lightning Detection Network contains sensors that detect the electric and magnetic radiation field and uses the magnetic direction finding method. The magnetic direction finders consist of two orthogonal magnetic-loop antennas, an electric field antenna, associated electronics to process the incoming signals, and an antenna to communicate via satellite with the National Lightning Detection Network operations center in Tucson, Arizona. The bandwidths of the antenna systems receiving the lightning signals are wide (approximately 1–380 kHz), so that the shapes and polarities of the radiation field waveforms are preserved. The orthogonal magnetic-loop antennas sense the magnetic field from lightning, and a voltage is induced in each loop that is proportional to the magnetic field derivative multiplied by the cosine of the angle between the plane of the loop and the direction of propagation of the incoming field. The ratio of the integrated voltages in the orthogonal

loops at the time of the peak voltage field provides the direction to the lightning flash. A 180° ambiguity in direction is removed by the electric field antenna that senses the polarity of the field (and the polarity of the lightning current). The processing electronics is designed to respond to only those waveforms that are characteristic of return strokes in cloud-to-ground flashes.

Information from all the sensors detecting the lightning is sent via satellite to the operations center. When a lightning flash is detected by a sensor, the time, angle, signal amplitude, and polarity of all strokes are stored until the information is electronically requested by a computer in the operations center, typically every 10 s. When two or more sensors detect a flash within a programmed time interval, the location of the flash is computed and plotted using the time-of-arrival and direction finding information. All the sensor information is used to plot the optimal location of the flash.

The sensors in the National Lightning Detection Network use magnetic direction finding and time-of-arrival techniques. The detection efficiency of the network is estimated to be approximately 80–90%, with an accuracy of approximately 500 m (over 1640 ft).

Positive and negative flashes. Although lightning to ground normally lowers negative charge (negative flashes), a small but significant number of flashes involve the lowering of positive charge to ground (positive flashes). Consequently, study of ground flashes must separate the characteristics of these two kinds of lightning. Negative flashes are known to have a median peak current in first return strokes of 30 kA, but positive flashes have a median peak current that is approximately 30% higher. Fortunately, the occurrence of positive lightning to ground is a small percentage of the total number of flashes, typically 10% for the entire year. In some regions of the United States, however, the percentage of positive lightning may exceed 25%.

An annual summary masks some of the interesting polarity variations that have been discovered. For example, the percentage of positive lightning flashes has been shown to vary with season, latitude, and storm. At higher latitudes, characteristic of New England and the upper Midwest, the percentage of positive lightning flashes in winter storms normally exceeds 50% and may be 100% in periods of a storm. At lower latitudes, characterized by Florida, the percentage of positive flashes rarely exceeds 20%. *See* LIGHTNING AND SURGE PROTECTION; STORM DETECTION.

Sprites, elves, and jets. Red sprites, elves, and blue jets are upper atmospheric optical phenomena associated with thunderstorms and have only recently been documented using low-light-level television technology. Since the first sprite images were obtained accidentally in 1989, thousands of images have been obtained, including over 20 from the space shuttle. They show massive but weak luminous flashes appearing directly above active thunderstorms coincident with cloud-to-ground or intracloud lightning. They extend from the cloud tops to about 95 km (59 mi) and are predominantly red. High-speed photometer measurements show that the duration of sprites is only a few milliseconds. Their brightness is comparable to a moderately bright auroral arc. The optical energy is roughly 10–50 kJ per event, with a corresponding optical power of 5–25 MW. Elves are associated with sprites and are a recent discovery. They are optical emissions of approximately 1 millisecond, with a fast lateral, horizontal expansion that emits more red than blue light. They occur at altitudes of 75–95 km (47–59 mi). *See* SPACE SHUTTLE.

Numerous images have been obtained from aircraft of blue jets. They are a second high-altitude optical phenomenon, distinct from sprites and observed above thunderstorms using low-light television systems. Blue jets are optical ejections from the top of the electrically active core regions of thunderstorms. Following the emergence from the top of the thundercloud, they typically propagate upward in narrow cones of about 15° full width at vertical speeds of roughly 100 km/s (60 mi/s), fanning out and disappearing at heights of about 40–50 km (25–30 mi).

Richard E. Orville

Bibliography. *The Earth's Electrical Environment*, National Research Council Studies in Geophysics, 1986; D. R. MacGorman and W. D. Rust, *The Electrical Nature of Storms*, 1998; M. A. Uman, *All About Lightning*, 1986; M. A. Uman, *The Lightning Discharge*, 1987; M. A. Uman and E. P. Krider, Natural and artificially initiated lightning, *Science*, 246:457–464, 1989.

Lightning and surge protection

Means of protecting electrical systems, buildings, and other property from lightning and other high-voltage surges.

The destructive effects of natural lightning are well known. Studies of lightning and means of either preventing its striking an object or passing the stroke harmlessly to ground have been going on since the days when Franklin first established that lightning is electrical in nature. From these studies, two conclusions emerge: (1) Lightning will not strike an object if it is placed in a grounded metal cage. (2) Lightning tends to strike, in general, the highest objects on the horizon. *See* ATMOSPHERIC ELECTRICITY; LIGHTNING.

One practical approximation of the grounded metal cage is the well-known lightning rod or mast (**Fig. 1***a*). The effectiveness of this device is evaluated on the cone-of-protection principle. The protected area is the space enclosed by a cone having the mast top as the apex of the cone and tapering out to the base. Laboratory tests and field experience have shown that if the radius of the base of the cone is equal to the height of the mast, equipment inside this cone will rarely be struck. A radius equal to twice the height of the mast gives a cone of shielding within which an object will be struck

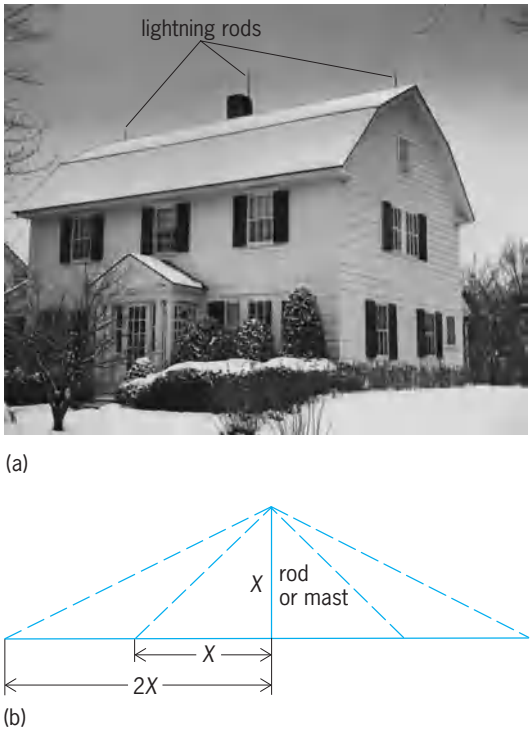

Fig. 1. Lightning rod cone of protection. (*a*) Configuration of rods on a house. (*b*) Geometry of the principle.

occasionally. The cone-of-protection principle is illustrated in Fig. 1*b*.

Another criterion for cone of protection of a lightning mast is based on the distance over which the final lightning stroke breakdown occurs. As the stroke can contact any point within striking distance of this final breakdown, the configuration of a sphere with a radius of the striking distance, conservatively taken as 100 ft (30 m), defines the vulnerable area, and locations outside the sphere would be protected. A different visualization of this would be a ball having a 100-ft radius, rolled on the ground toward a mast; when it contacts the mast, all points between the mast and the point where the ball contacts the ground, outside and below the ball, would be protected.

A building which stands alone, like the Empire State in New York City, is struck many times by lightning during a season. It is protected with a mast, and the strokes are passed harmlessly to ground. However, lightning has been observed to strike part way down the side of this building (**Fig. 2**). This shows that lightning does not always strike the highest object but rather chooses the path having the lowest electrical breakdown.

The probability that an object will be struck by lightning is considerably less if it is located in a valley. Therefore, electric transmission lines which must cross mountain ranges often will be routed through the gaps to avoid the direct exposure of the ridges. *See* ELECTRIC DISTRIBUTION SYSTEMS; ELECTRIC POWER SYSTEMS.

Overhead lines of electric power companies are vulnerable to lightning. Lightning appears on these lines as a transient voltage, which, if of sufficient magnitude, will either flash over or puncture the weakest point in the system insulation.

Many of the troubles that cause service interruptions on electrical systems are the results of flashovers of insulation wherein no permanent damage is done at the point of fault, and service can be restored as soon as the cause of the trouble has disappeared. A puncture or failure of the insulation, on the other hand, requires repair work, and damaged apparatus must be removed from service.

There are a number of protective devices to limit or prevent lightning damage to electric power systems and equipment. The word protective is used to connote either one or two functions: the prevention of trouble, or its elimination after it occurs. Various protective means have been devised either to prevent lightning from entering the system or to dissipate it harmlessly if it does. *See* ELECTRIC PROTECTIVE DEVICES.

Overhead ground wires and lightning rods. These devices are used to prevent lightning from striking the electrical system.

The grounded-metal-cage principle is approached by overhead ground wires, preferably two, installed over the transmission phase conductors and grounded at each tower (**Fig. 3**). The ground wires must be properly located with respect to the phase conductors to provide a cone of protection and have adequate clearance from them, both at the towers and throughout the span. If the resistance to ground of the tower is high, the passing of high lightning currents through it may sufficiently elevate the tower in potential from the transmission line conductors so that electrical flashover can occur. Since the magnitude of the lightning current may be defined in terms of probability, the expected frequency of line flashover may be predicted from expected storm and lightning stroke frequency, the current magnitude, and the tower footing resistance. Where

Fig. 2. Multiple lightning stroke A to Empire State and nearby buildings, August 23, 1936. Single, continuing stroke B to Empire State Building, August 24, 1936.

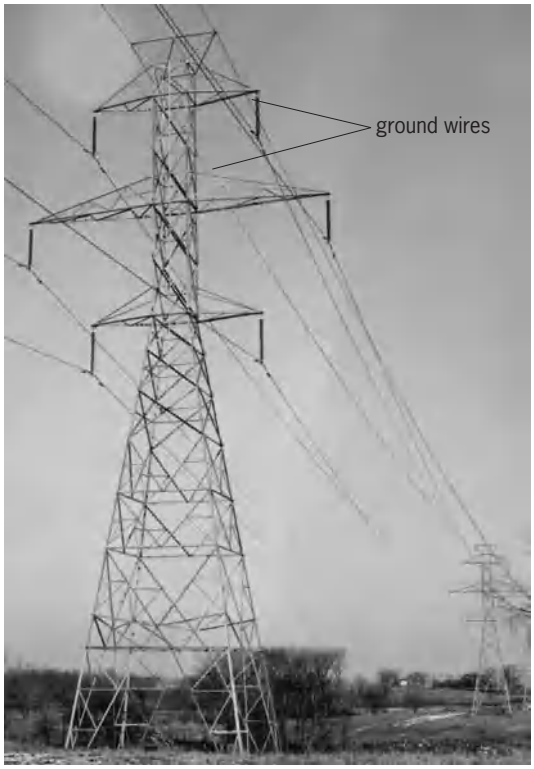

Fig. 3. Double-circuit suspension tower on the Olive–Gooding Grove 345-kV transmission line, with two circuits strung and with two ground wires. (*Indiana and Michigan Electric Co.*, *American Electric Power Co.*)

the expected flashover rate is too high, means to lower the tower footing resistance are employed such as driven ground rods or buried wires connected to the base of the tower. Applications of zinc oxide surge arresters across line insulator strings in areas of high tower footing resistance have been effective in lowering line flashover frequency.

The ground wires are often brought in over the terminal substations. For additional shielding of the substations, lightning rods or masts are installed. Several rods are usually used to obtain the desired protection. *See* ELECTRIC POWER SUBSTATION.

Lightning arresters. These are protective devices for reducing the transient system overvoltages to levels compatible with the terminal-apparatus insulation. They are connected in parallel with the apparatus to be protected. One end of the arrester is grounded and also connected to the case of the equipment being protected; the other end is connected to the electric conductor (**Figs. 4** and **5**).

The nonlinearity of current with respect to voltage of a lightning arrester provides a relatively low discharge path to ground for the transient overvoltages, and a relatively high resistance to the power system follow current, so that their operation does not cause a system short circuit.

In selecting an arrester to protect a transformer, for example, the voltage levels that can be maintained by the arrester both on lightning surges and surges resulting from system switching must be coordinated with the withstand strength of the transformers to these surges. Arrester discharge voltages on various magnitudes and wave shapes of discharge currents, the inductance of connections to the arrester, voltage wave shape, and other factors must all be evaluated. *See* SURGE ARRESTER.

Rod gaps. These also are devices for limiting the magnitude of the transient overvoltages. They usually are formed of two $^1/_2$-in.^{2} (3-cm^2) rods, one of which is grounded and the other connected to the line conductor but may also have the shape of rings or horns. They have no inherent arc-quenching ability, and once conducting, they continue to arc until the system voltage is removed, resulting in a system outage.

These devices are applied on the principle that, if an occasional flashover is to occur in a station, it is best to predetermine the point of flashover so that it will be away from any apparatus that might otherwise be damaged by the short-circuit current and the associated heat.

The flashover characteristics of rod gaps are such that they turn up (increase of breakdown voltages with decreasing time of wavefront) much faster on steep-wavefront surges than the withstand-voltage characteristics of apparatus, with the result that if a gap is set to give a reasonable margin of protection on slow-wavefront surges, there may be little or no protection for steep-wavefront surges. In addition, the gap characteristics may be adversely affected by weather conditions and may result in undesired flashovers.

Immediate reclosure. This is a practice for restoring service after a fault occurs by immediately reclosing automatically the line power circuit breakers that have been tripped. The protective devices involved are the power circuit breaker and the fault-detecting and reclosing relays.

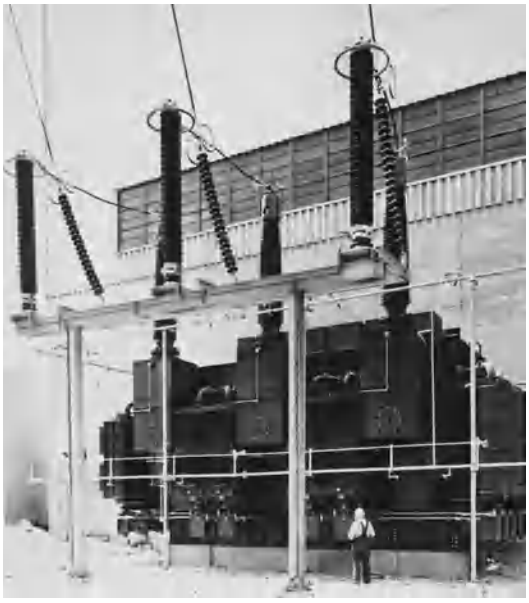

Fig. 4. Installation of three single-pole station lightning arresters rated 276 kV for lightning and surge protection of large 345-kV power transformer. (*General Electric Co.*)

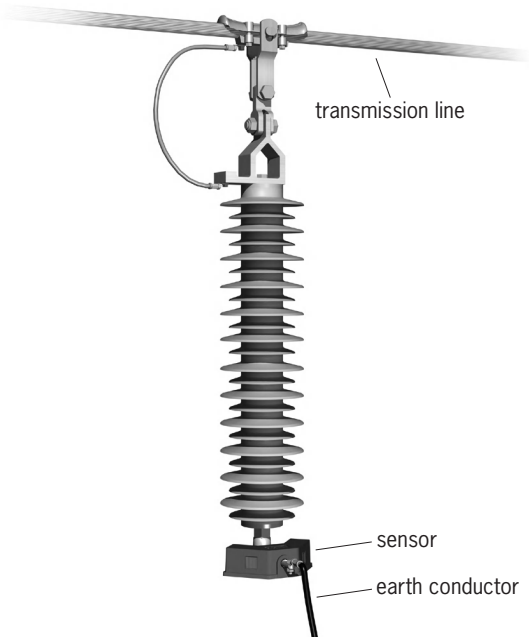

Fig. 5. PEXLINK® high-voltage surge arrester in silicone housing, equipped with special link arrangement for installation on a transmission line. The arrester protects the line from overvoltages such as lightning. The EXCOUNT-II sensor monitors the health of both the transmission line and the surge arrester. Data from the sensor can be read with a wireless transceiver and then transferred to a computer for statistical analysis. (*ABB Ltd.; photograph by Mats Findell*)

This practice is successful because the majority of the short circuits on overhead lines are the result of flashovers of insulators and there is no permanent damage at the point of fault. The fault may be either line-to-ground or between phases. Reclosing relays are available to reenergize the line several times with adjustable time intervals between reclosures.

If the relays go through the full sequence of reclosing and the fault has not cleared, they lock out. If the fault has cleared after a reclosure, the relays return to normal.

Permanent faults must always be removed from a system and the accepted electric protective devices are power circuit breakers and suitable protective relays.

Glenn D. Breuer

Bibliography. Electric Power Research Institute, *EPRI AC Transmission Line Reference Book: 200kV and Above*, 3d ed., 2005; D. G. Fink and H. W. Beaty (eds.), *Standard Handbook for Electrical Engineers*, 14th ed., 2000; M. M. Frydenlund, *Lightning Protection for People and Property*, 1993; T. Hovrath, *Computation of Lightning Protection*, 1991; National Fire Protection Association, *NFPA 780, Standard for the Installation of Lightning Protection Systems, 2004 Edition*, 2004.

Lignin

A polymer found extensively in the cell walls of all woody plants; is one of the most abundant natural polymers. Lignin, which constitutes one-fourth to one-third of the total dry weight of trees, combines with hemicellulose materials to help bind the cells together and direct water flow. *See* CELL WALLS (PLANT); HEMICELLULOSE.

Isolation. Several methods have been devised for isolating lignin from wood; isolated lignins are frequently named for the persons who developed the procedures. Brauns lignin is obtained by exhaustively extracting wood meal with 95% ethanol and then diluting the extract with water; the resulting precipitate is taken up in dioxane and reprecipitated with ether. Freudenburg lignin is obtained by a similar process, except the initial extraction is done with 90% acetone and the final purification with ethyl acetate.

Some isolation methods are based on acid treatments in which the carbohydrate components (cellulose and hemicelluloses) are hydrolyzed to water-soluble materials. Klason lignin (72% sulfuric acid) and dioxane lignin (hydrochloric acid) are produced in this way. A much milder and more popular isolation method gives Björkman or "milled wood" lignin. Here, wood meal is ground in a ball mill to break down the cell structures and then extracted with dioxane-water. This procedure, like most of the others, suffers from a poor yield (50%) of lignin. With all these procedures, serious doubts exist as to whether the isolated lignin is representative of the "native" lignin.

Enzymatic digestion of the carbohydrate in wood meal is a lengthy, tedious procedure but offers the greatest promise of leaving lignin unaltered during isolation. The isolated lignin contains some chemically bonded hemicellulose materials known as lignin-carbohydrate complexes.

Structure. Structural studies on lignin have been hampered by the random, cross-linked nature of the polymer. The relative proportions of the monomers which make up lignin [structures (**1**) and (**2**)] vary

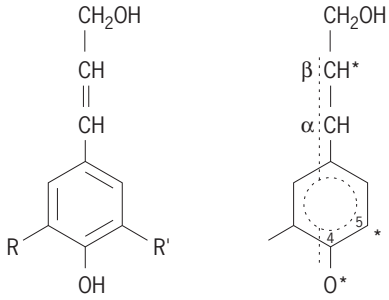

(**1**) (**2**)

with the plant species. In general, lignins in softwoods (pine, spruce, fir) are derived principally from coniferyl alcohol (R = OCH_3, R′ = H), with a few percent sinapyl alcohol (R = R′ = OCH_3) and trace amounts of *p*-coumaryl alcohol (R = R′ = H) structures. The precursors of lignins in hardwoods (oak, maple, birch) are coniferyl alcohol and sinapyl alcohol in roughly equal amounts.

Lignin is formed in the plant by an enzymatic dehydrogenation of the monomers. The * designations shown on the structure (**2**) indicate the principal sites for coupling monomers. The **illustration** presents a possible partial lignin structure. There are

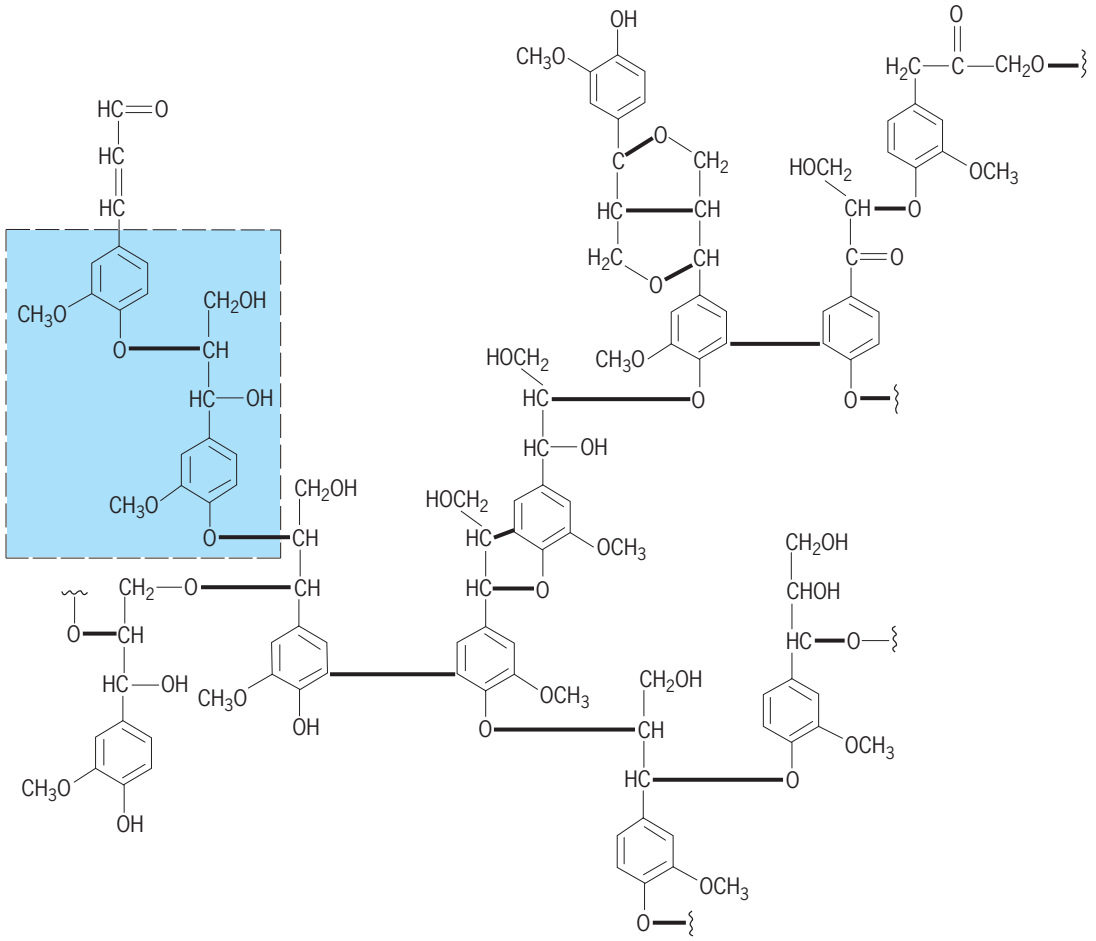

Chemical formula representation of lignin, in which bold lines represent linkages between individual phenylpropane lignin monomer units, and shaded area represents the structure of a typical lignin model compound.

occasional multiple (or secondary) linkages between units, especially at the α-carbon position. Research on lignin chemistry is often done with models of lignin. These models are typically dimers, joined by a β-aryl ether bond (see illus.). Unlike lignin, the model and its reaction products are easily characterized. Chemical reactions of lignin are assumed to parallel those of the models. The goal of chemical pulping is to break down and solubilize the lignin (delignify the wood and, thus, liberate its cellulose fibers for re-formation into paper products). *See* PAPER.

Uses. Very little lignin is isolated from pulp liquors and sold as such. In general, the markets for lignin products are not large or attractive enough to compensate for the cost of isolation and the energy derived from its burning. An exception is lignosulfonate, which is obtained either directly from sulfite pulping liquors or by sulfonation of acid-precipitated kraft lignin; its markets include a dispersant in carbon black slurries, clay products, dyes, cement, oil drilling muds, an asphalt emulsifier, a binder for animal feed pellets, a conditioner for boiler water or cooling water, and an additive to lead-acid storage battery plate expanders. *See* WOOD CHEMICALS.

Donald R. Dimmel

Bibliography. J. P. Casey (ed.), *Pulp and Paper Chemistry and Technology,* 3d ed., vol. 1, 1980; R. L. Crawford, *Lignin Biodegradation and Transformation*, 1981; D. Fengel and G. Wegener, *Wood*: *Chemistry, Ultrastructure, Reactions*, 1989; W. G. Glasser and S. Sarkanen (eds.), *Lignin: Properties and Materials*, 1989; I. A. Pearl, *The Chemistry of Lignin*, 1967; E. Sjöström, *Wood Chemistry*: *Fundamentals and Applications*, 2d ed., 1993.

Lignite

A brownish-black, low-rank coal defined in the engineering sense by the American Society for Testing and Materials as having a heating value of less than 8300 Btu/lb (4611 kcal/kg), determined on a moist, mineral-matter-free basis. Lignite occurs in two subclasses: lignite A [8300–6300 Btu/lb (4611–3500 kcal/kg)] and lignite B [less than 6300 Btu/lb (3500 kcal/kg)]. Vitrinite reflectance of lignite is 0.25–0.38%; however, vitrinite reflectance may be more suitably applied to higher-rank coals. Outside North America, low-rank coal is classified as brown coal, which includes lignite, subbituminous, and most high-volatile C bituminous coal of the North American classification system. Brown coal is divided into soft and hard coal; hard coal is subdivided into dull and bright coal. *See* COAL.

Generally, the fixed-carbon content of lignite is 60–68%, and volatile-matter content exceeds 50% (on dry, ash-free basis). The oxygen-to-carbon and hydrogen-to-carbon ratios (calculated on an atomic basis) are greater in lignite than in higher-rank coals. Porosity of lignite is about 25–30%, highest of all coals. Moisture ranges 30–75%; water occurs in pores and capillaries and is bound to organic molecules. Porosity, and thus moisture-holding capacity, decreases with increasing rank in lignite.

In the United States, lignite contains more alkali and alkaline-earth metals (especially sodium in the Northern Great Plains Region) than higher-rank coals. Relative to higher-rank coals, lignite is more reactive and commonly lower in sulfur content; and the contained inorganic matter is more likely to be organically bound (complexed) than in discrete minerals. *See* ALKALI METALS; ALKALINE-EARTH METALS.

Because lignite has undergone less coalification than higher-rank coals, the organic precursor constituents are more easily recognized than those in high-rank coals, and lignite serves as an invaluable link between peat and high-rank coals in studying the coal origin. *See* COAL PALEOBOTANY; PEAT.

Occurrences. World resources of lignite are difficult to assess because of the different classification systems for low-rank coal in North America and elsewhere. However, the world's greatest in-place resources of low-rank coal (lignite and subbituminous coal in the United States and brown coal elsewhere) occur in the United States, Russia, Australia, Germany, and the former Yugoslavia.

The lignite resource in the United States, primarily lignite A, is 5.19×10^{11} short tons (4.71×10^{11} metric tons), which is about 30% of the total identified United States coal resource. United States lignite occurs primarily in the Northern Great Plains Region, which has 4.65×10^{11} short tons (4.22×10^{11} metric tons) [90%], and the Gulf Coast Basin, which has 5.3×10^{10} short tons (4.8×10^{10} metric tons) [10%] the lignite resource. The major lignite-producing state is Texas, followed by North Dakota. Nearly all lignite in the United States is produced by surface mining. *See* SURFACE MINING.

Transportation. Lignite is difficult to store and transport. Its high moisture content adds to cost of transportation, and its high reactivity causes spontaneous combustion. Experiments with drying, spraying with oil, briquetting, and use of a slurry pipeline as alternatives or improvements in the transport and storage performance have shown that these techniques are not cost-effective.

Uses. Therefore, production is usually for use at short distances. In the United States, as elsewhere, lignite is used primarily to generate electricity at mine-mouth power plants. Lignite has been successfully used as a feedstock for gasification, liquefaction, and pyrolysis. Minor uses of lignite are montan wax, activated carbon, firing kilns, and home heating. *See* ACTIVATED CARBON; COAL CHEMICALS.

Lignite has certain utilization advantages over higher-rank coal. Because of its high reactivity, which is due in part to high oxygen content, lignite does not have to be ground as finely as higher-rank coal to ensure complete combustion in pulverized coal systems. Advantages for gasification and liquefaction are high reactivity, low sulfur content, and noncaking properties. Alkali and alkaline-earth elements have catalytic properties in gasification and possibly liquefaction. *See* COAL GASIFICATION; COAL LIQUEFACTION.

Disadvantages of lignite use in combustion, relative to higher-rank coals, are low heating value and the fact that fly ash from lignite may have high electrical resistivity, making it difficult to collect in electrostatic precipitators. Mineral matter in lignite is largely organically bound and inseparable by standard washing techniques; the high sodium content of some lignite contributes to boiler fouling and slagging problems; and the quartz content, where high, accelerates erosion of coal-feed systems and furnace burners. In gasification, moisture acts as a diluent.

Walter B. Ayers

Bibliography. American Society for Testing and Materials, *1991 Annual Book of ASTM Standards*, pt. 12: *Gaseous Fuels; Coal and Coke; Atmospheric Analysis*, 1991; N. Berkowitz, *The Chemistry of Coal: Coal Science and Technology, 7*, 1985; D. J. Trantolo and D. L. Wise (eds.), *Energy Recovery from Lignin, Peat, and Lower Rank Coals*, 1989.

Lignumvitae

A tree, *Guaiacum sanctum*, also known as holywood lignumvitae, which is cultivated to some extent in southern California and tropical Florida. Lignumvitae is native in the Florida Keys, Bahamas, West Indies, and Central and South America. It is an evergreen tree of medium size with abruptly pinnate leaves. The tree yields a resin or gum known as gum guaiac or resin of guaiac which is used in medicine. The very heavy black heartwood is used in bowling balls, blocks and pulleys, and parts of instruments. *See* FOREST AND FORESTRY; SAPINDALES; TREE.

Arthur H. Graves; Kenneth P. Davis

LIGO (Laser Interferometer Gravitational-wave Observatory)

A physics research facility developed to detect cosmic gravitational waves and to measure these waves for scientific research. It consists of two installations within the continental United States, located in the states of Washington and Louisiana, operated in unison as a single observatory. Funded by the National Science Foundation (NSF), LIGO was designed and constructed by a team of scientists from the California Institute of Technology and the Massachusetts Institute of Technology, and by industrial contractors. Construction of the facilities was completed in 1999, and operation of the detectors began

in 2001. LIGO is the leading member in a developing global network of gravitational-wave observatories.

Operating principles. Gravitational waves are emitted by accelerating masses much as electromagnetic waves are produced by accelerating charges. Unlike electromagnetic waves, astrophysical-sized objects, such as massive stars, are required to produce gravitational waves that are strong enough to be detectable. Such a source of waves may be in our galaxy, the Milky Way, or in a relatively nearby galaxy. As the wave propagates away from its source, it produces small oscillations in the space-time nature of gravity. To measure these oscillations, widely separated test masses have been set up, each hung by fibers to form a pendulum, as probes of the oscillating space-time (**Fig. 1**). The test masses are constructed as mirrors and arranged along the two arms of an L-shape, so that their separations can be monitored using a specialized type of Michelson interferometer. The interferometer is illuminated with a powerful laser, and at the vertex of the L-shape the laser beam is split into two beams, so that half the laser light travels down one arm of the L and half down the other. At the ends of the arms, each beam is reflected on itself by the end test masses, such that the two beams recombine at the vertex beam splitter. At the output port of the beam splitter, a photodetector monitors how much light exits the instrument. Nominally, when the two arms are of equal length, the two beams destructively interfere at the beam splitter, and no light reaches the photodetector. If a gravitational wave passes through the interferometer, the light travel time down and back one arm will be longer than that of the other, and the beams will no longer completely destructively interfere when they recombine at the beam splitter. Thus some light will exit the output port and be detected by the photodetector, indicating the presence of a gravitational wave. *See* ELECTROMAGNETIC RADIATION; INTERFEROMETRY.

The challenge is to make the instrument as sensitive as possible because the scale of the distance changes is incredibly small. A gravitational wave produces an oscillating strain in space, implying that the magnitude of the arm length change, dL, is proportional to the length of each arm. This fact provides the motivation for making the arms as long as possible, specifically 4 km (2.5 mi) long in LIGO. Even at this scale, the motion that must be measured is extremely small: gravitational waves passing through Earth are expected to carry strain amplitudes of order 10^{-21} or smaller, and the resulting arm length change, dL, is of order 10^{-18} m, 1000 times smaller than the diameter of a nucleus.

Refinements. Many refinements have been made to the basic interferometer to increase the sensitivity. One of these is to increase the interaction time of the light with the gravitational wave beyond the round-trip time down and back an arm. This is done by effectively folding the beams multiple times within each arm, by having the two test masses in each arm form a resonant optical cavity. Laser photons entering an arm cavity make, on average, 50 round trips

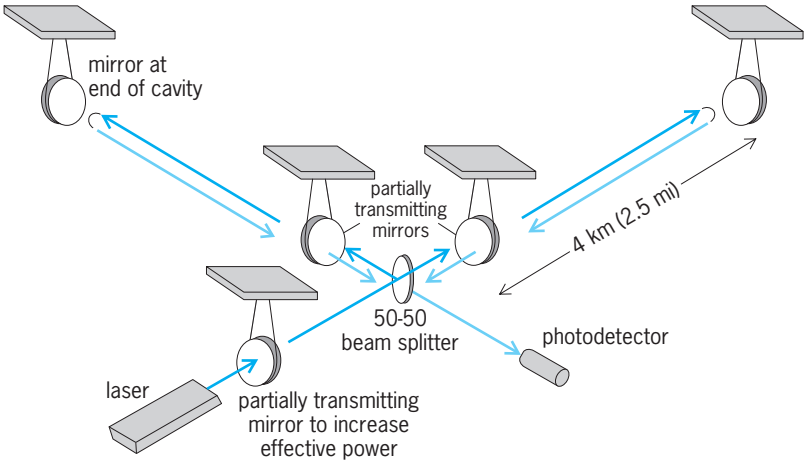

Fig. 1. Experimental setup of LIGO. The interferometric gravitational-wave detector is an equal-arm Michelson laser interferometer whose hanging mirrors serve as gravitational test masses. Beam paths and all optics are enclosed in a high-vacuum system. Each 4-km-long (2.5-mi) arm contains a resonant optical cavity in which each photon, on average, makes about 50 round trips before recombining with photons from the other arm of the beam splitter. The interference is measured with a photodetector, which is sensitive enough to detect phase shifts to a few times 10^{-10} of an interference fringe, such as might be produced by a passing gravitational wave.

in the arm before recombining with photons from the other arm cavity. This increases the interaction time of the light with the gravitational wave to about 1 millisecond, increasing the phase delay difference between the two arms and ultimately increasing the light power at the output photodetector.

Another special technique increases the effective light power by making the entire interferometer a resonant optical cavity. Because the two arms beams interfere destructively at the output port, most of the incident laser light interferes constructively on the input side of the beam splitter and actually returns toward the laser. This makes it possible to achieve a significant gain by placing a partially transmitting mirror between the laser and the beam splitter. By properly positioning this mirror, one can arrange that no light is reflected back toward the laser, so that all the light is resonantly built up in the interferometer. This technique, called power recycling, increases the laser power at the beam splitter by a factor of about 40. *See* CAVITY RESONATOR.

Increasing the interaction time and the effective power serves to mitigate a type of detector noise that is due to the quantum nature of light, often referred to as shot noise. Another type of detector noise that must be addressed is fluctuating random forces applied to the mirrors, which could be from a variety of sources. Isolation from motions of the ground, for example, is provided by cascaded stages of vibration isolation, both passive and active. A more fundamental type of noise is Brownian motion driven by thermal excitations; this is controlled largely by careful choice of materials and engineering. *See* BROWNIAN MOVEMENT; ELECTRICAL NOISE; VIBRATION ISOLATION.

Siting and status. LIGO consists of three of these interferometers, two located at the Hanford, Washington, site (**Fig. 2**) and one at the Livingston,

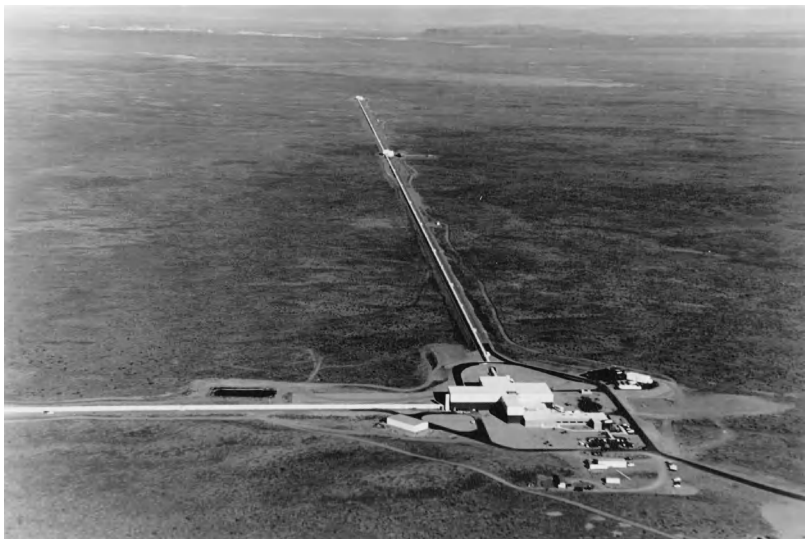

Fig. 2. Aerial photograph of the LIGO at Hanford, Washington. This facility houses two interferometers (a nearly identical facility, with a single interferometer, is in Livingston, Louisiana). The lasers and optics are contained in the white buildings; the 4-km-long (2.5-mi) vacuum tubes are covered by the arched concrete enclosure.

Louisiana, site. At least two detectors located at widely separated sites are essential for the certain detection of gravitational waves. Regional phenomena such as micro-earthquakes, acoustic noise, and laser fluctuations can cause disturbances that simulate a gravitational wave event. Such perceived events may happen locally at one site, but such disturbances are unlikely to happen simultaneously at two widely separated sites.

The LIGO detectors achieved their design sensitivity to gravitational waves near the end of 2005 and began an extended data collection phase. The next generation of LIGO interferometers is being designed and planned for implementation after 2010; these will provide an order of magnitude (10 times) greater sensitivity to gravitational waves. *See* GRAVITATIONAL RADIATION.

Peter K. Fritschel

Bibliography. B. Barish and R. Weiss, LIGO and the detection of gravitational waves, *Phys. Today*, 52(10):44–50, October 1999; M. Bartusiak, Catch a gravity wave, *Astronomy*, 28(10):54–59, October 2000; M. Bartusiak, *Einstein's Unfinished Symphony: Listening to the Sounds of Space-Time*, Joseph Henry Press, Washington, DC, 2000; G. H. Sanders and D. Beckett, LIGO: An antenna tuned to the songs of gravity, *Sky Telesc.*, 100(4):40–48, October 2000.

Liliales

An order of monocotyledons, the well-known lilies or family Liliaceae of many previous botanists, actually consisting of 9 families and about 1600 species. Liliales are clearly circumscribed in deoxyribonucleic acid (DNA) sequence analyses, but are difficult to define on the basis of morphological characters, resulting in varying family composition in different classifications. Separation of Liliales from the lilylike Asparagales has proved particularly problematic, but they differ in nectary position (septal in Asparagales) and absence of phytomelan, a dark seedcoat pigment present in most families of Asparagales. Nearly all features marking the families of Liliales are micromorphological (for example, perigonal nectaries, nuclear endosperm formation).

Many members of the order are herbaceous perennials, but there are also some vines, including the greenbriar (*Smilax*, Smilaceae) and *Lapageria* (the national flower of Chile, Philesiaceae). Liliaceae include species with some of the largest genomes recorded in the angiosperms, the record being held by *Fritillaria syriaca*. Many taxa are extremely poisonous. Most Colchicaceae, for example, possess colchicine-type alkaloids. *Lilium* (lilies), *Tulipa* (tulips), and *Fritillaria* (fritillaries) in Liliaceae, *Colchicum* (autumn crocuses, Colchicaceae), and *Alstroemeria* (Peruvian lilies, Alstroemeriaceae) are well-known horticultural plants. *Trillium* (wakerobin, Melanthiaceae) and *Erythronium* (troutlilies, Liliaceae) are familiar United States wildflowers. *See* ASPARAGUS; COLCHICINE; GARLIC; LILIIDAE; LILIOPSIDA; MAGNOLIOPHYTA; ONION; ORCHIDALES; ORNAMENTAL PLANTS; PLANT KINGDOM; SISAL.

Michael F. Fay; Mark W. Chase

Liliidae

A subclass of the class Liliopsida (monocotyledons) of the division Magnoliophyta (Angiospermae), the flowering plants, consisting of 2 orders (Liliales and Orchidales), 19 families, and about 25,000 species. The Liliidae are syncarpous monocotyledons with both the sepals and the petals usually petaloid. The seeds are either nonendospermous or have an endosperm with various sorts of reserve foods such as cellulose, fats or protein, and only seldom starch. The stomates are without subsidiary cells or, in a few small families, have two subsidiary cells. The pollen is binucleate. The vast majority of the species have the vessels chiefly or wholly confined to the roots. The flowers generally have well-developed nectaries, and pollination is usually by insects or other animals. *See* LILIALES; LILIOPSIDA; MAGNOLIOPHYTA; ORCHIDALES; PLANT KINGDOM.

Arthur Cronquist; T. M. Barkley

Liliopsida

One of the two classes which collectively make up the division Magnoliophyta (Angiospermae), the flowering plants. The Liliopsida, often known as Monocotyledoneae, or monocotyledons, embrace 5 subclasses (Alismatidae, Commelinidae, Arecidae, Zingiberidae, and Liliidae), 18 orders, 61 families, and about 55,000 species.

All of the characters which collectively distinguish the Liliopsida from the Magnoliopsida (dicotyledons) are subject to exception, but most of the Liliopsida

have parallel-veined leaves, and when the embryo is differentiated into recognizable parts, there is only a single cotyledon. The vascular bundles are generally scattered or borne in two or more rings, so the stems and roots do not have a well-defined pith and cortex.

Monocotyledons never have an intrafascicular cambium, and most of them have no secondary growth at all. Some few of them have an unusual type of cambium which produces vascular bundles toward the inside and usually only a small amount of parenchyma toward the outside. Woody monocots such as palms become woody by lignification of the ground tissues in which the vascular bundles of the stem are embedded. The mature root system of monocots is wholly adventitious. The floral parts of monocots, when of definite number, are most often borne in sets of 3, seldom 4, never 5. The pollen is uniaperturate or of uniaperturate-derived type.

It is generally agreed that the monocotyledons are derived from primitive dicotyledons. The solitary cotyledon, the parallel-veined leaves, the absence of a cambium, the dissected stele, and the adventitious root system of monocotyledons are all regarded as secondary rather than primitive characters in the angiosperms as a whole, and any plant which was more primitive than the monocotyledons in these several respects would certainly be a dicotyledon. The monocotyledons are more primitive than the bulk of the dicotyledons in having uniaperturate pollen, but several of the archaic families of dicotyledons also have uniaperturate pollen. *See* ALISMATIDAE; ARECIDAE; COMMELINIDAE; LILIIDAE; MAGNOLIOPHYTA; MAGNOLIOPSIDA; PLANT KINGDOM; ZINGIBERIDAE.

Arthur Cronquist; T. M. Barkley

Lime (botany)

An acid citrus fruit, *Citrus aurantifolia*, usually grown in tropical or subtropical regions because of its low resistance to cold. The two principal groups of limes are the West Indian or Mexican and the Tahiti or Bearss. The West Indian lime (see **illus.**) is a medium-sized, spreading tree with numerous willowy branches densely armed with short, stiff spines. Flowers are small and flowering occurs throughout the year, but mainly in the spring. The fruit is very small (walnut size) and strongly acid, and drops when fully colored. The West Indian lime is more sensitive to cold than the Tahiti lime, which is a more vigorous tree, bearing fruits of lemon size. The Tahiti lime is seedless and its aroma is less pronounced.

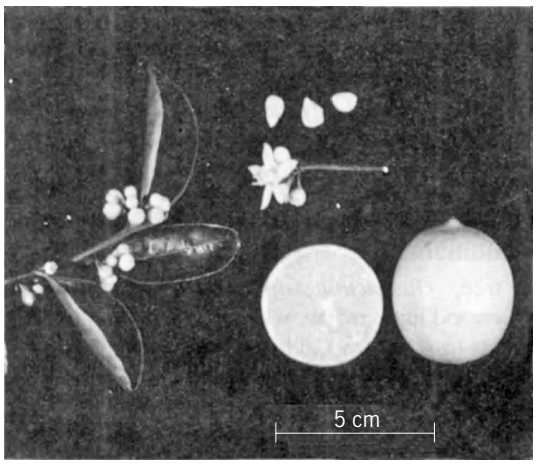

Foliage, seeds, flower, and fruit of the West Indian or Mexican lime.

The limes are believed to have originated in northeastern India or adjoining portions of Burma or northern Malaysia. It probably was introduced into Europe by the Arabs and was brought to the Americas by the Spanish and Portuguese explorers in the sixteenth century. It escaped cultivation and became feral in parts of the West Indies, some Caribbean countries, and southern Florida.

Except in the United States, the commercial lime industry is restricted to the West Indian group, which has a high total heat requirement for good-sized fruit. The major producing areas are India, Mexico, Egypt, and the West Indies. Plantings are scattered and production statistics uncertain.

Commercial production of the Tahiti lime is more recent and largely confined to the United States. It is grown mainly in Florida, with some plantings in the warmer areas of southern California. A little over half of the crop is processed, with the remainder utilized fresh. Fruits are harvested before turning yellow because they have maximum aroma and storage life. *See* FRUIT; FRUIT, TREE.

R. K. Soost

Lime (industry)

A general term for burned (or calcined) limestone, also known as quicklime, hydrated lime, and unslaked or slaked lime. Use of lime as a building material in mortar and plaster coincides with earliest recorded history. However, since development of the chemical process industries, its predominant usage is as a basic industrial chemical, where it ranks second to sulfuric acid in tonnage. It still enjoys its traditional building uses, but more than 90% is used as a chemical. Uses in order of decreasing size are steel fluxing, water treatment, nonferrous metals (alumina, magnesium, copper, and others), pulp and paper, refractories, soil stabilization, sewage and trade waste treatment, chemicals, and glass manufacture.

Lime is not a mineral; it is manufactured from a mineral—limestone, coral, oystershell, all being sources of calcium carbonate. Dolomite, a calcium-magnesium carbonate, is used to produce dolomitic (magnesium) lime. Only the purest types of stone or shell are used for lime. *See* LIMESTONE.

The quarried or mined limestone raw material is crushed and screened to produce either pebble size ($^1/_2$–2 in. or 1.3–5 cm) for charging into rotary kilns or lump size (3–8 in. or 7.5–20 cm) for vertical

kilns. At high temperatures of 2000–2500°F (1100–1400°C), the limestone is decomposed, evolving carbon dioxide gas that constitutes 44% of the weight of the limestone, with calcium oxide remaining. *See* KILN.

The resulting lime, depending upon degree of burn, is chemically reactive with water and acids. Soft-burned limes literally explode on contact with water. If the lime is hard-burned, its reactivity is retarded. One lime product is dead-burned dolomite that has no reactivity with water, making it useful as a refractory material. Unlike conventional limes, hydraulic lime is made from impure limestone that contains considerable silica, alumina, and iron. Calcination causes the lime to combine chemically with these impurities, forming silicates and aluminates. Such limes when hydrated will harden under water, somewhat like cement.

When lime hydrates in water, considerable heat is generated, enough for 1 lb of quicklime to heat 2 lb of water from 0°F (−18°C) to boiling. The lime manufacturer produces hydrated lime (calcium hydroxide), an ultrafine, fluffy, dry powder by controlled addition of water to ground quicklime. Hydrated lime is 25% chemically combined water by weight. Lime users also hydrate or slake quicklime with excess water into slurries or "milk of lime" of various concentrations. Dolomitic lime does not slake as readily as high-calcium types. Under normal conditions, only the calcium oxide component hydrates, yielding $Ca(OH)_2 \cdot MgO$. If slaking occurs under pressure, a highly hydrated dolomitic lime is produced.

Hydrated lime, as a base, is a strong alkali and neutralizes the strongest acids, forming neutral salts, such as the sulfates and chlorides of calcium and magnesium.

Robert S. Boynton

Bibliography. R. Boynton, *Chemistry and Technology of Lime and Limestone*, 2d ed., 1980; D. D. Carr (ed.), *Industrial Minerals and Rocks*, 6th ed., 1994; K. A. Gutschick (ed.), *Lime for Environmental Uses*, 1987; S. J. Lefond (ed.), *Industrial Minerals and Rocks*, 5th ed., AIME, 1983; U.S. Bureau of Mines, Lime, *Minerals Yearbook*, 1988.

Limestone

A common sedimentary rock composed predominantly of carbonates of calcium and magnesium. Limestones are the most voluminous of the nonsiliciclastic sedimentary rocks. In the strict sense, limestones refer to sedimentary rocks composed of the calcium carbonate mineral calcite ($CaCO_3$). Those rocks, dominated by the magnesium-calcium carbonate mineral dolomite [$CaMg(CO_3)_2$], are known as dolomites or dolostones. Although most limestones are similar in chemical and mineralogical composition, the complex organic and chemical origins of carbonate sediments lead to a wide range of textures and fabrics in the resulting limestones. These textures and fabrics share significant parallels with those found in siliciclastic rocks, and they are quite useful for the classification and determination of depositional environments for limestones. Limestones and dolomites are used commercially as building materials (**Fig. 1**) and as a source for industrial and agricultural lime. In addition, limestones and dolomites are important reservoirs for oil and gas and are the hosts for important mineral deposits, including lead, zinc, silver, and fluorite. *See* LIME (INDUSTRY); ORE AND MINERAL DEPOSITS; PETROLEUM GEOLOGY; STONE AND STONE PRODUCTS.

Fig. 1. Surface of a Lower Cretaceous limestone exposed in a quarry just north of Austin, Texas. The limestone is composed predominantly of fossil fragments. The large ribbed fossils are *Trigonia* sp., a common Cretaceous mollusk. This limestone is used extensively as a decorative building stone.

Chemical composition. Limestones are composed principally of calcium oxide (CaO) and carbon dioxide (CO_2). They may contain magnesium oxide (MgO) of up to several weight percent, in which case they are termed magnesian limestones. Limestones constitute the single largest carbon reservoir. Iron (Fe) may be present as an oxide or may (in its reduced state) substitute for magnesium (Mg) or calcium (Ca) in the calcite lattice. Iron commonly substitutes for magnesium in the dolomite lattice. Iron may also occur in association with limestones as a carbonate (siderite) or as a sulfide (pyrite). Strontium (Sr) is a common, important trace element in limestones, occurring at a level of 100–200 ppm. Strontium is a major trace element in aragonite skeletons of shallow marine, limestone-forming organisms (6000–10,000 ppm). Strontium is released into diagenetic waters during the conversion of aragonite into calcite, and is used extensively as a tracer in diagenetic studies of limestones. Isotopic composition of limestones and limestone components, such as fossil fragments, varies widely in response to rock–water interaction, during the extensive diagenetic changes suffered by most limestones as a consequence of their high chemical reactivity. Stable isotopes of oxygen, carbon, and sulfur, and the radiogenic isotopes of strontium are commonly used in diagenetic

studies of limestones. *See* ARAGONITE; CALCITE; DIAGENESIS; PYRITE; SIDERITE.

Mineralogy. Calcite and dolomite are the chief minerals found in ancient limestones and dolomitic limestones. Modern shallow marine carbonate sediments, however, are composed of aragonite, a more soluble polymorph of calcite, and magnesian calcite, a highly soluble form of calcite containing 4–16 mol % $MgCO_3$. This dramatic difference between the mineralogy of carbonate sediments and the mineralogy of ancient limestones suggests that during lithification processes leading to the formation of limestone and dolomitic limestone, a major mineralogical conversion, from relatively soluble aragonite and magnesian calcite to more stable calcite and dolomite, is accomplished. Studies have indicated that aragonite and magnesian calcite sediments were present throughout the Phanerozoic.

This stabilization process takes place relatively early in the burial history of carbonate sediments and generally is completed during the first million years of the limestone's history, as observed by the progressive loss of aragonic and magnesian calcite in Pleistocene limestones. The mineralogical stabilization process is a major factor in early freshwater limestone diagenesis and is extremely important in the porosity evolution of ancient limestone oil and gas reservoirs.

Deep-water carbonate sediments, however, consist of the skeletal remains of planktonic organisms composed of calcite, and they do not undergo the massive mineralogical conversion of their shallow marine counterparts.

Ancillary minerals commonly found in association with limestones include dolomite [$Ca(CO_3)_2$]; celestite ($SrSO_4$); strontianite ($SrCO_3$); anhydrite ($CaSO_4$); fluorite (CaF_2); pyrite (FeS_2); and quartz (SiO_2). *See* ANHYDRITE; CARBONATE MINERALS; CELESTITE; DOLOMITE; FLUORITE; MINERAL; QUARTZ; STRONTIANITE.

Origin. Most marine limestones (perhaps 90% or more) originate as calcium carbonate skeletal elements of various organisms, including both plants (marine algae such as *Lithothamnion* and phytoplankton such as coccoliths) and animals (such as corals, clams, snails, and oysters; Fig. 1). The larger organisms are broken down into cobble-to-silt-sized sediments by biological processes, such as boring, browsing, and grazing, in the environment. Many of the calcareous algae, such as *Halimeda*, and the smaller animals, such as juvenile formanifera, break down into mud-sized carbonate sediments upon death. Once formed, these sediments react to environmental processes as do their siliciclastic counterparts. High-energy conditions in carbonate depositional environments such as a tidal channel are marked by cross-bedded carbonate sands. Low-energy carbonate environments, such as a sheltered lagoon, are characterized by burrowed mud-dominated sediments. Calcareous organisms of pelagic environments are dominated by tiny phytoplankton (coccoliths) and zooplankton (foraminifera). Deep marine limestones, therefore, are very fine-grained and are generally termed chalks. Coccoliths and calcareous pelagic foraminifera became dominant in the Mesozoic. In the Paleozoic, the plankton were dominated by siliceous organisms, so that Paleozoic pelagic sequences are composed of massive cherts. *See* ALGAE; CHALK; CHERT; COCCOLITHOPHORIDA; DEPOSITIONAL SYSTEMS AND ENVIRONMENTS; FORAMINIFERIDA; MARINE SEDIMENTS; MARL; STRATIGRAPHY.

Some limestones and limestone components are formed by direct chemical precipitation from marine and meteoric waters. Most modern, tropical, marine surface water is supersaturated with respect to calcium carbonate. If CO_2 is removed from this water by warming, agitation, or photosynthesis, there is a tendency for calcium carbonate to be precipitated. This precipitation can take several forms: an aragonite or magnesian calcite cement, which lithifies carbonate sediment, such as the beach rock commonly found along tropical beaches; an aragonite precipitate on a moving nucleus in a high-energy environment, forming highly polished, round, sand-sized particles termed ooids; or clouds of spontaneously precipitated, clay-sized aragonite, forming on shallow carbonate platforms or in restricted bays. *See* OOLITE.

Finally, some limestones are formed in freshwater environments associated with caves (speleothems, such as stalactites and stalagmites), springs (tufa and travertine), and lakes (almost always chemically precipitated fine muds of calcite, dolomite, or alkali-carbonates). *See* CAVE; STALACTITES AND STALAGMITES; TRAVERTINE; TUFA.

Consequences of biological origin. Most carbonate sediments are forming in place in the depositional environment and generally suffer little transport. This fact, coupled with very high rates of sediment production, generally results in vertical sedimentation and in the common stacking of shoaling-upward cycles on carbonate-dominated marine shelves. This pattern of sedimentation is in direct contrast with siliciclastics, where the source of sediments is outside the basin of deposition, sediment transport to the basin is extremely important, and shoreline progradation is the major pattern of siliciclastic sedimentation on the shelf.

Textures and fabrics in limestones are much more difficult to interpret than in siliciclastics, because of the organic origin of most carbonate grains. While grain size distribution in siliciclastics is controlled by the flow velocity at the site of deposition, grain size distribution in carbonates may be controlled by the types of organisms present in the environment that furnishes the grains. As an example, an environment dominated by large mollusks will tend to produce a sediment characterized by coarse grain sizes, whereas a benthic foraminiferal community will tend to produce grain sizes that are much finer. Roundness in siliciclastic deposits may be used to infer transport and depositional processes. Roundness in the individual grains of a limestone, however, may reflect only the original shape of the organism (that is, a foraminifer or gastropod) or the architecture of its

Classification of carbonate rocks according to depositional texture*

Depositional texture recognizable					Depositional texure not recognizable
Original components not bound together during deposition				Original components were bound together during deposition as shown by intergrown skeletal matter, lamination contrary to gravity, or sediment-floored cavities that are roofed over by organic or questionably organic matter and are too large to be interstices	Crystalline carbonate
Contains mud (particles of clay and fine silt size)		Grain-supported	Lacks mud and is grain-supported		
Mud-supported					
Less than 10% grains	More than 10% grains				(Subdivide according to classifications designed to bear on physical texture or diagenesis)
Mudstone	Wackestone	Packstone	Grainstone	Boundstone	

*After R. J. Dunham, Classification of carbonate rocks according to depositional texture, in W. E. Ham (ed.), *Classification of Carbonate Rocks,* Amer. Ass. Petrol. Geol. Mem. 1, pp. 108–121, 1962.

skeleton. For example, coral septa are composed of spherical bodies. Coral skeletons tend to break down into these spheres during biological erosion after the death of the coral.

Finally, carbonate environments of deposition are characterized by unique faunal and floral communities. Because these organisms give rise to the sediments that ultimately form limestones, the grain composition of a detrital limestone composed of recognizable fossil fragments may directly reflect its environment of deposition. *See* FOSSIL.

Reefs. Certain carbonate-secreting organisms display ability to modify their environment by encrusting, binding, and building a solid organic framework that possesses the strength to resist wave attack and may act as a trap for sediments being transported across the shelf. These important solid limestone structures are known as reefs. **Figure 2** illustrates a schematic reef structure and its major components. Major reef builders today consist of corals and coralline algae. In the past, important reef formers included mollusks, sponges, and algae. Reef masses are important reservoirs for oil and gas. *See* CORALLINALES; MOLLUSCA; REEF.

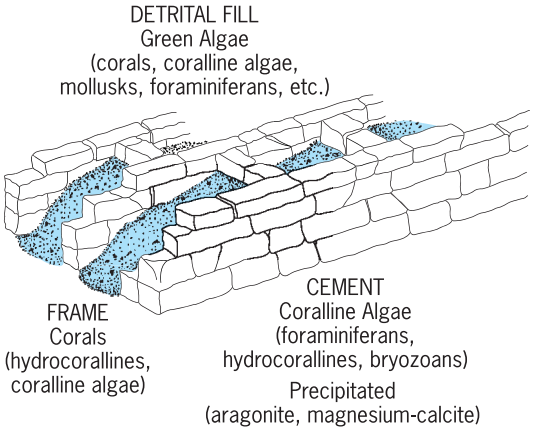

Fig. 2. Schematic rendering of a reef illustrating the complex interaction of biologic framework growth, sedimentation, and chemical precipitation in the formation of reef limestones. (*After R. N. Ginsberg and H. A. Lowenstam, The influence of marine bottom communities on the depositional environment of sediments, J. Geol., 66:310–318, 1958*)

Consequences of high chemical reactivity. Limestones are considerably more soluble and hence maintain a much higher chemical reactivity than their siliciclastic counterparts during burial and lithification. This higher chemical reactivity is reflected in the propensity of limestones to exhibit dramatic, early, surface-related, diagenetic overprints, including extensive dissolution, dolomitization, and massive, pore-filling calcite cements. In contrast, siliciclastics generally exhibit little early diagenetic activity and are buried into the subsurface relatively intact. During subsequent burial, pore space is lost much more rapidly in limestones than in siliciclastics because of pressure solution resulting from steadily increasing lithostatic pressures. Limestones dissolve more readily under pressure because of the high relative solubility of calcite as compared to quartz. As a result, successful exploration for oil and gas in limestone reservoirs has a severe depth constraint not shared by their siliciclastic counterparts.

Classification. The first practical, widely used limestone classification was developed by R. L. Folk in 1959. This classification encompasses the common textural classifications used in siliciclastics, as well as a strong grain compositional component. Folk's classification is complex, is difficult to use in detail, and generally is best used with a petrographic microscope. The most widely used classification is the simple, field-oriented, textural classification published by R. Dunham in 1962 (see **table**). Dunham's major rock classes are based on the presence or absence of organic binding, presence or absence of mud, and the concept of grain versus mud support. The first four major rock types, mudstone, wackestone, packstone, and grainstone, directly parallel common siliciclastic textural divisions and represent a gradient from low energy (mudstone) to high energy (grainstone). The boundstone category emphasizes the unique characteristics of organic

binding and framework construction. *See* DOLOMITE ROCK; SEDIMENTARY ROCKS; SEDIMENTOLOGY.

Clyde H. Moore

Bibliography. R. G. C. Bathurst, *Carbonate Sediments and Their Diagenesis*, 2d ed., 1975, *Developments in Sedimentology*, vol. 12, 1975; L. Glaister, *Limestone and Clay*, 1994; P. A. Scholle, D. G. Bebout, and C. H. Moore (eds.), *Carbonate Depositional Environments*, Amer. Ass. Petrol. Geol. Mem. 33, 1983; J. L. Wilson, *Carbonate Facies in Geologic History*, 1975.

Limiter circuit

A device whose purpose is to ensure that the amplitude of a sensed variable (referred to as a signal) is constrained or limited to lie within prescribed maximum and minimum values. It is more properly termed an amplitude limiter, although convention usually dispenses with the important modifier. Also, unless specified otherwise, the limiting is applied to voltage.

Function. Strictly speaking, the limiter should behave as a perfectly linear device (such as an ideal amplifier or even a piece of wire) until the amplitude of the input signal reaches the upper or lower limit values. In other words, the output of an ideal limiter matches the input perfectly when the input is between the limit values. If the input is greater than the upper limit, the output equals the upper limit; if the input is less than the lower limit, the output equals the lower limit. If the upper and lower limits are equal in magnitude, the limiting is symmetrical. In the past, one or two stages of high-gain amplification would often precede a limiter in order to obtain clean limiting. *See* LINEARITY.

The term limiter is often used to mean sign detector, so that when the input is greater than zero, the output equals some fixed positive value; when the input is less than zero, the output is the negative of this value. This usage is sometimes employed in discussing frequency-modulation (FM) radio receivers.

Mechanization. Discrete-component limiters have become rare. The cost/performance ratio of integrated circuits makes them the only rational choice for commercial applications. Most often, integrated circuits now contain limit operations that are both functionally and physically integrated with companion operations to form a higher-level function. The isolated need for a limit-only function is almost never encountered. Limiting within an integrated circuit is usually obtained by designing an amplifier to be heavily overdriven and therefore to quickly enter the saturation (limiting) range. *See* AMPLIFIER; INTEGRATED CIRCUITS.

The conceptual nonlinear mechanics of limiting are very simple. An ideal situation (**illus.** *a*) can be approximated with readily available components. The signal voltage is generated by a source, which has a resistance. For the sake of clarity, reactance will be ignored; that is, it will be assumed that all impedances are resistive. Two diodes are each back-biased by voltage sources. The backward resistance of each diode is much greater than the source resistance; and in turn, the source resistance is much greater than the forward resistance of each diode. *See* DIODE.

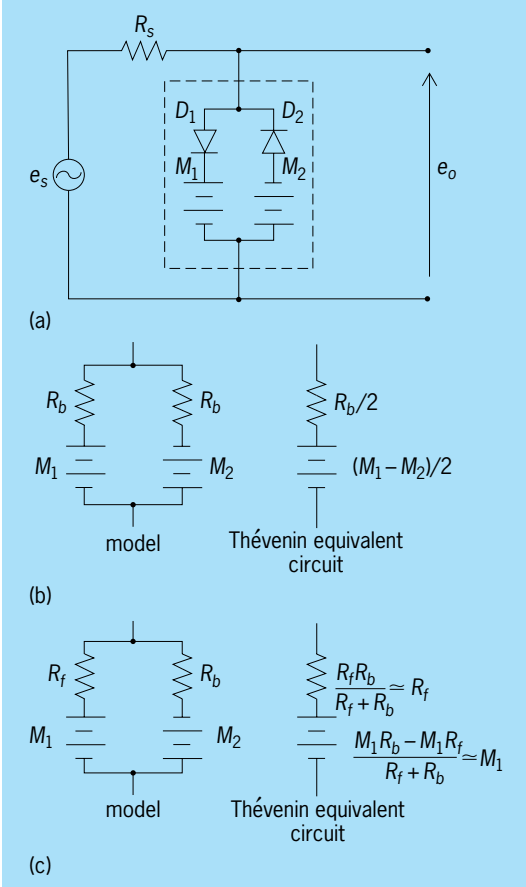

Limiter circuits. (*a*) Generic limiter. The broken line encloses the part of the circuit described by models. e_s = signal voltage; R_s = source resistance; e_o = output voltage. Diodes D_1 and D_2 are back-biased by voltage sources M_1 and M_2, respectively. (*b*) Model and Thévenin equivalent circuit for diodes and their biasing voltage sources when both diodes are back-biased. R_b is the back resistance of both diodes. (*c*) Model and Thévenin equivalent circuit for diodes and their biasing voltage sources when diode D_1 is forward-biased and D_2 is back-biased. R_f is the forward resistance of both diodes.

In order to easily and simply determine the operation of the circuit, the two diodes and two bias sources are combined into an equivalent circuit (consisting of the series combination of one resistor and one voltage source, as given by Thévenin's theorem) for the case when both diodes are back-biased (illus. *b*), and for the case when the first diode is forward-biased and the second diode is back-biased (illus. *c*). If the second diode is forward-biased and the first diode is back-biased, the roles of its corresponding voltage source and the negative of the other voltage source are exchanged. Never can both diodes be forward-biased simultaneously. *See* THÉVENIN'S THEOREM (ELECTRIC NETWORKS).

When both diodes are back-biased (illus. *b*), the output voltage is approximately equal to the signal voltage. When the first diode is forward-biased (illus. *c*), the output voltage is very nearly equal to its corresponding voltage source. Similarly, when the second diode is forward-biased, the output voltage is very nearly equal to the negative of its corresponding voltage source.

Virtually all limiter circuits, upon final analysis, reduce to this simple configuration. Digital limiting can be performed by a comparator and a logic statement.

Limiting for FM reception. The operation of FM detectors (discriminators) requires that the amplitude envelope of the frequency-modulated information signal be held nearly constant. The purpose of this limitation is to remove (or at least seriously reduce) additive noise and amplitude modulation from the signal. These unwanted envelope effects produce undesirable noise components at the output of the FM receiver. Some FM detectors provide internal limiting, but others require that the signal envelope be separately amplitude-limited.

If the FM detector is of the slope-detector type, additional filtering of the amplitude-limited signal is necessary. Because the limiting action modifies the signal wave shape, the frequency content of the signal is also changed by the creation and addition of high-frequency distortion components. Because the frequency content of the signal before limiting consists of the information energy tightly clustered around the carrier frequency, adequate waveform correction and high-frequency removal can be performed by applying the amplitude-limited signal across the terminals of a simple resonant circuit which has been tuned to the carrier frequency. *See* DISTORTION (ELECTRONIC CIRCUITS).

The effectiveness of the limiting is measured by a quieting criterion. When the input signal to the receiver is low, the limiting action does not occur and the receiver output is noticeably noisy. As the strength of the signal increases and limiting action begins to occur, the reduction in the noise level is immediately noticeable. As the strength of the signal continues to grow, the output signal-to-noise ratio continues to grow correspondingly. The level of input signal necessary to achieve a 30-decibel signal-to-noise ratio is called the receiver's sensitivity. Of course, extremely large input signals can also create problems. In practice, the limiter provides automatic-gain-control effects; however, separate automatic-gain-control circuits in the early (radio-frequency) stages of the receiver often are used to regulate the input signal to the limiter by boosting the amplitude of the signal so that amplitude lies in the most effective range for the limiter. *See* AUTOMATIC GAIN CONTROL (AGC); FREQUENCY-MODULATION DETECTOR; SIGNAL-TO-NOISE RATIO.

Stanley A. White

Bibliography. A. B. Carlson, *Communications Systems*, 3d ed., 1986; R. C. Dorf (ed.), *The Electrical Engineering Handbook*, 2d ed., 1997; D. Roddy and J. Coolen, *Electronic Communications*, 4th ed., 1995; R. A. Williams, *Communication System Analysis and Design*, 1987.

Limits and fits

The extreme permissible values of a dimension are known as limits. The degree of tightness or looseness between two mating parts that are intended to act together is known as the fit of the parts. The character of the fit depends upon the use of the parts. Thus, the fit between members that move or rotate relative to each other, such as a shaft rotating in a bearing, is considerably different from the fit that is designed to prevent any relative motion between two parts, such as a wheel attached to an axle.

In selecting and specifying limits and fits for various applications, it is essential in the interests of interchangeable manufacturing that (1) standard definitions of terms relating to limits and fits be used; (2) preferred basic sizes be selected wherever possible to reduce material and tool costs; (3) limits be based upon a series of preferred tolerances and allowances; and (4) a uniform system of applying tolerances (bilateral or unilateral) be used.

Nominal size. The basic size or dimension of a screw thread or machine part is the theoretical nominal standard size from which variations are made. For example, a shaft may have a basic diameter of 2.000 in. with a maximum variation of ±0.010 in. (5.060 ± 0.025 cm). The nominal size is generally the size used for purposes of general identification (see **illus.**)

Tolerance. A tolerance is the amount of variation permitted on dimensions or surfaces of machined parts. The tolerance is equal to the difference between the maximum and minimum limits of any specified dimension. For example, if the maximum limit for the diameter of a shaft is 2.000 in. (5.060 cm) and the minimum limit is 1.990 in. (5.055 cm), the tolerance for this diameter is 0.010 in. (0.025 cm). Any component-part tolerance is mainly decided by the functional requirement of the part as well as the capability of the manufacturing process.

A unilateral tolerance means that the total tolerance, as related to a basic dimension, is in one direction only. For example, if the basic dimension is 1.000 in. (2.540 cm) and the tolerance is expressed as 1.000 − 0.002, or as 1.000 + 0.002, these would be unilateral tolerances, because the total tolerance in each case is in one direction. If the tolerance is divided into plus and minus, for example, 1.000 ± 0.001, it is classified as a bilateral tolerance because the total tolerance of 0.002 is given in two directions. The limits (maximum and minimum) are obtained by adding or subtracting the tolerance from the basic dimension.

Allowance. An allowance is a prescribed difference between the maximum material limits of two mating parts. It is a minimum clearance (positive allowance) or a maximum interference (negative

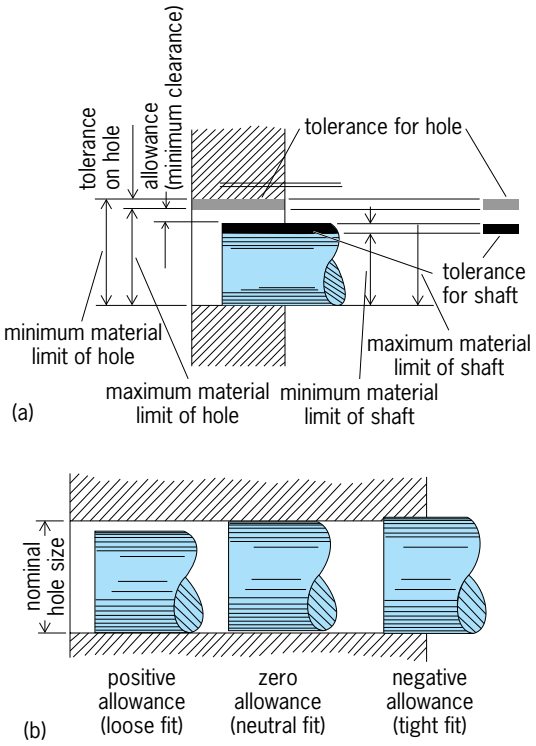

Limits and fits in machine parts. (*a*) Limits, tolerances, and allowance for a shaft. (*b*) Three types of allowances.

allowance) between the parts. Fit is the general term used to signify the range of tightness that may result from the application of a specific combination of allowances and tolerances in the design of mating parts. The actual fit between two mating parts is the relationship existing between them with respect to the amount of clearance or interference that is present when they are assembled.

Type of fit. In selecting limits of size for any application, the type of fit is determined based upon the use or service of the parts being designed. Then the limits of size of the mating parts are established to ensure that the desired fit will be produced. In general, fits may be considered as positive, negative, or zero allowances (illus. *b*).

The classes of fits are arranged in three general groups: running and sliding fits, locational fits, and force fits. Running and sliding fits are intended to provide a similar running performance with suitable lubrication allowances throughout the range of sizes. They range from close sliding fits (for the accurate location of parts that must be assembled without perceptible play between them) to loose running fits, where wide commercial tolerances are acceptable. Locational fits are intended to determine only the location of the mating parts. They may provide rigid or accurate location as in the case of interference fits, or some freedom of location as with clearance fits. Accordingly, they are divided into three groups: clearance fits, transition fits, and interference fits. Force or shrink fits constitute a special type of interference fit normally characterized by maintenance of constant bore pressures throughout the range of sizes. The interference varies almost directly with the diameter of the part and the difference between its minimum and maximum value in order to maintain the resulting pressure between the two mating parts within reasonable limits. The range is from light drive fits that require light pressure, to force fits that are more suitable for parts that can be highly stressed by a given force or load applied to the two parts. *See* DESIGN STANDARDS; ENGINEERING DESIGN; MACHINE DESIGN; MACHINE ELEMENTS; MACHINING. Joseph Elgomayel

Bibliography. E. A. Avallone and T. Baumeister III (ed.), *Marks' Standard Handbook for Mechanical Engineering*, 10th ed., 1996; A. Parrish (ed.), *Mechanical Engineer's Reference Book*, 12th ed., 1994; H. A. Rothbart, *Mechanical Systems Reference Guide*, 1989; R. A. Walsh, *McGraw-Hill Machining and Metalworking Handbook*, 2d ed., 1998.

Limnology

The study of lakes, ponds, rivers, streams, swamps, and reservoirs that make up inland water systems. Each of these inland aquatic environments is physically and chemically connected with its surroundings by meteorologic and hydrogeologic processes (**Fig. 1**). Precipitation and runoff, combined with the gradient and watershed characteristics of a river or stream, provide the physicochemical environment

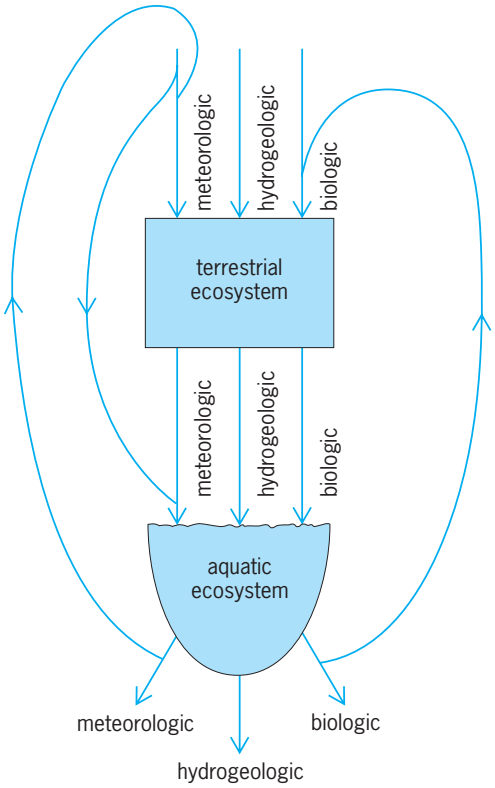

Fig. 1. Diagrammatic model of the functional linkages between terrestrial and aquatic ecosystems. Vectors may be meteorologic, hydrogeologic, or biologic components moving nutrients or energy along the pathway shown.

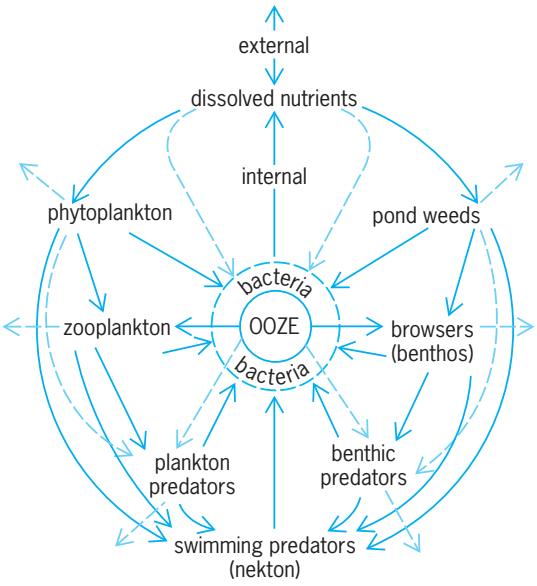

Fig. 2. Diagram of food webs in a lake, showing the interdependence of organisms. Broken lines depict the energy pathways and solid lines the food source.

for the organisms of flowing water (lotic) systems. The frequency and stability of thermal stratification and mixing in standing water (lentic) systems such as lakes, ponds, and reservoirs are determined by the seasonal balance of heating and cooling, the unique temperature-density characteristics of pure water, and the energy of the wind.

Solar energy supply and distribution, physical mixing processes, and nutrients supplied by the surrounding watershed and lake sediments determine how much organic matter is produced by photosynthesis in aquatic environments. That autotrophic production, combined with leaves and other organic matter produced outside the system, supports heterotrophic activities of aquatic communities.

Biogeochemical processes. Food webs are used to illustrate interactions between plants and animals in aquatic communities. The trophic-dynamic approach (**Fig. 2**) traces the energy fixed by photosynthesis through trophic levels from herbivores to top carnivores. The flow of energy and the return of minerals to inorganic nutrient pools maintain internal biogeochemical cycles of aquatic environments. *See* BIOGEOCHEMISTRY; FOOD WEB.

General habitats of aquatic environments. Aquatic organisms are grouped into categories according to where they live within a particular system. Habitats of aquatic systems are defined by unique physical conditions. The open water (limnetic zone) of lentic environments is inhabited by microscopic plants (phytoplankton) and animals (zooplankton). Shallows around the edge of the lake that are limited by light penetration (littoral zone) are occupied by rooted plants (aquatic macrophytes). These plants provide habitats for other plants and animals. The deepest area (profundal zone) is bounded by the limnetic zone on the top and the littoral zone on the sides. Benthic organisms such as insects, oligochaetes, and microorganisms occupy the profundal zone. Insects and free-swimming animals such as fish (nekton) are not restricted to any particular zone of a lentic environment. The feeding behavior of fish and other carnivores influences many food web interactions by removing large herbivores from the food web. The loss of large herbivores alters feeding relationships at the base of the food web, because small herbivores cannot eat large phytoplankton. This cascade of feeding interactions alters the structure of aquatic communities by permitting the accumulation of large phytoplankton and small herbivores. *See* PHYTOPLANKTON; ZOOPLANKTON.

Lotic environments also are divided into zones created by water velocity, bottom conditions, and stream gradients. In mountainous areas, rapids and turbulent water zones (riffles) are contrasted with sluggish water zones (pools); each of these habitats has characteristic organisms. Streams and rivers in valleys and on plains have many meanders, oxbows, and braids developed by the balance of erosion and

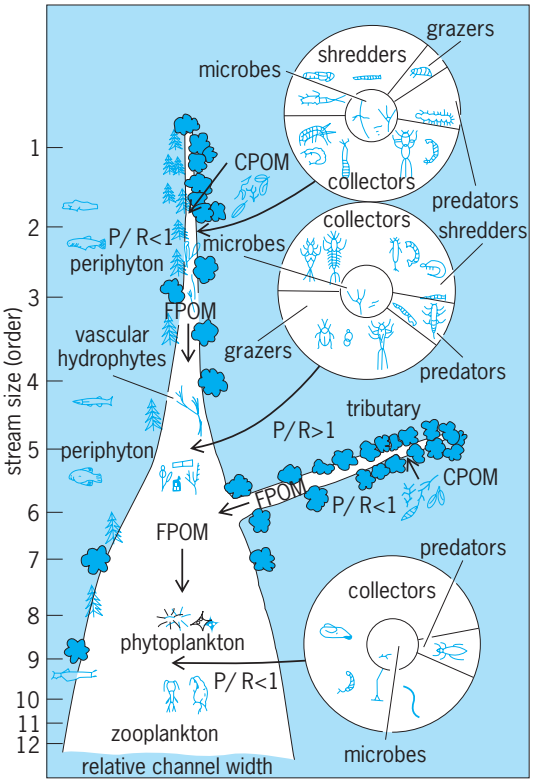

Fig. 3. A proposed relationship between stream size and the progressive shift in structural and functional attributes of lotic communities. Coarse particulate organic material (CPOM) that enters a stream from the watershed is shredded by organisms to form fine particulate organic matter (FPOM). Some organisms collect the fine material, and others graze on autotrophic organisms to sustain the food web of the stream. Production (P) and respiration (R) responses are used to detect changes in autotrophic and heterotrophic processes in the biotic community. (*After R. L. Vannote et al., The river continuum concept, Can. J. Fish. Aquat. Sci., 37:130–137, 1980*)

deposition of the riverbed. When studying the linkage between streams and their terrestrial setting, scientists consider the gradient of physical factors formed by drainage networks. Fluvial geomorphic processes are then integrated with community ecology principles to develop an understanding of functional processes that contribute to mineral cycling and organic matter utilization (**Fig. 3**). *See* FRESHWATER ECOSYSTEM.

Eutrophication and toxic materials. Aquatic systems with excellent physical conditions for production of organisms and high nutrient levels often show signs of eutrophication. Eutrophic lakes are generally identified by large numbers of phytoplankton and aquatic macrophytes and by low oxygen concentrations in the profundal zone. Eutrophication is accelerated by poor watershed management, by runoff from overfertilized lands, and by poor septic facilities. *See* EUTROPHICATION; WATER CONSERVATION.

Organisms of aquatic environments are also affected by metals such as lead and mercury, or pesticides that enter the aquatic environment from poor watershed management practices. These toxic materials alter food webs of aquatic systems by destroying sensitive organisms. Tolerant organisms concentrate toxic elements by feeding and absorption. Toxic elements are concentrated in tolerant organisms by a process called biomagnification. These organisms acquire levels of toxicity that make them dangerous for human consumption. Lakes and rivers are also influenced by changes in the chemical composition of rain. Acid runoffs cause stress to the biota of aquatic systems in many ways, including direct toxicity of hydrogen ions, disruption of normal food web relations, alterations of behavioral patterns of animals, and modification of biogeochemical cycles. *See* ACID RAIN; ECOLOGY; HYDROLOGY; LAKE; RIVER; WATER POLLUTION.

James E. Schindler

Bibliography. S. R. Carpenter (ed.), *Complex Interactions in Lake Communities*, 1988; A. J. Horne and C. R. Goldman, *Limnology*, 2d ed., 1994; D. W. Schindler et al., Long-term ecosystem stress: The effects of years of experimental acidification on a small lake, *Science*, 228:1395–1401, 1985; J. V. Ward, *Aquatic Insect Ecology*, 1992; R. G. Wetzel and G. E. Likens, *Limnological Analysis*, 3d ed., 2000.

Limonite

A field or generic term for natural hydrous iron oxides, the most common phase being the mineral goethite, α-FeO(OH). Limonite occurs as a low-temperature mixture of phases and includes the so-called bog iron ores. It is the characteristic brown stain which coats rocks containing sulfide ores, such as pyrite and pyrrhotite, in the zone of weathering of these ores referred to as a gossan. A vast list of pseudonyms, such as limnite, hypoxanthite, and xanthosiderite, plague the earlier literature. Limonite is most commonly a mixture of greater or lesser fractions of goethite, hematite, ferric oxyhydroxide colloids, clays, and manganese oxides. It is formed by biogenic or inorganic precipitation in bog, spring, lacustrine, or marine deposits. *See* GOETHITE; IRON METALLURGY; ORE AND MINERAL DEPOSITS.

Paul B. Moore

Limpet

Name given to a variety of species of aquatic gastropod mollusks, all with a characteristic conical shell (see **illus.**) and a suckerlike foot. Limpets (like chitons) are well adapted for life on rocky surfaces exposed to wave action and, in the higher levels of the littoral zone, to alternating tidal submergence and aerrial drying. Apparently the coiled gastropod shell has evolved in many different stocks into the conical shell with a wide opening (the limpet form) by a rapid enlargement of the mantle-shell edge so that the snail is completely accommodated in one open half-whorl. In many cases the initial coiling (recognizable in larval stages) is entirely lost in the adult shell, which is a wide cone. In a few others, initial coiling (termed a protoconch) remains obvious at the apex of the shell throughout adult life. The gastropod crawling foot is greatly enlarged and flattened into a round muscular sucker. All limpets move relatively slowly over rock or other hard surfaces, protecting themselves (against wave action or desiccation or predation) by clamping down the shell opening against the substrate by contraction of the enlarged shell muscles. There is never an operculum on the foot, and limpets are defenseless once detached.

Although not all limpets retain a recognizable anterior mantle cavity, all have a pallial groove between the circular outer edge of the foot and the concentric mantle edge lining the shell. This mantle edge may bear obvious sensory tentacles, but it and the pedal edge always contain tactile receptors and chemoreceptors (used by several different stocks of limpets in "homing" behavior). Limpets usually graze slowly and continously by radular scraping of attached algae and diatoms from rock surfaces. The structural and functional adaptations of the limpet form have arisen in many distinct groups of gastropods.

Limpets among the most primitive snails (those Archaeogastropoda with two aspidobranch ctenidia) include slit shells (*Emarginula*) and keyhole limpets

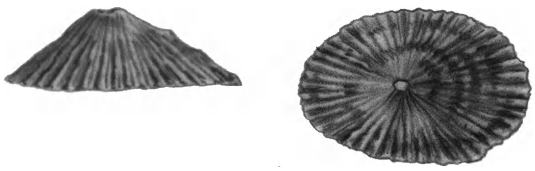

***Diodora aspera*, the rough-keyhole limpet of the Pacific coast of North America. All limpets have this shell shape as a widely open cone, but only a few genera have an apical "keyhole."**

(*Fissurella*). Other limpets, belonging to archaeogastropod stocks with marked asymmetry of gills and internal organs but with no openings or slits in the conical shell, include *Acmaea* (the most common limpet of the American Atlantic coast), which has a single aspidobranch ctenidium in a small anterior mantle cavity, and *Patella* (the dominant European limpet genus), which has no true ctenidium but a series of respiratory outgrowths (secondary or neomorphic gills) along each pallial groove. The closely related giant owl limpet (*Lottia*) of Californian shores, which can reach a diameter of 4 in. (10 cm), has both a ctenidium and neomorphic gills. Such acmaeids and patellids of the intertidal are often referred to as "true limpets." The more distantly related archaeogastropod family Lepetidae comprises rarer species of tiny limpets (up to 0.3 in. or 8 mm) without any gills, found only offshore in depths of more than 20 ft (6 m).

In the Mesogastropoda (with a pectinibranch ctenidium, or comblike "half-gill" with its axis fused to the mantle-cavity wall), limpets include the filter-feeding slipper limpets (*Crepidula*) and the fool's-cap limpets or capulids, some genera of which have become ectoparasites on echinoderms and on other mollusks. Among the higher gastropods, the subclass Opisthobranchia has a few limpet-shelled forms (*Tylodina*, *Umbraculum*), and the subclass Pulmonata has at least five distinct lines of limpets. Two of these are intertidal: in the Trimusculidae (=Gadiniidae) and Siphonariidae or false limpets, common on Gulf of Mexico and Caribbean shores, the air-breathing lung has been supplemented by secondary gills developed from its roof. Finally there are at least three stocks of fresh-water pulmonate limpets. These include the stream limpets, such as *Ancylus fluviatilis* in Europe and *Ferrissia rivularis* in North America, found abundantly clinging to rocks in swiftly flowing streams (even in waterfalls), and the pond limpets, such as *Acroloxus lacustris* in Europe and *Laevapex fuscus* in North America, which live on reed stalks. All such fresh-water limpets are derived from air-breathing "diving" snails which have developed, along with the limpet form, secondary (neomorphic) gills derived, in part, from ciliated rectal tissues. Outside gastropod stocks, there are the untorted limpets of the class Monoplacophora, and in the class Bivalvia the anomiid saddle oyster (*Enigmonia*), which inhabits mangrove swamps, has resumed a crawling habit on an enlarged foot as a bivalve turned "limpet," although it still filter-feeds as a typical lamellibranch.

This acquisition, occurring independently in so many diverse stocks of gastropods, of the structural and functional adaptations which make up the limpet form provides, as does the similar polyphyletic occurrence of certain structural adaptations to specific habitats in bivalves, a striking example of evolutionary convergence. *See* BIVALVIA; GASTROPODA; MOLLUSCA; MONOPLACOPHORA; OPISTHOBRANCHIA; PROSOBRANCHIA; PULMONATA.

W. D. Russell-Hunter

Line integral

The line integral of a vector function **F** of position over a path C is represented by Eq. (1), where F_x, F_y,

$$\int_C \mathbf{F} \cdot d\mathbf{r} = \int_C F_x(x, y, z)\, dx + \int_C F_y(x, y, z)\, dy + \int_C F_z(x, y, z)\, dz \qquad (1)$$

F_z are the scalar components of **F** along the coordinate axes. The path C is supposed to be a curve, smooth at least in part, defined parametrically by equations of form (2) for each smooth portion. The

$$x = x(p) \qquad y = y(p) \qquad z = z(p) \qquad (2)$$

functions $F_x(x,y,z)$, etc., must be defined at all points of C. When this is so, the line integral can be evaluated by writing Eq. (3), where the prime means dif-

$$\int_c \mathbf{F} \cdot d\mathbf{r} = \int_{p_1}^{p_2} F_x(p)x'(p)dp + \int_{p_1}^{p_2} F_y(p)y'(p)dp + \int_{p_1}^{p_2} F_z(p)z'(p)\, dp \qquad (3)$$

ferentiation with respect to the parameter, and p_1, p_2 are values of the parameter at the end points of the path C or of a smooth piece. The integral has been converted into an ordinary definite integral.

When C is a closed curve, the line integral is called a circuit integral, and is written as notation (4).

$$\oint \mathbf{F} \cdot d\mathbf{r} \qquad (4)$$

Some physical applications of the line integral follow. If **F** is a force, the line integral is the work done in moving a mass along the curve C. If **F** is the velocity of flow of a fluid, the line integral is the circulation of the fluid along the curve. If **F** is the electrostatic field strength, the integral is the electric potential difference between the end points of the curve. If **F** is the electric field strength of an electromagnetic field, the circuit integral is the electromotive force of the circuit. In each example $d\mathbf{r}$ is physically a length. *See* INTEGRATION.

McAllister H. Hull, Jr.

Line spectrum

A discontinuous spectrum characteristic of excited atoms, ions, and certain molecules in the gaseous phase at low pressures, to be distinguished from band spectra, emitted by most free molecules, and continuous spectra, emitted by matter in the solid, liquid, and sometimes gaseous phase. If an electric arc or spark between metallic electrodes, or an electric discharge through a low-pressure gas, is viewed through a spectroscope, images of the spectroscope slit are seen in the characteristic colors emitted by the atoms or ions present.

To avoid the overlapping of close spectral images, the slit illuminated by the light source is made very

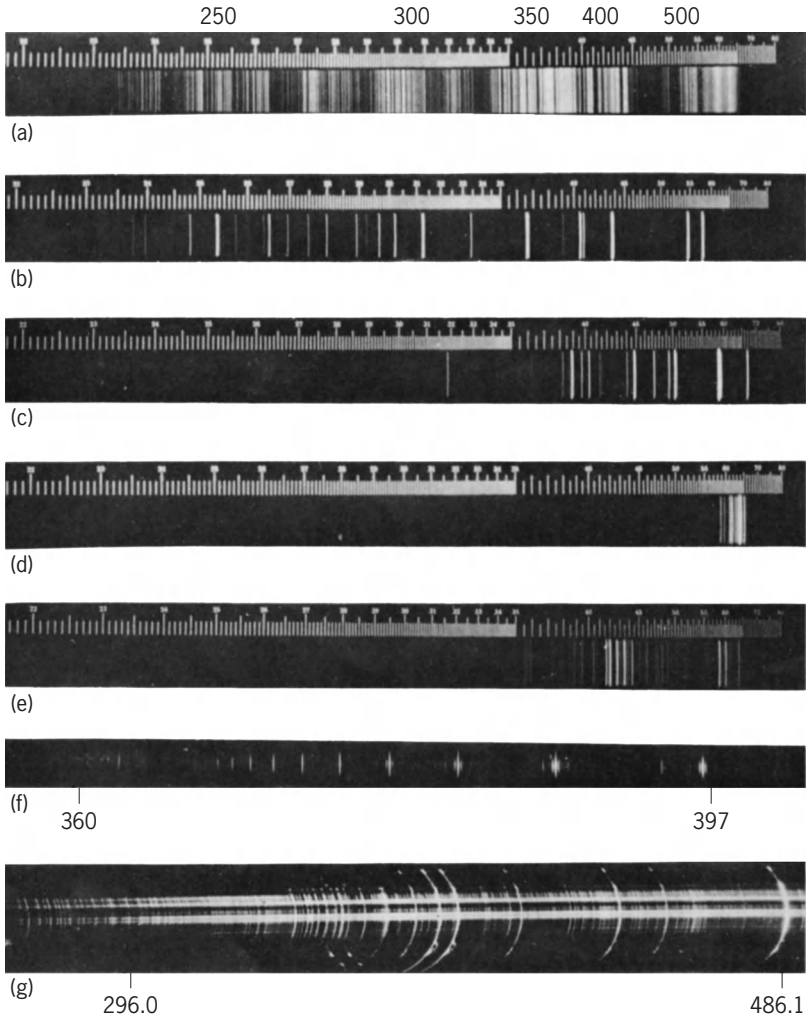

Photographs of common line spectra, wavelengths given in angstroms; emission spectra (*a*–*e*) all taken with the same quartz spectrograph. (*a*) Spectrum of iron arc. (*b*) Mercury spectrum from an arc enclosed in quartz. (*c*) Helium in a glass discharge tube. (*d*) Neon in a glass discharge tube. (*e*) Argon in a glass discharge tube. (*f*) Balmer series of hydrogen in the ultraviolet, photographed with a grating spectrograph. (*g*) Emission spectrum from gaseous chromosphere of the Sun, a grating spectrum taken without a slit at the instant immediately preceding a total eclipse, when the rest of the Sun is covered by the Moon's disk. Two strongest images, H and K lines of calcium, show marked prominences, or clouds, of calcium vapor. Other strong lines are caused by hydrogen and helium. 1 angstrom unit = 0.1 nanometer. (*From F. A. Jenkins and H. E. White, Fundamentals of Optics, 4th ed., McGraw-Hill, 1976*)

narrow. The spectrum then appears as an array of bright line slit images on a dark background (see **illus.**). Under certain conditions spectra show dark absorption lines against a bright background. *See* ATOMIC STRUCTURE AND SPECTRA; SPECTROSCOPY.

George R. Harrison

Linear algebra

That branch of mathematics which deals with solutions of systems of linear equations and the related geometric notions of vector spaces and linear transformations. It is fundamental in the theory of the calculus of functions of several variables and hence is of great importance in the application of mathematics to physical and biological sciences, economics, and so on.

The word linear is derived from the fact that the equation of a line in two-dimensional analytic geometry has the form shown in Eq. (1) and a system of lin-

$$ax + by = c \tag{1}$$

ear equations has the corresponding form shown in Eq. (2), where $i = 1, 2, \ldots, m$. The a_{ij} and b_i are fixed

$$a_{i1}x_1 + a_{i2}x_2 + \cdots + a_{in}x_n = b_i \tag{2}$$

quantities belonging to a specified field, for example, the field of real numbers, and solutions $(x_1, x_2, \ldots, x_n)$ are sought in the same field. If $m = n = 2$, the problem of solving the equations is equivalent to the geometric one of finding the points common to two lines (which may be coincident).

Basic concepts. Let R denote the field of real numbers and let R^2 be the set of pairs (x,y) of real numbers x, y. Such a pair can be regarded as the

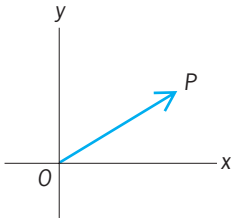

Geometric representation of a vector OP.

coordinates of a point P in a two-dimensional euclidean space. The point P determines a vector, or directed segment **OP** with initial point the origin O and terminal point P, as shown in the **illustration**.

Such vectors are basic in representing certain physical entities, for example, acceleration, velocity, force. Addition of these physical entities corresponds to the addition of vectors. If $\mathbf{v} = \mathbf{OP}$ and $\mathbf{v}' = \mathbf{OP}'$ where P' is the point (x',y'), then $\mathbf{v} + \mathbf{v}' = \mathbf{OQ}$, where $Q = (x + x', y + y')$. If t is a real number, a stretching of the vector $\mathbf{v}$ in the ratio t: 1 gives rise to the vector $t\mathbf{v} = \mathbf{OM}$, where $M = (tx,ty)$.

On the algebraic side these considerations generalize from pairs of real numbers (x,y) to n-tuples of real numbers $(x_1,x_2, \ldots, x_n)$, and one can replace the field R of real numbers by any field F, for example, the field of rational numbers.

Accordingly, let F^n denote the set of n-tuples $\mathbf{x} = (x_1,x_2, \ldots, x_n)$; where the x_i are in a given field F. Such an n-tuple is called a vector. If $\mathbf{y} = (y_1,y_2, \ldots, y_n$; then one defines the sum of x and y by Eq. (3).

$$\mathbf{x} + \mathbf{y} = (x_1 + y_1, x_2 + y_2, \ldots, x_n + y_n) \tag{3}$$

See ABSTRACT ALGEBRA.

The elements of the field F are called scalars. If t is such an element, one defines the multiplication of the vector x by the scalar t by means of Eq. (4).

$$t\mathbf{x} = (tx_1, tx_2, \ldots, tx_n) \tag{4}$$

The basic properties of addition of vectors and multiplication of vectors by scalars are listed below.

A_1. $(\mathbf{x} + \mathbf{y}) + \mathbf{z} = \mathbf{x} + (\mathbf{y} + \mathbf{z})$
A_2. $\mathbf{x} + \mathbf{y} = \mathbf{y} + \mathbf{x}$
A_3. There exists a vector $\mathbf{O}$ such that $\mathbf{x} + \mathbf{O} = \mathbf{x} = \mathbf{O} + \mathbf{x}$ for all $\mathbf{x}$.
A_4. For any vector $\mathbf{x}$ there exists a vector $-\mathbf{x}$ such that $\mathbf{x} + (-\mathbf{x}) = \mathbf{O} = (-\mathbf{x}) + \mathbf{x}$.
S_1. $t(\mathbf{x} + \mathbf{y}) = t\mathbf{x} + t\mathbf{y}$
S_2. $(s + t)\mathbf{x} = s\mathbf{x} + t\mathbf{x}$
S_3. $(st)\mathbf{x} = s(t\mathbf{x})$
S_4. $1\mathbf{x} = \mathbf{x}$

Here $\mathbf{x}$, $\mathbf{y}$, $\mathbf{z}$, are vectors, s, t are scalars, and 1 is the unit element of F. These properties are immediate consequences of the definitions and the properties of the field F. If one defines unit vectors $\mathbf{e}$ by means of Eq. (5), where the 1 occurs in the ith place, then

$$\mathbf{e}_i = (0, \ldots, 0, 1, 0, \ldots, 0) \tag{5}$$

a consequence of the definition of vector addition is that any vector $\mathbf{x} = (x_1,x_2, \ldots, x_n)$ can be expressed as the sum shown in Eq. (6). In addition, this way of

$$\mathbf{x} = x_1\mathbf{e}_1 + x_2\mathbf{e}_2 + \cdots + x_n\mathbf{e}_n \tag{6}$$

presenting the vector $\mathbf{x}$ as a linear combination of the vectors $\mathbf{e}_i$ is unique.

Axiomatic formulation. It is possible to obtain better insight and power in dealing with vectors if one axiomatizes the situation described above. Accordingly, one defines the notion of a vector space V over a field F as a set V with an addition composition $\mathbf{x} + \mathbf{y}$, and a multiplication $t\mathbf{x}$ of elements $\mathbf{x}$ of V by scalars t(elements of F). These are required to satisfy the axioms A_2 through A_4 and S_1 through S_4. It is worth noting that conditions A_1 through A_4 state that V and its addition composition constitute a commutative group. A subset B of V is called a base if every vector $\mathbf{x}$ can be written in one and only one way as a linear combination $\mathbf{x} = x_1\mathbf{b}_1 + x_2\mathbf{b}_2 + \cdots + x_m\mathbf{b}_m$, where the $\mathbf{b}_i$ are in B and the x_1 are in F. Every vector space has a base and any two bases have the same cardinal number which is called the dimension of V. The vector space F^n of n-tuples of elements of the field F has dimension n with base B = base B = $\{\mathbf{e}_1,\mathbf{e}_2, \ldots, \mathbf{e}_n\}$ defined above. *See* GROUP THEORY.

A subset U of V is called a subspace if the element $s\mathbf{u} + t\mathbf{v}$ is in U whenever $\mathbf{u}$ and $\mathbf{v}$ are in U and s and t are in F. The factor space V/U is the set of cosets $\mathbf{x} + \mathbf{u}$ where $\mathbf{x}$ is fixed and $\mathbf{u}$ ranges over U. Addition and scalar multiplication in V/U are defined by $(\mathbf{x} + U) + (\mathbf{y} + U) = \mathbf{x} + \mathbf{y} + U$, $t(\mathbf{x} + U) = t\mathbf{x} + U$, respectively.

Linear transformations. If U and V are vector spaces over the same field F, then one defines a linear transformation $\mathbf{A}$ of U into V as a correspondence $x \to \mathbf{Ax}$ (also written as $\mathbf{xA}$) of U into V such that Eqs. (7)

$$\begin{aligned} \mathbf{A}(\mathbf{x} + \mathbf{y}) &= \mathbf{Ax} + \mathbf{Ay} \\ \mathbf{A}(t\mathbf{x}) &= t(\mathbf{Ax}) \end{aligned} \tag{7}$$

is satisfied for any $\mathbf{x}$, $\mathbf{y}$ in U and any t in F. The image $\mathbf{A}U$ of U under the linear transformation $\mathbf{A}$ is the set of all vectors $\mathbf{Ax}$ where $\mathbf{x}$ ranges over all of U. $\mathbf{A}U$ is a subspace of V. The kernel of $\mathbf{A}$ is the set of vectors $\mathbf{z}$ in U such that $\mathbf{Az} = 0$. This is also a subspace of U. If U and V are finite dimensional and b is vector in V, then the determination of the vectors x of U such that $\mathbf{Ax} = \mathbf{b}$ is equivalent to the determination of the set of solutions of a system of linear equations.

If $\mathbf{A}$ and $\mathbf{B}$ are linear transformations of a vector space U into another vector space V and if t is in F, then one defines $\mathbf{A} + \mathbf{B}$ and $t\mathbf{A}$ by $(\mathbf{A} + \mathbf{B})\mathbf{x} = \mathbf{Ax} + \mathbf{Bx}$, $(t\mathbf{A})\mathbf{x} = t(\mathbf{Ax})$, respectively. If $\mathbf{C}$ is a linear transformation of V into a third vector space W, then one defines $\mathbf{AC}$ by $(\mathbf{AC})\mathbf{x} = \mathbf{A}(\mathbf{Cx})$. The mappings $\mathbf{A} + \mathbf{B}$, $t\mathbf{A}$, $\mathbf{AC}$ are all linear transformations. One denotes the set of linear transformations of U into V by hom (U,V). This is itself a vector space relative to the addition $\mathbf{A} + \mathbf{B}$ and the multiplication $t\mathbf{A}$ defined above. In the special case in which $V = F$, the vector space V^* = hom (V,F) is called the conjugate space of V or the space of the linear functions on V. If $\mathbf{A}$, $\mathbf{B}$, $\mathbf{C}$

are in hom(U,U), then $(\mathbf{AB})\mathbf{C} = \mathbf{A}(\mathbf{BC})$, $\mathbf{A}(\mathbf{B} + \mathbf{C}) = \mathbf{AB} + \mathbf{AC}$, $(\mathbf{B} + \mathbf{C})\mathbf{A} = \mathbf{BA} + \mathbf{CA}$, $t(\mathbf{AB}) = (t\mathbf{A})\mathbf{B} = \mathbf{A}(t\mathbf{B})$. These properties imply that hom (U,U) is an algebraic system of a type called an associative algebra.

If U and V are vector spaces over F with bases $\{\mathbf{u}_1,\mathbf{u}_2, \ldots, \mathbf{u}_m\}$ and $\{\mathbf{v}_1,\mathbf{v}_2, \ldots, \mathbf{v}_n\}$, respectively, and $\mathbf{A}$ is a linear transformation of U into V, then according to the definition of a base, one can write

$$\mathbf{A}\mathbf{u}_i = \sum_{j=1}^{i} a_{ji}\mathbf{v}_j$$

In this way one can associate with $\mathbf{A}$ the n by m matrix (a_{ji}). The correspondence between hom (U,V) and the set of n by m matrices with entries in F is 1-1 and preserves addition and multiplication by scalars. That is, to each transformation in hom (U,V) there corresponds one and only one matrix, and the matrix which corresponds to the sum of two transformations is the sum of the matrices corresponding to the separate transformations. Also if $V = U$ then the correspondence preserves multiplication. In this way one sees that the theory of linear transformations between finite-dimensional vector spaces is equivalent to matrix theory. *See* MATRIX THEORY.

Multilinear algebra and tensors. Linear algebra is generally regarded as including also multilinear algebra, the basic notion of which is that of a bilinear mapping of the pair of vector spaces U, V into a third vector space W (over the same field F). This is a mapping B of the set of pairs $(\mathbf{x},\mathbf{y})$ with $\mathbf{x}$ in U and $\mathbf{y}$ in V into W such that Eqs. (8) are satisfied for $\mathbf{x}$, $\mathbf{x}'$ in U;

$$\begin{aligned} B(\mathbf{x} + \mathbf{x}', \mathbf{y}) &= B(\mathbf{x}, \mathbf{y}) + B(\mathbf{x}', \mathbf{y}) \\ B(\mathbf{x}, \mathbf{y} + \mathbf{y}') &= B(\mathbf{x}, \mathbf{y}) + B(\mathbf{x}, \mathbf{y}') \\ B(t\mathbf{x}, \mathbf{y}) &= tB(\mathbf{x}, \mathbf{y}) = B(\mathbf{x}, t\,\mathbf{y}) \end{aligned} \tag{8}$$

$\mathbf{y}$, $\mathbf{y}'$ in V; and t in F. This leads to the notion of the tensor product $U \otimes V$, which is a vector space together with a bilinear mapping of U and V into this space which is maximal in a certain sense. One can iterate the construction of $U \otimes V$ to obtain tensor spaces of higher degree. Such spaces are fundamental for applications of algebra to differential geometry and relativity theory.

Quadratic forms. An important part of linear algebra is concerned with the study of a vector space relative to a given quadratic form. This is defined to be a correspondence Q: $\mathbf{x} \to Q(\mathbf{x})$ of V into F such that $Q(t\mathbf{x}) = t^2Q(\mathbf{x})$ and such that $B(\mathbf{x},\mathbf{y}) = Q(\mathbf{x} + \mathbf{y}) - Q(\mathbf{x}) - Q(\mathbf{y})$ is bilinear from the pair V, V to F. If $F = R$, the field of real numbers, and V is complete in the topology defined by Q as a norm (an absolute value), then a real Hilbert space is obtained. Replacement of Q by a hermitian form defines a (complex) Hilbert space. The theory of finite-dimensional real Hilbert spaces is equivalent to the study of n-dimensional euclidean geometry. Infinite-dimensional Hilbert spaces and their generalization called Banach spaces play an important role in modern analysis.

Nathan Jacobson

Bibliography. H. Anton, *Elementary Linear Algebra*, 8th ed., 2000; J. B. Fraleigh and R. A. Beauregard, *Linear Algebra*, 3d ed., 1995; P. R. Halmos, *Finite Dimensional Vector Spaces*, 2d ed., 1958, reprint 1993; S. A. Lang, *Linear Algebra*, 3d ed., 1994; S. J. Leon, *Linear Algebra with Applications*, 5th ed., 1997; W. K. Nicholson, *Linear Algebra with Applications*, 3d ed., 1994.

Linear energy transfer (biology)

A physical factor which is significant in biology because, in many biological actions of high-energy radiations, linear energy transfer (LET) strongly and characteristically modifies the quantitative relations between dose and effect. *See* RADIATION BIOLOGY.

When a moving charged particle (for example, an electron or proton) traverses matter, it progressively loses kinetic energy which is gained, in diverse amounts, by individual molecules along its path. The amount of energy thus transferred, per unit length of path, is the LET. It is roughly proportional, at least in gases, to ionization per unit path (specific ionization; ion density). LET increases as the velocity of the particle decreases; accordingly it varies greatly along any individual path and is maximal near the end. Also, LET increases as the square of the charge on the particle; for example, the LET of an alpha particle is four times that of an electron or proton of the same instantaneous velocity.

For experimental purposes, different values of LET can be obtained in two general ways. In the track-segment method, a beam is used made up of particles (protons) that have uniform initial velocity and produce substantially straight tracks. The experiment is so arranged that they all traverse a sample of biological objects with the same linear segment of their paths. Different LET values are obtained by using suitably different path segments. In the track-average method, either entire paths are spent within the biological object or random linear segments of different paths traverse it. Different average values of LET are obtained by using radiations that produce suitably different spectra of LET. Although the average usually used is the arithmetic mean, other averages will probably be found to be more meaningful as greater understanding of radiobiological mechanisms is achieved.

In some radiobiological actions the shape of the dose-effect curve is changed as LET is varied. However, these cases are rare in comparison with those in which only the slope is changed. In the latter case the effect of LET can be expressed by a single parameter (relative biological effectiveness, RBE) which varies as the slope (or as the reciprocal of the dose, in rads, required to produce a given degree of effect).

For some radiobiological actions, RBE decreases with increase in LET; this is exemplified by inactivation of macromolecules, viruses, and certain bacteria. For other actions, RBE increases with LET; in some of these cases, RBE has been shown to pass through a maximum; there are theoretical reasons

to believe that maxima would be observed for all of them if larger values of LET were available.

The distribution of individual energy transfers along a path corresponds to the distribution of ionized and excited molecules, production of which is believed to initiate the radiobiological mechanism. Because of diffusion, this distribution in space lasts only 1 microsecond or less. Thus the observed variation of RBE with LET demonstrates that some essential part of the radiobiological mechanism is completed in a very short time.

Among other interesting facts are the following: (1) In at least some radiobiological actions, the influence of LET is modified by other factors, such as concentration of molecular oxygen. (2) Influence of LET is also encountered in radiation chemistry. For instance, the decomposition of liquid water depends strongly on LET, and this dependence is modified by oxygen. Facts such as these make LET of prime interest in attempts to understand radiobiological mechanisms. *See* RADIATION; RADIATION INJURY (BIOLOGY).

Raymond E. Zirkle

Bibliography. T. Alper, *Cellular Radiology*, 1979; W. Harm, *Biological Effects of Ultraviolet Radiation*, 1980; D. J. Pizzarello and R. L. Witcofski, *Basic Radiation Biology*, 2d ed., 1975; C. Von Sonntag, *The Chemical Basis for Radiation Biology*, 1987.

Linear momentum

Isaac Newton's "quantity of motion," defined as the product of a particle's mass and velocity, whose time rate of change equals the applied force; in modern physics, the rate of change of energy with respect to velocity. The law of conservation of linear momentum states that the total linear momentum of an isolated system remains constant. *See* ANGULAR MOMENTUM; CONSERVATION OF MOMENTUM; ENERGY; MOMENTUM.

Role in classical mechanics. The linear momentum of a particle is the vector quantity $\mathbf{p}$ given by Eq. (1),

$$\mathbf{p} = m\mathbf{v} \tag{1}$$

where m is the particle's mass and $\mathbf{v}$ is its velocity. *See* MASS; VELOCITY.

Newton's second law of motion states that the rate of change of linear momentum is proportional to the applied force $\mathbf{F}$, Eq. (2).

$$\mathbf{F} = \frac{d\mathbf{p}}{dt} \tag{2}$$

See FORCE.

This is actually the definition of force in terms of the fundamental quantities of physics: mass, length (here, position), and time. If more than one force acts on the particle, then $\mathbf{F}$ is the (vector) sum of the forces. Newton's first law of motion is implied because if $\mathbf{F} = \mathbf{0}$, then $\mathbf{p}$ is constant. *See* DIMENSIONS (MECHANICS); DYNAMICS; EQUILIBRIUM OF FORCES; INERTIA; RESULTANT OF FORCES.

Newton based his laws on a number of assumptions he took for granted. These are (1) total mass is constant (this is sometimes called Newton's zeroth law of motion); (2) masses (which are scalar quantities) add linearly; (3) velocities (which are vector quantities) and forces (also vectors) add linearly, implying that momenta must add linearly; (4) forces do not depend on velocity; (5) forces between particles are directed along the line that connects them; (6) all physical interactions are completely deterministic; and (7) mass, energy, and momentum are infinitely subdivisible. *See* CONSERVATION OF MASS; DETERMINISM; RELATIVE MOTION.

In addition to the above assumptions are others regarding the reference frames: the coordinate systems for specifying positions and velocities. By definition, inertial reference frames are those in which Newton's laws are true; this implies that the frames are neither rotating nor accelerating, but are only moving at a constant velocity with respect to the observer. Newton's laws also assume that all the reference frames are Newtonian, meaning that measurements of position and time are completely independent; there is one absolute universal time measurement; and influences act across all distances instantaneously (the speed of light is infinite). *See* FRAME OF REFERENCE.

The various branches of modern physics are characterized by the extent to which one or more of the above assumptions are dropped. For example, assumptions (1), (2), and (3) are not true for relativistic velocities; assumptions (4) and (5) are not true for magnetic forces between particles; (6) is not true for quantum-mechanical systems; and (7) is not true for atomic, nuclear, and subnuclear physics. General relativity describes physics in accelerating frames of reference.

The total linear momentum of a multiparticle system equals the sum of the linear momenta of its constituent particles. If the system's configuration is not important, then it can be modeled as a single particle, having the same mass as the system, located at the system's center of mass, and subjected to the sum of the external forces. If there are no external forces (or if they always sum to zero), then by Newton's first law, the center of mass will move at a constant velocity. *See* CENTER OF MASS; COLLISION (PHYSICS).

Expanding Eq. (3) by the usual rules of differentiation shows that, in general, change in linear momentum can be caused by (nonrelativistic) change in mass. An example would be in the analysis of rocket flight wherein the total mass of the rocket decreases as its propellants are ejected.

$$\frac{d\mathbf{p}}{dt} = \frac{d}{dt}(m\mathbf{v}) = m\frac{d\mathbf{v}}{dt} + \mathbf{v}\frac{dm}{dt} \tag{3}$$

When mass is constant, Eq. (3) simplifies to Eq. (4),

$$\mathbf{F} = m\frac{d\mathbf{v}}{dt} = m\mathbf{a} \tag{4}$$

where $\mathbf{a}$ is the acceleration of the particle. *See* ACCELERATION.

The units of measure for linear momentum are the Newton second (in SI units) and pound-force second (in U.S Customary units). *See* UNITS OF MEASUREMENT.

Linear momentum in continuous media. Continuous media include deformable solids, fluids (liquids and gases), plasmas, and "empty" space. For such media, it is more appropriate to use momentum density, defined as momentum per unit volume of the medium. Two examples are given here.

Fluid mechanics. The Navier-Stokes equations describe the dynamics of fluids in terms of conservation of momentum. Linear momentum appears as the density (mass per unit volume) times velocity at a given point in the fluid, that is, the momentum density at that point. *See* FLUID-FLOW PRINCIPLES; NAVIER-STOKES EQUATIONS.

Classical electromagnetic theory. Electromagnetic waves transport energy according to the Poynting vector $\mathbf{S} = \mathbf{E} \times \mathbf{H}$, where $\mathbf{E}$ and $\mathbf{H}$ are the electric and magnetic field vectors, respectively. The energy propagates in the direction of $\mathbf{S}$ at the speed of light, suffusing the (lossless) medium with electromagnetic momentum $\mathbf{g} = (1/c^2)\,\mathbf{S}$, measured in N-s/m^3, that will exert radiation pressure on matter. The pressure is very small: for sunlight, it is about 0.44 kg-force/(km)^2, or 2.5 lb-force/(mi)^2, on the Earth's surface. *See* POYNTING'S VECTOR; RADIATION PRESSURE.

Role in relativistic mechanics. Relativistic effects become important when velocities approach the speed of light c. In particular, a particle moving with speed v appears more massive by the factor $\gamma(v)$, Eq. (5). However, an isolated system will retain the

$$\gamma(v) = (1 - v^2/c^2)^{-\frac{1}{2}} \tag{5}$$

same form of law of conservation of linear momentum provided we use the relativistic momentum, Eq. (6), of each constituent particle.

$$\mathbf{p} = \gamma(v) m_0 \mathbf{v} = m(v)\mathbf{v} \tag{6}$$

Relativistic momentum is sometimes called the 3-momentum because its three components plus an energy term constitute the momentum-energy 4-vector, or 4-momentum, much used in high-energy particle physics. Although different observers will obtain different measurements of a particle's energy and momentum, they will all agree on the value of its rest mass. Mathematically stated, the magnitude of the 4-momentum $c^2 m_0$ (the momentum-energy, or momenergy), given by Eq. (7), is invariant and so

$$c^2 m_0 = \sqrt{E^2 - |\mathbf{p}|^2 c^2} \tag{7}$$

relates any observer's own measurements of the particle's energy E and momentum $\mathbf{p}$. For a particle at rest in the observer's frame, Eq. (7) yields Einstein's famous equation for rest energy: $E_{\text{rest}} = m_0 c^2$. *See* RELATIVISTIC MECHANICS; RELATIVITY.

Linear momentum in quantum theory. Quantum mechanics differs radically from classical mechanics in several ways. With specific regard to linear momentum in nonrelativistic quantum theory:

1. A particle's linear momentum and position cannot both be precisely measured at the same time. Heisenberg's uncertainty principle specifies the lower limit on the product of the uncertainties (probable range of errors) of the two measurements by Eq. (8) where $\hbar = h/(2\pi)$ and h is Planck's constant. *See* PLANCK'S CONSTANT; UNCERTAINTY PRINCIPLE.

$$\Delta p_x \Delta x \geq \frac{\hbar}{2} \tag{8}$$

2. Electromagnetic radiation is quantized into photons whose linear momentum is given by Eq. (9),

$$p = \frac{h}{\lambda} \tag{9}$$

where λ is the electromagnetic wavelength. When a photon loses some of its momentum to a subatomic particle, its wavelength increases correspondingly. *See* COMPTON EFFECT; QUANTUM (PHYSICS).

3. Particles have wavelike properties and their momentum is also given by Eq. (9), where λ is now the particle's de Broglie wavelength. *See* DE BROGLIE WAVELENGTH; WAVE MECHANICS.

4. The Lagrangians and Hamiltonians of classical mechanics are invalid since they are premised on the observer being able to accurately measure momentum and position simultaneously. However, the same form of Hamiltonian is used, but with the dynamic variables replaced by their analogous Hamiltonian operators. For example, the momentum operator $\hat{p}$ in the one-dimensional form of Schrödinger's equation is given by Eq. (10), where i is the "imaginary" unit $\sqrt{-1}$. *See* HAMILTON'S EQUATIONS OF MOTION; LAGRANGE'S EQUATIONS OF MOTION.

$$\hat{p} = \frac{\hbar}{i}\frac{\partial}{\partial x} \tag{10}$$

By applying the momentum operator in the appropriate way to the wave function, one obtains the probability of obtaining any given value of measured momentum. Although repetition of the experiment will yield different results in detail, nevertheless the total linear momentum will always be found to be conserved. *See* NONRELATIVISTIIC QUANTUM THEORY; QUANTUM MECHANICS; SCHRÖDINGER'S WAVE EQUATION.

Role in relativistic quantum theory. When relativistic effects become important, the total momentum-energy of a system is still conserved. However, tools such as Schrödinger's equation become invalid because they use time independently of space and one must instead use the methods of quantum field theories. Among these methods are the diagrammatic momentum-space Feynman rules of quantum electrodynamics. *See* FEYNMAN DIAGRAM; QUANTUM ELECTRODYNAMICS; QUANTUM FIELD THEORY; QUANTUM GRAVITATION; RELATIVISTIC QUANTUM THEORY.

Andrej Tenne-Sens

Bibliography. R. P. Feynman, R. B. Leighton, and M. L. Sands, *The Feynman Lectures on Physics: The Definitive and Extended Edition*, 3 vols., Addison-Wesley, Reading, MA, 2005; H. Goldstein, C. P. Poole, and J. L. Safko, *Classical Mechanics*, 3d ed., Pearson Education, San Francisco, 2002; J. Griffiths, *Introduction to Quantum Mechanics*, Prentice Hall,

Englewood Cliffs, NJ, 1994; J. D. Jackson, *Classical Electrodynamics*, 3d ed., Wiley, 1999; R. Penrose, *The Road to Reality: A Complete Guide to the Laws of the Universe*, Jonathan Cape, London, 2004; M. E. Peskin and D. V. Schroeder, *An Introduction to Quantum Field Theory*, Westview Press, 1995; A. Sommerfeld, *Lectures on Theoretical Physics*, vol. 1: *Mechanics*, Academic Press, New York, 1964; E. F. Taylor and J. A. Wheeler, *Spacetime Physics: Introduction to Special Relativity*, 2d ed., Freeman, New York, 1992.

Linear programming

An area of mathematics concerned with the minimization (or maximization) of a linear function of several variables subject to linear equations and inequalities. Linear programming developed from three main areas: transportation problems, game theory, and input-output models. Work on all these areas took place before and during World War II, with major contributions by L. V. Kantorovich, J. von Neumann, and W. Leontief. The subject in its present form was created in 1947, when G. B. Dantzig defined the general model and proposed the first, and still the most widely used, method for its solution: the simplex method.

Although the linearity assumptions are restrictive, many algorithms for extensions of linear programming, such as problems with nonlinear or integer restrictions, involve successively solving linear programming problems. With a result in 1979 giving a polynomially bounded ellipsoid method, an alternative to the simplex method, linear programming became the focus of work by computer scientists, and nonlinear methods have been refocused on solving the linear programming problem. Work by N. K. Karmarkar announced in 1984 attracted much attention because of claims of vastly improved performance of a new interior method. The relative merits of Karmarkar's method and the simplex method remain to be determined, but there seems to be a place for both methods. Karmarkar's work stimulated considerable activity in linear programming methodology. *See* NONLINEAR PROGRAMMING; OPTIMIZATION.

General problem. The linear programming problem is to minimize linear objective function (1) subject to restrictions (2). The variables $x_1 \ldots, x_n$ are required to take on real values, and the coefficients a_{ij}, c_j, and b_i are real constants. The objective could be to maximize rather than minimize, and among constraints (2) the equations could be replaced by inequalities of the form less-than-or-equal-to or greater-than-or-equal-to. The set of x_j's satisfying constraints (2) form a convex polyhedron, and the optimum value of the objective function will always be assumed at a vertex of the polyhedron unless the objective function is unbounded. The simplex method works by moving from vertex to vertex until the vertex yielding the optimum value of the objective function is reached, while interior methods stay inside the polyhedron. *See* LINEAR SYSTEMS OF EQUATIONS.

$$c_1x_1 + \cdots + c_nx_n \tag{1}$$
$$x_1 \geq 0, \ldots, x_n \geq 0$$

$$\begin{aligned} a_{11}x_1 + \cdots + a_{1n}x_n &= b_1 \\ \vdots \qquad\qquad\quad & \vdots \\ a_{m1}x_1 + \cdots + a_{mn}x_n &= b_m \end{aligned} \tag{2}$$

Transportation problem. The transportation problem is an example of a linear programming model. In this model, there are supply amounts $S_1 \ldots, S_K$ of a given product at supply points $1, \ldots, K$ and demand amounts $D_1, \ldots, D_L$ at demand points $1, \ldots, L$. The variables x_{ij} are associated with a supply point i and demand point j and represent the amount to be shipped from i to j. The constraints are $x_{ij} \geq 0$ and inequalities (3), and the objective is to minimize

$$\begin{aligned} x_{11} + \cdots + x_{1L} &\leq S_1 \\ \cdots & \\ x_{K1} + \cdots + x_{KL} &\leq S_K \\ x_{11} + \cdots + x_{K1} &\geq D_1 \\ \cdots & \\ x_{1L} + \cdots + x_{KL} &\geq D_L \end{aligned} \tag{3}$$

$\Sigma c_{ij}x_{ij}$, the total cost of shipping, where c_{ij} is the per unit cost of shipping from supply point i to demand point j. Variants include bounds and costs on storage at the supply points and penalties for shortages at the demand points.

Dual problem. For every linear programming problem with objective function (1) and constraints (2), there is a dual linear program in variables $y_1, \ldots, y_m$, one variable for each equation in (2). The objective is to maximize function (4), subject to linear inequalities (5). In this form, the y_i's are not constrained to

$$y_1b_1 + \cdots + y_mb_m \tag{4}$$

$$\begin{aligned} y_1a_{11} + \cdots + y_ma_{m1} &\leq c_1 \\ y_1a_{1n} + \cdots + y_ma_{mn} &\leq c_n \end{aligned} \tag{5}$$

be nonnegative, although the problem can be stated so that the dual is more symmetric by changing the equations in (2) to inequalities. The duality theorem states that the maximum value of function (3) is equal to the minimum value of function (1), provided both constraints (2) and (5) have solutions. The dual variables are related to Lagrange multipliers, and can be interpreted as prices on resources constrained by restrictions (2). The duality theorem is mathematically equivalent to the result that any point not in the convex polyhedron defined by constraints (2) can be separated from it by a hyperplane. The original problem with constraints (2) is referred to as the primal problem, and the x_j's are called primal variables. *See* CALCULUS OF VARIATIONS.

Simplex method. The simplex method in its usual form is a primal feasible method; that is, it maintains constraints (2) while working toward optimality. The method must find a solution satisfying

constraints (2), and one way to do this is to initially solve the problem of finding a solution to these constraints while ignoring the original objective function. Such a problem is itself a linear programming problem and is called the phase-one problem. Then, the minimization of the original objective function becomes phase two. The algorithm in phase two maintains primal feasibility, that is, constraints (2), while working toward satisfying inequalities (5) in such a way that once these inequalities are satisfied the solutions x and y to the primal and dual problems will be optimal with regard to these respective problems.

Interior method. Interior methods were proposed at the same time as the simplex method, but were not pursued because they did not prove to be faster than the simplex method. The first promise of success for nonlinear methods was the proof of a polynomial upper bound for the ellipsoid method of L. G. Khatchian in 1979; that is, this method was guaranteed to find a solution in a time bounded by a polynomial function of the data. Despite the theoretical interest in Khatchian's breakthrough, the method proved to be much slower, on the average, than the simplex method, at least for problems of the size encountered in practice. Karmarkar's method in 1984 proved to be competitive with the simplex method and perhaps better on large problems and on certain classes of problems. Karmarkar also gave a smaller polynomial bound. The interior methods led to renewed research. In particular, bounds have been improved, variants developed, prior work (in particular, by Russian mathematicians) rediscovered, and computational experimentation carried out. The three basic interior methods are Karmarkar's method, affine scaling, and barrier methods.

Integer programming. An important extension in practice is to require some of the x_j's to take on integral values. The most common case in practice is where the integer x_j must be 0 or 1, representing decision choices such as to whether to switch from production of one product to another or whether to expand a warehouse to allow for larger throughput. Whereas linear programming solution times tend to be less than an hour, adding the constraint that some or all of the x_j's must be integral may cause the running time to be very long. Work in the 1950s established the usefulness of linear programming in solving the so-called traveling salesman problem. Around the same time, cutting-plane methods were shown to be a convergent process for solving general integer programs, in which all of the variables x_j are required to take on integer values. Cutting-plane methods attempt to adjoin new inequality constraints to constraints (2) so that all integral solutions remain feasible and the optimum solution is integral. Some linear programs have the property that the optimum vertex is already an integral solution, but in practice the main class of such problems is the transportation problem mentioned above. *See* DECISION THEORY.

Although cutting-plane methods offered the hope of converting integer programs to larger linear programs by adjoining more constraints, the simpler branch-and-bound method became more common and was incorporated into commercial codes, perhaps largely due to the fact that the important mixed 0–1 case, where some of the variables must be 0 or 1, is not yet adequately treated by cutting-plane methods. The branch-and-bound method is simple in its original form. The linear programming relaxation (in which the constraints are relaxed by not requiring the x_j's to be integers) is solved, and a branching procedure is carried out with regard to some 0–1 variable that is at a fractional value. Two problems are created: In one the variable is forced to be 0 and in the other it is forced to be 1. The difficulty with the method is its explosive growth in the number of problems to be solved. The "bound" part of branch-and-bound comes from using the objective value of the linear programming relaxation to terminate further exploration of a problem when its objective value is worse than the objective value of some integer solution previously found or given. In its more refined variations, branch-and-bound may employ many heuristics to guide the search and elaborate improvements to the linear programming relaxation in order to improve the bound given by the value of the linear programming objective function.

Computation. Early work on computer programs was done in the 1950s. Commercial computer codes implementing the simplex method have been used in industry since the mid-1960s. Efficient methods for handling the structures encountered have been developed. In particular, the matrices tend to be very sparse, that is, most (usually over 99%) of the a_{ij}'s are zeroes. Efficient methods for basis inversion and update have been the main numerical focus of code developers. Up until the early 1980s, most problems solved by commercial codes were in the range of several hundred to several thousand equations and variables. A typical time on a mainframe computer might have been several seconds to an hour. In the 1980s, intense development in software was begun because of changed hardware and new algorithmic developments. The hardware changes included both larger supercomputers and more powerful workstations. The algorithmic developments were mainly the interior methods as well as improvements in the simplex method. In integer programming, the main algorithmic focus has been on improving the linear programming relaxation to give better bounds in branch-and-bound. *See* MATRIX THEORY; SUPERCOMPUTER.

Applications. Following the early work on codes, the petroleum industry quickly became the major user of linear programming, and still is an important user, especially for blending models in petroleum refining. Commercial codes are used in industry and government for a variety of applications involving planning, scheduling, distribution, manufacturing, and so forth. In universities, linear programming is taught in most business schools, industrial engineering departments, and operations research departments, as well as some mathematics departments. The model is general enough to be useful in the physical and social sciences. The improved

computational efficiency achieved in the 1980s has gone hand-in-hand with expanded applications, particularly in manufacturing, transportation, and finance. *See* OPERATIONS RESEARCH. Ellis L. Johnson

Bibliography. V. Chvatal, *Linear Programming*, 1983; G. B. Dantzig and M. N. Thapa, *Linear Programming*, 2 vols., 1997, 2003; J. P. Ignizio and T. M. Cavalier, *Introduction to Linear Programming*, 1994; G. L. Nemhauser and L. Wolsey, *Integer and Combinatorial Programming*, 1988; A. Sultan, *Linear Programming: An Introduction with Applications*, 1993; R. J. Vanderbei, *Linear Programming: Foundations and Extensions*, 2d ed., 2001; L. N. Vaserstein, *Introduction to Linear Programming*, 2002.

Linear system analysis

The study of properties and behavior of a system using a body of mathematical techniques based on linear system theory. A system can be defined as a set or arrangement of things related in such a way as to form a whole. Linear system analysis is concerned with the study of equilibrium and change in dynamical systems, that is, in systems that contain variables that may change with time. These variables include system inputs (external causes of change or excitation), outputs (measurable results or effects of the behavior, response, or dynamics of the system), as well as variables describing internal states of the system. To perform the analysis, relationships between these variables are described by a set of equations known as the model. In order for linear system analysis to be applicable, the model must possess the linearity property: it must be a linear model. Linearity simplifies the analysis of systems significantly, and hence there is a large body of mathematical techniques and results, referred to as linear system theory, that can be used to study linear systems. *See* LINEARITY; SYSTEMS ENGINEERING.

Examples of systems studied include both natural (biological or environmental) systems and artificial or engineered systems, such as spacecraft, aircraft, and electronic circuits. Models describing such systems can be derived from the laws of physics or fitted empirically by using input and output data. A simple mathematical model of a linear dynamical system can be obtained by applying Newton's second law to the motion, in a single dimension, of a system (**Fig. 1**), which consists of a mass M that may represent a car or a train, as given in Eq. (1). Here $u(t)$ is

$$u(t) = M\frac{d^2y}{dt^2} \tag{1}$$

the net force applied in the direction of movement, and $y(t)$ is the displacement at time t. If the only forces considered are that of the engine $f(t)$ and a viscous friction opposed to the motion whose magnitude is proportional to the velocity of the mass, then Eq. (2) holds, where K is a constant. The model

$$u(t) = f(t) - K\frac{dy}{dt} \tag{2}$$

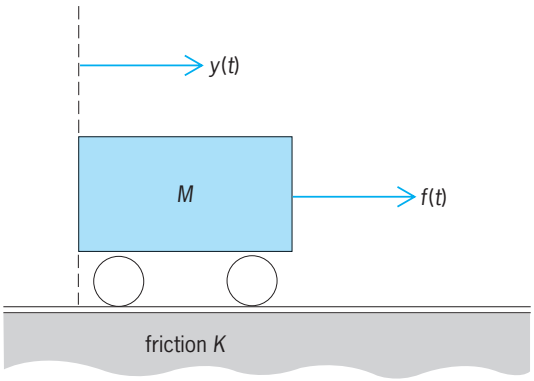

Fig. 1. A simple mass–friction dynamical system.

is then described by the second-order ordinary differential equation (3). In spite of the obvious simplicity

$$M\frac{d^2y}{dt^2} + K\frac{dy}{dt} = f(t) \tag{3}$$

of this model, it is useful in studying many practical situations.

The linearity property implies that the response of a system to the sum of several inputs is equal to the sum of its responses due to each of the individual inputs, and that the response of a system to an input multiplied by a scale factor is equal to the same scale factor times the response of the system to that input. In mathematical terms, linearity can be expressed through the use of Eq. (4), where the

$$y = F(u) \tag{4}$$

operator $F(.)$ describes the relationship between the system input and output. Here, y is the system output, u the system input, and F a mapping from input to output. In general, y and u are functions of time. The operator F is said to be linear if Eq. (5) is valid,

$$F(a_1u_1 + a_2u_2) = a_1F(u_1) + a_2F(u_2) \tag{5}$$

where u_1 and u_2 are two arbitrary inputs, and a_1 and a_2 are arbitrary real or complex numbers.

Although most systems in reality are nonlinear, it is possible to study their behavior in a limited range of values of inputs and outputs around an operating point with the help of linear approximations. By using Taylor's expansion, a nonlinear system $y = F(u)$ can be expressed in the neighborhood of an operating point u_0 as in Eq. (6), or as in Eq. (7), where F' is

$$y = F(u_0) + F'(u_0)(u - u_0) + R \tag{6}$$

$$\delta y = A\delta u + R \tag{7}$$

the first derivative of F with respect to u, $\delta y = y - F(u_0)$, $\delta u = u - u_0$, $A = F'(u_0)$ is a constant, and R is a residue which contains higher-order terms in δu that can be ignored if δu is small to achieve a linear approximation. An electronic amplifier, for example, can be approximated by a linear model for analysis of response to small signals around an operating point defined by dc bias voltages. *See* AMPLIFIER; DIFFERENTIATION.

Mathematical models. Mathematical models of dynamical systems can be divided into linear and nonlinear, time-invariant and time-varying, lumped-parameter and distributed-parameter, continuous-time and discrete-time, and so forth. The behavior of linear, continuous-time systems can be described by a set of differential equations. If the system parameters are time-invariant (that is, do not change value with time) and are lumped, then the model consists of a set or ordinary linear differential equations for continuous-time systems and difference equations for discrete-time systems. These equations can be solved, and the values of all variables at any moment in time t starting from any given initial time t_0 can be found, if all input functions are known from t_0 to t and if the initial conditions (the values at time t_0) of a minimal set of variables, referred to as the state variables of the system, are known. The state variables contain all the information about the history of the system needed to solve its equations. No knowledge of input or state values at time prior to t_0 is needed. Hence the state variables completely characterize the state of the system at any time t. *See* DIFFERENCE EQUATION; DIFFERENTIAL EQUATION.

If the state variable vector is a column vector comprising all the state variables of the system, the state vector for a second-order system is expressed by Eq. (8).

$$x(t) = \begin{bmatrix} x_1(t) \\ x_2(t) \end{bmatrix} \tag{8}$$

The state vector is a point in a linear algebraic space referred to as the state space. It is possible to describe the behavior of any linear system by using a specific form of mathematical models that expresses relationships between system inputs, state variables, and system outputs. This form is called the state-variable model or the state-space description. For continuous time it can be expressed as in Eqs. (9) and (10), where $x(t)$ is an n-component state vector, $\dot{x}(t)$ the derivative of this vector with respect to t, $u(t)$ a p-component input vector, $y(t)$ an m-component output vector, and $A(t)$, $B(t)$, $C(t)$, and $D(t)$ matrices of appropriate dimensions. The corresponding model for discrete-time systems is given by Eqs. (11) and (12), where $t = kT$, $k = 0, 1, 2, \ldots$,

$$\dot{x}(t) = A(t)x(t) + B(t)u(t) \tag{9}$$

$$y(t) = C(t)x(t) + D(t)u(t) \tag{10}$$

$$x(k+1) = A(k)x(k) + B(k)u(k) \tag{11}$$

$$y(k) = C(k)x(k) + D(k)u(k) \tag{12}$$

and T is the sampling period. *See* LINEAR ALGEBRA; LINEAR SYSTEMS OF EQUATIONS; MATRIX THEORY.

If the system is linear, the coefficients of these matrices do not depend on the values of the states. If the system is time-invariant, elements of the matrices are constants and the matrices are expressed simply as A, B, C, and D. Only continuous-time systems will be treated in this section; results for discrete-time systems are discussed below.

A set of state variables is defined in Eqs. (13) and (14) for the mass motion example given above. A

$$x_1(t) = y(t) \tag{13}$$

$$x_2(t) = \frac{dy}{dt} = \dot{x}_1(t) \tag{14}$$

state-space model can be formulated using these definitions as in Eqs. (15) and (16).

$$\begin{bmatrix} \dot{x}_1(t) \\ \dot{x}_2(t) \end{bmatrix} = \begin{bmatrix} 0 & 1 \\ 0 & \dfrac{-K}{M} \end{bmatrix} \begin{bmatrix} x_1(t) \\ x_2(t) \end{bmatrix} + \begin{bmatrix} 0 \\ \dfrac{1}{M} \end{bmatrix} f(t) \tag{15}$$

$$y(t) = [\,1\ 0\,] \begin{bmatrix} x_1(t) \\ x_2(t) \end{bmatrix} \tag{16}$$

It is possible to describe relationships between inputs and outputs of a linear system by using another type of mathematical model known as a transfer-function model. For systems with single input and single output (SISO systems), the transfer function is the ratio between the Laplace transform of the output and the input. For multiinput–multioutput systems (multivariable or MIMO), the transfer function may be put in matrix form. The element in the ith row and jth column is a scalar transfer function describing how the jth input influences the ith output.

The system transfer function can be obtained from the state-space model by taking the Laplace transform, setting the initial value of $x(t)$ to zero, and solving for $Y(s)$ as in Eq. (17), where $Y(s)$ and $U(s)$

$$Y(s) = [C(sI - A)^{-1}B + D]U(s) \tag{17}$$

are the Laplace transforms of $y(t)$ and $u(t)$, and I is an $n \times n$ identity matrix. *See* LAPLACE TRANSFORM; MODEL THEORY.

Behavior of a linear system. In order to understand the behavior of a linear system, its response to a specified input is often calculated. The output can be calculated by solving the differential equations describing the model. Solution of the state equations provides a systematic way of solving the model equations to calculate the output as a function of time. The state equations can be solved analytically or by computer simulation techniques involving numerical integration. The closed-form solution of the state equations is given by Eq. (18), and the output by Eq. (19), where the $n \times n$ state-transition matrix $\Phi(t,\tau)$ satisfies differential equation (20).

$$x(t) = \Phi(t, t_0)x(t_0) + \int_{t_0}^{t} \Phi(t, \tau)B(\tau)u(\tau)d\tau \tag{18}$$

$$y(t) = C(t)x(t) + D(t)u(t) \tag{19}$$

$$\frac{d\Phi(t, t_0)}{dt} = A(t)\Phi(t, t_0) \qquad \Phi(t_0, t_0) = I \tag{20}$$

See INTEGRAL EQUATION.

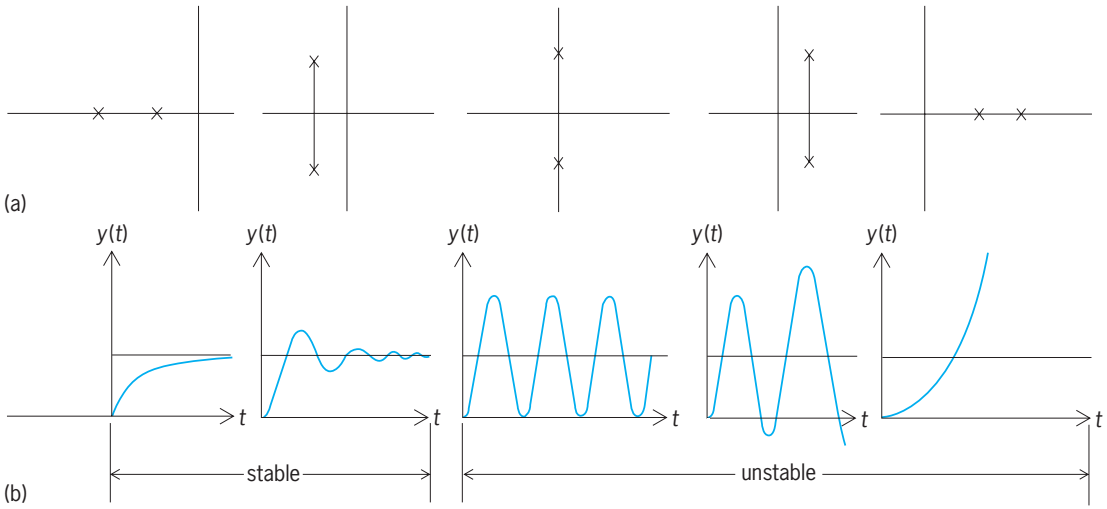

Fig. 2. Dependence of response of linear, second-order, single-input single-ouput system on location of eigenvalues of *A* matrix. (*a*) Locations of eigenvalues in complex plane. (*b*) Corresponding system response to a unit step input (a sudden change from zero to one at $t = 0$).

For time-invariant systems the state-transition matrix is found in closed form as in Eq. (21). The matrix

$$\Phi(t, t_0) = e^{A(t-t_0)} \tag{21}$$

e^{At} can be calculated by one of many possible methods, as shown in Eqs. (22) and (23), where $\mathscr{L}^{-1}$ is the inverse Laplace transform.

$$e^{At} = I + At + \frac{A^2t^2}{2!} + \frac{A^3t^3}{3!} + \cdots \tag{22}$$

$$e^{At} = \mathscr{L}^{-1}[sI - A]^{-1} \tag{23}$$

If the eigenvalues of A, λ_i $(i = 1, \ldots, n)$, are distinct and $\Lambda = \text{diag}(\lambda_1, \lambda_2, \ldots, \lambda_n)$ there is a similarity transformation Q that relates A to Λ by Eq. (24). In this case Eq. (25) holds.

$$A = Q\Lambda Q^{-1} \tag{24}$$

$$e^{At} = Qe^{\Lambda t}Q^{-1} \tag{25}$$

See EIGENFUNCTION.

Several commercial software packages and mathematical software libraries provide efficient numerical algorithms for calculation of e^{At} and for solution of the model using simulation involving numerical integration. *See* NUMERICAL ANALYSIS; SIMULATION.

Characteristics. By using the mathematical model of a linear system, a great deal of information about its behavior can be obtained. Stability, controllability, and observability can be deduced from a system model. There are many mathematical definitions and tests for stability. The bounded-input bounded-output definition is commonly used, which states simply that a system is stable if its output remains bounded for any bounded input applied to it. A continuous-time system is stable if all eigenvalues of the A matrix of its state-space model are in the left side of the complex plane, in other words if all eigenvalues have negative real parts. *See* COMPLEX NUMBERS AND COMPLEX VARIABLES.

The shape of the response of a linear single-input single-output system as a function of time is determined by the location of the eigenvalues of the A matrix in the complex plane (**Fig. 2**). This is due to the fact that all elements of the matrix e^{At} consist of linear combinations of terms of the form $t^k e^{\lambda_i t}$ called the modes of the system, where the λ_i $(i = 1, \ldots, n)$ are eigenvalues of A. For a multivariable system the eigenvalues and eigenvectors of A determine the shape of the response.

A system is controllable if it is possible to cause its state to move from an initial value $\boldsymbol{x}(t_0)$ at time t_0 to a specified final value $x(t_1)$ at a finite time t_1 by using an appropriate control input. A linear, time-invariant system is controllable if the $n \times pn$ controllability matrix of Eq. (26) has rank n.

$$U = [B|AB|A^2B| \cdots |A^{n-1}B] \tag{26}$$

Only the input and output of a system are measurable. The states are, in general, not accessible unless some of them are also outputs. It is sometimes necessary to generate an estimate of the state vector by using the input and output measurement values. This is possible if the system is observable. A linear, time-invariant system is observable if the $n \times mn$ observability matrix of Eq. (27) has rank n, where the

$$V = \left[C^T|A^TC^T|(A^2)^TC^T| \cdots |(A^{n-1})^TC^T\right] \tag{27}$$

superscript T stands for transpose of the matrix.

State feedback control. It is often desired to cause the system response to meet given specifications. This can be achieved by using state feedback of the form of Eq. (28) to place, or assign, the poles of the

$$u(t) = r(t) - Kx(t) \tag{28}$$

resulting (closed-loop) system (which are the same as the eigenvalues of the closed-loop A matrix) to desired locations in the complex plane, where $r(t)$ is a reference input and K a matrix of feedback gains.

It is possible to assign the poles of the closed-loop system (eigenvalues of the matrix A–BK) arbitrarily in the complex plane if the system is controllable. Furthermore, it is possible to design a state estimator of the form of Eq. (29), with arbitrarily chosen poles

$$\dot{\hat{x}}(t) = A\hat{x}(t) + Bu(t) + L[y(t) - C\hat{x}(t)] \qquad (29)$$

(eigenvalues of A–LC), if the system is observable. It can be shown that, under appropriate conditions, the design of a system combining state-feedback control and state estimation (**Fig. 3**) can be separated into two problems, one for control design and one for estimator design. This is known as the principle of separation between estimation and control. *See* ESTIMATION THEORY.

Computer assistance. There are many public-domain and commercial software packages and subroutine (or procedure) libraries that assist in implementing linear system analysis on digital computers. These typically include many collections of matrix and polynomial manipulation functions, such as finding matrix eigenvalues or exponential and polynomial roots. They usually also contain simulation routines based on numerical integration and graphics routines for plotting the outcome of the simulation. Numerical robustness and stability of the algorithms used become very important in computer-assisted analysis. The effect of round-off error resulting from the finite number of bits used to represent numbers in a computer can be significant. How round-off error, stability, and robustness are dealt with determines the quality of the software used. *See* ALGORITHM; CONTROL SYSTEMS.

Hany K. Eldeib

Discrete-time linear systems. A discrete-time system is one whose input and output responses evolve at discrete time instants rather than in continuous time. A discrete-time linear system is a discrete-time system that obeys the superposition property; that is, its response to a linear combination of two inputs is the same linear combination of the responses to the inputs applied separately. It is usually assumed that a discrete-time system is also a quantized system (not explicitly included in the definition), which means that the quantities, or signals, processed can take on only values from a finite set. In that case, a discrete-time system can be implemented by means of either finite-state processing components or a general-purpose or specialized signal-processing computer. One reason for the importance and increasing use of discrete-time (quantized) systems is the ease with which they can be realized and modified simply by programming a signal-processing computer. Other reasons are the great generality of functions that can be implemented, and the lower cost relative to implementation of continuous-time (or analog) processors for comparable signal-processing functions. Applications of discrete-time linear systems include control of a process, data manipulation, and signal processing such as filtering.

Numerical solutions. A discrete-time algorithm can also be used for the numerical solution of a continuous-time model for a system. An example is the simple

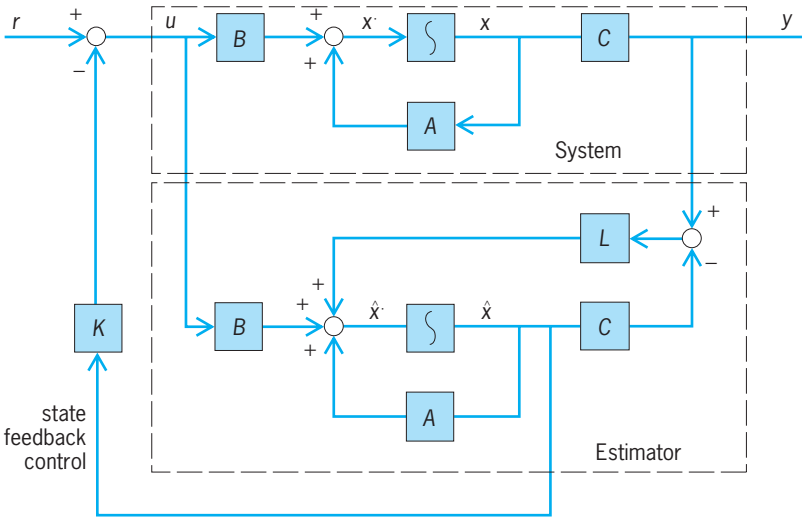

Fig. 3. State-space model of a system that combines state feedback control and state estimation.

first-order linear differential equation (30) with con-

$$\frac{dy(t)}{dt} + ay(t) = bu(t) \qquad (30)$$

stant coefficients a and b, which might relate the response of a system, $y(t)$, to a forcing function or input, $u(t)$. This equation can be put into standard state-variable form (although that would be unnecessary in this simple case) as Eq. (31), where $x(t)$ is

$$\frac{dx(t)}{dt} = -ax(t) + bu(t) \qquad y(t) = x(t) \qquad (31)$$

a state variable. The state equation [the first equation of Eq. (31)] can be approximated by a discrete-time equivalent equation by using a rectangular approximation for integration at the nth step given by Eq. (32). In this equation, the overdot denotes differ-

$$x_{n+1} = x_n + T\dot{x}_n \qquad (32)$$

entiation, T is the step size, and the subscript n denotes evaluation at the nth time instant, nT. Equation (32) is known as the Euler integration formula. The state equation (31) provides a means for eliminating $\dot{x}_n$ in Eq. (32). Rewriting it for the nth time instant gives Eq. (33). This equation can be substituted into Eq. (32) to yield Eq. (34). This first-order difference

$$\dot{x}_n = -ax_n + bu_n \qquad (33)$$

$$\left.\begin{aligned} x_{n+1} &= (1 - aT)x_n + bu_n \\ y_n &= x_n \end{aligned}\right\}, \quad n = 0, 1, 2, \ldots \qquad (34)$$

equation provides an algorithm for a numerical approximation to the solution of Eq. (30). Under the restriction that $aT \ll 1$, the sequence of numbers computed from Eq. (34) for a given input sequence $\{u_n\}$ provides a close approximation to the values of $y(t)$ at the sequence of time instants $\{nT\}$.

The advantage of recasting the original differential equation (30) in state-variable form is that the same form is obtained no matter what the order of the

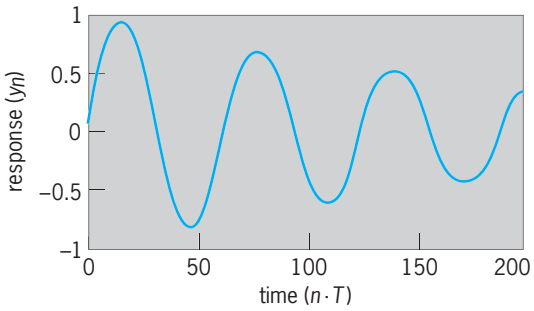

Fig. 4. Response to a unit step of a discrete-time approximation to a second-order system given by Eq. (37) with $T = 1$, $a = 0.02$, $b = 0.01$, $c = 0.1$.

system (or describing differential equation). For example, a continuous-time second-order linear system represented by the differential equation (35), where

$$\frac{d^2y(t)}{dt^2} + a\frac{dy(t)}{dt} + by(t) = c\frac{du(t)}{dt} \tag{35}$$

a, b, and c are constants, can be represented as the state-variable equations (36). The same approach to

$$\begin{aligned} \frac{dx_1(t)}{dt} &= -ax_1(t) - x_2(t) + cu(t) \\ \frac{dx_2(t)}{dt} &= bx_1(t) \\ y(t) &= x_1(t) \end{aligned} \tag{36}$$

numerical integration of these equations [or, equivalently, the second-order differential equation (35)] can be used as for the first-order example of Eq. (30), except that the numerical integration formulas are now matrix equations. The discrete-time equivalents to Eqs. (36) are given by Eqs. (37), where

$$\begin{aligned} x_{1,n+1} &= (1 - aT)x_{1,n} - Tx_{2,n} + cTu_n \\ x_{2,n+1} &= bTx_{1,n} + x_{2,n} \\ y_n &= x_{1,n} \end{aligned} \tag{37}$$

$x_{1,n} = x_1(nT)$, and so forth (**Fig. 4**). As these examples suggest, state-space methods for the description of nth-order systems of difference equations are closely related to those used for similar systems of linear differential equations.

Digital filters. Discrete-time linear systems find application in filtering, that is, the passing of certain frequency components of a signal and the attenuation or blockage of others. In general, a digital filter can be represented by the difference equation (38),

$$y(nT) = \sum_{i=0}^{r} L_i u[(n-i)T] - \sum_{j=1}^{m} K_j y[(n-j)T] \tag{38}$$

where the independent variable is now shown explicitly as integer multiples of the sampling interval to emphasize the fact that this application often concerns sampled continuous-time signals. The second term on the right-hand side of Eq. (38) involves past samples of the output, y, which will generate an infinitely long response for a finite-length input. Thus, with this term nonzero, Eq. (38) represents an infinite impulse response (IIR) filter. If this term is zero, the filter is known as a finite impulse response (FIR) filter, for the response will die out at a time rT after the input goes away.

Taking the z transform of Eq. (38) and solving for the ratio of $Y(z)$ to $X(z)$ gives the transfer function in Eq. (39). The substitution $z = e^{j\omega T}$ gives the frequency response. The magnitude of the frequency response function shows how the frequency components of the input signal are attenuated or enhanced, and it is this function that is often used for design purposes.

$$H(z) = \frac{Y(z)}{X(z)} = \frac{\sum_{i=0}^{r} L_i z^{-i}}{1 + \sum_{j=1}^{m} K_j z^{-j}} \tag{39}$$

An often used approach for designing IIR filters is to choose an analog (linear, continuous-time) prototype filter that has the frequency response properties desired for the application at hand, and transform the transfer function of the prototype filter to the discrete-time domain. One such technique, called invariance design, holds a time-domain response function the same between the analog and digital domains. For example, with an impulse-invariant design, the impulse responses of analog and

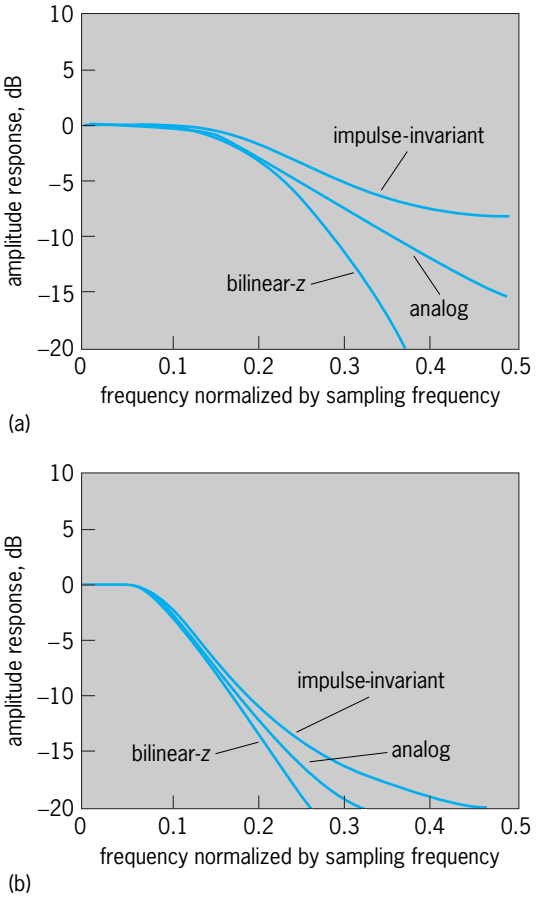

Fig. 5. Comparison of the amplitude response (that is, magnitude of frequency response) of a second-order Butterworth low-pass analog filter with responses of impulse-invariant and bilinear-z discrete-time filter approximations. (*a*) Cutoff frequency/sampling frequency = 0.2. (*b*) Cutoff frequency/sampling frequency = 0.1.

digital filters are proportional. Because invariant filter designs are prone to aliasing distortion, a bilinear-z designed filter is often favored. This filter has a zero in its frequency response at half the sampling frequency, which guarantees no aliasing, at the expense of distortion of the frequency-response function. However, for a sufficiently large ratio of sampling frequency to cutoff frequency of the filter, this distortion is small. (**Fig. 5**). *See* DIGITAL FILTER; DISTORTION (ELECTRONIC CIRCUITS); ELECTRIC FILTER.

Rodger E. Ziemer

Bibliography. C. T. Chen, *Linear System Theory and Design*, 3d ed., 1998; E. P. Cunningham, *Digital Filtering: An Introduction*, 1994; J. J. D'Azzo and C. H. Houpis, *Linear Control System Analysis and Design*, 4th ed., 1995; T. Kailath, *Linear Systems*, 1980; J. G. Proakis and D. G. Manolakkis, *Introduction to Digital Signal Processing*, 1992; R. E. Ziemer, W. H. Tranter, and D. R. Fannin, *Signals and Systems: Continuous and Discrete*, 4th ed., 1998.

Linear systems of equations

Systems of mathematical equations of the form of system (1), where the a_{ij}, $i = 1, 2, \ldots, m$, $j = 1, 2, \ldots, n$, and the b_1, $i = 1, 2, \ldots, m$, are constants, or fixed numbers, and the x_i, $i = 1, 2, \ldots, n$ are called unknowns. System (1) is referred to as m linear equations in n unknowns. A solution of system (1) is a set of numbers $c_1, c_2, \ldots, c_n$ such that when x_1 is replaced by c_1, x_2 by $c_2, \ldots, x_n$ by c_n every equation of system (1) becomes a true equality. The problem posed by such a system of equations is to find criteria for the existence of a solution and, when solutions exist, to obtain systematic methods for finding the solutions.

$$\begin{aligned} a_{11}x_1 + a_{12}x_2 + \cdots + a_{1n}x_n &= b_1 \\ a_{21}x_1 + a_{22}x_2 + \cdots + a_{2n}x_n &= b_2 \\ \cdots\cdots\cdots\cdots\cdots\cdots\cdots\cdots & \\ a_{m1}x_1 + a_{m2}x_2 + \cdots + a_{mn}x_n &= b_m \end{aligned} \tag{1}$$

An example of such a linear system of equations is system (2). System (2) has infinitely many solutions which can be given in the form $x_1 = -c_5 - {}^4/_7c_3 - {}^6/_7$, $x_2 = {}^1/_3c_5 - {}^8/_7c_3 + {}^8/_{21}$, $x_3 = c_3$, $x_4 = -{}^1/_3c_5 - {}^2/_3$, $x_5 = c_5$, where c_3 and c_5 are arbitrarily chosen numbers.

$$\begin{aligned} 2x_1 - x_2 \qquad\quad - x_4 + 2x_5 &= 2 \\ x_1 + 3x_2 + 4x_3 - 3x_4 - x_5 &= 4 \\ 3x_1 + 2x_2 + 4x_3 + 2x_4 + 3x_5 &= 2 \end{aligned} \tag{2}$$

Two linear systems of equations are equivalent if every solution of one of the systems is a solution of the other and vice versa. System (1) is replaced by an equivalent system, for which the solutions, if they exist, are easily found by performing certain elementary operations on the equations. These operations are interchanging two equations, adding to one equation another equation multiplied by a constant, or multiplying an equation by a nonzero constant. By a sequence of such operations, system (1) can be replaced by equivalent system (3). If $e_{r+1} = e_{r+2} = \cdots = e_m = 0$, then the solutions of the system can be obtained by choosing arbitrary values for the unknowns other than

$$x_{n_1}, x_{n_2}, \ldots, x_{n_r}$$

and solving the equations in turn, beginning with the last equation, for

$$x_{n_r}, x_{n_{r-1}}, \ldots, x_{n_2}, x_{n_1}$$

$$\begin{aligned} x_{n_1} + d_{1,n_1+1}x_{n_1+1} + d_{1,n_1+2}x_{n_1+2} + \cdots & \\ + d_{1,n}x_n &= e_1 \\ x_{n_2} + d_{2,n_2+1}x_{n2_1+1} + \cdots + d_{2,n}x_n &= e_2 \\ \cdots\cdots\cdots\cdots\cdots\cdots\cdots\cdots & \\ x_{n_r} + d_{r,n_r+1}x_{n1_r+1} + \cdots\cdots + d_{r,n}x_n &= e_r \\ 0 &= e_{r+1} \\ \cdots\cdots & \\ 0 &= e_m \end{aligned} \tag{3}$$

When the system has solutions it is said to be consistent. If any one of $e_{r+1}, e_{r+2}, \ldots, e_m$ is not zero, then the equations do not have a solution and are inconsistent. In example (2), the system is equivalent to the system

$$\begin{aligned} x_1 + 3x_2 + 4x_3 - 3x_4 - x_5 &= 4 \\ x_2 + {}^8/_7x_3 - {}^5/_7x_4 - {}^4/_7x_5 &= {}^6/_7 \\ x_4 + {}^1/_3x_5 &= -{}^2/_3 \end{aligned}$$

Arbitrary values c_5 and c_3 can be chosen for x_5 and x_3, respectively, and the equations can be solved successively for x_4, x_2, and x_1.

The operations used in reducing system (1) to system (3) can be most effectively performed on the rows of the matrix of system (4), and they are precisely the elementary row transformations of a matrix. *See* MATRIX THEORY.

$$A* = \begin{pmatrix} a_{11}\ a_{12} \cdots a_{1n}\ b_1 \\ a_{21}\ a_{22} \cdots a_{2n}\ b_1 \\ \cdots\cdots\cdots\cdots \\ a_{m1}\ a_{m2} \cdots a_{mn}\ b_m \end{pmatrix} \tag{4}$$

Matrix (4) is called the augmented matrix of the system, and matrix (5) is called the matrix of the coefficients. A necessary and sufficient condition for the existence of a solution of system (1) is that the rank of the augmented matrix A^* be the same as the rank of the matrix of coefficients A. (In general, the rank of a matrix A may be defined as the largest order r of a nonvanishing minor of A, where a minor of order r is the determinant of an $r \times r$ matrix that

$$A = \begin{pmatrix} a_{11}\ a_{12} \cdots a_{1n} \\ a_{21}\ a_{22} \cdots a_{2n} \\ \cdots\cdots\cdots\cdots \\ a_{m1}\ a_{m2} \cdots a_{mn} \end{pmatrix} \tag{5}$$

consists of the elements common to r rows and r columns selected from A.) In example (2), the rank of the augmented matrix

$$A^* = \begin{pmatrix} 2 & -1 & 0 & -1 & 2 & 2 \\ 1 & 3 & 4 & -3 & -1 & 4 \\ 3 & 2 & 4 & 2 & 3 & 2 \end{pmatrix}$$

as well as the rank of

$$A = \begin{pmatrix} 2 & -1 & 0 & -1 & 2 \\ 1 & 3 & 4 & -3 & -1 \\ 3 & 2 & 4 & 2 & 3 \end{pmatrix}$$

is equal to 3. Therefore the system is consistent and has the solutions given earlier.

If $m = n$ in system (1) and if the determinant $|A|$ of the matrix of the coefficients A is not zero, then system (1) has a unique solution which can be obtained by Cramer's rule, which gives the values of the unknowns $x_1, x_2, \ldots, x_n$ as the ratio of two determinants. *See* DETERMINANT.

Specifically, Cramer's rule gives

$$x_1 = \begin{vmatrix} b_1 & a_{12} & a_{1n} \\ b_2 & a_{22} & a_{2n} \\ \cdots & \cdots & \cdots \\ b_n & a_{n2} & a_{nn} \end{vmatrix} \Big/ |A|$$

$$x_2 = \begin{vmatrix} a_{11} & b_1 & a_{13} & \cdots & a_{1n} \\ a_{21} & b_2 & a_{23} & \cdots & a_{2n} \\ \cdots & \cdots & \cdots & \cdots & \\ a_{n1} & b_n & a_{n3} & \cdots & a_{nn} \end{vmatrix} \Big/ |A|$$

.....

$$x_n = \begin{vmatrix} a_{11} & \cdots & a_{1n-1} & b_1 \\ a_{21} & \cdots & a_{2n-1} & b_2 \\ \cdots & \cdots & \cdots & \cdots \\ a_{n1} & \cdots & a_{nn-1} & b_n \end{vmatrix} \Big/ |A|$$

In every case the determinant in the denominator is $|A|$, and for the value of the unknown x_i, the determinant in the numerator is the determinant of the matrix obtained from A by replacing the ith column of A by $b_1, b_2, \ldots, b_n$. If $|A| = 0$ in this case of n equations in n unknowns, the system may either be inconsistent or it may have infinitely many solutions. In the example

$$\begin{aligned} x_1 - 4x_2 + 5x_3 &= 6 \\ 2x_1 - 11x_2 + 10x_3 &= -1 \\ 4x_1 - x_2 + 5x_3 &= 0 \end{aligned}$$

$$|A| = \begin{vmatrix} 1 & -4 & 5 \\ 2 & -11 & 10 \\ 4 & -1 & 5 \end{vmatrix} = 45$$

and the unique solution is given by

$$x_1 = \begin{vmatrix} 6 & -4 & 5 \\ -1 & 11 & 10 \\ 0 & -1 & 5 \end{vmatrix} \Big/ 45 = -{}^{285}/_{45} = {}^{19}/_{3}$$

$$x_2 = \begin{vmatrix} 1 & 6 & 5 \\ 2 & -1 & 10 \\ 4 & 0 & \end{vmatrix} \Big/ 45 = {}^{194}/_{45} = {}^{13}/_{3}$$

$$x_3 = \begin{vmatrix} 1 & -4 & 6 \\ 2 & -11 & -1 \\ 4 & -1 & 0 \end{vmatrix} \Big/ 45 = {}^{267}/_{45} = {}^{89}/_{15}$$

If in system (1), $b_1 = b_2 = \cdots = b_m = 0$, system (6)

$$\begin{aligned} a_{11}x_1 + a_{12}x_2 + \cdots + a_{1n}x_n &= 0 \\ a_{21}x_1 + a_{22}x_2 + \cdots + a_{2n}x_n &= 0 \\ \cdots\cdots\cdots\cdots\cdots\cdots\cdots\cdots & \\ a_{m1}x_1 + a_{m2}x_2 + \cdots + a_{mn}x_n &= 0 \end{aligned} \tag{6}$$

is called homogeneous. Since the augmented matrix of system (6) differs from the matrix of the coefficients by an additional column of zeros, these matrices always have the same rank, so that a homogeneous system is always consistent. It has the obvious solution $x_1 = 0, x_2 = 0, \ldots, x_n = 0$, which is called the trivial solution. Any solution with at least one $x_i \neq 0$ is called nontrivial. A homogeneous system of m equations in n unknowns has a nontrivial solution if and only if the rank of the matrix of coefficients A is less than n. In particular, if m is less than n, the rank of A is at most m, and the system has a nontrivial solution. Further, if $m = n$, the system has a nontrivial solution if and only if the determinant $|A| = 0$. In system (7)

$$\begin{aligned} 3x_1 + 4x_2 - 2x_3 &= 0 \\ -2x_1 + 3x_2 - 4x_3 &= 0 \\ 5x_1 + x_2 + 2x_3 &= 0 \\ -9x_1 + 5x_2 - 10x_3 &= 0 \end{aligned} \tag{7}$$

the rank of A is 2, so that system (7) has a nontrivial solution:

$$A = \begin{pmatrix} 3 & 4 & -2 \\ -2 & 3 & -4 \\ 5 & 1 & 2 \\ -9 & 5 & -10 \end{pmatrix}$$

The rank of A is seen to be 2 by performing elementary row transformations on A to reduce it to the form

$$\begin{pmatrix} 1 & {}^{4}/_{3} & -{}^{2}/_{3} \\ 0 & 1 & -{}^{16}/_{17} \\ 0 & 0 & 0 \\ 0 & 0 & 0 \end{pmatrix}$$

System (7) is equivalent to the system

$$\begin{aligned} x_1 + {}^{4}/_{3}x_2 - {}^{2}/_{3}x_3 &= 0 \\ x_2 - {}^{16}/_{17}x_3 &= 0 \end{aligned}$$

The solutions are given by $x_1 = -{}^{10}/_{\sqrt{17}}c_3, x_2 = {}^{16}/_{\sqrt{17}}c_3$, $x_3 = c_3$, where c_3 is an arbitrarily chosen number.

In the event that a linear system (1) has infinitely many solutions, they can be given as in example (2) or, alternatively, a finite number of solutions can be listed in terms of which all solutions can be conveniently obtained. Any one fixed solution of system (1) is called a particular solution. In example (2), $x_1 = {}^{6}/_{\sqrt{7}}$, $x_2 = {}^{8}/_{\sqrt{21}}$, $x_3 = 0$, $x_4 = -{}^{2}/_{3}$, $x_5 = 0$ is a particular solution. If system (1) is consistent, every solution is of the form $x_1 = c_1 + c_1^{(0)}, x_2 = c_2 + c_2^{(0)}, \ldots, x_n = c_n + c_n^{(0)}$, where $c_1, c_2, \ldots, c_n$ is a fixed particular solution of system (1) and $c_1^{(0)}, c_2^{(0)}, \ldots, c_n^{(0)}$ is any solution of the corresponding homogeneous system (6). By virtue of this result, it is sufficient to investigate the solutions of the homogeneous system (6).

Let $C^{(1)} = (c_1^{(1)}, c_2^{(1)}, \ldots, c_n^{(1)})$ and $C^{(2)} = (c_1^{(2)}, c_2^{(2)}, \ldots, c_n^{(2)})$ be solutions of the homogeneous system (6), written as n-tuples. Then $C^{(1)} + C^{(2)} = (c_1^{(1)} + c_1^{(2)}, c_2^{(2)} + c_2^{(2)}, \ldots, c_n^{(1)} + c_n^{(2)})$ is the sum of the solutions, and $eC^{(1)} = (ec_1^{(1)}, ec_2^{(1)}, \ldots, ec_n^{(1)})$ where e is a fixed number and is a scalar multiple of the solution $C^{(1)}$. It is evident that any linear combination $e_1C^{(1)} + e_2C^{(2)} + \cdots + e_sC^{(s)}$ of solutions $C^{(1)}, C^{(2)}, \ldots, C^{(s)}$, of system (6) is again a solution of system (6). A set of solutions $C^{(1)}, C^{(2)}, \ldots, C^{(s)}$, of the homogeneous system (6) is called a linearly independent set if $e_1C^{(1)} + e_2C^{(2)} + \cdots + e_sC^{(s)} = (0, 0, \ldots, 0)$ implies that $e_1 = e_2 = \cdots = e_s = 0$. Otherwise the solutions form a linearly dependent set, that is, there exist numbers $e_1, e_2, \cdots, e_s$, not all zero such that $e_1C^{(1)} + e_2C^{(2)} + \cdots + e_sC^{(s)} = (0, 0, \ldots, 0)$. A set of solutions is a maximal linearly independent set if the set is linearly independent and if a set formed by adding any other solution of system (6) is linearly dependent. If the rank of the matrix A of system (6) is r, then the number of solutions in a maximal independent set is $n - r$. Every solution of system (6) is a linear combination $e_1C^{(1)} + e_2C^{(2)} + \cdots + e_{n-r}C^{(n-r)}$ of the solutions in a maximal independent set. In example (2), the corresponding homogeneous system is system (8). The rank of the matrix A of system (8)

$$\begin{aligned} 2x_1 - x_2 \quad\quad - x_4 + 2x_5 &= 0 \\ x_1 + 3x_2 + 4x_3 - 3x_4 - x_5 &= 0 \\ 3x_1 + 2x_2 + 4x_3 + 2x_4 + 3x_5 &= 0 \end{aligned} \tag{8}$$

is 3. Thus there are $5 - 3 = 2$ solutions in a maximal linearly independent set. They can be given as $C^{(1)} = (-4, -8, 7, 0, 0)$ and $C^{(2)} = (-3, 1, 0, -1, 3)$. Every solution of system (8) is given by $e_1C^{(1)} + e_2C^{(2)} = (-4e_1 - 3e_2, -8e_1 + e_2, 7e_1, -e_2, 3e_2)$ for arbitrary e_1 and e_2. Every solution of the original system is given by $({}^{6}/_{\sqrt{7}} - 4e_1 - 3e_2, {}^{8}/_{\sqrt{21}} - 8e_1 + e_2, 7e_1, -{}^{2}/_{3} - e_2, 3e_2)$.

In example (7), the rank of the matrix is 2, and there is $3 - 2 = 1$ solution in a maximal linearly independent set. It can be given as $C^{(1)} = (-10, 16, 17)$, and every solution of (7) is a multiple of $C^{(1)}$.

If the system of equations (1) has a solution, then it has a rational solution. This means that there is a solution which is obtained by employing only the rational operations of addition, subtraction, multiplication, and division on the coefficients of the system. The particular solution as well as the linearly independent solutions of the corresponding homogeneous system can always be selected rationally. This is evident since the operations performed on the system to obtain a solution are rational operations. *See* EQUATIONS, THEORY OF; POLYNOMIAL SYSTEMS OF EQUATIONS.

Ross A. Beaumont

Bibliography. J. B. Fraleigh and R. A. Beauregard, *Linear Algebra*, 3d ed., 1995; P. K. Rees et al., *College Algebra*, 10th ed., 1990.

Linearity

A relationship between two or more quantities which can be expressed in terms of linear algebraic, differential, or integral equations. A system in which all quantities (or variables) can be described in terms of such equations is said to be a linear system. By definition, linear systems satisfy the principle of superposition. By this principle, the response of a linear system to multiple inputs is given simply by the sum of the responses due to each individual input. In addition, if all inputs are multiplied by a common constant factor, the resulting response is multiplied by the same factor. *See* DIFFERENTIAL EQUATION; INTEGRAL EQUATION; LINEAR ALGEBRA; LINEAR SYSTEMS OF EQUATIONS.

As an example of a simple linear relationship, the voltage V across an ideal (ohmic) resistor is directly proportional to the current I through it, as given by Eq. (1), where R is the constant of proportionality.

$$V(I) = IR \tag{1}$$

Here, the customary notation $V(I)$ is used to denote V as a function of I. The voltage corresponding to a scaled input current, kI, is obtained by applying Eq. (2). A sum of input currents, $I_1 + I_2 + I_3$, gives

$$V(kI) = kIR = kV(I) \tag{2}$$

Eq. (3). Clearly, the principle of superposition is ob-

$$\begin{aligned} V(I_1 + I_2 + I_3) &= (I_1 + I_2 + I_3)R \\ &= I_1R + I_2 + I_3R \\ &= V(I_1) + V(I_2) + V(I_3) \end{aligned} \tag{3}$$

served in this case. *See* OHM'S LAW; SUPERPOSITION THEOREM (ELECTRIC NETWORKS).

In contrast, a semiconductor diode has a nonlinear I–V relationship of the form of Eq. (4), where V_0 and I_0 are constants. In this case, inequalities (5) and (6)

$$V(I) = V_0 \ln \frac{I}{I_0} \tag{4}$$

$$V(kI) \neq kV(I) \tag{5}$$

$$V(I_1 + I_2 + I_3) \neq V(I_1) + V(I_2) + V(I_3) \tag{6}$$

hold, and the superposition principle does not apply. *See* SEMICONDUCTOR DIODE.

Linearity is a desirable characteristic of all systems where an output response is required to be a faithful reproduction (except for a constant scale factor) of one or more inputs. For example, electronic amplifiers used in measurement and signal transmission and reproduction systems are designed with linearity as a primary goal. Although physical systems are generally nonlinear to some degree, in practice the objective is to realize a good approximation to an ideal linear system by minimizing nonlinearities as far as possible. Any departure from linearity in these systems causes unwanted distortion of the original signal and results in a degraded and erroneous response. *See* AMPLIFIER; DISTORTION (ELECTRONIC CIRCUITS).

Ashok P. Nedungadi

Bibliography. J. D. Bell, *Mathematics of Linear and Nonlinear Systems for Engineers and Applied Scientists*, 1990; N. K. Sinha, *Linear Systems*, 1991.

Linen

A widely used cloth made from flax fibers. Linen is noted for its evenness of thread, fineness, and density. Its uses include garments, tablecloths, sheeting, towels, and thread.

The flax plant which supplies the fiber needs a short, cool growing season with plenty of rainfall. Russia leads the world in growing flax for fiber. The manufacture of the fiber into fabric requires unusual care during each process to retain the strength and beauty of the fiber. *See* FLAX.

Processing the fiber. Seeds and leaves are removed from the stems of the flax plant by passing the stalks through coarse combs, a process called rippling. Bundles of stems weighted down with heavy stones to ensure complete immersion are then steeped in water. The wetting allows the bark surrounding the hairlike flax fibers to decompose, thus loosening the gums that hold the fibers. This decomposing, or fermentation, is called retting.

After removal from water the stems may be spread out on the ground for a week or more. After the woody tissue has become dry, it is crushed by fluted iron rollers. Then there remain only small pieces of wood called shives. The shives are removed by means of rotating beaters, thus finally releasing the flax fibers. This can be done by hand or with machinery. The simple combing process, known as hackling, straightens the flax fibers, separates the short from the long staple, and leaves the longer fibers in parallel formation. For coarse linen, hackling is usually done by hand. Fine linen is also hackled by machine, a finer comb being used with each hackling treatment.

Properties of flax fiber. Under a microscope the flax fiber shows hairlike cylindrical filaments with fine pointed ends. The filaments are cemented together by gummy pectin. The long flax filaments contain a lumen, or central canal. The fiber resembles a straight, smooth bamboo stick, with joints producing a slight natural unevenness that cannot be eliminated. Chemically the flax fiber is about 70% cellulose, 25% pectin, and the remainder of woody tissue and ash. From such fibers linen yarns are produced with a smooth, straight, compact, and lustrous appearance. *See* CELLULOSE; NATURAL FIBER; PECTIN; TEXTILE.

Elton G. Nelson

Lines of force

Imaginary lines in fields of force **F** whose tangents at any point *P* give the direction of the field at *P* and whose number through unit area perpendicular to this direction represents the intensity of the field at *P* (see **illustration**). The concept of lines of force is perhaps most common when dealing with electric or magnetic fields.

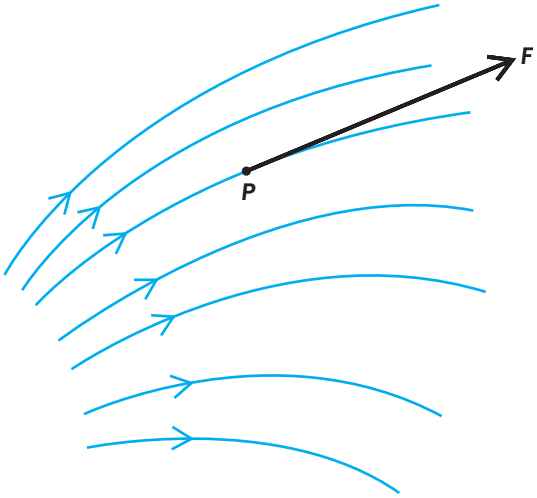

Definition of lines of force.

Electric lines of force. These are lines drawn to represent, or map, an electric field graphically in the space around a charged body. They are of great help in visualizing an electric field and in quantitative thinking about such a field. The direction of an electric line of force at any point is drawn parallel to the direction of the electric field intensity **E** at that point. The quantitative convention is that the number of electric lines of force drawn through an imaginary unit area of surface perpendicular to the field shall be numerically equal to **E** at that area. From this quantitative convention, and using International System (SI) units, in free space q/ϵ_0 lines of force originate on a positive charge q (in coulombs) and a like number terminate on a negative charge $-q$ of the same magnitude. Here $\epsilon_0 = 8.85 \times 10^{-12}$ farad/m is the permittivity of empty space. *See* ELECTRIC FIELD.

Magnetic lines of force. A magnetic field of strength **H** may also be represented by lines called lines of force. The number of lines of force per unit area of a surface perpendicular to **H** is numerically equal to the value of **H**. The lines of magnetic force due to currents are closed curves, as are the lines of magnetic induction. Magnetic lines of force due to magnets originate on north poles and terminate on south poles, both inside and outside the magnet. *See* MAGNETIC FIELD.

Ralph P. Winch; Bryan P. Kibble

Bibliography. D. J. Griffiths, *Introduction to Electrodynamics*, 3d ed., 1999; A. F. Kip, *Fundamentals of Electricity and Magnetism*, 2d ed., 1969; E. M. Purcell, *Electricity and Magnetism*, Berkeley Physics Course, vol. 2, 2d ed., 1985; W. T. Scott, *The Physics of Electricity and Magnetism*, 2d ed., 1966, reprint 1976.

Linewidth

A measure of the width of the band of frequencies of radiation emitted or absorbed in an atomic or molecular transition. One of the dominant sources of electromagnetic radiation of all frequencies is transitions between two energy levels of an atomic or molecular system. The frequency of the radiation is related to the difference in the energy of the two levels by the Bohr relation, Eq. (1), where ν_0 is the frequency

$$\nu_0 = \frac{E_1 - E_2}{h} \tag{1}$$

of the radiation, h is Planck's constant, and E_1 and E_2 are the energies of the levels. This radiation is not monochromatic, but consists of a band of frequencies centered about ν_0 whose intensity $I(\nu)$ can be characterized by the linewidth. The linewidth is the full width at half height of the distribution function $I(\nu)$. The simplest case is for a transition from an excited state to the ground state for an atom or molecule at rest. For this case, the normalized distribution function is the lorentzian line profile given by Eq. (2). Here $\Delta\nu$ is the full width at half maximum

$$I(\nu) = \frac{1}{\pi}\frac{\Delta\nu/2}{(\nu - \nu_0)^2 + (\Delta\nu/2)^2} \tag{2}$$

(FWHM). The FWHM is related to the lifetime τ of the excited level through Eq. (3). This is a manifestation of the quantum-mechanical uncertainty principle, and the linewidth $\Delta\nu$ is referred to as the natural linewidth. For a transition between two unstable levels with lifetimes τ_1 and τ_2, the FWHM is given by Eq. (4).

$$(\Delta\nu)(\tau) = \frac{1}{2\pi} \tag{3}$$

$$\Delta\nu = \frac{1}{2\pi}\left(\frac{1}{\tau_1} + \frac{1}{\tau_2}\right) \tag{4}$$

See ENERGY LEVEL (QUANTUM MECHANICS); QUANTUM MECHANICS; UNCERTAINTY PRINCIPLE.

Another major source of line broadening for atomic and molecular transitions is the Doppler shift due to thermal motion. To first-order in v/c, the frequency of the radiation depends upon whether the radiating object is moving away from or toward the observer according to Eq. (5). Here v is the component of the velocity along the line joining the observer and the radiating object taken as positive when the separation is increasing, and c is the speed of light. For a gaseous radiator whose velocity distribution is a maxwellian one characterized by a most probable velocity given by Eq. (6), where k is the Boltzmann constant, T the absolute temperature, and M the mass of the radiating molecule, the distribution of radiation is given by Eq. (7). This is a gaussian line profile with FWHM given by Eq. (8). For most situations the Doppler width is greater than the natural linewidth. A more accurate line profile is the Voigt line profile, a convolution of the lorentzian and gaussian profiles given by Eq. (9).

$$\nu = \nu_0\left(1 - \frac{v}{c}\right) \tag{5}$$

$$v_p = \left(\frac{2kT}{M}\right)^{1/2} \tag{6}$$

$$I(\nu) = I_0 \exp\{-[c(\nu - \nu_0)/\nu_0 v_p]^2\} \tag{7}$$

$$\begin{aligned}(\Delta\nu)_D &= \frac{(2\sqrt{\ln 2})\nu_0 v_p}{c} \\ &= \left(\frac{v_0}{c}\right)\left(\frac{8kT\ln 2}{M}\right)^{1/2}\end{aligned} \tag{8}$$

$$I(\nu) = (\text{const})\int_0^\infty \frac{\exp\{-[c(\nu' - \nu_0)/\nu_0 v_p]^2\}}{(\nu - \nu')^2 + (\Delta\nu/2)^2}\,d\nu' \tag{9}$$

See BOLTZMANN STATISTICS; DISTRIBUTION (PROBABILITY); DOPPLER EFFECT.

A third major source of line broadening is collisions of the radiating molecule with other molecules. This broadens the line, shifts the center of the line, and shortens the lifetime of the radiating state. The net result is a lorentzian line profile of the form of Eq. (10), where Γ is given by Eq. (11). Here $(\Delta\nu)_N$ is the natural linewidth, $(\Delta\nu)_{IC}$ the width due to inelastic collisions, $(\Delta\nu)_{EC}$ the width due to elastic collisions, and $(\delta\nu)_{EC}$ the shift of the center due to elastic collisions. The combination of the collision width, the natural width, and the Doppler width yields a generalized Voigt profile. This form is used to analyze data from plasmas and stellar atmospheres to determine the temperature of the radiator and the density of the perturbers. *See* PLASMA DIAGNOSTICS.

$$I(\nu) = I_0\frac{\Gamma^2}{[\nu - \nu_0 - (\delta\nu)_{EC}]^2 + \Gamma^2} \tag{10}$$

$$\Gamma = \frac{(\Delta\nu)_N + (\Delta\nu)_{IC}}{2} + (\Delta\nu)_{EC} \tag{11}$$

In many measurements the linewidth limits the precision with which the center of the line can be determined. A number of techniques have been invented to circumvent the limitation due to the Doppler width. One technique, called Dicke narrowing, is to confine the radiating atoms to a volume whose characteristic dimensions are much less than the wavelength of the radiation. *See* LASER SPECTROSCOPY.

For radiating atoms in a liquid or solid the width is usually dominated by the strong interaction of the radiator with the surrounding molecules. This usually results in a spectrum with a wide distribution which cannot be characterized by a simple lorentzian or

gaussian line profile. The inelastic interactions of the excited molecule with its surroundings produce radiationless transitions and shorten the lifetime of the excited state. There are often a variety of radiation sites with different characteristic frequencies. The net result is a broad line profile with a complex structure. *See* BAND THEORY OF SOLIDS; CRYSTAL ABSORPTION SPECTRA.

The above discussion deals principally with the situations where radiation is emitted by an excited molecule. The considerations are similar for the inverse reaction where a ground-state molecule absorbs radiation and makes a transition to an excited state. *See* ATOMIC STRUCTURE AND SPECTRA; MOLECULAR STRUCTURE AND SPECTRA. Francis M. Pipkin

Bibliography. R. C. Breen, Jr., *Theories of Spectral Line Shape*, 1981; W. Demtröder, *Laser Spectroscopy*, 2d ed., 1994.

Linguistics

The science, that is, the general and universal properties, of language. Interest in language seems to have arisen in the earliest history of the human species. Every culture has left records that reveal philosophical or practical concerns for this unique human characteristic, and these concerns have varied over time. The middle of the twentieth century saw a shift in the principal direction of linguistic inquiry from one of data collection and classification to the formulation of a theory of generative grammar, which focuses on the biological basis for the acquisition and use of human language and the universal principles that constrain the class of all languages.

Generative grammar distinguishes between the knowledge of language (linguistic competence), which is represented by mental grammar, and the production and comprehension of speech (linguistic performance). Theories of generative grammar include Government and Binding or Principles and Parameters Theory, Generalized Phrase Structure, and Lexical Functional Grammar, among others.

Grammar. If grammar is defined as the mental representation of linguistic knowledge, then a general theory of language is a theory of grammar. A grammar includes everything one knows about a language; its phonetics and phonology (the sounds and the sound system), its morphology (the structure of words), its lexicon (the words or vocabulary), its syntax (the structure of sentences and the constraints on well-formed sentences), and its semantics (the meaning of words and sentences).

Phonetics and phonology. Different languages use different inventories of discrete speech sounds. Speech is, however, a continuous acoustic signal, not a string of separate sounds. Yet speakers know that a word like "cat" is composed of three sounds represented by the letters c, a, and t. This illustrates in a simple way the difference between knowledge of language and linguistic performance. Phonetics is the study of the production or articulation and perception of speech as well as the acoustic characteristics of the sounds produced. *See* PSYCHOACOUSTICS; SPEECH; SPEECH PERCEPTION.

Speech reflects the more abstract system of phonological knowledge that determines, for example, why the letter g is pronounced in "signature" but not in "sign" or why stress is placed on the first word in the "White House," the official residence of the President of the United States, and on the second in "white house" a designation for any residence that is white.

Morphology. Morphology determines how words are constructed. The word "undesirability," for example, is a complex structure composed of the prefix "un," the root "desire," the suffix "able," and the final suffix "ity."

Syntax. Syntax, an important component of grammar and linguistic theory, concerns the structure of sentences, that is, the order and ways in which words, phrases, and clauses can be combined. It accounts for the ability of speakers to produce and comprehend an infinite number of sentences. Knowledge of syntax accounts for an English speaker knowing that a sentence such as "Linguistics is interesting" is acceptable but "interesting linguistics is" is not; it also explains why and how a sentence can be lengthened indefinitely; for example, "I know that linguistics is interesting," "You know that I know that linguistics is interesting," and so on. Syntactic principles account for the fact that in a sentence such as "Mary thinks that she is pretty," the word "she" may refer to Mary or to someone else, but in the sentence "She thinks that Mary is pretty," the word "she" cannot refer to Mary. Syntax also explains why the sentence "George put the book on the shelf," is grammatical but "George put the book" is not. The words in the mental lexicon contain syntactic information in addition to information about word meanings and pronunciation. Thus, a word like "put" must be followed by both an object and a prepositional phrase.

Semantics. Semantics is the study of the meaning of words and sentences and the relationship between logic and language, a subject of great interest in the Middle Ages and the seventeenth century. Semantics cannot be independent of syntax because meaning often depends on syntactic structure. Thus, a sentence like "John likes Mary more than Joan" has two meanings because of its structure and not because any of the words has two meanings. The semantic component of grammar accounts for the fact that sentences may be paraphrases of each other (that is, are semantic equivalents), as in "Look up the word in the dictionary" and "Look the word up in the dictionary"; or may be anomalous, as in "My sister is an only child"; or may entail other sentences (for example, "It is a red flower" entails the sentence "It is a flower").

Branches. Liquistics is not limited to grammatical theory. Descriptive linguistics analyzes the grammars of individual languages; for example, Indo-European linguistics, Romance linguistics, and African linguistics refer to the studies of particular languages and

language families, both from historical and synchronic points of view. In a more general sense, this area of linguistics investigates why and how languages develop.

Anthropological linguistics, or ethnolinguistics, and sociolinguistics focus on languages in relation to culture, social class, race, and gender. Dialectologists investigate how these factors fragment one language into many. In addition, sociolinguists and applied linguists examine language planning, literacy, bilingualism, and second-language acquisition. The study of Creoles and pidgins, languages that develop out of the need for speakers of different languages to communicate, has proved to provide important insights into language structure and change.

Computational linguistics encompasses automatic parsing, machine processing, and computer simulation of grammatical models for the generation and parsing of sentences. If viewed as a branch of artificial intelligence, computational linguistics has as its goal the modeling of human language as a cognitive system. *See* ARTIFICIAL INTELLIGENCE.

Historically, language has been considered a window into the mind. Whether language ability is distinct or arises in the human species out of more general cognitive capacities has yet to be determined. A branch of linguistics concerned with that question and with the biological basis of language development is neurolinguistics. Research on aphasia (language disorders following brain injury) reveals that damage to specific brain areas results in the disruption of distinct cognitive functions, as well as different motor and perceptual abilities, and that language may be disordered without disruption of other cognitive abilities. Furthermore, different parts of the language system (or grammar) may themselves be uniquely disturbed, a phenomenon that supports a modular concept of the brain, the mind, and the grammar itself in which the components interact but are independent. *See* INFORMATION PROCESSING (PSYCHOLOGY).

The form of language representation in the mind, that is, linguistic competence and the structure and components of the mental grammar, is the concern of theoretical linguistics. The branch of linguistics concerned with linguistic performance, that is, the production and comprehension of speech (or of sign language by the deaf), is called psycholinguistics. Psycholinguists also investigates how children acquire the complex grammar that underlies language use. *See* PSYCHOLINGUISTICS.

Children are not taught a language in the same way they are taught, for example, how to add. Nor are they taught the rules of grammar; those are acquired unconsciously. A child who incorrectly says "mouses" instead of "mice" or "bringed" instead of "brought" has learned the rules and is applying them to a case that is an exception to these rules. The fact that the complex grammar is acquired at a very early age, without being taught and before other seemingly simpler cognitive abilities are developed, supports the view that a child is genetically programmed for language acquisition. *See* COGNITION; LEARNING MECHANISMS.

Victoria A. Fromkin

Bibliography. N. Chomsky, *Knowledge of Language: Its Nature, Origin, and Use*, 1986; N. Chomsky, *Syntactic Structures*, 1957; V. Fromkin and R. Rodman, *An Introduction to Language*, 6th ed., 1998; F. J. Newmeyer, *Linguistic Theory in America*, 2d ed., 1986; F. J. Newmeyer (ed.), *Linguistics: The Cambridge Survey*, vols. 1–4, 1988.

Lingulida

An order of inarticulated brachiopods consisting of an exclusively marine group of lophophorate animals (animals with a tentacular food-gathering, respiratory, and protective organ): sessile benthic suspension-feeders possessing a chitinophosphatic shell. Representatives occur throughout the Phanerozoic Era (from the Early Cambrian to the present). Three superfamilies are recognized: Linguloidea, with the family Lingulidae, extends from the Middle Ordovician to the present; Discinoidea, with the family Discinidae, extends from the Early Ordovician to the present; and Acrotheloidea is known from the Early Cambrian to the Early Ordovician. *See* BRACHIOPODA; INARTICULATA.

General morphology. Shells are tongue-shaped (linguliform) to circular in outline. The valves are separate and lack articulation but possess a complex arrangement of muscles formed by paired anterior adductor muscles and single or paired posterior adductor muscles, and three or four pairs of oblique muscles. The pedicle emerges posteriorly between valves or through a foramen.

Lingulids are suspension feeders. The tentacular feeding organ (lophophore) occupies the mantle cavity. The digestive system consists of a mouth, pharynx, esophagus, stomach, digestive diverticula, pylorus, and intestine, and terminates in a functional anus. Four digestive diverticula open through ducts to the stomach. The excretory system consists of a pair of ciliated funnels (metanephridia) that act as gonoducts during spawning and allow the discharge of gametes from the coelom into the lophophoral cavity. Solid waste, enmeshed in mucus, is also ejected through the nephridiopores, while the excretory product ammonia is voided through the tissues of the mantle and lophophore.

Lingulids possess an open circulatory system of blood vessels and coelomic canals containing a faintly pigmented fluid, which is coagulable and contains free cellular inclusions consisting of blood cells and coelomocytes. In *Lingula*, the blood cells are somewhat round in shape and contain a respiratory protein that consists of hemoerythrins.

Lingulids have a central nervous system containing unsheathed nerves with no obviously differentiated sense organs, although statocysts have been reported in Lingulidae.

All extant members of this order are dioecious (that is, male and female reproductive organs are on separate individuals) and their larval development is

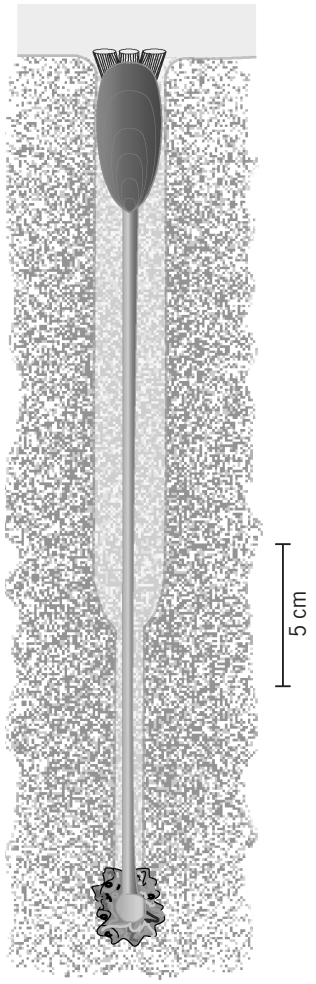

View of living *Lingula anatina* in its burrow. (*Courtesy of C. C. Emig*)

planktotrophic. They extend generally from inshore waters, mainly subtidal, to the bathyal zone.

Linguloidea. Shells are linguliform to circular in outline and are generally biconvex. The two extant genera belong to the family Lingulidae: *Lingula*, wrongly considered as "living fossils" from the Paleozoic, and *Glottidia*. Both genera originated at the beginning of the Tertiary. They have a long, fleshy extensible pedicle and burrow in soft sediments (see **illustration**). Their complex arrangement of muscles consists of two pairs of anterior and one single posterior adductor muscles, unpaired oblique muscles (three pairs and an single additional one), and a longitudinal lateral muscle, which help with movement of the valves.

Discinoidea and Acrotheloidea. Most shells are circular or subcircular in outline. The dorsal valve is usually larger than the ventral valve, and is convex and often conical. The ventral valve is flattened and disklike. Paired anterior and posterior adductor muscles and three pairs of oblique muscles make up the complex arrangement of muscles. A short pedicle in the postlarval stage emerges through a foramen in the ventral valve, but the adults lack a pedicle notch and pedicle. Christian C. Emig; Mark A. James

Bibliography. C. C. Emig, Ecology of inarticulated brachiopods. Biogeography of inarticulated brachiopods, in R. L. Kaesler (ed.), *Treatise on Invertebrate Paleontology*, pt. H revised: *Brachiopoda*, vol. 1, pp. 473–502, Geological Society of America, Boulder, and University of Kansas, Lawrence, 1997; C. C. Emig, Tools for linguloid taxonomy: The genus *Obolus* (Brachiopoda) as an example. *Carnets de Géologie-Notebooks on Geology*, Article 2002/01 (CG2002_A01_CCE), 2002; C. C. Emig, Proof that *Lingula* (Brachiopoda) is not a living-fossil, and emended diagnoses of the Family Lingulidae, *Carnets de Géologie-Notebooks on Geology*, Letter 2003/01 (CG2003_L01_CCE), 2003; R. L. Kaesler (ed.), *Treatise on Invertebrate Paleontology*, pt. H revised: *Brachiopoda*, vols. 1 and 2, Geological Society of America, Boulder, and University of Kansas, Lawrence, 1997 and 2000.

Link

An element of a mechanical linkage. A link may be a straight bar or a disk, or it may have any other shape, simple or complex. It is assumed, for simple analysis, to be made of unyielding material; that is, its shape does not change. The frame, or fixed member, of a linkage is one of the links, whether the frame is fixed relative to the Earth or relative to a movable body such as the chassis of an automobile.

Two links of a kinematic chain meet in a joint, or pair, by which these links are held together. Just as each joint is a pair having two elements, one from each link, so a link in a kinematic chain is the rigid connector of two or more elements belonging to different pairs.

Each free link has three degrees of freedom in the plane (two translational and one rotational). If the tail of one link is pin-joined to the head of its predecessor two degrees of freedom are lost. If several links are joined so as to form a closed loop, $2g$ degrees of freedom are lost, where g is the number of lower pair joints. If one member of an n-member chain is fixed, all three degrees of freedom of the fixed member are eliminated, the remaining degrees of freedom F being given by Eq. (1). Hence for a tri-

$$F = 3(n - 1) - 2g \tag{1}$$

angle $F = 0$ and for a chain of four links called simply a four bar linkage, $F = 1$. *See* DEGREE OF FREEDOM (MECHANICS).

Assuming that $F = 1$ is stipulated for a mechanism, and investigating n in Eq. (1), it is found that Eq. (2)

$$3n = 4 + 2g \tag{2}$$

results. Because 4 is even and $2g$ is even, n must always be even. There can be no pin-joint mechanism with five links; the next highest must have six links. *See* FOUR-BAR LINKAGE; LINKAGE (MECHANISM); MECHANISM. Douglas P. Adams

Bibliography. J. Bickford, *Mechanism for Intermittent Motion,* 1972; R. S. Hartenberg and J. Denavit,

Kinematic Synthesis of Linkages, 1964; G. D. Hiscox, *Mechanical Movements, Powers, and Devices,* 1983.

Linkage (genetics)

Failure of two or more genes to recombine at random as a result of their location on the same chromosome pair. Among the haploid products of a cell which has gone through meiosis, two genes located in the same chromosome pair remain in their two original combinations of alleles (parental) unless an odd number of exchanges of homologous segments occurred within the interval bounded by their loci. The incidence of exchanges of homologous segments at meiosis is roughly proportional to the length of the chromosome segment between two loci. The percentage of recombinants thus provides an estimate of this length and a basis for constructing gene maps on which linked loci are arranged in linear order and spaced out in proportion to the recombination percentages between them. The analogy is with a linear map of the stations along a railway line spaced out according to the time of travel between any two or more of them. By extension of the meaning of linkage to bacterial transduction or transformation, two bacterial genes are said to be linked when both are incorporated together in the chromosome of recipient cells more often than would be expected from mere coincidence of two separate incorporations. This is the consequence of their being frequently carried on the same transducing or transforming DNA fragment. *See* DEOXYRIBONUCLEIC ACID (DNA); MEIOSIS; TRANSDUCTION (BACTERIA); TRANSFORMATION (BACTERIA).

If at meiosis in an individual heterozygous at two loci on the same chromosome pair—for example, *AB*—less than one exchange occurs on the average between them, the proportions of haploid recombinant meiotic products—*aB* and *Ab*—will be less than 50%, and that of the parental meiotic products—*AB* and *ab*—correspondingly more than 50%. This defines the two loci as linked. If, however, two loci on the same chromosome pair are so far apart that on the average one or more exchanges occur between them at meiosis, the proportions of parental and recombinant meiotic products will be equal, that is, 50%. This is the same as for two loci on different chromosome pairs. Thus for two loci between which recombination is 50% there are no means of deciding, on the basis of the recombination percentage alone, whether they are on one and the same chromosome pair but sufficiently far apart, or on different pairs. For an explanation of why 50% is the upper limit of recombination *see* RECOMBINATION (GENETICS).

Thus, while evidence of linkage—less than 50% recombination—implies that two loci are on the same chromosome pair, absence of linkage—50% recombination—does not imply that they are not. Further evidence may reveal that two loci showing no linkage to each other are both linked to a third locus, and so on. This additional evidence permits the construction of linkage maps of all the loci belonging to one and the same linkage group. Linkage groups can then be homologized to chromosome pairs.

In human genetics, since the introduction of the techniques of somatic cell and molecular genetics, very often loci can be assigned to one and the same chromosome pair well before knowing anything about the recombination percentages between any two of them at gametogenesis, this is, before knowing whether or not they are linked in the precise arithmetical sense of the word. To overcome this ambiguity, the term syntenic, proposed by J. Renwick, is now in general use to define two loci carried on the same chromosome pair, irrespective of what is the recombination percentage between them at meiosis. *See* SOMATIC CELL GENETICS.

Genetic linkage is a structural relationship between two genes, that is, a restriction on their recombination at meiosis. It does not necessarily imply a functional relationship. However, in bacteria some of the structural and regulatory genes controlling enzymes sequentially involved in a metabolic pathway often turn out to be closely linked. With very few exceptions, such as homeobox gene clusters, this is not so in eukaryotes.

The biochemical and evolutionary significance of linkage is poorly understood. In the cases just mentioned in bacteria, linkage permits coordinated regulation of enzyme synthesis. In eukaryotes several linkages have been preserved over long periods of evolution, but it cannot be excluded that for some at least this is simply a matter of historical accident. The fact that more and more cases of linkage disequilibrium are coming to light, on the other hand, reflects selective advantages, possibly related to the preservation of genetic variation in natural populations.

G. Pontecorvo

Linkage (mechanism)

A set of rigid bodies, called links, joined together at pivots by means of pins or equivalent devices. A body is considered to be rigid if, for practical purposes, the distances between points on the body do not change. Linkages are used to transmit power and information. They may be employed to make a point on the linkage follow a prescribed curve, regardless of the input motions to the linkage. They are used to produce an angular or linear displacement $f(x)$, where $f(x)$ is a given function of a displacement x. *See* LINK.

If the links are bars the linkage is termed a bar linkage. In first approximations a bar may be treated as a straight line segment or a portion of a curve, and a pivot may be treated as a common point on the bars connected at the pivot. A common form of bar linkage is then one for which the bars are restricted to a given plane, such as a four-bar linkage (**Fig. 1**). A body pivoted to a fixed base and to one or more

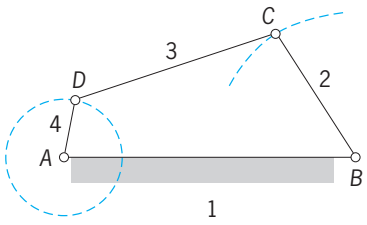

Fig. 1. Four-bar linkage.

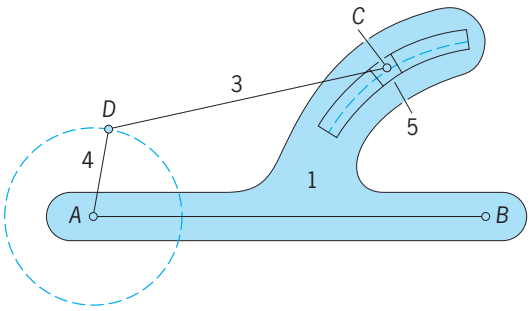

Fig. 2. Equivalent of four-bar linkage.

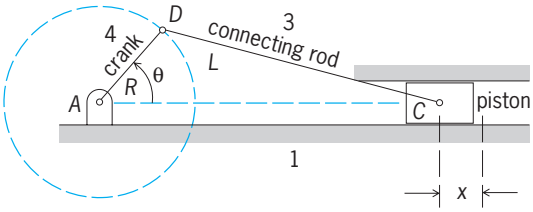

Fig. 3. Slider crank mechanism.

other links is a crank. As crank 4 in Fig. 1 rotates, link 2 (also a crank) oscillates back and forth. This four-bar linkage thus transforms a rotary motion into an oscillatory one, or vice versa. Link AB, marked 1, is fixed. Link 2 may be replaced by a slider 5 (**Fig. 2**). As end D of crank 4 rotates, pivot C describes the same curve as before. The slider moves in a fixed groove. *See* FOUR-BAR LINKAGE.

A commonly occurring variation of the four-bar linkage is the linkage used in reciprocating engines (**Fig. 3**). Slider C is the piston in a cylinder, link 3 is the connecting rod, and link 4 is the crank. This mechanism transforms a linear into a circular motion, or vice versa. The straight slider in line with the crank center is equivalent to a pivot at the end of an infinitely long link. Let R be the length of the crank, L the length of the connecting rod, while θ denotes the angle of the crank as shown in Fig. 3. Also, let x denote the coordinate of the pivot C measured so that $x = 0$ when $\theta = 0$. Length L normally dominates radius R, whence the approximate relation in Eq. (1) holds.

$$x = R(1 - \cos\theta) + \frac{R^2}{2L}\sin^2\theta \qquad (1)$$

A Scotch yoke is employed to convert a steady rotation into a simple harmonic motion (**Fig. 4**). The angle of the crank 2 with respect to the horizontal is denoted by θ, and the coordinate of the slider 4 by x. If R again denotes the length of the crank, Eq. (2) holds. In computer mechanisms, slider 3 can

$$x = R\cos\theta \qquad (2)$$

be moved along the crank so that the component of a vector can be obtained mechanically. *See* SLIDER-CRANK MECHANISM.

A lever is normally understood to be a bar connected to three other links. A lever is often used for addition (**Fig. 5**). Point B is at the center of lever AC. It is assumed that x and y are numerically small compared to the length of the lever. Levers with a fixed pivot (fulcrum) are very useful for amplifying or attenuating linear displacements and forces. *See* LEVER.

The pantograph shown in **Fig. 6** is a five-link mechanism employed in drafting to magnify or reduce diagrams. As point Q on link 5 describes a curve, point P on link 4 will describe a similar but enlarged curve. Here $ABCD$ is a parallelogram. Pivot A is fixed. *See* PANTOGRAPH.

A mechanism composed of six links, introduced by Joseph Whitworth (1803–1887), makes the return stroke of a body in oscillatory linear motion faster than the forward stroke. Universal joints for

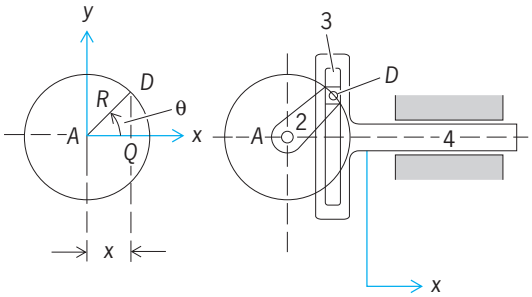

Fig. 4. Scotch yoke.

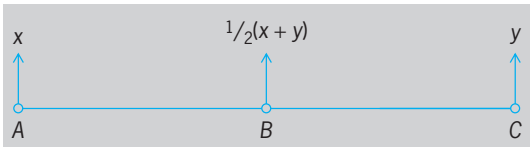

Fig. 5. Addition with a lever.

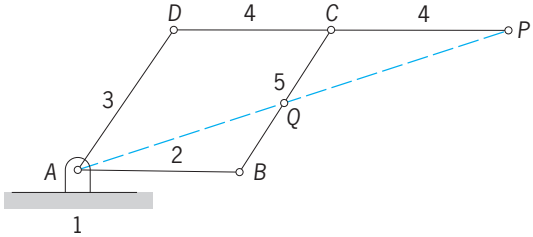

Fig. 6. Pantograph.

transmitting motion between intersecting axes and escapements permitting rotation about an axis in one direction only are examples of the many kinds of linkages used in machines. However, complicated linkages are becoming obsolete because of the ease with which information and power can be transmitted by electrical, hydraulic, and pneumatic means. *See* MECHANISM.

Rufus Oldenburger

Bibliography. N. P. Chironis, *Mechanisms and Mechanical Devices Sourcebook*, 3d ed., 2001; H. H. Mabie and C. F. Reinh, *Mechanisms and Dynamics of Machinery*, 4th ed., 1987; J. E. Shigley and C. R. Mischke, *Mechanisms: A Mechanical Designer's Workbook*, 1990; J. E. Shigley and J. J. Viker, *Theory of Machines and Mechanisms*, 2d ed., 1994; C. H. Suh and C. W. Radcliffe, *Kinematics and Mechanisms Design*, 1978, reprint 1983.

Lipid

One of a class of compounds which contains long-chain aliphatic hydrocarbons (cyclic or acyclic) and their derivatives, such as acids (fatty acids), alcohols, amines, amino alcohols, and aldehydes. The presence of the long aliphatic chain as the characteristic component of lipids confers distinct solubility properties on the simpler members of this class of naturally occurring compounds. This led to the traditional definition of lipids as substances which are insoluble in water but soluble in fat solvents such as ether, chloroform, and benzene. However, those lipids (particularly glycolipids and phospholipids) which contain polar components in the molecule may be insoluble in these solvents, and some are even soluble in water. Most of the phosphatides are good emulsifying agents. *See* EMULSION; SOLVENT.

Classification. The lipids are generally classified into the following groups:

A. Simple lipids
   1. Triglycerides or fats and oils are fatty acid esters of glycerol. Examples are lard, corn oil, cottonseed oil, and butter.
   2. Waxes are fatty acid esters of long-chain alcohols. Examples are beeswax, spermaceti, and carnauba wax.
   3. Steroids are lipids derived from partially or completely hydrogenated phenanthrene. Examples are cholesterol and ergosterol.

B. Complex lipids
   1. Phosphatides or phospholipids are lipids which contain phosphorus and, in many instances, nitrogen. Examples are lecithin, cephalin, and phosphatidyl inositol.
   2. Glycolipids are lipids which contain carbohydrate residues. Examples are sterol glycosides, cerebrosides, and plant phytoglycolipids.
   3. Sphingolipids are lipids containing the long-chain amino alcohol sphingosine and its derivatives. Examples are sphingomyelins, ceramides, and cerebrosides.

The classification scheme is not rigid since sphingolipids are found which contain phosphorus and carbohydrate, and glycolipids which contain phosphorus. Those lipids not included in the above groupings are of the chemically simpler type and include the fatty acids, alcohols, ethers such as batyl and chimyl alcohols, an hydrocarbons such as the terpenes and carotenes.

The fatty acids found in lipids may be saturated or unsaturated, cyclic or acyclic, and contain substituents such as hydroxyl or keto groups. They are combined in ester or amide linkage. The alcohols, likewise, may be saturated or unsaturated and are combined in ester or ether linkages; in the case of α-β unsaturated ethers, these are best considered as aldehyde derivatives.The amino alcohols found in lipids are linked as amides, glycosides, or phosphate esters. Sphingosine is the predominant amino alcohol found in animal tissue lipids, and phytosphingosine is its equivalent in the plant kingdom.

Occurrence. Lipids are present in all living cells, but the proportion varies from tissue to tissue. The triglycerides accumulate in certain areas, such as adipose tissue in the human being and in the seeds of plants, where they represent a form of energy storage. The more complex lipids occur closely linked with protein in the membranes of cell and of subcellular particles. More active tissues generally have a higher complex lipid content; for example, the brain, liver, kidney, lung, and blood contain the highest concentration of phosphatides in the mammal. Fish oils are important sources of vitamins A and D, and seed-germ oils contain quantities of vitamin E. The vitamins K occur chiefly in plants and microorganisms, and carotenoids are widely distributed in both the plant and animal kingdoms. Waxes are found in insects and as protective agents on plant leaves and the cuticles of fruits and vegetables (for instance, the bloom on grapes and plums). Soybeans are used for the commercial preparation of phosphatides. *See* CELL MEMBRANES.

Extraction. Many of the lipids, particularly glycolipids, phosphatides, and steroid esters, are present in the tissue in association with other cell components, such as protein. The nature of the linkages in these complexes is not fully understood although they are most certainly not covalent. Combinations of lipid and protein, like lipoproteins and proteolipids, have been isolated from sources such as blood serum and egg yolk. For the efficient extraction of lipids from tissues, these complexes must first be disrupted, and this is usually accomplished by dehydration procedures such as freeze-drying or acetone extraction, or by denaturation with alcohol before extracting the tissue with suitable lipid solvents. The use of mixed solvents, such as ethanol and ether, ethanol and benzene, or chloroform and methanol, allows disruption, dehydration, and extraction in one operation. Partial fractionation of lipids may

be effected by successive extractions with different solvents.

Separation. Prior to 1948, solvent fractionations or the use of specific complexing agents, such as cadmium chloride for the separation of lecithin, were the only methods available for the separation of lipids, and progress in the chemical identification of individual lipids was slow. Since then, the use of column chromatography (particularly on alumina, silicic acid, and diethylaminoethyl cellulose), thin-layer chromatography, countercurrent distribution, and gas-phase chromatography has allowed rapid progress in separation, and many new classes of lipid have been discovered as a result of the application of these techniques. Other methods which allow selective degradation of certain lipids either chemically (for example, the use of dilute alkali to cause preferential hydrolysis of esters) or enzymatically are also being used successfully for the separation of certain lipids. *See* CHROMATOGRAPHY.

Identification. Most of the conventional analytical procedures are used in the identification of lipid samples. Physical methods, such as infrared and ultraviolet spectroscopy, optical rotation, proton magnetic resonance, and mass spectrometry, have been used. The advent of gas-phase chromatography allowed a major advance in lipid chemistry by providing a complete analysis of the fatty acid content of lipid mixtures. The high resolving power of thin-layer chromatography has accelerated the routine analysis of the mixture of lipids from many natural sources; qualitative and quantitative methods for the determination of esters, aldehydes, carbohydrates, long-chain bases, and the other important components of lipids such as glycerol, glycerophosphate, ethanolamine, choline, serine, amino sugars, and inositol; and elementary analyses for nitrogen and phosphorus. The nitrogen-to-phosphorus ratio of a phosphatide sample was once used as a criterion of purity because carbon and hydrogen analyses on a single phosphatide species are not highly revealing, owing to the spectrum of fatty acids that may be present. The degree of unsaturation is determined by hydrogenation or iodine number determination, and free hydroxyl groups are expressed by the acetyl. Lipid samples also may be hydrolyzed under a variety of acid or alkaline conditions and the products investigated by paper chromatography. *See* CARBOXYLIC ACID; FAT AND OIL; FAT AND OIL (FOOD); GLYCOLIPID; LIPID METABOLISM; PHOSPHOLIPID; SPHINGOLIPID; STEROID; TERPENE; TRIGLYCERIDE; VITAMIN; WAX, ANIMAL AND VEGETABLE.

Roy H. Gigg

Bibliography. W. W. Christie, *High Performance Liquid Chromatography and Lipids: A Practical Guide*, 1987; F. D. Gunstone et al., *The Lipid Handbook*, 2d ed., 1994; N. F. Hadley, *The Adaptive Role of Lipids in Biological Systems*, 1985; J. L. Harwood and N. J. Russell, *Lipids in Plants and Microbes*, 1984; M. Horisberger and V. Bracco (eds.), *Lipids in Modern Nutrition*, 1987; J. J. Kabara (ed.), *The Pharmacological Effects of Lipids II*, 1985; J. F. Mead et al., *Lipids: Chemistry, Biochemistry, and Nutrition*, 1986; R. Paoletti et al. (eds.), *Drugs Affecting Lipid Metabolism*, 1988.

Lipid metabolism

Lipids form a class of compounds composed of neutral fats (triglycerides), phospholipids, glycolipids, sterols, and fat-soluble vitamins (A, D, E, and K). As a group they share the common physical property of insolubility in water. This article describes the assimilation of dietary lipids and the synthesis and degradation of lipids by the mammalian organism.

Fat digestion and absorption. The principal dietary fat is triglyceride, an ester of three fatty acids and glycerol. This substance is not digested in the stomach and passes into the duodenum, where it causes the release of enterogastrone, a hormone which inhibits stomach motility. The amount of fat in the diet, therefore, regulates the rate at which enterogastrone is released into the intestinal tract. Fat, together with other partially digested foodstuffs, causes the release of hormones, secretin, pancreozymin, and cholecystokinin from the wall of the duodenum into the bloodstream.

Secretin causes the secretion of an alkaline pancreatic juice rich in bicarbonate ions, while pancreozymin causes secretion of pancreatic enzymes. One of these enzymes, important in the digestion of fat, is lipase. Cholecystokinin, which is a protein substance chemically inseparable from pancreozymin, stimulates the gallbladder to release bile into the duodenum. Bile is secreted by the liver and concentrated in the gallbladder and contains two bile salts, both derived from cholesterol: taurocholic and glycocholic acids. These act as detergents by emulsifying the triglycerides in the intestinal tract, thus making the fats more susceptible to attack by pancreatic lipase. In this reaction, which works best in the alkaline medium provided by the pancreatic juice, each triglyceride is split into three fatty acid chains, forming monoglycerides. The fatty acids pass across the membranes of the intestinal mucosal (lining) cells. Enzymes in the membranes split monoglyceride to glycerol and fatty acid, but triglycerides are reformed within the mucosal cells from glycerol and those fatty acids with a chain length greater than eight carbons: Short- and medium-chain fatty acids are absorbed directly into the bloodstream once they pass through the intestinal mucosa.

The triglycerides formed in the mucosal cells are associated with proteins and phospholipids and pass into the intestinal lymphatics as the lipoproteins called chylomicrons. The thoracic duct, the main lymphatic channel, carries the chylomicrons to the great veins, where they enter the circulatory system and can be taken up and metabolized by most tissues. *See* CHOLESTEROL; DIGESTIVE SYSTEM; GALLBLADDER; LIVER; PANCREAS.

The bile salts are absorbed from the ileum, together with dietary cholesterol. They enter the portal circulation, which carries them to the liver, where they can be reexcreted into the duodenum. The

bile also contains pigments which are derived from hemoglobin metabolism. *See* BILIRUBIN; HEMOGLOBIN.

Abnormalities in the pancreatic secretions, bile secretion, or intestinal wall can lead to either partial or complete blockage of fat absorption and an abnormal excretion of fats in the stool.

Adipose tissue. Accumulations of fat cells in the body are called adipose tissue. This is found beneath the skin, between muscle fibers, around abdominal organs and their supporting structures called mesenteries, and around joints. The fat cell contains a central fat vacuole so large that it fills the cell, pushing the nucleus and cytoplasm to the periphery. The adipose tissue of the body is of considerable magnitude and is quite active metabolically, functioning as a buffer in energy metabolism. *See* ADIPOSE TISSUE.

During meals carbohydrates, amino acids, and fats which are absorbed in excess of immediate energy requirements are converted and stored in the fat-cell vacuoles as triglycerides. These fat depots provide an economical storage form for energy requirements and serve as the source of energy between meals and during periods of fasting.

Triglycerides cannot traverse the cell membrane until they are broken down into glycerol and fatty acids. Lipoprotein lipase, an enzyme which catalyzes the hydrolysis of lipoprotein triglycerides, controls entry of triglycerides into the cell; it is induced by feeding and disappears during periods of fasting. The lipase which breaks down triglycerides before they leave the cell is controlled by hormones. Norepinephrine, a hormone released from sympathetic nerve endings, is probably the most important factor controlling fat mobilization. Epinephrine from the adrenal medulla also activates lipase, as do adrenocorticotropic hormone (ACTH) and glucagon. Growth hormone and a separate fat-mobilizing factor released from the pituitary gland of some species also stimulate lipolysis and release of fatty acids from adipose tissue. While the fat-mobilizing factor may activate the same enzyme as the hormones cited above, growth hormone appears to function through a different mechanism, probably requiring protein synthesis. *See* ADENOHYPOPHYSIS HORMONE; ENDOCRINE MECHANISMS; GLUCAGON.

Obesity is a condition in which excessive fat accumulates in the adipose tissue. One factor responsible for this condition is excessive caloric intake. The metabolic and psychological factors are under investigation. In starvation, uncontrolled diabetes, and many generalized illnesses the opposite occurs and the adipose tissue becomes markedly depleted of lipid. *See* DIABETES; METABOLIC DISORDERS.

Blood lipids. Lipids are present in the blood in the form of lipoproteins and as free fatty acids (FFAs), which are bound to albumin. The FFAs originate in adipose tissue and are mobilized for oxidation in other tissues of the body. The lipoproteins are small droplets of lipids complexed with proteins dispersed in the blood. They originate in the liver, with the exception of the small droplets, called chylomicrons, derived from the intestinal tract. The lipoproteins have been divided into arbitrary classes based upon their physical properties. The two methods of classification separate them according to density by ultracentrifugation and according to electrical charge by electrophoresis. The classes of lipoproteins defined by either of these methods differ in their content of triglycerides, cholesterol, and phospholipids. Some disorders of lipid metabolism are manifested in the blood by an abnormality in the pattern of lipoprotein classes. *See* CENTRIFUGATION; CLINICAL PATHOLOGY; ELECTROPHORESIS.

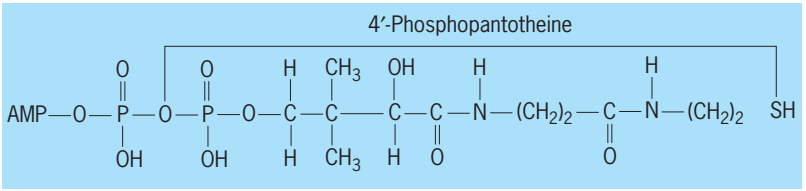

Fig. 1. Structural formula for coenzyme A.

Fatty acid oxidation. Fatty acids are oxidized to meet the energy requirements of the body by a β-oxidation pathway, that is, the second or β-carbon from the carboxyl group is oxidized. Before oxidation can proceed, the fatty acid must be coupled with coenzyme A (CoA), a compound containing adenosine monophosphate (AMP), two molecules of phosphate, and the complex nitrogen derivative pantotheine (**Fig. 1**).

In reaction (1), showing activation, the fatty acid is as shown in **Fig. 2**, in which only the terminal 4-carbon atoms are given. The initial activation proceeds in two steps. First, as shown in reaction (1*a*), the fatty acid reacts with adenosine triphosphate (ATP) to form fatty acid adenylate (fatty acid–AMP). This in turn reacts with CoA to form acyl CoA, as shown in reaction (1*b*). The enzyme that catalyzes reactions (1*a*) and (1*b*) is called the activating enzyme or thiokinase. The fatty acid–CoA cannot penetrate the mitochondrial membrane to gain access to the oxidative enzymes. To traverse the membrane, fatty acid must be esterified with the hydroxyl group of carnitine (**Fig. 3**), a reaction catalyzed by carnitine acyl transferases. The carnitine–fatty acid

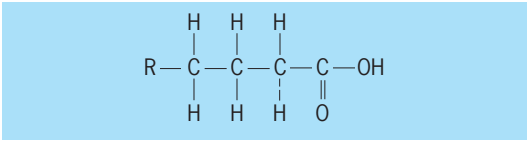

Fig. 2. Structural formula for a fatty acid. R represents chain of up to 14 carbon atoms.

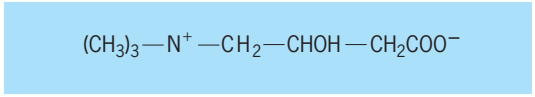

Fig. 3. Structural formula for carnitine.

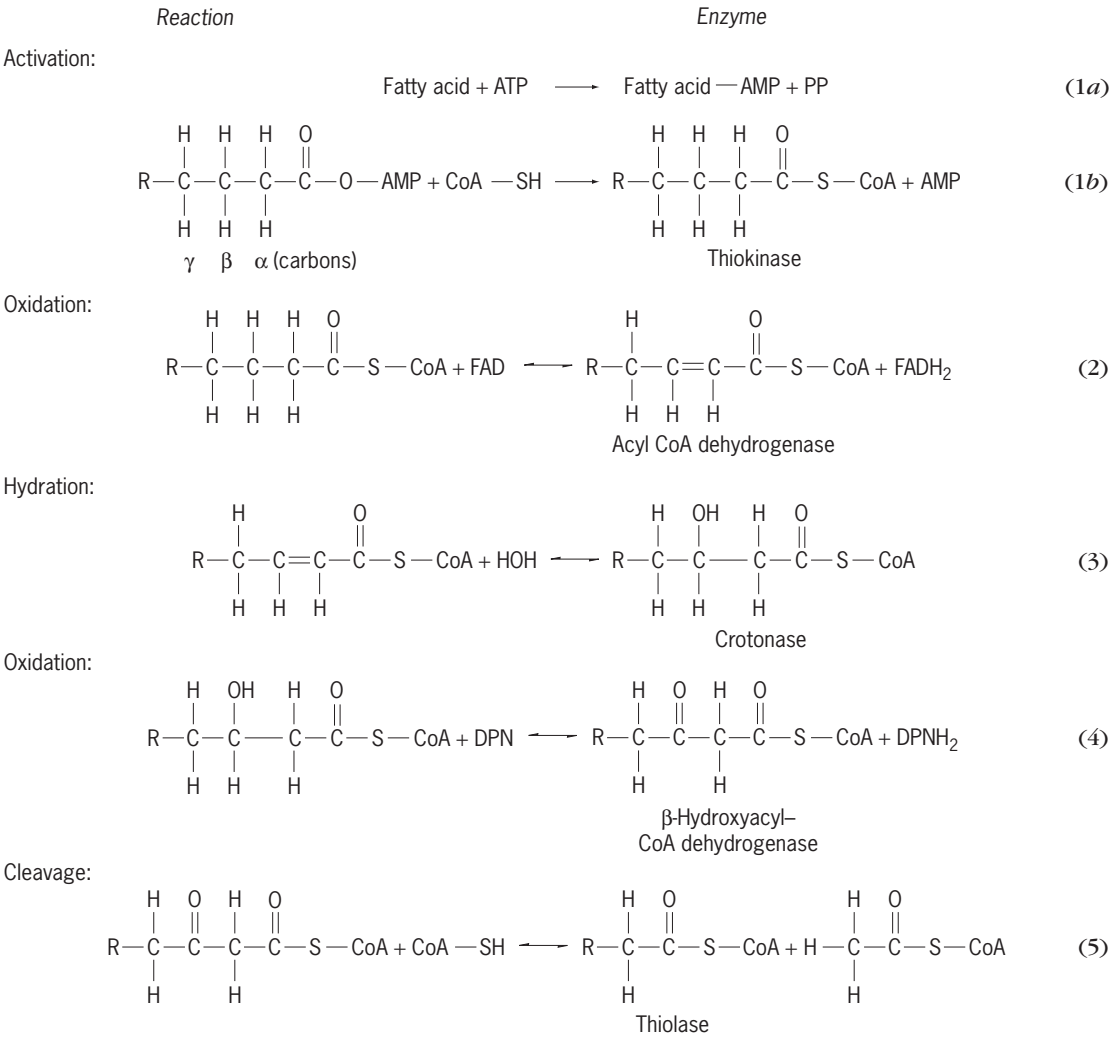

ester traverses the membrane, and the fatty acid is again coupled to CoA by a transferase on the other side.

In reaction (2), the first of two oxidation reactions, one hydrogen is removed from the α-carbon and one is removed from the β-carbon, producing an unsaturated fatty acid analogous to crotonic acid. The enzyme is called acyl CoA dehydrogenase, and the cofactor which acts as the oxidizing agent and accepts the hydrogen is flavin adenine dinucleotide (FAD).

In reaction (3), hydration, hydrogen and the hydroxyl group (from water) are introduced at the α- and β-carbons, respectively; a β-hydroxy acid is formed; the enzyme is crotonase.

In reaction (4), the second oxidation, two hydrogens are removed from the α and β carbons of the β-hydroxy acid to form a keto acid. The oxidizing agent is nicotinamide adenine dinucleotide (NAD), also called diphosphopyridine nucleotide (DPN). *See* NICOTINAMIDE ADENINE DINUCLEOTIDE (NAD).

In reaction (5), showing cleavage, acetyl CoA is split off. Thus a fatty acid two carbons shorter than the original one is formed. Simultaneously, the shortened fatty acid combines with another molecule of CoA at the newly formed carboxyl group to yield a new activated fatty acid. The enzyme is β-ketothidase. The new activated fatty acid undergoes the same series of reactions, and this process is repeated until the entire fatty acid molecule has been reduced completely to acetyl CoA. Oxidation of the higher fatty acids, such as palmitic acid with 16 carbon atoms, yields eight molecules of acetyl CoA. Two fates of acetyl CoA formed in the liver are of immediate interest (**Fig. 4**): (1) oxidation through the Krebs cycle to carbon dioxide and (2) condensation of two molecules of acetyl CoA with the splitting off of the CoA forming so-called ketone bodies. *See* BIOLOGICAL OXIDATION; CITRIC ACID CYCLE.

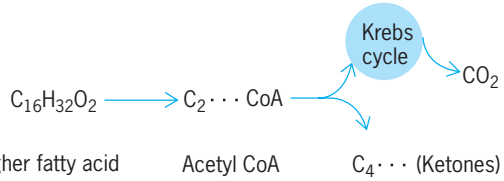

Fig. 4. Fates of acetyl CoA from fatty acid oxidation.

Ketone body formation. If excessive amounts of fatty acids are mobilized from the depots and metabolized by the liver, as occurs in starvation or diabetes, all the acetyl CoA formed cannot be oxidized. Instead, two molecules of acetyl CoA may form acetoacetic acid, which cannot be further oxidized by the liver but is transformed into β-hydroxybutyric acid or acetone according to reactions (6) and (7).

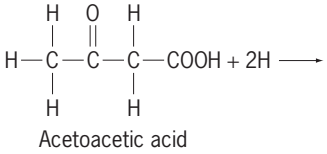

Acetoacetic acid

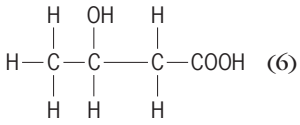

(6)

β-Hydroxbutyric acid

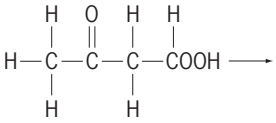

Acetoacetic acid

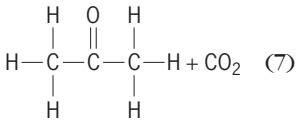

(7)

Acetone

These three compounds, acetoacetic acid, acetone, and β-hydroxybutyric acid, called the ketone bodies, are formed in excessive amounts in the liver not only because of the excess acetyl CoA present but also because the metabolic disturbances caused by such conditions reduce the capacity of the Krebs cycle for oxidation by diverting oxaloacetate, a key intermediate, to gluconeogenesis (synthesis of glucose from noncarbohydrate precursors).

The excessive formation of ketone bodies leads to a high concentration in the blood—a condition called ketonemia. This causes ketone body excretion in the urine, together with water, sodium, and potassium. These losses, along with the excessive acidity of the blood caused by the high concentration of ketone bodies (ketoacidosis), can lead to coma and death if uncorrected. Such fatal acidosis was quite common in diabetics before the advent of insulin. During starvation or diabetic ketosis, muscles are capable of deriving the major portion, if not all, of their energy from oxidizing the ketone bodies. However, in the uncontrolled diabetic subject, the formation of ketone bodies may greatly exceed the utilization of them by the muscle or other tissues, so that ketoacidosis results.

Lipotropic factors. A diet high in fat results in fat accumulation in the liver. This can be prevented by feeding choline, a phosphatide base; the effect has been termed a lipotropic effect. If methionine is present in the diet, it can substitute for choline, since enzymes are present in the liver which can transfer methyl groups from methionine to ethanolamine to form choline, as shown in reaction (8).

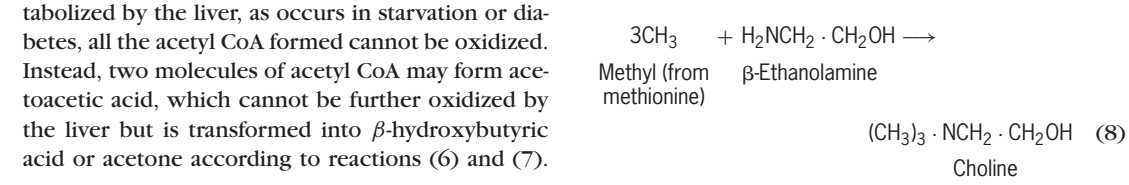

Methyl (from methionine)

β-Ethanolamine

Choline

(8)

Fatty livers can also occur when large amounts of depot fat are mobilized in starvation and diabetes. This type of fatty liver is not affected by choline. Since choline is a constituent of the phospholipid lecithin, it has been suggested that the lipotropic effect of choline is exerted through lecithin. Evidence to support this suggestion has not been forthcoming.

Fatty acid synthesis. Certain carbohydrates, such as glucose and fructose, yield simpler substances, such as lactic acid, pyruvic acid, and acetic acid, as do proteins, which are potential precursors of acetyl CoA. The acetyl CoA molecules thus formed are used to synthesize higher fatty acids.

The initial reaction in fatty acid synthesis is the carboxylation of acetyl CoA to form malonyl CoA. This reaction is catalyzed by acetyl CoA carboxylase, a biotin-containing enzyme (enz-biotin) and probably proceeds in two steps. In the first, reaction (9*a*), biotin is carboxylated in the 1′-nitrogen position in an ATP-dependent reaction to form 1′-*N*-carboxamide biotin. In the second step, reaction (9*b*), the carboxyl group is transferred to acetyl CoA to form malonyl CoA.

For the synthesis to proceed, the malonyl group must be transferred from CoA to a specific carrier protein called the acyl carrier protein (ACP). The compound with which the malonyl group is to be condensed is similarly transferred from CoA to ACP to form an acyl ACP. The acyl group can be acetate or any fatty acid less than 16 carbons in length, depending upon the species. The enzyme catalyzing the transfer from CoA to ACP is specific for each compound and is called a CoA-ACP transacylase. The active group of both CoA and ACP is 4′-phosphopantotheine (**Fig. 5**). This group is linked to the protein through the hydroxyl group of serine by a phosphodiester bond. The sulfhydryl group is the functional group of both CoA and ACP linkage occurring through sulfur (thiol ester).

The joining of malonyl ACP with an acyl ACP, as shown in reaction (10), is catalyzed by the acylmalonyl ACP condensing enzyme. Since carbon dioxide

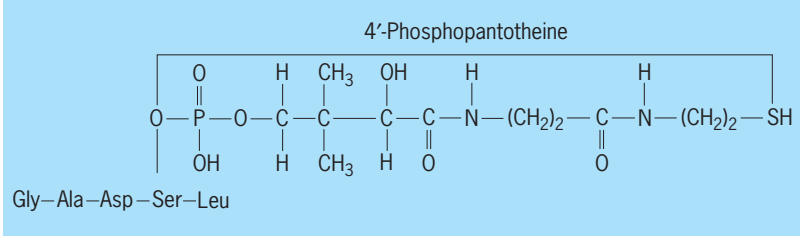

Fig. 5. Active site of acyl carrier protein (ACP). Gly, glycine; Ala, alanine; Asp, aspartic acid; Ser, serine; and Leu, leucine.

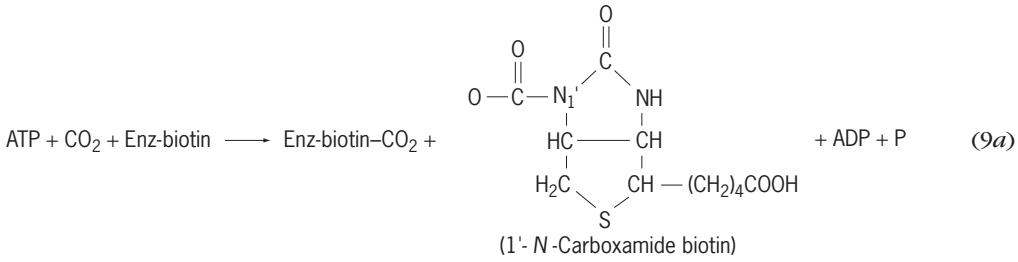

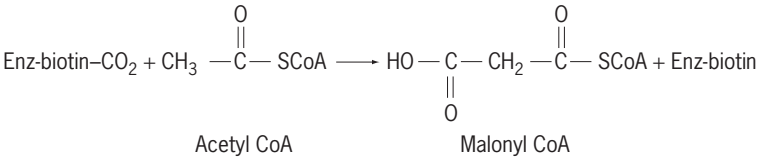

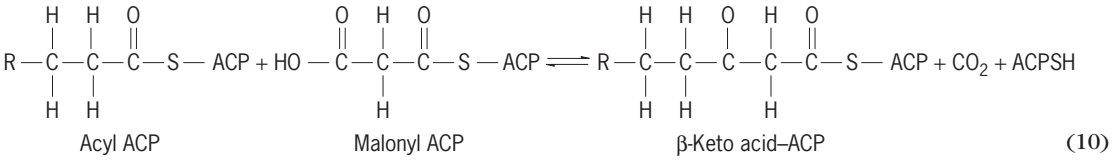

is released in this reaction, the acyl carbon chain is lengthened by two, resulting in a β-keto acid linked to ACP. This compound is converted to a fatty acid by the reverse of reactions (4), (3), and (2). These reactions are catalyzed by a series of enzymes which are associated in a complex protein called fatty acid synthase in yeast and pigeon liver. The individual enzymes have been isolated from bacterial systems and are specific for ACP compounds, in contrast to the specificity of oxidative enzymes for CoA compounds. The reverse reaction (4) is catalyzed by β-keto ACP reductase and the cofactor is nicotinamide adenine dinucleotide phosphate (NADP), also known as triphosphopyridine nucleotide (TPN), rather than NAD. Reverse reaction (3) is catalyzed by enoyl ACP dehydrase and reverse reaction (2) by enoyl ACP reductase. *See* NICOTINAMIDE ADENINE DINUCLEOTIDE PHOSPHATE (NADP).

Repetition of this series of reactions leads to a building up of the fatty acid molecule to a chain containing 16 or 18 carbons. When the fatty acid reaches this length, it is transferred from ACP to CoA. The CoA is split off by an enzyme, deacylase, yielding the free fatty acid, which in turn combines with glycerol to form phospholipids and the triglyceride that is stored in depots and circulates in lipoproteins.

Triglyceride synthesis. Triglycerides, which consist of three fatty acids joined to glycerol by ester bonds (**Fig. 6**), are synthesized in the liver from glycerol phosphate and CoA derivatives of fatty acids. A series of enzymes called transferases catalyze the joining of the first two fatty acids with glycerol phosphate to form a phosphatidic acid (**Fig. 7**). The phosphate group must be removed to form a 1,2-diglyceride before the third fatty acid can be transferred to form a triglyceride. The removal of phosphate is catalyzed by a specific phosphatase. In the intestinal mucosa, triglycerides can be synthesized from monoglycerides without passing through phosphatidic acid as an intermediate.

Modification of dietary lipids. The fatty acids in the depots of each mammalian species have a characteristic composition. The chain length of ingested fat is either lengthened or shortened by the same pathways used for the synthesis and degradation of fatty acids so that the composition of the depots remains constant. However, when large amounts of a fat of markedly different composition from the animal's depot fat is ingested, the depots slowly change to reflect the characteristics of the ingested fat. The ability to introduce double bonds or reduce them in order to form an unsaturated or a saturated fatty acid is limited; highly unsaturated fatty acids can only be derived from dietary sources.

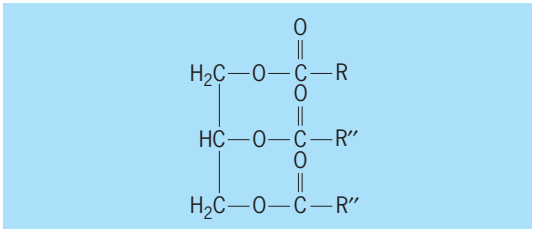

Fig. 6. General structural formula for a triglyceride.

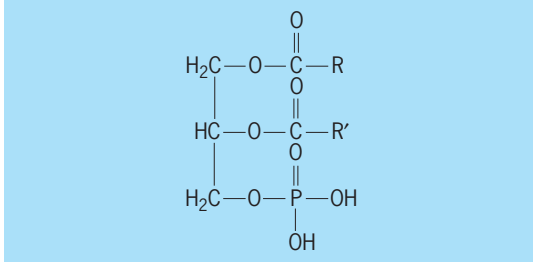

Fig. 7. Structural formula for a phosphatidic acid.

Essential fatty acids. Most mammals, including humans, probably require arachidonic acid for normal growth and for maintenance of the normal condition of the skin, although the mechanism of these effects has not been elucidated. Linoleic acid, a precursor of arachadonic acid in mammals, is the usual dietary source of unsaturated fatty acid. Highly unsaturated fatty acids cannot be synthesized by mammals from either saturated fatty acids or their precursors. Hence, the so-called essential fatty acids must be present in the diet.

Role of phosphatides. The phosphatides are compounds of glycerol, fatty acids, phosphate, and certain bases containing nitrogen, namely, ethanolamine, serine, and choline, the so-called phosphatide bases. When combined with fatty acids, they tend to make the insoluble fatty acids soluble in water. They are important constituents of both outer cell membranes (plasma membranes) and the network of cytoplasmic membranes (endoplasmic reticulum). *See* CELL MEMBRANES.

Phospholipid synthesis. In the liver, phospholipid synthesis follows the same pathway as triglyceride synthesis to the point of diglyceride formation. The nitrogenous base to be coupled at the 3 position of glycerol must first be phosphorylated by ATP and then reacted with cytidine triphosphate to form a cytidine diphosphoryl derivative. This derivative can then be coupled with the diglyceride in a reaction catalyzed by a specific transferase to form a phospholipid. *See* LIPID.

Martin A. Rizack

Bibliography. M. J. Halpern, *Lipid Metabolism and Its Pathology*, 1986; M. Horisberger and V. Bracco (eds.), *Lipids in Modern Nutrition*, 1987; J. F. Mead et al., *Lipids, Chemistry, Biochemistry, and Nutrition*, 1986; R. Paoletti et al., *Drugs Affecting Lipid Metabolism*, 1988; R. Salvayre et al. (eds.), *Lipid Storage Disorders: Biological and Medical Aspects*, 1988.

Lipid rafts (membranes)

Microdomains of the cell surface that play key roles in promoting information transfer across the membrane bilayer. The plasma membrane is composed of a lipid bilayer into which are inserted various essential proteins, such as transmembrane ion-channel and transporter proteins (which allow for the movement of small molecules into and out of the cell) and signaling proteins. Many of these proteins are found associated with domains on the surface of the membrane which are rich in free cholesterol (FC) and sphingolipids (lipids containing the amino acid sphingosine or its derivatives); some lipid components of transmembrane signaling pathways are also found here. It seems likely that both leaflets of the bilayer contribute to the structure of the microdomains. It is now evident that these rafts consist of a mixture of two quite different types of FC- and sphingolipid-rich domains: bowl-shaped caveolae and flat lipid rafts. Both caveolae and lipid rafts act as assembly sites (scaffolds) for signaling complexes, and may have important roles in signal transduction and other crucial intracellular functions. *See* CELL MEMBRANES.

Caveolae and lipid raft morphology. The general structures of caveolae and lipid rafts are shown in the **illustration**. Caveolae are invaginated membrane pockets 60–90 nanometers in diameter. They are stabilized by low-molecular-weight structural proteins, called caveolins, which are essential for their formation. In contrast to lipid rafts, caveolae are deficient in GPI-anchored proteins. (GPI stands for glycosylated derivatives of phosphatidylinositol; these are lipid molecules that insert into the membrane lipid bilayer, so that proteins attached to them are held at the membrane surface.) Caveolae and caveolins are abundant in differentiated cells but are relatively deficient (or absent) in cells transformed by cancer. Caveolae are relatively immobile, semipermanent features of the cell surface with a half-life of many hours.

Flat lipid rafts are planar, microdomains rich in FC, sphingolipids, and GPI-anchored proteins, and lacking caveolins. Mean diameters of 10–250 nm have been reported. The rafts are abundant in nonadherent cells, such as lymphocytes, but are probably present to some extent in all vertebrate cells. Lipid rafts are mobile and short-lived, with a half-life estimated by different biophysical techniques to be between a few seconds and several minutes. Microdomains with a composition similar to that of natural lipid rafts are formed spontaneously in synthetic lipid membranes containing FC and sphingolipids. *See* CHOLESTEROL; SPHINGOLIPID.

Presence in cells. There is no evidence that caveolae and lipid rafts are interconvertible, though most cells probably contain both. Depletion of lipid rafts in living cells is associated with an upregulation of the expression of caveolin and caveolae, and vice versa. In caveolin-deficient cells, signaling complexes normally associated with caveolae are found associated with lipid rafts. This may explain why, despite well-defined physiological roles for caveolae, cells from mice in which the caveolin gene has been deleted seem relatively normal. Conversely, in the absence of lipid rafts, signaling proteins that are generally present in the rafts are recruited to caveolae in the course of signal transduction.

Targeted protein assembly. One way in which proteins can be targeted to membrane domains is by covalent binding of long-chain fatty acids (acylation). These increase the association of proteins with membrane lipids. Lipid rafts support the assembly of many cytokine- and chemokine-dependent signaling complexes containing acylated proteins. Caveolae support the assembly of protein complexes that are active in signal transduction and those involved in cell attachment. In addition to acylation, these signaling proteins are bound to caveolin by a motif (local pattern of amino acids) that is rich in aromatic amino acids.

The high FC content of both flat lipid rafts and caveolae appears to be another major factor in targeting proteins to these microdomains. Depleting

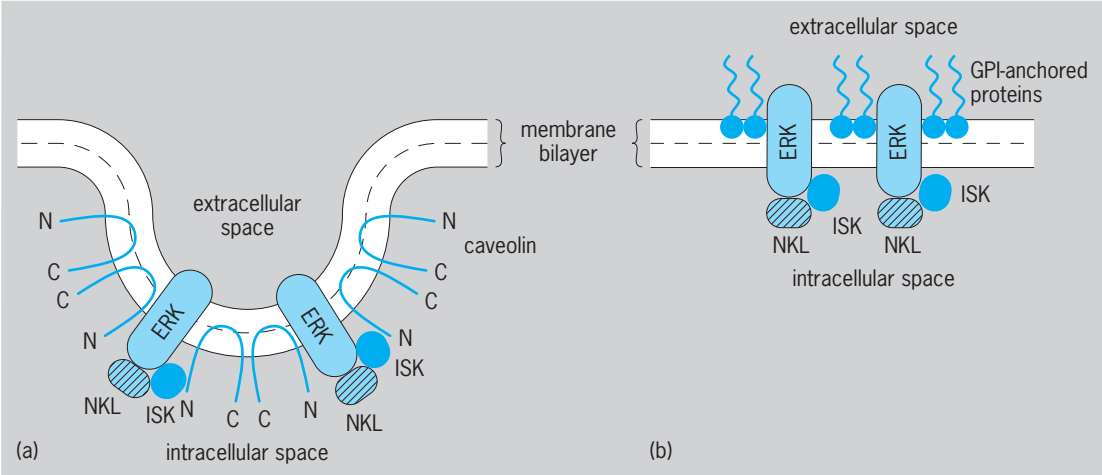

Cholesterol-rich membrane microdomains. (*a*) Caveola. (*b*) Lipid raft. ERK (extracellular receptor kinase), ISK (intracellular signaling kinase), and NKL (nonkinase linker protein) are microdomain-associated proteins that are important in signal transduction and protein complex assembly. N and C refer to the NH_2 and COOH termini of the caveolin protein primary sequence.

membrane FC by using extracellular lipid acceptors such as cyclodextrins (soluble synthetic FC acceptors) favors the transfer of signaling proteins to other parts of the membrane.

Signal transduction. In addition to their activity in assembling of signaling complexes, FC-rich microdomains can play more complex roles. For example, in the case of signaling initiated by the extracellular signaling protein called platelet-derived growth factor (PDGF), which stimulates cell growth and division and is essential to wound healing, FC is required for the initial assembly of the PDGF receptor complex in caveolae, but the FC must be expelled for subsequent steps in the pathway to proceed effectively. Linkage between loss of FC and signal transduction is also shown by the fact that the presence of extracellular FC-binding proteins stimulates both FC efflux and kinase activities in response to PDGF. Far from being inert, FC in caveolae can be dynamically regulated.

Endothelial nitric oxide synthase (e-nos) is an enzyme which regulates production of vascular nitric oxide production, an important mediator of blood vessel contraction. E-nos is localized within a signaling module (a complex of signaling molecules working together) in endothelial cell caveolae. Depletion of FC displaces e-nos from caveolae, rendering it inactive, an effect opposed by the delivery of FC to the caveola.

The signaling kinase Lyn is part of the B-cell antigen receptor (BCR) pathway which mediates the inflammatory response in lymphocytes, where it is mainly localized to lipid rafts. Raft FC mediates Lyn activity by protecting certain Lyn protein phosphoamino acids within rafts from hydrolysis. *See* SIGNAL TRANSDUCTION.

Caveolae, rafts, and cellular FC homeostasis. In addition to activities related to protein assembly and signal transduction, other roles for caveolae and rafts in FC homeostasis have been proposed.

FC efflux. The accessibility of caveolar FC is borne out by its rapid transfer from the cell surface to extracellular lipid acceptors such as plasma lipoproteins, particularly high-density lipoprotein (HDL), and cyclodextrin. The caveolar FC pool has been shown to contribute preferentially to such lipid transfer from caveola-rich primary smooth muscle cells and fibroblasts. This effect was not found in virus-transformed or other continuously dividing cell lines, probably because of the much smaller numbers of caveolae present.

Owing to their short life, a possible contribution of lipid rafts to FC efflux has not been quantified, though FC from rafts, like that from caveolae, is easily transferred to cyclodextrin.

Intracellular FC. An additional role has been suggested for caveolae and caveolin as intracellular mediators of FC transfer between membrane-bound organelles and storage areas. Caveolin has been identified in the perinuclear trans-Golgi fraction, in lipid storage droplets, in a weakly acidic recycling endosome fraction, and in a chaperone complex proposed as a carrier for the newly synthesized FC originating from the endoplasmic reticulum. Many transformed cells transfected with caveolin complementary DNA (cDNA) retain the protein within such intracellular pools.

Lipid rafts and viral infectivity. A recent development is the recognition that signaling proteins in lipid rafts are the binding sites by which many viruses gain entry to cells. The same structures can contribute coat lipids to newly synthesized virions. Lymphocyte raft signaling proteins CD4 and CCR5 are among the contributors to human immunodeficiency virus (HIV-1) binding. Depletion of FC in these microdomains via cyclodextrin significantly reduces infectivity in vitro. Other viruses shown to utilize lipid raft pathways for infection include Echovirus and Ebola virus. Details of the linkage between virus binding and internalization have not yet

been worked out. Preliminary data suggest that caveolae may contribute to the internalization of other microorganisms.

Answers to the many questions remaining about caveolae, lipid rafts, and their functions may be gained from their tertiary structure, when this information becomes available. Present data suggest that structural differences might contribute significantly to heterogeneity within plasma membranes, generating the unique lipid and protein structures that play important roles in cellular transport and communication. *See* VIRUS.

Christopher J. Fielding

Bibliography. C. J. Fielding (ed.), *Lipid Rafts and Caveolae: From Membrane Biophysics to Cell Biology*, Wiley-VCH, Weinheim, Germany, 2006; R. G. Parton, Caveolae—from ultrastructure to molecular mechanisms, *Nat. Rev. Mol. Cell Biol.*, 4:162–167, 2003; L. J. Pike, Lipid rafts: Bringing order to chaos, *J. Lipid Res.*, 44:655–667, 2003.

Lipoprotein

Classes of conjugated proteins consisting of a protein combined with a lipid. The normal functioning of higher organisms requires movement of insoluble lipids between tissues. These lipids include cholesterol, used for cell membranes, steroid hormones, and bile; and triglyceride, a major form of dietary and stored energy. To accomplish this movement, lipids are incorporated into macromolecular complexes called lipoproteins.

Structure and metabolism. All major types of lipoproteins share a general structure (see **illus.**). The core of these spherical particles contains primarily cholesteryl ester and triglyceride. These insoluble molecules are surrounded by a coating of proteins and phospholipids that are amphipathic; that is, they have both polar and nonpolar regions. Lipoproteins vary by size and density. The largest lipoproteins, chylomicrons, are up to 500 nanometers in diameter, and since they contain primarily triglyceride they are so buoyant that they float in plasma. Very low density lipoproteins (VLDL) also primarily transport triglyceride; low-density lipoproteins (LDL) and the smallest, most dense lipoproteins, high-density lipoproteins (HDL), transport cholesterol. The interactions of these particles with cell surface receptors and with metabolic enzymes are mediated by the protein components of the particles that are termed apolipoproteins. *See* CHOLESTEROL; TRIGLYCERIDE.

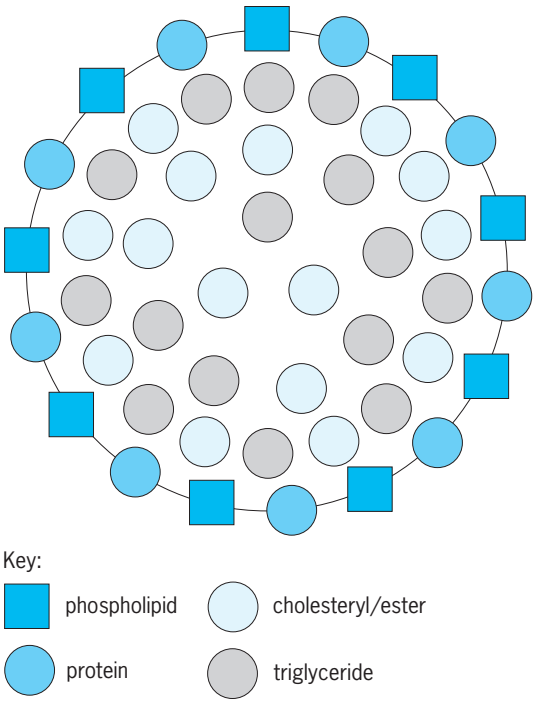

Structural model of a lipoprotein. PL, phospholipid; P, protein; CE, cholesteryl ester; TG, triglyceride.

Chylomicrons and VLDL. These two lipoproteins transport triglyceride. Chylomicrons contain triglyceride (fat) from the diet. In addition, they are the lipoproteins that carry fat-soluble vitamins, such as vitamin A and E, into the circulation. Chylomicrons are produced in the intestine, enter the body via the lymphatic system, and then enter the bloodstream. Very low density lipoproteins are made in the liver and contain triglyceride that is synthesized either from excess carbohydrate sources of calories or from fatty acids that enter the liver and are reassembled into triglyceride. Lipoprotein lipase (LpL) is an enzyme found on the surface of blood vessels that is responsible for the breakdown of triglyceride in lipoproteins. This enzyme is made in muscle and fat. It requires an activator protein, apoCII, that is carried on very low density lipoproteins and chylomicrons. Through this system, energy is supplied to muscle for motion and to fat for storage.

The partially degraded lipoproteins are termed remnants. They are ultimately removed from the circulation by the liver. Two receptors on liver cells, the LDL receptor and the LDL receptor–related protein, recognize apoE on the surface of the remnant lipoproteins.

LDL and HDL. Low-density lipoproteins constitute a metabolic product that results after triglyceride is removed from very low density lipoproteins. This leaves a smaller, denser particle that primarily contains cholesteryl ester as its core lipid and a single protein called apoB. Cells throughout the body contain an LDL receptor that recognizes apoB. This allows the uptake of low-density lipoproteins into cells, supplying them with cholesterol. When sufficient low-density lipoproteins and cholesterol are available, cells use them in preference to synthesizing new cholesterol from precursors.

In contrast, high-density lipoproteins both deliver and remove cholesterol from tissues. In animals that have very little circulating low-density lipoproteins, such as rodents, high-density lipoproteins deliver cholesterol to steroid-producing tissues. Its major protein, apoAI, is made in both the intestine and the liver and is secreted with a small amount of lipid. These small HDL precursors acquire additional cholesterol from other tissues. Via the actions of lecithin cholesterol acyl transferase (LCAT),

the cholesterol is converted to cholesteryl ester—a process that makes it more hydrophobic and allows it to create a lipoprotein with a cholesteryl ester core. High-density lipoproteins have at least one receptor, scavenger receptor B-1 (SRB-1). High-density lipoproteins bind to SRB-1 in the liver and in adrenal cells; and via a poorly understood process, cholesteryl ester, but not HDL protein, is transferred to cells. This process can supply cholesterol for steroid hormones and for bile. A plasma lipid transport protein called cholesteryl ester transfer protein (CETP) exchanges cholesteryl ester in high-density lipoproteins for triglyceride in very low density lipoproteins, thus reducing the size and cholesterol content of high-density lipoproteins. CETP is not produced by rodents.

Lipoprotein(a). Apo(a) is a large protein with homology to the blood-clotting protein plasminogen. Apo(a) complexes with low-density lipoproteins via a disulfide linkage and forms a lipoprotein called Lp(a). Lp(a) contains added protein and is denser than low-density lipoproteins.

Medical significance. Blood levels of lipoproteins are major factors regulating risk for development of coronary artery atherosclerosis, the most common form of heart disease in the western world. Via unknown mechanisms, low-density lipoproteins and remnant lipoproteins infiltrate and then become attached to extracellular matrix molecules within the artery. Some of the lipoproteins are internalized by macrophages and smooth muscle cells. This might first require chemical modification such as oxidation of the lipids. The resulting pathological findings are deposition of cholesterol in cells and matrix within the vessel wall, leading to a decrease in the diameter of the artery.

LDL cholesterol is a major predictor of the development of atherosclerosis in humans and in animals. Moreover, dietary and genetic modifications of animals have conclusively shown that elevated cholesterol in low-density lipoproteins or remnant lipoproteins is the only alteration required to convert a nonatherogenic animal into one that gets this disease.

In contrast, high-density lipoproteins appear to prevent atherosclerosis formation. The reasons are not entirely understood. Most likely, high-density lipoproteins remove excess cholesterol that accumulates in the artery, or high-density lipoproteins prevent the oxidation of low-density lipoproteins.

Lp(a) levels are also correlated with the development of atherosclerosis. This relationship is most evident in Caucasian populations. Blood Lp(a) concentrations are primarily genetically determined; individuals with smaller forms of apo(a) produce a greater number of these molecules. Lp(a) particles may alter blood clotting or have alternative molecular interactions that make them more likely to accumulate in arteries. *See* ARTERIOSCLEROSIS.

Regulation of levels. Diet, exercise, and genetic factors control the levels of lipoproteins in the blood. Diets containing more cholesterol and saturated fats increase the amounts of LDL cholesterol. Lipoproteins containing primarily triglyceride are increased with obesity, diabetes, and intake of foods such as simple sugars and alcohol that are readily converted to triglyceride in the liver. Exercise lowers triglyceride.

HDL levels are increased by high cholesterol–high saturated fat diets, but low-density lipoproteins are increased at the same time. In addition, alcohol, oral estrogen, and exercise raise high-density lipoproteins.

Lp(a) is reduced by estrogen.

Disorders. In most people the concentrations of blood lipoproteins are modulated by lifestyle and by poorly defined polygenetic factors. ApoB is produced in greater amounts in people with familial combined hyperlipoproteinemia. These people have increased very low density lipoproteins and low-density lipoproteins in their blood. Familial hypercholesterolemia is a disease due to a defect in removal of low-density lipoproteins from the bloodstream. This is either due to a defect in the LDL receptor or to a mutation in apoB that prevents low-density lipoproteins from being recognized by the receptor. Defects in lipoprotein lipase or its activator apoCII lead to very high blood levels of triglyceride. Defects in almost all the other apos and lipoprotein-metabolizing enzymes have been described and lead to diseases in humans.

Treatments. A number of medical therapies have been developed to reduce blood concentrations of lipoproteins. Medications that reduce LDL cholesterol are effective in reducing atherosclerosis complications such as heart attacks and strokes. Bile acid–binding resins reduce low-density lipoproteins by absorbing cholesterol in the gastrointestinal tract and augmenting its removal. The vitamin niacin decreases liver production of very low density lipoproteins and low-density lipoproteins. HMG CoA reductase inhibitors, also known as statins, are inhibitors of the cholesterol synthesis in the liver. In turn, the liver increases the number of LDL receptors, leading to greater removal of low-density lipoproteins from the bloodstream.

Ira J. Goldberg

Bibliography. H. N. Ginsberg and I. J. Goldberg, Lipoproteins disorders, in *Harrison's Principles of Internal Medicine,* 13th ed., edited by Fauci et al., pp. 2138–2149, 1997; M. Rosseneu (ed.), *Structure and Function of Apolipoproteins*, CRC Press, Boca Raton, FL, 1992.

Liposomes

Aqueous compartments enclosed by lipid bilayer membranes; liposomes are also known as lipid vesicles. Phospholipid molecules consist of an elongated nonpolar (hydrophobic) structure with a polar (hydrophilic) structure at one end. When dispersed in water, they spontaneously form bilayer membranes, also called lamellae, which are composed of two monolayer layer sheets of lipid molecules with their nonpolar (hydrophobic) surfaces facing each other and their polar (hydrophilic) surfaces facing the

aqueous medium. The membranes enclose a portion of the aqueous phase much like the cell membrane which encloses the cell; in fact, the bilayer membrane is essentially a cell membrane without its protein components.

Liposomes are often used to study the characteristics of the lipid bilayer. Properties of liposomes have been characterized by a variety of techniques: molecular organization by x-ray diffraction, nuclear magnetic resonance, electron paramagnetic resonance, and Raman spectroscopy; melting behavior (that is, crystal to liquid-crystal transition) by calorimetry; net electric surface charge by microelectrophoresis; size by light scattering and electron microscopy. *See* LIPID.

Liposomes are most easily formed by hand-shaking a solution of anhydrous lipids with water for seconds to hours (depending on the natures of the lipid or aqueous phases). This simple procedure spontaneously yields large, multilamellar liposomes or vesicles with diameters of 1–10 micrometers, which are composed of a few to hundreds of concentric lipid bilayers alternating with layers of aqueous phase. The thickness of the aqueous layers and, hence, the total amount of aqueous phase trapped by the vesicle, depends on the balance of electrostatic repulsion forces between charged lipids and van der Waals attractive forces between bilayers as a whole. Thus, aqueous layer spacing (and hence, volume trapped) increases with increasing proportion of charged lipids in the membrane and with decreasing concentrations of electrolyte (charged ions) in the aqueous phase. The smallest unilamellar vesicles of 20-nanometer diameter can be produced by subjecting multilamellar vesicles to ultrasound. Unilamellar vesicles of somewhat larger (0.1–1 μm) diameter result when lipid is solubilized in organic solvent or in detergent, and the solubilizing agent removed by evaporation or by dialysis, respectively. Fusion of small unilamellar vesicles by methods requiring particular lipids or stringent dehydration-hydration conditions can yield unilamellar vesicles as large as or larger than cells.

Although hydration of anhydrous phospholipids was long known to generate sheets of lipid bilayer, it was not established until the 1960s that the aqueous volume trapped by the hydrated lipid is totally enclosed. Since the vesicles are continent and can be loaded with almost any water-soluble molecule, it was possible to measure bilayer permeability to ions and metabolites present in cells. It was soon demonstrated that liposome membranes have low permeability to polar metabolites; this is also an essential material property of the similarly constructed matrix of the cell membrane, which means that liposomes can be used to reproduce various cell membrane functions. For example, the criterion for the isolation of membrane transport proteins is usually their incorporation into liposomes in a functional form.

Liposomes have numerous uses as biochemical and biophysical tools: (1) as vehicles for the delivery of both water- and oil-soluble materials to the cell, (2) as immunological adjuvants, (3) as substrates for the study of membrane properties such as rotational or translational diffusion in the plane of the membrane, and (4) as intermediates in the construction of bilayers large enough for the study of electrical properties of membranes. The great interest in liposomes as therapeutic agents was stimulated by the administration to animals of liposomes containing anticancer drugs, which suggested that such an innovation could decrease a person's exposure to toxic compounds while delivering a high dose of the compound to the diseased site. The targeting of drug-containing vesicles to specific sites by modification of the liposome surface—for example, by attaching site-specific antibodies—has met with limited success, however. A notable exception has been the treatment of parasitic diseases of the liver, in which most unmodified liposomes naturally accumulate, since most of the scavenging of particulate matter occurs in the liver. *See* LIVER.

Other medical applications that have been studied include the enhancement of x-ray imaging by radiopaque liposomes; heavy-metal toxicity therapy with liposomes containing chelating agents; protection of otherwise digestible dietary supplements and drugs to enable their oral administration; and preparation of artificial blood composed of hemoglobin-loaded liposomes. Technological applications of liposomes have also been the subject of study. Notable among these are (1) diagnostic assays featuring liposomes constructed to signal formation of antibody-antigen complexes; and (2) artificial photosynthesis by appropriately constructed liposomes, in which a light-driven reaction leads to the release of hydrogen from water. *See* CELL MEMBRANES.

Robert C. MacDonald; Ruby I. MacDonald

Bibliography. A. D. Bangham (ed.), *The Liposome Letters*, 1983; G. Gregoriadis (ed.), *Liposome Technology*, vols. 1–3, 1984; E. D. Korn (ed.), *Methods in Membrane Biology*, vol. 1, 1974.

Liquefaction of gases

The process of refrigerating a gas to a temperature below its critical temperature so that liquid can be formed at some suitable pressure, also below the critical pressure.

Thus gas liquefaction is a special case of gas refrigeration and cannot be separated from it. In both cases, the gas is first compressed to an elevated pressure in an ambient-temperature compressor. This high-pressure gas is passed through a countercurrent heat exchanger to a throttling valve or expansion engine. Upon expanding to the lower pressure, cooling may take place, and some liquid may be formed. The cool, low-pressure gas returns to the compressor inlet to repeat the cycle. The purpose of the countercurrent heat exchanger is to warm the low-pressure gas prior to recompression, and simultaneously to cool the high-pressure gas to the lowest temperature possible prior to expansion. Both refrigerators and liquefiers operate on this same basic principle.

See COMPRESSOR; CRITICAL PHENOMENA; GAS; HEAT EXCHANGER; REFRIGERATION.

There is nonetheless an important distinction between refrigerators and liquefiers: In a continuous refrigeration process, there is no accumulation of refrigerant in any part of the system. This contrasts with a gas-liquefying system, where liquid accumulates and is withdrawn. Thus, in a liquefying system, the total mass of gas that is warmed in the countercurrent heat exchanger is less than the gas to be cooled by the amount that is liquefied, creating an unbalanced flow in the heat exchanger. In a refrigerator, the warm and cool gas flows are equal in the heat exchanger. This results in balanced flow condition. The thermodynamic principles of refrigeration and liquefaction are identical. However, the analysis and design of the two systems are quite different due to the condition of balanced flow in the refrigerator, and unbalanced flow in liquefier systems.

Liquefaction principles. The prerequisite refrigeration for gas liquefaction is accomplished in a thermodynamic process when the process gas absorbs heat at temperatures below that of the environment. As mentioned above, a process for producing refrigeration at liquefied gas temperatures usually involves equipment at ambient temperature in which the gas is compressed and heat is rejected to a coolant. During the ambient-temperature compression process, the enthalpy and entropy, but usually not the temperature of the gas, are decreased. The reduction in temperature of the gas is usually accomplished by heat exchange between the cooling and warming gas streams followed by an expansion of the high-pressure stream. This expansion may take place either through a throttling device (isenthalpic expansion) where there is a reduction in temperature only (when the Joule-Thomson coefficient is positive) or in a work-producing device (isentropic expansion) where both temperature and enthalpy are decreased. *See* ENTHALPY; ENTROPY; ISENTROPIC PROCESS; THERMODYNAMIC PRINCIPLES; THERMODYNAMIC PROCESSES.

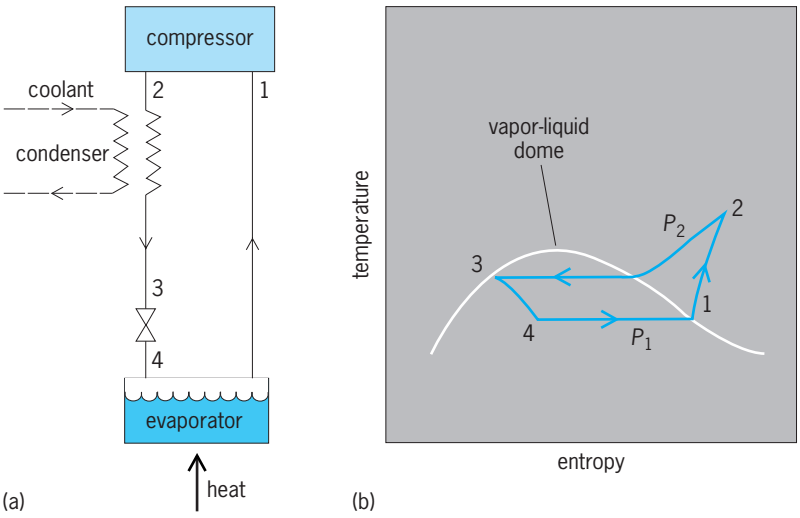

Fig. 1. Compressed-vapor refrigerator. (*a*) Arrangement of equipment. (*b*) Temperature-entropy diagram of process. Numbers indicate corresponding points in the cycle.

Maximum inversion temperatures of frequently liquefied gases*

Fluid	Maximum inversion temperature, °R (K)
Oxygen	1370 (761)
Argon	1300 (722)
Nitrogen	1120 (622)
Air	1085 (603)
Neon	450 (250)
Hydrogen	364 (202)
Helium	72 (40)

*After R. Barron, *Cryogenic Systems*, 1966.

For reasons of efficiency alone, isentropic expansion devices might be preferred for gas liquefaction. However, expansion engines have yet to be developed which can operate with more than a few percent of liquid present, due to erosion. Therefore, simple throttling devices are employed at some point in nearly all gas-liquefaction systems. Throttling is an isenthalpic process, and the slope at any point on an isenthalpic curve (constant enthalpy h) in a pressure-temperature diagram is a quantitative measure of how the temperature T will change with pressure P. This slope is called the Joule-Thomson coefficient and is usually denoted by μ given mathematically by Eq. (1).

$$\mu = \left(\frac{\partial T}{\partial P}\right)_h \tag{1}$$

The Joule-Thomson coefficient is a property of each specific gas, is a function of temperature and pressure, and may be positive, negative, or zero. For instance, hydrogen, helium, and neon have negative Joule-Thomson coefficients at ambient temperature. Consequently, to be used as refrigerants in a throttling process, they must first be cooled either by a separate precoolant fluid or by a work-producing expansion engine to a temperature (called inversion temperature) below that at which the Joule-Thomson coefficient is positive. Only then will throttling cause a further cooling rather than a heating of these gases.

Nitrogen, methane, and other gases, on the other hand, have positive Joule-Thomson coefficients at ambient temperatures and hence produce cooling when expanded through a valve. Accordingly, they may be liquefied directly in a throttling process without the necessity of a precooling step or expansion through a work-extracting device. Maximum inversion temperatures for some of the more frequently liquefied gases are given in the **table**.

Liquefaction methods. General principles of the more useful liquefaction methods are given below.

Vapor compression. In a typical single-stage compressed-vapor refrigerator (**Fig. 1***a*), heat is absorbed by evaporation of a suitable liquid at temperature T_1 and pressure P_1 in an evaporator. In a dry

compression cycle, saturated vapor is compressed to pressure P_2, and superheated vapor at the compressor outlet is condensed in a condenser at temperature T_2 by exchanging heat with a suitable coolant. A throttling valve allows the saturated liquid formed in the condenser to expand approximately isenthalpically from 3 to 4 to the evaporator, completing the cycle. Figure 1*b* shows the states of the refrigerant in this compressed-vapor process on a temperature-entropy diagram.

Certain criteria can be established to aid in choosing a gas for this type of liquefier.

1. The temperature of the evaporator is usually near the normal boiling point of the gas so that the pressure of the evaporator may be approximately atmospheric. Temperatures lower than the normal boiling temperature can be used; however, care must be taken to prevent air leaking into the subatmospheric parts of the cycle.

2. The gas must be chosen with a small compression ratio. This is necessary because the work of compression increases rapidly with the compression ratio. High discharge pressures require massive equipment for proper containment of the refrigerant and result in costly and heavy refrigerators.

3. The ambient temperature must be less than the critical temperature of the gas to effect condensation while using the environment as a coolant.

The efficiency of the compressed-vapor refrigerator is generally higher than that of other methods discussed below because heat is transferred nearly isothermally, and the compression process can be made nearly reversible. Thus, the main deviation of this cycle from a Carnot cycle is the isenthalpic expansion at the throttling valve.

Cascade vapor compression. It is possible to cascade several vapor-compression systems, each containing different refrigerants, to reach lower temperatures (**Fig. 2**). Cascading is necessary because the gases with the lower boiling points have critical temperatures well below the ambient temperature. Thus, it is necessary to provide condenser temperatures for these vapor-compression cycles by the evaporators of other vapor-compression cycles, which reject heat at higher temperatures. The efficiency of cascade systems is greatly improved by the use of heat exchangers which cool the incoming warm gases. The exchangers warm the cool gases before they reach the compressor intake.

Isenthalpic expansion. In a thermodynamic process to obtain cryogenic temperatures, known as the simple Linde cycle (**Fig. 3**), the gas is compressed at ambient temperature approximately isothermally from 1 to 2, rejecting heat to a coolant. The compressed gas is cooled in a heat exchanger by the stream returning to the compressor intake until it reaches the throttling valve. Joule-Thomson cooling upon expansion from 3 to 4 further reduces the temperature until, in the steady state, a portion of the gas is liquefied.

For the simple Linde liquefier shown, the liquefied portion is continuously withdrawn from the reservoir and only the unliquefied portion of the fluid is

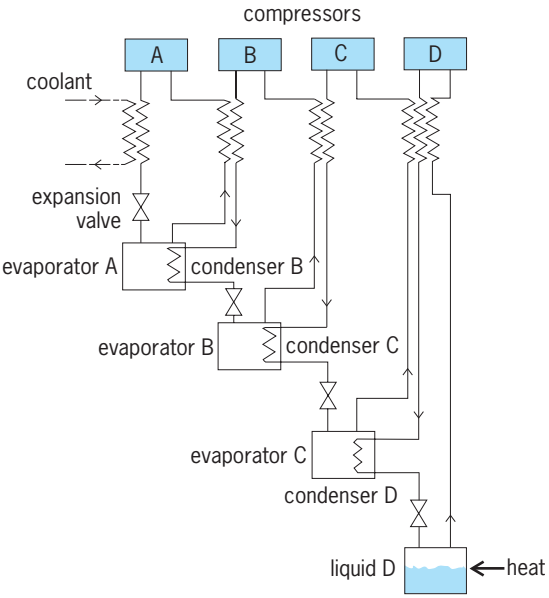

Fig. 2. Cascade compressed-vapor refrigerator.

warmed in the countercurrent heat exchanger and returned to the compressor. The fraction y that is liquefied is obtained by applying the first law of thermodynamics to the heat exchanger, Joule-Thomson valve, and liquid reservoir. This results in Eq. (2),

$$y = \frac{h_1 - h_2}{h_1 - h_f} \tag{2}$$

where h_f is the specific enthalpy of the liquid being withdrawn. Maximum liquefaction occurs when h_1 and h_2 refer to the same temperature.

Gases used in this process have a critical temperature well below the ambient temperature; consequently, liquefaction by direct compression is not possible. In addition, the inversion temperature must be above the ambient temperature to provide

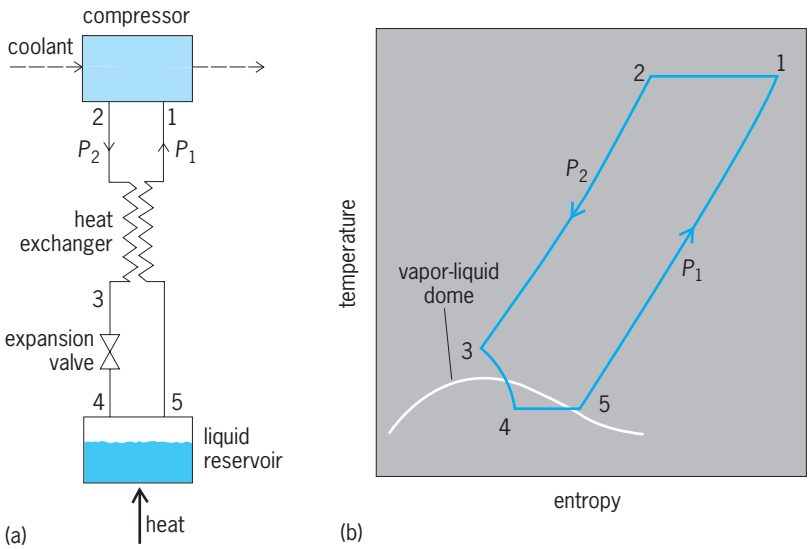

Fig. 3. Refrigerator using simple Linde cycle. (*a*) Arrangement of equipment. (*b*) Temperature-entropy diagram of process.

cooling as the process is started. Auxiliary refrigeration is required if the simple Linde cycle is to be used to liquefy gases whose inversion temperature is below the ambient temperature. Liquid nitrogen is the optimum refrigerant for hydrogen and neon liquefaction systems, while liquid hydrogen is the normal refrigerant for helium liquefaction systems.

Dual-pressure process. To reduce the work of compression, a two-stage or dual-pressure process may be used whereby the pressure is reduced by two successive isenthalpic expansions. Part of the gas is returned to the compressor after the first expansion, providing some precooling for the full high-pressure stream. The remainder of the gas proceeds to the second isenthalpic expansion. Since the work of compression is approximately proportional to the logarithm of the pressure ratio, and the Joule-Thomson cooling is roughly proportional to the total pressure difference, there is a much greater reduction in compressor work than in refrigerating performance. Hence, the dual-pressure process produces a given amount of liquefaction with less energy input than the simple Linde process.

Isentropic expansion. Refrigeration can always be produced by expanding the process gas in an engine and causing it to do work. In a simple refrigerator using this principle (**Fig. 4**), gas compressed isothermally from 1 to 2 at ambient temperature is cooled in a heat exchanger by gas being warmed on its way to the compressor intake. Further cooling takes place during the engine expansion from 3 to 4. In practice, this expansion is never truly isentropic, and this is reflected by the curved path 3–4 in Fig. 4*b*. The net cooling effect is shown between T_4 and T_5 in Fig. 4*b*.

In a work-producing expansion, the temperature of the gas is always reduced; hence, cooling does not depend on being below the inversion temperature prior to expansion. In large machines the work produced during expansion is conserved. In small liquefiers, the energy from the expansion is usually expended in a gas or hydraulic pump, or other suitable device.

Path 3–4 seldom dips very far into the liquid-vapor region because of technical problems associated with forming liquid in the expansion engine. Since a liquid product is the objective, an isentropic expansion for precooling is combined with isenthalpic expansion for forming liquid, as discussed below.

Combination of isenthalpic and isentropic expansion. It is not uncommon to combine the isentropic and isenthalpic expansions to allow the formation of liquid in the refrigerator. The Claude cycle is an example of a combination of these methods. All of the high-pressure gas is first expanded isentropically to produce cooling. A portion of this cooled gas is bypassed to the low-pressure stream to help precool the incoming high-pressure stream. The remainder of the cooled, high-pressure stream is expanded isenthalpically to produce liquid.

Modifications of Claude cycle. One modification of the Claude cycle that has been used extensively in high-pressure liquefaction plants for air is the Heylandt cycle. In this cycle, the first warm heat exchanger is eliminated, allowing the inlet of the expander to operate at ambient temperatures and thereby minimizing lubrication problems that are often encountered at lower temperatures.

Another modification of the basic Claude cycle is the dual-pressure Claude cycle, similar in principle to the dual-pressure Linde system discussed above. In the dual-pressure Claude cycle, only the gas which is sent through the expansion valve is compressed to the high pressure; this reduces the work requirement per unit mass of gas liquefied. When the Claude dual-pressure cycle is selected in the liquefaction of air, the liquid yield can be doubled while the work per unit mass liquefied can be halved in comparison to the dual-pressure Linde cycle.

Still another extension of the Claude cycle is the Collins helium liquefier. Depending upon the helium inlet pressure, from two to five expansion engines are used in this system. The addition of a liquid-nitrogen precooling bath to this system results in a two- to threefold increase in liquefaction performance. *See* LIQUID HELIUM.

Mixed refrigerant cycle. The mixed refrigerant cycle is a variation of the cascade cycle described above and involves the circulation of a single refrigerant stream which might be a mixture of refrigerants. The simplification of the compression and heat exchange services in such a cycle may, under certain circumstances, offer potential for reduced capital expenditure over the conventional cascade cycle. This cycle is widely used to liquefy natural gas. *See* AIR SEPARATION; CRYOGENICS; LOW-TEMPERATURE PHYSICS.

Thomas M. Flynn

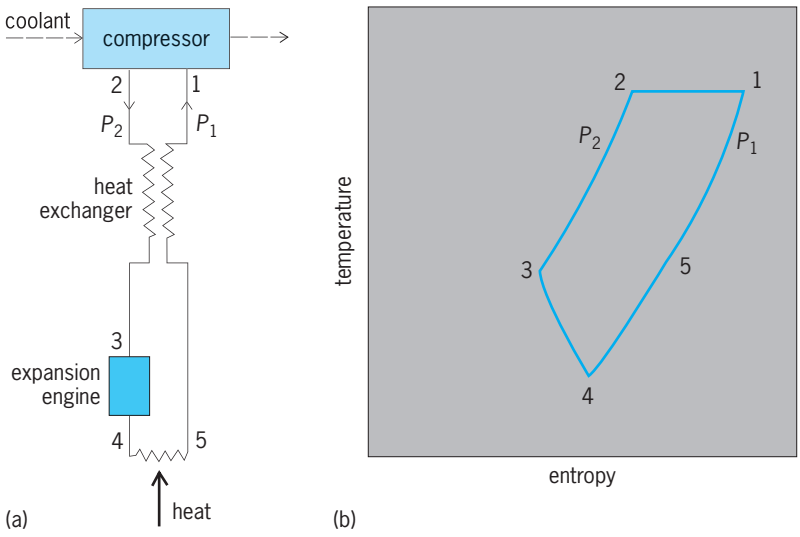

Fig. 4. Isentropic-expansion refrigerator. (*a*) Arrangement of equipment. (*b*) Temperature-entropy diagram of process.

Bibliography. *Advances in Cryogenic Engineering*, vols. 1–40, 1954–1994; R. Barron, *Cryogenic Systems*, 2d ed., 1985; T. M. Flynn and K. D. Timmerhaus, *Cryogenic Process Engineering*, 1989.

Liquefied natural gas (LNG)

Natural gas, usually consisting primarily of methane, that has been processed into liquid form. It is increasingly used for transporting large quantities of natural gas across oceans with specially designed ships. The properties of LNG are those of liquid methane, slightly modified by minor constituents. Natural gas must be cooled to cryogenic temperatures to be liquefied and then stored in well-insulated containers. More than 600 ft^3 (17 m^3) of natural gas condense into 1 ft^3 (0.028 m^3) of liquid at about −258°F (−161°C). In this form, the gas can be conveniently stored and transported. At the receiving end, LNG is revaporized and then compressed and put into the natural gas distribution system. *See* CRYOGENICS; NATURAL GAS.

Contribution to gas supply. By 2005, natural gas became the world's number two source of energy supply (behind oil but surpassing coal) with 23% of the total. Estimates vary but point toward an increasing market share for natural gas over the next several decades. While world energy demand is slated to increase by at least 50%, natural gas will provide at least 28% and as much as 45%.

For the United States, estimates suggest that there will be a need to import 8 trillion cubic feet (Tcf; 2.2×10^{11} m^3) by 2015 and 15 Tcf (4.2×10^{11} m^3) by 2015.

The earliest commercial use for LNG was to supply winter peak demands for home heating fuel. Such a peak management system was constructed in Cleveland, Ohio, in the early 1940s. However, several years of successful operation ended in disaster when a storage tank developed a leak and escaping liquid spread through city streets, producing a very destructive fire. Nearly two decades passed before another LNG plant was built in the United States.

In modern design, dikes separate storage tanks and equipment to ensure that liquid leaks will be confined. An accident or fire in one unit would not be likely to damage any other area of the plant or its surroundings.

Insulated storage tanks constitute the main cost element in LNG plants. Novel approaches have attempted to reduce this cost. Frozen earth can form the lining of an excavated reservoir. As tank size increases, the ratio of wall surface area to container volume declines. With large tanks, the heat conduction rate of natural soil results in tolerable evaporation. However, water flowing through the earth in contact with the frozen soil lining increases heat flow to intolerable levels.

Modern LNG schemes involve four distinct parts: supply of natural gas (likely from a country in South America, Africa, or the Middle East), liquefaction, transportation, and regasification. The relative costs for the four phases, respectively, for 1 Bcf/day (2.86×10^7 m^3/d) are $1.5 billion, $2 billion, $1–2 billion (depending on the distance), and $0.5 billion. These figures lead to a price per Mcf of $2–2.45 from South America, $2.25–3.25 from Africa, and $2.85–3.60 from the Middle East. Such prices make LNG affordable.

Specialized tanker ships can transport LNG over long distances. Modern LNG tankers transport about 3 Bcf of gas. Storage and regasification facilities are required to reconvert to a gas that can then be fed into the gas distribution system. Worldwide, there are about 17 natural gas liquefaction plants and 40 regasification plants in operation today, and several new liquefaction and regasification plants are under construction. Regasification facilities in the United States are expected to increase from 2 Bcf/d capacity in 2004 to at least 12 Bcf/d by 2010. *See* OIL AND GAS STORAGE.

Use. In 2004, about 27% of the global natural gas trading was done through LNG technology. This constitutes roughly 7% of total world production. Most of the current LNG transactions occur from Asia to Japan. Early on, the Japanese government realized the immense potential of natural gas in their energy mix and began construction of LNG facilities in the 1970s. Today Japan imports 47% of the world's LNG production.

Natural gas demand is fast increasing worldwide. As the United States increases its natural gas import capacity, Canada, its main outside source, will no longer be able to satisfy demand. Thus, LNG terminals are an increasingly viable alternative.

Ocean transport. Gas-producing areas remote from demand centers can ship LNG overseas—Japan is supplied by plants in Abu Dhabi, Alaska, Borneo, Brunei, Indonesia, and the Middle East. Western Europe and the United States receive LNG from the Middle East, Algeria, and Libya. Many other countries, such as Russia, Trinidad, and Australia, have embarked upon ambitious LNG projects. It is likely that China will soon become a major market for LNG imports.

In early 2005, the Atlantic Basin had 14.5 Bcf/d proposed and committed liquefaction plants for shipment to consumers. The numbers for the Middle East and Asia-Pacific were 12.5 Bcf/d and 14.2 Bcf/d, respectively. These projects would increase the total installed capacity in the world from 17 Bcf/d in 2003 to 30 Bcf/d by 2008 and 41 Bcf/d by 2010. Moreover, the world fleet for LNG tankers increased from 90 in 1995, to 128 in 2001, to 174 in 2004. By 2009, this number is estimated to exceed 300.

LNG ships are equipped with specially designed insulated storage tanks of three general types. Balsa wood has been used extensively as an effective insulation. Membrane, or integral, tanks contain LNG within a thin metallic liner, which is supported by load-bearing insulation, which in turn receives its support from the ship's structure. Stand-alone prismatic tanks conform to the hull contour but are self-supporting. Both membrane and prismatic tanks require special design at tank edges and corners to accommodate contraction during cool-down to LNG temperature. Spherical stand-alone cargo tanks minimize thermal problems. However, with spherical tanks the hull volume is poorly utilized. Ship design is influenced by the height of tanks above the

water line. Both LNG and its insulating material have densities significantly less than seawater. Therefore, all LNG vessels carry most of their cargo above the waterline. This design necessity is complemented by spherical tanks. Stability and wind load factors become more important in design and operation. *See* MARINE REFRIGERATION; MERCHANT SHIP.

Challenges. Normally, the composition of LNG is over 97% methane. Heat leak into storage tanks may vaporize essentially pure methane, causing enrichment of the remaining liquid in ethane and propane. At the same time, density increases and boiling temperature rises. Composition, density, and temperature of liquid added to the tank may be significantly different. Mixing large quantities of liquids of differing composition may cause very rapid vaporization. If the rate exceeds the capacity of relief devices, tank facilities may be damaged. *See* ETHANE; METHANE; PROPANE.

Large-scale spills of LNG present unique hazards. As very cold methane vapor mixes with air, the density of the mixture increases. Absorption of heat from contact with surfaces decreases mixture density. As a result, a cloud of cold gas may form and hover near the ground. Since dispersion is slow in relatively still air, combustible mixtures may travel considerable distances before achieving safe dilution.

Michael J. Economides; Arthur W. Francis

Bibliography. M. J. Economides, K. Sun, and G. Subero, *Compressed Natural Gas (CNG): An Alternative to Liquid Natural Gas (LNG)*, Pap. SPE 92047, 2005; C. H. Gatton, *Liquefied Natural Gas Technology and Economics*, 1967; LNG scorecard, *Pipeline Gas J.*, November 1982; National Fire Protection Association, *Liquefied Natural Gas: Production, Storage and Handling*, 1972; G. Subero et al., *A Comparative Study of Sea-Going Natural Gas Transport*, Pap. SPE 90243, 2004; U.S. Department of Energy, *An Approach to LNG Safety*, DOE/EV 002, February 1978.

Liquefied petroleum gas (LPG)

A product of petroleum gases, principally propane and butane, which must be stored under pressure to keep it in a liquid state. At atmospheric pressure and above freezing temperature, these substances would be gases. Large quantities of propane and butane are now available from the gas and petroleum industries. These are often employed as fuel for tractors, trucks, and buses and mainly as a domestic fuel in remote areas. Because of the low boiling point (−47 to 32°F or −44 to 0°C) and high vapor pressure of these gases, their handling as liquids in pressure cylinders is necessary. Owing to demand from industry for butane derivations, LPG sold as fuel is made up largely of propane.

Operating figures for gasoline, diesel, and LPG fuels show that LPG compares favorably in cost per mile. LPG has a high octane rating, making it useful in engines having compression ratios above 10:1.

Another factor of importance in internal combustion engines is that LPG leaves little or no engine deposit in the cylinders when it burns. Also, since it enters the engine as a vapor, it cannot wash down the cylinder walls, remove lubricant, and increase cylinder-wall, piston, and piston-ring wear. Nor does it cause crankcase dilution. All these factors reduce engine wear, increase engine life, and keep maintenance costs low. However, allowances must be made for the extra cost of LPG-handling equipment, including relatively heavy pressurized storage tanks, and special equipment to fill fuel tanks on the vehicles. *See* GAS TURBINE; INTERNAL COMBUSTION ENGINE; PETROLEUM PRODUCTS.

Mott Souders

Liquid

A state of matter intermediate between that of crystalline solids and gases. Macroscopically, liquids are distinguished from crystalline solids in their capacity to flow under the action of extremely small shear stresses and to conform to the shape of a confining vessel. Liquids differ from gases in possessing a free surface and in lacking the capacity to expand without limit. On the scale of molecular dimensions liquids lack the long-range order that characterizes the crystalline state, but nevertheless they possess a degree of structural regularity that extends over distances of a few molecular diameters. In this respect, liquids are wholly unlike gases, whose molecular organization is completely random.

Thermodynamic relations. The thermodynamic conditions under which a substance may exist indefinitely in the liquid state are described by its phase diagram, shown schematically in the **illustration**. The area designated by *L* depicts those pressures and temperatures for which the liquid state is energetically the lowest and therefore the stable state. The areas denoted by *S* and *V* similarly indicate those pressures and temperatures

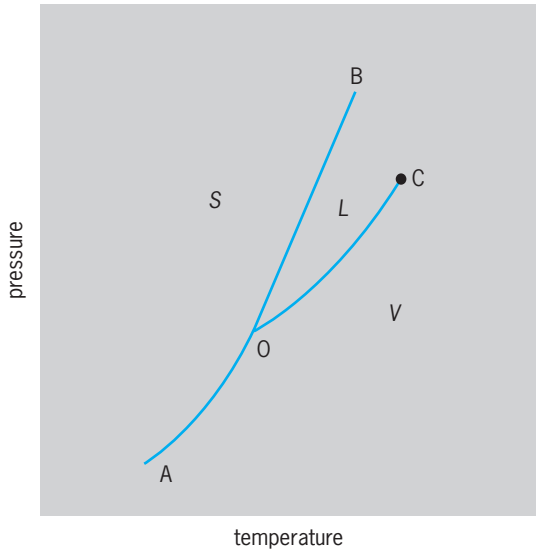

Phase diagram of a pure substance.

for which only the solid or vapor phase may exist. The connecting lines OC, OB, and OA define pressures and temperatures for which the liquid and its vapor, the solid and its liquid, and the solid and its vapor, respectively, may coexist in equilibrium. They are usually termed phase boundary or phase coexistence lines. The intersection of the three lines at O defines a triple point which, for the three states of matter under discussion, is the unique pressure and temperature at which they may coexist at equilibrium. Other triple points exist in the phase diagram of a substance that possesses two or more crystalline modifications, but the one depicted in the figure is the only triple point for the coexistence of the vapor, liquid, and solid. Line OA has its origin at the absolute zero of temperature and OB, the melting line, has no upper limit. The liquid-vapor pressure line OC is different from OB, however, in that it terminates at a precisely reproducible point C, called the critical point. Above the critical temperature no pressure, however large, will liquefy a gas. *See* TRIPLE POINT.

Along any of the coexistence curves the relationship between pressure and temperature is given by the Clausius-Clapeyron equation: $dP/dT = \Delta H/T\Delta V$, where ΔV is the difference in molar volume of the corresponding phases (gas-liquid, gas-solid, or liquid-solid) and ΔH is the molar heat of transition at the temperature in question. By means of this equation the change in the melting point of the solid or the boiling point of the liquid as a function of pressure may be calculated. When a liquid in equilibrium with its vapor is heated in a closed vessel, its vapor pressure and temperature increase along the line OC. ΔH and ΔV both decrease and become zero at the critical point, where all distinction between the two phases vanishes. *See* PHASE EQUILIBRIUM.

Transport properties. Liquids possess important transport properties, notably their capacity to transmit heat (thermal conductivity), to transfer momentum under shear stresses (viscosity), and to attain a state of homogeneous composition when mixed with other miscible liquids (diffusion). These nonequilibrium properties of liquids are well understood in macroscopic terms and are exploited in large-scale engineering and chemical-process operations. Thus, the rate of flow of heat across a layer of liquid is given by $\dot{Q} = \kappa\ dT/dx$, where $\dot{Q}$ is the heat flux, dT/dx is the thermal gradient, and κ is the coefficient of thermal conductivity. Similarly, the shearing of one liquid layer against another is resisted by a force equal to the momentum transfer: $F = \dot{P} = \eta\ dv/dx$, where dv/dx is the velocity gradient and η is the coefficient of viscosity. Likewise, the rate of transport of matter under nonconvective conditions is governed by the gradient of concentration of the diffusing species: $J = -D\ dC/dx$, where J is the matter flux and D is the coefficient of diffusion. Each of these transport coefficients depends upon temperature, pressure, and composition and may be determined experimentally. An a priori calculation of κ, η, and D is a very difficult problem, however, and only approximate theories exist.

Theoretical explanations. In fact, although a great deal of effort has been expended, there still exists no satisfactory theory of the liquid state. Even so commonplace a phenomenon as the melting of ice has no adequate theoretical explanation. The reason for this state of affairs lies in the tremendous structural and dynamical complexity of the liquid state. To understand this, it is useful to compare the structural and kinetic properties of liquids with those of crystalline solids on the one hand and with those of gases on the other.

In crystals, atoms or molecules occupy well-defined positions on a three-dimensional lattice, oscillating about them with small amplitudes; their kinetic energy is entirely distributed among these quantized vibrational states up to the melting point. This nearly perfect spatial order is revealed by diffraction techniques, which utilize the coherent scattering of x-rays or particles have wavelengths comparable with interatomic spacings. The structural and dynamical properties are sufficiently tractable mathematically so that the theory of solids is quite well understood.

The theory of gases is also simple, but for quite a different reason. No vestige of positional regularity of atoms remains in gases, and their energy resides entirely in high-speed translational motion. Except for collisions, which deflect their motions into new straight-line trajectories, atoms in gases do not interact with one another; vibrational modes in monatomic gases are absent.

Liquids, by contrast, lie intermediate between gases and crystals from both a structural and dynamic point of view. Kinetic energy is partitioned among translational and vibrational modes, and diffraction studies reveal a degree of short-range order that extends over several molecular diameters. Moreover, this "structure" is continually changing under the influence of vibrational and translational displacements of atoms. Physical reality may be attributed to this short-range structure, nevertheless, in the sense that a time average over the huge number of possible configurations of atoms may show that a fairly definite number of neighboring atoms lie close to any arbitrary atom. At a somewhat greater distance from this reference atom, the density of neighbors oscillates above and below the average density of atoms in the liquid as a whole.

Information about the degree of local order is contained in the radial distribution function, a mathematical property which may be deduced from diffraction measurements. This is the starting point for a theory of the liquid state, and although research efforts have yielded partial successes, prodigious mathematical difficulties lie in the path of an entirely satisfactory solution. *See* BOILING POINT; KINETIC THEORY OF MATTER; LIQUEFACTION OF GASES; MELTING POINT; VISCOSITY; X-RAY DIFFRACTION.

Norman H. Nachtrieb

Bibliography. J. P. Hansen and I. R. McDonald, *The Theory of Simple Liquids*, 2d ed., 1987, reprint 1990; P. Kruus, *Liquids and Solutions: Structure and Dynamics*, 1977; G. W. Rothschild, *Dynamics*

of Molecular Liquids, 1984; D. Tabor, *Gases, Liquids, and Solids: And Other States of Matter*, 3d ed., 1991.

Liquid chromatography

A method of chemical separation that involves passage of a liquid phase through a solid phase and relies on subtle chemical interactions to resolve complex mixtures into pure compounds. A small amount of the sample to be separated is injected onto the top of a column that is densely packed with spherical particles of small diameter, that is, the stationary phase. A liquid solvent, the mobile phase, flows through the column continuously to carry the sample from the top to the bottom of the column. During passage through the column, the components of the sample are transferred back and forth continuously between the two phases, and small thermodynamic differences in the chemical interactions of the various sample components with the mobile and stationary phases slow the passage of some solutes more than others and lead to their separation. The technique can be performed on very small scales for chemical analysis, dealing with micrograms or even nanograms of sample, or it can be performed on an industrial scale for purification of commercial products. The technique has great resolving power (see **illus.**).

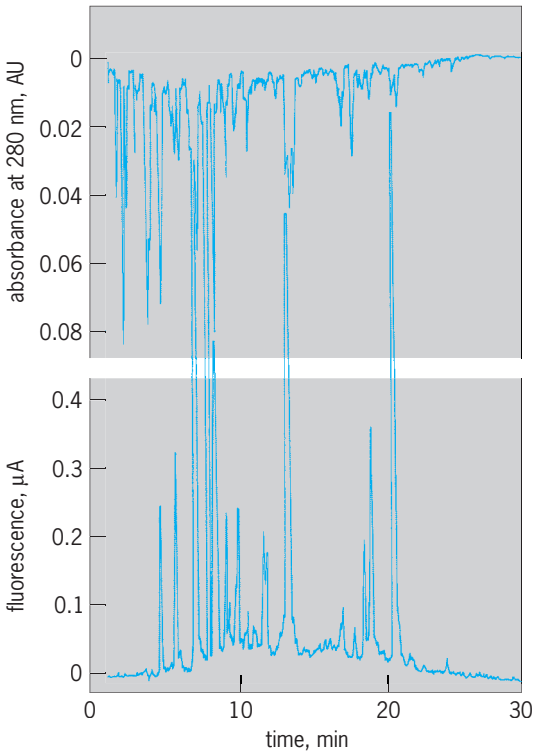

Chromatogram of a urine sample with added aromatic acids. Ten microliters of sample was separated on a 10-in. (25-cm) reversed-phase column using gradient elution. The separation was monitored with both fluorescence and absorbance detectors, and 119 compounds were separated in an analysis time of just under 30 min. (*After I. Molnar, C. Horvath, and P. Jatlow, Separation of urinary aromatic acids and measurement of vanilmandelic acid by high performance liquid chromatography, Chromatographia, 11:260–265, 1978*)

Liquid chromatography as practiced today differs only in detail from the technique as first described by its inventor, M. Tswett, a Russian botanist, in 1906. Many advances in instrumentation and understanding of the chemistry of the interactions involved have led to improvements in the separations, but the fundamental idea of the technique has not changed. This method of chemical analysis is widely used in the pharmaceutical, biomedical, biotechnology, chemical, oil, and polymer industries and to some extent in virtually every other chemical-based industry. *See* CHEMICAL SEPARATION TECHNIQUES.

Instrumentation. In the late 1960s, workers realized that to achieve maximum performance they needed to make the stationary-phase particles very small. As the stationary-phase particles became smaller, they packed too densely to permit gravity-driven flow of the mobile phase. It was necessary to force the mobile phase through the column under high pressure, and the technique was named high-pressure liquid chromatography (HPLC). The meaning of the acronym has been changed to high-performance liquid chromatography, for the elegant separations that are possible. Typical stationary-phase particles are monodisperse, macroporous silica particles either 3 or 5 micrometers in diameter, and the column lengths for analytical scale separations are on the order of 2–10 in. (5–25 cm), with inside diameters of about 0.16 in. (4 mm). The columns are made of stainless steel, which is relatively inert chemically and able to withstand the high pressures applied to the top of the column. Since these columns require pressures of a few hundred to a few thousand pounds per square inch, depending on the mobile-phase flow velocity desired, a high-pressure metering pump is an integral part of a modern liquid chromatograph. Most instruments include a means of performing gradient elution, that is, making a continuous change in the composition of the liquid mobile phase during the separation process. Gradient elution can be performed by using a separate pump for each solvent and changing the relative proportions during the separation, or by using a proportioning valve between the solvent reservoirs and the pump. An injector valve is used to introduce a small volume of sample, typically 5–100 microliters, onto the top of the column without interrupting the mobile-phase flow. These valves can be operated manually, or they can be programmed to perform injections from a tray of samples for routine analyses. After the sample traverses the column, a flow-through detector is employed to generate the chromatogram, which is the visual representation of the separation. Detectors can provide both quantitative and qualitative information about the separated components. Temperature control of the column and detector is important; they are generally operated at or near room temperature, and temperature fluctuations can adversely affect the reproducibility of the separation and detection steps.

Separation modes. Liquid chromatography very much depends on the highly selective chemical interactions that occur in both the mobile and stationary phases. Rapid separations have become possible for compounds whose difference in free energy of transfer between the two phases is only a few calories per mole. Columns exhibiting virtually every type of possible selectivity exist, including selectivity by shape, charge, size, and optical activity. Additional selectivity can be generated through manipulations of the mobile phase; additives that interact with the solute in the mobile phase can create unique selectivities in columns that do not normally show that type of selectivity.

Ion exchange. This is a popular mechanism for the separation of charged solutes. Ion-exchange chromatography involves the reversible exchange of ions between mobile and stationary phases. The stationary phase most often consists of beads of a polymer with charge-bearing functional groups, and the sample's ions compete with a mobile-phase ion for the ionic sites on the ion exchanger. This separation mode is frequently used in the electronics industry, for environmental analysis, and for the separation of proteins and biopolymers that have charged groups. *See* ION EXCHANGE.

Size exclusion. This type of chromatography involves separation based on the molecular size of the solutes. Exclusion columns contain porous stationary-phase materials, usually silica gel or a porous polymer, with different pore diameters. A solute injected onto such a column will diffuse into those pores that have a diameter greater than the effective diameter of the solute's molecules (under solvent conditions at that instant), and the effective diameters of the various solutes control elution order. The solute whose molecules have the largest effective diameter will elute first, since there are fewer pores that it can fit into. A smaller solute will diffuse into many more of the stationary-phase pores and will require a much larger volume of solvent to achieve elution. This separation mode is heavily used in the petrochemical and polymer industries for characterization of molecular weights and sizes of synthetic and natural polymers.

Bonded phases. In the early 1970s, technology was developed to chemically bond functional groups onto spherical silica particles, providing the efficient and highly reproducible stationary phases needed for liquid chromatography to gain acceptance as a routine method of chemical analysis. This bonding technology has the advantage of allowing researchers to tailor the surface chemistry of small-diameter silica particles to give virtually any desired interaction. There are reports of almost every conceivable functional group's being bonded to the surface, both alone and in mixtures to yield mixed interaction phases. *See* SURFACE AND INTERFACIAL CHEMISTRY.

Normal and reversed phase. Polar groups can be bonded to the surface of silica beads and used with nonpolar mobile phases for a separation mechanism known as normal-phase chromatography. The latter is best suited for separating polar compounds and geometrical isomers and for performing class separations. These separations are similar to those obtained on bare silica. The most popular mode of liquid chromatography is reversed-phase. Here a molecule with nonpolar functionality, typically a fully saturated 18-carbon hydrocarbon chain, is bonded to the silica surface, giving the stationary phase a highly nonpolar character. Aqueous-based mobile phases are used, and it is estimated that this mode of separation is used in 75% or more of analytical scale chromatography. The reversed-phase method has a number of advantages. The aqueous-based mobile phases provide good compatibility with many detection techniques and are also compatible with biological samples. The interactions of the solute with the stationary phase are weak. This provides rapid mass transfer and sharp chromatographic peaks, as well as rapid equilibrium with solvent changes, making the technique ideal for gradient elution methods. A very powerful advantage of aqueous-based mobile phases is the ability to control pH and other mobile-phase-based equilibria for additional separational selectivity. Weak acids and bases are retained very differently in their charged and uncharged forms, so pH control is a powerful means of modulating selectivity and of moving ionizable compounds relative to uncharged species. Complexation equilibria can also be advantageously used, such as with cyclodextrins for the separation of optical isomers.

One of the most popular types of chromatography that uses secondary equilibria is ion-pairing chromatography. This involves the addition of a hydrophobic counter-ion to the mobile phase, which is adsorbed onto the surface of the stationary phase and makes the reversed-phase stationary phase into a dynamic ion exchanger. Ion-pairing chromatography is popular because it allows the separation of charged and neutral species in the same sample. It is frequently used in pharmaceutical analysis.

Hydrophobic interaction. A variation on the reversed-phase mode is hydrophobic interaction chromatography. Nonpolar groups are bonded onto the silica surface at very low densities (number of groups per unit surface area). This technique is used mostly for protein separations, with mobile-phase conditions generally of a descending salt gradient. Retention is controlled by interactions between the hydrophobic ligands of the stationary phase and the hydrophobic entities of the protein. While interactions of small molecules are relatively well understood, the mechanism of protein separations is still largely unknown.

Affinity chromatography. This is the most highly selective chromatographic method. The technique closely mimics the types of binding processes found in nature, including antigen-antibody, enzyme-substrate, and hormone-receptor. Whereas most chromatographic methods are aimed at separating all solutes present in the sample, affinity chromatography attempts to retain only one solute on the column, while all undesired components are swept through. The mobile-phase conditions are then changed, and the desired analyte is eluted in a single peak. Affinity chromatography, really a form of digital chromatography, is useful for both analysis and purification of

biological materials. In affinity chromatography the solute is retained completely; the mobile phase is changed and the solute is instantly eluted. This is analogous to the "on" or "off" in digital electronics.

Other applications. In addition to facilitating chemical analysis, liquid chromatography can be used to obtain physicochemical information. Diffusion coefficients, kinetic parameters, critical micelle concentrations of surfactants, and other information have been estimated from chromatographic data. The most common application is the estimation of hydrophobic parameters, especially as models of biological or environmental partitioning processes (most frequently, of octanol-water partitioning). Bioavailability, bioaccumulation, soil sorption, and various other factors are estimated based on linear free-energy relationships. *See* CHROMATOGRAPHY.

John G. Dorsey

Bibliography. U. D. Neue, *HPLC Columns: Theory, Technology, and Practice*, 1997; P. C. Sadek, *The HPLC Solvent Guide*, 1996; L. R. Snyder, J. J. Kirkland, and J. L. Glajch, *Practical HPLC Method Development*, 2d ed., 1997.

Liquid crystals

A state of matter with an orientational order of building units—individual molecules or their aggregates—and complete or partial absence of the long-range positional order. Liquid crystals, discovered more than 100 years ago, are one of the best-studied classes of soft matter, along with colloids, polymer solutions and melts, gels, and foams.

The liquid-crystalline state, also known as the mesophase, is in between that of a regular solid having long-range positional order of atoms (or molecules which are also orientationally ordered in crystals) and an isotropic fluid in which the molecules show neither positional nor orientational order. Liquid crystals can flow, adopt the shape of a container, and form drops as regular isotropic fluids do; however, the molecules in the liquid-crystal sample are ordered. The direction of average orientation in liquid crystals is called the director **n**.

Molecular interactions responsible for the orientation order in liquid crystals are relatively weak, as most liquid crystals melt into the isotropic phase below 100–150°C (212–300°F). As a result, the structural organization of liquid crystals, most importantly the spatial configuration of the director and thus the optical properties, are very sensitive to the external factors such as electromagnetic field, shear deformations, and type of molecular orientation on bounding walls. This sensitivity allows for numerous applications of liquid crystals, including liquid-crystal displays (LCDs). In these devices, weak electric voltage pulses reorient the director and change the optical appearance of the liquid-crystal cell. *See* OPTICAL MATERIALS.

Classification. Depending on the way the liquid-crystalline state is produced, one distinguishes thermotropic and lyotropic liquid crystals.

Thermotropic (solvent-free) liquid crystals form either by heating a solid crystal or by cooling an isotropic fluid. They exist in a certain temperature range for the materials made of strongly anisometric (elongated or disklike) molecules. An individual substance forming a thermotropic liquid crystal does not require any solvent to exhibit the mesophase. In practical applications, a number of liquid-crystal materials are often mixed together to improve their functional properties (such as their useful temperature range) or doped with additives that are not necessarily mesomorphic (such as dyes, chiral molecules, and polymer inclusions).

Lyotropic liquid crystals form only in the presence of a solvent, such as water or oil. Most commonly, lyotropic mesophases are formed by solutions of amphiphilic molecules (such as soaps, phospholipids, and surfactants). Amphiphilic molecules have two distinct parts: a hydrophilic (polar) head and a hydrophobic (nonpolar) tail, which is generally an aliphatic chain. As a result, amphiphilic molecules in solvents give rise to "self-organization," as manifested by the formation of micelles and bilayers. Mesomorphic states (between liquid and solid) may also form in solutions of certain polymers; polymers may also form thermotropic liquid crystals. *See* MICELLE.

Phases. There are four basic types of liquid-crystalline phases, classified according to the dimensionality of the positional order of building units: nematic (only orientational order and no positional order), smectic (orientational and 1D positional order, caused by a periodic variation of the molecular densities), columnar (orientational and 2D positional order), and various 3D-correlated structures (such as cubic phases and blue phases).

Upon heating, many thermotropic substances, such as octylcyanobiphenyl (8CB) [**Fig. 1**], yield the following phase sequence: solid crystal > smectic (or columnar phase) > nematic > isotropic fluid. On cooling, the sequence is generally reversed, although it often includes phases that are absent during heating.

Nematics. There are three different variations of the nematic phase: uniaxial nematic (UN), biaxial nematic (BN), and cholesteric (Ch). The UN is formed by the molecules of a rodlike or disklike shape that can easily rotate around one of the axes. The average orientation of these axes of rotation coincides with the director **n** (**Fig. 2***a*). Even when the molecules are polar, as the 8CB molecules are, their

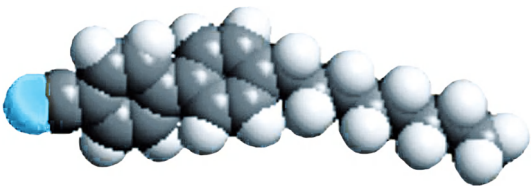

Fig. 1. A rodlike molecule of octylcyanobiphenyl (8CB), where the phases formed with increasing temperature are solid crystal > smectic A (24°C) > nematic (34°C) > isotropic fluid (42.6°C).

head-to-head overlapping and flip-flops establish centrosymmetric arrangement in the nematic bulk. The UN is an optically anisotropic medium; the optic axis coincides with the director (Fig. 2*a*). The speed of light propagation in the nematic medium depends on how the polarization of light is directed with respect to the optic axis, giving rise to the phenomenon of birefringence. *See* BIREFRINGENCE.

In BN, the shape of building units significantly deviates from axially symmetric and can be more appropriately described as boxlike. These materials exhibit the orientational order of all three axes and have three directors (Fig. 2*b*).

When the building unit (molecule or aggregate) is not equal to its mirror image (chiral), the director **n** might show a twisted structure. Most often, the twist is unidirectional and the director forms a helicoid by rotating around a single axis in space, which is the case of the Ch phase (Fig. 2*c*). The UN, BN, Ch, and blue phases are liquid phases (no correlations in molecular positions over large distances). However, Ch shows a periodic structure associated with the spatial twist of molecular orientation (Fig. 2*c*). The pitch (period) of this twist is much larger than the molecular size, as molecular interactions responsible for the twist are weak as compared to the interactions responsible for the mesomorphic state itself. With a typical molecular size of a liquid crystal being 1–10 nanometers, the pitch is often in the range of 0.1–1 micrometer, which overlaps with the range of the visible part of optical spectrum.

Smectics. Smectics are layered phases with a quasi-long-range 1D translational order of centers of molecules in a direction normal to the layers. This positional order is not exactly the long-range order as in a regular 3D crystal. As shown by L. D. Landau and R. E. Peierls, the fluctuative displacements of layers in 1D lattice diverge with the linear size of the sample. However, for typical smectic materials with a period of the order of 1 nm, the effect is noticeable only on scales of 1 mm and larger; it is thus not noticeable in samples that are normally 1–100 μm thick. In smectic A (SmA), the molecules within the layers show fluidlike arrangement, with no long-range in-plane positional order; it is a uniaxial medium with the optic axis and the director perpendicular to the layers (Fig. 2*d*).

In the lyotropic version of SmA, the lamellar L_α phase, the amphiphilic molecules arrange into bilayers. If the solvent is water, the exterior surfaces of the bilayer are formed by polar heads; the hydrophobic tails are hidden in the middle of the bilayer. (The membranes of many biological cells are organized in the similar way.) The periodic structure of alternating surfactant and water layers gives rise to the L_α phase (Fig. 2*e*). The lamellar structure may retain its smectic order, even when strongly diluted, as it is stabilized by thermal fluctuations of bilayers.

Other types of smectics show in-plane order, caused, for example, by a collective tilt of the rodlike molecules with respect to the normals to the layers (the so-called SmC) [Fig. 2*f*]. In chiral materials, the tilt of the molecules might lead to the helicoidal structure. The resulting chiral SmC phase is of considerable interest for applications in fast-switching optical devices (Fig. 2*g*).

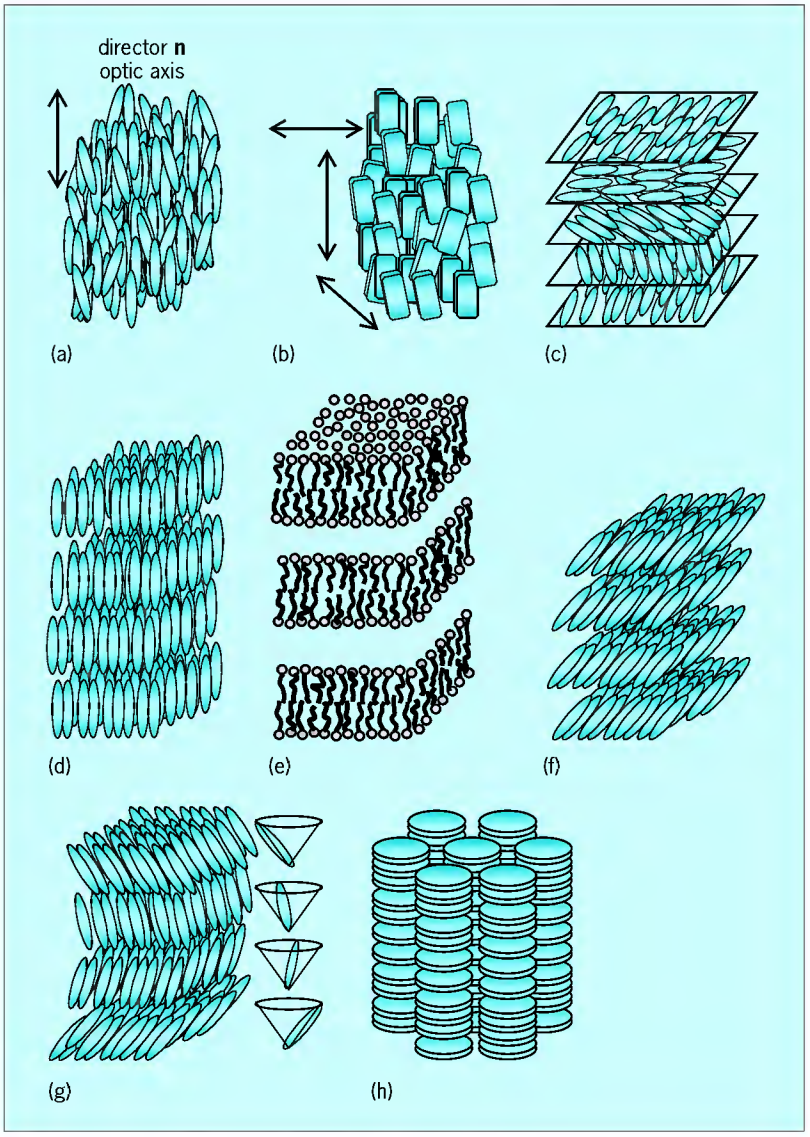

Fig. 2. Liquid-crystalline phases. (*a*) Uniaxial nematic; the molecular long axes are on average aligned along the director n which is also the optic axis. (*b*) Biaxial nematic; three molecular axes are on average aligned along three directors. (*c*) Cholesteric: the local nematic director rotates in space forming a helicoid. (*d*) Smectic A type of ordering in the thermotropic liquid crystal; the molecular axes are perpendicular to the plane of layers. (*e*) Smectic A type of ordering in the lyotropic L_α phase formed by equidistant arrangement of amphiphilic bilayers in water. (*f*) Smectic C; the molecular axes within the layers are tilted. (*g*) Chiral smectic C; the molecular axes are tilted and the direction of tilt forms a helicoid. (*h*) Columnar liquid crystal.

Columnar. Columnar phases are most frequently formed by hexagonal packing of cylindrical aggregates, as in the case of thermotropic materials formed by disklike molecules. The positional order is 2D only, as the intermolecular distances along the axes of the aggregates are not regular (Fig. 2*h*).

3D-correlated structures. These demonstrate a periodic structure along all three coordinates, but they are still different from the 3D crystals, as the periodicity is associated with repetition of the local director patterns rather than with a regular positional order of the molecular centers of mass. The molecules are

free to move around, adjusting to the local director orientation. For example, in cubic lyotropic phases the 3D network is formed by periodically curved layers of amphiphilic molecules. Another example is the blue phases that occur in the narrow temperature range between the isotropic fluid phase and Ch phase, in which the director forms double-twisted structures. The double twist cannot expand through the entire volume of the material and must be accompanied by a 3D periodic lattice of defects.

Order parameter. The director specifies only the direction of average orientation, not the degree of orientational order. For the latter, one can chose the temperature-dependent quantity $s(T) = \frac{1}{2}\langle 3\cos^2\theta - 1\rangle$, where θ is the angle between the axis of an individual molecule and the director, and $\langle \ldots \rangle$ means an average over molecular orientations. The term s is often called the scalar order parameter, where $s = 1$ corresponds to an ideal order with all the molecules rigidly aligned along one direction and $s = 0$ corresponds to absence of orientational order (in which case one deals with regular isotropic fluids).

The order parameter of the liquid crystal can be related to the anisotropy of macroscopic properties such as diamagnetic or dielectric susceptibility. Measuring these anisotropies allows one to determine the degree of orientational order. The magnetic measurements are especially convenient compared with their electric counterparts, as in this case the local field acting on the molecules differs very little from the external field. In uniaxial nematics (UNs), the values of the magnetic susceptibility measured in the direction parallel to the director and perpendicular to it are different. This difference $\chi_a = \chi_\parallel - \chi_\perp$ is called the anisotropy of the magnetic susceptibility. In most thermotropic UNs, $\chi_\parallel < 0$ and $\chi_\perp < 0$ (diamagnetism), and $\chi_a > 0$, so that the director orients along the applied magnetic field. In the isotropic phase, $\chi_a = 0$. For practical applications of UNs, of prime importance is the anisotropy of two other properties: the anisotropy of dielectric permittivity $\varepsilon_a = \varepsilon_\parallel - \varepsilon_\perp$ and optical birefringence—that is, the difference in the refractive indices for light polarized parallel to the director (the extraordinary index of refraction $n_e = n_\parallel$) and for light polarized perpendicularly to the director (the ordinary index of refraction $n_o = n_\perp$), i.e., $\Delta n = n_e - n_o$. When $\varepsilon_a > 0$, the director reorients along the applied electric field; and when $\varepsilon_a < 0$, the director realigns perpendicularly to the field. Because the director is simultaneously the optical axis, and because of the nonzero birefringence, $\Delta n \neq 0$, these field-induced reorientations change the optical properties of the sample, such as the effective value of the refractive index. The latter effect is at the core of numerous devices that use the dielectric response of the UN to display information or to control optical properties of the liquid crystal cell. *See* ELECTRIC SUSCEPTIBILITY; MAGNETIC SUSCEPTIBILITY; REFRACTION OF WAVES.

Elasticity and the free energy of the nematic phase. The molecular orientation in a liquid-crystal sample might change from point to point because of the external fields, boundary conditions, presence of foreign particles, and so on. The order parameter becomes spatially nonuniform. In most problems of practical interest, the typical scale of distortions is much larger than the molecular scale. The deformations are thus weak in the sense that the scalar part of the order parameter, $s(T)$, remains constant despite the spatial gradients of the director $\mathbf{n}(\mathbf{r})$.

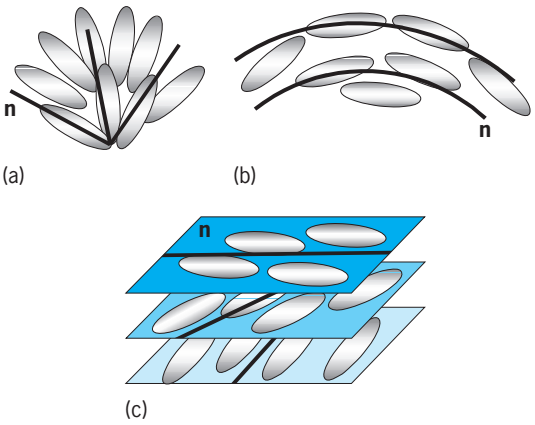

Fig. 3. Basic types of director distortions in the bulk of the uniaxial nematic: (*a*) splay, (*b*) bend, and (*c*) twist.

There are three basic types of director distortions in uniaxial nematics, called splay, twist, and bend (**Fig. 3**). The free-energy density associated with these three types of (small) deformation is written in terms of the spatial director gradients

$$n_{i,j} = \frac{\partial n_j}{\partial x_j}$$

as Eq. (1) and is known as the Frank-Oseen energy

$$f_{\mathrm{FO}} = \frac{1}{2}K_1(\mathrm{div}\,\mathbf{n})^2 + \frac{1}{2}K_2(\mathbf{n}\cdot\mathrm{curl}\,\mathbf{n})^2 + \frac{1}{2}K_3(\mathbf{n}\times\mathrm{curl}\,\mathbf{n})^2 \quad (1)$$

density, with Frank elastic constants of splay (K_1), twist (K_2), and bend (K_3); all three are necessarily positive-definite and the dimensionality is that of a force. The elastic constants can be estimated as the typical energy of molecular interactions responsible for the orientational order divided by the characteristic length, which is the molecular size

$$K \sim U/l \sim k_B T/l \sim 4\times 10^{-21}\mathrm{J}/10^{-9} \sim 4\ \mathrm{pN}$$

which is a very good estimate for many thermotropic uniaxial nematic materials, as the experimental values are between 1 and 10 piconewtons (pN). The energy density [Eq. (1)] is often supplemented with the so-called divergence terms that can influence the equilibrium director through boundary conditions at the surface. In the presence of an external field, the free-energy density acquires additional terms; for example, a diamagnetic term $f_{\mathrm{field}} = -\frac{1}{2}\mu_0^{-1}\chi_a(\mathbf{B}\cdot\mathbf{n})^2$ in the magnetic field $\mathbf{B}$; here $\mu_0 = 4\pi\times 10^{-7}$ henry/m is the magnetic permeability of free space.

Another important contribution to the free energy is related to the phenomenon of director anchoring at the bounding surfaces. Any actual liquid-crystal cell is confined, say, by a pair of parallel glass plates.

The molecular interactions between the liquid crystal and the boundary substrates are anisotropic. This anisotropy establishes one (sometimes more) preferred orientation of $\mathbf{n}$ at the boundary, the "easy axis." The phenomenon is called surface anchoring. Orienting action of the substrates usually keeps the director uniform if the external field is absent. To change this orientation, one needs to perform some work.

The equilibrium of a uniaxial nematic sample of a given shape in an external field is determined by the minimum of the functrional, Eq. (2),

$$F = \int_v (f_{\mathrm{FO}} + f_{\mathrm{field}})dV + \int_S F_{\mathrm{anch}}dS \qquad (2)$$

where f_{anch} is the surface-anchoring energy density, often represented by the simple potential $f_{\mathrm{anch}} = \frac{1}{2}W_a\alpha^2$, with W_a being the surface-anchoring coefficient and α the angle between the easy axis and the actual director orientation at the surface.

Elasticity of the smectic A phase. For the smectic A (SmA) phase, the elastic free-energy density, Eq. (3),

$$f = \tfrac{1}{2}K_1(\mathrm{div}\,\mathbf{n})^2 + \tfrac{1}{2}B\gamma^2 \qquad (3)$$

is different from Eq. (1) because of certain restrictions that the layered structure imposes onto the director distortions and the elastic cost of changes in the thickness of the layers. Here B is the Young modulus (layers compressibility modulus) and $\gamma = (d - d_0)/d_0$, the relative difference between the equilibrium period d_0 and the actual layer thickness measured along the director $\mathbf{n}$. The ratio of K_1 to B defines an important length scale, Eq. (4),

$$\gamma = \sqrt{K_1/B} \qquad (4)$$

called the penetration length γ, and is of the order of the layer separation but diverges when the system approaches the SmA-nematic transition. One expects that a SmA would have K_1 of the same order as in a nematic phase stable at higher temperatures. With $\lambda \approx d_0 \approx (1-3)$ nm, one finds $B \sim 10^6 \div 10^7$ N/m^2, a value that is 10^3 to 10^4 times smaller than the compressibility modulus in a solid.

Dynamics. Liquid crystals are fluids. They can flow while preserving the orientational order. Flow imposes an orientational torque on $\mathbf{n}$. Most often, $\mathbf{n}$ tends to realign along the direction of flow. There is also a reverse effect by which director distortions can cause the flow. This "backflow" effect is of importance in liquid-crystal displays. In the approximation of a constant scalar order parameter, the hydrodynamics of liquid crystals is described in terms of seven variables: (1) mass density, (2) three components of the velocity field, (3) energy density, and (4) two components of the director field $\mathbf{n}(\mathbf{r},t)$. In contrast to an isotropic fluid, the stress tensor depends not only on the gradients of the velocity but also on the director components. The uniaxial nematic phase should be characterized by five different viscosity constants. The number of viscosities reduces to three when the director distortions are

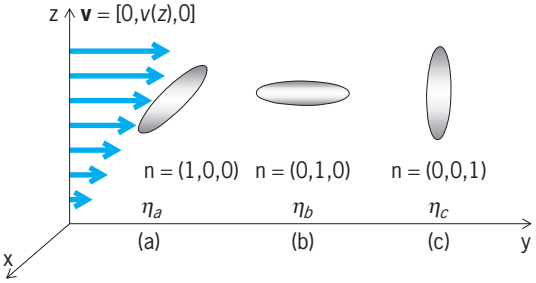

Fig. 4. Miezowicz geometries for effective viscosities of the uniaxial nematic.

small. These three can be chosen as the effective viscosities for three idealized geometries of flow, also known as Miezowicz geometries, in which one assumes that the director is fixed (for example, by a strong magnetic field): (a) When $\mathbf{n} = (1,0,0)$ is perpendicular to both the flow direction and the velocity gradient, the UN behaves as an isotropic fluid with a viscosity η_a; however, director fluctuations coupled with the certain values of the viscosity coefficients might destabilize the initial orientation. (b) When $\mathbf{n}$ is parallel to the flow or (c) when $\mathbf{n}$ is parallel to the velocity gradient (**Fig. 4**), the corresponding viscosities η_b and η_c are generally different from η_a and from each other; $\eta_b < \eta_a < \eta_c$ for a typical uniaxial nematic material composed of rodlike molecules; the result $\eta_b < \eta_c$ can be explained by assuming that the friction correlates with the cross section of the molecules seen by the flow.

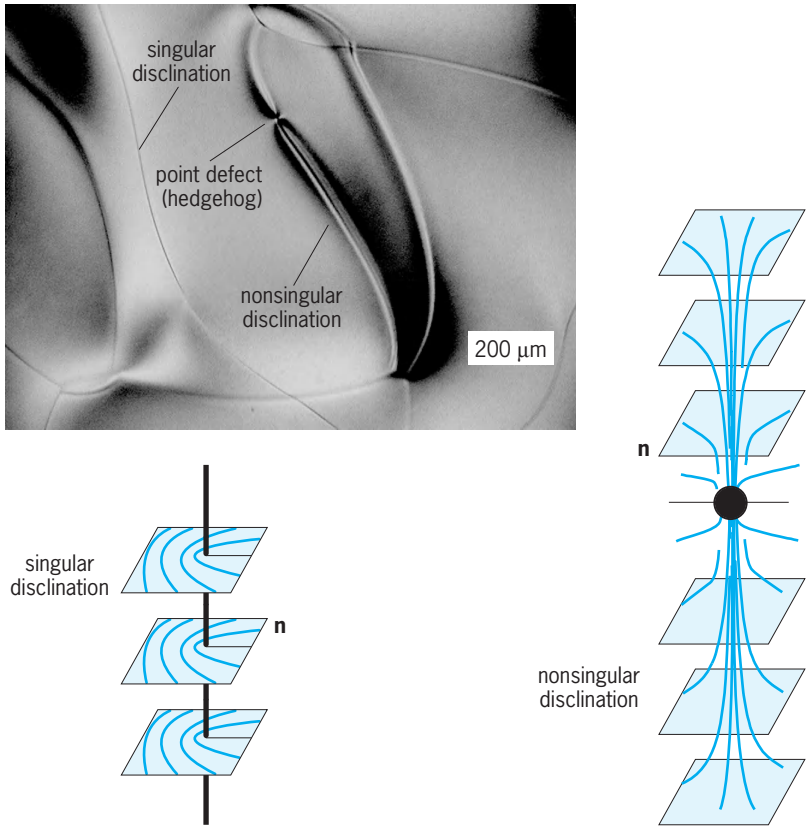

Fig. 5. Thin singular disclinations and thick nonsingular threads in the nematic [*n*-pentylcyanobiphenyl (5CB)] bulk, as observed under the microscope with crossed polarizers, and the corresponding director configurations.

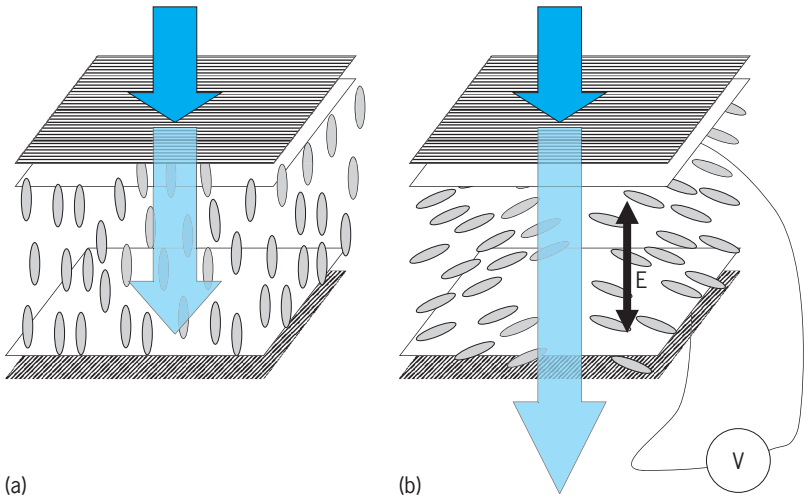

Fig. 6. Electrically controlled uniaxial nematic cell between a pair of crossed linear polarizers that either (*a*) blocks the transmitted light field off state or (*b*) allows the light to pass through the field on state.

Topological defects. When a thick (100-μm) nematic sample with no special aligning layers is viewed with a microscope, one usually observes a number of mobile flexible lines, called disclinations. The disclinations are seen as thin and thick threads (**Fig. 5**). Thin threads strongly scatter light and show up as sharp lines. These are truly topologically stable defect lines, along which the nematic symmetry of rotation is broken. The disclinations are topologically stable in the sense that no continuous deformation can transform them into a state with the uniform director field, $\mathbf{n}(\mathbf{r}) = \text{const}$. Thin disclinations are singular in the sense that the director is not defined along the line. Thick threads are line defects only in appearance; they are not singular disclinations. The director is smoothly curved and well defined everywhere, except for a number of point defects in the nematic bulk, called hedgehogs.

Applications of liquid crystals. The possibility to orient the director by an applied electric field leads to numerous practical applications. In a flat cell, the orienting action of the homogeneously treated substrate usually keeps the director uniform if the external field is absent. However, if the liquid crystal is dielectrically anisotropic, a sufficiently high electric field can overcome both the anchoring effect and the elasticity of the nematic bulk and reorient the director, either parallel ($\varepsilon_a > 0$) to the field or perpendicular to it ($\varepsilon_a < 0$). This is the Frederiks effect, first discovered for the magnetic case. When the field is removed, the surface anchoring and bulk elasticity restore the original director structure. Thus, one can use the electric field and surface anchoring to switch the elastic liquid crystal back and forth.

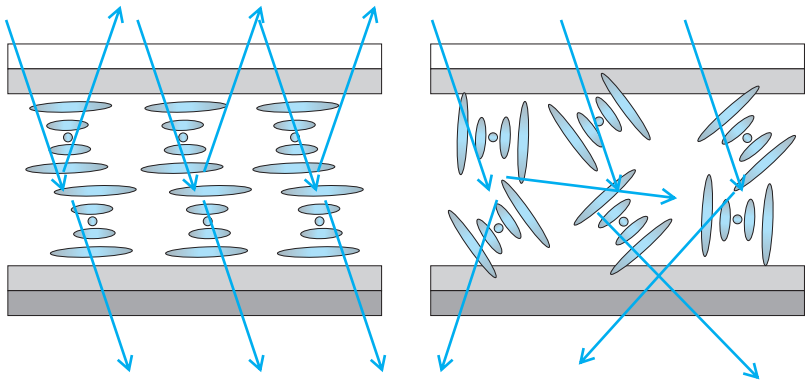

Fig. 7. Ch bistable display based on electrically controlled light scattering.

Various implementations of the Frederiks effect in uniaxial nematic (UN) and cholesteric (Ch) are widely used in electrooptic devices, including displays. The liquid crystal is usually sandwiched between two transparent electroconductive plates (for example, glass covered with indium tin oxide) coated with a suitable alignment layer, most often chosen from the polyimide family. The voltage across the cell controls the director configuration and thus the optical properties of the cell. In one of the most recent and commercially successful embodiments, the initial field-free state is the one in which $\mathbf{n}$ is perpendicular to the bounding plates with electrodes (**Fig. 6**). The cell is sandwiched between two crossed light-polarizing films. The light beam becomes linearly polarized after passing the first polarizer. This state of polarization is not changed by the liquid crystal, and the light beam is thus blocked by the second polarizer. The UN material is of a negative dielectric anisotropy, $\varepsilon_a < 0$. When the electric field is applied across the cell, the director deviates from the vertical axis. In this "field-on" state, because of the finite birefringence, the cell allows the light beam to pass through the second polarizer. The direction of director tilt in the plane of the UN cell can be controlled by using specially patterned electrodes; thus the mode is known as the patterned vertical alignment (PVA) mode. The field can also be applied in the plane of the sample, comprising a layer of a UN with $\varepsilon_a > 0$, thus forming the in-plane switching (IPS) mode. Finally, the polarization of light can be controlled by using the so-called twisted nematic (TN) cell, in which the electric field switched the twisted (chiral) nematic structure into a vertically aligned director configuration, thus altering the appearance of the UN cell between two polarizers, either crossed or parallel. To create a full-color display using the PVA, IPS, or TN techniques, one adds a pixelized color filter with red, blue, and green pixels to the glass plate facing the viewer. The panel that controls the voltage across the liquid crystal also is pixelized, so that the intensity of light transmitted by each pixel and the corresponding color filter is controlled independently of other pixels. The most advanced scheme of electric-addressing the liquid crystal display is the active matrix scheme, based on the array of thin-film transistors (TFTs). The operating voltage needed in liquid-crystal displays is relatively low, usually between 1 and 10 V. *See* ELECTRONIC DISPLAY; ELECTROOPTICS; FLAT-PANEL DISPLAY DEVICE.

The flexibility of molecular architectures of liquid crystals allows many other types of applications, including the information displays based on the effects of light scattering rather than the changes in

polarization state. Historically, one of the first liquid-crystal devices was the cholesteric thermometer that changed colors as the function of temperature. In Ch, the helicoidal pitch is often in the range of 0.1–1 μm (the molecular interactions responsible for the chiral structure are relatively weak, thus the pitch is much larger than the size of an individual molecule). The well-aligned periodic director structure is thus capable of selective reflection in the visible part of the spectrum, which brings a "colored" appearance to the sample viewed in the white light. The spectral range of this selective reflection is related to the value of the cholesteric pitch and can be changed by changing the pitch. Ch materials with electrically controlled orientation of the helicoids axis are used in bistable light-reflective liquid-crystals displays (**Fig. 7**). The Ch is switched by the electric voltage pulses between a well-aligned (planar) light-reflecting state and a disoriented light-scattering state with numerous defects of the director configuration. By adding a black absorbing layer to the bottom of the Ch film, one creates a bistable Ch display with a bright colored appearance in the planar state and black appearance in the distorted state. The field is needed only to switch the Ch sample from one state to another, which greatly reduces energy consumption. Although only the planar state is truly stable, the distorted state is relatively stable, as its relaxation into the planar state is hindered by a large energy barriers associated with the helix distortions. As the display works in the light-reflective mode, it does not need a special illuminating panel beneath the liquid-crystal layer, as most other liquid crystals displays do. The Ch reflective displays are used in "electronic books" and in development of flexible displays in which the traditional glass panels are replaced with plastic films.

Some applications use composite materials in which the liquid crystal is a component. Polymer-dispersed liquid crystals are one example. By dispersing the UN droplets in a polymer matrix (through a phase separation process), one can create an effective light-scattering medium, provided the effective index of the liquid-crystal droplet is different from the refractive index of the polymer. By applying the electric field, the droplets and the director inside them reorient along the field. If the materials are selected in such a way that the ordinary index of refraction of the UN matches the refractive index of the polymer, the composite film becomes transparent. The composite film thus represents an electrically switchable light-scattering panel and can be used in large-area (square meters) "privacy windows."

Oleg D. Lavrentovich

Bibliography. L. M. Blinov and V. G. Chigrinov, *Electrooptic Effects in Liquid Crystal Materials*, Springer, 1996; S. Chandrasekhar, *Liquid Crystals*, Cambridge University Press, 1992; P. G. de Gennes and J. Prost, *The Physics of Liquid Crystals*, Oxford Science, 1993; M. Kleman and O. D. Lavrentovich, *Soft Matter Physics: An Introduction*, Springer, 2003; R. G. Larsen, *The Structure and Rheology of Complex Fluids*, Oxford University Press, 1999; E. Lueder, *Liquid Crystal Displays: Addressing Schemes and Electro-optical Effects*, Wiley, 2001; S. T. Wu and D. K. Yang, *Reflective Liquid Crystal Displays*, Wiley, 2001.

Liquid helium

Helium boils at a substantially lower temperature, 4.2 K (−452°F or −269°C), than any other substance; and below 2.172 K (−455.76°F) the liquid exhibits the extraordinary properties of superfluidity, notably the ability to flow through narrow channels with complete absence of friction. In addition to the common isotope of atomic weight 4, helium has a rare isotope of atomic weight 3 with a normal boiling point of 3.2 K (−454°F) and a superfluid transition at a very much lower temperature near 0.001 K. Both forms of helium remain in a liquid state at absolute zero. All of these characteristics are due to the weakness of the attractive force between two helium atoms and to the small atomic mass, which according to the laws of quantum mechanics makes the atoms difficult to localize.

At 4.2 K (−452°F) liquid ^{4}He is colorless and of low refractive index ($n = 1.024$), with a density of 0.125 g/cm^3 (0.125 times that of water). The latent heat of vaporization, 5 cal/g (21 J/g), is very small, and so care must be taken to reduce the heat input by conduction and radiation into the storage container. The classical container consists of two vacuum-insulated vessels of silvered glass (Dewar flask) or metal, with the inner vessel containing the liquid helium immersed in a larger outer vessel filled with liquid nitrogen. Modern superinsulated Dewars are able to dispense with the liquid nitrogen.

The phase diagram of ^{4}He (**Fig. 1**) shows several remarkable characteristics. Helium remains a liquid down to absolute zero unless a pressure greater than 2.53 megapascals (25.0 atm or 367 lb/in.^{2}) is applied. A more subtle feature is a transition between two different liquid phases. This λ-transition is so named

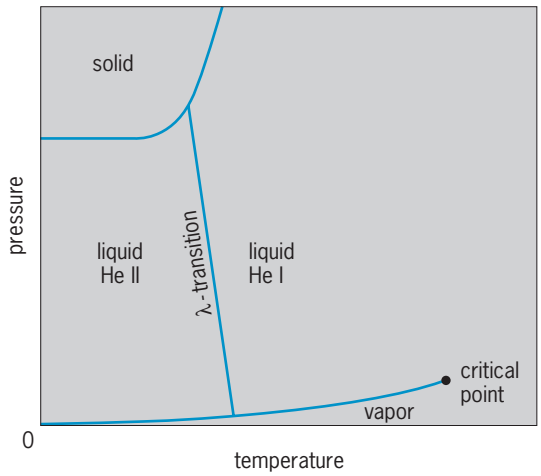

Fig. 1. Phase diagram for ^{4}He. The critical point is at $T_c = 5.20$ K (−450.3°F), $P_c = 229$ kPa (2.26 atm or 33.2 lb/in.^{2}).

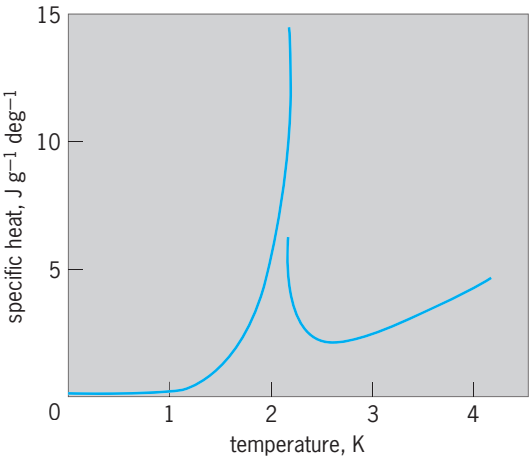

Fig. 2. Specific heat of liquid helium at saturated vapor pressure as a function of temperature °F = (K × 1.8) − 459.67. (*After K. Atkins, Liquid Helium, Cambridge University Press, 1959*)

because the specific heat (**Fig. 2**) has a singularity resembling the Greek letter lambda. There is no latent heat; such a transition is called second-order. The high-temperature liquid phase, called helium I, is a rather ordinary liquid. The λ-transition at 2.172 K or −455.76°F (at vapor pressure) marks the onset of superfluidity, which is the characteristic property of the low-temperature phase, helium II.

Liquid Helium II

When liquid helium is cooled by pumping, it boils vigorously until the λ-temperature is reached at a vapor pressure of 5.0 kilopascals (0.05 atm or 0.7 lb/in.^{2}). The λ-transition is manifest by a sudden cessation of bubbling, and the liquid becomes completely quiescent. Helium II has an enormous effective thermal conductivity, hundreds of times larger than that of the best metallic conductors. This explains the absence of bubbling, as evaporation need occur only at the surface; but it raises the problem of discovering the heat transport mechanism.

Superfluidity. Helium II flows thousands of times faster than He I at low pressure, and behaves as though turbulent. Thus, He II should be considered a superfluid state analogous to the superconducting state which appears in certain metals at low temperatures. *See* SUPERFLUIDITY.

When currents of helium are made to circulate around annular containers packed with fine powder or other porous material (provided that the initial speed of the helium is not too great), the helium continues to circulate for hours with no measurable loss of angular momentum. From these measurements an upper limit can be placed of the order of 10^{-19} cgs unit (1 cgs unit = 0.1 Pa · s) on the viscosity of the circulating superfluid at low speeds (about 10^{-15} that of air). *See* VISCOSITY.

However, a paradox exists because a different type of viscosity measurement, based on the drag torque on a cylinder rotating in the liquid, shows that the viscosity of He II is only about three times smaller than that of He I.

Thermomechanical effect. If two vessels partially filled with He II are connected by narrow channels and heat is supplied to one vessel, helium will flow into the warmer vessel and cause the level to rise against gravity. There is a converse mechanocaloric effect: if He II is forced by pressure through narrow channels, such as a porous plug, the upstream liquid becomes warmer and the downstream liquid becomes colder.

Ions in liquid helium. Electrons or positive ions injected into liquid helium form rather large complexes. An electron, which interacts repulsively with helium atoms, reduces its zero point energy by forming a cavity or bubble of 1.7-nm radius, within which it is confined. Thus the negative ion bubble displaces about 480 helium atoms. A He^+ ion attracts neutral helium atoms to form a "snowball" with an effective radius of 0.6 nm and an effective mass of about 44 helium atoms.

Critical velocities. Superfluid flow is frictionless only if the velocity is not too large. Above some "critical" velocity a pressure drop (or more precisely, a chemical potential difference) appears along the flow channel. The magnitude of the critical velocity may be less than 0.04 in./s (1 mm/s) in a wide channel (near 1-mm diameter) or as large as 70 ft/s (21 m/s) in a very short, narrow channel at very low temperatures. The value may depend on temperature; on approaching the λ-temperature the critical velocity decreases to zero. *See* CRITICAL PHENOMENA.

Film flow. Liquid helium was long thought to wet all solid surfaces, because a helium atom is more strongly attracted to other substances, which have molecules that are more polarizable than helium atoms. Consequently the surface of any solid in contact with liquid helium or its saturated vapor is covered, in thermodynamic equilibrium, by a helium film a few tens of nanometers thick. What is unique in the case of He II is that the film, like the bulk liquid, is superfluid and can flow as fast as about 1 ft/s (30 cm/s) without friction. It has been found that helium does not wet metallic cesium, and a cesium layer can interrupt superfluid film flow.

Thinner helium films are formed on solid surfaces exposed to helium vapor at less than the saturated vapor pressure. As the film becomes thinner, the onset of superfluidity is depressed progressively farther below the λ-temperature of the bulk liquid. Superfluid flow has been observed in films as thin as two atomic layers, at temperatures well below 1 K (−458°F). *See* PHASE TRANSITIONS.

Liquid Helium-3

The stable isotope ^{3}He occurs naturally as about 1 part per million (ppm) of atmospheric helium and 0.1 ppm of well helium. Commercial ^{3}He is obtained from beta decay of tritium.

Liquid ^{3}He-^{4}He mixtures. The addition of ^{3}He to liquid ^{4}He depresses the λ-transition to lower temperatures (**Fig. 3**). Below 0.87 K (−458.1°F) the

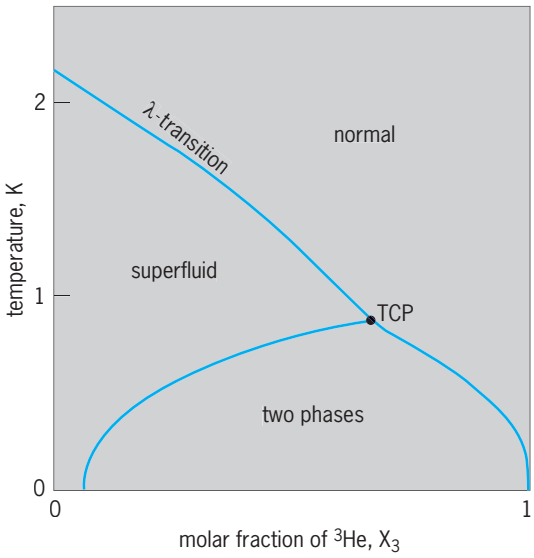

Fig. 3. Phase diagram for ^{3}He-^{4}He mixtures at saturated vapor pressure in the temperature-^{3}He concentration plane. The tricritical point (TCP) is at $X_3 = 0.67$, $T = 0.87$ K (−458.1°F). °F = (K × 1.8) − 459.67.

homogeneous solution is unstable and separates into a nonsuperfluid ^{3}He-rich phase floating on top of a superfluid ^{4}He-rich phase. In the superfluid phase, ^{3}He acts as part of the normal fluid.

Usually when a two-component system exhibits a liquid-liquid phase separation, the top of the phase-separation curve is rounded and the highest point is a critical point. By contrast in the helium isotope case, the two branches of the phase-separation curve meet in an angular contact with the λ-line. The junction, called a tricritical point, marks the change of the second-order λ-transition into a first-order phase-separation transition. Singularities in various thermodynamic functions at the tricritical point (in addition to those associated with the λ-line) have drawn considerable theoretical interest.

As the temperature is lowered toward absolute zero, the ^{3}He-rich phase rapidly becomes pure ^{3}He, but ^{3}He remains soluble up to a concentration of about 6% in the ^{4}He-rich phase. An insignificant number of phonons and rotons remain in the ^{4}He at temperatures well below 0.5 K (−458.8°F), and it is essentially in its ground state. This pure superfluid ^{4}He acts as an inert background for a gaslike solute of ^{3}He atoms, except that it increases the effective mass of the ^{3}He atoms and weakens the ^{3}He-^{3}He interaction. This has a very important practical consequence: It is possible to "evaporate" ^{3}He into superfluid ^{4}He with absorption of latent heat far below the temperature at which the true vapor pressure of ^{3}He becomes insignificant. Helium-3 dilution refrigerators based on this principle can attain temperatures less than 3 mK in continuous, recirculating operation.

Pure liquid helium-3. Liquid ^{3}He solidifies at absolute zero only at a pressure of 3.4 MPa (34 atm or 500 lb/in.^{2}). There is no λ-transition, because the exclusion principle prevents condensation of particles with half-integer spin such as ^{3}He atoms into a macroscopic quantum state, as occurs in superfluid ^{4}He. Instead, below about 0.5 K (−458.8°F) the liquid gradually becomes "degenerate" in the same sense as the electrons in a normal metal are degenerate. That is, a ^{3}He atom with each of the two allowed nuclear spin directions occupies each of the lowest momentum quantum states. Practically all the quantum states with energies up to the so-called Fermi level are occupied, and practically all above this energy are empty. The system is described in terms of the coordinates of weakly interacting quasiparticles, each moving in the mean field of the rest of the system. This Fermi liquid theory works well below about 100 mK. The mean field for nuclear spin interaction is such that the liquid is nearly ferromagnetic.

One consequence of the Fermi degeneracy is that the liquid has lower entropy than the solid, in which the nuclear spins are randomly oriented down to about 1 mK, where nuclear antiferromagnetic ordering occurs. In accord with the Clausius-Clapeyron equation of thermodynamics, the melting curve then has negative slope. This has an application known as Pomeranchuk cooling: if liquid ^{3}He at the solidification pressure in the region of negative slope is further compressed adiabatically, it begins to solidify, and this is accompanied by cooling. The amount of cooling can be very substantial if the initial temperature is sufficiently low. *See* FERMI-DIRAC STATISTICS; FREE-ELECTRON THEORY OF METALS; VAPOR PRESSURE.

Superfluid ^{3}He. The BCS theory explains how superconductivity occurs in certain metals, by a mechanism of electron pairing. Electrons of opposite spin and momentum become bound in pairs, of zero net spin, which condense into a macroscopic quantum state responsible for superconductivity. It became apparent that a similar pairing mechanism might result in a superfluid transition in liquid ^{3}He, which was studied at progressively lower temperatures, using an ^{3}He-dilution refrigerator and an additional cooling stage involving either Pomeranchuk cooling or adiabatic demagnetization. *See* ADIABATIC DEMAGNETIZATION; SUPERCONDUCTIVITY.

Sound propagation. Like ^{4}He-II, the superfluid phases of ^{3}He support first, second, third, and fourth sound waves. In the low-temperature limit, there are no collisions between the particles and the first sound mode is highly damped. However, a new mode called zero arises in the normal Fermi liquid because of the strong effective interactions between the ^{3}He quasiparticles. This mode is present in the superfluid phases also and, through its coupling to other excitations in the superfluid, demonstrates the triplet nature of the Cooper pairs in many dramatic ways.

Bellave S. Shivaram

Bibliography. K. H. Benneman and J. B. Ketterson (eds.), *The Physics of Solid and Liquid Helium*, 2 vols., 1976, 1978; K. Mendelssohn, *The Quest for Absolute Zero*, 2d ed., 1977; D. R. Tilley and J. Tilley, *Superfluidity and Superconductivity*, 3d ed., 1990; G. E. Volovik, *Exotic Properties of Superfluid Helium Three*, 1992; J. C. Wheatley, Helium three, *Phys. Today*, 29(2):32–42, 1976; J. Wilks and D. S. Betts, *An Introduction to Liquid Helium*, 2d ed., 1987.

Lissajous figures

Plane curves traced by a point which executes two independent harmonic motions in perpendicular direction, the frequencies of the motion being in the ratio of two integers. Such figures, produced on the screen of a cathode-ray tube, are widely used in frequency and phase measurements. *See* HARMONIC MOTION.

Methods of constructing. Mechanical, optical, and electronic methods may be used to construct Lissajous figures. Blackburn's pendulum consists of one ordinary pendulum hung from another with the two axes of rotation at right angles. The Lissajous figure is traced by the bob. An example of an optical method is afforded by a beam of light reflected successively from two small mirrors, each mounted on the prong of a separate tuning fork; the forks vibrate in perpendicular directions, and the image of the light source, focused on a screen, traces out the figure.

The cathode-ray oscilloscope furnishes the most important and practical means for the generation of the figures. The x-deflection plates of the tube are supplied with one alternating voltage, and the y-deflection plates with another. If the frequencies are incommensurable, the figure is not a closed curve and, except for very low frequencies, will appear as a patch of light because of the persistence of the screen. On the other hand, if the frequencies are commensurable, the figure is closed and strictly periodic; it is a true Lissajous figure, stationary on the screen and, if the persistence is sufficient, visible continuously as a complete pattern. *See* OSCILLOSCOPE.

Frequency measurements. Measurement of frequency in sinusoidal wave motion (for example, in alternating electric current) may be accomplished with an oscilloscope if one of the alternating voltages is derived from a variable-frequency calibrated oscillator. The standard is adjusted until a stationary figure results; if f_v is the frequency of the signal on the vertical deflection plates, and f_h that on the horizontal plates, then f_v/f_h equals the number of times a side of the figure is tangent to a vertical line divided by the number of times the top or bottom is tangent to a horizontal line. The shape of the figure depends also on the relative phase of the signals (**Fig. 1**), and in the case where one-half of the figure coincides with the other, the rule just stated does not hold. This situation is not troublesome in practice because unavoidable slow-frequency drifts of the signals prevent the figure from being exactly stationary; instead, the shape of the figure changes as though the relative phase of the signals were slowly changing.

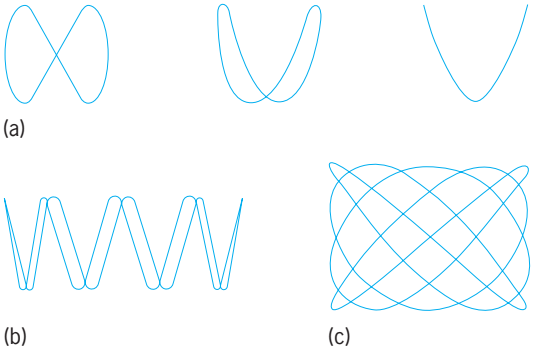

Fig. 1. Typical Lissajous figures for ratios of vertical frequency to horizontal frequency. (*a*) 2:1, with various phase relations. (*b*) 8:1. (*c*) 5:4. (*After F. E. Terman, Radio Engineers' Handbook, McGraw-Hill, 1943*)

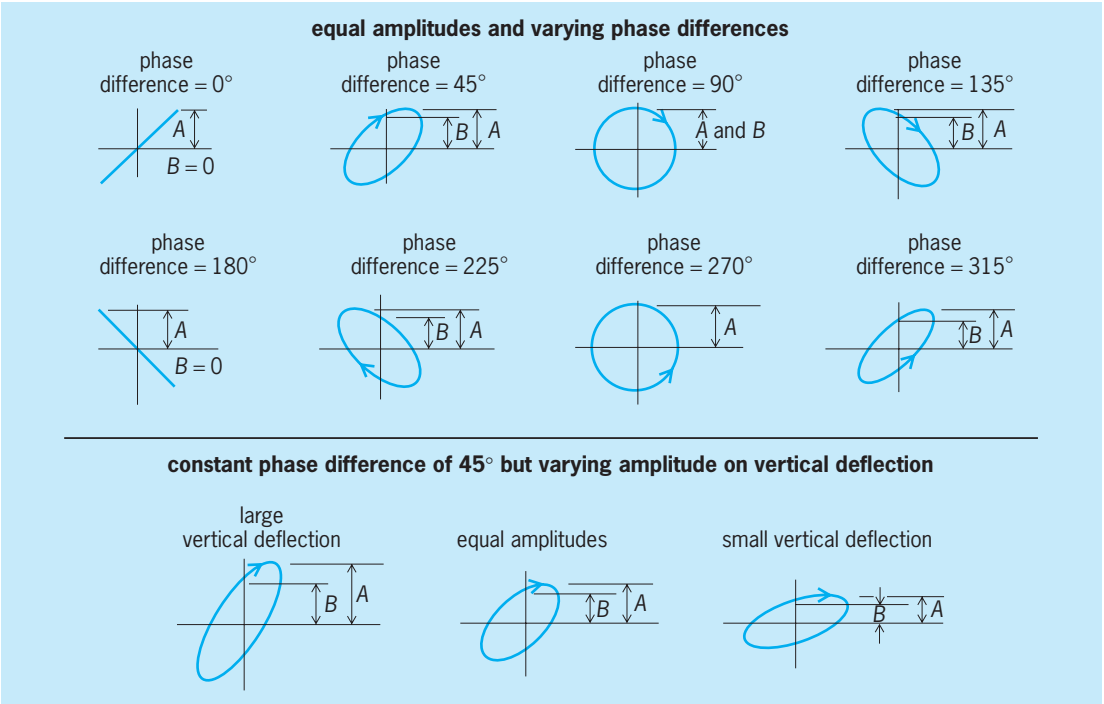

Fig. 2. Typical Lissajous figures of 1:1 frequency ratio. (*After F. E. Terman, Radio Engineers' Handbook, McGraw-Hill, 1943*)

In some cases, the standard is of fixed frequency and the unknown is nearly equal to the standard (or to some multiple or submultiple thereof). The figure will drift slowly through the various aspects it can assume for the nominal ratio involved. The actual ratio can be obtained from the nominal ratio, and a correction determined by the rate and direction of drift of the figure. This method is particularly valuable for the intercomparison of standards.

Phase measurements. These usually involve two signals of the same frequency. In this case, the Lissajous figure is an ellipse of which the shape and orientation depend on the relative phase and relative amplitudes of the signals, as shown in **Fig. 2**. The relative phase θ is given by the equation below,

$$\sin\theta = \pm\frac{B}{A}$$

in which A is the maximum half-height and B is the intercept on the y axis. Figure 2 shows how the quadrant in which θ lies is determined by the orientation of the major axis of the ellipse and the direction of motion of the spot. If the latter is unknown, the resulting ambiguity amounts to that in the sign of $\sin\theta$, once it is decided which signal is the reference. The ambiguity can be resolved by shifting the phase of either signal in a known direction and noting whether the phase shift indicated by the figure increases or decreases.

The most precise comparison can be made when the ellipse degenerates into a straight line. This condition is therefore used as a null in measurements made with a calibrated phase shifter. The unknown phase shift disturbs the null, and the calibrated phase shifter restores it.

More complicated figures are employed in the calibration of phase shifters. A signal at the desired frequency is connected through the phase shifter to the y plates of an oscilloscope and also through a frequency multiplier to the x plates. If the frequency multiplication is 8, for example, the Lissajous figure will appear as in Fig. 1*b*. The phase shifter is then successively set to the various positions for which one-half of the figure coincides with the other; these positions will correspond to phase differences of, in this case, $\pi/8$. *See* PHASE-ANGLE MEASUREMENT.

Martin Greenspan

Bibliography. A. D. Helfrick and W. D. Cooper, *Modern Electronic Instrumentation and Measurement Techniques*, 1990; J. D. Lenk, *Handbook of Oscilloscopes*, 1982; Lord Rayleigh, *Theory of Sound*, vol. 1, reprint 1945.

Lissamphibia

The subclass of Amphibia including all living amphibians (frogs, toads, salamanders, and apodans). The other two subclasses are the Labyrinthodontia and the Lepospondyli, predominantly Paleozoic fossil groups lacking recent representatives. *See* LABYRINTHODONTIA; LEPOSPONDYLI.

Morphology. Living amphibians are grouped together by possession of a unique series of characters, the most important of which are (1) pedicellate teeth; (2) an operculum-plectrum complex of the middle ear; (3) the papillar amphibiorum, a special sensory area of the inner ear; (4) green rods in the retina of the eye; (5) similar skin glands; and (6) a highly vascular skin used in respiration (cutaneous respiration). Only the first two characters can be used to separate the Lissamphibia from the other two subclasses, because the other characters are soft anatomy features not ordinarily preservable as fossils. *See* EAR (VERTEBRATE); EYE (VERTEBRATE); RESPIRATION.

Dentition. The pedicellate condition of the lissamphibian tooth is formed by a separation of the tooth into two segments, a crown and a pedicel (**Fig. 1**). The pedicel is usually fused to the jaw, but crown and pedicel are separated by uncalcified or fibrous material, which in effect functions as a hinge in the tooth. In at least some lissamphibians the tooth bends inward more easily than outward. This indicates that it may be an adaptation for allowing prey to enter the mouth easily, but tends to prevent its escape. Some teleost fishes also have such a hinged tooth that bends inward toward the throat and is relatively rigid when bent back; however, there the hinge is between tooth and jaw, without an intervening pedicel, and is not comparable with the

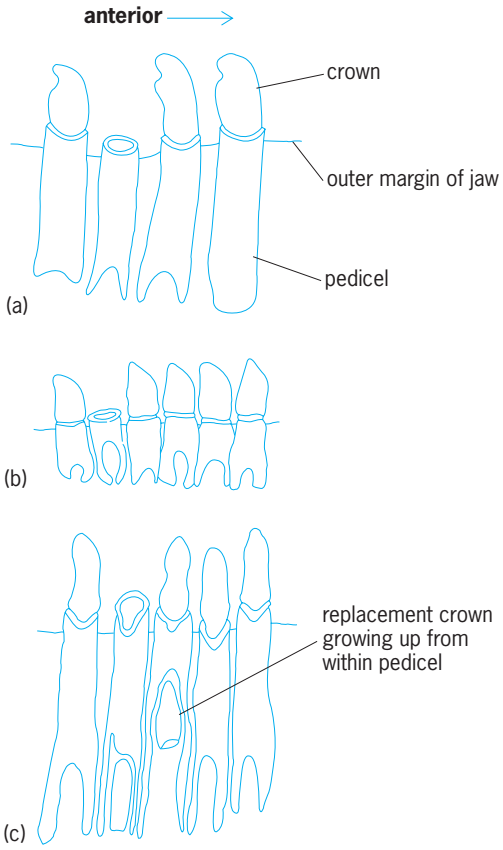

Fig. 1. Pedicellate teeth in Lissamphibia. (*a*) Salamander. (*b*) Apodan. (*c*) Frog. Teeth are from the lower jaw and are viewed from inside the mouth. (*After T. Parsons and E. Williams, J. Morphol., 110:375–390, 1962*)

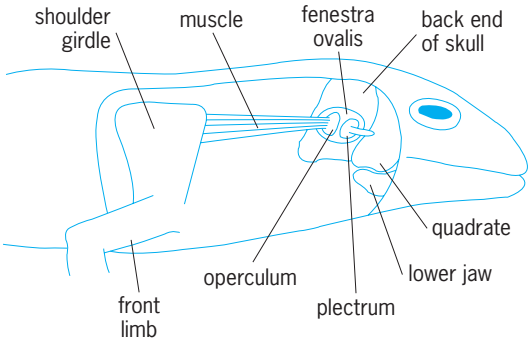

Fig. 2. Operculum-plectrum complex of a primitive salamander (skin removed to show internal structures).

lissamphibian condition except perhaps in function. *See* TOOTH.

Sound perception. The operculum-plectrum complex of the middle ear is an unusual feature unknown in other tetrapods. In the characteristic tetrapod condition a single sound-transmitting bone, the stapes, fills the opening (fenestra ovalis) of the middle ear and connects to the inner ear. In lissamphibians two structures occur in the fenestra ovalis: plectrum (stapes) and operculum (**Fig. 2**). The plectrum has the usual tetrapod connections to tympanic membrane or to quadrate. The operculum is connected to the shoulder girdle by a specialized shoulder muscle that may provide passage to the ear for vibrations traveling through the front limb from the substrate. Thus the animal may receive both airborne and ground-borne sounds.

Phylogeny and fossil record. Apodans lack a fossil record; frogs and salamanders go back to the Jurassic. There is a Triassic fossil from Madagascar that may be near the ancestry of frogs, but it does not indicate the group of origin. Except for this Triassic fossil, the ancient amphibians and the lissamphibians do not overlap in their geological ranges. On the basis of vertebral similarities (solid, spool-shaped centrum), lissamphibians have often been thought to be lepospondyl descendants, but in the skull (especially the palate) there are similarities to temnospondyl labyrinthodonts.

Pedicellate teeth and the operculum-plectrum complex are characters that form the best evidence for close relationship of modern amphibians to each other. Pedicellate teeth and the possible presence of an operculum have been found in one family of primitive rhachitome labyrinthodonts. These two occurrences may indicate that lissamphibians are derived from the latter group, although new fossil finds are necessary to clarify lissamphibian ancestry. *See* AMPHIBIA; ANURA; APODA; URODELA.

Richard Estes

Bibliography. E. Jarvik, *Basic Structure and Evolution of the Vertebrates*, 2 vols., 1981; T. Monath, The opercular apparatus of salamanders, *J. Morphol.*, 116:149–170, 1965; T. Parsons and E. Williams, The relationships of the modern Amphibia, *Quart. Rev. Biol.*, 38:26–53, 1963; A. Romer, *Vertebrate Paleontology*, 3d ed., 1966.

Listeriosis

An infectious disease of humans and animals caused by the bacteria *Listeria monocytogenes* and *L. ivanovii*. Both humans and animals can be carriers, which excrete the bacterium in feces. Sheep, goats, and cattle can excrete the bacteria in milk, without clinical symptoms of mastitis. The most important pathway of infection is probably through food. *Listeria monocytogenes* has frequently been isolated from grass silage (fermented fodder), especially from silage of inferior quality, which is an important source of infection in ruminants. Relatively few animals develop clinical disease, but a high proportion can be latent carriers. Farm leys often are fertilized with manure, and the bacteria in infected manure may be distributed on plants and in soil. During forage harvesting, soil and dung may be brought into the silo together with the grass, thus introducing the bacteria into the silage. *Listeria monocytogenes* is able to multiply in silage with a high pH, which probably is the main source of infection in ruminants.

Humans most likely ingest the bacteria with contaminated food, such as meat and meat products, raw milk and milk products, and unwashed vegetables. *See* FOOD MICROBIOLOGY.

Virulence and pathogenesis. Virulence depends upon attachment of the bacterium to a tissue cell, entrance into and multiplication in the cell, resistance to host defense, and damage to host mechanisms. Cells of *L. monocytogenes* are hydrophobic, which can be an attachment factor. They produce phospholipases which can disrupt cell surfaces, and catalase and superoxide dismutase to inactivate lethal enzymes in the macrophages. They also produce a hemolysin which disrupts the phagolysosomal membrane and releases the bacterium into the cytoplasm, where it can grow and multiply.

The *L. monocytogenes* organism usually enters the body by way of the alimentary route. The number of bacteria is substantially reduced after passing through the gastric acid, but bacteria that reach the intestine may attach to a portion of the epithelium. They rapidly infect the lymphoid tissue and may extend to other internal organs.

In ruminants, another mechanism seems more important. The bacteria pass the buccal mucosa and reach one or several of the brain nerves. They proceed to the brain through an intracellular route, and during this process they are shielded from the host's defense mechanisms. After about 2 weeks, they reach the brainstem and cause lesions within a fairly local area, with damage of neurons.

Clinical symptoms. Encephalitis is the most common form of disease in ruminants, and septicemia with involvement of several organs, including the pregnant uterus, occurs most commonly in monogastric animals, including very young sheep, goats, and calves.

Symptoms of encephalitis are dullness, and facial paralysis with dropping ear and lowered eyelid on the affected side. The head is often tilted to one side,

with slight paralysis of the tongue and loss of ability to salivate or swallow. The animal may walk in circles, become recumbent after a while and, if not recovering, pass into coma and die. About 40% of sheep and goats will recover if treated with antibiotics. The prognosis is better for cattle.

In cases of septicemia the animal looks depressed, with reduced appetite, high fever, and often diarrhea. Pregnant animals may abort, especially in the last trimester. They usually respond well to treatment with antibiotics.

Most human cases are sporadic, but food-borne epidemics occur. Abortions, perinatal disease, and disease in immunosuppressed individuals are most common. Perinatal disease is dominated by septicemia, widespread microscopic abscesses, and meningitis. In adults, meningitis is by far the most common manifestation, but in immunosuppressed individuals encephalitis occurs, possibly with a pathogenesis similar to encephalitis in ruminants.

Immunity. Cell-mediated immunity is the main defense against *L. monocytogenes*, and activated macrophages are the main effector cells. Neutrophils play an important part in defense before cell-mediated immunity has been developed. They destroy infected nonphagocytic cells in various organs, leaving the bacteria open for inactivation by other defense mechanisms. Immunity can be strengthened by use of a vaccine that is available for sheep in several countries. *See* IMMUNITY.

Diagnosis. Clinical diagnosis is based on symptoms, on isolation of *L. monocytogenes*, and on histopathological examination of affected tissue, especially brain tissue. Food samples are examined for the bacteria. The bacteria can be further identified in biochemical tests, by sero- and phagetyping, and by techniques such as gene probes, deoxyribonucleic acid (DNA) fingerprinting, isoenzyme typing, and ribosomal ribonucleic acid (rRNA) typing. *See* MEDICAL BACTERIOLOGY.

Hallstein Gronstol

Bibliography. J. M. Farber and P. I. Peterkin, *Listeria monocytogenes*: A food-borne pathogen, *Microbiol. Rev.*, 55:476–511, 1991; A. L. Miller, J. L. Smith, and G. A. Somkuti (eds.), *Foodborne Listeriosis*, 1990.

Literature of science and technology

The accumulated body of scientific-technical writings published to serve the informational needs of, primarily, scientists, engineers, and research workers, and, to the extent that it can be understood, the general public. This vast literature is worldwide in origin, international in language, diverse in subject content, varied in form, uneven in quality, and expensive. An ever-increasing portion of it is being produced, stored, and retrieved or published electronically, and is being made available on film, tape, CD-ROM or magnetic disk, or through remote terminals as well as in print-on-paper format. *See* COMPACT DISK; COMPUTER STORAGE TECHNOLOGY.

The primary sources of scientific-technical information are the first (and often the only) published records of original research and development, and accounts of new applications of science and engineering to technology and industry. These unorganized and usually not closely related contributions appear almost exclusively in periodicals, topical compilations such as Festschriften, and independently published proceedings of conferences, separate research reports or monographs, patents, standards, dissertations, or manufacturers' literature.

Organized works and compilations that derive from or refer to the primary-source literature make up the secondary sources of scientific-technical information: the handbooks, encyclopedias, treatises, bibliographies, reviews, abstracting and indexing serials, machine-readable bibliographic databases and databanks, other reference works, and, of course, all translations.

Guides to the literature, directories (of persons, organizations or products, for example), and textbooks are often looked upon as tertiary sources. Popularizations, biographies, histories, and similar relatively nontechnical publications are thought of as being about science rather than of science.

Primary Sources

These are the records of original research, patents, standards, and manufacturers' literature.

Periodicals. These publications traditionally make up the bulk of the primary-source literature of science and technology. Periodicals include journals, bulletins, transactions, proceedings, or other serial publications that appear regularly and continuously in numbered sequence, but not newspapers or annuals. More than 20,000 scientific and technical periodicals are published worldwide.

At least 150 countries regularly publish research journals in science-technology, and these may appear in many different languages. The growth of English as the major language of science has not displaced the considerable body of material in other languages, but the importance of language varies from subject to subject, and the importance of subject varies from country to country.

Current issues of some periodicals are available on black-and-white or colored microfiche as well as in print-on-paper format, and complete volumes of many periodicals are available on microfilm for space-saving storage. Some periodicals are available online in electronic form, although most have printed counterparts. Many authors are still reluctant to publish in nonprint formats alone, but electronic peer-reviewed journals with graphics and searchable text are an alternative. *See* PHOTOCOPYING PROCESSES; PRINTING.

The contents of periodicals vary considerably in the kind of material included as well as in the technical level. Professional, scientific, and technical societies, for example, tend to emphasize basic research and the more technical aspects to a subject, while industrial and trade associations lean toward the practical, personal, and popular side. Societies, too, almost uniformly make use of highly qualified subject experts, called referees, to evaluate critically all

original contributions before they are published, thus imparting reliability, authoritativeness, and prestige to their publications. Other organizations, such as research institutes, university experiment stations, and government agencies, publish periodicals comparable with those published by the societies, but such organizations are more likely to emphasize their own work. There are, of course, noteworthy exceptions.

Conference papers. Papers presented at national and international scientific conferences, symposia, colloquia, seminars, and other technical meetings often are important contributions to the primary-source literature of science and technology but are also often uneven and elusive. At widely varying intervals following their presentation they may be published as complete (or partial) collections by the convening bodies themselves, by the parent scientific societies, or by private publishers; they may appear as articles in, or supplements to, regular journals; or they may only be noted or at most abstracted. Audiotapes are sometimes available as supplements to, or substitutes for, printed proceedings. Sometimes papers are preprinted and not later published at all, thus being made available only to those who attend the meetings or who write for them in time. Announcements of forthcoming scientific meetings as well as of resulting technical publications are now published regularly. *World Meetings*, for example, is a 2-year registry of such meetings, and *Index to Scientific and Technical Proceedings* is one of several indexes to the resulting publications.

Research monographs. These are separately published reports on original research that are too long, too specialized, or otherwise unsuitable for publication in one of the standard journals. Each monograph is self-contained, frequently summarizes existing theory or practice before presenting the author's original and previously unpublished work, and is likely to be one of a series in the same field. Research monographs are also being published on microfiche with paper copies available on demand, a practice which may escalate as costs of print-on-paper publishing continue to rise.

Research reports. Reports from research and development projects make up another important part of the primary-source literature of science and technology. Reports are a more primitive form of literature because they are produced earlier in the research program, often as progress reports. While a progress report is only a temporary reference, it is important because it may include negative results and incidental data which may be missing from a final report.

Research reports originate in all research organizations doing work under contract to the United States government and are in turn distributed to all installations (including designated depository libraries) that have an interest in them. Classified reports, those containing data having some bearing on national security, are distributed only to properly cleared individuals or organizations. Since distribution of even the unclassified reports is somewhat limited, few of them are indexed, abstracted, or even listed by the standard services which cover other parts of the primary literature.

The National Technical Information Service (NTIS) of the U.S. Department of Commerce (Springfield, Virginia) is the agency responsible for the announcement, sales, and distribution of unclassified research, development, and engineering reports, translations, and other analyses prepared by United States and foreign government agencies, by their contractors or grantees, or by special technology groups, including many information analysis centers. NTIS also is the source for federally generated machine-processable data files and software. Since 1981, it has had the additional responsibility of operating an indexing service covering ongoing federally sponsored research projects, a service previously provided by the Smithsonian Science Information Exchange (SSIE). Established in 1970, NTIS superseded the Clearinghouse for Federal Scientific and Technical Information.

Summaries of unclassified government research reports and of available translations of foreign research reports are published in the comprehensive biweekly *Government Reports Announcements & Index (GRA&I)* and in the 27 *NTIS Alerts*, each covering a different subject area. Copies of the full reports are available from NTIS in paper copy or microform, and the NTIS database can be searched online through major vendors. Other more specific current awareness services are also available.

While the *GRA&I* and the 27 *NTIS Alerts* cover most government unclassified research reports, several government agencies also publish their own more specialized announcements and abstracts. Examples include *Scientific and Technical Aerospace Reports (STAR)*, published by the National Aeronautics and Space Administration (NASA), and *Energy Research Abstracts (ERA)*, published by the U.S. Department of Energy.

Preprints. Preprints are research-in-progress reports to the small but often international group of fellow scientists working in the same relatively narrow research specialty, somewhat after the fashion of seventeenth-century "invisible colleges." Like government research reports, the preprint is a primitive form of technical literature, unrefereed and unannounced but historical. In the past, preprints were far more elusive than conference papers since only those on particular "preprint circuits" knew of their existence, even though they may have been cited as references (for example, "in preparation"). However, now that many scientists are conferring with each other via computer conferencing and electronic mail, paper preprints are becoming obsolete except for possible record purposes. Preprint databases are being developed with abstracts distributed via electronic mail to announce the availability of new titles and the full text available for downloading via a computer network. To scientists on the research frontiers, paper preprints or preprint electronic reports are vital (and quite conventional); to others they may be stimulating or perhaps just interesting. Yet even mere identification of specific areas of ongoing research can help research and

development managers and policy makers to avoid unwarranted duplication of research effort and expense as well as to suggest other areas where research could be more profitable. *See* ELECTRONIC MAIL.

Patents. Patents are considered part of the primary-source literature, since an invention must be new in order to be patented and more often than not there will be no other published description either of the idea or of its application. Patents are sources of information about new products, processes, plants, microorganisms, and chemical compositions. Announcement publications, abstracts journals, and the individual patents are available from the various national patent offices and in selected depository libraries, but extensive patent searches require knowledge of both the subject field and patent law, as well as much time. There are more than 130 patenting authorities in the world. *See* PATENT.

Standards. Often a standard is a pamphlet describing acceptable levels of dimension, quality, performance, or other attributes of materials, products, or processes. Standards are established by general agreement among representatives of concerned groups, such as manufacturers and consumers, and may be issued by companies, trade associations, technical societies, government agencies, and national or international organizations. Technical societies also often issue statements of recommended practice as followed by competent practitioners.

Dissertations. Doctoral dissertations and master's theses are reports of original research. Although the research may later be reported in one or more periodical articles, dissertations and theses may still be consulted for their comprehensive literature reviews and for details not included in subsequent publications.

Festschriften. Compilations of scholarly papers memorializing a distinguished scientist, scientific society, or important scientific event often contain accounts or results of original research, the significance of which may well be comparable with that of the person, society, or event being commemorated. Each paper usually is related to some aspect of the subject's work or professional interests.

Manufacturers' literature. These publications are often the only source of specific information about particular products or their development; if the information is not published elsewhere, this source becomes a primary source. Technical service bulletins, data sheets, price lists, catalogs, and other specialized publications describing a manufacturer's equipment or processes are typical examples.

Secondary Sources

Reference works, which make up the bulk of the secondary literature, are of three types:

1. Those which in effect index selected portions of the primary literature and which thus aid in finding what has been published on a given subject (and where) generally or specifically, recently or retrospectively; for example, indexes themselves, bibliographies, indexing serials, and under certain conditions, abstracting serials, all of which, if computer-compiled, may become machine-readable bibliographic databases.

2. Those which survey selected portions of the primary literature and which thus aid in acquiring state-of-the-art, recent background, or comprehensive and definitive information on a given subject; for example, reviews, treatises, monographs, and again under certain conditions, abstracting serials.

3. Those which themselves contain the desired information (but rather concisely presented), such as established facts, formulas, procedures, equations, meanings, theories, history, and biography. All this information is compiled selectively from the primary literature and arranged in some definite manner for convenience in finding; for example, dictionaries, encyclopedias, handbooks, and compilations of tables. An increasing amount of the statistical, numerical, and structural data found in these works is also available from machine-readable data banks.

4. Technical translations are another important (and expensive) part of the secondary literature of science and technology. For all practical purposes these take on the characteristics of the particular primary-, secondary-, or tertiary-source literature that was translated, and they are often treated as if they were in fact the original publications. Translations, of course, are not new to science and technology, but since 1957 a crash program to disseminate scientific-technical information has encouraged many more government, society, academic, and private organizations throughout the world to produce English translations of works published originally in Russian, Chinese, Japanese, and other languages; translation from English into these languages is also occurring.

Some 500 periodicals translated into English are now available in cover-to-cover, selected articles, or abstract form, and additional thousands of separate articles, monographs, and other works translated into English are available from commercial sources, from NTIS, from the National Translations Center (U.S. Library of Congress), and from similar agencies in Canada and elsewhere. Many authors of research papers still prefer to cite original sources, so translations tend to serve largely as a kind of monitoring system with an inherent time delay for non-Western science and technology. *World Translations Index*, published by the International Translations Centre, announces translations in all fields of science and technology.

Index types. The following subsections discuss the various indexing services.

Indexes. An index is a detailed alphabetical list of the names, terms, topics, places, formulas, numbers, or other significant items in a completed work (such as a book, set, or bound journal) with exact page references to material discussed in that work. It may be part of the work or it may be published separately. Rather than alphabetically, it may be arranged chronologically, geographically, numerically, or in some other fashion. No reference work except, of course, a dictionary and possibly an

encyclopedia is any better than its index; a properly compiled index is the information hunter's most useful tool.

Bibliographies. A bibliography is a list of references to primary or other sources relating to some given subject or person; it is usually arranged chronologically or alphabetically by authors. It may be comprehensive or selective and annotated or otherwise evaluative. It may be published separately or as a part of a larger work to acknowledge information sources, recommend additional reading, or direct attention to more detailed treatment elsewhere. Almost always the time span and the subject coverage are well defined, so that a good bibliography represents a definitive coverage of the literature within the defined limits and makes retrospective literature searching that much easier.

Indexing serials. An indexing serial, sometimes called a current bibliography, is a regularly issued compilation of titles of articles (or of subsequent references to them) that appear in current primary-source journals; titles of new books and of other separately published material are often also included. In each issue the titles usually are listed alphabetically by subject; but they may be listed by both subject and author in one alphabet, or the authors may be indexed separately. Issues are published with a specific frequency, weekly or monthly, for example, and they may cumulate. Some indexing serials aim to cover only selected journals in their fields but to do it comprehensively, listing all articles of any possible interest; others aim to cover all journals in their fields but to do it selectively, listing only articles of real substantive interest. Current issues of typical indexing serials aid in finding recent articles, while bound sets are helpful in searching older literature, especially that published before the advent of machine-readable bibliographic databases in the 1970s.

Express services (such as *Current Contents*), which reproduce, often translate, and index the tables of contents of selected current primary-source journals and then distribute the usually weekly compilations by air mail or computer networks, are important current awareness aids as well as pertinent leads to reprint sources.

Most indexing serials are now being compiled and printed with the aid of computers, and the tapes become available for custom literature searches by the producer or for online searches through vendors of information services which lease them. In some cases the tapes may also be purchased.

Abstracting serials. An abstracting serial, also at times called a current bibliography, is a regularly issued compilation of concise summaries of (1) significant articles (often in a very limited subject field) that appear in current primary-source journals and (2) important new research monographs, reports, patents, and other primary-source publications in that field. In each issue the summaries usually are arranged by rather broad subjects followed by an author index, but some abstracting serials also include report number, corporate author, and more exact subject indexes as well. Most abstracting serials aim at selective substantive coverage of all known and available journals in their fields. Issues may be published with almost any specific frequency, but usually they do not cumulate. Instead, exhaustive annual or multiple-year indexes according to author, subject, patent, formula, or report number are published. Most abstracting serials are now being compiled and printed with the aid of computers, and the tapes become available for custom or online searches or for purchase. Long runs of many abstracting serials are available in microform.

Abstracts, however published, are likely to be further behind the current primary literature than title compilations are, but they also cover much more primary literature and give much more subject information per reference. Serious research workers find lengthy runs of abstracts, properly indexed, particularly suitable for in-depth searching of the older subject literature, especially that published before the advent of the applicable subject machine-readable bibliographic database. They find the current issues to be particularly suitable for keeping abreast of worldwide scientific progress in their chosen fields. Abstracts thus serve both as indexes to specific information and as surveys of particular subject areas.

Bibliographic databases. A bibliographic database is essentially a current bibliography or an indexing or abstracting serial in machine-readable form. It may be used to print paper copies in journal format, or it may be used to provide online (user-interactive) or batch (custom once-only) search service by the producer or by an information service vendor. Bibliographic databases are also distributed on CD-ROM, searchable by using a microcomputer. Some databases cover the literature of a subject, while others cover particular types of primary literature (dissertations, standards, patents, conference papers). References may be retrieved online or from CD-ROMs by using sophisticated search strategies, including terms from title and abstract as well as index terms. *See* DATABASE MANAGEMENT SYSTEM.

Survey types. The following subsections discuss the various survey types of reference works.

Reviews. A review is a subject survey of the primary literature usually covering the material that was published since the most recent review on the same subject. A good review accumulates, digests, and correlates the current literature and indicates the direction future research might take. A critical or evaluative review by a competent author is an important aid in keeping up with the work being done in a particular field and in spotting the outstanding developments. A review may appear as one of a collection of more or less related papers in an annual, a quarterly, or a monthly series, or it may appear as an article in a regularly issued primary-source subject journal.

Review reference lists are often extensive and, in a way, form a definitive bibliography of the subject for the period covered. One shortcoming of a review, though, is the inevitable delay before comprehensive and critical coverage of the primary literature can be obtained; one hindrance in getting a good

review is the difficulty in finding a qualified specialist with both the time and the literature-searching competence to do the job. Nevertheless, information experts believe that reviews are and will continue to be an important part of the literature of science and technology.

Treatises. A treatise is a comprehensive, authoritative, systematic, well-documented compilation or summary of known information on a subject, covering it so completely that the work becomes definitive at the time of writing. Thus a treatise is an aid in acquiring a foundation in a subject adequate to enable a trained individual to carry on advanced research; at the same time, it is a source of facts, procedures, theories, and other important data, presented in such a way as to show their development, correlation, and probable reliability. A treatise combines characteristics of an advanced textbook and a handbook; in fact, certain multivolume German *Handbücher* and certain multivolume British textbooks are good examples of treatises. One drawback to a treatise is that it is soon out of date. By the time the last part of a multipart treatise is published, the first parts are already quite old. Here, too, the time lag is unavoidable because of the scholarly inventory nature of the work itself. Periodic supplements and occasional new editions of the whole or of consecutive parts help overcome this lack of recency of the basic work, and so long as the dates of publication and the probable value of the original sources are clearly brought out, the usefulness of a treatise will not be impaired.

Monographs. A monograph, in effect, is a short treatise on a particular subject, a single division or part of a larger branch of knowledge. Hence it can be more up to date when it is published and can be brought up to date more easily for a revised edition; it frequently is published as part of a series. Almost any book on a special topic may be called a monograph unless obviously it is something else, for example, a research monograph, part of the primary literature already discussed, or a textbook, discussed later.

Reference tools. Five major types of reference tools are encyclopedias, dictionaries, handbooks, critical tables, and machine-readable data banks.

Encyclopedias. An encyclopedia is an idea book. It deals with concepts and is usually arranged alphabetically by separate subjects, those parts of all knowledge or of a branch of knowledge which are considered to be significant by the compilers. Treatment is as thorough as space will permit and may be descriptive, explanatory, statistical, historical, or evaluative, but it should be impartial and should summarize the information thought to be of the most general value at the time of writing. Illustrations, tables, drawings, and photographs are often used, lavishly on occasion. Source references may or may not be given, so authoritativeness depends largely on the reputations of the publisher and of the authors of the individual articles. The large-subject approach usual in a multivolume set requires a competent index, while the small-subject approach usual in a one-volume work does not; however, if the subject arrangement is not alphabetic, an index is indispensable.

An encyclopedia is designed to give a summary of background knowledge and a discussion of concepts in a particular field, useful for orientation in a strange subject area and for determining key words for more specific searching. One-volume encyclopedias give something less than this and tend to be considered and used as expanded dictionaries.

Dictionaries. A dictionary is a word book. In science and technology its purpose is to define commonly used terms as simply as possible, preferably without much recourse to other technical terms and, in addition, with some indication of the specific subject field in which a given definition is the accepted one. Etymology and pronunciation of terms may also be included. Terms may be illustrated to show shape or use, and the treatment of terms may be expanded beyond simple definitions to include information bordering on encyclopedic or handbook coverage. A good technical dictionary always gives the generally accepted correct spellings of the words it defines, and it often notes variants. For acronyms and abbreviations, the fully spelled out terms are given. Bilingual and polylingual dictionaries normally give just the direct equivalent word in the other language with no definition other than identifying the subject field in which it is used.

Handbooks. A handbook (or manual) in science and engineering usage is a compact, fairly up-to-date, relatively complete, authoritative compilation of specific data, procedures, and professional principles of a subject field. Much of the information is given in tables, graphs, and diagrams, and illustrations are freely used. Symbols, equations, formulas, abbreviations, and concise technical language all help condense much practical information into a handbook, but they also require that the reader already have rather broad knowledge of the field in order to use the work effectively. Hallmarks of a good handbook are an exhaustive index, up-to-date references, expert editorial staff, easy-to-read printing, and convenient format. The term handbook implies ready reference in a technical subject field. The term manual in common usage implies instruction in how to do something with the aid of very explicit step-by-step directions.

Critical tables. A collection of standard reference data (for example, physical and chemical properties of materials) that has been compiled, documented, evaluated, published, and kept up-to-date by reputable and responsible specialists is an essential reference tool to the working scientist or engineer. The compilation of a directory of critical (that is, critically evaluated) tables of standard reference data from worldwide sources is the responsibility of the World Data Referral Centre in Paris, established by the international Committee on Data for Science and Technology (CODATA). The National Standard Reference Data System of the National Institute of Standards and Technology is the United States affiliate.

Data banks. A data bank is a compilation of numerical, statistical, or structural (for example, chemical)

data in machine-readable form. Advances in instrumentation in all fields of science and technology have led to dramatic increases in the amount of data available, from gene sequences to space-based Earth measurements. When data banks are accessed online, numerical data may be retrieved and manipulated using available computer programs.

Tertiary Sources

These sources include textbooks, directories, and literature guides.

Textbooks. A textbook is a standard work used for instruction, arranged so as to develop an understanding of a branch of knowledge rather than to impart information for its own sake. Textbooks characteristically are graded in difficulty and are, therefore, suitable for either introductory or advanced study at almost any level, depending on the background of the reader. The most elementary textbooks assume no prior subject knowledge or experience at all; they work with and build on long-established (and sometimes already superseded) theories and concepts and proceed logically to newer and more advanced ideas as the student learns to master the material. The most advanced textbooks, on the other hand, take on the aspects of monographs or treatises in the thorough coverage, systematic development, and rigorous treatment of their subjects.

Directories. A directory is an alphabetical listing of at least the names and addresses of persons, organizations, manufacturers, or periodicals belonging to a particular class or group. The directory may include indexes or supplementary lists by subject field, geographical location, product, or some other desirable classification. It may be published separately in one or more volumes, or it may appear as a part in, an issue of, or a supplement to another work such as a journal or the proceedings of a society; it may be revised from time to time or not at all.

Biographical directories vary in coverage from annual membership lists with only the briefest information about the persons listed to the specialized compendiums of the *Who's Who* type. Trade and product directories, often appearing as annual buyers' guide issues of certain industrial and trade periodicals, frequently contain an unsuspected variety of information, such as sources, producers, dealers, properties, hazards, shipping instructions, trade names, and trademarks. Industrial directories—city, state, national, and international—often contain considerable data on manufacturers and their officials, subsidiaries, plants, dealers, capitalization, trade names, and products.

Organization directories of learned societies, professional associations, research establishments, trade groups, educational institutions, and government agencies, for example, usually give at least the officers, the address, the functions, and the date of establishment of each organization listed; coverage varies from community-size to worldwide. Periodicals directories include full bibliographical information, frequency, publisher, and price of each title listed; some also include index coverage, advertising arrangements, and availability in libraries. The more complete periodicals directories and lists are often considered to be national or subject bibliographies rather than directories.

Literature guides. A literature guide is a reference manual designed to aid research workers or other prospective users in finding their way into and through the literature of a specific subject field. Its purpose is to acquaint its readers with the important types of information sources available to satisfy their needs and to help them make fruitful current or retrospective literature searches. Library resources and services are discussed, and all important specific and related titles of works in the field are cited and many are described quite fully. Guides also exist, in both print and audiovisual forms, to assist users of specific reference tools, searching aids, or information services.

Information Science

Collecting, organizing, and providing easy access to the literature are generally performed by libraries with the aid of the tools produced by professional, governmental, academic, trade, and other members of the international information industry.

Role of libraries. The library has long been the institution most concerned with the methods, skills, and systems for the acquisition, storage, preservation, retrieval, and use of literature. The depth of a library's concern has always been determined primarily by the needs of those it serves and by the fields of literature it handles.

A subject-specialized research library acquires, classifies, catalogs, stores, and supplies both whole works and bits of information as precisely as possible, combining library practice with the techniques of documentation or information science.

But science-technology literature is vast, polylingual, expensive, and only imperfectly distributed or indexed (although better than most other subject literatures). No large research library can have everything published in even a relatively narrow subject field, to say nothing of the broader subject disciplines.

To the serious research worker, to industry, and to science itself, this present inability of libraries (however large, rich, dedicated, or specialized) to cope with the literature of science and technology is a very critical matter. In an attempt at solving this problem, local, regional, national, and international networks have been developed among libraries of various types, with members associated electronically in order to share resources, services, or internal technical procedures. Thus anyone in need of specialized information can get help from the total resources of a particular network or, if need be, any other network, by inquiring first at the local public, academic, or special library.

Role of information technology. Of even greater help to the serious research worker is the rapid development of electronic information and telecommunication systems combined with improvements in input and output devices and storage media. The *Gale*

Directory of Databases lists over 2200 databases of all types in science and technology. In addition to the bibliographic databases and data banks listed as separate categories above, many other databases are machine-readable counterparts of various primary, secondary, or tertiary sources. Examples include the full text of several periodicals dealing with chemistry and medicine, an encyclopedia of chemical technology, chemical dictionaries, biographical and organization directories, textbooks in emergency medicine, and the full text of technical reports. At present, most databases are equivalent to or supplements of their printed counterparts rather than total replacements. In the case of full text in electronic form, text can be searched for combinations of key words, and retrieved text can be displayed or printed on demand at remote terminals, or it may be produced in microform (computer output microfiche, or COM).

The kinds of information needed by research workers and now found in the present varied literature of science and technology probably will not change much over the years. But the form and manner in which information is produced, published, stored, retrieved, and analyzed certainly will change as information science and technology and the information industry (1) find out more about how information really is used by research workers, and (2) find ways to solve problems that seem to beset the new electronic information systems: reliability, security, access vocabulary, copyright, archiving, and user visual fatigue, among others. Some solutions to these problems are emerging. For example, the Copyright Clearance Center operates a centralized photocopy authorization and payment system on behalf of copyright owners, both foreign and domestic, providing a practical means for organizations to comply with copyright law in the use of scientific-technical information.

New technologies continue to be introduced. CD-ROMs offer the possibility of high-volume, low-cost storage of databases, including multimedia. Microcomputers are proving to be versatile devices, used by individual scientists and engineers for both document creation and retrieval of information from databases. The Internet, a worldwide system of interconnected computer networks, allows access to information resources all over the world from a desktop computer workstation. Software tools for navigation and retrieval improve access to distributed resources, including data, images, sounds, text, and computer programs. *See* MICROCOMPUTER; MULTIMEDIA TECHNOLOGY; OPTICAL RECORDING.

Documenting progress. Research, development, and state-of-the-art reports and current news items covering all aspects of the science information field may be found through *Library and Information Science Abstracts* (an abstracting serial) and *Library Literature* (an indexing serial). Machine-readable database material is featured in *Online*, *Online & CD-ROM Review,* and *Database*.

George S. Bonn; Linda C. Smith

Bibliography. C. D. Hurt, *Information Sources in Science and Technology*, 3d ed., 1998; H. R. Malinowsky, *Reference Sources in Science, Engineering, Medicine, and Agriculture*, 1994; E. Mount and B. Kovacs, *Using Science and Technology Information Sources*, 1995; National Academy of Sciences, *Realizing the Information Future: The Internet and Beyond*, 1994; G. Stix, The speed of write, *Sci. Amer.*, 271(6):72–77, December 1994; R. D. Walker and C. D. Hurt, *Scientific and Technical Literature: An Introduction to Forms of Communication*, 1990.

Lithium

A chemical element, Li, atomic number 3, and atomic weight 6.939. Lithium heads the alkali metal family in the periodic table. In nature it is a mixture of the isotopes ^{6}Li and ^{7}Li. Lithium, the lightest solid element, is a soft, low-melting, reactive metal. In many physical and chemical properties it resembles the alkaline-earth metals as much as, or more than, it does the alkali metals. *See* ALKALINE-EARTH METALS; PERIODIC TABLE.

1																	18
1 H	2											13	14	15	16	17	2 He
3 Li	4 Be											5 B	6 C	7 N	8 O	9 F	10 Ne
11 Na	12 Mg	3	4	5	6	7	8	9	10	11	12	13 Al	14 Si	15 P	16 S	17 Cl	18 Ar
19 K	20 Ca	21 Sc	22 Ti	23 V	24 Cr	25 Mn	26 Fe	27 Co	28 Ni	29 Cu	30 Zn	31 Ga	32 Ge	33 As	34 Se	35 Br	36 Kr
37 Rb	38 Sr	39 Y	40 Zr	41 Nb	42 Mo	43 Tc	44 Ru	45 Rh	46 Pd	47 Ag	48 Cd	49 In	50 Sn	51 Sb	52 Te	53 I	54 Xe
55 Cs	56 Ba	71 Lu	72 Hf	73 Ta	74 W	75 Re	76 Os	77 Ir	78 Pt	79 Au	80 Hg	81 Tl	82 Pb	83 Bi	84 Po	85 At	86 Rn
87 Fr	88 Ra	103 Lr	104 Rf	105 Db	106 Sg	107 Bh	108 Hs	109 Mt	110 Ds	111 Rg	112	113					

lanthanide series	57 La	58 Ce	59 Pr	60 Nd	61 Pm	62 Sm	63 Eu	64 Gd	65 Tb	66 Dy	67 Ho	68 Er	69 Tm	70 Yb
actinide series	89 Ac	90 Th	91 Pa	92 U	93 Np	94 Pu	95 Am	96 Cm	97 Bk	98 Cf	99 Es	100 Fm	101 Md	102 No

The major industrial use of lithium is in the form of lithium stearate as a thickener for lubricating greases. Other important uses of lithium compounds are in ceramics, specifically in porcelain enamel formulation; as an additive to give longer life and higher output in alkaline storage batteries; and in welding and brazing fluxes.

Lithium is a moderately abundant element and is present in the Earth's crust to the extent of 65 parts per million (ppm). This places lithium a little below nickel, copper, and tungsten, and a little above cerium and tin in abundance.

Noteworthy among lithium's physical properties are the high specific heat (heat capacity), large temperature range of the liquid phase, high thermal conductivity, low viscosity, and very low density. Lithium metal is soluble in liquid ammonia and is slightly soluble in the lower aliphatic amines, such as ethylamine. It is insoluble in hydrocarbons. The physical properties of lithium metal are summarized in the **table**.

Lithium undergoes a large number of reactions with both organic, and inorganic, reagents. It

Physical properties of lithium metal

Property	Temperature, °C (°F)	Metric (scientific) units	British (engineering) units
Density	20 (68)	0.534 g/cm^3	33.7 lb/ft^3
	400 (752)	0.490 g/cm^3	30.6 lb/ft^3
	800 (1472)	0.457 g/cm^3	28.6 lb/ft^3
Melting point	179 (354)		
Boiling point	1317 (2403)		
Heat of fusion	179 (354)	103.2 cal/g	186 Btu/lb
Heat of vaporization	1317 (2403)	4680 cal/g	8420 Btu/lb
Viscosity	200 (392)	5.62 millipoises	11.1 kinetic units
	400 (752)	4.02 millipoises	8.2 kinetic units
	600 (1112)	3.17 millipoises	6.7 kinetic units
Vapor pressure	727	0.78 mm	0.015 lb/in.^{2}
	1077	91.0 mm	1.76 lb/in.^{2}
Thermal conductivity	216 (420)	0.109 cal/(s)(cm^2)(cm)(°C)	26.5 Btu/(h)(ft^2)(°F)
	539 (1002)	0.073 cal/(s)(cm^2)(cm)(°C)	17.6 Btu/(h)(ft^2)(°F)
Heat capacity	100 (212)	0.90 cal/(g)(°C)	0.90 Btu/(lb)(°F)
	300 (573)	1.02 cal/(g)(°C)	1.02 Btu/(lb)(°F)
	800 (1472)	0.99 cal/(g)(°C)	0.99 Btu/(lb)(°F)
Electrical resistivity	0 (32)	1.34 microhm-cm	
	100 (212)	12.7 microhm-cm	
Surface tension	200–500 (392–932)	About 400 dynes/cm	

reacts with oxygen to form the monoxide, Li_2O, and the peroxide, Li_2O_2. Lithium is the only alkali metal that reacts with nitrogen at room temperature to form a nitride, Li_3N, which is black. Lithium reacts readily with hydrogen at about 930°F (500°C) to form lithium hydride, LiH. The reaction of lithium metal with water is exceedingly vigorous. Lithium reacts directly with carbon to form the carbide, Li_2C_2. Lithium combines readily with the halogens, forming halides with the emission of light. While lithium does not react with paraffin hydrocarbons, it does undergo addition reactions with arylated alkenes and with dienes. Lithium also reacts with acetylenic compounds, forming lithium acetylides, which are important in the synthesis of vitamin A.

The most important lithium compound is lithium hydroxide. It is a white powder, and the material of commerce is actually lithium hydroxide monohydrate, $LiOH \cdot H_2O$. Lithium carbonate, $LiCO_3$, finds application in the ceramic industries and in medicine as an antidepressant. Both lithium halides, lithium chloride and lithium bromide, form concentrated brines with ability to absorb moisture over a wide temperature range; these brines are used in commercial air conditioning systems.

Marshall Sittig

Bibliography. F. A. Cotton et al., *Advanced Inorganic Chemistry*, 6th ed., Wiley-Interscience, 1999; D. R. Lide, *CRC Handbook Chemistry and Physics*, 85th ed., CRC Press, 2004; G. N. Schrauzer and K. F. Klippel (eds.), *Lithium in Biology and Medicine*, 1991.

Lithosphere

The rigid or mechanically strong outer layer of the Earth that can support stress. The lithosphere is divided into 12 major plates, the boundaries of which are zones of intense activity that produce many of the large-scale geological features that characterize the Earth. These plates move as coherent units with velocities of up to several centimeters per year, and their relative movement and interaction form the foundation for the theory of plate tectonics.

The lithosphere comprises the crust (either continental or oceanic) and a portion of the upper mantle that together overlie a zone of relative weakness termed the asthenosphere (**Fig. 1**). The boundary between the crust and the mantle is known as the Mohorovičić discontinuity (Moho), and is compositional in origin—that is, the crust and mantle are distinguished by fundamental differences in rock chemistry. In contrast, the boundary between the lithosphere and the asthenosphere represents an isotherm that separates a conductively cooling lithosphere from a quasi-isothermal convecting asthenosphere. The asthenosphere differs from the overlying lithosphere principally in its ability to flow on geological time scales. These differences arise from the fact that temperature (and thus the fluid or flow properties of rocks) increases as a function of depth in the Earth. Whereas the lithosphere tends to be resistant to deformation, the asthenosphere deforms by flowing. A complication arises when the geothermal temperature is sufficiently high to

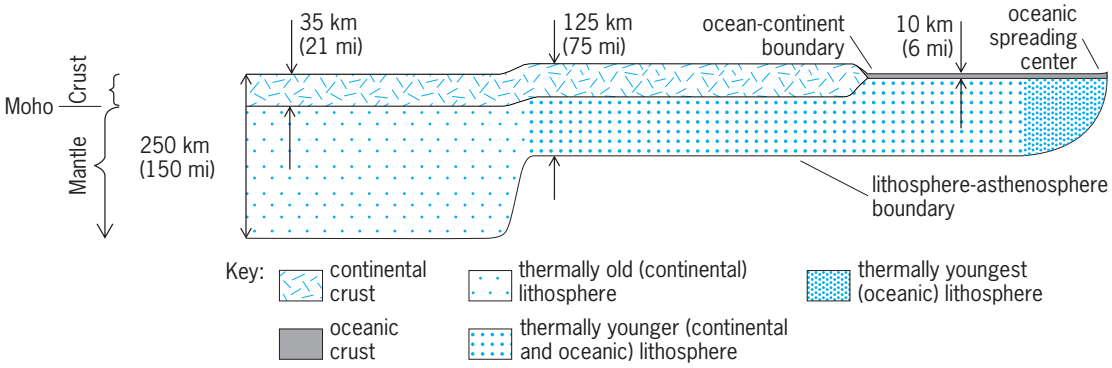

Fig. 1. Representation of oceanic and continental lithosphere as defined by thermal structure. Also shown are representative crustal and lithospheric thicknesses.

induce the lower crust to flow while the upper mantle is still relatively strong (for example, the Basin and Range Province of the western United States). Even in this case, a lithosphere-asthenosphere boundary still exists at depth. The lithosphere is either oceanic or continental, each type being fundamentally different in terms of the formation and composition of the rocks that constitute the crust and upper mantle. While the most common definition of the lithosphere is in terms of its temperature structure, there exist a whole range of alternative definitions that consider the seismic, mechanical, rheological, and chemical characteristics of the crust and mantle. *See* ASTHENOSPHERE; EARTH CRUST; MOHO (MOHOROVICIC DISCONTINUITY); PLATE TECTONICS; RHEOLOGY.

Oceanic lithosphere. The oceanic lithosphere ranges in thickness from near zero (young lithosphere at an oceanic spreading center) to 125 km (75 mi) within the oldest existing ocean basins ($\sim 2 \times 10^8$ years). Ages for oceanic lithosphere indicate not only their absolute age but their temperature state as well. Thus, young oceanic lithosphere refers to the new, hot lithosphere created at a spreading center as part of the plate tectonic cycle. In turn, the spreading center is the region where mantle (asthenosphere) material rises, melts, and is emplaced to produce new lithosphere. The thickness of oceanic crust typically ranges 5–10 km (3–6 mi), although thickness can approach 20 km (12 mi) when the normal oceanic crustal formation process is augmented thermally by the presence of hot spots (for example, Iceland). The oceanic lithosphere consists of a basaltic crust created at spreading centers by the passive emplacement of magma and an underlying mantle component. The new crustal material (oceanic crust) is extracted from the decompressive melting of the underlying asthenosphere. The mantle component consists of the residuum of this melting process (harzburgite rocks) and pristine upper-mantle material (lherzolite rocks) created by the transformation of asthenosphere to lithosphere by conductive cooling. Lherzolite is considered pristine because it is chemically indistinguishable from the composition of the underlying asthenosphere. The thickness of the oceanic crust is a function of the temperature of the underlying asthenosphere: the hotter the asthenosphere, the thicker the oceanic crust. *See* HOT SPOTS (GEOLOGY); MAGMA.

The oceanic lithosphere cools and thickens as it moves away from the spreading center, and ultimately it is consumed or recycled as it descends back into the asthenosphere in collisions with other plates to form subduction zones. The relatively young age of oceanic lithosphere ($\leq 0.2 \times 10^9$ years) compared to that of continental lithosphere ($\leq 3.8 \times 10^9$ years) is a direct consequence of this recycling process. *See* SUBDUCTION ZONES.

Continental lithosphere. The continental lithosphere ranges in thickness from approximately 50 to 250 km (30 to 150 mi), with crustal thicknesses ranging 20–70 km (12–40 mi). It consists of a crust created by the accretion of older, relatively low-density continental fragments augmented by the ascent and emplacement of new igneous material or even slivers of oceanic crust at subduction zones, and a mantle component that has been created by a range of processes. These processes include (1) the fracturing and emplacement of older continental mantle during plate collisions, (2) the fracturing and emplacement of older oceanic mantle during subduction, (3) the accretion of low-density depleted mantle derived from melting of the mantle that overlies subducted oceanic lithosphere, and (4) the transformation of asthenosphere to pristine lithosphere by long-term conductive cooling.

New continental crust is derived by partial melting of both the mantle overlying subducted oceanic lithosphere and the sediments that are transported along with the subducted plate during the formation of island arcs and continental arcs. In turn, island arcs are accreted to the continents during plate collisions. The decompressive melting of mantle material associated with hot spots and plumes is an important intraplate process for incorporating spatially extensive and thick basalts into the continental crust. *See* BASALT; OCEANIC ISLANDS.

Continental crust generally contains relatively light, granitic and gneissic rocks, and it tends to be thicker than its oceanic counterpart. While the upper continental crust is lithologically and chemically heterogeneous, it has an average composition

equivalent to granodiorite. The lower continental crust is significantly more mafic (containing magnesium and iron), with an average composition similar to that of oceanic crust (that is, basaltic). Because of their buoyancy, continental crust and strongly depleted continental mantle are difficult to subduct, and thus they are perpetually reincorporated into the structure of the interacting plates. It is this inability to subduct continental crust that helps explain the apparent logevity of the continents with respect to the oceans. *See* GNEISS; GRANITE; GRANODIORITE.

The continental crust is characterized by relatively abundant concentrations of long-lived radioactive isotopes of uranium (^{235}U and ^{238}U), potassium (^{40}K), and thorium (^{232}Th). Subduction recycling, surficial weathering, and magmatic and hydrothermal differentiation processes all help to concentrate these elements into the upper crust. The observed linear relationship between surface heat flow and radioactive heat content of surface rocks is satisfactorily explained by a distribution of radioactivity that decreases exponentially with depth. The contribution of radioactive heating to the mantle heat flux in the continents can be as high as 50%. *See* RADIOISOTOPE (GEOCHEMISTRY).

Other definitions. Although the most common and important definition of the lithosphere is in terms of its deformation properties, other definitions exist; they depend on identifying the differences between the lithosphere and the asthenosphere.

Thermal lithosphere. This is a thermal boundary layer between the surface of the Earth, which cools by conduction, and the asthenosphere, which cools by convection. In contrast, the underlying asthenosphere is characterized by convective stirring such that it is approximately isothermal, with a temperature of 1200–1400°C (2200–2600°F). The lithosphere is related to the asthenosphere by a physical change of state in that the boundary between them demarcates the onset of minor amounts of mantle melting (partial melting). Thus the asthenosphere has the ability to flow. It is precisely for this reason that the lithosphere-asthenosphere boundary represents the boundary between convective and conductive thermal processes.

The thickness of the oceanic thermal boundary layer (that is, oceanic lithosphere) is estimated by using the observed subsidence and heat flow as a function of crustal age. Typically, the thermal boundary layer thickness is 125 ± 10 km (75 ± 6 mi). In contrast, it is significantly more difficult to estimate the thickness of the continental thermal boundary layer (that is, the continental lithosphere) because of the effects of radioactive heating. The usual method for determining the thickness of the continental thermal boundary layer is to measure the length of time over which a sedimentary basin forms (known as the thermal time constant of the lithosphere). The thermal time constant estimated from continental sedimentary basins spans $6.5–26 \times 10^7$ years, implying that the continental lithosphere thickness ranges 125–250 km (75–150 mi). The thicker lithospheres tend to be associated with old, stable continental cratons. Their increased depth to the 1200–1400°C (2200–2600°F) isotherm (that is, the base of the lithosphere) is consistent with the temperature and pressure conditions obtained from studies on diamonds and their inclusions. *See* DIAMOND.

Two competing models have been used to explain the temperature behavior of the lithosphere: a cooling half-space model and a cooling plate model. For the cooling half-space model, it is assumed that conductive cooling progressively thickens the lithospheric mantle without limit; that is, the longer the interval of cooling, the thicker the lithosphere. By contrast, the cooling plate model assumes that there is a maximum thickness that limits conductive cooling. While observations of basement subsidence and heat-flow history favor the cooling plate model for the oceanic lithosphere (and by inference, the continental lithosphere), the subsidence data used for the model calibration may be biased by the effects of thermal plumes in the asthenosphere. This issue has not been resolved. It is probably fair to say that thermal steady state is never achieved in either the oceanic or continental lithosphere. In the continents, the complicating effects of erosion, radioactive heating, crustal thickening by the stacking of thrust sheets during broad continent-continent collisions (for example, the Himalayas and the Tibetan Plateau; the Hercynian orogeny of Europe), and the perpetual recycling of continental crust all mitigate against a simple application of the same techniques to estimate continental lithosphere thickness. Nevertheless, the general correlation between surface heat flow and the age of the last thermal event that affected the continental crust suggests that the temperature structure of the continents is primarily conductive, although it is not possible to discriminate between the applicability of the half-space or plate cooling models. *See* EARTH, CONVECTION IN; EARTH, HEAT FLOW IN.

Seismic lithosphere. The seismic lithosphere is that region between the surface of the Earth and the asthenosphere that is characterized by the efficient propagation of seismic waves. Since seismic velocity and attenuation are sensitive to temperature and melt content, the base of the lithosphere can be mapped using the variations in seismic P (longitudinal) waves and S (shear) waves. The lithosphere-asthenosphere boundary is marked by an abrupt decrease in shear-wave velocity. This low-velocity zone is 50–100 km (30–60 mi) thick and represents a region of incipient partial melting (approximately 1%). In effect, the velocities and efficient propagation of seismic body waves define a high-velocity "lid" that lies above the low-velocity asthenosphere. Surface wave studies also indicate that the depth to the low-velocity zone associated with relatively old oceanic lithosphere is approximately 100–125 km (60–75 mi). It has proved difficult to recognize the low-velocity zone beneath continental regions.

A subregion of the seismic lithosphere in which intraplate earthquakes are generated is termed the seismogenic zone. The seismogenic zone represents

those layers of the crust and mantle that are sufficiently cool that they can rupture by brittle fracture. *See* EARTHQUAKE; SEISMOLOGY.

Mechanical lithosphere. The mechanical lithosphere, also known as the elastic lithosphere, is a mechanical analog used to simulate the flexural deformation or response of the Earth to applied geological loads such as seamounts, subducted slabs, mountain ranges and thrust sheets, and deltas. Similarly, the Earth can be unloaded by processes such as lithosphere extension and erosion. The mechanical analog is a thin elastic plate overlying a fluid substratum. The flexural properties of the plate are characterized by its flexural rigidity, or equivalently by its thickness. When applied to the lithosphere, this thickness is termed the effective elastic thickness (T_e) of the lithosphere because it reflects the mechanical strength of the lithosphere in a depth-averaged sense. Even though the effective elastic thickness is a parametrization of real lithosphere behavior, its use does not imply that the lithosphere is necessarily elastic or that a geological or rheological boundary occurs at a specific depth in the lithosphere. In general, the effective elastic thickness should be thought of as an empirical parameter representing the integrated rheological strength of the entire lithosphere, with all its complexity, at a given time and location. Thus, the deformed shape of an elastic plate of thickness T_e is the same as the deformation of the lithosphere for the same load.

Three classes of studies have been used to determine the effective elastic thickness for the oceans and continents: (1) inverse gravity admittance techniques, which exploit the statistical relationship between topography and gravity anomalies; (2) forward modeling of the crustal shape and stratigraphy of extensional basins and their respective free-air gravity anomalies; and (3) determining the relationship between the basement relief and the Moho topography. Critical in these analyses is the fact that the wavelength of flexure indicates the strength of the lithosphere—a strong lithosphere produces a long-wavelength deformation of small amplitude, while a weaker lithosphere results in a shorter-wavelength deformation but of larger amplitude. *See* MODEL THEORY; SIMULATION.

In the oceans, a simple straightforward application of the admittance between bathymetry and free-air gravity (that is, the ratio of the gravity and bathymetry power spectra) has proved valuable in defining both the spatial and temporal variations of the effective elastic thickness. Most importantly, the effective elastic thickness tends to be a function of the age (and hence temperature structure) of the lithosphere at the time that it was loaded. The flexural strength of the oceanic lithosphere, as expressed by the effective elastic thickness, ranges 5–40 km (3–24 mi) and correlates with the depth to the 300–600°C (570–1110°F) isotherm as determined from thermal models for the lithosphere. The continents are somewhat more problematic. An implicit assumption in the interpretation of admittance functions is that the topography is the load responsible for deforming the crust and lithosphere. When the topography (or surface load) is augmented with subsurface loads, the effective elastic thickness estimates are suspect and are biased toward low values. This problem of subsurface loading seems most prevalent in the continents. When allowance is made for subsurface loads, the admittance technique predicts a range of the values of the effective elastic thickness for the Australian and North American continents [15 km (9 mi) $< T_e <$ 135 km (81 mi) and 4 km (2.4 mi) $\leq T_e \leq$ 128 km (79 mi), respectively] that correlates with the age range of orogenic events across each continent. Extremely low values of T_e are invariably related to regions that have recently undergone or are presently undergoing tectonic deformation involving large amounts of heat (for example, the Basin and Range Province of the western United States).

The flexural strength of the lithosphere can be determined by forward-modeling the topographic relief across regions of continental extension and compression. For example, in extensional settings the topography flanking rift basins is produced by the flexural rebound of the lithosphere in response to its tectonic unloading (that is, lateral removal of crustal and mantle material) during extension. Lithospheric flexural strength is maintained despite localized but intense fracturing of the crust by normal faults that penetrate to lower crustal levels.

Within compressional settings, studies of the gravity anomaly over mountain belts (that is, the load) and their associated foreland basins (that is, the flexural response or deformation of the lithosphere) indicate that the continental lithosphere in these tectonic settings has significant flexural strength. Estimated effective elastic thicknesses range 20–150 km (12–90 mi) and suggest that, in a broad way, the continents behave in a manner similar to the flexural deformation of oceanic lithosphere. The relationship between the flexural strength and the thermal age for the continental lithosphere appears similar to that found in the oceans as evidenced by the widths of foreland basins, given that foreland basin width is primarily controlled by the flexural strength of the lithosphere. Foreland basins on relatively young crust (for example, Molasse basin/Hercynian crust with an age of $2.45–2.6 \times 10^8$ years is 200 km or 120 mi wide) are narrower than foreland basins on relatively old crust (for example, Ganges basin/Archean crust with an age of 2.5×10^9 years is 400 km or 240 mi wide). The Molasse basin of Switzerland, southern Germany, and Austria represents the sediment-filled flexural deflection of the European crust, the deflection being produced in response to the weight and subsequent loading of the Alpine mountain thrust load. Similarly, the Ganges basin of northern India represents the sediment-filled flexural deflection of the Indian shield produced by the lateral emplacement of the thrust sheets that constitute, in part, the Himalayan Mountains. The thermal states of the European and northern Indian lithospheres are very different. Whereas the Indian lithosphere consists of extremely old, cold, crustal

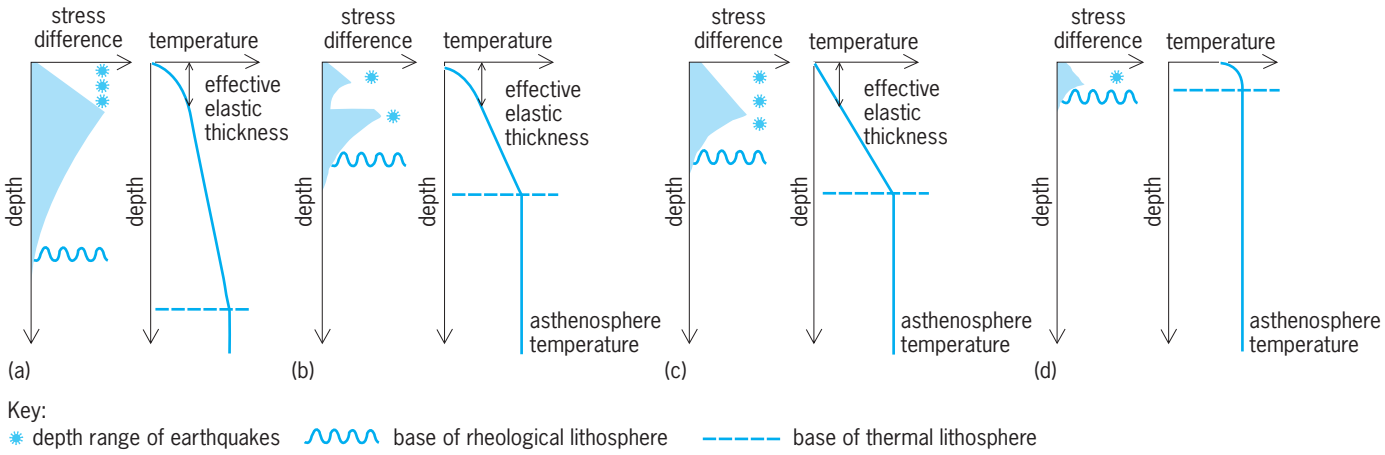

Fig. 2. Representation of oceanic and continental lithosphere as defined by thermal structure. Also shown are representative crustal and lithospheric thicknesses.

and mantle material, the European crust and mantle were severely deformed and heated during a major period of mountain building known as the Hercynian orogeny. The flexural response of the two lithospheres to thrust sheet loading (that is, the widths of their foreland basins) reflects the difference in their thermal states. *See* OROGENY.

While the importance of the free-air gravity cannot be overstated, there are some precautions that should be taken when using gravity to assess the flexural strength of the lithosphere. For example, a common misconception is that extensional basins are characterized by low-amplitude free-air gravity anomalies and thus the extended lithosphere has low flexural strength. A comparison of the similarly dimensioned Central Graben of the North Sea (−10 milligals) with the Tucano basin of Brazil (−140 milligals) indicates that the statement on gravity amplitude is incorrect. Another problem is that the gravity anomaly does not necessarily reflect details of the basement geometry because of the effects of compaction. As sediments compact, the density contrast with respect to the basement decreases, resulting in a decrease in the amplitude of the gravity anomaly. Thus, low-amplitude gravity anomalies over extensional basins do not necessarily reflect the flexural strength of the lithosphere, which is in marked contrast to basins that exhibit large negative gravity anomalies. Such gravity anomalies are indicative of high flexural strength.

Rheological lithosphere. This is the region of the crust and mantle over which the rheological or flow properties of rocks are insufficient to relieve stresses (primarily elastic). In general terms, stress is the pressure being sustained or supported within a material, whereas strain is the degree of deformation suffered by that material. Since by definition the lithosphere represents that region of the crust and mantle that can support significant stress, the more fluidlike the rocks become with increasing depth and temperature, the less shear stress they can support. A level of 10–50 megapascals is arbitrarily assigned to define the base of the rheological lithosphere.

Rock strength varies with depth in the lithosphere in response to changes in ambient temperature, confining pressure, and compositional variations. At shallow depths in the lithosphere, rock strength depends mainly on confining pressure, and yielding occurs as frictional sliding on fracture surfaces (that is, brittle deformation). It is this episodic stick-and-slip nature of frictional sliding that produces earthquakes. With increasing depth in the lithosphere, rock strength is expected to decrease as increasing temperatures and confining pressure promote thermally activated creep processes (that is, the rocks deform plastically). A particularly useful representation of the rheological lithosphere that incorporates these processes is in terms of a yield-stress envelope (**Fig. 2**). The yield-stress envelope defines the depth dependence of the maximum supportable stress difference in the lithosphere as a function of depth and composition. The continental yield-stress envelope has an additional region of low strength within the lower crust caused by the plastic deformation of the quartz-rich rocks that characterize this type of crust. The integral of the yield-stress envelope as a function of depth is a proxy for the total strength of the lithosphere, and it represents the force (per unit length) that opposes the breaching or breaking of the lithosphere due to horizontal forces.

According to the concept of the yield-stress envelope, even small levels of applied force are expected to produce yielding at the top and bottom of the lithosphere by brittle faulting and ductile creep, respectively (Fig. 2). The intervening core region can support large stress differences elastically without yielding on geological time scales, and correlates in a general way with the effective elastic thickness of the lithosphere. As with effective elastic thickness, it is this core region that controls the wavelength of flexural deformation in response to applied forces and loads, this wavelength being on the order of tens to hundreds of kilometers. In contrast, the brittle deformation associated with yielding in the top portion of the lithosphere might not have any preferential length scale, depending instead on the distribution

of existing faults and fractures in the crust and their orientation in relation to the applied force. *See* RHEOLOGY; STRESS AND STRAIN.

Chemical lithosphere. This lithosphere is defined as a chemical boundary layer between the surface of the Earth and the asthenosphere that cools by conduction and contains both the material differentiated or extracted from the mantle (for example, oceanic and continental crust) and mantle material modified by various degrees of depletion.

In general, the continental chemical lithosphere represents (1) the accretion of low-density depleted mantle originally associated with the formation of oceanic crust but remobilized by mantle convection systems, (2) the accretion of low-density depleted mantle derived from melting of the mantle overlying subducted oceanic lithosphere, and (3) the fracture and emplacement of older continental crust and mantle during plate collisions. As such, these magmatic differentiation processes explicitly result in chemical heterogeneities within the lithosphere. Perhaps more importantly, the low-density accreted mantle material is crucial in offsetting the subsidence engendered by the continued cooling and contraction of the lithosphere, thus for example helping to maintain cratons at relatively low but broadly distributed elevations (200–800 m or 660–2640 ft). The degree to which the lithospheric mantle is chemically distinct from the asthenosphere mantle is controversial. Seismic tomographic imaging of the mantle has revealed large velocity anomalies that correlate with the past location of subduction zones. Presumably, the subduction recycling process is conducive to a heterogeneous mantle asthenosphere with some affinity to the chemical composition of the lithosphere. *See* COMPUTERIZED TOMOGRAPHY.

Estimates for the thickness of old continental lithosphere are constrained primarily from the existence and composition of carbonatitic intrusions, particularly kimberlites, and the diamonds they may contain. Kimberlites are of special significance because they contain xenoliths of ultramafic rocks and eclogite from the upper mantle. Kimberlitic magmas result from the low partial melting of upper-mantle rocks (garnet lherzolites) at depths of 50–300 km (30–180 mi) and are rapidly emplaced. Kimberlites range in age from 20 to 1750 million years and occur in all major Precambrian cratons, suggesting that they are generated within the lower continental lithosphere. This implies that the lithospheric mantle of old continental terranes is chemically distinct from either younger continental terrane or the oceanic lithosphere. *See* ECLOGITE; KIMBERLITE; PRECAMBRIAN; XENOLITH.

Lithosphere interrelationships. A useful way to view the relationships between the various definitions for the lithosphere is by considering the depth distribution of earthquakes, temperature, and stress differences within old and young oceanic and continental lithosphere: old, cold continental lithosphere; relatively young continental lithosphere; relatively old, cold oceanic lithosphere; and young, hot oceanic lithosphere (Fig. 2).

The base of the thermal lithosphere is defined by T_m, which is the temperature of the asthenosphere at which olivine-bearing rock begins to flow easily. This boundary thus seperates material that remains in place and cools by heat conduction from material that moves as it is stirred by convection. The change in the rheological properties between old and young continental lithosphere is a function of the increased temperature gradient associated with the younger continental lithosphere and the accompanying creep activation of the quartz-rich rocks that compose the continental crust. As the lithosphere cools, this creep component becomes subordinate to the brittle deformation process, causing the yield-stress envelope bite within the lower crust to systemically diminish. It is the absence of this quartz-rich component in oceanic crust that results in the brittle-dominated segment of the yield-stress envelope observed for both old and young oceanic lithosphere.

Because of the pivotal role played by temperature in controlling the flow of rocks, there is a general temporal relationship between thermal lithospheric thickness, temperature gradients, brittle failure within the crust and upper mantle (defining the seismogenic layer), and the effective elastic thickness of the lithosphere. *See* EARTH.

Garry D. Karner

Bibliography. M. H. P. Bott, *The Interior of the Earth: Its Structure, Constitution and Evolution*, 2d ed., 1982; K. C. Condie, *Plate Tectonics and Crustal Evolution*, 3d ed., 1989; C. M. R. Fowler, *The Solid Earth: An Introduction to Global Geophysics*, 1990; H. L. Levin, *The Earth Through Time*, 3d ed., 1988.

Litopterna

Hoofed herbivores confined to the Cenozoic of South America. The order was well represented from the Paleocene to the Pleistocene, and apparently arose on that continent from a condylarth ancestry. By later Paleocene time two main lines of descent were clearly demarcated. The Proterotheriidae (**Fig. 1**) displayed a remarkable evolutionary convergence with the horses in their dentition and in reduction of the lateral digits of their feet. In one group the foot was reduced to a single median toe by early Miocene time. The members of the Macraucheniidae (**Fig. 2**) were proportioned much as in the camels and by late

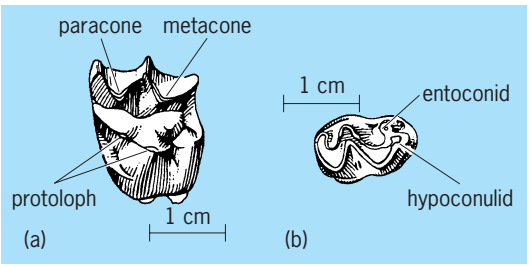

Fig. 1. Molars, (*a*) upper and (*b*) lower, of *Proterotherium*, an early Miocene proterotheriid litoptern from the Santa Cruz Formation of Patagonia, Argentina.

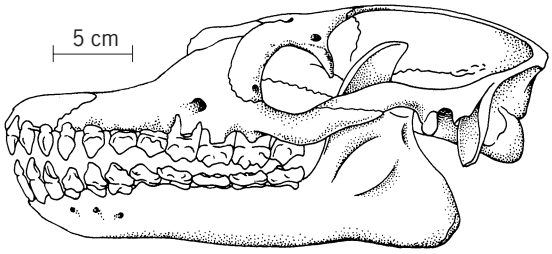

Fig. 2. Skull and jaw of *Theosodon garrettorum,* an early Miocene macraucheniid litoptern, Santa Cruz Formation, Patagonia, Argentina.

Tertiary time had similarly lost the vertebral arterial canal of the cervical vertebrae. They early developed a tendency toward retraction of the nasal bones; by late Tertiary time, the nasal opening was situated above the eyes on top of the skull. This specialization has been thought to indicate the presence of a trunk or perhaps dorsally situated nostrils adapted for a submerged amphibious existence. Three functional digits remain in the feet of even the most advanced macraucheniids. *See* ARCHAIC UNGULATE.

Both groups share the following characters held typical for the order. The skull was without expansion of the temporal or squamosal sinuses, as in the notoungulates; a postorbital bar was present. Dentition was primitive, with full eutherian formula and a tendency to reduce incisors and upper canine teeth; cheek teeth were unreduced, low- to high-crowned, the posterior premolars becoming molariform. The upper molars were quadrate, the paracone and metacone were crescentic, the protoloph was present and the metaloph was absent. The lower molars were bicrescentic; the entoconid was not isolated but joined to the posterior end of the tooth. The feet were functionally three-toed or reduced to a single digit, the weight borne by digit three. *See* DENTITION.

The earliest known mammalian faunas in South America (later Paleocene) contained representatives of both groups of litopterns. By Oligocene and Miocene time the litopterns reached their greatest recorded abundance. The proterotheres did not survive the Pliocene, and of the macraucheniids only the large *Macrauchenia* survived until Pleistocene time. *See* MAMMALIA.

Richard H. Tedford

Bibliography. M. J. Benton, *Vertebrate Paleontology*, 1991; R. L. Carroll, *Vertebrate Paleontology and Evolution*, 1988.

Liver

A large gland found in all vertebrates. It consists of a continuous parenchymal mass forming a system of walls (muralium) through which venous blood from the gut must pass. This strategic localization between nutrient-laden capillary beds and the general circulation is associated with hepatic regulation of metabolite levels in the blood through storage and mobilization mechanisms controlled by liver enzymes.

The liver is the sole source of such necessary constituents of the blood as fibrinogen, serum albumin, and cholinesterase (an enzyme which may prevent harmful buildup of the neuronal transmitter agent acetylcholine). In the embryonic stage of most vertebrates the liver serves as the major manufacturing site of erythrocytes, a process known as erythropoiesis. The liver also removes toxins from the systemic circulation and degrades them, as well as excess hormones, by oxidation, hydroxylation or conjugation. Particulate material may be removed through a phagocytic action of specialized cells (Kupffer cells) lining the lumen of the hepatic "capillary spaces," or sinusoids. In addition to the products which the liver delivers directly to the general circulation (endocrine function), it secretes bile through a duct system which, involving the gallbladder as a storage chamber, eventually passes into the duodenum (exocrine function). Bile functions as an emulsifier of fats to facilitate their digestion by fat-splitting lipases, and may also activate the lipase directly.

The liver does not exist in invertebrates except as the smaller analogous hepatopancreas of the crustaceans. In the vertebrate embryo the liver is a rapidly growing organ, but it rarely undergoes cellular division in the adult unless a portion is removed. Excision leads to such rapid restoration that regenerating mammalian liver has been used as a model in growth studies. As the largest discrete internal organ, it may make up more than 5% of total body weight in rodents and up to 3% in humans. Though the liver is highly variable in shape in different vertebrate groups, the basic features of circulation are probably similar in all livers.

The major afferent blood supply (70%) is from the hepatic portal vein, carrying blood from the spleen and digestive organs, with a smaller contribution from the hepatic artery. The smaller branches of these vessels join with the bile ductules and, as portal canals, reach the sinusoids. The major efferent vessel is the hepatic vein, whose smaller processes are known as central veins. Drainage is into the inferior vena cava.

Within the liver there are small branches of both the hepatic artery and portal vein supplying an elaborate network of capillaries apposed to the bile canaliculi (minute channels coursing in a continuous network between the parenchymal cells of the liver). These capillaries drain into the portal vein to form a minute portal system. This subsidiary system, supplying the liver cells directly with nutrient and oxygen, may represent a significant site for hepatic artery function in some species. In a number of mammalian species, for example, the pig, a discrete connective tissue boundary demarcates the liver mass into hexagonal bundles or lobules with portal canals arranged peripherally and central veins occupying the center. Even those forms lacking patent lobular arrangements demonstrate lobular distribution of key metabolites.

Comparative Anatomy

The liver is found only in vertebrates and is ubiquitous in this group. Despite the variations in embryonic hepatic development encountered in the

various vertebrate prototypes, all adult livers are essentially similar. This phenomenon is at sharp variance with Haeckel's biogenetic law, which stresses the similarity of embryonic structures and the divergence of adult structures. It also attests to the evolutionary success of the basic pattern of hepatic architecture: a continuous convoluted wall of functional parenchymal cells tunneled by passageways which contain a network of blood vessels and biliary tracts in homogeneous fashion within the organ.

In *Branchiostoma* (*Amphioxus*) a hollow outpocketing of the foregut, called a hepatic cecum, receives veins from the intestine. This may presage the portal system and liver of higher forms, and many consider this structure the first true homolog of the vertebrate liver.

Humans. Knowledge of the precise connections between liver and intestine and of liver and systemic circulation provides the mechanical basis for understanding hepatic function (**Fig. 1**). Although complex biochemically, the human liver is extremely simple structurally; it will be used here as a model for the vertebrates in terms of gross anatomic features, blood supply, and intrahepatic morphology. The liver is a remarkably plastic structure, and its general contour varies greatly from one class to another; however, the underlying features that determine function are sufficiently similar to justify selection of a single prototype.

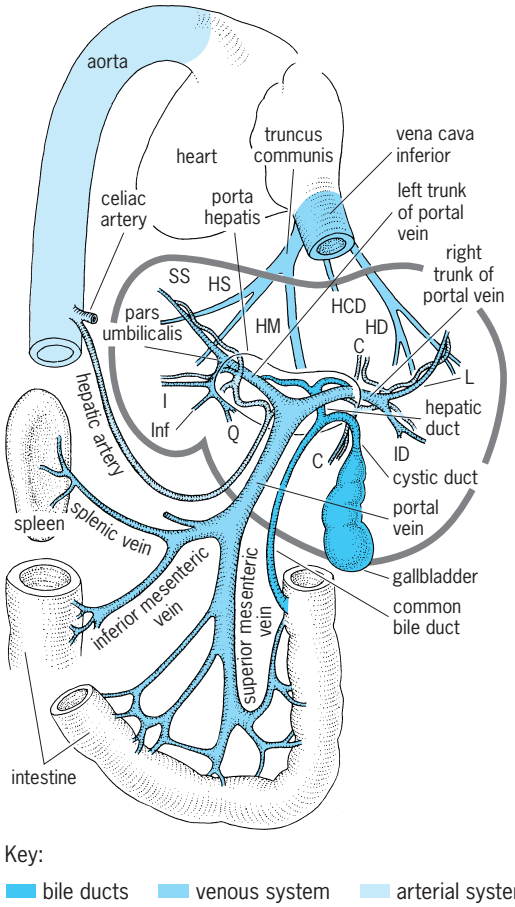

Fig. 1. Human liver and its major dorsal connections. Rami venae portae: C, centralis; I, intermedius; ID, inferior dexter; Inf, inferior sinister; L, lateralis; Q, quadratus; and SS, superior sinister. Venae hepaticae: HCD, dorsocaudalis; HD, dextra; HM, media; and HS, sinister.

General features. The human liver is a massive wedge-shaped organ divided into a large right lobe and a smaller left lobe. Its anterior surface underlies the diaphragm. The upper portion of the liver is partially covered ventrally by the lungs, whereas the lower portion overhangs the stomach and intestine. Both liver and gallbladder are innervated by the right phrenic nerve and by branches of the sympathetic fibers arising from the celiac ganglion. The vagus constitutes the parasympathetic source. The entire liver is covered by Glisson's capsule, an adherent membranous sheet of collagenous and elastic fibers.

Blood supply. Venous blood from the intestine, and to a lesser extent from spleen and stomach, converges upon a short broad vessel, called the hepatic portal vein, which enters the liver through a depression in the dorsocaudal surface termed the porta hepatis. There the hepatic portal vein divides (Fig. 1) into a short right branch (truncus dexter) and a longer left branch (truncus sinister). These vessels then ramify into the small branches which actually penetrate the functional parenchymal mass as the inner tubes of the portal canals (**Fig. 2**).

The hepatic artery, which is a branch of the larger celiac artery, also enters at the porta hepatis and ramifies unto smaller branches, which flank the portal venules within the portal canals (Figs. 1 and 2). Anastomoses of these arterial pairs result in the formation of a loose arterial plexus around each portal-vein branch. Arterial blood is also brought to the bile ducts and the lining cells of the portal canals by other sets of arterioles branching from tributaries of the hepatic artery.

The branches of the portal vein and hepatic artery then empty into the sinusoids (Fig. 2), the specialized capillaries lying within the spaces (lacunae hepatis) of the hepatic muralium. The sinusoids, which are major regions of hepatovascular exchange, communicate with small branches of the hepatic veins and, through the hepatic vein, the blood is returned to the heart by way of the vena cava. *See* CARDIOVASCULAR SYSTEM.

The hepatic canals house the hepatic venous branches in a manner similar to the containment of portal-vein and hepatic-artery branches within the portal canals. These respective canal systems are independent and are separated by the parenchymal cells (**Fig. 3**). Sinusoidal elements provide a functional continuum between afferent and efferent vascular systems. The absence of anastomoses within the portal canal system, as well as within the hepatic canal system, leads to a highly discrete pattern of vascular supply and drainage. This is of particular importance in surgical manipulations of the liver, since collateral circulation is of little significance in providing connections to those lobes whose vessels have been ligated.

Bile ducts. The tiny bile canaliculi, which lie between grooves in adjacent parenchymal cells, communicate with tiny intralobular bile ducts

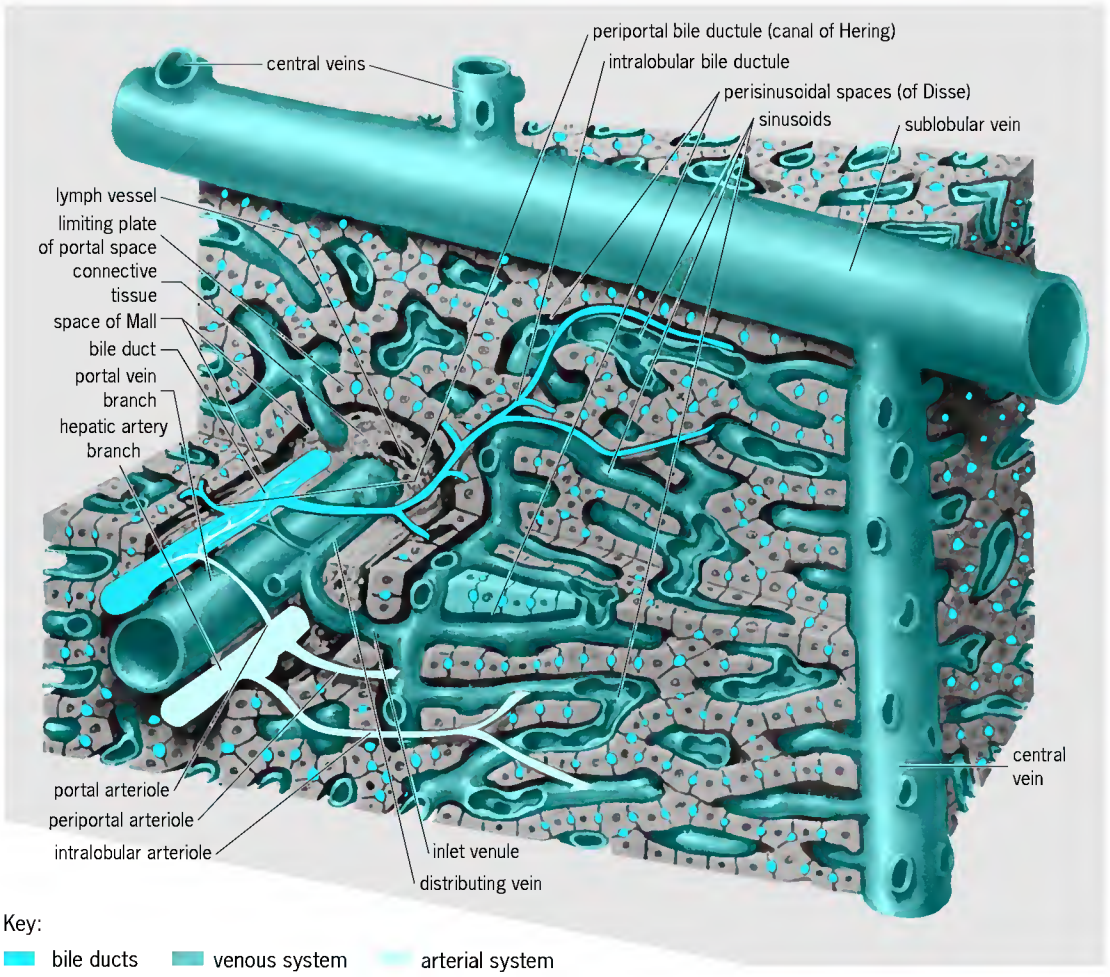

Fig. 2. Liver structure. ***(After E. Oppenheimer, ed., The Ciba Collection of Medical Illustrations, vol. 3: Digestive System, pt. 3: Liver, Biliary Tract and Pancreas, Ciba, 1957)***

(cholangioles or ductules), termed the canals of Hering (Fig. 2 and **Fig. 4**). These intralobular bile ducts empty into increasingly larger interlobular bile ducts which lie within the portal canals and make up the third element of the so-called portal triad (**Fig. 5**).

Although the biliary system is intimately associated with the portal system anatomically, even in terms of egress through the porta hepatis, it should be stressed that bile flow within this biliary system is in the opposite direction from that of blood flow. The hepatic duct arises in the region of the porta from the confluence of the largest bile ducts.

Gallbladder. A large outpouching of the hepatic duct forms the gallbladder (vesica fellea) and its cystic duct. Beyond the bifurcation the common bile duct enters the duodenum, thus serving as a conduit for bile from both the liver and its bile storage organ. Several mammals (for example, the horse and rat) do not possess gallbladders, and large numbers of humans have had their gallbladders removed surgically, thus indicating that the gallbladder is not essential for life. Electron microscopy studies indicate that the tall columnar cells which line the lumen of the gallbladder contain many microvilli. These may function in the concentration of bile, a significant function of gallbladder epithelium involving the active transport of sodium and potassium.

In addition to acting as a reservoir for the bile synthesized by the liver, the gallbladder plays a significant role in controlling the flow of bile to the intestine, when needed, because of its exquisite sensitivity to ingested fat or meat. Following a high-fat meal, up to three-fourths of gallbladder bile is expelled in less than 1 h as a result of contraction of the musculature of that organ and the concomitant relaxation of the sphincter choledochus (a ring of muscle) at the terminus of the common bile duct. Spasms of the sphincter may lead to abdominal pain and respiratory distress, symptoms which may be confused with those of heart seizures. *See* GALLBLADDER.

Vertebrata. The primitive vertebrate group Agnatha is represented by the extant cyclostomes: hagfishes and lampreys. The cyclostome liver is extremely small and consists of only a single lobe in the adult lamprey. The bilobed structure of the hagfish is more typical of the vertebrate archetype. The livers of higher fish are relatively large and lobated.

In some forms the gallbladder and even the bile duct may degenerate during metamorphosis and thus may be absent in the adult. A gallbladder is generally

present, although a few species of cartilaginous fish (shark) may lack this structure. In the teleosts (bony fish), the gallbladder is often quite large.

The economic importance of fish liver (oils and vitamins) stems in part from the capacity of this organ to synthesize and store lipids. Researchers hypothesized that in lower vertebrates the liver carries out synthetic functions, particularly of a lipid nature, which are delegated to the increasingly important adipose-tissue mass in birds and mammals. Shape and pancreatic relationship are quite variable for teleost liver.

Amphibians. The large liver of the amphibians, which is lobed and possesses a gallbladder, receives venous blood from the abdominal vein as well as the hepatic portal vein. Some variation in lobation patterns are encountered in the members of this class. *See* AMPHIBIA.

Reptiles. Reptiles demonstrate typical patterns of hepatic topography. In snakes (Squamata) one elongated lobe is found, whereas turtles (Chelonia) and crocodiles (Crocodylia) have two lateral masses connected by a thin isthmus. The gallbladder is invariably present. *See* REPTILIA.

Birds. The liver of birds is invariably lobed, but quite compact. The gallbladder is often absent but may exist as primordium in the embryo. In the pigeon two separate bile ducts lead from each lobe of the liver to the duodenum. *See* AVES.

Mammals. A great deal of variation characterizes the lobation of mammals (**Fig. 6**). Two major lobes may be subdivided in a variety of ways. If the lobations are superficial, the liver is classed as unified, as in the case of humans, whales, and many of the ruminants. In these livers the portal and hepatic canals tend to run at right angles to each other, whereas markedly lobated livers show a parallel arrangement of the large branches of these canals. Removal of a portion of a unified liver is a more difficult procedure than similar extirpation from a lobated liver.

Many mammals lack a gallbladder (rat, whale, coney, some of the artiodactyla, and all hoofed animals). In humans, those individuals who carry typhoid fever usually harbor the typhoid bacilli within the gallbladder and discharge the organisms in their feces. *See* ARTIODACTYLA; MAMMALIA.

Histology

In all vertebrates, with the exception of the adult lamprey, the liver is essentially a three-dimensional lattice of interconnected walls or plates made up of epithelial cells (hepatic parenchyma) [**Fig. 7**]. The cylindrical spaces (lacunae hepatis) which tunnel within this parenchymal mass interconnect to form a continuous maze of corridors known as the labyrinthus hepatus. Suspended in the lacunae hepatis are the sinusoids, or liver capillaries. These are relatively large, irregular, anastomosing vessels lined discontinuously with a specialized endothelial layer. Each functional unit of the liver is in contact with terminal branches of the two pervasive tunnel systems traversing the liver: the portal and hepatic canals. The branches of these two systems never

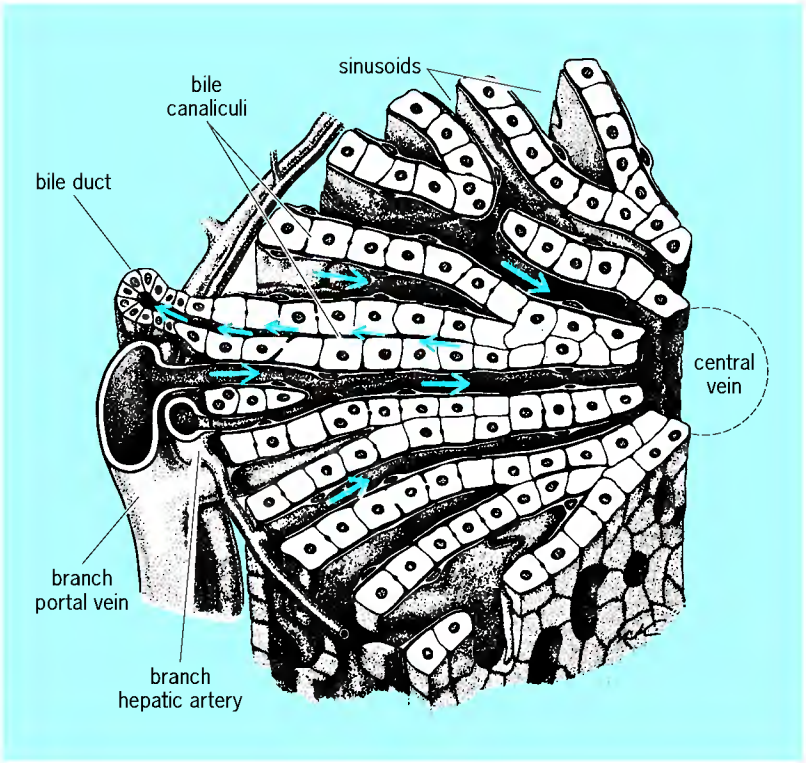

Fig. 3. Radial disposition of the liver-cell plates and sinusoids around the terminal hepatic venule or central vein, showing centripetal flow of blood from branches of the hepatic artery and portal vein and centrifugal flow of bile (small arrows) to the small bile duct in the portal space. (*After W. Bloom and D. W. Fawcett, A Textbook of Histology, 9th ed., Saunders, 1968*)

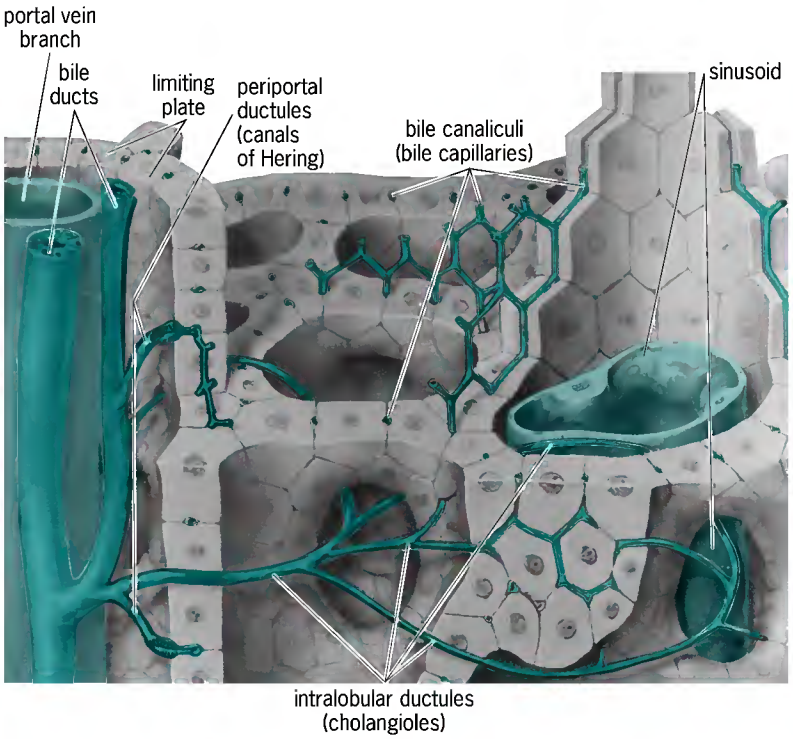

Fig. 4. Intrahepatic biliary system showing the arrangement of the bile ducts and the venous system. (*After E. Oppenheimer, ed., The Ciba Collection of Medical Illustrations, vol. 3: Digestive System, pt. 3: Liver, Biliary Tract and Pancreas, Ciba, 1957*)

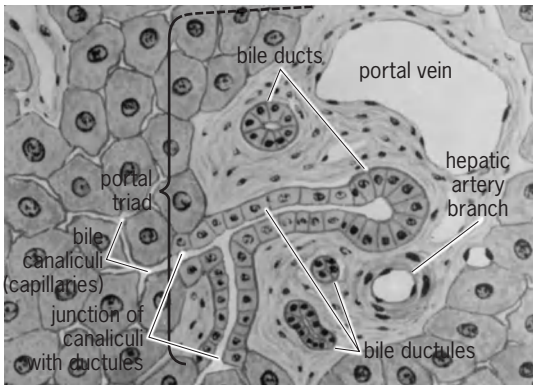

Fig. 5. Liver section, with components of portal triad. (*After E. Oppenheimer, ed., The Ciba Collection of Medical Illustrations, vol. 3: Digestive System, pt. 3: Liver, Biliary Tract and Pancreas, Ciba, 1957*)

communicate directly, but each is dovetailed into the sinusoid, the site of functional linkage between the two arborescent systems.

Limiting plate. The external surface of the liver is covered by a single layer of thin parenchymal cells lying immediately beneath the fibrous Glisson's capsule. This limiting plate is continuous with the hepatic muralium. It is reflected inward at the porta hepatis to form a fenestrated wall around the portal canals. In a similar manner the hepatic canals are also lined with a limiting plate (Figs. 2 and 4). Thus the external and internal limiting plates make up a continuum which is in intimate association with the internal muralium. The fibrous capsule is also reflected into the interior of both canal systems and provides a matrix for bringing blood vessels, lymph channels, nerves, and ducts into the interior of the liver.

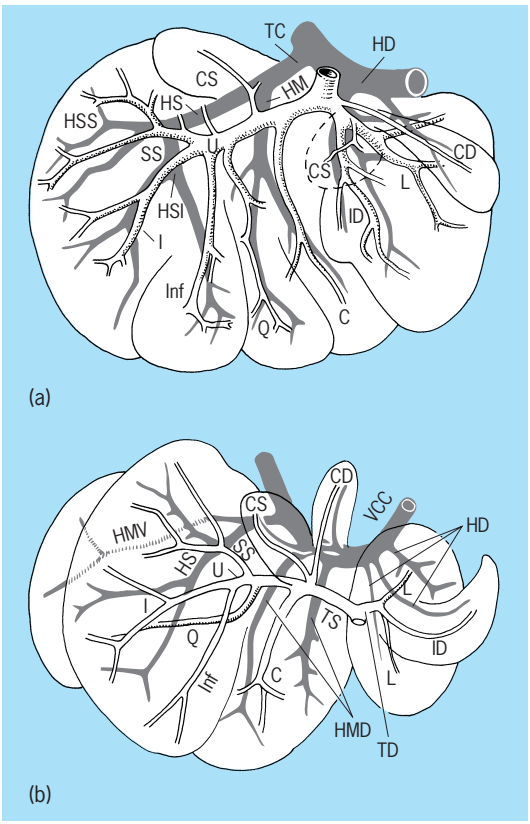

Fig. 6. Dorsal aspect of (*a*) liver of dog, (*b*) liver of rat. Rami venae portae: C, centralis; I, intermedius; ID, inferior dexter; Inf, inferior sinister; L, lateralis; Q, quadratus; SS, superior sinister. Venae hepaticae: HD, dextra; HM, media; HMV, ventral division of media; HMD, dorsal division of media; HS, sinister; HSI, sinistrae radix inferior; HSS, sinistrae radix superior. Ramuli: CD, caudatus dexter; CS, caudatus sinister; TC, truncus communis. Trunci venae portae: TD, dexter; TS, sinister; U, pars umbilicalis; VCC, vena cava inferior.

Sinusoids. The lining of these specialized capillaries has been the subject of considerable debate. Older theories postulated a syncytium (absence of individual cell boundaries), but electron micrographs show separate cells present. These lining cells were once hypothesized to be of only one type, the Kupffer cells, with a great capacity for engulfing foreign material (phagocytosis). It is now thought that there may be as many as three distinct types making up the lining, although transformation of one type to another is possible. The large macrophages (Kupffer cells) engulf degenerative erythrocytes as well as foreign or unassimilated material, thus "straining" the blood which moves through the liver sinusoids from the vessels of a portal canal to the central veins. Once again electron microscopy has clearly demonstrated that, although some of these lining cells tend to overlap one another, others have margins which are separated by as much as 0.5 μm. Some animals, for example, the calf, do not demonstrate this discontinuity; this raises the interesting problem of possible species differences. The regulation of blood flow within the hepatic lobule is achieved in part through a swelling of the macrophages lining the sinusoid.

A patent space, called the space of Disse, stands between sinusoid cells and the liver parenchymal cells (Fig. 2). Irregularly arranged projections, or microvilli, extend from the parenchymal cell and lie within the space of Disse. No limiting basement membrane blocks the free interchange between sinusoid gaps and the parenchymal cell. Futhermore, the villi of the parenchymal cell lying within the perisinusoidal space increase parenchymal cell surface across which exchanges may occur with the lymph-like fluid emanating abundantly from the sinusoid. This increase in the area of exchange is particularly important in terms of the rapid transfer of metabolites that must occur between the liver and portal blood.

Biliary system. The bile canaliculi are found between parenchymal cells throughout the liver. They are composed of a continuous network of polyhedral links associated with the convoluted muralium. If a single parenchymal cell is isolated, a hexagonal mesh of bile canaliculi appears to surround it. Although the specialized membranes of adjacent liver cells appear to extend into the lumen of the bile canaliculus in the form of microvilli, it is quite clear that no intracellular channels extend from the canaliculus into the parenchymal cytoplasm. Older studies suggested that the canalicular apparatus contained discrete walls which reinforced the histoarchitecture of the parenchymal mass. However, it is now

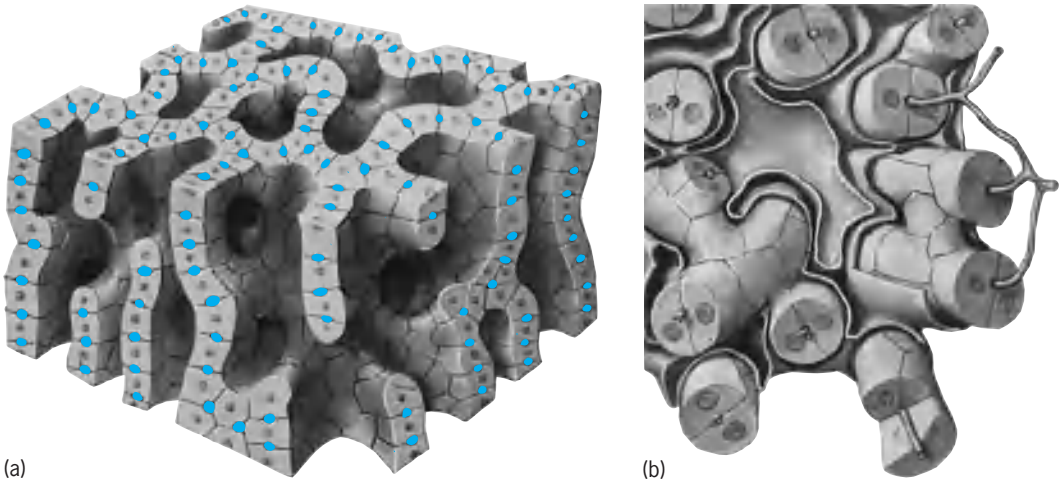

Fig. 7. Liver structure. (*a*) Stereogram of liver-cell plates after removal of ducts, vessels, and connective tissue. (*b*) A former concept of liver structure which was thought to be composed of cell cords. (*After E. Oppenheimer, ed., Ciba Collection of Medical Illustrations, vol. 3: Digestive System, pt. 3: Liver, Biliary Tract and Pancreas, Ciba, 1957*)

believed that the lumen of the canaliculus is merely an expansion of the parenchymal intercellular space, with fibrous reinforcement of the cytoplasm immediately surrounding the lumen. In the normal liver no communication exists between the canaliculi and the Disse space; under pathological conditions, however, the microvilli may swell and obstructive pressure may then lead to passage of bile into the Disse spaces. The high levels of the enzyme adenosinetriphosphatase (ATPase) found around the lumen of the bile canaliculi serve as a histochemical marker for these tiny structures.

Comparative histology. In early radiations of the vertebrate group, a parenchymal muralium two cells in thickness developed. In mammals, songbirds, and several primitive bird groups, a single-cell-thick muralium (simplex) is found. This mammalian pattern is more efficient in increasing the blood–parenchymal cell interface area and affords a more rapid exchange between blood and liver, which is appropriate to the metabolically more active homeotherms. Exchange is also facilitated by the microvilli which extend from parenchymal cell surfaces apposed to sinusoidal spaces.

Cyclostomes. This group is sufficiently different from other vertebrate groups to justify a separate categorization of their cellular arrangement: large bile canaliculi lined by parenchymal cells demonstrating polarity (structural and functional specialization in relation to the cell axis).

Fishes. The elasmobranchs (sharks) show bile canaliculi tubules of smaller bore lined by large, fat-laden cells. Some degree of polarity persists in the hepatocytes of teleosts. The lobular arrangement of higher forms, involving centripetal flow of blood through the sinusoid from peripheral vessels of portal triad to central veins, is absent. During vitellogenesis (egg development) or pregnancy in many teleosts, a marked reduction of hepatic lipid and hepatocyte volume is found, which suggests a calorie storage function for the liver in lower vertebrates.

Great variations in liver cell nuclei size have been reported in several teleosts, with some indications of a rhythmic alternation. This alternation of size may be related to the mitotic periodicities of higher vertebrate forms, such as the circadian (24-h) rhythms of the cortical liver cells in certain amphibians; namely, salamanders and newts.

Amphibians and reptiles. The capillaries between portal and hepatic channels are not arranged in typical radial fashion in the frog, so that a lobular pattern is not discernible. In addition, there are marked seasonal variations in the appearance of the liver cells and in their content of glycogen and fat. Large lymphatic channels are a characteristic of many amphibian livers, and cells within these ducts, as well as the hepatocytes themselves, are often pigmented. Similar pigmentation is encountered in the reptiles, whose livers also lack the clear-cut lobular pattern of birds and mammals.

Birds and mammals. In birds and mammals the classical lobular pattern is usually a distinguishing feature, although the absence of connective tissue boundaries may obscure this basic recurrent form of peripheral portal triads, radial sinusoids, and central veins. Some investigators maintain that the classical lobule is merely an artifact of blood flow patterns within the liver, and attempts to construct a functional unit in which the portal triad is the center of a smaller "acinar" lobule have received considerable support. In a number of mammalian species vinyl-injection techniques have provided histological evidence for such a pattern; this would also accord with the more usual glandular arrangement of secretory drainage ducts standing in the center of the lobule.

Cytology

The significant functional cell of the liver is the hepatic parenchymal cell (**Fig. 8**). The sinusoids and a small amount of connective tissue also contribute distinctive cell types.

Parenchymal cells. These are polyhedral units of at least six sides; varying in volume from less than

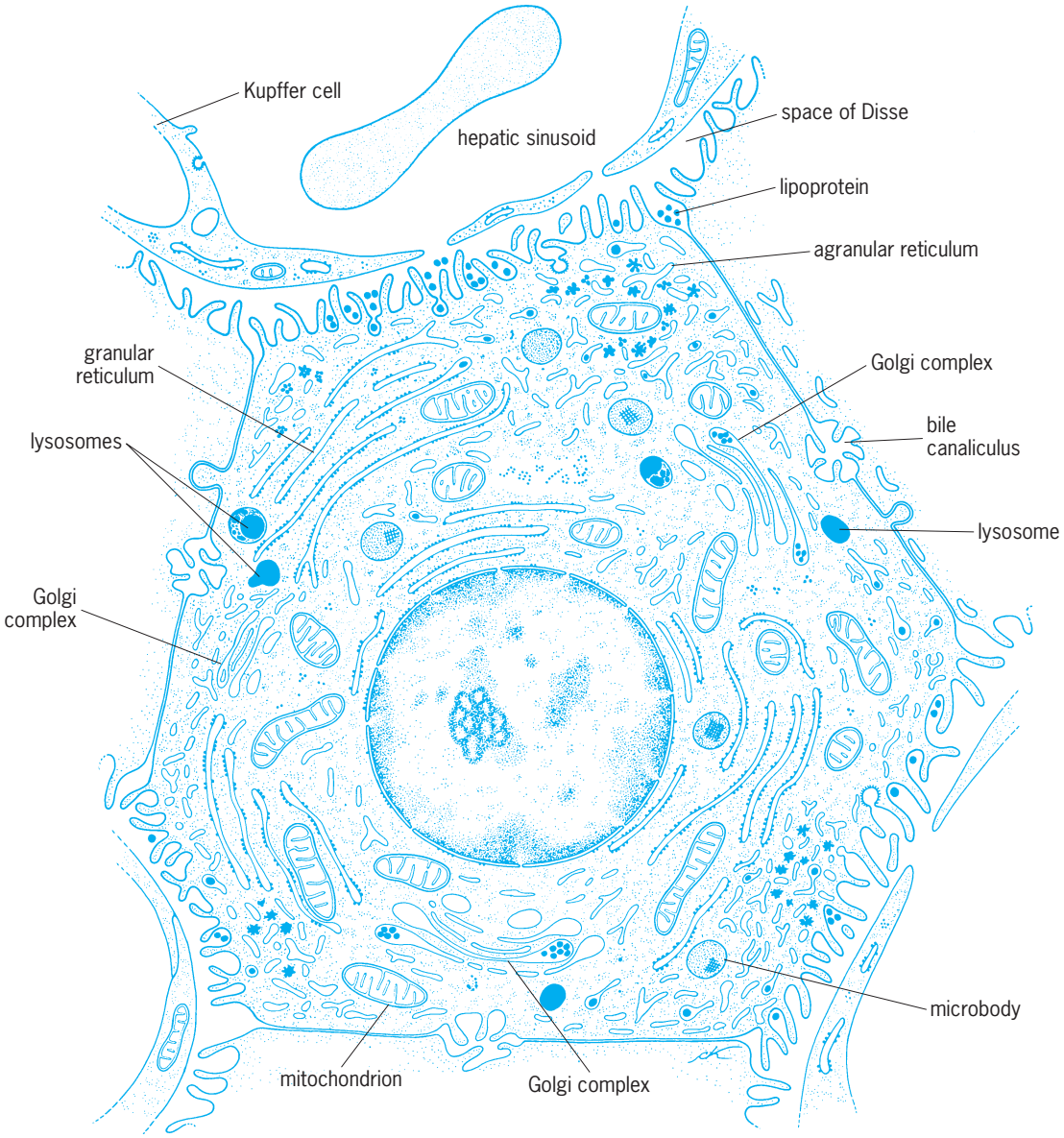

Fig. 8. Relationship of the liver cells to each other and to the sinusoids, with principal components of the hepatic cell as seen in electron micrographs. (*After W. Bloom and D. W. Fawcett, A Textbook of Histology, 9th ed., Saunders, 1968*)

10,000 to 35,000 cubic micrometers. The surfaces may be in contact with the perisinusoidal space; the lumen of a bile canaliculus; or an adjacent parenchymal cell.

The round nucleus may be quite large and variable, a consequence of the polyploidy (containing more than two sets of chromosomes) which characterizes many liver cells. Occasionally two nuclei are found. Nucleoli are prominent, and scattered chromatin clumps may be seen within the smooth nucleus. The cytoplasm varies with the nutritional state and general health of the animal, particularly in terms of glycogen space and fat vacuoles. Numerous mitochondria (filamentous) are present. A compact series of vesicles, the Golgi complex, is discernible near the bile canaliculus, where it probably acts to concentrate and "package" the bile. *See* CELL (BIOLOGY).

Electron microscopy. Electron micrographs have extended the understanding of hepatic ultrastructure. Thus both smooth- and rough-surfaced types of endoplasmic reticulum (tubular cytoskeleton) are present, with the rough-surfaced type being a major site of protein synthesis. The endoplasmic reticulum is continuous with the external membrane of the double nuclear envelope and possibly with the cytoplasmic membrane, so that a continuous system of channels may completely traverse the cell. Glycogen appears as single granules 40 nanometers thick, or in conglomerates up to 0.2 micrometer across, in close association with the smooth endoplasmic reticulum. *See* ELECTRON MICROSCOPE.

Distributed in the region of the bile canaliculus are dense rounded bodies, called lysosomes, containing several hydrolytic enzymes. The peroxisomes are similar in structure but contain crystalline inclusions rich in the enzyme uricase, which splits uric acid. They are also rich in enzymes which split hydrogen peroxide or use it to effect oxidations.

Adjacent parenchymal cells are reciprocally attached through tiny projections in one that fit snugly into recesses of the other in a manner analogous to snap fasteners.

Fractionation techniques. The region of cytoplasm immediately surrounding the bile canaliculus is fibrillar and probably gelated and may persist as tubular fragments even when the liver is macerated or homogenized. The homogenizing process involves the breakdown and dispersal of the cellular elements of a tissue to yield a homogeneous mixture for assay of enzymes, metabolites, and so forth. Differential centrifugation may then yield fractions which are particularly rich in mitochondria, other cellular organelles, or the nonparticulate cell sap. These fractionation techniques were originally developed with mammalian liver as the test material and sharply increased understanding of the biochemical patterns of liver organelles. *See* CENTRIFUGATION.

Sinusoidal lining cells. A great deal of variation is characteristic of these "littoral" cells, and even the shape and texture of the nucleus differs from one preparation to the next. Mitochondria have been noted, but not in all cells. Lipid has been demonstrated in these cells, but the existence of glycogen is in doubt. Lysosome activity has been indirectly demonstrated. The phagocytosing cells are believed to contain lysosomes and are characterized by long cytoplasmic extensions which prompted earlier investigators to call them the stellate (starlike) cells of Kupffer. Some of the living endothelial cells are vacuolated and are believed to serve as fat-storing cells, whereas others are highly granular. About 15% of the human liver cell population is made up of littoral cells.

Connective tissue. Although the liver is the largest internal organ in the body, it contains only slight amounts of supporting connective tissue, averaging less than 1%. Connective tissue is found in the capsular material, the sheath which surrounds the vessels and ducts of the portal canal system, and in lesser amounts within the hepatic canal system. *See* CONNECTIVE TISSUE.

Collagenous fibers are found within the canal systems, whereas delicate reticular fibers extend between the parenchymal cells of the muralium and the endothelial cells within the space of Disse. These fibers, appearing early in embryonic development, probably arise from the sinusoidal living cells. The connective tissue in the perisinusoidal space, which is continuous with the dense connective material of the portal sheath, is believed to function in channeling the large amount of lymph which arises as tissue fluid in the liver.

Embryology

The liver arises initially as a thickening and then an outpocketing of the ventral surface of that portion of the gut destined to become the duodenum. Two branches are quickly formed: an anterior portion from which the liver parenchyma develops; and a posterior portion giving rise to the gallbladder, its cystic duct, and the common bile duct.

Morphogenesis. The liver parenchyma develops as a series of cords or strands which are essentially tubular. At first these proliferating cords lie alongside the vitelline vessels of the yolk sac; then they are found ramified within these vessels to form an intermingled mass of epithelial cords and tiny channels, or sinusoids, representing subdivisions of the original larger venules. *See* FETAL MEMBRANE; YOLK SAC.

Alternative explanations for sinusoid development have been offered. Branching of the cords takes place in a manner characteristic of each vertebrate group and results in the varied hepatic architectures found in the adult. There may be as many as 12 basic patterns of hepatic development among vertebrates and the proliferation of hollow cords may be characteristic of only a few species.

The parenchymal cells, which are arranged in a continuous muralium (lamina) either two cells thick (lower vertebrates) or one cell thick (mammals and songbirds), are mainly derived from the endoderm. In early states the muralium may be several cells thick. The sinusoidal elements are chiefly derived from mesenchyme, but the origin of the blood-forming cells that characterize the embryonic liver is not fully known.

The bile canaliculi, which also form a continuous network in the liver, arise as a result of parenchymal cell differentiation. They are probably formed even before the liver is capable of producing bile and ramify into ductules and ducts which join the hollow posterior pouch, or future gallbladder. One contribution of electron microscopy has been the finding that the walls of the bile canaliculi do not exist as separate structures but simply represent differentiated surfaces of apposed hepatic cells.

Metabolic aspects. Although the liver plays a key role in assuring carbohydrate homeostasis (dynamic steady-state conditions) through the storage of sugar as glycogen, the embryonic livers of most species are incapable of synthesizing glycogen until a precise point is reached, rather late in development, which varies with different species. In most mammals a maximum reserve is achieved at birth, with a rapid falling off soon after. In amphibians glycogen build up is associated with metamorphosis, whereas in birds several cycles are apparent. Control is probably achieved through hormonal action of the pituitary-adrenal axis, although the role of enzyme activation has also been explored.

Much less is known about the handling of lipids, although it is clear that hepatic fat appears quite early in most mammalian embryos and is extremely high in the newborn. High lipid reserves exist in chick livers at hatching but diminish sharply thereafter. Protein incorporation, as measured by the uptake of radioactive-labeled amino acids, is extremely high in the livers of rat embryos despite the generally lower protein levels in comparison to adults. These livers also demonstrate an early competence for the synthesis of histamine.

Many of the enzymes which play a key role in the metabolic transformations of the adult mammalian liver are either low or absent at birth. The synthesis of

these enzymes at term may explain the sharp changes at birth in the levels of such metabolites as glycogen. Iron reserves also tend to increase late in embryonic life, and the storage in the liver of histologically identifiable iron is associated with the gradual diminution of the erythropoietic function. Electron microscopy studies have received an interest in the nature of the hemopoietic (blood-forming) function of the nature and origin of the blood-forming island cells which proliferate within the parenchymal elements early in embryonic life.

Physiology

The large size of the liver is matched by its functional complexity and involvement in a diverse array of regulatory mechanisms. Although said to perform over 100 specific functions, the liver's key physiological role may be delineated under seven major headings.

Control of carbohydrate metabolism. Following the ingestion of food, blood entering the liver from the hepatic portal vein is rich in glucose and other monosaccharides (simple sugars). The parenchymal cells, which are freely permeable to these sugars, remove them from the general circulation and store them as a complex insoluble polymer, glycogen. Since glycogen is a polysaccharide made up of glucose subunits, the liver must first convert other dietary monosaccharides (fructose, galactose) to glucose prior to glycogen synthesis (glycogenesis). As a result of this storage mechanism, the blood leaving the liver through the hepatic veins contains normal levels of glucose. In the intervals between ingestion of food, liver glycogen is broken down. This process, known as glycogenolysis, tends to maintain blood sugar levels between 80 and 100 mg per 100 ml of blood. *See* CARBOHYDRATE METABOLISM; GLUCOSE; GLYCOGEN; MONOSACCHARIDE.

Blood sugar level. Since the brain and other vital central nervous system structures are almost entirely dependent on the glucose fuel of the blood, hepatic regulation of circulating carbohydrate is necessary to life. Under conditions of prolonged fast, where glycogen stores are exhausted, the liver is capable of converting noncarbohydrate metabolites into glucose to maintain blood sugar levels. This process, by which amino acids, fats, glycerol, and other metabolites are converted enzymatically to glucose, is called gluconeogenesis. It represents a significant metabolic pathway for the regulation of carbohydrate metabolism by the liver, although the kidney is also capable of carrying out gluconeogenesis in mammals.

All of the processes involved in the manipulation of carbohydrate by the liver are active constantly, but the relative rates of individual pathways vary in response to food intake, tissue uptake, hormone levels, and so on. The maintenance of constancy through the dynamic balance of opposing metabolic forces is called homeostasis, a concept which was first developed a century ago by Claude Bernard in his studies of the biochemical competency of the liver. *See* HOMEOSTASIS.

Endocrine regulation. It has long been recognized that the pancreatic hormone insulin is necessary for the utilization and storage of glucose, while hormones of the adrenal cortex are involved in the gluconeogenic process. The actions of epinephrine and glucagon in enhancing hepatic glycogenolysis have been elucidated. Thus the complex steps involved in maintaining carbohydrate homeostasis are subject to endocrine control, with the liver serving as a particularly sensitive target organ for the hormone regulators. *See* INSULIN.

Enzyme systems. The precise nature of these hepatic responses are being explored, and emphasis is placed upon the role of specific enzyme systems which are rate-limiting in some overall pathway or which occupy a branch position serving to divert metabolites from one major pathway to another. *See* ENZYME.

1. *Gene activation*. George Weber showed that insulin, which is known to enhance uptake of glucose by muscle and adipose tissue, tends to increase the formation of three "bottleneck" enzymes in the liver which act to degrade glucose (glycolysis) and prepare its carbon skeletons for eventual oxidation by the mitochondria. On the other hand, insulin inhibits formation of a quartet of hepatic enzymes which act to bring the degradation products of glucose back to free monosaccharide. Hormones of the adrenal cortex have a completely opposite effect on these same target enzymes, thus explaining the opposing actions of cortisone (which increases blood sugar) and insulin (which decreases blood sugar) on carbohydrate balance. Presumably these hormones act on a specific gene which is responsible for the synthesis of a particular group of enzymes influencing a single effect. *See* GENE ACTION.

2. *Enzyme targets*. Direct action on an enzyme already present in the liver cell is also utilized. Thus epinephrine and glucagon (a pancreatic hormone that is antagonistic to insulin) each act to produce increased quantities of cyclic adenosine monophosphate (cAMP), which activates the hepatic enzyme involved in the cleavage of glycogen bonds to yield glucose. The rise in blood sugar associated with increased circulating levels of epinephrine is effected through this mechanism. Thyroxine also influences blood sugar levels, but its mode of action is unclear.

Negative feedback mechanisms. These provide a fine-control system for the hormones themselves in carbohydrate regulation. Thus insulin release is enhanced by high blood sugar levels (hyperglycemia), but its release brings into play mechanisms which tend to lower blood sugar levels and hence dampen the evoking stimulus. Long-term heavy ingestion of carbohydrate may exhaust the insulin-producing tissue of the pancreas and lead to diabetes—a complex disease usually involving insulin deficiency with concomitant disturbances of carbohydrate and fat metabolism. *See* DIABETES; ENDOCRINE MECHANISMS; LIPID METABOLISM.

In genetic obesity in mice, characterized by a seemingly paradoxical situation of high insulin levels and hyperglycemia, elevations in hepatic glycolytic

enzymes are found. This is consistent with Weber's findings of a similar hepatic glycolytic enzyme increase in animals injected with insulin. The relatively high fasting levels of liver glycogen also associated with this syndrome may be attributed to the induced synthesis of glycogen synthetase (glycogen-forming enzyme). This synthesis has been shown to occur with insulin and is related to the action of insulin in promoting carbohydrate storage in the liver. The liver possesses an enzyme, called insulinase, which degrades insulin. Its importance under physiological conditions is not clear; however, with overproduction of insulin, insulinase may prevent excessive buildup of the hormone in the bloodstream.

Interconversion of metabolites. The liver is a major site of the production of both fatty acids and neutral fats (triglycerides—three fatty acids joined to glycerol). Under conditions of adequate feeding and high carbohydrate intake, a significant proportion of the food entering the liver through the portal vein, or coming in from the systemic cirulation through the hepatic artery, will be converted to fatty acids and neutral fat. The liver possesses enzyme systems which activate both fatty acids and glycerol to facilitate their conversion to the less soluble triglycerides. In addition, the manipulation of carbohydrate in the liver leads to the formation of substrates and coenzymes (accessory molecules for enzyme action) necessary for fat synthesis, although an increasingly important role in fat metabolism is being assigned to the adipose tissue mass in mammals.

The link between the pathways of carbohydrate and fat metabolism is the probable basis for the disruption of fat synthesis and storage which occurs when carbohydrate metabolism is impaired. Synthesis of the phospholipids, which are readily transportable lipids, also occurs in the liver. The production of fatty infiltrations in the livers of animals deficient in choline or methionine may be associated with an impairment in phospholipid metabolism, since these substances are necessary for their formation. Inability to form lipoproteins has also been suggested as a factor. Agents which increase fatty acid transport to the liver or decrease hepatic fatty acid oxidation may also bring about fatty degeneration. Chronic accumulation of lipid in the liver leads to fibrotic changes and eventual cirrhosis, a condition in which the liver loses its resiliency and gradually ceases to function as the parenchymal mass is replaced by connective tissue. A variety of hepatotoxins (alcohol, chloroform, carbon tetrachloride, lead, and others) also produce fatty livers. *See* COENZYME; LIPID; LIVER DISORDERS.

Ketone bodies. Representing partial oxidation products of fatty acid degradation, these are produced by the liver and utilized as a rapid short-term energy source by extrahepatic tissues. In starvation and advanced cases of diabetes, the excess production of acidic ketone bodies poses a serious threat to life. It has been shown that hepatic glutamine production is markedly augmented in these circumstances, presumably to meet the increased needs of extrahepatic tissues. *See* KETONE.

Sterols and steroids. Cholesterol is also synthesized by the liver, although small amounts are ingested. High levels of cholesterol are believed to be associated with atherosclerosis (hardening of the arteries) by some investigators, but the relationship is a complex one. Cholesterol is excreted in the feces following its conversion to bile salts, but considerable recycling of these sterol compounds may occur between intestine and liver. Steroid hormones, which resemble cholesterol in their chemical structure, are degraded in the liver and may then be excreted in the bile. *See* CHOLESTEROL; STEROID; STEROL.

Amino acids. From the gut amino acids reach the liver through the portal circulation, and a small portion may be incorporated into hepatic structural protein to serve as a labile reserve. Protein is not generally regarded as being stored in animal tissues. During gluconeogenesis, which is enhanced by glucagon as well as the adrenal steroids, amino acids are stripped of their nitrogen and the remainder of the carbon skeleton is utilized for the production of glucose. The nitrogen arising from this deamination process may be secreted into the blood as ammonia, or the ammonia may be converted by the liver to urea or uric acid. The latter two nitrogenous end products are associated with vertebrates inhabiting marine or terrestrial environments. Nitrogen, or more specifically amino groups, may also be shifted from one organic molecule to another through the process of transamination. High levels of the enzymes mediating these transfers (transaminases) are found in the liver, and they may pass into the bloodstream during hepatic degeneration, where they serve as a clinical sign of liver damage. *See* AMINO ACIDS; CLINICAL PATHOLOGY; EXCRETION; PROTEIN METABOLISM; TRANSAMINATION.

Blood protein manufacture. The liver is the only source of plasma cholinesterase, albumin, prothrombin, and fibrinogen. Most of the globulins also arise in the liver, but gamma globulin is produced in plasma cells found principally in the spleen with only a minor contribution coming from the lymphoid tissue of the liver. On the basis of the hepatic contribution to the pool of blood proteins, a significant role may be averred for the liver in maintaining the osmotic pressure of the blood, preventing hemorrhage, providing a reserve of body protein (7 g per 100 ml of blood), promoting the transport of lipids, and preventing excess buildup of acetylcholine. *See* ACETYLCHOLINE; BLOOD; GLOBULIN; HEMORRHAGE.

Erythropoietic function. In almost all vertebrates the liver is the predominant embryonic source of red blood cells. Thrombocytes (platelets) are also produced in this organ, and in embryonic forms other than man the liver may be an important region for lymphocyte and granulocyte production as well. In urodeles the cortical region of the liver continues its erythropoietic function throughout the life cycle. *See* HEMATOPOIESIS.

Detoxification. Many poisons are rendered harmless by degradation reactions in the liver. These reactions involve conjugation, methylation, oxidation, reduction, and complex syntheses. The

microsomes (endoplasmic reticulum and ribosomes) are particularly active in neutralizing potentially harmful drugs, for example, barbiturates, tranquilizers, and hallucinogens such as lysergic acid diethylamide (LSD). Detoxification mechanisms are also involved in the formation of bile pigments, the esterification of cholesterol, and the conjugation or oxidation of steroid hormones. A diseased liver cannot carry out these functions, which lowers the body threshold to most toxic materials.

Bile formation. Bile is formed at the rate of about a quart per day. It consists of bile pigments, bile salts, protein, cholesterol, and inorganic salts. The pigments, bilirubin and biliverdin, arise from the breakdown of heme in those tissues (spleen, bone marrow) where erythrocytes are usually broken down, and then are conjugated with glucuronic acid by the liver. Bile salts and cholesterol are formed in the liver. The significance of bile release into the intestine lies in the ability of the bile salts to emulsify fats, activate lipase, and promote the uptake of the fat-soluble vitamins by the intestine. *See* BILIRUBIN.

Vitamin storage. The liver stores vitamins A and D and is apparently a reservoir for iron as well. Some of the B vitamins are also at high levels in liver tissue, suggesting a possible storage mechanism. Carotene in the liver is converted to vitamin A. *See* DIGESTIVE SYSTEM; VITAMIN A.

George H. Fried

Bibliography. D. Fawcett, *Bloom and Fawcett: A Textbook of Histology*, 12th ed., 2001; A. Francavilla et al. (eds.), *Liver and Hormones*, 1987; M. F. Heyworth and A. L. Jones (eds.), *Immunology of the Gastrointestinal Tract and Liver*, 1988; H. A. Harper et al., *Review of Physiological Chemistry*, 17th rev. ed., 1979; L. Weiss (ed.), *Cell and Tissue Biology: A Textbook of Histology*, 6th ed., 1988.

Liver disorders

A heterogeneous group of diseases that affect the liver and are of particular importance because of the many essential functions of the liver. It is a large organ (50–63 oz or 1400–1800 g), and it is involved in the metabolism of proteins, fats, and carbohydrates; in the production of bile and blood clotting substances; and in the metabolism and detoxification of many hormones and drugs. Because of the numerous functions of the liver, persons with liver disorders can develop a number of different signs and symptoms. One common symptom of liver disease is fatigue, although some people are entirely asymptomatic. A striking sign of liver disease is jaundice (yellowing of the skin and eyes) due to abnormal production or transport of bile. The presence of liver disease can be confirmed by performing liver function tests on the blood. Such tests can sometimes indicate the severity of the disease and occasionally even the exact type of abnormality. Usually, however, liver function tests can indicate only the presence of a liver abnormality. But a needle biopsy, in which a small amount of tissue is removed through a needle puncture for microscopic examination, can be done safely with minimal pain and inconvenience to the patient. A needle biopsy can help determine the type of liver disorder and the extent of organ damage. *See* JAUNDICE.

Fatty metamorphosis. This common condition is characterized by accumulation of fat (lipid) within the liver cells. The individual cells become engorged with fat, and overall liver size can increase to two or three times normal size. Persons who develop fatty metamorphosis may have no signs or symptoms except for a vague feeling of increased "fullness" in the right upper quadrant of the abdominal area, which is the location of the liver. An enlarged liver may also be diagnosed during a routine physical examination. In the United States the most common cause of a fatty liver is excessive alcohol intake, which appears to cause a change in the metabolism of the liver cells. In the developing areas of the world, malnutrition is the major cause of a fatty liver. The cause in this case is not a lack of calories but a deficiency in specific amino acids that are necessary for normal metabolism. Some obese persons also develop a fatty liver, perhaps as a manifestation of their overall excess body fat. Fatty liver caused by excess alcohol may progress to cirrhosis. *See* ADIPOSE TISSUE; ALCOHOLISM; MALNUTRITION; OBESITY.

Hepatitis. Hepatitis, which is an inflammation of the liver, has a variety of causes. The specific type of hepatitis present is usually determined by studies of serum, which identify the type of antibody directed against a component of the causative virus, or by liver biopsy. The prognosis for otherwise healthy persons who develop hepatitis is excellent: even those with hepatitis B have a greater than 85% survival rate. *See* HEPATITIS.

Cirrhosis. Cirrhosis is a disease in the liver that is characterized by scarring, which produces a marked nodularity of the liver. Cirrhosis has a variety of causes, although in the United States the most common by far is excessive alcohol intake. Cirrhosis caused by alcohol has been referred to as nutritional cirrhosis because it was originally believed to be related to a deficiency of certain dietary substances relating to the alcoholic condition. However, studies of the disease suggest that alcohol is a direct liver toxin and is itself responsible for the changes that eventually lead to cirrhosis. Cirrhosis may also result from almost any type of injury to the liver that does not heal but instead leads to progressive inflammation and scarring. Some cases of viral hepatitis progress to cirrhosis, as can obstruction of the bile duct. When the duct cannot drain bile from the liver, the result is a form of the disease that is referred to as secondary biliary cirrhosis. In general, cirrhosis is a devastating disease and has many serious complications due to increased pressure in the portal venous system, with shunting of blood through the systemic venous circulation. This shunting of blood frequently results in rupture of blood vessels near surfaces of various organs and can cause, for example, bleeding into the intestine. *See* CIRRHOSIS.

Neoplasms. Most neoplasms in the liver are malignant and are metastatic from a primary site. Because the liver receives the entire venous drainage from the intestine and thus is a common site for the spread

of tumors from the intestine. Lung and breast cancer also frequently metastasize to the liver. Primary tumors of the liver are rare in the United States, although in some parts of Africa they are the most common type of tumor. Usually their cause is unknown, but in the United States primary malignant tumors are most frequently associated with cirrhosis. Primary liver cancers are difficult to treat because they usually grow rapidly and involve other structures, preventing total surgical removal. *See* CANCER (MEDICINE); ONCOLOGY.

Uncommon or rare disorders. Reye's syndrome is a liver disorder that affects primarily infants and young children; it usually occurs during or after an episode of viral influenza and it has been causally related to the ingestion of aspirin for treatment of influenza. The effects of Reye's syndrome include a finely vacuolated fatty change in the liver. Wilson's disease, also called hepatolenticular degeneration, is a rare inherited disorder of copper metabolism in which cirrhosis of the liver is associated with degeneration of certain regions of the brain. Hemochromatosis, another hereditary disease, is marked by excessive deposition of iron in the liver because of faulty iron metabolism. It causes cirrhosis and is frequently associated with primary cancer of the liver. In alpha-1 antitrypsin deficiency, a disease characterized by an absence of an antienzyme in the blood, the liver can show extensive fibrosis and even cirrhosis. Some cases of primary cancer of the liver have been associated with an alpha-1 antitrypsin deficiency. *See* LIVER.

Samuel P. Hammar

Bibliography. J. H. Alter (ed.), Viral hepatitis, *Semin. Liver Dis.*, 6:1–95, 1986; J. R. Hodges et al., Chronic active hepatitis: The spectrum of disease, *Lancet*, 1:550–553, 1982; J. Ludwig and R. Axelsen, Drug effects on the liver: An updated tabular compilation of drugs and drug-related hepatic diseases, *Dig. Dis. Sci.*, 28:651–666, 1983; S. Sherlock, *Diseases of the Liver and Biliary System*, 10th ed., 1997; S. N. Zama et al., Risk factors in development of carcinoma in cirrhosis: Prospective study of 613 patients, *Lancet*, 1:1357–1359, 1985.

Living fossils

Living species very closely resembling fossil relatives in most anatomical details. The term is a relative one and, applied loosely, could embrace nearly all extant animals and plants. In its more restricted usage, the term applies to living species with four additional characteristics: (1) truly close anatomical similarity to (2) an ancient fossil species—generally at least 1×10^8 years old; (3) living members of the group are represented by only a single or at best a few species, which are (4) often found in a very limited geographic area. Examples are horseshoe crabs (found on the eastern shores of the two Northern Hemisphere continental landmasses, with closely similar relatives over 2×10^8 years old); ginkgo trees, dating from the Mesozoic era, which, until their recent introduction over the world, were restricted to Asia; and coelacanth fish, which have not changed much since the Devonian and which today are found only between eastern Africa and Madagascar and the Comoro Islands.

Living fossils are important because they retain many primitive traits, hence their study helps elucidate the anatomy of their fossil relatives. Living fossils also raise the issue of the lack of evolutionary change. Survival of primitive organisms in an unchanged state over many millions of years implies a low rate of evolution. Evidence suggests that slowly evolving groups speciate at a lower rate than faster-evolving groups. Such slowly evolving groups are frequently ecologically generalized, that is, able to exploit a wide variety of food resources and withstand large-scale fluctuations in the physical and chemical characteristics of their habitats. Organisms so adapted are unable to withstand competition from closely related species with similar habits. This factor reduces the number of available habitats and hence reduces the chance of new species evolving. Without speciation there can be little evolution, and as long as the habitat persists, so will the organisms, surviving virtually unchanged for millions of years. *See* SPECIATION.

Niles Eldredge

Bibliography. N. Eldredge, Survivors from the good old, old, old days, *Nat. Hist.*, 74(2):60–69, 1975; J. Martin, *Living Fossils*, 1997.

Llama

A member of the camel family (Camelidae) found only in South America. The llama is an artiodactyl, or even-toed ungulate, with two toes on each foot. The upper lip is cleft and prehensile. The animal has a

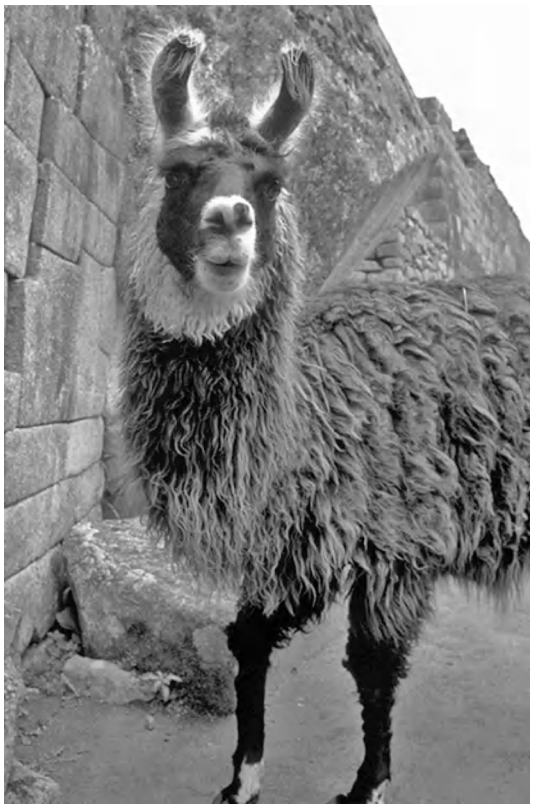

The llama of South America.

Hybrids produced by crossing different llamas

Male	Female	Hybrid
Llama	Alpaca	Huarizo
Alpaca	Llama	Misti; machurga
Vicuna	Llama	Llamavicuna
Guanaco	Llama	Llamahuanaco
Vicuna	Alpaca	Vacovicuna

long neck, and attains a maximum length of less than 8 ft (2.4 m) and a maximum weight of nearly 300 lb (135 kg; see **illus.**). A single young is born after a gestation period of about 11 months. The maximum life-span is about 20 years. Like other members of the family, the llama is herbivorous. It has 36 teeth with the dental formula I 1/3 C 1/1 Pm 3/3 M 3/3. These animals lack a gallbladder. Many interesting crosses have occurred among the different breeds in South America (see **table**). *See* ARTIODACTYLA.

Lama glama has been domesticated since the Inca civilization by the Peruvian Indians, who still keep large herds. While the fur provides material for rugs, rope, and cloth, the main use of this animal is as a beast of burden, especially in mining areas. The males are used as pack animals and the females are kept for breeding and wool production. The alpaca (*L. pacos*) is more restricted in its distribution and is specialized in wool production.

There are two species of wild llama, the guanaco or huanaco (*L. guanicoe*) and the vicuna (*L. vicugna*). The most widespread is the guanaco, which stands about 4 ft (1.2 m) at the shoulder and just over 5 ft (1.5 m) at the top of the head. The guanacos live in small herds composed of a male, several females, and the young. It was formerly thought that this stock represented the forerunner of the domestic breeds. The vicuna is becoming rare because of overshooting for its pelt of soft wool. *See* ALPACA; VICUNA.

Charles B. Curtin

Bibliography. R. M. Nowak, *Walker's Mammals of the World*, 6th ed., 1999.

Loads, dynamic

Forces which are derived from moving loads such as wind, earthquakes, machinery, vehicles, trains, cranes, and hoists. Analysis techniques which take into account the vibrations of the structures are required for loads which are repeated many times, such as machinery in motion, and produce harmonic motions of equal amplitude and constant frequency (cyclic loading); loads such as the motion produced by earthquakes (random motion); and varied loads, such as that of the wind, which produce gusts or short-duration impulses.

Repeated loads applied to a structural member can cause failure by fracture of the material. This fracture can occur at various stress levels depending upon the amplitude or acceleration of the motion, frequency, and duration. Often the stress level is below that of the design level for statically applied loads, and is referred to as the fatigue strength of the material for that application. The fatigue strength may vary for different applications of dynamic loadings and configurations of the structures or components. The fatigue strength will be lowered in the presence of localized stress concentrations.

Cycle of stress. The variation of stress S during one typical fluctuation when the load is repeatedly applied and removed or when the load fluctuates continuously from tension to compression is a stress cycle (see **illus.**). A fluctuating or pulsating stress varies between maximum and minimum values of the same sign; this condition is called repeated if the stress reduces to zero in each cycle. Reversed stress varies between values of opposite signs and is partly reversed when the opposite stresses are unequal, and completely reversed when the opposite stresses are equal.

Stress variation is described either by the maximum stress, its type (tension or compression), and the range of fluctuations, or by the mean or steady stress (S_m in illus.) together with the magnitude of the superimposed alternating stress producing the cyclic variation. Repeated loads superimposed on a constant load, such as dead weight of the structure, may produce fluctuation without reversal. Engine crankshafts and parts, rails, and axles are subjected to the reversed-type cyclic loading, which may involve billions of repetitions in the life of the member.

Stress raisers. Dimensional changes, internal discontinuities, or other conditions causing localized disturbance of the normal stress distribution, with increase of stress over that normally produced, are termed stress raisers. The maximum stress is called a stress concentration. High local stresses exist at bolt threads, abrupt change of shaft diameter, notches, holes, keyways, or fillet wells. Internal discontinuities, such as blowholes, inclusions, seams or cracks, ducts and knots in wood, voids in concrete, and variable stiffness of component constituents, cause stress concentrations. At points of contact of ball or roller bearings, gear teeth, or other local load applications, the stress may be greatly increased. Maximum stress is obtained by multiplying the nominal stress, computed without regard to the modifying effect of the stress raiser, by a stress concentration factor. This factor, found experimentally, depends on the type

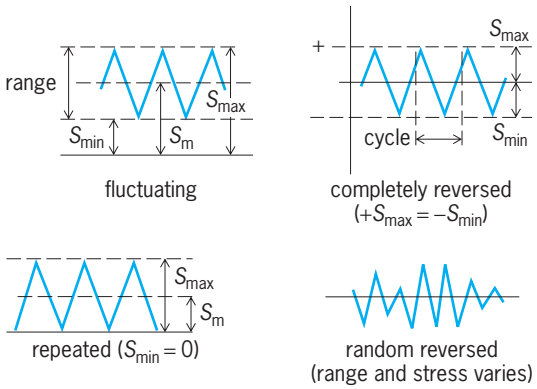

Types of repeated stress.

of discontinuity and the properties of the material under static load. Ductile material relieves most of the stress concentration by plastic yielding. Stress raisers contribute to failure under high stress rates and low temperatures, which tend to inhibit plastic flow, and are of great importance under repeated loads, which produce progressive fracture, called fatigue failure. *See* STRESS AND STRAIN. John B. Scalzi

Loads, transverse

Forces applied perpendicularly to the longitudinal axis of a member. Transverse loading causes the member to bend and deflect from its original position, with internal tensile and compressive strains accompanying change in curvature.

Concentrated loads are applied over areas or lengths which are relatively small compared with the dimensions of the supporting member. Often a single resultant force is used to analyze effects on the member. Examples are a heavy machine occupying limited floor area, wheel loads on a rail, or a tie rod attached locally. Loads may be stationary or they may be moving, as with the carriage of a crane hoist or with truck wheels.

Distributed loads are forces applied completely over large areas with uniform or nonuniform intensity. Closely stacked contents on warehouse floors, snow, or wind pressures are considered to be uniform loads. An equivalent uniform load may represent multiple closely spaced, concentrated loads. Variably distributed load intensities include foundation soil pressures and hydrostatic pressures.

Bending and shear. Transverse forces produce bending moments and transverse (shearing) forces at every section which must be balanced by an internal couple or resisting moment M and an internal shear force V (**Fig. 1***a*). These component forces are evaluated by free-body analysis. The bending moment and resultant shear force can be expressed analytically as functions of the loads and the distance locating the section from a reference origin. The magnitude and distribution of internal stresses associated with the external force system are calculated by the theory of flexure.

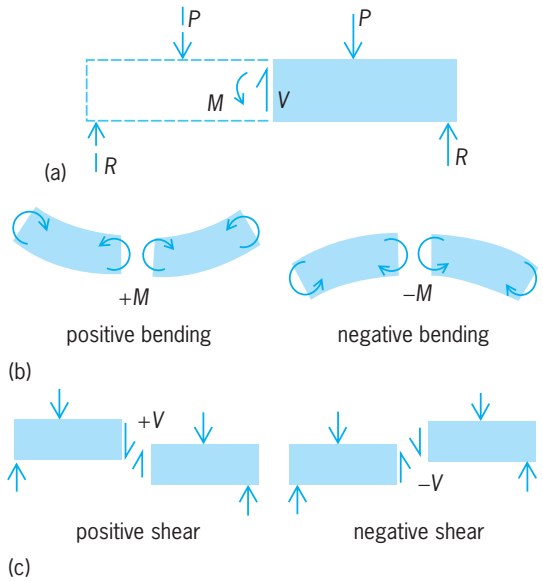

Fig. 1. Beam loading analysis. (*a*) By free-body analysis of beam. (*b*) Conventions of sign for bending moment. (*c*) Conventions of sign for shear.

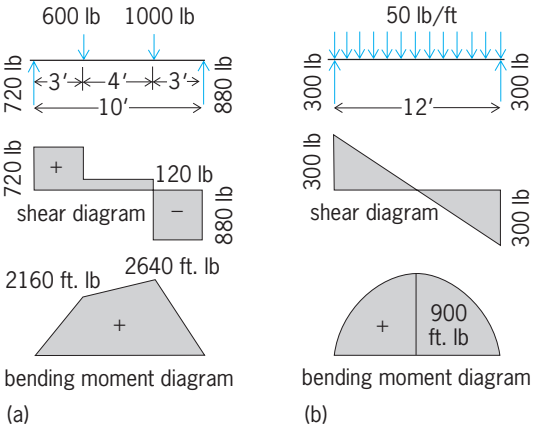

Fig. 2. Typical shear and bending moment diagrams for (*a*) concentrated and (*b*) uniformly distributed loads. 1 ft = 0.3 m; 1 lb = 4.45 N; 1 ft-lb = 1.36 N-m.

Bending moment diagram. A graphical representation indicates the bending moment produced at all sections of a member by a specified loading. The bending moment is the sum of the moments of external forces acting to the left or right of the section, taken about the section. The sign of the curvature is related to the sign of the bending moment (Fig. 1*b*).

Typical bending moment and shear diagrams are shown in **Fig. 2** for concentrated and uniformly distributed loads on a simply supported beam. The reactions and moments are calculated for equilibrium. *See* STATICS.

Shear diagram. A graphic representation of the transverse (shearing) force at all sections of a beam produced by specified loading is called a shear diagram. The shear at any section is equal to the sum of the forces on a segment to the left or right of the section considered (Fig. 1*c*). Positive shears are produced by upward forces on the left section (Fig. 2).

Relationships between shear and bending moment that assist in construction of diagrams are the following: (1) maximum moment occurs where shear is zero; (2) area in the shear diagram equals change of bending moment between sections; (3) ordinates in the shear diagram equal slope of moment diagram; (4) shear is constant between concentrated loads and has constant slope for uniformly distributed loads. Combined loading can be represented by conventional composite moment diagrams or by separate diagrams, called diagrams by parts.

Beams. Members subjected to bending by transverse loads are classed as beams. The span is the unsupported length. Beams may have single or multiple spans and are classified according to type of support, which may permit freedom of rotation or furnish restraint (**Fig. 3**).

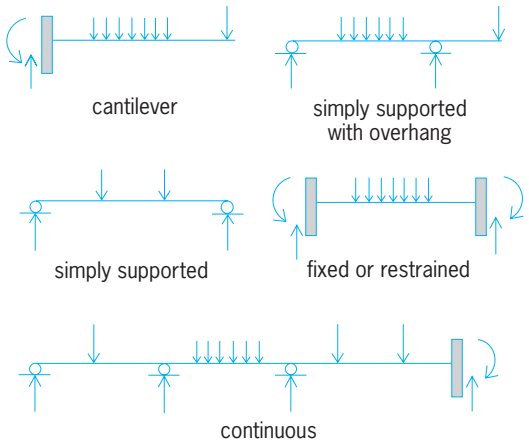

Fig. 3. Diagrams showing types of beams.

The degree of restraint at supports determines the stresses, curvature, and deflection. A beam is statically determinate when all reaction components can be evaluated by the equations of statics. Two equations are available for transverse loads and only two reaction components can be found. Fixed-end and continuous beams are statically indeterminate, and additional load deformation relationships are required to supplement statics.

Bending stresses are the internal tensile and compressive longitudinal stresses developed in response to curvature induced by external loads. Their magnitudes depend on the bending moment and the properties of the section. The theory of flexure assumes elastic behavior. No stresses act along a longitudinal plane surface within the beam called the neutral surface. A segment subjected to constant bending moment, as when bent by end couples, is in pure bending, and stresses vary linearly across the section which remains plane. Simultaneous shear causes warping and nonlinear stress distribution. The flexure stress is maximum at boundary surfaces of sections where bending moment M is greatest. Maximum stress σ at distance c from the neutral axis to the extreme element of a section having a moment of inertia I is $\sigma = Mc/I = M/S$, where $S = I/c$ is called the section modulus, a measure of the section depending upon shape and dimensions. Greatest economy results when the section provides the required section modulus with least area. The common theory of flexure applies only to elastic stresses. Stresses exceeding the elastic limit involve plastic strains producing permanent deflections upon load removal.

Inelastic stresses are first produced at surface elements of sections resisting maximum moment. A distinct yield point in materials, such as structural grade steel, causes stresses near the surface to remain constant, while interior stresses increase with increasing load. Redistribution of stress continues until the entire section behaves plastically. The fully plastic resisting moment of a standard rolled, wide-flange section is about 12% greater than the moment just producing yield point at the surface. Where small increases in deflection can be tolerated, this plastic-hinge moment is used in design.

Shearing stresses are intensities of the shear force distributed over a beam cross section. At any point in the beam, the vertical and longitudinal shear stresses are equal. They are zero at the boundary surfaces and maximum at the neutral axis. The shear stress according to the common theory of flexure is $S_s = VQ/Ib$, where V is total shear force, Q is statical moment about the neutral axis of that area of the beam section between the level of investigation and the top or bottom of the section, I is moment of inertia, and b is width. In rectangular sections the distribution is parabolic, and maximum S_s is one and one-half times the average stress.

Shear flow is the shear force per unit length acting along component areas of the section. The concept of flow is derived from the distribution of unit shear forces represented by vectors pointing in the same direction along the median line of a thin element, and the similarity of the expression for unit shear to the equation for quantity of liquid flowing in a pipe or channel. The direction of unit shear forces acting in typical structural shapes is shown in **Fig. 4**. *See* TORSION.

Deflection. A beam is said to undergo deflection when the displacement is normal to the original unloaded position and is due to curvature produced by loads. Deflections may be limited to less than structurally safe values in buildings to avoid cracking the ceiling or in machines because of necessary clearances.

Elastic curve is the curved shape of the longitudinal centroidal surface when loads produce elastic stresses only. Deflection at any point is calculated from the equation of this curve. Shear forces contribute additional deflection.

Radius of curvature depends on the moment and stiffness of the beam and is constant, with bending to a circular arc, when the moment is constant. This is simple bending. Curvature varies under variable moment.

Statically indeterminate beam. In the presence of more reaction components than can be determined by the equations of statics alone, a beam is statically indeterminate. The first step in analysis is to find the reactions. Equations of statics are supplemented by additional equations relating external forces to slope and deflection.

The curvature and accompanying stresses depend on the loads and the restraint imposed by the

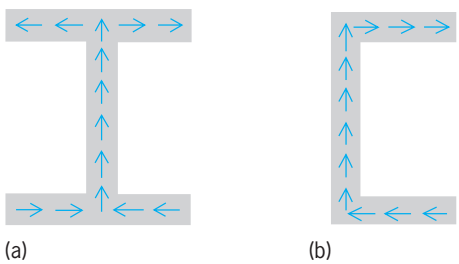

Fig. 4. Shear flow in (*a*) a wide-flange section and (*b*) a channel section.

supports. In a simply supported beam, only vertical displacement is prevented at the supports, whereas when the beam is fixed, rotation is also prevented at the ends. Similarly, beams with overhanging ends and beams continuous over multiple supports are partially restrained. Introduction of the boundary conditions describing the conditions imposed by the supports in the solution of the basic differential equation for the elastic curve furnishes relations between the loads, reaction components, and properties of the beam. For elastic behavior these relations, together with the equations of statics, evaluate the indeterminate reactions. Inelastic behavior is caused by plastic deformations at critical sections of high flexural stress when the yield point of the material is exceeded. When a fully plastic condition is reached, the section acts as a plastic hinge, with constant resisting moment during unrestrained rotation. These known moments at supports or intermediate points permit determination of the reactions by the equations of statics. Advantage is taken of this inelastic action in plastic design.

Unsymmetrical bending. Loads that produce bending moments in planes oblique to the principal axes of a section cause unsymmetrical bending. Components of the applied moment produce curvature and deflection in planes perpendicular to these bending axes; the stresses produced by these components acting separately can be superimposed. To avoid torsional twist, the oblique forces must pass through either the geometric center of symmetrical sections or a particular point called the shear center for unsymmetrical sections.

Lateral buckling of beams is caused by instability of the compression flange, which results in lateral deflection and twist of the section. The action corresponds to buckling of long columns. The critical compressive stress producing buckling depends on the sectional dimensions and type of loading, which in turn determine the flange stresses and torsional rigidity of the section. Beams having small moments of inertia about the weak axis with low torsional resistance are susceptible to buckling. For rolled beams, buckling resistance is related approximately to the Ld/A_f ratio, where L is span, d is beam depth, and A_f is the area of the flange.

Buckling of beam webs is caused by excessive diagonal compression induced by the shear stresses in the web or by the combined shear and bending stresses in the web acting as an edge-supported plate. Because the web is relatively thin, it tends to buckle laterally in a series of waves. For deep beams the shear stress must be reduced by increased web thickness or reinforcement in the form of stiffener angles or plates added to increase resistance to lateral buckling.

Variable cross sections make more efficient use of material in beams by providing resisting moment at all sections more nearly equal to the applied moment. If the section modulus varies directly as the bending moment, stress M/S will be constant at all sections, and the beam is said to have constant strength. Dimensions of the section can be varied by tapering the width and depth or by adding cover plates to a built-up section to vary the section modulus. Common examples of beams with variable section are tapered cantilevers, plate girders with multiple cover plates, forgings, and other machine elements. A leaf spring is a tapered beam in which uniform stress increases energy absorption. *See* PLATE GIRDER; SHEAR CENTER.

Beams on elastic foundation. These members are subjected to transverse loads while resting either on a continuous supporting foundation or on closely spaced supports which behave elastically. The curvature, deflection, and bending moment depend upon the relative stiffness of the beam and supporting foundation. Beams of this type include railroad rails on ties, a timber resting on level ground, a long pipe supported by closely spaced hanger rods or springs, and a concrete footing on a soil foundation. The unknown reactive force per unit length of beam is assumed to be proportional to the deflection, and the solution of this statically indeterminate problem requires derivation of the equation of the elastic curve whose differential equation is $EI(d^4y/dx^4) = -ky$, where k is the spring constant per unit length of support and ky is the elastic force exerted per unit length of beam. Solution of this equation determines the distribution of reactive forces from which the shear and moments can be calculated. *See* STRENGTH OF MATERIALS.

John B. Scalzi

Bibliography. S. Berkowitz, *Introduction to Structural Analysis*, 2d ed., 2000; R. N. White, P. Gergely, and R. G. Sexsmith, *Structural Engineering*, vol. 1: *Introduction to Design Concepts and Analysis*, 2d ed., 1976.

Lobata

An order of the phylum Ctenophora (comb jellies) comprising the families Bathocyroidae, Bolinopsidae, Eurhamphaeidae, Kiyohimeidae, Leucotheidae, and Ocyropsidae. Lobate ctenophores are characterized by large winglike lobes on the oral end of the body that are used for capturing food. All species are predators on zooplankton. Lobates are among the largest ctenophores; some epipelagic species attain an oral-aboral height of 8 in. (20 cm), and some deep-sea species have lobes nearly 39 in. (1 m) across. Most species are transparent, but some have conspicuous brown, blue, or purple spots on the lobes. Deep-sea forms often have red pigment surrounding the stomodeum. Lobates are bioluminescent, like other ctenophores. Bright blue-green light is produced in the meridional canals, and some species also release a cloud of luminous material into the water when disturbed, probably as part of an escape response.

The upper body is usually compressed in the tentacular plane. The comb (ctene) rows in this plane are short, but the substomodeal comb rows extend onto the outer surface of the lobes. Meridional canals are long and interconnected; the substomodeal canals often make complex loops in the

lobes that are characteristic for different species. Pendant structures called auricles extend from the oral end of the body into the space enclosed by the oral lobes. Auricles may be short and stubby or long and sinuous in different species. Locomotion is produced by the comb rows, but some genera (*Ocyropsis*, *Bathocyroe*) can also swim by flapping the oral lobes.

Except for the genus *Ocyropsis*, all lobate ctenophores are simultaneous hermaphrodites, and have ovaries and testes situated along the meridional canals. The gonads open to the outside by way of numerous gonopores along the comb rows, and many species are thought to be self-fertilizing. Coastal species can produce thousands of eggs per day, but oceanic and deep-sea species probably produce fewer. Eggs develop into the cydippid larva typical of most ctenophores. After a variable length of time of swimming and feeding as a cydippid, the larva metamorphoses into the adult form, passing through intermediate larval stages in some species (for example, *Leucothea*, *Mnemiopsis*). Metamorphosis from the cydippid form involves loss of the primary tentacles, development of the oral lobes and auricles, and growth of secondary tentacles near the mouth.

In most lobate ctenophores, feeding is accomplished by swimming slowly forward with the lobes spread open around the mouth. The secondary tentacles give off numerous fine side branches that cover the inner surface of the lobes. Movement of the auricles may startle the crustacean copepods and other small zooplankton so that they try to escape but instead swim into an outspread oral lobe. On contact, the lobe closes over the prey, which becomes tangled in the tentilla and is then transported to the mouth. In some species both lobes contract to enclose the prey, and in others the lobes operate independently. Species of *Ocyropsis* lose their tentacles entirely during metamorphosis and rely on their muscular lobes alone to catch and hold prey before transferring it to the mouth. This mechanism enables them to catch larger and more active prey than other species. Many deep-sea species have exceptionally large, flimsy oral lobes, presumably to increase the chance of capturing sparsely distributed prey.

Lobate ctenophores are found in both coastal and oceanic waters at all latitudes and depths. In coastal waters and estuaries, their high fecundity, efficient feeding, and rapid growth rates can lead to extremely dense seasonal populations that have a significant impact as predators on smaller zooplankton and competitors for young fish. Lobate ctenophores are parasitized by hyperiid amphipods and preyed upon by medusae, the ctenophore *Beröe*, and various fishes. *See* CTENOPHORA; CYDIPPIDA. Laurence P. Madin

Bibliography. G. R. Harbison, L. P. Madin, and N. R. Swanberg, On the natural history and distribution of oceanic ctenophores, *Deep-sea Res.*, 25:233–256, 1978; F. W. Harrison and J. A. Westfall (eds.), *Microscopic Anatomy of Invertebrates*, vol. 2, 1991; S. P. Parker (ed.), *Synopsis and Classification of Living Organisms*, 1982.

Lobosia

A subclass of Rhizopodea characterized by lobopodia predominantly, although certain of these protozoan species also may form slender pseudopodia, or even develop several different kinds. Lobosia are divided into two orders which differ in presence or absence of a test. The Amoebida include the amebas, which do not produce a test. The Arcellinida possess a one-chambered test ranging from a predominantly chitinous to a mainly siliceous covering. Pseudopodia emerge through the aperture of the test. *See* AMOEBIDA; ARCELLINIDA; PROTOZOA; SARCODINA; SARCOMASTIGOPHORA. Richard P. Hall

Local-area networks

Computer networks that usually cover a limited range, say, within the boundary of a building. A computer network is two or more computers that communicate with each other through some physical medium. The primary usage of local-area networks (LANs) is the sharing of hardware, software, or information, such as data files, multimedia files, or electronic mail. Resource sharing provided by local-area networks improves efficiency and reduces overhead. *See* DIGITAL COMPUTER; ELECTRONIC MAIL; MULTIMEDIA TECHNOLOGY.

A local-area network can be thought of as similar to a telephone network which uses phone wires installed in a star topology. A local-area network must also use some transmission medium installed with a selected topology.

Transmission media. Four basic types of media are used in local-area networks: coaxial cable, twisted-pair wires, fiber-optic cable, and wireless. Each medium has its advantages and disadvantages relative to cost, speed, and expandability. Originally, most local-area networks used coaxial cables. A coaxial cable consists of one or two conducting wires encapsulated by several layers of insulation and shielding (**Fig. 1***a*). Coaxial cables provide high speed and low error rates. Twisted-pair wires (Fig. 1*b*) are cheaper than coaxial cables, can sustain the speeds common to most personal computers, and are easy to install. Fiber-optic cable (Fig. 1*c*) is the medium of choice for high-speed local-area networks, operating at speeds of 100 megabits per second or higher. A fiber-optic cable uses light pulses to represent data. Because light signals are not distorted by electric or magnetic fields, fiber-optic cables provide excellent error characteristics. The disadvantages of fiber-optic cables include their high cost and the difficulty of adding or removing stations. Messages in wireless local-area networks are transferred through the air as radio waves rather than through a conductive cable or wire. Hence, wireless local-area networks have the advantage of expandability. *See* COAXIAL CABLE; COMMUNICATIONS CABLE; FIBER-OPTIC CIRCUIT; OPTICAL COMMUNICATIONS; OPTICAL FIBERS.

Topology. The topology of a local-area networks is the physical layout of the network. For wired

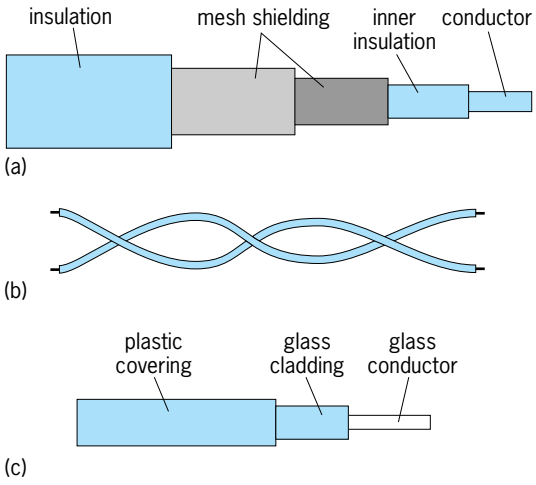

Fig. 1. Media used in local-area networks. (*a*) Coaxial cable. (*b*) Twisted-pair wires. (*c*) Fiber-optic cable.

local-area networks, there are four basic topologies: bus, ring, star, and mesh (**Fig. 2**). The most widely used local-area network topology is the bus (Fig. 2*a*), where the medium consists of a single wire or cable to which nodes are attached. A message transmitted over a bus propagates in both directions along the bus, passing each tap until it is finally absorbed at the ends. In a ring topology (Fig. 2*b*), the medium forms a closed loop, and all stations are connected to the loop or ring. Data propagate in one direction. The star topology (Fig. 2*c*) has a central node to which the computers and devices are separately connected. All the network traffic passes through the central node. In a mesh topology (Fig. 2*d*), messages are transmitted through several switches that connect nodes. The asynchronous-transfer-mode (ATM) technology favors the use of mesh topology. Modifying and combining some of the characteristics of these basic network topologies may result in hybrid topologies, which often provide greater network efficiency.

Circuit versus packet switching. There are a number of ways in which nodes can communicate over a network. The simplest is to establish a dedicated link between the transmitting and receiving stations. This technique is known as circuit switching. In the topologies outlined above, this would involve dedicating the medium to communication between the nodes. However, data communications over a local-area network tend to be bursty; that is, they are characterized by periods of intensive data transfer, followed by lulls. During this period of inactivity, precious bandwidth capability is being wasted.

A better way of communicating is to use a technique known as packet switching, in which a dedicated path is not reserved between the source and the destination. Data are wrapped up in a packet and launched into the network. In this way, a node only has exclusive access to the medium while it is sending a packet. During its inactive period, other nodes can transmit. Thus, the available bandwidth can be better utilized. The problem of sharing access to the network is reduced to establishing some rules that will allow each node on the network to launch its packet in a fair manner. This is achieved by access protocols, discussed below. *See* PACKET SWITCHING.

Packet format. A typical packet is divided into preamble, address, control, data, and error-check fields. The field of the preamble contains some bit sequence that never occurs in normal data. It serves to inform all other nodes on the network that transmission of a packet has begun. The address field contains addresses of both the sender node and receiver

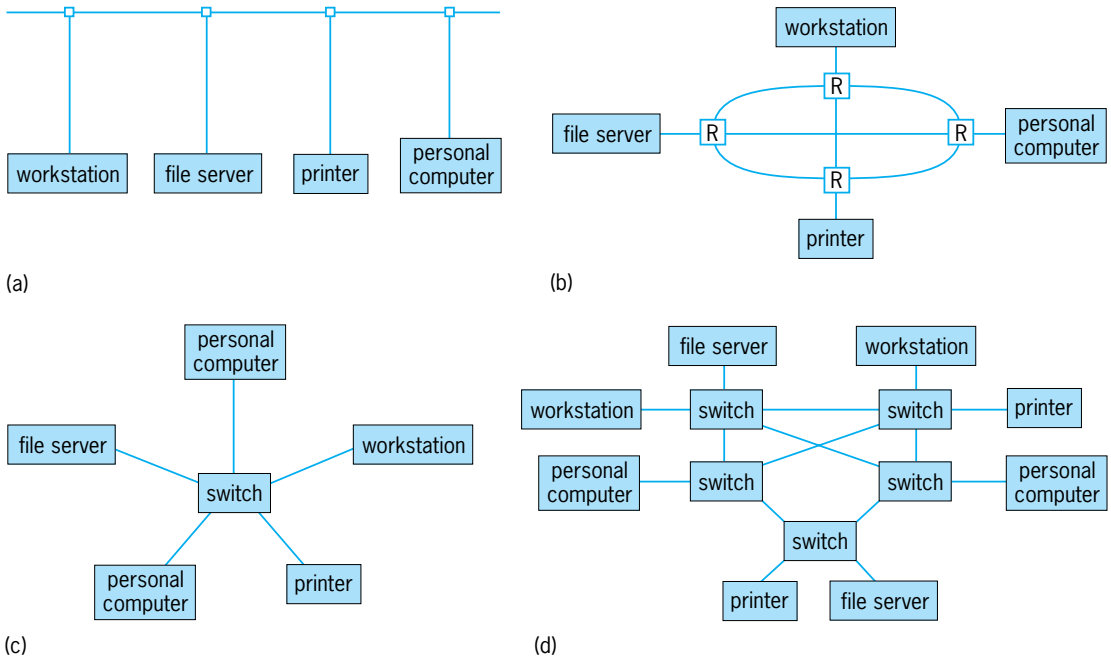

Fig. 2. Local-area network topologies. (*a*) Bus. (*b*) Ring; R = ring repeater. (*c*) Star. (*d*) Mesh.

node. This allows the nodes on the network to recognize where the packet comes from and who should receive it. The control field identifies the purpose of the packet as normal data transmission or a special management purpose. Although a packet usually contains normal data, it can also be sent for a network management purpose (for example, to discover the status of nodes and medium). The data field contains the actual data to be transferred. Although the error rate in a local-area network is typically very low, a packet usually has an error-check field that allows the receiver node to detect or recover transmission errors. The sizes of all these fields are usually fixed except for the data field, which may have a variable length, depending on the amount of data to be transferred.

Access protocols. An access protocol is a set of rules observed by all the nodes in a local-area network so that one node can get the attention of another and its data packet can be transferred. Two common protocols are carrier sense multiple access with collision detection (CSMA/CD) and token passing.

With the CSMA/CD protocol, a node that wants to transmit its data must first listen to the medium to hear if any other node is using the medium. If not, the node may transmit immediately. However, while the transmission is taking place, the transmitting node must continue listening to ascertain if anyone else has begun transmitting. This is possible because, with the propagation delay over the medium, two or more nodes could simultaneously decide that the medium is idle and start transmission virtually at the same time. Then, data transmitted by the nodes collide and get garbled. Hence, if the transmitting node detects that someone else is also transmitting, the node aborts its own transmission, waits for a random amount of time, and then restarts the process until its data transmission succeeds.

With the token-passing protocol, the right to transmit is granted by a token, a predefined bit pattern that is recognized by each node. The token is passed for one node to another in a pre-determined order. For example, in a ring network the token passes from one node to its adjacent node. When a node obtains the token, it has two options: it can transmit a message, if any, or it can pass the token to the next node. If the node transmits a message, then at the end of its transmission it releases the token to the next node. When a token network starts up, an initial token must be generated, and when the token is damaged because of node and transmission errors, a token must be regenerated. This function is usually carried out by a designated monitor node. If the token does not arrive at the monitor node within a certain time, it generates a new token. this technique works because the token traveling time around the network is usually predictable.

Software. The success of the local-area network depends on how application and system software interacts with the hardware in setting up the communication capability. Application software is designed to solve users' problems. It is assisted in this goal by supporting system software. Local-area network system software is essentially an extension of the operating system. It insulates applications from hardware details and carries out hardware-oriented local-area network tasks, such as interfacing to the medium, directing printing jobs, and sending and receiving service requests. That is, the applications can make requests for services, and system software contains the logic to carry out these requests for a specific type of hardware. *See* OPERATING SYSTEM; SOFTWARE.

Network services. The primary usage of local-area networks is resource sharing. The resources can be information, such as data files, multimedia files, electronic mail, or software. They can also be hardware devices such as printers, plotters, scanners, or storage devices. Resource sharing is realized by services provided by the local-area network. Usually some nodes in the network function as file servers. File services provide the central repository of data or application programs, and offer consistent and easy-to-use file access to all the users and applications. Management services provide uniform interfaces so that a small central staff can monitor and control end-user activities, network changes, security, and system performance across an entire corporate network. Security services aim at establishing consistent security across a variety of network resources. Usually these services are integrated with other network services and are enforced transparently with every network activity. Time services synchronize enterprise-wide services and applications, making network events temporally consistent. *See* COMPUTER PERIPHERAL DEVICES; COMPUTER SECURITY.

Connection-oriented communications. While the packet-switching method is cost-effective and acceptable for many common applications such as electronic mail and file transfer, it does not provide a prior guarantee regarding the quality of service that an overlying application may receive. Hence, it is insufficient for applications such as multimedia and teleconferencing. *See* TELECONFERENCING.

Connection-oriented communication technology has been developed to improve the packet-switching method. A connection is an abstract communication service provided by the network to a particular application. It can be considered as a two-way contract: The communicating applications specify the characteristics of traffic which they may generate (say, the maximum rates), and the network agrees to provide the requested quality of service to the applications. The network may disallow a connection if it cannot provide the requested quality-of-service guarantees. Thus, a connection may be viewed as a virtual link that is dedicated for the use of an application and that has a certain traffic-carrying capacity. Connection-oriented communication technology exploits the advantages of packet switching while overcoming its weaknesses.

Development of networks. A representative of the first generation of local-area networks is the Ethernet, a CSMA/CD bus. It uses coaxial cable with a maximum data rate of 10 megabits per second. The best-known second-generation local-area network is

the Fiber Distributed Data Interface (FDDI), a token-ring network using optical fibers with a data rate of 100 megabits per second.

Another local-area network technology, which uses the asynchronous transmission mode, is ATM LAN. An ATM LAN is a mesh-based network using the optical-fiber medium with data rates of the order of 150 megabits to 10 gigabits per second. With the high bandwidth provided by ATM LANs, many applications such as integrated real-time data and multimedia services become possible.

The basic premise of virtual local-area networks is to separate logical work groups from physical constraints. This enables devices that are connected to different components throughout the network to be logically grouped into communities of interest. Thus, virtual local-area networks are built by administrative and functional needs rather than attachment. Virtual local-area network technology provides scalability, flexibility, and policy-based management. *See* DATA COMMUNICATIONS.

Wei Zhao

Bibliography. N. Malcolm and W. Zhao, Hard real-time communication in multi-access networks, *J. Real-time Syst.*, 8(1):35–77, January 1995; W. Stallings, *Data and Computer Communications*, 6th ed., 1999; A. Tanenbaum, *Computer Networks*, 3d ed., 1996.

Local Group

The small cluster of galaxies that contains the Milky Way Galaxy. Galaxies exhibit a pronounced tendency to clump together on a variety of scales. It is assumed that gravitational attraction draws galaxies together. On a very large scale, this attractive process may still be at an early stage, resulting in filamentary structures which are only mildly perturbed in their motions from the general expansion of the universe. On a smaller scale, the process has led to collapse. Galaxies have fallen together, though with enough angular momentum that they usually orbit each other rather than collide.

Collapsed structures that contain a few dozen to a few thousand substantial galaxies are called clusters; collapsed structures that contain a few but less than 10 or 20 big galaxies are called groups. The Milky Way Galaxy is a large but not exceptional spiral galaxy and one of two dominant members of a small assemblage referred to as the Local Group.

Environment. On successively larger scales, the Local Group is a member of the Coma-Sculptor Cloud and the Local Supercluster. The Coma-Sculptor Cloud contains several hundred galaxies in an extremely flattened distribution that extends across 4×10^7 light-years (1 light-year equals 9.46×10^{12} km or 5.48×10^{12} mi), in the general direction toward the Virgo cluster at the center of the Local Supercluster. The dominant members of the nearest-neighboring groups (see **illus.**) are New General Catalogue (NGC) 253, Maffei 1, Index Catalogue (IC) 342, Messier (M) 81, and the prominent source of radio emission, Centaurus A. The closest galaxies

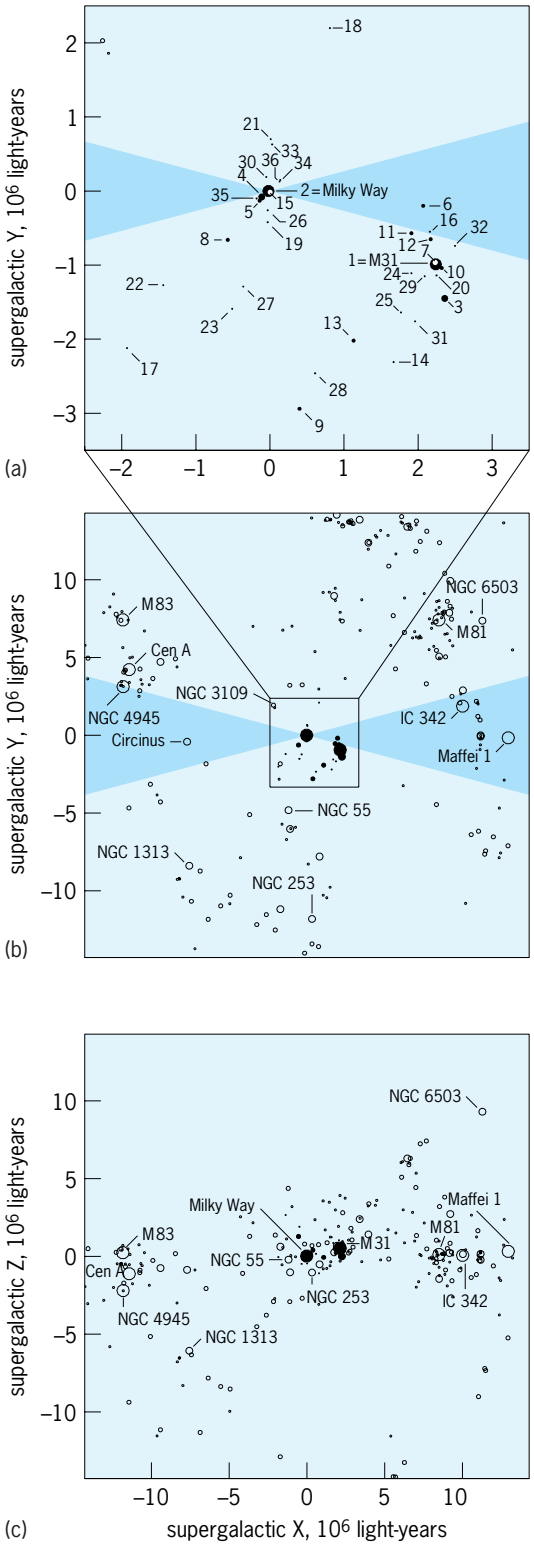

Neighborhood of the Local Group. Shaded wedges indicate the zone partially obscured by the Milky Way Galaxy. Filled circles denote members of the Local Group. Open circles locate galaxies beyond the Local Group. Members of the Local Group are identified by the running number given in the table. Several prominent galaxies beyond the Local Group are identified by name. (*a*) Blowup of the Local Group. (*b*) View down onto supergalactic equatorial plane ($Z = 0$) of the region around the Local Group. (*c*) View edge-on to the supergalactic plane, showing that most nearby galaxies lie near this plane.

Local Group Galaxies*

Name	Type	Distance, 10^6 light-years	Luminosity (X Sun)
1. M31 = Andromeda	Spiral	2.5	3×10^{10}
2. Milky Way Galaxy	Spiral	—	2×10^{10}
3. M33 = Triangulum	Spiral	2.8	6×10^{9}
4. Large Magellanic Cloud	Irregular	0.16	3×10^{9}
5. Small Magellanic Cloud	Irregular	0.19	7×10^{8}
6. IC 10	Irregular	2.2	3×10^{8}
7. NGC 205	Elliptical	2.5	3×10^{8}
8. NGC 6822	Irregular	1.6	2×10^{8}
9. WLM	Irregular	3.0	2×10^{8}
10. M32	Elliptical	2.6	2×10^{8}
11. NGC 185	Elliptical	2.0	2×10^{8}
12. NGC 147	Elliptical	2.3	1×10^{8}
13. IC 1613	Irregular	2.3	9×10^{7}
14. Pegasus	Dwarf irregular	3.1	3×10^{7}
15. Sagittarius	Dwarf spheroidal	0.08	2×10^{7}
16. Cassiopeia	Dwarf spheroidal	2.5	1×10^{7}
17. Tucana	Dwarf spheroidal	2.6	9×10^{6}
18. Leo A	Dwarf irregular	2.6	8×10^{6}
19. Fornax	Dwarf spheroidal	0.48	7×10^{6}
20. Andromeda I	Dwarf spheroidal	2.6	6×10^{6}
21. Leo I	Dwarf spheroidal	0.83	6×10^{6}
22. SagDIG	Dwarf irregular	3.4	5×10^{6}
23. DDO 210	Dwarf irregular	2.6	4×10^{6}
24. Andromeda II	Dwarf spheroidal	2.2	4×10^{6}
25. Andromeda VI	Dwarf spheroidal	2.6	3×10^{6}
26. Sculptor	Dwarf spheroidal	0.26	2×10^{6}
27. Phoenix	Dwarf irregular	1.4	2×10^{6}
28. Cetus	Dwarf spheroidal	2.5	2×10^{6}
29. Andromeda III	Dwarf spheroidal	2.4	1×10^{6}
30. Sextans	Dwarf spheroidal	0.26	1×10^{6}
31. LGS 3	Dwarf irregular	2.6	8×10^{5}
32. Andromeda V	Dwarf spheroidal	2.6	7×10^{5}
33. Leo II	Dwarf spheroidal	0.65	6×10^{5}
34. Ursa Minor	Dwarf spheroidal	0.22	4×10^{5}
35. Carina	Dwarf spheroidal	0.35	4×10^{5}
36. Draco	Dwarf spheroidal	0.26	3×10^{5}

*Ordered from brightest to faintest.

beyond the Local Group are at a distance of 7×10^6 light-years.

Members. The Local Group has 36 known or suspected members (see **table**). The only system larger than the Milky Way Galaxy is M31, the Andromeda Nebula. These two giant galaxies generate 80% of the light of the group. There are also two intermediate-scale galaxies: M33, the Triangulum Nebula near Andromeda; and the Large Magellanic Cloud, a close companion of the Milky Way and a conspicuous feature of the night sky in the Southern Hemisphere. Fainter than these are 32 small systems. The smallest among them are identified only because they are so close. Many would not be detected in even the nearest adjacent groups. The census of Local Group members may be very incomplete at the faint end and in the zones obscured by the plane of the Milky Way. *See* ANDROMEDA GALAXY; MAGELLANIC CLOUDS; MILKY WAY GALAXY.

Subclustering. The two giant galaxies have entourages of small systems. The Large and Small Magellanic clouds are so close that they may be in the process of merging with the Milky Way Galaxy. The Milky Way also has the nine dwarf satellites: Fornax, Sculptor, Leo I, Leo II, Sextans, Draco, Carina, Ursa Minor, and Sagittarius. These are gas-depleted spheroidal systems with essentially no ongoing star formation. The Sagittarius dwarf is in the process of being absorbed by the Milky Way Galaxy.

In any photograph of M31 the high surface-brightness companions M32 and NGC 205 are clearly visible. In addition, M33 is within 6.5×10^5 light-years of M31, and in proximity there are NGC 147, NGC 185, IC 10, and the very small systems LGS 3 and Andromeda I, II, III, V, and VI.

In another part of the sky, NGC 6822, David Dunlap Observatory (DDO) 210, SagDIG (Sagittarius Dwarf Irregular Galaxy), and Phoenix are close together. The nearest neighbors to the Local Group are four other dwarf irregular systems close enough to each other that they could be thought of as a distinct entity: NGC 3109, Sextans A, Sextans B, and Antlia. A rigorous criterion for group membership might require total or continuing collapse toward the common potential of the group. However, the distances and three-dimensional motions of each of the systems or of the underlying mass distribution are not well enough known to identify with certainty which systems are bound and which are separating.

Types of galaxies. Galaxies within the Local Group, as with most others, can be assigned to one of two families. Some have substantial reservoirs of hydrogen and are actively forming new stars; others are

gas-depleted and contain only old stars. The three spirals and the Magellanic or dwarf irregulars have young stars and gas as well as old constituents. The elliptical, lenticular, and dwarf spheroidal systems are all deficient in interstellar gas and have the smooth textures of old, dynamically relaxed galaxies.

All the known gas-poor systems in the Local Group lie close to one of the giant galaxies and to each other. In contrast, the gas-rich systems tend to be farther apart, even though still identified with the group. Tidal or direct collisional stripping has probably affected the systems in crowded regions and deprived them of the gas reserves necessary for continued star formation.

Distances. The galaxies in the Local Group are so close that individual stars can be resolved with modern detectors on large telescopes. More massive young stars are easily observed in the spiral and irregular galaxies. Among the populations of old stars, only the brightest of those in a certain phase of their evolution called red giants are visible in the more distant parts of the Local Group. In each case, all well-studied systems contain stars with familiar properties that give an indication of their distances. The most useful are the Cepheid and RR Lyrae stars because they pulsate with frequencies that are related to their intrinsic luminosities. With the Hubble Space Telescope, red giant stars are easily observed, and accurate distances can be determined from the properties of the brightest of these. It has been established that the distances measured in the first half of the twentieth century were badly underestimated. The current estimates (see table) are fundamental for the calibration of the extragalactic distance scale. *See* CEPHEIDS; GIANT STAR; VARIABLE STAR.

Mass. Assuming that the galaxies within 3×10^6 light-years of either the Milky Way or M31 are part of a dynamically collapsed system, the mass of the unit can be estimated with the virial theorem. This theorem specifies the relationship between the mass, dimensions, and motions in an isolated, relaxed system of gravitating particles. In practice, there are problems because not all the velocity and position information is available, and the assumption that the system has collapsed and relaxed is probably poorly satisfied. Nevertheless, the results of such an analysis are consistent with similar analyses of other groups and can be taken to be valid in a statistical sense. It is estimated that the mass of the Local Group is roughly 10^{12} times the mass of the Sun (2×10^{42} kg or 4×10^{42} lb). Hence, the ratio of the mass to light of the Local Group is 20 in solar units. This value is lower than a more typical value of 100 for galaxy groups, but much larger than the value of about 5 for the luminous parts of individual galaxies. It is supposed that in the Local Group, as in many other environments, the potential well is dominated by a component of invisible matter, so-called dark matter. The mass contributed by the stars that produce the light and by the interstellar hydrogen are relatively insignificant. *See* COSMOLOGY; GALAXY, EXTERNAL. R. Brent Tully

Bibliography. P. Hodge, Populations in Local Group galaxies, *Annu. Rev. Astron. Astrophys.*, 27:139–159, 1989; A. Layden, R. C. Smith, and J. Storm (eds.), *The Local Group: Comparative and Global Properties*, 3d CTIO/ESO Workshop, La Serena, Chile, Jan. 25–28, 1994; M. L. Mateo, Dwarf galaxies of the Local Group, *Annu. Rev. Astron. Astrophys.*, 36:435–506, 1998; A. R. Sandage and J. Bedke, *The Carnegie Atlas of Galaxies*, 2 vols., 1994; R. B. Tully and J. R. Fisher, *Nearby Galaxies Atlas*, 1987; S. van den Bergh, *The Galaxies of the Local Group*, Cambridge Astrophysics Series 35, 2000.

Location fit

Mechanical sizes of mating parts such that, when assembled, they are accurately positioned in relation to each other. Locational fits are intended only to determine the orientation of the parts. For normally stationary parts that require ease of assembly or disassembly, for parts that fit snugly, and for parts that move yet fit closely as in spigots, slight clearance is provided between parts. Where accuracy of location is important, transition fits are used. In these fits the holes and shafts are normally nearly the same diameter. For greater accuracy of location, the shafts are made slightly larger than the holes; such fits are termed location interference fits. *See* ALLOWANCE. Paul H. Black

Locomotive

A machine mounted on flanged wheels which converts some form of potential energy into the mechanical work of propelling itself and other, nonpowered vehicles over a railroad track. The dimensions and weight of a locomotive are restricted by the presence of stationary structures adjacent to and above the track, such as overhead bridges and tunnels, and by the strength of the track and bridges that support it.

Economics demands that locomotives use an available and plentiful form of potential energy; that they convert it to useful work efficiently; that they be capable of applying sufficient force to overcome the resistance of the loaded vehicles they are to move, and they do so in the time allotted; and that they be durable, reliable, and relatively easy to maintain.

Characteristics. Locomotives are described in terms of the type of energy they consume; their size and weight; the tractive effort, that is, the force they are capable of exerting; and their power, that is, the rate at which they convert energy to work. Locomotive tractive effort varies with speed, so it is often described by a curve that shows the relationship between speed and the force applied to the leading coupler of a train. The force at zero speed is known as the starting tractive effort and is related to the locomotive's weight on driving wheels by the factor of adhesion. The factor of adhesion can exceed the nominal coefficient of friction by employing sophisticated antislip technologies.

The coefficient of friction between a steel wheel

and a steel rail depends upon the surface conditions of both and varies considerably even over short distances and at different times. The nominal coefficient of friction is therefore only an average value. Railroads have used a number of techniques to enhance friction levels. Spreading sand ahead of driving wheels has been used for years. Antislip controls that detect slipping wheels and momentarily reduce power to those wheels have been developed. The use of alternating-current (ac) synchronous traction motors where speed is strictly controlled by current frequency has further raised the effective coefficient of friction. In such cases the locomotive wheels improve the surface conditions of wheels and rails by instantaneous slippage or stick-slip phenomena, which burn off contaminants that would otherwise lower the friction coefficient by lubricating the contacting surfaces. Thus, nominal coefficients of friction of the order of 20–30% can be raised to factors of adhesion well above 40%. *See* FRICTION.

Steam models. The first locomotives (around 1830) were steam propelled. The first successful steam locomotives employed a multiple fire-tube boiler in which the hot gases from the combustion of coal or wood were passed through submerged pipes (flues) to heat water to or above its boiling point. The resulting steam was expanded against pistons connected to driving wheels, the linear reciprocating motion of the pistons being converted to rotation by a system of cranks. Over the first 100 years or so of railroad history, steam locomotives were the primary source of power for railroads throughout the world. The basic concept of firebox, boiler, and smoke box arranged longitudinally from rear to front and cylinders under the smoke box lasted throughout the history of steam with some minor exceptions. Within this concept, however, many changes and improvements were made. In particular, as rail and track strength were increased, locomotive size and weight did as well. The first steam locomotives were restricted to weights of about 10 tons (9 metric tons), but by the 1940s huge machines weighing over 300 tons (270 metric tons) were being produced. These locomotives were equipped with superheaters and feedwater heaters to improve their efficiency, sanders to reduce wheel slippage in situations requiring high tractive effort, mechanical stokers and lubricators, and electric generators for lighting; they used specially treated water; at speed, they could produce upward of 6000 horsepower. Because of the many advantages of other forms of motive power, steam locomotives began to be replaced shortly after World War II and had virtually disappeared in the United States by the late 1950s. However, steam power is still used in China on some railways preserved as attractions for tourists and railroad enthusiasts. *See* STEAM ENGINE.

Electric models. Electric locomotives draw electricity from a third rail set alongside the running rails of track through a sliding shoe that transmits electric power to the locomotive, or from a configuration of overhead wires known as a catenary by means of a pantograph that raises or lowers to compensate for wire height variations. The cost of these electric distribution systems has restricted the use of electric motive power to only very high traffic routes such as the Northeast Corridor of Amtrak in the United States, commuter lines, and some routes in Japan, Russia, England, and continental Europe.

Electric locomotives can be designed and constructed to use a wide variety or even combinations of voltages and either direct or alternating currents. Low-voltage direct current (dc) is often distributed over relatively short distances by a third rail. High-voltage direct or alternating current (1500 dc, 3000 dc, 11,000 ac, 15,000 ac, 25,000 ac) is distributed by overhead catenary.

Electric locomotives can be overloaded for short periods of time so that a nominal 4000–5000–hp locomotive can produce 7000–8000 hp during acceleration or when climbing grades.

Therefore, since locomotives do not require their maximum power at all times, electrification permits a railroad to purchase a smaller quantity of total locomotive horsepower than would be required for other types of power. Besides the high cost of electric distribution systems, the disadvantages of electrification include reduced overhead clearance where a catenary is used, danger to employees working on or around the third rail or catenary, and generally lower utilization factors for locomotives. Utilization factors are the measures used by railroads to describe the percentage of time that a locomotive (or other piece of equipment) is actually in service. The utilization of electric locomotives is restricted by the limits of the power distribution system. Electric locomotives can go only where the electrification system goes. This differs from availability factors (which are high for electric locomotives) that measure the percentage of time that a locomotive is ready for service. Thus an electric locomotive may be available (that is, may be functional and serviced) but cannot be assigned since there are no trains destined to locations on the electrified lines. *See* ALTERNATING-CURRENT MOTOR.

Diesel models. Individual diesel-electric locomotive units are produced in a number of sizes, with corresponding power (**Fig. 1**). Switching or shunting locomotives are of approximately 1000 hp and

Fig. 1. Modern 4000-hp diesel-electric ac locomotive. (*Electro-Motive Division of General Motors Corp.*)

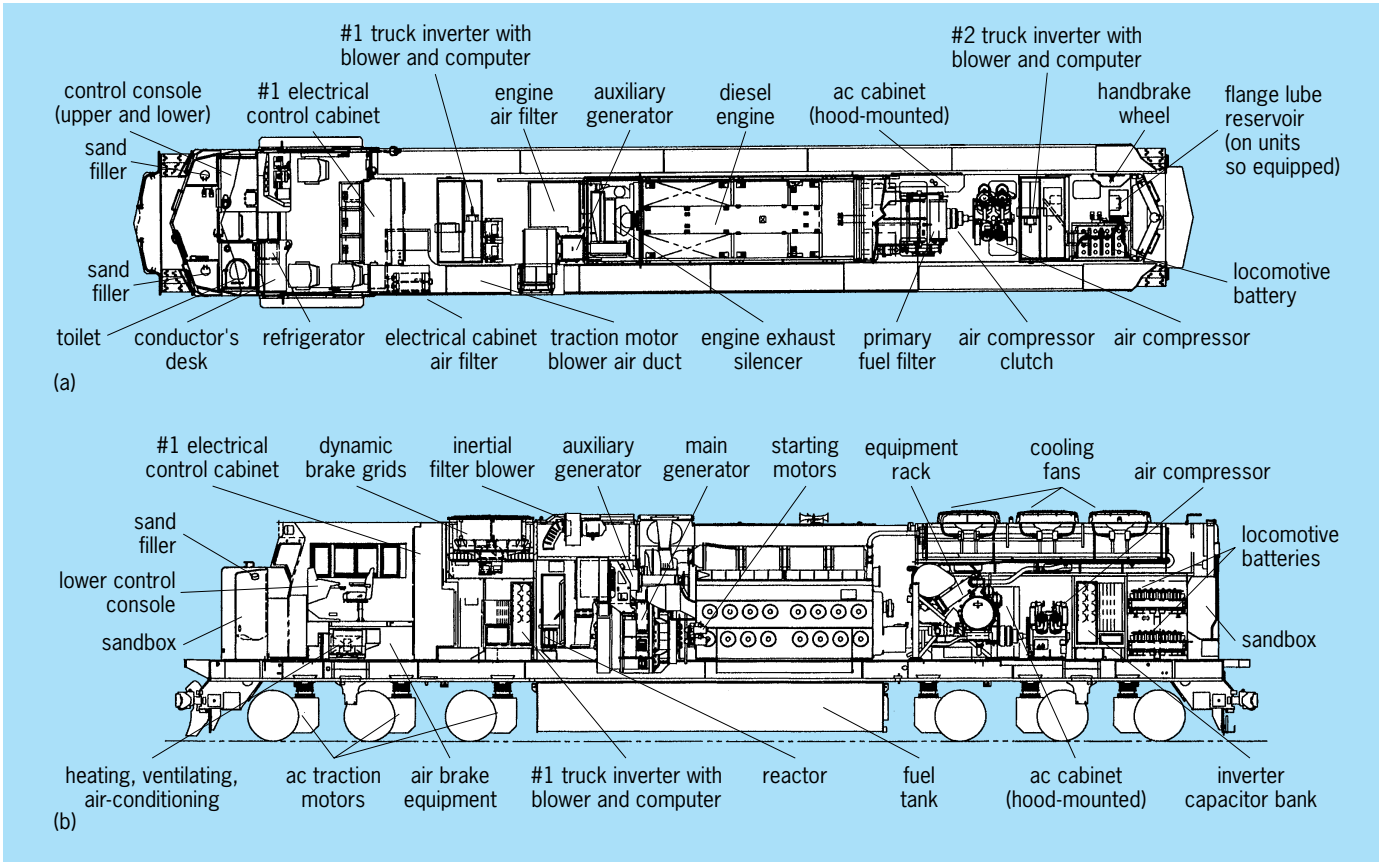

Fig. 2. Major components of a modern diesel-electric locomotive. (*a*) Plan view. (*b*) Cross section. (*Electro-Motive Division of General Motors Corp.*)

low maximum speed, while mainline passenger and freight units are being designed to produce 5000–6000 hp. Several diesel-electric units are most often coupled together to produce a single locomotive of as much as 15,000 hp or more. In such cases the entire locomotive assembly is controlled from the leading unit.

The diesel engines are designed either as two- or four-cycle (**Fig. 2**). They are most often of the vee configuration of 12–20 cylinders 9–11 in. (23–28 cm) in diameter. Most are turbo-supercharged and operate at approximately 1000 rpm. The lubricating oil system on a diesel unit ensures a supply of clean, cool oil to the engine, and it provides for extracting carbon deposits left by combustion along with some heat from the engine. The oil is circulated by engine-driven pressure pumps through removable filter elements, strainers, and a water-cooled heat exchanger. The engine cooling system also uses engine-driven centrifugal pumps to circulate treated water through cylinder heads, liners, and the oil cooler to banks of radiator units. The large fans that force air through the radiators are driven mechanically from the engine or by electric motors. *See* TURBOCHARGER.

The fuel system includes a motor-driven pump to deliver fuel oil from a storage tank, usually mounted under the carbody between the trucks, with a capacity of about 4000 gal (15,000 liters). The oil is forced through a strainer and filter to the injectors, where it is sprayed into the cylinders by high-pressure pumps and nozzles. The quantity of fuel delivered for each stroke of the engine piston is regulated by a mechanical linkage connected to the engine governor. This device keeps engine speed constant for each throttle setting, regardless of load. *See* GOVERNOR; LINKAGE (MECHANISM).

These engines turn an alternator, which produces the electricity to power the traction motors. The traction motors are mounted in the truck assemblies with their armature shafts parallel to the locomotive's driving axles. A pinion gear on the armature shaft turns a bull gear on the axle to propel the locomotive. Traction motors are cooled by fan-driven air through ducts. There may be four or six such motor-driven axles per locomotive unit, and the gear ratio between pinion and bull gear teeth is varied according to the locomotive's intended use.

At one time, all traction motors were dc, series-wound machines, and motor speed had to be limited to prevent damage to the commutator and armature from centrifugal force. However, low motor speed for extended periods is associated with high current flow and damage from excessive heat. Thus, gear ratio has been critical, and it determined the speed range of the locomotive. With the advent of ac squirrel-cage motors, gear ratio is less critical, and locomotive assignments can be more flexible as these ac machines are equally suited to both high-speed

passenger or merchandise service and lower-speed heavy-tonnage assignments. *See* DIESEL ENGINE.

Braking. Both diesel-electric and straight electric locomotives can be equipped with dynamic brakes where traction motors act as generators resisting rotation, thus slowing the train. In the straight electric locomotive the current produced is fed back into the catenary, while in the diesel-electric the generated current is fed to high-resistance grids, which must be cooled by fan-driven air. Dynamic braking can be advantageous in reducing wear and tear on train brakes and wheels, but it must be used judiciously to avoid excessive longitudinal train forces. *See* BRAKE; DYNAMIC BRAKING; GAS TURBINE; RAILROAD ENGINEERING; TURBINE PROPULSION. George H. Way

Bibliography. H. I. Andrews, *Railway Traction: The Principles of Mechanical and Electrical Railway Traction*, 1986; J. H. Armstrong, *The Railroad, What It Is, What It Does*, 4th ed., 1990; W. W. Hay, *Railroad Engineering*, 2d ed., 1982; C. J. Riley, *The Encyclopedia of Trains and Locomotives*, 1994.

Locust (forestry)

A name commonly applied to two trees, the black locust (*Robinia pseudoacacia*) and the honey locust (*Gleditsia triacanthos*). Both of these commercially important trees have podlike fruits similar to those of the pea or bean. *See* LEGUME.

The black locust, which may attain a height of 75 ft (22 m), is native in the Appalachian and the Ozark regions and is now widely naturalized in the eastern United States, southern Canada, and Europe. It is characterized by odd-pinnate leaves, fragrant white blossoms like those of pea plants in long clusters, flat brown pods 2–4 in. (5–10 cm) long, and a pair of stipular thorns at the base of each leaf. In winter these paired thorns and the superposed buds hidden under the leaf scar are important distinguishing features (see **illus.**).

The wood is hard and durable in the soil and is used for fence posts, mine timbers, poles, and railroad ties. It is the principal wood for insulator pins on utility poles. Because of its wide-spreading, fibrous root system which supports nitrogen-fixing nodules, the black locust is well adapted to erosion control and soil reclamation. Many varieties are planted as shade or ornamental trees. *See* SOIL CONSERVATION.

The honey locust, which reaches a height of 135 ft (41 m), is native in the Appalachian and the Mississippi Valley regions, but is also widely naturalized in the eastern United States and southern Canada. The flowers are inconspicuous, but the large brown fruit pods (12–18 in. or 30–45 cm long) are striking. The tree may be easily recognized at any season of the year by the branched thorns growing on the trunk or branches. The leaves are either pinnate or bipinnate. The reddish wood is hard, strong, and coarse-grained and takes a high polish. Because it is durable in contact with soil, it is used for fence posts and railroad ties; it is also used for construction, furniture, and interior finish. Although it belongs to the legume family, the roots do not possess nitrogen-fixing bacteria. The tree is often used for hedges, as an ornamental, and for shade. *See* FOREST AND FORESTRY; TREE. Arthur H. Graves; Kenneth P. Davis

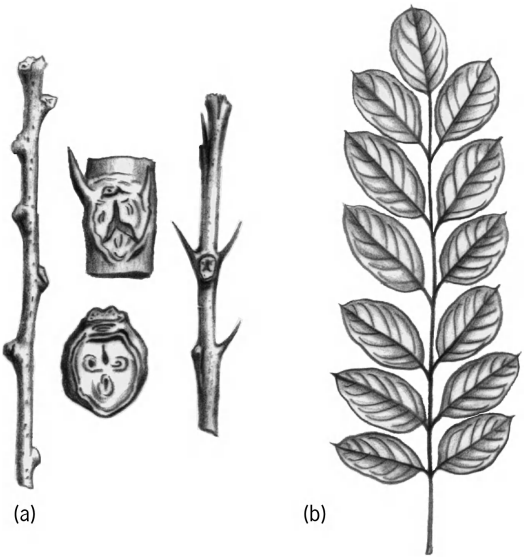

Black locust (*Robinia pseudoacacia*). (*a*) Branches, with and without thorns, and enlarged views of leaf scars. (*b*) Odd-pinnate leaves.

Loess

Deposits of windblown fine-grained angular particles that are produced by the breakdown of larger particles at desert or glacial margins. Suspension and transport by the wind produces particularly homogenous and well-sorted loess upon deposition. Loess is dominated by silt-sized (2–63 micrometers in diameter) particles of quartz, with smaller amounts of feldspars, calcium carbonate, and clay minerals, and can form successive, blanketing layers of thickness from centimeters to hundreds of meters, as in the Loess Plateau region of north-central China (**Fig. 1**). Loess occurs globally, encompassing the pampas of Argentina, the central and east European and Russian steppe, and the midcontinent United States, to name some locations. It is porous and unconsolidated, making it a valuable agricultural resource. Loess is highly erodible in wet conditions, although often mechanically strong when dry because calcium carbonate and clay aggregates bind the silt particles together. *See* CALCITE; CLAY MINERALS; DEPOSITIONAL SYSTEMS AND ENVIRONMENTS; EOLIAN LANDFORMS; FELDSPAR; QUARTZ.

Paleoclimate and the Chinese Loess Plateau. In addition to its agricultural importance, loess is of key geological significance. Thick sequences of loess and their interbedded buried soils (Fig. 1) are the subject of intense scientific attention because they contain the longest, most detailed record of Quaternary climatic changes yet found on land. In China, these sediments span at least the last 2.5 million years of the Earth's history, and cover some 500,000 km^2 (193,000 mi^2) of land (**Fig. 2**). The vertical loess

Fig. 1. Loess/paleosol sequence in the central Loess Plateau of China. The paler layers of loess are interbedded with the darker paleosol units, two of which are indicated by arrows.

thickness is ~350 m (1150 ft) near the nothern and western Plateau edges, bordering Mongolia and Tibet, ~150 m (490 ft) in the central area, and thins out towards the southern and eastern cities of Xi'an and Beijing.

Sediment source. Because the Chinese loess is thickest and its particle size coarsest toward the northwest (**Fig. 3**), it was thought that the northwestern deserts were the source of the loess, blown by winter monsoon winds. There is a good match of the geochemical "fingerprints," including strontium and neodymium isotopic compositions and rare-earth and trace-element concentrations, between the loess and desert sands. However, the loess is often much

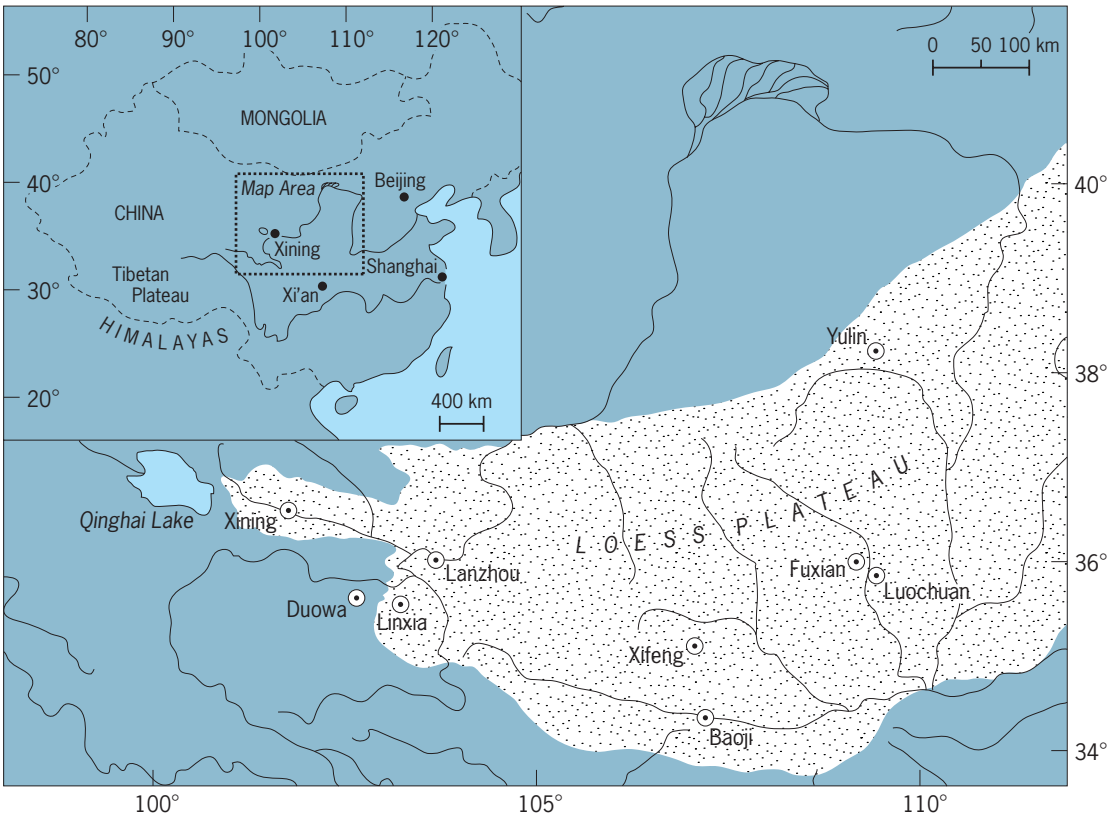

Fig. 2. Loess Plateau, north-central China.

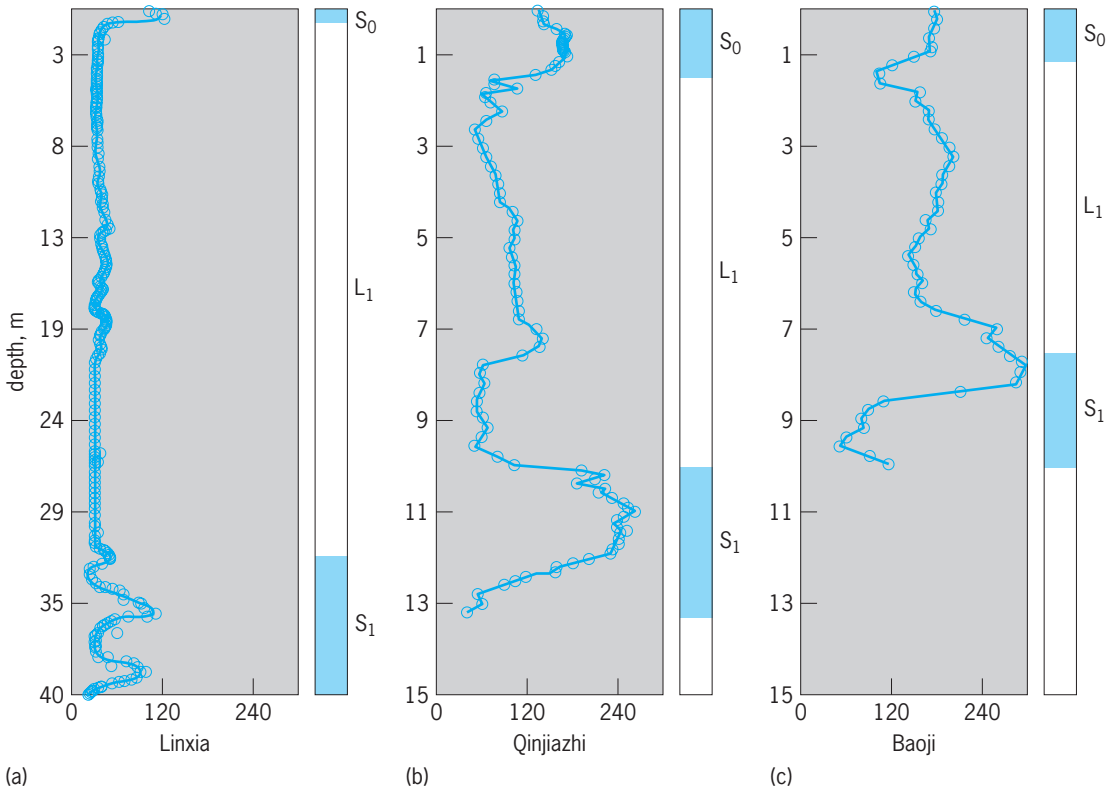

Fig. 3. Loess/paleosol stratigraphy (modern soil—S_0; last glacial loess unit—L_1; and last interglacial paleosol—S_1) and magnetic susceptibility (10^{-8} m^3 kg^{-1}). (*a*) A western Loess Plateau site (note 40 m or 131 ft of sediment spanning the soil/loess/paleosol units, and a maximum paleosol susceptibility value of 120 × 10^{-8} m^3 kg^{-1}). (*b*) A central site (note 13 m or 43 ft of sediment for the same time span as *a*, and maximum paleosol susceptibility value of 245 × 10^{-8} m^3 kg^{-1}). (*c*) A southern site (10 m or 33 ft of sediment for the same time span as *a* and *b*, and maximum paleosol susceptibility value of 300 10^{-8} m^3 kg^{-1}). The higher the susceptibility, the higher the paleo-rainfall.

more magnetic than modern desert sand. It also has variable but often very high values of beryllium-10, which forms in the atmosphere through nuclear reactions caused by cosmic rays and is brought down to the Earth's service by precipitation, indicating a source area with moderate to high rainfall such as the Himalayas or Tibetan Plateau. The loess transport path might originate with winter surface winds, blowing from the western Himalayas to the northeast, and supplying Himalayan dust to the deserts to the north and west of the Loess Plateau. During the spring months of the winter monsoon, the dust is blown from these deserts to the Loess Plateau to the southeast. *See* ASIA; BERYLLIUM; COSMIC RAYS; COSMOGENIC NUCLIDE; MAGNETIC SUSCEPTIBILITY; MONSOON METEOROLOGY; QUATERNARY; RADIOISOTOPE (GEOCHEMISTRY); SEDIMENTOLOGY.

Paleosols and climate. Interlayered within the "buff"-colored loess are buried soils (paleosols), traceable over hundreds of kilometers as near-horizontal, reddened layers (Fig. 1). These ancient soils formed when the climate became warmer and wetter so that at successive intervals the loess surface became vegetated and weathered. More than 30 alternations between cooler, drier periods (during which loess was transported and deposited) and warmer, wetter, soil-forming periods have occurred. These climatic variations have occurred over the past 2.5 million years. The basal age of the Chinese sequences has been defined paleomagnetically, and the central area of the Chinese Loess Plateau has recorded the last six major reversals of the Earth's magnetic field. *See* CLIMATE HISTORY; MAGNETIC FIELD; PALEOMAGNETISM; PALEOSOL; ROCK MAGNETISM; SOIL.

Magnetic variations. It may be possible to quantify these monsoon rainfall variations from the mineral magnetic properties of the loess and paleosol units. The paleosols are much more magnetic than the loess layers. In terms of their response to an applied magnetic field (that is, their magnetic susceptibility), paleosol layers have values 2–5 times higher than the loess layers (Fig. 3). In modern soils, strongly magnetic minerals (magnetite and maghemite) are formed in situ in well-drained, moderately acidic soils (pH ~5.5–7) on iron-bearing, weatherable parent materials. Magnetic measurements of modern soils across the Chinese Loess Plateau and Russian steppe show that the amount of magnetic material formed is strongly correlated with annual rainfall. The numerical relationship between magnetic susceptibility and rainfall defined from modern soils can be used to calculate paleo-rainfall from the magnetic susceptibility values of the buried soils in the Chinese loess/soil sequences. This approach identifies high rainfall (more intense summer monsoons) in the early Holocene (8000 to 6000 years ago) and late Holocene (5000 to 3000 years ago) and the last interglacial, especially in the presently semiarid western Plateau. During the last glacial stage, rainfall was

reduced across the whole region. Controversially, G. Kukla and colleagues believe that the susceptibility variations are mostly controlled not by rainfall but by the rate of deposition of the magnetically poor dust. *See* GLACIOLOGY; MAGNETITE.

Multiproxy climate indicators. In addition to geochemical and paleomagnetic indicators, other proxy climate indicators retrieved from global loess/soil sequences include fossil snails, plant phytoliths (silicate exudates from plant roots), loess particle size, and carbonate content. It is possible to extract preserved fossil snails from loess/paleosol sequences, with different ecological groups reflecting different temperature and moisture requirements of each taxon. Phytolith analysis provides information on vegetation changes, with trees and grasses forming differently shaped phytoliths, but phytoliths can also record isotopic information relating to changes in temperature and rainfall. As with the fossil snails, the phytoliths have to be extracted from the loess and both are subject to dissolution in some sequences. Particle-size variations in the loess can record the strength of the winter monsoon winds. Larger detrital grain sizes may indicate periods of increased wind strength (or increased proximity to dust sources), and smaller sizes may indicate periods of decreased winter monsoon intensity (or increased distance from dust sources). Carbonate content may reflect variations in summer monsoon moisture, causing dissolution of detrital carbonate and its reprecipitation in lower soil horizons. High-resolution studies of the loess/soil sections in the western Chinese Loess Plateau, where the sequences are at their thickest, show that the intensities of the summer and winter monsoons are not directly coupled. From about 12,000 to 8000 years ago the summer monsoon was generally strong and the winter monsoon was weak, while about 8000 years ago both the winter and summer monsoons were strong.

Magnetic susceptibility/climate relationships. Thinner, less complete loess/soil sequences occur around the globe. Those in Alaska, Siberia, and Poland show the opposite pattern of magnetism, with low susceptibility values associated with the paleosols and higher values for the loess layers. One reason for this is that the loess in these regions is very strongly magnetic (much more magnetic than the Chinese loess). Also, modern soils show that arid conditions prevent formation of new magnetic material, while waterlogging and acidification of soils not only inhibit magnetic mineral formation but also destroy detrital magnetic minerals. Thus, we can infer that the climate at soil-forming intervals in these locations was not conducive to in situ magnetic mineral production.

Barbara A. Maher

Bibliography. F. Heller and M. E. Evans, Loess magnetism, *Rev. Geophys.*, 33:211–240, 1995; H. Y. Lu et al., Seasonal climatic variation recorded by phytolith assemblages from the Baoji loess sequence in central China over the last 150 ka, *Past Global Changes Newslett*, 6:4–5, 1998; B. A. Maher, Magnetic properties of modern soils and loessic paleosols: Implications for paleoclimate, *Palaeogeog. Palaeoclimatol. Palaeoecol.*, 137:25–54, 1998; B. A. Maher and R. Thompson, Palaeomonsoons I: The magnetic record of palaeoclimate in the terrestrial loess and palaeosol sequences, in B. A. Maher and R. Thompson, *Quaternary Climates, Environments and Magnetism*, pp. 81–125, Cambridge University Press, 1999; B. A. Maher, A. Alekseev, and T. Alekseeva, Variation of soil magnetism across the Russian steppe: Its significance for use of soil magnetism as a palaeorainfall proxy, *Quat. Sci. Rev.*, 21:1571–1576, 2002.

Logarithm

An exponent of a suitably chosen positive number (base) larger than unity. Logarithms are of value in mathematical computation and in the equations and formulas used in expressing natural phenomena.

The invention of natural logarithms (base $e = 2.718\ldots$) is usually attributed to John Napier, who published a table of logarithms in Edinburgh in 1614 under the title *Mirifici Logarithmorum Canonis Descriptio*, even though the functions tabulated by Napier are merely related to, and not identical with, natural logarithms.

The invention of common logarithms (base 10) is generally attributed to Henri Briggs; Napier's share is acknowledged, however, by Briggs himself in his *Arithmetica Logarithmica* in 1624.

Theory. If $b_l = n$, where b is a positive number larger than unity, then l is called the logarithm of n to the base b and is written $l = \log_b n$. From this definition it follows at once that all positive numbers larger than unity have positive logarithms, all positive numbers smaller than unity have negative logarithms, and the logarithm of unity is equal to 0. Since $b^0 = 1$ irrespective of the value of b, it follows that the logarithm of unity is equal to 0. From the known properties of exponentials expressed by relations (1), it follows immediately that (a) the log-

$$\begin{aligned} b^{l_1} \cdot b^{l_2} &= b^{l_1+l_2} \qquad b^{l_1} \div b^{l_2} = b^{l_1-l_2} \\ \left(b^l\right)^m &= b^{lm} \qquad \sqrt[m]{b^l} = b^{l/m} \end{aligned} \tag{1}$$

arithm of a product of two or more factors is equal to the sum of the logarithms of the factors; (b) the logarithm of the ratio of two numbers is equal to the difference between the logarithm of the numerator and the logarithm of the denominator; (c) the logarithm of the mth power of a number is the product of m and the logarithm of the number; and (d) the logarithm of the mth root of a number is equal to the logarithm of the number divided by m. These properties are responsible for the great simplification in the task of carrying out numerical computations involving multiplication, division, raising numbers to certain powers, or extracting the roots of a certain order of given numbers. It also follows from these properties that in constructing a table of logarithms to a certain base from the beginning, the computer need only compute the logarithms of prime numbers, because the logarithm of any number which is

not prime can be obtained from the logarithms of its prime factors by simple operations of addition and multiplication. *See* EXPONENT.

Although any positive number b larger than unity might have been chosen as the base of a system of logarithms, actually two numbers have been chosen in the construction of tables of logarithms, namely, the number $b = 10$ and the number e defined as the sum of infinite series (2). The system of logarithms

$$1 + \frac{1}{1} + \frac{1}{1 \cdot 2} + \frac{1}{1 \cdot 2 \cdot 3} + \cdots + \frac{1}{1 \cdot 2 \cdot 3 \cdots n} + \cdots \quad (2)$$

to the base 10 is usually referred to as common logarithms; the system of logarithms to the base e is called natural logarithms.

Common logarithms have certain obvious advantages not shared by natural logarithms. All numbers between 1 and 10 have logarithms between 0 and 1, all numbers between 10 and 100 have logarithms between 1 and 2, and so on. Thus the integral part of the common logarithm of a number larger than unity is one unit less than the number of digits before the decimal point. This integral part is called the characteristic; the decimal part is called the mantissa. Similarly, because the common logarithms of 0.1, 0.01, and 0.001 are -1, -2, and -3, it follows that the logarithm of a number smaller than unity having p zeros after the decimal point may be expressed as the sum of a negative characteristic equal to $-(p + 1)$ and a positive mantissa.

Natural logarithms. Because the number $e = 2.718 \ldots$, the base of the system of natural logarithms is irrational; that is, it cannot be expressed as the ratio of two integers (and therefore when expressed as a decimal number, it involves an infinite number of decimals with no repeating groups of decimals). It might seem odd, therefore, that it has been chosen as the base of a system of logarithms. The primary motivation for this choice lies in the fact that the solutions of numerous problems in applied mathematics are most naturally expressed in terms of powers of e. Thus, for instance, the solutions of the problems of equilibrium of a flexible cable, the transient flow of electric current in a circuit, and the disintegration of radioactive elements are expressed in terms of e^x, where x is either positive or negative and depends on the physical parameters of the problem in question. Thus, the tabulation of the function e^x for both positive and negative values of x was an indispensable aid in obtaining the solutions of many physical problems. Because the logarithmic function is the inverse of the exponential function, a table of natural logarithms can be constructed with relative ease from a table of e^x by the process of inverse interpolation. Another motivation for constructing tables of natural logarithms is the fact that natural logarithms arise in the integration of quotients of polynomials and of functions which may be approximated by quotients of polynomials. Indeed, it is a well-known fact that if the n roots of a polynomial $Pn(x)$ are known so that $Pn(x) = a_0(x - x_1)(x - x_3) \cdots (x - x_n)$ and if $Q(x)$ is a polynomial of degree smaller than n, then the quotient $Q(x)/Pn(x)$ may be expressed in the form of expression (3) when the A_ks may be easily determined. Accordingly Eq. (4) may be written.

$$\sum_{k=1}^{n} \frac{A_k}{x - x_k} \quad (3)$$

$$\int \frac{Q(x)}{Pn(x)}\, dx = \sum_{k=1}^{n} A_k \int \frac{dx}{x - x_k} = \sum_{k=1}^{n} A_k \log_e (x - x_k) \quad (4)$$

Table of logarithms

Number	Natural logarithm	Common logarithm
0.01	5.586–10	−2 (8 − 10)
1.0	0	0
$e = 2.718 \ldots$	1	0.4343
10	2.303	1
1000	6.909	3

Relation between logarithm bases. Let l_1 be the known natural logarithm of a number N. What is the common logarithm of N? Clearly $N = e_1^l$, and therefore $\log_{10} N = l_l \log_{10} e$. Since $\log_{10} e = 0.43429$ (to five decimals) it can be concluded that natural logarithms are converted into common logarithms by multiplying the natural logarithm by the factor 0.43429, which is called the modulus. Similarly the common logarithm is converted into a natural logarithm by division by the modulus 0.43429 or multiplication by 2.303. The **table** shows natural and common logarithms for some numbers from 0.01 to 1000.

Logarithms of complex numbers. Since b^l is positive when b is positive, negative numbers have no real logarithms. Nevertheless, Euler's famous formula $e^{i\theta} = \cos\theta + i \sin\theta$, where $i = \sqrt{-1}$, makes it possible to define not only the logarithm of a negative number but also the logarithm of a complex number. Indeed, any complex number $a + ib$ may be written in the form $\rho e^{i\theta}$, where $\rho = \sqrt{a^2 + b^2}$ and $\theta = \arctan(b/a)$. It follows that the logarithm of a complex number $a + ib$ is a complex number whose real part is the logarithm of its modulus ρ and whose imaginary part is its phase (or argument) ρ. Because $e^{i\theta} = e^{i(\theta + 2n\pi)}$, it follows that a complex number has an infinite number of logarithms given by Eq. (5), where

$$\log(a + ib) = \log \sqrt{a^2 + b^2} + i(\theta + 2n\pi) \quad (5)$$

n is a positive or negative integer.

As previously mentioned, the evaluation of natural logarithms may be based on inverse interpolation in a table of e^x. For small values of x, positive or negative, it is possible to use expansion (6). This expan-

$$\log_e(1 + x) = x - \frac{x^2}{2} + \frac{x^3}{3} - \cdots + (-1)^{n+1} \frac{x^n}{n} + \cdots \quad (6)$$

sion may be derived from Taylor's series, notation (7),

$$f(x+a) = f(a) + \frac{x}{1}f'(a) + \frac{x^2}{1\cdot 2}f''(a) + \cdots + \frac{x^n}{1\cdot 2\cdot 3\cdot m}f^{(n)}(a) + \cdots \quad (7)$$

by writing $f(x) = \log_e x$. After a sufficiently accurate table of $\log(1 \pm x)$, for $x = k10^{-n}$, $k = 1, 2, 3, \ldots, 9$, and $n = 1, 2, 3, \ldots, N$, where N is sufficiently large (perhaps 15) has been computed, this table may be used to compute the logarithm of any number. From the expansion (6) for $\log_e(1 + x)$ it is easy to derive expansion (8), where Eq. (9) holds; this has the

$$\log_e p = {}^1/_2\{\log_e(p-1) + \log_e(p+1)\} + S(p) \quad (8)$$

$$S(p) = \frac{1}{2p^2-1} + \frac{1}{3(2p^2-1)^3} + \cdots + \frac{1}{(2n+1)(2p^2-1)^{2n+1}} + \cdots \quad (9)$$

virtue that $S(p)$ converges quite rapidly. Thus for $p >$ 10,000 the error resulting from neglecting all but the first term in $S(p)$ is considerably less than 10^{-20}. *See* E (MATHEMATICS); NUMBER THEORY; NUMERICAL ANALYSIS.

Arnold N. Lowan; Solomon Bochner

Logging

Those processes required to bring all or a portion of a tree from the stump to the mill facilities. Logging (tree harvesting) processes are clustered into tree conversion, woods transport (off-road transportation), landing operations (wood transfer), transport from landing to mill facility (truck, water, or rail), and unloading at the mill facility (wood transfer).

Logging systems are networks that connect harvesting processes so that the whole operation is physically feasible, economically efficient, environmentally sound, and institutionally feasible. They are usually characterized by the degree of tree conversion before off-road transportation: cut-to-log-length, tree-length, or full-tree. Off-road transportation options are the decisive factors for the use of equipment, and restrict the possible configuration of harvesting systems. The major off-road transportation options include ground-based transportation (vehicles operating on the surface using unpaved "skid trails" through the forest), cable systems, and airships (such as helicopters).

Logging operations around the world vary with the level of industrial development of the local forest industry. Logging in some countries is done by hand tools and human or animal power (biomechanical). In other countries, machines with on-board computers and microprocessors carry out the harvesting activities without workers setting foot on the forest floor (mechanized logging).

Logging is both a transportation process and an allocation process. The allocation process relates how the various parts of the tree can meet a product or environmental need. Depending upon the forest management plan, some trees or parts of trees are removed to make some of the many wood products such as fuelwood, materials for housing, and furniture. Other trees are left in the forest for wildlife, forest renewal, or soil nutrient reasons. The transportation process moves the logs (woody stems), chips, chunks, flakes, or biomass (whole or parts of the tree destined to be used for energy) from the forest to mill facilities. *See* FOREST TIMBER RESOURCES; PAPER; PLYWOOD; WOOD PRODUCTS.

Felling (tree conversion). The start of harvesting is the cutting down of trees with hand tools, chain saws, or mechanized felling machines (using chain saws, circular saws, or hydraulic shears to cut the tree at the base). The tree may be further cut into suitable lengths (bucking), or it may be transported whole or in tree-lengths. Tree products may be allocated during bucking with the aid of a computer on the felling and bucking machine or by a faller using a log order list or a hand-held computer to help decide the log products to make.

Felling is the most dangerous part of the harvesting operation. Larger trees generally must be felled manually with a chainsaw. Manual fallers often work under difficult conditions and must possess stamina, dexterity, skill with hand tools, mechanical ability, tree identification skills, and a thorough understanding of the rules involved in bucking. Mechanized felling operators must be adequately literate; have good dexterity, mechanical ability, tree identification skills, and decision-making skills; and be able to follow complex plans while working independently.

The objective of the tree falling operation is to fell the tree with minimum damage, to avoid damaging surrounding trees, to minimize soil and water impacts, and to position the tree or logs for the next phase of harvesting (**Fig. 1**). The goal of bucking is to produce the most valuable assortment of logs from the tree while considering the physical

Fig. 1. Feller-buncher cutting tree. (*John Deere*)

capability of the skidding (log-dragging), yarding (moving of logs to a landing), or forwarding (log-carrying) equipment.

Woods transport (off-road transport). Logs in lengths from about 1 to 10 m (3 to 33 ft) or other products must be transported from the stump to a place where they are further processed (often called a landing). In some cases, entire trees are pulled to the landing. Humans, animals (for example, oxen, horses, and elephants), crawler tractors and wheeled skidders (machines that drag the logs), forwarders (machines that carry loads of logs), farm tractors with winches or trailers, cable logging systems, balloons, or even helicopters transport logs and tree products to landings.

Normally, logs are hooked to the skidding animal or vehicle using wire rope (choker) or chains, or by a grapple arm. Forwarders use a hydraulic grapple to load the forwarder in the woods and unload it at the landing (**Fig. 2**).

The choice of the transport system depends on topography, roads and other transport options, size of products, economics, environmental considerations, soil types, weather, and the development stage of transport systems for the region or country. It may also depend upon the subsequent silvicultural activities. In some situations, soil disturbance may be encouraged to provide beds for seedlings; while in other situations, soil disturbance may be minimized to prevent erosion.

Where terrain (soil and slopes) is unsuitable for machines to operate on the ground surface for environmental or economic reasons, cable systems may be used to lift and drag or fly logs or felled trees to a landing area. Skyline systems may use wire rope 10–40 mm (0.4–1.6 in.) in diameter suspended between a steel tower 9–35 m (30–115 ft) high and a stump or tree to carry a load of logs connected to a carriage (device that rides on the skyline on pulley blocks) from where the tree was cut to the landing. The distance may be as short as 200 m (660 ft) or as long as 1700 m (5600 ft) depending on roads and terrain. Intermediate supports may be needed to provide necessary skyline clearance over the terrain. Alternately, helicopters used for heavy lifting may carry logs or trees by flying them to landings up to 2 km (1.2 mi) away.

Fig. 2. Forwarder loading logs for transport to landing. (*John Deere*)

Yarding productivity depends upon the system, equipment, yarding distance, and other circumstances. Equipment factors include the pulling power, load capacity, and speed. Environmental factors affecting productivity include tree characteristics; stand characteristics of size, shape, and location; the volume of timber to be harvested; yarding distance and direction; terrain conditions; and weather. Other productivity factors include the harvesting method, type of cutting (manual or mechanized), and skill and organization of the crew.

Landing operations. At the landing, the logs or trees may be stored or directly processed for transport. They may be loaded onto trucks, trains, barges, or ships, or prepared for water transport. Whole trees brought to a landing may have limbs and bark removed, and then be chipped and loaded into chip vans for transport to a pulp mill. Tree-length segments may be delimbed and bucked into logs for different market destinations. Trees may be shredded, chunked, or processed through machines for use as fuel. The allocation process may include measurement by volume or weight of the products. In some cases, logs can be offloaded from a woods transport vehicle, such as a forwarder, directly to a trailer, minimizing rehandling.

Loading. Because logs are heavy, they are normally loaded mechanically, although some regions still use manual or animal methods involving ramps. There are two general types of mechanical loaders used at roadside: swingboom loaders with grapples, and front-end loaders fitted with a log fork or grapple. Both are mobile, mounted on tracked or rubber-tired carriers. Forwarders usually unload themselves either into log decks for storage or onto setout trailers. For log products, loads are usually secured by using wire rope wrappers and binders to hold logs on the trailer during transport. Loader operators must be highly skilled. They are responsible for sorting logs on the landing, loading trucks heading for different destinations, carefully building stable loads for transport, without overloading the truck or injuring landing personnel.

Transportation (landing to mill facility). Trucks are most commonly used to transport log products to mill facilities (**Fig. 3**). They vary from small vehicles hauling 5–8 tons on straight beds to large specialized off-highway vehicles hauling 50 tons or more. A variety of truck trailers are used depending upon the type of product. Trees or long logs may be loaded onto pole trailers. Short logs, 2.5 m (8 ft) and less, are often stacked sideways on flat-bed trailers with bunks. Chips or flakes are hauled in specially designed chip vans. Many pole-trailers permit the trailer to be loaded onto the truck tractor for the return trip to improve traction and reduce tire wear. Logging trucks need to be stronger than normal highway trucks because they travel on lower-quality roads. Truck components must be suitably matched, including engines, brakes, transmissions, differentials, and tires. Drivers must be especially skilled in

Fig. 3. Heavy-duty log truck-trailer being loaded with a grapple. Part of a steel yarding tower is visible at the left and is rigged with a skyline cable system. (*Kenworth Truck Co., Division of PACCAR*)

maneuvering under adverse forest conditions as well as on public highways.

Water transport in barges, as log rafts, and as free-floating logs is used in some areas. Where water transport is consistent with environmental concerns, it is often the most economical alternative. It also may be used in conjunction with truck transport. Logs can be banded on the truck trailer before they are lifted from the truck and placed in the water. Bundles of logs form rafts which are then towed to processing destinations or to sites for loading onto seagoing vessels.

At one time, railroads were one of the principal methods of moving timber from the forest to a river landing or to the sawmill. With the development of modern road construction, improved road maintenance, and more powerful and reliable trucks, rail transport has declined.

Unloading. Log products can be unloaded from truck trailers by lifting, rolling, or dumping over the side or end, depending upon the type of trailer. Trees and long logs are usually lifted from trailers by a grapple on mobile wheel loaders or overhead cranes (which can unload the entire truck in one pass). Shorter logs are often unloaded using slings. In some cases, short wood for pulp is swept directly off the trailer and fed into a debarking machine to eliminate rehandling. Chip trailers are often tilted and end-dumped on large hydraulic ramps.

Not all logs are processed in the countries where they were harvested. Sometimes logs are shipped from countries with greater forest resources to those needing logs for their processing facilities.

Loggers. The people who conduct tree harvesting operations are called loggers. In some countries, loggers are farmers for part of the year who then use their tractors for logging in the forests adjacent to their farms. In others, loggers are highly skilled technicians operating from computerized cabs. Loggers may be self-employed and own their own equipment, or they may be employed by logging contractors or companies. Logging work is characterized as difficult and dangerous. In most countries, logging has one of the highest accident rates of any industrial activity. Most of the accidents occur from the use of chain saws. When mechanized harvesting operations replace manual harvesting, accidents decrease dramatically. Loggers implement the silvicultural prescriptions of forestry professionals. Logging contractors provide logging services to governmental and large and small forest owners, often using capital equipment worth millions of dollars.

Logging is a means of resource development that can be abused if modern forestry practices are not regulated or enforced. Throughout the world, many communities and cultures are dependent on the forest resource and its utilization that starts with the process of logging. Developed countries have forest practices regulations that are strongly enforced to protect environmental and societal values.

Environmental effects. Potential risks from logging within the natural environment include loss, destruction, and compaction of soils; damage to residual trees; disturbance of flora and fauna; and pollution of water. Risks in the social setting are to human health and safety, disturbance of landscape esthetics, and disturbance of cultural heritage. At present, a major emphasis of the logging industry worldwide is on reducing environmental impacts. Environmental as well as safety and health standards are prescribed in codes of practices to help control and reduce risks.

When logging is done poorly and without regard for environmental concerns, resource damage to trees, soil, water, and wildlife can occur. When environmental concerns are accommodated, such as careful selection of roads and landings, control over the season of operation, minimizing the area where machines travel, minimizing damage to surrounding trees, careful activities around streams, and controlled waste disposal from operations, logging can be conducted as part of a sustainable basis of development.

Planning for logging operations. An adequate plan is essential for a successful logging operation. Logging operations are expensive and if done incorrectly can be costly to correct. The logging plan often specifies the type of equipment used, the location and size of roads and landings, the location of skid trails, the felling pattern, and the season of operation. Logging planning must consider subsequent forestry operations such as site preparation.

The tools to plan and organize a logging operation include on-the-ground reconnaissance and computer programs that assess logging feasibility, equipment performance, environmental impacts, and economic performance. Planning is often conducted by professional forest engineers.

Training and supervision. Good plans and technical solutions require effective training and on-site supervision. On-site supervision and communication with loggers are vital in controlling soil and water impacts and minimizing resource problems. In many cases, small adjustments by equipment operators can produce significant benefits. For example, skidder

operators can keep the front end of the log fully suspended and not use the skidder blade as a brake to avoid disturbing the soil. Careful supervision is especially important when operating during wet weather or on weak soils to avoid soil and water damage. Trained loggers blend harvesting and environmental knowledge into safe and effective forest operations.

[The authors thank the Forest Engineering Department, Oregon State University, for cooperation in the preparation of this article.]

John Sessions; John Garland

Bibliography. S. Conway, *Logging Practices*, Miller Freeman, 1982; *Model Code of Forest Harvesting Practice*, Food and Agriculture organization of the United Nations, 1996; L. Pancel (ed.), *Tropical Forestry Handbook*, Springer-Verlag, 1993; Planning Forest Roads and Harvesting Systems, *FAO Forestry Pap.*, no. 2, Food and Agriculture Organization of the United Nations, 1977; U. Sundberg and C. Silversides (eds.), *Operational Efficiency in Forestry*, Kluwer Academic, 1988; Workers Compensation Board of British Columbia, *Handbooks for Falling, Skidding, Yarding, Loading, Helicopter Logging*.

Logic

The subject that investigates, formulates, and establishes principles of valid reasoning.

The first attempt to investigate systematically acceptable modes of reasoning was made by Aristotle, in whose *Organon* reasoning was recognized as the subject of a special science. He formulated three basic "laws of thought": (1) the law of contradiction (no proposition is both true and false), (2) the law of excluded middle (each proposition is either true or false), and (3) the law of identity (each proposition implies itself). Advanced as his views of logic were, it seems doubtful that the idea of axiomatizing it ever occurred to him, despite the success of his contemporary Euclid in organizing geometry. That aspect of logic which enunciates or establishes valid reasoning (rather than merely investigating it) began with the publication in 1854 of George Boole's *An Investigation of the Laws of Thought*. The partly abstract treatment of logic presented in this work initiated the completely abstract developments that were to follow. In it the laws of thought are regarded as mere conventions which, like the postulates of euclidean geometry, might be modified or even rejected to create new logics. The only requirement that a "new" logic must satisfy is the one demanded of every deductive system—consistency. Just as different geometries are useful for different purposes, a logic that is appropriate in one environment might not be so in another. There are a growing number of competent individuals, for example, who consider that any logic containing Aristotle's law of excluded middle is not suitable for mathematics. *See* BOOLEAN ALGEBRA; EUCLIDEAN GEOMETRY; GEOMETRY.

This article discusses some of the principles for testing inferences, the use of formal procedures in clarifying arguments, and how important parts of logic have been developed axiomatically. The classical theory of the syllogism will be examined, and the deductive theory of truth functions (the calculus of propositions) will be presented in some detail. Finally, mathematical logic, which arose from work on the foundations of mathematics and encompasses proof theory, set theory, model theory, and recursion theory, will be discussed. For the most part, the discussion will be limited to what is called symbolic logic, for a special set of symbols is employed to exhibit in the clearest way the (at times) complicated logical relations involved. The advantages of a thoroughgoing use of a good symbolization are enormous. It is by such means that modern logic is able to solve problems that were quite beyond the power of logicians of an earlier time, and to render some of the achievements of those logicians almost trivial by comparison.

The syllogism. The formulation of the syllogism is contained in Aristotle's *Organon*. It had a great fascination for medieval logicians, for almost all their work centered about ascertaining its valid moods. The three characteristic properties of a syllogism are as follows:

1. It consists of three statements, the third one (conclusion) being a logical consequence of the first two (the premises).

2. Each of the three sentences has one of the following four forms.

(A) All X is Y (universal affirmative judgment).
(E) No X is Y (universal negative judgment).
(I) Some X is Y (particular affirmative judgment).
(O) Some X is not Y (particular negative judgment).

3. The three sentences contain altogether three terms, S (the subject of the conclusion), P (the predicate of the conclusion), and M (the middle term), that occur in each of the premises. P is called the major term, S the minor term, and a premise is called major or minor depending on whether it contains P or S, respectively. It is by virtue of the middle term, M, which occurs in both premises, that a relation between S and P can be asserted. Thus the three statements

No professors are rich.
All handsome men are professors.
No handsome men are rich.

form a syllogism in which M stands for professors, P for rich, and S for handsome men. This particular syllogism is valid (that is, the conclusion is a consequence of the premises), and hence the validity of a syllogism is seen to be independent of the truth or falsity of its conclusion. Notice that the major premise, minor premise, and conclusion of the above syllogism are statements of type (E), (A), and (E), respectively.

The four figures of the syllogism are represented

by notation (1). Each symbol *MP*, *SM*, and so on

(I)	(II)	(III)	(IV)	
MP	*PM*	*MP*	*PM*	(1)
SM	*SM*	*MS*	*MS*	
SP	*SP*	*SP*	*SP*	

stands for one of the four statements (A), (E), (I), and (O); for example, *MP* might symbolize the statement "No M is P." Hence each figure has $4^3 = 64$ possible forms, and consequently there are $4 \cdot 4^3 = 256$ possible forms for a syllogism. The great attention given the syllogism by logicians of the Middle Ages resulted in establishing that only 19 of the possible 256 forms that a syllogism might take are admissible (that is, yield valid conclusions). It should be noted that the result they obtained is correct provided one accepts the Aristotelian principle that the statement "All X is Y" implies that "There are X's." It was also maintained that "No X is Y" implies that "Some X is not Y." Thus, according to early logicians, universals have existential implications. Modern logicians do not take this point of view. This results in eliminating 4 of the 19 admissible forms (moods). Three-syllable mnemonic words were coined in which the vowels indicated, in order, those combinations of the statements (A), (E), (I), and (O) that resulted in valid syllogisms. For figure (I) they are *Barbara*, *Celarent*, *Darii*, *Ferio*; figure (II), *Cesare*, *Camestres*, *Festino*, *Baroco*; figure (III), *Datisi*, *Feriso*, *Disamis*, *Bocardo*, *Darapti*, *Felapton;* and figure (IV), *Calemes*, *Fresison*, *Dimatis*, *Bamalip*, and *Fesapo*. The illustrative syllogism given above is Celarent, figure (I). The four moods that depend for their validity on the classical assumption that universals imply existence (and which must be eliminated if that assumption is not made) are *Darapti*, *Bamalip*, *Fesapo*, and *Felapton*.

The syllogism is now of little more than historical interest. Its limitations were recognized quite early, for it was clear that few of the inferences needed in mathematics could be put in syllogistic form. As remarked by Hans Reichenbach, "It is only the combination of a logic of functions of several variables with the logic of propositions that leads to the full understanding of conversational language as well as of mathematics."

Propositional calculus. The unit of the propositional calculus is the proposition, which may be defined as the meaning of an indicative or declarative sentence. Each proposition has a truth-value; it is either true or false in the classical logic, but may assume other truth-values (for example, uncertain) in some of the new logics. Thus, "To err is human" is a proposition, whereas "Lead us not into temptation" is not a proposition. It is convenient to use letters p, q, r, and so on to denote propositions. Propositions are combined by logical connectives to form other propositions. Chief among these are (1) negation (the negation of a proposition p, symbolized by p', may be formed verbally by writing "It is not the case that" before p); (2) conjunction (a binary operation symbolized by $\cdot$ or &, for example, $p \cdot q$, read "p and q"); (3) disjunction (a binary operation symbolized by $+$ or $\vee$; for example, $p \vee q$, read "p or q"); (4) implication (a binary operation symbolized by $\supset$ or $\rightarrow$, for example, $p \rightarrow q$, read "p implies q"); and (5) equivalence (a binary operation denoted by $\equiv$ for example, $p \equiv q$, read "p is equivalent to q," means that each proposition implies the other). The proposition $p \cdot q$ asserts that both p and q are true. It is important to note that the disjunctive "or" is always used in the inclusive sense; that is, $p \vee q$ asserts that at least one, possibly both, of the propositions p and q is true. In addition, the meaning of "implication" in logic differs markedly from the ordinary sense of that term. The proposition $p \rightarrow q$ asserts merely that it is not the case that p is true and q is false; that is, in classical logic $p \rightarrow q$ means that either p is false or q is true. Thus any false proposition (for example, Napoleon Bonaparte was born in the year 1600) implies any proposition whatever. It implies, New York is a large city, or Cleopatra was queen of France. Similarly, any true proposition is implied by any proposition whatever. In an implication $p \rightarrow q$, p is called the antecedent and q the consequent. The logical connectives introduced above are examples of logical constants. They are not independent notions. Implication may be defined in terms of negation and conjunction, and this is true for all of the connectives. By use of the symbol $\equiv_D$ to mean "is defined," notation (2) follows, for example.

$$\begin{gathered} p \cdot q \equiv_D (p' \vee q')' \qquad p \supset q \equiv_D p' \vee q \\ p \equiv q \equiv_D [(p' \vee q)' \vee (q' \vee p)']' \end{gathered} \tag{2}$$

In fact, all the connectives can be defined in terms of one binary operation, the so-called Scheffer stroke function $p|q$, which may be read "p is false or q is false." Therefore, notation (3) follows.

$$\begin{gathered} p' \equiv_D p|p \qquad p \cdot q \equiv_D (p|q)|(p|q) \\ p \vee q \equiv_D (p|p)|(q|q) \\ p \supset q \equiv_D [(p|p)|(p|p)]|(q|q) \end{gathered} \tag{3}$$

The logical connectives, the letters p, q, r, and so on, that stand for propositions (propositional variables), and the parentheses, brackets, and braces needed for punctuation are formal concepts. A propositional function is a combination of concepts, formal or nonformal, involving at least one variable, which is not a proposition but becomes one when all the variables are given specified values. Examples are (1) p and q, (2) $x^2 + y^2 = 1$, and (3) x is president of the United States. Unlike a proposition, a propositional function has no truth-value. On the other hand, the statement "for every integer x, $x^2 + 2 = 0$" is a proposition (not a propositional function) even though it contains a (bound) variable. A formal function is a propositional function that contains only formal concepts—for example $[(p \vee q) \cdot r] \supset s$. The form of a given proposition is the formal function obtained from it by substituting formal concepts for all nonformal ones. Thus $p \cdot q$ is the form of the proposition "Leonard is happy and the moon is blue." Notice that in formalizing the above proposition, different propositions were replaced by

different propositional variables. A truth function is a propositional function in which only propositional variables occur, and such that the truth value of each proposition obtained from the function by substituting specific propositions for the variables depends only on the truth values of those propositions. Examples are (1) $(p \cdot q) \vee r'$, (2) Napoleon was a great general and p (where p is a propositional variable). On the other hand, "Jones stated that p" is not a truth function.

This article is concerned principally with the class of formal truth functions (that is, those containing only formal concepts) and with an important subclass called tautologies [that is, those formal truth functions such that every proposition obtained from them by substituting specific values (propositions) for the variables they contain has the truth value T (true)]. A truth function is contingent provided it assumes both truth values T and F (false)—here only the classical two-valued (Aristotelian logic) truth functions are considered—and self-inconsistent provided it has only the value F. The character of a truth function is determined when it is shown to be self-inconsistent, contingent, or a tautology.

Character of a truth function. A truth function may be analyzed by means of a truth table, or matrix. Such tables are made first for the elementary truth functions p', $p \vee q$, $p \cdot q$, $p \supset q$ as follows:

(I)

p	p'
T	F
F	T

(II)

p	q	$p \vee q$
T	T	T
T	F	T
F	T	T
F	F	F

(III)

p	q	$p \cdot q$
T	T	T
T	F	F
F	T	F
F	F	F

(IV)

p	q	$p \supset q$
T	T	T
T	F	F
F	T	T
F	F	T

In every table each row of the last column gives that truth value of the function which is determined by those truth values (assigned to the variables) that are entered in the preceding columns of that row. For example, the second row of table (IV) states that the truth function $p \supset q$ has value F. Since all logical connectives are used in the logic of propositions are expressible in terms of negation and disjunction, only tables (I) and (II) are really essential, but tables (III) and (IV) are convenient when analyzing complicated truth functions. Although the character of any truth function may be determined by constructing its truth table, the method is tedious when the function contains a large number of variables, since the truth table of a truth function of n variables has 2^n rows. As an example, the character of the truth function $(p \supset q) \supset (q' \supset p')$ may be determined. Using tables (I) and (IV), the truth table of the function is found to be

p	q	p'	q'	$p \supset q$	$q' \supset p'$	$(p \supset q) \supset (q' \supset p')$
T	T	F	F	T	T	T
T	F	F	T	F	F	T
F	T	T	F	T	T	T
F	F	T	T	T	T	T

Since every entry in the last column is T, the function $(p \supset q) \supset (q' \supset p')$ is seen to be a tautology. It may also be observed that in each row the entries in columns 5 and 6 are the same; that is, for any given values of p and q, the functions $p \supset q$ and $q' \supset p'$ assume the same truth value. Hence $(q' \supset p') \supset (p \supset q)$ and the two functions are logically equivalent. The principle embodied in this equivalence (the law of contraposition) is often used in mathematics.

Another device for ascertaining the character of a truth function is the method of negation. It sometimes happens that the character of the function obtained by negating a given function can be easily established, and since a function is contingent if and only if its negation is, self-inconsistent if and only if its negation is a tautology, and a tautology provided its negation is self-inconsistent, a knowledge of the character of the negated function solves the problem. The method makes use of the so-called De Morgan formulas $(p \vee q)' = p' \cdot q'$, $(p \cdot q)' = (p' \vee q')$, in which the sign $=$ signifies that an expression appearing on one side of it may be replaced by the expression appearing on the other side, and the boolean expansion of a truth function. This is an expansion that exhibits all of the conjunctive possibilities for truth value T; It is a disjunction of mutually exclusive (incompatible) conjuncts. For example, $p \vee q$ assumes truth value T if and only if the function $(p \cdot q') \vee (p \cdot q) \vee (p' \cdot q)$ does. The latter function is the boolean expansion of $p \vee q$. The method of negation can be illustrated first by considering the same truth function $(p \supset q) \supset (q' \supset p')$ analyzed by the matrix method. Writing Eq. (4) and noting that

$$\begin{aligned}[(p \supset q) \supset (q' \supset p')]' &= (p \supset q) \cdot (q' \supset p')' \\ &= (p' \vee q) \cdot (q \vee p')' \\ &= (p' \vee q) \cdot (p' \vee q)' \end{aligned} \quad (4)$$

$(p' \vee q) \cdot (p' \vee q)'$, as the conjunction of a proposition and its negation, is self-inconsistent, it follows that $[(p \supset q) \supset (q' \supset p')]'$ is self-inconsistent, and so $(p \supset q) \supset (q' \supset p')$ is a tautology. A second example, using the boolean expansion of $p \vee q$, is Eq. (5). Clearly, the truth function $p \cdot q'$ is

$$\begin{aligned}[(p \vee q) \supset q]' &= (p \vee q) \cdot q' \\ &= [(p \cdot q) \vee (p \cdot q') \vee (p' \cdot q)] \cdot q' \\ &= p \cdot q' \end{aligned} \quad (5)$$

contingent, and consequently so is the function $(p \vee q) \supset q$.

Tautologies and forms of argumentation. One truth function T_1 necessarily implies another T_2 provided the truth function $T_1 \supset T_2$ is a tautology. For example, $(p \supset q) \supset (q' \supset p')$ is a tautology, and so the truth function $p \supset q$ necessarily implies the truth function $q' \supset p'$. On the other hand, neither of those two truth functions is a tautology, and so the implications they exhibit are not necessary implications. Valid forms of argumentation are based on the notion of necessary implication. Two such forms were known to classical logic as *modus ponendo ponens* and *modus tollendo tollens*. The first states that if an implication

$p \supset q$ and its antecedent p are asserted, then the consequent q may be asserted; that is, the truth function $(p \supset q) \cdot p$ necessarily implies q. This is established by proving that the truth function $[(p \supset q) \cdot p] \supset q$ is a tautology. The *modus tollendo tollens* form of argument permits the denial of the antecedent of an asserted implication when its consequent is denied. The validity of the argument rests upon the tautology $[(p \supset q) \cdot q'] \supset p'$. A common fallacy (fallacy of the consequent) is to assert the antecedent of an implication whose consequent has been asserted. This is not permissible since the truth function $[(p \supset q) \cdot q] \supset p$ is not a tautology. Although such an argument is logically unwarranted, it is frequently invoked in testing experimentally a hypothesis p, for if q follows from p, numerous instances of the validity of q are sometimes taken to furnish strong evidence of the validity of p.

A traditional form of argumentation known as the dilemma is an application of *modus ponendo ponens* or *modus tollendo tollens*. Consider an example:

1. If I speak the truth, men will hate me; if I lie, the gods will hate me.
2. I must either speak the truth or lie.
3. Therefore, either men will hate me, or the gods will hate me.

The form of this dilemma is as follows:

1. $(p \supset q) \cdot (r \supset s)$
2. $p \vee r$
3. $q \vee s$

The argument is valid by *modus ponendo ponens,* for since premise (2) affirms the antecedent of at least one of the implications of premise (1), at least one of the consequents may be asserted, which is what the conclusion (3) does.

Deductive theory. The intent of this section is to sketch the procedure by which all tautologies are deducible from a set of just four of them. This is analogous to what is done in an axiomatic geometry in which all the theorems of the geometry are deduced from a selected set of axioms or postulates that are assumed to be true. The nature of the geometry is fully determined by the set of statements forming the postulates.

Let P denote a nonempty abstact set whose elements, denoted by *p, q, r,* and so on, are called propositions (for suggestiveness), and suppose P is closed with respect to a unary operation, denoted by $(')$, and a binary operation, denoted by $\vee$; that is, if p and q are any elemets of P, then p' and $p \vee q$ must be unique elemets of P. An additional binary operation, denoted by $\supset$ and read "implies" is defined in P:

If p, q are elements of P, $p \supset q \equiv_D p' \vee q$.

An expression formed by elements of P and the operations $(')$, $\vee$ is a truth function if and only if it conforms to the following syntactical rules: (1) *p, q, r,* and so on are truth functions; (2) if A and B are truth functions, then so are A' and $\vee B$; (3) no sequence of symbols denotes a truth function unless it is constructed according to (1) or (2), or unless it is replaceable by definition by a truth function. A subclass of the class of truth functions constitutes the class of tautologies. It is assumed that the following four truth functions are tautologies (these are the postulates):

P1 $(p \vee p) \supset p$
P2 $q \supset (p \vee q)$
P3 $(p \vee q) \supset (q \vee p)$
P4 $(q \supset r) \supset [(p \vee q) \supset (p \vee r)]$

These simple tautologies were selected by Alfred North Whitehead and Bertrand Russell in their monumental work *Principia Mathematica* as the basic set from which all tautologies can be derived. They had an additional postulate

P5 $[p \vee (q \vee r)] \supset [q \vee (p \vee r)]$

which was later shown by Paul Bernays to be deducible from the first four postulates, and hence may be deleted as a postulate. None of the three Aristotelian principles (laws of identity, contradiction, and excluded middle) are in the basic set. They are all deduced as theorems.

Before any theorems can be deduced there must be available rules that make it possible to go from one step in a proof to another. Among such rules are those of formal substitution, according to which any truth function may be substituted for any of the variables occurring in a postulate or theorem, provided the substitution is carried out completely, and any expression may be replaced by one definitionally identical. Among the rules of formal assertion are the principle of inference (that is, if P and $P \supset Q$ are postulates or proved theorems, then Q is a theorem) and the principle of adjunction (that is, if P, Q are postulates or theorems then $P \cdot Q$ is a theorem).

It was proved by E. L. Post that postulates P1–P4 are consistent; that is, it is impossible to deduce from them truth functions X and X'. He also proved that the four postulates form an independent set; that is, no one of the postulates can be deduced from the others.

Non-Aristotelian logics. In these logics the principle of the excluded middle (that is, each proposition is either true or false) is not valid. There are, then, at least truth values possible for a proposition, and for this reason such logics are known as many-valued. In a many-valued logic the *reductio ad absurdum* procedure that is so frequently used in mathematics is much less effective than it is in two-valued classical logic, for if it is not possible to conclude (as is permissible in Aristotelian logic) that the proposition is true. The Aristotelian tautology $(p')' \equiv p$ is not a tautology in a logic with at least three truth values. Doubts that the classical logic is an appropriate one to use in mathematics stem from the modern view that the concepts and the relationships dealt

with in mathematics have no real existence in the external world. It would seem to follow that the a priori nature of "true" or "false" then disappears and with it the law of excluded middle! If "true" is interpreted in mathematics to mean "provable," and a proposition is called false provided its negation is provable, then the law of excluded middle is demonstably false, since it has been shown that mathematics contains propositions p such that neither p nor its negation p' is provable. The intuitionistic school of the Dutch mathematician L. E. J. Brouwer rejected the excluded middle law, and it forms no part of the logic of that school, formulated by A. Heyting. *See* FUZZY SETS AND SYSTEMS. Leonard M. Blumenthal

Mathematical logic. Mathematical logic is an area of research that has emerged from the study of formal systems. It has its roots in work on the foundations of mathematics in the nineteenth and early twentieth centuries, showing that the customary forms of mathematical reasoning can be adequately expressed in formal (purely symbolic) systems. Mathematical logic contains four areas of research: proof theory, set theory, model theory, and recursion theory.

Formal systems. The original objective of work in the foundations of mathematics was the analysis and precise formulation of mathematical concepts, such as "limit," "function," and "differential manifold," as well as a complete and explicit determination of the valid forms of mathematical argument. This goal was achieved by the formalization of mathematics.

A formal system consists of a symbolic notation (or language) with rules for constructing expressions using the specified notation, axioms (expressions taken as given), and rules of inference used to derive additional expressions from a given set of expressions. To formalize an area of mathematics means to give a procedure for representing proofs in the specified area within a definite formal system. The process of formalization requires the construction of a formal language in which all the fundamental concepts of the theory can be adequately represented, as well as the specification of appropriate axioms and rules of inference. One formal system that is adequate for the formalization of all existing mathematics is the language of set theory, which can be set up in a variety of ways. There are various standard systems of axioms for set theory, notably the axiom system ZFC, consisting of axioms proposed by E. Zermelo and A. Fränkel, with the addition of the axiom of choice. A typical formalized axiom, the power set axiom of ZFC, is displayed in notation (6).

$$(\forall u)(\exists v)(\forall w)((w \in v) \iff (\forall x)(x \in w \implies x \in u)) \tag{6}$$

Proof theory. Proof theoretic research continues the study of formal systems that are adequate for the formalization of various parts of mathematics. Two basic results, due to K. Gödel, relate to the adequacy of formal systems in general: the so-called completeness and incompleteness theorems.

The completeness theorem essentially states that the laws of inference are adequately mirrored in the usual formal systems in the sense that any law of inference that is in fact valid in all mathematical contexts is derivable in any of these systems.

The incompleteness theorem, on the other hand, can be interpreted as stating that it is impossible to give a completely satisfactory axiom system for any theory that can serve as a formal foundation for mathematics. More precisely, for any axiom system that is adequate for the development of number theory and that is explicitly presented, it is possible to write down a true sentence of number theory that is not derivable from the given axioms. As a result, although the logic actually used by mathematicians in their proofs can be fully captured by a single formal system, at a certain theoretical level any formalization is necessarily incomplete. One way to prove the incompleteness theorem is to show that, for any explicitly given formal system T capable of formalizing number theory, the statement "T is a consistent system" can be formalized in T, and this formalized consistency statement is not provable within the system T.

Modern proof theory studies the strength of a variety of formal systems, generally using a convenient formalism due to G. Gentzen.

Axiomatic set theory. Axiomatic set theory was developed in part as a way of obtaining a formalism adequate for all of mathematics, and also for concrete mathematical reasons connected with the development of general topology and measure theory around 1900. Set theory is probably the most active research area within mathematical logic. It has been shown that a variety of problems in analysis, general topology, and algebra (especially homological algebra) cannot be settled within the framework of any of the standard set theoretic systems like ZFC. Thus such questions cannot be settled rigorously unless additional axioms of set theory (or equivalent methods of proof) are accepted. Many such axioms have been proposed, and their relationships intensively investigated, but no consensus has emerged as to which additional axioms should be accepted. *See* SET THEORY.

Model theory. The development of formal systems in logic is related to the development of axiomatic systems in modern algebra, although the motivation is very different. Model theory combines the algebraic and logical points of view. In applied model theory, the tools of mathematical logic are applied to problems arising in algebra. In pure model theory, axiomatic systems are studied as if they were algebraic systems, and the class of all models of a given axiomatic system is investigated.

The basic result in model theory is the compactness theorem, stating that an infinite axiom system will have a model whenever all of its finite subsystems have models. This follows from the completeness theorem. One curious consequence of the compactness theorem is the existence of mathematical structures that have all the formal properties

of the real number system but contain so-called infinitesimal elements as well; this gives a rigorous foundation for differential and integral calculus that appears closer in spirit to the original seventeenth-century viewpoint than the so-called (ϵ, δ) formulation of A. Cauchy and K. Weierstrass. *See* CALCULUS; DIFFERENTIATION; INTEGRATION.

Recursion theory. The notion of a computable function was defined rigorously in connection with problems in formal logic prior to the development of electronic computers. Such a definition is needed, for example, in order to state precisely what is meant by an explicitly given axiom system. A wide variety of noncomputable functions arise in mathematics; many of them correspond to concrete problems that cannot be solved algorithmically.

For example, the Diophantine problem, associated with Diophantos of Alexandria in the third century and reformulated by D. Hilbert in 1900, asks for a procedure to determine whether an arbitrary polynomial equation in several variables with integer coefficients has an integer solution. It was shown in 1970 that this problem has no algorithmic solution; in other words, it is not possible to write a computer program that solves all instances of this problem correctly. This result depends on a substantial refinement of the encoding technique used by Gödel in the proof of his incompleteness theorem, and the proof also requires a precise notion of computability. The theoretical analysis of the notion of computability was also of some importance in developing the electronic computer, particularly in connection with the work of A. Turing and J. von Neumann during World War II.

Given two functions, f and g, from the natural numbers to the natural numbers, f is said to be reducible to g if there is an algorithm that will compute f by using information about g. For example, any function is reducible to itself, and a computable function is reducible to any other function. Two functions are equivalent if each can be reduced to the other. The equivalence classes are called degrees; they can be thought of as degrees of complexity. Modern recursion theory has produced a very detailed picture of the structure of the degrees and the reducibility relation. Modified notions of reducibility are used also in theoretical computer science, in which all algorithms are assumed to satisfy additional restrictions in the amount of time or space used in the computation. *See* DIGITAL COMPUTER; MATHEMATICS; SCIENCE; SCIENTIFIC METHODS. Gregory Cherlin

Bibliography. S. Barker, *Elements of Logic*, 5th ed., 1989; I. M. Copi and C. Cohen, *Introduction to Logic*, 10th ed., 1998; H. J. Gensler, *Introduction to Logic*, 2002; D. L. Johnson, *Elements of Logic via Numbers and Sets*, 2001; E. Lepore, *Meaning and Argument: An Introduction to Logic Through Language*, 2d ed., 2003; E. Mendelson, *Introduction to Mathematical Logic*, 4th ed., 1997; E. Nagel, J. R. Newman, and D. R. Hofstadter, *Gödel's Proof*, 2d ed., 2002; G. Takeuti, *Proof Theory*, 2d ed., 1987; J. van Heijenoort, *From Frege to Gödel: A Source Book in Mathematical Logic, 1879–1931*, 1967.

Logic circuits

The basic building blocks used to realize consumer and industrial products that incorporate digital electronics. Such products include digital computers, video games, voice synthesizers, pocket calculators, and robot controls. *See* CALCULATORS; DIGITAL COMPUTER; ROBOTICS; VIDEO GAMES; VOICE RESPONSE.

The change that has enabled widespread economical use of digital logic once found only in very expensive, room-sized computers has been a dramatic evolution in device technology. Logic circuits which comprise several basic electronic devices (typically transistors, resistors, and diodes) were once designed with each device as a separate physical entity. Now, very large scale integration delivers millions of equivalent basic devices on one piece of silicon typically rectangular with maximum dimensions of a few tenths of an inch (0.1 in. = 2.5 mm) per side. *See* INTEGRATED CIRCUITS.

This dramatic reduction in size and concomitant increase in integrated circuit capabilities has been accompanied by a number of effects. Both the cost and power consumption per logic device have been greatly reduced, while increasingly powerful computing capability has been incorporated into ever smaller packages. The modestly priced, multicapable, digital watch that can run for over a year on a tiny battery exemplifies this progression.

Logic circuit operation. Logic circuits process information encoded as voltage or current levels. The adjective "digital" derives from the fact that symbols are encoded as one of a limited set of specific values. While it would be feasible to encode information using many distinct voltage levels (for example, each of 10 voltage levels might correspond to a distinct decimal digit value), there are several reasons for using binary, or two-valued, signals to represent information: the complexity of the sending and receiving circuit is reduced to a simple on-off-switch type of operation corresponding to the two-valued signals; the speed of operation is far greater since it is not necessary to wait until a changing signal has had time to converge to a final value before interpreting its binary value; and the on-off operation makes the circuitry very tolerant of both changing characteristics of devices due to aging or temperature–humidity environment and electromagnetically induced noise added to the voltage levels.

Since signals are interpreted to be one of only two values (denoted as 0 and 1), these binary digits, or bits, are used in a number system with digit weights that change by multiples of 2 rather than multiples of 10 as in the decimal system. In this system, successive digits or bits have weights of 1, 2, 4, 8, . . . , in contrast to the decimal system where successive digits have weights of 1, 10, 100, ... *See* NUMBER SYSTEMS.

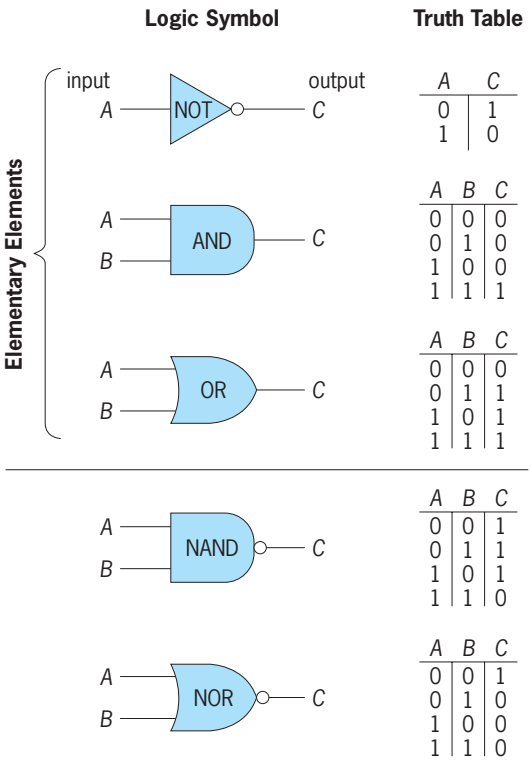

Fig. 1. Logic elements.

Bit patterns also are used in computers to represent alphanumeric characters. A very useful character-encoding convention, called Unicode®, uses a standard collection of 8, 16, or 32 of these binary signals to represent all keyboard-derived symbols in any of the world's languages.

Types of logic functions. All logic circuits may be described in terms of three fundamental elements (**Fig. 1**). The NOT element has one input and one output; the output generated is the opposite of the input in binary. In other words, a 0 input value causes a 1 to appear at the output; a 1 input results in a 0 output. Two NOT elements in series, one output driving the input to the other, simply reproduce a copy of the input signal.

The AND element has an arbitrary number of inputs and a single output. (Electrical characteristics of devices used or physical packaging of devices result in some practical limit to the number of inputs allowed.) The output becomes 1 if, and only if, all of the inputs are 1; otherwise the output is 0. The AND together with the NOT circuit therefore enables searching for a particular combination of binary signals. If, for example, a signal is needed that goes to 1 only when signals *A*, *B*, and *C* are 1, 0, and 1, respectively, then the circuit indicated in **Fig. 2** will generate the desired output.

The third element is the OR function. As with the AND, an arbitrary number of inputs may exist and one output is generated. The OR output is 1 if one or more inputs are 1.

The operations of AND and OR have some analogies to the arithmetic operations of multiplication and addition, respectively. The collection of mathematical rules and properties of these operations is called Boolean algebra. *See* BOOLEAN ALGEBRA.

While the NOT, AND, and OR functions have been designed as individual circuits in many circuit families, by far the most common functions realized as individual circuits are the NAND and NOR circuits of Fig. 1. A NAND may be described as equivalent to an AND element driving a NOT element. Similarly, a NOR is equivalent to an OR element driving a NOT element. (The reason for this strong bias favoring inverting outputs is that the transistor, and the vacuum tube which preceded it, are by nature inverters, or NOT-type circuit devices, when used as signal amplifiers.) An interesting property of the NAND or NOR circuits is that all logic functions may be accessed using either type of circuit. A NOT element, for example, is realized as a one-input NAND. An AND element is realized as NAND followed by a NOT element. An OR element is realized by applying a NOT to each input individually and then applying the resulting outputs to the NAND as inputs.

Combinational and sequential logic. Logic circuits respond to combinations of input signals. In an arithmetic adder, for example, a network of logic elements is interconnected to generate the sum digit as an output by monitoring combinations of input digits; the network generates a 1 for each output only in response to those combinations in the addition table that call for it. Logic networks which are interconnected so that the current set of output signals is responsive only to the current set of input signals are appropriately termed combinational logic.

A further capability for processing information is memory, or the ability to store information. In digital systems, the memory function has been provided for by a variety of technologies, including magnetic cores, stored charge, magnetic bubbles, and magnetic tape. The logic circuits themselves must provide a memory function if information is to be manipulated at the speeds the logic is capable of. The logic elements defined above may be interconnected to provide this memory by the use of feedback. *See* COMPUTER STORAGE TECHNOLOGY.

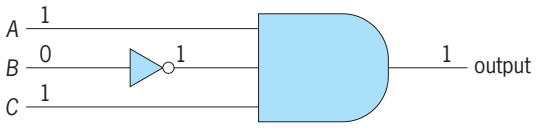

Fig. 2. Logic circuit whose output is 1 only when input signals *A*, *B*, and *C* are 1, 0, and 1, respectively.

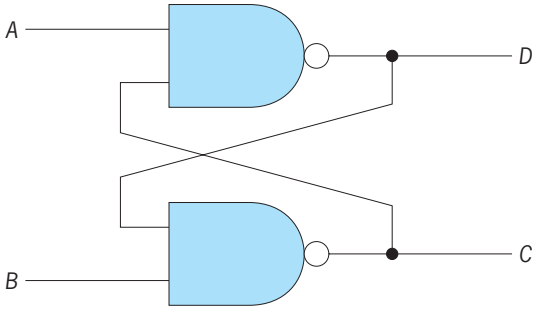

Fig. 3. A memory element.

The circuit in **Fig. 3** illustrates a basic and perhaps the most commonly used form of memory circuit. Normally both inputs *A* and *B* to the cross-coupled NAND gates are at the voltage corresponding to logic 1; if a 0 is applied to signal *A*, outputs *C* and *D* assume the values 0 and 1, respectively, based on the definition of NAND operation; the outputs retain these values after input *A* is returned to the quiescent value of 1. Conversely, if *B* is set to 0 while *A* is 1, the outputs *C* and *D* become 1 and 0, respectively, and again retain these values after *B* is returned to a value of 1. In the jargon of logic circuit design, this circuit is called a flip-flop, toggle, or trigger. Like the light switch on the wall, the circuit retains one of two stable states after the force initiating change to that state is removed. This circuit is therefore well matched to the storage of binary, or two-valued, signals. Logic circuit networks that include feedback paths to retain information are termed sequential logic networks, since outputs are in part dependent on the prior input signals and in particular on the sequence in which the signals were applied. *See* SWITCHING CIRCUIT.

Logic circuit embodiment. Alternatives exist for the digital designer to create a digital system, and seven are summarized below.

1. Ready-made catalog-order devices can be combined as building blocks. In this case, manufacturers have attempted to provide a repertoire of logic networks that will find common usage and generality. Some examples of the types of circuits in digital circuit manuals or catalogs are arrays of individual logic gates (typically four to six) with outputs and inputs available as external connections to the device; arrays of memory elements (flip-flops) used to hold a collection of binary signals or digits; arithmetic adders capable of adding four corresponding binary digits from each of two binary numbers and of being cascaded to produce an adder for any multiple of four digits; and multipliers capable of forming the product of two 16-bit numbers in a single step (that is, a combinational multiplier).

The significance of these examples is that the number of gates or logic elements realized on individual devices ranges from a few to several thousand. Clearly, a design that can use the devices with larger gate counts is likely to be more compact and more economical.

2. An increasingly common realization of logic gates is custom-designed devices. Two factors which make this practical are computer-aided-design (CAD) tools and libraries of subnetworks that can be used as building blocks. Custom design of a logic network implies the generation of highly complicated artwork patterns, called masks, for use in photographic-development-like steps used to produce the integrated circuit networks. The availability of a library of subnetworks for which this artwork has already been generated reduces the additional artwork required to interconnection patterns among these library elements to set up the desired logic network. *See* COMPUTER-AIDED DESIGN AND MANUFACTURING.

3. Another option is gate-array devices. In this case, the device vendor manufactures devices comprising a two-dimensional array of logic cells. Each cell is equivalent to one or a few logic gates. The final layers of metallization that determine the exact function of each cell and interconnect the cells to form a specific network are deferred until the customer orders such a device. This procedure uses mass production for the majority of processing steps necessary to manufacture a device, including most of the necessary artwork. Since the interconnecting metallization layers are a relatively small and simple part of the total device fabrication, the customization cost and time can be reduced significantly by this method relative to a totally custom fabrication. The sacrifice in this approach is that the packing density of the two-dimensional array will tend to be less than a custom-designed layout, since routing channels must allow for reasonably general interconnection patterns.

4. An additional option in realizing logic functions is programmable logic arrays (PLAs). The manufactured part has the potential for realizing any of a large number of different sets of logic functions; the particular functions produced are determined by actually blowing microscopic fuses built into the device, in effect removing unwanted connections. In one device, each of 16 device-input signals is an input to each of 48 AND gates; the 48 AND outputs are input signals to 8 OR gates that generate the device outputs. Selective removal of inputs to the AND gates, and between the AND and OR gates, enables implementation of a wide variety of functions.

5. Another embodiment of logic network functions involves the use of table look-up. A logic network has several binary input signals and one or more binary outputs. The transformation of input-signal combinations to output-signal values need not be realized by AND-OR-type logic elements; instead, the collection of input signals can be grouped arbitrarily as address digits to a memory device. In response to any particular combination of inputs, the memory device location that is addressed becomes the output. For example, a logic network function involving 10 binary inputs and 8 binary output signals could be realized with a single memory device that holds 1024 memory cells, with 8 bits stored in each cell. (Ten bits address 2^{10} or 1024 locations.)

The form of memory device used for table look-up is usually read-only; that is, memory contents are defined as part of the manufacturing process by means of the last layer of metallization, or one of a number of other means is used to fix the memory cell contents so that it is not necessary to reload the memory after each turn-off of power. Typically, this approach may lead to slower operation than the use of logic circuits, but in some cases can lead to very significant economies.

6. The field-programmable gate array (FPGA) is another embodiment of logic functions. The logic network on an FPGA is configured by loading gate interconnection data over certain FPGA pins after power is applied. The FPGA retains this configuration until its power source is disconnected or until it is reprogrammed. Powerful high-end FPGAs can include onboard microcomputers in addition to their

usual arrays of reconfigurable logic gates. *See* FIELD-PROGRAMMABLE GATE ARRAYS.

7. The last form of logic network embodiment that will be discussed is the microcontroller. A microcontroller is a single device that includes a read-only memory to hold a program, a processor capable of reading and executing that program, and a small read-write memory for scratch working space. Just as a memory device provides an efficient realization of a combinational network, the equivalent of a highly complex sequential network can be had with a microcontroller. Two advantages of this approach are that little or no custom-device fabrication is required and that the programmability permits utilization of complicated and modifiable equivalent networks. As with table look-up, the principal disadvantage is that the speed of operation may be slower than if an actual network of high-speed logic circuits was used. *See* MICROCOMPUTER; MICROPROCESSOR.

Technology. There are basically two logic circuit families in use: bipolar and metal-oxide-semiconductor (MOS), with MOS technology the dominant one.

The basic MOS device is formed by using a silicon substrate which has been doped in such a way as to greatly increase the hole/electron relative density, forming a *p*-type substrate. In addition to the substrate, two diffused *n*-type regions are formed. A layer of metal, insulated from the substrate by a deposit of oxide, is situated between the two *n* regions. This metal connection is known as the gate, and the two *n* regions are called the source and drain; since the device is symmetrical in every respect, source and drain are functionally interchangeable. When a sufficient voltage exists between the metal gate and the substrate, electrons are conducted between the drain and source connections, essentially shorting the two together. Otherwise, a high resistance exists between the two. Thus, the gate input is analogous to the control lever of a switch. In like manner, an *n*-type doping of the substrate, along with a *p*-type source and drain, may be used to implement the switch. This will result in hole migration between source and drain when the gate is turned on. *See* SEMICONDUCTOR; TRANSISTOR.

The simplest MOS logic structure is the transmission gate (also known as pass transistor and steering logic). Only one transistor is used to implement the function, where source and gate leads represent the two input variables, and the drain becomes the output value. The transistor is turned on when the gate voltage is above the threshold voltage, assuring sufficient current flow through the channel; in other words, it acts as a short between source and drain. This is analogous to a mechanical switch in the "on" position. When the gate is below the threshold potential, the switch is opened, thus performing an AND-like function on the inputs.

The NAND logic function is also easily derived with MOS circuits. **Figure 4** shows a sample NAND circuit in which the transistors *A*, *B*, and *C* are configured in series and must therefore all be in the "on" state for a conduction path from output *Z* to ground to be established. If *A*, *B*, and *C* are all above threshold, output *Z* is shorted to ground or is forced to logical zero. On the other hand, if any of *A*, *B*, or *C* is off, an open circuit essentially exists between *Z* and ground. In this case, output node *Z* exhibits much less resistance to the power source ($R \ll R_a + R_b + R_c$) and therefore will be at the voltage potential of the power source. (The resistance *R* is commonly formed by a type of MOS device known as a depletion-mode transistor.)

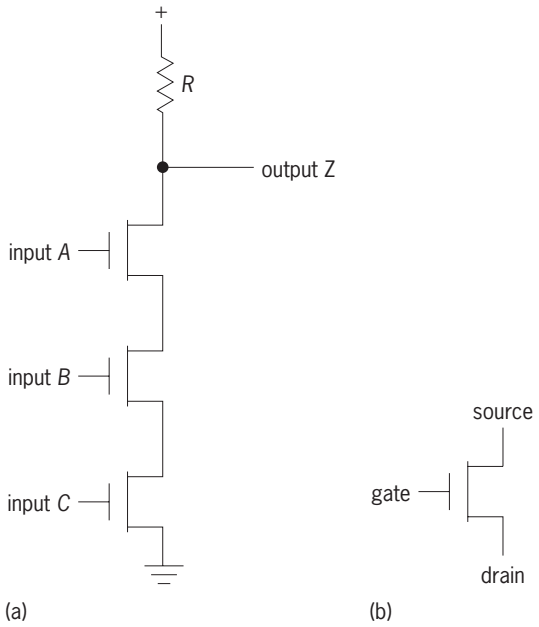

Fig. 4. MOS NAND gate. (*a*) Circuit configuration. (*b*) MOS transistor (*n* or *p*), the basic circuit device.

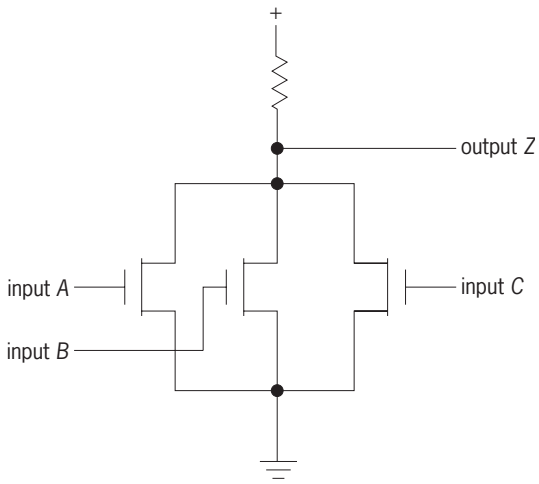

Fig. 5. MOS NOR gate.

This NAND circuit can be reconfigured into the NOR circuit of **Fig. 5**. Here, the transistors are in parallel instead of in series, and when any of the inputs are turned on, the output will be grounded. Otherwise, *Z* will be pulled up to the power supply voltage.

Another useful MOS logic structure is the AND-OR-INVERT, which performs the logic functions exactly as stated in the name. The A-O-I is shown in **Fig. 6** to be a combination of the NAND and NOR configurations.

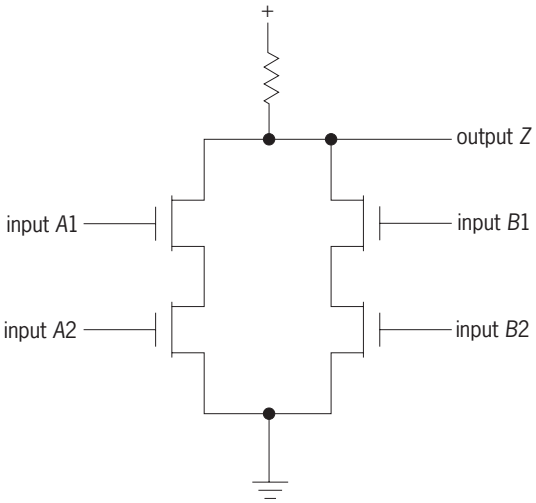

Fig. 6. MOS A-O-I (AND-OR-INVERT) gate.

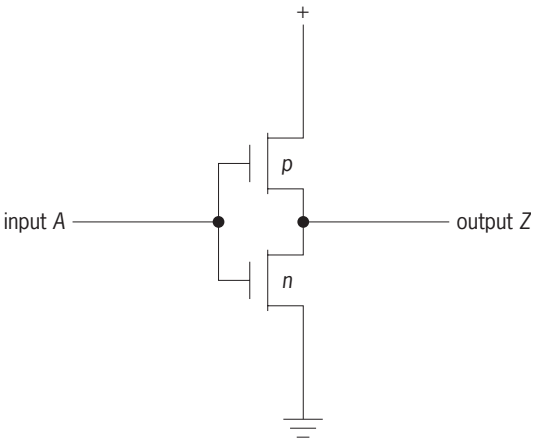

Fig. 7. CMOS inverter.

Output Z is low only if the function ($A1$ AND $A2$) OR ($B1$ AND $B2$) is high.

As described earlier, either an n-channel substrate (NMOS) or a p-channel substrate (PMOS) may be used to implement the logic structures. Additionally, both types may be used concurrently in the logic circuit to fabricate a more sophisticated device. **Figure 7** shows an inverter built with both NMOS and PMOS devices. When the input is low, the NMOS transistor is cut off and the PMOS transistor conducts, shorting the output to the power source. On the other hand, when the input is high, the PMOS gate is shut off and the NMOS gate shorts the output to ground, thus performing the inverter function. The advantage of such a complementary configuration, known as CMOS, is primarily power dissipation. Owing to the fact that only one complementary transistor conducts at any time (other than the short overlap during switching), there is always a very high resistance from the power source to ground, and therefore very little current flows through the pair. The primary disadvantage of CMOS over the common MOS circuit is the increased fabrication complexity due to the n and p substrates occupying the same chip, and the secondary disadvantage is the increased area needed to build the CMOS structure because of the use of complementary pairs.

The charge carriers in an MOS transistor are either free electrons or holes. For this reason, MOS is known as a unipolar device. In contrast, devices that utilize both free electrons and hole migration, such as the junction transistor, are known as bipolar devices. Although general comparisons are hard to make, bipolar devices typically exhibit much less input resistance and demand a more sophisticated fabrication technique than do MOS devices. In terms of logic realization, the bipolar family encompasses many common circuit types. Perhaps the best-known and most widely used implementation of bipolar logic switches is transistor-transistor logic (TTL). The basic TTL NAND gate (**Fig. 8**) is formed by a multiemitter transistor (turned on only if every input is high) followed by an output transistor that acts as a pullup/buffer. Thus, the first transistor performs an AND operation on the inputs and the second transistor

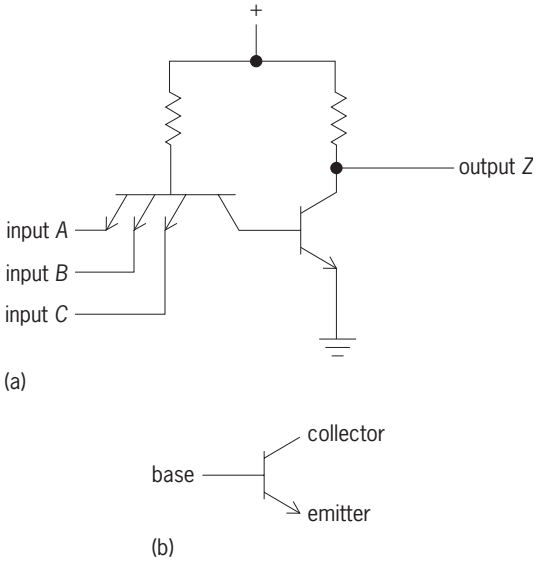

Fig. 8. Simplified TTL (transistor-transistor-logic) NAND gate. (*a*) Circuit configuration. (*b*) Bipolar junction transistor (*npn*), the basic circuit device.

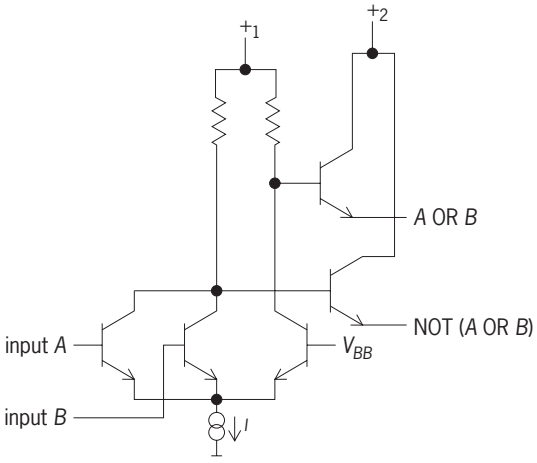

Fig. 9. Simplified ECL (emitter-coupled-logic) OR/NOR gate.

completes the NAND by performing an inversion. *See* JUNCTION TRANSISTOR.

TTL transistors are operated in the saturation mode; in other words, the transistors are driven hard to either the cutoff or the saturation limits. This overdriving introduces a time delay that does not exist if the transistors are operated in the nonsaturated mode. Such nonsaturating logic, while inherently faster, is more susceptible to noise since it is biased in the linear region.

Current-mode logic (CML) is a popular form of nonsaturation logic, and most often takes the configuration of emitter-coupled logic (ECL). The basic ECL gate (**Fig. 9**) is composed of current-steering transistors that perform an OR operation on the inputs. Typically, the gate output is amplified by an emitter-follower transistor, and both the true and complement signals are available simultaneously. *See* EMITTER FOLLOWER.

Speed and power. Historically, the operational speeds achievable with MOS, TTL, and ECL logic have been well ordered, that is, ECL is the fastest, MOS the slowest, and TTL in between. Power levels vary inversely with gate delays, so that the compensating advantage of MOS is low power. CMOS in particular has the advantage that virtually no power is dissipated (typically microwatts per device) during periods when no switching is taking place, and power consumption in general is directly proportional to the frequency of operation.

With the advent of very large scale integration (VLSI) and corresponding fine-line lithography with feature sizes on digital chips of 90 nanometers or less, the speed categorization described above is less well defined. As a result of the smaller feature sizes, gate delays achievable in all three technologies typically are below 1 nanosecond. MOS technology is now the choice for even very high speed digital systems because its reduced power levels and simpler fabrication procedure enable placing more devices in the same area on individual chips.

R. R. Shively; W. V. Robinson; Philip V. Lopresti

Bibliography. R. J. Baker, *CMOS: Circuit Design, Layout, and Simulation*, 2d ed., 2004; R. H. Katz and G. Borriello, *Contemporary Logic Design*, 2d ed., 2005; J. M. Rabaey, A. Chandrakasan, and B. Nikolic, *Digital Integrated Circuits*, 2d ed., 2003; A. S. Sedra and K. C. Smith, *Microelectronic Circuits*, 5th ed., 2004; J. F. Wakerly, *Digital Design: Principles and Practices*, 4th ed., 2006.

Lophiiformes

The anglerfishes and their relatives. This highly modified order of antinopterygian fishes, also known as the Pediculati, is thought to have been derived from a stock close to the Batrachoidiformes, or toadfishes, at least as early as Eocene time. The first dorsal fin is reduced to a few flexible rays, of which the first is placed on top of the head and bears a terminal bulb or tassel and functions as a fishing lure (see **illus.**). The epiotics are large and meet behind the supraoccipital. There are no ribs or epipleurals, and the gill opening is small and placed far back. Pelvic fins, if present, are thoracic, and the pectoral girdle is notably modified. *See* BATRACHOIDIFORMES.

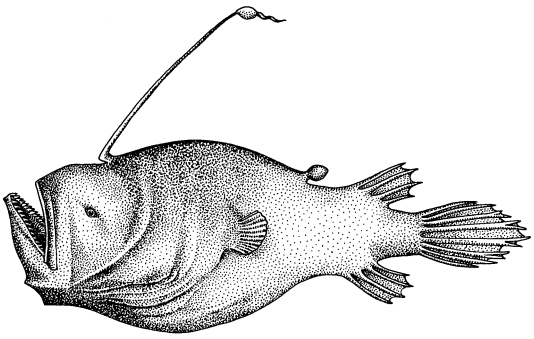

Anglerfish (*Cryptopsaras couesi*). (*After G. B. Goode and T. H. Bean, Oceanic Ichthyology, U.S. Nat. Mus. Spec. Bull. 2, 1985*)

There are 3 suborders, 15 families, nearly 60 genera, and about 195 known species. All are marine. Most species inhabit deep seas or tropical shore waters; the shore forms are commonly sedentary in habit. Luminescent organs may be present, and in some deep-sea species the males are dwarfed and attached as ectoparasites on the females. *See* ACTINOPTERYGII.

Reeve M. Bailey

Bibliography. E. Bertelsen, *The Ceratioid Fishes: Ontogeny, Taxonomy, Distribution and Biology,* Dana Rep. 39, 1951.

Lophophore

The crown of tentacles which surrounds the mouth in the Bryozoa, Phoronida, and Brachiopoda. Other groups of invertebrates also have tentacle crowns used in feeding, but the term lophophore is limited to the structure common to these three phyla in which the numerous ciliated tentacles arise from a circular or horseshoe-shaped fold of the body wall (see **illus.**). The tentacles are hollow outgrowths of the body wall, each containing fluid-filled extensions of the body cavity and extended hydraulically.

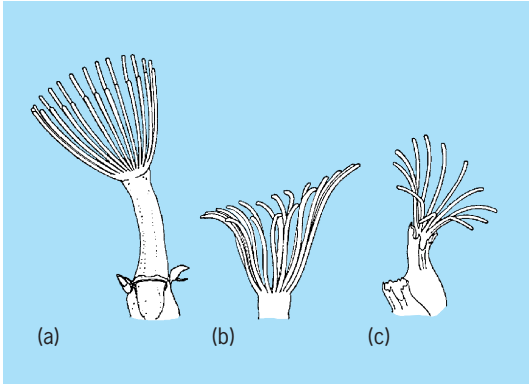

Examples of lophophores. (*a*) Equitentacled (*Beania intermedia*). (*b*) Scalloped (*Trematooecia turrita*). (*c*) Bent-tentacled (*Reteporellina evelinae*). (*After J. E. Winston, Polypide morphology and feeding behavior in marine ectoprocts, Bull. Mar. Sci., 28(1):1–31, 1978*)

The lophophore surrounds the mouth but not the anus of the animals. The primary function of the lophophore is to gather food. On the tentacles are ciliary tracts which drive a current of food-particle-bearing water through the lophophore. The action of the cilia, the flow of the current, and the movements of the flexible tentacles (which are provided with muscles under control of the nervous system) combine to collect food and deliver it to the mouth, where it is ingested. While the lophophore is primarily a feeding organ, it may also play a role in reproduction, respiration, and larval locomotion.

Bryozoa. Bryozoans are microscopic colonial animals. Marine bryozoans (gymnolaemates and stenolaemates) have the simplest lophophores: circular funnels which have the tentacles either equal in length or obliquely truncate, have their edges straight or curving, and are usually less than a millimeter in size. The lophophore of bryozoans can be protruded from the body and opened like an umbrella for feeding, or the tentacles may be furled and the whole lophophore drawn back into the zooid. In the gymnolaemates the lophophore is also important in reproduction. Sperm are liberated through pores in the tentacle tips. Some species have special male zooids with lophophores bearing only a few long tentacles. Species which do not brood their eggs have a vase-shaped structure between two tentacles. The eggs pass from the body cavity of the zooid into this intertentacular organ to be shed into the sea.

One fresh-water (phylactolaemate) bryozoan has a round lophophore, similar to that of marine bryozoans, but most have large horseshoe-shaped lophophores with a double series of tentacles arranged in a crescent and the mouth in the bend of the U. Their lophophores can also be retracted. *See* BRYOZOA.

Phoronida. Phoronids are larger tube-dwelling animals. The lophophore of phoronids is similar to that of the phylactolaemate bryozoans, with the tentacles arranged around the perimeter of the crescent. In some species the ends of the lophophore may be spirally coiled. The cilia of the tentacles create a current directed toward the groove between the two ridges of tentacles. This current moves toward the mouth and exits dorsally over the anus. Food particles carried by the current are entangled with mucus from the tentacles and carried by cilia on the basal groove to the mouth. The lophophores of phoronids cannot be introverted, but the animals can draw them back into their tubes. Phoronids can orient their expanded lophophores in various directions to take advantage of the water currents where they live. Phoronids also utilize the lophophore in reproduction. In *Phoronis viridis* sperm packages freed into seawater by a male dissolve a pore in a tentacle of a female, and the sperm travel down the tentacle and penetrate into the main body cavity to fertilize the eggs. The eggs of some species of phoronids are brooded between the two arms of the lophophore. *See* PHORONIDA.

Brachiopoda. Within their bivalved shells the brachiopods have the largest, most complicated lophophores, coiled and drawn out into two complex arms or lobes called brachia. Often this lophophore is provided with a rigid coiled support or brachidium. The tentacles of brachiopods are aligned in rows along the brachia. The lophophore divides the "mantle cavity" into incurrent and excurrent areas. The mouth is located medially in the incurrent area, in a groove which extends along both brachia below the tentacle-bearing ridges. Food is transported by cilia to the mouth. In the shelled planktonic larval stage of some inarticulate brachiopods, the tentacles of the lophophore may be used temporarily for swimming as well as for feeding. *See* BRACHIOPODA; FEEDING MECHANISMS (INVERTEBRATE).

Judith E. Winston

Loran

A navigation system from which hyperbolic lines of position are determined by measuring the difference in times of arrival of pulses from widely spaced, synchronized transmitting stations. Since radio waves travel at the speed of light, a line of position represents a constant range difference from two transmitters. Loran is used by commercial and military ships and aircraft. The name is derived from "long-range navigation." *See* HYPERBOLIC NAVIGATION SYSTEM.

In **Fig. 1**, it is assumed that the master station M transmits a pulse signal at time $t = 0$, and that the secondary station S transmits a similar pulse signal Δ microseconds after receiving the master pulse signal. The secondary station receives the master signal at time $t = \beta$ microseconds, and therefore transmits its pulse at time $t = \beta + \Delta$ microseconds. A receiver at R measuring the difference in the times of arrival of the signals from the secondary and master stations measures the time difference TD $= (\beta + \Delta) + t_{SR} - t_{MR}$. The locus of all points with this common time difference is a hyperbola through the receiver

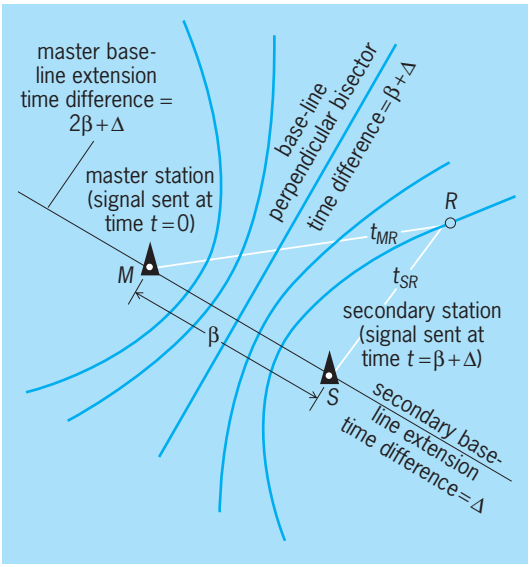

Fig. 1. Principle of position fixing by hyperbolic navigation systems. (*After J. P. Van Etten, Navigation systems: Fundamentals of low- and very-low-frequency hyperbolic techniques, Electr. Commun., 45(3):192–212, 1970*)

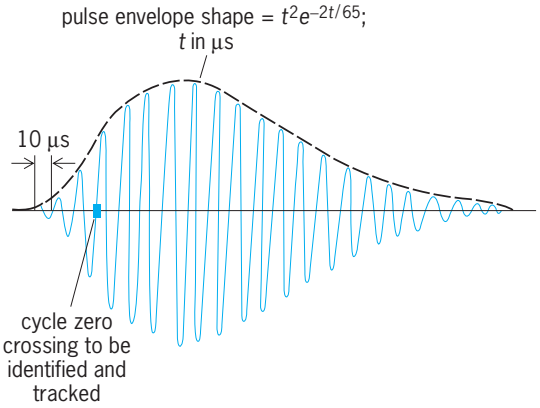

Fig. 2. Loran C pulse. (*After U.S. Coast Guard, Department of Transportation, Loran-C User Handbook, COMDTPUB P16562.6, 1992*)

position R. Similarly, every hyperbolic line of position is uniquely defined by a time difference. The intersection of two such lines of position gives a navigational fix, or location. Historically, maritime charts were printed with these lines of constant time difference and fixes were manually plotted. Since it is common for a Loran receiver to be able to receive the signals from four or more transmitters, there will exist more than two hyperbolic lines of position and they will intersect at many different locations. More recently, techniques have been developed to both automatically convert receiver observations into position and to utilize this redundant information to improve the accuracy and integrity of the fix obtained.

Development. The Loran position-fixing system was originally developed during World War II as an aid to the navigation of Allied aircraft and the North Atlantic convoys. Following the war, its use was extended by the U.S. Coast Guard to aid marine navigation. Operating at a frequency of about 2 MHz, this system was subsequently known as Loran A. The Loran B system, a high-accuracy cycle-matching version of Loran A, was not implemented because propagation disturbances rendered cycle selection unreliable. The Loran C system evolved from Loran A to provide greater range and more precise, repeatable, and accurate navigation. By the end of 1980, all Loran A service operated by the U.S. government had been terminated. Loran D, which evolved as a tactical (short-range transportable) version of Loran C that could be more quickly deployed, is no longer in use.

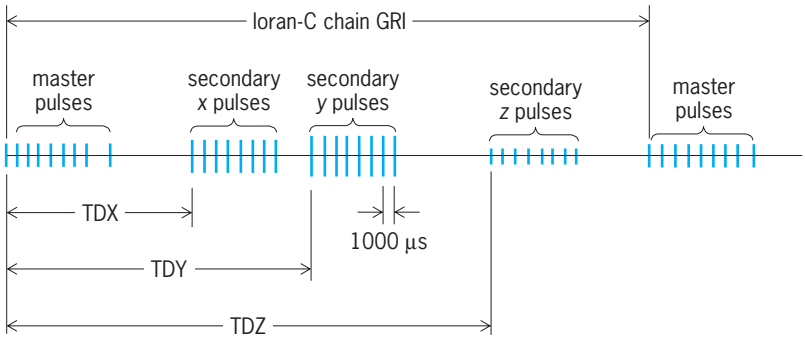

Fig. 3. Loran C signal format. (*After U.S. Coast Guard, Department of Transportation, Loran-C User Handbook, COMDTPUB P16562.6, 1992*)

Loran C. Loran C uses ground-wave transmissions at low frequencies to give an operating range in excess of 1000 nautical miles (1800 km). Sky-wave contamination is avoided by using pulse techniques. High accuracy is obtained by carrier-phase comparison, and cycle identification is accomplished by measurement of the pulse envelope. Operation is possible in poor signal-to-noise conditions by using correlation techniques and time-domain filtering. Loran C has been conservatively evaluated as providing an absolute accuracy of better than 0.25 nmi (500 m) at least 95% of the time with better than 165 ft (50 m) repeatable accuracy from day to day throughout 80% of the fishing grounds, where repeatable accuracy is desired for economic reasons. In the United States, differential Loran is being developed such that the 95% accuracy will be improved to approximately 65 ft (20 m) in areas that have been surveyed and are near a differential monitor site. In the United States the Loran C system is operated and maintained by the Coast Guard.

Transmission. Loran C chains are composed of a master transmitting station and two or more secondary transmitting stations. Master and secondary stations are generally separated by about 600 mi (970 km). Peak power of up to 2 MW is generated by the transmitter. Most stations use top-loaded monopole antennas up to 720 ft (220 m) in height. Six sites have multitower antenna arrays. *See* ANTENNA (ELECTROMAGNETISM).

All Loran C transmitters operate at a fixed frequency of 100 kHz and confine 99% of their radiated energy within the 90–110-kHz band. Each radiated pulse is designed, therefore, to build up quickly and decay slowly (**Fig. 2**). The radio frequency within each pulse is coherent with the repetition frequency.

Each Loran C transmitting station transmits a group of these pulses at a specified group repetition interval (GRI; **Fig. 3**). The master pulse group consists of eight pulses spaced 1000 microseconds apart, and a ninth pulse 2000 μs after the eighth. Secondary pulse groups contain eight pulses spaced 1000 μs apart.

Multiple pulses are used so that more signal energy is available at the receiver, improving significantly the signal-to-noise ratio without an increase in the peak transmitted power capability of the transmitters. The master station transmits a ninth pulse that can be used for visual identification. In the event that a baseline is unusable for navigation, the secondary transmitter of the affected baseline notifies the navigator by blinking the first two pulses off and on.

Each pulse within a group may have its radio-frequency cycles in phase or 180° out of phase with an established reference. The phase coding identifies master or secondary transmissions so that automatic signal acquisition can be accomplished unambiguously; coding is chosen so that the effects of long sky-wave pulse trains (over 1000 μs) cancel, thus permitting ground-wave accuracy to be retained under all conditions.

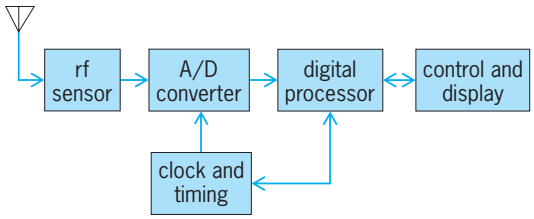

Fig. 4. Loran C navigation receiver.

Reception. High accuracy is obtained in the receiver by measuring the crossover time of individual radio-frequency (rf) cycles on the leading edge of the pulse envelope. Because of the longer propagation path of the sky wave, sky-wave contamination does not start until at least 30 μs after the beginning of the ground-wave pulse. Therefore, the first three cycles of the received signal are always stable ground waves. Tracking is accomplished on the third rf cycle of each pulse in the group to obtain the greatest measurement precision and stability. Cycle identification requires integration or filtering of measurements of the pulse envelope to permit a reliable decision as to whether the correct third cycle or an earlier or later cycle is being tracked. Once this decision is made, the correct cycle can be selected. Continuous monitoring of this cycle selection process is generally implemented, with an alarm if correction is required. *See* RADIO-WAVE PROPAGATION.

There are five major sections of a modern Loran C automatic acquisition and tracking, cycle-matching receiver (**Fig. 4**): the rf sensor, the analog-to-digital (A/D) converter, a Loran clock and timing circuits, a digital processor, and appropriate operator controls and displays. *See* ANALOG-TO-DIGITAL CONVERTER.

The rf sensor receives and processes the signal to provide adequate overall signal-to-interference protection, to "notch out" severe continuous-wave interferences, and, if necessary, to provide amplification to a suitable level for digital sampling. The analog-to-digital converter is used to convert the analog rf signal information from the rf sensor to digital samples associated with each Loran pulse or pulse group. The digital samples so obtained are then processed in the digital-processor. *See* SIGNAL PROCESSING.

Technology that emerged during 1972–1975 made it possible to incorporate tracking-loop algorithms, search algorithms, cycle identification algorithms, and so on, in digital software using inexpensive read-only memory for control of an inexpensive microprocessor. As a result, fully automatic microprocessor-based Loran C receivers were produced at a user cost comparable to that of the manual, and comparatively crude, predecessor Loran A equipment. *See* MICROPROCESSOR.

Operator controls and displays can take many forms, depending on the application. The navigation display, in its simplest form, is time-difference line-of-position numbers in microseconds for two signal pairs. More useful navigation outputs in terms of latitude-longitude coordinates, course-to-steer and distance-to-go to a selected destination, along-track and cross-track error, and so on, are generally provided in avionics equipment configurations and are generally offered as options in marine equipment configurations. Map displays with automatic Loran C position plot are also available.

Enhancements in the United States. Considerable effort and funding has been expended since the mid-1990s, to recapitalize the infrastructure and enhance the performance of Loran in the United States. All of the cesium atomic clocks have been replaced with newer versions. New timing and control equipment has been installed to enable precise synchronization to Universal Time Coordinated (UTC). Transmitter uninterruptible power supplies (UPS) have been installed to eliminate temporary loss of signal when commercial power is lost. New solid-state transmitters have replaced all tube transmitters in the contiguous 48 states and will replace those in Alaska as additional funding becomes available. *See* ATOMIC CLOCK; TIME; UNINTERRUPTIBLE POWER SUPPLY.

The Coast Guard has begun implementation of a Loran data channel to improve the accuracy, integrity, and availability for aviation, maritime, and timing users. The data channel consists of an additional ninth pulse in each group for data purposes only. This pulse is pulse position modulated in 32 possible states to transmit five bits per group. A message consists of 24 words: 15 words are Reed-Solomon parity and nine words or 45 bits are data. Several types of messages have been designed.

One type of message transmits absolute time, station identification, and leap-second information. Historically, since Loran signals are periodic and synchronized to UTC, they have been used as a source of frequency and of time modulo the period of the signal. They can now be used as a source of absolute time as well. Since the periodicity of all Loran signals in North America is in multiples of 200 μs, an inherent 200-μs lane ambiguity can hinder attempts to combine observations from more than one Loran chain. In addition, since all secondary signals are of the same format, if a receiver can successfully track a Loran secondary but not the corresponding master, there can be uncertainty as to which secondary is being tracked. Transmitting absolute time to resolve the interchain lane ambiguities, as well as station identification, enables master independent, multichain navigation with high integrity.

A second type of message transmits differential Loran corrections. Local monitors measure the times of arrival (TOAs) of the various Loran signals and offsets from nominal TOAs are broadcast. These corrections remove the effects of diurnal and seasonal variations in phase propagation velocity for maritime and timing users. For maritime users it is also necessary to conduct precise surveys of a harbor and its approaches to account for spatial variations in propagation as well. By removing errors due to both spatial and temporal variations in phase it is possible to obtain 2DRMS or 95% accuracies of 65 ft (20 m) or better.

Another message warns users of anomalous propagation caused by solar disturbances resulting in abnormally low ionospheric layers and early sky-wave

interference. These solar disturbances are usually referred to as polar-cap disturbances (PCDs), which affect only those paths in the auroral zone, and sudden ionospheric disturbances (SIDs), which affect paths at all latitudes. These disturbances will be detected by the monitor network. The warning message will transmit the geomagnetic latitude of the lower limit of the auroral zone. This will be set to 90° during times of no warning, to 0° during SIDs, and to the geomagnetic latitude of the lower limit of the auroral zone during PCDs. Receivers should not use signals when the midpoint of the path exceeds this geomagnetic latitude, the propagation distance exceeds 500 mi (800 km), and the midpoint of the propagation path is illuminated by the Sun. *See* GEOMAGNETIC VARIATIONS; IONOSPHERE; SOLAR WIND.

Other messages will be used to transmit system status, monitor locations, and other data channel information. In early 2006 the Loran data channel was being transmitted only on secondary signals. Whether to, and if so how to, implement it on master signals was under discussion.

EUROFIX. Beginning in the late 1980s, at the Delft University of Technology in the Netherlands, a group led by Durk van Willigen developed a Loran communications scheme called EUROFIX. In EUROFIX, the last six navigational pulses in a group are pulse-position modulated, resulting in one seven-bit word per group. A complete message contains 30 words: 20 words are Reed-Solomon parity and 10 words or 70 bits are data. The system was originally designed to transmit differential Global Positioning System (DGPS) corrections, and a message type has been added to transmit absolute time as well. As of January 2006, there were EUROFIX broadcasts of both DGPS and time from four European stations (Lessay, France; Sylt, Germany; and Vaerlandet and Boe, Norway) and DGPS-only broadcasts from three Saudi stations. *See* SATELLITE NAVIGATION SYSTEMS.

Status. The 2005 edition of the (U.S.) Federal Radionavigation Plan states "The Government continues to operate the Loran-C system in the short term while evaluating the long-term need for the system. If a decision is made to discontinue Loran as a result of these evaluations, then at least 6 months notice will be provided to the public prior to the termination of service." In 2002, a team was chartered by the Federal Aviation Administration's Loran evaluation program to determine if a modernized Loran system could meet aviation nonprecision approach (NPA), maritime harbor entrance and approach (HEA), and time and frequency dissemination requirements in the event of a GPS outage. This team's report,

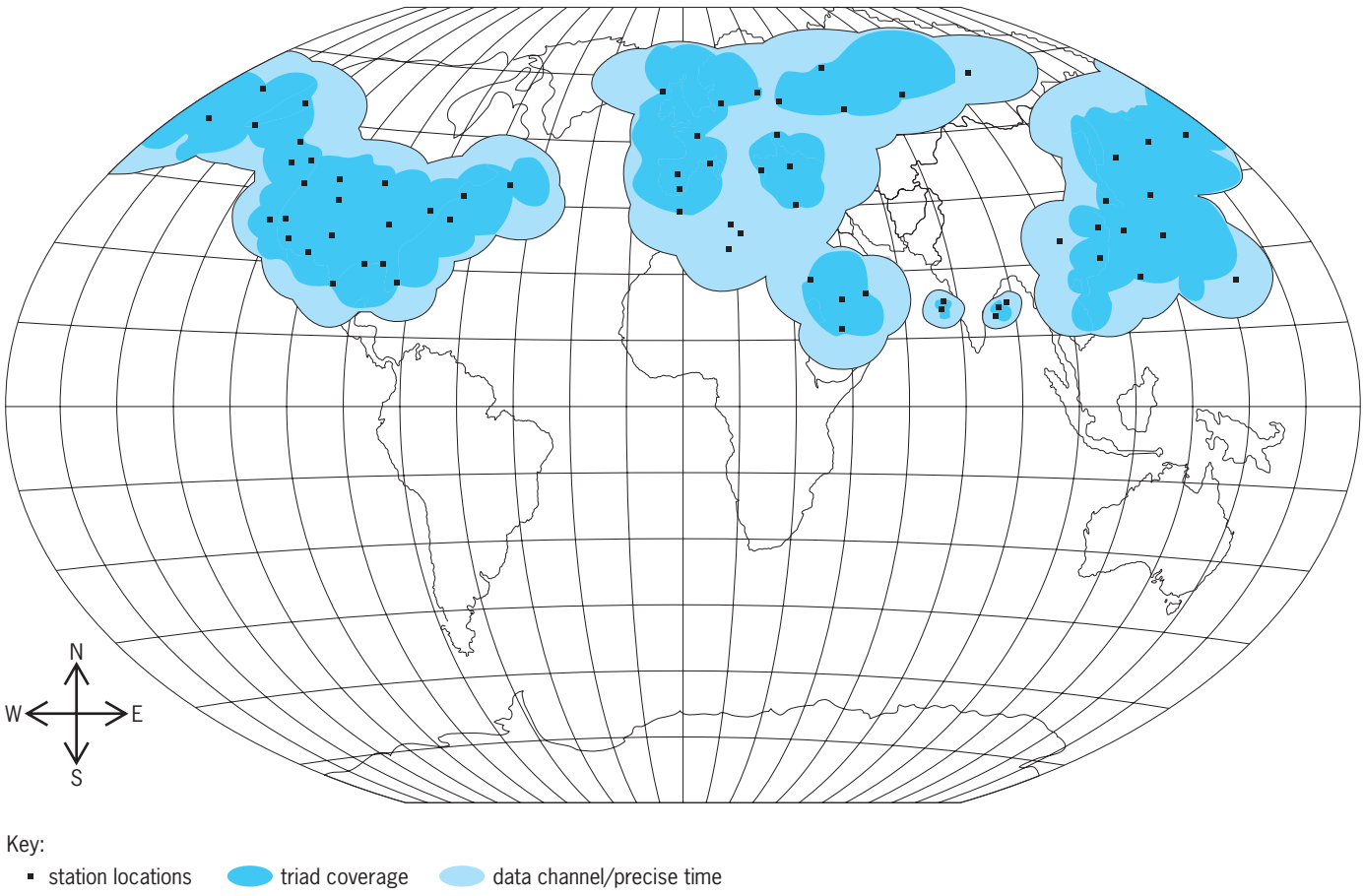

Fig. 5. Locations of Loran C transmitting stations and predicted coverage throughout the world as of 2006. (*Produced by and used with the permission of Megapulse, Inc.*)

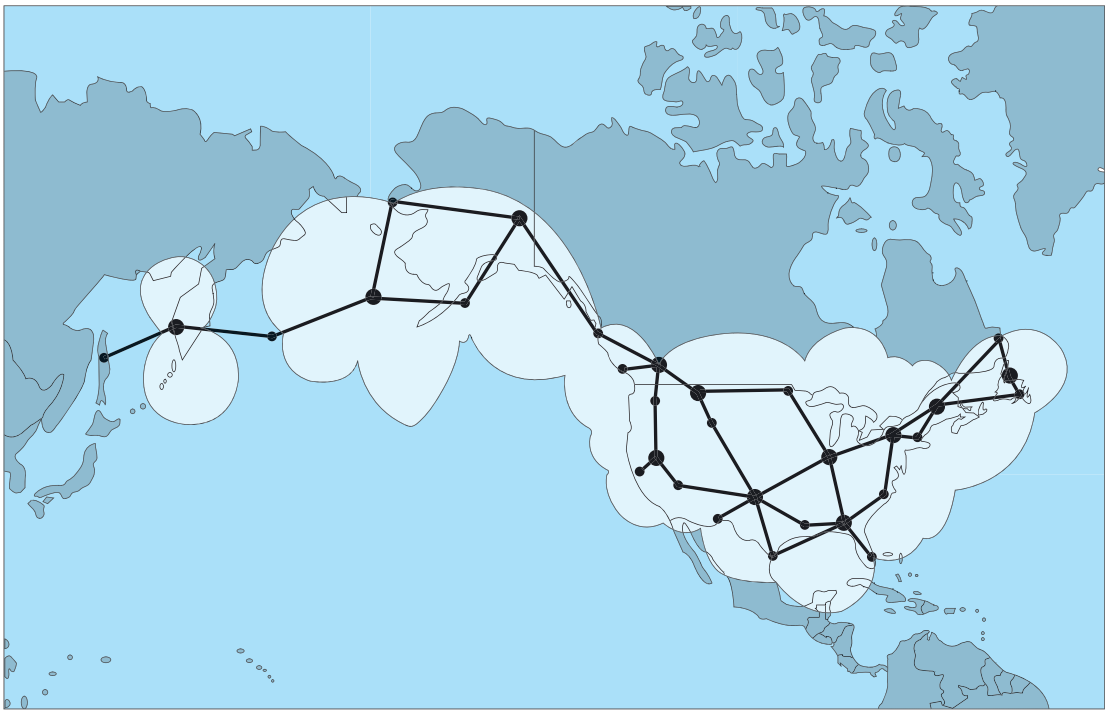

Fig. 6. Coverage provided by Loran C stations operated or supported by the United States as of 2006. Master stations are larger black dots. (*After 1999 Federal Radionavigation Plan, DOT-VNTSC-RSPA-98-1, U.S. Department of Transportation and U.S. Department of Defense, 1999*)

released in 2004, concluded that an enhanced Loran can meet all of these requirements. However, in early 2006 there was still no U.S. decision on the long-term future of Loran.

For a 10-year period ending January 1, 2006, the Northwest European Loran C System (NELS) was the operator of Loran in Western Europe. The NELS member nations included Germany, France, the Netherlands, Norway, Denmark, and Ireland. In 2005, the French Navy committed to operate the two French stations (Lessay and Soustons) for its own needs until 2015 and to enter into bilateral agreements with the goal of maintaining service of as many of the existing stations as possible. Also in 2005, the United Kingdom established a station at Rugby for testing purposes. However, Germany said it would terminate transmissions from Sylt, and Norway announced that it would demolish its stations, although both governments said that they would delay implementation of these plans. The Danish station at Ejde in the Faroe Islands probably will continue operations with financial support from the French government.

Coverage. **Figure 5** illustrates the worldwide distribution of Loran C transmitters as of January 2006. The inner area labeled "triad coverage" indicates where navigation fixes from Loran are available. In the outer area labeled "data channel/precise time," at least one signal can be received, and Loran is a source of frequency. It would potentially be the area of coverage for a data channel and absolute time if all signals were modulated, which at present they are not. **Figure 6** illustrates Loran C coverage provided or supported by the United States as of 2006. This includes Loran C sites operated in cooperation with Canada and Russia. Additional stations are operated by India, China, Japan, Korea, and Saudi Arabia. Russia with partner nations operates Chayka stations, which broadcast navigation signals that are very similar to Loran C. Transmitters for the Chayka "European" chain are located within Russia, Ukraine, and Belarus; transmitters for the "Eastern" chain are located within Russia and include two stations that operate cooperatively with the Loran C station operated by the United States at Attu, Alaska.

Applications. Although originally implemented as an electronic aid to marine navigation, the Loran C system can serve diverse airborne and land position location and navigation applications as well.

In the late twentieth century, technological advances rapidly lowered receiver costs, and coastal coverage limitations were eliminated or reduced by system improvements and expansion; consequently, there was a high degree of user acceptance by fishing crews and other commercial marine users, by the marine recreational community, and by civil aviation. In 1990, there were over 400,000 civil maritime users and approximately 75,000 civil aviation users of Loran C worldwide.

The determination of atmospheric winds using retransmission with navigational aids is accepted as economically and technically viable. For this application, meteorological probes, in the form of balloon-borne radiosondes, retransmit narrow-band Loran C signals to be processed at the tracking facility. Accurate velocity (not accurate position) is the sought-after parameter; hence narrow-banding of the Loran signals prior to retransmission is permissible; this has the advantage of greatly reduced

out-of-band interference and an improved signal-to-noise ratio. The improved Loran C worldwide coverage makes extensive use of this technique. *See* WIND MEASUREMENT.

There is also potential terrestrial use of Loran C for radiolocation, such as automatic vehicle monitoring in both rural and urban environments, and for precise determination of time and time intervals.

However, since the 1990s, actual use of Loran has diminished due to the better performance of GPS. The major argument for retaining Loran has become the vulnerability of GPS and other satellite-based navigation systems to jamming or interference, both intentional and unintentional. The major issue regarding Loran facing the United States and other governments are whether these vulnerabilities justify the costs of a terrestrial backup to satellite-based navigation systems; and, if so, if Loran is the appropriate backup. *See* AIR NAVIGATION; ELECTRONIC NAVIGATION SYSTEMS; MARINE NAVIGATION.

Benjamin B. Peterson; James P. Van Etten

Bibliography. *Loran-C and the Northwest European Loran-C System*, NELS Coordinating Agency, Oslo, 1998; *LORAN-C User Handbook*, COMDTPUB P16562.6, U.S. Coast Guard, Department of Transportation, 1992; L. Melton, *The Complete Loran-C Handbook*, International Marine Publishing Co., McGraw-Hill, 1987; *2005 Federal Radionavigation Plan*, DOT-VNTSC-RITA-05-12, U.S. Department of Transportation and U.S. Department of Defense, 2005; U.S. Federal Aviation Administration, *Loran's Capability to Mitigate the Impact of a GPS Outage on GPS Position, Navigation, and Time Applications*, March 2004.

Lorentz transformations

The relationship in the special theory of relativity between the sets of coordinates (t, x, y, z) and (t', x', y', z') used to label events in spacetime by two inertial observers, O and O', who are moving with respect to each other. Many of the effects predicted by special relativity can be derived in a direct manner from the Lorentz transformation formulas.

By definition, an event in spacetime is a point of space at an instant of time. It is an empirical fact that the collection of events in spacetime constitutes a four-dimensional continuum. This means that it takes four numbers to specify a particular event: one number to specify its "time" and three numbers to specify its spatial position.

Construction of coordinate systems. In both prerelativity physics and in special relativity, an inertial observer, O, is one who is not acted upon by any external forces and thus undergoes straight-line motion. It is assumed in prerelativity physics and in special relativity that any inertial observer, O, can use the following procedure to assign four numbers (t, x, y, z) to each event in spacetime: First, O builds a rigid cartesian grid of meter sticks, all of which intersect each other at right angles. Each point on this meter-stick grid may then be labeled by the three numbers (x, y, z) representing the distance of this point from O along each of the three orthogonal directions of the cartesian grid. The observer O may then carry the grid without rotating it, so that each point on the grid undergoes inertial motion. Next, O may arrange to have a clock placed at each point of this grid. Finally, O may synchronize all of the clocks placed on the grid. In prerelativity physics, this clock synchronization can, in principle, be achieved in a very straightforward manner because there is no limit to the speed at which a material body can move. Thus, at time $t = 0$ on O's clock, O could send off an assistant to visit and start each of the clocks on the grid and return to O before any appreciable time has elapsed on O's clock. *See* COORDINATE SYSTEMS.

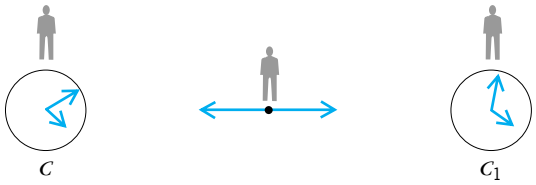

Fig. 1. Procedure that can be used in special relativity to synchronize clocks that are at rest with respect to each other.

However, in special relativity this straightforward (in principle) synchronization procedure cannot be used because the velocity of the assistant (or any other material body) is limited to be less than the velocity of light, c. Nevertheless, any clock, C_1, on the grid can be synchronized with O's clock C by stationing an assistant half-way between C_1 and C, and having the assistant send a signal (such as a light ray) simultaneously toward C_1 and C in a symmetrical manner (**Fig. 1**). Another assistant who is stationed at C_1 is instructed to record the reading of C_1 at the event at which the signal is received. Finally, yet another assistant may travel from O to C_1 (at a speed less than c) carrying the information of the reading on O's clock, C, when O received the signal. The assistant stationed at C_1 is then instructed to correct the "zero" of the clock reading there (by setting it forward or backward, but not changing its rate) by the amount of the difference of the readings of C_1 and C at the time the signal was received. By performing the same procedure with all the clocks on his grid, an observer O in special relativity can achieve the desired clock synchronization.

After performing this clock synchronization, an inertial observer in both prerelativity physics and in special relativity can label any event by the four numbers (t, x, y, z) as follows: The numbers (x, y, z) assigned to the event are the spatial coordinates of the meter-stick gridpoint at which the event occurred, while t is the time of the event as determined by the (synchronized) clock located at that gridpoint. This correspondence of the numbers (t, x, y, z) to events in spacetime is called the global inertial coordinate system associated with observer O.

Relationship of coordinate systems. Another inertial observer, O', who moves with respect to O at velocity v in the x direction, may also construct a global inertial coordinate system by using exactly the same procedure as O. The observer O' can thereby label events in spacetime by the numbers (t', x', y', z').

It is of interest to compare the way the same events are labeled by O and O'. For simplicity, it is assumed that O and O' meet at an event A, and that they adjust their clocks so that $t = t' = 0$ at this event. It is also assumed for simplicity that the axes of the grid of meter sticks carried by O' are aligned (that is, not rotated) with respect to the axes of O when they meet.

In prerelativistic physics, the relationship between the global inertial coordinate systems of O and O' is given by a galilean transformation defined by Eqs. (1).

$$t' = t \tag{1a}$$

$$x' = x - vt \tag{1b}$$

$$y' = y \tag{1c}$$

$$z' = z \tag{1d}$$

Equation (1a) states that O and O' agree on the time labeling of any two events. In particular, if two events are judged to be simultaneous by O (that is, if $t_1 = t_2$ for the two events), they also will be judged to be simultaneous by O' (that is, $t_1' = t_2'$). This reflects the fact that the notion of simultaneity is an absolute one in prerelativistic physics. The observers O and O' disagree only about the x-labeling of events, and this disagreement is readily understood as resulting from their relative motion.

In special relativity the corresponding relationship between the global inertial coordinates of O and O' is a Lorentz transformation, defined by Eqs. (2). The

$$t' = \frac{t - \frac{xv}{c^2}}{\sqrt{1 - \frac{v^2}{c^2}}} \tag{2a}$$

$$x' = \frac{x - vt}{\sqrt{1 - \frac{v^2}{c^2}}} \tag{2b}$$

$$y' = y \tag{2c}$$

$$z' = z \tag{2d}$$

Lorentz transformation differs dramatically from the galilean transformation in that O and O' disagree over the time labeling of events (**Fig. 2**). In particular, two events judged by O to be simultaneous (that is, $t_1 = t_2$) will not, in general, be simultaneous according to O'. This reflects the fact that simultaneity is not an absolute notion in special relativity.

General transformation. Equation (2) gives the Lorentz transformation for the simple case where O' moves in the x direction with respect to O, and O and O' have their axes aligned. The general Lorentz transformation allows for an arbitrary velocity, $\vec{v}$, of O and an arbitrary rotation of the axes of O and O'. For a general Lorentz transformation, Eq. (3) is satisfied. [It is readily verified that this relationship holds for the particular Lorentz transformation given in Eq. (2).] Indeed, the collection of all possible Lorentz transformations is composed precisely by the linear transformations of coordinates which satisfy Eq. (3). The mathematical role played by Lorentz transformations in special relativity thus is closely analogous to the mathematical role played by rotations in ordinary euclidean geometry in four dimensions, since a rotation may be defined to be a linear transformation of the coordinates (x_1, x_2, x_3, x_4) for which $x_1^2 + x_2^{\prime 2} + x_3^{\prime 2} + x_4^{\prime 2} = x_1^2 + x_2^2 + x_3^2 + x_4^2$. *See* EUCLIDEAN GEOMETRY.

$$x'^2 + y'^2 + z'^2 - c^2t'^2 = x^2 + y^2 + z^2 - c^2t^2 \tag{3}$$

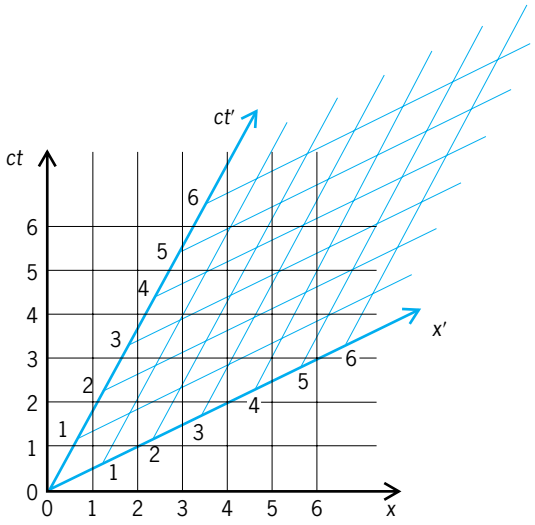

Fig. 2. Spacetime diagram illustrating the Lorentz transformation for the case $v = c/2$. The black lines indicate the (t, x) labels given to events in spacetime by inertial observer O, whereas the color lines indicate the corresponding (t', x') labeling given by inertial observer O'.

Transformation of physical quantities. All quantities of interest in special relativity which have an intrinsic, observer-independent meaning have well-defined transformation properties under Lorentz transformations. A good example is provided by the energy and momentum of a particle. In special relativity the energy, E, and 3-momentum, $\vec{p}$, of a particle are combined into a spacetime 4-vector, $(E/c, p_x, p_y, p_z)$. In order to get simple Lorentz transformation properties it is necessary to choose the "zero" of energy so that this vector is tangent to the worldline of the particle in spacetime. This implies that a particle of mass m which is at rest with respect to a particular global inertial coordinate system is assigned the energy $E = mc^2$ in that system. Under a Lorentz transformation of the form given by Eq. (2), these quantities transform in the same way as the spacetime position 4-vector (ct, x, y, z). Then Eqs. (4) are obtained. In particular, if the particle is

$$E' = \frac{E - p_x v}{\sqrt{1 - \frac{v^2}{c^2}}} \tag{4a}$$

$$p_x' = \frac{p_x - E\frac{v}{c^2}}{\sqrt{1 - \frac{v^2}{c^2}}} \tag{4b}$$

$$p_y' = p_y \tag{4c}$$

$$p_z' = p_z \tag{4d}$$

at rest with respect to O, the energy and magnitude of momentum of the particle as seen by O' are given by Eqs. (5).

$$E' = \frac{mc^2}{\sqrt{1 - \frac{v^2}{c^2}}} \tag{5a}$$

$$|\vec{p}| = \frac{mv}{\sqrt{1 - \frac{v^2}{c^2}}} \tag{5b}$$

See RELATIVISTIC MECHANICS.

Another interesting example of the behavior of quantities under Lorentz transformations is provided by the electromagnetic field. In special relativity, the electric field vector $\vec{E}$ and magnetic field vector $\vec{B}$ are combined into a single spacetime tensor with simple properties under Lorentz transformation. Under the Lorentz transformation (2), the electric and magnetic fields at the event where O and O' meet transform as Eqs. (6). Thus, for example, if according to O only an

$$E'_x = E_x \qquad B'_x = B_x \tag{6a}$$

$$E'_y = \frac{E_y - \frac{v}{c}B_z}{\sqrt{1 - \frac{v^2}{c^2}}} \qquad B'_y = \frac{B_y + \frac{v}{c}E_z}{\sqrt{1 - \frac{v^2}{c^2}}} \tag{6b}$$

$$E'_z = \frac{E_z + \frac{v}{c}B_y}{\sqrt{1 - \frac{v^2}{c^2}}} \qquad B'_z = \frac{B_z - \frac{v}{c}E_y}{\sqrt{1 - \frac{v^2}{c^2}}} \tag{6c}$$

electric field is present, then, in general, according to observer O' a magnetic field also will be present. However, it can be verified from Eq. (6) that the quantities $\vec{E} \cdot \vec{B}$ and $(|\vec{E}|^2 - |\vec{B}|^2)$ remain unchanged under Lorentz transformations, so all observers agree on the values of these quantities. *See* CALCULUS OF VECTORS; RELATIVISTIC ELECTRODYNAMICS; RELATIVITY.

Robert M. Wald

Bibliography. H. Bondi, *Relativity and Common Sense*, 1964, reprint 1980; R. M. Wald, *Space, Time, and Gravity*, 2d ed., 1992.

Loricifera

A phylum of multicellular invertebrates. These marine organisms are entirely meiobenthic; that is, they never exceed a maximum dimension of 400 micrometers and live in sediments ranging from deep-sea red clay to coarse sand or shell hash. They have some of the smallest known cells in the animal kingdom. Although they have been found throughout the world, only 10 species representing three genera and two families have been described: the first described species (*Nannaloricus mysticus*) from shallow coastal waters near Roscof, France; eight species (including the first loriciferan seen, *Pliciloricus enigmaticus*) off North Carolina, and a single species

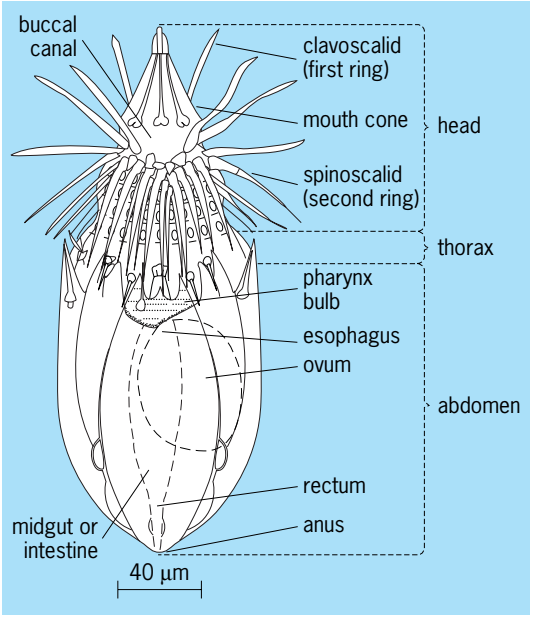

Ventral view of adult female loriciferan (*Nannaloricus mysticus*). (*After R. M. Kristensen, Loricifera, a new phylum with Aschelminthes characters from the meiobenthus, Z. Zool. Syst. Evolutionsforsch., 21(3):163–180, 1983*)

from the western Pacific. Well over 50 species thought to represent several additional genera are known but remain undescribed.

Adult loriciferans are bilaterally symmetrical. The body is regionated into a mouth cone which telescopically protrudes anteriorly from the center of a spherical, appendage-ringed (up to 400 rings may be present) head; a short, usually plated neck region; and a distinctively loricated (thick-cuticled) thorax-abdomen (see **illus.**). The head, along with its withdrawn mouth cone, may be inverted into the thorax-abdomen, which is then closed anteriorly by the cuticle of the neck region.

The first ring of appendages of the head comprises clavoscalids. They usually consist of eight club-shaped structures that extend anteriorly, similar to the arrangement of less prominent scalids in the Priapulida. Up to eight additional rings of posteriorly directed scalids follow in posterior progression. When the head is inverted into the lorica, the scalids fold together like the ribs of an umbrella, closing the wrong way in a manner similar to the scalids of the Kinorhyncha, a postulated close relative.

Internally, an eight-lobed brain surrounds the anterior part of the alimentary tract. Ten nerve cords extend posteriorly. At various places on the cuticle are special receptor organs called flosculi. The digestive system consists of a terminal mouth, followed by a cuticular buccal tube, muscular pharynx, and a short cuticle-lined esophagus. The esophagus opens into a large midgut, which is followed by a cuticle-lined hindgut opening dorso- or ventrocaudally. Sexes are separate in the Loricifera; clavoscalids of some may exhibit dimorphic characters. Females have dorsal ovaries and laterodorsal oviducts that open caudally. Males have two saccate testes, each with large seminal vesicles. The excretory system consists of a single

pair of protonephridia uniquely located within the gonads.

Two to five immature stages (called Higgins larvae) precede the adult. Higgins larvae have the same body regions as adults and range from 50 to 385 μm long. The structure of the mouth cone, the morphology and number of rings of head appendages, a thinner and slightly modified cuticular pattern of the remaining body, and presence of two posterior toes are characters that identify the immature stages. The toes may be used for locomotion or possibly for adhesion to the substrate.

Loriciferans appear to be closely related to the Priapulida and perhaps less so to the Kinorhyncha. Certain structures of the mouth cone suggest affinities to the Tardigrada. Their presence may support the idea that proarthropods could have been developed from aschelminth ancestral stock. *See* ANIMAL KINGDOM; ARTHROPODA; KINORHYNCHA; PRIAPULIDA; TARDIGRADA.

Robert P. Higgins

Bibliography. R. P. Higgins and R. M. Kristensen, New Loricifera from southeastern United States coastal waters, *Smithson. Contrib. Zool.*, 438:1–70, 1986; R. P. Higgins and H. Thiel (eds.), *Introduction to the Study of Meiofauna*, 1988; E. E. Ruppert and R. D. Barnes, *Invertebrate Zoology*, 6th ed., 1994.

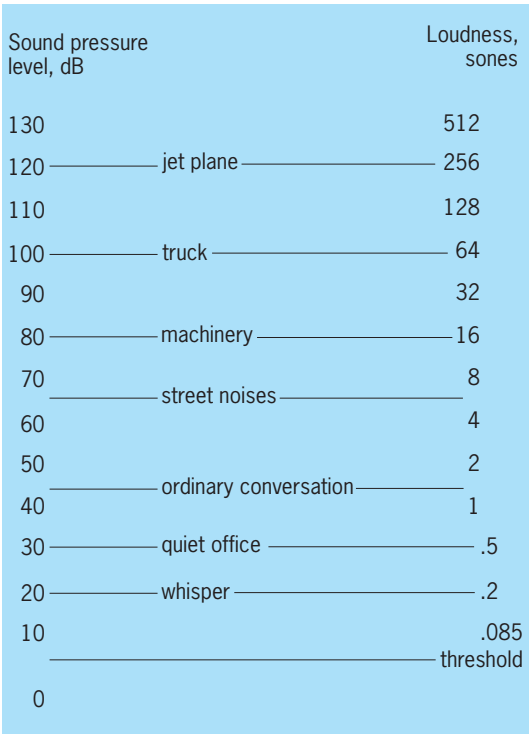

Fig. 1. Decibel and loudness scales of common sounds.

Loudness

The perceptual intensity of sound. Loudness depends importantly on the physical intensity of sound, increasing when physical intensity increases and decreasing when physical intensity decreases. But loudness also depends on other physical properties of sound, such as frequency and duration. Sound waves with frequencies between 1000 and 5000 Hz are louder than sound waves that have the same intensity but lower or higher frequencies. Very brief bursts of sound are less loud than are longer bursts, loudness increasing regularly as duration increases up to about 0.1–0.2 s, beyond which point in time, loudness no longer increases with increasing duration.

Decibels. In most work, the physical level of sound is expressed in decibels (dB). Decibels are units that denote relative intensity or pressure of a sound. One bel is defined as the logarithm to the base 10 of the ratio of a given sound intensity to a reference intensity. A decibel is one-tenth of a bel. Hence, a decibel level of 10 dB means an intensity 10 times that of the reference; a level of 20 dB means an intensity 100 times the reference.

Although decibels are defined primarily in terms of relative intensity, sound levels are usually measured in units of sound pressure. Under most circumstances, the intensity of a sound wave is proportional, not to its pressure, but to the square of its pressure. A sound whose pressure is 10 times that of the reference, therefore, has an intensity 100 times the reference, and decibel level of 20 dB. The most commonly used reference level for decibel scales is a sound pressure of 0.00002 newton/m^2. When expressed in terms of this reference a decibel level is called sound pressure level (SPL). Typical SPLs of some ordinary sounds are: a whisper, 20 dB; a quiet office, 30 dB; street noises, 60–70 dB; a truck, 100 dB; a jet plane, 120 dB (**Fig. 1**).

Phons. Because loudness depends on sound frequency as well as sound intensity or pressure, different stimuli with the same SPL may not be equally loud. One type of decibel scale, called the phon scale, overcomes this deficiency. The level of a sound in phons is the SPL in decibels of an equally loud 1000-Hz tone. Thus a 1000 Hz-tone at 40-dB SPL has a level of 40 phons, as do all other sounds that equal its loudness, even though these other sounds may have SPLs much greater than 40 dB. **Figure 2** shows the relationship between decibels SPL and phons in terms of several equal-loudness contours. The lowest curve is the audibility function, the absolute threshold for sound. Note that the equal-loudness curves become flatter and flatter at higher and higher levels of loudness. This flattening is most evident at low frequencies. In other words, the higher the intensity, the more closely phon levels correspond with SPL throughout the range of audible frequencies.

Loud sounds (70–100 phons) with the same frequency spectrum can be discriminated on the basis of their loudness if they differ by about 0.5 dB. Soft sounds (10–40 phons) must differ by 1–1.5 dB to be discriminated.

Sones. The phon scale is often designated as a scale of loudness level. It is a scale of equal loudness, in that all equally loud sounds take the same level in phons, regardless of the SPL. Nevertheless, the phon scale is not a true scale of loudness, because it is a physical (decibel) scale. That is, a sound of 80 phons is not necessarily twice as loud as a

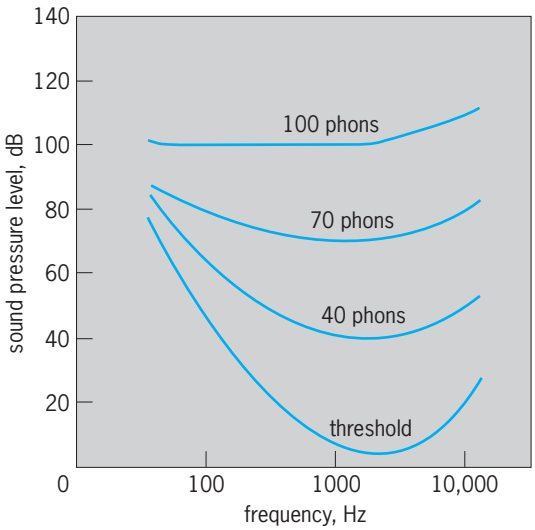

Fig. 2. Relationship between loudness level in phons and sound pressure level for audible frequencies.

sound of 40 phons. In order to determine a scale of perceived loudness, observers were asked to set the level of one sound to make it appear twice or half as loud as standard sounds. Observers were also asked to make numerical judgments of the degree of loudness. From such judgments a scale of loudness in sones was established. One sone is defined as the loudness of a 1000-Hz tone at 40-dB SPL heard with both ears. (When heard with one ear, loudness is half as great.) Above 40 dB, loudness in sones doubles with every 10-dB increase in the level of sound. Below 40 dB, loudness falls by half with decrements smaller than 10 dB (Fig. 1).

The loudness of complex sounds depends on how the sound energy is distributed across the frequency range. If components are sufficiently separated in frequency, the loudness of the total complex in sones equals the linear sum of the loudnesses of the components presented separately. If the components are not widely separated, the total loudness in sones is smaller than the sum of the component loudnesses.

Several methods exist to calculate the loudness in sones or the loudness level in phons of any complex sound. Sound-level meters essentially use the ear's equal-loudness curves (Fig. 2) to weigh the spectrum and produce an estimate of the overall loudness level in phons. Most often used is the A scale, the weighting that corresponds to the 40-phon curve. More accurate methods for computing loudness and loudness level require the individual evaluation of partial loudnesses in many frequency bands across the spectrum, together with complex rules for combining the partial loudnesses.

Noise. The problem of unwanted noise in the environment often reduces largely to a question of loudness. Judgments of noisiness, unpleasantness, and annoyance of sound correspond closely, in most instances, with judgments of perceived loudness, though other acoustical properties, such as impulsiveness, as well as nonacoustical factors, such as predictability, are also important. *See* ACOUSTIC NOISE; HEARING (HUMAN).

Lawrence E. Marks

Bibliography. K. K. Charan, *Fundamentals of Hearing: A Textbook on Acoustics and Psychoacoustics*, 1989; T. N. Decker (ed.), *Introduction to Audiology and Hearing Science*, 1990; G. M. Edelman et al., *Auditory Function: Neurobiological Bases of Hearing*, 1988; J. Katz (ed.), *Handbook of Clinical Audiology*, 4th ed., 1994; K. D. Kryter, *The Handbook of Hearing and the Effects of Noise*, 1994; J. O. Pickles, *An Introduction to the Physiology of Hearing*, 2d ed., 1988.

Loudspeaker

A device that converts an electrical signal from an amplifier into sound. A loudspeaker driver is an electromechanical-acoustic device with two electrical input terminals, to which an electrical signal is applied, and a diaphragm which vibrates and radiates sound. An electromechanical motor mechanism exerts a force on the diaphragm to cause it to vibrate. By far the most common type of motor mechanism, the electromagnetic-mechanical transducer, employs a coil of wire immersed in a magnetic field; electric current flowing through the coil causes a force to be exerted on the coil which is mechanically coupled to the diaphragm. A less common type of motor mechanism is the electrostatic-mechanical transducer. It uses a capacitor to which an electric voltage is applied, causing a force to be exerted between the capacitor plates, which is mechanically coupled to the diaphragm. Two types of electrostatic transducers are used: the piezoelectric transducer and the condenser transducer. The piezoelectric transducer uses a piezoelectric crystal between the capacitor plates. The condenser transducer uses an air dielectric. One plate of the capacitor is a flexible membrane which serves as the diaphragm. *See* AUDIO AMPLIFIER.

A loudspeaker system employs one or more loudspeaker drivers in a common enclosure. A one-way loudspeaker system employs a full-range driver to cover the full audio spectrum. A two-way system employs a low-frequency driver called a woofer and a high-frequency driver called a tweeter. An electrical low-pass filter is used in series with the woofer and a high-pass filter is used in series with the tweeter. These filters are commonly referred to as the crossover networks. A three-way system adds a mid-frequency driver called the midrange or squawker. The crossover network for this driver is a band-pass filter. In some systems, a driver called a supertweeter is used to reproduce audio frequencies into the ultrasonic range. A driver called a subwoofer is used to reproduce audio frequencies into the infrasonic range. *See* ELECTRIC FILTER; NETWORK THEORY.

Crossover networks can be either passive or active. Passive filters contain inductors, capacitors, and resistors, which are commonly mounted inside the loudspeaker enclosure. Active filters contain operational amplifier circuits, and must precede the power amplifiers that drive the loudspeakers.

A biamplified system uses two power amplifiers, one for the woofer and another for the midrange and tweeter. Passive networks are used between the midrange and tweeter. A triamplified system is one in which three power amplifiers are used, one for the woofer, one for the midrange, and one for the tweeter. *See* OPERATIONAL AMPLIFIER; POWER AMPLIFIER.

Loudspeaker drivers can also be operated either as direct-radiator or horn-loaded. A direct-radiator driver is one whose diaphragm radiates directly into the external air load. A horn-loaded driver has an acoustic horn between the diaphragm and the air load. A horn can be used to improve the efficiency and to control the directional pattern of the radiated sound at the expense of frequency response. *See* DIRECTIVITY; SOUND-REINFORCEMENT SYSTEM.

Dynamic drivers. A driver that uses an electromagnetic-mechanical transducer is called a dynamic or moving-coil driver. (**Fig. 1**). The moving surface which radiates sound is called the diaphragm. It is also called the cone because of its shape. Some drivers are designed with flat diaphragms. However, the cone shape exhibits better rigidity and is preferred.

The diaphragm is usually made of paper or paper-felt. Where deterioration due to weather or direct sunlight is a problem, a plastic is used. Paper-felt usually exhibits better damping of mechanical resonant modes that can cause peaks and dips in the response in the upper frequency range. The diaphragm is supported by an inner suspension, called the spider, and an outer suspension. These permit diaphragm motion in the axial direction when a signal is applied, while providing the restoring force to keep it centered in the absence of a signal. *See* DAMPING.

There are two basic types of outer suspensions, rolled and accordion. A rolled suspension has an arc-shaped cross section and is very compliant, allowing

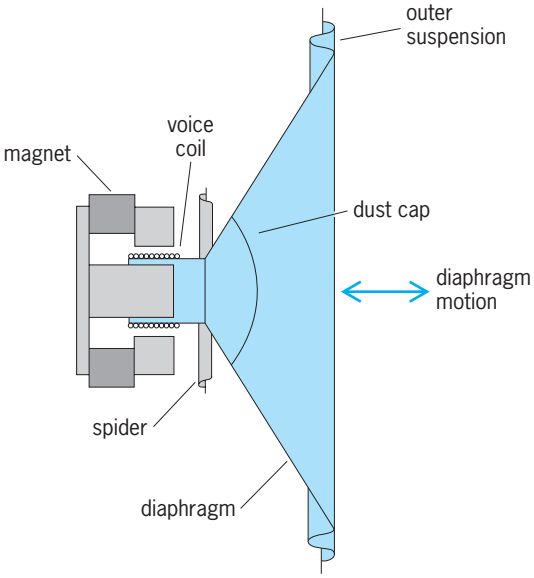

Fig. 1. Cross section of a typical dynamic loudspeaker driver.

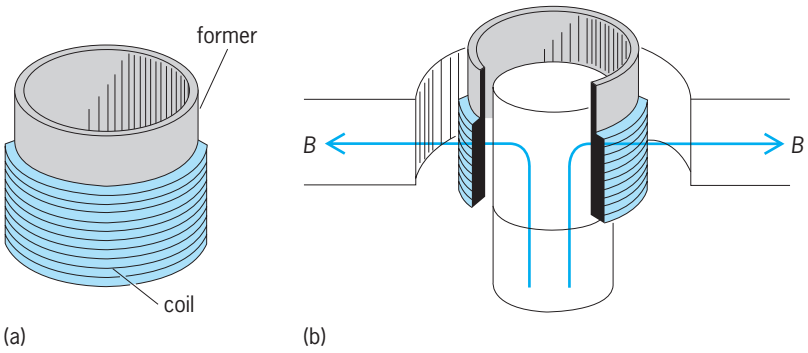

Fig. 2. Voice coil. (*a*) Coil wound on a former. (*b*) Magnetic flux, *B*, through an air gap in the magnet assembly where the voice coil is located. The force generated is in the axial direction when a current flows in the voice coil.

the diaphragm to move with relatively little restoring force. The suspension is usually made of thin foam rubber or butyl rubber. Drivers with rolled suspensions are better suited for closed-box systems where the spring constant of the air inside the enclosure dominates over the spring constant of the driver suspension. An accordion suspension has a cross section that resembles the folds of an accordion. It is stiffer than the rolled suspension and is used primarily for drivers designed for open-back and vented-box systems. The suspension is made of paper-felt or lacquered cloth.

The electrical input signal is applied to the voice coil, a coil of wire wound on a cylindrical form, called the voice-coil former (**Fig. 2***a*), which is glued to the diaphragm. The voice-coil former is usually made of paper in low-power drivers. In high-power drivers, it may be made of aluminum or some other heat resistant material. A dome-shaped cover prevents dust from entering the driver through the voice coil.

When current flows through the voice coil, a force is generated, which causes the diaphragm to move and radiate sound. The interaction of the current and the magnetic flux through the voice coil produces the force. For maximum force, the magnetic field must be perpendicular to the direction of the current flow. The field is set up by a permanent magnet that is part of a magnet assembly which focuses the field through the voice coil (Fig. 2*b*). *See* MAGNETISM.

The magnet assembly consists of a permanent magnet and several pole pieces. The magnet is normally made of either an alnico (aluminum-nickel-cobalt) alloy or ceramic. The pole pieces, made of a high-permeability metal, form a low-reluctance path to focus the magnetic field through the air gap (**Fig. 3**). Ceramic magnets are normally donut-shaped (Fig. 3), while alnico magnets have a slug shape and occupy the position of the center pole piece. *See* MAGNETIC MATERIALS; RELUCTANCE.

Figure 4 illustrates how the force is generated through the voice coil. The direction of the force is that of the vector cross product of the direction of current flow and the magnetic flux B ($\vec{n} \times \vec{B}$, where $\vec{n}$ is in the direction of positive current flow). Because an audio signal is an ac signal, the force reverses direction each time the current reverses, so that the

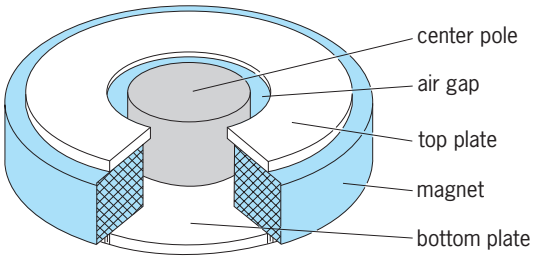

Fig. 3. Typical magnet assembly. The cylindrical, donut-shaped magnet is sandwiched between top and bottom pole plates. The air gap is the space between the center pole and the top pole plate.

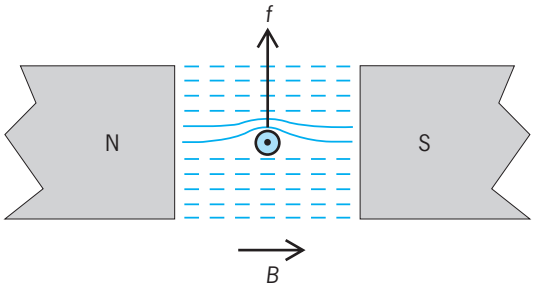

Fig. 4. Cross section of one turn of voice-coil wire with the current flowing, for illustration, in the direction out of the page. $\vec{B}$ is the direction of the magnetic flux. For current flowing out of the page, the force *f* generated on the voice coil is upward.

force causes the diaphragm to move in and out with the signal.

The force on the diaphragm is linearly related to the current in the voice coil only if the total number of turns of wire in the magnetic field does not change when the diaphragm moves. There are two methods by which this may be achieved. The long voice coil (**Fig. 5*a***) is wound so that there is an overhang on each side of the air gap. When the voice coil moves, turns of wire leave the gap on one side while simultaneously the same number of turns enter the gap on the other side so that the total number of turns in the gap remains constant. The long voice coil is preferred in woofers and higher-power drivers because a greater diaphragm excursion can be obtained and its heat dissipation is better than for the short voice coil.

In the short voice coil (Fig. 5*b*), all turns of wire are located in the central portion of the air gap, so that no turns leave the gap when the diaphragm moves. Because all the turns are in the magnetic field, the efficiency of the driver is improved. However, heat dissipation is poor because of overlapping turns. Thus, the short voice coil is usually not used in high-power drivers.

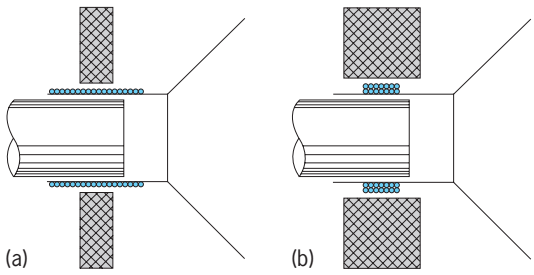

Fig. 5. Voice-coil configurations. (*a*) Long voice coil. (*b*) Short voice coil.

There is a maximum distance that the voice coil can move for either geometry before the number of turns in the magnetic field no longer remains constant. When this occurs, the driver becomes nonlinear and produces a distorted output. The maximum distance that the diaphragm can move from its rest position (zero), either inward or outward, before it becomes nonlinear is usually denoted by the symbol x_{max}. *See* DISTORTION (ELECTRONIC CIRCUITS).

Another nonlinear effect is caused by the driver's inner (spider) and outer suspensions (Fig. 1). The spring constant of these materials is constant only for small diaphragm displacements. As the displacement increases, the suspension become nonlinear. When the suspension bottoms out, the diaphragm cannot move further. In a well-designed driver, the voice coil displacement limit x_{max} is reached before the suspension bottoms out.

In modeling the acoustic radiation from a driver, it is common to assume that the diaphragm is a flat piston. The piston radius of the driver is measured by taking one-half the diameter of the diaphragm aperture, measured half-way into the outer suspension on each side. As a rule, a driver's piston radius in centimeters is numerically approximately equal to its advertised diameter in inches.

The flat piston approximation fails at high frequencies. The frequency at which this occurs is a function of the piston radius, the depth of the diaphragm, and the diaphragm material. Although it is impossible to specify an exact relation for the upper-frequency limit, it is normal to take it to be the frequency at which the circumference of the equivalent flat piston is somewhere between $\lambda/2$ and λ, where λ is the wavelength. The depth of the diaphragm should not exceed about $\lambda/10$ at this frequency. Unless specified otherwise, the upper frequency limit is usually taken to be the frequency at which the circumference is λ. Above this frequency, the radiation from the diaphragm can become directional and exhibit undesirable peaks and dips as the frequency is increased.

Small-signal parameters. The basic parameters commonly specified for dynamic drivers (see **table**) are called small-signal parameters because they assume the diaphragm is not driven into nonlinear operation. Knowledge of these parameters is necessary to design system enclosures, particularly woofer enclosures because the lower cutoff frequency of a system is determined by the woofer. A typical value for the voice-coil resistance is in the range from 4 to 8 ohms. This resistance value is commonly used in specifying the rated impedance of a system. The other parameters determine the optimum enclosure volume for the driver and its lower cutoff frequency. For woofer drivers, the resonance frequency is typically in the range of 20 to 40 Hz. For woofer drivers made for musical instruments, it is typically 40 to 80 Hz. For tweeter drivers, it is typically in the range

Loudspeaker parameters

Parameter	Symbol
Voice-coil resistance	R_E
Resonance frequency	f_s
Electrical quality factor	Q_{ES}
Mechanical quality factor	Q_{MS}
Total quality factor	Q_{TS}
Volume compliance	V_{AS}

from 1 to 2 kHz. Midrange drivers have intermediate values. *See* MUSICAL INSTRUMENTS.

The total quality factor Q_{TS} is related to the mechanical and electrical quality factors by Eq. (1). Q_{TS}

$$Q_{TS} = \frac{Q_{MS}Q_{ES}}{Q_{TS} + Q_{ES}} \tag{1}$$

has a typical value of 0.2 to 0.5 for woofers intended for use in enclosures and a value of 0.7 to 1.0 for woofers intended for use in walls or open-back enclosures. The electrical quality factor is typically 5 to 20% greater than the total quality factor. The mechanical quality factor is typically 5 to 20 times the electrical quality factor. If a resistor R is inserted in series with the driver voice coil, the electrical quality factor is increased to an effective value Q'_{ES} given by $Q'_{ES} = Q_{ES}(1 + R/R_E)$, where R is the value of the added resistor. For example, R might be the dc resistance of any passive crossover network elements in series with the driver. *See* Q (ELECTRICITY).

Driver sensitivity. The sensitivity of a driver is usually defined as the on-axis sound pressure level (SPL) 1 m (3.3 ft) in front of the driver with an electrical input power of 1 W. The frequency at which the sensitivity is measured should be stated as part of the driver's specification. The voice-coil voltage is usually calculated assuming the voice coil is a resistor having a value equal to the dc resistance of the driver. For 1 W of input power, the root-mean-square (rms) voice coil voltage has the value $\sqrt{R_E}$ V. For example, a driver with $R_E = 8$ ohms would require 2.83 V rms. Typical sensitivity values are in the range from 85 to 95 dB. When comparing drivers with different voice-coil resistances, the sensitivities must be referenced to the same voice-coil voltage. For example, the sensitivity for $\sqrt{R_E}$ V rms across the voice coil can be converted to a sensitivity for 1 V rms by subtracting $10 \log_{10}(R_E)$ from the 1-W specification. *See* SOUND PRESSURE.

Closed-box systems. A closed-box system is one in which the woofer is mounted in a sealed box (**Fig. 6***a*). When the diaphragm vibrates, it compresses and rarefies (expands) the air in the box, causing an increase in the effective spring constant of the driver suspension. This causes an increase in the driver resonance frequency and quality factors. If the spring constant of the air in the enclosure dominates over the spring constant of the driver suspension, the system is called an acoustic-suspension or air-suspension system. If the spring constant of the diaphragm suspension dominates over that of the air in the enclosure, the system is called an infinite-baffle system. Closed-box systems are usually loosely filled with an absorbing material such as fiberglass. This has the beneficial effect of damping standing waves inside the box. In addition, it increases the effective internal volume of the box. This occurs because the filling acts as a heat reservoir to maintain the air at constant temperature in the box as it is compressed and rarefied, thus decreasing the change in pressure as the diaphragm vibrates.

Vented-box systems. A vented-box or ported system is one in which the woofer is mounted in a box with a vent connecting the air inside the box to the outside. The vent can be a rectangular or cylindrical tube installed in the front panel of the enclosure (Fig. 6*b*). Sometimes it is formed by a shelf across the width of the box below the driver so that the volume of air in the vent is the air between the shelf and the bottom of the box. Vented-box systems are

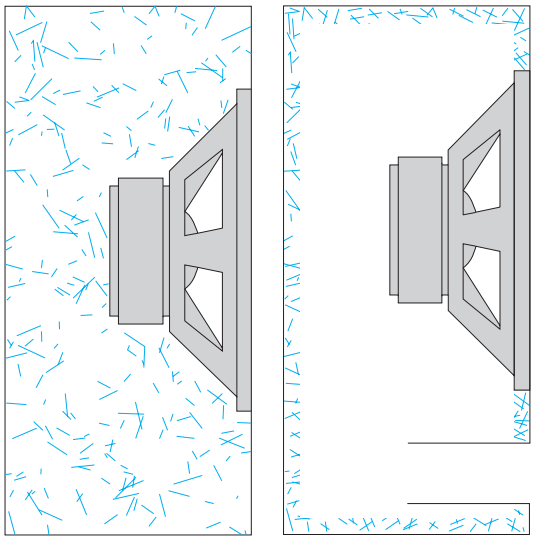

Fig. 6. Driver mountings. (*a*) Mounting in a filled closed box. (*b*) Mounting in a lined vented box in which the vent is a tube installed in the front panel of the enclosure.

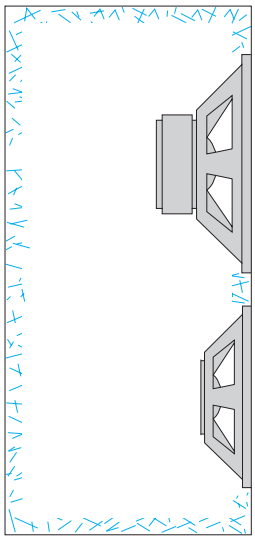

Fig. 7. Passive radiator (passive lower driver) system.

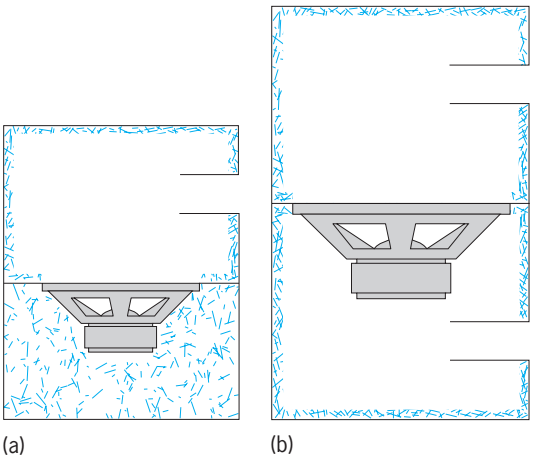

Fig. 8. Band-pass systems. (*a*) Fourth-order system. (*b*) Sixth-order asymmetrical system.

usually lined with a 1-in. (2.5-cm) thickness of filling material such as fiberglass. This helps absorb standing waves inside the box but has little effect on the effective volume of air in the box.

The air in the vent and the air trapped in the box form an acoustical resonator called a Helmholtz resonator that is used to extend the response of the system to lower frequencies. At the Helmholtz resonance frequency, the mass of the air in the vent resonates with the spring constant of the air in the box to cause strong radiation from the vent. At the same time, the pressure of the air in the box tends to oppose motion of the driver diaphragm so that little radiation comes from the driver. If the system is driven hard at the Helmholtz frequency, the airflow in the vent can become so great that noise can be generated by turbulent airflow. To minimize this noise, the vent area should be as large as possible. For a given Helmholtz frequency, the vent length must be made longer if its area is increased. However, increasing the vent's area may require a vent longer than the depth of the box, which can be accomplished using a vent tube with a 90° angle inside the box. *See* ACOUSTIC RESONATOR.

An aperiodic vented-box system has some type of acoustical damping material, such as fiberglass, placed inside the vent. This tends to damp the radiation from the vent at the Helmholtz frequency, thus decreasing the output from the system at low frequencies. A properly designed vented-box system does not require such damping. It is useful only if the box is too small, thus causing an undesirable peak in the frequency response at the Helmholtz frequency.

Passive-radiator systems. A passive-radiator system replaces the vent in a vented-box system with a passive radiator, that is, a driver having no voice-coil and magnet assemblies (**Fig. 7**). The advantage is that the Helmholtz frequency of the system can be controlled by varying the mass of the passive radiator diaphragm instead of the length of a vent tube.

Like the vented-box system, the passive-radiator system exhibits a Helmholtz resonance frequency at which the mass of the passive radiator diaphragm resonates with the spring constant of the air in the enclosure. This resonance can be used to improve the low-frequency response of the system. However, there is a second resonance frequency at which the radiation from the passive radiator tends to cancel that from the driver. At this frequency, the system exhibits a null in its frequency response. In a properly designed system, this resonance should be well below the Helmholtz resonance so that is has a minimal effect on the lower half-power or −3-dB cutoff frequency of the system. *See* RESONANCE (ACOUSTICS AND MECHANICS).

Band-pass systems. A band-pass enclosure is often used for subwoofers. In such a system, the loudspeaker driver is mounted on a shelf inside the enclosure, which divides the enclosure into two parts. For the system of **Fig. 8***a*, one of the two enclosures is coupled to the outside of the box through a vent. The frequency response of this system is that of a fourth-order band-pass filter which rolls off at a rate of 12 dB per octave or 40 dB per decade below its lower cutoff frequency and above its upper cutoff frequency. In the system of Fig. 8*b*, the two enclosures are coupled to the outside of the box through separate vents. The frequency response of this system is that of a sixth-order asymmetrical band-pass filter which rolls off at a rate of 24 dB per octave or 80 dB per decade below its lower cutoff frequency and a rate of 12 dB per octave or 40 dB per decade above its upper cutoff frequency. **Figure 9** compares the responses of the two systems, and illustrates why the sixth-order system is said to have an asymmetrical response. Both of the curves exhibit a maximally flat response in the midband range that is typical of a Butterworth response. (A Chebyschev response would exhibit peaks at the edges of the midband range.)

Horn-loaded drivers. A driver may be connected to an acoustic horn (**Fig. 10**). The sound radiated by the driver enters the throat of the horn and propagates to the mouth, where it is radiated. The acoustic impedance seen by the diaphragm of the driver is much higher with the horn than for a direct-radiator driver. This improves the efficiency so that less power is required to drive the system. In addition, the radiation from the mouth is more directional than for a direct-radiator driver. This is advantageous in public address systems in large rooms, where it is desirable to direct the sound to

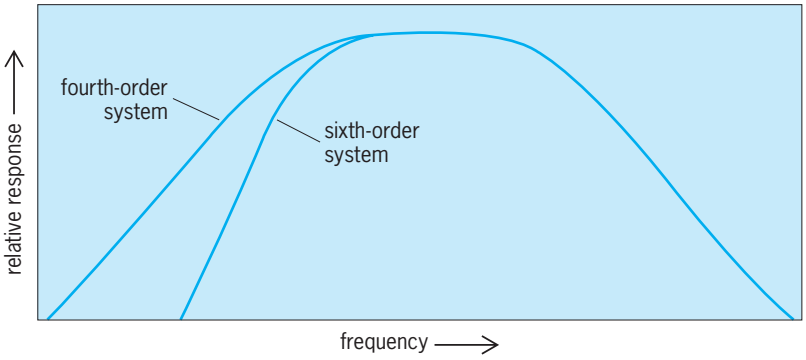

Fig. 9. Comparison of the low-frequency responses of fourth-order and sixth-order band-pass systems.

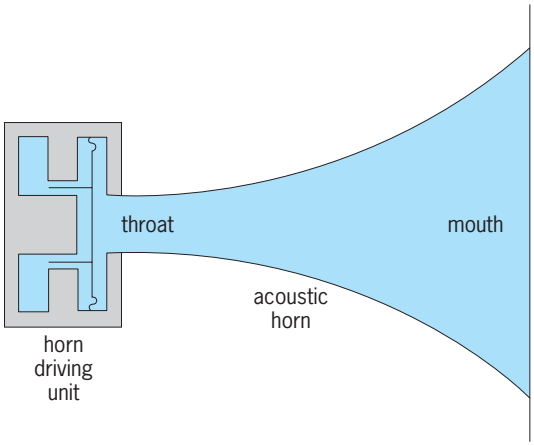

Fig. 10. Horn-loaded driver.

listeners at the back of the room without reflections from the side walls. Horn-loaded systems become physically very large when designed for low-frequency applications. For this reason, horns are normally used with midrange and tweeter drivers. *See* ACOUSTIC IMPEDANCE. W. Marshall Leach, Jr.

Bibliography. F. V. Hunt, *Electroacoustics*, American Institute of Physics for the Acoustical Society of America, 1982; W. M. Leach, Jr., *Introduction to Electroacoustics and Audio Amplifier Design*, 2d ed., Kendall/Hunt, 1999; *Loudspeakers*, vols. 1–4, Audio Engineering Society Anthology Series; L. L. Beranek, *Acoustics*, rev. ed., Acoustical Society of America, 1986; H. F. Olson, *Acoustical Engineering*, Van Nostrand, New York, 1957.

Louping ill

A viral disease of sheep, capable of producing central nervous system manifestations. It occurs chiefly in the British Isles. Infections have been reported, although rarely, among persons working with sheep.

In sheep the disease is usually biphasic with a systemic influenzalike phase, which is followed by encephalitic signs. In infected humans the first phase is generally the extent of the illness.

The virus is a member of the Russian tick-borne complex of the group B arboviruses. Characteristics, diagnosis, and epidemiology are similar to those of other viruses of this complex. *See* ANIMAL VIRUS; ARBOVIRAL ENCEPHALITIDES. Joseph L. Melnick

Low-level counting

The measurement of very small amounts of radioactivity. This can be achieved by measuring radioactivity in large samples or modifying conventional radiation-detection instruments for greater detection sensitivity, or both. All approaches must take into account the characteristics of the radiations, notably the very short range and intense energy deposition of alpha particles, intermediate range and energy deposition of beta particles, and high penetration of matter with low linear energy transfer by gamma rays. These techniques are important for measuring radionuclides from naturally occurring terrestrial and cosmic-ray-produced sources, and anthropogenic radionuclides to characterize the decay schemes of newly formed isotopes and analyze environmental and biological samples. *See* ALPHA PARTICLES; BETA PARTICLES; GAMMA RAYS.

Statistical error. Accurate measurements are defined by a small statistical error E, in percent, for the net sample count rate R, in inverse seconds (s^{-1}). Because the statistical error depends both on R and on the radiation background count rate R_b, in s^{-1}, both measured for the counting period t, in seconds (s), the value of R_b must be kept as low as possible. When R_b is much greater than R, E can be estimated from Eq. (1). For example, a sample counted for 5000 s

$$E = 100(2R_b t^{-1} R^{-2})^{0.5} \quad (1)$$

at a net count rate of 0.001 s^{-1} in a low-background beta-particle detector with a background count rate of 0.02 s^{-1} has an unacceptably high error of 283%. To reduce this error tenfold, Eq. (1) indicates that the background count rate has to be reduced by a factor of 100, or the time increased by a factor of 100, or the sample net count rate increased by a factor of 10. If R and R_b are of the same magnitude, the statistical uncertainty of both the gross count rate and the background must be considered. *See* BACKGROUND COUNT; STATISTICS.

Concentration. The concentration C, in units of s^{-1} kg^{-1}, of a sample is related to R by Eq. (2). Here e is

$$C = R(efdm)^{-1} \quad (2)$$

the overall fractional counting efficiency of the detector for the sample, f is the fraction of the counted radiation type relative to the emitted radiation, d is the fraction of the radionuclide remaining after radioactive decay during the interval between sample collection and counting, and m is the sample mass (in kg). For measuring very low concentrations, the values of e, f, and d should be as near unity as possible, and m should be large.

Radiation detectors. These concepts apply to a variety of radiation detectors for counting solid, liquid, and gaseous samples. Commonly used radiation detectors are gas-ionization systems operating in the ionization, proportional, or Geiger-Müller regions; scintillation systems with scintillators that are inorganic solids, organic solids, or organic liquids; and solid-state systems with germanium or silicon detectors. If possible, the various factors cited above are combined to improve the detection sensitivity, although some circumstances require a compromise between factors—for example, balancing the advantages of large sample mass and a counting efficiency near unity—if the two cannot be achieved simultaneously. *See* GEIGER-MÜLLER COUNTER; IONIZATION CHAMBER; JUNCTION DETECTOR; PARTICLE DETECTOR; SCINTILLATION COUNTER.

Sample preparation. Radionuclides in very large samples may be measured directly by counting the

energetic gamma rays they emit, for example in whole-body counting. If such samples emit only alpha particles, beta particles, or weak gamma rays (x-rays), then the radionuclides must be extracted and concentrated by chemical or physical processes. Radionuclides can be concentrated from water on ion-exchange resins or by precipitation, and from air by sorption on materials such as charcoal or molecular sieves. Filtering will collect radioactive solids from both media. Other processes include condensation of gases from air and volatilization from liquids or solids. The radionuclides must then be prepared for counting as thin solids, as solutes in a liquid scintillation cocktail, or as gases that are part of an ionization-detector filling. *See* ADSORPTION; CHARCOAL; FILTRATION; ION EXCHANGE; MOLECULAR SIEVE; PRECIPITATION (CHEMISTRY); VOLATILIZATION.

Detection efficiency. To maximize the detection efficiency, the intrinsic efficiency for recording the radiation should be near unity and the detector should view the sample from as large a solid angle as possible. Even relatively thin detectors have intrinsic efficiencies near unity for alpha particles, beta particles, and x-rays, but energetic gamma rays are detected with much lower intrinsic efficiency, except by very thick detectors. In general, the larger the sample, the smaller the angle subtended by the detector, although large detectors have been made for large samples. Relatively small samples can be surrounded more easily by a detector.

Radiation background. Achieving a low and stable radiation background is one basic aim in low-level counting. Stability is necessary because the detector background generally is determined by counting blanks between samples and subtracting these blank counts from the sample count on the assumption that the background is invariant. The counting facility must be situated to avoid fluctuating external radiation fields at nuclear facilities or near radiation sources. Airborne radon and progeny may have to be controlled by air-cleaning processes to avoid radiation background fluctuations. *See* RADON.

Shielding. The detector background from ambient radiation is reduced by shielding and by anticoincidence systems. A typical shield consists of 2 in. (5 cm) of a heavy metal such as lead or mercury, or thicker iron, to surround a beta-particle detector, or at least twice that thickness for a gamma-ray detector. This shielding absorbs all beta particles and most gamma rays. Water or paraffin is added to shield against neutrons (**Fig. 1**). For ultralow-level counting, the entire system can be shielded with massive amounts of iron and buried below ground to reduce the cosmic-ray background. *See* NEUTRON; RADIATION SHIELDING.

Radioactive contamination. The shielding materials and the detector plus ancillary equipment such as supports and cryostat within the shield must be as free as possible of radioactive contamination. Small amounts of natural and anthropogenic radionuclides may be in the mineral from which the metal is refined, may be added during production of detector-system components, or may be deposited on a surface within the shield. Contaminants that have been found include thorium-232 in aluminum, cobalt-60 and ruthenium-106 in steel, and lead-210 in lead. These radionuclides may be at low levels that are difficult to detect until they are used in the low-level counter.

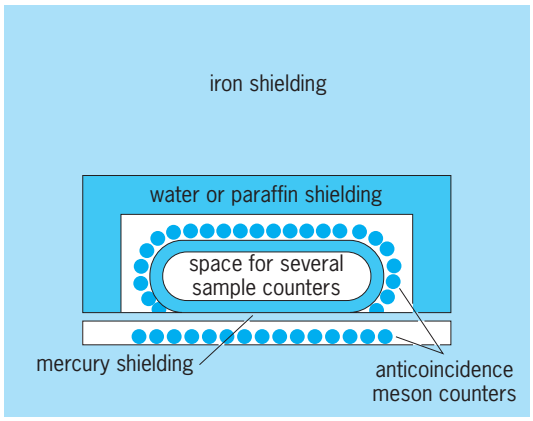

Fig. 1. Cross section of the shielding used for large-volume ultralow-level gas counters.

Interfering radionuclides. Radionuclides in the sample that interfere with measuring the radionuclide of interest can be considered another component of the background. These interfering radionuclides may be removed during the chemical and physical separations for extracting the radionuclide of interest from a large sample and for preparing the radionuclide in dimensions that are suitably thin and have been calibrated for counting. In addition, or as an alternative, electronic discrimination may be used to prevent or reduce such interference.

Electronic discrimination. An anticoincidence detector system, either surrounding the detector (Fig. 1) or part of it (**Fig. 2**), is used to reduce the count rate due to external beta particles and gamma rays. The electronic system cancels a pulse from the detector when a simultaneous pulse is recorded in an anticoincidence detector. It must be realized that the system also cancels pulses due to radiations emitted by the source that are counted both in the detector

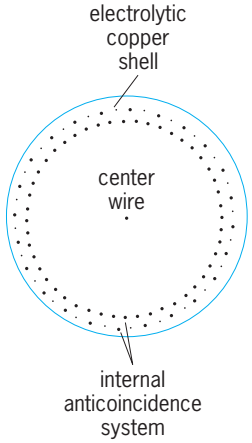

Fig. 2. Cross section of a proportional gas counter with an internal anticoincidence system.

and the anticoincidence detector.

Coincidence systems are used to detect selectively any radionuclide that emits without delay two or more successive radiations. They reverse the anticoincidence mode, accepting only pulses that are recorded simultaneously in two detectors. The two radiations may be an alpha particle, a beta particle, or a gamma ray followed by the same or a different radiation, each counted by a detector that responds preferentially to the radiation of interest. In a different context, liquid scintillation counters couple two photomultiplier tubes and only accept pulses due to scintillations recorded by both tubes in coincidence, to eliminate noise pulses from the individual tubes.

Pulse-height discrimination removes pulses due to radiations that have energies other than those of the radionuclide of interest. This approach is most effective for discriminating among alpha particles, which are emitted typically at one to three discrete energies per radionuclide. It is also effective for gamma rays, which deposit in the detector by photoelectric and multiple interactions discrete energies that correspond to those of emitted gamma rays, in addition to other energies deposited by Compton scattering and pair production. Various detector systems include spectrometers for pulse-height analysis. The pulse height is calibrated in terms of gamma-ray energy, and the area beneath the peak is calibrated for counting efficiency. The peak energies are used to identify the radionuclide, while the areas beneath the peaks give the amount present.

Simple pulse-height analysis is not feasible for beta particles because they are emitted in an energy continuum, with a characteristic maximum energy. It is possible to distinguish among beta-particle groups that have widely different maximum energies and to exclude beta particles beyond the maximum energy of the radionuclide of interest. Pulse-height discrimination also is used to avoid recording low-energy noise, and to separate different types of radiations, for example, alpha particles from beta particles, when the energy deposited in a detector by the different radiations differs widely.

Pulse-shape discrimination is also used to distinguish among types of radiations in a single detector or among pulses detected in different detectors within a counting system. This process can reduce the background by removing noise or pulses from interfering radiations.

Track-detection systems. These can be particularly useful for low-level measurements because they permit detection over periods of months with materials that respond only to specific types of radiation. Selected photographic films are used to record alpha-particle tracks. Alpha-particle tracks are also formed in certain plastics and some natural substances, and can be made visible under a microscope by etching with a strong base. *See* PARTICLE TRACK ETCHING.

Mass measurement. Special mass-measurement techniques can reach levels of activity per atom (that is, per unit mass) of the isotope too low for low-level counting. The activity A, in disintegrations per unit time, is related to the number of atoms N and the half-life of the radionuclide T, in the same units of time, according to Eq. (3). When the half-life

$$A = 0.693NT^{-1} \tag{3}$$

of the radionuclide is much longer than a day, the number of its atoms present is much greater than the number of radiations emitted in a day. By separating the atoms of such a long-lived radionuclide from interfering atoms, ionizing them, and counting them in an ionization detector, the detection sensitivity is lowered by orders of magnitude compared to counting the emitted radiations. Atoms have been separated for this purpose by mass spectrometer, accelerator, and laser excitation. A technique for the chemical analysis of elements at the picogram level that can be applied to measuring low levels of radioisotopes that have half lives in excess of about 10,000 years is inductively-coupled plasma mass spectrometry. The activity can be calculated from the mass according to Eq. (3). *See* ACCELERATOR MASS SPECTROMETRY; ISOTOPE SEPARATION; MASS SPECTROMETRY; RADIOACTIVITY. Bernd Kahn

Bibliography. National Council on Radiation Protection and Measurements, *A Handbook of Radioactivity Measurement Procedures*, 2d ed., 1985.

Low-temperature acoustics

The application of acoustics to research on the properties of condensed matter at low temperatures. Acoustic techniques are readily adaptable to the cryogenic environment and make possible many measurements of the structural and thermodynamic properties of materials at temperatures approaching absolute zero (0 K, which is −460°F or −273°C). The study of sound propagation has also yielded major insights into the low-temperature phenomena of superconductivity in metals and superfluidity in liquid helium.

Low-Temperature Properties of Solid Materials

Acoustic measurements have been used to characterize the properties of a wide variety of solid-state materials, such as metals, dielectric crystals, amorphous solids, and magnetic materials. A measurement of the velocity of sound in a substance gives information on its elastic properties, while the attenuation of the sound characterizes the interaction of the lattice vibrations with the electronic and structural properties of the material.

Experimental methods. Ultrasonic frequencies, in the range from 20 kHz to 100 MHz and above, are commonly employed in these measurements because of the ease of generating and detecting the sound with piezoelectric quartz crystals. In a typical experimental arrangement (**Fig. 1**), the opposite sides of the material being investigated are cut flat and the surfaces polished. Two quartz transducers are cemented to the flat sides. The sound is generated by exciting the quartz with a short voltage pulse at its resonant frequency. The pulse of sound propagates

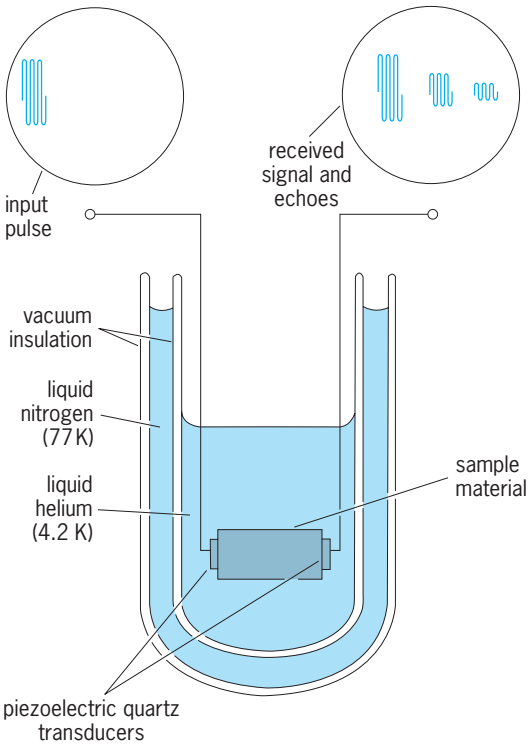

Fig. 1. Experimental arrangement to measure the velocity and attenuation of sound in a sample cooled to 4.2 K (−452°F) using liquid helium.

through the sample and is detected by the receiver-transducer. By measuring the time of flight across the sample, the sound velocity can be obtained. As the sound then reflects back and forth across the sample, the attentuation of the wave is found by measuring the rate of decay of the echo pulses. The temperature of the sample can be varied by bringing it into contact with cryogenic fluids such as liquid nitrogen (77 K or −321°F) or liquid helium (1–4.2 K or −458 to −452°F). Various refrigeration techniques using these liquids allow measurements over the entire range from room temperature (300 K or 80°F) down to well below 1 K (−458°F). *See* ULTRASONICS.

Metals and crystals. Because the sound velocity effectively measures elastic constants, such measurements are used to characterize phase transitions in crystals where the structure of the lattice changes. For example, in solid metallic sodium there is a transition near 36 K (−395°F), where the crystal lattice changes from body-centered cubic to hexagonal close-packed. Both the sound velocity and the attenuation change abruptly when the transition occurs, and provide a means of monitoring the nature of the transition. *See* CRYSTAL STRUCTURE; PHASE TRANSITIONS.

The attenuation of sound in many crystals is due to defects and impurities in the crystal lattice and provides information on such structures. If there is a line of missing atoms (a line dislocation), the stress from the sound field causes it to move back and forth. However, because of pinning forces, the dislocation cannot freely follow the sound oscillation and hence absorbs energy from it. In a metal at very low temperatures, the dominant source of attenuation is the interaction of the sound with the conduction electrons. Oscillations of the positively charged ions making up the crystal lattice couple to the negatively charged electrons. When the mean free path of the electrons becomes longer than the acoustic wavelength (which occurs at low temperatures), the sound wave loses energy to the electrons. Studies of this process are important in determining the strength of the electron-phonon coupling in a material (phonons are thermally excited quantized lattice vibrations). The coupling between the electrons and phonons is responsible for superconductivity. *See* CRYSTAL DEFECTS; LATTICE VIBRATIONS; PHONON; SOUND ABSORPTION.

A large variety of magnetoacoustic effects are observed in metals and crystals. In these measurements, changes in the sound attenuation occur as the strength of a magnetic field applied to the sample is increased. One example is the phenomenon of nuclear acoustic resonance. The nuclear spins in a crystal interact with vibrations of the lattice. When the frequency of the sound matches the Larmor frequency of the spins (which is determined by the magnetic field), the sound can induce transitions in the spin states to higher energies. This results in absorption of the sound, and a resonance is observed in the graph of attenuation versus field. Other magnetoacoustic effects in metals are useful in determining the orbits followed by the conduction electrons in the metal. *See* DE HAAS-VAN ALPHEN EFFECT; LARMOR PRECESSION.

Amorphous materials. Sound propagation is useful for studying amorphous materials. In materials such as silica glass (amorphous silicon dioxide, SiO_2), only two quantum energy levels are found to be important at low temperatures. These levels correspond to two nearly equivalent arrangements of the atoms, with one arrangement having slightly higher energy. An imposed sound field can cause a transition from one arrangement to the other. If the relaxation rate back to the original configuration is comparable to the sound frequency, there will be a net absorption of energy from the sound wave. A peak in the attenuation in silica glass near 50 K (−370°F) has been identified as being due to this process, and measurements as a function of frequency allow a determination of the relaxation rate. *See* AMORPHOUS SOLID.

Superconductors. When a metal is cooled below its superconducting transition temperature, there are striking changes in the attenuation of sound. At the transition some of the electrons near the Fermi surface begin to pair together, because of the attractive electron-phonon coupling. Once this occurs, the electrons can no longer exchange momentum with the lattice, and hence have zero resistance. This also means that the paired electrons no longer absorb energy from the sound wave, and the attenuation is from the remaining unpaired normal electrons. As the temperature is lowered well below the transition, the density of the unpaired electrons drops rapidly, and the attenuation becomes very small. The

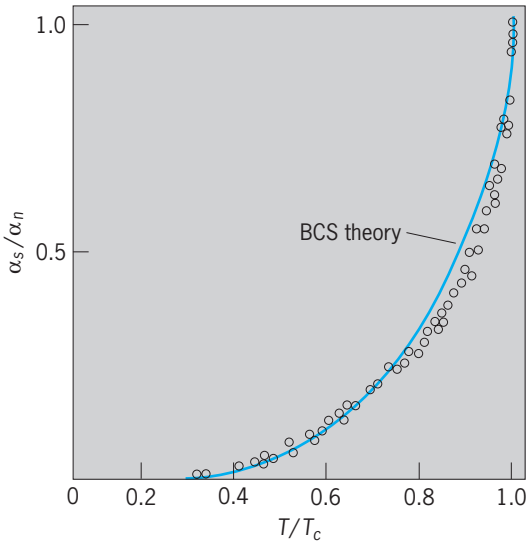

Fig. 2. Ratio of the sound attenuation α_s in the superconducting state to that in the normal state α_n for metallic tin, as a function of temperature T. The superconducting transition temperature T_c is 3.71 K (−453.0°F) for tin.

exponential drop in attenuation is well predicted by the Bardeen-Cooper-Schrieffer (BCS) theory of superconductivity, in substances such as metallic tin (**Fig. 2**). From attenuation measurements, values of the energy gap of the electrons (Δ) can be obtained, and this is the fundamental parameter characterizing the superconducting state.

The sound attenuation is also used to study the characteristics of type II superconductors. In these superconductors the magnetic flux applied to a sample is expelled until a critical field H_{c1} is reached. Above that field the flux enters the sample by threading the materials with an array of flux tubes known as quantized vortex lines. The motion of these pinned vortex lines contributes to the sound attenuation. As the magnetic field is increased, there is a further sharp increase in the attenuation at the second critical field H_{c2}, where the superconductivity is destroyed.

Acoustic techniques play a major role in understanding the unconventional properties of two material systems, the heavy-fermion superconductors and the high-T_c superconductors (where T_c is the superconducting transition temperature). The heavy-fermion metals are transition-metal compounds such as UBe_{13}, $CeCuSi_2$, and UPt_3, in which the conduction electrons are found to have effective masses as much as a thousand times greater than ordinary electrons. The discovery of superconductivity in these systems was quite unexpected, and a number of observations have shown that the predictions of the BCS theory are not followed for these materials. Ultrasonic attenuation measurements show an unusual peak in the attenuation just below the transition temperature, and at lower temperatures the attenuation follows a power-law behavior versus temperature rather than the exponential behavior discussed above. This indicates that the electrons may be paired in an unusual state where their spins point in the same direction (a spin triplet state), rather than in opposite directions (spin singlet state) as assumed by the BCS theory.

The discovery in 1986 of the high-T_c ceramic superconductors [such as $YBa_2Cu_3O_7$ with $T_c = 94$ K (−290°F)] generated intense research activity into the possible mechanisms that could account for such high transition temperatures. By using acoustic measurements of velocity and attenuation, features have been observed at and below the transistion temperature that are connected with the superconducting transition, but a clear interpretation of the data has not yet emerged. *See* SUPERCONDUCTIVITY.

Superfluid Helium

Sound propagation has been extensively used to probe many of the unusual properties of superfluid helium. When liquid ^{4}He is cooled below $T_\lambda = 2.17$ K (−455.76°F), it undergoes a phase transition into the superfluid state. In the two-fluid model the liquid helium below T_λ is treated as being a mixture of two fluids, a superfluid component with density ρ_s and a normal fluid component with density ρ_n. Just below the transition at T_λ, the superfluid density ρ_s is nearly zero, but it increases rapidly as the liquid is cooled, and below 1 K (−458°F) ρ_s is nearly equal to ρ.

The superfluid component has the unusual property that its viscosity is identically zero, and it is able to flow through the tiniest of capillaries. The normal fluid component, on the other hand, has the properties of an ordinary viscous liquid and is completely immobilized in a small capillary. A second characteristic of the superfluid is that it has zero entropy because it is an ordered quantum system, and all of the liquid's entropy is carried by the normal fluid component. This leads to an unusual flow property of the superfluid, namely, that it flows in response to both pressure gradients and temperature gradients in the liquid. An ordinary fluid is accelerated only by pressure gradients. These novel features of the superfluid (zero viscosity and entropy) give rise to a rich variety of different types of sound which can propagate in the superfluid helium. Five distinct sound modes have been identified and observed experimentally (**Fig. 3**).

First sound. First sound is a pressure wave which propagates in the bulk liquid. It is quite similar to sound in ordinary fluids. The velocity C_1 is given by Eq. (1), where B is the adiabatic bulk modulus of

$$C_1^2 = \frac{B}{\rho} \tag{1}$$

the helium. The velocity is relatively temperature-independent at a value of about 778 ft/s (237 m/s), except for the region near T_λ. At that point the velocity dips in a sharp cusp. High-resolution measurements of the sound velocity and attenuation in this region yield valuable information on the critical properties of the superfluid transition.

An important application of first sound is the acoustic microscope using liquid helium at 0.1 K (−459.5°F) as the coupling fluid for imaging.

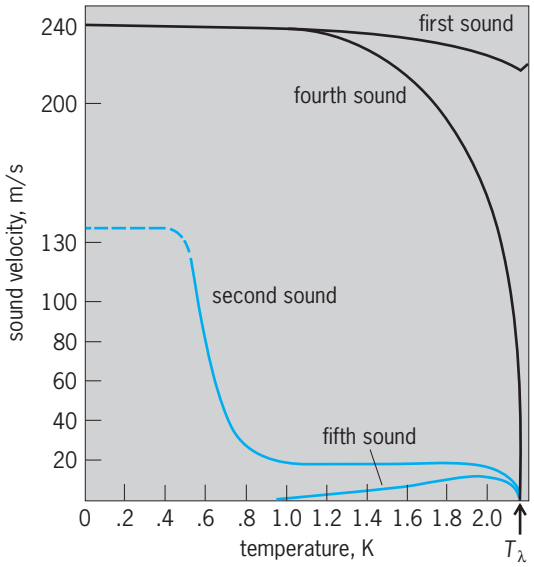

Fig. 3. Velocity of the various types of sound in superfluid ^{4}He as a function of temperature. 1 m/s = 3.28 ft/s. °F = (K × 1.8) − 459.67.

Because of the very low attenuation of first sound at this temperature, it was possible to use higher ultrasonic frequencies (up to 10 GHz) than can be achieved with similar microscopes that operate with water. The higher frequencies resulted in an image resolution of less than 20 nanometers, more than an order of magnitude better than can be obtained with light microscopes. *See* ACOUSTIC MICROSCOPE.

Second sound. Second sound is an unusual type of wave: it is a temperature wave in the bulk superfluid. In this mode the normal fluid and superfluid move in opposite directions. This keeps the density constant, and hence there are no pressure oscillations in the wave (as in first sound); but because only the normal fluid carries entropy, there are oscillations in the entropy and thus in the temperature of the liquid. The second sound can be generated with a heater wire and detected with a carbon resistance thermometer. According to the theory, the sound velocity is given by Eq. (2), where T is the temperature, S the specific entropy, and C the specific heat. The velocity is zero at T_λ (since $\rho_s/\rho = 0$ there), and then increases at lower temperatures to a value of about 65 ft/s (20 m/s). Below 1 K (−458°F) there is a further rapid increase to a value $C_2 = C_1\sqrt{3} = 460$ ft/s = 140 m/s, but in this region the mean free path of the normal fluid phonon excitations becomes longer than the sound wavelength, and the second sound can no longer be observed below about 0.6 K (−458.6°F). *See* SECOND SOUND.

$$C_2^2 = \frac{\rho_s}{\rho_n}\frac{TS^2}{C} \tag{2}$$

Third sound. Third sound is a wave which propagates in very thin films of helium. If helium gas is introduced into a chamber at low temperatures, some of the helium atoms are attracted to solid surfaces within the chamber by van der Waals forces, forming a thin layer of liquid on all of the surfaces. The thickness of the film can be varied between about 0.5 and 30 nm by adjusting the pressure of the gas in the chamber. The third sound is a wave in which the thickness of the film varies, somewhat like waves in a tank of water. Because the films are so thin, only the superfluid can move, the normal fluid being immobilized by its viscosity. The van der Waals force is the restoring force for the wave, and the velocity is given by Eq. (3), where α is the van der Waals coefficient and d is the film thickness. Experiments have verified this formula. *See* INTERMOLECULAR FORCES.

$$C_3^2 = \frac{\rho_s}{\rho}\frac{3\alpha}{d^3} \tag{3}$$

Third sound has been used to investigate the superfluid transition in thin films, which occurs at temperatures lower than T_λ and is found to depend on the exact thickness of the helium film. These observations have served to verify a general theory of two-dimensional matter, which predicts that ρ_s should drop discontinuously from a finite value to zero at the transition in the thin films.

Fourth sound. Fourth sound is a pressure wave which propagates in superfluid helium when it is confined in a porous material such as a tightly packed powder. In such a situation the normal fluid is immobilized, and only the superfluid can flow freely because of its zero viscosity (the porous materials are often called superleaks for this reason). The fourth sound is analogous to first sound because it involves density and pressure oscillations. Because only the superfluid component can move in the superleak, the velocity is modified from that of first sound and is given by Eq. (4). Because C_1 is known quite accurately, measurements of C_4 can be used with Eq. (4) to obtain highly precise values of ρ_s/ρ as a function of temperature.

$$C_4^2 = \frac{\rho_s}{\rho}C_1^2 \tag{4}$$

Fifth sound. Fifth sound is a temperature wave which can propagate in helium confined in a superleak. It is analogous to second sound, except that again only the superfluid component can flow. This modifies the velocity from that of second sound to Eq. (5). This velocity is zero both at T_λ (where C_2 is zero) and $T = 0$ (where $\rho_n/\rho = 0$). The fifth sound is quite a low-velocity mode, reaching a maximum value of about 40 ft/s (12 m/s) at 1.9 K (−456.2°F).

$$C_5^2 = \frac{\rho_n}{\rho}C_2^2 \tag{5}$$

Detailed measurements of both fourth and fifth sound in a variety of different porous materials have shown that these sound modes can be used to characterize the hydrodynamic flow in the pores. One application of the sound modes has been to study the properties of the interconnected pores in ceramic materials. It is found that the fourth sound velocity of helium in these materials decreases substantially as they are made denser by stronger sintering, allowing a study of the structural changes in the ceramic

as complete solidification is approached. These techniques also have possible applications to the oil industry, where fluid flow in porous rocks is an important technical problem. Fourth sound measurements in porous sandstones can yield parameters that help to interpret data from the logging of the size of oilfield reservoirs.

Superfluid ^{3}He. Acoustic methods have also been very important in determining the superfluid properties of the isotope ^{3}He. A phase transition was discovered in liquid ^{3}He in 1973 at ultralow temperatures, below 0.003 K. The first conclusive evidence that this was a transition to a superfluid state came when it was discovered that fourth sound can propagate in a superleak filled with the ^{3}He. The fourth sound exists only if there is a frictionless superfluid component, and the measurements of ρ_s derived from C_4 were in general agreement with theoretical predictions.

When the sound frequency is increased to a value greater than the rate of collisions between the ^{3}He atoms, the characteristics of the wave change from first sound to what is known as zero sound, where the velocity is slightly higher and the attenuation is reduced. At the superfluid transition there is a sharp peak in the attenuation as a function of temperature, and further variation is found at lower temperatures. In the magnetic A phase, the zero sound attenuation is found to depend on the angle between the direction of the sound beam and the direction of a magnetic field applied on the liquid. This anisotropy is an unusual feature, and the zero sound measurements are able to probe the microscopic structure of the paired ^{3}He atoms. *See* LIQUID HELIUM.

Gary A. Williams

Bibliography. W. P. Mason (ed.), *Physical Acoustics*, vols. 1–5, 1964–1969; W. P. Mason and R. N. Thurston (eds.), *Physical Acoustics*, vols. 6–18, 1970–1988; S. J. Putterman, *Superfluid Hydrodynamics*, 1974; R. N. Thurston and A. D. Pierce (eds.), *Physical Acoustics*, vols. 19–22, 1990–1992.

Low-temperature physics

A branch of physics dealing with physical properties of matter at temperatures such that thermal fluctuations are greatly reduced and effects of interactions at the quantum-mechanical level can be observed. As the temperature is lowered, order sets in (either in space or in motion), and quantum-mechanical phenomena can be observed on a macroscopic scale. As an example, consider a magnetic system. In a sample at high temperatures, there is a high degree of disorder (**Fig. 1***a*) corresponding to a large entropy because of the random orientations of its magnetic moments, the sample being in a paramagnetic state. At low temperatures (Fig. 1*b*), the sample is in a highly ordered state, the ferromagnetic state (lower entropy), and the details of the interactions responsible for this state can be studied. *See* ENTROPY; MAGNETISM.

Some of the most interesting manifestations of low

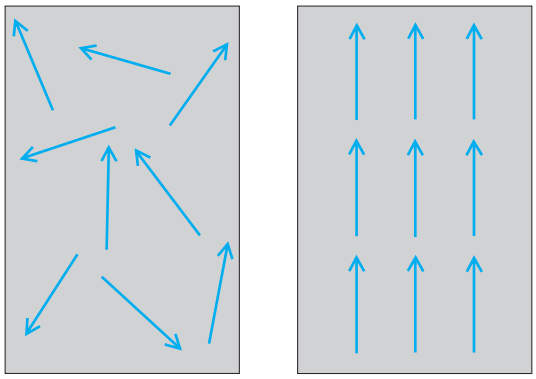

Fig. 1. Ordering of a magnetic system at (*a*) high temperatures and (*b*) low temperatures.

temperatures have been investigated in the temperature range from 4 K (−452°F) down to less than a nanokelvin above absolute zero. (1 K is equal to 1.8°F above absolute zero, or −459.67°F.) Certain metals become superconducting, losing their electrical resistance entirely; hence persistent currents can flow indefinitely in a superconducting ring or coil, displaying quantum-mechanical coherence over large distances. The liquids helium-3 (^{3}He) and helium-4 (^{4}He) remain liquid down to absolute zero under their own vapor pressure due to the large zero-point energy of these light atoms. (To overcome the large zero-point energy in liquid ^{3}He and liquid ^{4}He, a large pressure, approximately 30 atm or 3 megapascals, must be applied to cause these systems to solidify.) Liquid ^{4}He becomes superfluid, exhibiting no resistance to flow under certain conditions; when set in circulation, the fluid current persists indefinitely. Liquid ^{3}He also becomes superfluid at a much lower temperature with interesting magnetic and orbital effects. At sufficiently low temperatures, nuclear magnetic ordering has been observed in solid ^{3}He, in magnetic insulators, and in metallic systems. Silver becomes a nuclear antiferromagnet in the nanokelvin range as a result of quantum-mechanical exchange interactions. Considerable attention has been addressed to the general problem of ordering in disordered systems leading to studies of spin glasses, localization, and lower dimensionality. Quantum statistics are investigated in atomic hydrogen and deuterium, stabilized in states known as spin-polarized hydrogen (H↓) and spin-polarized deuterium (D↓). Because of its light mass and weak interactions, spin-polarized hydrogen is expected to remain gaseous down to absolute zero, whereas spin-polarized deuterium might liquefy at low temperatures. *See* HYDROGEN; LIQUID HELIUM; SUPERFLUIDITY.

Low-temperature research also deals with problems of thermometry and heat transfer between systems and within systems. Many practical applications have emerged, including the use of superconductivity for large magnets, ultrafast electronics for computers, and low-noise and high-sensitivity instrumentation. This type of instrumentation has

opened new areas of research in biophysics, and in fundamental problems such as the search for magnetic monopoles, gravity waves, and quarks. *See* LOW-TEMPERATURE THERMOMETRY; SUPERCONDUCTING DEVICES.

Production of low temperatures. Because of the need for small quantities of liquid ^{4}He in superconducting instrumentation and electronics, small cyclic heat engines are needed for continuous refrigeration. For lower temperatures, the refrigeration is produced by a variety of methods (depending on the experiment) in the research apparatus itself, called the cryostat. Some of the most important ones are described below.

Liquefaction of helium. Liquid helium at its normal boiling point of 4.2 K (−452.1°F) is a basic working substance used as a platform for many experiments and for attaining lower temperatures. Liquid is produced from the gas phase by a combination of adiabatic work on a piston and expansion through a Joule-Thompson valve; the cycle is maintained by use of a compressor, liquid-nitrogen precooling, and heat exchangers.

Since ^{3}He is rare and hence expensive, small quantities are liquefied in the cryostat in a closed cycle using liquid ^{4}He whose temperature is reduced by adiabatic evaporation. *See* LIQUEFACTION OF GASES.

Adiabatic evaporation. Evaporation is one of the most powerful methods of producing cooling, and it is used for reducing the temperature of liquid ^{4}He or liquid ^{3}He. **Figure 2** shows a typical arrangement where the liquid is in a container, isolated by a vacuum. Cooling results when the vapor pressure in the container is reduced by a pump. The rate of energy extraction by this refrigerator depends on the latent heat of the liquid and the pumping speed. The lowest temperatures achieved are typically 0.8 K (−458.2°F) for liquid ^{4}He and 0.2 K (−459.3°F) for liquid ^{3}He. At these temperatures, the vapor pressure is so low that the slow rate at which atoms can be removed from the liquid phase sets the limit.

^{3}He–^{4}He dilution refrigerator. This is an important method for producing low temperatures continuously by dissolving ^{3}He in liquid ^{4}He. This process is analogous to the above evaporation process but with an inverted geometry (**Fig. 3**), and relies on the fact that a mixture of ^{3}He–^{4}He separates into two phases below 0.87 K (−458.10°F). In a container, the mixing chamber, liquid ^{3}He is diluted in ^{4}He, since it has a finite solubility in ^{4}He, being 6.4% at 0 K (−459.67°F). Because liquid ^{4}He is a superfluid, it acts like a mechanical vacuum wherein ^{3}He atoms behave like an ideal gas. On passing from the ^{3}He-rich phase to the ^{4}He-rich phase, ^{3}He atoms produce cooling. To maintain continuous cooling, ^{3}He is extracted from the ^{4}He-rich phase at a still by means of a pump; it is then recondensed at a 1 K liquid-^{4}He evaporator and dissolved again in the mixing chamber, the ^{4}He being stationary in the cycle. Efficiency is improved by the use of heat exchangers. Temperatures as low as 2 millikelvins (3.6×10^{-3}°F above absolute zero) can be achieved continuously. The limiting temperature is determined by the decreasing entropy available and the intrinsic limitations due to viscous heating of the circulating ^{3}He and other heat influxes.

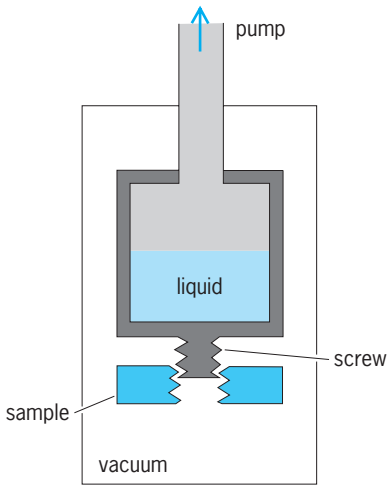

Fig. 2. Liquid-helium evaporator with screw for attaching sample.

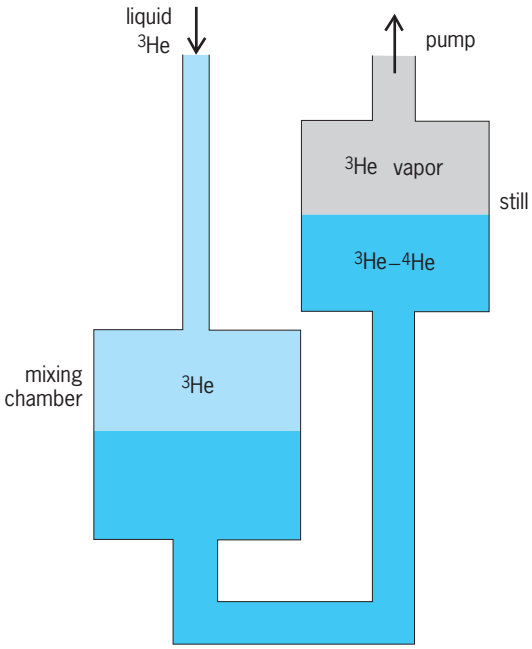

Fig. 3. Basic ^{3}He–^{4}He dilution refrigerator.

Adiabatic compression of ^{3}He. This method of refrigeration is based on the fact that below 0.32 K (−459.09°F) the entropy of solid ^{3}He is larger than that of the liquid. Liquid ^{3}He is a Fermi liquid with a high degree of motional order (because of quantum statistics); the solid has a high degree of disorder due to the random orientations of the ^{3}He nuclear magnetic moments. Changing the liquid to the solid under adiabatic conditions below 0.32 K (−459.09°F) leads to cooling of the solid-liquid mixture to temperatures as low as 1 mK (1.8×10^{-3} °F above absolute zero). The conversion to solid is achieved by applying pressure at the melting curve of ^{3}He. In accord with the Clausius-Clapeyron equation, the slope of the melting curve is negative below 0.32 K (−459.09°F), and hence solid is produced.

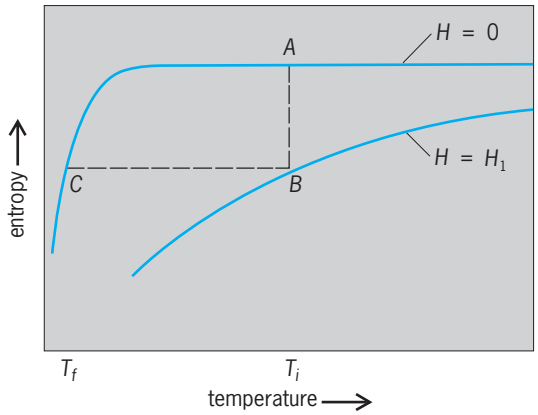

Fig. 4. Magnetic cooling process on entropy-temperature diagram.

This method is particularly interesting for cooling solid ^{3}He and even liquid ^{3}He.

Adiabatic demagnetization. This is a method of producing temperatures much below 1 K (−458°F) using a paramagnetic system whose entropy can be reduced by a magnetic field. **Figure 4** shows the entropy due to random orientations of magnetic moments in a paramagnet for zero magnetic field, $H = 0$. In a magnetic field and at low temperatures, the entropy is reduced and it is shown for some value of the field, H_1. As the system follows the path from A to B at constant temperature T_i, heat is given off during magnetization. Then, by an adiabatic (isentropic) demagnetization from B to C, the system cools to T_f. The limiting temperature is determined by the internal magnetic fields in the system. With an electronic paramagnet such as cerium magnesium nitrate, temperatures of approximately 1 mK (1.8×10^{-3} °F above absolute zero) can be reached from 1 K (−458°F). With a nuclear paramagnet, much lower temperatures can be achieved since the internal fields are much weaker than in electronic systems. Usually, metallic copper is used, and submicrodegree temperatures have been achieved in the spin system. Starting conditions require a large magnetic field and low temperatures. For work just below 1 mK (1.8×10^{-3} °F above absolute zero), it is easier to use hyperfine-enhanced nuclear cooling with a system such as $PrNi_5$. The strong coupling between electronic and nuclear magnetic moments enhances the entropy reduction with modest magnetic fields, and hence the initial conditions are less stringent. *See* ADIABATIC DEMAGNETIZATION.

Low-temperature phenomena. At a temperature of 2.17 K (−455.76°F), liquid ^{4}He undergoes a phase transition to a state characterized by flow without any resistance under certain conditions. The liquid then has very large heat conductivity (much better than many metals), peculiar film-flow behavior, and interesting and unusual sound and thermal propagation properties. Quantized vortices can exist in the rotating fluid at certain speeds, and above a certain critical velocity dissipation sets in. Rotating superfluid ^{4}He provides the best testing ground for theories of vortex dynamics. Numerous experiments demonstrate the unusual behavior of a superfluid, including photographic recordings of vortices. *See* QUANTIZED VORTICES.

The explanation for this behavior is that liquid ^{4}He obeys Bose-Einstein statistics and that a condensation to the ground state is expected. Liquid ^{3}He obeys Fermi-Dirac statistics, and its behavior is different than ^{4}He. After much theoretical and experimental work, it was discovered that liquid ^{3}He also undergoes a superfluid transition at 0.93 mK (1.67×10^{-3} °F above absolute zero) under zero pressure. The behavior is comparable to superconductivity, but instead of having pairing in a nonmagnetic singlet state, the ^{3}He spins pair in triplet states. Unusual behavior occurs in liquid ^{3}He as a result of the magnetic and nonmagnetic triplet pairs. The pairing explains the three known superfluid phases: A_1, A, and B near the melting curve. Many experimental and theoretical investigations of these ordered phases of the magnetic superfluid have discovered unexpected behavior in their magnetic properties, flow characteristics, and sound propagation, where collective excitations contribute from zero sound to fourth sound. *See* BOSE-EINSTEIN STATISTICS; FERMI-DIRAC STATISTICS; LOW-TEMPERATURE ACOUSTICS.

Superconductivity. This phenomenon is another manifestation of superfluidity, the fluid here being the conduction electrons in certain metals and compounds. Below a critical temperature T_c ranging from 133 K (−220°F) for Hg-Ba-Ca-Cu-O to 0.325 mK (5.85×10^{-4} °F above absolute zero) for rhodium, the materials show no electrical resistance as a result of quantum-mechanical phase coherence over macroscopic distances. The impetus provided by the BCS (Bardeen-Cooper-Schrieffer) theory of superconductivity led to investigations of a variety of phenomena such as tunneling, flux quantization, very sensitive devices called SQUID (superconducting quantum interference devices), new materials, amorphous superconductors, vortex flow and dissipation, and magnetic superconductors. The BCS theory led to the suggestion that electron pairing could occur in media of high electrical polarizability. This suggestion of possible superconductivity in organic molecules has stimulated a great deal of research in the field of conducting organic molecular solids. Consequently, materials such as $(TMTSF)_2ClO_4$ (TMTSF = tetramethyltetraselenafulvalene) have been found to be superconducting below 1 K (−458°F). The discovery of the Josephson effect and flux quantization in superconductors has led to the development of devices of extremely high sensitivity. *See* JOSEPHSON EFFECT; SQUID.

Because the cost of refrigeration is an important factor in the applications of superconductivity, there has always been interest in trying to find superconductors with high transition temperatures. For many years, Nb_3Ge had the highest transition temperature, 23.3 K (−417.7°F). In 1986 a new class of materials was discovered to have high critical temperatures ranging from 40 to 93 K (−388 to −292°F). These materials are oxides, usually in ceramic form, $YBa_2CU_3O_7$ being a typical example with

temperature of 92 K (−294°F). Transition temperatures as high as 133 K (−220°F) have been observed. Such unexpected behavior attracted much interest with the hope of achieving even higher transition temperatures and hence using cheaper refrigeration. The mechanism responsible for superconductivity in these materials is not clear; based on experimental facts, the applicability of the BCS theory to the high-T_c materials has been questioned. Although at the present there are problems of material preparation and of physical understanding of their behavior, these materials have great potential for a variety of applications ranging from high magnetic fields to electronics. The field of high-T_c superconductors is still part of low-temperature physics since it deals with a quantum-mechanical system on a macroscopic scale. *See* SUPERCONDUCTIVITY.

Quantum crystals. The amplitude of quantum-mechanical zero-point vibrations is especially large in crystals of light elements. It can become comparable to the lattice parameters. As a consequence of these vibrations, there is a high quantum-mechanical probability of particles tunneling into the neighboring lattice sites. This leads to quantum-mechanically delocalized particles in the crystal, similar to a quantum fluid. The largest effects occur for ^{3}He, followed by ^{4}He, hydrogen, and neon. Such effects are responsible for the direct-exchange interactions which influence the nuclear magnetism of ^{3}He. Nuclear-magnetic-resonance measurements of spin diffusion and relaxation, as well as susceptibility measurements, substantiate such a model. The antiferromagnetic phase structure found in solid ^{3}He around 1 mK (1.8×10^{-3}°F above absolute zero) is attributed to such many-particle exchange. *See* EXCHANGE INTERACTION; NUCLEAR MAGNETIC RESONANCE (NMR); QUANTUM SOLIDS.

Lower dimensionality and localization. These phenomena involve electrical conduction in thin films behaving as two-dimensional systems and in one-dimensional-like long narrow channels. This subject is of great theoretical importance, and is also of great importance in the development of very small circuits and devices in the submicrometer limit. Localization theory argues that a wave cannot propagate through a disordered one-dimensional system. In a disordered system, electrons can be localized in regions of disorder, and hence electrical conductivity will be strongly affected at very low temperatures. Quantum-mechanical effects govern the behavior, one being the exponential increase of resistance with the length of a very thin wire. Fundamental questions of electrical conduction are studied, experimentally and theoretically, with benefits for the design of very small circuits.

Lower-dimensionality magnetism. In order to understand three-dimensional systems, models in one dimension (for example, the Ising model) have been proposed and studied. The results are extremely interesting, and they have been applied to real systems of long chains and two-dimensional arrays of magnetic moments. The absence of phase transitions in one dimension has led to a more fundamental understanding of magnetic ordering at low temperatures. *See* ISING MODEL.

Dilute magnetic alloys. The study of dilute alloys was originally proposed to help solve the problem of magnetism in metals, but it became a fundamental problem in itself. The basic question deals with the behavior of a magnetic impurity in a nonmagnetic metallic host. A wide spectrum of behavior is observed from the nonmagnetic behavior of the impurity in one host to strong magnetic behavior in others. The electrical resistance, after going through a minimum, shows a logarithmic rise as the temperature is lowered; this is the Kondo effect. At higher magnetic impurity levels, the exchange coupling between the impurities, being of random strength and sign, leads to spin-glass freezing below a certain temperature, and to irreversible behavior. A question of fundamental interest is the nature of the freezing and the type of order that sets in at lower temperatures. This problem has been extended to semiconductors and insulators where randomness in the impurity interactions has also led to spin-glass behavior. *See* KONDO EFFECT; SPIN GLASS.

Spin-polarized hydrogen and deuterium. When atomic hydrogen and deuterium are stabilized (so as not to form molecules), interesting quantum gas behavior is observed. Stabilization can be achieved by large magnetic fields, and the systems are then called spin-polarized hydrogen and spin-polarized deuterium. Spin-polarized hydrogen provides a gas for which Bose-Einstein condensation is expected, while spin-polarized deuterium is expected to produce superfluidity due to fermion pairing, similar to liquid ^{3}He. Working with a gas provides researchers with the possibility of studying weakly interacting systems for which theories exist. Actually it has never been shown that liquid ^{4}He is really a Bose-Einstein system since the interactions are so strong. Research in this area, which is usually at temperatures below 1 K (−458°F), deals with fundamental questions of quantum statistics.

Magnetic superconductors. The observation of the coexistence of superconductivity and magnetism, made possible by the discovery of superconducting stoichiometric rare-earth compounds, has in turn opened the possibility of observing a wide range of phenomena. The occurrence of antiferromagnetic order in the superconducting state is deduced from the presence of a lambda-type anomaly in the specific heat and a cusp in the magnetic susceptibility. In some ternary rare-earth compounds, superconductivity is destroyed at a second lower critical temperature by the onset of long-range ferromagnetic ordering.

Quantum Hall effect. This is a form of the Hall effect observed in semiconductors with thin-film structure. At low temperatures and in high magnetic fields, the Hall conductance is quantized in integral multiples of e^2/h, where e is the electronic charge and h is Planck's constant, varying as the number of electrons is changed and dependent on localized states. Experiments have shown that the Hall conductance below 2 K (−456°F) exhibits also odd-denominator

and even-denominator simple fractions of e^2/h, attributed to two-dimensional quantum fluid behavior of electrons. This fractional quantum Hall effect is a many-particle effect that is based on electron-electron correlations. *See* HALL EFFECT.

Tunneling. According to quantum mechanics, particles trapped between potential barriers can escape by tunneling due to the wave nature of the particles. At low temperatures, thermal processes are reduced, making it possible to observe such tunneling. For very small structures, such as a junction formed by two electrodes separated by an insulator, single-electron tunneling effects can be observed when the electron electrostatic energy is larger than its thermal energy. This effect has been applied to single-electron transistors and quantum dots. On a larger scale, the applicability of quantum mechanics to macroscopic objects is being studied in macroscopic quantum tunneling experiments on two systems, Josephson junctions and small magnetic particles. *See* QUANTIZED ELECTRONIC STRUCTURE (QUEST); TRANSISTOR.

When the dissipation is reduced, tunneling of a macroscopic variable can be observed. At very low dissipation, there is a chance of seeing macroscopic quantum coherence in the tunneling experiments. *See* NONRELATIVISTIC QUANTUM THEORY; TUNNELING IN SOLIDS.

Other phenomena. The development of low-temperature techniques has revealed a wide range of other phenomena. The behavior of oriented nuclei is studied by observing the distribution of gamma-ray emission of radioactive nuclei oriented in a magnetic field. Other areas of study include surfaces of liquid ^{3}He and liquid ^{4}He, ^{3}He–^{4}He mixtures, cryogenics, acoustic microscopy, phonon spectroscopy, monolayer helium films, molecular hydrogen, determination of the voltage standard, and phase transitions. *See* ACOUSTIC MICROSCOPE; CRYOGENICS; ELECTRICAL UNITS AND STANDARDS; NUCLEAR ORIENTATION; PHASE TRANSITIONS.

Orest G. Symko

Bibliography. D. S. Betts, *Introduction to Millikelvin Technology*, 1989; D. F. Brewer (ed.), *Progress in Low Temperature Physics*, vols. 7–12, 1982–1989; W. G. Clark, Proceedings of the 16th International Conference on Low Temperature Physics, *Physica*, vols. 109, 110 B and C, 1982; R. P. Hudson, *Principles and Application of Magnetic Cooling*, 1972; O. Lounasmaa, *Experimental Principles and Methods Below 1 K*, 1974; K. Mendelssohn, *The Quest for Absolute Zero*, 1977; F. Pobell, *Matter and Methods at Low Temperatures*, 2d ed., 1996; G. K. White, *Experimental Techniques in Low-Temperature Physics*, 3d ed., 1987.

Low-temperature thermometry

The measurement of temperature below 0°C (32°F). Very few thermometers are truly wide-range, and hence most of the conventional methods of thermometry tend to fail the further the temperature drops below room temperature (see **table**). The defining instrument for a great part of the International Temperature Scale, the platinum resistance thermometer, rapidly loses sensitivity below 30 K, and its official limit is set at 13.81 K, the triple point of equilibrium hydrogen. This scale is based upon measurements of thermodynamic temperature made with the gas thermometer; the gas thermometer may be used down to about 2 K, for which purpose it is usually filled at, and "piggybacked" upon, a temperature in the region of the normal boiling point of equilibrium hydrogen, about 20.28 K. Liquid-in-glass thermometers may be used down to about −39°C or −38°F (mercury), about −100°C or −148°F (ethyl alcohol), and almost down to 70 K with various organic fluids. A liquid becomes sluggish at the lower end of its range, and also, with the exception of mercury, it presents problems of wetting the capillary wall and draining. Thermocouples are quite commonly encountered as temperature sensors down to 77 K and below, and thermistors and semiconductor diode sensors are used down to the liquid helium region, all three being available commercially in conjunction with linearizing electronics. Certain thermocouples have been developed especially for use in the 1–20 K region, and others with enough sensitivity for use in the millikelvin region. The electronic thermometer based upon the thermal expansion of a quartz frequency-controlling element may be used down to −40°C (−40°F). *See* GAS THERMOMETRY; THERMISTOR; THERMOCOUPLE.

In the liquid cryogen region, the saturation vapor pressure is used as a convenient and sensitive indicator of temperature. The usable range from 10 pascals pressure, for example, up to the critical point for the "permanently" liquid heliums corresponds to a temperature range from 0.45 to 3.32 K (at 1.15 atm or 116.5 kilopascals) for ^{3}He and 0.95 to 5.20 K (at 2.26 atm or 229.0 kPa) for ^{4}He. The method is also quite commonly used for equilibrium hydrogen between the triple point and the normal boiling point or above, but not much in modern times for liquid nitrogen (triple point of 63.15 K, normal boiling point of 77.35 K). *See* LIQUID HELIUM; VAPOR PRESSURE.

Thermometry below 1 K. The region below 1 K is special, not only because quantum phenomena are present on a macroscopic scale, but also because of the intrusion of a thermodynamic uncertainty principle: the small heat capacities of many systems studied preclude measurement techniques which gratuitously introduce energy and modify the state of the subject. In addition, relaxation times are long, and a system, once perturbed, may take minutes, hours, or even days to return to a state of equilibrium. Thus it is difficult to find an accurate, reproducible, and "well-behaved" thermometer that is very sensitive, small, and of low heat capacity, and the investigator is inclined to discount cost and complexity. The magnitude of a temperature, or a temperature change, is significant only in relation to the quantity E/k, or $\Delta E/k$, where k is Boltzmann's constant, and E and ΔE are energies which characterize the phenomenon under investigation. Thus, to a nuclear spin system

Ranges and sensitivities of low-temperature thermometers

Thermometer	Temperature range, K	Typical sensitivity or precision at low-temperature limit
Thermocouples		
300 to 700 ppm Fe in Au/Ag + 0.37 at. % Au	1–25	10 $\mu V \cdot K^{-1}$
Chromel/300 to 700 ppm Fe in Au	1–300	10 $\mu V \cdot K^{-1}$
Chromel/Constantan	20–1100	8.5 $\mu V \cdot K^{-1}$
Resistance thermometers		
Platinum (capsule)	4–500	±3 mK [3.3 $\mu V \cdot K^{-1}$ at 10 mA]
Rhodium + 0.5 at. % Fe	0.5–300	±30 μK [350 $\mu V \cdot K^{-1}$ at 0.5 mA]
Carbon	0.01–300	~5 μK
Germanium	0.01–30	~5 μK
Saturation vapor pressure thermometers		
Hydrogen	14–21	1 mK [dT/dp ~30 mK $(mmHg)^{-1}$~0.23 mK $\cdot Pa^{-1}$]
Helium-4	1.0–5.2	20 mK [dT/dp ~0.85 K $(mmHg)^{-1}$ ~6.4 mK $\cdot Pa^{-1}$]
Helium-3	0.5–3.3	10 mK [dT/dp ~0.44 K $(mmHg)^{-1}$ ~3.3 mK $\cdot Pa^{-1}$]
Noise thermometer*	0.002–0.1	1–5%
Magnetic thermometers		
Gadolinium metaphosphate, $Gd(PO_3)_3$	2–100	100 nK
Cerous magnesium nitrate (CMN), $Ce_2Mg_3(NO_3)_{12} \cdot 24H_2O$; single crystal	0.003–4	5 nK
CMN powder sphere or cylinder	0.002–4	1 nK
Copper (and other nuclear paramagnets)	0.001–0.01	100 nK
Gamma-ray anisotropy thermometers*	0.002–0.05	1–10%
^{60}Co in hexagonal close-packed cobalt single crystal	0.002–0.04	
^{54}Mn in iron	0.003–0.03	
^{54}Mn in nickel	0.004–0.045	
^{3}He melting-curve thermometer	0.001–1	1 μK
Nuclear resonance thermometer	310 nK–2 K	1–20%

*Primary thermometer.

which might become ferromagnetic at 10^{-6} K, a temperature change of 1 microkelvin is very large, while room temperature would be much as the Sun's interior is to a human being. *See* ADIABATIC DEMAGNETIZATION.

For many years, the traditional method for measuring temperature below 1 K was that of magnetic thermometry, wherein the susceptibility χ of paramagnetic salts which closely obey the Curie law, $\chi \propto T^{-1}$, is utilized. A sample is calibrated at a known temperature in the 1–4 K region, and then, for lower temperatures, a "magnetic temperature" T^* is extracted from the inversion of Curie's law. The establishment of the exact relationship between T^* and T, which is of greatest importance at the low end of the range, where the simple law begins to break down, was a lengthy and difficult process. The magnetic thermometer is still used because of its basic simplicity, and also as a verifier and "smoother" of temperature scales derived by other methods. Enhanced detection sensitivity is available through superconducting quantum interference device (SQUID) technology, so that very much smaller sensors can be employed, always an important advantage for low-temperature research. The magnetic-thermometry technique has also been adapted to nuclear spin systems for measurements in the microkelvin region (discussed below). *See* CURIE-WEISS LAW; LOW-TEMPERATURE PHYSICS; MAGNETIC THERMOMETER; PARAMAGNETISM; SQUID; SUPERCONDUCTING DEVICES.

Although primary in principle, the ^{3}He melting-curve thermometer seems to deliver the highest accuracy as a secondary instrument, making use of a pressure-temperature relation obtained by temperature calibration. It is used over the range 1 mK to 1 K and offers very high precision (better than 1 μK at the low-temperature end). The accuracy remains somewhat uncertain, especially at the lowest temperatures, and has been the subject of intensive research. *See* QUANTUM SOLIDS.

As at room temperature and above, resistance thermometers tend to be accorded highest favor as far as practicality is concerned, but very few types having adequate sensitivity exist. Doped germanium semiconductors and carbon resistors are much in use down to temperatures as low as a few millikelvins, the germanium being somewhat more reproducible, if much more costly. A normally resistive rhodium-iron alloy (0.5% Fe) is also useful for the region above 0.1 K (and up to 300°C), and serve, in fact, as an extremely important transfer standard for use in thermometry calibration service.

Superconducting transitions have been developed for temperature reference points between 15 mK (tungsten) and 9.3 K (niobium).

Primary thermometers. The low-temperature region is unique in having available several different types of primary thermometers, all of which are quite practical. The least practical, perhaps, is the acoustic thermometer, which uses the property that, extrapolated to zero pressure, the speed of sound in a gas is proportional to $T^{1/2}$. This has been used in the range 2–20 K as an alternative to, and check upon, the gas thermometer. The Johnson noise in a resistor can be used with particular advantage at low temperatures when allied with SQUID detector technology. This yields a value of temperature through a restricted form of the Nyquist relation $\overline{P(t)} = 4kTR\Delta f$, where $\overline{P(t)}$ is the mean noise power (averaged over

infinite time, to be rigorous), R the resistance, k the Boltzmann constant, and Δf the frequency bandwidth. *See* ELECTRICAL NOISE; SOUND.

In suitable systems it is possible to spatially orient atomic nuclei at very low temperatures, and if these nuclei are emitters of gamma rays, the emission pattern is anisotropic to a degree which is a measure of the thermodynamic temperature. Finally the magnetic susceptibility of suitable atomic nuclei may also be employed via the Curie law. This magnetism is very weak, which gave it the disadvantage that it was difficult to measure accurately, prior to the advent of modern technologies, and the advantage that the Curie law validity persists down to the microkelvin region. Nuclear magnetic resonance or static SQUID-based techniques may be employed, but the former is preferable in being unaffected by magnetic impurities, to which the second method falls hostage.

The nuclear magnetic resonance thermometer needs one calibration point, and since this calibration cannot be performed at the kelvin-defining triple point of water, but must be carried out at 1 K or lower, some deny it primary thermometer status. *See* NUCLEAR MAGNETIC RESONANCE (NMR); NUCLEAR ORIENTATION.

Revision of IPTS-68. In 1990, the International Committee of Weights and Measures promulgated an extensively revised version (ITS-90) of the scale that it recommended 22 years earlier, the IPTS-68. Two significant features are an extension down to 0.65 K (far below the earlier limit of 13.81 K) and improved approximation to thermodynamic temperature in all ranges. In this effort, input data came from many sources. A magnetic thermometer was used between 1 and 83 K to detect irregularities in the 1968 scale. Values for defining fixed points were improved by using acoustic, constant-volume gas, and gas-isotherm thermometry over the range 1–30 K. The role of the high-temperature thermocouple has been eliminated, and the platinum resistance thermometer has been adopted as the recommended interpolation instrument for the entire temperature region between the freezing point of silver (961.78°C) and the triple point of hydrogen (13.81 K). The most striking change is that, for the first time, alternative realizations of the scale are permitted, for operational convenience and when no significant discrepancies arise from those alternatives. Thus, for example, the lowest region of the scale, 0.65 K–3.2 K, utilizes the saturation vapor pressure of ^{3}He, while the next higher range, 1.25 K–5.0 K, is realized in terms of the saturation vapor pressure of ^{4}He, with evident overlap between 1.25 K and 3.2 K. *See* TEMPERATURE; TEMPERATURE MEASUREMENT; THERMOMETER.

Ralph P. Hudson

Bibliography. R. P. Hudson et al., Recent advances in thermometry below 300 mK, *J. Low Temp. Phys.*, 20:1, 1975; B. W. Mangum and G. T. Furukawa, *Guidelines for Realizing the International Temperature Scale of 1990 (ITS-90)*, NIST Tech. Note 1265, 1990; F. Pobell, *Matter and Methods at Low Temperatures*, 2d ed., 1996.

Lubricant

A gas, liquid, or solid used to prevent contact of parts in relative motion, and thereby reduce friction and wear. In many machines, cooling by the lubricant is equally important. The lubricant may also be called upon to prevent rusting and the deposition of solids on close-fitting parts.

Liquid hydrocarbons are the most commonly used lubricants because they are inexpensive, easily applied, and good coolants. In most cases, petroleum fractions are applicable, but for special conditions such as extremes of temperature, select synthetic liquids may be used. At very high temperatures, or in places where renewal of liquid lubricants is impossible, solid lubricants (graphite or molybdenum disulfide) may be used.

Petroleum lubricants. Crude petroleum is an excellent source of lubricants because a very wide range of suitable liquids, varying in molecular weight from 150 to over 1000 and in viscosity from light machine oils to heavy gear oils, can be produced by various refining processes. Crude petroleum fractions consist of saturates (normal, iso-, and cyclo- paraffins); monoaromatics which may contain saturated rings as well as saturated side chains; substituted polyaromatics; hetero compounds containing sulfur, nitrogen, and oxygen; and asphaltic material made up of polycondensed aromatics and hetero compounds. Of these, the wax-free saturates and monoaromatics are desired in the finished oil in order to obtain the desired viscometric properties and oxidation and thermal stability. So far as possible, the other types of compounds are generally removed. Classically, only those crudes (so-called paraffinic crudes) relatively rich in the desired type of hydrocarbons were used in lubricating oil manufacture. By atmospheric distillation, neutrals were produced as distillates and the residual fractions were treated with activated clays, which removed asphaltic and hetero material to produce bright stock.

In modern refining, vacuum distillation removes the desired hydrocarbons from the asphaltic constituents (which may be present in amounts up to 40% of the total) and gives oils in the required viscosity and boiling range. Extraction of the distilled fractions with solvents such as liquid sulfur dioxide, furfural, and phenol permits the removal of the polyaromatic and hetero compounds to improve viscosity-temperature characteristics (viscosity index, VI) and stability of the oil. Dewaxing removes the high-melting paraffins. *See* DEWAXING OF PETROLEUM.

If the viscosity index of the oil is not important for a particular application, the most reactive polyaromatics and hetero compounds may be removed by treatment with concentrated sulfuric acid. In either case, the oil is treated finally with an active clay to remove trace amounts of residual acids and resins (heterocyclics).

Small amounts of heterocyclics, such as substituted benzthiophenes, quinolines, and indoles, may remain in the finished oil. The sulfur-containing

Viscosity of oils for various applications

Application	Viscosity in centistokes at 77°F (25°C)	Primary function
Engine oils		
SAE 10W	60–90	Lubricate piston rings, cylinders, valve gear, bearings; cool piston; prevent deposition on metal surfaces
SAE 20	90–180	
SAE 30	180–280	
SAE 40	280–450	
SAE 50	450–800	
Gear oils		
SAE 80	100–400	Prevent metal contact and wear of spur gears, hypold gears, worm gears; cool gear cases
SAE 90	400–1000	
SAE 140	1000–2200	
Aviation engine oils	200–700	Same as engine oils
Torque converter fluid	80–140	Lubricate, transmit power
Hydraulic brake fluid	35	Transmit power
Refrigerator oils	30–260	Lubricate compressor pump
Steam-turbine oil	55–300	Lubricate reduction gearing, cool
Steam cylinder oil	1500–3300	Lubricate in presence of steam at high temperatures

compounds serve the useful purpose of acting as natural antioxidants. The nitrogen compounds may be harmful in certain applications because of their propensity to form deposits on hot surfaces and are generally reduced to low concentrations.

The **table** lists typical specification data for lubricants in several applications. Viscosity is a determining factor in lubricant selection. Machines are generally designed to operate on the lowest practicable viscosity, since the lighter fluids give lower friction and better heat-transfer rates. However, if loads or temperatures are high, more viscous and less volatile lubricants are required. Change of viscosity with temperature is often of considerable practical importance and is customarily expressed in terms of viscosity index, an arbitrarily chosen scale on which an oil from a Pennsylvania crude, high in saturate and monoaromatic content, is assigned a value of 100, and those containing a relatively large amount of cyclohydrocarbons, both paraffinic and aromatic (from naphthenic crudes) are in the 0–50 viscosity-index range. As already described, the refiner can produce oils of high viscosity index from naphthenic stocks, but yields may be low.

Multigrade oils. In order to standardize on nomenclature for oils of differing viscosity, the Society of Automotive Engineers (SAE) has established viscosity ranges for the various SAE designations (see table). By the use of relatively large amounts of additives for improving viscosity index, it is possible to formulate one oil which will fall within the range of more than one SAE viscosity grade, the so-called multigrade oils, illustrated by **Fig. 1**. Since all viscosity-index improvers also increase viscosity, it is necessary to use a base oil of low viscosity to formulate such oils. Since the viscosity-increasing effect of the additive decreases with increase in shear rate, an artificially thickened oil of this type behaves as a light oil in engine parts under high shear, and thereby friction is low, but acts as a heavier oil in low-shear regions or at higher temperatures. However, volatility and ability to protect high shear parts from rubbing set limits to the use of light oils in these formulations.

Additives for lubricating oils. It is often desirable to add various chemicals to lubricating oils to improve their physical properties or to obtain some needed improvement in performance.

Viscosity-index improvers. The fall in viscosity with increase in temperature of oils of a given grade, or viscosity level, can be made less steep by thickening lighter oils with polymeric substances such as polybutenes and copolymers of polymethacrylates. The polymer may increase in solubility as the temperature increases, and correspondingly, the molecules uncoil and thicken the base oil more at high than at low temperatures and thus counteract, to some extent, the natural decrease in viscosity the base oil would undergo (Fig. 1).

Pour-point depressants. The dewaxing process removes the higher melting hydrocarbons, but some components remain which may solidify and gel the oil, and thus reduce its fluidity at low temperatures. Small amounts of chemicals, such as metallic soaps, condensation products of chlorinated wax and alkyl naphthalenes or phenols, polymethacrylates, and a host of others, increase fluidity at low temperatures. The mechanism of their action is still uncertain, but

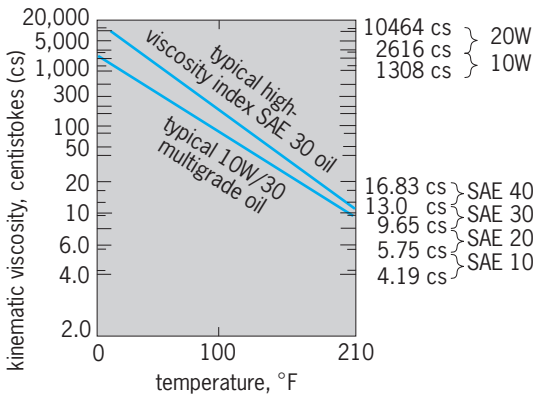

Fig. 1. Viscosity-temperature relationships indicated for additive-thickened multigrade oils. °C = (°F − 32)/1.8.

it probably involves adsorption of additive molecules on the surface of the growing wax crystals. The adsorbed layer either reduces intercrystal forces or modifies crystal growth.

Antioxidants. Lubricants are exposed to oxidation by atmospheric oxygen in practically all of their applications. This results in formation of acids and sludges which interfere with the primary function of the lubricant. Substantial increases in service life can be obtained by using small amounts (0.1–1.0%) of antioxidants. For lighter, more highly refined oils such as steam turbine oils, hindered phenols such as dibutyl-*p*-cresol are very effective. In heavy lubricants, such as engine oils, amines (phenyl-α-naphthylamine), metal phenates (alkali-earth salts of phenol disulfides), and zinc salts of thiophosphates and carbamates are used.

Antiwear and friction-reducing additives. If sliding surfaces can be completely separated by an oil film, friction and wear will be at a minimum. There are many systems, however, in which the combination of component geometry and operating conditions is such that a continuous oil film cannot be maintained. If no separating film of any kind were interposed, however, complete seizure would result. If the pressures and temperatures between such contacting surfaces are moderate, the provision of a boundary lubricating film will suffice, whereas if, as in some gears, conditions of both temperature and pressure are severe, some form of extreme pressure (EP) lubrication may be necessary.

The form in which wear manifests itself in machine components varies widely with the conditions, from the catastrophic welding together of gear-tooth surfaces to the slow continuous removal of material from an engine cylinder; even within the same mechanical system, it may change profoundly with changes in operating and environmental conditions.

In internal-combustion engines operating at low cylinder temperatures, for instance, condensation of acids from the gaseous combustion products on the cylinder and ring surfaces results in corrosive wear; in such cases, the addition of alkaline-earth phenates to the lubricating oil to neutralize the acids has succeeded in reducing wear rates.

Extreme pressure additives. Certain types of gears, particularly the hypoids used in automotive rear-axle transmissions, operate under such severe conditions of load and sliding speed, with resulting high temperature and pressure, that ordinary lubricants cannot provide complete protection against metal contact; this leads to welding, transfer of surface metal, and ultimate destruction of the gears. Also, in certain machining operations, it is necessary to prevent the chip from welding to the cutting tool. For such applications, lubricants containing sulfur and chlorine compounds are used. At the temperatures developed in the contact, these react chemically with the metal surfaces; the resulting sulfide and chloride films provide penetration-resistant, low-shear-strength films which prevent damage to the surfaces. Care in formulating these lubricants must, however, be exercised to ensure that corrosion of metal at normal temperatures does not occur. **Figure 2** shows the damage which may occur in the absence of protective additives.

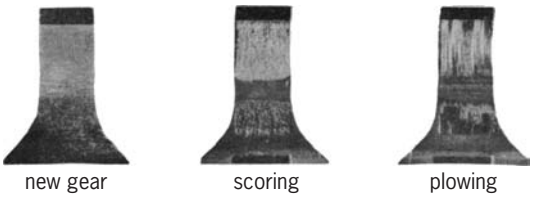

Fig. 2. Two examples of gear damage.

Dispersants. In internal combustion engines, some of the products of combustion, which include carbonaceous particles, partially burnt fuel, sulfur acids, and water, enter the oil film on the cylinder walls. These materials may react to form lacquers and sludges which are deposited on the working parts of the engine. The lubricant is called upon to keep engine parts (oil screens, ring grooves) clean, and this is accomplished by the use of so-called detergent oils (**Fig. 3**).

The most commonly used dispersants are alkaline-earth salts. Of these, the most successful have been the salts of petroleum sulfonic acids, phenates, salicylates, thiophosphates, and oxidized olefinphosphorus pentasulfide reaction products. These materials owe their effectiveness partly to their surface activity, which ensures that foreign particles are kept in suspension in the lubricating oil, and partly to their alkalinity, which enables them to neutralize combustion acids that would otherwise catalyze the formation of lacquers.

Polymeric additives have been introduced for dispersancy. They are copolymers of a long-chain methacrylate, for example, lauryl methacrylate, and a nitrogen-containing olefin, such as vinyl pyrrolidone. These nonash dispersants are superior to the metal-containing additives for low-temperature operation and can be used very effectively in motor oils. Because they are less alkaline than metallic additives, the polymeric additives are less effective in diesel engines whose fuels often lead to combustion products which are much more acid than those from gasoline.

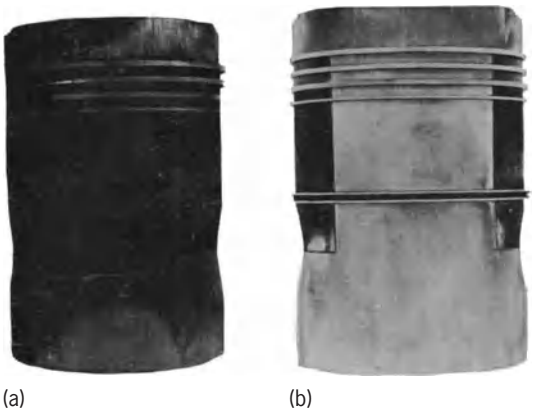

Fig. 3. Effect of dispersant on cleanliness. (*a*) Ordinary oil. (*b*) Oil containing dispersant additive.

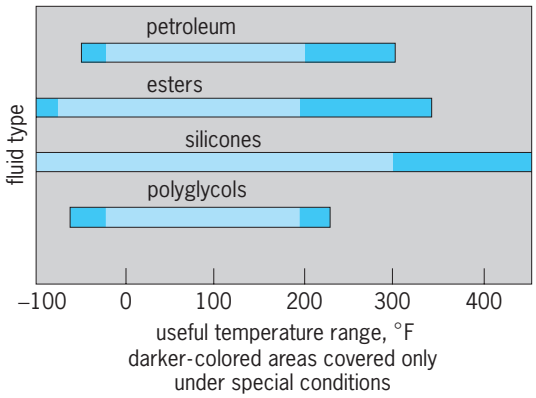

Fig. 4. Useful temperature range of synthetic oils. °C = (°F − 32)/1.8.

Boundary lubricants. Boundary conditions are encountered in many metal-forming processes in which the pressures required to deform the metal are too high to allow an oil film to form. In such applications, fatty oils, such as palm oil, or lubricants containing fatty materials are employed to reduce the friction and wear; the fatty acids react with the metal surface to form a tenacious soap film which provides lubrication up to temperatures near the melting point of the soap, usually about 250°F (120°C). *See* MACHINABILITY OF METALS.

Synthetic oils. During World War II, synthetic lubricants were extensively employed by Germany as substitutes for mineral lubricants which were in short supply. Some of these, such as the ester oils, were in fact superior to mineral lubricants in some applications. After the war, the use of synthetics for special applications, where their performance justifies the higher costs, steadily increased. Their main advantage is that they have a greater operating range than a mineral oil (**Fig. 4**). Esters such as 2-ethylhexyl sebacate, containing oxidation inhibitors and sometimes mild extreme pressure additives, are used as lubricants for aircraft jet engines. Silicones, although ideal with regard to thermal stability and viscosity characteristics, are poor lubricants for steel on steel, and this has restricted their use, although they are invaluable in some applications. Another class of widely used synthetic oils are the polyglycols, such as polypropylene and ethylene oxides. These polymers are available in a wide molecular-weight range, and they vary considerably in solubility in water and hydrocarbons. Thus, water-base lubricants may be formed which are used when a fire hazard exists.

Solid lubricants. The most useful solid lubricants are those with a layer structure in which the molecular platelets will readily slide over each other. Graphite, molybdenum disulfide, talc, and boron nitride possess this property.

The principal difficulty encountered with the use of solid lubricants is that of maintaining an adequate lubricant layer between the sliding metal surfaces. If the solid lubricant is applied as a suspension in a fluid, there is a tendency for the particles to settle out, and they may not reach the region where they are required. If they are applied as a thick paste to overcome the tendency to settle out, it is frequently difficult to force the paste through the narrow clearances between the sliding surfaces. A third method is to pretreat the surfaces with a relatively thick film of solid lubricant suspended in a resin and bake it on. Difficulties may then arise through progressively increasing clearances as the film wears, and there is no method for its continuous renewal. Materials such as graphite and molybdenum disulfide oxidize quite rapidly in air at 750°F (400°C). Unless air can be excluded, therefore, alternative solid lubricants will be required at temperatures greatly in excess of this.

A unique type of solid lubricant is provided by the plastic polytetrafluoroethylene (PTFE). At low speeds, PTFE slides on itself or on metals with a coefficient of friction in the lowest range observed for boundary lubrication (about 0.05). The friction rises to values common for other plastics after the sliding speed passes a critical value, and this high friction tends to persist when returning to low speeds.

It is likely that this is a thermal effect, the incidence of which is promoted by the extremely low thermal conductivity of PTFE, and it can be combated to a considerable extent by using the PTFE in a copper matrix. The use of such a matrix also reduces the wear which would occur with PTFE alone. This type of structure is used as a self-lubricated bearing material.

Greases. A lubricating grease is a solid or semifluid lubricant comprising a thickening (or gelling) agent in a liquid lubricant. Other ingredients imparting special properties may be included. An important property of a grease is its solid nature; it has a yield value. This enables grease to retain itself in a bearing assembly without the aid of expensive seals, to provide its own seal against the ingress of moisture and dirt, and to remain on vertical surfaces and protect against moisture corrosion, especially during shutdown periods.

The gelling agents used in most greases are fatty acid soaps of lithium, sodium, calcium, and aluminum. Potassium, barium, and lead soaps are used occasionally. The fatty acids employed are oleic, palmitic, stearic, and other carboxylic acids derived from animal, fish, and vegetable oils. The use of soaps in greases is limited by phase changes (or melting points) that occur in the range 120–390°F (50–200°C). Because many applications require operation above this temperature, greases have been introduced which are thickened by high-melting solids such as clays, silica, organic dyes, aromatic amides, and urea derivatives. In these cases, the upper limit of application is set by the volatility or by the oxidation and thermal stability of the base oil. To extend the operating range to extremes of high and low temperatures, synthetic oils may be used as the substrate. Silicones, esters, and fluorocarbons have all been employed for this purpose. As in the case of liquid lubricants, various additives such as oxidation inhibitors, EP agents, and antirust additives are frequently used in greases. Volatility of the base oil is

particularly important in greases, because it is constantly exposed as a thin film on the bearing surfaces.

Structure. The gelling agent in most soap-base greases is present as crystalline fibers having lengths of 1–100 micrometers and diameters $^1/_{10}$ to $^1/_{100}$ of their lengths. The fibers thicken the oil by forming a network or brush-heap structure in which the oil is held by capillary forces. For a given concentration of soap, the larger the length-to-diameter ratio of the fibers, the greater is the probability of network junction formation and the harder is the grease. However, not all soaps form such crystalline fibers; aluminum soap is a notable exception. There is evidence that aluminum soap molecules form a network akin to that formed by polymer molecules.

Nonsoap thickeners are present as small isometric particles much smaller than 1 μm in linear size. Silica particles are round, and some clay particles are plates. Forces of interaction between silica, clay particles, and oil are easily destroyed by water, so it is necessary to waterproof the primary particles by special treatments. Electron micrographs of various types of greases are shown in **Fig. 5**.

Mechanical properties. When the applied stress exceeds the yield stress, the grease flows and the viscosity falls rapidly with further increase of stress until it reaches a value only a little higher than that of the base oil. This fall in viscosity is largely reversible, since it is caused by the rupture of network junctions which, following the release of stress, can reform. However, continued vigorous shearing usually results in the rupture of fibers and permanent softening of the grease. Here, certain greases such as those derived from lithium salts of hydroxy acids are superior to other types, although the manner of grease preparation exercises considerable influence.

In a major grease application, for example, ball and roller bearings, shearing between the races and rolling elements is extremely severe. The reason that a good bearing grease does not soften and run out lies in the fact that only a very small fraction of the grease put in the bearing is actually subjected to shearing. As soon as a freshly packed bearing is set in motion, most of the grease is redistributed to places where it can remain static in the cover plate recesses and attached to the bore of the cage between the balls or rollers. The small amount of grease remaining on the working surfaces of the bearing is quickly broken down to a soft oily material which lubricates these parts, and because it has only a low viscosity, it develops very little friction. *See* ANTIFRICTION BEARING.

A number of methods exist for the measurement of yield stress and viscosity at various temperatures. One of the oldest of grease tests, still universally used, is a consistency (hardness) test in which the depth of penetration of a cone of standard weight and dimensions is determined. However, few of the many tests used are helpful in predicting the performance of a grease. Consequently, in development work, recourse is made to actual performance data and to the use of rigs that simulate field conditions. *See* GEL; PETROLEUM PROCESSING AND REFINING.

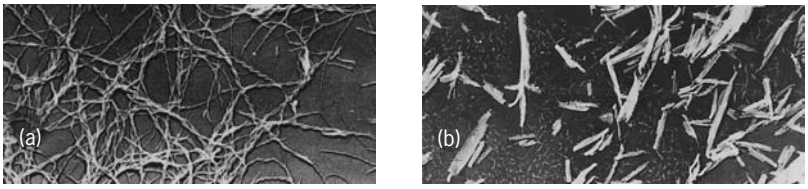

Fig. 5. Electron micrographs showing (*a*) soap-thickened grease and (*b*) dye-thickened grease.

Robert G. Larsen

Bibliography. J. Bruce, *Synthetic Functional Fluids and Lubricants*, 1994; Business Trend Analysts, *Lubricating Oils and Greases*, 1992.

Lubrication

The use of lubricants to reduce friction and wear. Whenever two bodies in contact are made to slide relative to one another, a resistance to the motion is experienced. This resistance, called friction, is present in all machinery. Approximately 30% of the power of an automobile engine is consumed by friction. Friction and wear can be significantly reduced, and thus relative motion of machine parts made possible, by interposing a lubricant at the interface of the contacting surfaces; the machine elements designed to accomplish this are called bearings. Bearings can be lubricated by solids such as graphite or, more commonly, by liquids and gases. *See* ANTIFRICTION BEARING; FRICTION; GRAPHITE; LUBRICANT; SURFACE AND INTERFACIAL CHEMISTRY; WEAR.

Conventionally, lubrication has been divided into (1) fluid-film lubrication (hydrostatic, hydrodynamic, and elastohydrodynamic), where the sliding surfaces are separated by a relatively thick, continuous film of lubricant; and (2) boundary lubrication, where contact surface separation is but a few molecular layers and asperity contact is unavoidable. Under conditions of boundary lubrication, solid lubricants are often used as films, or in particulate form as dispersions in oils, greases, and gases, to provide relatively stress-free surface conditions. Solid lubricants are also employed in very high temperature or very low pressure environments. The solid lubricants most commonly employed in particulate form are graphite and molybdenum disulfide (MoS_2), but polytetrafluoroethylene (Teflon) and lead compounds are also used. Another method of application of solid film lubricants is through bonded films; these are solid lubricants, such as molybdenum disulfide, graphite, Teflon, and tungsten disulfide, (WS_2), attached to the metal surface by means of a binder material such as a resin, a silicate, or a ceramic.

Lubricant films. When the lubricant film in a bearing is discontinuous, partial or boundary lubrication results. In this case, the coefficient of friction $f = F/N$, where F represents tangential (frictional) and N normal components of the contact force, depends on the characteristics of both the lubricant and the

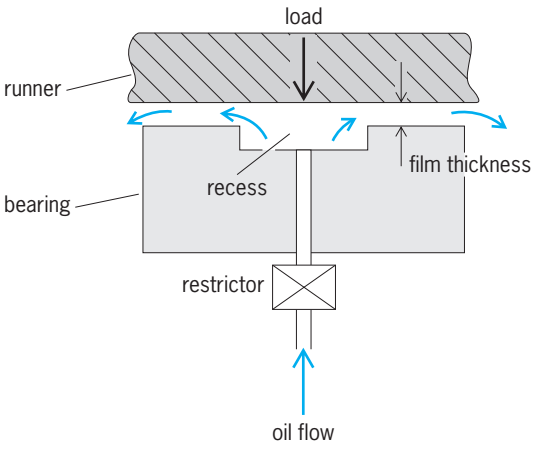

Fig. 1. Hydrostatic bearing pad.

contacting surfaces. The coefficient of friction can be analyzed by the methods of surface chemistry and physics. When the lubricant film is continuous, such as in the case of fluid film lubrication, frictional characteristics are defined solely by the material properties of the lubricant but not of the bounding surfaces. Continuous lubricant films can be generated in either of two modes, termed hydrostatic (externally pressurized) and hydrodynamic (self-acting).

Hydrostatic bearings. Hydrostatic films are created when a high-pressure lubricant is injected between opposing (parallel) surfaces (pad and runner), thereby separating them and preventing their coming into direct contact. Hydrostatic bearings require external pressurization. The film is 5–50 micrometers thick, depending on application. Though hydrostatic lubrication does not rely on relative motion of the surfaces, relative motion is permitted and can even be discontinuous. **Figure 1** is a schematic of a hydrostatic bearing pad. To handle asymmetric loads, hydrostatic systems generally employ several evenly spaced pads. The pads are usually supplied from a common reservoir and are equipped with flow restrictors. Flow restrictors are flow control devices, such as orifices and capillaries, across which minute changes in flow rate cause large changes in pressure drop. Thus, if variation in the load vector causes even a small variation in film thickness over a particular pad, a large change in the recess pressure of that pad will result, yielding a righting moment on the runner. Hydrostatic bearings find application where relative positioning is of extreme importance; machine tools using this type of bearing can grind parts round within 5 μm, with a 2.5-μm surface finish.

Hydrostatic bearings are also applied where a low coefficient of friction ($\sim 10^{-6}$ to 10^{-4}) at vanishing relative velocity is required. The 200-in. (5-m) optical telescope at Mount Palomar, which weighs 500 tons (454 metric tons), is supported on hydrostatic pads and kept synchronized with the aid of a $^1/_4$-hp (190-W) clock motor. Hydrostatic lifts are often built into the hydrodynamic bearings of a large rotating apparatus to facilitate starting and stopping, when a continuous hydrodynamic film is absent. The advantages of hydrostatic bearings are low friction, exact relative positioning of the bearing surfaces, and insensitivity to magnitude and continuity of relative motion. Among their disadvantages is the need for auxiliary equipment, the high risk of failure in the absence of a back-up system, and the high capital cost. Because of these disadvantages, hydrostatic bearings are used less frequently than are hydrodynamic bearings.

Hydrodynamic bearings. Hydrodynamic bearings are self-acting. To create and maintain a load-carrying hydrodynamic film, it is necessary only that the bearing surfaces move relative to one another and ample lubricant is available. The surfaces must be inclined to form a clearance space in the shape of a wedge, which converges in the direction of relative motion. The lubricant film is then created as the lubricant is dragged into the clearance by the relative motion. This viscous action results in a pressure build-up within the film (**Fig. 2**). The fact that hydrodynamic bearings are self-generating and do not rely on auxiliary equipment makes these bearings very reliable. Hydrodynamic lubrication can be found to operate even when highly undesirable; on the rain-covered pavement, an automobile tire rides on a hydrodynamic film, thereby reducing friction between road and tire by orders of magnitude compared to dry conditions.

Hydrodynamic journal bearings (**Fig. 3**) and thrust bearings (**Fig. 4**) are designed to support radial and axial loads, respectively, on a rotating shaft. The film thickness (h) in these bearings is in the $\sim$10–200-μm range, and the coefficient of friction $\sim 10^{-2}$ to 10^{-3}. Because of their relatively large contact area, the pressures generated in hydrodynamic bearings are low, in the range of 1–10 megapascals (10–100 atm). They operate with the bearing surfaces remaining rigid, although at higher speeds and loads both thermal and elastic deformations can be considerable. Hydrodynamic bearings are usually lubricated with liquids (such as mineral oil), but for light loads and high speeds, as in sophisticated navigational equipment, gas lubrication is preferred.

Intense development of gas lubrication technology was spurred, beginning in the 1950s, by the demands of sophisticated navigation systems, by the operation of gas-cooled nuclear energy sources, and by the quest for exotic machinery in aerospace applications. The magnetic recording industry has

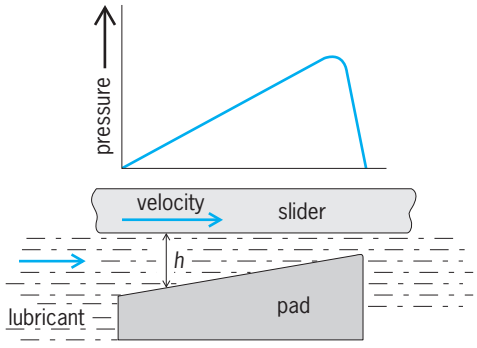

Fig. 2. Hydrodynamic film formation.

further emphasized the importance of this technology; the pursuit of ever-increasing densities of information storage has led to the design of disk drives with slider bearings, or "sliders," that carry the read/write head, allowing it to skim over disk surfaces at minuscule distances, a fraction of the mean free path (the average distance traveled by gas molecules between collisions, about 60 nm for air). *See* COMPUTER STORAGE TECHNOLOGY; MAGNETIC RECORDING.

Shaped bearings. Journal and thrust bearings are conformal bearings; that is the opposing bearing surfaces conform in shape. Ball and roller bearings, also known as rolling contact bearings, are counterformal. Counterformal bearings always operate in the hydrodynamic mode, but because the contact area in these bearings is small the pressure attains high values, in the range of 1–3 gigapascals (10,000–30,000 atm). In consequence, the surfaces deform elastically and the lubricant viscosity increases by several orders of magnitude—the variation of lubricant viscosity, μ, with pressure, P, approximately follows the law $\mu = \mu_0 \exp(\alpha p)$, where μ_0 represents viscosity at atmospheric pressure and α is a material constant. Conformal bearings are said to operate in the elastohydrodynamic (EHD) mode. The schematic of a ball bearing is shown in the **Figure 5**. Rolling contact bearings can be designed to support either radial or axial loads or any combination thereof. The greatest disadvantage of rolling contact bearings is that they posses little or no damping, necessary to dissipate the vibrational energy when approaching system resonance. The friction coefficient of rolling contact bearings is about the same as journal bearings, but the film thickness is two orders or magnitude smaller; compared to this film thickness, the roughness of the bearing surfaces can no longer be neglected, unless the surfaces are made particularly smooth. *See* VIBRATION.

Lubricants. Lubricants that are liquids at normal temperatures played a minor role until the industrial revolution; before then greases and pastes of animal and vegetable origin were the principal lubricants. Today, mineral oils manufactured from petroleum are the most common liquid lubricants. The manufacturer of petroleum lubricants can choose from a wide variety of crude oils, and the choice is of great importance because the lubricating oil fraction of crude oils varies widely. Petroleum oils are excellent lubricants because they wet metal surfaces, are available in a wide range of viscosities, and have viscosity that increases with pressure faster than that of almost all other fluids (of great importance in rolling contact bearings). The next important property of petroleum oils is their ability to resist oxidation. For most applications of petroleum oil lubricants, however, certain materials must be added to provide a new and desirable property that was not originally present, to enhance a desirable property already possessed in some degree, or to overcome some natural dificiency. Additives are used to reduce thermal and oxidative degradation, lessen the accumulation of harmful deposits, change the viscosity characteristics, minimize rust and corrosion, control frictional behavior, reduce wear, prevent bacterial growth, prevent destructive metal to metal contact, and control foaming. *See* PETROLEUM; VISCOSITY.

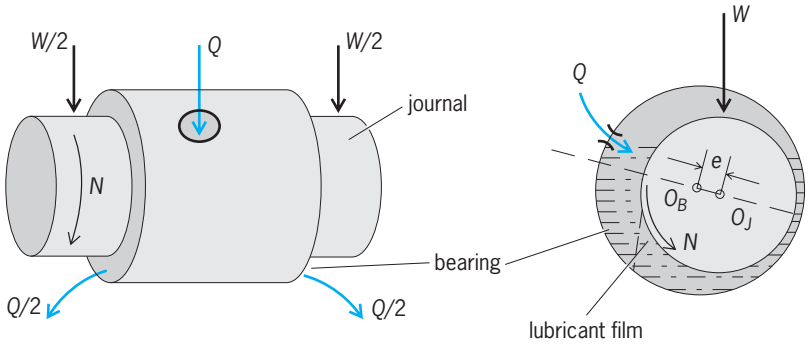

Key:

Q = oil flow	N = shaft rotation	O_B = center of bearing
W = load	e = bearing eccentricity	O_J = center of journal

Fig. 3. Journal bearing.

Bearing materials. The selection of the bearing material for a particular application depends on the type of bearing, the type of lubricant, and environmental conditions. For hydrodynamic bearings, babbitts are among the most widely used materials. They are either tin- or lead-base alloys, having excellent embeddability (the ability to embed dirt or other foreign material so that damage to the shaft is minimized) and conformability (to misalignment)

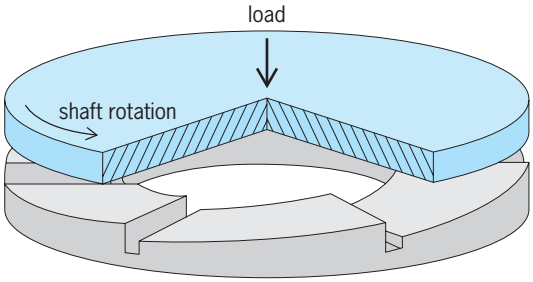

Fig. 4. Thrust bearing.

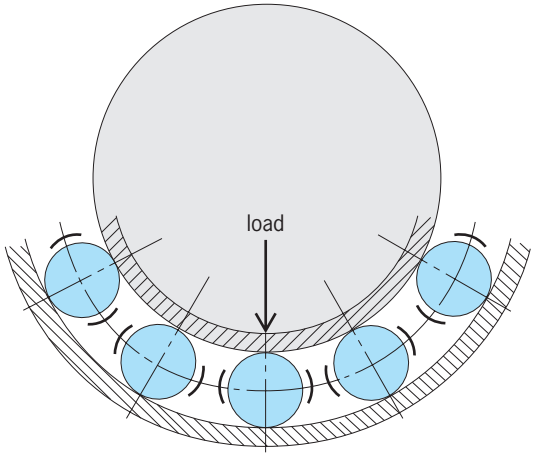

Fig. 5. Ball bearing.

characteristics. Babbitts, however, have relatively low load-carrying capacity. To increase their load capability, these alloys are metallurgically bonded to stronger backing materials such as steel, cast iron, and bronze. Rolling contact bearings operate under conditions that impose high compressive stress for millions of stress cycles as the balls or rollers rotate through the loaded zone of the bearing. For such applications, the materials of the races and balls should be hard and have high fatigue resistance. The most common material used is hardened chrome steel. In high-temperature applications, high-speed tool steels with better hardness retention are used. In any high-temperature application, it is normally the thermal stability of lubricants, rather than the bearing materials, that limits the maximum operating temperature. *See* ALLOY; BRONZE; IRON; LEAD; METALLURGY; STEEL; TIN.

Andras Z. Szeri

Bibliography. K. E. Bannister, *Lubrication for Industry*, Industrial Press, 1996; B. Bhuushan (ed.), *Modern Tribology Handbook*, CRC Press, 2000; B. Bhushan, *Principles and Applications of Tribology*, Wiley, 1999; B. J. Hamrock, *Fundamentals of Fluid Film Lubrication*, McGraw-Hill, 1993; K. C. Ludema, *Friction, Wear, Lubrication: A Textbook in Tribology*, CRC Press, 1996; M. J. Neale (ed.), *The Tribology Handbook*, 2d ed., Butterworth-Heinemann, 1995; B. N. J. Persson, *Sliding Friction: Physical Principles and Applications (Nanoscience and Technology)*, 2d ed., Springer-Verlag, 2000: A. Z. Szeri, *Fluid Film Lubrication: Theory & Design*, Cambridge University Press, 1998.

Lumber

Timber sawed or split into planks, boards, and similar products. Lumber can come in many forms, species, and types from a wide variety of commercial sources. Because most lumber is manufactured similarly and graded by standardized rules, it is fairly uniform throughout the United States. This article describes the manufacturing, processing, and grading of commercial lumber and the effects of moisture content. *See* WOOD PRODUCTS.

Manufacturing and processing. Lumber is manufactured from round logs primarily in rectangular shapes of different dimensions. Lumber length is recorded in actual dimensions. Width and thickness are traditionally recorded in nominal dimensions, which are somewhat more than actual dimensions. Softwood lumber is manufactured in length multiples of 305 mm (1 ft) as specified in various grading rules. In practice, 610-mm (2-ft) multiples are most common. Lumber width commonly varies from 38 to 387 mm (nominal 2 to 16 in.). Lumber is classified by thickness into three categories: (1) board, lumber less than 38 mm (nominally 2 in.) thick; (2) dimension, lumber from 38 mm to, but not including, 114 mm (nominally 5 in.) thick; and (3) timber, lumber 114 mm (nominally 5 in.) or more in thickness in the least dimension. *See* LOGGING.

Lumber can be produced with either a rough or surfaced (dressed) finish. Rough-sawn lumber has surface imperfections caused by the primary sawing operations. Surfaced lumber is smoothed on either one or both sides and one or both edges.

Grades. In general, the grade of a piece of lumber is based on the number, character, and location of features that may lower the strength, durability, or utility value of the wood. Lumber grading can be divided into two main categories: remanufacture "shop grade" and structural "stress grade."

Shop grade. Sorting of lumber for remanufacture is based on visual inspection. The wood is designated shop grade on the proportion of defect-free or clear cuttings of a certain size that can be made from a piece of lumber. The larger volume and more frequent number of clear cuttings, the higher the grade. The rules adopted by the National Hardwood Lumber Association are considered standard in grading hardwood lumber intended for cutting into smaller pieces to make furniture or other fabricated products. Some shop grades commonly used for this material are Select, No. 1 Common, and No. 2A Common.

Stress grade. Pieces of lumber graded for structural uses are put into classes with similar mechanical properties called stress grades. Stress grades are characterized by (1) one or more sorting criteria, (2) a set of allowable properties for engineering design, and (3) a unique grade name. The allowable properties depend on the particular sorting criteria and additional factors that are independent of sorting criteria. Allowable properties are usually much lower than the properties of clear, straight-grained wood. The allowable properties are inferred through visual grading criteria or are determined nondestructively by machine-grading criteria.

Visually graded. Visual grading is the oldest stress-grading method. It is based on the premise that mechanical properties of lumber differ from mechanical properties of clear wood. Growth characteristics, which affect properties and can be seen and judged by eye, are used to sort the lumber into stress grades. Typical visual sorting criteria include density, decay, proportion of heartwood and sapwood, slope of grain, knots, shake, checks and splits, wane, and pitch pockets. Some grades commonly used for this material are Select Structural, No. 1, No. 2, and Construction. Two species with the same grade look alike but may have different individual properties.

Machine graded. Machine-graded lumber is evaluated by a machine using a nondestructive test followed by visual grading to evaluate certain characteristics that the machine cannot or may not properly evaluate. Machine-stress-rated (MSR), machine-evaluated (MEL), and E-rated lumber are three types of machine-graded lumber. Machine-graded lumber allows for better sorting of material for specific applications in engineered structures. The basic components of a machine-grading system are as follows: (1) sorting and prediction of strength through machine-measured nondestructive testing coupled with visual assessment of growth characteristics; (2) assignment of design properties based on

strength prediction; and (3) quality control to ensure that assigned properties are being obtained. The MSR and MEL systems differ in grade names, quality control, and coefficient of variation (COV) for modulus of elasticity (E) values. Grade names for MSR lumber are a combination of the design bending stress and average modulus of elasticity (such as 1650F 1.5E), whereas grade names for MEL lumber start with an M designation (such as M-14). Machine grading is species-independent because grading is based on properties.

Moisture content. Clear, straight-grained lumber can be about 50% stronger when dry than when wet. For lumber containing knots, the increase in strength with decreasing moisture content is dependent on lumber quality. As the frequency and size of knots increase, the reduction in strength resulting from the knots begins to negate the increase in strength in the clear wood portion of the lumber. Very low quality lumber, which has many large knots, may be insensitive to changes in moisture content. Some strength values may decrease with decreasing moisture content (less than about 8%), and care should be exercised in these situations. For timber, often no adjustment for moisture content is made because properties are assigned on the basis of wood in the green condition. Timber is usually put into service without drying, and it is assumed that drying degrade offsets the increase in strength normally associated with loss in moisture. *See* WOOD PRODUCTS; WOOD PROPERTIES.

David E. Kretschmann

Bibliography. *Rules for the Measurement and Inspection of Hardwood and Cypress*, National Hardwood Lumber Association, Memphis, TN, 1990; *Wood Handbook: Wood as an Engineering Material*, Gen. Tech. Rep. FPL-GTR-113, U.S. Department of Agriculture, Forest Service, Forest Products Laboratory, Madison, WI, 1999.

Luminance

The luminous intensity of any surface in a given direction per unit of projected area of the surface viewed from that direction. The International Commission on Illumination defines it as the quotient of the luminous intensity in the given direction of an infinitesimal element of the surface containing the point under consideration, by the orthogonally projected area of the element on a plane perpendicular to the given direction. Simply, it is the luminous intensity per unit area. Luminance is also called photometric brightness.

Since the candela is the unit of luminous intensity, the luminance, or photometric brightness, of a surface may be expressed in candelas/cm^2, candelas/in.^{2}, and so forth.

Mathematically, luminance L may be found from the equation below, where θ is the angle between

$$L = \frac{dI}{dA \cos\theta}$$

the line of sight and the normal to the surface area A considered, and I is the luminous intensity.

The stilb is a unit of luminance (photometric brightness) equal to 1 candela/cm^2. It is often used in Europe, but the practice in America is to use the term candela/cm^2 in its place.

The apostilb is another unit of luminance sometimes used in Europe. It is equal to the luminance of a perfectly diffusing surface emitting or diffusing light at the rate of 1 lumen/m^2. *See* LUMINOUS INTENSITY; PHOTOMETRY.

Russell C. Putnam

Luminescence

Light emission that cannot be attributed merely to the temperature of the emitting body. Various types of luminescence are often distinguished according to the source of the energy which excites the emission. When the light energy emitted results from a chemical reaction, such as in the slow oxidation of phosphorus at ordinary temperatures, the emission is called chemiluminescence. When the luminescent chemical reaction occurs in a living system, such as in the glow of the firefly, the emission is called bioluminescence. In the foregoing two examples part of the energy of a chemical reaction is converted into light. There are also types of luminescence that are initiated by the flow of some form of energy into the body from the outside. According to the source of the exciting energy, these luminescences are designated as cathodoluminescence if the energy comes from electron bombardment; radioluminescence or roentgenoluminescence if the energy comes from x-rays or from gamma rays; photoluminescence if the energy comes from ultraviolet, visible, or infrared radiation; and electroluminescence if the energy comes from the application of an electric field. By attaching a suitable prefix to the word luminescence, similar designations may be coined to characterize luminescence excited by other agents. Since a given substance can frequently be made to luminesce by a number of different external exciting agents, and since the atomic and electronic phenomena that cause luminescence are basically the same regardless of the mode of excitation, the classification of luminescence phenomena into the foregoing categories is essentially only a matter of convenience, not of fundamental distinction.

When a luminescent system provided with a special configuration is excited, or "pumped," with sufficient intensity of excitation to cause an excess of excited atoms over unexcited atoms (a so-called population inversion), it can produce laser action. (Laser is an acronym for light amplification by stimulated emission of radiation.) This laser emission is a coherent stimulated luminescence, in contrast to the incoherent spontaneous emission from most luminescent systems as they are ordinarily excited and used. *See* LASER; OPTICAL PUMPING.

Fluorescence and phosphorescence. A second basis frequently used for characterizing luminescence is its persistence after the source of exciting energy is removed. Many substances continue to luminesce

for extended periods after the exciting energy is shut off. The delayed light emission (afterglow) is generally called phosphorescence; the light emitted during the period of excitation is generally called fluorescence. In an exact sense, this classification, based on persistence of the afterglow, is not meaningful because it depends on the properties of the detector used to observe the luminescence. With appropriate instruments one can detect afterglows lasting on the order of a few thousandths of a microsecond, which would be imperceptible to the human eye. The characterization of such a luminescence, based on its persistence, as either fluorescence or phosphorescence would therefore depend upon whether the observation was made by eye or by instrumental means. These terms are nevertheless commonly used in the approximate sense defined here, and are convenient for many practical purposes. However, they can be given a more precise meaning. For example, fluorescence may be defined as a luminescence emission having an afterglow duration which is temperature-independent, while phosphorescence may be defined as a luminescence with an afterglow duration which becomes shorter with increasing temperature. *See* BIOLUMINESCENCE; CATHODOLUMINESCENCE; CHEMILUMINESCENCE; ELECTROLUMINESCENCE; FLUORESCENCE; PHOSPHORESCENCE; PHOTOLUMINESCENCE; THERMOLUMINESCENCE.

Type of radiation emitted. Because of their many practical applications, materials that give a visible luminescence have been studied and developed more intensively than those which emit in other spectral regions. Luminescence, however, may consist of radiation in any region of the electromagnetic spectrum. The production of x-radiation by the bombardment of a metal target by a fast electron beam is an example of luminescence. Certain fluorescent lamps, called black-light lamps, are coated with a luminescent powder chosen for its ability to emit ultraviolet light of approximately 360 nanometers rather than visible light. A number of luminescent solids have been developed which luminesce in the near infrared under excitation by visible light, by a cathode-ray beam, or by electric fields. *See* ULTRAVIOLET LAMP.

Luminescent substances. The ability to luminesce is not confined to any particular state of matter. Luminescence is observed in gases, liquids, and amorphous and crystalline solids. The passage of an electrical discharge through a gas will excite the gaseous atoms or molecules to luminesce under certain conditions. An example of such a gaseous luminescence is the mercury-vapor lamp, in which an electrical discharge excites the mercury vapor to emit both visible and ultraviolet light. Many liquids, such as oil or solutions of certain dyestuffs in various solvents, luminesce very strongly under ultraviolet light. A large number of solids, including many natural minerals as well as thousands of synthetic inorganic and organic compounds, luminesce under various types of excitation. Applications of gas luminescence, formerly confined to advertising signs (neon signs) and fluorescent lamps, have multiplied greatly with the invention of the laser, many atomic and molecular gases providing the laser-active materials. The same is true of dye solutions and inorganic glasses. The major nonlaser applications of luminescence involve solid luminescent materials. *See* MERCURY-VAPOR LAMP.

The term phosphor, originally applied to certain solids that exhibit long afterglows, has been extended to include any luminescent solid regardless of its afterglow properties. Other terms sometimes used synonymously with phosphor are luminophor, fluor, or fluorphor. The term luminophor is preferable, since it carries no connotation that afterglow times are long or short. In conformity with current usage, however, the term phosphor is used in the succeeding discussion of solid materials.

Comparatively few pure solids luminesce efficiently, at least at normal temperatures. In the category of organic solids, the pure aromatic hydrocarbons, such as naphthalene and anthracene, which consist exclusively of condensed phenyl rings, are luminescent, as are many heterocyclic closed-ring compounds. However, the closed phenyl ring structure is not in itself a guarantee of efficient luminescence, since certain substituents for hydrogen in the structure, particularly halogens, tend to reduce luminescence efficiency. This quenching of efficiency is called internal conversion. Among the pure inorganic solids that luminesce efficiently at room temperature are the tungstates, uranyl salts, platinocyanids, and a number of salts of the rare-earth elements.

Activators and poisons. The development of a large number of inorganic phosphors is due to the discovery that certain impurities, called activators, when present in amounts ranging from a few parts per million to several percent, can confer luminescent properties on the compounds (host or matrix compounds) in which they are incorporated. The activator and its nearby atoms are often referred to as the luminescent center.

By the same token, small amounts of other impurities or imperfections, called poisons or quenchers, can inhibit or destroy the luminescence, evidently by providing alternative mechanisms for the radiationless dissipation of the energy imparted to the phosphor or by emitting radiation characteristic of the poison itself which may not be in a spectral region of interest for the purpose at hand.

Manganese is a particularly effective activator in a wide variety of matrices when incorporated in amounts ranging from a small trace up to the order of several percent. The emission spectrum of these manganese-activated phosphors generally lies in the green, yellow, or orange spectral regions. Other frequently used activators are copper, silver, thallium, lead, cerium, chromium, titanium, antimony, tin, and the rare-earth elements. Poisons in inorganic phosphors generally are from the iron-nickel-cobalt group. The most important host materials are silicates, phosphates, aluminates, sulfides, selenides, the alkali halides, and oxides of calcium, magnesium, barium, and zinc. Preparation of phosphors

and the incorporation of the activators is generally done by high-temperature reaction of well-mixed, finely ground powders of the components. A number of semiconducting compounds such as gallium phosphide (GaP) and gallium arsenide (GaAs) can be made to luminesce and display laser action when prepared so that charges can be injected into the semiconductor. *See* JUNCTION DIODE; SEMICONDUCTOR; SEMICONDUCTOR DIODE.

In order for ultraviolet light to provoke luminescence in a substance, the substance must be able to absorb it. Because of variations in its ability to absorb ultraviolet light of different wavelengths, a material may be nonluminescent under ultraviolet light of one wavelength and strongly luminescent under a different wavelength in the ultraviolet region. For a similar reason a substance may not luminesce under ultraviolet light at all and yet be strongly luminescent under x-ray irradiation.

Luminescence in Atomic Gases

The processes that occur in luminescence may be most simply illustrated in the case of an atom in a gas. The atom can exist only in certain specific states of energy, some of which are shown schematically in **Fig. 1**. The lowest energy level of the atom, E_1, corresponds to the atom in its unexcited, or ground, state, and the higher energy levels, E_2 and E_3, represent electronically excited states of the atom. The excitation of the atom from state E_1 to state E_2 requires the absorption of an amount of energy $\Delta E = E_2 - E_1$. If this excitation is to be produced by the absorption of light, the energy of the acting light photon, E_{absorbed}, must equal ΔE. The frequency of the exciting light must therefore be $\nu = E_{\text{absorbed}}/h = (E_2 - E_1)/h$, and the wavelength of the exciting light must be $\lambda_{\text{absorbed}} = hc/(E_2 - E_1)$, where h is Planck's constant and c is the velocity of light. In an isolated atom this extra energy cannot be dissipated and is emitted as radiation when the atom eventually returns to its ground state. The emitted light will therefore again correspond in energy to ΔE and it will have a wavelength $\lambda_{\text{emitted}} = \lambda_{\text{absorbed}}$. When $\lambda_{\text{emitted}} = \lambda_{\text{absorbed}}$, the emitted light is sometimes referred to as resonance luminescence or resonance radiation. *See* ATOMIC STRUCTURE AND SPECTRA.

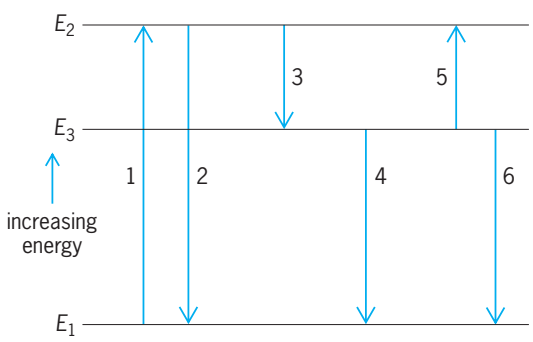

Fig. 1. Schematic representation of energy levels and electronic transitions in an atomic gas. E_1, ground state; E_2 and E_3, excited states; 1, excitation; 2, emission of resonance luminescence; 3, radiationless transition to lower excited state; 4, luminescence emission, if transition $E_3 \rightarrow E_1$ is allowed (if it is not allowed, 4 does not occur and E_3 is called a metastable state); 5, stimulation of atom back to emitting state; 6, radiationless transition of atom back to ground state (quenching).

If a large number of atoms are excited and the excitation then removed, the luminescence intensity will decrease with time exponentially according to the equation $I_t = I_0 e^{-t/\tau_l}$, where I_t is the intensity of luminescence at a time t after removal of the excitation, I_0 is the intensity at $t = 0$, and τ_l is the average time required by an atom to make a spontaneous luminescent transition. The quantity τ_l, called the radiative lifetime, is independent of temperature, and it is this temperature independence that is emphasized in the more precise definition of fluorescence given earlier. If the transition between the energy levels E_1 and E_2 is highly probable (a so-called permitted or allowed transition), τ_l is very small, of the order of 10^{-8} s for transitions involving visible light.

The excited atom can also lose a certain amount of energy and fall to an energy state E_3, of intermediate energy between E_1 and E_2. This can happen, for example, if the excited atom collides with another atom. If the transition from state E_3 to the ground state E_1 can occur with a reasonably high probability, fluorescence will occur starting from this intermediate excited state. In this case the fluorescent wavelength $\lambda_{\text{emitted}} = hc/(E_3 - E_1)$. Since $(E_3 - E_1)$ is smaller than $(E_2 - E_1)$, the fluorescence in this case will be of longer wavelength than the resonance radiation. Although the quantum efficiency of luminescence is unity (one photon of emitted light per photon of absorbed light), the energy efficiency is less than unity.

If, however, a transition between state E_3 and state E_1 is highly improbable (a so-called forbidden transition), state E_3 is known as a metastable state. The atom can remain in this state for long periods of time and cannot return to the ground state with the emission of radiation. Luminescence can occur under these circumstances only if the atom regains the energy $(E_2 - E_3)$ by a collision with another atom or by some other process. Once the atom has been brought back to state E_2, a transition to the ground state is again allowed, and luminescence corresponding to $(E_2 - E_1)$ will be emitted. The existence of metastable states like E_3 explains the delayed emission termed phosphorescence. The atom may spend a considerable amount of time in such a state before some external influence causes it to return to an emitting state such as E_2, in which case the luminescence is correspondingly delayed and appears as an afterglow. In order for the atom to get from E_3 to E_2 it must absorb energy somehow. The rate of return to the emitting state, and hence the duration of the afterglow, will therefore depend to a very large extent on temperature. At high temperatures the atoms will be excited back to the emitting state rapidly, and there will be a bright afterglow of short duration. At lower temperatures the atoms will be raised back to the emitting state very slowly, and the afterglow will be of long duration but of low intensity. This temperature dependence is the basis for the more precise definition of phosphorescence that was given earlier.

As an alternative to regaining the energy ($E_2 - E_3$), the atom may lose the energy ($E_3 - E_1$) by a competing radiationless process, for example, by collision with another atom. The energy of excitation is thus dissipated without luminescence, and the quantum yield of luminescence is zero (quenching).

The principles illustrated in the foregoing discussion may be extended with little modification to the case where the primary absorption or excitation act completely removes an electron from an atom (that is, ionizes the atom) instead of merely raising the atom to an excited state. Under these conditions the electron can be trapped temporarily by other atoms, and its return to the parent atom can also be delayed by this mechanism.

The same principles are also operative in the case of complex configurations of atoms, such as in organic molecules or solids. However, the forbiddenness of radiative transitions can be modified in these cases, and efficient luminescent emissions can consequently be observed due to radiative transitions from metastable states, albeit with longer afterglows.

When nonlinear optics conditions exist, luminescence can be excited in certain systems by multiphoton absorption, the resulting luminescence being of higher frequency than the exciting light because the energy of two or more photons of the latter are combined to give one photon of emitted light. There are also cases where a single photon is absorbed by a pair of activator atoms or ions, each of which then emits a luminescence photon, leading to a quantum efficiency of 2. However, the preceding discussion and the exposition of those principles which follow deal primarily with the more usual case of single-photon absorption and emission. *See* NONLINEAR OPTICS.

Configuration Coordinate Curve Model

Luminescence in atomic gases is adequately described by the concepts of atomic spectroscopy, but luminescence in molecular gases, in liquids, and in solids introduces two major new effects which need special explanation. One is that the emission band appears on the long wavelength (low-energy) side of the absorption band; the other is that emission and absorption often show as bands tens of nanometers wide instead of as the lines found in atomic gases.

Both of these effects may be explained by using the concept of configuration coordinate curves illustrated in **Fig. 2**. As in the case of atomic gases, the ground and excited states represent different electronic states of the luminescent center, that is, the region containing the atoms, or electrons, or both, involved in the luminescent transition. On these curves the energy of the ground and excited state is shown to vary parabolically as some configuration coordinate, usually the distance from the activator to its nearest neighbors, is changed. There is a value of the coordinate for which the energy is a minimum, but this value is different for the ground and excited states because of the different interactions of the activator with its neighbors. Absorption of light gives rise to the transition from A to B. This transition occurs so rapidly that the ions in the luminescent center do not have time to rearrange. Once the system is at B it gives up heat energy to its surroundings by means of lattice vibrations and reaches the new equilibrium position at C. Emission occurs when the system makes the transition from C to D, and once again heat energy is given up when the system goes from D back down to A. This loss of energy in the form of heat causes the energy associated with the emission $C \rightarrow D$ to be less than that associated with the absorption $A \rightarrow B$. *See* FRANCK-CONDON PRINCIPLE; LATTICE VIBRATIONS.

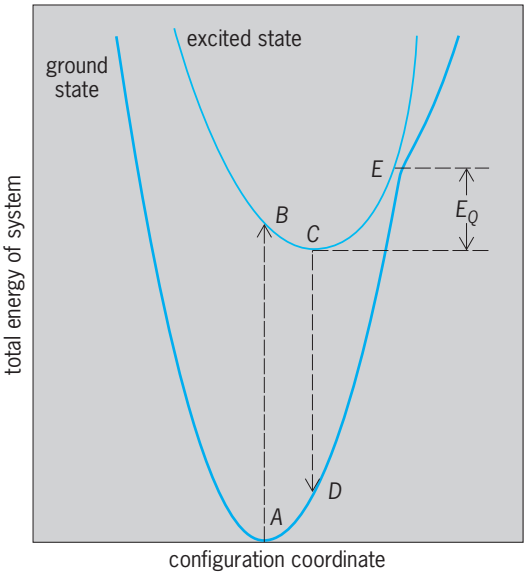

Fig. 2. Configuration coordinate curves for a simple luminescence center. Transition $A \rightarrow B$ shows absorption, and transition $C \rightarrow D$ shows emission. Energy E_Q is that necessary for the excited state to reach point E, from which a transition to the ground state can be made without luminescence.

When the system is at an equilibrium position, such as C of the excited-state curve, it is not at rest but migrates over a small region around C because of the thermal energy of the system. At higher temperatures these fluctuations cover a wider range of the configuration coordinate. As a result, the emission transition is not just to point D on the ground state curve but covers a region around D. In the vicinity of D the ground state curve shows a rapid change of energy, so that even a small range of values for the configuration coordinate leads to a large range of energies in the optical transition. This explains the broad emission and absorption bands that are observed. An analysis of this sort predicts that the widths of the band (usually measured in energy units between the points at which the emission or absorption is half its maximum value) should vary as the square root of the temperature. For many systems this relationship is valid for temperatures near and above room temperature. At low temperatures, quantum-mechanical effects, described below, become dominant.

Two other phenomena which can be explained on the basis of the model described in Fig. 2 are temperature quenching of luminescence and the variation of the decay time of luminescence

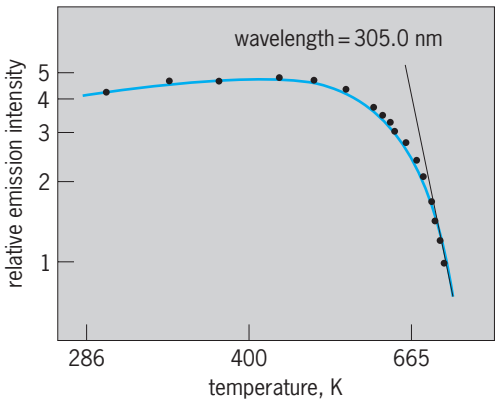

Fig. 3. Variation of the brightness of a thallium-activated potassium chloride phosphor with temperature. °F = (K × 1.8) − 459.67.

with temperature. In **Fig. 3** a curve of temperature quenching for the emission in thallium-activated potassium chloride is shown. At low temperatures there is very little change in brightness with temperature, but at elevated temperatures the luminescence efficiency decreases rapidly (so-called thermal quenching). On the scheme of Fig. 2 this is interpreted as meaning that the thermal vibrations become sufficiently intense to raise the system to point E. From point E the system can fall to the ground state by emitting a small amount of heat, or infrared radiation. If point E is at an energy E_Q above the minimum of the excited state curve, it may be shown that the quantum efficiency, η, of luminescence is given by Eq. (1), where C is a constant, k is Boltzmann's con-

$$\eta = 1 + C \exp\left(-\frac{E_Q}{kT}\right)^{-1} \tag{1}$$

stant, and T is the temperature on the Kelvin scale. By fitting an expression of this form to the data of Fig. 3, a value of 0.60 eV is obtained for E_Q.

Another result of the onset of thermal quenching is that the luminescence decays faster, since the excited state is now depopulated by two processes simultaneously—a dissipative process in parallel with the luminescent process.

Quantum-mechanical corrections. Although the configuration coordinate curve model of Fig. 2 is successful in describing many aspects of luminescence in solids, it predicts that emission and absorption bands should become narrow lines as the temperature is reduced to absolute zero (0 K). This is not the case, as is shown in **Fig. 4**, which gives the width of the absorption band of the *F*-center in potassium chloride as a function of the square root of the temperature. (An *F*-center is the simplest type of color center, a color center being a lattice defect which can absorb light.) At high temperatures the previously quoted results are valid, but at low temperatures the width of the band is constant. *See* COLOR CENTERS.

This phenomenon may be explained by treating the configuration coordinate curves quantum mechanically. The curves have the energy versus displacement characteristics of the simple harmonic oscillator. For this case the quantum-mechanical analysis shows that there is a series of equally spaced energy levels separated by an energy of $h\nu$, where h is Planck's constant and ν is the frequency of vibration. The lowest of these levels occurs at a value of $^1/_2\ h\nu$ above the minimum of the classical curve, and this energy is called the zero point energy. Its importance is that even at absolute zero the system is not at rest but varies over a range of configuration coordinates characteristic of this lowest vibrational level. Analysis shows that under these conditions the widths of the bands, ΔE, vary as in Eq. (2), where A is

$$\Delta E = A\left[\coth\left(\frac{h\nu}{2kT}\right)\right]^{1/2} \tag{2}$$

a constant. A curve of this form is drawn through the experimentally obtained points of Fig. 4 and shows satisfactory agreement.

One other result of the introduction of quantum mechanics is that this simple model predicts that both absorption and emission bands should be gaussian in shape at all temperatures; that is, they should be of the form of Eq. (3), where I is the emission

$$I = I_0\ \exp\left[-A(E - E_0)^2\right] \tag{3}$$

intensity or absorption strength for light of energy E, and I_0 and E_0 refer to corresponding quantities at the maximum of the curve. **Figure 5** shows the emission spectrum of thallium-activated potassium chloride plotted in such a way that the expression of Eq. (3) would give two straight lines making equal angles with the horizontal. Although there is some disagreement in the wings of the emission spectrum, and although the lines are not quite at the same angle, there still is fairly good agreement with the predictions of Eq. (3).

High dielectric constant materials. The use of configuration coordinate curves is justifiable only when the electron taking part in an optical transition is tightly bound to a luminescent center and interacts primarily with its nearest neighbors. This

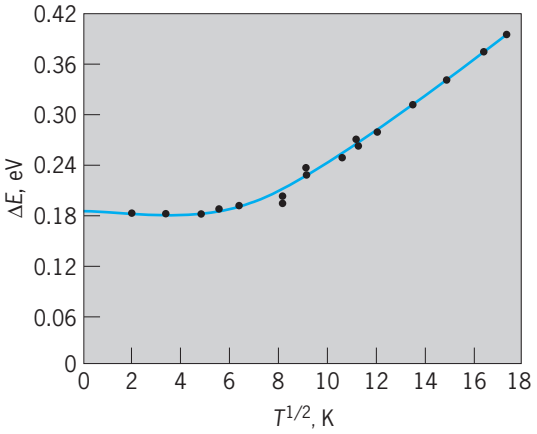

Fig. 4. Variation of the width of the *F*-center absorption band in potassium chloride at its half-maximum points, *FE*, as a function of the square root of the temperature. °F = (K × 1.8) − 459.67.

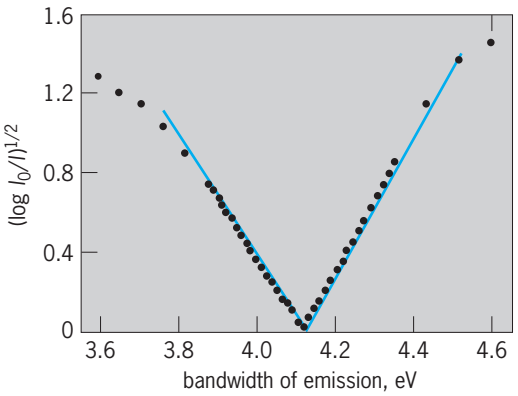

Fig. 5. Emission of thallium-activated potassium chloride at 4 K (−452°F). In a plot of this particular form, a gaussian curve would consist of two straight lines which make equal angles with the abscissa.

appears to be generally the case in materials with low dielectric constants such as the alkali halides. For high dielectric constant materials the situation is very different. It has been estimated that for boron in silicon the electron is spread over about 500 atoms so that its interaction with the nearest neighbors is small. In these cases the center interacts with the lattice during an optical transition through the creation of many vibrational phonons (sound quanta) at relatively large distances from the center. A case of this sort is illustrated in **Fig. 6**, which shows edge emission in cadmium sulfide near the absorption edge of the material. The major peaks correspond to an optical transition with simultaneous emission of 0, 1, 2, and 3 phonons, respectively, starting with the highest peak. The peaks are equidistant in energy, and the spacing is just that to be expected for the creation of phonons. Although both short- and long-range interactions of a center with its environment occur in all cases, the short-range interaction dominates for tightly bound electrons in low dielectric constant materials, while the long-range interaction dominates for loosely bound electrons in high dielectric constant materials. *See* DIELECTRIC MATERIALS; PHONON.

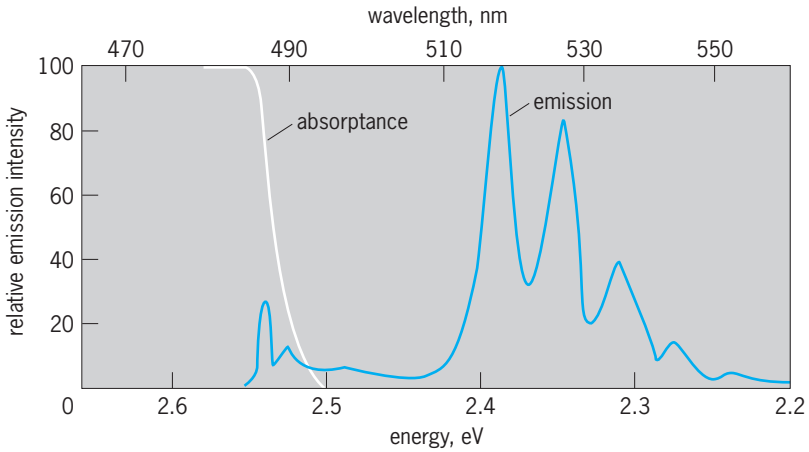

Fig. 6. Graph showing the absorptance (100 minus percent of transmission) and edge emission of cadmium sulfide at 4 K (−452°F).

Sensitized Luminescence

A process of considerable interest occurs in systems where one type of activator absorbs the exciting light and transfers its energy to a second type of activator which then emits. The transfer does not involve motion of electrons. This process is often called sensitized luminescence, and it is widespread in both inorganic and organic luminescent systems. The principal phosphors used in fluorescent lamps are of this type. The results on calcium carbonate ($CaCO_3$) shown in **Fig. 7** illustrate this kind of

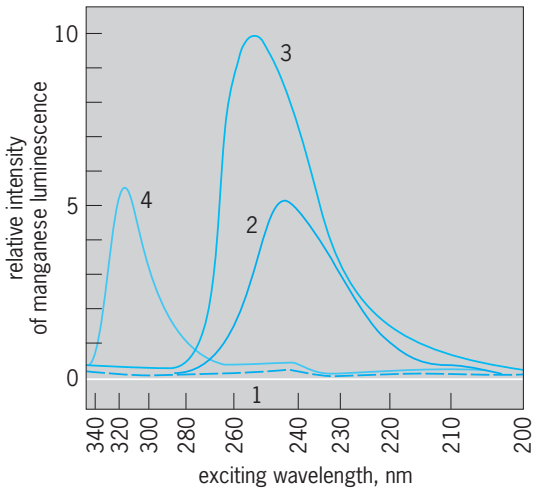

Fig. 7. Excitation spectra for emission of calcium carbonate phosphors, using manganese as an activator, with different impurity sensitizers: 1, no sensitizer; 2, thallium; 3, lead; and 4, cerium.

system. If divalent manganese (Mn^{2+}) alone is incorporated as an activator into $CaCO_3$, the system gives only a very weak Mn^{2+} emission for all wavelengths of exciting ultraviolet light. This is because the Mn^{2+} ion has only forbidden transitions in this spectral region, as shown by its very low absorption strength and slow decay of luminescence. In other words, the Mn^{2+} does not absorb very much ultraviolet light. Bright phosphors may be prepared by incorporating divalent lead (Pb^{2+}), monovalent thallium (Tl^{+}), or trivalent cerium (Ce^{3+}) along with Mn^{2+} in $CaCO_3$. In each case the Mn^{2+} emission is the same, but the wavelengths which excite these phosphors vary as the other activator (called the sensitizer) is changed. All these absorptions occur for energies well below the energy at which free electrons are formed in the solid. The ultraviolet light is absorbed by the Pb^{2+}, Tl^{+}, or Ce^{3+} sensitizers, which have allowed transitions leading to strong absorption of the light; this absorbed energy is then passed on to nearby Mn^{2+} activators and excite the Mn^{2+} emission. It is important to know over what distances the energy may be transferred from absorber to emitter. Experiments on calcium silicate with Pb^{2+} and Mn^{2+} as added impurities have shown that if a Mn^{2+} ion is in any one of the 28 nearest lattice sites around the Pb^{2+} ion, the energy transfer may take place.

Resonant transfer. The transfer of energy has been treated theoretically using quantum mechanics and

assuming a model of resonance between coupled systems. A number of cases have been examined; in each case the sensitizer has an allowed transition since only in this case will it absorb the exciting light appreciably.

The first case is one in which the activator undergoes an allowed transition. The probability of energy transfer, P (defined as the reciprocal of the time required for a transition to occur), varies as in expression (4). Here R is the distance between sensitizer

$$P \propto \frac{1}{R^6 n^4} \int f_s F_A dE \qquad (4)$$

and activator; n is the index of refraction of the host material, which may be liquid or solid; f_s is a function describing the emission band of the sensitizer as a function of energy, and is normalized so that the area under the curve is unity; and F_A is a function describing the absorption band of the activator, also normalized to unity. The integral of expression (4) measures the overlap of these bands and determines the resonance transfer. In typical cases the sensitizer will transfer energy to an activator if the activator occupies any one of the 1000–10,000 nearest available sites around the sensitizer. Another case is that of a forbidden quadrupole transition in the activator; in this case the number of sites for transfer would be about 100. If the transition in the activator is even more strongly forbidden, quantum-mechanical "exchange" effects predominate and the number of available sites for transfer should be reduced to 40 or less. In both of the cases just mentioned the integral measuring the overlap enters in the same way as it does in expression (4). From this theoretical treatment it appears that phosphors with Mn^{2+} as the activator probably receive their energy by exchange interactions.

Concentration quenching. Another phenomenon related to the resonant transfer of energy is that of concentration quenching. If phosphors are prepared with increasing concentrations of activators, the brightness will first increase but eventually will be quenched at high concentrations. It is believed that at high concentrations the absorbed energy is able to move from one activator to a nearby one by resonant transfer and thus migrate through the solid or liquid. If there are "poisons," or quenching sites, distributed in the material, the migrating energy may reach one of these, be transferred to it, and dissipate without luminescence. Impurity atoms, vacancies, jogs at dislocations, normal lattice ions near dislocations, and even a small fraction of the activator ions themselves, when associated in pairs or higher aggregates, can act as poisons. As the concentration is increased, the speed of migration is increased, and the quenching process becomes increasingly important.

Luminescence Involving Electron Motion

In an important group of luminescent materials the transfer of energy to the luminescent center is brought about by the motion of electrons. Many

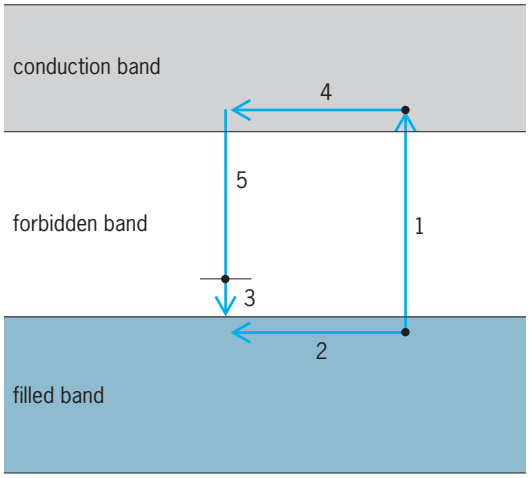

Fig. 8. Energy-band model for luminescence processes in zinc sulfide. Electron energy increases vertically.

oxides, sulfides, selenides, tellurides, arsenides, and phosphides are of this type, and of these, zinc sulfide has been most widely studied. It is frequently used as the luminescent material in cathode-ray tubes and electroluminescent lamps.

Electronic processes in insulating materials are described by a band model such as that illustrated in **Fig. 8**. The electron energy increases vertically and the horizontal dimension shows position in a crystal. In the shaded areas, called the filled band, or the valence band, all the energy levels are filled with electrons. No electron can be accelerated or moved to higher energies within this band since the higher levels are already filled. Thus the material is an insulator. Above the valence band is an energy region called the forbidden band, which has no energy levels in it for pure materials. However, imperfections may introduce a local energy level in this region, as illustrated by the short line above 3 in Fig. 8. Above the forbidden band is an energy region called the conduction band. Here there are energy levels but, in an insulator, no electrons. If an electron in the filled band absorbs light of sufficiently high energy, it may jump up into the conduction band, as shown in 1 of Fig. 8. The empty position left behind in the filled band, called a hole, has properties which allow it to be described as an electron except that it has a positive charge. Both the electron in the conduction band and the hole in the filled band are free to move and gain energy. As a result, current can flow when a voltage is applied externally. The electron and hole can also diffuse far from their origin and can thus transport energy to a distant luminescent center. *See* HOLE STATES IN SOLIDS.

A simple luminescent transition is illustrated in Fig. 8. Assume that the impurity level (black dot in the forbidden band) is due to a luminescent center and that there is an electron in the level at the beginning of the process. Transition (1) shows the creation of a free electron and hole due to the absorption of light. The hole migrates to the center (2), and the electron in the impurity level falls into the hole (3),

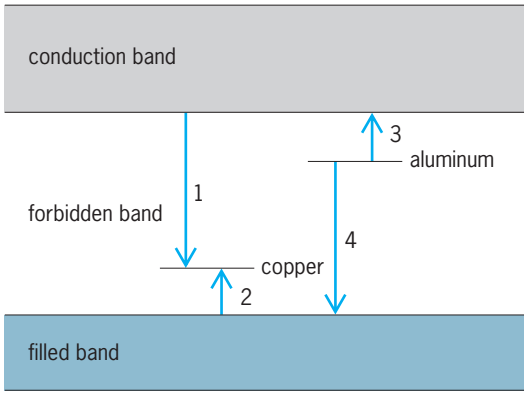

Fig. 9. Energy-band model for luminescence processes in zinc sulfide which uses copper as the activator and aluminum as the coactivator.

thus destroying it. The free electron now migrates toward the center (4) and falls into it (5), giving off luminescence. The cycle is complete and the center once again has an electron. It is important to note that in this process both electrons and holes must be assumed to move.

In zinc sulfide the normal activators are monovalent metals such as Ag^+ or Cu^+. They replace Zn^{2+} ions. To maintain electrical neutrality it is necessary also to incorporate into the lattice ions such as Cl^- for S^{2-} or Al^{3+} for Zn^{2+}. These additional ions are called coactivators. The situation is now quite complex, and is illustrated for ZnS with Cu and Al as added impurities in **Fig. 9**. The various arrows in this figure show some of the electronic transitions that give rise to observable effects. Arrows 1 and 4 show two different luminescent transitions. Arrow 2 shows the excitation of an electron into the luminescent center, which may occur by absorption of infrared light or by thermal fluctuations. In either case the center is prevented from luminescing and thus is quenched. Transition 3 is the excitation of an electron into the conduction band. The electron may be excited by thermal energy and its appearance may be detected by the appearance of transition 1. This process is called thermoluminescence.

The wide variety of luminescence phenomena, the insight they give into the constitution of very different classes of materials, and their many important applications to light production, imaging devices, and radiation detectors make luminescence a perennially challenging field of study.

Clifford C. Klick; James H. Schulman

Bibliography. H. J. Cantow et al. (eds.), *Luminescence*, 1981; J. D. Dunitz et al. (eds.), *Luminescence and Energy Transfer*, 1981; A. H. Kitai (ed.), *Solid State Luminescence: Theory, Materials, and Devices*, 1993; R. P. Rao (ed.), *Luminiscence: Phenomena, Materials and Devices*, 1991; D. Rendell, *Fluorescence and Phosphorescence Spectroscopy*, 1987; R. C. Ropp, *Luminescence and the Solid State*, 1991; S. G. Schulman (ed.), *Molecular Luminescence Spectroscopy*, 3 vols., 1985, 1988, 1993.

Luminescence analysis

Methods of chemical analysis in which analyte concentration is related to luminescence intensity or some other property of luminescence. Photoluminescence, particularly fluorescence, is the most widely used type of luminescence for chemical analysis. However, there are also important analytical applications of both chemiluminescence and bioluminescence.

Principles. Luminescence is light that accompanies the transition from an electronically excited atom or molecule to a lower energy state. The forms of luminescence are distinguished by the method used to produce the electronically excited species. When produced by absorption of incident radiation, the light emission is known as photoluminescence. Photoluminescence that is short-lived (10^{-8} s or less between excitation and emission) is known as fluorescence. Photoluminescence that is longer-lived (from 10^{-6} s all the way up to seconds) is known as phosphorescence. The reason for the difference in lifetime is that fluorescence involves an allowed, high-probability transition while phosphorescence involves a forbidden, low-probability transition. *See* FLUORESCENCE; LUMINESCENCE; PHOSPHORESCENCE; PHOTOLUMINESCENCE; SELECTION RULES (PHYSICS).

Chemiluminescence is observed when the electronically excited atom or molecule is formed as the product of a chemical reaction. If the light-producing reaction occurs in nature, such as the light emitted by fireflies, it is known as bioluminescence. *See* BIOLUMINESCENCE; CHEMILUMINESCENCE.

Spectra. Photoluminescence excitation spectra are determined by measuring emission intensity at a fixed wavelength while varying the wavelength of the incident light used to produce the electronically excited species responsible for emission. The excitation spectrum is a measure of the efficiency of electronic excitation as a function of excitation wavelength. Photoluminescence emission spectra are determined by exciting at a fixed wavelength and varying the wavelength at which emission is observed. **Figure 1** shows typical excitation and fluorescence and phosphorescence emission spectra for a molecule in solution. Between excitation and emission, electronically excited molecules normally lose some of their energy because of relaxation processes. As a consequence, the emission spectrum is at longer wavelengths, that is, at lower energy, than the excitation spectrum. Because the magnitude of the energy loss due to relaxation processes is greater for phosphorescence than for fluorescence, phosphorescence occurs at longer wavelengths than fluorescence. The spectra extend over a range of wavelengths, because in solution, molecules exist in a continuous distribution of vibrational and rotational energy levels. *See* ENERGY LEVEL (QUANTUM MECHANICS).

Chemiluminescence and bioluminescence spectra are equivalent to photoluminescence emission spectra for the electronically excited reaction products. The difference between these forms of luminescence

lies only in the method of production of the excited state.

Methods based on chemiluminescence and bioluminescence are restricted in scope because relatively few reactions produce light.

Intensities. Observed luminescence intensities depend on three factors: (1) the number of electronically excited molecules or atoms produced by the excitation process; (2) the fraction of electronically excited molecules that emit light as they relax to a lower energy state; and (3) the fraction of the emitted luminescence that impinges on the detector and is measured. In the case of photoluminescence, the number of excited molecules is proportional to incident excitation intensity, the concentration of the luminescent species, and the efficiency with which the luminescence species absorbs the incident radiation. In the case of chemiluminescence and bioluminescence, the number of excited molecules depends on reactant concentrations and the efficiency with which the reaction pathway leads to production of the excited state. The dependence of intensity on concentration is the basis for chemical analysis based on luminescence.

The fraction of excited species emitting light depends on the rate of the emission process relative to the rates of competing nonemissive processes and is expressed as the quantum yield of fluorescence or phosphorescence.

The fraction of the emitted light that is observed by the detector is a function of the optics of the instrumentation.

Instrumentation. Measurements of photoluminescence require a source of radiation to excite the sample and a detection system to measure the intensity of the resulting emission (**Fig. 2**). The most common radiation source is a xenon-arc lamp, which emits strongly throughout the ultraviolet and visible regions of the electromagnetic spectrum. Lasers provide high performance for specialized applications, but are not widely used for routine work because they are expensive to purchase and maintain and they emit at a limited number of wavelengths. Mercury-arc lamps provide high intensity at mercury emission lines and are relatively inexpensive. A filter or monochromator is used to transmit the excitation radiation of the desired wavelength selectively and to reject all other wavelengths. The light is focused on the sample. *See* SPECTROSCOPY.

As shown in Fig. 2, the detection system is usually placed at right angles to the incident light beam. This arrangement is employed to minimize the amount of excitation radiation that enters the detection system. A second filter or monochromator is used in the detection system to reject scattered excitation radiation selectively and transmit the desired photoluminescence that is at a longer wavelength. A photomultiplier tube detects and amplifies the luminescence signal. *See* PHOTOMULTIPLIER.

Instrumentation designed for phosphorescence measurements also includes provisions for exciting the sample sequentially and then measuring photoluminescence intensity after the source radiation is no longer incident on the sample. This arrangement discriminates temporally against scattered excitation radiation, making it easier to measure small luminescence signals. The same approach can also be applied to fluorescence measurements; but because fluorescence is so short-lived, the required instrumentation is too complex and expensive to be practical for most analytical applications.

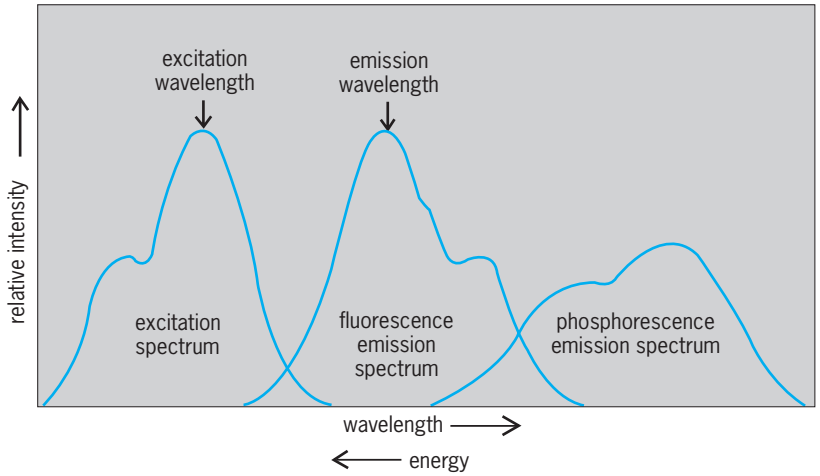

Fig. 1. Typical photoluminescence excitation and emission spectra for molecules in solution.

Chemiluminescence and bioluminescence measurements do not require excitation radiation or a means of resolving the emission of interest from scattered excitation radiation. Instead they require a system for initiating the reaction that gives rise to light production. Most frequently, this is accomplished by placing one component of the reaction in a sample container positioned in front of a photomultiplier tube that measures light intensity. The reaction is initiated by injecting a known volume of solution containing the other components required for light production.

Analytical variables. To maximize the observed intensity, most analytical photoluminescence

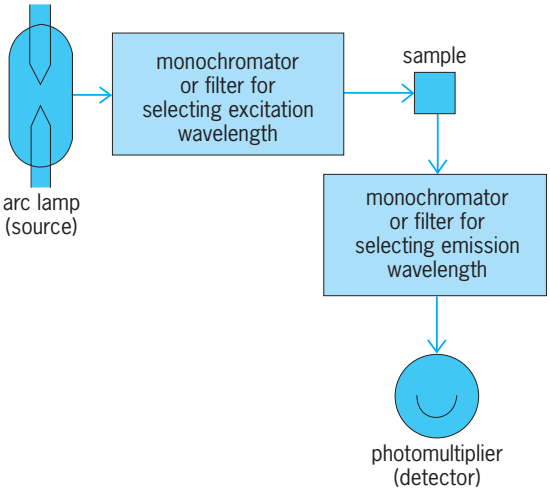

Fig. 2. Components of instrumentation for luminescence measurements.

measurements are made by exciting at the maximum point in the excitation spectrum and observing emission at the maximum point in the emission spectrum. These points are indicated in Fig. 1. However, if the sample contains multiple photoluminescent species, wavelengths may be chosen on the basis of selectivity. The goal is to maximize the signal for the photoluminescent species of interest relative to the signals for other interfering species.

Samples that are colored attenuate the excitation radiation as it passes through, thereby affecting the observed intensity. Therefore, they are avoided where possible for analytical photoluminescence measurements. This is most easily accomplished by diluting the sample with solvent until there is no longer any observable color. Dilution with solvent also reduces the likelihood that interaction between the luminescent species and other components of the sample will lead to quenching of fluorescence.

Colloidal samples scatter excitation radiation, and can be used for analytical photoluminescence measurements only with instrumentation that includes an emission monochromator of sufficiently high quality to resolve a relatively weak luminescence signal from a much stronger signal due to scattered excitation. *See* COLLOID.

Because solutions are clear and homogeneous, they are the preferred media for most analytical photoluminescence measurements. However, they are also subject to some drawbacks. The motion of molecules in liquids causes them to collide with each other, which can lead to quenching. This is rarely a serious problem for fluorescence, because it occurs on such a rapid time scale. However, phosphorescence is rarely observed from solution, because quenching processes occur more rapidly than light emission. Dissolved oxygen, in particular, is extremely effective at quenching phosphorescence. As a consequence, it is usually necessary to work with deoxygenated solid-phase samples to observe phosphorescence. The sample can be prepared by freezing a solution of analyte or by spotting analyte solution on an appropriate solid substrate and allowing the solvent to evaporate. Because of the inconvenience of working with solid-phase samples, phosphorescence is much less widely used for analysis than fluorescence.

Luminescent molecules in a solid phase can exist only in a limited number of unique environments rather than in a continuum of environments as is the case in solution. This leads to excitation and emission spectra that consist of a series of narrow lines rather than the broad bands illustrated in Fig. 1. By using solid-phase measurements to get narrow-line spectra, it is possible to identify individual components of mixtures of complex molecules that fluoresce (fluorophors), for example, polynuclear aromatic hydrocarbons in fossil fuels.

Chemiluminescence and bioluminescence measurements are usually made in solution or the gas phase. After the reaction is initiated, intensity decreases with time as reactants are consumed. The measured parameter can be the initial intensity or the intensity integrated over a specified time interval after the reaction has been initiated. An alternative approach is to mix the reactants required for light emission continuously in a flow system and to measure steady-state light output. In all cases, reactant concentrations need to be chosen so that the observed intensities depend on the concentration of analyte.

Applications. By far the most important advantage of luminescence methods of chemical analysis is their ability to measure extremely low concentrations. Analyte levels in the range of 0.001 to 10 micrograms per liter are readily measured by luminescence techniques. This advantage arises because luminescence is measured relative to weak background signals. In contrast, methods based on the absorption of light require that a small difference between two large signals be measured. Detection limits for luminescence methods are established by the magnitude of the luminescence relative to the background signal, which can arise from several sources including fluorescence from impurities in the solvent, Raman scattered light, detector dark current, and stray excitation light that is not eliminated by the emission filter or monochromator. *See* RAMAN EFFECT.

Compounds that are intrinsically luminescent may be determined directly. Polynuclear aromatic hydrocarbons are an important example. While most intrinsically luminescent compounds are aromatic organic substances, some inorganic compounds also luminesce. Uranium salts are an important example.

Luminescence methods may be extended to nonluminescent analytes by using reagents that react with the analyte to form a luminescent derivative. There is a vast number of such reactions. Some are specific for a particular analyte. Others are generic for a particular type of compound, such as amines or aldehydes. The generic reactions are often applied in combination with chemical separations. An important example is the analysis of amino acids by ion-exchange chromatography coupled to fluorescence derivatization and detection. *See* ION EXCHANGE.

Luminescence methods are particularly important in the life sciences. For example, sensitive measurements of enzyme activities may be made by using substrates that are converted to fluorescent products by the action of the enzyme. Immunological assays, which are based on the highly specific interaction between an antibody and an antigen, are frequently coupled to fluorescence measurements by chemical bonding of a high-efficiency fluorophor to either the antibody or the antigen. *See* ENZYME; IMMUNOASSAY.

W. Rudolf Seitz

Bibliography. M. A. DeLuca and W. D. McElroy (eds.), *Bioluminescence and Chemiluminescence, Basic Chemistry and Analytical Applications*, 1981; P. J. Elving (ed.), *Treatise on Analytical Chemistry*, 2d ed., pt. 1, vol. 7, 1981; G. G. Guilbault, *Practical Fluorescence: Theory, Methods and Techniques*, 1973; D. M. Hercules, *Fluorescence and Phosphorescence Analysis*, 1966; J. R. Lackowicz, *Principles of Fluorescence Spectroscopy*, 2d ed., 1999; C. S. Parker, *Photoluminescence of Solutions*, 1968; S. G. Schulman (ed.), *Molecular Luminescence Spectroscopy, Methods and Applications*, pt. 2, 1988.

Luminous efficacy

There are three ways this term can be used: (1) The luminous efficacy of a source of light is the quotient of the total luminous flux emitted divided by the total lamp power input. Light is visually evaluated radiant energy. Luminous flux is the time rate of flow of light. Luminous efficacy is expressed in lumens per watt. (2) The luminous efficacy of radiant power is the quotient of the total luminous flux emitted divided by the total radiant power emitted. This is always somewhat larger for a particular lamp than the previous measure, since not all the input power is transformed into radiant power. (3) The spectral luminous efficacy of radiant power is the quotient of the luminous flux at a given wavelength of light divided by the radiant power at that wavelength. A plot of this quotient versus wavelength displays the spectral response of the human visual system. It is, of course, zero for all wavelengths outside the range from 380 to 760 nanometers. It rises to a maximum near the center of this range. Both the value and the wavelength of this maximum depend on the degree of dark adaptation present. However, an accepted value of 683 lumens per watt maximum at 555 nm represents a standard observer in a light-adapted condition. The reciprocal of this maximum spectral luminous efficacy of radiant power is sometimes referred to as the mechanical equivalent of light, with a probable value of 0.00147 W/lm.

If the spectral luminous efficacy values at all wavelengths are each divided by the value at the maximum (683 lm/W), the spectral luminous efficiency of radiant power is obtained. It is dimensionless.

For purposes of illuminating engineering, light is radiant energy which is evaluated in terms of what is now simply and descriptively the spectral luminous efficiency curve, V_λ. In this case it is the intent that an illuminating engineer have a measure for the capacity or capability for the production of luminous flux from radiant flux, or that radiant flux has efficacy for the production of luminous flux.

Since the human eye is sensitive only to radiations of wavelengths between about 400 and 700 nm, it follows that the sensation of sight evoked by a radiator is due only to the radiation within this limited wavelength band. If all the wavelengths within this band were equally effective for the purpose of vision, then the area under the graph of radiant power distribution would be a measure of the light output.

The **illustration** shows the spectral distribution curve for an electric tungsten filament lamp. The total area under the curve between the wavelength limits $\lambda = 0$ and $\lambda = \infty$ is proportional to the power of the total radiation. In illus. *a* the shaded area between the limits of $\lambda = 400$ and $\lambda = 700$ nm is a measure of the power of visible radiation. However, this is not the same thing as luminous efficacy because of the variable sensitivity of the eye with respect to wavelength. If each ordinate, say at 10-nm wavelength intervals, is multiplied by the appropriate value of V_λ a new distribution is obtained, as shown in the shaded area of illus. *b*. This area is a measure of the light output of the source. The ratio of the shaded area of illus. *b* to the area under the larger curve is the luminous efficacy in terms of lumens per watt, and this is the method of determination that is generally used. The name luminous efficacy expresses exactly what is meant by the effectiveness of 1 watt of radiant power in producing luminous flux. *See* ILLUMINATION; LUMINOUS EFFICIENCY; LUMINOUS FLUX; PHOTOMETRY.

G. A. Horton

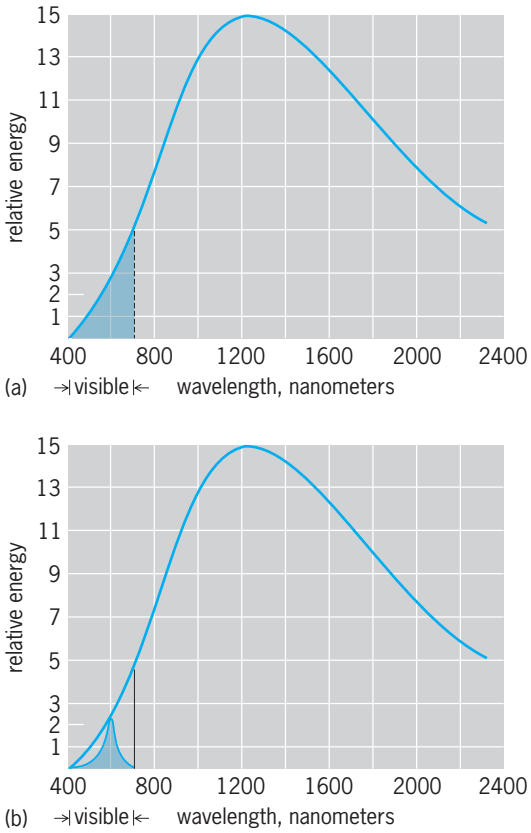

Spectral energy distribution of electric filament lamp. (*a*) Colored area is measure of power of visible radiation. (*b*) Colored area is measure of light output.

Luminous efficiency

Visual efficacy of visible radiation, a function of the spectral distribution of the source radiation in accordance with the "spectral luminous efficiency curve," usually for the light-adapted eye or photopic vision, or in some instances for the dark-adapted eye or scotopic vision. Account is taken of this fact in photometry, or the measurement of light. Actually, instead of indicating directly the physical radiant power of light, photometers are designed to indicate the corresponding luminous flux of the visually effective value of the radiation.

The spectral luminous efficiency of radiant flux is the ratio of luminous efficacy for a given wavelength to the value of maximum luminous efficacy. It is a dimensionless ratio. Values of spectral luminous efficiency for photopic vision V_λ at 10-nanometer-wavelength intervals were provisionally adopted by the International Commission on Illumination in

1924 and by the International Committee on Weights and Measures in 1933, as a basis for the establishment of photometric standards of types of sources differing from the primary standard in spectral distribution of radiant flux. These standard values of spectral luminous efficiency were determined by visual photometric observations with a 2° photometric field having a moderately high luminance (photometric brightness); photometric evaluations based upon them, consequently, do not agree exactly with other conditions of observations, such as in physical radiometry. Watts weighted in accordance with these standard values are often referred to as light-watts.

Values of spectral luminous efficiency for scotopic vision V'_λ at 10-nm intervals were provisionally adopted by the International Commission on Illumination in 1951. These values of spectral luminous efficiency were determined by visual observations by young, dark-adapted observers, using extra-foveal vision at near-threshold luminance.

The main difference between the terms luminous efficacy and luminous efficiency is that the latter came into use a century or so before the former. It should also be noted that in engineering, general values of efficiency never exceed 1.0, and illuminating engineers were the only ones who had values of efficiency up to 683, but this has now been changed by the usage of the term luminous efficacy. In view of the above discussion, the term luminous efficiency is evidently a misnomer. *See* ILLUMINATION; LUMINOUS EFFICACY; PHOTOMETRY.

G. A. Horton

Bibliography. Illuminating Engineering Soc., *American National Standard Nomenclature and Definitions for Illuminating Engineering*, ANSI/IES R16–1986.

Luminous energy

The radiant energy in the visible region or quantity of light. It is in the form of electromagnetic waves, and since the visible region is commonly taken as extending 380–760 nanometers in wavelength, the luminous energy is contained within that region. It is equal to the time integral of the production of the luminous flux. *See* PHOTOMETRY.

Russell C. Putnam

Luminous flux

The time rate of flow of light. It is radiant flux in the form of electromagnetic waves which affects the eye or, more strictly, the time rate of flow of radiant energy evaluated according to its capacity to produce visual sensation. The visible spectrum is ordinarily considered to extend from 380 to 760 nanometers in wavelength; luminous flux is radiant flux in that region of the electromagnetic spectrum. The unit of measure of luminous flux is the lumen. *See* PHOTOMETRY.

Russell C. Putnam

Luminous intensity

The solid angular luminous flux density in a given direction from a light source. It may be considered as the luminous flux on a small surface normal to the given direction, divided by the solid angle (in steradians) which the surface subtends at the source of light. Since the apex of a solid angle is a point, this concept applies exactly only to a point source. The size of the source, however, is often extremely small when compared with the distance from which it is observed, so in practice the luminous flux coming from such a source may be taken as coming from a point. For accuracy, the ratio of the diameter of the light source to the measuring distance should be about 1:10, although in practice ratios as large as 1:5 have been used without excessive error.

Mathematically, luminous intensity I is given by the equation below, where ω the solid angle is through

$$I = \frac{dF}{d\omega}$$

which the flux from the point source is radiated, and F is the luminous flux. The luminous intensity is often expressed as candlepower. *See* CANDLEPOWER; PHOTOMETRY.

Russell C. Putnam

Lung

Paired, air-filled respiratory sacs, usually in the anterior or anteroventral part of the trunk of most tetrapods. Many elongated tetrapods, such as snakes, possess a simple lung, and one group of salamanders have lost their lungs completely with gas exchange occurring through the skin of the back. Lungs originated, however, early in fish evolution, presumably in the placoderms, as an adaptation to obtain atmospheric oxygen required for life in stagnant, oxygen-depleted waters. Lungs are still found in a few living species of freshwater fishes (such as lungfish) in which they may fuse to form a single organ and may come to lie well dorsally in the body; in many fishes the lungs have evolved into the swim bladder, a dorsal hydrostatic organ. *See* DIPNOI; SWIM BLADDER.

Lungs develop as outgrowths of the anterior end of the digestive tract, from the pharynx or throat, and remain connected to it by the trachea or windpipe. They lie within the coelom and are covered by peritoneum. In mammals they are within special chambers of the coelom known as pleural cavities and the peritoneum is termed pleura.

Amphibian lungs are often simple sacs, with only small ridges on the internal walls. In higher forms the lungs become more and more subdivided internally, thus increasing greatly the surface areas across which the respiratory exchange takes place. However, even in many reptiles the lungs may be quite simple. Birds have especially complex lungs with a highly differentiated system of tubes leading into and through them to the air sacs which are contained in many parts of the bird's body. Mammalian lungs are simpler, but in them the internal subdivision into tiny sacs or alveoli

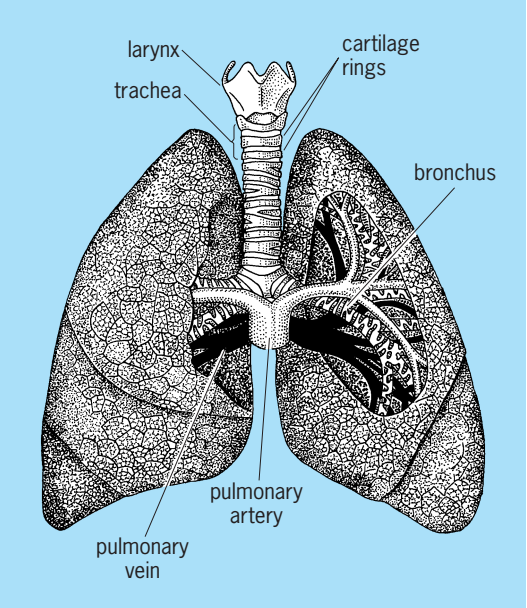

Human lungs. (*After T. I. Storer and R. L. Usinger, General Zoology, 4th ed., McGraw-Hill, 1965*)

is extreme; there may be over 350 million of them in one human lung.

In humans the two lungs lie within the chest, separated by the heart and mediastinum. The right lung has three lobes and the left lung two. A bronchus, an artery, and a vein enter each lung medially at the hilum; each branches again and again as it enters the lobules and smaller divisions of the lungs (see **illus.**). The terminal airways or bronchioles expand into small clusters of grapelike air cells, the alveoli. The alveolar walls consist of a single layer of epithelium and collectively present a huge surface. A small network of blood capillaries in the walls of the alveoli affords surfaces for the actual exchange of gases. *See* RESPIRATION; RESPIRATORY SYSTEM.

Thomas S. Parsons

Lupine

A cool-season legume with an upright stem, leaves divided into several digitate leaflets, and terminal racemes of pea-shaped blossoms. Three species, yellow, blue, and white, each named for the color of its blossoms, are cultivated as field crops; several hybrids are grown as ornamentals; and many species occur as wild plants. The yellow crop varieties are usually the earliest and smallest, the whites latest and largest. Field crop lupines have been grown in Europe since early Roman times as a soil-improving crop. The older varieties could not be used as forage since the plants contained a bitter, water-soluble, toxic alkaloid. However, since 1912, plant breeders have developed "sweet" varieties with only traces of alkaloid. *See* LEGUME.

Blue lupine was grown extensively as a winter cover crop in the southeastern United States during the 1940s. From the 1950s, however, lupine culture declined, partly because cheap nitrogen fertilizer competes with the nitrogen-fixing value of the cover crop, and also because diseases and winter killing of lupines increased.

The ornamental lupines are perennials unsuited to areas with hot summers. The many kinds of wild lupines which occur in the western part of the United States vary greatly in length of life, size, and site requirement. In the East a few small perennial wild lupines are found on deep sands. *See* BREEDING (PLANT); COVER CROPS; LEGUME FORAGES. Paul Tabor

Lutetium

A chemical element, Lu, atomic number 71, atomic weight 174.97, a very rare metal and the heaviest member of the rare-earth group. The naturally occurring element is made up of the stable isotope ^{175}Lu, 97.41%, and the long-life β-emitter ^{176}Lu with a half-life of 2.1×10^{10} years. *See* PERIODIC TABLE.

1																	18
1 H	2											13	14	15	16	17	2 He
3 Li	4 Be											5 B	6 C	7 N	8 O	9 F	10 Ne
11 Na	12 Mg	3	4	5	6	7	8	9	10	11	12	13 Al	14 Si	15 P	16 S	17 Cl	18 Ar
19 K	20 Ca	21 Sc	22 Ti	23 V	24 Cr	25 Mn	26 Fe	27 Co	28 Ni	29 Cu	30 Zn	31 Ga	32 Ge	33 As	34 Se	35 Br	36 Kr
37 Rb	38 Sr	39 Y	40 Zr	41 Nb	42 Mo	43 Tc	44 Ru	45 Rh	46 Pd	47 Ag	48 Cd	49 In	50 Sn	51 Sb	52 Te	53 I	54 Xe
55 Cs	56 Ba	71 Lu	72 Hf	73 Ta	74 W	75 Re	76 Os	77 Ir	78 Pt	79 Au	80 Hg	81 Tl	82 Pb	83 Bi	84 Po	85 At	86 Rn
87 Fr	88 Ra	103 Lr	104 Rf	105 Db	106 Sg	107 Bh	108 Hs	109 Mt	110 Ds	111 Rg	112	113					

lanthanide series	57 La	58 Ce	59 Pr	60 Nd	61 Pm	62 Sm	63 Eu	64 Gd	65 Tb	66 Dy	67 Ho	68 Er	69 Tm	70 Yb
actinide series	89 Ac	90 Th	91 Pa	92 U	93 Np	94 Pu	95 Am	96 Cm	97 Bk	98 Cf	99 Es	100 Fm	101 Md	102 No

Lutetium, along with yttrium and lanthanum, is of interest to scientists studying magnetism. All of these elements form trivalent ions with only subshells which have been completed, so they have no unpaired electrons to contribute to the magnetism. Their radii with regard to the other rare-earth ions or metals are very similar so they form at almost all compositions either solid solutions or mixed crystals with the strongly magnetic rare-earth elements. Therefore, the scientist can dilute the magnetically active rare earths in a continuous manner without changing appreciably the crystal environment. *See* MAGNETOCHEMISTRY; RARE-EARTH ELEMENTS. Frank H. Spedding

Bibliography. F. A. Cotton et al., *Advanced Inorganic Chemistry*, 6th ed., Wiley-Interscience, 1999; R. J. Elliott (ed.), *Magnetic Properties of Rare Earth Metals*, 1972.

Lychee

The plant *Litchi chinensis*, also called litchi, a member of the soapberry family (Sapindaceae). It is a native of southern China, where it has been cultivated for more than 2000 years. It is now being grown successfully in India, Republic of South Africa, Hawaii,

Burma, Madagascar, West Indies, Brazil, Honduras, Japan, Australia, and the southern United States. *See* SAPINDALES.

The fruit is a one-seeded berry. The thin, leathery, rough shell or pericarp of the ripe fruit is bright red in most varieties. Beneath the shell, completely surrounding the seed, is the edible aril or pulp. The fruit may be eaten fresh, canned, or dried. In China the fresh fruit is considered a great delicacy. *See* FRUIT.

Perry D. Strausbaugh; Earl L. Core

Lycophyta

A division (formerly Lycopodiophyta) of the subkingdom Embryobionta which represents one of two main lineages that evolved during the Early Devonian from the earliest land plants to develop vascular tissue and multiple sporangia. Integration of living and fossil taxa has allowed tentative reconstruction of the evolutionary history of the lycophyte group (**Fig. 1**), which is generally regarded as monophyletic (includes all the descendants of a single putative ancestor). The division Lycophyta contains two classes: the extinct Zosterophyllopsida (zosterophylls; **Fig. 2**) and the Lycopsida (clubmosses; **Fig. 3**), which contains 10 extant genera. *See* LYCOPSIDA; ZOSTEROPHYLLOPSIDA.

Living and fossil taxa. Living lycophytes are confined to the Lycopsida and are of far less phenotypic diversity and ecological significance than the fossils; most are small-bodied rhizomatous herbs or tuberous pseudoherbs occupying moist niches of low interspecific competition. Their economic significance is confined to various industrial applications of the abundant, small, and unusually uniformly sized spores of *Lycopodium*.

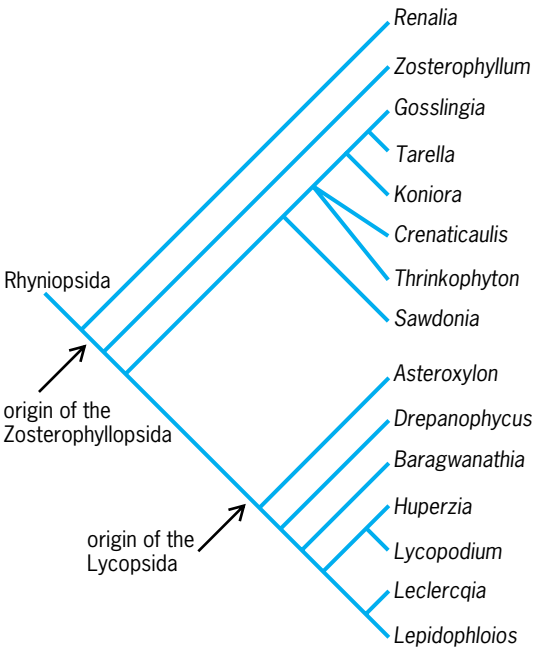

Fig. 1. Cladistic phylogeny of the Lycophyta. Only *Huperzia* and *Lycopodium* include extant species. (*After P. G. Gensel, Phylogenetic relationships of the zosterophylls and lycopsids, Ann. Mo. Bot. Gard., 79:450–473, 1992*)

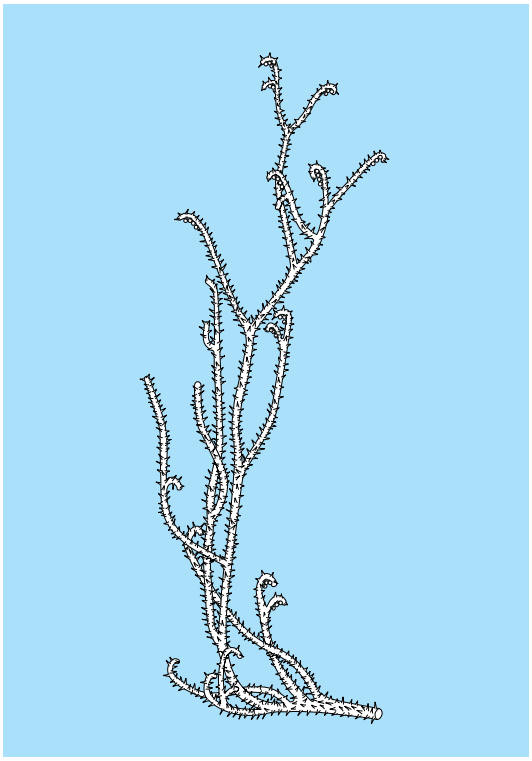

Fig. 2. Reconstruction of *Sawdonia ornata*. (*After Ananiev and Stopanov, Finds of sporogenous organs of Psilophyton princeps, Treat. Tomsk Lab. St. Univ. Geol. Ser., 202:30–46, 1968*)

The extant genera represent perhaps half of the major lycopsid groups known in the fossil record. Although living genera such as the lycopsid *Lycopodiella* (Fig. 3) and fully reconstructed fossils such as the zosterophyllopsid *Sawdonia* (Fig. 2) provide a strong phylogenetic framework, some key inferences of relationship depend on poorly known fossils, such as the putative rhyniopsid *Renalia*, which has been implicated as a potential ancestor of the Lycophyta. *See* RHYNIOPSIDA.

Characteristics. The lycophytes have a small gametophyte that is morphologically distinct from, and physically independent of, the larger sporophyte. Gametophytes are either supraterranean and photosynthetic or subterranean and saprophytic. The primitive growth habit is unipolar; rhizomes periodically generate adventitious roots and aerial branches. Vegetative branches are small, nonwoody, dichotomously branched, and either naked or, more commonly, scattered with cortical projections. The latter are termed emergences if unvascularized and microphyllous if supplied by a typically small and unbranched vascular strand. The primary xylem undergoes external maturation. Other key features of the Lycophyta are unvascularized, kidney-shaped eusporangia that are positioned laterally rather than terminating axes. The spores are released through distal lateral dehiscence slits.

Evolutionary pattern. The evolutionary history of the lycophytes generally is documented by increases

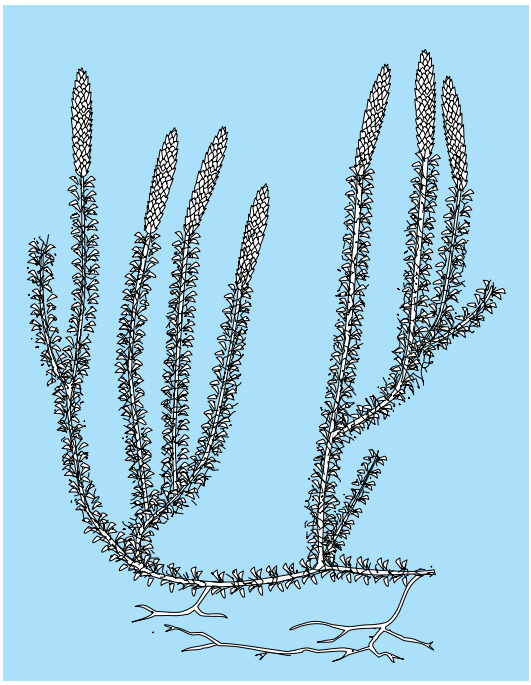

Fig. 3. ***Lycopodiella annotina*****, an extant club moss. (*After W. N. Stewart and G. W. Rothwell, Paleobotany and the Evolution of Plants, 2d ed., Cambridge University Press, 1993*)**

in body size, vegetative complexity, and reproductive sophistication. Sporangia were borne on naked axes in zosterophyllopsids, but in the lycopsids were produced on the upper surface of the sporophylls. The sporophylls increasingly diverged in morphology from the leaves and became terminally concentrated as cones.

Primitive lycophytes produced only one size of spore. However, the most advanced lycopsid orders (selaginellaleans, lepidodendraleans, and isoetaleans) are uniformly heterosporous, producing microspores that form male gametophytes and megaspores that form female gametophytes. Further evolution in the rhizomorphic lycopsids led to retention of the megaspore in the megasporangium, in a structure analogous to a true seed. The rhizomorphic groups were also characterized by a centralized rootstock (rhizomorph), bipolar growth, large medullated protosteles, and wood production. These characters allowed growth to tree-sized dimensions, producing the most sophisticated of all pteridophytes. Richard M. Bateman; William A. DiMichele

Bibliography. D. W. Bierhorst, *Morphology of Vascular Plants*, 1971; W. N. Stewart and G. W. Rothwell, *Paleobotany and the Evolution of Plants*, 2d ed., 1993.

Lycopodiales

An order of the class Lycopsida (clubmosses) that is evolutionarily positioned between two extinct orders. The Lycopodiales are more advanced than the Asteroxylales because their sporangia are unequivocally positioned on the upper surface of modified leaves, but less advanced than the Protolepidodendrales because they lack a uniquely lycopsid feature termed the ligule. All have steles with metaxylem toward the center of the axis, but otherwise show considerable variation. All are perennial nonwoody herbs. *See* ASTEROXYLALES; PROTOLEPIDODENDRALES.

The fossil record of lycopodialeans begins with *Baragwanathia*. Its earliest occurrence, in Australia, has been controversially dated as Late Silurian or Early Devonian. Unlike most other lycopsid orders, the range of variation observed among the fossils is well reflected by the extant genera. Eight genera (of approximately 350 extant species) are recognized: the widespread *Huperzia, Phlegmariurus, Lycopodium, Diphasiastrum, Pseudolycopodiella, Lycopodiella*, and *Palhinhaea*, together with the enigmatic antipodean endemic *Phylloglossum* (see **illus.**).

Phylloglossum drummondii is one of the great curiosities of modern botany. Found in shrubland habitats in Australia and New Zealand, it does not resemble other lycopodialeans because of its apparently highly reduced morphology and centralized tuberous growth. Each growing season, the short underground stem branches to generate a new fleshy tuberous storage organ that in turn produces up to 10 quill-like leaves at the soil surface. From the center of this winter-green pseudowhorl emerges a single naked cone axis up to 2 in. (5 cm) long, with an unusual stelar morphology (mesarch siphonostele), and bears at its apex a small dense cone of up to 20 sporophylls. Each sporophyll bears a single kidney-shaped sporangium on its upper surface. Like all lycopodialeans, the plant produces only one size of spore. These spores generate gametophytes that initially are subterranean, but later grow to the soil surface and become photosynthetic. The highly specialized

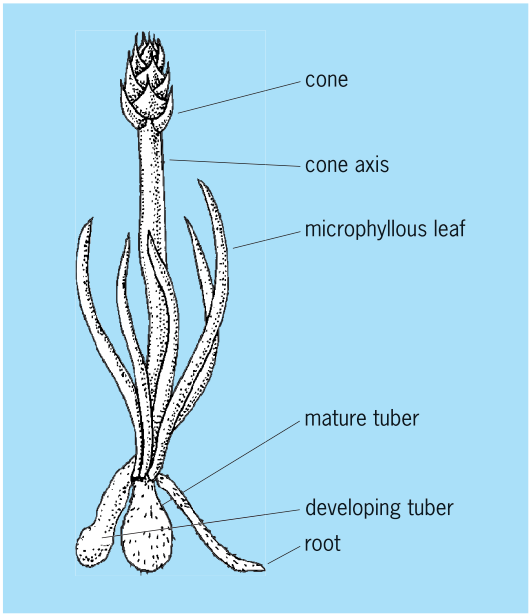

Fertile sporophyte of *Phylloglossum drummondii*. (*After A. W. Haupt, Plant Morphology, McGraw-Hill, 1953*)

morphology of *Phylloglossum* makes a comparison with other lycopsids difficult. Thus, its evolutionary position within the Lycopodiales, and even its inclusion in the Lycopodiales, remains questionable.

Phylogeny of extant genera. *Huperzia* and *Phlegmariurus* are the most primitive of the living genera. They have non-rhizomatous aerial axes with undivided, star-shaped actinosteles. Sporangia are simple in construction and positioned on sporophylls that resemble leaves; they do not form cones. In contrast, the remainder of the genera have rhizomatous growth and possess thin-walled sporangia and sporophylls that are aggregated into cones. *Lycopodium* and *Diphasiastrum* gametophytes share an annular meristem, and the stem vascular system is partially dissected into a plectostele. In *Pseudolycopodiella, Lycopodiella*, and *Palhinhaea*, the vascular system is further dissected into an annulus of apparently discrete but actually interconnected strands, and axial branching is more complex. Because gametophytes are lobed and occur on the soil surface, they are able to photosynthesize, thus reducing their dependence for nutrition on symbiotic mycorrhizal fungi. Also, the deciduous sporophytes of *Lycopodiella* and *Palhinhaea* develop from a protocorm and produce globose sporangia.

Habitats and life history. *Phlegmariurus* species grow hanging from other plants; *Pseudolycopodiella* and *Lycopodiella* are semiaquatics. The remaining genera are dominantly terrestrial. Lycopodialeans tend to prefer habitats where interspecific competition is low; few clubmoss species form a major proportion of the biomass in their preferred communities. Nonetheless, together they have a global distribution. Species-level diversity is greatest in the tropics, although a few species reach the Arctic Circle.

Lycopodialeans have a large and long-lived diploid sporophyte, which alternates with the wholly physiologically independent, smaller, and generally shorter-lived haploid gametophyte. The sporophyte produces spores that are released from the sporangium and germinate to produce gametophytes, which in most genera are subterranean and rely for nutrition on mycorrhizal fungi. The large gamete-producing sex organs are borne terminally. Antheridia produce biflagellate spermatozoids, which swim to archegonia and fuse with the egg to form a diploid zygote that develops into a juvenile sporophyte.

Fossil record. Many fossils of a wide age range have been assigned to the Lycopodiales. However, most are poorly understood vegetative fragments that often prove to belong to other orders of the Lycopsida, notably the Asteroxylales for Devonian material, Lepidodendrales for the upper Carboniferous, and Selaginellales for the Mesozoic. Identification as lycopodialean rests primarily on demonstrating the absence of wood, ligules, and megaspores—features of the more evolutionarily derived orders Protolepidodendrales, Selaginellales, Lepidodendrales, and Isoetales. The generic radiation within the Lycopodiales may have occurred in the Late Jurassic and Cretaceous periods, contemporaneously with the major radiations of the polypodiaceous ferns and angiosperms. *See* LYCOPHYTA; LYCOPSIDA. Richard M. Bateman; William A. DiMichele

Bibliography. B. A. Thomas, Paleozoic herbaceous lycopsids and the beginnings of extant *Lycopodium* and *Selaginella, Ann. Mo. Bot. Gard.*, 79:623–631, 1992; W. H. Wagner, Jr., and J. M. Beitel, Generic classification of modern North American Lycopodiaceae, *Ann. Mo. Bot. Gard.*, 79:676–686, 1992; D. P. Whittier and J. E. Braggins, The young gametophyte of *Phylloglossum* (Lycopodiaceae), *Ann. Mo. Bot. Gard.*, 79:730–736, 1992.

Lycopsida

A class (formerly Lycopodiopsida) of the division Lycophyta. It probably evolved in the Early Devonian from a zosterophyllopsid ancester; all six constituent taxonomic orders had probably evolved by the end of the Devonian. *See* ZOSTEROPHYLLOPSIDA.

Since this early and rapid radiation, lycopsids have always been globally distributed, with peak diversity in the tropics. In terms of both species diversity and biomass, lycophytes dominated many Devonian and Carboniferous plant communities, including the classic coal-swamp forests. Living lycopsids are of far less phenotypic diversity and ecological significance than the fossils; most are small-bodied rhizomatous perennial herbs (see **illus.**) or tuberous pseudoherbs

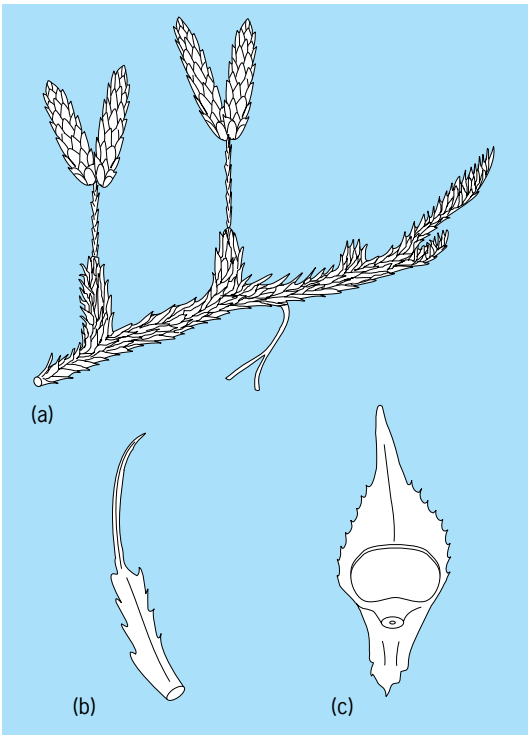

***Lycopodium clavatum*, a representative homosporous lycopsid. (*a*) Sporophyte showing typical rhizomatous growth and paired cones. (*b*) Microphyllous leaf. (*c*) Sporophyll bearing a sporangium on the upper surface. (*From K. R. Sporne, The Morphology of Pteridophytes, 2d ed., Hutchinson, 1975*)**

occupying moist niches of low interspecific competition. Many are polyploids.

Extant genera are relatively evenly distributed from a phylogenetic viewpoint. Fourteen representative genera of lycopsids belong to six orders, which either lack living species (Asteroxylales, Protolepidodendrales, Lepidodendrales) or possess them (Lycopodiales, Selaginellales, Isoetales). *See* ASTEROXYLALES; ISOETALES; LEPIDODENDRALES; LYCOPODIALES; PROTOLEPIDODENDRALES; SELAGINELLALES.

Because the prelycopsids of the Asteroxylales are treated as the most primitive lycopsids rather than as the most advanced zosterophyllopsids, characters delimiting the lycopsids concern vasculature. The inception of the order Lycopodiales was marked by vascularization of the microphylls and by the unequivocal sharing of a single vascular trace by the sporangium and the subtending microphyll. The Lycopodiales achieved considerable phenotypic diversity that is well represented in the extant flora although all remained rhizomatous herbs. Sporangia of the Protolepidodendrales remained adaxial but were situated farther from the axis; they were also radially elongate and had a longitudinal dehiscence slit. This group also showed the earliest evidence of a uniquely lycopsid feature, the ligule.

All the preceding orders are homosporous; that is, they generate only one spore type. However, the Selaginellales are heterosporous and produce large megaspores and small microspores that generate male and female gametophytes. Megasporangia and microsporangia are borne together in bisporangiate cones.

The Lepidodendrales and the Isoetales are characterized by finite growth from a centralized axial rooting structure termed the rhizomorph. All rhizomorphic species undergo at least some secondary thickening to generate wood and bark. These characters probably first appeared in the Lepidodendrales, allowing the development of large trees as well as shrubs and pseudoherbs which together could occupy a wide range of habitats.

The lycopsids illustrate the value of integrating evolutionary data from living and fossil plants. The fossils provide characters and, more importantly, combinations of characters that do not occur in the living genera, thereby bridging apparent evolutionary discontinuities. However, many fossils provide tantalizingly limited ranges of characters and so are problematic, both phylogenetically and taxonomically. Although some lineages remain geographically widespread and speciose, most species are only trivially distinct in morphological terms; many are polyploid. Also, they are biased toward morphologically simple but ecologically specialized species that occupy low-stress habitats, where they are interstitial elements in communities dominated by other plant groups. *See* LYCOPHYTA.

Richard M. Bateman; William A. DiMichele

Bibliography. W. N. Stewart and G. W. Rothwell, *Paleobotany and the Evolution of Plants*, 2d ed., 1993.

Lyme disease

A multisystem illness caused by the tick-borne spirochete *Borrelia burgdorferi*. The disease, also known as Lyme borreliosis, generally begins with a unique expanding skin lesion, erythema migrans, which is often accompanied by symptoms resembling those of influenza or meningitis. During the weeks or months following the tick bite, some individuals may develop cardiac and neurological abnormalities, particularly meningitis or inflammation of the cranial or peripheral nerves. If the disease is untreated, intermittent or chronic arthritis and progressive encephalomyelitis may develop months or years after primary infection. *See* NERVOUS SYSTEM DISORDERS.

Human. Erythema migrans, which occurs in about 60% of persons with the disease, is a unique clinical marker. It can be characterized by a small red papule or macule, often considered the site of the tick bite, that 3 to 23 days later spreads centrifugally, with induration up to 0.8 in. (2 cm) wide and usually flat borders. The centers of early lesions are usually erythematous and indurated but may also be vesicular or necrotic. As the lesions expand, the centers clear. Annular secondary lesions appear in almost half the individuals within several days of the initial lesion.

Causative agent. The causative agent, *B. burgdorferi*, is a helically shaped bacterium with dimensions of 0.18–0.25 by 4–30 micrometers (see **illus.**). An outer membrane surrounds the protoplasmic cylinder, which consists of a peptidoglycan layer, a cytoplasmic membrane, and enclosed cytoplasmic contents. Seven to eleven periplasmic flagella are attached subterminally and overlap at the central region of the cell; they are responsible for the organism's rotational and translational movements. *Borrelia burgdorferi* is gram-negative and uses carbohydrates such as glucose as energy and carbon sources.

Epidemiology. Once thought to be limited to the European continent, Lyme borreliosis and related disorders are now known to occur also in North

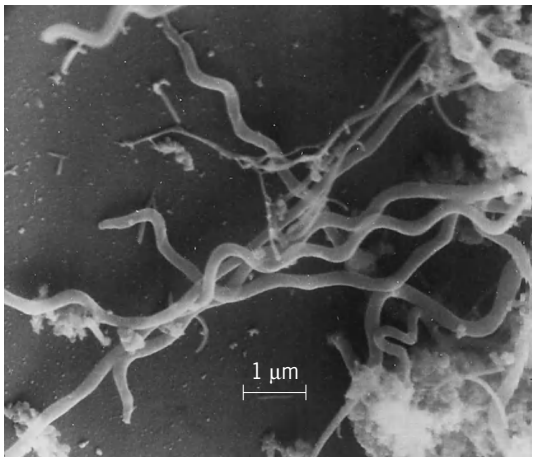

Scanning electron micrograph of *Borrelia burgdorferi*.

America, Russia, Japan, China, Australia, and Africa, where *B. burgdorferi* is maintained and transmitted by ticks of the genus *Ixodes*, namely *I. dammini, I. pacificus*, and possibly *I. scapularis* in the United States, *I. ricinus* in Europe, and *I. persulcatus* in Asia. *See* IXODIDES.

In the United States, Lyme borreliosis is the most prevalent arthropod-borne illness, affecting thousands of children and adults. Because of variations in case definition, no accurate data on its incidence are available.

Reports of Lyme disease in areas where neither *I. dammini* nor *I. pacificus* is present suggest that other species of ticks or possibly other bloodsucking arthropods such as biting flies or fleas may be involved in maintaining and transmitting the spirochetes.

Diagnosis and treatment. Diagnosis of Lyme borreliosis is based chiefly on clinical and epidemiologic evidence, particularly the presence of the unique skin lesion, erythema migrans. However, in as many as 40% of patients, that pathognomonic sign does not develop, rendering an early diagnosis only suggestive. Serologic tests such as indirect fluorescent antibody staining and enzyme-linked immunosorbent assay have been applied successfully in differentiating Lyme disease in its later stages from aseptic meningitis, rheumatoid arthritis, and other nervous system disorders such as multiple sclerosis. Both methods, however, lack sensitivity and specificity during the early course of the illness, and they have been shown to produce false-positive reactions. Because the procedures for both assays have not yet been standardized, differences in test results (serovariability) are common. The use of pathogen-specific antigens of *B. burgdorferi* should facilitate serologic diagnosis of Lyme disease.

All stages of Lyme borreliosis may respond to antibiotic therapy. Early treatment with oral tetracycline, doxycycline, penicillin, amoxicillin, or erythromycin can shorten the duration of symptoms and prevent later disease. Optimal treatment for arthritis, carditis, and neurological involvement is not yet clear, but intravenous penicillin and the cephalosporin, ceftriaxone, are highly promising. *See* ANTIBIOTIC.

Prevention and control. Prevention and control of Lyme borreliosis must be directed toward reduction of the tick population. This can be accomplished through reducing the population of animals that serve as hosts for the adult ticks, elimination of rodents that are not only the preferred hosts but also the source for infecting immature ticks with *B. burgdorferi*, and application of tick-killing agents to vegetation in infested areas. The Damminix method, a commercially available regimen that uses permethrin-impregnated cotton fibers, involves application directly to tick-infested rodents. Personal protection methods, including the use of effective tick repellents and toxins such as Permanone, are also recommended. *See* INFECTIOUS DISEASE; INSECTICIDE.

Animal. Lyme disease affects not only humans but also domestic animals such as dogs, horses, and cattle that serve as hosts for the tick vectors. Animals affected show migratory, intermittent arthritis in some joints similar to that observed in humans. In horses and cattle the most frequently observed clinical signs are lameness and swollen joints, although stiffness, inflammation of the hoof, abortion, and fever may occur. Spirochetes in the urine of such animals are said to be responsible for transmission of the disease by direct contact of an infected animal with an uninfected one. Birds also have been shown susceptible to *B. burgdorferi*, but their potential role in the epidemiology of the agent is still a matter of conjecture.

The disease is called canine Lyme borreliosis when it affects dogs. The transmission of *B. burgdorferi* from the tick to its host is minimal during the first 48 h of attachment; therefore, daily inspection and removal of ticks should be performed on dogs that have been in a tick habitat. A vaccine for the prevention of canine Lyme borreliosis is available, which is meant to be administered prior to *B. burgdorferi* exposure. In endemic areas, minimizing a dog's exposure to potentially infected ticks though the use of tick collars, sprays, and dips can be of value. Tick repellents containing DEET (*N,N*-diethyl-*meta*-toluamide) or permethrin are approved for veterinary use, and dog owners are advised to consult with their veterinarians before using these repellents and acaricides.

Because of the highly regional nature of canine Lyme borreliosis, dog owners considering either the vaccine or chemical tick-control measures should learn about the incidence of the disease in those areas that will be frequented by the dog. State health departments can provide information on the incidence of indigenously acquired Lyme disease and the presence of vector ticks in the geographic area of interest. Willy Burgdorfer; James J. Kasmierczak

Bibliography. M. J. Appel et al., Experimental Lyme disease in dogs produces arthritis and persistent infection, *J. Infect. Dis.*, 167:651–664, 1993; J. L. Benach and E. M. Bosler (eds.), Lyme disease and related disorders, *Ann. N.Y. Acad. Sci.*, 539:180–191, 1988; R. C. Johnson et al., *Borrelia burgdorferi* sp. nov.: Etiologic agent of Lyme disease, *Int. J. Syst. Bacteriol.*, 34:496–497, 1984; J. J. Kazmierczak and F. E. Sorhage, Current understanding of *Borrelia burgdorferi* infection, with emphasis on its prevention in dogs, *J. Amer. Vet. Med. Ass.*, 203:1524–1528, 1993; A. C. Steere, Lyme disease, *N. Engl. J. Med.*, 321:586–596, 1989.

Lymphatic system

A system of vessels in the vertebrate body, beginning in a network of exceedingly thin-walled capillaries in almost all the organs and tissues except the brain and bones. This network is drained by larger channels, mostly coursing along the veins and eventually joining to form a large vessel, the thoracic duct, which runs beside the spinal column to enter the left subclavian vein at the base of the neck. The lymph fluid originates in the tissue spaces by filtration from

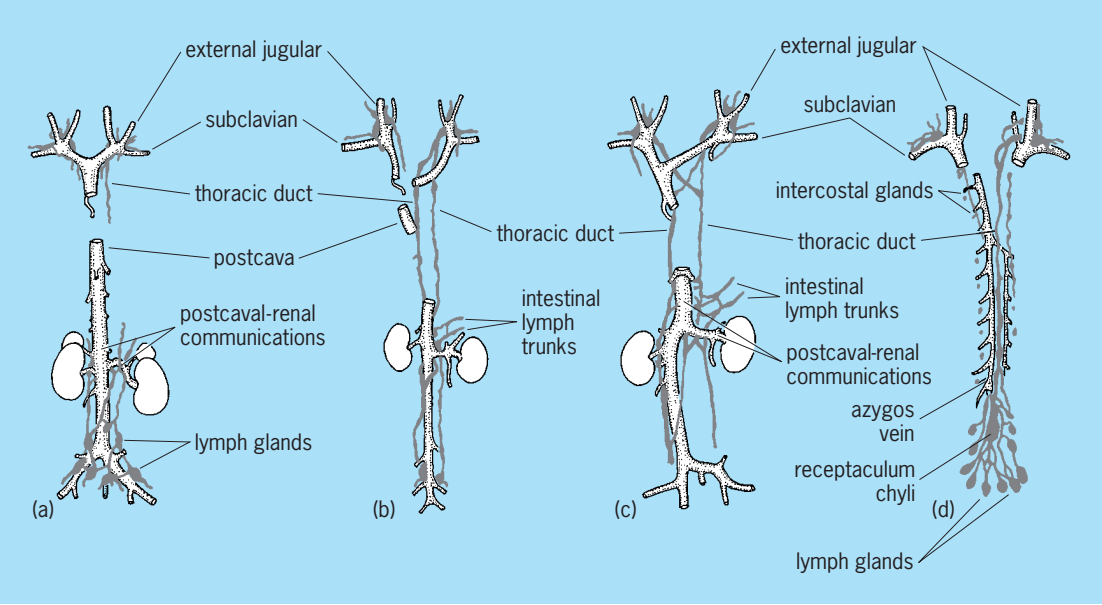

Fig. 1. Chief mammalian lymphatic trunks and their relations to the veins; ventral views. (*a*) South American monkeys. (*b*) Mammals (*Lepus*) in which postcaval-renal communications are wanting. (c) Mammals in general. (*d*) Humans (postcava and kidneys not shown). In all mammals the lymph enters the veins at the point of junction between the jugular and the subclavian veins. In most mammals there is also communication between the lymph vessels and the postcaval and renal veins. In humans the right thoracic duct degenerates in part and the only communication with veins is at the root of the jugulars. (*After H. V. Neal and H. W. Rand, Chordate Anatomy, Blakiston–McGraw-Hill, 1939*)

the blood capillaries. While in the lymphatic capillaries, it is clear and watery. However, at intervals along the larger lymphatic vessels, the lymph passes through spongelike lymph nodes, where it receives great numbers of cells, the lymphocytes, and becomes turbid. The lymphatic vessels other than capillaries contain numerous valves preventing backflow of the lymph. The functions of the lymphatic system are to remove particulate materials such as molecular proteins and bacteria from the tissues, to transport fat from the intestine to the blood, and to supply the blood with lymphocytes.

This article contains sections on the comparative anatomy, histology, embryology, and physiology of the lymphatic system.

Comparative Anatomy

It is disputable how far down in the animal series lymphoid tissue is found. Some researchers speak of lymphocytic cells in annelid worms, in mollusks, and in other invertebrates.

In general, the more primitive and less differentiated blood cells resemble more closely the lymphocytes of vertebrates. This is true also of the lower chordates in which so-called lymphocytes of the tunicates are said to differentiate into any of the other cell types of the body. Lymph nodules are described in some species of tunicates in the body wall and in the gut wall.

In the nonchordates it is difficult or impossible to make a distinction between blood vessels and lymphatic vessels. Probably the two systems had a common type of origin.

In *Branchiostoma* (*Amphioxus*), however, among the lower chordates, lymphatic vessels can be identified surrounding the blood vessels, and are seen also around the central nervous system, in the dorsal fin, and in the metapleural folds.

The lymphatics of vertebrates are distributed in somewhat the same manner as are the veins (**Fig. 1**). Thus they are divided into a deep and a superficial set. The deep set develops in relation to the cardinal veins and then makes connection with them and with the superficial set.

Fishes. In fishes the lymphatic system varies in degree of development in different species. In some, the veins seem to carry on the function of lymphatic drainage, but in a number of species of ganoids, teleosts, and elasmobranchs a well-developed lymphatic system is seen. The lymphatic vessels surround the veins in the elasmobranchs; in other fishes they are not so closely related to the blood vessels. In the elasmobranchs, also, there may be one or two large trunks which run parallel with the aorta and are comparable to the thoracic duct or ducts of humans and other mammals. Pulsating organs called lymph hearts, which assist in driving the lymph along the vessels, occur in some fishes (**Fig. 2**). The lymph vessels lack valves. Lymph nodes are absent, although there are collections of lymphoid tissue, chiefly close to mucosal surfaces. Nodules are found in these collections but they lack germinal centers.

The organ of Leydig of the selachian fishes consists of two large accumulations of lymphoid tissue which run longitudinally the whole length of the esophagus and even extend into the stomach. Although the cells of this organ are primarily lymphocytic, they apparently serve as stem cells for all the types of white blood corpuscles in these fishes, and hence the tissue perhaps should be spoken of as lymphomyeloid,

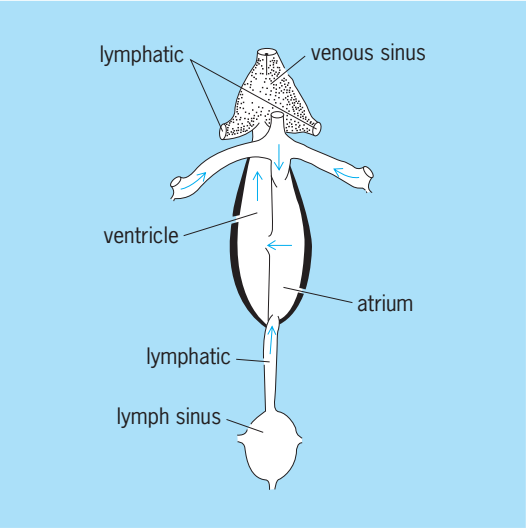

Fig. 2. Lymph heart in the tail of a teleost. (*After G. C. Kent, Comparative Anatomy of the Vertebrates, 2d ed., Blakiston–McGraw-Hill, 1965*)

indicating its hematopoietic as well as lymphoid character.

In the sturgeon a mass of lymphoid tissue has been described which occurs near the heart and resembles a lymph node, but its homologies are doubtful.

Amphibia. In the Amphibia the lymphatic system often includes very large subcutaneous sinuses, probably to protect against the danger of loss of moisture. Dilatations of the lymphatics, or lymph sacs, occur frequently. Lymph hearts are common in various parts of the body and a thoracic duct is present. Accumulations of lymphoid tissue are often present adjacent to the lymph sacs, but are not comparable in architecture to the lymph nodes of higher vertebrates. They may, however, represent an early stage in the development of such nodes.

Reptiles. Reptiles have a well-developed lymphatic system but lack the special features seen in amphibians. In the crocodiles true lymph nodes have been described in the mesentery.

Birds. The birds present a special condition in relation to the development of a lymphatic system. Here, as in other vertebrates, the more fluid portions of the blood readily leave the capillaries to diffuse among the tissue cells. This exudate is collected into lymphatic capillaries which join to form larger lymphatic vessels. The entire system converges toward the two superior (or anterior) venae cavae into which the main lymphatic trunks (thoracic ducts) empty. These veins bring the blood from the head, neck, and wings of the bird. The description of the lymphatic system of birds resembles that of mammals, even to the union of lymphatic with venous system.

The lymphatic vessels of birds are similar in structure to those of mammals and are provided with valves to help ensure one-way flow. However, the number of vessels is less than in mammals.

Lymph nodes are absent in vertebrates lower than the birds; that is, they are lacking in cold-blooded animals. Lymph nodes are not present in the common fowl (*Gallus domesticus*), but plexuses of lymphatic vessels do occur in the places where nodes are found in some other birds. Nodes are developed only in certain families of birds. This is not to say, however, that lymphatic tissue is lacking in birds without lymph nodes, for such tissue occurs in both diffuse and nodular form in the walls of the alimentary and respiratory systems: "Tonsillar" structures occur in the upper parts of these tracts; a large "esophageal tonsil" is found in the common domestic fowl; the bursa of Fabricius is a lymphoid organ in the wall of the posterior part of the alimentary tract; and the thymus appears to be an important producer of lymphocytes.

Early studies demonstrated that the quantity of lymphatic tissue increases, in general, toward the anal region in all birds studied. The avian cecum, in such mammals as the rabbit, is particularly rich in lymphoid tissue and may be said to constitute an "intestinal tonsil."

According to other findings, true lymph nodes probably occur only in water, shore, and swamp birds. Even when present, they are few, two pairs being found for the cervical-thoracic and two for the lumbar region. The nodes generally are elongated and spindle-shaped and lack a hilum. Capsule and trabeculae are lacking or very poorly developed.

Lymph nodes arise in birds about midway in embryonic life. The wall of the lymphatic vessel in the region of development becomes surrounded by a thick mass of mesenchyme which sends cordlike growths into the lumen of the vessel and eventually leaves only the central portion free, to serve as a central sinus into which the peripheral spaces open. Infiltrating lymphocytes transform the mesenchyme into truly lymphoid tissue. Nodules are formed, and in the centers of these nodules the germinal, or reaction, center develops, which is not found in fishes, amphibians, or reptiles.

These centers contain many phagocytic cells, or macrophages, as well as lymphocytes, some of which are undergoing mitotic division. These new centers in birds are found not only in the lymph nodes but also in individual nodules in other locations.

The lymph hearts, which are prominent features in cold-blooded vertebrates, were described in a number of species of birds, including the ostrich, cassowary, goose, swan, stork, and dove. The lymph hearts are paired structures in close relation to the kidneys and are true pulsatile organs provided with striated muscle. Two additional lymph hearts have been described in the goose; these have delicate, bladderlike walls which lie close under the hypogastric veins and are places of convergence for lymphatic vessels coming from several directions. From each of these hearts, a lymphatic vessel passes forward to the lumbar lymph nodes, and in its course receives tributaries from the pelvis and lower extremities.

In the fowl (*Gallus*) genuine lymph hearts with striated muscle are found only in the embryo. They

do not degenerate completely, however, until after hatching, and traces may be seen up to the thirty-fifth day after hatching.

Lymph hearts are said to occur in the embryos of all birds and are found on either side of the last sacral vertebrae. After hatching they disappear in some birds, as in the fowl, but are retained to some degree in the majority. They seem to be most prominent in the ostrich.

There does not appear to be a regular pulsation in the lymph hearts of birds but rather a contraction initiated by stretching of the wall due to filling. In the birds as a class the lymph hearts appear to be in a regressive condition when compared with such structures in amphibians and reptiles.

Mammals. The lymph nodes of mammals vary in number, size, form, and structure in different species. There appear to be some rather surprising differences in numbers of lymph nodes in different kinds of mammals. For example, the dog is said to have about 60, the cow 300, human 465, and the horse 8000. In the dog and cow, however, the lymph nodes are relatively large; in humans and the horse, they are relatively small. Their shape also varies. In the cow, for instance, the mesenteric nodes are long and narrow, attaining a length of several decimeters. In the rabbit the mesenteric nodes seem to have fused into one huge node, the pancreas aselli, weighing several times as much as all the other nodes combined. There is a similar arrangement for the mesenteric nodes in some other rodents and in some carnivores. These species include the mole, the dolphin, the seal, and the narwhal.

The amount of connective tissue of the lymph nodes, that is, the degree of development of the capsule and trabeculae, varies in different mammals. It is weakly developed in the pig, dog, sheep, rabbit, guinea pig, and rat. In humans and in the horse the trabeculae of the medullary part are more strongly developed than those of the cortex. Many mammals show a strong development of smooth muscle in the capsule and trabeculae, for instance, the horse, sheep, cow, and dog. The cow has an especially thick capsule and trabeculae.

In some lymph nodes the cortex, with its nodules, is very sharply set off from the medulla, with its more diffuse lymphoid tissue. This is true of the cow. In other animals the nodes seem to vary in this respect in different parts of the body or even in a rather haphazard manner, whereas in still others, such as the pig, there may seem to be almost a reversal of arrangement, with the nodular tissue situated centrally and the diffuse tissue peripherally.

Other lymphoid organs. These include the tonsils, thymus gland, and spleen, and in certain classes and groups of animals, structures which are confined to such groups, for instance, the bursa of Fabricius in the birds, a diverticulum from the lower end of the alimentary canal. *See* SPLEEN; THYMUS GLAND; TONSIL.

Tonsils. The tonsils seem to be represented in the frog and toad by two large fossae palatinae, invaginations of epithelium surrounded by dense masses of lymphoid tissue. Smaller structures of simple construction also are present.

In the posterior part of the buccal cavity of *Proteus* and *Salamandra* there are areas in which the epithelium is thickly infiltrated by lymphocytes.

Among the reptiles, *Lacerta agilis* shows definite tonsils in the pharynx, with elongated lymph nodules occurring along epithelial invaginations and with an apparent lack of basement membrane and a complete intermingling of epithelial and lymphoid tissue near the surface. Tonsils are seen also in the crocodiles.

Birds not only have large aggregations of lymphoid tissue in the pharynx but often also a large esophageal tonsil. The light-staining germinal centers are seen for the first time in birds.

A ring of lymphoid tissue, known as Waldeyer's ring, consisting of palatine, pharyngeal, and lingual tonsils, is present in many mammals, for instance, humans. Other mammals, however, may lack one or more of its component parts. In the rat and mouse, there are no palatine tonsils. In the hare and rabbit, pharyngeal tonsils are lacking. The rabbit, hare, dog, cat, and sheep apparently lack lingual tonsils.

Tonsils of the horse are peculiar in that they contain structures apparently identical with the Hassall's corpuscles of the thymus gland.

Spleen. The spleen is an organ of dual nature, belonging to both the blood-vascular and the lymphatic system. In the lower vertebrates it is actually within the wall of the alimentary canal. In cyclostomes it lies in the submucosa of stomach and intestine. In the lamprey it is within the spiral valve. Among the Dipnoi it is found within the stomach wall, but in elasmobranchs and ganoids it is a separate structure attached to the mesentery. In fishes and amphibians it is active as an erythrocytopoietic and lymphocytopoietic organ. Its function of forming lymphocytes is important also in higher vertebrates (including humans and other mammals), but its blood-cell-forming function is lost and replaced by one of destruction of "old" or worn-out red corpuscles and, to some degree, of blood storage. *See* HEMATOPOIESIS.

The lymphoid tissue of the spleen in higher vertebrates contains many nodules known as Malpighian bodies. These usually contain active germinal centers.

Histology

Lymphoid tissue is a tissue in which the predominant cell type, under normal conditions, is the lymphocyte. Lymphocytes are associated with reticular fibroblasts which form a delicate framework of fibers which can be demonstrated by their affinity for silver. There usually are cells of other types present also, including macrophages (fixed and free), plasma cells, and occasional eosinophile granulocytes.

Function. The chief function of the lymphoid tissue is to produce lymphocytes. In efferent lymphatic vessels, those leaving the lymph nodes, lymphocytes are considerably more abundant than in afferent lymphatics. Lymphocytes are added to the

lymph as it flows through the lymph nodes. The lymphocyte content of veins coming from the nodes also is greater than that of arteries going to them. Apparently newly formed lymphocytes also migrate into the capillaries and small veins. A second function of lymphoid tissue is protection against infection, which it carries out by means of its phagocytic and antibody-producing activity.

Cellular composition. Lymphocytes are of different sizes, small, medium, and large. The range in size of these three kinds, however, varies with different classes and even species of animals. The large lymphocyte resembles very closely the stem cell of blood-forming tissue; the hemocytoblast. In fact, lymphoid tissue itself bears a considerable resemblance to hematopoietic tissue, and in lower vertebrates it is not always possible to distinguish one from the other.

The function of the lymphocytes themselves is imperfectly known. The study of comparative histology, however, seems to throw light on their probable role in higher forms. In many invertebrates, the regenerative powers are much greater than in higher vertebrates. It has been shown that primitive mesenchymatous and free lymphoid cells often aggregate to form the various organ primordia and eventually even a completely differentiated animal. In some flatworms it has been found that not only do new parts arise from such elements (cells with conspicuous nucleoli and basophilic cytoplasm comparable to the large lymphocyte) but that the relative power of regeneration in different species may be correlated with the relative numbers of such cells. Thus, where they are numerous, as in *Planaria*, regenerative power is high. When they are not so common, as in *Procotyla*, regenerative power is low. In flatworms these cells will form such varied structures as epithelium of the gut, germ cells, and brain.

Although the lymphocytes of mammals do not have such remarkable potentialities, many workers have shown that they can develop into various other types of cells, including macrophages, which are large phagocytic cells; some types of granular white cells of the blood; red blood cells; and fibroblasts, or fiber-forming cells. The suggestion has been made also that they may metamorphose into epithelial cells in some locations. Thus one of their important roles in the higher vertebrates is still a regenerative or cell-replacing one.

Lymph vessels. The lymph capillaries, the smallest lymph vessels, form a dense network in almost every portion of the body. They appear to end blindly and consist only of an endothelial layer. As they unite to form larger vessels, connective tissue appears in the wall. The blind, rounded ends of lymphatic capillaries are easily seen in the lacteals in the villi, which receive the fatty foods from the intestinal lumen and hence contain chyle, a fluid made milky by the presence of multitudes of minute droplets of fat (**Fig. 3**).

In larger lymphatic vessels there are more collagenous fibers and also some elastic and smooth muscle fibers. In vessels with a diameter of more than

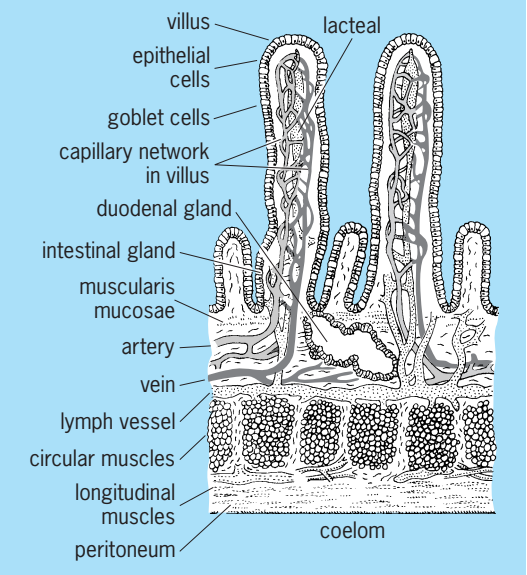

Fig. 3. Cross section of duodenum. (*After T. I. Storer and R. L. Usinger, General Zoology, 4th ed., McGraw-Hill, 1965*)

0.008 in. (0.2 mm), the wall generally shows three layers which bear the same names as those in the blood vessels, namely, intima, media, and adventitia. In lymph vessels the adventitia is usually the thickest layer and often contains smooth muscle cells as well as collagenous and elastic connective tissue fibers. In the largest lymphatic vessels, the right lymphatic duct and the thoracic duct, the media is more fully developed and contains considerable smooth muscle.

Lymph nodes. The lymph nodes are masses of lymphoid tissue with a special type of architecture. They are interposed as way stations in the course of the lymphatic stream. The vessels entering the node are called afferent; those leaving it are the efferent vessels.

The cortex usually consists of rather dense lymphoid tissue composed of rounded nodules, made up chiefly of small lymphocytes. In the centers of the nodules are lighter-staining portions, the germinal centers with macrophages and lymphocytes of medium and large size, frequently seen in mitosis.

The medulla of the lymph node consists of anastomosing channels or sinusoids, through which the lymph is coursing toward the efferent vessels and of cords of lymphoid tissue. It is more spongy than the cortex.

The lymph node is surrounded by a capsule consisting of collagenous and elastic connective tissue fibers and often containing some smooth muscle. At the hilum, where the blood vessels of the node enter and leave and from which the efferent lymphatics emerge, the connective tissue of the capsule penetrates well into the node.

Warren Andrew

Embryology

The mode of development of the lymphatic system, in contradistinction to the arterial and venous

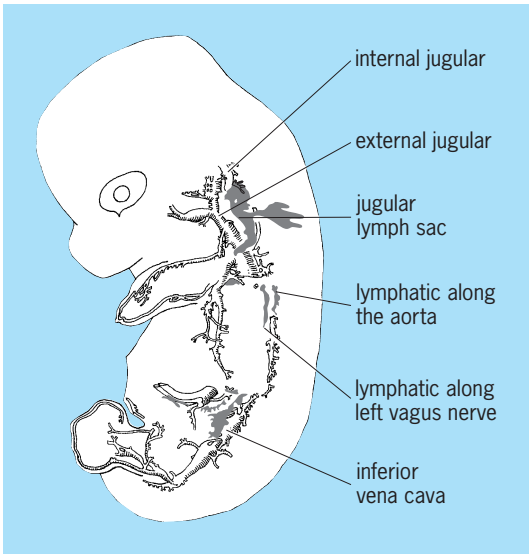

Fig. 4. Lymphatic vessels and veins in a 14.5-mm rabbit embryo. (*After R. O. Greep, ed., Histology, 2d ed., Blakiston-McGraw-Hill, 1966*)

systems, has been elucidated only since about 1910. Embryos of representative species from all classes of vertebrates have been studied, and as yet there is no agreement on fundamental questions pertaining to the early embryology of this elusive system. The unsolved status appears to rest more on differences of interpretations than on sufficient observations and facts.

A sharp distinction must be made between the processes of the earliest formation of discrete lymph vessels and those leading merely to an extension of once-established channels. The former entail actual genesis of endothelium (vasculogenesis); the latter merely represent growth. Growth by budding and branching of newly established vessels occurs throughout the vascular system, whether hemal (arterial and venous) or lymphatic. The controversial aspects mainly concern the earliest beginnings of lymph vessels.

Theories. There are two conflicting concepts. One is that all lymph channels develop by centrifugal outgrowth from embryonic veins, specifically from their endothelial lining. In the neck and loin regions, as well as in the posterior abdominal wall and at the root of the intestinal mesentery, such outgrowths form saclike expansions (**Fig. 4**; this figure, as well as **Fig. 5** and Fig. 7, shows general topography and structural plan in schematic form, but in detail these situations are not precisely as shown in the diagrams). These are, respectively, the jugular and iliac (lumbar) lymph sacs, the future cisterna chyli (pool of chyle near the base of the abdominal aorta), and the mesenteric lymph sac. All the body-pervading lymphatics are said to be formed by sprouting from these sacs and thus to be derived indirectly from the lining epithelium of blood vessels. The original points of budding from certain veins (cardinals, for instance) either could be retained or lost, and secondary evacuation taps for the lymph could be established.

The opposing view holds that the lymphatics arise directly from mesenchymal spaces, either adjacent to decadent venules or unassociated with veins. During early embryonic development, some rich and temporary venous plexuses become reorganized. Certain venules atrophy and disappear, particularly in regions of the developing lymph sacs. The drainage function is taken over by a lymphatic network which temporarily may carry blood cells received either from degenerative venules or from blood islands in the surrounding mesenchyme. The ultimate connection with major stem veins is always secondary. The system arises in a discontinuous manner and independently of the endothelium of veins. The overall direction of its development is centripetal. The isolated and discrete spaces converge and fuse to form continuous lymphatic trunks and networks. The main connection of the jugular lymph sacs with the venous system develops early, before the more distal lymphatic primordia have interconnected or joined the sacs. This link between two drainage systems, lymphatic and venous, occurs near the base of the neck (Fig. 4) at the jugulosubclavian junction.

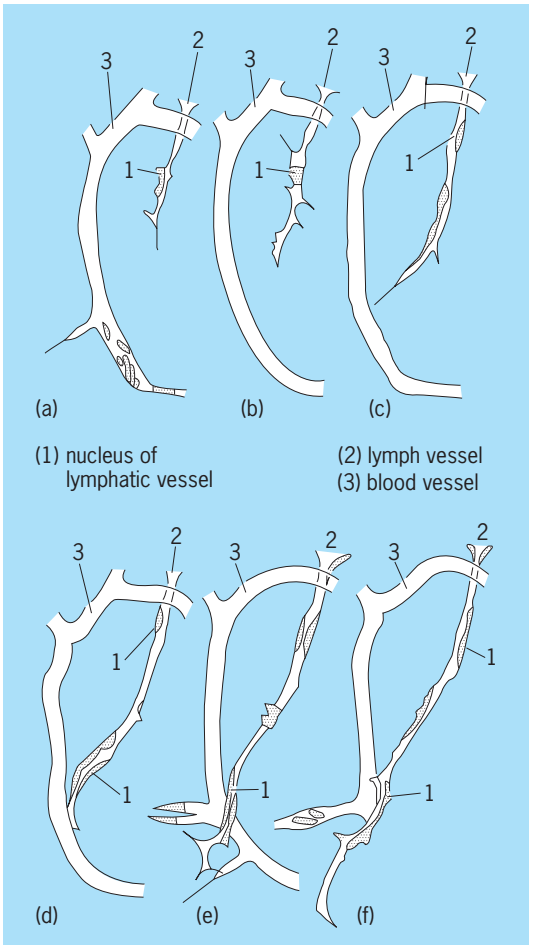

Fig. 5. Successive stages *a-f* in growth of lymphatic vessel in tail of tadpole during 72 h. (*After R. O. Greep, ed., Histology, 2d ed., Blakiston-McGraw-Hill, 1966*)

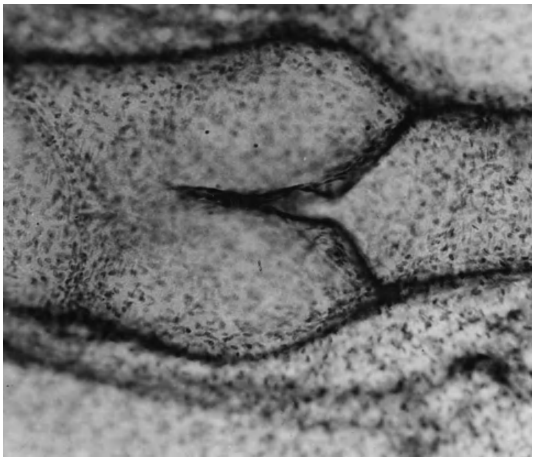

Fig. 6. Valve in lymph vessel to prevent backflow of blood. (*General Biology Supply House, Inc.*)

Investigative methods. There are two general methods for the investigation of lymphatic genesis; each has serious limitations. They consist either of the study of serial sections of well-preserved embryos or of injections of the developing lymphatics (Fig. 5). Crucial events in that development take place very early, in human embryos, for instance, when they measure only about 0.5 in. (10 mm). Obviously it is impossible to detect discontinuous segments of developing lymphatics by the injection method. Serial sections, on the other hand, can be obtained of uninjected as well as of injected embryos. This method in its turn presents difficulties in regard to fixation effects, shrinkage of the delicate embryonic tissues, and interpretive errors in reconstructions.

Evidence strongly supports the centripetal view of the origin of the lymphatic system. According to this view, the very first beginnings are identical with those of the arterial and venous components of the vascular system. All vasculogenesis appears to occur through the same fundamental transformation of mesenchymal cells into endothelial cells. The lymphatic precursor stages, succeeding the development of veins, as a rule are less distinct, evanescent, and therefore difficult to recognize. This has caused differing interpretations.

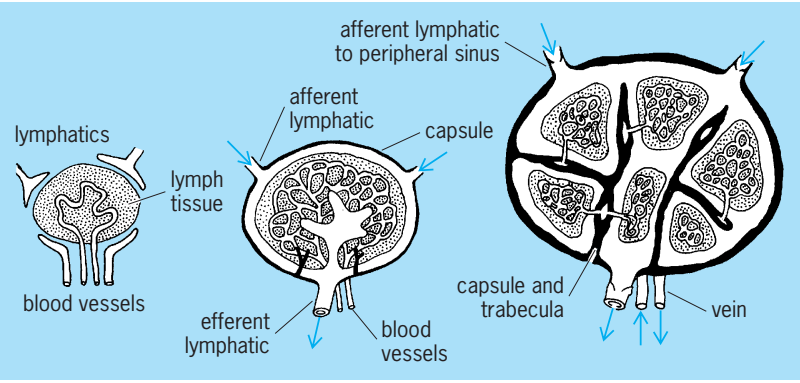

Fig. 7. Development of a lymphatic gland, with ingrowth of connective tissue strands. (*After L. B. Arey, Developmental Anatomy, 7th ed., Saunders, 1965*)

Embryonic phase. In human embryos of about 1 in. (20–30 mm) a connected primitive lymph system is already established. The main lymph channel ascending through the thorax in front of the vertebral column (thoracic duct) has joined the jugular lymph sac. At its distal end, it is continuous with the cisterna chyli, into which converge the lymphatics from the intestinal tract and those of the lower trunk and limbs. The jugular lymph sacs also receive lymphatic drainage from the developing upper limbs through the primitive ulnar lymphatics. Other lymph trunks develop in the head and neck regions, so that the jugular lymph sacs soon receive returning tissue fluids from all body regions. Lymph thereby is returned to the economy of the blood vascular system.

In early stages, the thoracic ducts are paired and symmetrically developed. Some animals retain double thoracic ducts. In many mammals and in humans the thoracic duct system becomes asymmetrical through the formation of interconnecting links and atrophy of certain segments. Henceforth, lymph drainage from the lower body regions occurs through a single main trunk, which terminates at the left jugulosubclavian junction.

Fetal phase. During early fetal months, the main lymph trunks, as well as the peripheral lymph vessels, become provided with valves which arise earlier in lymphatic vessels than in veins. Their structural arrangement enhances centripetal flow of lymph. By the fifth month, valves are present throughout the system (**Fig. 6**).

By ingrowth of connective tissue strands, the lymph sacs become transformed into a lacy plexus or fenestrated structure. In the meshes between the remaining lymph spaces the mesenchymal cells proliferate rapidly. Blood capillaries pervade the tissue bridges and immature lymphocytes appear in great numbers. The whole represents the beginning of a lymph node (**Fig. 7**). True lymphocytes further infiltrate the structure and produce compact cellular masses surrounded by lymph vessels. The complex may become subdivided to form groups of smaller lymph nodes. By the middle of fetal life the surrounding lymph vessels form a characteristic peripheral sinus, and an investing capsule is formed by the adjacent connective tissue. The full differentiation of lymph nodes is attained only after birth.

Arnold A. Zimmermann

Physiology

In any given region the fluid which enters a lymphatic capillary may be that which is close to the arteriolar or to the venous end of a blood capillary, or it may be fluid relatively distant from either. There exists a gradient of pressure from the tissue fluid to the lumen of the lymphatic capillary. In edema such as can be brought about experimentally by treatment with xylol or by heat, the gradient is increased. This pressure gradient is known to be an important factor in the formation of lymph. *See* EDEMA.

TABLE 1. Average values for the concentrations of electrolytes in lymph and plasma

Substance or property	Source of lymph	Subject*	Plasma	Lymph	Anesthetic
Sodium, meq/liter	Thoracic duct	Human (5)	127	127	
	Cervical duct	Dog	163	157	Nembutal
Potassium, meq/liter	Thoracic duct	Human (5)	5.0	4.7	
	Right lymph duct	Dog (5)		5.4	Nembutal
Calcium, meq/liter	Thoracic duct	Human (5)	5.0	4.2	
	Thoracic duct	Dog (1)	5.2	4.6	Amytal
	Cervical duct	Dog (11)	5.8	4.9	Nembutal
Chloride, meq/liter	Thoracic duct	Human (5)	96	98	
	Thoracic duct	Dog (1)	110	116	Amytal
	Cervical duct	Dog (7)	116	122	Nembutal
Inorganic phosphorus, mg %	Thoracic duct	Human (5)	4.5	4.4	
	Thoracic duct	Dog (1)	4.3	3.6	Amytal
	Cervical duct	Dog (3)	5.6	5.9	Nembutal
Carbon dioxide, ml %	Cervical duct	Dog (7)	56.8	58.8	Nembutal
Carbon dioxide tension, mmHg	Cervical duct	Dog (7)	46.4	40.3	Nembutal
pH	Cervical duct	Dog (7)	7.34	7.41	Nembutal

*Number of subjects studied is shown.

Any fluid in which filtration exceeds absorption through the wall of the blood capillary is normally drained by the lymphatics. Experimentally, this drainage is demonstrated where the filtration rate is increased by intravenous transfusions or by warming of parts.

Lymph collection. The function of the lymphatics is to remove such excess fluid and also to return to the bloodstream the protein which has escaped from the blood capillaries. Lymph collected from lymphatics of the kidney, leg, and cervical region, as well as from the thoracic duct, has been shown to contain this protein which has been "leaked" from the blood-vascular system. These proteins include serum globulin, serum albumin, and fibrinogen. The filtrate from the blood capillaries consists of water and of sugar and salts in concentrations found within the bloodstream, plus these proteins in low concentration. The salts and much of the water are reabsorbed by blood vessels, whereas the protein, together with some water and salt, enters the lymphatics. When the normal drainage of protein from the tissue spaces is prevented, elephantiasis may result, as when the lymphatics are obstructed in filariasis. The result is massive edema of a part, with dilatation and thickening of the lymphatic capillaries and an overgrowth of connective tissue.

In addition to water, ions, small molecules, and the large molecules of extravascular protein, particles such as injected graphite or extravasated red cells also enter the lymphatic capillaries. Such relatively huge structures pass between the cells.

Composition and properties of lymph. Basically, the composition of lymph closely resembles that of the plasma. Chemical and electrophoretic studies show that lymph contains all of the types of protein found in plasma, but in lower concentration. The composition of lymph varies to some extent from one part of the body to another. Thus, the lymph from the liver contains more protein than that from the skin.

The ability of lymph to coagulate depends largely on its content of fibrinogen and prothrombin, and this varies rather markedly. In dogs the mean prothrombin level is 7.6 for leg lymph, 51.2 for thoracic duct lymph, and 93.2 for liver lymph. There are no blood platelets in lymph, and it is thought that thromboplastin, generally considered necessary in clotting, is formed at the time of clotting from precursors present in the lymph. Calcium, also needed in clotting, is present in the lymph in slightly lower concentration than in the blood.

The ionic content of lymph does not vary much from that of plasma **(Table 1)**. Chloride and bicarbonate levels are higher in the lymph than in the plasma, whereas total base is slightly lower.

The glucose content usually is essentially the same in the lymph as in the blood. Curiously, the lymph of the kidney has a lower concentration of glucose. When carbohydrate is fed or when an intravenous injection of glucose is made, the concentration of this sugar in the lymph lags behind that in the plasma, but eventually catches up when an equilibrium between plasma and lymph is attained. Concentrations of amino acid, creatinine, and urea are approximately equal in lymph and plasma, but in the kidney the urea of the lymph is slightly higher than that of the plasma. It seems probable that some of the renal lymph comes from fluid reabsorbed from the distal and collecting tubules.

The lipids consist of neutral fat forming the chylomicrons, and of cholesterol and phospholipid, the latter two kinds of compounds being associated chiefly with proteins to form lipoproteins. The quantity of neutral fat depends on the fat absorption by the lacteals of the intestine, and the amounts of cholesterol and phospholipid vary with the amounts of protein present.

Lymph flow. Contractility of the walls of lymphatic vessels in humans and other mammals appears to be only slight and to play a minor role in lymph flow. This is in marked contrast to the condition in some lower vertebrates, particularly the

TABLE 2. Average flow and protein content of lymph from various lymph ducts in dogs under nembutal anesthesia*

Lymph duct†	Lymph flow, ml/h (in.^{3}/m)	Lymph protein		
		g %	g/day (oz/day)	% of total intravascular plasma protein
Thoracic duct (4)	26.0 (1.6)	4.1	26.1 (0.92)	47.5
Right lymph duct (21)	2.3 (0.14)	3.7	2.0 (0.07)	3.6
Cervical ducts (18)	2.2 (0.13)	2.8	1.3 (0.05)	2.4
Foreleg ducts (5)	3.8 (0.23)	1.3	1.2 (0.04)	2.2
Hindleg ducts (17)	2.2 (0.13)	1.8	1.0 (0.04)	1.8

*After C. K. Drinker and J. M. Yoffey, *Lymphatics, Lymph and Lymphoid Tissue,* 2d ed., Harvard University Press, 1956. Average weight of each animal in each group was approximately 46 lb (21 kg) and average intravascular plasma protein 1.9 oz (55 g). Total lymph protein from leg and cervical ducts includes both sides.

† In parentheses is the number of animals in each group.

Amphibia, in which well-developed pulsatile lymph hearts occur along the course of the lymphatic channels (Fig. 2). The lymph flow in mammals appears to be very sluggish compared with that in the frog. The rather slow rate of flow of the lymph in dogs is seen in **Table 2**. It is calculated that extravascular circulation involves 50–100% of the plasma proteins each day.

The pressure of the lymph flow is variable, even in any given lymphatic vessel. Because lymph flows centripetally, it is clear that the peripheral lymph is under higher pressure than that farther along the vessels. Muscle contractions, such as those of the legs in walking, may greatly increase the pressure of the lymph in an individual region. During contraction of the muscle the lymphatics tend to empty, whereas during relaxation they fill again. In one experiment no pressure was recorded from a lymphatic just below the popliteal lymph node of a dog when the animal was at rest; but during rapid flexion and extension of the leg, the pressure rose to 27 in. (68 cm) of water.

Measurements of lymph pressure usually are made under standard conditions of rest. Pressure in a major division of the thoracic duct of the dog has been recorded as 2.6 in. (6.4 cm) of water, compared with a pressure of 1 in. (2.4 cm) in the internal jugular vein of the same dog. Such a pressure difference promotes flow from the thoracic duct into the venous system. Pressures have been recorded from a number of different lymphatic vessels. That of the lymphatic capillaries is rather high, having been recorded as 17 in. (42.6 cm) of water or 1.25 in. (31.3 mm) of mercury in the capillary of the villus.

Immunity. The lymph nodes serve as filtering-out places for foreign particles, including microorganisms, because the lymph comes into intimate contact with the many phagocytic cells of the sinusoids. These macrophages are of both the fixed and free wandering types. *See* PHAGOCYTOSIS.

In addition to the phagocytic function, experimental studies have demonstrated that lymphoid tissue produces antibodies. If antigens such as typhoid bacilli or sheep erythrocytes are injected into the pad of the foot of an experimental animal, antibodies begin to appear in the efferent lymph vessels of the popliteal node a few days later and their titer rapidly increases to a maximum and then declines. Some investigators have found that most of the antibody is within the lymphocytes rather than in the fluid. Germinal centers of the lymph node increase in size, and there is an increased output of lymphocytes. *See* ANTIBODY.

The actual process of antibody formation in lymphoid tissue is not well understood. A considerable body of evidence would assign the chief role to the plasma cell, generally abundant in lymphoid tissue, rather than to the lymphocyte. Antigen injection has been shown to bring about an intense plasma cell response in many instances.

The use of fluorescent antigens and antibodies offers evidence that antigen is fixed by plasma cells in lymph nodes which are forming antibodies, but is not fixed by lymphocytes. The increased numbers of lymphocytes in infection and their passage into the bloodstream may thus have some significance not connected with antibody formation.

Lymphocyte transformations. A large body of evidence supports the view that lymphocytes undergo transformations. Tracer studies combined with tissue culture methods for peripheral blood seem to show conclusively that the large proliferating cells in such cultures originate from small lymphocytes. Phytohemagglutinin acting on cultures of peripheral blood induces a transformation of small lymphocytes into large stem-type cells, which then become active mitotically.

A profound modification occurs in the ultrastructure of human lymphocytes cultured with phytohemagglutinin: New organelles increase in number in the cytoplasm of such cells; mitochondria become more numerous; the Golgi apparatus enlarges; and a variety of vesicles is seen. A transformation of small lymphocytes (parental strain) into larger cells of pyroninophilic type has been shown in F_1 hybrid rats. Cytochemical studies on lymphocytes and large blast cells in short-term culture show the dehydrogenase system highly active in glycolysis.

Cerebrospinal fluid. The cerebrospinal fluid fills the ventricles of the brain and the space between the arachnoid mater and the pia mater. Cerebrospinal fluid is a clear liquid derived from the capillary

vessels of the choroid plexuses which permit the passage of water, electrolytes, and small molecules, but hold back the proteins of the blood. Fluid passing through the walls of the capillaries must also go through a layer of epithelium covering the capillaries. Traces of protein are found in the normal cerebrospinal fluid. *See* NERVOUS SYSTEM (VERTEBRATE).

By far the greater part of the cerebrospinal fluid is absorbed into the veins of the arachnoid villi. The relationship between the cerebrospinal fluid and the lymphatic system is found in certain regions in which the fluid escapes from the meninges and enters lymphatic capillaries. Thus it may pass by way of the arachnoid sheaths of the olfactory nerves into the submucosa of the nasal cavity, and so reach the cervical lymphatic vessels. Arachnoid coverings of the sensory ganglia also are locations where cerebrospinal fluid may reach the lymphatics in the normal animal.

Clinically, such connections may serve as routes by which bacteria or viruses can enter the central nervous system. They may also, in cases of meningitis or of hemorrhage, help to clear the cerebrospinal fluid of cells and of plasma proteins.

Cerebrospinal fluid differs from other lymph in its low protein content, low cell content, and lower specific gravity (1.004–1.008). It contains no fibrinogen.

The cerebrospinal fluid has at least three functions: (1) It acts as a fluid buffer against shocks and jars of the central nervous system. (2) It serves as a reservoir in regulation of the cranial contents. (3) It acts as a mechanism for exchange of gases and nutrients in the nervous system. In relation to these functions, its properties are particular, but it may be considered as a specialized type of lymph.

Warren Andrew

Bibliography. J. A. Barrowman, *Physiology of the Gastro-Intestinal Lymphatic System,* 1978; G. F. Bastian, *Lymphatic and Immune System,* 1993; M. Battezzati and I. Donini, *The Lymphatic System,* 1974; R. C. Myall and M. H. White, *Progress in Lymphology,* 1977; M. Nishi, S. Uchino, and S. Yabuki (eds.), *Progress in Lymphology,* no. 12, Proceedings of the 12th International Congress on Lymphology, 1990.

Lymphoma

Any of a group of malignant neoplasms derived from cells endogenous to lymphoid tissue. Lymphomas are grouped into two major categories: Hodgkin's disease and non-Hodgkin's lymphomas. Lymphomas usually originate in the lymph nodes located throughout the body, but they can arise from lymphoid tissue that does not form distinct nodes, such as that in the gastrointestinal tract or lung. Determination of the specific variety of Hodgkin's disease or non-Hodgkin's lymphoma was formerly based on the appearance of the cells when examined under a light microscope. Identification now relies on the nature of the cells with respect to certain substances (antigens) that they have on their surface or within their cytoplasm. For clinical purposes, lymphomas are categorized into three grades, low, intermediate, and high, with low-grade lymphomas having the best prognosis. *See* HODGKIN'S DISEASE.

Etiology. The etiology of most lymphomas is unknown. In experimental and domestic animals, viruses can cause lymphomas. Burkitt's lymphoma, a type of lymphoma that is rare in the United States but relatively common in children of central Africa, is thought to be caused by Epstein-Barr virus, a member of the herpes virus group. Electron microscopic studies of Burkitt's tumor cells have shown intracellular viral particles; Burkitt's lymphoma produces elevated serum antibody levels against Epstein-Barr virus. A form of T-cell lymphoma that has been identified in southern Japan has been attributed to a retrovirus referred to as human T-cell lymphoma-leukemia virus type 1 (HTLV-1). *See* EPSTEIN-BARR VIRUS; RETROVIRUS.

Clinical features of lymphomas. Patients with lymphomas may have painless swelling of various lymph nodes, such as those in the neck or near the armpit. Some patients, especially those with Hodgkin's disease, are referred to as B symptoms (fever, malaise, and weight loss). If the lymphoma originates in lymphoid tissue outside the lymph nodes, abdominal pain will signal lymphoma of the gastrointestinal tract and a cough will point to lymphoma of the lung.

Pathologic features. Lymph nodes involved by lymphoma are characteristically enlarged. They may be firm and have a consistency resembling fish flesh. In rare cases they are rock hard and they may show areas of cellular death (necrosis).

The appearance of lymphomas under a light microscope is highly variable. They can range from neoplasms composed of cells that very closely resemble normal lymphocytes, to tumors that are composed of large neoplastic cells. Hodgkin's disease has four microscopic subtypes, although the malignant cell in all of these subtypes is what is referred to as a Reed-Sternberg cell. The Reed-Sternberg cell is a tumor giant cell that frequently measures as large as 40 micrometers. It can have different forms, depending on the histologic subtype of Hodgkin's disease.

Cells of origin. Advances in the understanding of immunology have led to new concepts concerning lymphomas. It has long been known that there are two major classes of lymphocytes, referred to as B lymphocytes and T lymphocytes (B cells and T cells), both of which are formed in bone marrow. B lymphocytes differentiate into cells called plasma cells, which produce immunoglobulin. T lymphocytes are involved in cell-mediated immunity; before entering lymph nodes and other lymphoid organs, they are processed by the thymus gland to become functional, mature lymphocytes. Macrophages, sometimes referred to as histiocytes or M cells, are also of bone marrow origin, and are involved in a

number of functions, such as antigen presentation to the lymphocytes. By using modern immunologic techniques, most lymphomas can be identified as B-cell, T-cell, or M-cell type; about 90% of lymphomas are of B-lymphocyte origin. A T-cell lymphoma that occurs in the skin, referred to as mycosis fungoides, is a lymphoma of a specific subtype of lymphocyte labeled a T-helper/inducer lymphocyte. It is that subtype that is depleted in patients with acquired immune deficiency syndrome (AIDS). *See* ACQUIRED IMMUNE DEFICIENCY SYNDROME (AIDS); CELLULAR IMMUNOLOGY; IMMUNOLOGY.

It is not always clear whether a lymph node shows the microscopic changes of a lymphoma or is a benign, reactive type of lymphoid cell proliferation. By using immunologic techniques with antibodies directed against various types of lymphocytes, the malignancy of the cells can often be determined. Other available techniques can ascertain whether the cells are of clonal origin, suggesting they are neoplastic, by determining that specific changes have taken place in their genes.

Evaluation of patients. Most diagnoses of lymphoma are made by surgical removal of a lymph node. The pathologist slices a thin section of the node, stains it with dyes, and examines it under a light microscope. If the lymph node shows a malignancy and is a lymphoma, then the type of lymphoma is determined by the appearance of the cells. Once a diagnosis of lymphoma is established, the patient usually must undergo a series of staging studies. These include a liver-spleen scan to determine if those organs are involved as well as a bone marrow biopsy to check for the presence of malignant cells. Some patients with Hodgkin's disease undergo exploratory abdominal surgery, at which time their spleen is removed for examination, and their liver and abdominal lymph nodes are biopsied and examined for evidence of the disease. *See* ONCOLOGY.

Treatment and prognosis. The treatment of lymphomas depends on the type of lymphoma diagnosed. Lymphomas in the low-grade group are usually not treated, since treatment does not increase life expectancy. Patients who have Hodgkin's disease or who have intermediate or high-grade non-Hodgkin's lymphoma are usually treated with chemotherapy with or without concurrent radiation.

Most cases of Hodgkin's disease and more than half the cases of intermediate and high-grade non-Hodgkin's lymphomas are potentially curable. Persons with low-grade non-Hodgkin's lymphomas usually have a life expectancy of 7–10 years, although some live considerably longer. Treatment protocols are now being developed for the low-grade lymphomas in the hope of increasing life expectancy. Among the experimental therapies that have been under investigation are treatment with interferon and with antibodies directed against tumor cells. *See* CHEMOTHERAPY AND OTHER ANTINEOPLASTIC DRUGS; LYMPHATIC SYSTEM.

Samuel P. Hammar

Bibliography. A. R. Moossa et al. (eds.), *Comprehensive Textbook of Oncology*, 2d ed., 1991; P. K. Pattengale, R. J. Lukes, and C. R. Taylor (eds.), *Lymphoproliferation Diseases*: *Pathogenesis, Diagnoses, Therapy*, 1985.

Lyophilization

Solvent removal from the frozen state by sublimation; commonly referred to as freeze-drying. The dried material, a porous solid, is sealed under vacuum or inert-gas atmosphere and retains its physical and biological characteristics indefinitely. When reconstituted for use, the porous product readily readmits solvent; hence the term lyophile, or solvent-loving.

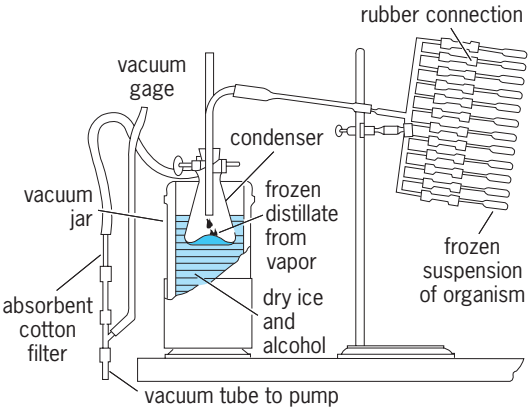

Apparatus for rapid high-vacuum desiccation of frozen suspensions of biologic materials. (*After A. J. Salle, Fundamental Principles of Bacteriology, 4th ed., McGraw-Hill, 1954*)

Lyophilization is accomplished by freezing the material to be dried below its eutectic point and then providing the latent heat of sublimation. Precise control of heat input permits drying from the frozen state without product melt-back. In practical application, the process is accelerated and more precisely controlled under reduced pressure conditions.

Several forms of apparatus are in use, ranging from the small laboratory equipment in the **illustration** to large chamber-type installations for preservation of serums, vaccines, blood plasma, soluble beverages, and foodstuffs.

Samuel C. Tease

Lyra

The Lyre (a stringed musical instrument), a small northern constellation (see **illustration**). It is marked by the fifth brightest star in the sky, Vega. In Greek mythology, the god Mercury made the first lyre by placing strings across a turtleshell. The constellation commemorates the lyre that the god Apollo gave to Orpheus, a gifted musician who used it to induce Pluto to release Orpheus's wife, Eurydice, from the underworld. Orpheus, warned not to look backward while liberating Eurydice, could

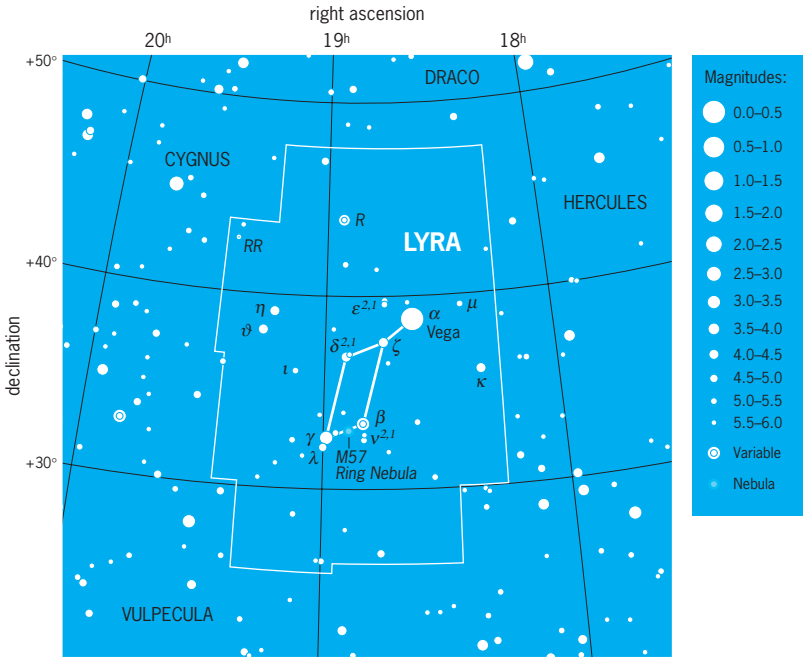

Modern boundaries of the constellation Lyra, the Lyre. The celestial equator is 0° of declination, which corresponds to celestial latitude. Right ascension corresponds to celestial longitude, with each hour of right ascension representing 15° of arc. Apparent brightness of stars is shown with dot sizes to illustrate the magnitude scale, where the brightest stars in the sky are 0th magnitude or brighter and the faintest stars that can be seen with the unaided eye at a dark site are 6th magnitude. (*Wil Tirion*)

not help himself from doing so, and lost her again. *See* VEGA.

Lyra contains the Ring Nebula, the most famous example of a planetary nebula, the gas given off by dying sunlike stars. Deneb in Cygnus, Vega in Lyra, and Altair in Aquila make the "summer triangle." Epsilon Lyrae, the "double-double" (that is, a multiple star system with two widely spaced components, each of which has two closely spaced stars), is a popular object for amateur astronomers. *See* BINARY STAR; CYGNUS; PLANETARY NEBULA.

The modern boundaries of the 88 constellations, including this one, were defined by the International Astronomical Union in 1928. *See* CONSTELLATION.

Jay M. Pasachoff

Lysin

A term used in biology to describe substances that will disrupt a cell, with the release of some of its constituents. Unless the damage is minor, this action leads to the death of the cell. Lysins vary in the range of host species whose cells they will attack and in their requirements for accessory factors for lysis; the immune lysins are strictest in their requirements. Erythrocytes are lysed by a wide variety of chemicals, including water and hypertonic salt solutions, which displace the osmotic pressure from that of isotonicity. They are also susceptible to surface-active substances, such as saponin. Many bacteria, such as the staphylococcus and the streptococcus, elaborate one or more hemolysins that will lyse erythrocytes from certain, although not all, species of animals. These patterns may be used in the taxonomic classification of microorganisms. There are a number of other lytic substances, such as lysozyme, an enzyme in the eye aqueous humor and to some extent the bacteriophages, which attack diverse species of bacteria. These actions are not entirely nonspecific since they depend on the presence of common cell constituents or receptors which need not, however, coincide with those involved in immune lysis. *See* BACTERIOPHAGE; LYSOGENY; STAPHYLOCOCCUS; STREPTOCOCCUS.

Immune lysin is a term used in serology to designate an antibody that, in the presence of complement and cofactors, such as Mg^{2+} (magnesium ion) and Ca^{2+} (calcium ion), will disrupt a particular type of cell, with the release of some of its constituents. This action is in accord with the principles of serologic specificity and is to be distinguished from the more general actions of other lytic chemicals. Immune lysins are also classified according to the general class of cell attacked: Hemolysins are antibodies lysing erythrocytes, while bacteriolysins cause the lysis of bacterial cells. Hemolysins against various foreign erythrocytes occur normally in many sera; the Forssman and other heterophile antibodies and the blood group isoantibodies constitute special instances. High titers of hemolysins may also be produced by immunization with erythrocytes, and rabbit antibody against sheep erythrocytes is an important laboratory reagent, the so-called amboceptor, in complement-fixation tests. For example, sheep erythrocytes injected into a rabbit produce antibodies in the rabbit against the sheep red blood cells. The lysis of erythrocytes releases hemoglobin,

which may be quantitated by eye or by a colorimeter. *See* ANTIBODY; ANTIGEN; COMPLEMENT; COMPLEMENT-FIXATION TEST; HETEROPHILE ANTIGEN; LYTIC REACTION; SEROLOGY. Henry P. Treffers

Lysogeny

Almost all strains of bacteria are lysogenic; that is, they have the capacity on rare occasions to lyse with the liberation of particles of bacteriophage (see **illus.**). Such particles can be detected by their ability to form plaques (colonies of bacteriophage) on lawns of sensitive (indicator) bacteria. The genetic determinant of the capacity of lysogenic bacteria to produce bacteriophage is a repressed phage genome (provirus) which exists in the bacterium in one of two states: (1) integrated into the bacterial chromosome (most cases), or (2) occupying some extrachromosomal location (rare cases).

Bacteriophages which have the potential to exist as provirus are called temperate phages. When the provirus is integrated into the bacterial genome, it is called prophage. When the germinal substance (deoxyribonucleic acid, DNA, or deoxyribonucleoprotein) of certain temperate phages (for example, wild type of coliphage λ) enters a sensitive bacterium, the outcome may be death (lysis) for the bacterium as a result of phage multiplication, or it may result in the integration of the phage nucleic acid into the host genome (as a prophage), with the formation of a stable lysogenic bacterium. The lysogenic strain is designated by the name of the sensitive strain, followed, in parentheses, by the strain of lysogenizing phage, for example, *Escherichia coli* (λ). Such a bacterium differs from its nonlysogenic ancestor in one special way: It is immune to lysis by phage homologous to its carried prophage. *See* DEOXYRIBONUCLEIC ACID (DNA).

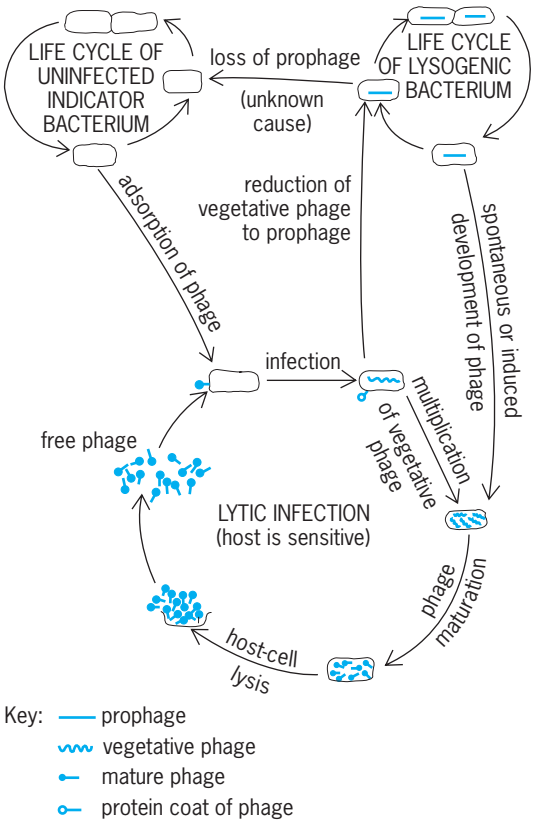

Life cycles of phage and bacterial host. (*After E. Jawetz, J. L. Melnick, and E. A. Adelberg, Review of Medical Microbiology, 2d ed., Lange, 1956*)

Repression. The conversion of a nonlysogenic cell to an immune lysogenic state by its resident prophage is the essential element of lysogeny, and is related to the regulatory mechanism by which the lysogenic state is maintained stably. When a prophage becomes part of the bacterial genome, most of the prophage genes, especially those having to do with DNA replication and the synthesis of viral protein, are repressed. This repression is attributed to the synthesis, under the direction of the prophage genome, of a repressor substance; thus at least one gene of prophage is expressed. This process is responsible for the immunity of lysogenic bacteria to lytic superinfection.

Immunity. The immunity conferred by prophage explains the fact that in most lysogenic cultures, while the host bacteria multiply normally, mature phage particles of the kind for which the host is lysogenic can be found in the surrounding medium. In a very few cells in any lysogenic population, the repressive mechanism fails to function, and prophage initiates replication and the host cell undergoes productive lysis. Since the population as a whole is immune, free virus merely persists in the environment. Under certain conditions, of which irradiation and the introduction of certain chemicals into the medium have been the best studied, a lysogenic culture may be induced to shift from the prophage to the lytic cycle; that is, the regulatory mechanism in the majority of cells is caused to break down and mass lysis of the culture occurs, with the production of many infectious phage particles. *See* LYTIC INFECTION.

Not all genes of the prophage are repressed, and a number of properties of lysogenic bacteria, assumed to be solely under the genetic control of the host cell, have been shown to be the expression of genes of the harbored prophage. Thus, the synthesis of diphtherial toxin by the diphtheria bacillus is controlled by the tox^+ gene of several corynebacteriophages, which render nontoxinogenic diphtheria bacilli both lysogenic and toxinogenic. Certain strains of *Salmonella* synthesize one kind of antigen when they are nonlysogenic, while when they harbor a specific prophage, antigen synthesis is altered by an expressed prophage enzyme, giving rise to another kind of antigen.

In one well-studied case, the origin of viral genes expressed in the lysogenic host cell is clear. Coliphage λ, liberated from galactose-fermenting *E. coli* (λ) has, sometimes, in the process of prophage integration, exchanged λ genes having to do with capsid production with host cell genes having to do with the enzymes of galactose utilization. When the repression mechanism for prophage fails, copies of λDNA

now contain genes for galactose fermentation. The DNA of this mutant, λdg, converts *E. coli* cells unable to utilize galactose into *E. coli* (λdg), the cells of which are lysogenic for λdg and able to utilize galactose. This galactose-positive state results from the expression of bacterial genes that have become an integral part of a viral DNA. *See* BACTERIOPHAGE; COLIPHAGE. Lane Barksdale

Bibliography. E. A. Birge, *Bacterial and Bacteriophage Genetics*, 4th ed., 2000; R. Dulbecco and H. Ginsberg, *Virology*, 2d ed., 1988; M. Dworkin, *Developmental Biology of the Bacteria*, 1985; W. Hayes, *The Genetics of Bacteria and Their Viruses*, 2d ed., 1976; W. K. Jokklik et al., *Zinsser Microbiology*, 20th ed., 1995.

Lysorophia

An order and clade of elongate lepospondyls with highly reduced limbs and a lightly built, open skull known from the Middle Pennsylvanian to Lower Permian (305–270 million years ago) of North America and the British Isles. Unlike other lepospondyls, no lysorophians have been found in continental Europe. The vast majority of specimens come from two localities: the coal deposits of Linton, Ohio, and the Clear Fork redbeds of north central Texas. They were aquatic in their lifestyle, and are frequently found in large numbers curled in burrows. These burrows are believed to be estivation chambers, structures constructed by animals for periods of dormancy associated with suboptimal living conditions. *See* LEPOSPONDYLI.

Features. Three species from one family are currently recognized: *Brachydectes newberryi, B. elongatus*, and *Pleuropteryx clavatus*, ranging in size from a few centimeters to about 1.5 m (4.5 ft). All possess the same unique anatomical features. The skull of lysorophians has a large opening inside the skull that extends the orbit back to the bones of the jaw articulation. The jaw articulation is inclined in a forward direction, and the lower jaw is short. Lysorophians have highly ossified remnants of the gill support skeleton, unique in lepospondyls, that could have supported three sets of gills, but it is unclear whether gills were present or if these bones performed other functions such as anchoring the tongue muscles. Vertebrae are distinctive, having neural arches that do not meet dorsally and are sutured, not fused as in other lepospondyls, to the single, spool-shaped vertebral body (or centrum). There are between 69 and 97 presacral vertebrae, and tails were probably relatively short. Limbs are short, about as long as four vertebrae, and probably had four fingers and five toes, but they are very poorly preserved so certainty is impossible.

Phylogeny. Relationships of lysorophians are very unclear. Traditionally they have been placed within the microsaurs, a group of salamander-like lepospondyls. In recent analyses of relationship they are frequently placed next to other elongate, limbless lepospondyls such as aistopods and adelospondylids, but many of the uniting features can easily be associated with being long and limbless and not recent shared common ancestry. Recently a small number of scientists have hypothesized that lysorophians are connected to the origins of modern amphibians (frogs, salamanders, and caecilians). Critics of this idea point out that most of the features that link lysorophians and modern amphibians are shared absences, which is not strong evidence. However, this idea is driving much new research on the question of the origins of modern amphibians. *See* AISTOPODS; AMPHIBIA; MICROSAURIA. Jason S. Anderson

Bibliography. M. J. Benton, *Vertebrate Palaeontology*, 3d ed., Blackwell Press, London, 2004; R. L. Carroll, Lepospondyls, in H. Heatwole and R. L. Carroll (eds.), *Amphibian Biology*, vol. 4: *Palaeontology: The Evolutionary History of Amphibians*, pp. 1198–1269, Surrey Beatty, Chipping Norton, NSW, Australia, 2000; R. L. Carroll, *Vertebrate Paleontology and Evolution*, Freeman, New York, 1988; C. F. Wellstead, Taxonomic revision of the Lysorophia, Permo-Carboniferous lepospondyl amphibians, *Bull. Amer. Mus. Nat. Hist.*, 209:1–90, 1991; C. F. Wellstead, Order Lysorophia, in P. Wellnhofer and R. L. Carroll (eds.), *Encyclopedia of Paleoherpetology*, vol. 1: *Lepospondyli*, pp. 133–148, Verlag Dr. Friedrich Pfeil, München, 1998.

Lysosome

A digestive structure found within virtually all types of animal cells. Lysosome sizes, microscopic appearances, and other properties vary among different cell types and circumstances owing, in part, to differences in their functions and states. Typical lysosomes (**Figs. 1** and **2**) are roughly spherical or elongate

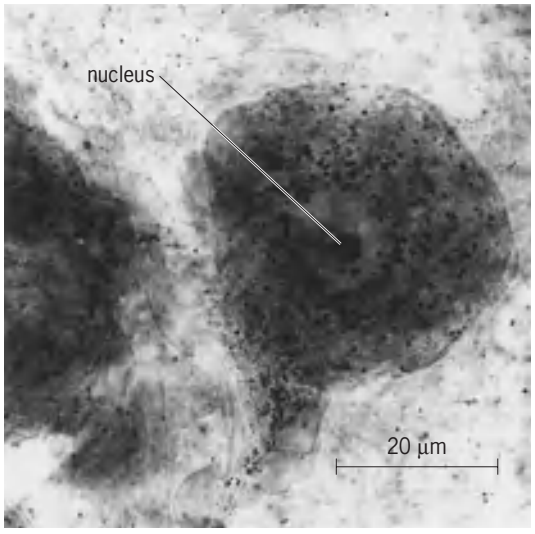

Fig. 1. Light microscope image of a nerve cell treated to show the locations of the lysosomal enzyme aryl sulfatase. The lysosomes show as small dark granules in the cell's cytoplasm. (*From E. Holtzman, Lysosomes in the physiology and pathology of neurons, in J. T. Dingle and H. B. Fell, eds., Lysosomes in Biology and Pathology, vol. 1, North Holland, 1969*)

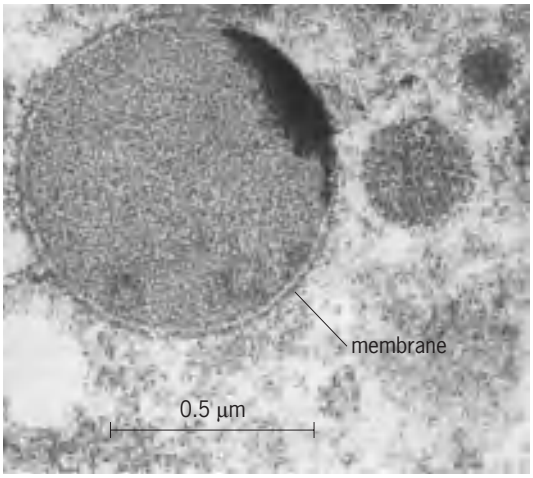

Fig. 2. Electron microscope image of a lysosome from the adrenal gland after treatment to reveal the lysosomal enzyme aryl sulfatase. The membrane bounding a mature secondary lysosome surrounds contents that appear moderately dark and heterogeneous. The very dark patch results from the cytochemical reaction that demonstrates the presence of the sulfatase enzyme. (*Reproduced, with permission, from E. Holtzman and R. Dominitz, Cytochemical studies of lysosomes, Golgi apparatus and endoplasmic reticulum in secretion and protein uptake by adrenal medulla cells of the rat, J. Histochem. Cytochem., 16:320–326, 1968*)

bodies with largest dimensions of 0.1–1 micrometer or greater; tens to hundreds are present in a single cell.

Enzymes. Each lysosome is bounded by a membrane and contains several dozen different species of digestive enzymes, each of which can sever (by hydrolysis) particular chemical bonds found in natural materials. Collectively, the enzymes are capable of splitting most of the large molecules of living systems—proteins, nucleic acids, complex lipids, polysaccharides—into their component parts, such as amino acids. The enzymes are made by the ribosomes of the rough endoplasmic reticulum and pass to the Golgi apparatus before being sorted to the lysosomes. In cells of higher animals, this sorting depends partly on the enzyme molecules being tagged with the sugar derivative mannose-6-phosphate. Specific membrane-associated proteins, known as mannose phosphate receptors, recognize and bind to molecules carrying the mannose-6-phosphate tag and segregate them into membrane-bounded transport vehicles, such as vesicles, for eventual delivery to digestive bodies. The transport vehicles for newly made hydrolases are sometimes called primary lysosomes to distinguish them from late endosomes and other secondary vacuoles, in which the enzymes have been mixed with materials undergoing digestion or with indigestible residues of earlier digestion. *See* CELL MEMBRANES; ENDOPLASMIC RETICULUM; ENZYME; GOLGI APPARATUS.

Most lysosomal enzymes function best in an acid environment, and the interior of the endosomal-lysosomal system displays a pH gradient (pH 5–6 or less) with the lysosome itself exhibiting the greatest acidity. This acidification is accomplished by an energy-dependent mechanism, a proton pump, which is built into the membrane surrounding the lysosome and which effects the transport of hydrogen ions into the lysosomes. *See* ION TRANSPORT.

Principal roles. Lysosomes digest materials taken into the cell from the outside (a process known as heterophagy) as well as other materials that originate in the cell's own cytoplasm (autophagy) [**Fig. 3**]. The materials to be digested are ultimately incorporated into the same membrane-bounded compartments as the lysosomal enzymes. Selective degradative products can pass out of the lysosome by crossing the membrane, but the enzymes cannot. This sequestration, which protects the cell, persists because the admixture of the enzymes and the materials to digest takes place through fusion of membrane-bounded compartments.

In heterophagy, the cell takes up particles or molecules by the process of endocytosis, engulfing them in membrane-bounded vesicles or vacuoles that are formed at the cell surface. The endocytosed material enters lysosomes via intermediate compartments known as endosomes. These are membrane-bounded bodies with moderately acidic interiors that possess limited digestive capacities at some stages of their life histories. One role of endosomes is the separation of endocytosed materials destined for lysosomal degradation from membrane-associated molecules which are sent back to the cell surface to be reused. Trafficking of molecules through the endosomal-lysosomal system may have significant influence over receptor-mediated signaling and signal transduction. *See* ENDOCYTOSIS.

Heterophagy is employed by many protozoa to obtain nutrients. In multicellular organisms, it is used to process some nutrients. For example, cholesterol can enter mammalian cells by uptake and lysosomal hydrolysis of particulate complexes of lipids and proteins that circulate in the blood. In higher animals, however, heterophagy is most prominently used by leukocytes and macrophages. These specialized cells endocytose invasive microorganisms and use endocytosis in clearing debris and disposing of dead or senescent cells that result from injury or from natural processes such as the regression of tadpole tails or the aging of red blood cells. *See* CELL SENESCENCE AND DEATH; PHAGOCYTOSIS.

Other cell types call upon elements of the endocytic and heterophagic systems for other specialized functions. The thyroid gland produces hormones by using heterophagy to release them from large proteins. Cells of the immune system employ endocytosis and endosome- or lysosome-related structures to fragment some of the foreign materials (antigens) that the immune system is designed to eliminate; the molecular fragments are then moved to the cell surface, where they take part in processes of antibody production. *See* CELLULAR IMMUNOLOGY.

In autophagy (Fig. 3), cells segregate regions of their own cytoplasm within compartments that come to be bounded by single membranes and to receive lysosomal enzymes. Autophagic lysosomes take part in the remodeling of cells as part of

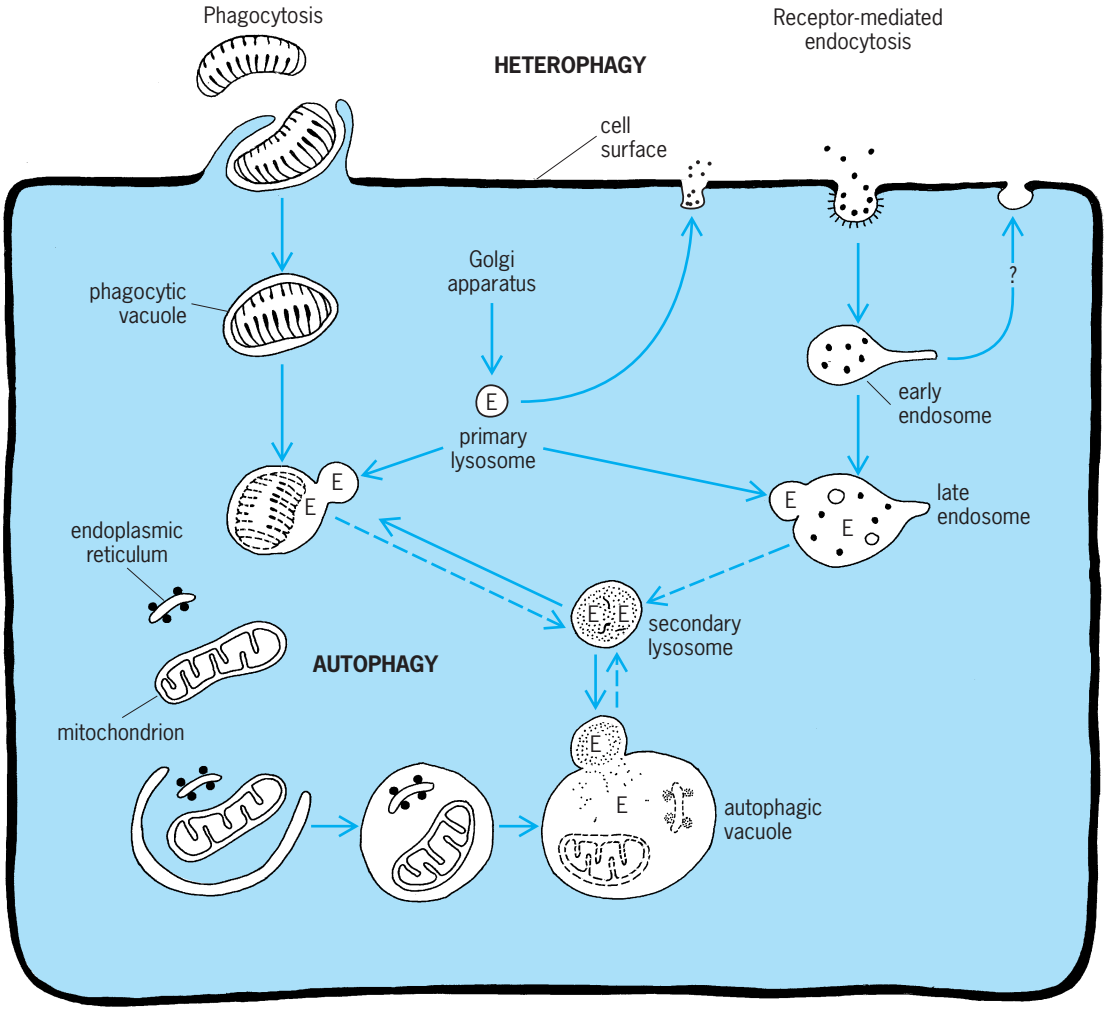

Fig. 3. Intracellular digestive phenomena. In one form of heterophagy, phagocyte cells take up particles into vacuoles arising from the plasma membrane. In receptor-mediated endocytosis, another form of heterophagy, molecules bind to receptors in the plasma membrane. After internalization by the cell, the molecules are delivered to an endosome where the receptors may be freed to return to the cell surface while other endocytosed molecules undergo digestion by lysosomal enzymes (E). In autophagy, the cell sequesters and digests portions of its own cytoplasm. Both autophagic and heterophagic lysosomes may evolve (broken arrows) into bodies containing lysosomal enzymes and indigestible residues.

the processes of development and during stressful circumstances. They also participate, along with nonlysosomal enzymes and heterophagic lysosomes, in normal turnover of the body's constituents—the balanced synthesis and destruction through which most molecules of most cells are replaced by new molecules over periods of hours to weeks.

Older lysosomes can recycle by fusing with newer digestive structures (Fig. 3). Lysosomes also sometimes fuse with the cell surface, releasing their contents to the extracellular space, and differential lysosomal enzyme secretion may be a common feature in many cell types. Cells known as osteoclasts use such fusion to help create extracellular digestive chambers for sculpting and remodeling of bone during growth and development. *See* SKELETAL SYSTEM.

Involvement in disease. Genetic defects in lysosomal enzymes and related proteins are known to be associated with a large number of rare disorders in humans and animals (such as Tay-Sachs disease and Niemann-Pick disease type C). Defective lysosomal function leads to storage of particular classes of molecules that cannot be degraded and, in long-lived cells such as neurons, to complex pathogenic cascades with widespread impact on endosomal-lysosomal function, membrane trafficking, and signal transduction. Such disorders are most often fatal. Lysosomes or prelysosomal structures also have been "adopted" as intracellular homes by certain pathogenic microorganisms that avoid or survive the attacks of the lysosomal system. Some strains of viruses, and toxins such as the one responsible for diphtheria, may use endosomes as their route of entry into the cell, penetrating through the endosomal membrane into the surrounding cytoplasm.

Plants, yeast, and fungi. In plant cells, yeast, and fungi, many of the structures that are known as vacuoles are closely related to lysosomes in that they are acidified and contain degradative enzymes. In some plant cells, a single vacuole is the largest intracellular compartment, occupying as much as 90%

of the cell's volume. Less is known about the digestive functions of vacuoles than of the lysosomes of animal cells, but vacuoles can be used for extensive storage of amino acids, proteins, pigments, and other molecules. In addition, they play a central role in the osmotic regulation of water balances, which is crucial to plant cell architecture and growth. *See* CELL (BIOLOGY); VACUOLE.

Eric Holtzman; S. U. Walkley

Bibliography. E. Holtzman, *Lysosomes*, 1989; J. B. Lloyd and R. W. Mason (eds.), Biology of the Lysosome, *Subcellular Biochemistry*, vol. 27, 1996; B. Storrie and R. F. Murphy (eds.), *Endosomes and Lysosomes*: *A Dynamic Relationship*, 1993.

Lysozyme

An enyme that was first identified and named by Alexander Fleming, who recognized its bacteriolytic properties. It has been designated muramidase, since it is known to facilitate the hydrolysis of a β-1-4-glycosidic bond between *N*-acetylglucosamine and *N*-acetylmuramic acid in bacterial cell walls; it also hydrolyzes similar glycosidic bonds in fragments of chitin. In recognition of this enzyme function, the International Enzyme Commission assigned the official chemical name of *N*-acetylmuramide glycanohydrolyase, coded as 3.2.1.17.

The most detailed studies have been performed on hen egg-white lysozyme, because this product is readily available. However, enzymes possessing lysozyme activity have been found in bacteria, bacteriophages, and plants and in human leukocytes, nasal secretions, saliva, and tears. People with a certain type of monocytic leukemia excrete large quantities of lysozyme in their urine. This excretion is presumed to be secondary to the synthesis of the enzyme by the large mass of leukemic cells.

The three-dimensional structure of the protein has been defined by x-ray crystallography. Additional data are available for the amino acid sequence of human lysozyme and also for a bacteriophage lysozyme. These results have given rise to speculation concerning the origin of the lysozyme gene during evolution.

Amino acid sequence. The complete amino acid sequence of hen egg lysozyme was determined independently by P. Jollès and by R. E. Canfield with their respective coworkers. The molecule consists of a single polypeptide chain containing 129 amino acid residues. The complete structure is illustrated in **Fig. 1**. This was determined by a technique which involved splitting the reduced alkylated lysozyme molecule into small peptide fragments with the proteolytic enzymes trypsin, chymotrypsin, and pepsin. The precise sequence of amino acids in each of the isolated fragments was then determined by the Edman degradation technique.

There are eight half-cystine residues in hen egg lysozyme, arranged in the native molecule as four cystine bridges. M. Inouye and A. Tsugita reported the amino acid sequence of a lysozyme synthesized by T4 bacteriophage that facilitates the penetration of phage deoxyribonucleic acid (DNA) through the bacterial cell wall. The protein is a single polypeptide chain containing 160 amino acid residues and no cystine bridges.

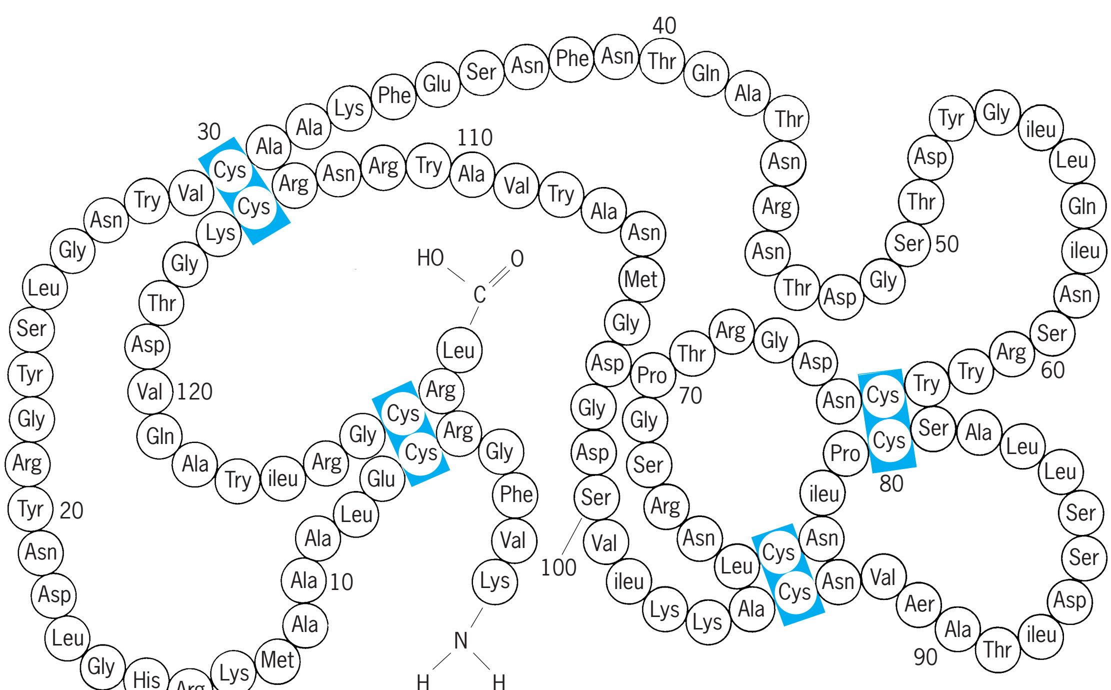

Fig. 1. Amino acid sequence of hen egg lysozyme. Four rectangles indicate cystine bridges. Ala, alanine; Arg, arginine; Asn, asparagine; Asp, aspartic acid; Cys, half-cystine; Gln, glutamine, Glu, glutamic acid; Gly, glycine; His, histidine; Ilen, isoleucine; Leu, leucine; Lys, lysine; Met, methionine; Phi, phenylalanine; Pro, proline; Ser, serine; Thr, threonine; Try, tryptophan; Tyr, tyrosine; Val, valine. (*After R. E. Canfield and A. K. Liu, J. Biol. Chem., 240:1997, 1965*)

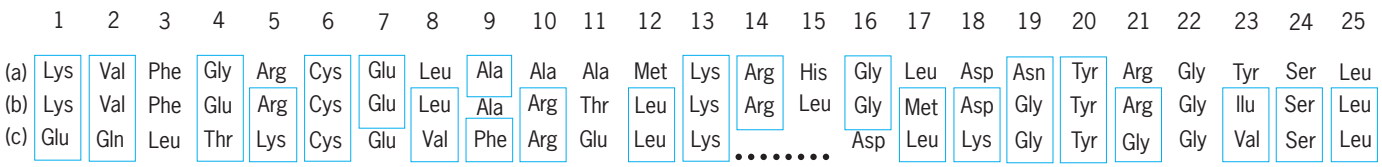

Fig. 2. Amino acid terminal sequences for (*a*) hen egg lysozyme, (*b*) human lysozyme, and (*c*) α-lactalbumin from cow milk. Rectangles identify common structural features. Dotted line for milk α-lactalbumin at positions 14-15 indicates gene deletion. Abbreviations are as in Fig. 1.

A portion of the structure of human lysozyme, described by Canfield, is illustrated in **Fig. 2**.

X-ray crystallography. D. C. Phillips and coworkers constructed a model of hen egg lysozyme based on a detailed x-ray crystallographic study of the three-dimensional structure of the enzyme at a resolution that permitted discrimination of structural features that were separated by a distance of 2 angstroms (0.2 nanometer). This model agreed with the primary structure shown in Fig. 1, including the location of the disulfide bonds. The lysozyme molecule appears to be folded in a fashion that accommodates most of the hydrophobic amino acid side chains inside the molecule, where they are removed from contact with the aqueous solvent, while most of the polar groups are distributed at the surface.

A unique aspect of the hen egg lysozyme model is the presence of a long cleft in the surface of the molecule. A trisaccharide inhibitor of lysozyme (tri-*N*-acetylglucosamine) can be bound in the cleft. This binding occurred at the same location when the inhibitor was diffused into crystals of lysozyme and when lysozyme was crystallized in the presence of the inhibitor. This unique binding of the inhibitor in the cleft may serve to localize the region of the active site of lysozyme. Of the various ways in which a model of the enzyme's substrate can be fitted into the region of the active site, the most favorable arrangement places the β-1-4-glycosidic bond that is hydrolyzed by lysozyme directly between the carboxyl group of the aspartic acid in position 52 and the carboxyl group of the glutamic acid in position 35 (Fig. 1). Structural observations indicate that these two amino acids have an important function in the mechanism of action of lysozyme.

Evolution. Certain enzyme functions appear to be widely distributed in nature. The amino acid sequences of proteins possessing these functions reflect changes that have occurred in the course of evolution. The structures of lysozymes from three sources, distant in evolution, have been carefully examined. Hen egg lysozyme (Fig. 1) has no structural elements in common with bacteriophage lysozyme. Thus it must be concluded that these two enzymes emerged in evolution completely independent of each other. Preliminary studies of the structure of human lysozyme reveal considerable similarity to the structure of hen egg lysozyme. In fact, the resemblance is so great, including the strategically placed aspartic and glutamic acids in the active site, that it can be concluded that these proteins evolved from the same gene and have an essentially identical mechanism of action. Figure 2 illustrates this similarity, or homology, for the first 25 amino acid residues of these two lysozymes, where 18 of the first 25 are identical.

The amino acid composition of α-lactalbumin, a protein in cow's milk, is quite similar to that of hen egg lysozyme; nearly half of the amino acid positions in these two proteins are identical (Fig. 2). This is surprising since hen egg lysozyme operates to hydrolyze a β-1-4-glycosidic bond between amino sugars in bacterial cell walls, while α-lactalbumin facilitates the synthesis of β-1-4-glycosidic bond between glucose and galactose to form lactose. One possible explanation is that the lysozyme gene was accidentally duplicated at some point in evolution and that subsequently one of the genes acquired lactose synthetase function. This new function seems to have appeared late in evolution, and is coincident with the development of breast feeding.

It is postulated from a comparison of the amino acid sequences of hen egg lysozyme, human lysozyme, and α-lactalbumin (Fig. 2) that a "deletion" occurred during evolution in the α-lactalbumin gene with a resulting loss of information for two amino acids near position 13. In addition, positions 10, 12, and 19 in human lysozyme and α-lactalbumin are identical, so it is possible to see remnants of a common ancestral gene in all three proteins. These data illustrate the manner in which amino acid sequence information is being used as a molecular reflection of the paths of evolution. *See* PROTEINS, EVOLUTION OF.

Experimental approach. One approach to the problem of determining the mechanism of action of the enzyme is to determine the structure of other lysozymes that derive their catalytic activity from amino acid sequences different from that of hen egg lysozyme. An examination of the structure of the active sites in these other lysozymes will permit the exploration of the common features that are essential for enzyme activity. If the present hypothesis based on the location of the active site for the mechanism of lysozyme action is correct, then the finding of two carboxyl groups immediately adjacent to the substrate bond that is hydrolyzed is to be expected. The data for human lysozyme appear to follow this pattern.

The synthesis of various substrate analogs will also be important in future work, because as these are fitted into the model of the lysozyme cleft, it should be possible to predict their chemical behavior and

verify the predictions by experiments. *See* BACTERIA; CRYSTALLOGRAPHY; ENZYME; LYSIN; LYTIC REACTION; POLYSACCHARIDE.

Robert E. Canfield

Bibliography. K. Hayashi and N. Sakamoto (eds.), *Dynamic Analysis of Enzyme Systems*, 1985; C. P. Hollenberg and H. Sahm (eds.), *Microbial Genetical Engineering and Enzyme Technology*, 1987; S. Smith-Gill and E. Sercarz (eds.), *The Immune Response to Structurally Defined Proteins*: *The Lysozyme Model*, 1989.

Lytic infection

Infection of a bacterium by a bacteriophage with subsequent production of more phage particles and lysis, or dissolution, of the cell. The viruses responsible are commonly called virulent phages. Lytic infection is one of the two major bacteriophage–bacterium relationships, the other being lysogenic infection. *See* BACTERIOPHAGE; COLIPHAGE; LYSOGENY.

Philip B. Cowles

Lytic reaction

A term used in serology to describe a reaction that leads to the disruption or lysis of a cell. The best example is the lysis of sheep red blood cells by specific antibody and complement in the presence of Ca^{2+} (calcium ion) and Mg^{2+} (magnesium ion), a reaction that forms the indicator system of the standard Wassermann test for syphilis, as well as other complement-fixation reactions. In this example, lysis results in the release of cellular hemoglobin into the medium; the reaction may be followed by visual or instrumental estimation of the decreased cell turbidity or the increased color of the medium due to the free hemoglobin. The initiation of lysis by complement can apparently proceed after the attachment of only one molecule of IgM or two molecules of IgG antibody to the red blood cell. IgM and IgG are both immunoglobulins. *See* IMMUNOGLOBULIN.

Pfeiffer reaction. This is an example of a bacteriolytic reaction, carried out with gram-negative bacteria, such as cholera vibrios, which are especially susceptible to the lytic action of specific antibody, complement, and Mg^{2+} and Ca^{2+}. This reaction may be carried out in the living subject (Pfeiffer's system) or in the test tube, and is a valuable aid in diagnosis. An analogous reaction is given by the spirochetes of relapsing fever. Although demonstrable instances of bacteriolysis occur, it is not clear whether all the bactericidal actions of antibody and complement are necessarily preceded by lysis.

Phagocytic reaction. The engulfment of microorganisms by phagocytic cells is often accompanied by their digestion and lysis. The initial stages of this reaction are aided by specific antibody and by complement. It has been estimated that no more than 8 molecules of IgM or 2200 molecules of IgG are needed for the phagocytosis of a typical enteric bacterium. *See* PHAGOCYTOSIS.

Cytotoxic assays. A variety of reactions have come into use because of the necessity of detecting tissue incompatibilities before transplantation. The cell damage, including permeability changes resulting from the actions of antibody and complement, can be estimated from the differential staining by dyes or by assay of the release of tracers. *See* COMPLEMENT; COMPLEMENT-FIXATION TEST; SEROLOGY.

Henry P. Treffers

Bibliography. P. Agre and J. C. Parker, *Red Blood Cell Membranes*: *Structure*, *Function*, *Clinical Implications*, 1989; J. Bryant, *Laboratory Immunology and Serology*, 2d ed., 1986; M. L. Turgeon, *Immunology and Serology in Laboratory Medicine*, 2d ed., 1996.

Macadamia nut

The fruit of a tropical evergreen tree, *Macadamia ternifolia*, native to Queensland and New South Wales and now grown commercially in Australia and Hawaii. The trees grow to 50 ft (15 m) in height and have dense foliage of glossy, leathery leaves. They bear many small white or pinkish flowers in drooping racemes, each of which may mature from 1 to 20 fruits. These consist of a leathery outer husk (pericarp) which splits along one side at maturity, freeing the very hard-shelled, nearly round seed or nut about an inch in diameter. Two types of nuts are recognized: the most important commercially having a smooth shell and the other having a rough shell and sometimes referred to another species, *M. integrifolia* (see **illus.**).

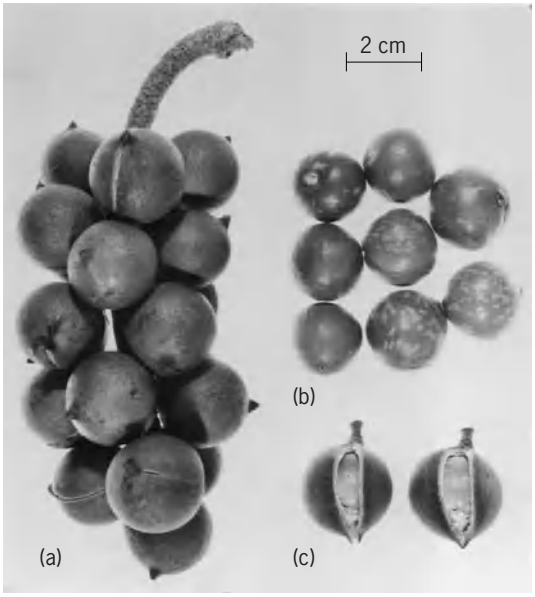

***Macadamia integrifolia*. (*a*) Mature nuts. (*b*) Nuts without husks. (*c*) Nuts in husk showing method of dehiscence. (*From R. A. Jaynes, ed., Handbook of North American Nut Trees, Humphrey Press, 1969*)**

Successful culture of the trees as an orchard crop requires a tropical climate, good well-drained soil, abundant rainfall (50 in. or 1.3 m or more), and soil management to control competing vegetation. Protection from strong winds is essential. Trees have been grown successfully in Florida and California, but the nuts are commercially important only in Hawaii.

Macadamia nuts ripen over a period of several months: As immature nuts they are of little value; the nuts are allowed to mature on the trees and fall to the ground, where they are picked up by hand, machine-hulled, dried, and stored for processing. After machine-cracking, the kernels are graded by floating in water, where the high-quality kernels float and are skimmed off. They are then roasted, usually in oil, salted, and packed, with glass jars being used for best-grade nuts. The processed nuts are of high quality and find a ready market. *See* NUT CROP CULTURE.

Laurence H. MacDaniels

Mach number

In the flow of a fluid, the ratio of the flow velocity, V, at a given point in the flow to the local speed of sound, a, at that same point. That is, the Mach number, M, is defined as V/a. In a flowfield where the properties vary in time and/or space, the local value of M will also vary in time and/or space. In aeronautics, Mach number is frequently used to denote the ratio of the airspeed of an aircraft to the speed of sound in the freestream far ahead of the aircraft; this is called the freestream Mach number. The Mach number is a convenient index used to define the following flow regimes: (1) subsonic, where M is less than 1 everywhere throughout the flow; (2) supersonic, where M is greater than 1 everywhere throughout the flow; (3) transonic, where the flow is composed of mixed regions of locally subsonic and supersonic flows, all with local Mach numbers near 1, typically between 0.8 and 1.2; and

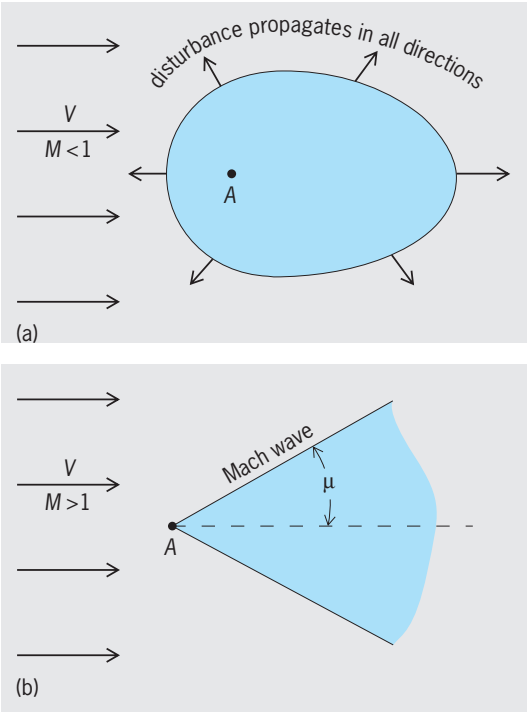

Propagation of disturbances from a stationary source in (*a*) subsonic flow and (*b*) supersonic flow.

(4) hypersonic, where (by arbitrary definition) M is 5 or greater.

Perhaps the most important physical aspect of Mach number is in the completely different ways that disturbances propagate in subsonic flow compared to that in a supersonic flow. Consider an initially uniform flow from left to right in the plane of this page, as shown in the **illustration**. First consider a subsonic flow. Imagine that you jab the subsonic flow in illus. *a* with a needle perpendicular to the page at point A. The weak disturbance created will propagate in all directions at the local speed of sound relative to the flow. Because the initially uniform flow is moving at less than the speed of sound, the disturbance will work its way upstream, eventually covering the entire extent of the flow. The shaded region in illus. *a* is a qualitative sketch of the subsonic flow region affected by the disturbance at some instant after you have jabbed it at point A. In illus. *b*, when you jab the supersonic flow with the needle at point A, once again the disturbance will want to propagate in all directions at the local speed of sound. However, because the initially uniform flow is already moving at a velocity greater than the speed of sound, the disturbance will not be able to work its way upstream; rather, it will be swept downstream, affecting only the conical shaded region. This region is bounded by a Mach wave at an angle μ to the freestream direction. The angle μ is defined as the Mach angle, given by $\mu = \sin^{-1}(1/M)$. If the disturbance at point A is strong (not weak, as in the example), the disturbed region is bounded by an oblique shock wave which is at an angle larger than μ. Severe, almost discontinuous changes take place across shock waves; for example, the pressure, density, and temperature increase across a shock wave, sometimes dramatically. Shock waves are a ubiquitous aspect of supersonic flows. Because of the phenomena in the illustration, the physical aspects of subsonic and supersonic flows are quite different.

The physical importance of the ratio of flow velocity to the speed of sound was recognized and studied as early as 1887 by the scientist and philosopher Ernst Mach in Prague. The term "Mach number" for this ratio was coined in 1929 by Jakob Ackeret in Zurich, and did not find its way into the English literature until the late 1930s. *See* COMPRESSIBLE FLOW; SHOCK WAVE; SONIC BOOM; SUPERSONIC FLIGHT.

John D. Anderson, Jr.

Bibliography. J. D. Anderson, Jr., *Fundamentals of Aerodynamics*, 2d ed., McGraw-Hill, 1991; J. D. Anderson, Jr., *A History of Aerodynamics*, Cambridge University Press, 1997; J. D. Anderson, Jr., *Modern Compressible Flow, with Historical Perspective*, 2d ed., McGraw-Hill, 1990; L. W. Reithmaier, *Mach 1 and Beyond*, McGraw-Hill, 1994.

Machinability of metals

The ease and economy with which a metal may be cut under average conditions. Frequently no truly quantitative assessment is made, but rather a rating or an index is established vis-à-vis a reference material. More quantitative comparisons are based on tool life. For example, maximum cutting speeds for a given tool life may be used as a rating of machinability. Alternatively, tool wear rate may be the basis for a machinability rating. Surface finish is sometimes used for assessing machinability.

Machining process. The wide range of metal-cutting processes may be represented, with some oversimplification, by the orthogonal cutting process (**Fig. 1**). A rectangular metal workpiece is machined by a tool with a face at a rake angle γ_c measured from the normal of the surface to be machined. A clearance angle Θ exists between the flank of the tool and the machined surface of the workpiece. The

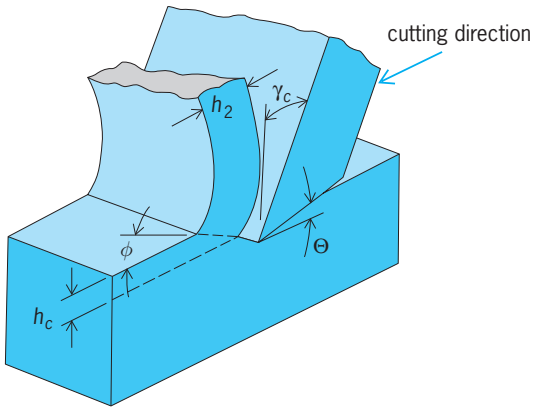

Fig. 1. Orthogonal cutting process: a simplified view of machining. (*After J. A. Schey, Introduction to Manufacturing Processes, McGraw-Hill, 1977*)

tool cuts into the workpiece to a depth h_c. However, the emerging chip is thicker than h_c. The chip thickness h_2 reflects intense shearing that takes place at an angle ϕ to the workpiece surface.

Cutting speed. The machining response of ductile metals is very sensitive to cutting speed (**Fig. 2**). Below about 0.06 ft/s (0.02 m/s), chips form discontinuously, metal chunks are lifted out of the surface, and the surface is scalloped or pockmarked (Fig. 2*b*). When the speed is in the 0.1 m/s range, chips are formed continuously, the shear zone is narrow, and the chip slides on the tool face (Fig. 2*b*). Under these conditions a cutting fluid can lubricate both the rake and flank faces of the tool. If the speed is increased to 1.0 ft/s (0.3 m/s) or so, sticking starts to occur at the tool-workpiece interface due to the increased heat generation. The metal begins to shear along a built-up edge of metal which is stuck to the tool face (Fig. 2*c*). The appearance of the built-up edge has several practical consequences. The effective rake angle becomes quite large, and energy consumption drops. The surface finish is poor, however, owing to the ill-defined tool tip and sporadic breakdowns in the builtup edge. At much higher speeds (above 3.2 ft/s or 1.0 m/s), heat generation is even more intense, and temperature increases of several hundred degrees Celsius may occur. Under these conditions the built-up edge disappears, and the chip makes full, sticking contact with the tool face (Fig. 2*d*). The chip moves by shearing along the so-called secondary shear zone. With the high temperature, workpiece strength may be so low that power consumption is lower in spite of the extensive shearing. The most serious problem associated with the high temperature may be the possibility of diffusional bonding occurring between the tool and workpiece. If alloying elements of the tool material diffuse into the workpiece, very rapid wear (called crater wear) develops.

Cutting fluid. The interaction of the tool and the workpiece is considerably affected by the presence of cutting fluids. Cutting fluid has two primary functions. First, as long as the cutting speed is slow, the cutting fluid can act as a lubricant between the chip and the tool face. Even at higher speeds some lubricating effect at the flank face may be present. Second, and perhaps more importantly, the cutting fluid serves as a coolant. In most instances the cutting fluid will be an emulsion of a lubricating phase (oil, graphite, and so on) in water, since water is the best heat-transfer medium readily available. Beyond lubrication and cooling, the cutting fluid can be used to flush out the cutting zone.

Surface quality and tool wear. Cutting speed thus affects the all-important machinability considerations of surface quality and tool wear. As implied by Fig. 2, surface finish is best with well-lubricated, moderately low-speed operation or high-speed cutting with no built-up edge. The high pressures and temperatures of operation, abetted by shock loading and vibrations, can lead to rapid tool wear. Tool wear is often sufficiently rapid to make tool replacement a major factor in machining economics. Tools must

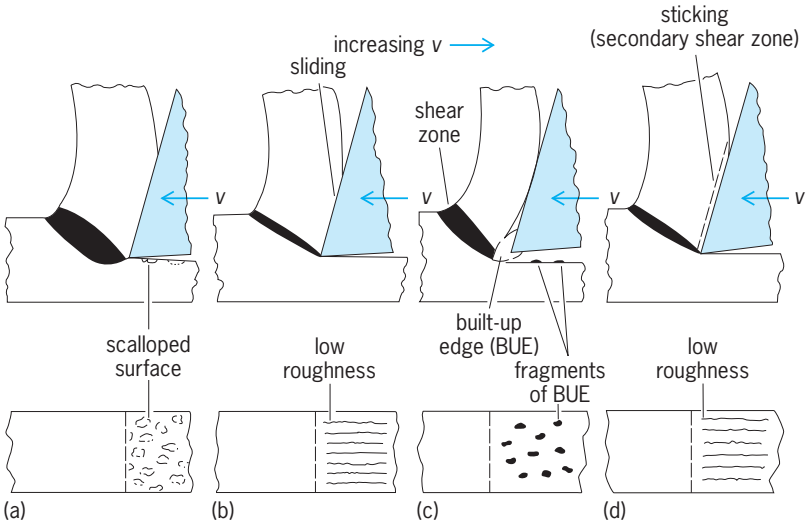

Fig. 2. Changes in chip formation and surface finish with increasing cutting speed: (*a*) 0.02 m/s; (*b*) 0.1 m/s; (c) 0.3 m/s; and (*d*) above 1.0 m/s. (*After J. A. Schey, Introduction to Manufacturing Processes, McGraw-Hill, 1977*)

be replaced when they break or when they have worn to the point of producing an unacceptable surface finish or an unacceptable degree of surface heating. Whereas cracking and chipping occur suddenly, other forms of wear occur gradually. Gradual wear is related to rubbing distance and temperature, and thus to speed v. It often follows the Taylor power law, $C = vt^n$, where C is the cutting speed leading specifically to 1 minute of tool life, t is actual tool life in minutes, and n is the Taylor exponent. Both C and n reflect the tool and workpiece combination.

Metal properties. A machining operation can be optimized to effect metal removal with the least energy, or the best surface, or the longest tool life, or a reasonable compromise among these factors. Even so, it remains that the optimum ease and economy of machining some alloys is vastly different from that of others, and some basic attributes of easily machined alloys can be set forth.

Toughness. To ensure that chip separation occurs after minimum sliding, low ductility is required. To minimize cutting force, low strength and low ductility combine to mean low toughness. Toughness is generally defined as energy per unit volume consumed en route to fracture. Ironically, materials of maximized toughness are desirable for most engineering applications and, thus, some of the most attractive alloys, such as austenitic stainless steels, are difficult to machine.

Adhesion. The degree to which the metal adheres to the tool material is important to its machinability. Actually this attribute can work to advantage or disadvantage. If diffusion results, the tool can be weakened, and rapid wear occurs. Otherwise, high adhesion will stabilize the secondary shear zone.

Workpiece second phases. Small particles or inclusions in the metal can have a marked effect on machinability. Hard sharp oxides, carbides, and certain intermetallic compounds abrade the tool and accelerate

tool wear. On the other hand, soft second phases are beneficial because they promote localized shear and chip breakage.

Thermal conductivity. In some cases, workpiece thermal conductivity can be important to machinability. A low thermal conductivity generally results in high shear-zone temperature. This can be advantageous in reducing the strength of the metal or in softening second-phase particles. Of course, if adhesion and diffusional depletion of tool alloy content result, the high temperature is a problem. The workpiece temperature can be managed by cutting-speed and cutting-fluid manipulation.

Alloy systems. Commercial alloys can be grouped into two categories, namely those designed for ease of machining (so-called free machining grades), and the vast majority which are of widely varying but generally less than optimum machinability. Considering these latter, ordinary alloys, it can be shown that their machinability may be considerably improved by metallurgical operations which limit strength or ductility or both. Of course, it is not often possible to simultaneously reduce both strength and ductility. Even so, machinability often can be improved by grossly reducing one or the other property.

Consider the range of plain carbon steels represented in **Fig. 3**. In each case, the steel can be produced in three relevant forms: fully annealed (pearlitic), spheroidized, or cold-worked. For steel in the 0.20% C range, the annealed and spheroidized conditions involve too much ductility for optimum machinability. Better machinability can be had by reducing the ductility through cold work, even if strength is increased. In the 0.45% C range, the cold-worked material is too strong, and the intermediate strength and ductility of the annealed condition is optimum. In the 0.70% C range, the large quantities of lamellar carbide in the annealed pearlitic form are too abrasive and promote tool wear. Better machinability is possible with the globular carbides and lower strength of the spheroidized condition despite its high ductility. *See* STEEL.

Similar cases may be cited for other alloy systems, and the following principles are fairly general: (1) soft, ductile materials are more machinable when work-hardened; (2) hard materials with hard second phases are best machined in the well-annealed or overaged condition where globular particle shapes are developed; (3) moderate-strength age-hardenable alloys (such as age-hardenable Al alloys) are best machined in the aged and strengthened condition. *See* ALLOY.

Cast iron. Cast iron is a "natural" free-machining material. Gray cast iron with its large graphite flakes produces short chips without extra alloying or further process control. Moreover, the graphite itself serves as a lubricant. However, the machined surface is somewhat roughened by the breaking out of graphite particles. The machinability of gray iron may be further enhanced with a subcritical anneal (1 h at about 1380°F or 750°C) to graphitize the carbide that exists in the pearlite lamellae. The resultant structure is totally iron and flake graphite. *See* CAST IRON.

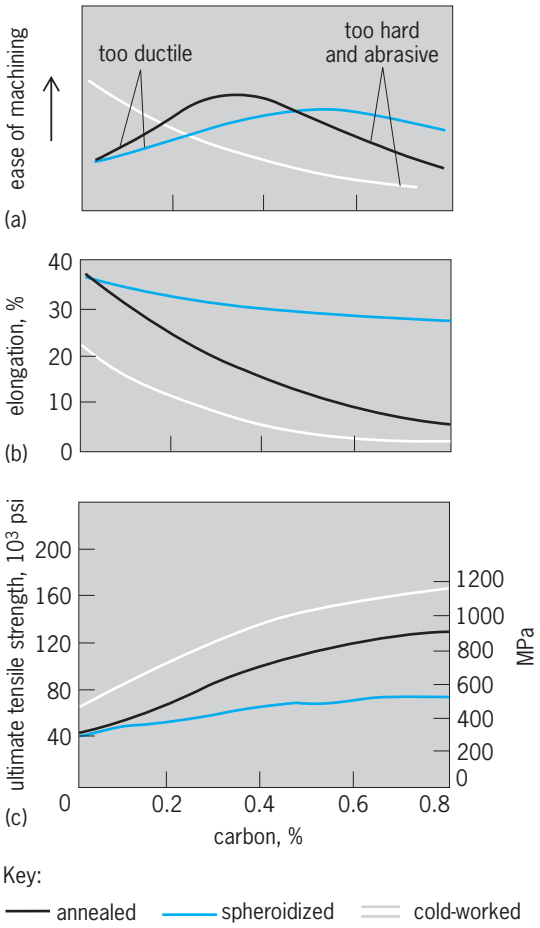

Fig. 3. The ease of machining carbon steels as a function of their metallurgical condition. (*a*) Ease of machining versus carbon content. (*b*) Elongation versus carbon content. (*c*) Ultimate tensile strength versus carbon content. (*After J. A. Schey, Introduction to Manufacturing Processes, McGraw-Hill, 1977*)

Lead additive. One of the most universal free-machining additives is lead. Lead is insoluble in iron, copper, aluminum, and alloys thereof. It can be finely dispersed as a soft second phase, which helps to break up the chips and, furthermore, lubricates the tool-workpiece interface. *See* LEAD ALLOYS; METAL, MECHANICAL PROPERTIES OF; PLASTIC DEFORMATION OF METAL.

Roger N. Wright

Bibliography. American Society for Metals, *Metals Handbook*, 9th ed., vol. 16: *Machining*, 1989; R. Baril, *Modern Machining Technology*, 1987; J. N. Harris, *Mechanical Working of Metals: Theory and Practice*, 1983; J. A. Schey, *Introduction to Manufacturing Processes*, 2d ed., 1987, rev. 2000; R. Stevenson and D. A. Stephenson (eds.), *Materials Issues and Physics of Machining Processes*, 1992.

Machine

A combination of rigid or resistant bodies having definite motions and capable of performing useful work. The term mechanism is closely related but applies only to the physical arrangement that provides for the definite motions of the parts of a machine. For

example, a wristwatch is a mechanism, but it does no useful work and thus is not a machine. Machines vary widely in appearance, function, and complexity from the simple hand-operated paper punch to the ocean liner, which is itself composed of many simple and complex machines. No matter how complicated in appearance, every machine may be broken down into smaller and smaller assemblies, until an analysis of the operation becomes dependent upon an understanding of a few basic concepts, most of which come from elementary physics. *See* MECHANISM; SIMPLE MACHINE. Richard M. Phelan

Bibliography. K. Sherwin, *Engineering Design for Performance*, 1982; J. E. Shigley and L. Mitchell, *Mechanical Engineering Design*, 6th ed., 2000.

Machine design

Application of science and invention to the development and construction of machines. An understanding of the basic laws of nature is essential to a proper perspective in the approach to machine design. Knowledge of the past development of machine elements makes possible their effective application. Inventiveness consists of producing new combinations of old elements or, where extreme need arises, of exercising genius either in breaking the bounds of convention, or in evolving new principles not hitherto applied or known.

In machine design, accomplishment takes on two forms: one is the drawings and blueprints, which completely describe the machine, and the other is the assembled product. In addition, most machines go through periods of evolution, and later models may show little outward similarity to the original design. *See* ENGINEERING DRAWING.

Machine design consists of the conception of a machine that will meet a specific need. Before constructing a machine to fulfill the need, the designer must thoroughly understand the application, and mentally modify an old machine or devise a new machine as required. A certain cost for the machine and a probable time for its construction are estimated. These estimates consider the materials required, the equipment necessary for its manufacture and testing, and the final operation in meeting the original need. If the machine is desirable, construction of the unit follows. In time the machine may become obsolete due to advances in the technology; it may then be rebuilt or replaced, possibly under the direction of the original designer.

The working tools in machine design are an understanding of the basic elements of machines that have been developed in the past and a thorough knowledge of the mechanical fields of science including mathematics, physics, statics and dynamics, strength of materials, kinematics, mechanisms, and the laboratories associated with them. *See* DYNAMICS; KINEMATICS; MATHEMATICS; MECHANISM; PHYSICS; STATICS; STRENGTH OF MATERIALS. James J. Ryan

Bibliography. R. H. Creamer, *Machine Design: Mechanical Engineering Technology*, 3d ed., 1983.

Machine elements

Elementary mechanical parts used as building blocks for the construction of most devices, apparatus, and machinery. The gradual development of these building blocks, following the invention of the roller or wheel and the arm or lever in ancient times, brought about the Industrial Revolution, starting with the assembly of James Watt's engine for harnessing the force of steam and proceeding into the advanced mechanization of present automatic control.

The most common example of a machine element is a gear, which, fundamentally, is a combination of the wheel and the lever to form a toothed wheel (see **illus.**). The rotation of this gear on a hub or shaft drives other gears which may rotate faster or slower, depending upon the number of teeth on the basic wheels. The material from which the gear is made establishes its strength, and the hardness of its surface determines its resistance to wear. Knowledge of the forces on the gear makes possible the determination of its size. Changes in its shape allow modifications in its use. These applications, as in most machine elements, have developed into many standard forms, such as spur, bevel, helical, and worm gears. Each of these forms has required the development of a special technology for its production and use. *See* GEAR.

Other fundamental machine elements have evolved from wheels and levers. A wheel must have a shaft on which it may rotate. The wheel is fastened to the shaft with a key, and the shaft is joined to other shafts with couplings. The shaft must rest in bearings, such as journal bearings, ball bearings, or roller bearings. The shaft may be started by a clutch or stopped with a brake. It may be turned by a pulley with a flat belt, a V belt, or a chain or a rope connecting it to a pulley on a second shaft. The supporting structure may be assembled with bolts or rivets or by welding. Proper application of these machine elements depends upon a knowledge of the forces on the structure and the strength of the materials employed. In the design, calculations must accommodate the forces to the materials in the simplest construction. Other machine elements have been evolved whose applications are more specific in construction. *See* ANTIFRICTION BEARING; BRAKE; CAM

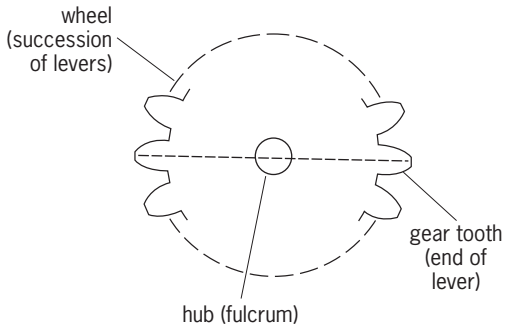

The gear, a machine element which combines features of the wheel and the lever.

MECHANISM; CLUTCH; COUPLING; FLYWHEEL; FOUR-BAR LINKAGE; GOVERNOR; MACHINE KEY; SCREW FASTENER; SHAFTING; SPRING (MACHINES); WHEEL AND AXLE.

Machine parts which are commonly used have been developed into standardized designs. Manufacturing specialists have concentrated upon the development of standard elements and have mass-produced these parts with a high degree of perfection at reduced cost. Standard elements, as applied in machine design, may be modified as desired, although certain ones, through the hazards to safety under improper use, must be modified only in line with the requirements of codes established by regulating bodies. *See* DESIGN STANDARDS. James J. Ryan

Bibliography. E. Oberg et al., *Machinery's Handbook*, 26th ed., 2000.

Machine key

The most common function of a key is to prevent relative rotation of a shaft and the member to which it is connected, such as the hub of a gear, pulley, or crank. Many types of keys are available, and the choice in any installation depends on such factors as power requirements, tightness of fit, stability of connection, and cost. For light power requirements a setscrew may be tightened against the round shaft or against a flat spot on the shaft. For most requirements a positive connection, such as by a key, is necessary. A setscrew is frequently used to seat the key and to prevent axial motion.

Square keys are common in general industrial machinery (**Fig. 1***a*). Flat keys are used where added stability of the connection is desired, as in machine tools (Fig. 1*b*). Square or flat keys may be of uniform cross section or they may be tapered. In tapered keys the width is uniform and the height of the key tapers. Tapered keys may have gib heads to facilitate removal (Fig. 1*c*).

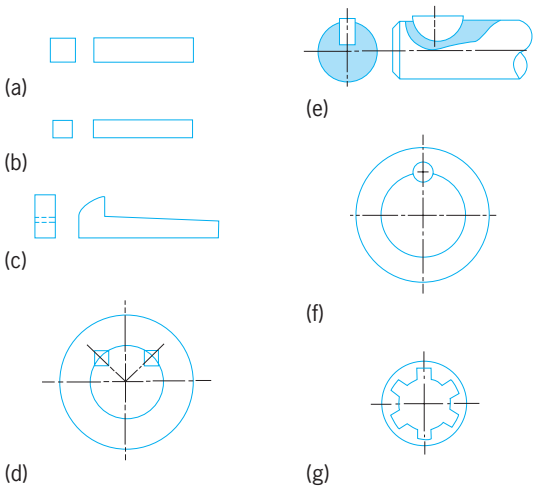

Fig. 1. Types of keys. (*a*) Square key. (*b*) Flat key. (*c*) Taper key with gib head. (*d*) Kennedy key. (*e*) Woodruff key. (*f*) Round key. (*g*) Spline fitting. (*After P. H. Black and O. E. Adams, Jr., Machine Design, 3d ed., McGraw-Hill, 1968*)

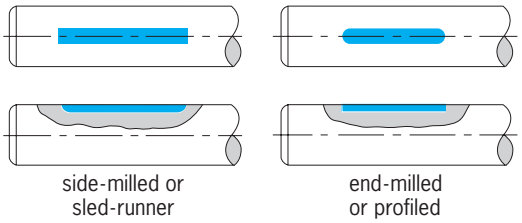

Fig. 2. Types of keyways. (*After P. H. Black and O. E. Adams, Jr., Machine Design, 3d ed., McGraw-Hill, 1968*)

The Kennedy key is used for heavy duty and consists of two keys driven 90° apart (Fig. 1*d*). The hub is bored to fit the shaft and is then rebored slightly off center. The keys force the shaft and hub into concentric position.

The Woodruff key requires a key seat formed by a special side-milling cutter (Fig. 1*e*). This key will align itself in the key seat. It has the disadvantage of weakening the shaft more than a straight key.

The round key, or pin, introduces less stress concentration at the key seat in the shaft and is satisfactory except for the necessity of drilling the hole to accommodate the pin after assembly of the hub and shaft (Fig. 1*f*). This may be a disadvantage in production and prevents interchangeability.

A spline fitting is composed of a splined shaft formed by milling and a mating hub with internal splines formed by broaching (Fig. 1*g*). The splines in reality are a number of keys integral with the shaft. Splined fittings are adaptable to mass production and are used where radial space must be conserved.

Straight-side splines are being replaced at an increasing rate by stub involute splines. These splines have the advantages of greater strength, a self-centering feature, and production economy.

Keyways for straight keys are formed either by a side-milling cutter which forms a sled-runner keyway, or by an end-milling cutter which forms profiled keyways (**Fig. 2**). The sled-runner keyway requires a longer space between the end of the key and the end of the keyway than does an end-milled keyway. This favors the end-milled keyway in locations near a shoulder. However, the end-milled keyway reduces the endurance limit of a shaft more than does the sled-runner type.

Feather keys are used where it is necessary to slide a keyed gear or pulley along the shaft. The key is generally tight in the shaft and with clearance between key and hub keyway. When a gear or pulley must be moved axially along the shaft while power is being transmitted, it is desirable to provide for a minimum of force necessary to move the hub along the shaft. The use of two feather keys equally spaced reduces the necessary axial force to half that for one key. *See* SHAFTING. Paul H. Black

Bibliography. P. H. Black and O. E. Adams, Jr., *Machine Design*, 3d ed., 1968; A. D. Deutschman et al., *Machine Design: Theory and Practice*, 1975; E. Oberg et al., *Machinery's Handbook*, 26th ed., 2000; J. Shigley, *Machine Design*, 1989.

Machinery

A group of parts arranged to perform a useful function. Normally some of the parts are capable of motion; others are stationary and provide a frame for the moving parts. The terms machine and machinery are so closely related as to be almost synonymous; however, machinery has a plural implication, suggesting more than one machine. Common examples of machinery include automobiles, clothes washers, and airplanes; machinery differs greatly in number of parts and complexity.

Some machinery simply provides a mechanical advantage for human effort. Other machinery performs functions that no human being can do for long-sustained periods. A jackscrew does nothing until a person pulls on a lever; then they are able to move objects many times their weight. Conversely, an internal combustion engine can run unattended for hours, requiring only the press of a button to start it.

The need for machinery usually stems from a desire to do a job at less cost. Evolution of machinery for a certain function may be gradual or rapid. If only small quantities of a product are needed, it is likely that machinery used in making the product will not change rapidly or possess the highest degree of automation. On the other hand, machinery used in making automobiles has evolved into some of the most complex automatic machines in existence. *See* AUTOMATION; MACHINE; MACHINE DESIGN; MECHANICAL ENGINEERING; SIMPLE MACHINE.

Robert S. Sherwood

Machining

Any one of a group of operations that change the shape, surface finish, or mechanical properties of a material by the application of special tools and equipment. Machining almost always is a process where a cutting tool removes material to effect the desired change in the workpiece. Typically, powered machinery is required to operate the cutting tools. *See* PRODUCTION METHODS.

Although various machining operations may appear to be very different, most are very similar: they make chips. These chips vary in size from the long continuous ribbons produced on a lathe to the microfine sludge produced by lapping or grinding. These chips are formed by shearing away the workpiece material by the action of a cutting tool. Cylindrical holes can be produced in a workpiece by drilling, milling, reaming, turning, and electric discharge machining. Rectangular (or nonround) holes and slots may be produced by broaching, electric discharge machining, milling, grinding, and nibbling; and cylinders may be produced on lathes and grinders. Special geometries, such as threads and gears, are produced with special tooling and equipment utilizing the same turning and grinding processes mentioned above. Polishing, lapping, and buffing are variants of grinding where a very small amount of stock is removed from the workpiece to produce a high-quality surface.

In almost every case, machining accuracy, economics, and production rates are controlled by the careful evaluation and selection of tooling and equipment. Speed of cut, depth of cut, cutting-tool material selection, and machine-tool selection have a tremendous impact on machining. In general, the more rigid and vibration-free a machining tool is, the better it will perform. Jigs and fixtures are often used to support the workpiece. Since it relies on the plastic deformation and shearing of the workpiece by the cutting tool, machining generates heat that must be dissipated before it damages the workpiece or tooling. Coolants, which also act as lubricants, are often used.

Boring. This machining operation increases the size of an existing hole in a workpiece. The usual purpose of boring is to produce a hole with an accurate diameter and good surface finish. Boring can be performed on a special machine or a lathe, with either the workpiece or the boring tool being on a movable table. A rotating spindle, holding either a single-point cutting tool or the workpiece, is fed into the work. As the spindle rotates, the cutting tool engages the interior of the existing hole, and chips are formed as the tool cuts into the workpiece. The actual cutting action of a boring tool is very similar to a lathe turning tool. Both the dimensional quality and the surface finish of the hole are determined by the rigidity and accuracy of the machine spindle and tool holder. The more rigid the machine is, and the more precisely the boring tool and spindle are controlled, the more precise the hole will be, both as to dimension and surface finish.

Broaching. This is the removal of material to produce a slot (or other formed shape) in a workpiece by moving a multiple-tooth, barlike tool across the workpiece. The cutting action results from the configuration of each tooth being progressively higher than the preceding one. Each tooth of the broach removes a small, predetermined amount of stock, the chip (**Fig. 1**). The peripheries or cutting edge of the broach are shaped to give a desired surface contour. Often a slot, it may also be almost any geometric shape desired. Broaching is usually performed on special machines that pull or push the broach across the workpiece. Internal broaching utilizes an existing hole to provide clearance for the broaching tool. External broaches do not require existing slots,

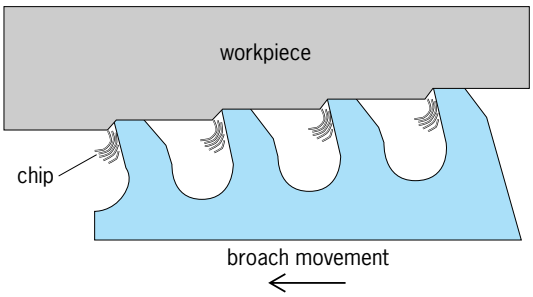

Fig. 1. Broach cutting a small chip from a workpiece.

but they may have guide bushings to support the broaching tool and a fixture to hold the workpiece. Broaching is a very economical machining operation, although tool costs can be high; accordingly, it is applied most often to high-volume production.

Drilling. One of the most common machining operations, drilling is a method of producing a cylindrical hole in a workpiece. A typical twist drill consists of a helically grooved steel rod with two cutting edges on the end. The helical flutes or grooves in the drill allow the chips to be removed from the cutting edge, conduct coolant to the cutting lips, and form part of the cutting edge geometry. Although drills may appear to be simple, their geometries are carefully controlled. Chisel angle, point angle, and web thickness, for example, are optimized to speed drilling and maximize tool life (**Fig. 2**). If this geometry is significantly altered during resharpening, drill life and hole quality may be compromised.

Drilling can be performed on special machines, which range in size and complexity from small sensitive drill presses through upright and multiple-spindle models designed for mass production. Jigs are often used to guide and support the drill. The use of a bushing to guide the drill into the workpiece can significantly improve drilling accuracy and tool life by improving the rigidity of the drill and assisting in properly locating it in relation to the workpiece. Of course, drilling can also be performed with simple hand drills. Drilling is a very fast and economical process, but it usually does not produce a very accurate hole diameter or a fine surface finish.

Turning. This type of machining is performed on a lathe. The process involves the removal of material from a workpiece by rotating the workpiece under power against a cutting tool. The cutting tool is held in a tool post that is supported on a cross slide and carriage. The tool may be moved radially or longitudinally in relation to the turning axis of the workpiece (**Fig. 3**). Forms such as cones, spheres, and related workpieces of concentric shape as well as true cylinders can be turned on a lathe. Machining operations such as facing and boring are variations of the turning process, and they can also be performed on a lathe.

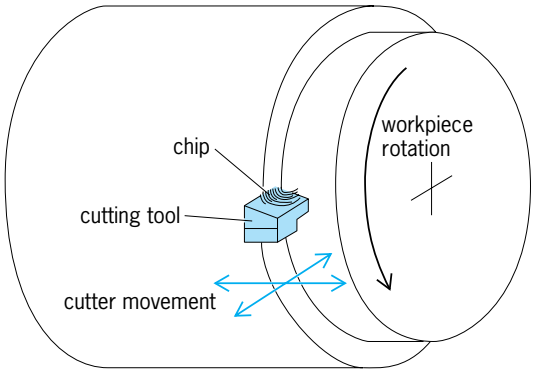

Fig. 3. Formation of turning chips as a single-point tool contacts the exterior of the spinning workpiece.

The most common lathe is an engine lathe, where the workpiece may be rotated and held between tapered centers or by means of a collet or chuck. A turret lathe is an engine lathe that has a multisided, indexing tool holder, or turret, instead of a tailstock center. This adds to the versatility of the machine by allowing a greater variety of cutting tools to be applied to the rotating workpiece. In addition to the turning tools used on an engine lathe, the turret lathe has tool holders that can be set up to drill, tap, and bore the workpiece.

Automatic screw machines. Automatic screw machines are sophisticated lathes that have been designed to perform several turning operations automatically in rapid succession without removing the workpiece from the machine. They are used when the volume and complexity of the required workpieces justifies the expense of setting up and operating these very versatile but complex machines. A screw machine (named for the screw manufacturing role for which is was created) is cam controlled or driven by computer numerical control (CNC). Several individually controlled slides are provided to hold turning, grooving, or cutoff tools. The machines also have turrets that hold drills, reamers, hollow mills, and counterboring tools. Special attachments permit performance of operations such as milling, index drilling, or thread chasing. *See* COMPUTER NUMERICAL CONTROL.

Milling. This process removes material by feeding a workpiece through the periphery of a rotating circular cutter. Each tooth of the rotating multitoothed milling cutter removes a portion of material from the passing workpiece.

Milling cutters are designed for particular operations and are classified as either shell type or end type. Shell mills are disk shaped and usually produce continuous slots. When well supported in the

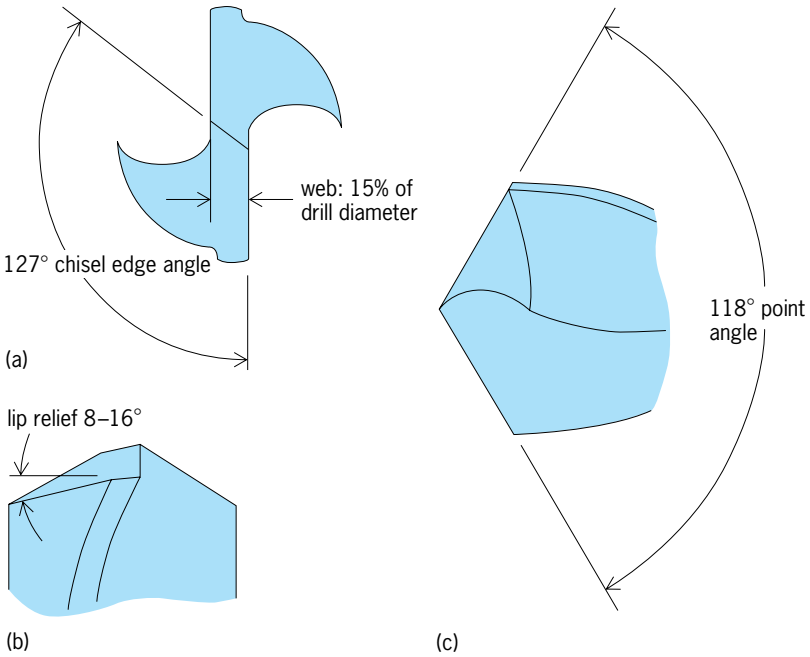

Fig. 2. Critical items on a drill point and their geometry. (*a*) End view. (*b*) Side view. (*c*) Side view, with drill rotated 90° about its axis from the position shown in *b*.

machine tool to minimize vibration, they perform well and economically. The more versatile end mill is held by its shank only. End mills can be used for slotting just like a shell mill, but they also can cut pockets, contours, and even cylindrical holes. End mills with four or six flutes are stronger and more rigid than two-flute mills, and so are better able to machine tougher materials. They have less flute room to allow chips to be removed, however, so they do not perform well on soft material at high speeds. Two-flute end mills are typically used for high production rates on soft materials such as aluminum. Ball-nose end mills, which have round ends, can be used to machine complex three-dimensional contours.

Reaming. This machining operation enlarges an existing hole by a few thousandths of an inch and produces a hole whose diameter is very accurately controlled. The cutting edges of a reamer may be ground on the apexes between longitudinal flutes or grooves, or cutting may take place on chamfered edges at the end of the reamer. Reaming is performed either manually or by machine, often as a finishing operation after drilling. Reamed holes have good surface finish. Hand reamers have a slight end taper to aid in starting. Fluted machine reamers for finishing work remove material by both end and side cutting, while the heavier tools known as rose reamers cut only on their chamfered ends.

Sawing. This is the parting of material by using blades, bands, or abrasive disks as the cutting tools. In the most common type of saw, a toothed blade is passed across the workpiece in either a reciprocating or continuous motion. The teeth can be mounted on continuous bands, short steel blades, or the periphery of a disk. Friction sawing is a rapid process used to cut steel as well as certain plastics. A very high speed blade softens the workpiece material with frictional heat. The material is then wiped away from the workpiece by the cutting blade. Since many teeth engage the workpiece, no single tooth overheats. Abrasive sawing looks similar to friction sawing, except that a thin rubber or bakelite bonded abrasive disk grinds the material away instead of simply softening and wiping it.

Shaping. This process cuts flat or contoured surfaces by reciprocating a single-point tool across the workpiece. The tool is mounted on a hinged unit known as a clapper box, which lifts up to disengage the tool from the surface on the return stroke. The cutting action of a shaper is actually similar to turning, except that the single-point cutting tool moves straight across a workpiece, instead of having the workpiece rotate against the cutting tool. Because shapers have a limited stroke, shaping is usually performed on small pieces requiring a short cutter stroke. Larger pieces requiring longer strokes are usually milled or planed.

By and large, shaping is obsolete except in small shops; shapers are no longer being produced. Planing, when employed to substitute for shaping, is done by reversing the relative motion between tool and workpiece; that is, the tool is stationary during the cut, and is fed incrementally between cuts, while the workpiece is reciprocated past the stationary tool.

Nibbling. Nibbling is the operation that cuts away small pieces of material by the action of a reciprocating punch. A nibbler takes repeated small bites from the workpiece (which is usually a thin sheet of material) utilizing a quickly reciprocating punch system. As the work is passed beneath the punch, a small nibble of material is removed by the punch during each punch cycle. After each quick nibble, the workpiece is advanced under the punch to allow another small bite to be taken away. In this manner, a great deal of material can be removed from the workpiece after several tens or hundreds of individual punching cycles. By controlling the movement of the workpiece under the reciprocating punch, slots, profiles, and radii may be cut into the workpiece. Additionally, since there is a great deal of versatility in workpiece movement, complex or irregular shapes may easily be produced. Duplicate pieces may be made simultaneously by stacking the sheet workpieces and allowing the punch to cut several sheets at a time. Templates are also used as guides to direct the material movement beneath the punch to produce large predetermined shapes.

Nibbling machines are constructed with considerable distance, or throat, between the punch and its drive and support mechanism. This distance allows relatively large workpieces to be machined. The punches themselves are frequently round or square, but also may have complex shapes if special detailed shapes are desired on the workpiece.

Grinding. This process removes material by the cutting action of a solid, rotating, grinding wheel. The abrasive grains of the wheel perform a multitude of minute machining cuts on the workpiece. Although grinding is sometimes used as the sole machining operation on a surface, it is generally considered a finishing process used to obtain a fine surface and extremely accurate dimensions.

Grinding is used to machine a wide range of metals, carbide materials, stone, and ceramics. The grinding process may be used on metals too hard to machine otherwise because commercial grinding abrasives are many times harder than the metals to be machined.

Grinding wheels are composed of abrasive grains plus a bonding material (**Fig. 4**). The wheels are often very porous, with homogeneous open areas between the grains. The abrasives most commonly used are silicon carbide (SiC) and aluminum oxide (Al_2O_3). Coarse-grained wheels are used for rapid removal of stock; wheels with fine grains cut more slowly but give smoother finishes. Coolants are applied to the grinding point to dissipate the heat generated and to flush away the fine chips. *See* ABRASIVE.

Cylindrical grinding is performed on the peripheries or shoulders of workpieces such as shafts, cylinders, rolls, and axles. They rotate the workpiece from a power headstock while it is held between centers, gripped in a jawed chuck, or fastened to a faceplate. Centerless grinding is similar to cylindrical grinding, except that the work is supported on

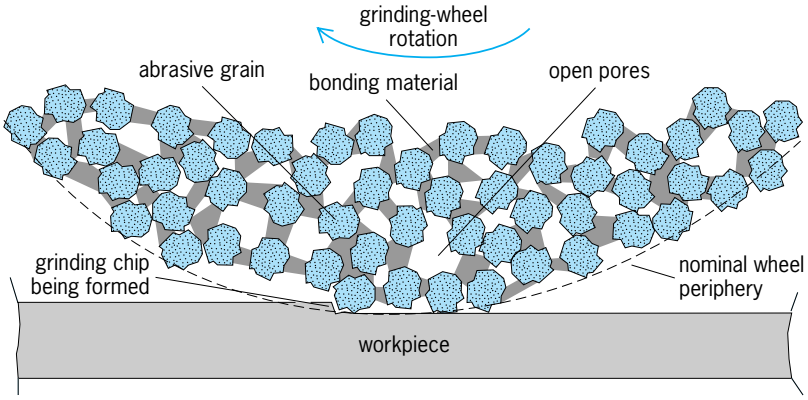

Fig. 4. Action of a grinding wheel, showing how individual grains of the wheel produce chips from a workpiece.

a blade between two abrasive wheels. One wheel is a regular grinding wheel rotating at normal grinding speed, while the second is a rubber-bonded regulating wheel that causes the workpiece to rotate against the grinding wheel (**Fig. 5**). Centerless grinders are faster than cylindrical grinders, but they do not provide the accurate concentricity that cylindrical grinders provide. Surface grinding is accomplished by holding one or several workpieces on a reciprocating or rotating horizontal table and feeding them through the cutting path of a rotating grinding wheel.

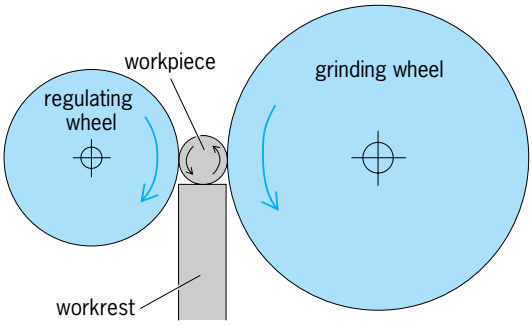

Fig. 5. Configuration of a centerless grinding wheel.

Creep-feed grinding is an abrasive machine process capable of removal of heavy stock in working difficult-to-machine materials. The process has the ability to hold both size and form to very close tolerances (**Fig. 6**). Specialized equipment and grinding wheels are required to properly perform creep-feed grinding. Creep-feed grinding is analogous to shell milling except that a grinding wheel is used in place of the milling cutter. The multitude of abrasive grains acts as the cutting teeth of a shell mill. The cutting forces are very high in the creep-feed grinding process; therefore the machine tool must be designed for rigidity and must be capable of closely controlled slow table speeds. Creep-feed grinding also requires special wheels. These grinding wheels are very soft, and have pores in the wheel that allow the cutting fluid to be taken up and into the arc of the cut. Superabrasive wheels are sometimes used, because their high initial cost is justified by their long life and high grinding productivity.

Cubic boron nitride and polycrystalline diamond are classified as superabrasives. Cubic boron nitride was discovered as the product of a failed attempt to make diamonds in the laboratory. It is almost as hard as diamond. Since cubic boron nitride is a synthetic material, the structure and size of the grains can be closely controlled and optimized for specific applications. Polycrystalline diamond is a synthetic diamond that cleaves as it fractures under load, thus exposing a new, sharp cutting edge instead of simply dulling as other abrasives do. Therefore polycrystalline diamond provides longer cutting life compared to other abrasives.

Honing. Honing is a grinding process that removes a small amount of material from a workpiece by means of abrasive stones. It is able to produce extremely close dimensional tolerances and very fine surface finishes. The abrading action of the fine grit stones occurs on a wide surface area rather than on a line of contact as in grinding. A hone floats as it moves across the workpiece. The hone removes high spots and smooth surface inaccuracies. It is well suited to smoothing and improving the roundness of a hole, but it will not correct the position of a hole or establish its alignment.

Lapping. This is precision abrading process used to finish a surface to a desired state of refinement or dimensional accuracy by removing an extremely small amount of material. Lapping is accomplished by abrading a surface with a fine abrasive grit rubbed about it in a random manner. A loose unbonded grit is used. It is traversed about on a lap, made of a somewhat softer material than the workpiece. The unbonded grit is mixed with a vehicle such as oil, grease, or soap and water. When a bonded grit is used, it may be in the form of a bonded abrasive lap or a charged lap such as cast iron or copper with the lapping compound embedded in it. In some cases, abrasive-covered paper laps are used.

Polishing. This is the smoothing of a surface by the cutting action of an abrasive grit that is either glued to or impregnated in a flexible wheel or belt. Polishing is not a precision process; it removes stock until the desired surface condition is obtained. Polishing

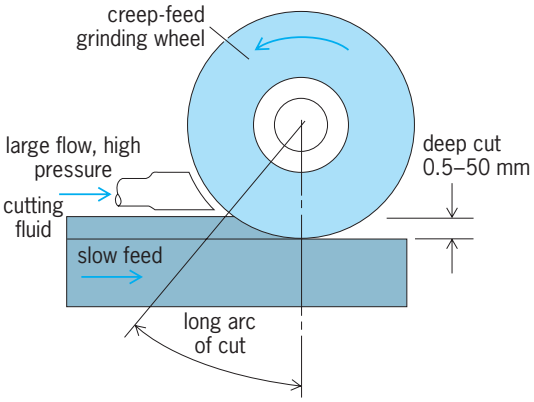

Fig. 6. Creep-feed grinding process.

wheels are built up from layers of soft material such as wood or leather.

Superfinishing. For mirrorlike surface, a precision abrading process known as superfinishing is used. Superfinishing removes minute flaws or inequalities because it is performed with an extremely fine-grit abrasive stone, shaped to match and cover a large portion of work surface. As the workpiece turns, the stone reciprocates across the work under a flood of lubrication. The process is usually performed on cylindrical pieces.

Buffing. This is the smoothing and brightening of a surface by rubbing it with a fine abrasive compound carried in a soft wheel or belt. The abrasive is a fine powder or flour mixed with tallow or wax to form a smooth paste. Buffing is performed on the same types of machines as polishing; frequently both buffing and polishing wheels are included on the same machine. Buffing differs from polishing in that a finer grit is used and less material is removed from the workpiece. Although some material is removed, the amount is almost undetectable.

Ultrasonic machining. In this process, material is removed by abrasive bombardment and crushing in which a vibrating tool drives an abrasive grit against a workpiece. In ultrasonic machining, the tool never directly contacts the workpiece; rather, the vibrations (typically 20,000 Hz) drive the abrasive, which is suspended in a liquid, against the workpiece. Impressions may be economically sunk in glass, ceramics, carbides, and hard brittle metals by this method. The shape of the tool basically determines the shape of the impression. Often, several cuts will be required, with progressively finer abrasive grit sizes, to obtain the desired dimensional accuracy and surface finish. *See* ULTRASONICS.

Electric-discharge machining. This is a machining process in which electrically conductive materials can be removed by repeated electric sparks. Electric-discharge machining is used to form holes of varied shape in materials of poor machinability. Unlike other machining operations, it does not rely on a cutting tool to shear away the workpiece. Instead, it uses electrical energy to melt or vaporize small areas on the workpiece. The sparks created by an electric-discharge machining unit (at a rate greater than 20,000 per second) are discharged through the space between the tool (cathode) and the workpiece (anode; **Fig. 7**). The small gap between the tool and workpiece is filled with a circulating dielectric hydrocarbon oil, which serves as a cooling medium and flushes away metal particles. Although not as fast as other machining processes, electric-discharge machining has the unique ability to remove hard materials that otherwise would not be machinable. Electric-discharge machining was originally developed as a method of removing broken taps or drills from holes.

Gear cutting. This operation results in a uniform series of toothed projections on the surface of a workpiece, the teeth being designed to mesh with a mating tooth series in order to transmit power or motion. Gear-cutting machines may use either conventional

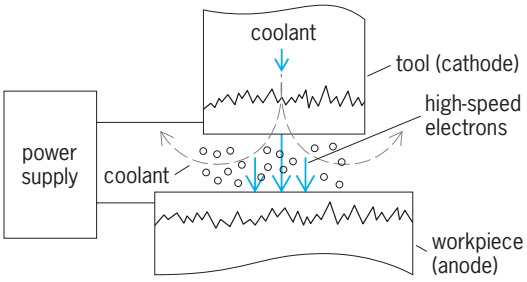

Fig. 7. Electric-discharge, or electric-spark, machining process. (*Elox Corporation of Michigan*)

cutting tools or grinding wheels to produce the desired gear shape.

Gear forms may be generated by the total cutting action of the tool plus the rotation of the workpiece, or they may be formed by a tool whose cutting profile matches the tooth form. Frequently, gear teeth may be rough-cut by a generating method and finished to size with a form tool.

Gear hobbing machines revolve the gear blank while the rotating hob, or cutter, moves across the face of the gear to generate the teeth (**Fig. 8**). A system of index gearing maintains the relative positions of the blank and the hob and controls the number

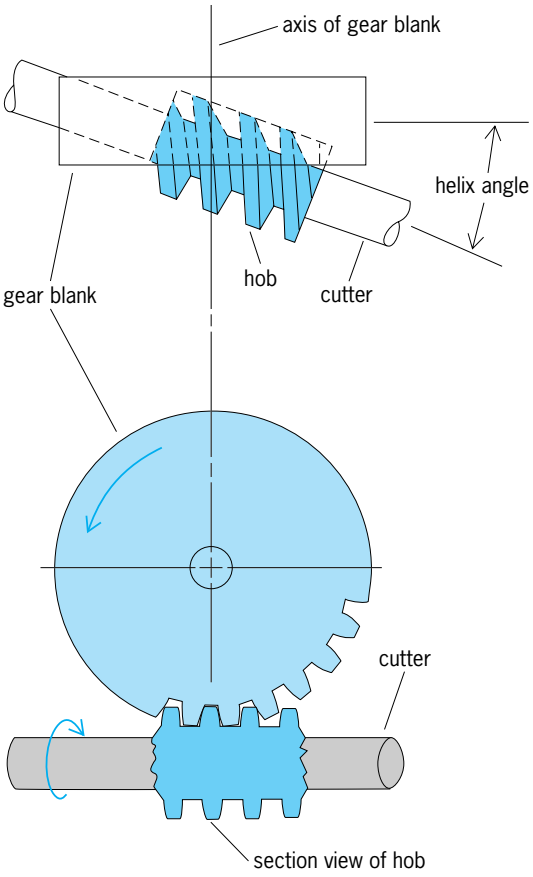

Fig. 8. Gear hobbing operation; rotation of the hob and gear blank is synchronized and continuous. (*After J. G. Bralla, ed., Handbook of Product Design for Manufacturing, McGraw-Hill, 1986*)

of teeth to be cut. In addition to use of specialized hobbing machines, gears can be formed by milling and broaching.

Gear-grinding machines produce gear teeth by using preformed grinding wheels. Although some fine-pitch gear teeth are finish-ground from solid stock, gear grinding is primarily a finishing operation. Grinding is the only way to finish gears that have been brought to a high degree of hardness. A grinding wheel, which has an involute tooth form dressed into both sides, grinds both sides of the space between the two gear teeth as it moves across the face of the gear. *See* GEAR.

Threading. Threading is the forming of a ridge and valley of uniform cross section that spiral about the inner or outer diameter of a cylinder or cone in an even, continuing manner. The work must be produced with sufficient uniformity and accuracy that the resulting threaded part will accomplish its intended purpose of fastening, transmitting motion or power, or measuring.

Threads are produced by several machining methods. External threads may be chased by preformed cutting dies, turned with single-point turning tools on a lathe, milled, hobbed, ground, or rolled. Most internal threading is cut with a preformed tap although turning, hobbing, grinding, and milling are also used. *See* SCREW THREADS.

Peening. This is a metal-finishing operation, also known as shot peening. During a peening operation, small steel shot is driven against a workpiece to plastically deform its surface to a depth of a few thousandths of an inch, producing residual compressive stress. The material is thus made more resistant to fatigue failure. Surface hardness of the material is also increased slightly by the cold working produced by shot peening. The shot is driven at high velocity against the work by centrifugal force or by an air blast.

Cutting-tool coatings. To increase the life and speed of cutting tools, they are often coated with a thin layer of extremely hard material such as titanium nitride or zirconium nitride. These materials, which are applied over the cutting edges, provide excellent wear resistance. They are also relatively brittle, so they rely on the toughness of the underlying cutting tool to support them. Coated tools are more expensive than conventional tools, but they can often cut at much higher rates and last significantly longer. When used properly on sufficiently rigid machine tools, they are far more economical than conventional tooling. *See* METAL COATINGS.

Jig and fixture design. Successful machining usually requires that the workpiece be securely presented to the cutting tool. In machines such as lathes or cylindrical grinders, the holding device is typically a chuck, collet, or center driver. Often, however, special devices must be constructed to position and support the workpiece, especially for drilling, milling, welding, and assembly operations. Jigs and fixtures provide this function. Jigs support the workpiece and provide locating guides for the cutting tool. Fixtures support the workpiece but do not provide locating guides. The workpiece is held against one or more reference surfaces, from which all machining cuts are measured. Some type of clamping device, such as a toggle clamp or locking screw, is also frequently used. The most common locating guide is a drill or reamer bushing, which is a hardened steel tube whose inside diameter is just slightly larger than the cutting-tool diameter. The bushing guides the drill or reamer to the workpiece and helps to prevent deflection of the cutting tool under load, thereby improving cutting accuracy and extending cutting tool life.

J. R. Casey Bralla

Bibliography. W. E. Boyes (ed.), *Jigs and Fixtures*, 3d ed., Society of Manufacturing Engineers, 1989; J. G. Bralla (ed.), *Product Design for Manufacturing*, 1986; R. J. Christoforo, *Jigs, Fixtures, and Shop Accessories*, 1993; S. F. Krar, *Grinding Technology*, 2d ed., 1994; S. F. Krar, *Machine Tool Operations*, 1983; R. L. Little, *Metalworking Technology*, 1976; Society of Manufacturing Engineers, *SME Tool and Manufacturing Engineers Handbook*, vols. 1–5, 1983–1987; R. A. Walsh, *McGraw-Hill Machining and Metalworking Handbook*, 2d ed., 1998.

Mackerel

A fish which is a member of the order Perciformes, family Scombridae. There are about 50 carnivorous species found in the middle layer or near the surface of tropical and temperate seas.

Mackerel are characterized by a long slender body, pointed head, and large mouth. The dorsal fin is spinous, the anal fin is soft-rayed, and the tail fins are widely forked and powerful. The teeth are feeble, and the maxillary bones are fused to the premaxillaries.

Scomber scombrus, the common mackerel (see **illus.**), is an important fish commercially. It does not have a swim bladder and can move from the depths to the surface rapidly. It is a migratory species that is found on both sides of the North Atlantic. It swims in large schools, which approach the coast in the early summer to spawn, and then return to the ocean. This mackerel is about 2 ft (0.6 m) long when mature.

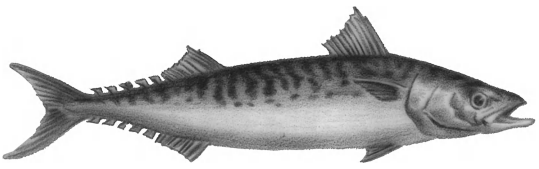

Common mackerel (*Scomber scombrus*).

The Pacific mackerel (*Pneumatophorous diego*) is also an important commercial fish but differs from the common mackerel in having a swim bladder. The American Spanish mackerel (*Scomberomorus maculatus*) is a choice food fish that may attain a weight of 10 lb (4.5 kg). *See* PERCIFORMES; SWIM BLADDER.

Charles B. Curtin

Macrocyclic compound

An organic compound that contains a large ring. In the organic chemistry of alicyclic compounds, a closed chain of 12 carbon (C) atoms is usually regarded as the minimum size for a large ring; crown ethers are similarly defined. Macrocyclic compounds may be a single, continuous thread of atoms, as in cyclododecane [$(CH_2)_{12}$], or they may incorporate more than one strand or other ring systems (subcyclic units) within the macrocycle or macroring. In addition, macrocycles may be composed of aromatic rings that confer considerable rigidity upon the cyclic system. These aromatic rings may be joined together or coupled by spacer units consisting of one or more carbon atoms. The compounds generally thought of as macrocycles include crown ethers, cryptands, spherands, carcerands, cyclodextrins, cyclophanes, and calixarenes. *See* AROMATIC HYDROCARBON.

Classes of macrocyclic polyethers. Crown ethers are generally composed of repeating ethylene (CH_2CH_2) units separated by noncarbon atoms such as oxygen (O), nitrogen (N), sulfur (S), phosphorus (P), or silicon (Si). Cryptands are similar to crown ethers but have a third organic chain attached at two points on the crown ring, usually trivalent nitrogen. Although other carbon-containing subunits such as propylene ($CH_2CH_2CH_2$) or methylene (CH_2) may be included, these subunits are less common. The conformations of the ethylene unit are more favorable than those of propylene, and the ethylene unit is more stable to hydrolysis than is the O—CH_2—O linkage (an acetal). Organic units sterically equivalent to the ethylene unit, such as 1,2-benzo, have been incorporated, as have units sterically equivalent to two ethyleneoxy units, such as 2,6-bis(hydroxymethyl)pyridine. Replacement of an OCH_2CH_2O unit by the 1,2-dihydroxyethyl unit of tartaric acid (HOOC—CHOH—CHOH—COOH) or by the adjacent hydroxyl groups of carbohydrates (sugars) alters hydrophobicity and introduces chirality. By far, the most common heteroatom present in the macrorings of crowns [X in $(XCH_2CH_2)_n$] is oxygen; but as more intricate structures are prepared, nitrogen, sulfur, phosphorus, silicon, or siloxy residues are becoming much more common. *See* STEREOCHEMISTRY.

The name crown ether is informal, developed to bypass the complex systematic names that these compounds are given under traditional nomenclature rules. A simple formal system of nomenclature for compounds of this type has yet to be developed, although several systems have been suggested. Of these, the names coronand for a cycle and coronates for its complex have been most widely adopted. By tradition, however, crown ethers are named according to the total number of atoms composing the macrocyclic ring and the number of heteroatoms contained within it (**Fig. 1***a*). A crown composed of five ethyleneoxy [CH_2CH_2O] units would be called 15-crown-5. Substitution of one ethyleneoxy unit by a 1,2-benzo unit would lead to benzo-15-crown-5.

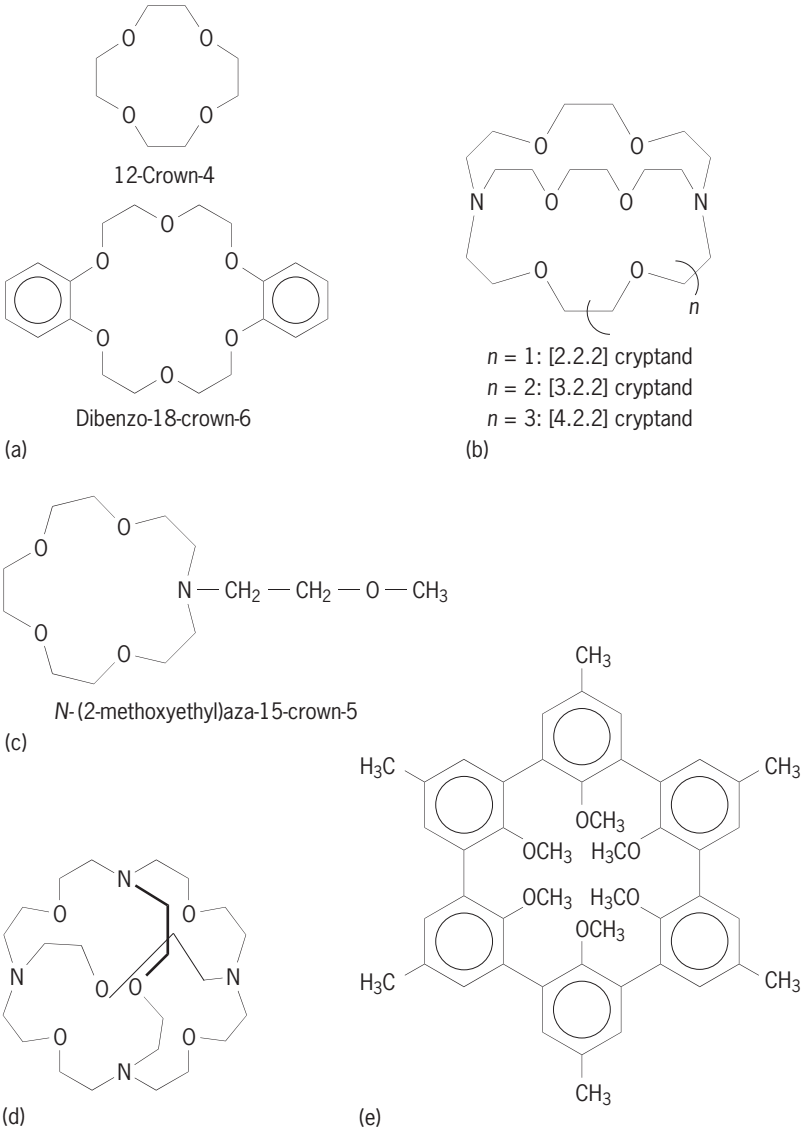

Fig. 1. Macrocyclic structures. (*a*) Two crown ethers. (*b*) A basic structure for three cryptands. (*c*) A lariat ether. (*d*) All-aliphatic spherand. (*e*) All-aromatic spherand.

Substitution of a nitrogen atom for an oxygen would transform 15-crown-5 into aza-15-crown-5.

Crown ether variants. Numerous structural features have been incorporated into the crown ether ring system. The simplest variation is substitution of nitrogen, sulfur, phosphorus, silicon, or other heteroatom for oxygen. Such substitution leads, respectively, to azacrowns, thiacrowns, phosphacrowns, and silacrowns. Multiple substitution of heteroatoms is also possible. A 14-membered ring containing 4 oxygen heteroatoms is called 14-crown-4. The all-nitrogen analog may be called tetraaza-14-crown-4, or 14-ane-4 and has the trivial name cyclam. Such compounds are of special interest to inorganic chemists, as these analogs of crown ethers bind transition and coinage metals. When the —CH_2—O—(ether) link is replaced by a —CO—O—(ester) unit, the crown ether is transformed into a crown ester. Likewise the interchange (ether for amide) of reaction (1) affords macrocyclic

$$—CH_2—O— \longrightarrow — CO—NH— \qquad (1)$$

lactams. Crown ethers have also been prepared that incorporate subcyclic units such as benzene, furan, and pyridine. *See* ESTER; ETHER; LACTAM; LACTONE.

Cryptands. By adding a third strand to the simple macrocyclic polyethers, three-dimensional compounds based on the crown framework are formed. Typically, two of the oxygen atoms across the ring from each other are replaced by nitrogens, and a third ethyleneoxy chain is attached to them. Known as cryptands (Fig. 1*b*), these structures completely encapsulate cations smaller than their internal cavities and strongly bind the most similar in size. Systematic nomenclature of cryptands is complicated. A cryptand is usually presumed to be composed of ethyleneoxy chains attached to a nitrogen atom at either end. A typical cryptand would be $N[(CH_2CH_2O_2)\ CH_2CH_2]_3N$. Since each chain contains two oxygen heteroatoms, it is referred to as [2.2.2]-cryptand, or simply [2.2.2]. A cryptand composed of chains having two, three, and four ethyleneoxy units tied to nitrogen atoms at either end has one, two, and three oxygens respectively in the chains and is called [3.2.1] cryptand.

Lariat ethers. The name lariat ether (Fig. 1*c*) has been given to compounds that, like the cryptands, have a ring and a third strand, but the additional chain is attached at only one point. This permits three-dimensional encapsulation of a cation while retaining a high degree of flexibility. Two-armed lariat ethers are referred to as bibracchial lariat ethers or BiBLEs. Three-armed systems are TriBLEs, and so forth.

Spherands. Compounds other than simple cryptands have been developed that are capable of either partially (cavitands) or completely (spherands) enveloping cations. The donor atoms (O, N, S) are arranged so that they provide a solvation sphere to the encapsulated cation. The earliest example of a spherand is Lehn's all-aliphatic spherand (Fig. 1*d*). An all-aromatic spherand (Fig. 1*e*) is a compound that can envelop a guest three-dimensionally to an even greater extent than can a cryptand. When a crown ether ring is attached to three of the six aromatic rings shown for the all-aromatic spherand, a cryptaspherand results. If only an ethyleneoxy chain, rather than a crown ether, is appended to the aromatic unit, a hemispherand results.

Calixarenes, cavitands, and carcerands. Calixarenes are cyclic oligomers of phenol and formaldehyde. Calix[*n*]arenes from *p-tert*-butylphenol have been developed in which *n* is 4, 6, or 8, corresponding to that number of aromatic rings and CH_2 units (Fig. 2*b*). Less common but also available are the five- and seven-ring calix[*n*]arenes. All these compounds have aromatic walls and a hydrophobic interior. The larger molecules are more flexible than the smaller ones, but both are capable of including a variety of organic guest molecules.

An extension of calixarenes to a more rigid, basket-shaped system can be accomplished by the reaction of resorcinol and acetaldehyde. Subsequent reaction with formaldehyde gives the enforced-cavity structure called a cavitand (Fig. 2*c*), a structure that possesses a molecular void (cavity) that is invariably filled by solvent when the molecule crystallizes.

An even greater level of encapsulation (incarceration) of a molecular guest is possible when two cavitands are combined as top and bottom shells of a carcerand (Fig. 2*d*). These compounds can effectively isolate the bound guest from the chemical environment (solvent) in which the host·guest (solvent·carcerand) complex exists. In keeping with nomenclature traditions, the complexes of these two structures are referred to as cavitates and carcerates. *See* SUPRAMOLECULAR CHEMISTRY.

Cyclophane is the name given to macrocyclic compounds that contain organic (usually aromatic) rings as part of a cavity-containing structure (Fig. 2*e*). The first such compound was [2.2]-paracyclophane. In it, two benzene rings are joined by ethylene (CH_2CH_2) chains in their para positions. *See* CYCLOPHANE.

Bicyclic cryptands. Two crown ether rings may be held together by a crown-ether-like strand to give a bicyclic cryptand (**Fig. 2***a*). These have sometimes been referred to as ditopic receptors because they possess two distinct binding sites. The cryptands and spherands differ from the ditopic or bicyclic cryptands in that they normally possess a three-dimensional array of binding sites focused for a single guest.

Host-guest chemistry. The terms host and guest designate a pair of molecular species, comprising one molecule that can bind another. In principle, either molecule of the pair may be the host or the guest. The distinction between host (receptor) and guest (substrate) is arbitrarily made based upon size. The larger (higher molecular weight) molecule is the host (receptor) and is the compound that is deliberately prepared by chemical synthesis or that has evolved to complexity in nature for example, (proteins, DNA). In chemistry the host or receptor molecule (especially for a cation) is called a ligand, but in biology it is the substrate or guest that is often called a ligand.

Calixarene is representative of a growing family of diverse molecular receptors in which four, six, and eight aromatic rings are common in otherwise analogous structures (**Fig. 3**). As with crown ethers, assorted molecular species may be complexed by these diverse receptors. In many cases, the focus will be on a single receptor molecule and many potential substrates in order to define the efficacy and selectivity of the host. Natural receptors such as proteins have been studied in order to understand which guest molecules are bound and transformed (enzymatic catalysis) by them. Other families of receptor molecules have been devised which are based upon the sugar oligomers called cyclodextrins containing five to seven glucose molecules in a cyclic array. These natural and semisynthetic hosts bind a variety of organic substrates (guests) in water solution.

Complexation phenomena. It is the ability of these macrocyclic host compounds to complex a variety of guest species that makes these structures interesting.

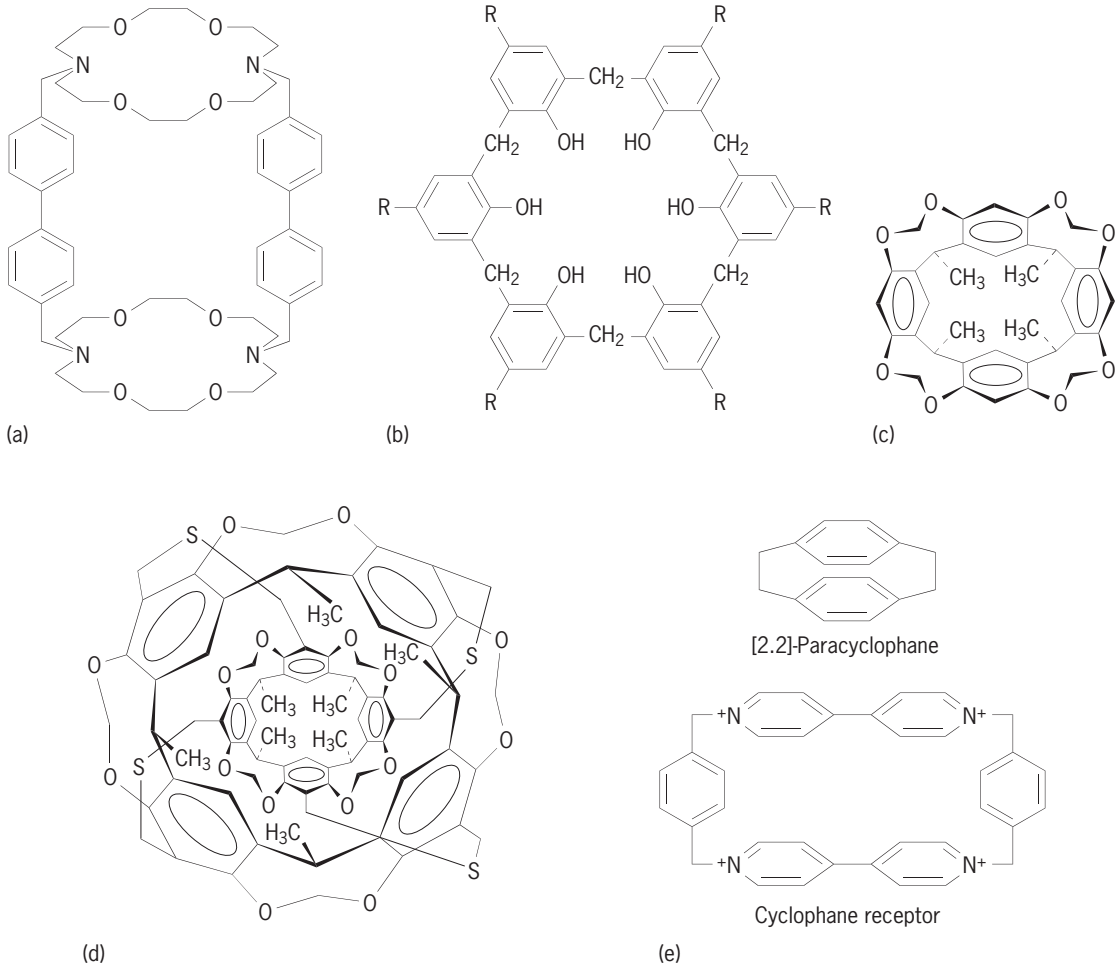

Fig. 2. Macrocycles with various structural features. (*a*) Bicyclic cryptand (ditopic receptor). (*b*) Calix[6]arene; R represents a functional group. (*c*) Cavitand. (*d*) Carcerand. (*e*) Cyclophanes.

A crown ether can be described as a doughnut with an electron-rich and polar hole and a greasy or lipophilic (hydrophobic) exterior. As a result, these compounds are usually quite soluble in organic solvents but accommodate positively charged species in their holes. The complexation process is usually characterized by a binding or stability constant (K_s) of the form $K_s = k_c/k_d$, where k_c represents the rate constant for complex formation (k_{complex}) and k_d represents the rate of decomplexation ($k_{\text{decomplex}}$ or k_{release}).

The two important components of complexation are the magnitude of the equilibrium constant and the kinetics of the process. For simple crown ethers, k_c is usually very large and k_d is also large. These rate constants are solvent-dependent, but k_d decreases more in nonpolar solvents than does k_c. Thus, K_s is smaller in polar solvents and larger in nonpolar solvents. Both k_c and k_d are lower for cryptands and spherands than for crowns, but k_d is lowered more. As a result, binding constants (K_s) for the three-dimensional hosts are generally higher (they bind cations more strongly) than for simple two-dimensional crowns.

Binding constants. Binding or stability constants can be assessed by several methods. One approach is to dissolve in water a cation such as Li^+ or Na^+ paired with a colored organic anion such as picrate. Shaking with an equal volume of organic solvent does not extract the salt. When a crown ether is added, the cation is complexed and transported into the organic phase. The crown cation–complex is accompanied by the colored anion, so the extent of extraction can be determined by colorimetric analysis. The extraction constants are expressed numerically as the percent of total salt extracted.

Homogeneous binding constants are determined for a ligand and a cation present simultaneously in solution. These K_s values may be determined by a variety of techniques (nuclear magnetic resonance, conductometric methods, calorimetry), but are most often obtained from either calorimetric or ion-selective electrode studies.

The interior cavity (hole) of a crown ether or cryptand varies in size depending upon the compound's structure. The series of compounds 12-crown-4, 15-crown-5, 18-crown-6, and so forth, increase in size. Thus, the hole of 15-crown-5 is about 0.20 nanometer, almost the same size as the ionic diameter of the sodium ion (Na^+). Likewise, the hole of 18-crown-6 and the potassium ion (K^+) are similar at about 0.27 nm. This similarity has given rise to

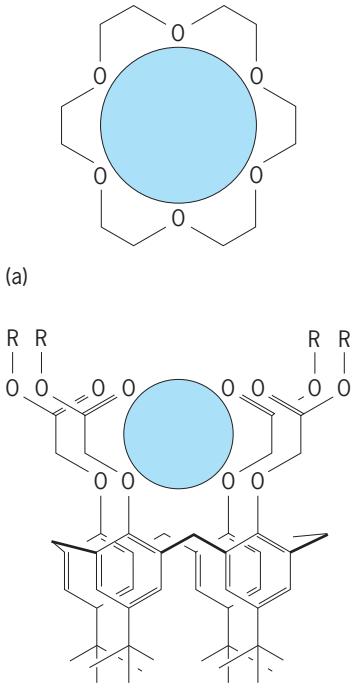

Fig. 3. The metal cation is the great and the organic structure is the host in (*a*) 18-crown-6 complex of potassium cation (K^+) and (*b*) sodium (Na^+) complexed by a calix[4]arene.

the hole/size relationship, which holds that binding is at a maximum when the cation and crown ether's hole are similarly sized. This principle is valid for the cryptands, which select cations on the basis of size. The correlation is tenuous for crown ethers in solution.

Complexing species. A variety of organic cations have been found to complex with crown ethers and related hosts. It has been suggested that for a host-guest interaction to occur, the host must have convergent binding sites and the guest must have divergent sites. This is illustrated by the interaction between optically active dibinaphtho-22-crown-6 (**Fig. 4***a*) and optically active phenethylammonium chloride. The crown ether oxygen atoms converge to the center of a hole and the ammonium hydrogens diverge from nitrogen. Three complementary O—H—N hydrogen bonds stabilize the complex (Fig. 4*b*). In this particular case, different steric interactions between the optically active crown and the enantiomers of the complex permit resolution of the salt.

Other organic cations have also been complexed, either by insertion of the charged function in the crown's polar hole or by less distinct interactions observed in the solid state. *See* COORDINATION CHEMISTRY; COORDINATION COMPLEXES.

Applications. Macrocyclic compounds have numerous interesting properties that have led to many applications.

Cation complexation. The striking ability of neutral macrocyclic polyethers to complex with alkali and alkaline-earth cations as well as a variety of other species has proved of considerable interest to the chemistry community. Crown ethers may complex the cation associated with an organic salt and cause separation of the ions. In the absence of cations to neutralize them, many anions show considerably enhanced reactivity. *See* ORGANIC REACTION MECHANISM.

By far, the most common effect of crown or cryptand compounds is to enhance the reactivity of counteranions by complexation of cations. There are two notable exceptions. First, when complexed by crowns, the normally unstable or explosive arenediazonium cations exhibit remarkably enhanced stability. More dramatic is the complete isolation of sodium cation, which allowed the preparation of the sodium anion (Na^-) for the first time. The crystals of cryptated Na^+ in the presence of Na^- are deep gold in color. This ability of cryptands to surround and protect the cation also allowed the preparation of the first electride, a cation salt of a lone electron. *See* ALKALI METALS; ALKALINE-EARTH METALS.

Phase-transfer catalysis. One of the important modern developments in synthetic chemistry was the use of the phase-transfer technique. Nucleophiles such as cyanide are often insoluble in media that dissolve organic compounds with which they react. Thus 1-bromooctane may be heated in the presence of sodium cyanide for days with no product formation. When a crown ether is added, two things change. First, solubility is enhanced because the crown wraps about the cation, making it more lipophilic. This, in turn, makes the entire salt more lipophilic. Second, by solvating the cation, the association between cation and anion and the interactions with solvent are weakened, thus activating the anion for reaction. This approach has been used to assist the

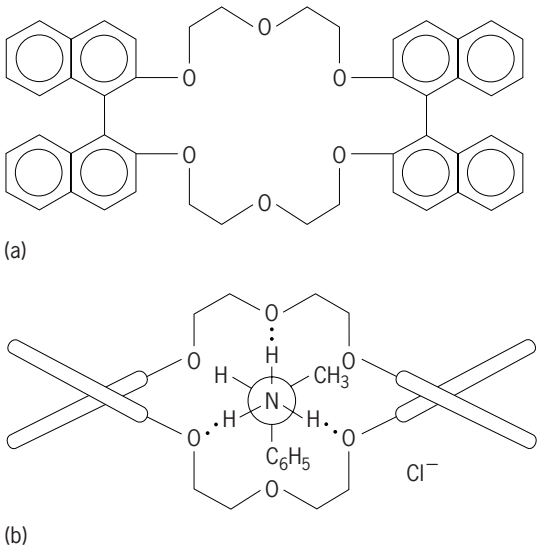

Fig. 4. Complexing species. (*a*) Dibinaphtho-22-crown-6. (*b*) R,R-dibinaphtho-22-crown-6 complex of phenethylammonium chloride.

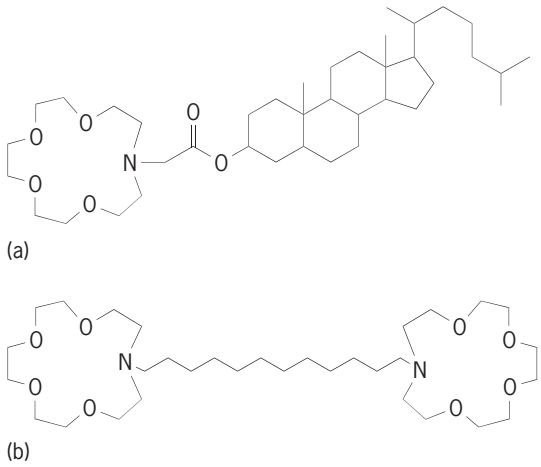

Fig. 5. Amphiphiles. (*a*) Crown ether-steroid amphiphile. (*b*) Crown ether bolaamphiphile.

dissolution of potassium permanganate ($KMnO_4$) in benzene (to give so-called purple benzene) in which solvent permanganate is a powerful oxidizing agent. One striking example of solubilization is the displacement of chloride (Cl^-) by fluoride (F^-) in dimethyl 2-chloroethylene-1,1-dicarboxylate by using the KF complex of dicyclohexano-18-crown-6, reaction (2).

$$ClHC{=}C(COOCH_3)_2 \longrightarrow FHC{=}C(COOCH_3)_2 \qquad (2)$$

In reaction (2), a crown provides solubility for an otherwise insoluble or marginally soluble salt. Use of crowns to transfer a salt from the solid phase into an organic phase is often referred to as solid-liquid phase-transfer catalysis. *See* CATALYSIS; PHASE-TRANSFER CATALYSIS.

Indicators and sensors. Since crown ethers and related species complex cations selectively, they can be used as sensors. Crowns have been incorporated into electrodes for this purpose, and crowns having various appended chromophores have been prepared. When a cation is bound within the macroring, a change in electron density is felt in the chromophore. The chromophores are often nitroaromatic residues and therefore highly colored. The color change that accompanies complexation can be easily detected and quantitated. *See* ION-SELECTIVE MEMBRANES AND ELECTRODES.

Membrane formation. Lipid bilayer membranes form from compounds that have polar head groups and nonpolar tails. Such compounds are known as amphiphiles. Crown ethers are capable of serving as the head group in a family of compounds that form membranes. The crown ether-steroid compound (**Fig. 5***a*) forms traditional bilayers, but the bis(crown) compound (Fig. 5*b*), which has two head groups (a bolaamphiphile), forms ultrathin monolayer membranes in which a single covalent chain spans the entire membrane. *See* MICELLE; MONOMOLECULAR FILM.

Toxicity. Some crowns and cryptands, like many other organic compounds, are irritants or toxic. 15-Crown-5 has produced a slight redness in skin tests and is reported to be toxic in mice at a level of about 0.01 oz/lb (800 mg/kg) of body weight. This means that a 150-lb (70-kg) human would have to ingest about 2 oz (56 g) of this compound to be in danger. The toxicity of simple aspirin is about half this (that is, twice as much aspirin, 0.0267 oz/lb or 1.75 g/kg, is required for the same toxic effect), so the toxicity level of this crown is not high. Of course, not all crowns have been tested, and some may be dangerous. *See* TOXICOLOGY.

George W. Gokel

Bibliography. V. Balzani and F. Scandola, *Supramolecular Photochemistry*, 1991; D. J. Cram and J. M. Cram, *Container Molecules and Their Guests*, 1994; F. Diederich, *Cyclophanes*, 1991; B. Dietrich, P. Viout, and J.-M. Lehn, *Macrocyclic Chemistry*, 1992; G. W. Gokel, *Crown Ethers and Cryptands*, 1991; C. D. Gutsche, *Calixarenes*, 1989; Y. Inoue and G. W. Gokel (eds.), *Cation Binding by Macrocycles*, 1990; C. M. Starks, C. L. Liotta, and M. Halpern, *Phase Transfer Catalysis*, 1993; J. W. Steed and J. L. Atwood, *Supramolecular Chemistry*, 2000.

Macrodasyida

An order of the phylum Gastrotricha. Members all have pharyngeal lumina that are inverted-Y–shaped, and most have pharyngeal pores. They inhabit marine or brackish waters, seldom fresh waters. Some do not exceed 0.5 mm (0.02 in.) in length, and most are not more than 1–1.5 mm (0.04–0.06 in.);

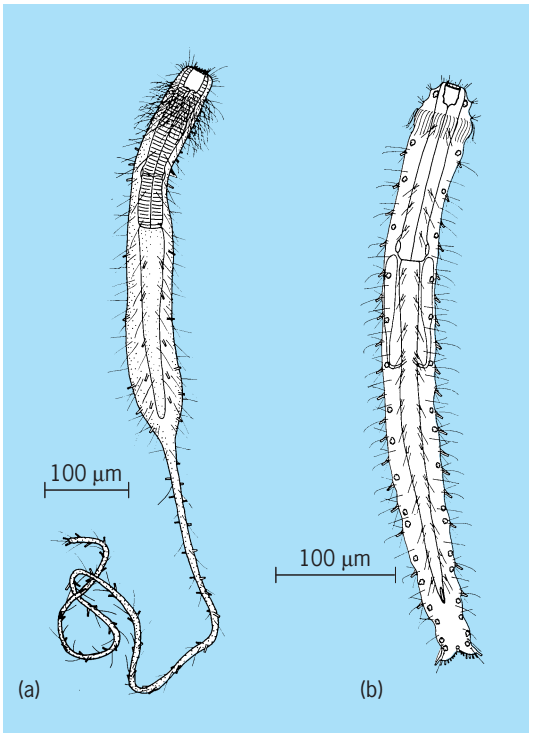

Marine gastrotrichs of the order Macrodasyida; dorsal views. (*a*) *Urodasys (courtesy of W. D. Hummon*). (*b*) *Turbanella (after W. D. Hummon, Intertidal marine Gastrotricha from Colombia, Bull. Mar. Sci., 24:396–408, 1974*).

these live in clean to detritus-rich marine sands of littoral or sublittoral areas. Both *Dolichodasys*, which reaches 2.5 mm (0.1 in.), and *Megadasys*, which reaches 4 mm (0.16 in.), inhabit black sulfide zones beneath quiet waters. All have front and rear groups of adhesive tubes; most also have tubes along their sides. Some have cuticular thickenings (*Lepidodasys* in one family) or scales or hooks (*Acanthodasys, Diplodasys, Tetranchyroderma*, and *Thaumastoderma* in another family). *Macrodasys* has a pointed rear, *Urodasys* has a tail (**illus.** *a*). Dactylopodolids, planodasyids, and turbanellids all have bilobed rear ends; lepidodasyids have rounded ones. *Turbanella* (illus. *b*) and *Tetranchyroderma* are the most common and most abundant of macrodasyids, with numbers of 50–100 per cubic centimeter of sand (800–1600 per cubic inch) not being unusual. *See* GASTROTRICHA.

William D. Hummon

Macroevolution

Large-scale patterns and processes in the history of life, including the origins of novel organismal designs, evolutionary trends, adaptive radiations, and extinctions. Macroevolutionary research is based on phylogeny, the history of common descent among species. The formation of species and branching of evolutionary lineages mark the interface between macroevolution and microevolution, which addresses the dynamics of genetic variation within populations. The term macroevolution was used by the geneticist Richard Goldschmidt around 1940 to challenge the then prevailing notion that major features of evolutionary history could be understood as simple extrapolations of population genetic principles. The term still often implies this challenge and the expansion of Darwinian evolutionary theory to include evolutionary processes emerging above the species level on time scales encompassing multiple millions of years. Phylogenetic reconstruction, the developmental basis of evolutionary change, and long-term trends in patterns of speciation and extinction among lineages constitute major foci of macroevolutionary studies.

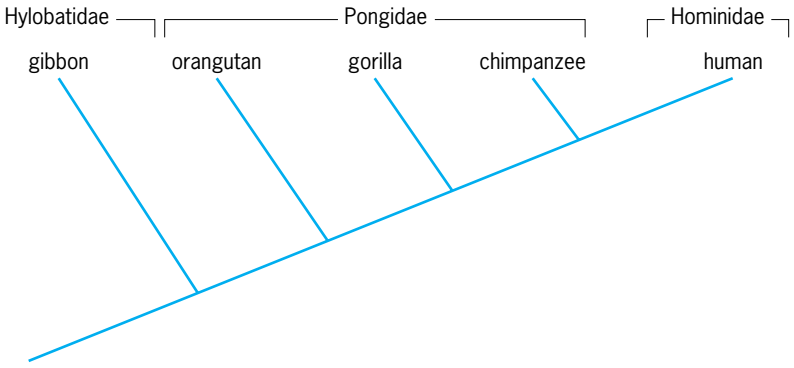

Fig. 1. Phylogenetic relationships of anthropoid primates showing traditional family-level taxa. All apes and humans together form a monophyletic group. The family Pongidae is paraphyletic, and therefore considered invalid by cladistic taxonomists. (*After C. P. Hickman, Jr., L. S. Roberts, and A. Larson, Integrated Principles of Zoology, 9th ed., 1993*)

Systematics and phylogeny. The goals of systematics are to reconstruct the phylogeny of species and to produce a taxonomy of species that reflects their phylogenetic relationships. Phylogenetic relationships are revealed by the sharing of evolutionarily derived characteristics among species, which provides evidence for common ancestry. Shared derived characteristics are termed synapomorphies, and are equated by many systematists with the older concept of homology. Characteristics of different organisms are homologous if they descend, with some modification, from an equivalent characteristic of their most recent common ancestor. Closely related species share more homologous characteristics than do species whose common ancestry is more distant. Species are grouped into clades according to patterns of shared homologies. The clades form a nested hierarchy in which large clades are subdivided into smaller, less inclusive ones, and are depicted by a branching diagram called a cladogram. A phylogenetic tree is a branching diagram, congruent with the cladogram, that represents real lineages of past evolutionary history; that is, it has a time division.

A cladogram or phylogenetic tree is necessary for constructing a taxonomy, but the principles by which higher taxa are recognized remain controversial. The traditional evolutionary taxonomy of G. G. Simpson recognizes higher taxa as units of adaptive evolution called adaptive zones. Species of an adaptive zone share common ancestry, and distinctive morphological or behavioral characteristics associated with use of environmental resources. Higher taxa receive Linnean categorical ranks (genus, family, order, and so forth) reflecting the breadth and distinctness of their adaptive zones. All taxa must have a single evolutionary origin, which means that the taxon must include the most recent common ancestor of all included species. A taxon is monophyletic if it contains all descendants of the group's most recent common ancestor, or paraphyletic if some descendants of the group's most recent common ancestor are excluded because they have evolved a new adaptive zone. For example, evolutionary taxonomy of the anthropoid primates groups the orangutan, gorilla, and chimpanzee in the paraphyletic family Pongidae and the humans in the monophyletic family Hominidae. Although the humans and chimpanzees share more recent common ancestry than either does with the gorilla or orangutan, the chimpanzees are grouped with the latter species at the family level and the humans are placed in a different family because they are considered to have evolved a new adaptive zone. The Hominidae and Pongidae together form a monophyletic group at a higher level (**Fig. 1**). *See* ANIMAL SYSTEMATICS.

Cladistic taxonomy or phylogenetic systematics accepts only monophyletic taxa because these alone are considered natural units of common descent. Such taxa form a nested hierarchy of groups within groups corresponding to the structure of the cladogram or phylogenetic tree. Linnean rankings are

considered unimportant. Taxa recognized using both the Simpsonian and cladistic taxonomies are standardly used in macroevolutionary analyses of extinction and patterns of diversity through time. The Simpsonian versus cladistic taxonomies often lead to fundamentally different interpretations, however. For example, extinction of a paraphyletic group, such as dinosaurs, would be considered pseudoextinction by cladists because some descendants of the group's most recent common ancestor survive. Birds are living descendants of the most recent common ancestor of all dinosaurs. The dinosaurs as traditionally recognized, therefore, do not form a valid cladistic taxon. *See* AVES; DINOSAURIA; PHYLOGENY.

Origins of evolutionary novelty. Comparative studies of organismal ontogeny are used to find where in development the key features of higher taxa appear and how developmental processes differ between taxa. Evolutionary developmental biologists denote the characteristic body plans of taxa by the term Bauplan, and the developmental stage during which key features of the Bauplan are formed by the term phylotypic stage. Developmental stages preceding and following phylotypic stages are subject to profound modification among species, but the phylotypic stages are evolutionarily stable. Specific patterns of gene expression that characterize some phylotypic stages in animal development have been identified through molecular genetics. The major characteristics of animal phyla and their developmental and molecular attributes appear to have arisen and stabilized early in the history of life, during the Cambrian Period. Subsequent evolutionary diversification builds upon the Baupläne established early in animal evolution. *See* CAMBRIAN.

Heterochrony. Particularly important to the evolutionary diversification of life are historical processes that generate change by altering the timing of organismal development, a phenomenon called heterochrony. Heterochronic changes may alter the ontogeny and life history of the organism as a whole or may be limited to certain structures or organs. The different heterochronic processes are described by using an ontogenetic trajectory that describes changes in form occurring throughout the organism's life. Ontogenetic changes are measured relative to the timing of reproductive maturation.

Heterochronic changes can produce either paedomorphic or peramorphic results. Paedomorphosis denotes the retention of preadult characteristics of ancestors in the adult stages of descendants; peramorphosis is the opposite outcome, in which the descendant ontogeny transcends that of the ancestor, adding new features at the final stages. Heterochronic changes can be produced by changing the rates of developmental processes or the times of their onset or termination. Axolotls of the salamander genus *Ambystoma* illustrate paedomorphosis produced by the heterochronic process neoteny, in which the rate of morphological development is decreased relative to reproductive maturation. The ancestral life history of *Ambystoma* is biphasic, possessing an aquatic larval stage followed by a metamorphosed, terrestrial adult. In the axolotl, reproductive maturity proceeds normally, but metamorphosis does not occur and the adult retains the morphological characteristics of the aquatic larva, including gills and tail fin.

Developmental dissociation occurs when different kinds of heterochronic change alter the development of different parts of the organism independently. Extensive dissociation can fundamentally restructure organismal ontogeny, producing ontogenetic repatterning. However, it is rare that a single heterochronic transformation affects all parts of the organism simultaneously, as seen in the axolotl example above. Dissociation and paedomorphosis together refute the statement that ontogeny recapitulates phylogeny, a claim that preadult stages of organismal development correspond to adult morphologies of ancestors. Ontogeny recapitulates phylogeny only in the unusual event that evolutionary change produces peramorphosis affecting all parts of the organism simultaneously. Ontogeny recapitulates phylogeny for individual structures or organs experiencing peramorphic evolution, whereas reverse recapitulation characterizes paedomorphic transformations. For most taxa, novel morphologies are produced by a mosaic of different heterochronic processes and by changes in the physical location of developmental events within the organism. *See* HETEROCHRONY.

Key innovation. A novel morphological or behavioral feature that alters the functional relationship between organisms and their environments is called a key innovation. A key innovation changes the selective factors acting on populational variation and leads to new directions of adaptive evolution. The trophically diverse cichlid fishes illustrate the concept of a key innovation and its evolutionary consequences. The key innovation in this group constitutes changes in the structure of the pharyngeal jaws that permit them to process food. Without the modified pharyngeal jaws, the maxillary and mandibular jaws must both obtain and process food items, preventing the jaws from becoming specialized for obtaining food. The cichlid pharyngeal jaws permit the maxillary and mandibular jaws to specialize for obtaining food in diverse ways, and this has produced an enormous diversity in feeding morphology and ecology among cichlid species. A key innovation or Bauplan of a taxon is evolutionarily stable because many subsequently evolved features are built upon it, causing it to become developmentally and functionally burdened; any major alteration would disrupt the adaptive system and have disastrous consequences. A trophically specialized cichlid fish would be unable to survive, for example, if its pharyngeal jaws lost their ability to process food.

Hierarchical expansion. Traditional Darwinian theory emphasizes natural selection acting on varying organisms within populations as the main causal factor of evolutionary change. Over many generations, the accumulation of favorable variants by natural selection produces new adaptations and new species. Macroevolutionary theory postulates two additional

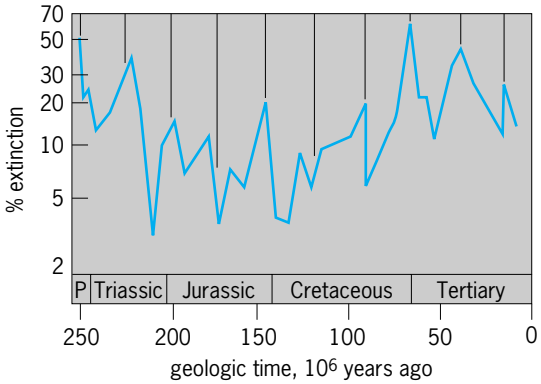

Fig. 2. Simpsonian patterns of mass extinction in the post-Permian fossil record of marine invertebrates. Mass extinctions (peaks) correspond approximately to 26-million-year intervals (vertical bars). (*After D. M. Raup and J. J. Sepkoski, Jr., Periodicity of extinctions in the geologic past, Proceedings of the National Academy of Sciences USA, 81:801–805, 1984*)

processes analogous to natural selection that act above the species level and on much longer time scales. An evolving lineage ultimately experiences one of two fates, branching speciation or extinction. Lineages that have a high propensity to produce new species and an ability to withstand extinction will dominate evolutionary history to the detriment of lineages that are prone to extinction and that have low rates of speciation. Biological characteristics are transmitted from ancestral to descendant species, and characteristics associated with lineages having high rates of speciation and low rates of extinction will prevail, even if they do not experience variation and selection within populations.

The higher-level process of differential speciation and extinction caused by the varying characteristics of species or lineages has been called species selection. Because the precise meaning of the term species is controversial, the more neutral terms lineage selection and clade selection are sometimes substituted for species selection. Most species show an evolutionary duration from a few million to approximately 10 million years in the fossil record between geologically instantaneous events of branching speciation. Species selection therefore generally occurs on a time scale of millions of years, rather than the generational time scale of natural selection. Species selection may be the primary factor underlying morphological evolutionary trends at this scale if lineages evolve by punctuated equilibrium, in which most morphological evolutionary change accompanies branching speciation, and species remain morphologically stable between speciational events. *See* SPECIATION.

The fossil record reveals mass extinctions in which enormous numbers of species from many different taxa are lost within a relatively short interval of geological time. For example, approximately 90% of the species and half of the families of shallow-water marine invertebrates were lost within a few million years during the Permian mass extinction (225 million years ago). A major recent discovery is that mass extinctions may occur at a periodicity of approximately 26 million years in the post-Permian fossil record of marine invertebrates (**Fig. 2**). This periodicity may represent periodic bombardment of the Earth by asteroids, causing massive environmental destruction. Some lineages may be better able to survive mass extinction events than others, and the characteristics that make a lineage prone to survive mass extinction may be very different from those that influence species selection between events of mass extinction. Catastrophic species selection denotes differential survival and extinction of lineages during events of mass extinction as determined by character variation among lineages. Prior to the Cretaceous mass extinction, dinosaur taxa dominated mammalian taxa, whereas mammals survived the mass extinction and then diversified extensively. The characteristics of the ancestral mammals may have permitted them to survive environmental challenges to which dinosaurs were susceptible. *See* EXTINCTION (BIOLOGY); FOSSIL; MAMMALIA; PALEONTOLOGY; PERMIAN.

Because natural selection, species selection, and catastrophic species selection can differ in the biological characteristics they promote, higher-level processes may undo or reverse evolutionary trends arising from lower-level processes. For this reason, macroevolutionists often resist attempts to explain evolutionary trends strictly from the occurrence of natural selection acting within populations. Species selection and catastrophic species selection are being investigated by paleontological research where processes occurring on geological time scales of multiple millions of years can be investigated. *See* ORGANIC EVOLUTION.

Allan Larson

Bibliography. W. Alvarez and F. Asaro, An extraterrestrial impact, *Sci. Amer.*, 263(4):78–84, 1990; N. Eldredge and J. Cracraft, *Phylogenetic Patterns and the Evolutionary Process*, 1980; S. J. Gould, Darwinism and the expansion of evolutionary theory, *Science*, 216:380–387, 1982; S. J. Gould, The paradox of the first tier: An agenda for paleobiology, *Paleobiology*, 11:2–12, 1985; S. J. Gould and N. Eldredge, Punctuated equilibrium comes of age, *Nature*, 366:223–227, 1993; S. J. Gould, N. L. Gilinsky, and R. Z. German, Asymmetry of lineages and the direction of evolutionary time, *Science*, 236:1437–1441, 1987; B. K. Hall, *Evolutionary Developmental Biology*, 2d ed., 1998; J. Levinton, *Genetics, Paleontology, and Macroevolution*, 2d ed., 2001; M. H. Nitecki, *Evolutionary Innovations*, 1990; R. M. Ross and W. D. Allmon, *Causes of Evolution*, 1990; A. Somit and S. A. Peterson, *The Dynamics of Evolution*, 1989.

Macromolecular engineering

The process of designing and synthesizing well-defined complex macromolecular architectures. This process allows for the control of molecular parameters such as molecular-weight/molecular-weight distribution, microstructure/structure, topology,

and the nature and number of functional groups. In addition, macromolecular engineering is the key to establishing the relationships between the precise molecular architectures and their properties. The understanding of the structure–property interplay is critical for the successful use of these elegantly tailored structures in the design of novel polymeric materials for applications such as tissue engineering, drug delivery, molecular filtration, micro- and optoelectronics, and polymer conductivity. Complex architectures, including star-shaped, branched, grafted, and dendritic-like polymers, have been prepared using living polymerization methods (for which there is no termination step to stop chain growth) such as anionic, cationic, living radical, metal-catalyzed polymerization, or combinations of these methods. *See* POLYMER; POLYMERIZATION.

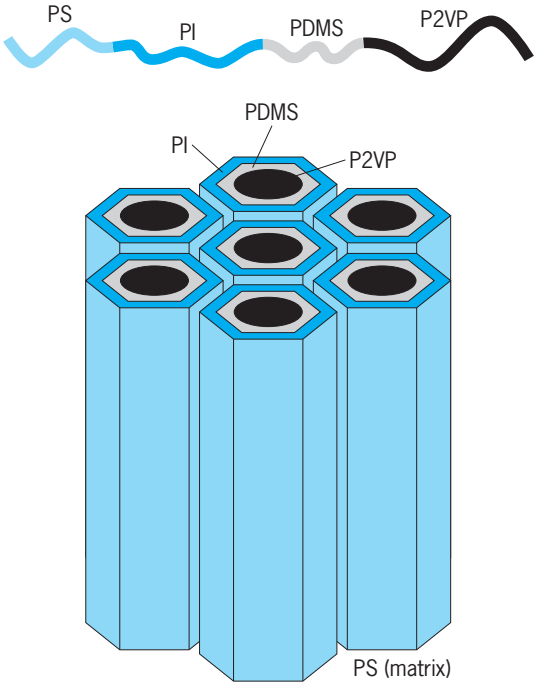

Fig. 1. Hexagonal triple coaxial cylindrical structure observed in PS-*b*-PI-*b*-PDMS-*b*-P2VP found by transmission electron microscopy. (*Reprinted with permission from Macromolecules, 35:4859–4861, 2002. Copyright 2002 American Chemical Society*.)

Anionic polymerization. The first organometallic miktoarm (mikto is from a Greek word meaning mixed) star copolymer of the AB_3 type, where A is polyferrocenyldimethylsilane (PFS) and B is polyisoprene-3,4 (PI), was synthesized by I. Manners and coworkers by anionic polymerization. The synthetic approach involved the anionic ring-opening polymerization of ferrocenophane, followed by reaction with excess silicon tetrachloride. After the removal of the excess of the volatile linking agent, the resulting macromolecular linking agent PFS-$SiCl_3$ was reacted with excess of living polyisoprenyllithium. The desired product (PFS)Si$(PI)_3$ was separated from

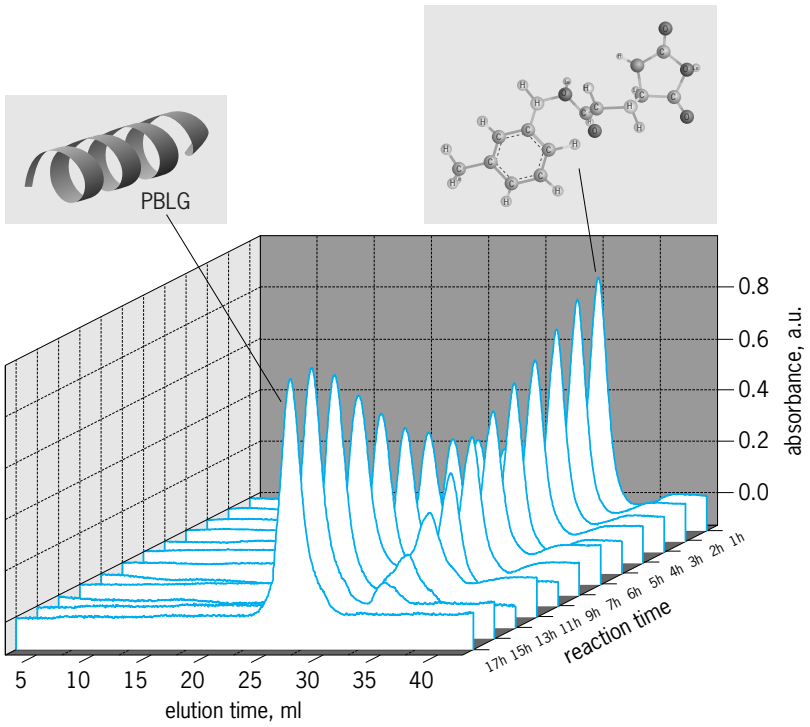

Fig. 2. Monitoring the living polymerization of γ-benzyl-L-glutamate NCA with *n*-hexylamine by size exclusion chromatography with a UV detector. The monomer is transformed 100% to polypeptide. (*Reprinted with permission from Biomacromolecules, 5(5):1653–1656, 2004. Copyright 2004 American Chemical Society*.)

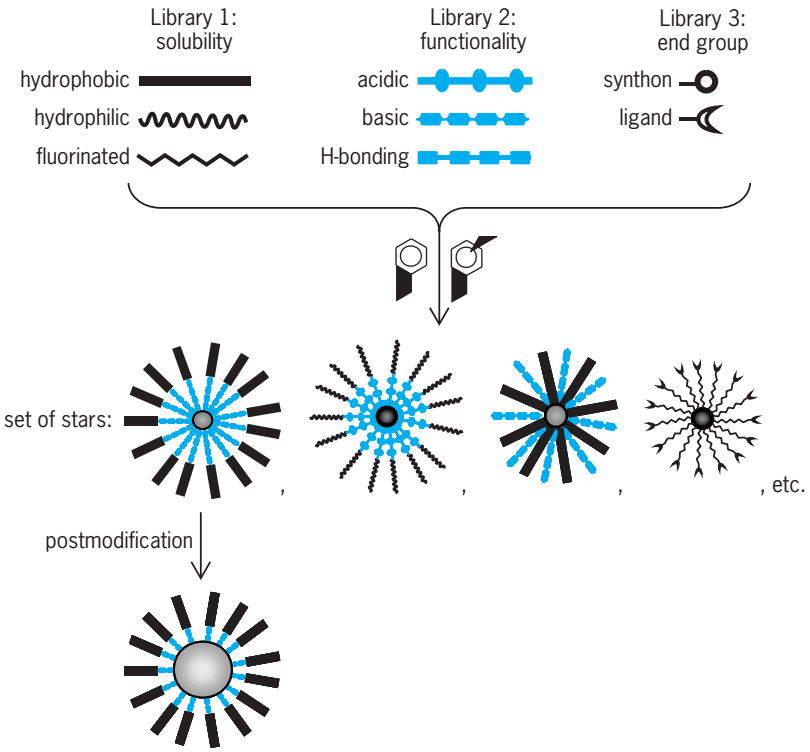

Fig. 3. Schematic representation of the modular approach to star polymers by nitroxide-mediated living radical polymerization. (*Reprinted with permission from J. Amer. Chem. Soc., 125:715–728, 2003. Copyright 2003 American Chemical Society*.)

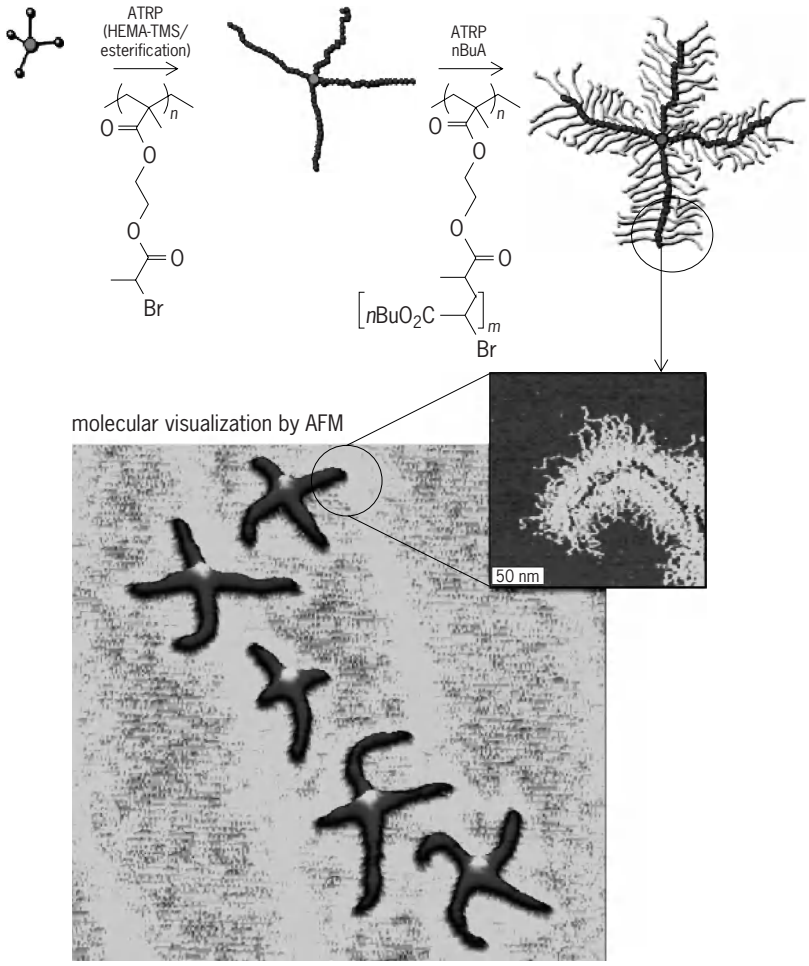

Fig. 4. Reaction sequence for the synthesis of four-arm star brushes, and AFM images. (*Reprinted with permission from Macromolecules, 36:1843–1849, 2003. Copyright 2003 American Chemical Society.*)

the excess PI arm by preparative size exclusion chromatography to yield a near-monodisperse miktoarm star copolymer. The presence of a metallopolymeric block can give redox activity, as well as semiconducting and preceramic properties, to these materials. *See* BRANCHED POLYMER; COPOLYMER; RING-OPENING POLYMERIZATION.

The first tetrablock quaterpolymers of polystyrene (PS), polyisoprene (PI), polydimethylsiloxane (PDMS), and poly(2-vinylpyridine) [P2VP] having different total molecular weights and compositions were synthesized by N. Hadjichristidis and coworkers. The synthetic strategy relied on recent advances in the living anionic polymerization of hexamethylcyclotrisiloxane and the use of a heterofunctional linking agent. This heterofunctional linking agent contains two functional groups, one of which reacts selectively with the polydimethylsiloxanyl lithium. The synthetic approach involved the sequential polymerization of styrene, isoprene, and hexamethylcyclotrisiloxane, followed by reaction with a stoichiometric amount of the heterofunctional linking agent 2-(chloromethylphenyl)ethyldimethyl chlorosilane. A slight excess of living poly(2-vinylpyridine) lithium was then added to react with the functional group of the resulting macromolecular linking agent PS-PI-PDMS-Ph-CH_2Cl. The excess P2VP was removed by fractional precipitation to give the pure tetrablock quaterpolymers. Due to the incompatibility of the four different blocks, these new quaterpolymers gave a unique four-phase triple coaxial cylindrical microdomain morphology never obtained before (**Fig. 1**). These structures could be used, for example, as multifunctional sensors or multiselective catalysts for sequential or simultaneous chemical reactions.

New ways of living ring-opening polymerization of α-amino acid-*N*-carboxy anhydrides (NCA) to yield polypeptides have been presented, thereby resolving a problem which had existed for more than 50 years. H. Schlaad and coworkers synthesized polystyrene-*b*-poly(γ-benzy-L-glutamate) block copolymers by using the hydrochloric salt of an ω-functionalized —NH_2 polystyrene as the macroinitiator of the ring-opening polymerization of γ-benzy-L-glutamate NCA. The use of the hydrochloric acid, instead of the free amine, suppressed the termination reactions. Hadjichristidis and coworkers synthesized well-defined di- and triblock copolypeptides, as well as star-shaped homo- and copolypeptides, by extensively purifying the solvent (dimethylformamide), the monomers (NCAs), and initiator (primary amines) in order to maintain the conditions necessary for the living polymerization. A variety of NCAs, such as γ-benzy-L-glutamate NCA, ϵ-carbobenzoxy-L-lysine NCA, glycine NCA, and *O*-benzyl-L-tyrosine NCA, were used to synthesize several combinations of block copolypeptides, showing that this is a general methodology (**Fig. 2**). The combination of the self-assembly of block copolymers and the highly ordered three-dimensional structures of proteins is expected to give novel supramolecular structures. *See* SUPRAMOLECULAR CHEMISTRY.

Living radical polymerization. A modular strategy for preparing functional multiarm star polymers by using nitroxide-mediated, living radical polymerization was proposed by J. M. Fréchet, C. Hawker, and coworkers. The approach used a variety of alkoxyamine-functional initiators for the polymerization of several vinyl monomers. These linear chains, containing a dormant chain end, were coupled with a crosslinkable monomer, such as divinylbenzene, resulting in a star polymer. The ability of this initiator to polymerize a great variety of vinyl monomers, along with the great diversity of the block sequence, led to the synthesis of a myriad of functionalized three-dimensional star polymers. A few examples are given in **Fig. 3**. The diversity of the method becomes even higher when performing postpolymerization reactions on specific blocks of the stars. These unique structures are useful in a range of applications such as supramolecular hosts, catalytic scaffolds, and substrates for nanoparticle formation.

K. Matyjaszewski and coworkers synthesized a series of three- and four-arm stars of poly(bromo-

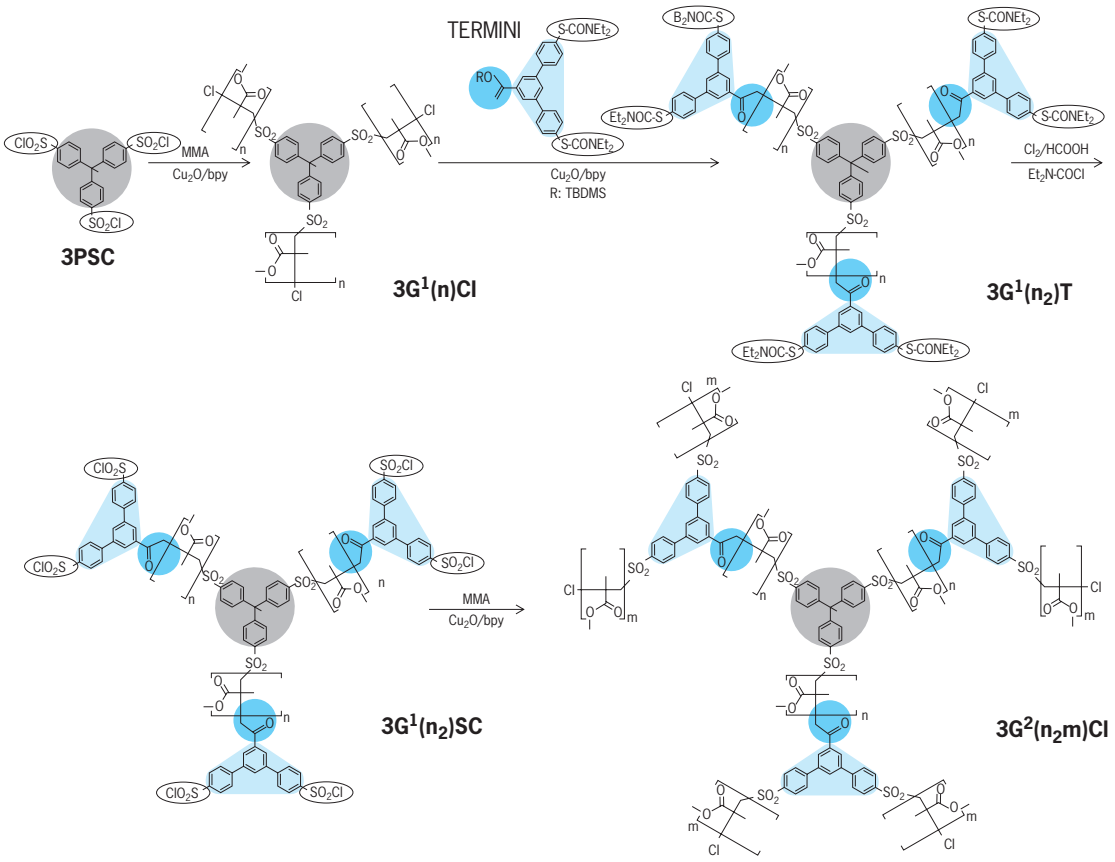

Fig. 5. Divergent iterative synthetic strategy for synthesis of dendritic PMMA. (*Reprinted with permission from J. Amer. Chem. Soc., 125:6503–6516, 2003. Copyright 2003 American Chemical Society.*)

propionylethyl-methacrylate-*g*-*n*-butyl acrylate) by using atom transfer radical polymerization (ATRP). The synthetic approach involved the use of tri- and tetrafunctional initiators for the ATRP of a 2-(trimethylsiloxyethyl)ethyl methacrylate (HEMA-TMS), which is a monomer containing protected hydroxyl groups. After the polymerization, the hydroxyl groups were deprotected and transformed to new bromine-containing groups, which are initiating sites of ATRP. The three- and four-arm star multifunctional macroinitiators were subsequently transformed to the densely grafted molecular brushes of poly(bromopropionylethyl-methacrylate-*g*-*n*-butyl acrylate), after the ATRP of poly(*n*-butyl acrylate) [Fig. 4]. The researchers were able to see the actual stars by atomic force microscopy (AFM). The synthesis of four-arm star brushes is given in **Fig. 4**.

A universal iterative strategy for the divergent synthesis of dendritic macromolecules was presented by V. Percec and coworkers. They used living radical polymerization of conventional monomers, such as methyl methacrylate (MMA), to synthesize the polymeric blocks of the dendrimers, followed by reaction with a specially designed compound, called TERMINI (from TERminator Multifunctional INItiator). TERMINI acts both as a terminator of the living polymer chains and as a masked difunctional initiator. Consequently, after terminating the living polymer and demasking, TERMINI is able to reinitiate the polymerization of MMA by ATRP, generating two new PMMA branches per TERMINI unit with nearly 100% efficiency. Using this methodology, dendrimers with up to four generations were synthesized (**Fig. 5**). The dendrimers were extensively characterized, showing that they exhibited high-molecular-weight homogeneity. *See* DENDRITIC MACROMOLECULE.

Catalytic polymerizations. Living polymerization of propylene was achieved by T. Fujita and coworkers

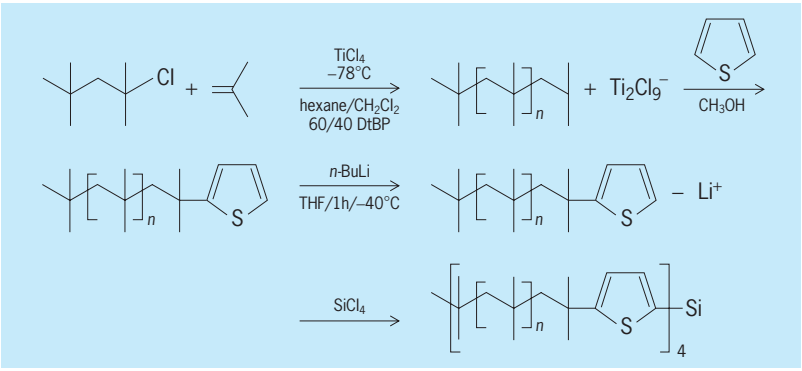

Fig. 6. Synthesis of four-arm PIB stars by site transformation of thiophene end-capped PIB chain ends.

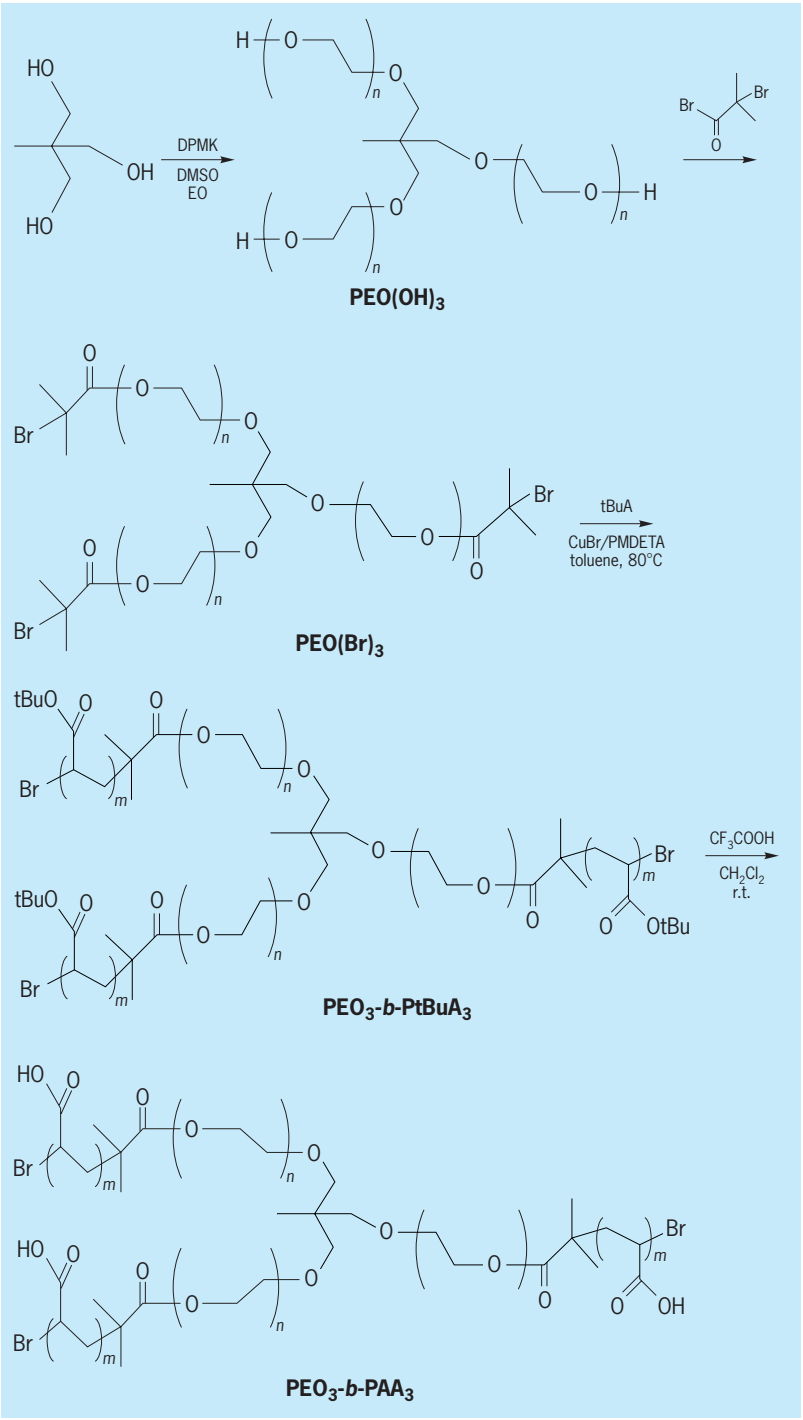

Fig. 7. Synthesis of PEO_3-*b*-PAA_3 star block copolymers.

using a series of titanium (Ti) complexes featuring fluorine-containing phenoxy-imine chelate ligands in the presence of methylaluminoxane (MAO). Despite the fact that the Ti catalyst possesses C_2 symmetry, the polypropylene produced is syndiospecific, through a chain-end control mechanism. Highly syndiotactic and monodisperse polypropylenes were synthesized at the temperature range between 0 and 50°C (32 and 122°F).

Well-defined poly(*n*-butyl methacrylate-*b*-methyl methacrylate) block copolymers were prepared by Hadjichristidis and coworkers, using zirconocene catalysts, fluorophenyl borate cocatalysts, and sequential addition of monomers, starting from the polymerization of *n*-butyl methacrylate. The success of the procedure was based on previous kinetic investigations that have revealed the exact experimental conditions (such as the temperature, nature of catalytic system, catalyst and cocatalyst concentration, and time for the completion of polymerization) under which the polymerization is controlled and the termination reactions are minimized.

Combinations of techniques. Specific polymerization techniques are applicable to a limited number of monomers. Therefore, the combination of different polymerization methods is expected to lead to new and unique macromolecular architectures. A new and efficient procedure for the synthesis of polyisobutylene (PIB) stars and PIB-poly(*t*-butyl methacrylate) block copolymers was developed by A. Müller, R. Faust, and collaborators by combining living carbocationic and anionic polymerizations. Monoaddition of thiophene to living PIB leads to the formation of 2-polyisobutylene-thiophene macroinitiator, which was subsequently metalated with *n*-butyllithium to transform the living cations to the respective anions. The stable carbanionic species were then used to initiate the polymerization of *t*-butyl methacrylate. PIB four-arm stars were also prepared via coupling of the living macrocarbanions with $SiCl_4$ as a coupling agent (**Fig. 6**).

Y. Gnanou and coworkers prepared double hydrophilic star-block (PEO_3-*b*-PAA_3) and dendrimer-like copolymers (PEO_3-*b*-PAA_6) consisting of three inner poly(ethylene oxide) [PEO] arms and either three or six outer poly(acrylic acid) [PAA] arms. Three arm PEO stars, having terminal —OH groups, were prepared by anionic polymerization using a suitable trifunctional initiator. The hydroxyl functions were subsequently transformed to either three or six bromo-ester groups, which were used to initiate the polymerization of *t*-butyl acrylate by ATRP. Subsequent hydrolysis of the *t*-butyl groups yielded the desired products (**Fig. 7**). These double hydrophilic block copolymers exhibit stimuli-responsive properties with potential biotech applications.

Graft copolymers having poly(methyl methacrylate) [PMMA] backbone and polystyrene [PS], polyisoprene [PI], poly(ethylene oxide) [PEO], poly(2-methyl-1,3-pentadiene) [P2MP], and PS-*b*-PI branches were prepared by Hadjichristidis and coworkers using the macromonomer methodology. The methacrylic macromonomers were synthesized by anionic polymerization, whereas their homopolymerization and copolymerization with MMA were performed by metallocene catalysts. Relatively high macromonomer conversions were obtained in all cases. Parameters such as the flexibility, structure, and molecular weight of the macromonomer as well

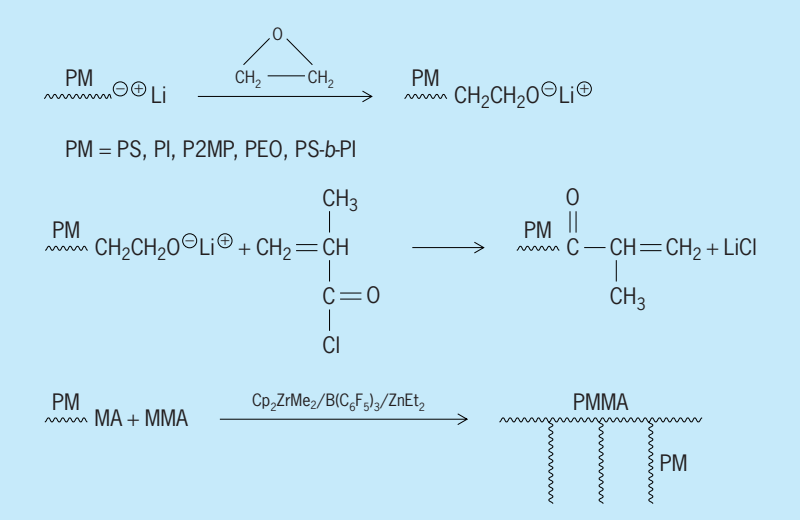

Fig. 8. Synthesis of graft copolymers by combination of anionic and metallocene-catalyzed polymerizations.

as the nature of the catalytic system were found to affect the copolymerization behavior (**Fig. 8**).

Nikos Hadjichristidis; Hermis Iatrou; Marinos Pitsikalis

Bibliography. J. M. Fréchet et al., A modular approach toward functionalized three-dimensional macromolecules: From synthetic concepts to practical applications, *J. Amer. Chem. Soc.*, 125:715–728, 2003; T. Fujita et al., Syndiospecific living propylene polymerization catalyzed by titanium complexes having fluorine-containing phenoxy-imine chelate ligands, *J. Amer. Chem. Soc.*, 125:4293–4305, 2003; Y. Gnanou et al., Synthesis and surface properties of amphiphilic star-shaped and dendrimer-like copolymers based on polystyrene core and poly(ethylene oxide) corona, *Macromolecules*, 36:8253–8259, 2003; Y. Gnanou et al., Synthesis of water-soluble star-block and dendrimer-like copolymers based on poly(ethylene oxide) and poly(acrylic acid), *Macromolecules*, 36:3874–3881, 2003; N. Hadjichristidis et al., *Block Copolymers: Synthetic Strategies, Physical Properties and Applications*, Wiley-Interscience, 2003; N. Hadjichristidis et al., Complex macromolecular architectures utilizing metallocene catalysts, *Macromolecules*, 36:9763–9774, 2003; N. Hadjichristidis et al., Four-phase triple coaxial cylindrical microdomain morphology in a linear tetrablock quarterpolymer of styrene, isoprene, dimethylsiloxane and 2-vinylpyridine, *Macromolecules*, 35:4859–4861, 2002; N. Hadjichristidis et al., Living polypeptides, *Biomacromolecules*, 5(5):1653–1656, 2004; N. Hadjichristidis et al., Synthesis and characterization of linear tetrablock quaterpolymers of styrene, isoprene, dimethylsiloxane and 2-vinylpyridine, *J. Polym. Sci., Polym. Chem.*, 42:514–519, 2004; I. Manners et al., Synthesis of the first organometallic miktoarm star polymer, *Macromol. Rapid Commun.*, 24:403–407, 2003; K. Matyjaszewski et al., Effect of initiation conditions on the uniformity of three-arm star molecular brushes, *Macromolecules*, 36:1843–1849, 2003; A. Müller et al., Polyisobutylene stars and polyisobutylene-block-poly(*tert*-butyl methacrylate) block copolymers by site transformation of thiophene end-capped polyisobutylene chain ends, *Macromolecules*, 36:6985–6994, 2003; V. Percec et al., Universal iterative strategy for the divergent synthesis of dendritic macromolecules from conventional monomers by a combination of living radical polymerization and irreversible terminator multifunctional initiator (TERMINI), *J. Amer. Chem. Soc.*, 125:6503–6516, 2003; H. Schlaad et al., Synthesis of nearly monodisperse polystyrene-polypeptide block copolymers *via* polymerisation of *N*-carboxyanhydrides, *Chem. Commun.*, 23:2944–2945, 2003.

Macroscelidea

An order of mammals containing the single family Macroscelididae (elephant shrews). Although formerly thought to be most closely associated with shrews, ungulates, and rabbits and hares, they are now thought to be most closely associated with elephants, aardvarks, golden moles, hyraxes, and sea cows on the basis of DNA investigations. *See* MAMMALIA.

General morphology. The 15 species of elephant shrews have chubby, soft-furred bodies, long hindlegs, and a long, slender, ratlike tail usually covered with knobbed bristles (see **illustration**). The fur is brownish or grayish. A gland on the underside of the tail produces a musky odor, especially in males. The hindlegs are much longer than the front limbs. Four or five toes are present on each foot. They may walk on all four feet, or when alarmed or pursued they hop on their hindlegs like a kangaroo. The eyes are large, the ears are well developed, and the elongated, trunklike snout is flexible and sensitive. The nostrils are located at the end of the snout. All

Elephant shrew, *Elephantulus*. (*Photo by Dr. Lloyd Glenn Ingles; © 2001 California Academy of Sciences*)

elephant shrews have long tongues that extend beyond the tips of their noses and are used to flick small food items into their mouths. The dental formula is I 1-3/3, C 1/1, PM 4/4, M 2/2-3 × 2 for a total of 36 to 42 teeth. Females have two or three pairs of mammae. The head and body length ranges 95–315 mm (3.5–12 in.) and the tail 80–265 mm (3–10 in.) The largest species is the checkered elephant shrew (*Rhynchocyon*) whose back is marked like a checkerboard, with four or five rows of evenly spaced light and dark square spots.

Behavior and habitats. Elephant shrews are found throughout Africa in a variety of habitats from the deserts of the Sahara to grassy plains, to rocky outcrops and boulder fields, to the well-forested regions of the Congo. They are primarily diurnal, but may be nocturnal during hot weather and on moonlit nights. They often bask and stretch out in the warm sunshine. While not a typical burrowing animal, as judged by its claws, the elephant shrew can quickly dig its way out of sight in reasonably soft soil or sand. The den may be a crevice in the rocks, a depression beneath a log, or a burrow it has dug in the ground. All burrows have a perpendicular emergency exit situated on the surface a few feet from the main entrance.

Food consists primarily of ants, termites, beetles, centipedes, spiders, and earthworms. The large checkered elephant shrew may also consume small mammals, birds, eggs, and mollusks. Some, like the short-eared elephant shrew (*Macroscelides*), may include shoots, roots, and berries in their diet. The elephant shrew, like most insect-eating animals, is not a particularly sociable creature: most species live either singly or in pairs. Several species including the golden-rumped elephant shrew (*Rhynchocyon chrysopygus*), the four-toed elephant shrew (*Petrodomus tetradactylus*), the short-eared elephant shrew (*Macroscelides proboscideus*), the rufous elephant shrew (*Elephantulus rufescens*), and the western rock elephant shrew (*Elephanteus rupestris*) are monogamous.

Reproduction. Breeding in some species may be continuous throughout the year, whereas in others it is seasonal. Following a gestation period of about 2 months, a litter of one or two young is born. Newborn elephant shrews are well developed, covered with fur, and usually have their eyes open. They can move about shortly after birth, and they nurse for a relatively short period of time. Sexual maturity is attained at 5 to 6 weeks.

Threats. Longevity in some species in the wild may be up to 4 years. Some of the larger species, such as the golden-rumped elephant shrew and the four-toed elephant shrew, may be taken for food in Kenya. Several species are classified as vulnerable or endangered by the International Union for the Conservation of Nature and Natural Resources (IUCN) primarily due to restricted areas of suitable habitat that are expected to decline due to human activity for subsistence farming, exotic tree plantations, and urban developments.

Donald W. Linzey

Bibliography. D. Macdonald (ed.), *The Encyclopedia of Mammals*, Andromeda Oxford Limited, 2001; R. M. Nowak, *Walker's Mammals of the World*, 6th ed., Johns Hopkins University Press, 1999.

Macrostomorpha

More than 300 species of small (mostly 1 mm size) flatworms usually with a ventral mouth situated about one quarter distant from the rostral tip of the body. A ciliated tubular foregut leads into a ciliated gut. Except for the Haplopharyngida, an anus is lacking. A hindgut is never differentiated. Macrostomorpha are covered by a single-layered, ciliated epidermis; they move by ciliary gliding and have special duo-gland adhesive papillae, at least in the tail region, which they use for temporary adhesion to and quick release from the substrate (only the marine, pelagic microstomid *Alaurina* does not possess papillae). The space between epidermis and gut is filled with parenchymal cells and muscle cells among others. The animals are hermaphroditic; sexual reproduction is typical. Larval stages are not known. Many species are found in marine sand and mud, and in various freshwater habitats. These flatworms were formerly members of the Turbellaria-Rhabdocoela, but are now included in the Rhabditophora, which is one of three monophyletic taxa constituting the Platyhelminthes (Acoelomorpha, Catenulida, and Rhabditophora). *See* PLATYHELMINTHES.

Taxonomy. Macrostomorpha are subdivided into two taxonomic groups of equal rank:

The Haplopharyngida are more than 5 mm (0.2 in.) long. They have a particularly pronounced glandular (sometimes highly muscular) proboscis-like organ in front of the mouth. Only two marine species in one family (Haplopharyngidae) are known.

The Macrostomida include all other Macrostomorpha. Three families are distinguished: (1) Microstomidae (three genera with 35 species) is known from many marine and freshwater habitats worldwide. The genus *Microstomum* (with 29 species) is characterized by asexual reproduction through transverse fission in addition to sexual reproduction. (2) Dolichomacrostomidae (35 species in three

subfamilies) is known only from marine sediments. The genus *Paromalostomum* shows worldwide distribution. These animals exhibit very complicated reproductive organs and an unpaired, common gonopore through which eggs are laid and sperm is transferred during copulation. (3) Macrostomidae includes most of the 11 genera of widely recognized species. Marine, brackish-water, and freshwater forms are found in all regions of the world. The best-known genus of Macrostomorpha is *Macrostomum*. The species *M. lignano* from the northern Adriatic can be cultured in large numbers and is a new model organism for developmental and evolutionary studies (see **illustration**). Another species with worldwide distribution, *M. orthostylum*, is cultured as food for fish larvae in India.

In the illustration, the general body plan of the Macrostomorpha is shown in *Microstomum lignano*, with hermaphroditic reproductive structures.

Based on body plan and molecular data, the Macrostomorpha are considered to be a basalmost branch of the Rhabditophora. Above Macrostomorpha, the following branches form a sequence from basal to most derived: Polycladida, Lecithoepitheliata, Prolecithophora, Proseriata, Tricladida, Rhabdocoela, and the parasitic Neodermata (with the Trematoda, Monogenea, and Cestoda).

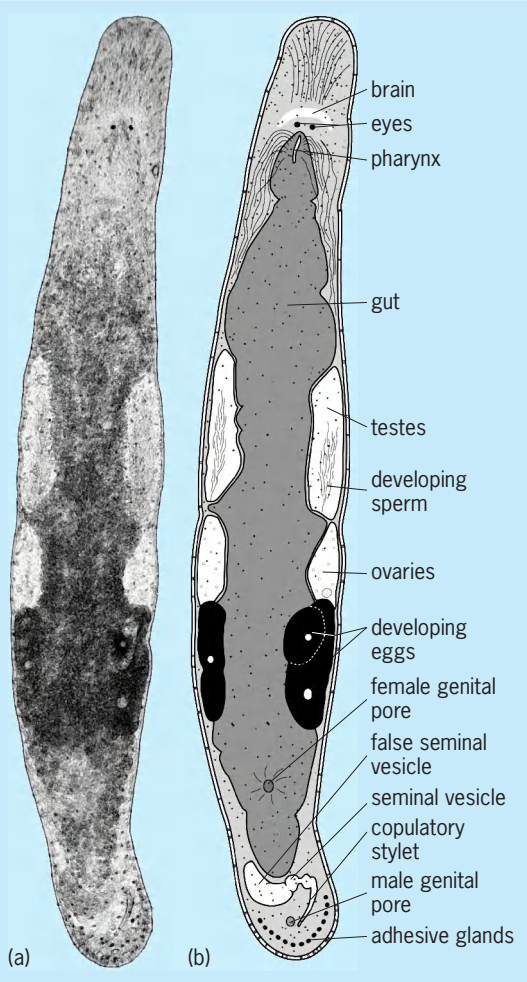

***Macrostomum lignano*, a new species from the northern Adriatic near Lignano, Italy. (*a*) Photomicrograph of a living, slightly squeezed worm. (*b*) Diagram showing the major organ systems. (*From L. Schärer, G. Joss, and P. Sandner, Mating behavior of the marine turbellarian Macrostomum sp., Mar. Biol., 145:373–380, 2004; with kind permission of Springer Science and Business Media*)**

Reinhard Rieger

Bibliography. L. R. G. Cannon, *Turbellaria of the World: A Guide to Families & Genera*, Queensland Museum Cultural Centre, Brisbane, 1986; M. Crezee, Turbellaria, in S. P. Parker (ed.), *Synopsis and Classification of Living Organisms*, pp. 718–740, McGraw-Hill, New York, 1982; R. Rieger, Phylogentic systematics of the Macrostomorpha, in D. T. J. Littlewood and R. A. Bray (eds.), *Interrelationship of the Platyhelminthes*, pp. 28–38, Taylor and Francis, New York, 2001.

Madelung constant

A numerical constant α_M in terms of which the electrostatic energy U of a three-dimensional periodic crystal lattice of positive and negative point charges q_+, q_-, N in number, is given by Eq. (1), where d is

$$U = -\frac{1}{2}\frac{Nq_+q_-}{d}\alpha_M \tag{1}$$

the nearest-neighbor distance between positive and negative charges and N is large. Knowledge of such electrostatic energies as given by the Madelung constant is of importance in the calculation of the cohesive energies of ionic crystals and in many other problems in the physics of solids. *See* IONIC CRYSTALS.

Designate the lattice sites by indices i or j, and let the distance between sites i and j be given by r_{ij}. Then U is given by the sum of the Coulomb interaction energies of all pairs of charges as shown in Eq. (2). In the summation, i and j range over all sites

$$U = \frac{1}{2}\sum_{i,j}{}' \frac{q_iq_j}{r_{ij}} \tag{2}$$

in the lattice, and the prime on the summation sign indicates the exclusion of terms for which $i = j$. The factor $^1/_2$ avoids counting pairs of charges twice. In Eq. (2) $q_i = q_+$ or q_-, depending upon whether the lattice site i is occupied by a positive or a negative ion. From this expression for U it can be seen by comparison of Eq. (2) with Eq. (1) that Eq. (3) holds.

$$\alpha_M = -\frac{1}{2}\sum{}' \left(\frac{q_i}{q_+}\right)\left(\frac{q_j}{q_-}\right)\left(\frac{d}{r_{ij}}\right) \tag{3}$$

This number is called the Madelung constant after E. Madelung, who first calculated the sum in connection with the cohesive energies of ionic crystals. It is characteristic of the lattice structure but independent of the dimensions of the lattice. Its numerical value does, however, depend on the

Madelung constants for some common ionic crystals

Name and formula	Madelung constant, α_M
Sodium chloride, NaCl	1.7476
Cesium chloride, CsCl	1.7627
Zinc blende, α-ZnS	1.6381
Wurtzite, β-ZnS	1.641
Fluorite, CaF_2	5.0388
Cuprite, CuO_2	4.1155
Rutile, TiO_2	4.816
Anatase, TiO_2	4.800
Corundum, Al_2O_3	25.0312

choice of the unit distance within the crystal, d. In Eq. (1), d has been chosen to be the nearest-neighbor positive-negative charge separation. Occasionally other choices of d are used instead, such as the cube root of the molecular volume or the unit cube edge in cubic crystals.

The calculation of Madelung constants requires some care since they are given by slowly and conditionally convergent series. Attempts at direct summation can involve thousands of terms without impressive accuracy. Various ingenious schemes for calculation have been used, but the most general and powerful is Ewald's method, also called the theta function method.

The Madelung constants for a number of common ionic crystal structures are given in the **table**. For these cases d is chosen as the nearest-neighbor distance. *See* CRYSTAL STRUCTURE.

B. Gale Dick

Magellanic Clouds

Two small, irregular galaxies that are close companions of the Milky Way Galaxy. Both are nearby galaxies that are located in the southern sky, not far from the south celestial pole. When viewed without a telescope, they resemble small sections of the Milky Way that might have drifted away from the main arc of that soft, glowing belt of light. On a very dark clear night the Magellanic Clouds can also be mistaken for small atmospheric clouds because of their diffuse appearance. *See* MILKY WAY GALAXY.

The Large Magellanic Cloud (LMC) subtends an angular extent of about 5° in the sky (**Fig. 1**), and the Small Magellanic Cloud (SMC) is about 3° across. Telescopic studies show, however, that each is really much larger than it appears. Outer stars are detected over 10° and 6°, respectively, and there is even a faint bridge of stars that joins them tenuously together.

Because they are not visible from the Northern Hemisphere, the Magellanic Clouds were not known to European astronomers until Portuguese explorers brought back word of them from their travels down the coasts of Africa. They were given their names when Antonio Pigafetta, Ferdinand Magellan's navigator, published his description of the circumnavigation of the world, suggesting that these celestial objects be named for Magellan as a memorial. (Magellan did not complete his journey, having been killed in the Philippines.)

Distances. The Magellanic Clouds are now known to be rather small irregular-type galaxies. The Large Magellanic Cloud is at a distance of 160,000 light-years (1.5×10^{18} km or 9×10^{17} mi), and the Small Cloud is about 10% farther away. Their distances have been measured by many methods, including observations of Cepheid and RR Lyrae variables and (for the Large Magellanic Cloud) Supernova 1987A. The explosion of the supernova was seen in February 1987, and then several days later the effects were detected of its burst of light on a circumstellar ring of material that had been formed around the star before its final explosion. The time difference, combined with the angular size of the ring, provided a measurement of the distance to the Large Magellanic Cloud. *See* CEPHEIDS; SUPERNOVA; VARIABLE STAR.

Motions. The motions of the Magellanic Clouds across the sky have been measured by precise astrometry over many years. Combined with radial velocities measured spectroscopically, they provide knowledge of the motion of the Clouds in space. In both cases it is clear that these galaxies are satellites of the Milky Way Galaxy, with orbits that bring them close enough to the Milky Way and to each other to provide strong tidal effects. Indications are that such close encounters have led to periods of enhanced star formation.

Star clusters. In addition to some 5×10^9 ordinary stars, the Large Magellanic Cloud has a suite of about 10 massive old globular star clusters and several thousand smaller, younger star clusters. It was shown in 1998, using Hubble Space Telescope measurements, that the oldest globular clusters in the Large Magellanic Cloud have the same ages as the oldest such clusters in the Milky Way Galaxy, indicating that both galaxies must have formed at nearly the same time.

The Small Magellanic Cloud may have formed more recently, perhaps 10×10^9 rather than

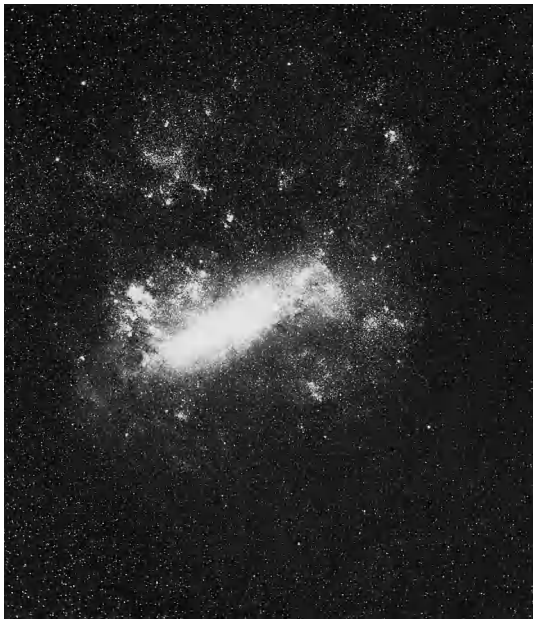

Fig. 1. Large Magellanic Cloud. (*Harvard Observatory photo by P. Hodge*)

Fig. 2. Giant gas cloud centered on 30 Doradus in the Large Magellanic Cloud. (*Cerro Tololo Interamerican Observatory photo by P. Hodge*)

15×10^9 years ago, as no very old clusters have yet been identified among its several hundred star clusters. It is less massive than the Large Magellanic Cloud, with a total content of about 5×10^8 stars. Both Magellanic Clouds have large numbers of very young stars, most of which are located in stellar associations, each of which contains several hundred recently formed stars in loose aggregates about 200 light-years (2×10^{15} km or 1.2×10^{15} mi) across. *See* STAR CLUSTERS.

Gas and nebulae. Both objects also are rich in gas, mostly neutral hydrogen gas, detected by radio telescopes, such as the giant Australia Telescope array. In certain areas the gas is heated by nearby bright stars, producing brilliant glowing nebulae. The brightest and biggest is the 30 Doradus nebula (see **Fig. 2**), one of the most remarkable objects of the nearby universe. It extends over 500 light-years (5×10^{15} km or 3×10^{15} mi), and its primary source of energy is the ultraviolet light from many very young, massive stars, including about 10 extreme stars that are clustered together so compactly that ordinary ground-based telescopes mistakenly led astronomers to think that only one immense star was involved. Special interferometry techniques and the Hubble Space Telescope resolved this remarkable object in the 1990s, providing an example of a rare phenomenon: a "nursery" for the formation of supergiant stars. *See* INTERSTELLAR MATTER; NEBULA; SUPERGIANT STAR; SUPERMASSIVE STARS.

The gas clouds of both galaxies can be used to measure their chemical compositions, which are different from that of the Sun and the nearby stars. The Small Magellanic Cloud is depleted in heavy elements by a factor of about 6, and the Large Magellanic Cloud by a factor of about 2. *See* GALAXY, EXTERNAL.

Paul Hodge

Bibliography. P. Hodge and F. Wright, The Large Magellanic Cloud, *Smithson. Publ.*, no. 4699, 1967; P. Hodge and F. Wright, *The Small Magellanic Cloud*, University of Washington Press, 1977; B. Westerlund, *The Magellanic Clouds*, Cambridge University Press, 1998.

Magic numbers

The number of neutrons or protons in nuclei which are required to fill major quantum shells. They occur at particle numbers 2, 8, 20, 50, and 82.

In atoms, the electrons that orbit the nucleus fill quantum electron shells at atomic numbers of 2 (helium), 10 (neon), 18 (argon), 36 (krypton), and 54 (xenon). These elements are chemically inert and difficult to ionize because the energies of orbits are grouped in bunches or shells with large gaps between them. In nuclei, an analogous behavior is found; quantum orbits completely filled with neutrons or protons result in extra stability. The neutrons and protons fill their quantum states independently, so that both full neutron and full proton shells can occur as magic nuclei. In a few cases, for example oxygen-16 ($^{16}_{8}O_8$) and calcium-40 ($^{40}_{20}Ca_{20}$), doubly magic nuclei have full neutron and proton shells. Between the major shell gaps, smaller subshell gaps cause some extra stabilization and semimagic behavior is found at particle numbers 14, 28, 40, and 64. *See* ATOMIC STRUCTURE AND SPECTRA; ELECTRON CONFIGURATION.

In very heavy nuclei the Coulomb repulsion between the protons results in a different sequence of states for neutrons and protons and different major shell gaps. For neutrons the magic sequence continues at $N = 126$; the next shell gap is predicted at $N = 184$. For protons the next major shell gap is anticipated at $Z = 114$. The latter shell gaps lie beyond the heaviest nuclei known, but calculations indicate that the extra stability gained by producing nuclei with these particle numbers may result in an island of long-lived superheavy nuclei.

The closing of nuclear quantum shells has many observable consequences. The nuclei are more tightly bound than average, and the extra stability leads to anomalously high abundances of magic nuclei in nature. The full shells require unusually high energies to remove the least bound neutron or proton, and the probability of capturing extra particles is lower than expected. Furthermore, the full shells are spherically symmetric, and the nuclei have very small electric quadrupole moments. Many of these properties were known before the nuclear shell model was developed to account for quantum-level ordering and gaps between major shells. The different shell closures for atomic and nuclear systems reflect the differences between the Coulomb force that binds electrons to nuclei and the strong force that holds the nucleus together. An important component of the strong force in nuclei is the spin-orbit term, which makes the energy of a state strongly dependent on the relative orientation of spin and orbital angular momentum. *See* ANGULAR MOMENTUM; ELEMENTS, COSMIC ABUNDANCE OF; ISOTOPE; NUCLEAR MOMENTS; STRONG NUCLEAR INTERACTIONS.

Unlike atoms, nuclei that have both neutrons and protons in excess of magic closings are not confined to sphericity and can be polarized to exotic shapes. The bunching of quantum states into shells is

removed by a small deformation and the influences of shell gaps disappear. However, if the deformation becomes very large and nuclei become polarized to ellipsoidal shapes with axis ratios 2:1, 3:1, and so on, new symmetry is then imposed and the quantum states bunch into new shell groups with large gaps between them. Hence, deformed gaps and magic numbers appear which help stabilize these highly eccentric shapes. The production of nuclei in these highly elongated shapes is difficult and requires the fusion of heavy ions at high rotational frequency. The population of these superdeformed nuclei, the position of the deformed gaps and magic numbers, and the degree of stabilization they cause are of great interest. *See* EXOTIC NUCLEI; NUCLEAR STRUCTURE.

C. J. Lister

Bibliography. W. E. Burcham and M. Jobes, *Nuclear and Particle Physics*, 1994; A. De Shalit, *Theoretical Nuclear Physics*, 1990; K. S. Krane, *Introduction to Nuclear Physics*, 1987.

Magma

The hot material, partly or wholly liquid, from which igneous rocks form. Besides liquids, solids and gas may be present in magma. Most observed magmas are silicate melts with associated crystals and gas, but some inferred magmas are carbonate, phosphate, oxide, sulfide, and sulfur melts.

Strictly, any natural material which contains a finite proportion of melt (hot liquid) is a magma. However, magmas which contain more than about 60% by volume of solids generally have finite strength and fracture like solids.

Hypothetical, wholly liquid magmas which develop by partial melting of previously solid rock and segregation of the liquid into a volume free of suspended solids and gas are called primary magmas. Hypothetical, wholly liquid magmas which develop by crystallization of a primary magma and isolation of rest liquid free of suspended solids are called parental (or secondary) magmas. Although no unquestioned natural examples of either primary or parental magmas are known, the concepts implied by the definitions are useful in discussing the origins of magmas.

Bodies of flowing lava and natural volcanic glass prove the existence of magmas. Such proven magmas include the silicate magmas corresponding to such rocks as basalt, and andesite, dacite, and rhyolite as well as rare carbonate-rich magmas and sulfur melts. Oxide-rich and sulfide-rich magmas are inferred from textural and structural evidence of fluidity as well as mineralogical evidence of high temperature, together with the results of experiments on the equilibrium relations of melts and crystals. *See* LAVA.

Temperatures. The temperatures observed for silicate magmas flowing on the surface (lavas) range from slightly greater than 2200°F (1200°C) for basalts to about 1500°F (800°C) for rhyolites. The lower temperatures reflect both the nonequilibrium persistence of supercooled liquid and a lower temperature of melting at equilibrium for rhyolite than for basalt. Temperatures inferred for intrusive magmas vary widely and are both higher and lower than those observed for lavas. Both relations are possible, because some very hot magmas may cool before reaching the surface and because pressure enhances the solubility in melts of H_2O and other volatile substances which lower the equilibrium temperature of freezing. The volatile substances may largely escape during crystallization, and the minerals in a rock may interact during slow cooling; therefore, it is generally impossible to infer, with certainty, the temperatures of intrusive magmas.

Density. The mass density of silicate magmas (about 2.7 to 2.4 g/cm^3 or 1.6 to 1.4 oz/in^3) depends upon composition and temperature. In general, the density of the melt is less than that of crystals forming from it. Thus, buoyance forces lead to gravitative settling of crystals. In hot fluid basaltic magmas, millimeter-sized crystals may settle at rates of centimeters per hour. Indeed, some pillows of basalts 8 in. (20 cm) in diameter are known to contain accumulations of olivine crystals in their lower parts. In some iron-rich melts, feldspar crystals may float. Flotation of feldspar may occur on Earth rarely and probably has occurred on the Moon.

Many basaltic magmas are denser than continental crustal material and are necessarily forced to the surface either by hydrostatic head in the mantle, where the encasing rock is denser than the melt, or by gas propulsion. Most other magmas are less dense than most rock types and are buoyant everywhere within the crust and upper mantle. *See* BASALT.

Viscosity. Silicate magmas are variably viscous, ranging from about 100 poise (10 N·s/m^2) to more than 100,000 poise (10,000 N·s/m^2). Viscosity of magmas increases with decrease in temperature, with decrease in dissolved H_2O, with increase in crystal fraction, and with increase in fraction of SiO_2. In natural magmas the above variables are not independent; the viscosity of silicate magmas generally increases with fraction of SiO_2 in the melt. Thus, basaltic magmas produce flat-lying lava fields, whereas rhyolitic magmas commonly yield mounds and domes. Magmas with more than a few percent of crystals may have a finite yield strength.

Structure. Silicate melts are ionic solutions and have significant electrical conductivity (100 ohm^{-1}·cm^{-1}). Melts rich in silica are highly polymerized, which fact accounts for their high viscosity. Following the practice used in studies of slags, siliceous melts are commonly termed acidic (low activity of oxygen anion), and melts rich in basic oxides such as MgO and CaO are termed basic (high activity of oxygen anion).

Crystallization. Magmas crystallize as a consequence of cooling or effervescence, or both. Minerals grow in crystallizing magmas according to mass-action principles whereby the most abundant, least soluble constituents crystallize first, followed by less abundant, more soluble substances. With crystallization, most magmas display progressive enrichment to both crystals and residual melts in soda relative to lime and ferrous iron relative to magnesia. In many systems an immiscible sulfide melt develops

at an early stage. Minerals (such as apatite and zircon) which contain high concentrations of minor elements generally crystallize late and tend to have comparatively high ratios of surface area to volume. However, minerals which crystallize early in one magma may form later or not at all in other magmas. *See* PETROLOGY.

Magmas which cool and crystallize quickly (in a few decades or less) develop small crystals (a few millimeters in diameter or smaller). Magmas which cool and crystallize slowly (hundreds of thousands of years) develop large crystals (up to a few centimeters, rarely many tens of centimeters).

Occurrence. Magma is presumed to underlie regions of active volcanism and to occupy volumes comparable in size and shape to plutons of eroded igneous rocks. However, it is not certain that individual plutons existed wholly as magma at one time. Some catastrophic eruptions have yielded up to about 250 mi^3 (1000 km^3) of material on a void-free basis in a single event of short duration (few weeks or years), it is certain that some large bodies of magma have existed at one time, and presumably exist today. Magma may underlie some regions where no volcanic activity exists, because many plutons appear not to have vented to the surface.

Remote detection of bodies of magma is difficult because the properties of magma are closely approximated by hot fractured rock filled with water or water vapor. Seismic, gravimetric, and magnetic data are consistent with the existence of major bodies of magma beneath Yellowstone Park; Katmai-Trident, Alaska; several regions in Kamchatka; Japan; and elsewhere.

Origin. Diverse origins are probable for various magmas. Basaltic magmas because of their high temperatures probably originate within the mantle several tens of kilometers beneath the surface of the Earth. Experiments at high pressure have led many scientists to conclude that most basaltic magmas are modified by crystallization and separation of residual liquid from crystals between the site of melting in the mantle and the place of crystallization within the crust. Rhyolitic magmas may originate through crystallization differentiation of basaltic magmas or by melting of crustal rock. Intermediate magmas may originate within the mantle or by crystallization of basaltic magmas, by melting of appropriate crustal rock, and also by mixing of magmas or by assimilation of an appropriate rock by an appropriate magma. *See* IGNEOUS ROCKS; VOLCANO.

Alfred T. Anderson

Bibliography. M. G. Best, *Igneous and Metamorphic Petrology,* 1982; L. Civetta et al., *Physical Volcanology,* 1974; C. J. Hughes, *Igneous Petrology,* 1982; A. R. McBirney, *Igneous Petrology*, 2d ed., 1992.

Magnesite

A member of the calcite-type car-bonates having the formula $MgCO_3$. It forms dolomite [$CaMg(CO_3)_2$] with calcite ($CaCO_3$) in the system $CaCO_3$—$MgCO_3$. Pure magnesite is not common in nature because there exists a complete series of solid solutions between $MgCO_3$ and $FeCO_3$, which is constantly present in magnesite in its natural occurrence. *See* CARBONATE MINERALS; MAGNESIUM.

The calcite-type structure of magnesite has $a = 0.4632$ nm, $c = 1.5032$ nm, $z = 6$, and space group $R\bar{3}c$. The interatomic distances are C—O, 0.12851 nm, and Mg—O, 0.21018 nm, which produce a MgO octahedron with less distortion than that of CaO_6 in calcite. Magnesite decomposes to MgO and CO_2 in the temperature range of 625–643°C as determined by differential thermal analysis. Crystallization of magnesite in aqueous solution is inhibited by species of magnesium in solution and strong positive catalysis by ionic strength and CO_2 pressure. Therefore, highly saline conditions provide a favorable environment for magnesite crystallization.

Magnesite is uniaxial and optically negative with extreme birefringence (0.191). Refractive indices are $\epsilon = 1.509$ (extraordinary index) and $\omega = 1.700$ (ordinary index). Magnesite is usually white, but it may be light to dark brown if iron-bearing. The hardness of magnesite is $3\frac{1}{2}$–$4\frac{1}{2}$ on the Mohs scale, and the specific gravity is 3.00. *See* BIREFRINGENCE; CRYSTAL OPTICS; HARDNESS SCALES.

Magnesite deposits are of two general types: massive and crystalline. Massive magnesite is an alteration product of serpentine which has been subjected to the action of carbonate waters. Crystalline magnesite is usually found in association with dolomite. It is generally thought to be a secondary replacement of magnesite in preexisting dolomite by magnesium-rich fluids. Massive magnesite deposits are found in Greece, Turkey, India, China, North Korea, and Australia, while those of crystalline magnesite occur in the United States, Austria, Spain, Russia, and the Czech Republic.

Magnesite is an important industrial mineral. Various types of magnesite or magnesia (MgO) are produced by different thermal treatment. The caustic-calcined magnesite or magnesia is used in the chemical industry for the production of magnesium compounds, while dead-burned or sintered magnesite or magnesia is used in refractory materials. Fused magnesia is used as an insulating material in the electrical industry because of its high electrical resistance and high thermal conductivity. Luke L. Y. Chang

Bibliography. L. Chang, R. A. Howie, and J. Zussman, *Rock-Forming Minerals*, vol. 5B: *Non-Silicates*, 2d ed., Geological Society Publishing House, 1998.

Magnesium

A metallic chemical element, Mg, in group 2 of the periodic system, atomic number 12, atomic weight 24.312. Magnesium is silvery white and extremely light in weight. The specific gravity is 1.74, and the density is 1740 kg/m^3 (0.063 $lb/in.^3$ or 108.6 lb/ft^3). Because of this lightness combined with alloy strength suitable for many structural

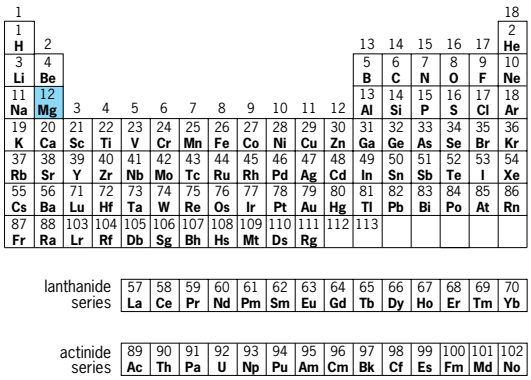

uses, magnesium has long been known as industry's lightest structural metal. *See* PERIODIC TABLE.

With a density only two-thirds that of aluminum, magnesium is used in countless applications where weight saving is an important consideration. The metal also has, however, many desirable chemical and metallurgical properties which account for its extensive use in a variety of nonstructural applications.

Magnesium is very abundant in nature, occurring in substantial amounts in many rock-forming minerals such as dolomite, magnesite, olivine, and serpentine. In addition, magnesium is also found in sea water, subterranean brines, and salt beds. It is the third most abundant structural metal in the Earth's crust, exceeded only by aluminum and iron.

Some of the properties of magnesium in metallic form are listed in **Table 1**. Magnesium is very active chemically. It will actually displace hydrogen from boiling water, and a large number of metals can be prepared by thermal reduction of their salts and oxides with magnesium. The metal will combine with most nonmetals and with practically all acids. Magnesium reacts only slightly or not at all with most alkalies and many organic chemicals, including hydrocarbons, aldehydes, alcohols, phenols, amines, esters, and most oils. As a catalyst, magnesium is useful for promoting organic condensation, reduction, addition, and dehalogenation reactions. It has long been used for the synthesis of complex and special organic compounds by the well-known Grignard reaction. Principal alloying ingredients include aluminum, manganese, zirconium, zinc, rare-earth metals, and thorium. *See* MAGNESIUM ALLOYS.

Magnesium compounds are used extensively in industry and agriculture. **Table 2** lists the major magnesium compounds and indicates some of their more significant applications.

William H. Gross; Stephen C. Encleson

TABLE 1. Physical properties of primary magnesium (99.9% pure)

Property	Value
Atomic number	12
Atomic weight	24.312
Atomic volume, cm^3/g-atom	14.0
Crystal structure	Close-packed hexagonal
Electron arrangement in free atoms	(2) (8) 2
Mass numbers of the isotopes	24, 25, 26
Percent relative abundances of ^{24}Mg, ^{25}Mg, ^{26}Mg	77, 11.5, 11.5
Density, g/cm^3 at 20°C	1.738
Specific heat, cal/g/°C at 20°C (1 cal = 4.2 joules)	0.245
Melting point, °C	650
Boiling point, °C	1110 ± 10

TABLE 2. Principal magnesium compounds and uses

Compound	Uses
Magnesium carbonte	Refractories, production of other magnesium compounds, water treatment, fertilizers
Magnesium chloride	Cell feed for production of metallic magnesium, oxychloride cement, refrigerating brines, catalyst in organic chemistry, production of other magnesium compounds, flocculating agent, treatment of foliage to prevent fire and resist fire, magnesium melting and welding fluxes
Magnesium hydroxide	Chemical intermediate, alkali, medicinal
Magnesium oxide	Insulation, refractories, oxychloride and oxysulfate cements, fertilizers, rayon-textile processing, water treatment, papermaking, household cleaners, alkali, pharmaceuticals, rubber filler catalyst
Magnesium sulfate	Leather tanning, paper sizing, oxychloride and oxysulfate cements, rayon delustrant, textile dyeing and printing, medicinal, fertilizer ingredient, livestock-food additive, ceramics, explosives, match manufacture

The magnesium ion (Mg^{2+}) is an essential component of all living systems; it is the second most abundant positive ion within cells and the fourth most common cation in the body. Magnesium plays a structural role in bones and teeth. More importantly, magnesium ion is involved in a variety of cellular biochemical processes. Intracellular magnesium ion either is present in its free form or is bound to biomolecules such as adenosine triphosphate (ATP), nucleic acids, chlorophyll, and Mg^{2+}-activated enzymes. The bound form of intracellular magnesium ion predominates over its free from because of the high charge density of this metal ion. The partitioning of intracellular magnesium ion between bound and free forms regulates the biological activity of many Mg^{2+}-dependent enzymes, which participate in glycolysis, muscle contraction, ion transport, protein synthesis, respiration, photosynthesis, and signal transduction. The free intracellular magnesium ion concentration, unlike that of the calcium ion (Ca^{2+}), is well maintained within the cell; it has therefore been suggested that magnesium ion is not a trigger of cell activity but a static regulator. *See* BIOINORGANIC CHEMISTRY.

Duarte Mota de Freitas

Bibliography. B. Alberts et al., *Molecular Biology of the Cell*, 4th ed., Garland Publishing, 2002; F. A. Cotton et al., *Advanced Inorganic Chemistry*, 6th ed., Wiley-Interscience, 1999.

Magnesium alloys

Solid solutions of magnesium and aluminum, zinc, manganese, silicon, zirconium, rare-earth metals, thorium, or yttrium. The specific gravity of magnesium alloys ranges from 1.74 to 1.83. This low specific gravity has led to a great many structural applications in the aircraft, transportation, materials-handling, and portable-tool and -equipment industries. *See* MAGNESIUM.

The magnesium-aluminum-zinc (Mg-Al-Zn) alloys are the most important commercial alloys. These alloys are produced in the form of sand, permanent-mold, and die castings; extrusions; rolled sheet and plate; and forgings. They are also cast by some of the less common methods, including plaster-molding, centrifugal-molding, shell-molding, and investment-molding processes. Their properties may be modified by appropriate heat treatments. Sand and permanent-mold castings are used primarily in the solution heat-treated condition and in the solution heat-treated plus artificially aged condition. The alloys are used in the solution heat-treated condition, where maximum ductility and toughness with adequate strength are required, and in the artificially aged condition, where maximum strength is needed and somewhat lower ductility can be tolerated. Die castings are used in the as-cast condition. Extrusions and forgings are used either as fabricated or after an artificial aging treatment. Sheet and plate are produced primarily in two tempers, annealed and strain-hardened plus partially annealed.

Magnesium-zinc-zircon alloys. The magnesium-zinc-zircon alloys are high-strength alloys with good ductility and toughness. They are generally used in the artificially aged condition, but for maximum strength in forgings they are solution-heat-treated followed by artificial aging.

Some magnesium-zinc-zircon alloys can also be used as sand castings. These alloys are high-strength, having an excellent combination of mechanical strength, ductility, and toughness. However, they are poor in overall castability, having a high tendency toward hot cracking and microshrinkage porosity. They are suitable only for producing relatively simple castings which do not have pressure-tightness requirements and which are not intended for use at temperatures above 250°F (121°C). The addition of misch metal and thorium to these alloys greatly improves their castability and weldability. *See* ZINC; ZIRCONIUM.

Rare-earth and thorium alloy ingredients. The alloys described thus far have the disadvantage of losing their strength rapidly with increasing temperature, especially above 300°F (149°C). The need for magnesium alloys with improved strength and creep resistance at elevated temperatures has been met by the development of alloys containing rare-earth metals or thorium, or both, as the principal alloying constituents. The temperature range over which magnesium alloys exhibit structurally useful mechanical strength has been markedly extended by the use of rare-earth metals and thorium. Magnesium-thorium alloys, for example, are used up to temperatures in the range of 700–900°F (371–482°C) and even higher, depending on the time duration of exposure at the elevated temperature.

The most effective rare earth is neodymium, and it is economically available in the form of didymium, which is also referred to as neodymium-rich rare-earth metal. Didymium is the rare-earth mixture remaining when both cerium and lanthanum are separated from misch metal. It consists of 80–85% neodymium, and the balance is substantially praseodymium with small amounts of samarium, gadolinium, cerium, and lanthanum. Didymium is used in two commercial casting alloys. Silver is a major alloying constituent, and zirconium is added for grain refinement and improved castability and weldability. Both alloys have exceptionally high strength from ambient temperature up to 600°F (316°C). There are no rare-earth alloys used for wrought products.

Several magnesium alloys containing thorium as the principal alloying ingredient can be used for wrought products and for cast products. The wrought and magnesium-thorium alloys are used for all applications involving exposure to temperatures above 250–300°F (121–149°C). An important consideration for an elevated temperature application, especially for long time exposure, is resistance to creep. Another characteristic important in structural design is modulus of elasticity. Magnesium alloys containing thorium and rare-earth metals retain a high modulus over a wide temperature range. The combination of light weight, high strength and modulus, and good creep resistance permits the design of structures having the highest stiffness-to-weight ratio over a wide temperature range. The use of rare earths and thorium has expanded markedly the applicability of magnesium alloys in the rather limited field of missiles and spacecraft and has retained a position for magnesium in aircraft engine applications.

The need for die-casting alloys with improved creep resistance at temperatures in the range of 275–375°F (135–190°C) has produced a magnesium-aluminum-silicon (Mg-Al-Si) alloy, that requires the use of higher casting temperatures; but at the same time the presence of silicon improves fluidity and results in overall better castability. It is especially suitable for automotive engines and power-train housings.

A little-known advantage of magnesium over other common structural materials is its inherently high damping capacity, that is, its capacity to absorb mechanical vibrations. In general, addition of alloying elements decreases this property. *See* THORIUM.

Magnesium-yttrium alloys. A family of magnesium alloys based on the addition of yttrium has surpassed the performance of all previous magnesium-based casting alloys, particularly in the areas of temperature tolerance and corrosion resistance. In fact, the general corrosion resistance of one member of this family is more comparable to aluminum alloys than to the less corrosion-resistant magnesium alloys. In

addition, the room-temperature tensile strength of this particular alloy exceeds proposed specification minimums.

Alloy preparation. Metal for the production of either shape castings or ingots for subsequent fabrication is prepared by melting and alloying in either stationary or tilting iron pots or crucibles. The capacity of the pots may vary from a few hundred pounds to 6000 lb (2700 kg). Induction furnaces or ceramic-lined reverberatory or muffle furnaces may also be used.

The surface of the molten metal is protected from atmospheric oxidation by a cover of flux consisting of a mixture of alkali and alkaline-earth halides. A technique for protecting the surface of molten magnesium involves the use of an atmosphere of air containing a few tenths of one percent sulfur hexafluoride. Elimination of the use of halide fluxes greatly alleviates environmental control problems and reduces metal loss and processing costs. Aluminum, zinc, thorium, misch metal, and didymium are usually added in the elemental form. Manganese and zirconium are alloyed by the addition of a proprietary fused salt containing either the chloride or fluoride of the desired metal which is reduced by the molten magnesium. Zirconium and thorium may be added in the form of magnesium hardeners containing 20–35% of the alloying element. Beryllium in amounts of 0.0003–0.001% is added particularly to magnesium die-casting alloys in order to minimize oxidation in the molten state during melting and casting operations.

Mg-Al-Zn alloys are grain refined either by superheating or by the addition of a carbonaceous material. Alloys containing zirconium are inherently fine grained. Molten magnesium alloys are transferred from one pot to another or from pot to mold by air-driven mechanical pumps through steel pipes.

Fabricability. In addition to being adaptable to all the primary working operations already mentioned, magnesium alloys can be fabricated by all the common metalworking processes such as stamping, deep and shallow drawing, blanking, coining, spinning, impact extrusion, and forging. For forging operations both press and hammer equipment are used, but the former is more commonly used because the physical structure of magnesium alloys makes the metals better adapted to the squeezing action of the forging press. *See* FORGING.

Magnesium alloys exhibit excellent machinability. They can be machined at higher speeds and with larger feeds and depths of cut than is possible with most other commonly used metals. Power requirements needed in machining are the lowest for magnesium among all structural metals. *See* MACHINABILITY OF METALS.

Magnesium alloy parts can be joined by any of the common methods. Inert-gas, shielded-arc, and electrical-resistance welding, adhesive bonding, and riveting are in daily production use. Brazing and gas welding, although not as frequently used as the other methods, are also suitable for joining magnesium alloys. *See* ADHESIVE BONDING; BRAZING; WELDING AND CUTTING OF MATERIALS.

A wide variety of protective and decorative surface-finishing systems can be applied to magnesium alloys. They can be treated chemically and electrochemically to produce a protective and paint-adherent surface. In addition they can be painted, electroplated, anodized, and clad with plastic sheathing. *See* METAL COATINGS.

Uses. Reviewing the nonstructural uses of magnesium gives an accurate perspective of the entire industry. Nonstructural uses are those in which magnesium is used for its particular chemical, electrochemical, and metallurgical properties. The principal nonstructural uses are as alloying constituent in other metals (principally aluminum); nodularizing agent for graphite in cast iron; reducing agent in the production of other metals, such as uranium, titanium, zirconium, beryllium, and hafnium; desulfurizing agent in iron and steel production; sacrificial anode in the protection of other metals against corrosion; and anode material in reserve batteries and dry cells.

As structural materials, magnesium alloys are best known for their light weight and high strength-to-weight ratio. Accordingly, they are used generally in applications where weight is a critical factor and where high mechanical integrity is needed. Magnesium alloys are most commonly used in the form of die casting. Of all the metalworking and fabricating processes, die casting is the most readily adaptable to the specific characteristics of magnesium. Magnesium has a relatively low melting point, low heat content per unit volume, and low reactivity toward ferrous materials. Coupling these characteristics with the high productivity of the die-casting process results in the most economical technique for the mass production of a large number of complex parts of the same configuration. Magnesium die castings are produced on hot-chamber die-casting machines. The hot-chamber machine is even more amenable to automation than the cold-chamber machine and is capable of higher production rates and overall lower operating costs.

The hot-chamber machine has greatly enhanced the potential for expansion of the use of magnesium die castings in the automotive and appliance industries. Some automobiles contain magnesium parts such as the distributor diaphragm, steering column brackets, and a lever cover plate. Magnesium-alloy die castings are also used on chain saws, portable power tools, cameras and projectors, office and business machines, tape reels, sporting goods, luggage frames, and many other products.

Uses of sand and permanent mold castings are confined largely to aircraft engine and airframe components. Engine parts include gearboxes, compressor housings, diffusers, fan thrust reversers, and miscellaneous brackets. On the airframe, magnesium sand castings are used for leading edge flaps, control pulleys and brackets, entry door gates, and various

cockpit components. This is a small market in volume, but one requiring highly technical skills in production.

The use of magnesium wrought products has become rather limited. Magnesium sheet, extrusions, and forgings continue to be used in a few limited air-frame applications. The high-temperature alloys are used in at least 20 different missiles (including ICBMs) and on various spacecraft. *See* ALLOY; HEAT TREATMENT (METALLURGY); METAL CASTING; METAL FORMING.

Thomas E. Leontis

Bibliography. American Foundrymen's Society, *Conference on Recent Advances in Magnesium Technology*, 1987; *Annual Book of ASTM Standards*, vol. 2.02: *Die-Aluminum and Magnesium Alloys*, 1993; National Fire Protection Association, *Storage, Handling, and Processing of Magnesium*, 1987; H. Paris and W. H. Hunt (eds.), *Advances in Magnesium Alloys and Composites*, 1989.

Magnet

An object or device that produces a magnetic field. Magnets are essential for the generation of electric power and are used in motors, generators, labor-saving electromechanical devices, information storage, recording, and numerous specialized applications, for example, seals of refrigerator doors. The magnetic fields produced by magnets apply a force at a distance on other magnets, charged particles, electric currents, and magnetic materials. *See* GENERATOR; MAGNETIC RECORDING; MOTOR.

Magnets may be classified as either permanent or excited. Permanent magnets are composed of so-called hard magnetic material, which retains an alignment of the magnetization in the presence of ambient fields. Excited magnets use controllable energizing currents to generate magnetic fields in either electromagnets or air-cored magnets. Most electromagnets use iron or its alloys, allowing efficient generation of fields up to 2 teslas. Air-cored magnets often are used to generate fields above the saturation of ferromagnetic materials. The power requirements of excited magnets can be reduced by using superconducting wire to carry the current. *See* ELECTROMAGNET; FERROMAGNETISM; SUPERCONDUCTIVITY.

Theory and design. Flux density B (in teslas), field strength H (in amperes/meter), and magnetization M are related by Eq. (1), where μ_0 is the permeability

$$\vec{B} = \mu_0(\vec{H} + \vec{M}) \tag{1}$$

of free space ($4\pi \times 10^{-7}$ henry/meter). In ferromagnetic materials, M is a nonlinear and hysteretic function of B.

Field strength H is related to current I by Ampère's law, Eq. (2). Here the integral of the scalar product is

$$\int \vec{H} \cdot \vec{ds} = I \tag{2}$$

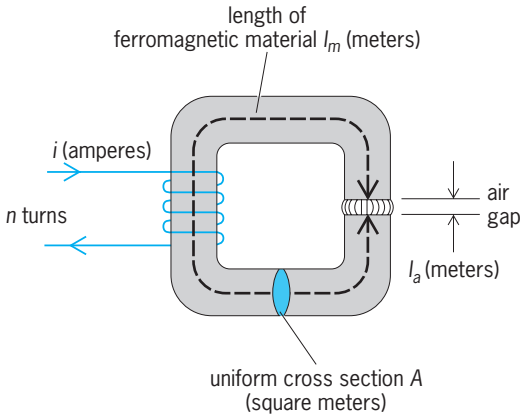

Fig. 1. Simple electromagnetic circuit.

taken around any path s encompassing the currents whose sum is I.

The relation between B and H for a ferromagnetic material is a property of the material expressed graphically and known variously as a magnetization curve, demagnetization curve, or hysteresis loop.

The procedure for calculating B in electromagnets is illustrated by an electromagnetic circuit containing an air gap (**Fig. 1**). A simplified analysis reveals the following features:

1. The relation between the field strength in the ferromagnetic material H_m and the flux density in the air gap B is defined simultaneously by the properties of the material and by Eq. (3), where l_m is the length

$$H_m = \left(ni - \frac{Bl_a}{\mu_0}\right) l_m \tag{3}$$

of the ferromagnetic material (in meters), l_a is the distance across the air gap (in meters), i is the current through the coil (in amperes), and n is the number of turns in the coil.

2. The energy density in the air gap is given by Eq. (4). This is also the force of attraction per unit area in pascals acting on the magnet pole faces.

$$W = \frac{B^2}{2\mu_0} \qquad \text{joules/m}^3 \tag{4}$$

If the ferromagnetic material is magnetically hard and i is zero, then the electromagnet becomes a permanent magnet and Ampère's law shows that H_m must be negative. It follows that the volume of ferromagnetic material equals $-2E/BH_m$, where E is the air gap energy. Hence for economic reasons, permanent-magnet designs should maximize the product $(-BH_m)$. Moreover, the maximum attainable value of this product, $(-BH_m)_{\max}$, is an important property of a material.

In air-cored magnets, flux density may be computed by using the Biot-Savart law or one of its many derivatives.

For discussion of the theory underlying the functioning and design of magnets *see* AMPÈRE'S LAW; BIOT-SAVART LAW; MAGNETISM; MAGNETIZATION.

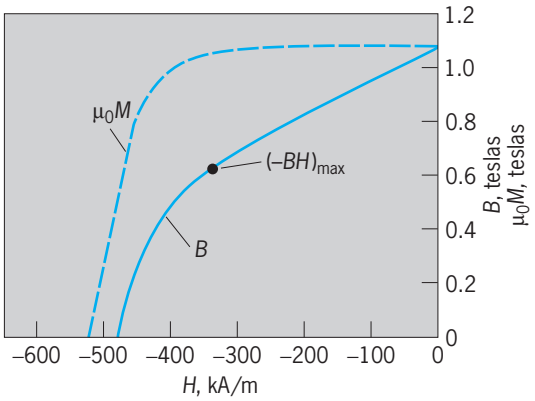

Fig. 2. The variation of *B* (the demagnetization curve) and $\mu_0 M$ as *H* is increased in the negative direction (opposite to *B* and *M*) for the permanent-magnet material $Sm_2(Co, Cu,Fe,Zr)_{17}$. B_r is the remanence, H_c the coercive force, and $(-BH)_{max}$ the optimum operating point. (*After Z. A. Abdelnour, H. F. Mildrum, and K. J. Strnat, Properties of various sintered rare earth–cobalt permanent magnets between −60° and +200°C, IEEE Trans. Magnet., MAG-16:944–996, 1980*)

Materials for magnets. The essential characteristic of permanent-magnet materials is an inherent resistance to change in magnetization over a wide range of field strength H (**Fig. 2**). Resistance to change in M in this type of material and in a great many of its predecessors is due to two factors: (1) the material consists of particles smaller than the size of a domain, a circumstance which prevents the gradual change in M which would otherwise take place through the movement of domain wall boundaries; and (2) the particles exhibit a marked magnetocrystalline anisotropy. During manufacture the particles are aligned in a magnetic field before being sintered or bonded in a soft metal or polyester resin. Compounds of neodymium, iron, and boron have the highest known values of $(-BH_m)_{max}$. *See* IRON ALLOYS.

Electromagnets rely on magnetically soft or permeable materials which are well annealed and homogeneous so as to allow easy motion of domain wall boundaries. Ideally the coercive force H_c should be zero, permeability should be high, and the flux density saturation level should be high. Coincidentally the hysteresis energy loss represented by the area of the hysteresis curve is small. This property and high electrical resistance (for the reduction of eddy currents) are required where the magnetic field is to vary rapidly. This is accomplished by laminating the core and using iron alloyed with a few percent silicon that increases the resistivity.

Electromagnets. Electromagnets usually have an energizing winding made of copper and a permeable iron core. Applications include relays, motors, generators, magnetic clutches, switches, scanning magnets for electron beams (for example, in television receivers), lifting magnets for handling scrap, and magnetic recording heads. *See* CATHODE-RAY TUBE; CLUTCH; ELECTRIC SWITCH; RELAY.

Special iron-cored electromagnets designed with highly homogeneous fields are used for special analytical applications in, for example, electron or nuclear magnetic resonance, or as bending magnets for particle accelerators. *See* MAGNETIC RESONANCE; PARTICLE ACCELERATOR.

Normal-conductor air-cored magnets. Air-cored electromagnets are usually employed above the saturation flux density of iron (about 2 T); at lower fields, iron-cored magnets require much less power because the excitation currents needed then are required only to generate a small field to magnetize the iron. The air-cored magnets are usually in the form of a solenoid with an axial hole allowing access to the high field in the center. The conductor, usually copper or a copper alloy, must be cooled to dissipate the heat generated by resistive losses. In addition, the conductor and supporting structure must be sufficiently strong to support the forces generated in the magnet. The effective pressure in the magnet bore is approximately $B^2/2\mu_0$, or 40 megapascals (6000 lbf/in.^{2}) for a flux density of 10 T. *See* SOLENOID (ELECTRICITY).

Bitter design. A design for high-field solenoids developed by F. Bitter, which addresses these problems, employs a stack of mass-produced and interchangeable slit disks (**Fig. 3***a*). The Bitter stack is interleaved with insulation and compressed axially so as to form a compact helical conductor structurally bonded by friction. Hole patterns punched through the conducting plates and insulators are carefully aligned to allow axial flow of the cooling water. A modification of this helical structure (Figs. 3*b* and *c*) employs two

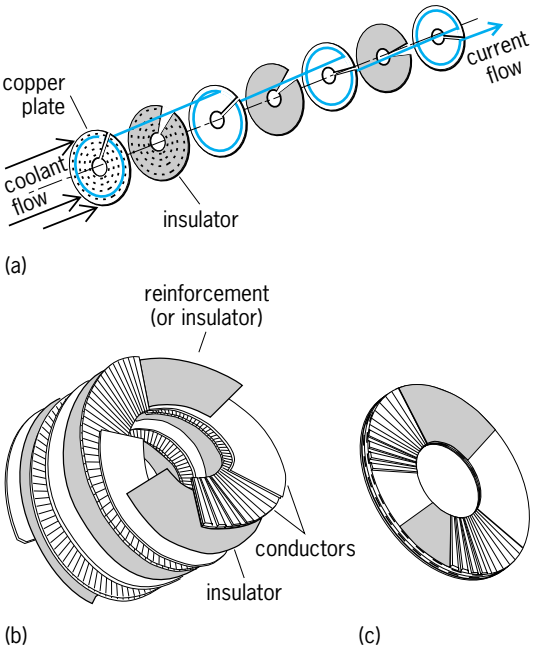

Fig. 3. Bitter magnet stacks. (*a*) Exploded view of helical current path through slotted plates in a stack. (*b*) Expanded view of a stack that has a similar current path shared by the two conductors in a helical plate structure, but has radial grooves in one of them for cooling. (c) Assembled view of a few plates. (*After D. B. Montgomery, The Magnetic and Mechanical Aspects of Resistive and Superconducting Systems, Robert E. Krieger Publishing Co., 1980*)

parallel slit copper-plate structures as conductors (one with etched radial cooling channels). A reinforcing plate structure may also be included in either design. Radial cooling is used when higher power dissipation is required. A Bitter magnet produced a sustained field of 30 T and required 30 MW of power. A slightly more efficient but more complex magnet is composed of parallel-connected nested coils with water-cooling passages between them.

Pulsed magnets. Higher fields can be generated by limiting the excitation to short pulses (usually furnished by the energy stored in a capacitor bank) and cooling the magnet between pulses. The pulse length is limited by the heat capacity of the magnet and the resistive losses in the conductor. The highest fields are generally achieved in small volumes. The fundamental limit for an efficient magnet generating pulsed fields repeatedly is set by the conductivity and strength of the conductor. Often additional structures are required to support the large forces generated. A field of 75 T has been generated for 120 microseconds. Special high-strength, high-conductivity conductors for such magnets include a copper-niobium microcomposite and a copper-silver alloy. Pulse durations of 100 ms or more require very large volume magnets and large energies.

The highest fields are generated in magnets which fail during the pulse. Over 200 T is generated for a few microseconds in a single-turn magnet which explodes radially outward. Even higher fields (over 1500 T) are generated by explosive compression of magnetic flux trapped in a single-turn coil.

Superconductor air-cored magnets. Large-volume or high-field magnets are often fabricated with superconducting wire in order to avoid the large resistive power losses of normal conductors. The two commercially available superconducting wire materials are (1) alloys of niobium-titanium, a ductile material which is used for generating fields up to about 9 T; and (2) a brittle alloy of niobium and tin (Nb_3Sn) for fields above 9 T. Practical superconducting wires use complex structures of fine filaments of superconductor that are twisted together and embedded in a copper matrix. Practical superconducting wires can carry current densities of 10^8 A/m^2 with no resistive power loss. However, at sufficiently high fields the superconductor becomes resistive. The conductors are supported against the electromagnetic forces and cooled by liquid helium at 4.2 K (−452°F). A surrounding thermal insulating enclosure such as a dewar minimizes the heat flow from the surroundings.

Superconducting magnets operating over 20 T have been made with niobium-titanium outer sections and niobium-tin inner sections. Niobium-titanium is used in whole-body nuclear magnetic resonance imaging magnets for medical diagnostics. Other applications of superconducting magnets include their use in nuclear magnetic resonance for chemical analysis, particle accelerators, containment of plasma in fusion reactors, magnetic separation, and magnetic levitation. The nuclear magnetic resonance magnets are usually operated as permanent magnets. Once the excitation current reaches the appropriate value, it is switched through a superconducting joint between the magnet leads so that current flows continuously with no resistive loss as long as the conductor is cooled to maintain superconductivity. *See* MAGNETIC LEVITATION; MAGNETIC SEPARATION METHODS; MEDICAL IMAGING; NUCLEAR FUSION; NUCLEAR MAGNETIC RESONANCE (NMR); SUPERCONDUCTING DEVICES.

Hybrid air-cored magnets. The highest continuous fields are generated by hybrid magnets. A large-volume (lower-field) superconducting magnet that has no resistive power losses surrounds a water-cooled inner magnet that operates at the highest field. The fields of the two magnets add. Over 35 T has been generated continuously.

There are active world-wide efforts to increase the high field capabilities of the various air-cooled magnets.

Simon Foner

Bibliography. B. I. Bleaney and B. Bleaney, *Electricity and Magnetism*, 3d ed., 1976, paper 1989; J. E. Evetts (ed.), *Encyclopedia of Magnetic and Superconducting Materials*, 1992; D. C. Jiles, *Introduction to Magnetism and Magnetic Materials*, 2d ed., 1998; D. B. Montgomery, *Solenoid Magnet Design*, 1969, reprint 1980; S. G. Sankar, *Permanent Magnet Materials and Devices*, 2000; E. P. Wohlfarth et al. (eds.), *Ferromagnetic Materials*, vols. 1–5, 1980–1990.

Magnet wire

The insulated copper or aluminum wire used in the coils of all types of electromagnetic machines and devices. It is single-strand wire insulated with enamel, varnish, cotton, glass, asbestos, or combinations of these. To meet the immense variety of uses and to gain competitive advantage, a great number of kinds of enamel and of fiber insulations have been developed and are widely available. And to ensure that the many synthetic materials and combinations are properly applied, many elaborate test procedures have been devised to evaluate heat shock, solubility, blister and abrasion resistance, flexibility, and so on as covered in the National Electrical Manufacturers Association (NEMA) Standards. Most important, the thermal endurance is determined by repeated exposure to high temperature, moisture, and electrical stress, as specified in the American Society for Testing and Materials (ASTM).

The Institute of Electrical and Electronics Engineers (IEEE) thermal classes of insulation, defined by upper temperature limits at which the untreated insulation will have a life expectancy of at least 20,000 h, are O (176°F or 80°C), A (221°F or 105°C), B (266°F or 130°C), F (311°F or 155°C), and H (356°F or 180°C). In general, materials such as cotton, paper, and silk are class O. Organic materials, such as oleoresinous and Formvar enamels, varnish-treated cotton, paper, and silk are class A, and asbestos, mica, silicone varnishes, and polyimide are class H, while

Data on film- and fiber-insulated magnet wire

Type	Shape	Size range, mils*	NEMA spec.	Thermal class	Applications	Qualities
Formvar coated	Round Rectangular	1–204 2100–65,000†	MW15 MW18	A 105°C	Universal use for 105°C limit	Tough, high dielectric strength, chemical stability, but crazes in polar solvents
Alkanex coated	Round Rectangular	1–204 2100–65,000†	MW5	F 155°C	Motors, transformers, control coils for 130° and 155°C limits	Same as Formex, but higher thermal endurance
Polyurethane coated	Round	1–102	MW2	A 105°C	Automatic coil winding	Solderable, low dielectric losses, chemical stability, but low abrasion resistance
Nylon coated	Round	1–102	MW6	A 105°C	Automatic winding with varnish treatment	Solvent resistant, solderable, but high electrical losses and moisture-absorbent
Fluoropolymer resin coated	Round	2–57	MW10	H 180°C	High-temperature and corrosive ambients	Thermal and chemical stability, but low abrasion resistance, and cold flow
Butvar coated	Round	2–64	MW19	A 105°C	Self-supporting coils	Self-bonding, no varnish required for physical support
Imidex E or Isomid coated	Round	2–64	—	180–200°C	High-temperature ambients	No extractibles and highly Freon-resistant
Glass fiber, varnish-treated	Round Rectangular	36–258 2400–93,000†	MW41 MW42	B 130°C	Traction motors and high-temperature windings	Thermal endurance, good dielectric, positive spacing
Dacron and glass fiber, varnish-treated	Round Rectangular	36–258 2400–93,000†	MW45 MW46	B, F, or H, depending on varnish	Machine windings and control coils	Good flexibility and temperature endurance, tough, smooth surface
Asbestos with varnish impregnation	Round Rectangular	18–258 2400–166,000†	MIL-W-583A	B, F, or H, depending on varnish	Large machine windings and traction motors	Good resistance to forming stresses and temperature endurance

*1 mil = 25 μm.
†In mils^2: 1 mil^2 = 645 μm^2.

various synthetic enamels fall in the B and F classes. The polyesterimide enamels, however, are capable of withstanding temperatures of 356–392°F (180–200°C).

The **table** provides a summary of the most widely used types of film- and fiber-insulated magnet wire.

Almost all magnet wire is insulated soft-drawn electrolytic copper, but aluminum is being used more, especially in times when copper is scarce or high-priced and where space is not limiting. Round aluminum wire, being soft, flattens under pressure, giving a higher space factor in coils than might be expected. At temperatures above 392°F (200°C) copper oxidizes rapidly; it also becomes brittle when under stress at such temperatures. Its high-temperature strength is increased considerably by adding a small amount of silver (about 30 oz/ton or 1 kg/metric ton). Anodized aluminum is preferred for higher temperatures, up to 572°F (300°C) or more, while copper nickel wire with an anodized aluminum coating may be operated at still higher temperatures.

The increase in wire diameter due to a single coat of enamel varies from about 1 mil (25 micrometers) for a wire diameter of 80 mils (2 mm) to about 5 mils (15 μm) for a wire diameter of 200 mils (5 mm). The double coating that is frequently called for is not quite twice as thick. The fiber coatings are about three times as thick as the enamel, and they too can be obtained in double thickness. *See* ELECTRICAL INSULATION; MAGNET. Philip L. Alger; C. J. Herman

Bibliography. American Society for Testing and Materials, *Test Method for Relative Thermal Endurance of Film-Insulated Round Magnet Wire*, Stand. ASTM-D2307-94, 1994; D. G. Fink and H. W. Beaty (eds.), *Standard Handbook for Electrical Engineers*, 14th ed., 2000; National Electrical Manufacturers Association, *Magnet Wire*, Stand. MW 1000-1993.

Magnetic compass

A compass depending for its directive force upon the attraction of the Earth's magnetism for a magnet free to turn in any horizontal direction. A compass is an instrument used for determining horizontal direction.

Principle of operation. The magnetic compass operates on the principle that like magnetic poles repel each other whereas unlike poles attract each other. The Earth has internal magnetism similar to that which would result from a short, powerful bar magnet at the center of the Earth. The lines of force connecting the two poles are vertical at two points on the surface of the Earth, called magnetic poles,

and horizontal along the magnetic equator, a line approximating a great circle nearly midway between the magnetic poles. The horizontal component of the Earth's magnetic field varies from a maximum on or near the magnetic equator to zero at the magnetic poles. *See* GEOMAGNETISM; MAGNET; MAGNETIC FIELD; MAGNETISM.

A simple magnetic compass consists of a magnetized needle mounted so as to be free to align itself with the horizontal component of the Earth's field. A magnetic compass is unreliable or inoperative in the vicinities of the magnetic poles. Other sources of error are described below.

Uses. Compasses are used to determine the direction in which a craft is pointed, the direction of travel on land, the direction or bearing of an object, and for other purposes. Mariners, aviators, explorers, guides, scouts, and surveyors have need for a compass. *See* NAVIGATION; SURVEYING.

Direction. The primary function of a compass is to indicate a reference direction, from which all other directions are derived. South is the usual reference direction for astronomers and surveyors; north is the reference direction for others.

Compasses are generally graduated so that, when the north and south graduations on the compass readout are aligned with the north-seeking and south-seeking ends of the compass needle, respectively, other directions are shown in their correct positions as seen from the center of the compass. Most modern navigational compasses mounted permanently in ships, aircraft, and land vehicles are graduated in degrees, from 0° at north clockwise through 360°; the graduations are found on a lightweight compass card attached to the directive element. Pocket or wrist compasses are usually graduated in compass points; the graduations in this instance are found in the case.

Errors. In addition to such errors as faulty alignment or inaccurate graduation, magnetic compasses are subject to two principal errors if the instruments are to be used to determine geographical north and south: variation and deviation.

Variation. This is the angle between geographic and magnetic meridians. The magnetic needle of a compass tends to align itself with the magnetic meridian, which is the horizontal component of a line of force of the magnetic field of the Earth. Magnetic meridians do not, in general, coincide with the geographic meridians, which converge at the geographical poles. The magnetic meridians converge at the magnetic poles, some distance away. The magnetic meridians, unlike the geographic meridians, are not great circles. This is true because the magnetic field is not uniform; it is distorted considerably by irregularities in the magnetic properties of the materials forming the Earth's crust.

Variation of the compass, called declination by magneticians, depends upon the location of the compass. It is determined by magnetic surveys and is published on charts and elsewhere. It varies somewhat with time, both diurnally (daily) and secularly (long-term).

Deviation. The angle between a magnetic meridian and the axis of a compass needle is termed deviation. It is caused by local magnetic effects, such as magnetism of a ship, the magnetic field around a nearby conductor of direct-current electricity, or induced magnetism in a nearby tool or pocketknife.

This source of error generally can be eliminated in a portable compass by using it in a position free from such disturbing influences. For permanent installations in ships, aircraft, and land vehicles, provision is generally made for setting up equal and opposite forces near the compass to neutralize the effects of magnetic influences at the compass. The process is called compass adjustment or compass compensation. In case the deviation cannot be eliminated completely, a deviation table is made up listing the residual deviation on each of a number of headings of the craft. Each deviation table applies only to the compass installation for which it was compiled, since the deviations are caused by local magnetic effects.

Marine compass. The magnetic compass has been largely replaced by the gyrocompass, which is not subject to variation or deviation, as the primary source of directional information at sea. However, the magnetic compass, which does not require an external source of electric power and does not have a mechanism subject to mechanical failure, is still standard equipment aboard ship (**illus.** *a*), and small

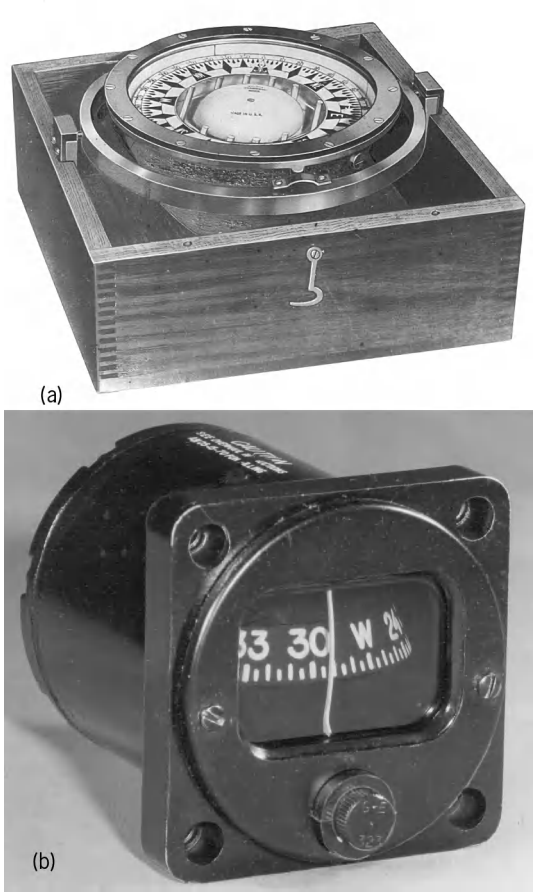

Typical magnetic compasses. (*a*) Marine. (*b*) Aircraft (*Aviation Electric, Ltd.*).

craft almost universally use the less expensive magnetic compass exclusively. The directional element of a marine compass is mounted in a bowl generally filled with liquid (usually a petroleum distillate) that reduces friction on the pivot, thus making the directional force more effective, and damps oscillations of the card. The entire compass is mounted in a stand called a binnacle (or box for small craft) that has provision for magnets and perhaps electric currents to largely neutralize deviation. It may also have a device to facilitate use of the compass for observing bearings of external objects. *See* GYROCOMPASS.

Aircraft compass. Aircraft compasses (illus. *b*) are generally smaller than those used aboard ship and may be mounted in the instrument panel, with graduations on the after (rear) side of the compass card. However, because of the adverse effects of inertial errors related to motions of the aircraft and magnetic disturbances from electric currents and other instruments in the instrument panel, most aircraft compasses are installed in a more favorable location such as a wing or the tail, with remote indicators where needed. A widely used type of remote-indicating aircraft compass is known as a gyro fluxgate compass, or simply fluxgate compass. The entire system consists of a magnetic compass stabilized by means of a gyroscope to reduce the inertial and magnetic errors (which are particularly severe when the aircraft tilts or turns), a transmitter, an amplifier, and one or more remote indicators. The fluxgate itself consists of a fixed soft-iron-core artificial magnet energized by an alternating electric current of suitable strength to saturate the coil with magnetism at each maximum current. The addition of the horizontal component of the Earth's magnetism distorts the core response in such a way that the Earth's horizontal lines of force can be duplicated, making possible the rotation of a moving coil to align itself with the magnetic meridian of the Earth. This alignment can be transmitted to remote indicators throughout the aircraft. *See* AIRCRAFT INSTRUMENTATION; GYROSCOPE.

Alton B Moody

Bibliography. W. Denne, *Magnetic Compass Deviation and Correction*, 3d ed., 1979; J. Klinkert, *Compass-wise or Getting to Know Your Compass*, 1976.

Magnetic ferroelectrics

Materials which display both magnetic order and spontaneous electric polarization. Research on these materials has enabled considerable advances to be made in understanding the interplay between magnetism and ferroelectricity. The existence of both linear and higher-order coupling terms has been confirmed, and their consequences studied. They have given rise, in particular, to a number of magnetically induced polar anomalies and have even provided an example of a ferromagnet whose magnetic moment per unit volume is totally induced by its coupling via linear terms to a spontaneous electric dipole moment.

Most known ferromagnetic materials are metals or alloys. Ferroelectric materials, on the other hand, are nonmetals by definition since they are materials which can maintain a spontaneous electric moment per unit volume (called the polarization) which can be reversed by the application of an external electric field. It therefore comes as no surprise to find that there are no known room-temperature ferromagnetic ferroelectrics. In fact, there are no well-characterized materials which are known to be both strongly ferromagnetic and ferroelectric at any temperature. This is unfortunate since not only would a study of the interactions between ferromagnetism and ferroelectricity be valuable as basic research but such interplay could well give rise to important device applications.

Most antiferromagnetic materials, however, are nonmetals, so there is no apparent reason why ferroelectricity and antiferromagnetism should not coexist. A study of antiferromagnetic ferroelectrics would also provide much information concerning the interplay of magnetic and ferroelectric characteristics even if the device potential were very much reduced. Somewhat unaccountably, antiferromagnetic ferroelectrics are also comparative rarities in nature. Nevertheless, a few are known, and among them the barium–transition-metal fluorides are virtually unique in providing a complete series of isostructural examples. First characterized in the late 1960s, they have the chemical composition $BaXF_4$ in which X is a divalent ion of one of the 3*d* transition metals, manganese, iron, cobalt, or nickel. Nonmagnetic, but still ferroelectric, isomorphs (that is, isostructural equivalents) also exist in the series in which X is magnesium or zinc.

The antiferromagnetic ferroelectrics $BaMnF_4$, $BaFeF_4$, $BaNiF_4$, and $BaCoF_4$ and their nonmagnetic magnesium and zinc counterparts are orthorhombic and all spontaneously polar (that is, pyroelectric) at room temperature. For all except the iron and manganese materials, which have a higher electrical conductivity than the others, the polarization has been reversed by the application of an electric field, so that they are correctly classified as ferroelectric, although their ferroelectric transition (or Curie) temperatures are in general higher than their melting points. The elementary magnetic moments of the manganese, iron, cobalt, and nickel structures are thermally disordered at room temperature, and long-range antiferromagnetic ordering sets in at temperatures somewhat below 100 K (−280°F). Structurally the materials consist of XF_6 octahedra which share corners to form puckered *xy* sheets which are linked in the third dimension *z* by the barium atoms. The magnetic interactions are very dominantly within the *xy* layers, leading to two-dimensional magnetic characteristics, with the magnetic spins eventually aligning themselves antiferromagnetically within the planes. The axis of the spontaneous polarization is also contained within the planes. *See* CRYSTAL STRUCTURE.

The importance of these magnetic ferroelectrics is the opportunity they provide to study and to

separate the effects of a variety of magnetic and nonmagnetic excitations upon the ferroelectric properties and particularly upon the spontaneous polarization. Measurements are often made via the pyroelectric effect p, which is the variation of polarization P with temperature T; that is, $p = dP/dT$. This effect is an extremely sensitive indicator of electronic and ionic charge perturbations in polar materials. Through these perturbations the effects of propagating lattice vibrations (phonons), magnetic excitations (magnons), electronic excitations (excitons), and even subtle structural transitions can all be probed with precision. *See* PYROELECTRICITY.

Phonons. At sufficiently low temperatures the dominant contribution to the pyroelectric effect p comes from thermal excitation of acoustic-phonons, with p varying as T^3. At higher temperatures optic-phonon-mode excitations contribute additional components of exponential form and tend to dominate the acoustic terms. In the magnetic ferroelectrics these contributions must compete with the components arising from the thermal disruption of the ordered antiferromagnetic state. These low-temperature magnetic components take different forms depending on the character of the low-temperature magnetic ordering (in particular, depending on whether the magnetic anisotropy is large, as in the iron and cobalt systems, or small as in the manganese and nickel analogs). The two types of phonon terms are present, of course, in both the magnetic and the nonmagnetic materials, with the additional magnon contributions present only in the magnetic systems. Although the basic contributions are readily detectable in the pyroelectric response, a full separation of all three contributions has not yet been convincingly obtained at low temperatures. *See* LATTICE VIBRATIONS; PHONON.

Magnons. The magnetic contributions to p are seen most easily near the magnetic transitions (that is, the Néel points). Since the magnetic systems undergo very drastic changes, here the perturbation of p is large and easily recognizable. The Néel temperature anomalies take on a cusplike form and arise physically because both the polarization and the magnetic interactions couple strongly to crystal strain, the former via the piezoelectric effect and the latter via magnetostriction. The details of the magnetically produced cusps differ for the different magnetic materials depending on the details of the magnetic anisotropy, but they are now very well understood. Detailed theories have been given, and the quality of agreement between theory and experiment indicates that the magnetic to ferroelectric coupling mechanisms are now known in considerable detail. Since the magnetism is basically of a two-dimensional nature, a significant vestige of the Néel point p-anomalies persists to temperatures well in excess of the transition. This reflects the well-known persistence of short-range spin correlations in two dimensions. *See* MAGNETOSTRICTION; MAGNON; PHASE TRANSITIONS; PIEZOELECTRICITY.

Excitons. The optical absorption spectrum in the magnetic ferroelectrics $BaXF_4$ is dominated throughout the visible region by the d-state-to-d-state localized electronic excitations on the magnetic ions. The approximately cubic crystal field environment splits the magnetic d states into two subgroups which are typically separated in energy by values corresponding to the visible or near-visible range. The excited states on the individual magnetic ions tend to be long-lived at low temperatures, and the excitation can propagate through the crystal via magnetic (exchange) interactions with its magnetic neighbors. These excitations are known as Frenkel excitons, and they couple to the spontaneous polarization via the elementary electric moment perturbation associated with each exciton due to the different charge distributions in the ground and excited d states. The electrical response of the magnetic crystals to short-duration optical pulses clearly shows the exciton contributions to p and their relaxation as the excitations gradually decay back to their ground states. In $BaMnF_4$, for which the most detailed exciton work has been performed, the excited-state polarization is of opposite sign to the spontaneous polarization, enabling a particularly convincing verification of the exciton origin of the effect to be made. *See* CRYSTAL ABSORPTION SPECTRA; EXCHANGE INTERACTION; EXCITON.

Structural transitions. Of all the X ions present in the series $BaXF_4$, the largest is Mn^{2+}. As the temperature is reduced from room temperature, the fluorine cages contract and eventually the divalent manganous ion becomes too big for its cage, precipitating a structural transition at 250 K (-10°F). For the rest of the X ions this overcrowding effect does not occur. The resulting transition in $BaMnF_4$ is quite a complicated one, and produces a cell doubling in the xz plane and a repeat distance in the y direction which is incommensurate with the high-temperature unit cell. The transition involves a complex series of rigid rotations of the fluorine octahedral cages. The subtle atomic rearrangements which take place perturb the local charge environment in such a way that the response is again easily picked up by the pyroelectric effect. A pronounced but rather diffuse peak is seen in p, although the structural transition is known to be sharp from the findings of other probes such as neutron or light scattering, and fluorine nuclear magnetic resonance. A detailed interpretation of this pyroelectric response has not yet been forthcoming.

Magnetoelectric effect. One of the more interesting effects of the incommensurate phase transition at 250 K (-10°F) in $BaMnF_4$ is that it produces a lower-temperature phase with a crystal symmetry low enough to support the existence of the linear magnetoelectric effect. The couplings between magnetism and ferroelectricity discussed above all involve quadratic spin terms. The magnetoelectric effect in contrast is a linear coupling between magnetization and polarization. It is forbidden by symmetry in most magnetic systems, but its presence when allowed always raises the possibility of pyroelectrically inducing a ferromagnetic moment in an antiferromagnetically ordered system. Below the

antiferromagnetic transition at 26 K in $BaMnF_4$ this linear coupling does indeed produce a canting of the antiferromagnetic sublattices through a very small angle (of order 0.2 degree of arc). The result is a spontaneous, polarization-induced magnetic moment. At low temperatures $BaMnF_4$ is therefore technically a weak ferromagnet, although the resultant magnetic moment is extremely small, and it is more usually referred to as a canted antiferromagnet. Pyroelectrically driven ferromagnetism is extremely rare, and this is the only well-categorized example. The magnetoelectric effect also produces additional perturbations of the dielectric susceptibility near the magnetic Néel temperature for the manganese material which are not seen in the other magnetic ferroelectrics of the series for which the linear coupling term is absent for symmetry reasons. *See* ANTIFERROMAGNETISM; FERROELECTRICS; FERROMAGNETISM; MAGNETISM.

Malcolm E. Lines

Bibliography. M. E. Lines and A. M. Glass, *Principles and Applications of Ferroelectrics and Related Materials*, 1977; X. Yuhuan, *Ferroelectric Materials and Their Applications*, 1991.

Magnetic instruments

Instruments designed for the measurement of magnetic field strength or magnetic flux density, depending on their principle of operation.

Hall-effect instruments. Often called gaussmeters, these instruments measure magnetic field strength. They have a useful working range from 10 A/m to 8 MA/m (0.125 oersted to 100 kOe). When a magnetic field, H_z, is applied in a direction at right angles to the current flowing in a conductor (or semiconductor), a voltage proportional to H_z is produced across the conductor in a direction mutually perpendicular to the current and the applied magnetic field (**Fig. 1**). This phenomenon is called the Hall effect. The output voltage of the Hall probe is proportional to the Hall coefficient, which is a characteristic of the Hall-element material, and is inversely proportional to the thickness of this material. *See* HALL EFFECT.

For a sensitive Hall probe, the material is thin with a large Hall coefficient. The semiconducting materials indium arsenide and indium antimonide are particularly suitable. Because of the small size of the Hall element (usually of the order of 2 mm square), it is difficult to align the voltage contacts exactly opposite each other. A compensating network comprising a resistive divider (with the addition of a variable capacitor if ac excitation is used) is connected (Fig. 1) to counteract the voltage drop produced by the current flowing in the region between the voltage contacts. The temperature coefficient (about 0.05% per Celsius degree for indium arsenide) can be compensated by the addition of a suitable thermistor. The Hall probe is connected by a flexible cable to a control unit housing the current supply and Hall voltage detection unit. At high magnetic field strengths (above 1.2 MA/m or 15 kOe), the linearity of the Hall-effect device falls off because of the deflection of the electrons within the sensor by the strong magnetic field. By calibrating the instrument, its useful range can be extended. *See* THERMISTOR.

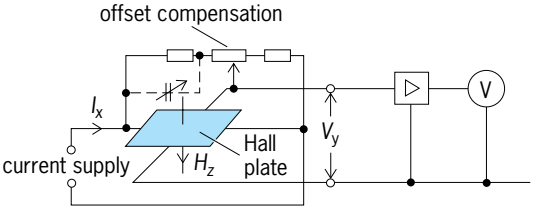

Fig. 1. Principle of the Hall-effect gaussmeter.

Hall-effect gaussmeters are calibrated at low magnetic field strengths by mounting the probe at the center of a long solenoid or pair of Helmholtz coils for which the field-to-current ratio has been determined. At higher magnetic field strengths, the probe is mounted in the gap of a large electromagnet having a uniform magnetic field which is measured by a magnetic resonance magnetometer. *See* HELMHOLTZ COILS; NUCLEAR MAGNETIC RESONANCE (NMR); SOLENOID (ELECTRICITY).

Fluxgate magnetometer. This instrument is used to measure low magnetic field strengths. It is usually calibrated as a gaussmeter with a useful range of 0.2 millitesla to 0.1 nanotesla (2 gauss to 1 microgauss).

Fluxmeter. This instrument is designed to measure magnetic flux. A fluxmeter is a form of galvanometer in which the torsional control is very small and heavy damping is produced by currents induced in the coil by its motion. This enables a fluxmeter to accurately integrate an emf produced in a search coil when the latter is withdrawn from a magnetic field, almost independently of the time taken for the search coil to be moved. A fluxmeter comprises a rectangular coil of wire held between the poles of a permanent magnet. To minimize the torsional control, the suspension is either by an unspun silk fiber or, in the case of more robust instruments, jeweled bearings. Connection between the coil and fluxmeter terminals is made through thin spirals of strip silver, copper, or gold. Assuming the torsional control is negligible and no air damping exists, the fluxmeter receives an impulse and the coil moves through an angle independent of the rate of change of magnetic flux. In practice, there is a small torsional control and some air damping; these cause the instrument to drift slowly toward zero after the maximum deflection has been attained. In the case of Grassof fluxmeters, the resistance of the external circuit should be less than 10 ohms. Some types of light-spot fluxmeters require an external circuit of resistance exactly 30 ohms to maintain the marked calibration. Fluxmeters can be calibrated in a similar way to electronic charge integrators. *See* GALVANOMETER.

Electronic charge integrators. Often termed an integrator or gaussmeter, an electronic charge integrator, in conjunction with a search coil of known effective area, is used for the measurement of magnetic flux density. Integrators have almost exclusively replaced

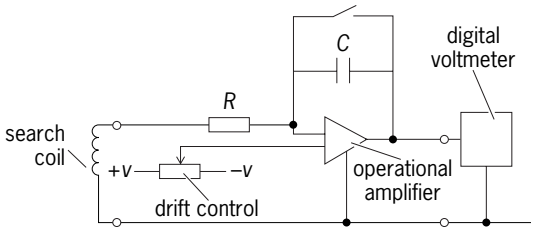

Fig. 2. Arrangement of an electronic charge integrator.

fluxmeters because of their independence of level and vibration. The instrument (**Fig. 2**) consists of a high-open-loop-gain (10^7 or more) operational amplifier with capacitive feedback and resistive input. The value of the input resistor is high (10 kΩ) compared with that of the search coil. The feedback capacitor is chosen to give a convenient time constant and is typically 0.1 or 1 microfarad. The output voltage is proportional to the product of the effective area of the search coil and the change in the magnetic flux density. In practice, consideration must be given to the insulation resistance of the feedback capacitor and any parallel circuits, to thermal and stray pick-up voltages arising in the input circuit, and to changes in the input offset current of the operational amplifier. *See* OPERATIONAL AMPLIFIER.

Electronic charge integrators may be calibrated in one of several ways, as follows:

1. The input can be connected to the secondary of a mutual inductor of known value, and a measured change made in the primary current. The integrator will be direct-reading if the product of the mutual inductance in henrys and the primary current in amperes is equal to the product of the change in the magnetic flux density in teslas and the effective area of the search coil in square meters.

2. A capacitor of known value can be charged up to a known voltage and discharged into the integrator.

3. A linear ramp voltage generator can be connected to the input of the integrator for a measured period of time, t.

If the search coil is wound onto a specimen of ferromagnetic material, it will measure the magnetic flux induced in that material by a known magnetic field strength. Using a Hall-effect instrument in conjunction with an electronic integrator and search coil enables the magnetization curve and hysteresis loop of the magnetic material to be measured. *See* MAGNETIZATION.

Rotating-coil gaussmeter. This instrument measures low magnetic field strengths and flux densities. It comprises a coil mounted on a nonmagnetic shaft remote from a motor mounted at the other end (**Fig. 3**). The motor causes the coil to rotate at a constant speed δ and, in the presence of a magnetic field or magnetic flux density, a voltage is induced in the search coil. The magnitude of the voltage is proportional to the effective area of the search coil and the speed of rotation.

The output of the search coil is taken via slip rings on the driving shaft, rectified by using a synchronous cam-driven switch and measured by using a dc voltmeter. The linearity is exceptionally good over the whole working range from below the Earth's magnetic field strength up to very high magnetic field strengths, limited only by the design of the search coil. Calibration of the instrument is achieved by inserting the rotating coil in a uniform field, for example in the gap of a large electromagnet, the value of which is determined by using a magnetic resonance magnetometer.

Alternating magnetic field meters. These instruments essentially comprise a search coil connected to a root-mean-square (rms) sensing voltmeter and frequency meter. The search coil may be a single turn of calculable area, or a coil of many turns in one or more layers. Alternating magnetic field meters are used extensively in measuring magnetic field strengths from power frequencies up to very high radio frequencies (in the megahertz region), in particular where the effects of stray electromagnetic radiation are of concern. They can be calibrated as an entity over a wide frequency range by mounting the search coil in a specially constructed high-frequency Helmholtz coil system for which the field-to-current and the frequency characteristics have been determined. For an alternating magnetic field of sine-wave form, the magnetic field strength, H (A/m), is given by

$$H = \frac{2\sqrt{2}V}{\pi \mu_o f(AN)}$$

where V is the rms value of the induced voltage in the search coil (V), μ_o is the magnetic constant ($= 4\pi \times 10^{-7}$ H/m), f is the frequency of the alternating magnetic field (Hz), and AN is the effective area-turns product of the search coil (m^2). The measurement of complex waveforms can be achieved by the use of a search coil connected to an oscilloscope with the facility for fast Fourier transform analysis. *See* HELMHOLTZ COILS.

Permeability indicators. These are instruments used for the measurement of the relative magnetic permeability, μ_r, of low-magnetic-permeability materials, for instance stainless steel, in order to assess the effect of the material on the ambient magnetic field. The range of permeability covered is typically 1.001–2. The simplest form of permeability indicator

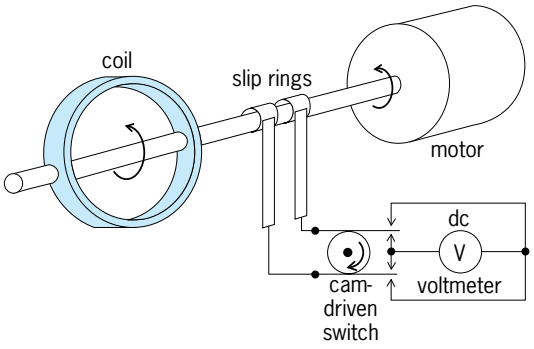

Fig. 3. Arrangement of a rotating-coil gaussmeter. (*M. Lush*)

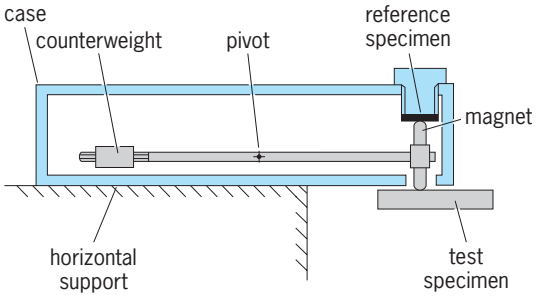

Fig. 4. A typical magnetic balance, side view.

is the magnetic balance (**Fig. 4**). The balance comprises a rod pivoted at its center with a hemispherically ended cylindrical permanent magnet at one end and a counterweight at the other. A number of reference specimens are supplied in the form of discs which can be screwed into the balance case above the upper end of the permanent magnet. Starting with the reference disc of lowest relative magnetic permeability in place, a test specimen is brought into contact with the lower end of the permanent magnet. If the magnet is attracted to the test specimen, then higher values of reference disc are sequentially inserted into the balance until the magnet is attracted to the reference disc. The relative magnetic permeability of the test specimen is then in the range between the values of this disc and the previous reference disc of lower value.

Another type of instrument is based on a fluxgate magnetometer. The permeability-measuring probe includes a permanent magnet, one end of which is placed in contact with the test specimen (**Fig. 5**). The change in the magnetic field around this magnet due to the presence of the test specimen is detected by a pair of fluxgate magnetometer elements. The magnetometer is scaled in terms of $(\mu_r - 1)$, and its advantage over the magnetic-balance type of instrument is that it has a continuous scale.

Both instruments can be calibrated using specially prepared certified reference materials available from some National Standards Laboratories. *See* MAGNETISM; MAGNETOMETER. A. E. Drake

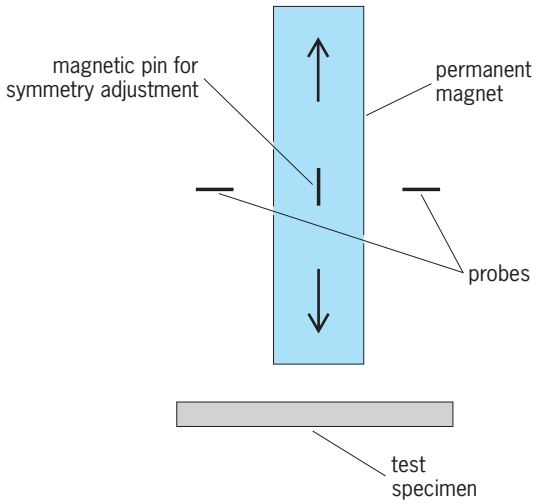

Fig. 5. Arrangement of the permeability meter probe.

Bibliography. E. W. Golding and F. C. Widdis, *Electrical Measurements and Measuring Instruments*, 1963; M. J. Hall et al., Low magnetic permeability reference standards with improved high magnetic field strength performance, *IEE Proc. Sci. Meas. Technol.*, vol. 145, no. 4, July 1998; F. K. Harris, *Electrical Measurements*, 1952, reprint 1975; M. Lush, *Rotating Coil Gaussmeters*, 1964; D. A. Rollett and A. E. Drake, Traceable magnetic field strength measurements to 120 kHz, *IEE Proc. Sci. Meas. Technol.*, vol. 143, no. 4, July 1996.

Magnetic lens

A magnetic field with axial symmetry capable of converging beams of charged particles of uniform velocity and of forming images of objects placed in the path of such beams. Magnetic lenses are employed as condensers, objectives, and projection lenses in magnetic electron microscopes, as final focusing lenses in the electron guns of cathode-ray tubes, and for the selection of groups of charged particles of specific velocity in velocity spectrographs.

As shown in the **illustration**, magnetic lenses may be formed by solenoids or helical coils of wire traversed by electric current, by axially symmetric pole pieces excited by a coil encased in a high-permeability material such as soft iron, or by similar pole pieces excited by permanent magnets. In the last two instances the armatures and pole pieces serve to concentrate the magnetic field in a narrow region about the axis.

Magnetic lenses are always converging lenses. Their action differs from that of electrostatic lenses and glass lenses in that they produce a rotation of the image in addition to the focusing action. For the simple uniform magnetic field within a long solenoid the image rotation is exactly 180°. Thus a uniform magnetic field forms an erect real image of an object on its axis. This image has unity magnification and is at a distance from the object equal to $(8\pi^2 m\phi/eB^2)^{1/2} = 21.08\phi^{1/2}/B$, where m is the mass of the particles, e their charge, ϕ the accelerating potential of the particles, and B the magnetic induction on an axis of symmetry of the field. The numerical coefficient 21.08 applies for electrons, with ϕ in volts and B in gauss.

For short magnetic lenses, or lens fields which are short compared to the focal length, both the magnification and image position depend on the position of the object. The focal length f is given by Eq. (1). The

$$\frac{1}{f} = \frac{e}{8m\phi}\int B^2\,dz = \frac{0.022}{\phi}\int B^2\cdot dz \quad \text{cm}^{-1} \qquad (1)$$

integration is carried out over the extent of the lens field along the axis of symmetry (the z axis). The numerical coefficient 0.022 again applies for electrons. At the same time the field produces an image

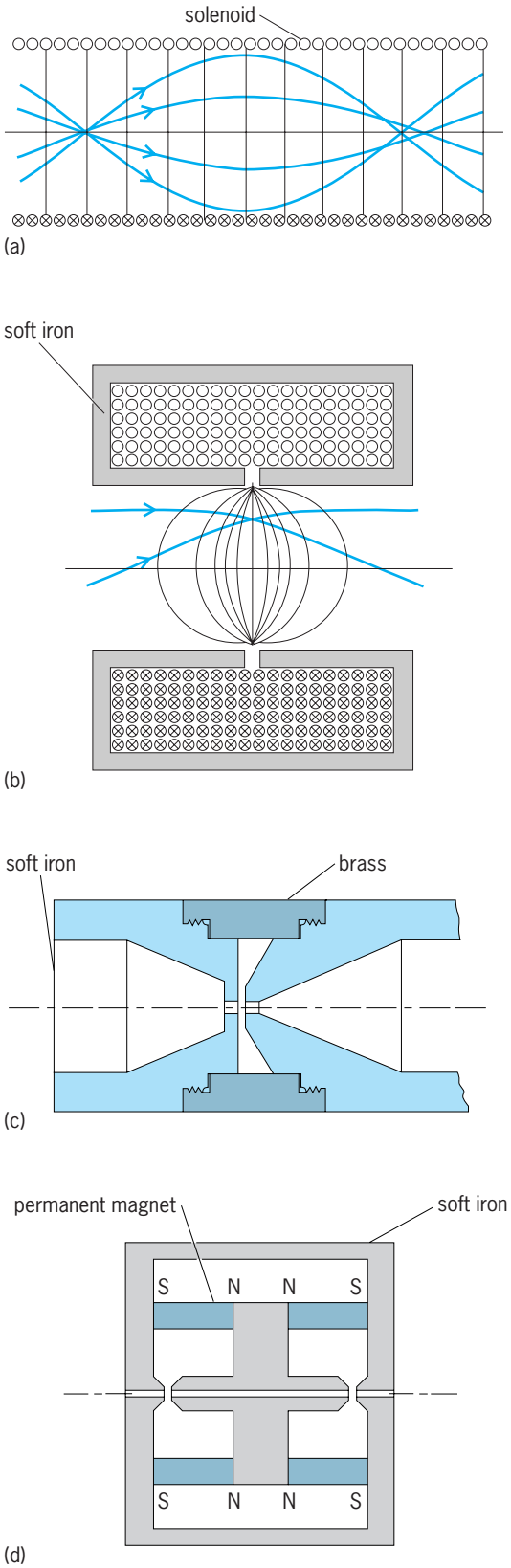

Magnetic lenses. (*a*) Uniform magnetic field. (*b*) Short magnetic lens formed at gap in soft-iron casing about coil. (*c*) Pole pieces for magnetic electron microscope objective. (*d*) Double magnetic lens excited by permanent magnets. (*After E. G. Ramberg and G. A. Morton, J. Appl. Phys., vol. 10, 1939, and J. Hillier and E. G. Ramberg, J. Appl. Phys., vol. 18, 1947*)

rotation through an angle ϕ, as given in Eq. (2). Thus

$$\theta = \left(\frac{e}{8m\phi}\right)^{1/2} \int B\,dz = \frac{0.147}{\phi^{1/2}} \int B\,dz \qquad (2)$$

the magnetic lens field formed by two identical coils in tandem, traversed by oppositely directed currents, is rotation free. As a specific example of a short lens, a single circular loop of wire of radius r traversed by current I produces a lens with focal length $f = 96.8r\phi/I^2$ cm. Here ϕ is in volts and I in amperes. The image rotation for this lens is $\theta = 0.185I/\phi^{1/2}$ radian. *See* ELECTRON MOTION IN VACUUM. E. G. Ramberg

Bibliography. D. A. DeWolf, *Basis of Electron Optics*, 1990; P. W. Hawkes and E. Kaspar (eds.), *Principles of Electron Optics*, 2 vols., 1989; M. Szilagyi, *Electron and Ion Optics*, 1988.

Magnetic levitation

A method of supporting and transporting objects or vehicles which is based on the physical property that the force between two magnetized bodies is inversely proportional to their distance. By using this magnetic force to counterbalance the gravitational pull, a stable and contactless suspension between a magnet (magnetic body) and a fixed guideway (magnetized body) may be obtained. In magnetic levitation (maglev), also known as magnetic suspension, this basic principle is used to suspend (or levitate) vehicles weighing 40 tons or more by generating a controlled magnetic force. By removing friction, these vehicles can travel at speeds higher than wheeled trains, with considerably improved propulsion efficiency (thrust energy/input energy) and reduced noise. In maglev vehicles, chassis-mounted magnets are either suspended underneath a ferromagnetic guideway (track), or levitated above an aluminum track. *See* MAGNET; MAGNETISM.

Attraction-type suspension system. In the attraction-type system, a magnet-guideway geometry, (**Fig. 1***a*) is used to attract a direct-current electromagnet toward the track. This system, also known as the electromagnetic suspension (EMS) system, is suitable for low- and high-speed passenger-carrying vehicles and a wide range of magnetic bearings. The electromagnetic suspension system is inherently non-linear and unstable, requiring an active feedback to maintain an upward lift force equal to the weight of the suspended magnet and its payload (vehicle). The upward life force, $F(i,z,t)$, is given by Eq. (1), where i is the current and z is the

$$F(i,z,t) = \frac{B^2A}{\mu_0} = \frac{\mu_0 N^2 A}{4}\left(\frac{i}{z}\right)^2 \qquad (1)$$

airgap, which both depend on time t, B is the airgap flux density, N is the number of turns in the magnet winding, A is the pole-face area of the magnet, and μ_0 is the permeability of free space. A basic form of state feedback controller which maintains a constant clearance (airgap) between the guideway and the magnet is shown in Fig. 1*b*. The position feedback

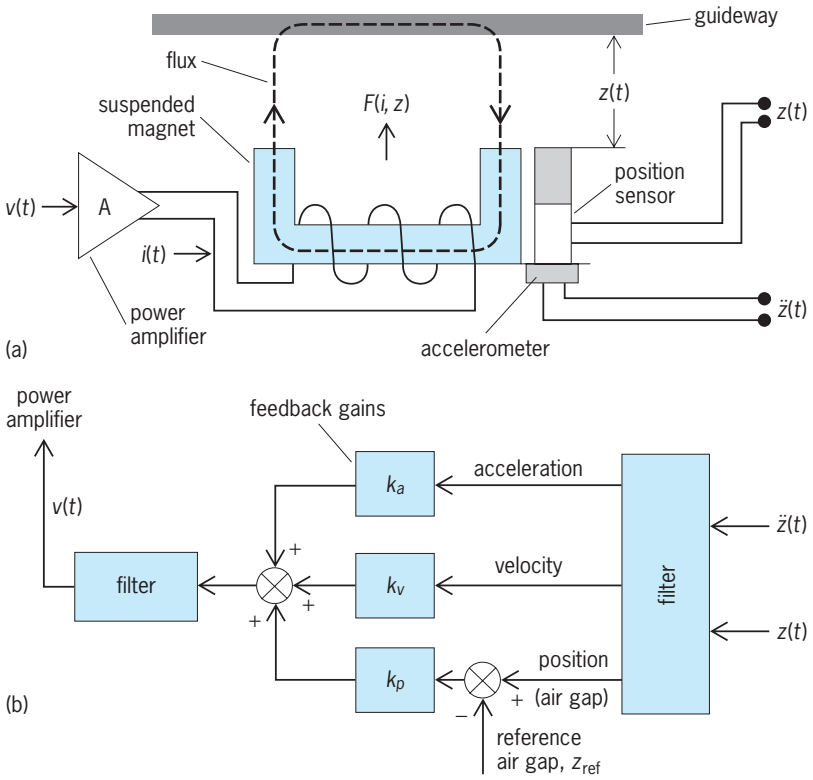

Fig. 1. Attraction-type suspension system. (*a*) Electromagnet-guideway (track) geometry with flux linkages between the magnet and the track. (*b*) Basic state feedback controller. Here, $v(t)$ is the voltage input to the power amplifier, and $z(t)$ is the second time derivative (acceleration) of the airgap or clearance, $z(t)$. Other symbols are explained in the text. (*After P. K. Sinha, Electromagnetic Suspension: Dynamics and Control, Institution of Electrical Engineers, London, 1987*)

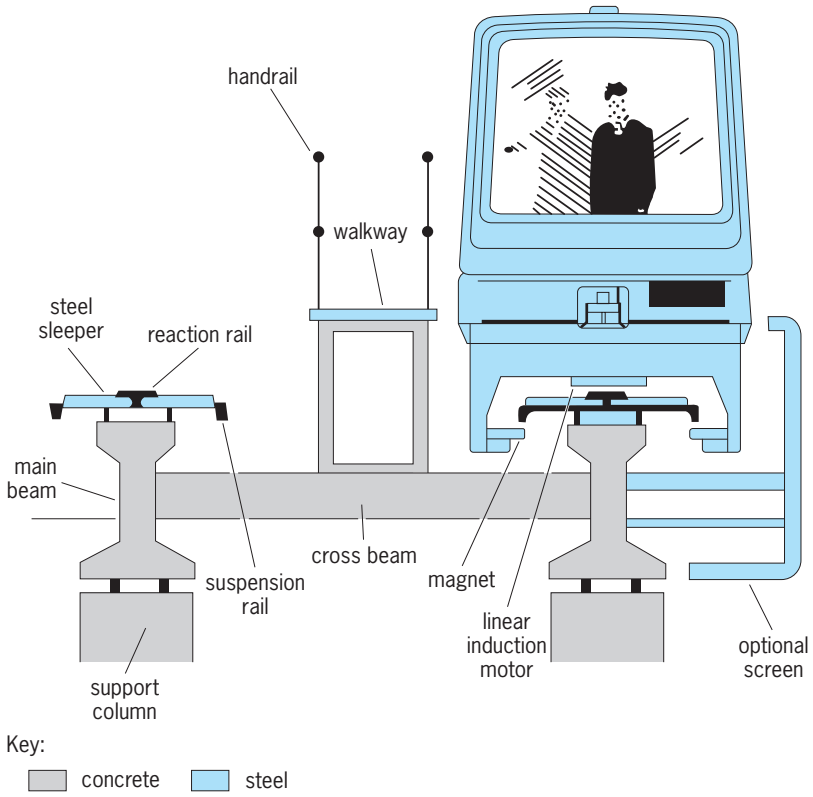

Fig. 2. Sectional view of the Birmingham system, with key components marked. (*After P. K. Sinha, Electromagnetic Suspension: Dynamics and Control, Institution of Electrical Engineers, London, 1987*)

maintains a constant airgap (z_{ref}) and suspension stiffness, the velocity feedback introduces damping, while the acceleration feedback controls damping and ride quality. High-performance microprocessors and digital signal processors are used to implement this and other forms of advanced control laws to provide a very high degree of suspension stability and ride characteristics. For vehicle suspension applications, the airgap is kept in the range of 12–15 mm (0.5–0.6 in.), with airgap flux densities varying from 0.8–1 tesla. For other applications, such as magnetic bearings, the airgaps can be as small as 1 mm (0.04 in.) with considerably lower flux densities. *See* CONTROL SYSTEMS; ELECTROMAGNET; MICROPROCESSOR.

Development of electromagnetic suspension technology for vehicle suspension has been actively pursued since the 1960s, with several experimental and demonstration vehicles running at various locations. The first public system was installed in 1984 at the Birmingham International airport in England to connect the inter-city railway station to the expanded airport. During its operation over several years, this kilometer-long (0.6-mi) system established the electromagnetic suspension technology and its role in public transport. The Birmingham system (**Fig. 2**) used a set of staggered magnets to generate vertical suspension and lateral guidance forces, and linear induction motors for propulsion.

Since the Birmingham system, several full-scale prototype vehicles have been exhibited. Germany leads the technology with the Transrapid series of vehicles (**Fig. 3**) and the construction of a 500-km/h (300-mi/h) maglev link between Hamburg and Berlin. Development of a 100-km/h (60-mi/h) system has been undertaken in Japan for use in urban transit systems.

Repulsion-type levitation system. Most conductors exhibit a reduction in resistance with decreasing temperature; some "lose" their resistance completely below the critical temperature (T_c) to become ideal conductors (superconductors). An electric current set up in a superconducting coil will thus continue to flow and produce a magnetic field as long as the coil remains below T_c (around 20 K or −424°F for copper). This low-temperature condition is achieved by immersing the coil in a coolant (typically, liquid helium) stored in a specially constructed chamber (cryostat). This persistent current makes the superconducting coil behave like a high-field permanent magnet. *See* SUPERCONDUCTIVITY.

In the repulsion-type system, also known as the electrodynamic levitation system (EDS or EDL), a superconducting coil operating in persistent-current mode is moved longitudinally along a conducting surface (an aluminum plate fixed on the ground and acting as the guideway) to induce circulating eddy currents in the aluminum plate. These eddy currents create a magnetic field which, by Lenz's law, oppose the magnetic field generated by the travelling coil. This interaction produces a repulsion force on the moving coil. At lower speeds, this vertical force is not sufficient to lift the coil (and its payload), so

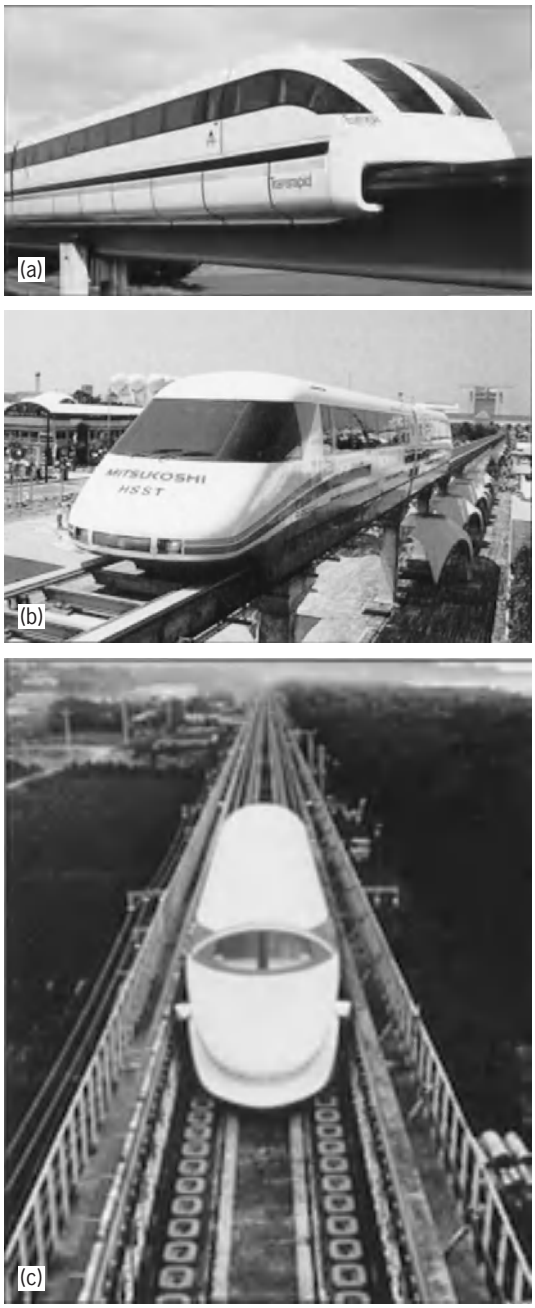

Fig. 3. Magnetic levitation systems and vehicles. (*a*) German Transrapid TR07 vehicle (*Thyssen Henschel, Munich*). (*b*) Japanese HSST system. (*c*) Japanese superconducting test vehicle MLU-002 (*HSST Corporation, Tokyo*).

supporting auxiliary wheels are needed until the net repulsion force is positive. The speed at which the net upward lift force is positive (critical speed) is dependent on the magnetic field in the airgap and payload, and is typically around 80 km/h (50 mi/h). To produce high flux from the travelling coils, hard superconductors (type II) with relatively high values of the critical field (the magnetic field strength of the coil at 0 K) are used to yield airgap flux densities of over 4 tesla. With this choice, the strong eddy-current induced magnetic field is rejected by the superconducting field, giving a self-stabilizing levitation force at high speeds (though additional control circuitry is required for adequate damping and ride quality). For mathematical analysis, the interaction between the two fields is expressed as the repulsive force between the moving superconducting coil above the aluminum track and an imaginary image coil of opposite polarity located at an equal distance below the track. *See* EDDY CURRENT.

Only direct-current superconducting magnets are suitable for this system because of the relatively high hysteresis loss in hard superconductors with alternating-current excitation. In practice, there is some residual resistance in the direct-current superconducting loop, which, although very small, eventually reduces the amplitude of the persistent current. In addition, the coolant in the cryostat needs replacing to keep the coil temperature below T_c. Thus some charging-up current as well as coolant topping up are required from time to time to sustain the levitation force on the moving magnet. Also, there is a certain amount of ohmic loss in the aluminum track, which generates heat and a magnetic drag force as the magnet travels along. In the simplest form, the lift and the drag forces due to a single-turn coil, at any values of the longitudinal velocity v and the airgap z [100 mm (4 in.) or more], are given by Eqs. (2), with $w = 2/(\mu_0 \sigma b)$, where b is

$$F_{\text{drag}}(v,z,t) = \frac{w}{v} F_{\text{lift}}(v,z,t) \qquad (2a)$$

$$F_{\text{lift}}(v,z,t) = \left[\frac{v^2}{v^2 + w^2}\right] F_{\text{coil}}(I,z,t) \qquad (2b)$$

the thickness of the aluminum plate and σ is the conductivity of the superconducting coil material. Here, $F_{\text{coil}} = \mu_0 I^2/(4\pi z)$ is the repulsive force between the levitated coil with a persistent current of I amperes and its image at a distance of $2z$.

The first fully operational supeconducting maglev vehicle was demonstrated by the Japanese National Railways in 1972. This was followed by systems from Germany and the United States. Speeds of up to 517 km/h (321 mi/h) were recorded on the Myazaki test track, in Japan in 1980, and in 1998 a three-car 80-m-long (260-ft) long test vehicle operating on the Yamanashi test track near Tokyo achieved a speed of 550 km/h (342 mi/h).

Linear motors. Due to their contactless operation, linear motors are used to propel maglev vehicles: linear induction motors for low-speed vehicles and linear synchronous motors for high-speed systems. Although their performance parameters are different, operationally they are the unrolled versions of the conventional rotary motors. For linear synchronous motors, three-phase windings are mounted on the guideway, and propulsion force is generated by the interaction between these long stator windings and vehicle-borne direct-current electromagnets (field coils). In the electrodynamic repulsion system, field coils are made of a separate set of superconducting loops. In high-speed electromagnetic attraction systems, such as the Transrapid vehicles, the lift magnets are constructed to provide

the vertical suspension force and act as the field coils of the linear synchronous motor. *See* INDUCTION MOTOR; SYNCHRONOUS MOTOR.

While high-speed vehicles have a restricted magnet-guideway configuration, several types of low-speed systems with different magnet-guideway geometries have been developed. The Berlin Magnetbahn uses a combination of small wheels and permanent magnets for suspension and a linear synchronous motor for propulsion, while the Tokyo continuous transit magnet (CTM) vehicles are supported by rubber wheels and propelled by the coupling force between the vehicle-mounted permanent magnets and a series of linear magnetic belts.

Magnetic bearings. Suspending the rotating part of a machine in a magnetic field may eliminate the contact friction present in conventional mechanical bearings. Magnetic bearings may be based on either attractive or repulsive forces. While the attraction type offers the advantage of controlling the suspension dynamics (stiffness in particular), it is inherently more complex and is used in high-performance and heavy-duty applications. A repulsion system may be very compact and is better suited where physical size is more important than flexibility in the choice of suspension characteristics. Although well developed, radial magnetic bearings are relatively expensive and complex, and are used in specialized areas such as vibration dampers for large drive shafts for marine propellers. In contrast, the axial versions of magnetic bearings are in common use in heavy-duty applications, such as large pump shafts and industrial drums. *See* ANTIFRICTION BEARING.

Maglev technology has evolved from tabletop demonstrations, through high-speed passenger trains traveling at over 550 km/h (342 mi/h), to contactless bearings to support a 3-m-long (10-ft) pump shafts in hazardous environments. As the demand for precise, quiet, and efficient drives grows, the concepts of magnetic suspension and linear motors are likely to find new applications such as the clean-room wafer carrying mechanism, reusable space rocket launchers, and even household appliances.

P. K. Sinha

Bibliography. IEEE Magnetics Society, *Intermag, 2000*, 2000; P. K. Sinha, *Electromagnetic Suspension: Dynamics and Control*, Institution of Electrical Engineers, London, 1987.

Magnetic materials

Materials exhibiting ferromagnetism. The magnetic properties of all materials make them respond in some way to a magnetic field, but most materials are diamagnetic or paramagnetic and show almost no response. The materials that are most important to magnetic technology are ferromagnetic and ferrimagnetic materials. Their response to a field H is to create an internal contribution to the magnetic induction B proportional to H, expressed as $B = \mu H$, where μ the permeability, varies with H for ferromagnetic materials. Ferromagnetic materials are the elements iron, cobalt, nickel, and their alloys, some manganese compounds, and some rare earths. Ferrimagnetic materials are spinels of the general composition MFe_2O_4, and garnets, $M_3Fe_5O_{12}$, where M represents a metal. *See* FERRIMAGNETISM; FERROMAGNETISM; MAGNETISM; MAGNETIZATION.

Ferromagnetic materials are characterized by a Curie temperature, above which thermal agitation destroys the magnetic coupling giving rise to the alignment of the elementary magnets (electron spins) of adjacent atoms in a crystal lattice. Below the Curie temperature, ferromagnetism appears spontaneously in small volumes called domains. In the absence of a magnetic field, the domain arrangement minimizes the external energy, and the bulk material appears unmagnetized. *See* CURIE TEMPERATURE.

Magnetic materials are further classified as soft or hard according to the ease of magnetization. Soft materials are used in devices in which change in the magnetization during operation is desirable, sometimes rapidly, as in ac generators and transformers. Hard materials are used to supply a fixed field either to act alone, as in a magnetic separator, or to interact with others, as in loudspeakers and instruments. Both soft and hard materials are characterized by their magnetic hysteresis curve (see **illus.**). *See* ELECTRIC ROTATING MACHINERY; ELECTRICAL MEASUREMENTS; GENERATOR; INDUCTOR; LOUDSPEAKER; MAGNETIC SEPARATION METHODS; MICROPHONE; TRANSFORMER.

Soft magnetic materials. These materials are characterized by their low loss and high permeability. There are a variety of alloys used with various combinations of magnetic properties, mechanical properties, and cost (**Table 1**). There are seven major groups of commercially important materials: iron and low-carbon steels, iron-silicon alloys, iron-aluminum-silicon alloys, nickel-iron alloys, iron-cobalt alloys, ferrites, and amorphous alloys.

The behavior of soft materials is controlled by the pinning of domain walls at heterogeneities such as grain boundaries and inclusions. Thus the common goal in their production is to minimize such heterogeneities. In addition, eddy-current loss is minimized through alloying additions which increase the electrical resistivity. Initial permeability, important in electronic transformers and inductors, is improved by minimizing all sources of magnetic anisotropy, for example, by using amorphous metallic alloys and by using zero magnetostrictive alloys. A high maximum permeability, which is necessary for motors and power transformers, is increased by the alignment of the anisotropy, for example, through development of crystal texture or magnetically induced anisotropy. *See* EDDY CURRENT; MAGNETOSTRICTION.

The class of alloys used in largest volume is by far iron and 1–3.5% silicon-iron for applications in motors and large transformers. In these applications the cost of the material is often the dominant factor, with losses and excitation power secondary

but still important. Thus, the improvement over the years in these alloys has been in developing lower losses without increases in cost. A major improvement in these alloys occurred around 1940 with the development of a $\{110\}\langle 001\rangle$ crystal texture in 3.2% silicon-iron which greatly reduced losses and increased permeability. Since 1880 the losses have decreased steadily through alloying, texture improvements, decreasing the thickness of the strip, and application of stressed insulating coatings. *See* IRON ALLOYS.

Many special alloys find their use in special devices designed to exploit unusual properties. These include materials with high-saturation induction B_s (the magnetic induction at very large values of H), usually cobalt-iron alloys; and alloys with high permeability μ, most often nickel-iron alloys. These alloys are the mainstay of the telecommunications industry. Some of the devices require high initial permeability μ_0 (the permeability at very low fields), and others may depend on high values of μ_{max}, the maximum permeability.

In power equipment the major consideration is the power lost in the magnetic circuit under operating conditions. The total core loss P_c consists of the hysteresis loss P_h and eddy-current loss P_e. The hysteresis loss represents the energy lost at each cycle in the magnetization process. It is proportional to the area of the hysteresis loop and is directly dependent on the frequency f. The loss due to eddy currents depends on the square of the elecromotive force (emf) developed in the conducting magnetic material, that is, B^2f^2, and inversely on the electrical resistivity ρ of the material. By combining geometric factors into constants, the equation below is obtained.

$$P_{c(B,f)} = P_h + P_e = \text{const} \times f + \text{const} \times \frac{B^2 f^2}{\rho}$$

The hysteresis loss may be kept low by using a material with a narrow hysteresis loop (one with low coercive force H_c, the value of H required to reduce B to zero). The low H_c is obtained by choosing an alloy with zero stress sensitivity or by minimizing mechanical strain after the final stress-relief anneal. Eddy-current loss may be reduced by breaking up eddy-current paths, for example, by using laminations rather than solid cores.

Audio-frequency devices require very thin laminations or resin-bonded alloy powder cores. The very high electrical resistivity ($1–10^6$ ohm-cm) qualifies many ferrites and garnets for very high-frequency applications, for example, in cores, transformers, phase shifters, and isolators. *See* FERRITE.

Hard magnetic materials. Permanent magnets, or hard magnetic materials, strongly resist demagnetization once magnetized (**Table 2**). They are used, for example, in motors, loudspeakers, meters, and holding devices, and have coercivities H_c from several hundred to many thousands of oersteds (10 to over 100 kA/m). The bulk of commercial permanent magnets are of the ceramic type, followed by the Alnicos and the cobalt-samarium, iron-neodymium, iron-chromium-cobalt, and elongated single-domain (ESD) types in decreasing sequence of usage. The overall quality of a permanent magnet is represented by the highest-energy product $(BH)_m$; but depending on the design considerations, high H_c, high residual induction B_r (the magnetic induction when H is reduced to zero), and reversibility of permeability may also be controlling factors. *See* MAGNET.

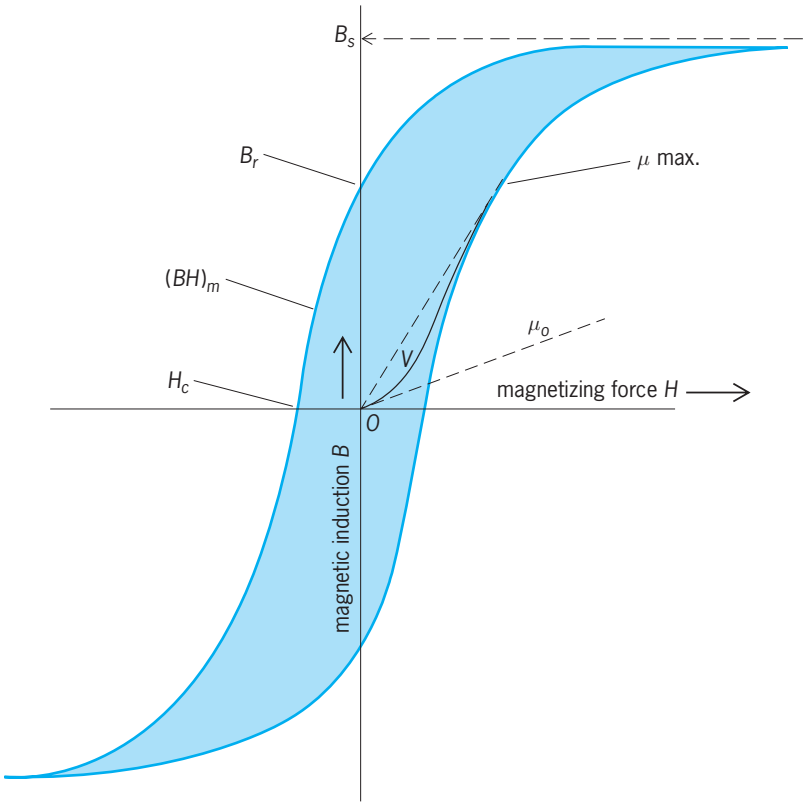

Identification of properties related to the magnetic hysteresis loop. Colored area is the magnetization energy lost in every cycle (hysteresis loss).

To understand the relation between the resistance to demagnetization, that is, the coercivity, and the metallurgical microstructure, it is necessary to understand the mechanisms of magnetization reversal. The two major mechanisms are reversal against a shape anisotropy and reversal through nucleation and growth of reverse magnetic domains against crystal anisotropy. The Alnicos, the iron-chromium-cobalt alloys, and the elongated single-domain Lodex alloys are examples of materials of the shape anisotropy structure, while barium ferrites, the cobalt-samarium alloys, and the iron-neodymium-boron alloys are examples of the crystal anisotropy-controlled materials.

Recording materials. Recording tapes and disks for many years were mostly coated with δ–Fe_2O_3, but a variety of new materials have been introduced, for example, metallic particles, chrome oxide, metallic alloy tapes, and cobalt-doped Fe_2O_3. The forming of uniform, and often oriented, dispersions of these materials on flexible (tapes) or rigid (disks)

TABLE 1. Some properties of selected soft magnetic materials

Material or trade name	Composition % by weight, remainder Fe	Relative permeability: Initial μ_0	Relative permeability: Max. μ_{max}	Coercive force H_c, A/m (oersteds)	Saturation induction B_s, teslas (gauss)	Curie temperature T_c, °F (°C)	Electrical resistivity ρ, microhm-cm	Core loss at 60 Hz, 1.5 teslas (15 kilogauss), W/lb (W/kg)	Sample thickness, in. (mm)
Iron, high-purity	0.05 impurity	10,000	200,000	88 (1.1)	2.15 (21,500)	1420 (770)	10	5.9 (13)	0.025 (0.64)
Iron, commercial-purity	0.2 impurity	250	9,000	72 (0.9)	2.14 (21,400)	1420 (770)	12	3.7 (8.1)	0.019 (0.47)
Carbonyl iron powder	—	60	150	—	—	—	10×10^6		
Armature M-43	0.95Si	—	4,100	75 (0.94)	2.13 (21,300)	1400 (760)	24	2.3 (5.1)	0.019 (0.47)
Electric M-36	2Si	—	7,500	40 (0.5)	2.11 (21,100)	1390 (755)	41	1.9 (4.2)	0.014 (0.36)
Dyname M-22	2.8Si	—	9,400	32 (0.4)	2.03 (20,300)	1365 (740)	49	1.7 (3.7)	0.014 (0.36)
Transformer, M-15	2.2Si	1,500	7,000	28 (0.35)	1.95 (19,500)	1345 (730)	53	1.4 (3.0)	0.014 (0.36)
Oriented cube-on-edge texture, M-4	3.2Si	7,500	55,000	8 (0.1)	2.01 (20,100)	1365 (740)	48	0.55 (1.2)	0.011 (0.27)
High-permeability G.O.	3.2Si	—	—	—	2.01 (20,100)	1365 (740)	45	0.35 (0.77)	0.008 (0.20)
Low-aluminum iron (3.5%)	3.5Al	500	19,000	24 (0.3)	1.90 (19,000)	1380 (750)	47		
16% Al-Fe	16.0Al	3,900	110,000	1.2 (0.015)	0.50 (5,000)	840 (450)	153		
Sendust	5.0Al, 10.0Sl	30,000	120,000	4 (0.05)	1.00 (10,000)	930 (500)	45		
Thermoperm	30Ni	—	—	—	0.203 (2,030)	120 (50)	—		
45 Permalloy	45Ni	2,500	25,000	8 (0.10)	1.60 (16,000)	750 (400)	45		
50–50 Ni-Fe	50Ni	4,000	100,000	4 (0.05)	1.60 (16,000)	930 (500)	45		
Mumetal	77Ni,5Cu,2Cr	20,000	100,000	4 (0.05)	0.65 (6,500)	— 62			
78 Permalloy	78.5Ni	8,000	100,000	4 (0.05)	1.08 (10,800)	1110 (600)	16		
Supermalloy	79Ni,5Mo	100,000	1,000,000	0.32 (0.004)	0.78 (7,800)	750 (400)	60		
2–81 Moly permalloy powder	81 Ni,2Mo	125	130	—	—	—	16×10^6		
27% Co-Fe	27Co, 1Cr	650	10,000	56 (0.70)	2.42 (24,200)	— 28			
50% Co-Fe	49Co,2V, or 2Cr	800	5,000	160 (2.0)	2.45 (24,500)	1800 (980)	7		
Supermendur	49Co,2V	800	70,000	24 (0.3)	2.40 (24,000)	1800 (980)	40		
45–25 Perminvar	45Ni,25Co	400	2,000	95 (1.2)	1.55 (15,500)	1320 (715)	19		
Mn-Zn Ferrite	Mn-δZn-δFe_2O_4	1,500	2,500	16 (0.2)	0.34 (3,400)	265 (130)	20×10^6		
Ni-Zn Ferrite	—	2,500	5,000	8 (0.1)	0.32 (3,200)	285 (140)	10^{11}		
Amorphous Fe-B-Sl, METGLAS 2605S-2	4B,3Sl	15,000	300,000	1.6 (0.02)	1.56 (15,600)	780 (415)	130	0.1 (0.2) at 1.4 T (14 kG)	0.001 (0.025)

TABLE 2. Representative permanent-magnet properties*

Material	Composition % by weight	Curie temperature T_c: °F	Curie temperature T_c: °C	Coercive force H_c: kA/m	Coercive force H_c: Oe	Residual induction B_c: T	Residual induction B_c: G	Max. energy product $(BH)_m$: kJ/m³	Max. energy product $(BH)_m$: MGOe	Preparation	Mechanical properties
Ba ferrite	$BaO \cdot 6Fe_2O_3$	840	450	170	2,100	0.43	4,300	36	4.5	Press, sinter	Brittle
Sr ferrite	$SrO \cdot 6Fe_2O_3$	860	460	250	3,100	0.42	4,200	36	4.5		
Alnico 5	50Fe,24Co,15Ni, 8Al,3Cu	1650	900	58	620	1.25	12,500	42	5.3	Cast, anneal	Hard, brittle
Alnico 8	34Fe,35Co,15Ni, 7Al,5Ti,4 Cu	1580	860	130	1,600	0.83	8,300	40	5.0		
Alnico 9	34Fe,35Co,15Ni, 7Al,5ti,4Cu			120	1,450	1.05	10,500	68	8.5		
Fe-Cr-Co	63Fe,22Cr,15Co	1165	630	51	640	1.56	15,600	66	8.3	Cast, anneal	Hard
Fe-Cr-Co-Cu	42Fe,33Cr,23Co,2Cu			86	1080	1.30	13,000	78	9.8	Roll, anneal	Hard
Co_5Sm	66Co,34Sm	1290	700	665	8,300	0.91	9,050	160	20	Press, sinter,	Brittle
Co_{17} Sm_2	77Co,23Sm	1470	800	670	8,400	1.08	10,800	223	28	Press, sinter	Brittle
Elongated single domain (ESD) Fe-Co(Lodex)	9.9Fe,5.5Co,77Pb, 8.6Sn	1795	980	70	870	0.8	8,000	25	3.2	Electroplate, distill, press	Soft
Mn-Al-C	70Mn,29Al0.5Ni,0.5C	570	300	220	2,700	0.61	6,100	56	7.0	Cast, extrude, anneal	
Co-Pt	77Pt,23Co	895	480	360	4,500	0.65	6,500	73	9.2	Cast, anneal	Hard, strong
Fe-Nd-B	66Fe,33Nd,1B	570	300	905	11,300	1.21	12,100	280	35	Press, sinter, anneal	Brittle

*Oe = oersteds, T = teslas, G = gauss, MGOe = megagauss-oersteds.

substrates is a challenging manufacturing problem. *See* ALLOY; AMORPHOUS SOLID; MAGNETIC RECORDING.

F. E. Luborsky

Bibliography. American Society for Metals, *Metals Handbook, Desk Edition*, 1985; K. M. Buschow et al. (eds.), *Ferromagnetic Materials*, vols. 1–6, 1980–1991; P. Campbell, *Permanent Magnetic Materials and Their Application*, 1994; C. W. Chen, *Magnetism and Metallurgy of Soft Magnetic Materials*, 1977, reprint 1986; J. Crangle, *Solid State Magnetism*, 1991; J. E. Evetts (ed.), *Concise Encyclopedia of Magnetic and Superconducting Materials*, 1992; J. P. Jakubovics, *Magnetism and Magnetic Materials*, 2d ed., 1994; D. C. Jiles, *Introduction to Magnetism and Magnetic Materials*, 1991; C. Kittel, *Introduction to Solid State Physics*, 6th ed., 1986; P. Robert, *Electrical and Magnetic Properties of Materials*, 1988; S. G. Sankar, *Permanent Magnet Materials and Devices*, 1995.

Magnetic monopoles

Magnetically charged particles. Such particles are predicted by various physical theories, but so far all experimental searches have failed to demonstrate their existence.

Theoretical basis. The fundamental laws governing electricity and magnetism become symmetric if particles exist that carry magnetic charge. Current understanding of electromagnetic physical phenomena is based on the existence of electric monopoles, which are sources or sinks of electric field lines (**Fig. 1***a*), and which when set into motion generate magnetic fields. The magnetic field lines produced by such a current have no beginning or end and form closed loops (Fig. 1*a*). All magnetic fields occurring in nature can be explained as arising from currents. However, theories of electromagnetism become symmetric if magnetic charges also exist. These would be sources or sinks of magnetic field and when set into motion would generate electric fields whose lines would be closed without ends (Fig. 1*b*). *See* ELECTRIC FIELD.

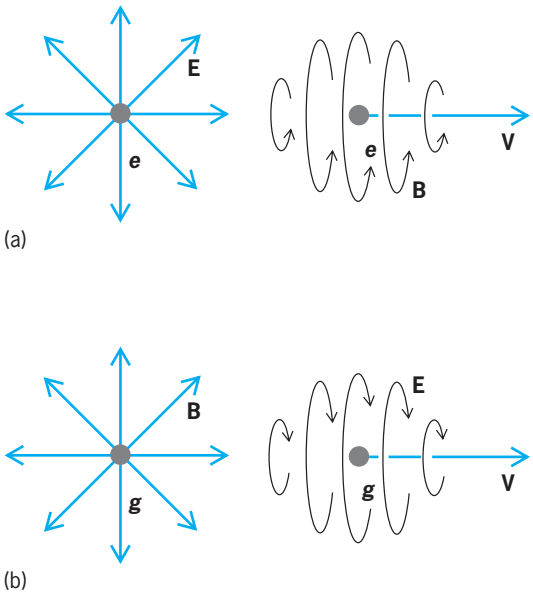

Fig. 1. Electric (*E*) and magnetic (*B*) field lines generated by monopoles and by their motion with velocity *v*. (*a*) Electric monopole with electric charge *e*. (*b*) Magnetic monopole with magnetic charge *g*.

J. C. Maxwell's equations describing electromagnetism can be generalized by adding the magnetic charge density ρ_m and the magnetic current density $\mathbf{j}_m$. The generalized Maxwell equations are Eqs. (1)

$$\begin{aligned} \nabla \times \mathbf{B} - \frac{1}{c}\frac{\partial \mathbf{E}}{\partial t} &= \frac{4\pi}{c}\mathbf{j}_e \\ \nabla \cdot \mathbf{E} &= 4\pi\rho_e \\ \nabla \times \mathbf{E} + \frac{1}{c}\frac{\partial \mathbf{B}}{\partial t} &= -\frac{4\pi}{c}\mathbf{j}_m \\ \nabla \cdot \mathbf{B} &= 4\pi\rho_m \end{aligned} \tag{1}$$

in cgs units, where c is the speed of light. The first equation (Ampère's law) says that electric currents ($\mathbf{j}_e$) and time-varying electric fields ($\mathbf{E}$) produce magnetic fields ($\mathbf{B}$); the second (Gauss's law), that electric charges (with density ρ_e) produce electric fields with strength inversely proportional to the square of the distance from the charge; the third (Faraday's law), that electric fields are produced by time-varying magnetic fields and by magnetic charge currents (if they exist); and the fourth (Gauss's law for magnetic monopoles), that magnetic charges would produce magnetic fields with strength inversely proportional to the square of the distance from the charge. *See* AMPÈRE'S LAW; ELECTROMAGNETIC INDUCTION; GAUSS' THEOREM; MAXWELL'S EQUATIONS.

However, this symmetrization of Maxwell's equations is not a strong reason for suggesting the existence of magnetic charges. New electric and magnetic fields can be defined as linear combinations of the present fields in such a way that Maxwell's equations become symmetric but no new physics is introduced.

Dirac's theory. In 1931 P. A. M. Dirac found a more fundamental reason for hypothesizing magnetic charges, when he showed that this would explain the observed quantization of electric charge. He showed that all electric and magnetic charges e and g must obey Eq. (2), where k must be an integer and is Planck's constant divided by 2π. Equation (2) can be satisfied only if all electric and magnetic charges are integer multiples of an elementary electric charge e_0 and an elementary magnetic charge g_0. Since the size of the elementary electric charge, the charge carried by an electron or proton, is known experimentally, Dirac's equation predicts the size of the elementary magnetic charge to be given by Eq. (3). Since the fine structure constant α is given by Eq. (4), the elementary magnetic charge g_0 is about 68.5 times larger than the elementary electric

$$eg = k(^1/_2\hbar c) \tag{2}$$

$$g_0 = \frac{1}{2}\frac{\hbar c}{e_0} \tag{3}$$

$$\alpha = \frac{e_0^2}{\hbar c} \approx \frac{1}{137} \tag{4}$$

charge e_0. *See* FINE STRUCTURE (SPECTRAL LINES); FUNDAMENTAL CONSTANTS.

Grand unification theories. In 1983 a successful theoretical unification of the electromagnetic and weak forces culminated in the detection of the W^+, the W^-, and the Z^0 particles predicted by the theory. This success has encouraged the search for a grand unification theory that would include the electroweak force and the nuclear or color force under one consistent description. In 1974 G. 't Hooft and independently A. M. Polyakov showed that magnetically charged particles are necessarily present in all true unification theories (those based on simple or semisimple compact groups). These theories predict the same long-range field and thus the same charge g_0 as the Dirac solution; now, however, the near field is also specified, leading to a calculable mass. The SU(5) model predicts a monopole mass of 10^{16} GeV/c^2, while theories based on supersymmetry or Kaluza-Klein models yield even higher masses up to the Planck mass of 10^{19} GeV/c^2. *See* ELECTROWEAK INTERACTION; FUNDAMENTAL INTERACTIONS; GRAND UNIFICATION THEORIES; QUANTUM GRAVITATION; SUPERGRAVITY; SUPERSYMMETRY.

Astrophysical limits. Although grand unification theories clearly predict the existence of monopoles, cosmological models based on these theories lead to impossibly high or unobservably low predictions for monopole fluxes. However, the low predictions are based on the inflationary model, involving an exponential expansion of the early universe followed by a reheating. In this model, the number of monopoles depends exponentially on the reheating energy, and thus small changes in this energy, which cannot be calculated in detail, can result in observable monopole fluxes. *See* INFLATIONARY UNIVERSE COSMOLOGY.

An upper bound (the Parker bound) of 10^{-15} cm^{-2} sr^{-1} s^{-1} is obtained, assuming an isotropic flux, from arguments based on the existence of the 3-microgauss (3×10^{-10} tesla) galactic magnetic field. The Parker bound becomes less severe linearly with monopole mass for masses above 10^{17} GeV/c^2. In addition, models incorporating monopole plasma oscillations would allow a much larger particle flux. All of these bounds assume particle velocities in gravitational virial equilibrium, that is, very near 10^{-3} c.

It has been shown theoretically that the supermassive monopoles arising from many grand unification theories would catalyze nucleon decay processes. Arguments based on x-ray flux limits from galactic neutron stars, which assume a strong-interaction cross section for proton decay catalysis, lead to an upper bound for magnetic particle flux of about 10^{-21} cm^{-2} sr^{-1} s^{-1}, which would make direct detection of monopoles virtually impossible. However, the incomplete understanding of both the catalysis cross section and neutron stars, and the failure to observe proton decay, make this bound highly uncertain. *See* NEUTRON STAR; PROTON.

Detectors. There are two classes of magnetic monopole detectors, superconducting and conventional.

Superconducting detectors. These are based on Faraday's generalized law of induction [the third of Maxwell's equations in (1)], where a magnetic charge passing through a conducting coil will induce a current, in the same way that passing one end of a solenoid through a conducting coil induces a current. If the coil is superconducting, the current never dies away so that the passage of a magnetic charge would show itself as a step in the persistent current of the coil. This type of detector directly measures the magnetic charge of a particle, independent of particle velocity and other properties. Because of their velocity-independent response, these detectors are a natural choice in searches for supermassive (and therefore slow) magnetically charged particles. *See* SUPERCONDUCTING DEVICES; SUPERCONDUCTIVITY.

In addition, the detector response is based on simple, fundamental, and extremely convincing theoretical arguments.

The remarkable theoretical similarities between flux quantization in superconductors and Dirac magnetic monopoles make superconducting systems natural detectors for these particles. The magnetic flux emanating from a Dirac charge g_0 is exactly twice the flux quantum of superconductivity. Since no magnetic field line can pass through a superconductor, when a magnetic charge passes through a superconducting ring (**Fig. 2**), every flux line emanating from the pole must leave a closed loop around the ring wire as the particle moves through. Thus, the magnetic flux change through the ring must exactly equal

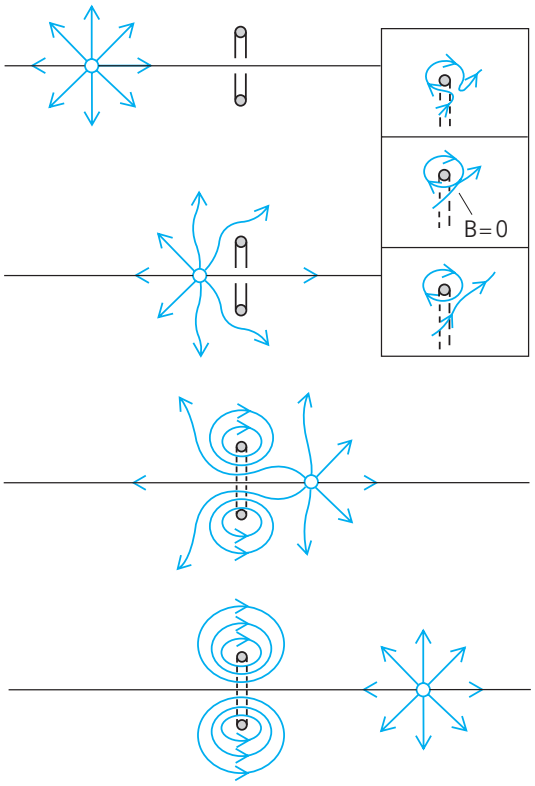

Fig. 2. Successive configurations of magnetic field lines as a monopole passes through a superconducting ring. Inset shows detail of a single magnetic field line leaving a closed loop around the ring; *B* is the magnetic flux density.

the total flux from the pole: two flux quanta for a monopole of unit Dirac charge. No net flux change results form trajectories that miss the ring.

On February 14, 1982, a prototype superconducting detector operating at Stanford University observed a single candidate event. Since then a number of groups have operated larger second- and third-generation detectors, and their combined data have placed a limit on the monopole flux more than 3000 times lower than the value from the data set that included the original event. Thus the possibility that this event was caused by the passage of a magnetic monopole has been largely discounted.

Another single event was observed in a second-generation detector at Imperial College, London, on August 11, 1985. The possibility of the event having been caused by the passage of a magnetic monopole also has been largely discounted because it was a noncoincident signal observed by only one SQUID, and thus more susceptible to a spurious cause. All other second-generation detectors have used fully coincident multiple-loop detection schemes. *See* SQUID.

Several groups have operated larger third-generation detectors. The detector shown in **Fig. 3**, with a sensing area greater than 1.5 m^2 (16 ft^2) times 4π sr, is composed of eight planar superconducting detection coils arranged around a cylinder with an octagonal cross section. Each coil is a gradiometer connected to a high-sensitivity radio-frequency SQUID current sensor.

The gradiometer winding pattern is an important design feature for superconducting monopole detectors. For example, a figure-eight coil couples no net magnetic flux for any change in a uniform applied field. The sensitivity of a gradiometer to external magnetic field changes is substantially reduced over that from a simple coil, whereas the sensitivity to the passage of a magnetic charge remains high since the particle passes through only one element of the gradiometer pattern. A further improvement was achieved by breaking the loop up into a number of separate elements that are connected to one SQUID in parallel, thereby reducing coupling losses to the SQUID.

The monopole flux limit from the combined data of all detectors is below 3×10^{-13} cm^{-2} sr^{-1} s^{-1} (90% confidence limit). Each of the third-generation detectors is capable of surpassing the peak of the mass-dependent Parker bound in 3 years of operation, or convincingly discovering magnetic monopoles in cosmic rays. If magnetic monopoles exist in cosmic rays, they are rare and very large detectors are required to observe them.

Conventional detectors. These measure the weak ionization of matter expected along the trajectory of a magnetic charge. Particle detectors such as scintillators, which collect the fluorescent light from the ionization, and proportional counters, which collect the electrons produced by the ionization, can be used. The signature of a monopole in these conventional detectors would be that of a massive particle moving a thousand times slower than the speed of light. Such a signature would not directly measure a magnetic charge, but the detection of any massive ionizing particle, whether electrically or magnetically charged, would be highly significant. The primary advantage of conventional detectors over superconducting ones is that sensing areas roughly 10 times larger can be instrumented for the same costs. In addition, the conventional detectors are also sensitive to known particles such as cosmic-ray neutrinos, allowing other experiments to be run simultaneously. *See* IONIZATION CHAMBER; PARTICLE DETECTOR; SCINTILLATION COUNTER.

Blas Cabrera

Bibliography. A. S. Goldhaber and W. P. Trower (eds.), *Magnetic Monopoles: Selected Reprints*, 1990; P. A. Horvathy, *Introduction to Monopoles*, 1988.

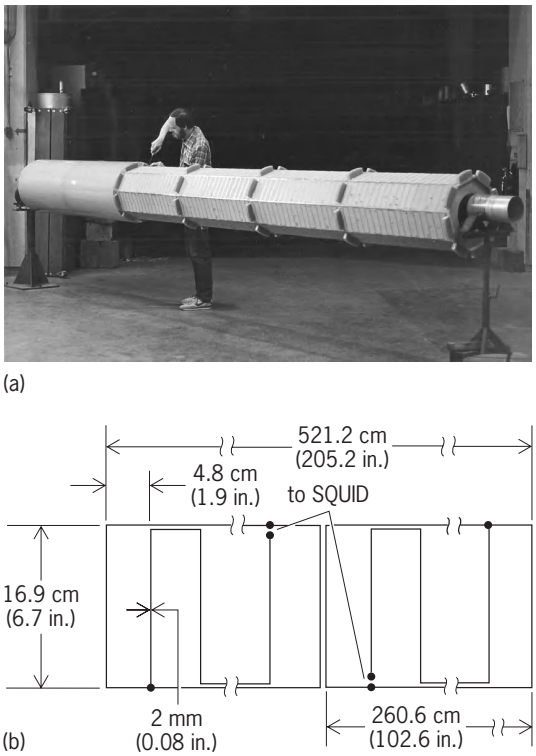

Fig. 3. Eight-SQUID 1.5-m^2 (16-ft^2) octagonal detector in operation at Stanford University. (*a*) Detector being adjusted. (*b*) Schematic diagram of detector.

Magnetic reception (biology)

Sensitivity to magnetic stimuli. For more than a century, biologists have speculated whether any living organism can detect magnetic stimuli, especially the very weak ones occurring naturally in the environment (the intensity of the Earth's magnetic field, the geomagnetic field, is roughly 0.5 gauss). A great variety of biological effects resulting from exposure to fields many thousands of times more intense than Earth's have been reported. Among these are changes in plant growth rates, retardation of embryo development, changes in enzyme activity, alterations of tumor growth, and other indications of stress. While the evidence for some of the reported

effects is not very convincing, it does seem likely that, under certain conditions, such intense fields can indeed produce stress effects in living tissues similar to the effects of factors such as extremes of heat, cold, or starvation. This article is primarily concerned with sensory detection, not with stress effects, and focuses primarily on fields of geomagnetic intensities.

Invertebrates. Most of the evidence for magnetic detection comes from experiments performed during the 1960s and 1970s. During the first half of this period most of the experiments were performed by F. A. Brown and colleagues, who reported turning or orientational responses to weak magnetic fields in a variety of invertebrates, including protozoa, flatworms, and snails.

In the late 1960s and early 1970s a number of other laboratories began to find evidence of responses to weak magnetic fields. Attracting special attention were experiments on insects and on birds (and later, on fish and on bacteria). In 1968 Martin Lindauer and Herman Martin first published extensive data showing that the geomagnetic field influences the orientation of the waggle-run dance by which a scout honeybee communicates the distance and direction of a food source to the forager bees. Later, Lindauer and Martin showed that honeybees are so sensitive to magnetic stimuli that fluctuations of less than 10^{-4} gauss (roughly 1/10,000 of the Earth's field) can influence their behavior. Other investigators found evidence of magnetic detection in other kinds of insects, including termites, beetles, and fruit flies (*Drosophila*).

Birds. Most of the evidence for magnetic detection by birds has come from studies of their migratory and homing behavior. Experiments on birds exhibiting oriented migratory restlessness in circular test cages and experiments on the initial orientation of homing pigeons have yielded results strongly suggesting that birds possess a magnetic compass, that is, they can determine compass bearings from the geomagnetic field. Evidence indicates that birds' sensitivity to magnetic stimuli is roughly similar to the honeybees'; they too can probably detect fluctuations of less than 10^{-4} gauss. It appears that the tiny fluctuations in the Earth's magnetic field caused by solar flares and other solar disturbances have a detectable effect on birds' navigation.

Although behavioral effects of magnetic stimuli have been found in many kinds of animals, no one has yet succeeded in conditioning an animal to a magnetic stimulus in the laboratory. There is abundant evidence that the detection process is not quick, usually taking 15 min or more; hence, the flash stimuli presented in most classical conditioning attempts may be undetectable.

It appears that birds do not read the magnetic compass from its horizontal component the way people do. Rather, they probably rely on the angle between gravity and the magnetic total vector (which points north and down in the Northern Hemisphere); for a bird in the Northern Hemisphere, north is apparently that direction in which the gravity and magnetic vectors form the most acute angle. Only the magnetic vector itself, not its polarity, is important. Moreover, the detection system probably has a narrow range of sensitivity; magnetic fields much stronger or weaker than the Earth's probably cannot be detected. *See* MIGRATORY BEHAVIOR.

Mechanisms. The physical mechanism for magnetic detection by living organisms is unknown, though a variety of possibilities have been put forward, such as an induced electromotive force (emf) as a result of motion through the magnetic field; deflection of moving charges by means of the Hall effect; distortions of molecular bond angles; nuclear magnetic resonance effects; direct deflection of ferromagnetic particles; and many others. But the evidence is still so scanty that any choice between them is more theoretical than empirical. What does seem very likely, in view of the sensitivity of detection already demonstrated, which is at a level where thermal noise becomes a major problem, is that the process must involve extensive integration across sites or across time, or both.

William T. Keeton

Bibliography. M. F. Barnothy (ed.), *Biological Effects of Magnetic Fields*, 1964, vol. 2, 1969; W. T. Keeton, Magnets interfere with pigeon homing, *Proc. Nat. Acad. Sci.*, 68:102–106, 1971; C. Walcott and R. P. Green, Orientation of homing pigeons altered by a change in the direction of an applied magnetic field, *Science*, 184:180–182, 1974; W. Wiltschko, in *Orientation and Navigation: Birds, Humans, and Other Animals*, Paper No. 12, 1993; W. Wiltschko and R. Wiltschko, Magnetic compass of European robins, *Science*, 176:62–64, 1972.

Magnetic recording

The technique of storing information as a magnetic pattern on a moving magnetic medium. The medium may be a disk, either flexible (floppy) or rigid, or a tape. There are various techniques for "writing" the patterns, including the use of the magnetic field generated by an electric current in a miniature coil, or the use of a laser beam to heat the material. There are several techniques for "reading" the pattern, such as measuring the voltage induced in the same or different coil by the magnetic fields associated with the pattern, measuring the change in the resistance of a metal stripe due to this field, or measuring the polarization of a laser beam upon reflection from the medium.

This combination of formats and techniques has given rise to a variety of products with applications ranging from audio recorders to large optical data files.

Magnetic medium. All materials respond in some way to an applied magnetic field, but the term "magnetic material" generally means one that maintains a magnetic polarization in the absence of an applied field. This remanence depends upon the magnetic field history to which the material was exposed. This history can be plotted on a graph of magnetization

versus magnetic field, giving rise to hysteresis loops (**Fig. 1**). If the material is initially completely demagnetized (A in Fig. 1, sometimes referred to as the ac erase state), and the applied field is increased to some intermediate value and then reversed, a minor loop (BCDEB) is obtained. At zero magnetic field there is a remanence. If the field is increased to the point that further increases in the field result in no further increases in magnetization, the material is said to be saturated. The remanence, at zero magnetic field, is a function of the maximum magnetic field to which the material has been exposed (Fig. 1). Also, it takes a finite field in the reverse direction to drive the magnetization to zero. This field is called the coercivity of the material, and is an important parameter in magnetic recording. *See* MAGNETIC MATERIALS; MAGNETIZATION.

Audio recording. The hysteretic behavior of magnetic materials, and in particular, the field dependence of the remanence (Fig. 1), is the basis for recording sound. The basic idea is to use the electric current from a microphone to generate a magnetic field (Ampère's law) that magnetizes portions of a magnetic medium (originally, segments of a steel wire) in proportion to this current. The resulting magnetic pattern along the medium can then be read back as a voltage induced in a pick-up coil (Faraday's induction law) as the fringing fields from the magnetic medium pass by. *See* AMPÈRE'S LAW; FARADAY'S LAW OF INDUCTION.

The writing field associated with a coil can be enhanced by filling the coil with a magnetic material. The reason is that the magnetic flux density generated by an electric current is proportional to the current through a constant of proportionality called the permeability. In free space, this quantity is usually denoted by μ_0. The permeability of a magnetic material, μ, however, is much larger. For example, the nickel-iron alloy permalloy has a relative permeability, μ/μ_0, of the order of 10,000. Therefore, the magnetic flux density inside a permalloy core would be 10,000 times that of an air core.

A high-permeability core also serves to confine the flux density. The field in a very narrow gap in the magnetic material can therefore be relatively large. Thus, recording generally employs an electromagnet with a narrow gap (**Fig. 2**). The writing and reading element is referred to as the head.

The relationship between the remanence and the field is very nonlinear (Fig. 1), which led to a good deal of distortion in early recorders. However, if an alternating current (ac) is added to the signal current, the resulting remanence, called the anhysteretic remanence, becomes linear at low fields. The amplitude of this bias must be sufficient to produce a field greater than the coercivity, and the bias frequency must be higher than the highest signal frequency. This ac-biasing technique, which makes magnetic recording practical, was discovered in 1927 but was not widely applied to recording until the 1940s. The first magnetic tape, also introduced in 1927, consisted of paper coated with a magnetic powder. *See* SOUND RECORDING.

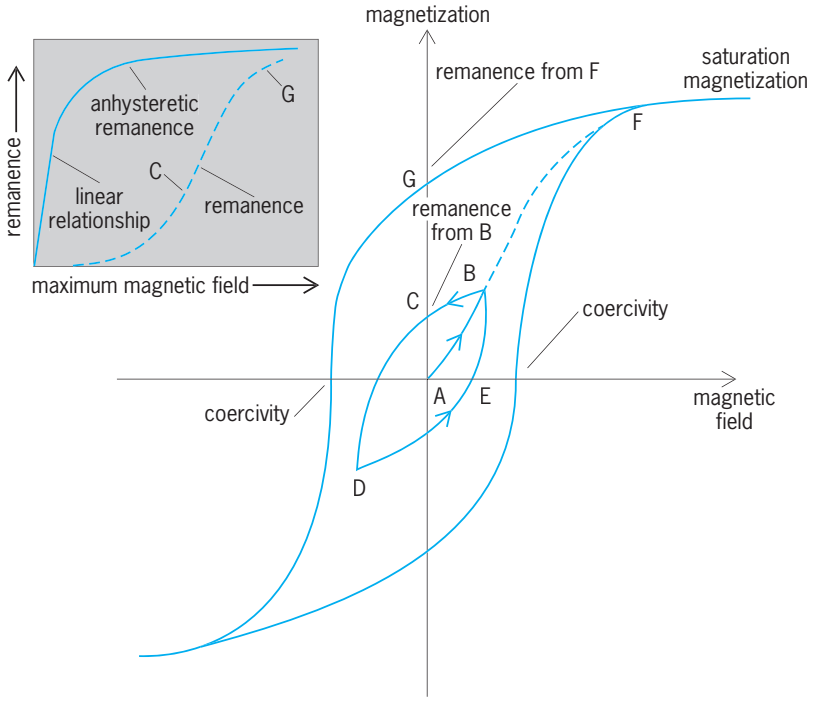

Fig. 1. Typical magnetization curves. At A, material is completely demagnetized. If the magnetic field is increased to B and then reversed, the minor loop BCDE is obtained. The inset shows remanence as a function of maximum field; points C and G correspond to the hysteresis loops shown.

Video and data recording. To extend magnetic recording to video recording with signals as high as 5 MHz requires increasing the speed between the tape and the recording head. Video recording is based on an approach in which a number of heads are mounted on the face of a drum that rotates rapidly in a direction transverse to the direction of the tape motion. The first commercial broadcast product, a video tape recorder (VTR), introduced in 1956, used a rotating drum mounted with four heads; this became known as the quadruplex head. *See* TELEVISION.

In order to reduce flicker, television systems interlace two scans down the screen. Each scan is called a field. To record one field continuously on a tape, the video track is recorded diagonally. This is accomplished by a helical-scan approach, in which the tape is wrapped around the rotating-head drum in a helical path.

In order to adapt this commercial technology for home recording (that is, video cassette recorders or VCRs), it is necessary to provide a longer playing time, and this requires a better utilization of the tape area. This is accomplished by azimuthal recording, in which two heads are used whose gaps are inclined at different angles to the direction of the track. This gives a herringbone recording pattern with very low crosstalk between the two tracks, and eliminates the need for guard bands between them.

Magnetic recording was applied to the storage of data in the early 1950s. Data generally means information represented in a digital form, that is, a sequence of 0's and 1's. In the first tape system for data storage, the data were recorded longitudinally along seven tracks. In a disk system, data are stored along

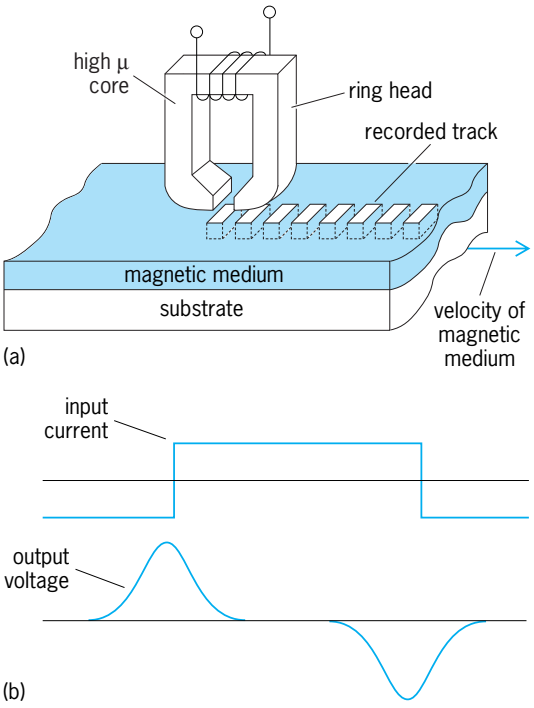

Fig. 2. Writing and reading process. (*a*) Motion of the magnetic medium past the electromagnet in the form of a ring head. (*b*) Variation with time of input current and output voltage.

concentric tracks. The figure of merit is the areal bit density, which is the product of the linear density along a track and the track density. *See* COMPUTER STORAGE TECHNOLOGY.

Digital recording. The three basic types of signals for magnetic recording are audio, video, and digital (**Fig. 3**). The audio signal contains a high-frequency ac bias, and the video signal is frequency-modulated. In the video and digital cases the maximum current is sufficient to produce a field that takes the medium to saturation magnetization (Fig. 1). The video signal is analog in that the location of the zero-crossings is continuous. In the digital signal the zero-crossings occur, or do not occur, in synchronization with a clock signal. *See* FREQUENCY MODULATION.

If an analog signal is sampled at short time intervals and the measured amplitude expressed digitally, it is possible to take advantage of digital processing techniques to eliminate many of the sources of degradation of the analog signal. This is the reason for the widespread use of compact-disk read-only memories (CD-ROMs) and digital audio tapes (DATs). Professional video recorders have also made the transition to a digital format. Consumer digital VCRs are technically feasible. The remainder of this article discusses digital systems. *See* ANALOG-TO-DIGITAL CONVERTER; COMPACT DISK.

The digital input signal, consisting of 1's and 0's, must be represented in the magnetic medium. A straightforward method would be to associate a 1 with one direction of the magnetization and a 0 with the opposite direction. This is referred to as non-return-to-zero (NRZ) recording. A major disadvantage of this approach is that if there is an error in one bit it will propagate indefinitely. Also, large strings of 1's or 0's require very accurate clocking to assure that a bit is not lost. The approach that is now commonly used is to associate a 1 with a transition, and a 0 with the absence of a transition. To avoid the clocking problem, the incoming data are precoded such that after a certain number of 0's, denoted by k, a 1 is inserted into the data stream. Likewise, a string of 1's is not desirable since the associated transitions interfere with one another. Therefore, some number of 0's, denoted d, is inserted between consecutive 1's. The result is that n bits of coded data are used to represent m bits of original data. The ratio m/n is called the code rate, and the code is indicated by m/n (d,k). For finite k, the code is said to be run-length-limited (RLL). Thus, the fundamental physical object in magnetic recording is the magnetic transition.

Writing. When current passes through the coil (Fig. 2), a magnetic field is created in the vicinity of the gap. In magnetic recording systems the magnetization of the medium lies in the plane of the medium. Therefore, this writing is carried out by the longitudinal component of the magnetic field. The contours of constant longitudinal field ($H_{\parallel}$) form nested circles.

The region of the medium that experiences fields exceeding the coercivity (H_c) will be reoriented in the direction of the field. As the medium passes under the head, this reversed region grows out behind the trailing edge of the head. The coercivity

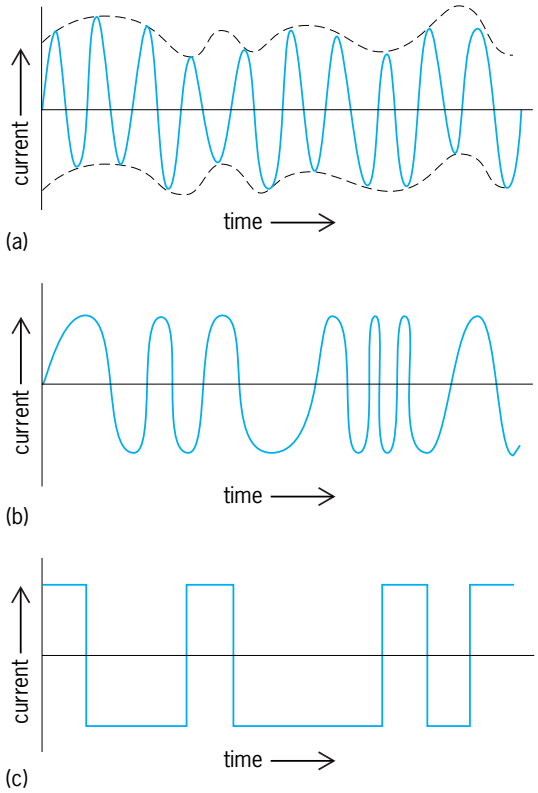

Fig. 3. Three types of input current signals. (*a*) Analog signal (audio with ac bias). (*b*) Frequency-modulated (FM) video signal. (*c*) Digital signal.

cannot be too high or the head will not be able to switch the medium.

Head materials are also characterized by a hysteresis loop (Fig. 1), but for a head material a small remanance is desirable (so the head does not write when the signal current is zero), as well as a large saturation magnetization. Once the core saturates, a larger signal current has little effect on the field produced. Thus, the maximum head field is of the order of half the saturation magnetization of the head material. Earlier heads were commonly of the form called ring heads (Fig. 2), where the electromagnet was machined out of a ceramic made from a class of magnetic oxides known as ferrites. Today the electromagnet is fabricated as a thin-film coil using photolithographic techniques (**Fig. 4**). *See* FERRITE.

Since heads saturate at the pole tips where the field is strongest, one way of extending the maximum field of a ring head is to line the gap with a material having a higher saturation magnetization. This is usually a metallic material, and thus the head is called a metal-in-gap (MIG) head.

Even though the current in the head can be switched virtually instantaneously, the resulting transition in the magnetic medium is not correspondingly sharp. The reason is that like magnetic poles repel. As a result, the transition spreads out over a distance, a, that depends upon the characteristics of this hysteresis loop (Fig. 1), the saturation magnetization, M_s, and the coercivity, H_c, as given by the equation below. Here δ is the thickness of the medium.

$$a = \frac{M_s \delta}{4\pi H_c}$$

The parameter a is important because it determines how closely transitions can be placed and therefore limits the recording density.

Media. The equation for a defines the strategy for achieving higher recording densities. To reduce a, thinner media with higher coercivity are needed. Reducing the saturation magnetization also reduces the readout, so this is not an option. In fact, a larger magnetization is generally desired to give a larger signal.

Particulate media. Early tapes and disks utilized particulate media in which the magnetic ingredient consisted of microscopic particles of a magnetic oxide. These particles were immersed in a polymeric binder that served to separate the particles from one another and bind them to the substrate. The particles first used were the gamma form of iron oxide. These particles are needle-shaped, with a length-to-width ratio of 5-to-1 and a length less than 1 micrometer, and have a coercivity of the order of 200 oersteds (16 kA/m). If the particles are randomly oriented in the tape, the coercivity of the tape is half that of an individual particle. To recover this factor of 2, the particles are physically oriented by exposing them to a magnetic field during the coating process. The search for higher coercivity led to the discovery that impregnating the surfaces of iron oxide particles with cobalt gave coercivities in the range 550–750 Oe (44–60 kA/m). These cobalt-modified particles are widely used in high-performance audio and video tapes.

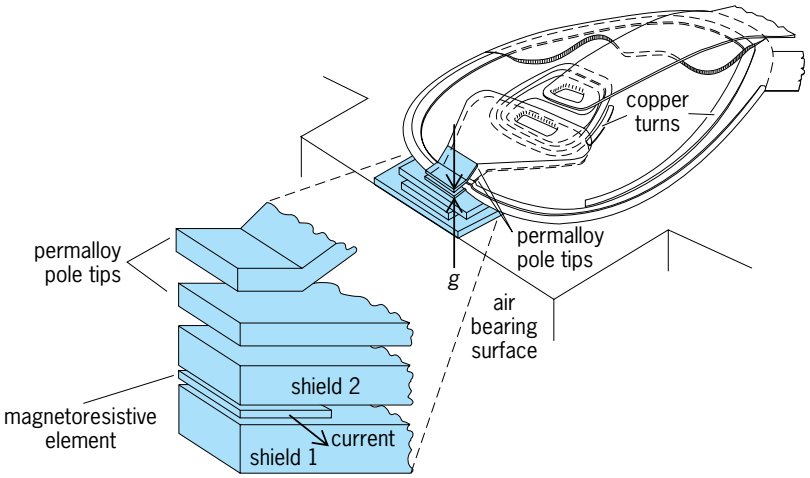

Fig. 4. Thin-film head, showing incorporation of a magnetoresistive read element. Copper turns are a two-dimensional version of the coil in a conventional head. (Not shown are the leads attached to the magnetoresistive element.)

Higher levels of magnetization and coercivity can be obtained in particles made of the ferromagnetic elements, iron and cobalt, and their alloys than is possible with oxide particles. Offsetting these advantages are some serious disadvantages. Metal particles tend to corrode in the atmosphere and to react with binders and so must be passivated at some cost in saturation magnetization. The particles are also difficult to disperse and are much more expensive than particles of iron oxide. Metal particles having coercivities in the range 700–1150 Oe (56–92 kA/m) are used in premium audio tapes, and particles with coercivities of 1350–1550 Oe (107–123 kA/m) are used in 8-mm video tapes.

Metallic films. These are used on magnetic disks to reduce the thickness of the magnetic medium and retain a large magnetization. Among the magnetic elements (iron, cobalt, and nickel), cobalt has a hexagonal crystalline structure that leads to a large coercivity. Therefore, many metallic media consist of cobalt with additional elements to stabilize the hexagonal phase, and also, for longitudinal recording, to ensure that the hexagonal axis lies in the plane of the film. Cobalt-rhenium (Co-Re) is an example. The addition of 10% rhenium stabilizes the hexagonal phase. Another widely used alloy is cobalt-chromium-tantalum (CoCrTa). In many ways, metallic films resemble particulate media. They consist of grains typically 30 nanometers in size. The magnetic properties are strongly dependent upon the size of these grains and the strength of the magnetic coupling between them.

Two techniques are used to deposit magnetic films, sputtering and electron-beam evaporation. Sputtering is primarily used for disks. In this process, the material to be deposited, identified as the target, is placed in a vacuum chamber opposite the disk substrate to be coated. The chamber is filled with argon gas, and a voltage is applied between the target and anode. This forms a plasma of argon ions.

These ions strike the target, knocking out atoms that travel through the plasma and deposit on the substrate. This technique is particularly well suited for the deposition of alloys. *See* SPUTTERING.

A magnetic recording disk actually consists of many layers. The aluminum substrate is first coated with a nickel-phosphorus sublayer to provide hardness. Then a 100-nm chromium underlayer is deposited in order to provide the proper crystallographic texture for the 30-nm magnetic layer, which is deposited next. A 25-nm carbon overcoat is then added for protection.

Because sputtering is a relatively high energy process, this technique does not work well for organic substrates such as the polyethyleneterephthalate (PET) used in most tapes. Therefore, the cobalt-nickel (Co-Ni) films on 8-mm tape, for example, are obtained by electron-beam evaporation of the alloy. The geometry is such that the metal vapor strikes the tape at an oblique angle. As a result, the crystallites making up the film grow as columns at an angle to the film surface. The angle of incidence and the amount of oxygen present during deposition govern the magnetic properties of the tape.

Inductive readout. According to a basic law of physics, any spatial change in the magnetization becomes a source of magnetic fields. Thus, each transition in the medium produces a fountain of magnetic field lines emanating from the surface of the medium. One way of detecting these fields is to use the same transducer that is used to write these data, but in an open-circuit configuration. As the transition sweeps under the head, this magnetic field is attracted into the core because of its large permeability. As the field lines thread through the coils at the back of the head, they induce a voltage in accordance with Faraday's law of induction. *See* MAGNETISM.

As a function of time, this voltage appears as a bell-shaped pulse (Fig. 2). The height of this pulse is proportional, among other factors, to the relative velocity between the head and the medium, the track width, and the number of turns of the coil. The width of this pulse, at half its maximum, depends upon the various geometrical parameters such as the gap between the pole tips, the magnetic spacing between the head and the surface of the magnetic medium, the transition length, and the thickness of the medium.

The linear recording density along a track is limited by the width of this pulse. The interdependence of these geometrical parameters means that to achieve higher densities all these dimensions must be reduced together. Rigid-disk systems use media with a thickness of 30 nm and heads with a gap of 0.2 μm. The magnetic spacing is of the order of 20 nm.

In the early 1980s, most heads consisted of ferrite cores with coils that were hand-wound. In 1989 a thin-film version of an inductive head was introduced. This thin-film structure is deposited on the trailing edge of a slider that is mounted at the end of a swing arm. This slider is designed to create an air bearing between the air-bearing surface (Fig. 4) and the surface of the recording medium. One of the attractive features of a thin-film head is that its pole material, permalloy, has a higher saturation magnetization than ferrite, and therefore can write on higher-coercivity media, which translates to sharper transitions and higher densities.

Magnetoresistive readout. The thin-film head was later modified by the addition of a strip of magnetoresistive material. Magnetoresistance is the phenomenon in which the resistance of a material depends upon the direction in which the current flows relative to the direction of the magnetization. If, in zero magnetic field, the magnetization makes some angle with respect to the current, then in the presence of the field from the media the magnetization will, in general, be tipped away from this direction, producing a change in the resistance (Fig. 4). The magnetoresistive strip is bounded by two layers of soft magnetic material which, like the pole tips themselves, draw in magnetic flux. This has the effect of shielding the magnetoresistive strip so that it senses a magnetic transition only when the transition is directly under the strip; that is, the shields enhance the resolution of the magnetoresistive element. The magnetoresistive effect provides higher sensitivity than inductive readout, and therefore quickly became the preferred readout approach for high-density drives. The separation of the writing and reading functions also means that each can be optimized independently.

In 1988 it was discovered that the resistance of a sandwich of two magnetic films separated by a thin (1-nm) copper layer is dramatically different depending upon the relative orientation of the magnetization in the two films. Thus, if the magnetization in one of the films is pinned while that of the other is free to be oriented by the magnetic field from a transition, the resistance of the sandwich may change by as much as 10% in a field as small as 10 Oe (0.8 kA/m). This giant magnetoresistance (GMR) effect can provide heads with much greater sensitivity than single-strip magnetoresistive heads. *See* MAGNETORESISTANCE.

Recording systems. The major applications for magnetic recording are audio, video, and data storage. A widely used audio system was the compact cassette. This has been largely replaced by the digital compact disk. Digital audio type systems are another viable technology, for example, the rotary digital audio tape (R-DAT) system.

R-DAT. This system uses the helical scan technology developed for video systems (**Fig. 5**). The rotating drum contains two MIG heads. The tape is a metal-particle medium, 0.16 in. (4 mm) wide. R-DAT uses an 8/10 code, which suppresses the low-frequency crosstalk that survives the azimuthal recording.

In the write mode, R-DAT uses a 48 kilosample-per-second sampling rate with a 16-bit analog-to-digital conversion. This leads to a digital signal at 61,000 bits/in. (2400 bits/mm). With the 8/10 code, this means 76,000 magnetic flux transitions per inch (3000 per millimeter). The cassette has dimensions

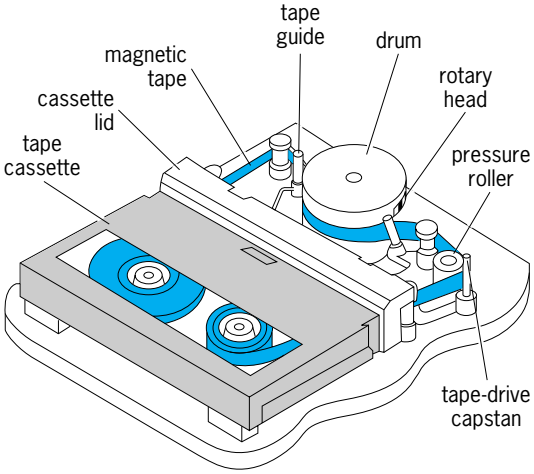

Fig. 5. R-DAT recorder. (*After J. Watkinson, An Introduction to Digital Audio, Focal Press, Butterworth-Heinemann Ltd., 1994*)

of 2.9 × 2.1 × 0.4 in. (74 × 53 × 10 mm) and a volume storage density of 2×10^{11} bits/in.^{3} (1.2×10^7 bits/mm^3). Because of this very high packaging density, this technology is used for data storage in the form of disk backup. Cassettes holding 12 gigabytes are available.

Home video recorders have long been based on a 0.5-in.-wide (13-mm) tape cartridge format. Improvements in heads and media over the years contributed to better picture quality, and in 1984 an 8-mm (0.3-in.) video technology was introduced. The Hi-Band 8-mm VCR uses MIG ferrite heads with metal-evaporated media. Being incompatible with the 0.5-in. format, this technology found success in video camcorders. As with the R-DAT technology, the 8-mm technology was also adapted for digital data storage backup. Cartridges capable of holding 20 gigabytes of data are available.

Rigid-disk drives. Tape systems are inherently sequential and therefore appropriate for audio and video applications. For data applications, however, it is necessary to access data from any location in the file. For this purpose, a disk format is preferable (**Fig. 6**). Data are recorded on concentric tracks on the surfaces of the disks. The heads are mounted at the end of arms that are positioned over the disks by an electromagnetic actuator. Since rapid access to data is important, the disks rotate at high speeds, up to 10,000 revolutions per minute in some drives. In order to reduce wear and prevent contamination, the heads ride above the surface of the disk on a cushion of air, or air bearing; flying heights are of the order of 10 nm. Heights less than this require ultrasmooth surfaces. The typical roughness on a nickel-phosphorus/aluminum (NiP/Al) disk might be 25 nm, while ultrasmooth surfaces require roughnesses less than 0.5 nm. The requirement for extreme cleanliness means the head-disk assembly must be enclosed in its own clean environment. Thus, the disks in high-performance rigid-disk systems are not removable, unlike the diskettes in lower-performance flexible-disk drives.

Track widths are of the order of 3 or 4 μm. To follow such narrow tracks, one approach has been to dedicate one of the surfaces in the stack of disks (Fig. 6) to positional information which is fed back to the actuator. It is then assumed that the other heads on the actuator will be aligned with this servo head. However, as track widths decrease, uneven thermal expansion of the actuator comb can lead to track misregistration. One solution is to dedicate certain sectors on each disk to positional information, thereby embedding the servo information within the data itself.

Various technologies have increased the areal density of rigid-disk systems a millionfold since the first disk system in 1954. This increased areal density has meant that larger capacities can be achieved with smaller disk sizes. The dominant disk size is 3.5 in. (90 mm). One 3.5-in. system, for example, stores 36.7 gigabytes on 6 disks and uses magnetoresistive heads and thin-film media to achieve an areal density of 6 gigabits/in.^{2} (9.3 megabits/mm^2).

At sufficiently low recording densities, the precoding leads to separated output pulses (Fig. 2) that may be detected by looking for peaks in the signal. Most high-performance disk systems use a 1/2 (2,7) or 2/3 (1,7) code. However, the system discussed above has a bit density of 344,000 bits per inch (13,150 bits per millimeter), and at this density the output pulses overlap, resulting in intersymbol interference. The addition of noise further complicates the output signal. To recover the data from such a signal, techniques that were originally developed for communication channels have been adopted.

Magnetic recording channel. The magnetic recording channel behaves almost like an ideal channel studied in signal processing called a class IV partial response (PR4) channel. The advantage of this behavior is that if the isolated pulse shape of a PR4 channel is sampled at time intervals equal to the channel bit period T, all values are zero except those at $t = 0$, the time when the transition was written, and $t = T$. These two nonzero values are equal and assigned the value 1. Thus, the samples of an isolated pulse are $- - - 0\ 0\ 1\ 1\ 0\ 0\ 0 - - -$. If an opposite transition is written at time $t = T$, the linear superposition of the two transitions (called a dibit) gives the samples $- - - 0\ 0\ 1\ 0 {-} 1\ 0\ 0\ 0 - - -$. The samples of an arbitrary stream of data will consist of 1's, 0's, and −1's.

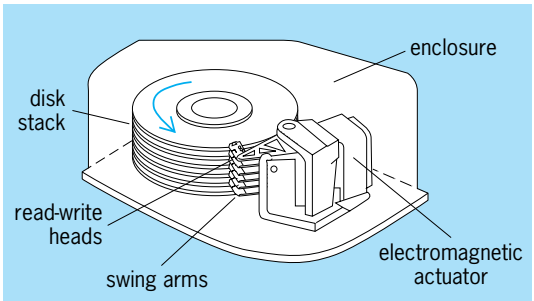

Fig. 6. Rigid-disk drive. (*After C. D. Mee and E. D. Daniel, eds., Magnetic Recording Handbook: Technology and Applications, McGraw-Hill, 1990*)

Since the magnetic recording channel is not an ideal PR4 channel, and since there is obviously noise present, there will be some uncertainty. Rather than trying to decide whether one sample is a 1, 0, or −1, a sequence of samples is examined and the sequence with the maximum likelihood is determined. For example, the sequence − − − 1 1 1 − − − cannot exist since transitions must alternate. The algorithm used to establish the most likely sequence was developed by Andrew Viterbi, and is implemented as a Viterbi detector. The use of such a partial-response maximum-likelihood (PRML) technique provides a 1.5-dB signal-to-noise gain over peak detection. *See* ELECTRICAL NOISE; SIGNAL-TO-NOISE RATIO.

Limits to recording density. Magnetic recording has been a remarkably resilient technology, and hard-disk areal densities have increased over a million times since the first product. The nature of the ultimate limits to recording density has occupied engineers since the technology was introduced. Today, the major challenge is thought to arise from thermal effects. Thin-film media are composed of crystalline grains. As the recording density increases, the number of grains contributing to a bit must at least stay the same in order to maintain a given signal-to-noise ratio. This entails the preparation of media with smaller grains. However, as the grains become smaller, they eventually reach a size where their magnetic properties decrease with time due to thermal fluctuations. Such fluctuating magnetic particles are said to be superparamagnetic. The result is that the data decay with time, a very undesirable situation. Various approaches have been proposed to stabilize media at high densities. One is to place the recording medium on top of an antiferromagnetic underlayer, which serves to increase the volume of the bit cell. Another approach is to record perpendicular to the plane of the media, which also allows somewhat thicker media. It is believed that these approaches may extend the superparamagnetic limit well beyond 100 gigabits/in.^{2} (150 megabits/mm^2).

Perpendicular recording. As discussed above, the transition length arises from the demagnetizing fields associated with the opposing magnetic alignments. If, however, the alternating magnetic regions are perpendicular to the plane of the medium, the north and south poles of these regions occur next to one another. Since this is a favorable situation, the transition length in this case actually becomes smaller with increasing recording density. This was the basis for early interest in perpendicular recording. However, a small transition length by itself is not advantageous. A small gap, thin media, and a small head-to-medium spacing are also necessary. While the fringing field from a ring head (Fig. 2) has a vertical component that can be used to write on perpendicular media, it is more efficient to use a pole head in connection with a magnetically soft (that is, low-coercivity) underlayer.

Optical storage. Optical storage encompasses read-only optical systems such as the CD-ROM, write-once systems, and erasable optical systems. In the CD-ROM systems, the data are impressed on a disk by a stamping process and read out by means of a solid-state laser. This medium is widely used for distributing system documentation and software. In write-once systems the user is provided with a medium whose state may be irreversibly changed by the application of local heating by a focused laser beam. This change may be from an amorphous to a crystalline state, or it may involve actual deformation of the material by local melting. The medium is typically an alloy of tellurium. Once created, the data may be read many times by a lower-power laser.

Phase-change recording. The tellurium-based materials used for write-once read-many-time (WORM) systems may also be modified for erasable applications. As an alloy such as germanium-antimony-tellurium (Ge-Sb-Te) of suitable composition is rapidly cooled from above its melting point, it solidifies into a glassy, or amorphous, state in which the atoms are randomly arranged. If this amorphous material is heated, it crystallizes before it melts. Thus, by controlling the power level and the pulse length of a laser beam, it is possible to reversibly alter the state of such materials. The reflectivities of these two states are generally quite different. Therefore, the readback signal is much larger than that obtained, for example, in a magnetooptic system. The challenge is to find materials that can be crystallized quickly with a laser but are thermally stable at room temperature.

Magnetooptic effect. Another widely used technology for erasable optical storage is based on the magnetooptic effect. Since light consists of oscillating electric and magnetic fields, when light passes through a magnetic material it undergoes change. One of the features of light that is affected is polarization. When a laser beam is emitted from a solid-state laser, its electric field oscillations lie in a plane governed by the geometry of the laser, and the beam is said to be linearly polarized. When such a beam passes through a magnetic material in which the direction of the magnetization is parallel (or antiparallel) to the beam, the plane of the polarization of the light is rotated clockwise (or counterclockwise). This magnetooptic effect is called the Faraday effect. A similar change that occurs when light is reflected from the surface of a metallic magnetic material (**Fig. 7**) is the magnetoopic Kerr effect. For typical materials, this rotation is of the order of 1°. *See* FARADAY EFFECT; MAGNETOOPTICS.

Perpendicular magnetization. To utilize this magnetoopic effect on a storage system requires a medium with a perpendicular magnetization. Amorphous films containing the rare-earth elements, such as gadolinium and terbium, together with the transition-metal elements iron, cobalt, and nickel, can be prepared with a perpendicular magnetic orientation. Furthermore, the coercivities of these materials are very temperature dependent. These properties are the basis for the use of these materials in optical storage.

A composition is found for which the coercivity at room temperature is very high but decreases with increasing temperature. Typical materials are terbium-iron-cobalt (TbFeCo) and gadolinium-terbium-iron

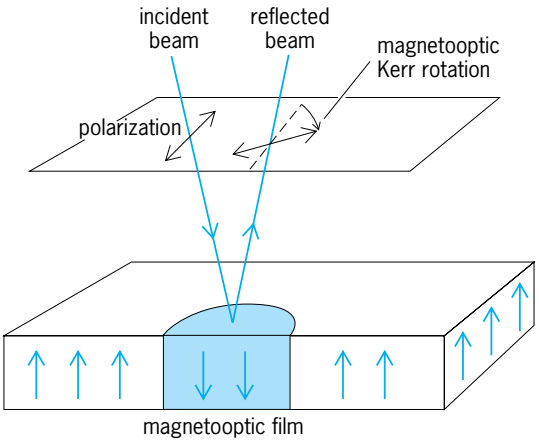

Fig. 7. Cross section of a magnetooptic film showing rotation of polarized light upon reflection.

(GdTbFe). If the material is heated with a laser beam in the presence of a magnetic field, then as the coercivity decreases, the heated region within the laser spot will align with the applied field. When the heating is removed, the coercivity again increases, freezing in the cylindrical domain. Assuming that the disk was initially all polarized, say, "down," an "up" region would be identified as a 1, in analogy with the magnetic transition on a rigid disk. Magnetooptic systems therefore also precode the signals with a run-length-limited code such as the (2,7) code.

Areal densities. Since the power in the laser beam has a bell-shaped profile, the size of the recorded spot will depend on the corresponding temperature profile in the medium and can therefore be made arbitrarily small. However, the detection of spots is limited by the diffraction that takes place during readout. Assuming that the diffraction spots just touch, their separation becomes the limiting diameter of a bit cell. Since current solid-state lasers for recording have infrared wavelengths, spot sizes are of the order of 1 μm. This gives areal densities in the range of 540 megabits/in.^{2} (0.8 megabit/mm^2) and total capacities on a 5.25-in. (130-mm) removable cartridge of 1.3 gigabytes. Optical storage was once favored for its high areal densities, but magnetoresistive heads and thin-film media enabled conventional magnetic recording densities to surpass optical densities. However, optical densities will increase with higher-frequency lasers. Magnetooptical disks also have the attractive feature of being removable. *See* LASER.

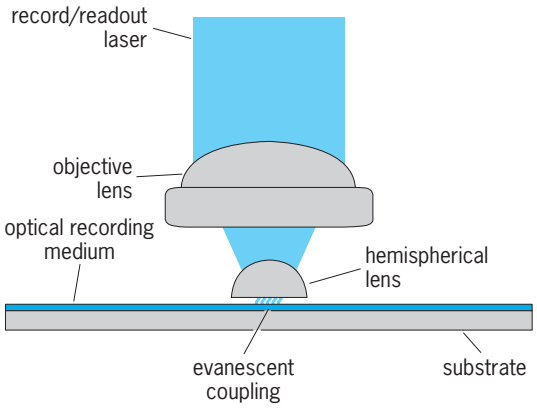

Fig. 8. Near-field optical recording system.

Biasing and direct overwrite. One of the challenges in a magnetooptic system is to generate the biasing magnetic field. Early designs used an electromagnet. However, since it is difficult to switch such a magnet at recording data rates, these systems required two revolutions to rewrite data, a distinct disadvantage. Of course, it is possible to use a conventional recording head flying close to the disk, but this compromises the advantage of optical systems, which is their beam-addressable nature, the fact that the head is a focal length away from the medium. This is what makes it possible to encapsulate the medium, so that it is removable.

Approaches to achieving direct overwrite in magnetooptic systems involve additional layers of material. For example, if a memory layer, with a relatively high coercivity that is sensitive to temperature, is placed on top of a reference layer, with a low coercivity that is relatively insensitive to temperature, then as the bilayer passes through an initializing field, the reference layer is polarized by this field. However, the data in the memory layer are unaffected. If the bilayer now moves into a region with a reverse-bias field and is simultaneously exposed to a low-power laser pulse that reduces the coercivity of the memory layer, this layer will be oriented by the strong field from the reference layer. If, however, the laser pulse has enough power to reduce the coercivities of both layers, both will be aligned by the bias field. Thus, by modulating the laser power, direct overwrite can be achieved.

Near-field recording. It is possible to improve on the diffraction limit if a very small head-to-disk spacing is acceptable. The idea is to focus the optical beam through a hemispherical lens to a point at the back (flat) face of the lens (**Fig. 8**). This arrangement reduces the diffraction limit by the index of refraction of the lens (typically a factor close to 2). The beam is "immersed" in the solid lens, which is therefore called a solid immersion lens (SIL). The disadvantage of this scheme is that in focusing a broad beam within the lens some of the light is internally reflected. It is a property of internally reflected light that the field of the light actually extends beyond the boundary; this extension is called an evanescent wave, or near-field. If the medium is placed within this near-field, it interacts with the beam and utilizes the higher resolution. *See* OPTICAL RECORDING.

Robert M. White

Bibliography. R. L. Comstock, *Introduction to Magnetism and Magnetic Recording*, Wiley, 1999; E. D. Daniel, C. D. Mee, and M. H. Clark (eds.), *Magnetic Recording: The First 100 Years*, IEEE Press, 1999; C. D. Mee and E. D. Daniel (eds.), *Magnetic Recording Technology*, 2d ed., McGraw-Hill, 1996; S. X. Wang and A. M. Taratorin, *Magnetic Information Storage Technology*, Academic Press, 1999.

Magnetic relaxation

The relaxation or approach of a magnetic system to an equilibrium or steady-state condition as the magnetic field is changed. This relaxation is not instantaneous but requires time. The characteristic times involved in magnetic relaxation are known as relaxation times.

Magnetism is associated with angular momentum called spin, because it usually arises from spin of nuclei or electrons. The spins may interact with applied magnetic fields, the so-called Zeeman energy; with electric fields, usually atomic in origin; and with one another through magnetic dipole or exchange coupling, the so-called spin-spin energy. Relaxation which changes the total energy of these interactions is called spin-lattice relaxation; that which does not is called spin-spin relaxation. (As used here, the term lattice does not refer to an ordered crystal but rather signifies degrees of freedom other than spin orientation, for example, translational motion of molecules in a liquid.) Spin-lattice relaxation is associated with the approach of the spin system to thermal equilibrium with the host material; spin-spin relaxation is associated with an internal equilibrium of the spins among themselves. *See* MAGNETISM; SPIN (QUANTUM MECHANICS).

The measurement of relaxation times is of interest in the study of molecular motions and interactions. An important practical application of magnetic relaxation is the attainment of very low temperatures. For example, a sample of a paramagnetic salt can be cooled by liquid helium to about 1 K (2°F above absolute zero, −459.67°F), then subjected to a magnetic field. Heat, evolved in the magnetization, will be dissipated into the liquid helium. If thermal contact to the helium is broken, and the magnetic field is then removed, the relaxation of the sample to more random orientation will be accompanied by a further decrease in temperature, in some cases to 0.01 K (0.02°F above absolute zero). A similar adiabatic demagnetization of copper, in this case involving nuclear spin, has cooled the sample to 0.00002 K (0.00004°F above absolute zero). *See* ADIABATIC DEMAGNETIZATION.

Relaxation process. In an unmagnetized sample (ferromagnets are excluded for the moment) the spin orientations are random. In the presence of a static magnetic field and at thermal equilibrium, an excess of the spin vectors points in the lower energy orientation along the field. The buildup of magnetization following application of the field requires that some of the spins turn from antiparallel to parallel orientations. The energy given up in this turning process may go to either or both of two reservoirs. If the applied field is weak, the spin-spin energy constitutes an effective reservoir. If the applied field is strong, the spin-spin (free) energy is negligible and magnetization requires an interchange with the lattice. At low fields the transfer of energy into the spin-spin reservoir may be thought of as corresponding to a heating of the spin system. The spin-lattice coupling will eventually bring the spins into thermal equilibrium with the lattice (by changing either the spin "temperature" or the lattice temperature, or both). Thus for low fields the process of magnetization would exhibit two stages: (1) the redistribution of energy in the spin system, or spin-spin relaxation, and (2) equilibration of the spin system with the lattice, or spin-lattice relaxation. For high fields, only spin-lattice relaxation plays a role in establishing the magnetization.

Although relaxation exhibits itself in a macroscopic manner, an explanation of the rates of relaxation requires consideration of atomic processes. Two requirements must be met for spin-lattice relaxation: (1) There must be a coupling of the spin to the lattice, and (2) the coupling must be time-dependent, its frequency spectrum containing natural frequencies of the spin system (for example, the precession frequency of the spins in the applied field).

Types of relaxation. Relaxation has been studied for nuclear magnetism, electron paramagnetism, and ferromagnetism.

Nuclear relaxation. For nuclei, the Zeeman and spin-spin interactions are always important, and in some cases, the nonspherical charge distribution (electric quadrupole moment) of a nucleus affects the relaxation time. When the quadrupolar energy may be neglected, the magnetization usually approaches thermal equilibrium exponentially after application of a strong static field, the time constant being the spin-lattice relaxation time. Nuclear relaxation is almost invariably studied by magnetic resonance; the weak nuclear paramagnetism cannot be detected by other methods. *See* MAGNETIC RESONANCE.

If bulk nuclear magnetization **M** is tilted away from the direction of the static field **H**, the **M** vector precesses about **H**. The component of **M** parallel to **H** returns to its thermal equilibrium value by means of spin-lattice relaxation. The spin-spin coupling gives a spread in precession frequencies, causing the nuclei to get out of step with one another, as manifested by the decay of the components of **M** perpendicular to **H** without energy exchange with the lattice (spin-spin relaxation).

Rapid motion of a nucleus relative to its neighbors lengthens the spin-spin relaxation. The times range from tens of microseconds, in almost all solids, to several seconds, in cases of rapid nuclear motion. Measurement of spin-spin relaxation has been extensively used to study atomic motion.

Spin-lattice relaxation arises from magnetic dipole coupling with electrons in the case of metals, paramagnetic substances, or diamagnetic insulators possessing paramagnetic impurities; with other nuclear moments when the relative nuclear positions undergo large changes due to sufficiently rapid self-diffusion or molecular rotation in liquids, gases, or even some solids; or from the nuclear electric quadrupole coupling to the electric fields of the host material. Spin-lattice relaxation times range from less than 1 ms to several hours.

Paramagnetic relaxation. Resonance methods can be used for the study of paramagnetic relaxation. However, the observation of the ability of the

magnetization to follow a changing field and even the observation of the change in the lattice temperature brought about by spin-lattice relaxation have also been used. The first interest in magnetic relaxation, in fact, stemmed from the desire to cool the lattice by adiabatic demagnetization of the spins of paramagnetic ions. Large electrostatic interactions between the ions and their surroundings make major contributions to the total spin energy, and it is rarely possible to neglect this effect. Other important contributions to the spin energy arise from dipolar coupling to applied fields, spin-spin coupling by both magnetic dipole and exchange mechanisms, and magnetic coupling to nuclei, particularly the nuclei of the paramagnetic ions.

The principal spin-lattice relaxation mechanisms involve modulation of the spin-orbit coupling by lattice motion, modulation of the magnetic coupling to nuclei by lattice motion, and coupling with paramagnetic impurity atoms. Typical spin-lattice relaxation times vary from less than 10^{-8}s at room temperature to tens of seconds at liquid helium temperature. Although the study of paramagnetic relaxation was begun in the 1930s, it is not as thoroughly understood as the more recently studied nuclear relaxation, primarily because of the complexity of the electronic energy levels of the paramagnetic ions.

Ferromagnetic relaxation. In ferromagnetic substances, strong exchange coupling between electron spins, causing them to prefer an alignment parallel to one another, and demagnetizing effects cause ferromagnetic relaxation to differ from paramagnetic relaxation.

The strong tendency of ferromagnetic spins to remain parallel makes it convenient to distinguish between two types of relaxation: (1) that in which the total magnetization changes direction but not magnitude, thereby keeping the exchange energy constant, and (2) that in which the magnitude of the magnetization changes, producing a change in the exchange and also in the demagnetizing energies. The second mechanism depends on the sample shape and may arise from irregularities in the ferromagnetic lattice (impurities and nonstochiometric composition, as in ferrites) as well as from thermal vibrations. Ferromagnetic relaxation has been studied primarily by magnetic resonance. Charles P. Slichter

Magnetic resonance

A phenomenon exhibited by the magnetic spin systems of certain atoms whereby the spin systems absorb energy at specific (resonant) frequencies when subjected to alternating magnetic fields. The magnetic fields must alternate in synchronism with natural frequencies of the magnetic system. In most cases the natural frequency is that of precession of the bulk magnetic moment **M** of constituent atoms or nuclei about some magnetic field **H**. Because the natural frequencies are highly specific as to their origin (nuclear magnetism, electron spin magnetism, and so on), the resonant method makes possible the selective study of particular features of interest. For example, it is possible to study weak nuclear magnetism unmasked by the much larger electronic paramagnetism or diamagnetism which usually accompanies it.

Nuclear magnetic resonance (that is, resonance exhibited by nuclei) reveals not only the presence of a nucleus such as hydrogen, which possesses a magnetic moment, but also its interaction with nearby nuclei. It has therefore become a most powerful method of determining molecular structure. The detection of resonance displayed by unpaired electrons, called electron paramagnetic resonance, is also an important application. These two phenomena, as well as other related resonance phenomena, are discussed in this article. *See* MAGNETISM.

Origin. Because **M** has its origin in circulating currents or intrinsic spins, there is always an angular momentum **J** associated with it. The vector quantities **M** and **J** are related by Eq. (1), where γ is called the gyromagnetic ratio.

$$\mathbf{M} = \gamma \mathbf{J} \tag{1}$$

For a system to exhibit a magnetic resonance, it must possess a magnetic moment, possess angular momentum, and experience torques. The magnetic moment may arise from nuclei of atoms, from orbital electronic motion, from electronic spins, or from moving nuclear charges during molecular rotation. The angular momentum arises from the same sources. The torques may arise from externally applied magnetic fields; from magnetic dipole fields exerted by neighboring nuclei, atoms, or molecules; from electric fields acting on, for example, a nuclear electric quadrupole moment or the nonspherical electron cloud of an atom; or from electron exchange coupling. In any given case it is necessary to decide which interactions are large and which are small. Thus, for a paramagnetic atom possessing a nuclear magnetic moment, a distinction might be made between small applied static fields, in which the coupled nucleus and electron angular momenta act as a unit, and large magnetic fields, which decouple them so that they act independently. An effective angular momentum and magnetic moment can often be defined, giving an effective γ (in analogy to the Landé g factor of optical spectroscopy).

Several types of resonances have been observed; these differ in one or more of the three basic requirements. However, the principal features can be understood by assuming that the torques arise from an effective static applied magnetic field **H**. The torque $\mathbf{M} \times \mathbf{H}$ causes the angular momentum to change with time according to Eq. (2). The resultant motion

$$\frac{d\mathbf{J}}{dt} = \mathbf{M} \times \mathbf{H} \qquad \text{or} \qquad \frac{d\mathbf{M}}{dt} = \gamma \mathbf{M} \times \mathbf{H} \tag{2}$$

of **M** is a precession at angular frequency γH about the direction of **H**. At thermal equilibrium, **M** is parallel to **H**, and no precession occurs. Application of an alternating magnetic field $H_x \cos \omega t$ perpendicular to **H** causes **M** to tilt away from **H** with a consequent absorption of energy, provided the resonant condition

$\omega = \gamma H$ is satisfied. In practice, the absorption takes place over a narrow range of frequency on both sides of γH. The magnetization M_x parallel to H_x obeys Eq. (3), where $\chi'(\omega)$ and $\chi''(\omega)$ are the real and imag-

$$M_x = H_x\chi'(\omega)\cos\omega t + H_x\chi''(\omega)\sin\omega t \qquad (3)$$

inary parts of the complex magnetic susceptibility $\chi = \chi'(\omega) - j\chi''(\omega)$ ($j = \sqrt{-1}$), and characterize dispersion and absorption respectively. For a typical resonance, $\chi''(\omega)$ attains maximum value for a region of frequencies near $\omega = \gamma H$.

For many cases, it is necessary to analyze magnetic resonance by quantum theory. Consider a system composed of many (weakly interacting) identical parts (atoms or nuclei), each with angular momentum quantum number F (total angular momentum $= \sqrt{F(F+1)}\,\hbar$, where $\hbar$ is Planck's constant h divided by 2π). The spatial quantization in the magnetic field H gives $2F + 1$ equally spaced energy levels labeled by the quantum number $M_F = (F, F-1, \ldots, -F)$ and energy spacing between adjacent levels of $\gamma\hbar H$. The field $H_x \cos \omega t$ produces transitions with the selection rule $\Delta M_F = \pm 1$. To satisfy the Bohr frequency condition, $\hbar w = \gamma\hbar H$, in agreement with the classical result, $\omega = \gamma H$.

According to quantum theory, the probability of transition from any energy level A to any other B is the same as that from B to A; thus a net absorption of energy requires that the population of the lower energy states be greater than that of the upper. The reverse situation in which the upper states are more populated leads to an induced emission and is the basis for the operation of the solid-state maser. At thermal equilibrium, as a result of spin-lattice relaxation, the lower energy states are more heavily populated in accordance with the classical Maxwell-Boltzmann statistics (ordinarily it is unnecessary to use either Fermi-Dirac or Bose-Einstein statistics). When H_x becomes sufficiently large, the level populations become disturbed from thermal equilibrium. The population difference between states joined by H_x decreases, a phenomenon known as saturation, because it causes χ' and χ'' to diminish with increasing H_x. Population differences between pairs of states other than A and B may simultaneously be increased, or even inverted, as in the three-level maser. The intensity of the alternating field necessary to produce saturation depends on the width of the absorption line and on the spin-lattice relaxation time (wider lines or shorter times require larger H_x). *See* MAGNETIC RELAXATION; MASER; NONRELATIVISTIC QUANTUM THEORY.

Observation. Experimentally it is possible to detect magnetic resonance by measuring the absorption of magnetic energy of a circuit containing the magnetic material or by measuring the change in inductance or resonant frequency of the circuit. The two methods measure $\chi''(\omega)$ or $\chi''(\omega)$, respectively. The resonant condition $\omega = \gamma H$ may be produced by varying ω, or more customarily, by changing H. In some experiments, one tilts **M** away from the direction of **H** by alternating fields of short duration and then observes voltages induced by the subsequent free precession of **M**. This method is particularly useful for studying relaxation times.

Nuclear magnetic resonance (NMR). The nuclei of many atoms possess angular momentum (spin) and nonvanishing magnetic moments. The former may be characterized by an angular momentum quantum number I (integer or half integer) of the nuclear particles. As far as is known, stable nuclei with an even number of neutrons and even number of protons have zero spin and magnetic moment, and hence are incapable of exhibiting magnetic resonance. *See* NUCLEAR MOMENTS.

Nuclear resonances have been observed in insulators, metals, paramagnetic salts, antiferromagnetic substances, and other solids, and in gases and liquids. Often, to observe NMR a sample is placed between the poles of an electromagnet (**Fig. 1**) which in addition to the main winding carries a small auxiliary winding or sweep. A coil connected to an oscillator surrounds the sample, as does a second coil at right angles to both the oscillator coil and the sweep winding, to avoid direct coupling. The oscillator frequency is fixed and the sweep circuit is used to vary the magnetic field strength continuously. When a resonance frequency of the sample is reached, a signal induced in the second coil is detected and amplified. Typical resonance frequencies in a field of 10,000 gauss lie in the radio-frequency region (1–45 MHz). For example, the H^1 nucleus shows a resonance frequency of 42.6 MHz at this field strength. ^{13}C nuclei give a much weaker signal, further decreased in a sample containing this isotope in its natural abundance of 1.1%.

Nuclei with quadrupole moments. If a nucleus has a spin $\geqq 1$, it generally has a nonvanishing electric quadrupole moment, expressing the deviation of its spatial change distribution from spherical symmetry (there are good grounds for believing that all nuclei have zero electric dipole moments). The electrical interaction between the nucleus and electric potentials $V(x,y,z)$ from other charges depends on the nuclear orientation (specified by the direction of nuclear spin) and on the spatial second derivatives of

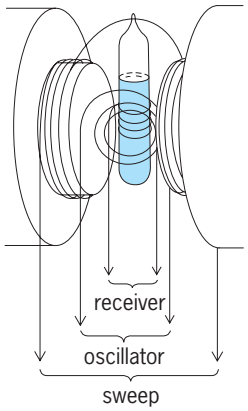

Fig. 1. Arrangement of a sample and coils in a nuclear induction apparatus. (*After J. D. Roberts, Nuclear Magnetic Resonance, McGraw-Hill, 1959*)

the potential $\partial^2 V/\partial x^2$, $\partial^2 V/\partial x\,\partial y$, and so on, at the position of the nucleus. For potentials of spherical, tetrahedral, or cubic symmetry, the interaction energy is independent of orientation and may be disregarded. When the electric quadrupole interaction is nonzero but nevertheless much weaker than the static magnetic interaction, the unique resonance condition $\omega = \gamma H$ is changed, and the resonance line splits into $2I$ components centered around γH. A convenient method of determining the nuclear spin is thereby provided.

The name "nuclear quadrupole resonance" is used when one dispenses with the static field H and observes the reorientation of the nucleus among its various quantized orientations with respect to the electric potential alone. Classically, the nonspherical nuclear charge experiences a torque which causes precession. This technique is particularly useful when the electric quadrupole coupling is large and the sample is available only in powder form. For such a sample, the NMR lines tend to be broad, owing to the distribution of the orientations of the powder granules with respect to the direction of the applied magnetic field. No such broadening arises in the absence of a magnetic field since the frequency of the nuclear quadrupole resonance does not depend on spatial orientation.

Applications. Nuclear magnetic resonance has been used widely to measure nuclear magnetic moments, electric quadrupole moments, and spins. Because the resonance lines may be on occasion very sharp (1 cycle wide at 40 MHz), nuclear resonance is frequently employed to measure magnetic fields with great precision. For an example *see* MAGNETOMETER.

The extensive use of NMR in molecular structure determinations arises from the slight shift in the resonance frequency of an atom—commonly that of a proton—due to the environment of neighboring atoms. Because the magnitude of this shift depends on the type of environment, it is called the chemical shift. **Figure 2** shows the NMR spectrum of ethyl alcohol, CH_3CH_2OH. The three main resonance frequencies are due to protons in the OH, CH_2, and CH_3 groups, respectively, and the spacing between them (which varies with the field strength) shows the chemical shift characteristic of the protons in these three typical structural groups.

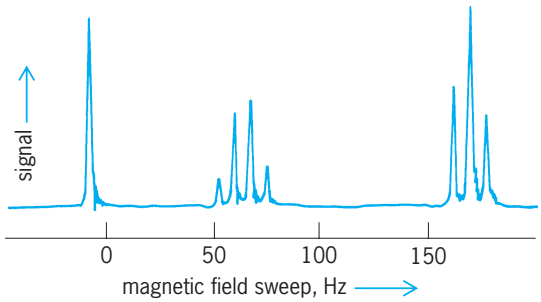

Fig. 2. Proton resonance spectra of ethyl alcohol at 40 MHz. (*After J. D. Roberts, Nuclear Magnetic Resonance, McGraw-Hill, 1959*)

The separate peaks at each frequency are due to spin-spin splitting. Often, the presence of n protons will split the frequency of a given, structurally different proton into $n + 1$ peaks, in direct analogy to ordinary spectral lines. The triplet in the NMR spectrum of ethyl alcohol results from the splitting of the frequency of the CH_3 protons by the two adjacent CH_2 protons; the quadruplet is at the typical CH_2 frequency and is split into four peaks by the three protons of the CH_3 group. *See* MOLECULAR STRUCTURE AND SPECTRA.

Because the time required for nuclear transitions is relatively long, substances undergoing fast reactions show altered NMR spectra, and rates of such rapid processes as ionization or intramolecular rotation can be measured. *See* NUCLEAR MAGNETIC RESONANCE (NMR).

Magnetic resonance imagining (MRI). Ordinarily in magnetic resonance, it is desirable to have the static field, H_0, as uniform as possible in order that the NMR lines reveal the detailed structure originating in the chemical shifts and spin-spin coupling. In 1973, Paul Lauterbur and Peter Mansfield independently realized that by making the field nonuniform in a controlled manner one could form spatial images of the number density and other properties of nuclei in a sample. This method is the basis for MRI.

The general principles of MRI are as follows. In order to image a sample, it is placed in a strong uni-form laboratory magnetic field oriented in the z direction, of strength H_0. Added to that field is a second one, called the gradient field, whose z component, H_G, at spatial position specified by coordinates (x,y,z), is a linear function of those coordinates [Eq. (4), where a, b, and c are constants controlled

$$H_G(x, y, z) = ax + by + cz \tag{4}$$

by the experimenter]. Such a gradient is called a linear gradient. The resonance angular frequency, ω, now becomes a function of position, obeying the law shown in Eq. (5). Choice of the constants a, b, and

$$\omega(x, y, z) = \gamma\,[H_0 + H_G(x, y, z)] \tag{5}$$

c defines planes in space over which the resonance frequency has the same value, and how rapidly the magnetic field changes when one moves from one plane to another. For example, if only a is nonzero, all nuclei with the same coordinate x have the same resonance frequency, independent of their y or z coordinates. The nuclei between two planes $x = x_1$ and $x = x_2$ would produce a resonance extending from frequency $\omega(x_1) = g[H_0 + ax_1]$ to frequency $\omega(x_2) = g[H_0 + ax_2]$ whose total intensity is proportional to the number of nuclei in the sample between these two planes. The size of a determines how big a change in frequency accompanies a change in x. Since a is controlled by the experimenter, it is a known quantity, and thus the relationship between frequency and x is also known.

The NMR absorption is recorded as a function of frequency. A plot of NMR signal strength versus ω can

thus be converted to a plot of NMR signal strength versus x. It gives one the number of nuclei per unit distance in the x direction versus x. By varying the quantities a, b, and c, one can change the spatial orientation of the planes over which the magnetic field values are uniform (that is, one can change the direction of the field gradient). One proceeds to gather data for a variety of directions of gradient. These data can then be processed in a computer using well-known mathematical methods (such as Fourier transforms) to obtain n (x,y,z), the number of nuclei per unit volume at position x,y,z in the sample. *See* FOURIER SERIES AND TRANSFORMS.

Such results for planes in space (called slices) are often displayed as images whose darkness at a particular spatial position corresponds to the numerical value of n at that position. The resulting pattern of varying lightness and darkness gives an "image" of n (x,y,z). A given set of experimental data can be used to display slices of any orientation.

A unique feature of NMR images is that the strength of the NMR signal may be adjusted to tell more than just the spatial distribution of the number density of nuclei n (x,y,z). For example, a so-called T_1 weighted image shows how the spin-lattice relaxation time, T_1, varies with position. One may also give a T_2-weighted image to show spatial variation of the transverse relaxation time, T_2. Or one can pick a given region of space to display the chemical shift data. Using these methods, it is possible to use NMR images to display flow patterns of fluids, such as blood, or to show the existence of spatial diffusion of nuclei. These latter quantities are useful in diagnosis of stroke.

Two quantities of great interest are the spatial resolving power of the imaging method and apparatus and the length of time required to form an image. In general, the higher the spatial resolution, the longer the time to form the image. In practice, the sequence of gradients which are employed (through the sequence of values of a, b, and c employed to form the image) and the method of recording the NMR spectra control how quickly an image can be formed and how high its spatial resolution will be. The method of choice depends on the purpose for which the image is being obtained. For some medical applications, for instance, one may wish to emphasize speed of data acquisition (reducing data acquisition times to minutes rather than hours) at the expense of spatial resolving power. A research area of growing importance is "functional imaging," in which the goal is to locate where in the brain the response occurs to an external stimulus.

Electron-nuclear double resonance (ENDOR). In this technique the magnetic resonance of a nucleus is detected by observing that of a nearby electron. The magnetic coupling between the nuclear and electronic magnetic moments gives rise to a back reaction on the electron resonance when the nuclei are brought into resonance. The sample under study is placed in a conventional electron resonance apparatus. In addition, an oscillator drives a coil to produce alternating magnetic fields at the sample under study, the frequency of alternation being in an appropriate range to produce nuclear transitions. Typically, the static magnetic field is adjusted to produce electron resonance. With the static magnetic field and the frequency of the electron resonance apparatus held fixed, the frequency of the nuclear resonance oscillator is then swept. As it passes through the resonant frequency of any nucleus that is coupled to the electron, a change in the electron absorption occurs.

The electron resonance and the nuclear resonance both represent transitions between energy levels of the combined system of electron and nucleus, each resonance being between a pair of levels. The strength of the electron resonance depends on the difference in population between its two levels. Thus, if one of these levels takes part in both resonances, the nuclear resonance may influence the electron resonance by changing the population of the common energy level.

Since the individual quanta absorbed in an electron resonance are much larger in energy than those absorbed in a nuclear resonance, the double resonance often permits the detection of the resonant absorption of a smaller number of nuclei than it would be possible to detect by a direct observation of the nuclear resonance. Since ENDOR requires both electron and nuclear resonances, it is applicable only to systems possessing both. It has been used, for example, to study the nuclear resonance associated with impurity atoms in semiconductors and that associated with F-centers in alkali halides, as well as to measure nuclear moments of rare elements. Important results have included the determination of the electronic structure of point imperfections and the measurement of nuclear magnetic moments and hyperfine anomalies.

Paramagnetic resonance. Magnetic resonance arising from electrons in paramagnetic substances or from electrons in paramagnetic centers in diamagnetic substances is called paramagnetic resonance. For applied fields of several thousand gauss, the electron paramagnetic resonance (EPR) experiments are done at microwave frequencies, commonly at 3-cm (1.2-in.) or at 1-cm (0.4-in.) wavelengths. In some instances, nuclear resonance apparatus has been used with correspondingly lower applied fields. The most sensitive apparatus detects approximately 10^{12} electron spins for a line 1 gauss broad, a sensitivity far greater than that obtained by nonresonant methods, such as those utilizing paramagnetic susceptibility.

Resonances have been observed in atoms of the iron group, rare earths, and other transition elements; in paramagnetic gases; in organic free radicals; in color centers in crystals (such as F- and V-centers); in metals (conduction electron spin); and in semiconductors (both conduction electron and impurity center spins).

When two paramagnetic ions or molecules approach one another, the spins become coupled via the exchange interaction. Much weaker couplings than the usual exchange interactions within atoms, in chemical bonds, or in ferromagnets produce pronounced effects. For additional information on this

phenomenon and its applications . *See* ELECTRON PARAMAGNETIC RESONANCE (EPR) SPECTROSCOPY.

Ferromagnetic resonance. In the case of both nuclear and paramagnetic resonance, the spins of neighboring atoms are nearly randomly oriented with respect to one another. In contrast, the electron spins in one domain of a ferromagnet are nearly all parallel for temperatures sufficiently below the Curie point. The alignment may be described in terms of the exchange coupling between neighboring spins, or equivalently in terms of the Weiss molecular magnetic field $\mathbf{H}_w$.

It is simplest to consider the case where magnetization is uniform throughout the sample. Neglecting relaxation effects, the equation of motion is still Eq. (2), but an effective field is substituted for $\mathbf{H}$, consisting of the applied static and alternating fields, the demagnetizing corrections (from the electron magnetic dipolar fields), and the effects of crystalline anisotropy. Because the Weiss molecular field is always parallel to $\mathbf{M}$, $\mathbf{H}_w$ exerts no torque and plays no role as long as the magnetization is uniform throughout the sample. (The exchange energy between spins does not change as long as their relative orientation does not change.)

The crystalline anisotropy can be shown to be equivalent to a magnetic field $\mathbf{H}_A$ along the direction of easy magnetization as long as $\mathbf{M}$ points nearly in that direction.

Because of the demagnetizing effects, the resonant frequency depends on sample geometry. For an infinite plane perpendicular to the applied field, the resonant angular frequency ω is given by $\omega = \gamma\sqrt{BH}$, but for a sphere, $\omega = \gamma H$.

The large demagnetizing and exchange fields are the principal difference between ferromagnetic and paramagnetic resonance. The demagnetizing field has components $-N_x M_x$, $-N_y M_y$, and $-N_z M_z$, where N_x, N_y, and N_z are the demagnetizing coefficients. Thus, suppose the static field and $\mathbf{M}$ lie along the z direction. Application of the alternating field tilts $\mathbf{M}$ away from z, changing the effective z field. If the change brings the spins closer to resonance, $\mathbf{M}$ may tilt out more. It is possible for such a nonlinear effect to be unstable for sufficiently large alternating fields. This instability is utilized in the Suhl ferromagnetic amplifier.

Antiferromagnetic resonance. The two sublattices of spins in an antiferromagnet are strongly coupled together by exchange forces. If both magnetizations ($\mathbf{M}_1$ and $\mathbf{M}_2$) are tilted together, away from the normal direction of magnetization in the crystal (call this the z direction), the only change in energy results from the anisotropy fields. However, because the anisotropy fields are reversed in direction for the two lattices, the magnetizations $\mathbf{M}_1$ and $\mathbf{M}_2$ tend to precess in opposite directions, bringing about a change in the exchange energy. An external field along the z direction aids one anisotropy field but opposes the other. The resonant angular frequency ω for a sphere is given by Eq. (6), where H is the applied field, H_A the equivalent anisotropy field, and H_E the equivalent exchange field. The plus and minus signs refer to two opposite directions of rotating magnetic fields which may be used to observe the resonance. If H_E is 10^6 oersteds, and H_A is 10^4 oersteds, the corresponding frequency is 3×10^{11} Hz.

$$\omega = \gamma\left[H \pm \sqrt{H_A(H_A + 2H_E)}\right] \qquad (6)$$

Ferrimagnetic resonance. Magnetic resonance in ferrites is called ferrimagnetic resonance. Ferrites are the natural generalization of antiferromagnets, containing two or more sublattices which may differ in magnetization. The basic coupling terms are still anisotropy fields, exchange fields, and the applied fields. The resonant angular frequency ω for the case of two sublattices is given by Eq. (7), where η is

$$\omega = \gamma\left[H - \frac{\eta H_E}{2} \pm \sqrt{\left(\frac{\eta H_E}{2}\right)^2 + H_E H_A(2-\eta) + {H_A}^2}\right] \qquad (7)$$

a parameter measuring the relative sizes of the two magnetization vectors. Taking $\mathbf{M}_1$ to be the smaller magnetization, η is defined by Eq. (8). This equation

$$\mathbf{M}_1 = (1-\eta)\mathbf{M}_2 \qquad (8)$$

assumes the magnetizations to be at saturation and the two sublattices to have the same γ (deviations might differ from spin-orbit coupling). *See* MOLECULAR BEAMS.

Charles P. Slichter

Bibliography. R. J. Abraham, J. P. Fisher, and P. Loftus, *Introduction to NMR Spectroscopy*, 1992; H. Friebolin, *Basic One- and Two-Dimensional NMR Spectroscopy*, 2d ed., 1993; J. W. Hennel and J. Klinowski, *Fundamentals of Nuclear Magnetic Resonance*, 1993; C. P. Poole and H. A. Farach, *Theory of Magnetic Resonance*, 2d ed., 1987; C. P. Slichter, The golden anniversary of nuclear magnetic resonance, NMR—Fifty years of surprises, *Proc. Amer. Phil. Soc.*, 142:533–556, 1998; C. P. Slichter, *Principles of Magnetic Resonance*, 3d ed., 1990, reprint 1992; W. S. Warren (ed.), *Advances in Magnetic Resonance*, vols. 1–14, 1965–1990.

Magnetic reversals

The Earth's magnetic field has reversed polarity hundreds of times. That is, at different times in Earth's past, a compass would have pointed south instead of north. Recognition that the geomagnetic field has repeatedly reversed polarity played a key role in the revolution that transformed the geological sciences in the 1960s—the acceptance of the theory of plate tectonics. It is generally accepted that the geomagnetic field is generated by motion of electrically conducting molten metal in Earth's outer core. However, the mechanism by which the field decays and reverses polarity remains one of the great unknowns in geophysics. *See* GEOMAGNETISM; PLATE TECTONICS.

The last magnetic field reversal occurred long before humans were aware of the geomagnetic field

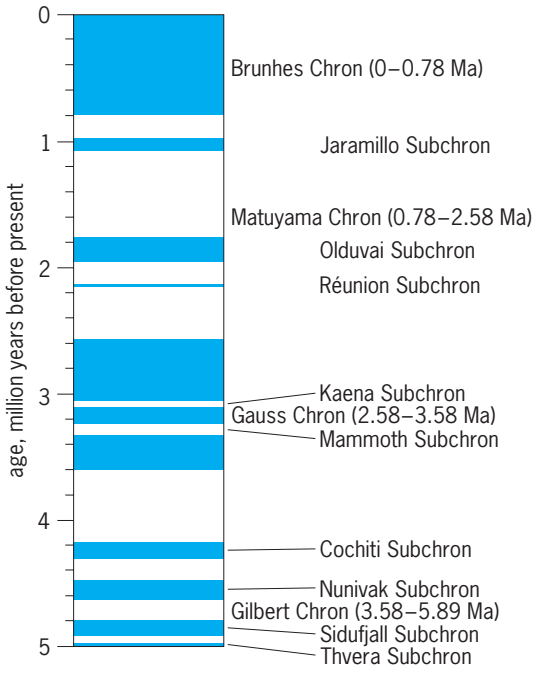

Fig. 1. Time scale of reversals of Earth's magnetic field for the last 5 million years. Color intervals represent periods when Earth's magnetic field was in the same state as the present field (called the normal polarity state) when a compass would point north. White intervals represent periods when Earth's magnetic field was in the opposite state as the present field (called the reversed polarity state) when a compass would point south. The boundaries between these polarity intervals represent short periods of geological time. Long intervals of nearly constant polarity are termed chrons, while shorter periods of opposite polarity within a chron are termed subchrons. The last four chrons are named after famous contributors to geomagnetism (Brunhes, Matuyama, Gauss, and Gilbert), while the subchrons in these intervals are named after the locations at which they were first discovered. (*From S. C. Cande and D. V. Kent, Revised calibration of the geomagnetic polarity time scale for the Late Cretaceous and Cenozoic, J. Geophys. Res., 100:6093–6095, 1995*)

(780,000 years ago; **Fig. 1**), so it is necessary to study geological records to understand the process by which the field reverses. The ability of rocks to act as fossilized compasses, which record a permanent "memory" of Earth's magnetic field at the time of rock formation, makes them suitable for detailed studies of ancient geomagnetic field behavior. *See* PALEOMAGNETISM; ROCK MAGNETISM.

In order to understand the mechanism of field reversal, it is necessary to develop a realistic view of the geometry of the field during polarity transitions. The interval of time required for the field to switch polarity is between about 5000 and 10,000 years. In a typical sedimentary rock unit, a polarity transition is recorded across a thin interval of strata, generally less than a meter thick. Many detailed studies have been undertaken from closely spaced samples through such intervals. During the early 1990s, a compilation of existing records indicated a distinct pattern in the way the field behaves during reversals. In particular, if the position of the magnetic pole was plotted as it progressed through a reversal (**Fig. 2**), it seemed that a large proportion of the poles tracked across a longitudinal band through the Americas. A second set of poles followed a path on the other side of the Earth (180° from the first) through western Australia and east Asia. This compilation suggested that the transitional field was dominantly dipolar and that biased field configurations may have persisted for several reversals during the last 10 million years. The time constants of convective motion in Earth's fluid outer core are a great deal shorter than in the solid overlying mantle. The persistence of these patterns over such long time intervals therefore suggested that fluid motion in the core is strongly affected by Earth's mantle and that the proposed bias may reflect long-term characteristics of deep-Earth dynamics. The coincidence in the location of transitional geomagnetic poles and other geophysical observations, such as anomalously cool lower-mantle temperatures, fluid flow patterns at the top of Earth's outer core, and significant features in the present geomagnetic field, excited a great deal of interest. As a result, the nature of transitional geomagnetic field behavior became one of the most hotly debated issues in geophysics in the 1990s. *See* EARTH, CONVECTION IN.

When observations concerning transitional geomagnetic field behavior were subjected to more rigorous statistical analysis, it was concluded that it is premature to accept the hypothesis of lower-mantle control of the geodynamo. Despite the compilation of many polarity transition records, there is an uneven distribution of sites around the world from which polarity transition records are available. A much wider distribution of sites is required for adequate testing of current hypotheses concerning

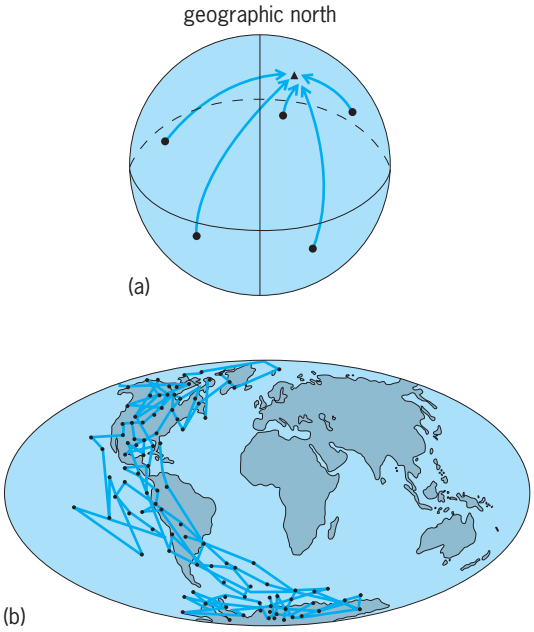

Fig. 2. Position of the magnetic pole plotted as it progresses through a reversal. (*a*) In a purely dipole field, such as that produced by a bar magnet, paleomagnetic data from any site on Earth's surface will describe a single pole (Fuller et al., 1996). (*b*) An example of a series of poles determined from a detailed paleomagnetic study of a polarity transition (Tric et al., 1991). When a number of such records were plotted together, the majority of poles plotted over a longitudinal band across the Americas (Laj et al., 1991), which indicated that the transitional field was dominantly dipolar.

transitional field behavior. In addition, there is considerable concern about the ability of some geological materials, particularly sediments, to record the geomagnetic field during periods when the field is extremely weak (such as during a reversal when the field decays to about one-tenth of its nontransitional value). Thus, rigorous methods must also be developed for assessing the reliability of the records used to make inferences about transitional field behavior. *See* GEODYNAMO.

Major advances in understanding geomagnetic field behavior have recently been made using numerical models that require thousands of hours of super-computer processing. The models provide fairly realistic simulations for how the geomagnetic field is generated, and a polarity reversal has been simulated. This simulation displays many features in common with paleomagnetic records of reversals, but much more work is needed to get a more realistic match. Paleomagnetic observations of polarity transitions are still required from widely distributed sites around the world. Debate concerning geomagnetic field behavior during polarity transitions is therefore far from settled and is likely to rage for some time to come. Andrew P. Roberts

Bibliography. S. C. Cande and D. V. Kent, Revised calibration of the geomagnetic polarity time scale for the Late Cretaceous and Cenozoic, *J. Geophys. Res.*, 100:6093–6095, 1995; M. Fuller, C. Laj, and E. Herrero-Bervera, The reversal of the Earth's magnetic field, *Amer. Sci.*, 84:552–561, 1996; G. A. Glatzmaier and P. H. Roberts, A three-dimensional self-consistent computer simulation of a geomagnetic field reversal, *Nature*, 377:203–209, 1995; J. A. Jacobs, *Reversals of the Earth's Magnetic Field*, Cambridge University Press, 1994; C. Laj et al., Geomagnetic reversal paths, *Nature*, 351:447, 1991; P. L. McFadden, C. E. Barton, and R. T. Merrill, Do virtual geomagnetic poles follow preferred paths during geomagnetic reversals?, *Nature*, 361:342–344, 1993; A. P. Roberts, Polarity transitions and excursions of the geomagnetic field, *Rev. Geophys. Suppl.*, 35:153–160, 1995; E. Tric et al., High-resolution record of the Upper Olduvai transition from Po Valley (Italy) sediments: Support for dipolar transition geometry?, *Phys. Earth Planet. Inter.*, 65:319–336, 1991.

Magnetic separation methods

All materials possess magnetic properties. Substances that have a greater permeability than air are classified as paramagnetic; those with a lower permeability are called diamagnetic. Paramagnetic materials are attracted to a magnet; diamagnetic substances are repelled. Very strongly paramagnetic materials are classified as ferromagnetic and include such metals as iron, nickel, and cobalt, and such minerals as magnetite, pyrrhotite, and ilmenite. Such substances can be separated from weakly or nonmagnetic materials by the use of low-intensity magnetic separators. Minerals such as hematite, limonite, and garnet are weakly magnetic and can be separated from nonmagnetics by the use of high-intensity separators.

Magnetic separators are widely used to remove tramp iron from ores being crushed, thereby protecting the crushers; to remove contaminating magnetics from food and industrial products; to recover magnetite and ferrosilicon in the float-sink methods of ore concentration; and to upgrade or concentrate ores. Tramp iron may be removed by a stationary magnet suspended over a conveyor belt or the material may be passed over a magnetic pulley; in both cases, magnetics are attracted by the magnetic field and separated.

Magnetic separators are extensively used to concentrate ores, particularly iron ores, when one of the principal constituents is magnetic. When the chief economic mineral is magnetite, iron ores can be cheaply and effectively separated by low-intensity separators. Such separators may be dry or wet. If an ore can be crushed to give substantial liberation of minerals at sizes coarser than $^1/_4$ in. (0.6 cm), separations can be made on the $+^1/_4$-in. (0.6-cm) sizes on a belt-type magnetic cobber (see **illus.**). Such a machine is usually used to cob out or reject waste materials. If clean mineral occurs at this size, it can be recovered by splitting the discharge or by retreatment on a lower strength machine. Wet magnetic separators are usually used to treat ore finer than $^1/_8$ in. (0.3 cm). These separators may be of the belt type or of the more common rotating-drum type. Drum-type separators consist of one or more rotatable drums having inner nonrotatable magnet elements with 3–7 poles. The magnets may be either electromagnets or permanent magnets. After the feed enters the machine as a slurry, the magnetics are attracted to the pole pieces and are carried to a discharge point on the surface of the drum. Many types of box designs are in use. The concurrent type is frequently used on relatively coarse material to reject a clean waste product. The countercurrent type is employed on fine ore to give a clean concentrate. Magnets may be of either the electromagnetic or permanent type. Electromagnets were formerly used almost exclusively but are now used mainly when exceptionally high

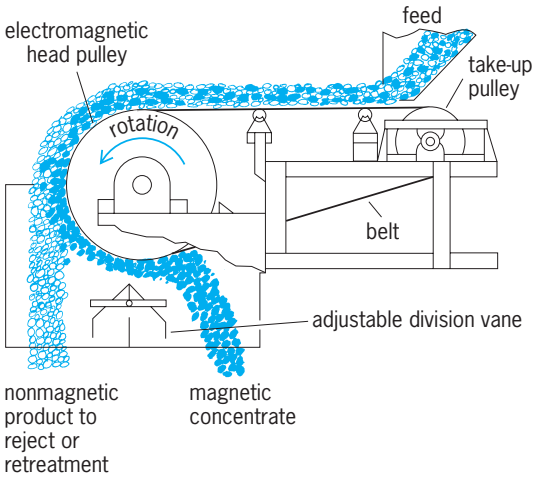

Belt-type magnetic cobber. (*Stearns Magnetic Products*)

field strengths are required or when it is desirable to vary magnet strength. Permanent magnets are now widely used since modern materials permit charging and retaining high field strengths permanently. Most permanent magnets are of the alnico type but the ceramic types containing barium ferrites are coming into use. Several types of magnetic separators employing alternating current have been devised but have found little commercial use.

High-intensity separators for the separation of weakly magnetic minerals are usually of the dry type. Surface-tension effects usually rule out wet separations. Since magnetic attraction varies inversely as the square of the distance, weakly magnetic minerals must be brought close to the magnets if they are to be separated. Both belt-type and induced-roll machines are used. The ore must be fully dried and closely sized for best results. *See* CHEMICAL SEPARATION TECHNIQUES; MAGNETISM; MECHANICAL SEPARATION TECHNIQUES; ORE DRESSING.

Fred D. DeVaney

Bibliography. A. Grandison and M. Lewis, *Separation Processes*, 1993; C. J. King, *Separation Processes*, 2d ed., 1980; R. H. Perry and D. Green (eds.), *Perry's Chemical Engineers' Handbook*, 7th ed., 1997; J. A. Wesselingh and R. Krishna, *Mass Transfer*, 1991.

Magnetic susceptibility

The magnetization of a material per unit applied field. It describes the magnetic response of a substance to an applied magnetic field. If M is the magnetization and H the applied magnetic field, then the magnetic susceptibility, denoted by χ, is given by Eq. (1). In the case that M is not parallel to H,

$$\chi = \frac{M}{H} \tag{1}$$

χ is a tensor. Otherwise, it is a simple number. For a crystalline material, χ may depend upon the direction of H with respect to the axes of the crystal because of anisotropic effects. For an elementary discussion of M and H *see* MAGNETISM; MAGNETIZATION.

The magnetic susceptibility is expressed in a variety of ways: per gram, per atom, per unit volume, and per mole. In this article, electromagnetic units are used. In Eq. (1), the units of χ are ergs per oersted per unit volume. **Figure 1** shows the atomic susceptibilities χ_A (ergs per oersted per atom) of the elements. The static susceptibility is measured in constant applied magnetic fields. The frequency-dependent susceptibility is measured in alternating magnetic fields. It is usually a complex quantity in which both the real and imaginary parts are functions of frequency.

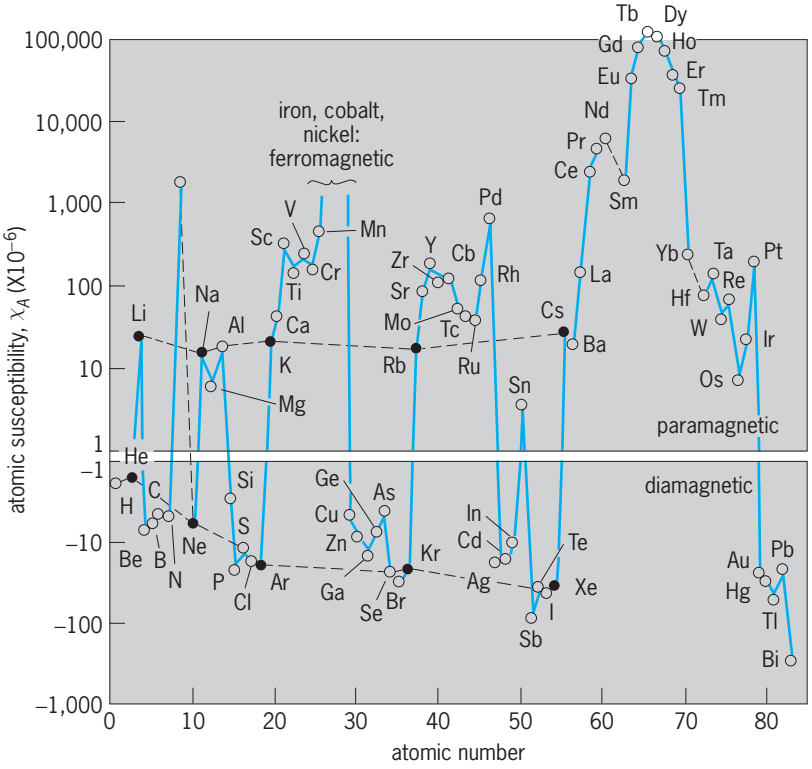

Fig. 1. Atomic susceptibilities of the elements at room temperature. The broken lines connect the alkali metals (paramagnetic) and the rare gases (diamagnetic).

Ferromagnetic susceptibility. The general behavior of the susceptibility of ferromagnetic materials above the Curie temperature follows the Curie-Weiss law, Eq. (2). This behavior is followed in the region well

$$\chi = \frac{C}{T - \theta} \tag{2}$$

above the ferromagnetic Curie temperature T_c. The paramagnetic Curie temperature θ is usually slightly greater than the temperature of transition T_c. Comparison of θ and T_c for three ferromagnetic metals is given in the **table**.

Comparison of θ and T_c

Parameter	Fe	Co	Ni
θ, K	1093	1428	650
T, K	1043	1393	631

All ferromagnetic materials exhibit paramagnetic behavior above their ferromagnetic Curie points. The magnitude of the paramagnetic susceptibility is determined by the Curie constant C, as in Eq. (2). A typical value of C is 0.2 K/cm^3 for iron. For the theory of ferromagnetic susceptibility *see* CURIE TEMPERATURE; CURIE-WEISS LAW; FERROMAGNETISM.

In the region just a fraction of a degree above the "critical point," or Curie temperature T_c, the susceptibility is found to approximate Eq. (3),with γ generally very close to 1.33. The theory is extremely complicated and not entirely satisfactory.

$$\chi = \frac{C'}{(T - T_c)^{\gamma}} \tag{3}$$

Below the Curie point, the static susceptibility is not usually defined for a ferromagnetic substance, since the ferromagnet may have a finite magnetization in zero applied field.

The initial permeability is the slope of the magnetization curve (B plotted against H) for magnetic field strength $H = 0$. Initial permeabilities vary from almost 300 (platinum-cobalt) to 100,000 (supermalloy).

The frequency-dependent permeability is that measured in an alternating magnetic field. The experiments are usually carried out in small magnetic fields so that it is the frequency dependence of the initial permeability which is measured. Such experiments give information on the structure of ferromagnetic domains and the motion of domain walls.

Paramagnetic susceptibility. Most paramagnetic substances at room temperature have a static susceptibility which follows a Langevin-Debye law, Eq. (4),

$$\chi = \frac{Np^2\mu_B^2}{3kT} + N\alpha \tag{4}$$

where N is the number of magnetic dipoles per unit volume, p is the effective magneton number, μ_B is the Bohr magneton, k is Boltzmann's constant, T is the absolute temperature, and α is the temperature-independent contribution of Van Vleck paramagnetism. The first term of Eq. (4) is referred to as the Curie law because of its $1/T$ dependence. Experimental results are often expressed in terms of what the effective magneton numbers must be in order to account for the variation of χ with $1/T$. The interpretation of the experimental data reveals the nature of the energy levels of the paramagnetic ions, the symmetry of paramagnetic crystals, the effects of crystalline electric fields on the energy levels, and the influence of the paramagnetic ions on one another.

Saturation of the paramagnetic susceptibility occurs when a further increase of the applied magnetic field fails to increase the magnetization, because practically all the magnetic dipoles are already oriented parallel to the field. Saturation will occur either at very strong fields or at very low temperatures; that is, in cases when the approximation leading to the Langevin-Debye formula fails. Some paramagnetic solids have susceptibilities which follow a Curie-Weiss law rather than a Curie law. *See* PARAMAGNETISM.

Diamagnetic susceptibility. The susceptibility of diamagnetic materials is negative, since a diamagnetic substance is magnetized in a direction opposite to that of the applied magnetic field. The diamagnetic susceptibility is independent of temperature.

Diamagnetic susceptibility depends upon the distribution of electronic charge in an atom and upon the energy levels. Interpretation of the experimental data reveals the nature of the atomic wave functions of the atom in question. For the theory of diamagnetic susceptibility and a listing of values of the molar diamagnetic susceptibilities of several rare gases and ions in crystals *see* DIAMAGNETISM.

Antiferromagnetic susceptibility. The susceptibility of antiferromagnetic materials above the Néel point, which marks the transition from antiferromagnetic to paramagnetic behavior, follows a Curie-Weiss law with a negative paramagnetic Curie temperature $-\theta$, as in Eq. (5). The Néel temperature is always somewhat less than θ.

$$\chi = \frac{C}{T + \theta} \tag{5}$$

The antiferromagnetic susceptibility is a maximum at the Néel temperature. Below the Néel temperature, it behaves in a way determined by the angle between the field direction and the crystal axes—it usually decreases as the temperature lowers. For the theory of antiferromagnetic susceptibility *see* ANTIFERROMAGNETISM.

Measurement of susceptibility. Magnetic susceptibilities may be measured by several methods, depending upon the quantity sought. Ferromagnetic static permeabilities may be measured by the Rowland ballistic method. In this technique, the specimen is cut in the shape of a ring, and a magnetic field is applied by means of a primary winding on the ring. A secondary winding is connected to a ballistic galvanometer. The current through the primary is changed suddenly. The resulting abrupt change in magnetic field H causes a change in magnetic induction B ($B = H + 4\pi M$) in the specimen, which in turn induces a voltage in the secondary. Thus, the galvanometer suffers a deflection proportional to the change in B. One starts with a known value of B (usually zero) and plots the magnetization curve in this way.

Paramagnetic and diamagnetic susceptibilities may be measured by the balance method. A magnetized substance in an inhomogeneous magnetic field experiences a force given by Eq. (6).

$$F = {}^1/_2 \operatorname{grad} \int M \cdot H \, dV \tag{6}$$

The integral is over the volume of the specimen. The susceptibility is $\chi = M/H$. Therefore Eq. (7) holds.

$$F = {}^1/_2 \chi \operatorname{grad} \int H^2 \, dV \tag{7}$$

If the magnetic field now varies only in one direction, say the z direction, then Eq. (8) is valid,

$$F = {}^1/_2 \chi A \int \frac{d}{dz}(H^2)\, dz = {}^1/_2 \chi A (H_1^2 - H_2^2) \tag{8}$$

where the specimen is in the shape of a rod of cross-sectional area A and is suspended in the z direction in the inhomogeneous field (**Fig. 2**). In Fig. 2, H_1 and H_2 are the values of the magnetic field strength at the two ends of the rod. The force is measured and, when H_1 and H_2 (or H and dH/dz) are known, the susceptibility can be determined. This is known as the Gouy balance method. Note that the total magnetic susceptibility is measured, both para- and diamagnetic contributions.

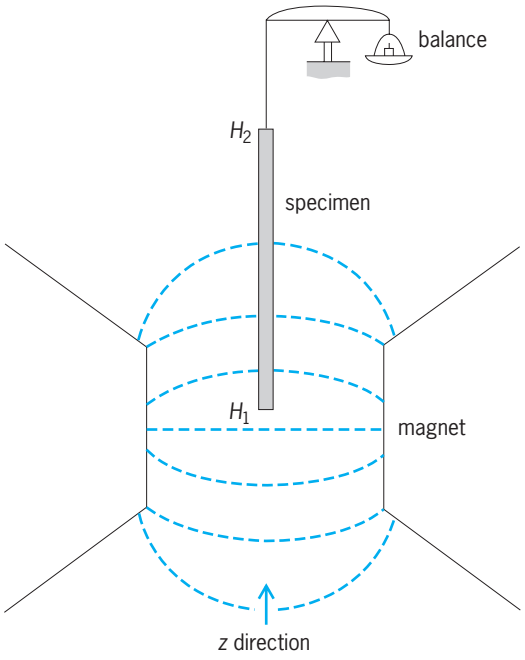

Fig. 2. Gouy balance method for measurement of magnetic susceptibilities. (*After C. Kittel, Introduction to Solid State Physics, 3d ed., John Wiley and Sons, 1966*)

The paramagnetic susceptibility may sometimes be measured separately by spin-resonance techniques. This is especially true of the Pauli paramagnetic susceptibility of conduction electrons in alkali metals. *See* MAGNETIC RESONANCE.

At low temperatures, relative measurements of paramagnetic susceptibility are very simple in comparison with absolute measurements and yet can provide much of the ionic and crystal-field information referred to above. Such measurements are most commonly carried out using an audio-frequency mutual-inductance technique. Exactly the same procedure can be employed for another important purpose—namely, low-temperature thermometry—making use of the Curie law (with or without refinements). *See* LOW-TEMPERATURE THERMOMETRY; MAGNETIC THERMOMETER; SQUID. Elihu Abrahams; Frederic Keffer

Bibliography. R. A. Hein, T. L. Francavilla, and D.H. Liebenberg (eds.), *Magnetic Susceptibility of Superconductors and Other Spin Systems*, 1992; J. R. Hook and H. E. Hall, *Solid State Physics*, 2d ed., 1995; C. Kittel, *Introduction to Solid State Physics*, 7th ed., 1996.

Magnetic thermometer

A thermometer whose operation is based on Curie's law, which states that the magnetic susceptibility of noninteracting (that is, paramagnetic) dipole moments is inversely proportional to absolute temperature. Magnetic thermometers are typically used at temperatures below 1 K (−458°F). The magnetic moments in the thermometric material may be of either electronic or nuclear origin. Generally the magnetic thermometer must be calibrated at one (or more) reference temperatures. *See* ELECTRON; NUCLEAR MOMENTS; PARAMAGNETISM.

Principle. In a magnetic field H, paramagnetic moments are polarized so that the vectorial sum of the individual dipole moments μ produces a magnetization M. At absolute temperatures T that are relatively high compared to the magnetic energy of the dipole (that is, at temperatures at which k_BT is much greater than μH, where k_B is Boltzmann's constant), the magnetization obeys the Curie-Weiss law, Eq. (1). Here χ is the magnetic susceptibility of the

$$M = \chi H = \frac{C}{T - \Delta} H \tag{1}$$

thermometric material, C its Curie constant, and Δ a small correction which becomes important only at the low-temperature end of the thermometer's working range. *See* CURIE-WEISS LAW.

For an actual device, C in Eq. (1) becomes the so-called thermometer constant C', comprising the Curie constant multiplied by detection-sensitivity parameters. By measuring the magnetization M in a constant polarizing field H, the absolute temperature T can be determined if the thermometer constant C is known from a calibration with some other thermometer.

Toward high temperatures, the useful temperature range is limited by the decreasing sensitivity (since the increment in M for a unit change in T is proportional to $1/T^2$). Toward low temperatures, the measurement sensitivity increases, but at the lowest temperatures the range is restricted, first by the need to calibrate the correction term Δ, and finally by the breakdown of the Curie-Weiss behavior. Even at the expense of a reduced signal amplitude, it is therefore preferable to use both a small polarizing field H and a low measuring frequency, well below the equivalent of the spin-lattice relaxation time (to avoid loss of thermal contact between the magnetic moments and their environment in the crystalline lattice). *See* MAGNETIC SUSCEPTIBILITY; MAGNETIZATION.

Electronic magnetic thermometer. At temperatures from a few millikelvins upward, the thermometric material is preferably an electronic paramagnet, typically a nonconducting hydrous rare-earth salt. For higher temperatures, an ion is selected with a large magnetic moment in a crystalline environment with a high density of magnetic ions. In contrast, for low temperature use the magnetic exchange interactions between the magnetic ions should be small, which is accomplished by selecting an ion with a well-localized moment and by maintaining a large separation between the magnetic ions by means of diamagnetic atoms. This is the case in cerium magnesium nitrate (CMN) $[2Ce(NO_3)_3 \cdot 3Mg(NO_3)_3 \cdot 24H_2O]$. Here, the Ce^{3+} ion is responsible for the magnetic moment, which is well localized within the incompletely filled $4f$ shell relatively deep below the outer valence electrons. To reduce the magnetic interactions between the Ce^{3+} ions further, Ce^{3+} may be partly substituted with diamagnetic La^{3+} ions. Lanthanum-diluted CMN has been used for

thermometry to below 1 mK. *See* EXCHANGE INTERACTION.

A mutual-inductance bridge, originally known as the Hartshorn bridge, has been the most widely employed measuring circuit for precision thermometry (**Fig. 1**). The bridge is driven by a low-frequency alternating-current source. The inductance at low temperatures consists of two coils, which are as identical as possible. The voltages induced across them by the drive current are compared by means of a high-input-impedance ratio transformer. The output level of this voltage divider is adjusted to equal that of the midpoint between the two coils, using as null indicator a narrow-band preamplifier and a phase-sensitive (lock-in) detector. Thus, without a paramagnetic specimen, the bridge is balanced with the decade divider adjusted at its midpoint, while with the specimen inside one of the coils the change in the divider reading at bridge balance is proportional to the sample magnetization. For high-resolution thermometry it has become standard practice to replace the room-temperature zero detector with a SQUID magnetometer circuit. This also allows the mass of the sample to be reduced from several grams to the 1-mg level. *See* INDUCTANCE MEASUREMENT; SQUID.

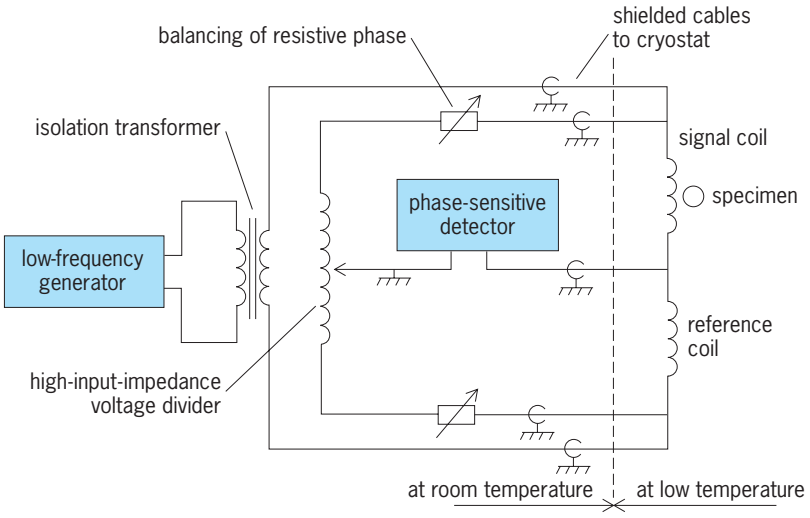

Fig. 1. Low-frequency (10–10^4 Hz) inductance bridge for the measurement of the susceptibility of an electronic paramagnet. The two identical solenoidal coils with three shielded cables are located at low temperatures, with the thermometric specimen in good thermal contact with the body whose temperature is measured.

Nuclear magnetic thermometer. Nuclear magnetic moments are smaller by a factor of 10^3 and are used for thermometry only in the ultralow-temperature region. For this the Curie-law behavior with $\Delta = 0$ in Eq. (1) is generally sufficient down to the lowest temperatures. The nuclear paramagnetic thermometer loses adequate sensitivity for calibration purposes above 50–100 millikelvins, unless it is operated in a high polarizing field (H greater than 0.1 tesla). It can be utilized as a self-calibrating primary thermometer if the spin-lattice relaxation time is measured in parallel with the nuclear Curie susceptibility. In metals where the temperature-independent Pauli paramagnetism of the conduction electrons is predominant and which are not in the superconducting state, the nuclear spin-lattice relaxation time τ_1 is controlled by the conduction electrons according to Korringa's relation, Eq. (2). Here, κ is the Korringa constant,

$$\tau_1 T = \kappa \tag{2}$$

which for platinum is 30 ms·K and for copper 1.2 s·K. The thermometric specimen is in metallic form in order to secure fast spin-lattice relaxation and adequate thermal homogeneity through electronic

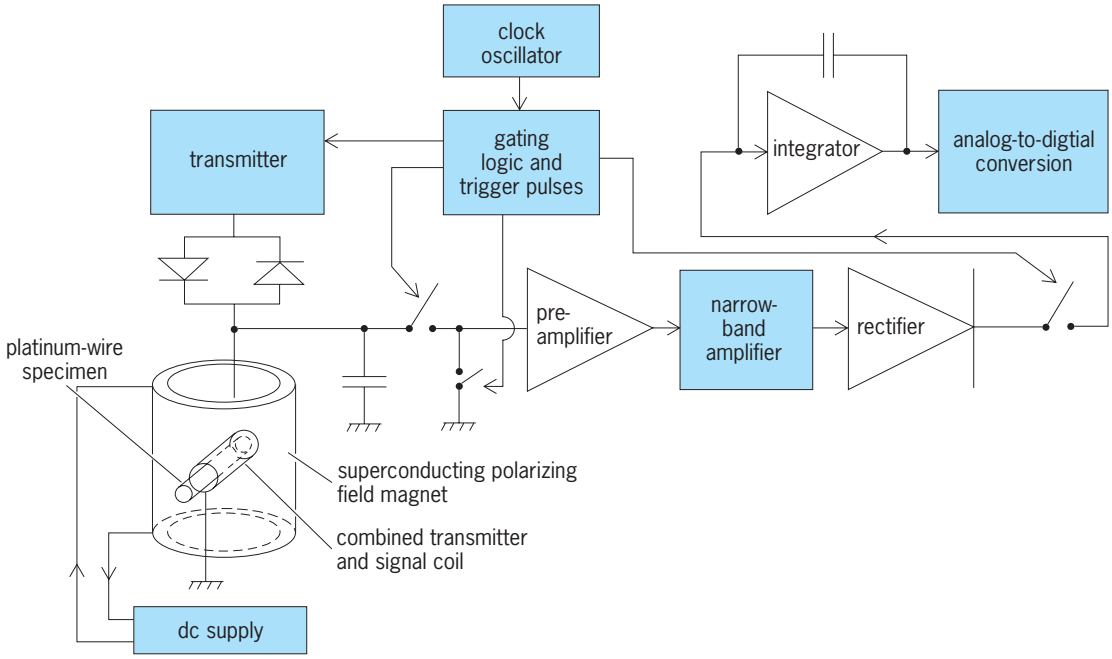

Fig. 2. Pulsed nuclear magnetic resonance (NMR) thermometer for the measurement of the nuclear paramagnetic susceptibility and spin-lattice relaxation time of a metallic wire or powder sample at temperatures below 100 mK and magnetic fields less than 50 millitesla. (*PicoWatt, Inc., Finland*)

thermal conduction. Extreme purity with respect to electronic magnetic impurities is important. With nuclear magnetic resonance (NMR) techniques the measurement can be restricted to probe only the magnetism of one nuclear spin species in the specimen. Pulsed NMR measurement on the ^{195}Pt isotope in natural platinum metal provides presently the most widely used thermometry at temperatures below 1 mK. In the Curie-susceptibility measuring mode, it has been extended down to 10 μK. *See* MAGNETIC RELAXATION.

NMR measurement is selectively sensitive only to those paramagnetic nuclei for which the Larmor frequency in the externally applied polarizing field H coincides with the frequency of the rf excitation field (oriented transverse to the steady field H), which is also the frequency of the tuned amplifier chain (**Fig. 2**). This property is important for reducing the influence from electronic-impurity magnetism. Measurement in the pulsed mode reduces problems associated with heating from the resonance excitation field and makes it possible to measure the spin-lattice relaxation time. The rectified and integrated value of the NMR free-induction-decay (FID) signal is usually treated without any corrections as inversely proportional to absolute temperature. *See* LOW-TEMPERATURE THERMOMETRY; NUCLEAR MAGNETIC RESONANCE (NMR).

Matti Krusius

Bibliography. D. S. Betts, *Refrigeration and Thermometry Below 1 K*, 1976; R. P. Hudson, *Principles and Applications of Magnetic Cooling*, 1972; O. V. Lounasmaa, *Experimental Principles and Methods Below 1 K*, 1974; F. Pobell, *Matter and Methods at Low Temperatures*, 2d ed., 1996; R. C. Richardson and E. N. Smith, *Experimental Techniques in Condensed Matter Physics at Low Temperatures*, 1988.

Magnetic thin films

Sheets of magnetic material with thicknesses of a few micrometers or less, used in the electronics industry. Magnetic films can be single-crystal, polycrystalline, amorphous, or multilayered in the arrangement of their atoms. Applications include magnetooptic storage, inductive recording media, magnetoresist sensors, and thin-film heads. *See* COMPUTER STORAGE TECHNOLOGY; MAGNETIC RECORDING; MAGNETOOPTICS; MAGNETORESISTANCE.

Fabrication. Thin films are usually directly deposited on a substrate. The techniques of deposition vary from high-temperature liquid-phase epitaxy such as that used in the fabrication of garnet films, through electroplating, to computer-controlled vapor deposition and sputtering. Permalloy, for example, can be both electroplated and sputtered or vapor-deposited. Magnetooptic films for storage applications are usually sputtered. *See* CRYSTAL GROWTH; ELECTROPLATING OF METALS; SPUTTERING.

Magnetic order. Both ferro- and ferrimagnetic films are used. The ferromagnetic films are usually transition-metal-based alloys. For example, permalloy is a nickel-iron alloy. The ferrimagnetic films, such as garnets or the amorphous films, contain transition metals such as iron or cobalt and rare earths. The ferrimagnetic properties are advantageous in magnetooptic applications where a low overall magnetic moment can be achieved without a significant change in the Curie temperature. *See* FERRIMAGNETISM; FERROMAGNETISM.

Magnetic anisotropy. In an isotropic bulk magnetic sample the overall magnetization does not prefer a particular direction. However, the same material in the form of a thin film has a lower energy when the magnetization lies in the plane of the film. This shape-induced anisotropy is useful in applications such as permalloy drive or sensor patterns used in magnetoresist-head technology. However, there are other situations where it is advantageous to have perpendicular rather than in-plane anisotropy. For example, magnetooptic memory materials have perpendicular anisotropy. This is obtained by using anisotropic crystals, by growing films in a magnetic field or directional deposition, and by annealing in a magnetic field or applying an anisotropic stress. A preferred direction of magnetic bias in multilayer films can also be achieved through exchange coupling.

Domain structure. Depending upon the nature of anisotropy (perpendicular to planar), a variety of domain patterns can be obtained. For example, when the perpendicular anisotropy is large relative to shape-induced anisotropy, stripe domains are observed. These form cylindrical domains if an external magnetic field is applied perpendicular to the plane of the films. Such cylindrical domains are used to represent bits of information in magnetooptical storage. The domain structure can be observed in an optical microscope with polarized light by using either the Faraday or Kerr effect. This effect is also used to sense a bit of information in magnetooptic storage. Domains can also be observed by using ferrofluids. Domains and domain wall structure are also observable by electron microscope techniques. *See* DOMAIN (ELECTRICITY AND MAGNETISM); FARADAY EFFECT; KERR EFFECT.

Coercivity. The coercivity of thin film varies with applications. For most applications a low coercive force is desired. Coercivity is generally associated with inhomogeneities such as stress fields, compositional fluctuations, defects, and surface roughness. *See* MAGNETISM; MAGNETIZATION.

Magnetotransport. The change in electrical properties, such as the electrical resistance, with a magnetic field is used in sensor elements. The most notable of these in semiconductor technology is the magnetoresist head used in disk storage technology. Very large magnetoresist signals (called giant magnetoresistance) are observed in magnetic multilayers and composites containing a magnetic and nonmagnetic material.

Praveen Chaudhari

Bibliography. J. A. Bland and H. Bretislav (eds.), *Ultrathin Magnetic Structures I: Introduction to Electronic, Magnetic, and Structural Properties*,

1994; P. Chaudhari and D. Turnbull, Structure and properties of metallic glasses, *Science*, 199:11–21, 1978; L. M. Falicov, Metallic magnetic superlattices, *Phys. Today*, 45(10):46–51, October 1992; I. S. Jacobs, Magnetic materials and applications: Quarter century overview, *J. Appl. Phys.*, 50:7294–7306, 1979; D. L. Smith, *Thin Film Deposition and Applications*, 1995.

Magnetism

The branch of science that describes the effects of the interactions between charges due to their motion and spin. These may appear in various forms, including electric currents and permanent magnets. The interactions are described in terms of the magnetic field, although the field hypothesis cannot be tested independently of the electrokinetic effects by which it is defined. The magnetic field complements the concept of the electrostatic field used to describe the potential energy between charges due to their relative positions. Special relativity theory relates the two, showing that magnetism is a relativistic modification of the electrostatic forces. The two together form the electromagnetic interactions which are propagated as electromagnetic waves, including light. They control the structure of materials at distances between the long-range gravitational actions and the short-range "strong" and "weak" forces most evident within the atomic nucleus. *See* ELECTROMAGNETIC RADIATION; RELATIVITY.

The term "magnetism" originates in the material magnetite, an iron ore, which produces weak natural magnets in the form of lodestones, exerting forces on each other and on pieces of iron. Peregrinus showed in 1269 that the behavior can be described in terms of magnetic poles on opposite end surfaces. The analogy between magnetic poles and electric charge greatly influenced the later development of the subject. The Earth provides an example of the subsequent explanation of magnetic behavior in terms of the flow of current and movement of charge, including the quantum state described as spin. This leaves open the question of whether or not isolated magnetic poles, or monopoles, exist as separate physical entities. *See* MAGNETIC MONOPOLES; MAGNETITE.

The magnetic field can be visualized as a set of lines (**Fig. 1**) illustrated by iron filings scattered on a suitable surface. The intensity of the field is indicated by the line spacing, and the direction by arrows pointing along the lines. The sign convention is chosen so that the Earth's magnetic field is directed from the north magnetic pole toward the south magnetic pole. The field can be defined and measured in various ways, including the forces on the equivalent magnetic poles, and on currents or moving charges. Bringing a coil of wire into the field, or removing it, induces an electromotive force (emf) which depends on the rate at which the number of field lines, referred to as lines of magnetic flux, linking the coil changes in time. This provides a definition of flux,

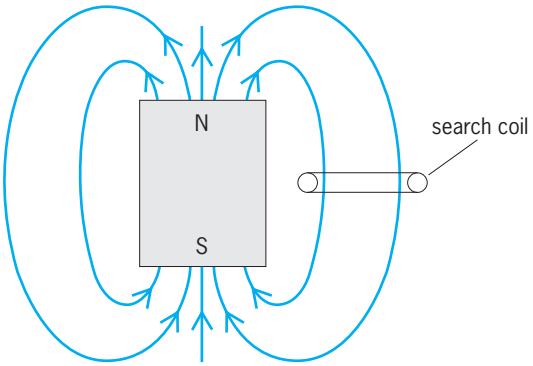

Fig. 1. Magnetic lines of a bar magnet.

Φ, in terms of the emf, e, given by Eq. (1) for a coil

$$e = -N\, d\Phi/dt \qquad \text{volts} \qquad (1)$$

of N turns wound sufficiently closely to make the number of lines linking each the same. The International System (SI) unit of Φ, the weber (Wb), is defined accordingly as the volt-second. The symbol B is used to denote the flux, or line, density, as in Eq. (2), when the area of the coil is sufficiently small

$$B = \Phi/\text{area} \qquad (2)$$

to sample conditions at a point, and the coil is oriented so that the induced emf is a maximum. The SI unit of B, the tesla (T), is the Wb/m^2. The sign of the emf, e, is measured positively in the direction of a right-hand screw pointing in the direction of the flux lines. It is often convenient, particularly when calculating induced emfs, to describe the field in terms of a magnetic vector potential function instead of flux.

Magnetic circuits. The magnetic circuit provides a useful method of analyzing devices with ferromagnetic parts, and introduces various quantities used in magnetism. It describes the use of ferromagnetic materials to control the flux paths in a manner analogous to the role of conductors in carrying currents around electrical circuits. For example, pieces of iron may be used to guide the flux which is produced by a magnet along a path which includes an air gap (**Fig. 2**), giving an increase in the flux density, B, if the cross-sectional area of the gap is less than that of the magnet. *See* MAGNET; MAGNETIC MATERIALS.

The magnet may be replaced by a coil of N turns carrying a current, i, wound over a piece of iron, or ferromagnetic material, in the form of a ring of uniform cross section (**Fig. 3**). The flux linking each turn of the coil, and each turn of a secondary coil wound

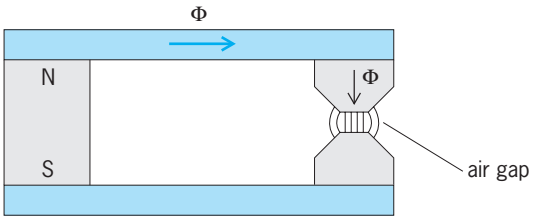

Fig. 2. Magnetic circuit with an air gap.

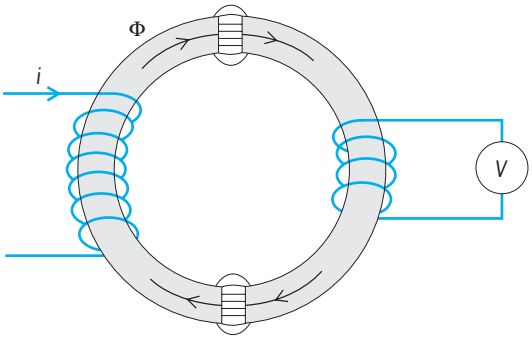

Fig. 3. Coils coupled by a ring of ferromagnetic material of uniform cross section.

separately from the first, is then approximately the same, giving the same induced emf per turn [according to Eq. (1)] when the supply current, i, and hence the flux, Φ, changes in time. The arrangement is typical of many different devices. It provides, for example, an electrical transformer whose input and output voltages are directly proportional to the numbers of turns in the windings. Emf's also appear within the iron, and tend to produce circulating currents and losses. These are commonly reduced by dividing the material into thin laminations. *See* EDDY CURRENT; TRANSFORMER.

The amount of flux produced by a given supply current is reduced by the presence of any air gaps which may be introduced to contribute constructional convenience or to allow a part to move. The effects of the gaps, and of different magnetic materials, can be predicted by utilizing the analogy between flux, Φ, and the flow of electric current through a circuit consisting of resistors connected in series (**Fig. 4**). Since Φ depends on the product, iN, of the winding current and number of turns, as in Eq. (3),

$$iN = \Phi\Re \tag{3}$$

the ratio between them, termed the reluctance, $\Re$, is the analog of electrical resistance. It may be constant, or may vary with Φ. The quantity iN is the magnetomotive force (mmf), analogous to voltage or emf in the equivalent electrical circuit. The relationship between the two exchanges the potental and flow quantities, since the magnetic mmf depends on current, i, and the electrical emf on $d\Phi/dt$. Electric and magnetic equivalent circuits are referred to as duals. *See* RELUCTANCE.

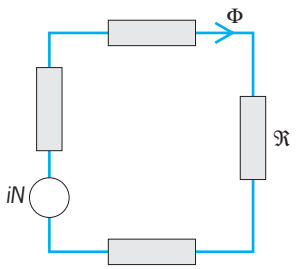

Fig. 4. Circuit analogy. Components of a magnetic circuit carrying a flux Φ, analogous to current i. The reluctances $\Re$ of the components are analogous to resistance, R.

Any part of the magnetic circuit of length l, in which the cross section, a, and flux density, B, are uniform has a reluctance given by Eq. (4). This equation parallels Eq. (5) for the resistance, R, of a con-

$$\Re = l/(a\mu) \tag{4}$$

$$R = l/(a\sigma) \tag{5}$$

duct or of the same dimensions. The permeability, μ, is the magnetic equivalent of the conductivity, σ, of the conducting material. Using a magnet as a flux source (Fig. 2) gives an mmf which varies with the air gap reluctance. In the absence of any magnetizable materials, as in the air gaps, the permeability is given by Eq. (6) in SI units (Wb/A-m). The quantity μ_0

$$\mu = \mu_0 = 4\pi \times 10^{-7} \tag{6}$$

is sometimes referred to as the permeability of free space. Material properties are described by the relative permeability, μ_r in accordance with Eq. (7), The

$$\mu = \mu_r\mu_0 \tag{7}$$

materials which are important in magnetic circuits are the ferromagnetics and ferrites characterized by large value of μ_r, sometimes in excess of 10,000 at low flux densities.

The various reluctances, $\Re_1, \Re_2, \ldots$, forming the different parts of the magnetic circuit can be added, yielding Eq. (8), when each part carries the same

$$\Phi = iN/(\Re_1 + \Re_2 + \Re_3 + \cdots) \tag{8}$$

flux, Φ. The largest reluctances are often those of the air gaps. In iron the nonlinear relationship between mmf and flux may produce large variations in $\Re$, and it is then convenient to specify B, and use the magnetization surve, relating B to the mmf per meter, to obtain the mmf, iN. Fringe fields in air may cause significant differences in fluxes in the different parts of the circuit, referred to as flux leakage, and these usually require corresponding adjustments to B. Greater accuracy is obtained by using numerical methods to compute the field.

The analogy between magnetic and electric circuits fails in that energy is dissipated in resistance but not in reluctance. Equations (1) and (3) show that a coil of N turns magnetizing a magnetic circuit of reluctance $\Re$ absorbs an energy given by Eq. (9)

$$ei\,dt = iN\,d\Phi = \Re\Phi\,d\Phi \qquad \text{joules} \tag{9}$$

in time dt, where $d\Phi$ is the flux change [Eq. (1)]. Summing shows that, if $\Re$ is constant, then the total energy required to increase the flux from zero to Φ is given by Eq. (10), and this energy, measured in

$$\int ei\,dt = \Re\Phi^2/2 \qquad \text{joules} \tag{10}$$

joules, is stored, not dissipated, since it is recovered when the flux is driven back to zero.

The storage of energy is a key property of a magnetic circuit or, more generally, of a magnetic field.

Since the flux $\delta\Phi$ in a volume element of cross-sectional area δa is $B\ \delta a$, and the reluctance $\delta\Re$ is proportional to the length δl [Eq. (4)], the energy required to magnetize the element is proportional to its volume. Substituting in Eq. (10) shows that the energy per unit volume is given by Eq. (11).

$$\mathfrak{E} = B^2/2\mu \qquad \text{J/m}^3 \qquad (11)$$

The high permeability, μ, of the iron causes a high concentration of energy, $\mathfrak{E}$, in the air gaps of a magnetic circuit in which B is uniform. This is recovered if the iron surfaces are allowed to come together, while B is kept constant. Hence, the force per unit area is given by Eq. (12) when the flux density, B,

$$f = B^2/2\mu_0 \qquad (12)$$

in the air is in the direction normal to the surface. The force of attraction between the two halves of the magnetic circuit in Fig. 3 is obtained by summing f over the areas of both air gaps. The attraction is important in many magnetic devices. An example is the use of electromagnets to lift steel scrap. *See* ELECTROMAGNET.

The highest fields obtainable in air, using superconducting coils, give B values in excess of 1 tesla, at which the energy density is approximately 4×10^5 J/m^3, or 0.4 J/cm^3. The recovery of the energy takes the form of an arc if any attempt is made to reduce the current to zero by opening a switch. Some arcing occurs across the contacts of any switch which energizes a magnetic circuit, or field, and protective measures may be necessary to prevent damage.

Comparing energy properties makes $\Re$ the magnetic equivalent of an electrical capacitor. The magnetic "flow" quantity, or "current," becomes $d\Phi/dt$ instead of Φ and describes the movement of poles, corresponding to the flow of charge in the electrical equivalent. Although this analogy is helpful, and more systematic (including aspects such as the modeling of eddy currents), the comparison of $\Re$ with electrical resistance is more usual.

Magnetic field strength. It is convenient to introduce two different measures of the magnetic field: the flux density, B, and the mmf per meter, referred to as the field strength, or field intensity, H. The field strength, H, provides a measure of the currents and other magnetic field sources, excluding those representing polarizable materials. It may also be defined in terms of the force on a unit pole.

A straight wire carrying a current I sets up a field (**Fig. 5**) whose intensity at a point at distance r is given by Eq. (13). The field strength, H, like B, is a

$$H = \frac{I}{2\pi r} \qquad (13)$$

vector quantity pointing in the direction of rotation of a right-hand screw advancing in the direction of current flow. The intensity of the field is shown by the number of field lines intersecting a unit area. The straight wire provides one example of the circuital

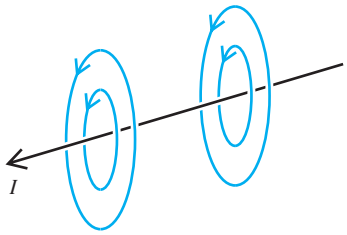

Fig. 5. Magnetic field of a straight wire.

law, known as Ampère's law, given in vector notation by Eq. (14). Here, θ is the angle between the vector

$$\oint H \cdot dl = \oint H \cos\theta\, dl = I \qquad (14)$$

H and the element **dl** of any closed path of summation, or integration, and H and d denote magnitudes. I is the current which links this path. Choosing a circular path, centered on a straight wire, reduces the integral to $H\,(2\pi r)$. Equation (4) cannot be applied unless a path can be found along which H is uniform, or the way in which H varies with position is known.

A long, straight, uniformly wound coil (**Fig. 6**), for example, produces a field which is uniform in the interior and zero outside. The interior magnetic field, H, points in the direction parallel to the coil axis. Applying Eq. (14) to the rectangle $pqrs$ of unit length in the axial direction shows that the only contribution is from pq, giving Eq. (15), where $\boldsymbol{n}$ is the number

$$H = In \qquad (15)$$

of turns, per unit length, carrying the current, I. The magnetic field strength, H, remains the same, by definition, whether the interior of the coil is empty or is filled with ferromagnetic material of uniform properties. The interior forms part of a magnetic circuit in which In is the mmf per unit length. H is the analog of the electric field strength E, in the conductors of an electric circuit. The flux density, B, describes the effect of the field, in the sense of the voltage which is induced in a search coil by changes in time [Eq. (1)]. The ratio of H to B is the reluctance of a volume element of unit length and unit cross section in which

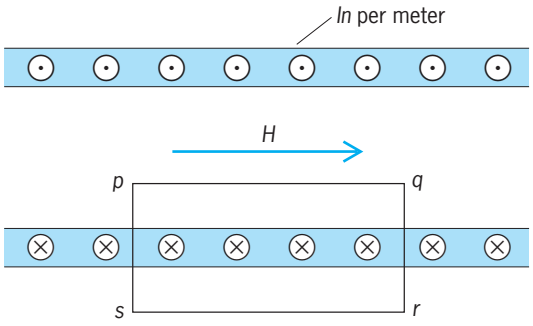

Fig. 6. Cross section of part of a long, straight uniformly wound coil. Black circles indicate current flowing out of the plane of the page, and crosses indicate flow in the opposite direction. Rectangle *pqrs* is used to calculate magnetic field strength, *H*, within the coil.

the field is uniform. Equation (4), shows that the two quantities are related by Eq. (16). The energy density in the field [Eq. (11)] is given by Eq. (17).

$$B = \mu H \tag{16}$$

$$\mathfrak{E} = HB/2 \qquad \text{J/m}^3 \tag{17}$$

The permeability, μ, is defined by Eq. (16). The relative permeability, μ_r, of polarizable materials [Eq. (7)] is measured accordingly by subjecting a sample to a uniform field inside a long coil such as that shown in Fig. 6 and using the emf induced in a search coil wound around the specimen to observe the flux in it.

The magnetic field due to current-carrying conductors in air may also be found by dividing the circuit into elements and summing the contributions from each. Provided that I is constant, or varies only slowly in time, the field, dH, at a point, P, due to a short length, dl, of a thin wire carrying a current, I, is given by the Biot-Savart law, Eq. (18), where θ is

$$dH = \left(\frac{I\,dl}{4\pi r^2}\right)\sin\theta \tag{18}$$

the angle between the axis of the wire, in the current flow direction, and the line of length r joining P to the current element. The field lines form circles centered on the current element axis, directed according to the right-handed screw rule. The field due to a point charge, q, moving at velocity u is likewise given by Eq. (19) at points close enough to make the

$$H = \left(\frac{qu}{4\pi r^2}\right)\sin\theta \tag{19}$$

propagation delay negligible.

Magnetic flux and flux density. Magnetic flux is defined in terms of the forces exerted by the magnetic field on electric charge. The forces can be described in terms of changes in flux with time [Eq. (1)], caused either by motion relative to the source or by changes in the source current, describing the effect of charge acceleration.

Since the magnetic, or electrokinetic, energy of current flowing in parallel wires depends on their spacing, the wires are subject to forces tending to change the configuration. The force, dF, on an element of wire carrying a current, i, is given by Eq. (20), and this provides a definition of the flux

$$dF = Bi\,dl \qquad \text{newtons} \tag{20}$$

density, B, due to the wires which exert the force. The quantity B is sometimes referred to as magnetic induction. The SI unit, called the tesla, or Wb/m^2, is the N/A-m. The flux density, B, equals $\mu_0 H$ in empty space, or in any material which is not magnetizable [Eq. (16)]. An example is the force which is exerted by a long straight wire on another which is parallel to it, at distance r. Equation (13) shows that the force, F, per meter length, between wires carrying currents I and i is given by Eq. (21). when the wires carry currents I and i. F is accounted for by the electrokinetic interactions between the conduction charges, and describes the relativistic modification of the electric forces between them due to their motion. In consequence, F is small when the currents are of the order of 1 A, but is sufficient to cause damage in high-power devices, particularly when the currents are of an impulsive nature, due to fault conditions or lightning strokes. *See* LIGHTNING AND SURGE PROTECTION.

$$F = \frac{\mu_0 Ii}{2\pi r} = 2\times 10^{-7}\,Ii/r \qquad \text{newtons} \tag{21}$$

In general, any charge, q, moving at velocity u is subject to a force given by Eq. (22), where $\mathbf{u}\times\mathbf{B}$ denotes the cross-product between vector quantities. That is, the magnitude of $\mathbf{f}$ depends on the sine of the angle θ between the vectors $\mathbf{u}$ and $\mathbf{B}$, of magnitudes u and B, according to Eq. (23). The force

$$\mathbf{f} = q\,\mathbf{u}\times\mathbf{B} \qquad \text{newtons} \tag{22}$$

$$f = quB\sin\theta \tag{23}$$

on a positive charge is at right angles to the plane containing $\mathbf{u}$ and $\mathbf{B}$ and points in the direction of a right-handed screw turned from $\mathbf{u}$ to $\mathbf{B}$.

The same force also acts in the axial direction on the conduction electrons in a wire moving in a magnetic field, and this force generates an emf in the wire. The emf in an element of wire of length dl is greatest when the wire is at right angles to the $\mathbf{B}$ vector, and the motion is at right angles to both. The emf is then given by Eq. (24). More generally, u is

$$\text{emf} = uB\,dl \tag{24}$$

the component of velocity normal to $\mathbf{B}$, and the emf depends on the sine of the angle between $\mathbf{dl}$ and the plane containing the velocity and the $\mathbf{B}$ vectors. The sign is given by the right-handed screw rule, as applied to Eq. (23).

Since the wire moves through a distance $u\,dt$ in time dt, and B denotes flux density, the element dl "cuts through" an amount of flux given by Eq. (25).

$$d\Phi = uB\,dl\,dt \tag{25}$$

It follows that the motion of any closed loop generates a net emf given by the rate of change of flux linkage, $d\Phi/dt$, with the loop, in accordance with Eq. (1). The concept of motion relative to the field which is implied by "flux cutting" has caused much debate in applications such as homopolar devices in which B is uniform. The difficulty originates in the interpretation of velocity in Eq. (22). In general, the Lorentz force, Eq. (26), depends on the definition of

$$\mathbf{f} = q(\mathbf{E} + \mathbf{u}\times\mathbf{B}) \tag{26}$$

$\mathbf{u}$ as relative to any specified inertial reference frame in which the electric field is $\mathbf{E}$. The magnetic field

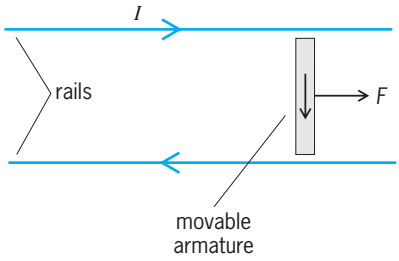

Fig. 7. Electromagnetic railgun. Passing a large current, *I*, along the rails and through the movable armature produces force, *F*, on the armature.

sources are not necessarily stationary in this reference. They may contribute to **E**, so that the electric field is not, in general, confined to electrostatics. **E** depends on the velocity of the observer, as does **B**, since the magnetic field of a moving charge is zero in the reference in which the charge is stationary [Eq. (19)].

A small search coil provides a convenient way of measuring B [Eq. (2)]. Either removing or inserting it, or changing the source current, induces an emf in accordance with Eq. (1). The change in Φ is obtained by integrating the induced voltage in time as, for example, with a ballistic galvanometer, with an integrating amplifier, or by digital processing. The transverse Hall voltage which appears in a stationary current-carrying conductor as a consequence of the Lorentz forces on the moving electrons is also commonly used to measure B. *See* GALVANOMETER; HALL EFFECT.

Since the forces on current elements are in the direction at right angles to the element, the action and reaction forces between two elements are not in opposite directions. A force balance is obtained only between total forces on closed circuits. The electromagnetic railgun (**Fig. 7**) provides an example. Passing a large current, I, from a source to the left along the rails and through a movable armature propels the armature to the right. The source of the action is the B field of the rail currents, but these are not subject to any recoil since the forces on them are at right angles to the rails. The equilibrium is accounted for locally by attributing a state of stress to the magnetic field in the gun interior, producing an outward pressure on each of the conductors. The concept of stress, due to James Clerk Maxwell, describes the flux lines as in tension, producing the force per unit area given by Eq. (12), together with a transverse pressure of the same magnitude. The stress is commonly used to predict forces in magnetic devices, particularly when the field is calculated by numerical methods.

Equation (22) shows that any charge which moves freely in a magnetic field is subjected to a force at right angles to its motion, tending to drive it into a closed circular path. This force, quB, is balanced by the centrifugal force mu^2/r on a particle of mass m, causing it to travel in a circle whose radius is given by Eq. (27) [with a transit time which is independent of u], unless there is a component of the velocity, u, in the direction of B. Since this component causes no interaction, the charges then tend to spiral along the flux lines. The behavior is characteristic of charged particles entering the Earth's magnetic field from outer space, and is utilized in many applications requiring the control of moving electrons, such as the magnetic focusing of electron beams. *See* ELECTRON MOTION IN VACUUM; VAN ALLEN RADIATION.

$$r = \frac{mu}{qB} \qquad \text{meters} \qquad (27)$$

Magnetic flux linkage. The magnetic flux linking any closed path is obtained by counting the number of flux lines passing through any surface, s, which is bounded by the path. Stated more formally, the linkage depends on the sum given in Eq. (28), where B_n

$$\Phi = \iint B_n \, ds \qquad \text{webers} \qquad (28)$$

denotes the component of B in the direction normal to the area element, ds. The rate of change of linkage gives the emf induced in any conducting wire which follows the path [Eq. (1)].

The flux linkage with a coil (**Fig. 8**) is usually calculated by assuming that each turn of the coil closes on itself, giving a flux pattern which likewise consists of a large number of separate closed loops. Each links some of the turns, so that the two cannot be separated without breaking, or "tearing," either the loop or the turn. The total linkage with the coil is then obtained by adding the contributions from each turn.

Linkage can be defined only when both the flux lines and the conductors form closed paths, so that its use depends on the absence of magnetic monopoles, since these terminate flux lines. The linkage concept cannot be applied to circuits which are not closed, such as some forms of wire antenna, and it may be difficult to apply to conductors of complex shape, as in coils that are not closely wound but form an open spiral (Fig. 8), producing a flux pattern in which the flux lines likewise form spirals. The concept of linkage attributes the induced emf to flux which may be remote from the wire in which the emf is induced, and this action-at-a-distance effect has been the source of much discussion in some applications. One such application is the magnetic Aharonov-Bohm effect, which describes the effect of the flux linkage on quantum phase. All of the actions attributed to flux linkage can be described more directly in terms of the magnetic vector potential. *See* AHARONOV-BOHM EFFECT.

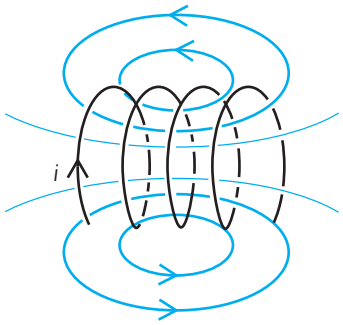

Fig. 8. *B* (magnetic flux) field of a short coil.

The inductance, L, is a property of a circuit defined by the emf which is induced by changes of current in time, as in Eq. (29). The SI unit of inductance is

$$e = -L\,di/dt \tag{29}$$

the henry (H), or V-s/A. The negative sign shows that e opposes an increase in current (Lenz's law). From Eq. (1) the inductance of a coil of N turns, each linking the same flux, Φ, is given by Eq. (30), so that

$$L = N\,\Phi/i \qquad \text{henrys} \tag{30}$$

the henry is also the Wb/A. When different turns, or different parts of a circuit, do not link the same flux, the product $N\Phi$ is replaced by the total flux linkage, Φ, with the circuit as a whole. Applying the result to a air-cored coil of N turns whose length, d, is sufficient to give an approximately uniform field, H, in the interior [Eq. (15)] gives Eq. (31), if all of the

$$L = \mu_0 N^2\,\pi r^2/d \qquad \text{henrys} \tag{31}$$

turns (Fig. 6) are circular in shape with a common radius, r. Doubling the number of turns produces a fourfold increase in L because the same current produces twice as much flux, linking twice as many turns. *See* INDUCTANCE.

Reducing the length brings the turns closer together and increases the inductance, since this consists of the sum of the mutual interactions between the various parts. The mutual inductance, M, between any two coils, or circuit parts, is defined by emf which is induced in one by a change of current in the other. Using 1 and 2 to distinguish between them, the emf induced in coil 1 is given by Eq. (32*a*),

$$e_1 = -M_{12}\,di_2/dt \tag{32a}$$

$$e_2 = -M_{21}\,di_1/dt \tag{32b}$$

where the sign convention is consistent with that used for L when the coils are connected in the series. The quantity L is referred to as the self-inductance. Likewise, the emf induced in coil 2 when the roles of the windings are reversed is given by Eq. (32*b*). The interaction satisfies the reciprocity condition of Eq. (33), so that the suffixes may be omitted. If coil

$$M_{21} = M_{12} \tag{33}$$

1 consists of N_1 turns wound sufficiently closely together to link the same flux, then the mutual inductance is given by Eq. (34).

$$M = N_1\,\Phi_1/i_2 \qquad \text{henrys} \tag{34}$$

The choice of winding role may sometimes simplify the calculation. For example, a short coil of N_2 turns, each in the form of a circle of radius r_2, will link a flux which is proportional to the circles area when placed inside, and coaxial with, the coil whose self-inductance is given by Eq. (31). Applying Eq. (15) shows that the mutual inductance between the two is given by Eq. (35) if the larger coil consists of N_1 turns wound over a length d_1. Reversing the roles makes it more difficult to calculate the mutual flux linkage when the smaller coil is too short to produce a uniform field. The mutual inductance between two coils which have approximately the same length and radius, and are sufficiently close, is given by Eq. (36). This equation applies more generally to

$$M = \mu_0 N_1 N_2\,\pi r_2^2/d_1 \qquad \text{henrys} \tag{35}$$

$$M = L_1\,N_2/N_1 \tag{36}$$

any two coils whose turns share the same flux, usually because they are linked by a common flux path of a sufficiently high permeability (Fig. 3).

Parallel wires whose length is sufficient to ignore axial variations in the field provide another important example. Current flowing in any one of them produces a magnetic field strength, H, varying inversely with the distance, r, from it [Eq. (13)]. Hence, the total flux per meter length linking two other wires, at distances r_1 and r_2 from the source, is given by Eq. (37). Dividing by the current, i, gives the mutual inductance in H/m. Any assembly of wires can be treated by superposition.

$$\Phi = \int B\,dr = (\mu_0/2\pi)i\,\log_e\,[r_2/r_1] \qquad \text{Wb/m} \tag{37}$$

The field conditions are similar between the core and sheath of a coaxial cable consisting of a core conductor of circular cross section, with radius r_1, inside a sheath of radius r_2 carrying the return current. Equation (14) shows that the field, H, varies inversely with radius in the annular space between the two. Hence Eq. (37) gives the flux, and inductance per meter, when the frequency is sufficiently high to confine the current to the surface layers of the conductors. *See* COAXIAL CABLE.

Current flow paths inside the core add to the flux, giving these paths a higher inductance than those on the surface. This increases their inductive impedance, defined as the ratio of the induced emf, e, to the current. The increase is typical of internal paths, in all problems of alternating currents flowing in solid conductors, and tends to confine the currents to a surface layer whose thickness diminishes as the frequency rises. The same effect may also restrict the current to a more limited path within the layer, as when a wire carries a current, I, at high frequency close to a conducting plate (**Fig. 9**). The requirement that the inductance, and hence the magnetic flux linkage, is a minimum produces a concentration of induced current in a path immediately beneath the wire, known as the shadowing effect. The local heating may raise the temperature of the strip sufficiently to make it glow, and provides a method of controlled welding. *See* SKIN EFFECT (ELECTRICITY).

Magnetostatics. The term "magnetostatics" is usually interpreted as the magnet equivalent of the electrostatic interactions between electric charges. The

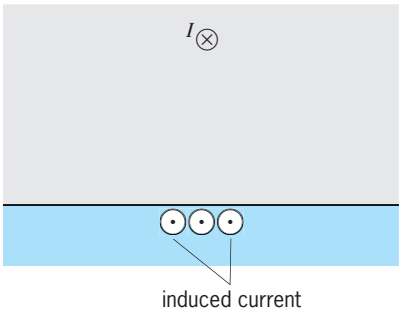

Fig. 9. Current shadowing.

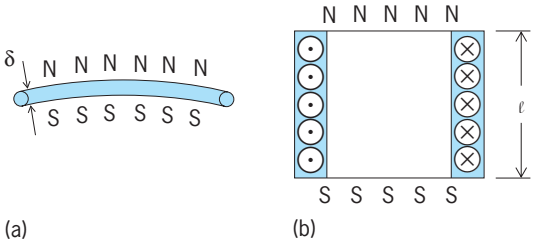

Fig. 10. Magnetic shell equivalents for (*a*) wire loop and (*b*) multiturn coil.

equivalence is described most directly in terms of the magnetic pole, since the forces between poles, like those between charges, vary inversely with the square of the separation distance. Although no isolated poles, or monopoles, have yet been observed, the forces which act on both magnets and on coils are consistent with the assumption that the end surfaces are equivalent to magnetic poles.

This follows from the magnetic shell principle. Separating two surfaces of magnetic charge of opposite sign by a small distance, δ (**Fig. 10***a*), creates a constant difference in potential, or mmf, if the charges, or poles, are uniformly distributed. A current flowing in a loop which bounds the edge of the sheets produces the same magnetic field, other than in the space between the sheets. Superposing turns shows that a uniformly wound coil of N turns of wire carrying a current, i (Fig. 10*b*), can be replaced by two sheets of magnetic charge of opposite sign, each uniformly distributed over surfaces bounded by the end turns of the coil. Both the turns and the pole sheets are shown plane in Fig. 10*b*, but in general the magnetic shell of a single turn can have any shape which is bounded by the turn, and this applies by superposition to larger coils.

The pole density, per unit area, is given by Eq. (38) for a single turn, or by Eq. (39) for a coil of N turns and length l. The total force, or torque, acting on the shell is the same as that on the loop or coil, where the force on a pole of strength q_m is given by Eq. (40). Figure 10*b* also illustrates the two alternative models of a uniformly polarized magnet, one consisting of surface currents representing the sum of the "Ampèrean currents," and the other the surface poles. Equations (14) and (40) show that the work done in carrying a unit pole around any closed path is equal to the current I, or iN, which is linked by the path.

$$\rho_m = \mu_0 i/\delta \tag{38}$$

$$\rho_m = \mu_0 iN/l \tag{39}$$

$$f = q_m H \tag{40}$$

Replacing currents by poles is useful for computational purposes since it replaces the mmf by a magnetic scalar potential, analogous to the electrostatic potential. Both are conservative; that is, the work required to move a pole, or charge, between any two points is independent of the path taken.

Magnetic moment. The magnetic moment of a small current loop, or magnet, can be defined in terms of the torque which acts on it when placed in a magnetic flux density, B, which is sufficiently uniform in the region of the loop. Equal but opposite forces then act on opposite sides of length a of a rectangular loop of N turns (**Fig. 11**) carrying a current, i. The force is $iNBa$ [Eq. (20)], and the torque, given by Eq. (41), depends on the effective

$$T = iNBa\,b \sin\theta \qquad \text{N-m} \tag{41}$$

distance, $b \sin\theta$, between the wires. It is proportional to the area ab, and is a maximum when the angle θ between B and the axis of the loop is 90°. A current loop of any other shape can be replaced by a set of smaller rectangles placed edge to edge, and the torques of these added to give the total on the loop. The magnetic moment, m, of any loop of area s is defined as the ratio of the maximum torque to the flux density, so that m is given by Eq. (42). This

$$m = iNs \tag{42}$$

is the magnitude of a vector quantity $\mathbf{m}$ pointing in the direction of a right-handed screw turned in the direction of current flow. It gives the torque $\mathbf{T}$ in Eq. (43) in vector cross-product notation.

$$\mathbf{T} = \mathbf{m} \times \mathbf{B} \tag{43}$$

See TORQUE.

The coil, or magnet, may also replaced by its magnetic pole, or magnetic shell, equivalent. The torque is then accounted for by the forces on poles of strength q_m at opposite ends distance l apart, where q_m is the pole density times the area, s. Hence, from

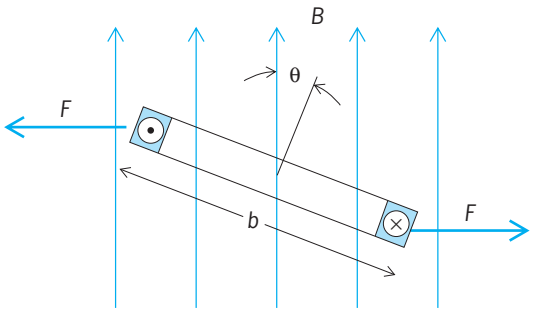

Fig. 11. Forces acting on rectangular current loop, shown in cross section, due to the magnetic flux density *B*. Current flow direction is shown in the same way as in Fig. 6.

Eqs. (39) and (40), the torque is given by Eq. (44),

$$T = \mu_0 iNH\, s \sin\theta \tag{44}$$

and this comparison demonstrates the equivalence. The moment, m^*, may be defined by describing the torque in terms of H instead of B, giving Eq. (45).

$$m^* = \mu_0 m \tag{45}$$

An electron of charge of $q_e$orbiting at frequency f is the equivalent of a current $i = q_e f$, giving Eq. (46)

$$m_0 = q_e f s \tag{46}$$

for the moment, where s is the area of the orbit. The permissible values are determined by the quantum energy levels. The electron spin is a quantum state which can likewise be visualized as a small current loop. Atomic nuclei also possess magnetic moments. *See* ELECTRON SPIN; MAGNETON; NUCLEAR MOMENTS.

Magnetic polarization. Materials are described as magnetic when their response to the magnetic field controls the ratio of B to H. The behavior is accounted for by the magnetic moments produced mainly by the electron spins and orbital motions. These respond to the field and contribute to it in a process referred to as magnetic polarization. The effects are greatest in ferromagnetics and in ferrites, in which the action is described as ferrimagnetic. *See* FERRIMAGNETISM; FERRITE; FERROMAGNETISM.

Current-based model. The sources are the equivalent of miniature "Ampèrean currents" whose sum, in any volume element, is equivalent to a loop of current flowing along the surface of the element. The flux density, B, depends on the field intensity, H, which is defined so that its value inside a long ferromagnetic rod of uniform cross section placed inside a long coil (Fig. 6) is not affected by the rod. It is given by Eqs. (14) and (15) and is the same inside the material as in the annular gap between the rod and the coil, in accordance with Eq. (15). If the field is not sufficiently uniform, H can be measured by using a search coil to observe the flux density, $\mu_0 H$, in the gap. The flux density inside the rod is given by Eq. (47), where

$$B = \mu_r B_0 \tag{47}$$

B_0 denotes $\mu_0 H$, and μ_r is the relative permeability [Eqs. (7) and (16)]. The same flux, B, is obtained by replacing the material by a coil in which the current in amperes per unit length is given by Eq. (48).

$$\begin{aligned} J_s &= (B - B_0)/\mu_0 \\ &= (1 - 1/\mu_r)B/\mu_0 \end{aligned} \tag{48}$$

The magnetic moment, [Eq. (42)], of a volume element of length dz, due to the current J_s flowing over the surface enclosing the area, $dx\, dy$, is given by Eq. (49). The moment per unit volume defines

$$dm = (J_s\, dz)\, dx\, dy \tag{49}$$

the magnetic polarization, as in Eq. (50). The polarization, $\mathbf{M}$, is a vector pointing in the direction of $\mathbf{dm}$ with magnitude J_s. The surface current accounts for $\mathbf{B}$ but produces an $\mathbf{H}$-like, or $\mathbf{B}/\mu_0$, field which is entirely different from $\mathbf{H}$ in the material. Substituting from Eq. (48) gives Eq. (51).

$$M = dm/dx\, dy\, dz \tag{50}$$

$$\mathbf{H} = \frac{\mathbf{B}}{\mu_0} - \mathbf{M} \tag{51}$$

This model of the material gives the flux field, $\mathbf{B}$, as observed by the voltage induced in a search coil wound around the specimen, and $\mathbf{H}$, becomes an auxiliary quantity representing the difference between $\mathbf{B}/\mu_0$ and the polarization, $\mathbf{M}$. $\mathbf{B}$ is the magnetizing field to which $\mathbf{M}$ responds. The polarization, $\mathbf{M}$, contributes to that field, when B is greater than B_0 [Eq. (47)], since the equivalent surface current is then in the same direction as the current in the magnetizing coil.

Pole-based model. The rod may also be replaced by equivalent magnetic poles distributed over the two end surfaces (Fig. 10*b*), and this alternative likewise applies to its volume elements. Since the flux lines are continuous, by definition, the component of $\mathbf{B}$ normal to the surface is the same on both sides, and the relationship $B = \mu H$ requires a change in H. The change, from H_0 on the outside to H, given by Eq. (52), in the interior, is accounted for by the

$$H = H_0/\mu_r \tag{52}$$

magnetic poles. The pole density, ρ_s^*, per unit surface area is given by Eq. (53).

$$\begin{aligned} \rho_s^* &= \mu_0(H_0 - H) \\ &= (\mu_r - 1)\mu_0 H \end{aligned} \tag{53}$$

Each volume element $dx\, dy\, dz$ acquires a magnetic moment given by Eq. (54), and a corresponding magnetic moment, $\mathbf{M}^*$, per unit volume. The equivalent poles are defined so as to produce the same field, $\mathbf{H}$, as in the material, and the corresponding $\mu_0\mathbf{H}$ flux field is entirely different from $\mathbf{B}$, which is obtained by adding $\mathbf{M}^*$ to $\mu_0\mathbf{H}$, as in Eq. (55). It is B which be-

$$dm^* = (\rho_s\, dx\, dy)\, dz \tag{54}$$

$$\mathbf{B} = \mu_0\mathbf{H} + \mathbf{M}^* \tag{55}$$

comes the auxiliary vector in the pole-based model, whose polarization vector, $\mathbf{M}^*$, is $\mu_0\mathbf{M}$, in accordance with Eq. (45). If a sample of the material is placed in an air gap, the surface poles acquire an opposite sign to those on the iron surfaces adjacent to them.

Additional equivalent sources appear inside the material when the changes in permeability are not confined to the surfaces. The customary use of $\mathbf{H}$ as the "magnetizing field" follows from the historical role of the pole as the magnetic analog of electric charge, and the corresponding comparison between the treatment of magnetic materials, in terms of displaced poles, with dielectrics, whose behavior depends on the displacement of charge. Both $\mathbf{B}$ and $\mathbf{H}$ represent averages of the complex field conditions

which are produced by arrays of dipoles, and are difficult to observe since local measurements require cavities whose shape determines the result. The potential functions provide more meaningful measures, in terms of the array energy, and provide a definition of the vector **B** as the differential of the magnetic vector potential, **A**, discussed below.

Magnetic hysteresis. The relationship between the flux density, B, and the field intensity, H, in ferromagnetic materials depends on the past history of magnetization. The effect is known as hysteresis. It is demonstrated by subjecting the material to a symmetrical cycle of change during which H is varied continuously between the positive and negative limits $+H_m$ and $-H_m$ (**Fig. 12**). The path that is traced by repeating the cycle a sufficient number of times is the hysteresis loop. The sequence is counterclockwise, so that B is larger when H is diminishing than when it is increasing, in the region of positive H. The flux density, B_r, which is left when H falls to zero is called the remanence, or retentivity. The magnetically "hard" materials used for permanent magnets are characterised by a high B_r, together with a high value of the field strength, $-H_c$, which is needed to reduce B to zero. The field strength, H_c, is known as the coercive force, or coercivity. Cycling the material over a reduced range in H gives the path in Fig. 12 traced by the broken line, lying inside the larger loop. The locus of the tips of such loops is known as the normal magnetization curve. The initial magnetization curve is the B-H relationship which is followed when H is progressively increased in one direction after the material has first been demagnetized ($B = H = 0$).

A magnet which forms a part of a magnetic circuit (Fig. 2) is driven to the point, P, in the part of the hysteresis loop in which B and H are in opposite directions. The mmf of the magnet of length l is Hl if the field intensity, H, is the same through the volume of the material. The reluctance $\Re$ of the rest of the magnetic circuit produces an equal but opposite mmf in response to the flux, Φ, obtained by multiplying B by the magnet cross-sectional area, a. Hence, Eq. (56) holds.

$$Hl = \Re Ba \tag{56}$$

This approximation to the position of P can be expressed graphically by observing that the slope, B/H, of the line OP is inversely proportional to $\Re$. Reducing the reluctance does not, in general, return the magnet to the point B_r, but establishes a path, PQ, known as a recoil curve, forming a part of a minor hysteresis loop.

Materials that are easily demagnetized are referred to as magnetically soft. When these are used in applications in which the supply current alternates in time, the hysteresis action changes the time phase between B and H, producing losses in the form of heat. The field strength, H, is a measure of the current, i, flowing in a single turn of suitable shape which is required to magnetize a volume element of material of unit size. Since the flux linking the coil, of unit

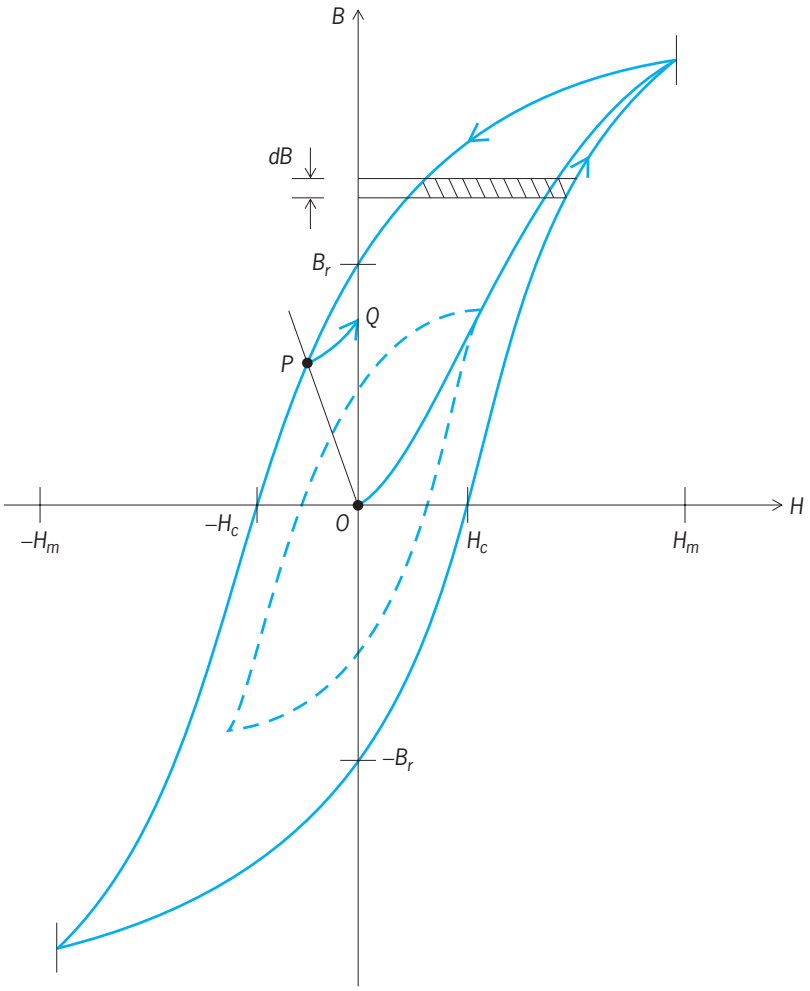

Fig. 12. Hysteresis behavior of a ferromagnetic material.

area, is B, the voltage, e, induced in the coil [Eq. (1)] is given by dB/dt, and the energy supplied to the element during any interval of time, t, is given by Eq. (57). In the last integral, $H\,dB$ is the area of a

$$\int ei\,dt = \int (dB/dt)H\,dt = \int H\,dB \tag{57}$$

strip of width dB drawn between the B-H curve and the $H = 0$ axis (Fig. 12), so that the energy injected is the area over the curve. When B varies linearly with H, up to the values B_m and H_m, the area forms a triangle, and the input, given by Eq. (58), is recov-

$$\int ei\,dt = H_m B_m/2 \tag{58}$$

ered when the line retraced is in accordance with the stored energy density in Eq. (17). Retracing the magnetization curve along a different path results in a hysteresis loop whose area is the loss, W, per unit volume per cycle. The Steinmetz coefficient, η, gives the net loss in terms of the empirical relationship of Eq. (59). The exponent n may vary between 1.5 and

$$W = \eta(B_m)^n \tag{59}$$

2.5. The Steinmetz value of 1.6 is appropriate for many materials.

Vector potential. The use of magnetic poles provides a treatment of magnets and current-carrying coils in terms of a magnetic scalar potential, but the application is limited by the need to replace current sources by magnetic pole equivalents. The more direct description of moving charges, or currents, as field sources requires the magnetic vector potential, **A**, whose significance is illustrated by its application to the calculation of induced emf's. A magnetic field which changes in time induces an emf in an element of wire of length dl given by Eq. (60), where θ is the

$$de = -(dA/dt)\, dl\, \cos\theta \tag{60}$$

angle between the vectors **dl** and **A**. The total, e, for any wire, or conducting path, is obtained by summation. The quantity $N\Phi$ in Eq. (1) can therefore be replaced by the symbol Ψ, defined by Eq. (61), without reference to flux or flux linkage, as in Eq. (28). The integral may extend around the N turns of a coil by adding the contributions of each, but does not require that the path, or any part of it, closes on itself. Other advantages include the description of emf in terms of the local values of **A** at the wire, in place of flux linkages requiring the summation of remote values of B over surfaces bounded by the wire [Eq. (28)].

$$\Psi = \int A\, \cos\theta\, dl \tag{61}$$

The relationship between the magnetic field and the source currents is described most directly by treating an element, dl, of a wire carrying a current, i, as the magnetic analog of electric charge. The magnitude of **A**, like the electric potential, φ, of a point charge, varies inversely with the distance, r, from the source in accordance with Eq. (62). **dA** points

$$\mathbf{dA} = \frac{\mu_0 i\, \mathbf{dl}}{4\pi r} \tag{62}$$

in the direction of current flow in the element. This is an example of the more general relationship given by Eq. (63) between the vector potential, at point

$$\mathbf{A} = \mu\varphi/c^2 \tag{63}$$

P, due to any group of charges moving at velocity u and the potential, φ, of the same group at P. Here, c is the velocity at which changes in both potentials propagate in empty space (the velocity of light). It follows that the constant μ_0 is given by Eq. (64) in

$$\mu_0 = 1/\varepsilon_0 c^2 \tag{64}$$

terms of ε_0, sometimes known as the permittivity of free space.

The mutual inductance between any two wires, as defined by Eqs. (32) and (60), is given by Eq. (65)

$$M = \Psi_2/i_1 \tag{65}$$

in terms of the summation along wire 2 of the contributions to **A** from the current, i_1, flowing in wire 1.

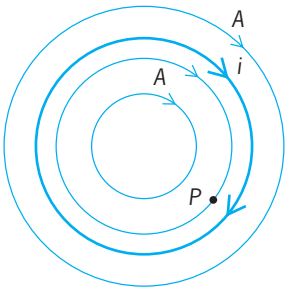

Fig. 13. Magnetic vector potential, *A*, due to a loop of wire.

The calculation cannot be expressed in terms of flux linkage if wire 2 does not form a closed circuit. The two summations can be combined to give Eq. (66)

$$M = \mu_0 \int_1 \int_2 (1/r)\, dl_1\, dl_2\, \cos\theta \tag{66}$$

in terms of elements dl_1 and dl_2 at distance r and angle θ to each other. The result, due to Franz Neumann, is limited to circuits in air formed from wires, or filaments, in which the current is everywhere the same. In general, it is necessary to calculate **A** explicitly, particularly when considering the effects of induced currents and of ferromagnetic materials.

The magnetic field due to currents flowing in parallel straight wires is described by an **A** vector which points everywhere in the axial direction. Equation (63) shows that an equipotential map of the surfaces on which the magnitude **A** is constant is identical to the map of the φ equipotentials when the same wires carry charge instead of current. Hence the inductances between various conductors, when the currents are confined to the surface layers, are proportional to the reciprocal of the capacitances between the same conductors. Closing up any current-carrying wire into a loop (**Fig. 13**) likewise "curls up" its **A** vector, since Eq. (62) requires that the direction of **A** at any point, P, close to the wire is that of the nearest current. If the frequency is sufficiently low to give the same current at all points in the wire, then **A** likewise forms closed loops. Equations (28) and (61) can be expressed in the differential form of Eq. (67), and this provides an alternative definition

$$\mathbf{B} = \text{curl}\, \mathbf{A} \tag{67}$$

of magnetic flux density. The "general equations of the electromagnetic field" set out by Maxwell in his *Treatise* depend on this use of **A** as the principal measure of the magnetic field, and **B** as a symbol for its differential. Maxwell's approach is reversed in modern practice, in which **B** is treated as the source and **A** derived from it, leaving open the choice of the vector property of divergence, div **A**, or gauge. Equation (62) describes the magnetic field of a current element in terms of an **A** vector which does not necessarily close on itself, but satisfies the Lorentz condition, given by Eq. (68).

$$\text{div}\, \mathbf{A} = -(1/c^2)\, \partial\varphi/\partial t \tag{68}$$

The emf, *de*, in Eq. (60) is an example of the force given by Eq. (69), which acts on any charge,

$$\mathbf{f} = -q d\mathbf{A}/dt \qquad (69)$$

q, due to a change of **A**. This provides a description of charge behavior in terms of an electrokinetic momentum, *q***A**, predicting forces which tend to oppose any change. Interrupting the movement of the conduction charges in a current-carrying winding, for example, by opening a switch, causes an arc to form across the contacts due to a rise in electrical potential which is analogous to the rise in pressure when the flow of a fluid through a pipeline is suddenly blocked. The comparison illustrates the physical significance of the circuit inductance. The quantity *q***A** describes the sum of the interactions between all of the moving electrons and *q*, and is thus a property of the system as a whole. The magnetic, or electrokinetic, energy is likewise obtained by summing the energy density, $\mathbf{J} \cdot \mathbf{A}/2$, over all of the currents, of density **J**, and it is this from which the alternative description of energy as a property of the field [Eq. (17)] is derived. The vector **A** is sufficient to describe many magnetic, or electrokinetic, effects without reference to the vector **B**. *See* POTENTIALS. C. J. Carpenter

Bibliography. W. Berkson, *Fields of Force: Development of a World View from Faraday to Einstein*, 1974; B. I. Bleaney and B. Bleaney, *Electricity and Magnetism*, 3d ed., 1976; J. D. Buchwald, *From Maxwell to Microphysics*, 1985; H. E. Burke, *Handbook of Magnetic Phenomena*, 1986; W. J. Duffin, *Electricity and Magnetism*, 4th ed., 1990; I. S. Grant and W. R. Phillips, *Electromagnetism*, 2d ed., 1990; D. Halliday, R. Resnick, and J. Walker, *Fundamentals of Physics*, 6th ed., Wiley, 2000; P. Hammond, *Electromagnetism for Engineers: An Introductory Course*, 4th ed., Oxford University Press, 1997; Y. Ishikawa and Miura (eds.), *Physics and Engineering Applications of Magnetism*, 1991; J. D. Jackson, *Classical Electrodynamics*, 3d ed., 1998; J. D. Krauss, *Electromagnetism*, 4th ed., McGraw-Hill, 1991; P. F. Mottelay, *Biographical History of Electricity and Magnetism*, 1975, reprint 1991; R. G. Powell, *Electromagnetism*, 1990; J. R. Reitz, F. J. Milford, and R. W. Christy, *Foundations of Electromagnetic Theory*, 4th ed., Addison-Wesley, 1993; M. N. O. Sadiku, *Elements of Electromagnetism*, 1995; M. Sibley, *Introduction to Electromagnetics*, 1996; J. Vanderlinde, *Classical Electromagnetic Theory*, 1993; E. Whittaker, *History of Theories of Aether and Electricity*, reprinted 1987; H. D. Young and R. A. Freedman, *University Physics*, 9th ed., 1998.

Magnetite

A cubic mineral and member of the spinel structure type, space group Fd3m, with composition $[Fe^{3+}]^{IV}[Fe^{2+}Fe^{3+}]^{VI}O_4$. It possesses the inverse spinel structure, in which half the ferric iron is tetrahedrally coordinated and the remaining half as well as all ferrous iron are octahedrally coordinated by the cubic close-packed oxygen atoms. The color is opaque iron-black and streak black, the hardness is 6 (Mohs scale), and the specific gravity is 5.20. The habit is octahedral (see **illus.**), but the mineral usually occurs in granular to massive form, sometimes of enormous dimensions. Though possessing no cleavage, some specimens show an octahedral parting. Limited Al^{3+} may substitute for Fe^{3+}; and Ca^{2+}, Mn^{2+}, and Mg^{2+} for Fe^{2+}.

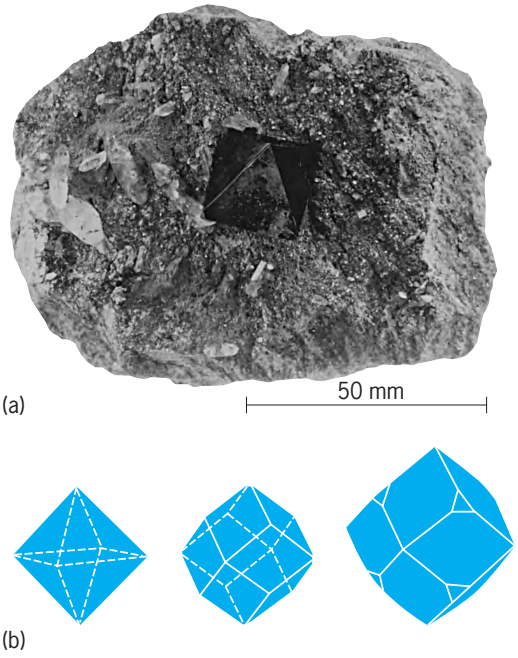

Magnetite. (*a*) Crystal on block of mica schist with small quartz crystals on left, Binnenthal, Switzerland (*American Museum of Natural History specimens*). (*b*) Crystal habits (*after C. Klein and C. S. Hurlbut, Jr., Manual of Mineralogy, 21st ed., John Wiley and Sons, 1993*).

Magnetite is a natural ferrimagnet, but heated above 578°C (1072°F; the Curie temperature) it becomes paramagnetic. It can be prepared by heating hematite (α-Fe_2O_3) in a reducing atmosphere, by heating hematite in air above 1400°C (2552°F), or by the oxidation of iron at high temperatures. Oxidation of magnetite leads to maghemite (γ-Fe_2O_3), which gradually inverts to hematite.

The major magnetic ore of iron, magnetite may be economically important if it occurs in sufficient quantities. It often occurs as an early magmatic segregation in basic rocks, such as anorthosites and norites where it has accumulated in bands by gravity settling. It is also a contact metamorphic product, occurring with limestones, leptites, and so forth. Moderately resistant to weathering, magnetite sometimes accumulates in detrital sands. The most spectacular ore body occurs at Kiruna in northern Sweden, where the magnetite fluid differentiate was injected into syenitic rocks. Other important occurrences are in Norway, Russia, and Canada. Magnetite is common as an accessory mineral in igneous

rocks throughout the world. *See* EMERY; HEMATITE; ILMENITE; IRON METALLURGY; MAGNETIZATION; ORE AND MINERAL DEPOSITS; SPINEL. Paul B. Moore

Magnetization

The process of becoming magnetized; also the property and in particular the extent of being magnetized. Magnetization has an effect on many of the physical properties of a substance. Among these are electrical resistance, specific heat, and elastic strain. *See* MAGNETOCALORIC EFFECT; MAGNETORESISTANCE; MAGNETOSTRICTION.

The magnetization **M** of a body is caused by circulating electric currents or by elementary atomic magnetic moments, and is defined as the magnetic moment per unit volume of such currents or moments. In the electromagnetic system of units (emu), **M** is measured in gauss; in the mks system, **M** is measured in webers per square meter. For **M**, 1 weber/m^2 = $10^4/4\pi$ gauss.

The magnetic induction or magnetic flux density **B** is given by Eq. (1), where **B** and **M** are in gauss,

$$\mathbf{B} = \mathbf{H} + 4\pi\mathbf{M} \text{ (emu)} \tag{1}$$

and **H**, the applied magnetic field, is in oersteds (equivalent to gauss); or by Eq. (2), where **B** and

$$\mathbf{B} = \mu_0\mathbf{H} + \mathbf{M} \text{ (mks)} \tag{2}$$

M are in webers/m^2, **H** is in ampere-turns/m, and μ_0, the permeability of free space, is defined as $4\pi \times 10^{-7}$ henry/m, that is, webers/(ampere-turn)(m). *See* ELECTRICAL UNITS AND STANDARDS.

The permeability μ of a substance is defined as the ratio **B**/**H** (in emu) or $\mathbf{B}/\mu_0\mathbf{H}$ (in mks). The magnetic susceptibility χ is defined as the ratio **M**/**H** (in emu) or $\mathbf{M}/\mu_0\mathbf{H}$ (in mks). From Eqs. (1) and (2) Eq. (3) is

$$\mu = 1 + (4\pi)\chi \tag{3}$$

obtained, where the 4π is to be used only in the emu system. It is to be noted that the magnitude of μ is the same in both systems of units, but the magnitude of χ differs by a factor of 4π. Both μ and χ may be tensors, although usually they are simple numbers. *See* MAGNETIC SUSCEPTIBILITY.

The topic of magnetization is generally restricted to materials exhibiting spontaneous magnetization, that is, magnetization in the absence of **H**. All such materials will be referred to as ferromagnets, including the special category of ferrimagnets. A ferromagnet is composed of an assemblage of spontaneously magnetized regions called domains. Within each domain, the elementary atomic magnetic moments are essentially aligned, that is, each domain may be envisioned as a small magnet. An unmagnetized ferromagnet is composed of numerous domains, oriented in some fashion as shown in **Fig. 1**, so that the total magnetization is zero.

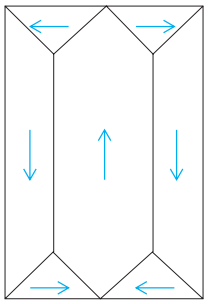

Fig. 1. Possible arrangement of domains in an unmagnetized single crystal. The arrangement is much more haphazard in polycrystals.

The process of magnetization in an applied field **H** consists of growth of those domains oriented most nearly in the direction of **H** at the expense of others (**Fig. 2***a*), followed by rotation of the direction of magnetization against anisotropy forces (Fig. 2*b*). For discussions of anisotropy and of domains *see* FERROMAGNETISM

On removal of the field **H**, some magnetization will remain, called the remanence $\mathbf{M}_r$.

Magnetization curves. These curves, sometimes called *B-H* curves, are used to describe magnetic materials. They are plotted with **H** as abscissa and with either **M** or **B** as ordinate. In **Fig. 3**, $\mathbf{B}_r$ is the remanent induction ($\mathbf{B}_r = 4\pi\mathbf{M}_r$); $\mathbf{H}_c$ is the coercive force, or reverse field required to bring the induction **B** back to zero; and $\mathbf{M}_s$ is the saturation magnetization, or magnetization when all domains are aligned. The saturation magnetization is equal to the spontaneous magnetization of a single domain, except that it is possible to increase this magnetization slightly by application of an extremely large field. Saturation magnetization is temperature dependent, and disappears completely above the Curie temperature T_c where a ferromagnet changes into a paramagnet. The **table** lists $\mathbf{M}_s$ and T_c for a few ferromagnetic materials. *See* CURIE TEMPERATURE.

The initial permeability μ_i of a substance is the slope of the magnetization curve at $\mathbf{H} = 0$. There is a definite correlation between initial permeability and coercive force; that is, materials of large μ_i have small $\mathbf{H}_c$ and vice versa.

The relationship between **B** and **H** may be studied

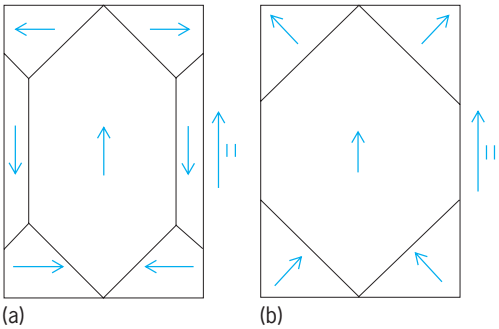

Fig. 2. Process of magnetization. (*a*) Domain growth. (*b*) Rotation.

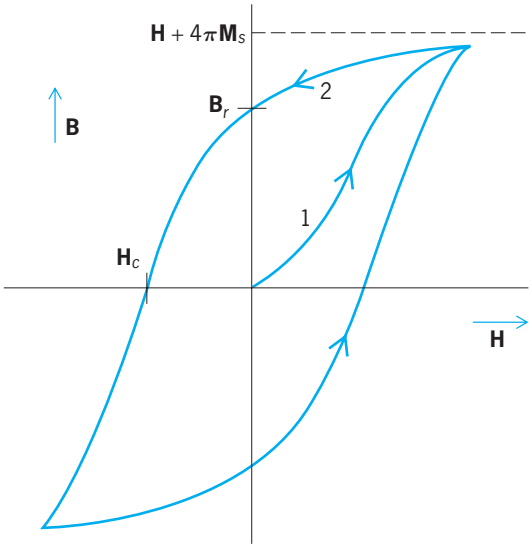

Fig. 3. Magnetization or *B-H* curves.

Values of saturation magnetization M_s and ferromagnetic Curie temperature T_c

Substance	M_s at 293 K (68°F), gauss	M_s at 0 K (−460°F), gauss	T_c, K (°F)
Fe	1707	1752	1043 (1418)
Co	1400	1446	1394 (2050)
Ni	485	510	631 (676)
Gd	0	1980	293 (68)
MnBi	600	675	670 (746)
Fe_3O_4	480	510	858 (1085)
EuO	0	1910	77 (−321)
$Y_3Fe_5O_{12}$	135	195	560 (548)

by means of a Rowland ring or toroid in which the core is the material to be studied. For this arrangement, the numerical value of **H** can be computed from the relation in Eq. (4), where N is the number

$$H = \frac{NI}{l} \tag{4}$$

of turns of the coil, I is the current in the coil, and l is the length of the mean circumference of the coil. If the radius of the ring is large compared to the radial distance across the core, the flux density will be nearly uniform.

The flux density **B** is not a linear function of **H**, and furthermore, its value depends not only upon **H** but upon the previous magnetic history of the sample used.

The ferromagnetic core of the Rowland ring may be demagnetized by successive reversals of the current as the current is gradually reduced from a sufficiently high initial current to a current that will produce a magnetizing force less than any value to be used subsequently. *See* DEMAGNETIZATION.

Changes in **B**, but not **B** itself, can be measured by wrapping a search coil on the toroid and observing the throw of a ballistic galvanometer.

Normal magnetization curve. When the core of the Rowland ring is initially demagnetized, $\mathbf{B} = 0$ and $\mathbf{H} = 0$. If the current is quickly increased to give a predetermined value $\mathbf{H}_1$, a flux $\Phi_1 - 0$ will be measured by the throw of the ballistic galvanometer. From the flux and the area A of cross section of the core, the value of $\mathbf{B} = \Phi/A$ corresponding to the selected **H** is computed. Then, without reducing the current, a second increase in current is made to reach $\mathbf{H}_2$. Again, the throw of the galvanometer measures the change in flux $\Phi_2 - \Phi_1$, and hence Φ_2 is found and $\mathbf{B}_2$ is computed corresponding to $\mathbf{H}_2$. By continuing this process for as many pairs of **B** and **H** as are necessary, points on the magnetization curve are obtained. The curve obtained starting with the core demagnetized is called the normal magnetization curve (**Fig. 4**). If the specimen were not initially demagnetized, the process here described would yield a magnetization curve that would differ in shape from the normal magnetization curve and, in general, would not pass through the origin.

In the curve of Fig. 4, **B** increases slowly at first as **H** rises, then increases rapidly until the "knee" of the curve is reached. Here, the rate of change of **B** with respect to **H** decreases and becomes small as saturation is approached.

Single crystals. Magnetization curves of single crystals depend upon the direction of **H** with respect to the crystallographic axes. If a weak field is applied to a crystal, those domains whose magnetic moments are most nearly parallel to **H** increase in size at the expense of those in other directions. There is then a small net contribution of the domains to the flux. As the field increases, the boundaries of the domains continue to change, and **B** increases rapidly along the steep part of the curve. Near the end of this change, all the magnetic moments in the domains rotate in a direction parallel to those that have been increasing. The rotation within the domains requires greater change in **H**, and thus the slope changes at the knee. As **H** is further increased, the domains rotate until their magnetic moments are all parallel to the field

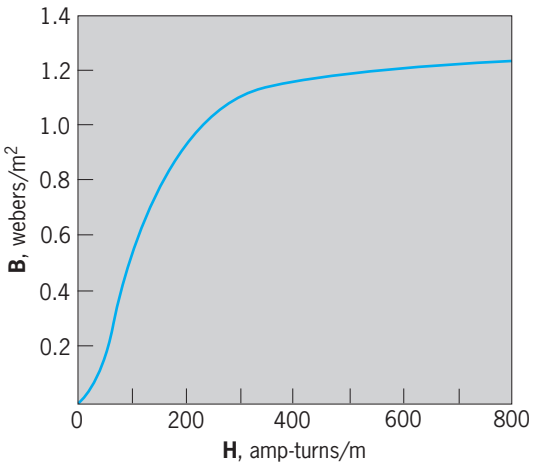

Fig. 4. Normal magnetization curve.

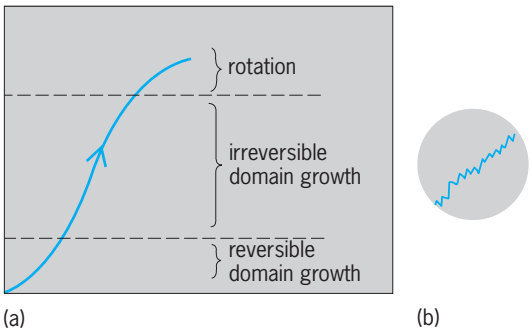

Fig. 5. Process of magnetization. (*a*) Portion of a magnetization curve, showing magnetization processes. (*b*) Enlarged section of path, showing Barkhausen effect.

and saturation has been reached. *See* SINGLE CRYSTAL.

The ferromagnetic materials in common use are polycrystalline; that is, a piece of the material consists of a tremendous number of single crystals of random orientation. In each single crystal, there are many domains. The magnetization of the whole body consists of the magnetization of the various single crystals within that body.

Domain growth. The process of magnetization is shown in **Fig. 5***a*. Domain growth proceeds by movement of the so-called Bloch wall between domains. This takes place reversibly at first, then irreversibly. Irreversible motion causes sudden almost discontinuous changes in magnetization, called the Barkhausen effect (Fig. 5*b*). *See* BARKHAUSEN EFFECT.

Hysteresis. The irreversible nature of magnetization is shown most strikingly by the fact that the path of demagnetization does not retrace the path of magnetization—path 2 of Fig. 3 does not retrace path 1. There is a tendency for the magnetization to show hysteresis, that is, to lag behind the applied field, and the loop of Fig. 3 is called a hysteresis loop. The area of the loop is a measure of the energy lost to heat, per cycle, in going around the loop, and therefore is related to the energy lost by a magnet in an alternating field. An additional energy loss is that from eddy currents; this is absent in the nonconducting ferrites and may be minimized in metals by lamination.

Demagnetizing fields. The effect of an applied field **H** on a sample is always reduced by a demagnetizing field $-N\mathbf{M}$ coming from the surface "poles," where N, the demagnetizing factor, depends upon the sample shape and orientation with respect to **H**. It varies from nearly 0 in a sample long and thin in the direction of **H**, to nearly 4π (in emu) in a sample short and fat, like a disk of revolution about **H**. Magnetization curves are generally obtained from long, thin samples to avoid demagnetization. The demagnetization effects are extremely important in ferromagnetic resonance. *See* MAGNETIC RESONANCE.

Elihu Abrahams; Frederick Keffer; Kenneth V. Manning

Bibliography. B. I. Bleaney and B. Bleaney, *Electricity and Magnetism*, 3d ed., 1976, paper 1989; D. Craik, *Magnetism*, 1995; W. J. Duffin, *Electricity and Magnetism*, 4th ed., 1990; J. D. Jakubovics, *Magnetism and Magnetic Materials*, 2d ed., 1994.

Magneto

A type of permanent-magnet alternating-current generator frequently used as a source of ignition energy on tractor, marine, industrial, and aviation engines. The higher cost of magneto ignition is not warranted in modern automobiles, where storage batteries are required for other electrically operated equipment. Hand-operated magneto generators were once widely used for signaling from local battery telephone sets. *See* GENERATOR.

Modern induction-type magnetos consist of a permanent-magnet rotor and stationary low- and high-tension windings, also called the primary and secondary windings. The **illustration** shows two induction-type magnetos in a dual-ignition circuit for a nine-cylinder aircraft engine. The two magnetos are identical, but only magneto no. 1 is shown schematically. The ignition system may receive energy from either or both magnetos, according to the position of the switch.

The energy output of a magneto is obtained as a result of a rapid rate of change of flux through the stationary windings. The primary winding has comparatively few turns and the secondary winding has many thousand turns of fine wire. One end of the secondary winding is connected to an end of the primary winding and grounded to the frame of the magneto. The primary winding is closed on itself through a breaker mechanism actuated by a cam on the magneto shaft. The breaker is mechanically set to interrupt the primary circuit each time the flux

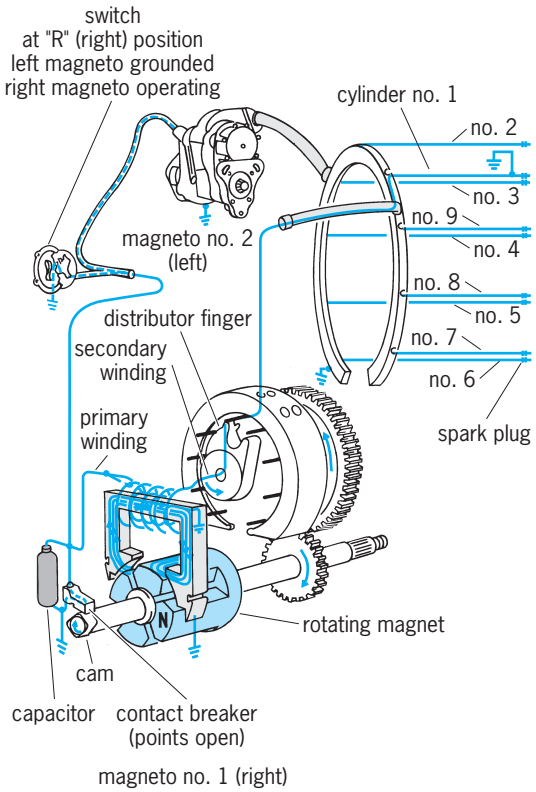

Multipolar aviation magneto in dual-ignition circuit for nine-cylinder radial engine. (*Bendix Aviation Corp.*)

through the winding is changing at its greatest rate. The sudden collapse of the primary current induces a very high voltage in the secondary winding.

Magnetos are always geared to the engine shaft and timed to open the breaker at the proper instant. Magneto speed depends on the number of poles of the magneto and the number of engine cylinders. The distributor finger speed is always one-half engine speed. *See* IGNITION SYSTEM; INTERNAL COMBUSTION ENGINE.

Robert T. Weil, Jr.

Bibliography. E. A. Avallone and T. Baumeister III (eds.), *Marks' Standard Handbook for Mechanical Engineers,* 10th ed., 1996; D. Fink and H. W. Beatty (eds.), *Standard Handbook for Electrical Engineers,* 14th ed., 1999.

Magnetocaloric effect

The reversible change of temperature accompanying the change of magnetization of a ferromagnetic or paramagnetic material. Thermodynamics theory shows that, for an adiabatic change of field ΔH, the change of temperature ΔT is given by the equation below, where c_H is the specific heat per unit volume

$$\frac{\Delta T}{\Delta H} = -\frac{T}{c_H}\left(\frac{\partial M}{\partial T}\right)_H$$

at constant H, and M is the magnetization.

This change in temperature may be of the order of 2°F (1°C), and is not to be confused with the much smaller hysteresis heating effect, which is irreversible. *See* THERMAL HYSTERESIS.

Except in antiferromagnets, $(\partial M/\partial T)_H$ is negative and an adiabatic decrease in H causes T to drop. This is the basis of the Giauque-Debye adiabatic demagnetization of paramagnetic salts, a technique which has achieved extremely low temperatures. *See* ADIABATIC DEMAGNETIZATION.

Elihu Abrahams; Frederick Keffer

Magnetochemistry

The study of magnetic properties of materials by analyzing the interactions between a magnetic field and chemical substances, which include both molecular and extended structures. All substances respond to a magnetic field. Some materials, called permanent magnets, generate magnetic fields.

Magnetic properties. When a substance is placed in a magnetic field **H**, its response **B**, called magnetic induction, is given by Eq. (1). Here **M** is the

$$\mathbf{B} = \mu\mathbf{H} = (1 + 4\pi\kappa)\mathbf{H} = \mathbf{H} + 4\pi\mathbf{M} \qquad (1)$$

magnetization, which is total magnetic moment per volume in the material, **H**, **B**, and **M** are vector quantities; their corresponding magnitudes (intensities or strengths) are symbolized as H, B, and M. The permeability μ is the tensor relationship between the external field and induction; the volume susceptibility κ is the tensor relationship between the external field and magnetization ($\mathbf{M} = \kappa\mathbf{H}$). When magnetic measurements are made on single crystals with well-defined directions, the tensor properties of κ can be obtained. Susceptibilities measured along different crystal axes are called principal susceptibilities, and the difference between principal susceptibilities is called the magnetic anisotropy of the substance. However, measurements are usually made on powders, so κ is typically reported as a single number (a scalar quantity), which is the average of the three principal susceptibilities and represents the ratio M/H. More frequently, the molar susceptibility is reported, which is $\chi_M = \kappa \cdot \mathrm{FW}/d$, where FW is the formula weight and d is the density of the substance.

The susceptibility can be negative, zero, or positive: when negative, $B < H$ and the substance is repelled by a magnet (diamagnetic); when zero, $B = H$ (nonmagnetic and highly unusual); when positive, $B > H$ and the substance is attracted by a magnet (paramagnetic). *See* MAGNETIC SUSCEPTIBILITY.

Magnetism originates in matter from the intrinsic spin of nuclei (protons and neutrons) and electrons, as well as from the orbital motion of electrons. The spins of protons, neutrons, and electrons create magnetic moments. The magnitudes of these moments are related inversely to their masses, so the electronic magnetic moment is about 2000 times larger than that of a proton or neutron. Therefore, macroscopic magnetic behavior arises essentially from electronic properties. The magnetism associated with nuclei is used in nuclear magnetic resonance (NMR) and is very useful for structural information and analysis. *See* ATOMIC STRUCTURE AND SPECTRA; MAGNETIC RESONANCE; NUCLEAR MAGNETIC RESONANCE (NMR); NUCLEAR MOMENTS.

The orbital motion of electrons can also create a magnetic moment if the orbital angular momentum is not quenched. The combination of electron spin and orbital momenta produces a local magnetic moment assigned to each atom in a chemical structure. These local moments can interact with one another and with an external magnetic field, leading to the substance's magnetic behavior and response. If the orbital angular momentum for an atom is quenched, which is often the case, then the local moment comes entirely from the total electron spin. If all electron spins are paired, an atom or ion has no local magnetic moment. Therefore, local magnetic moments primarily arise from unpaired electrons. *See* ELECTRON SPIN; MAGNETISM; MOLECULAR ORBITAL THEORY.

Units. Magnetic moments are given in units of Bohr magnetons, $\mu_B = (e/2mc) = 9.274 \times 10^{-21}$ erg/gauss $= 9.274 \times 10^{-24}$ joule/tesla. The Bohr magneton is not an SI unit but corresponds to the magnetic moment of a 1s electron in hydrogen. Magnetic field strengths and inductions are given in units of gauss, Oersted, or tesla (1 gauss = 1 Oersted = 10^4 tesla). Volume magnetic susceptibility is dimensionless; molar susceptibility has the units emu/mole $= 4\pi$ cm^3/mole.

Measurements. Magnetic susceptibilities are commonly determined by measuring a material's response to an external magnetic field. The Gouy and Faraday methods rely on measuring the weight difference for a sample in and out of a magnetic field. A SQUID (superconducting quantum interference device) uses changes in magnetic fluxes in a superconducting ring and is a sensitive instrument for measuring magnetic responses. NMR studies of solutions can also be used to approximate susceptibilities. Magnetic susceptibilities are typically measured over a range of temperature, typically from about 4 to 300 K. In some cases, magnetization is recorded as a function of external magnetic field. *See* SQUID.

Magnetic states of matter. The nature of a material's response to an external magnetic field essentially depends on the number of unpaired electrons. In an external magnetic field, all electrons, as charged particles, will develop trajectories that create an induced magnetic field opposing the applied field, according to Lenz's law. The presence of unpaired electron spins will create local moments that counteract this induced field. If these local moments interact strongly with one another within the material in the absence of the external field, there can be cooperative behavior. The commonly observed magnetic states are diamagnetism, paramagnetism, ferromagnetism, antiferromagnetism, ferrimagnetism, and superconductivity. *See* LENZ'S LAW.

Diamagnetism. This is a property of a material which is repelled by an external magnetic field due to the induced motion of electrons. All electron spins are paired giving a net spin of zero. This is the most common behavior for main-group molecules and solids. The susceptibility is independent of temperature and field strength and is usually of the order of magnitude 10^{-6} to 10^{-5} emu/mole. *See* DIAMAGNETISM.

Paramagnetism. This is the property of a material which is attracted by an external magnetic field. There are unpaired electrons, which are commonly observed for transition-metal and rare-earth metal complexes. The susceptibility is inversely proportional to temperature but independent of field strength, and is usually of the order of magnitude 10^{-4} to 10^{-3} emu/mole. *See* PARAMAGNETISM.

Ferromagnetism. This property is exhibited by materials that are strongly attracted by an external magnetic field and can produce a permanent magnet. There are unpaired electron spins that are held in parallel alignment between adjacent magnetic atoms (**Fig. 1**). Ferromagnets show paramagnetic behavior above a critical temperature called the Curie temperature. *See* CURIE TEMPERATURE; FERROMAGNETISM.

Antiferromagnetism. This property is exhibited by materials that are weakly attracted by an external magnetic field because there are unpaired electrons that are held in antiparallel alignment between different atoms, and there is no net magnetization (**Fig. 2**). If the external field is oriented parallel to the direction of these local moments (called the easy axis of magnetization), the material would be repelled by the field. Antiferromagnets show paramagnetic behavior above a critical temperature called the Neél temperature. *See* ANTIFERROMAGNETISM.

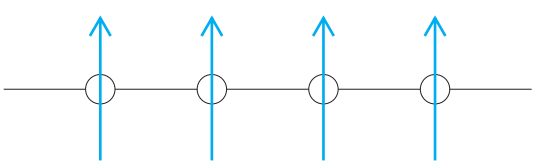

Fig. 1. Diagram of ferromagnetism.

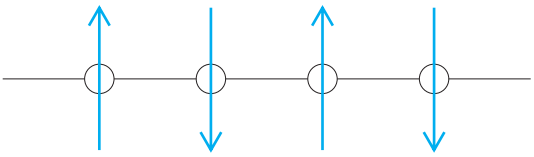

Fig. 2. Diagram of antiferromagnetism.

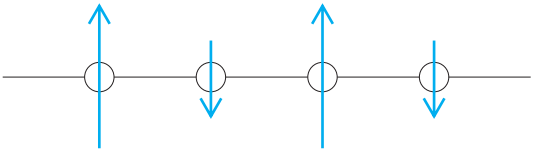

Fig. 3. Diagram of ferrimagnetism.

Ferrimagnetism. This is a property of materials that are attracted by an external magnetic field as there are unpaired electrons with antiparallel alignment, but there is an overall net magnetization (**Fig. 3**). Ferrimagnets show paramagnetic behavior above a critical temperature. *See* FERRIMAGNETISM.

Superconductors. These are "perfect" diamagnets with an immeasurably small electrical resistivity. Electrons are coupled into Cooper pairs, and the material completely repels an external magnetic field. Superconductors adopt "normal" behavior above a critical temperature. *See* SUPERCONDUCTIVITY.

Understanding magnetic behavior. One appeal of magnetochemistry is the ability to construct accurate mathematical models to understand magnetic responses. These models rely on constructing expressions for the spectrum of energy levels of the chemical system in the presence of a magnetic field. From a thermodynamic perspective, an external magnetic field does work on the system of electrons that is at thermal equilibrium. Therefore, the magnetic field affects the spectrum of electronic energy states, while the temperature controls how these states are occupied by electrons. Quantum mechanics provides the physical and mathematical machinery for interpreting measurements of magnetic susceptibilities with the Van Vleck equation. If a substance has unpaired spins (total spin S), the ground electronic state is split into $2S + 1$ levels by a magnetic field according to the Zeeman energy term in Eq. (2), and g is about 2. The occupation of the ex-

$$E(H) = -g\mu_B H M_S \qquad (2)$$
$$M_S = S, S-1, \ldots, -S$$

cited energy levels at temperature T are determined by the factor $\exp(-g\mu_B H/kT) = \exp(-1.34H/T)$ [H in tesla, T in K]. Since H is typically less than 10 tesla, magnetic fields place a small perturbation on

the occupation of electronic states until very low temperatures are reached. *See* MOLECULAR STRUCTURE AND SPECTRA.

Noninteracting magnetic atoms. If local magnetic moments are widely separated, they do not interact with one another, and the molar susceptibility has three components $\chi_M = \chi_{dia} + \chi_{TIP} + \chi_{Curie}$. The first, χ_{dia}, is the diamagnetic (Langevin) susceptibility due to the induced magnetic field from the circulating electrons. This term is negative. It increases with the size of the atom/ion and is additive over all atoms making up the chemical substance. For a molecule or unit cell, the Pascal relation approximates the diamagnetic contribution $\chi_{dia} = \Sigma n_A \chi_{dia}(A) + \Sigma n_B \chi_{dia}(B)$, where A = atoms, B = bonds, n_A = number of A atoms, n_B = number of B bonds. $\chi_{dia}(A)$ and $\chi_{dia}(B)$ are empirical constants derived from measured susceptibilities. The second, χ_{TIP}, is Van Vleck (temperature-independent) paramagnetism and occurs when the external magnetic field causes excited electronic states to mix with the ground state. Molecular ions, such as $(CrO_4)^{2-}$ and $(MnO_4)^-$, show temperature-independent paramagnetism. The third, χ_{Curie}, is the typical temperature-dependent paramagnetism. As temperature increases, the magnetic susceptibility decreases; thus $\chi_{Curie} = 0.125\mu_{eff}^2/T$, where μ_{eff} is the effective magnetic moment per atom/ion (χ_{Curie} in cgs units emu/mol; T in K). When orbital angular momentum is quenched, $\mu_{eff} = g[S(S+1)]^{1/2} \cong [n(n+2)]^{1/2}$ [$n = 2S$ = number of unpaired electrons] in units of Bohr magnetons, called spin-only magnetic moments. For rare-earth ions and certain transition-metal complexes, the total orbital angular momentum is not quenched, and through spin-orbit coupling we must consider the total angular momentum $\mathbf{J} = \mathbf{L} + \mathbf{S}$, so that $\mu_{eff} = g[J(J+1)]^{1/2}$, where g = Landé g-factor. One of the early major successes of quantum mechanics, this formula successfully explained the observed magnetic behavior of rare-earth salts. At low temperatures or high magnetic fields (that is, large H/T), the Curie expression breaks down because only the very lowest electronic energy levels are occupied. In this regime, the molar susceptibility follows the approximate relation $\chi_M = M_{sat}/H$, where M_{sat} is saturation magnetization—the largest possible magnetization for the substance. *See* RARE-EARTH ELEMENTS.

Interacting magnetic atoms. Magnetic centers are never truly isolated from one another in any substance. The interaction between two centers of unpaired spins, $\mathbf{S}_1$ and $\mathbf{S}_2$, is called exchange and the potential energy is $-J_{12}\,\mathbf{S}_1 \cdot \mathbf{S}_2$, where J_{12} is the exchange constant (given in units of K), and called the Heisenberg exchange model. If $J_{12} > 0$, the preferred interaction is ferromagnetic; if $J_{12} < 0$, the interaction is antiferromagnetic. When exchange is included in the Van Vleck equation, the temperature-dependent molar susceptibility becomes $\chi_{Curie\text{-}Weiss} = 0.125\mu_{eff}^2/(T - \Theta)$, called the Curie-Weiss law, where Θ, the Weiss constant, is proportional to J_{12}. Plots of $1/\chi_{Curie\text{-}Weiss}$ versus T are linear, and the slopes allow determination of μ_{eff} and the intercepts along the T axis tell the sign and magnitude of the exchange constant (**Fig. 4**). *See* CURIE-WEISS LAW.

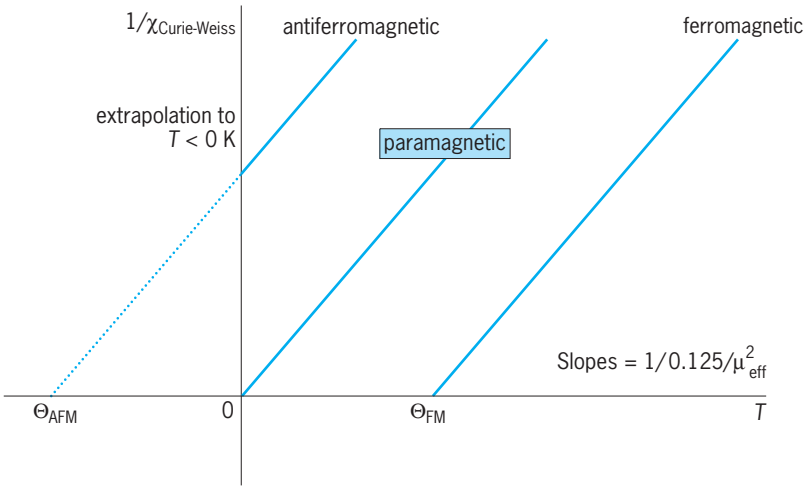

Fig. 4. Qualitative plots of $1/\chi_{Curie\text{-}Weiss}$ versus T.

Exchange is a purely quantum-mechanical phenomenon and arises as a consequence of the Pauli exclusion principle. Intra-atomic exchange (within the atom) is responsible for Hund's rule, which creates special stability to half-filled orbital subshells. Interatomic exchange (between atoms) can be characterized as direct or indirect. Direct exchange involves overlapping electronic wavefunctions, and its magnitude decreases rapidly with distance. The sign of the exchange interaction is related to the strength of the orbital overlap [strong overlap, negative exchange (antiferromagnetic); weak overlap, positive exchange (ferromagnetic)]. Indirect exchange produces an interaction between magnetic moments through an intermediary. In molecules and magnetic insulators, superexchange is the coupling of magnetic moments via bridging ligands. J. B. Goodenough and J. Kanamori developed a series of rules for transition-metal oxides based on the electronic configuration at the metal atoms and the metal-oxide-metal (M-O-M) angle for whether the exchange is ferromagnetic (parallel) or antiferromagnetic (antiparallel). In metals, magnetic moments associated with atoms, such as rare-earth elements, can interact via the spins of the conduction electrons. This mechanism is called RKKY exchange (for Ruderman, Kittel, Kasuya, and Yosida, who developed the model). *See* EXCHANGE INTERACTION.

Examples of magnetism for chemical substances. Molecular oxygen (O_2) has two unpaired electrons in its ground state and is paramagnetic. This is clearly observed when blue, liquid oxygen is poured between the poles of a magnet. Its molar susceptibility over a wide range of pressures and temperatures is $\chi_{Curie} = 0.993/T$. Other paramagnetic molecules include NO, NO_2, ClO_2, and ClO_3.

Most organic compounds are diamagnetic, but there are some, called free radicals, with one or two unpaired electrons. One example is hexaphenylethane, which dissociates in benzene

solution to give the triphenylmethyl radical. Aromaticity assists to stabilize the unpaired electrons. *See* FREE RADICAL.

Numerous monatomic transition-metal complexes, especially those involving the 3*d* metal ions, show paramagnetic behavior. Often the orbital angular momentum is quenched, and these ions exhibit spin-only magnetic moments. The number of unpaired electrons depends on the strength of the ligand field created by the coordination environment, where strong ligand fields generate low-spin configurations, and weak ligand fields generate high-spin configurations. Most tetrahedral complexes show high-spin behavior. The nature of ligand field strength is given by the spectrochemical series: cyanide (CN^-), carbonyl (CO), and nitrosyl (NO^+) are strong-field ligands; iodide (I^-) and bromide (Br^-) are weak-field ligands. In certain cases of octahedral or tetrahedral coordination, there can be some orbital effects via spin-orbit coupling. The 4*d* and 5*d* transition metals often show low-spin configurations and greater effects of ligand orbitals mixing into the valence orbitals, which complicate the magnetic response. Rare-earth ions show significant

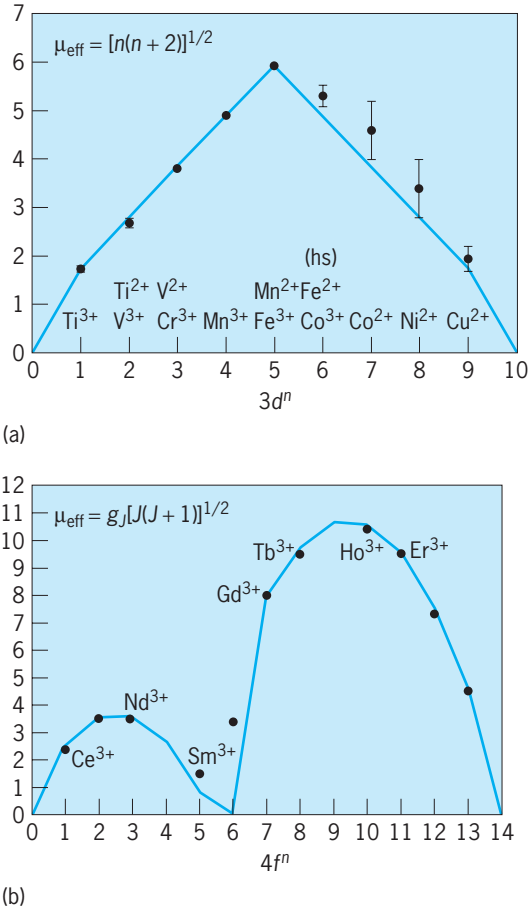

Fig. 5. Plots of effective magnetic moments versus numbers of valence electrons for (*a*) 3*d* ions, where theory uses the spin-only model; and (*b*) 4*f* ions, where theory uses the total angular momentum for each electronic configuration. Lines correspond to theoretically predicted values; dots with error bars indicate experimentally measured values.

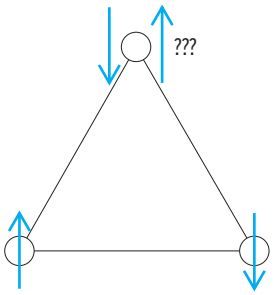

Fig. 6. Diagram of antiferromagnetic frustration.

magnetic behavior which utilizes their total angular momentum. **Figure 5** illustrates the variation in theoretical and experimental magnetic moments for 3*d* transition-metal ions and 4*f* rare-earth ions to show how successful these two interpretations are. *See* LIGAND FIELD THEORY.

Clusters of magnetic ions can lead to interesting magnetic behavior because the magnetic exchange interaction can vary with temperature to show high-spin to low-spin transitions. If the exchange interaction is antiferromagnetic and the cluster contains triangles, then frustration arises, as complete antiferromagnetic coupling between magnetic centers cannot be sustained by the structure (**Fig. 6**). Large clusters can lead to superparamagnetism, in which molecules can behave as classical magnets with large magnetic moments.

Metals typically show Pauli paramagnetism. In the presence of an external magnetic field, the energy bands associated with spin-up electrons are separated from the energy bands of the spin-down electrons (Zeeman interaction), resulting in more spin-up than spin-down electrons and an induced, temperature-independent magnetization. This effect is observed for sodium, magnesium, and aluminum (Al becomes superconducting at low temperatures). In poor metals (for example, graphite) and semimetals (such as antimony and bismuth), the induced magnetic field from the trajectories of the conduction electrons in the external magnetic field create a net diamagnetic response called Landau diamagnetism. In anisotropic materials, such as graphite, this diamagnetism shows that the principal susceptibility perpendicular to the hexagonal axis of a single crystal of graphite at room temperature is about -0.5×10^{-6} emu/mol, but parallel with the hexagonal axis, it is -21.5×10^{-6} emu/mol. The enhanced diamagnetism when the field is parallel to the hexagonal axis is thought to arise from the trajectories of the conduction electrons in the graphite planes. Some metallic elements, such as iron, cobalt, nickel, gadolinium, and dysprosium, are ferromagnetic, which means they show net magnetization in the absence of a magnetic field. A few elements are antiferromagnetic, such as manganese and chromium. Recent investigations with possible applications to magnetic storage and retrieval involve half-metallic ferromagnets, in which only the spin-up electrons contribute to electronic conduction.

Gordon J. Miller

Bibliography. R. L. Carlin, *Magnetochemistry*, Springer-Verlag, Berlin, 1986; P. Day (ed.), *Electronic Structure and Magnetism of Inorganic Compounds*, vols. 1–7, Chemical Society, London, 1970–1982; J. B. Goodenough, *Magnetism and the Chemical Bond*, R.E. Krieger Publishing, 1976; A. F. Orchard, *Magnetochemistry*, Oxford University Press, 2003; G. T. Rado and H. Suhl (eds.), *Magnetism: A Treatise on Modern Theory and Materials*, 5 vols., Academic Press, 1963–1973; É. du Trémolet de Lacheisserie, D. Gignoix, M. Schlenker (eds.), *Magnetism: I, Fundamentals, and II, Materials and Applications*, Kluwer Academic, Dordrecht, 2002.

Magnetohydrodynamic power generator

A system for the generation of electrical power through the interaction of a flowing, electrically conducting fluid with a magnetic field. As in a conventional electrical generator, the Faraday principle of motional induction is employed, but solid conductors are replaced by an electrically conducting fluid. The interactions between this conducting fluid and the electromagnetic field system through which power is delivered to a circuit are determined by the magnetohydrodynamic (MHD) equations, while the properties of electrically conducting gases or plasmas are established from the appropriate relationships of plasma physics. Major emphasis has been placed on MHD systems utilizing an ionized gas, but an electrically conducting liquid or a two-phase flow can also be employed. *See* ELECTROMAGNETIC INDUCTION; GENERATOR; MAGNETOHYDRODYNAMICS; PLASMA (PHYSICS).

Principle. Electrical conductivity in an MHD generator can be achieved in a number of ways. At the heat-source operating temperatures of MHD systems (1300–5000°F or 1000–3000 K), the working fluids usually considered are gases derived from combustion, noble gases, and alkali metal vapors. In the case of combustion gases, a seed material such as potassium carbonate is added in small amounts, typically about 1% of the total mass flow. The seed material is thermally ionized and yields the electron number density required for adequate electrical conductivity above about 4000°F (2500 K). With monatomic gases, operation at temperatures down to about 2200°F (1500 K) is possible through the use of cesium as a seed material. In plasmas of this type, the electron temperature can be elevated above that of the gas (nonequilibrium ionization) to provide adequate electrical conductivity at lower temperatures than with thermal ionization. In so-called liquid metal MHD, electrical conductivity is obtained by injecting a liquid metal into a vapor or gas stream to obtain a continuous liquid phase.

The conversion process in the MHD generator itself occurs in a channel or duct in which a plasma flows usually above the speed of sound through a magnetic field. The power output per unit volume W_e is given by the equation below, where σ is the

$$W_e = \sigma v^2 B^2 k(1 - k)$$

electrical conductivity of the gas, v the velocity of the working fluid, B the magnetic flux density, and k the electrical loading factor (terminal voltage/induced emf).

With a conductivity of 10 siemens, a value typical for fossil fuel combustion, $B = 6$ teslas, $v = 600$ m/s = 1970 ft/s, and $k = 0.75$, the power density is 24 MW/m^3 (680 kW/ft^3). Increasing the plasma values to $\sigma = 120$ S and $v = 1000$ m/s = 3280 ft/s and setting $k = 0.5$ yields a power density of 1.08 GW/m^3 (30.6 kW/ft^3). High power densities are one of the attractive features of MHD power generators.

Under the magnetic field strengths required for MHD generators, the plasma displays a pronounced Hall effect. To permit the basic Faraday motional induction interaction and simultaneously support the resulting Hall potential in the flow direction, a linear channel requires segmented walls comprising alternately electrodes (anode or cathode) and insulators. Various connections are possible to combine the outputs of the individual anode-cathode pairs thus formed. These are (1) Faraday, with individual loading of each anode-cathode pair or cell; (2) diagonal loading, with cells series-connected along diagonal equipotentials; and (3) Hall, involving direct loading of the Hall potential with short-circuiting of the individual Faraday anode-cathode pairs. From an electrical machine viewpoint, both individual cells and the complete generator may be regarded as a gyrator. Indeed, the optimum loading of the MHD channel is achieved by extracting power from both the Faraday and Hall terminals, and this is most readily accomplished through consolidation of the dc outputs of individual electrode pairs using power electronics (**Fig. 1**), rather than by the direct physical connections just described. *See* GYRATOR; HALL EFFECT.

For most applications, a superconducting magnet system is needed to provide the 4–6-T field, which is at least twice the value utilized in conventional machines. *See* MAGNET; SUPERCONDUCTING DEVICES.

System considerations. The MHD generator is a heat engine or electromagnetic turbine which

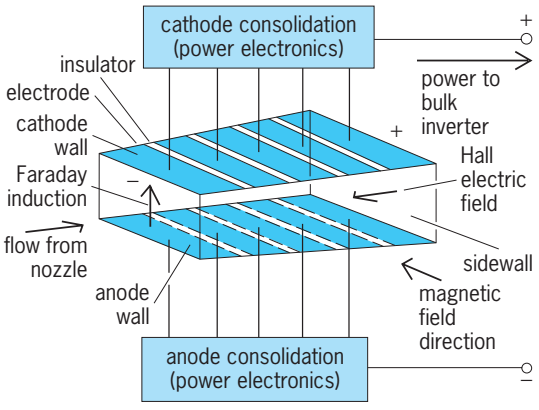

Fig. 1. MHD generator with five electrode segments.

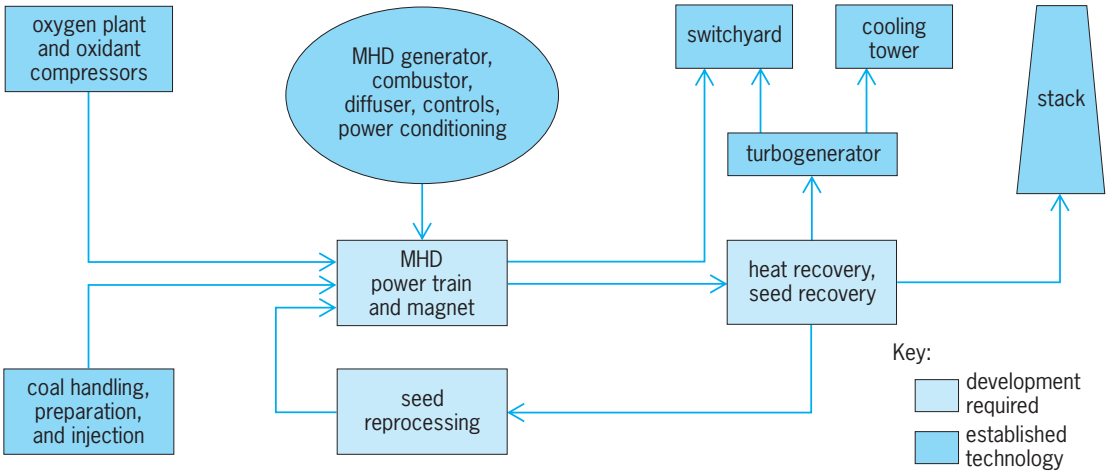

Fig. 2. Major subsystems of an MHD-steam combined-cycle plant.

converts thermal energy to a direct electrical output via the intermediate step of the energy of the flowing working fluid. As such, it must be embedded in a complete power train comprising a heat source, a nozzle for fluid acceleration, the channel itself, a diffuser for pressure recovery, a magnet subsystem, and the power conditioning subsystem to combine the many direct-current outputs resulting from segmentation and match them to the voltage and frequency requirements of the load or system to which the generator is connected. Fuel, oxidizer, and ionizing seed supplies complete the basic MHD power generating system (**Fig. 2**). *See* ENGINE; THERMODYNAMIC PROCESSES.

The gas exhausted from an MHD system generally contains significant recoverable energy. A combined cycle, generally with a steam turbine, is advantageous when the objective, as is the case for electrical utility application, is to take advantage of the higher thermodynamic efficiency available with a 4600°F (2800 K) inlet temperature to the conversion system (Fig. 2).

Improvement of the overall thermal efficiency of central station power plants has been the continuing objective of power engineers. Conventional plants based on steam turbine technology are limited to about 40% efficiency, imposed by a combination of working-fluid properties and limits on the operating temperatures of materials. Application of the MHD interaction to electrical power generation removes the restrictions imposed by the blade structure of turbines and enables the working-fluid temperature to be increased substantially. This enables the working fluid to be rendered electrically conducting and yields a conversion process based on a body force of electromagnetic origin.

When combined with a steam turbine system to serve as the high-temperature or topping stage of a binary cycle, an MHD generator has the potential for increasing the overall plant thermal efficiency to around 50%, and values higher than 60% have been predicted for advanced systems. *See* ELECTRIC POWER GENERATION; STEAM TURBINE.

Types. When this generator is embedded in an overall electrical power generation system, a number of alternatives are possible, depending on the heat source and working fluid selected. The temperature range required by MHD can be achieved through combustion with oxygen or compressed preheated air. The association of MHD with nuclear heat sources has also been considered, but in this case limitations on the temperature of nuclear fission heat sources with solid fuel elements has thus far precluded any practical scheme being developed where a plasma serves the working fluid. The possibility of coupling MHD to a fusion reactor has been explored, and it is possible that twenty-first-century central station power systems will comprise a fusion reactor and an MHD energy conversion system. *See* NUCLEAR FUSION; NUCLEAR REACTOR.

MHD power systems are classified into open- or closed-cycle systems, depending respectively on whether the working fluid is utilized on a once-through basis or recirculated via a compressor. For fossil fuels, the open-cycle system offers the inherent advantage of interposing no solid heat-exchange surface between the combustor and the MHD generator, thus avoiding any limitation being placed on the cycle by the temperature attainable over a long period of operation by construction materials in the heat exchanger. Closed-cycle systems were originally proposed for nuclear heat sources, and the working fluid can be either a seeded noble gas or a liquid metal-vapor mixture.

Features and applications. The greatest development effort in MHD power generation has been applied to fossil-fired open-cycle systems, but sufficient progress has been made in closed-cycle systems to establish their potential and to identify the engineering problems which must be solved before they can be considered practical.

In addition to offering increased power plant efficiencies, MHD power generation also has important potential environmental advantages. These are of special significance when coal is the primary fuel, for it appears that MHD systems can utilize coal directly

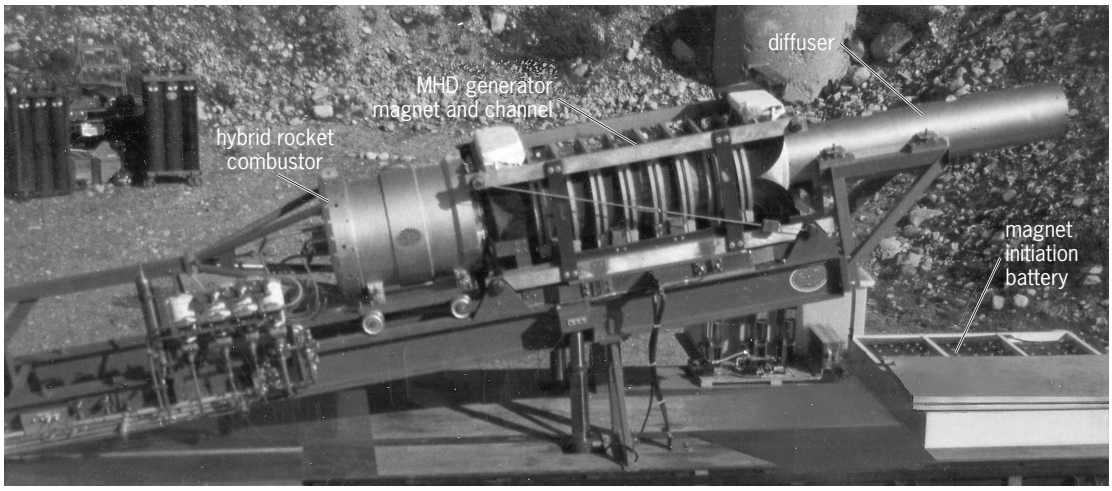

Fig. 3. Self-excited, rocket-motor–driven, pulsed MHD generator. (*STD Research Corp.*)

without the cost and loss of efficiency resulting from the processing of coal into a clean fuel required by competing systems. The use of a seed material to obtain electrical conductivity in the working fluid also places the requirement on the MHD system that a high level of recovery be attained to avoid adverse environmental impact and also to ensure acceptable plant economics. The seed recovery system required by an MHD plant also serves to recover all particulate material in the plant effluent. A further consequence of the use of seed material is its demonstrated ability to remove sulfur from coal combustion products. This occurs because the seed material is completely dissociated in the combustor, and the recombination phenomena downstream of the MHD generator favor formation of potassium sulfate in the presence of sulfur. Accordingly, seed material acts as a built-in vehicle for removal of sulfur. Laboratory experiments have shown that the sulfur dioxide emissions can be reduced to levels experienced with natural-gas–fired plants. A further important consideration is the reduction of the emission of oxides of nitrogen through control of combustion and the design of component operating conditions. Tests at the 30-MW (thermal) Coal-Fired Flow Facility in Tennessee have shown that these emissions can be held to about 10% of the values allowed by the New Source Performance Standards of the Environmental Protection Administration. *See* AIR POLLUTION.

While not a property of the MHD system in itself, the potential of MHD to operate at higher thermal plant efficiencies has the consequence of substantial reduction in thermal waste discharge, following the relationship that the heat rejected per unit of electricity generated is given by $(1 - \eta)/\eta$, where η is the plant efficiency. As the technology of MHD is developed along with that of advanced gas turbines, it is also possible that MHD systems can dispense entirely with the need for large amounts of cooling water for steam condensation through the coupling of MHD generators with closed-cycle gas turbines. *See* GAS TURBINE; WATER POLLUTION.

The high-power-density feature has led to MHD being considered for situations where compact electrical sources, usually of the pulse power type, are required. Energy storage in high-energy fuel, together with the rapid start-up capability of a rocket engine–type combustor, leads to the possibility of pulsed systems (1 s or less) at powers up to at least 1 GW. *See* PLASMA PROPULSION.

An experimental pulse MHD generator of 10-MW electrical output, driven by a solid-fuel rocket motor, is shown in **Fig. 3**. It is self-excited, and the combustion gas plasma has an electrical conductivity greater than 100 S/m.

One application of MHD results from the advantages inherent in using a liquid metal as the heat-transfer medium in a solar central receiver system. The liquid-metal type of MHD is readily coupled to this type of power tower. Liquid-metal systems have also been considered for long-duration space power applications. *See* SOLAR ENERGY; SPACE POWER SYSTEMS.

State of development. Development efforts on MHD have been mainly focused on fossil-fired systems, the fossil fuel selected being determined by national energy considerations. Coal is particularly attractive as a fuel for MHD plants because the basic electromagnetic interaction process is not compromised by ash, slag, or combustion products. Efforts in the United States, China, India, Australia, and the European community have centered on open-cycle systems utilizing this fuel. In Russia, the large reserves of natural gas have led to its extensive use in MHD research and development, although emphasis on coal-fired systems is increasing. Work in Japan was originally based on petroleum-based fuels, but now is also oriented toward coal firing with closed-cycle systems.

The most complete MHD plant constructed to date is the open-cycle U-25 installation near Moscow. As first constructed, it operated with natural gas and achieved a maximum power output of 25 MW and continuous operation for 250 h at low power levels. In both cases, the electrical output was delivered to the Moscow grid. This plant has been extensively

modified and, as the U-25M, resumed operation in 1989.

In the United States, important engineering progress has been achieved on coal-fired systems. A 50-MW coal-fired combustor has been developed, and over 1000 h of operation of an open-cycle channel have been completed. A large experimental generator in Tennessee reached an electrical power above 30 MW. A 6-T superconducting magnet has been constructed and operated by the Argonne National Laboratory. Design studies have dealt with the feasibility of retrofitting existing plants with an MHD generator of about 25-MW electrical output. Electrical power conditioning has been addressed, and a 3.5-MW inverter has been successfully coupled to an MHD generator at a Department of Energy development facility.

Pulsed MHD has also been applied to geophysical research in Russia. Up to 100 MW peak power is delivered in 1–3 s through suitably placed electrodes to the Earth's crust, and electrical conductivity in the surrounding region is recorded by stations which pick up the transmitted pulse. Detection of impending earthquakes and the location of minerals have been achieved by this method. *See* GEOPHYSICAL EXPLORATION; ROCK, ELECTRICAL PROPERTIES OF.

William D. Jackson

Bibliography. H. K. Messerle, *Magnetohydrodynamic Electrical Power Generation*, 1995; R. J. Rosa, *Magnetohydrodynamic Energy Conversion*, 1968, reprint 1987; P. E. Sens (ed.), *Coal-Fired Magnetohydrodynamic (MHD) Electric Power Generation*, 1992.

Magnetohydrodynamics

The interaction of electrically conducting fluids with magnetic fields. The fluids can be ionized gases (commonly called plasmas) or liquid metals. Magnetohydrodynamic (MHD) phenomena occur naturally in the Earth's interior, constituting the dynamo that produces the Earth's magnetic field; in the magnetosphere that surrounds the Earth; and in the Sun and throughout astrophysics. In the laboratory, magnetohydrodynamics is important in the magnetic confinement of plasmas in experiments on controlled thermonuclear fusion. Magnetohydrodynamic principles are also used in plasma accelerators for ion thrusters for spacecraft propulsion, for light-ion-beam powered inertial confinement, and for magnetohydrodynamic power generation. Magnetic fields can also be spontaneously generated in inertial confinement experiments, making magnetohydrodynamics relevant in this area. *See* COSMIC RAYS; GEOMAGNETISM; ION PROPULSION; MAGNETOHYDRODYNAMIC POWER GENERATOR; MAGNETOSPHERE; NUCLEAR FUSION; PLASMA (PHYSICS); SOLAR WIND; SUN.

The conducting fluid and magnetic field interact through electric currents that flow in the fluid. The currents are induced as the conducting fluid moves across the magnetic field lines. In turn, the currents influence both the magnetic field and the motion of the fluid. Qualitatively, the magnetohydrodynamic interactions tend to link the fluid and the field lines so as to make them move together. *See* ELECTRIC CURRENT.

The generation of the currents and their subsequent effects are governed by the familiar laws of electricity and magnetism. The motion of a conductor across magnetic lines of force causes a voltage drop or electric field at right angles to the direction of the motion and the field lines; the induced voltage drop causes a current to flow as in the armature of a generator.

The currents themselves create magnetic fields which tend to loop around each current element. The currents heat the conductor and also give rise to mechanical ponderomotive forces when flowing across a magnetic field. (These are the forces which cause the armature of an electric motor to turn.) In a fluid, the ponderomotive forces combine with the pressure forces to determine the fluid motion. *See* ELECTRICITY; GENERATOR; MAGNETISM; MOTOR.

Magnetohydrodynamic phenomena involve two well-known branches of physics, electrodynamics and hydrodynamics, with some modifications to account for their interplay. The basic laws of electrodynamics as formulated by J. C. Maxwell apply without any change. However, Ohm's law, which relates the current flow to the induced voltage, has to be modified for a moving conductor. *See* ELECTRODYNAMICS; HYDRODYNAMICS; MAXWELL'S EQUATIONS; OHM'S LAW.

It is useful to consider first the extreme case of a fluid with a very large electrical conductivity. Maxwell's equations predict, according to H. Alfvén, that for a fluid of this kind the lines of the magnetic field **B** move with the material. The picture of moving lines of force is convenient but must be used with care because such a motion is not observable. It may be defined, however, in terms of observable consequences by either of the following statements: (1) a line moving with the fluid, which is initially a line of force, will remain one; or (2) the magnetic flux through a closed loop moving with the fluid remains unchanged.

If the conductivity is low, this is not true and the fluid and the field lines slip across each other. This is similar to a diffusion of two gases across one another and is governed by similar mathematical laws.

As in ordinary hydrodynamics, the dynamics of the fluid obeys theorems expressing the conservation of mass, momentum, and energy. These theorems treat the fluid as a continuum. This is justified if the mean free path of the individual particles is much shorter than the distances that characterize the structure of the flow. Although this assumption does not generally hold for plasmas, one can gain much insight into magnetohydrodynamics from the continuum approximation. The ordinary laws of hydrodynamics can then easily be extended to cover the effect of magnetic and electric fields on the fluid by adding a magnetic force to the momentum-conservation equation and electric heating and work to the energy-conservation equation.

Ideal magnetohydrodynamics. Ideal magnetohydrodynamics refers to the study of magnetohydrodynamics for a perfectly conducting fluid, that is, one obeying the form of Ohm's law, given by Eq. (1), where

$$0 = \mathbf{E} + \mathbf{v} \times \mathbf{B} \tag{1}$$

E is the electric field, **B** the magnetic field, and **v** the center-of-mass velocity of the fluid. This equation means that the electric field in the rest frame of the fluid is zero. *See* ELECTRIC FIELD; RELATIVISTIC ELECTRODYNAMICS.

Frozen flow. Equation (1) can be combined with Faraday's law, Eq. (2), to give Eq. (3), which shows

$$\nabla \times \mathbf{E} = -\frac{\partial \mathbf{B}}{\partial t} \tag{2}$$

$$\begin{aligned} \frac{d}{dt}\int \mathbf{B}\cdot d\mathbf{S} &= \int \frac{\partial \mathbf{B}}{\partial t}\cdot d\mathbf{S} + \int \mathbf{B}\cdot\frac{\partial}{\partial t}d\mathbf{S} \\ &= -\int \nabla\times\mathbf{E}\cdot d\mathbf{S} + \oint \mathbf{B}\cdot\mathbf{v}\times d\mathbf{l} \\ &= -\oint (\mathbf{E}+\mathbf{v}\times\mathbf{B})\cdot d\mathbf{l} = 0 \end{aligned} \tag{3}$$

that the magnetic flux, $\int \mathbf{B}\cdot d\mathbf{S}$, where $d\mathbf{S}$ is an element of area in the fluid, is conserved in the frame of reference of the fluid. *See* CALCULUS OF VECTORS; FARADAY'S LAW OF INDUCTION.

It can thus be said that the magnetic field and the fluid are frozen together. This result also implies that magnetic field lines immersed in a perfectly conducting fluid cannot change their topology.

Alfvén waves. If a uniform plasma of density ρ_0 is immersed in a uniform magnetic field $\mathbf{B}_0$, then if there is a periodic transverse displacement of the frozen-in plasma and magnetic field (**Fig. 1**), it can be shown that the displacement propagates as a wave with a velocity $c_A = (B^2{}_0/\mu_0\rho_0)^{1/2}$, where μ_0 is the permeability of empty space. This is called an Alfvén wave. Physically this is analogous to a wave on a loaded string, the magnetic field lines being the string with tension $B^2{}_0/\mu_0$, and the mass loading of the string being ρ_0 per unit volume [Eq. (16)]. This result can easily be derived by using perturbation techniques.

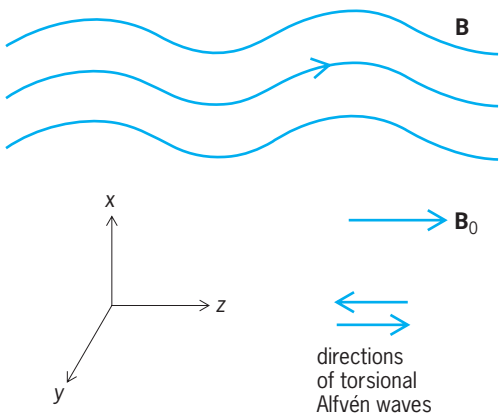

Fig. 1. Periodic transverse displacement of a uniform magnetic field B_0 and a uniform, frozen-in plasma.

The equation of motion for the plasma is Eq. (4),

$$\rho\frac{d\mathbf{v}}{dt} = -\nabla p + \mathbf{J}\times\mathbf{B} \tag{4}$$

where p is the pressure and **J** is the current density. For the situation shown in Fig. 1 this becomes Eq. (5),

$$\rho_0\frac{\partial v_{x1}}{\partial t} = J_{y1}B_{z0} \tag{5}$$

where J_{y1} is the perturbed current density and v_{x1} is the x-component of the perturbed velocity. The plasma pressure p does not contribute to Eq. (5) for purely transverse motion. Ampère's law (neglecting the displacement current which is negligible at such low frequencies) is Eq. (6), and relates the perturbation current of the wave with the perturbed magnetic field through Eq. (7). Combining Eqs. (1)

$$\nabla\times\mathbf{B} = \mu_0\mathbf{J} \tag{6}$$

$$\frac{\partial B_{x1}}{\partial z} = \mu_0 J_{y1} \tag{7}$$

and (2) yields Eq. (8), and in perturbation form this becomes Eq. (9). Differentiating Eq. (9) with respect to time t and employing Eqs. (5) and (7) gives Eq. (10), which is the wave equation for a wave propagating in the $\pm z$ direction with a wave velocity c_A, the Alfvén speed. *See* ALFVÉN WAVES; AMPÈRE'S LAW; WAVE MOTION.

$$\frac{\partial \mathbf{B}}{\partial t} = \nabla\times(\mathbf{v}\times\mathbf{B}) \tag{8}$$

$$\frac{\partial B_{x1}}{\partial t} = B_{z0}\frac{\partial v_{x1}}{\partial z} \tag{9}$$

$$\frac{\partial^2 B_{x1}}{\partial t^2} - \frac{B^2_{z0}}{\mu_0\rho_0}\frac{\partial^2 B_{x1}}{\partial z^2} = 0 \tag{10}$$

Magnetosonic waves. For the more general case when the wave vector **k** is at some arbitrary angle θ to the equilibrium magnetic field $\mathbf{B}_0$, the plasma pressure also contributes to the restoring force of the waves because, in general, compression of the plasma now occurs. Therefore, in addition to the Alfvén wave there are two magnetosonic waves with phase velocity given by Eq. (11), where $c_s = (\gamma p_0/\rho_0)^{1/2}$ is the sound speed, γ being the ratio of specific heats. The plus sign refers to the fast magnetosonic wave in which the plasma pressure perturbations and the magnetic force perturbations act in phase, while the minus sign refers to the slow magnetosonic wave in which the two forces are out of phase. The first (+) magnetosonic wave is the only one that can propagate perpendicular to $\mathbf{B}_0$, and then both the magnetic pressure $B^2_0 2\mu_0$ [Eq. (16)] and the plasma pressure p_0 contribute to the restoring force of this compressional longitudinal wave, and it propagates with a velocity $(c^2_A + c^2_S)^{1/2}$. *See* SOUND.

$$v_\pm = \left\{ {}^1\!/_2\left[c_A^2 + c_s^2 \pm \sqrt{\left(c_A^2 + c_s^2\right)^2 - 4c_A^2c_s^2\ \cos^2\ \theta}\right]\right\}^{1/2} \tag{11}$$

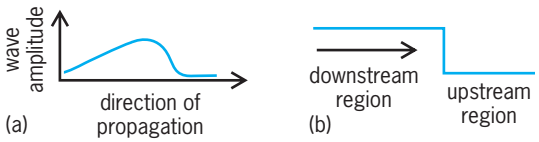

Fig. 2. Evolution of a large-amplitude wave. (*a*) Steepening of wave. (*b*) Formation of shock wave.

Shock waves. When the amplitude of a wave is large, it tends to steepen in the direction of propagation (**Fig. 2***a*). The reason is that the local phase velocity increases where the temperature and magnetic field are higher. The steepening process increases with wave amplitude until a sharp shock (Fig. 2*b*) occurs. The shock thickness and structure are determined by dissipative processes such as viscosity, thermal conduction, and electrical resistivity, discussed below. Conservation laws for mass, momentum, energy, and magnetic flux can be applied in the frame of reference of the shock front in which a steady state can be assumed. For a shock in which the magnetic field is transverse to the direction of propagation, the conservation relations between the upstream region (indicated by subscript 1) and downstream region (indicated by subscript 2) are given by Eqs. (12). The

$$\begin{aligned} \rho_1 v_1 &= \rho_2 v_2 \\ \rho_1 v_1^2 + p_1 + \frac{B_1^2}{2\mu_0} &= \rho_2 v_2^2 + p_2 + \frac{B_2^2}{2\mu_0} \\ {}^1\!/_2 \rho_1 v_1^3 + \frac{\gamma}{\gamma - 1} p_1 v_1 + \frac{B_1^2 v_1}{\mu_0} &= {}^1\!/_2 \rho_2 v_2^3 + \frac{\gamma}{\gamma - 1} p_2 v_2 + \frac{B_2^2 v_2}{\mu_0} \\ v_1 B_1 &= v_2 B_2 \end{aligned} \tag{12}$$

first three of these equations describe conservation of mass, momentum, and energy in that order, the fourth relation being conservation of magnetic flux, derived from Eq. (8). *See* CONSERVATION OF ENERGY; CONSERVATION OF MASS; CONSERVATION OF MOMENTUM.

The shock velocity v_1 in the laboratory frame can be found from Eqs. (12) in terms of the density ratio ρ_1/ρ_2 from Eq. (13). An important result from this is

$$v_1^2 = \frac{2}{\gamma + 1} \cdot \frac{c_s^2 + c_A^2 \left[1 + \left(1 - {}^1\!/_2\gamma\right)(\rho_2/\rho_1 - 1)\right]}{\rho_1/\rho_2 - (\gamma - 1)/(\gamma + 1)} \tag{13}$$

that the maximum density ratio that can occur in a single shock compression is a factor of 4 for $\gamma = {}^5\!/_3$. For this reason the high compression that is required in inertial confinement fusion cannot be attained by a single shock wave, but requires a tailored compression wave that is equivalent to many weaker shocks following each other.

More generally, it is possible to drive a current in the shock front which causes other components of the magnetic field to be generated or removed. Such shocks are called switch-on or switch-off shocks, respectively. *See* SHOCK WAVE.

Collisionless shock. At low density and high temperature the mean free path of electrons and ions is too large for collisional processes to determine the shock structure. Instead, within the shock structure microscopic kinetic instabilities occur because the relative drift velocity of electrons and ions (associated with the net current density in the shock) exceeds some critical value such as the ion sound speed, c_S [Eq. (11)]. These instabilities grow to give a turbulent state yielding corresponding anomalous transport coefficients. *See* TRANSPORT PROCESSES; TURBULENT FLOW.

Magnetostatic equilibria. If the center-of-mass velocity $\mathbf{v}$ is very small, a stationary equilibrium can exist in which the pressure gradient in Eq. (4) is balanced by the magnetomotive force, $\mathbf{J} \times \mathbf{B}$; that is, Eq. (14)

$$\nabla p = \mathbf{J} \times \mathbf{B} \tag{14}$$

is satisfied. This nonlinear equation together with Eq. (6) represents the set of equations describing magnetostatic equilibria.

Two important results follow from Eq. (14). Taking the scalar product first with $\mathbf{B}$ and then with $\mathbf{J}$ yields Eqs. (15), which shows that the pressure is constant

$$\mathbf{B} \cdot \nabla p = 0 \qquad \mathbf{J} \cdot \nabla p = 0 \tag{15}$$

along both a magnetic field line and the current density direction. Applying this to the case of a toroidal axisymmetric equilibrium (**Fig. 3**), it is found that magnetic field lines with toroidal B_ϕ and poloidal B_p components form nested surfaces on each of which the pressure is constant. The current density $\mathbf{J}$ lies in the plane of each magnetic surface and is related to $\mathbf{B}$ through Eq. (6). Thus Eq. (14) can be written as Eq. (16), where $\perp$ signifies the component perpendicular to the magnetic field, and $\mathbf{b} = \mathbf{B}/|B|$ is the unit vector in the direction of the magnetic field. Then it is possible to identify the magnetic pressure, $B^2/(2\mu_0)$, and the tension in the magnetic field lines, B^2/μ_0, which causes a force through the curvature of the lines of force, $(\mathbf{b} \cdot \nabla)\mathbf{b}$. The quantity $2\mu_0 p/B^2$ defines β, the ratio of plasma pressure to magnetic pressure.

$$\begin{aligned} \nabla p &= \frac{(\nabla \times \mathbf{B}) \times \mathbf{B}}{\mu_0} \\ &= -\nabla_\perp \left(\frac{B^2}{2\mu_0} \right) + \frac{B^2}{\mu_0} (\mathbf{b} \cdot \nabla)\mathbf{b} \end{aligned} \tag{16}$$

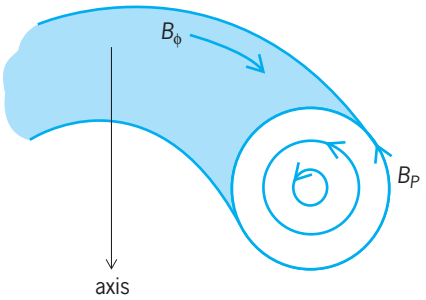

Fig. 3. Perfectly conducting fluid in toroidal axisymmetric equilibrium.

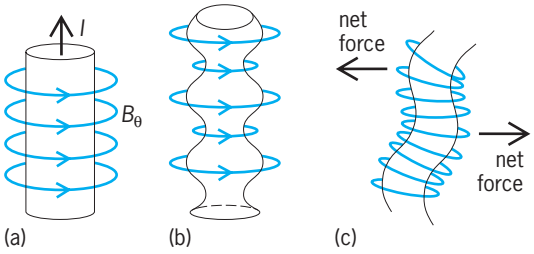

Fig. 4. Instabilities of a Z-pinch configuration. (*a*) Initial configuration of magnetically confined plasma. (*b*) Sausage instability. (*c*) Kink instability.

The solution of Eq. (16) for the axisymmetric large aspect ratio toroidal equilibrium shown in Fig. 3 gives nested circular magnetic surfaces that are not concentric; the inner ones are shifted out, away from the major axis of the torus, so that the surfaces are closer together on the outside of the torus. The physical reason for this is that the toroidal current I_θ which produces the poloidal magnetic field B_p flows as in a hoop, leading to an outward force on the plasma. (Each current segment experiences a repulsive force from the oppositely flowing current in the segment opposite it.) This toroidal configuration is the basis of the tokamak approach to magnetic fusion energy.

Stability of ideal plasmas. An equilibrium state as described above is not necessarily stable. The most elementary configuration of a magnetically confined plasma is a Z-pinch (**Fig. 4***a*) in which a cylindrical column carrying an axial current I is confined by the self-magnetic field produced by the current I itself. This was the earliest concept for confinement of plasma for controlled fusion. Consider an azimuthally symmetric perturbation (Fig. 4*b*) that makes the configuration look rather like a string of sausages. The magnetic field B_θ at the surface of radius a is $\mu_0 I/2\pi a$, so that the magnetic field is stronger where the radius a is narrower, and vice versa. Hence the plasma column (unless it is very diffuse) can be unstable to this perturbation because of the enhanced $\mathbf{J} \times \mathbf{B}$ force where a is small. *See* PINCH EFFECT.

Another type of instability is the kink mode (Fig. 4*c*) where the column is bent one way and the other in an alternating way. Again the driving force for the instability can be seen from an examination of the magnetic lines of force. In the kink mode they are concentrated together on the concave side and are further apart on the convex side of each kink. This leads to a net force (as shown in Fig. 4*c*) which increases the amplitude of the kink.

Such instabilities have been seen experimentally, and led to the introduction of another magnetic field component, an axial magnetic field B_z, in order to stabilize the configuration. With both B_z and B_θ components present, the magnetic field lines are now helices. If the pitch of the helices varies across the radius of the plasma column, then this shear of the field can stabilize the discharge against localized modes.

The necessary stability criterion is given by Eq. (17), where r is the distance from the axis of the column and μ, the pitch, is defined by Eq. (18).

$$\left(\frac{1}{\mu}\frac{d\mu}{dr}\right)^2 + \frac{8\mu_0}{rB_z{}^2}\frac{dp}{dr} \geq 0 \tag{17}$$

$$\mu = \frac{B_\theta}{rB_z} \tag{18}$$

For a confined plasma the second term involving the pressure gradient, dp/dr, is always a negative contribution, and so this condition determines the shear $d\mu/dr$ required for stability. When the configuration is bent into a torus, the second term is multiplied by a factor $(1 - q^2)$, where q, the safety factor, is rB_ϕ/RB_θ; this leads to stability of these internal modes for $q > 1$. Here R is the major radius of the torus, and B_ϕ is the toroidal component of magnetic field.

A purely hydrodynamic instability, found also in dynamic Z-pinches and exploding supernovae, but also of vital concern in the concept of inertial confinement, is the Rayleigh-Taylor instability. The original problem concerned the stability of a heavy fluid above a light fluid under gravitational acceleration g. A small perturbation of the interface (**Fig. 5**) is clearly unstable, and one with a wave number k (where the wavelength $\lambda = 2\pi/k$) can be shown to have a growth rate $\gamma = (kg)^{1/2}$. Short wavelengths thus have the highest growth rates, and in inertial confinement the shell thickness is likely to determine the most dangerous mode. The reason why the Rayleigh-Taylor instability applies here is that the effect of g is the same as a fluid acceleration in the opposite direction.

Energy principle. Two theoretical methods have been developed for examining the linear stability of an equilibrium configuration; one is a normal mode analysis which directly determines the growth rate, and the other uses an energy principle. When more complex physical processes such as the nonvanishing ion Larmor radius or the Hall effect are included, the former method is applicable; but where the complexity is entirely in the geometrical configuration of the magnetically confined plasma, the energy principle is the more appropriate technique. In ideal magnetohydrodynamics, Eqs. (1), (2), (4), and (6) can be combined to linearly relate the acceleration $\ddot{\boldsymbol{\xi}}$ of a fluid element to the force $\mathbf{F}(\boldsymbol{\xi})$, where $\boldsymbol{\xi}$ is the local fluid displacement and the two dots above $\boldsymbol{\xi}$ means the second derivation with respect to time. Because of the adjointness of $\mathbf{F}$, the stability is ensured if the change in potential energy associated with the

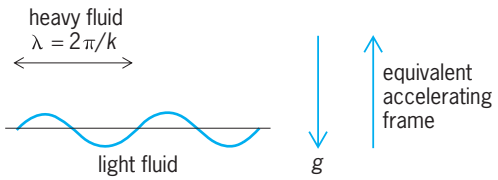

Fig. 5. Rayleigh-Taylor instability, involving a perturbation in the interface between a light fluid and a heavy fluid above it.

displacement, given by Eq. (19), is positive, where

$$\delta W = -\frac{1}{2}\int \ddot{\xi}\cdot \mathbf{F} d^3r \tag{19}$$

the integral is taken over the entire volume of the configuration. Equation (17) was derived from the energy principle. [By adjointness is meant that $\mathbf{F}$ satisfies Eq. (20), where η obeys the same boundary conditions as ξ.] Thus the rate of increase of kinetic energy (that is, the rate of doing work) is $\int \xi \cdot \mathbf{F}(\xi) d^3r$. By virtue of conservation of total energy and the adjointness of $\mathbf{F}(\xi)$, it follows that the corresponding change in potential energy δW is given by Eq. (19). If the kinetic energy is increasing through growth of the instability, there is a corresponding decrease in potential energy. Conversely, if δW is positive, the system is stable. More strictly, if δW is found to be positive for all allowable displacements ξ, the plasma is stable; but if δW is negative for any allowable displacement ξ, the plasma is unstable.

$$\int \xi \cdot F(\eta)\, d^3r = \int \eta \cdot \mathbf{F}(\xi) d^3r \tag{20}$$

The most simple example of the use of the energy principle is the interchange mode. **Figure 6** illustrates two flux tubes each having a magnetic flux $\delta\phi = B\delta A$, where δA is the local area of cross section. The volume of a flux tube, δV, is the integral $\int \delta A dl$, where dl is an element of length along the tube, and therefore the plasma thermal energy in a flux tube is given by Eq. (21). When the plasma on the two

$$\frac{p}{\gamma - 1} dV = \frac{p}{\gamma - 1}\delta\phi \int \frac{dl}{B} \tag{21}$$

flux tubes is interchanged, δW is found to be positive if $\int dl/B$ decreases with the spatially decreasing plasma pressure as one moves toward the walls of the confining vessel. This leads to the concept of a minimum-B confinement configuration, that is, one in which the magnitude of the magnetic field is a minimum at the center of the plasma and increases in all directions away from the center.

Resistive magnetohydrodynamics. An electrically conducting fluid acquires new properties when its resistivity is taken into account.

Stability of resistive plasmas. While the resistivity η of thermonuclear plasmas at a temperature of 10 keV is very low (approximately 10^{-9} ohm·m), it is nevertheless sufficient to permit the magnetic field configuration to change its topology in a thin layer inside which the wave number $\mathbf{k}$ of the perturbation mode

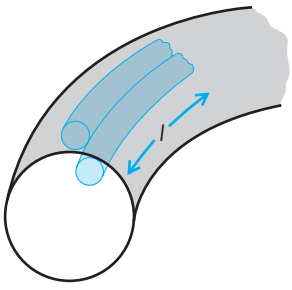

Fig. 6. Two flux tubes in a magnetic field configuration.

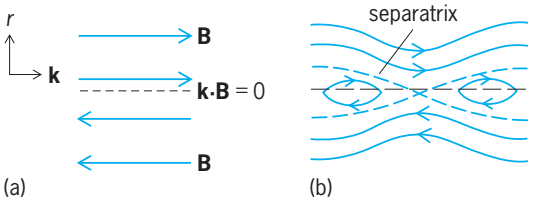

Fig. 7. Effect of nonvanishing resistivity on plasma stability. (*a*) Location of resonant surface k · B = 0. (*b*) Breaking and reconnection of magnetic field lines about the resonant surface in a resistive plasma.

and the magnetic field vector $\mathbf{B}$ satisfy the condition $\mathbf{k}\cdot\mathbf{B} = 0$. The surface that satisfies this condition is called a resonant surface since the magnetic field lies in a plane of constant phase of the plasma displacement. In a torus, such resonant surfaces occur at rational values of q, the safety factor.

Figure 7*a* illustrates the plane containing $\mathbf{k}$ and the coordinate r perpendicular to the magnetic surface, surrounding the resonant surface, $\mathbf{k}\cdot\mathbf{B} = 0$. With nonvanishing resistivity η, Ohm's law is given by Eq. (22), replacing Eq. (1). With the presence of

$$\eta\mathbf{J} = \mathbf{E} + \mathbf{v}\times\mathbf{B} \tag{22}$$

the $\eta\mathbf{J}$ term, the magnetic field lines can break and reconnect to form a different configuration consisting of magnetic islands centered on the $\mathbf{k}\cdot\mathbf{B} = 0$ surface. There are corresponding X-type and O-type neutral points (Fig. 7*b*), the former lying at the intersection of the separatrix and the $\mathbf{k}\cdot\mathbf{B} = 0$ surface. The growth of such a magnetic island structure to a finite size is of major importance in understanding the magnetohydrodynamic behavior of toroidal magnetically confined plasma, particularly with regard to disruptions in tokamaks. The phenomenon of magnetic reconnection is also important in the evolution of solar flares. The nonlinear evolution of the new closed magnetic lines topology, called magnetic islands, is the subject of much research. For example, the Sweet-Parker model suggests that the open field lines drift slowly in toward the $\mathbf{k}\cdot\mathbf{B} = 0$ plane, while the plasma flows in the $\pm\mathbf{k}$ direction within the reconnection layer have an amplitude of the order of the Alfvén velocity. It is also possible that the high current density induced in the reconnection layer will, as in collisionless shocks, lead to the triggering of microinstabilities with an associated anomalous resistivity, resulting in a fast reconnection. This is particularly applicable to astrophysical reconnection processes.

Helicity. The possibility of magnetic reconnection even when the resistivity is small but nonzero allows the overriding thermodynamic tendencies to dominate. Hence, for example, in the toroidal reversed-field pinch, the plasma and magnetic field can relax to a state of minimum energy. In doing so, a three-dimensional dynamo occurs as a result of the resistive MHD instabilities and the associated plasma flows, causing the toroidal magnetic field to peak on the minor axis and to reverse in direction at the plasma edge. During this process, it can be reasonably postulated that the magnetic helicity. $\int \mathbf{A}\cdot\mathbf{B}\, dV$ is approximately conserved. Here $\mathbf{A}$ is the magnetic

vector potential defined by $\mathbf{B} = \nabla \times \mathbf{A}$. The reason for this conservation is that the local helicity density $\mathbf{A} \cdot \mathbf{B}$ obeys Eq. (23), where Φ is the electrostatic

$$\frac{\partial}{\partial t}(\mathbf{A} \cdot \mathbf{B}) + \nabla(\Phi \mathbf{B} + \mathbf{E} \times \mathbf{A}) = -2\mathbf{E} \cdot \mathbf{B} \qquad (23)$$

potential. If the flux of helicity, (Φ $\mathbf{B}$ + $\mathbf{E}$ × $\mathbf{A}$), is zero, then the source or sink of helicity is the term $-2\mathbf{E} \cdot \mathbf{B}$, which is small everywhere for a plasma of high conductivity, and is only significant in the reconnection layer associated with resistive MHD instabilities. (In evaluating helicity, care must be taken with the choice of gauge for $\mathbf{A}$.)

Diffusion. Finite resistivity also allows the plasma to diffuse across magnetic field lines. Classical diffusion of a low β plasma across an axial magnetic field B_z can be described in terms of the pressure balance of Eq. (14), which here becomes Eq. (24). In this

$$\frac{\partial p}{\partial r} = J_\theta B_z \qquad (24)$$

the azimuthal current density is driven by the radial diffusion velocity v_r through Ohm's law, Eq. (22), which here becomes Eq. (25). Thus, the flux of par-

$$\eta J_\theta = -v_r B_z \qquad (25)$$

ticles of density n in an isothermal plasma is given by Eq. (26). This is Fick's law of diffusion, with a dif-

$$nv_r = -\frac{\eta p}{B^2}\frac{\partial n}{\partial r} \qquad (26)$$

fusion coefficient $D = \eta p/B^2$. The B^{-2} dependence is characteristic of classical diffusion. Plasmas that are microscopically turbulent tend to obey Bohm diffusion where the diffusion coefficient $k_B T/(16eB)$ [where k_B is Boltzmann's constant, T the absolute temperature, and e the electronic charge] is larger by a factor of $\omega_e \tau_e/16$; ω_e is the electron cyclotron frequency, τ_e is the electron-ion collision time, and the product, $\omega_e \tau_e$, is called the Hall parameter, being equal to $B/(ne\eta)$. *See* DIFFUSION; ELECTRON MOTION IN VACUUM; HALL EFFECT; PARTICLE ACCELERATOR; RELAXATION TIME OF ELECTRONS.

In a toroidal configuration with high safety factor q, greater than 1 (usually called a tokamak), classical diffusion is enhanced by two effects. The first is connected with the magnetohydrodynamic equilibrium itself, as defined by Eq. (14), in which, to balance the outward hoop force of the toroidal current itself, a vertical magnetic field component is required which causes the magnetic surfaces to be shifted outward. Consistent with this, the toroidal current must increase with increasing distance R from the major axis. However, the applied electric field E_ϕ (equal to $-\partial A_\phi/\partial t$, where A_ϕ is the toroidal component of the electromagnetic vector potential) varies as R^{-1}. Therefore an outward diffusion velocity v_R occurs, so that the current density J_ϕ in Ohm's law, here given by Eq. (27), has the required spatial depen-

$$\eta J_\phi = E_\phi + (\mathbf{v} \times \mathbf{B})_\phi \qquad (27)$$

dence. This diffusion is $2q^2$ times the classical value. *See* POTENTIALS.

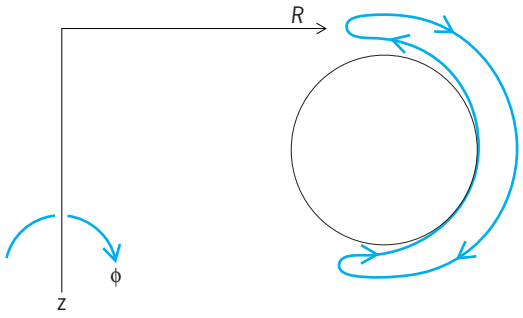

Fig. 8. Projection of a guiding center orbit onto a poloidal plane of a tokamak.

The second effect is important at high temperature when the plasma is relatively collisionless, and when the trajectories of particles have large excursions from magnetic surfaces. Because the toroidal magnetic field varies as $1/R$, the magnitude of the total field is greater near the inside of the torus. A guiding center for the motion of a particle can therefore be reflected near the inside of the torus and, in continuing its drift motion, executes a trajectory which is banana-shaped when projected onto a poloidal plane (**Fig. 8**). The width of the "banana" is $2mv_{||}/(ZeB_p)$, where B_p is the poloidal component of the magnetic field, m and Z are the particle's mass and charge number, and $v_{||}$ is the component of its velocity parallel to the magnetic field. This width is much greater than the Larmor radius $mv_\perp/(ZeB_\phi)$, and when such particles have even only weak collisions, an enhanced diffusion occurs; here $v_\perp$ is the component of velocity perpendicular to the magnetic field. *See* CHARGED PARTICLE OPTICS.

Magnetic Reynolds number. The relative strength of the $\mathbf{v} \times \mathbf{B}$ and $\eta\mathbf{J}$ terms in Ohm's law can be written with the aid of Eq. (6) as the ratio R_M given by Eq. (28),

$$R_M = \frac{\mu_0 vL}{\eta} \qquad (28)$$

the magnetic Reynolds number, where L is a characteristic length. When R_M is much greater than 1, the magnetic field is frozen to the conducting fluid, while for R_M much less than 1 the fluid very easily penetrates an applied magnetic field (as in magnetohydrodynamic power generators). When resistive damping is included in the theory of Alfvén waves and magnetohydrodynamic stability theory, a corresponding dimensionless parameter, the Lundquist parameter, given by Eq. (29), occurs, where λ is the wavelength.

$$S = \frac{\mu_0 c_A \lambda}{\eta} \qquad (29)$$

When S is much greater than 1 the resistive damping or thickness of the tearing layer is small, while for S less than 1 no Alfvén wave propagation occurs. *See* DIMENSIONLESS GROUPS.

Electrically conducting fluids. Electrically conducting fluids are either liquid metals or plasmas.

Liquid metals. Mercury and liquid sodium are two familiar examples of electrically conducting, incompressible fluids. The core of the Earth is also

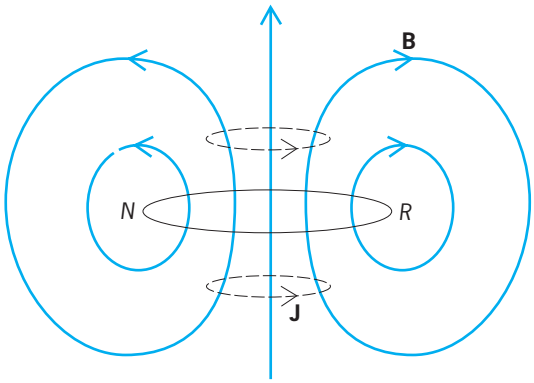

Fig. 9. Axisymmetric, two-dimensional, liquid-metal system in which only an azimuthal current and poloidal magnetic field components exist.

interpreted to be in the liquid-metal state and able to generate currents and magnetic fields. In particular, in a three-dimensional interaction involving the Coriolis force and the $\mathbf{v} \times \mathbf{B}$ force associated with the Earth's rotation, a dynamo action is postulated to account for the Earth's magnetic field. A similar mechanism could generate the solar magnetic field. *See* CORIOLIS ACCELERATION.

The necessity of involving a three-dimensional model for dynamo action can be seen from consideration of an axisymmetric, two-dimensional system (**Fig. 9**), in which only an azimuthal current and poloidal magnetic field components exist. It has been shown that such a system cannot be sustained by fluid motion alone in a steady state. The argument is as follows: the azimuthal electric field must vanish in a steady state so that $\eta\mathbf{J} = \mathbf{v} \times \mathbf{B}$; therefore the neutral ring NR where $\mathbf{B}$ is zero will also have $\mathbf{J} = 0$ and hence $\nabla \times \mathbf{B} = 0$. If this condition is satisfied—for example, if, in the vicinity of the neutral ring, $|B| \propto r^{\alpha}$ for $\alpha > 1$, where r is the distance from the neutral ring—then Ampère's law gives $J \propto r^{\alpha-1}$, but Ohm's law then yields $\upsilon \propto 1/r$ which is an impossible singularity.

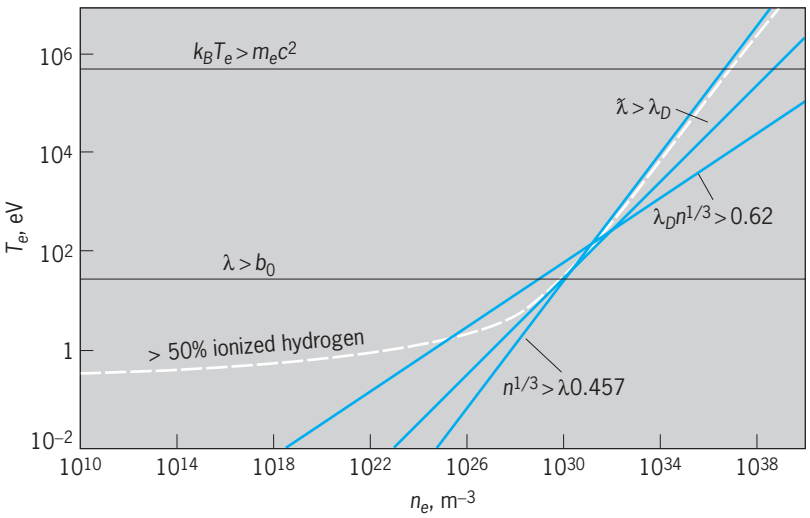

Fig. 10. Plot of electron temperature T_e and density n_e in a plasma, showing values of these parameters where various types of behavior occur.

Another theorem for the same axisymmetric system is as follows: Because the current is purely azimuthal, the curl of $\mathbf{J}$ has no azimuthal component. For uniform resistivity, this means that the azimuthal component of curl $(\mathbf{v} \times \mathbf{B})$ vanishes, which, with the Maxwell equation (30), gives $\mathbf{B} \cdot \nabla\Omega = 0$, where

$$\nabla \cdot \mathbf{B} = 0 \tag{30}$$

$r\Omega = \upsilon_\theta$. This means that the fluid at all points on a magnetic field line rotates about the axis with a uniform angular velocity Ω, r being the distance from the axis.

Plasmas. Most work in magnetohydrodynamics has concerned ionized gases or plasmas. Plasma physics concerns the collective interaction of ions and electrons in a usually quasi-neutral system. In such a plasma there are many particles in a Debye sphere. This follows from the condition that for the gas to remain fully ionized, the mean kinetic energy k_BT_e (where k_B is Boltzmann's constant, and T_e is the electron temperature) must be larger than the mean potential energy $n_e^{1/3}e^2/\epsilon_0$, where ϵ_0 is the permittivity of empty space, and n_e is the number of electrons per cubic meter, so that the average distance between particles is $n^{-1/3}{}_e$. Raising this condition to the power $^3/_2$ yields the condition $n_e\lambda^3{}_D \gg 1$, where λ_D (the Debye length) is $[\epsilon_0 k_B T_e/(n_e e^2)]^{1/2}$. In contrast to this condition, there is increasing interest in "strongly coupled" plasmas where $n_e\lambda^3{}_D \lesssim 1$, as these are relevant to the early stages of inertial confinement when the plasma is very dense and relatively cold. **Figure 10** illustrates the regimes in $n_e - T_e$ parameter space, and shows three quantum-mechanical effects: (1) The classical minimum impact parameter b_0 (the Landau parameter), given by Eq. (31), is less than the de Broglie wavelength, given by Eq. (32), where $\hbar$ is Planck's constant h divided

$$b_0 = \frac{Ze^2}{4\pi\epsilon_0 k_B T_e} \tag{31}$$

$$\lambda\!\!\!^{-} = \frac{\hbar}{(m_e k_B T_e)^{1/2}} \tag{32}$$

by 2π, and m_e is the electron mass, above a temperature of 27 eV (1 eV $= 1.16 \times 10^4$ K). [The effective minimum impact parameter is then the de Broglie wavelength, though strictly the reason for the departure from classical Rutherford scattering is that the presence of Debye shielding modifies the r^{-1} dependence of the Coulomb potential to $r^{-1}\exp(-r/\lambda_D)$, which quantum-mechanically leads to the maximum impact parameter being reduced from λ_D to $\lambda_D\, b_0/\lambda\!\!\!^{-}$. Furthermore, electrons colliding with ions with an impact parameter of $\lambda\!\!\!^{-}$ have a maximum cross section for radiating their energy due to their large acceleration during the collision. This radiation loss is hence called bremsstrahlung, literally, braking radiation. The radiation is characterized by photon energy $h\nu$ of order k_BT.] (2) Below 1 eV a typical gas is only weakly ionized. (3) For dense plasmas when $n_e^{-1/3}$ is less than $\lambda\!\!\!^{-}$, the electron gas becomes degenerate. Above 0.5 MeV the electron energy is relativistic ($k_BT_e > m_ec^2$, where m_e is the electron mass and c is

the speed of light). *See* BREMSSTRAHLUNG; NONRELATIVISTIC QUANTUM THEORY; QUANTUM MECHANICS; RELATIVISTIC QUANTUM THEORY.

The classical collision cross section for a single 90° deflection of an electron by an ion is πb_0^2. However, since there are many particles in a Debye sphere, each particle simultaneously interacts with $n\lambda^3{}_D$ particles. This leads to an increase in collision cross section by a factor 8 ln Λ, where Λ is λ_D/b_0 (or λ_D/λ for $T_e > 10^5$ K). Apart from the weak logarithmic dependence, the mean free path is then found to be proportional to T^2/n and the mean collision frequency $\bar{\nu}$ to $nT^{-3/2}$; for an electron of velocity v, the mean free path is proportional to v^4/n, and its collision frequency (with stationary ions) ν is proportional to nv^{-3}. This velocity dependence of the collision frequency is responsible for the penetration and preheating by more energetic electrons in laser-induced compression experiments, for so-called runaway electrons in ohmically heated toroidal plasmas, and in linear transport theory for the existence of large thermoelectric and Nernst terms in Ohm's law, discussed below. When the plasma is only partially ionized (for example, in a magnetohydrodynamic power generator), the effective collision frequency is the sum of the electron-ion and electron-neutral collision frequencies. *See* KINETIC THEORY OF MATTER.

For a fully ionized plasma the electrical conductivity σ (equal to η^{-1}) is $ne^2/(m_e v)$ and therefore is independent of electron density and proportional to $T^{3/2}$. Similarly the thermal conductivity and the viscosity are proportional to $T^{5/2}$ in the absence of a magnetic field. *See* CONDUCTION (ELECTRICITY); CONDUCTION (HEAT); VISCOSITY.

Fluid equations for a plasma. The full set of fluid equations for a plasma in a magnetic field displays a large number of terms which give many interesting effects in magnetohydrodynamics. This set can be derived from the Boltzmann kinetic equation. *See* BOLTZMANN TRANSPORT EQUATION.

Conservation equations. The first of these equations, Eq. (33), describes the conservation of mass, where

$$\frac{\partial \rho}{\partial t} + \nabla \cdot (\rho \mathbf{v}) = 0 \tag{33}$$

ρ is the mass density and $\mathbf{v}$ is the fluid center-of-mass velocity. That this does indeed give conservation, which means no creation or destruction of mass, can be shown by integrating Eq. (33) over a volume V and employing Gauss' theorem, Eq. (34), so that the mathematical result of Eq. (35) means that the rate

$$\int \nabla \cdot (\rho \mathbf{v})\, dV = \oint \rho \mathbf{v} \cdot d\mathbf{S} \tag{34}$$

$$\frac{d}{dt} \int_V \rho\, dV = -\oint \rho \mathbf{v} \cdot d\mathbf{S} \tag{35}$$

of change of mass in the volume V is equal to the net inward flux, $-\rho\mathbf{v}$, integrated over the closed surface $d\mathbf{S}$ enclosing the volume V. *See* EQUATION OF CONTINUITY; GAUSS' THEOREM.

The conservation of total momentum is of similar form, given by Eq. (36). Here $\rho\mathbf{v}$ is the momentum of

$$\frac{d}{dt}(\rho \mathbf{v} + \mathbf{D} \times \mathbf{B}) + \nabla \cdot (\rho \mathbf{v}\mathbf{v} + \mathbf{P} + \mathbf{T}) = 0 \tag{36}$$

the fluid per unit volume, and to this must be added the momentum of the electromagnetic fields themselves per unit volume, $\mathbf{D} \times \mathbf{B}$. Since flux is a vector and momentum is also a vector, the flux of momentum is in general a tensor. For example, there can be a momentum component ρv_x transported with a velocity component v_y. Thus the terms in the divergence operator are tensors: $\rho\mathbf{v}\mathbf{v}$ is the flux of momentum associated with the center-of-mass velocity; $\mathbf{P}$, called the stress tensor, is the flux of momentum associated with the random or thermal motion of the fluid particles; and $\mathbf{T}$ is the flux of electromagnetic momentum usually called the Maxwell stress tensor. In most cases, Eq. (36) can be reduced to a more simple form that does not involve tensors, as given in Eq. (40). *See* TENSOR ANALYSIS.

The conservation of total energy also obeys a similar equation, Eq. (37), where $^1/_2\rho v^2$ and $^1/_2\rho v^2\mathbf{v}$ are

$$\frac{\partial}{\partial t}(^1/_2\rho v^2 + U + {}^1/_2\mathbf{E} \cdot \mathbf{D} + {}^1/_2\mathbf{H} \cdot \mathbf{B}) + \nabla \cdot (^1/_2\rho v^2 \mathbf{v} + U\mathbf{v} + \mathbf{P} \cdot \mathbf{v} + \mathbf{q} + \mathbf{E} \times \mathbf{H}) = 0 \tag{37}$$

the kinetic energy per unit volume and flux of kinetic energy, respectively; $U = {}^3/_2 n k_B T$ is the internal energy density, n being the particle number density, k_B Boltzmann's constant, and T the temperature; and $\mathbf{q}$ is the heat flux. The terms $^1/_2\mathbf{E} \cdot \mathbf{D}$ and $^1/_2\mathbf{H} \cdot \mathbf{B}$ are the energy per unit volume in electric and magnetic fields, respectively, and $\mathbf{E} \times \mathbf{H}$ is the electromagnetic energy flux, commonly called Poynting's vector, and equal to $c^2\mathbf{D} \times \mathbf{B}$ for vacuum fields. *See* POYNTING'S VECTOR.

Application of Maxwell's equations. Maxwell's equations are Eqs. (38), (2), (39), and (30), where q_v is the

$$\nabla \cdot \mathbf{D} = q_v \tag{38}$$

$$\nabla \times \mathbf{E} = -\frac{\partial \mathbf{B}}{\partial t} \tag{2}$$

$$\nabla \times \mathbf{H} = \mathbf{J} + \frac{\partial \mathbf{D}}{\partial t} \tag{39}$$

$$\nabla \cdot \mathbf{B} = 0 \tag{30}$$

charge density. From these equations it can be shown that the electromagnetic force per unit volume is given by Eq. (40), where $\mathbf{T}$ is given by Eq. (41) and

$$q_v\mathbf{E} + \mathbf{J} \times \mathbf{B} = -\frac{\partial}{\partial t}(\mathbf{D} \times \mathbf{B}) - \nabla \cdot \mathbf{T} \tag{40}$$

$$\mathbf{T} = -\mathbf{E}\,\mathbf{D} + {}^1/_2\mathbf{E} \cdot \mathbf{D}\mathbf{1} - \mathbf{H}\,\mathbf{B} + {}^1/_2\mathbf{H} \cdot \mathbf{B}\,\mathbf{1} \tag{41}$$

$\mathbf{1}$ is the unit tensor. The left-hand side of Eq. (40) can also be considered as the rate at which electromagnetic momentum per unit volume is given to the fluid or plasma, or minus the rate at which fluid momentum density is given to the electromagnetic fields. Through the effects of magnetic field tension

and pressure, the electromagnetic stress **T** provides the means, for example, of transferring the equal and opposite momentum onto a field coil when a plasma is being accelerated.

Using Eq. (40) and subtracting **v** times Eq. (33), Eq. (36) can now be written simply as Eq. (42),

$$\rho\frac{\partial \mathbf{v}}{\partial t}+\rho(\mathbf{v}\cdot\nabla)\mathbf{v}=\rho\frac{d\mathbf{v}}{dt}=-\nabla p+\mathbf{J}\times\mathbf{B} \qquad (42)$$

where the stress tensor has been approximated by the isotropic scalar pressure $p = nk_BT$. It has also been assumed here that the plasma is quasi-neutral, that is, that there are many particles in a Debye sphere so that the residual charge density q_v is small, causing $q_v\mathbf{E}$ to be a negligible force per unit volume. For this reason Eq. (38) is employed only for describing high-frequency phenomena. The operator d/dt refers to the absolute rate of change with time as seen by a moving fluid element.

Maxwell's equations can also be used to derive Eq. (43) for $\mathbf{J}\cdot\mathbf{E}$, the rate of transfer of energy per

$$\mathbf{J}\cdot\mathbf{E}=-\frac{\partial}{\partial t}({}^1/_2\mathbf{E}\cdot\mathbf{D}+{}^1/_2\mathbf{H}\cdot\mathbf{B})-\nabla\cdot(\mathbf{E}\times\mathbf{H}) \qquad (43)$$

unit volume from electromagnetic to plasma energy. For a dynamo or a generator (for example, a magnetohydrodynamic generator) $\mathbf{J}\cdot\mathbf{E}$ must be negative, while for dissipation in or Joule heating of a stationary plasma, $\mathbf{J}\cdot\mathbf{E}$ will be positive.

Viscous effects. When the stress tensor is retained in the equation of motion, kinetic theory shows that in addition to the isotropic pressure there are contributions proportional to gradients or shear in velocity **v**. For an isotropic plasma (that is, one without large magnetic field effects) the equation of motion (42) is modified to give Eq. (44), where μ is the ion

$$\rho\frac{\partial \mathbf{v}}{\partial t}+\rho(\mathbf{v}\cdot\nabla)\mathbf{v}=-\nabla p+\mathbf{J}\times\mathbf{B}+\mu\nabla^2\mathbf{v}+{}^1/_3\mu\nabla(\nabla\cdot\mathbf{v}) \qquad (44)$$

viscosity, equal to the ion pressure divided by the collision frequency for ion-ion collisions. The viscous terms in Eq. (44) are the characteristic Navier-Stokes terms, the second one vanishing for an incompressible fluid. *See* FLUID-FLOW PRINCIPLES; NAVIER-STOKES EQUATION; VISCOSITY.

Other dimensionless numbers. The ratio of $\rho(\mathbf{v}\cdot\nabla)\mathbf{v}$ to $\mu\nabla^2\mathbf{v}$ in Eq. (44) gives Eq. (45) for the (viscous) Reynolds number, where L is the characteristic length over which the velocity shear exists. R describes the ratio of convection of vorticity, $\nabla\times\mathbf{v}$, to diffusion. A large value of R of the order of 10^3 leads to hydrodynamic turbulence. *See* REYNOLDS NUMBER.

$$R=\frac{\rho vL}{\mu} \qquad (45)$$

The Peclet or thermal Reynolds number R_T is the ratio of the enthalpy flow $(U + p)\mathbf{v}$ to the heat flow **q**. If **q** is given by Fourier's law, Eq. (46), where κ is the thermal conductivity, the thermal Reynolds number R_T describes in Eq. (47) the ratio of convection of temperature to diffusion.

$$\mathbf{q}=-\kappa\nabla T \qquad (46)$$

$$R_T=\frac{5}{2}\frac{nk_Bv L}{\kappa} \qquad (47)$$

The combined effect of convection and diffusion can lead to boundary layers being established. The relative thickness of the thermal viscous and magnetic (or skin current) boundary layers is described by Prandtl numbers which are the ratio of the various Reynolds numbers or diffusivities. The original Prandtl number is R_T/R, while the magnetic Prandtl number is R_M/R, where R_M is the magnetic Reynolds number defined in Eq. (28). *See* BOUNDARY-LAYER FLOW; SKIN EFFECT (ELECTRICITY).

The relative strength of $\mathbf{J}\times\mathbf{B}$ and $\mu\nabla^2\mathbf{v}$ in Eq. (44) leads to the definition of the Hartmann number H by Eq. (48), where **J** is taken to be of order $\mathbf{v}\times\mathbf{B}/\eta$. Setting H approximately equal to 1 defines the scale length over which magnetic and viscous forces are comparable in magnitude.

$$H^2=\frac{B^2L^2}{\mu\eta} \qquad (48)$$

Diamagnetism. The mean center-of-mass velocity **v** for a species should not be confused with the mean guiding-center velocity $\mathbf{v}_{gc}$ associated with the motion of individual particles of the species. Ignoring inertial effects and collisions, **v** in Eq. (34) can be shown to be the sum of $\mathbf{v}_{gc}$ and the diamagnetic velocity $1/Zen\ \mathrm{curl}_\perp\,(p_\perp\mathbf{B}/B^2)$, where $\mathrm{curl}_\perp$ is the component of the curl perpendicular to the magnetic field, and $p_\perp$ is the component of the anisotropic pressure perpendicular to the magnetic field. The physical meaning of the diamagnetic velocity can be understood from **Fig. 11**, which shows particle orbits in the plane perpendicular to the magnetic field B_z in a frame of reference in which the mean guiding-center motion is zero. It can be seen that if the density or temperature increases in the x direction, or if B_z decreases in the x direction, there will be a net contribution to momentum in the y direction in the shaded element due to the time-averaged statistical contribution from particles whose orbits intersect the element.

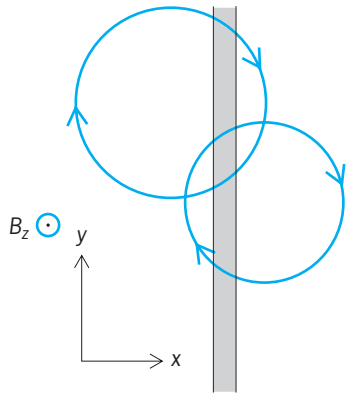

Fig. 11. Particles orbits in the plane perpendicular to a magnetic field B_z in a frame of reference in which the mean guiding center motion is zero.

Transport equations for a two-fluid plasma in a magnetic field. By solving the Boltzmann equation for the case when the electric field **E** and gradients of pressure, temperature, and velocity are small, transport equations can be derived relating the current density **J** and the heat flux **q** to these quantities. Thermodynamically the fluxes **J** and **q** are driven by the thermodynamic forces, **E** and ∇T, so that the irreversible generation of entropy is always positive locally. *See* ENTROPY.

In general, cross-phenomena occur; for example, current can flow as a result of a temperature gradient. The physical reason for this is that the collision frequency is velocity-dependent. Thus, when a temperature gradient exists, higher-velocity particles in the hotter region will flow with fewer collisions, so that there will be not only a heat flow but also a current. If a current is prevented from flowing, as in the symmetric radially inward heat flow in laser fusion targets, an electric field will develop instead to retard the hotter electrons and also to drive an equal and opposite cold electron current. The presence of the electric field will also affect the heat flow. *See* THERMOELECTRICITY.

If there is also a magnetic field which is orthogonal to an electric field or to a temperature gradient, the electrons will cause a current or heat flow not only parallel to **E** or ∇T but also orthogonal to both **E** or ∇T and the magnetic field. This is because of the cycloidal motion of charged particles in a magnetic field. *See* GALVANOMAGNETIC EFFECTS; THERMOMAGNETIC EFFECTS.

When the center-of-mass velocities and temperature of the electrons and ions are considered to be different, separate equations for the two fluids have to be employed. Using the notation of Braginskii, the transport equations for the electron fluid (subscript *e*) can be written as Eqs. (49) and (50), where $\mathbf{E}^*$ is a generalized electric field given by Eq. (51); **b** is

$$n_e e\mathbf{E}^* = \frac{\alpha_\parallel \mathbf{J}_\parallel + \alpha_\perp \mathbf{J}_\perp - \alpha_\wedge \mathbf{b}\times\mathbf{J}}{n_e e} - n_e\left(\beta_\parallel \nabla_\parallel T_e + \beta_\perp \nabla_\perp T_e + \beta_\wedge \mathbf{b}\times\nabla T_e\right) \quad (49)$$

$$\mathbf{q}_e = -\left(\kappa_\parallel \nabla_\parallel T_e + \kappa_\perp \nabla_\perp T_e + \kappa_\wedge \mathbf{b}\times\nabla T_e\right) - \frac{\left(\beta_\parallel \mathbf{J}_\parallel + \beta_\perp \mathbf{J}_\perp + \beta_\wedge \mathbf{b}\times\mathbf{J}\right) T_e}{e} \quad (50)$$

$$\mathbf{E}^* = \mathbf{E} + \mathbf{v}\times\mathbf{B} - \frac{\mathbf{J}\times\mathbf{B}}{n_e e} + \frac{\nabla p_e}{n_e e} \quad (51)$$

the unit vector in the direction of the magnetic field; the coefficients $\alpha_\perp$, $\alpha_\wedge$, and so forth are functions of $(\omega_e\tau_e)$, the Hall parameter; $\alpha_{||}$ is the value of $\alpha_\perp$ when $\omega_e\tau_e = 0$, and so forth; and $\mathbf{J}_{||}$, $\mathbf{J}_\perp$, $\nabla_{||}T_e$, and $\nabla_\perp T_e$ are given by Eqs. (52)–(55).

$$\begin{aligned} \mathbf{J}_\parallel &= \mathbf{b}(\mathbf{J}\cdot\mathbf{b}) \\ \mathbf{J}_\perp &= \mathbf{b}\times(\mathbf{J}\times\mathbf{b}) \\ \nabla_\parallel T_e &= \mathbf{b}(\nabla T_e\cdot\mathbf{b}) \\ \nabla_\perp T_e &= \mathbf{b}\times(\nabla T_e\times\mathbf{b}) \end{aligned} \quad (52)$$

In Eq. (49) the Hall electric field is principally included in the $\mathbf{J}\times\mathbf{B}$ term in the definition of $\mathbf{E}^*$ [Eq. (51)], while the correction $\alpha_\wedge$ has been shown to vary as $(\omega_e\tau_e)^{-2/3}$ for values of $(\omega_e\tau_e)$ much greater than 1. The main property of the Hall effect comes from a comparison of the $\alpha_\perp$ term and the $\mathbf{J}\times\mathbf{B}$ term in $\mathbf{E}^*$: This is that the components of current density **J** and the general electric field $\mathbf{E}+\mathbf{v}\times\mathbf{B}+\nabla p_e/(n_e e)$ in the plane perpendicular to the magnetic field are at an angle $\theta \simeq \tan^{-1}(\omega_e\tau_e)$ to each other. Thus in a magnetically confined plasma there is an electric field component orthogonal to the magnetic surface. In magnetohydrodynamic power generators the electrodes have to be segmented in order that the current flow is orthogonal to the gas flow, so that the $\mathbf{J}\times\mathbf{B}$ force is directed to oppose this flow, and the generator impedance is minimized. The segmentation of the electrodes permits an electric field to be set up between the segments.

When an electric field **E** is applied to a plasma in a direction orthogonal to a magnetic field so that the current can flow freely at the angle $\tan^{-1}(\omega_e\,\tau_e)$ to **E**, the component of current density orthogonal to **E** is called the Hall current. This can be used to give a $\mathbf{J}\times\mathbf{B}$ acceleration of the ions in a suitable magnetic field configuration such as in magnetically insulated diodes (as used for light ion-beam production). The Hall term modifies the ideal magnetohydrodynamic frozen-flow motion so that magnetic fields are now frozen to the electron center-of-mass velocity.

The last term in Eq. (49) describes the thermoelectric term, and through this it is possible to generate a current parallel to ∇T_e (Seebeck effect) or perpendicular to ∇T_e (Nernst effect). The Nernst effect can approximately be represented as an electic field equal to $\mathbf{q}_e\times\mathbf{B}/(\frac{3}{2}n_e k_B T_e)$ showing by analogy with Eqs. (1) and (3) that the magnetic field is convected in the direction of heat flow with a velocity given by Eq. (56). In the case of laser fusion, this

$$\mathbf{v}_T = \frac{\mathbf{q}_e}{\frac{3}{2}nk_B T_e} \quad (56)$$

can lead to a magnetic field being convected from the critical surface to the ablation surface, and, furthermore, amplified because of the increase in number density *n* which reduces the velocity $\mathbf{v}_T$ causing the transverse magnetic field lines to bunch up. This further modification of frozen flow implies that the magnetic field is frozen to the hotter (and less collisional) electrons that carry the heat. Indeed, it is a special feature of inertial confinement fusion that megagauss magnetic fields can spontaneously be generated in nonuniformly irradiated targets through the $\nabla p_e/(n_e e)$ term in $\mathbf{E}^*$ [Eq. (50)] from Eq. (2), so that Eq. (57) holds. (In laser fusion the ideal situation is one in which laser radiation is uniformly irradiated onto and absorbed by a perfectly symmetrical spherical target. The above magnetic fields are generated only through a lack of symmetry arising from nonuniform irradiation or through instabilities such as the Rayleigh-Taylor instability discussed above.)

$$\frac{\partial \mathbf{B}}{\partial t} = -\nabla\times\mathbf{E} = k_B \nabla T_e \times \frac{\nabla n_e}{n_e e} \quad (57)$$

In Eq. (50), it is found that while $\kappa_{||}$ is proportional to $T^{5/2}_e$, $\kappa_\perp$ varies as $\kappa_{||}(\omega_e\tau_e)^{-2}$ for values of $\omega_e\tau_e$ much greater than 1. Therefore, in magnetically confined plasmas the electron thermal conduction across magnetic surfaces is considerably reduced, and indeed ion thermal conduction across field lines is $[m_i/(Zm_e)]^{1/2}$ times larger. The heat flow parallel to a current flow essentially represents the flux of enthalpy of the current carriers and is called the Peltier effect. The heat flux defined by Eq. (50), however, is defined in the center-of-mass frame of the electrons, and so the $\beta_{||}$ and $\beta_\perp$ terms refer to the corrections to the enthalpy flow caused by the velocity dependence of the collision frequency. The Ettingshausen effect is the heat flow in the direction of the Hall electric field, while the Righi-Leduc effect is the heat flow orthogonal to ∇T_e and $\mathbf{B}$. $\kappa_\wedge$ and $\beta_\wedge$ are proportional to $\omega_e\tau_e$ for $\omega_e\tau_e$ much less than 1, and to $(\omega_e\tau_e)^{-1}$ for $\omega_e\tau_e$ much greater than 1, while $\beta_\perp$ varies as $(\omega_e\tau_e)^{-5/3}$ for $\omega_e\tau_e$ much greater than 1. It follows that $\alpha_\wedge$, $\beta_\wedge$, and $\kappa_\wedge$ all vanish as the magnetic field tends to 0. The peculiar fractional powers in $\alpha_\wedge$ and $\beta_\perp$ occur because for a value of $\omega_e\tau_e$ much larger than 1 it is found that a fraction of electrons with a velocity less than $(\omega_e\tau_e)^{-1/3}$ times the mean thermal speed $\sqrt{(2k_BT_e/m_e)}$ have in fact unmagnetized orbits. This is because they have a low velocity υ so that their collision frequency which is proportional to υ^{-3} exceeds their cyclotron frequency.

The ion stress tensor is also modified by a strong magnetic field, and for $\omega_i\tau_i \gg 1$ leads to the persistence of terms in velocity gradients with a coefficient p_i/ω_i, where p_i is the ion pressure and ω_i the ion cyclotron frequency. These residual terms describe finite ion Larmor radius effects, which can be a beneficial correction to ideal magnetohydrodynamic stability theory.

Malcolm G. Haines

Bibliography. G. Bateman, *MHD Instabilities*, 1980; D. Biskamp, *Nonlinear Magnetohydrodynamics*, 1993; F. F. Chen, *Introduction to Plasma Physics and Controlled Fusion*, vol 1: *Plasma Physics*, 2d ed., 1984; E. M. Epperlein and M. G. Haines, *Physics of Fluids*, 29:1029, 1986; N. A. Krall and W. Trivelpiece, *Principles of Plasma Physics*, 1973, reprint 1986; K. Miyamoto, *Plasma Physics for Nuclear Fusion*, 1976, rev. ed.1989; J. A. Wesson, *Tokamaks* 1987, 2d ed., 1997.

Magnetometer

An instrument that measures the magnitude and/or direction of a magnetic field. A magnetometer can be either a scalar instrument that measures the magnitude of the total field or a vector instrument that measures one or more vector components of the field. Some magnetometers are relative devices that are calibrated with respect to a known field. Others are absolute devices that yield magnetic-field values without calibration. Arrays of magnetometers can be configured as gradiometers that suppress or enhance far-field magnetic sources while enhancing or suppressing near-field sources. Magnetometer technology is available for detecting a range of magnetic fields (**Fig. 1**).

Induction. Perhaps the simplest magnetometer is an induction coil that employs the Faraday effect, a voltage induced in a conductor by a time-varying magnetic flux. Induction magnetometers are generally multiturn coils that are either air-wound or wound around a ferromagnetic core to increase flux through the coil. Fixed coils can measure only time-varying fields, but static fields can be measured using moving induction coils that rotate, vibrate, or deform. Their sensitivity is governed by the time rate of change of the magnetic flux change in the coil, the number of turns in the coil, the magnetic permeability of the core, the electrical resistance and parasitic capacitance of the coil, and thermal noise. Induction coils are usually vector sensors that require external calibration. *See* FARADAY EFFECT.

Hall effect. In the presence of a magnetic field, moving charge carriers in a current-carrying solid conductor or semiconductor are subjected to a Lorentz force that depends upon their charge, velocity, and magnitude and direction of the magnetic field. This force deflects the charge carriers and produces a voltage difference on opposite sides of the solid known as the Hall effect. *See* HALL EFFECT; MAGNETIC FIELD.

Modern Hall-effect sensors are made from InSb or InAs alloy thin films produced by vacuum deposition or molecular-beam epitaxy. These solid-state vector devices can be fabricated as integrated circuit packages that can measure alternating-current and direct-current magnetic fields. By combining multiple calibrated sensors into a single package, the total magnetic field and magnetic-field gradients can be measured. Hall-effect magnetometers are usually used to measure relatively strong magnetic fields.

Magnetoresistance and SDT. Magnetoresistance is the dependence of the electrical resistance of a solid upon an applied magnetic field. A wide variety of magnetoresistive sensors have been designed and constructed for medium field strengths. They can be manufactured in integrated circuit packages in small sizes at relatively low cost and used for magnetic detection and navigation. *See* MAGNETORESISTANCE.

Thin-film alloys of iron, nickel, and/or cobalt are used to measure magnetic fields using anisotropic magnetoresistance (AMR). The more recently discovered giant magnetoresistive (GMR) effect sensors are made of sandwiched layers of ferromagnetic iron-nickel-cobalt alloy and a nonferromagnetic material. A recent variant of this type of sensor is the spin-dependent tunneling (SDT) device (**Fig. 2**), where the nonferromagnetic layer is replaced by an insulator (commonly aluminum oxide) yielding up to 20 times the sensitivity of a GMR device and perhaps 200 times the sensitivity of an AMR sensor. *See* MAGNETIC THIN FILMS.

Fluxgate. The fluxgate (saturable-core) sensor is constructed from a pair of high-magnetic-permeability cores. Wound around each core in opposite directions is a primary field core driven to

magnetic saturation by an audio-frequency current. The primary coils are connected in series. A secondary field core wound collectively around both cores is connected to a detector circuit.

When a core reaches magnetic saturation, the driving current waveform is distorted by a change in self-inductance in the primary coil. In the absence of an external magnetic field, both cores saturate at the same instant and no voltage is developed in the secondary coil. In the presence of a biasing external magnetic field, one core comes to saturation before the other, producing a pair of voltage pulses in the secondary coil at twice the driving frequency. For small fields, the amplitude of this pulse is proportional to the strength of the ambient field, and thus the device is a sensitive magnetometer capable of measurement precision better than 0.1 nanotesla over a frequency range from direct current to low audio frequencies.

All fluxgate magnetometers are relative vector instruments that require calibration in a known magnetic field to produce accurate results. Orthogonal sets of fluxgate sensors can be used to measure all three field components and thereby the total field vector.

Resonance. Two general classes of resonance magnetometers are proton precession magnetometers and optically pumped magnetometers. Both are absolute instruments that measure total field strength without the need for calibration using a known magnetic field.

Proton precession magnetometer. The proton precession magnetometer employs nuclear magnetic resonance to measure magnetic-field strength. The sensor contains a reservoir of a proton-rich fluid (water or a low-density hydrocarbon like kerosene or decane) surrounded by a magnetic-field coil. The coil initially produces a direct-current magnetic field that aligns the magnetic moments of the protons. The direct-current field is abruptly turned off, whereupon the proton magnetic moments precess about the ambient magnetic-field direction for a few seconds, and produce an alternating-current signal in the coil whose frequency is directly proportional to the intensity of the ambient magnetic field. The Overhauser magnetometer is a variant of this design that aligns the protons by radio-frequency electron spin resonance coupling. This technique requires far less power and is well suited for spacecraft.

The precession signal is essentially independent of the orientation of the sensor, and accuracy is limited by the magnitude of the precession signal and the accuracy of the frequency counter connected to the coil. Typical precision is on the order of 0.01 nT. Using a larger Helmholtz coil to null one component of the ambient field allows the proton precession magnetometer to be converted to a vector magnetometer that can measure components of a magnetic field. The measurement bandwidth of the proton magnetometer is limited to low frequencies because the polarization/frequency counting sequence can take several seconds. *See* NUCLEAR MAGNETIC RESONANCE (NMR).

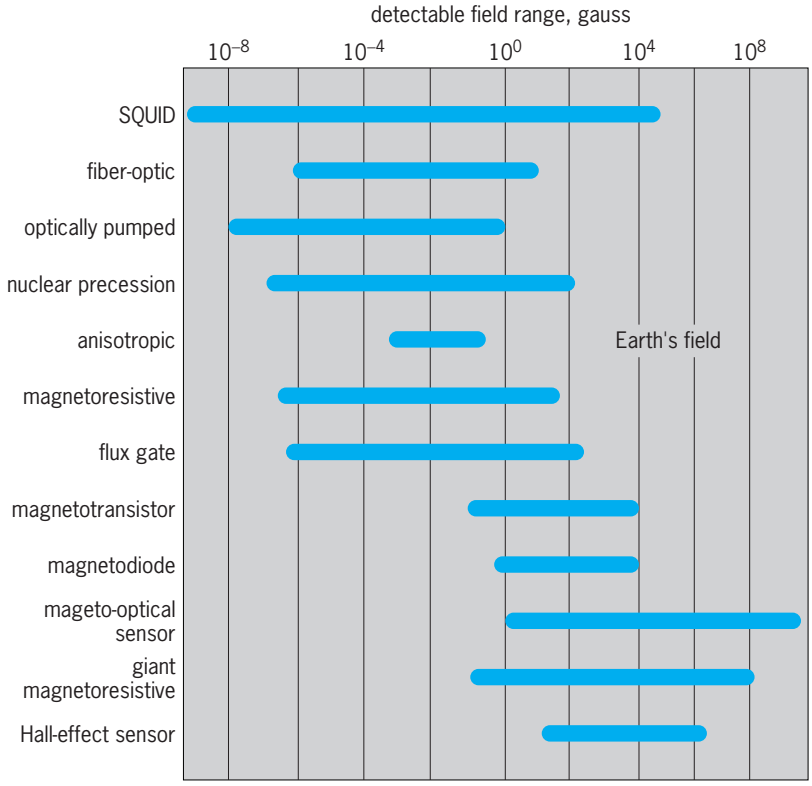

Fig. 1. Magnetic sensor technologies and ranges. 1 gauss = 10^{-4} tesla = 10^{5} gamma.

Optically pumped magnetometer. This device is analogous to the proton magnetometer in that it employs optical pumping to cause atomic or electron spin precession. A sealed glass cell containing an alkali vapor (typically cesium, rubidium, or potassium) is placed next to a lamp containing the same alkali vapor, and produces light at a characteristic frequency (**Fig. 3**). Opposite the lamp is a photodetector whose output is connected through an amplifier to a coil surrounding the cell. Resonance absorption and reradiation of optical energy from the cell produce oscillation in a feedback loop whose frequency is proportional to the intensity of the ambient magnetic field, as in the case of the proton magnetometer. A variant is the metastable ^{4}He magnetometer, where the alkali vapor cell is replaced by

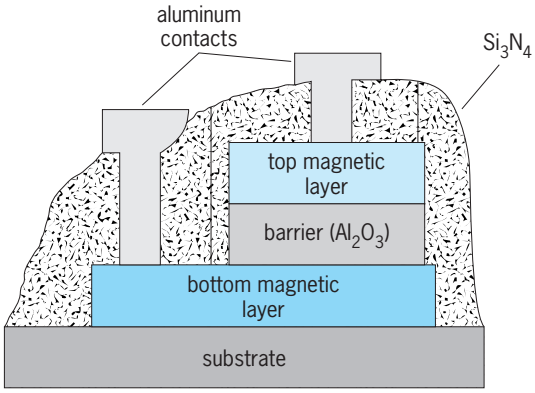

Fig. 2. Schematic cross section of the STD structure.

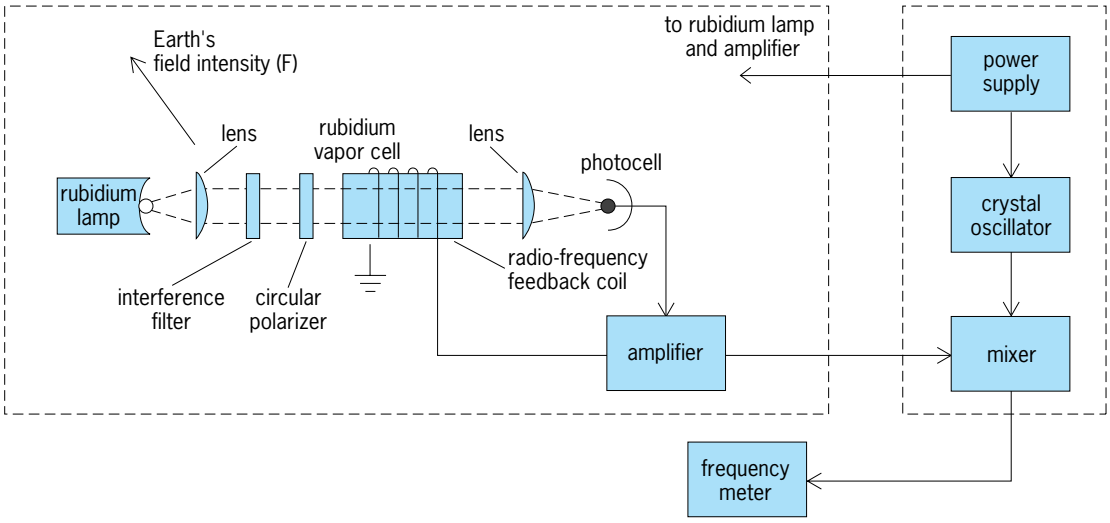

Fig. 3. Rubidium vapor magnetometer. The rubidium vapor cell, photocell, amplifier, and feedback coil constitute an oscillator whose frequency is proportional to the ambient magnetic field.

a helium gas cell. In the most modern designs, the lamps are replaced by lasers and the cells contain an alkali metal vapor and helium, providing vastly increased sensitivity and spatial resolution.

The sensitivity of most optically pumped magnetometers is superior to that of proton precession magnetometers. A typical cesium vapor magnetometer has a measurement precision better than 0.001 nT, but the absolute accuracy is on the order of 1 nT because of field-dependent complexities in the energy transitions in the cell. In contrast to the proton magnetometer, the measurement bandwidth of optically pumped magnetometers is quite broad (from direct current up to several megahertz) because the pumped energy transitions occur over very short time intervals. *See* OPTICAL PUMPING.

Superconducting. The cryogenic or SQUID magnetometer uses one or more Josephson junctions as a magnetic-field sensor. A Josephson junction is a zone of weak magnetic coupling (a weak link) between two regions of superconducting material in which current will flow without resistance. A change in the magnetic field applied to the weak link produces a proportional change in magnetic flux within the Josephson junction (**Fig. 4**). The SQUID is the most sensitive magnetometer in general use, capable of measuring flux changes only a small fraction of a flux quantum Φ (2.07×10^{-15} weber), but its capabilities are now rivaled by modern spin-polarized alkali vapor magnetometers. *See* JOSEPHSON EFFECT; SUPERCONDUCTIVITY.

Two types of SQUID are in common use. The radio-frequency SQUID employs a single weak link, whereas the direct-current SQUID uses a pair of Josephson junctions. Flux changes can be introduced directly to the SQUID, but more commonly a flux transformer is used, where external sensing coils are inductively linked to the SQUID. The external coils are made of superconducting material and can be configured as a single-turn or multiturn coil, a Helmholtz pair, or even a first- or second-order gradiometer. The practical noise limits of conventional niobium SQUID devices are on the order of 10^{-6} nT, orders of magnitude better than other devices. *See* HELMHOLTZ COILS.

All SQUID magnetometers are relative, vector instruments. The principal advantages of the SQUID magnetometer over proton, optically pumped, and fluxgate magnetometers are sensitivity and frequency response. The principal disadvantage of the SQUID magnetometer is that it must be kept in a

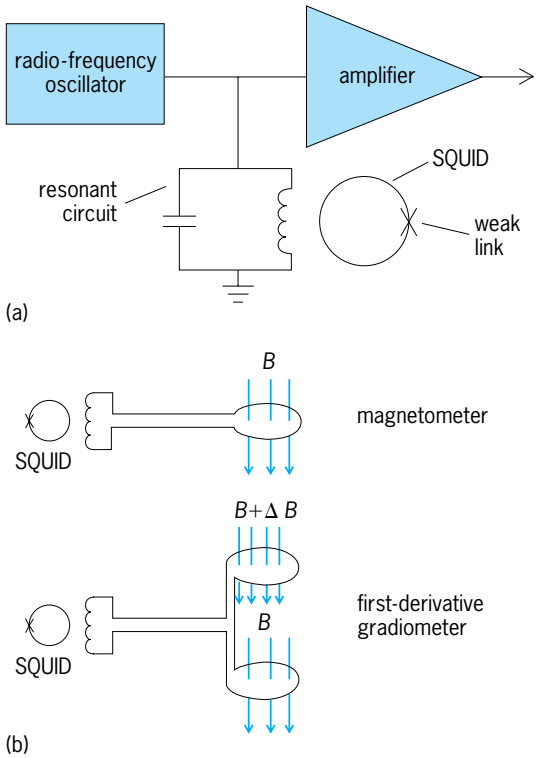

Fig. 4. SQUID magnetometer. (*a*) Conventional radio-frequency SQUID electronics. (*b*) Sensing-coil configurations.

superconducting state. At one time, this meant that the sensor had to be maintained at 4.2 K (−452°F) by using liquid helium as a cryogen. Now inexpensive direct-current SQUID devices can be made from a thin-film substrate of YBCO ($Y_1Ba_2Cu_3/SO_7$), which use liquid nitrogen (77 K or −321°F) as a cryogen. The performance of the high-temperature SQUID device does not yet match that of the conventional liquid-helium-cooled niobium SQUID. *See* SQUID.

Fiber-optic. Some ferromagnetic materials exhibit magnetostriction, the dependence of the state of strain of a solid (and hence its dimensions) on magnetic-field strength. By bonding a magnetostrictive material to an optical fiber, its optical path length can be made to change in response to a magnetic field. Sensitive magnetometers have been constructed that employ a Mach-Zehnder interferometer to measure the optical path length difference between the sensor fiber and a reference fiber at mechanical resonance. *See* FIBER-OPTIC SENSOR; MAGNETOSTRICTION.

Other magnetometers. Classical mechanical magnetometers employ small magnets suspended on balances or torsion fibers. The first absolute device was probably constructed by K. F. Gauss in 1832 and consisted of a magnet suspended by a torsion fiber and free to rotate about a vertical axis. The absolute value of the horizontal magnetic-field component is estimated by measuring the period of oscillation of the magnet. The field inclination is measured with a dip needle, resulting in a complete specification of the vector field.

Other devices that employ suspended or balanced magnets are the dip needle, sine galvanometer, Schmidt vertical balance, quartz horizontal magnetometer, astatic magnetometer, and magnetometer zero balance. Compared to modern instruments, their main disadvantages include the time required to make a measurement, temperature dependence of the sensor, and reduced sensitivity. *See* GEOPHYSICS; MAGNET.

Michael McWilliams

Bibliography. D. Grundler, Highly sensitive YBCO DC SQUID magnetometer with thin-film flux transformer, *Appl. Phys. Lett.*, 63:2700–2702, 1993; D. A. Konotop, Development of high T_c superconductor SQUID-based magnetometer, *Cryogenics*, 33:632–636, 1993; P. Ripka, *Magnetic Sensors and Magnetometers*, Artech House, 2001; S. Tanaka, Four-channel YBCO DC SQUID magnetometer for biomagnetic measurements, *Appl. Phys. Lett.*, 64:514–516, 1994; W. M. Telford, L. P. Geldart, and R. E. Sheriff, *Applied Geophysics*, 2d ed., 1990.

Magneton

A unit of magnetic moment used to describe atomic, molecular, or nuclear magnets. More precisely, one unit, the Bohr magneton, is used at the atomic and molecular levels, and another unit, the nuclear magneton, is used at the nuclear level. Still another unit (which might be called the muon magneton, but is usually not named) is used to describe the magnetic moment of the muon.

Bohr magneton. The Bohr magneton μ_B is defined and its value given in Eq. (1), where $-e$ and m are the

$$\mu_B = \frac{e\hbar}{2m} = (9.274\ 009\ 49 \pm 0.000\ 000\ 80) \times 10^{-24}\ \text{joule/tesla} \quad (1)$$

charge and mass of the electron respectively and $\hbar$ is Planck's constant divided by 2π. In Dirac's theory the magnetic moment of the electron is exactly $-\mu_B$, but according to the theory of quantum electrodynamics the electron has a small anomalous magnetic moment. (The anomalous magnetic moment of a particle of spin $^1/_2$ is the deviation of its magnetic moment from the value given by the Dirac equation.) The experimental value of the electron magnetic moment μ_e is given by Eq. (2), in agreement with the pre-

$$\mu_e = -(1.001\ 159\ 652\ 185\ 9 \pm 0.000\ 000\ 000\ 003\ 8)\mu_B \quad (2)$$

diction of quantum electrodynamics within the errors. The minus sign in Eq. (2), which arises from the fact that the electron has negative charge, is usually omitted, and just the magnitude of the electron magnetic moment is given. According to quantum electrodynamics, the magnetic moment of the positron is equal in magnitude to the magnetic moment of the electron but positive in sign. More generally, the magnetic moments of any particle and its antiparticle are expected to be equal in magnitude and opposite in sign. *See* ELECTRON SPIN; QUANTUM ELECTRODYNAMICS; RELATIVISTIC QUANTUM THEORY.

The magnetic moment of a composite particle results from contributions from both orbital angular momentum and spin of its constituents. In the case of atoms and molecules, by far the major contribution comes from the electrons, the contribution from the atomic nuclei usually being neglected. If an atom is regarded as having an infinitely heavy nucleus, the contribution from the orbital angular momentum of an electron is an integral number of Bohr magnetons.

Muon magnetic moment. The unit of magnetic moment to describe the muon is obtained from the Bohr magneton by replacing m in Eq. (1) by the muon mass m_μ. The value of the muon magnetic moment is given in Eq. (3). The deviation of the muon magnetic

$$\mu_\mu = (1.001\ 165\ 919\ 81 \pm 0.000\ 000\ 000\ 62)\frac{e\hbar}{2m_\mu} \quad (3)$$

moment from its Dirac value can also be accounted for by the theory of quantum electrodynamics. *See* LEPTON.

Nuclear magneton. The nuclear magneton is obtained from the Bohr magneton by replacing m by the proton mass m_p. The value of the nuclear magneton is given in Eq. (4). The nuclear magneton is used

$$\mu_N = (5.050\ 783\ 43 \pm 0.000\ 000\ 43) \times 10^{-27}\ \text{joule/tesla} \quad (4)$$

not only as the unit for the magnetic moment of the proton but also for the neutron and other hadrons and for atomic nuclei. If the proton and neutron were Dirac particles, the proton's magnetic moment would be one nuclear magneton (except for a small correction arising from quantum electrodynamics) and the neutron's magnetic moment would be zero (because the neutron is uncharged). However, the proton and neutron have large anomalous magnetic moments. The magnetic moments of the proton and neutron are given in Eqs. (5).

$$\mu_p = (2.792\,847\,351 \pm 0.000\,000\,028)\mu_N$$
$$\mu_n = (-1.913\,042\,73 \pm 0.000\,000\,45)\mu_N \quad (5)$$

See NEUTRON; NUCLEAR MOMENTS; PROTON.

Origin of anomalous moments. According to present theory, the proton, neutron, and other hadrons have large anomalous magnetic moments because these particles are not elementary but composite. In the theory of quantum chromodynamics, the principal constituents of a baryon, such as the proton or neutron, are three quarks. In a simple model that neglects the contributions from quark orbital angular momenta, from relativistic effects, and from higher-order effects of quantum chromodynamics, the magnetic moment of a baryon can be calculated in terms of the magnetic moments of its three constituent quarks. These calculations give the remarkably good prediction that $\mu_p/\mu_n = -1.5$, a value only 3% from the measured value. In the case of the higher-mass baryons (Λ, Σ, Ξ), the predicted magnetic moments are all of the correct sign, but the disagreement with experiment is up to 20%. Inclusion of contributions from quark orbital angular momentum and other higher-order effects improves the agreement with experiment, but a residual disagreement remains. *See* BARYON; ELEMENTARY PARTICLE; FUNDAMENTAL CONSTANTS; QUANTUM CHROMODYNAMICS; QUARKS.

Don B. Lichtenberg

Bibliography. S. Eidelman et al., Review of particle physics, *Phys. Lett. B*, 592:1–1109, 2004; K. J. Heller (ed.), *High-Energy Spin Physics 8th International Symposium*, Amer. Inst. Phys. Conf. Proc. 187, 1989; P. J. Mohr and B. N. Taylor, CODATA recommended values of the fundamental physical constants: 2002, *Rev. Mod. Phys.*, 77:1–107, 2005.

Magnetooptics

That branch of physics which deals with the influence of a magnetic field on optical phenomena. Considering the fact that light is electromagnetic radiation, an interaction between light and a magnetic field would seem quite plausible. It is, however, not the direct interaction of the magnetic field and light that produces the known magnetooptic effects, but the influence of the magnetic field upon matter which is in the process of emitting or absorbing light.

Zeeman effect. This produces a splitting of spectrum lines when the emitting light source is placed in a magnetic field. The inverse Zeeman effect refers to a similar splitting of absorption lines when the absorbing substance is in a magnetic field. The Zeeman effect for spectrum lines originating from closely spaced levels is called the Paschen-Back effect. The explanation of most other magnetooptical phenomena is based on the Zeeman effect, which therefore may be regarded as the basic magnetooptic effect. *See* PASCHEN-BACK EFFECT; ZEEMAN EFFECT.

Faraday effect. This is the rotation of the plane of polarization of light when light traverses certain substances in a magnetic field. *See* FARADAY EFFECT.

Voigt effect. An anisotropic substance placed in a magnetic field becomes birefringent (doubly refracting), and its optical properties are similar to those of a uniaxial crystal. The Faraday effect is the result of this birefringence when observations are made parallel to the magnetic field. The analogous observations perpendicular to the magnetic lines of force are more difficult and were not successfully carried out until 1898 because of the smallness of the effect. The transverse magnetooptic birefringence is called the Voigt effect after its discoverer, W. Voigt.

The Voigt effect (also called magnetic double refraction) can easily be calculated for substances having a normal Zeeman effect. For more complicated Zeeman effects the results can also be theoretically predicted but are less simple quantitatively, though not essentially different from those in the simpler cases.

The Voigt effect depends on the fact that the indices n_s and n_p for light polarized perpendicular or parallel to the magnetic lines of force respectively are different from one another in a magnetic field where the absorption line shows a Zeeman effect. The value of n_p is independent of the magnetic field because the central component does not change while $n_s = {}^1/_2(n^+ + n^-)$. The appropriately labeled curve in the **illustration** gives $n_s - n_p$, on which the observed effects of the transverse magnetic double refraction depend.

The theoretical formulas which represent the double refraction, though readily derived, are quite complicated. When the wavelength is considerably

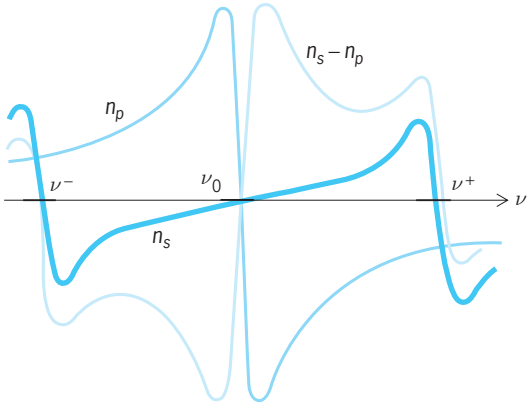

Index of refraction of light polarized parallel (n_p) and perpendicular (n_s) to the magnetic field in the vicinity of a Zeeman triplet. The Voigt effect is proportional to $n_s - n_p$ (shown as a curve).

removed from the Zeeman triplet, the phase difference is as given by Eq. (1), where ν_0 is absorption

$$\delta = \frac{2\pi x}{c}(n_p - n_s) = \frac{e^4 f x}{32\pi^2 c^3 n_0 (\nu - \nu_0)^3} NH^2 \quad (1)$$

line frequency, ν is frequency of transmitted light, e is charge of electron, x is path length, c is velocity of light, n_0 is index of refraction without field, N is number of absorbing atoms per unit volume, H is magnetic field strength, and f is so-called oscillator strength, measure of strength of absorption.

Contrary to the situation existing in the Faraday effect, first-order effects of magnetic double refraction are canceled out because of the presence of two perpendicular, symmetrically placed Zeeman components of combined strength equal to that of the parallel component. Because of this the Voigt effect can be observed only in the vicinity of sharply defined absorption lines, that is, in gases and in certain crystals having sharp lines, such as rare-earth salts. In the case of the rare-earth salts a linear Voigt effect is also possible at extremely low temperatures.

Since the formula for phase difference contains the oscillator strength f, the Voigt effect may be used to measure this important quantity.

Cotton-Mouton effect. This effect is concerned with the double refraction of light in a liquid when the liquid is placed in a transverse magnetic field. It is analogous to the electrooptical Kerr effect and is observed in liquids with complicated molecular structure. If the molecule has a magnetic moment, the field tries to orient the molecule, but the thermal motion tends to oppose this action. There is thus a degree of orientation, which is dependent on the temperature. If the molecule itself is optically anisotropic, the liquid also will be anisotropic and will exhibit double refraction. *See* KERR EFFECT.

The Cotton-Mouton effect is observed chiefly in nitrobenzene and aromatic organic liquids. Aliphatic compounds have a considerably smaller effect.

The phase difference of the Cotton-Mouton effect is expressed by Eq. (2), where x is the path length

$$\delta = C_m x H^2 \quad (2)$$

and C_m is called the Cotton-Mouton constant. For nitrobenzene at a temperature of 61.3°F (16.3°C) and a wavelength λ of 578 nanometers, $C_m = 2.53 \times 10^{-2}/(\text{m} \cdot \text{T}^2) = 2.53 \times 10^{-12}/(\text{cm} \cdot \text{gauss}^2)$. With large magnets ($H = 4.65$ teslas $= 46{,}500$ gauss) under the most favorable circumstances, rotations of the plane of polarization up to 27° have been observed.

The dispersion of the Cotton-Mouton effect is given by Havelock's law as in the Kerr effect.

Magnetooptic Kerr effect. This deals with the changes that are produced in the optical properties of a reflecting surface of a ferromagnetic substance when the substance is magnetized. In a typical case this will result in elliptically polarized light appearing in reflection, when the ordinary rules of metallic reflection would given only plane-polarized light. The component produced by the magnetic field when the magnetization is close to saturation is only of the order 10^{-3} of that normally present. The explanation must be sought in the fact that the conduction electrons made to vibrate by the incident light will have a curved path in the magnetic field.

Majorana effect. This deals with optical anisotropy of colloidal solutions. The effect probably is caused by the orientation of the particles in the magnetic field.

Magnetooptic effects have played an increasingly important role in microwave spectroscopy, where transitions between the Zeeman components of a single level can be observed directly. *See* MICROWAVE SPECTROSCOPY.

G. H. Dieke; William W. Watson

Magnetoresistance

The change of electrical resistance produced in a current-carrying conductor or semiconductor on application of a magnetic field H. Magnetoresistance is one of the galvanomagnetic effects. It is observed with H both parallel to and transverse to the current flow. The change of resistance usually is proportional to H^2 for small fields, but at high fields it can rise faster than H^2, increase linearly with H, or tend to a constant (that is, saturate), depending on the material. In most nonmagnetic solids the magnetoresistance is positive. *See* GALVANOMAGNETIC EFFECTS.

In semiconductors, the magnetoresistance is unusually large (especially in indium antimonide) and is highly anisotropic with respect to the angle between the field direction and the current flow in single crystals. When the magnetoresistance is measured as a function of field, it is the basis for the Shubnikov–de Haas effect, much as the field dependence of the magnetization gives rise to the de Haas–van Alphen effect. Measurement of either effect as the field direction changes with respect to the crystal axes serves as a powerful probe of the Fermi surface. Magnetoresistance measurements also yield information about current carrier mobilities. Important to practical applications is the fact that the geometry of a semiconductor sample can generate very large magnetoresistance, as in the Corbino disk. *See* CORBINO DISK; DE HAAS-VAN ALPHEN EFFECT; FERMI SURFACE; SEMICONDUCTOR.

In some effectively two-dimensional systems, such as GaAs-AlGaAs field-effect transistors, the high-field magnetoresistance goes to zero in fields at which the Hall resistance exhibits plateaus. The Hall resistance is then independent of H and its value is $h/(e^2 i)$, where h is Planck's constant, e is the electronic charge, and i is an integer or, in some cases, a simple fraction. This behavior is known as the quantum Hall effect. *See* HALL EFFECT.

Multilayered structures composed of alternating layers of magnetic and nonmagnetic metals, such as iron/chromium or cobalt/copper, can feature very large, negative values of magnetoresistance. This effect, called giant magnetoresistance, arises from the spin dependence of the electron scattering which causes resistance. When consecutive magnetic layers have their magnetizations antiparallel

(antiferromagnetic alignment), the resistance of the structure is larger than when they are parallel (ferromagnetic alignment). Since the magnetic alignment can be changed with an applied magnetic field, the resistance of the structure is sensitive to the field. Giant magnetoresistance can also be observed in a simpler structure known as a spin valve, which consists of a nonmagnetic layer (for example, copper) sandwiched between two ferromagnetic layers (for example, cobalt). The magnetization direction in one of the ferromagnetic layers is fixed by an antiferromagnetic coating on the outside, while the magnetization direction in the other layer, and hence the resistance of the structure, can be changed by an external magnetic field. Films of nonmagnetic metals containing ferromagnetic granules, such as cobalt precipitates in copper, have been found to exhibit giant magnetoresistance as well. *See* ANTIFERROMAGNETISM; FERROMAGNETISM; MAGNETIC THIN FILMS; MAGNETIZATION.

Magnetoresistors, especially those consisting of semiconductors such as indium antimonide or ferromagnets such as permalloy, are important to a variety of devices which detect magnetic fields. These include magnetic recording heads and position and speed sensors. *See* MAGNETIC RECORDING.

J. F. Herbst

Magnetosphere

A comet-shaped cavity or bubble around the Earth, carved in the solar wind. This cavity is formed because the Earth's magnetic field represents an obstacle to the solar wind, which is a supersonic flow of plasma blowing away from the Sun. As a result, the solar wind flows around the Earth, confining the Earth and its magnetic field into a long cylindrical cavity with a blunt nose (**Fig. 1**). Since the solar wind is a supersonic flow, it also forms a bow shock a few earth radii away from the front of the cavity. The boundary of the cavity is called the magnetopause. The region between the bow shock and the magnetopause is called the magnetosheath. The Earth is located about 10 earth radii from the blunt-nosed front of the magnetopause. The long cylindrical section of the cavity is called the magnetotail, which is on the order of a few thousand earth radii in length, extending approximately radially away from the Sun. *See* SOLAR WIND.

The concept of the magnetosphere was first formulated by S. Chapman and V. C. A. Ferraro in 1931, but the term magnetosphere was introduced in 1959 by T. Gold, who defined it as "the region above the ionosphere in which the magnetic field of the Earth has a dominant control over the motions of gas and fast charged particles." It was, however, only during the 1970s that the magnetosphere was extensively explored by a number of satellites carrying sophisticated instruments. This exploration was a part of the effort to understand that region of the Earth's environment above the level where most meteorological phenomena take place, namely, the space between the Sun and the stratosphere/mesosphere. The space which surrounds the magnetosphere is often referred to as geospace. *See* IONOSPHERE; SCIENTIFIC AND APPLICATIONS SATELLITES.

Plasma. The satellite observations have indicated that the cavity is not an empty one, but is filled with plasmas of different characteristics (Fig. 1). Just inside the magnetopause some solar wind plasma blows; this particular plasma region is called the plasma mantle. There are also two funnel-shaped regions (one in each hemisphere), extending from the front magnetopause to the polar ionosphere, which are also filled with solar wind plasma; these regions are called the cusp. The extensive tail region of the magnetosphere is divided into the northern and southern halves by a thin sheet of plasma, called the plasma sheet. The distant tail region (beyond the lunar distance) has been infrequently explored when it was traversed by space probes on their way to the planets. The inner magnetosphere is occupied by the Van Allen belts, the ring current belt, and the plasmasphere. All of them are doughnut shaped and surround the Earth. The ring current belt is colocated with the Van Allen belts and is so named because it carries a large amount of a westward-directed electric current around the Earth.

It is generally believed that the main part of the plasma sheet is of solar origin; the mantle plasma may be an important source of it. The plasmasphere is formed mainly by ionospheric plasma which diffuses outward along magnetic field lines. At times the ring current belt contains heavy ions of ionospheric origin, such as helium and oxgen ions, as well as protons of solar origin. The heavy ions are found also in the plasma sheet.

The Earth's dipolar magnetic field is considerably deformed by these plasmas and the electric currents generated by them. The dipolar field is compressed in the dayside part of the magnetosphere, mainly by the action of the impacting solar wind, whereas it is considerably stretched along the equatorial plane in the magnetotail (Fig. 1). *See* VAN ALLEN RADIATION.

Solar wind–magnetosphere generator. If there were no magnetic field in the solar wind, the Earth's magnetic field would simply be confined by the solar wind into a teardrop-shaped cavity (rather than a comet-shaped cavity), and the cavity would be

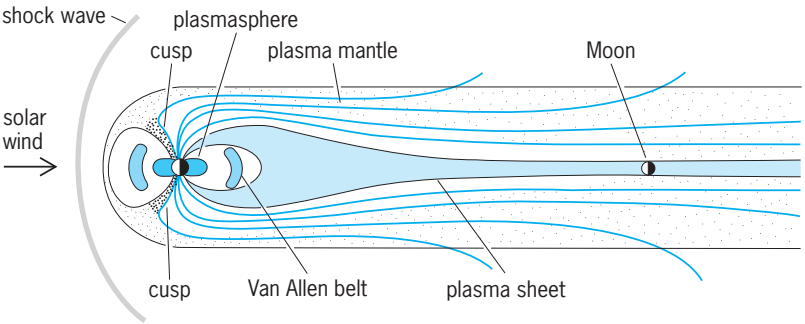

Fig. 1. Noon-midnight cross section of the magnetosphere and the distribution of various plasmas inside it.

almost empty. It is the magnetic field of the solar wind which introduces considerable complexity in the interaction between the solar wind and the magnetosphere. Some of the magnetic field lines originating from the polar region are almost always connected to the solar wind magnetic field lines across the magnetopause (**Fig. 2**). In fact, because the solar wind magnetic field lines originate from the Sun, it may be said that the Sun and the Earth are connected by magnetic field lines. More specifically, the connected field lines originate from an oval area in the polar region. This area is called the polar cap and is bounded by a belt of the aurora called the auroral oval. The magnetic field lines originating from the northern polar cap are stretched along the northern half of the magnetotail as a bundle of magnetic field lines and are connected to the solar wind magnetic field lines across the magnetopause. Similarly, the magnetic flux from the southern polar cap occupies the southern half of the magnetotail.

This connection between the solar wind magnetic field lines and the Earth's magnetic field lines provides the most important aspect of the solar wind–magnetosphere interaction. Since the solar wind (a fully ionized plasma and thus a conductor) must blow across the connected magnetic field lines as it flows along the magnetopause (Fig. 2), an electromotive force is generated. This force powers the solar wind–magnetosphere generator and thus provides practically all the electric power for various magnetospheric processes, such as auroral phenomena and magnetospheric disturbances, including geomagnetic storms. It is precisely in this way that the solar wind (a flow of magnetized plasma) couples its energy to the magnetosphere. Therefore, if there were no connection of the field lines, there would be no energy transfer from the solar wind to the magnetosphere, and thus there would be no auroral phenomena, which are one of the most spectacular wonders of nature.

Because the solar wind–magnetosphere generator is operated on the magnetopause, where the solar wind blows across the connected field lines, the whole cylindrical surface of the magnetotail can be considered to be the generator in which the current flows from the duskside magnetopause to the dawnside magnetopause along the cylindrical surface. Much of the current thus generated flows in the plasma sheet across the magnetotail; this part of the circuit may be called the cross-tail circuit (**Fig. 3**). Thus, the magnetotail may be viewed as two long solenoids, producing two bundles of magnetic field lines separated by the plasma sheet. As a result, the Earth's dipolar field is stretched along the magnetotail in the antisolar direction. The generator also powers a large-scale motion of plasmas in the magnetosphere. In the main part of the plasma sheet, the plasma flows toward the Earth. *See* GEOMAGNETIC VARIATIONS; GEOMAGNETISM; SOLAR MAGNETIC FIELD.

Auroral phenomena. Another important circuit that is connected to the generator consists of a current flow along magnetic field lines from the morning side of the magnetotail to the morning half of the auroral oval, a flow along the auroral ionosphere (the auroral oval), and a flow along magnetic field lines from the evening half of the auroral oval to the evening side of the magnetotail. This discharge circuit may be called the auroral circuit because it is responsible for causing acceleration of current-carrying charged particles (Fig. 3). When the accelerated particles collide with upper atmospheric particles, they excite or ionize them. The auroral lights are emitted by those excited or ionized particles when they return to a lower or the ground state.

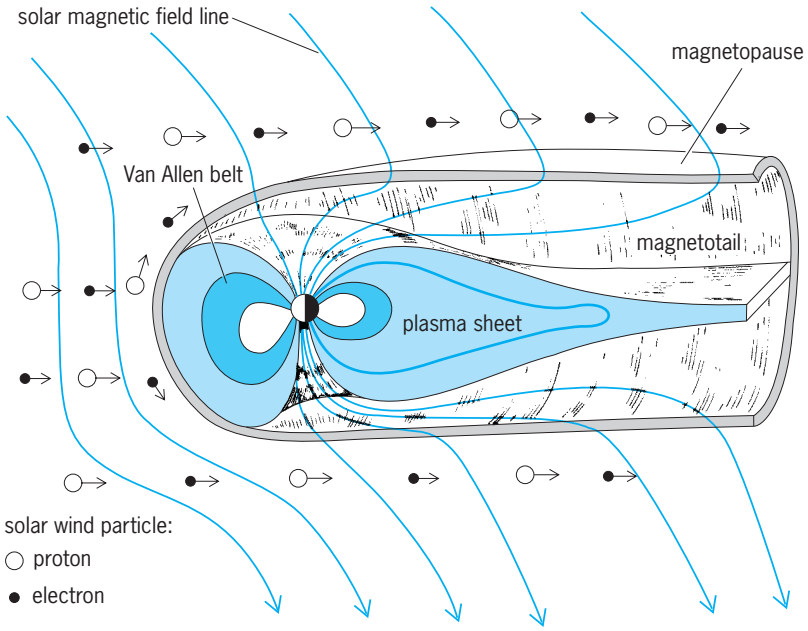

Fig. 2. Internal structure of the magnetosphere (noon-midnight cut). Motions of solar wind protons and electrons around the magnetopause and the linkage of the solar wind magnetic field lines and Earth's magnetic field lines are also shown.

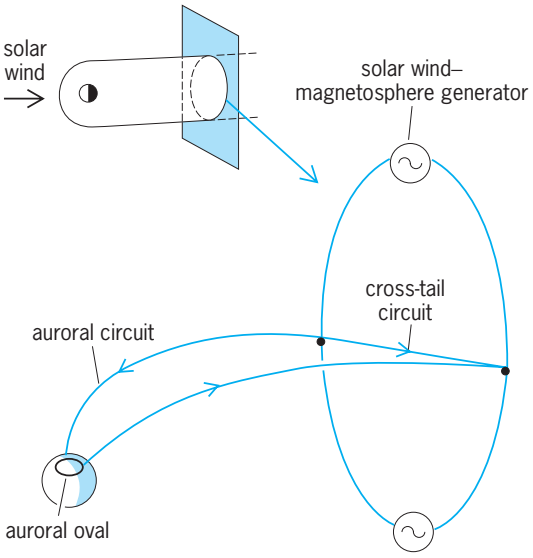

Fig. 3. The solar wind–magnetosphere generator located on the magnetopause (one cross section is shown) and its two main circuits: the cross-tail circuit and the auroral circuit.

The total power generated by the solar wind–magnetosphere generator depends on the magnitude and direction of the solar wind magnetic field, as well as on the speed of the solar wind. In particular, when the solar wind magnetic field is directed southward, the generated power becomes maximum. On the other hand, when the solar wind magnetic field is directed northward, the power becomes minimum. The power is also greater if the magnitude of the solar wind magnetic field B and the speed of the solar wind V are higher. The power P is given by the equation below, where θ is the polar angle of the

$$P = VB^2 \sin^4\left(\frac{\theta}{2}\right) l_0^2$$

solar wind vector projected to a plane perpendicular to the Sun-Earth line and l_0 is a constant of about 7 earth radii.

When the solar wind magnetic field vector turns gradually from a northern to a southern direction in the vicinity of the magnetosphere, the power generated by the dynamo begins to increase. As a result, the cross-tail electric current in the plasma sheet is increased. As the generated power is very high, the consumption of the power by the magnetosphere also becomes high. An indication of this high consumption rate is the phenomenon called the magnetospheric substorm which manifests itself in various magnetospheric and polar upper-atmospheric disturbances. As a result of this process, the earthward edge of the plasma sheet is suddenly pushed toward the Earth, and the plasma thus injected into the inner magnetosphere forms the ring current belt.

At the same time, the electric current along the auroral circuit is also intensified. As a result, the aurora becomes bright and active. The enhanced ionospheric portion of the auroral circuit is called the auroral electrojet. Intense magnetic field variations are experienced under and near the auroral electrojet. In this way, effects of the enhanced power of the solar wind–magnetosphere generator are manifested most conspicuously in the polar region. An intense auroral activity associated with this phenomenon is called the auroral substorm. The associated intense magnetic disturbances are called polar magnetic substorms. The ionosphere is also greatly disturbed in this period, and this phenomenon is called the ionospheric substorm. The ionospheric disturbances greatly affect high-frequency and very high-frequency radio communication in high latitudes. Even satellite microwave communication is at times disturbed by auroral activity.

Because the Earth is a good conductor, the auroral electrojets induce a potential difference on the Earth's surface. Therefore, if two points, along which the potential difference is present, are connected by a conductor, an electric current flows along it. It is for this reason that electric currents are induced in oil and gas pipelines and in power transmission lines in high latitudes during auroral activity. In the power lines there are severe power fluctuations when the electrojets are particularly intense.

Various solar activities are responsible for the time variations of the three solar wind quantities which determine the power of the generator. In particular, an intense explosion on the solar surface, a solar flare, causes a gusty solar wind and a large-scale deformation of the solar wind magnetic field. If this deformation happens to produce a large southward-directed magnetic field around the magnetosphere for an extended period (approximately 6 to 24 h), the generated power is considerably enhanced, and intense magnetospheric substorms occur. As a result, an unusually intense ring current grows, carrying a westward current surrounding the Earth and producing a southward-directed magnetic field around the Earth. Since the Earth's magnetic field is directed northward, this addition of the southward field is observed as a decrease of the Earth's magnetic field, one typical aspect of geomagnetic storms.

The Sun has also a few regions from which a high-speed stream is generated, particularly during the declining epoch of the 11-year sunspot cycle. Such a stream lasts for an extended period, from several months to more than 1 year. The solar wind magnetic field is markedly variable in the high-speed stream. As the Sun and the stream rotate with a period of about 27 days, the Earth is immersed in the stream once each period. As a result, the power of the solar wind–magnetosphere dynamo is increased and fluctuates considerably, causing magnetospheric substorms and auroral activity. *See* AURORA; SUN.

Planets. All other magnetic planets, such as Mercury, Jupiter, and Saturn, have magnetospheres which are similar in many respects to the magnetosphere of the Earth. The magnetosphere of Mercury is much smaller than that of the Earth. Since the solar wind pressure is higher at Mercury's than at the Earth's distance and since the magnetic field of Mercury is weaker than that of the Earth, the blunt-nosed front of the magnetosphere of Mercury is located at a distance of only 0.5 Mercury radius from its surface. On the other hand, because of a weak solar wind, a very strong magnetic field, and a fast rotation, the magnetosphere of Jupiter is gigantic and has an extensive current disk which lies along its equator. The distance to the blunt-nosed front is about 100 Jupiter radii. The *Voyager 2* space probe found that the magnetosphere of Jupiter is filled with sulfuric ions, presumably injected from one of its satellites, Io. The space probe also traversed its gigantic magnetotail. The magnetosphere of Saturn is a little smaller than that of Jupiter, but extends well beyond its rings. *See* JUPITER; MERCURY (PLANET); PLANETARY PHYSICS; SATURN.

A great variety of plasma processes, plasma waves, and plasma instabilities are involved in all magnetospheric phenomena. Some of them occur commonly in a thermonuclear machine. The magnetosphere provides a natural laboratory in which these plasma behaviors can be studied without the so-called wall effects. Among a variety of astrophysical conditions, the magnetospheres of the Earth and the planets are the only regions in which plasma behaviors can be studied in natural conditions. Therefore, a study of

the magnetosphere provides an important foundation upon which astrophysical plasma theories can be tested and constructed. It has also been speculated that many magnetic stars, pulsars, and even some galaxies have structures similar to the Earth's magnetosphere. Since a magnetosphere results from an interaction of magnetized plasma flow and a magnetized celestial body, it is likely that it is of common occurrence in galaxies. *See* MILKY WAY GALAXY; PLASMA (PHYSICS); PULSAR.

S.-I. Akasofu

Bibliography. S.-I. Akasofu, *Physics of Magnetospheric Substorms*, 1977; S.-I. Akasofu and S. Chapman, *Solar-Terrestrial Physics*, 1972.

Magnetostriction

The change of length of a ferromagnetic substance when it is magnetized. More generally, it is the phenomenon that the state of strain of a ferromagnetic sample depends on the direction and extent of magnetization. The phenomenon has an important application in magnetostriction transducers.

Physical cause. Magnetostriction results from the dependence of the crystalline anisotropy energy upon the state of strain of the crystalline lattice. If the crystal deforms (for example, suffers a change in length), the anisotropy energy may be lowered more than the elastic energy is raised. Thus, a strained state will be favored. For a discussion of crystalline anisotropy energy *see* FERROMAGNETISM.

The total energy of a ferromagnetic substance depends upon the state of strain and the direction of magnetization through three contributions. The first two consist of the crystalline anisotropy energy of the unstrained lattice plus a correction which takes into account the dependence of the anisotropy energy on the state of strain. The third contribution is that of the elastic energy, which is independent of magnetization direction and is a minimum in the unstrained state. The state of strain of the crystal will be that which makes the sum of the three contributions to the energy a minimum. The result is that, when magnetized, the lattice is always distorted from the unstrained state, unless there is no anisotropy.

Since spontaneous magnetization occurs below the Curie temperature, there will always be a spontaneous lattice distortion which depends on magnetization direction in the ferromagnetic state. In nickel, the lattice spacing parallel to the magnetization is always smaller than the lattice spacing perpendicular to the magnetization. *See* CURIE TEMPERATURE.

Magnetoelastic coupling constants. These determine the magnitude of the correction arising from strains to the anisotropy energy. In cubic crystals, there are two magnetoelastic coupling constants B_1 and B_2. The constant B_1 determines the change in anisotropy due to a diagonal component of strain, and B_2 that due to a mixed component. The values of the strain components which lead to a minimum in the total magnetoelastic energy are given in terms of the magnetoelastic coupling constants, the elastic constants, and the direction cosines of the magnetization with respect to the crystal axes, α_1, α_2, α_3. In the strain state of lowest magnetoelastic energy, that part of the energy which depends upon magnetization direction is given by the equation below, where

$$U = (K_1 + \Delta K) \times (\alpha_1{}^2\alpha_2{}^2 + \alpha_2{}^2\alpha_3{}^2 + \alpha_3{}^2\alpha_1{}^2) + \cdots$$

ΔK is a correction to the first-order anisotropy constant K_1. The quantity ΔK depends only upon the magnetoelastic constants and the elastic constants.

When a high permeability (soft) magnetic material is required, the magnetostriction should be small in order that anisotropy not be induced by lattice distortions. Magnetostriction appears to be a major source of transformer hum. As the silicon content of soft magnetic steel is increased toward 6.5%, the magnetostriction disappears. Unfortunately, the metal becomes excessively brittle.

Applications. The magnetostrictive effect is exploited in transducers used for the reception and transmission of high-frequency sound vibrations. Nickel is often used for this application. *See* ELASTICITY; SONAR; ULTRASONICS.

Elihu Abrahams; Frederick Keffer

Bibliography. D. Craik, *Magnetism*, 1994; E. Du Tremolet de Lacheisseri, *Magnetostriction: Theory and Applications—Magnetoelasticity*, 1993.

Magnetron

The oldest of a family of crossed-field microwave electron tubes wherein electrons, generated from a heated cathode, move under the combined force of a radial electric field and an axial magnetic field. By its structure a magnetron causes moving electrons to interact synchronously with traveling-wave components of a microwave standing-wave pattern in such a manner that electron potential energy is converted

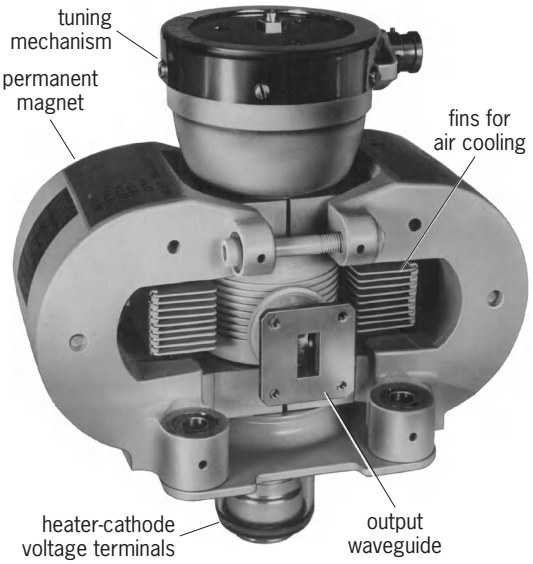

Fig. 1. Coaxial cavity magnetron with horseshoe-shaped magnets. (*After J. W. Gewartowski and H. A. Watson, Principles of Electron Tubes, Van Nostrand, 1965*)

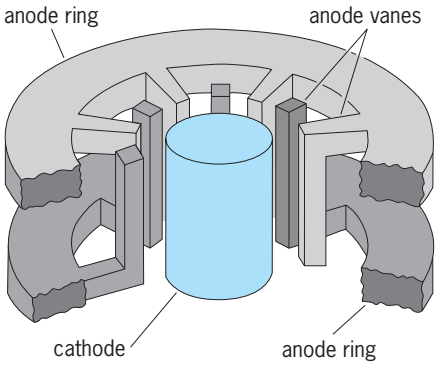

Fig. 2. Interdigital-vane anode circuit and cathode, indicating the basic cylindrical geometry. (*After G. D. Sims and I. M. Stephenson, Microwave Tubes and Semiconductor Devices, Blackie and Son, London, 1963*)

to microwave energy with high efficiency. Magnetrons have been used since the 1940s as pulsed microwave radiation sources for radar tracking. Because of their compactness and the high efficiency with which they can emit short bursts of megawatt peak output power, they have proved excellent for installation in aircraft as well as in ground radar stations. In continuous operation, a magnetron can produce a kilowatt of microwave power, which is appropriate for rapid microwave cooking.

The magnetron in an oscillator; it generates radio-frequency energy, usually over limited portions of the microwave frequency range of 1–40 gigahertz. It can produce microsecond pulses of peak power as high as 10 megawatts but with low duty-cycle ratios (ratio of pulse length of pulse repetition period). Mechanical tuning of the magnetron microwave circuit can change the center frequency of the output radiation by about ±5%.

Configuration. Raw materials of a magnetron are chiefly copper, iron, and ceramic welded and brazed together to form a vacuum tube. A slow-wave microwave circuit, made of copper to reduce ohmic losses, serves to provide a traveling wave that can interact with the electrons. Iron pole pieces guide the magnetic flux from externally attached horseshoe-shaped magnets (**Fig. 1**). Pole pieces shape the kilogauss magnetic field in the electron-microwave interaction region to be perpendicular to the electric field and to constrain the electrons to the interaction region. Ceramic (or sometimes glass) serves as a standoff insulator for the tens of kilovolts applied between cathode and anode. Ceramic is also used as the microwave window to couple the power generated inside the magnetron through the vacuum enclosure to externally attached waveguides. The breakdown limit of this window may be the chief factor in setting the peak power output obtainable from a magnetron.

The magnetron is a device of essentially cylindrical symmetry (**Fig. 2**). On the central axis is a hollow cylindrical cathode. The outer surface of the cathode carries electron-emitting materials, primarily barium and strontium oxides in a nickel matrix. Such a matrix is capable of emitting electrons when current flows through the heater inside the cathode cylinder. *See* VACUUM TUBE.

At a radius somewhat larger than the outer radius of the cathode is a concentric cylindrical anode. The anode serves two functions: (1) to collect electrons emitted by the cathode and (2) to store and guide microwave energy. The anode consists of a series of quarter-wavelength cavity resonators symmetrically arranged around the cathode. *See* CAVITY RESONATOR.

A radial dc electric field (perpendicular to the cathode) is applied between cathode and anode. This electric field and the axial magnetic field (parallel and coaxial with the cathode) introduced by pole pieces at either end of the cathode, as described above, provide the required crossed-field configuration.

Microwave generation. Provided that the magnitudes of the electric field and the magnetic field are properly adjusted, an electron emerging from the heated cathode proceeds to orbit the cylindrical cathode, moving on the average in a direction perpendicular to both applied fields (**Fig. 3**). The totality of electrons emitted by the cathode form a swarm or hub of negative charge rotating about the cathode axis. The hub thickness extends from the cathode surface outward to a radius intermediate between cathode and anode radii. Motion of the rotating swarm of electrons past the surface of the concentric-anode microwave circuit induces a noise current in the copper circuit. This noise shock excites the resonators so that microwave fields build up at the resonant frequency. The velocity of the electrons, as determined by the applied voltage and magnetic field, is made to be close to or synchronous with the slow-wave phase velocity characteristic of the microwave circuit. Consequently, as the electron swarm rotates, it concentrates into bunches that deliver microwave energy to the resonators. Thus, as in most oscillators, the process begins with noise; then electromagnetic fields build up at the resonant

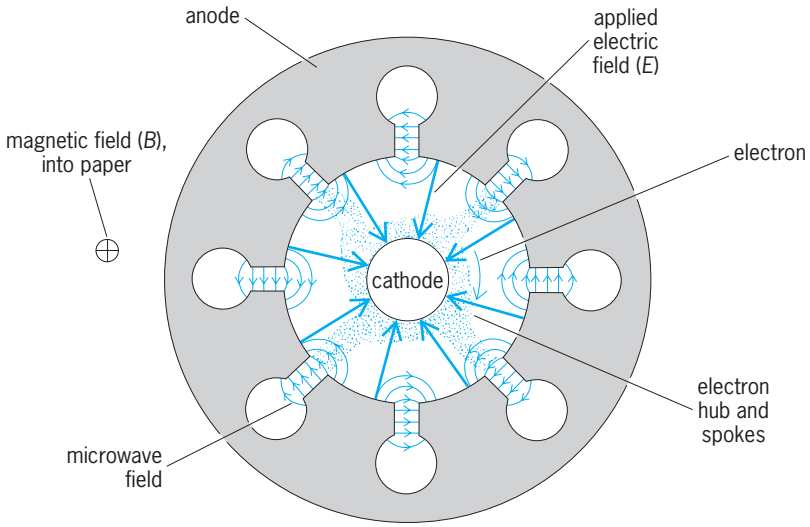

Fig. 3. Electron motion in magnetron interaction region under action of applied electric and magnetic fields and generated microwave field. (*After C. H. Dix and W. H. Aldous, Microwave Valves, Illiffe Books, London, 1966*)

frequency. These fields react, in turn, upon the electrons, remove some of their potential energy, and cause them to approach the circuit more closely, whereupon the process intensifies. Buildup of the microwave field is limited by internal ohmic losses in the circuit, external loading of the output coupling, and the electron energy available for conversion to microwave energy.

Electron bunching. Bunching of electrons plays a prominent role in the generation of microwave power in the magnetron, as it does in most microwave tubes. The applied radial electric field E and the axial field B constrain the average motion of the hub electrons to a direction perpendicular to both fields and hence circumferential about the cathode. (There is cycloidal motion superimposed on the average, as well.) The average circumferential electron velocity, called drift velocity, has a magnitude $u = E/B$. The microwave circuit is designed to support a traveling wave whose phase velocity v is equal to u. If $u = v$, the electron hub rotation is said to be synchronous with the rotating traveling wave. Under these conditions, one can consider the interaction of electrons with microwave fields from the anode in a frame of reference which rotates at the synchronous velocity.

The quarter-wave cavity resonators, which support the rotating microwaves and surround the electron hub, present at the hub a rotating microwave field configuration consisting of electric fields having strong circumferential components. These components are 180° out of phase (oppositely directed) for neighboring cavities, as shown in Fig. 3. This set of alternating fields can be considered as composed of two sets of uniformly directed fields (each internally inphase), one set 180° out of phase with the other and the two interlaced. (Such a microwave field configuration is called a π mode, the two sets of fields being phased π radians from each other.) In the frame of reference rotating in synchronism with these two sets of microwave fields, the circumferential components of the microwave electric fields can be regarded as steady or static fields crossed with the applied axial magnetic field.

Those hub electrons rotating in phase and under the influence of one of the sets of microwave fields, because of the crossed-field situation, are constrained to move radially toward the anode (average electron motion is always perpendicular to both electric and magnetic crossed-field directions). In doing so they contribute to the strength of the microwave field, converting their potential energy in the applied electric field to microwave energy. The process continues until the electrons finally fall through the entire hub-to-anode potential and are collected on the anode. As a consequence, the distribution of electrons in the interaction region between cathode and anode looks like a hub with spokes, all rotating together at drift velocity E/B (Fig. 3). In this sense the electrons are bunched. Throughout the interaction the electrons continue to rotate at close to synchronous velocity, remaining in phase with the wave and continuing to convert dc potential energy into microwave energy until striking the anode. This staying-in-synchronism results in high energy conversion efficiency (values may be as high as 65–75%) of the magnetron in contrast to those microwave tubes that depend on differential velocities of electrons for bunching. It also means that the anode must be rugged enough to absorb the full kinetic energy of the electrons ($mu^2/2$, where m is the electron mass). *See* KLYSTRON.

Those electrons in phase with the remaining set of microwave fields (the set 180° out of phase with the first) will be constrained to move radially back through the hub toward the cathode. This motion results in an increase of electron potential energy at the expense of the microwave field. However, the loss in microwave energy is small because such electrons move out of high microwave field regions toward weaker ones and so move to minimize their interaction. On striking the cathode these electrons heat up the cathode and reduce the required heater power. The phenomenon of electron bunching, wherein certain in-phase electrons give up their potential energy to the microwave field while other out-of-phase electrons are forced out of the microwave field region to prevent their extracting microwave energy, is further abetted by the shape of the microwave fields near the anode. The field shape is such as to cause electrons approaching the anode to become even more closely in phase so as to deliver maximum power to the circuit.

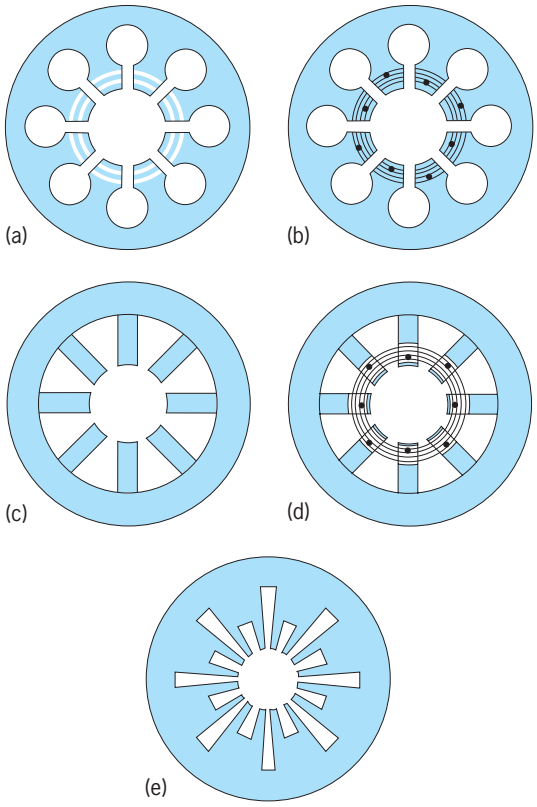

Fig. 4. Magnetron slow-wave circuits. (*a*) Unstrapped cavity. (*b*) Strapped cavity. (*c*) Unstrapped vane block. (*d*) Strapped vane block. (*e*) Rising-sun block. (*After C. H. Dix and W. H. Aldous, Microwave Valves, Illiffe Books, London, 1966*)

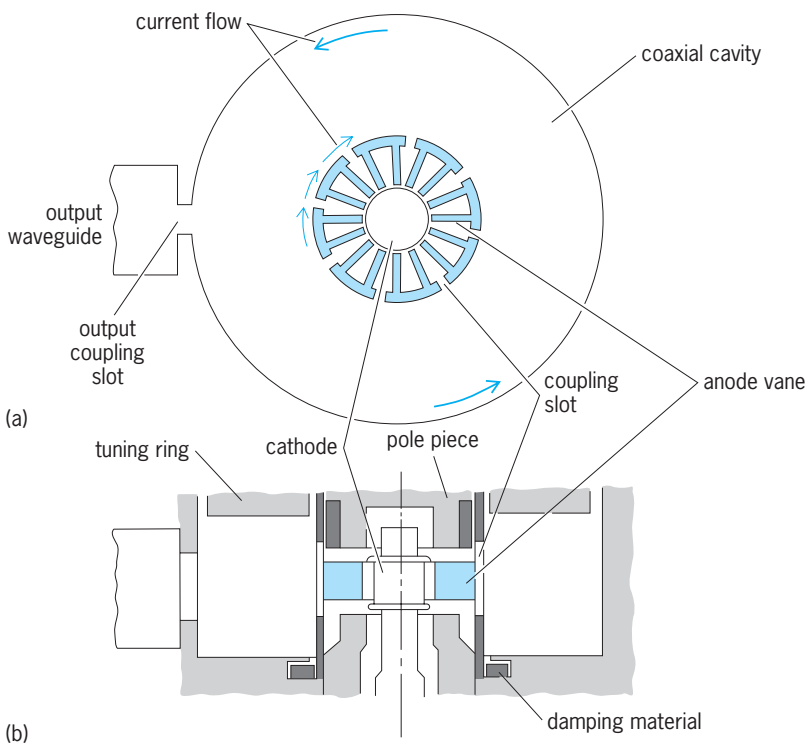

Fig. 5. Coaxial cavity magnetron. (*a*) End view. (*b*) Cross-sectional view. (*After J. W. Gewartowski and H. A. Watson, Principles of Electron Tubes, Van Nostrand, 1965*)

Microwave circuit. The only aspect of the magnetron that is not symmetric is the output coupler. Being an oscillator and generating its own signal starting from noise-induced fields, the magnetron must maintain enough energy in its resonant circuit to keep the generation process going. On the other hand, only the microwave energy coupled out of the magnetron is useful to the radar operator. Thus some compromise must determine the fraction of the generated power which is coupled out through the output coupling slot, the ceramic window, and output waveguide.

The π-mode electromagnetic field configuration is desirable for interaction with the electrons as described above, and the output coupling is generally designed for such a resonant condition. However, the microwave circuit can sustain other resonant modes which can interact with the electrons and which are generally less efficient. Some of these undesirable modes can so orient themselves as to present a null in the microwave field pattern at the output. All the energy converted from interaction with electrons is then stored inside the magnetron in such modes, and none is usefully coupled out. The fields in the interaction region can become high enough to block operation in the π mode. Such undesirable modes can be close in frequency to the π mode, and unless special circuit design is incorporated, they are difficult to discriminate against. Much of the design of magnetron microwave structures has to do with maximizing efficiency of π-mode interaction while inhibiting electron interaction with other undesirable modes.

A variety of shapes have been used in the design of the quarter-wavelength cavities whose open-end, capacitative section provides the electric fields for interaction with the electrons. There are vane-type cavities and hole-and-slot versions (**Fig. 4**). These may be strapped (alternate cavities tied together with a copper strap to promote π-mode operation), or alternate cavities can be elongated (rising-sun configuration) to separate the undesirable modes from the π mode. Such circuits are generally tuned in frequency by inserting copper pins into the induction sections of the quarter-wave cavities. Voltage tuning has been achieved in certain low-power magnetrons.

Coaxial cavity magnetron. A more recent magnetron design, the coaxial cavity magnetron (**Fig. 5**), achieves mode separation, high efficiency, stability, and ease of mechanical tuning by coupling a coaxial high-Q cavity to a normal set of quarter-wavelength vane cavities. *See* CAVITY RESONATOR; Q (ELECTRICITY).

The high-Q cavity is resonant in the TE_{011} mode, a mode in which current flow on the inner conductor is circumferential and phase is not a function of circumferential position. To couple microwave energy from the slow-wave circuit into the coaxial cavity, slots are cut into the backs of alternate quarter-wavelength cavities. If the rotation of the electron hub induces current flow on the vanes, so that a π-mode resonant buildup of microwave fields commences there, the slot coupling geometry is correct to also stimulate the buildup of the TE_{011} mode in the outer coaxial cavity. Because alternate vane cavities are in phase in π-mode operation, the current coupled into the high-Q cavity through slots cut only in alternate cavities will also be in phase. This is the condition required to induce the TE_{011} mode in the coaxial cavity. The output frequency can be tuned merely by altering the axial length of the outer coaxial cavity (a tuning piston is employed). Most stored microwave energy is in the coaxial cavity, and its high Q ensures efficient storage. The coaxial cavity magnetron has replaced many earlier designs for airborne radar.

Some characteristics typical for the coaxial cavity magnetron are as follows.

Frequency (tunable)	15.5–17.5 GHz
Peak output power	125 kW
Peak applied voltage	17.5 kV
Peak anode current	19 A
Pulse duration	3μs
Duty cycle	0.001s
Magnetic field	0.74 weber/in.^{2} (1150 teslas)
Overall efficiency	43

Other crossed-field tubes. The magnetron is a member of the crossed-field family of devices. Other members are platinotrons, amplitrons, forward-wave crossed-field amplifiers, non-reentrant-beam crossed-field amplifiers, and carcinotrons. Some of these devices are oscillators and others amplifiers (**Fig. 6**).

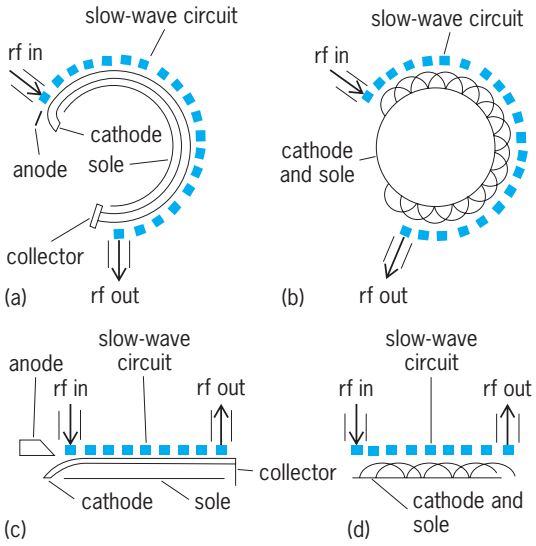

Fig. 6. Magnetron amplifiers. (*a*) Circular type with beam injection. (*b*) Circular type with continuously emitting sole. (*c*) Linear type with beam injection. (*d*) Linear type with continuously emitting sole.

Some interact with backward slow waves, others with forward waves. Some employ an electron gun, others an emitting sole. The magnetron oscillator itself has both a reentrant electron beam and a reentrant microwave circuit. (The electron flow is continuous in the circumferential direction, orbiting the axial cathode, while the quarter-wavelength cavities are symmetrically disposed around the cathode with no beginning or end.)

Power generation in an oscillator begins with noise, and the resonant nature of the circuit produces the high electric fields required to further react with the electrons. Amplifiers, on the other hand, have non-reentrant circuits with a definite input and output. The input signal provides the initial microwave field to begin interaction between electrons and circuit. The electron beam may be reentrant or not, depending upon the geometry of the circuit, that is, whether the cavities are arranged with cylindrical or linear symmetry.

The magnetron and related crossed-field amplifiers and oscillators are rather noisy devices and operate best in the high-output-power region. As amplifiers, they have generally low gain, but their output power is high. Compactness and high efficiency are the most attractive features of crossed-field electron tubes. Conversion of electron potential energy to microwave energy in characteristic of all crossed-field devices (M-type carcinotrons) in contrast to conversion of kinetic energy in the case of traveling-wave tubes (O-type devices). *See* TRAVELING-WAVE TUBE.

R. J. Collier

Bibliography. R. E. Collin, *Foundations for Microwave Engineering*, 2d ed., 2000; A. S. Gilmour, *Microwave Tubes*, 1986; J. Helszajn, *Microwave Engineering*, 1992; C. A. Lee and G. C. Delman, *Microwave Devices, Circuits and Their Interaction*, 1994; S. Liao, *Microwave Devices and Circuits*, 3d ed., 1996.

Magnification

A measure of the effectiveness of an optical system in enlarging or reducing an image. For an optical system that forms a real image, such a measure is the lateral magnification m, which is the ratio of the size of the image to the size of the object. If the magnification is greater than unity, it is an enlargement; if less than unity, it is a reduction.

The ratio of the longitudinal (with respect to the optical axis) dimensions of the image to the corresponding dimensions of the object is known as longitudinal magnification, which in first order equals the square of the lateral magnification.

The angular magnification γ is the ratio of the angles formed by the image and the object at the eye. The relation $n'\gamma m = n$ relates angular to lateral magnification. Here n and n' are the refractive indices of the media containing the object and image, respectively. In telescopes the angular magnification (or, better, the ratio of the tangents of the angles under which the object is seen with and without the lens, respectively) can be taken as a measure of the effectiveness of the instrument.

A small off-axis element is imaged with different magnification in both the meridional and sagittal directions. This may be called differential magnification.

Magnifying power is the measure of the effectiveness of an optical system used in connection with the eye. The magnifying power of a spectacle lens is the ratio of the tangents of the angles under which the object is seen with and without the lens, respectively. The magnifying power of a magnifier or an ocular is the ratio of the size under which an object would appear seen through the instrument at a distance of 10 in. (25 cm; the distance of distinct vision) divided by the object size.

E. Abbe suggested defining the magnifying power of an optical system as the ratio of the tangent of the visual angle under which the object appears to the object size. This quantity is approximately equal to the power of the system, which is the reciprocal of the focal length, $1/f'$. *See* DIOPTER; LENS (OPTICS); OPTICAL IMAGE.

Max Herzberger

Bibliography. M. Born and E. Wolf, *Principles of Optics*, 7th ed., 1999; M. Herzberger, *Modern Geometrical Optics*, 1958, reprint 1980; F. A. Jenkins and H. E. White, *Fundamentals of Optics*, 4th ed., 1976; J. R. Meyer-Arendt, *Introduction to Classical and Modern Optics*, 4th ed., 1995.

Magnitude (astronomy)

The brightness of an astronomical object, expressed on a unique numerical scale. The stellar magnitude scale is logarithmic and is inverted in that fainter objects have numerically larger magnitudes. The term "magnitude" in this context refers to brightness only and has nothing to do with the size or other quantities. Although used primarily for stars, the stellar magnitude scale can also be used to

express the brightness of the Sun, planets, asteroids, comets, nebulae, galaxies, and even background radiation.

Since the brightness of any object varies with wavelength, many different magnitude scales have been defined corresponding to different spectral regions, bandwidths, and methods of observation. Visual magnitudes, corresponding to the sensitivity of the human eye centered in the yellow part of the spectrum, are usually implied if the type is unspecified. A distinction is made between the apparent magnitude of an object viewed from the Earth and its absolute magnitude, which measures the object's intrinsic luminosity by indicating its apparent magnitude as seen from a standard distance.

Development. The star catalog of Hipparchus (about 150 B.C.) is thought to have contained approximately 850 naked-eye stars classified according to brightness. The 15 or so brightest stars were referred to as stars of the first magnitude, while second-magnitude stars were on the average two or three times fainter, and so on. The scale is logarithmic because intervals that are perceived as equal intervals are, in fact, equal brightness ratios.

Measurements of brightness ratios in the nineteenth century showed that, on average, stars of the sixth magnitude (near the limit of naked-eye vision) were about 100 times fainter than those of the first. On the scale introduced by N. R. Pogson in 1856 and universally adopted, an interval of 5 magnitudes corresponds to a factor of exactly 100, so that each magnitude corresponds to a factor of $\sqrt[5]{100} \approx 2.512 \ldots$. The zero point of the Pogson scale was set so that most stars retained their customary magnitudes.

Mathematical properties. The stellar magnitude scale has many convenient properties. Its logarithmic character means that brightness ratios can be calculated by simple subtraction, and that the entire range of astronomical brightnesses can be represented in terms of small numbers, ranging from −27 (the apparent magnitude of the Sun) to approximately +31 (the faintest objects detected with confidence on deep-field images taken with the *Hubble Space Telescope*). Its inverted nature seems natural to observers, who are apt to think in terms of a star's faintness, that is, how hard it is to make a particular observation. It is particularly convenient in that the most familiar stars have magnitudes near zero.

The correspondence between magnitude interval and brightness ratio is shown in **Table 1**. In general, an interval of n magnitudes corresponds to a factor of 2.512^n in brightness. A factor of 10 corresponds to exactly 2.5 magnitudes, a factor of 100 to exactly 5 magnitudes. Any linear measure of brightness X can be expressed as a magnitude m through Eq. (1), where the negative sign is needed to produce

$$m = -2.5 \log_{10} X + \text{ constant} \qquad (1)$$

an inverted scale and the constant can be evaluated by measuring X for any star of known magnitude. *See* LOGARITHM.

TABLE 1. Magnitude scale

Magnitude difference	Brightness ratio
0.00	1
0.01	1.01
0.05	1.05
0.30	1.32
0.753	2
1.000	2.512 . . . (= $\sqrt[5]{100}$)
1.5	~4
2	6.31 . . . (=2.512^2)
2.5	10 exactly
3	~16 (=2.512^3)
3.5	25.12 . . .
4	~40
5	100 exactly
10	10^4
15	10^6
50	10^{20}

An attractive feature of the magnitude scale is the ease with which fractional magnitudes can be interpreted. Each change of 1% in the brightness of an object corresponds to a change of 0.01 in the magnitude, and this numerical correspondence holds to good accuracy for changes up to about 30%.

Absolute magnitude. The apparent magnitude m of a star observed from the Earth depends upon both its absolute magnitude M (an intrinsic property of the star) and its distance d from Earth. The difference $m - M$ between the apparent and absolute magnitude is thus a function of the distance, given by Eq. (2), and is sometimes called the distance modulus. Here the distance d is expressed in parsecs (1 pc = 3.26 light-years = 1.92×10^{13} mi = 3.09×10^{13} km). The constants in the formula come from the inverse-square law of light, the definition of a magnitude, and the choice of $d = 10$ pc as the standard distance at which the apparent and absolute magnitudes are defined to be equal. Thus the absolute magnitude may be defined as the apparent magnitude an object would have if viewed from a distance of 10 pc. *See* PARSEC.

$$m - M = 5 \log_{10} d - 5 \qquad (2)$$

The absolute magnitude can thus be found for any astronomical object whose distance has been measured (**Table 2**). The Sun has an absolute visual magnitude of +4.79; that is, it would appear as about a fifth-magnitude star to an observer 10 pc away. The brightest stable stars in the Milky Way Galaxy and in external galaxies have absolute magnitudes about −9, while the faintest are near +20 or even fainter. Supernova 1987A in the Large Magellanic Cloud ($m - M \approx 18.5$) reached an absolute magnitude of −15.5 at its maximum of May 1987; more typical supernovae attain even higher luminosities. *See* STAR; SUPERNOVA.

It is often possible to assign an absolute magnitude to a star on the basis of its spectral classification, in which case its distance can be calculated from Eq. (2). The problem of determining absolute

TABLE 2. Apparent and absolute visual magnitudes and distances of familiar stars

Name	m	M	d, pc	Comment
Sun	−26.78	4.79	$\frac{1}{206{,}265}$	
Barnard's star	9.54	13.25	1.81	Nearby red dwarf
Sirius	−1.46	1.42	2.65	The brightest star
Arcturus	−0.06	−0.3	11	Red giant
Betelgeuse	0.5 var.	−5.2	130	Cool supergiant
Deneb	1.25	−7.2	500	Very bright supergiant
SN 1987A (maximum)	3.0	−15.5	50,000	Supernova in Large Magellanic Cloud

magnitudes is thus equivalent to that of determining distances.

Absorption by interstellar dust affects the apparent magnitudes of distant stars, particularly those lying in the plane of the Milky Way. If the absorption A is expressed in magnitudes, Eq. (2) may be rewritten as Eq. (3).

$$m - M = 5 \log_{10} d - 5 + A \tag{3}$$

See INTERSTELLAR EXTINCTION.

Visual magnitudes. The scale of visual magnitudes was originally established with the dark-adapted eye as the detector. Visual magnitudes can be measured photographically (in which case they are called photovisual) by using an emulsion sensitive to yellow light and a filter to block the shorter wavelengths. However, most modern measurements of visual magnitudes are done photoelectrically, with either a photomultiplier or a charge-coupled device (CCD), in combination with a suitable filter; the symbol V is reserved for photoelectrically determined visual magnitudes. Eye estimates are often employed to monitor the visual magnitudes of variable stars. *See* CHARGE-COUPLED DEVICES; PHOTOELECTRIC DEVICES; PHOTOMETRY; VARIABLE STAR.

Photographic magnitudes. Magnitudes of stars can be determined from image sizes on astronomical photographs. Magnitudes can be found by interpolation if they are known for a sequence of stars appearing on the same photograph. The advantage of photographic photometry is that many thousands of stellar images can often be recorded on a single exposure.

The basic photographic emulsion is sensitive to blue light, and the term photographic magnitude (designated m_{pg}) specifically means a wideband blue magnitude that includes the near-ultraviolet but excludes the yellow region and all longer wavelengths. Star catalogs usually list either m_{pg} or the visual magnitude m_v. When both are known, the difference can be used as a quantitative measure of the color of the star, given by Eq. (4). The zero point of the m_{pg} scale

$$\text{Color index} = m_{pg} - m_v \tag{4}$$

has been set so that $m_{pg} - m_v = 0.0$ for stars similar to Vega, of spectral type A. The color index is positive for stars redder than Vega, negative for bluer stars. Although colors can be affected by interstellar absorption, they serve primarily as indicators of surface temperature; cooler stars have redder (numerically larger) colors. *See* ASTRONOMICAL PHOTOGRAPHY.

Multicolor photoelectric photometry. Magnitudes can be measured accurately and conveniently with a photomultiplier tube and a filter to limit the bandpass. Aperture photometry, the traditional method by which stars are measured one at a time through a small circular aperture, is now used primarily when the number of filters is large; by measuring a star through n filters, a magnitude and $n - 1$ color indices are obtained. The various color indices of a star are normally well correlated, but they often provide additional information because of the presence of absorption features in the stellar spectrum. An accuracy of 0.01 magnitude or better is routinely achieved in this work. *See* PHOTOMULTIPLIER; RADIOMETRY.

Most photometry today is done with CCD detectors. In this case, an image of the field is recorded through each filter at the telescope, and the photometry is done digitally on the computer. The advantages of CCDs are particularly great for faint stars in crowded fields.

Many multicolor photometric systems have been defined with wide, intermediate, and narrow bandpass filters. One of the first and still the most widely used is the wideband UBV (ultraviolet, blue, visual) system introduced by H. L. Johnson about 1950. The B and V filters are the photoelectric equivalents of m_{pg} and m_v, respectively (the most significant difference being that the B filter excludes the ultraviolet light that contributes to the photographic magnitude), and B − V has replaced $m_{pg} - m_v$ as the general-purpose color index most commonly employed. The addition of the U filter, placed in a spectral region strongly affected by absorption by neutral hydrogen in hot stars, makes it possible to determine the intrinsic properties of stars from UBV photometry alone, even in the presence of interstellar absorption.

Measurements in red and near-infrared (R,I) filters are often added to UBV photometry, especially when the object is to determine stellar temperatures without relying on the U and B filters, which are strongly affected by absorption lines in the stellar spectrum.

Infrared magnitudes. With the improvement of infrared detectors and the development of telescopes

TABLE 3. Filter characteristics for standard wideband multicolor photometric system

Filter	Central wavelength, μm	Bandwidth μm	Flux density* for Magnitude = 0.00	Thermal sources peaking in filter: Temperature, K†	Thermal sources peaking in filter: Example
U	0.36	0.07	4350	8500	Fairly hot star
B	0.44	0.10	7200	7000	
V	0.55	0.08	3920	5500	Solar-type star
R	0.70	0.21	1760	4300	
I	0.90	0.22	830	3300	Typical red giant
J	1.25	0.4	340	2400	
H	1.6	0.5	120	1900	Very cool star
K	2.2	0.6	39	1400	
L	3.4	0.7	8.1	900	Circumstellar dust
M	5.0	1.2	2.2	600	
N	10	5	0.12	300	Room temperature

*Unit = 10^{-15} W·cm^{-2}·μm^{-1}.

optimized for infrared work, Johnson was able to extend the wideband UBVRI photometric system to much longer wavelengths. Filters were chosen to match the windows between bands of atmospheric absorption. The 11 filters of the standard multicolor system, as originally defined by Johnson, have the central wavelengths and bandwidths given in **Table 3**. (These bandwidths are the full widths at one-half the peak transmission.) Subsequent observers have often used somewhat narrower bands. The magnitude scale for each filter has an arbitrary zero point, and these have been set by requiring a typical star of type A0 (such as Vega) to have the same magnitude in each filter.

Applications of multicolor infrared photometry have included refinement of the stellar temperature scale, especially for cool stars, and the determination of "bolometric magnitudes." Unlike other magnitudes, which refer to particular wavelength regions, the bolometric magnitude is an integrated quantity referring to the total radiative energy output of the star. That is, it represents, on the magnitude scale, the area under the flux curve. The absolute bolometric magnitude (referred to a distance of 10 pc) represents the intrinsic luminosity of the star. *See* INFRARED ASTRONOMY.

Robert F. Wing

Bibliography. E. Budding, *Introduction to Astronomical Photometry*, 2d ed., 2006; A. A. Henden and R. H. Kaitchuck, *Astronomical Photometry*, 1982, reprint 1990; S. B. Howell, *Handbook of CCD Astronomy*, 2d ed., 2006; J. R. Percy (ed.), *The Study of Variable Stars Using Small Telescopes*, 1986; C. Sterken and J. Manfroid, *Astronomical Photometry, a Guide*, 1992.

Magnolia

A genus of trees with large, chiefly white flowers, and simple, entire, usually large alternate leaves. In the winter the twigs may be recognized by their aromatic odor when bruised, by the encircling stipule scars at the nodes, and by the chambered pith (see **illus.**).

The most important species industrially is *Magnolia acuminata*, commonly called cucumber tree, which grows in the Appalachian and Ozark mountains and may reach a height of 80 ft (20 m), rarely 100 ft (30 m). The fruit is red when ripe and resembles a small cucumber in shape.

The wood of the magnolia is similar to that of the tulip tree and is rather soft, but it is of such wide

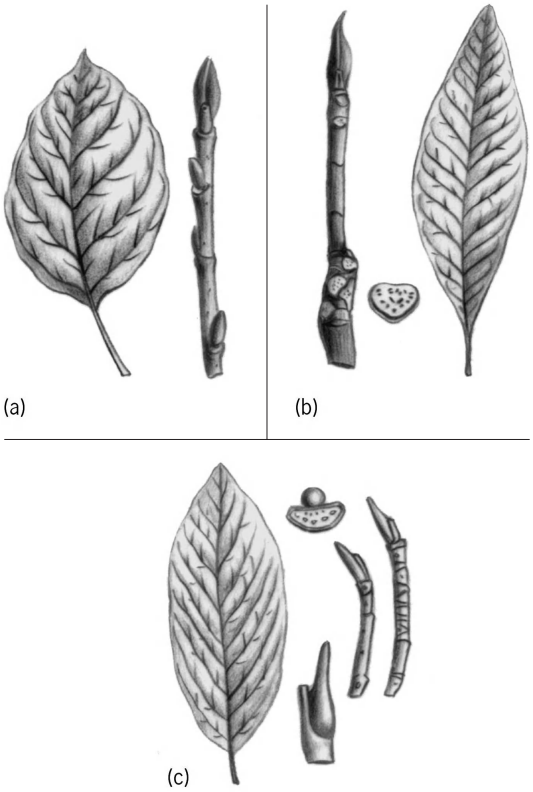

Magnolia leaves and twigs. (*a*) Cucumber tree (*Magnolia acuminata*). (*b*) Umbrella magnolia (*M. tripetala*). (*c*) Sweetbay (*M. virginiana*). In *b* and *c*, note the chambered pith of twig cross sections.

natural dimensions that it is valued for furniture, cabinetwork, flooring, and interior finish. The annual cut amounts to several million board feet. *See* MAGNOLIALES; RANUNCULALES; TULIP TREE.

Magnolia species occur naturally in a broad belt in the eastern United States and Central America, with a similar region in eastern Asia and the Himalayas. With a few exceptions the Asiatic species bloom early, before the leaves appear. These are valued as ornamental trees in the United States. *Magnolia stellata* is shrubby with white or pinkish flowers; *M. yulan* is a small tree with cream-colored flowers; *M. kobus* is similar to *M. yulan*; and *M. soulangeana*, the saucercup magnolia, has pink flowers and is supposedly a hybrid. The species of the eastern United States, all important ornamentals, bloom after the leaves appear and include *M. tripetala*, the umbrella magnolia; *M. virginiana*, the sweetbay; *M. macrophylla*, the big-leaf magnolia; and *M. grandiflora*, the southern magnolia. *See* FOREST AND FORESTRY; TREE. Arthur H. Graves; Kenneth P. Davis

Magnoliales

An order of flowering plants consisting of six families, the best known of which are Magnoliaceae (220 species) and Annonaceae (2200 species). The others contain some botanically interesting and peculiar plants (305 species), but none besides Myristicaceae (300 species) are commonly encountered. Previously, many authors have considered these families as among the most primitive of the flowering plants, but in all cases the plants exhibit some highly derived traits. Although their fruits are often cited as the most primitive in the flowering plants, their carpels are not fused but the edges are sealed, unlike those of Nymphaeaceae and Chloranthaceae, which are not sealed at maturity. Their "primitiveness" has been overemphasized; studies of sequences of deoxyribonucleic acid (DNA) demonstrate that Magnoliales are closely related to Laurales, Piperales, and Winterales, and then more distantly to the monocotyledons.

Some species are of minor economic importance in various parts of the tropics: Annonaceae contain the custard apple, soursop, and sweetsop (*Annona* species), ylang-ylang (an aromatic oil is produced by the flowers of *Canaga odorata*), and *Mkilua fragrans* is the source of a perfume. *Myristica fragrans* (Myristicaeae) is the source of nutmeg and mace, and seeds of several species in this family are used locally to produce consumable oils that are sometimes also used for candle making. Of Magnoliaceae, many species of *Magnolia* (tulip trees) are used as ornamental trees in the temperate and tropical zones, and *Liriodendron* (yellow poplar or green tulip tree) is a commonly planted shade tree throughout the north temperate region. The latter is also a valuable timber-producing genus. *See* LAURALES; PIPERALES; PLANT KINGDOM; TULIP TREE. Mark Chase

Magnoliidae

A subclass of the class Magnoliopsida (dicotyledons) in the division Magnoliophyta (Angiospermae), the flowering plants. The subclass consists of 8 orders, 39 families, and more than 12,000 species. The Magnoliidae are the most primitive subclass of flowering plants, being essentially coextensive with what has often been called the Ranalian complex. In general, they have a well-developed perianth, which may or may not be numerous, centripetal stamens, and they are apocarpous. Their ovules are bitegmic and crassinucellate, and their seeds usually have a small embryo and copious endosperm. All of these characters are subject to exception, however, and there is no one character or easy set of characters by which the group can be formally defined. Various other putatively primitive characters, such as vesselless xylem, laminar stamens, laminar placentation, and the presence of more than two cotyledons, are largely or wholly restricted to this subclass, but are not standard features. *See* ARISTOLOCHIALES; ILLICIALES; LAURALES; MAGNOLIALES; MAGNOLIOPHYTA; MAGNOLIOPSIDA; NYMPHAEALES; PAPAVERALES; PIPERALES; PLANT KINGDOM; RANUNCULALES. Arthur Cronquist; T. M. Barkley

Magnoliophyta

A division of seed plants consisting of about 250,000 species, which form the bulk and most conspicuous element of the land plants. Often called flowering plants or angiosperms, they have several unique characteristics, the most prominent of which are their reproductive structure, flowers, and covered seeds. The other obvious woody land plants are the gymnosperms, which have cones instead of flowers and have naked seeds. Another trait distinguishing the angiosperms is the presence of double fertilization, which results in the production of stored food (starch or oils) within their seeds.

Angiosperms range from some of the smallest plants known to large forest trees, and they occur in all habitats, including the oceans, where they are only a minor element in most marine ecosystems. Some are capable of growing directly on rock surfaces as well as on the limbs of trees (*Tillandsia*, the so-called Spanish moss of the family Bromeliaceae, even grows on telephone wires). *Borya* (of the family Boryaceae from Australia) grows in rock crevices; during the dry season, it dries down to a fraction of its fresh weight and, like many mosses, is a "resurrection plant" that quickly resumes photosynthesis once rain occurs. The flowering plants thus have become masters of the world in many ways. The success of humankind is completely dependent on them, and if human activities alter their success the results will be catastrophic. Mark W. Chase

The angiosperms may be characterized as vascular plants with roots, stems, and leaves, usually with well-developed vessels in the xylem and with

companion cells in the phloem. The central cylinder has leaf gaps or scattered vascular bundles; the ovules are enclosed in an ovary; and the female gametophyte is reduced to a few-nucleate embryo sac without an archegonium. The male gametophyte is reduced to a tiny pollen grain that gives rise to a pollen tube containing a tube nucleus and two sperms; one sperm fuses with the egg in the embryo sac to form a zygote, and the other fuses with two nuclei of the embryo sac to form a triple fusion nucleus that is typically the forerunner of the endosperm of the seed. *See* LEAF; PHLOEM; POLLEN; ROOT (BOTANY); SEED; STEM; XYLEM.

Life cycle. The angiosperms are often called flowering plants because the flower is a characteristic feature not found in other groups of plants. A flower is a special sort of short shoot with modified leaves, some of which produce sexual reproductive structures, leading ultimately to the formation of seeds. A flower typically has four kinds of modified leaves—the sepals, petals, stamens, and carpels—attached to a stem tip called the receptacle. The sepals are on the outside, the petals next, and then the stamens, and the carpels are in the center. One or more of these kinds of parts may be missing, but the order (in normal specimens) is invariable. Typically the sepals are greenish and protective in function, whereas the petals are larger, brightly colored, and serve to attract insects or other pollinators. The sepals collectively constitute the calyx, the petals collectively constitute the corolla, and the calyx and corolla together constitute the perianth. *See* FLOWER.

Sporophyte generation. The stamens, collectively constituting the androecium, are essentially microsporophylls which have been modified to the point that they do not resemble leaves in structure. Typically a stamen has a slender stalk (filament) and a thicker, terminal anther with two pollen sacs (microsporangia), in which the pollen grains (young male gametophytes) are produced.

The carpels, collectively constituting the gynoecium, are essentially megasporophylls. The carpels may be separate from each other, each one folded and joined at the margins to form a simple pistil, or they may all be united to form a compound pistil. A pistil is usually differentiated into three externally visible parts: the ovary, style or styles, and stigma or stigmas. The ovary, at the base, contains the ovules (essentially megasporangia, with some additional outer coats). The stigma, which receives the pollen, is usually elevated above the ovary on a slender style. Each ovule typically contains a single embryo sac, representing the female gametophyte.

Gametophyte generation. The pollen grains are transported to the stigma (often of a different flower) by one means or another, often incidentally by insects seeking nectar. Birds, bats, wind, and even water may also serve as pollinating agents for some species. Some kinds of flowers are self-pollinated, the pollen being deposited directly on the stigma as the flower develops. The pollen grain germinates on the stigma, producing a pollen tube which grows down through the style into the ovary, eventually delivering its two sperms into the embryo sac of an ovule. The ovule develops into the seed, the fertilized egg in the embryo sac develops into the embryo (young sporophyte) of the seed, the triple fusion nucleus (resulting from the fusion of the second sperm with two nuclei of the embryo sac) is the forerunner of the endosperm in the seed, and the integuments (outer coatings) of the ovule develop into the seed coat.

The endosperm typically serves as a food storage tissue for the seed, but in some kinds of seeds the food is absorbed by the embryo during early development so that the ripe seed has no endosperm. Food may also be stored in the nucellus, which is the megasporangium wall that encloses the embryo sac and is in turn largely enclosed by the integuments of the ovule. A small opening through the integuments to the nucellus in the young ovule is called the micropyle. The pollen tube may enter the ovule through the micropyle, or it may digest its way through at some other point. *See* REPRODUCTION (PLANT).

Evolutionary position. Among plants with alternation of sporophyte and gametophyte generations, the angiosperms represent the most extreme stage in reduction of the gametophyte, which in effect is reduced to a mere stage in the reproduction of the sporophyte. The pollen grain, with its associated pollen tube, and the embryo sac represent the male and female gametophyte generations; the endosperm is a new structure not referable to either generation; and the remainder of the plant throughout its life cycle is the sporophyte. Many angiosperms can also propagate asexually by means of creeping stems or roots or by other specialized vegetative structures such as bulbils.

The angiosperms are usually considered to be the most highly evolved division of the subkingdom Embryobionta. Their highly specialized and relatively efficient conducting tissues, combined with the protection of their ovules in an ovary, give them a competitive advantage over most other groups of land plants in most regions. This general advantage is reflected in their abundance and in their great diversification, with different species adapted to a wide range of ecological niches. *See* EMBRYOBIONTA.

It is obvious to biologists that the angiosperms must have evolved from gymnosperms, but beyond this the facts are obscure. They appear in the fossil record early in the Cretaceous Period as obvious angiosperms, without any hint of a connection to any particular group of gymnosperms. Many believe that among the gymnosperms the seed ferns provide the most likely ancestors. *See* PALEOBOTANY; PINOPHYTA.

Arthur Cronquist; T. M. Barkley

The Magnoliophyta consist of two large groups that have not been formally named: eudicots (formerly considered dicotyledons with triaperturate pollen, and the magnoliids (including the monocotyledons) with uniaperturate pollen. Although the difference in pollen formation has been known for

a long time, the significance was not appreciated until deoxyribonucleic acid (DNA) studies produced results that clearly reflect this difference. The eudicots are characterized by flowers that are highly organized in terms of the number and orientation of parts whereas the magnoliids have many parts without any particular fixed patterns among the parts—except for the monocots, in which the most developed groups, like the eudicots, exhibit developed flowes with highly organized patterns. *See* LILIOPSIDA; MAGNOLIOPSIDA. Mark W. Chase

Economic importance. The vast majority of conspicuous land plants with green leaves—other than the ferns and the evergreen, needle-leaved trees—are angiosperms. Their significance to humans is more than proportional to their abundance. All the important staples of the human diet are either angiosperms or are derived from animals (except for fish) which feed largely on angiosperms. In addition to food, they provide clothing and shelter and furnish raw materials for countless industrial processes. Even the air has its oxygen supply constantly replenished by angiosperms (and other plants) as a result of their food-making processes. Angiosperms are so essential to human life that they may properly be said to be the foundation of human existence. *See* PHOTOSYNTHESIS; PLANT KINGDOM. Arthur Cronquist; T. M. Barkley

Bibliography. Angiosperm Phylogeny Group (K. Bremer, M. W. Chase, and P. Stevens, eds.), An ordinal classification for the families of flowering plants, *Ann. Missouri Bot. Garden*, 85:531–553, 1998; A. Cronquist, *The Evolution and Classification of Flowering Plants*, 1968; A. Cronquist, *Integrated System of Classification of Flowering Plants*, 1981; A. Cronquist, *Introductory Botany*, 1961; A. Eames, *Morphology of Angiosperms*, 1961; P. Maheshwari, *An Introduction to the Embryology of Angiosperms*, 1950.

Magnoliopsida

One of the two classes of flowering plants which collectively make up the division Magnoliophyta (Angiospermae). The Magnoliopsida, often known as Dicotyledoneae or dicotyledons, embrace 6 subclasses, 64 orders, 318 families, and about 165,000 species.

All of the characters which collectively distinguish the Magnoliopsida from the Liliopsida (monocotyledons) are subject to exception, but in general the Magnoliopsida have two cotyledons and net-veined leaves. The vascular bundles are typically borne in a ring (or cylinder) enclosing a pith. Increase in thickness of stems and roots, after the primary tissues have matured, results from meristematic activity of a cambial layer which passes through the vascular bundles. In about half of the species of the group, the cambium of the stem forms a continuous cylinder which produces a new layer of wood (secondary xylem) and bark (secondary phloem) each growing season for year after year. Such plants become trees or shrubs.

Some other species have an active cambium and are potentially woody, but the stem or the whole plant dies at the end of the year. In still other species the cambium is confined to the vascular bundles and produces relatively little secondary tissue, or there may be no cambium at all. The root system in many species is derived wholly from the primary root; in others it is partly or wholly adventitious.

The floral parts of dicotyledons, when of definite number, are most often borne in sets of five, less often four, and seldom only three (except that there are often only two carpels, or even only one). The pollen is typically triaperturate or of triaperturate-derived type, except in a few of the more primitive families in which it is uniaperturate.

It is widely agreed that the most existing angiosperms belong to the dicotyledons (especially the order Magnoliales) and that most of the characters which distinguish the monocotyledons as a group are derived rather than primitive. *See* ASTERIDAE; CARYOPHYLLIDAE; DILLENIIDAE; HAMAMELIDAE; LILIOPSIDA; MAGNOLIALES; MAGNOLIIDAE; MAGNOLIOPHYTA; PLANT KINGDOM; ROSIDAE.

Arthur Cronquist; T. M. Barkley

Magnon

A quantum of a spin wave; an elementary excitation of a magnetic system which is usually long-range-ordered, such as a ferromagnet. *See* ANTIFERROMAGNETISM; FERRIMAGNETISM; FERROMAGNETISM.

In the lowest energy state of a simple ferromagnet, all the magnetic moments of the individual atoms are parallel (say, to the z axis). Each atomic moment derives mainly from the electron spin angular momentum of the atom. In the next-to-lowest energy state (first excited state), the total z component of spin angular momentum, S_z, is reduced by one unit of $\hbar = h/2\pi$, where h is Planck's constant. In the case of a crystalline material, this unit is shared equally by all the spins, each of which lies on a cone (see **illus.**), precessing at an angular rate ω. These spins form a wave, known as a spin wave, having a repeat distance or wavelength, λ. The wave amplitude (that is, the cone angle) is extremely small, because of the sharing among all the spins whose number N is very large, roughly 10^{23}. Thus, each atom's share of the reduction in S_z, labeled Δ, is only $\hbar/N$, whereas the z component of the atomic spin in the fully aligned state is typically 1–10 times $\hbar$. It follows from simple geometry that the cone half-angle is of order 10^{-11} to 10^{-12} radian. The state with this value of the amplitude is said to be a one-magnon state with wave number $k = 1/\lambda$. If Δ is doubled to $2\hbar/N$, the state is a two-magnon state, and so forth. The integer values of $N\Delta/\hbar$ correspond to the possible changes in S_z being integral multiples of $\hbar$. *See* ELECTRON SPIN; WAVE MOTION.

While the spin waves associated with energy states, that is, stationary states, in crystals vary

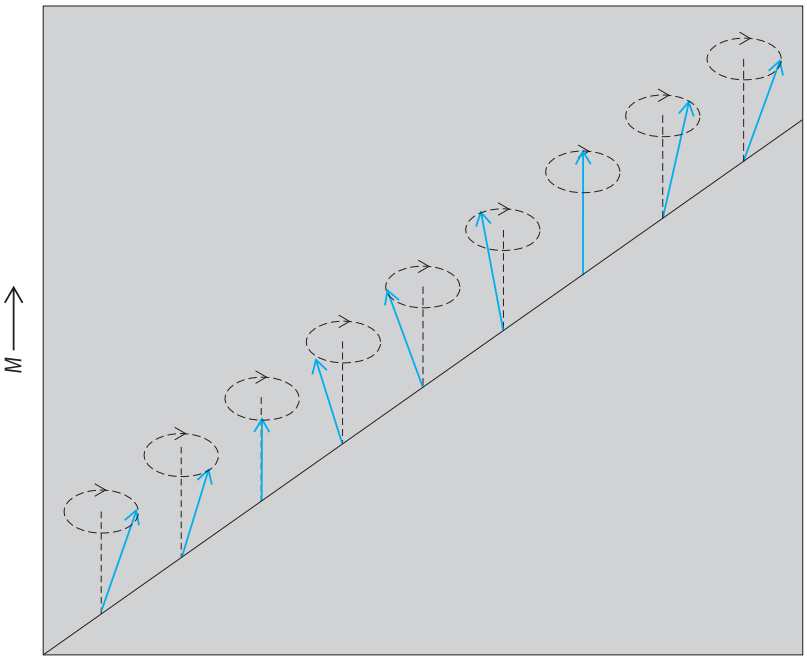

Spin wave in a linear ferromagnetic array of precessing atomic spins of equal magnitude, represented as arrows (vectors) in perspective. The axis of precession is along the vertical direction of the total magnetization, *M*.

sinusoidally in space (see illus.), magnons can be associated, instead, with nonstationary states (wave packets) in some situations. Closely analogous to magnons are phonons and photons, quanta of mass-density waves and electromagnetic waves, respectively. *See* ELECTROMAGNETIC WAVE; PHONON; PHOTON; QUANTUM MECHANICS.

Energy of magnon states in ferromagnets. For a ferromagnet the energy is minimum when the spins are parallel; in the spin-wave state shown (see illus.), the energy is raised by an amount ΔE that depends both on the wavelength and on the amplitude. In the Heisenberg model where the energy (called exchange energy) is proportional to the cosine of the angle between neighboring spins, ΔE for one-magnon states is proportional to k^2 when the wave number (k) is small (that is, for long wavelengths). To determine this energy more generally, it is usually necessary to resort to approximations. A rather broadly applicable one is the semiclassical spin-wave approximation, which assumes that the x and y components of the spins are much smaller than the z components. Then ΔE for an n-magnon state with wave number k is $n\epsilon_k$, where ϵ_k is the energy increase for a single-magnon state. The linear dependence on n follows from the energy being proportional to the cosine of the angle between neighboring spins, $\mathbf{S}_1$ and $\mathbf{S}_2$, or to $\mathbf{S}_1 \cdot \mathbf{S}_2$, with the two spins lying on the surface of the cone, and the cone angle being extremely small. Then (see illus.) it is found that $\mathbf{S}_1 \cdot \mathbf{S}_2 - S^2$ is proportional to the square of the cone angle, which is linear in n. Also, the energy, ϵ_k, of a single-magnon state is equal to $\hbar\omega$, where ω is the precession frequency. When there are magnons with different wave numbers (k) simultaneously present, it is found that they contribute additively to the total increase in energy.

Energy in other magnets. For magnons in antiferromagnets and ferrimagnets, the properties observed in ferromagnets still hold, with two principal exceptions, as follows:

1. The excitation energy ϵ_k can be very different. For example, in antiferromagnets, ϵ_k is proportional to k when k is small, rather than k^2; for ferrimagnets the lowest values of ϵ_k go as k^2.

2. Whereas in the ground state of a Heisenberg ferromagnet each atomic spin has its maximum allowed z component (S), in an antiferromagnet or ferrimagnet this full value cannot be achieved, the expectation value being reduced from S in general. In the latter ground states, the number of magnons present is still zero, but there is a nonzero cone angle φ_0 for each spin. Excited states have nonzero values of the magnon numbers, n_k, as with ferromagnets, which now increase the cone angles beyond the zero-point value φ_0. The ground-state reduction of the z component of each spin is said to be due to zero-point quantum spin fluctuations, in close analogy to zero-point lattice vibrations and vacuum fluctuations of the electromagnetic field (related to phonons and photons, respectively). *See* LATTICE VIBRATIONS; QUANTUM ELECTRODYNAMICS.

These concepts of magnon or spin-wave theory have been applied with remarkable success to many experimentally observed properties.

Thermal properties. The fact that magnons with different wave numbers contribute additively to the total energy increase, plus the fact that the numbers n_k of magnons with wave number k take on the values 0, 1, 2, . . . , imply that the average values of the magnon numbers, denoted $\langle n_k \rangle$, in thermal equilibrium at absolute temperature T, are given by the Bose-Einstein distribution. For this reason, magnons can be considered particles of the type called bosons. From the values of $\langle n_k \rangle$ are found the internal energy and therefore the specific heat. Also, for a ferromagnet, for example, the average spin, $\langle S_z \rangle$, can be found. These results imply particular behaviors with T at low temperature, depending on the form of ϵ_k at small k, and the dimensionality of the structure. For a typical ferromagnet or ferrimagnet with essentially three-dimensional bonding, for example, the cubic materials europium oxide (EuO) and magnetite (Fe_3O_4), the decrease in $\langle S_z \rangle$ from S is proportional to $T^{3/2}$. The magnetic specific heat for these cases is proportional to $T^{3/2}$, whereas for cubic antiferromagnets the magnetic specific heat goes as T^3. *See* BOSE-EINSTEIN STATISTICS; SPECIFIC HEAT OF SOLIDS; STATISTICAL MECHANICS.

Neutron scattering. Elastic or Bragg scattering of neutrons via their magnetic moment helps determine the type of ordering of the atomic moments, while inelastic scattering measures the magnon energy ϵ_k. The particle nature of magnons is reinforced by the fact that the assignment of momentum a $\hbar$ (related to $\vec{k}$) to a magnon leads to the conservation of energy and momentum of the system of neutron

and magnons in the scattering process. The intensities of the Bragg peaks are related to the strength of the ordered moments; they consequently give information about the zero-point spin fluctuations. These are particularly large in the antiferromagnets La_2CuO_4 and $YBa_2Cu_3O_4$ (the insulating parents of high-temperature superconductors) due to the essentially two-dimensional structure of these layered materials and the fact that for the magnetic ion (Cu^{2+}), $S = {}^1/_2$, the smallest possible nonzero value. *See* NEUTRON DIFFRACTION; SLOW NEUTRON SPECTROSCOPY; SUPERCONDUCTIVITY. Thomas A. Kaplan

Bibliography. C. Kittel, *Introduction to Solid State Physics*, 7th ed., 1996; D. C. Mattis, *The Theory of Magnetism*, 2d ed., 1987.

Mahogany

A hard, red or yellow-brown wood which takes a high polish and is extensively used for furniture and cabinetwork. The West Indies mahogany tree (*Swietenia mahagoni*), a native of tropical regions in North and South America, is a large evergreen tree with smooth pinnate leaves (see **illus.**). Together

Leaf and fruit of the West Indies mahogany (*Swietenia mahagoni*).

with other species it yields the world's most valuable cabinet wood. Varieties with ornamental figures in the grain are highly prized. In the United States it occurs naturally only in the extreme southern tip of Florida, but it is planted elsewhere in the state as an ornamental and shade tree. The cigarbox or West Indian cedar (*Cedrela odorata*) belongs to the same family. *See* FOREST AND FORESTRY; GERANIALES; TREE. Arthur H. Graves; Kenneth P. Davis

Maillard reaction

A nonenzymatic chemical reaction involving condensation of an amino group and a reducing group, resulting in the formation of intermediates which ultimately polymerize to form brown pigments (melanoidins). It was named for the French biochemist Louis-Camille Maillard, who published initial studies of the reaction between 1912 and 1916. The reaction is of extreme importance to food chemistry, especially because of its ramifications in terms of food quality. *See* AMINE; REACTIVE INTERMEDIATES.

Mechanism. There are three major stages of the reaction. The first comprises glycosylamine formation and rearrangement to *N*-substituted-1-amino-1-deoxy-2-ketose (Amadori compound). The second phase involves loss of the amine to form carbonyl intermediates, which upon dehydration or fission form highly reactive carbonyl compounds through several pathways. Three of these pathways are given in the **illustration**.

Pathway (1) leads to the formation of fission product reductones such as pyruvaldehyde, diacetyl, and hydroxyacetone; pathway (2) forms 2-furfural or its derivatives by dehydration; and pathway (3) is responsible for forming flavor compounds such as maltol, isomaltol, and 4-hydroxy-5-methyl-3(2H)-furanone by dehydration.

Another degrading pathway is the Strecker degradation of amino acids by α-dicarbonyls produced in the above pathways, which by decarboxylation and oxidation forms aldehydes with one less carbon atom than the original amino acid.

The third phase of the Maillard reaction occurring upon subsequent heating involves the interaction of the carbonyl flavor compounds (see illus.) with other constituents to form brown nitrogen-containing pigments (melanoidins) by aldol condensation, carbonyl-amine polymerization, and the production of *N*-, *O*-, and *S*-heterocyclic compounds such as furans, furanones, pyrazines, thiazoles, thiophenes, oxazolines, and polysulfides responsible for heated-food flavors (corny, nutty, bready, and roasted). These are highly desirous compounds in certain foods browned by heating in the presence of oxygen.

Antioxidant properties. Melanoidins or pre-melanoidins resulting from heating various sugar-amine mixtures have strong antioxidant properties in certain lipid mixtures. The use of these high-molecular-weight compounds and their intermediates have tremendous potential as antioxidants in food systems. *See* ANTIOXIDANT.

Undesirable aspects. The Maillard reaction is considered undesirable in some biological and food systems. The interaction of carbonyl and amine compounds might damage the nutritional quality of proteins by reducing the availability of lysine and other essential amino acids and by forming inhibitory or antinutritional compounds. The reaction is also associated with undesirable flavors and colors in some foods, particularly dehydrated foods. Some of the Maillard interaction products are also possibly toxic to animals. Maillard-type carbonyl–amine reactions in living organisms have specific physiological effects that may influence human health.

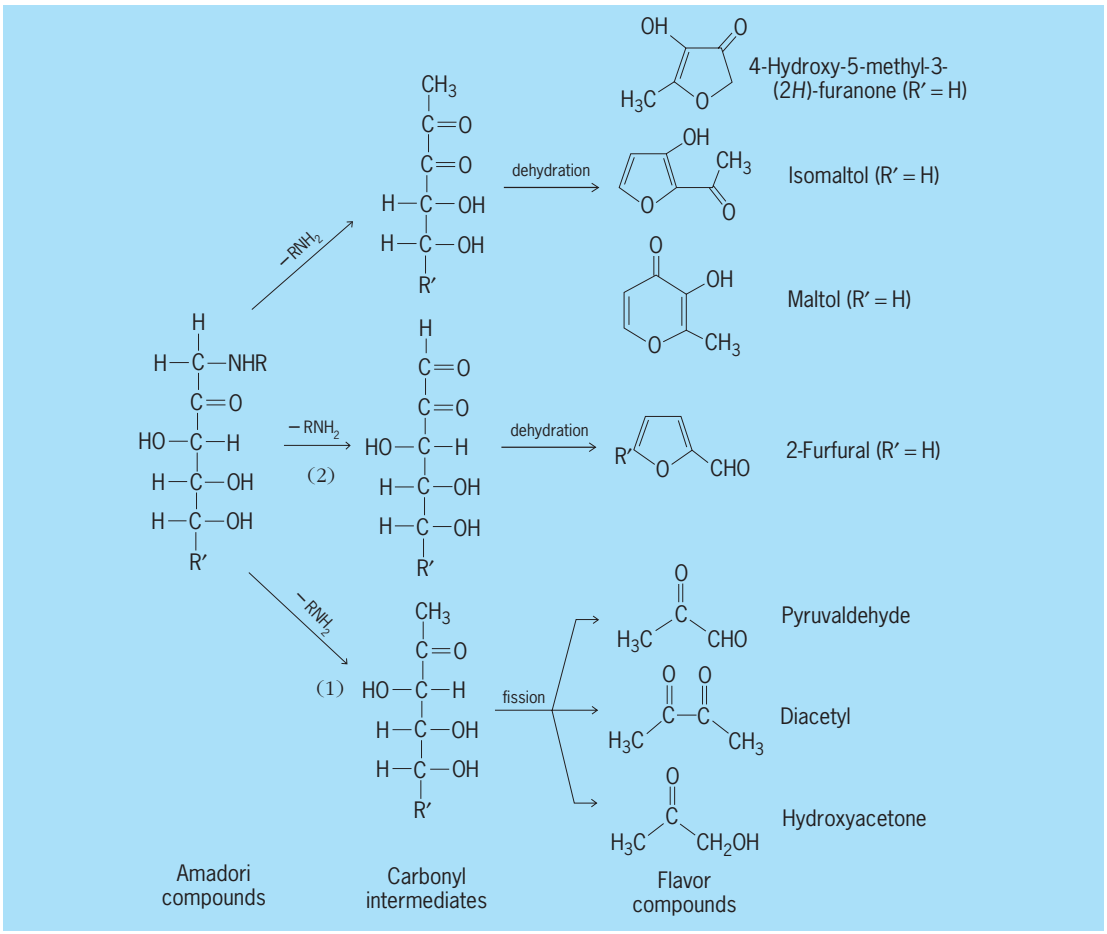

Degradation of Amadori compounds to carbonyl intermediates in Maillard browning reactions.

See AMINO ACIDS; CARBONYL; FOOD MANUFACTURING.

Milton E. Bailey

Bibliography. C. E. Eriksson, Maillard reactions in food, *Prog. Food Nutrit. Sci.*, vol. 5, 1981; P. A. Finot et al. (eds.), *The Maillard Reaction in Food Processing, Human Nutrition, and Physiology*, 1990; T. M. Reynolds, Chemistry of nonenzymic browning II, *Adv. Food Res.*, 14:167–283, 1965; R. Waller and M. S. Feather, *The Maillard Reaction in Foods and Nutrition*, ACS Symp. Ser. 215, 1982.

Maintenance, industrial and production

The actions taken to preserve the operation of devices, particularly of electromechanical equipment, to ensure that the devices can perform their intended functions when needed. The field of maintenance science is an interdisciplinary research area that employs techniques from physics, engineering, and decision analysis to develop methods for the safe and reliable performance of devices and equipment. Traditionally, the focus of maintenance has been on equipment availability—the ratio of operating time less downtime to total available time. Modern maintenance practices focus on increasing equipment effectiveness, that is, making sure that the equipment is both available and capable of producing superior-quality products. *See* SYSTEMS ENGINEERING.

Life-cycle considerations. It has been estimated that up to 50% of all life-cycle equipment costs are attributable to operation and maintenance. As customers recognize that their options are to "pay now" (higher purchase price) or "pay later" (increased maintenance costs), maintenance considerations are increasingly important at the design phase. Equipment buyers are now requiring better information on time to failure and repair. Suppliers have responded by including such things as failure mode and effects analysis, statistical information on failure times, cost-effective maintenance procedures, and better customer training with their products. Additionally, many companies emphasize design enhancements to improve maintainability, such as built-in diagnostics, greater standardization and modularity, and improved component accessibility. While these enhancements may add to the purchase price of equipment, in most cases they more than offset this price in reduced operating and maintenance costs over the equipment's life cycle. *See* ENGINEERING DESIGN; MACHINE DESIGN.

Categories of maintenance activities. Maintenance activities can be classified into several broad

categories, depending on whether they respond to failures that have occurred or whether they attempt to prevent failures.

Reactive maintenance. The simplest and least sophisticated maintenance strategy still used by many companies is reactive maintenance or breakdown maintenance. Equipment is operated until it fails, then repaired or replaced. No effort is expended on activities that monitor the ongoing "health" of the equipment, and maintenance is focused on quick repairs that return the equipment to production as soon as possible. This type of maintenance has two significant drawbacks: (1) repairs are unpredictable and often result in significant unplanned downtime, and (2) equipment often experiences accelerated degradation as a result of interactions at the subsystem or component level within the equipment.

Preventive maintenance. A slightly more sophisticated maintenance strategy is preventive maintenance, also known as calendar-based maintenance. This system involves detailed, planned maintenance activities on a periodic basis, usually monthly, quarterly, semiannually, or annually. As in reactive maintenance, preventive maintenance does not monitor information on equipment status. Rather, it attempts to avoid unplanned failures through planned repairs or replacements. The advantage to this strategy is that one knows in advance when repairs are to be made, but a big drawback is that properly working components may actually be replaced with defective ones. Moreover, operating equipment is taken offline while such repairs are made, and a large spare parts inventory may be required.

Predictive maintenance. Also known as condition-based maintenance, predictive maintenance is based on an ongoing (continuous or periodic) assessment of the actual operating condition of equipment. The equipment is monitored while in operation, and repair or replacement is scheduled only when measurements indicate that it is required. Predictive maintenance programs seek to control maintenance activities to avoid both unplanned equipment outages and unnecessary maintenance and overhauls. An important aspect of predictive maintenance strategies is the use of sophisticated sensoring technologies in combination with data-driven models to characterize equipment degradation. Among the new sensoring technologies for monitoring critical parameters are acoustic sensors for vibration analysis, microelectronic devices for gas analysis, sensors for oil wear analysis, infrared thermography to locate aberrantly high temperatures indicative of excessive wear, ultrasound for detection of incipient cracks, fiber optics for strain gauge measurements, high-speed video, and laser alignment. *See* FIBER-OPTIC SENSOR; MICROSENSOR.

Industry-driven maintenance initiatives. The importance of equipment maintenance for product quality and plant safety has long been recognized. Recently, industry has begun to understand the impact of maintenance practice on the broader elements of manufacturing productivity, such as factory output and product cycle time, as well as on product yield. In equipment-intensive industries, such as the semiconductor industry and the electric utility industry, even small improvements in equipment use can result in an immediate competitive advantage.

Reliability-centered maintenance. Developed in the late 1960s by the aerospace industry, and since then widely adopted in the passenger airline industry and in the nuclear power industry, reliability-centered maintenance (RCM) involves the use of reliability methods, such as failure mode, effects and criticality analysis (FMECA), to identify and prioritize component failures in a systematic and structured way. Key equipment components are then selected and monitored, and appropriate maintenance actions are determined for all components based on cost, safety, environmental, and operational requirements. The rationale behind reliability-centered maintenance is that most vendor-supplied recommendations for fixed, time-in-service maintenance intervals are overly conservative, and are applied to individual components without consideration of their overall system functions. The focus of reliability-centered maintenance is on failure "triage," that is, on identifying and avoiding machine conditions that are likely to be the most serious and lead to expensive equipment failures. For critical equipment, reliability-centered maintenance replaces fixed maintenance intervals with intervals that depend on use and condition, as determined by analysis of past performance and machine diagnostics. For noncritical equipment, cost analysis is performed to determine an appropriate balance between reactive and preventive maintenance. Maintenance tasks are not performed unless they affect system availability, safety, or overall cost. Companies that have introduced reliability-centered maintenance report significant savings in maintenance costs and improved equipment effectiveness. Moreover, the data collected as part of the reliability-centered maintenance program are valuable in guiding ongoing maintenance improvements.

Total productive maintenance. Total productive maintenance (TPM), developed in Japan in the 1980s, has been adopted by many industries, notably by semiconductor manufacturers. The development of total productive maintenance stems from the recognition that production-level cost, inventory, safety, and product quality depend directly on equipment performance. The goals of total productive maintenance—zero unplanned downtime, zero equipment-caused product defects, and zero loss of equipment speed—are approached via a continuous improvement strategy that involves all workers. Managers, engineers, production operators, and maintenance personnel are organized into small autonomous groups and charged with maintenance responsibility for a machine or set of machines. Machine operators are assigned certain routine maintenance tasks, such as cleaning, lubrication, calibration, and bolt tightening, while maintenance personnel have responsibility for larger, less frequent tasks, such as overhauls and component replacements. Their activities are directed toward five

main categories of equipment losses that reduce equipment effectiveness: set-ups and adjustments, equipment failures, idling and minor stoppages, reductions in equipment speed, and process defects. Total productive maintenance prescribes a data collection strategy that ensures a consistent set of metrics and allows groups to prioritize improvements.

Integrated production operations. As the impact of equipment maintenance on plant productivity has become better understood, recent interest has focused on integrating production and maintenance decisions. While the initiatives described above have been successful in reducing processing time variability due to unplanned equipment downtime, maintenance activities are still largely scheduled independently of the production status (the amount and location of work) of the plant. As a result, planned maintenance activities have the potential for significant disruptions in product flow. Many companies now employ strategies to execute maintenance activities "opportunistically," that is, when production status allows, subject to achieving certain performance objectives. The performance objective may involve meeting targeted equipment availability or minimizing total expected production and maintenance costs. The long-term goal of this approach is to develop controllers that schedule appropriate production and maintenance actions based on the combined input of a shop-floor control system and condition-monitoring sensors. Georgia-Ann Klutke

Bibliography. B. S. Blanchard, D. Verma, and E. L. Peterson, *Maintainability: A Key to Effective Serviceability and Maintenance Management*, Wiley, New York, 1995; J. Douglas, The maintenance revolution, *EPRI J.*, January–February 1995; R. K. Mobley, *An Introduction to Predictive Maintenance*, Van Nostrand Reinhold, New York, 1990; S. Nakajima, *Introduction to TPM*, Productivity Press, Cambridge, MA, 1988; A. M. Smith, *Reliability-Centered Maintenance*, McGraw-Hill, New York, 1993.

Malachite

A bright-green, basic carbonate of copper [$Cu_2CO_3(OH)_2$]. Malachite is the most stable copper mineral in natural environments in contact with the atmosphere and hydrosphere. It occurs as an ore mineral in oxidized copper sulfide deposits; as a stain on fractures in rock outcrops; as a corrosion product of copper and its alloys (except in industrial-urban environments, where the basic copper sulfate dominates); as suspended particles in streams and in alluvial sediments; and as encrustations on bronze artifacts in seawater and on coccoliths floating in the oceans. It can be distinguished from other green copper minerals by its effervescence in acid. The combination of hardness (3.5–4 on Mohs scale) ideal for carving, color variation in concentric layers, and adamantine-to-silky luster has made malachite a highly prized ornamental stone. Its rare blocky-tabular crystals up to 5 mm (0.2 in.), its pseudomorphs after azurite crystals to 2 cm (0.8 in.), and its more common felty tufts perched on bright blue azurite are eagerly sought by mineral collectors.

Malachite is an important copper ore mineral in supergene copper oxide deposits formed by weathering of primary copper sulfide deposits. The high acidity necessary for dissolution of sulfide minerals and solution transport of copper (pH = 2–3) occurs with the oxidation of pyrite followed by generation of sulfuric acid in the unsaturated zone above the water table. Malachite, stable in oxidized ground waters at pH > 5, readily precipitates in large amounts in places where copper-laden, acidic waters from a nearby sulfide deposit encounter a neutralizer that also can supply carbonate ion, such as limestone wall rocks or calcite gangue. If cupric solutions are neutralized in the absence of carbonate, chrysocolla ($CuSiO_3 \cdot 2H_2O$) or tenorite (CuO) may form; in arid climates, the soluble basic copper sulfates are stable (chalcanthite, antlerite, brochantite). Azurite may form rather than malachite if the concentration of carbon dioxide (CO_2) gas is high (as in soils producing CO_2 by oxidation of organic matter) or if the relative humidity is low (as in arid climates), as shown by the reaction below.

$$\underset{\text{Malachite}}{3Cu_2CO_3(OH)_2} + \underset{\text{Carbon dioxide}}{CO_2} \longrightarrow \underset{\text{Azurite}}{2Cu_3(CO_3)_2(OH)_2} + \underset{\text{Water}}{H_2O}$$

Copper oxide deposits with malachite as an important ore mineral include N'Changa and Chambishi in the Zambian copperbelt, Tsumeb in Namibia, Mount Isa in Australia, Bisbee in Arizona, and oxidized portions of copper-bearing skarn and vein deposits in limestone throughout the world. *See* AZURITE; CARBONATE MINERALS; COPPER. Marco T. Einaudi

Bibliography. L. L. Y. Chang, R. A. Howie, and J. Zussman, *Rock Forming Minerals,* vol. 5B: *Nonsilicates: Sulfates, Carbonates, Phosphates, Halides*, 1995; C. Palache, H. Berman, and C. Frondel, *The System of Mineralogy of James Dwight Dana and Edward Salisbury Dana*, 7th ed., vol. 2, 1951.

Malacostraca

The largest and most diversified class of the Crustacea; includes the shrimps, lobsters, crabs, sow bugs, beach hoppers, and their allies. The shell or carapace may be large, small, vestigial, or absent; the tail or abdomen is long or short; the eyes are generally set on movable stalks but may be sessile or even coalesced. Despite this diversity, the unity of the group is demonstrated by the following characteristics which all share. The maximum number of appendages is 19 pairs, even where there is an additional body segment such as is found in the Phyllocarida and embryonic Mysidacea. The trunk limbs are sharply differentiated into a thoracic series

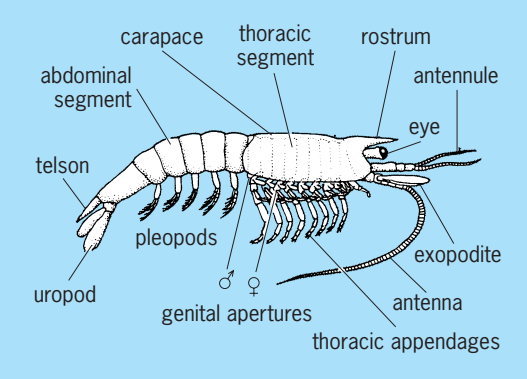

Fig. 1. Caridoid facies. (*After E. R. Lankester, ed., A Treatise on Zoology, pt. 7, fasc. 3, A. and C. Black, 1909*)

of eight pairs and an abdominal series of six pairs. The female genital duct always opens at the level of the sixth thoracic segment, whereas those of the male open at the level of the eighth. Additionally, the frontal organs of malacostracans differ significantly from nonmalacostracans. Even greater, more fundamental differences between malacostracans and nonmalacostracans have been found in their compound eyes.

Classification. Malacostraca are divided into three subclasses, the Phyllocarida, Hoplocarida, and Eumalacostraca. Central to the classification of the Eumalacostraca has been the concept of the "caridoid facies" (**Fig. 1**). This term refers to a series of morphological attributes generally common to the three orders, Syncarida, Peracarida, and Eucarida. Those attributes are a well-developed carapace covering the cephalothorax; stalked and movable eyes; biramous antennules; the exopod of the antenna developed as a blade or scale; natatory exopods on the thoracic appendages; a long, ventrally flexing abdomen; and a tail fan formed by the uropods and telson. Other shared characteristics include a complex set of intertwining abdominal muscles that provide the flexing mechanism seen in escape reactions, internal organs located primarily in the thorax, and a similarity in pleopod structure and function. *See* EUCARIDA; PERACARIDA; SYNCARIDA.

Although they share some of the more primitive aspects of the caridoid facies, the Phyllocarida are distinguished by their retaining the primitive condition of a seventh abdominal somite, the presence of caudal rami on the telson, and a bivalve shell-like carapace held together by an adductor muscle. Similarly, aspects of Hoplocarida morphology have led some researchers to suggest the Hoplocarida represents another lineage within the Malacostraca that has evolved independently of the Eumalacostraca.

Evolution. The first unequivocal malacostracan fossil is that of a phyllocarid. Comparative functional morphology of extant malacostracans, however, suggests that the phyllocarids, and the hoplocarids as well, were early offshoots from the basically eumalacostracan stem. Although conflicting theories regarding a eumalacostracan precursor are numerous, it is probable that possession of a carapace represents the primitive condition and its loss in such groups as the Syncarida and some Peracarida is a derived condition. Other caridoid features, such as the antennal scale, tail fan, and abdominal musculature, appear to have played important roles in eumalacostracan evolution, but radiation also seems to have been dependent upon a change in feeding strategies from primitive thoracopodan phyllopod filter feeding to maxillary feeding and concurrent development of the stenopodial limb for locomotion. The more anterior (thoracic) and more posterior (abdominal) appendages have become specialized, whereas the central pairs, which are also thoracic, have developed as locomotory limbs. Walking legs, for example, have evolved through the reduction or loss of the exopod.

Terminology. The terminology applied to the thoracic appendages and their segments in the various orders differs widely. From one to three of the anterior pairs may be called maxillipeds and the other seven to five pairs pereopods. The second and third (rarely also the fourth) pairs in some orders are known as gnathopods. In Stomatopoda the first five pairs are often termed maxillipeds, although gnathopods would be more appropriate. The abdominal appendages are called pleopods, unless they are modified for reproductive purposes. In the latter, they are referred to as gonopods.

The basis malacostracan appendage is made up of a basal protopod and two terminal rami. The protopod is usually divided into a coxa and a basis, one or both of which may have mesial (endites) or

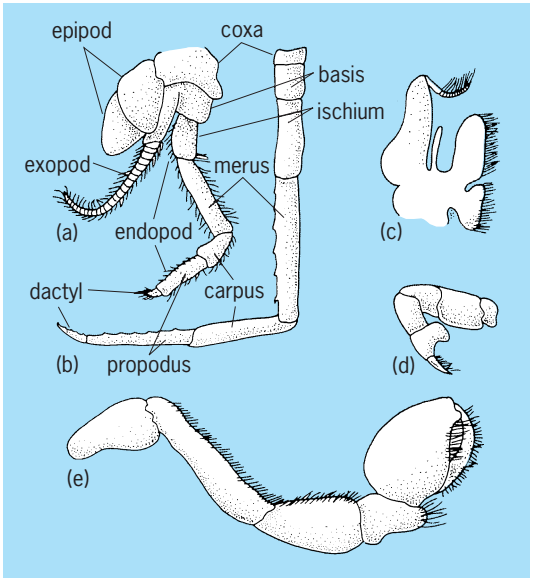

Fig. 2. Representative malacostracan thoracic appendages: (*a*) biramous ambulatory thoracic appendage of an Anaspidacea; (*b*) uniramous thoracic walking leg of a Stenopodidea; (*c*) first maxilliped of a Paguroidea; (*d*) third maxilliped of a Thalassinoidea; (*e*) raptorial appendage ("maxilliped") of a Stomatopoda. (*After P. A. McLaughlin, Comparative morphology of crustacean appendages, in L. G. Abele, ed., The Biology of Crustacea, vol. 2: Embryology, Morphology, and Genetics, Academic Press, 1982*)

lateral (epipods) protrusions. An exception exists in the Stomatopoda, where a precoxal segment may also present. Endites function primarily in food transport or in mastication; epipods, on the other hand, most often are specialized as respiratory structures, or gills. The exterior ramus (exopod), if not reduced or absent, consists of two segments, with the distal segment often multiarticulate or annulated. Exopods may be modified for feeding or for facilitating movement in water, but more often they function as swimming appendages. The inner ramus (endopod) is usually the best developed and consists of five segments: ischium, merus, carpus, propodus, and dactyl (**Fig. 2**). The endopods may be unspecialized locomotive limbs or may be transformed into highly specialized appendages used in sensory detection, feeding, grasping, walking, or burrowing. *See* CRUSTACEA; EUMALACOSTRACA; HOPLOCARIDA; PHYLLOCARIDA. Patsy A. McLaughlin

Bibliography. L. G. Abele (ed.), *The Biology of Crustacea*, vol. 2: *Embryology*, *Morphology*, *and Genetics*, 1982; F. R. Schram (ed.), *Crustacean Phylogeny*, *Crustacean Issues*, vol. 1, 1983.

Malaria

A disease caused by members of the protozoan genus *Plasmodium*, a widespread group of sporozoans that parasitize the human liver and red blood cells. Four species can infect humans: *P. vivax*, causing vivax or benign tertian malaria; *P. ovale,* a very similar form found chiefly in central Africa that causes ovale malaria; *P. malariae,* which causes malariae or quartan malaria; and *P. falciparum,* the highly pathogenic causative organism of falciparum or malignant tertian malaria. Malaria is characterized by periodic chills, fever, and sweats, often leading to severe anemia, an enlarged spleen, and other complications that may result in loss of life, especially among infants whose deaths are almost always attributed to falciparum malaria. The infective agents are inoculated into the human bloodstream by the bite of an infected female *Anopheles* mosquito, more than 60 species of which can carry the infection to humans. The disease is found in all tropical and some temperate regions, but it has been eradicated in North America, Europe, and Russia. Despite control efforts, malaria has probably been the greatest single killer disease throughout human history and continues to be a major infectious disease. An estimated 1 million children die of malaria in Africa each year, and estimates of the world's malaria death toll vary from 1.5 to 2 million cases annually. *See* EPIDEMIC.

Life cycle. The vast reproductive capacity of *Plasmodium* parasites is illustrated by their life cycle, which begins as a series of asexual divisions in human liver and then red blood cells. Transfer of the parasites to the mosquito host depends on the rate of sexual multiplication that begins in the infected human red blood cells and is completed in the mosquito stomach, followed by asexual multiple division of the product of sexual fusion. During the developmental stage, enormous numbers of the sporozoites are produced in cysts massed on the stomach wall of the mosquito. These elongated microscopic forms break out of their cysts and concentrate in the mosquito salivary glands, from which they are pumped into another human when the mosquito next takes a blood meal. In a matter of minutes, the sporozoites enter human liver cells, where they divide many times in each infected cell. However, this does not initiate any host recognition or disease response. The progeny, called merozoites, burst out of the infected liver cells and may invade more liver cells for another generation or two, but most leave the liver and invade red cells in the bloodstream. Only then does the body respond with fever and other symptoms associated with the disease.

Clinical malaria usually begins 7–18 days after infection with sporozoites. Progression to that phase is most rapid with *P. falciparum* and slowest with *P. malariae*. In *P. vivax* and *P. ovale,* some of the invading sporozoites from the infective mosquitoes enter liver cells but do not develop or divide. These "sleeping" parasites (hypnozoites) can remain unchanged for months or years. They eventually grow, divide, and infect the blood cells to initiate bouts of clinical malaria up to 3 years after the initial infection (relapse malaria). Red cell infections tend to follow a remarkably synchronous division cycle. The parasite progresses from merozoite to a vegetative phase (trophozoite) to a division stage (schizont), ending with the new generation of merozoites ready to break out in a burst of parasite releases and initiate the chills–fever–sweat phase of the disease. This symptomatic period takes place in a 48-h pattern, at the start of the third day (hence tertian), with *P. vivax* and *P. ovale.* With *P. falciparum,* an extended fever phase occurs during the 48-h cycle, with the fever lasting 1–8 h rather than 30 min to 1 h, as in the others. *Plasmodium malariae* has a 72-h, or quartan (at the start of fourth day), periodicity. Synchronous schizogony continues for 3 to 6 weeks, up to about 3 months, depending upon the host's acquired or genetic resistance. *See* HAEMOSPORINA; SPOROZOA.

Clinical malaria. Clinical malaria begins with the erythrocytic cycle, and the sequence of chills, fever, and sweats is the result of simultaneous red cell destruction at 48- or 72-h intervals. Bouts of chills and fever often begin irregularly but usually revert to the synchronous pattern. *Plasmodium falciparum* is the most uncertain and variable of the four species, and it is by far the most dangerous. The period from infective mosquito bite to onset of symptoms (incubation period) varies from about 12 days for falciparum malaria (range 6–25 days), to 14 days (range 8–27 days) for vivax and ovale malaria, to 4 weeks (range 16 days–8 weeks) for quartan malaria. The incubation period may be extended to several months with resistant or partially resistant falciparum malaria when prophylactic drugs have been used. Early symptoms, usually 1 or 2 days before the start of an acute attack, include headache, low fever

with chills, and muscle aches and pains. The full attack generally begins with shaking chills, followed by intermittent fever bouts up to 105.8°F (41°C), followed by the 1–2-h sweating stage. The entire attack usually lasts 4–8 h, the longer period usually due to *P. falciparum*. Associated signs and symptoms may include severe headache, abdominal pain with nausea and sometimes forceful vomiting, joint pain, extreme fatigue, and various signs and symptoms that suggest a number of other conditions. Hence, malaria is frequently called the great mimic. High fever with chills and headache are the most consistent symptoms. After about a week, a soft, enlarged, and sometimes tender spleen can usually be detected. The liver may also become enlarged and tender. Between malarial bouts, the patient is fatigued but usually asymptomatic.

A thick blood smear is preferred for diagnosing malaria, but a thin blood smear is essential for reaching a definitive or species diagnosis, particularly for identifying a life-threatening case of falciparum malaria. Frequently, many smears must be made at various periods of the erythrocytic cycle to confirm the diagnosis.

Pathogenesis. The destruction of red cells results in anemia, which is the most characteristic cause of malarial pathology. An enlarged spleen develops because the spleen has the burden of filtering out the many red cells that are burst or damaged because of the disease, as well as removing the characteristic pigment clusters that are present in all red cells infected with *Plasmodium*. Fatalities from falciparum malaria can be directly traced to any or all of three factors: (1) destruction of stem cells in the bone marrow; (2) infection of large numbers of red cells (50,000–2,000,000 or more infected cells per cubic millimeter of blood, rather than the 10,000–35,000 that is indicative of the other three species); and (3) induction of "knobby" or sticky infected red cells, which then adhere to endothelial linings of blood vessels. Should the stickiness lead to vessel blockage in the brain, cerebral malaria, the primary cause of death, can rapidly result from brain anoxia. Similar blockage of essential circulatory vessels in the intestine, lungs, liver, and kidneys can also cause rapid death from falciparum malaria. Death may follow this severe form of attack in 6–12 h. Hence, falciparum malaria should be considered a medical emergency.

Chemotherapy. Chloroquine remains the drug of choice for prevention as well as treatment of vivax, ovale, and malariae malaria. However, most strains of falciparum malaria have become strongly chloroquine-resistant, with the sole remaining chloroquine-sensitive areas being the Caribbean region and the Arabian peninsula.

For prevention of chloroquine-resistant falciparum malaria (and in some areas vivax malaria is now chloroquine-resistant as well) a weekly dose of mefloquine beginning a week before, then during, and for 4 weeks after leaving the endemic area is recommended. Resistance to mefloquine is a major concern in Southeast Asia and other countries. The tetracycline doxycycline can be used in mefloquine-resistant areas, except by pregnant women and children under 8. Possible relapse from latent liver infections with vivax or ovale malaria in travelers can be prevented by administration of primaquine upon return.

Chloroquine-resistant malaria is chiefly treated with the oldest known malaricide, quinine, in the form of quinine sulfate, plus pyrimethamine-sulfadoxine. If sulfa-based compounds cannot be used (in cases such as pregnancy), tetracycline and clindamycin (though even here pregnancy may rule out their use) may be used with quinine. Mefloquine, halofantrine, a phenanthrine-methanol compound, or a herbal drug used for many years in China, qinghaosu (the active agent is artemesin, from the plant *Artemisia*), are effective against chloroquine-resistant strains of *Plasmodium*. *See* DRUG RESISTANCE; QUININE.

Eradication efforts. Malaria is perhaps the most urgent problem in tropical medicine. Failure of earlier efforts to eradicate malaria and the rapid spread of resistant strains of both parasites and their mosquito vectors necessitated renewed interest in prevention of exposure by avoidance of mosquito bites using pyrethrin-treated bednets, coverage of exposed skin during active mosquito periods (usually dawn, dusk, and evening hours), and use of insect-repellent lotions. A balance between epidemiological and immunological approaches to prevention, and the continued development of new drugs for prophylaxis and treatment are recognized as the most effective means to combat one of the most dangerous and widespread threats to humankind from an infectious agent. *See* MEDICAL PARASITOLOGY.

Donald Heyneman

Bibliography. P. Gardner (ed.), *Health Issues of International Travelers*, 1992; H. M. Gilles, *Management of Severe and Complicated Malaria: A Practical Handbook*, 1991; F. J. López-Antuñano and G. Schmunis (eds.), *Diagnosis of Malaria*, 1990; S. C. Oaks, Jr., et al. (eds.), *Malaria: Obstacles and Opportunities*, 1991; R. S. Phillips, Vaccination against malaria, *Immunobiology*, 184:240–262, 1992; F. O. Ter Kuile et al., Halofantrine versus mefloquine in treatment of multidrug-resistant falciparum malaria, *Lancet*, 341:1044–1049, 1993; M. V. Valero et al., Vaccination with SPf66, a chemically synthesized vaccine, against *Plasmodium falciparum* malaria in Colombia, *Lancet*, 341(8847):705–710, 1993; D. J. Wyler, Malaria chemoprophylaxis for the traveler, *New Engl. J. Med.*, 329:31–37, 1993.

Malnutrition

Impaired health caused by a dietary deficiency, excess, or imbalance. To support human life, energy (from fat, carbohydrate, and protein), water, and more than 40 different food substances must be obtained from the diet in appropriate amounts. Malnutrition can result from the chronic intake of any

of these substances at levels above, as well as below, ranges that are adequate and safe, but commonly, the term refers only to deficient intake.

Primary (diet-induced) malnutrition. The number of people throughout the world who suffer from nutritional deficiencies as a result of inadequate dietary intake is uncertain, but even the most conservative estimates place that figure at hundreds of millions; many experts consider the actual number to approach 1 billion. Most malnourished people live in developing countries where income, education, and housing are inadequate to buy, transport, store, and prepare food and where nutritional deficiencies are almost always related to poverty. All but the very poorest nations produce enough food to meet the energy requirements of their populations, but the food that is produced is either inadequately distributed or too expensive.

In industrialized countries, chronic conditions of deficient dietary intake occur far less frequently but are reported occasionally among people who are dieting to lose weight, fasting, or on an unusually restrictive ("fad") diet. The widening gap in income between rich and poor has focused attention on inadequate food intake among low-income populations. Hunger—when defined as inadequate access to food assistance—has been reported to affect 20 million children and adults in the United States, and many surveys have identified substandard levels of dietary intake (below the levels generally recommended for prevention of nutritional deficiencies) among participants in assistance programs. *See* OBESITY.

Pregnant women, infants, and children are most at risk for inadequate dietary intake because their nutritional requirements are relatively high. Surveys also have identified dietary deficiencies among older adults who do not consume enough food to meet nutritional requirements. Their inadequate food intake often is associated with unemployment, reduced access to health care, low levels of education, and other factors that adversely affect health.

Secondary (illness-induced) malnutrition. Nutritional deficiencies also occur as a result of illness, injury, or alcohol or drug abuse that interferes with appetite; the inability to eat; defective digestion, absorption, or metabolism of food molecules; or disease states that increase nutrient losses. Secondary malnutrition has been observed frequently among medical and surgical patients who are treated in hospitals for prolonged periods of time. Hospital malnutrition can be prevented or corrected through appropriate nutritional support, which is a major reason for efforts to improve the nutrition training of physicians and other health professionals. Regardless of cause, the effects of malnutrition can range from minor symptoms to severe syndromes of starvation, protein-calorie malnutrition, or single-nutrient deficiencies. *See* METABOLIC DISORDERS.

Starvation. The chronic intake of energy below the level of expenditure induces rapid losses in body weight and muscle mass accompanied by profound changes in physiology and behavior. Together, these effects cause a starving person to become weak, apathetic, depressed, and unable to work productively and to do whatever is necessary to reverse the malnutrition. The consequences of nutritional deficiencies are seen first in tissues that are growing rapidly. These changes are most evident in the gastrointestinal tract, skin, blood cells, and nervous system as indigestion, malabsorption, skin lesions, anemia, or neurologic and behavior changes.

Of special concern is the loss of immune function that accompanies severe malnutrition. Malnourished individuals lose cellular immune competence and are less resistant to infectious disease. Because infections interfere with the body's ability to digest, absorb, and use food, they increase nutritional requirements. This cyclical interaction of malnutrition and infection produces the greatest damage among people in developing countries, where water supplies are contaminated with disease-causing microorganisms and where that interaction is the principal cause of death in young children and a chief cause of illness in adults.

Protein-calorie malnutrition. The combined effects of malnutrition and infection in young children are referred to as protein-calorie malnutrition. Because breast milk contains immune substances that fight infection, the children most likely to become malnourished are those who are not breast-fed. Not only do infant formulas lack the immune factors, but they also must be diluted in clean water and stored under refrigeration—conditions often unavailable in developing countries. For these reasons, the World Health Organization has developed guidelines to regulate the promotion of infant formulas in these countries by their manufacturers. Children who have just been weaned are also at high risk, because traditional weaning foods may lack essential nutrients and sufficient protein or calories.

Protein-calorie malnutrition usually is classified into two entities, marasmus and kwashiorkor, on the basis of physical appearance and the relative proportions of protein and calories in the diet. Children with the marasmus form appear generally wasted as a result of diets that are chronically deficient in calories as well as protein and other nutrients. Children with kwashiorkor are also very thin but have characteristically bloated bellies due to fluid retention and accumulation of fat in the liver, symptoms attributed to diets relatively deficient in protein. These distinctions are not precise, however; undernourished children raised on similar diets may exhibit signs characteristic of either form of the disease. In any case, children who survive protein-calorie malnutrition display the typical effects of starvation: depression, apathy, irritability, and growth retardation. *See* ADIPOSE TISSUE; PROTEIN METABOLISM.

Deficiencies of single nutrients. Deficiency conditions due to lack of a single vitamin or mineral occur rarely and usually reflect the lack of the most limiting nutrient in a generally deficient diet. In industrialized countries, single-nutrient deficiencies are most evident in individuals who abuse alcohol or drugs.

Classic conditions of deficiency of niacin (pellagra), thiamine (beriberi), vitamin C (scurvy), and vitamin D (rickets) have virtually disappeared as a result of food fortification programs and the development of food distribution systems that provide fresh fruits and vegetables throughout the year. Iron-deficiency anemia also has declined in prevalence, although children in low-income families remain at risk. *See* ANEMIA.

In developing countries, however, such conditions are still observed among people whose diets depend on one staple food as the major source of calories.

Beriberi, for example, was common among Japanese sailors whose diets were based mainly on white rice that had been milled to remove the outer thiamine-containing bran layer. The sailors developed disorders of the heart muscle and of neurologic function. The disease declined in prevalence when the diet became more varied and when it was discovered that par-boiled rice retains thiamine. However, it still occurs in parts of the world where milled rice is the principal source of calories.

Pellagra is caused by a deficiency of the vitamin niacin. Because some niacin can be synthesized from the amino acid tryptophan, pellagra is also considered to be a disease of protein deficiency. Pellagra was common through the 1930s in parts of the southern United States where the diet consisted mainly of corn. Corn is low in tryptophan, and its niacin occurs in an unavailable form. Increasing the variety of foods in the diet and fortifying corn meal and flour with niacin have effectively eliminated pellagra from industrialized countries.

Scurvy was observed often among sailors who were unable to obtain vitamin C from fresh fruits and vegetables during long sea voyages. Providing limes on board ship prevented this condition. Scurvy is reported occasionally in the United States among alcoholics and among infants born to mothers who consume unusually restricted diets. *See* ALCOHOLISM.

The characteristic bowed legs of children with rickets are rarely seen in countries where milk is fortified with vitamin D. This vitamin is synthesized in the body by the action of sunlight on skin, and rickets continues to occur among children who live in parts of the world where sunlight is limited and among those confined indoors.

A condition of substantial current public health importance is vitamin A deficiency, which is the principal cause of blindness and a major contributor to illness and death among children in developing countries. The carotene precursors of vitamin A are readily available in the local fruits and vegetables, but custom dictates that those foods are inappropriate for young children. Education and various forms of fortification and supplementation can serve as preventive measures, but because children with vitamin A deficiency are generally undernourished, the most effective form of prevention is improvement of the overall diet. *See* VITAMIN.

Marion Nestle

Bibliography. J. L. Brown, Hunger in the U.S., *Sci. Amer.*, 256(2):37–41, 1987; L. C. Chen and N. S. Scrimshaw (eds.), *Diarrhea and Malnutrition: Interactions, Mechanisms, and Interventions*, 1983; W. A. Coward and P. G. Lunn, The biochemistry and physiology of kwashiorkor and marasmus, *Brit. Med. Bull.*, 37(1):19–24, 1981; P. R. Kerndt et al., Fasting: The history, pathophysiology, and complications, *West. J. Med.*, 137:379–399, 1982; F. M. Lappe and J. Collins, *World Hunger: Twelve Myths*, 2d ed., 1998; R. Roubenoff et al., Malnutrition among hospitalized patients: A problem of physician awareness. *Arch. Int. Med.*, 147:1462–1465, 1987; N. S. Scrimshaw, The politics of starvation, *Technol. Rev.*, 87:19–27,50, 1984; R. R. Watson (ed.), *Nutrition, Disease Resistance, and Immune Function*, 1984; World Bank staff, *Poverty and Hunger: Issues and Options for Food Security in Developing Countries*, 1986.

Malpighiales

One of the largest orders of the rosid eudicotyledons, comprising more than 30 families. Distributed worldwide, this order has never before encompassed this composition. Recent analyses of deoxyribonucleic acid (DNA) sequences, both plastid and nuclear, led to its recognition, even though the group is highly heterogeneous and difficult to characterize. The largest families are Euphorbiaceae (8000 species), Clusiaceae (1400), Malpighiaceae (1100), Flacourtiaceae (900), and Violaceae (850). Most of the order is composed of woody species, many of regional importance as timber and medicines. Several of the smaller families are significant as well, including Salicaceae (used as coppice, and the original source of aspirin) and Rhizophoraceae (the ecologically significant mangroves). *See* MAGNOLIOPHYTA.

Mark W. Chase

Malt beverage

A fermented beverage produced from grain. Beer is a generic term used to describe alcoholic beverages made from cereal grains, especially barley, in the form of malt. Ale, lager, porter, and stout are different kinds of beer made by recognizably similar processes. The United States is the largest producer of beer in the world.

The manufacture of beer is a complex natural process of three general parts: the preparation of barley by germination, or the malting process; the actual digestion of barley (now malt) starch to produce a solution of sugars (called wort) and the adjustment of flavor with hops, which are the brewhouse processes (see **illus.**); and the fermentation of these sugars by yeast to yield alcohol, carbon dioxide gas, and flavor compounds to produce beer. *See* HOP.

Malting process. Barleys for malting in the United States are special varieties grown in the Middle West (six-rowed types) or the West (two-rowed types). Barley is a hard, flavorless grain with an incomplete

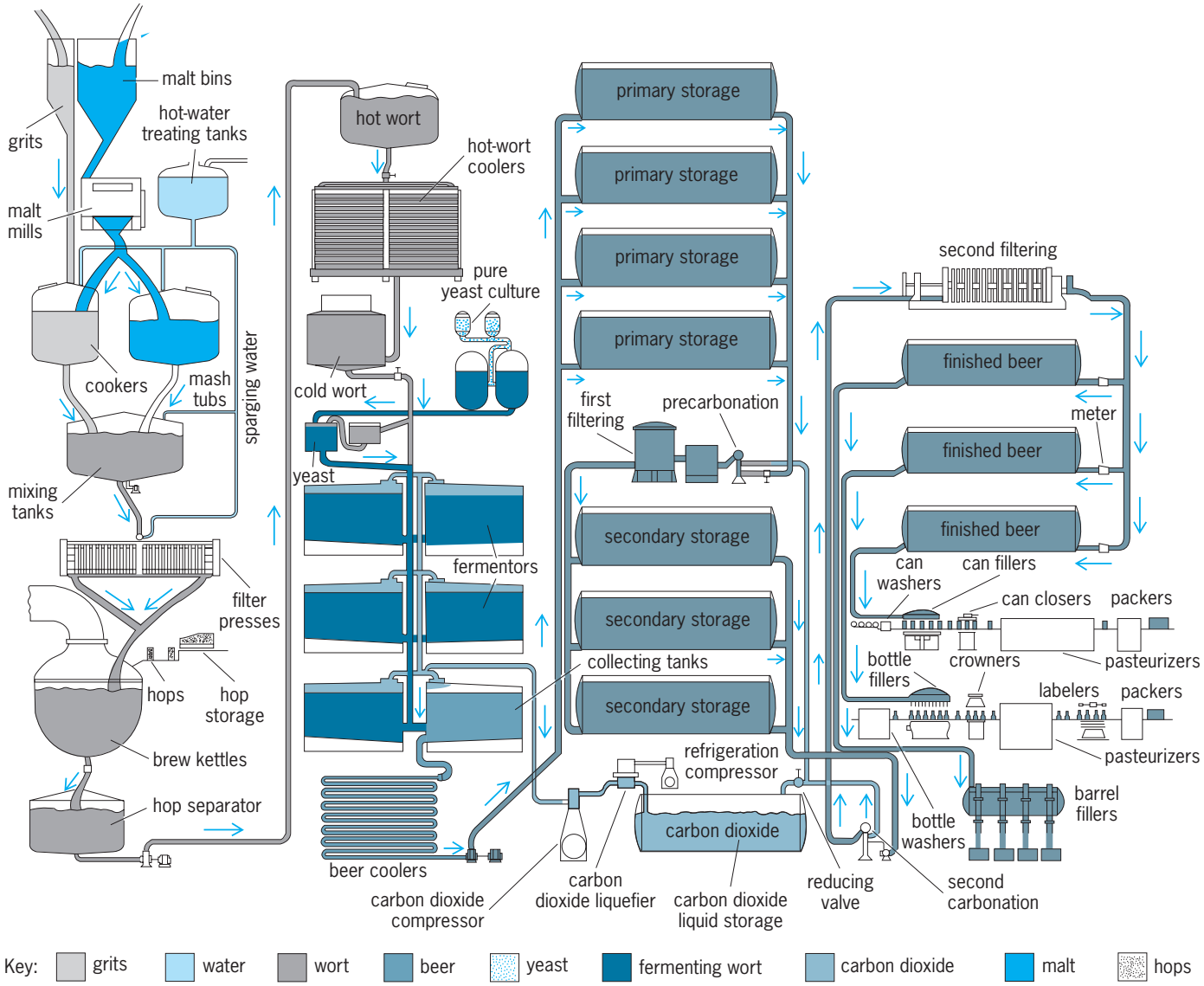

Flow chart of brewing process. (*Pabst Breweries*)

enzyme content (from the brewer's viewpoint), but malt is friable, flavorful, and has an enzyme complement necessary for brewing. The malting process contains three interrelated parts: steeping or soaking the grain, germination, and kilning. *See* BARLEY.

Steeping. When barley is harvested, it contains about 12% moisture and therefore cannot germinate. In large conical-bottomed vessels, barley and water at about 59°F (15°C) are mixed, and the grain rapidly absorbs water. The first steep water quickly becomes brown as the barley is washed. This cleaning is improved by forcing air through the grain and by changing the water often. The air also provides oxygen for germination which begins during steeping. After about 40 h or so, the barley contains about 45% moisture, and the root sheath begins to show.

Germination. The barley is now transferred to large vessels through which cooled humidified air is passed, and screwlike ploughs keep the rootlets from matting. The airflow and moisture are required for the grain to germinate optimally and allow the maltster to control temperature at about 68°F (20°C) and moisture at about 45%. Germination continues 3 to 5 days, depending on the variety of barley and the kind of malt being made.

Kilning. When germination is complete, as judged by the soft consistency of the contents of the kernels and by the growth of the shoot (about three-fourths the length of the kernel beneath the husk), germination is halted by a programmed process of heat and draft (kilning). There are three stages: At first, low heat and high draft reduce malt moisture to about 8 to 10%, then higher heat reduces moisture to about 5%. Finally, intense heat for a short time (called curing) drives the level of moisture to about 4% or less and induces good malt flavor. This heating schedule helps to preserve the enzymes present in the malt (which are heat-sensitive when wet) and to produce a flavorful, friable product (malt), the starch of which has been modified to render it more readily soluble in water. In addition, during the germination

process the starch-splitting enzyme α-amylase is created (β-amylase exists in barley), and substantial protein breakdown to amino acids is achieved.

Brewing. Malt is the main raw material of brewing. Corn (or cornflakes or a variety of corn syrups) or rice are used as adjuncts to provide 20 to 50% of the total raw materials. They provide cheaper starch than does malt, and (because they are low in nitrogenous compounds, color, and flavor) they permit pale-colored beers to be made which have a light and fresh flavor.

In a brewery two main processes occur: the transformation of the malt and other raw materials into a fermentable liquid in the brewhouse and the cellar operations of fermentation and finishing.

The objective of brewhouse operations is to extract the raw materials and to recover the desirable liquid (wort) from the insoluble solids (spent grain). These are the processes of mashing, lautering, and wort boiling.

Mashing. In the United States the adjunct (corn or rice containing a little malt) is gradually heated with water to boiling to gelatinize the starch of the adjunct. For the separate malt mash the malt is first milled, mixed with hot water, and stirred at about 100°F (38°C) for about 10 to 20 min. The boiling adjunct mash is then mixed into the malt mash, and the temperature of this combined mash is 158 to 160°F (70 to 71°C). The temperature is critical because it is here that the α- and β-amylases of the malt intensively digest the starch of the malt and adjunct to produce simple fermentable sugars (such as maltose) and unfermentable dextrins. This conversion takes 15 to 30 min. Many other compounds essential to fermentation and beer quality, including amino acids, vitamins, and minerals, are dissolved in this process.

Lautering. The converted mash is transferred to the lauter vessel—a wide, flat vessel with a slotted false bottom—where the wort can be filtered from the spent grains. The bed of spent grains is then sparged (rinsed) with hot water to recover the maximum amount of sugar.

Boiling. The sweet wort is collected in the kettle and boiled for up to 1 h with 0.25 to 0.35 lb/barrel (0.97 to 1.35 kg/m^3) of hops or extract of hops. The amount of hops used, the blend of foreign and domestic hops, and the time of their addition to the kettle are selected by the brewer. The hop resins, called α-acids, by boiling are extracted and isomerized to iso-α-acids, which impart bitterness to beer. Boiling also sterilizes the wort and precipitates some protein which otherwise would cause haze in the finished beer. After separation in a hop strainer or whirlpool, the wort is cooled, yeast is added, and the fermentation stage begins.

Sugar syrups of various kinds (made from cornstarch) do not have to be digested in brewing and are added directly to the boiling stage. This allows the brewer to produce a more concentrated wort (about 16 to 18% sugar) than is economically feasible with traditional processes (about 10 to 12% sugar). When fermented, this beer is high in alcohol and needs to be diluted to normal strength with deaerated, carbonated water. The advantage of this "high gravity brewing" is that the brewer can increase production without additional equipment.

Fermentation and finishing. Yeasts are unicellular fungi which are classified in 37 genera, but all brewers' yeasts are selected strains of only two species of one genus, namely *Saccharomyces carlsbergensis* (the lager yeast, presently called *S. uvarum*) and *S. cerevisiae* (the ale yeast; other strains of this yeast are used for winemaking and baking). A brewing strain may be unique to one company, though not necessarily, and is chosen because it ferments at the right speed, can be removed easily at the end of the process, and produces beer of the desired flavor.

Yeast is added to wort immediately after it is cooled to about 55–60°F (13–16°C) and as it is being run to a fermenter. A traditional fermenter is a horizontal cylinder of about 1000 barrels (117 m^3) capacity, but some major breweries now have additional vertical tanks of six to eight times this capacity. Fermentation takes approximately 1 week. During this time the yeast grows to about three to five times its original amount, using the sugar and other materials in wort as fuel and food for this growth. Beer flavor characteristics are largely created during fermentation and are the waste products of anaerobic yeast growth. Alcohol (ethanol) and carbon dioxide gas are obvious products of fermentation, but the yeast produces a host of additional materials, including many other alcohols, esters, aldehydes and ketones, sulfur-containing materials, and organic acids. The precise array of materials produced strongly affects beer flavor and is a function of wort composition, conditions of fermentation, and yeast characteristics.

Toward the end of fermentation, when the sugars are almost exhausted, the fermentation is cooled. This aids the yeast's natural tendency to settle out (flocculate). The cooled beer is then transferred off the settled yeast to tanks in the lager (resting) cellar which is kept at 35°F (2°C) or so. Here the beer is allowed to mature and clarify quietly for about 3 weeks in the presence of some yeast transferred from the primary fermentation. *See* FERMENTATION; YEAST.

After lagering, beer is filtered at 29°F (−2°C), usually through diatomaceous earth, carbonated, packaged, and pasteurized to complete the process. However, other treatments may variously be used in finishing. For example, many beers are treated with papain (a protease enzyme from papaya) or an insoluble absorbent (such as silica gel) to remove some protein which otherwise could cause haze in the beer when it is cooled. A fairly common practice at this stage is krausening, which is the addition of some freshly fermenting wort to the beer while it is in large tanks in cold storage to achieve natural carbonation. Beers that have been brewed at high gravity are adjusted with deaerated carbonated water en route to the bottle shop to achieve the required final level of alcohol and flavor components. Hops extract may be added at this point to adjust bitterness to a standard

value, and caramel (made from roasted sugar) may be added to produce dark beer.

Bottling or canning of beer is a highly developed technology. Speed and exclusion of air are the keys to successful packaging of beer, and great improvements have been made in recent years. Because beer does not improve in the package, it should be drunk fresh. Brewers therefore make every effort to get the beer to the consumer as rapidly and as cool as possible. About 80% of production is sold in the retail package; only 15% is marketed in kegs for draft sale.

Light (low-calorie) beer. The calories in beer (about 150 per 10-oz can or 630 joules per 283-g can) arise from the alcohol present (two-thirds) and the residual carbohydrates (one-third), which are flavorless unfermentable dextrins produced from starch during mashing. Low-calorie beer is made by eliminating these dextrins. This is achieved by controlling the amount of dextrins entering the wort, since in making light beer the adjunct used is fully fermentable (dextrin-free) corn syrup; and by converting the dextrins to fermentable sugar, which is done by adding to the cooled wort an enzyme of microbial origin (called amyloglucosidase or glucamylase). Fermentation of such wort converts all the carbohydrate to alcohol. This yields a beer of nearly 5% alcohol which (because the conversion of sugar to alcohol removes few calories) gives little saving of calories. Therefore the beer is diluted to a normal alcohol content (about 3.4 to 3.8% by weight) with pure water. The end product contains no dextrins, and almost all the calories (about 100 or 420 J) derive from an essentially normal content of alcohol. Any further savings in calories, to produce beers of 60 to 90 calories (250–380 J), can be made only by dilution below the normal alcohol content.

M. J. Lewis

Malvales

An order of flowering plants in the core eudicots. The order consists of 10 families and more than 5500 species. The circumscription of the order has been altered greatly in recent years, largely on the basis of deoxyribonucleic acid (DNA) sequence data. Of the five families in the traditional concept (Bombacaceae, Malvaceae, Sterculiaceae, Tiliaceae, and Elaeocarpaceae), the first four have been combined as Malvaceae, due to lack of monophyly of three of these families in their traditional circumscription; and Elaeocarpaceae are included in Oxalidales. In addition, other families have been transferred to Malvales, including Dipterocarpaceae and Thymelaeaceae. The expanded order is characterized by the presence of mucilage in epidermal cells and cavities; and of palmate leaves, stellate hairs, and numerous stamens with partially fused filaments occur frequently.

Malvaceae are cosmopolitan and include economic crops such as cotton (*Gossypium*), cocoa (*Theobroma*), and durian (*Durio*) and horticultural plants such as hollyhocks (*Althaea*) and rose of Sharon (*Hibiscus*). Dipterocarpaceae are important elements of tropical forests, especially in Southeast Asia, and provide hardwood timbers. Other horticultural genera in the order include *Cistus* and *Helianthemum* (Cistaceae) and *Daphne* (Thymelaeaceae). Several genera of Thymelaeaceae provide fibers used for making paper, and *Bixa* (Bixaceae) is the source of the orange dyestuff anatto. *See* CACAO; COTTON; EUDICOTYLEDONS.

Mark Chase

Mammalia

The class Mammalia is the dominant group of vertebrates today. They have ruled the planet since the extinction of the dinosaurs 65 million years ago. There are over 4200 living species of mammals, classified into over 1000 genera, 140 families, and 18 orders. However, the number of extinct mammals is at least five times that. Most living mammals are terrestrial, including such large beasts as elephants, rhinos, hippos, and giraffes, as well as a great diversity of smaller land animals. The largest known land mammal was the extinct 20-ton hornless rhino *Paraceratherium*. Many groups of mammals moved to the water from land-dwelling ancestors. These included manatees and dugongs (which are distantly related to elephants), otters (which are related to weasels), seals, sea lions, and walruses (which are distantly related to bears), and whales (which are distantly related to even-toed hoofed mammals), as well as numerous extinct groups. The living blue whale [reaching 30 m (100 ft) in length and 150 tons] is by far the largest animal that has ever lived. Mammals have also taken to the air, with over 920 living species of bats, as well as numerous gliding forms such as the flying squirrels, phalangerid marsupials, and flying lemurs or colugos. Mammals are even more successful at small body sizes, with hundreds of small species of rodents, rabbits, and insectivores. The smallest living mammal, the 1.5-g Kitti's hognosed bat, is at the lower limit of body size for mammals, since physiology and anatomy prevent them from thriving in the tiny-body-size niche inhabited by insects and other arthropods.

Anatomy and physiology. Mammals are distinguished from all other animals by a number of unique characteristics. These include a body covered with hair or fur (secondarily reduced in some mammals, particularly aquatic forms); mammary glands in the female for nursing the young; a jaw composed of a single bone, the dentary; and three middle ear bones, the incus, malleus, and stapes. All mammals maintain a constant body temperature through metabolic heat. Their four-chambered heart (two ventricles and two atria) keeps the circulation of the lungs separate from that of the rest of the body, resulting in more efficient oxygen transport to the body tissues. They have many other adaptations for their active life-style, including specialized teeth (incisors, canines, molars, and premolars) for biting, tearing, and grinding up food for more efficient digestion. These teeth

are replaced only once in the lifetime of the animal (rather than continuous replacement, found in other toothed vertebrates). Mammals have a unique set of muscles that allow the jaw to move in many directions for chewing and for stronger bite force. Their secondary palate encloses the internal nasal passage and allows breathing while they have food in the mouth. Ribs (found only in the thoracic region) are firmly attached to the breastbone (sternum), so that expansion of the lung cavity is accomplished by a muscular wall in the abdominal cavity called the diaphragm. *See* CARDIOVASCULAR SYSTEM; DENTITION; GHOST IMAGE (OPTICS); HAIR; LACTATION; MAMMARY GLAND; THERMOREGULATION; TOOTH.

All mammals have large brains relative to their body size. Most mammals have excellent senses, and some have extraordinary senses of sight, smell, and hearing. To accommodate their large brains and more sophisticated development, mammals are born alive (except for the platypus and echidnas, which lay eggs), and may require considerable parental care before they are ready to fend for themselves. Juvenile mammals have separate bony caps (epiphyses) on the long bones, separated from the shaft of the bone by a layer of cartilage. This allows the long bones to grow rapidly while still having a strong, bony articulation at the end. When a mammal reaches maturity, these epiphyses fuse to the shaft, and the mammal stops growing (in contrast to other vertebrates, which grow continuously through their lives). *See* BRAIN; NERVOUS SYSTEM (VERTEBRATE); SKELETAL SYSTEM.

Reproduction and classification. The living mammals are divided into three major groups: the monotremes (platypus and echidnas), which still lay eggs, retain a number of reptilian bones in their skeletons, and have other primitive features of their anatomy and physiology; the marsupials (opossums, kangaroos, koalas, wombats, and their relatives), which give birth to an immature embryo that must crawl into the mother's pouch (marsupium), where it finishes development; and the placentals (the rest of the living mammals), which carry the young through a long gestation until they give birth to relatively well-developed progeny. In addition to these three living groups, there were many other major groups, such as the rodentlike multituberculates, now extinct. The most recent classification of the mammals can be summarized as follows:

Class Mammalia
- Subclass Prototheria (monotremes)
- Subclass Theriiformes
  - Infraclass Holotheria
    - Cohort Marsupialia (marsupials or pouched mammals)
    - Cohort Placentalia (placentals)
      - Magnorder Xenarthra (sloths, anteaters, armadillos)
      - Magnorder Epitheria
        - Grandorder Anagalida (= Glires) (rodents, rabbits, elephant shrews)
        - Grandorder Ferae (carnivores, pangolins, many extinct groups)
        - Grandorder Lipotyphla (hedgehogs, shrews, moles, tenreces, and kin)
        - Grandorder Archonta
          - Order Chiroptera (bats)
          - Order Primates (lemurs, monkeys, apes, humans)
          - Order Scandentia (tree shrews)
        - Grandorder Ungulata (hoofed mammals)
          - Order Tubulidentata (aardvarks)
          - Order Artiodactyla (even-toed hoofed mammals: pigs, hippos, camels, deer, antelopes, cattle, giraffes, pronghorns, and relatives)
          - Order Cete (whales and their extinct land relatives)
          - Order Perissodactyla (odd-toed hoofed mammals: horses, rhinos, tapirs, and extinct relatives)
          - Order Hyracoidea (hyraxes)
          - Order Tethytheria (elephants, manatees, and extinct relatives)

This classification does not list all the extinct groups, which include at least a dozen more ordinal-level taxa. It is a considerable improvement over previous mammalian classifications, which used to list over 30 different orders with no indication of how they were related to one another. Although there are more ranks in this classification than is traditional, this nesting of groups within groups accurately reflects the evolutionary branching sequence (see **illus.**). *See* REPRODUCTIVE SYSTEM.

Evolution. Mammals evolved from the Synapsida, an early branch of the terrestrial amniotes that has been erroneously called the mammallike reptiles. This name is inappropriate because synapsids were never related to reptiles. Synapsids and reptiles originated independently from one another about 320 million years ago, and evolved separately ever since. Early synapsids, such as the finback *Dimetrodon*, show relatively few mammalian characteristics, but as their evolution progressed through the late Paleozoic, synapsids became progressively more mammallike.

The first undoubted mammals appeared in the Late Triassic (about 210 million years ago), and were tiny insectivorous forms much like living shrews. Through the rest of the age of dinosaurs, a number of different groups evolved over the next 145 million years of the Jurassic and Cretaceous. Most remained tiny, shrewlike animals, hiding from the dinosaurs in the underbrush and coming out mostly at night. The first two-thirds of mammalian history had passed before the dinosaurs became extinct 65 million years ago, and this allowed mammals to emerge from their shadow.

Opossumlike marsupials are known from the Early Cretaceous (about 110 million years ago), and they were more common than placentals just before the

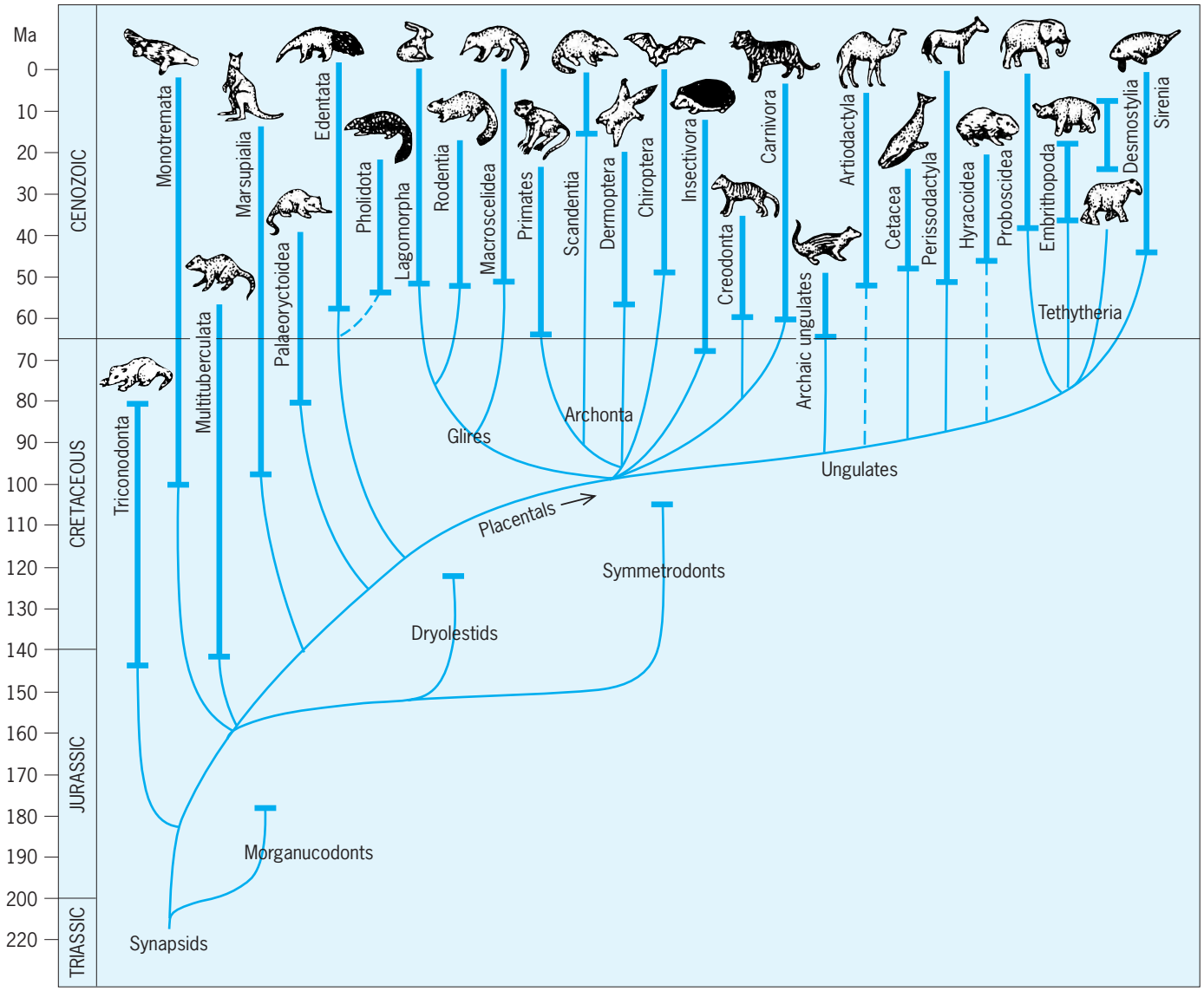

Evolutionary relationships of the major groups of mammals.

end of the age of dinosaurs. Although opossums were found on most continents during the Cenozoic, other marsupials diversified primarily on the southern continents of Australia or South America, which were isolated from the main developments in placental evolution. On both of these continents, marsupials evolved in parallel with placentals, so that Australia has marsupials shaped like woodchucks (wombats), rabbits (bandicoots), flying squirrels (phalangers), monkeys (cuscuses), dogs (Tasmanian wolf), wolverines (Tasmanian devil), anteaters (myrmecobiids), cats (dasyurines), moles (notoryctines), mice (dasycercines), as well as extinct marsupial lions and rhinosized diprotodonts. South America was once the home of marsupial sabertooths and hyaenalike marsupials known as borhyaenids, although they apparently became extinct about 3 million years ago when placental carnivores came from North America via the Panamanian land bridge.

Between 65 and 55 million years ago, a rapid adaptive radiation (see illus.) yielded all the living orders of placental mammals and many extinct forms as well. The Xenarthra, or edentates, were the first group of placentals to branch off. Although "edentate" means toothless, this is true only of anteaters; sloths and armadillos have simple peglike teeth lacking enamel. The archaic nature of edentates among the placentals is shown by a variety of characters, including a uterus simplex (divided by a septum and lacking a cervix), a slower, less well regulated metabolism, retention of several reptilian bones lost in all other placentals, and a primitive rodlike stapes in the middle ear. Like the marsupial carnivores, edentates evolved in isolation in South America throughout most of their history, developing into a variety of sloths (both tree sloths and huge ground sloths weighing up to 3 tons), anteaters, and armadillos [including the giant glyptodonts, which were

2 m (6.5 ft) long, had 400 kg (880 lb) of body armor, and a spiked club on the tip of the tail]. The long period of isolation in South America ended about 3 million years ago, and ground sloths and glyptodonts migrated to central America and parts of North America, but they disappeared at the end of the last ice age.

The remaining (nonedentate) placentals, or epitheres, diversified primarily in Eurasia and North America and spread throughout the world in the early Cenozoic. The true lipotyphlan insectivorans (represented by shrews, moles, and hedgehogs) continued to diversify all over the northern continents throughout the Cenozoic. Most remained small, and they ate insects, worms, and other small animals, although the extinct giant hedgehog *Dinogalerix* was as big as a large dog and killed sizable prey.

The archontan radiation began with an enormous expansion of primitive lemurlike primates in the early Cenozoic, when the world had dense jungle vegetation all the way to the Poles. Primates declined in the Oligocene, when their forest habitats disappeared, and they became restricted to Africa (Old World monkeys and apes) and South America (New World monkeys). The earliest bats (known from about 50 million years ago) already had fully developed wings. They are the second most diverse group of mammals, after the rodents.

The radiation of the Glires began in the Paleocene of Asia, where numerous primitive relatives of rodents and rabbits are found. In the Eocene, both groups migrated to Europe and North America, where they soon took over the niche of small-bodied fruit, seed, and nut eaters that had been occupied by multituberculates and primitive primates. Although rodents and rabbits are separate orders, they are both characterized by chisellike, ever-growing front incisors that are used in gnawing. However, rodents have only a single pair of incisors, while rabbits have two. The enormous diversification of the Rodentia since the Eocene has given rise to over 1700 species (about 40% of the Mammalia), with forms as large as the pig-sized capybara down to the tiny mice and voles.

Predatory mammals (the Ferae) include the extinct creodonts (an archaic group that were the dominant predators and scavengers of the early Cenozoic), and the living order Carnivora (cats, hyenas, mongooses, civets, dogs, bears, weasels and their kins, seals and sea lions, raccoons, and many extinct groups). All Carnivora are distinguished by distinctive shearing teeth, the carnassials, developed between the last upper premolar and first lower molar. True Carnivora began as weasellike forms in the early Eocene, but by the Oligocene they had taken over most of the predatory niches from the creodonts. By the Miocene, the ancestors of seals and sea lions had evolved from bearlike ancestors. Carnivorous mammals show remarkable examples of convergence on a limited number of body forms. For example, sabertoothed forms evolved four times: once in the creodonts, once in the true cats, and once in the extinct catlike nimravids, which are related to dogs (plus the extinct sabertoothed marsupial). In North America, the borophagine dogs converged on hyenas, with similar bone-crushing teeth.

The hoofed mammals, or ungulates, are first known from about 85 million years ago in central Asia. In the latest Cretaceous and Paleocene, archaic hoofed mammals ("condylarths") were among the most common forms in North America and Asia. From these roots, numerous orders evolved. The first to branch off were the even-toed Artiodactyla, which have two or four toes on each foot and a distinctive ankle structure. First appearing in Pakistan in the earliest Eocene, artiodactyls quickly diversified into a number of different groups, including suoids (pigs, peccaries, hippos), tylopods (camels and their extinct relatives), and ruminants (deer, giraffes, pronghorns, cattle, sheep, goats, antelopes). With their four-chambered stomachs for more efficient digestion, the ruminants became the dominant group of large herbivorous mammals as global climates became drier and grasslands expanded in the later Cenozoic.

The ancestors of whales were large hoofed predators known as mesonychids. Recently, transitional forms between mesonychids and primitive whales have been found in the Eocene of Pakistan. By the Oligocene, whales had diversified into the predatory toothed whales (dolphins, orcas, sperm whales) and filter-feeding baleen whales (blue, right, humpback, gray, and many other whales).

The Perissodactyla, or odd-toed ungulates, have one or three toes on each foot. Today they include horses, rhinos, and tapirs, but they were much more diverse in the past, with huge slingshot-horned brontotheres and bizarre clawed chalicotheres. Closely related to perissodactyls are the hyraxes or conies, and the tethytheres (elephants, sea cows, and their relatives). Tethytheres originated from late Paleocene ancestors that once lived along the Tethys Seaway (which stretched from Gibraltar to Indonesia). Although sea cows spread around the world by the Eocene, the early evolution of hyraxes, and of elephants and their kin was restricted to Africa until the middle Miocene, when both groups spread to Eurasia, and mastodonts even reached North America.

Donald R. Prothero

Bibliography. J. F. Eisenberg, *The Mammalian Radiations*, 1981; J. H. Honacki, K. E. Kinman, and J. W. Koeppl, *Mammal Species of the World*, 1982; D. Macdonald, *The Encyclopedia of Mammals*, 1984; M. C. McKenna and S. K. Bell, *Classification of Mammals above the Species Level*, 1997; R. M. Nowak, *Walker's Mammals of the World*, 1999; D. R. Prothero and R. M. Schoch, *Horns, Hooves, and Flippers: The Evolution of Hoofed Mammals and Their Relatives*, 2000; R. J. G. Savage and M. R. Long, *Mammal Evolution: An Illustrated Guide*, 1986; F. S. Szalay, M. J. Novacek, and M. C. McKenna (eds.), *Mammal Phylogeny*, 1993; J. Z. Young, *The Life of Mammals*, 1975.

Mammary gland

A unique anatomical structure of mammals that secretes milk for the nourishment of the newborn. The mammary gland contains thousands of milk-producing units called alveoli, each of which consists of a unicellular layer of epithelial cells arranged in a spheroid structure (**Fig. 1**). The alveolar epithelial cells take up a variety of nutrients from the blood that perfuses the outer surface of the alveolar structures. Some of the nutrients are then secreted directly into the alveolar lumen; other nutrients are used to synthesize the unique constituents of milk which are then secreted. Each alveolus is connected to a duct through which milk flows. The ducts from many alveoli are connected via a converging ductal system which opens externally by way of the lactiferous pore (**Fig. 2**).

Surrounding each alveolus and its associated small ducts are smooth muscle cells called myoepithelial cells. These cells contract in response to the posterior pituitary hormone oxytocin; milk is thus forced out of the alveoli, through the ductal system, and out the lactiferous pore for the nourishment of the newborn. The release of oxytocin is a neuroendocrine reflex triggered by the stimulation of sensory receptors by the suckling of the newborn. *See* ENDOCRINE MECHANISMS.

Embryology. Mammary glands are basically highly modified and specialized sebaceous glands which derive from ectoderm. In the embryo, mammary lines, formed on both sides of the midventral line, mark the location of future mammary glands. In some species (such as elephants, sirenians, and primates) mammary glands develop in the thoracic region, in others (ungulates, cetaceans) in the inguinal region; in litter-bearing animals they extend from the thoracic to the inguinal region. Along the mammary lines discrete ectodermal ingrowths, called mammary buds, produce a rudimentary branched system of ducts at birth. For each mammary gland, the ingrowths begin as primary sprouts which number from 1, as is the case in the cow, to as many as 20, as in humans. In all species (except the monotremes) a nipple or teat develops in concert with the mammary buds. The most common type of nipple proliferates outward as the primary sprouts grow downward. A second type, found in some marsupials, grows inward into a pocket and everts after sexual maturity. A third type, found in rats and mice, is formed by an epithelial ingrowth in the gland area, and at the time of puberty the nipple emerges as the mammary gland develops. Each teat or nipple has lactiferous pores from 1 to 20 excurrent ducts; the number is determined by the number of primary sprouts that develop in embryonic life. In the most primitive mammal (the duckbill or platypus), which lacks nipples or teats, milk simply oozes out of the two mammary gland areas and is lapped up by the young.

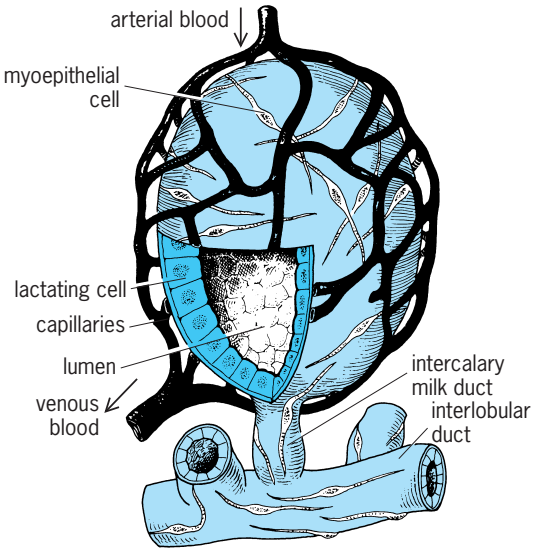

Fig. 1. An alveolus, the milk-producing unit of the mammary gland.

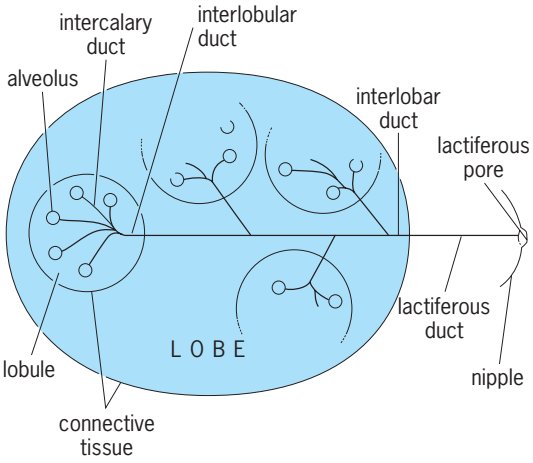

Fig. 2. Structural components of the human mammary gland.

Puberty. From birth to sexual maturity the mammary gland consists of a nipple and a rudimentary ductal system in both males and females. At the onset of puberty in the female, the enhanced secretion of estrogen causes a further development of the mammary ductal system and an accumulation of lipids in fat cells. After puberty in women, the mammary gland consists of about 85% fat cells and a partially developed ductal system. *See* ESTROGEN.

Pregnancy. During pregnancy the mammary gland comes under the influence of estrogen and progesterone which are derived from both the ovary and placenta. These hormones cause a further branching of the ductal system and the development of milk-secreting structures, the alveoli. In humans, approximately 200 alveoli are surrounded by a connective tissue sheath forming a structure called a lobule (Fig. 2). About 26 lobules are packaged via another connective tissue sheath into a larger structure called a lobe. Each of 15–20 lobes is exteriorized into the nipple via separate lactiferous pores. *See* PROGESTERONE.

A complement of hormones maximizes the development of the ductal and lobuloalveolar elements in the mammary gland. Optimal ductal growth is

attained with estrogen, a glucocorticoid, prolactin, and insulin. Maximal lobuloalveolar growth is obtained with estrogen, progesterone, growth hormone, prolactin, a glucocorticoid, and insulin. During pregnancy estrogen and progesterone stimulate mammary development but inhibit milk production.

During the final third of pregnancy, the alveolar epithelial cells begin secreting a fluid called colostrum. This fluid fills the alveoli and causes a gradual enlargement of the breast or udder. At parturition, the inhibitory influence of estrogen and progesterone is removed, and the gland can secrete milk under the influence of a further complement of hormones including prolactin, a glucocorticoid, insulin, and the thyroid hormones.

At birth the mammary glands of about 80% of human newborns are found to secrete a watery substance called witch's milk. During pregnancy the estrogen and progesterone in the mother pass into the fetal circulation and influence the mammary cells of the fetus. *See* GLAND; LACTATION; MAMMALIA; MILK; PREGNANCY.

James A. Rillema

Bibliography. T. C. Jones, U. Mohr, and R. D. Hun (eds.), *Integument and Mammary Glands*, 1989; M. C. Neville and C. W. Daniel (eds.), *The Mammary Gland: Development, Regulation, and Function*, 1987; T. B. Mepham, *Physiology of Lactation*, 1991.

Mammography

The radiological imaging of breast tissue. This procedure is used to identify cancer, preferably when still impalpable. Because of improved resolution in high-contrast film, only minor exposure of skin to x-rays is required, so that national screening programs have been set up in many western industrialized countries.

Mammography depends on the tumor being reflected as a dense focus in contrast to surrounding tissue or less dense glandular and ductal parts of the structure. Discrimination between benign and malignant lesions may sometimes be difficult, but may be aided by increased magnification of the image and by spot compression to confirm otherwise equivocally benign lesions. In addition, ultrasonography may be used to distinguish between cystic (mainly benign) and solid (possibly malignant) masses. Many women with impalpable cancers discovered through mammography have microcalcifications as the diagnostic feature; others are diagnosed by the presence of a distinct mass, architectural asymmetry of the glandular and ductal tissue, or tissue distortion.

Mammography has recognized limitations: the possibility exists that in some postmenopausal women it will fail to reveal cancer that is present. Similarly, in premenopausal women in whom the breast tissue is often dense, mammography can be falsely negative in some women with subsequently proven cancers.

National screening mammography programs in Europe have shown some reduction of mortality from breast cancer in screened women between 50 and 70 years of age. The value of screening mammography in women between 40 and 50 who have no family history of breast cancer is unknown.

Western experience suggests that of every 1000 women between the age of 40 and 70 initially screened, approximately 70 will be recalled for more meticulous diagnostic mammography, 15 will have surgical biopsy, and 6 will be found to have cancer. The confirmation necessary for the diagnosis may be made by surgical excision preceded by insertion of a wire under mammographic guidance for localization of the impalpable abnormal shadow or microcalcifications. Ultrasonographic or stereotactic guided core biopsy has also been investigated as a technique to prevent a surgical operation solely for diagnostic purposes.

By revealing unsuspected shadows due to early cancer in asymptomatic women, mammography is estimated to account for much of the apparent increase in incidence of breast cancer: A number of these lesions are still confined to the mammary duct and may be as small as 4 mm. As this type of lesion does not necessarily progress to invasive cancer, it is not certain whether mammography will improve outcome in this group of very small lesions. The ability of mammography to reflect breast changes over time and its value in the surveillance of women with breast cancer treated by conservation techniques (lumpectomy and radiation) has made mammography an invaluable clinical tool. Efforts to refine the technique still further include the exploration of digital mammography using computer-acquired data to provide more accurate stereotactic guidance to the biopsy of impalpable suspicious lesions. *See* BREAST DISORDERS; CANCER (MEDICINE); MEDICAL ULTRASONIC TOMOGRAPHY; RADIOGRAPHY.

Alexander J. Walt

Bibliography. D. B. Kopans, *Breast Imaging*, 2d ed., 1998; A. K. Tucker (ed.), *Textbook of Mammography*, 1993.

Mandarin

A name used to designate a large group of citrus fruits in the species *Citrus reticulata* and some of its hybrids. This group is variable in the character of trees and fruits since the term is used in a general sense to include many different forms, such as tangerines, King oranges, Temple oranges, tangelos (hybrids between grapefruit and tangerine), Satsuma oranges, and Calamondin, presumably a hybrid between a mandarin and a kumquat. *See* KUMQUAT; ORANGE; TANGERINE.

Many varieties of citrus falling in the mandarin classification are compact trees with willowy twigs and rather small, narrow, pointed leaves. The fruits are usually yellow, orange, or red and have loose skins which peel easily. A distinguishing feature common to the true mandarins and their hybrids is the chlorophyll in the cotyledons (seed leaves), giving them a pistachio-green color.

Although tangerines are the most extensively planted of the mandarin group, others, particularly the Temple orange, the Murcott orange, and the tangelos, of which there are several varieties, are important commercial fruits in the United States. *See* FRUIT; FRUIT, TREE; SAPINDALES. Frank E. Gardner

Mandibulata

A subphylum of the phylum Arthropoda in the long-established classification scheme which comprises three groups at subphylum level; it is almost certainly not a natural assemblage. Each of the other two subphyla (Trilobitomorpha and Chelicerata) is more likely to be monophyletic. *See* CHELICERATA; TRILOBITA.

The subphylum Mandibulata, defined as those arthropods possessing mandibles (lateral jaws) and antennae, includes the six classes Insecta, Chilopoda, Diplopoda, Symphyla, Pauropoda, and Crustacea. The subphylum could also be defined, more correctly, as comprising all classes of living arthropods that lack chelicerae and pedipalps. In fact, neither in their development nor in their functional morphology are the mandibles of crustaceans homologous with the mandibles of insects. The available fossil evidence for primitive crustaceans also supports a different phyletic origin for these appendages. In addition, insects have a single pair of antennae, while crustaceans have two pairs (borne on the second and third preoral segments of the head, with the second pair of antennae typically biramous). In contrast, most authorities agree on a closer relationship between the insects and the four myriapodous classes, and among these five classes the mandibles are almost certainly homologous. *See* ARTHROPODA; CHILOPODA; CRUSTACEA; DIPLOPODA; INSECTA; PAUROPODA; SYMPHYLA. W. D. Russell-Hunter

Manganese

A metallic element, Mn, atomic number 25, and atomic weight 54.9380 g/mole. Manganese is one of the transition elements of the first long period of the periodic table, falling between chromium and iron. The principal properties of manganese are given in the table. It is the twelfth most abundant element in the Earth's crust (approximately 0.1%) and occurs naturally in several forms, primarily as the silicate ($MnSiO_3$) but also as the carbonate ($MnCO_3$) and a variety of oxides, including pyrolusite (MnO_2) and hausmannite (Mn_3O_4). Weathering of land deposits has led to large amounts of the oxide being washed out to sea, where they have aggregated into the so-called manganese nodules containing 15–30% Mn. Vast deposits, estimated at over 10^{12} metric tons, have been detected on the seabed, and a further 10^7 metric tons is deposited every year. The nodules also contain smaller amounts of the oxides of other metals such as iron (Fe), cobalt (Co), nickel (Ni), and copper (Cu). The economic importance of the nodules as a source of these important metals is enormous. *See* HAUSMANNITE; MANGANESE NODULES; PERIODIC TABLE; PYROLUSITE.

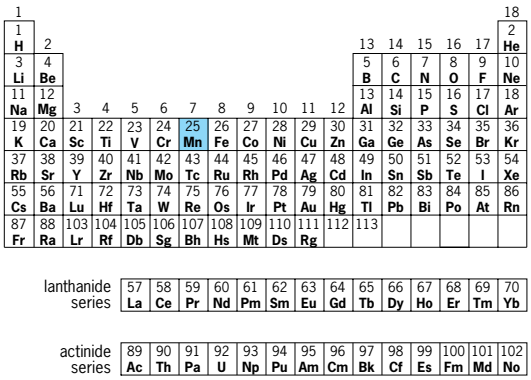

Manganese is more electropositive than its near neighbors in the periodic table, and consequently more reactive. The bulk metal undergoes only surface oxidation when exposed to atmospheric oxygen, but finely divided metal is pyrophoric.

Manganese is a trace element essential to a variety of living systems, including bacteria, plants, and animals. In contrast to iron (Fe), its neighbor in the periodic table, the exact function of the manganese in many of these systems was determined only recently. The manganese superoxide dismutases have been isolated from bacteria, plants, and animals, and are relatively small enzymes with molecular weights of approximately 20,000. The function of the enzyme is believed to be protection of living tissue from the harmful effects of the superoxide ion (O_2^-), a radical formed from partial reduction of O_2 in the cells of respiring (O_2-utilizing) cells.

The most important biological role yet recognized for manganese is in the enzyme responsible for photosynthetic water oxidation to oxygen in plants and certain photosynthetic bacteria. This reaction represents the source of oxygen gas on the Earth and is therefore responsible for the development of the most common forms of life.

All steels contain some manganese, the major advantage being an increase in hardness, although it also serves as a scavenger of oxygen and sulfur impurities that would induce defects and consequent

Properties of manganese

Property	Value
Atomic number	25
Atomic weight, g/mole	54.9380
Naturally occurring isotope	^{55}Mn (100%)
Electronic configuration	[Ar]$3d^5 4s^2$
Electronegativity	1.5
Metal radius, picometers	127
Melting point, °C (°F)	1244 ± 3 (2271 ± 5.4)
Boiling point, °C (°F)	1962 (3563)
Density (25 °C or 77°F), g/cm^3 (oz/in.^{3})	7.43 (4.30)
Electrical resistivity, ohm·cm	185×10^{-6}

brittleness in the steel. Manganese even has some use in the electronics industry, where manganese dioxide, either natural or synthetic, is employed to produce manganese compounds possessing high electrical resistivity; among other applications, these are utilized as components in every television set. *See* ELECTROLYSIS; GLASS; METAL; TRANSITION ELEMENTS.

George Christou

Bibliography. F. A. Cotton et al., *Advanced Inorganic Chemistry*, 6th ed., Wiley-Interscience, 1999; N. N. Greenwood and A. Earnshaw, *Chemistry of the Elements*, 2d ed., 1997; A. G. Sykes (ed.), *Advances in Inorganic Chemistry*, vol. 49, 1999.

Manganese nodules

Concentrations of manganese (Mn) and iron oxides found on the floors of many oceans. The complex growth histories of manganese nodules are revealed by the textures of nodule interiors (**Fig. 1**).

Nodules from certain regions are significantly enriched in nickel, copper, cobalt, zinc, molybdenum, and other elements so as to make them important reserves for these strategic metals. Modern oceanographic surveys have delineated areas of the world's sea floors where nodule abundances and metal concentrations are highest.

Regions of metal-rich nodules. Although manganiferous nodules and crusts have been sampled or observed on most sea floors, attention has focused on the nickel-copper–rich nodules (2–3 wt %) from the north equatorial Pacific belt stretching from southeast Hawaii to Baja California, as well as the high-cobalt nodules and crusts from seamounts in the central Pacific. Manganese nodules from the Atlantic Ocean and from higher latitudes in the Pacific Ocean have significantly lower concentrations of the minor strategic metals. Surveys of the Indian Ocean have revealed metal-enrichment trends comparable to those found in the Pacific Ocean nodules; high nickel-cobalt-copper–bearing nodules are found near the Equator. The ferromanganese nodules and crusts associated with submarine hydrothermal deposits have extremely low concentrations of nickel-cobalt-copper.

Fig. 1. Reflected-light photograph of the polished surface of a sectioned manganese nodule showing the complex growth history of the concretionary deposit (diameter 1.6 in. or 4 cm).

The metal-rich nodules of the north equatorial Pacific are underlain by siliceous ooze sediments composed primarily of skeletons of radiolarians and diatoms. The sea floor here is generally deeper than the carbonate compensation depth, below which the calcium carbonate ($CaCO_3$) in tests of foraminifera, coccoliths, and other calcareous organisms is dissolved at the high pressures (approximately 500 atm or 50 megapascals) and low temperatures (approximately 36°F or 2°C) of the deep ocean. South of the Equator, calcareous ooze sediments predominate and abundances of manganese nodules are considerably lower. At higher latitudes, away from the high biological productivity surface waters that occur near the Equator, pelagic red clays underlie the manganese nodules, which generally have lower Ni + Cu, but higher iron (Fe), contents than equatorial nodules.

The growth rate of marine manganese nodules, determined by decay measurements of traces of radioactive isotopes such as thorium-230 (^{230}Th), protactinium-231 (^{231}Pa), beryllium-10 (^{10}Be), and potassium-40 (^{40}K) contained in the nodules is very slow, averaging a few millimeters each million years. Since the sedimentation rates of accompanying siliceous ooze or pelagic red clay sediments are almost a thousand times faster than the nodule growth rates, an enigma in manganese nodule geochemistry is how they avoid being buried by sediment raining down on them. One explanation is the high populations of benthic organisms living in the inhospitable, dark, high-hydrostatic-pressure, low-temperature environment on deep sea floors which could periodically roll over the nodules and keep them at the sediment-seawater interface. Other possible mechanisms are winnowing of sediments by bottom currents, less dense nodules floating on top of denser sediments, and diagenetic remobilization of manganese in the sediment column, dissolving buried nodules and redepositing the manganese on surface nodules. *See* DEEP-SEA FAUNA.

Chemistry of nodules. Marine manganese nodules are usually classified by mode of formation into hydrogenetic, diagenetic, and hydrothermal types. A fourth, mixed type also exists. Hydrogenetic nodules form by direct precipitation of manganese–iron oxide phases onto an existing nucleus at the sediment-water interface; diagenetic nodules are believed to be biologically driven; and hydrothermal nodules form by submarine hydrothermal activity. Hydrothermal nodules are rarely reported; in submarine hydrothermal environments, manganese–iron oxides occur mainly as crusts. Cobalt is the only strategic metal reported in hydrogenetic nodules that have relatively low manganese/iron ratios. Nodules

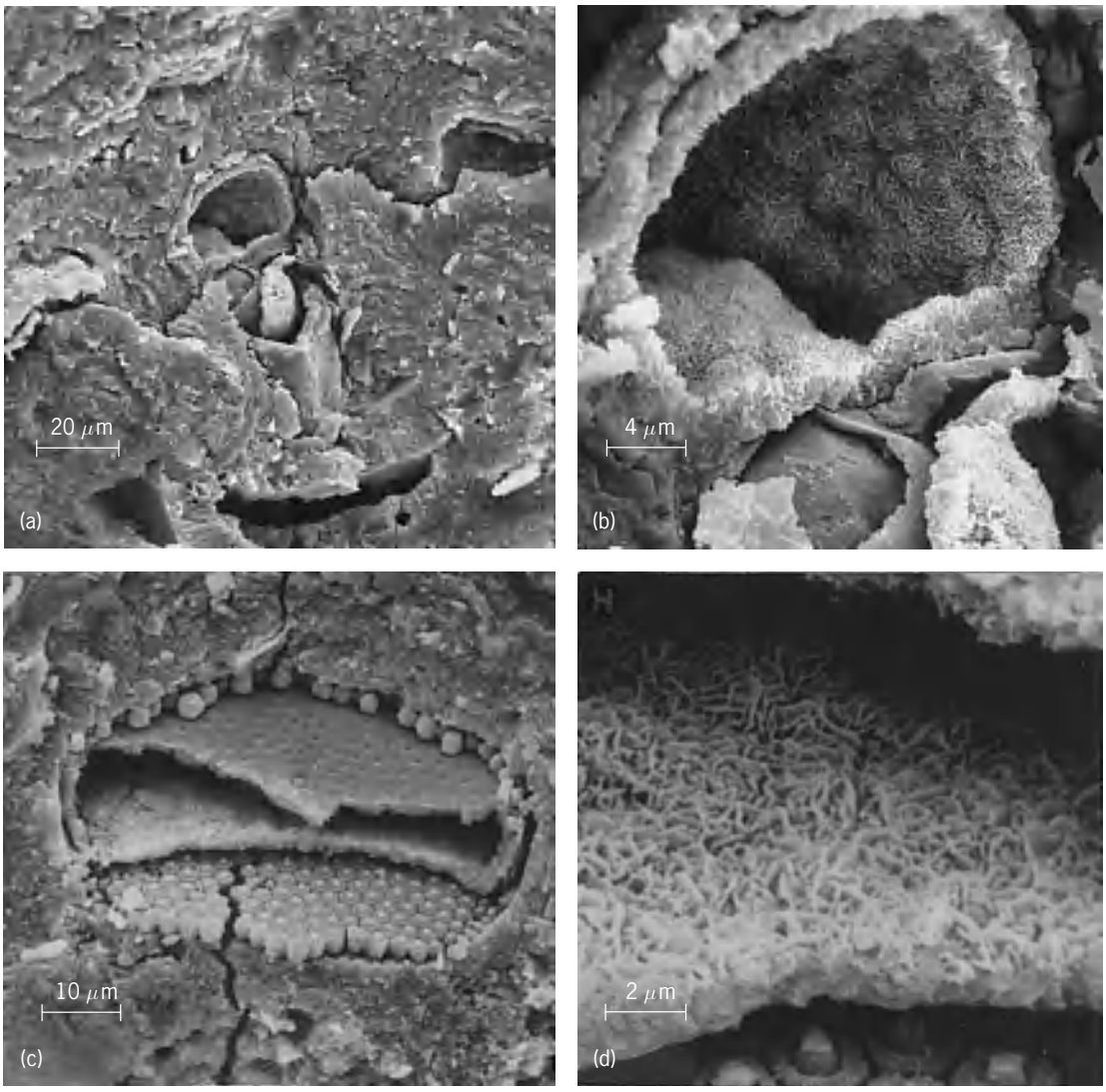

Fig. 2. Scanning electron microscopy photographs showing the growth of Ni + Cu–rich todorokite inside a manganese nodule from the north equatorial Pacific. The meshworks of tiny todorokite crystals (*a, b*) line a cavity and (*c, d*) replace biogenic debris in a fossil cast inside the nodule. (*From R. G. Burns and V. M. Burns, Manganese oxides, in R. G. Burns, ed., Marine Minerals, Mineralogical Society of America Publication Series Reviews in Mineralogy, vol. 6, pp. 1–46, 1979*)

with high nickel, cobalt, and copper contents are diagenetic and have relatively high manganese/iron ratios. Chemical differences exist between the outermost top layer (exposed to seawater) and bottom layer (immersed in sediment) of manganese nodules. Surfaces buried in underlying sediments are generally higher in manganese, nickel, and copper contents, compared to the more iron-cobalt–rich surfaces exposed to seawater. Episodic rolling-over of a nodule would account for fluctuating concentrations of manganese, iron, nickel, cobalt, copper, and other metals across sectioned manganese nodules.

There is a biological source of the metals and diagenetic remobilization of them in the underlying sediment (**Fig. 2**). Very fine grained, highly dispersed clay minerals and oxides of iron and manganese, derived from various sources, are buried with biogenic debris from deceased organisms living in the surface waters of the equatorial photic zone. Traces of the strategic metals, nickel, copper, cobalt, and so on, either are adsorbed onto the surfaces of clays or manganese and iron oxides or are organically complexed in biological matter settling to the sea floor. A reducing environment is set up at depths in the buried sediments, and organic debris is oxidized by the manganese(IV) and iron(III) oxides, leading to remobilization of soluble cations such as manganese, iron, nickel, and copper in pore waters of the sediments. Oxidation by aerated pore water or ocean bottom water near the sediment-seawater interface, first of iron and then of manganese, produces insoluble authigenic hydrated manganese(IV) and iron(III) oxide phases that accrete onto surfaces of manganese nodules lying in the sediments. Ions of nickel, copper, and other elements are bound as essential constituents in the crystal structures of these diagenetically formed manganese oxides. *See* AUTHIGENIC MINERALS; DIAGENESIS.

Minerals in manganese nodules. Manganese nodules contain extremely small, poorly crystalline

phases of minerals, often finely intermixed. In cobalt-rich nodules from seamounts and relatively shallow sea floors, vernadite (a manganese oxide; δ-MnO_2) accommodates cobalt(III) ions, which have ionic radii identical to those of manganese(IV) ions. Vernadite, which can incorporate iron into its structure, is the characteristic mineral phase in hydrogenetic nodules. The characteristic mineral in diagenetic nodules is todorokite, which concentrates nickel and copper ions in the metal-rich nodules. Todorokite has a framework structure consisting of long chains and tunnels that accommodates both divalent transition metals, and larger cations and water molecules. Ions such as nickel and copper stabilize the todorokite structure. In hydrothermal manganese nodules and crusts near hot-water sources, relatively well-crystallized todorokite occurs along with birnessite, a layer mineral. Iron occurs in nodules as feroxyhyte, which is usually so fine-grained as to be x-ray amorphous and may be epitaxially intergrown with vernadite, especially in hydrogenetic nodules from pelagic red clays and seamounts. Other minerals in low or trace amounts in manganese nodules include smectite, phillipsite, plagioclase, and quartz. *See* HYDROTHERMAL VENT; MARINE MINING; MARINE SEDIMENTS; ORE AND MINERAL DEPOSITS; TODOROKITE.

Roger G. Burns; Virginia Mee-Burns

Bibliography. R. G. Burns and V. M. Burns, The mineralogy and crystal chemistry of deep-sea manganese nodules, a polymetallic resource of the twenty-first century, *Phil. Trans. Roy. Soc. London*, A285:249–258, 1977; D. S. Cronan, *Marine Minerals in Exclusive Economic Zones*, 1991; A. Martin-Barajas, E. Lallier-Verges, and L. Leclaire, Characteristics of manganese nodules from the Central Indian Basin: Relationship with the sedimentary environment, *Mar. Geol.*, 101:249–265, 1991; P. A. Rona and S. D. Scott, A special issue on sea-floor hydrothermal mineralization: New perspectives, *Econ. Geol.*, 88:1935–1976, 1993.

Mango

A tree (*Mangifera indica*) of the family Anacardiaceae that originated in the Indo-Burma region and is now grown throughout the tropical and subtropical areas of the world. The mango is a medium to large evergreen tree; it produces a dense, round canopy, with leaves up to 15 in. (38 cm) long by 2.5 in. (10 cm) wide, which are reddish brown when young and dark green when mature. The tree puts down a deep taproot and has many fibrous roots near the surface. Small, pinkish-white flowers, numbering 600 to 2000 and mostly staminate (male), grow on large terminal panicles. *See* SAPINDALES.

In the United States, mangoes are grown only in Florida and on a small scale in Hawaii, usually as backyard trees. Their greatest importance is in India, which contains about 75% of the world's area of mango production. The ripe fruit is eaten raw as a dessert or used in the manufacture of juice, jams, jellies, and preserves. Unripe fruit can be made into pickles or chutneys. Mangoes are a good source of vitamins A and C.

Mango is grown from sea level to 4000 ft (1220 m) in the tropics. Optimum growth temperature is 75–80°F (24–27°C). Dry weather during flowering and fruiting is important. A high carbon/nitrogen ratio is required for flower initiation. Mangoes tend to bear fruit every two years.

Pollination, which is necessary for setting the fruit, is usually accomplished by flies. Rain and high humidity reduce the fruit set, especially if the anthracnose fungus (*Colletotrichum gloeosporioides*) is present. Benlate or captan sprays give control.

There are three groups of mangoes grown: (1) seedling races in the Western Hemisphere (such as Turpentine, Number 11, and Hawaiian), producing fruit of inferior quality and poor color; (2) Indochinese or Saigon, including Philippine, types which are also rather colorless but have flesh with practically no fiber and a delicate flavor (these are polyembryonic and seedlings come true to type); and (3) the Indian race which is better flavored, has brilliant red, purple, and yellow skins, and is good for commercial production. Practically all of these are monoembryonic and must be propagated asexually. Usually either a side wedge or a veneer graft is used.

Florida developed a large number of mango cultivars in a very short time. The Haden originated in Miami as a seedling of Mulgaba, an Indian cultivar introduced to Florida in 1883. Haden was the standard in commerce for more than 40 years. In Hawaii, Haden and Pirie are popular. Other cultivars include Irwin, Edward, Smith, Tommy Atkins, Kent, Keitt, Palmer, Sensation, Pope, Momi-k, Gouveia, and Ah Ping. *See* FRUIT, TREE.

Robert M. Warner

Bibliography. S. L. Kochhar, *Tropical Crops: A Textbook of Economic Botany*, 1989; S. E. Malo, Mango and avocado cultivars, *Fla. State Hort. Soc.*, 83:357–362, 1970.

Mangrove

A taxonomically diverse assemblage of trees and shrubs that form the dominant plant communities in tidal, saline wetlands along sheltered tropical and subtropical coasts. The development and composition of mangrove communities depend largely on temperature, soil type and salinity, duration and frequency of inundation, accretion of silt, tidal and wave energy, and such fortuitous factors as cyclone or flood frequencies (see **illus.**). Extensive mangrove communities seem to correlate with areas in which the water temperature of the warmest month exceeds 75°F (24°C), and they are absent from waters that never exceed 75°F (24°C) during the year. Intertidal, sheltered, low-energy, muddy sediments are the most suitable habitats for mangrove communities, and under optimal conditions, forests up to 148 ft (45 m) in height can develop, such as those in Ecuador, Thailand, and Malaysia. Where less

Mangroves, Great Barrier Reef, off northeast Australia. (*a*) Mangroves at northwestern corner of King Island. (*b*) Interior of mangrove swamp, Newton Island. (*c*) Mangroves on north side of Howick Island. (*From J. A. Steers, Salt marshes, Endeavour, 18(70):75–82, 1959*)

favorable conditions are found, mangrove communities may reach maturity at heights of only 3 ft (1 m). *See* ECOSYSTEM.

Approximately 58,000 mi^2 (150,000 km^2) of the land in the Americas, Africa, Asia, and Australia is occupied by mangrove communities, which show a great similarity in structure, flora, and function. Plants of the mangrove community belong to many different genera and families, many of which are not closely related to one another phylogenetically. However, they do share a variety of morphological, physiological, and reproductive adaptations that enable them to grow in an unstable, harsh, and salty environment. On the basis of the commonality of those various adaptations, approximately 80 species of plants belonging to about 30 genera in over 20 families are recognized throughout the world as being indigenous to mangroves. About 60 species occur on the east coasts of Africa and Australasia, whereas about 20 species are found in the Western Hemisphere.

At the generic level, *Avicennia* and *Rhizophora* are the dominant plants of mangrove communities throughout the world, with each genus having several closely related species in both hemispheres. At the species level, however, only a few species, such as the portia tree (*Thespesia populnea*), the mangrove fern (*Acrostichum aureum*), and the swamp hibiscus (*Hibiscus tiliaceus*), occur in both hemispheres. Such a present-day distribution can be satisfactorily explained only if the ancestors of the mangroves evolved in the Lower Cretaceous, were dispersed outward from their center of origin in the remnants of the Tethys Sea, and subsequently developed further as two isolated groups following the closure of the Mediterranean Sea as a dispersal route between the Eastern and Western hemispheres. *See* CRETACEOUS.

The mangrove community is often strikingly zoned parallel to the shoreline, with a sequence of different species dominating from open water to the landward margins. These zones are the response of individual species to gradients of inundation frequency, waterlogging, nutrient availability, and soil salt concentrations across the intertidal area, rather than a reflection of ecological succession, as earlier studies had suggested. Not surprisingly, the zonation patterns show some similarity between the Eastern and Western hemispheres. In the Americas and western Africa, *Rhizophora* forms the outermost (seaward) zone, followed by *Avicennia*, then *Laguncularia*, with a sporadic landward fringe of *Conocarpus*. In the Eastern Hemisphere, *Rhizophora* forms the outermost zone, although at some localities *Sonneratia* and *Avicennia* may also be present. *Avicennia* generally forms monospecific stands behind the outer zone, followed by mixed stands of *Bruguiera*, *Heritiera*, and *Xylocarpus*, with a landward zone of *Ceriops* mixed with *Lumnitzera* and *Avicennia*. *See* ECOLOGICAL SUCCESSION.

Most plants of the mangrove community are halophytes, well adapted to salt water and fluctuations of tide level. Many species show modified root structures such as stilt or prop roots, which offer support on the semiliquid or shifting sediments, whereas others have erect root structures (pneumatophores) that facilitate oxygen penetration to the roots in a hypoxic environment. Salt glands, which allow excess salt to be extruded through the leaves, occur in several species; others show a range of physiological mechanisms that either exclude salt from the plants or minimize the damage excess salts can cause by separating the salt from the sensitive enzyme systems of the plant. Several species have well-developed vivipary of their seeds, whereby the hypocotyl develops while the fruit is still attached to the tree. The seedlings are generally buoyant, able to float over long distances in the sea and rapidly establish themselves once stranded in a suitable habitat. *See* PLANTS, SALINE ENVIRONMENTS OF.

A mangrove may be considered either a sheltered, muddy, intertidal habitat or a forest community; consequently, the mangrove fauna comprises elements dependent on either of these habitats. The sediment surface of mangrove communities abounds with species that have marine affinities, including brightly colored fiddler crabs, mound-building mud lobsters (*Thalassina anomala*), and a variety of mollusks and worms, as well as specialized gobiid fish, whose ability to travel over the mud surface by using their fins has earned them the common name mudskippers. The waterways among the mangroves are important feeding and nursery areas for a variety of juvenile finfish as well as crustaceans such as portunid crabs and penaeid shrimps, all of which are important sources of protein for indigenous populations. Animals with forest affinities that are associated with mangroves include snakes, lizards, deer, tigers, crab-eating monkeys, bats, and many species of birds, including flamingos, ibis, sea eagles, herons, pelicans, and several species of kingfisher.

Economically, mangroves are a major source of timber, poles, thatch, and fuel. The bark of some trees is used for tanning materials, whereas other species have food or medicinal value. In Malaysia, Bangladesh, India, and Thailand, managed forest operations produce commercial timber, fuelwood, charcoal, or woodpulp. Subsistence harvesting of mangrove resources is widespread in Central America and parts of Asia and Africa. Elsewhere, mangroves are gathering areas for honey and fodder. Despite their obvious economic value, mangroves have often been considered wastelands and have been converted to other forms of land use. Gradually, however, opinion has changed, and mangrove communities are now recognized not merely for their economic value but also as living systems of major intrinsic scientific interest. *See* ECOLOGICAL COMMUNITIES; FOREST MANAGEMENT. Peter Saenger

Bibliography. P. Hutchings and P. Saenger, *Ecology of Mangroves*, 1987; V. Jaccarini and E. Martens (eds.), *The Ecology of Mangrove and Related Ecosystems*, 1993; P. B. Tomlinson, *The Botany of Mangroves*, 1994.

Manifold (mathematics)

A Hausdorff topological space with an n-dimensional atlas of charts for some integer n. The integer n is called the dimension of the manifold. If M is a Hausdorff space, an n-chart on M is a pair (U, φ) with U an open subset of M and φ a homeomorphism of U onto an open subset $\varphi(U)$ of n-dimensional euclidean space $\mathbf{R}^n$. An n-dimensional atlas for M is a system of n-charts (U, φ) such that the union of the sets U is all of M. *See* TOPOLOGY.

The terminology "charts" and "atlases" comes from the geographer's way of viewing the surface of the Earth. The manifold described in this case is the two-dimensional sphere $M = S^2$.

Many mathematicians include an additional restriction in the definition of manifold—sometimes the underlying topological space is connected, sometimes the topology is given by a metric, sometimes both.

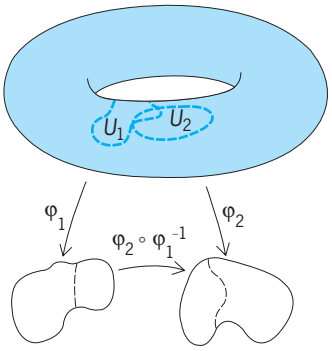

Sets and mappings defining compatible n-charts (U_1, φ_1) and (U_2, φ_2).

Differentiable structure. With an appropriate additional structure on a manifold, it is possible to speak of differentiability or smoothness of real-valued functions. In this setting, the notion of a smooth mapping between smooth manifolds can be defined, and the differential of a smooth mapping, which is a generalization of the derivative, can be introduced.

Two charts (U_1, φ_1) and (U_2, φ_2) in an atlas for an n-dimensional manifold M are compatible (for defining smoothness) if the mapping $\varphi_2 \circ \varphi_1^{-1}$ from the open set $\varphi_1(U_1 \cap U_2)$ in $\mathbf{R}^n$ to the open set $\varphi_2(U_1 \cap U_2)$ is infinitely differentiable and has an infinitely differentiable inverse function (see **illus.**). If all the charts in an atlas are compatible with one another, the atlas is said to determine a differentiable structure on M, and M with its atlas is then called a smooth manifold. Two atlases determine the same differentiable structure if all the charts in question are compatible with one another. Smooth manifolds are called also differentiable manifolds, differential manifolds, and C^∞ manifolds.

Examples. If M is an open subset of $\mathbf{R}^n$, then M and the identity mapping form a single chart, that is, an atlas of compatible charts for M. The resulting differentiable structure is the standard differentiable structure on this open subset of $\mathbf{R}^n$.

The unit sphere S^n in $\mathbf{R}^{n+1}$ can be made into a smooth manifold of dimension n by using the two charts given in Eqs. (1) and (2). The function φ_1 is defined on $U_1 = S^n - \{(0, \ldots, 0, -1)\}$, and the function φ_2 is defined on $U_2 = S^n - \{(0, \ldots, 0, -1)\}$.

$$\varphi_1(x_1, \ldots, x_{n+1}) = \left(\frac{x_1}{1 - x_{n+1}}, \ldots, \frac{x_n}{1 - x_{n+1}}\right) \quad (1)$$

$$\varphi_2(x_1, \ldots, x_{n+1}) = \left(\frac{x_1}{1 + x_{n+1}}, \ldots, \frac{x_n}{1 + x_{n+1}}\right) \quad (2)$$

The projective space $\mathbf{R}P^n$ is another example of a smooth manifold. A point of $\mathbf{R}P^n$ is all nonzero points on a line through the origin of $\mathbf{R}^{n+1}$ and is written $[(x_1, \ldots, x_{n+1})]$. The space $\mathbf{R}P^n$ is given the quotient topology. An atlas (U_j, φ_j), $1 \le j \le n + 1$, is defined

as follows: U_j is the set of members of $\mathbf{R}P^n$ whose jth coordinate is nonzero, and φ_j is given on U_j by Eq. (3). The space $\mathbf{R}P^2$ is the underlying set in which

$$\varphi_j[(x_1, \ldots, x_{n+1})] = x_j^{-1}(x_1, \ldots, x_{j-1}, x_{j+1}, \ldots, x_{n+1}) \quad (3)$$

two-dimensional projective geometry is studied. *See* GEOMETRY; PROJECTIVE GEOMETRY.

The product of two smooth manifolds is a smooth manifold. The torus $S^1 \times S^1$ (surface of a doughnut) is an example. *See* TORUS.

Nonsingular plane curves give examples of one-dimensional smooth manifolds, and nonsingular surfaces in $\mathbf{R}^3$ give examples of two-dimensional smooth manifolds. These facts can be proved from the implicit function theorem. *See* DIFFERENTIAL GEOMETRY; PARTIAL DIFFERENTIATION.

Smooth functions and mappings. Functions on a smooth manifold can be referred to functions on euclidean space by means of the charts, which can be regarded as supplying local coordinate systems for the manifold. A real-valued function on a smooth manifold or a mapping between smooth manifolds is said to be smooth if, when referred to local coordinates, it is infinitely differentiable.

Tangent space. The real-valued smooth functions on M form a real vector space. A linear functional L on this space is called a tangent vector at a point p of M if Eq. (4) is satisfied for all smooth f and g. In local co-

$$L(fg) = f(p)L(g) + g(p)L(f) \quad (4)$$

ordinates, L is a linear combination, with numerical coefficients, of first partial derivatives evaluated at p. The vector space of all tangent vectors at p is called the tangent space to M at p. If M has dimension n, its tangent space at p has dimension n. *See* LINEAR ALGEBRA; OPERATOR THEORY.

Differential. If $\varphi: M \to N$ is a smooth mapping between smooth manifolds, p is a point of M, and X is a tangent vector at p, then a tangent vector L to N at $\varphi(p)$ is defined by Eq. (5), where f is any smooth

$$Lf = X(f \circ \varphi) \quad (5)$$

real-valued function on N; $d\varphi_p(X)$ is written for L. The mapping $d\varphi_p$ defined in this way and carrying the tangent space to M at p to the tangent space to N at $\varphi(p)$ is linear and is called the differential of φ at p.

If M and N are both the real line, the differential of φ at p is a multiple of the differential of the identity mapping at p, and that multiple is exactly the derivative of φ at p. *See* DIFFERENTIATION.

Other structures. Alternate definitions of compatibility of charts lead to other classes of manifolds. Thus a manifold with its atlas is said to be piecewise linear (PL) or real analytic if all the mappings $\varphi_2 \circ \varphi_1^{-1}$ have the corresponding property.

If the dimension n is even, say $2m$, then the open sets in $\mathbf{R}^n$ can be regarded as open sets in the complex space $\mathbf{C}^m$ The manifold with its atlas is called a complex manifold of dimension m if the mappings $\varphi_2 \circ \varphi_1^{-1}$ are analytic functions of several variables. Complex manifolds are used in studying varieties in algebraic geometry. *See* ALGEBRAIC GEOMETRY; COMPLEX NUMBERS AND COMPLEX VARIABLES; SERIES.

Anthony W. Knapp

Bibliography. L. Conlon, *Differentiable Manifolds: A First Course*, 2d ed., 2001; G. de Rham, *Differentiable Manifolds*: *Forms*, *Currents*, *Harmonic Forms*, 1984; A. A. Kosinski, *Differential Manifolds*, 1997; S. Lang, *Differential and Riemannian Manifolds*, 3d ed., 1995; K. Shiohama (ed.), *Geometry of Manifolds*, 1989; F. W. Warner, *Foundations of Differentiable Manifolds and Lie Groups*, 1996.

Mantophasmatodea

An order of Insecta, known as heel-walkers or gladiators, occurring in Africa south of the Equator. Members of the 13 known species are 1–3 cm (0.4–1.2 in.) long, slender, moderately long-legged, and secondarily wingless. The habitus (general appearance) resembles a mixture of grasshopper, stick-insect, and praying mantis (see **illustration**).

While amber fossils were mentioned in the literature in 1997 (nymphs only), the first species was not described until 2001 (*Raptophasma*, adult specimens). The two first extant specimens, collected in Namibia and Tanzania, were found in the natural history museums of Berlin and London in 2001 and described in 2002 (*Mantophasma* and *Tanzaniophasma*). During 2002 and 2003 living specimens were reported from many places in Namibia and South Africa.

Morphology. The biting mouthparts are directed downward. The antennae are long and thin; the forelegs have a strong femur and two rows of spines on the tibia. The females possess a short ovipositor (egg-laying device) on the posterior abdominal segments. The cerci (appendages of last abdominal segment) are short and one-segmented, forming claspers in the male. Derived characters distinguishing Mantophasmatodea from other insects are

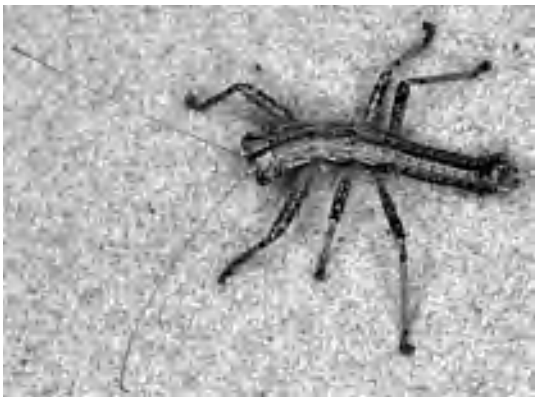

Male of *Karoophasma biedouwensis* from Succulent Karoo biome of western South Africa. (*Photo by M. Picker, University of Cape Town*)

(1) anterior tentorial pits (invagination points of the skeleton inside the head) located far above the base of the mandibles; (2) antennae differentiated into a sparsely setose, multijointed basal part and a wider, more strongly setose distal part with seven joints showing specific length ratios; (3) a huge lobe (arolium) between the claws of the legs. The coloration is patchy, mainly brown, yellow, grey, and green, varying among and within species.

Diversity and distribution. Four species occur in Namibia (genera *Mantophasma, Sclerophasma, Praedatophasma*, and *Tyrannophasma*), eight in western South Africa (*Austrophasma, Karoophasma, Lobophasma, Hemilobophasma*, and *Namaquaphasma*), and one in Tanzania (*Tanzaniophasma*). Species differ mainly in the structure of the male and female genitalia; *Praedatophasma* and *Tyrannophasma* are conspicuously spinose (hence the common name "gladiator"). The single species usually exhibit limited distribution. Mantophasmatodea inhabit several major biomes of southwestern Africa: the dry Nama Karoo and Succulent Karoo, and the more humid Fynbos. Fossils from the Lower Tertiary were found in Europe (*Raptophasma* and *Adicophasma* in Baltic amber).

Life history. The heel-walkers live singly and prey on insects, which they grasp using their strong, spiny forelegs. The terminal tarsomere (foot segment), with the claws and arolium, is usually held elevated (hence the common name). The males use a median projection of their subgenital plate to knock on the ground—probably for communication. To copulate, the male jumps onto the female and bends its abdomen aside and downward to bring the copulatory organs into contact. The female produces sausage-shaped egg pods, each containing 10–20 eggs, enclosed in a hard envelope made from gland secretions and sand. The nymphs, which resemble the adults (hemimetabolism), hatch in the early humid season and reach maturity near its end.

Phylogenetic relationships. Anatomical details of the spiracles, musculature, and ovipositor show that despite their lacking wings the Mantophasmatodea belong to the subclass Pterygota of the Insecta ("winged insects"). DNA studies suggest the wingless Notoptera (ice-crawlers) to be their closest relatives. The morphological evidence is conjectural: different characters point to a close relationship with Dictyoptera (cockroach-mantis-termite group) based on the structure of the male genitalia and spermatozoa, with Phasmatodea (stick-insects) based on the sclerotized process above the male genitalia, with Plecoptera (stoneflies) based on the median process on the male subgenital plate, or Notoptera based on the foregut structure.

Klaus-Dieter Klass

Bibliography. K.-D. Klass, Mantophasmatodea, pp. 182–184 in *2004 McGraw-Hill Yearbook of Science & Technology*, McGraw-Hill, New York, 2004; K.-D. Klass, Mantophasmatodea, pp. 677–678 in V. H. Resh and R. T. Cardé (eds.), *Encyclopedia of Insects*, Academic Press, San Diego, 2003; K.-D. Klass et al., Mantophasmatodea: A new insect order with extant members in the Afrotropics, *Science*, 296:1456–1459, 2002; K.-D. Klass et al., The taxonomy, genitalic morphology, and phylogenetic relationships of southern African Mantophasmatodea (Insecta), *Entomol. Abhandlungen*, 61:3–67, 2003.

Manufactured fiber

Any of a number of textile fibers produced from chemical substances of natural origin or synthetic origin; the latter are also known as synthetic fibers. Among the natural sources of manufactured fibers are plant cellulose and protein, rubber, metals, and nonmetallic inorganics. The synthetic fibers are produced from organic intermediates derived from petroleum, coal, and natural gas.

In addition to names based on their chemical composition, manufactured fibers may be known by the manufacturer's name or trademark; terms referring to characteristic properties, for example, thermoplastic fibers; and method of manufacture, for example, wet-spun fiber. In the United States, the Textile Fiber Products Identification Act (TFPIA) standardized the nomenclature. In the following discussions, each fiber will be defined according to the TFPIA. Fiber structures are shown in **Fig. 1**.

Manufacture

With the exceptions of glass and metal fibers, the manufactured fibers are made from very long chainlike molecules called linear polymers (**Fig. 2**). These polymers may be naturally occurring (cellulose from cotton or wood pulp) or may be synthetic (polyester). When the polymer is of biological origin, the problem is one of converting it from its natural form into a fiber. The synthetic polymers may be formed either by addition polymerization or by condensation polymerization. In the former process, small molecules (monomer) containing unsaturated carbon-carbon bonds are built into polymers by using catalysts to open the double bonds joining the carbon atoms of one molecule. This reactive molecule subsequently "attacks" a second molecule, joins with it, and propagates the reactive entity. Thus, a number of monomer units may be joined together in a single chain by the addition of links of monomer. The growing chains may be terminated by the joining of two growing chains or by the addition of substances which will combine with the reactive species to form inactive chain ends.

In condensation polymerization, molecules containing reactive groups at each end are combined, with the elimination of water as a by-product, to yield larger molecules which still contain reactive groups at each end. The reactive groups can continue to combine to build, step by step, a large polymer. The reaction may be terminated by the addition of a stopping agent, which will inactivate one or both of the reactive species. *See* POLYMERIZATION.

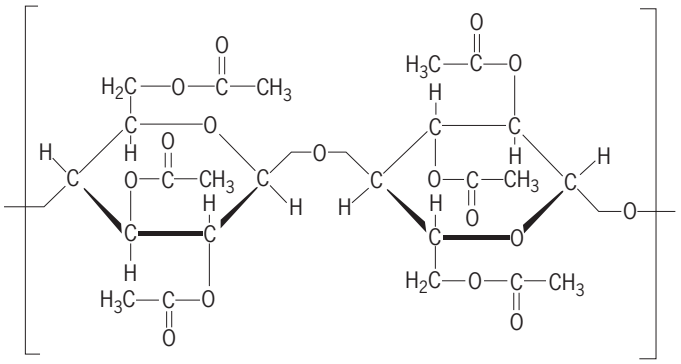

Cellulose triacetate

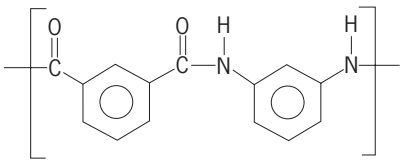

Aramid (Nomex)

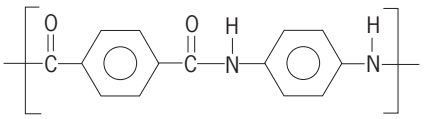

Aramid (Kevlar)

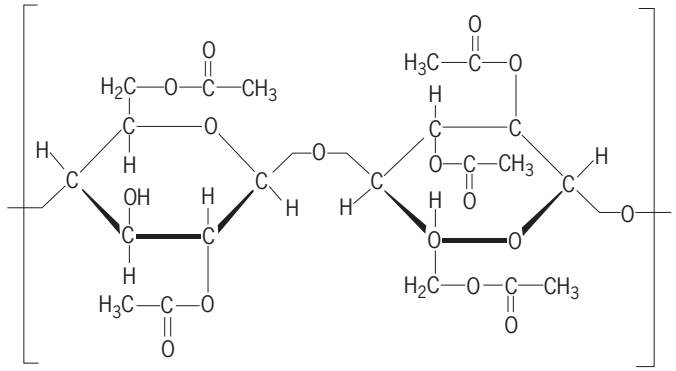

Cellulose acetate

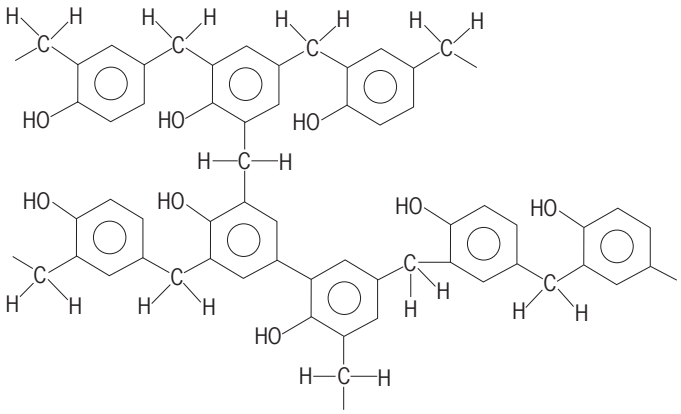

Novolac (Kynol)

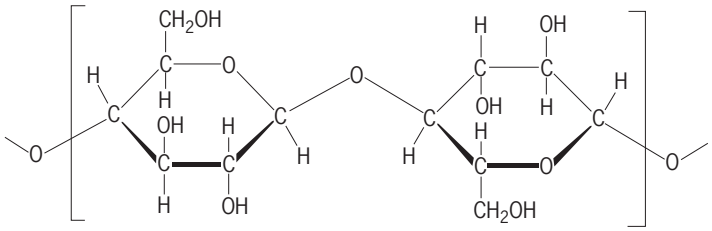

Rayon

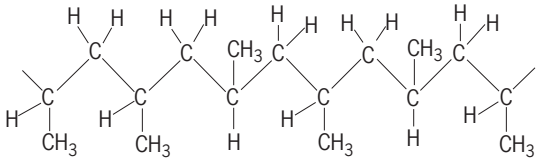

Polypropylene (olefin)

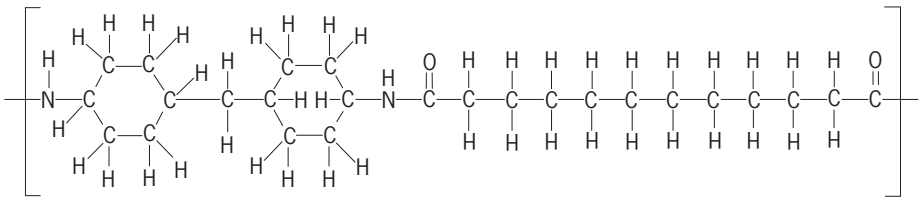

Qiana nylon

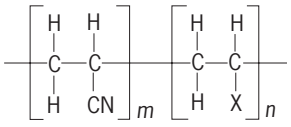

copolymer

Acrylic (X = –CN) and Modacrylic

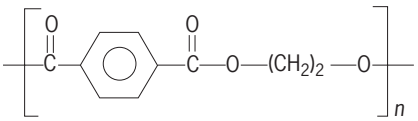

Polyester (PET)

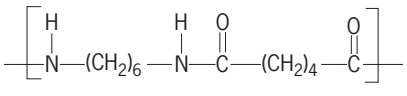

Nylon 6,6

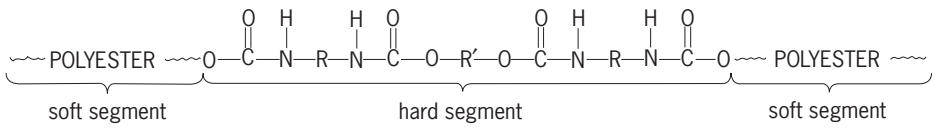

soft segment hard segment soft segment

Spandex

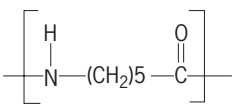

Nylon 6

Fig. 1. Structures of the manufactured fibers. (*After B. F. Smith and I. Block, Textiles in Perspective, Prentice-Hall, 1982*)

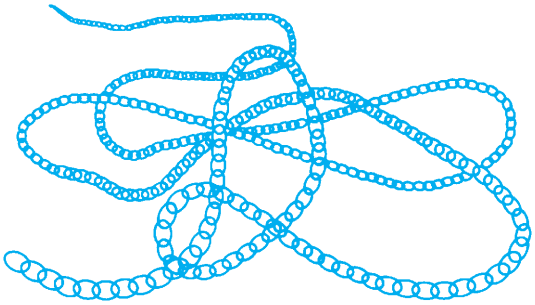

Fig. 2. Idealized polymer modeled as a chain of many identical links. The molecule tends to curl rather than stretch out. (*After B. F. Smith and I. Block, Textiles in Perspective, Prentice-Hall, 1982*)

Polymer characteristics. Irrespective of their chemical nature, fiber-forming polymers must possess the following characteristics: (1) great length—at least 200 monomer units must be joined in a chain; (2) a high degree of intramolecular and intermolecular attraction, whether through primary chemical bonds or other attractive forces; (3) the ability to be oriented along the axis of the fiber; and (4) the ability to form well-ordered crystals or pseudocrystals. All of these parameters are sensitive to the chemical nature of the polymer and the processes of manufacture of the fiber. In turn, they establish the properties of the fiber, such as strength, flexibility, resilience, and abrasion resistance, which contribute to their usefulness in various end uses for apparel, home furnishings, and commercial and industrial applications.

Only a fraction of those substances capable of forming fibers prove to have all of the characteristics necessary for commercial success. The fiber types of major importance in the United States are classified by composition as follows: cellulosic (composed of regenerated cellulose, cellulose diacetate, and cellulose triacetate); synthetic (composed of polyamide, polyester, polyacrylic, polyvinyl, and polyolefin resins); and inorganic (composed of glass and metal).

All of the manufactured fibers are produced according to the same principles: (1) the fiber-forming material must first be made fluid; (2) the fluid is forced under pressure (extruded) through tiny holes into a medium which causes it to solidify; and (3) the solid fibers are further processed to obtain their optimum properties.

Fiber production. Depending upon the starting materials, typically one of three procedures is used to produce fibers.

Wet spinning. The major example of this process is the production of rayon by the viscose process: the polymer is dissolved in an applicable reagent to form the fluid (dope). The fluid is then pumped through metal plates (spinnerets) containing many small holes into a liquid bath of appropriate composition. A chemical reaction between the spinning dope and the bath causes the fiber to solidify.

Dry spinning. In this process, the polymer is again dissolved in an appropriate solvent and extruded through a spinneret. However, the liquid bath is replaced by a stream of warm gas (usually air) which evaporates the solvent and allows the polymer to solidify as a filament. Cellulose diacetate and triacetate are produced in this manner.

Melt spinning. Nylon, polyester, and the other thermoplastic fibers are produced by melt spinning. No solvents or reagents are required since the polymer can be melted without appreciable decomposition. Thus, the fluid consists of hot molten polymer which, upon extrusion into a stream of cold air, solidifies into a filament. Depending upon the end use, filaments may be produced in various sizes ranging from finer than a human hair to thick bristles for toothbrushes. They may also be produced with different cross-sectional shapes, such as round, lobed, square, or dogbone (**Fig. 3**).

Filament drawing. After extrusion, filaments are usually stretched (drawn). Drawing causes an increase in order (crystallinity) by extending the molecules of the fiber so that they pack more closely together, and orients the molecules along the longitudinal axis of the fiber. Higher orientation and increased crystallinity raise the strength of the fiber, decrease its stretch, and improve its elasticity.

Texturing. Often, the manufactured fibers are textured to improve their comfort properties. Fabrics made from smooth, straight filament yarns are not as comfortable as those made from yarns spun from the shorter natural fibers. Spun yarns which are more open and have a higher surface area than the filament yarns trap air between the fibers. This trapped air acts as an insulator which improves winter comfort by retaining body heat. The higher surface area facilitates the transport of body moisture within and through a fabric and improves summer comfort by reducing dampness and enhancing evaporative cooling. Because the early manufactured fibers were straight and smooth, yarns made from them provided little insulation and poor moisture transport, so that the early fabrics were cold and clammy in winter and hot and sticky in summer.

Texturing introduces irregularities (crimp) along the length of the filament and leads to bulkier filament yarns which are closer to spun yarns in their performance (**Fig. 4**). There are a number of methods used to introduce crimp into manufactured filament yarns. The most widely used is the false twist method, in which the yarn traveling vertically is looped over a horizontal pin which rotates at very high speed about its vertical axis, or in which the yarn is passed through a set of rotating disks. In either method, the heated yarn is caused to twist as it enters and to untwist as it exits the device.

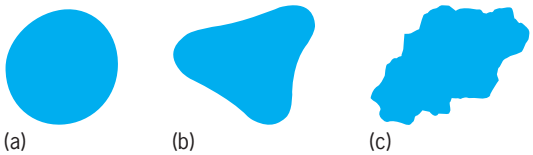

Fig. 3. Typical fiber cross sections. (*a*) Round. (*b*) Lobed. (*c*) Irregular. (*After B. F. Smith and I. Block, Textiles in Perspective, Prentice-Hall, 1982*)

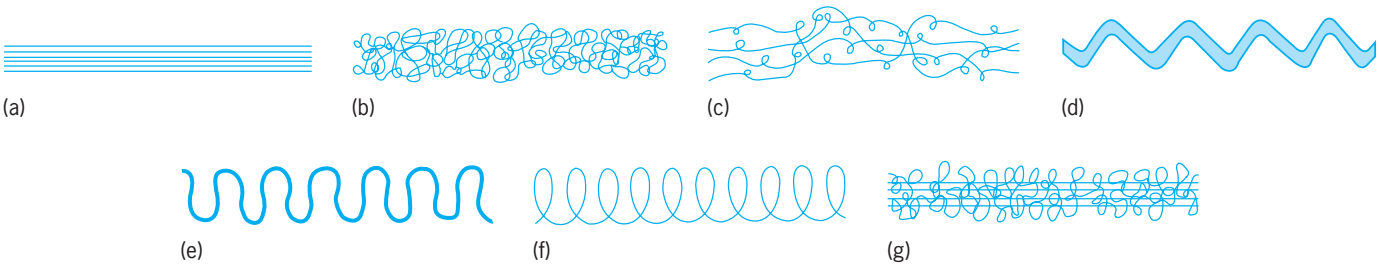

Fig. 4. Comparison of configurations of untextured and textured yarns. (*a*) Untextured filament yarn. (*b*) Entangled yarn. (*c*) Multifilament coil yarn. (*d*) Stuffer box crinkle yarn. (*e*) Knit-de-knit crinkle yarn. (*f*) Monofilament coil yarn. (*g*) Core-bulked yarn. (*After B. F. Smith and I. Block, Textiles in Perspective, Prentice Hall, 1982*)

Beyond the texturing apparatus, the yarn is cooled and the wavy crimp imparted to the individual filaments by the twisting while hot is permanently set. Other methods such as air jet, edge crimp, gear crimp, and stuffer box are also used, depending upon the nature of the fiber and the end use of the yarn (**Fig. 5**). Innovations in the spinning of filament fibers have led to filaments which are

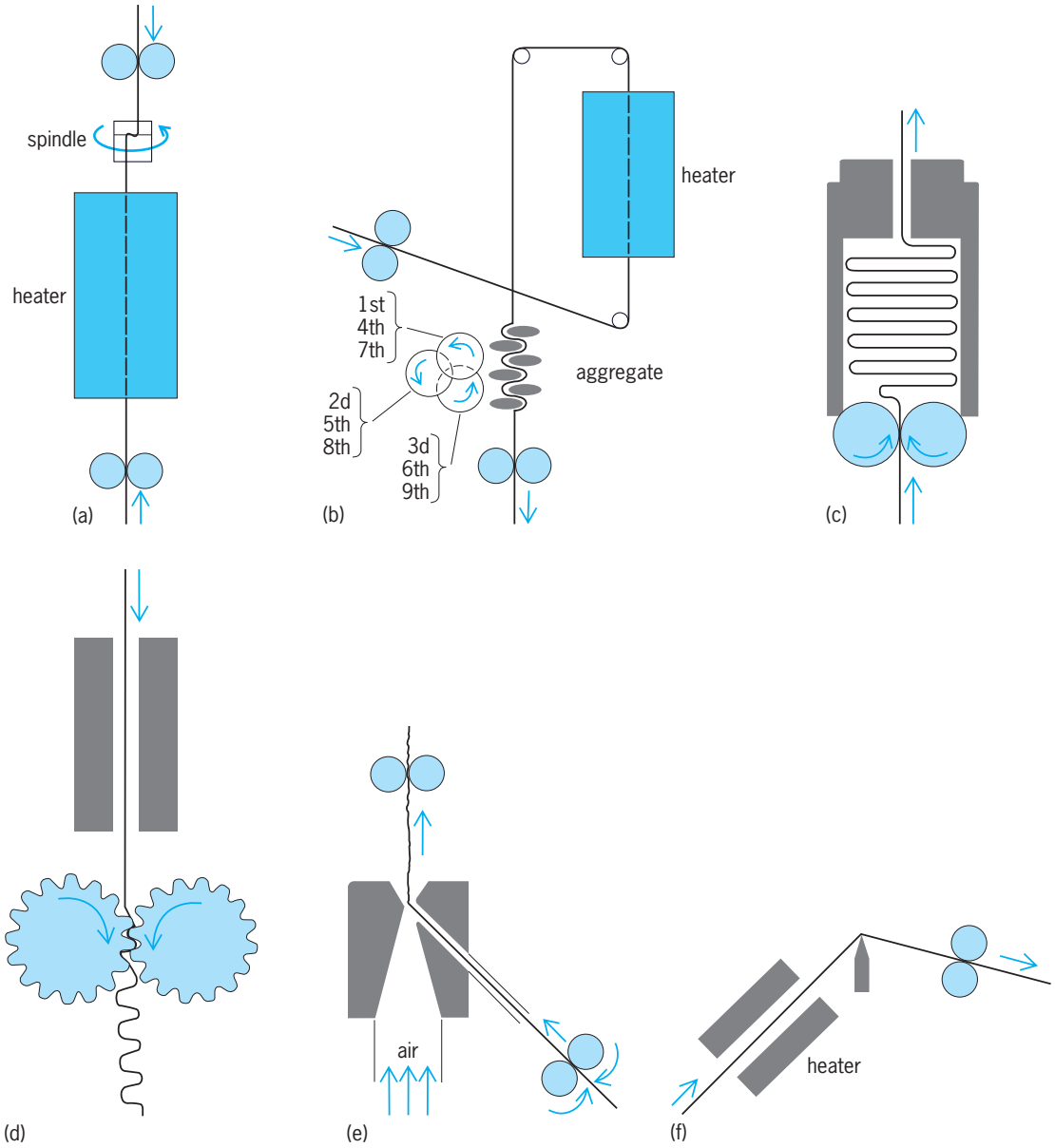

Fig. 5. Methods for crimping manufactured filament yarns. (*a*) Spindle false twisting. (*b*) Friction false twisting. (*c*) Stuffer box method. (*d*) Gear crimping. (*e*) Airjet method. (*f*) Edge crimp method. (*After B. F. Smith and I. Block, Textiles in Perspective, Prentice Hall, 1982*)

self-crimping. It is also possible to cut textured filament fibers to short (staple) length and to twist them into spun yarns, either as 100% manufactured fibers or in blends with natural fibers.

Cellulosic Fibers

These fibers are made from naturally occurring cellulose. They are found as (1) regenerated cellulose (rayon) in which the polymer is converted from the natural staple to manufactured filament while still maintaining its chemical structure; (2) cellulose diacetate (acetate) in which chemical modification converts about 80% of the hydroxyl (S—OH) groups on the cellulose to acetate (S—$OOCCH_3$) groups; and (3) cellulose triacetate in which at least 92% of the hydroxyl groups are converted to acetate. *See* CELLULOSE; WOOD CHEMICALS.

Rayon. Rayon is a manufactured fiber composed of regenerated cellulose in which substituents have replaced not more than 15% of the hydrogens of the hydroxyl groups. To spin these fibers from cotton linters or wood pulp, it is necessary to put the cellulose into fluid form without destroying its chain-like molecular structure. About 1885, Joseph Swan in England and Count Hilaire de Chardonnet in France conducted experiments leading to a process for extruding solutions of nitrocellulose and denitrating the filaments. In 1892, C. F. Cross and E. J. Bevan developed a better method using a solution of cellulose xanthate made from alkali cellulose and carbon disulfide. This is the basis of the viscose process used for the bulk of modern rayon production. Some is made by the regeneration of cuprammonium cellulose.

The viscose process consists of the following steps: steeping cellulose sheets in sodium hydroxide, shredding the sheets, aging the shredded materials to form alkali cellulose, treating it with carbon disulfide to form cellulose xanthate, ripening and filtering the spinning solution, extruding the solution through the small holes of the spinneret into an acid coagulating bath, stretching the filaments, and then washing, drying, and packaging.

Over the years, rayon has steadily improved in quality, versatility, and economic importance. Partly responsible for this expansion was the introduction of staple fiber that could be processed on the same types of equipment used for cotton and wool yarn spinning. For staple fiber, the number of holes in one spinneret is increased from the usual number (20–200) to as many as 20,000. Bundles of fibers from several spinnerets are combined into a rope (tow) which can be cut into short lengths and packaged in bulk. The second significant development was the attainment of high-strength yarns, which led to cords suitable for automobile and truck tires, and to textile yarns with sufficient wet strength for launderable fabrics.

Rayons now offer improved strength coupled with a higher level of comfort. Rayon fibers offer a high luster, a smooth silky hand, and excellent moisture absorption, although strength and abrasion resistance are only fair. The major disadvantages of rayon are its tendency to wrinkle and need for ironing.

Acetate and triacetate. These are manufactured fibers in which the fiber-forming substance is cellulose acetate. The term triacetate may be used as a generic description of the fiber when not less than 92% of the hydroxyl groups are acetylated.

Three hydroxyl groups on each glucose unit of the cellulose molecule can be esterified by acids, such as formic, acetic, propionic, and butyric. The resulting cellulose derivatives can be spun into fibers. Of these, cellulose acetate is most important.

To make acetate, the triacetate is formed first by treating cellulose with acetic anhydride. The triacetate is then converted back to diacetate by partial hydrolysis, precipitated with water, washed acid-free, dried, dissolved in a solvent (usually acetone), and then extruded by a dry-spinning process.

Cellulose triacetate (no hydroxyl groups) is less sensitive to hot water than the diacetate (one hydroxyl group), and garments made of it wrinkle less than those of regular acetate during laundering.

Both acetate and triacetate are less prone to wrinkling and have better wrinkle recovery than rayon. However, they are less durable and not as comfortable as rayon or the natural cellulosic fibers. Where good color, luster, and a silky hand are more important than durability, they have found a useful niche.

Petroleum-Based Fibers

In addition to its use as a fuel, petroleum is a major source of organic molecules which can be converted to synthetic polymers. The petroleum-based fibers constitute the largest class of the manufactured fibers because of the relative ease with which modern technology can prepare the polymers and convert them to fiber. In addition, since the chemical precursors, the polymers, and the fibers can be produced in highly integrated manufacturing plants insensitive to the vagaries of weather and less dependent upon human labor, yarns and cloth made from these fibers are usually less expensive than those produced from natural fibers or from the cellulosics. *See* PETROLEUM.

Nylon. Nylon is a manufactured fiber in which the fiber-forming substance is a long-chain synthetic polyamide having less than 85% of the amide linkages attached directly to two aromatic rings. These fibers are made from polymers based on the condensation polymerization of a dibasic acid with a diamine or of an amino acid with itself. The major one is nylon 6,6, which is made from a six-carbon acid (adipic acid) and a six-carbon diamine. In nylon 6, caprolactam molecules join together by self-condensation to form poly(caproamide). The fiber is produced by melt spinning of the molten polymer.

Nylon fibers have remarkable properties. After spinning, nylon can be drawn to about four times its original length. In addition to producing a finer fiber, the drawing process greatly increases the strength. Another unusual property of nylon fibers compared to earlier manufactured fibers is that nylon can be heat-set. That is, after manufacture of the cloth,

either by weaving or knitting, a heat treatment can be used to relax the residual stresses in the fibers and yarns. Heat setting provides an essentially permanent stability to the fabric so that shrinkage and wrinkling are almost eliminated.

Of major importance to consumers is the high strength, extreme abrasion resistance, excellent resistance to soiling and staining, and ease of care provided by nylon fibers. The major drawback is the slick, synthetic feel of the cloth. However, it is possible to alleviate this problem somewhat by texturing. Alone, or in combination with other fibers such as wool, nylon serves such diverse end uses as intimate apparel, daywear, home furnishings (particularly upholstery, draperies, and carpeting), tire cord, and industrial belting.

Because they are thermoplastic, nylon fibers can be readily spun with cross sections of many shapes. This property was originally exploited by the DuPont Company in its development of trilobal fibers which exhibited an interesting sparkle rivaled only by silk. Others have since developed fibers with Y-shaped, pentalobal and octagonal cross sections, each giving a subtly different combination of esthetics, hand, durability, and ease of care.

An interesting development in nylon technology was Qiana. This fiber, prepared from bis(*p*-aminocyclohexylmethane) and dodecandioic acid is made of molecules having both linear and cyclic components. The ring structures yield a polymer with the strength, durability, and ease of care of nylon, but a hand, luster, and drape which rivals silk. *See* POLYAMIDE RESINS.

Polyester. This is a manufactured fiber composed of at least 85% by weight of a substituted aromatic carboxylic acid, including but not restricted to substituted terephthalate units and parasubstituted hydroxybenzoate units. Although three types of polyester fibers have gained commercial status—poly(ethylene terephthalate) [PET], poly(1,4-cyclohexane dimethyl terephthalate) [PCDT], and poly(ethylene oxybenzoate) [PEB]—the first is by far the largest in sales volume in the United States. Manufactured in a manner similar to that of the nylons, PET is prepared by condensation polymerization of the dimethyl ester of terephthalic acid with ethylene glycol to produce the polymer, and is melt-spun to produce fibers. Like nylon, it is extruded with a variety of cross-sectional shapes and is usually textured prior to use.

Polyester fibers offer high strength and durability but suffer from a tendency to absorb oily stains and poor moisture absorption. Despite these problems, polyester has become the most ubiquitous of the manufactured fibers, appearing as textured filament in knitwear, and in spun blends along with either cotton or wool in both knit and woven apparel. In blends with natural fibers, polyester provides strength, abrasion resistance, and ease of care along with low cost. In home furnishings, polyester is greatly prized as a carpet fiber, but its tendency to absorb oils limits its utility for upholstery.

Acrylic. Acrylic is a manufactured fiber composed of at least 85% by weight of acrylonitrile units. Although the polymer of acrylonitrile had been known for many years, its successful use in fiber form depended upon the discovery of appropriate solvents for dry or wet spinning, and satisfactory methods to dye the fiber. The first commercial acrylic fiber was Orlon. Fibers of this type have attractive properties and a great deal of versatility.

Polyacrylonitrile (PAN) is prepared from the addition polymerization of acrylonitrile. However, the pure polymer is a brittle, glassy substance at room temperature and is not well suited for use as a textile fiber. It was found that by forming copolymers of acrylonitrile and other vinyl monomers the mechanical properties of the fiber would be greatly improved. The fiber is produced by either the wet-spun or the dry-spun process from solution in appropriate solvents. After drawing and texturing, the product is a soft, springy yarn with characteristics similar to wool. It takes dyes well, is extremely resistant to sunlight, is durable, and is relatively easy to maintain. It is widely used by itself and in blends with wool or nylon in sweaters, socks, robes, blankets, carpets, and other products where high bulk and good insulation are important. Because it does not absorb moisture, acrylic suffers from a high buildup of static electricity, particularly in dry weather, which can cause static cling and shock. *See* COPOLYMER; POLYACRYLATE RESIN.

Modacrylic. This is a manufactured fiber composed of less than 85% but at least 35% by weight of acrylonitrile units. The modacrylics are modified acrylic fibers. The addition of large amounts of comonomer with acrylonitrile allows the manufacturer to tailor the fiber to fit specific end-use requirements. These fibers are produced by dissolution of the copolymer in appropriate solvents followed by either wet or dry spinning. The most important uses of modacrylics have been in imitation hair for wigs and imitation furs and fleeces.

Olefin. Olefin is a manufactured fiber composed of at least 85% by weight of ethylene, propylene, or other olefin units. The most useful of the olefin fibers are those produced by the melt spinning of isotactic polypropylene. Because of their rather low melting temperature, these fibers are easily drawn and textured. The product yields fabrics with high bulk and good opacity. In addition, strength, abrasion resistance, and toughness are quite high. The major drawbacks are a slick waxy hand, very poor moisture absorption, and great difficulty in dyeing.

Because of the unappealing hand of cloth made from olefin fibers, they have not been accepted in the general wearing-apparel market. However, thermal undergarments of olefin fiber have been developed. Olefin's most important use is in upholstery and carpeting where its durability, resistance to staining, and ease of cleaning overcome its poor comfort properties and low melting temperature. *See* POLYOLEFIN RESINS.

Spandex. A manufactured fiber identified as spandex must be composed of at least 85% of a segmented polyurethane. In spandex, a long-chain polyester is combined with a short diisocyanate to produce a polymer containing long lengths of a relatively soft material joined by short lengths of a relatively hard material. This is the segmented polyurethane. In the relaxed state, the fibers are rather weak and easily stretched. However, as the fiber is elongated, the hard segments align and form strong, stiff crystals which prevent further extension. Thus, by appropriate combinations of hard and soft segments, these fibers can be engineered to provide any required degree of stretch and strength. The fibers are produced by the wet-spun process from appropriate solvents.

Spandex has found its greatest use as a replacement for rubber, both natural and synthetic. It is particularly useful in intimate apparel and sportswear, where its high elasticity give both figure control and a close fit without restricting the movements of the wearer. *See* RUBBER.

High-performance fibers. Advances in polymer and fiber technology have led to the development of fibers with exceptionally high temperature resistance and extremely high strength. These properties are desirable in applications such as upholstery and floor coverings in aircraft and other mass-transit vehicles, protective clothing for fire fighters and other emergency personnel, body armor for soldiers and police officers, tire cords, and industrial belting.

Aramid. Aramid is a manufactured fiber in which at least 85% of the amide linkages are attached directly to two aromatic rings. The aramids are similar to the nylons. However, the aromatic rings are more stable than linear arrangements of atoms and provide great strength and heat stability. The two most important aramid fibers are Nomex and Kevlar. Nomex is poly(*m*-phenylene isophthalamide), and Kevlar is poly(*p*-phenylene terephthalamide). Both fibers are highly crystalline and very strong—stronger than steel on a weight basis. Abrasion resistance is not very good, so these fibers are most important in specialty uses. Kevlar is also used as a tire cord.

Novoloid. This is a manufactured fiber containing at least 85% by weight of a cross-linked novolac. This fiber is claimed to be more comfortable than the aramids and although not as strong, has been used in clothing and upholstery where fire resistance is very important. Novoloid fiber was chosen for flight suits for astronauts.

Inorganic Fibers

Metallic fibers of silver and gold have been used for millennia to decorate fabrics. Today metallic fibers serve useful as well as decorative purposes. These fibers are formed by drawing metal wires through successively finer dies to achieve the desired diameter. Although gold and silver are the easiest to draw, modern methods have allowed the manufacture of steel, tantalum, and zirconium fibers. Because they are electrical conductors, metal fibers have been blended into fabrics to reduce the tendency to develop static electrical charges.

Glass

The art of heating sand and limestone to form a molten liquid has been known from the time of the ancient Egyptians. It was not until the 1930s, however, that glass fibers fine and flexible enough to be converted into textiles were produced. Glass fibers are prepared by the melt spinning of previously formed glass marbles, and the molten filaments are drawn down to very fine dimensions. It is the fineness of the fibers that gives them their flexibility and allows them to be used in textiles. Unfortunately, the fibers are so stiff that when broken they can penetrate human skin. Thus, they are not well suited to use in apparel or upholstery. Glass is widely used in curtains and drapery because of its total resistance to the degrading effects of sunlight, its low cost, and its flame resistance. It provides a nonrotting, nonsettling insulating material for homes and industrial uses. *See* GLASS.

Heterogeneous Fibers

These are fibers prepared from two or more chemical species which retain their identities after the fiber has been formed. These fibers may be spun with their components side by side, as a sheath of one material surrounding a core of another (sheath-core), or as a matrix of one material surrounding another (**Fig. 6**). The heterogeneous fibers can be tailored

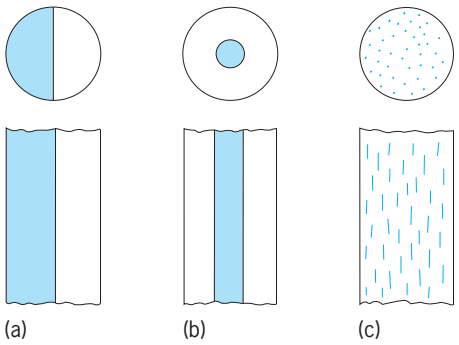

Fig. 6. Heterogeneous fiber types. (*a*) Side-by-side. (*b*) Sheath-core. (*c*) Matrix. (*After B. F. Smith and I. Block, Textiles in Perspective, Prentice Hall, 1982*)

to give a variety of performance properties, but the most notable are those which, because of differential response to moisture and temperature, form self-crimping fibers that do not require texturing, and those which incorporate a conductive component to reduce static buildup inhydrophobic fibers.

Fiber Properties

These are the physical, mechanical, chemical, biological, and geometrical characteristics of fibers. Some of the more important ones are tensile strength, elongation at break, modulus of elasticity or stiffness,

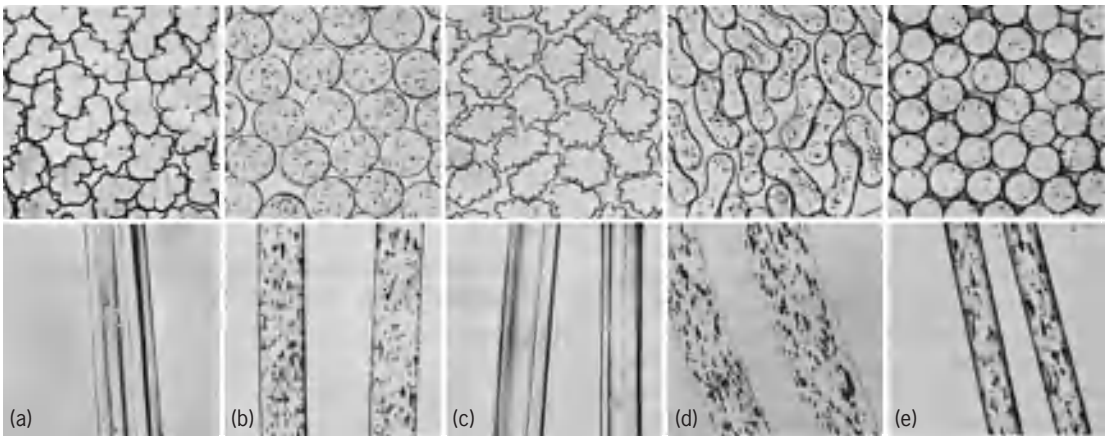

Fig. 7. Cross-sectional and longitudinal views of some typical fibers. (*a*) Acetate fiber. (*b*) Nylon fiber. (*c*) Rayon fiber. (*d*) Orlon fiber. (*e*) Dacron fiber. (*E. I. duPont de Nemours and Company*)

Characteristic attributes of manufactured fibers

Attribute	Properties required	Fiber recommended
Durability and abrasion resistance	High tenacity, high elongation at break	Nylon and polyester fibers
Resistance to soil particles	Smooth, round cross section	Melt-spun fibers
Quick drying	Low moisture content inside fiber	Hydrophobic fibers: polyesters, acrylics, nylon, triacetate
Winter warmth	Ability to entrap air spaces between resilient fibers; thick fabrics	Almost all textured synthetic fibers, the acrylics in particular
Summer comfort	Ability to wick perspiration from wet skin and dry quickly; thin but not-too-smooth fabrics	Acrylics and most rayon-synthetic blends
High resistance to light, solvents, acids, and bases	Compact chemical structure	Fluorocarbons and polyacrylics
Wrinkle resistance and wash-wear	High resilience both wet and dry	Polyesters outstanding; many others good, including acrylics, nylon, and triacetate
Freedom from static and hole melting	High moisture content	Rayon and rayon synthetic blends
Crease and pleat retention	Heat settability	Nylon and many other synthetic fibers

fatigue under repeated stress, resilience or ability to recover from deformation, moisture absorption and wettability, electrostatic properties, friction, color, luster, density, and resistance to light, heat, weathering, abrasion, laundering, mildew, insects, chemicals, and solvents; and finally a number of geometric features, such as diameter, cross-sectional shape, and crimp.

Figure 7 shows cross-sectional and longitudinal views of typical fibers. Such properties play an important part in determining whether or not the fiber can be made into a fabric that will be wrinkle-resistant, pleasing to the touch, comfortable, easy to clean, durable, and attractive in color, luster, drape, and general appearance. With a knowledge of the physical properties of the available fibers, the textile engineer can choose the best fiber or best blend of several fibers to fit the intended use. The final result, however, is also dependent upon the proper choice and control of additional factors such as the yarn and fabric structure, the weave pattern, and the finishing of the cloth.

In spite of the research efforts put into the development of improved fibers, no fiber is perfect for all uses. In many cases, perfect performance represents an incompatible and, therefore, impossible combination, exemplified by the desire for sheer hosiery with heavy-duty wear. Notable among existing deficiencies in some fibers both old and new are poor durability, soiling, static electricity, hole melting, yellowing with age, and poor shape retention. However, for each of these a manufactured fiber can be found which will solve the problem, as indicated in the **table**, which gives a partial listing of the major attributes of manufactured fibers.

All of the properties covered in the table deal with functional performance. An additional category of importance relates to the esthetic properties of fibers and fabrics—certain subtle qualities apparent to the hand, eye, and even to the ear (the whisper of silk or the rustle of a good taffeta). One of the reasons that cellulose acetate was able to compete successfully with its predecessor, viscose rayon, was its superior handle—a soft, luxurious feel—especially desirable in crepes and satins. As the result of much technical effort, manufactured fibers have been able to achieve those esthetic qualities referred to by textile experts in describing the characteristic handle of a cashmere sweater, a wool flannel, or a silk taffeta fabric. *See* NATURAL FIBER; POLYMER; TEXTILE. Ira Block

Bibliography. M. Grayson, *Encyclopedia of Textiles, Fibers, and Non-Woven Fabrics*, 1984; M. Lewin,

Handbook of Fiber Chemistry, 2d ed., 1998; Man-Made Fiber Producers Association, Inc., *Man-Made Fibers Guide*, 1988; H. L. Needles, *Textile Fibers, Dyes, Finishes, and Processes: A Concise Guide*, 1986; B. F. Smith and I. Block, *Textiles in Perspective*, 1996.

Manufacturing engineering

Engineering activities involved in the creation and operation of the technical and economic processes that convert raw materials, energy, and purchased items into components for sale to other manufacturers or into end products for sale to the public. Defined in this way, manufacturing engineering includes product design and manufacturing system design as well as operation of the factory. More specifically, manufacturing engineering involves the analysis and modification of product designs so as to assure manufacturability; the design, selection, specification, and optimization of the required equipment, tooling, processes, and operations; and the determination of other technical matters required to make a given product according to the desired volume, timetable, cost, quality level, and other specifications.

Manufacturing is one of the most complex of human group activities. It comprises hundreds or thousands of simultaneous and serial subactions, some of which occur in fractions of a second while others take hours, months, or even years to have full effect. These actions may be material, technical, informational, social, or economic.

Function. Historically, the function of manufacturing engineering was limited to developing and optimizing the production process. In brief, the manufacturing engineering function bridges the gap between the product design and full production. This can best be understood by considering the total process through which a designer's concept becomes a marketable product: (1) From the results of a needs analysis or market analysis, a product designer conceptualizes a product, and then drawings and one or more prototypes of this product are produced. (2) The finalized prototype and its part drawings are released to the group responsible for the manufacturing engineering function, which starts designing and building an economically justifiable process by which the product will be produced. (3) When the manufacturing process developed by manufacturing engineering has been thoroughly tried and proved workable, it is turned over to the production group, which assumes responsibility for product manufacture.

This method is known as the serial method of product production or the conventional product-production system design process (**Fig. 1**). A method developed after the serial method, known as concurrent design/concurrent engineering, has been practiced in Japan since the late 1950s and since around 1980 in the most progressive companies in the United States. Concurrent design/concurrent engineering means the consideration of issues of product design, manufacture, and use concurrently, but not necessarily simultaneously. As shown in the diagram in **Fig. 2**, a team is formed of all the necessary specialists who meet periodically to review the status of the design, report on the success or difficulties in satisfying their individual functional constraints, and collectively determine their next steps. An alternative arrangement has the team meeting continually. The starting point for a new design includes

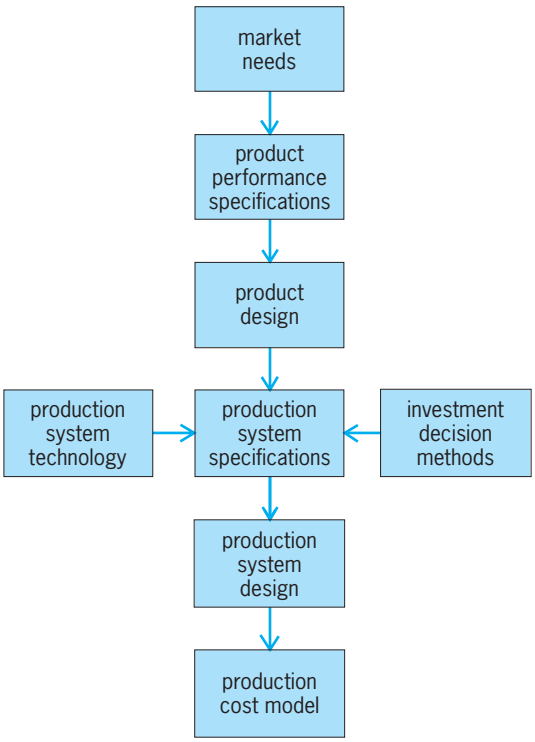

Fig. 1. Flow chart showing the components of the serial method of product production.

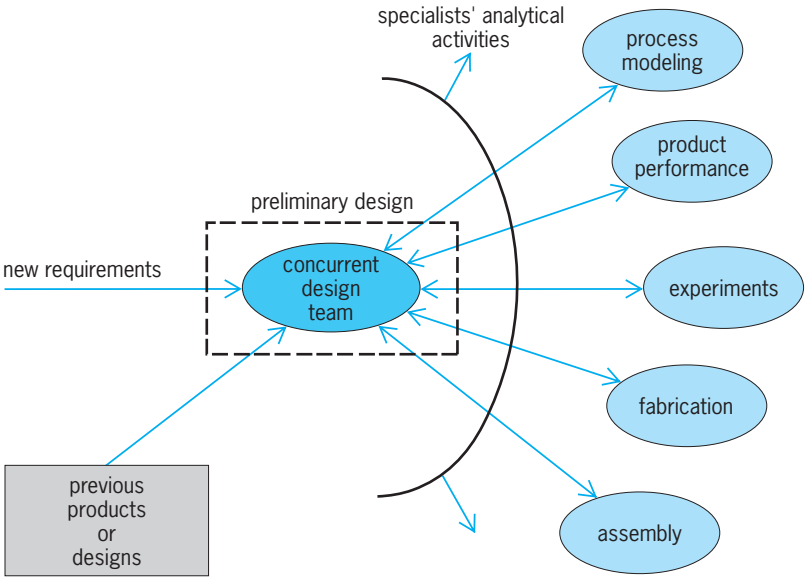

Fig. 2. Diagram showing the various elements of the concurrent design/concurrent engineering (CD/CE) process.

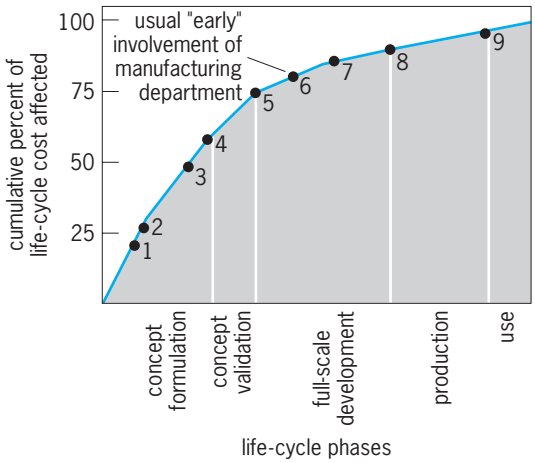

Fig. 3. Chart showing the cumulative percent of life-cycle cost of a product by individual phases of a product life cycle. Numbers represent the following phases: 1, define use patterns; 2, define alternatives; 3, develop alternatives; 4, freeze subsystems; 5, prove feasibility; 6, provide preliminary designs; 7, provide detail designs; 8, provide manufacturing plans; 9, product.

all the history of previous products, how they were designed and manufactured, as well as the institutions of people who did the work and who will do the next design. This concept is important, because, as shown in **Fig. 3**, by the time the concept validation phase is finished, 75% of the total life-cycle cost of a product has been determined. Thus any downstream function can optimize only the remaining 25%, no matter what it does or how much money it spends. *See* PROCESS ENGINEERING; PRODUCTION ENGINEERING.

Models. Manufacturing engineering involves technical as well as economic issues; these can be represented by models. Technical models usually comprise physical parameters, whereas economic models typically comprise time and money. In significant ways, the two types of models interact or may be linked, and in such cases they are known as economic-technical models.

A familiar technical model is that of metal cutting. The metal removal model represents the forces on a cutting tool while cutting a particular material. This model can be used to predict the quantity of heat delivered to the workpiece, the energy required for cutting, the resulting surface finish, and the risk of the tool breaking. A physical model of assembly relates the physical variables (size and shape of workpieces, friction during assembly, stiffness of tools and grippers, and relative error between parts) to the performance variables (likelihood of assembly failure and forces exerted on the parts by tools and each other).

A typical economic model of metal cutting predicts the tool's wear rate, given the same type of physical variables as the technical cutting model, but the quantities of interest are economic: how long the tool lasts, how much a new tool costs, how long it takes to change tools, and so on. The more intensive the cutting, the faster new workpieces are created. However, the work may not be cost-effective if it becomes necessary to stop often because of broken or worn tools.

At their most basic, technical models represent the physical response of machines and materials, perhaps in great detail, while economic models attempt to capture the economic consequences of those responses, typically with less detail. *See* MODEL THEORY.

Work content analysis. Economic models relate an amount of work to the amount of time or money or number of machines needed to do that work. The basic currency of such models is the work content inherent in a manufacturing task. In metal cutting or grinding, the content may be represented by the volume of material that must be removed; in assembly, it is the number of assembly operations needed to make one unit of the product. Since manufacturing may be regarded as a rate process governed by an output quantity in a given time, the work content is usually specified in productive units per unit time (assemblies per hour, for example). Determining the work content of a job is thus a basic step in manufacturing, whether the job is metal cutting, assembly, testing, or transport.

The objective of work content analysis, usually known as process planning, is to describe the elemental operations necessary to completely fabricate each part, to assemble parts into a whole or product, and to properly test the parts and assemblies to verify that the specified quality was achieved. A key aspect of process planning is that it results in an estimate of the time and the number of tools required to complete each fabrication operation. The amount of time that a specific individual piece of a product (piece-part) remains on a machine tool is known as the part cycle time. Part cycle times are used to determine the number of workstations that are necessary in the system in order to achieve a specific mix of parts or products. These times may also be used to determine the maximum allowable service or delivery rate and time available for the material-handling or parts supply system.

Process planning. The formulation of a process plan for a given part has seven aspects: (1) a thorough understanding of processing techniques, their yield and their reliability, precedences, and constraints (both economic as well as technical); (2) the material and tolerances of the part; (3) proper definition of machinability or process data; (4) proper workholding design of the stock or piece part during the fabrication process, a key consideration in generating piece parts of consistent quality; (5) proper tool selection for the task; (6) the capability of the equipment selected; and (7) personnel skills required and available.

Machinability or process data. The cycle times defined in the process plan for each operation are the sum of the cycle times for each tool used during that operation. The process planner determines the amount of time that a cutting tool is actually cutting the metal of a piece-part (in cut) based on the form of the raw material; dimension and surface finish of the final form of a specific feature (such as a hole or

a slot); tools necessary to generate that feature; and cutting speed and its relationship to the feed rate of the material being machined, based on the tool selected and the material to be cut. A principal cause of poor performance in existing systems is the incorrect choice of cutting speed and feed rate for the parts in the system.

Each fabrication process has similar issues and concerns, whether the process is metal forming, composite layup, near-net shape-forming techniques or others.

Work-holding alternatives. Proper conception and design of work-holding devices also known as fixtures are critical to the successful fabrication and assembly of any product. The system designer's objective with respect to fixture definition is to minimize the number of fixtures required throughout the system for fabrication of each component, while assuring proper control and orientation of the component. Adequate support and clamping force must be designed into every fixture. Additionally, the fixture's design should prevent the loading of incorrect parts into the fixture as well as improper orientation of the correct part in the fixture.

Tool selection. The process planner attempts to satisfy the following objectives when selecting tools for processing parts in a fabrication system: (1) accurately generate each feature as quickly as possible; (2) provide sufficient tool longevity to avoid an unnecessary amount of tool replacement (and machine downtime waiting for tools); (3) minimize the number of tools per part; and (4) maximize the commonality of tools among parts.

Cutting time and tool life are inversely related; the faster a tool cuts, the shorter its useful life (between resharpenings). The process planner must balance the speed at which parts are produced with the downtime on the equipment required to replenish tools because of wear. Almost all equipment in a fabrication system will change tools automatically to minimize the direct labor necessary to produce a part. Tool-changing machines have a limited capability for storing tools, often only 40 to 60 tools.

The fewer the tools required by each part, the greater the number of parts a machine can accommodate between tool exchanges. Using the same tools, where appropriate, on as many parts as possible also addresses this problem; as more parts share a greater number of tools, the total number of unique tools needed in the system is reduced. This allows more parts to be produced with less interruption of productive machine time. Additional benefits derived from tool standardization and consolidation include reduced tool-storage space and inventory-tracking requirements, higher-quantity purchases, and less potential for tool unavailability.

Scheduling and routing of parts are also simplified. A part does not have to visit a particular machine just because a unique tool is stored there. Instead, it may visit any available machine that has the common tools it needs.

Significant gains in production efficiency have been made since the mid-1970s. Ensembles of computer-controlled machines, known as flexible manufacturing systems, permit their individual machines to cut metal 65–85% of the time. Manually operated machine tools are much less efficient. *See* ASSEMBLY MACHINES; FLEXIBLE MANUFACTURING SYSTEM; COMPUTER NUMERICAL CONTROL.

Computer-aided process planning. Process planning aids based on computer programs that incorporate a type of spread sheet can be used to reduce significantly the time required to generate individual process plans. For example, systems have been developed that calculate the cycle time for each part as well as the number of tools used per part, the number of unique tools per part set, and the total time for cutting operations per tool type. *See* COMPUTER-AIDED DESIGN AND MANUFACTURING.

Materials-handling equipment selection. In parallel with the definition of process equipment, the manufacturing system designer must determine the most appropriate materials-handling techniques for the transfer of parts from machine to machine of each family of parts. During the manufacture of pieces, the parts are organized by the type of feature desired. The parts are then grouped and manufactured as a family, a method known as group technology. This includes the selection of storage devices appropriate for raw material, work in process, and finished-goods inventory as well as fixtures, gages, and tooling. Materials-handling equipment may be very different for each family, depending on part size and weight, aggregate production volume, part quality considerations during transfer, and ease of loading and unloading candidate machines. Different materials-handling approaches may also be appropriate within individual fabrication systems. *See* MATERIALS-HANDLING EQUIPMENT.

Process quality assurance. A quality assurance philosophy must be developed that emphasizes process control as the means to assure part conformance rather than emphasizing the detection of part nonconformance as a means of detecting an out-of-control process. The success of any fabrication process is based on rigid work-holding devices that are accurately referenced to the machine, accurate tool sizing, and tool position control. The basic way to determine if these three factors are functioning together acceptably is to measure a feature they produce as they produce it or as soon as possible after that feature is machined. The primary objective of this measurement is to determine that the combination is working within acceptable limits (statistical process control); the fact that the part feature is in conformance to print (conformance to tolerance specified on the print/drawing) is a by-product of a process that is in control. *See* QUALITY CONTROL.

Human resource considerations. In a modern manufacturing environment an organization's strategies for highly automated systems and the role for workers in these systems are generally based on one of two distinct philosophical approaches. One approach views workers within the plant as the greatest source of error. This approach uses computer-integrated

manufacturing technology to reduce the workers' influence on the manufacturing process. The second approach uses computer-integrated manufacturing technology to help the workers make the best product possible. It implies that workers use the technology to control variance, detect and correct error, and adapt to a changing marketplace. *See* COMPUTER-INTEGRATED MANUFACTURING.

The best approach utilizes the attributes of employees in the factory to produce products in response to customer demand. This viewpoint enables the employees to exert some control over the system, rather than simply serving it. The employees can then use the system as a tool to achieve production goals.

Prospects. As technology and automation have advanced, it has become necessary for manufacturing engineers to gain a much broader perspective. They must be able to function in an integrated activity involving product design, product manufacture, and product use. They also have to consider how the product will be destroyed as well as the efficient recovery of the materials used in its manufacture.

Manufacturing engineers must also be able to use an increasing array of computerized support tools, ranging from process planning and monitoring to total factory simulation—and in some cases, including models of the total enterprise. *See* SIMULATION.

Consideration is being given to redefine and enlarge the role of manufacturing engineers. There is a tendency to move away from the highly segmented array of specialists that requires industrial engineers to detail tasks, plant engineers to design facilities, engineers to design materials-handling systems, and so forth.

J. L. Nevins

Bibliography. B. H. Amstead et al., *Manufacturing Processes*, 8th ed., 1987; G. Boothroyd, P. Dewhurst, and W. Knight, *Product Design for Manufacture and Assembly*, 2d ed., 2001; Committee on the Effective Implementation of Advanced Manufacturing Technology of the Manufacturing Studies Board, *Human Resource Practices for Implementing Advanced Manufacturing Technology*, Commission on Engineering and Technical Systems, 1986; C. S. Draper Laboratory, *Flexible Manufacturing System Handbook*, CSDL Rep. R-1599, 1984; D. T. Koening, *Manufacturing Engineering: Principles for Optimization*, 2d ed., 1994; G. Taguchi et al., *Taguchi's Quality Engineering Handbook*, 2004.

Map design

In contrast to the creative freedom of painting or graphic illustration, map design must observe rigid limitations because the locations of geographic features such as rivers, national boundaries, and coastlines are tied to reality. Map design is defined as the systematic process of arranging and assigning meaning to elements on a map for the purpose of communicating geographic knowledge in a pleasing format. During the twentieth century, standardized symbols and designs evolved for reference maps such as topographic maps. However, nonstandard maps with unique purposes must be designed within a process that encompasses creativity, experimentation, and evaluation. Careful design is crucial to map effectiveness to avoid distorted or inaccurately represented information.

Design process. The first design stage involves determining the type of map to be created for the problem at hand. Decisions must be made about the map's spatial format in terms of size and shape, the basic layout, and the data to be represented. In this step, the experience, cultural background, and educational attainment of the intended audience must be considered. The second stage involves the exploration of preliminary ideas through the manipulation of design parameters such as symbols, color, typography, and line weight. In the third step, alternatives are evaluated and may be accepted or rejected. Under some circumstances, prototype maps may be developed for sample readers as a means of evaluating design scenarios. The last step involves the selection of a final design.

Design considerations include the selection of scale (the relationship between the mapping media format and the area being mapped), symbols to represent geographic features, the system of projection (the method used to translate Earth coordinates to flat media), titles, legends, text, borders, and credits. The process of arranging each map element is referred to as map composition. Success in map composition is achieved when design principles are applied to create a pleasing image with a high degree of information content and readability.

Design principles. Map design principles have emerged from the disciplines of cartography, graphic arts, and psychology. They include balance, the relationship between figure and ground, visual acuity, hierarchy, and contrast.

Balance. Balance refers to arranging major map elements within the map frame in a visually appealing manner. A map is off balance if all elements appear on one side of its frame, leaving a large amount of open space. The visual balance is closely tied to the map's optical center, located slightly above the center of the rectangle formed by the map border.

Figure and ground relationships. As discovered through the work of psychologists, the mind organizes a map's visual area into two separate perceptual fields—figures that the eye focuses on, and the background. The differentiation of land and water through the application of color or shading is a common method for helping to establish these two fields (**Fig. 1**).

Visual acuity. Map elements must be readable by most map users. Visual acuity refers to the threshold minimal size of objects that can be correctly identified. For example, what is the smallest size of lettering that can be interpreted on a map designed for a viewing distance of 18 in. (46 cm).

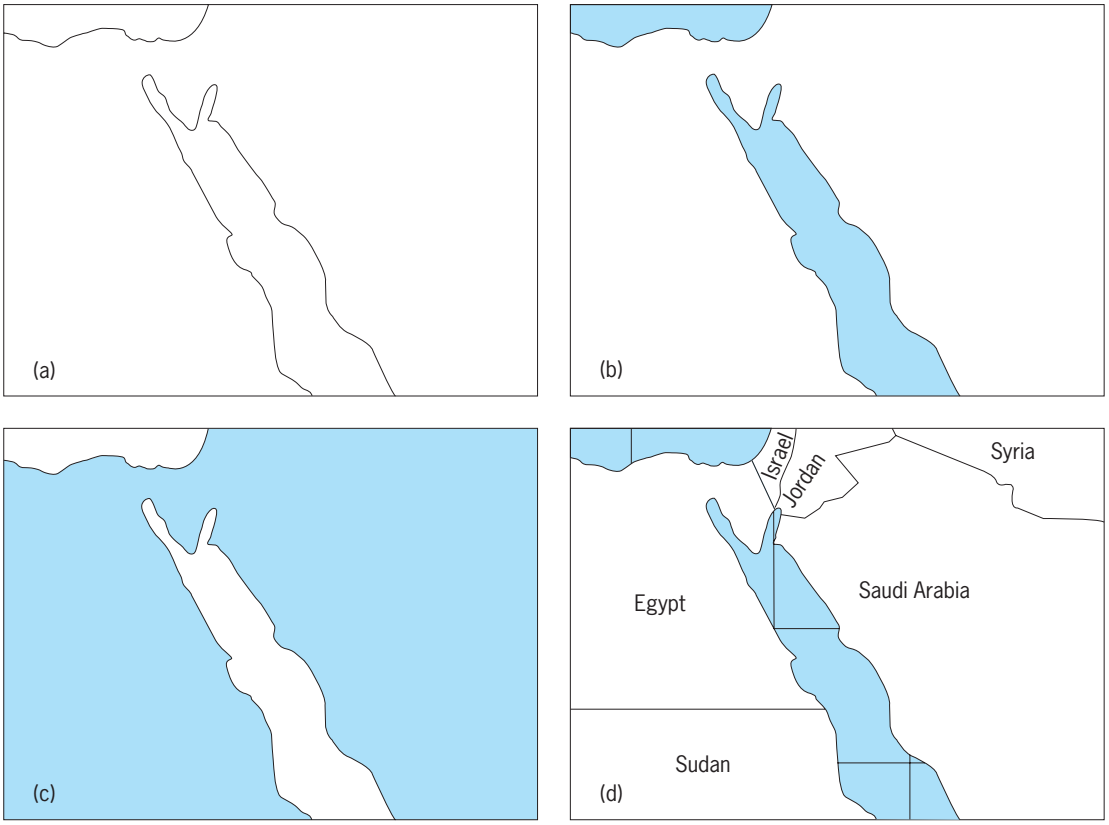

Fig. 1. Figure and ground relationship. (*a*) Map without shading does not assist the user in isolating the subject from the background. (*b*, *c*) Map shaded in two different ways improves definition. (*d*) Addition of labels to show place and of the graticule, clearly differentiates subject and background.

Hierarchy. Maps should exhibit a clear hierarchy of importance for each type of element, the most important elements having the greatest visual prominence. For example, the importance of places can be established using variation in sizes of point symbols or place names.

Contrast. An absence of contrast can result in a map element being lost in its surroundings. Contrast refers to variation in color, line weight, texture, or detail.

Computers. Computers now duplicate all capabilities of manual map design. Design iterations can be explored and evaluated faster and with lower cost, compared to manual drafting methods (**Fig. 2**). The digital environment facilitates the independent storage of map elements that can be combined to form composite images. Automated processes have also impacted map reproduction; it is now possible for the cartographer to prepare a map image for printing without a photographic step.

Research in cartographic design has recently focused on the application of artificial intelligence to the automation of text placement. Other computer innovations such as interactive mapping allow a map user to act as map creator in exploring geographic relationships by selecting and tailoring data sets available through software or the World Wide Web. In addition to its benefits to the design process, mapping software has brought challenges to the mapping

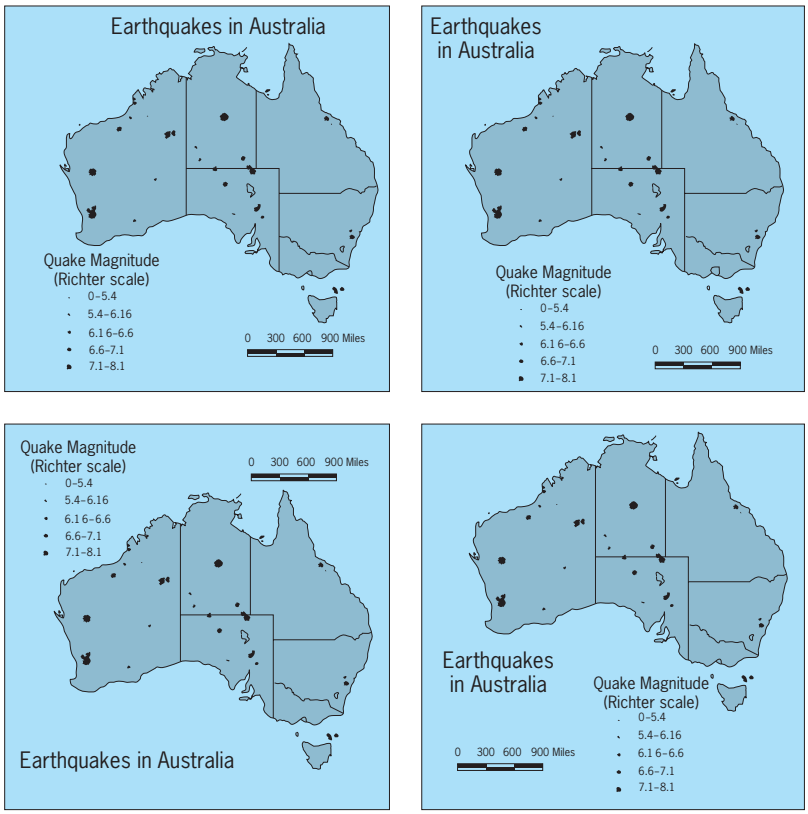

Fig. 2. Design iterations created by a computer.

sciences, including the proliferation of poorly designed maps constructed by persons untrained in cartography. *See* CARTOGRAPHY; COMPUTER GRAPHICS; MAP PROJECTIONS; MAP REPRODUCTION.

Thomas A. Wikle

Bibliography. A. H. Robinson et al., *Elements of Cartography*, 6th ed., Wiley, 1995; C. H. Wood and C. P. Keller, Design: Its place in cartography, *Cartographic Design: Theoretical and Practical Perspectives*, Wiley, 1996.

Map projections

Systematic methods of transforming the spherical representation of parallels, meridians, and geographic features of the Earth's surface to a nonspherical surface, usually a plane. Map projections have been of concern to cartographers, mathematicians, and geographers for centuries because globes and curved-surface reproductions of the Earth are cumbersome, expensive, and difficult to use for making measurements. Although the term "projection" implies that transformation is accomplished by projecting surface features of a sphere to a flat piece of paper using a light source, most projections are devised mathematically and are drawn with computer assistance. The task can be complex because the sphere and plane are not applicable surfaces. As a result, each of the infinite number of possible projections deforms the geometric relationships among the points on a sphere in some way, with directions, distances, areas, and angular relationships on the Earth never being completely recreated on a flat map.

Although the most commonly used map projections are accessible through mapping software, their fundamental attributes are best appreciated by considering the problem of the transformation of a spherical surface to a plane.

Deformation patterns. It is impossible to transfer spherical coordinates to a flat surface without distortion caused by compression, tearing, or shearing of the surface. Conceptually, the transformation may be accomplished in two ways: (1) by geometric transfer to some other surface, such as a tangent or intersecting cylinder, cone, or plane, which can then be developed, that is, cut apart and laid out flat; or (2) by direct mathematical transfer to a plane of the directions and distances among points on the sphere. Patterns of deformation can be evaluated by looking at different projection families. Whether a projection is geometrically or mathematically derived, if its pattern of scale variation is like that which results from geometric transfer, it is classed as cylindrical, conic, or in the case of a plane, azimuthal or zenithal. *See* CARTOGRAPHY; TERRESTRIAL COORDINATE SYSTEM.

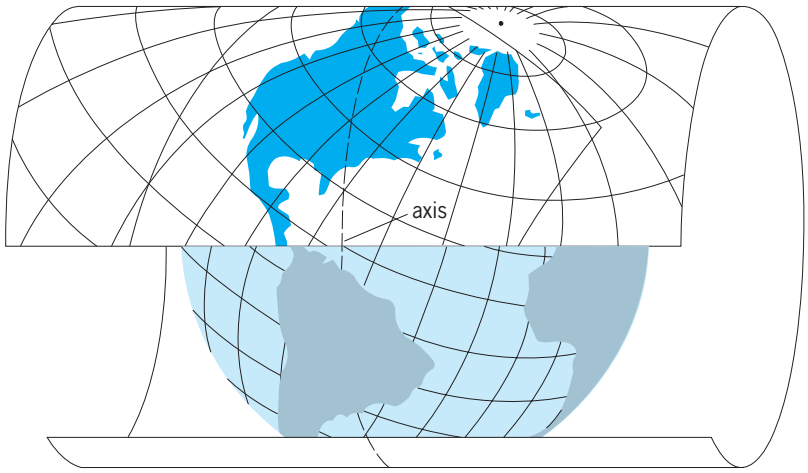

Fig. 1. Oblique Mercator projection on a cylinder. (*After American Oxford Atlas, Oxford, 1951*)

Cylindrical projections. These result from symmetrical transfer of the spherical surface to a tangent or intersecting cylinder. True or correct scale can be obtained along the great circle of tangency or the two homothetic small circles of intersection. If the axis of the cylinder is made parallel to the axis of the Earth, the parallels and meridians appear as perpendicular lines. Points on the Earth equally distant from the tangent great circle (Equator) or small circles of intersection (parallels equally spaced on either side of the Equator) have equal scale departure. The pattern of deformation therefore parallel the parallels, as change in scale occurs in a direction perpendicular to the parallels. A cylinder turned 90° with respect to the Earth's axis creates a transverse projection with a pattern of deformation that is symmetric with respect to a great circle through the Poles. Transverse projections based on the Universal Transverse Mercator grid system are commonly used to represent satellite images, topographic maps, and other digital databases requiring high levels of precision. If the turn of the cylinder is less than 90°, an oblique projection results (**Fig. 1**). All cylindrical projections, whether geometrically or mathematically derived, have similar patterns of deformation. *See* GREAT CIRCLE, TERRESTRIAL.

Conic projections. Transfer to a tangent or intersecting cone is the basis of conic projections. For these projections, true scale can be found along one or two small circles in the same hemisphere. Conic projections are usually arranged with the axis of the cone parallel to the Earth's axis. Consequently, meridians appear as radiating straight lines and parallels as concentric angles. Conical patterns of deformation parallel the parallels; that is, scale departure is uniform along any parallel (**Fig. 2**). Several important conical projections are not true conics in that their derivation either is based upon more than one cone (polyconic) or is based upon one cone with a subsequent rearrangement of scale variation. Because conic projections can be designed to have low levels of distortion in the midlatitudes, they are often preferred for representing countries such as the United States.

Azimuthal projections. These result from the transfer to a tangent or intersecting plane established perpendicular to a right line passing through the center of the Earth. All geometrically developed azimuthal projections are transferred from some point on this line. Points on the Earth equidistant from the point of tangency or the center of the circle of intersection

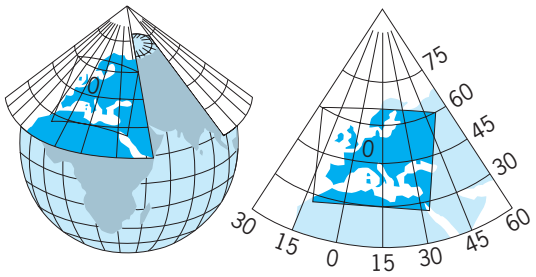

Fig. 2. Conical projection, based on origin 45°N, 10°E. (*After American Oxford Atlas, Oxford, 1951*)

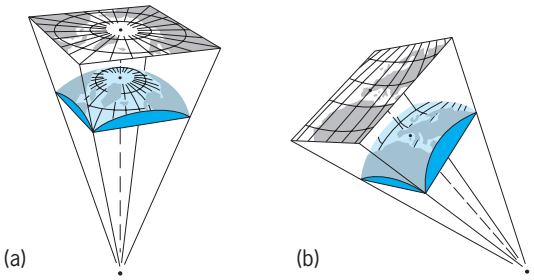

Fig. 3. Azimuthal projections with tangent planes have been raised above the sphere surface. (*a*) Polar azimuthal. (*b*) Oblique azimuthal. (*After American Oxford Atlas, Oxford, 1951*)

have equal scale departure. Hence the pattern of deformation is circular and concentric to the Earth's center. All azimuthal projections, whether geometrically or mathematically derived, have two aspects in common: (1) all great circles that pass through the center of the projection appear as straight lines; and (2) all azimuths from the center are truly displayed (**Fig. 3**).

Nongeometric projections show no consistency in their patterns of deformation; nevertheless, many are useful. One such group, called pseudocylindrical projections, is derived by mathematically arranging the spherical surface within a shape bordered by a series of specified smooth curves, such as ellipses, parabolas, or sine or quartic curves (**Fig. 4**).

Properties. The retention anywhere on the projection of some specific geometric quality of the sphere, such as uniformity of compass rose, or the creation of some useful attribute, such as straight rhumb lines, is called a property. Projections offer possibilities for maintaining single properties or combinations of properties. Ultimately, a map's intended use should determine the properties to be retained in the transformation process. All properties are the result of arranging the magnitudes and directions of scale variation.

Conformality. Conformality (orthomorphism) is the retention of angular relationships at each point, resulting in the preservation of the shapes of small features. It is obtained by arranging the scale so that at each point the scale is uniform in all directions. Since the spheroid and plane are not applicable, scale must change from point to point. Thus, all conformal projections deform the relative sizes of Earth areas (**Fig. 5**). Conformal projections are most widely used for navigational, engineering, and topographic maps, since observable angles may be measured on the map with a protractor.

Equivalence. Equivalence (equal-area) is the retention of the relative sizes of areas. It is obtained by arranging the scale at each point so that the product of the sides of an infinitesimal Earth rectangle projected anywhere on the map is the same. Since the two surfaces are nonapplicable, the scale at a point must be different in different directions. Therefore, the properties of conformality and equivalence are mutually exclusive. Equivalent projections are most widely used for mapping geographic, economic, and similar types of data whenever the areal extent of the phenomena is important. The extent of Earth

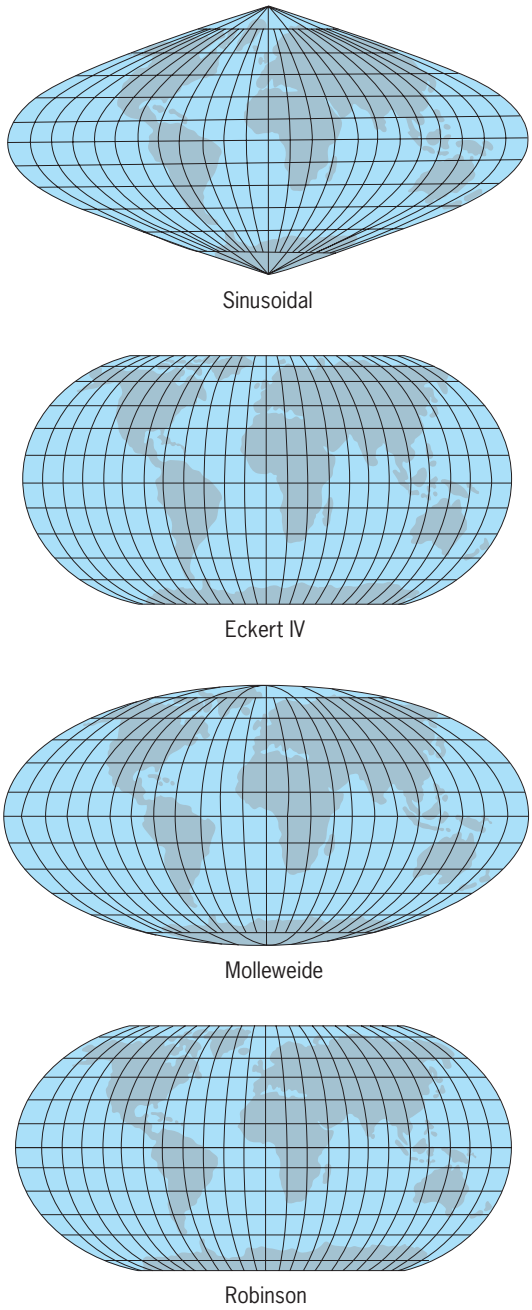

Fig. 4. Four pseudocylindrical projections. (*University of Wisconsin-Madison Cartographic Laboratory*)

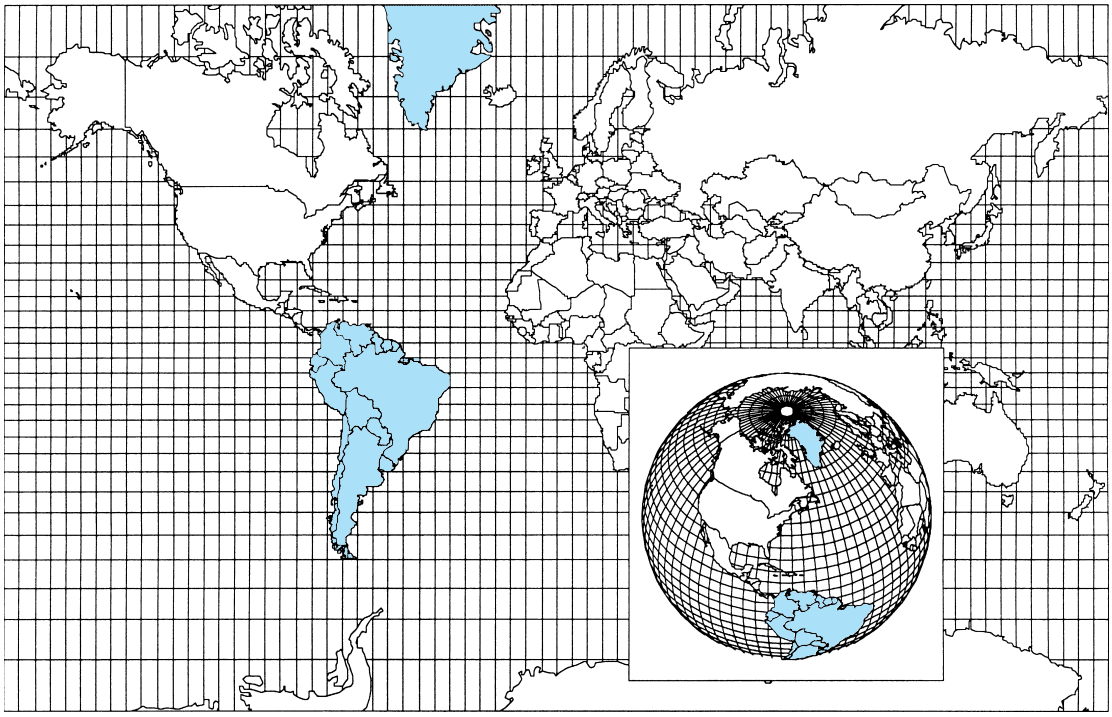

Fig. 5. The property of equivalence is not maintained on the Mercator projection, making Greenland and South America appear similar in size. The inset map shows that South America is actually about 15 times larger than Greenland.

area within administrative subdivisions can best be derived by measurement from equivalent projections.

Azimuthality. Azimuthality is the retention of azimuths (correct directional relations along a great circle bearing) from one point to another. Within limited areas, this, like all properties, can be approached on many projections but can be precisely retained from only one or two points. The centers of all projections theoretically or actually constructed on a tangent plane have this property. Azimuthality is useful in graphic aids to communication and for observations dealing with electronic impulses that travel along great circles.

Significant lines. Significant reference lines on the Earth include great circles, rhumb lines, and small circles, which are utilized in navigation, communication, and area and space analysis. By arranging the scale, these may be made to appear as straight or consistently curved lines on a map. Of special significance are great circles and rhumb lines in air and sea navigation. Because they represent the shortest distance between two locations on the Earth's surface, aircraft follow great circle routes. The practical requirement of guiding movement by compass angle requires that headings be along rhumb lines (loxodromes). Scale on projections can be arranged so that entire families of these kinds of critical lines may be made to appear as straight lines. Similarly, directional concepts, such as a specific cardinal direction, can be made parallel anywhere on the map. Any circle on the Earth can be made to appear as a circle on a map. Many other similar attributes are possible with map projections.

Examples. Although an infinite number of different projections is possible, only a relatively few are widely used. There is no best projection for any specific mapping problem, and in most cases several different projections can be applied to any given project.

Mercator. The Mercator projection is a mathematically derived, cylindrical-type, conformal projection that is conventionally based on the Equator as the tangent great circle. The projection was developed in 1569 by the Flemish cartographer Gerhardus Mercator to represent his world map. Linear scale on the Mercator increases in a direction perpendicular to the Equator as the secant of the latitude on a sphere. All rhumb lines are straight lines on the conventional form, making the Mercator the most widely used projection for nautical navigation. The transverse Mercator (and similar variants for the spheroid, for example, Gauss-Krüger) employs a meridian pair as the tangent great circle. Rhumb lines are not straight lines on the transverse form.

Sinusoidal. The sinusoidal, also called the Sanson-Flamsteed or Sanson-Mercator projection, is an equal-area projection with a straight central meridian and straight, equally spaced parallels. An area of least distortion is found along the Equator and central meridian, making it a popular projection for representing Africa and South America. Since the projection comes to a point at the Poles, shapes are distorted in the high latitudes.

Mollweide. An equal-area projection with straight parallels, the Mollweide resembles the sinusoidal but forms an ellipse without pointed poles. In contrast to the sinusoidal, low distortion is found along the 40th

parallels north and south latitude rather than at the center. When centered on the prime meridian, the Mollweide is a popular projection for representing continental Europe.

Gnomonic. The gnomonic (azimuthal) projection is obtained by geometric transfer from the center of a sphere to a tangent plane. Scale is greatly exaggerated away from its center, making the projection impractical for representing more than 45° of latitude in a single hemisphere. Because all arcs of great circles appear as straight lines, this projection is popular for navigation.

Azimuthal equidistant. The azimuthal equidistant projection is formed by straight meridians radiating from a single point of plane tangency with the surface. Parallels form concentric circles and, when measured from the point of tangency, all points are true in distance and global direction. Although commonly used to represent Arctic and Antarctic regions, the projection can be centered on any location, making it ideal for plotting seismic or radio waves.

Stereographic. The stereographic (azimuthal and conformal) projection is derived by geometric transfer to a tangent plane from a point opposite the point of tangency. All circles on the Earth appear as circles on the map. It is widely used as a framework for topographic maps of small areas and for navigation and grid systems in polar areas.

Lambert conformal conic. The Lambert conformal conic with two true-scale (standard) parallels is widely used for aeronautical and meteorological charts, as the framework for topographic series, and for rectangular grid systems of smaller areas. Scale increases away from the standard parallels, and great circles are nearly straight lines.

Albers equal-area conic. The Albers equal-area conic with two standard parallels is similar in appearance to the Lambert. The projection is commonly used to show middle latitudes for administrative and area research maps, especially for the United States, Europe, and Russia.

Polyconic. Although the polyconic (the ordinary, or American, polyconic) is neither equal-area or conformal; each parallel is true scale. It has been widely used for large-scale topographic maps, each sheet being individually developed and essentially error-free. Sheets fit together north-south but not east-west and cannot be mosaicked in all directions without gaps. The U.S. Geological Survey ceased using the polyconic for topographic maps in favor of either the transverse Mercator or the Lambert conformal conic. The modified polyconic employs straight meridians and distributes scale error over the map sheet.

Goode's homolosine. Interrupted projections, such as the Goode's homolosine, make it possible to maintain a degree of equivalence and conformality on a single world map. The projection is created by inserting breaks over land or ocean areas and is homolographic from 40° north to the North Pole and from 40° south to the South Pole. Elsewhere, from 40° north to 40° south, the projection is sinusoidal. Goode's homolosine is a popular projection for use in atlases and textbooks.

Most other forms of projection are used for small-scale, general or thematic maps. Most widely used for these are equivalent or near-equivalent varieties. The display of imagery from a satellite orbiting about the rotating Earth has required complex mathematical developments in map projections.

Computers. Computers have become extremely valuable tools for the assisting in selecting the most appropriate projection to fit the unique constraints of each mapping problem. Mapping software allows the cartographer to experiment with alternative projections or to make parameter adjustments after a projection has been selected.

Arthur H. Robinson; Thomas A. Wikle

Bibliography. B. D. Dent, *Cartography: Thematic Map Design*, 4th ed., 1996; D. H. Maling, *Coordinate Systems and Map Projections*, 2d ed., 1993; F. Pearson II, *Map Projection Methods*, 1984; A. H. Robinson, *Elements of Cartography*, 6th ed., 1995; J. P. Snyder and P. M. Voxland, *Album of Map Projections*, 1989.

Map reproduction

The processes of producing multiple copies of maps or map drawings. Reproductions are obtained by a number of procedures, including inked-plate printing, photographic processes, office copying equipment, and computers. Choosing a process depends on the use of the map, quality and quantity desired, cost, and availability of equipment. The reproduction process governs the techniques and media for preparing the original artwork. Some processes serve as intermediate stages in map reproduction. Finished reproductions can be on any material, but film and paper are most commonly used and are single color or multicolor.

Inked-plate processes. Of the three major kinds of printing—relief plate (letterpress), intaglio (engraving or gravure), and planographic (lithography or offset)—the planographic process is most commonly used for map reproduction. Before the development of photolithography, the majority of maps were made from engravings. Today, this method is not used, although photogravure maps are made in the printing of newspapers or reproductions of antique maps. Large printing runs of maps may call for use of the letterpress process.

With multicolor maps, registry of colors and images is of great importance both in the making of the artwork and in the printing. Each color is represented by one or more separate artwork overlays which must be matched in printing. Information on each overlay can be depicted by drawing with India ink and adding stick-on symbolization and lettering. The artwork is photographed on film, which is used to make the printing plate. To help reduce the steps leading to the printing plate and have better registry control, another method of preparing the artwork is used, called scribing. Overlays consist of clear, stable plastic coated with opaque material which is engraved (scribed) to establish a clear image. The

scribed overlay can then be used directly as a negative for plate making, bypassing the intermediate photographic process. *See* PRINTING.

Photographic processes. For photographic work, originals can be on transparent or opaque bases and the reproductions may be enlarged, same-size, or reduced copies of the original. Procedures involve a camera, exposure to light-sensitive film or paper as a negative or positive image, and wet developing. Silver salts provide the more common light-sensitive emulsion, although some other processes use different emulsions and light requirements. Reproductions are either single-color or multicolor prints or film transparencies. Often the photographic processes serve as intermediate steps toward the duplication of maps, that is, in the preparation of the artwork and in the production of printing plates. *See* PHOTOGRAPHY.

Diffusion transfer. A high-quality image is produced by first exposing negative paper in a camera or by contact with image light. The negative and receiver material are moistened in a liquid developer, followed by face-to-face contact which allows the image to be transferred from the negative to the receiver sheet. This process often serves as an intermediate step in the production of artwork and printing plates.

Electrostatic. This system, commonly called photocopying (or "xeroxing," from the proprietary name Xerox), uses a chemically coated plate which becomes light-sensitive when charged with electricity. The plate is put in the camera in place of film for exposure, after which the image is coated with a powder or liquid toner. The toner image is transferred to a paper or film and fused to the base by heat. The process can be used as an intermediate step in map production but more commonly serves to produce the printing plate. *See* PHOTOCOPYING PROCESSES.

Contact processes. Generally, these provide reproductions in the same size as the original, involve no optical equipment, and are of lower quality than the above processes.

Spirit duplicating. The map is drawn on a paper master, creating a carbon image on the reverse side. Alcohol is brushed over the carbon image and dissolves a small amount of the image with each revolution. The image is transferred in contact with each passing sheet of paper. This is the only mechanical process producing a multicolor image in one pass through the machine. Different-colored carbons can be combined on one master to prepare the image.

Mimeographing. The map is drawn on a wax-coated sheet of porous paper with styli which open segments of the stencil to allow ink to flow through when the stencil is mounted on a drum on the machine. Centrifugal force moves the ink from inside the drum and through the image area, depositing on the passing sheet of paper. Stencils can also be made from an original drawing by a heat development process and by the electrostatic process.

Diazo. This process produces a good-quality direct print, positive original to positive print, in one exposure and development. A positive transparent paper or film master containing an opaque image is placed in contact with a light-sensitive coated paper or film and exposed to ultraviolet light, neutralizing the coating except where hidden by the master's image. The copy is then passed through ammonia fumes for development, turning the image black.

Blueprinting. The master and exposure requirements are similar to those used with the diazo process. The light-sensitive coating is an iron compound which, after exposure, is washed and fixed in a chemical bath, turning deep blue. The unexposed coating behind the master's image is washed away, and the duplicate image becomes white. Diazo and blueprinting are the only processes to provide duplicate maps of a large size at low cost, limited only by the width of the machine and length of a roll of paper or film.

As an intermediate step in multicolor map construction, diazo or blueprinting serves to make registered duplicate compilation images on overlays to be scribed. Selected information is then scribed on each overlay, representing the color ultimately to be printed. This procedure assures that the various symbols and colors will print in register.

Computer-generated maps. Rapid developments in graphic software programming systems and the accompanying hardware have provided a number of possibilities in map compilation and reproduction of high quality and speed. Geographic information can be stored in data banks, to be called for later to plot images either for study and modification or for producing intermediates for printing plates. The information can be separated into overlays to produce the assigned colors for printing. Film negatives and positives drafted by plotters with ink, with a light beam, or by scribing are the common procedures. Such hardware is more limited to large mapping operations. *See* CARTOGRAPHY; COMPUTER GRAPHICS.

James A. Bier

Bibliography. I. S. Keates, *Cartographic Design and Production*, 2d ed., 1989; A. H. Robinson, *Elements of Cartography*, 6th ed., 1994; D. R. Taylor (ed.), *The Computer in Contemporary Cartography*, vol. 1, 1980.

Maple

A genus, *Acer*, of broad-leaved, deciduous trees including about 115 species in North America, Asia, Europe, and North Africa. This genus is characterized by simple, opposite, usually palmately lobed (rarely pinnate) leaves, generally inconspicuous flowers, and a fruit consisting of two long-winged samaras or keys. The winter buds have several overlapping scales, rarely only two. The most important commercial species is the sugar or rock maple (*A. saccharum*), called hard maple in the lumber market. This tree, attaining a height of 120 ft (37 m), grows in the eastern half of the United States and adjacent Canada. It can be recognized by its gray furrowed bark, sharp-pointed scaly winter buds, and symmetrical oval outline of the crown (**illus.** *a*). *See* SAPINDALES.

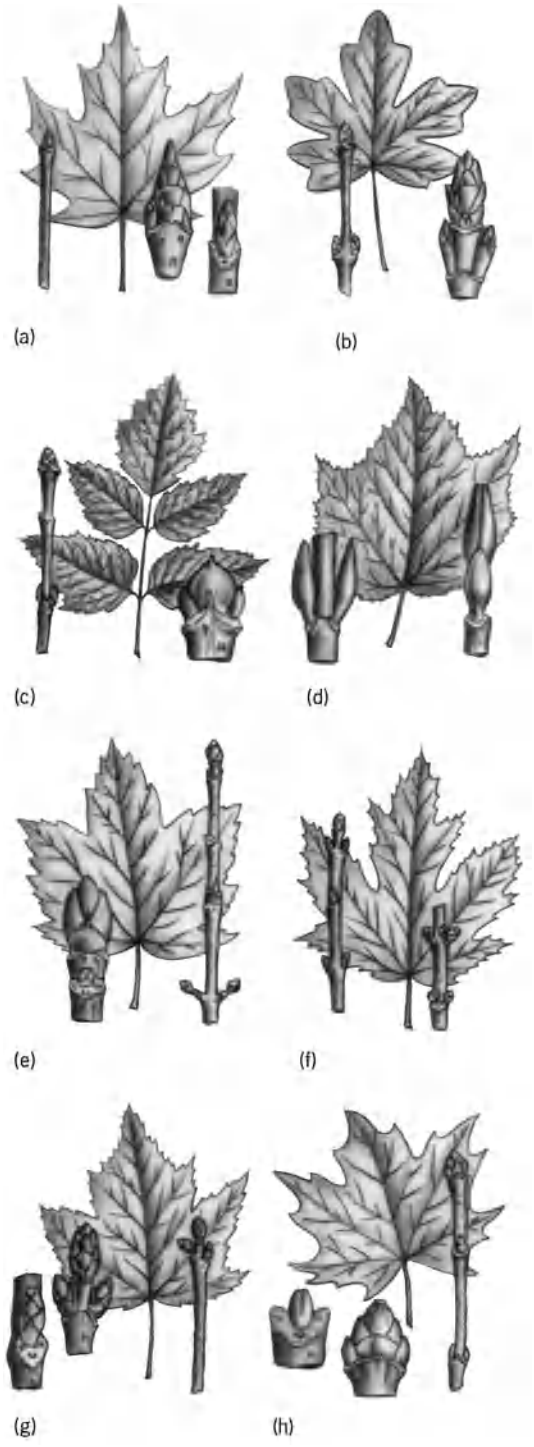

Characteristic maple leaves, twigs, and buds. (*a*) Sugar maple (*Acer saccharum*). (*b*) Hedge maple (*A. campestre*). (*c*) Box elder (*A. negundo*). (*d*) Striped maple (*A. pensylvanicum*). (*e*) Sycamore maple (*A. pseudoplatanus*). (*f*) Silver maple (*A. saccharinum*). (*g*) Red maple (*A. rubrum*). (*h*) Norway maple (*A. platanoides*).

Maple is an important source of hardwood lumber. Hard maple is used for flooring, furniture, boxes, crates, woodenware, spools, bobbins, motor vehicle parts, veneer, railroad ties, and pulpwood. It is the source of maple sugar and syrup and is planted as a shade tree.

The red maple (*A. rubrum*), with much the same botanical range as *A. saccharum*, is second commercially to sugar maple. It can be distinguished by fewer scales on the winter buds, scalier or flakier bark, and the red coloration of all parts of the shoot, leaves, flowers, fruits, and twigs. The leaf lobes are separated by sharp sinuses in contrast to the U-shaped ones of sugar maple (illus. *g*). Because it often grows in moist places, it is commonly known as swamp maple. In the lumber trade it is called soft maple.

The silver maple (*A. saccharinum*), with a range similar to *A. rubrum*, has more deeply cut leaves which are silvery beneath (illus. *f*). Its lumber and that of the red maple are used for furniture, boxes, crates, woodenware, spools, bobbins, railroad ties, and pulpwood. Both silver and red maples are planted as shade trees.

The bigleaf maple (*A. macrophyllum*), which attains a height of 90 ft (27 m) in the Pacific Coast region and north to Canada, can be recognized by its large leaves, which strongly resemble those of the eastern sugar maple, and by its long (about 1 ft or 0.3 m) leafstalks. The lumber is used for veneer, furniture, handles, fixtures, and woodenware. It is also planted as a shade tree.

The box elder (*A. negundo*), with pinnately compound leaves (illus. *c*), is native throughout most of the United States and part of Canada. It is often cultivated as a shade tree.

Two European species are popular street and shade trees: the Norway maple (*A. platanoides*), now becoming naturalized in North America, and the sycamore maple (*A. pseudoplatanus*). The former has copious milky sap in its leaves, twigs, and red bud scales, and close, nonscaly bark; the latter has green winter buds and bark which exfoliates in small polygonal plates (illus. *e* and *b*). *See* FOREST AND FORESTRY; TREE.

Arthur H. Graves; Kenneth P. Davis

Marattiales

An order (class Polypodiopsida) of primitive ferns that consists of about seven living genera and 150 species. They exist mostly in tropical regions. These large, coarse, sappy ferns usually have large, highly divided fronds. *Danaea simplicafolia*, however, has an undivided frond consisting of a single blade. Stems of living genera (*Angiopteris*, **illus. *a*;** *Marattia*) are short and bulbous, often a foot or more in diameter. Other genera have smaller, mostly horizontal, and somewhat more elongated stems. The internal vascular system (food and water conduction tissue) of the stems and fronds can be quite complex, apparently as a function of size. Marattialeans are included among the primitive ferns primarily because of the way that the sporangia (spore-bearing organs) arise from a mass of cells rather than from a single cell as in more highly evolved ferns. Sporangia are generally fused together into a synangium. Synangia are borne on the lower surface of the pinnules and are usually elongate. *Christensenia* differs from other genera in having palmately branched fronds (pinnate in other

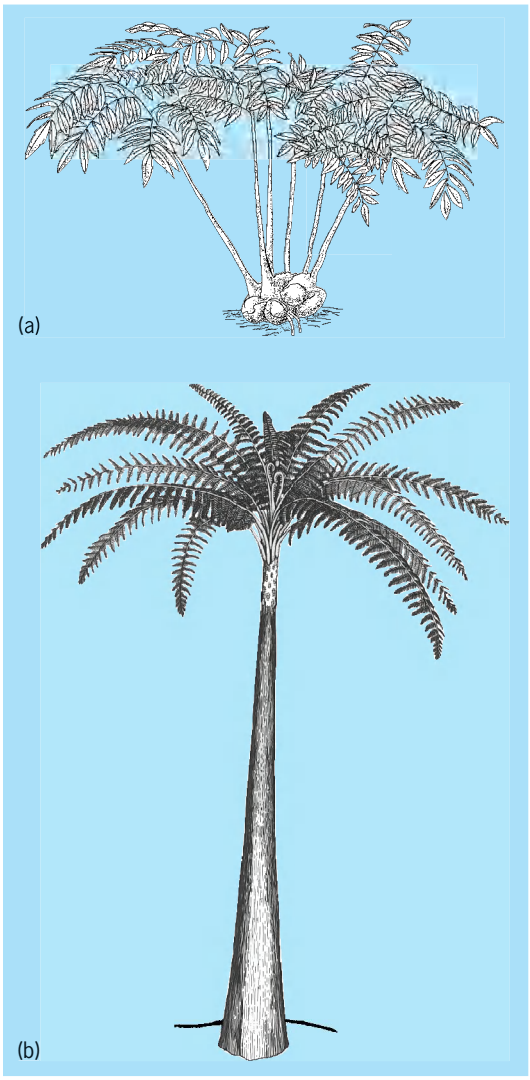

Typical marattialean ferns. (*a*) *Angiopteris*, an extant genus with a short bulbous stem. (*b*) *Psaronius*, a Carboniferous tree fern (*after B. M. Stidd, Morphology and anatomy of the frond of Psaronius, Palaeontographica B, 134:87–123, 1971*).

genera), net venation, and circular rather than linear synangia. Gametophytes (the small plant generation bearing egg- and sperm-producing organs) are large (among ferns) and thick and resemble thallose liverworts.

Psaronius is perhaps the best-known marattialean fern in the fossil record (illus. *b*). It was a prominent member of Carboniferous swamp forests, and much of the fern foliage (known as *Pecopteris*) found on coal mine spoil heaps represents portions of the large fronds borne on *Psaronius* stems. In contrast to most genera, *Psaronius* was more than 33 ft (10 m) tall. The stem was slender, 0.04 in. (1 mm) in diameter at the base, and increased upward, to about 6 in. (15 cm) or more. A plant so slender at the base could not stand erect while bearing the weight of a crown of fronds, each 10–16 ft (3–5 m) long. Consequently, the *Psaronius* trunklike support consisted mostly of a massive cylinder of roots that surrounded the stem. The roots arose from progressively higher levels on the stem as it grew upward; new roots grew downward over older ones and proliferating tissue from root surfaces bound the ensemble into a solid mass, at least in the inner portions of the root mantle. This system of stem encased in a solid layer of roots is highly unusual, if not unique, among plants, both living and fossil. Despite this distinctive feature of *Psaronius*, the anatomy of stem and frond vascular systems is fundamentally similar to that of living marattialean ferns. *See* PALEOBOTANY; PLANT KINGDOM; POLYPODIOPHYTA.

Benton M. Stidd

Bibliography. W. N. Stewart and G. W. Rothwell, *Paleobotany and the Evolution of Plants*, 1993; T. N. Taylor and E. L. Taylor, *The Biology and Evolution of Fossil Plants*, 1993.

Marble

A term applied commercially to any limestone or dolomite taking polish. Marble is extensively used for building and ornamental purposes. *See* LIMESTONE; STONE AND STONE PRODUCTS.

In petrography the term marble is applied to metamorphic rocks composed of recrystallized calcite or dolomite. Schistosity, often controlled by the original bedding, is usually weak except in impure micaceous or tremolite-bearing types. Calcite (marble) deforms readily by plastic flow even at low temperatures. Therefore, granulation is rare, and instead of schistosity there develops a flow structure characterized by elongation and bending of the grains concomitant with a strong development of twin lamellae. In calcite the twinning plane is the flat rhombohedron $\{01\bar{1}2\}$; in dolomite twinning is markedly less common and the plane is the steep rhombohedron $\{02\bar{2}1\}$. *See* METAMORPHIC ROCKS; MINERALOGY.

Regional metamorphic marbles are more or less deformed and therefore texturally marked by characteristic deformation patterns—parallel elongation of irregularly bounded lensoid grains of calcite (less typically of dolomite)—and by preferred orientation of mica flakes, if mica is present, producing a tightly woven, close fabric. This makes the rock, particularly the pure calcite (not dolomitic) marble, well suited for building purposes.

Contact metamorphism of limestones and of dolomites produces granoblastic rocks composed mainly of a mosaic of equant grains of calcite. The fabric is loose and the rock not suitable for use as building material.

Pure marbles attaining 99% calcium carbonate ($CaCO_3$) are often formed by simple recrystallization of sedimentary limestone. Dolomite marbles are usually formed by metasomatism. More interesting petrographically are impure marbles in which various reactions between silicates and carbonates have taken place.

If an impure carbonate rock is subjected to slowly increasing temperature at constant pressure, a series of reactions involving progressive elimination of carbon dioxide takes place. Each of these reactions is determined by the temperature, pressure, and bulk composition of the reacting system. In natural rocks,

water and traces of other fugitive compounds are usually present. These facilitate the metamorphism and permit certain reactions to take place at low temperatures. The pressure usually has not great influence.

If at the beginning of the reaction there is a dolomitic limestone at low temperature composed of the phases calcite + dolomite + quartz (+ traces of water), certain mineral sequences will develop at given stages in the metamorphism. If the temperature is raised only a moderate amount, talc will form, followed by tremolite, forsterite, diopside, and brucite, until eventually wollastonite forms according to the reaction shown here. This reaction

$$\underset{\text{Calcite}}{CaCO_3} + \underset{\text{Quartz}}{SiO_2} \rightarrow \underset{\text{Wollastonite}}{CaSiO_3} + \underset{\text{Carbon dioxide}}{CO_2}$$

has been carefully studied, and it can be shown that it takes place at about 840°F (450°C) [assuming no great buildup of CO_2 pressure]. At higher temperatures rare lime-silicates, such as monticellite, akermanite, tilleyite, spurrite, merwinite, and others, develop.

Examinations of natural occurrences show that at the relatively low temperatures of regional metamorphism the diopside stage is rarely passed. At the somewhat higher temperatures of the contact zones about granites, which come from the coolest of magmas, the wollastonite stage may be attained but not passed. It is only at the hotter contacts of syenitic or granodioritic masses that members higher in the series begin to form, and the highest members are associated only with basic, and usually basaltic, rocks.

T. F. W. Barth

Marchantiales

An order of the liverwort subclass Marchantiidae. Characteristic features include the differentiation of upper and lower tissues of the gametophyte, ventral scales, and rhizoids of two kinds. The sporophyte is considerably reduced, and the capsule dehisces irregularly. The archegonia, though dorsal, come to be pendant from an elevated receptacle because of differential growth resulting in decurved margins. The stalks of the receptacles are modified branches often with rhizoids in one, two, or rarely four furrows along their length. The order consists of 12 families grouped in two suborders, the more complex Marchantiineae and the simplified Ricciineae. *See* BRYOPHYTA; HEPATICOPSIDA; MARCHANTIIDAE.

Howard Crum

Marchantiidae

One of the two subclasses of liverworts (class Hepaticopsida). The gametophytes are ribbonlike or rosette-shaped thalli, usually showing considerable internal tissue differentiation. The rhizoids may be both smooth and internally pegged on the same thalli. Oil bodies, if present, are restricted to scattered cells that lack chloroplasts. The antheridia are usually ovoid, and the archegonia usually consist of six rows of cells. The sporophytes are generally reduced.

The subclass differs from the thallose Metzgeriales of the subclass Jungermanniidae in the internal differentiation of the thallose gametophytes, the smooth and pegged rhizoids, and the variation in the way the capsules dehisce. The subclass is divided into three orders, the Marchantiales, the Monocleales, and the Sphaerocarpales. *See* BRYOPHYTA; HEPATICOPSIDA; JUNGERMANNIIDAE; MARCHANTIALES; METZGERIALES; MONOCLEALES; SPHAEROCARPALES.

Howard Crum

Marcus equation

In the late 1950s and early 1960s Rudolph A. Marcus developed a theory for treating the rates of outer-sphere electron-transfer reactions. In outer-sphere reactions an electron is transferred from a donor to an acceptor without any chemical bonds being made or broken. (Electron-transfer reactions in which bonds are made or broken are referred to as inner-sphere reactions.) Marcus derived several useful expressions, one of which has come to be known as the Marcus cross-relation or the Marcus equation. It is widely used for correlating and predicting electron-transfer rates. For contributions to the understanding of electron-transfer reactions, Marcus received the 1992 Nobel prize in chemistry.

Like ordinary chemical reactions, an electron-transfer reaction can be described in terms of the motion of the system on an energy surface. As the reaction proceeds, the system moves from the reactant minimum (initial state) to the product minimum (final state). The nuclear configurations of the reactants and products and the configuration of the surrounding solvent are constantly changing as a consequence of thermal motion. Subject to certain assumptions, these fluctuations can be described in terms of displacements on harmonic free-energy curves that are a function of a single reaction coordinate. Two harmonic free-energy curves are needed to describe the reaction—one refers to the reactants plus surrounding medium, and the other to the products plus surrounding medium. The two free-energy curves have identical force constants, and the reaction coordinate is the difference between the reactant and product free energies at a particular nuclear configuration.

The free energy of the close-contact reactants plus surrounding medium (curve R) and the free energy of the close-contact products plus surrounding medium (curve P) are plotted versus the reaction coordinate (**Fig. 1**). The free-energy curves intersect where the reactants plus surrounding solvent and the products plus surrounding solvent have the same nuclear configurations and energies. This intersection defines the transition state for the reaction: the energy required to reach the intersection is the

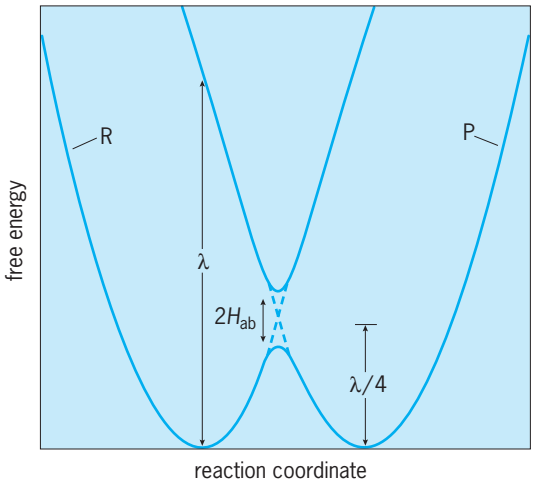

Key:
R = reactants
P = products
λ = reorganization parameter
H_{ab} = electronic coupling matrix element

Fig. 1. Free-energy plot for an electron-transfer reaction with zero standard free-energy change (an electron self-exchange reaction).

free energy of activation for the reaction. The reorganization parameter, λ, is the vertical difference between the free energies of the (noninteracting) reactants and products of a self-exchange reaction at the reactants' equilibrium configuration. Electronic interaction of the reactants gives rise to the splitting of the energy curves (noncrossing) at their intersection. This splitting is equal to $2H_{ab}$, where H_{ab} is the electronic coupling matrix element. The coupling of the reactants is assumed large enough that the electron transfer occurs with unit probability at the transition-state configuration but not large enough to lower the barrier significantly. The splitting is usually neglected in calculating the free energy of activation for the electron transfer.

Self-exchange reactions. The reactants and products of an electron self-exchange reaction are identical. An example is reaction (1), where phen = 1,10-phenanthroline. In terms of the Marcus formalism, the rate constant for a self-exchange reaction is given by Eqs. (2) and (3), where A is the collision

$$\mathrm{Fe(phen)_3^{2+} + Fe(phen)_3^{3+} = Fe(phen)_3^{3+} + Fe(phen)_3^{2+}} \quad (1)$$

$$k = A\exp(-\Delta G^*/RT) \quad (2)$$

$$\Delta G^* = \lambda/4 \quad (3)$$

frequency of the reactants in solution, ΔG^* is the activation free energy for the electron transfer with the two reactants in contact, R is the gas constant, T is the absolute temperature, and λ is the reorganization parameter. The reorganization parameter or intrinsic barrier comprises solvational and intramolecular (vibrational) components. The solvational contribution depends upon the solvent dielectric properties, on the distance separating the donor and acceptor sites and, for a given separation, on the shape of the reactants. The intramolecular contribution depends upon the bond length changes and force constants and is generally treated within a harmonic approximation.

Net electron-transfer reactions. The oxidation of $Ru(NH_3)_6^{2+}$ by $Fe(phen)_3^{3+}$ in reaction (4) is an example of an electron-transfer reaction accompanied by a net chemical change (most electron-transfer reactions fall into this category). Because the reactants and products of a net reaction differ, there is a net free-energy change in the reaction. The free-energy curves for the reactants and products of an exergonic electron-transfer reaction, that is, a reaction accompanied by a decrease in free energy, may be plotted (**Fig. 2**). The free energy of activation for such a reaction is given by Eq. (5), where ΔG° is the standard

$$\mathrm{Ru(NH_3)_6^{2+} + Fe(phen)_3^{3+} = Ru(NH_3)_6^{3+} + Fe(phen)_3^{2+}} \quad (4)$$

$$\Delta G^* = \frac{(\lambda + \Delta G^\circ)^2}{4\lambda} \quad (5)$$

free-energy change for the reaction with the two reactants in contact. Equation (5) reduces to the expression for the free energy of activation for a self-exchange reaction, Eq. (3), when $\Delta G^\circ = 0$. $|\Delta G^\circ|$

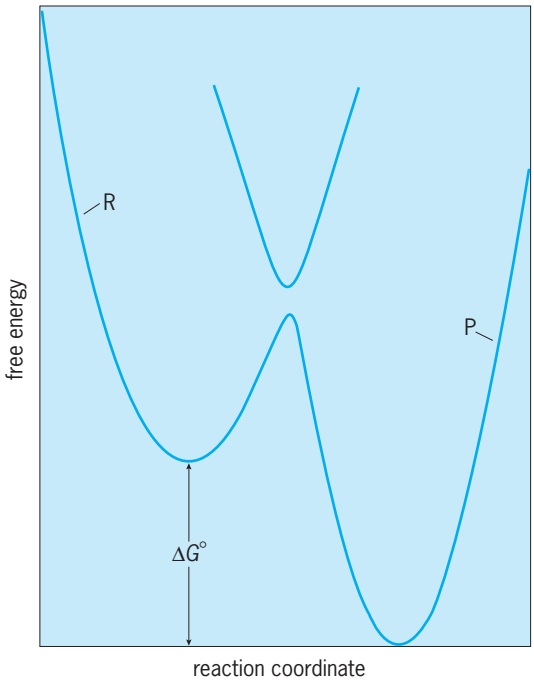

Key:
R = reactants
P = products
ΔG° = standard free-energy change

Fig. 2. Free-energy plot for an electron-transfer reaction when the free-energy change ($|\Delta G^\circ|$) is less than the reorganization parameter (λ).

may be viewed as the driving force for an exergonic electron-transfer reaction.

Three free-energy regimes can be distinguished depending on the relative magnitudes of the reorganization parameter and the driving force. When $|\Delta G^\circ| < \lambda$, the reaction is in the normal regime where ΔG^* decreases, and the rate constant increases, with increasing driving force (as is the case in Fig. 2). The reaction becomes barrierless ($\Delta G^* = 0$) when $|\Delta G^\circ| = \lambda$. If the driving force is increased even further, then $|\Delta G^\circ| > \lambda$ and ΔG^* increases, and the rate constant decreases, with increasing driving force. This is the nonintuitive inverted regime.

Marcus cross-relation. Marcus showed that the rate constant k_{12} for an electron-transfer reaction accompanied by a net chemical change is related to the rate constants k_{11} and k_{22} for the component self exchanges by Eq. (6). Here K_{12} is the equilibrium

$$k_{12} = (k_{11}k_{22}K_{12}f_{12})^{1/2}W_{12} \tag{6}$$

$$\ln f_{12} = \frac{[\ln K_{12} + (w_{12} - w_{21})/RT]^2}{4\left[\ln\left(\frac{k_{11}k_{22}}{Z^2}\right) + \frac{w_{11} + w_{22}}{RT}\right]}$$

$$W_{12} = \exp[-(w_{12} + w_{21} - w_{11} - w_{22})/2RT]$$

constant for the cross-reaction, f_{12} is a factor that becomes significant at large driving forces, W_{12} is a factor that corrects for differences between the electrostatic work terms for the various reactions, w_{12} (w_{21}) is the electrostatic work required to bring together the reactants (products) of the cross-reaction, w_{11} (w_{22}) is the corresponding work to bring together the reactants in the self-exchange reaction, and Z is the collision frequency of two uncharged molecules in solution (10^{11} M^{-1} s^{-1}). Equation (6) is based upon the assumption that the reorganization parameter for a cross-reaction is equal to the average of the reorganization parameters for the component self-exchange reactions, Eq. (7).

$$\lambda_{12} = \frac{\lambda_{11} + \lambda_{22}}{2} \tag{7}$$

For example, if the oxidation of $Ru(NH_3)_6^{2+}$ by $Fe(phen)_3^{3+}$ [reaction (4)] is the cross-reaction (k_{12}, λ_{12}), then the $Ru(NH_3)_6^{2+}$–$Ru(NH_3)_6^{3+}$ reaction (8) and

$$Ru(NH_3)_6^{2+} + Ru(NH_3)_6^{3+} = Ru(NH_3)_6^{3+} + Ru(NH_3)_6^{2+} \tag{8}$$

$Fe(phen)_3^{2+}$–$Fe(phen)_3^{3+}$ reaction (1) are the component self-exchange reactions (k_{11}, λ_{11} and k_{22}, λ_{22}). When the driving force is not too large and the work terms cancel, then $\ln f_{12} \approx 0$ and $W_{12} = 1$. Under these conditions, Eq. (6) reduces to Eq. (9).

$$k_{12} = (k_{11}k_{22}K_{12})^{1/2} \tag{9}$$

Equation (9) is often referred to as the Marcus equation. It has been extensively applied to electron-transfer reactions involving metal complexes. The stable oxidation states of transition-metal complexes generally differ by one electron, and the metal centers and surrounding ligands can be independently varied to encompass a wide range of electron-transfer rates and driving forces. For moderately exergonic electron-transfer reactions between similarly charged complexes, the agreement of the observed rates with those calculated from Eq. (9) is often remarkably good. At high exergonicities or when the net electron transfer involves oppositely charged complexes, it is necessary to use Eq. (6). The rates of highly exergonic reactions calculated with the extended equation are usually somewhat higher than the observed rates in the normal free-energy regime and are slower than the observed rates in the inverted regime. Reasons advanced for the failure of the cross-relation include changes in reaction mechanism, anharmonicity contributions, nuclear tunneling contributions, and noncancellation of nonelectrostatic contributions to the work terms.

Examples of the application of the Marcus equation to organic or organometallic systems include the oxidation of tetraalkyltin, tetraalkyllead, and dialkylmercury by $Fe(phen)_3^{3+}$; the oxidation of various methylarenes, $ArCH_3$, by substituted $Fe(phen)_3^{3+}$ complexes, reaction (10); and the oxidation of

$$ArCH_3 + Fe(phen)_3^{3+} = ArCH_3^+\cdot + Fe(phen)_3^{2+} \tag{10}$$

N-alkylpyridinyl radicals by [Ir(1,5-cyclooctadiene)(μ-pyrazolyl)]$_2^+$, reaction (11), where very good

$$C_6H_5N\text{–}R\cdot + Ir_2^+\cdot = C_6H_5N\text{–}R^+ + Ir_2 \tag{11}$$

agreement with the predictions for highly exergonic electron transfer is obtained. The Marcus equation has also been succesfully applied to reactions of alkylhydrazines, ferrocene derivatives, and *p*-phenylenediamine derivatives.

Because the reorganization barrier is an intrinsic property of a redox couple and independent of its reaction partner, a simple relationship should exist between the homogeneous self-exchange rate constant of a redox couple and its exchange rate constant at an electrode. The relationship between homogeneous and heterogeneous electron-transfer rate constants predicted by the Marcus formalism also holds up well in practice.

Proton, hydride, atom, and group transfers. Although originally derived for electron-transfer reactions, the Marcus formalism can also be applied to reactions in which bond making and bond breaking occur. If the net reaction involves transfer of a covalently attached X from a donor to an acceptor, then the cross-reaction and self-exchanges need to be redefined in terms of X-transfer reactions as shown in Eqs. (12).

$$\begin{aligned} AX + B &= A + XB \\ AX + A &= A + XA \\ BX + B &= B + XB \end{aligned} \tag{12}$$

For example, the oxidation of a methylarene, reaction (10), is followed by proton transfer from the methylarene cation radical to a substituted pyridine,

reaction (13). In this case, $X = H^+$, $A = ArCH_2^{\cdot}$, and

$$ArCH_3^+\cdot + Y\text{-}py = ArCH_2\cdot + Y\text{-}pyH^+ \qquad (13)$$

B = Y-py. The Marcus formalism yields a consistent value for the intrinsic barrier for the proton transfer. Other applications include hydride transfers, reaction (14), where A_iN^+R is a nitrogen heterocycle; gas-phase atom transfers, reaction (15); and nucleophilic displacements (methyl transfers), reaction (16).

$$A_1(H)NR + A_2N^+R = A_1N^+R + A_2(H)NR \qquad (14)$$

$$RH + CH_3\cdot = R\cdot + CH_4 \qquad (15)$$

$$ClCH_3 + F^- = Cl^- + CH_3F \qquad (16)$$

Since the transfer of the heavier particles generally involves strong electronic interactions, the X transfers are not well described by intersecting harmonic free-energy curves. Use of a bond-energy bond-order (BEBO) model for the X transfers results in a free-energy expression similar to Eq. (5) when $|\Delta G^\circ|/\lambda$ is small, but differs from it in not predicting an inverted regime at large $|\Delta G^\circ|/\lambda$. The λ parameter is found to have the same property as Eq. (5), and a cross-relation analogous to Eq. (6) is obtained.

The expression for the free-energy of activation, Eq. (5), is applicable to reactions that can be described in terms of two weakly interacting harmonic free-energy curves. It does not apply when there is an appreciable contribution from bond making or rupture in the rate-determining step. The barrier averaging relation, Eq. (7), is, however, more general: intrinsic barrier additivity obtains in both electron and heavier-particle transfers. The factors determining reaction rates, particularly the additivity of intrinsic barriers, have proved invaluable in understanding and predicting the rates of a variety of electron-, atom-, and group-transfer reactions. Norman Sutin

Bibliography. D. A. Astruc, *Electron Transfer and Radical Processes in Transition-Metal Chemistry*, 1995; L. Eberson, *Electron Transfer Reactions in Organic Chemistry*, 1987; R. A. Marcus, *Annu. Rev. Phys. Chem.*, 15:155–196, 1964; R. A. Marcus, *Pure Appl. Chem.*, 69:13–29, 1997; R. A. Marcus and N. Sutin, *Biochim. Biophys. Acta*, 811:265–322, 1985; S. F. Nelsen et al., *J. Amer. Chem. Soc.*, 119:5900–5907, 1997; N. Sutin, *Prog. Inorg. Chem.*, 30:441–498, 1983.

Margarine

An emulsified fatty food product used as a spread and a baking and cooking fat, consisting of an aqueous phase dispersed in the fat as a continuous phase. Hyppolyte Mège-Mouriés invented margarine in 1869 and won the prize offered by Louis Napoleon for the development of an inexpensive butter substitute. Margarine is now considered a food in its own right and is manufactured in forms unknown to butter, such as plastic, soft, or fluid. However, the interrelationship is still acknowledged since margarine is colored, flavored, fortified with vitamins, and otherwise formulated to have the same or similar taste, appearance, and nutritional value as butter. *See* BUTTER.

Margarine is regulated by law in practically every country in which it is manufactured or sold. In 1977 the U.S. Food and Drug Administration revised and broadened its margarine Standards of Identity to conform to the agreements reached by the Codex Alimentarius Commission, an international body of food and legal authorities charged with the responsibility of unifying foods sold in international trade.

Margarine produced in the United States must contain not less than 80% fat. The fats and oils must be edible but may be from any vegetable or animal carcass source, natural or hydrogenated. The required aqueous phase may be water, milk products, or solutions of dairy or vegetable protein, and must be pasteurized. Milk may be cultured after pasteurization. Vitamin A must be added to yield a finished margarine with not less than 15,000 international units per pound (0.45 kg). Optional ingredients include salt or potassium chloride for low-sodium diets, nutritive carbohydrate sweeteners, fatty emulsifiers, antioxidants, preservatives, edible colors, flavors, vitamin D, acids, and alkalies. *See* PASTEURIZATION.

Margarines are formulated by blending two or more fats and oils in proportions designed to obtain the desired texture, consistency, and melting characteristics in the finished product. The various types of components include unhydrogenated or liquid, lightly, moderately, and highly hydrogenated oils. Meat fats are used in various bakery margarine formulations. *See* FAT AND OIL (FOOD).

Low-calorie spreads designed to resemble margarine contain only 40–60% fat. The higher level of aqueous phase in the product requires the addition of emulsion stabilizers. These may be high levels of milk solids, casein, vegetable proteins, vegetable gums, or various emulsifiers. Low-fat spreads are not covered by U.S. Standards of Identity and cannot be labeled as margarine. *See* FOOD ENGINEERING. Theodore J. Weiss

Bibliography. *Code of Federal Regulations*, 21, 166.110, 1983; H. Lawson, *Food Oils and Fats: Technology, Utilization, and Nutrition*, 1994; T. J. Weiss, *Food Oils and Their Uses*, 2d ed., 1983.

Marine biological sampling

The collection and observation of living organisms in the sea, including the quantitative determination of their abundance in time and space. The biological survey of the ocean largely depends on specially equipped vessels. Sampling in intertidal regions at low tide is one of the few instances where it is possible to observe and collect marine organisms without special apparatus.

A primary aim of marine biology is to discover how ocean phenomena control the distribution of organisms. Sampling is the means by which this aim is accomplished. Suppositions about the dynamics of

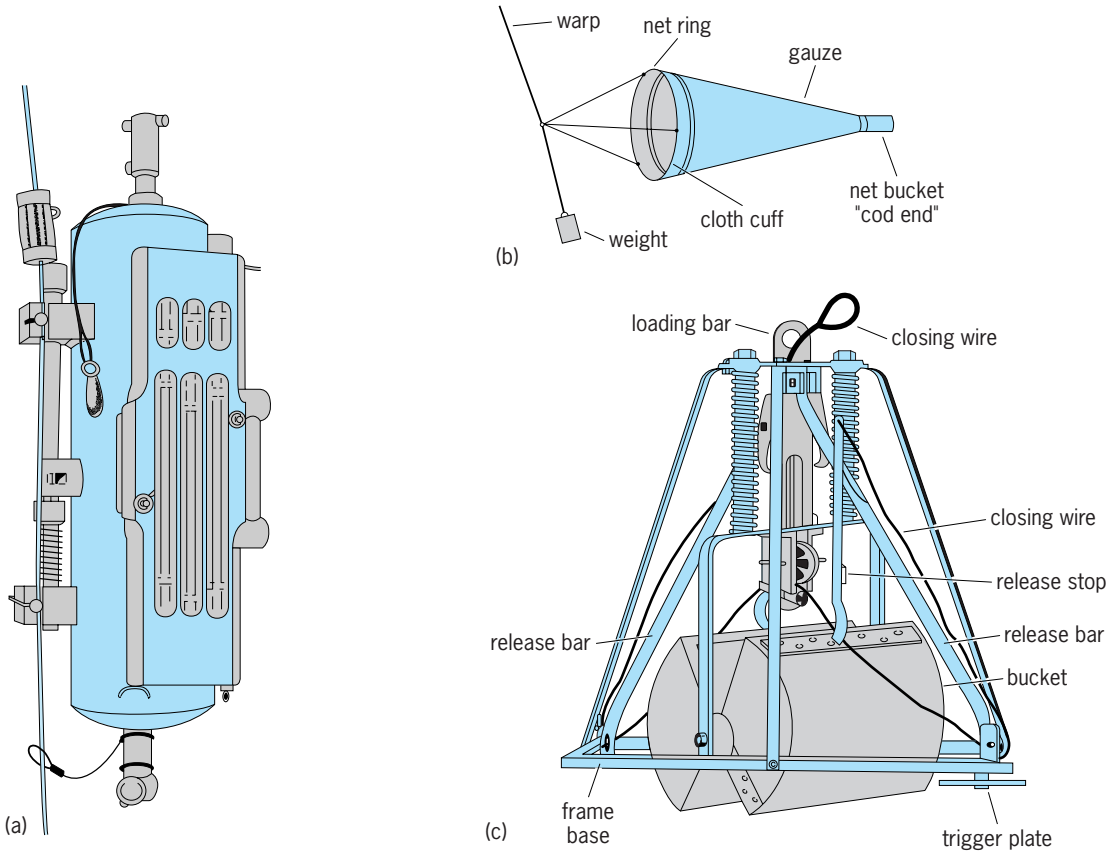

Fig. 1. Marine sampling devices. (*a*) Water sampling bottle with attached thermometer rack for recording water temperature at sampling depth. The brass messenger on the wire has just tripped the spring-loaded end closures (*after S. Niskin, A reversing-thermometer mechanism for attachment to oceanographic devices, Limnol. Oceanogr., 9:591–594, 1964*). (*b*) Conventional plankton net (*after C. Schlieper, ed., Research Methods in Marine Biology, University of Washington Press, pp. 46–63, 1972*). (*c*) Spring-loaded grab sampler (*after W. Smith and A. D. MacIntyre, J. Mar. Biol. Ass. U.K., 33:257–264, 1954*).

ocean life rest entirely on sampling methodology. Traditional techniques use samplers attached to wires lowered over the side of a ship by hydraulic winches (**Fig. 1**). These samplers include bottles designed for collecting seawater samples from particular depths, fine-meshed nets that are towed behind the ship to sieve out plankton and fish, and grabs or dredges that collect animals inhabiting the ocean bottom. These types of gear are relied upon in many circumstances; however, they illustrate some of the problems common to all methods by which the ocean is sampled. First, sampling is never synoptic, which means that it is not possible to sample an area of ocean so that conditions can be considered equivalent at each point. Usually, it is assumed that this is so. Second, there are marine organisms for which there exists no sampling methodology. For example, knowledge of the larger species of squid is confined to the few animals that have been washed ashore, or to the rare video recording. Third, the representativeness of the samples collected is problematic. The open ocean has no easily definable boundaries, and organisms are not uniformly distributed. The actual sampling is regularly done out of view of the observer; thus, sampling effectiveness is often difficult to determine. Furthermore, navigational systems are not error-free, so the position of the sample is never precisely known. All developments in methods for sampling the ocean try to resolve one or more of these difficulties by improving synopticity, devising more efficient sampling gear, or devising methods for observation such that more meaningful samples can be obtained.

Plankton. Single samples for phytoplankton and zooplankton are obtained by using sampling bottles or by towing a plankton net through the water horizontally, vertically, or obliquely (Fig. 1). These samples are preserved and then counted and identified using a microscope. Two developments in sampling planktonic organisms are continuous-recording systems, and multiple-net systems that collect zooplankton from various depths. *See* PHYTOPLANKTON; ZOOPLANKTON.

Continuously recording systems. These methods for phytoplankton take advantage of the fact that chlorophyll *a*, the primary light-sensitive pigment used in photosynthesis, is a fluorescent molecule. This means that when chlorophyll-containing plant cells are illuminated (excited) by a particular wavelength of light, they reemit (fluoresce) light at another wavelength. Chlorophyll is excited by blue light and fluoresces red. Seawater is pumped aboard ship and passed through an instrument called a fluorometer that illuminates the water and records the level of fluorescence due to chlorophyll *a* in the

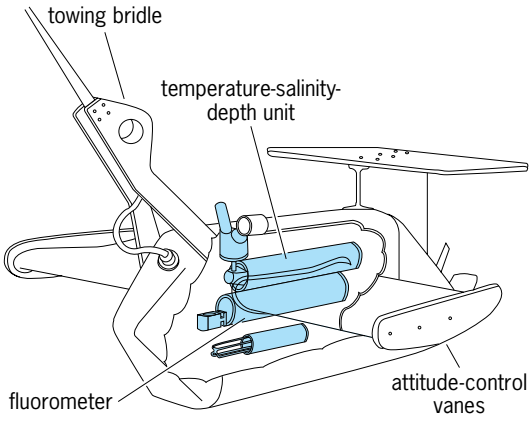

Fig. 2. Towed undulating vehicle system with some of its sensors. (*Chelsea Instruments, Ltd., United Kingdom*)

phytoplankton. This technique thus provides a continuous estimate of the total amount of plant biomass as the water is pumped through the fluorometer. Some fluorometers can be lowered over the side of the ship to measure directly the fluorescence in the water. A strobe light is used to illuminate a small volume near the device, the fluorescence is sensed, and a signal is sent up a conducting cable to shipboard recording devices. *See* CHLOROPHYLL; FLUORESCENCE; LUMINESCENCE ANALYSIS.

Acoustic methods and video cameras can be used for estimating zooplankton abundances continuously. The sound sources used are derived from fish-finder sonars developed for commercial fishing. Sound energy is transmitted at multiple ultrahigh frequencies, usually between 10 kHz and 1 MHz, insonifying a volume of water within 1–2 m (3.3–6.6 ft) of the transducer; and the sound that is reflected, or backscattered, from the organisms is then

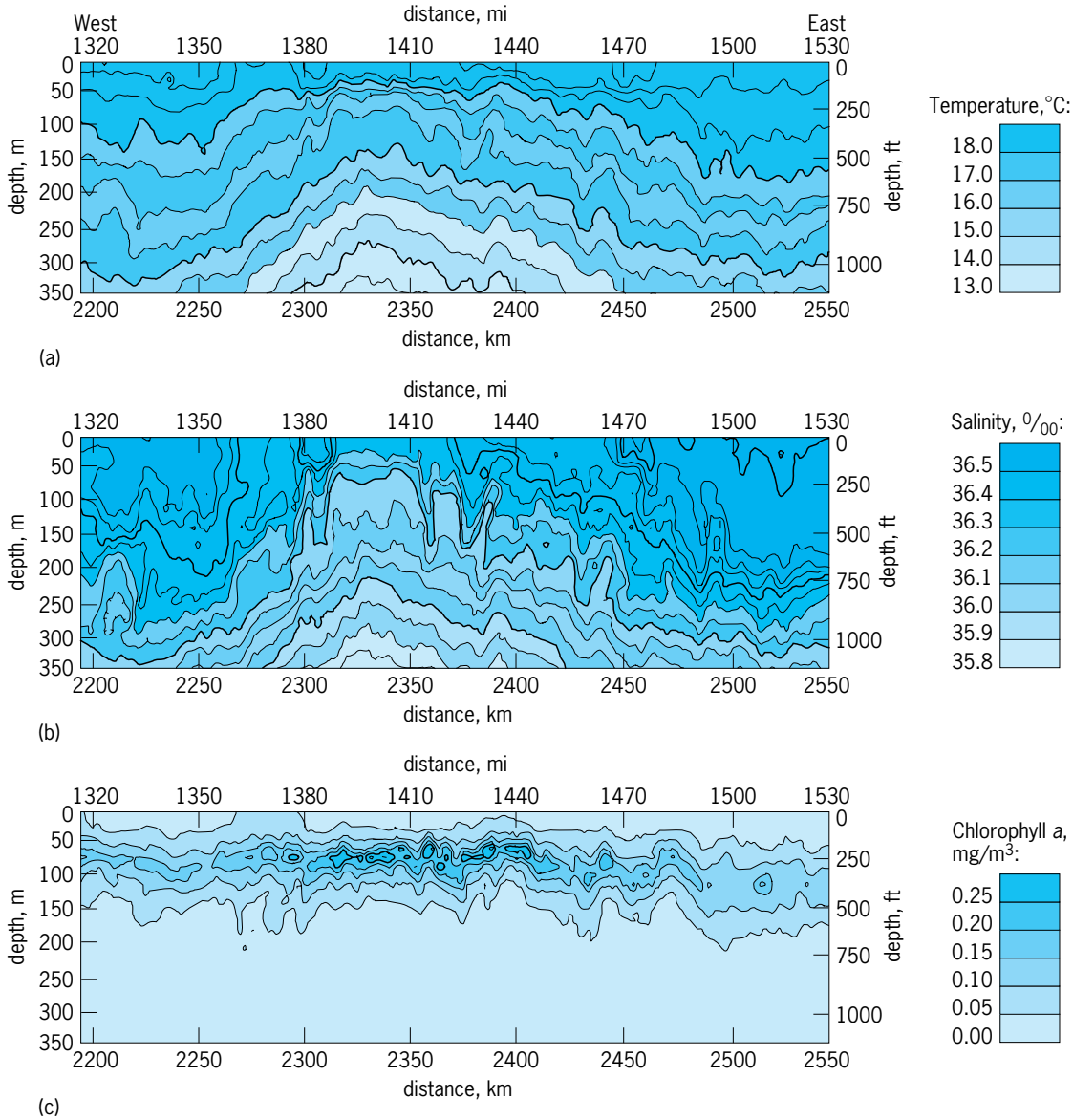

Fig. 3. Data collected by a towed undulating vehicle along a transect in the ocean. (*a*) Temperature; $^{\circ}F = (^{\circ}C \times 1.8) + 32$. (*b*) Salinity. (*c*) Chlorophyll *a*. (*Chelsea Instruments, Ltd., United Kingdom*)

recorded electronically. In this range, organisms 0.1–10 mm (0.004–0.4 in.) in size can be detected. Usually, the transducers for each frequency are triggered sequentially, and the acoustic backscatter measured from each. Backscattered sound depends on size. Smaller organisms can be detected only with high frequencies, while larger organisms can be detected at all frequencies. In the video method, a video camera with a synchronized strobe light is used to sample a volume of water at 60 frames per second. The recorded images are digitized and scanned for zooplankton.

The fluorescence method for phytoplankton and the acoustic and video methods for zooplankton can be used while the ship is under way. For phytoplankton, water is normally pumped continuously to shipboard labs, whereas acoustic transducers are mounted to the hull or are towed just behind the ship near the surface. *See* SCATTERING LAYER; SONAR.

The towed-undulating vehicle instrument can incorporate all three of the continuous-recording techniques as an undulating instrument package towed behind the ship (**Fig. 2**). Variations in plankton abundance (as acoustic backscatter or optical images for zooplankton, and as chlorophyll *a* for phytoplankton) along with environmental parameters such as temperature and salinity are recorded simultaneously in two dimensions (**Fig. 3**).

These techniques are indirect and, with the exception of video methods, provide little information on what species are present. They do provide a detailed, nearly synoptic estimate of the small-scale variation in abundances of plankton over wide areas and with depth. Species analysis of phytoplankton requires bottle sampling (or in special cases, nets). Study of particular zooplankton organisms or groups can be accomplished by use of multiple-net systems.

Multiple-net systems. These types of sampling gear are used to characterize the small-scale vertical distribution of zooplankton species. There are several designs in use. One of the most successful is the multiple opening/closing net environmental sensing system (MOCNESS). MOCNESS carries nine nets that are sequentially opened and closed at desired depths by sending electrical command signals down a conducting cable. The system is deployed with one net opened and is lowered to the desired depth. As MOCNESS is hauled in, nets are opened and closed sequentially at desired depths. The opening of one net automatically closes the previous net. For example, MOCNESS can be sent down to 1000 m (3000 ft) with one net open, and the remaining eight nets could be opened/closed at increments of 125 m (400 ft) as the net is hauled in. An electronic instrument package is mounted on the main frame and contains salinity, temperature, pressure (depth), light, and dissolved oxygen sensors for the recording of environmental data, as well as sensors that detect the flow of water through the net and the attitude of the net as it is towed. During a tow, all this information is recorded on a computer on the ship for later analysis. Every tow provides a series of eight zooplankton samples, each from a different stratum, and one sample representing organisms collected over the entire depth that the net fished.

Nekton. For catching the more active fishes and cephalopods and the larger crustaceans, large-sized nets are essential. The mouth opening of the MOCNESS has been enlarged for this purpose, to 215 ft^2 (20 m^2) for example, and represents an advance in nekton sampling because multiple depths can be fished. A similar design is the rectangular midwater trawl, combining multiple nets of 11 ft^2 (1 m^2) and others of 88 ft^2 (8 m^2), the two-sized nets being used to sample plankton and nekton, respectively. Other enhancements to these nets include specially designed cod ends that maintain the pressure and temperature of the sample as it is collected. By using this last modification, deep-living fish and crustaceans can be brought to the surface alive. A net that will catch larger squids and fishes inhabiting the deep has yet to be developed. For these organisms, video recording and direct viewing from deep-sea vehicles are the best options. *See* DEEP-SEA FAUNA.

Benthos. Organisms that live on the bottom are sampled by grabs, dredges, trawls, and box corers. Grabs are basically a pair of jaws, triggered in various ways to close when they touch bottom, capturing a small (about 0.1 m^2 or 3.3 ft^2) sample of sediment. Several designs are available, depending on bottom type and depth of water (Fig. 1). The sample, after being returned to the deck, is washed and sieved for the organisms it contains.

Dredges have a bag of coarse-meshed netting attached to a rectangular wrought-iron frame (0.6–0.9 m or 2-3 ft wide) that forms the mouth of the net. The dredge is towed along the bottom by means of a movable bridle arrangement, while the lower side of the frame digs into the sediment to scoop up organisms living just below the surface.

Bottom trawls are baglike nets tapering to a cod end. The mouth is kept open by otter boards, to which the two towing warps are attached. The otter boards also serve to disturb organisms off the bottom so that they become trapped in the net. Sometimes, counting wheels are fitted to trawls or dredges to give an indication of distance traveled.

The box corer (**Fig. 4**) is a sediment-coring device. However, the same features that make it useful for the study of ocean sediments make it a valuable piece of equipment for benthic biological research as well. The advantages of the box corer over grabs and dredges are the precision with which it can obtain a bottom sample and the fact that it can bring a largely undisturbed sediment sample to the surface. Therefore, a better characterization of the environment of the organisms can be obtained. In addition, there is little bow wave as the corer approaches the bottom, and it can work in all types of sediment. The disadvantage is that it is large and heavy and thus requires handling by the most powerful winches.

The box corer is allowed to free-fall to the ocean bottom. As the weight of the corer drives it into the bottom, the wire slackens. This action releases the spade, which swings to close off the bottom

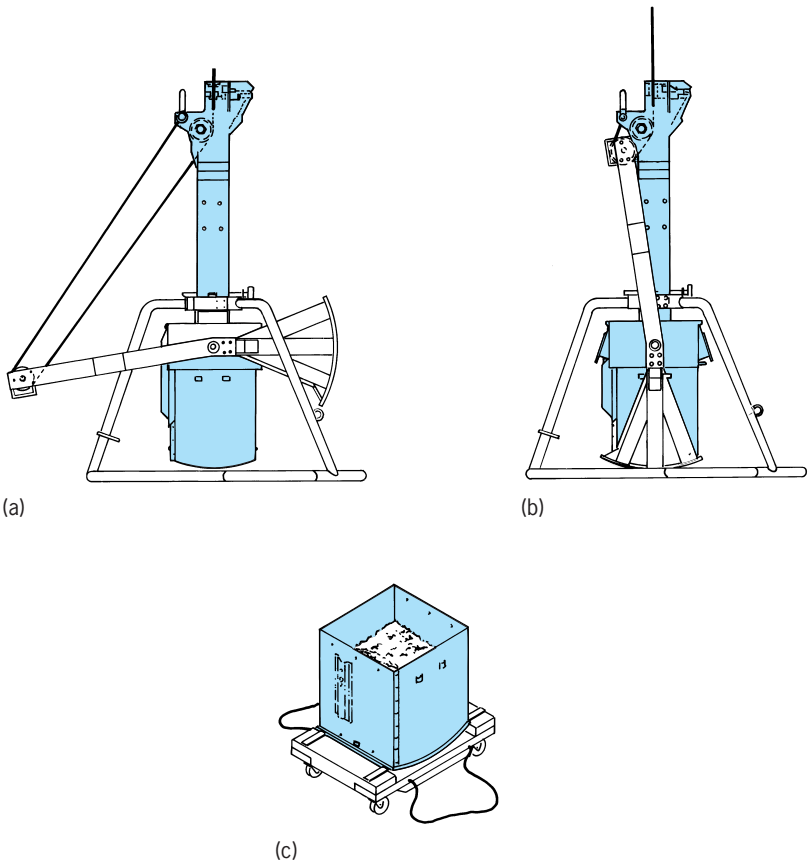

Fig. 4. United States Naval Electronics Laboratory box corer. (*a*) Side view with spade in open position. (*b*) Side view with spade in closed position. (c) Disengaged core box for processing sample. (*After R. R. Hessler and P. A. Jumars, Abyssal community analysis from replicate box cores in the central North Pacific, Deep-Sea Res., 21:185–209, 1974*)

of the corer. The box corer is then brought to the surface. *See* MARINE SEDIMENTS.

Bacteria and viruses. The use of fluorescent dyes, or fluorochromes, simplifies sampling and enumeration of marine bacteria. For this technique, a known volume of uncontaminated seawater or sediment (collected by water sampling bottles, grabs, or corers) is incubated for a short time with the fluorochrome, while bacteria cells absorb some of the dye. The cells are then collected on a filter and viewed under a high-powered microscope equipped with a light source that causes the dye to fluoresce. The bacteria appear as bright objects against a dark background and are counted directly. Acridine orange, a fluorochrome that binds to nucleic acids (RNA and DNA), is commonly used for enumerating marine bacteria. Not all bacterial cells seen under the fluorescent microscope are alive or capable of growth in laboratory culture, although the abundances measured correlate with other plankton variables. Viruses must be enumerated with an electron microscope, usually on samples that have been concentrated and filtered for larger forms. *See* MARINE ECOLOGY; MARINE MICROBIOLOGY; STAIN (MICROBIOLOGY).

Other methods and observations. Direct and remote observation methods provide valuable information on the undersea environment and thus on the representativeness of various sampling techniques. Personnel-operated deep-submergence research vessels (DSRVs) are increasingly used to observe ocean life at depth and on the bottom, and to determine appropriate sampling schemes. The deep-submergence research vessels are used with cameras and television recording equipment and are fitted with coring devices, seawater samplers, and sensors of various types. Other cameras are operated unattended at the bottom for months at a time, recording changes occurring there. Scuba diving is playing a larger role, especially in open-ocean areas, and is used to observe marine organisms in their natural habitat as well as to collect the more fragile marine planktonic forms such as foraminifera, radiolaria, and jellyfish. Autonomous underwater vehicles (AUVs) continue to assume greater importance in sampling programs since they can go to greater depths than can divers, and they overcome a limitation in diving in that AUVs can be operated at night and can sample extensively under ice. Optical sensors carried aboard Earth-orbiting satellites can provide images of ocean color over wide areas. Ocean color is related to the turbidity as well as the amount of plant material in the seawater. This establishes a means by which sampling programs from ships can be optimized. *See* DIVING; SEAWATER FERTILITY; UNDERWATER PHOTOGRAPHY; UNDERWATER TELEVISION; UNDERWATER VEHICLE.

John Marra

Bibliography. P. F. Brodie, D. D. Sameoto, and R. W. Sheldon, Population densities of euphausiids off Nova Scotia as indicated by net samples, whale stomach contents, and sonar, *Limnol. Oceanog.*, 23:1264–1267, 1978; C. S. Davis et al., Rapid visualization of plankton abundance and taxonomic composition using the Video Plankton Recorder, *Deep Sea Res. II*, 43:1947–1970, 1996; K. L. Denman and D. L. Mackas, Collection and analysis of underway data and related physical measurements, pp. 85–109 in J. H. Steele (ed.), *Spaital Pattern in Plankton Communities*, Plenum, New York, 1978; L. R. Haury, J. A. McGowan, and P. H. Wiebe, Patterns and processes in the time-space scales of plankton distributions, pp. 277–327 in J. H. Steele (ed.), *Spaital Pattern in Plankton Communities*, Plenum, New York, 1978; J. C. Kelly, Sampling the sea, pp. 361–387 in D. H. Cushing and J. J. Walsh (eds.), *The Ecology of the Seas*, W. B. Saunders, Philadelphia, 1976; J. Sherman et al., The autonomous underwater glider "Spray," *IEEE J. Oceanic Eng.*, 26:437–446, 2001.

Marine boiler

A steam boiler designed to suit the marine environment and generally arranged to supply steam to the main propulsion machinery, ship's service electric generators, feed-pump drivers, and other auxiliary services. *See* MARINE MACHINERY.

Types of units. Marine boilers are usually of the two-drum water-tube type with water-cooled furnaces, superheaters, desuperheaters, and heat

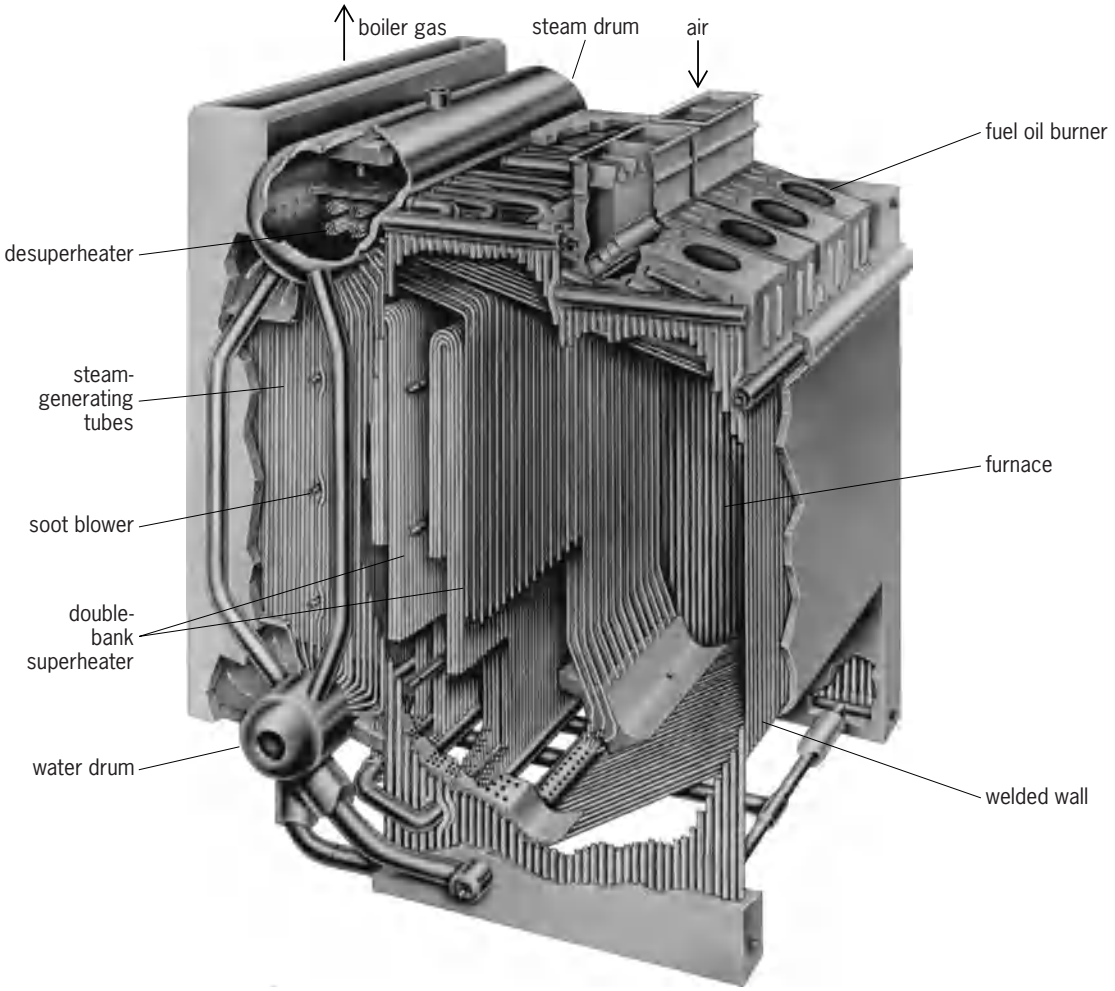

Fig. 1. Typical nonreheat, two-drum, down-fired welded-wall, double-superheater marine boiler. (*Foster Wheeler Boiler Corp.*)

recovery equipment of the economizer or air-heater type. The older fire-tube boilers, commonly referred to as Scotch boilers, and water-tube header types are no longer manufactured for marine service, although some of these boilers are still in use on older ships. *See* FIRE-TUBE BOILER; WATER-TUBE BOILER.

The majority of ships are fitted with two boilers, although some large passenger ships may have three or more. Some cargo ships are fitted with only one boiler, and in some of these cases a smaller auxiliary boiler may be fitted for emergency or in-port steaming use.

Design considerations. The pressure and temperature of the steam produced by marine boilers are dependent upon the steam cycle selected, which in turn relates to economic considerations such as the cost of fuel and the installed cost for the equipment for the propulsion power plant. Since the cost of fuel (energy) is high and rising as it relates to the installed cost of the equipment, there is a need for efficient steam plants, which in turn require high steam pressures and temperatures and efficient boilers. To attain high boiler efficiency it is necessary to minimize the heat loss up the boiler stack. This can be accomplished by utilizing heat recovery equipment such as economizers or air heaters. *See* AIR HEATER; BOILER ECONOMIZER.

Worldwide, most modern ships generate steam at a pressure of 850 lb/in.^{2} gage (5.86 megapascals) and a temperature of 955°F (513°C) at the superheater outlet and employ rotary regenerative air preheaters for the heat recovery equipment. However, in the United States most power plants employ the less efficient economizer as the heat recovery unit.

Figure 1 shows a cutaway view of a typical two-drum marine boiler. It has a welded wall construction in way of the furnace and superheater; that is, the tubes are welded together and joined by ligaments so as to make the furnace and area in way of the superheaters gas- and airtight. *See* SUPERHEATER.

In the upper boiler drum a submerged desuperheater is shown. The purpose of the desuperheater is to lower the steam temperature for a portion of the superheated steam that may be used for auxiliary purposes.

Although they are not popular in the United States, a number of marine power plants employ a steam cycle using boiler steam reheaters. With this arrangement, steam that has passed through a portion of the turbine is directed back into the boiler for

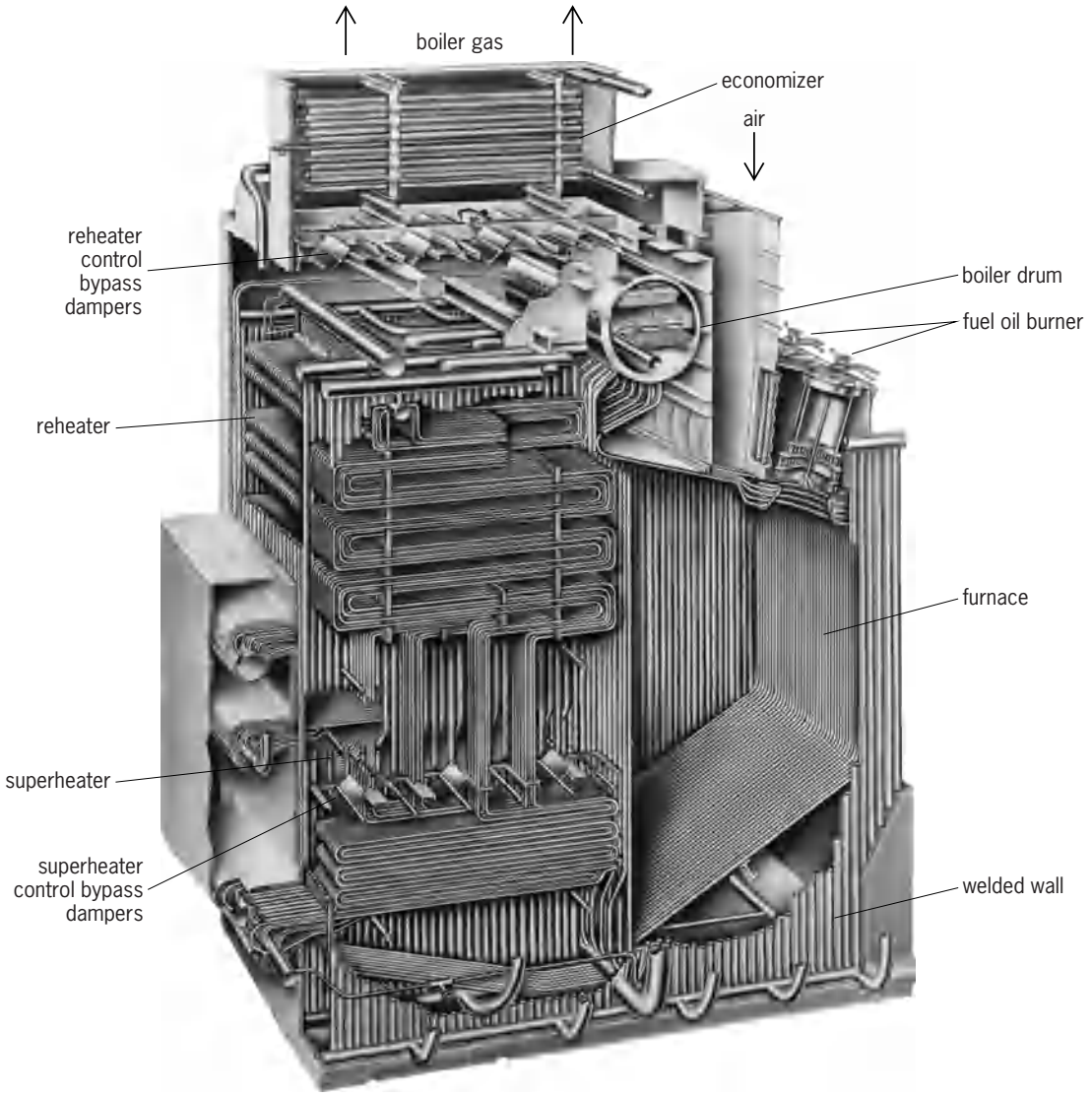

Fig. 2. Typical reheat, down-fired, welded-wall marine boiler containing primary superheater and reheater with economizer and gas damper control. The boiler gas air heater is not shown. (*Foster Wheeler Boiler Corp.*)

reheating in a device similar to the initial boiler superheater, except that the pressure is lower. The advantage of using this arrangement is that higher initial steam pressure may be employed, generally around 1450 lb/in.^{2} gage (10.0 MPa), and this advantage, coupled with the advantage of reheating the steam, can result in propulsion power plants where the fuel consumption may be 5–8% less than the conventional arrangement discussed above. *See* REHEATING.

Figure 2 shows an economizer in the gas path; this would be installed in series with a gas air heater of the type shown in **Fig. 3**. The air heater shown is a rotary regenerative type and consists of a drum filled with a plate-type heat exchange surface that is rotated first through the boiler exhaust gas path, which heats the surface while cooling the gas, and then through the air that is discharged from the boiler-forced draft fan, which heats the air while cooling the surface. The heated air then passes to the boiler, where it supplies the air necessary for combustion. The use of an air heater of this type can permit boiler efficiencies to be in the range of 91%, based on the lower heating value of the fuel.

Although the heat exchange surfaces are coated with acid-resistant enamel, they deteriorate in time and must be replaced, particularly in the colder part of the heater. Thus arrangements must be made for easy replacement of the surfaces.

Where economizers alone are fitted to serve as the boiler heat-recovery equipment, it is common to use steam air heaters. With this arrangement the air for combustion is forced through a heat exchanger containing extended surface tubes where heat is extracted from the steam to warm the combustion air.

Special design requirements. In the design of marine boilers, special requirements must be considered. The units must be compact and economical with regard to space and weight. Also, they must be built to withstand the effect of the pitching and rolling motions of the ship, as well as vibration which is caused by the ship's propeller. Reliability must be inherent in the design because of the requirements of safety at sea.

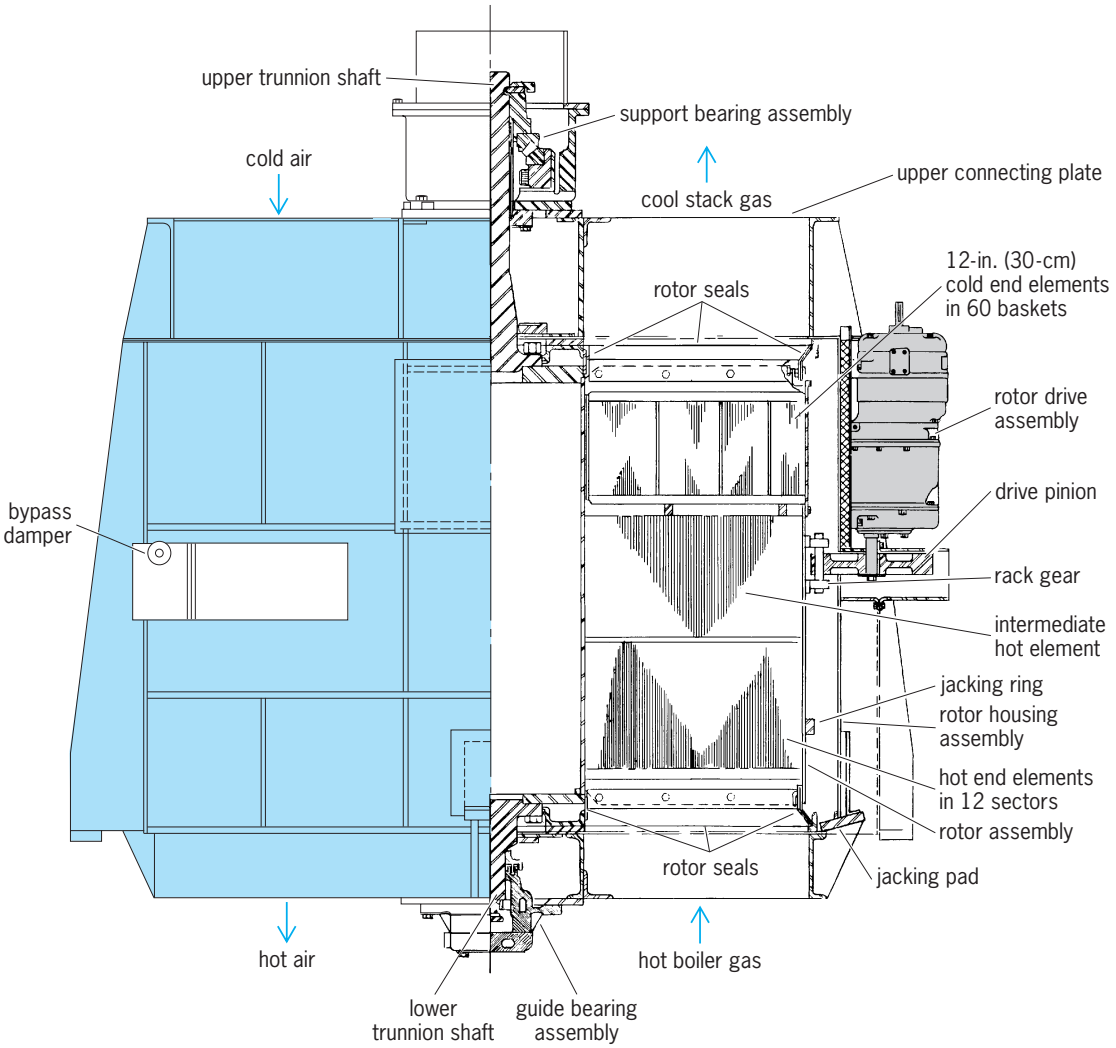

Fig. 3. Vertical rotary regenerative gas air heater. (*Air Preheater Company, Inc.*)

Fuels. Marine boilers are generally arranged for oil firing. Oil is used extensively because of its simplicity of handling and storing and the fact that it can be stored in spaces that often cannot be used for carrying cargo. For economic reasons, coal was used in the United States for boats operating on the Great Lakes, but most of these installations have been converted to use oil as a fuel.

Oil-fired boilers are arranged for forced draft; that is, the air for combustion is blown or forced into the boiler furnace by use of centrifugal, motor-driven fans. Coal firing generally uses a combination of forced and induced draft fans, and these boilers are operated such that the gas pressure in the boiler furnace is slightly negative with respect to the surrounding atmosphere.

The oil normally burned is a residual fuel called No. 6 fuel oil or sometimes referred to as Bunker C. This fuel has the lowest cost of liquid fuel since it is what is left over after the refining process, which has extracted better and cleaner products such as gasoline, diesel oil, and home heating oil.

The fuel from the ship's bunker tanks is generally transferred to a settling tank, which contains about a day's supply. While in the tank, the fuel is heated, and water and heavy solids such as sand can be removed by settling before the fuel is pumped at high pressure through fuel oil heaters and to the burners. The purpose of the fuel oil heaters is to reduce the viscosity of the oil so that it may be atomized for burning. To assist this mechanical atomizing process, most fuel oil burners utilize steam under pressure to further break down the oil particles so as to provide better combustion characteristics. The oil being atomized at the burner is then mixed with the heated combustion air so that the combustion process can take place in the furnace.

Coal is normally burned by using mechanical stokers and moving chain grates, although some consideration is being given to burning powdered coal, either in the solid form or as a powder mixed with oil in the form of a slurry.

Automatic controls. Automatic controls regulate the feedwater flow to the boiler, the superheater outlet steam pressure and temperature, the fuel oil flow, and the quantity of combustion air. Generally the controls are of the solid-state electric type that sends signals to the electric or air power devices for positioning of valves and dampers. *See* BOILER

FEEDWATER REGULATION; STEAM TEMPERATURE CONTROL.

Maintenance and repairs. Reliable and efficient performance of the boiler is required over the economic life of the ship, which is considered to be about 25 years. Normal maintenance and repairs are generally made while the ship is in port, while major repairs are made in a shipyard during the annual inspection periods. *See* DRYDOCKING.

Boiler firesides must be cleaned of soot and ash deposits to obtain high boiler efficiency and proper superheater steam temperature. For this purpose soot blowers using steam as cleaning media are fitted in the superheater and the steam-generating and heat recovery sections of the boiler. These surfaces also must be water-washed periodically.

Scale deposits and corrosion of the water sides of the boiler must be avoided. To accomplish this, chemically treated distilled water must be used for boiler makeup, and leaks of seawater to the boiler feedwater must be avoided. Periodic chemical testing of the boiler water and the feedwater must be conducted by manual or automatic means. *See* BOILER; BOILER FEEDWATER; STEAM-GENERATING UNIT.

Robert P. Giblon

Marine conservation

The management of marine species and ecosystems to prevent their decline and extinction. As in terrestrial conservation, the goal of marine conservation is to preserve and protect biodiversity and ecosystem function through the preservation of species, populations, and habitats. The importance of conserving marine species and ecosystems is growing as a consequence of human activities. Negative impacts on marine biological systems are caused by such actions as overfishing; overutilization, degradation, and loss of coastal and marine habitats; introduction of nonnative species; and intensification of global climate change, which alters oceanic circulation and disrupts existing trophic relationships. Such factors contribute to species decline and extinction in the sea. The growing human population puts direct pressure on marine biological resources through extraction of food and natural resources from the ocean; conversion of coastal habitats for housing, marinas, and other purposes; use of waterways for shipping and recreational purposes; intentional and unintentional translocation of exotic marine species; and pollution of coastal waters and their underlying sediments. In addition, humans put indirect pressure on coastal and marine systems through runoff, erosion, pollution, and eutrophication from terrestrial sources. Additional indirect pressures are imposed on marine systems, and on the entire biosphere, by the production of atmospheric emissions that contribute to global warming and increased penetration of ultraviolet radiation. Marine conservation biologists seek to reduce the negative effects of all these factors by conducting directed research and helping to develop management strategies for particular species, communities, habitats, or ecosystems.

The discipline of marine conservation has lagged behind terrestrial conservation in its development and application. This is due to many factors, including the logistic difficulties of working in the marine environment; practical difficulties of observing, counting, and tracking marine organisms and their offspring; and a relative lack of knowledge concerning many marine communities and habitats, especially those of the open ocean and deep sea.

A variety of approaches and tools are used in marine conservation. These include population assessment; mitigation, recovery, and restoration efforts; establishment of marine protected areas; and monitoring programs. Many of these approaches overlap with those in terrestrial conservation. However, fundamental differences between terrestrial and marine environments in spatial dimension, habitat type, and organismal life history require that basic conservation techniques be modified for application to the marine environment. *See* BIODIVERSITY; ECOSYSTEM; MARINE ECOLOGY; OCEANOGRAPHY.

Population assessment. Effective management requires knowledge of the size and status of populations. Trends in abundance can be detected through stock assessment methods first developed for marine fisheries and subsequently modified for application to other marine organisms. These methods use estimates of population size, reproduction, survivorship, and immigration to determine whether populations are increasing, decreasing, or stable. Small populations and populations with steeply declining numbers are typically thought to be at greater risk of extinction than larger, more stable populations. Population viability analysis is a specialized statistical assessment in which demographic and environmental information is used to determine the probability that a population will persist in a particular environment for a specified period of time. Population viability analysis can be used to guide management decisions, and has been used in efforts to manage marine mammals, turtles, seabirds, and other species. *See* ECOLOGICAL COMMUNITIES; ECOLOGICAL METHODS; POPULATION ECOLOGY.

Mitigation, recovery, and restoration. Depleted, threatened, or endangered populations are often subject to mitigation or recovery efforts. The purpose of these efforts is to reduce the immediate threat of extinction or extirpation. This is typically achieved by direct human intervention to increase the size of a population or to prevent further decline in population size. Recovery can be promoted by reducing juvenile and adult mortality and by restoring critical habitat (that is, areas essential for feeding or reproduction). Methods used to achieve recovery of fish and marine invertebrate populations include reducing fishing quotas, restricting the use of certain types of fishing gear, restricting the seasonal or annual distribution of a fishery, or closing fisheries altogether. For species such as some marine mammals, recovery has been effected by legislation that greatly limits or prohibits their capture or lethal take. The eastern North Pacific stock of gray whale and the Bering-Chucki-Beaufort stock of bowhead whale, both of which suffered severe depletion due to

overexploitation in the nineteenth and twentieth centuries, are examples of successful recovery efforts. In contrast, for reasons that are not fully understood, attempts to increase the number of Hawaiian monk seals have been largely unsuccessful, and the species remains in danger of extinction. *See* ENDANGERED SPECIES; FISHERIES ECOLOGY.

Recovery efforts can be most successful if they are based on multispecies or ecosystem-level management strategies. These strategies take into account positive and negative interactions between species, such as facilitation, competition, and predation. They further take into account interactions between species and their environment. An example of a multispecies interaction comes from the red sea urchin and the abalone, both of which have been the target of commercial and recreational fisheries in California. Juvenile abalone recruit most successfully beneath the spine canopies of adult urchins; thus, efforts to aid the recovery of abalone are most effective when the abundance of urchins is sufficiently high. An example of ecosystem-level interactions comes from the Steller sea lion, which has shown continued population decline in the Gulf of Alaska. Despite ongoing research and recovery efforts, the causes of this decline remain unknown, and attempts to increase the number of sea lions have been mostly unsuccessful. However, some believe that the decline has been caused in part by the combined effects of commercial fisheries that target the forage fish required by the sea lions, and by climate change, which has altered oceanic circulation patterns and thereby altered the distribution and reduced the availability of suitable prey.

Key to the success of assessment and recovery programs is identification of the appropriate biological unit for conservation (for example, population, subspecies, stock, or evolutionarily significant unit). Maintaining genetic diversity is an important goal of conservation biology, because genetic diversity confers evolutionary potential. Thus, conservation efforts often are aimed at populations that are genetically distinct from other populations of the same species. Species become and remain genetically distinct through reproductive isolation (that is, by lack of interbreeding). A good example of reproductive isolation in marine species is found among salmon stocks in the Pacific Northwest of the United States. In this region, salmon of diverse stocks and species intermingle while they are feeding at sea. However, members of each stock return to a particular stream or river system to reproduce, thereby creating a high degree of genetic isolation between groups. Effective conservation strategies must take into account this genetic distinction by managing distinct stocks separately.

Restoration efforts are aimed at returning habitats to an ecologically functional condition, usually consistent with some previous, more pristine condition. In the marine realm, restoration efforts have been limited to certain coastal and estuarine habitats. Seagrasses provide an important example of restoration efforts in coastal areas. Seagrasses are marine flowering plants that grow in large stands, or "meadows," in shallow bays and inlets. Seagrass communities are highly productive, and they perform essential ecosystem functions through provision of nursery areas for juvenile fish and other animals, and as feeding areas for both fish and birds. However, seagrass communities are being lost rapidly through coastal development. To offset these losses, restoration activities have been initiated in California, Texas, Florida, and other places. These efforts include transplanting seagrasses from healthy populations to sites where they can replace plants that were lost; regulating activities that contribute to habitat loss, such as the dredging or filling of tidelands; and modifying the design of docks and marinas to have a less deleterious effect on existing seagrass populations. *See* MARINE FISHERIES.

Marine protected areas. Marine protected areas are set aside for the protection or recovery of species, habitats, or ecosystems. They include marine parks, marine reserves, marine sanctuaries, harvest refugia, and voluntary or legislated no-take areas. Some marine protected areas allow for consumptive use (such as fishing) or extraction of resources (for example, oil drilling), while others are closed to most human activities.

The number of marine protected areas is growing. Two of the largest are Great Barrier Reef Marine Park in Australia, established to protect coral reef ecosystems, and the Galápagos Marine Park in Ecuador, which protects a unique temperate ecosystem. In the Antarctic, protection is provided to living and nonrenewable marine resources by principles codified in several international treaties. Other, smaller marine protected areas have been established to protect or promote the recovery of individual species or groups of species such as seahorses, dugongs, sea turtles, Mediterranean monk seals, Hawaiian monk seals, southern sea otters, rockfish, abalone, and seagrasses. However, many of these marine protected areas are so new that their effectiveness has not yet been demonstrated.

Monitoring programs. Monitoring programs are necessary to determine the outcome of specific conservation actions and to guide future conservation decisions. Monitoring programs vary according to the objectives of specific conservation projects but typically include such activities as long-term surveys of population size and status, and the development of mathematical models to help predict specific outcomes. A good example of monitoring efforts are those concerned with the California gray whale. Repeated surveys of migrating whales allowed observers to estimate the number of animals in the population as well as trends in abundance over a 30-year period. The data showed the California gray whale population to be growing steadily and sufficiently large to allow its removal from the U.S. List of Endangered and Threatened Wildlife in June 1994.

Terrie Klinger

Bibliography. T. S. Agardy, *Marine Protected Areas and Ocean Conservation*, Academic Press, San Diego, 1977; E. A. Norse (ed.), *Global Marine Biological Diversity*, Island Press, Washington, DC, 1993.

Marine containers

Standardized rectangular boxes for the transport of marine cargo. Ocean transportation of cargo containers began in 1956, when the converted tanker *Ideal-X* of Pan-Atlantic Steamship Company left Newark, NJ, for Houston, TX, for the first time. On the vessel's deck were fifty-nine 35-ft (11-m) containers holding cargo that until then had been brought to piers by truck or train, placed on pallets or in cargo slings, and lifted into the ships' holds. This method of handling cargo, called break-bulk, was slow and labor-intensive. Containers, in contrast, can be loaded at a remote site, sealed, moved to the pier, and lifted into the ship without the need for intermediate handling. The principal benefits other than reduced pierside handling cost are less cargo damage and reduced pilferage. *See* MERCHANT SHIP.

Containerization has been the most significant change ever made to cargo transportation by sea. The now ubiquitous container transportation system has made break-bulk shipping almost obsolete on the major trade routes of the world. Even on routes serving minor outports, where cargo volumes have been insufficient to justify the landside infrastructure required for the container system, the phenomenon of containerization is increasingly important.

Development. One aspect of the success of container transportation has centered on the standardization of equipment, which has allowed virtually any container to be carried anywhere in the world—by road, rail, or sea or any combination of these modes—without concern for the ability of the transport facilities to deliver the cargo, safely and untouched, to the ultimate destination, however remote it might be.

The predominant materials of construction are steel and aluminum, although a small number of containers have included reinforced plastic side panels. All are built around a steel frame to provide the requisite strength for lifting and stacking, in vessel holds and on deck, as well as during intermodal portions of the journey.

Through the mid-1960s, container transportation was marked by the use of boxes of a variety of lengths according to the needs of individual vessel operators and local statutory limits on over-the-road transportation. Containers with a length of 17, 20, 24, 30, and 35 ft (5.2, 6, 7.3, 9, and 11 m) were used during this period. These soon gave way to containers of International Standards Organization (ISO) dimensions, wherein lengths of 20 and 40 ft (6 and 12 m) were specified with heights of 8, 8.5, and 9.5 ft (2.4, 2.6, and 2.9 m). Width was standardized at 8 ft (2.4 m).

At a later date, containers 45 ft (14 m) long were introduced, and later still, the length was increased to 48 ft (15 m) and finally 53 ft (16 m). The width of the 48- and 53-ft containers is 8.5 ft (2.6 m). Although these non-ISO boxes originated in the United States, where highway transportation practices and most state laws permit their use, they are now common in many other parts of the world. In addition, attempts are being made to adapt the ISO standard containers to accommodate European standard pallets more efficiently; however, these have not been widely used in international shipping.

An increasing number of containers are specially fitted with racks and other devices for dedicated services, of which the transport of motor vehicles and vehicle components is the most common. When completed vehicles are carried in ISO standard containers, they are usually stowed on movable racks to accommodate the maximum load per box. A low-height 53-ft (16-m) container has been developed to permit motor cars to be driven in and secured without the need for special interior fittings.

Where wider-than-ISO containers [mainly 48-ft (15-m) boxes] are to be carried below deck, it has been necessary to construct dedicated cellular guides to accommodate these boxes. On deck, the problem is less onerous, for container support points on deck and on hatch covers can readily be installed. In intermodal traffic, a number of special rail cars will accept containers of either width by the use of adjustable corner fittings.

Although a majority of containers are used for general cargo, an increasing number of specialized boxes carry refrigerated or frozen meats, fish, fruit, and other foods. Refrigerated boxes are also used to carry critical medical supplies such as blood plasma and insulin. These containers are equipped with self-contained refrigeration units powered from the ship's electrical system. Instrumentation systems are used to monitor and control cargo temperature.

Tank containers are used to transport a vast array of oils, chemicals, and other liquids. Notable among these liquids are certain potable commodities and cryogenic gases, the latter typically carried in insulated, double-wall tanks.

High-cube boxes are widely used for low-density commodities such as apparel. Apparel is carried on hangers that may be moved direct to retail outlets without the need for packaging.

Half-height containers are used for special ladings, such as dense commodities. Open-top and open-flat containers are used for outsized loads, while a few double-height boxes have been used for the movement of outsized aircraft components.

Stowage and handling. Containers are carried below deck on ships having cellular holds fitted with steel guides at the four corners, which provide longitudinal and transverse restraint as the ship rolls and pitches at sea. No other restraint is required. Stacking containers up to nine high is common in the holds of the largest ships.

Deck loading, a unique characteristic of container ships, had been unavailable for most cargoes on break-bulk vessels. In the pioneering days of container transportation, deck stacks generally were limited to two tiers. As lashing methods and equipment were perfected, stack heights eventually rose to six high, consistent with adequate ship stability and unimpeded visibility from the wheelhouse. Many operators use the sixth tier to transport empty containers.

Common to all containers are standardized corner fittings, which not only provide structural strength to permit stacking but also provide anchoring points for lashing. Lockable fittings are employed at each corner to provide rigidity throughout the entire stack.

Lashings are conventionally chain or steel rods, with appropriate fittings at each end to mate with deck lashing points or container corners. The lashing assemblies include toggle or turnbucklelike devices to assist in securing the stack as an integral unit.

Several ship operators have substituted structural frames for a portion of the conventional lashing devices in order to minimize time and labor in making deck-loaded containers ready for sea. These lashing frames are anchored to fixed ship structure and typically are placed between the lowermost and second tier of a deck stack, thus eliminating the need for chain or rod lashings on these tiers.

A number of "hatch-coverless" container ships have been built for the purpose of reducing port time and the expense of handling hatch covers while loading and discharging. On such vessels, cell guides are extended upward above the hatch coamings to secure containers stowed above deck.

The carriage of hazardous cargo in containers has received much attention. Regulatory requirements and common sense dictate how and where containers loaded with such commodities should be stowed. An important consideration in transporting hazardous cargo in this manner is to ensure that cargo manifests are accurate and the guidelines for stowage are strictly followed.

Shoreside handling. In loading or discharging a container ship, individual boxes are typically lifted by shoreside or ship-mounted cranes using spreader frames having locking devices at the corners that engage the container corner fittings. The remote-operated locking devices are under the control of the crane operator. Under certain circumstances, two containers are handled simultaneously; two 20-ft (6-m) boxes in tandem may be lifted using a single 40-ft (12-m) spreader frame, or two empty boxes, one above the other and secured to one another by locking fittings, may be lifted.

Shoreside cranes are of the gantry type, capable of reaching to the extreme far side of the ship being worked. Over the first 30 years of the container era, shoreside cranes evolved to the centerpiece of an efficient handling for vessels of up to Panamax (106 ft or 32.2 m) beam, then the industry-wide standard. From the mid-1980s on, ships with a beam of up to 138 ft (42 m) have been built, making them unable to traverse the Panama Canal. As a result, the maximum outreach of newer shoreside cranes has been increased to handle these larger vessels. Cranes with an outreach of up to 180 ft (55 m) are being installed at major terminals, anticipating dimensions of future vessels. *See* HOISTING MACHINES.

Geared container ships, that is, vessels having shipboard cranes, are generally limited to feeder vessels and smaller line-haul ships that call at ports not having extensive container-handling terminals. Although some multipurpose vessels, which may also be used to carry break-bulk or bulk cargoes, have center-line mounted cranes, the cranes of geared container ships are typically installed on one side of the ship so that the vessel may be moored with cranes away from the pier in order to eliminate interference while containers are loaded or discharged by shoreside cranes.

Handling and movement of containers at shore terminals has received close attention in an effort to reduce terminal dwell time. Two separate systems have evolved: placing each container on its own tractor-drawn chassis for eventual dispatch by road, and handling the containers within the terminal with specially designed straddle carriers, some of which can transport two containers one above the other. At some terminals, on-pier marshaling yards permit the loading of rail cars direct from the vessel for intermodal shipment. In-terminal transfer of containers from ship to ship or barge is also used extensively.

The use of containers as an integral part of military logistics systems has received much attention, having been proven in both simulated and actual operations. Prepositioned military support vessels utilize containers for a major part of their cargo stowage. *See* HARBORS AND PORTS.

Intermodalism. The concept of intermodalism, by which containers may be transported successively by sea, rail, and road, was the premise upon which containerization was conceived and achieved its greatest success. Intermodalism was most emphatically demonstrated in the United States, where the growth of the industry coincided with the establishment of the interstate federal highway network.

The railroads, previously handicapped because of the atmosphere engendered by an archaic regulatory climate, eventually assembled an efficient container-on-flat-car transport system by which transocean containers could be carried between ocean terminals and inland points. Special rail cars were devised to permit up to two 40-ft (12-m) containers to be carried on each piece of rolling stock, and dedicated inland terminals were able to handle transfers between rail and road vehicles.

Although the rail system was reasonably efficient, it was not until the development of the double-stack rail car fleet that per-mile costs were decreased sufficiently to make rail transport a truly competitive alternative. Articulated, drop-center cars permitted containers (including high-cube boxes) to be carried one atop the other, thus doubling the load carried per unit of train length. The western railroads of the United States, enjoying more liberal loading-gauge restrictions, were the earliest beneficiaries of this concept. Many eastern railroads, with their more congested facilities, found it necessary to alter bridges, tunnels, and other lineside impediments to take advantage of the double-stack equipment. The concept is in use with success over much of the United States, bringing the heartland within easy reach of deepwater ports. *See* RAILROAD ENGINEERING.

Prospects. It is predicted that there will be significant increases in the level of both international and domestic container trade. Among the developments

in container transportation that must accompany increased traffic will be further increases in the size of the container ship fleet, individual ship capacity, more efficient terminals and intermodal connections, and changes in container technology.

Maximum ship capacity, now around 7000 TEU (twenty-foot equivalent units), may soon reach 8000 to 9000 TEU, and it is possible that true megacarriers, which carry over 10,000 TEU, may become the standard for major line-haul routes.

Maximum ship capacity is closely tied to the ability of shore terminals and intermodal facilities to handle container throughput efficiently. Hence, improvements in the way that containers are handled throughout the landside transportation system, including ship loading and discharging, will be made.

Critical to the ability of developed countries to handle increased traffic is the provision of adaquate and efficient port facilities. Assuming that container dwell time is constant, throughput at a terminal is a function of terminal area. The question must be raised: is sufficient additional area available at existing container ports to accommodate future growth? If not, is the construction of new ports, with appropriate intermodal connections, a viable alternative?

Heretofore, the physical size of container ships has permitted the operation of port-to-port services, in which vessels call at multiple ports at each end of an ocean voyage. Ship size has increased significantly from the mid-1980s, leading to the emergence of hub- and-spoke operations, in which large line-haul ships call at a limited number of hub ports. From these, smaller feeder ships (which may be as large as yesterday's line-haul vessels) distribute containers to nearby smaller outports. The expansion of the hub-and-spoke concept will continue as line-haul ship capacities increase to megacarrier (about 10,000 TEU) dimensions. The success of the hub port concept will depend upon the ability of the ship-port interface to decrease terminal dwell time to a commercially acceptable amount.

There is also likely to be a substantial increase in development of intermodal systems in parts of the world where rail and highway facilities are being expanded. Similarly, the intermodal system will need to be made more efficient in developed countries as cargo volume increases and existing road and rail facilities become overloaded.

Other changes are likely to be seen in the containers themselves. It is foreseen that collapsible containers will be developed for certain commodity loading to minimize the volume occupied in repositioning empty boxes, and specialized containers for dedicated cargoes will be utilized to a greater degree than that at present.

Rod Vulovic

Marine ecology

An integrative science that studies the basic structural and functional relationships within and among living populations and their physical–chemical environments in marine ecosystems. Although an outgrowth of natural history and the life sciences, marine ecology draws on all the major fields within the biological sciences as well as oceanography, physics, geology, and chemistry. *See* ENVIRONMENT.

Historically, and to some extent today, emphasis within the field has been directed at the gathering and analysis of data and descriptive information about taxonomy, species distributions and abundances, natural history and population biology, and the physical–chemical characteristics of marine environments. However, emphasis has evolved toward understanding the rates and controls on ecological processes that govern both short- and long-term events, including population growth and survival, primary and secondary productivity, and community dynamics and stability.

Marine ecology focuses on specific organisms as well as on particular environments or physical settings. Mangrove forests, salt marshes, seagrasses and seaweeds, and coral reefs form unique ecosystems defined by the dominant biological community. Lagoons, estuaries, bays, and the principal ocean environments of continental shelf, slope, abyssal plain, and mid-oceanic ridges form ecosystems based on physical–geological features. Together, these ecosystems occur in water depths ranging from the intertidal zone to the deepest ocean depths, about 33,000 ft (10,000 m), and encompass temperature extremes of 27°F (−3°C) in the deepest ocean waters to 104°F (40°C) in some tropical lagoons. *See* ATOLL; MID-OCEANIC RIDGE.

Marine environments. Classification of marine environments for ecological purposes is based very generally on two criteria, the dominant community or ecosystem type and the physical–geological setting. Those ecosystems identified by their dominant community type include mangrove forests, coastal salt marshes, submersed seagrasses and seaweeds, and tropical coral reefs. Plankton are a principal component in all marine ecosystems and include organisms ranging in size from viruses to larval fishes that permanently, or at some stage in their life cycle, reside in the water column. Other communities include benthic (bottom–dwelling) communities in shallow and deep water, occupants of upwelling areas, and the specialized community that inhabits deep-sea hydrothermal vents. Marine environments identified by their physical–geological setting include estuaries, coastal marine and nearshore zones, and open-ocean–deep-sea regions (**Fig. 1**). *See* DEEP-SEA FAUNA; ECOLOGICAL COMMUNITIES; HYDROTHERMAL VENT; PHYTOPLANKTON; ZOOPLANKTON.

Estuarine ecosystems. An estuary is a semienclosed area or basin with an open outlet to the sea where fresh water from the land mixes with seawater. The ecological consequences of fresh-water input and mixing create strong gradients in physical–chemical characteristics, biological activity and diversity, and the potential for major adverse impacts associated with human activities. Because of the physical forces of tides, wind, waves, and freshwater

input, estuaries are perhaps the most ecologically complex marine environment. They are also the most productive of all marine ecosystems on an area basis and contain within their physical boundaries many of the principal marine ecosystems defined by community type. *See* ESTUARINE OCEANOGRAPHY.

Salinity, temperature, submarine irradiance, that is, underwater light, and dissolved inorganic nutrients determine to large extent the biological composition of estuarine communities. In estuaries, salinity ranges from nearly fresh-water to oceanic concentrations. The actual salinity structure of estuaries varies both among and within estuaries and is determined by fresh-water inflow, tidal energy, and general estuarine circulation patterns. Estuaries are often classified into three groups, based on salinity structure (**Fig. 2**). The ecological significance of this is that most estuarine populations of plants and animals are physiologically limited by their salinity tolerance range, which restricts their distribution to particular zones. Temperature and submarine light play similarly important ecological roles by limiting or controlling important ecological processes. Temperature extremes generally limit the global distribution of species and seasonally determine the rates of metabolic processes within a given ecosystem. Submarine light plays an equally important role in governing both the rates of photosynthesis and the distribution of photosynthetic organisms. Dissolved inorganic nutrients, particularly nitrogen and phosphorus, not only limit the level of primary production but can influence species composition of estuarine communities. *See* SEAWATER.

Estuaries are further characterized by their principal ecosystem components, which often form the basic ecological unit of study. Salt marshes, mangroves, seagrasses, plankton, and benthic ecosystems are principal components of estuaries and vary in relative importance or even occurrence within specific estuaries. Salt marshes and mangroves are ecosystems that are dominated by vascular plants, occur worldwide, and occupy the intertidal zone. Salt marshes have their greatest distribution and abundance in the temperate latitudes, whereas mangroves are restricted to the tropics. Both play important roles in aquatic productivity, trophic structure, and nutrient cycling and serve as natural erosion-control structures. Seagrasses, which are submersed aquatic vascular plants, occur subtidally throughout the world and grow at depths ranging from just below the water surface to more than 30 ft (10 m) in some tropical areas. These plants, evolved from terrestrial ancestors, play many of the same ecological roles as the intertidal salt marsh and mangrove ecosystems, and are limited principally by the availability of submarine light. Planktonic and benthic ecosystems occur in all aquatic systems and for most estuarine environments have the greatest areal extent. Both are important for aquatic productivity and nutrient cycling and support, at least in part, economically valuable fisheries resources. *See* MANGROVE; SALT MARSH.

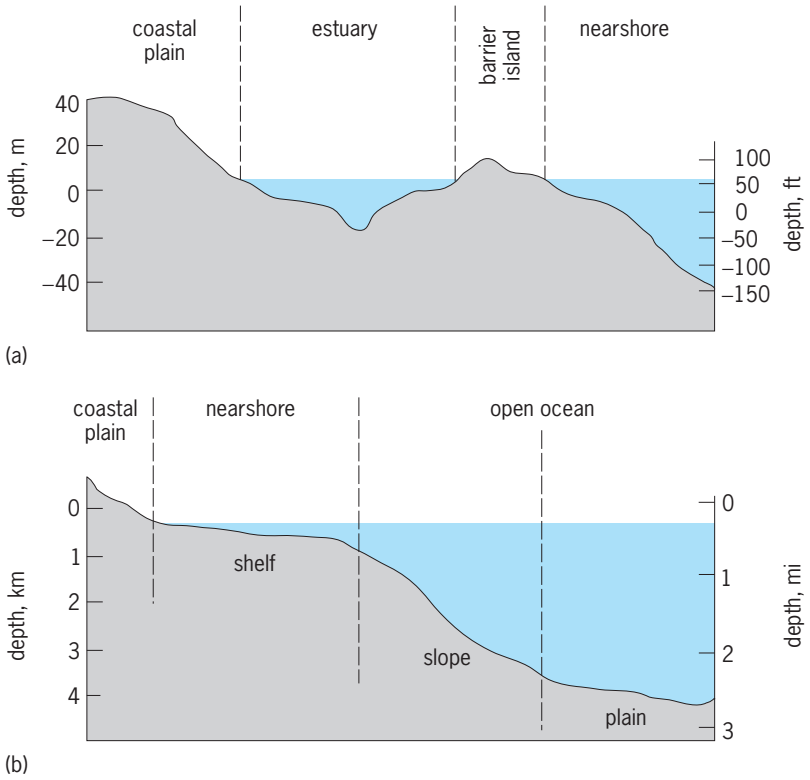

Fig. 1. Cross-sectional profile of (*a*) estuarine and nearshore and (*b*) coastal and open-ocean marine environments. The nearshore region, although not precisely defined, is generally within kilometers of the coastline. 1 m = 3.3 ft.

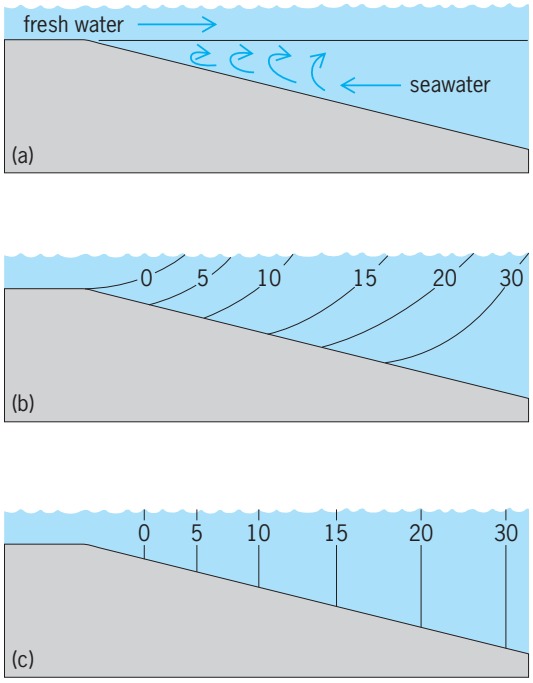

Fig. 2. Salinity structure of the three general types of estuaries found throughout the world. (*a*) Strongly stratified system due to high surface fresh-water inflow. (*b*) Moderated stratified system showing lines of equal salinity in parts per thousand. (*c*) Well-mixed estuary showing vertically homogeneous salinity structure in parts per thousand.

Coastal and nearshore ecosystems. Coastal and nearshore marine ecosystems are generally considered to be marine environments bounded by the coastal land margin (seashore) and the continental shelf 300–600 ft (100–200 m) below sea level. The continental shelf, which occupies the greater area of the two and varies in width from a few to several hundred kilometers, is strongly influenced by physical oceanographic processes that govern general patterns of circulation and the energy associated with waves and currents. *See* CONTINENTAL MARGIN.

Ecologically, the coastal and nearshore zones grade from shallow water depths, influenced by the adjacent landmass and input from coastal rivers and estuaries, to the continental shelf break, where oceanic processes predominate. Biological productivity and species diversity and abundance tend to decrease in an offshore direction as the food web becomes supported only by planktonic production.

Estuarine–nearshore couplings include the advective transport of nutrients and organic matter into nearshore waters, and seasonal migrations of ecologically and economically important species between coastal waters and estuaries. Advective transport contributes organic matter and nutrients, particularly nitrogen, which are thought to augment both primary and secondary production. Net primary production in nearshore waters has often been shown inadequate to support estimated secondary production, and so riverine and estuarine sources provide organic matter and nutrients. In seasonal migrations, many species of shellfish and finfish that spawn offshore migrate or are transported by water into estuaries during the larval or juvenile stage. There, they grow and mature and then migrate offshore as adults to complete the cycle.

Among the unique marine ecosystems associated with coastal and nearshore water bodies are seaweed-dominated communities (for example, kelp "forests"), coral reefs, and upwellings. Seaweed communities are distributed worldwide and occupy coastal areas from the intertidal zone to depths exceeding 30 ft (10 m). Green (Chlorophyceae), brown (Phaeophyceae), and red (Rhodophyceae) macroscopic algae dominate seaweed communities and show strong depth-dependent zonation patterns in response to various physical stresses, light requirements, and grazing pressure. Coral reefs are calcium carbonate structures made by reef-building (hermatypic) corals and crustose coralline algae and are best known for their high species diversity and structural complexity. They are limited to the tropical regions and require high light and temperature environments (greater than 68°F or 20°C). Upwelling regions are coastal areas where nutrient-rich bottom waters are moved toward the surface by persistent winds blowing parallel to the coast. As a result of the Coriolis effect and the Ekman spiral, surface water is transported offshore and replaced by bottom or middepth water, leading to a relatively continuous supply of nutrients to enhance primary production. Upwelling regions have historically been areas of economically important fisheries. *See* REEF; UPWELLING.

Open-ocean–deep-sea environments. Approximately 70% of the Earth's surface is covered by oceans, and more than 80% of the ocean's surface overlies water depths greater than 600 ft (200 m), making open-ocean–deep-sea environments the largest—yet the least ecologically studied and understood— of all marine environments. The major oceans of the world differ in their extent of landmass influence, circulation patterns, and other physical–chemical properties. Other major water bodies included in open-ocean–deep-sea environments are the areas of the oceans that are referred to as seas. A sea is a water body that is smaller than an ocean and has unique physical oceanographic features defined by basin morphology. Because of their circulation patterns and geomorphology, seas are more strongly influenced by the continental landmass and island chain structures than are oceanic environments.

Within the major oceans, as well as seas, various oceanographic environments can be defined. A simple classification would include water column depths receiving sufficient light to support photosynthesis (photic zone); water depths at which light penetration cannot support photosynthesis and which for all ecological purposes are without light (aphotic zone); and the benthos or bottom-dwelling organisms. Occupying the depths between the surface and the average depth of the world's oceans (12,000 ft or 4000 m) are a diverse group of organisms that include microbes, invertebrates, and vertebrates. Classical oceanography defines four depth zones; epipelagic, 0–450 ft (0–150 m), which is variable; mesopelagic, 450–3000 ft (150–1000 m); bathypelagic, 3000–12,000 ft (1000–4000 m); and abyssopelagic, greater than 12,000 ft (4000 m). These depth strata correspond approximately to the depth of sufficient light penetration to support photosynthesis; the zone in which all light is attenuated; the truly aphotic zone; and the deepest oceanic environments. The benthic fauna are classified in a similar manner as continental shelf and slope fauna, ocean basin or abyssal fauna, and fauna unique to the deep ocean basins and trenches.

The open-ocean–deep-sea environments present themselves as both a challenge scientifically and as a world resource that demands cooperative international research and attention. Estuaries and coastal ecosystems, as defined previously, are more localized and lend themselves to regional scientific exploration and understanding. Oceans and seas, on the other hand, are a global resource, crossing all political and national boundaries and requiring international cooperation and participation in ecological studies.

Marine ecological processes. Fundamental to marine ecology is the discovery and understanding of the principles that underlie the organization of marine communities and govern their behavior, such as controls on population growth and stability, quantifying interactions among populations that lead to persistent communities, and coupling of communities

to form viable ecosystems. The basis of this organization is the flow of energy and cycling of materials, beginning with the capture of radiant solar energy through the processes of photosynthesis and ending with the remineralization of organic matter and nutrients.

Photosynthesis and autotrophic production. Photosynthesis in seawater is carried out by various marine organisms that range in size from the microscopic, single-celled marine algae to multicellular vascular plants. Conversion of carbon dioxide into simple organic compounds and the subsequent synthesis of algal or vascular plant biomass forms the ultimate base of most food webs in the marine environment (omitted from this discussion are food webs based on chemosynthetic organisms). Because of that relationship, photosynthesis and primary production remain the focus of much marine ecological research. *See* FOOD WEB.

The rate of photosynthesis, and thus the growth and primary production of marine plants, is dependent on a number of factors, the more important of which are availability and uptake of nutrients, temperature, and intensity and quality of light. Of these three, the last probably is the single most important in governing primary production and the distribution and abundance of marine plants. Consequently, the optical physics of seawater has been an important component of much research on photosynthesis and primary production in marine environments.

The intensity and spectral quality of light in seawater is a function of incoming solar radiation, surface roughness, dissolved substances, suspended particulates, and water depth. Historically, measures of submarine light were based on photometric standards and units that had been developed for the human eye, such as footcandle, lumen, and lux, which have limited and questionable meaning in a biological context. Both physiologically and ecologically, light in the spectral region termed photosynthetically active radiation (PAR), at about 400–700 nanometers, is important and is measured as irradiance in units of energy flux (joules $\cdot$ m^{-2} $\cdot$ s^{-1}) or photon flux (microeinsteins $\cdot$ m^{-2} $\cdot$ s^{-1}), where one einstein (1 E) equals one mole of quanta or photons (6.02×10^{23}). As solar radiation passes through a water column, it is reduced in energy content and changed in spectral quality because of absorption and scattering. The total effect on intensity, termed attenuation, is probably the most common optical property of water reported and is derived according to the exponential decay function expressed in the equation

$$k_{1,2} = \frac{\ln (I_2) - \ln (I_1)}{z_2 - z_1}$$

where k is the attenuation coefficient between depths 1 and 2, I is the irradiance intensity at depths 1 and 2, and z is the depth. Generally, all depths are measured in meters below the water surface, and the attenuation coefficient is expressed in units of per-meter (m^{-1}). PAR attenuation varies considerably depending on water type, with attenuation coefficients of 0.03–0.04 for the clearest open-ocean waters and 3–4 for the most turbid coastal and estuarine waters. PAR attenuation determines water depths at which light intensity can support photosynthesis (photic zone) and ranges from a few meters in estuaries and turbid coastal waters to approximately 450–600 ft (150–200 m) in the clearest open-ocean waters (**Fig. 3**).

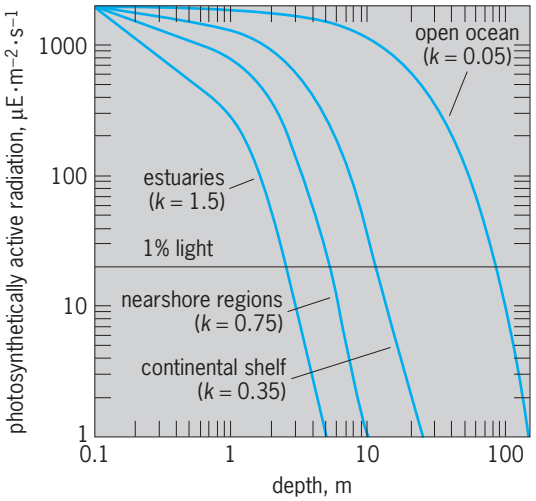

Fig. 3. Photosynthetically active radiation intensity at depth for various values of the attenuation coefficient (*k*). The intersection of the 1% light level (the limiting light intensity for photosynthesis) with the decay curves marks the depth limit for the photic zone. In these examples, the depth limit ranges from approximately 300 ft (100 m) in the open ocean to 10 ft (3 m) in estuaries. 1 m = 3.3 ft.

The relationship between photosynthesis and light intensity varies among the different primary producers in marine environments but can be defined generally by a hyperbolic relationship. Characteristic of this relationship is (1) an initial positive, linear increase in photosynthesis with increasing light; (2) a nonlinear response above a threshold light intensity where photosynthesis does not increase linearly with increasing light; and (3) an upper limit to the rate of photosynthesis (P_{max}) at which increasing light has no effect and, if light intensity becomes high enough, may actually reduce or inhibit photosynthesis in some plants. **Figure 4** illustrates the photosynthesis–light relationships for two hypothetical marine plants that differ in these fundamental characteristics.

Autotrophic or primary production is the direct result of the biochemical and physiological processes of photosynthesis, but it is not equal to it, and results from the net positive growth of marine plants. Considering the high attenuation of light in water and the relationships between light intensity and photosynthesis, net autotrophic production is confined to relatively shallow water depths. The major primary producers in marine environments are intertidal salt marshes and mangroves, submersed seagrasses and seaweeds, phytoplankton, benthic and attached microalgae, and—for coral reefs—symbiotic algae (zooxanthellae). These principal autotrophic components of marine ecosystems differ in geographic distribution and abundance, rates of organic matter

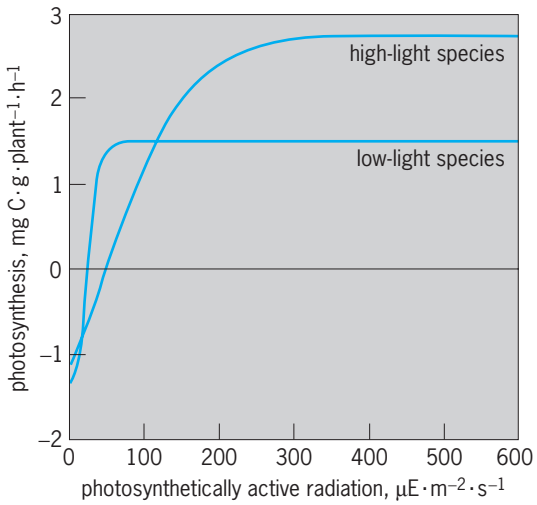

Fig. 4. Photosynthesis–photosynthetically active radiation curves for two marine plants with fundamentally different light relations. The high-light plant, which has a higher P_{max} but requires much more light, is typical of high-light environments such as those of the tropics and shallow water. The low-light plant has a lower P_{max} but requires much less light and photosynthetically saturates more quickly. These plants are typical of more turbid environments or environments where light is limiting for significant portions of the photoperiod.

production, and the food webs they support relative to secondary or heterotrophic production, including fishery yields. Though imprecisely known and highly variable for specific environments, net primary production for the principal marine environments of the world's oceans is summarized in the **table**. On an areal basis, estuaries and nearshore marine ecosystems have the highest annual rates of primary production. From a global perspective, the open oceans are the greatest contributors to total marine primary production because of their overwhelming size.

The two other principal factors that influence photosynthesis and primary production are temperature and nutrient supply. Temperature affects the rate of metabolic reactions, and marine plants show specific optima and tolerance ranges relative to photosynthesis. Nutrients, particularly nitrogen, phosphorus, and silica, are essential for marine plants and influence both the rate of photosynthesis and plant growth. For many phytoplankton-based marine ecosystems, dissolved inorganic nitrogen is considered the principal limiting nutrient for autotrophic production, both in its limiting behavior and in its role in the eutrophication of estuarine and coastal waters. *See* PHOTOSYNTHESIS.

Food webs and heterotrophic production. The concept of a marine food web and heterotrophic, or secondary, production is based on the view that energy, as well as organic matter and nutrients, is transferred between organisms that occupy different levels in a heirarchical trophic or feeding structure. The complexity and specific interactions among populations within this conceptual framework form the basis of much marine ecological research and are a source of controversy among marine ecologists. What has evolved is that marine food webs and the processes leading to secondary production of marine populations can be divided into plankton-based and detritus-based food webs. They approximate phytoplankton-based systems and macrophyte-based systems.

The classical view of the open-ocean food web involved planktonic algae (diatoms) being grazed by planktonic crustaceans (copepods), which were in turn preyed upon by other invertebrates and fish. Based on size, the final links in the food chain were relatively large organisms, and the classical view dictated that both energy flow and productivity in the oceans were due to these larger populations. To a large extent, this view resulted from the sampling gear and techniques available at the time. This simple, linear food-chain model has been replaced by recognition of the role played by smaller organisms, both autotrophic and heterotrophic, in primary and secondary production, and the cycling of carbon and nutrients. For planktonic food webs, current evidence suggests that primary production is partitioned among groups of variously sized organisms, with small organisms, such as cyanobacteria, playing an equal if not dominant role at times in aquatic productivity. The smaller autotrophs, both through excretion of dissolved organic compounds to provide a substrate for bacterial growth and by direct grazing by protozoa (microflagellates and ciliates), create a microbially based food web in aquatic ecosystems that had once been largely ignored. The consequences of the revised view are that the major portion of autotrophic production and secondary utilization in marine food webs may be controlled,

Areal and total estimates for net primary production in the principal marine environments of the world

Region	Area 10^6 km^2*	Net primary production, g · m^{-2} · yr^{-1}	Total net primary production 10^9 t · yr^{-1}	Percent of area	Percent of total net primary production
Open ocean	332	125	41.5	91.9	77.7
Continental shelf	27	300	8.1	7.5	15.2
Estuaries	1.4	1500	2.1	0.4	3.9
Seaweeds and coral	0.6	2500	1.5	0.2	2.6
Upwelling regions	0.4	500	0.2	0.1	0.4
Total	361.4		53.4		

*1 km^2 = 0.4 mi^2.

not by the larger organisms typically described as supporting marine food webs (including those leading to the major coastal and oceanic fisheries), but by microscopic populations, thus giving rise to the paradigm of the so-called microbial loop.

Macrophyte-based food webs, such as those associated with salt marsh, mangrove, and seagrass ecosystems, are not supported by direct grazing of the dominant vascular plant but by the production of detrital matter through plant mortality. The classic example is the detritus-based food webs of coastal salt marsh ecosystems. These ecosystems, which have very high rates of primary production (see table), enter the marine food web as decomposed and fragmented particulate organics. The particulate organics of vascular plant origin support a diverse microbial community that includes bacteria, flagellates, ciliates, and other protozoa. These organisms in turn support higher-level consumers, which include gastropods, mollusks, polychaetes, crustaceans, and fish. The high productivity of estuaries, particularly those in the Mid-Atlantic temperate regions of North America and Europe and the northern coasts of the Gulf of Mexico, results not only from phytoplankton production in the estuaries themselves but also from the contribution of surrounding salt marsh ecosystems.

The highest levels of both primary and secondary production are associated with estuarine and nearshore coastal marine ecosystems. Open-ocean systems are less productive on a per-area basis, and both pelagic (water column) and benthic food webs in deep ocean environments depend on primary production in the overlying water column. For benthic communities, organic matter must reach the bottom by sinking through a deep water column, a process that further reduces its energy content. Thus, in the open ocean, high rates of secondary production, such as fish yields, are associated with areas in which physical–chemical conditions permit and sustain high rates of primary production over long periods of time, as is found in upwelling regions.

Regardless of specific marine environment, microbial processes provide fundamental links in marine food webs that directly or indirectly govern flows of organic matter and nutrients that in turn control ecosystem productivity and stability. *See* BIOLOGICAL PRODUCTIVITY; ECOLOGY; ECOSYSTEM; SEAWATER FERTILITY.

Richard Wetzel

Bibliography. J. W. Day, Jr., et al., *Estuarine Ecology*, 1989; M. L. Dring, *The Biology of Marine Plants*, 1982; J. W. Nybakken, *Marine Biology: An Ecological Approach*, 5th ed., 2000; I. Valiela, *Marine Ecological Processes*, 2d ed., 1995.

Marine engine

An engine that propels a waterborne vessel. In all except the smallest boats, the engine is but part of an integrated power plant, which includes auxiliary machinery for propulsion engine support, ship services, and cargo, trade, or mission services. Marine engines in common use are diesel engines, steam turbines, and gas turbines. Gasoline engines are widely used in pleasure craft. Only the propulsion engine will be discussed in this article. *See* BOAT PROPULSION; INTERNAL COMBUSTION ENGINE; MARINE MACHINERY.

Factors in engine selection. The engine type selected for an application should depend on its characteristics, usually with reliability of prime importance. Other factors may include weight, volume, quality and type of fuel required, efficiency, maintenance requirements, durability, simplicity in installation and operation, noise and vibration, initial cost, and ability to sustain the required power levels. In some applications, selection has been made on the basis of expedience or convenience, usually because of the ready availability of an engine type; this explains the continued use of gasoline engines in pleasure craft.

Weight and volume. These are usually the dominant criteria in warship applications and are also very important in fast merchant ships. Efficiency, or fuel economy, is tied to weight and volume of the machinery, since it is the range of operation that determines the amount of fuel that must be carried, by which the ship's payload is correspondingly diminished. In large, relatively slow merchant ships, machinery weight and volume are less important.

Fuels. Mostly, liquid petroleum fuels are used, with distillate fuels (including diesel fuel and gas oil) being the highest quality but most expensive, and residual fuel the cheapest but most difficult to use. Blended fuels of intermediate characteristics are often used, generally tending more toward the residual in cost and difficulty of use. While fuel-oil costs have varied widely over time, heavy blends and residuals have tended to cost about half as much as distillates, although experience has demonstrated an inverse correlation between maintenance cost and fuel quality. Coal and natural gas have application in certain trades, and the use of both is considered likely to increase in the future. Nuclear fuel is no longer considered viable for merchant ships, for economic and social reasons, but remains the dominant choice for the largest surface warships and for long-range submarines. *See* DIESEL FUEL; FUEL OIL; SHIP NUCLEAR PROPULSION.

Power level. Power-level requirements depend on the application. One extreme is represented by most merchant trades, where an engine is required to sustain high power output between ports, without relief until arrival, and yet be capable of fairly rapid response over the whole power range while the ship is maneuvered. Another extreme exists with warships, where sustained performance is usually required at a low power level yielding a modest cruise or endurance speed, as well as at a much higher power for high speeds. The difference in power requirements is so great that two engines of different type may be selected. *See* SHIP POWERING, MANEUVERING, AND SEAKEEPING.

Propellers. Most often, marine engines drive propellers, which must be operated at rotative speeds lower than those of turbines and of all but the

largest diesel engines. A speed-reducing transmission is therefore inherent with most marine engines, with reduction gearing the most common type, and electric drive or, in some small installations, belt or hydraulic drive also used. *See* PROPELLER (MARINE CRAFT).

Diesel engines. Diesel engines of all types and power outputs are in use for propulsion of most merchant ships from the smallest to the largest, most service and utility craft, most naval auxiliary vessels, and most smaller surface warships and shorter-range submarines.

The diesel engines most commonly used fall into either a low-speed category or the medium- and high-speed category. Low-speed engines (**Fig. 1**) are generally intended for the direct drive of propellers without any speed reduction, and therefore are restricted to a range of rotative speeds for which efficient propellers can be designed, generally below 300 revolutions per minute (rpm), and as low as 50 rpm at rated power. Low-speed engines are two-stroke, crosshead engines, with 4–12 cylinders, which are always in-line, turbocharged, and aftercooled. The stroke-to-bore ratio of low-speed engines in current production is about 3:1. The largest engines are rated for power output of over 5000 kW (almost 7500 horsepower) per cylinder at about 100 rpm. These engines are heavy and very large, but they are well suited to operation on low-quality fuels and generally require only modest levels of maintenance. *See* TURBOCHARGER.

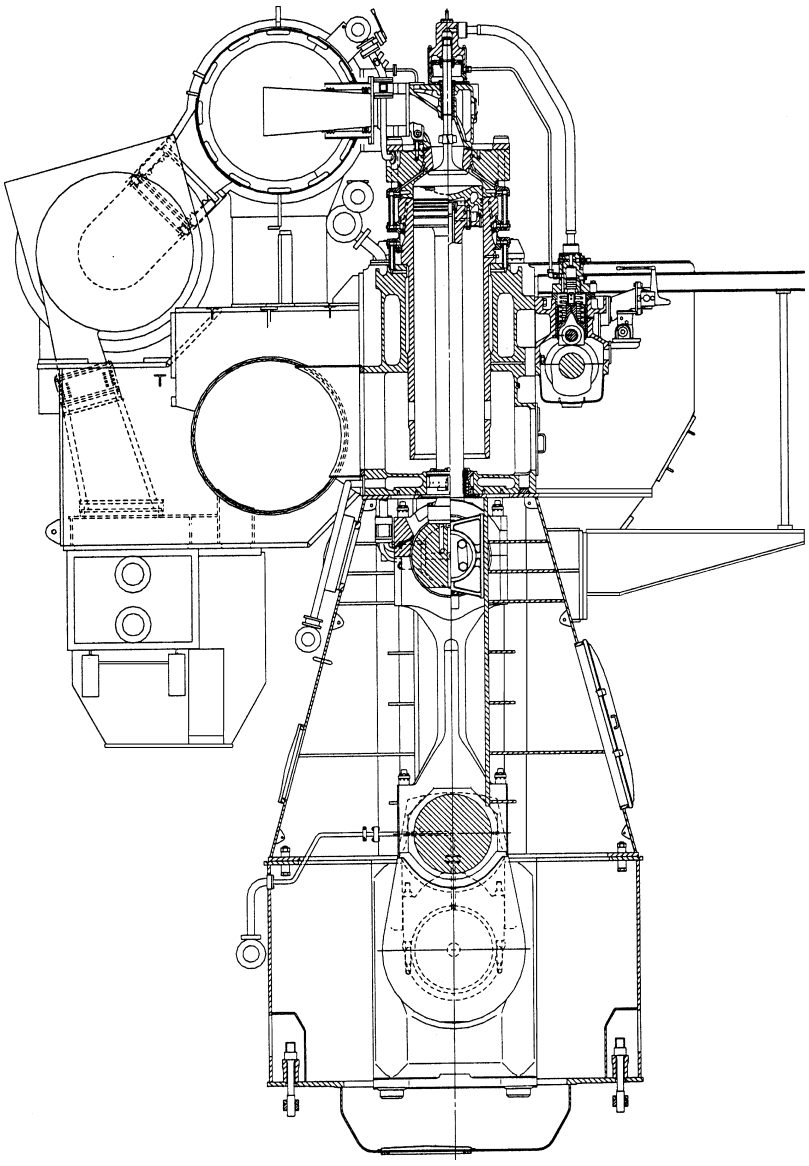

Fig. 1. Cross section of a low-speed diesel engine.

Because of their higher rotative speeds, medium- and high-speed engines (**Fig. 2**) drive propellers through speed-reduction gears, but they are directly connected for driving generators in diesel-electric installations. With few exceptions, these are four-stroke, trunk-piston engines, which have up to 10 cylinders in-line or up to 24 in a V configuration and are mostly turbocharged and aftercooled. Stroke-to-bore ratios range from 1:1 to 1.5:1. Large medium-speed engines are capable of over 1500 kW (2000 hp) per cylinder at about 400 rpm. The upper limit of the medium-speed category, and the start of the high-speed category, is generally placed in the range of 900–1200 rpm, but there are no clear physical features that enable the distinction to be made. Many of these engines have a proven heavy-fuel capability, but most evidence indicates that maintenance costs are higher than those of low-speed engines that are run on fuels of similar poor quality. Some engines, especially those in the higher-speed category, are restricted to distillate fuels.

Outside of the typical categories cited above are four-stroke, trunk-piston engines that are designed to be directly connected to propellers, and are indigenous, in both manufacture and application, to the Far East. These engines are built with six or eight cylinders in-line; they are rated for 70–700 kW (95–950 hp) per cylinder at speeds of 200–500 rpm. Another exception is a series of two-stroke, trunk-piston, medium-speed engines that dominate their field of application in United States waters, despite their requirement for distillate fuels. The highest rated of these engines, with 20 cylinders, has an output of more than 3500 kW (over 4500 hp) at 900 rpm.

All of the low-speed diesel engines and many of the medium- and high-speed engines are direct-reversing engines, that is, capable of being adjusted, after being stopped, so that they can be started and run in the opposite direction. Nonreversing engines use reversing gearing, if reversing is not provided by electric drive or a controllable-pitch propeller.

Most diesel engines have complex vibration characteristics and a tendency toward noisy operation, but much can be done to prevent these characteristics from becoming problematic. All diesel engines consume lubricating oil, generally at a rate of less than 1% of the fuel consumption. The thermal efficiency, which in the largest engines can exceed 45% even without the heat-recovery equipment generally used, is the highest of all current alternatives. The largest, low-speed engines offer this efficiency from

low-quality fuel oils, with modest maintenance requirements and relative simplicity but with penalties of high weight, high volume, and high initial cost. The largest medium-speed engines offer comparable efficiencies but with lower weight, volume, and cost, and with a trade-off between fuel quality and maintenance costs. High-speed engines are lighter and more compact and have good efficiency, but generally require good fuels if intensive maintenance is to be avoided. *See* DIESEL ENGINE.

Steam turbines. While steam-turbine plants cannot achieve the thermal efficiency of diesel engines, steam turbines of moderately high power levels (above about 7500 kW or 10,000 hp) offer efficient energy conversion from steam, which can in turn be produced by combustion of low-quality fuel oil, coal, or natural gas in boilers, or from a nuclear reactor. For high efficiency, high turbine speeds are required, typically 3000–10,000 rpm, with reduction gearing or electric drive used to achieve low propeller rotative speeds. The combination of turbine and reduction gear or electric drive has usually proven robust and durable, so that most oil-fueled steamships currently in service are held over from an earlier era. Others, more recently built, are capitalizing on the availability, in their trade, of a fuel unsuitable for diesel engines.

In modern merchant ship plants, typical steam conditions at the turbine are a pressure of about 6 megapascals (870 lb/in.^{2}), superheated to about 510°C (950°F), with exhaust to a vacuum condenser at about 5 kilopascals (1.5 in. Hg). Some high-powered plants have used reheat turbines, but generally cycle improvements are confined to two to four stages of regenerative feed heating from turbine extractions, and to economizers or rotary regenerative air heaters. *See* MARINE BOILER.

In some applications, especially with electric drive, single-cased turbines are used, but more common is the division of the turbine into a small, high-speed, high-pressure unit and a larger, lower-speed, low-pressure unit, each with 8–10 stages, independently connected to a single propulsion gear set (**Fig. 3**). This arrangement, known as a cross-compound turbine, provides more flexibility in design, allowing the high- and low-pressure stages to be better matched to the properties of the steam, which expands to about 400 times its initial volume from the throttle conditions cited above, to exhaust. For related reasons, impulse blading is favored for the high-pressure stages, with lower-pressure stages having increasing reaction. The first high-pressure stage is the control stage, and has partial admission, with the nozzles in groups, each controlled by a valve, enabling power output to be regulated by the number of nozzles in use. Throttle valve control is reserved for maneuvering. For reversing, separate astern stages are usually incorporated in the casing of the low-pressure turbine (Fig. 3), if reversing is not provided by an electric drive. *See* IMPULSE TURBINE; REACTION TURBINE; STEAM TURBINE.

Gas turbines. Aircraft-derivative gas turbines have become the dominant type of propulsion engine for medium-sized surface warships, including frigates, destroyers, cruisers, and small aircraft carriers. In all cases the turbines are multishaft, simple-cycle engines, with the power turbine geared to the propeller. In some installations, two to four turbines are the sole means of propulsion; in other cases, one or two turbines provide high-speed propulsion, while

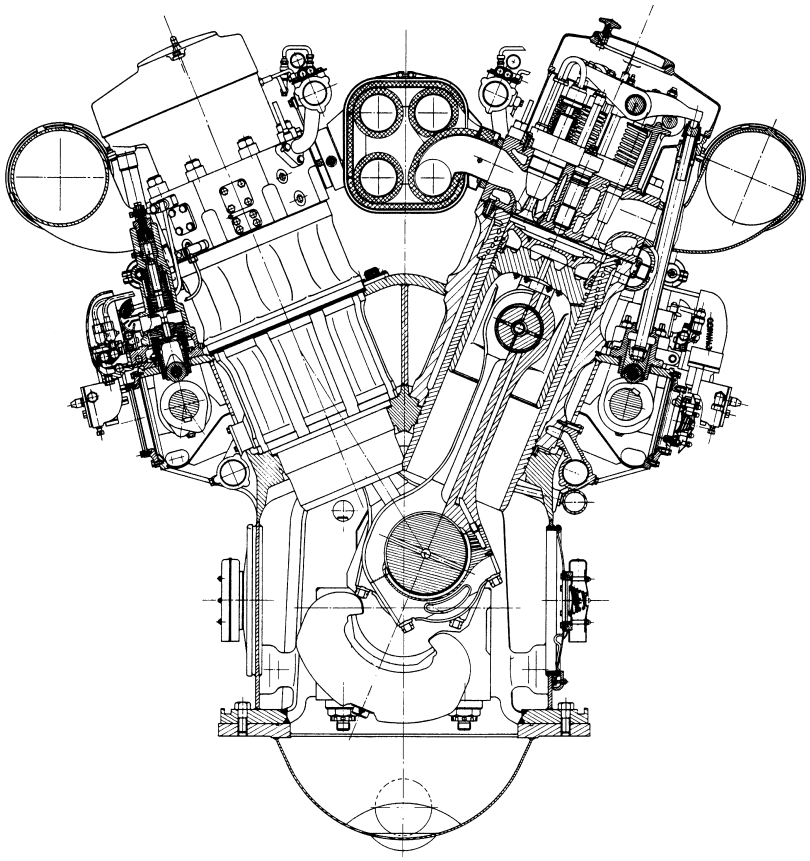

Fig. 2. Cross section of a four-stroke-cycle V-engine.

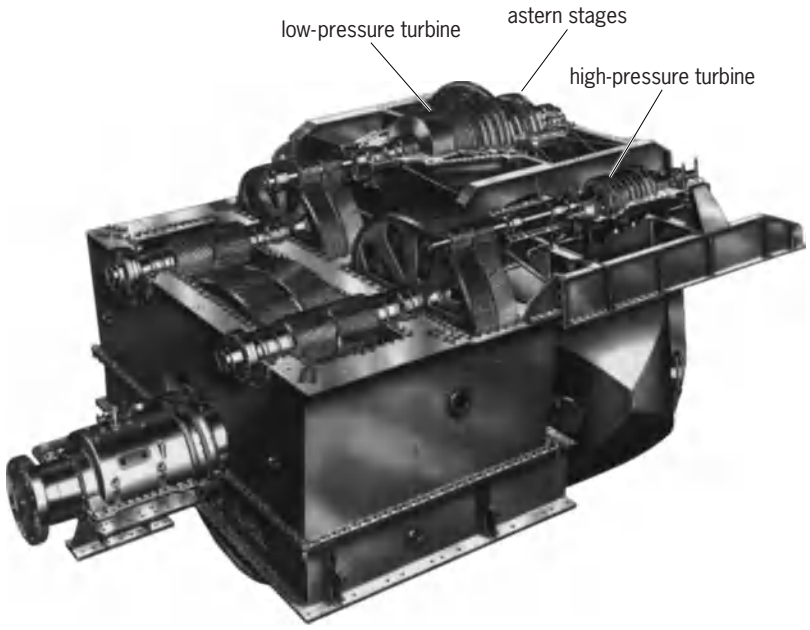

Fig. 3. Typical cross-compound steam turbine, with a double reduction gear, shown with upper halves of the turbine and gear casings removed. (*Westinghouse Electric Corp.*)

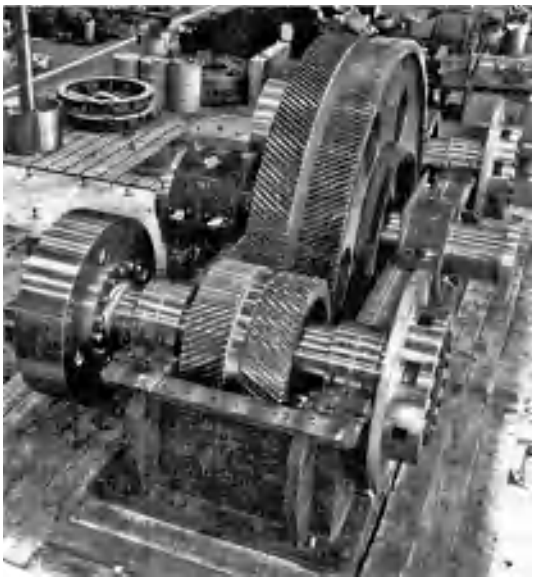

Fig. 4. Gearset for a twin-engine, single-screw ship. (*Philadelphia Gear Corp.*)

diesel engines or smaller gas turbines are used for cruising speeds.

Factors favoring the aircraft-derivative gas turbine in this application are low weight, compact dimensions, high power, rapid start and response, standardization of components, and maintenance by replacement. The last two features are especially important in warships, since an engine can be exchanged in 2 days or less and overhauled by civilian experts ashore, permitting a smaller on-board crew. A major disadvantage of aircraft-derivative gas turbines, their requirement for high-quality distillate fuels, is of diminished importance in the warship application, since most warships, including steamships, use these fuels anyway. Other disadvantages include poorer performance in warmer climates, decreased efficiency at power levels below maximum, large air intake and exhaust ducts, and high exhaust temperatures. Reversing thrust must be provided in the gearbox, by electric drive, or by a controllable-pitch propeller.

A further evolution of the aircraft-derivative gas turbine is an intercooled, regenerative-cycle unit, which offers higher thermal efficiency across the entire upper power output range, while retaining the other advantages cited above. Past applications of aircraft-derivative gas turbines and of simple-cycle and regenerative-cycle heavy-duty gas turbines to ships other than warships have had only limited success, and many of these ships were later converted to diesel propulsion. More recently, gas turbines have been used for very fast merchant ships. *See* GAS TURBINE; TURBINE PROPULSION.

Mechanical reduction gears. Marine propulsion gearing is usually of the parallel-shaft, helical-tooth type. Single-reduction gearing (**Fig. 4**) is usually

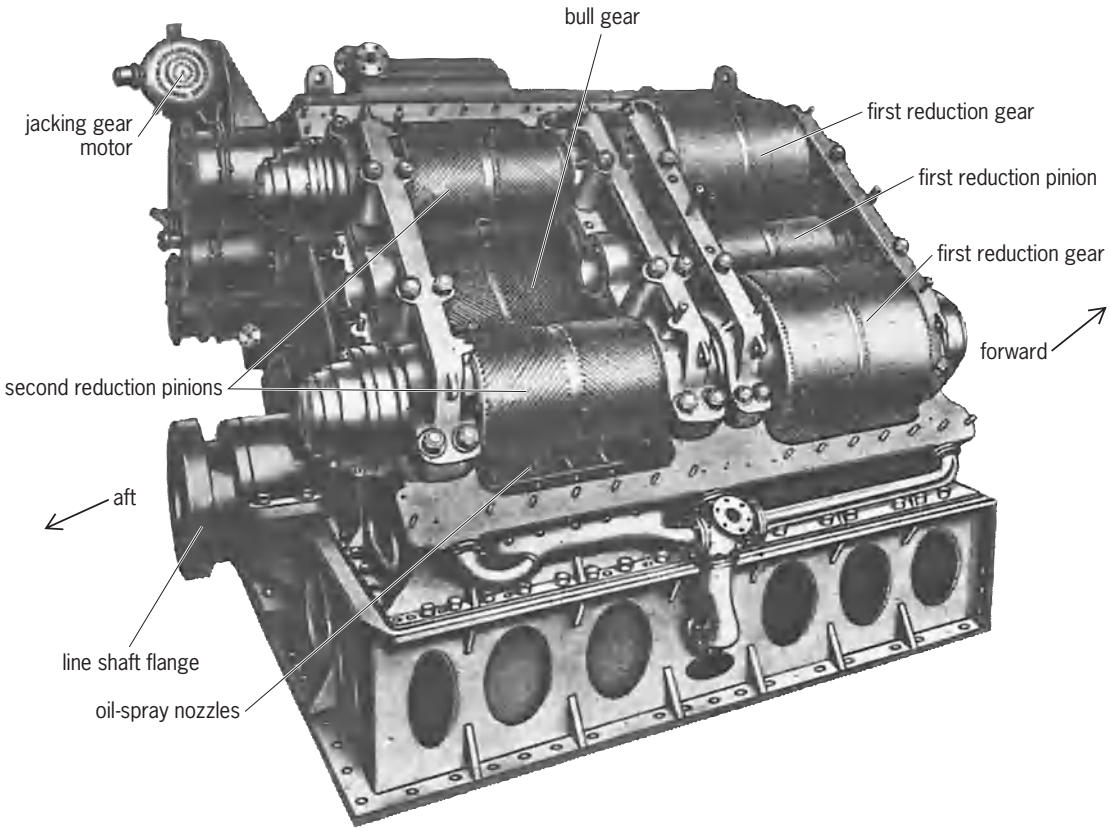

Fig. 5. Locked-train, double-reduction gearing for use with a cross-compound steam turbine or twin gas turbines. (*Naval Machinery, U.S. Naval Academy, 1946*)

adequate for medium- and high-speed diesels, where the rotative speed ratio ranges from about 2:1 to 10:1. In a typical arrangement (Fig. 4), two engines drive a single propeller, with each engine connected to its pinion via one or more flexible couplings to reduce torsional vibration, and a clutch, which is usually pneumatic or hydraulic. Both double-helical teeth (Fig. 4) and single-helical teeth are common.

The high speed of steam and gas turbines requires rotative speed ratios which can reach 100:1, so that double-reduction gearing is necessary (Fig. 3). For higher powers, with both steam and gas turbines, locked-train, double-reduction gearing is used (**Fig. 5**), which divides the input torque into parallel paths, permitting smaller, if more numerous, gears than would otherwise be required. Couplings of limited flexibility are provided between the first and second stages.

Epicyclic gearing has been successfully used in propulsion applications, most often for high-speed stages in double- or triple-reduction steam turbine gearing. Two-speed gears, permitting a selection of rotative speed ratio, have been fitted in low-power applications, with diesel engines, where there is a large range of required ship speeds.

Propulsion gearing is constructed to extremely close tolerances, with teeth of modified involute form, formed by hobbing or grinding processes, and either through-hardened or case-hardened, depending on the severity of the stresses. Forced lubrication of bearings, meshing teeth, and mechanical couplings is provided. Transmission efficiencies are high, with losses rarely exceeding 1–2% per stage. *See* GEAR; GEAR TRAIN.

Electric drive. In this arrangement, the engine is directly coupled to a generator, and the electricity produced drives an electric motor, which is most often of sufficiently low rotative speed to be directly connected to the propeller shaft. Any number of engine-generator sets may be connected to drive one or more propulsion motors. Electric drive has been used with engines of all types, including low-speed diesels. Advantages of electric drive include flexibility of machinery arrangement, elimination of gear noise, high propeller torque at low speed, and inherent reversing capability. In ships with high electric requirements for cargo, mission, or trade services—for example, passenger ships, tankers with electric-motor-driven cargo pumps, or warships with laser weapons—there is an advantage in integrating propulsion and ship service support through a common electric distribution system. However, electric drive is usually heavier, higher in initial cost, and less efficient than direct or geared drive.

Control arrangements. Automation has been widely applied to marine vehicles of all types; propulsion is normally under direct control from the wheelhouse.

Alan L. Rowen

Bibliography. R. L. Harrington (ed.), *Marine Engineering*, 1992; S. H. Henshall, *Medium and High Speed Diesel Engines for Marine Use*, 1972; E. C. Hunt et al., (eds.), *Modern Marine Engineer's Manual*, vol. 1, 3d ed., 1999, vol. 2, 2d ed., 1991; C. M. Plumb, *Warship Propulsion System Selection*, 1987; D. A. Taylor, *Introduction to Marine Engineering*, 2d rev. ed., 1996.

Marine engineering

The engineering discipline concerned with the machinery and systems of ships and other marine vehicles and structures. Marine engineers are responsible for the design and selection of equipment and systems, for installation and commissioning, for operation, and for maintenance and repair. They must interface with naval architects, especially during design and construction.

Marine operating engineers form part of the crew of large ships, where they are responsible for the operation and maintenance of the machinery. Aboard merchant ships, operating engineers are ship's officers licensed by government agencies (in the United States, by the Coast Guard).

Marine engineers are likely to have to deal with a wide range of systems, including diesel engines, gas turbines, steam turbines, boilers, heat exchangers, and pumps and compressors; electrical machinery; hydraulic machinery; refrigeration machinery; steam, water, fuel oil, lubricating oil, compressed gas, and electrical systems; equipment for automation and control; equipment for fire fighting and other forms of damage control; and systems for cargo handling. Many marine engineers become involved with structural issues, including inspection and surveying, corrosion protection, and repair.

Marine engineers are generally mechanical engineers or systems engineers who have acquired their marine orientation through professional experience, but programs leading to degrees in marine engineering are offered by colleges and universities in many countries. Most marine operating engineers are graduates of these programs, although others have obtained their training through experience aboard ship. *See* BOAT PROPULSION; MARINE BOILER; MARINE ENGINE; MARINE MACHINERY; MARINE REFRIGERATION; NAVAL ARCHITECTURE; PROPELLER (MARINE CRAFT); SHIP DESIGN; SHIP POWERING, MANEUVERING, AND SEAKEEPING.

Alan L. Rowen

Bibliography. C. Drummond, *The Remarkable Life of Victoria Drummond, Marine Engineer*, 1995; R. L. Harrington (ed.), *Marine Engineering*, 1992; E. C. Hunt (ed.), *Modern Marine Engineer's Manual*, 1991; D. A. Taylor, *Introduction to Marine Engineering*, 1990.

Marine fisheries

The harvest of animals and plants from the ocean to provide food and recreation for people, food for animals, and a variety of organic materials for industry. Important products in marine capture fisheries include fish; mollusks such as oysters, clams, and squid; and crustaceans such as crabs and shrimps.

Marine mammals (whales) and reptiles (turtles) have been important historically in marine landings (the weight of the catch landed at the whart); and some plants, mostly seaweeds, are harvested in significant amounts. World landings began to increase substantially during the industrial revolution and rose at a rapid rate after World War II before leveling off in recent years.

Marine Resources

The oceans' fish resources were once thought to be inexhaustible, essentially immune to the effects of fishing. As technological advances were made, bigger, more powerful vessels ranged ever farther from their home ports to exploit valuable fishery resources. The advent of steam and diesel engines, freezing capacity, and fish-finding capabilities added to the fishing power of specialized fleets, which by the 1960s fished for extended periods throughout the world's oceans. By then, it was clear that fishing was a major factor controlling abundances of fish in the sea.

Fishing is the last major food-hunting industry in the world in which wild animals are exploited in large quantities by nations with market economies. Marine fisheries provide >10% annually of animal protein consumed by humans, and additional large amounts of fish are processed to be fed to domestic livestock. As practiced in recent decades, unregulated or poorly managed fisheries can lead to collapse of major fish stocks. *See* FISHERIES ECOLOGY; FOOD MANUFACTURING.

The annual marine fish catch, not including aquaculture and exclusive of plants and marine mammals, increased from 18.5 million metric tons (MMT) in 1950 to more than 93 MMT in 1997. Increases were particularly rapid in the 1960s as the rich ocean upwelling regions off Peru came under exploitation, primarily for anchoveta (*Engraulis ringens*). Global fleets capable of industrial-scale fishing anywhere in the world dominated during this expansion phase (**Fig. 1**). Marine fisheries landings increased 7.2% per year during the 1960s, spurring false optimism that marine fish catches would ensure animal protein for a fast-growing human population. In the period 1969–1973, temporary drops in global landings were recorded, a reflection of combined heavy fishing and unfavorable El Niño climate conditions that devastated the anchoveta population off Peru, which had supported the world's largest single-species fishery, peaking at more than 12 MMT in 1970. Subsequently, marine fish catches rose again, increasing at 1.3% annually in the period 1985–1997 (see **table**). This rate is less than the rate of human population growth in that period. *See* EL NIÑO; SEAWATER FERTILITY; UPWELLING.

Most scientists believe that the global potential for marine fish catches has essentially been reached unless there is a major shift in fishing strategy. For traditional fisheries, approximately 100 MMT appears to be the limit of sustainability, and even that level depends upon effective habitat management and protection. A shift from fishing mostly large, carnivorous species to primarily species lower on the food chain that feed on plants or small animal plankton (which is already occurring to an extent) potentially could increase global landings. Targeting resources now hardly exploited, such as lanternfishes (family Myctophidae) in the deep sea or the shrimplike krill (euphausids) in the Antarctic, could also increase global landings. Whether developing such technologies will allow such shifts in strategy, whether the economics and marketing will be favorable, and whether it is ethically acceptable to develop these

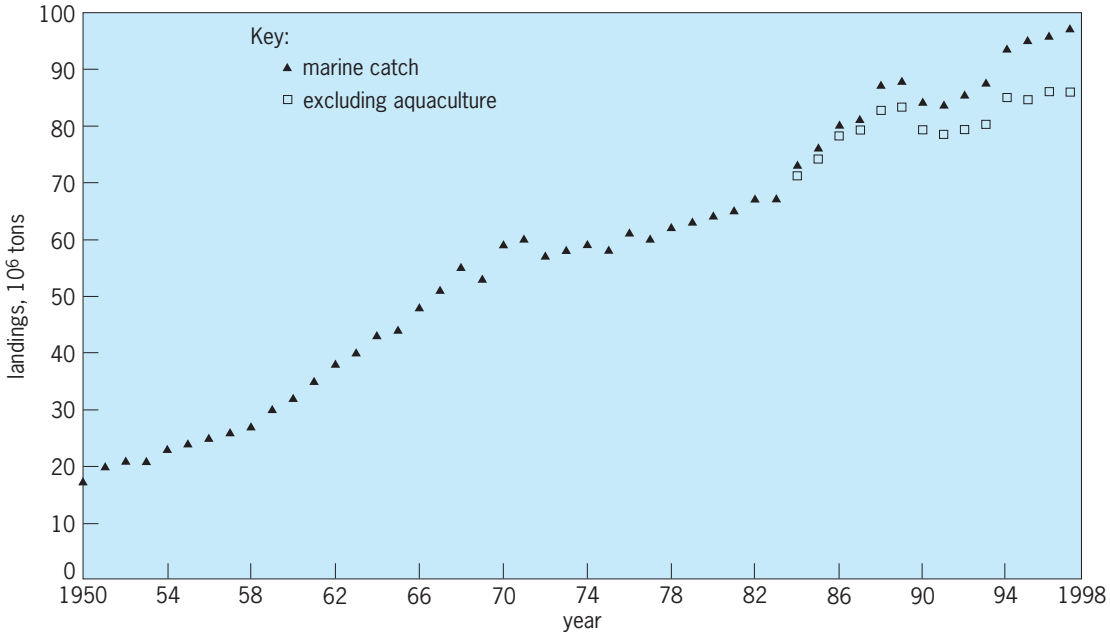

Fig. 1. Global landings from marine capture fisheries and marine aquaculture production, 1950–1997. Marine aquaculture contributed only small amounts until the mid-1980s. Marine plants (8.4 million tons harvested, mostly from aquaculture, in 1997) are not included in the graph. (*Data from United Nations, Food and Agriculture Organization, Rome*)

World fisheries, 1985–1997, in millions of tons*

	1985	1990	1995	1997	Rate of increase, % per year
Inland					
Capture	5.7	6.5	7.2	7.7	2.5
Aquaculture	5.0	8.2	13.8	17.1	10.5
Marine					
Capture	73.2	79.0	84.7	86.0	1.3
Aquaculture	2.7	4.2	7.2	11.2	11.9
Total world	86.6	98.0	112.9	122.0	2.9
Human population (in billions)	4.9	5.3	5.7	6.0	1.7

*Fisheries data from FAO (*http://www.fao.org/docrep/w9900e/9900e00.htm*). Data for 1997 are preliminary and subject to change.

fisheries in sensitive marine ecosystems, are questions that must be answered. To most scientists, it seems unlikely that the sustainable level of marine capture fisheries will be much higher than 100 MMT. *See* ANTARCTIC OCEAN; FOOD WEB.

Biological productivity of ocean regions varies greatly, controlling the potential to produce fisheries products. Coastal regions and estuaries are more productive than the open ocean, which has been described in a comparative sense as a desert. Coastal areas of the sea where nutrient-rich water upwells, especially on the west coasts of continents, support many of the world's greatest fisheries for sardinelike and anchovy species, even though these areas constitute less than 2% of the sea. Despite the infertility and low productivity of the open ocean, some of the world's most valuable fisheries, for example tuna, are found there, often in weak but geographically extensive upwelling regions of the subtropical gyres in the world oceans.

Most of the sea is being fished to some extent today. The deep sea has been relatively untouched because of technological challenges and dilute fish resources. But new fisheries at greater depths are developing that may change this situation. The vast expanses of the southern ocean support major krill (*Euphausia superba*) resources, which have been exploited only lightly to date because they are regulated by international treaties. If these krill were exploited heavily, the annual yield could be millions of tons. However, the role of krill as prey for fish, birds, and mammals in the Antarctic marine ecosystem is critical, and it seems unlikely that krill will support large fisheries in the near future.

Marine aquaculture has become a major factor in marine fisheries production since the 1980s. The marine aquaculture sector has had the greatest relative increase in fisheries production since 1985 (Fig. 1; table) and will continue to increase during the twenty-first century. Ironically, the rapid rise in marine aquaculture production depends in part on landings of marine-capture fish, which are processed into fish meal, a major constituent of aquaculture feeds. Aquaculture is the sector of fisheries where large increases in production remain possible over the next 25 years. *See* AQUACULTURE.

The character of fishing has changed significantly since 1950. Traditional artisanal fisheries still exist in many parts of the world, although developing market economies have transformed these fisheries from subsistence fisheries to market industries. Since 1985, catches by developing nations have exceeded those of developed nations. Industrial fishing, dependent on fleets of large vessels and supported by sophisticated technologies, expanded primarily in developed nations, mostly in the Western Hemisphere, Japan, and the former Soviet Union. It was this sector of marine fisheries, especially its distant-water fleets, that was responsible for the rapid global expansion of fisheries.

Marine recreational fishing has increased in importance. Statistics for recreational fishing are seldom accurate, but these fisheries account for a major fraction of landings for some species. While most recreational fishing is practiced in developed nations, its importance to tourist economies in developing nations has contributed to its increasing popularity. Recreational fishing is a major industry in the United States, where annual landings of recreationally caught marine fish have averaged more than 90,000 tons in recent years, and marine recreational anglers spent more than $7 billion dollars in 1997. Recreational fishers outnumber commercial fishers and have a powerful influence on fisheries management in the United States.

Major components in the catch. The global catch (capture plus aquaculture) consists of hundreds of species partitioned into categories by the Food and Agriculture Organization (FAO). However, on a global basis 40% of the world landings and production of fish products (combined fresh-water, marine, and aquaculture) come from only 20 species. Thus, very few species dominate the marine capture fisheries. In 1997 five species contributed 22.1% to the marine landings: Peru anchoveta 7.7 MMT, Alaska pollock (*Theragra chalcogramma*) 4.4 MMT, Chilean jack mackerel (*Trachurus symmetricus*) 3.6 MMT, Atlantic herring (*Clupea harengus*) 2.5 MMT, and chub mackerel (*Scomber japonicus*) 2.4 MMT. All of these species are small, shoaling fishes that feed on plankton.

Herrings, sardines, and anchovies make up the largest FAO category in global landing and production statistics, with more than 20 MMT landed

annually in recent years. Other major categories include cods, hakes, and pollocks (10 MMT), flatfishes and flounders (1 MMT), salmons (>2 MMT), and tunas, billfishes, and swordfish (nearly 5 MMT). Among the invertebrates, shrimps (>3 MMT), oysters (>3 MMT), squids (>3 MMT), and clams (nearly 3 MMT) are major contributors to these relatively high-value fisheries.

The largest fraction of landings (70–75%) is consumed directly by humans. However, an important component, ranging 25–30% in recent years, is reduced to fishmeal and oil, which is used primarily as feed for domestic livestock. Small, oily fishes with low market value, such as sardines, anchovies, and capelin (*Mallotus villosus*), contribute most to these industrial meal and oil fisheries. A significant fraction of these landings and products are processed as feed for fish and shrimp in the aquaculture industry. Thus, inexpensive fish are converted into products that are used to produce cultured shrimp and salmon which have high market value. Some scientists question the wisdom of this approach, which requires heavy exploitation of small fishes to support a relatively small production of valued aquaculture products.

Global status. Many marine fisheries are overexploited and less productive than they could be if managed better. On a global basis, FAO indicates that approximately 25% of the world's fisheries were overexploited, depleted, or recovering during the mid-1990s. Another 44% were heavily or fully exploited, while approximately 31% were believed to be capable of sustaining heavier fishing. In the United States, the situation was similar in 1999, when 27% of its marine fisheries were known to be overexploited, 37% were heavily or fully exploited, and 15% were capable of sustaining heavier exploitation. The status of 21% of the United States stocks was unknown in 1999.

Global demand. It is estimated that annual demand for fish to be consumed by humans will reach 95 MMT by the year 2010 if per capita consumption (15.7 kg in 1996) is maintained. Approximately 58 MMT of marine capture fish and 7 MMT of marine aquaculture fish are consumed annually in addition to approximately 25 MMT of fresh-water fish (aquaculture plus capture). Increased demand will require an additional 5 MMT to maintain the per capita consumption level. There is concern that wild fish stocks cannot meet that demand, given present fishing strategies and management problems. Marine aquaculture production will continue to increase, although its ultimate potential is uncertain and dependent to an extent upon landings of wild fish. Many authorities believe that an additional 5–10 MMT of marine capture fish could be landed sustainably if fishery management improved and overfished stocks were restored.

Major Fishing Nations

Major marine fishing nations fall into two categories: recent entrants and historical fishing nations. Each of the top five marine fishing nations landed more than 5 MMT in marine capture fisheries in 1997. In that year, the top five nations were China (13.8 MMT), Peru (7.8 MMT), Japan (5.8 MMT), Chile (5.8 MMT), and the United States (5.0 MMT).

Beginning in the 1980s, China has emerged as the number one fishing nation. China also has a major fresh-water and marine aquaculture industry. China's total catch and production of fishery products was 35 MMT in 1997 (28.6% of world total). Although China has a long history of fishing and fresh-water aquaculture, its marine catch increased rapidly in recent years and continues to increase. In contrast, Peru was not a major fishing nation until the 1960s, when its anchoveta stocks came under exploitation. Peruvian fisheries concentrate on small pelagic fishes, including anchoveta, sardines, and jack mackerel, much of which is reduced to meal and oil. Landings and fish production fluctuate significantly under the positive influence of upwelled nutrients and are negatively affected by periodic El Niño oceanographic conditions. As a consequence, annual landings fluctuate markedly in Peru. Chile also is a recent entrant into the major fishing nation category, with landings resembling those of Peru, but with added diversity.

Japan has a long history of fishing and was the number one fishing nation until the 1980s. Traditional fisheries in Japan are characterized by their diversity. Declaration of 200-nautical-mile Exclusive Economic Zones by most maritime nations in the 1970s had a negative impact on Japan's distant-water fisheries. The United States, with extensive coastlines on both the Atlantic and Pacific coasts, also has a long history as a major fishing nation. Although levels of marine landings changed little in the 1990s (4–5 MMT), the United States has maintained its position among the top five or six fishing nations, which it has held for many decades.

Many other nations have economies that depend significantly upon marine fisheries and marine aquaculture or have high per capita consumption of marine fishery products. These nations and their 1997 landings include the Russian Federation (4.4 MMT), Iceland (2.2 MMT), Norway (3.2 MMT), Thailand (3.5 MMT), Indonesia (3.3 MMT) and the Republic of Korea (2.6 MMT). In the past 25 years, there has been a significant shift in the dominance nations producing the most fish products. Historically, nations with developed economies landed the highest percentage of fish, but a shift occurred in the mid-1980s when nations with developing economies became the largest producers annually catching or producing approximately 70% of the global fish.

Managing the Fisheries

Managing marine fisheries is complex and often uncertain. Managers and the agencies or institutions that support them have jurisdiction over living resources that fluctuate naturally in abundance, often are highly mobile, and are only rarely privately owned. Many species (for example, tunas and billfishes) have ranges that extend over thousands of kilometers during their annual migratory cycle. The common property nature of marine fisheries

complicates conventional management approaches that allow open access and require agreement among jurisdictions, and consensus on the best methods to regulate fishing and the allocation of the catch.

Total Allowable Catch versus fishing effort control. The most common management approach is to assign an annual Total Allowable Catch (TAC). This requires setting a quota that, if exceeded, will terminate the fishery for that year. The TAC is set at a level to prevent a catch so large that the stock will be overfished. In an open-access fishery, there may be competition among fishers to secure a large fraction of the TAC, which can lead to "derby" fishing that is difficult to control. In international fisheries, the TAC is commonly apportioned among participating nations based on negotiated allocations and historical landings. Many variations of quota assignments, including dividing the TAC into seasonal allocations or apportioning it among areas, have been used. For example, in Pacific salmon management, individual TACs may be assigned to stocks that are fished near the mouths of spawning rivers. In this way, sufficient adults escape to insure the continued reproductive success of the individual stocks.

A second common management approach is to control the amount of fishing effort. Controlling effort nominally limits the mortality rate attributable to fishing, which is presumed to be directly proportional to fishing effort. Effort regulation, when effective, fixes the fraction of a stock that is caught. Consequently, the number of fish landed may vary among years, with high catches during years of high abundance and lower catches when the stock is less abundant. Many fishery scientists and managers argue that effort management is preferred over TACs because TACs may allow landings that are too high in years when the stock is at low levels. Fishing effort can be controlled by limiting numbers of participants, by limiting amounts of fishing time or amounts of gear, or by legislating inefficiencies into the fisheries. Prohibiting fishing gears or methods that may, because of their efficiency, catch fish too rapidly or effectively may control fishers and allow an even distribution of landings throughout the fishing year.

Frequently, TAC (output) and fishing effort (input) controls are applied together, especially in heavily fished stocks, for example, northwestern Atlantic stocks, such as cod (*Gadus morhua*) and haddock (*Melanogrammus aeglefinus*). Other, less direct methods may be applied as well. For example, size limits may be imposed to protect young fish, allowing them to mature and spawn. In some species (for example, some sturgeons), very large individuals may be protected from fishing to maintain the fecundity and spawning potential of a stock. Other controls which are becoming common include time and area restrictions, such as closure of nursery areas, protection of spawning habitats, and exclusion of fishers from polluted areas. In some cases, managers attempt to maximize the quality of the catch by specifying a fishing season when the resource is at its best condition (for example, oysters). Daily landing quotas, called bag limits, may be assigned to spread the TAC over a season or to ensure that the catch is spread among numerous fishers, rather than being taken by the most powerful fishing vessels. In some managed stocks, only males are allowed to be landed—females carrying eggs must be released to protect spawning potential of the stock. Such measures are particularly popular in some crustacean (crab and lobster) fisheries.

Maximizing sustainable yields. An objective of fisheries management is to achieve yields from a fishery that are both high and sustainable. In marine commercial fisheries, that objective historically was translated into a fishing strategy that allowed a maximum sustainable yield (MSY) from a stock that is in balance with the stock's reproductive and growth capacities under a given set of environmental conditions. If the population growth rate of a species is known and is presumed to be primarily a function of the population's size (expressed as its aggregate weight, or biomass), then the MSY can be predicted in relation to fishing effort (or fishing mortality rate) [**Fig. 2**]. *See* POPULATION ECOLOGY.

For many years, MSY was set as a management target, which in retrospect often allowed catches that were too high, precipitating declines in the stock, leading to an unsustainable, overfished condition.

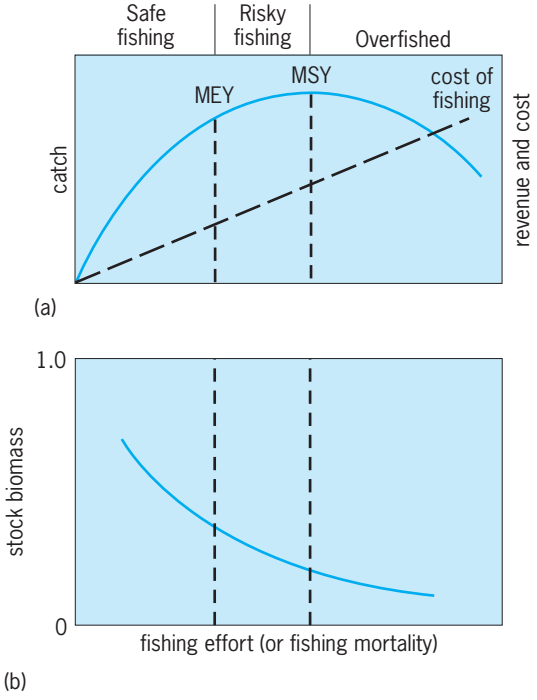

Fig. 2. Concept of maximum sustainable yield (MSY). (*a*) Catch and revenue and cost versus fishing effort. (*b*) Stock biomass versus fishing effort. In a developing fishery, catch increases in relation to fishing effort. At an intermediate level of effort and stock biomass, the MSY can, in theory, be caught. At higher levels of effort, the sustainable level of catch declines and the stock is overfished. Fishing at effort levels near MSY is risky. Safe fishing is practiced at considerably lower levels of effort. The maximum economic yield (MEY) is taken at a level of effort where net profit is maximum. The MEY is taken at effort levels lower than the effort level associated with MSY. In unregulated, open-access fisheries, the level of effort may increase to the point where the "cost of fishing" line intersects the catch (=revenue) line.

Environmental variability and failed reproduction in years of unfavorable conditions make MSY an undesirable and risky strategy. However, estimating MSY remains an important objective, and recent management advice usually sets MSY as a threshold, a level of catch that, if approached, should signal caution rather than being considered a target for the fishery.

Maximizing yield per recruit. A second common management goal has been to maximize or optimize the catch with respect to a given level of recruitment (production of young fish). In this approach, the size (or age) at which fish first enter the fishery is adjusted by regulating mesh sizes of fishing gears, and the fishing mortality rate is controlled by adjusting the amount of fishing effort. Given a fundamental knowledge of fish growth and an estimate of natural mortality rate, maximizing the yield per recruit can be easily achieved in theory, although it may be achieved at the risk of catching too many adults, thus reducing the biomass of the spawning stock to a level so low that future recruitment success is jeopardized (**Fig. 3**). Thus, fishing at a level that takes maximum yield per recruit is risky, and is now considered to be a threshold associated with too high a level of fishing mortality.

The yield-per-recruit model also can be used to estimate spawning biomass per recruit relative to its level if there were no fishing mortality and under specified levels of fishing mortality (Fig. 3). Spawning biomass of a stock falls rapidly as fishing mortality rate increases, indicating that fishing mortalities must be set at relatively low levels to conserve high spawning potential and ensure future recruitment success.

Biological reference points. Managing marine fisheries generally requires the designation of reference points, which serve as targets and thresholds. Biological reference points most often are specified fishing mortality rates, spawning stock biomasses associated with fishing mortality rates, or catch levels relative to specified fishing mortality rates or stock biomass levels. Precautionary management rests on selecting target reference points that allow sustainable fishing at profitable levels, yet do not endanger the stock's capacity to reproduce. In many fisheries, experience has demonstrated that fishing mortality rates must be limited to levels that maintain spawning biomass at levels at least 20–40% of that in an unfished stock. Thus, safe fishing may require limiting yields to levels that are less than the maximum sustainable yield and less than the maximum yield per recruit (Figs. 2 and 3).

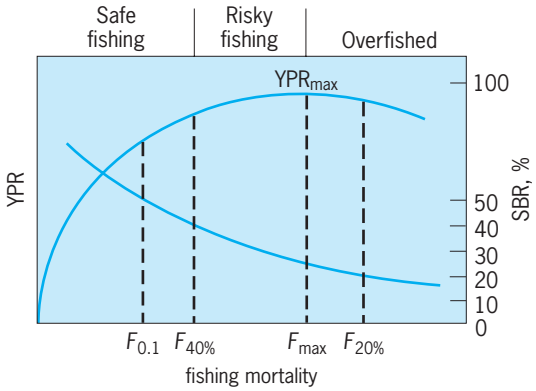

Fig. 3. Concept of maximizing yield per recruit (YPR$_{max}$). Yield per recruit increases as fishing mortality (or effort) increases until a maximum is reached, beyond which increases in effort result in declining YPR as the stock is overfished. Biological reference points ($F_{\%}$) are fishing mortality rates associated with specified yields per recruit. A stock is overfished at F levels higher than F_{max}. Spawning biomass per recruit (SBR) declines as F increases. Safe fishing may require a relatively low F that ensures higher SBR ($\geq$40% in the example). The $F_{0.1}$ reference point, historically considered a safe target level, sets F at a level where the slope of the YPR curve is 1/10 of that at the origin.

Economics. To be profitable, revenues from catches obviously must exceed costs, although governments often have subsidized fishing, an industry that provides human food. In a simple model, the maximum economic yield, or level of catch that provides the largest net profit, is achieved at an effort level where revenues most exceed costs of fishing. This effort level is considerably lower than the effort required to obtain maximum sustainable yield (Fig. 2). In this sense, it is a safer level at which to fish, in addition to maximizing profits. In open-access fisheries, without strong management control, economists argue that effort will increase in a fishery until it equilibrates at a high level where net profits are zero (Fig. 2)—a clearly undesirable circumstance that also risks the biological collapse of the stock.

Recreational fisheries. Marine recreational fishing is a valuable industry in many developed countries. Allocations of catch to recreational fishers are controversial in fisheries with competing users and different values, althouth principles of conservation and management for recreational and commercial sectors often are similar. In some cases, reference points in fisheries dominated by the recreational sector may be set conservatively to maintain quality (many and big fish) in the fishery. As marine recreational fishing increases in importance globally and contributes significantly to the economies of developing nations, conflicting management philosophy and practice between the recreational and commercial sectors seem certain to increase.

Allocating rights and privileges. Many scientists and managers believe that to secure and stabilize marine fisheries their historical common property nature must be transformed to selectively grant user rights or privileges to participants in the fishery. Many examples of rights-based management are in effect throughout the world, such as licensing and permitting systems, and limiting entry to already overcapitalized fisheries to reduce or place a cap on the numbers of participants. An increasingly common but controversial management approach to limit access is the Individual Fishing Quota, which allocates shares to selected fishers based on their historical presence in a fishery. These shares of the Total Allowable Catch are often treated as a commodity that can be traded or sold. Management by Individual Fishing Quota, works on the assumption that participants,

because they hold access rights and in a sense share ownership of the resource, will not engage in behavior that promotes overfishing or damages the marine environment.

Institutions and agencies. A complex of local, regional, national, and international institutions is charged with management of marine fisheries. Many fish stocks are migratory. Fish stocks do not recognize jurisdictional boundaries and cannot be assessed or managed effectively if some jurisdictions are not included in management plans. The classic case exemplifying the need for interjurisdictional management is that of tunas, swordfish, and billfishes, which have been called "fish without countries" because of their migratory behaviors.

International commissions provide management advice and in some cases hold management authority for highly migratory species, such as tunas, or for less migratory fish stocks in international waters, such as cod, haddock, and herring in the North Sea, Barents Sea, or Baltic Sea ecosystems. Examples of international commissions are the International Commission for the Conservation of Atlantic Tunas (ICCAT) and the Northwest Atlantic Fisheries Organization (NAFO). International commissions vary with respect to their research responsibilities and with respect to their advisory or regulatory roles relative to authority exercised by the signatory nations. *See* ARCTIC OCEAN; BALTIC SEA; NORTH SEA.

Marine fisheries of most nations are usually managed by a national authority. In the United States, that authority rests in the Department of Commerce and its National Marine Fisheries Service. Nations with large, geographically dispersed fisheries may have regional management institutions responsibe for particular fish stocks. In the United States, regional management is vested in eight Regional Fisheries Management Councils, which develop management plans to govern particular fisheries. In addition, other regional institutions may manage marine fisheries in particular zones. For example, in the United States, the Atlantic States Marine Fisheries Commission is responsible for managing migratory stocks, such as striped bass (*Morone saxatilis*) and American shad (*Alosa sapidissima*), that primarily reside within 3 nautical miles of shore, but which may be fished along the coastlines of many states. There are also agencies within individual regions or states (or in local waters) that have authority to regulate fishing. These jurisdictional units sometimes have conflicting goals and approaches to fish stock management. In many cases, conflicts are resolved or avoided by agreements that ensure joint management responsibility among agencies. For example, in the United States, Atlantic coastal stocks of bluefish (*Pomatomus saltatrix*) are jointly managed by the Atlantic States Marine Fisheries Commission, the states, and three Regional Fisheries Management Councils.

Ecosystem Approaches to Management

During the 1990s there was increasing public concern about the status of marine fisheries and exploitation practices. As more fisheries were overexploited, more habitats came under stress, and water quality issues came to the forefront. Most nations and management agencies adopted, at least nominally, precautionary approaches to the exploitation and management of marine fisheries. There emerged a sense that the burden of proof with respect to effects of heavier fishing pressure or implementation of new marine fisheries ought to be borne by fishers and not by management agencies. This shift in philosophy gained a foothold in the 1990s and has slowly become a guiding framework for marine fisheries management. The approach recognizes that fishing is a significant presence in marine ecosystems and that its ecosystem-level effects must be considered.

Multispecies management. New models are emerging to account for multispecies interactions in marine fisheries that previously were neglected in traditional, single-species management. Predatorprey relationships dominate interactions among marine species and are emphasized in these models. Most fish die from being consumed by larger fish. Fishing that significantly alters abundances of predator and prey species can affect productivities of the stocks and their potentials to provide sustainable catches. In cases where several species of fish interact through predator-prey and competitive relationships, the effects of fishing on those interactions and on potential yields of individual species are difficult to predict and not always intuitive. Consequently, managers have been reluctant to adopt complex multispecies models as the basis for management. However, it is probable that such models will become a tool that managers regularly use to forecast potential effects of different fishing strategies on fisheries productivity and marine ecosystem structure.

Ecosystem principles and fisheries management. Beyond multispecies management, the broader consequences of ecosystem effects of fishing need to be addressed. Consideration of fishing practices and their effects must be included in fisheries management plans. Water quality and critical spawning and nursery areas, or areas with critical habitats for prey or predators of a target species, must be protected. Catches of nontargeted organisms, called bycatch, whether they are unwanted species or are small individuals of a targeted species, must be reduced. The bycatch issue extends to the capture of birds, turtles, and marine mammals, adding impetus to solve the problem. The magnitude of the problem is highlighted by records that indicate more than 25 MMT annually of marine bycatch has been caught and discarded in recent years. *See* WATER CONSERVATION.

Accounting for effects of fishing on ecosystems will depend on development of ecosystem models that not only examine a multispecies complex exploited by a fishery but include other components and aspects of ecosystems. In future management scenarios, ecosystem-level effects of fishing practices and alternatives will be explored by running ecosystem models in which fishing is simulated and ecosystem responses are evaluated. Such

integrated management of marine fisheries will depend on developing new ecosystem models and on applying new tools. The concepts of marine protected areas and no-take reserves have become popular, and under some circumstances they promise to conserve, restore, and improve fisheries. Moving toward ecosystem-level management of marine fisheries requires a rigorous hypothesis-based, experimental approach. In this sense, adaptive management, which to date has mostly meant remaining flexible in management responses, will take on a more important role as ecosystem-level models are developed to guide marine fisheries management. *See* MARINE ECOLOGY; MATHEMATICAL ECOLOGY.

Edward D. Houde

Fishing Technology

Fishing technology is the rational application of practical experience together with engineering and related natural sciences (such as physics, chemistry, mathematics, biology, and hydrology) to fishing vessels, gears, and operations.

Until the 1930s the technical development of fishing was largely left to the fishers, the ship builders, and the supplying industry. In industrialized countries the overall technical development has had a significant impact on fishing in terms of increased size, power mechanization, range, complexity, and costs. Consequently the traditional trial-and-error approach had to be replaced by systematic research and development. Industrialized countries with important fisheries have, therefore, established specific government- and industry-sponsored research and development capacities, and fishing technology has thus become a fisheries discipline in its own right.

The introduction of engine power to fishing vessels at the end of the last century considerably increased the range and flexibility of fishing operations. It also enabled the development of auxiliary machinery such as winches and haulers to improve efficiency and safety and to reduce hard labor.

Fig. 4. Example of a long-distance factory trawler (3177 ft or 95 m long, 5000 hp or 3.7 MW) capable of bottom and midwater trawling anywhere in the world. (*Hansetische Hochseefischerei, Germany*)

Trawling. This mechanization—from which all fishing techniques benefited to various degrees—started a spectacular development of trawling which became one of the most productive fishing methods. In trawling, a conical net bag is towed over the ground (bottom trawling) or through the free water at any depth (midwater trawling) and scoops up the fish in its path. The net is usually towed by a vessel called a trawler; sometimes two vessels are used. Trawlers range from outboard-powered canoes, operating on lakes or in coastal waters, to long-distance factory trawlers that are more than 330 ft (100 m) long and have main engines with more than 5000 hp (3.7 MW) (**Fig. 4**). These are among the most expensive and sophisticated commercial vessels of their size. The most common trawl gear is the otter trawl, for which special shearing devices (otter boards) are used to spread the net opening horizontally. Otter boards range from flat rectangular plates to hydrofoil curved designs up to 129 ft^3 (12 m^2) each. Bottom trawl nets have a mouth opening of up to about 2700 ft^2 (250 m^2) and a total net length of about 260 ft (80 m), and midwater trawl nets can be even larger, up to 22,000 ft^2 (2000 m^2) and 590 ft (180 m), respectively. Commercial bottom trawling goes down to more than 3300 ft (1000 m) depth, and midwater trawling to about 2600 ft (800 m). Towing speed is between about 2.5 and 5 knots (4.5 and 9 km/h). As exploitation of ocean resources has grown more intense, trawling in the deep sea (depths >400 m) has been increasingly common.

Aimed trawling. Technical progress in trawlers, trawl gears, and underwater acoustics led during the 1960s to the development of aimed trawling (**Fig. 5**). The gear requires a horizontal echo sounder or sonar to detect and select suitable fish schools ahead of the trawler, the ship's echo sounder to further assess the depth and quantity of the school and the bottom conditions, and a net sounder to monitor the net depth, the opening height, and the fish in, below, and above the net opening. This combination of echo-sounding (acoustic) devices with modern navigational aids such as gyro compass, sensitive speed log, radar, decca navigator, loran, or even satellite navigation significantly improved the chances of hitting a fish school with the trawl gear and of counteracting escape reactions. Aimed trawling is mainly applied in midwater trawling, but the technology is increasingly also used in bottom trawling. *See* UNDERWATER SOUND.

Integrated trawling systems supplement aimed trawling by adding electronic data processing and computer control of certain parts of the aiming process. A virtually automatic interception of trawl and fish and optimum operational efficiency are achieved by computer processing. This processing includes adjustment of course and speed of the trawler and the trawl gear to the position and the movements of selected fish schools, the fixing of sonar to the target, and the adjustment of the trawl winch operation

and the towing speed to correct the net depth. Such complex systems are mainly meant for midwater trawling. Other applications are being developed. *See* SONAR.

Echo sounding. One of the major problems of fishing is to find the fish when they are not visible at the surface. This was largely solved when, starting in the late 1930s, echo sounding was developed not only to measure the water depth but also to show fish. The principle of echo sounding consists in measuring the time that a sound impulse takes to travel to a target and the reflected echo to come back. Half the total time multiplied by the speed of sound (in water, about 0.9 mi/s or 1500 m/s) gives the distance. The echo strength depends, among other things, on the reflection properties of the target; for example, rocks reflect better than sand or mud and large fish (particularly with swim bladder), or fish schools better than small or single fish. Fish-finding echo sounders need more transmission power and echo amplification than purely navigational echo sounders and also a suitable monitor display, Historically, echograms were presented on recording or cathode-ray-tube (CRT) displays for echo discrimination of bottom and various fish sizes and concentrations.

The normal echo sounder, covering the water column below the vessel, is applicable to all fishing methods. Horizontal, or, rather, oblique, echo sounding at various angles between the surface and the bottom forward and around the vessel is also known as sonar (sound navigation and ranging). It mainly serves in midwater trawling and purse seining (see below), for which the advance detection of fish is quite essential. Depending on type and power, the range for fish detection of echo sounders is down to about a 3300-ft (1000-m) depth, and of sonar up to about 9900 ft (3000 m) away from the vessel. The net sounder developed for midwater trawling is an echo sounder with the transducers or sounding units at the net rather than in the ship's bottom (Fig. 3). The connection from net to trawler may be by cable or by an acoustic link (wireless). The more complex multinet sounder equipment for commercial fisheries includes forward transducers in addition to the down and up transducers, a net filling meter, and a thermometer at the net to check whether the water temperature is according to the preference of the species sought. Scientific multi-net sounder equipment has additional transducers across the trawl opening and further aft in the bag, a speed-through-water meter, and a transponder to study gear performance and fish reactions in detail.

Purse seining. In addition to giving all fishers an eye to see under water and paving the way for aimed trawling, the development of underwater acoustics also opened a new dimension to purse seining. This fishing method uses a net which may be 490 to 4900 ft (150 to 1500 m) long and 100 to 660 ft (30 to 200 m) deep which is set in a circle around a fish school and then closed at the bottom like a purse, catching all fish inside. Unless it is done in connection with fish attraction (such as with light), purse seining is completely dependent on finding suitable

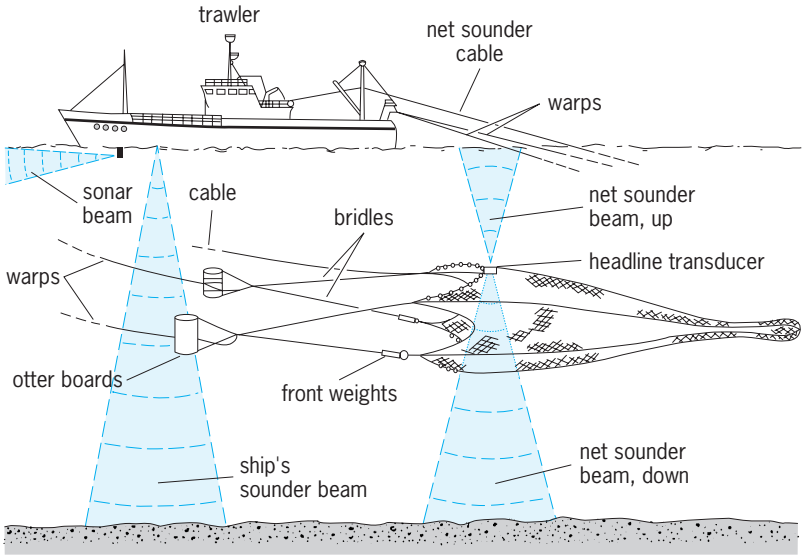

Fig. 5. Typical arrangements of fishing gear and acoustic instrumentation for aimed midwater trawling.

fish schools. Schools of fish may be sited from the vessel or from airplane spotters who locate the schools and direct the vessel to them. For fish which are not visible at the surface, sonar-guided purse seining is the only solution and quickly led to a very significant expansion of this fishery, which is the largest bulk fish producer in the world. As in aimed trawling, the success of sonar-guided purse seining is largely dependent on the skill of the individual skipper. Consequently, computerized systems have been developed to assist the skipper and also improve the complex tasks of detecting and approaching a fish school, assessing its size and depth, and coordinating the relative movements of vessel and fish school during actual fishing. One such system employs a television screen (**Fig. 6**) to show the situation in the horizontal in relative or true motion as desired. The computer can also link the sonar to a selected fish school and calculate the depth of the school.

Longlining. Longlines range (from a few hundred meters to many kilometers in length and carry baited hooks set at intervals. This gear has been adapted since the 1950s to effectively catch migratory species such as tunas and swordfish in the open sea. Development of accurate navigation and the Global Positioning System, and acquisition of sensors to detect temperature and other oceanographic features, have increased the ability of longliners to locate and remain in the environment of the target species. In addition, the use of chemiluminescent sticks light as a fish attractant has increased the effectiveness of the longline technique. *See* REMOTE SENSING; SATELLITE NAVIGATION SYSTEMS.

Vessel trends. In addition to increases in size and horsepower, vessels in modern industrial fishing fleets have become more diversified to allow participation in fisheries that use more than one type of gear and target different kinds of fish. For example, in the Gulf of Alaska and Bering Sea fisheries, vessels may be rigged to alternatively trawl for groundfish, set

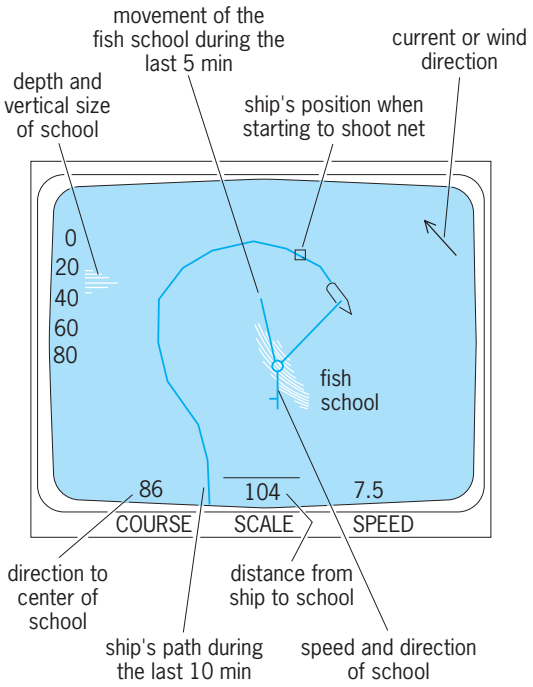

Fig. 6. Automatic tracking and true-motion situation display by a computer-integrated purse-seining system. Course is indicated in degrees, scale in meters, and speed of vessel in knots. Depth scale at left is in meters. 1 m = 3.3 ft. (*SIMRAD AS, Norway*)

traps for crab, or longline for halibut, depending on the season and potential profitablility of a particular fishery. Such versatility often is required to remain profitable in modern, highly competitive fisheries. *See* BERING SEA; OCEANOGRAPHIC VESSELS.

Synthetic fibers. Apart from these special developments in trawling and purse seining, the introduction of synthetic materials for yarns, netting, and ropes had an even more general impact on fishing gears and fishing than the introduction of echo sounding, which started at about the same time. The main advantages of synthetics such as polyamide (for example, nylon), polyethylene, and polypropylene are their strong resistance against rotting. Some also have higher breaking strength, elasticity, and abrasion resistance than natural fibers such as cotton, manila, and sisal used hitherto. Higher breaking strength enables the use of thinner yarns, and synthetic monofilaments are almost invisible in water. This can significantly improve the catching efficiency of, for instance, trawls and other bag nets, gill nets, or angling gear. These advantages compensate for the higher price of synthetics, which have now almost completely replaced the traditional natural-fiber materials. *See* MANUFACTURED FIBER.

Joachim Schärfe

Bibliography. *Ecosystem-Based Fishery Management*, National Oceanographic and Atmospheric Administration, National Marine Fisheries Service, Silver Spring, MD, 1999; *Fisheries of the United States*, National Marine Fisheries Service, Silver Spring, MD, annually; National Research Council, *Improving Fish Stock Assessments*, National Academy Press, Washington, DC, 1998; National Research Council, *Sustaining Marine Fisheries*, National Academy Press, Washington, DC, 1999; *Our Living Oceans 1999*, National Oceanographic and Atmospheric Administration, National Marine Fisheries Service, Silver Spring, MD, 1999; *Yearbook of Fishery Statistics*, Food and Agriculture Organization, Rome, annually.

Marine geology

The study of the portion of the Earth beneath the oceans. Approximately 70% of the Earth's surface is covered with water. Marine geology involves the study of the sea floor; of the sediments, rocks, and structures beneath the sea floor; and of the processes that are responsible for their formation. For the marine geologist, the presence of the oceans masks the principal features of interest. The average depth of the ocean is about 3800 m (12,500 ft), and the greatest depths are in excess of 11,000 m (36,000 ft; the Marianas Trench). The study of the sea floor necessitates employing a complex suite of techniques to measure the characteristic properties of the Earth's surface beneath the oceans. Contrary to popular views, only a minority of marine geological investigations involve the direct observation of the sea floor by scuba diving or in submersibles. Instead, most of the ocean floor has been investigated by surface ships using remote-sensing geophysical techniques, and more recently by satellite observations.

In the mid-1960s to the mid-1970s, the theory of plate tectonics was developed and verified based on geological and geophysical observations of the ocean floor and crust. Key observations included the magnetic characteristics of rocks, the disposition of submarine landforms, the distribution and ages of marine sediments, and the locus and nature of zones of earthquake and volcanic activity. Earthquakes served to define the principal plate boundaries. The axes of mid-oceanic ridges mark sites of plate divergence; trenches mark sites of plate collisions (subduction zones). Diverging plates allow for the birth of new oceanic crust, whereas colliding plates accommodate the destruction of equivalent amounts of crust. Large strike-slip faults exist (such as the San Andreas Fault) where plates slide by one another (**Fig. 1**). *See* EARTHQUAKE; PLATE TECTONICS.

The ocean crust is relatively young, having been formed entirely within the last 200 million years (m.y). The process of renewing or recycling the oceanic crust is the direct consequence of plate tectonics and sea-floor-spreading processes. It is therefore logical, and perhaps essential, that the geologic history of the sea floor be outlined within the framework of plate tectonic tenets. Where plates move apart, molten lava reaches the surface to fill the voids, creating new oceanic crust. Where the plates come together, oceanic crust is thrust back within the interior of the Earth, creating the deep oceanic trenches. These trenches are located primarily around the rim of the Pacific Ocean (Fig. 1). The down-going material can be traced by using the distribution of earthquakes to depths of about 700 km (420 mi). At that level, the character of the subducted lithosphere

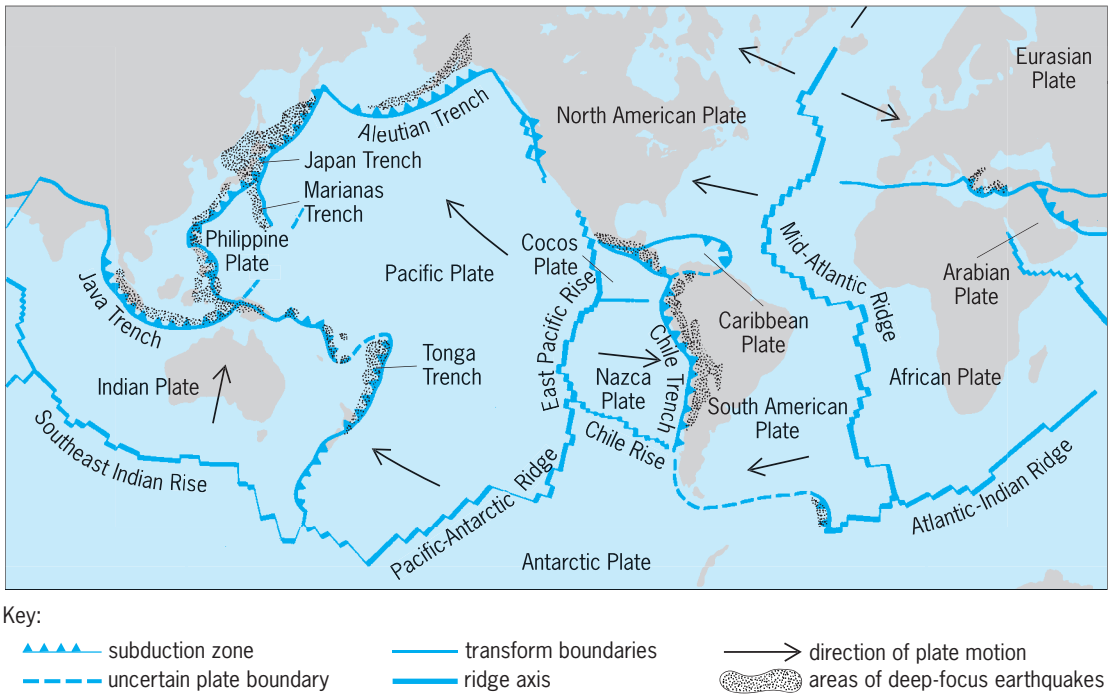

Fig. 1. Map showing the tectonic structure of the Earth's lithosphere, which is composed of about 10 rigid plates, each moving as a distinct unit. (*After J. F. Dewey, Plate tectonics, Sci. Amer., 226(5):56–68, 1972*)

is lost, and this material is presumably remelted and assimilated with the surrounding upper-mantle material. *See* GEODYNAMICS; LITHOSPHERE.

Major Morphologic and Sediment Provinces

The major features of the sea floor are the mid-oceanic ridges, basins, continental margins, large igneous provinces, marginal seas, and anomalous features.

Mid-oceanic ridges. Most of the ocean floor can be classified into three broad physiographic regions, one grading into the other (**Fig. 2**). The approximate centers of the ocean basin are characterized by spectacular, globally encircling mountain ranges, the mid-oceanic ridge (MOR) system, which formed as the direct consequence of the splitting apart of oceanic lithosphere. The small-scale morphologic characteristics of these mountain ranges depend somewhat upon the rate of separation of the plates involved. As is shown in **Fig. 3**, abyssal hill relief, especially within 500 km (300 mi) of ridge crest, is noticeably rougher on the slow-spreading Mid-Atlantic Ridge than on the

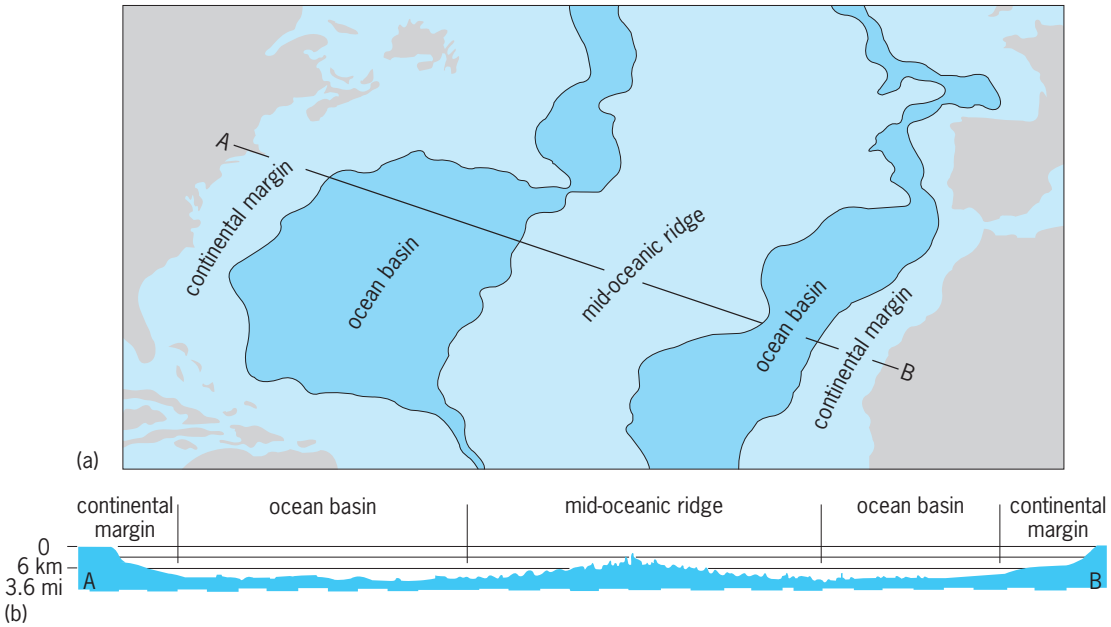

Fig. 2. Geology of the North Atlantic Ocean. (*a*) Physiographic divisions of the ocean floor. (*b*) Principal morphologic features along the profile between North America and Africa. (*Modified from B. C. Heezen et al., GSA Spec. Pap. 65, 1959*)

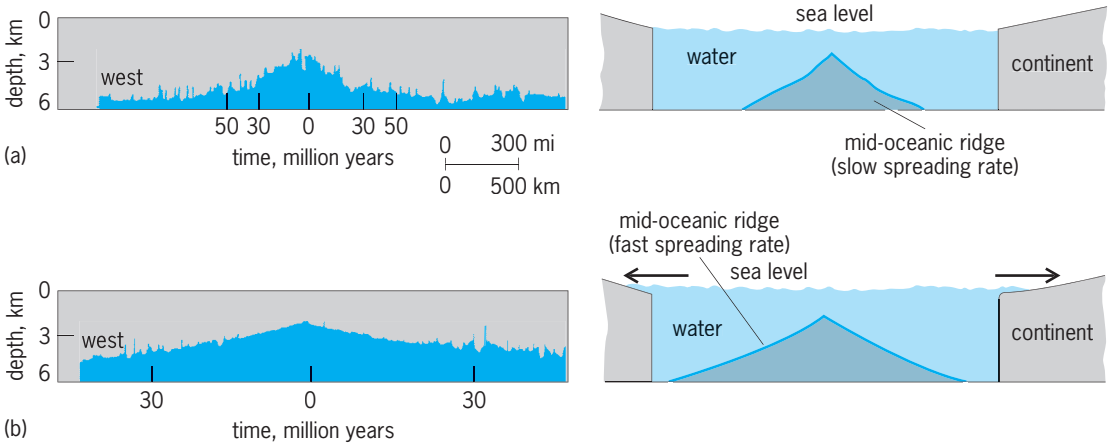

Fig. 3. Topography of the mid-oceanic ridge. (*a*) Mid-Atlantic Ridge (25°N), spreading rate 2.6 cm (1.0 in.) per year. (*b*) East Pacific Rise (55°S), spreading rate 8.8 cm (3.5 in.) per year; sea-level rises causing transgression (arrows). 1 km = 0.6 mi.

fast-spreading East Pacific Rise. The profile of the East Pacific Rise is also broader and shallower than for the Mid-Atlantic Ridge. If the entire mid-oceanic ridge system were spreading rapidly, the expanded volume of the ridge system would displace water from the ocean basins onto the continents, and this may explain a well-known incident of marine transgression during the Cretaceous Period.

The broad cross-sectional shape of this mid-ocean mountain range can be related directly and simply to its age. The depth of the mid-oceanic ridge at any place is a consequence of the steady conduction of heat to the surface and the associated cooling of the oceanic crust and lithosphere. As it cools, contracts, and becomes denser, the oceanic crust plus the oceanic lithosphere sink isostatically (under its own weight) into the more fluid asthenosphere. The depth to the top of the oceanic crust is a predictable function of the age of that crust; departures from such depth predictions represent oceanic depth anomalies (**Fig. 4**). These depth anomalies are presumably formed because of processes other than lithospheric cooling, such as intraplate volcanism. The Hawaiian island chain and the Polynesian island groups are examples of this type of volcanism. *See* ASTHENOSPHERE; ISOSTASY.

Very detailed surveys have been completed for modest sized pieces of the mid-ocean ridge system in the North Pacific, South Pacific, and South Atlantic in an effort to compare and contrast the morphologic features of the crestal zones at fast-, intermediate-, and slow-spreading ridges. The amplitude of the small-scale component of relief is somewhat dependent on the associated rate of sea-floor spreading. This small-scale relief is born at the axis of the ridge. As it moves laterally by spreading, it evolves gradually, becoming more subdued as it is slowly draped by a "snowfall" of pelagic sediments. The resulting sea floor abyssal hills constitute the largest morphologic province in the world.

The mapping studies have revealed that the mid-ocean ridges are characteristically segmented at a variety of along-axis scales ranging from about 10 km (6 mi) up to about 1000 km (600 mi). The depth of the near crestal regions and the degree of segmentation are thought to reflect the relative amount of magmatic melt available for injection and its temporal variability. Mid-ocean ridges' variable subsidence character captures the largest scale component of ridge segmentation. The smaller scales of segmentation are manifest as contrasts in the along-axis depths and in their near-crestal morphology (**Fig. 5**).

The loci of sea-floor volcanic activity create, most notably at or near the axis of the MOR system, an extreme environment of chemistry and temperature, with hydrothermal plumes (vents) having temperatures often in excess of 400°C (750°F) and containing dissolved and particulate minerals such as sulfides, lead, copper, and others but devoid of free oxygen and sunlight. These conditions define an environment previously presumed unsuitable for supporting life. Numerous diving vessel expeditions to these environments have sampled the fluids and mineral particles emanating like "black smoke" from large chimneylike structures. They have also recovered strange life-forms such as enormous clams and giant tubeworms that symbiotically exist with a type of bacteria called chemoautotrophs. Such observations have required geobiologists to reevaluate their presumptions about what other extreme environmental conditions may sustain life-forms. *See* HYDROTHERMAL VENT; MID-OCEANIC RIDGE; OCEANIC ISLANDS; VOLCANOLOGY.

Basins. The deep ocean basins, which lie adjacent to the flanks of the mid-oceanic ridge, represent the older portions of the sea floor that were once the shallower flanks of the ridge (Fig. 2). The bulk of sediments found on the ocean floor can be broadly classified as terrigenous or biogenic. Terrigenous sediments are derived from drainage of adjacent landmasses and are brought to the sea floor through river systems. This sediment load is sometimes transported across the continental shelves, often using as pathways the submarine canyons that dissect the shelves, the continental slope, and the continental rise. Biogenic sediments are found in all parts of the

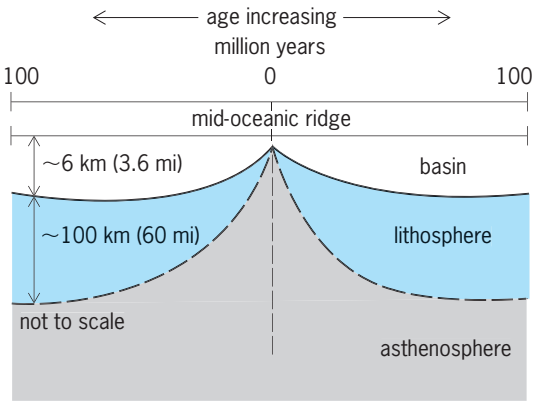

(a)

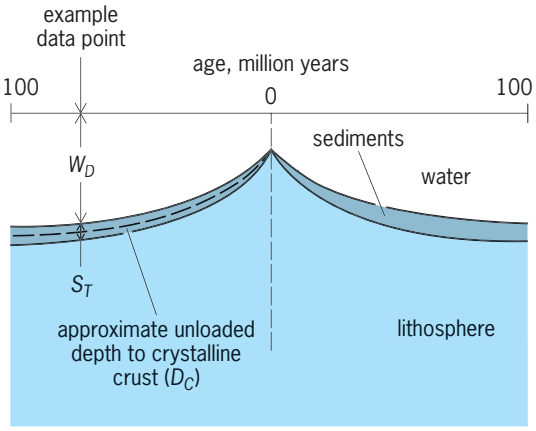

(b)

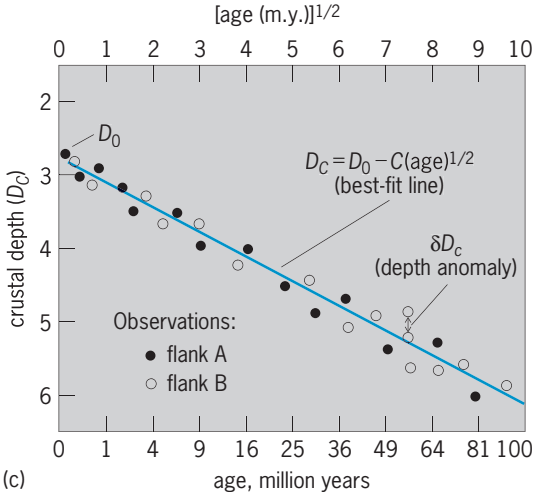

(c)

Fig. 4. Ocean depth anomalies. (*a*) Schema of the lithosphere, asthenosphere, and varying ocean depths away from the axis of mid-oceanic ridge spreading system. (*b*) Parameters used to compute adjusted crustal depths and to analyze depth-age relationships. (*c*) Hypothetical crustal depth (D_C) versus (age)$^{1/2}$ plot showing linear relationship predicted by theory. Differences between the actual observations and the statistically best-fitted line represent residual depth anomalies. D_C (predicted) yield positive or negative depth anomalies. W_D = water depth; S_T = sediment thickness; D_0 = crustal depth at zero age crust; δD_C = depth anomalies (difference between the observed and predicted crustal depths). (*After D. E. Hayes, Mapping oceanic depth anomalies: In search for indicators of asthenospheric convection, Lamont-Doherty Geological Observatory Yearbook, 1982–1983*)

ocean, intermixed either with terrigenous sediments or in near "pure form" in those areas inaccessible to terrigenous sedimentation.

Biogenic sediments are composed mostly of the undissolved tests of siliceous and calcareous microorganisms, which settle slowly to the sea floor. This steady so-called pelagic rain typically accumulates at rates of a few centimeters per thousand years. The composition and extent of the input to the biogenic sediment depend upon the composition and abundances of the organisms, which in turn are largely reflective of the water temperature and the available supply of nutrients. The Pacific equatorial zones and certain other regions of deep ocean upwelling are rich in nutrients and correspondingly rich in the microfauna and flora of the surface waters. Such regions are characterized by atypically high pelagic sedimention rates. *See* UPWELLING.

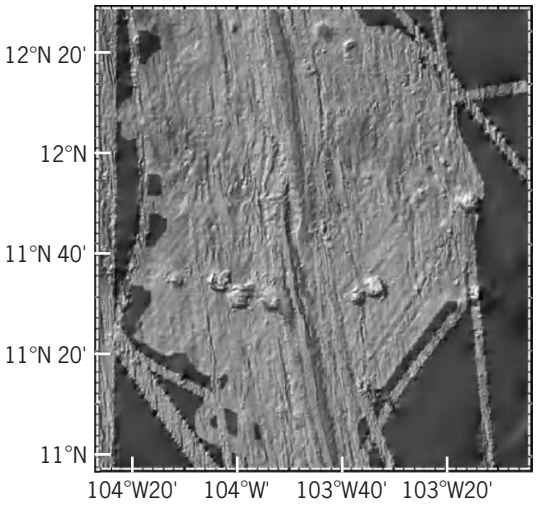

Fig. 5. Digitized contoured map of a ~200 km (120 mi) stretch of the East Pacific Rise (Ridge) near 11°N, 104°W. The data were collected using a multibeam swath mapping system. The depth of the ridge crest varies from south to north and illustrates an intermediate scale segmentation of the ridge. The area slightly north of the map center shows an overlapping spreading center, another example of ridge segmentation. (*Taken from Ridge 2000 MBS data and displayed using GeoMapApp software*)

As the ridge flanks subside to great depths, often in excess of 6 km (4 mi) over a period of 100 m.y., the small-scale topography is gradually modified by pelagic sediments. Once sediments reach the sea floor, their ultimate disposition depends on local environment. Fine sediments can be held in suspension for long periods or can be transported along the bottom, ultimately to be deposited in a more tranquil environment. Spectacular bedforms such as sediment waves sometimes result and provide important information regarding the nature and vigor of present and ancient bottom-current activity. In some cases, the bottom currents can be so strong as to prevent the deposition of fine-grained sediments altogether, essentially scouring the sea floor free of any significant sediment. Over most of the deep-sea floor, bottom currents are sluggish, and most pelagic sediments

are deposited in a relatively tranquil environment as a uniform blanket of sediments on the existing sea-floor relief. If steep sea-floor slopes exist, some sediments may slump off to the sides, effectively smoothing the primary topography upon which they are deposited.

Where the processes of sedimentation have been acting long enough and the deposition locale is accessible to the sediments derived from the continents, the original relief of the ocean crust can become completely buried. Many terrigenous deposits represent relatively impulsive events (for example, major submarine landslides on the continental margin or large turbidity flows), where large volumes of material are transported great distances over very short periods. The principal mechanism of deposition is a leveling process that fills first the topographic lows and, ultimately, can lead to burial of the entire initial sea-floor relief. This result is an extremely flat, topographically featureless abyssal plain. Such abyssal plains characteristically lie between the continental margins and the exposed flanks of the mid-oceanic ridge system. The abyssal plains areas have gradients that are less than 1:1000 and are typically underlain by a variety of discrete layers of transported sediments. *See* BASIN; MARINE SEDIMENTS; TURBIDITY CURRENT.

Continental margins. The continental margins lie at the transition zone between the continents and the ocean basins and mark a major change from deep to shallow water and from thin to thick continental crust. The continental margins consist of two broad categories: rifted margins and convergent margins.

Rifted margins. Good examples of rifted margins are found bounding the Atlantic Ocean (Fig. 2). These margins represent sections of the South American and North American continents that were once contiguous to west Africa and northwest Africa, respectively. These supercontinents were rifted apart 160–200 m.y. ago as the initial stages of sea-floor spreading and the birth of the present Atlantic Ocean sea floor (Fig. 2). *See* CONTINENTS, EVOLUTION OF; SUPERCONTINENT.

Continental margins are proximal to large sources of terrestrial sediments that are the products of continental erosion. The margins are also the regions of very large vertical motions through time. This vertical motion is a consequence of heating and subsequent cooling of the rifted continental lithosphere and subsidence. During initial rifting of the continents, fault-bound rift basins are formed that serve as sites of deposition for large quantities of sediment (**Fig. 6**). These sedimentary basins constitute significant loads on the underlying crust, giving rise to an additional component of margin subsidence. The continental margins are of particular importance also because, as sites of thick sediment accumulations (including organic detritus), they hold considerable potential for the eventual formation and concentration of hydrocarbons. As relatively shallow areas, they are also accessible to offshore exploratory drilling and oil and gas production wells.

Also found in selected continental margin environments are the unusual formations known as gas hydrates. Hydrates are frozen gases, typically composed of methane, higher-order hydrocarbons, and carbon dioxide, which exist in a stable state only within a relatively narrow range of temperature and pressure. The occurrence of such hydrates is now believed to be far greater than past estimates. Hydrates are often associated with a bottom-simulating reflector, which is thought to represent a sharp drop in acoustic impedance created by accumulations of free methane gas just below the base of the gas hydrate zone. *See* HYDRATE.

There is growing evidence that the hydrocarbon gases (mostly methane), entrapped in sub-sea floor gas hydrates, constitute a significant component of global methane and is likely to be the focus of intense ongoing investigations. The potential of gas hydrates to contribute to the global energy inventory of recoverable hydrocarbons remains the subject of debate. *See* OIL AND GAS, OFFSHORE.

Many sedimentary aprons or submarine fans are found seaward of prominent submarine canyons that incise the continental margins. Studies of these sedimentary deposits have revealed a number of unusual surface features that include a complex system of submarine distributary channels, some with levees. The channel systems control and influence sediment distribution by depositional or erosional interchannel flows. Fans also result from major instantaneous sediment inputs caused by large submarine mass slumping and extrachannel turbidity flows. *See* SUBMARINE CANYON.

The present coastline shows no particular geological significance as a boundary, and continental and oceanic crustal structures may or may not lie close to the present shoreline. It has been well established that the sea level has changed many times, fluctuating by as much as 300–400 m (980–1300 ft) during the last 200 m.y. Such changes in sea level are primarily due to the presence or absence of major continental ice sheets, which store vast quantities of water, thereby reducing the total water available to fill the ocean basins. During periods of glaciation, sea level falls. *See* GLACIAL EPOCH.

Low stands of sea level coincide with times of rapid transport of terrestrial sediments across the continental shelves and into the deep ocean basins. During interglacial periods, when little water is stored as continental ice sheets, sea level rises. Accordingly, much of the terrestrial material transported to

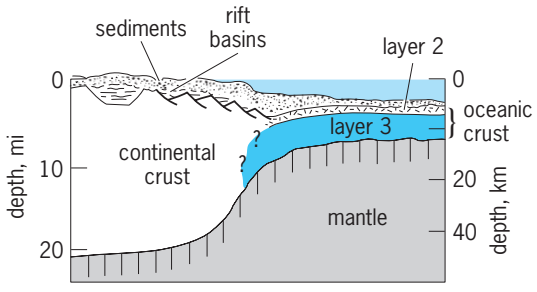

Fig. 6. Schematic cross section of a rifted continental margin. Note dramatic change in total crustal thickness across the margin, fault-bounded sedimentary basins, and large thicknesses of land-derived sediments making up the continental rise.

the sea is trapped on the broad continental shelves, and results in the outbuilding or progradation that characterizes many present-day continental margins. The interplay between sea-level changes and sedimentation yield gives rise to the complicated interfingering of sediment deposits along the continental margins.

Another method of significantly altering sea level is related to large, global differences in the rate at which sea floor is created at the mid-oceanic ridge systems. When sea floor is created extremely rapidly, that is, the plates are moving apart very rapidly, the profile of the mid-oceanic ridge is relatively broad. Because the depths of the mid-oceanic ridges are a direct function of crustal age, fast spreading results in a greater fraction of the ridge appearing at shallow elevations than for a mid-oceanic ridge created by very slow spreading (Fig. 3). Hence, a mid-oceanic ridge system with a broad profile will effectively displace more water from the ocean basin regions than one with a steep profile. The displaced water must move onto the adjacent continents in association with the eustatic sea-level rise. This is one explanation for the occurrence of a major global transgression of the ocean onto the continental areas during the middle Cretaceous period (85–115 m.y.a.). *See* RIFT VALLEY.

Convergent margins. In contrast to the rifted margins, the continental margins that typically surround the Pacific Ocean represent areas where plates are colliding (Fig. 1). As a consequence of these collisions, the oceanic lithosphere is thrust back into the interior of the Earth; the loci of underthrusting are manifest as atypically deep ocean sites known as oceanic trenches (**Fig. 7**). The processes of subducting the oceanic lithosphere give rise to a suite of tectonic and morphologic features characteristically found in association with the oceanic trenches. An upward bulge of the crust is created seaward of the trench that represents the flexing of the rigid oceanic crust as it is bent downward at the trench. The broad zone landward of most trenches is known as the accretionary prism and represents the accumulation of large quantities of sediment that was carried on the oceanic crust to the trench. Because the sediments have relatively little strength, they are not underthrust with the more rigid oceanic crust, but they are scraped off. In effect, they are plastered along the inner wall of the trench system, giving rise to a zone of highly deformed sediments. These sediments derived from the ocean floor are intermixed with sediments transported downslope from the adjacent landmass, thus creating a classic sedimentary melange. *See* CONTINENTAL MARGIN; SEDIMENTOLOGY.

Anomalous features. In addition to the major morphologic and sediment provinces, parts of the sea floor consist of anomalous features that obviously were not formed by fundamental processes of seafloor spreading, plate collisions, or sedimentation. Such features are nonetheless important and represent significant components of the ocean-floor relief. Examples are long, linear chains of seamounts and islands. Many of these chains are thought to reflect

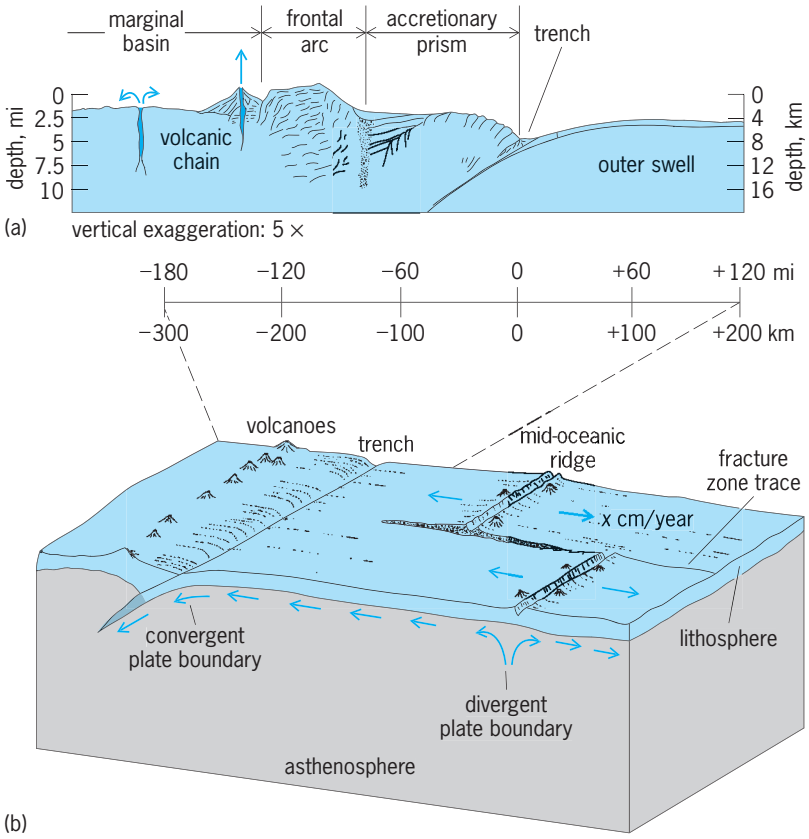

Fig. 7. Oceanic trench and associated tectonic and morphologic features. (*a*) Cross section of typical island arc system showing tectonic units and terminology (*after D. E. Karig and G. E. Sharma III, Subduction and accretion at trenches, Geol. Soc. Amer. Bull., 86:377–389, 1975*). (*b*) Schematic cross section showing the relationship of relative plate motions to plate boundaries and associated sea-floor features. At divergent plate boundaries (mid-oceanic ridges), shallow earthquakes occur. At convergent plate boundaries (trenches), shallow, intermediate, and deep earthquakes occur. Shallow earthquakes occur along active transform zones; fracture zones represent the relict traces of crustal discontinuities originally formed within a transform zone (*after B. Isacks, J. Oliver, and L. R. Sykes, Seismology and the new global tectonics, J. Geophys. Res., 73:5855–5900, 1968*).

the motion of the oceanic plates over hot spots that are fixed within the mantle. Hot spots carry magma through the oceanic crust to the surface, resulting in volcanic trails, which serve to define the relative motion of the plate over the hot spot. *See* MAGMA; SEAMOUNT AND GUYOT.

The presence of large, anomalously shallow regions known as oceanic plateaus may also represent long periods of anomalous regional magmatic activity that may have occurred either near divergent plate boundaries or within the plate. Alternatively, many oceanic plateaus are thought to be small fragments of continental blocks that have been dispersed through the processes of rifting and spreading, and have subsequently subsided below sea level to become part of the submarine terrain.

Large igneous provinces (LIPs) are noteworthy examples of vast outpourings of mafic lava that are found both on continents as large flood basalts and on the ocean floor primarily as large oceanic plateaus. While the existence of these features has been known for some time, their genesis was largely assumed to be the result of perturbations to normal plate tectonic processes. It is now believed that the

emplacement of many LIPs was so rapid (<1–2 my) and the volume of material so large, that creation of new oceanic crust as attributed to sea-floor spreading could not accommodate the rate of magma production represented by the LIPs.

It has been proposed by some investigators that the LIPs were formed by major rising plumes created when rapid overturn of the mantle was initiated by sinking of accumulated "cold material" from the upper mantle at about 650 km (400 mi). These rising plumes then poured out at the Earth's surface, creating LIPs. The last major episode of LIP formation was during the Cretaceous Period. Examples of oceanic LIPs are Kerguelen Plateau, Ontong-Java Plateau, Rio Grande Rise, and Broken Ridge. The reason these and similar features have been the subject of renewed interest is the realization that such huge outpourings of basalt would be accompanied by the extensive release of associated gases (such as CO_2 and SO_2), which in turn could have profoundly impacted the environment and initiated mass extinctions of various life-forms.

Other important features of the ocean floor are the so-called scars represented by fracture zone traces that were formed as part of the mid-oceanic ridge system, where the ridge axis was initially offset. Oceanic crusts on opposite sides of such offsets have different ages and hence they have different crustal depths. A structural-tectonic discontinuity exists across this zone of ridge axis offset known as a transform zone (Fig. 7*b*). Although relative plate motion does not occur outside the transform zone, the contrasting properties represented by the crustal age differences create contrasting topographic and subsurface structural discontinuities, which can sometimes be traced for great distances. Fracture zone traces define the paths of relative motion between the two plates involved. Those mapped by conventional methods of marine survey have provided fundamental information that allows rough reconstructions of the relative positions of the continents and oceans throughout the last 150–200 m.y. The study that deals with the relative motions of the plates is known as plate kinematics. *See* TRANSFORM FAULT.

In 1978, precise satellite altimeter observations from the *SEASAT* mission, coupled with similar but more precise measurements from a later *GEOSAT* mission in 1987, revealed the detailed variations in sea-surface height over the entire water-covered surface of the Earth. The relief of the sea surface responds to lateral variations of mass within the crust below the ocean. These lateral variations in mass are due to the topography of the sea floor, to the crustal structure associated with such topographic variations, and to other lateral subsurface variations in density. Through sophisticated analysis of the *SEASAT* and *GEOSAT* data, it is possible to create a map of subtle gravity variations (of the order of 1 part in 100,000) over the entire water-covered surface of the Earth.

The resultant gravity maps largely mimic the major topographic and structural features of the sea floor, which lie hundreds to thousands of meters below the ocean surface (**Fig. 8**). Because gravity maps represent not only the major relief features of the sea floor but also the associated subsurface structures, various large-scale topographic features may be manifest in different ways. For example, the fast-spreading mid-oceanic ridge system of the South Pacific shows a far less conspicuous gravity signal associated with it than the more slowly spreading mid-oceanic ridge system found in the South Atlantic (Figs. 1 and 8).

The extraordinary success of this satellite altimeter technique has provided enough detailed information that many fracture zone traces can now be followed, unequivocally, across entire basins. Hence, the earlier relative positions of the plates throughout the last 200 m.y. can be determined with much greater accuracy than was previously possible. Because the satellite coverage is global and consists of fairly closely spaced ground tracks, many features of the ocean floor that were previously unrecognized, because of limited surface-ship data, are now being predicted by utilizing the satellite observations; many have subsequently been verified by conventional surface-ship surveys.

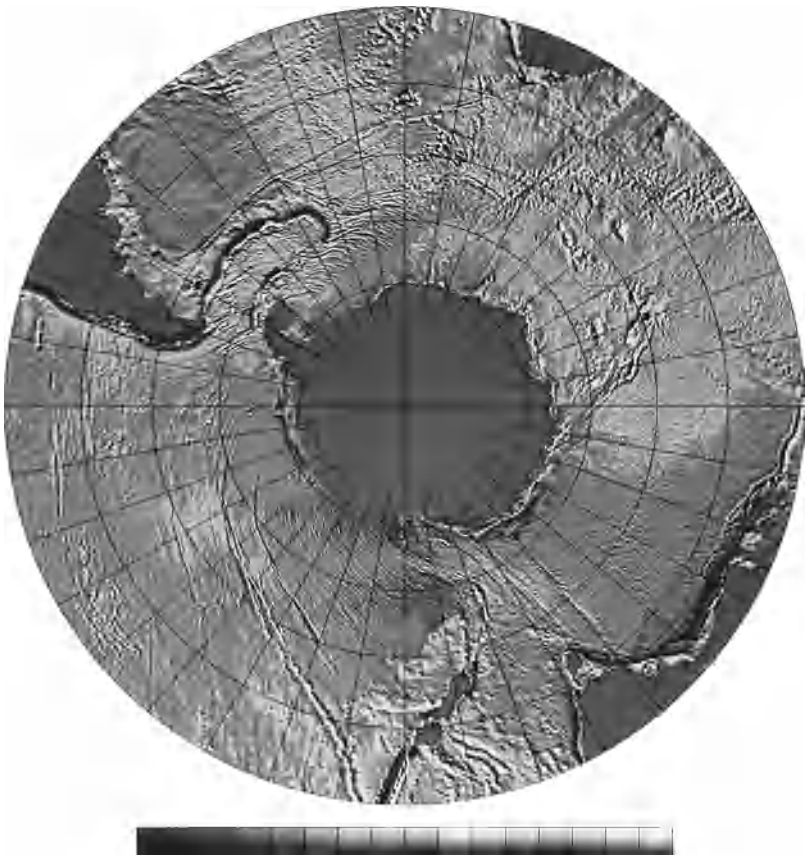

Fig. 8. Free-air gravity map of the Southern Ocean derived from analysis of *SEASAT* and *GEOSAT* altimeter data. Light areas represent positive anomalies; dark areas represent negative anomalies. Note long linear expressions of fracture zone traces. (*From W. Haxby and D. E. Hayes, The Gravity Field of the Circum-Antarctic, Antarctic Research Series, 1990, copyright by the American Geophysical Union*)

Marginal seas. The sea-floor features described so far are representative of the main ocean basins and reflect their evolution mostly through processes of plate tectonics. Other, more complicated oceanic

regions, typically found in the western Pacific, include a variety of small, marginal seas (back-arc basins) that were formed by the same general processes as the main ocean basins. These regions define a number of small plates whose interaction is also more or less governed by the normal tenets of plate tectonics. One difficulty in studying these small basins is that they are typified by only short-lived phases of evolution. Frequent changes in plate motions interrupt the process, creating tectonic overprints and a new suite of ocean-floor features. Furthermore, conventional methods of analyzing rock magnetism, heat flow, or depths of the sea floor to roughly date the underlying crust do not work well in these small regions. The small dimensions of these seas bring into play relatively large effects of nearby tectonic boundaries and render invalid key assumptions of these analytical techniques. The number of small plates that actually behave as rigid pieces is not well known, but it is probably only 10–20 for the entire world.

Exemplary Techniques

A number of advances have permitted detailed studies and detailed mapping of the sea floor. These include accurate determination of a ship's position and velocity, scanning systems, and comprehensive geophysical measurements.

Determination of ship's position and velocity. The ability to determine a ship's position and velocity is often the factor that controls the scale of features that can be mapped on the sea floor. Since the 1950s, the development of electronic navigational tools has greatly enhanced positioning capabilities. The introduction of navigational satellites (Transit Satellite System) and their availability to the research community in the mid-1960s allowed approximately 10 ship fixes to be obtained each day with an accuracy of about 0.5 km (0.3 mi) or better. This was a vast improvement over the celestial navigation and electronic systems in use at the time.

The Global Positioning System (GPS) now exists which uses a constellation of 24 satellites orbiting the Earth at high elevations. The concept involved is that at any point on the Earth's surface, three or four of these satellites would be in view at all times, thereby allowing position ranging on them. The satellites' positions are known from ground-tracking stations. The Global Positioning System provides continuous position fixing that is accurate to much better than 0.16 km (0.1 mi) [for surface vessels] and is available at all times, under all weather conditions, and over the entire surface of the Earth. This system will allow marine geologists to study effectively features on the sea floor whose horizontal dimensions are of the order of tens of meters or smaller. *See* SATELLITE NAVIGATION SYSTEMS.

Multibeam and side-scan swath systems. Since the mid-1970s very significant improvements have been made in the instruments available for investigating the sea floor and its subsurface structures. The analytical techniques that can be applied to quantitative interpretation and understanding of the key operative processes that shape the Earth have also improved. Since World War II, the conventional method of determining the depth of the ocean has been by the transmission of acoustic signal pulses from the ship to the sea floor, where they are reflected to the sea surface and detected. The elapsed travel time is measured, and either by assuming the velocity of sound in the water or by measuring it, the depths of the ocean can be determined with a relative accuracy of approximately 1 m (3.3 ft) and with an absolute accuracy of a few tens of meters. Historically, the acoustic pulses used have not been very directional, so that the sound waves that reached the sea floor were actually reflected off a fairly large area (the footprint) of the sea floor. Hence, some average depth, taken over the scale of that footprint, was measured. Interpretations of the returning echo were further complicated by the presence of side echos reflected from sea-floor features off to the side of the ship.

Today's advanced systems, generically known as multibeam echo sounders, provide marine scientists with the ability to measure the sea-floor depth with greater precision and over smaller acoustic footprints. The ability to generate an array of directed acoustic pulses, subtending 45 to 90°, across the ship's track (**Fig. 9**) provides a means for the simultaneous measurement of the ocean depths across a swath up to twice the water depth. Because the individual soundings making up this swath are fixed with respect to one another, the details of the sea-floor relief can be determined with remarkable clarity. The data can be analyzed onboard the survey ship in near-real time.

The output of multibeam echo sounders can be displayed as a bathymetric contour map centered on the ship's track (Fig. 9). Contours are generated

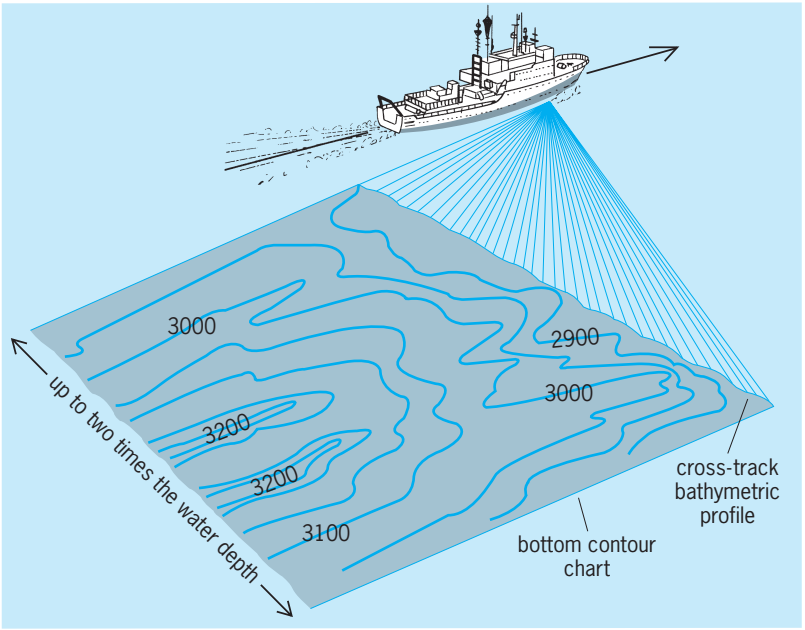

Fig. 9. A multibeam bathymetric swath mapping system. The bottom contour chart is produced on board the vessel in real time. The width of the mapped swath depends on the specific system used but can be up to two times the water depth. Contours are given in meters. 1 m = 3.3 ft. (*Krupp-Atlas Elektronik*)

continuously onboard within a few minutes of the acquisition of the soundings. If a survey is conducted so that tracks are spaced no greater than the swath width, complete sounding coverage of the sea floor is obtained, and small-scale features with bathymetric relief of a few meters can be identified and mapped over large areas in a manner not possible with the older techniques (Fig. 5). *See* ECHO SOUNDER; HYDROPHONE.

Side-scan sonars constitute a similar family of deep- or shallow-towed survey instruments. These systems emit sound at a much higher frequency than conventional single-beam or multibeam echo sounders, and the swaths can extend to several kilometers on either side of the towed instrument. The returned acoustic signals result from backscattering of the sound pulses due to variations in the small-scale roughness and to the varying reflective properties of the sea floor. Side-scan sonar instruments provide a qualitative picture of the sea floor. The near-surface texture and the planform of the sea-floor relief is recorded over a large area, but there is virtually no subsurface information measured. Side-scan instruments provide for maximum areal mapping coverage at minimal expense. The side-scan acoustic image of the sea floor is analogous to an aerial photograph or radar image of a land area. *See* ACOUSTIC SIGNAL PROCESSING; SONAR; UNDERWATER SOUND.

Comprehensive geophysical measurements. Many geophysical properties of the sea floor and its underlying materials are not very diagnostic. For example, a variety of rocks may exhibit the same seismic-wave velocity, the same magnetic properties, or the same density. Gravity variations occur because of lateral differences in the near-surface distribution of mass caused by different rock types, by different structures, and by sea-floor relief. Gravity measurements alone cannot reveal a unique causative geological feature for each observed gravity anomaly, since several different mass distributions could give rise to the same observed variations in gravitational field. But, by adopting reasonable constraints and using a general knowledge of geology and geophysical properties of the Earth, interpretations of a collection of different types of observations can be reduced to a few possibilities with geological plausibility. *See* GEOPHYSICAL EXPLORATION.

Gravity. The ability to measure small variations in the Earth's gravitational field to a few parts in a million in the presence of large disturbing accelerations due to the ship's motion requires very sophisticated instrumentation. Because the measurement of gravity is difficult and the instrumentation expensive, most ships do not carry gravimeters. Consequently, the total gravity track coverage for the entire world oceans is relatively limited.

Satellite observations have allowed the indirect measurement of subtle variations in the Earth's gravitational field over almost the entire world ocean. These variations have been important in refining knowledge about the details of plate kinematics and in identifying the presence of unknown or anomalous topographic or subsurface ocean-floor structures that were previously unknown. The satellites *SEASAT* and *GEOSAT* measure with great accuracy the distance between the satellite and the ocean

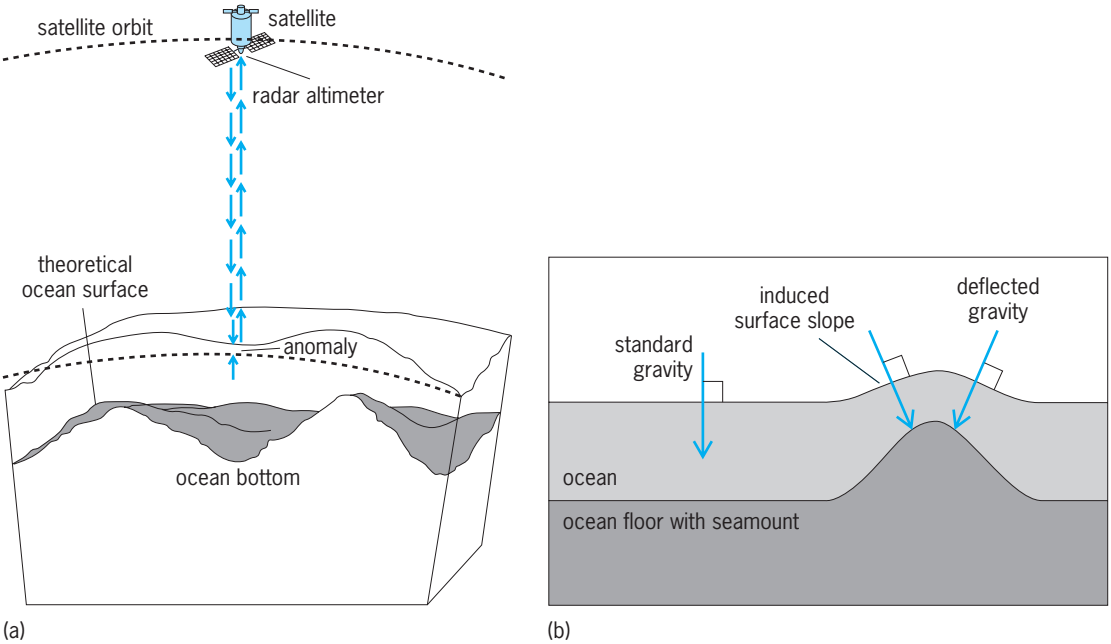

Fig. 10. Satellite-derived bathymetry. (*a*) An Earth-orbiting radar in space cannot see the ocean bottom, but it can measure ocean surface height variations induced by ocean floor topography. A mountain on the ocean floor adds to the pull of Earth's gravity and changes its direction subtly, causing extra water to pile up around the mountain. For example, a mountain on the ocean floor that is 2000 m (6600 ft) tall produces a sea surface bump only 20 cm (8 in.) tall; this is measurable from space. The ultimate resolution of this method is limited by regional ocean depth. (*b*) The tilt in the direction of gravity, called a "deflection of the vertical," is equal to the slope of the sea surface. (*After D. T. Sandwell, S. T. Gille, and W. H. F. Smith, eds., Bathymetry from Space: Oceanography, Geophysics, and Climate, Geoscience Professional Services, Bethesda, MD, June 2002, http://www.igpp.ucsd.edu/bathymetry_workshop*)

surface heights. The detailed shape of the ocean surface is in large part a response to small variations in the Earth's gravitational field. Variations of gravity over distances longer than about 30 km (18 mi) and shorter than about 2000 km (1200 mi) can be determined with a reliability of a few milligals (1 mgal $\simeq 10^{-6}$ of the Earth's average gravity value). This range scale encompasses many of the tectonic and structural and topographic features of interest in the sea floor.

Bathymetry from space. The recent novel applications of satellite altimeter measurements have led to the modeling and prediction of submarine topographic features with wavelengths of 15–2000 km (9–1240 mi). D. T. Sandwell and W. H. F. Smith have applied this analysis on a global basis. By combining this intermediate-scale (interpreted) topography with the deterministic regional topography obtained by ships equipped with echo sounders, a comprehensive model of the sea-floor topography that combines the two approaches can be generated. These model results can be stored digitally for related studies or future revisions.

The Sandwell and Smith methodology involves calculating the free-air gravity anomalies from actual measurements of sea surface undulations. This is accommodated by presuming the sea surface represents a specific gravity equipotential surface known as the geoid. Using the N-S and E-W gradients of the geoid (that is, the surface undulations mapped) the vertical gradient of the geoid can be calculated, thus providing the free-air gravity anomaly. Variations in the free-air gravity anomaly are caused in part by lateral and vertical variations of mass represented by sea-floor topography (for example, seamounts) and the variable subsurface structures associated with them (**Fig. 10**). The degree of "correlation" of free-air anomalies with topography depends greatly on the horizontal dimensions (scale) of the topographic features in question. Generally, the greater the width of the feature, the smaller the correlation between gravity and topography. The transfer functions used to "convert" gravity anomalies to predicted causative topography are dependent on the wavelengths of the features in question. The remote sensing of sea-floor features using satellite altimetry measurements constitutes a significant advance in our knowledge of small- to intermediate-scale submarine topographic relief. This advance is especially significant for the high latitude regions of the Southern Ocean (south of ~30°S) where the bathymetry mapped by conventional ship-borne echo sounders is poorly defined due to the sparseness of survey ship tracks. *See* EARTH, GRAVITY FIELD OF.

Magnetics. Measuring the variation of the magnitude of the Earth's magnetic field is a routine part of most marine survey operations. To make measurements, a simple sensor, usually a nuclear precession magnetometer, is towed several hundred yards behind the vessel. The magnetometer can provide an absolute measure of the total magnetic field strength every few seconds. The reduction and interpretation of the magnetic data can be complicated in part because the Earth's magnetic field undergoes a variety of temporal variations not directly related to the magnetic properties of the Earth's crust.

Magnetic surveys of the world ocean and their subsequent interpretations have provided perhaps the most conclusive evidence for sea-floor spreading and plate tectonics. The Earth's magnetic field is known to reverse its polarity every few hundred thousand years (although not exactly regularly). Newly formed ocean crust at the axis of the mid-oceanic ridge acts like a magnetic tape recorder of the direction and magnitude of the Earth's field at the time the volcanic rocks cool below about 500°C (930°F; the Curie temperature) [**Fig. 11**]. This has led to the creation of small systematic anomalies in the Earth's magnetic field that, when mapped, describe a series of distinctive magnetic lineations (stripes) that are oriented parallel to the axis of the mid-oceanic ridge system. Such magnetic stripes are generally symmetrically disposed about the axis of the mid-oceanic ridge and are offset across transform faults and fracture zones. Because the lineations record the variations

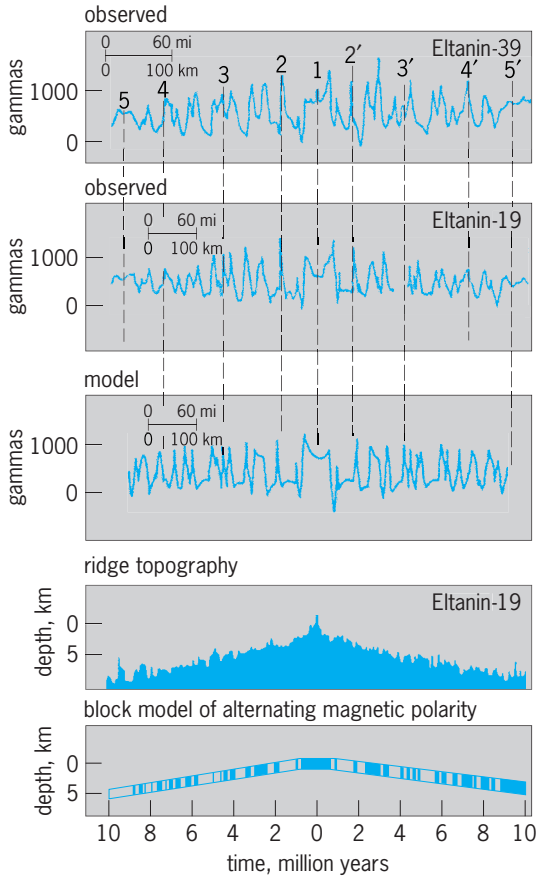

Fig. 11. Observed magnetic anomalies from two *Eltanin* cruises and ridge topography from cruise 19. The theoretical magnetic anomaly (model) computed from the simple block model of alternating magnetic polarity (near the bottom) can be easily correlated with the observed profiles. Profiles Eltanin-39 and Eltanin-19 are from areas more than 10,000 km (6000 mi) apart. Note symmetric distribution of characteristic peaks (2 and 2′, 3 and 3′, and so forth) about the ridge axis. 1 km = 0.6 mi. (*After D. E. Hayes and W. C. Pitman III, Marine geophysics and seafloor spreading in the Pacific-Antarctic area: A review, Antarc. J., 5(3):70–72, 1970*)

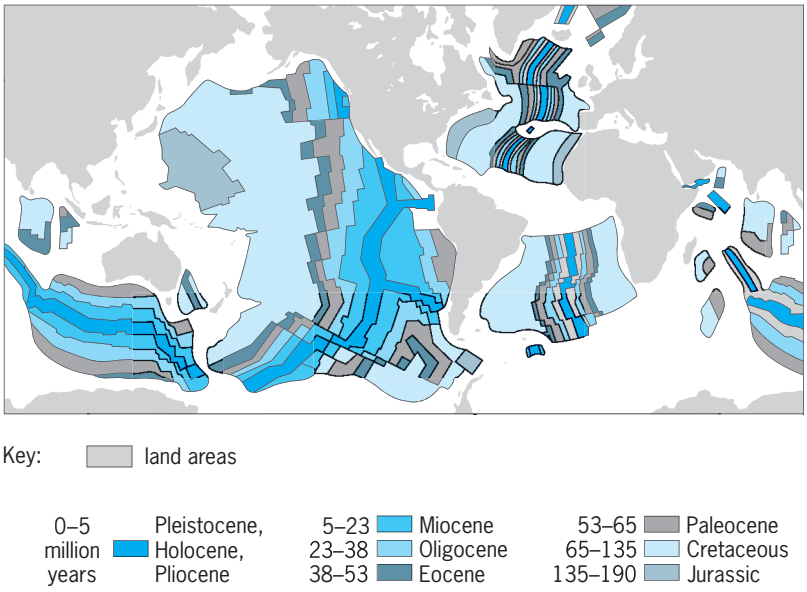

Fig. 12. Map showing age of the ocean crust based on interpretation of magnetic anomaly patterns such as shown in Fig. 10. (*After W. C. Pitman, R. L. Larson, and E. M. Herron, The age of the ocean basins, Geol. Soc. Amer. Map and Chart. Ser. MC-6, 1974*)

in the magnetic polarity of the Earth over time, a sequence of these anomalies can be used to date the formation of the anomalies. Relatively large time slices of the geological polarity history of the Earth can be distinguished from one another. The slightly different pattern of Earth polarity reversals allows the observation of magnetic anomalies to determine when in geologic time the crust underlying those magnetic anomalies was created. This technique has allowed the age of the ocean crust to be mapped on a global basis (**Fig. 12**). *See* CURIE TEMPERATURE; GEOMAGNETISM; PALEOMAGNETISM; ROCK MAGNETISM.

Heat flow. For the deep ocean basins, there are good theoretical and empirical models to account for the observed heat flow from measured geothermal gradients in the ocean sediment and crust. In general, heat flow decreases as a simple function of the age of the crust. Predictable variations in heat flow reflect the heat lost through conductive cooling since the initial time of formation of the underlying crust at the axis of the mid-oceanic ridge system. Young ocean crust is characterized by high heat flow, approximately 500 mW/m^2, whereas old (>100 m.y.) oceanic crust has heat flow that asymptotically approaches a value of about 50 mW/m^2.

In relatively young ocean crust, some heat may be transported by processes other than conduction. Global observations of heat flow suggest that for crust younger than about 40 m.y., observed heat flow often falls well below that predicted by simple conductive cooling models. Hydrothermal circulation in the uppermost parts of the crust may serve to remove significant amounts of heat, thereby resulting in artificially low values of conductive heat flow. As the crust ages and gradually becomes covered by sediments, the effective plumbing system for hydrothermal circulation, the fractured upper crust, eventually becomes sealed, thereby preempting any additional heat loss except by conduction. The amount of heat lost through hydrothermal processes is unknown and can be estimated only by comparing observations with theoretical predictions. Hence, the total integrated annual heat flow through the sea floor is still somewhat uncertain. *See* EARTH, HEAT FLOW IN.

Seismic reflection. The most commonly used technique for investigating the subsurface structure of the sea floor is seismic profiling. In principle, this technique is like depth sounding, but it involves the transmission of low-frequency acoustic energy to the sea floor and subsurface horizons. Low-frequency acoustic energy (about 10–100 Hz) is less rapidly attenuated within the sediments than the high-frequency energy of depth-sounding instruments. Hence, a portion of the outgoing acoustic signal penetrates the sea floor, eventually to be reflected to the surface at major geologic (lithologic) boundaries. Geologic materials with contrasts in density and seismic-wave velocity give rise to the seismic reflections.

Modern seismic techniques involve the recording of the reflected energy at a large number of receiver locations, fixed within a seismic streamer that is towed behind the ship (**Fig. 13**). A typical streamer may consist of 240 or more independent recording channels, equally spaced in the streamer and extending 6 km (3.6 mi) or more behind the vessel. Information from different shots fired along the track and recorded at the various receivers can be gathered

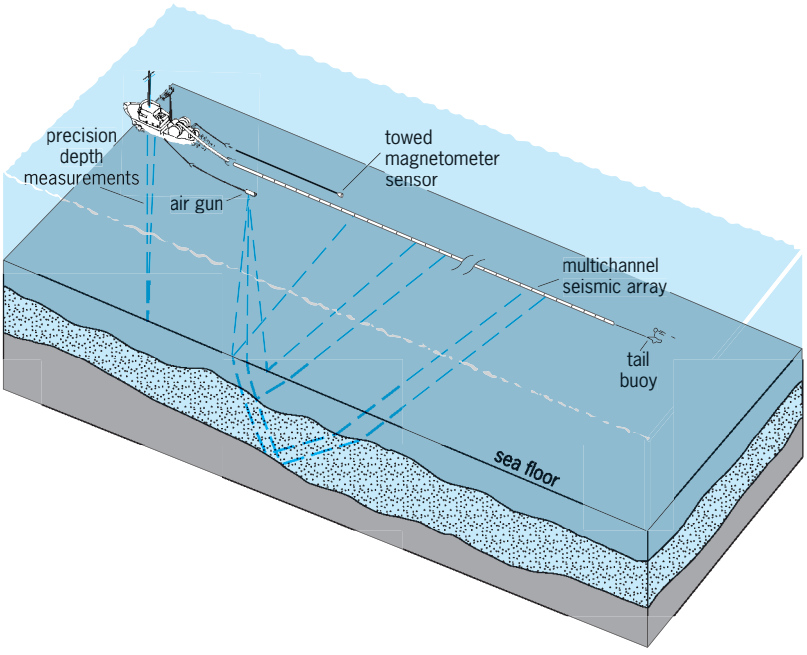

Fig. 13. Diagram of a fully equipped geophysical vessel and the subsurface geology, showing a few selected seismic-ray paths from the source (air gun) to individual sections of the receiving (multichannel seismic) array, whose length is in the range 2.5–6.0 km (1.5–3.6 mi). Precision depth measurements are made by using a high-frequency, hull-mounted single-beam transducer. The gravimeter is mounted in the ship, near its center of rotation. (*After Acquisition of Marine Surveying Technologies, United Nations Publication ST/ESA/17B*)

together by considering signals traveling through different offset distances but reflected from a subsurface common midpoint. This process is used to calculate velocity as a function of depth and to convert the reflection times of key reflecting horizons to depth. Also, by gathering, correcting, and adding the individual receiver signals (stacking), very weak or deep reflecting horizons can be detected.

The common midpoint technique is the most popular method used in offshore oil exploration. It is also used extensively for seismic imaging of the structures of the deep ocean crust and the continental margins. Subsurface structures to depths of several kilometers below the sea floor can be imaged. It is the crustal layer thicknesses, the disposition of the reflecting horizons, and the relative amplitudes of the seismic returns that allow the acoustic properties of the oceanic sediments and crust to be interpreted in terms of geological properties and of marine geological history.

Changes in the chemistry of the seawater, in bottom circulation, and in surface productivity, and impulsive sedimentation events can give rise to abrupt and dramatic changes in the sedimentary environment. Sedimentary deposits bounding such changes are usually characterized by contrasting physical properties. These contrasts in physical properties mark important events in the sedimentary history that give rise to discrete horizons that can be detected with seismic reflection techniques. Seismic techniques not only provide information regarding the total distribution of sediments but also allow correlation of key sedimentological events throughout time. Seismic horizons sampled in a small number of localities, but correlated and traced over very large regions, can be used to extrapolate limited sample results and to interpret the depositional history throughout entire ocean basins. *See* SEISMOLOGY.

Seismic exploration technology continues to produce new and better tools for imaging the sub-sea floor. The Global Positioning System (GPS) has facilitated a higher quality and better resolution of surveys.

The transition from conventional (2D) seismic surveys [Fig. 13] to 3D [**Fig. 14**] has been rapidly incorporated for use in offshore oil exploration. This precise and rapid acquisition methodology has in turn led logically to the time-dependent characterization (that is, 4D seismics) of known oil fields by seismic surveys. The availability of GPS now makes it practical to resurvey areas periodically and to reliably attribute observed differences in the images obtained to the temporal evolution of an oil field or perhaps to structural changes of an area of the sea floor following a tectonic event.

New implications of remote sensing. Ongoing studies of the sea floor and sub-sea floor involve largely the application of sophisticated remote-sensing techniques. Most notable is the use of a variety of high-frequency seismic instrumentation designed to provide higher resolution of acoustic images of the sub-sea floor. Surveys using side-scan tools now have the capacity to map the fine details of the sea floor and its shallow subsurfaces over much greater areal extent than before. Some of these tools provide deeper looks into the structure beneath the sea floor.

Similarly, the improvement of multibeam topographic swath-mapping and associated side-scan sonar has allowed detailed features of the sea floor to be mapped over extensive areas. These map results are helping scientists to discriminate between competing models of volcanism and faulting regarding the formation of the relief of the small-scale topographic features (such as abyssal hills) characteristic of mid-ocean ridges.

Paleobathymetry. Scientists are giving more attention to the importance of sea-floor relief in controlling the pathways of both shallow- and deep-ocean circulation. This circulation largely governs the meridional exchange of heat, which affects the pattern of global climate. With the advent of digital data files for bathymetry, crustal age, and sediment thickness, it is now possible to analyze the third dimension

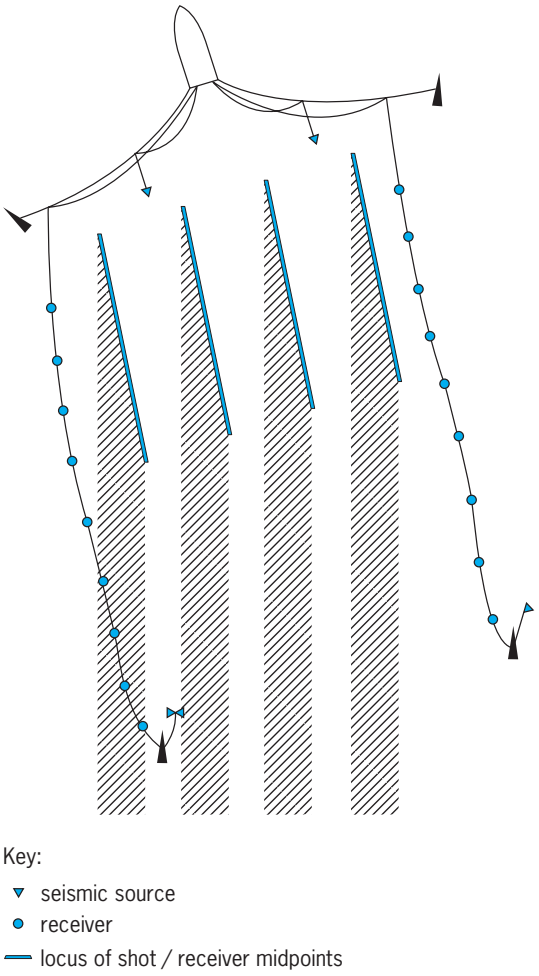

Fig. 14. Seismic profiling using four source arrays and two streamers (*courtesy of Western Geophysical*); hachured areas represent zones of the sea floor "swept over" by lines of shot/receiver midpoints, thereby creating an effective three-dimensional seismic reflection survey. (*E. J. W. Jones, Marine Geophysics, Wiley, 1999*)

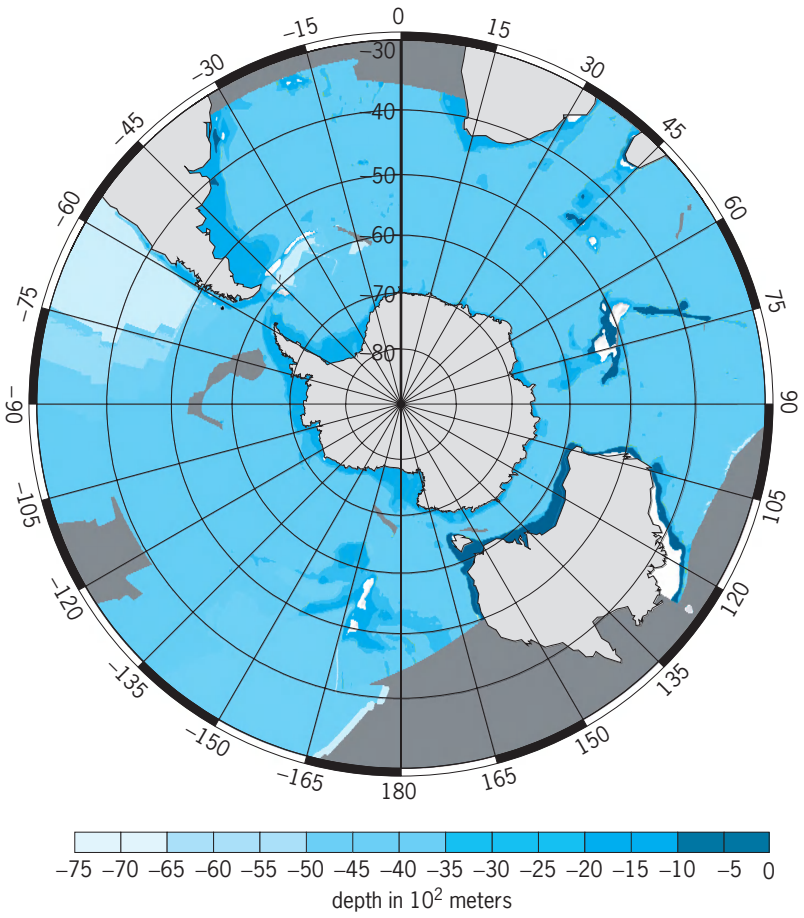

Fig. 15. Paleobathymetry of the circum-Antarctic at 50 m.y. Selected isobaths (in meters) are color-coded. Note the presence of major ocean circulation barriers between Australia and Antarctica, between Cape Horn and the Antarctic Peninsula, and between Antarctica and the Kerguelen Plateau. (*Dennis E. Hayes, Paleobathymetry of the Circum-Antarctic, in prep.*)

of plate reconstructions—paleobathymetry. Such reconstructions reveal the evolution of ridges, basins, and gateways and suggest their influences on variable paleoclimates. For example, although the Antarctic continent was located in a high-latitude position at least for the last 200 m.y., it has only been covered with ice for only about the last 35 m.y. The changing bathymetry of the circum-Antarctic must have played a profound role in modulating the climate in Antarctica and beyond (**Fig. 15**).

Sampling. The ability to sample reflecting horizons, especially deep horizons, is limited. Standard piston cores recover only the 10–20 m (30–60 ft) of the near-surface sediment. Several thousand piston cores have been taken from the world ocean floor. In order to sample horizons lying deep beneath the sea floor, drilling/coring techniques must be used. The initial drilling program began in 1968 as the Deep Sea Drilling Project (DSDP), which transitioned in 1984 into the IPOD (International Phase of Ocean Drilling Program). The most recent phase of cooperative marine geological drilling in the deep sea floor is the Integrated Ocean Drilling Program (IODP). It continues with the goals of solving key problems of Earth science that are best (perhaps only) addressed by direct deep sampling of the sub-sea floor using drilling. The IODP uses a dynamically positioned drilling vessel (the *JOIDES Resolution*) to drill into and sample the sediments and crystalline rock lying as much as 2000 m (6000 ft) below the sea floor.

Over 35 years of international collaborative research is attributable to the ocean drilling program. Since its inception, nearly 800 sites and more than 1700 holes have been drilled. They provide the only direct sampling of the deep sediments and basement rocks that compose the sea floor. These drilling sites have led to breakthrough findings, including evidence of the nature and pattern of paleoclimate change, confirmation of the Earth's paleomagnetic reversal time scale to ~200 mybp, the composition of the upper oceanic crust, the history of deep-sea sedimentation, the nature of past ocean circulation, hydrothermal processes at mid-ocean ridges and within the accretionary sediment wedges associated with subduction, and many others.

The principal difference in the new IPOD phase of the program will be the incorporation of more than one drilling platform. The most dramatic addition will be the Japanese vessel, *CHIKYU* [over 200 m (650 ft) long], that will be capable of riser drilling. Riser drilling includes the ability to "seal off" the drill hole if dangerous conditions are encountered. Riser drilling capability opens up a variety of new target areas previously considered unsafe to drill because of the possibility of unstable sub-sea-floor conditions (such as hydrocarbons or other fluids/gases under high pressure).

The next decade of research will see the implementation of "semipermanent" undersea observatories designed to make *in-situ*, real-time measurements of chemical, biological, and geophysical parameters relevant to sea-floor processes and phenomena. One specific example, the "Neptune Project," will focus on monitoring the activities on and around the Juan de Fuca Plate, offshore NE Pacific Ocean. The proposed network will include ~3000 km (2000 mi) of data and power cables laid on the sea floor which will service some 50 experimental sites through nodes onto the main cable network. Unmanned underwater vehicles will traverse the areas between experiment sites, and can be "repowered" from the cable nodes. They can also be deployed automatically or on command to sites of volcanic or tectonic events, relaying information to shore in real-time via direct links to the internet and facilitating control activities from shore-based labs. *See* UNDERWATER VEHICLES.

The long-term unmanned sea-floor observatories, judiciously deployed in geologically active seafloor regions, will mark one important new approach to marine geological research in the coming decades.

Dennis E. Hayes

Bibliography. C. Emiliani (ed.), *The Sea,* vol. 7: *The Oceanic Lithosphere*, 1981; B. C. Heezen and C. D. Hollister, *The Face of the Deep*, 1971; J. Kennett, *Marine Geology*, 1982; E. Seibold and W. H. Berger, *The Sea Floor: An Introduction to Marine Geology*, 3d ed., 1996.

Marine machinery

All machinery installed on waterborne craft, including engines, transmissions, shafting, propulsors, generators, motors, pumps, compressors, blowers, eductors, centrifuges, boilers and other heat exchangers, winches, cranes, steering gear, and associated piping, tanks, wiring, and controls, used for propulsion, for ship services, and for cargo, trade, or mission services.

Practically all marine machinery elements have nonmarine counterparts; in some cases, the latter were developed from marine applications, while in other cases specific equipment was "marinized." For marine service, machinery may have to meet higher standards of reliability and greater demands for weight and volume reduction and access for maintenance. Marine machinery must be capable of withstanding the marine environment, which tends toward extreme ambient conditions, high humidity, sea-water corrosion, vibration, sea motions, shock, variable demand, and fluctuating support services. Even higher standards may apply for warship machinery. To improve system reliability, essential equipment may be fitted in duplicate or provided with duplicated or alternative support or control systems, while nonessential equipment may be fitted with bypasses, to permit continued operation of a system following a component failure. Isolation valves or circuit breakers are common, enabling immediate repair.

Machinery on modern ships is highly automated, with propulsion usually directly controlled from the wheelhouse, and auxiliary machinery centrally controlled from an air-conditioned, sound-proofed control room, usually in the engine room. In the typical modern merchant ship (but not in passenger ships), the machinery operates automatically, and the controls are unattended at sea, with engineers called out by alarm in the event of malfunctions.

Propulsion Machinery

Propulsion machinery comprises an engine, usually a diesel engine, steam turbine, or gas turbine, with required gearing or other transmission system, and, for steam plants, steam generators. *See* BOAT PROPULSION; MARINE BOILER; MARINE ENGINE; PROPELLER (MARINE CRAFT); SHIP NUCLEAR PROPULSION.

Shafting. Shafting (**Fig. 1**) is of steel, usually solid for fixed-pitch propellers. In modern practice, the propeller is fitted to a matched taper on the propeller shaft by a hydraulic press fit, without a key, since a keyway would be a source of stress concentrations. Shafting sections are flanged and bolted together. For controllable-pitch propellers, the shaft is hollow to accommodate the hydraulic or mechanical linkage, and the propeller is bolted to an outboard flange on the propeller shaft. Because the propeller shaft must then be withdrawn outboard, the inboard connection to the remaining shafting is usually made by a removable sleeve coupling. In modern commercial practice, all bearings, including those in the stern tube, are oil-lubricated, with special seals at both ends of the stern tube; but in many applications, including warships, the stern-tube bearings have nonmetallic linings and are lubricated by water allowed to leak in around the shaft. *See* ANTIFRICTION BEARING; MACHINE KEY.

Shafting is subject to large cyclic variations in load induced by the propeller and, in diesel plants, by the engines. An important consideration in shafting design is to prevent resonant frequencies of the shafting from coinciding with these cyclic variations, within the operating range of shaft speeds.

Thrust bearing. The thrust developed by the propeller is transmitted through the shafting to the hull via a thrust bearing, comprising a collar on the shaft (Fig. 1) and a stationary housing mounted on a substantial foundation integral with the hull structure. For low-speed diesel engines, which are directly coupled to the shaft, the thrust bearing is built into the engine at its after end. In geared installations the bearing may be separate from or integral with the gear case, and forward or aft of the gear. Except in the lowest-powered installations, the bearings are of the pivoted-shoe, oil-lubricated type.

Auxiliary Machinery

In all but the smallest boats, the propulsion machinery is but part of an integrated power plant, which includes auxiliary machinery for propulsion-engine support and other ship services.

Electric generating plant. The electric power required for all continuous or recurring purposes on a ship is about 5% of the propulsion power, when restricted to the supply of motor-driven auxiliaries, lighting, other hotel services including high-voltage alternating current and provision refrigeration, communication, navigation, and control equipment of simple cargo ships. Much higher percentages are required when such services as cargo refrigeration or cargo hold ventilation are provided. On passenger ships the electric load can rival or exceed the propulsion power. Peak power demand may occur intermittently if motor-driven thrusters are fitted for maneuvering.

Ocean-going ships are required to have a minimum of two generators, with either one capable of supporting the essential electrical load, but most ships have at least three in order to improve ship reliability. A ship with a high electrical load may have three or more generators, with two or more operated in parallel to support the load. In addition, most ships are required to have a separate emergency source, usually a diesel generator, located outside the engine room, for emergency lighting, communication, navigation and control services, fire fighting, and often, steering.

Power from the generators is distributed to motors, lighting, and other consumers through switchboards and distribution boards.

On steamships, at least one of the generators, acting as the normal electricity source, is driven by an independent turbine supplied with steam from the same source as the propulsion turbines, and at least one will be a diesel generator. Most diesel-driven

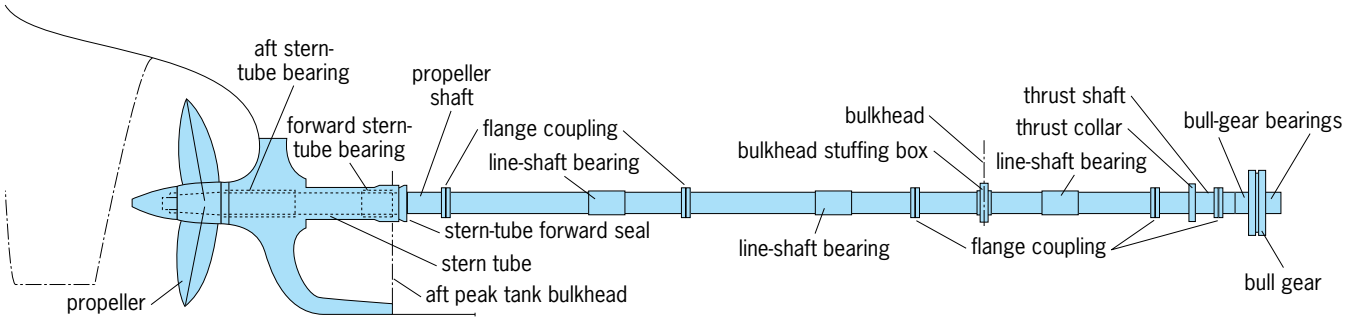

Fig. 1. Propeller shafting for a single-screw merchant ship. (*After R. L. Harrington, ed., Marine Engineering, Society of Naval Architects and Marine Engineers, 1992*)

ships have diesel generators, as do many gas turbine–driven ships, although others have gas turbogenerators. Many ships are fitted with a generator driven from the propulsion gearing or shafting as the normal electricity source. In many high-powered diesel-engine ships, sufficient waste heat can be recovered by an exhaust gas boiler to support a steam turbine, adequate for the normal load. Ships with alternating-current electric drive may take power for ship services from the propulsion generator. *See* DIESEL ENGINE; GAS TURBINE; GENERATOR; STEAM TURBINE.

Fuel systems. Generally, fuel is bunkered into tanks dispersed through the hull of a ship, using centrally controlled piping, and brought daily to settling tanks in or near the engine room by motor-driven transfer pumps, usually located in the engine room and using the same piping. Fuel systems are most complex on merchant ships with diesel engines, burning heavy fuel oil. On these ships, the fuel is heated in the tanks to facilitate pumping, then kept hot in the settlers to encourage the settling, by gravity, of water and solids. After further heating, settled fuel is passed through centrifugal separators to a day tank, from which it is supplied by motor-driven service pumps, through final heaters and fine filters, to the engine. The heating is done by steam in immersed coils in the tanks and in shell-and-tube or plate heat exchangers. In parallel with the heavy fuel system is an abbreviated diesel fuel system supplying the generator engines and package boiler if these are not run on heavy fuel, and supplying the propulsion engine when necessary. The diesel fuel is not heated but is pumped to a settling tank, a centrifugal separator, a day tank, and filters.

For ships using diesel fuel only, fuel heating is usually unnecessary and the system is simplified. Smaller plants are often not fitted with centrifugal separators, eliminating the need for a separate day tank. On steamships burning residual fuel, the fuel must be heated in the tanks, but is not centrifuged, so that the service pumps draw fuel directly from the settling tanks for supply to the burners via heaters and a fine strainer. *See* CENTRIFUGATION; DISPLACEMENT PUMP; HEAT EXCHANGER; PUMPING MACHINERY.

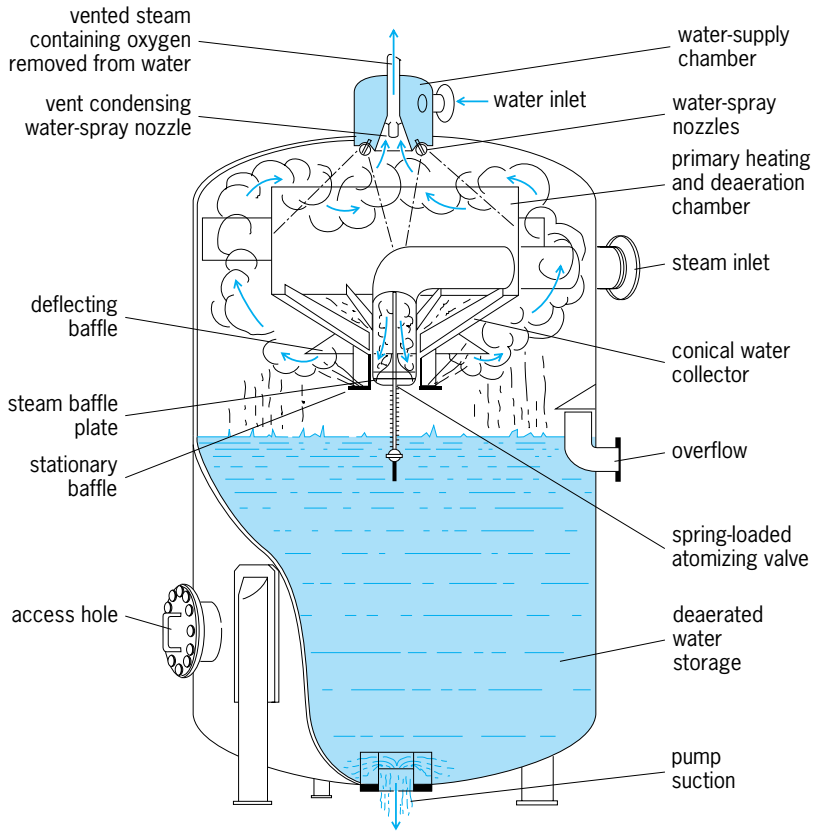

Fig. 2. Deaerating feed heater. (*After R. L. Harrington, ed., Marine Engineering, Society of Naval Architects and Marine Engineers, 1992*)

Steam and feedwater systems. On steamships, superheated steam passes to the propulsion turbine and to the turbogenerator, then exhausts to the condenser, a shell-and-tube heat exchanger, which is cooled by seawater inside the tubes. The condenser is maintained under a vacuum, usually 5 kilopascals (1.5 in. Hg), by air ejectors to extend the useful range of energy recovery from the steam. Condensate is drawn from the condenser by motor-driven condensate pumps and discharged through one or more shell-and-tube heaters, each heated regeneratively by steam extracted from the propulsion turbine, to a deaerating feed tank. *See* STEAM CONDENSER; VAPOR CONDENSER.

The deaerating feed tank (**Fig. 2**) uses extraction steam to heat the condensate, now called feedwater, to saturation temperatures, at which air and other noncondensable gases approach insolubility and can be vented from the system. This tank is also a surge

tank to accommodate differences in total volume of water and steam in the system as the ship is maneuvered. The deaerating feed tank distinguishes the marine steam plant from shoreside steam plants, which are not routinely subject to large load changes, where deaeration and limited surge can be achieved in a large condenser drainwell, not feasible aboard ship because of limited depth below the condenser. The deaerating feed tank is usually located high in the ship to provide a static head at the feedwater pumps, thereby preventing the hot feedwater from flashing to steam. On warships where this location is considered too vulnerable, the tank is lower, and feed booster pumps substitute for the static head. *See* BOILER FEEDWATER.

Feed pumps are usually multistage centrifugal pumps directly driven by compact steam turbines. For boilers fitted with economizers, the feedwater passes directly to the economizer, but when air heaters are fitted the feedwater passes through one or more shell-and-tube, high-pressure heaters, heated regeneratively by steam extracted from the propulsion turbine. *See* AIR HEATER; BOILER ECONOMIZER.

Often the turbogenerator has its own condenser and condensate pump. Sometimes the turbogenerator exhausts to the deaerating feed tank via an auxiliary exhaust line.

Steam for some auxiliary services, such as for fuel heating and the distilling plant, is supplied from turbine extractions as the most efficient source. Steam for the feed-pump turbine is taken from the superheated steam line, in some cases directly, but more frequently via a desuperheater. All exhaust steam and all drains are collected to appropriate points in the cycle to recover the heat and the water.

Steam systems on diesel-powered ships usually comprise a waste-heat boiler in the main engine uptake, in parallel with an oil-fired package boiler. Unless heat recovery is to be maximized, as when a waste-heat turbogenerator is fitted, the steam generated is saturated and is sufficient for fuel heating and other needs. Condensate is collected in a tank for return to the boiler via a motor-driven feed pump.

On tankers, steam may be used for cargo pumps and for heating of the cargo. On steamships the cargo-pump turbines are supplied from the propulsion boilers directly, but to avoid contamination the cargo-heating steam may be supplied indirectly from a steam-to-steam heat exchanger. On diesel-powered tankers, large auxiliary, oil-fired boilers may be used for these services. On ships with no heating requirements for fuel, a low-pressure package boiler may be fitted or an alternative heating plant may be provided.

Water-cooling systems. For steamships, very large quantities of seawater are required for the condensers. The seawater can be pumped through the condenser by large motor-driven centrifugal pumps, or induced to flow by pressure differences across the hull, which may have to be augmented or even created by a protruding lip at the outlet. Other cooling requirements, such as those for lubricating-oil coolers and refrigeration condensers, are also met with seawater, directly or via an intermediate heat exchanger that cools freshwater for circulation to the auxiliaries. *See* CENTRIFUGAL PUMP.

Except for the smallest engines, diesel-engine jackets are fresh-water-cooled in closed circuit, with the fresh water cooled in turn by seawater in a heat exchanger. Engine lubricating-oil coolers and aftercoolers and other auxiliaries may be circulated with seawater directly or via an intermediate freshwater loop. Cooling for gas turbines is largely internal, and cooling-water requirements are limited to lubricating-oil coolers for the engine and its reduction gear, and to the auxiliary machinery.

Seawater and fresh water are circulated by centrifugal pumps, usually motor-driven, but often driven from the engine they serve. Heat exchangers of both shell-and-tube type and plate type are used. The selection of materials for equipment that handles seawater is critical, tending toward bronze pumps with stainless-steel impellers, and nonferrous or plastic-lined piping and heat-exchanger waterboxes. Heat-exchanger tubes are usually copper-nickel, but titanium has been used in naval applications. Plate-type heat exchangers are usually fitted with stainless steel or titanium plates.

Lubricating-oil systems. The most complex systems are those on merchant ships burning heavy fuel in diesel engines. In general, large engines are operated with a dry crankcase, the oil draining to a sump tank below the engine, usually built into the double bottom. The oil is drawn from the sump by circulating pumps, which discharge through a cooler and a fine filter to bearings, pistons (if oil-cooled), camshaft, governor, and valve gear, from which the oil drains to the sump. Each engine has its own lubricating-oil system. Oil is drawn continuously to a centrifugal separator via a heater and then returned to the sump. Low-speed engines are fitted with a separate cylinder lubrication system, storing and supplying a high-viscosity oil of injection directly into the cylinders, where it lubricates the piston rings and cylinder liners before it burns. In trunk-piston engines, some of the circulating oil is used for this purpose.

Reduction gearing is usually fitted with an independent sump, circulating pumps, filter, and cooler. Steam-turbine bearings are supplied from the same system that serves the reduction gear, but gas turbines usually use a different grade of oil and require separate pumps, coolers, and filters. Turbines and connected gearing, which unlike diesels cannot be brought to an immediate stop following an oil failure, are fitted with a gravity tank or other means of maintaining oil flow in an emergency.

Stern tubes, line-shaft bearings, air compressors, auxiliary steam turbines, and some other auxiliaries may use the same grade of oil as the reduction gear on ships with turbines or medium- or high-speed diesel engines, or the same oil as the bearings of low-speed engines. However, diesel generators and refrigeration compressors each require a different grade of

oil. Storage tanks of adequate capacity for several voyages must be provided for each grade of oil, as well as settling tanks for used oils that can be renovated onboard by settling and centrifuging, and used-oil storage tanks and a transfer pump for oils that must be discharged ashore after use.

Lubricating-oil pumps are most often motor-driven rotary types, but centrifugal pumps are occasionally used. Some medium- and high-speed diesel engines are arranged to drive their own oil pumps, as are some reduction gears. Oil coolers may be shell-and-tube or plate type.

Compressed-air systems. Each of these systems comprises one or more motor-driven air compressors and one or more receivers. Most diesel propulsion and auxiliary engines and many gas turbines are started by using compressed air which, because of the volume required, is stored at medium or high pressures, typically 3 megapascals (435 lb/in.^{2}) or higher. Air for miscellaneous services, such as for operating pneumatic hoists and tools, for recharging accumulators, and for supplying pneumatic controls, is usually stored at about 700 kilopascals (100 lb/in.^{2}). The air for pneumatic controls is usually separately compressed and stored, and passed to services via a dryer. Compressors are usually motor-driven reciprocating units, but other types have been used for low-pressure service. *See* COMPRESSOR.

Distilling plants. Fresh water is required for making up losses in steam systems and freshwater cooling circuits, as well as for drinking, washing, and cooking. Most modern ships also use freshwater for toilet flushing. Other ships, such as chemical tankers, require fresh water for cleaning of cargo tanks. In short voyages and in journeys on lakes and rivers, some of these needs might be met by taking water from shore, but most ocean-going ships generate their own freshwater from seawater. Steamships generally use multistage, low-pressure evaporators, heated by steam extracted from the turbine. Diesel-powered ships generally have single-stage evaporators heated by engine cooling water. Gas turbine ships with diesel generators may use the diesel cooling water or steam produced in a waste-heat boiler or an oil-fired package boiler. Alternatives to low-pressure evaporators are vapor-compression plants and reverse-osmosis units. High-pressure evaporators are generally obsolete because of seawater scaling. *See* DISTILLATION.

Bilge and ballast systems. Bilge systems consist of pumps, sometimes assisted by eductors, to remove water and other accumulated liquids from the engine room and other compartments in the ship, other than oil tanks. Where bilge water may be contaminated by oil, it is first pumped to a holding tank and discharged overboard slowly through an oil-and-water separator. Ballast systems comprise the pumps and piping used to fill and empty ballast tanks. (Ballast tanks are filled to improve the trim or stability of a ship which is not carrying cargo.) To reduce pollution, past practices of filling empty fuel and cargo tanks with ballast are no longer allowed. Bilge and ballast pumps are usually motor-driven centrifugal pumps, although steam-reciprocating pumps are sometimes fitted for bilge service, while tanker ballast pumps are often steam-turbine-driven centrifugal units. In smaller plants the bilge pump may be driven via a clutch from the propulsion engine, and may double as a fire pump.

Fire-fighting and inert-gas systems. In addition to portable extinguishers, a ship will be fitted with at least two centrifugal seawater pumps and a fire main to supply hose connections and sprinklers throughout the ship. Fire pumps are usually motor-driven, but in smaller plants a fire pump may be driven via a clutch from the propulsion engine and may double as a bilge pump. Most ships are required to have an emergency fire pump in a separate compartment, driven from the emergency generator or by an independent diesel engine. A separate system is fitted for smothering fires in machinery spaces and dry cargo holds, most often using bottled carbon dioxide and piping for gas distribution. On tankers and other ships with flammable liquid cargoes, a foam system is installed, with tanks of foam concentrate to be injected into seawater from the fire pumps and distributed via nozzles and monitors.

On oil tankers, the space above the cargo in the tanks, or the whole tank when empty, is kept full of inert gas. Most often, the inert gas is boiler exhaust gas, passed through a seawater spray to remove sulfur and then blown into the tanks, but on tankers without boilers of adequate size an oil-burning inert-gas generator is fitted.

Refrigeration, heating, and ventilation. Refrigeration for provisions and air conditioning is generally provided by vapor-compression units, each consisting of a motor-driven compressor and a water-cooled condenser. The halogenated hydrocarbon refrigerants are being replaced by partially chlorinated refrigerants, which have lower ozone-depletion potentials, or by ammonia, previously considered obsolete. In systems suitable for most merchant ships, the refrigerant is expanded directly in evaporator coils in the provision store rooms or in the air-conditioning ducts; but for larger, more distributed systems, as on passenger ships, refrigerated-cargo ships, and fishing boats, an intermediate refrigerant, usually brine, is circulated through piping to the coils. *See* MARINE REFRIGERATION.

Much refrigerated cargo is containerized, with each container equipped with its own motor-driven vapor-compression unit. Ships intended to carry such cargo have increased electrical generating capacity, sockets at the container locations, and increased ventilation capacity for containers carried below deck. *See* MARINE CONTAINERS.

Heating for air conditioning is usually by steam or electric coils in the ducts, supplemented by local convectors. Ventilation systems on all ships are extensive, using motor-driven fans to force airflow through machinery, accommodation, and work spaces, and through cargo areas when appropriate, such as the enclosed vehicle decks of ferries and roll-on/roll-off ships. *See* AIR CONDITIONING; COMFORT HEATING; VENTILATION.

Sewage treatment plants. Overboard discharge of raw sewage is no longer permitted, and craft for which holding tanks are impractical must be fitted with treatment plants. Most installations are of the biological type. In order to reduce the volume of sewage to be treated, clean drains from wash basins and showers are passed directly overboard. Further reductions can be made by using vacuum-flush systems, which are common on ships with large complements or with passenger accommodation. *See* SEWAGE TREATMENT.

Incinerators. Garbage can no longer be dumped overboard, and most ships are therefore fitted with incinerators, most of which burn the garbage in a diesel oil-fired furnace. Most incinerators are equipped to burn used oil and sludge collected at the centrifugal fuel and lubricating-oil separators.

Deck Machinery

This machinery is more appropriately described as hull machinery, as it could encompass all machinery outside the engine room, including much of that cited above as auxiliary machinery. Much of the machinery described below is hydraulic. Such machinery is driven by electrohydraulic power packs, centered about a motor-driven hydraulic pump which supplies fluid under sufficient pressure to operate the rams or rotating hydraulic motors. Direct electric drive is also common, but steam-driven deck machinery is rarely found on modern ships.

Steering machinery. Except for those of the smallest craft, rudders are turned by hydraulic power, usually rams operating directly on the rudder stock. The rams are under command of a telemotor, which transmits the motion of the manually operated steering wheel or lever in the wheelhouse, or signals from the automatic pilot. In general, steering machinery incorporates redundant systems and emergency controls. *See* SHIP POWERING, MANEUVERING, AND SEAKEEPING.

Windlasses, capstans, and mooring winches. A windlass is a power-driven sprocket, permanently meshed to the anchor chain, used to raise the anchor; it is equipped with a brake to allow the anchor to be dropped in an orderly fashion. Capstans are vertical, power-driven drums around which wire or rope lines may be wrapped to assist in pulling and hoisting tasks. Mooring winches are power-driven horizontal spools, equipped with brakes, on which the wire or rope line for securing the craft to a dock is stored, and which are used to pay out the line and draw it taut as required. Some mooring winches are automatic, able to maintain a constant tension in the line. Most mooring winches are fitted with an auxiliary drum, called a warping or gypsy head, which is used like a horizontal capstan to assist in handling loose lines.

Derricks and cranes. These are fitted for cargo handling and utility services on many types of ships, and may range from a boom pivoted at the base of a mast, used in conjunction with winches, to swiveling jib cranes with self-contained hoisting, luffing, and slewing drives, operated from an enclosed cab (**Fig. 3**).

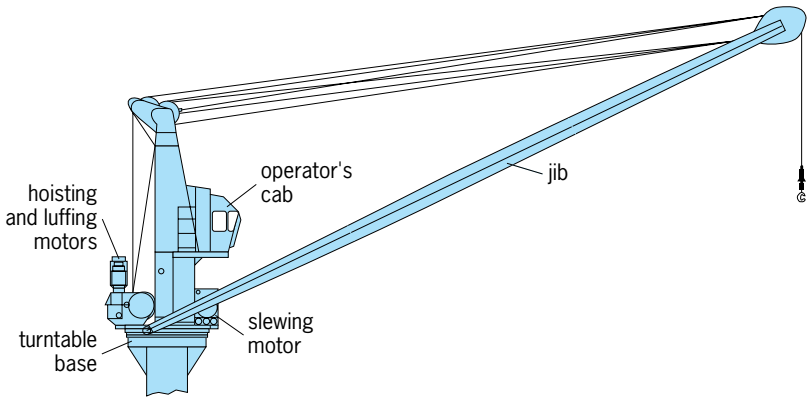

Fig. 3. General-purpose deck crane. (*After D. A. Taylor, Introduction to Marine Engineering, 2d ed., Butterworth, 1990*)

Power may be direct-electric or electrohydraulic. *See* DERRICK; HOISTING MACHINES.

Boats, including lifeboats, are usually handled by davits, which are pairs of dedicated cranes that enable a loaded boat to be lowered safely to the surface of the sea. Specialized lifeboats, called free-fall lifeboats, are designed to be launched, fully loaded, from inclined ramps built onto a ship's superstructure.

Access and overhauling equipment. Apart from cargo handling, most ships are designed with carefully considered provisions to facilitate moving stores, garbage, and equipment on and off the ship and about the ship to locations such as workshops. These provisions include stores cranes, hatches or bolted plates, vertical trunks, side ports, monorails with trolleys, ramps for hand trucks or battery-powered forklift trucks, elevators, and strategically located pad eyes. Naval vessels are usually equipped with specialized equipment for underway replenishment of fuel, provisions, ammunition, and spares.

Cargo pumping systems. These systems are installed in tankers and other ships carrying liquid cargo. In a large oil tanker, centrifugal pumps are located at the bottom of a pump room, which is located forward of the engine room bulkhead and extends the full height of the hull. The pumps are usually driven by steam turbines, but in some tankers by electric motors located in the engine room, with the shafts penetrating the bulkhead. The pumps are used to discharge the cargo, via mains with branches from each cargo tank, to flanged connections amidships, at both sides of the main deck, where hoses from the shore can be attached. During discharge, some of the oil is recirculated to tank cleaning machines, which spray it in a pattern to wash residue to the bottom of the tanks. At all times the space above the oil is kept full of inert gas. Stripping eductors, driven by the oil discharged from the pumps, are used to remove the last of the oil from the tanks. The ship is loaded through the same piping, with the oil under pressure from pumps ashore. All valves in the system are remotely controlled from a console in a cargo control room.

Some tankers, generally carriers of refined products or chemicals, have no pump room, but use individual pumps submerged at the bottom of each tank. These pumps may be driven by motors on deck via long shafts, or by hydraulic motors submerged in the tanks with the pumps.

Stabilizers. Many types of ships are fitted with these units, including warships and passenger ships, intended to reduce the rolling motions of the ship by generating a moment to oppose the roll. Fin stabilizers are short, swiveling, streamlined blades which protrude from both sides of the hull, pivoted by hydraulic actuators controlled by a gyroscope. They may retract or fold back against the hull, or they may protrude at all times. Tank stabilizers are pairs of tanks, one on each side of the ship, which are kept half full of water and connected by a large pipe through which water is transferred. They may be passive, relying on gravity to transfer the water as the ship rolls, or active, using a gyroscope-controlled pump or compressed air.

Thrusters. All types of ships are fitted with these units, usually at the bow but often at the stern as well, which function as maneuvering aids by providing a transverse thrust on command. The most common arrangement uses a propeller mounted in a transverse tunnel through the hull, driven by bevel gearing from an electric motor or diesel engine. Other thruster types, which may be rotated, are used for special applications, including dynamically positioned ships.

Alan L. Rowen

Bibliography. R. L. Harrington (ed.), *Marine Engineering*, 1992; E. C. Hunt (ed.), *Modern Marine Engineer's Manual*, vol. 2, 2d ed., 1990; A. B. Neild, Jr. (ed.), *Modern Marine Engineer's Manual*, vol. 1, 2d ed., 1965; D. W. Smith, *Marine Auxiliary Machinery,* 1983; D. A. Taylor, *Introduction to Marine Engineering*, 2d ed., 1990.

Marine microbiology

An independent discipline applying the principles and methods of general microbiology to research in marine biology and biogeochemistry. Dealing, by definition, with organisms of microscopic dimensions, marine microbiology focuses primarily on prokaryotic organisms, mainly bacteria.

Every cubic centimeter (0.06) of seawater contains about 1000–100,000 bacteria, and this to 1 million or more in nutrient-rich inshore waters. Because of their small size and easy dispersability, bacteria are virtually ubiquitous in the marine environment. Furthermore, natural populations of marine bacteria comprise a large variety of physiological types, can survive long periods of starvation, and are able to start their metabolic activity as soon as a substrate (food or growth-limiting nutrient) becomes available. As a result, the marine environment, similar to soil, possesses the potential of a large variety of microbial processes that degrade (heterotrophy) but also produce (autotrophy) organic matter. Considering the fact that the marine environment represents about 99% of the biosphere, marine microbial transformations are of tremendous global importance. If the deep sea is defined as waters below 1000 m (0.62 mi), this area still comprises 75% of the global biosphere, with temperatures of 2–4°C (34–39°F), total darkness, and high hydrostatic pressures. *See* BIOSPHERE.

Heterotrophic transformations. Quantitatively, the most important role of microorganisms in the marine environment is heterotrophic decomposition and remineralization of organic matter. It is estimated that about 95% of the photosynthetically produced organic matter is recycled in the upper 300–400 m (1000–1300 ft) of water, while the remaining 5%, largely particulate matter, is further decomposed during sedimentation. Only about 1% of the total organic matter produced in surface waters arrives at the deep-sea floor in particulate form. In other words, the major source of energy and carbon for all marine heterotrophic organisms is distributed over the huge volume of pelagic water mass with an average depth of about 3800 m (2.5 mi). In this highly dilute medium, particulate organic matter is partly replenished from dissolved organic carbon by microbial growth, the so-called microbial loop.

The rate of heterotrophic microbial decomposition of organic matter is primarily affected by three factors: nutrient concentration, temperature, and pressure. As a low-nutrient medium, seawater offers a growth advantage to bacterial populations that are characterized by high enzymatic affinities for their particular growth substrates. Morphological structures, such as increased surface area or stalks and organelles for the attachment of cells to solid surfaces, are other means of coping with the low-nutrient environment. Below depths of 300–400 m (1000–1300 ft) the temperature is uniformly in the range of 2–4°C (34–39°F), furthering growth, and hence creating a predominance of low-temperature-adapted or psychrophilic microorganisms. While most surface-born mesophilic bacteria grow optimally within a range of 20–35°C (68–95°F), marine psychrophilic bacteria have growth optima of 8–16°C (46–61°F), and they are commonly killed at temperatures above 20°C (68°F). *See* SEAWATER.

Hydrostatic pressure increases approximately 1 atm (100 kilopascals) for every 10 m (33 ft) of water depth. Most bacteria, marine and nonmarine, are barotolerant to various degrees and still grow at pressures of 300–600 atm (30–61 megapascals), corresponding to water depths of approximately 3000–6000 m (2–4 mi). Pressure-adapted (barophilic) microorganisms grow beyond these pressures and are characterized by having growth optima at pressures higher than 1 atm (100 kPa). Obligately barophilic bacteria are species that are unable to grow at 1 atm (100 kPa). The various types and degrees of pressure adaptation (**Fig. 1**) do not eliminate a general gradual decrease of microbial metabolic activity with increasing pressure or depth in the ocean. In consideration of microbial adaptations for a deep-sea existence, temperature- and pressure-retaining samplers have been developed (**Fig. 2**).

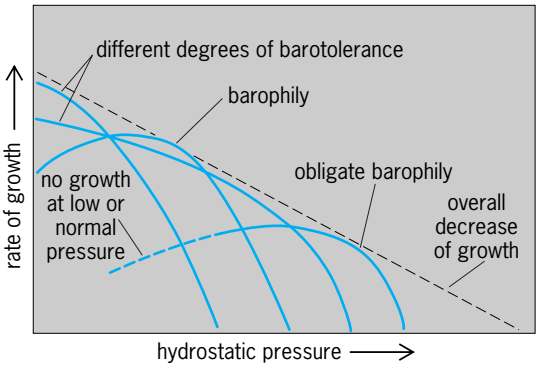

Fig. 1. Pressure-adapted growth in marine bacteria. The broken line represents a general decrease of microbial metabolic activity with increasing hydrostatic pressure (or water depth). (*After H. W. Jannasch, R. E. Marquis, and A. M. Zimmerman, eds., Current Perspectives in High Pressure Biology. Academic Press, 1987*)

Most microorganisms in a given sample of seawater lack their particular growth substrate or are not adapted to the prevailing environmental conditions and are therefore metabolically inactive. As a consequence, the mere number of microorganisms (as determined microscopically or by colony counts on agar plates) provides less information than direct testing of metabolic activity. The latter is done by measuring the rate of incorporation or turnover of a suitable radiolabeled substrate by the natural microbial population under natural conditions. The use of non-growth-stimulating labeled indicators, such as adenine or thymidine as precursors of nucleic acid production, is one of the attempts to assess the unaltered natural activity of whole microbial populations.

Fig. 2. Pressure- and temperature-retaining bacteriological water sampler during recovery from a depth of 6000 m (about 4 mi). Transfer into prepressurized reaction vessels permits the measurement of microbial activity under field conditions. (*Courtesy of S. Molyneaux*)

Of the large variety of organic material decomposed by marine heterotrophic bacteria, oil and related hydrocarbons are of special interest. Other environmentally detrimental pollutants (such as inorganic acids, organic solvents, pesticides, and herbicides) that are directly dumped or reach the ocean as the ultimate sink by land runoff are microbiologically degraded at varying rates. Techniques of molecular genetics are aimed at encoding genes of desirable enzymes into organisms for use as degraders of particular pollutants.

A specifically marine microbiological phenomenon is bacterial bioluminescence, which may function as a respiratory bypass of the electron transport chain. Free-living luminescent bacteria are distinguished from those that live in symbiotic fashion in light organelles of fishes or invertebrates. *See* BIOLUMINESCENCE.

Photoautotrophs and chemoautotrophs. The type of photosynthesis carried out by purple sulfur bacteria is an anaerobic process. It uses hydrogen sulfide (in contrast to water, which is used in green plant photosynthesis) as a source of electrons and thus produces sulfur, not oxygen. Photoautotrophic bacteria are therefore limited to environments where light and hydrogen sulfide occur simultaneously, mostly in lagoons and estuaries. In the presence of sufficient amounts of organic substrates, heterotrophic sulfate-reducing bacteria provide the necessary hydrogen sulfide where oxygen is depleted by decomposition processes. Anoxygenic photosynthesis is also carried out by some blue-green algae, which are now classified as cyanobacteria. A genus of oxygenically photosynthesizing cyanobacteria (*Synechococcus*) was discovered to be common in surface seawater. *See* CYANOBACTERIA; PHOTOSYNTHESIS.

Chemoautotrophic bacteria are able to reduce inorganic carbon to organic carbon (chemosynthesis) by using the chemical energy liberated during the oxidation of inorganic compounds (hydrogen, hydrogen sulfide, elemental sulfur, thiosulfate, ammonia, nitrite, and reduced iron and manganese). Their occurrence, therefore, is not light-limited but depends on the availability of oxygen and the suitable inorganic electron source. Their role as producers of organic carbon is insignificant in comparison with that of photosynthetic producers (exempting the processes found at deep-sea hydrothermal vents). The oxidation of ammonia and nitrite to nitrate (nitrification) furnishes the chemically stable and biologically most available form of inorganic nitrogen for photosynthesis. Genera of nitrifying bacteria include *Nitrosomonas, Nitrosococcus, Nitrosospira, Nitrobacter*, other *Nitrosovibrio, Nitrosolobus*, and *Nitrospina*. *See* NITROGEN CYCLE.

In contrast to soil and fresh water, the effect of acidification by the microbial formation of sulfate and nitrate is minimized in the marine environment by the high buffering capacity of seawater.

By the same token, highly acidophilic sulfur-oxidizing bacteria lose out in competition with facultatively chemoautotrophic bacteria, which produce nonacidifying polythionates as their end product of sulfur oxidation. The generation of methane and acetic acid from hydrogen and carbon dioxide stems from anaerobic bacterial chemosynthesis, and is common in anoxic marine sediments. *See* METHANOGENESIS (BACTERIA).

Marine microbial sulfur cycle. Sulfate is quantitatively the most prominent anion in seawater. Since it can be used by a number of heterotrophic bacteria as an electron acceptor in respiration following the depletion of dissolved oxygen, the resulting sulfate reduction and the further recycling of the reduced sulfur compounds make the marine environment microbiologically distinctly different from freshwater and most soils. Sulfate is far more important in seawater for microbial anaerobic respiration, than nitrate (denitrification, resulting in nitrogen gas production) or carbonate (methanogenesis, resulting in methane production). The assimilatory reduction of sulfate to organic sulfur compounds is quantitatively of minor importance in the marine environment compared to the bacterial respiration of sulfate. The resulting hydrogen sulfide is reoxidized to sulfate in the presence of oxygen with the concomitant production of organic carbon. This chemosynthetic production is considered secondary, since it depends on the primary photosynthetic production of organic carbon and oxygen.

The marine anaerobic, heterotrophic sulfate-reducing bacteria are classified in three genera; *Desulfovibrio, Desulfotomaculum*, and *Clostridium*. Microbial sulfate reduction is particularly important in the Black Sea, the world's largest anoxic basin with a maximum depth of 2000 m (6000 ft), where the oxygen-sulfide interface lies at a depth of about 100 m (300 ft). This microbially produced phenomenon has turned the Black Sea into one of the most studied marine environments. *See* BLACK SEA.

The marine aerobic sulfur-oxidizing bacteria fall into two groups: the thiobacilli (*Thiobacillus* and *Thiomicrospira*) and the morphologically conspicuous filamentous or unicellular organisms (*Beggiatoa, Thiothrix, Thiovulum, Thiospira, Thioploca*, and *Achromatium*). While the former comprise a wide range from obligately to facultatively chemoautotrophic species (requiring none or some organic compounds), few of the latter have been isolated in pure culture, and chemoautotrophy has been demonstrated in only a few. *Thioploca* and *Beggiatoa* have been observed to form massive microbial mats on the sea floor, the former off the coast of Chile in depths of 60–200 m (80–600 ft), the latter in the vicinity of sediment-covered hydrothermal vents at a depth of 2000 m (6000 ft).

Deep-sea hydrothermal vent bacteria. Two types of hydrothermal vents have been investigated: warm vents (8–25°C or 46–77°F) with flow rates of 1–2 cm (0.4–0.8 in.)/s, and hot vents (260–360°C or 500–600°F) with flow rates of 2 m (6.5 ft)/s. In their immediate vicinity, dense communities of benthic invertebrates are found with a biomass that is orders of magnitude higher than that normally found at these depths and dependent on photosynthetic food sources. This phenomenon has been explained by the bacterial primary production of organic carbon through the chemosynthetic oxidation of reduced inorganic compounds. The chemical energy required for this process is analogous to the light energy used in photosynthesis and is provided by the geothermal reduction of inorganic chemical species. The specific compounds contained in the emitted vent waters and suitable for bacterial chemosynthesis are mainly hydrogen sulfide, hydrogen, methane, and reduced iron and manganese.

There appear to be three major sites where microbial growth takes place: within the subsurface vent system, in microbial mats covering surfaces exposed to the vent plume, and in various symbiotic associations. In the first case, bacterial cells and visible cell aggregations are emitted with the vent waters and become available to filter-feeding sessile and planktonic animals; *Thiomicrospira* is the most commonly isolated genus. In the second case, grazing animals can be observed on various types of surfaces feeding on *Beggiatoa* and *Thiothrix*-like filamentous bacteria. Isolated from mat material are manganese-oxidizing, extremely thermophilic methanogenic as well as methylotrophic bacteria (**Fig. 3**). The third case leads to the production of the major portion of animal biomass: prokaryotic chemoautotrophic symbiosis is found in the gill tissue of the vent clam (*Calyptogena magnifica*) and mussel (*Bathymodiolus*), as well as in a special tissue, the trophosome, of

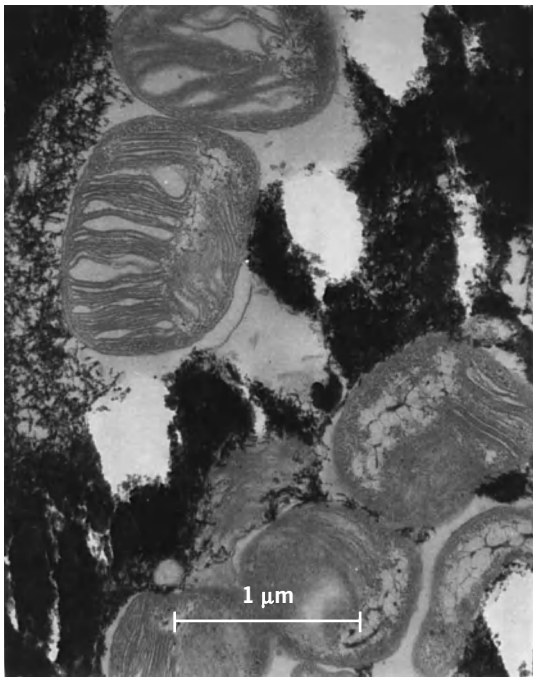

Fig. 3. Transmission electron micrograph of methylotrophic bacteria within iron-manganese deposits of microbial mats from deep-sea hydrothermal vents. (*From P. A. Rona et al., eds., Hydrothermal Processes at Seafloor Spreading Centers, Plenum Press, 1984*)

the mouthless and gutless pogonophoran tubeworm (*Riftia pachyptila*). Similar symbiotic systems have subsequently been found in estuarine environments, where hydrogen sulfide occurs as a product of bacterial sulfate reduction.

The extremely thermophilic microorganisms isolated from hydrothermal vents belong, with the exception of the genus *Thermotoga,* to the Archaebacteria. Of eight archaeal genera, growing within a temperature range of about 75–110°C (165–230°F), three are able to grow beyond the boiling point of water, if the necessary pressure is applied to prevent boiling. These organisms are strictly anaerobic. However, unlike mesophilic bacteria, hyperthermophilic marine isolates tolerate oxygen when cooled below their minimum growth temperature. *See* ARCHAEA; HYDROTHERMAL VENT.

Virology. Observations have shown that seawater may contain 10^5–10^8 virus or phage particles per cubic centimeter (0.62 in.^{3}). While one hypothesis purports that up to 60% of bacterial mortality may by due to viral infection, it is generally assumed that bacterial communities are dominated by cells that are resistant to their co-occurring phages, the latter maintaining themselves by infecting relatively rare sensitive cells. *See* BACTERIOPHAGE.

Biotechnology. Marine microbial biotechnology is an applied science. As an example, thermostable deoxyribonucleic acid–cleaving polymerases from the above-mentioned hyperthermophilic vent bacteria are produced commercially and used extensively in molecular biology, particularly in the polymerase chain reaction. Another example is the use of thermostable enzymes in high-temperature processes, such as the use of amylases from hyperthermophilic archaea in the conversion of cornstarch to glucose and fructose in the beverage industry. *See* BACTERIA; BIOTECHNOLOGY; MICROBIOLOGY.

Holger W. Jannasch

Bibliography. R. M. Atlas and R. Bartha, *Microbial Ecology*, 4th ed., 1997; A. T. D. Brock (ed.), *Thermophiles: General, Molecular and Applied Microbiology*, 1986; R. A. Herbert and G. A. Codd, *Microbes in Extreme Environments*, 1986; G. Rheinheimer, *Aquatic Microbiology*, 4th ed., 1993; H. G. Schlegel and B. Bowien, *Autotrophic Bacteria*, 1989.

Marine mining

The process of recovering mineral wealth from seawater and from deposits on and under the seabed. While the world's demand for mineral commodities is increasing at a rapid rate, most of the developed countries have been thoroughly explored for surface outcroppings of mineral deposits. The mining industry has needed to improve its capabilities for exploring and exploiting low-grade and unconventional sources of ore. Corresponding advances in oceanography have highlighted the importance of the ocean as a source of minerals and indicated that the technology required for their exploitation is in some cases already available.

Manganese nodules. Undersea mining became an important, but unsuccessful, diversification for many major oil and aerospace companies in the late 1960s. Over 80 separate exploration activities were reported in shallow coastal areas worldwide, but few resulted in new operating mines. Attention turned to the deep seabeds, and much of the debate and controversy in the deliberations of the United Nations Conference on the Law of the Sea (UNCLOS) revolved around the exploitation of manganese nodules. Conflicts over the rights of management of these minerals in international waters led to attempted moratoria on deep-seabed mining activities. Anticipating agreement, several countries, including the United States and Germany, prepared interim legislation to permit nationals of the respective countries and reciprocating states to mine the deep seabed for nodules containing manganese, copper, nickel, and cobalt. Several major multinational consortia were active in testing deep-seabed mining systems, including companies from the United States, Canada, United Kingdom, Australia, Germany, France, Belgium, Netherlands, and Japan. *See* MANGANESE NODULES.

Metalliferous sulfides. In 1979, an extraordinary discovery of massive deposits of metalliferous sulfides containing zinc, copper, silver, and gold was made at 21°N on the East Pacific Rise at a depth of 3000 m (10,000 ft). This confirmed projections, based on previous discoveries of metalliferous muds in the Red Sea, that the boundaries between spreading oceanic plates would be host to similar hydrothermal mineral deposits. As oceanic plates move apart, molten basaltic magma is thrust up between them, resulting in extensive fracturing of the adjacent flanks as much as several kilometers from the axis. Cold seawater percolates through the fractures, deep into the oceanic crust, and in its then superheated state dissolves many of the metals contained in the basalt. Normal convection causes the now hot, metal-rich solution to rise back to the seabed along the axis. The temperature and pressure decrease as the solution rises, and the contained minerals may be differentially precipitated as they pass through the cooler rocks. The fluids rise from the seabed at 300–350°C (570–660°F) into cold seawater at 4°C (37°F) to form black or gray smokers (hydrothermal vents), from which the remaining minerals are precipitated to form vent chimneys or to rain down as fine particles of mineral-rich sediments. Intensive examination of parts of the Juan de Fuca/Gorda Ridge spreading centers off the northwestern United States resulted in further discoveries, including gold-rich sulfide deposits off Papua, New Guinea. *See* HYDROTHERMAL VENT; ORE AND MINERAL DEPOSITS; PLATE TECTONICS.

With commercial interest in the manganese nodules waning, because of depressed metal markets and continuing uncertainties over the terms of the UNCLOS, and claims of 370-km (200-nautical-mile) exclusive economic zones (EEZ) proliferating, emphasis changed during the 1980s to assessing the potential of minerals within the EEZs. Prime targets

were the high-cobalt manganese crusts, containing up to 2% cobalt, which were found to be widely distributed throughout the Pacific basin on the flanks of islands and seamounts at depths between 800 and 2400 m (2600 and 7900 ft). Others were the metalliferous sulfide deposits formed at spreading centers and in back-arc basins within the economic zones, as well as the more traditional nearshore deposits of unconsolidated heavy minerals containing gold, tin, and titanium, and extensive bedded deposits of phosphorites projected in the U.S. Atlantic margin (**Fig. 1**). Meantime in certain countries, government interests in the manganese nodules was maintained, mainly in connection with environmental issues. In 1988, France, India, Japan, and the Soviet Union registered as pioneer investors under the terms of the United Nations convention. Since then, China and Korea have been added.

Hydrates. More recently, there has been widespread interest in the research, identification, assessment, exploration, and development of methane hydrate resources. In the United States, methane hydrates had been regarded as an academic curiosity, or as an expensive nuisance causing the clogging of oil and gas pipelines. The frozen, crystalline gas hydrates, also known as clathrates, have been demonstrated to be more widely distributed in the marine environment than was originally anticipated, and that this ubiquitous material represents a potential source of energy, on a global scale, that is significantly greater than all other forms of fossil fuel energy combined. The formation and stability of the crystals are dependent on the combination of high pressure, low temperature, and a source of gas. Fossil hydrates formed during the ice age are found onshore and throughout the continental shelf in high

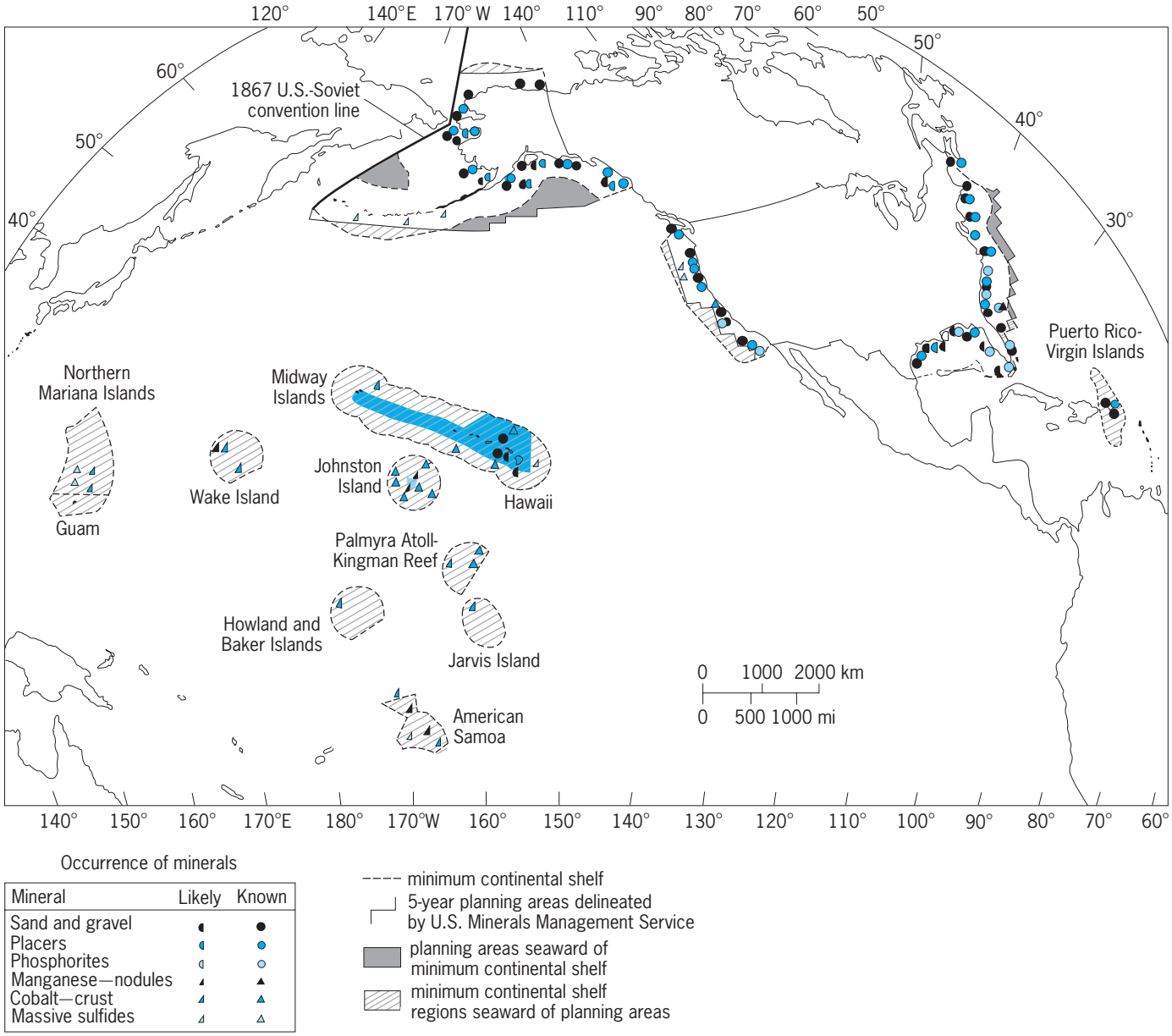

Fig. 1. Offshore mineral areas of the United States.

latitudes. The deep seabeds are host to hydrate deposits that are forming now. Methods of extraction of these deposits, which may be up to hundreds of meters thick over areas of tens of square kilometers, are being studied in India and Japan, where they are considered serious contenders as national sources of energy. One proposed method of recovery would be to drill underneath the deposit and remove the gas below the hydrates. The subsequent reduction in gas pressure would lead to sublimation of the crystalline hydrate cap, resulting in a continuous release of additional gas. The hydrate deposits may also constitute a hazard to oil and gas operations in terms of sea-floor instability, and it is suggested that they may be a significant factor in the presence of atmospheric greenhouse gases as the result of temperature changes in the oceanic environment, causing major gaseous releases from the seabed and influencing global climate. *See* HYDRATE.

Environment and minerals. While mineral resources to the value of trillions of dollars do exist in and under the oceans, their exploitation will not be simple. Many environmental problems must be overcome and many technical advances must be made before the majority of these deposits can be mined in competition with existing land resources. The International Seabed Authority (ISA) has prepared environmental guidelines for the development of manganese nodules and the International Marine Minerals Society (IMMS) has compiled similar guidelines for the development of metalliferous sulfides.

The marine environment may be logically divided into four significant areas: waters, deep seabeds, continental shelf and slope, and seacoast. Of these, the waters are the most significant, both for their mineral content and for their unique properties as a mineral overburden. Not only do they cover the ocean floor with a fluid medium quite different from the solid earth or atmosphere and require entirely different concepts of ground survey and exploration, the constant and often violent movement of the surface waters combined with unusual water depths presents formidable deterrents to the use of conventional seagoing techniques in marine mining operations.

The mineral resources of the marine environment are of three types: dissolved minerals of the ocean waters; unconsolidated mineral deposits of marine beaches, continental shelf, and deep seabed; and consolidated deposits contained within the bedrock underlying the seas. These are described in the classification outline below, which shows also subclasses of seabed and subseabed deposits, characteristics that have a very great influence on the economics of exploration and mining.

I. FLUID
  Seabed
    Freshwater
    Seawater
      Magnesium
      Sodium
      Uranium
      Bromine
      Salts of 26 other elements
  Subseabed
    Hydrothermal fluids
II. UNCONSOLIDATED
  Seabed
    Industrial materials
      Sand and gravel
      Shells
      Aragonite
    Heavy-mineral placers
      Magnetite
      Ilmenite, rutile
      Chromite, monazite
    Nodules
      Manganese
      Phosphorite
    Muds and oozes
      Metalliferous
      Carbonaceous
      Siliceous
      Calcareous
      Barite
  Subseabed
    Heavy-mineral placers
      Gold
      Platinum
      Cassiterite
      Gemstones
    Bedded deposits
      Phosphorites
III. CONSOLIDATED
  Seabed
    Crusts
      Phosphorite
      Cobalt
      Manganese
    Mounds and stacks
      Metallic sulfides
  Subseabed
    Disseminated, stratified, vein, or massive deposits
      Coal
      Sulfur
      Phosphates
      Carbonates
      Potash
      Ironstone
      Limestone
      Metallic sulfides
      Metallic salts
      Gas hydrates

See MARINE GEOLOGY; SEAWATER.

As with land deposits, the initial stages preceding the production of a marketable commodity include discovery, characterization of the deposit to assess its value and exploitability, and mining, including beneficiation of the material to a salable product.

Exploration. Initial requirements of an exploration program on the continental shelves are a thorough study of the known geology of the shelves and adjacent coastal areas and the extrapolation of known

metallogenic provinces into the offshore areas. The projection of these provinces, characterized by relatively abundant mineralization, generally of one predominant type, has been practiced with some success in the localization of certain mineral commodities, overlain by thick sediments. As a first step, the application of this technique to the continental shelf, overlain by water, is of considerable guidance in localizing more intensive operations. Areas thus delineated are considered to be potentially mineral bearing and are subject to prospecting by geophysical and other methods.

A study of the oceanographic environment may indicate areas favorable to the deposition of authigenic deposits in deep and shallow water. Some deposits may be discovered by chance in the process of other marine activities.

Field exploration prior to or following discovery will involve three major categories of work: ship operation, survey, and sampling.

Ship operation. Conventional seagoing vessels are used for exploration activities with equipment mounted on board to suit the particular type of operation. The use of remotely operated vehicles (ROVs) will eventually augment or replace existing techniques, but they are not yet advanced sufficiently for commercial exploration. *See* UNDERWATER VEHICLE.

One of the most important factors in the location of undersea minerals is accurate navigation. Ore bodies must be relocated after being found and must be accurately delineated and defined. The accuracy of survey required depends upon the phase of operation. Initially, errors of 300 m (1000 ft) or more may be tolerated.

However, once an ore body is believed to exist in a given area, maximum errors of less than 30 m (100 ft) are desirable. These maximum tolerated errors may be further reduced to centimeters in detailed ore-body delineation and extraction.

A variety of types of electronic navigation systems is available, with accuracies from 900 m (3000 ft) down to approximately 1 m (3 ft). Loran, Lorac, and Decca are permanently installed in various locations throughout the world but are becoming obsolete as the differential Global Positioning System (GPS) has completely revolutionized the capabilities for positioning with high accuracy in any part of the world's oceans. *See* SATELLITE NAVIGATION SYSTEMS.

During sampling and mining operations, the vessel must be held steady over a selected spot on the ocean floor. Two procedures that have been fairly well developed for this purpose are multiple anchoring and dynamic positioning.

A three-point anchoring system is of value for a coring vessel working close to the shore. A series of cores may be obtained along the line of operations by winching in the forward anchors and releasing the stern anchor. Good positive control over the vessel can be obtained with this system, and if conditions warrant, a four-point anchoring system may be used. Increased holding power can be obtained by multiple anchoring at each point.

Dynamic positioning is useful in deeper water, where anchoring may not be practical. The ship is kept in position by use of auxiliary outboard propeller drive units or transverse thrusters. These can be placed both fore and aft to provide excellent maneuverability. Sonar transponders are placed on the bottom or held submerged at a depth of minimum disturbance, or the system may be tied to shore stations. The auxiliary power units are then controlled manually or by computer to keep the ranges at a constant value. *See* MARINE NAVIGATION; SONAR; UNDERWATER NAVIGATION.

Survey. The primary aids to exploration for mineral deposits at sea are depth recorders, side scan sonars, subbottom profilers, magnetometers, and bottom and subbottom sampling systems. Their use is dependent upon the characteristics of the ore being sought.

For the initial topographic survey of the seabed, and as an aid to navigation in inshore waters, the depth recorder is indispensable. It is usually carried as standard ship equipment, but precision recorders having a high accuracy are most useful in survey work.

Integrated equipment packages to record bathymetric features using side-scan sonar similar to radar imagery, and precision contouring using multiple, narrow-beam depth recorders have been among the most significant advances in seabed mapping. By using sophisticated image enhancement, a direct fallout from the space program, these systems are able to map in real time at rates up to 25,000 km^2 (9700 mi^2) a day, depending on the precision required. Combined with the GPS, these developments have brought seabed mapping much closer to the capabilities attained in terrestrial mapping from the air, at least where the water is deep enough to allow relatively wide swaths to be recorded.

In the search for marine placer deposits of heavy minerals, the subbottom profiler is probably the most useful of all the exploration aids. It is one of several systems utilizing the reflective characteristics of acoustic or shock waves, and is a development of standard geophysical seismic systems for reflection surveys, used in the oil industry. Profilers for shallow penetration use a variety of energy sources including electric sparks, compressed air, gas explosions, acoustic transducers, and electromechanical (boomer) transducers. The return signals as recorded show a recognizable section of the subbottom. Shallow layers of sediment, configurations in the bedrock, faults, and other features are clearly displayed and require little interpretation. The maximum theoretical penetration is dependent on the time interval between pulses and the wave velocity in the subbottom. A pulse interval of 0.5 s and an average velocity of 2400 m/s (8000 ft/s) will allow a penetration of 600 m (2000 ft), the reflected wave being recorded before the next transmitted pulse. *See* SEISMIC STRATIGRAPHY.

Penetration and resolution are widely variable features on most models of wave velocity profiling systems. In general, high frequencies give high resolution with low penetration, while low frequencies

give low resolution with high penetration. The general range of frequencies for mineral exploration varies from 1 to 10 kHz (typically 3.5 kHz), and the general range of pulse energy is 100–25,000 joules for nonexplosive energy sources. The choice of system will depend very much on the requirements of the survey, but for the location of shallow placer deposits on the continental shelf the smaller low-powered models have been used with considerable success.

With the advent of the flux gate, proton precession, and the rubidium vapor magnetometer, all measuring the Earth's total magnetic field to a high degree of accuracy, this technique has become much more useful in the field of mineral exploration. Anomalies indicative of mineralization such as magnetic bodies, concentrations of magnetic sands, and certain structural features can be detected. Although all three types are adaptable to undersea survey work, the precession magnetometer is more sensitive and more easily handled than the flux gate, and the rubidium vapor type has an extreme degree of sensitivity which enhances its usefulness when used as a gradiometer on the sea surface or submerged. *See* GEOPHYSICAL EXPLORATION.

Once an ore body is indicated by geological, geophysical, or other means, the next step is to sample it in area and in depth. Mineral reserves cannot be confirmed without collecting samples.

Sampling. Mineral deposit sampling involves two stages. First, exploratory or qualitative sampling to locate mineral values and allow preliminary judgment to be made. For marine deposits, this will involve such simple devices as snappers, drop corers, drag dredges, and divers. Accuracy of positioning is not critical at this stage, but of course is dependent on the type of deposit being sampled. Second, the deposit must be characterized in sufficient detail to determine the production technology requirements and to estimate the profitability of its exploitation. This quantitative sampling requires much more sophisticated equipment than does the qualitative type, and for marine work few systems in existence can be considered reliable and accurate. However, in particular cases, systems can be put together using available hardware that give the accuracy required. Specifically, qualitative sampling of any mineral deposit offshore can be carried out with existing equipment. Quantitative sampling of most alluvial deposits of heavy minerals (specific gravity less than 8) can be carried out at shallow depths (less than 107 m or 350 ft overall) using existing equipment, but cannot be carried out with reliability for higher-specific-gravity minerals such as gold (specific gravity 19). Advances have been made in sampling for diamonds.

Any system that will give quantitative samples can be used for qualitative sampling, but in many cases heavy expenses could be avoided by using the simpler equipment.

To obviate the effects of the sea surface environment, the trend is toward the development of fully submerged systems, but the deficiencies in sampling heavy placer minerals are not due to the marine environment. Even on land, the accuracy of placer deposit evaluation is not high and the controlling factors not well understood. There is still a need for more intensive research in this area.

Quantitative sampling of consolidated deposits offshore has been confined to water depths of no more than a few hundred feet mainly because of the expense. Whereas the Ocean Drilling Program has the capability to drill in thousands of meters of water, only one system presently exists that can be placed on the bottom from a conventional vessel, to drill small holes in the rock to depths of about 50 m (165 ft), which is a prerequisite for even the most simple deposit characterization of metalliferous sulfides. Similarly, the characterization of metalliferous crust deposits depends on multiple, accurately positioned samples of the crust material and the underlying bedrock. Until such systems are better developed, the true nature of the many discoveries of deep-seabed consolidated deposits will remain speculative.

Evaluation of surficial nodule deposits on the deep seabed at depths of 5000–6000 m (16,500–19,800 ft) may be carried out by using combinations of optical or acoustic imagery and sampling. Except for box corers that are used for geotechnical sampling, devices lowered from a stationary vessel have given way to the use of free-fall (boomerang) samplers equipped with corers, grabs, or cameras, and discharged at preselected points in groups of 8–12 for later retrieval. Also widely used are towed-television or multiple-shot photographic cameras that give a fully or nearly continuous coverage along selected tracks. Nodules are commonly assayed aboard ship and the data from all systems analyzed with onboard computers. A variety of seabed maps showing bathymetry, seabed topography, nodule distribution, and grade may be produced while the vessel is still on site. Ultimately, methods for continuous in-place assaying while under way should be perfected, which will allow the requisite data maps to be produced in real time.

Exploitation. Despite the intense interest in undersea mining, new activities have been limited mostly to conceptual studies and exploration. The volume of production has shown little change, and publicity has tended to overemphasize some of the smaller, if more newsworthy, operations. All production to date has come from nearshore sources, namely, seawater, beach and nearshore gold and diamond placers, and nearshore-consolidated deposits of coal, sulfur, and potash.

Minerals dissolved in seawater. Commercial separation techniques for the recovery of minerals dissolved in seawater are limited to chemical precipitation and filtration for magnesium and bromine salts and solar evaporation for common salts and freshwater production on a limited scale. Other processes developed in the laboratory on pilot plant scale include electrolysis, electrodialysis, adsorption, ion exchange, chelation, oxidation, chlorination, and solvent extraction. The intensive interest in the extraction of fresh water from the sea has permitted

TABLE 1. Mining regions for dissolved mineral deposits offshore

Mineral	Location
Sodium, NaCl	Worldwide
Magnesium, metal Mg, MgO, $Mg(OH)_2$	United States, United Kingdom, Germany, Russia
Bromine, Br	Worldwide
Freshwater	Middle East, Atlantic region, United States
Heavy water	Canada

additional research on the recovery of minerals, but successful commercial operations will require continued development of the combination of processes involved for each specific mineral.

Three minerals or mineral suites are extracted commercially from seawater: sodium, magnesium, and bromine (**Table 1**). Of these, salt evaporites are the most important. Japan's total production of salt products comes from the sea. Magnesium extracted from seawater accounts for 75% of domestic production in the United States. Freshwater compares with bromine in total production value, and heavy water, or deuterium oxide, has been produced from seawater in Canada for many years. Extensive work has been carried out in Japan on the extraction of uranium.

Unconsolidated deposits. Unconsolidated deposits include all the placer minerals, on the seabed and in the subseabed, as well as the authigenic deposits of manganese nodules found at moderate to great depths. *See* AUTHIGENIC MINERALS.

The mining of unconsolidated deposits became widely publicized with the awareness of the potential of manganese nodules as a source of manganese, copper, nickel, and cobalt, and because of developments in the exploitation of offshore diamonds in South-West Africa in the late 1960s. Unconsolidated deposits for many years presented a major source of tin offshore in South East Asia.

So far, the methods of recovery (which have been used or proposed) have been conventional; that is, dredging using draglines, clamshells, bucket dredges, hydraulic dredges, or airlifts. All these methods (**Fig. 2**) have been used in mining to maximum depths of 60 m (200 ft), and hydraulic dredges for digging to 90 m (300 ft) have been built. Extension to depths much greater than this does not appear to present any insurmountable technical difficulties, and in Japan, reserves of sand and gravel are being mapped for exploitation to depths of 300 m (1000 ft). In the deep ocean three industrial consortia successfully tested dredge systems for manganese nodules in water depths over 4500 m (15000 ft).

Dredging operations have exploited such diverse products as diamonds, gold, heavy mineral sands, iron sands, tin sands, lime sand, and sand and gravel. The most important of all of these commodities is the least exotic; 60% of world production from marine unconsolidated deposits is involved in dredging and mining operations for sand and gravel. Other major contributors to world production are the operations for heavy mineral sands (ilmenite, rutile, and zircon), mostly in Australia, and the tin operations in Thailand and Indonesia, which account for more than 10% of the world's tin.

Economics of these operations are dictated by many conditions. The spectacular range of costs offshore results from the effects of different environmental conditions. In general, offshore operations are more costly than similar operations onshore, but the factoring of secondary environmental costs may change this.

Offshore diamonds represent a $1.5 billion per year industry along the coasts of Namibia and South Africa. Most of the marine diamonds are high-quality gemstones, having traveled thousands of kilometers from their source inland and then been subjected to intensive wave action over several cycles of sea-level change.

Much of the world's heavy mineral sand production is from beach sand operations in Australia, Sri Lanka, and India. Only two oceangoing dredges are used. Most of the others are pontoon-mounted hydraulic dredges, or draglines, with separate washing plants.

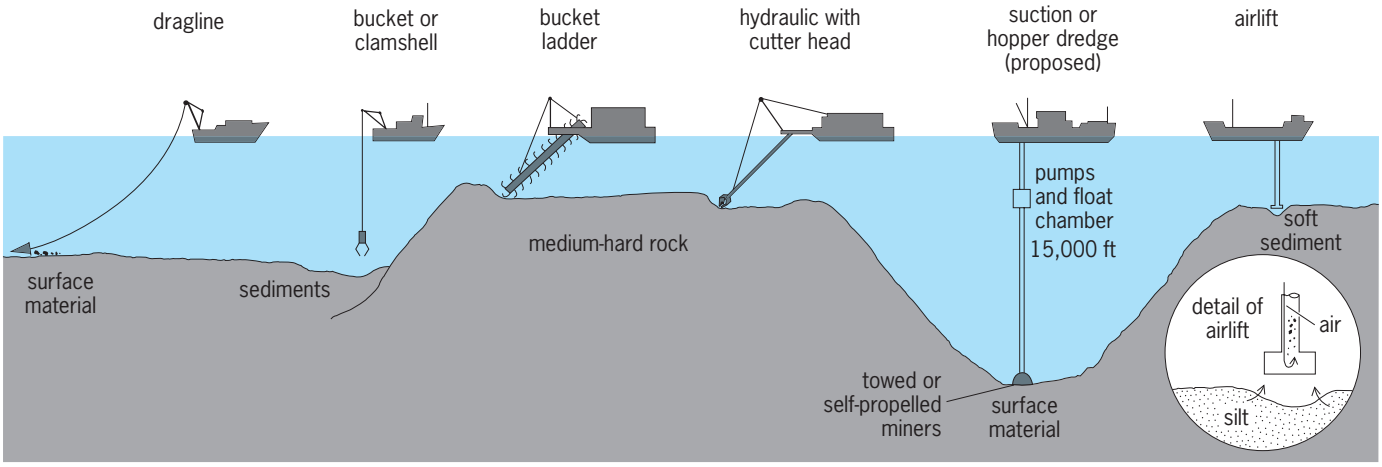

Fig. 2. Methods of dredging used in the exploitation of unconsolidated mineral deposits offshore.

Lime shells are mined as a raw material for portland cement. Two U.S. operations for oyster shells in San Francisco Bay and Louisiana employed barge-mounted hydraulic cutter dredges of 41- and 46-cm (16- and 18-in.) diameter in 9–15 m (30–50 ft) of water. The Iceland Government Cement Works in Akranes uses a 46-m (150-ft) ship to dredge seashells from 40 m (130 ft) of water, with a 61-cm (24-in.) hydraulic drag dredge.

In the United Kingdom, hopper dredges are used for mining undersea reserves of sand and gravel. Drag suction dredges up to 97 cm (38 in.) in diameter are most commonly used with the seagoing hopper hulls. Similar deposits have been mined in the United States, and the same type of dredge is employed for the removal of sand for harbor construction or for beach replenishment. Some sand operations use beach-mounted draglines for removal of material from the surf zone or beyond.

For deep-seabed mining at depths below 5000 m (3 mi), systems have been tested using airlift or suction lift and a mechanical system using a continuous loop of synthetic line from which buckets are suspended every 100 m (330 ft) or so. The gathering devices tested on the bottom with hydraulic systems include towed and self-propelled miners (**Fig. 3**), the latter incorporating a means to crush and slurry the nodules before pumping. Tests to identify the environmental effects of mining have not been conclusive, but tend to indicate that adverse effects are minor and can be mitigated.

Consolidated deposits. The third and last area of offshore mineral resources has an equally long history. The production from in-place mineral deposits under the sea is quite substantial, particularly in coal deposits. Undersea coal accounts for almost 30% of the total coal production in Japan and just less than 10% in Great Britain.

For most of the bedded deposits that extend from shore workings a shaft is sunk on land with access under the sea by tunnel (**Fig. 4*a***). Massive and vein deposits are also worked in this manner. Normal mining methods are used, but precautions must be taken with regard to overhead cover. Near land and in shallow water a shaft is sunk at sea on an artificial island (Fig. 4*b*). The islands are constructed by dredging from the seabed or by transporting fill over causeways. Sinking through the island is accompanied by normal precautions for loose, waterlogged ground, and development and mining are thereafter conventional. The same method is also used in oil drilling. Offshore drilling and in-place mining (Fig. 4*c*) are used only in the mining of sulfur, but this method has considerable possibilities for mining other minerals (such as hydrates, metalliferous sulfides, or deep placers) for which leaching or slurrying are applicable. Petroleum drilling techniques are used throughout, employing stationary platforms constructed on piles driven into the sea floor or floating drill rigs. *See* OIL AND GAS, OFFSHORE; UNDERGROUND MINING.

Minerals produced by offshore mining include dissolved minerals, unconsolidated minerals, and consolidated minerals (**Table 2**). Though this is only a fraction of world mineral production, the percentages will increase as problems of technology, environment, and infrastructure are resolved.

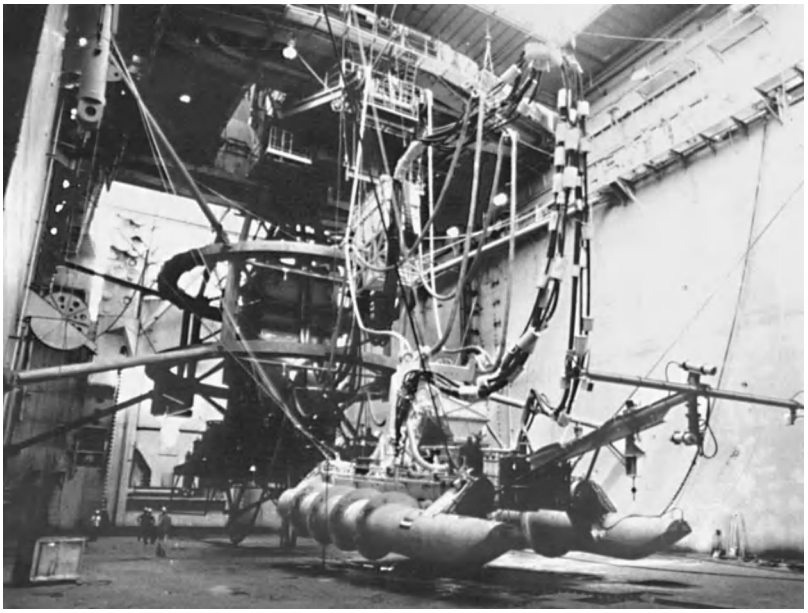

Fig. 3. One-tenth-scale remotely piloted vehicle test miner; note Archimedes' screw drive cyclinders. (*Ocean Mineral Company*)

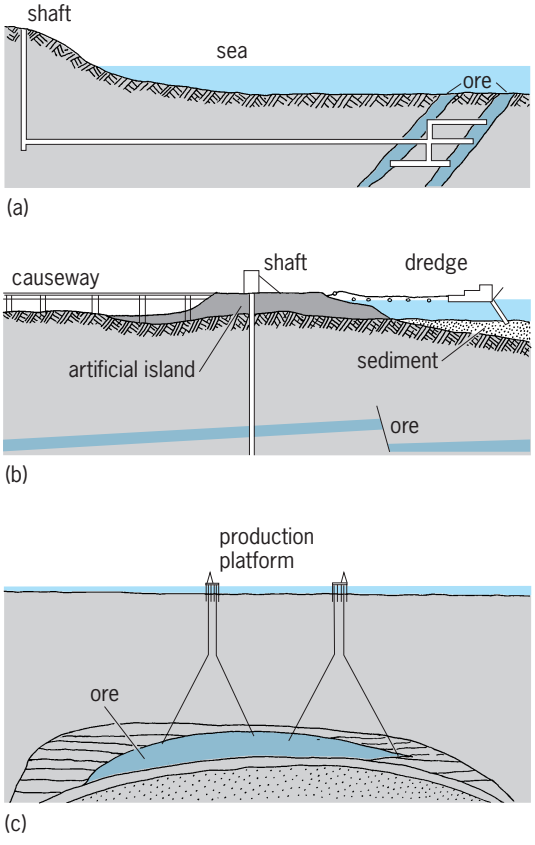

Fig. 4. Methods of mining for exploitation of consolidated mineral deposits offshore. (*a*) Shaft sunk on land, access by tunnel. (*b*) Shaft sunk at sea on artificial island. (*c*) Offshore drilling and in-place mining.

TABLE 2. Summary of production from mineral deposits offshore

Type	Minerals	Percent of world production value
Dissolved minerals	Sodium, magnesium, calcium, bromine	25
Unconsolidated minerals	Diamonds, gold, heavy mineral sands, iron, sands, tin sands, lime shells, sand and gravel	<1
Consolidated minerals	Iron ore, coal, sulfur, hydrates	<1

The future. Despite the technical problems to be overcome, the future of the undersea mining industry is potent. With the advent of national exclusive economic zones claimed by most sovereign coastal states, there is a strong impetus to understand the nature of the resources that are potentially available from these vast new jurisdictional areas. The distinction between shallow and deep-water seabed minerals is no longer political, as in continental-shelf and international seabeds, because many of the exclusive economic zones extend to abyssal depths. The most significant discoveries of marine minerals since the early 1970s have included metalliferous muds in the Red Sea, manganese nodules in the Pacific and Indian oceans, massive metalliferous sulfide deposits in the Atlantic and Pacific oceans, widespread seabed encrustations of high-cobalt metalliferous oxides in the Pacific, and gas hydrates in continental margins and deep ocean basins.

Seawater represents the greatest accessible resource of many elements known and dissolved mineral extraction from seawater by conventional means results in a significant portion of the world's mineral production. As appropriate technology is developed, it is likely that the extraction of minerals directly from the sea will increase. The presence of hydrothermal fluids rich in minerals, associated with sea-floor spreading centers and other volcanic phenomena, presents an additional potential for the production of minerals and geothermal energy.

The mining of unconsolidated deposits nearshore will continue to be significant for the supply of construction materials and heavy minerals and will benefit from improved technology, particularly as deposits are sought in deeper water, further from shore, and in high latitudes. In the deep seabeds, extensive testing of systems for recovering manganese nodules, during the late 1970s, indicated almost conclusively that the nodules are a recoverable resource that await only a suitable economic climate and political infrastructure. Similar conclusions may be drawn from the successful testing of systems to mine the metalliferous muds in the Red Sea.

Consolidated deposits may call for a variety of new mining methods that will depend on the type, grade, and chemistry of the deposit, its distance from land, and the depth of water (**Fig. 5**). The possibility of direct sea-floor access at remote sites through shafts drilled in the sea floor was given consideration under the U.S. Navy's Rocksite program during the 1960s and will be directly applicable to some undersea mining operations. In relatively shallow water, shafts could be sunk by rotary drilling with caissons. In deeper water, the drilling equipment could be placed on the sea floor and the shaft collared on completion. The laying of large-diameter undersea pipelines has been accomplished over distances of 40 km (25 mi) and has been planned for greater distances. Subestuarine road tunnels have been built using prefabricated sections. The sinking of shafts in the sea floor from the extremities of such tunnels should be technically feasible under certain conditions.

The most likely methods for the development of hard-rock submarine ore bodies will be some variation of solution mining technology, involving fracturing of the rock mass in place and removing the valuable materials in solution through a pattern of boreholes. Major problems to be overcome include the control of the fracture pattern and the selective extraction of the desired elements from complex ores. *See* SOLUTION MINING.

In the late 1990s, Australian scientists discovered rich deposits of gold, silver, copper, and zinc sulfide in water at a depth of 1200–1700 m (4000–5700 ft) in the Manus Basin off the coast of Papua New Guinea.

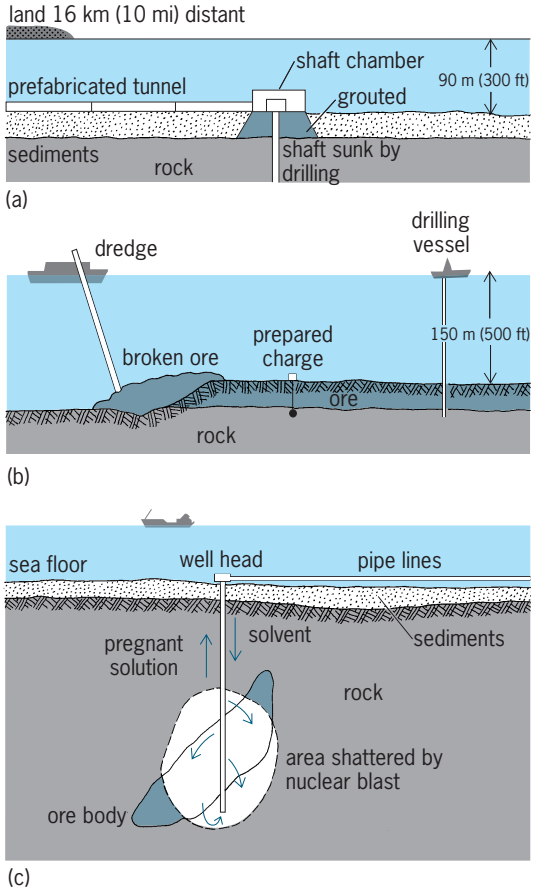

Fig. 5. Possible future methods of mining consolidated mineral deposits under the sea. (*a*) Shaft sinking by rotary drilling from tunnels laid on the seabed. (*b*) Breaking by nuclear blasting and dredging. (*c*) Shattering by nuclear blasting and solution mining.

Metal content of samples from the areas being studied have ranged 10–15% copper, 3–26% zinc, 15–21 g of gold per ton, and 130–200 g of silver per ton. The deposits are surficial masses and chimneys formed around high-temperature hydrothermal vents of mineralized fluids or smokers resulting from tectonic activity associated with the movement of oceanic plates. With drilling for oil and gas now becoming state of the art in similar water depths, the transition to active mining development using off-the-shelf equipment appears likely in the near future. Exploration for similar deposits is being carried out in other areas.

Major technological advances achieved will enhance the possibility of mining in the future, including underwater surveying, advanced underwater vehicle systems, and hydrometallurgical processing. The most important of these may be in the combination of seabed imagery and global positioning, for without adequate maps the characterization and development of the resources of the seabed could not be reasonably pursued.

Outlook. There have been some significant advances in understanding minerals of the seabeds. The ability to manage these minerals as sustainable resources has been enhanced by the passage of legislation. The most important understanding is that, despite the difference in the geological environment of the seabeds compared to land, the potential for mineral occurrence, hectare for hectare, is equivalent in both. On this basis, the global mineral resource base has recently been increased by a factor of 4, and three-quarters of it is underwater. The most important legislation has been the Law of the Sea, in what is probably the most far-reaching redistribution of natural resources in human history. This law has resulted in a peaceful subdivision of jurisdictions, which should significantly affect the world's mineral markets and the balance of economic powers, at least in the Pacific, for as long as humans are dependent on the use of mineral raw materials.

Michael J. Cruickshank

Bibliography. H. R. Cooper, *Practical Dredging*, 1981; D. S. Cronan, *Underwater Minerals*, 1980; M. J. Cruickshank, Law of the Sea and minerals development, *Ocean Yearbook*, vol. 13, pp. 80–106, Dalhousie Law School, 1998; M. J. Cruickshank, Marine mining, in *SME Mining Engineering Handbook*, pp. 1985–2027, 1992; M. J. Cruickshank, Mining, and mineral recovery, *U.S.T. Handbook Directory*, pp. A/15–A/28, 1973; M. J. Cruickshank and C. L. Morgan, *Synthesis and Analysis of Existing Information Regarding Environmental Effects of Marine Mining*, Consulting Report to Continental Shelf Associates for U.S. Department of the Interior, Minerals Management Service, OCS Study MMS 93-0006, 1992; Deep Seabed Polymetallic Nodule Exploration: Development of Environmental Guidelines, *Proceedings of the International Seabed Authority's Workshop*, Sanya, Hainan Island, People's Republic of China, June 1–5, 1998; F. C. F. Earney, *Marine Mineral Resources*, Routledge, 1990; P. Hoagland III and J. Broadus, *Seabed Material Commodity and Resource Summaries*, Woods Hole Oceanog. Inst. Tech. Rep. WHOI-87-43, October 1987; R. H. Joynt, R. Greenshields, and R. Hodgen, Advances in sea and beach diamond mining techniques, *S.A. Min. Eng. J.*, p. 25 ff., 1977; A. Krull, *Ocean Mining and Engineering: New Directions and Opportunities*, 1983; Society of Mining Engineers, *Mineral Resources of the Pacific Rim*, 1982; United Nations (ed.), *Seabed Minerals Series*, 3 vols., 1983; U.S. Congress, Office of Technology Assessment, *Marine Minerals: Exploring Our Ocean Frontier*, 1987.

Marine navigation

The process of directing a watercraft to a destination in a safe and expeditious manner. From a known present position, a course is determined that avoids dangers, and on this course estimates are made of time schedules. The task is to make periodic adjustments using en route measurements of position or heading and speed.

The method used will depend on the type of vessel and on its role or mission. The devices available range from a simple compass to a host of sophisticated electronic systems. In all cases, the navigator must plan and prepare by setting instruments in order and by checking for predictable current and tidal effects and hazards to navigation en route. This preparation includes having the latest, correct charts and reviewing pertinent sections of sailing directions, tabulations of navigational lights, and tide and current tables.

The prudent navigator of a ship planning to cross an ocean will consider the particular requirements of each segment of the voyage. A voyage may be broken into six phases: preparatory, departure, confluence area after departure, high seas, confluence near destination, and terminal.

The methods used to fulfill the requirements of these phases fall under one of the following broad categories of navigation: dead reckoning, piloting, celestial navigation, and electronic navigation. The first three categories have become somewhat standardized; the fourth category has been under constant and innovative development. Electronic navigation is rapidly evolving into integrated systems providing all navigation functions. The publishing of full portfolios of electronic navigational charts and related publications, and the establishment of international standards for systems that display and integrate information, have allowed navigators and maritime administrators to consider reliance on full electronic solutions. The following discussion covers the methods and technologies, and how they may be applied onboard ships.

Dead reckoning. A navigator maintains a reckoning of present and future positions of a ship that is deduced from measurements of direction and speed along the track. In the absence of systems that provide position-fixing capability, this reckoning may be the only way of estimating position on a voyage.

Position fixing is always a past event. Hence, a projection of position requires the use of dead reckoning. It is customary to do this by hand by using pencil, paper, and plotting instruments. However, there are computerized electronic devices that have brought dead reckoning to a high state of sophistication. Among these are marine course computers that will automatically provide such positions besides indicating the command heading, speed made good, distance to destination, estimated time of arrival, and steering signal to gyropilot. *See* DEAD RECKONING.

Inertial navigation is a position-fixing technique that estimates current position by accumulating position changes since the last known position. This self-contained method of navigation eliminates the need for any external references and is passive, that is, nonradiating. The basic principle of inertial navigation is to measure the components of a craft's acceleration along precisely defined axes. If the initial conditions are known, successive integration will produce the velocities and distances along those axes. The key inertial component is the gyroscope with its characteristic "rigidity in space" and its phenomenon of precession. The basic instrument for measuring acceleration is the accelerometer. A digital computer is used for converting accelerations into position. *See* ACCELEROMETER; GYROSCOPE; INERTIAL GUIDANCE SYSTEM.

Another self-contained positioning system is the Doppler sonar navigator. In this system, ultrasonic beams are transmitted to the ocean floor in the forward, aft, starboard, and port directions, and reflected by the ocean floor. Relative motion between the craft and the ocean floor produces Doppler shifts in the frequencies of the reflected signals, the amount of the shift of each beam being directly proportional to the speed of the craft in the direction of that beam. A digital computer converts the Doppler shift of each frequency to speed, and if a reliable reference direction indicator is available, the resultant velocity—speed and direction—of the craft is determined. Distance traveled is determined by integration of the speed with respect to time. Velocity thus determined is with respect to the ocean floor. If the depth of water is greater than about 400 m (220 fathoms or 1320 ft), signals are returned by water reverberation rather than by reflection from the ocean floor, and the velocity is therefore relative to the water. The system can be adapted as an aid in the docking maneuvers of ships. In this use, additional transducers are employed to provide bow, stern, and athwartships velocities. *See* DOPPLER EFFECT; SONAR.

Piloting. This method of navigation is used when the ship is close to land and involves the use of landmarks and seamarks for frequent determination of position. Such marks may be observed by visual, radio, or sound techniques. Visual piloting consists of sighting identifiable landmarks at known positions. The radio system most widely used in this piloting sequence is radar that, besides giving a chartlike pictorial display, can provide bearings and distances for position fixing. The acoustical approach utilizes ultrasonic depth finders. These instruments provide depth measurements that may be compared with those on the chart. Such comparisons can be used to confirm positions or can be used as forewarnings of possible stranding. *See* PILOTING; RADAR.

Celestial navigation. The high-seas phase of a voyage involves the use of either celestial navigation or satellite navigation systems. Sometimes a combination of the two is used. Celestial navigation was formerly considered the primary method of fixing the position of a craft when it was out of sight of land. When using celestial navigation, the navigator follows a routine schedule of a morning twilight observation for a fix, a morning Sun observation of both altitude and azimuth for a morning Sun line of position from which an estimated position can be determined using the dead-reckoning plot, as well as a check on the errors of magnetic compasses and gyrocompasses, an observation of the Sun at meridian transit for a latitude line, and afternoon and evening twilight observations similar to those in the morning. Altitude observations are made with a marine sextant and are timed to the nearest second. For each body observed, the altitude, time, assumed position, and pertinent data from a nautical almanac are converted to a line of position by using prepared tables or a computer. Although two lines of position suitably distributed in azimuth can provide a fix, mariners typically require at least four lines of position unless that is not possible under the prevailing conditions. The celestial bodies observed are the Sun, stars, planets, and the Moon when it is in favorable position relative to other bodies. The principal limitations of celestial navigation are the need for a well-defined natural horizon and for visible celestial bodies. Celestial navigation serves as a backup technique on most vessels and is usually practiced by aficionados or students. The practice of celestial navigation is of value in educating mariners to better understand satellite navigation, since the effects of geometry and measurement quality are similar whether one is navigating by a constellation of satellites or a collection of celestial objects. *See* CELESTIAL NAVIGATION.

Electronic navigation. This division of navigation previously encompassed only radio navigation systems. It now includes navigation involving any electronic device or instrument. A system that utilizes radio signals to provide lines of position or to fix the position of a craft involves the use of transmitters at accurately defined positions on the surface of the Earth or in satellites. Most common today is the use of satellite navigation using the Global Positioning System (GPS). In the near future new signals will be added to GPS, and the European Union is building a compatible system called Galileo. *See* ELECTRONIC NAVIGATION SYSTEMS.

Loran C. Loran C is a hyperbolic system operating at 100 kHz. It combines the pulse-matching techniques of the former Loran A with phase comparison for greater accuracy. Each chain of Loran C stations consists of a master station operating with two or more secondary stations that transmit synchronized

signals. The useful range extends outward to the limit of ground-wave reception, about 1500–2200 km (810–1190 nmi) from the transmitters. Increased accuracy can be obtained by using Loran C in the differential mode. In this mode the reading of a monitor receiver at a known position is compared with the predicted reading, and any difference is then transmitted to vessels in the vicinity and applied as a correction to their readings. Loran C can also be used in a range-range mode, in which position is determined from the ranges to two transmitters, if the user has a stable, accurate time indicator synchronized with the time sources at the transmitters. Loran C has been designated the official system for the United States confluence and coastal regions. In the mid-1990s the advent of satellite navigation led to decisions by the federal government to decommission Loran C by the year 2000. However, the lifetime of the system has now been extended indefinitely. The need for Loran C as a backup system for navigation and timing is being examined by the U.S. Department of Transportation. The Northwest European Loran-C System (NELS) organization is undertaking a similar examination regarding future operations, with further complications arising from the circumstance that several countries host stations. *See* LORAN.

Global Positioning System. The United States' Global Positioning System (GPS) is an advanced navigation satellite system whose space segment consists of 24 satellites in 12-h orbits, 20,200 km (10,907 nmi) above the surface of the Earth. The control segment consists of several monitor stations to continuously track the satellites above the horizon, a master control station (with one or more additional for redundancy) to receive the tracking data and update the orbital data and satellite clock drifts, and upload stations to transmit the data to the satellites daily or more often. The user segment receives the signals transmitted by the satellites and computes pseudorange and pseudorange rate, which it converts to three-dimensional position of the craft. The average velocity of the craft during a measurement interval is the change in carrier phase of the GPS signal averaged over that interval. Time is available to 0.1 microsecond.

With 24 functioning satellites in orbit, five or more are above the horizon virtually all the time. Signals from four satellites are sufficient for computation of three-dimensional positions. Users authorized to have access to the Precise Positioning Service (PPS) can expect absolute accuracy of positions of 5–10 m (16–32 ft). Other users have access to Standard Positioning Service (SPS), providing 20 m (65 ft) accuracy. In the differential mode an accuracy of 3–5 m (10–16 ft) can be achieved. The GPS can be integrated with other systems for redundancy and integrity measurement. *See* SATELLITE NAVIGATION SYSTEMS.

Galileo. The European Union is building a satellite navigation system called Galileo. Galileo is generally similar to GPS. Significant differences in the programs are the level of civilian control of policy in Galileo, a greater number of available services, and the upfront development of applications that take advantage of Galileo.

Automatic Identification System. The Automatic Identification System (AIS) was developed under the guidance of the International Maritime Organization (IMO), primarily to improve maritime safety by assisting the navigation of ships, the protection of the environment, and the operation of vessel traffic services (VTS). AIS serves in a vessel-to-vessel mode for collision avoidance, as a means for coastal states to obtain information about a ship and its cargo, and as a ship-to-shore method for vessel traffic management.

The AIS device includes a Global Positioning System (GPS) receiver, a microprocessor, and a very high frequency–frequency-modulation (VHF-FM) transceiver. The microprocessor takes data from a ship's sensors and packages it with the vessel's identification into a digital signal. The signal is automatically broadcast. When other broadcasts are received, the processor prepares the received data for display. Each device determines its own transmission schedule, and, in the presence of other stations, uses receipt of previous messages to ensure that stations do not transmit simultaneously. This self-organizing logic allows many AIS units to operate without interfering with one another. AIS information includes static, dynamic, and voyage-related elements. Static information is manually entered on installation and seldom changed. Dynamic information is automatically entered from ship sensors, while voyage-related information is manually entered and updated as appropriate. The primary emphasis of AIS is collision avoidance.

AIS is expected to improve vessel-operator situational awareness. In comparison to radar and automatic radar plotting aids ("own ship" information), AIS information is provided directly from the "other" ship's sensors with each vessel's name and call sign. AIS will also provide an efficient method to monitor vessel movements for purposes of environmental safety, coastal security, or traffic management. Though there is as yet no agreement on the definition of an AIS base station, coastal and harbor monitoring will probably be accomplished through a local network of AIS stations forming an "AIS Reception Network." On a regional or national level, the multiple, local networks might be linked through a wide-area network.

Vessel traffic services. Vessel traffic services (VTS) have been established in a number of heavily trafficked ports throughout the world in an attempt to reduce the number of collisions and strandings and safeguard the environment. Generally the service provides marine traffic management of an advisory nature, but in an especially hazardous situation it may be necessary for the VTS to exercise emergency control of vessel movements. The usual system components of such a service include AIS base stations, high-resolution radars, general-purpose computers, and synthetic video displays, all combined to provide real-time forecasts of vessel movements, lane stray alerts, collision and grounding warnings, and a

description of potential congestion areas. A ship-to-shore voice communications link permits information to flow between VTS operations personnel and identified ships within the traffic surveillance area. These voice communications are often recorded on audio tape units. The system tracks stationary and moving traffic to establish position coordinates, and monitors the position of floating navigational aids in the surveillance area to permit detection of misplaced or drifting buoys. *See* VESSEL TRAFFIC SERVICE.

Traffic-separation schemes. Traffic-separation schemes have been established in a number of high-traffic density areas throughout the world, primarily to decrease the risk of collision at sea. International navigation rules govern the operation of vessels within these traffic separation schemes. A typical scheme consists of the establishment of parallel traffic lanes separated by an intervening buffer zone, analogous to a divided freeway on land. In some areas, surveillance centers provide information on the positions and movements of vessels in the area, and other hazards. Although compliance with such schemes is generally advisory only, a dramatic reduction in collisions in the areas where they have been established has contributed to increased acceptance by mariners, and the present trend is toward mandatory compliance, analogous to air-traffic control, but generally leaving the mariner greater freedom of selection of route, speed, and time of encounter of other craft.

Shipboard systems. The human–machine interface for the practice of marine navigation is evolving. Once the navigator was an expert on a complex set of publications, making precise optical measurements, and plotting the results with the accuracy of a draftsman. Now the navigator retains these skills and must also learn to work with complex computer-based systems that integrate several sources of real-time information and compare the results to large quantities of stored hydrography and cartography. The trend is toward more integration with an accompanying assessment of the integrity or quality of separate information sources. This integration is becoming possible through redundancy of the essential information regarding one's own ship and other nearby ships. For example, a crossing situation with another ship can be evaluated with both radar and AIS information. Basic sensors in these systems include GPS receivers, radar, AIS transceivers, a gyrocompass or transmitting magnetic compass, and normally some type of autopilot for steering and perhaps speed control. In ascending order of sophistication, a brief description of the major systems follows:

Electronic chart system. An electronic chart displays on a video screen the same type of hydrographic information that mariners seek in a traditional nautical chart. Both electronic and paper charts offer graphic representations of water depths, shorelines, topographical features, aids to navigation, and hazards.

An electronic chart database and display offers improvement over the paper chart when it is combined with other information. At a minimum, the ship's position (from electronic navigation) and planned track are needed. With such a display, the navigating officer can determine at a glance the ship's position relative to its intended track, the shoreline, the waterway, and any hazards or threats.

Electronic charts integrated with a range of information, and with hardware and software that can process a hydrographic database to support decision making, are classified as electronic chart display and information systems (ECDIS). Thus, electronic charts are a component of an ECDIS. In addition to displaying a real-time picture of the vessel's position in the waterway, an ECDIS manages navigational and piloting information (typically, vessel-route-monitoring, track-keeping, and track-planning information) to support navigational decision making. The term ECDIS is specifically used to indicate an approved device for carriage onboard internationally regulated commercial vessels. The term "electronic chart system" (ECS) is somewhat more generic and is used to indicate a range of systems on various vessels.

Collision avoidance systems. Collision avoidance systems (CAS), also known as automatic radar plotting aids (ARPA), of varying degrees of sophistication have been developed to reduce the work load of the navigator and eliminate human error. Typically, such a system consists of a digital computer that receives inputs from the ship's radar, compass, and log, and determines and displays collision threats, and in some installations provides a recommended avoiding action.

Integrated navigation systems. Integrated navigation systems integrate the functions of the electronic chart system and collision avoidance systems, and normally some level of automated control of vessel course and speed. The advent of the AIS gives a big technical push towards integration in order to correlate the AIS-derived collision avoidance information with the traditional radar tracks. Automation of navigation tasks through an ECDIS combined with the accuracy of plotting intercepts in an integrated collision avoidance system gives the navigator better information and more time to consider and act versus manually plotting and correlating disparate sources. Some systems may provide a visual display of traffic lanes and possible navigation hazards. They may also perform prevoyage route planning and then continuously maintain a dead-reckoning position. Other features available in some are the computation of course to steer to the next waypoint and the use of adaptive automatic steering wherein the vessel's reaction to the outside environment is translated into corrective steering changes designed to optimize the track and decrease the possibility of damage to the ship and its cargo.

Intelligent systems. There are a variety of intelligent systems deployed aboard automated ship's bridges: piloting expert systems, engineering and vibration expert systems, neutral network systems for adaptive and intelligent steering control, and automated intelligent docking systems. Piloting expert systems provide advice for navigation and collision avoidance by

combining the knowledge and reasoning processes of expert ship's captains, ship's officers, and pilots so as to assist navigators during trips. Such systems make use of real-time positioning information, nautical rules of the road, local knowledge, and organizational procedures and regulations to recommend best courses of action for the navigator. *See* EXPERT SYSTEMS; NEURAL NETWORK.

Shipboard piloting expert systems are integrated into conventional and advanced bridge designs so as to provide intelligent ship control systems. Such systems use input from radar, automated radar plotting aid (ARPA), ECDIS, and bridge instrumentation, and employ heuristic or qualitative reasoning, rather than strict application of deterministic rules.

Integrated bridge systems. These systems are designed to allow the wheelhouse to function as the operational center for navigational and supervisory tasks aboard the ship. These bridges in many cases become ship's operations centers, incorporating controls and monitors for all essential vessel functions, including navigation, engine control, and communications. Other ship functions such as cargo loading, monitoring, and damage control may be included. Many routine navigational tasks, such as chart updating, position plotting, and steering, may be automated. The integrated ship's bridge is thus a unified federation of systems supporting vessel navigation, communications, steering, administration, collision avoidance, safety, and monitoring and control of ship's systems. *See* NAVIGATION.

Jay Spalding; Alton B Moody; Martha R. Grabowski; Richard Greenspan

Bibliography. S. F. Appleyard, *Marine Electronic Navigation*, 2d ed., 1988; N. Bowditch, *American Practical Navigator: An Epitome of Navigation*, National Imagery and Mapping Agency, H. O. Publ. 9, 2002; T. J. Cutler, *Dutton's Nautical Navigation*, 15th ed., 2004; R. R. Hobbs, *Marine Navigation*, 4th ed., 1998; F. J. Larkin, *Basic Coastal Navigation*, 2d ed., 1998; A. B Moody, *Navigation Afloat: A Manual For the Seaman*, 1980; National Research Council, *Minding the Helm: Marine Navigation and Piloting*, 1994; H. H. Shufeldt, G. D. Dunlap, and B. A. Bauer, *Piloting and Dead Reckoning*, 4th ed., 1999.

Marine refrigeration

Marine refrigerating equipment is used for shipboard refrigeration of products as well as for air conditioning the quarters of passengers and crew. Shipboard refrigeration is necessary for the preservation of perishables in transit and foodstuffs to be used by passengers and crew. Marine refrigeration is also used for maintaining certain cargo products in liquid form that would otherwise evaporate when stored at ambient conditions. A typical ship stores or cargo refrigeration plant consists of a compressor, motor, condensor, receiver, evaporators, and controls. A typical air-conditioning unit consists of a compressor, motor, condenser, receiver, water chiller, and controls. *See* AIR CONDITIONING; REFRIGERATION.

Refrigerants. The common refrigerants that have been in use for years, known as CFCs (chlorofluorocarbons) and HCFCs (hydrochlorofluorocarbons), are still being phased out because they contain chlorine, which depletes Earth's stratospheric ozone layer. The stratospheric ozone layer protects all life from ultraviolet radiation. In recent years, holes have been detected in the ozone layer in both hemispheres in late winter and early spring. CFC and HCFC refrigerants have been determined to be major contributors to the holes. Common CFC refrigerants include R-11 and R-12. R-22 is a common HCFC refrigerant.

Replacements for these refrigerants known as HFCs, which are non-ozone-depleting, have been developed. These refrigerants contain fluorine in place of chlorine, and do not destroy the ozone layer. The replacement HFC refrigerants normally provide similar to slightly better efficiencies than the CFC refrigerants they replace. The exception is that HFC-134a, which replaces CFC-12 (R-12) in low-temperature applications, decreases plant capacity approximately 35%. This problem is solved by increasing the compressor speed or changing the compressors. For some systems, the cargo itself is used as the refrigerant, such as when carrying ammonia or petroleum products such as propane or butane.

Preservation of perishables. Cargoes such as perishable foodstuffs and chemicals requiring refrigeration are normally carried in insulated holds. The holds are usually cooled by direct-expansion evaporators which may be gravity-type cooling coils or forced-convection cooling units located in the holds. As an alternative to this system, cargoes may be carried in insulated containers stowed on deck.

Liquid cargoes. Liquid cargoes, such as ammonia, and low-pressure petroleum gases, such as propane and butane, are carried in insulated tanks kept cool by allowing the cargo to evaporate. This process involves drawing off the vapors from the tanks, compressing and condensing the fluids, and returning them to the tanks. Hydrocarbon cargoes of very low temperature, such as liquefied natural gas, are stowed in well-insulated tanks and also are kept cold by allowing the cargo to evaporate. The gases are drawn off and may be burned in the ship's power plant as a partial source of energy for propulsion, or used to power an engine-driven refrigerating unit to assist in keeping the product cold while minimizing the amount of product that must be evaporated for cooling.

Refrigerating systems. For refrigerating systems using insulated holds, liquid refrigerant is delivered to cooling coils, where the refrigerant is expanded, and enters the evaporator as a low-pressure liquid. There it evaporates by absorbing heat from the space being cooled. The refrigerant vapor is then drawn from the evaporator by a compressor, which delivers the refrigerant to a condenser as a high-pressure, high-temperature vapor. The condenser, normally a shell-and-tube heat exchanger cooled by seawater flowing through the tubes, removes the heat

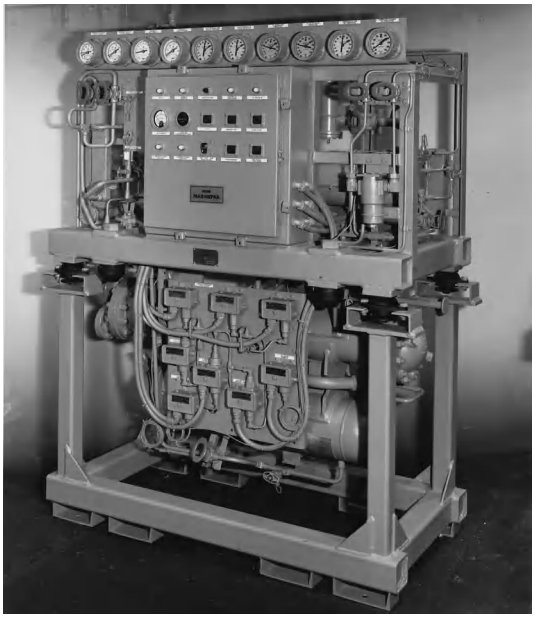

Modern rotary vane HFC-143a ship stores refrigeration unit. (*York International Corp.*)

absorbed in the evaporator and the heat of compression from the refrigerant as it condenses to a high-pressure liquid. The refrigerating cycle is then repeated. For the deck-stowed container system, each container has its own refrigeration system consisting of a compressor, air-cooled condenser, cooling coil, and circulating fan. For liquid cargoes in insulated tanks, the latent heat of vaporization is released as the evaporating liquid changes state to a gas. This is the refrigeration system used in liquid cargo systems.

Ship stores. A modern ship stores refrigeration unit is shown in the **illustration**. Refrigeration systems for ship stores are relatively small compared to cargo refrigeration systems or air-conditioning systems. The refrigerant is circulated through evaporators to maintain the desired temperatures in the various storerooms needed for chilled and frozen products. Two complete refrigeration units are usually employed, with one unit operating and the second on standby.

Air conditioning. For air-conditioning applications, the cooling coils used for refrigeration are replaced with a water chiller. The water chiller is the evaporator where water that is circulated throughout the ship is cooled. The chilled water is circulated to cooling coils situated in various fan rooms for passenger comfort as well as the cooling of equipment. Multiple air-conditioning units are normally employed, and sometimes the units are located in different areas or zones of the ship. For large ships with many passengers, reciprocating compressors are too small; high-tonnage centrifugal-compressor air-conditioning plants are used instead. Reciprocating compressors are normally less than 100 tons, whereas centrifugal compressors can have several hundred tons capacity. Screw compressors can be used for moderate- as well as high-capacity air-conditioning plants.

John H. Merold

Marine sediments

The accumulation of minerals and organic remains on the sea floor. Marine sediments vary widely in composition and physical characteristics as a function of water depth, distance from land, variations in sediment source, and the physical, chemical, and biological characteristics of their environments. The study of marine sediments is an important phase of oceanographic research and, together with the study of sediments and sedimentation processes on land, constitutes the subdivision of geology known as sedimentology. *See* MARINE GEOLOGY; OCEANOGRAPHY; SEDIMENTOLOGY.

Environments of Deposition

Traditionally, marine sediments are subdivided on the basis of their depth of deposition into littoral (0–66 ft or 0–20 m), neritic (66–660 ft or 20–200 m), and bathyal (660–6600 ft or 200–2000 m) deposits. This division overemphasizes depth. More meaningful, although less rigorous, is a distinction between sediments mainly composed of materials derived from land, and sediments composed of biological and mineral material originating in the sea. Moreover, there are significant and general differences between deposits formed along the margins of the continents and large islands, which are influenced strongly by the nearness of land and occur mostly in fairly shallow water, and the pelagic sediments of the deep ocean far from land.

Sediments of continental margins. These include the deposits of the coastal zone, the sediments of the continental shelf, conventionally limited by a maximum depth of 330–660 ft (100–200 m), and those of the continental slope. Because of large differences in sedimentation processes, a useful distinction can be made between the coastal deposits on the one hand (littoral), and the open shelf and slope sediments on the other (neritic and bathyal). Furthermore, significant differences in sediment characteristics and sedimentation patterns exist between areas receiving substantial detrital material from land, and areas where most of the sediment is organic or chemical in origin. *See* DEPOSITIONAL SYSTEMS AND ENVIRONMENTS.

Coastal sediments. These include the deposits of deltas, lagoons, and bays, barrier islands and beaches, and the surf zone. The zone of coastal sediments is limited on the seaward side by the depth to which normal wave action can stir and transport sand, which depends on the exposure of the coast to waves and does not usually exceed 66–99 ft (20–30 m); the width of this zone is normally a few miles. The sediments in the coastal zone are usually land-derived. The material supplied by streams is sorted in the surf zone; the sand fraction is transported along the shore in the surf zone, often over long distances, while the silt and clay fractions are carried offshore into deeper water by currents. Consequently, the beaches and barrier islands are constructed by wave action mainly from material from fairly far away, although local erosion may make a contribution, while the lagoons and

bays behind them receive their sediment from local rivers. The types and patterns of distribution of the sediments are controlled by three factors and their interaction: (1) the rate of continental runoff and sediment supply; (2) the intensity and direction of marine transporting agents, such as waves, tidal currents, and wind; and (3) the rate and direction of sea level changes. The balance between these three determines the types of sediment to be found. *See* DELTA.

On the Texas Gulf Coast, rainfall and continental runoff decrease gradually in a southwesterly direction. The wind regime favors considerable wave action and a southwesterly drift of the nearshore sand from abundant sources in the east. Since sea level has been stable for several thousand years, the conditions have been favorable for the construction of a thick and nearly closed sand barrier that separates a large number of bays from the open Gulf. This barrier is constructed by marine forces from sediments from distant sources and varies little in characteristics along its length. The bays, on the other hand, receive local water and sediment. In the east, the supply of both is fairly abundant, and since the streams are small, the sediment is dominantly fine; the bays have muddy bottoms and brackish waters. Conditions are fairly stable, and a rich, but quantitatively not large fauna is present, including oyster banks. At the southwestern end, continental runoff and sediment supply are negligible.

The only sediment received by the bays comes from washovers from the barriers and is therefore mainly sandy, and the virtually enclosed bays with no runoff are marine to hypersaline. Locally, this yields chemical precipitates such as gypsum and calcium carbonate, and is also conducive to the development of a restricted but very abundant fauna, which produces significant deposits of calcareous material. The sediments of bays and lagoons are often more stratified than those of the open sea as a result of fluctuating conditions. The textural and compositional characteristics depend on local conditions of topography, shore development, and wave and current patterns. They range from coarse gravel and cobbles on rocky beaches fronting the open sea to very fine clayey silt in the interior of quiet lagoons. *See* ESTUARINE OCEANOGRAPHY.

The effects of sea-level changes are imperfectly known, but it is easily comprehended that the development of coastal sediments is to a large extent a function of the duration of this environment in a particular place. Thus if sea level rises or falls rapidly, there is no time for extensive development of beach, barrier, and lagoon deposits, and discontinuous blankets of nearshore sands, with muds behind them, are formed. As the rate of change decreases, open barriers, consisting of widely spaced low sand islands, tend to form, which imperfectly isolate open shallow lagoons in which essentially marine conditions prevail. A prolonged stability is required to produce thick, closed barriers and completely isolate the lagoon environment.

Entirely different nearshore deposits are found on shoals where supply of sediment and freshwater from the land is absent, either because land areas are small (Bahamas), the drainage is directed elsewhere (southern Cuba), or there is no rainfall (Arabian Peninsula). Calcareous muds and coarse calcareous sands then make up the lagoon and beach deposits. If, in addition, the shoal borders directly on the deep ocean without transitional shelf (**Fig. 1**), cool water is driven onto the shoal, where it warms up and precipitates calcium carbonate. In the turbulent water of the shoal, this precipitation either takes place in the form of oolites or it cements organic debris together in small aggregates (grapestone). At the edge of the shoal, the presence of cool, nutrient-rich ocean water is favorable for the growth of coral and algal reefs that are bordered by a zone of skeletal sand derived from broken calcareous organisms. The inner sheltered portions receive the finest calcareous sediments. The types of sediment and their distribution patterns are controlled mainly by the shape of the shoal, in particular the position of its edge, by the prevailing wind, and by the location of sheltered or somewhat deeper quiet areas.

Shelf and slope sediments. The continental shelf is a gently seaward sloping plain of greatly varying width,

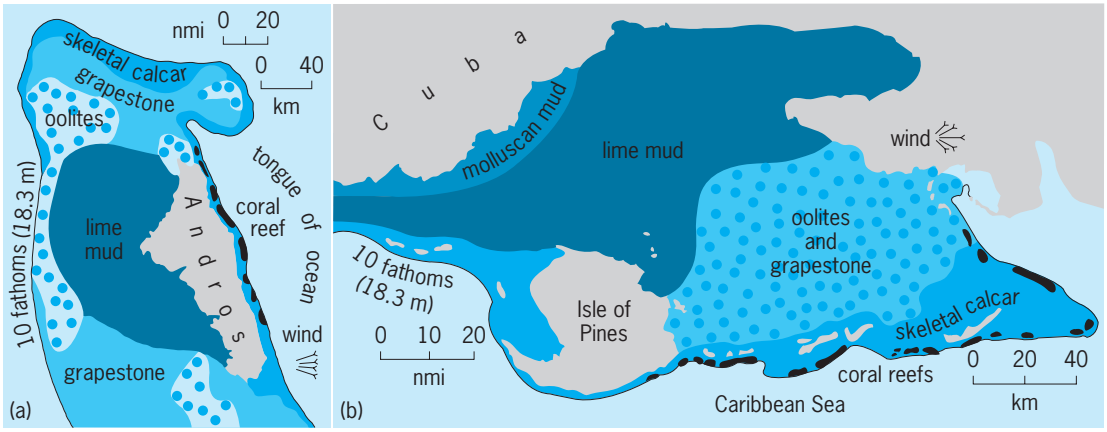

Fig. 1. Shoal water sediments as examples of sedimentation without supply of land-derived sediment. (*a*) The Bahamas. (*b*) The Gulf of Batabano, which is in southwestern Cuba. Both of these shoals border directly on the deep ocean.

ranging from less than a mile (1.6 km) along steep rocky coasts to several hundred miles, for example, in the western Gulf of Mexico. A distinct break in slope at 330–1600-ft (100–500-m) depth marks the transition to the continental slope which descends somewhat more steeply (5–10°) to the deep-sea floor. In areas of active tectonism, for example, off the coast of southern California, the shelf is narrow and separated from the continental slope by a wide zone of deep basins alternating with shallow banks and islands. Submarine canyons cut the edge of the continental shelf in many places and sometimes reach back into the nearshore zone. *See* SUBMARINE CANYON.

During the Pleistocene, the continental shelf was subjected to repeated transgressions and regressions. During each interglacial, sea level was high and the shoreline was located near its present position; during each glacial period, much water was withdrawn from the ocean and the shoreline occurred near the edge of the shelf. The last low sea-level stand occurred approximately 19,000 years ago, and the present shoreline was established as recently as 3000–5000 years ago. On most shelves, equilibrium has not yet been fully established and the sediments reflect to a large extent the recent rise of sea level. Only on narrow shelves with active sedimentation are present environmental conditions alone responsible for the sediment distribution.

Sediments of the continental shelf and slope belong to one or more of the following types: (1) biogenic (derived from organisms and consisting mostly of calcareous material); (2) authigenic (precipitated from seawater or formed by chemical replacement of other particles, for example, glauconite, salt, and phosphorite); (3) residual (locally weathered from underlying rocks); (4) relict (remnants of earlier environments of deposition, for example, deposits formed during the transgression leading to the present high sea-level stand); (5) detrital (products of weathering and erosion of land, supplied by streams and coastal erosion, such as gravels, sand, silt, and clay). *See* AUTHIGENIC MINERALS.

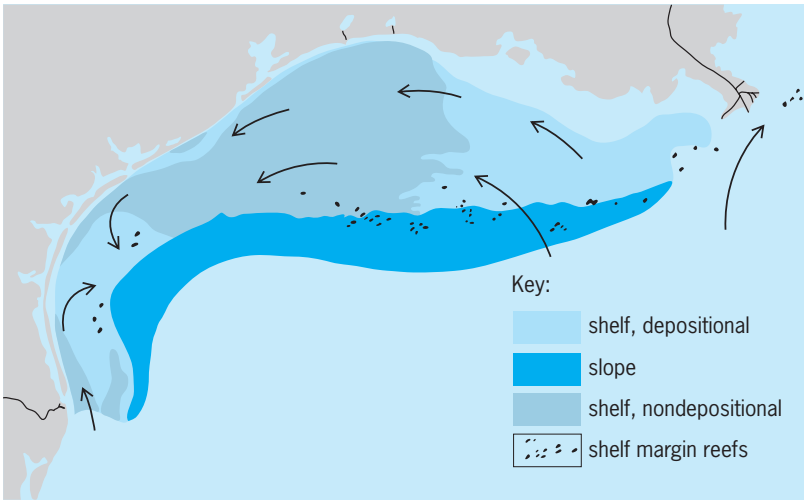

Fig. 2. Sediment distribution of the northwestern Gulf of Mexico as an example of the sediments of a shelf with abundant land-derived sediment. Shelf depositional sediments and slope deposits are silty clays; nondepositional area is covered with relict sediments. Arrows show generalized circulation.

On shelves with abundant land-derived sediment, the coastal zone is composed of deltas, lagoons, bays, and beaches and barriers. Outside the beaches and barriers, a narrow strip of wave-transported sand, usually less than 2 or 3 mi (3 or 5 km) wide, fringes the coast. On the open shelf, the sediment deposited under present conditions is a silty clay, which, near deltas, grades imperceptibly into its bottomset beds. Usually, the silty clay, which results from winnowing near the coast, is carried no more than 20–30 mi (32–48 km) offshore by marine currents, so that the zone of active deposition is restricted. If the shelf is narrow, all of it will fall into this zone, but if it is wide, the outer part will be covered by relict sediments resulting from the recent transgression. These relict sediments were deposited near the migrating shoreline and consist of beach sands and thin lagoonal deposits. They have been extensively churned by burrowing animals and wave action, resulting in a mottled structure, and authigenic glauconite has formed in them. *See* TRACE FOSSILS.

On many shelves, small calcareous reefs (shelf-edge reefs) occur at the outer edge. These reefs apparently depend on the presence of deep water for their growth, although it is not certain that they are growing vigorously at the present time. In the Gulf of Mexico, where they are particularly abundant, they mark the tops of salt domes in the subsurface. Beyond the reefs begins the zone of slope deposition, where in deeper and quiet water silty clays with abundant calcareous remains of open water organisms are being slowly deposited. Thus, there are in principle four parallel zones on each shelf: an inner sandy zone; an intermediate zone of clay deposition; an outer shelf zone of no deposition, where relict sediments occur, terminating in edge reefs; and a slope zone of calcareous clays. This parallel zonation is often strongly modified by special current patterns, which carry fine sediments farther out across the shelf, as in the western Gulf of Mexico; by rapidly advancing deltas that provide a sediment source far out on the shelf, as in the Mississippi delta; or by exposure to unusually vigorous wave action that prevents fine sediments from being deposited, even though a supply is present.

The fine-grained deposits that are being formed tend to be deposited more rapidly near the source than farther away, and as a result contain more biogenous material with increasing distance from the source, so that they become more calcareous (**Fig. 2**). On shelves with little or no land-derived material, the only available sources of sediment are biogenous and authigenic. These sources provide far less material than rivers do, and as a result sedimentation rates are much lower. Even on shelves with abundant supply of land-derived material, the areas of nondeposition are extensive, often 40–50% of the total area. On the calcareous shelves, relict sediment may cover up to 75% of the entire area. Near the shelf

edge, these relict sediments are shallow-water deposits formed during the last low stand of the sea, and consist of small algal reefs and oolites as described for the Bahamas. *See* OOLITE.

Landward of this zone, the deposits, formed when sea level rose rapidly, are thin blankets of calcareous debris, consisting of shell material, bryozoa, coral debris, and so forth (**Fig. 3**). The only active sedimentation zones occur very near the shore, where calcareous and sometimes land-derived sand, silt, and clay are being deposited at present, and at the outermost shelf margin and continental slope, where a blanket of fine-grained calcareous mud very rich in planktonic Foraminiferida is found (foraminiferid calcilutite and calcarenite). Calcareous shelves occur in the Persian Gulf and off the coasts of Australia.

The rise of sea level has, in many regions, severely restricted the supply of sediment to the continental shelf. Along the eastern coast of the United States, the valleys of many rivers have been flooded, and during the present stable sea level, barriers have been built across them which restrict the escape of sediment from the estuaries. As a result, sedimentation on this shelf is slow, and relict transgressive sands occur nearly everywhere at the surface.

Much of the fine-grained sediment transported into the sea by rivers is not permanently deposited on the shelf but kept in suspension by waves. This material is slowly carried across the shelf by currents and by gravity flow down its gentle slope, and is finally deposited either on the continental slope or in the deep sea. If submarine canyons occur in the area, they may intercept these clouds, or suspended material, channel them, and transport them far into the deep ocean as turbidity currents. If the canyons intersect the nearshore zone where sand is transported, they can carry this material also out into deep water over great distances. *See* SUBMARINE CANYON; TURBIDITY CURRENT.

Complex sediment patterns form in areas of considerable relief, for example, the borderland off southern California, where very coarse relict and residual sediments on shallow banks alternate rapidly with silty clays and calcareous deposits in the deep troughs. Such cases, however, are rare along the continental margins. Unimportant, but striking and geologically interesting, are the calcareous sediments associated with coral reefs and atolls. Usually, they occur on islands in mid-ocean, where clear water with abundant nutrients is available, and land-derived sediments are absent; but fringing and barrier reefs with associated calcareous sediments also occur along coasts with low sediment supply. *See* CONTINENTAL MARGIN; REEF. Tjeerd H. Van Andel

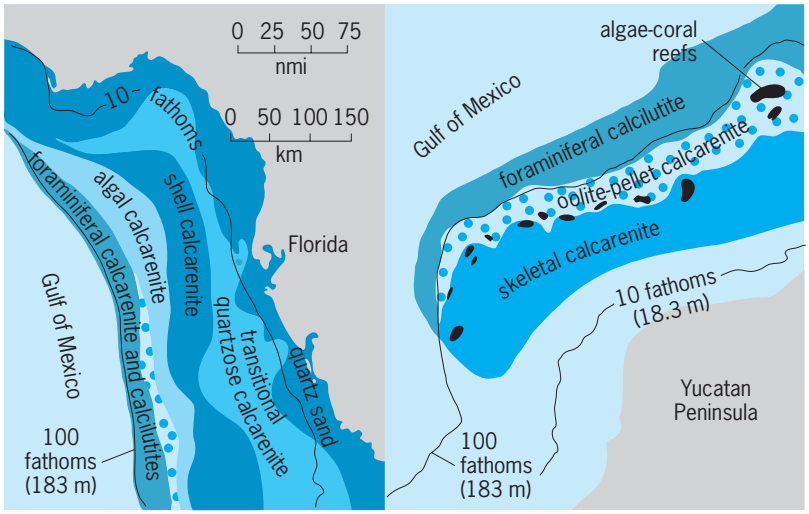

Fig. 3. Sediments on shelves with little land-derived sediment supply. (*a*) Off western coast of Florida. (*b*) Off northwestern Yucatan Peninsula.

Deep-sea sediments. Sediments covering the floor of the deep sea were first systematically described and classified during the late nineteenth century by J. Murray and A. F. Renard (1884, 1891) after their observations during the Challenger Expedition (1872–1876). Their classification included two principal sediment types, terrigenous (sediments deposited near to and derived from continental areas) and pelagic (sediments, principally fine grained, accumulated slowly by settling of suspended material in those parts of the ocean farthest from land). Both categories include biogenic and nonbiogenic material, as well as sediment derived from continents, that is, terrigenous, making the classification, at best, difficult to apply. Some of the terms, such as pelagic red clay, however, have remained in general usage but with meanings somewhat modified from the original definitions. A problem with most classifications has been in distinguishing descriptive categories, for example, red clay, from genetic categories, that is, those that include an interpretation of sediment origins, for example, volcanic mud. In addition, classifications are difficult to apply because so many deep-sea sediments are widely ranging mixtures of two or more end-member sediment types. The following sections will briefly describe the most important end members, their manner of origin, and some of the factors that control their distribution.

Biogenic sediments. Biogenic sediments, those that were formed from the skeletal remains of various kinds of marine organisms, may be distinguished according to the composition of the skeletal material, principally either calcium carbonate or opaline silica. The most abundant contributors of calcium carbonate to the deep-sea sediments are the planktonic foraminiferids, coccolithoforids, and pteropods. Organisms that extract silica from the seawater and whose hard parts eventually are added to the sediment are radiolaria, diatoms, and to a lesser degree, silicoflagellates and sponges. The degree to which deep-sea sediments in any area are composed of one or more of these biogenic types depends on the organic productivity of the various organisms in the surface water, the degree to which the skeletal remains are redissolved by seawater while settling to the bottom, and the rate of sedimentation of other types of sediment material. Where sediments are composed largely of a single type of biogenic

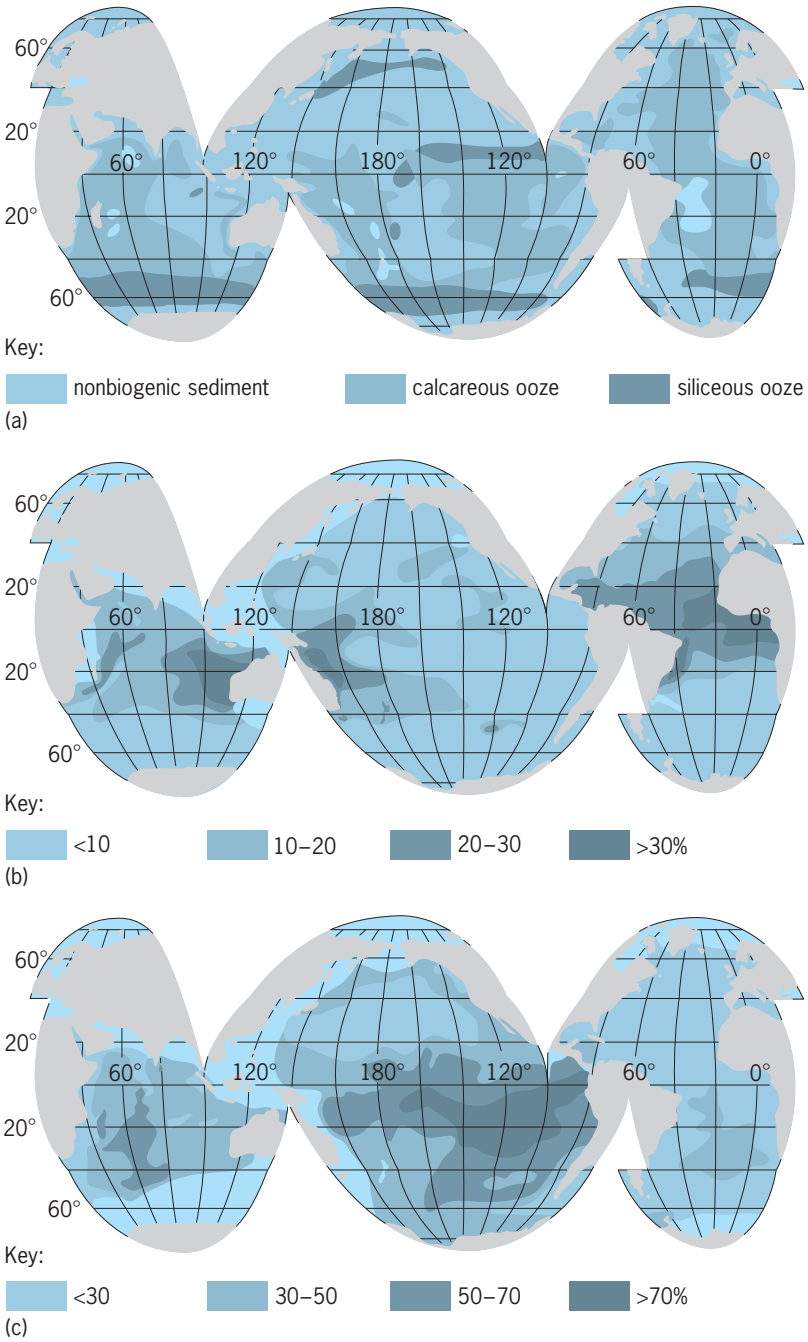

Fig. 4. Distribution of deep-sea sediments. (*a*) Major types. (*b*) Kaolinite concentration. (*c*) Montmorillonite concentrations. The concentrations are in the <2-μm-size fraction on a carbonate-opaline-silica-free basis.

material, it is often referred to as an ooze, after its consistency in place on the ocean floor. Thus, depending on the organism, it may be called a foraminiferal ooze (or globigerina ooze, after one of the most abundant foraminiferid genera, *Globigerina*), coccolith ooze, pteropod ooze, or for the siliceous types, diatomaceous or radiolarian ooze. The distribution map of major sediment types (**Fig. 4***a*) does not distinguish the several types of organism, but indicates that the siliceous oozes are most abundant at high latitudes and in the highly productive areas of upwelling such as the Equatorial Pacific. Calcareous oozes are also abundant beneath zones of upwelling and along topographic highs such as the Mid-Atlantic Ridge. Their relative abundance in shallower water is due to an increased tendency for calcium carbonate (calcite) to redissolve at ocean depths greater than about 13,000 ft (4000 m) because of lower water temperature, greater pressure, and increased dissolved carbon dioxide in the water.

Nonbiogenic sediments. The nonbiogenic sediment constituents are principally silicate materials and, locally, certain oxides. These may be broadly divided into materials which originate on the continents and are transported to the deep sea (detrital constituents) and those which originate in place in the deep sea, either precipitating from solution (authigenic minerals) or forming from the alteration of volcanic or other materials. The coarser constituents of detrital sediments include quartz, feldspars, amphiboles, and a wide spectrum of other common rock-forming minerals. The finer-grained components also include some quartz and feldspars, but belong principally to a group of sheet-silicate minerals known as the clay minerals, the most common of which are illite, montmorillonite, kaolinite, and chlorite. The distributions of several of these clay minerals have yielded information about their origins on the continents and, in several cases, clues to their modes of transport to the oceans. For example, the distribution map of kaolinite concentrations in the less than 2-micrometer fraction (Fig. 4*b*) shows that this mineral occurs in the deep sea principally adjacent to continental areas, mostly at low latitudes, where it is a common constituent of tropical soils. Its distribution indicates that it occurs only in the deep sea as a detrital phase and, in the western Equatorial Atlantic, appears to be carried to the ocean only by rivers. On the eastern side of the Equatorial Atlantic, however, its more widespread distribution corresponds with a region of frequent dust storms and suggests that its transport there is both by rivers and by the Northeast Trade Winds.

One of the common clay minerals, montmorillonite, has both a detrital and volcanogenic origin in different parts of the deep sea. In the Atlantic Ocean, its distribution is controlled by its relative abundance in the soils of adjacent continental areas, whereas in the South Pacific Ocean its great abundance results from its formation, along with authigenic minerals called zeolites, as an alteration product of widespread volcanic glass (Fig. 4*c*). The reason these materials—both the volcanic glass shards and their alteration products—are so abundant in the South Pacific is that they are relatively undiluted by detrital constituents, the South Pacific being so large and rimmed by numerous deep trenches which act as traps for seaward-moving detrital sediments. *See* CLAY MINERALS; ZEOLITE.

An authigenic constituent of deep-sea sediments that has received much attention, because of the potential economic value of trace elements that occur with it (principally copper), is manganese oxide (MnO_4). This material occurs in many areas

as manganese-iron nodules. These are spheroidal pellets of MnO_4 and iron(III) oxide (Fe_2O_3), ranging in size from microscopic to tens of centimeters in diameter and covering thousands of square miles of the deep-sea floor, principally in areas where both biogenic and nonbiogenic sedimentation rates are very slow. *See* MANGANESE NODULES.

Both in the case of biogenic and nonbiogenic sedimentation, the old concept of a slow, gentle "snowfall" of sediment particles to the sea floor where they remain forever buried, has been shown to be untrue in many parts of the ocean. Agencies are at work within the deep sea capable of distributing and redistributing sediment from its point of origin or entry in the ocean. Turbidity currents, high-density clouds of entrained sediment, are responsible for rapidly moving downward vast amounts of sediment from the continental slopes and other topographic highs. In addition, the deep oceanic current systems have been shown to be capable of eroding and transporting sediment along the ocean floor. The evidence for this comes from deep-sea photographs that show current ripple marks and scour marks in many parts of the ocean as well as measurements of relatively turbid zones of water traveling near the bottom (the nepheloid layer) in many parts of the ocean; this research suggests a rather continuous process of sediment erosion and redeposition. This process is discussed in a later section on transport and rate of sedimentation.

Ancient sediments. Because intensive studies of deep-sea sediments are a relatively recent phenomenon in the study of the Earth, and because the surface layer of sediment covers nearly two-thirds of the Earth's surface, investigators have only begun to understand the factors that presently control the distribution of sediments. An entire additional dimension, however, is introduced by extending these studies down through the sediment column, that is, back through geologic time. Samples of sediment have been taken in deep-sea cores back through the Pleistocene, Tertiary, and as old as Jurassic, or more than 130,000,000 years old. The studies on these older deep-sea sediments show that sedimentary conditions were very different from those that now obtain. Several studies in the Pacific Ocean and results from the Atlantic Ocean suggest that sediments derived from volcanic sources were possibly much more important in late Mesozoic and during most Tertiary time, and that the importance of detrital sediment sources is a relatively recent phenomenon, beginning as late as Pliocene or Pleistocene time. *See* JURASSIC; MESOZOIC; PLEISTOCENE; PLIOCENE; TERTIARY.

Pierre E. Biscaye

Physical Properties

Physical properties of marine sediments, such as density and the elastic constants, depend on many factors. These include grain shapes, sizes, and compositions; the amount of interstitial fluid and its properties; the nature of grain-to-grain contacts; the degree of compaction and consolidation; and the age. Measurable physical quantities appear to be affected to a much greater extent by the fractional volume of fluid in the sediment (porosity) than by sediment type. This is to be expected since density and elastic constants do not differ much for the principal constituents of sediments (silica, calcium carbonate, clay minerals). Water depth affects physical properties only to a slight extent.

Some measurements of physical properties are made on samples recovered from the ocean bottom by coring devices or in sufficiently shallow water by divers. Such observations are limited to sediments lying within a few tens of feet of the water-sediment interface. Properties of deeper-lying sediments are known from seismic refraction measurements of the velocities of elastic waves, by inference from dispersion of surface waves, or from gravity data (**Table 1**).

TABLE 1. Typical measurements of selected properties of marine sediments

Property measured	Fine sand, 17-station average[a]	Clayey fine silt[a]	Gray clay or silt[b]		Cream calcisiltite[c]		Gray clay[c]	Artificially compacted globigerina ooze pressure,[d] kg/cm^2		
								512	768	1024
Medium grain diameter, mm	0.19	0.02			[0.01][e]	[0.01]				
ρ, g/cm^3	1.93	1.60	1.72	1.58	1.60	1.71	1.46	2.14	2.22	2.26
ϕ, %	46.2	65.6	[56]	[65]	65	57	74	[32]	[28]	[26]
α, km/s	[1.68]	[1.46]			1.59	1.68	1.49	2.68	2.89	3.06
β, km/s								1.20	1.42	1.57
σ (Poisson's ratio)	0.44[f]	0.50[f]						0.37	0.34	0.32
κ, 10^{-11} dyne/cm^2	[0.472]	[0.342]						1.13	1.25	1.38
μ, 10^{-11} dyne/cm^2	[0.06][g]	[0.00][g]						0.31	0.45	0.56
Thermal conductivity, 10^{-4} cal/(cm)(°C)(s)			26.8	23.1						
Approximate water depth, fathoms	15	15	1000	1000	2300	1600	2550			

[a]After E. L. Hamilton et al., 1956. [b]After E. Bullard, 1954. [c]After G. H. Sutton et al., 1957. [d]After A. S. Laughton, 1957. [e]Brackets indicate conversion of units from those used in the original publication. [f]fLower limit. [g]Upper limit.

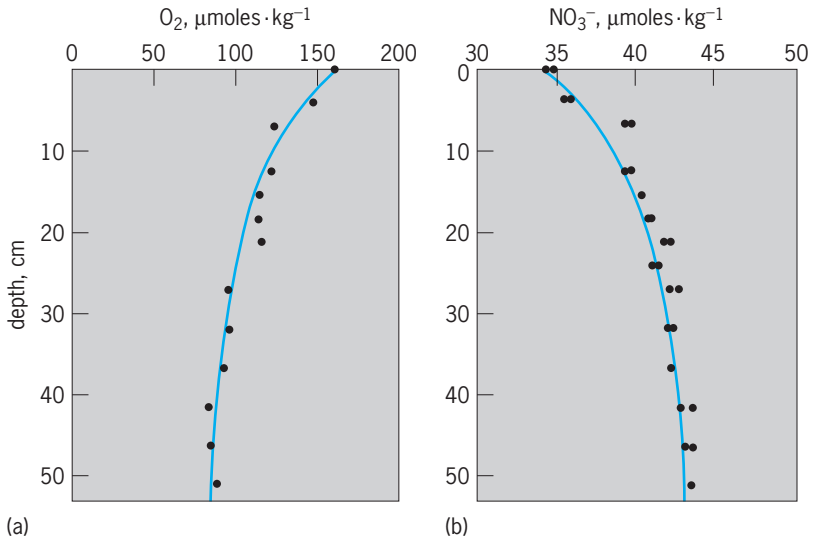

Fig. 5. Dissolved (*a*) oxygen (O_2) and (*b*) nitrate (NO_3^-) in the interstitial water of a pelagic marine sediment. 1 cm = 0.4 in.

Definitions and some useful interrelationships among measurable quantities are given by Eqs. (1)–(5), where ρ_1 and ρ_2 are fluid and average particle densities, respectively, ϕ is the porosity ($\phi = 1$ at 100% fluid, $\phi = 0$ at 0% fluid), μ is rigidity, and σ is Poisson's ratio.

$$\rho = \rho_1\phi + \rho_2(1-\phi) \quad \text{(bulk density)} \tag{1}$$

$$\alpha = \sqrt{(k + {}^4/_3\mu)/\rho} \quad \text{(compressional wave velocity)} \tag{2}$$

$$\beta = \sqrt{\mu/\rho} \quad \text{(shear wave velocity)} \tag{3}$$

$$\left(\frac{\alpha}{\beta}\right)^2 = \frac{2(1-\sigma)}{(1-2\sigma)} \tag{4}$$

$$k = \frac{1}{C} \quad \text{(incompressibility = 1/compressibility)} \tag{5}$$

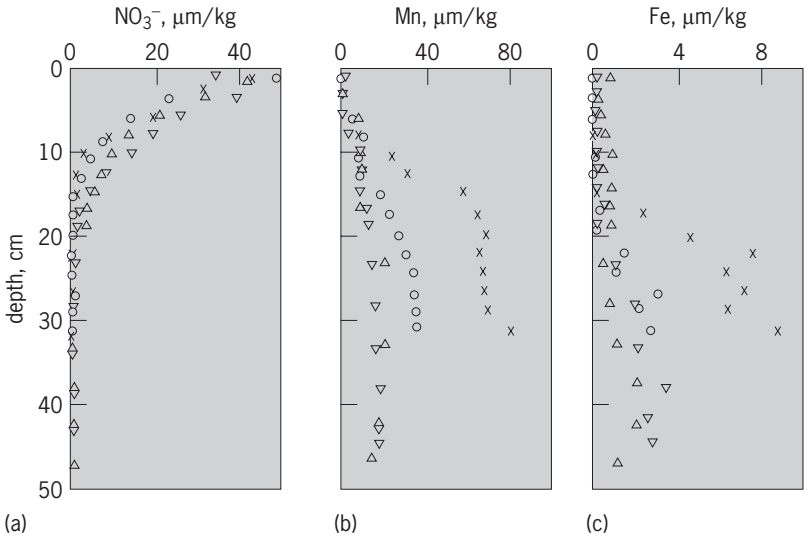

Fig. 6. Dissolved (*a*) nitrate (NO_3^-), (*b*) manganese (Mn), and (*c*) iron (Fe) in the interstitial water from a hemipelagic marine sediment. Symbols represent different cores. 1 cm = 0.4 in.

Several general conclusions may be drawn from observations. Density and porosity are nearly linearly related and for most ocean sediments observations lie between the two lines, as in Eq. (6). Compressional wave velocities for $\phi > 0.6$ agree well with the predictions, or equation, of A. B. Wood. This is obtained by inserting into Eq. (2) $\mu = 0$ and $C = 1/k = C_1\phi + C_2(1-\phi)$, where C_1 and C_2 are compressibilities of fluid and particles, respectively. At smaller porosities compressional velocity rises more steeply, the $\phi = 0$ limit being near 6 km/s. Poisson's ratio may be expected to vary from a value near 0.25 at zero porosity to 0.5 at $\mu = 0$. Good agreement of α with the Wood equation for $\phi > 0.6$ indicates that σ reaches its upper limit near $\phi = 0.6$.

$$\rho_{cgs} = 1.03 + (1.67 \pm 0.05)(1-\phi) \tag{6}$$

Seismic refraction measurements indicate that compressional velocity increases with depth in the sedimentary column, the gradient being from 0.5 to 2.0/s. Thus ρ, μ, k, β should also increase with depth and ϕ and σ decrease.

John E. Nafe

Sediment Chemistry

The chemical compositions of interstitial waters are modified from seawater by reactions with organic matter and with the silicate, carbonate, and oxide solid phases in the sediments. While research was formerly concerned primarily with the major ions and silica, emphasis has shifted to the diagenesis of organic matter in marine sediments.

Interstitial waters. Respiration of sedimentary organic matter influences the concentrations of nutrients, alkalinity, and pH. The sequence of reactions for the oxidation of organic matter follows the order of free energy that can be gained during bacterial metabolism. Oxygen is the thermodynamically favored electron acceptor, followed by nitrate, manganese(IV), iron(III), and sulfate. To a first degree, these metabolic processes are segregated into vertically isolated zones. In nature, the boundaries between these zones are obscured by interdiffusion and, in some cases, bioturbation.

Oxidation and nitrification. In the deep sea, little metabolizable organic matter reaches the sediments, the sedimentation rate is slow, and thus the effects of early diagenesis in the top 20 in. (50 cm) of sediments are small. Results on in-place samples from pelagic red clay and carbonate ooze sediments in the Central Equatorial Pacific reveal that aerobic respiration with nitrification is the dominant microbial process. In these sediments, oxygen decreases with depth and the nitrate increases with depth (**Fig. 5**). The stoichiometry of the oxidation reactions must be considered approximate because of uncertainty in the composition of the decomposing organic matter. In all cases from this region, the oxygen profiles level off at some constant value that is greater than 50 μmoles · kg^{-1}.

These profiles can be used to calculate the diffusive flux from the overlying water into the sediments. This steady-state flux can be estimated by using Fick's

first law, as given by Eq. (7), where $D_{O_2,pw}$ is the dif-

$$\text{Flux } O_2 = -D_{O_2,pw}\,\phi\left(\frac{dO_2}{dz}\right)_{z=0} \qquad (7)$$

fusion coefficient for oxygen in the pore water, ϕ is the porosity, and $(dO_2/dz)_{z=0}$ is the gradient at the sediment-water interface. The average diffusive flux of oxygen from seawater into the sediments at these locations was 9.0×10^{-14} moles · cm^{-2} · s^{-1}. The location for aerobic respiration also indicates that alkalinity and pH will decrease during oxygen consumption in red clay sediments. In carbonate ooze sediments, the carbon dioxide (CO_2) produced during respiration dissolves calcium carbonate ($CaCO_3$), and thus the alkalinity will increase. Both of these predicted changes in alkalinity have been observed in pelagic aerobic red clay and carbonate ooze sediments respectively. *See* PH.

Denitrification. Proceeding from aerobic sediments with low organic carbon to sediments with higher sedimentation rates and organic carbon, oxygen is reduced to lower values until it is completely removed. In the absence of dissolved oxygen, bacteria turn to nitrate (NO_3^-) as an electron acceptor and reduce it to nitrogen (N_2) [denitrification]. For example, nitrate decreases to zero by about 8 in. (20 cm) in organic-rich hemipelagic sediments of the Eastern Tropical Pacific (**Fig. 6**). The gradient in NO_3^- results in a flux of NO_3^- from seawater into the sediments, where it is reduced to nitrogen gas. Similar nitrate gradients have been observed in the Equatorial Atlantic. Calculations of the resulting diffusive fluxes of nitrate indicate that hemipelagic sediments may be important sites of marine denitrification.

Manganese and iron reduction. Manganese(IV) reduction and iron(III) reduction are the major microbiologically mediated reactions that follow the reduction of NO_3^-. Thermodynamic calculations suggest that Mn(IV) reduction should precede Fe(III) reductions. These predictions appear to be borne out when the reactions are suitably well spaced over the sediment column. As seen in the hemipelagic sediments of the Eastern Tropical Pacific (Fig. 6), dissolved manganese ion (Mn^{2+}) begins to build up in the interstitial waters after NO_3^- has been almost completely removed. Reduced Fe(II) does not appear until further down in the sediments. The buildup of reduced forms of manganese and iron creates concentration gradients in the interstitial waters that result in a flux toward the sediment–water interface for both metals. Both metals reoxidize when they reach oxidizing conditions. The diagenetic remobilization and upward flux of reduced manganese has been proposed as a source for manganese in ferromanganese nodules, as well as causing an excess of solid manganese in the surface layers of some marine sediments.

The reduction of Mn(IV) and Fe(III) oxides appears to control the interstitial water profiles of other trace metals as well. In particular, copper (Cu) and nickel (Ni) appear to be released when Mn(IV) is reduced, and cadmium (Cd) when Fe(III) is reduced. These metals also diffuse toward the sediment-water interface, where they may accumulate in manganese nodules, readsorb on Mn(IV) and Fe(III) oxides in the sediments, or enter the water column.

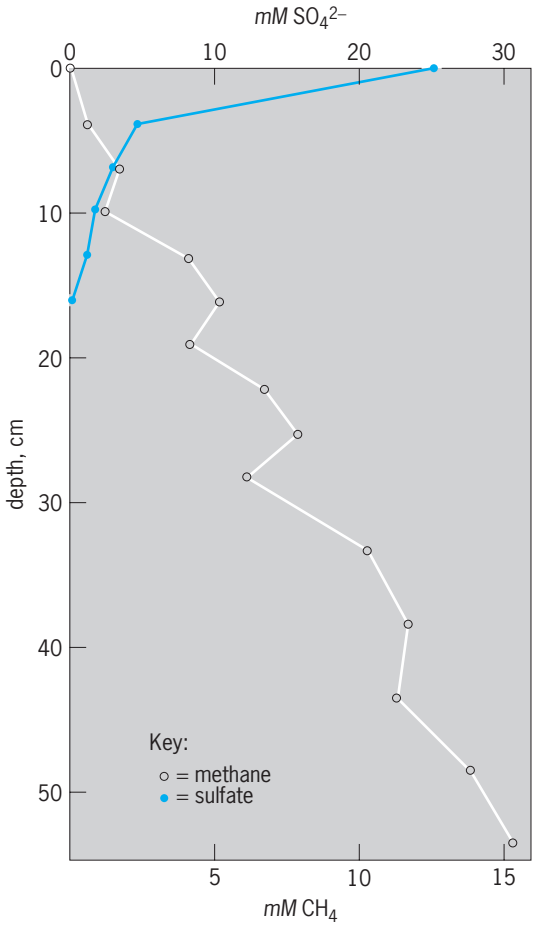

Fig. 7. Dissolved sulfate (SO_4^{2-}) and methane from extremely reducing sediments in Saanich Inlet. 1 cm = 0.4 in.

Sulfate reduction. Following Mn(IV) and Fe(III), sulfate (SO_4^-) is the energetically most favorable electron acceptor. Sulfate reduction is especially intense in rapidly accumulating sediments, rich in organic matter. Sulfate reduction has been intensively studied in the sediments of Long Island Sound and Saanich Inlet (British Columbia, Canada). Sulfate decreases rapidly in these sediments and in some cases is completely consumed by 5.9 in. (15 cm) [**Fig. 7**]. As sulfate is reduced, hydrogen sulfide ion (HS^-) accumulates in the sediments and diffuses toward the sediment–water interface. In some fiords with restricted circulation (such as Saanich Inlet), the HS^- that diffuses out of the sediments can accumulate in the bottom waters.

Following sulfate reduction, methane (CH_4) formation can proceed by two possible pathways: acetic acid fermentation [reaction (8)] and CO_2 reduction [reaction (9)]. The methane produced by these

$$CH_3COOH \longrightarrow CH_4 + CO_2 \qquad (8)$$

$$CO_2 + 8H_2 \longrightarrow CH_4 + 2H_2O \qquad (9)$$

reactions will also diffuse upward and may accumulate in the overlying water (Fig. 7).

Silicate and carbonate reactions. It has been suggested that reactions with silicates and carbonate control the interstitial water concentrations of sodium (Na^+), potassium (K^+), Ca^{2+}, and Mg^{2+} and also influence the alkalinity. Samples have shown that diagenesis leads to the uptake of Mg^{2+} and K^+ and the release of Ca^{2+}, bicarbonate ion (HCO_3^-), and Na^+ by the solid phases. The exact nature of the reactions is uncertain, but reverse weathering reactions may play a role. The calculated fluxes across the sediment–water interface are of the same order of magnitude as river inputs for these ions. In the case of Mg^{2+} and K^+, 60–100% of the river input to the ocean can be balanced by diagenetic uptake in the sediment. Ca^{2+} and HCO_3^- additions to seawater augment the river supply by 25 to 50%.

James W. Murray

Carbonate and opal dissolution. Skeletal remains of calcareous planktonic organisms such as foraminifera, coccoliths, and pteropods, and of siliceous planktonic organisms such as radiolarians and diatoms, dissolve partially or entirely in ocean water as they settle through the water column or after they are deposited on the ocean floor. This dissolution, along with that of the remains of benthic shell-secreting organisms, constitutes a major chemical feedback mechanism in the material cycle of calcium, carbon, and silica in the oceans.

Distribution. The concentration of $CaCO_3$ (calcite and aragonite) in recent pelagic sediments (excluding those near the continents and islands) have been measured in various regions of the world oceans as a function of water depth (**Fig. 8**). In shallower depths, down to about 13,000 ft (4000 m), it is nearly constant at about 90 wt % (as $CaCO_3$), and gradually decreases to 5 wt % or less at a water depth of 15,000–16,000 ft (4500–5000 m). The water depth at which the $CaCO_3$ content starts to decrease has been called the sedimentary lysocline, and that at which the $CaCO_3$ content is reduced to 5% or less is called the carbonate compensation depth (CCD). When morphological changes of the tests of certain biological species are used to identify the beginning of $CaCO_3$ loss, the water depth that marks the first appearance of such changes is called the

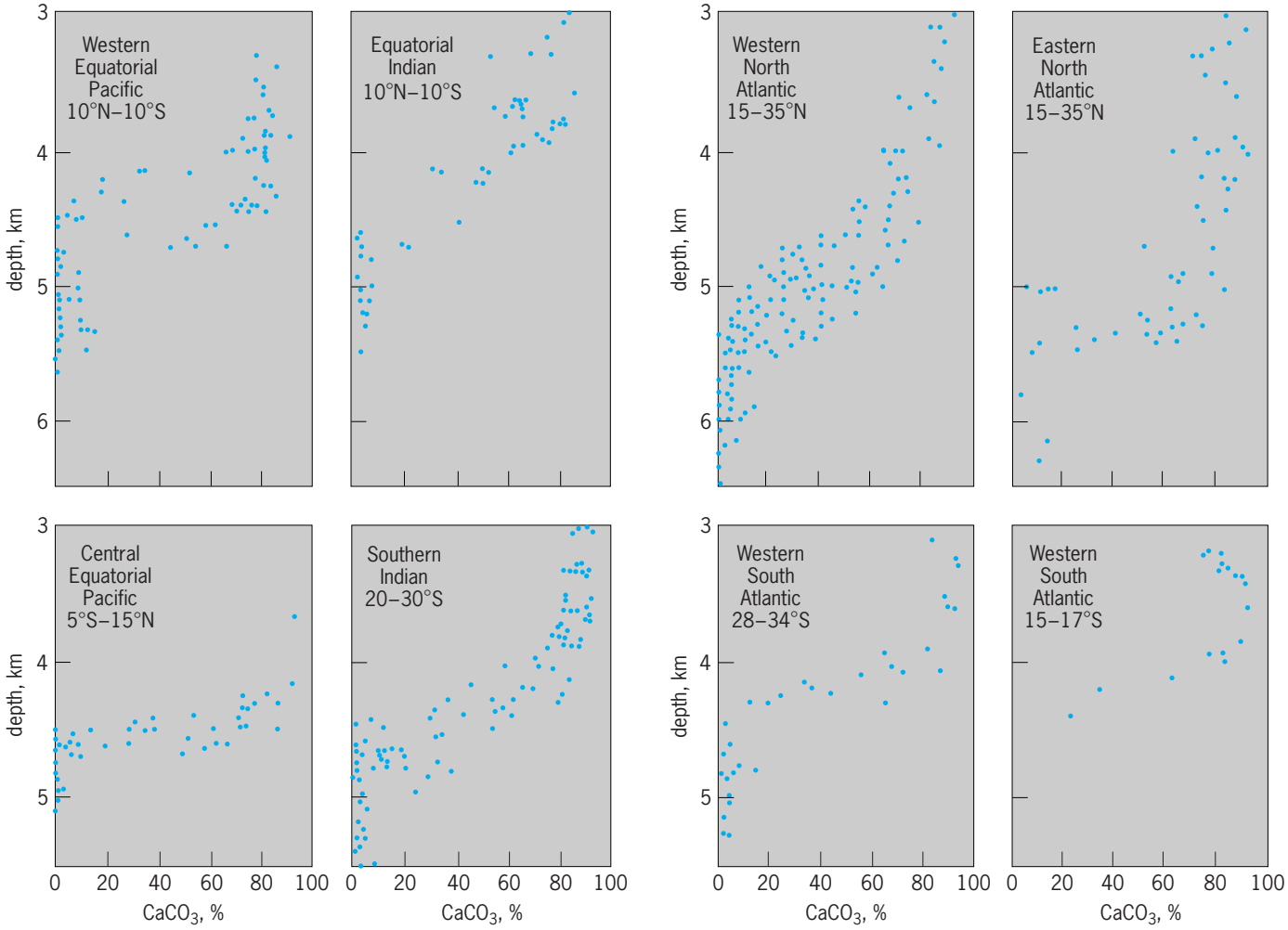

Fig. 8. $CaCO_3$ concentration in recent deep-sea sediments in eight regions of the world oceans as a function of water depths. Both aragonite and calcite are included as $CaCO_3$. 1 km = 0.6 mi. (*After N. Andersen and A. Malahoff, eds., The Fate of Fossil Fuel Carbon Dioxide in the Oceans, Plenum Press, 1977*)

foraminifera or pteropod lysocline according to the organisms used for its identification. Such distinctions are necessary since the lysocline identified on the basis of the $CaCO_3$ content in sediments does not necessarily coincide with that determined on the basis of morphological observations. Such a discrepancy may be attributed to the dissolution of tests that occurs in the guts of some feeders or in the sediments.

In contrast to the clear dependence of the $CaCO_3$ distribution on the water depth, the distribution of opaline silica does not depend upon the water depth. Instead, it appears to correlate well with the biological productivity of silica-secreting organisms in the surface water, which, in turn, depends on the intensity of the vertical circulation and the upwelling of deep waters rich in silica and other nutrient salts. Thus, sediments rich in siliceous tests are found in the belt around the Antarctica continent, in the northernmost Pacific, and in the equatorial zone of the world oceans.

Solubility. The observed decrease in $CaCO_3$ content in pelagic sediments with increasing water depths can be mainly attributed to the undersaturation of the deep waters with respect to calcium carbonate minerals, aragonite (pteropod shells), and calcite (foraminifera and coccolith tests). This undersaturation is caused by increased solubilities of these minerals with increasing pressure and decreasing temperature, and the lower pH. The smaller concentrations of CO_3^{2-} ion in deep waters are therefore caused by the greater concentration of CO_2 that is produced by microbial oxidation of the falling organic debris in the water column.

The concentration of calcium ion in ocean water is nearly constant (10.26 m*M*/kg), and the solubility of aragonite and calcite is expressed in terms of the CO_3^{2-} concentration in seawater. Pressure (or the water depth) affects the solubilities of calcite and aragonite (**Fig. 9**). Waters in the upper layer of the oceans down to about 1600 ft (500 m) in the Pacific and 9800 ft (3000 m) in the Atlantic are supersaturated with respect to aragonite, and below these water depths the water is undersaturated and becomes corrosive to aragonite. Therefore, the aragonitic tests of such organisms as pteropods are dissolved in seawater and are not found in sediments located at water depths greater than several hundred meters in the Pacific and 9800 ft (3000 m) in the Atlantic, although aragonitic organisms appear to be as equally abundant as calcitic ones in plankton tow samples collected in surface waters. Deep ocean waters below 13,000 ft (4000 m) in the Pacific and 15,000 ft (4500 m) in the Atlantic are undersaturated with respect to calcite, the less soluble form of $CaCO_3$. This accounts for the decrease in $CaCO_3$ content in deep-sea sediments. The rate of calcite dissolution increases as a third- to fourth-power function of the degree of saturation, and it increases rapidly with the water depth below the saturation level (see Fig. 9). At the carbonate compensation depth, the rate of deposition of calcite tests becomes equal to (or compensated by) the rate of dissolution, and thus little or no accumulation of $CaCO_3$ takes place below (**Table 2**).

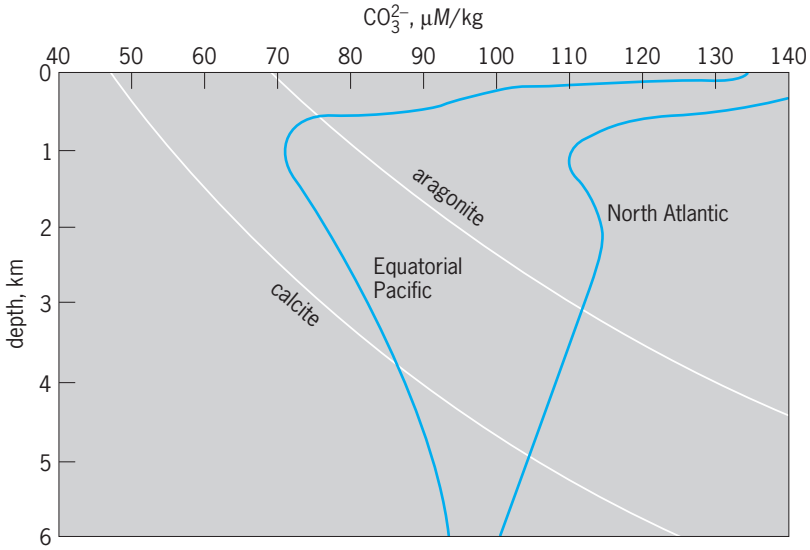

Fig. 9. Solubility of aragonite and calcite [expressed in terms of carbonate (CO_3^{2-}) ion concentration] in seawater at 2°C (36°F) as a function of water depths in the North Atlantic and the eastern Equatorial Pacific. The intersections of the solubility curves with the curves for the concentration of the CO_3^{2-} ion indicate the water depths at which the ocean water is saturated with the respective minerals. 1 km = 0.6 mi.

The solubility of opaline silica, the major constituent of siliceous tests, has not been determined exactly due to its variable stoichiometry, its slow reaction kinetics, and the presence of metastable silica species in seawater. However, it is in the range of 1.7 to 2.3 m*M*/kg at 25°C (77°F) and 1 atm (101 kilopascals) based on measurements made on amorphous silica and silica gel. The solubility increases slightly with increasing pressure. Since the concentration of silica dissolved in ocean water ranges from nearly zero in surface waters to about 0.17 m*M*/kg in the deep water of the North Pacific Ocean, the entire ocean is undersaturated with respect to opaline silica. Thus, the siliceous tests which form in the biologically active surface water dissolve during descent to the ocean floor and while they lie on the sea floor. It has been estimated that only about 4% of the siliceous tests formed in surface waters

TABLE 2. Estimated calcium carbonate balance in the Atlantic and Pacific oceans

Processes	Rates, $CaCO_3$ mg/(cm^2)(yr)	
	Atlantic	Pacific
Production of calcitic tests	1.3	0.9
Production of aragonitic tests	1.3	0.9
Total biogenic calcareous test production (aragonite + calcite)	2.6	1.8
Dissolution of calcareous tests in the oceans (aragonite + calcite)	1.9	1.5
Accumulation of calcareous tests on the ocean floor	0.7	0.3

TABLE 3. Silica budget in the oceans

Processes	Rates (10^{13} g/yr)
Supplies from rivers	43
Addition from alteration of basalts	8
Diffusion out of sediments	57
Burial of silica tests in sediments	104
Loss by inorganic silica adsorption	4
Biological fixation of silica	2500
Dissolution of tests in water column	2155
Dissolution of tests on sea floor	240

escape dissolution and become incorporated permanently into sediments (**Table 3**). Taro Takahashi

Organic geochemistry. Knowledge of the geochemistry of organic matter in sediments is important to the understanding of the global cycle of carbon in both ancient and modern times. Specific topics of importance are the origin of oil and gas, the climatic effects of perturbing the carbon cycle (for example, the CO_2 problem), contemporary sediments as temporary or permanent sinks for pollutant organic compounds (for example, pesticides and petrochemicals), and organic matter in ancient sediments as molecular paleontological markers and even as indicators of the origin of life on Earth.

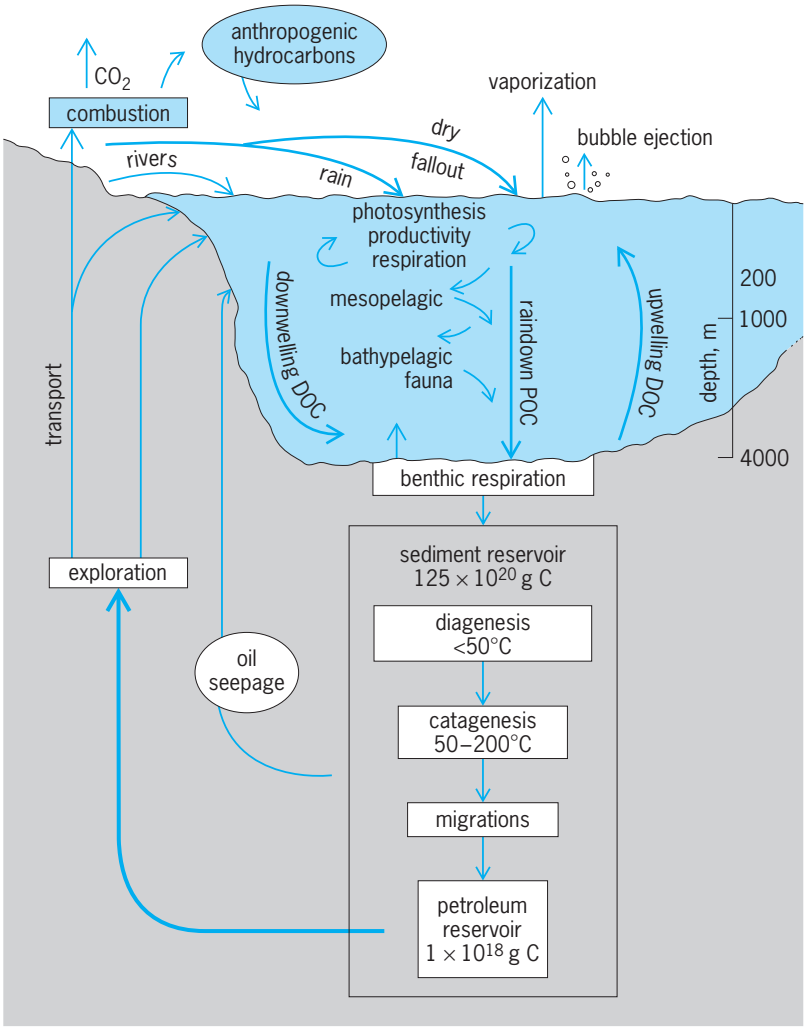

Fig. 10. Global organic carbon cycles. DOC = dissolved organic carbon; POC = particulate organic carbon. °F = (°C × 1.8) + 32; 1 m = 3.3 ft.

Sources of organic matter. In the contemporary marine environment, the carbon cycle involves certain mechanisms (**Fig. 10**). Organic matter in sediments is derived primarily from photosynthesis in the upper layers of the oceans or on land. A portion of this material escapes remineralization processes on land and in the upper layers of the ocean, and is transported by a variety of processes to sediments. Chemosynthesis by bacteria- and mineral-catalyzed reactions are very minor sources of organic matter synthesis.

Organic matter deposited to surface sediments undergoes a complex series of biotic and mineral-catalyzed reactions known as diagenesis (**Fig. 11**). Biologically synthesized polymers, carbohydrates, proteins, and lipids (fats) are broken apart to yield their constituent smaller molecules. Other organic polymers produced by biological systems such as chitinous skeletons of zooplankton and lignin from plants on land are less susceptible to breakdown to their constituent smaller molecules. Bacterial metabolism in sediments contributes other low-molecular-weight organic compounds such as phenols and aldehydes. It is thought that this complex assemblage of low-molecular-weight organic compounds and higher-molecular-weight biopolymers such as chitin and lignin react to produce humic and fulvic materials similar to humic and fulvic materials in soils. The exact mechanisms, rates of reaction, and even the structures of the humic and fulvic acid type of materials are not known. Some evidence is available to support the general scheme (Fig. 11). *See* DIAGENESIS.

Oil and gas formation. Microbial activity decreases and the relative importance of chemical reactions increases as sediments accumulate and the organic matter is buried deeper (Fig. 11). Over periods of thousands to millions of years the humic and fulvic type of materials plus other organic matter are converted to kerogen, itself an ill-defined polymeric structure (Fig. 11). If conditions of heat input, clay catalysis, kerogen composition, and geological structures are appropriate, oil can be formed. Other, slightly different conditions can yield gas. Sometimes the process does not go to completion because of a change in geological conditions, for example, uplifting near the Earth's surface after millions of years of burial. This is exemplified by the oil shales in Colorado and Wyoming. Humans will complete the process of oil formation by heating the shale to drive out oil already trapped and to convert more of the kerogen to oil. *See* KEROGEN; OIL SHALE; PETROLEUM.

Cycle of organic matter. Knowledge of the source of organic matter in sediments is of importance in elucidating the cycle of organic matter in the oceans and sediments. Measurements of stable isotope ratios of carbon to $^{13}C/^{12}C$ have been used extensively for determining the relative importance of land plants and marine plants as sources of organic matter found in

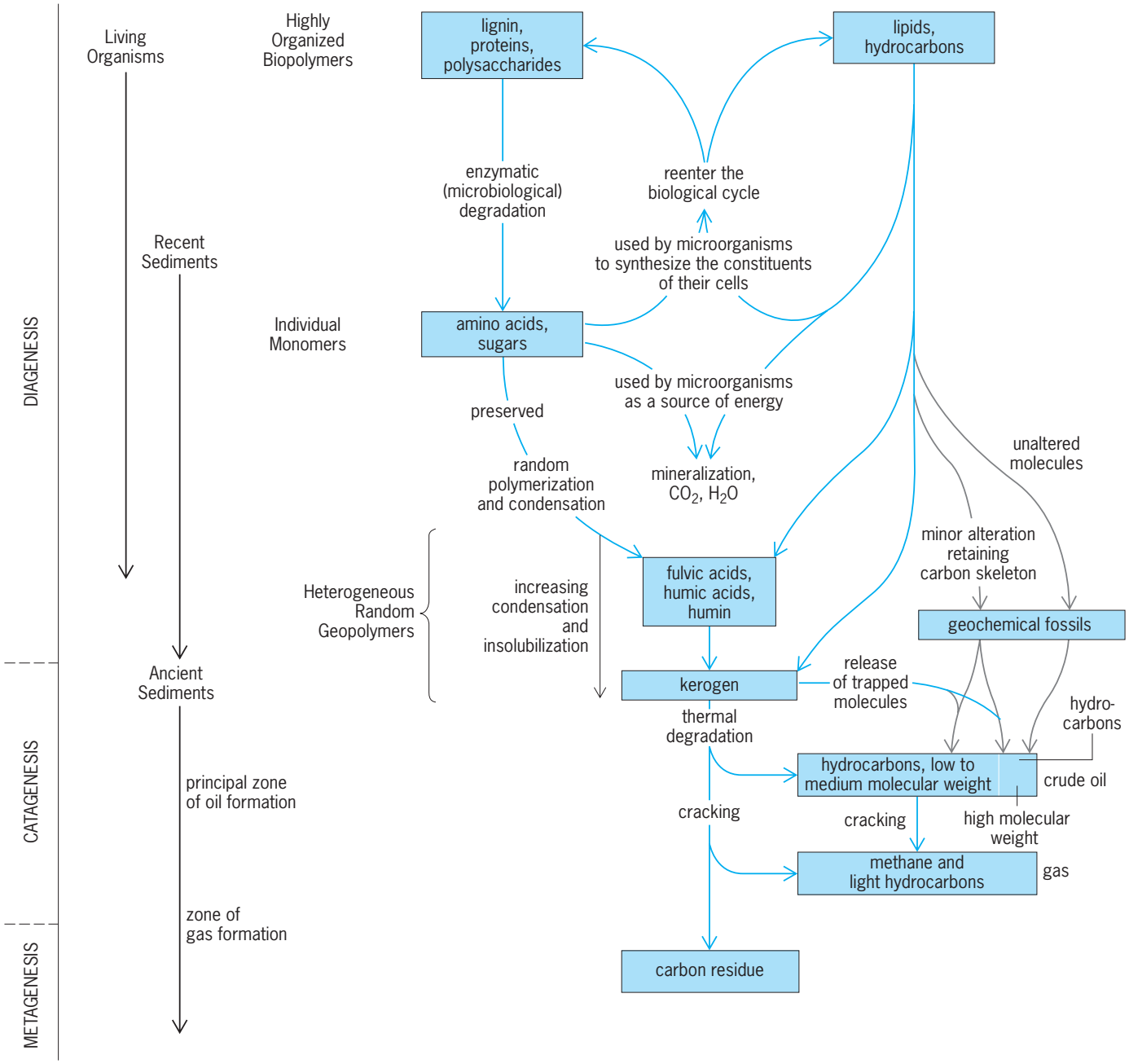

Fig. 11. Processes of change in marine sediments. (*After B. P. Tissot and D. H. Welte, Petroleum Formation and Occurrence, Springer-Verlag, 1978*)

sediments. These ratios are conventionally expressed as shown in Eq. (10). [The standard commonly used

$$\delta^{13}C‰ = \frac{(^{13}C/^{12}C \text{ sample} : ^{13}C/^{12}C \text{ standard}) \times 1000}{^{13}C/^{12}C \text{ standard}} \quad (10)$$

is the Peedee Belemnite, or PDB—a particular carbonate rock formation.] Terrestrial plant organic matter is usually 5 to 10‰ lighter than marine plant organic matter. This is the result of the differences in the $\delta^{13}C$ value of atmospheric carbon dioxide, the source of land plant carbon, and the carbon dioxide–carbonate–bicarbonate source of carbon in marine plants. The differences between land-derived organic matter and marine-derived organic matter become less marked as diagenesis in young sediments and catagenesis in ancient sediments proceeds. Isotope fraction can accompany biochemical reactions in early diagenesis. Biogenic methane is produced with a $\delta^{13}C$ of -30 to $-50‰$, that is, encriched in the light ^{12}C isotope, while carbon dioxide produced by the same assemblage of microorganisms is enriched in ^{13}C. Different classes of organic matter, for example, lipids, proteins, or carbohydrates, generally have different ^{13}C values. The former class is usually enriched in ^{12}C relative to the latter two classes. Even within a given molecule such as an amino acid, the carbon atom of the carboxyl group has a different ^{13}C value than the other carbon atoms. By carefully

studying the carbon isotope ratios, some of the biological and geological processes which have acted on organic matter in a given sample can be inferred. The radioactive isotope ^{14}C is used to date organic matter in samples ranging from contemporary to 50,000 to 75,000 years old. *See* RADIOCARBON DATING.

Organic structures. The detailed chemical structure of organic matter in sediments is poorly known relative to knowledge of the chemical structure of organic matter in organisms. Various estimates of 10 to 30% are given for that portion of organic matter in seawater or sediments for which information on chemical structures is available since fulvic acid, humic materials, and kerogen are very complex assemblages of organic matter. Nevertheless, sophisticated, sensitive, highly selective analytical chemical tools such as high-resolution gas chromatography–mass spectrometry of the organic compounds in that 10 to 30% of the organic matter has provided a wealth of information about the sources of the organic matter and the processes acting on it prior, during, and after deposition in sediments. Biosynthetic pathways in organisms lead to some very specific structural configurations for the molecules. This structural specificity was a major clue that led to the conclusion that oil in ancient sediments had a biological origin (Fig. 11). Several compounds serve as markers of a particular source of organic matter input, for example, bacterial fatty acids, land-plant *n*-alkanes, land-plant lignin, marine phytoplankton fatty acids and sterols, and amino acids from bacteria. *See* BIOSYNTHESIS.

Geochemical transformations. During diagenesis, several types of geochemical transformations of structures can take place. Some, such as the amino acid racemization, have fairly predictable rates if the thermal history of a sample is known, and thus the ratios of particular isomers give an indication of the age of the sample or at least of the organic matter in the sample. Other reactions convert biological compounds such as sterols and fatty acids to hydrocarbons—aromatic hydrocarbons, steranes (cycloalkanes derived from sterols), and alkanes found in petroleum. *See* AMINO ACID DATING.

Much more research is necessary to unravel the wealth of information about processes active in modern and ancient sedimentary environments that is contained collectively and individually in the many thousands of organic compounds found in ancient and modern sediments. A major advance in analytical chemistry allowed scientists to combine stable isotope measurement with specific compound analyses to determine the isotope ratios of individual compounds in a wide range of biological and geological samples. This approach has provided powerful new information about the carbon cycle and about the processes that yield oil and gas. *See* ORGANIC GEOCHEMISTRY.

John W. Farrington

Transport and Rate of Sedimentation

Rivers, glaciers, wind, and ocean waves and currents carry particles from continents and continental margins to the various environments of deposition in the ocean. The rates of sedimentation can be determined by study of the micropaleontology, radioactivity, or paleomagnetism of the sediments.

Transport of sediments. Most of the sediment eroded from continents enters the oceans at its margins, though some is delivered to the open sea by the wind or by icebergs. Much of this material, and some of the pelagic sediment produced by the life processes of marine plankton, is redistributed by currents within the ocean basins. *See* NEARSHORE PROCESSES.

Turbidity currents. Density flows that derive their energy from high concentrations of suspended sediment are efficient but episodic agents of downslope sediment transport. Their most important role is dispersing sediment from continental margins to abyssal plains and deep-sea fans, but they also may be effective in locally redistributing pelagic sediment in mid-ocean areas of high relief. Turbidity currents are thought to have velocities of several meters per second, especially where they are channelized in submarine canyons and fan valleys, and are competent to transport sediment grains of up to coarse gravel size. Larger blocks of sediment move downslope in debris flows.

Thermohaline currents. Branches of the general oceanic circulation that are driven by pressure differences caused by temperature and salinity distributions transport large amounts of fine sediment in some parts of the deep ocean. They are slower (generally less than 20 in./s or 50 cm/s) but much steadier than turbidity currents, and carry sediment both in suspension, as a so-called bottom nepheloid layer, and as bed load (**Fig. 12**). Because these currents typically flow along rather than across bottom contours, geologists often refer to them as contour currents. They may transport fine suspended clay for hundreds of kilometers along the basin margins even where current velocities are low (<4 in./s or 10 cm/s); bed-load transport, for most of the cohesionless particles available in the deep sea (for example, foraminiferal shells) requires speeds of about 8 in./s (20 cm/s). Where thermohaline currents are locally accelerated, as in constricted passages

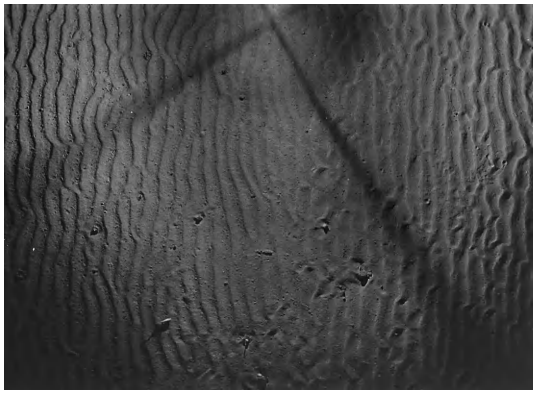

Fig. 12. Rippled sea floor of sand being transported along the bed of a thermohaline current. From a water depth of 8900 ft (2700 m) on the northwest side of the Rockall Plateau, North Atlantic.

between basins, they may attain speeds high enough for effective erosion of their beds.

Tidal currents. These currents are fast enough to entrain and transport silt and sand in some parts of the ocean, even at abyssal depths. Their effects are best known from shallow continental shelves, where alternating ebb and flood currents may build sand ridges and other bedforms. Oscillating sea-bed currents capable of moving sediment are also caused by the passage of surface waves and internal waves. Geological effects of internal waves are poorly known, but may be important at all water depths; normal wind-driven waves have no effect below a depth of about 660 ft (200 m), but tsunamis (seismic waves) can infrequently stir up sediment several kilometers below the ocean surface. *See* TSUNAMI.

Significance. The importance of sediment transport in the ocean is that the thickness of sediment on any part of the floor reflects past and present current regimes, not just crustal age and location of terrigenous and biogenous sediment sources. Some styles of erosion, transport, and deposition produce distinctive types of sediment (for example, turbidites and contourites) and distinctive topographic forms (for example, ripples and mud waves). *See* OCEAN CIRCULATION; TIDALITES; TURBIDITE. P. Lonsdale

Rates of sedimentation. The accumulation rates of sediments in the deep sea are determined either directly or indirectly through the use of natural radioactive nuclides. There are three sources of these nuclides: members of the decay series of the two uranium isotopes ^{235}U and ^{238}U dissolved in seawater; radioactive nuclides, such as carbon-14 (^{14}C), silicon-32 (^{32}Si), beryllium-10 (^{10}Be), and aluminum-26 (^{26}Al), produced in the atmosphere by cosmic rays and delivered to the ocean; and long-lived radionuclides, in particular potassium-40 (^{40}K) and ^{238}U, found in volcanic mineral and glass ejecta from explosive volcanoes (**Table 4**).

In addition to the direct use of radioactive nuclides, the magnetic reversal history of the Earth, as chronicled by the potassium-argon dating of basaltic lava flows on land, is commonly recorded in accumulating deep-sea sediments. So long as the pattern is preserved as a continuous record, sedimentary layers can be dated from the magnetic orientation pattern of the successive layers of sediment. *See* PALEOMAGNETISM; ROCK AGE DETERMINATION.

Sediment type and region. The sediment accumulation rates in the oceans vary depending on sediment type and region. Sediments dominated by clay-size grains are delivered to the ocean surface by streams (passing through estuaries) or winds and accumulate at a rate of about 0.1 in. (0.3 cm)/1000 years. Foraminiferan and coccolith-rich sediments (sometimes called ooze) accumulate at a rate of about 0.8 in. (2 cm)/1000 years. Diatom- and radiolarian-rich sediments also accumulate at these high rates. Detrital sediments supplied from the continental margins to the deep sea by turbidity currents and other forms of bottom transport accumulate in abyssal plains and associated areas at an average rate of about 2 in. (5 cm)/1000 years with a wide range around this value. As a crude estimate, the average rate of sediment accumulation in the deep sea is about 0.4–0.8 in. (1 to 2 cm)/1000 years. Additional sediments accumulate on the continental margins, and the two environments are the repositories of material derived from continental denudation.

Sediment activity. Sediments, once deposited on the sea floor, are hardly inactive. They are subject to biological and physical mixing at the interface, chemical dissolution and mobilization, and perturbation by slumping and scouring by bottom processes such as currents and sediment avalanches. These can affect both the rates of sediment accumulation as compared to the rate of sedimentation and the estimation of rates of accumulation using radionuclides.

Bioturbation. Bioturbation can be identified and its rate determined by the distribution in a sediment core of natural short-lived [lead-210 (^{210}Pb); half-life = 22 years] nuclides sequestered from the water column (**Fig. 13**) or recently introduced radionuclides (plutonium) produced by human activities. The depth of bioturbation is indicated by the effective homogenization of the concentration of the long-lived diagnostic radionuclides used for dating (such as ^{14}C; **Fig. 14**). The rates and depths of bioturbation vary throughout the deep ocean basin, but the average diffusionlike constant is about 8×10^{-8} in.^{2}/s (5×10^{-9} cm^2/s) and the average depth of mixing about 3 in. (8 cm).

Time scales of stability. Sediments can be lost or gained episodically to and from surrounding areas over a range of time scales. The bottoms of fracture zones commonly receive cascades of carbonate-rich sediments from the cliffs above. The stochastics of sediment perturbation on the ocean floor have not yet been studied adequately. Results based on thorium-230 (^{230}Th), ^{14}C, and ^{10}Be indicate time scales of stability ranging from less than 100,000 years (along the Mid-Atlantic Ridge) to 3,000,000 years (on the North Pacific ocean floor). The frequency of postdepositional sediment mobilization by episodic events will influence the geologic record in deep-sea sediments. The understanding

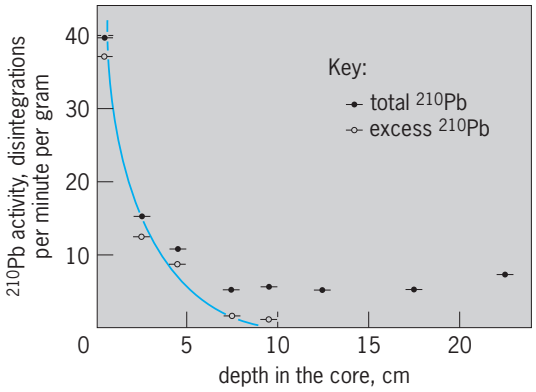

Fig. 13. Lead-210 (^{210}Pb) distribution in a sediment core (527-3) obtained by the research submersible *Alvin* from the *Famous* site (36°48.5′N, 33°15.3′W) on the Mid-Atlantic Ridge. The fit of the excess ^{210}Pb [that is, unsupported by radium-226 (^{226}Ra)] distribution to a diffusion equation yields a constant of 6×10 cm^2/s. 1 cm = 0.4 in. (*After Y. Nozaki et al., Earth Planet Sci. Lett., 34:167, 1977*)

TABLE 4. Radionuclides used in the chronology of deep-sea sediments

Radionuclides	Half-life, years	Useful range, years	Types of sediment
1. Uranium-decay-series nuclides			
Uranium-234 (from ^{238}U)	250,000	0–400,000	All
Thorium-230 (from ^{230}U)	74,500	0–300,000	All
Protactinium-231 (from ^{235}U)	32,000	0–120,000	All
2. Cosmic-ray-produced			
Silicon-32	277 (possibly 100)	0–2,000	Diatom and radiolarian deposits
Carbon-14	5,720	0–40,000	1. Principally calcareous (foram and coccolith deposits) 2. Organic fraction of deposits
Aluminum-26	0.72×10^6	$0–4 \times 10^6$	All
Beryllium-10	1.5×10^6	$0–8 \times 10^6$	All
3. Long-lived from volcanoes on land or tektites			
Potassium-40 (decay to ^{40}Ar)	1.25×10^{16}	>60,000	Feldspars, volcanic glass, tektites
Uranium-238 (fission tracks)	1.01×10^{16} (spontaneous fission)	$>10^6$	Volcanic glass, tektites
4. Magnetic reversal	—	$0–5 \times 10^6$	All with magnetic minerals

of the time scales of stability of sediment piles is also important for engineering uses of the deep-sea floor, such as platform construction and burial of radioactive wastes. Karl K. Turekian

Climatic Record in Sediments

Undisturbed sediments that accumulate at the ocean floor preserve important information regarding past processes in the overlying water column, on adjacent continents, in the atmosphere, as well as on the Earth as a whole. Sediments for climate-change studies are recovered by a variety of coring methods, from piston coring to drilling. The drilling vessel *JOIDES Resolution*, using advanced piston-coring and drilling techniques, has recovered continuous sequences of sediments extending to 100 million years ago (Ma). Typical pelagic sediments accumulate at rates of centimeters every 1000 years, although at some locations pelagic and hemipelagic sediments accumulate much more rapidly, preserving high-resolution records of climate change. Both slowly and rapidly accumulating marine sediments provide important information regarding past patterns of oceanographic and climatic change. Studies of the climate record preserved in marine sediments are collectively referred to as paleoceanography or paleoclimatology. *See* PALEOCEANOGRAPHY; PALEOCLIMATOLOGY.

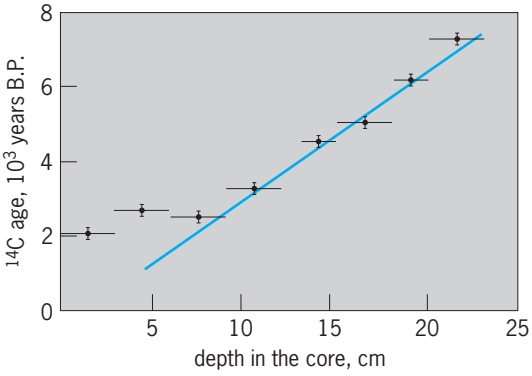

Fig. 14. Distribution of ^{14}C ages with depth in *Famous* core 527-3. The top 3.5 in. (9 cm) yield a constant age of 2400 years before present (B.P.) because of bioturbation. The deeper points define a line yielding a sediment accumulation rate of 2.9 cm/10^3 years. 1 cm = 0.4 in. (*After Y. Nozaki et al., Earth Planet. Sci. Lett., 34:167, 1977*)

Sediment indicators of climatic change. Information from marine sediments regarding past climate change can be inferred from measurements made from marine sediments. These measurements act as indicators, or proxies, of past climate. Proxy indicators for paleoceanographic processes are derived from the lithologic and biotic composition of sediments and from geochemical indices preserved in sedimentary components. Geochemical and isotopic proxies for climate processes are often derived from measurements made by using the microfossil

Problems	Successes
Assume either constant nuclide flux or invariant initial specific activity over time.	^{234}U: Not generally successful in sediment dating by itself but important adjunct to other decay-series nuclides. ^{230}Th: Established glacial climatic chronology of the last 300,000 years from fossiliferous deep-sea sediments in conjunction with uranium-decay-series chronometric studies of fossil hermatypic corals. ^{231}Pa: In conjunction with ^{230}Th, helps distinguish dilution versus decay in sediments.
Time scale comparable to bioturbation time scale. Useful for accumulation rate studies only in fast accumulating (> 0.8 in. or 2 cm/1000 years) sediments.	Established possibility of fast rates of siliceous sediment accumulation around Antarctica and in Gulf of California over hundreds of years.
Assumes constancy of initial $^{14}C/^{12}C$ ratio. Assumes no detrital organic matter. Also needs high organic content in sediment.	Established breaks in sediment accumulation rates of various components over the Pleistocene-Holocene boundary. Fast rates of accumulation in Argentine Basin and abyssal plains determined from organic matter.
Very low activity. Difficult to measure. Assume either constant flux or invariant initial specific activity over time.	Established that ^{26}Al primarily produced in atmosphere. Awaits future uses.
Low activity but successfully measured. Assume either constant nuclide flux or invariant initial specific activity over time.	Showed accumulation rates in North Pacific effectively constant over 3,000,000 years. Confirms magnetic stratigraphy. Also useful for establishing breaks in record due to episodic sediment loss or long-term nondeposition.
Suitable volcanic materials occur only at ocean basin margins close to subduction zones. Record more subject to destruction with increasing age due to subduction.	Useful for calibrating magnetic stratigraphy. Also dating beyond 1,000,000 years.
Depends on preservation of a binary signal without distortion. Signal lost where magnetic minerals absent.	Where applicable, establishes long-term faunal chronologies.

skeletons of foraminifera, a calcareous organism. Although the utility, understanding, and independence of different proxies vary, a number of proxies are available to study different climatic processes. Paleoceanographic and paleoclimatic processes that are studied include past glaciations, surface ocean characteristics, oceanic production and nutrient cycles, deep-ocean circulation, atmospheric circulation, and continental weathering. *See* MICROPALEONTOLOGY.

Ice volume. The ratio of the stable isotopes oxygen-18 (^{18}O) and oxygen-16 (^{16}O) in skeletons of foraminifera records the isotopic composition of the seawater in which the foraminifera lived. The seawater $^{18}O/^{16}O$ ratio is related to local water temperature and to the amount of ^{18}O-depleted water stored as ice on land, a global effect. The $^{18}O/^{16}O$ ratio preserved in foraminifera is dominated by the ice-volume effect and is only secondarily affected by temperature and other factors. Evidence for this is the global similarity of planktonic (surface-dwelling) and benthic (deep-dwelling) foraminiferal $^{18}O/^{16}O$ ratios as well as the similarity of the $^{18}O/^{16}O$ record to sea-level reconstructions. The $^{18}O/^{16}O$ patterns recorded globally in marine sediments are a key indicator of the cyclicity of glaciations of the late Neogene (26–0 Ma; late Oligocene to present). It has also enabled development of a common time scale for marine sediments.

Surface ocean conditions. Estimates of sea surface temperature and surface ocean characteristics such as oceanic upwelling are provided by several proxies. Modern distributions of microfaunal and microfloral assemblages are used to infer past surface ocean conditions. Primary faunal indicators are planktonic foraminifera and radiolaria, and floral indicators are coccolithophorids and diatoms. Foraminifera and coccolithophorids are composed of calcite, while radiolaria and diatoms are composed of opal. Statistical analyses of these microfossil assemblages are used to reconstruct past surface ocean conditions (**Fig. 15**). If the ice-volume component of the $^{18}O/^{16}O$ ratio and vital effects of planktonic foraminifera are accounted for, the planktonic $^{18}O/^{16}O$ ratio yields information about the temperature of the water in which the organisms lived. It is possible to determine oceanic mixed-layer structure from combined assemblage and isotopic compositions of planktonic foraminifera. The isotopic composition of organic matter preserved in marine sediments provides another independent estimate of past temperatures of the surface layer. *See* BACILLARIOPHYCEAE; COCCOLITHOPHORIDA; FORAMINIFERIDA; RADIOLARIA.

Oceanic productivity, CO_2, and nutrients. Multiple sediment proxies yield information regarding the past productivity of surface waters and past oceanic nutrient distributions. A frequently used proxy is the carbon

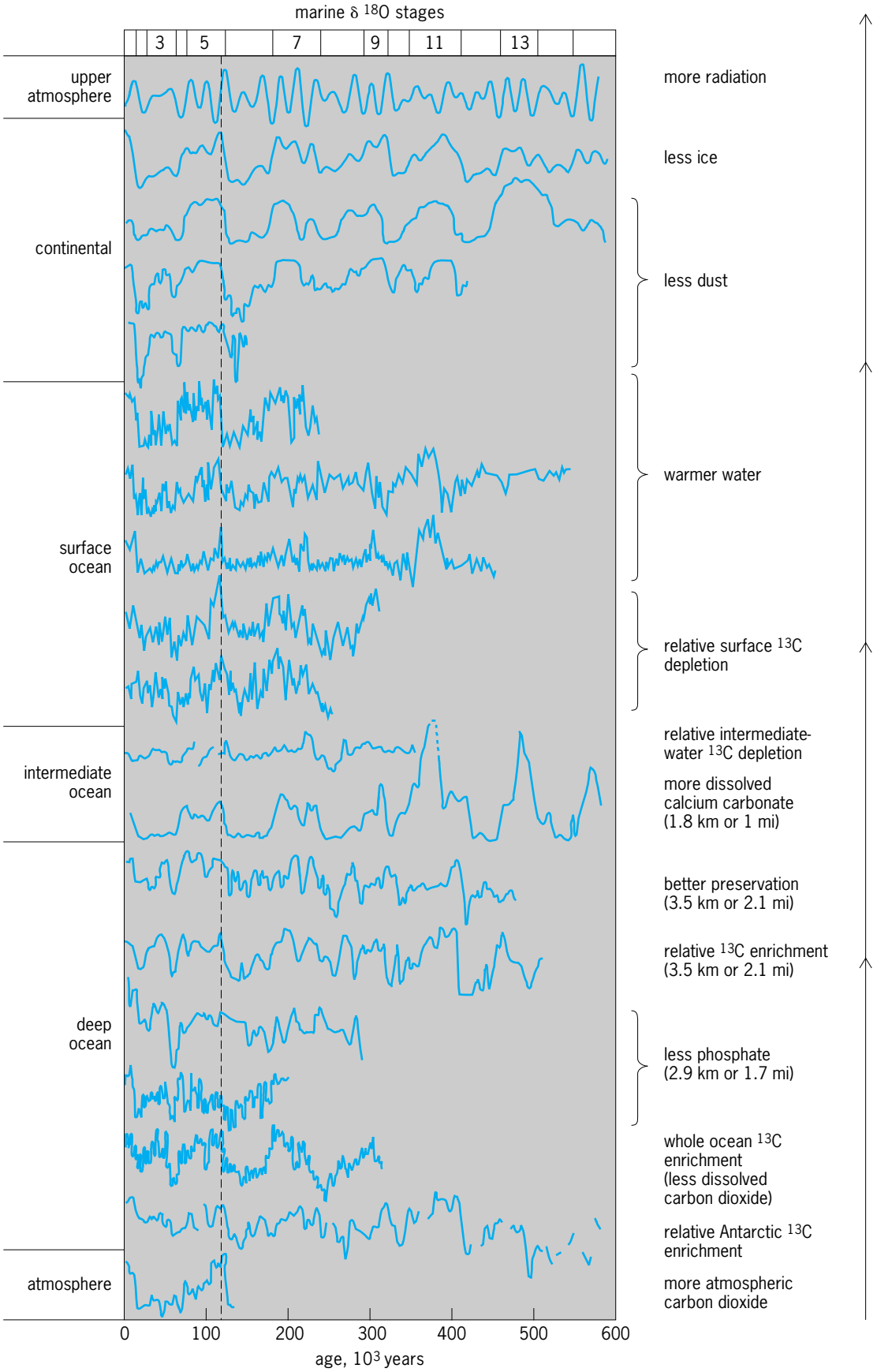

Fig. 15. Summary of major changes in the climate system over the past 800,000 years from a set of 18 proxy indicators. Coherent variations are evident in all components. (*After J. Imbrie et al., On the structure and origin of major glaciation cycles, 1. Linear responses to Milankovitch forcing, Paleoceanography, 7:701–1738, 1993*)

isotopic composition of skeletons of foraminifera. Photosynthetic processes preferentially incorporate ^{12}C and exclude ^{13}C from organic matter; thus changes in oceanic carbon reservoirs are reflected in $^{13}C/^{12}C$ ratios from foraminifera. The $^{13}C/^{12}C$ in benthic and planktonic foraminifera from marine sediments have been used to infer paleoproductivity. Other indicators of past oceanic production are sedimentary organic carbon content, microfossil assemblages, bulk calcite and opal accumulation, and stable nitrogen isotope ratios in organic carbon. Oceanic productivity strongly affects dissolved carbon dioxide (CO_2) levels in the ocean, and hence CO_2 levels in the atmosphere. Past levels of atmospheric CO_2 have been inferred from carbon isotope gradients in planktonic and benthic foraminifera and from specific components of sedimentary organic material. Sedimentary proxies for past nutrient distributions include the above indicators as well as trace-element measurements from fossil foraminifera.

Deep-water circulation. As deep water masses slowly circulate through the world's oceans, their chemistry changes as the waters age. Past patterns and rates of deep-ocean circulation can be inferred from past chemistry changes. Comparison of stable carbon isotope ratios ($^{13}C/^{12}C$) between planktonic and benthic foraminifera, and the geographical variation in these ratios, is a means for reconstructing variations in deep-ocean chemistry and circulation.

Atmospheric circulation. Away from continents and from ocean-bottom thermal vents, the primary source of nonbiogenic materials to the deep sea is wind-borne deposition of terrigenous material or hydrothermal deposition. Terrigenous sediment flux, terrigenous grain size, and the mineralogy of terrigenous sediments provide clues to the strength and location of winds over the ocean, continental aridity, and source regions of terrigenous material.

Weathering fluxes to the ocean. Continental weathering rates are a product of both orogeny (tectonic uplift) and climatic changes. Information regarding past weathering is given by geochemical proxies in marine sediments that indicate the discharge of elements from the continents to the ocean. Proxies for weathering fluxes include ratios of strontium-87/strontium-86 ($^{87}Sr/^{86}Sr$) and germanium/silicon (Ge/Si) in biogenic sediments, accumulation rates of biogenic and terrigenous sediments, and the mineralogical composition of terrigenous sediments. *See* OROGENY.

Climate since the last ice age. On continental margins and in sediment drift deposits where marine sediments accumulate rapidly, detailed studies of climate changes associated with the last ice age are possible. Sediments at these locations fall within the range of radiocarbon dating and can be closely tied to continental and ice-core climate records. Paleoclimate proxies from these sediments indicate that climate has been highly variable, punctuated by rapid cooling events in surface waters, large changes in deep-water circulation, and major iceberg discharges on time scales of centuries to thousands of years. In some marginal basins, where oxygen levels in bottom waters are low, sediments are undisturbed by burrowing organisms and are often laminated. In these specialized settings, the sediments preserve climate records on annual-to-decadal time scales. Climate changes associated with the Little Ice Age and El Niño–Southern Oscillation phenomena have been recorded. *See* EL NIÑO.

Pleistocene climates. The climatic record preserved in marine sediments of the past 2 Ma is dominated by ice ages. Measurements of climate proxies from a wide geographic distribution of sediment cores has documented the timing, amplitude, and spatial sequence of glacial and interglacial cycles (Fig. 15). At the forefront of this effort was the establishment of a consistent time scale for correlations between different sediment cores. This was accomplished by using the global ice-volume signal preserved in oxygen isotope ratios from foraminifera, combined with radiometrically dated magnetic reversals. The ice-volume proxy records indicate that over the past 1 Ma glacial intervals occur cyclically at periods of 100,000 years, 41,000 years, 23,000 years, and 19,000 years. Statistical analyses have demonstrated a strong connection between these major climate cycles and changes in the amount of insolation received by the Earth because of changes in the Earth's orbit. This is the foundation for the astronomical theory of climate change, also known as the Milankovitch hypothesis. Acceptance of this theory led to improvements in the Pleistocene time scale. Variations in every component of the climate system occur sequentially at these astronomically driven periods (Fig. 15). Previous to 1 Ma, the dominance of 100,000-year cycles was diminished, but strong variations in ice volume and other climatic proxies occurred at cycles of 41,000 years, 23,000 years, and 19,000 years. The patterns and amplitudes of Pleistocene (1.88–0 Ma) climatic change can be to first order modeled as a linear response of the climate system to orbitally driven insolation changes. *See* CLIMATE HISTORY; GLACIAL EPOCH; INSOLATION.

Pre-Pleistocene climates. A continuous sequence of marine sediments from the Cretaceous (~136–~66 Ma) through the Holocene (10,000 years ago to present) has been recovered through advanced drilling efforts. The undisturbed nature of some sediment sequences has facilitated extension of the astronomically calibrated time scale. The climatic record preserved in pre-Pleistocene sediments documents a progressive cooling of global climate beginning in the Eocene (57.8–36.6 Ma). It is hypothesized that this cooling is ultimately caused by tectonic boundary condition changes, including uplift of the Tibetan plateau during the past 40 Ma, as weathering associated with these tectonic changes impacts global geochemical cycles. Superimposed on this cooling trend are cycles of warming and cooling both before and after the onset of Northern Hemisphere glaciation at about 2.4 Ma. Despite large boundary condition changes, variations in insolation reaching the Earth have influenced climate variability throughout the Cenozoic (~66–0 Ma). Several periods of abrupt climatic transitions have also occurred during

the Cenozoic. Rapid warming of surface and deep waters occurred in the latest Paleocene, ~55 Ma, whereas global cooling and Antarctic glaciation occurred during the early Oligocene, ~35 Ma. Broad climate studies are focused on understanding the evolution, sensitivity, and variability of climate systems from the beginning of the Cenozoic through today. *See* CENOZOIC; GEOLOGIC THERMOMETRY; GEOLOGIC TIME SCALE.

Teresa King Hagelberg

Bibliography. W. S. Broecker and T. H. Peng, *Tracers in the Sea*, 1982; H. Charnock and J. Edmond (eds.), *The Deep Sea Bed: Its Physics, Chemistry, and Biology*, 1991; R. Chester, *Marine Geochemistry*, 2d ed., 2003; R. M. Cline and J. D. Hays (eds.), *Investigation of Late Quaternary Paleoceanography and Paleoclimatology*, Geol. Soc. Amer. Mem. 145, 1976; W. W. Hay (ed.), *Studies in Paleo-Oceanography*, Soc. Econ. Paleontol. Mineralog. Spec. Publ. 20, 1974; B. C. Heezen and C. D. Hollister, *The Face of the Deep*, 1971; J. M. Hunt, *Petroleum Geochemistry and Geology*, 2d ed., 1995; J. Imbrie et al., On the structure and origin of major glaciation cycles, 1. Linear responses to Milankovitch forcing, *Paleoceanography*, 7:701–738, 1992; J. Imbrie and K. P. Imbrie, *Ice Ages: Solving the Mystery*, 1986; J. Kennett, *Marine Geology*, 1982; F. J. Millero and M. L. Sohn, *Chemical Oceanography*, 3d ed., 2005; H. C. Nelson and T. H. Nilsen, *Modern and Ancient Deep Sea Fan Sedimentation*, 1984; Open University Course Team Staff (ed.), *Ocean Chemistry and Deep-Sea Sediments*, vol. 5, 1989; K. E. Peters et al., *The Biomaker Guide*, 2d ed., 2005; M. E. Raymo and W. F. Ruddiman, Tectonic forcing of late Cenozoic climate, *Nature*, 359:117–122, 1992; J. P. Riley (ed.), *Chemical Oceanography*, vol. 9, 1989; B. P. Tissot and D. H. Welte, *Petroleum Formation and Occurrence*, 2d ed., 1984; J. C. Zachos et al., Abrupt climate change and transient climates during the Paleogene: A marine perspective, *J. Geol.*, 101:191–213, 1993.

Maritime meteorology

Those aspects of meteorology that occur over, or are influenced by, ocean areas. Maritime meteorology serves the practical needs of surface and air navigation over the oceans. Phenomena such as heavy weather, high seas, tropical storms, fog, ice accretion, sea ice, and icebergs are especially important because they seriously threaten the safety of ships and personnel. The weather and ocean conditions near the air–ocean interface are also influenced by the atmospheric planetary boundary layer, the ocean mixed layer, and ocean fronts and eddies.

Meteorological phenomena. These include heavy weather, tropical storms, fog, ice accretion, and the atmospheric planetary boundary layer.

Heavy weather. Stormy weather at sea outside the tropics is primarily associated with cyclones that form in certain geographical regions where cold, dry air of continental origin and warm, moist air of tropical origin come together during winter (**Fig. 1**). These extratropical storms are especially dangerous to ships at sea because of their relatively high frequency of occurrence and the fact that they can develop extremely rapidly, reaching full force in less than 24 h. A common storm of this type in high latitudes is known as a polar low. Polar lows are relatively small in size (300–500 km or 180–300 mi in diameter) and quite shallow, extending from the sea surface to a height of only 1 or 2 km (0.6 or 1.2 mi). Sudden, explosive storm development (that is, cyclogenesis) is also very common off the east coast of North America in winter. A mature east coast storm is much larger (1000 km or 600 mi in diameter) and deeper (8–10 km or 5–6 mi deep or more) than a polar low. Mature extratropical storms that bring most of the heavy weather at sea include gale and hurricane force winds, heavy rains, and high seas.

The fact that such powerful and dangerous marine storms can develop so rapidly presents an especially challenging forecasting problem for meteorologists. The explosive cyclogenesis that occurs off the east coast of North America takes place during winter over the warm Gulf Stream waters east of Cape Cod and south of Nova Scotia. The conditions that are most favorable for such explosive cyclogenesis include a strong, horizontal temperature contrast in the lower atmosphere between the cold continent and the warm Gulf Stream; low vertical stability of the air due to the movement of cold, dry continental air out over the warm water; and the release of latent heat of condensation in the ascent of warm, moist air ahead of the developing storm. Since these conditions are usually prevalent throughout the winter, meteorologists consider the movement of an upper-level (midtropospheric) disturbance over the region favorable for cyclone development to be a key ingredient to triggering the growth of such rapidly developing storms. *See* CYCLONE; STORM.

Tropical storms. Cyclones (that is, storms) with very warm, moist air in the center develop in low latitudes over the warmest parts of the tropical oceans (**Fig. 2**). These violent and dangerous storms obtain their energy from the latent heat of condensation that is released in deep, convective rain clouds that form in unstable tropical air. They form when this deep convection becomes organized by the inward-spiraling low-level winds associated with an initially weak tropical disturbance. *See* CLOUD PHYSICS.

The winds in a mature tropical storm in the Northern Hemisphere spiral inward and counterclockwise (clockwise in the Southern Hemisphere) in the lower atmosphere and outward and clockwise (counterclockwise in the Southern Hemisphere) aloft. In intense storms, known as hurricanes in the North Atlantic, Gulf of Mexico, and eastern North Pacific, and typhoons in the western North Pacific, the winds can reach up to 320 km/h (200 mi/h) or more, with a central calm area or eye roughly 25–80 km (15–48 mi) in diameter. These storms generally move from east to west in the trade wind belt, but they occasionally curve poleward into middle latitudes, making forecasting difficult. When a tropical storm

Fig. 1. Cloud patterns in developing extratropical cyclones. (*a*) Photograph (100 mm) taken during a United States space shuttle mission, showing the typical comma-shaped cloud pattern associated with a developing storm off the coast of Nova Scotia (55°N, 50°W). (*b*) Satellite infrared image of a rapidly developing storm in the eastern Atlantic Ocean. The speckled clouds to the northwest of the storm center are seen to originate as thin cloud lines farther upwind to the northwest of the storm (upper left). Such cloud lines are indicative of very cold air that is being drawn into the storm from the northwest by the storm's own cyclonic circulation. (*C. H. Wash, Naval Postgraduate School*)

moves inland, the source of low-level moisture is greatly reduced, and the storm usually weakens or dissipates—however, not without damage and sometimes loss of life due to the strong winds, heavy rains, and flooding storm tides. With modern technology, tropical storms are easily located and tracked by meteorological satellites. However, their movement can be very difficult to predict because of the strong interaction that occurs between the storm and the larger-scale winds in which the storm is embedded. Also, the reason why so few tropical disturbances actually develop into full-fledged hurricanes is still one

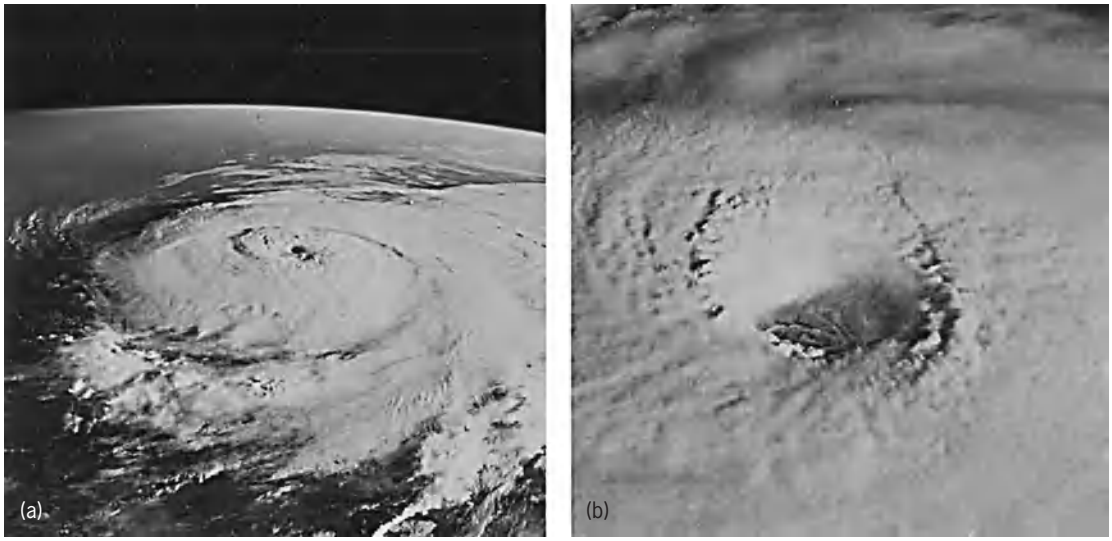

Fig. 2. Photographs (50 mm) of Hurricane Elena in the Gulf of Mexico on September 1, 1988, taken during a United States space shuttle mission. The low viewing angle and sun angle reveal the different cloud structures and heights in this mature hurricane. (*a*) Inward-spiraling cloud bands. (*b*) Close-up of the eye of the storm. (*C. H. Wash, Naval Postgraduate School*)

of the most important unanswered questions in meteorology. *See* HURRICANE; METEOROLOGICAL SATELLITES; SATELLITE METEOROLOGY; STORM DETECTION; TROPICAL METEOROLOGY.

Fog. Fog is important to all seagoing activities because it restricts visibility, making navigation (and aircraft operations from navy aircraft carriers) extremely hazardous. Certain types of marine fog can be very thick and persistent. Steam fog is produced when cold air flows over a warmer water surface. Evaporation of the relatively warm water into the overlying, cooler air, followed by condensation into minute liquid droplets, produces the fog. In high northern latitudes, steam fog is referred to as arctic sea smoke, and it is very common in the marginal ice zone in winter and early spring (**Fig. 3**). Advection fog occurs when relatively warm, moist air flows over cooler water, cooling the air to saturation. Extensive areas of advection fog can develop when warm air flows poleward over colder water at higher latitudes or when such air flows eastward over the cold, coastal ocean currents that usually exist in midlatitudes off the west coast of continents. Advection fog in such coastal regions is especially pronounced in the summer, when the normally cold ocean currents are made even colder by upwelling of cold water near the coast. *See* FOG; UPWELLING.

Ice accretion. Ice accretion, which may occur on ships as well as aircraft, not only decreases the efficiency of operation but also may be extremely hazardous, especially to small vessels. The accumulation of ice reduces freeboard and, more importantly, the stability of the ship by making it top-heavy. Ice accretion affects all exposed equipment on ships, including missile launchers and gun systems on navy ships and radar and radio antennas on all ships. Heavy ice accretion can render such equipment completely inoperable. Ice formation occurs primarily from freezing rain and freezing spray from the sea. The most dangerous accumulations of ice develop with freezing spray, which can occur when the air temperature is several degrees or more below freezing. The colder the air and the sea and the stronger the wind, the more rapid is the accumulation of ice. As much as 45 metric tons (50 tons) or more of ice can accumulate in 24 h depending on the size of the ship, which creates a serious hazard to the ship and crew.

Atmospheric planetary boundary layer. Since the atmosphere is semitransparent to incoming solar radiation, about 50% of the Sun's energy passes directly through the atmosphere to be absorbed at the surface. [Some of the energy in the other 50% is reflected (albedo).] This heat energy is transferred to the atmosphere in the form of sensible and latent heat by conduction and by long-wave radiation, although a large part of the long-wave radiation from the Earth's surface is lost to space and therefore does not affect the atmosphere. The lowest kilometer or so of the atmosphere, in which the air and ocean (or Earth) exchange heat, moisture, and momentum, is known as the atmospheric planetary boundary layer (**Fig. 4**). Except for the lowest millimeter above the sea, the air flow in the atmospheric planetary boundary layer is fully turbulent. This means that the air flow is unsteady, that is, it fluctuates rapidly in space and time; fluid properties mix, that is, they are readily transported from one place to another within the boundary layer; and the forces of inertia dominate those of molecular viscosity. The turbulent nature of the boundary layer greatly increases the vertical transport and the exchange of heat, moisture, and momentum between the atmosphere and the ocean. *See* HEAT BALANCE, TERRESTRIAL ATMOSPHERIC; TURBULENT FLOW.

The atmospheric planetary boundary layer consists of two distinct regions that are of great scientific interest and practical importance to maritime meteorology (Fig. 4). In the lowest 50 m (165 ft) or so, in what is called the surface layer, the vertical

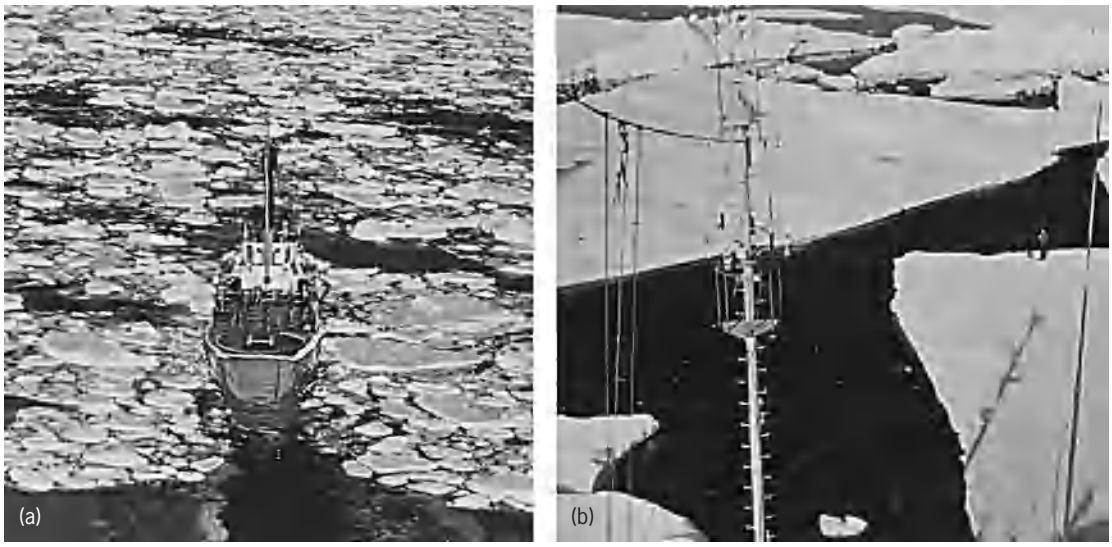

Fig. 3. Sea ice in the marginal ice zone. (*a*) Relatively small cakes of thin ice near the seaward edge of the marginal ice zone. (*b*) Much larger and thicker floes farther back from the edge. (*P. S. Guest, Naval Postgraduate School*)

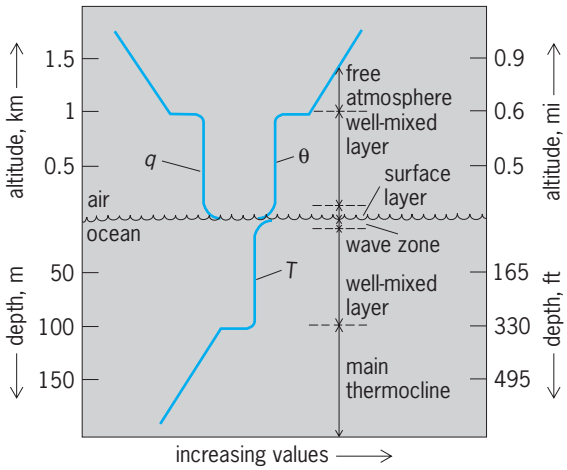

Fig. 4. Schematic drawing of the atmospheric planetary boundary layer and the ocean mixed layer. In the atmosphere, θ is potential temperature (temperature adjusted for the compressibility of the atmosphere), and q is specific humidity (ratio of the mass of water vapor to the mass of air in a unit volume of air). In the ocean, T is temperature. The quantity θ generally increases with height in the atmosphere, while T decreases with depth in the ocean. The wind speed and ocean currents are not shown, but an idealized profile of the winds and currents would tend to follow the θ and T lines, respectively.

turbulent transport of heat, moisture, and momentum is essentially constant in the vertical. As a result, the mean temperature, humidity, and horizontal velocity vary approximately logarithmically with height above the sea surface. Above the surface layer, and extending throughout the rest of the boundary layer, the turbulence is so strong that the mean temperature, moisture, and momentum themselves are well mixed and nearly uniform with height. If the air in the boundary layer is sufficiently moist, clouds (mostly stratocumulus) form in the upper part of the boundary layer, and these clouds sometimes drop to the sea surface as fog. When clouds are present in the boundary layer, both the temperature and the turbulence are affected. Whether the boundary layer is cloudy or not, it usually is capped by a rather thin inversion above which the air is warmer, drier, and much less turbulent. This region above the boundary layer is called the free atmosphere, meaning that the flow there is essentially free of turbulence and largely free from the effects of the underlying surface of the land or ocean. *See* ATMOSPHERE.

Oceanic phenomena. These include high seas, sea ice and icebergs, the mixed layer, and fronts and eddies.

High seas. Winds blowing over the sea generate waves and ocean currents. Waves generated by the wind vary in height, length, and period, depending on the wind speed, the length of water over which the wind is blowing in a more or less uniform direction (fetch), and the duration of time the wind has blown. The winds in a mature extratropical cyclone over the ocean can generate waves 10–15 m (33–49 ft) high. Such high seas can cause great damage to ships, harbors, and beaches, and they produce a large amount of ambient noise (sound) in the ocean that hinders naval antisubmarine warfare operations. Because of the importance of high seas to all seagoing activities, oceanographers have developed numerical wave prediction models to forecast the state of the sea. These models include such processes as wave growth, propagation, and dissipation. Their success depends on an accurate analysis and forecast of the surface wind field. Such wave forecasts are used by private companies and government agencies for various purposes, including merchant marine operations, navy tactics and ship maneuvers, refueling at sea, amphibious landing exercises, oil drilling and oil spill operations, and search and rescue. *See* OCEAN WAVES.

Sea ice and icebergs. Sea ice, formed by the freezing of seawater and floating at the surface of the ocean, is of keen scientific interest and importance to marine meteorology and oceanography. Sea ice plays a key role in air–sea interaction. Since it reflects much of the solar radiation reaching the surface, sea ice greatly reduces the sensible and latent heat exchange between the atmosphere and the ocean, and it severely alters the wind stress acting on the water. At high latitudes, the open and ice-covered regions of the ocean meet in a narrow zone, known as the marginal ice zone (Fig. 3). Environmental parameters of importance in the marginal ice zone include the location, concentration, and thickness of sea ice, and, for naval operations, the small-scale roughness of the top and bottom surfaces of the ice. The ability to predict these parameters depends on a full understanding of how the ocean and the ice exert drag on one another, and how they exchange heat and mass through melting and freezing. Since sea ice rejects most of the salt in the seawater as it freezes, the melting and freezing of sea ice changes the salinity, and hence the density and vertical stability, of the sea immediately below the ice. This, in turn, modifies the dynamic and thermodynamic interaction between the ice and the underlying ocean. In the marginal ice zone, sea ice often drifts, or is episodically forced by the wind, into water that is above freezing, resulting in a rapid melting of the ice. Icebergs, masses of land ice that have broken away from land and are floating on the sea, are of less scientific interest to marine meteorology, but they present a threat to the safety of some ships. They are readily identified and routinely tracked by satellites. *See* ICEBERG; SEA ICE; WIND STRESS.

Mixed layer. Over most of the ocean at low and middle latitudes, solar radiation that penetrates the atmosphere is absorbed in the upper ocean, forming a warm, stable, surface layer (Fig. 4). When the wind blows over the surface of the ocean, or when the surface of the ocean is cooled by heat loss to the atmosphere, turbulent motions are generated which mix the warmed and stably stratified surface waters down into the cooler, denser water below. This one-sided mixing process is called entrainment, and it leads to the formation of a well-mixed upper layer in which the temperature is essentially uniform and at the bottom of which there is a sharp temperature drop (density increase). The situation is analogous to the stable inversion that is formed at the top

of the atmospheric planetary boundary layer. The only difference is that in the atmospheric boundary layer, active entrainment advances upward from below while in the ocean it works downward from above.

When the winds decrease, turbulence in the upper ocean quickly decays, and active entrainment ceases. The absorption of solar radiation along with lower levels of turbulence then can cause a new mixed layer to form at a shallower depth. Over much of the world's ocean, pronounced deepening and shallowing of the mixed layer takes place over an annual cycle, with warm, shallow mixed layers in summer and cold, deep mixed layers in winter. A less pronounced daily cycle of mixed layer deepening at night and shallowing during the day also occurs. Both of these cycles are greatly modified by episodes of strong winds and high surface-heat losses associated with tropical and extratropical cyclones over the ocean. Because turbulence in the upper ocean is so strongly dependent on the local atmospheric forcing, the vertical density structure of the upper ocean preserves a fairly accurate record of the wind and weather of the recent past, modified of course by such factors as horizontal and vertical transports within the upper ocean. Fluctuations in the depth of the mixed layer, and in the magnitude of the temperature drop at the base of the mixed layer, are especially important to many tactical naval operations.

Fronts and eddies. Maritime meteorology is concerned about fronts and eddies in the ocean because of their effect on the overlying atmosphere and because they are associated with significant fluctuations in ocean currents, temperature, salinity, and other ocean variables. These fluctuations have horizontal scales of 10–500 km (6–300 mi), vertical scales of 1–2 km (0.6–1.2 mi), and time scales of several days to several weeks or more. Ocean fronts and eddies are commonly referred to as oceanic weather, because of their dynamic and kinematic similarity to atmospheric weather.

Ocean fronts and eddies come in a wide variety of types. The most significant ones are meanders or cut-off eddies (cold and warm core rings) in major ocean current systems such as the north wall of the Gulf Stream or other strong western boundary current systems. Also, there are eddies in the open ocean driven directly by the wind, eddies generated by the interaction of ocean currents with bottom topography, and fronts in the coastal zones caused by upwelling or by cooling of the shallow water on the continental shelf. The meandering of major western boundary currents and the subsequent pinching-off of eddies and rings occur through mixed baroclinic and barotropic instability in the way that midlatitude cyclones develop and occlude in the atmosphere, but the exact mechanisms responsible for these ocean developments are not completely understood. Variations in ocean depth can influence the direction of propagation of preexisting waves and eddies, and cause eddies to be generated locally when water is forced to flow up or down a topographic slope, and they can significantly modify the dynamic stability of major current systems. Oceanic weather associated with upwelling fronts in coastal regions often takes the form of long filaments or dipole (counterrotating) eddies that extend seaward for several hundred kilometers. The origin and dynamics of many of these features are not completely understood, but they are the subject of active research. *See* FRONT; OCEAN CIRCULATION.

Analysis and forecasting. This involves observations and numerical prediction.

Observations. To support the analysis and forecasting of many meteorological and oceanographic elements over the globe, observations are needed from a depth of roughly 1 km (0.6 mi) in the ocean to a height of 30 km (18 mi) in the atmosphere. In addition, the observations must be plentiful enough in space and time to keep track of the major features of interest, that is, tropical and extratropical weather systems in the atmosphere and fronts and eddies in the ocean. Over populated land areas, there is a fairly dense meteorological network; however, over oceans and uninhabited lands, meteorological observations are scarce and expensive to make, except over the major sea lanes and air routes. Direct observations in the ocean, especially below the sea surface, are insufficient to make a synoptic analysis of the ocean except in very limited regions. Fortunately, remotely sensed data from meteorological and oceanographic satellites are helping to fill in some of these gaps in data. Satellite data can provide useful information on the type and height of clouds, the temperature and humidity structure in the atmosphere, wind velocity at cloud level and at the sea surface, the ocean surface temperature, the height of the sea, and the location of sea ice. Although satellite-borne sensors cannot penetrate below the sea surface, the height of the sea can be used to infer useful information about the density structure of the ocean interior. *See* REMOTE SENSING.

Numerical prediction. The motion of the atmosphere and the ocean is governed by the laws of fluid dynamics and thermodynamics. These laws can be expressed in terms of mathematical equations that can be put on a computer in the form of a numerical model and used to help analyze the present state of the fluid system and to forecast its future state. This is the science of numerical prediction, and it plays a very central role in marine meteorology and physical oceanography.

The first step in numerical prediction is known as data assimilation. This is the procedure by which observations are combined with the most recent numerical prediction valid at the time that the observations are taken. This combination produces an analysis of the present state of the atmosphere and ocean that is better than can be obtained from the observations alone. Data assimilation with a numerical model increases the value of a piece of data, because it spreads the influence of the data in space and time in a dynamically consistent way.

The second step is the numerical forecast itself, in which the model is integrated forward in time

to predict the state of the atmosphere and ocean at a future time. Models of the global atmosphere and world ocean, as well as regional models with higher spatial resolution covering limited geographical areas, are used for this purpose. In meteorology and oceanography the success of numerical prediction depends on collecting sufficient data to keep track of meteorological and oceanographic features of interest (including those in the earliest stages of development), having access to physically complete and accurate numerical models of the atmosphere and ocean, and having computer systems powerful enough to run the models and make timely forecasts. *See* WEATHER FORECASTING AND PREDICTION.

Applications. Two important applications of maritime meteorology are ship routing and tactical naval environmental support.

Ship routing. The headway made by a ship transiting the ocean depends to a great extent on the state of the sea, as well as the force of the winds. The larger the waves and the more directly into the waves, or winds, the ship is headed, the slower the headway. Hence, it is clearly desirable to avoid heavy seas and strong winds, not only to avoid damage and possible injuries but also to save time and fuel in ocean crossing. Empirical data collected from ships' logs have enabled researchers to relate ship speed to sea state and, from such relationships, to construct a least-time track for a ship crossing the ocean. This requires an accurate forecast of the weather along all possible routes the ship might take made several weeks in advance. Since this is generally beyond state-of-the-art forecast skill, preliminary ship tracks are recommended based on 5–7-day predictions and climatology; and then they are modified, if necessary, as the voyage progresses. Ship routing based on weather and sea conditions has been found to improve the efficiency and reduce the cost of shipping; consequently, it has been widely used for both commercial and naval ships of the United States and other countries. *See* SHIP ROUTING.

Tactical naval environmental support. Tactical environmental support refers to describing and predicting those meteorological and oceanographic phenomena that affect the performance of naval weapons systems on time and space scales that are important to tactical naval operations. This aspect of marine meteorology and oceanography is becoming increasingly important to the modern navy because of the increased sophistication and range of naval weapons systems, and the great sensitivity of those systems to variations in the environment. Thus, an accurate knowledge of present and future meteorological and oceanographic conditions can be a significant asset to the operating navy in its conduct of command, control and communication, antisubmarine and electronic warfare, navigation, search and rescue, and many other tactical operations at sea. *See* ANTISUBMARINE WARFARE; NAVIGATION.

The physical environment affects communications and weapon systems primarily by refracting, scattering, and attenuating electromagnetic waves (microwaves, optical, and radio waves) in the atmosphere and acoustic (sound) waves in the ocean. Atmospheric refraction is caused by vertical variations in temperature and humidity, primarily in the lower part of the atmosphere. Such variations can be especially significant in the first few tens of meters above the sea surface and in the sharp transition region between the atmospheric planetary boundary layer and the free atmosphere. As a result, the structure and variability of the atmospheric planetary boundary layer are extremely important to naval meteorology.

An important application of maritime meteorology to naval operations is the prediction of radar (or other electromagnetic or optical) wave propagation in the atmosphere and sound-wave propagation in the ocean (**Fig. 5**). Sound waves can travel great distances through the ocean, at a speed that depends on the temperature, pressure, and salinity

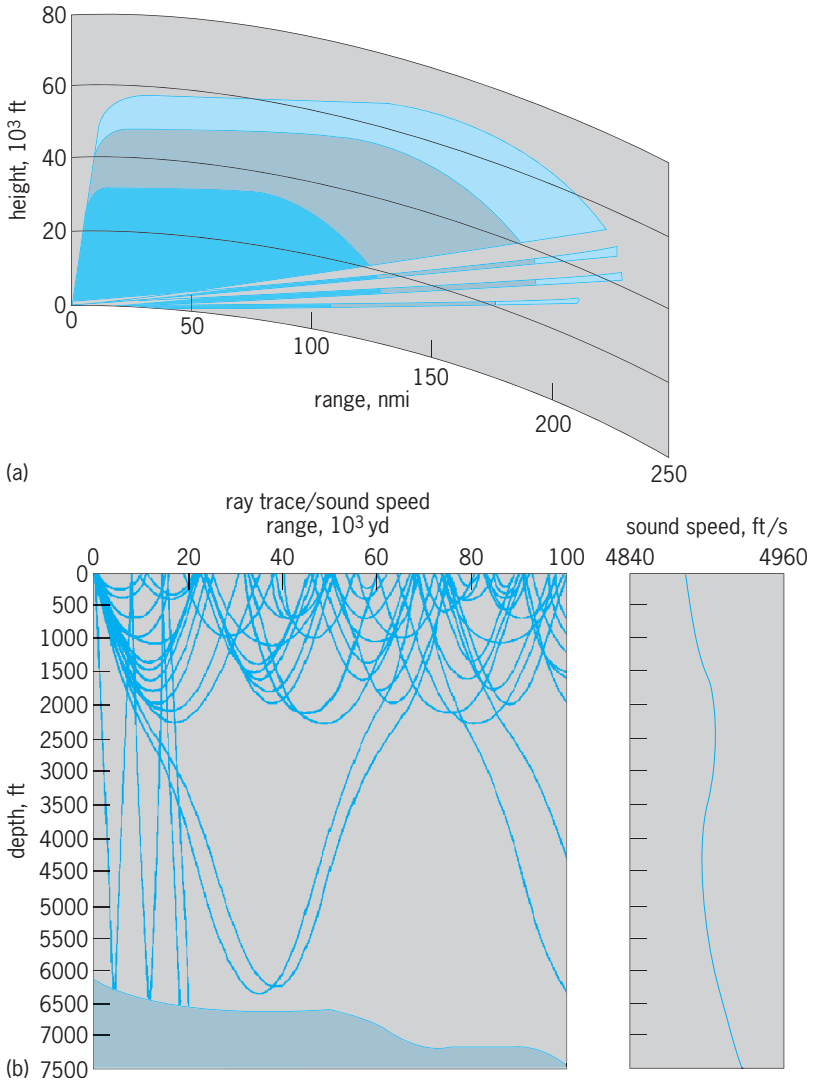

Fig. 5. Prediction of (*a*) radar (or other electromagnetic or optical) wave propagation in the atmosphere and (*b*) sound wave propagation in the ocean. 1 ft = 0.3 m. 1 nautical mile = 1852 m. (*LCDR W. T. "Kim" Curry, U.S. Navy*)

of the water through which the waves are propagating. As a result, variations in these quantities refract sound waves in the ocean in the same way that variations in temperature and humidity refract electromagnetic waves in the atmosphere. Because of refraction, the sound waves emitted from a given location in the ocean will travel along a curved path that depends on the ocean thermal structure. When the waves reach the top or bottom of the ocean, they are reflected into the ocean interior in ways that depend on the properties of the sea surface or sea floor. Because of the variable nature of these environmental factors, acoustic waves leaving a particular sound source will tend to converge into certain areas and diverge from others. The places where sound waves come together because of refraction are called convergence zones, and they represent optimal locations to "listen" for enemy ships. Likewise, places where sound waves tend to diverge from are called shadow zones, and they are good places to "hide" from enemy ships. The location and intensity of convergence zones and shadow zones are strongly affected by ocean fronts and eddies, by fine structure and turbulence in the upper ocean, and by the properties of the sea floor and sea surface. In very high latitudes, the sea ice concentration and the surface wave conditions strongly affect the ambient noise in the ocean, while the roughness of the underside of sea ice is important for acoustic propagation. The application of the science of maritime meteorology and oceanography to naval tactics is a very important aspect of most naval operations at sea. *See* METEOROLOGY; OCEANOGRAPHY; UNDERWATER SOUND.

Robert L. Haney

Bibliography. A. E. Gill, *Atmosphere-Ocean Dynamics*, 1982; G. J. Haltiner and R. T. Williams, *Numerical Prediction and Dynamic Meteorology*, 2d ed., 1988; E. B. Kraus and J. A. Businger, *Atmospheric-Ocean Interaction*, 2d ed., 1994; A. R. Robinson (ed.), *Eddies in Marine Science*, 1983; R. B. Stull, *An Introduction to Boundary Layer Meteorology*, 1988.

Marjoram

The aromatic herb *Majorana hortensis*, a common plant in Mediterranean areas. The spicy camphoraceous odor of marjoram has long been cherished as an addition to a wide variety of foods; in the Middle Ages marjoram was used as an air freshener.

Marjoram is in the mint family (Lamiaceae) and is a close relative of European or Greek oregano, with which it is often confused. There is still controversy concerning the proper taxonomic classification of this plant. Some authors place it in the genus *Origanum*, while others continue to separate it into its own genus *Majorana*. Many ecotypes or varieties of marjoram exist, both in wild populations and under cultivation. *See* OREGANO.

Marjoram is a small perennial (1–2 ft or 30–60 cm tall), and has ovate leaves up to 1 in. (2.5 cm) long. The leaves are slightly hairy, as are the erect somewhat woody stems. Marjoram flowers are white to very light lavender or pink in color but are very small and usually go unnoticed; the entire flower spike or inflorescence is, however, easily noticeable.

Marjoram is native to North Africa and southern Europe; its range stretches into southern Germany. It is cultivated in numerous locations throughout the world, including Europe, Egypt, Israel, Mexico, India, and the United States. Cultivation is best accomplished in a warm environment with a low relative humidity. Marjoram will tolerate a frost, but prolonged cold and dampness will weaken or kill it. Well-drained fertile soil produces the most vigorous plants. In the United States it is grown primarily in California due to the mild winters and low humidity needed for dehydration.

Marjoram is usually directly seeded into the field at a rate of 5–15 lb of seed per acre (2.3–6.8 kg/ha). It will grow enough the first year to be cut twice, and is usually cut three times a year in subsequent years. After 4 years, yields drop off, and it is usually plowed under and then replanted in a new location to avoid disease buildup in the soil. Harvesting is accomplished mechanically or by hand, after which the leaves are dried as quickly as possible at low temperatures (100°F or 37.7°C) to preserve color and flavor.

Because it is a perennial, marjoram is more likely to become infected with soil-borne diseases than annual spices such as basil and savory. Both Phytophora and Verticillium wilt sometimes infect this crop, with resulting dieback and death of individual stems that eventually spreads to whole plants and fields. *See* PLANT PATHOLOGY.

The dried and fresh leaves are used as flavoring for meats (sausage), vegetables, cheeses, poultry stuffing blends, and sauces, especially tomato-based sauces. *See* LAMIALES; SPICE AND FLAVORING.

Seth Kirby

Marl

In the most general use of this term, a sediment that consists of a mixture of calcium carbonate ($CaCO_3$) and any other constituents in varying proportions. Marls usually are fine-grained, so that most marls consist of $CaCO_3$ mixed with silt and clay. The dominant carbonate mineral in most marls is calcite ($CaCO_3$), but other carbonate minerals such as aragonite (another form of $CaCO_3$), dolomite [Ca, Mg $(CO_3)_2$], and siderite ($FeCO_3$) may be present also. *See* ARAGONITE; CALCITE; CARBONATE MINERALS; DOLOMITE; SIDERITE.

Frequently, particularly in North America, the name marl is limited to a lake deposit that is rich in $CaCO_3$, but usually the term is extended to include marine deposits. Deep-sea marls consist of mixtures of clay and the $CaCO_3$ skeletons of microscopic planktonic animals (foraminiferans) and plants (coccoliths and discoasters). Marls deposited in the deeper parts of lakes consist of fine-grained

$CaCO_3$, but marls deposited in shallow water may contain $CaCO_3$ in the form of shells of mollusks and fragments of calcareous algae such as *Chara* (stonewort) mixed with fine-grained $CaCO_3$ that is precipitated on the leaves of rooted aquatic vegetation. The $CaCO_3$ from these various sources is then mixed with sand, silt, or clay brought in by streams from the surrounding drainage basin. *See* MARINE SEDIMENTS.

Although the term marl has been applied to sediments with a greatly variable content of $CaCO_3$, strictly speaking the $CaCO_3$ content should range between 30 and 70%. Because of the high $CaCO_3$ content, most marls are light to medium gray, although they can be almost any color. The high $CaCO_3$ content also tends to make dried marl earthy and crumbly.

The indurated rock equivalent of marl is marlstone. Equivalent terms range from calcareous claystone to argillaceous or impure limestone, depending on the amount of $CaCO_3$ that is present. Marlstone is common in marine sequences of all ages, and is particularly common in ancient lake sequences of Tertiary age in the western United States. For example, the famous "oil shale" of the Green River Formation of Wyoming, Colorado, and Utah is not a shale at all but a marlstone in which the dominant carbonate mineral is dolomite. *See* LIMESTONE; OIL SHALE; SEDIMENTARY ROCKS.

Walter E. Dean

Marmot

A member of the genus *Marmota* in the squirrel family Sciuridae. Fourteen species occur mainly in mountainous areas in the northern hemisphere (see **table**). *See* RODENTIA; SQUIRREL.

General morphology. Marmots are large, heavy-bodied rodents attaining weights of 3–7.5 kg (6.6–16.5 lb) and total lengths of 400–820 mm (16–32.8 in.). Fur color varies considerably among the different species. The upper parts may be gray, brown, or yellowish. The underside, although paler, normally differs little in color from the upper parts, although in *M. flaviventris* the belly is yellow (see **illustration**). Some species have white markings. *Marmota vancouverensis* is melanistic. The texture of the fur varies from thin to long and thick. The head is short and broad, the legs are short, and the densely haired, slightly flattened tail is one-fifth to one-third of the total length. The eyes are small, and the ears are short, broad, rounded, and well haired. The feet have five digits, each terminating in a thick, slightly curved claw. The palms and soles are naked. The dental formula is I 1/1, C 0/0, Pm 2/1, M 3/3 × 2 for a total of 22 teeth.

Habitats and behavior. Marmots are found in open habitats such as pastures, forest edges, alpine meadows, and steppes. Most of their life is spent in burrows, which they excavate in well-drained soil. A mound of fresh soil at the entrance and numerous trails radiating to and from feeding areas is characteristic. Burrows may be as deep as 5–7 m (16–23 ft) and have several entrances. Tunnels measuring over 100 m (330 ft) have been recorded. Winter dens of *M. monax* are normally in wooded or brushy habitats on sloping ground and have only one entrance, whereas summer dens are most often in open areas and have several entrances. Marmots are primarily diurnal and terrestrial, but occasionally climb into shrubs and trees, especially when being pursued. Some are known to be good swimmers. Marmots are herbivorous. Food consists mainly of green vegetation such as grasses and forbs as well as fruits, grains, and legumes. Marmots use visual and auditory senses for the main contacts between members of a group, with some olfactory and tactile cues. A sharp whistle, which functions as an alarm call, is one of several types of vocalizations. Some species sun themselves on warm days near their burrow entrances.

Social behavior varies between the different species. Some, such as *M. monax*, are usually solitary, but sometimes are found in small family groups. Others such as *M. olympus* are highly sociable.

Hibernation. Most marmots inhabit northern mountainous areas where food is unavailable during the winter, thus making hibernation a necessity. They are true hibernators: they do not store food for winter but subsist entirely on fat reserves stored in their bodies. Fat reserves are accumulated during the summer and may account for as much as 20% of the animal's weight when it enters dormancy. Hibernation may last as long as 9 months in some species.

Yellow-bellied marmot, *Marmota flaviventris*. (*Photo by Dr. Lloyd Glenn Ingles, © 1999 California Academy of Sciences*)

Members of the genus *Marmota* and their geographical distribution

Species	Range
M. marmota, alpine marmot	Mountains of Europe
M. camtschatica, black-capped marmot	Mountains of NE Siberia
M. menzbieri, Menzbier's marmot	Mountains of Kyrgyzstan and Kazakhstan
M. bobak, Steppe or Siberian marmot	Poland and Romania to Manchuria and China
M. baibacina, gray marmot	Siberia, Kazakhstan, Kyrgyzstan, Mongolia
M. himalayana, Himalayan marmot	Himalayan region of China, India, Nepal
M. sibirica, Mongolian bobak	Siberia, Mongolia, China
M. broweri, Alaskan marmot	Northern Alaska, Yukon
M. caudata, red marmot	Mountains of Kyrgyzstan, Tajikistan, Afghanistan, India, Pakistan, Tibet
M. monax, woodchuck, groundhog, whistle pig	Alaska to Newfoundland and eastern United States
M. flaviventris, yellow-bellied marmot	SW Canada, western United States
M. caligata, hoary marmot	Alaska to Washington and Montana
M. olympus, Olympic marmot	Olympic Peninsula of western Washington
M. vancouverensis, Vancouver Island marmot	Vancouver Island

In southern parts of its range, the woodchuck may hibernate for only several weeks or not at all. *See* HIBERNATION AND ESTIVATION.

Reproduction and life. Periods of mating, gestation, parturition, and litter size vary as a result of latitude and altitude. Most marmots do not breed until they are 2 to 3 years of age. Breeding normally occurs shortly after emergence from hibernation with a single litter of 4 to 6 young being born annually after a gestation period of approximately 30 days. Female *M. olympus* usually produce a litter every other year. Young marmots are born in a grass-lined nest within the burrow. The young emerge from the burrow at about 4 weeks of age and are weaned at about 6 weeks. The young of some species may disperse as early as 6 weeks of age, whereas others may remain with their parents until their second summer when they are just over 1 year old. Life expectancy in wild *M. marmota* is 4 to 6 years, although one individual in captivity lived for almost 10 years.

Threats. Major natural predators include cougars, coyotes, dogs, foxes, bears, and golden eagles. Young animals are most susceptible to predation since adults are generally able to defend themselves against most natural predators.

Deforestation along with the subsequent expansion of pastureland and the elimination of large predators in the eastern United States has allowed populations of *M. monax* to greatly expand. Some, however, consider it a pest because of its damage to crops and that its burrows pose potential damage to livestock and farm machinery. For example, in agricultural areas, where groundhogs are often considered a pest because of crop depredation and burrowing, they may be shot, trapped, or gassed. Other species have experienced drastic population declines due to loss of subalpine habitat to ski resorts. *Marmota vancouverensis* is classified as Endangered by the International Union for the Conservation of Nature and Natural Resources (IUCN) and the U. S. Department of the Interior. In Central Asia, *M. menzbieri* is classified as vulnerable and *M. caudata* as near threatened by the IUCN.

Donald W. Linzey

Bibliography. G. A. Feldhamer, B. C. Thompson, and J. A. Chapman, *Wild Mammals of North America: Biology, Management, and Conservation*, 2d ed., Johns Hopkins University Press, 2003; D. Macdonald (ed.), *The Encyclopedia of Mammals*, Andromeda Oxford Limited, 2001; R. M. Nowak, *Walker's Mammals of the World*, 6th ed., Johns Hopkins University Press, 1999; D. E. Wilson and S. Ruff (eds.), *The Smithsonian Book of North American Mammals*, Smithsonian Institution Press, 1999.

Mars

The fourth planet outward from the Sun. Mars is the planet most like Earth in terms of geology, climate, and suitability for life. It is also the world that has been most thoroughly studied by interplanetary spacecraft.

Orbital characteristics. Mars has a mean heliocentric distance (semimajor axis) of 1.524 astronomical units, equivalent to 141.6×10^6 mi (227.9×10^6 km). Its orbit plane is inclined 1.85° to the ecliptic plane. Its orbital eccentricity of 0.093, one of the largest of the major planets, causes Mars's distance to the Sun to vary from 128×10^6 mi (207×10^6 km) at perihelion to 155×10^6 mi (249×10^6 km) at aphelion. *See* PLANET.

Mars revolves around the Sun with a sidereal period of 1.881 years or 686.93 days at a mean orbital velocity of 15.0 mi/s (24.1 km/s). The planet comes closest to Earth, reaching opposition, every 780 days on average.

The globe. The mean diameter of Mars is 4212 mi (6780 km), or about 53% that of the Earth. The planet has a mass of 7.08×10^{20} tons (6.42×10^{23} kg), about 11% of Earth's. The mean density is thus about 3.91 g/cm^3, less than that of any other terrestrial planet. At the equator the surface gravity is 12.1 ft/s^2 (369 cm/s^2), about 38% of Earth's, and the escape velocity is 3.1 mi/s (5.0 km/s).

Astronomers long ago determined the planet's rotation period very accurately by watching surface markings cross the disk. The sidereal period is 24h

37m 22.7s, corresponding to a mean solar day of 24h 39m 35.2s. Consequently, there are about 669 Martian mean solar days (called sols) in the planet's year. The obliquity of Mars, that is, the inclination of its polar axis to a line perpendicular to the orbital plane, is 25.2°. This value is only slightly greater than that of Earth, so the seasons are similar but longer and also more unequal because of the planet's greater orbital eccentricity. Theoretical work has shown that the obliquity of Mars undergoes large, irregular variations that have ranged from 15° to 35° during the last 10^6 years and from 0° to 60° over geologic time. These chaotic shifts occasionally expose the polar caps to much more direct sunlight and trigger major climatic changes.

Telescopic appearance. Mars appears to the unaided eye as a bright, slightly reddish star. Viewed through a telescope, Mars usually appears as a salmon-hued disk marked by mottled dark regions and white, seasonally variable polar caps (**Fig. 1**). The atmosphere occasionally displays clouds of dust and water ice. In the late 1800s, some telescopic observers mapped a multitude of surface formations that were believed to be canals and oases due to vegetation responding to the Martian seasons. As revealed by spacecraft, however, these features are now known to be complexes of dark rock and light-collored sand whose contrast changes with the introduction of clouds and airborne dust driven by seasonal winds.

The apparent diameter of the disk of Mars varies from 3.5 seconds of arc at conjunction (when on the far side of the Sun) to 25.1 seconds of arc at the most favorable perihelic (near-perihelion) oppositions, when the distance to the Earth is only 35×10^6 mi (56×10^6 km). Perihelic oppositions with Mars occur every 15 to 17 years. During the perihelic opposition on August 27, 2003, Mars was marginally closer to Earth—34,646,418 mi (55,758,006 km)—than at any time in nearly 60,000 years.

As a superior planet (that is, a planet that moves outside Earth's orbit), Mars presents only gibbous phases when it is not in opposition to or conjunction with the Sun; the maximum phase angle (Sun-Mars-Earth angle) is 48°, when Mars is in quadrature. The apparent visual magnitude of Mars in conjunction averages −1.5, but it brightens to −2.7 at perihelic opposition, when Mars is brighter than any other planet except Venus. *See* MAGNITUDE (ASTRONOMY).

The visual albedo of Mars is about 0.15. The planet's reflectivity increases rapidly from a low value of only 5% in the near ultraviolet to more than 30% in the near infrared. This variation accounts for the reddish color of Mars. In the infrared, at wavelengths between 1 and 2 μm, the spectral reflectivity of Mars resembles that of iron oxides, especially goethite and hematite. *See* ALBEDO.

Interior. Measurements of the planet's gravitational field made by orbiting spacecraft have shown that Mars has a dense core and thus is differentiated into a core, mantle, and crust. The crust, composed of silicate rocks, varies irregularly in thickness from about 22 mi (35 km) near the north pole to 45 mi (70 km) near the south pole. The reason for this gradation is not well understood. The surface exhibits no obvious evidence of terrestrial-style plate tectonism.

At present Mars does not have a global magnetic field of appreciable strength. Spacecraft measurements suggest that the equivalent dipole field is at most 30 nanoteslas at the equator, corresponding to a magnetic moment 5000 times weaker than Earth's. However, early in its history Mars must have had a more substantial magnetic field, because its near-surface rocks exhibit strong remanent magnetism. Based on the absence of a remanent magnetic signature in the vicinity of large impact basins, geophysicists believe that the internal dynamo responsible for the planet's intrinsic global magnetic field must have ceased activity about 4×10^9 years ago. *See* ROCK MAGNETISM.

Geology. The Martian surface has been modified extensively by the processes of impact cratering, volcanism, faulting, and fluvial erosion. The terrain in the southern hemisphere is very heavily cratered and thus quite old, having formed some 3.8×10^9 years ago. Much of it stands 1 to 2 mi (1 to 4 km) higher than the planet's mean radius (**Colorplate 1**). Although volcanic sources are not common at southern latitudes, maps of spectral reflectivity made by orbiting spacecraft show that surface rocks in the southern hemisphere are predominantly basaltic (silicon-poor) in mineralogy. The northern hemisphere is dominated by vast, lava-covered plains with relatively few impact craters and an average elevation about 3 mi (5 km) below the mean radius. Mineral compositions are typically andesitic (silicon-rich). This puzzling hemispheric dichotomy has no well-accepted explanation but may be related to the large-scale interior movement early in Martian history.

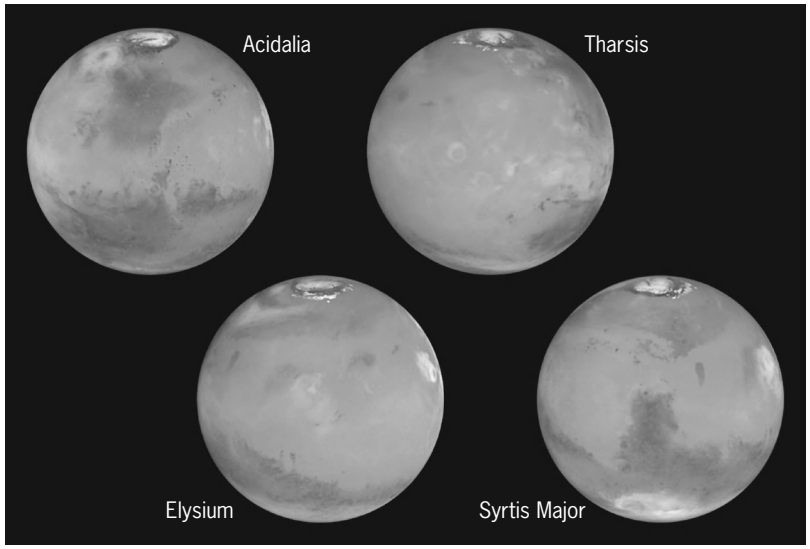

Fig. 1. Images of Mars in 90° longitude steps through one complete rotation. When the *Hubble Space Telescope* obtained these views in 1999, the planet was 54×10^6 mi (87×10^6 km) from Earth. Note the bright and dark albedo markings and bright polar caps. (*NASA/Space Telescope Science Institute*)

Fig. 2. The huge Martian shield volcano Olympus Mons covers an area the size of Arizona. Its peak is 13.2 mi (21.3 km) above Martian "sea level." Somewhat north of the summit is a conspicuous caldera, a complex nest of collapse craters 55 mi (90 km) across. (*NASA*)

The surface also exhibits numerous impact basins. The largest of these, Hellas, is approximately 2500 mi (4000 km) across and 6 mi (9 km) deep; it ranks as the largest known impact structure in the solar system.

The Tharsis ridge, or bulge, is an uplifted portion of the surface that stands several kilometers above the mean elevation of the planet. Most of Mars's tectonic features are associated with Tharsis, which affects approximately one-quarter of the entire surface. The formation of the ridge appears to have begun more than 3×10^9 years ago, long before the volcanoes that now dot its crest and surroundings. The height and mass of Tharsis may be supported below either by an extremely thick, rigid lithosphere or by the force from an upwelling mantle plume.

Volcanoes. The Martian surface exhibits several enormous shield volcanoes. The largest and perhaps the youngest is Olympus Mons, which is nearly 370 mi (600 km) across at its base and stands approximately 16 mi (26 km) above the surrounding terrain (**Fig. 2**). Three other large shield volcanoes—Ascraeus Mons, Pavonis Mons, and Arsia Mons—lie along the nearby Tharsis ridge. The Tharsis volcanoes are approximately 250 mi (400 km) across and 12 mi (20 km) high. By comparison, the largest volcanic constructs on Earth—Mauna Loa and Mauna Kea in Hawaii—together are approximately 125 mi (200 km) across and stand 5.5 mi (9 km) above the ocean floor.

In shape and structure, the Martian shield volcanoes bear a strong resemblance to their Hawaiian counterparts. At the summit of each shield is a complex of calderas, collapsed craterlike features that were once vents for lava. The central smooth-floored caldera of Arsia Mons is the largest, about 80 mi (130 km) in diameter.

About 3000 mi (5000 km) to the west of the Tharsis area is another volcanic field, dominated by the symmetrical shield volcano, Elysium Mons, approximately 140 mi (225 km) across. Many other volcanoes with dimensions of up to 60 mi (100 km) and in various states of preservation are found scattered over the Martian surface, mostly in the northern hemisphere.

A volcanic formation known as a patera (Latin for "saucer"), a shallow, complex crater with scalloped edges, occurs on Mars but has not been observed on any other planet. Alba Patera, northeast of Olympus Mons, is between 900 and 1200 mi (1500 and 2000 km) across but rises only 2 to 3 mi (3 to 5 km) above the surrounding plains. Enormous quantities of highly fluid lava must have emerged from its central caldera, flowing to great distances along channels and tubes. *See* VOLCANO.

Canyons. Perhaps the most spectacular features on the Martian surface are the huge canyons located primarily in the equatorial regions. Valles Marineris, actually a system of canyons, extends for over 3000 mi (5000 km) along the equatorial belt (**Colorplate 2**). In places, the canyon complex is as much as 300 mi (500 km) wide and drops to more than 4 mi (6 km) below the surrounding surface. Dwarfing the Grand Canyon, Valles Marineris is comparable in size to the great East African Rift Valley. In general, the walls of the canyon are precipitous and show evidence of slumping and landslide activity (**Fig. 3**). The principal canyons of Valles Marineris appear to be linked with the formation of the Tharsis uplift. They may

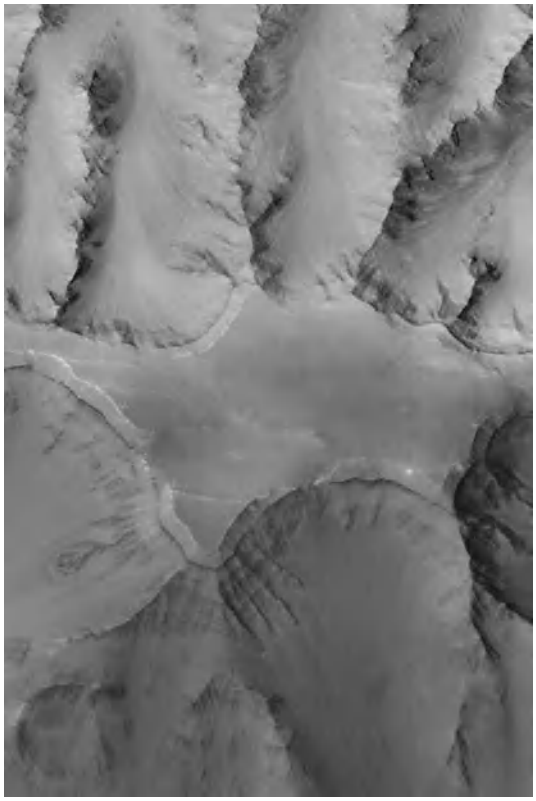

Fig. 3. An image from the *Mars Global Surveyor* resolves features as small as 20 ft (6 m) in a 6-mi-wide (10-km) portion of Coprates Chasma, which is located in the middle of Mars's vast Valles Marineris canyon complex. The high-standing plateau is underlain by multiple rock layers that may be volcanic or sedimentary in nature. (*NASA/Malin Space Science Systems*)

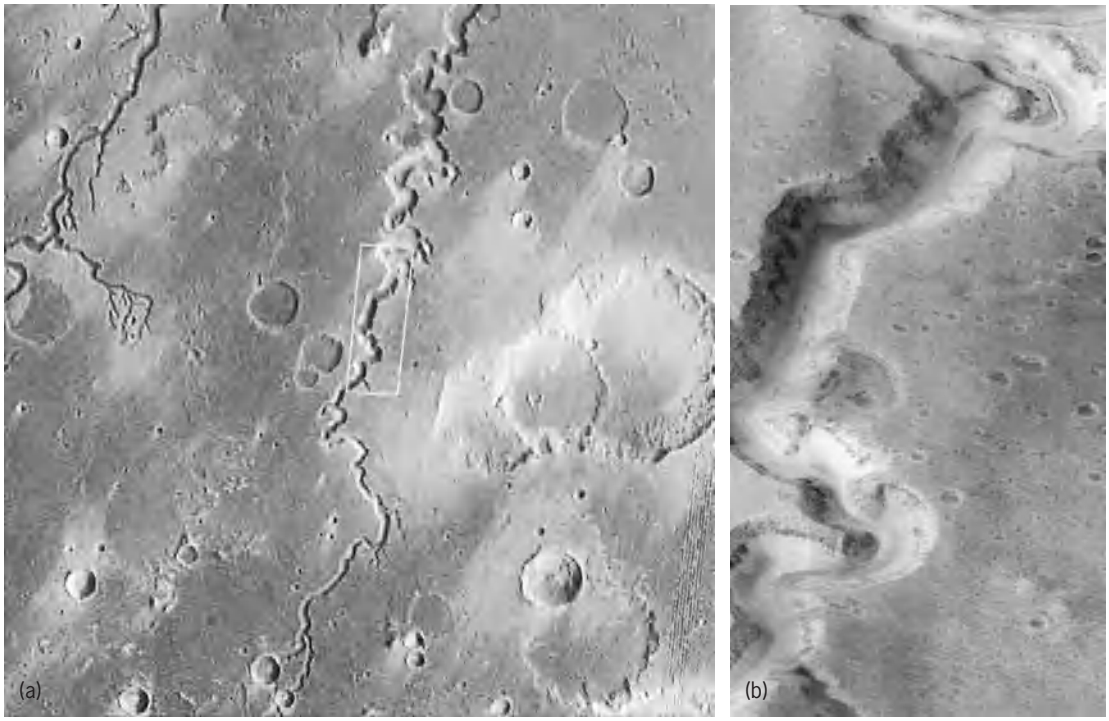

Fig. 4. Nanedi Vallis, a long, water-cut canyon on Mars, which is 1.5 mi (2.5 km) wide. (*a*) Canyon and surrounding terrain. (*b*) Detailed view of area in white rectangle in part a. Rocky outcrops jut from the canyon's walls, and a secondary rivulet is seen in its floor. (*NASA/Malin Space Science Systems*)

have formed by faulting along lines of tension within the crust. In essence, such canyons (called graben) are pairs of parallel faults with a sunken area between them.

Channels. An astonishing class of features on the Martian surface is a widespread network of channels that bear a very strong resemblance to dry river beds (**Fig. 4**). These channels do not coincide with the channels or canals which, in the past, were frequently reported by telescopic observers of Mars.

Ranging in size from broad, sinuous features nearly 40 mi (60 km) wide to small, narrow networks less than 300 ft (100 m) wide, the channels appear to have been created by water erosion. Early analysis assumed the apparently dendritic nature of some channels to be evidence of watershed rain collection and episodic flow. On closer inspection, however, many systems previously considered dendritic now appear to result from more gradual formation through ground-water sapping, not rainfall.

The largest channels must have been formed by enormous torrents of water, presumably released in some catastrophic manner (**Fig. 5**). Yet liquid water at present cannot exist on the surface of Mars, because the atmospheric pressure and surface temperature keep most available water trapped as subsurface ice or locked up in the permanent polar caps.

As a way out of this enigma, it has been suggested that the long-term climate of Mars is variable, and that in the past the planet might have had conditions suitable for free running water over its surface. Alternatively, episodic volcanic activity may have rapidly melted buried ice and disgorged torrents of water. According to some estimates, liquid-water reservoirs could have been maintained under relatively thin ice covers for up to 700×10^6 years after the mean global temperature fell below the freezing point of water. Some geologic evidence indicates that huge lakes and glaciers of ice were present on the Martian surface many millions of years ago.

Images from the *Mars Global Surveyor* spacecraft have revealed the existence of more than 120 small gullies cascading down the slopes of hillsides and crater rims that appear to have been carved by flowing water or mud. These features are typically about 1500 to 3000 ft (0.5 to 1 km) long and usually form on slopes facing away from the equator, which receive less sunlight than their surroundings and are thus colder. Because the gullies appear to be extremely fresh, they imply that liquid water in some form has flowed on the Martian surface within the past 10^6 years and perhaps much more recently. Some scientists have argued that the gullies result from springs or pressurized underground flows, while others believe they were created by trickling water from melting snow packs.

Sedimentary layering. Spacecraft images show that many canyon walls and crater floors exhibit extensive exposures of layered rock, up to 2.5 mi (4 km) thick in some places. Although their stratigraphic age is uncertain, these layers imply that the deposition of sediment was widespread early in Martian history. The frequent presence of layering within craters argues for repeated episodes of deposition in standing water. However, it is also possible that the sediments were transported by the atmosphere, either as massive amounts of windblown dust or as airborne volcanic ash.

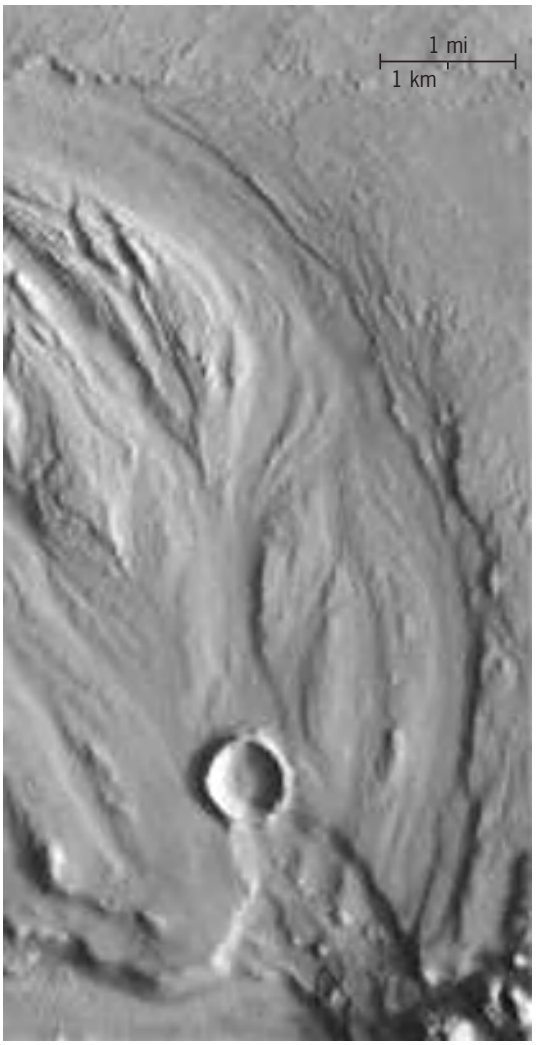

Fig. 5. Section of the Martian flood channel Hrad Vallis, showing streamlined flow features. (*NASA/Malin Space Science Systems*)

Surface characteristics. Five spacecraft have landed safely on the Martian surface and returned significant scientific data about its properties. *See* SPACE PROBE.

Two American *Viking* landers arrived in 1976. *Lander 1* set down in a region known as Chryse Planitia (22.3°N, 48.0°W) on July 20, and *Lander 2* arrived at Utopia Planitia (47.7°N, 225.7°W) on September 3. *Lander 1* sits in a moderately cratered, low-lying volcanic plain near the mouth of a large outflow channel. Numerous rocks of varying size litter the surroundings, and fine-grained material is occasionally seen in large drifts. *Lander 2* is situated in a region of fractured plains about 125 mi (200 km) south of the large crater Mie; it probably sits atop a lobe of the crater's ejecta blanket. This site is very flat and sparsely cratered, though rocks cover a higher proportion of the surface than at the other *Viking* site.

Most of the data concerning the composition of the surface came from x-ray fluorescence spectrometers, which showed that small particles were remarkably similar at both sites, with silicon and iron accounting for about two-thirds of the samples' content. The sulfur content was unexpectedly high, 100 times greater than in the Earth's crust, an indication that much of the surface is coated with very fine grain weathering by-products enriched in salts. In general, the surface material at both sites can be characterized as iron-rich clays. Small particles also clung to magnets on each spacecraft, and these are probably composed of the mineral maghemite. *See* X-RAY FLUORESCENCE ANALYSIS.

On July 4, 1997, *Mars Pathfinder* also landed in Chryse Planitia about 500 mi (800 km) east-southeast of *Viking 1*, near the mouth of the Ares Vallis flood channel at 19.3°N, 33.6°W. The lander's stereo camera recorded a dense accumulation of sizable rocks (**Fig. 6**), which lay on gently sloping ridges and troughs presumably shaped by the flood waters. *Mars Pathfinder* also carried a small, instrumented rover, *Sojourner*, which was directed from Earth via remote control to several rocks and fine-grained drifts in the lander's immediate vicinity.

The most extensive surface exploration has been conducted by two Mars Exploration Rovers (MERs) that landed on Mars in early 2004. *Spirit* arrived on January 3, landing in the large crater Gusev (14.6°S, 184.5°W). *Opportunity* reached the flatland known as Meridiani Planum (2.0°S, 5.5°W) on January 25. Each rover was equipped with panoramic and microscopic cameras, three different spectrometers to characterize surface composition, magnets to collect metallic particles, and a grinding tool to expose fresh rock surfaces. Although the MERs had been designed to operate for 3 months, both were still fully functional in early 2006, more than 2 years after their arrival. In that time *Spirit* traveled more than 3.8 mi (6.1 km) and *Opportunity* logged 4.0 mi (6.5 km).

Both MER landing sites were chosen in the hope of finding evidence for the presence of liquid water at ground level in the geologically recent past. Scientists had chosen Gusev, which is 103 mi (170 km) across, because its floor was once flooded and appeared to be covered with water-borne sediment. Although *Spirit* initially found no evidence of lakebed deposits, it later identified an iron oxide called goethite, which forms only in the presence of water, in elevated terrain called the Columbia Hills about 2 mi (3 km) from its landing site.

Meridiani Planum was chosen for *Opportunity* because its spectral reflectivity strongly implied the presence of coarse-grained hematite, another iron oxide, which forms only in wet environments. After *Opportunity* arrived, scientists discovered that its landing site exhibited countless millimeter-size concretions, nicknamed blueberries, scattered across the ground and embedded in the exposed bedrock (**Fig. 7**). These spherules are the source of the hematite detected spectroscopically from orbit. *Opportunity* also found that the outcrops are rich in sulfate minerals, evidence that the rock had been saturated by salt-laden water; one of these minerals, jarosite, requires highly acidic conditions to form.

Meteorites from Mars. Geologists have come to recognize that a small number of meteorites have reached Earth after being violently ejected from Mars

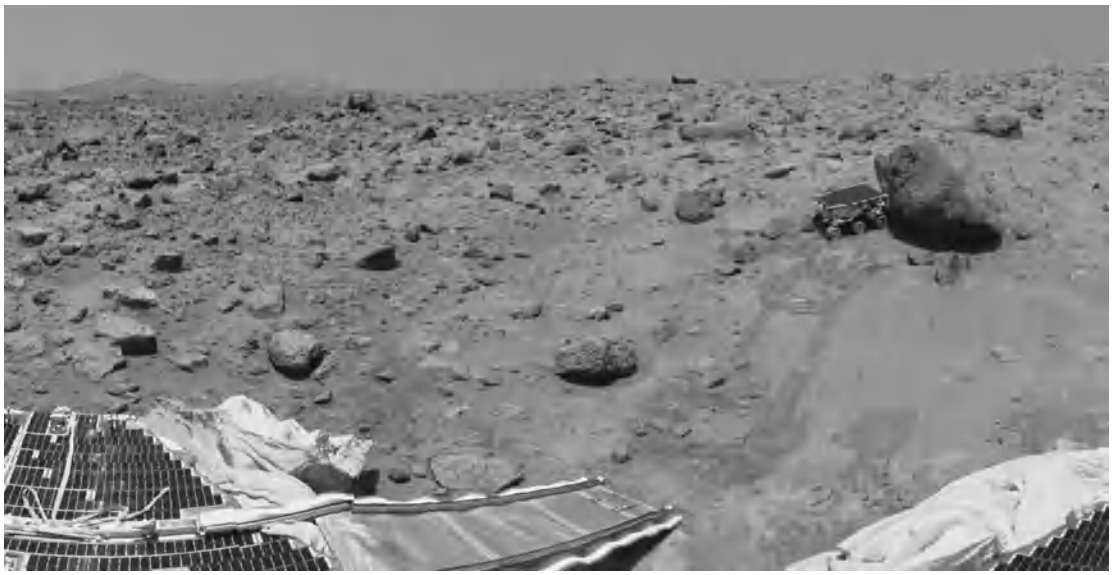

Fig. 6. View of the Ares Vallis flood plain, as recorded by *Mars Pathfinder* in July 1997. The hill on the horizon, near the left edge, is 0.6 mi (1 km) from the lander. At right, the rover *Sojourner* is analyzing the elemental composition of a large boulder nicknamed Yogi. (*NASA*)

during the collision of sizable asteroids or comets. The meteorites are thus samples from Mars itself. The first of these meteorites was recognized in 1982, and 36 distinct falls (some represented by multiple samples) were known by early 2006. They are sometimes collectively termed the SNC meteorites, representing their three subclasses: shergottites, nakhlites, and chassignites. The Martian meteorites contain a distinctive ratio of the isotopes of oxygen found nowhere on Earth, on the Moon, or in other meteorites. Almost all of them crystallized from molten rock 1.3×10^9 years ago, far more recently than the usual 4.6×10^9 years (the age of the solar system) found in all other meteorites. The lone exception to date, designated ALH 84001, crystallized 4.5×10^9 years ago during the planet's infancy.

All but one of the Martian meteorites are basaltic, as would be expected from volcanic flows with relatively young geologic ages. By contrast, ALH 84001 is an igneous rock whose large crystals argue that it cooled slowly within the crust. Some of the Martian meteorites contain tiny amounts of water, hydrated minerals, and carbonates that must have become trapped within the rocks while still on Mars. *See* METEORITE.

Atmosphere. The Martian atmosphere is very thin, with surface pressure averaging about 6.5 millibars (650 Pa), or less than 1% of the pressure at Earth's surface. Atmospheric pressure, temperature, wind velocity, and direction were monitored by both *Viking* landers for more than a full Martian year and by the *Mars Pathfinder* lander for 4 months. Temperatures during these missions ranged from a low of −190°F (−123°C) to a high exceeding 0°F (−18°C), though dust storms tend to moderate these extremes. The globally averaged surface temperature is −81°F (−63°C).

Composition. The atmosphere consists principally of carbon dioxide (95.3%) but contains nitrogen, argon, oxygen, and a trace of water vapor totaling 4.7%. In 2004 a spectrometer aboard *Mars Express*, a spacecraft orbiting the planet, discovered trace amounts of methane in the Martian atmosphere. The mixing ratio of methane varies from 0 to 30 parts per billion by volume, depending on location. Methane cannot exist in equilibrium with the other gases, and scientists are unsure of its source. Speculations include delivery to Mars by a comet, release during a volcanic eruption or by the decomposition of stored methane hydrates, or production by methane-excreting (methanogenic) organisms either at present or in the past.

Clouds. Both carbon dioxide and water form clouds in the Martian atmosphere. Certain water-ice condensations are associated with the largest volcanic

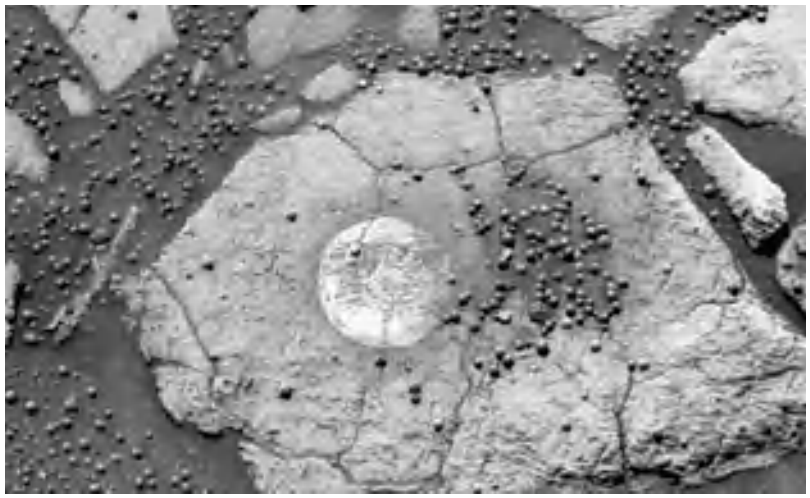

Fig. 7. Image from the roving spacecraft *Opportunity* showing a rock outcrop at Meridiani Planum strewn with small spherical concretions, nicknamed blueberries, that contain the iron-bearing mineral hematite. This hematite type forms only in the presence of water. The light-colored circle, 2 in. (5 cm) across, was created by the rock abrasion tool on *Opportunity*. (*NASA*/*USGS*)

peaks, while carbon dioxide clouds occur frequently over the polar regions during local winter, when the region is in continuous darkness. Often clouds appear during or just after sunrise, either because vapor has condensed in the atmosphere during the cold night, or because frosts that were deposited on the surface overnight are warmed by the Sun and sublime back into the atmosphere, saturating it with vapor.

Early history. The oldest terrains, in Mars's southern hemisphere, bear systems of small, interconnected channels as well as craters and other landforms that have been heavily eroded and degraded. These features suggest that early in its history the planet had a much thicker atmosphere. However, most or perhaps virtually all of the original atmosphere disappeared beginning about 4×10^9 years ago. The loss of gas was probably due to a combination of impact events, stripping by the solar wind, and chemical reaction with surface rocks.

Dust storms. Localized dust storms appear quite frequently on Mars. Because the Martian atmosphere is extremely thin, wind velocities greater than 90–110 mi/h (40–50 m/s) are needed to set surface dust grains in motion. The most abundant particles in a typical Martian dust storm are estimated to be about 10 μm in diameter, similar to finely powdered talc. The very smallest particles may be carried to heights as great as 30 mi (50 km) above the surface. Localized "dust devils" are apparently widespread and occur frequently.

Some dust storms develop with such intensity that their total extent may be hemispheric or even global. Such was the case of the great dust storm of 1971, which began in September and completely enshrouded the planet by the time *Mariner 9* arrived in November. Major dust storms tend to begin at the end of spring in the southern hemisphere, when Mars is near perihelion. The initial dust-raising disturbance is probably related to temperature instabilities in the Martian atmosphere at a time when solar heating is greatest. Once the dust is in the air, increased absorption of solar energy causes the dust-laden air to rise, producing strong surface winds that rush in to replace the rising air mass. Thus the storm propagates, growing in intensity and extent. When the distribution of dust finally reaches global dimensions, the temperature differences over the planet are diminished, winds correspondingly subside, and dust begins to settle out of the atmosphere. The settling process may take weeks or, in the case of a severe storm, several months. The 1971 storm lasted for approximately 5 months.

Water inventory. If all the water currently present in the atmosphere of Mars were to condense onto the surface, it would form a film only 10 μm thick. This is inconsistent with the amount of water needed to form the planet's huge eroded channels. For example, the volume of water needed to form the flood-related features in and near Chryse Basin alone is roughly 1.0×10^6 mi^3 (4.2×10^6 km^3). Therefore a much larger source of water must exist now or must have existed in the geologically distant past.

However, the surface of Mars exhibits widespread exposures of olivine, an iron-magnesium silicate mineral that readily reacts with water to form other compounds. The frequent occurrence of olivine implies that much of the Martian surface has not been exposed to liquid water for billions of years and argues that Mars has been cold and dry for much of its history.

Polar caps. The seasonal cycle of growth and decay of the bright polar caps has long been taken as evidence of the presence of water on Mars. However, evidence from the *Mariner* spacecraft identified carbon dioxide as the principal constituent of the polar snow, with lesser amounts of water ice also present. Formed during autumn and winter by condensation and deposition of the icy mist covering the polar regions, the polar caps at the end of winter cover a vast area extending to latitude 60° in the southern hemisphere and 70° in the northern hemisphere. The surfaces covered are, respectively, 0.4 and 1.7×10^6 mi^2 (1 and 4.5×10^6 km^2).

During spring and summer the edges of the caps retreat, reaching minimum diameters of about 400 and 300 mi (650 and 450 km), respectively. The north pole's residual cap consists almost entirely of water ice; although likely to be dominated by water ice, the southern cap is covered with frozen carbon dioxide (**Fig. 8**). Measurements by the *Mars Global Survevor* spacecraft showed that both were broad, elevated domes. The volume of water ice within the northern residual cap is likely 290,000–430,000 mi^3 ($1.2–1.7 \times 10^6$ km^3); the estimate for the southern residual cap is 480,000–720,000 mi^3 ($2–3 \times 10^6$ km^3). If all the water present in the polar caps were distributed uniformly over the surface of Mars, it would produce a layer 70–110 ft (22–33 m) deep.

Subterranean ice. Although no spacecraft to date has detected the presence of liquid water directly, there is ample evidence that a great volume of ice lies beneath the surface. Broad, flat plains regions

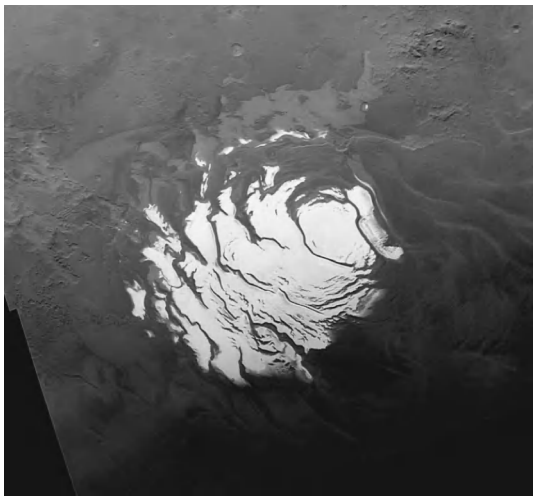

Fig. 8. Mars's south polar cap as it appears near its minimum size, about 250 mi (400 km) across, during local summer. (*NASA/USGS*)

surround each residual cap. This terrain is characterized by stacks of evenly spaced layers from 60 to 150 ft (20 to 50 m) in thickness. Although ice is absent in these layered terrains at ground level, a gamma- ray spectrometer on the 2001 *Mars Odyssey* spacecraft has detected areally extensive subsurface layers enriched in hydrogen. The only plausible source of this hydrogen is water ice, which apparently exists in concentrations of 40 to 73% by volume. The ice-rich layers are located poleward of about latitude 60° in both the northern and southern hemispheres, and the estimated volume of ice exceeds 2400 mi^3 (10,000 km^3), enough to fill Lake Michigan twice. However, *Mars Odyssey's* gamma-ray spectrometer could detect the presence of hydrogen to a depth of only about 3 ft (1 m), so the ice-rich layer may extend to much greater depths. By early 2006 a radar instrument on *Mars Express* had detected the likely presence of massive ice reservoirs buried beneath the plains surrounding both polar caps.

Hypothesized ocean. Even though at present liquid water cannot exist on the Martian surface, the planet's numerous large flood channels suggest that vast amounts of water flowed on the surface early in Martian history. This conclusion, together with water bound in the polar caps and evidence for widespread deposits of subsurface ice, suggests that the total volume of water on Mars would likely cover the planet to a depth of about 0.1–0.3 mi (0.2–0.5 km). The corresponding value for Earth is 1.7 mi (2.7 km). Circumstantial evidence implies that much of the low-lying northern hemisphere was covered with an ocean roughly 4×10^9 years ago. Although unproven, this hypothesis suggests that 10^7 mi^2 (27×10^6 km^2) of the northern plains were inundated. The total volume would have been roughly 3.6×10^6 mi^3 (15×10^6 km^3), about one-third of the water in the Atlantic Ocean.

Possibility of life. The ample evidence that early Mars had an abundance of liquid water, a thicker atmosphere, and a more clement environment has raised speculation that the planet may have once been, or may still be, an abode for primitive life forms.

In 1976, the twin *Viking* landers conducted experiments on the Martian surface to test for the existence of life. Three biological instruments and a gas chromatograph/mass spectrometer sampled the soil within reach of the 10.5-ft (3.2-m) mechanical arm aboard each spacecraft. The spectrometer detected no organic compounds at all (within the limits of its sensitivity). One of the biological experiments gave a positive result—the release of oxygen from a soil sample when humidified—but there is no consensus as to the source of this reaction. Some scientists have suggested inorganic superoxides or other catalysts as the substances involved. *See* GAS CHROMATOGRAPHY; MASS SPECTROMETRY.

Twenty years later, a scientific team claimed that it had found evidence of fossilized microbes within a known Martian meteorite (ALH 84001). They reported that tiny carbonate beads within the meteorite had chemical and mineral characteristics most logically explained by biological activity. However, other research groups dispute this conclusion and have offered various nonbiological explanations for the same features. After years of intensive study, scientists have reached no consensus; the mineral associations within ALH 84001 and other Martian meteorites neither confirm the presence of once-living organisms nor exclude it.

Satellites. Mars has two small satellites, Phobos and Deimos, discovered by Asaph Hall in 1877. Their apparent visual magnitudes at mean opposition are relatively bright, 11.3 and 12.4, respectively, but a large telescope is required to see them because of the bright glare surrounding the planet.

The outer satellite, Deimos, moves at a mean distance from the planet's center of 14,580 mi (23,460 km) in a sidereal period of 30h 18m, only slightly longer than a period of rotation of Mars. The orbital plane of Deimos is inclined to the equatorial plane of Mars about 1.8°. The inner satellite, Phobos, orbits only 3700 mi (6000 km) from the surface of Mars and 5830 mi (9380 km) from the planet's center. The inclination of its orbital plane is 1.9°. Phobos has a sidereal orbital period of 7h 39m, less than one-third of the mean Martian solar day. Thus, as seen from the surface of Mars, Phobos rises in the west and sets in the east twice daily, moving apparently in the direction opposite to all other celestial bodies, including Deimos. Seen overhead near the Martian equator, Phobos would appear less than half the size of the Moon viewed from Earth, and Deimos would be a barely discernible disk.

Neither satellite is massive enough to be gravitationally contracted to a spherical shape (**Fig. 9**). Phobos measures only $11 \times 14 \times 17$ mi ($18 \times 22 \times 27$ km), and Deimos just $6 \times 8 \times 9$ mi ($10 \times 12 \times 15$ km). These tiny satellites have very low surface gravity and an escape velocity of only about 30 ft/s (10 m/s). A person standing on Deimos or Phobos could quite easily throw rocks that would leave the satellite forever.

Both satellites are saturated with impact craters; the largest is Stickney, a 6-mi-diameter (10-km) crater located on Phobos. Had the impacting object that excavated Stickney been much larger, it probably would have destroyed Phobos. In fact, it has been suggested that Deimos and Phobos may be the shattered and, perhaps, partially reconstituted remains

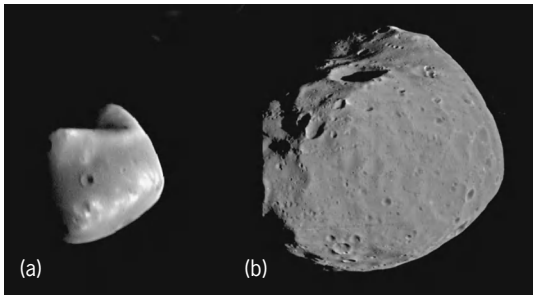

Fig. 9. The two Martian moons, (*a*) Deimos and (*b*) Phobos, have irregular outlines shaped by past collisions. (*NASA*)

of an earlier, single, large satellite of Mars. Both satellites have the same low albedo, approximately 0.05, so that surfaces are as dark as the very darkest asteroids. This low reflectivity suggests that the Martian satellites may have originated in the asteroid belt and been captured by Mars long ago. *See* ASTEROID.

J. Kelly Beatty

Bibliography. A. Albee, The unearthly landscapes of Mars, *Sci. Amer.*, 288(6):44–53, June 2003; J. K. Beatty, C. C. Petersen, and A. Chaikin (eds.), *The New Solar System*, 4th ed., Sky Publishing, Cambridge, MA, and Cambridge University Press, England, 1999; M. H. Carr, *Water on Mars*, Oxford University Press, New York, 1996; W. Sheehan, *The Planet Mars: A History of Observation and Discovery*, University of Arizona Press, Tucson, 1996; S. Squyres, *Roving Mars: Spirit, Opportunity, and the Exploration of the Red Planet*, Hyperion, New York, 2005.

Marsileales

A small order of heterosporous, leptosporangiate ferns (division Polypodiophyta) which grow in water or wet places and are rooted to the substrate. The leaves arise on long stalks from the rhizome and typically have floating blades with four leaflets, suggesting a four-leaved clover. The sporangia are enclosed in modified folded leaves or leaf segments called sporocarps. Megasporangia and microsporangia are borne in the same sporocarp. The order contains a single family and only 3 genera, about 50 species in all, most of them belonging to the widespread genus *Marsilea* (water clover). *See* POLYPODIOPHYTA.

Arthur Cronquist

Marsupialia

An order of animals, long considered the only order of the mammalian infraclass Metatheria.

Morphology. The marsupials are characterized by the presence of a pouch (marsupium) in the female, a skin pocket whose teat-bearing abdominal wall is supported by epipubic bones. The young are born in an embryonic state and crawl unaided to the marsupium, where they attach themselves to the teats and continue their development. In a few species the pouch is vestigial or has disappeared completely. The most complete dental formula for the living genera is exemplified by that of the family of American opossums (Didelphidae): I 5/4 C 1/1 Pm 3/3 M 4/4. The number of teeth may be reduced in other genera. Diprotodonty, or enlargement of the lower median incisors, is characteristic of the Australian herbivorous marsupials (**Fig. 1**). The last (third) premolar is the only replacement tooth in the cheek tooth row. The angle of the mandible is usually inflected. The five-toed plantigrade condition of the hindfeet in most marsupials is curiously modified in some Australian families to the syndactylous condition, in which the second and third digits are contained in a common web of skin (**Fig. 2**). *See* DENTITION.

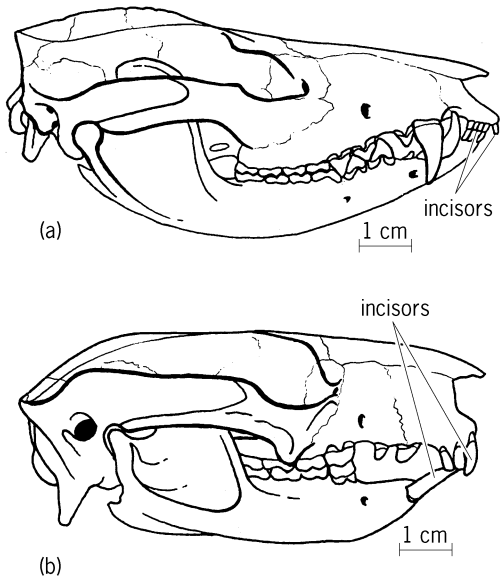

Fig. 1. Skull and jaws of marsupials. (*a*) Didelphidae, *Didelphis* (the carnivorous opossum of North America), Recent, with polyprotodont incisors (I 5/4). (*b*) Phalangeridae, *Trichosurus* (the herbivorous opossum of Australia), Recent, with diprotodont incisors (I 3/1).

A wide variety of terrestrial adaptations are found among the 82 genera of living marsupials. Some spectacular examples of evolution convergent upon placental modes of life are exemplified by the Australian marsupial "moles" (*Notoryctes*), "wolves" (*Thylacinus*), and "flying squirrels" (*Petaurus*). For the most part, the adaptive radiation of the marsupials has paralleled that of the placentals, yielding many ecological analogs, such as kangaroos and wallabies, which are the counterparts of the placental deer and antelopes, although these groups differ widely in structure. *See* EUTHERIA.

Phylogeny. The marsupials and placentals share a common Middle Cretaceous ancestor, and both were undergoing vigorous adaptive radiation in the Late Cretaceous, when the fossil record of the marsupials begins in North America. In the Cenozoic the marsupials diversified most extensively in the southern continents, such as Australia, where they lacked

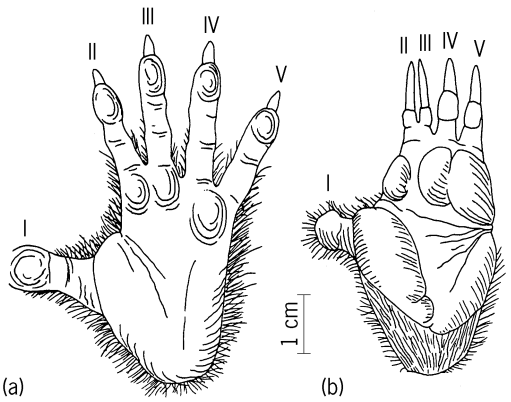

Fig. 2. Views of the soles of the left hindfoot of marsupials. (*a*) Didelphidae, *Didelphis*, representing the five-toed, polydactylous condition. (*b*) Phalangeridae, *Trichosurus*, representing the five-toed, syndactylous condition (digits II and III are bound in one web of skin).

effective placental competition, and South America, where they had only partial competition. Northern Hemisphere Cenozoic records represent only a single family (Didelphidae, the opossums), which is known in North America and Europe from the Paleocene into the early Miocene. The living American opossum (*Didelphis*) is a Pleistocene immigrant from Central and South America. There are no later records of marsupials in Europe and no Cenozoic records at all in Asia and Africa.

The marsupials were well represented during the Cenozoic in South America, where they underwent an adaptive radiation limited by direct competition with contemporary placental herbivores; consequently, the marsupials entered only a restricted number of adaptive zones. The carnivorous families (Borhyaenidae, Didelphidae) were dominant, but insectivorous groups (Caenolestidae, Necrolestidae) were present, and in the early Cenozoic some rodentlike types (Polydolopidae, Groeberiidae) evolved before the appearance of placental rodents in the Oligocene. The extinct carnivorous borhyaenids converged with placental carnivores in hyenalike (*Borhyaena*), wolflike (*Lycopsis*), and saber-toothed (*Thylacosmilus*) adaptations, and even more closely paralleled the carnivorous marsupials of Australia (especially the Thylacinidae). Late in the Cenozoic a curious group of saltatorial caenolestoids (Microtraguliidae) appeared which paralleled the smaller kangaroos of Australia. Only the families Didelphidae and Caenolestidae survived the Pleistocene invasion of South America by the placental carnivores.

It is not known when or how marsupials reached Australia, but evidence from the late Cenozoic faunas indicates that 10 of the 12 recognized families have experienced an evolutionary history that probably extends back into early Cenozoic or even Cretaceous time. Only three families, Thylacoleonidae, Diprotodontidae, and Wynyardiidae, became extinct by the end of Pleistocene time, and the last-mentioned is known only from the early Miocene. The Australian adaptive radiation is often cited as an excellent example of that evolutionary process, since a wide range of adaptive zones were invaded. Families of carnivorous (some Dasyuridae, Thylacinidae, Thylacoleonidae), insectivorous (some Dasyuridae, Peramelidae, Notoryctidae), herbivorous (Phalangeridae, Phascolarctidae, Vombatidae, Wynyardiidae, Diprotodontidae, Macropodidae), and nectar-feeding (Tarsipedidae) marsupials are represented. In addition to almost all the living genera, the Australian Pleistocene fauna included many very large extinct forms, such as giant kangaroos (Sthenurinae) and wombats (*Phascolonus*), diprotodonts such as *Diprotodon*, which was as large as living rhinoceroses, and the so-called marsupial lion *Thylacoleo*.

Taxonomy. Although the marsupials traditionally have been arranged as a single order, Marsupialia, it has long been recognized that their diversity of adaptations and length of geological history parallels that of all 30 orders of placentals. Reviews of living and fossil marsupials and the serology of the living species have given impetus to the formalization of various arrangements of the marsupial families as orders and consequently to the elevation of the term Marsupialia to superordinal rank. The proposed schemes agree in uniting the polydactylous and polyprotodont carnivorous superfamilies (Didelphioidea, Borhyaenoidea, and Dasyuroidea) either as a separate order, Marsupicarnivora Ride (1964), or with the syndactylous and polyprotodont Perameloidea as order Polyprotodonta Owen (1866). The Perameloidea are sometimes separated as order Peramelina Gray (1825). The South American diprotodont and the polydactylous, insectivorous, and rodentlike Caenolestoidea are grouped as order Paucituberculata Ameghino (1894). Most of the diprotodont, syndactylous, herbivorous marsupials of Australia (superfamilies Vombatoidea, Phalangeroidea, and Tarsipedoidea) are placed in the order Diprotodonta Owen (1866). *See* ANTEATER; KANGAROO; KOALA; MAMMALIA; METATHERIA; OPOSSUM.

Richard H. Tedford

Bibliography. M. J. Benton, *Vertebrate Paleontology*, 1991; R. L. Carroll, *Vertebrate Paleontology and Evolution*, 1988; R. M. Nowak, *Walker's Mammals of the World*, 6th ed., 1999.

Marten

One of eight groups of carnivorous mammals in the family Mustelidae along with the fisher, weasels, mink, polecats, wolverines, otters, and badgers. Six are found in Europe and Asia and two (marten and fisher) are found in North America (see **table**). The stone marten (*Martes foina*) inhabits coniferous and deciduous woodlands, while the European pine marten (*M. martes*), sable (*M. zibellina*), Japanese marten (*M. melampus*), and American pine marten (*M. americana*) are restricted to northern coniferous forests.

General morphology. The marten (*Martes*) is a medium-sized, dark-colored, semiarboreal mustelid with a moderately elongated shape, sharply pointed face, rounded ears, and a bushy tail (see **illustration**). Some members of this genus possess a white

Geographic distribution of martens

Name	Range
European pine marten *Martes martes*	Central and Northern Europe to western Siberia
Japanese marten *Martes melampus*	Japan, South Korea
Yellow-throated marten *Martes flavigula*	SE Asia, Korea, Borneo, Sumatra, Java
American pine marten *Martes americana*	N. North America to Sierra Nevada and Rockies
Sable *Martes zibellina*	Scandinavia to N. Asia, N. Japanese islands
Stone marten *Martes foina*	Denmark and Spain to Mongolia and Himalayas
Fisher *Martes pennanti*	N. North America to California and West Virginia
Nilgiri marten *Martes gwatkinsi*	Nilgiri Mountains of southern India

American pine marten, *Martes americana*. (*Photo by Gerald and Buff Corsi; © 2001 California Academy of Sciences*)

throat patch. The throat patch in the American pine marten is reddish-orange, while the yellow-throated marten (*M. flavigula*) and the Nilgiri marten (*M. gwatkinsi*) have yellow throat patches. The fisher (*M. pennanti*) lacks a throat patch. Martens are digitigrade (that is, they walk on the digits with the posterior part of the foot raised from the ground) with five toes on each foot. The large paws possess hairy soles and semiretractile claws that are not sheathed. A pair of elongated abdominal scent glands and paired anal scent glands are present in both sexes and are used for marking. Martens range in head-body length 30–75 cm (12–45 in.) and have a 12–45 cm (5–18 in.) tail. They weigh 0.5–6 kg (1–13 lb). Males are considerably larger than females in all species.

Behavior and habitats. Martens are generally solitary. They are among the most agile and graceful members of the weasel family and are able to leap effortlessly from branch to branch. Martens are opportunistic hunters and kill their prey with a bite to the back of the neck.

Martens are crepuscular and are primarily nocturnal, although they may be active any time of the day during all seasons. Dens may be in hollow trees or on or under the ground in rock crevices, hollow logs, tree roots, or under the snow. Squirrel nests and woodpecker holes are important den sites. Red-backed voles (*Clethrionomys*) and red squirrels (*Tamiasciurus*) are its chief prey, although other small mammals such as flying squirrels and shrews, birds, fish, earthworms, insects, and fruit may also be consumed. Martens have few enemies. Coyotes, fisher, foxes, lynx, cougars, eagles, and owls may take an occasional young marten, but humans are the greatest enemy through trapping and habitat destruction. American martens have been known to survive in captivity up to 17 years and in the wild for 19 years.

American pine marten. The American pine marten is about the size of a small house cat. Its pelage, which ranges in color from yellowish brown to dark brown, is soft and lustrous. The tooth formula is I 3/3, C 1/1, Pm 4/4, M 1/2 × 2 for a total of 38 teeth. Formerly found in the northern spruce and balsam fir forests and the mixed deciduous-coniferous forests south to Virginia and California, the species is now extirpated over much of this area due to habitat destruction and overtrapping. It avoids early and mid-successional forests, as well as forest openings.

Reproduction. They are polygamous with one female accepting more than one male. Most species breed in late summer, with litters of 1–5 sparsely furred, blind, and deaf kits being born during early spring. Delayed implantation is known to occur in some northern species (yellow-throated marten, American marten, sable, fisher). In the American marten, for example, gestation is 220–276 days, although the period of active pregnancy is about 27 days. Weaning occurs between 6 and 8 weeks of age. Kits are able to kill prey when 3–4 months old. Sexual maturity is attained at about 15 months.

Fur. The fur of some martens, especially the sable and fisher, is highly valued. It is used in the manufacture of coats, capes, and jackets as well as for trim and for linings for luxury garments. The fur of the American pine marten is sometimes referred to as "American sable." Overharvesting along with habitat destruction has caused some populations to decline. The status of the Nilgiri marten is considered vulnerable. *See* CARNIVORA; FISHER; SABLE. Donald W. Linzey

Bibliography. S. Buskirk et al. (eds.), *Martens, Sables, and Fishers: Biology and Conservation*, Cornell University Press, Ithaca, New York, 1994; T. W. Clark et al., *Martes americana, Mammalian Species*, no. 289, pp. 1–8, American Society of Mammalogists, 1987; G. A. Feldhamer, B. C. Thompson, and J. A. Chapman, *Wild Mammals of North America: Biology, Management, and Conservation*, 2d ed., Johns Hopkins University Press, 2003; R. M. Nowak, *Walker's Mammals of the World*, 6th ed., Johns Hopkins University Press, 1999.

Maser

A device for coherent amplification or generation of electromagnetic waves by use of excitation energy in resonant atomic or molecular systems. "Maser" is an acronym for microwave amplification by stimulated emission of radiation. The device uses an unstable ensemble of atoms or molecules that may be stimulated by an electromagnetic wave to radiate energy at the same frequency and phase as the stimulating wave, thus providing coherent amplification. Amplifiers and oscillators operating on the same principle as the maser exist in many regions of the electromagnetic spectrum. Those operating in the optical region were once called optical masers, but they are now universally called lasers (the "l" stands for "light"). Amplification by maser action is also observed arising naturally from interstellar gases. *See* COHERENCE; LASER.

Maser amplifiers can have exceptionally low internally generated noise, approaching the limiting effective input power of one-half quantum of energy per unit bandwidth. This limit is often described as one quantum per unit bandwidth, but the other half quantum is better attributed to a zero-point input noise field. The limit is consistent with Heisenberg's uncertainty principle, which prohibits exact simultaneous determination of the amplitude and phase of a wave. Their inherently low noise makes maser oscillators that use a narrow atomic or molecular resonance extremely monochromatic, providing a basis for frequency standards. The hydrogen maser, which uses a hyperfine resonance of a gas of hydrogen atoms as the amplification source, is the prime example of this use. Also because of their low noise and consequent high sensitivity, maser amplifiers are particularly useful for reception and detection of very weak signals in radio astronomy, microwave radiometry, and the like. A maser amplifier was used in the experiments that detected the cosmic microwave radiation left over from the big bang that created the universe. *See* COSMIC BACKGROUND RADIATION; ELECTRICAL NOISE; FREQUENCY MEASUREMENT; RADIO ASTRONOMY; UNCERTAINTY PRINCIPLE.

Principle of operation. The quantum theory describes discrete particles such as atoms or molecules as existing in one or more members of a discrete set of energy levels, corresponding to the various possible internal motions of the particle (vibrations, rotations, and so forth). Thermal equilibrium of an ensemble of such particles requires that the number of particles n_1 in a lower energy level 1 be related to the number of particles n_2 in a higher energy level 2 by the Boltzmann distribution, given by Eq. (1), where E_1 and E_2 are the respective energies

$$\frac{n_1}{n_2} = \exp \frac{(E_2 - E_1)}{kT} \tag{1}$$

of the two levels, k is Boltzmann's constant, and T is the absolute (Kelvin) temperature. Thermal equilibrium also requires that the phases of oscillation of the particles, or the relative phases of the quantum-mechanical wave functions of the various states, be random. A collection of such particles in thermal equilibrium absorbs electromagnetic energy at their resonance frequencies $\nu_{21} = (E_2 - E_1)/h$, where h is Planck's constant. Maser amplification requires upset of the thermal equilibrium condition. *See* BOLTZMANN STATISTICS; NONRELATIVISTIC QUANTUM THEORY; QUANTUM MECHANICS.

Particles may be stimulated by an electromagnetic wave to make transitions from a lower energy level to a higher one, thereby absorbing energy from the wave and decreasing its amplitude, or from a higher energy level to a lower one, thereby giving energy to the wave and increasing its amplitude. These two processes are inverses of each other, and their effects on the stimulating wave add together. The upward and downward transition rates are the same, so that, for example, if the number of particles in the upper and lower energy states is the same, the stimulated emission and absorption processes just cancel. For any substance in thermal equilibrium at a positive (ordinary) temperature, the Boltzmann distribution requires that n_1 be greater than n_2 resulting in net absorption of the wave. If n_2 is greater than n_1, however, there are more particles that emit than those that absorb, so that the particles amplify the wave. In such a case, the ensemble of particles is said to have a negative temperature T, to be consistent with the Boltzmann condition. If there are not too many counterbalancing losses from other sources, this condition allows net amplification. This is the basic description of how a maser amplifies an electromagnetic wave. An energy source is required to create the negative temperature distribution of particles needed for a maser. This source is called the pump.

Gas masers. The first known maser of any kind was realized in 1954. The amplifying medium was a beam of ammonia (NH_3) molecules, and the molecular resonance used was the strongest of the rotation-inversion lines, at a frequency near 23.87 GHz (1.26-cm wavelength). Molecules from a pressurized tank of ammonia issued through an array of small orifices to form a molecular beam in a meter-long vacuum chamber. Spatially varying electric fields in the vacuum chamber created by a cylindrical array of electrodes formed a focusing device, which ejected from the beam the molecules in the lower energy level and directed the molecules in the upper energy level into a metal-walled electromagnetic cavity resonator. When the cavity resonator was tuned to the molecular transition frequency, the number of molecules was sufficiently large to produce net amplification and self-sustained oscillation. This type of maser is particularly useful as a frequency or time standard because of the relative sharpness and invariance of the resonance frequencies of molecules in a dilute gas. *See* CAVITY RESONATOR; MOLECULAR BEAMS.

The condition for oscillation to occur is given by Eq. (2), where m and e are respectively the mass and

$$n_2 - n_1 \geq \frac{\pi m V \nu \Delta\nu}{f e^2 Q} \tag{2}$$

charge of an electron, V and Q are the volume and quality factor of the cavity resonator, while the resonant molecular response is described by its resonant frequency ν, its full width at half maximum $\Delta\nu$, and its oscillator strength f. The quality factor Q is defined as $2\pi\nu$ divided by the fractional rate of loss of field energy stored in the cavity, due to both internal losses and losses through coupling holes. Low loss translates into high Q. The oscillator strength f is the ratio of the integrated response of a molecule in its lower state to that of a harmonically bound electron. Small oscillator strength requires a proportionately greater number of molecules. The maximum power output is the quantum energy $h\nu$ multiplied by the rate at which molecules enter the cavity (for the ammonia maser, this amounted to a few nanowatts). A wave impinging on the cavity at the molecular transition

frequency is amplified in transmission or reflection if Eq. (2) is satisfied, with Q_0 replacing Q, where $Q_0 > Q$ is the quality factor of the cavity representing only its internal losses.

A gas maser that is currently used as a particularly valuable frequency standard is the hydrogen maser mentioned above. First reported in 1960, this maser is similar to the ammonia maser. A beam of hydrogen atoms in a vacuum chamber passes through a state selector, this time using a magnetic field, which directs the upper-state atoms into a small opening in a quartz bulb. The bulb sits in a silver-plated cavity resonator tuned to the hyperfine transition frequency near 1.42 GHz (21.1-cm wavelength). The inside walls of the quartz bulb are specially coated so that the hydrogen atoms can bounce off them many times with little disturbance of the transition frequency or phase. This property leads to an exceptionally narrow resonance line and thus an exceptionally stable frequency of oscillation. *See* ATOMIC CLOCK.

Solid-state masers. Solid-state masers usually involve the electrons of paramagnetic ions in crystalline media immersed in a magnetic field. At least three energy levels are needed for continuous maser action. The energy levels are determined both by the interaction of the electrons with the internal electric fields of the crystal and by the interaction of the magnetic moments of the electrons with the externally applied magnetic field. The resonant frequencies of these materials can be tuned to a desired condition by changing the strength of the applied magnetic field and the orientation of the crystal in the field. An external oscillator, called the pump, excites the transition between levels 1 and 3 [at the frequency $\nu_{31} = (E_3 - E_1)/h$], equalizing their populations. Then, depending on other conditions, the population of the intermediate level 2 may be greater or less than that of levels 1 and 3. If greater, maser amplification can occur at the frequency ν_{21}, or if less, at the frequency ν_{32}. Favorable conditions for this type of maser are obtained only at very low temperature, as in a liquid-helium cryostat. A typical material is synthetic ruby, which contains paramagnetic chromium ions (Cr^{3+}), and has four pertinent energy levels. *See* PARAMAGNETISM.

The important feature of solid-state masers is their sensitivity when used as amplifiers. Such masers have been made with effective input noise temperatures less than about 5 K. They have usually been made using traveling-wave structures rather than resonant cavities. In this case, the gain per unit length (α) produced by the maser medium placed in the structure is given by Eq. (3), where n_2 and n_1 are the numbers

$$\alpha(\nu) = \frac{2f(n_2 - n_1)\pi^2 e^2}{Amv_g} g(\nu) \tag{3}$$

of ions per unit length, A is the cross-sectional area of the waveguide structure, v_g is the group (energy) velocity of the microwaves in the waveguide, and $g(\nu)$ is the line shape function, normalized so that its integral over frequency is unity. The other symbols are as in Eq. (2). Slow-wave waveguide structures can increase the gain by reducing the group velocity to about one-hundredth of the velocity of light. Typical values of the other parameters can give amplifier gains of a few decibels per centimeter of length, and maximum output powers in the microwatt range. *See* WAVEGUIDE.

Astronomical masers. Powerful, naturally occurring masers have probably existed since the earliest stages of the universe, though that was not realized until a few years after masers were invented and built on Earth. Their existence was first proven by discovery of rather intense 18-cm-wavelength microwave radiation of the free radical hydroxyl (OH) molecule coming from very localized regions of the Milky Way Galaxy.

Microwave radiation of OH reaching the Earth from various directions in outer space had already been studied for a few years before discovery that some of this radiation comes from areas in the Milky Way Galaxy which are very limited in size. This means that in its own locality the radiation is much too intense to be simply due to warm molecules; it had to be brought up to the observed intensity by the process of stimulated emission, or maser-type action. Soon after recognition that OH radiation came from astronomical masers, it was found that the water molecule in interstellar clouds of gas is also producing intense 1.35-cm-wavelength radiation by maser action. This radiation from water and from OH reaches the Earth from many directions in the Milky Way Galaxy, such as from the Orion Nebula, and from many stars that are surrounded by dust particles and gas. Microwave radiation from water molecules has been found to come even from distant galaxies, some of which are broadcasting this radiation at an intensity as large as a few hundred times that of the total radiation at all wavelengths produced by the Sun.

Continued studies of microwave radiation from outer space have revealed many additional masers in various astronomical sources and from a wide variety of molecules. Radiation by astronomical masers at more than 120 different frequencies is now known, produced by more than a dozen different molecules such as OH, water, ammonia, methyl alcohol, and hydrogen cyanide. Masers due to excited hydrogen atoms are also found. Some of these naturally occurring amplifying systems are also at wavelengths shorter than microwaves. In the infrared region, they are generally called lasers rather than masers. There are even lasers in the atmosphere of Mars, due to carbon dioxide that is excited to high energy levels by solar radiation. *See* INTERSTELLAR MATTER.

Although the natural occurrence of masers in astronomical sources had not been considered before they were discovered somewhat accidentally, in hindsight it should have been expected that conditions in astronomical sources would produce them. Radiation from stars, molecular collisions in stellar clouds that are not in thermal equilibrium, and other sources of energy in astronomical objects can easily excite molecules and atoms. It can produce energy

distributions in them that are very different from those of normal materials in thermal equilibrium, and thus provide conditions for maser-type amplification of waves. Some of the mechanisms for this excitation in astronomical situations are understood. An example is the ionization of hydrogen by ultraviolet stellar radiation and subsequent recombination of protons and electrons into excited energy states of hydrogen. In the case of water-vapor masers, it appears that molecular collisions in strong shock waves of rarefied gases are probably the source of their often very powerful maser action. Some masers are recognized to be characteristic of particular types of astronomical locations. For example, masers produced by silicon monoxide (SiO) molecules are found almost always in gas produced by and closely surrounding stars. However, there are also many astronomical masers for which the mechanisms involved are not yet well understood, and undoubtedly there are a number of new types still to be discovered. These masers have existed for many billions of years, and humans have just recently begun to know of them.

Masers in astronomical objects differ from those generally used on Earth in that they involve no resonators or slow-wave structures to contain the radiation and so increase its interaction with the amplifying medium. Instead, the electromagnetic waves in astronomical masers simply travel a very long distance through astronomical clouds of gas, far enough to amplify the waves enormously even on a single pass through the cloud. It is believed that usually these clouds are large enough in all directions that a wave passing through them in any direction can be strongly amplified, and hence astronomical maser radiation emerges from them in all directions. Although some amplifying clouds may be thinner in one direction than in others, and thus amplify unequally in different directions, it is believed that most astronomical masers radiate broadly in a wide range of directions, and it is on this basis that their total power is estimated.

Naturally occurring masers have been important tools for obtaining information about astronomical objects. Since they are very intense localized sources of microwave radiation, their positions around stars or other objects can be determined very accurately with microwave antennas separated by long distances and used as interferometers. This provides information about the location of stars themselves as well as that of the masers often closely surrounding them. The masers' velocity of motion can also be determined by Doppler shifts in their wavelengths. The location and motion of masers surrounding black holes at the centers of galaxies have also provided information on the impressively large mass of these black holes. Astronomical masers often vary in power on time scales of days to years, indicating changing conditions in the regions where they are located. Such masers also give information on likely gas densities, temperature, motions, or other conditions in the rarefied gas of which they are a part. *See* BLACK HOLE; DOPPLER EFFECT.

Charles H. Townes; James P. Gordon

Bibliography. A. W. Clegg and G. E. Nedoluha (eds.), *Astrophysical Masers*, Springer-Verlag, 1993; T. K. Ishii, *Maser and Laser Engineering*, 1983; A. E. Siegman, *An Introduction to Lasers and Masers*, 1971; A. E. Siegman, *Microwave Solid-State Masers*, 1964; A. Yariv, *Quantum Electronics*, 3d ed., John Wiley, 1989.

Masking of sound

Interference with the audibility of a sound caused by the presence of another sound. More specifically, the number of decibels (dB) by which the intensity level of a sound (signal) must be raised above its threshold of audibility, to be heard in the presence of a second sound (masker), is called the masking produced by the masker on the signal. The masker and the signal may be identical or may differ in frequency, complexity, or time.

Masking between pure tones. Masking effects when both the masker and signal are pure tones and are presented simultaneously are shown in **Fig. 1**. The three curves represent cases in which the frequency of the signal is 300, 1000, or 3000 Hz. The tonal signal is brief, and it is presented at a low sensation level in the temporal middle of a longer-duration tonal masker. The level of the tonal masker required for threshold detection of the signal is the dependent variable shown on the ordinate. As the masker is moved through the range of frequencies shown on the abscissa, the amount of masking (or threshold shift) is plotted in the curves. When the tonal signal and masker have the same frequency, a very low level masker is required to mask the signal, indicating significant masking. As the difference in the frequency between the signal and masker increases, the signal is easier to detect, requiring a higher-level masker to mask the signal. Results from these psychophysical tuning curve measures of masking agree very well with data obtained from single auditory neurons in

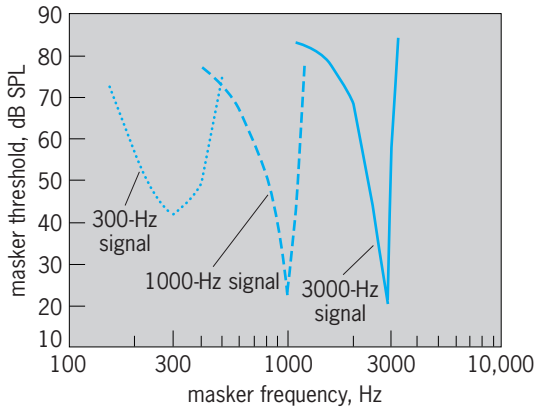

Fig. 1. Three psychophysical tuning curves, showing the tonal masking effects for tonal signals of 300, 1000, or 3000 Hz. (*After F. L. Wightman et al. Factors influencing frequency selectivity in normal and hearing-impaired listeners, in E. F. Evans and J. Wilson, eds., Psychophysics and Physiology of Hearing, Academic Press, London, 1977*)

the auditory periphery, suggesting that tonal masking is mediated by the activity of these peripheral neurons.

Masking between complex sounds. The most widely studied complex masking sound is random noise which has energy at all frequencies and is said to be flat if the level for each 1-Hz bandwidth of the noise is the same. When random-flat noise is used to mask a pure tone, only a narrow frequency band (critical band) of the noise centered at the tonal frequency causes masking. If the bandwidth of the noise is narrower than this critical bandwidth, the tone's intensity can be lowered before the tone is masked. If the bandwidth is wider than this critical bandwidth, further widening of the bandwidth causes no changes in the detectability of the signal. The width of the critical band increases proportionally to its center frequency, that is, to the signal frequency (**Fig. 2**). When noise masks speech, either the detectability of speech or speech intelligibility can be measured. The level for speech intelligibility is about 10–14 dB higher than for speech detectability. Masking by other complex sounds leads to results such as would be expected from the principles shown in Fig. 1 and those based on the existence of critical bands.

Temporal masking. Masking can occur when the signal either precedes or follows the masker in time. In backward masking the signal precedes the masker, while in forward masking the signal follows the masker. **Figure 3** shows the relative amount of masking which exists if the masker is presented for a brief time and the signal is of a shorter duration and appears at various times before, during, and after the masker. As is shown, signal threshold is highest at the temporal edges of the masker (masking overshoot), while more masking is obtained at longer temporal separations between the masker and signal in forward than in backward masking. **Figure 4***a* shows an example of another forward-masking phenomenon. The signal is 1000 Hz and the masker is two tones: a 1000-Hz tone and a second tone whose frequency is shown on the abscissa (Fig. 4*b* shows the temporal relationships). The solid line on the ordinate of Fig. 4*a* represents the signal threshold when only the 1000-Hz tone is the masker (approximately 65 dB). When the frequency of the second tone in the complex two-tone masker is less than 1100 Hz, the second tone yields masking in addition to that obtained for the 1000-Hz masker. When the second tone in the complex two-tone masker is between 1100 and 1600 Hz, the signal threshold is less than that obtained when only the 1000-Hz masker produced the masking. In this frequency region, then, the addition of a second tone to the 1000-Hz masker yields a signal which is easier to detect, and thus its threshold is lower. It is as if the second tone reduces the effectiveness of the 1000-Hz masking stimulus. The physiological basis for this effect, as well as its implications for auditory processing of complex stimuli, is of great interest to the auditory scientist. *See* ACOUSTIC NOISE; HEARING (HUMAN); SOUND. William A. Yost

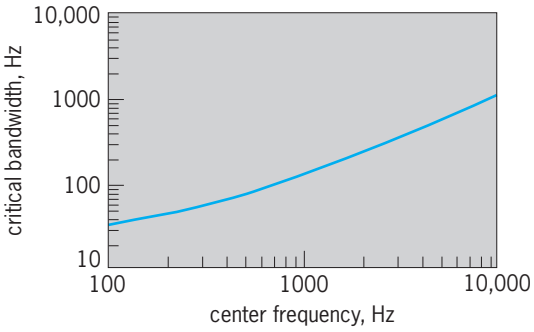

Fig. 2. Width of the critical band in hertz as a function of signal frequency.

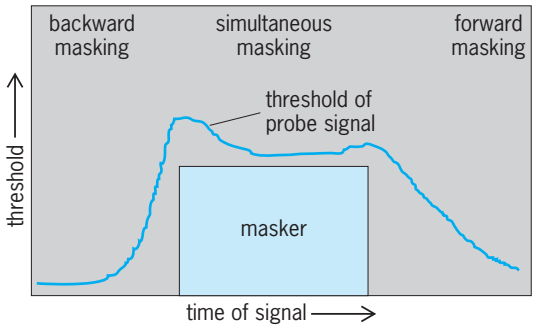

Fig. 3. Relative amount of masking obtained in forward, simultaneous, and backward masking. (*After W. A. Yost, Fundamentals of Hearing: An Introduction, 4th ed., Academic Press, New York, 2000*)

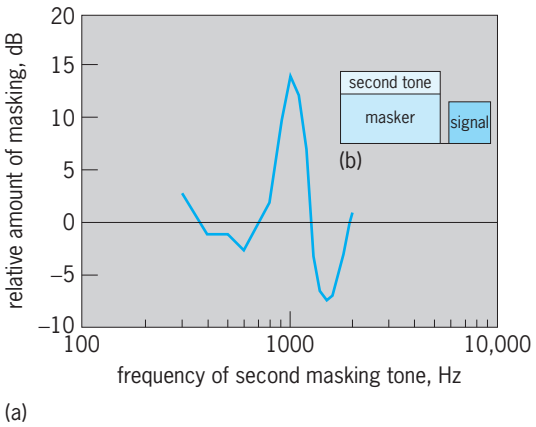

Fig. 4. Masking of a 1000-Hz pure-tone signal in forward masking when the masker is a two-tone complex consisting of a 1000-Hz masker and a second tone. (*a*) Threshold of signal for the two-tone masker relative to that obtained when only the 1000-Hz tone served as the masker, plotted against the frequency of the second masking tone. (*b*) Temporal relationship of signal and maskers. (*After R. V. Shannon, Two-tone unmasking and suppression in a forward-masking situation, J. Acous. Soc. Amer., 59:1460–1471, 1975*)

Bibliography. W. M. Hartmann, *Signal, Sounds, and Sensation*, Springer-Verlag, New York, 1998; B. C. J. Moore, *Introduction to the Psychology of Hearing*, 4th ed., Academic Press, London, 1997; W. A. Yost, *Fundamentals of Hearing: An Introduction*, 4th ed., Academic Press, New York, 2000.

Masonry

Construction of natural building stone or manufactured units such as brick, concrete block, adobe, glass block, or cast stone that is usually bonded with mortar. Masonry can be used structurally or as cladding or paving. It is strong in compression but requires the incorporation of reinforcing steel to resist tensile and flexural stresses. Masonry veneer cladding can be constructed with adhesive or mechanical bond over a variety of structural frame types and backing walls.

Masonry is noncombustible and can be used as both structural and protective elements in fire-resistive construction. It is durable against wear and abrasion, and most types weather well without protective coatings. The mass and density of masonry also provide efficient thermal and acoustical resistance.

Materials. Brick, concrete block, and stone are the most widely used masonry materials for both interior and exterior applications in bearing and nonbearing construction. Stone masonry can range from small rubble or units of ashlar (a hewn or squared stone) embedded in mortar, to mechanically anchored thin slabs, to ornately carved decorative elements. Hardness dictates both form and cost, and it also affects durability and weathering. Granite, marble, and limestone are the most commonly used commercial building stones. Glass block can be used as security glazing or as elements to produce special daylighting effects. Both clear, colored, and reflective coated glass-block units in smooth and textured surfaces are available. *See* GLASS; GRANITE; LIMESTONE; MARBLE.

Masonry mortar is made from cement, sand, lime, and water. Masonry grout, a more fluid mixture of similar ingredients, is used to fill hollow cores and cavities and to embed reinforcing steel. Anchors and ties are usually of galvanized or stainless steel. Flashing may be of stainless steel, coated copper, heavy rubber sheet, or rubberized asphalt. Weepholes are formed by leaving the mortar out of head joints just above flashing. *See* GROUT; MORTAR.

Wall types. Both brick and concrete block are available in hollow units suitable for walls that are a single unit thick (single wythe). Steel reinforcing bars can be grouted vertically in the hollow cores and horizontally in U-shaped bond beam units. Where walls are required to accommodate electrical conduit or plumbing piping, double-wythe walls with an open or grouted cavity are more appropriate. The backing and facing wythe may be of the same or dissimilar types of masonry.

Veneer applications of masonry are appropriate when the visual appearance of a masonry structure is desired, but a load-bearing wall design is not considered appropriate. Masonry veneers may be used on buildings of wood, steel, or concrete structural frames, as well as cladding on load-bearing masonry buildings. Anchored veneers must be designed with an open cavity for drainage, and require the installation of flashing and weepholes for collection and discharge of moisture.

Important considerations. Masonry walls are permeable. Even when the design is adequate and the workmanship is acceptable, some wind-driven moisture can still penetrate the face shell of single-wythe units or the full thickness of a 4-in. (10-cm) exterior wythe. Cavity walls were initially conceived to provide drainage for this moisture through a system of flashing and weepholes. Cavity walls and anchored veneer walls should have an open separation of at least 2 in. (5 cm) between the exterior masonry wythe and the backing. The open cavity, when it is properly fitted with flashing and weepholes, functions as a drainage system for moisture that penetrates from the exterior or is condensed from water vapor within the wall section. Single-wythe walls and multiwythe solid walls must also be designed with a system of flashing and weepholes to divert moisture to the outside. Moisture protection is maximized when the flashing membrane is continuous, without gaps or voids, and is turned up to form pans at terminations.

Masonry walls are also relatively brittle and contain thousands of linear feet of joints along which cracks can open because of thermal and moisture movements and dissimilar movement between adjacent materials. Concrete products shrink, clay products expand, and metals expand and contract reversibly. Such movement is accommodated through flexible anchorage and the installation of control joints in concrete masonry and expansion joints in clay masonry. Coefficients of thermal expansion and coefficients of moisture expansion can be used to estimate the expected movement of various materials, so that movement joints can be sized and joint sealants selected accordingly. If details do not accommodate the necessary wall movement, excessive moisture can penetrate through the resulting cracks. *See* BRICK; CLAY, COMMERCIAL; CONCRETE; STONE AND STONE PRODUCTS.

Christine Beall

Bibliography. C. Beall, *Masonry Design and Detailing*, 4th ed., 1997; Brick Institute of America, *Technical Notes*; National Concrete Masonry Association, *TEK Notes*; F. A. Robert, R. Schneider, and W. L. Dickey, *Reinforced Masonry Design*, 2d ed., 1987.

Mass

The quantitative measure of the inertia of an object, that is, of its resistance to being accelerated. Thus, the more massive an object is, the harder it is to accelerate it (change its state of motion). Isaac Newton described mass as the "quantity of matter" when formulating his second law of motion. He observed that the rate of change of motion is proportional to the impressed force and in the direction of that force. By "motion" he meant the product of the quantity of matter and the velocity. In modern terms Newton's "motion" is known as momentum. The second law is expressed by Eq. (1), where **F** is the

$$\frac{d\mathbf{p}}{dt} \propto \mathbf{F} \tag{1}$$

applied force, t the time, and $\mathbf{p}$ the momentum. If the mass of the object is constant, then the rate of change of momentum with time is just the product of the mass with the rate of change of the velocity with time, the acceleration $\mathbf{a}$. For this situation the second law may be written as Eq. (2).

$$\mathbf{a} \propto \frac{\mathbf{F}}{m} \tag{2}$$

See FORCE; LINEAR MOMENTUM; MOMENTUM.

By suitable choice of units the proportionality becomes an equality as shown in Eq. (3). In particular, the equality holds in the International System of Units (SI), in which acceleration is measured in meters/second, force is in newtons, and the unit of mass is the kilogram (kg). *See* ACCELERATION; UNITS OF MEASUREMENT.

$$\mathbf{a} = \frac{\mathbf{F}}{m} \tag{3}$$

The primary standard of the unit of mass is the international prototype kilogram kept at Le Bureau International des Poids et Mesures in France. The prototype kilogram is a cylinder of a platinum-iridium alloy, a material chosen for its stability. The standard of mass is kept under conditions specified initially by the first Conférence Général des Poids et Mesures in 1889. Secondary standards are maintained in laboratories around the world and are compared with the mass of the prototype by means of balances whose precision reaches 1 part in 10^8 or better. *See* PHYSICAL MEASUREMENT.

Measuring mass. The mass that is described through the second law is known as inertial mass. The inertial mass of any object may be measured by comparing it to the inertial mass of another object. For example, two objects may be made to collide and their accelerations measured. According to Newton's third law of motion, both objects experience forces of equal magnitude. Consequently the ratio of their masses will be related to their accelerations through Eq. (4), where a_1 and a_2 are the magnitudes of accelerations. Thus, if the value of one mass is known, the value of the other mass may be determined by experiment.

$$\frac{m_1}{m_2} = \frac{a_2}{a_1} \tag{4}$$

Masses may be compared or measured by means other than collisions. Systems that oscillate do so with a frequency that depends on their mass. For example, the frequency of a mass oscillating at the end of a spring decreases as the mass is increased. This behavior is utilized to construct inertial balances, devices that measure the inertial mass. *See* HARMONIC MOTION.

Mass and weight. The most common way of measuring mass is by weighing, a process that involves the effect of gravity. With a simple two-pan balance, two masses are compared by comparing their weights. The weight of an object on Earth is the gravitational force of attraction exerted on it by the Earth. The response of the balance to the two masses is really a response to their weights. As a result, in commercial and common use, weight is often expressed in units of kilograms instead of the correct units of newtons. *See* GRAVITATION; WEIGHT.

The gravitational force that leads to weight is not confined to just the interaction between the Earth and objects at its surface. Indeed, the law of universal gravitation, first formulated by Newton in 1684, describes an attractive force that exists between all objects and is proportional to the product of their masses. In effect, mass is the source of the gravitational force of attraction. Consequently, there is another interpretation of mass, one that is based on gravitational force and not on inertia. It is called gravitational mass to distinguish it from inertial mass.

Newton recognized that he had two distinct concepts of mass and devised an experimental test of the equivalence of inertial and gravitational mass. Using crude methods he was unable to detect any difference between the two types of mass. In 1890, Lorand Eötvös devised a sensitive method to test the equivalence of inertial and gravitational mass. He used objects of different materials to compare the effect of the Earth's gravitational force on them with the inertial effects of the Earth's rotation. Eötvös concluded that the two types of mass were the same. More recent experiments with even greater sensitivity continue to support the idea that inertial mass and gravitational mass are identical. The principle of equivalence is the assertion that both masses are exactly equal. Albert Einstein employed the principle of equivalence in his development of the general theory of relativity. *See* RELATIVITY.

Weightlessness and microgravity. Near the Earth's surface, when air resistance is removed, all objects fall with the same acceleration. This constant acceleration is known as the acceleration of gravity, g, and has the standard value 9.80665 m/s^2. Although g is the same for all objects in a given locality, it does vary slightly with altitude and latitude. Newton's second law may be used to relate the gravitational force (the weight) to the acceleration. Thus, the weight w may be expressed by Eq. (5), which gives the relationship between mass and weight. Weight is a force proportional to the mass of an object and g is the constant of proportionality.

$$w = mg \tag{5}$$

When you stand on a scale, the scale reading gives the magnitude of your weight. Most of the force that comprises your weight is due to the gravitational attraction between you and the Earth. However, because the Earth rotates, your weight is slightly less than it would be if the Earth were not rotating. Consequently, a more precise definition of weight is as follows: The weight of a object in a specified reference frame is the force that, when applied to the object, would give it an acceleration equal to the local acceleration of free fall in that reference frame. On the Earth, the local acceleration of free fall is g. If an object is taken to the Moon, the force of gravity

exerted on it by the Moon is less than the force of gravity on it when it was on Earth. Thus, its weight on the Moon is less than its weight on Earth, even though its mass remains unchanged. *See* REFERENCE FRAME.

An astronaut inside an orbiting spacecraft experiences a condition called weightlessness. In orbit, both the spacecraft and the astronaut are in free fall. They are both being accelerated by gravity at the same rate and there is no noticeable attraction between them. The astronaut floats around freely within the spacecraft. If the astronaut were to stand on a scale attached to the spacecraft, the scale would record essentially zero weight. If an object (including the astronaut) is placed at a location a meter or so from the center of mass of the spacecraft, it will actually drift slightly relative to the center of mass. The drift occurs because the object and the spacecraft experience slightly different accelerations due to the Earth's gravity because of the slight difference in radial distance from the Earth and the corresponding slight difference in orbital path. For the astronaut in a low Earth orbit, 300 km (186 mi) above the surface, this relative motion would seem to be due to a very small force. An object displaced a few meters from the center of mass of the spacecraft would have an acceleration relative to the spacecraft of approximately one millionth the value of g at the Earth's surface. Consequently, this condition of near weightlessness is known as microgravity. *See* FREE FALL; WEIGHTLESSNESS.

In monitoring the health of the crew in sustained orbit, the body mass of the astronauts provides important information. On Earth, their weight would be measured using scales. In the microgravity of orbit, their weight is meaningless. Instead, astronauts measure their mass with an inertial balance that consists of a chair that moves relative to the spacecraft with a simple back-and-forth motion similar to that of a porch glider. The mass is computed from measurements of the frequency of the chair's motion.

Mass and energy. For many years it was thought that mass was a conserved quantity; that is, that it can neither be created nor destroyed. During the eighteenth and nineteenth centuries much of the development of chemistry was based on the conservation of mass. Careful measurements of the mass of constituents of chemical reactions and their products showed that the quantity of matter was unchanged by chemical reactions. However, in the twentieth century, observations and measurements in nuclear and particle physics demonstrated conclusively that mass is not a conserved quantity. For example, radioactive polonium-210 decays into lead-206 by the emission of an energetic alpha particle (a helium nucleus). The combined mass of the lead nucleus and the alpha particle is less than the mass of the original polonium nucleus. The difference in the masses appears as the kinetic energy of the alpha and the lead nucleus. This correspondence between mass and energy was shown by Einstein in Eq. (6). In the case of the alpha decay of polonium, the loss of mass during the decay results an increase in the kinetic energy of the decay products. *See* CONSERVATION OF MASS.

$$E = mc^2 \tag{6}$$

There are many other examples that demonstrate the nonconservation of mass. One of these is the annihilation process that occurs when matter and antimatter combine. An electron can combine with its antiparticle, a positron, and the two annihilate each other. The two massive particles disappear and a pair of massless photons (the quanta of light) emerge. In a coordinate system in which the electron-positron pair is at rest, the two photons are emitted in opposite directions with identical energies as required by momentum conservation. These two photons carry away the energy that was present in the form of the mass of the electron and the positron. As a result, each photon has an energy equivalent to the mass of a single electron. That energy may be found from Eq. (6). Inserting $m = 9.11 \times 10^{-31}$ kg and $c = 2.997 \times 10^{8}$ m/s gives an energy value of 8.19×10^{-14} joules. In units of electronvolts (eV) the photon energy is 5.11×10^{5} eV or 0.511 MeV. *See* ANTIMATTER; ELECTRONVOLT.

The energies released in chemical reactions are typically a fraction of an electronvolt and the resulting mass changes are thus approximately a millionth of the mass of an electron. Because the electron mass is only a small fraction of the atomic mass, the change in mass-energy in chemical reactions is only at the level of parts per billion. The practical result is that on the scale of chemical reactions mass appears to be conserved. At much higher energies, however, the changes in mass-energy become significant. It is the energy release in the fission of heavy elements such as uranium and plutonium that makes nuclear reactors practical sources of energy. *See* NUCLEAR FISSION.

In the present model for understanding fundamental particles and their interactions, that is, the standard model, the masses of particles arise from the energy of the force fields of their constituents. The masses of the nuclear particles, the protons and neutrons, are thought to arise from the interactions of subnuclear particles called quarks. The mass of a proton, for example, comes at least in part from the energy of the force fields of the quarks.

When a particle is accelerated it gains kinetic energy as its speed and momentum increase. As its speed approaches the speed of light, its momentum increases without limit. Further increases in kinetic energy result in increases in momentum but the speed changes more slowly as it approaches the limiting speed, the speed of light. A change of kinetic energy (or work done on the particle) at high speeds does not produce the same change of speed that would result from the identical increment of energy when the particle is moving at a lower speed. In the early twentieth century, the particle was generally regarded as becoming more massive as its speed approached the speed of light. However, the current practice is to take the view that the mass is invariant, unlike the m used in Eq. (6), and is related to

the energy through Eq. (7). Here, E represents the

$$m = \sqrt{\frac{E^2}{c^4} - \frac{p^2}{c^2}} \tag{7}$$

total energy of the particle of mass m moving with momentum p. As the energy, and hence the speed, of the particle increases, the momentum changes according to Eq. (8). In this view, the mass m is the

$$p = \frac{mv}{\sqrt{1 - v^2/c^2}} \tag{8}$$

invariant mass and is a constant. Then at speeds near the speed of light, changes in energy result in negligible changes in speed even though the changes in momentum are large. *See* FLIGHT; MOMENTUM.

Edwin R. Jones

Bibliography. A. Hobson, Teaching $E = mc^2$: Mass without mass, *Phys. Teacher*, 43(2):80–82, 2005; K. R. Symon, *Mechanics*, 3d ed., Addison-Wesley, Boston, 1971; B. N. Taylor (ed.), *The International System of Units (SI)*, NIST Spec. Publ. 330, 2001; E. F. Taylor and J. A. Wheeler, *Spacetime Physics*, 2d ed., Freeman, New York, 1992; F. Wilczek, Whence the force of $F = ma$? II: Rationalizations, *Phys. Today*, 57(12):10–11, December 2004.

Mass defect

The difference between the mass of an atom and the sum of the masses of its individual components in the free (unbound) state. The mass of an atom is always less than the total mass of its constituent particles; this means, according to Albert Einstein's well-known formula, that an energy of $E = mc^2$ has been released in the process of combination, where m is the difference between the total mass of the constituent particles and the mass of the atom, and c is the velocity of light.

The mass defect, when expressed in energy units, is called the binding energy, a term which is perhaps more commonly used. *See* NUCLEAR BINDING ENERGY.

W. W. Watson

Mass–luminosity relation

The relation, observed or predicted by theory, between the quantity of matter a star contains (its mass) and the amount of energy generated in its interior (its luminosity). Because of the great sensitivity of the rate of energy production in a stellar interior to the mass of the star, the mass–luminosity relation provides an important test of theories of stellar interiors. This predicted relation is a corollary of the more general principle that if a star is in equilibrium—it is neither expanding nor contracting—all its other properties depend only on its mass and the distribution of chemical elements within it. For a family of stars with different masses but with the same mixture of chemical elements uniformly distributed throughout the stellar volumes, there should be a unique mass–luminosity relation. The observed relation, obtained from binary stars for which masses and luminosities can be observationally evaluated, is shown in the **illustration**. The majority of stars placed on such a plot are found along this relation, called the main sequence, and it implies that all stars begin their lives with roughly the same chemical composition. It conforms reasonably well to theory. It was this agreement that showed the pioneering studies of stellar structure by A. S. Eddington in the 1920s to be on a sound basis. *See* BINARY STAR; STAR.

Effects of stellar evolution. There are classes of stars not on the main sequence that depart markedly from the mass–luminosity relation for main-sequence stars. The theory of stellar evolution predicts that a star's interior chemical composition will change as a result of the conversion of hydrogen into helium and heavier elements in the process of nuclear energy generation, which is the source of stellar luminosity. Accompanying these changes in composition, there will be changes in luminosity. Examples are the three stars in the illustration lying below the smooth relation. These are white dwarf stars, which are known to be extremely underluminous for their masses, and are thought to be stars in which all sources of nuclear energy have been exhausted. Giants and supergiants are thought to be in an intermediate state of evolution, between main-sequence stars and white dwarfs, with central nuclear energy generation that is markedly different from main-sequence stars. One of the triumphs of twentieth-century astrophysics was the establishment and exploration of stellar evolution theory, which sees stars evolving off the main sequence as they age, and links an individual star's entire evolutionary roadmap to its initial mass and composition. *See* CARBON-NITROGEN-OXYGEN CYCLES; GIANT STAR; HERTZSPRUNG-RUSSELL DIAGRAM; NUCLEOSYNTHESIS; PROTON-PROTON CHAIN; SUPERGIANT STAR; WHITE DWARF STAR.

Stellar mass and luminosity determination. Stellar masses are determined observationally from binary stars. By mapping the orbits of the two components of a binary system, the mass of each star (subject to a correction for the angle at which we are viewing) may be determined from the dynamics of the orbit. Additionally, through comparison of the appearance of that orbit upon the sky with its true physical size, the distance to the binary system may be established. From the apparent brightness and the distance, the actual brightness of the system can be determined, which gives a measure of the luminosity of each component. *See* CELESTIAL MECHANICS; KEPLER'S LAWS; ORBITAL MOTION.

Historically, binary star orbits have been determined though observations of eclipsing binary stars, since we know the angle at which we are observing them. More recently, astronomical interferometers have enabled high-resolution (at scales of milliarcseconds to microarcseconds) mapping of binary

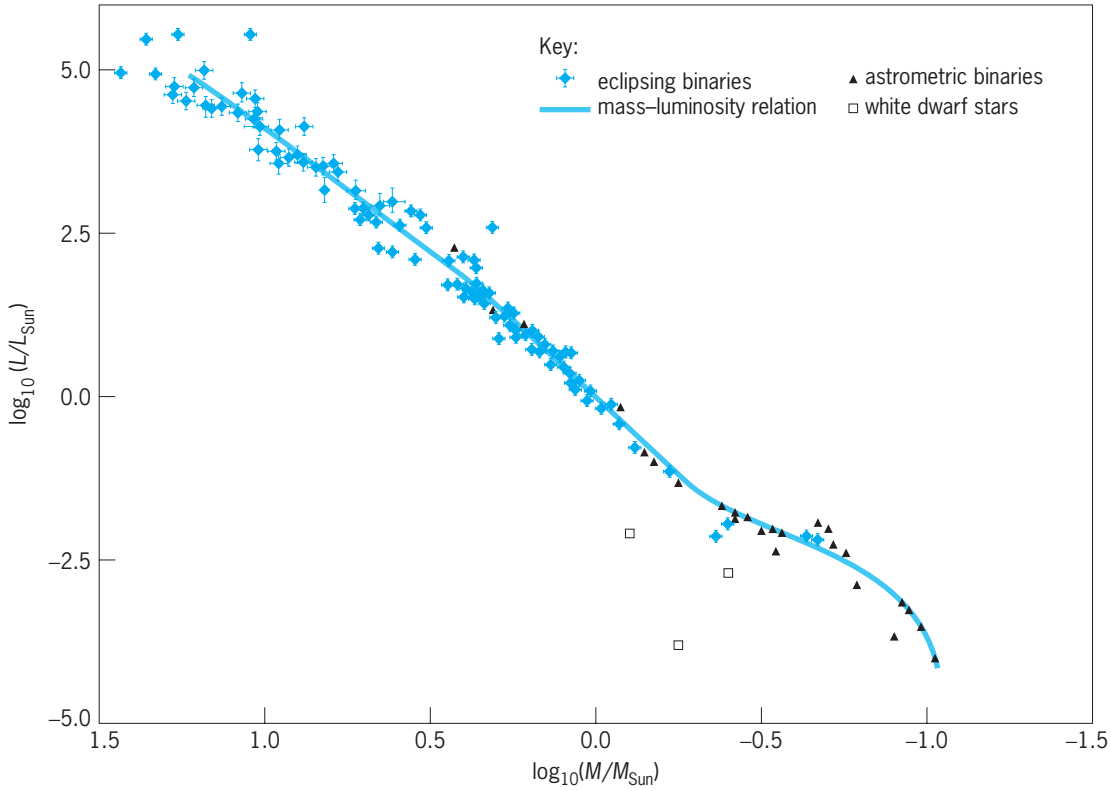

Mass-luminosity relation, where the abscissa is the logarithm of mass *M* and the ordinate is the logarithm of luminosity *L*, both relative to the Sun as unit. This relation is typically plotted with the brightest, most massive stars at the upper left, and the dimmer, least massive stars at the lower right.

star orbits for those binaries that do not happen to eclipse, which has allowed greater discretion in selecting binary stars for observation. Observations of these astrometric binaries (also referred to as visual binaries) has assisted in the observation of orbits of lower-mass binary stars, which are populous in the galaxy, but dim and limited to the few nearest examples for observation. Agreement with the observed mass–luminosity relation is one of the key tests of stellar models that are produced in modern astrophysics. *See* ASTROMETRY; ECLIPSING VARIABLE STARS.

Evolution of close binary systems. If a star is a member of a close binary system, it may be prevented by the presence of its companion from evolving by expansion into a giant star. The evolutionary histories of stars in such systems are predicted to involve mass exchange between the components. The relation between masses and luminosities will depend upon the state of evolution of the individual system. In some cases, gross departures from the mass–luminosity relation for main-sequence stars are predicted and observed. A star that has lost the bulk of its mass to its companion may radiate as much energy as a normal star, even though its mass is much less. X-ray binaries are thought to be extreme examples of advanced evolution of close binary systems. Application of the mass–luminosity relation to the visible components in x-ray binaries leads to the conclusion that in a couple of cases the invisible component may well be a black hole; these systems are the best candidates known for this extreme among stellar configurations. A number of the predictions of the evolution of close binaries appear to be verified observationally. *See* ASTROPHYSICS, HIGH-ENERGY; BLACK HOLE; STELLAR EVOLUTION; X-RAY ASTRONOMY.

Daniel M. Popper; Gerard van Belle

Bibliography. C. W. De Loore, *Structure and Evolution of Single and Binary Stars*, 1992; R. Kippenhahn and A. Weigert, *Stellar Structure and Evolution*, 1991; D. Prialnik, *An Introduction to the Theory of Stellar Structure and Evolution*, 2000; J. Sahade (ed.), *The Realm of Interacting Binary Stars*, 1993.

Mass number

The mass number *A* of an atom is the total number of its nuclear constituents, or nucleons, as the protons and neutrons are collectively called. The mass number is placed before and above the elemental symbol, as in ^{238}U. Because of the approximate equality of the proton and neutron masses, and the relative insignificance of that of the electron, the mass number gives a useful rough figure for the atomic mass; for example, ^{1}H = 1.00783 atomic mass units (amu), ^{238}U = 238.051 amu, and so on. The mass number is reduced by four during alpha emission, but is not altered during beta decay or electron capture. *See* ATOMIC NUMBER.

Henry E. Duckworth

Mass spectrometry

An analytical technique for identification of chemical structures, determination of mixtures, and quantitative elemental analysis, based on application of the mass spectrometer. Determination of organic and inorganic molecular structure is based on the fragmentation pattern of the ion formed when the molecule is ionized; further, because such patterns are distinctive, reproducible, and additive, mixtures of known compounds may be analyzed quantitatively. Quantitative elemental analysis of organic compounds requires exact mass values from a high-resolution mass spectrometer; trace analysis of inorganic solids requires a measure of ion intensity as well. *See* MASS SPECTROSCOPE.

Methods of ion production. For analysis of organic compounds the principal methods are electron impact, chemical ionization, field ionization, field desorption, particle bombardment, laser desorption, and electrospray.

Electron impact. When a gaseous sample of a molecular compound is ionized with a beam of energetic (commonly 70-V) electrons, part of the energy is transferred to the ion formed by the collision, as shown in reaction (1). For most molecules, the pro-

$$A—B—C + e \longrightarrow A—B—C^+ + e + e \qquad (1)$$

duction of cations is favored over the production of anions by a factor of about 10^4, and the following discussion pertains to cations. The ion corresponding to the simple removal of the electron is commonly called the molecular ion and normally will be the ion of greatest m/e ratio in the spectrum. In the ratio, m is the mass of the ion in atomic mass units (daltons) and e is the charge of the ion measured in terms of the number of electrons removed (or added) during ionization. Occasionally the ion is of vanishing intensity, and sometimes it collides with another molecule

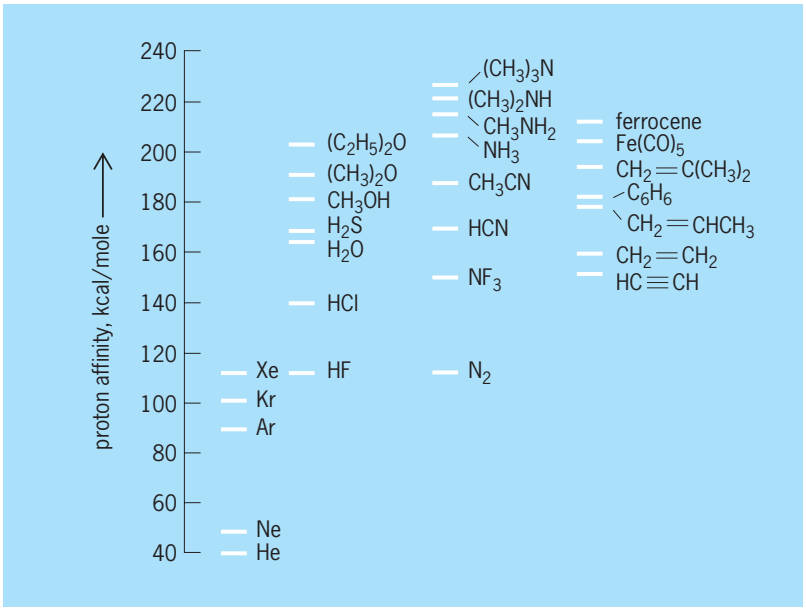

Fig. 1. Representative gas-phase proton affinities of molecules.

to abstract a hydrogen or another group. In these cases, an incorrect assignment of the molecular ion may be made unless further tests are applied. Proper identification gives the molecular weight of the sample.

The remaining techniques were devised generally to circumvent the problem of the weak or vanishingly small intensity of a molecular ion.

Chemical ionization. Here the ions to be analyzed are produced by transfer of a heavy particle (H^+, H^-, or heavier) to the sample from ions produced from a reactant gas. Frequently the reactant gas is methane at pressures of 0.2–2.0 torr (27–270 pascals). As above, the initial process in methane (CH_4) upon electron impact is ionization to yield CH_4^+ ions; some of these have enough energy to fragment to $CH_3^+ + H$. These ions in turn react with neutral methane as in reactions (2) and (3). The resulting ions are strong

$$CH_4^+ + CH_4 \longrightarrow CH_5^+ + CH_3 \qquad (2)$$

$$CH_3^+ + CH_4 \longrightarrow C_2H_5^+ + H_2 \qquad (3)$$

Brønsted acids and react by proton transfer as in reactions (4) and (5) to ionize the molecule of in-

$$CH_5^+ + A—B—C \longrightarrow H—A—B—C^+ + CH_4 \qquad (4)$$

$$C_2H_5^+ + A—B—C \longrightarrow H—A—B—C^+ + C_2H_4 \qquad (5)$$

terest. The $C_2H_5^+$ ion also reacts by hydride abstraction, as in reaction (6). Other gases may also be used

$$C_2H_5^+ + A—B—C—H \longrightarrow A—B—C^+ + C_2H_6 \qquad (6)$$

for ionization; hydrogen (H_2), water (H_2O), ammonia (NH_3), and isobutane (C_4H_{10}) are common. In these the reactive ions are H_3^+, H_3O^+, NH_4^+, and $C_4H_9^+$ [the conjugate acid of $(CH_3)_2C{=}CH_2$], respectively. The proton affinity (**Fig. 1**) is the negative of the enthalpy change for the solvation of a proton by the compound, as in reaction (7). It follows

$$A—B—C + H^+ \longrightarrow A—B—C—H^+ \qquad (7)$$

that $A—B—C—H^+$ protonates molecules with greater proton affinities in the absence of kinetic complications; such reactions are exothermic. Proton affinities have been determined both by high-pressure techniques akin to chemical ionization and by the ion cyclotron resonance technique. Thus H_3^+ transfers the most energy when it protonates a molecule; NH_4^+ transfers the least of the four examples. If the energy transferred (typically 10–50 kcal/mole or 40–200 kilojoules/mole) is great enough, fragmentation can occur, but there is much less in chemical ionization than in electron impact mass spectra.

In addition to heavy-particle transfer of other types (transfer of CH_3^+, $C_2H_5^+$, Cl^-), another important method is charge exchange. For a gas with an ionization potential greater than that of the molecule of interest, reaction (8) is exothermic, and the excess

$$G^+ + A—B—C \longrightarrow A—B—C^+ + G \qquad (8)$$

energy is transferred as internal energy. Helium ion

(He^+), neon ion (Ne^+), and argon ion (Ar^+) transfer large amounts of internal energy and molecular ions are weak; carbon monoxide (CO) and nitrogen monoxide (NO) are useful gases for this process. Occasionally a combination of chemical ionization and charge exchange is used, with mixtures of Ar and H_2O yielding information about both the molecular weight and important fragments, for example.

The term negative chemical ionization is usually intended to include all ionization processes yielding negative ions under source pressure conditions characteristic of chemical ionization. In some cases, ions may be formed by a true chemical ionization process like proton transfer, as in reaction (9), in

$$RCOOH + OH^- \longrightarrow RCOO^- + H_2O \qquad (9)$$

which OH^- is the reagent ion, produced from H_2O or $N_2O + CH_4$. In others, the reagent gas only mediates the energy of free electrons to low values compatible with capture by neutral molecules to yield negative molecular ions. Molecules with several electronegative atoms have large cross sections for this latter process. Thus the direct analysis of polychlorinated aromatics, and the analysis of small peptides after derivatization by pentafluorobenzoylation, are possible in the femtogram region.

There are applications of ions formed by chemical ionization (atmospheric pressure ionization; plasma chromatography, in which the drift time of the ion through a flowing gas is measured) in which the sample is not depleted before ionization. Because of this preservation of sample molecules, they also have femtogram sensitivities. *See* IONIZATION POTENTIAL; REACTIVE INTERMEDIATES.

Field ionization and field desorption. For less volatile material, the sample is ionized when it is in a very high field gradient (several volts per angstrom) near an electrode surface. The molecular potential well is distorted so that an electron tunnels from the molecule to the anode. The ion thus formed is repelled by the anode (**Fig. 2**). Typically, the lifetime of the ion in the mass spectrometer source is much less (10^{-12} to 10^{-9} s) than in electron impact. Because little energy is transferred as internal energy and the ion is removed rapidly, little fragmentation occurs, and the molecular weight is more easily determined. Field ionization is also used in the time-resolved study of ion fragmentation and rearrangement called field ionization kinetics. This technique permits determination of the fragmentation products at specific times from about 10^{-11} to 10^{-8} s after ionization by energy-focusing of ions at different points in the field ionization source. In this way, simple fragmentations uncomplicated by rearrangements of hydrogen or other atoms in the molecular ion may be observed at the shortest times yet used for sampling ions, and complex rearrangements of ions may be defined from studies over a range of times.

Cations, most commonly lithium ion (Li^+) but often other alkali metals, may be field-desorbed from a salt coating on a wire and pass through a gaseous or adsorbed sample M. MLi^+ ions are produced in some cases where simple field desorption fails.

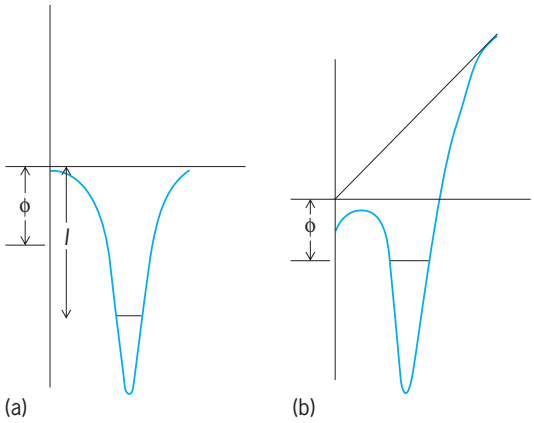

Fig. 2. Potential well of a molecule: (*a*) undistorted, with ionization potential *I* near a metal with work function ϕ in the absence of a field gradient; and (*b*) in a strong field gradient. Near the metal surface the external field raises the most weakly bonded electron to the Fermi level so that tunneling through the small barrier may occur.

Electrohydrodynamic ionization. A high electric-field gradient induces ion emission from a droplet of a liquid solution, that is, the sample and a salt dissolved in a solvent of low volatility. An example is the sample plus sodium iodide (NaI) dissolved in glycerol. The spectra include peaks due to cationized molecules of MNa^+, $MNa(C_3H_8O_3)_n^+$, and $Na(C_3H_8O_3)_n^+$.

Rapid heating methods. A sample heated very rapidly may vaporize before it pyrolyzes. Techniques for heating by raising the temperature of a source probe on which the sample is coated by 200 K (360°F)/s have been developed. Irradiation of an organic sample with laser radiation can move ions of mass up to 1500 daltons into the gas phase for analysis. This technique is the most compatible with analyzers that require particularly low pressures such as ion cyclotron resonance. Time-resolved spectra of surface ejecta are proving to be the most useful kinds of laser desorption spectra available.

Particle bombardment techniques. A solid sample or a sample in a viscous solvent such as glycerol may have ions sputtered from its surface by bombardment with accelerated electrons, ions, or neutrals. Bombardment by electrons is achieved simply by inserting a probe with the sample directly into the electron beam of an electron impact source (in-beam electron ionization). The energetic ions may likewise be the plasma in a chemical ionization source (in-beam chemical ionization), or alternatively, ions in a beam of 2.5-kV Ar^+ directed to a surface coated with the sample (without the coating, this is the inorganic surface analysis technique of secondary ion mass spectrometry). With charge exchange between accelerated Ar^+ (most commonly 6–8 keV) and thermal Ar, a beam of accelerated Ar atoms is produced; desorption of surface layers of glycerol solutions of biological molecules up to 40,000 molecular weight or inorganic salts $(Cs_xI_{(x-1)})^+$ up to 100,000) produces useful spectra by fast atom bombardment. The simplicity of application of this broadly useful technique is

associated with the long duration of spectra because of the constantly regenerated surface of the solution after bombardment, and not so much (as originally thought) with the avoidance of surface charging by using atoms instead of molecules; beams consisting partially or wholly of accelerated Ar^+ ions produce spectra from viscous solutions in techniques more precisely called liquid secondary ion mass spectrometry (SIMS), or liquid-target SIMS. The most powerful method of this variety is the californium-252 (^{252}Cf) plasma desorption source. It must be noted that nomenclature is not unified in this area; some authors also refer to ion-beam chemical ionization as plasma desorption.

The ^{252}Cf source produces fission fragments that penetrate a thin foil on which a film of sample has been coated. The fission fragment deposits energy by electronic excitation in a cylindrical track with a 20-nanometer diameter. Molecular, $(M + 1)^+$, and $(M - 1)^-$ ion ejection from the surface then occurs as the energy is dissipated through the remaining lattice in a shock wave. Molecular ions of mass up to 40,000 daltons have been observed with this technique. *See* SHOCK WAVE.

Laser desorption. The energy of laser photons may be used to remove an analyte from a surface and ionize it for mass-spectrometric analysis. In virtually all cases involving polar compounds of high molecular weight, the analyte is prepared in or on an organic matrix that is coated on the surface to be irradiated. The matrix material assists in the ionization process; the technique is known as matrix-assisted laser desorption ionization (MALDI). Numerous organic materials have been investigated. Molecular weights in excess of 700,000 have been measured with this technique, and the technique is particularly suited for the molecular-weight determination of large polar biological molecules; for example, enzymes and intact antibodies have been analyzed.

Electrospray ionization. A solution sprayed through a nozzle of very small diameter into a vacuum with an electric field having a gradient of several hundred to a thousand volts per centimeter produces gaseous ions from solutes effectively. Electrospray ionization is the only mass-spectrometric technique that produces a large fraction of multiply charged ions from an organic or biological analyte. Since mass spectrometers measure mass-to-charge ratios of ions, not simply their mass, electrospray ionization has the advantage of permitting ions of very high mass to be analyzed without special mass-analysis instrumentation; for example, an ion of mass 120,000 daltons carrying 60 positive charges appears at mass-to-charge 2000, within the range of many mass analyzers. This technique has been used to measure the masses of ions from molecules of masses up to about 200,000 daltons. Since the distribution of charged species reflects to some extent the degree of protonation in solution, a signal that reflects the folding of a protein, there is evidence that solution conformations of proteins can be studied by electrospray ionization mass spectrometry.

Multiphoton ionization of gaseous molecules. If absorption of several photons from a laser produces an excited state of the molecule, molecules accumulate in this state so that absorption of further photons produces especially abundant ions (resonant multiphoton ionization) in contrast to the case where no excited state is reached as an intermediate (nonresonant multiphoton ionization). This tunability for a certain energy to achieve selective ionization of a particular molecule suggests that analysis of mixtures for especially targeted components would be possible. The difficulty is that for even modestly complex molecules the number of states in rotationally and vibrationally broadened bands is large, and the search for selectivity for target molecules has led to use of supersonic nozzle introduction of the sample, where extreme cooling will yield states with insignificant population of higher rotational and vibrational levels, and ideally, electronic levels of nearly line width; thus interference due to excitation of bands of contaminants of the target will be greatly reduced.

Assignment of empirical formula. If the spectrum is a high-resolution spectrum, the deviation of the molecular weight from an integral value is used to determine the elemental composition (for example, $^{12}C_{12}{}^{1}H_{10}$ has molecular weight 154.0782; $^{12}C_9{}^{1}H_{14}{}^{16}O_2$, 154.0994; $^{12}C_{10}{}^{1}H_{16}{}^{16}O$, 154.1358; and $^{12}C_{11}{}^{1}H_{22}$, 154.1721). If it is low-resolution, then the worker takes advantage of the natural abundances of isotopes (for example, ^{12}C, 98.9%; ^{13}C, 1.1%; ^{35}Cl, 75.4%; ^{37}Cl, 24.6%; ^{79}Br, 50.6%; and ^{81}Br, 49.4%) to calculate at least part of the empirical formula by application of the binomial coefficients. For example, if the intensity of the $(M + 1)$ peak in such a spectrum (**Fig. 3**) is 11% that of the M peak, only ions containing one ^{13}C ion contribute to the $(M + 1)$ peak, and the probability that any C chosen randomly is ^{13}C is 1.1%. If 10 C atoms are examined as a group, the probability that one is ^{13}C is 10 times greater, or 11%; hence the molecule contained 10 carbons.

Fragmentation patterns. Since the amount of energy transferred to the molecule is much more than that required simply to ionize it or to break some of the bonds in the remaining ion, some of the molecules fragment after ionization, by competing consecutive decompositions, as indicated in reactions

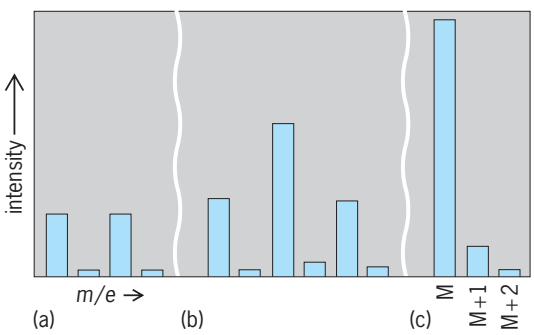

Fig. 3. Use of isotope distribution to determine elemental composition. (*a*) Molecular ion for a compound containing one bromine atom. (*b*) Molecular ion for a compound containing two bromine atoms. (*c*) Molecular ion for a compound containing neither bromine nor chlorine.

(10)–(15). These ions are separated by mass in

$$A—B—C^{+\cdot} \longrightarrow A—B^{+} + C\cdot \quad (10)$$

$$A—B—C^{+\cdot} \longrightarrow A—B\cdot + C^{+} \quad (11)$$

$$A—B—C^{+\cdot} \longrightarrow A\cdot + B—C^{+} \quad (12)$$

$$A—B^{+} \longrightarrow A + B^{+} \quad (13)$$

$$B—C^{+} \longrightarrow B^{+} + C \quad (14)$$

$$A—B—C^{+\cdot} \longrightarrow A—C^{+\cdot} + B \quad (15)$$

the spectrometer and produce the mass spectrum. Although fragments at almost every mass are usually produced, the most favorable routes for decomposition, which give the most intense peaks in the spectrum, are characteristic of the functional groups in the molecule. Therefore, the intense ions, particularly those at the high-mass end of the spectrum, are used in the assignment of structure to compounds. The common mechanistic rationalizations used for interpretation assume that the charge is localized at the functional group, because the electron lost is most likely to be a π electron or a nonbonding electron. Other less empirical explanations, notably the statistical approach of the quasi-equilibrium theory of mass spectra, have been outlined in the literature. *See* CHEMICAL BONDING.

The reactions of functional groups bearing electronegative atoms are typically loss of the electronegative atom or the group containing it [X = Cl, Br, I, OR, SR, acyl, in reaction (16)] or loss of a substituent group on the α-carbon [R = H or alkyl, X = OR, NR_2, SR, Cl, Br, in reaction (17); R = H, alkyl, or aryl, X = H, OH, OR, NR_2, Cl, Br, I, alkyl, or aryl, in reaction (18)]. These are simple fragmentations

$$R—\overset{+\cdot}{X} \longrightarrow R^{+} + X\cdot \quad (16)$$

$$R—\!-\!-CH_2—\overset{+\cdot}{X} \longrightarrow R\cdot + CH_2{=}X^{+} \quad (17)$$

$$R—\overset{\overset{O^{+}\cdot}{\|}}{C}—X \longrightarrow R—C{=}O^{+} + X\cdot \quad (18)$$

[reactions (10)–(12)] corresponding to losses of a free radical; the remaining ion is an even-electron ion. Except for the molecular ion, which is an odd-electron ion, the principal ions in a spectrum are even-electron ions unless special structural requirements are met. In these less common cases, prominent odd-electron ions, formed by the loss of a molecule, are found. *See* FREE RADICAL.

The most general case of odd-electron ion formation is illustrated in reaction (19), where in general a

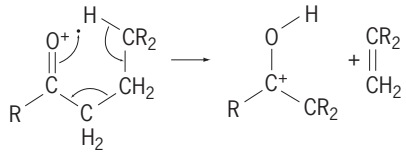
(19)

γ-hydrogen is abstracted by a multiply bonded electronegative atom with rupture of the β bond; this reaction is called the McLafferty rearrangement. Other cases of odd-electron ion formation involve interactions of ortho substituents on aromatic systems and certain decompositions of cyclic molecules, which may or may not be rearrangements [reaction (15)]. The spectrum of the volatile compound acetophenone (**Fig. 4***a*) is characterized only by simple bond-cleavage reactions, but there is an intense peak in the spectrum of valerophenone (Fig. 4*b*) corresponding to a McLafferty rearrangement in which the C_4H_8 group is lost from the molecule.

Even-electron ions, such as many fragment ions found in electron-impact spectra and also (M + 1) ions from chemical ionization, decompose most often to smaller even-electron ions by loss of a small molecule. Illustrations are given by reactions (20) and (21), from the chemical ionization of small peptides. Complex rearrangements are more competitive with simple cleavages in ions of low internal energy than in ions of higher internal energy; so in chemical ionization spectra, though only a few pathways for loss of small molecules may exist, some of the pathways may be found to be quite remarkable. Occasionally the fragmentations involve rearrangements so poorly understood that the fragment peaks are not of much use in establishing the structure of the molecule.

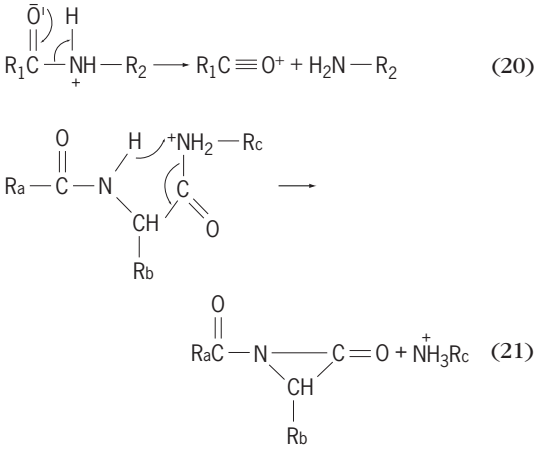
(20)

(21)

Spectra of the involatile compound creatine are typical for the various techniques discussed (**Fig. 5**); both the molecular ion (Fig. 5*a*) and the (M + 1) ions (Fig. 5*b–d*) lose water by a rearrangement process. It is not universally true that the chance of finding the molecular ion increases as the experiment progresses from electron impact to chemical ionization, field ionization, and field desorption, but these results are typical.

Further useful information about fragments is obtained, first, from the potentials required to ionize the molecule and to form fragments and, second, from observations of shifts of peaks with isotopic labeling techniques. For example, in reaction (19), substitution of D for H at the β position does not increase the mass of the product ion, but when H at the γ position is replaced by D, the mass of

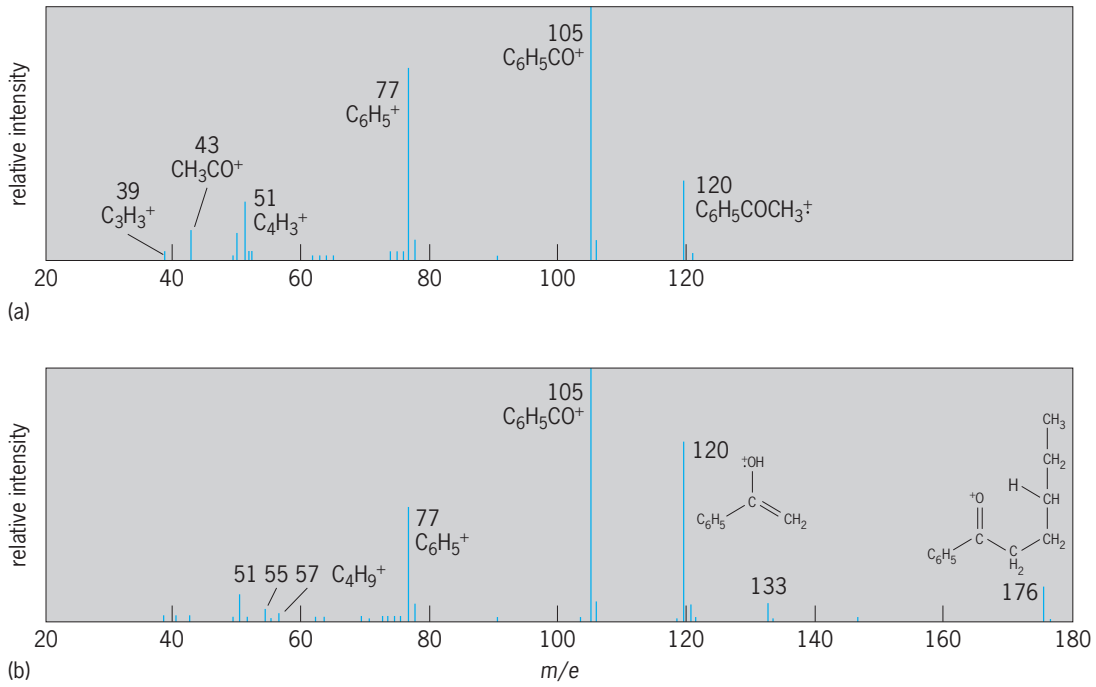

Fig. 4. Mass spectra of (*a*) acetophenone and (*b*) valerophenone, using electron impact.

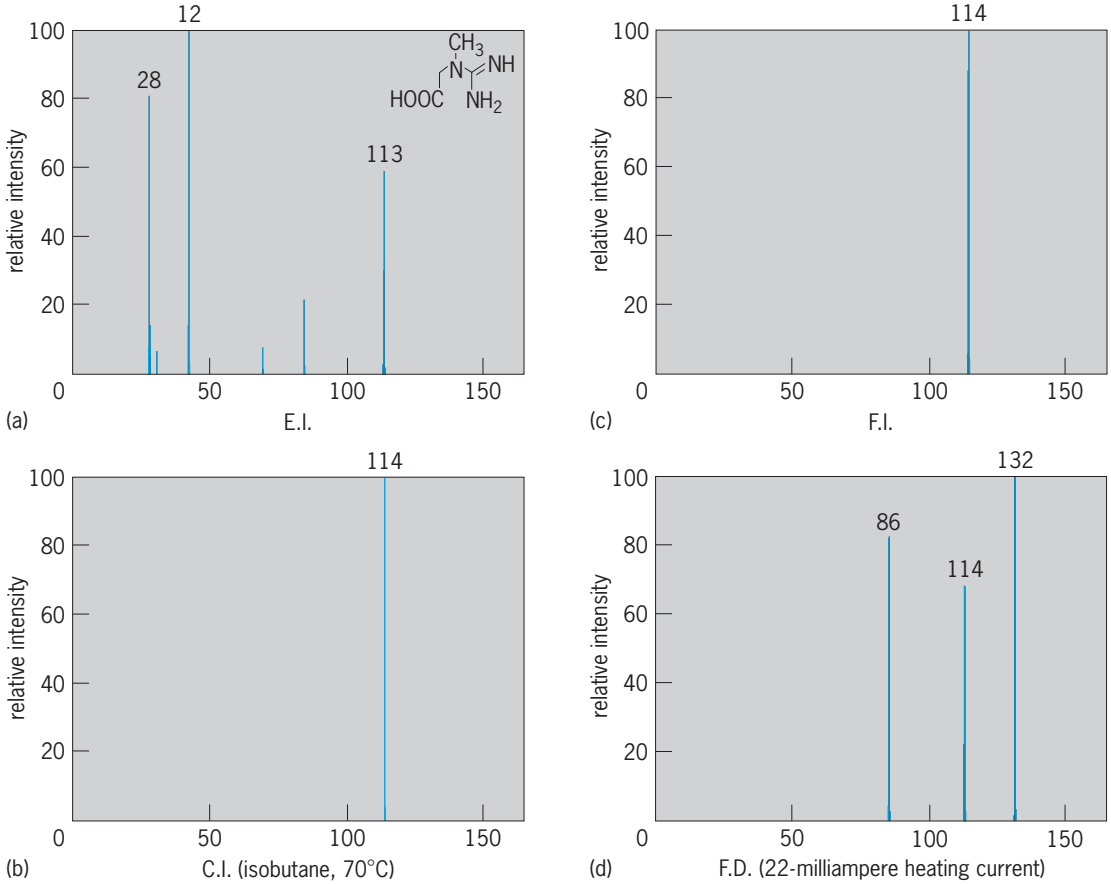

Fig. 5. Mass spectra of creatine (molecular weight 131) obtained by (*a*) electron impact, (*b*) chemical ionization, (*c*) field ionization, and (*d*) field desorption with moderate heating. Both the molecular ion (not observed in *a*) and the M + 1 ion in *b*, *c*, and *d* undergo a loss of water. Field desorption does not always produce the largest ion related to the molecular weight on comparing the four techniques, but this result is typical. (*After H. M. Fales et al., Comparison of mass spectra of some biologically important compounds as obtained by various ionization techniques, Anal. Chem., 47:207–219, 1975*)

the product is shifted to higher mass by one unit. Finally, correlations with trends observed in ordinary chemical reactions yield information. For example, in both aromatic and aliphatic systems, orders of reactivities depending on substitution patterns show correspondence; in some aromatic systems, the correlation is quantitative. If an unknown compound is suspected of belonging to a certain group of compounds, then its structure may often be established by comparison of its spectrum with spectra of compounds of known structure. This technique is particularly valuable in the study of natural products. The shift technique, the interpretation of substitution patterns when the molecular ion and some fragments are shifted by the same amount, for example, 30 units by a methoxy group, is helpful in studying alkaloid spectra. In addition to correlation with typical solution phenomena, relation of fragmentations to pyrolytic reactions and to photochemical processes is studied. The McLafferty reaction is analogous to a well-known photochemical reaction of ketones, the Norrish type II rearrangement, in which an olefin molecule is lost from the alkyl ketone while the enol form of a smaller ketone is produced by the influence of light. Other ionization techniques (by large electric-field gradients, by photons, or by other ions) produce different types of spectra useful in structural analysis. *See* PHOTOCHEMISTRY.

Metastable ions. Correlation of spectra with structure requires the additional use of further decomposition products beyond the first fragmentation steps, but it is difficult to define the origin of products possibly arising by more than one path, for example, B^+ in reactions (13) and (14). A clue to origin of fragments is given by metastable ions: If in reaction (13) some AB^+ ions decompose after they are accelerated but before they are magnetically deflected, a broad peak (**Fig. 6**) appears at an m/e value numerically equal to m_B^2/m_{AB}. The value 56.5 (Fig. 6) equals $77^2/105$; therefore, the metastable peak corresponds to the reaction $105 \rightarrow 77$ and indicates that at least part of the $C_6H_5^+$ ion is formed by the loss of CO from $C_6H_5CO^+$. The order of the decomposition steps is suggested by the collection of metastable ions and bears on the organization of the parts of the molecule into the whole.

Study of metastable ions and other ions that can be made to decompose between acceleration and mass analysis has been carried out through ion kinetic energy spectroscopy (IKES) and mass-analyzed ion kinetic energy spectroscopy (MIKES), also called direct analysis of daughter ions (DADI). In the ion kinetic energy spectroscopy technique, which may be studied with a conventional double-focusing mass spectrometer, those ions which decompose between the accelerating region and the electric sector will form ionic fragments with only a fraction of the kinetic energy imparted to the original ions. The fraction is the ratio of the mass of the fragment to that of the original ion. Scanning the voltage of the electric sector and detecting the ions that leave it provides a scan of ions according to their kinetic energy. Frequently intensities of ions differ substantially for even

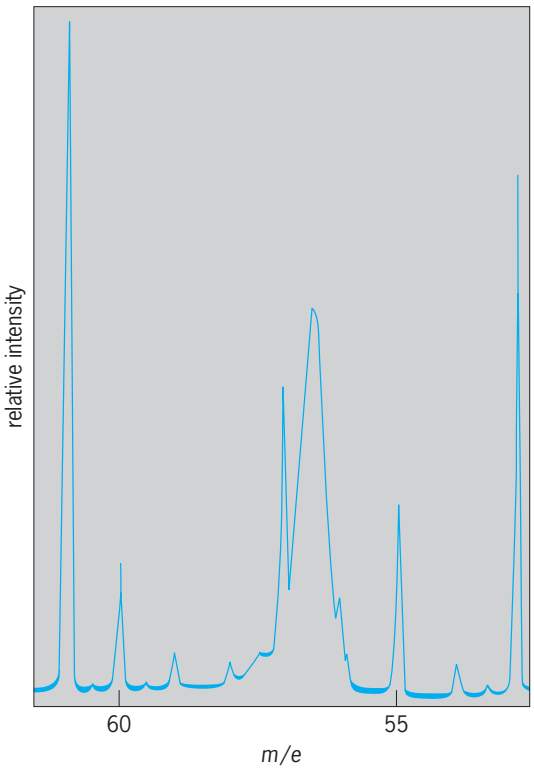

Fig. 6. Scale-expanded portion of acetophenone spectrum showing a broad metastable ion at *m/e* 56.5.

closely related isomers; thus this technique is useful for fingerprinting difficult compounds.

In mass-analyzed ion kinetic energy spectroscopy, the electric sector and the magnetic sector in the double-focusing mass spectrometer are reversed, so that the ions, after acceleration, enter the magnetic sector and are analyzed according to mass before they enter the electric sector. By setting the magnetic field, ions of a certain mass are chosen for study; those that decompose before entering the electric sector have only the fraction of the kinetic energy according to the ratio of fragment and original mass noted above, and by sweeping the electric sector, the amounts of daughter ions from this one particular precursor may be observed. The intensities of ions are useful for structure determination, although they are somewhat affected by the distribution of energies within the fragmenting ion. Much information about energetics of decomposing ions has been gained from studies of the width of peaks due to their products in mass-analyzed ion kinetic energy spectroscopy, for these are always broadened because kinetic energy T is released in the fragmentation. It has been shown that T is a characteristic of molecular structure; for example, the McLafferty product ion formed by the loss of C_2H_4 from the molecular ion of butyrophenone, as in reaction (19), fragments by loss of CH_3, releasing 48 meV (4.6 kilojoules/mole) of T. Since the molecular ion of acetophenone releases 7 meV (0.7 kJ/mole) energy, the McLafferty product does not have the acetophenone structure. Further studies of rearrangements have led to analyses of the partitioning of energy between internal and kinetic

energy in fragmentation as a function of geometry of the activated complex and other parameters. The study of metastable peak shape as a function of ion lifetime, or of ion internal energy, provides information on ion structure.

Unimolecular mass-analyzed ion kinetic energy spectra, that is, those involving metastable ions, are somewhat dependent on ion internal energy. A less energy-dependent method, and therefore a surer guide to structure, is that of collisionally activated decomposition, occasionally also known as collisionally induced dissociation. In this, a collision gas is admitted at a low pressure to the region between the magnetic and electric sector of the reversed instrument. As mass-selected ions travel from the magnetic sector, they collide with the gas molecules, and a fraction of their kinetic energy is transformed into internal energy sufficient to cause rapid decomposition of the ions. The spectra are recorded as in mass-analyzed ion kinetic energy. Charge-exchange processes may also occur on collision, as in reactions (22)–(24). If the electric sector is set at

$$\mathrm{A{-}B{-}C^{2+} + N \longrightarrow A{-}B{-}C^{+} + N^{+}} \qquad (22)$$

$$\mathrm{A{-}B{-}C^{+} + N \longrightarrow A{-}B{-}C^{2+} + N + e} \qquad (23)$$

$$\mathrm{A{-}B{-}C^{+} + N \longrightarrow A{-}B{-}C^{-} + N^{2+}} \qquad (24)$$

twice, one-half, or minus the voltage which transmits normal ions, the products of reactions (22)–(24) can be detected. Thus mass spectra of ions produced by special routes are generated, and the utility of these spectra for interpretive purposes is being explored.

The spectra have been found to depend on the angle by which the products are deflected from their path in the absence of collision, deflections of only a half degree to one degree producing major changes in the spectra in the direction of more energy content in the ions (angle-resolved mass spectrometry).

Collision-induced dissociations in mass-analyzed ion kinetic energy spectrometers involve ion accelerations of 4–8 kV. A similar experiment can be carried out in a triple quadrupole instrument, in which the acceleration is 2–100 eV. In the former, energy transfer is through electronic modes; in the latter through vibrational modes. Because the kinetic energy of the ion strongly influences the collisionally activated decomposition product distribution in the latter experiment, studies of energy-resolved mass spectra of ions by this technique are of much interest, especially in comparison to the angle-resolved mass spectra.

These techniques for producing mass spectra from mass-resolved ions have become of paramount importance to establishing the structures of small ions, particularly in combination with more advanced methods of measuring heats of formation of ions and onset energies for ion formation. Maurice M. Bursey

Analysis techniques. Measurement using a mass spectrometer takes advantage of the mass dependency in the equations of motion of an ion in an electric or magnetic field. Three common mass analyzers are magnetic-sector, quadrupole, and time-of-flight. An ion traversing the magnetic field of a sector instrument successfully reaches the detector when its mass, m, corresponds to $m/z = r^2B^2/2V$, where z is the charge of the ion, r is the radius of the flight tube, B is the magnetic field strength, and V is the acceleration voltage. A mass spectrum can be recorded by varying B or V. A quadrupole is an array of four parallel rods electronically connected such that a radio frequency (RF) is applied to opposing rods, and the waveforms applied to adjacent rods are out of phase. In addition, a direct-current (DC) component is added to the rods such that one opposing pair has +DC and the other −DC. Ions entering the quadrupole follow complex sinusoidal paths. An ion successfully traversing the rods to the detector is mass-selected by the amplitude of the applied radio frequency and the amount of resolution from adjacent masses by the DC/RF ratio. A spectrum is detected by scanning the RF amplitude and the DC voltage in a fixed ratio. The time-of-flight analyzer is a tube with an acceleration field at one end and a detector at the other. Ions are pulsed and accelerated down the tube, starting a clock. Arrival times at the detector are converted to mass by solving the equation $m/z = 2V(t/L)^2$, where V is the acceleration potential, t is the arrival time, and L is the flight tube length.

The mass analyzers are characterized by their mass resolving power (RP), scan or acquisition rate, and mass range. Sector instruments are usually assembled with an additional energy filter and can be operated up to 100,000 RP. Resolving power is defined as $M/\Delta M$, where M is the mass number of the observed mass and ΔM is the mass difference in two signals with a 10% valley between them. Increased resolution in sectors comes at the sacrifice of sensitivity. To increase resolution, the slits are narrowed on the ion beam. It is typical to lose 90% of the signal going from 1000 to 10,000 RP. Magnetic instruments are available with mass ranges up to 10,000 atomic mass units (amu) for singly charged ions at full acceleration potential. To obtain good quality, data sectors are scanned relatively slowly—a practical rate is 5 s per decade (1000–100 amu). Quadrupoles are usually operated at unit resolution. For example, 100 is resolved from 101, or 1000 from 1001. Quadrupoles can be scanned at 2000 amu/s and are available with mass range up to 4000 amu. Fast scanning and high-gas-pressure tolerance make quadrupoles popular for mass spectrometer–chromatographic hybrid systems. Modern time-of-flight analyzers are capable of 10,000 RP, with 50% valley definition of ΔM. Acquisition rates can be 100 spectra per second. The time-of-flight mass range is theoretically unlimited, and singly charged ions over 100,000 amu have been observed. *See* ATOMIC NUMBER; MASS NUMBER. Todd D. Williams

Applications of computers. The principal applications of computers to analysis have been to data acquisition and structure interpretation. High-resolution spectra contain so much data that the

rapid acquisition and presentation of data in a form easily assimilated by the operator has been adapted to the computer. Similarly, in cases where a gas chromatograph effluent passes through the source of the mass spectrometer, the generation of even low-resolution data is so rapid that a dedicated computer is appropriate. A variety of data displays are useful for interpretation. The plot of total ion current versus time produces a reconstructed chromatogram; the plot of ions of a single mass versus time, called a mass fragmentogram, is useful in identifying compound classes among the gas chromatogram peaks if the appropriate mass is chosen, or in identifying compounds directly if some other mass like the molecular weight of a desired component is chosen.

For interpretation, two approaches have been used: library searching and training. Library searches of large collections (over 25,000 spectra) by comparison of the spectrum with known spectra yield degrees of closeness of agreement of the unknown and known spectra. Various algorithms for spectral comparison, using the 10 most intense peaks in the spectrum or the two most intense peaks in each 14-mass-unit segment, for example, have been devised, and the minimum amount of information to be supplied for a good chance of identification has been studied. The other approach involves several pattern recognition approaches in which various features of the spectra are correlated with structural characteristics by methods independent of formal theories of mass spectral interpretation; these include learning-machine and factor-analysis approaches. Hybrid techniques, in which the self-trained computer approach is augmented by selected tests derived from the fragmentation theory noted previously, have also been devised.

Hybrid techniques. The coupling together of different kinds of mass and energy analyzers for specialized purposes produces hybrid mass spectrometers. For example, to achieve unit resolution after collisional activation in a collision cell, an instrument may be designed with a magnetic sector before the collision cell (to choose ions by mass before they enter the collision cell) and a quadrupole mass filter to separate collision products by mass. Another intermediate quadrupole is used between these two analyzers to separate the product–mass-analyzing quadrupole from the high electric field associated with the magnetic sector analysis; ions that have fallen through a high electric field have kinetic energy too great for good separation by a quadrupole. This intermediate quadrupole is operated with only radio-frequency voltages on the rods ("RF-only" mode) and then serves only to collect and move ions of all masses away from the high field, instead of mass-analyzing them. Other hybrid combinations of sectors and assemblies are electric-magnetic-quadrupole-quadrupole (which provides high resolution before the collision cell and unit resolution after) and magnetic-quadrupole–ion cyclotron resonance (which provides high resolution and high mass range after collision). Another instrument related to this discussion contains two electric sectors, so that energy analysis before and after collision, but no mass analysis, can be studied for well-understood systems. Some of these elaborate instruments are commercially available, but they are much more expensive than simpler instruments.

Another use of the term hybrid involves mass spectrometry coupled to a chromatograph or other device for separating compounds; these constitute a major fraction of the so-called hyphenated techniques. The information contained in a rapidly acquired mass spectrum of a chromatographic peak is often enough to identify the structure of the compound eluting from the chromatograph. Among the separation methods that use mass spectrometry for identification are gas chromatography, liquid chromatography, supercritical fluid chromatography, and capillary zone electrophoresis.

Typically, the selective removal of the mobile phase in which the eluting sample is contained is necessary before the mass spectrum is obtained. This may be accomplished by techniques based in part upon rapid pumping. In gas chromatography–mass spectrometry, the gases exiting the chromatograph are also accelerated through a nozzle into the pumping region; the light helium atoms are scattered and pumped away, while the heavier solute molecules tend to stay aligned in a linear path from the nozzle until they enter the orifice of a carefully aligned skimmer, through which they pass to the mass spectrometer source. In liquid chromatography–mass spectrometry a small fraction of the solution exiting the chromatograph may be sprayed into the source, often through a heated nozzle; or it may be deposited on the surface of a moving belt that passes through several vacuum locks into the source, where the sample is evaporated and ionized by heating or particle bombardment. The sample may also be removed from solvent through a selective membrane, or the solution may be mixed with glycerol in a moving stream and subjected to fast atom bombardment in the source. Electrospray methods also serve as a method to interface liquid chromatography and mass spectrometry. The interfaces used for supercritical fluid chromatography–mass spectrometry resemble those for gas chromatography–mass spectrometry, and those for capillary zone electrophoresis–mass spectrometry resemble methods for liquid chromatography–mass spectrometry. *See* ELECTROPHORESIS; GAS CHROMATOGRAPHY; LIQUID CHROMATOGRAPHY; SUPERCRITICAL-FLUID CHROMATOGRAPHY.

Ion cyclotron resonance. In ion cyclotron resonance spectrometry the ions, as charged particles in a magnetic field, complete circular orbits. Their frequency depends upon the strength of the magnetic field and their mass-to-charge ratio [Eq. (25)],

$$\omega = \frac{zB}{m} \tag{25}$$

where ω = frequency, z = charge of the ion, B = magnetic flux density, and m = mass of the ion, and the signal produced by the packet of ions is

detected by tracking of ion motion by image currents in a detector plate. At first, ion cyclotron resonance spectrometry was used for the study of ion–molecule reactions at low pressures because of the long lifetimes of ions in the ion cyclotron resonance cell; it has evolved to serve as the fundamental technique upon which Fourier-transform mass spectrometry is based. In this type of mass spectrometry, ions of all masses are excited by a rapidly swept excitation pulse, so that ions of each mass have coherent motion. The image current consists of a sum of sinusoidal waves of different frequencies; it can be transformed into a spectrum in the frequency domain, and thus by Eq. (25) into a spectrum in the mass domain. Loss of coherence of ion motion results from collisions of ions with neutrals. Although arbitrarily high resolution and mass range are expected, collisions reduce the time available for observation and thus limit resolution. Ions of mass greater than 20,000 daltons have been detected by Fourier-transform mass spectrometry, though other analyzers have also gone above this limit. Resolution greater than 3,000,000 daltons has also been observed in Fourier-transform mass spectrometry, and this is the record for all analyzers. *See* CYCLOTRON RESONANCE EXPERIMENTS; INFRARED SPECTROSCOPY.

Analysis of inorganic solids. The analysis of solid inorganic samples can be made either by vaporization in a Knudsen cell arrangement at very high temperatures or by volatilization of the sample surface so that particles are atomized and ionized with a high-energy spark (for example, 20,000 eV). The wide range of energies given to the particles requires a double-focusing mass spectrometer for analysis. Detection in such instruments is by photographic plate; exposures for different lengths of time are recorded sequentially, and the darkening of the lines on the plate is related empirically to quantitative composition by calibration charts. The method is useful for trace analysis (parts per billion) with accuracy ranging from 10% at higher concentration levels to 50% at trace levels. Methods for improving accuracy, including interruption and sampling of the ion beam, are under development.

Secondary ion mass spectrometry is most commonly used for surface analysis. A primary beam of ions accelerated through a few kilovolts is focused on a surface; ions are among the products sputtered from this surface, and they may be directly analyzed in a quadrupole filter. Sputtered material may also be analyzed by ionization of the neutrals in an inductively coupled plasma and subsequent mass analysis. This method produces ions with a lower energy spread than spark source mass spectrometry and, since detection then becomes less of a problem, has been supplanting spark source methods. *See* LASER SPECTROSCOPY; SECONDARY ION MASS SPECTROMETRY (SIMS); SPECTROSCOPY; SPUTTERING.

Maurice M. Bursey

Bibliography. J. R. Chapman, *Practical Organic Mass Spectrometry: A Guide of Chemical and Biochemical Analysis*, 2d ed., 1993; S. Gaskell (ed.), *Mass Spectrometry in Biomedical Research*, 1986; E. de Hoffmann and V. Stroobant, *Mass Spectrometry: Principles and Applications*, 2d ed., 2001; S.-T. F. Lai, *Gas Chromatography/Mass Spectrometry*, 1988; F. W. McLafferty and F. Turecek, *Interpretation of Mass Spectra*, 4th ed., 1992; J. Throck Watson, *Introduction to Mass Spectrometry*, 3d ed., 1997.

Mass spectroscope

An instrument used for determining the masses of atoms or molecules found in a sample of gas, liquid, or solid. It is analogous to the optical spectroscope, in which a beam of light containing various colors (white light) is sent through a prism to separate it into the spectrum of colors present. In a mass spectroscope, a beam of ions (electrically charged atoms or molecules) is sent through a combination of electric and magnetic fields so arranged that a mass spectrum is produced. If the ions fall on a photographic plate which after development shows the mass spectrum, the instrument is called a mass spectrograph; if the spectrum is allowed to sweep across a slit in front of an electrical detector which records the current, it is called a mass spectrometer.

Operation. A typical mass spectroscope has a continuously pumped vacuum chamber, commonly called the spectrometer tube, into which the gas or vapor to be investigated flows at such a rate that the equilibrium pressure in the chamber is of the order of 10^{-6} mm of mercury (10^{-8} lbf/in.^{2} or 10^{-4} pascal). **Figure 1** is a schematic drawing of a type of mass spectrometer tube widely used for making gas and isotope analyses. The pumping system consists of a mechanical vacuum forepump followed by either an oil or mercury diffusion pump and a cold trap maintained at dry ice or liquid air temperature. A sufficient quantity of the gas to be analyzed is placed in a

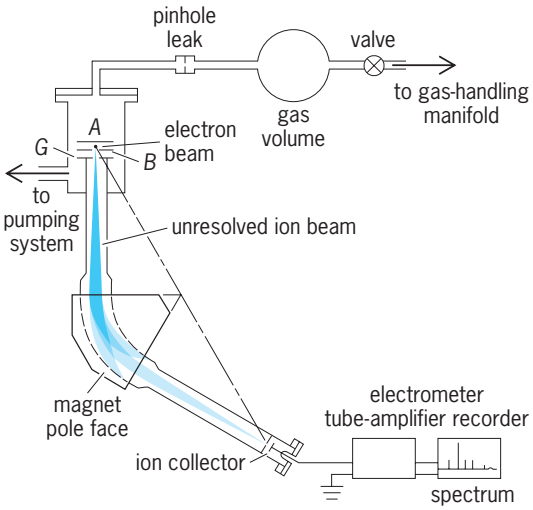

Fig. 1. Schematic diagram of mass spectrometer tube. Ion currents are in the range 10^{-10} to 10^{-15} A and require special electrometer tube amplifiers for their detection. In actual instruments the radius of curvature of ions in a magnetic field is 4–6 in. (10–15 cm).

vacuum chamber, whose pressure is approximately 0.05 mmHg (10^{-3} lbf/in.^{2} or 7 Pa). A pinhole having a diameter of approximately 0.001 in. (0.025 mm) permits this gas to leak continuously into the mass spectrometer tube.

A heated tungsten or rhenium filament, not shown in the diagram, produces an electron beam normal to the plane of the diagram, as shown. The electrons in the beam collide with the molecules of gas present and knock off one or more electrons, thus creating positive ions. *See* ION SOURCES.

In a monatomic gas such as argon, multiply charged positive ions, designated as Ar^+ (singly charged), Ar^{2+} (doubly charged), and so on, are formed. In the case of polyatomic molecules, ionized fragments may also be formed. For example, for methane, CH_4, the ions CH_4^+, CH_3^+, CH_2^+, CH^+, C^+, and H^+ are found. In some cases, negative ions are also created as a result of an electron capture process. Thus for CO, in addition to the ions CO^+, C^+, O^+, the ions C^- and O^- are observed. *See* ELECTRON CAPTURE.

An electric field resulting from the application of a potential difference of several volts between A and B draws the ions through the slit in plate B. Further energy is given the ions by allowing them to fall through an electric potential of several hundreds or thousands of volts applied between plates B and G. In such an instrument setup, plate G is grounded.

The beam of ions travels downward and because of the finite width of the slits in plates B and G, diverges lightly, as shown. The beam passes between the poles of a magnet as indicated. The magnetic field is perpendicular to the plane of the diagram. In the magnetic field the ions experience a force at right angles to their direction of travel given by Eq. (1),

$$f = Bev \tag{1}$$

where f is the force, B the magnetic field intensity, e the charge on the ion, and v its speed, all in SI units. This force results in a circular trajectory, whose radius r is found by equating the force to the product of mass and acceleration according to Newton's laws of motion, as in Eq. (2).

$$Bev = \frac{mv^2}{r} \tag{2}$$

Equation (2) may be put in the more convenient form of Eq. (3) by equating the kinetic energy gained

$$\tfrac{1}{2}mv^2 = eV \tag{3}$$

to the potential energy lost and expressing v in terms of potential difference V through which the ion fell. By combining Eqs. (2) and (3), solving for r, and substituting units which are more convenient for actual calculation, Eqs. (4) are obtained, where r' is now

$$r' = 57(MV/e)^{1/2}B \tag{4a}$$

$$r = \frac{144(mV/e)^{1/2}}{B} \tag{4b}$$

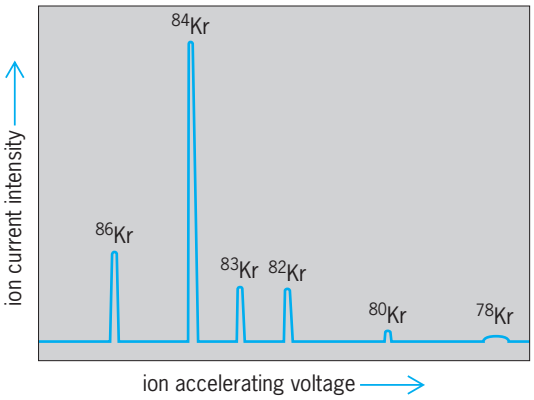

Fig. 2. Mass spectrum of krypton isotopes obtained with an instrument such as that shown in Fig. 1.

in inches, r is in cm, B in gauss (1 gauss = 10^{-4} tesla), V in volts, e is the charge of the ion measured in terms of the number of electrons removed (or added) during ionization, and m is the mass measured in atomic mass units; that is, for hydrogen $m = 1$, for the most abundant isotope of oxygen, ^{16}O, $m = 16$, and so on.

Figure 1 shows the paths of ions having three different masses. Only the intermediate group has the proper mass to reach and pass through the collector slit and to be measured.

If the source of ions, the apex of the wedge-shaped field, and the collector slit all lie on a straight line, the diverging beam of ions is focused as shown. This property of a wedge-shaped magnetic field is analogous to the focusing property of a convex lens in optics.

From Eqs. (4) it is clear that if either B or V is varied continuously, a mass spectrum may be swept. **Figure 2** is a recording of such a spectrum for krypton. The abundances of the several isotopes are proportional to the recording pen deflection.

Routine gas or isotope analyses may be made on 10^{-3} in.^{3} (10^{-2} cm^3) of gas at normal pressure and temperature (NTP), and in special cases as little as 10^{-9} in.^{3} (10^{-8} cm^3) of gas at NTP suffices. Some solids, such as alkali metals or alkali earths, give off ions directly when heated; therefore a filament coated with a salt containing these elements may serve as a source of ions. With this method, analyses have been made on samples as small as 3×10^{-14} oz (10^{-12} g). Electric sparks may also serve as sources of ions in solid analyses. Because of the unsteady nature of a spark, photographic recording of the spectra is generally employed.

In order to obtain higher resolution and a more definite relation between mass and position in a spectrum, an electric field region is employed in series with the magnetic field region. With this arrangement, called double focusing, resolutions of the order of 1 part in 50,000 are obtained, and masses can be determined to 1 part in 10^7, or better. **Figure 3** is a mass spectrum obtained with a double-focusing mass spectrograph.

Applications. Mass spectroscopes are used in both pure and applied science. Atomic masses can be

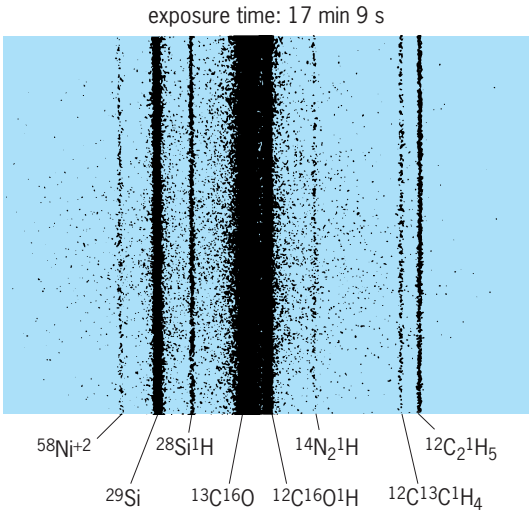

Fig. 3. Mass spectrum observed at mass number 29 when several substances are present simultaneously in a mass spectrograph. Resolution is sufficient to completely separate two close lines such as $^{12}C^{13}C^{1}H_4$ and $^{12}C_2{}^{1}H_5$, which differ in mass by only 1 part in 75,000.

measured very precisely. Because of the equivalence of mass and energy, knowledge of nuclear structure and binding energy of nuclei is thus gained. The relative abundances of the isotopes in naturally occurring or artificially produced elements can be determined. Thus nuclear processes occurring either in nature or in the laboratory may be investigated. Isotopic analyses of elements such as lead, argon, or strontium, which may result from the radioactive decay of other elements, are of particular interest because they make possible the determination of the geological age of the minerals from which the elements are extracted. Other geological effects which cause variations in relative abundances of isotopes may also be investigated.

Empirical and theoretical studies have led to an understanding of the relation between molecular structure and the relative abundances of the fragments observed when a complex molecule, such as a heavy organic compound, is ionized. When a high-resolution instrument is employed, the masses of the molecular or fragment ions can be determined so accurately that identification of the ion can frequently be made from the mass alone. Thus, although $C_2H_4N_4$ and $C_2H_4N_2O$ have molecular weights of approximately 84 when made up of the most abundant isotope in each of the elements concerned, the deviation from integral numbers of the constituents is sufficiently different to cause the exact masses to be 84.04359 and 84.03236 atomic mass units (amu), respectively ($^{12}C = 12.00000$ amu). If the isotopic nature of the elements is also taken into account, additional ions will be observed whose relative abundances depend upon the relative abundances of the isotopes. This fact provides another powerful tool in determining the identification of the ion in question. These methods, supplemented by others, frequently make the determination of the molecular formula of a compound relatively easy. Once this has been accomplished, the actual structure can usually be found by considering the relative abundances of the fragment ions.

Mass spectrometers also make possible isotopic analyses of compounds which have reacted chemically with other compounds containing elements with artificially altered isotopic abundance ratios. Thus the instruments make possible tracer studies of chemical or biochemical reactions.

Because chemical compounds may have mass spectra as unique as fingerprints, mass spectroscopes are widely used in industries such as oil refineries, where analyses of complex hydrocarbon mixtures are required. For further information on applications *see* BETA PARTICLES.

Miscellaneous types. In the instruments thus far discussed, a mass spectrum is obtained by making use of the fact that ions of different mass are deflected through different angles in passing through a magnetic field. In one important modification a superimposed electric and magnetic field is used, resulting in a trochoidal ion path. This has certain advantages, especially in that high resolution is obtained in a very compact apparatus. Various time-of-flight mass spectrometers are also employed. In some of these, ions are accelerated in pulses or by potentials varying sinusoidally with time and then sent through a system of grids where potentials also vary with time. A separation according to mass is effected because ions of different mass require different times to traverse the arrangement. In still others, use is made of the cyclotron principle; that is, the time for an ion to traverse a complete circle in a magnetic field is independent of the energy of the ion and depends only on its mass. In the quadrupole spectrometer, or *Massenfilter*, ions pass along a line of symmetry between four parallel cylindrical rods. An alternating potential superimposed on a steady potential between pairs of rods filters out all ions except those of a predetermined mass.

Alfred O. Nier

Tandem accelerator mass spectrometers. Mass spectrometers of the type described above have limitations in certain circumstances. For example, they may not be able to resolve molecules from equivalent mass number atoms, although the double-focusing mass spectrometers described above generally have sufficient mass resolution to avoid this problem. Such high resolution (1 part in 50,000 or better) is achieved, however, with a sacrifice in efficiency. A more serious problem is the separation of the wanted atom from its isobars. For example, ^{14}C and ^{14}N differ in mass by 1 part in 100,000.

Both these problems are overcome by the use of a tandem electrostatic accelerator as a mass spectrometer (**Fig. 4**). The system starts with negative ions (neutral atoms to which an extra electron is attached) produced in a sputter ion source. These are mass-analyzed to about 1 part in 200 and injected into the low-energy end of a tandem electrostatic accelerator. They are accelerated to the central positive terminal whose voltage can be adjusted up to 12 MV. In the terminal they pass through a differentially pumped

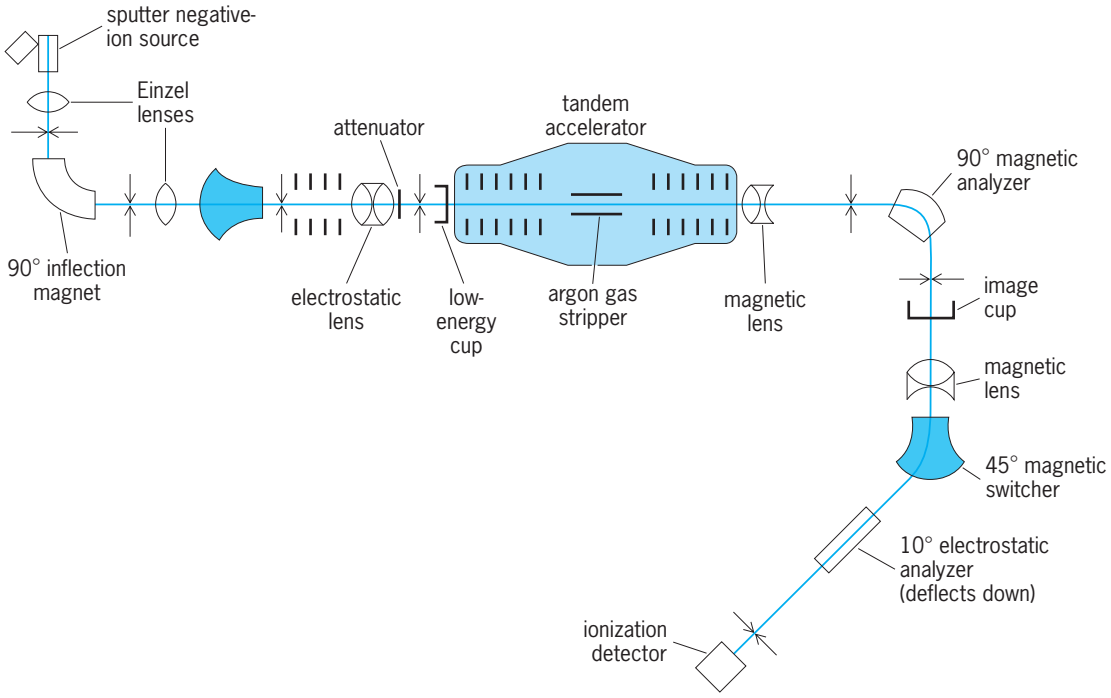

Fig. 4. Typical arrangement of a tandem accelerator mass spectrometry system.

argon gas stripper and emerge with several electrons removed. These positive ions are then accelerated through the second half of the machine and exit at the high-energy end. Here they are subjected to a series of magnetic and electrostatic deflections and finally pass into an ionization detector. Molecules are dissociated in the terminal stripper, and isobars are separated by their different rates of energy loss in the ionization detector due to their different atomic number.

Such systems are used to measure cosmogenic radioisotopes in a wide variety of naturally occurring material as well as stable isotopes in matrices of much more abundant elements. The **table** lists some of the radionuclides that have been measured. The limit of detection is listed in the last column. This limit is the ratio of the number of atoms of the radionuclide to the number of atoms of the stable isotopes. For ^{14}C and ^{16}Cl, the detection limit approaches 1 part in 10^{16}. Such detection limits never have been, and probably never will be, achieved by conventional mass spectrometers.

Radioactive isotopes are normally measured by detecting their decay products. For example, the amount of ^{14}C in a carbonaceous artifact can be used to determine the age of that artifact. To make such a measurement by radioactive decay counting, because of the relatively long half-life of 5730 years, requires carbon samples in the range of 1 to 10 grams. The tandem accelerator technique can measure the ^{14}C contents of a carbon sample by using 10 micrograms to a few milligrams of carbon. There are innumerable examples of carbonaceous artifacts which it would be of great interest to date but whose carbon content or the sample size is much too small to permit radioactive decay counting. The accelerator technique makes their age measurement possible. *See* RADIOCARBON DATING.

Many of the other radioisotopes listed in the table have much larger half-lives than ^{14}C and thus are even more difficult to measure by decay counting. The accelerator mass spectrometry technique, which does not require that the isotope be measured by radioactive decay, can readily be used.

Radionuclides studied in tandem accelerator mass spectrometer

Radionuclide	Half-life, years	Stable isotopes	Stable isobars	Chemical form	Charge state	Energy, MeV	Limit of detection
^{10}Be	1.6×10^6	^{9}Be	^{10}B	BeO	3+	33†	7×10^{-5}
^{14}C	5730	$^{13,13}C$	^{14}N*	C	4+	40	0.3×10^{-15}
^{26}Al	7.2×10^5	^{27}Al	^{26}Mg*	Al	5+	48	10×10^{-15}
^{32}Si	108	$^{28,29,30}Si$	^{32}S	SiO_2	5+	55	7×10^{-12}
^{36}Cl	3.0×10^5	$^{35,37}Cl$	^{36}Ar*, ^{36}S	AgCl	7+	80	0.2×10^{-15}
^{129}I	15.9×10^6	^{127}I	^{129}Xe*	AgI	5+	30	0.3×10^{-12}

*Does not form negative ions.
†BeO from source.

Carbon-14 has now been measured by tandem accelerators in a wide variety of important archeological, anthropological, and geological samples. For example, the date of the Turin Shroud was measured by accelerator mass spectrometry. This cloth, believed by many to have been Christ's burial shroud, could not have been dated by the conventional decay-counting technique because a sample the size of a handkerchief would have been required. Three laboratories made the measurements independently, using only a few square centimeters of cloth. They ascertained that the flax from which the linen cloth was made was harvested in A.D. 1325 ± 30.

Chlorine-36 has been measured in meteorites, lunar rocks, ice cores, ground water, and many other naturally occurring materials. Beryllium-10 has been measured in lake and ocean cores, a Moon core, rainwater, ice, and manganese modules. Iodine-129, which is the longest-lived cosmogenic radioisotope, has been measured in meteorites and in lunar rocks and ground water.

The accelerator mass spectrometry technique has also been applied to the measurement of stable isotopes. In particular, platinum and iridium have been measured in samples of geological and anthropological interest.

Accelerator-based ultrasensitive mass spectrometry finds applications in quite different areas of research than conventional mass spectrometry. The two techniques complement one another. *See* MASS SPECTROMETRY.

Harry E. Gove

Bibliography. J. Barker, *Mass Spectrometry*, 2d ed., John Wiley, 1999; J. R. Chapman, *Practical Organic Mass Spectrometry*, 2d ed., Wiley, 1993; E. de Hoffman and V. Stroobart, *Mass Spectrometry Principles and Applications*, 2d ed., Wiley, 2002; H. E. Gove, *From Hiroshima to the Iceman: The Development and Applications of Accelerator Mass Spectrometry*, Institute of Physics, Bristol and Philadelphia, 1998; H. E. Gove, *Relic, Icon or Hoax? Carbon Dating the Turin Shroud*, Institute of Physics, Bristol and Philadelphia, 1996; F. W. McLafferty and F. Turaček, *Interpretation of Mass Spectra*, 4th ed., University Science Books, 1993; C. Tuniz et al., *Accelerator Mass Spectrometry: Ultrasensitive Analysis for Global Science*, CRC Press, Boca Raton, FL, 1998; J. T. Watson, *Introduction to Mass Spectrometry*, 3d ed., Lippincott Williams & Wilkins, 1997.

Mass wasting

A generic term for downslope movement of soil and rock, primarily in response to gravitational body forces. Mass wasting is distinct from other erosive processes in which particles or fragments are carried down by the internal energy of wind, running water, or moving ice and snow. Mass wasting generally creates colluvium, a type of deposit over or at the bottom of many slopes and with characteristics as varied as the mass-wasting processes.

Shear strength and stress. The stability of slope-making materials is lost when their shear strength (or sometimes their tensile strength) is overcome by shear (or tensile) stresses, or when individual particles, fragments, and blocks are induced to topple or tumble. The shear and tensile strength of earth materials depends on their mineralogy and structure. Processes that generally decrease the strength of earth materials include one or more of the following: structural changes, which promote fracturing and faulting, hence, weakening of the mass; weathering, which changes mineralogy and promotes further breakdown; ground water, which softens clays, dissolves some minerals, and, more importantly, develops pressures that oppose the frictional resistance of the mass—a main component of its shear strength; and meteorological changes, which result in melting of ice and snow. Stresses in slopes are increased by steepening, heightening, and external loading due to static and dynamic forces. Processes that increase stresses can be caused by natural or human means. Thus, steepening and heightening may result from erosion or from mining activity; static loading of slopes may be caused by snow, rain, or fill placement; dynamic loading may be the consequence of earthquakes or blasting. Although other classifications exist, these movements can be conveniently classified according to their velocity into two types: creep and landsliding. *See* SOIL MECHANICS.

Creep. Geologically, creep is the imperceptible downslope movement at rates as slow as a fraction of a millimeter per year; its cumulative effects are ubiquitously expressed in slopes as the downhill bending of bedded and foliated rock, bent tree trunks, broken retaining walls, and tilted structures. There are two varieties of geologic creep. Seasonal creep is the slow, episodic movement of the uppermost several centimeters of soil, or fractured and weathered rock. This type of creep occurs when particles or fragments are heaved perpendicular to the slope surface by freezing and allowed to come down roughly in a vertical direction during thawing; the resulting cycle gives the movement a lateral component. Seasonal creep is especially important in regions where the ground is permanently frozen. *See* PERMAFROST.

The second variety, rheologic creep, is sometimes called continuous creep. It is a time-dependent deformation at relatively constant shear stress of masses of rock, soil, ice, and snow. This type of creep affects rock slopes down to depths of a few hundred meters, as well as the surficial layer disturbed by seasonal creep. Continuous creep is most conspicuous in weak rocks and in regions where high horizontal stresses (several tens of bars or several megapascals) are known to exist in rock masses at depths of 300 to 600 ft (100 to 200 m). These conditions are found in shale sections of those parts of the north-central United States, Ontario, and New York adjacent to the Great Lakes. In this region, shales are known to have crept several tens of centimeters into valleys and excavations. In this process, interbeds of sandstone are stretched, fractured, and separated into discrete blocks by the creeping shale above and below

Fig. 1. Landslide of slump type in bank along Mississippi River. (*U.S. Soil Conservation Service*)

the interbeds. Deep-seated creep also occurs along narrow weakness zones in rock masses before such zones become ruptured and the moving masses become landslides.

Landsliding. This includes all perceptible mass movements. Three types are generally recognized on the basis of the type of movement: falls, slides, and flows. Falls involve free-falling material; in slides the moving mass displaces along one or more narrow shear zones (**Fig. 1**); and in flows the distribution of velocities within the moving mass resembles that of a viscous flow. Sometimes flows are not included as a type of landslide but as a separate type of mass movement. All three types can occur in different earth materials and can affect small hill slopes or high mountainsides; often, more than one type occur in a single event. In many instances, a very large rock mass begins to displace as a slide but soon breaks down into progressively smaller blocks and fragments which tend to move very much like sand poured from a container. The most disastrous mass movements in history (debris avalanches) have evolved in this manner (**Fig. 2**).

Fig. 2. Rockslide debris avalanche at Mount Huascaráan, Peru, 1970. The large scar on the side of Mount Huascaráan (background) marks initiation of the rockslide. Santa Valley is seen in the foreground.

Mass wasting is an important consideration in the interaction between humans and the environment. Deforestation accelerates soil creep. Engineering activities such as damming and open-pit mining are known to increase landsliding. On the other hand, enormous natural rock avalanches have buried entire villages and claimed tens of thousands of lives. *See* LANDSLIDE.

Alberto S. Nieto

Bibliography. M. J. Crozier, *Landslides*: *Causes, Consequences, and Environment*, 1986; R. L. Schuster and R J. Krizek (eds.), *Landslides*: *Analysis and Control*, NAS-NRC Spec. Rep. 176, 1978; B. Voight (ed.), *Rockslides and Avalanches*, pt. 1, Developments in Geotechnical Engineering, vol. 14a, 1978.

Massif

A block of the Earth's crust commonly consisting of crystalline gneisses and schists, the textural appearance of which is generally markedly different from that of the surrounding rocks. Common usage indicates that a massif has limited areal extent and considerable topographic relief. Structurally, a massif may form the core of an anticline or may be a block bounded by faults or even unconformities. In any case, during the final stages of its development a massif acts as a relatively homogeneous tectonic unit which to some extent controls the structures that surround it. Numerous complex internal structures may be present; many of these are not related to its development as a massif but are the mark of previous deformations.

Philip H. Osberg

Mastigophora

A superclass of the Protozoa also known as the Flagellata. The flagellates make up a large and heterogeneous group of Protozoa, varying in size from *Noctiluca*, 1500 micrometers in diameter, to monads, barely 3 micrometers long. The common morphological flagellate type is spherical to cylindrical on an anteroposterior axis. They are probably more nearly representative of the primitive protozoan type than Sarcodina or Ciliophora, but exhibit a more evident relationship to the former. Despite their common morphological plan, based on the flagellum as a means of locomotion, Flagellata are very diverse in shape, colony formation, internal structure, external shell or test, color, physiology, reproduction, and choice of environment. *See* CILIOPHORA; SARCODINA.

The Mastigophora exhibit marked plantlike characteristics, so that texts and references in botany always treat at least some of them. Some workers include all colorless flagellates in the algae; however, flagellates display many distinctly animal features

and sometimes are treated as Protozoa. Thus, flagellates are regarded as a link between the plant and animal kingdoms. *See* PHYTAMASTIGOPHOREA; ZOOMASTIGOPHOREA.

Morphology. Mastigophora possess one common feature, locomotion by means of one or more whiplike protoplasmic extrusions termed flagella. A few have secondarily lost this organelle. In some it is single and directed anteriorly; in a few it is directed posteriorly. Others have one anterior and one trailing flagellum, but there are numerous combinations such as one anterior and two trailing (*Amphimonas*), or up to eight anterior (*Polyblepharides*). Dinoflagellates customarily have two laterally inserted flagella, one posteriorly directed, the other encircling the cell. *Trepomonas* and its relatives have two lateral sets, and the Hypermastigina, symbiotic in termites and wood roaches, have large numbers of very long flagella, mostly lateral. The flagella may be equal or subequal. Usually the flagellar equipment is handed on to one daughter cell at division, a new set being produced in the other. In some species (*Mastigamoeba reptans*) the flagellum may be temporarily withdrawn, at which time the organism moves by ameboid action. Flagella are usually few in number, except in Hypermastigina.

Body form. The flagellate body is typically monaxial and elongate to some degree. Cells are practically spherical in *Monas*, but ovoid, cordiform, pyriform, fusiform, acicular, tubular, or flattened cells are more common. Flattened species typically glide along a surface rather than swim. A particular shape is normally maintained by *Ochromonas* (see **illus.**), whereas *Mastigamoeba* and some others form pseudopodia, and certain species (*Euglena agilis*) undergo frequent distortions termed euglenoid or metabolic changes of shape.

Structurally the flagellate cell is not simple. The cytoplasm is sometimes quite vacuolated (*Collodictyon* or *Trepomonas*) and occasionally colored, although color is generally confined to chromatophores when these are present. One or more contractile vacuoles may be located near the flagellar base.

Colony formation. Most flagellates are single-celled but colony formation is frequent. Cells may be naked (*Oicomonas*), enclosed in a thick cellulose cell wall or pellicle (*Euglena spirogyra*), or in a chitinous, calcareous, or silicious test, the lorica or shell (*Trachelomonas, Distephanus speculum*). The lorica may be smooth, spiny, sculptured, or with attached foreign bodies (*Urceolus sabulosus*). Tests may be clear or colored by impregnated iron. Colony forms are variously flattened (*Platydorina*), spherical (*Volvox*), irregular (*Cladospongia*), linear (*Desmarella*), catenate (*Gonyaulax*), tubular (*Stelexomonas*), or dendroid. Colony walls are usually gelatinous in texture but vary. Single cells are frequently attached by a stalk to some substrate, especially those living in cup-shaped tests. The cell proper rarely shows protuberant parts other than flagella and pseudopodia, but the Protomonadina include many species showing one (*Monosiga, Proterospongia*), or two (*Dicraspedella*) protoplasmic collars ringing the base of the flagellum.

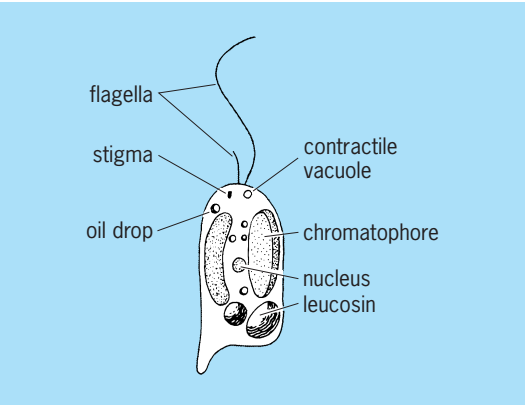

***Ochromonas ludibunda*, showing component parts.**

Flagellum. The flagellum contains a structurally complex longitudinal axial fibril or axoneme. Along its length numerous short lateral hairlike mastigonemes occur which can be seen only in special preparations. The flagellum originates in a kinetic body, the blepharoplast, usually close to the outer surface of the cell. Blepharoplasts for each flagellum are connected by fibrils termed paradesmoses. Another fibril, the rhizoplast, may extend from the blepharoplast to the centriole or to the nucleus. There may be still other structures in the flagellar complex, demonstrable by special techniques. The whole flagellar apparatus produces coordinated movement. Red eye spots (stigmas) may occur near the base of the flagellum. They are considered photoreceptors, and are sometimes accompanied by a lenslike structure; the whole is important in phototactic orientation. *See* CILIA AND FLAGELLA; PHOTORECEPTION.

Nucleus. Nuclei are single except in the distomates (*Hexamitus, Giardia*) and each undergoes mitosis in division. Some contain endosomes of unknown function but which do not contribute directly to chromosome formation. Others contain nucleoli which apparently are identical with, or contribute to, chromatin. Dinoflagellate nuclei are large and vesicular; each chromosome apparently retains its identity during the interphase. In the Euglenoidina the chromatin granules are typically scattered with one or more centrally located endosomes. Nuclei are large in Chloromonadida and are small in Chrysomonadida, Cryptomonadida, Phytomonadida, Zoomastigophorea, Rhizomastigida, and some Protomonadida. In these the chromatin tends to peripheral location with central endosomes.

Nuclear and cell division. In species whose nuclear division is mitotic, details vary, but definite and species-characteristic chromosome numbers occur. In some cases (*Bodopsis godboldi, Dimorpha mutans*), well-defined spindles, within or without the original nuclear membrane, are present. Blepharoplasts function as centrioles. Other mitoses may lack spindles or centrioles (*Oxyrrhis marina, Entosiphon sulcatum*). Mitosis in Hypermastigida is extremely complicated. Most flagellates are haploid; gamete

formation is the exception although sexual processes are known for Phytomonadina. *Pleodorina californica* has visibly different somatic and reproductive cells.

Cell division is generally longitudinal binary fission which sometimes occurs while the organism is encysted, but more often while it is active. Occasionally, multiple fission occurs as in *Chlorogonium* whose trophozoites are sometimes seen to be divided into eight daughter cells. *See* MITOSIS.

Cell inclusions. Flagellates contain various cell inclusions, such as mitochondria and Golgi apparatus. Conspicuous inclusions are chromatophores and reserve food materials. Chromatophores are discoid, cup-shaped, or irregular networks containing one or more of the chlorophylls and often carotene, xanthophyll, or other pigments. Green is characteristic for Phytomonadida and Euglenida, yellow for Chrysomonadida. Cryptomonadida and Dinoflagellida are blue, brown, olive green, pink, or red. Chromatophores may contain pyrenoids as centers of starch formation. Other supposed reserve food inclusions are paramylum (Euglenida); leucosin and volutin (Chrysomonadida); and glycogen (Chloromonadida). Lipids are widely distributed. Occasionally hematochrome granules are sufficiently abundant to color the cell, as when blooms of *Euglena haematoides* redden the surfaces of ponds in hot summer weather. *See* CAROTENOID; CHLOROPHYLL; CHROMATOPHORE; GOLGI APPARATUS; MITOCHONDRIA.

Nematocysts, trichocysts, and trichites occur in flagellates. In *Polykrikos* (Dinoflagellida) nematocysts lie free in the cytoplasm, but their function is unknown. Trichocysts in *Polykrikos*, in *Euglena* species, and in *Chilomonas* may be discharged as long threads by various stimuli, but here too their function is open to speculation.

Nutrition. Nutrition is holophytic when food is manufactured from inorganic substances by those species containing chlorophyll; saprozoic, when dissolved organic materials are absorbed and resynthesized; and holozoic, when solid food is ingested. *Euglena gracilis*, which is holophytic in the light, may become saprozoic in the dark. *Euglena acus* may become saprozoic in the light in a rich organic medium. *Ochromonas ludibunda* apparently is simultaneously holophytic and holozoic. Flagellata perhaps more than any other group vary widely in nutritive processes from those involving intake of specific chemical entities to those of synthesis. Their requirements of trace elements, vitamins, and amino acids vary almost from species to species, as shown by precise experimental investigation. *See* NUTRITION; PHOTOSYNTHESIS.

Respiration. Respiration is complex. Many flagellates adjust to wide oxygen-tension ranges; probably most are facultative (*Peranema trichophorum*), but some (*Gonyostomum semen*) appear to be obligate aerobes, others (*Trepomonas rotans*) obligate anaerobes. Carbon dioxide is excreted through the contractile vacuole as is oxygen. Dense blooms of *Chlamydomonas* or *Euglena* will supersaturate surface waters with oxygen within a few hours after daybreak. Excretion of other metabolites such as antibiotics is demonstrable. Circulation by cyclosis is sometimes observable.

Ecology. Flagellates adjust to wide ranges of pH, osmotic pressure, light, and temperature but optima are found upon investigation. *Euglena mutabilis* grows at pH 0.9–7.2, but densest blooms occur about pH 3.5–4.0. Some flagellate species occur in both fresh and seawater, but cannot be transferred directly from fresh to seawater.

Almost any aqueous ecological niche contains Flagellata. Dense fresh-water blooms of *Euglena* or *Platymonas* are matched by blooms of *Eutreptia* or *Gymnodinium breve* in the ocean. *Trentonia flagellata* is the only green flagellate occurring abundantly in Warm Mineral Springs, an anaerobic sulfur spring of southern Florida. Euglenida and Phytomonadida grow profusely in barnyard pools, Chloromonadida in weakly acid cedar and cypress swamp water, and Phytomastigida and Cryptomonadida in lower-nutrient levels of oceans, streams, and lakes. Dinoflagellida abound in the oceans; Chrysomonadida tend to live in clean water; Zoomastigida and Rhizomastigida favor organically polluted water. There is much overlapping because many are ubiquitous.

Flagellata are near the base of the food pyramid, probably next to bacteria. Their varied synthetic abilities, fast reproductive rate, and huge numbers in both fresh and salt water compensate for their usual small size. The oceanic blooms which kill fish and other animals are principally flagellates, but green flagellates reaerate polluted water. They often cause tastes and odors in potable water, but they readily attack organic matter in natural water as do bacteria. They include many parasites dangerous to humans and animals and are themselves frequently parasitized. *See* FOOD WEB; PROTOZOA. James B. Lackey

Mastitis

Inflammation of the mammary gland. This condition is most frequently caused by infection of the gland with bacteria that are pathogenic for this organ. It has been described in humans, cows, sheep, goats, pigs, horses, and rabbits. Mastitis causes lactating women to experience pain when nursing the child, it damages mammary tissue, and the formation of scar tissue in the breast may cause disfigurement. It also is the most economically important disease of dairy cows.

The mammary gland is composed of a teat and a glandular portion. The number of glands varies with the species. The glandular portion consists of lobules of secretory tissue and a series of collecting ducts. The teat is composed of an external orifice, teat duct, and teat lumen. In humans there are a series of lactose-secreting ducts opening on the nipple surface. The gland has defensive mechanisms to prevent and overcome infection with bacteria. Nonspecific defense mechanisms include teat duct keratin, lactoferrin, lactoperoxidase, and complement. Specific

defense mechanisms are mediated by antibodies and include opsonization, direct lysis of pathogens, and toxin neutralization. Milk contains epithelial cells, macrophages, neutrophils, and lymphocytes. To induce mastitis, a pathogen must first pass through the teat duct to enter the gland, survive the bacteriostatic and bactericidal mechanisms, and multiply. Bacteria possess virulence factors such as capsules and toxins which enable them to withstand these protective mechanisms. *See* LACTATION.

Agents and mode of transmission. Mammary infections in humans are usually caused by *Staphylococcus aureus*. The source of infection is typically the nasopharynx of the infant, although mass outbreaks of mastitis have been documented in maternity wards, suggesting spread between nursing women. Bovine mastitis is classified as either contagious or environmental in nature. Contagious mastitis is caused by *Streptococcus agalactiae* and *Staphylococcus aureus*. The term contagious reflects the role of infected glands as the critical reservoir of infection, with transmission occurring at milking. Environmental mastitis is caused by *Streptococcus uberis, Escherichia coli*, and *Klebsiella* spp., bacteria that are found on other parts of the cow and in bedding, manure, and soil. *Streptococcus aureus* frequently induces mastitis in goats, sheep, and rabbits, with *Pasteurella haemolytica* also being a prime culprit in sheep. In pigs *Escherichia coli* and *Klebsiella* spp. are isolated, while the occasional equine case usually yields streptococci. *See* ESCHERICHIA; KLEBSIELLA; PASTEURELLA; STAPHYLOCOCCUS; STREPTOCOCCUS.

Clinical signs. When bacteria multiply within the gland, there is a release of inflammatory mediators and an influx of neutrophils. The severity of mammary infection is classified according to the clinical signs. In humans, infection occurs during lactation, with clinical episodes most frequent during the first 2 months of lactation. In acute puerperal mastitis the tissue becomes hot, swollen, red, and painful, and a fever may be present. In the absence of treatment, this may progress to a pus-forming mastitis, with the development of breast abscesses.

Clinical mastitis in ruminants causes inflammatory changes as described above, and the milk may contain clots and be discolored. In severe cases the cow may display fever, anorexia, and depression. In subclinical mastitis the milk appears grossly normal, but analysis reveals an elevated cell count and the presence of bacteria. In cows the different etiologic agents vary in the severity of the disease they cause. Coliform bacteria cause a peracute mastitis which can be fatal. Infection with *Staphylococcus aureus* and streptococci often commences with an initial acute clinical episode that subsides into a chronic subclinical state. Occasional clinical flare-ups occur. In rabbits the disease occurs as either a gangrenous or abscess form.

Diagnosis. Clinical mastitis can be diagnosed by examination of the gland and its secretion. Subclinical mastitis cannot be identified by this means but relies on bacteriologic and cytologic analysis. Bacteria cultured from aseptically collected secretion are identified by cultural morphology and biochemical tests. In uninfected glands the predominant cell type in milk is the macrophage. Neutrophils are attracted once bacteria invade the gland, and these neutrophils cause the cell count to increase. The cell count thus serves as an indicator of the health of the gland. Mastitic milk possesses increased levels of sodium and chlorine ions, albumin, and acetylglucosiminidase, and displays altered electrical conductivity.

Treatment. In acute puerperal mastitis of humans suitable antibiotics are administered by the intravenous or intramuscular route, while in the abscess form surgical drainage is provided in addition to antibacterial therapy. In dairy cows the continuous manual removal of the secretion of infected quarters is usually replaced by antibiotic use. Penicillins, cephalosporins, and erythromycin are administered locally into the infected gland after milking for 1–2 days. Additional antibiotics are given systemically, that is, intravenously or intramuscularly, in severe cases of mastitis, and also to improve bacteriologic cure rates. Certain forms of bovine mastitis are unresponsive to therapy, and the animals are isolated from the herd. The milk from cows undergoing treatment is discarded to prevent contamination of milk for human consumption. The pathogenic effects of coliform mastitis in cows are mediated in part by the release of endotoxin from the bacterial cell which induces macrophages to secrete inflammatory cytokines, which in turn cause fever, hypotension, and shock. In this type of mastitis, antibiotics have a secondary role to the administration of fluids and anti-inflammatory agents, and the continuous removal of secretion from the infected gland after injection of oxytocin. *See* ANTIBIOTIC.

Prevention. Proper hygiene during nursing helps prevent breast infections in humans. In cows, good milking practices, milking machine maintenance, and the dipping of teats with disinfectant after milking help reduce infections caused by staphylococci and streptococci. However, these steps have no impact on infection with environmental organisms. For the last 2 months of pregnancy, cows are not milked; this is the so-called dry or nonlactating period during which infections commonly occur. Administering long-acting antibiotic formulations at drying-off helps to prevent new infections and to eliminate existing ones without the need to discard milk. Proper hygiene and sanitary housing are critical in the prevention of environmental mastitis. In the United States, immunization to increase resistance to infection is possible with a vaccine containing killed *Escherichia coli* bacteria.

Neil L. Norcross

Matched-field processing

A set of related signal processing techniques for remote sensing that involve matching measured signals obtained from an array of sensors to synthesized signals obtained from signal propagation

simulations conducted in a model of the actual environment. Here the signals are typically acoustic or electromagnetic waves, but they may be water waves, seismic waves, structural waves, or any other measurable phenomenon that travels in a predictable manner from its source to a distant receiver. Matched-field processing is the extension of elementary sensor-array signal processing techniques for line-of-sight signal propagation in uniform unbounded environments to complicated, but predictable, signal propagation in nonuniform bounded environments. Matched-field processing is superior to these elementary techniques because it can explicitly account for reflection, refraction, and scattering of the signal as it propagates from its source to the sensors. However, this superior performance is possible only when the signal propagation simulations are accurate and the model environment matches the environment in which the signal propagation took place. *See* ACOUSTIC SIGNAL PROCESSING; SIGNAL PROCESSING; SIMULATION; WAVE MOTION.

Remote sensing is common for military, biomedical, surveillance, quality control, and nondestructive evaluation purposes. The primary remote-sensing tasks are typically detection, localization, tracking, and identification of signal sources (or scatterers). These tasks all become more difficult when the environment is complicated and multiple signal-propagation paths are possible between distant signal sources (or scatterers) and the sensors. Such environments occur in applications of radar and sonar where naturally occurring or artificial obstacles and surfaces cause signal echoes and reflections. Matched-field processing is utilized primarily for detection and localization of signal sources, with a greater emphasis on localization. *See* RADAR; REMOTE SENSING; SONAR; UNDERWATER SOUND.

Techniques for remote source localization from sensor-array measurements exist for a variety of remote-sensing scenarios involving different kinds of sources, propagation physics, and environments. For example, signal sources may be relatively small or large compared to the propagation distances, sensor-array size, or average signal wavelength; signal wave fronts may be planar, spherical, or more complicated; and environments may or may not include reflecting surfaces and refraction. Matched-field processing is the preferred source localization technique for small sources, complicated wave fronts, and environments with known reflection and refraction.

Homer Bucker is generally credited with putting matched-field processing into its current form in 1976. He studied remote acoustic source localization in the shallow ocean, and was the first to utilize a realistic environmental model and to introduce a two-dimensional surface as the matched-field processing output. In 1985, Richard Fizell and Stephen Wales reported the first matched-field processing localization results using field measurements of sound propagation under Arctic ice. From these beginnings in sonar, the development of matched-field processing has been boosted by incorporation of ideas from radar and astronomy, so that it is now used or being considered for applications in leak testing, noise-control engineering, seismology, structural monitoring, and even astrophysics.

Basic features. The capabilities of matched-field processing can be illustrated by comparing it to simple plane-wave sensor-array processing in a series of increasingly complicated environments. Consider first a uniform unbounded environment with a linear transducer array (**Fig. 1***a*). If a single plane-wave signal from a distant source propagates past the array at an angle $\theta = \theta_1$, then each transducer will record the same signal waveform at a slightly different time. When the signal propagation speed and the locations of the sensors are known, the recorded signal timing differences between sensors can be used to determine the propagation angle. Here, the plane-wave array-signal-processor output, $A(\theta)$, and the matched-field processing output, $B(\theta)$, will be equivalent and will involve only a single search coordinate, the angle θ (Fig. 1*b*). Both signal processor outputs will peak at the angle θ_1, and the width of this peak and its height relative to A or B values away from θ_1 will be determined by the number and spatial distribution of the array elements, the signal-to-noise ratio and timing accuracy of the signal recordings, and the signal processing algorithms. False peaks and unwanted nonzero values in an array signal processor's output are commonly called side lobes and clutter.

As a second step, consider the same source-array geometry when a reflecting surface causes the original signal to traverse the receiving array in two different directions, θ_1 and θ_2 (**Fig. 2***a*). In this case, the plane-wave array-signal-processor output, A, will indicate two possible source directions, but a matched-field processing scheme based on signal propagation in the actual environment will account for the reflecting surface and will correctly determine the true source direction (Fig. 2*b*). In fact, the matched-field processing scheme does a better job finding the source angle when the reflecting surface is present, compared to when it is absent, because matched-field processing utilizes the signal timing information from both signal paths.

As a final illustration consider an environment with

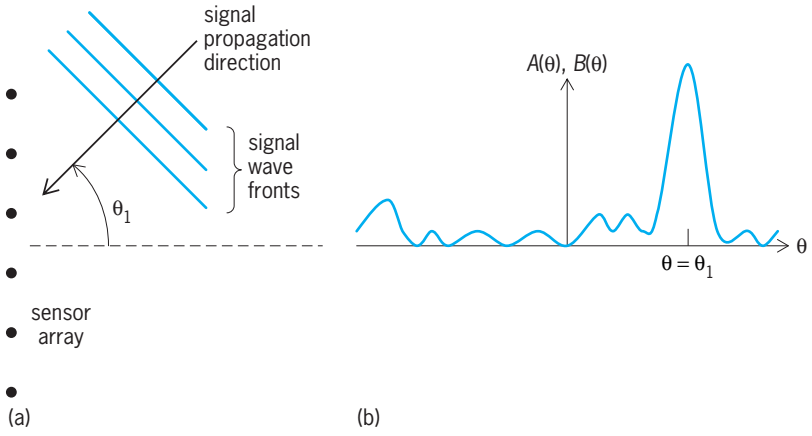

Fig. 1. Plane-wave signal incident on a linear sensor array without any reflections. (*a*) Signal and sensor-array geometry. (*b*) Typical plane-wave array-signal-processor output, $A(\theta)$, and the matched-field processing output, $B(\theta)$, versus signal incident angle, θ.

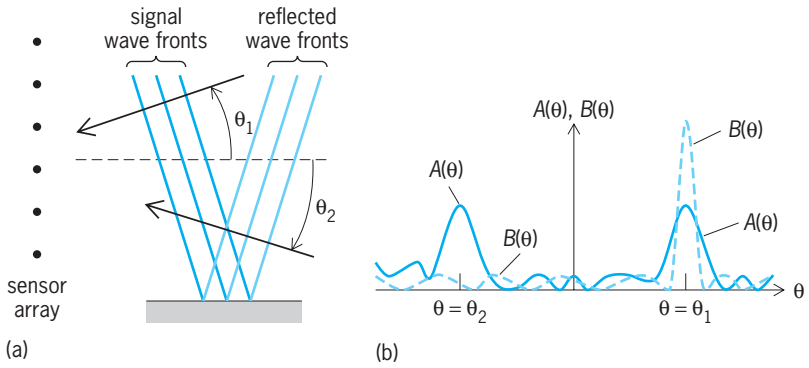

Fig. 2. Plane-wave signal incident on a linear sensor array with one reflection. (*a*) Signal and sensor-array geometry. (*b*) Typical plane-wave array-signal-processor output, $A(\theta)$, and the matched-field processing output, $B(\theta)$, versus signal incident angle, θ.

two parallel reflecting surfaces that form a waveguide with four signal paths connecting the source and the sensor array, each path having a different angle (**Fig. 3***a*). This situation is common for ocean sonar operations, but even more source-array paths may be involved. For the case depicted here, the plane-wave array signal processor will indicate four possible source directions (Fig. 3*b*). However, when the environment is known, matched-field processing can exploit the environmental complexity to determine both the horizontal and vertical location of the source. Thus, the matched-field processing output is commonly presented as a surface having two (or more) independent spatial dimensions with color or gray-scale indicating the peaks (Fig. 3*c*). Even though clutter and side lobes still occur with matched-field processing, this example shows how matched-field processing can improve source localization in a multipath environment by eliminating ambiguous source directions in favor of a single source localization peak in range and depth coordinates.

Algorithms. The actual signal processing algorithms used in matched-field processing fall into two broad categories: linear and adaptive (or nonlinear). The primary linear algorithm, often called the Bartlett processor, is implemented by placing a grid of points in the model environment in the region to be searched for the signal source. A synthetic test source is placed at each grid point and signals for each test source location are synthesized for each sensor of the receiving array using a signal propagation simulation. The measured signals are then compared with the synthetic signals. The test source location corresponding to the best match between measured and synthesized signals is the location of the source determined by matched-field processing. The Bartlett processor can also be described in terms of time-forward and time-reverse signal propagation. First, genuine signals travel in the actual environment from the source to the sensors where they are recorded with time increasing, as usual. Next, the direction of time is mathematically reversed for the measured signals and time-reverse propagation is simulated in the model environment. If the propagation simulations are accurate, and the actual and model environments are well matched, then the location in the model environment where the time-reversed signals converge, constructively interfere, and form a peak is the matched-field processing prediction of their source location (Fig. 3*c*). For an oscillating signal in an environment that supports multiple reflections from different directions, linear matched-field processing is capable of localizing a remote source to within a half wavelength. Bartlett matched-field processing is considered linear because the measured signals are directly correlated with the synthesized signals via simple multiplication and sum operations. *See* TIME-REVERSED SIGNAL PROCESSING.

Adaptive matched-field processing differs from linear matched-field processing in the way that the actual and synthetic signals are combined. Although there are many adaptive matched-field processing algorithms, their general intent is to improve source localization resolution and clutter and side-lobe suppression beyond that of linear matched-field processing. Hence, these algorithms are mathematically more complicated, so the descriptions above involving signal correlations and time reversal are no longer directly applicable. However, the implementation procedure for adaptive and linear matched-field processing is essentially the same, but the quality of the results from adaptive matched-field processing can be much better, especially when the signal-to-noise ratio of the original measured signals is high. Under the right conditions, adaptive matched-field processing routines may reduce localization uncertainty by

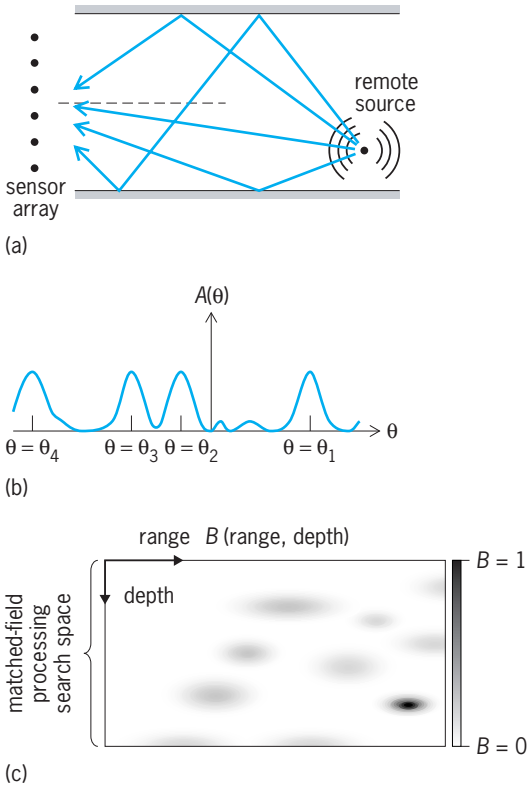

Fig. 3. Signals from a remote source incident on a linear sensor array in a waveguide with two reflecting surfaces and four signal paths connecting the source and the array. (*a*) Signal and sensor-array geometry. (*b*) Typical plane-wave array-signal-processor output, *A*. (*c*) Matched-field output, *B*, in grayscale as a function of range and depth.

a factor of 3 or more, and may suppress side lobes and clutter by more than a factor of 10, when compared to linear matched-field processing. These advantages may be tactically important for correctly discriminating between a single isolated source and two closely spaced sources, or for finding a weak target source in an environment dominated by loud interfering sources.

Limitations. The primary limitations of matched-field processing stem from differences between actual signal propagation in the real environment and simulated signal propagation in the model environment. Here, geometrical differences as small as a fraction of a signal wavelength in the placement of a reflecting surface can lead to erroneous source localization, or degradation (or even loss) of the localization peak in the matched-field processing output. Thus, there is a significant burden on the user to know the environment well and to faithfully simulate signal propagation. Yet, even when all the environmental-specification parameters are not known, matched-field processing is still possible by adding parameter searches to the preexisting search space, an extension of matched-field processing called focalization. However, the main computational burden of matched-field processing commonly results from repeated simulation of signal propagation in the model environment as the test source is moved through the search space. Thus, minimizing the number of signal propagation simulations is typically advantageous. David R. Dowling

Bibliography. A. Baggeroer, W. A. Kuperman, and P. N. Mikhalevsky, An overview of matched field methods in ocean acoustics, *IEEE J. Oceanic Eng.*, 18:401–424, 1993; F. B. Jensen et al., *Computational Ocean Acoustics*, chap. 10, AIP Press, 1994; A. Tolstoy, *Matched Field Processing for Underwater Acoustics*, World Scientific, Singapore, 1993.

Material resource planning

A formal computerized approach to inventory planning, manufacturing scheduling, supplier scheduling, and overall corporate planning. The material requirements planning (MRP) system provides the user with information about timing (when to order) and quantity (how much to order), generates new orders, and reschedules existing orders as necessary to meet the changing requirements of customers and manufacturing. The system is driven by change and constantly recalculates material requirements based on actual forecast orders. It makes adjustments for possible problems prior to their occurrence, as opposed to traditional control systems, which looked at more historical demand and reacted to existing problems. Material resource planning (MRP II) evolved from material requirements planning when it was recognized that most major data needed to manage a manufacturing or distribution firm could be obtained from the material requirements planning information. The ability of a material resource planning system to meet the various needs of manufacturing, materials, and marketing personnel within a changing business environment contributes to its growing implementation by manufacturing companies. *See* MANUFACTURING ENGINEERING.

Dependent and independent demand. The logic of the material requirements planning system is based on the principle of dependent demand, a term describing the direct relationship between demand for one item and demand for a higher-level assembly part or component. For example, the demand for the number of wheel assemblies on a bicycle is directly related to the number of bicycles planned for production; further, the demand for tires is directly dependent on the demand for wheel assemblies. In most manufacturing businesses, the bulk of the raw material and in-process inventories are subject to dependent demand. An important characteristic of dependent demand items that affects timing is known as lumpy demand. Since most manufacturers assemble their products in batches or specific lot sizes to fulfill customer requirements, dependent demand items at lower levels do not exhibit uniform usage but are subject to extreme fluctuation. This creates situations in which no demand exists for weeks, and then a large quantity is required. **Figure 1** illustrates the concept of lumpy demand on three styles of drills. While demand for the end drills is constant, the plant produces them in various lot sizes, thereby creating discontinuous and discrete demands. Applications by corporations of the just-in-time (JIT) philosophy will help smooth lumpiness to a certain extent since JIT argues for running smaller lot sizes. Lumpy demand is handled in material requirements planning through the calculation of future requirements at all levels of the assembled product. Dependent demand quantities are calculated, while independent demand items are forecast. Independent demand is unrelated to a higher-level item that the company manufactures or stocks. Generally, independent demand items are carried in finished goods inventory and subject to uncertain end-customer demand. Spare parts or replacement requirements for a drill press are an example of an independent demand item.

Material resource planning. In essence, material resource planning (also termed closed-loop material

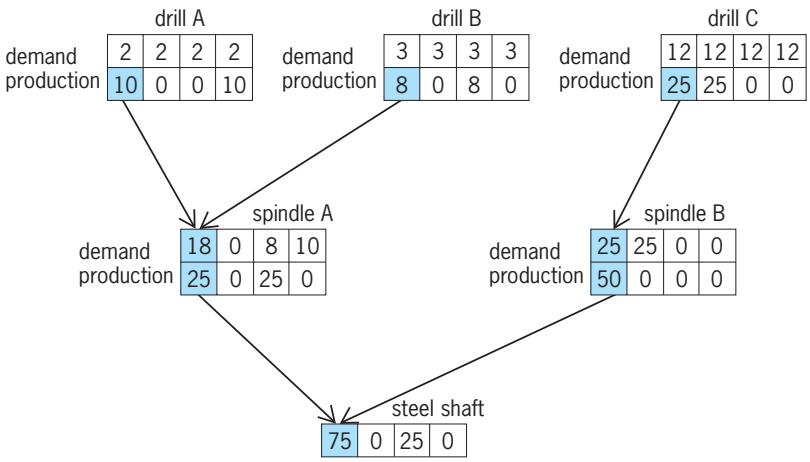

Fig. 1. Lumpy demand in manufacturing for three types of drills. The boxes represent equal time periods.

requirements planning) has the effect of extending the material requirements planning scheduling into all major functions of the firm. Material requirements planning provided firms with the ability to schedule and manage priorities. As the accuracy in material requirements planning increased, firms realized they could use these numbers in their business and financial plans. There was no longer a need for two sets of numbers. Operating and financial data are not kept on one system. Further, top management can use material resource planning as a system since it affects and is affected by sales, inventories, cash flow, production levels, and purchasing activities. Further, it ties key functional groups into the planning cycle.

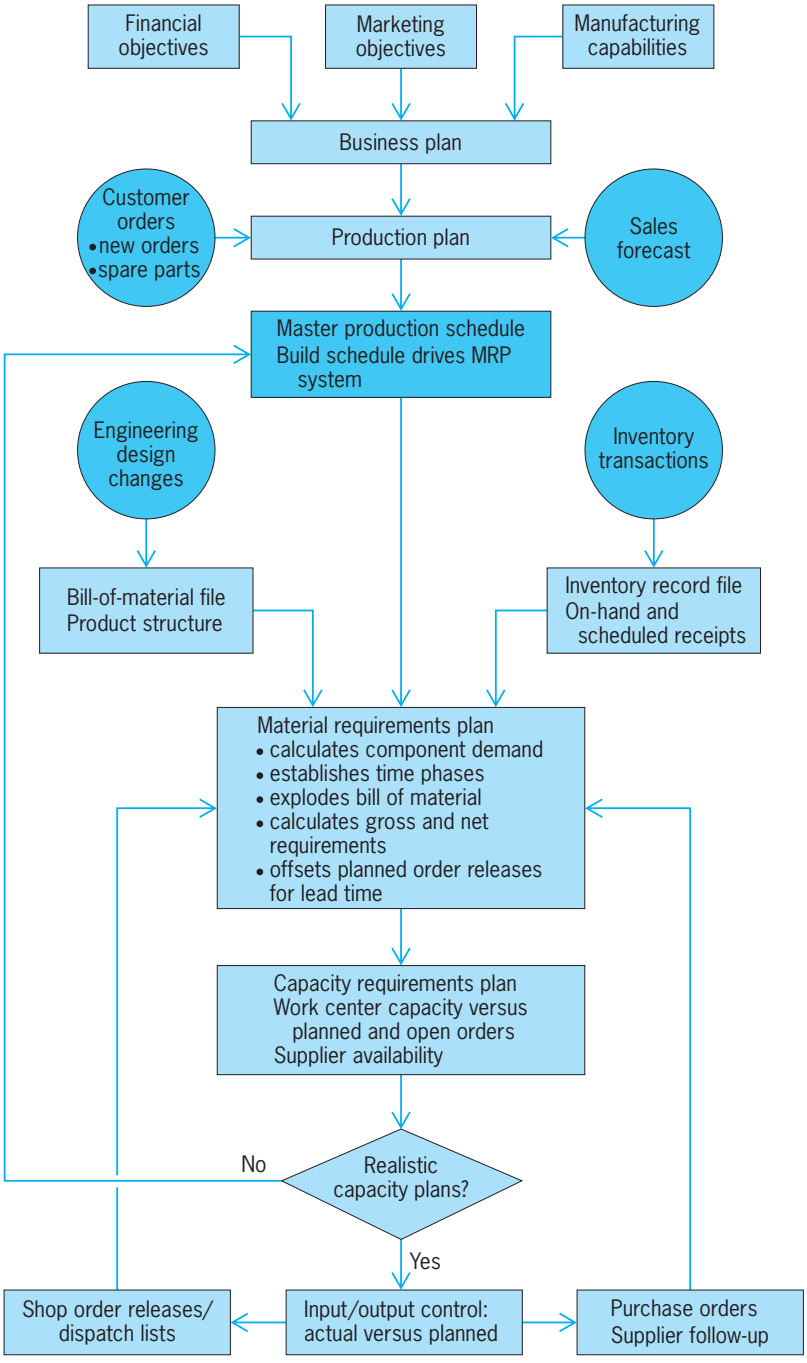

Fig. 2. Flowchart for a model material resource planning system.

For example, the marketing group can use data from master production schedules to plan and promise customer orders. The engineering group's impact on the system has become more visible since changes in design now are reflected by the information system. If drawings are not completed on time, the schedule delay will be visible on the material resource plan. Lastly, this plan permits firms to ask "what if" questions and analyze the effects of various factors on the overall operation.

Model system. A model material resource planning system is shown in **Fig. 2**. The business plan prepared by top management is based on certain expectations of sales from forecasts, firm orders, or a combination of sales forecasts and firm orders. The master production schedule refers to the products that are actually going to be produced in a particular time period. Demand inputs on the typical firm can originate from several sources: customers, warehouses, service parts, safety stock, and interplant orders. Except for make-to-order firms, the marketing forecast is adjusted periodically and reviewed by the plant manager as well as functional managers from the marketing, manufacturing, and materials groups. The marketing forecast is then translated into a production plan. This plan establishes an aggregate production rate which considers planned inventory increases or decreases. In a make-to-order company, production planning adjusts the customer order backlog; in a make-to-stock firm, the inventory levels are adjusted.

Master production schedule. While the production plan is a general plan, the master production schedule is the shop-build schedule which drives the material requirements planning system. The master production schedule is stated in bill-of-material numbers, and is used to generate the material requirements plan, and also generates the capacity requirements plan. This master schedule also lists all the end items (the items as sold by various users) by date (planned shipping period) and their quantity.

The master production schedule gives management an approximation of long-term capacity utilization, labor needs, the impact of new product plans in the shop load, and current priority status.

Bill-of-material file. This contains information about all parts and shows the dependent demand relationship of subassemblies or end items (finished product) down to components and raw material level. For example, a bill of material for a screwdriver would show the plastic handle, forged shaft, and steel from which the shaft was made. If users are to obtain valid system outputs, the bill-of-material file must be accurate and up to date, and must be suitably defined for customers, manufacturing, and purchasing. Users must ensure that the latest engineering changes are incorporated into the bill of material.

Inventory record file. This contains a record of the actual inventory level of each item and part as well as lead times. Inventory accuracy is critical in avoiding erroneous system outputs. Most users strive for 95–99% accuracy and monitor actual inventory through cycle counting, which involves periodically counting inventory.

Master Schedule		week 1	2	3	4	5	6
level 0 skateboards	Planned order release	40	0	50	0	0	60
level 1 axles lead time = 2	Project requirements	80	0	100	0	0	120
	Scheduled receipts						200
	On hand 200	120	120	20	0	0	80
	Planned order release				200	offset	
level 2 steel rod lead time = 3	Projected requirements	0	0	0	200	0	0
	Scheduled receipts				200		
	On hand 10	10	10	10	10	10	10
	Planned order release	200		offset			

Fig. 3. Material requirements plan mechanics and lead-time offsetting for skateboards.

Material requirements plan. The function of this plan is to explode the master schedule against the bill-of-material file to determine the gross requirements necessary to make the product. These gross requirements are then compared to inventory on hand to determine net requirements. The net requirements at the higher level become gross requirements at the next lower level, and so on, down through the bill of material. These requirements are offset for lead time by subtracting the lead time from the date of the net requirements. **Figure 3** shows the material requirements planning format and how lead times are offset. In Fig. 3 the term projected requirements refers to the number of items necessary to make up the next-higher assembly (for example, 40 skateboards require 80 axles). The term scheduled receipts refers to material already on order or scheduled to come in. The inventory of the item is represented by the term on hand. Planned order release (net requirements) means the number of items that manufacturing must make or purchasing must buy to meet higher-level requirements. Level 0 is the highest level and represents the end item. Lead time is the time required to acquire an item after it is ordered or manufactured.

Capacity requirements plan. This part of the system enables manufacturing to determine what capacity will be required by work centers during each time period to meet the master production schedule. The material requirements planning system will indicate which items are required and the timing of the items. The actual work load is then compared to work center capacity. If the available capacity falls short in meeting the master schedule, a decision must be made either to reduce the schedule or to expand capacity by working overtime, subcontracting, or purchasing additional capacity.

Input/output control. This part of the system monitors the levels of work into and out of each work center. Control is achieved by ensuring on-schedule job flow through various work centers. If a job slips behind schedule, its priority should be increased. When input to the factory begins to exceed output, this indicates that the production schedule has been overstated and should be reduced or the capacity expanded.

Dispatch lists and vendor follow-up lists. These help manufacturing and purchasing supervisors to determine accurate priorities. The dispatch list will print out jobs requested to be run and jobs available to be run, and the sequence in which to run them. Dispatch lists, usually generated daily, continually revise priorities on the shop floor. Follow-up lists give the purchasing department a tool to ensure that suppliers will deliver on time by providing information about requirements on a short- and long-term basis.

Advantages. Material requirements and material resource planning systems offer users multiple benefits. From a broad perspective, this type of system provides a tool for total business planning of sales, production, cash flow, and so forth. It also provides a tool for marketing and provides better customer service through higher on-time completion dates, accurate order promise dates, and follow-up information. Other productivity enhancers include more professional purchasing, lower inventories, improved planning by shop supervisors, and increased direct labor productivity. By use of the computer, material resource planning manipulates massive amounts of data to keep schedules up to date and priorities in order and valid.

The technological advances in computing and processing power, the benefits of on-line capabilities, and reduction in computing cost make computerized manufacturing planning and control systems such as material resource planning powerful tools in operating modern manufacturing systems productively. *See* ACTIVITY-BASED COSTING; INDUSTRIAL ENGINEERING; INVENTORY CONTROL; SYSTEMS ENGINEERING.

Larry C. Giunipero

Bibliography. R. B. Chase and N. J. Aquilano, *Production and Operations Management*, 8th ed., 1998; *J. N. Petroff Handbook of MRP II and JIT: Strategies for Total Manufacturing Control*, 1993; R. J. Schonberger and E. M. Knod, *Operations Management: Improving Customer Service*, 5th ed., 1993; O. W. Wight, *MRP II: Unlocking America's Productivity Potential*, 1983.

Materials handling

The movement, protection, storage, and control of materials and products throughout the process of their manufacture, distribution, consumption, and disposal, as defined by the Material Handling Industry of America. Materials handling is not just about equipment for storage and movement, it also includes controls that direct movement, packaging tools, and techniques that protect goods as they flow from point to point. However, no amount of equipment, automation, or information technology can take the place of a well-designed system that facilitates the steady flow of goods through manufacturing and distribution facilities. *See* INDUSTRIAL FACILITIES.

Materials-handling systems are designed to make sure that materials and goods are delivered to the right place, at the right time, in the right condition, with the correct information (labeling and invoices or other paperwork) in a safe and cost-effective manner as they flow through networks of suppliers and customers. Sometimes materials handling is not considered a value-added activity, but it adds value by putting things where they need to be for use at the right time. Items that are damaged or delivered to the wrong location have less value than those delivered when and where they are needed for further processing or use. This is known as the "time-and-place value" of goods and materials.

Types of handling. Materials handling is typically classified as bulk or discrete handling. Bulk handling deals with the controlled movement and storage of materials, such as coal, grains, liquids, or other types of materials, which flow from point to point and are measured in terms of their volume or mass. Mining operations, chemical processing facilities, and oil refineries are bulk-handling operations. Discrete handling deals with individual items or groups of items packaged together to form what is known as a unit load. Unit loads are stored and moved as if they were a single item. They can be items grouped together in a box, a group of boxes on a pallet, or simply one individual item. Unit-load formation is a fundamental concept of discrete handling. Many criteria influence the decision of how to form unit loads, such as size, weight, available equipment, and how often the goods are to be stored or moved. The design of manufacturing facilities, assembly lines, and warehouses are greatly influenced by the tradeoffs necessary in determining the quantity of a unit load. Examples of discrete handling are most often found in manufacturing, assembly, and warehouses. If you have ever picked up your bags from an airport luggage carousel, you have also experienced discrete-parts materials handling. *See* BULK-HANDLING MACHINES.

Equipment. The types of materials handling equipment applied depends on the goals of the facility.

Starting simple. The most common materials-handling equipment is the industrial truck (forklift), which picks up a pallet-load of goods and moves it from place to place, typically between a storage location and a truck at a loading dock. Despite its high labor cost, this is the simplest and most flexible point-to-point movement of goods. The corrugated boxes (cardboard is a different type of material) holding the goods are also part of materials handling. If they are shrink-wrapped to keep them secure, then yet another materials-handling product is being used. It is also possible to use manually powered devices, such as pallet jacks, carts, and many other kinds of equipment, to move the items. Lists of items coming into the facility, sitting in storage, being picked from storage, and being shipped out of the facility can be tracked or recorded on 3×5 index cards if the number of different kinds of items (also known as stock keeping units or SKUs) is small, the storage scheme is simple, and the flow of goods infrequent. However, as needs change and customer demands grow, the typical facility needs to consider other kinds of equipment, techniques, and information technology to meet the challenge. *See* INDUSTRIAL TRUCKS.

Growing complexity. When a facility runs out of space, it might stack pallets higher or consider adding industrial, steel storage racks to use vertical space rather than continuing to spread out horizontally. If customers would order more if they could buy smaller quantities of a greater number of items but shipped more often, then a facility might need to consider shelving, carton flow racks, carousels, and many other kinds of equipment that might better address individual items rather than pallet loads. For moving large, heavy, or bulky items, a facility might consider using cranes, hoists, and various types of attachments. To reduce the amount of packaging consumed to ship goods to regular customers, reusable pallets and containers should be considered. There is a wide range of equipment with features to fit a wide range of handling tasks. Fitting the right equipment and techniques to the task is part of materials handling. *See* ELEVATING MACHINES; HOISTING MACHINES.

New materials handling workhorses. The changing manufacturing and distribution environment requires the high-speed routing of goods through a facility's system of pathways, linking receiving and storage areas with manufacturing, packaging, assembly, and shipping points. The new workhorses of materials handling are "sortation" conveyors—equipment that makes materials flow, then diverts them to another section of conveyor—coupled with automatic identification equipment (for example, barcode scanners). Goods are free to flow to interconnected points because the identification equipment, sensors, controls, and software route and redirect them so they arrive at the right locations at the right time. Packages shipped through any of the major overnight delivery services likely have flowed through miles of conveyors and past many sensors and barcode readers. *See* CONVEYOR; MONORAIL.

Control and information systems. In addition to hardware, a materials-handling system has a control system, as well as information-gathering (sensors) and communication components. In a distribution network, manufacturing, warehousing, and transportation execution systems (often collectively

referred to as supply-chain execution system components) control the movement (when and where) of goods as they flow through the system. These systems not only track the goods in a facility, many of them also track the equipment resources used to move the goods and the labor used to perform tasks. *See* CONTROL SYSTEMS.

Planning and handling techniques. All the handling equipment and information technology must be coupled with good planning and the use of proven materials-handling techniques. For instance, nearly all manufacturing and distribution facilities tend to follow the 80/20 rule (Pareto's law); that is, 80% of the product flow will be the result of 20% of the types of items handled by the facility. As a result, it makes sense to locate the 20% of the fast-moving items closer to the people or machines performing the movements. In a technique called crossdocking, a facility is organized to coordinate the receipt and shipment of items, such that they can be taken directly to a staging area near a truck dock or put directly on a waiting truck, eliminating the need for storage. Another technique, known as task interleaving, alerts workers between tasks that there is a task, nearby or on the way to another, they could perform. Task interleaving increases worker, manufacturing, and distribution productivity. Theses are just a few examples of materials-handling techniques. There are nearly as many techniques as there are types of equipment for performing them. Applying the right equipment, information technologies, and techniques to ensure the timely, safe, and cost-effective delivery of goods and materials is the essence of materials-handling system design. *See* INDUSTRIAL ENGINEERING; PARETO ANALYSIS; PRODUCTION ENGINEERING; PRODUCTION PLANNING; TRANSPORTATION ENGINEERING.

Michael Ogle

Bibliography. R. G. Askin and C. R. Standridge, *Modeling and Analysis of Manufacturing Systems*, Wiley, 1993; S. Heragu, *Facilities Design*, PWS Publishing, 1997; F. E. Meyers and M. P. Stephens, *Manufacturing Facilities Design and Material Handling*, 2d ed., Prentice Hall, NJ, 2000; D. R. Sule, *Manufacturing Facilities: Location, Planning, and Design*, 2d ed., PWS Publishing, 1994; J. A. Tompkins et al., *Facilities Planning*, 3d ed., Wiley, New York, 2003.

Materials science and engineering

The term "materials science and engineering" emerged in the 1960s to represent how the engineering application of materials was increasingly based on scientific principles, rather than the empiricism typically used prior to World War II. Materials science focuses on understanding how the properties (or characteristics) of materials are based on their atomic- and microscopic-scale structure. The term microstructure refers to this microscopic-scale structure. Materials science grew out of the fields of physical chemistry, polymer chemistry, and condensed-matter physics. *See* PHYSICAL CHEMISTRY; SOLID-STATE PHYSICS.

The engineering of materials involves the processing, testing, and selection of materials for various design applications. Materials engineering grew out of the fields of metallurgy, plastics engineering, and ceramic engineering. *See* METALLURGY.

Types of materials. Most engineering designs incorporate a limited "menu" of materials, namely metals, polymers, and ceramics. As material properties are based on the structural arrangement of atoms, these categories follow directly from primary types of atomic bonding, namely metallic, covalent, and ionic.

Metals. Most of the elements in the periodic table exhibit atomic bonding that is metallic in nature. An alloy is a metal composed of more than one element. Copper and its alloys, such as brass (copper plus zinc), are common examples. The metallic bond involves a mobile "gas" of electrons that produces the electrical conductivity, thermal conductivity, and optical reflectivity characteristic of metals. The crystalline (regular and repeating) arrangement of atoms in metals generally provides attractive mechanical behavior in structural applications. Many alloys are reasonably strong and can be formed into practical shapes. *See* ALLOY; METAL; PERIODIC TABLE.

The dominant examples are the iron-based or ferrous alloys, which include carbon and alloy steels and the cast irons. Although ferrous alloys represent the majority of metal applications in engineering designs, nonferrous alloys also are widely used. Major examples include alloys of aluminum, magnesium, titanium, and copper. Other examples include alloys based on zinc, lead (including solders alloyed with tin), refractory metals such as tungsten, and precious metals such as gold, platinum, and silver. *See* FERROALLOY; IRON ALLOYS.

Although most commercial metal alloys are crystalline in nature, rapid processing techniques can produce noncrystalline (amorphous) alloys. The resulting lack of periodic crystalline structure provides these amorphous alloys with some attractive properties, such as high strength combined with high deformability and excellent corrosion resistance.

Polymers. Polymers are composed of a few elements in the periodic table (usually carbon and hydrogen and possibly a few of the nonmetallic elements such as oxygen, nitrogen, fluorine, and silicon) that exhibit covalent atomic bonding. Polymers with carbon backbones (a carbon-carbon bonded chain) are the most common. A very common polymer is polyethylene $(C_2H_4)_n$, where n is the degree of polymerization, a number around 1000 representing the number of ethylene monomers linked by covalent bonding. Other polymers can contain oxygen (for example, acrylics), nitrogen (for example, nylon), fluorine (for example, fluoropolymers), and silicon (silicones). *See* POLYACRYLATE RESIN; POLYAMIDE RESINS; POLYFLUOROOLEFIN RESINS; POLYMER; POLYOLEFIN RESINS; SILICONE RESINS.

Polymers are generally good electrical insulators because directional covalent bonding between adjacent atoms usually does not provide "free" electrons

for conduction. The use of polymeric insulation on electrical wires is a practical example. Polymers also can be optically transparent (for example, clear plastic wrap for food). The alternative name "plastic" comes from the extensive formability of many polymers during fabrication. *See* DIELECTRIC MATERIALS.

Polymers composed of high-molecular-weight molecules, such as $(C_2H_4)_n$ (for example, $n > 100$), often have a "spaghetti-like" structure, with weak secondary nonbonding interactions between molecules. The result is relatively low strength compared to metals. Nonetheless, many polymers have been engineered to have sufficient strength and stiffness which, when combined with their characteristically low density, allows them to be increasingly popular substitutes for traditional structural metals. Contemporary automotive design provides numerous examples of metal substitution by polymers.

Ceramics (and glasses). Ceramics can be defined as nonmetallic and inorganic materials. Ceramics are chemical combinations of at least one metallic and at least one nonmetallic element (especially oxygen, with others possibly including carbon, nitrogen, phosphorous, and sulfur). Aluminum oxide (Al_2O_3) is a common example in which the metallic element aluminum is combined with the nonmetallic element oxygen. In fact, such chemical combinations are a fundamental tendency in nature, where metals chemically combine with nonmetallic elements from the environment. The rusting of iron is an example, both familiar and costly. Engineers also use similar environmental reactions to their advantage. Aluminum is a durable metal for structural applications because it can be anodized, a process in which a thin layer of aluminum oxide is produced on its surface. The aluminum oxide layer, in turn, usually protects the aluminum from further environmental degradation. *See* CERAMICS.

The ionic bond between metallic and nonmetallic atoms is a strong one. In aluminum oxide, the aluminum is a cation, Al^{3+}, and oxygen is an anion, O^{2-}. These oppositely charged ions are strongly attractive in an ionic bond. The thermal stability associated with the ionic bond makes ceramics resistant to high temperatures. The melting point of aluminum is 660°C (1220°F), while the melting point of aluminum oxide is 2020°C (3670°F). This heat resistance leads to the use of ceramics in refractory applications such as furnaces and boilers. *See* REFRACTORY.

Ceramics usually are crystalline in nature. Compared with metals and alloys, the greater structural complexity of ceramic structures leads to generally brittle mechanical behavior, limiting the applications of ceramics in many structural designs. *See* BRITTLENESS.

Although forming amorphous alloys is difficult, forming noncrystalline ceramics, called glasses, is relatively easy, as the crystallization of molten oxides can be a sluggish process. The most common examples are the silicate glasses, based on the mineral silicon dioxide (SiO_2). After melting, many of the silicate materials can be cooled to a rigid state, while retaining the random atomic structure of the melt. Common window and container glasses are made in this way, with a typical composition (by weight) of roughly 75% SiO_2, 15% Na_2O, and 10% CaO. *See* GLASS.

A common theme in processing ceramics and glasses is the presence of porosity (in the form of tiny air bubbles). These small bubbles serve as light-scattering centers, and as little as 3% porosity can turn a transparent material into a completely opaque one. The chalky appearance of many ceramics is the result. Porosity also weakens the material under structural loads.

Composites. Metals, polymers, and ceramics, which are fundamentally based on atomic bonding, cover the basic categories of structural materials. Engineers have developed many advanced materials based on the microscopic-scale combinations of them, resulting in a fourth category called composites. A common example is fiberglass, a composite of glass fibers (a few micrometers in diameter) embedded in a polymer matrix. In this case, the high strength of the small-diameter glass fibers is combined with the flexibility of the polymer matrix. Typical of structural composites, the fiberglass has properties superior to either component by itself. (Compared to fiberglass, the pure glass is more brittle and the pure epoxy is weaker.) More sophisticated composites include poly(*p*-phenylene terephthalamide) [Kevlar®] fibers and graphite fibers in various polymeric matrices, such as epoxy, polyester, polyetheretherketone (PEEK™), and poly(phenylene sulfide) [PPS]. *See* COMPOSITE MATERIAL; METAL MATRIX COMPOSITE; POLYMERIC COMPOSITE.

Not all composites involve fiber reinforcement. Aggregate composites use particles embedded in a matrix. Concrete, with rock and sand in a calcium aluminosilicate (cement) matrix, is a common example. Tungsten carbide particles in a matrix of cobalt make excellent cutting tools. *See* CONCRETE.

Semiconductors. Many structural materials can be classified adequately by the four categories described above. Materials also can be classified based on electrical conductivity rather than atomic bonding. Electrical classification provides a fifth category of materials—semiconductors. While metals are typically good electrical conductors and polymers and ceramics/glasses are typically electrical insulators, composites tend to have electrical properties that are the average of their individual components. Since the invention of the transistor at Bell Labs in 1948, covalently bonded semiconductors, with intermediate levels of electrical conductivity, have played an increasingly critical role in modern technology. The primary example is silicon, a central component of modern, solid-state electronics. Germanium is chemically similar to silicon and is a semiconductor widely used for electronic devices. Chemical compounds of elements close to silicon and germanium in the periodic table often display semiconduction. For example, gallium arsenide (GaAs) is a high-temperature rectifier and laser material. *See* SEMICONDUCTOR.

Advances in materials science and engineering. The field of materials science and engineering is a

dynamic one, with new materials and processing technologies developed by materials scientists constantly being applied by materials engineers to new engineering designs. Recent examples include the application of certain materials with zero electrical resistance (superconductors) as thin-film filters for improved cellular-telephone base stations. Micro-electro-mechanical systems (MEMS) include microscopic-scale gear systems fabricated by technologies developed for integrated circuits. And, finally, nanotechnology involves structures developed on the nanometer (10^{-9} m) scale, rather than the micrometer (10^{-6} m) scale. The resulting nanomaterials can display significantly improved mechanical, electrical, magnetic, thermal, and optical properties, compared to their counterparts on a coarser scale. *See* MICRO-ELECTRO-MECHANICAL SYSTEMS (MEMS); NANOTECHNOLOGY; SUPERCONDUCTIVITY.

James F. Shackelford

Bibliography. M. F. Ashby, *Materials Selection in Mechanical Design*, 2d ed., Butterworth-Heinemann, 1999; W. D. Callister, Jr., *Materials Science and Engineering: An Introduction*, 6th ed., Wiley, 2003; J. F. Shackelford, *Introduction to Materials Science for Engineers*, 6th ed., Prentice-Hall, 2005; W. F. Smith, *Foundations of Materials Science and Engineering*, 3d ed., McGraw-Hill, 2005; M. A. White, *Properties of Materials*, Oxford University Press, 1999.

Maternal behavior

The pattern of care given an offspring by its mother. Many species reproduce generation after generation without receiving or providing any parental care. Insects and fish commonly produce vast numbers of offspring that they neither feed nor defend, resulting in the loss of many offspring to predators and to other hazards. Their great numbers, however, ensure that some will survive and reproduce. Also, if the young of a species are self-sufficient at birth or if they mature very rapidly after birth, they can often survive and reproduce with little parental care.

Biological need. Parental behavior is most highly developed in species that produce only a few offspring at once, mature slowly, and have complex behavior patterns that can be learned only through extended practice. Parental behavior can involve as little as hiding the young and never seeing them again or it can involve years of feeding, defending, and teaching. In most species that care for their young after birth, the female does most or all of the work. The biological explanation for this arises from the fact that a male can father vast numbers of offspring, whereas a female can bear only a few. Each offspring that fails to survive or reproduce can represent a significant proportion of the female's lifetime reproductive output. Thus, the females that pass their genes on to subsequent generations in greatest numbers are not those that bear the most young but those that invest more in caring for the few young they produce.

Active care of the young by the male is most common when males of a species limit themselves to one or a few female partners. That is, when males forego the strategy of having many offspring, there is a premium on the success of each one. Examples of paternal investment are seen in many bird species and in monogamous primates such as humans and marmosets. The extended period of infancy and childhood in humans has also favored the evolution of paternal care of offspring. Prolonged immaturity increases the amount of care that each child requires and the number of children that must be cared for at once. Nonetheless, in most human cultures and under most circumstances, mothers contribute more than fathers. *See* REPRODUCTIVE BEHAVIOR.

Eliciting and maintaining maternal behavior. Factors that influence the onset of maternal behavior include physiological and psychological factors related to pregnancy, hormonal influences associated with childbirth, the behavior of the newborn, and cultural factors such as learning and social traditions. Among rodents, exposure to female hormones (estrogens) can cause both females and males to display maternal behavior, but hormone exposure is not necessary. Females who have never given birth and whose estrogen production is blocked will display maternal behavior over a period of time if they are simply exposed to the young. With longer exposure to the young, even males will begin to lick them and retrieve them when they leave the nest. Since the males do not produce female hormones in response to the young, the behavior of the offspring is itself a powerful stimulus for care-giving behavior. *See* ESTROGEN.

Although hormones play necessary roles in recovery from pregnancy and in milk production, there is no evidence that they play a critical role in any other aspect of human maternal behavior. Cultural factors and the behavior of the newborn are the primary cues that prompt human mothers to care for their young. Many factors contribute to maternal competence, that is, the mother's skill and consistency in caring for her infant or child. Hormones may increase her readiness to respond to infant behavior for a short time after birth, but it also seems likely that species' learning abilities have evolved in such a way that patterns of maternal behavior are easily learned. Ultimately, experience and practice are the dominant factors in human maternal behavior.

Human infants have a wide range of behaviors that communicate what their needs are and how urgent they are at a given moment, including smiling, crying, grasping, cuddling against the mother, and even changes in skin color if the infant is cold or extremely upset. Infants do not necessarily perform these behaviors with the intention of securing the mother's care, but the behaviors have the predictable outcome of attracting the mother's attention and care. By the time the child is two years old, language becomes a powerful guide to maternal care. *See* DEVELOPMENTAL PSYCHOLOGY.

Mothers can often tell what a baby needs from the context in which the demand occurs. For example,

the cries of a recently fed baby are unlikely to stem from hunger. There is no evidence that human mothers are biologically endowed with knowledge of appropriate child care. Observation of other mothers, help from parents, and general problem-solving abilities are key factors in human maternal competence. In most cultures, females begin to learn maternal behavior in early childhood. Adults encourage an interest in infants and provide opportunities for girls to practice parental behavior in their play and in caring for younger children. Much of what a mother needs to know is learned by trial and error after the birth of her baby.

Dimensions of maternal behavior. Mothers differ in the patterns of care they provide. Maternal behavior with infants is usually measured in terms of timing and appropriateness, and in terms of cooperation versus interference with the baby's ongoing behavior. After infancy, maternal behavior is typically demonstrated in expressions of warmth rather than hostility, or restrictiveness rather than permissiveness. These variables are modest but consistent predictors of the child's later behavior, just as a lack of supervision is the strongest predictor of delinquency.

Parenting stress and parenting failure. If a mother is very young, living in isolation, under a great deal of stress, or impaired by drugs or mental disorder, she may find caring for her infant to be a difficult learning task, and those same factors are associated with child neglect and physical abuse. Neglect and abuse occur in all social classes, but a limited education, stress, drugs, and mental disorder are more common when families live in isolation and poverty. *See* INSTINCTIVE BEHAVIOR; PERSONALITY THEORY.

Everett Waters; German Posada

Bibliography. L. Hoffman, R. Gandelman, and H. R. Schiffman (eds.), *Parenting*: *Its Causes and Consequences*, 1982; M. Lamb et al. (eds.), *Infant-Mother Attachment*: *The Origins and Developmental Significance of Individual Differences in Strange Situations Behavior*, 1985; P. Mussen and E. M. Hetherington (eds.), *Handbook of Child Psychology*, 1983; R. Trivers, *Social Evolution*, 1985.

Maternal influence

Effects on development that are attributable specifically to the maternal parent or to maternally inherited factors. This influence can take a variety of forms, including maternal-specific inheritance of genetic material (for example, mitochondrial DNA), parent-specific epigenetic modification of genes (genomic imprinting), placement of molecules into the oocyte prior to fertilization, and interactions with the maternal parent during development.

The term "parent-of-origin effects" describes instances where an offspring's phenotype is asymmetrically dependent on the genotypes or phenotypes of its maternal and paternal parents. In most cases where such asymmetry exists, it is the maternal parent that wields the greater influence. This maternal advantage derives in part from the greater size of the oocyte, which means that the mother contributes more cytoplasmic material to the zygote than the father does. This asymmetry is enhanced in species where a part of the offspring's development occurs in physical contact with the mother, as in viviparous animals and many plants. Postnatal care, if present, is often provided preferentially by the mother.

Maternal DNA. One source of maternal influence is the inheritance of DNA specifically from the mother. Organelles that contain their own DNA, such as mitochondria and chloroplasts, are inherited cytoplasmically. Mitochondria are inherited predominantly, if not exclusively, from the mother. Many of the genes encoded by the mitochondrial DNA are involved in oxidative phosphorylation. A number of maternally transmitted diseases are characterized by oxidative phosphorylation defects; they affect in particular the central nervous system and muscle tissues.

The pattern of inheritance for chloroplasts varies, and apparently there may be different plant species in which chloroplasts are inherited exclusively maternally, exclusively paternally, and biparentally. The best-known phenotype associated with chloroplast inheritance occurs in the four-o'clock plant (*Mirabilis jalapa*), where leaf color varies depending on the ability of the chloroplasts to produce chlorophyll. In this species, chloroplasts, and therefore the leaf color trait, are always maternally inherited. *See* DEOXYRIBONUCLEIC ACID (DNA); MITOCHONDRIA; PLANT CELL.

Cytoplasmic factors. Many insect species possess cytoplasmic symbiotic bacteria, such as the well-known members of the *Wolbachia* and *Buchnera* genera. Inheritance of these bacteria bears some similarity to that of the cytoplasmic organelles, which may themselves be descended from bacteria that were once free-living. In many cases, these bacterial endosymbionts are restricted to specific host cells (bacteriocytes). Although cases of horizontal transfer have been documented, the predominant mode of propagation for these bacteria is maternal transmission. In this case, newly formed embryos are colonized by the bacteria present in the mother.

Maternal influence may also be exerted through molecules placed in the egg during oogenesis. Following fertilization, the newly formed genome in a zygote is not immediately transcriptionally active. In some cases, these genes are not transcribed until multiple rounds of cell division have occurred. During this earliest phase of development, the RNA and protein in the embryo predominantly reflect the genes of the mother. Small quantities of protein and mRNA are also carried into the zygote by the sperm, providing a possible source of paternal influence on early embryonic development. However, the much smaller size of the sperm makes the maternal contribution dominant in this context (**Fig. 1**).

Proteins in the egg that are active after fertilization are referred to as maternal-store proteins. In vertebrates, oogenesis is arrested in meiosis I, in some cases for years. These arrested oocytes still contain both of the mother's alleles at each diploid locus.

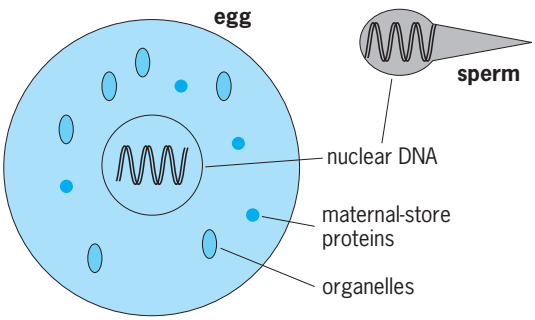

Fig. 1. In cytoplasmic inheritance, the gamete produced by the maternal parent is typically much larger than the gamete of the male parent. As a result, the egg contributes the majority of the cytoplasmic material to the zygote, including organelles that contain their own DNA as well as messenger RNA and proteins.

Maternal-store proteins are synthesized at this stage and inherited by the mature oocyte. In many invertebrates, polyploid "nurse cells" produce mRNA and proteins, which are transferred into oocytes through cytoplasmic bridges.

The reliance on maternal-store factors in early development means that there are certain phenotypes observable in offspring that depend on the genotype of the mother rather than that of the offspring itself. For instance, in preimplantation mouse embryos the maintenance of certain patterns of DNA methylation depends on the enzyme Dnmt1o, an oocyte-specific splice variant of the somatic maintenance methyltransferase Dnmt1. Homozygous knockout (*Dnmt1o*$^{-}$/*Dnmt1o*$^{-}$) offspring of a heterozygous (*Dnmt1o*$^{+}$/*Dnmt1o*$^{-}$) mother are phenotypically normal. Heterozygous offspring of a mother that is homozygous for the *Dnmt1o* knockout suffer methylation defects and embryonic lethality. *See* CELL ORGANIZATION; GENE ACTION; OOGENESIS; SPERMATOGENESIS.

Genomic imprinting. In some species, asymmetric parental influence derives from differential epigenetic modification of genes inherited by the offspring, or "genomic imprinting." An imprinted gene is one where an allele's pattern of expression differs depending on whether it was inherited from the mother or the father. In the simplest instances, one of the two alleles is active and one is transcriptionally silent (**Fig. 2**). In more complex cases, clusters of imprinted genes are coregulated, and various transcripts (including noncoding antisense RNA and splice variants) are produced from the maternally and paternally derived alleles.

The epigenetic modifications involved in imprinting include DNA methylation as well as histone modifications, such as methylation and acetylation. Epigenetic propagation mechanisms maintain these allele-specific modifications across cell divisions, so that each adult somatic cell contains two differentially marked alleles. These modifications are erased and reset in each generation in the germ line.

Genomic imprinting is the result of an evolutionary conflict between the maternally and paternally derived alleles within an individual. The optimal expression strategy for an allele may be different depending upon whether the allele is maternally derived or paternally derived. Alleles at an imprinted locus can be thought of as possessing a unique form of phenotypic plasticity—taking on different strategies depending on their parent of origin.

Imprinted genes have been identified in mammals and angiosperms, where the early part of development occurs in close physical contact with the maternal parent. In these cases, paternally derived genes are selected to place a greater demand for resources on the mother. Maternally derived genes favor more restraint, preserving maternal resources for the mother's other offspring. Many imprinted genes directly influence growth and resource demands during development. At loci where increased expression enhances growth, imprinted genes are paternally expressed and maternally silenced. At growth-suppressing loci, the opposite pattern of expression holds.

The pattern of allele silencing in genomic imprinting results in systematic functional differences between the maternally and paternally derived genomes in mammals and angiosperms. One consequence of this functional nonequivalence is that both the maternally derived and paternally derived chromosomes are required for successful development. Mouse zygotes formed from two maternally derived or two paternally derived pronuclei are not viable, and parthenogenesis (asexual female reproduction) is not seen in mammals. This contrasts with species that lack genomic imprinting, such as birds, amphibians, and insects, where it is possible to form viable offspring with two male or two female parents.

The dependence of normal development on particular epigenetic modifications produces one of the technical difficulties in mammalian cloning. Germ

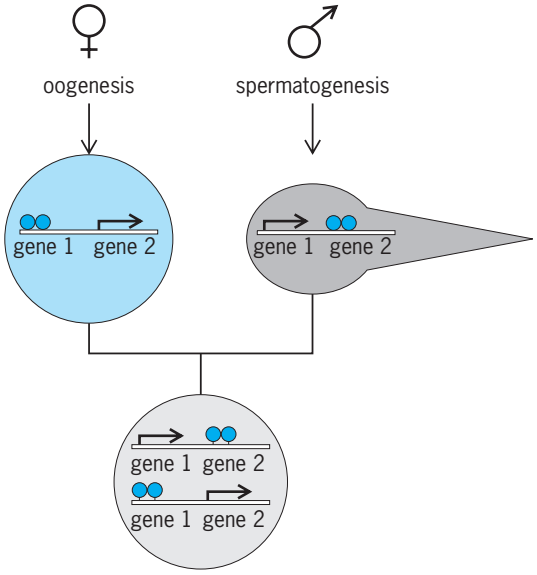

Fig. 2. In genomic imprinting in mammals and angiosperms, some genes are epigenetically modified in the germ line. Typically, only the copy inherited from one of the parents is transcriptionally active. This makes the offspring functionally haploid at these loci.

cells, which have been retained in or returned to a pluripotent state, contain only one of the two required patterns of imprinting. In many cases, the failure of cloning procedure to produce viable tissues or animals is associated with a failure of epigenetic reprogramming at imprinted loci.

Postfertilization influences. A final source of maternal influence results from interactions between the mother and offspring after fertilization. In many plants and in viviparous animals, the early part of development occurs in close physical contact with the mother. In the cases of mammals and angiosperms, specific organs exist (the placenta and endosperm, respectively) that mediate nutrient transfer from mother to offspring. Implantation experiments have demonstrated effects of the intrauterine environment on development in mice.

Further maternal influence arises in postnatal care. For instance, mammalian breast feeding involves the transfer of antibodies as well as nutrients to offspring. An offspring's immunity in the earliest stages of life therefore depends on its mother's genotype at various immune system loci, as well as her history of antigen exposure.

Where additional parental care is provided or where there is significant learning by offspring, the result is additional maternal or paternal influence. A trivial example might be the patrilineal "inheritance" of the last name in many human cultures. A more complex example would be song imitation and learning in songbirds. For example, in the zebra finch (*Taeniopygia guttata*), male birds' songs resemble those of their fathers as a result of cultural transmission. *See* DEVELOPMENTAL BIOLOGY; DEVELOPMENTAL GENETICS.

Bibliography. C. W. Birky, The inheritance of genes in mitochondria and chloroplasts: Laws, mechanisms, and models, *Annu. Rev. Genet.*, 35:125–148, 2001; A. Qvarnstrom and T. D. Price, Maternal effects, paternal effects and sexual selection, *Trends Ecol. Evol.*, 16(2):95–100, 2001; W. M. Rideout, K. Eggan, and R. Jaenisch, Nuclear cloning and epigenetic reprogramming of the genome, *Science*, 293(5532):1093–1098, 2001; W. Tadros and H. D. Lipshitz, Setting the stage for development: mRNA translation and stability during oocyte maturation and egg activation in *Drosophila*, *Dev. Dynamics*, 232(3):593–608, 2005; J. F. Wilkins and D. Haig, What good is genomic imprinting: The function of parent-specific gene expression, *Nat. Rev. Genet.*, 4(5):359–368, 2003.

Mathematical biology

The application of mathematics to biological systems. Just as physics underlies many engineering technologies, biology serves as a foundation for such disciplines as medicine, agriculture, animal husbandry, and environmental sciences, in which mathematical analyses have proved indispensable. Mathematical biology spans all levels of biological organization and biological function, from the configuration of biological macromolecules, as exemplified by the folding of proteins and the recognition properties of active sites in enzymes and receptors, to the entire ecosphere over the course of evolutionary time.

The important role of physics in the development of mathematical biology is natural, considering that physics is a much older science than biology. The influence of physics has been twofold. On the one hand, organisms simply are material systems, albeit of a very special kind, and presumably can be analyzed in the same terms and in the same way as any other material system. Reductionism, the theory that biological processes find their resolution in the particularities of physics, finds its practical embodiment in biophysics. Thus, one of the roots of mathematical biology is what was originally called mathematical biophysics. On the other hand, other early investigations in mathematical biology, such as population dynamics (mathematical ecology), did not attempt such a reductionistic analysis. Instead, they exploited the form of such analyses, such as using differential rate equations, but they expressed their analyses in frankly biological terms rather than physical terms. Such approaches were guided by analogy with mathematical physics rather than by reduction to physics and as a result rest on the form rather than the substance of physics. *See* BIOPHYSICS; PHYSICS.

Both of these approaches are important, especially since organisms possess characteristics (particularly in their development and evolution) that have no obvious counterpart in inorganic systems. As a result, mathematical biology has acquired an independent and unique character. In several important cases, these characteristics have required a reconsideration of physics itself, as in the impact of open systems on classical thermodynamics. *See* OPEN-SYSTEMS THERMODYNAMICS (BIOLOGY).

Surrogacy and models. The idea that something can be learned about a system by studying a different system, or surrogate, is central to all science, experimental as well as theoretical. Indeed, experimental or observational data would be useless if it pertained only to the specific system under observation. The relation between a system and its surrogates is embodied in the concept of a model. *See* MODEL THEORY.

For example, it is commonplace to use a laboratory animal such as a rat as a surrogate for a human. Data drawn from study of the rat can presumably be extrapolated to pertain to the human. It is likewise commonplace to treat a homogenate or extract as a surrogate for the intact material from which the extract was taken.

The basic idea of mathematical biology is that an appropriate formal or mathematical system may similarly be used as a surrogate for a biological system; that is, scientists can learn about an organism by interrogating an appropriate mathematical model the same way that they can learn about a human by interrogating a surrogate experimental animal. The use of mathematical models offers possibilities that, in many important ways, far transcend what can be

done on the basis of observation and experiment alone.

The richness of mathematical biology can become apparent if the mathematical roots of the concept of surrogacy itself are explored. For example, morphological differences between related species can be made to disappear by means of relatively simple coordinate transformations of the space in which the forms are embedded (**Figs. 1** and **2**). Surrogacy explicitly becomes a matter of intertransformability, or similarity, and what is true for morphology also holds true for other functional relationships that are characteristic of organisms, whether they be chemical, physical, or evolutionary. The concept of surrogacy is not confined to biology: the same kinds of ideas underlie the use of scale models in engineering design, the notions of congruence and symmetry in geometry and algebra, and the capability for analog computation in general.

In more modern terminology, these assertions of surrogacy and modeling can be restated: closely related implies similar. This is a nontrivial assertion: "closely related" is a metric relation pertaining to genotypes, whereas "similar" is an equivalence relation based on phenotypes. It is the similarity relation between phenotypes that, of course, provides the basis for surrogacy. Thus the question immediately arises: given a genotype, how far can it be varied or changed or mutated, and still preserve similarity?

Such questions fall mathematically into the province of stability theory, particularly structural stability. The interrelations between metric approximation and similarity is an exceedingly deep and subtle one. Under very general conditions, there exist many genomes that are unstable (bifurcation points) in the sense that however high a degree of metric approximation is chosen, the associated phenotypes may be dissimilar, that is, not intertransformable. That observation by R. Thom provides the basis for his theory of catastrophes and demonstrates the complexity of the surrogacy relationship. The fundamental importance of such ideas for phenomena of development, for evolution (particularly for macroevolution), and for the extrapolation of data from one species to another, or the relation between health and disease, is evident. It is also clear that a coherent mathematical framework is necessary for exploring these ideas. *See* CATASTROPHE THEORY.

Metaphor. A distinct but closely related group of ideas that are characteristic of mathematical biology may be described as metaphoric. One example of a metaphoric approach is the study of brain activities through the application of the properties of neural networks, that is, networks of interconnected boolean (binary-state) switches (**Figs. 3** and **4**). Appropriately configured switching networks are known to exhibit behaviors that are analogous to those that characterize the brain, such as learning, memory, and discrimination. That is, networks of neuronlike units can automatically manifest brainlike behaviors and can be regarded as metaphorical brains. Generally there is no attempt to explicitly model a particular brain as a particular neural network; the idea rather is to develop general properties of such networks, which might lead to a deeper understanding of those particular biological networks called brains.

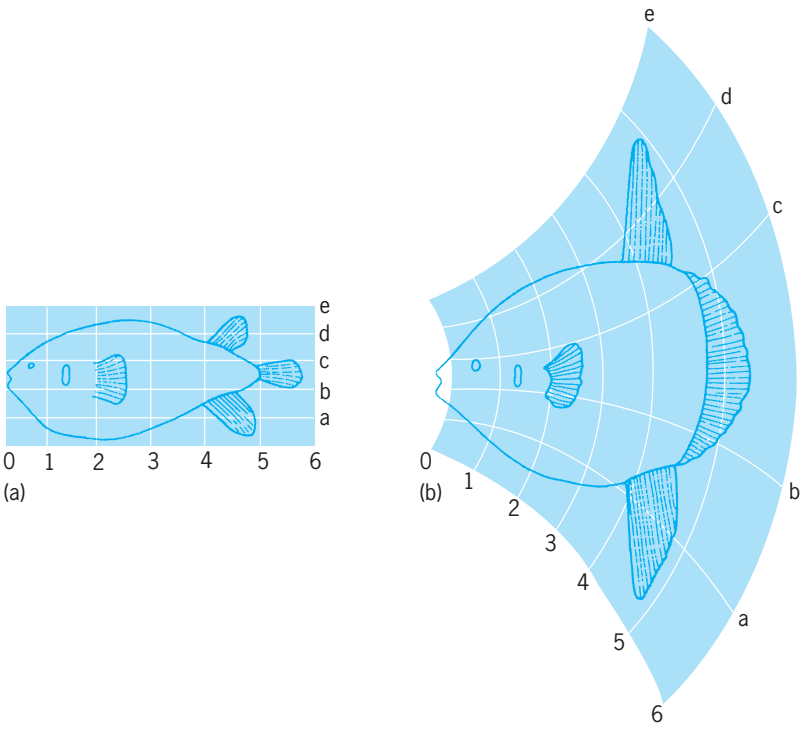

Fig. 1. The fishes (*a*) *Diodon* and (*b*) *Orthagoriscus*, showing the basic relatedness of the two genera by the superimposed grids. (*After D. W. Thompson, On Growth and Form, Cambridge University Press, 1917*)

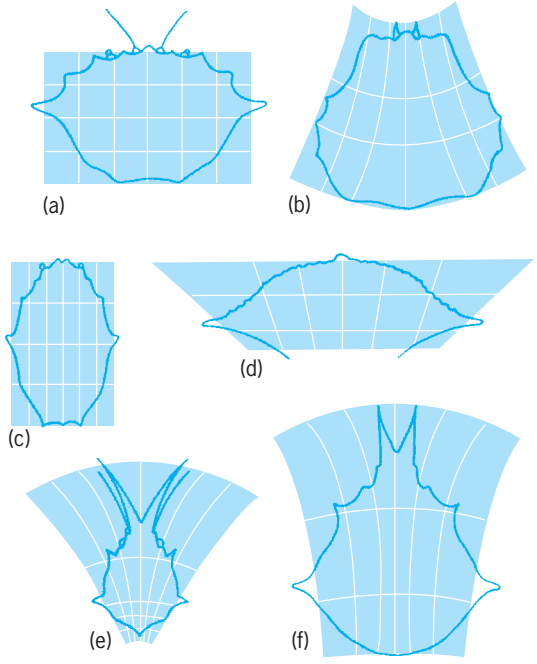

Fig. 2. Crab carapaces from species *b–f* as deformations of *a*. By transforming the grid coordinates, the variation in the shapes of the carapaces is minimized. (*After D. W. Thompson, On Growth and Form, Cambridge University Press, 1917*)

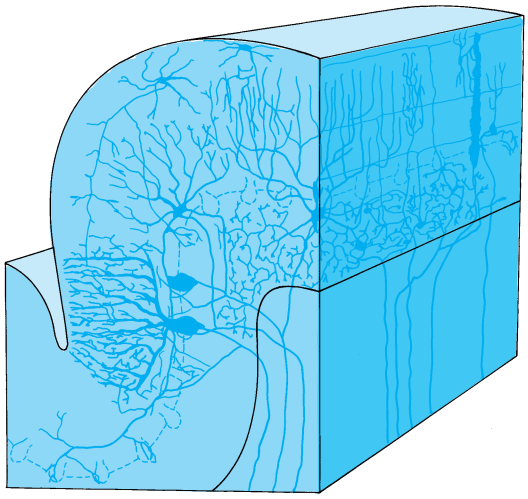

Fig. 3. Section of cerebellum, a "real" network of neurons. (*After K. N. Leibovic, ed., Symposium on Information Processing in the Nervous System, Springer-Verlag, 1969*)

Such metaphorical ideas lead to new ways of relating the behaviors of different biological systems and even of systems that have biological and nonbiological origins. For instance, the boolean neural nets also underlie digital computation, leading to the relationship that is noted between brains and computers. This relationship is explored in the hybrid area of artificial intelligence. The same mathematical formulation of switching networks arises in genetic and developmental phenomena, such as the concept of operon, and in other physiological systems, such as the immune system. *See* ARTIFICIAL INTELLIGENCE; NEURAL NETWORK; OPERON.

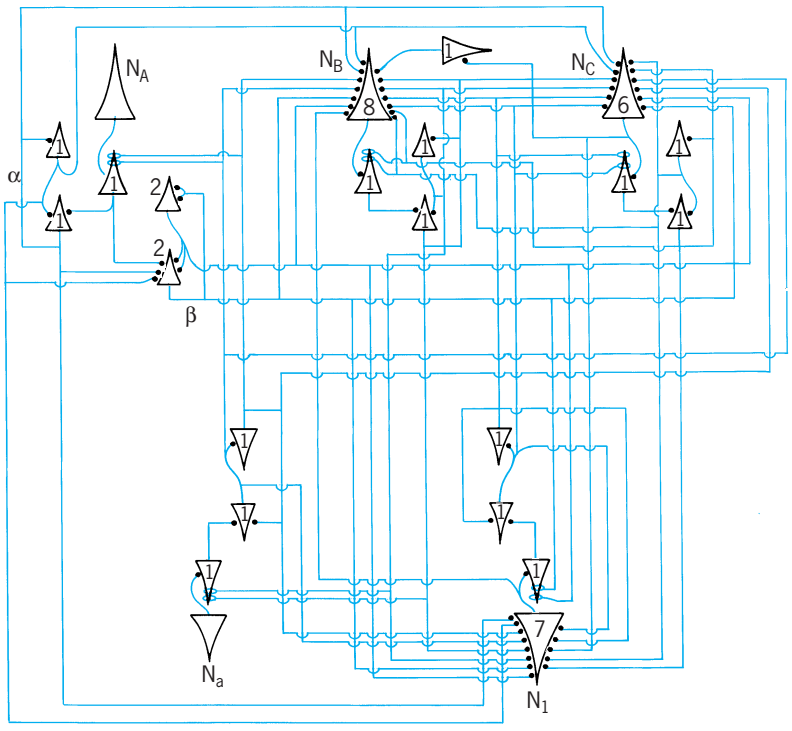

Fig. 4. Neural network that can "reason" syllogistically. Numbers inside neurons (triangles) indicate thresholds, the amount by which excitation must exceed inhibition at one instant in order to fire at the next instant. Triangles without numbers are delays. (*After N. Rashevsky, The neural mechanism of logical thinking, Bull. Math. Biophys., 8:29–40, 1946*)

Another important example of metaphor in biology is morphogenesis, or pattern generation, through the coupling of chemical reactions with physical diffusion. Chemical reactions tend to make systems heterogeneous, diffusion tends to smooth them out, and combining the two can lead to highly complex behaviors. Again, the intention is not to make specific models of specific pattern-generating systems. Rather, since reactions and diffusions typically occur together in biological systems, the idea is to explore the general properties of such systems to illuminate pattern generation in general.

Such ideas turn out to be closely related to those of bifurcation and catastrophe and have a profound impact on physics itself, since they are inherently associated with systems that are thermodynamically open and hence completely outside the realm of classical thermodynamics. The behavior of such open systems can be infinitely more complicated than those that are commonly explored in physics. Open systems may possess large numbers of stable and unstable steady states of various types, as well as more complicated oscillatory steady-state behaviors (limit cycles) and still more general behaviors collectively called chaotic. Changes in initial conditions or in environmental circumstances can result in dramatic switching (bifurcations) between these modes of behavior. *See* CHAOS.

Technological aspects. Biological science underlies a host of basic technologies. Perhaps the biotechnology that has affected everyone most directly is medicine. Medicine can be regarded as a branch of control theory, geared to the maintenance or restoration of a state of health. It is unique in that the systems needed for control are themselves control systems that are far more intricate and complex than any that can be fabricated. In addition to the light it sheds on the processes needed for control, mathematical biology is indispensable for designing the controls themselves and for assessing their costs, benefits, safety, and efficacy.

In general, any theory of control is a matter of design rather than of analysis, and its object is to produce an algorithm, or protocol, that will achieve optimal results. Mathematical biology allows one to relate, and learn about, systems of different characters through the exploitation of their mathematical commonalities. Biology has many optimal designs and optimal controls, which are the products of biological evolution through natural selection. In an exact sense, the design of optimal therapies, for example, is analogous to the generation of optimal organisms, making the concept of surrogacy even more significant. The mathematical theory appropriate for analyzing one discipline of biology, such as evolution, itself becomes transmuted into a theory of control in an entirely different realm.

The same holds true for other biotechnologies. The livelihood of entire nations can rest on

exploitation of biological populations, for example, of fish or forest timber. As with biomedicine, the object is to design strategies for optimally exploiting the resource in question, deriving the maximal economic benefit without irreversibly compromising the resource itself, or inadvertently, the larger system to which the resource belongs and on which it depends. Mathematical biology is called upon to play two roles: it is required to understand the basic biological nature of the resource itself, and to use that understanding in the design of optimal strategies for the harvesting and the maintenance of that resource. *See* MATHEMATICAL ECOLOGY. Robert Rosen

Bibliography. P. L. Antonelli (ed.), *Mathematical Essays on Growth and the Emergence of Form*, 1985; J. A. Metz and O. Diekmann (eds.), *Physiologically Structured Populations*, 1986; L. M. Ricciardi (ed.), *Biomathematics and Related Computational Problems*, 1988.

Mathematical ecology

The application of mathematical theory and technique to ecology. The earliest studies in ecology were by naturalists interested in organisms and their relationships to the environment. Such investigations continue to this day as an active and central part of the subject, and have focused attention on understanding the ecological and evolutionary relationships among species. A large mathematical literature has arisen as an aid to the formalization of concepts and ideas; the underlying goal has been to understand patterns of nature. For the most part, such approaches are retrospective, designed to help in understanding how current ecological relationships developed, and to place that development within appropriate evolutionary context.

The second major branch is applied ecology, and derives from the need to manage the environment and its finite resources. Fisheries, forestry, agriculture, and epidemiology are all highly developed subjects that have arisen from well-defined applied needs. Here the necessity for rigorous mathematical treatments is obvious, but the goals are quite different from those in evolutionary ecology. Management and control are the objectives, and the relevant time horizon lies in the future. The focus is no longer simply to derive understanding and explanation; rather, one seeks methods for prediction and algorithms for control.

That such a dichotomy exists does not mean that pure and applied investigations are disjunct, nor that they are as simply categorized as the above suggests. Yet an appreciation for these opposing tendencies can help to explain the differences among some of the major schools of thought.

Classical theory. The roots of mathematical ecology can be traced to demographic studies as early as the seventeenth century. The well-known arguments of Thomas Malthus and others, that a population growing without bound would soon outstrip the capability of the environment to support it, were based on detailed analyses of births and deaths in human populations. These analyses led to the first important mathematical efforts in ecology, namely those of P. F. Verhulst and others to describe the dependence of population growth rate on population size, and to infer the consequences of such relations. Models of the type developed by Verhulst are called nonlinear, because the graph of growth rate versus population size is not a straight line, but typically bends over due to increased competitive effects (see **illus.**).

The most basic models of growth are iterations, in which population size is recomputed at consecutive times in accordance with a basic underlying growth model. Such a model can be expressed in mathematical form by the difference equation (1), where

$$N(t+h) - N(t) = F[N(t)]h \qquad (1)$$

$N(t)$ is the population size at time t, $N(t+h)$ is the size h units later, and the function F defines the growth rule, as depicted, for example, in the illustration.

Despite the apparent simplicity of such models, their behavior can be exceedingly complex, and they have motivated mathematical investigations even until the present. The time period for which the population growth rate remains fixed determines the characteristics of growth. If the time period h is short, a population governed by such a law typically will come into balance with its environment, equilibrating at its carrying capacity K. However, if the time period is too long, the adjustment of the growth rate is delayed and the population may undergo oscillations, continuing to increase long after

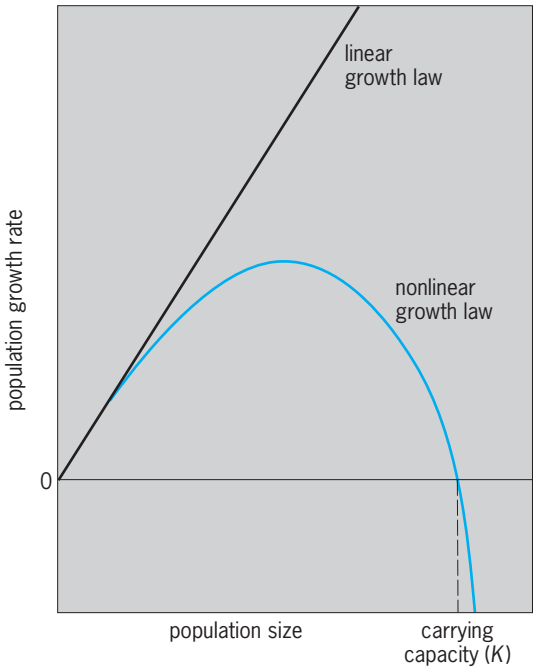

Typical nonlinear curve of population growth rate versus population size, compared with a linear growth law exhibiting the same initial slope (same growth rate at low densities). Note the existence of a carrying capacity, above which population growth rate will be negative.

the resources have been depleted, and then declining until resources recover. Such fluctuations, which may be seen in a variety of mathematical models, mimic the fluctuations observed in many natural populations. When a model based on simple principles gives rise to behavior similar to what is observed in nature, one has an analogy, not a definitive explanation. But such analogies are suggestive, and can be invaluable in helping to develop insights.

When h is small, a powerful approximation to Eq. (1) can be obtained by using differential calculus; in particular, the limiting form is the differential equation (2). If F is continuous, solutions to Eq. (2) never

$$\frac{dN}{dt} = F(N) \tag{2}$$

exhibit oscillations, since they approximate the situation for small h. *See* DIFFERENTIAL EQUATION.

Models of the sort just described are the simplest possible—they ignore all complications due to the fact that a population is composed of a heterogeneous assemblage of individuals, and further that it interacts with other populations and with its abiotic environment. Thus, although these simple models have found application in applied areas such as fishery science, in which one seeks to develop models relating one year's fish population size to the previous year's spawning stock, it is well recognized that more precise answers require consideration of various complications. *See* POPULATION ECOLOGY.

Age-structured models. Perhaps the most obvious potential complicating feature is the spread in ages that may be found within many natural populations. Typically, the production of offspring varies over the lifetime of an individual, as does mortality, the probability that an individual will not survive another year. Such variation is the basis of life tables constructed by life insurance companies to determine premiums; and thus it is not surprising that some of the most important advances in the theory of the dynamics of age-structured populations were made by an actuary, Alfred Lotka, in the early twentieth century. In the approach of Lotka, one describes a population not just by its total size, but also by the number of individuals of each age, summarized mathematically by a vector. This vector is a one-dimensional array [notation (3)], in which n_i denotes the number of

$$n = (n_1, n_2, \ldots, n_A) \tag{3}$$

individuals in age class i, for each i from 1 through the maximum age A.

The description of the dynamics of an age-structured population involves age-specific information concerning both fecundity and mortality. This information may also be expressed in a two-dimensional array, known as the Leslie matrix, which summarizes the contribution, through births or advancement in age, of each age class to each other one. One of the most fundamental results in mathematical ecology is that when the fecundity and mortality schedules for a population remain constant, the population will in general tend to a stable age distribution. In this distribution the relative proportions of the various age classes remain fixed while the population grows exponentially at a rate known as the intrinsic rate of natural increase. The only exception to this rule occurs in the unlikely situation that births are pulsed, taking place only at exact periodic (multiyear) intervals in the life of the organism.

Of course, the discussion above suffers from the same weakness as does discussion of exponential growth: In nature, birth and death parameters will not be constant, but will vary as population size changes. In such situations, the classical results do not apply, and the population may either attain balance or oscillate. As for the earlier case (without age structure), a continuous approximation may be derived, using the calculus of several variables; but unlike the previous case, the solutions to the limiting partial differential equation may sustain oscillations.

Competition and predation models. The most important extensions of these single-species models in the classical literature are to systems of interacting populations, especially the famous differential equations derived independently by Lotka and by the mathematician Vito Volterra. In this description, if X_1 and X_2 denote two interacting populations, the growth relationships are expressed by Eqs. (4), in which r_i de-

$$\begin{aligned} \frac{dX_1}{dt} &= r_1 X_1 \left(1 - \frac{X_1}{K_1} - \alpha_{12}\frac{X_2}{K_1}\right) \\ \frac{dX_2}{dt} &= r_2 X_2 \left(1 - \frac{X_2}{K_2} - \alpha_{21}\frac{X_1}{K_2}\right) \end{aligned} \tag{4}$$

notes the intrinsic rate of natural increase of species i, and K_i denotes its carrying capacity. Further, α_{ij} is a measure of the influence of species j on species i.

The two most important special cases of Eqs. (4) are competition (in which α_{12} and α_{21} are both positive) and predation (in which α_{12} is positive, but α_{21} is negative to reflect the positive effect of prey density, X_1, on predator growth rates).

The Lotka-Volterra equations have been analyzed in remarkable detail, and continue to fascinate mathematicians. In the case of competition, attention has focused on the conditions under which species can coexist; and when these conditions are violated, Eqs. (4) form the starting point for the theory of competitive exclusion and the closely related theory of the ecological niche. In the case of predation, the most powerful insight came from Volterra's original study, which was designed to show the similarity between the inherently oscillatory character of the solutions to Eqs. (4) and the fluctuations observed in the fisheries of the Adriatic. Later versions have embellished these results, and other models have been developed which demonstrate more stable oscillations, or which extend Eqs. (4) to systems of many interacting populations (this was actually done by the early masters), but no later work has come close to matching the influence of the seminal investigations of Lotka and Volterra.

Modern trends. The classical tradition has been carried into the present, especially regarding the development of an elegant theory of interspecific interactions and evolutionary relationships. Research has extended the theory to an examination of the structure of ecological food webs, and the factors governing their organization, and has taken the subject into diverse mathematical disciplines such as graph theory and dynamical systems theory.

Increasingly, however, mathematical approaches have been recognized as being valuable not only for theoretical investigations but also for the applied problems that society must confront. For example, mathematical descriptions of population dispersal, which are among the oldest models in theoretical ecology, are being used to quantify the movements of agricultural pest species and the rates of advance of exotic species invading new habitats. Also, the theory of island biogeography and more extensive mathematical models of spatially distributed populations are finding application in the design of reserves, in national park planning, and in regional landscape ecology. *See* ISLAND BIOGEOGRAPHY; POPULATION DISPERSAL.

Optimization and control theory are being applied as integral parts of programs for the management of renewable resources, especially fisheries and agricultural production. Such approaches wed biology and economics through mathematical models, and this marriage must become an increasing imperative for society as it faces shortages in energy and depletion of its limited resources. Inherent limitations to predictability are apparent in any rigorous mathematical analysis, and have made essential the development of adaptive management strategies, which couple short-term prediction with continually adjusted management rules. *See* OPTIMIZATION; QUALITY CONTROL.

Epidemiology is an area which has had a firm mathematical basis since the turn of the century. The impact of these models has been limited, although the problems society faces in combating the spread of diseases of humans and other animal and plant species are of overwhelming importance. There has been a dramatic increase in mathematical activity concerning the modeling and control of epidemics, and an increasing recognition of the need to view such problems in their proper ecological context as host-parasite interactions. Very likely this will be one of the most important growth areas in mathematical ecology over the next quarter century. Researchers are using mathematical models to help to understand the factors underlying disease outbreaks, and to develop methods for control such as vaccination strategies. *See* EPIDEMIOLOGY.

Finally, the need for environmental protection in the face of threats from such competing stresses as toxic substances, acid precipitation, and power generation has led to the development of more sophisticated models that address the responses to stress of community and ecosystem characteristics, for example, succession, productivity, and nutrient cycling. Such models, while owing much to their classical origin, typically differ substantially in form, and recognize the importance of explicitly considering environmental factors, physical characteristics of the environment, and nonbiotic system components, and of focusing attention on holistic measures of system response. Examples include large-scale models being developed to examine the likely effects of air pollution on regional patterns of forest productivity, or of power plants upon estuarine communities. *See* ENVIRONMENTAL ENGINEERING.

A major difference between such models and those discussed earlier is that they are in general too large to be fully analyzed, and one must rely heavily on the computer to simulate possible outcomes. However, in such applications, mathematical analyses are as essential as ever, since one must find ways to simplify, to guide simulations, and to derive understanding. Applications will increasingly be needed and will introduce new and vital challenges for mathematical ecology. *See* ECOLOGY; ECOLOGY, APPLIED; SIMULATION.

Simon A. Levin

Bibliography. Y. Cohn (ed.), *Application of Control Theory in Ecology: Lecture Notes in Biomathematics*, 1987; T. G. Hallam and S. A. Levin (eds.), *Mathematical Ecology*, 1986; C. J. Krebs, *Ecological Methodology*, 1988; L. Legendre and P. Legendre (eds.), *Developments in Numerical Ecology*, 1987; A. S. Podolsky, *New Phenology: Elements of Mathematical Forecasting in Ecology*, 1984.

Mathematical geography

The branch of geography that examines human and physical activities on the Earth's surface using models and statistical analysis. The primary areas in which mathematical methods are used include the analysis of spatial patterns, the processes that are responsible for creating and modifying these patterns, and the interactions among spatially separated entities.

What sets geographic methods apart from other quantitative disciplines is geography's focus on place and relative location. Latitude and longitude provide an absolute system of recording spatial data, but geographic databases also typically contain large amounts of relative and relational data about places. Thus, conventional quantitative methods are often insufficient for spatial problems, and geographers have devoted much effort to accounting for spatial interrelations while maintaining consistency with the assumptions of mathematical models and statistical theory. *See* GEOGRAPHY; MODEL THEORY; STATISTICS.

Quantitative methodology has long been part of physical geography due to its ties to geology and other physical sciences, but human geographers were slower in adopting and adapting quantitative methods. In the 1950s a growing dissatisfaction with traditional regional and descriptive approaches to geography, as well as an absence of theory, led geographers to incorporate statistical and mathematical methods and other theoretical models into geographic research. This methodological and philosophical shift is now known as the "Quantitative

Revolution," and quantitative methods remain a cornerstone of geographic research. *See* PHYSICAL GEOGRAPHY.

Spatial pattern. Spatial pattern methodologies attempt to describe the arrangement of phenomena over space. In most cases these phenomena are either point or area features, though computers now allow for advanced three-dimensional modeling as well. Point and area analyses use randomness (or lack of pattern) as a dividing point between two opposite pattern types—dispersed or clustered.

An important innovation in geographic modeling has been the development of spatial autocorrelation techniques. Unlike conventional statistics, in which many tests assume that observations are independent and unrelated, very little spatial data can truly be considered independent. Soil moisture or acidity in one location, for example, is a function of many factors, including the moisture or acidity of nearby points. Because most physical and human phenomena exhibit some form of spatial interrelationships, several statistical methods have been developed to measure this spatial autocorrelation. Once identified, the presence and extent of spatial autocorrelation can be built into the specification of geographical models to more accurately reflect the behavior of spatial phenomena.

Related to the search for spatial pattern is the concept of spatial hierarchy. With respect to cities, Zipf's law or rank-size rule presumes a direct relationship between a city's size and its relative national population rank. The standard form of this rule predicts that the second largest city in a nation should have half the population of the largest city, the third largest city one-third the population of the largest city, and so on. Studies have shown a clear relationship between a nation's conformity to this rule and its development level, with more developed nations more closely adhering to the rank-size rule.

Central place theory is a more comprehensive model of urban structure, focusing on the location and spacing of cities. This theory identifies three primary guiding principles for the arrangement of cities in an urban hierarchy, depending on whether retail, transportation, or administrative efficiency is being optimized. Precise mathematical relationships between the orders of the hierarchy indicate the expected relative market sizes, spacing, and numbers of cities at different levels of the hierarchy.

Analysis of hub-and-spoke networks has become an important field in spatial analysis, due to the proliferation of passenger and parcel transportation via air. Relative location is more important than site-specific characteristics of places, particularly because of the nature of air travel. Hence, a node's interconnections and links to other nodes determine its place in the hierarchy and the overall efficiency of the system.

Spatial processes. Analysis of spatial pattern is motivated by the desire to reveal the processes that create patterns. When central place theory reveals a retail, transportation, or administrative pattern in a landscape, for example, further analysis can uncover the behavioral forces that created such patterns, opening the way to a better understanding of human behavior or of physical properties.

A spatial process that underlies many spatial models is distance decay. Distance decay assumes that interactions diminish with distance, such that entities (cities, individuals, and so on) that are farther apart will interact less than entities in closer proximity. With the electronic and communications advances of the 1990s, though, the impact of distance is shrinking. New avenues of research in geography are exploring the impact of the Internet society on distance decay and on spatial interaction.

Spatial interaction. Perhaps the most frequent application of mathematical methods in geography has been to study the flows of goods, people, and ideas. Early in the Quantitative Revolution, social scientists looked to the physical sciences for analog models that could be adapted to human behavior, giving rise to the term "social physics." The most notable form of social physics has been the use of Newton's gravity model, in which the attraction (or interaction) between two places and the sizes of the places are directly proportional. Additionally, the distance decay effect plays a prominent role as more distant locations are expected to interact less than closer places. Travel time or cost can substitute for simple distance in this model, while some type of population statistic is the most common measure of the size of places.

While a simple gravity model allows for only two places to be modeled simultaneously, spatial interaction models represent an advancement by allowing multiple origins and destinations, multiple attributes of these origins and destinations, and varying effects of distance all to be incorporated into a model of flows or interactions. These models have been heavily used in migration, journey-to-work, and interregional flow studies.

Further integration of mathematics into spatial analysis includes fuzzy logic and chaos theory, better cohesion in spatial statistical theory, behavioral models of individual (as opposed to aggregate) choice, and decision support systems. *See* CHAOS; DECISION SUPPORT SYSTEM.

Jonathan C. Comer

Bibliography. B. Boots and A. Getis, *Spatial Point Pattern Analysis*, Sage Publications, Beverly Hills, CA, 1988; A. S. Fotheringham and M. E. O'Kelly, *Spatial Interaction Models: Formulations and Applications*, Kluwer Academic, Dodrecht, Netherlands, 1989; D. A. Griffith and C. G. Amrhein, *Statistical Analysis for Geographers*, Prentice Hall, Englewood Cliffs, NJ, 1991; J. Odland, *Spatial Autocorrelation*, Sage Publications, Newbury Park, CA, 1988; J. Odland, R. G. Golledge, and P. A. Rogerson, Mathematical and statistical analysis in human geography, in G. L. Gaile and C. J. Wilmott (eds.), *Geography in America*, Merrill Publishing, Columbus, OH, 1989.

Mathematical physics

An area of science concerned with the application of mathematical concepts to the physical sciences and the development of mathematical ideas in response

to the needs of physics. Historically, the concept of mathematical physics was synonymous with that of theoretical physics. In present-day terminology, however, a distinction is made between the two. Whereas most of theoretical physics uses a large amount of mathematics as a tool and as a language, Mathematical physics places greater emphasis on mathematical rigor, and devotes attention to the development of areas of mathematics that are, or show promise to be, useful to physics. Henri Poincaré likened physics to a large library in which the books are furnished by the experimenters, and the index, without which the collection would be inaccessible and useless, by the mathematical physicists (in the older sense of the word). If that simile is accepted, there remains the remarkable fact that most of the organization and structure of the library, and even the existence of many of the books, is determined by the nature of the index, since both the language and the content of mathematics continue to have a powerful influence on ideas of the structure of nature. The results obtained by pure mathematicians, with no thought to applications, are almost always found to be both useful and effective in formulating physical theories.

Mathematical physics forms the bridge between physics as the description of nature and its structure on the one hand, and mathematics as a construction of pure logical thought on the other. This bridge between the two disciplines benefits and strengthens both fields enormously. *See* MATHEMATICS; PHYSICS; THEORETICAL PHYSICS.

Historical examples. Isaac Newton invented the differential and integral calculus for the specific purpose of physical application, in the formulation of his equations of motion and for the law of gravitation as applied to extended bodies. In the course of the next two centuries, the calculus grew into the large branch of analysis in mathematics. Within that branch, the development of the science of differential equations was further propelled by the need for solving the equations of motion of objects in mechanics, and specifically the development of partial differential equations by their use in Maxwell's theory of electromagnetism, in continuum mechanics, and in the theory of sound. *See* CALCULUS; CLASSICAL FIELD THEORY; DIFFERENTIAL EQUATION; GRAVITATION; MAXWELL'S EQUATIONS; NEWTON'S LAWS OF MOTION; SOUND.

When the true complication of the newtonian mechanics of the solar system, in which each planet was gravitationally attracted not only by the Sun but also by all the others, became apparent, the urgent problem arose to ascertain mathematically whether this system was stable or whether it might be destined to collapse. The stability of the system was proved by J. L. Lagrange, whose method of proof engendered a new, fruitful branch of mathematics, perturbation theory.

Modern examples. W. Heisenberg's formulation of matrix mechanics included strange noncommuting entities (later called q-numbers by P. A. M. Dirac), which led to his principle of indeterminacy, thus beginning the large-scale introduction of the use of operators on Hilbert space in quantum mechanics. Although D. Hilbert had developed the theory of these infinite-dimensional function spaces, this theory was entirely unfamiliar to physicists at the time. Dirac formulated all of quantum mechanics in the language of that theory, and J. von Neumann put that formulation on a firm mathematical foundation. Today, most of the work of mathematical physicists is concerned with problems in either quantum mechanics or quantum field theory. *See* HILBERT SPACE; NONRELATIVISTIC QUANTUM THEORY; QUANTUM MECHANICS.

Stability of matter. A problem analogous to that of the stability of the solar system arose in the quantum mechanics of bulk matter: whether a solid (a system of a large number of atoms, consisting of many electrically charged particles, which attract or repel one another, as described by the equations and postulates of quantum mechanics) is stable or will collapse. Since matter is manifestly stable, the problem constituted a mathematically difficult test for quantum mechanics. The stability proof was given in the 1960s. *See* QUANTUM THEORY OF MATTER.

Phase transitions. Numerous other modern problems of mathematical physics also involve many-particle systems. One of these is the question of the existence of a critical temperature at which an abrupt phase transition takes place. Such a phase transition may, as the temperature is lowered or raised, change a liquid into a gas or a solid, cause a ferromagnet to lose its ferromagnetism, change an insulator into a superconductor, or cause any number of other sudden changes of properties. These problems are particularly difficult because such a discontinuous transformation can never occur so long as the number of particles is finite.

As in some other problems of mathematical physics, in the case of ferromagnetism it was the introduction of a very simplified but mathematically nontrivial model that led to a clearer understanding: the Ising model. It consists of a regular, infinite, two-dimensional lattice of elementary magnets that can point only up or down, and that interact with only their nearest neighbors, so as to favor alignment. The calculation of the partition function of statistical mechanics for this model led to a proof that there is, indeed, a Curie temperature, below which there is long-range order and above which that order disappears. However, there is still no proof that even this vastly simplified model has a phase transition when extended to three dimensions. The existence of the most common phase transitions, freezing and boiling of liquids, is an unsolved problem of mathematical physics and so is the problem of why most solid matter is in crystalline form. *See* ISING MODEL; PHASE TRANSITIONS; STATISTICAL MECHANICS.

Scattering theory. Mathematical physicists have also been very active in the development of the quantum theory of scattering, which deals with the scattering of particles under the influence of forces. The mathematical investigation of the analytic properties of wave functions, of the scattering amplitude,

and of the scattering matrix has led to important experimental predictions, such as dispersion relations. The inverse scattering problem is the mathematical question of whether it is possible to infer the interparticle forces from measurements of the scattering, and if so, whether such an inference is unique and how it can be implemented. *See* DISPERSION RELATIONS; INVERSE SCATTERING THEORY; SCATTERING MATRIX.

Quantum field theory. Theories of fundamental particles are all based on quantum field theory, which is fertile ground for problems in mathematical physics. Here the problems usually deal with the question of whether a given theory, formulated in mathematical language, makes mathematical sense. In particular, mathematical physicists investigate whether the postulated equations have solutions, what the properties of these solutions are, and how the solutions can be constructed for actual numerical calculations that can then be compared with experimental data. Sometimes, as in the case of string field theory, such investigations lead to deep new mathematical developments or even to the construction of entirely new areas of mathematics. (In this particular case, the theory of knots received an important stimulus and a new set of ideas.) To find a consistent theory that combines the quantum field theory of elementary particles with the force of gravity is one of the greatest challenges faced by mathematical physics. Entirely novel mathematical concepts have been proposed (such as noncommutative geometry) for this purpose. *See* QUANTUM FIELD THEORY; QUANTUM GRAVITATION; RELATIVITY; SUPERSTRING THEORY.

Quantum electrodynamics. In the instance of quantum electrodynamics (QED), the quantum theory of the interaction of the electromagnetic field and electrons, there is an unsolved puzzle: On the one hand, the theory has produced unprecedented precision in its agreement between calculations that are based on well-defined approximation schemes for solving the equations of QED and experimental results; on the other hand, all attempts at proving that the equations, in fact, have solutions have failed. If a proof should be forthcoming that the equations of QED have no solutions (and there are some indications that this may be the case), it will be the task of mathematical physics to lead to an understanding of what it is that has been calculated and that agrees with nature so remarkably well, if it is not a solution. In other words, the concept of what constitutes a solution of such equations will have to be appropriately altered. *See* QUANTUM ELECTRODYNAMICS.

Computer applications. The use of large-scale computers makes it possible to solve equations that were previously intractable. Even though the computer can rarely provide definitive proofs, it can often provide very fruitful clues to new effects and stimulate ideas. *See* DIGITAL COMPUTER; NUMERICAL ANALYSIS.

Nonlinear differential equations. The study of nonlinear differential equations is a case in point. The equations of classical mechanics are almost always nonlinear and therefore, in practice, unmanageable, with only some very special solutions either numerically calculable by hand or qualitatively comprehensible. In fact, most systems of classical particles evolve into chaos. However, the fact that Maxwell's equations of electromagnetism and those of quantum mechanics are linear led mathematical physicists for almost a century to pay almost exclusive attention to linear phenomena. The introduction of the computer changed this situation, and the study of nonlinear dynamical equations, with the quasi- universal development of chaos, became numerically feasible and consequently a fertile field of research for mathematical physicists. However, turbulence is a highly nonlinear phenomenon of great practical importance that has, so far, resisted the efforts of mathematical physicists. Yet, the borderline between those few solutions of a general nonlinear dynamical system that are said to be regular and those that are chaotic has been shown by the KAM theorem (due to A. N. Kolmogorov, V. I. Arnold, and J. Moser) to be surprisingly fuzzy: when parameters are changed from values for which the system is understood to be quasiperiodic and regular, however it starts, the system does not immediately become chaotic but retains its predictable character for a finite range of parameter values until it finally succumbs to chaos for all initial conditions. *See* CHAOS; NONLINEAR PHYSICS; TURBULENT FLOW.

Solar-system stability. One result of the computer development is that the question of the stability of the solar system has been reexamined without the use of linear methods. It is now feasible to check the stability numerically for several million years. This numerical work has shown that the stability of the orientation of the Earth's axis is assured only because of the presence of the moon.

Solitons. Another example of the influence of the computer upon the development of mathematical physics is the investigation of the Korteweg-De Vries equation, a nonlinear partial differential equation that was devised in the late nineteenth century to describe the motion of shallow water waves in a one-dimensional channel. Computer calculations in the 1960s led to the discovery of solitons, solutions that describe solitary bumps colliding with one another, causing, during the collision, distortions of their shape, but that, after the collision, emerge unscathed, with no change in shape, speed, or amplitude. This quite unexpected effect has subsequently been found for many other nonlinear equations, and its mathematical analysis (rather than numerical study) has given rise to a large field of applied mathematics as well as to an explanation of a number of natural phenomena. *See* SOLITON.

Methods. The methods employed in mathematical physics range over most of mathematics, the areas of analysis and algebra being the most commonly used. Partial differential equations and differential geometry, with heavy use of vector and tensor methods, are of particular importance in the formulation of field theories, and functional analysis as well as operator theory in quantum mechanics. Group theory has become an especially valuable tool in the construction of quantum field theories

and in elementary-particle physics. There has also been an increase in the use of general geometrical approaches and of topology. For solution methods and the calculation of quantities that are amenable to experimental tests, of particular prominence are Fourier analysis, complex analysis, variational methods, the theory of integral equations, and perturbation theory. *See* ABSTRACT ALGEBRA; COMPLEX NUMBERS AND COMPLEX VARIABLES; DIFFERENTIAL GEOMETRY; FOURIER SERIES AND TRANSFORMS; GROUP THEORY; INTEGRAL EQUATION; OPERATOR THEORY; TOPOLOGY; VARIATIONAL METHODS (PHYSICS); VECTOR METHODS (PHYSICS). Roger G. Newton

Bibliography. E. Butkov, *Mathematical Physics*, 1968; R. Geroch, *Mathematical Physics*, 1985; E. H. Lieb and D. C. Mattis, *Mathematical Physics in One Dimension; Exactly Solvable Models of Interacting Particles*, 1966; M. Reed and B. Simon, *Methods of Modern Mathematical Physics*, vol. 1, 2d ed., 1980, vol. 2, 1975, vol. 3, 1979, vol. 4, 1978; R. D. Richtmyer, *Principles of Advanced Mathematical Physics*, 2 vols., 1979, 1981.

Mathematical software

The collection of computer programs that can solve equations or perform mathematical manipulations. The developing of mathematical equations that describe a process is called mathematical modeling. Once these equations are developed, they must be solved, and the solutions to the equations are then analyzed to determine what information they give about the process. Many discoveries have been made by studying how to solve the equations that model a process and by studying the solutions that are obtained.

Before computers, these mathematical equations were usually solved by mathematical manipulation. Frequently, new mathematical techniques had to be discovered in order to solve the equations. In other cases, only the properties of the solutions could be determined. In those cases where solutions could not be obtained, the solutions had to be approximated by using numerical calculations involving only addition, subtraction, multiplication, and division. These methods are called numerical algorithms. These algorithms are often straightforward, but they are usually tedious and require a large number of calculations, usually too many for a human to perform. There are also many cases where there are too many equations to write down. *See* ALGORITHM; NUMERICAL ANALYSIS.

The advent of computers and high-level computer languages has allowed many of the tedious calculations to be performed by a machine. In the cases where there are too many equations, computer programs have been written to manipulate the equations. A numerical algorithm carried out by a computer program can then be applied to these equations to approximate their solutions. Mathematical software is usually divided into two categories: the numerical computation environment and the symbolic computation environment. However, many software packages exist that can perform both numerical and symbolic computation.

Characteristics. Mathematical software that does numerical computations must be accurate, fast, and robust. Accuracy depends on both the algorithm and the machine on which the software is run. Most computers follow the standards of the American National Standards Institute (ANSI) and the Institute of Electrical and Electronics Engineers (IEEE). Most mathematical software uses the most advanced numerical algorithms. Robustness means that the software checks to make sure that the user is inputting reasonable data, and provides information during the performance of the algorithm on the convergence of the calculated numbers to an answer. Mathematical software packages can approximate solutions to a large range of problems in mathematics, including matrix equations, nonlinear equations, ordinary and partial differential equations, integration, and optimization. Mathematical software libraries contain large collections of subroutines that can solve problems in a wide range of mathematics. These subroutines can easily be incorporated into larger programs.

Software packages. For many years, these subroutines were available only in Fortran. Almost all of the Fortran programs are now available in C. IMSL® is a mathematical software package that contains numerous numerical algorithms for solving linear and nonlinear mathematical problems. The IMSL® programs are written in both Fortran and C and are available for downloading. The Numerical Algorithms Group (NAG®) is an organization that puts out a mathematical software package of algorithms in Fortran and C. Two popular texts, *Numerical Recipes in Fortran* and *Numerical Recipes in C*, also contain numerous algorithms. The company The MathWorks has written the software package MATLAB® (Matrix Laboratory). MATLAB® was originally written in Fortran but now is in C. Its numerical software environment contains most of the algorithms in IMSL®, NAG®, and the two *Numerical Recipes* texts. The user of MATLAB® can develop software in MATLAB®. A programmer who has to use a numerical algorithm can save time and effort by using any of these products. *See* PROGRAMMING LANGUAGES.

Symbolic computation. Early computers were used mainly to perform numerical calculations, while the mathematical symbolic manipulations were still done by humans. Now software such as Derive®, Maple®, and Mathematica® is available to perform these mathematical manipulations. Most of the mathematical software packages that perform symbolic manipulations can also perform numerical calculations. Software can be written in the package to perform the numerical calculations, or the calculations can be performed after the symbolic manipulations by putting numbers into the symbolic formulas. Mathematical software that is written to solve a specific problem using a numerical algorithm is usually computationally more efficient than these software environments. However, these software environments can perform almost all the commonly

used numerical and symbolic mathematical manipulations. *See* SYMBOLIC COMPUTING.

Parallel computation. Since most of the problems of interest to society are modeled by complicated mathematical equations, they require a large number of calculations and storage of their results. This has led to industries of people working on building larger and faster computers. Different types of computers have also been developed. Parallel computers have more than one processor that can work on the same problem at the same time. Parallel computing allows a large problem to be distributed over the processors. This allows the problem to be solved in a smaller period of time. Many numerical algorithms have been converted to run on parallel computers. *See* MULTIPROCESSING.

A set of personal computers can be connected into an array that can perform parallel computations. Oak Ridge National Laboratory has developed a software package, Parallel Virtual Machine (PVM), which allows the user to divide a problem among several connected personal computers. The National Science Foundation spearheaded a worldwide operation that united computer scientists and mathematicians from universities and industries to develop a parallel software environment, Message Passing Interface (MPI), which is easy to use and incorporates the best properties of such an environment. Both PVM and MPI can be used with Fortran or C, and both provide users with the power of a supercomputer at a fraction of its cost. Fortran has also been upgraded to a parallel language called High-Performance Fortran (HPF). The National Aeronautics and Space Administration (NASA) has developed a parallel-personal-computer hardware-software environment called Beowulf. The Beowulf system is a configuration of personal computers with a communication environment between them. It can use HPF, PVM, or MPI. *See* COMPUTER PROGRAMMING; CONCURRENT PROCESSING; DIGITAL COMPUTER; DISTRIBUTED SYSTEMS (COMPUTERS); SOFTWARE. James Sochacki

Bibliography. W. J. Kaufmann and L. L. Smarr, *Supercomputing and the Transformation of Science* (*Scientific American Library*, no. 43), W. H. Freeman, 1993; W. H. Press et al., *Numerical Recipes in C: The Art of Scientific Computing*, 2d ed., Cambridge University Press, 1992; W. H. Press et al., *Numerical Recipes in Fortran 90: The Art of Parallel Scientific Computing* (*Fortran Numerical Recipes,* vol. 2), Cambridge University Press, 1996.

Mathematics

Mathematics is frequently encountered in association and interaction with astronomy, physics, and other branches of natural science, and it also has deep-rooted affinities to the humanities. Actually, it is a realm of knowledge entirely unto itself, and one of considerable scope; the word mathematics stems from a root which means learnable knowledge. Mathematical knowledge is commonly deemed to have a high degree of validity, irrespective of culture conditioning and predilection, although it can be argued that, in the past, cultural settings have affected its development noticeably.

Relation to science. As far as the scientist is concerned, mathematics is not a branch of natural science itself. It does not deal with phenomena and objects of the external world and their relations to each other but, strictly speaking, only with objects and relations of its own imagery. Mathematical figures in two- or three-dimensional geometry are largely idealizations of objects occurring in the physical world, but figures in n-dimensional space for general n no longer are such idealization. Integer numbers 1, 2, 3, ..., and even real numbers in general, can be claimed to be abstractions from quantities occurring in the physical world, but the "imaginary" number $i = \sqrt{-1}$ has received its name from the very fact that it has no basis in the material world, even though the use of complex numbers $a + bi$ is indispensable to science. If a laboratory experiment idealizes a physical system in order to eliminate secondary features not essential to the study at hand, its ultimate objective is an understanding of the unidealized physical system. But even if it were true that the five regular solids as investigated in the thirteenth book of Euclid's *Elements* (cube, tetrahedron, octahedron, icosahedron, and dodecahedron) had been found because of the occurrence of approximating crystals in nature, nevertheless, once found, the idealized geometric figures would still have become primary objects of study in mathematics.

Mathematics is not subordinate to natural science by being a handmaiden of it, and one can practice competently meaningful mathematics without being concerned with science at all. Especially, philosophical attempts to reduce all origin of mathematics to utilitarian motives are wholly unconvincing. However, it is fair to say that mathematics is the language of science in a deep sense. Mathematics is an indispensable medium by which and within which science expresses, formulates, continues, and communicates itself. And just as the language of true literacy not only specifies and expresses thoughts and processes of thinking but also creates them in turn, so does mathematics not only specify, clarify, and make rigorously workable concepts and laws of science, but also at certain crucial instances becomes an indispensable constituent of their creation and emergence as well. In Isaac Newton's formula for the motion of a particle on a straight line, Eq. (1), the mass m and the force F are nonmathematical objects, perhaps. But the instantaneous velocity $v = dx/dt$ and the instantaneous acceleration $a = dv/dt = d^2x/dt^2$ are wholly mathematical, and without a mathematical theory of the infinitesimal calculus, they are not conceivable. I. Newton, the physicist, was driven to creating his version of the calculus because of this. Also, Newton had to have not only the process of differentiation but also

$$m\frac{d^2x}{dt^2} = F \tag{1}$$

the concept of a mathematical function, because only a function can be differentiated. He required not only the path function $x = x(t)$, but, for the second derivative, he had to envisage the velocity $v = dx/dt$ itself, again as a function depending on t, even though by the definition of v this dependence had been reduced to "instantaneousness." This concept of function was given to Newton by the then new theory of analytic geometry of René Descartes, and it is a fact that after Archimedes' work on the motion of a lever, theoretical mechanics stood virtually still for almost 2000 years until the twin mathematical concepts of function and derivative were ready to emerge. *See* CALCULUS.

A striking case of the manner in which mathematics may shape physics has occurred in the theory of relativity. When A. Einstein was pondering the transition from special to general relativity, his attention was drawn to G. Ricci's work on tensor calculus. Einstein found it an excellent medium for his thoughts, adopted it, and made it widely known to mathematicians. In the 1920s the quantum theory could move as rapidly as it did only because certain prefabricated parts from the theory of matrices and differential equations were lying about somewhat idly. *See* DIFFERENTIAL EQUATION; MATRIX THEORY.

Creative formulas. A formula is a string of mathematical symbols subject only to certain general rules of composition. To a working mathematician a string of symbols is a formula if it is something worth remembering. Much mathematics is concentrated in and propelled by certain formulas of unusual import.

The oldest of these is the pythagorean theorem $c^2 = a^2 + b^2$, where a, b are the sides and c is the hypotenuse in a right-angled triangle. If a, b are rational numbers p/q, then c need not be so; for instance, when $a = b = 1$, $c = \sqrt{2}$ and is not a rational number. This compelled the Greeks to study ratios of incommensurable quantities and also quadratic irrationalities. In modern times the formula was extended to $c^2 = a_1{}^2 + \cdots + a_n{}^2$ for the diagonal of a rectangular parallelepiped in n-dimensional euclidean space, and gave Eq. (2) for the distance between two points

$$s^2 = (x^1 - y^1)^2 + \cdots + (x^n - y^n)^2 \qquad (2)$$

$x = (x^1, \ldots, x^n)$, $y = (y^1, \ldots, y^n)$ in cartesian coordinates there. For infinitesimally near points this becomes the line element $ds^2 = (dx^1)^2 + \cdots + (dx^n)^2$, which in the more general affine version, Eq. (3a), is the cornerstone of riemannian geometry. [Equation (3b) is discussed below.] On the other

$$ds^2 = \sum_{i,j=1}^{n} g_{ij}\, dx^i\, dx^j \qquad (3a)$$

$$ds^2 = \sum_{\alpha,\beta=1}^{n} g_{\alpha\bar{\beta}}\, dz^\alpha\, dz^{\bar{\beta}} \qquad (3b)$$

hand, analytic developments demanded the extension of Eq. (2) to a space of infinitely many dimensions and then even to the case in which coordinates are complex numbers; thus Eq. (4) may be written.

$$s^2 = |z^1 - w^1|^2 + |z^2 - w^2|^2 + \cdots \qquad (4)$$

With this definition of distance the space becomes a Hilbert space, the basis of operator theory and quantum mechanics. Finally, again for finite dimension but still complex coordinates, it became significant, in analogy to Eq. (3a), to introduce the line element in Eq. (3b). It is the basis for the study of riemannian geometry on complex manifolds, and the study of such manifolds is penetrating even relativity and field theory. *See* OPERATOR THEORY; QUANTUM MECHANICS; RIEMANNIAN GEOMETRY.

The simple relation $(1 + x)^2 = 1 + 2x + x^2$ was generalized by Newton to Eq. (5). The coefficients are the binomial coefficients, shown in Eq. (6), and

$$(1 + x)^n = 1 + \binom{n}{1} x + \binom{n}{2} x^2 + \cdots \qquad (5)$$

$$\binom{n}{k} = \frac{n(n-1)\cdots(n-k+1)}{1 \cdot 2 \cdots k} \qquad (6)$$

the formula is a generating relation for them. The expression in Eq. (6) can also be set up if n is any nonintegral number, real or complex, and it was indeed established that Eq. (5) holds for any n for $|x| < 1$. The expansion is usually an infinite series, and it is in fact the Taylor series of $(1 + x)^n$. By studying, for general n, the behavior of the series as $|x| \to 1$, H. Abel laid the foundation for the theories of summability of nonconvergent series. *See* SERIES.

Euclid's theorem that any integer is a unique product of primes (stated in Euclid only implicitly) can be expressed as a formula, Eq. (7). The concept of a

$$a = {p_1}^{n_1} \times {p_2}^{n_2} \times \cdots \times {p_k}^{n_k} \qquad (7)$$

prime factor and the quest for a theorem on unique decomposition into prime factors have been leading principles of arithmetic and algebra on all levels ever since. *See* NUMBER THEORY.

The constant π, widely known from antiquity through the formulas $l = 2\pi r$, $A = \pi r^2$ for a circle and $A = 4\pi r^2$, $V = 4/3\pi r^3$ for a sphere, also enters the sophisticated formula, Eq. (8), derived by G. W.

$$\frac{\pi}{4} = 1 - {}^1/_3 + {}^1/_5 - {}^1/_7 + \cdots \qquad (8)$$

Leibnitz. Both kinds of formulas were much used for the approximate computation of this transcendental number, and a great deal of computational technique (including the use of computing machines) was initiated in the course.

The transcendental number e, the basis of natural logarithms, appeared in the eighteenth century in the formulas given as Eqs. (9), which have been

$$e^{2\pi\sqrt{-1}} = 1 \qquad \cos\varphi + \sqrt{-1}\sin\varphi = e^{\varphi\sqrt{-1}} \qquad (9)$$

of immeasurable consequence to all of mathematics. Even the age-old plane trigonometry was greatly streamlined by them. *See* NUMERICAL ANALYSIS.

Near the end of the eighteenth century, L. Euler gave for convex polyhedrons the formula $e_0 - e_1 + e_2 = 2$, in which e_0 is the number of vertices, e_1 of edges, and e_2 of surfaces. This was a first step in function theory of closed Riemann surfaces and in algebraic geometry, and it was a starting point for H. Poincaré's combinatorial topology. Poincaré's own formula, $B_p = B_{n-p}$ for Betti numbers of compact manifolds, is even today one of the most arresting statements of the theory.

Cauchy's formula, Eq. (10), is a center point from

$$f(z) = \frac{1}{2\pi i} \oint_C \frac{f(\zeta)\, d\zeta}{\zeta - z} \tag{10}$$

which the theory of complex functions radiates. *See* COMPLEX NUMBERS AND COMPLEX VARIABLES.

Galileo's main achievement is embodied in the formula $s = 1/2gt^2$ for a falling body, and Newton's gravitational law in the formula $F = m_1 m_2 / r^2$, which also represents Coulomb's law of electricity. Einstein's daring formula $E = mc^2$ from special relativity created the atomic bomb, and W. Heisenberg's interpretation (1927) of the formula $pq - qp = h/2\pi i$ from quantum theory as an indeterminacy relation for physical observables has been an irritant to philosophers ever since. *See* RELATIVITY; UNCERTAINTY PRINCIPLE.

Foundations—mathematical logic. A prime demand on mathematics is that it be deductively rigorous, and a traditional model for intended rigor is Euclid's presentation of mathematical assertions in theorems. For the philosopher G. Spinoza in the seventeenth century, the phrase "more geometrico" is a synonym for "deductively rigorous." A theorem is a proposition which has been proved, excepting certain first theorems called axioms, which are admitted without proof; and to prove a theorem means to obtain it from other theorems by certain procedures of deduction or inference. It had long been commonplace that each branch of mathematics was based on its own axioms, but during the nineteenth century, mathematicians arrived at the insight that even the same branch might have alternate axioms. Specifically, there were envisaged alternate versions of two- and three-dimensional geometry, the axiom varied being the axiom on parallels. It was also recognized that a set of axioms becomes mathematically possible if it is logically consistent, that is, if one cannot deduce from the axioms to theorems one of which, as a proposition, is the negation of the other. *See* EUCLIDEAN GEOMETRY; NONEUCLIDEAN GEOMETRY.

At the same time certain developments led to the realization that not only the axioms but the rules of inference themselves might be, and even ought to be, subjected to variations. Now if axioms and rules of inferences are both viewed as subject to change, it is customary to speak of a mathematical system or also a formal system, and, of course, an irreducible first requirement is that the system be consistent after the manner just stated. Consistency alone is a somewhat negative property. There is a further property, called completeness, which is more positive, and which, if present, is very welcome. A system is complete if for any proposition which can be formulated it can be proved either that it holds or that its negation holds. If a theorem holds in a system and the system is altered, then the same proposition, or what corresponds to it in the new system, may become doubtful if not absolutely false; if it remains valid it may require a new proof because certain axioms or rules of inference are no longer available.

Some of the developments that led to doubt as to whether the traditional rules of inference are inviolate were the following.

1. G. Boole had found in 1854 that the classical Aristotelian connectives "and," "or," "negation of" for propositions follow rules similar to those which the operations addition, multiplication, "the negative of" obey in ordinary algebra (Boole's algebra of propositions); his conclusions took from rules of inference the status of untouchability.

2. G. Cantor, the founder of the theory of sets and operations between them, defined a set (intuitively or naïvely) as the collection of all objects having a certain property which is verbally expressible. Especially, "the set of all sets" is again a set and it has the peculiarity of being a set which contains itself as one of its elements. But this leads to the following contradictory situation (Russell's paradox): Divide the totality of all possible sets into two categories. A set shall belong to category I if it does not contain itself as an element, and to category II if it does contain itself as an element. Now form the set M whose elements are the sets of category I. It can now be reasoned by deductive steps admissible in Cantor's own theory that the set M cannot belong to either of the two categories, although the original division into categories did assign each set to one of them.

3. In 1904 E. Zermelo formulated the following axiom of choice: Given any family of nonvacuous sets $\{S\}$, no matter how (infinitely) large the family may be, it is possible to choose simultaneously an element $x = x_s$ from each given set S and thus to consider the set M consisting of precisely these elements. By the use of this axiom some striking theorems in classical mathematics could be proved which, without the use of the axiom, seemed to be logically out of reach entirely. Mathematicians began to wonder whether a theorem based on the axiom of choice is indeed valid or, at any rate, whether it has the same level of validity as one without it, and as a consequence, theorems employing the axiom of choice were frequently labeled as such. *See* SET THEORY.

Some of the doubts were resolved eventually; the most striking results are the following ones of K. Gödel. (1) Any consistent mathematical system which is sufficient for classical arithmetic must be incomplete. In other words, in a formal system which is expressible within the arithmetical language taught to a student of a secondary school in any country it is possible to formulate assertions which can be neither

proved nor disproved. (2) Any such system remains consistent if one adds to it the axiom of choice, so that working mathematics cannot disprove the axiom of choice. In 1963 P. Cohen showed that the axiom cannot be proved, either. (3) The so-called general continuum hypothesis is also consistent with ordinary mathematics, and, in fact, ordinary mathematics remains consistent if the axiom of choice and the general continuum hypothesis are added simultaneously. Cantor says that two sets A_1, A_2 have the same cardinal number if there exists a one-to-one correspondence between the elements of A_1 and A_2. Any infinite set has the same cardinal number as some proper subset of itself. For instance, the set of all integers $A_1 = \{1,2,3,\dots\}$ has the same cardinal number as the subset of all even integers $A_2 = \{2,4,6,8, \dots\}$ because the association of the number n in A_1 to the number $2n$ in A_2 is one-to-one. However, for a finite set this cannot happen, and the cardinal number of a finite set is the ordinary number of its elements. Next, Cantor says that a set A_2 has a larger cardinal number than A_1 if there is a one-to-one correspondence from A_1 to a subset of A_2 but not one from A_2 to A_1 or a subset of A_1. He then shows that if A is any set and S is the set of its subsets including the empty set, the cardinal number of S is greater than that of A. If A is finite and has n elements, then S has 2^n elements. Now 2^n is indeed greater than n, and for $n \geqq 2$ there are even other integer numbers between n and 2^n. This is true for finite sets. However, for infinite sets the situation seems to change radically, and the generalized continuum hypothesis asserts that there are no other cardinal numbers between those of A and S. *See* LOGIC.

Counterexamples. It follows easily from the definition of a derivative that a differentiable function $y = f(x)$ in $a < x < b$ is also continuous. K. Weierstrass deepened this statement considerably by demonstrating that the converse is not true. He constructed a function $f(x)$ that is continuous in $a < x < b$ but does not have a derivative at any point (his function does have right and left derivatives at all points). A construction of this kind is called a counterexample. Systematic preoccupation with counterexamples, which sometimes require considerable ingenuity, did not arise before the middle of the nineteenth century. Another early counterexample of considerable consequence referred to Fourier series. If $f(x)$ is periodic with period 2π, then its Fourier series is expression (11), from which, by definition, Eqs. (12) may be written. Fourier himself

$$\tfrac{1}{2}a_0 + \sum_{n=1}^{\infty}(a_n \cos nx + b_n \sin nx) \qquad (11)$$

$$\begin{aligned} a_n &= \frac{1}{\pi}\int_0^{2\pi} f(t)\ \cos nt\ dt \\ b_n &= \int_0^{2\pi} f(t)\ \sin nt \end{aligned} \qquad (12)$$

stated somewhat vaguely that for "any" function $f(x)$ the partial sums of the Fourier series are convergent to $f(x)$. P. G. L. Dirichlet was the first to give a specific criterion of convergence. In his criterion the function $f(x)$ may have certain simple discontinuities. But in the present discussion these discontinuities are excluded and $f(x)$ must first of all be continuous. Dirichlet proved that the Fourier series converged everywhere to $f(x)$, if $f(x)$ is piecewise monotone, that is, if the interval of periodicity $0 \leqq x < 2\pi$ can be divided into a finite number of smaller intervals such that in each of these the function is either monotonely increasing or monotonely decreasing. Then, P. du Bois Reymond demonstrated that the requirement of monotoneity cannot be dispensed with entirely. He constructed a continuous periodic function $f(x)$ for which the Fourier series fails to converge in at least one point. By a general principle developed by A. Harnack (condensation of singularities) it is then possible to construct a continuous function whose Fourier series fails to converge at countably many points even if they are everywhere dense, for instance, at all rational points $x = p/q$. But to this day it is not known whether there exists a continuous function whose Fourier series fails to converge at all points, or at least at all points with the only exception of a set of Lebesgue measure 0. *See* FOURIER SERIES AND TRANSFORMS.

Counterexamples frequently fall into patterns; that is, the same underlying construction is used over again for different but related purposes. A construction used in many counterexamples is Cantor's ternary set. Divide the closed interval $0 \leqq x \leqq 1$ into three equal parts $(0, \frac{1}{3}, \frac{1}{3}, \frac{2}{3})$, $(\frac{2}{3}, 1)$ and remove the middle one, but only the open inner part of it $\frac{1}{3} < x < \frac{2}{3}$. This leaves two closed intervals $0 \leqq x \leqq \frac{1}{3}$, $\frac{2}{3} \leqq x \leqq 1$. In each of these remove the open inner third, that is, $\frac{1}{9} < x < \frac{2}{9}$ and $\frac{2}{3} + \frac{1}{9} < x < \frac{2}{3} + \frac{2}{9}$. This leaves four closed intervals together. From each, remove the open inner third, and so on. After n steps the number of intervals removed is $1 + 2 + 2^2 + \cdots + 2^{n-1}$, and the sum of the length of the removed intervals is Eq. (13). This value is less than

$$\frac{1}{3} + \frac{2}{3^2} + \frac{2^2}{3^3} + \cdots + \frac{2^{n-1}}{3^n} = 1 - \left(\frac{2}{3}\right)^n \qquad (13)$$

1, which must be so, because the total interval has length 1 and the removed intervals do not overlap. However, if one lets n go to ∞ the $(\frac{2}{3})^n$ tends to 0, and the aggregate length of all infinitely many intervals which have been removed has value 1. Thus, the point set which is left over ought somehow to have a one-dimensional measure which has value 0. This is so indeed in the theory of Lebesgue. Also the leftover set is nowhere dense. However, it is a very big set, by a crude counting of its points, at any rate. More precisely, it turns out that its cardinal number is the same as for the entire interval $0 \leqq x \leqq 1$. This can be deduced from the following fact, which is interesting for many purposes: Any number $0 \leqq x \leqq 1$ can be represented by a ternary expansion instead of by a decimal expansion, that is, by an expansion $0.a_1a_2a_3\dots$ in which each symbol $a_1, a_2, a_3, \dots$, has

one of the values 0, 1, 2. Now the leftover set consists of precisely those points in whose expansion the symbols $a_1, a_2, a_3, \ldots$, assume only the values 0, 2 and not 1.

Constructiveness and approximations. Some mathematicians object to mere existence proofs, and they demand that any proof also be constructive. The interpretations of this demand differ widely. Some proofs closely approach what a practical mathematician welcomes; if, for instance, a theorem asserts the existence of a number or a function, then the proof must also embody a procedure for actual computation of the solution, approximately, at least. Other versions are little more than the negative requirement that certain combinations of inference be avoided. There are also views which combine both; the best known among the last is the intuitionist view. It firmly demands a certain kind of constructiveness, which, however, does not necessarily guarantee the calculation by present-day computing machines. However, the actual stricture by which intuitionism became widely known is that proof by contradiction is not admissible. It is also called proof by double negation, and it is equivalent to the Aristotelian *tertium non datur*. It assumes tentatively that the proposition to be proved is false and from this assumption deduces a contradiction to a previously established theorem.

There is one difference between practical and theoretical demands on constructiveness. Sometimes it is possible to prove the existence of a function nonconstructively and after that, based on the existence statement, to devise a procedure for a manageable construction. To practical mathematicians this is satisfactory; to theoretical mathematicians it is not.

A demand superficially related to constructiveness, and without any overtones of "logic," is a desire to estimate the degree of approximation, whenever a task of approximation is being performed. For instance, a classical result of J. L. Lagrange for the Taylor series with remainder term states that if $f(x)$ has n derivatives in the interval $0 \leqq x \leqq 1$, then $f(x) = P_n(x) + R_n(x)$, where $P_n(x)$ is the polynomial in Eq. (14), and the "error term" $R_n(x)$ is in numerical

$$P_n(x) = \sum_{m=0}^{n} \frac{f^{(m)}(0)}{m!} x^m \tag{14}$$

value bounded by $M_n/n!$, where M_n is the maximum of $|f(n)(x)|$ in $0 \leqq x \leqq 1$. This result leads to the following topic. The polynomial in Eq. (14) can be formed only if $f(x)$ has n derivations. However, there is a theorem of Weierstrass that states that any function $f(x)$ which is continuous in an interval $a \leqq x \leqq b$ (and nothing more) can be approximated uniformly by the polynomials in Eq. (15). Each proof for

$$P_n(x) = a_0 x^n + a_1 x^{n-1} + \cdots + a_n \tag{15}$$

this theorem produces its polynomials, and there is an extensive theory for securing those for which the approximation is a best possible one.

The parallel question of approximating not by ordinary polynomials, Eq. (15), but by trigonometric polynomials, Eq. (16), leads to mathematical procedures which pervade all of science. If one wishes to make the difference, shown as expression (17),

$$s_n(x) = {}^1\!/_2 a_0 + \sum_{m=1}^{n} (a_m \cos mx + b_m \sin mx) \tag{16}$$

$$\mathrm{Max}_{0 \leq x < 2\pi} \, |f(x) - s_n(x)| \tag{17}$$

rather small, then the partial sums of the Fourier series, Eq. (11), are not too good, meaning that it is not very advantageous to use the polynomials in Eq. (16) in which the coefficients a_m, b_m are the expressions (12). However, it improves the degree of approximation if one replaces the partial sums by their arithmetic means (Fejer sums), Eq. (18), which are again exponential polynomials, namely Eq. (19).

$$\sigma_n = \frac{s_0 + s_1 + \cdots + s_{n-1}}{n} \tag{18}$$

$$\sigma_n(x) = {}^1\!/_2 a_0 + \sum_{m=1}^{n} \left(1 - \frac{m}{n}\right) \cdot (a_m \cos mx + b_x \sin mx) \tag{19}$$

There are other averages which give even better approximations, and one is led to studying procedures of averaging and smoothing which are of importance to analysis, probability, and statistics. But a major development begins if, following F. W. Bessel and M. A. Parseval (nineteenth century), expression (17) is replaced by expression (20) as a measure for the degree of approximation. In this case the partial sums of the Fourier series are indeed the best approximating sums for any order n, not only for ordinary Fourier series but for so-called orthogonal series in general. Pertinent application to the theory of acoustical and then optical waves led to an interpretation of the Fourier series, Eq. (11), as a spectral resolution of its function $f(x)$, and this interpretation has been gradually extended to a host of related and analogous expansions in analysis, algebra, theory of probability, quantum theory, and other parts of physics. The measuring of approximation, deviation, and dispersion by a square of integral mean—which is expression (20)—has become a strong and pervasive influence on scientific thinking.

$$\left[\frac{1}{2\pi} \int_0^{2\pi} |f(x) - s_n(x)|^2 \, dx\right]^{1/2} \tag{20}$$

Space in mathematics. If geometry is the mathematics of space, then, in a superficial sense, all mathematics began with geometry, because apparently it began with measurements of figures: length, area, volume, and size of angles. It did not concern itself with questions of shape but with clarifying and deciding when figures are equal or substantially equal with regard to form. The first true theory of geometry was the great theory of the Greeks, whose primary concern was study of the basic concept of equality of figures—their congruence and similarity—and the

Greeks were so determined to dissociate their theory from the preceding phase of merely making measurements that Euclid's extensive work, for instance, avoids to a fault any kind of actual measurements. In the case of the Pythagorean theorem $c^2 = a^2 + b^2$, there is no hint that it might be an equality between numbers. It is only an equality between areas based on congruences, two of the squares being cut up into pieces and then put together into the third square after the manner of a jigsaw puzzle. But, for all its lofty purposes, Greek geometry was too rigid and circumscribed to be able really to cope with the mathematical problem of space. It came to a standstill and geometry did not progress further until, with the advent of coordinate systems, introduced by Descartes and his predecessors, a better mathematics of space could be initiated.

If a cartesian coordinate system is etched into two- or three-dimensional euclidean space, then the space becomes a point set, each point being a pair (x^1, x^2) or a triple (x^1, x^2, x^3) of real numbers, and any figure a suitable subset of it. This is a deliberate process of arithmetization of space which unifies space and number at the base. It does not hamper geometry in its task of pursuing problems of shape but instead aids it. In the cartesian plane, two figures are similar if the points of one can be obtained from the points of the other by means of a transformation, Eqs. (21), where Eq. (22) applies and where, for some $\rho > 0$, Eq. (23) can be written. The similarity is a congruence if, and only if, $\rho = 1$ (orthogonal transformation). Now this analytic representation of congruence and similarity suggests a geometric examination of the most general linear transformations, Eq. (21), which are nonsingular, that is, for which the determinant $|\alpha_q^p| \neq 0$. They were virtually unknown to the Greeks, although they highlight the axiom of parallels of Euclid's geometry. A one-to-one transformation of the cartesian plane is such a linear transformation if, and only if, it carries a straight line into a straight line and parallel straight lines into parallel straight lines. Thus, a parallelogram goes into a parallelogram, and, in fact, given any two parallelograms there is a linear transformation which carries the one into the other no matter what the angles and ratios of sides in the two figures are. There is a geometry, the so-called affine geometry, in which any two parallelograms are considered equal. It cannot measure angles, and nonparallel segments cannot be compared for length. This geometry does have conics, however, and it can separate them into ellipses, parabolas, and hyperbolas. *See* CONFORMAL MAPPING.

$$\begin{aligned} y^1 &= a^1 + \alpha_1{}^1 x^1 + \alpha_2{}^1 x^2 \\ y^2 &= a^2 + \alpha_1{}^2 x^1 + \alpha_2{}^2 x^2 \end{aligned} \tag{21}$$

$$\alpha_1{}^1 \cdot \alpha_1{}^2 + \alpha_2{}^1 \cdot \alpha_2{}^2 = 0 \tag{22}$$

$$(\alpha_1{}^1)^2 + (\alpha_2{}^1)^2 = (\alpha_1{}^2)^2 + (\alpha_2{}^2) = \rho^2 \tag{23}$$

The family of all linear transformations constitutes a transitive group, and the subfamily of orthogonal transformations is already a transitive group. F. Klein made the pronouncement, which is generally accepted, that there arises a geometry on a space if on the space there is given a transitive group of transformations; two figures are considered equal whenever one figure can be carried into the other figure by one of the transformations. For the noneuclidean geometries of Bolyai-Lobachevski-Gauss various models have been exhibited which conform to this view, and perhaps the most interesting one is the following. In the plane (x^1, x^2) introduce the complex variable $z = x^1 + ix^2$ and consider the family of transformations, Eq. (24), for all constant complex numbers

$$w = e^{i\theta} \frac{z - a}{1 - \bar{a}z} \tag{24}$$

a for which $|a| < 1$ and all real numbers θ. They give rise to the following noneuclidean geometry. The space is not the entire z plane but only the unit disk: $|z| < 1$. A "point" is an ordinary point in it and a "straight line" of the new geometry is in the euclidean geometry either a diameter of the disk or any circular arc inside the disk whose end points are on the boundary line of the disk and which meets the boundary line of the disk at right angles. Through a point outside a straight line of the geometry go infinitely many straight lines which are "parallel" to it; that is, they do not meet it inside the disk. This makes the geometry a hyperbolic one. If, however, in a geometry any two straight lines always intersect, the geometry is called elliptic. The prototype of an elliptic geometry is a geometry on a surface of a sphere (for example, the surface of the Earth) in which the straight lines are the great circles. As a matter of fact, the hyperbolic geometry just described is in a very precise sense a counterpart to the elliptic geometry of great circles on a sphere.

The arithmetization of space led to a purely mathematical creation of n-dimensional space, euclidean and other, for any integer dimension n, by defining its points generally as n-tuples of real numbers $(x^1, \ldots, x^n)$ with suitable definitions for various geometrical relations between such points. The most eye-catching consequence in science was the four-dimensional space of the theory of relativity, but actually multidimensional geometry had been playing a part in physics before that. If a mechanical system involves M mass points, it was customary in effect to introduce the space of dimension $n = 3M$, whose points are the states of the system, that is, the n-tuples of coordinates $\{x_m{}^1, x_m{}^1, x_m{}^3\}$, $m = 1, \ldots, M$, at any one time point. Also, if there are restraints operative in the system, then the Lagrange-Hamilton theory suitably reduced the dimension of the space by the use of the free parameters of the system instead of the original n coordinates themselves. The use of free parameters spread from mechanical systems to other systems in physics and chemistry, and all so-called equations of state are geared to this. Finally, in quantum theory a state of a system has infinitely many coordinates and the infinitely dimensional space representing it is a Hilbert space. Also, partly under the influence of Hilbert space, mathematicians have become fascinated with

infinitely dimensional spaces in general. They are being studied intensively, and large parts of mathematics are being pressed into these new frames of reference.

The arithmetization of space is also reflected in the ever-widening use of graphs and charts. Any tabulated dependence of a number y on a number is a function $y = f(x)$ and hence representable as a curve on graph paper; a great amount of information is thus illustrated and stored. This is nothing but a practical application of the concept of a manifold in modern topology and differential geometry, and, as is frequently true, the abstract formulation of a mathematical concept is but a circumlocution of what common sense dictates. *See* ALGEBRA; ANALYTIC GEOMETRY; CALCULUS OF VECTORS; COORDINATE SYSTEMS; PROBABILITY; STATISTICS; TOPOLOGY.

Salomon Bochner

Bibliography. N. I. Achiezer, *Theory of Approximation*, 1956, reprint 1992; W. Cheney, *Introduction to Approximation Theory*, 2d ed., 1991; I. M. Copi, *Introduction to Logic*, 9th ed., 1993; H. D. Ebbinghaus, J. Flum, and W. Thomas, *Mathematical Logic*, 1994; V. Klenk, *Understanding Symbolic Logic*, 3d ed., 1994; R. L. Vaught, *Set Theory: An Introduction*, 2d ed., 1994.

Matrix calculus

That branch of mathematics which deals with matrices whose elements are functions of one or more independent variables.

The derivative of a matrix $A(t)$ whose elements $a_{ij}(t)$ are functions of a variable t is defined in Eq. (1),

$$\frac{dA}{dt} = \lim_{\Delta t \to 0} \frac{A(t + \Delta t) - A(t)}{\Delta t} = \left(\frac{da_{ij}}{dt}\right) \tag{1}$$

where da_{ij}/dt represents the matrix whose elements are da_{ij}/dt. Thus dA/dt is formed by replacing the elements of $A(t)$ by their derivatives. *See* MATRIX THEORY.

If the matrices A and B are functions of t, then Eqs. (2) are satisfied by the operation of differentiation. In differentiating a product the order of the factors must be preserved. Thus Eq. (3) is obtained for

$$\frac{d}{dt}(A + B) = \frac{dA}{dt} + \frac{dB}{dt}$$
$$\frac{d}{dt}(AB) = \frac{dA}{dt}B + A\frac{dB}{dt} \tag{2}$$

$$\frac{d}{dt}A^2 = \frac{dA}{dt}A + A\frac{dA}{dt} \tag{3}$$

$(d/dt)A^2$ and not $2A(dA/dt)$. From $A^{-1}A = I$, Eq. (4) is found.

$$\frac{dA^{-1}}{dt} = -A^{-1}\frac{dA}{dt}A^{-1} \tag{4}$$

The integral of $A(t)$ is defined as the matrix whose elements are integrals of $a_{ij}(t)$.

Every square n by n matrix satisfies a polynomial equation of lowest degree, called its minimum equation, which is shown in Eq. (5). Equation (5) may be

$$A^m + a_1A^{m-1} + \cdots + a_mI = 0 \quad (m \le n) \tag{5}$$

used to express all powers of $A > m - 1$ in terms of $I, A, A^2, \ldots, A^{m-1}$. Therefore any matrix polynomial $f(A)$ of degree $k > m - 1$ may be replaced by a polynomial $F(A)$ of degree $< m$. If

$$f(z) = \sum_{k=0}^{\infty} c_k z^k$$

is a power series whose radius of convergence is r, and if all eigenvalues of A are less than r in absolute value, then (A) is defined as the matrix series shown in Eq. (6).

$$f(A) = c_0I + \sum_{k=0}^{\infty} c_kA^k \qquad |\lambda_A| < r \tag{6}$$

Thus the binomial series yields Eq. (7) for rational n; and since the exponential series for e^z converges for all z, Eq. (8) can be set up for arbitrary A. The matrix exponential has the properties $e^0 = I$, $e^Ae^{-A} = I$; also, $e^Ae^B = e^{A+B}$ when $AB = BA$. From the series for e^{tA}, $de^{tA}/dt = Ae^{tA}$.

$$(I + A)^n = I + \sum_{k=1}^{\infty} \left(\frac{n}{k}\right) A^k \qquad |\lambda_A| < 1 \tag{7}$$

$$e^A = I + \sum_{k=1}^{\infty} \frac{1}{k!}A^k \tag{8}$$

The minimum equation (5) may also be used to replace a power series for $f(A)$ by a polynomial $F(A)$. If Eq. (5) has distinct roots $\lambda_1, \lambda_2, \ldots, \lambda_m$ (eigenvalues of A), $F(A)$ has the eigenvalues $F(\lambda_i) = f(\lambda_i)$. The polynomial $F(\lambda)$ is completely determined by the m values $f(\lambda_i)$ that it assumes when $\lambda = \lambda_i$. Hence $F(\lambda)$, and also $F(A) = f(A)$, may be determined by Lagrange's interpolation formulas given in Eqs. (9) and (10), where each product has $m - 1$ factors.

$$f(A) = f(\lambda_1)C_1(A) + \cdots + f(\lambda_m)C_m(A) \tag{9}$$

$$C_j(A)\frac{\prod_{i \ne j}(A - \lambda_iI)}{\prod_{i \ne j}(\lambda_j - \lambda_i)} \tag{10}$$

When Eq. (5) has repeated roots, say $\lambda_1 = \lambda_2 = \lambda_3$, the corresponding terms in the modified equation (9) are given by formula (11), and Eq. (10) does

$$f(\lambda_1)C_1(A) + f'(\lambda_1)C_2(A) + f''(\lambda_1)C_3(A) \tag{11}$$

not apply. But since the $C_j(A)$ do not depend on f, they can be found by choosing m functions $f_i(\lambda)$ so that the m linear equations (9) and (10) in C_j have a nonzero determinant, and then solving them for the $C_j(A)$.

Consider, for example, a 4 by 4 matrix A with $\lambda_1 = \lambda_2 = \lambda_3$, $\lambda_4 \ne \lambda_1$. If $m = 4$, the basic equation (9) is

now Eq. (12). By choosing $f(\lambda) = 1, \lambda - \lambda_1, (\lambda - \lambda_1)^2$, and $(\lambda - \lambda_1)^3$, respectively, Eqs. (13) are obtained,

$$f(A) = f(\lambda_1)C_1 + f'(\lambda_1)C_2 + f''(\lambda_1)C_3 + f(\lambda_4)C_4 \quad (12)$$

$$\begin{aligned} I &= C_1 + 0 + 0 + C_4 \\ A - \lambda_1 I &= 0 + C_2 + 0 + (\lambda_4 - \lambda_1)C_4 \\ (A - \lambda_1 I)^2 &= 0 + 0 + 2C_3 + (\lambda_4 - \lambda_1)^2 C_4 \\ (A - \lambda_1 I)^3 &= 0 + 0 + 0 + (\lambda_4 - \lambda_1)^3 C_4 \end{aligned} \quad (13)$$

which give C_4, C_3, C_2, and C_1.

Eigenmatrices. Any n by n matrix A is reduced to its Jordan form J by finding its eigenmatrix E whose columns are the eigenvectors $e_1, \ldots, e_n$ belonging to the eigenvalues $\lambda_1, \lambda_2, \ldots, \lambda_n$. If λ_1 is simple, A has a proper eigenvector e_1 such that $(A - \lambda_1 I)e_1 = 0$. If λ_1 is k-tuple, with one proper eigenvector e_1 and $k - 1$ generalized eigenvectors $e_2, e_3, \ldots, e_k$ which satisfy Eqs. (14), then $E = (e_1|e_2| \ldots |e_n)$ and Eqs. (15) are valid.

$$(A - \lambda_1 I)e_j = e_{j-1} \qquad j = 2, 3, \ldots, k \quad (14)$$

$$E^{-1}AE = J \qquad A = EJE^{-1} \quad (15)$$

If $f(z)$ is an analytic function, then Eq. (16) holds,

$$f(A) = f(EJE^{-1}) = Ef(J)E^{-1} \quad (16)$$

which gives $f(A)$ when the simpler $f(J)$ is known. Thus, when A has distinct eigenvalues $\lambda_1, \ldots, \lambda_n$, J and $f(J)$ have the form shown in Eqs. (17).

$$\begin{aligned} J &= \text{diag}(\lambda_1, \ldots, \lambda_n) \\ f(J) &= \text{diag}[f(\lambda_1), \ldots, f(\lambda_n)] \end{aligned} \quad (17)$$

Equation (16) is an explicit formula for $f(A)$ and agrees with the former interpolation method; it requires, however, the eigenmatrix E and its reciprocal. Both methods are shown in the following example.

The eigenvalues of

$$A = \begin{pmatrix} 0 & 1 \\ -2 & 3 \end{pmatrix}$$

are $\lambda_1 = 1, \lambda_2 = 2$ and $e_1 = (1, 1)^\top, e_2 = (1, 2)^\top$. Then Eq. (16) gives Eq. (18).

$$f(A) = \begin{pmatrix} 1 & 1 \\ 1 & 2 \end{pmatrix} \begin{pmatrix} f(1) & 0 \\ 0 & f(2) \end{pmatrix} \begin{pmatrix} 2 & -1 \\ -1 & 1 \end{pmatrix}$$

$$= \begin{pmatrix} 2 & -1 \\ 2 & -1 \end{pmatrix} f(1) + \begin{pmatrix} -1 & 1 \\ -2 & 2 \end{pmatrix} f(2) \quad (18)$$

The interpolation method uses Eq. (9), which in this case reduces to Eq. (19). Choose $f(\lambda)$ as

$$f(A) = f(1)C_1 + f(2)C_2 \quad (19)$$

$\lambda - 1, \lambda - 2$, respectively; then C_2 and C_1 are given by Eqs. (20) in agreement with Eq. (18).

$$\begin{aligned} C_2 &= A - I = \begin{pmatrix} -1 & 1 \\ -2 & 2 \end{pmatrix} \\ -C_1 &= A - 2I = \begin{pmatrix} -2 & 1 \\ -2 & 1 \end{pmatrix} \end{aligned} \quad (20)$$

As an example with multiple eigenvalues, consider A given by Eq. (21). The modified Eq. (19) is now Eq. (22). Choose $f(\lambda)$ as $1, \lambda - 1, (\lambda - 1)^2$, respectively; then C_1, C_2, and C_3 are given by Eqs. (23).

$$A = \begin{pmatrix} 1 & 1 & 0 \\ 0 & 1 & 1 \\ 0 & 0 & 1 \end{pmatrix} \qquad \lambda_1 = \lambda_2 = \lambda_3 = 1 \quad (21)$$

$$f(A) = f(1)C_1 + f'(1)C_2 + f''(1)C_3 \quad (22)$$

$$I = C_1 \qquad A - I = C_2 \qquad (A - I)^2 = 2C_3 \quad (23)$$

Let $f(\lambda) = e^{\lambda t}$; then $f'(\lambda) = te^{\lambda t}$, $f''(\lambda) = t^2 e^{\lambda t}$, and so e^{tA} is given by Eq. (24), which can be expressed as Eq. (25).

$$e^{tA} = \begin{pmatrix} 1 & 0 & 0 \\ 0 & 1 & 0 \\ 0 & 0 & 1 \end{pmatrix} e^t + \begin{pmatrix} 0 & 1 & 0 \\ 0 & 0 & 1 \\ 0 & 0 & 0 \end{pmatrix} te^t + \begin{pmatrix} 0 & 0 & \frac{1}{2} \\ 0 & 0 & 0 \\ 0 & 0 & 0 \end{pmatrix} t^2 e^t \quad (24)$$

$$e^{tA} = \begin{pmatrix} 1 & t & \frac{1}{2}t^2 \\ 0 & 1 & t \\ 0 & 0 & 1 \end{pmatrix} e^t \quad (25)$$

Differential equations. Let $x_1(t), \ldots, x(t)$ be n unknown functions and $X(t)$ their column vector. Then if $A(t)$ is an n by n matrix whose elements are continuous functions of t, the system of n linear differential equations (26) may be solved by successive approx-

$$\frac{dX}{dt} = AX \qquad X(0) = X_0 \quad (26)$$

imations. The nth approximation is obtained from the $(n - 1)$th by integrating Eqs. (27) from $t = 0$ to t. Then a solution is obtained in the form of Eq. (28), where Ω is given by Eq. (29) and is called the matricant of A. When A has constant elements, Eq. (29) reduces to Eq. (30).

$$\frac{dX_n}{dt} = AX_{n-1} \qquad n = 1, 2, \ldots \quad (27)$$

$$X = \lim_{n \to \infty} X_n = \Omega X_0 \quad (28)$$

$$\Omega = I + \int_0^t A\,dt + \int_0^t A\,dt \int_0^t A\,dt + \cdots \quad (29)$$

$$\Omega = I + At + \frac{1}{2!}A^2 t^2 + \frac{1}{3!}A^3 t^3 + \cdots = e^{tA} \quad (30)$$

Consider, for example, the system given by Eqs. (31), or in matrix form by Eq. (32). Then

from Eq. (25) one obtains Eq. (33).

$$\begin{aligned} \frac{dx_1}{dt} &= x_1 + x_2 \\ \frac{dx_2}{dt} &= x_2 + x_3 \\ \frac{dx_3}{dt} &= x_3 \end{aligned} \tag{31}$$

$$\frac{dX}{dt} = \begin{pmatrix} 1 & 1 & 0 \\ 0 & 1 & 1 \\ 0 & 0 & 1 \end{pmatrix} X = AX \tag{32}$$

$$X = e^{tA}X_0 = e^t \begin{pmatrix} 1 & t & {}^1\!/_2 t^2 \\ 0 & 1 & t \\ 0 & 0 & 1 \end{pmatrix} X_0 \tag{33}$$

In a linear system with variable coefficients $p_{ij}(t)$, the differential Eq. (26) becomes Eqs. (34). If X_1,

$$\frac{dX}{dt} = P(t)X \qquad P(t) = [p_{ij}(t)] \tag{34}$$

X_2, X_3 are three linearly independent solutions of Eqs. (34), let $Y = (X_1|X_2|X_3)$ denote the 3 by 3 matrix whose columns are X_1, X_2, X_3. Then Eqs. (34) are equivalent to the matrix equation (35).

$$\frac{dY}{dt} = P(t)Y \tag{35}$$

If one differentiates det Y by rows and adds the resulting determinants, one obtains Eq. (36), where

$$\begin{aligned} \frac{d}{dt}(\det Y) &= (p_{11} + p_{22} + p_{33})\det Y \\ &= (\operatorname{tr} P)\ \det Y \end{aligned} \tag{36}$$

tr P denotes the trace of P and det Y is the determinant of Y. On integration this yields the Jacobi identity given in Eq. (37). Since det Y is not

$$\det Y = c \exp \int_{t_0}^{t} \operatorname{tr} P\, dt \tag{37}$$

identically zero, $c \neq 0$; hence the matrix integral $Y(t)$ is nonsingular; that is, det $Y \neq 0$.

If Y_1 is a particular solution of Eq. (35) and C is an arbitrary 3 by 3 constant matrix, then $Y = Y_1C$ is also a solution. Moreover, all solutions of Eq. (35) are contained in $Y = Y_1C$. For if Y is a solution of Eq. (35), then Eq. (4) gives Eq. (38), hence $Y_1^{-1}Y = C$ and $Y = Y_1C$.

$$\begin{aligned} \frac{d}{dt}({Y_1}^{-1}Y) &= \left(-{Y_1}^{-1}\frac{dY_1}{dt}{Y_1}^{-1}\right) Y + {Y_1}^{-1}\frac{dY}{dt} \\ &= -{Y_1}^{-1}PY + {Y_1}^{-1}PY = 0 \end{aligned} \tag{38}$$

If the coefficients $p_{ij}(t)$ are periodic with the same period ω, that is, $P(t + \omega) = P(t)$, then the system shown in Eq. (35) can be reduced to one with constant coefficients by a linear transformation $Y = L(t)Z$, where $L(t)$ is a nonsingular matrix of period ω. Let $Y_1(t)$ be the solution of Eq. (35) for which $Y_1(0) = I$; then $Y_1(t + \omega)$ is also a solution, and hence $Y_1(t + \omega) = Y_1(t)C$, where C is a nonsingular matrix of constants. If a matrix B is determined so that $e^{B\omega} = C$, then Eqs. (39) and (40) result, which reduce Eq. (35) to

$$Y = L(t)Z \tag{39}$$

$$L(t) = Y_1(t)e^{-Bt} = L(t + \omega) \tag{40}$$

$dZ/dt = BZ$, whose solution $Z_1(t)e^{Bt}$ corresponds to $Y_1(t)$. Note that $Y_1(t) = Y_1(t)e^{-Bt}Z_1(t)$ requires $Z_1(t) = e^{Bt}$, $dZ_1/dt = BZ_1$; and since all solutions of this equation have the form $Z(t) = CZ_1(t)$, $dZ/dt = BZ$.

Louis Brand

Bibliography. P. Bugl, *Differential Equations: Matrixes and Models*, 1994; R. A. Horn and C. R. Johnson, *Matrix Analysis*, 1985, paper 1990; A. W. Joshi, *Matrices and Tensors in Physics*, 1995; J. R. Magnus and H. Neudecker, *Matrix and Differential Calculus with Applications in Statistics and Econometrics*, 2d ed., 1999.

Matrix isolation

A technique for providing a means of maintaining molecules in an inert medium at low temperature for spectroscopic study. This method is particularly well suited for preserving reactive species in a solid, inert environment. Absorption (infrared, visible, and ultraviolet), electron-spin resonance, and laser-excitation spectroscopes can be used to examine elusive molecular fragments such as free radicals that may be postulated as important controlling intermediates for chemical transformations used in industrial reactions, high-temperature molecules that are in equilibrium with solids at very high temperatures, weak molecular complexes that may be stable at low temperatures, new reactive molecular species, and molecular ions that are produced in plasma discharges or by high-energy radiation. The matrix isolation technique enables spectroscopic data to be obtained for reactive molecular fragments, many of which cannot be studied in the gas phase. *See* ELECTRON PARAMAGNETIC RESONANCE (EPR) SPECTROSCOPY; INFRARED SPECTROSCOPY; SPECTROSCOPY.

Experimental apparatus. The experimental apparatus for matrix isolation experiments is designed with the method of generating the molecular transient and performing the spectroscopy in mind. **Figure 1** shows the cross section of a vacuum vessel used for absorption spectroscopic measurements (such as infrared, visible, and ultraviolet). The optical windows must be transparent to the examining radiation. The rotatable cold window is cooled to 4 to 20 K (−452 to −424°F) by closed-cycle refrigeration or liquid helium. The matrix sample is introduced through the spray-on line at rates of 1–5 millimoles per hour; argon is the most widely used matrix gas, although neon, krypton, xenon, and nitrogen are also used. The reactive species can be generated in a number of ways: mercury-arc photolysis of a trapped precursor molecule through the quartz window, evaporation from a Knudsen cell in the heater, chemical reaction of atoms evaporated from the Knudsen

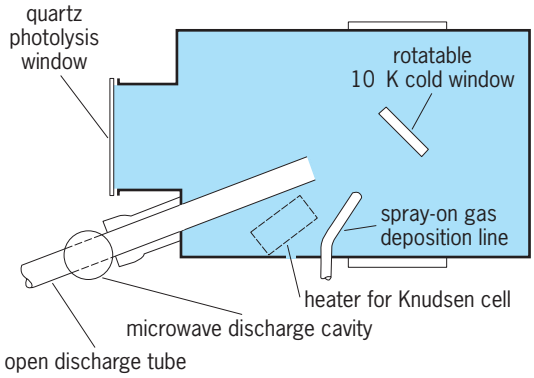

Fig. 1. Vacuum-vessel base cross section for matrix photoionization experiments. 10 K = −263°C or −442°F.

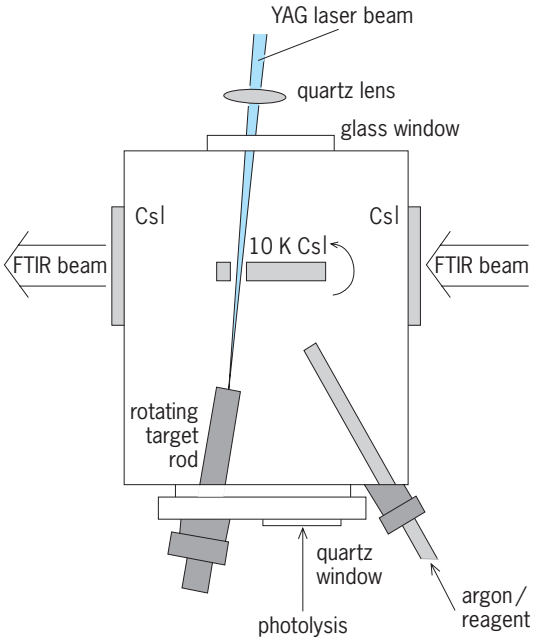

Fig. 2. Schematic plan view of the matrix assembly for pulsed-laser ablation.

cell with molecules deposited through the spray-on line, neodymium-yttrium aluminum garnet (Nd-YAG) laser evaporation of solids, and vacuum-ultraviolet photolysis of molecules deposited from the spray-on line by radiation from discharge-excited atoms flowing through the tube. The cold window is rotated for transmission absorption spectroscopic measurements using ultraviolet-visible or infrared spectrometers.

Figure 2 is a schematic diagram of the laser ablation matrix isolation apparatus. The ablated metal atoms intersect the gas sample during codeposition on the cold cesium iodide (CsI) window, where collisions and reactions occur. The Nd-YAG fundamental at 1064 nanometers in 5–50-millijoule pulses of 10-nanosecond duration was focused (spot size approximately 0.1 nm) onto a rotating metal target. For laser excitation studies, the sample is deposited on a tilted copper wedge which is grazed by the laser beam, and light emitted or scattered at approximately 90° is examined by a spectrograph. In electron-spin resonance studies, the sample is condensed on a sapphire rod that can be lowered into the necessary waveguide and magnet. The chemical versatility of the matrix technique can perhaps be best described by considering a number of important examples. *See* PHOTOLYSIS.

Applications. The first free radical stabilized in sufficient concentration for matrix infrared detection was formyl (HCO·). Hydrogen iodide (HI) was deposited in a carbon monoxide (CO) matrix and photolyzed with a mercury arc; hydrogen atoms produced by dissociation of HI reacted with CO in the cold solid to produce HCO. The infrared spectrum of HCO provided vibrational fundamentals and information about the chemical bonding in this reactive species. Free radicals have been produced in matrices with a variety of techniques such as ultraviolet photolysis [reaction (1)]; vacuum ultraviolet photolysis [reaction (2)]; fluorine atom [reaction (3)]; metal atom [reaction (4)]; and hydrogen atom [reaction (5)].

$$OF_2 + \text{ultraviolet light} \rightarrow OF\cdot + F\cdot \quad (1)$$

$$CHF_3 + \text{vacuum ultraviolet light} \rightarrow CF_3\cdot + H\cdot \quad (2)$$

$$C_2H_2 + F\cdot \rightarrow C_2H_2F\cdot \quad (3)$$

$$CCl_4 + Li \rightarrow CCl_3\cdot + LiCl \quad (4)$$

$$H\cdot + O_2 \rightarrow HO_2\cdot \quad (5)$$

See CHEMICAL BONDING.

The first molecular ionic species characterized in matrices, $Li^+O_2^-$ was formed by the cocondensation reaction of lithium (Li) atoms and oxygen (O_2) molecules at high dilution in argon. The infrared spectrum exhibited a weak $(O \leftrightarrow O)^-$ stretching vibration and two strong $Li^+ \leftrightarrow O_2^-$ stretching vibrations, as shown at the top of **Fig. 3** for the ^7Li and $^{16,18}O_2$ isotopic reaction. The 1-2-1 relative-intensity oxygen isotopic triplets in this experiment showed that the oxygen atomic positions in the molecule are equivalent and indicated an isosceles triangular structure. The ionic model for the bonding

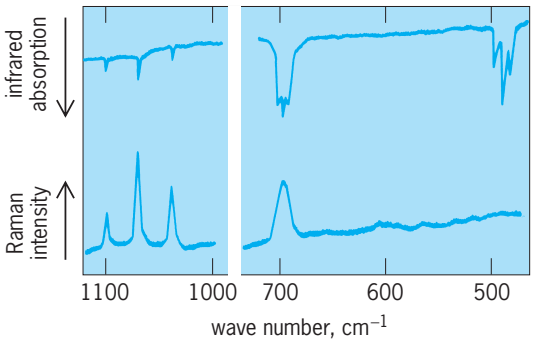

Fig. 3. Infrared and Raman spectra of lithium superoxide, $Li^+O_2^-$, using lithium-7 and 30% $^{18}O_2$, 50% $^{16}O^{18}O$, and 20% $^{16}O_2$ at concentrations of $Ar/O_2 = 100$. The Raman spectrum was recorded by using 200 mW of 488-nm excitation at the sample.

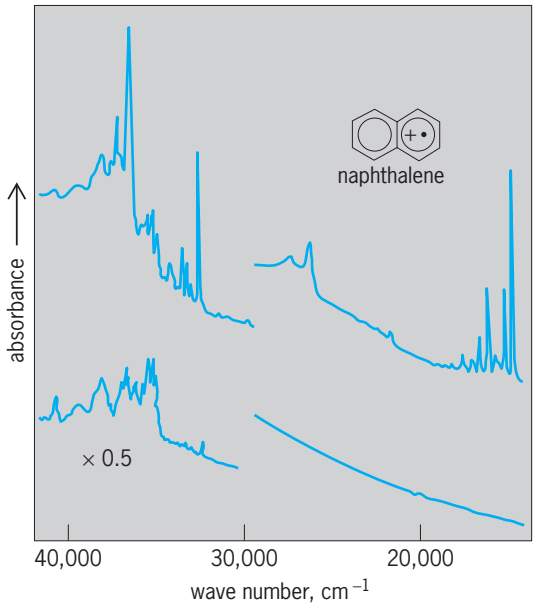

Fig. 4. Visible and ultraviolet absorption spectra of naphthalene samples in solid argon at 20 K. Upper curves show Ar/CCl_4/N = 3000/4/1, and lower curves show the same sample after 15 s of irradiation at 220–1000 nm from a high-pressure mercury arc.

in $Li^+O_2^-$ was confirmed by contrasting intensities between the laser-Raman and infrared-absorption spectra shown in Fig. 3. *See* RAMAN EFFECT.

High-temperature molecules like lithium fluoride (LiF) can be trapped in matrices by evaporating the molecule from the crystalline solid in a Knudsen cell at high temperature or by reacting lithium atoms with fluorine molecules during condensation. The latter method has been used to synthesize the calcium oxide (CaO) molecule from the calcium atom–ozone reaction, which gives the calcium ozonide ion pair $Ca^+O_3^-$ and CaO diatomic products.

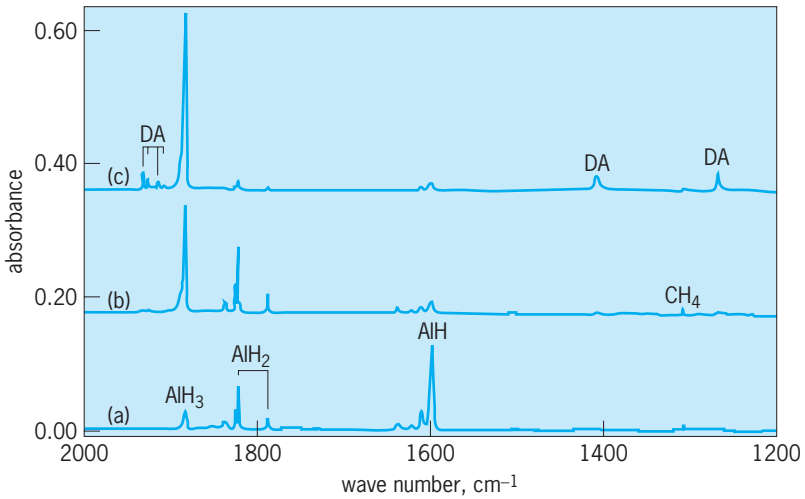

Fig. 5. Infrared spectra in the 2000–1200 cm^{-1} region for the products of the reactions of laser-ablated Al atoms with pure hydrogen co-deposited at 3.5 K. (*a*) Spectrum obtained from initial deposited sample. (*b*) Spectrum after >290 nm irradiation. (*c*) Spectrum after >220 nm irradiation.

Continuous exposure of a condensing sample to argon-resonance radiation during sample condensation has been used to produce molecular cations for spectroscopic study. In the case of fluoroform (CHF_3), photolysis produced the CF_3 · radical, which may be photoionized by a second 11.6-eV photon to give CF_3^+. The infrared spectrum of CF_3^+ revealed a very high C-F vibrational fundamental, which indicates substantial pi bonding in this planar carbocation.

The naphthalene ($C_{10}H_8$; mothballs) cation is an interesting case for matrix study since a wealth of data is available from other spectroscopic techniques. Vacuum ultraviolet photoionization of $C_{10}H_8$ during condensation with excess argon produced new absorption band systems at 14,810, 21,697, and 26,240 cm^{-1} for the naphthalene cation. Using a 15-s mercury-arc irradiation with an electron-trapping molecule (CCl_4) present, **Fig. 4** shows that the above three bands plus two others, at 32,510 and 36,417 cm^{-1}, were produced. In the latter case, one ultraviolet photon excited $C_{10}H_8$ and a second photon produced ionization, the removed electron being trapped by CCl_4 (as CCl_3· and Cl^-), and in the former case, one vacuum-ultraviolet photon ionized $C_{10}H_8$ directly to give the $C_{10}H_8^+$ cation trapped in solid argon for observation of its electronic absorption spectrum. Vibronic intervals (vibrational fine structure) in the absorption spectrum provide information on vibrational fundamentals in the cation excited states.

Molecular complexes involving hydrogen fluoride (HF) serve as useful prototypes for the understanding of the important phenomenon of hydrogen bonding. An interesting chemical case is ammonia (NH_3) and HF, which on the macroscopic scale produce the salt ammonium fluoride but on the microscopic scale give the NH_3-HF complex. The infrared spectrum of this complex reveals vibrations for NH_3 and HF perturbed by their association in the complex. Fourier-transformed infrared spectroscopy is particularly advantageous in these studies because of the high vibrational frequencies for HF species and low sample transmission in this region. The ammonia symmetric bending motion is considerably blue-shifted, and the hydrogen fluoride stretching fundamental is markedly redshifted. These shifts attest to a strong intermolecular interaction within the complex. *See* HYDROGEN BOND.

Ozone (O_3) is a very important molecule in the upper atmosphere, as it absorbs harmful ultraviolet radiation. In the laboratory, this ultraviolet dissociation of ozone provides oxygen atoms for chemical reactions. Photochemical reactions of elemental phosphorus (P_4), an extremely reactive molecule well suited for matrix isolation studies, and ozone produce a new low oxide of phosphorus, P_4O, which is involved as a reactive intermediate in the striking of a match. The infrared spectrum of P_4O shows a strong terminal PO bond-stretching fundamental and characterizes the P_4O structure as tetrahedral P_4 with an O atom cap. Further photochemical reactions

of phosphorus and oxygen produce and trap the reactive molecule PO_2·, which can also be formed by laser evaporation of red phosphorus followed by reaction with a stream of oxygen gas. *See* FREE RADICAL; REACTIVE INTERMEDIATES.

The use of pulsed laser ablation to produce metal atoms for reactions to make new chemical species is illustrated by investigations of metal carbonyls and nitrosyls and metal hydrides. When the cold window (Fig. 1) is cooled below 4 K, neon and pure hydrogen are condensed; and metal atom reactions can be done in an inert solid neon or a reactive solid hydrogen host. This is illustrated by reactions of aluminum (Al) atoms to form in solid hydrogen the dialane (Al_2H_6) molecule,

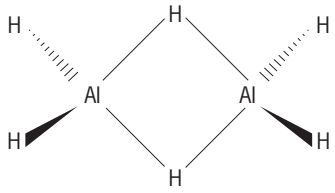

which is isostructural to diborane—a model for bridge bonding. Laser-ablated and excited Al atoms co-deposited with pure hydrogen at 3.5 K react with the hydrogen host to give absorptions for AlH (1599 cm^{-1}), AlH_2 (1822, 1788 cm^{-1}), and AlH_3 (1884 cm^{-1}), which are shown in **Fig. 5***a*. Irradiation of the sample with a mercury-arc lamp filtered by a Pyrex plate (wavelengths >290 nm) promotes the reaction of AlH with H_2 to form AlH_3 as shown in Fig. 5*b*. Further irradiation with the full arc (wavelengths >220 nm; Fig. 5*c*) almost destroys AlH_2, making more AlH_3 and new bands at 1932, 1915, 1408, and 1268 cm^{-1} (labeled DA). These bands shift when the reaction is done in pure D_2 and confirm that a new aluminum hydride species is formed. The important point is that the two higher frequency bands are due to terminal Al-H stretching modes and the 1408 and 1268 cm^{-1} bands are in the region for Al-H-Al bridge-bond-stretching modes, which characterizes a new molecule containing both terminal and bridge aluminum-hydrogen bonds. The new molecule $H_2Al(H)_2AlH_2$ is formed from the combination of two AlH_3 molecules [reactions (6)–(8)] and characterized experimentally from its infrared spectrum.

$$Al + H_2 \rightarrow AlH + H \quad (6)$$

$$AlH + H_2 \rightarrow AlH_3 \quad (7)$$

$$AlH_3 + AlH_3 \rightarrow H_2Al(H)_2AlH_2 \quad (8)$$

The vibrational frequencies assigned to new molecules through matrix isolation infrared spectroscopy can be determined with a high degree of accuracy using density functional theory calculations, a computational quantum-chemistry approach. Such calculations predict that the bridge-bonded dialane molecule has seven infrared active vibrational modes with observable infrared intensity. The above four stretching modes plus three lower-frequency bending modes are observed for dialane in solid hydrogen in excellent agreement with the calculated frequencies. This agreement between calculated and observed frequencies confirms the identification of the novel bridge-bonded dialane molecule in solid hydrogen. *See* BORANE; METAL CARBONYL; METAL HYDRIDES; MOLECULAR SIMULATION; QUANTUM CHEMISTRY.

Lester Andrews

Bibliography. L. Andrews, Fourier transform infrared spectra of HF complexes in solid argon, *J. Phys. Chem.*, 88:2940–2949, 1984; L. Andrews, Matrix infrared spectra and density functional calculations of transition metal hydrides and dihydrogen complexes, *Chem. Soc. Rev.*, 33:123–132, 2004; L. Andrews, W. D. Bare, and G. V. Chertihin, Reactions of laser-ablated V, Cr and Mn atoms with nitrogen atoms and molecules, *J. Phys. Chem.*, 101:8417–8427, 1997; L. Andrews and A. Citra, Infrared spectra and density functional calculations on transition metal nitrosyls, *Chem. Rev.*, 102:885–911, 2002; L. Andrews and M. Moskovits (eds.), *Chemistry and Physics of Matrix Isolated Species*, 1989; L. Andrews and X. Wang, The infrared spectrum of Al_2H_6 in solid hydrogen, *Science*, 299:2049–2052, 2003; V. E. Bondybey, A. M. Smith, and J. Agreiter, New developments in matrix isolation spectroscopy, *Chem. Rev.*, 96:2113–2134, 1996; M. Zhou, L. Andrews, and C. W. Bauschlicher, Jr., Spectroscopic and theoretical investigations of binary unsaturated transition metal carbonyl cations, neutrals, and anions, *Chem. Rev.*, 101:1931–1961, 2001.

Matrix mechanics

A formulation of quantum theory in which the operators are represented by time-dependent matrices. For a discussion of quantum-mechanical operators and other information essential to an understanding of this article *see* NONRELATIVISTIC QUANTUM THEORY

Matrix mechanics is not useful for obtaining quantitative solutions to actual problems; on the other hand, because it is concisely expressed in a form independent of special coordinate systems, matrix mechanics is useful for proving general theorems. For the purposes of the following brief discussion it is sufficient to consider a one-dimensional spinless system, described by a wave function $\psi(x,t)$.

A matrix A is a rectangular array of numbers; the number of rows or columns of the array may be finite or infinite; A_{mn} is the element (number) in the mth row and the nth column; m, n may be discrete or continuous indices.

Symbolic addition $C = A + B$ is defined as meaning that $C_{mn} = A_{mn} + B_{mn}$ for each m and n, with the implication that the rows of A, B have the same indexing m and that the columns also have the same indexing m. Symbolic multiplication $C = AB$ is defined to mean $C_{mn} = \Sigma_j A_{mj} B_{jn}$, summed over all values of j, again with the implication that the columns of A

and the rows of B have the same indexing j; when j is continuous, the sum in the definition of C_{mn} is replaced by an integral. The adjoint $A^\dagger$ of A is obtained by interchanging rows and columns of A and then taking the complex conjugate of each element, that is, ${A_{mn}}^\dagger = (A_{nm})^* \equiv {A_{nm}}^*$; $(AB)^\dagger = B^\dagger A^\dagger$. *See* MATRIX THEORY.

Suppose $\phi(x,t)$ is expanded in terms of any complete set of orthonormal functions u_n, as shown in Eq. (1). The matrix elements (in this u representation) of any quantum-mechanical operator A are defined by Eq. (2). For instance, when $A \equiv p_x$, A is

$$\psi(x, t) = \sum_n \psi_n(t) u_n(x) \tag{1}$$

$$A_{mn} = \int_{-\infty}^{\infty} dx\, {u_m}^*(x) A u_n(x) \tag{2}$$

replaced by $(\hbar/i)\,\partial/\partial x$ in Eq. (2). From Eqs. (1) and the orthonormality of $u_n(x)$, if Eq. (3) holds, then Eq. (4) can be obtained. This result shows that the

$$A\psi \equiv \phi = \sum_n \phi_n u_n \tag{3}$$

$$\phi_m = \sum_n A_{mn} \psi_n \tag{4}$$

equation $\phi = A\psi$, which states that ϕ is the function resulting from the operation A on ψ, can be interpreted equally well as a matrix equation, provided ψ, ϕ are represented by single-column matrices whose elements are respectively ψ_n, ϕ_n. Similarly, the expectation value of the operator A in the state ψ is given by Eq. (5), that is, in matrix notation $\langle A \rangle =$

$$\langle A \rangle = \int \psi^* A \psi = \int \psi^* \phi = \sum_{m,n} {\psi_m}^* A_{mn} \psi_n \tag{5}$$

$\psi^\dagger A \psi$; the adjoint of a column matrix ψ_{m} is the row $\psi_{\mathrm{m}}{}^*$.

The time-dependent Schrödinger equation implies $\psi(t) = \exp(-iHt/\hbar)\ \psi(0)$. Thus, noting that, because the operator H is hermitian, the matrix H is self-adjoint, $H^\dagger = H$, and the expectation value of A at time t is as shown in Eq. (6). Equation (6) shows

$$\langle A \rangle_t = \psi^\dagger(0) \exp(iHt/\hbar) \times A \exp -(iHt/\hbar)\psi(0) \tag{6}$$

that $\langle A \rangle_t$ can be computed in two equivalent ways: (i) the conventional Schrödinger representation, in which ψ is time-dependent and the A_{mn}'s are time-independent; (ii) the Heisenberg representation, in which ψ is time-independent and equal to $\psi(0)$ but A is represented by time-dependent matrix elements given in Eq. (7). Differentiating Eq. (7), one obtains Eq. (8); that is, $dA/dt = (i\hbar)^{-1}\,(A,H)$, where $(A,B) \equiv AB - AB$.

$$A_{mn}(t) = [\exp(iHt/\hbar)A(0)\ \exp -(iHt/\hbar)]_{mn} \tag{7}$$

$$\frac{d}{dt}A(t) = \frac{iH}{\hbar} \exp(iHt/\hbar)A(0) \exp -(iHt/\hbar) - \exp(iHt/\hbar)A(0) \exp -(iHt/\hbar)\frac{iH}{\hbar}$$

$$= \frac{1}{i\hbar}[A(t)H - HA(t)] \tag{8}$$

It can be proved that (i) operators can consistently be replaced by equivalent matrices, defined by Eq. (2); and (ii) the Heisenberg time-dependent matrix formulation of quantum theory is completely equivalent to the Schrödinger time-dependent wave function formulation.

Edward Gerjuoy

Matrix theory

The study of matrices and their properties, and of linear transformations on vector spaces, which can be represented by matrices.

Matrices. A matrix is a rectangular array of numbers, with the numbers that appear in the matrix being called entries. For example, A, given by Eq. (1), is a 2×3 matrix (that is, it has 2 rows and 3 columns). The first row of A is given by notation (2), and the second column of A is given by notation (3).

$$A = \begin{bmatrix} 1 & 2 & 3 \\ 4 & 5 & 6 \end{bmatrix} \tag{1}$$

$$[1 \quad 2 \quad 3] \tag{2}$$

$$\begin{bmatrix} 2 \\ 5 \end{bmatrix} \tag{3}$$

The entry in the ith row and jth column of a matrix is denoted by a_{ij}. For example, in the matrix A, $a_{21} = 4$ and $a_{12} = 2$.

Representation of rotations. Matrices arise naturally as concrete representations of certain geometric transformations in the cartesian plane. An example of such a transformation is one in which any point v in the plane (v is also called a vector) is rotated counterclockwise through 45° around the origin O to a new vector Tv (see **illus.**). The vectors

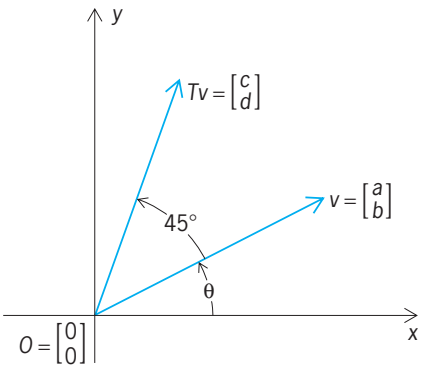

Vector rotation that rotates any vector *v* in the plane counterclockwise through 45° to a new vector *Tv*.

v and Tv can be represented as in Eqs. (4), where

$$v = \begin{bmatrix} a \\ b \end{bmatrix} \qquad Tv = \begin{bmatrix} c \\ d \end{bmatrix} \tag{4}$$

each vector is defined by a pair of numbers: a is the projection of v on the x axis, b is its projection on the y axis, and c and d are the corresponding projections of Tv. If v is a distance r from O and makes an angle θ with the x axis, then the rotated vector Tv is also a distance r from O and makes an angle $\theta + 45^\circ$ with the x axis. Thus, the projections are given by Eqs. (5), and the identities for

$$\begin{aligned} a &= r\cos\theta \\ b &= r\sin\theta \\ c &= r\cos(\theta + 45^\circ) \\ d &= r\sin(\theta + 45^\circ) \end{aligned} \tag{5}$$

the cosine and sine of a sum of angles can be applied to this equation, yielding Eqs. (6). If A is the 2×2 matrix given by Eq. (7), then Eqs. (6) can be conveniently summarized with Eq. (8). Thus, the transformation T is described completely by the matrix A, as in Eq. (8). *See* ANALYTIC GEOMETRY; TRIGONOMETRY.

$$\begin{aligned} c &= r\cos\theta\cos 45^\circ - r\sin\theta\sin 45^\circ \\ &= a\cos 45^\circ - b\sin 45^\circ \\ d &= r\sin\theta\cos 45^\circ + r\cos\theta\sin 45^\circ \\ &= a\sin 45^\circ + b\cos 45^\circ \end{aligned} \tag{6}$$

$$A = \begin{bmatrix} \cos 45^\circ & -\sin 45^\circ \\ \sin 45^\circ & \cos 45^\circ \end{bmatrix} \tag{7}$$

$$\begin{bmatrix} c \\ d \end{bmatrix} = A \begin{bmatrix} a \\ b \end{bmatrix} \tag{8}$$

If S is another counterclockwise rotation through 30°, then it follows similarly that S is described by the matrix B given by Eq. (9).

$$B = \begin{bmatrix} \cos 30^\circ & -\sin 30^\circ \\ \sin 30^\circ & \cos 30^\circ \end{bmatrix} \tag{9}$$

Clearly, the composition of S and T, that is, "T followed by S," denoted by ST, is a counterclockwise rotation through $(45 + 30)^\circ = 75^\circ$. The composition ST has a matrix representation C, which is denoted by Eq. (10). The entries of C can be

$$C = BA \tag{10}$$

conveniently computed directly from the entries of A and B as follows: if A and B are any two 2×2 matrices, given by Eq. (11), then the product of B and A is defined as the matrix in Eq. (12). If the definition in Eq. (12) is applied to the matrices (7) and (9), then Eq. (13) results, and the trigonometric formulas used previously yield Eq. (14). Thus the

$$A = \begin{bmatrix} a_{11} & a_{12} \\ a_{21} & a_{22} \end{bmatrix} \qquad B = \begin{bmatrix} b_{11} & b_{12} \\ b_{21} & b_{22} \end{bmatrix} \tag{11}$$

$$BA = \begin{bmatrix} b_{11}a_{11} + b_{12}a_{21} & b_{11}a_{12} + b_{12}a_{22} \\ b_{21}a_{11} + b_{22}a_{21} & b_{21}a_{12} + b_{22}a_{22} \end{bmatrix} \tag{12}$$

$$BA = \begin{bmatrix} \cos 30^\circ\cos 45^\circ - \sin 30^\circ\sin 45^\circ & \sin 30^\circ\cos 45^\circ + \cos 30^\circ\sin 45^\circ \\ -\cos 30^\circ\sin 45^\circ - \sin 30^\circ\cos 45^\circ & -\sin 30^\circ\sin 45^\circ + \cos 30^\circ\cos 45^\circ \end{bmatrix} \tag{13}$$

$$BA = \begin{bmatrix} \cos 75^\circ & -\sin 75^\circ \\ \sin 75^\circ & \cos 75^\circ \end{bmatrix} \tag{14}$$

definition in Eq. (12) yields the matrix $C = BA$ that represents the composition ST. The matrix C in Eq. (10) is the product of the matrices B and A.

Matrix multiplication. In general, if X is an $m \times n$ matrix and Y is an $n \times q$ matrix, then the product $P = XY$ is an $m \times q$ matrix whose entry in row i and column j is given by Eq. (15) for $i, \ldots, m$ and $j = 1, \ldots, q$.

$$p_{ij} = x_{i1}y_{1j} + x_{i2}y_{2j} + \cdots + x_{in}y_{nj} \tag{15}$$

The number of columns of X must be the same as the number of rows of Y in order that the product matrix P can be defined. Some examples of matrix products are given in Eqs. (16)–(20). The examples in Eqs. (16) and (17) show that, in general, XY and YX need not be the same matrix; that is, matrix multiplication is not always commutative. The examples in Eqs. (18) and (19) show that multiplication of a matrix X by the $n \times n$ matrix with 1 in row i and column i for $i = 1, \ldots, n$, and 0 elsewhere, does not change the matrix X. Finally, the example in Eq. (20) shows that the product of two matrices can have every entry 0 without this being the case for either factor.

$$\begin{bmatrix} 1 & 2 \\ 0 & 3 \end{bmatrix}\begin{bmatrix} 4 & 0 \\ 5 & 6 \end{bmatrix} = \begin{bmatrix} 1\cdot 4 + 2\cdot 5 & 1\cdot 0 + 2\cdot 6 \\ 0\cdot 4 + 3\cdot 5 & 0\cdot 0 + 3\cdot 6 \end{bmatrix} = \begin{bmatrix} 14 & 12 \\ 15 & 18 \end{bmatrix} \tag{16}$$

$$\begin{bmatrix} 4 & 0 \\ 5 & 6 \end{bmatrix}\begin{bmatrix} 1 & 2 \\ 0 & 3 \end{bmatrix} = \begin{bmatrix} 4\cdot 1 + 0\cdot 0 & 4\cdot 2 + 0\cdot 3 \\ 5\cdot 1 + 6\cdot 0 & 5\cdot 2 + 6\cdot 3 \end{bmatrix} = \begin{bmatrix} 4 & 8 \\ 5 & 28 \end{bmatrix} \tag{17}$$

$$\begin{bmatrix} 1 & 0 \\ 0 & 1 \end{bmatrix}\begin{bmatrix} 2 & 3 & 4 \\ 5 & 6 & 7 \end{bmatrix} = \begin{bmatrix} 2 & 3 & 4 \\ 5 & 6 & 7 \end{bmatrix} \tag{18}$$

$$\begin{bmatrix} 2 & 3 & 4 \\ 5 & 6 & 7 \end{bmatrix}\begin{bmatrix} 1 & 0 & 0 \\ 0 & 1 & 0 \\ 0 & 0 & 1 \end{bmatrix} = \begin{bmatrix} 2 & 3 & 4 \\ 5 & 6 & 7 \end{bmatrix} \tag{19}$$

$$\begin{bmatrix} 0 & 1 \\ 0 & 0 \end{bmatrix}\begin{bmatrix} 0 & 1 \\ 0 & 0 \end{bmatrix} = \begin{bmatrix} 0 & 0 \\ 0 & 0 \end{bmatrix} \tag{20}$$

Vector spaces. Vectors in the plane can be added and multiplied (scaled) by constants. For example, if the vectors u and v and the number c are given by Eq. (21), then $u + v$ is given by Eq. (22) and cu is given by Eq. (23).

$$u = \begin{bmatrix} 1 \\ 2 \end{bmatrix} \qquad v = \begin{bmatrix} 3 \\ 4 \end{bmatrix} \qquad c = -3 \tag{21}$$

$$u + v = \begin{bmatrix} 1+3 \\ 2+4 \end{bmatrix} = \begin{bmatrix} 4 \\ 6 \end{bmatrix} \tag{22}$$

$$cu = \begin{bmatrix} -3 \cdot 1 \\ -3 \cdot 2 \end{bmatrix} = \begin{bmatrix} -3 \\ -6 \end{bmatrix} \tag{23}$$

Axioms. There are a number of simple axioms that are satisfied by vector addition and scalar multiplication. If u, v, and w are vectors, then [1] Eqs. (24) and (25) are valid; [2] there exists a vector 0 such that Eq. (26) is satisfied; and there exists a unique vector $-u$ such that Eq. (27) is satisfied. If, in addition, c and d are numbers (also called scalars), then Eqs. (28)–(31) are satisfied. A set of vectors V together with a set of numbers F that satisfy these rules is called a vector space over F. The set of numbers F is a field. This means that F has many of the properties associated with rational numbers (fractions), real numbers (decimals), or complex numbers. There are many important mathematical systems that satisfy the preceding axioms for a vector space. Some examples are the two-dimensional space of plane geometry, the three-dimensional space of solid geometry, and polynomials with coefficients from F. *See* FIELD THEORY (MATHEMATICS).

$$u + v = v + u \tag{24}$$

$$u + (v + w) = (u + v) + w \tag{25}$$

$$u + 0 = u \tag{26}$$

$$u + (-u) = 0 \tag{27}$$

$$(cd)\, u = c\,(du) \tag{28}$$

$$1u = u \tag{29}$$

$$c(u + v) = cu + cv \tag{30}$$

$$(c + d)\, u = cu + du \tag{31}$$

Linear transformations. If V and W are vector spaces over F, then a linear transformation T on V to W is a function that assigns to each vector v in V a unique vector w in W, as in Eq. (32). Moreover, if u and v

$$Tv = w \tag{32}$$

are any vectors in V, and c and d are any scalars in F, then T satisfies Eq. (33). The vector rotation examples T and S described previously are linear transformations.

$$T(cu + dv) = cTu + dTv \tag{33}$$

A basis of the vector space V is an ordered sequence of vectors $v_1, \ldots, v_n$ in V such that any vector v in V can be written in only one way as in Eq. (34)

$$v = c_1 v_1 + c_2 v_2 + \cdots + c_n v_n \tag{34}$$

for appropriate scalars $c_1, \ldots, c_n$. For example, if V is the cartesian plane, then the vectors of notation (35) form a basis, as do the vectors of notation (36).

$$\begin{bmatrix} 1 \\ 0 \end{bmatrix}, \begin{bmatrix} 0 \\ 1 \end{bmatrix} \tag{35}$$

$$\begin{bmatrix} 1 \\ -1 \end{bmatrix}, \begin{bmatrix} 1 \\ 1 \end{bmatrix} \tag{36}$$

Once bases $v_1, \ldots, v_n$ and $w_1, \ldots, w_m$ for V and W respectively have been chosen, any linear transformation T on V to W can be completely and uniquely described in terms of the entries in an $m \times n$ matrix A by Eq. (37). In other words, each Tv_j, as a vector in

$$Tv_j = a_{1j} w_1 + a_{2j} w_2 + \cdots + a_{mj} w_m \tag{37}$$

$$j = 1, 2, \ldots, n$$

W, can be expressed uniquely as a sum of scalar multiples of the basis $w_1, \ldots, w_m$. The scalars $a_{1j}, \ldots, a_{mj}$ are the entries in column j of A; that is, the entry in row i and column j is a_{ij}. This observation is fundamental because it shows that the study of linear transformations is coextensive with the study of matrices.

Important problems. There are a number of important questions about linear transformations that have been studied extensively, as follows:

1. Given w in W, the problem of determining all vectors v in V (if any) for which Eq. (38) is satisfied.

$$Tv = w \tag{38}$$

2. If $V = W$, the problem of determining all scalars λ and nonzero vectors v for which Eq. (39) is satisfied.

$$Tv = \lambda v \tag{39}$$

3. If $V = W$ and F is any field, the problem of finding a basis of V such that the corresponding matrix representation A for T is as simple as possible.

4. If $V = W$ and F is either the real numbers or the complex numbers, the problem of determining the structure of all T that preserve the lengths of all vectors; that is, for all v, the vectors v and Tv have the same length. This property is possessed by rotations.

The set of all vectors Tv obtained as v varies over V is called the range of T. The range of T is always a vector space. Thus the first problem above is equivalent to determining the range of a linear transformation T. Once bases of V and W have been selected, Eq. (38) is readily seen to be equivalent to solving a system of linear equations of the form of Eqs. (40) for the

determination of the numbers $x_1, \ldots, x_n$.

$$\begin{aligned} a_{11}x_1 + \cdots + a_{1n}x_n &= b_1 \\ a_{21}x_1 + \cdots + a_{2n}x_n &= b_2 \\ &\vdots \\ a_{m1}x_1 + \cdots + a_{mn}x_n &= b_m \end{aligned} \tag{40}$$

Finding the numbers λ and vectors v that satisfy Eq. (39) is called the eigenvalue problem; the number λ in (39) is called an eigenvalue of T, and the corresponding vector v in Eq. (39) is called an eigenvector of T. Equation (39) leads to a system similar to Eqs. (40), but $m = n$ and each b_i must be replaced by λx_i for $i = 1, \ldots, n$. Moreover, both the eigenvalue λ and $x_1, \ldots, x_n$ must be determined. Because of the importance of Eqs. (38) and (39) in many areas of applied mathematics, special-purpose computer programs have been developed to deal with them. *See* EIGENFUNCTION; EIGENVALUE (QUANTUM MECHANICS); LINEAR SYSTEMS OF EQUATIONS.

The problem of finding the basis of a vector space that simplifies the matrix representation of a linear transformation on the vector space to itself was solved in a sequence of papers in the latter part of the nineteenth century and the early part of the twentieth century. *See* LINEAR ALGEBRA.

Results. Because of their applications in the physical and social sciences, certain special classes of linear transformations and matrices have been studied extensively. If A is an $m \times n$ matrix, then the transpose of A is the $n \times m$ matrix whose rows, in succession, are columns of A written as rows. The transpose of A is denoted by A^T. If A has complex number entries, then A^* is the matrix obtained from A^T by replacing each entry by its complex conjugate. An $n \times n$ matrix A is said to be nonsingular (or invertible) if there is a unique $n \times n$ matrix A^{-1} for which $AA^{-1} = A^{-1}A = I_n$; the matrix I_n is the identity matrix: $a_{ii} = 1$ for $i = 1, \ldots, n$, and $a_{ij} = 0$ if $i \neq j$. If $A^* = A$, then A is hermitian; if $A^* = A^{-1}$, then A is unitary; if $A^*A = AA^*$, then A is normal.

An important result is the polar decomposition theorem: if A is an $n \times n$ matrix with complex number entries, then $A = PH$, where P is unitary and H is hermitian with nonnegative real eigenvalues. A triangularization theorem due to I. Schur has many important applications. It states that any $n \times n$ matrix A with complex number entries can be written as $A = P^{-1}BP$, in which P is unitary, the entries b_{ii}, $i = 1, \ldots, n$, are the eigenvalues of A, and $b_{ij} = 0$ if $j > i$. The QR factorization theorem states that any $m \times n$ matrix A, $m \geq n$, can be factored into a product $A = QR$ in which Q is $m \times m$ unitary and R is $m \times n$ upper triangular (that is, $r_{ij} = 0$ if $j > i$). The QR factorization theorem is used to devise practical methods for finding mutually perpendicular vectors of length 1 that comprise a basis of the range of a linear transformation. The singular-value decomposition theorem states that any $m \times n$ matrix A can be factored into a product $A = UDV$, in which U is $m \times m$ unitary, V is $n \times n$ unitary, and D is an $m \times n$ matrix whose only (possibly) nonzero entries are $d_{11} \geq \ldots > d_{pp} \geq 0$, where p is the smaller of m and n. The numbers $d_{11}, \ldots, d_{pp}$ are called the singular values of A. The singular-value decomposition theorem is used extensively in solving least-squares problems.

Matrices whose entries are nonnegative real numbers are important in many applications of matrix theory to problems in the social sciences. The principal result about an $n \times n$ matrix A with positive entries is the Perron-Frobenius theorem: A possesses a unique positive eigenvalue λ and a corresponding eigenvector x with positive entries; that is, $Ax = \lambda x$. Moreover, any other eigenvalue of A is smaller in absolute value than λ.

Matrices with polynomial entries have been studied extensively because of their importance in control theory, systems theory, and other areas of applied mathematics and engineering.

If A is an $n \times n$ complex matrix and x is an $n \times 1$ matrix, then x^*Ax is a scalar (that is, a 1×1 matrix) called the hermitian form associated with A. As x runs over all $n \times 1$ matrices satisfying $x^*x = 1$, the corresponding set of numbers x^*Ax fills up a region in the complex plane called the numerical range or field of values of A, denoted by $W(A)$. The set $W(A)$ is an inclusion region for the eigenvalues of A; that is, every eigenvalue λ of A is contained in $W(A)$. Because of this fact, the set $W(A)$ has been extensively studied ever since the important discovery in 1918 and 1919 by F. Hausdorff and O. Toeplitz that $W(A)$ is always a convex set in the plane. A subset of the plane is convex if the line segment joining any two points in the subset is itself entirely contained in the subset.

Marvin Marcus

Bibliography. W. C. Brown, *Matrices and Vector Spaces*, 1991; I. Gohberg, P. Lancaster, and L. Rodman, *Matrix Polynomials*, 1982; P. R. Halmos, *Finite-Dimensional Vector Spaces*, 2d ed., 1958, reprint 1993; R. A. Horn and C. R. Johnson, *Matrix Analysis*, 1985, paper 1990; D. Lewis, *Matrix Theory*, 1991; M. Marcus and H. Minc, *A Survey of Matrix Theory and Matrix Inequalities*, 1964, reprint 1992; H. Minc, *Nonnegative Matrices*, 1988; D. J. Winter, *Matrix Algebra*, 1991.

Matter (physics)

A term that traditionally refers to the substance of which all bodies consist. In Aristotelian physics, each type (species) of material body had a distinct "essential form." Early modern scientists, however, asserted that there is one universal type of matter. For Isaac Newton, this matter consisted of "solid, massy, hard, impenetrable, movable," ultimate particles ("atoms"), which were discrete, localized, indivisible bodies. Modern analyses distinguish two types of mass in classical (Newtonian) matter: inertial mass, by which matter retains its state of rest or uniform rectilinear motion in the absence of external forces; and gravitational mass, by which a body exerts forces of attraction on other bodies and by which

it reacts to those forces. Expressed in appropriate units, these two properties are numerically equal—a purely experimental fact, unexplained by theory. Albert Einstein made the equality of inertial and gravitational mass a fundamental principle (principle of equivalence), as one of the two postulates of the theory of general relativity. In the equation $E = mc^2$ (where c is the velocity of light), Einstein recognized the equivalence (interconvertibility) of mass (m) and energy (E), which had been distinguished in classical theories. *See* GRAVITATION; INERTIA; MASS; RELATIVITY; WEIGHT.

Implications of quantum mechanics. Among the departures from classical thinking instituted by quantum mechanics with regard to matter are the following. Matter in classical mechanics is closely identified with mass; in quantum mechanics, mass is only one among many properties (quantum numbers) that a particle can have, for example, electric charge, spin, and parity. The nearest quantum-mechanical analogs of traditional matter are fermions, having half-integral values of spin. Forces are mediated by exchange of bosons, particles having integral spins (such as photons). Fermions correspond to classical matter in exhibiting impenetrability (a consequence of the exclusion principle), but the correspondence is only rough. For example, fermions can also be exchanged in interactions (a photon and an electron can exchange an electron), and they also exhibit wavelike behavior. States of classical matter-particles were given by their positions and momenta, but in quantum mechanics it is impossible to assign simultaneous precise positions and momenta to particles. Finally, two or more particles in quantum theory can become "entangled," so that, in the case of two particles that become entangled and separate by a very great distance, an operation on one particle will be immediately responded to by a corresponding change in the other. This "nonlocality" violates traditional notions of what a piece of matter must be, which led Einstein to refer to quantum mechanics as objectionable in implying a "spooky action at a distance." *See* EXCLUSION PRINCIPLE; NONRELATIVISTIC QUANTUM THEORY; QUANTUM ELECTRODYNAMICS; QUANTUM MECHANICS; QUANTUM STATISTICS.

Matter in the universe. Beginning in the 1920s, astronomers accumulated a vast amount of evidence leading to the conclusion that the density of matter in the universe was much larger than that of visible matter. Important steps in this direction were taken in 1933, when Fritz Zwicky found that the amount of visible matter in a number of galaxy clusters was far too small to hold the galaxies in the cluster, and in 1983, when Vera Rubin and colleagues found that the rotation curves of individual spiral galaxies implied that the galaxies must be surrounded by a sphere of unseen matter, ten times the amount in the visible galaxy itself. It began to appear that the visible matter might constitute less than 1%, or at most 3%, of the amount of matter required, in the simplest theories, to equal the critical density at which the geometry of the universe would be Euclidean ("flat"), and at which the expansion rate of the universe would gradually slow down, asymptotically approaching zero. Some scientists accepted the implication that the universe was "open," with a hyperbolic geometry and continued expansion forever at a rate that did not approach zero.

Others proposed that missing matter, undetectable by current techniques, might equal the critical density, and many proposals were made regarding the nature of the missing matter. The motivation for seeking the missing matter became stronger with the proposal of the theory of inflation, which required a critical density. However, visible matter is baryonic, consisting almost entirely by mass of protons and neutrons. With the total density of baryonic matter so low, the missing nonbaryonic dark matter would have to be some kind of exotic particle. Candidates for this status included axions and the lightest (nondecaying) supersymmetric particles, photinos or perhaps winos. None of these, nor many other candidates, have been observed. *See* DARK MATTER; SUPERSYMMETRY; WEAKLY INTERACTING MASSIVE PARTICLE (WIMP).

It was long realized that such exotic matter was still not enough for closure (critical density), however, and debates arose regarding the nature of the dark energy that was needed to provide the remainder. One popular proposal was that of quintessence, a negative-pressure energy field, perhaps created by particles that had not been suggested in current hypotheses. However, while quintessence theories have not been entirely ruled out, they have been replaced by a different approach. In 1998, results from studies of distant supernovae indicated strongly that the universe is not merely expanding: the rate of expansion is accelerating. It was found that this acceleration has been going on for approximately 5×10^9 years. The new view thus suggested was that some kind of dark antigravitational energy was at work, a product of the vacuum rather than, as with quintessence views, some unknown form of quasi-matter. It thus resembles the cosmological constant that Einstein had proposed as a term in his equations designed to preserve the universe from the possibility that it might expand or contract. He abandoned this term after the discovery of the expansion of the universe. *See* ACCELERATING UNIVERSE; COSMOLOGICAL CONSTANT; DARK ENERGY.

In 2003, one of the great achievements of the *Wilkinson Microwave Anisotropy Probe* (*WMAP*) was to pin down the distribution as follows: 4% of the matter in the universe is baryonic, 23% is dark nonbaryonic matter, and 73% is something else, generally known as dark energy. Though slightly different values have been proposed, all are within an estimated 5% error range. The *WMAP* results were bolstered by ones from the Sloan Digital Sky Survey (SSDS), also announced in 2003. Several future investigations, expanding and improving on these results, are in preparation. *See* COSMOLOGY; SLOAN DIGITAL SKY SURVEY; UNIVERSE; WILKINSON MICROWAVE ANISOTROPY PROBE.

Dudley Shapere

Bibliography. N. S. Hetherington (ed.), *Encyclopedia of Cosmology*, Garland Publishing, New York, 1993; M. Jammer, *Concepts of Mass in Classical*

and Modern Physics, 1961, reprint 1993; L. Krauss, *Quintessence: The Mystery of Missing Mass in the Universe*, 2000; E. McMullin, *The Concept of Matter*, 1963; H. C. Ohanian and R. Ruffini, *Gravitation and Spacetime*, 2d ed., 1994; U. Seljak et al., Cosmological parameter analysis including SDSS Lyalpha forest and galaxy bias: Constraints on the primordial spectrum of fluctuations, neutrino mass, and dark energy, *Phys. Rev. D*, 71:103515, 2005; Special issue: The dark side, *Science*, 300:1893–1918, 2003; D. N. Spergel et al., First-year *Wilkinson Microwave Anisotropy Probe* (*WMAP*) observations: Determination of cosmological parameters, *Astrophys. J. Suppl. Ser.*, 148(1):175–194, 2003.

Matthiessen's rule

An empirical rule which states that the total resistivity of a crystalline metallic specimen is the sum of the resistivity due to thermal agitation of the metal ions of the lattice and the resistivity due to the presence of imperfections in the crystal. This rule is a basis for understanding the resistivity behavior of metals and alloys at low temperatures.

The resistivity of a metal results from the scattering of conduction electrons. Lattice vibrations scatter electrons because the vibrations distort the crystal. Imperfections such as impurity atoms, interstitials, dislocations, and grain boundaries scatter conduction electrons because in their immediate vicinity the electrostatic potential differs from that of the perfect crystal. If lattice scattering and imperfection scattering are independent processes and are isotropic, it can be shown that Eq. (1) holds, where

$$\rho(T) = \rho_L(T) + \rho_1 \tag{1}$$

$\rho(T)$ is the resistivity at temperature T, $\rho_L(T)$ is the resistivity due to lattice scattering (the ideal resistivity, which is temperature-dependent), and ρ_1 is the so-called residual resistivity due to imperfections, which is presumably independent of temperature. An equivalent statement is given in Eq. (2).

$$\frac{\partial \rho(T)}{\partial T} = \frac{\partial \rho_L(T)}{\partial T} \tag{2}$$

As exemplified by the **illustration**, Matthiessen's rule is generally obeyed, although some deviations do occur. Such deviations arise for the following reasons: (1) The introduction of impurities generally alters the elastic properties, influences the lattice vibration spectrum, and thereby changes $\rho_L(T)$. (2) Some imperfections, such as dislocations, do not scatter isotropically. (3) Thermal expansion lowers the Fermi energy (since impurity scattering depends on the velocity of the electrons at the Fermi energy, the resistivity due to impurities depends also on the temperature through the thermal expansion). (4) The impurity ions also participate in the thermal vibrations of the crystal lattice. However, since the scattering potential of an impurity differs from that of a solvent ion, lattice scattering from the former also differs from that due to a solvent ion. Frank J. Blatt

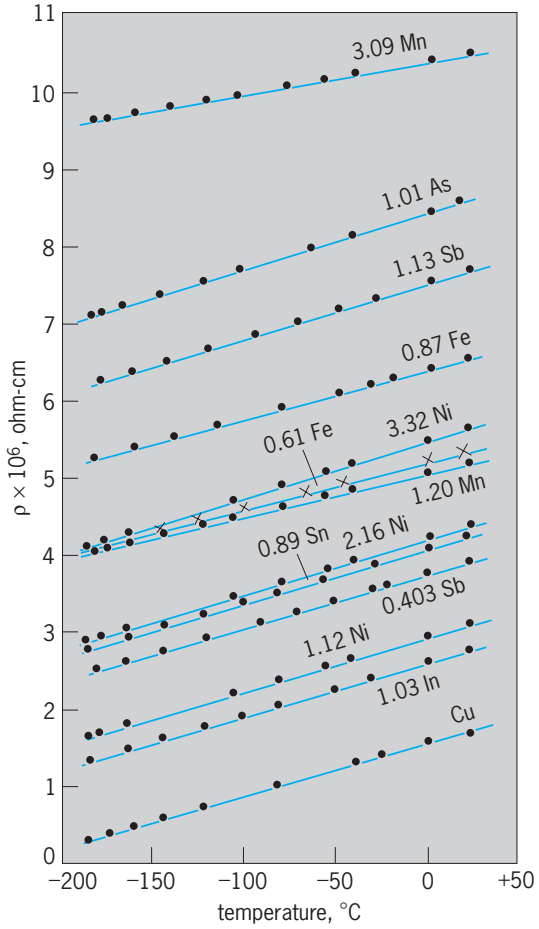

Resistivity of copper and copper alloys. Solute concentrations are given in atomic percent. °F = (°C × 1.8) + 32. (*After J. O. Linde*)

Maxillopoda

A class of Crustacea whose application is gaining moderately widespread use, despite the fact that its validity is not universally accepted by researchers. The constituent subclasses of the Maxillopoda also remain unsettled: before 1956, all major subclasses of the Crustacea were regarded as distinct taxa of equal rank. In addition to the Malacostraca, these included the Cephalocarida, Branchiopoda, Cirripedia, Copepoda, Mystacocarida, Branchiura, and Ostracoda. Use of cladistics, or phylogenetic analysis, has rekindled interest in phylogenetic relationships and hierarchy among the nonmalacostracan taxa.

The class Maxillopoda was proposed for those taxa with six thoracic somites (with some exceptions), a well-developed mandibular palp in adults, well-developed maxillules and maxillae adapted for filtering in filter feeders, and the lack of gnathobases on the appendages of the thorax. The Recent taxa included were the Copepoda, Branchiura, Mystacocarida, and provisionally, the Cirripedia. Subsequently the Cirripedia (subdivided into Cirripedia sensu stricto and Ascothoracida) were unequivocally incorporated. The Ostracoda are now included by some but excluded by others. More recent suggestions have included the Tantulocarida,

and even the probably noncrustacean Pentastomida, within the Maxillopoda. *See* BRANCHIURA; CIRRIPEDIA; COPEPODA; OSTRACODA; PENTASTOMIDA; TANTULOCARIDA.

In addition to the original characters used to diagnose the Maxillopoda, tagmosis (division of the body into five cephalic, six or seven thoracic, and five or four abdominal somites), gonopore position, form and structure of thoracic appendages, evidence from comparative spermatology, and the structure of the nauplius eye have been used to argue for the homogeneity of this class. Opponents have argued that the body segmentation presumed to be common to all subclasses had been misinterpreted and that heterogeneity is apparent during several developmental processes. When morphological characters of members of the various maxillopodan taxa are subjected to cladistic analyses, the results are dependent upon the investigator's interpretations of homologies as opposed to convergences, and primitive versus advanced character states, as well as the number of characters utilized. Whether the Maxillopoda is a monophyletic and meaningful taxon remains to be determined. *See* CRUSTACEA. Patsy A. McLaughlin

Bibliography. G. A. Boxshall and R. Huys, New tantulocarid, *Stygotantulus stocki*, parasitic on harpacticoid copepods, with an analysis of the phylogenetic relationships within the Maxillopoda, *J. Crust. Biol.*, vol. 9, 1989; F. R. Schram, *Crustacea*, 1986; F. R. Schram (ed.), Crustacean phylogeny, *Crust. Iss.*, vol. 1, 1983.

Maxwell's demon

An imaginary being whose action appears to contradict the second law of thermodynamics. The properties of bulk systems are explained in terms of contributions from their constituent molecules. The same, presumably, should be true of certain grand properties of nature, and in particular the second law of thermodynamics, which identifies the natural direction of change with the direction of increasing entropy. The statistical basis of this law, in which entropy is identified with molecular chaos, was established largely through the work of L. Boltzmann. However, there has always been a certain degree of discomfort associated with the acceptance of the law, particularly in relation to the time reversibility of physical laws and the role of molecular fluctuations. In 1867, J. C. Maxwell considered, in this connection, the action of "a finite being who knows the paths and velocities of all the molecules by inspection." This being was later referred to as a demon by Lord Kelvin, and the usage has been generally adopted. *See* ENTROPY; THERMODYNAMIC PRINCIPLES; TIME, ARROW OF.

Trapdoor model. The activity of Maxwell's demon can be modeled by a trapdoor in a partition between two regions full of gas at the same pressure and temperature. The trapdoor needs to be restrained by a light spring to ensure that it is closed unless it is struck by molecules traveling from the left (see **illus.**). Its hinging is such that molecules traveling from the right cannot open it. The essential point of Maxwell's vision was that molecules striking the trapdoor from the left would be able to penetrate into the right-hand region but those present on the right would not be able to escape back into the left-hand region. Therefore, the initial equilibrium state of the two regions, that of equal pressures, would be slowly replaced by a state in which the two regions acquired different pressures as molecules accumulated in the right-hand region at the expense of the left-hand region. Only a slightly more elaborate mechanical arrangement is needed to change the apparatus to one in which the temperatures of the two regions move apart. For this to be achieved, the trapdoor needs to admit faster molecules, but not slower molecules, into the right-hand region. In each case, the demonic trapdoor appears to be contriving a change that is contrary to the second law, for an implication of that law is that systems in either mechanical equilibrium (at the same pressure) or thermal equilibrium (at the same temperature) cannot spontaneously diverge from equilibrium.

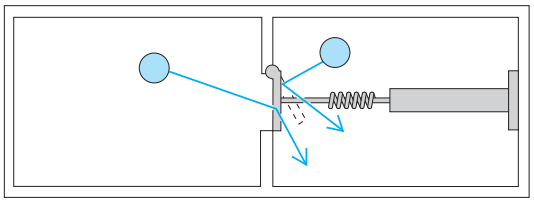

Type of device that emulates mechanically the actions of Maxwell's demon. Molecules traveling to the right can open the trapdoor and enter the right-hand compartment, but those striking it from the right cannot open it, so do not move into the left-hand compartment.

Resolution of paradox. As frequently occurs in science, the resolution of a paradox or the elimination of an apparent conflict with a firmly based law depends on a detailed analysis of the proposed arrangement. Numerous analyses of this kind have shown that the activities of Maxwell's demon do not in fact result in the overthrow of the second law. An indication of the thrust of these discussions can be obtained by noting that for the trapdoor to act as specified, it must close immediately after it has allowed a molecule to pass, for otherwise the "wrong" molecules will take advantage of its opening. However, the act of opening the door gives the door a certain additional energy, and it is possible for a molecule in the right-hand region to be struck by the door and batted into the left-hand region. Thus, the demonic door undoes what it achieved when it admitted a molecule, and the net effect is the maintenance of mechanical equilibrium. Similar remarks apply to the maintenance of thermal equilibrium.

It is sometimes argued that a true demon, one endowed with intelligence, would elude this argument. However, there are several rebuttals of this claim. One is that a truly intelligent demon would use its intelligence to construct a mechanical device that is equivalent to the trapdoor: hence, the same argument would apply, and the exercise of intelligence would not circumvent the second law. Even if the demon resorts to more elaborate inspection techniques, it fails to circumvent the law. For instance,

if it uses electromagnetic radiation to monitor the approach of candidate molecules for admission to the right-hand region, it needs to unleash and detect at least one photon. However, a photon carries energy, so its emission and detection involve the dissipation of energy and hence a contribution to the entropy.

P. W. Atkins

Bibliography. K. G. Denbigh and J. S. Denbigh, *Entropy in Relation to Incomplete Knowledge*, 1985; R. P. Feynman, *Lectures in Physics*, 1966; E. Garber, S. G. Brush, and C. W. F. Everitt (eds.), *Maxwell on Molecules and Gases*, 1985; H. S. Leff and A. F. Rex (eds.), *Maxwell's Demon: Entropy, Information, and Computing*, 1990.

Maxwell's equations

The four equations of electromagnetism completed by J. C. Maxwell in 1864. The equations govern a wide range of phenomena, including much of electronic technology. However, some modern technology requires the quantum-mechanical interpretation of the equations. In their most general form, Eqs. (1)–(4) relate four field quantities, the electric field **E**,

$$\nabla \times \mathbf{E} = -\frac{\partial \mathbf{B}}{\partial t} \tag{1}$$

$$\nabla \times \mathbf{H} = \mathbf{J} + \frac{\partial \mathbf{D}}{\partial t} \tag{2}$$

$$\nabla \cdot \mathbf{B} = 0 \tag{3}$$

$$\nabla \cdot \mathbf{D} = \rho \tag{4}$$

magnetic induction **B**, magnetic field **H**, and the electric displacement **D**, to the free charge and current densities ρ and **J**. Two auxiliary equations are needed. Microscopic displacements between bound positive and negative charges produce fields on a macroscopic scale when the displacements are the same throughout a macroscopic volume of material. Equation (5) relates **D** to **E** and the polarization **P**, which results from the bound charges within a material. The constant ϵ_0 is called the permittivity of free space, and its value is closely approximated by $10^{-11}/(36\pi)$ in SI (meter-kilogram-second-ampere or MKSA) units. The polarization can be a function of **E**, or it can be a spontaneous property of the material. In the latter case, the material is said to be ferroelectric. A material may also contain currents that arise in the atomic and nuclear structure of matter and do not flow over macroscopic distances. The other auxiliary equation (6) relates **B**

$$\mathbf{D} = \epsilon_0 \mathbf{E} + \mathbf{P} \tag{5}$$

$$\mathbf{B} = \mu_0(\mathbf{H} + \mathbf{M}) \tag{6}$$

to **H** and the magnetization **M**, which results from the bound currents. The constant μ_0 is called the permeability of free space, defined to be $4\pi(10)^{-7}$ in SI units. The magnetization can be a function of **H** or a spontaneous property in a ferromagnetic material. *See* CURRENT DENSITY; DIFFERENTIAL EQUATION; ELECTRIC CHARGE; ELECTRIC FIELD; FERROELECTRICS; FERROMAGNETISM; MAGNETIZATION; POLARIZATION OF DIELECTRICS.

Lorentz force law. When no polarizable or magnetizable materials are being considered, Maxwell's equations can be solved for the fields **E** and **B** in terms of the sources ρ and **J**. When the fields are known, the motion of charged particles may be found with the help of Eq. (7), which gives the force on a charge

$$\mathbf{F} = q(\mathbf{E} + \mathbf{v} \times \mathbf{B}) \tag{7}$$

q moving with velocity **v** as written by H. A. Lorentz. The Lorentz force law depends only on **E** and **B**. For this reason, the other two fields **D** and **H** are not considered fundamental, and in fact Maxwell's equations can be formulated without them. In this more fundamental formulation, there is only one constant in the equations instead of the two ϵ_0 and μ_0. Introducing a second constant, however, allows familiar units to be used for both types of fields. *See* ELECTRICAL UNITS AND STANDARDS.

Divergence and curl. Maxwell's equations can be manipulated easily when the various uses of the gradient operator are known. If $\hat{\boldsymbol{\imath}}$, $\hat{\mathbf{j}}$, and $\hat{\mathbf{k}}$ are defined to be unit vectors along the x, y, and z coordinate axes, then the gradient of a scalar function $\phi(x,y,z)$ is compactly written as in Eq. (8). Equation (9) defines the dot product of the gradient operator with a vector function of position $\mathbf{A}(x,y,z)$. It is called the divergence of **A**. The cross product of the gradient with **A**, Eq. (10), is called the curl of **A**. The curl of a curl simplifies to terms involving the gradient, divergence, and laplacian, as shown in Eq. (11). Finally, the laplacian, which is defined by Eq. (12), can be applied to both scalar and vector functions. A typical use of these rules with Maxwell's equations is to derive a wave equation that can be solved by familiar techniques. *See* CALCULUS OF VECTORS; GRADIENT OF A SCALAR; LAPLACIAN.

$$\nabla\phi = \hat{\mathbf{i}}\frac{\partial\phi}{\partial x} + \hat{\mathbf{j}}\frac{\partial\phi}{\partial y} + \hat{\mathbf{k}}\frac{\partial\phi}{\partial z} \tag{8}$$

$$\nabla \cdot \mathbf{A} = \frac{\partial A_x}{\partial x} + \frac{\partial A_y}{\partial y} + \frac{\partial A_z}{\partial z} \tag{9}$$

$$\nabla \times \mathbf{A} = \hat{\mathbf{i}}\left(\frac{\partial A_z}{\partial y} - \frac{\partial A_y}{\partial z}\right) + \hat{\mathbf{j}}\left(\frac{\partial A_x}{\partial z} - \frac{\partial A_z}{\partial x}\right) + \hat{\mathbf{k}}\left(\frac{\partial A_y}{\partial x} - \frac{\partial A_x}{\partial y}\right) \tag{10}$$

$$\nabla \times (\nabla \times \mathbf{A}) = \nabla(\nabla \cdot \mathbf{A}) - \nabla^2\mathbf{A} \tag{11}$$

$$\nabla^2 = \frac{\partial^2}{\partial x^2} + \frac{\partial^2}{\partial y^2} + \frac{\partial^2}{\partial z^2} \tag{12}$$

Coulomb's law. When there is no time dependence, the four equations uncouple into two for the electric field and two for the magnetic field. Also, some important and instructive special cases of Maxwell's equations can be solved by using symmetry to avoid tedious integrations. The electric field of a charged body with spherical symmetry (**Fig. 1**) can be found by integrating the fourth of Maxwell's

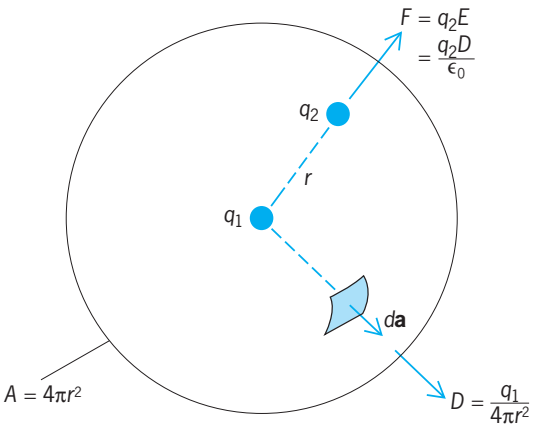

Fig. 1. Electric field of a spherically symmetric charge. Symbols are explained in text.

equations, yielding Eq. (13*a*). The left-hand side of

$$\int d^3x\rho = \int d^3x\Delta\cdot\mathbf{D} \qquad (13a)$$

$$q = \int_{\circ\!\!-} d\mathbf{a}\cdot\mathbf{D} \qquad (13b)$$

$$q = 4\pi r^2\epsilon_0 E(r) \qquad (13c)$$

this equation gives the total charge q, and the right-hand side is the integral of the divergence of **D** over some volume that includes the charge. By a theorem proved by K. F. Gauss, a volume integral of the divergence of a field can be replaced by an integral of the outward component of the field on the surface that encloses the volume. Thus, Eq. (13*b*) follows, where the closed surface is represented by the circle, and the arrow perpendicular to it represents the direction of the vector element of area $d\mathbf{a}$ perpendicular to the surface. If the closed surface is chosen to be a sphere of radius r, centered on the charge, the outward component of the field is constant on the sphere by symmetry. Therefore the integral reduces to the area of the sphere, $4\pi r^2$, times $\epsilon_0 E(r)$, yielding Eq. (13*c*). The force exerted by one charge on a second charge can then be found from the first term in the Lorentz force law. C. A. de Coulomb first determined experimentally that the force, as shown in Eq. (14), is proportional to both charges, inversely

$$F = \frac{q_1 q_2}{4\pi\epsilon_0 r^2} \qquad (14)$$

proportional to the square of the distance between them, and attractive when the charges are of opposite sign. *See* COULOMB'S LAW; ELECTROSTATICS; GAUSS' THEOREM.

Ampére's law. The magnetic field of a cylindrically symmetric, time-independent current distribution can also be found by symmetry. This is done by integrating the second Maxwell equation (**Fig. 2**), yielding Eq. (15*a*). The integral of the outward component of **J** over some surface gives the total current I intersecting that surface. The closed path that bounds the surface is represented by a circle, and the arrow perpendicular to the surface represents the direction of the vector element of area $d\mathbf{a}$. The curl of **H** appears on the right-hand side of Eq. (15*a*). The integral of the outward component of the curl of a vector field over a surface was simplified by G. G. Stokes. Stokes' theorem allows the surface integral of the curl of a vector field to be replaced by an integral of the tangential component of the field around the closed curve bounding the surface, yielding Eq. (15*b*). The right-hand rule is used to determine the direction of $d\mathbf{a}$ (the thumb) relative to the direction of the line integral (the fingers). This directional line integral is represented on the integral sign by a circle with an arrow head embedded in it. *See* STOKES' THEOREM.

$$\int_{\circ\!\!-} d\mathbf{a}\cdot\mathbf{J} = \int_{\circ\!\!-} d\mathbf{a}\cdot\nabla\times\mathbf{H} \qquad (15a)$$

$$I = \oint d\ell\cdot\mathbf{H} \qquad (15b)$$

$$I = \frac{2\pi r}{\mu_0}B(r) \qquad (15c)$$

Since the current distribution is symmetric, rotating it about its axis would not change the field. The magnetic field is therefore tangential in direction and constant in magnitude on any circle centered on the current. Therefore, in the case of such a circular closed path of radius r, the integral reduces to the circumference of the circle, $2\pi r$, times $H(r)$, so that Eq. (15*c*) holds. The second term in the Lorentz force law, Eq. (7), gives the force exerted by the current on a charge q moving with speed v along a parallel line a distance r away, Eq. (16). This force is attractive when the charge is positive and moving in the same direction as the current. When a number of particles are distributed along the line to make up a second current I_2, the charge per unit length is I_2/v. Thus the force per unit length is proportional to both currents and inversely proportional to the distance between them. Equation (17), discovered by A. M. Ampére, is a useful special case of the general rule for the force between two currents. *See* AMPÈRE'S LAW.

$$f = qv\frac{\mu_0 I}{2\pi r} \qquad (16)$$

$$\frac{df}{dl} = \frac{\mu_0 I_1 I_2}{2\pi r} \qquad (17)$$

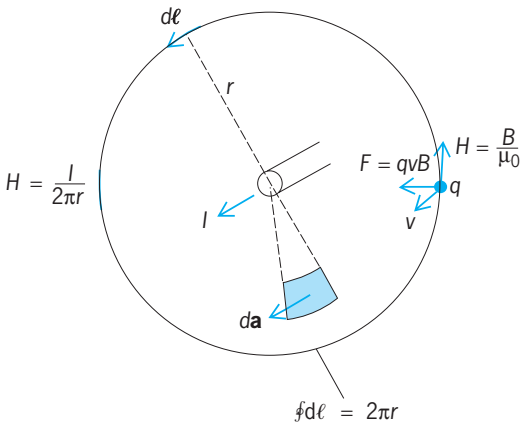

Fig. 2. Magnetic field of a cylindrically symmetric current. Symbols are explained in text.

Faraday's law and Ohm's law. The quantity **B** is also called the magnetic flux density. The reason can be explained by integrating the first Maxwell equation over some surface, yielding Eq. (18*a*). When Stokes'

$$\int_{\mathcal{S}} d\mathbf{a} \cdot \nabla \times \mathbf{E} == \int_{\mathcal{S}} d\mathbf{a} \cdot \frac{\partial \mathbf{B}}{\partial t} \tag{18a}$$

$$\oint dl \cdot \mathbf{E} = -\frac{dF}{dt} \tag{18b}$$

theorem is used, the left-hand side of this equation becomes the line integral of **E** around the path bounding the surface. This line integral known as the electromotive force (emf) is also equal to the work done on a unit charge that moves around the path. The quantity

$$\int_{\mathcal{S}} d\mathbf{a} \cdot \mathbf{B}$$

is called the flux F through the surface. The order of the time derivative and the integration is interchanged to show that the right-hand side of Eq. (18*a*) is the time rate of change of the flux intersecting the path, so that Eq. (18*b*) holds. This relationship between the electromotive force and rate of change of the flux was discovered by M. Faraday and is called electromagnetic induction. *See* ELECTROMAGNETIC INDUCTION; ELECTROMOTIVE FORCE (EMF); FARADAY'S LAW OF INDUCTION.

If the path around the surface in question were traced out by a conducting material, current would flow in response to the electromotive force. Often the current density is linearly related to the electric field, as in Eq. (19), and the coefficient σ is a constant

$$\mathbf{J} = \sigma \mathbf{E} \tag{19}$$

called the conductivity of the material. Integration of this equation around the path yields Eq. (20*a*).

$$\sigma \oint dl \cdot \boldsymbol{E} = \oint \mathbf{J} \cdot dl \tag{20a}$$

$$V = \frac{IL}{A\sigma} = RI \tag{20b}$$

If it is assumed, for simplicity, that the current density is constant over the cross section of the wire, then the path integral in Eq. (20*a*) relates the current I in the wire to the electromotive force V, as in Eq. (20*b*). The proportionality constant R is called the resistance of the path; it is proportional to the length L and inversely proportional to the cross section A. The unit of resistance is named the ohm, after G. S. Ohm, who formulated the relationship between I and V. *See* ELECTRICAL CONDUCTIVITY OF METALS; ELECTRICAL RESISTANCE; OHM'S LAW.

Continuity equation. By taking the divergence of the second Maxwell equation and the time derivative of the fourth, Eq. (21) is derived. This is called

$$\begin{aligned} 0 = \nabla \cdot (\nabla \times \mathbf{H}) &= \nabla \cdot \mathbf{J} + \nabla \cdot \frac{\partial \mathbf{D}}{\partial \mathbf{t}} \\ &= \nabla \cdot \mathbf{J} + \frac{\partial \rho}{\partial t} \end{aligned} \tag{21}$$

the continuity equation and shows that charge is conserved. This can be shown by integrating over some volume, as in Eq. (22). One term then becomes the

$$0 = \int_{\circ\!\!\rightarrow} \mathbf{J} \cdot d\mathbf{a} + \frac{d}{dt} \int d^3xp \tag{22}$$

time rate of change of the net charge in that volume. Gauss' theorem can be used to express the other term as the surface integral of the outward component of the current density. The latter is the net current flowing outward through the surface. Thus the continuity equation states that the quantity of charge present in a region can change only through the transport of charge across its boundaries. *See* EQUATION OF CONTINUITY.

Wave equation. Maxwell completed his equations by adding the displacement current, $\partial \mathbf{D}/\partial t$, to the second equation. As was shown above, this was necessary for charge conservation, but it had other far-reaching consequences. Maxwell's equations can be used to calculate the forces between charges and currents, but they also have nontrivial solutions in free space in the absence of sources. This can be seen by taking the curl of the first equation and the time derivative of the second. Indeed, taking the curl of Eq. (1) gives Eq. (23*a*),and applying Eq. (11) to the

$$\nabla \times (\nabla \times \mathbf{E}) = -\nabla \times \frac{\partial \mathbf{B}}{\partial t} \tag{23a}$$

$$\nabla(\nabla \cdot \mathbf{E}) - \nabla^2 \mathbf{E} = -\mu_0 \epsilon_0 \frac{\partial^2 \mathbf{E}}{\partial t^2} \tag{23b}$$

$$\left(\nabla^2 - \mu_0 \epsilon_0 \frac{\partial^2}{\partial t^2}\right) \mathbf{E} = 0 \tag{23c}$$

left-hand side of this equation and the time derivative of Eq. (2) to the right-hand side yields Eq. (23*b*). After setting the divergence of the electric field to zero and rearranging terms, Eq. (23*c*), called the wave equation, results. The wave equation contains only one parameter, and is the same in the fundamental units used by Maxwell. This equation has solutions that propagate with speed $1/\sqrt{\mu_0 \epsilon_0}$, which turned out to be numerically equal to the speed of light c, approximately 3×10^8 m/s. Light was identified as an electromagnetic wave, and the theories of electromagnetism and optics were thereby unified. *See* DISPLACEMENT CURRENT; ELECTROMAGNETIC RADIATION; LIGHT; WAVE EQUATION; WAVE MOTION.

Relativity. Maxwell's equations possess wavelike solutions that propagate at the speed of light. However, it was not immediately clear in what coordinate systems the equations should be applied. Two plausible alternatives were that the speed of light should be equal to the constant c (1) relative to the source and (2) relative to some hypothetical medium called ether that extends throughout all space. Experimental refutations of both alternatives were made. A. Einstein based his special theory of relativity on the idea that the speed of light should have the same value when measured by any observer who is not accelerating. Einstein generalized this to the principle of relativity, which states that all natural laws should have

the same form in all nonaccelerating coordinate systems. In Maxwell's equations, c appears as a parameter (which is more obvious in the fundamental formulation mentioned above). It turned out that Maxwell's equations also had the correct form required by the principle of relativity. However, the rules by which the fields transform from one coordinate system to another had to be worked out. *See* RELATIVISTIC ELECTRODYNAMICS; RELATIVITY. T. J. Nelson

Bibliography. R. H. Good, Jr., and T. J. Nelson, *Classical Theory of Electric and Magnetic Fields*, 1971; J. Hendry, *James Clerk Maxwell and the Theory of the Electromagnetic Field*, 1986; J. D. Jackson, *Classical Electrodynamics*, 3d ed., 1998; J. A. Kong, *Electromagnetic Wave Theory*, 3d ed., 2000; P. Lorrain, D. R. Corson, and F. Lorrain, *Electromagnetic Fields and Waves*, 3d ed., 1988; H. P. Neff, Jr., *Basic Electromagnetic Fields*, 2d ed., 1986.

McLeod gage

A type of instrument used to measure vacuum by application of the principle of Boyle's law. *See* BOYLE'S LAW.

A known volume of a gas whose pressure is to be measured is trapped by raising the level of a fluid (mercury or oil) by means of a plunger, by lifting a reservoir, by using pressure, or by tipping the apparatus. As the fluid level is further raised, the gas is compressed into the capillary tube (see **illus.**). Obeying Boyle's law, the compressed gas now exerts enough pressure to support a column of fluid high enough to read. Readings are somewhat independent of the composition of the gas under pressure.

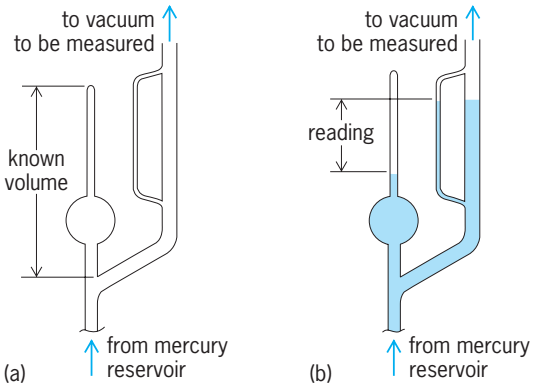

McLeod gage. (*a*) Filling (charging) position. (*b*) Measuring position.

The McLeod gage is simple and inexpensive. It is widely used as a standard of pressure between 10 torr (10^3 pascals) and 10^{-5} torr (10^{-3} pascal) and is often used to calibrate other vacuum instruments. Some disadvantages of this gage are that readings are not continuous, the operator must be skilled in taking visual readings, and mercury or oil vapor may diffuse into the gas being measured. Condensable gases cannot be measured with a McLeod gage, although use of a sorption trap or cold trap may allow some measurements. *See* VACUUM MEASUREMENT. Richard Comeau

Bibliography. T. A. Delchar, *Vacuum Physics and Technology*, 1993; J. F. O'Hanlon, *A User's Guide to Vacuum Technology*, 2d ed., 1989; A. Roth, *Vacuum Technology*, 3d ed., 1990, reprint 1998.

Mean effective pressure

A term commonly used in the evaluation for positive-displacement machinery performance which expresses the average net pressure difference in pounds per square inch (lb/in.^{2} or psi) on the two sides of the piston in engines, pumps, and compressors. It is also known as mean pressure and is abbreviated mep or mp.

In an engine (prime mover) it is the average pressure which urges the piston forward on its stroke. In a pump or compressor it is the average pressure which must be overcome, through the driver, to move the piston against the fluid resistance.

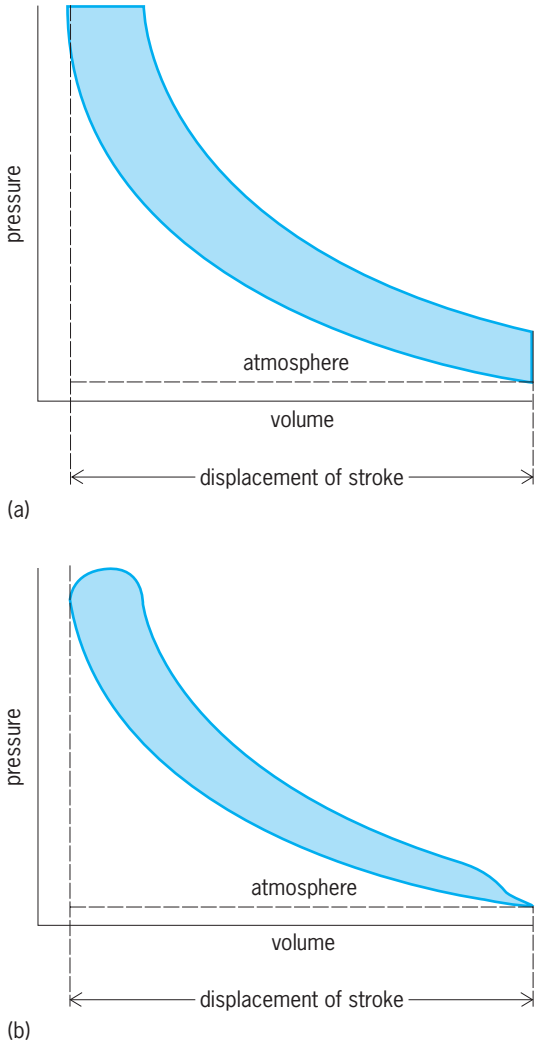

Pressure-volume diagrams (indicator cards) for diesel engine. (*a*) Theoretical (ideal) conditions. (*b*) Actual two-cycle engine card. The colored areas represent the effective work of the cycle.

Some representative values of mean effective pressures at full load

Unit	Value, lb/in.^{2}
Aircraft engine	100–200
Automobile engine	100–140
Diesel engine	75–150
Outboard engine	50–100
Steam engine	50–150
Air compressor	50–100

It can be a theoretic value obtained from the pressure-volume diagram of the thermodynamic or fluid dynamic cycle, such as Otto, diesel, or air-compressor cycle, or it may be the actual value, as measured by an instrument (generally called an engine indicator), which traces the real performance cycle diagram as the machine is running. The **illustration** shows the difference with a two-cycle diesel engine under ideal conditions and under real conditions. The colored area represents the effective work of the cycle. If the area is divided by the length of the diagram (the stroke of the engine), the result is an average height—the mean pressure or mean effective pressure acting throughout the cycle.

The mep can be applied to the cylinder dimensions and to the speed of the engine (or compressor) to give the horsepower. The equation is generally identified as the *plan* equation:

$$\text{Horsepower} = \frac{plan}{33{,}000}$$

$p =$ mep, lb/in.^{2}

$l =$ length of stroke, ft

$a =$ net area of piston, in.^{2}

$n =$ number of cycles completed per minute

Inspection of this equation shows that, for an engine cylinder of given size (l and a) and for a given operating speed (n), the higher the mean effective pressure (p) the greater will be the horsepower output, resulting in the most effective utilization of the engine bulk, weight, and investment. The criterion of mep thus is a vitally convenient device for the evaluation of a reciprocating engine, pump, or compressor design as judged by initial cost, space occupied, and deadweight. Some representative values of mep are given in the **table**. *See* COMPRESSOR; DIESEL CYCLE; THERMODYNAMIC CYCLE; VAPOR CYCLE.

Theodore Baumeister

Bibliography. E. A. Avallone and T. Baumeister III (eds.), *Marks' Standard Handbook for Mechanical Engineers,* 10th ed., 1996.

Mean free path

The average distance traveled between two similar events. The concept of mean free path is met in all fields of science and is classified by the events which take place. The concept is most useful in systems which can be treated statistically, and is most frequently used in the theoretical interpretation of transport phenomena in gases and solids, such as diffusion, viscosity, heat conduction, and electrical conduction. The types of mean free paths which are used most frequently are for elastic collisions of molecules in a gas, of electrons in a crystal, of phonons in a crystal, and of neutrons in a moderator.

An elementary formula for the mean free path for elastic collision of a molecule in a gas can be derived in the following way. In a gas at a pressure P, let n be the average number of molecules per unit volume and a the average radius of a molecule. The distance between centers of the molecules during a collision will be $2a$. Assume that one molecule has a radius $2a$ and travels with a velocity c, and that all other molecules are mass-points at rest. In a time t the moving molecule will "sweep out" a volume $4\pi a^2ct$, and since there are n molecules per unit volume, there will be $4\pi a^2ctn$ collisions. The distance traveled is ct; therefore the average distance between collisions is $1/(4\pi a^2n)$. Other more exact methods of taking averages give values which are closer to those determined experimentally. In hydrogen at normal temperature and pressure the mean free path is 1.7×10^{-5} cm. *See* KINETIC THEORY OF MATTER.

W. Dexter Whitehead

Measles

An acute, highly infectious viral disease with cough, fever, and maculopapular rash. It is of worldwide endemicity. The infective particle is a ribonucleic acid (RNA) virus. Measles, canine distemper, and bovine rinderpest viruses are antigenically related. *See* ANIMAL VIRUS.

The virus enters the body via the respiratory system, multiplies there, and circulates in the blood. Cough, sneezing, conjunctivitis, photophobia, and fever occur, with Koplik's spots in the mouth. Koplik's spots are small red spots containing a bluish-white speck in the center of each, and are located on the mucous membrane of the cheek. Koplik spots are seen early in measles, before the eruption of the skin, and are considered to be a diagnostic indicator of the disease.

A rash appears after 14 days' incubation and persists 5–10 days. Serious complications may occur in 1 out of 15 persons; these are mostly respiratory (bronchitis, pneumonia), but neurological complications are also found. Encephalomyelitis occurs rarely. Permanent disabilities may ensue for a significant number of persons.

Measles is one of the leading causes of death among children in the world, particularly in the developing countries. Complications are frequent, including pneumonia, diarrhea, encephalitis, and blindness, leaving thousands of children disabled each year. Children who survive acute measles have a greatly increased chance of dying from a variety of causes over the next year. The younger the age

at which measles occurs, the greater the effect in delayed mortality.

In unvaccinated populations, immunizing infections occur in early childhood during epidemics which recur after 2–3 years' accumulation of susceptible children. Transmission is by coughing or sneezing. Measles is infectious from the onset of symptoms until a few days after the rash has appeared. Second attacks of measles are very rare. Treatment is symptomatic.

At one time, prevention was limited to use of gamma globulin, which protects for about 4 weeks, and can modify or prevent the disease. *See* IMMUNOGLOBULIN.

Killed virus vaccine was once available, but it should not be used, as certain vaccinees become sensitized and develop local reactions when revaccinated with live attenuated virus, or develop a severe illness upon contracting natural measles. Live attenuated virus vaccine effectively prevents measles; vaccine-induced antibodies persist for years. *See* BIOLOGICALS; HYPERSENSITIVITY.

Measles antibodies cross the placenta and protect the infant during the first 6 months of life. Vaccination with the live virus fails to take during this period. Timely and sustained use of vaccine should lead to the eradication of measles. That goal has been thwarted, however, by repeated outbreaks among unvaccinated inner-city preschool-age children. Lowering the minimum age for routine vaccination from 15 months to 9 months of age could prevent measles outbreaks, but children who receive single-antigen vaccine before their first birthday should be revaccinated with trivalent measles-mumps-rubella (MMR) vaccine at 15 months of age. Vaccination for measles is not recommended in persons with febrile illnesses, with allergies to eggs or other products that are used in production of the vaccine, and with congenital or acquired immune defects. Joseph L. Melnick

Bibliography. F. L. Black, Measles active and passive immunity in a worldwide perspective, *Prog. Med. Virol.*, 36:1–33, 1989; F. T. Cutts et al., Principles of measles control, *Bull. WHO*, 69:1–7, 1991; M. Garenne et al., Child mortality after high-titre measles vaccines: Prospective study in Senegal, *Lancet*, 338:903–906, 1991; A. R. Hinman et al., Elimination of indigenous measles from the United States, *Rev. Infect. Dis.*, 5:538–545, 1983; A. R. Hinman and W. A. Orenstein, Immunization practices in developed countries, *Lancet*, 335:707–710, 1990; T. H. Tulchinsky et al., Measles control in developing and developed countries: The case for a two-dose policy, *Bull. WHO*, 71:93–103, 1993.

Measure

A reference sample used in comparing lengths, areas, volumes, masses, and the like. The measures employed in scientific work are based on the international units of length, mass, and time—the meter, the kilogram, and the second—but decimal multiples and submultiples are commonly employed. Prior to the development of the international metric system, many special-purpose systems of measures had evolved and many still survive, especially in Great Britain and the United States, where metric units have not come into common use. Multiples and submultiples in these systems are usually nondecimal; some are based on successive doubling or halving; others involve subdivision of 60 or 12; still others have multiples and submultiples of unknown origin. A few common systems are listed here; others can be found in engineering handbooks.

Length measures

12 inches = 1 foot (= 0.3048 meter)
3 feet = 1 yard
$5\frac{1}{2}$ yards = 1 rod
40 rods = 1 furlong = 220 yards
8 furlongs = 1 mile = 5280 feed
4 inches = 1 hand
9 inches = 1 span

(Surveyor's length measures)

7.92 inches = 1 link
100 links = 1 chain
10 chains = 220 yards = 1 furlong
8 furlongs = 1 mile

(Nautical length measures)

6080.26 feet = 1.15156 statute miles
= 1 nautical mile
3 nautical miles = 1 league
60 nautical miles = 1 degree at Equator
6 feet = 1 fathom
120 fathoms = 1 cable

Measures of area

1 acre = 160 square rods
= 4840 square yards
640 acres = 1 square mile

1 circular inch = area of circle 1 inch in diameter
= 0.7854 square inch
1 circular mil = area of circle 0.001 inch in diam.

Measures of mass (avoirdupois weight)

16 drams = 1 ounce
16 ounce = 7000 grains
= 1 pound (= 453.6 grams)
14 pounds = 1 stone
8 stones = 112 pounds
= 1 hundredweight (cwt)
20 cwt = 2240 pounds = long ton
2000 pounds = 1 short ton

[Troy weight (for gold and silver), carat weight (for precious stones), and apothecaries' weight (for

drugs) are other systems, in all of which the grain is the same as the avoirdupois grain.]

Measures of volume (Liquid measures)

4 gills = 1 pint
2 pints = 1 quart
4 quarts = 1 U.S. gallon
= 231 cubic inches
1 Imperial gallon = 1.20094 U.S. gallons

["Old Liquid Measures," involving 1 barrel = $31\frac{1}{2}$ gallons, and apothecaries' measures, involving 16 fluid ounces = 1 pint, are still in wide use.]

(*Dry measure*)

2 pints = 1 quart
8 quarts = 1 peck
4 pecks = 1 bushel
= 2150.42 cubic inches
105 quarts = 1 barrel
8 Imperial gallons = 1 Imperial bushel

Circular measure

60 seconds = 1 minute
60 minutes = 1 degree
90 degrees = 1 quadrant
360 degrees = 1 revolution
2π radians = 1 revolution

Time

60 seconds = 1 minute
60 minutes = 1 hour
24 hours = 1 day
7 days = 1 week
365 days, 5 hours, 48 min, 45.6 s = 1 year
1 sideral day = 86, 164 s

See METRIC SYSTEM; PHYSICAL MEASUREMENT; TIME; UNITS OF MEASUREMENT; WEIGHT. Dudley Williams

Bibliography. American National Metric Council, *Metric Reference for Consumers*, 1990; J. V. Drazil, *Quantities and Units of Measurement*, 1983.

Measure theory

A branch of mathematical analysis connected with the theory of integration. In order to discuss this subject, a formal definition of the term measure must be given.

Sigma algebras. Let X be an arbitrary set. Let $\mathcal{M}$ be a fixed collection of subsets of X satisfying the following conditions:

1. $\phi \in \mathcal{M}$. (ϕ is the empty set. The symbol $\in$ indicates that ϕ is an element of $\mathcal{M}$.)

2. If $A \in \mathcal{M}$, then $A^c \in \mathcal{M}$. (A^c is the complement of A. It consists of those elements of X which do not belong to A.)

3. If $A_1, A_2, \ldots \in \mathcal{M}$, then (1) is valid. (This set is

$$\bigcup_{k=1}^{\infty} A_k \in \mathcal{M} \tag{1}$$

the union of $A_1, A_2, \ldots$. It consists of those elements of X which belong to at least one of the sets $A_1, A_2, \ldots$.)

In this situation the collection $\mathcal{M}$ is called a σ-algebra. Here the term algebra refers to the various set operations (complementation, union, intersection), and the prefix σ to the fact that countably many such operations can be performed with sets in $\mathcal{M}$ and still result in sets in $\mathcal{M}$. For example, the three properties mentioned above imply another property:

4. If $A_1, A_2, \ldots \in \mathcal{M}$, then (2) is valid. (This set is

$$\bigcap_{k=1}^{\infty} A_k \in \mathcal{M} \tag{2}$$

the intersection of $A_1, A_2, \ldots$. It consists of those elements of X which belong to all of the sets $A_1, A_2, \ldots$.) *See* SET THEORY.

Some examples of σ-algebras will be given:

1. If $\mathcal{M}$ consists of all subsets of X, then $\mathcal{M}$ is a σ-algebra.

2. If $\mathcal{M}$ consists only of ϕ and X, then $\mathcal{M}$ is a σ-algebra.

These two examples are trivial. The next example is highly nontrivial.

3. Let $X = \mathbf{R}^n$ be n-dimensional euclidean space. Let $\mathcal{O}$ be the collection of all open subsets of $\mathbf{R}^n$. This is not a σ-algebra. However, it is contained in σ-algebras of subsets of $\mathbf{R}^n$ for example, the one mentioned in example. Among all σ-algebras which contain $\mathcal{O}$, there is a smallest one. Namely, it is the intersection of all σ-algebras which contain $\mathcal{O}$. This σ-algebra is said to be generated by $\mathcal{O}$. Let $\mathcal{B}_n$ designate this σ-algebra generated by the open sets of $\mathbf{R}^n$. It is called the Borel σ-algebra. A set in $\mathcal{B}_n$ is called a Borel set. $\mathcal{B}_n$ contains all the open sets in $\mathbf{R}^n$ and also all the closed sets in $\mathbf{R}^n$, but it also contains many more sets.

Measures. Now suppose that X is a set and $\mathcal{M}$ is a particular σ-algebra of subsets of X. A measure μ is a function which assigns to each set in $\mathcal{M}$ a certain nonnegative real number (or $+\infty$) and which satisfies the following conditions:

1. $\mu(\phi) = 0$.

2. If A and $B \in \mathcal{M}$ and are disjoint ($A \cap B = \phi$), then Eq. (3) holds.

$$\mu(A \cup B) = \mu(A) + \mu(B) \tag{3}$$

3. If $A_1, A_2, \ldots \in \mathcal{M}$, then Eq. (4) holds.

$$\mu\left(\bigcup_{k=1}^{\infty} A_k\right) \leq \sum_{k=1}^{\infty} \mu(A_k) \tag{4}$$

Various other properties can be derived from these conditions, such as:

4. If A and $B \in \mathcal{M}$ and $A \subset B$ (that is, A is a subset of B), then $\mu(A) \leq \mu(B)$.

5. If $A_1, A_2, \ldots \in \mathcal{M}$ and are mutually disjoint ($A_i \cap A_j = \phi$ if $i \neq j$), then Eq. (5) holds. The last property

$$\mu\left(\bigcup_{k=1}^{\infty} A_k\right) = \sum_{k=1}^{\infty} \mu(A_k) \tag{5}$$

is of crucial importance and is called the countable additivity property of the measure μ.

Some examples of measures will be given:

1. Let X be any set and let $\mathcal{M}$ consist of all subsets of X. For any $A \subset X$ define $\mu(A)$ by Eqs. (6). It is not difficult to see that μ is a measure. It is called counting measure.

$$\mu(A) = \begin{cases} \text{number of elements in } A, & \text{if } A \text{ is finite} \\ \infty, & \text{if } A \text{ is infinite} \end{cases} \tag{6}$$

2. Again, let $\mathcal{M}$ be the σ-algebra of all subsets of X. Let $a \in X$ be a fixed element. For any $A \subset X$, define $\mu(A)$ by Eqs. (7). This measure is called the Dirac measure concentrated at a, and is often denoted δ_a.

$$\mu(A) = \begin{cases} 0, & \text{if } a \notin A \\ 1, & \text{if } a \in A \end{cases} \tag{7}$$

The most important example is Lebesgue measure. It is much harder to describe than the previous examples and will be discussed separately.

Lebesgue measure. Let $\mathbf{R}^n$ be n-dimensional euclidean space. A measure λ will now be defined for certain subsets of $\mathbf{R}^n$. If $n = 1$, the measure $\lambda(A)$ will correspond to the length of A; if $n = 2$, $\lambda(A)$ will correspond to the area of A; if $n = 3$, $\lambda(A)$ will correspond to the volume of A. A standard unit of "measurement" must be chosen. To do this, arbitrarily say that the measure of an "interval" is the product of the lengths of its edges. In this discussion an interval is any set of the form given by Eq. (8). The definition is then given by Eq. (9). Thus, $\lambda(I)$ is the length, area, or volume of I if $n = 1$, 2, or 3, respectively.

$$I = \{x \in \mathbf{R}^n \mid a_i \leq x_i \leq b_i,\ i = 1, \ldots, n\} \tag{8}$$

$$\lambda(I) = (b_1 - a_1)(b_2 - a_2) \cdots (b_n - a_n) \tag{9}$$

The next step is to define the measure of an open set $G \subset \mathbf{R}^n$. This is done by approximating G by smaller finite unions of intervals, as follows. Consider any intervals $I_1, \ldots, I_m$ such that each pair is nonoverlapping and such that each $I_k \subset G$. Then form the number $\lambda(I_1) + \cdots + \lambda(I_m)$. A set of real numbers is obtained in this way. Then $\lambda(G)$ is simply the least upperbound of this set of numbers.

Now let A be any set in $\mathbf{R}^n$. The outer measure of A is defined by approximating A by larger open sets. Specifically, the outer measure of A, $\lambda^*(A)$, is the greatest lower bound of the measures $\lambda(G)$ of open sets G such that $A \subset G$.

It is not the case that λ^* is a measure on the σ-algebra of all subsets of $\mathbf{R}^n$. However, it is a measure on a smaller σ-algebra, which can be defined by a standard procedure that applies to all outer measures, and which will now be described.

Outer measures. Let X be an arbitrary set. An outer measure on X is a function α which assigns to each $A \subset X$ a number $\alpha(A)$ and which satisfies the following conditions:

1. $0 \leq \alpha(A) \leq \infty$

2. $\alpha(\phi) = 0$

3. $\alpha\left(\bigcup_{k=1}^{\infty} A_k\right) \leq \sum_{k=1}^{\infty} i\, \alpha(A_k)$

Every measure defined on the σ-algebra of all subsets of X is an outer measure. There are important outer measures which are not measures, for example, the Lebesgue outer measure λ^* defined above. (It can be verified that λ^* satisfies these conditions.)

Given an outer measure α, C. Carathéodory has defined an important collection of subsets of X associated with α: a set E is said to be measurable (with respect to α) if Eq. (10) is satisfied. The following two facts can then be proved:

$$\alpha(A) = \alpha(A \cap E) + \alpha(A \cap E^c) \quad \text{for all } A \subset X \tag{10}$$

1. The collection of measurable sets is a σ-algebra.

2. When α is restricted to the measurable sets, it is a measure.

Application to Lebesgue measure. As mentioned above, λ^* is an outer measure on $\mathbf{R}^n$. Let $\mathcal{L}_n$ denote the measurable sets which arise from this outer measure by means of the Carathéodory construction. It can be proved that every open set in $\mathbf{R}^n$ is measurable. Since $\mathcal{L}_n$ is thus a σ-algebra which contains all open sets, it also contains $\mathcal{B}_n$ (the smallest σ-algebra which contains all open sets).

This, finally, completes the definition of n-dimensional Lebesgue measure. The set is $\mathbf{R}^n$; the σ-algebra is $\mathcal{L}_n$ and the Lebesgue measure of a (measurable) set $A \in \mathcal{L}_n$ is defined by Eq. (11).

$$\lambda(A) = \lambda^*(A) \tag{11}$$

The importance of Lebesgue measure is due to three factors: (1) $\lambda(A)$ is what an n-dimensional measure should be if A is an open set; (2) a great collection of sets are measurable; and (3) λ is countably additive.

Integration. Measure theory has a great number of important applications. Undoubtedly, the most important is the application to integration.

Let μ be an arbitrary measure on a σ-algebra $\mathcal{M}$ of subsets of X. Let f be a nonnegative simple function on X. That is, there exist disjoint sets $A_1, \ldots, A_m \in \mathcal{M}$ such that Eq. (12) holds and f has a constant value c_k on A_k, where $0 \leq c_k \leq \infty$. Then the integral of f (with respect to μ) is defined by Eq. (13).

$$X = \bigcup_{k=1}^{m} A_k \tag{12}$$

$$\int_X f\, d\mu = \sum_{k=1}^{m} c_k\, \mu(A_k) \tag{13}$$

Now suppose f is a nonnegative measurable function on X. This means that for all $0 \le t < \infty$ the set $S(t)$, consisting of all elements $x \in X$ such that $f(x) \le t$, is a member of m. The integral of f is then defined by Eq. (14), where g is any nonnegative simple function

$$\int_X f\, d\mu = \text{least upper bound of } \int_X g\, d\mu \tag{14}$$

satisfying $g(x) \le f(x)$ for all $x \in X$.

Finally, an arbitrary real-valued function f defined on X is said to be integrable if the two nonnegative functions given by Eqs. (15) are themselves measur-

$$\begin{aligned} f_+(x) &= \max(f(x), 0) \\ f_-(x) &= \max(-f(x), 0) \end{aligned} \tag{15}$$

able and if their integrals are finite. In this case, the integral of f is defined to be the real number given by Eq. (16).

$$\int_X f\, d\mu = \int_X f_+ d\mu - \int_X f_- d\mu \tag{16}$$

In the case of counting measure, the integral is really an infinite sum given by Eq. (17). The function

$$\int_X f\, d\mu = \sum_{x \in X} f(x) \tag{17}$$

f is integrable if and only if it vanishes except on a countable set $\{x_1, x_2, \dots\}$ and Eq. (18) holds. In

$$\sum_{k=1}^{\infty} |f(x_k)| < \infty \tag{18}$$

the case of the Dirac measure concentrated at a, the integral is given by Eq. (19), and f is integrable if and

$$\int_X f\, d\delta_a = f(a) \tag{19}$$

only if $f(a)$ is a (finite) real number.

Connection with Riemann integration. The integration concept just defined is more valuable in many applications than Riemann integration (the technique discussed in most calculus texts) because more functions are integrable and there are more easily applied limit theorems of the form of Eq. (20).

$$\lim_{k \to \infty} \int_X f_K\, d\mu = \int_X \left(\lim_{k \to \infty} f_K\right) d\mu \tag{20}$$

In order to illustrate the first point, suppose that $n = 1$ and suppose all functions under consideration vanish outside a fixed interval $[a,b] \subset \mathbf{R}$. Also suppose f is a bounded function. In case f is integrable in the sense of Riemann (as defined in calculus texts), denote its Riemann integral as expression (21). In

$$R \int_a^b f(x)\, dx \tag{21}$$

case f is integrable in the sense of Lebesgue (as defined above), denote its (Lebesgue) integral as expression (22). It can then be proved that if the former

$$L \int_a^b f(x)\, dx \qquad \left(= \int_{[a,b]} f\, d\lambda \text{ in the above notation}\right) \tag{22}$$

integral exists, then so does the latter, and also that Eq. (23) holds. But also there are functions which are

$$R \int_a^b f(x)\, dx = L \int_a^b f(x)\, dx \tag{23}$$

Lebesgue-integrable and not Riemann-integrable. For example, if $f(x) = 0$ or 1 according as x is rational or irrational, then f is not Riemann-integrable, although the Lebesgue integral exists and is given by Eq. (24).

$$L \int_a^b f(x)\, dx = b - a \tag{24}$$

Lesbesgue measure also provides an answer to the question of Riemann integrability. The bounded function f on $[a,b]$ is Riemann-integrable if and only if the set of x at which f is discontinuous has zero Lebesgue measure. *See* INTEGRATION.

B. Frank Jones, Jr.

Bibliography. D. Cohn, *Measure Theory*, 1996; J. L. Doob, *Measure Theory and Probability*, 1993; P. R. Halmos, *Measure Theory*, 1950, reprint 1991; F. Morgan, *Geometric Measure Theory*, 3d ed., 2000; H. L. Royden, *Real Analysis*, 3d ed., 1988.

Measured daywork

A tool used primarily in manufacturing facilities as a control device to measure productive output in relation to labor input within a specific time period. The measurement of the work content is accomplished through the use of time standards (which are usually the result of a stopwatch time study), predetermined time standards (methods-time measurement, the work-factor system), or some other form of work-measurement technique designed to measure tasks of labor under normal and average conditions.

Characteristics. A measured daywork plan shares some characteristics of both incentive pay plans and unmeasured daywork plans, thus becoming a unique plan in itself. It is similar to incentive pay plans inasmuch as, in both plans, time standards are used as a device for measuring operator performance and also for various forms of management planning. There the similarity ends, for, with incentive plans, operator earnings are directly related to, and fluctuate accordingly with, productive output. In a measured daywork plan, worker income is based on a fixed hourly rate established by management, and is usually affected only by job classification, shift premiums, and overtime adjustments. Because of the fixed hourly rate in a measured daywork plan, there is a little incentive for a worker to exceed a normal or standard level of performance or productivity. On

the other hand, time standards are more readily acceptable, and become less an item of contention to the employee and bargaining unit (union).

The fixed hourly rate of measured daywork is also characteristic of an unmeasured daywork plan. However, unlike an unmeasured daywork plan, measured daywork does determine worker performance factually. Other advantages of measured daywork compared with unmeasured daywork are that costs can be readily identified for specific jobs or products, accurate estimated costs for new products can be derived if standard data have been compiled, and management planning and control are aided by use of time standards when planning for equipment and worker-power needs and scheduling work through the shop.

Operating principles. The term daywork as used in industry denotes a fixed hourly rate that is not raised or lowered by varying worker performance levels. The hourly rate for a particular job should be a fair one relative to other jobs in the shop, and should also be comparable to rates of pay for similar jobs in the industrial community. In order to ensure an equality of pay rates, a job-evaluation program should exist, and be reviewed and updated as required. Once it is established what a fair rate of pay should be for each job, measurements can be made regarding how long it should take under normal, average conditions to complete the job, task, or operation. Allowances should be made for personal time, unavoidable delays, and, when required, fatigue factors. The result is a time standard as it relates to a specific job, task, or operation. *See* PRODUCTIVITY.

Once measured labor time standards have been established for shop operations, in addition to evaluating operator performance and identifying labor costs, new-product costs can also be determined prior to release to production, worker-power planning and scheduling can be done, equipment capacity requirements can be identified, and planning and make/buy decisions can be facilitated. Most importantly, a system has also been established to aid in identifying those areas, operations, and tasks that offer cost reduction potential.

Program criteria. There are several key criteria that are essential to a sound measured daywork program. First, the labor standards must be realistic and kept current to reflect existing shop conditions. In addition, the labor standards must also be fair and attainable.

Second, the worker should be made aware of what is the standard or production rate/quota. This in itself will often aid in increasing productivity.

Third, since there is no pay incentive for the worker to exceed standard or normal performance, there is the inherent characteristic of employees in a measured daywork system to fall somewhat short of standard or 100% performance level. Consequently it is of the utmost importance to have strong, qualified, and aggressive first-line supervision, or a foreperson who will provide direct supervision to the employee. *See* PERFORMANCE RATING; WAGE INCENTIVES; WORK MEASUREMENT.

Dave H. Scott

Bibliography. C. R. Asfahl, *Industrial Safety and Health Management*, 4th ed., 1998; P. E. Hicks, *Industrial Engineering and Management: A New Perspective*, 2d ed., 1999; R. C. Vaughn, *Introduction to Industrial Engineering*, 1985.

Mechanical advantage

Ratio of the force exerted by a machine (the output) to the force exerted on the machine, usually by an operator (the input). The term is useful in discussing a simple machine, where it becomes a figure of merit. It is not particularly useful, however, when applied to more complicated machines, where other considerations become more important than a simple ratio of forces. *See* EFFICIENCY; SIMPLE MACHINE.

Richard M. Phelan

Mechanical alloying

A materials-processing method that involves the repeated welding, fracturing, and rewelding of a mixture of powder particles, generally in a high-energy ball mill, to produce a controlled, extremely fine microstructure. The mechanical alloying technique allows alloying of elements that are difficult or impossible to combine by conventional melting methods. In general, the process can be viewed as a means of assembling metal constituents with a controlled microstructure. If two metals will form a solid solution, mechanical alloying can be used to achieve this state without the need for a high-temperature excursion. Conversely, if the two metals are insoluble in the liquid or solid state, an extremely fine dispersion of one of the metals in the other can be accomplished. The process of mechanical alloying was originally developed as a means of overcoming the disadvantages associated with using powder metallurgy to alloy elements that are difficult to combine. Using powder metallurgy, homogeneity is dictated by the size of the particle, but contamination and fire hazards become a concern when particle size is very small. *See* POWDER METALLURGY; SOLID SOLUTION.

Process. The process of mechanical alloying consists of repeated flattening, fracture, and rewelding of the powder particles in a high-energy ball charge. Every time two steel balls collide, they trap powder particles between them. This deforms the particles and creates minimal foreign species on the surface so that welding together of adjacent surfaces can occur easily. The alloying is effected by the ball-powder-ball collisions in several stages. In the first stage, intense cold welding predominates, and layered composite particulates of the starting constituents form (**illus.** *a*). This is followed by a hardening of the particles and fracturing and cold welding leading to a finer composite particle size (illus. *b*). Solid-solution formation begins at this stage. Next, in a moderate cold-welding period, the microstructure of the particles gets finer, with a typical spacing between

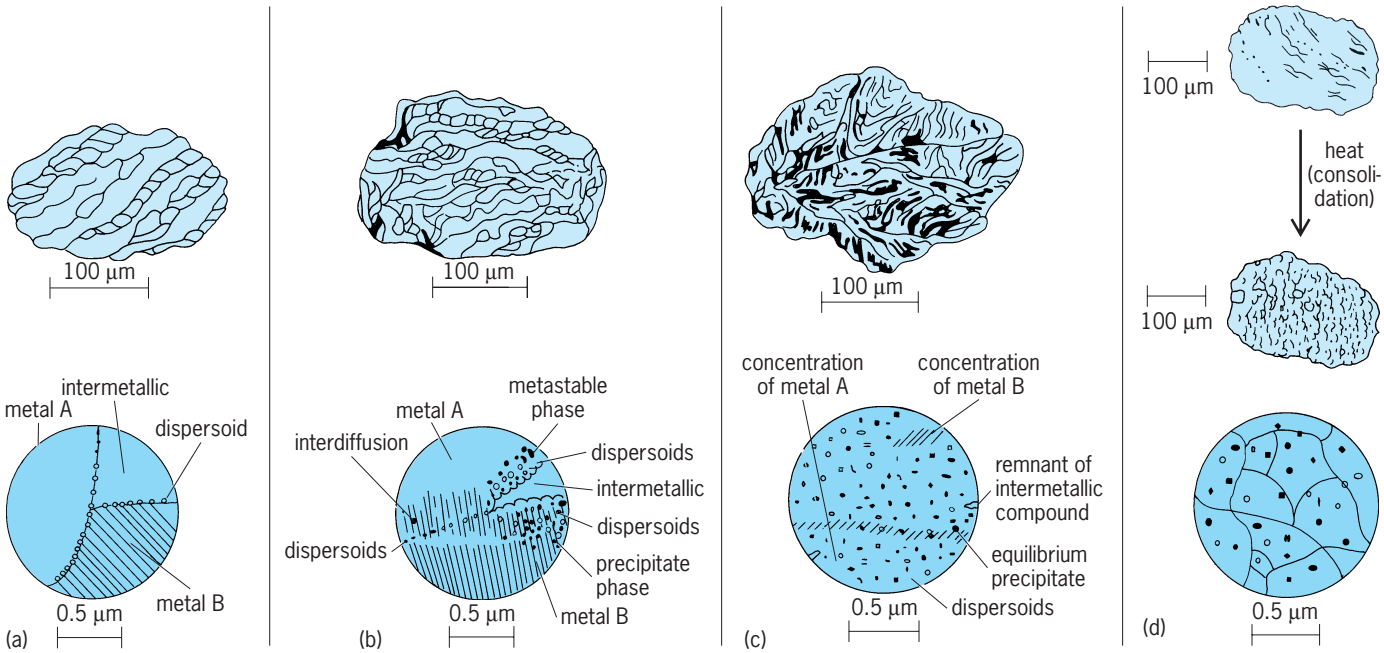

Diagrams showing mechanical alloying; the upper portion in each case represents low magnification, and the lower portion represents a higher magnification. (*a*) First stage of processing, intense cold welding; (*b*) intermediate stage of processing, rapid fracturing; (*c*) final stage of processing, moderate cold welding; (*d*) completion of processing, steady-state. The powder has an extremely deformed metastable structure with dispersoids, where the lamellae are no longer optically resoluble; that is, they cannot be resolved in the optical microscope (in contrast to having to go to a higher magnification using a transmission electron microscope). On consolidation, this leads to a fine grain size with equilibrium distribution of dispersoids.

adjacent regions of 1 micrometer (illus. *c*). The compositions of the individual particles converge to the original blend composition, with the rate of refinement of the internal structure (reduction in scale of the microstructure) of the particles approximately logarithmic with processing time. The final stage is a steady-state period (illus. *d*). By the time processing has been completed, the particles have an extremely deformed metastable structure, which can contain dispersoids. Generally, at this point the microstructural scale is significantly below the micrometer level.

Mechanical alloying can be carried out in small batches on shaker mills (few grams per run), high-energy stirred-ball millers known as attritors (1.1–220 lb or 0.5–100 kg of powder), or on a commercial scale in a ball mill (up to about 4400 lb or 2000 kg). The attritor is capable of generating high energies by utilizing a vertical drum with a series of impellers inside it. A powerful motor rotates the impellers, which in turn agitate the steel balls in the drum. The scaling-up from one process to the next is not direct, and it is considered an art rather than a science. The powders used in mechanical alloying are very hard because of their heavily worked condition; thus they must normally be consolidated to a useful form by hot-processing methods. The powders for mechanical alloying are hot-pressed followed by hot extrusion; in a number of situations this is followed by a hot-rolling operation. *See* CRUSHING AND PULVERIZING; EXTRUSION; METAL FORMING.

Applications. Some oxides are insoluble in molten metals. Mechanical alloying was originally developed to provide a means of dispersing these oxides in the metals. Examples are nickel-based superalloys strengthened with dispersed thorium oxide or yttrium oxide (Y_2O_3), the latter being preferred. These superalloys have excellent strength and corrosion resistance at elevated temperatures, making them attractive candidate materials for use in applications such as jet-engine turbine blades, vanes, and combustors. This class of alloys is known as oxide-dispersion-strengthened nickel-base superalloys. Iron- and aluminum-based dispersion-strengthened alloys have also been developed. Additionally, a number of other potential applications for mechanical alloying material are being explored, including powders for coating applications, alloys of immiscible systems, amorphous alloys, intermetallics, cermets, and organic-ceramic-metallic material systems in general. *See* AMORPHOUS SOLID; CERMET; INTERMETALLIC COMPOUNDS; METAL COATINGS.

Alloys like MA754 (Ni-20Cr-0.3Al-0.5Ti-0.6Y_2O_3) and MA6000 (Ni-15Cr-4W-2Mo-2Ta-4.5Al-2.5Ti-1.1Y_2O_3) are commercially available as bar and plate for use in gas turbine vanes and turbine blades and for other applications in oxidizing or corrosive atmospheres. The vane alloy MA754 is capable of a service temperature of about 2100°F (1100°C) and is used in military engines. The iron-base alloy MA956 (Fe-20Cr-4.5Al-0.5Ti-0.5Y_2O_3), available as plate sheet, bar, and wire, is capable of withstanding temperatures up to 2370°C (1300°C) or even higher in corrosive environments; it has applications in aircraft and industrial gas turbine combustors, in

swirlers and heat exchangers of power generation equipment, and in heat-treatment equipment.

Conventional coatings in advanced gas turbine engines fail by loss of aluminum in the coating or by interdiffusion between the coating and substrate. Coatings possessing a large amount of Y_2O_3, produced by mechanical alloying, could solve such problems. *See* METAL COATINGS.

Liquid or solid immiscible systems are difficult to process by conventional pyrometallurgy, for example, the copper-lead (Cu-Pb) or copper-iron (Cu-Fe) systems. In these cases, mechanical alloying provides a route to obtain a homogeneous distribution in the solid phase. Mechanical alloying has also been used to fabricate the superconducting intermetallic niobium-tin compound Nb_3Sn, which is difficult to produce conventionally because of the large melting-point difference between Nb and Sn. Mechanical alloying can also be used to produce supercorroding magnesium-base alloys. These alloys are designed to corrode at a controlled rate for release of deep-sea equipment at specific depths. The requirement is to have the anode and cathode in proximity by using mechanical alloying. In another interesting application of mechanical alloying, titanium (Ti) and magnesium (Mg) have been combined by using mechanical alloying; usually it is very difficult to produce such an alloy because the boiling point of Mg is lower than the melting point of Ti. This achievement could result in a lower-density titanium alloy for aerospace applications. *See* PYROMETALLURGY.

Amorphous alloys can also be produced by using the mechanical alloying technique. These include Nb_3Sn starting from elemental powders, various rare-earth/cobalt combinations, and titanium-copper (Ti-Cu) and titanium-copper-palladium (Ti-Cu-Pd) systems. *See* ALLOY; HIGH-TEMPERATURE MATERIALS; SOLID-STATE CHEMISTRY; WELDING AND CUTTING OF MATERIALS.

F. H. Froes

Bibliography. J. J. De Barbadillo, *Mechanical Alloying for Structural Applications*, 1993; B. L. Bramfitt et al. (eds.), *Oxide Dispersion Strengthened Alloys*, ASTM STP-979, 1988; R. M. German, *Powder Metallurgy Science*, 2d ed., 1994; P. H. Shingu (ed.), *Mechanical Alloying*, 1992; R. Sundaresan and F. H. Froes, Mechanical alloying, *J. Met.*, pp. 22–27, August 1987.

Mechanical classification

A sorting operation in which mixtures of particles of mixed sizes, and often of different specific gravities, are separated into fractions by the action of a stream of fluid. Water is ordinarily used as the sorting fluid, but other liquids or air or other gases may be used.

The main objective of classification is to separate the particles according to size. This function is identical to that of screening, but classification is applicable to smaller particles, especially those that are undersize. For small particles, it is more economical than screening. In classification, the oversize and undersize are called sands and slimes, respectively.

Material also may be mechanically classified by specific gravity, a method that separates substances differing in chemical composition. This is called hydraulic separation. Such classification is based on the fact that, in a fluid, particles of the same specific gravity but of different size or shape settle at different constant speeds. Large, heavy, round particles settle faster than small, light, needlelike ones. If the particles also differ in specific gravity, the speed of settling is further affected. This is the basis for the separation of particles by kind rather than by size alone.

Mechanical classifiers utilize the differences in settling velocities by bringing the feed mixture into contact with a continuous stream of fluid, and allowing the particles to reach their settling velocities with respect to the fluid. Then, by adjusting the rate of flow of the fluid, the small particles, which have the lower settling speeds, are removed from the classifier with the fluid stream before they have had time to settle out of the fluid. The larger particles, which settle through the fluid more rapidly, strike the wall or bottom of the classifier, collect in the bottom of the apparatus, and are rejected as sands.

When the particles in a classifier are so far apart that they do not interfere with one another, the action is called free settling; when they are so close together that they do interfere with one another, the action is called hindered settling. In hindered settling the velocities of settling are less than in free settling, but the capacity of the equipment, measured in tons per square foot per day, is much greater. Also, the separation by specific gravity is improved in hindered settling. This method is used in commercial classification.

Wet classifiers. These are built in two major categories—horizontal flow and vertical flow. The latter are more effective in separations by specific gravity, and the former have greater capacity in separation by size alone.

An example of a horizontal-flow classifier is the Dorr unit, shown in **Fig. 1**. It consists of a rectangular tank with a sloping bottom, a rake mechanism for moving sands uphill along the bottom, an inlet for feed, and outlets for sands and slimes. The feed is admitted in a stream of water behind a baffle and subjected to the action of the stream as it flows toward the slime overflow. Coarse solids (sands) settle

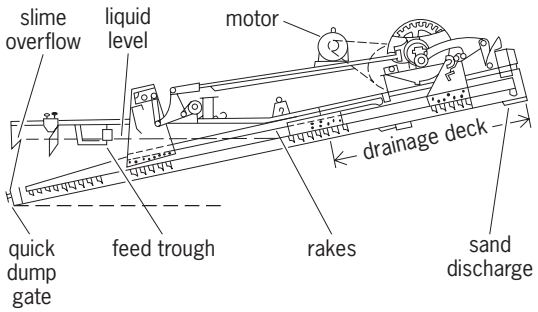

Fig. 1. Dorr classifier. (*After R. R. Perry, ed., Chemical Engineers' Handbook, 4th ed., McGraw-Hill, 1963*)

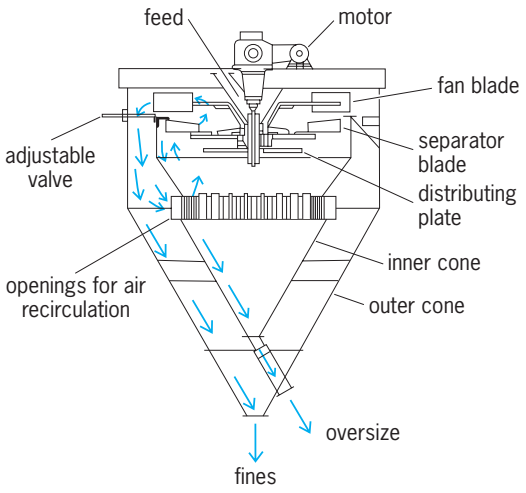

Fig. 2. Double-cone air separator. (*After W. L. McCabe and J. C. Smith, Unit Operations of Chemical Engineering, McGraw-Hill, 1956*)

rapidly enough to reach the bottom of the tank and are raked out of the classifier at the shallow end. The rakes accomplish this by moving slowly along the bottom, dragging the solids with them. After a short motion in this direction, the rakes are lifted clear of the sands by mechanical means, returned, and lowered for another stroke. The action is sufficiently gentle not to disturb the settling in the bulk of the liquid. Fines (slimes) overflow with the liquid at the deep end of the tank.

Vertical-flow classifiers are used when separation by specific gravity is important. These machines have been largely superseded by flotation, which can make closer separations of substances of different chemical composition. *See* FLOTATION.

Air classifiers. These are used to separate particles by size through the action of a stream of air. They make sharper and more accurate separations than wet classifiers. An example is the double-cone air separator in **Fig. 2**. The feed, consisting of a mixture of sizes, is dropped on a horizontal rotating distributor plate, which is driven by a vertical shaft that also carries fan blades. The plate disperses the particles into the air stream, and the fan maintains a circulation of air inside the separator. The air flows downward and then suddenly reverses to flow upward. The larger and heavier particles have sufficient momentum that they do not follow the air, but are thrown against the inner surface of the inner cone, from which they are collected and withdrawn. The smaller particles accompany the air into the annular space between the two cones, where the velocity is low enough to allow the particles to settle and be removed from the bottom of the outside cone. *See* MECHANICAL SEPARATION TECHNIQUES; UNIT OPERATIONS.

Warren L. McCabe

Bibliography. W. L. McCabe, J. C. Smith, and P. Hariott, *Unit Operations in Mechanical Engineering*, 7th ed., 2004; R. H. Perry and D. Green (eds.), *Perry's Chemical Engineers' Handbook*, 7th ed., 1997.

Mechanical engineering

The branch of engineering that deals with the generation, transmission, and utilization of heat and mechanical power, and with the production of tools and machines. This distinction begins in college where, after 1 year of common engineering studies, a person can be identified as a student of mechanical engineering. After college, mechanical engineers may enter many industries. Common areas of industrial employment for mechanical engineers are private electric power and machinery manufacturing.

To grasp the meaning of mechanical engineering, it is desirable to take a close look at what engineering really is. The Engineers' Council for Professional Development has defined engineering as the profession in which a knowledge of the mathematical and physical sciences gained by study, experience, and practice is applied with judgment to develop ways to utilize economically the materials and forces of nature for the progressive well-being of humankind. Here is a picture of a profession in which study in mathematics and science is blended with experience and judgment for the production of useful things.

Formal training of a mechanical engineer includes mastery of mathematics through the level of differential equations. Training in physical science embraces chemistry, physics, mechanics of materials, fluid mechanics, thermodynamics, statics, and dynamics. Enhancing these subjects are courses in the humanities: literature, economics, philosophy, and history.

Experience, for the mechanical engineer, is not gained solely by the passage of time. For experience to be added, the time spent in engineering must be meaningful. Projects must become more difficult and the consequences of error greater.

Judgment is the hallmark of any competent engineer in whatever specialized branch of engineering is pursued. The exercise of judgment requires the ability to assess and decide between alternate courses of action. In the application of judgment there is constant testing of the engineer's decisions against his or her knowledge of the laws of nature, his or her sense of right and wrong, and economics.

A further essential of an engineer is that efforts be devoted to matters which improve the well-being of humankind. This purpose is kindred to that of all learned professions and is closely allied to the professions of medicine and law.

In relation to other professions the mechanical engineer differs in one large measure. Whereas most doctors and many lawyers are self-employed, almost all engineers are employed by corporations, colleges, or government. This distinction exists for several reasons. Generally the doctor or lawyer is far more concerned with people and their actions than is the engineer. Also, an engineer dealing with machines requires larger sums of money to finance the equipment and facilities used than does the doctor or lawyer.

From the foregoing, a young person thinking of becoming a mechanical engineer should recognize that

there is a long period of preparation necessary. Starting in high school, a full, rigorous academic program should be pursued. Then careful self-examination of results in high school are in order. If high interest and success in mathematics, English, and science are demonstrated, there is room to consider the matter further. Finally, there must be evidence of willingness to work and patience to gain the experience and judgment required in any learned profession. *See* ENGINEERING; MACHINE DESIGN; MACHINERY; TECHNOLOGY.

Robert S. Sherwood

Bibliography. American Society of Mechanical Engineers, *Mechanical Engineering*, monthly; Engineer's Council for Professional Development (ECPD), *So You Want To Be an Engineer*, Pam. EC11; J. R. Henninger (ed. ECDP), *A Professional Guide for Young Engineers*, Pam. EC43; A. P. Johnson (ECPD), *Do I Have Engineering Aptitude*?, Pam. EC14.

Mechanical impedance

For a system executing simple harmonic motion, the mechanical impedance is the ratio of force to particle velocity. If the force is that which drives the system and the velocity is that of the point of application of the force, the ratio is the input or driving-point impedance. If the velocity is that at some other point, the ratio is the transfer impedance corresponding to the two points.

As in the case of electrical impedance, to which it is analogous, mechanical impedance is a complex quantity. The real part, the mechanical resistance, is independent of frequency if the dissipative forces are proportional to velocity; the imaginary part, the mechanical reactance, varies with frequency, becoming zero at the resonant and infinite at the antiresonant frequencies of the system. *See* ACOUSTIC IMPEDANCE; ELECTRICAL IMPEDANCE; FORCED OSCILLATION; HARMONIC MOTION.

Martin Greenspan

Bibliography. S. G. Kelly, *Fundamentals of Mechanical Vibrations*, 2d ed., 2000; W. T. Thomson, *Theory of Vibration with Applications*, 4th ed., 1992.

Mechanical separation techniques

A group of laboratory and production operations whereby the components of a polyphase mixture are separated by mechanical methods into two or more fractions of different mechanical characteristics. The separated fractions may be homogeneous or heterogeneous, particulate or nonparticulate. Mechanical separations are differentiated from two other classes of separations of major importance: those that depend on separation at the molecular level on the basis of thermodynamic or physicochemical properties and by means of such mass-transfer processes as evaporation, dissolution, precipitation, absorption, and intraphase or interphase diffusion; and those that depend on chemical reaction of a component and subsequent separation of the product by mass-transfer or mechanical methods. *See* CHEMICAL SEPARATION TECHNIQUES; UNIT OPERATIONS.

The techniques of mechanical separation are based on differences in phase density, in phase fluidity, and in such mechanical properties of particles as size, shape, and density; and on such particle characteristics as wettability, surface charge, and magnetic susceptibility. Obviously, such techniques are applicable only to the separation of phases in a heterogeneous mixture. They may be applied, however, to all kinds of mixtures containing two or more phases, whether they are liquid-liquid, liquid-gas, liquid-solid, gas-solid, solid-solid, or gas-liquid-solid.

Methods of mechanical separations fall into four general classes: (1) those employing a selective barrier such as a screen or filter cloth; (2) those depending on differences in phase density alone (hydrostatic separators); (3) those depending on fluid and particle mechanics; and (4) those depending on surface or electrical characteristics of particles.

Because of the extensive differences in the nature of mixtures to be separated, in the properties of the components, in the size of the particles, and in the functional character of the tasks performed by mechanical separators, a wide variety of separation devices have been devised and are in use. The more important kinds of equipment are listed in the **table**, grouped according to the phases involved.

Use of selective barriers. In liquid filters, including clarifying and gas (bag or air) filters, solids are removed from the fluid by pumping or drawing the fluid through a filter medium which retains the solids on or within itself. In a centrifugal filter the same process occurs (limited to liquid-solid suspensions), but the driving force is that of a centrifugal field. The solids are removed from the medium, continuously or intermittently, or are discarded with the medium when it is replaced. In screening, screen cloth or perforated sheet or plate is used to pass particles smaller than, and retain particles larger than, the screen aperture (normally performed dry), or to separate relatively large particles from a liquid (wet screening). A special case of separation by a selective barrier is the operation called expression, the squeezing of liquid from a nonfluid solid-liquid system (such as a cider press or cane mill). *See* CENTRIFUGATION; CLARIFICATION; FILTRATION; MEMBRANE SEPARATIONS; SCREENING.

Hydrostatic separators. Batch or continuous settling tanks are employed to retain liquid while an immiscible liquid, a gas, or a solid separates from it. A supernatant liquid or floating solid may be overflowed or skimmed away; a subnatant liquid or settled solid may be pumped away (the latter as a thick sludge). A sedimentation thickener is a continuous hydrostatic settling tank. Sedimentation centrifuges are substantially hydrostatic separators when used as liquid clarifiers or oil-water separators, since density difference is the prime quality that makes separation possible, provided sufficient residence time is allowed, as in settling tanks, to permit complete separation. The same is true of dense-medium separators, in which a pulp of controlled density carries

Types of mechanical separator

Materials separated	Separators
Liquid from liquid	Settling tanks, liquid cyclones, centrifugal decanters, coalescers
Gas from liquid	Still tanks, deaerators, foam breakers
Liquid from gas	Settling chambers, cyclones, electrostatic precipitators, impingement separators
Solid from liquid	Filters, centrifugal filters, clarifiers, thickeners, sedimentation centrifuges, liquid cyclones, wet screens, magnetic separators
Liquid from solid	Presses, centrifugal extractors
Solid from gas	Settling chambers, air filters, bag filters, cyclones, impingement separators, electrostatic and high-tension precipitators
Solid from solid	
By size	Screens, air and wet classifiers, centrifugal classifiers
By other characteristics	Air and wet classifiers, centrifugal classifiers, jigs, tables, spiral concentrators, flotation cells, dense-medium separators, magnetic separators, electrostatic separators

a low-density fraction of solids on its surface while allowing a higher-density fraction of solids to sink and be raked away. *See* SEDIMENTATION (INDUSTRY); THICKENING.

Fluid and particle dynamics. Most of the other methods listed in the table are based on movement of liquid drops or solid particles with respect to a suspending fluid (gas or liquid). Even most solid-solid separations require the presence of a fluid.

Drag forces and gravity, either natural or centrifugal, are the factors involved in establishing the trajectories that make wet and air classifiers, jigs, tables, spiral concentrators, cyclones, and classifying centrifuges effective.

Inertia differences between particles and the suspending fluid are the basis for the operation of impingement separators. When a fluid, ordinarily a gas, is given a sharp change in direction, any particulates therein, because of their inertia, do not conform to the new direction of flow, but continue to move nearly in their original direction. Then they strike the solid surfaces of the equipment, which may consist of a bed of solid shapes, a series of baffles, a bed of liquid-covered fibers, or other collecting surfaces. The particles striking these surfaces coalesce and are removed from the gas stream. *See* DUST AND MIST COLLECTION; MECHANICAL CLASSIFICATION.

Other methods. Froth flotation cells operate on the bases of selective wettability and density difference. Chemicals, called promoters or collectors, cause the particles of one fraction of a suspension to become air-avid and water-repellent. Air introduced to the suspension collects as bubbles on these particles, causing them to float to the surface, while the remaining solids sink and are withdrawn at the bottom.

Electrostatic and electrodynamic (current flow) forces are used in electrostatic precipitators to drive small dust particles or droplets to a collecting electrode, and thus to clean a smoky or foggy gas stream. Magnetic separators, batch or continuous, are used to separate iron-bearing or other magnetic particles from liquids in which they are suspended. *See* ELECTROSTATIC PRECIPITATOR; FLOTATION; MAGNETIC SEPARATION METHODS.

Shelby A. Miller

Bibliography. W. L. McCabe, J. C. Smith, and P. Hariott, *Unit Operations in Mechanical Engineering*, 7th ed., 2004; R. H. Perry and D. Green (eds.), *Perry's Chemical Engineers' Handbook*, 7th ed., 1997; R. W. Rousseau (ed.), *Handbook of Separation Process Technology*, 1987; J. D. Seader and E. J. Henley, *Separation Process Principles*, 2d ed., 2005.

Mechanical vibration

The continuing motion, repetitive and often periodic, of a solid or liquid body within certain spatial limits. Vibration occurs frequently in a variety of natural phenomena such as the tidal motion of the oceans, in rotating and stationary machinery, in structures as varied in nature as buildings and ships, in vehicles, and in combinations of these various elements in larger systems. The sources of vibration and the types of vibratory motion and their propagation are subjects that are complicated and depend a great deal on the particular characteristics of the systems being examined. Further, there is strong coupling between the notions of mechanical vibration and the propagation of vibration and acoustic signals through both the ground and the air so as to create possible sources of discomfort, annoyance, and even physical damage to people and structures adjacent to a source of vibration.

Mass-spring-damper system. Although vibrational phenomena are complex, some basic principles can be recognized in a very simple linear model of a mass-spring-damper system (**Fig. 1**). Such a system contains a mass M, a spring with spring constant k that serves to restore the mass to a neutral position, and a damping element which opposes the motion of the vibratory response with a force proportional to the

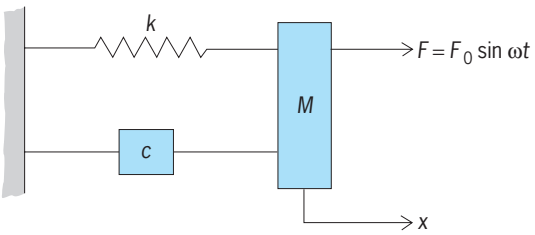

Fig. 1. Vibrating linear system (mass-spring-damper) with one degree of freedom.

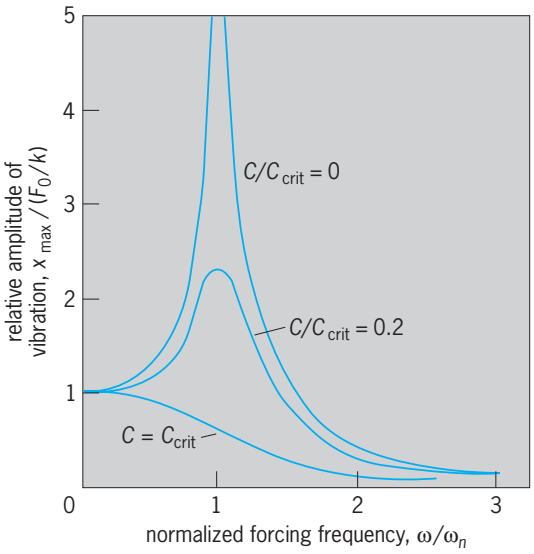

Fig. 2. Variation of amplitude of vibration with forcing frequency and damping. X_{max} = maximum displacement.

velocity of the system, the constant of proportionality being the damping constant c. This damping force is dissipative in nature, and without its presence a response of this mass-spring system would be completely periodic.

Free vibrations. In the absence of an exciting force and of the damping component, the spring-mass system can execute free, periodic vibration at a natural frequency ω_n given by Eq. (1). This is the so-called

$$\omega_n = \sqrt{k/M} \tag{1}$$

angular frequency and must be divided by 2π to get the actual frequency f_n in hertz (with dimensions time^{-1}). Equation (1) demonstrates that the natural frequency, also called the fundamental or resonant frequency, increases with the stiffness of the system and decreases as the mass of the system is increased. Thus, very stiff systems have high natural frequencies, and very massive systems could have very low natural frequencies. In some of the more complex structures referred to above, there are in fact multiple (and even infinite) resonant frequencies, but they all have in common the basic dependence upon the stiffness of the system and the system's mass. *See* HARMONIC MOTION.

Effect of damping. The inclusion of the damping element with the constant of proportionality c results in a change of the natural frequency of the system and of its response characteristics. If the damping is relatively small in magnitude (the scale against which smallness is to be measured will be given below), then the natural frequency of the system does not change substantially, and the free response of a perturbed mass-spring-damper system is periodic within the confines of a slow exponential decay. However, if the damping constant c becomes large, the motion of the system is not vibratory but is in fact one where the mass creeps back, along an exponential curve, to its initial position without any oscillation. The lowest value of damping for which this loss of vibratory response occurs is called critical damping, and it is defined by a damping constant, Eq. (2). Damping is

$$c_{crit} = 2\sqrt{kM} \tag{2}$$

considered to be small when the ratio C/C_{crit} is small compared to unity. *See* DAMPING.

Impedance and resonance. When the mass-spring-damper system is excited by a periodic force, for example, $F = F_0 \sin \omega t$, where the angular frequency ω $(= 2\pi f)$ can be chosen freely, the response of the system is such that it can be displayed in one of two commonly used forms. One of these (**Fig. 2**) is a plot of the relative amplitude of vibration (the dimensionless ratio of the actual motion of the perturbed system divided by the corresponding elastic response of the spring alone to the same force) against the normalized (dimensionless) frequency ratio of the forcing frequency divided by the undamped natural frequency. The curves shown in Fig. 2 indicate the response for no damping ($C/C_{crit} = 0$), small damping, and critical damping. It can be seen that in the undamped case ($C/C_{crit} = 0$), the amplitude of the response is infinite when the forcing frequency is identically equal to the natural frequency. This is the condition of resonance. It can also be seen that when there is damping, even though it may be small, the system responds so as to peak very near the undamped resonant frequency, but the response is not infinite in amplitude. Finally, if the damping is greater than or equal to C_{crit}, the response is simply the decaying curve that exhibits no peak at the resonant frequency.

Another way of presenting these results is to look at the quantity called the impedance Z, which may be defined here as the ratio of the magnitude of the input force to the magnitude of the velocity of the mass-spring system (**Fig. 3**). For the case where there is no damping, the impedance can be shown to be in the form of Eq. (3). It follows from

$$Z = k\left(\frac{1}{\omega} - \frac{M\omega}{k}\right) \tag{3}$$

Eq. (1), which relates the stiffness k and the mass M to the resonant frequency ω_n, and from the impedance formula that when the forcing frequency

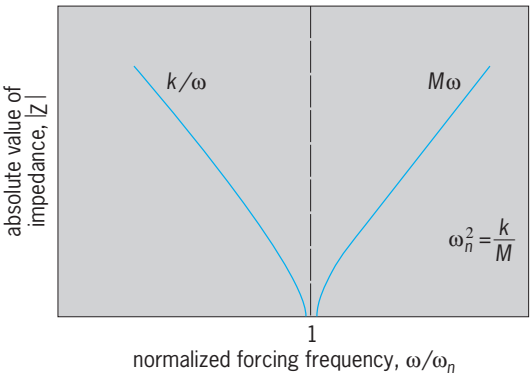

Fig. 3. Impedance of a simple oscillator.

is well below the resonant frequency, the impedance can be approximated by Eq. (4). This is considered

$$Z_k \cong \frac{k}{\omega} \qquad \omega \ll \omega_n \tag{4}$$

the stiffness-controlled region wherein the spring-mass system responds largely as a static spring. For frequencies that are significantly above the resonant frequency, the impedance can be written as Eq. (5).

$$Z_m \cong -M \quad \omega \gg \omega_n \tag{5}$$

In this regime the response of the system is said to be mass-controlled, and at high frequencies, well above the resonant frequency, the dynamics of the system are governed by the mass of the system. It follows from Eq. (3) that the impedance vanishes at resonance in the absence of damping. Thus resonance may also be defined as the condition where a very small input force produces an infinite response in the absence of damping. When damping is incorporated in the calculation of impedance, it then turns out that at resonance the impedance is exactly equal to the damping constant; that is, $Z_{\text{res}} = c$. *See* FORCED OSCILLATION; MECHANICAL IMPEDANCE; RESONANCE (ACOUSTICS AND MECHANICS).

Linear response. One other feature in the simple model is that the response is linear; that is, there is a direct proportionality of the magnitude of the input to the magnitude of the output, and signals of response for different inputs can be superposed to give the total response to a combined signal.

Relation to real systems. This simple model of the response of the single-degree-of-freedom system, as it is commony called, serves as a model or paradigm for almost all mechanical vibration problems. However, real systems are often extremely complex and involve multiple resonances and multiple sources of excitation. Further, the types of vibrational response that can be seen in different solid bodies are very much dependent not only on the nature of the excitation in terms of its time history, but also on the spatial distribution of the exciting force and the geometry of the system that is responding. There are many different ways in which a solid body can vibrate, and these different ways couple into vibratory and acoustic motions of surrounding media such as air or water in very different ways. Some of the sources of vibration, the types of vibrational response exhibited by solid bodies, and their interactions that result in perceptible, audible, and even dangerous vibration and acoustic signals will be discussed. First, however, some further comments about the general complexity of vibration problems are appropriate in order that the context of the above simple model be more clearly and sharply defined.

Analysis of complex systems. The foregoing model of the linear spring-mass-damper system contains within it a number of simplifications that do not reflect conditions of the real world in any obvious way. These simplifications include the periodicity of both the input and, to some extent, the response; the discrete nature of the input, that is, the assumption that it is temporal in nature with no reference to spatial distribution; and the assumption that only a single resonant frequency and a single set of parameters are required to describe the mass, the stiffness, and the damping. The real world is far more complex. Many sources of vibration are not periodic. These include impulsive forces and shock loading, wherein a force is suddenly applied for a very short time to a system; random excitations, wherein the signal fluctuates in time in such a way that its amplitude at any given instant can be expressed only in terms of a probabilistic expectation; and aperiodic motions, wherein the fluctuation in time may be some prescribed nonperiodic function or some other function that is not readily seen to be periodic.

However, in most cases the notions of periodic response to periodic excitation can be used because it is generally possible to describe the variation in time of a nonperiodic forcing function as a sum of periodic components using the tools of Fourier analysis and Fourier series. In such an approach, the nonperiodic signal is expressed as a sum of periodic signals, each of whose amplitudes and individual periods (or resonant frequencies) is tailored to represent the total nonperiodic signal being described. In such a Fourier analysis of a vibrating system, it is customary to look at the response of the complex system as a sum of responses of linear spring-mass-damper systems to each of the given periodic inputs, and then the simple model outlined earlier can be readily applied.

In any real system there are multiple resonances, each reflecting a different balance of stiffness and mass within a complex elastic system. Again, it is possible in general to describe the response of a complicated system in terms of individual spring-mass oscillators, the stiffness and mass of each of which represents some average of the overall stiffness and mass distributions of the complicated system. Thus, the analysis of complex systems can again be reduced to the superposition of systems of the elementary type. Very often this reduction of the complex to the simple not only involves Fourier analysis in time, but also represents a Fourier analysis in space, wherein spatial averages are used to reduce spatial variations of both excitation and response to the discrete forms in which they appear in the simple model. Thus, for a continuous system where the variables depend on space as well as time, a Fourier analysis can be used to generate a system that involves multiple degrees of freedom, each degree of freedom being a single discrete spring-mass-damper oscillator. *See* FOURIER SERIES AND TRANSFORMS.

Sources of vibration. There are many sources of mechanical and structural vibration that the engineer must contend with in both the analysis and the design of engineering systems. The most common form of mechanical vibration problem is motion induced by machinery of varying types, often but not always of the rotating variety; the machinery vibration thus induced can be a problem both for the machinery itself and in terms of vibration and noise propagated to adjacent systems. For example, the vibrations of a

compressor in an air-conditioning system in a building can create fatigue and stress problems for the compressor and adjacent piping itself, and can set into motion the floor and walls of the room wherein the compressor is housed. This in turn can set into vibrational motion other walls and components of the building and thus produce vibration and acoustic signals that are both perceptible and audible throughout the building. This simple example could thus run a gamut of problems from structural failure to human annoyance.

Such machinery-induced vibration can also be propagated into adjacent buildings through the coupling of a building foundation with the ground around it, and it is not uncommon for heavy machinery in a factory to produce perceptible vibration at considerable distances from the factory itself. This is more likely to be the case with extremely heavy pieces of equipment, for example a large-scale shredder used in a solid-waste disposal system.

Another source of vibration wherein groundborne propagation is important is vibration due to construction. Construction vibration is a major source of environmental concern, particularly in urban environments, and especially in the construction of large projects within these environments such as urban transportation systems.

Another source of vibration in urban environments is transportation systems themselves. Included may be vibration from heavy vehicles on conventional pavement as well as vibratory signals from the rail systems common in many metropolitan areas. For such rapid-transit system vibration, the sources include tunnels, at-grade rails, and elevated guideway systems. The propagation characteristics for each of these important vibration sources are different and have been the subject of extensive research.

Other vibrations are induced by natural phenomena, including earthquakes and wind forces. Wave motion is a source of vibration in mechanical and structural systems associated with offshore structures. In the analysis and design of systems that are used in environments where these natural phenomena are important, the basic principles of vibration analysis, such as the elementary model outlined above, remain the same. Thus, although such motion is not in a very strict sense due to ordinary mechanical excitation, it is in terms of practice and design a strongly related phenomenon.

Types of mechanical signals and waves. Due to the varying geometry both of the structural elements involved in a machine or structure and of the loading itself, several different types of vibratory motion may be induced in a solid body. Unlike the acoustic signals that are generated in air and water, wherein all the motion is in the form of waves termed body or compressional waves in which the fundamental mechanism is volumetric contraction or expansion, solid bodies support waves of several different varieties and thus produce several different mechanical vibratory signals. These include torsional vibration, longitudinal vibration, and the lateral vibrations of beams, plates, and membranes. The fundamental mechanisms in each case are different in that the elastic restoring forces that are analogous to the spring constant k in the simple model are very different and are produced by different physical effects in these bodies. Each type of vibration will be discussed briefly, although the major emphasis will be placed on vibrations of and in machinery.

Torsional vibration. An engine-driven system (usually diesel or internal combustion powering a generator, a ship's propeller, or other load) has many degrees of freedom and, hence, many natural frequencies of which only the lowest two or three are of practical importance. The installation may, if excited by alternating components in its torque, execute torsional vibrations between its various parts of a magnitude of a fraction of a degree. This relatively small alternating motion is superposed on, and independent of, the continuous rotation of the engine shaft. Whereas the continuous rotation causes no extreme stress in the shaft, the small (quarter degree) angles of vibration wind up the shaft and relax it, causing alternating stresses that on many occasions have caused failure.

The torque on a crankshaft caused by a single cylinder and piston having one explosion for each one or two revolutions has a highly irregular time history containing many harmonics. (Harmonics are integral multiples of the fundamental frequency.) The torques developed by the various cylinders of a multicylinder engine combine in accordance with their times of occurrences. Thus, the exciting torque contains components of the firing frequency (one cycle per one or two revolutions) and multiples of that firing frequency, which are of practical importance up to the 16th multiple or harmonic. Because these 16 exciting or forced frequencies are proportional to the engine speed and the two or three natural frequencies are independent of it, and each exciting frequency can resonate with each natual one, there are as many as 48 resonances or critical speeds to be considered. Many of these will lie outside the habitual running range of the engine.

The designer may shift the severity of the resonances by using flexible couplings or extra flywheels in the engine, or by changing the arrangement of the cylinders, the V-angle of the engine, and the firing order. These suffice to make an installation satisfactory for any one running speed, but it is usually not possible to avoid all dangerous resonances in a wide range of running speeds. The designer must then resort to dampers to keep the amplitude of motion and the stress down. Various types of dampers exist; the most familiar is the pulley in the front of an automobile engine which drives the fan belt. This pulley is usually a small flywheel coupled to the engine shaft through a rubber insert. The assembly serves simultaneously as a torsional spring and as a dashpot damper. The flywheel is so tuned that it holds the principal torsional critical speed of the engine below dangerous torsional stress levels. Fatigue failures of crankshafts and of other shafting due to torsional vibration were common in the past, but such failures

are avoidable by proper design and are now rare. *See* COUPLING; FLYWHEEL; SHAFTING.

By the principle of action equals reaction, the gas torque acting on the piston-crankshaft assembly is equal and opposite to the gas torque acting on the engine frame. Hence, when the engine frame is rigidly attached to a foundation, that foundation experiences an alternating torque. To protect the foundation and to prevent the vibration from spreading through the structure, the engine is often mounted on metal springs or on rubber bushings. This is now universal practice with automobile and aircraft piston engines. *See* AUTOMOTIVE ENGINE.

Longitudinal vibration. A large ship's shafting excited by the propeller blades may come to resonance. The shafting and propeller must be designed to allow for such resonance. This is one cause of vibration in passenger liners. It occurs at a frequency of the shaft revolutions multiplied by the number of propeller blades. *See* PROPELLER (MARINE CRAFT).

The air or gas column in the suction or discharge lines of internal combustion engines acted upon by the piston motions can come to resonance at certain speeds. This principle has been used to increase the power of the engine by designing those lines so that during the intake more air than usual enters the cylinder, and during exhaust more air than usual goes out, thereby decreasing the back-pressure. *See* INTERNAL COMBUSTION ENGINE.

In internal combustion engines the gas pressure exerted on the piston and thence on a crank throw tends to lengthen the crankshaft. Because this effect is periodic, longitudinal vibrations in internal combustion engine shafts have been observed; however, they are of less importance than the torsional ones and become serious only if a longitudinal and a torsional natural frequency fall close together, causing coupling oscillations.

Lateral vibrations. The most important of all machinery vibrations are the lateral or bending vibrations of shafts and other rotors caused by the centrifugal force of unbalance. The unbalance consists of a very small deviation of the center of gravity of the rotor from the geometric axis connecting the bearing centers, or of a small angular deviation between that bearing center line and a principal axis of inertia of the rotor. Thus the excitation always has the frequency of the shaft rotation, and when that coincides with one of the natural bending frequencies of the rotor, there is resonance or a critical speed where the bending stresses in the shaft can be a hundred times higher than those caused by the centrifugal force of the unbalance directly.

Slow-speed machines are always designed to run well below the lowest or first critical speed, but for high-speed ones this often is not possible. Steam turbines and electric generators of large power stations have for many years been designed to run between the first and second critical speeds; the newest and largest units are between their second and third criticals. The flexibility of the supporting (nonrotating) bearings is an important factor in the calculation of critical speeds or natural frequencies of rotors, because the flexible bearing decreases the natural frequencies by some 10% on the average below those that would be present if rigid bearings were used. For rotors of a high diameter-length ratio such as in steam turbines with large-diameter disks mounted on a comparatively thin shaft, the effect of rotating inertia, sometimes called the gyroscopic effect of the disks, is an important consideration.

Besides the classical unbalance critical speed, which always has a vibration frequency equal to that of the rpm, a number of secondary critical speeds have been observed and explained, in which the frequency of vibration is a multiple of, usually twice, the rpm. The practical importance of these is secondary with respect to the ordinary critical speed.

Beam vibration. Whenever a part of a structure or the entire structure itself has a natural frequency resonating with an alternating excitation, nearby (or sometimes far removed) severe vibrations may result. A typical example is an unbalanced piston machine, such as an air compressor, which frequently causes objectionable vibration in some locations in the building where it is installed. Another example is the vibration of an entire ship in the mode of a free-free (totally unsupported) beam, excited by the propeller blade frequency.

With the advent of jet engines, the effect of high-intensity airborne noise on the very light structures of airplanes and missiles has become important. It is characteristic of jet noise, or indeed of all cases of turbulent flow, that the excitation is distributed continuously over a wide band of frequencies. This type of excitation is random and is playing an increasingly important role in the design of aircraft and missiles.

Membrane vibration. A tightly stretched skin, which has negligible bending stiffness like a drumhead, is a membrane. (The diaphragm in a telephone receiver possesses considerable bending stiffness, and is not stretched; hence technically it is a plate, although sometimes it is also called a membrane.) The theory of vibration of a membrane of circular shape has been known for a century and is one of the more beautiful illustrations of the mathematics of Bessel functions. The lowest frequency of vibration corresponds to a shape where the entire membrane bulges in and out, without nodal lines, the periphery remaining fixed. The higher modes of motion possess nodal lines, which are concentric circles or angularly equidistant diameters. The frequency formula for the circular membrane vibration is given in Eq. (6). Here T is the tension in the membrane,

$$f = \alpha\sqrt{Tg/\gamma r^2} \tag{6}$$

g is the acceleration due to gravity, γ is the surface weight density of the membrane, r is the radius, and a is a numerical factor having the values shown in the **table**.

Plate vibration. Plate vibrations are very important for a variety of reasons. They occur in large, flat, solid surfaces that are excited in planes normal to that surface. The reason that such vibrations are important in mechanical systems is that they occur frequently

Numerical factor for membrane frequency

Number of nodal circles	Number of nodal diameters			
	0	1	2	3
0	0.383	0.610	0.819	1.02
1	0.880	1.12	1.34	1.55
2	1.38	1.62	1.85	2.08

in practice and in addition they are very good acoustical radiators; that is, they couple extremely well with the air around them and produce significant quantities of vibratory energy that can be both felt and heard as acoustic signals. The basic mechanism by which a plate operates is similar to a beam in that the action consists of the bending of the plate about its middle surface, except that whereas a beam is a one-dimensional element with bending in only one direction, a plate is a surface that has bending in two orthogonal directions as well as a torsional or twisting type of bending at angles between these two orthogonal directions. Thus, more complicated curvature and surface interaction effects are involved.

Self-excited vibrations. In the cases discussed so far, the existence of an alternating exciting force (or torque) has been assumed which would continue to exist by itself even after the vibratory motion was prevented or stopped. These are called forced vibrations. There is another class of motions, called self-excited, in which the exciting force is generated by the vibrating motion itself and hence disappears with that motion.

A familiar mechanical example of self-excited vibration is the piston of an engine. The back-and-forth motion (vibration) is maintained by an alternating gas or steam pressure steered by the valve mechanism. The initial source of energy is without alternating properties (the gasoline supply or the boiler steam) but is made alternating by the valves, which are operated by the vibratory piston itself.

A familiar electrical example is the self-oscillating electronic circuit which has a steady source of energy (for example, a battery), and a transistor that plays the role of the valve.

The oldest practical examples of useful self-excited vibrations are musical instruments. The violin operates on the behavior of the friction between the rosined bow and the string, which has aptly been described as stick-slip friction. Vibrations of this type have appeared repeatedly and still are often met within machinery with insufficient lubrication; the most vexing and difficult case is that of the chattering machine tool cutter which leaves a wavy cut instead of a smooth one. *See* MUSICAL INSTRUMENTS.

The clarinet operates on the passage of air (from the mouth to the instrument) though a narrow leakage opening whose width varies periodically with the vibration of the reed. Serious vibrations of this character occur in steam, gas, or hydraulic turbines, heat exchangers, and other apparatus in which a fluid or gas passes through narrow passages. Other self-excited vibrations are the pulsating flow sometimes observed in fans and blowers, and the shimmying motion of wheels, which has been a serious problem in automobiles and in the landing gear of aircraft. Self-excited vibrations appear in autopilots of aircraft and missiles, and in general are apt to occur in servomechanisms with high gain.

A class of dangerous vibrations is provided by the various phenonena of flutter, whereby an elastic system becomes self-excited in the stream of air, gas, or fluid of sufficient speed. This aviation problem first arose in airplane wings, but as speeds increased, other parts of airplanes and other machinery, such as turbine blades, displayed flutter. Flutter theory has grown into a subject by itself. *See* AEROELASTICITY; FLUTTER (AERONAUTICS).

Serious vibrations have occurred in rocket engines and other types of combustion chambers, whereby the combustion becomes unstable and the burning gas mass enters a state of self-excited vibration. These phenomena have been known for a century and still are not completely understood.

Effect of vibrations. The most serious effect of vibration, especially in the case of machinery, is that sufficiently high alternating stresses can produce fatigue failure in machine and structural parts. Less serious effects include increased wear of parts, general malfunctioning of apparatus, and the propagation of vibration through foundations and buildings to locations where the vibration or its acoustic realization is intolerable either for human comfort or

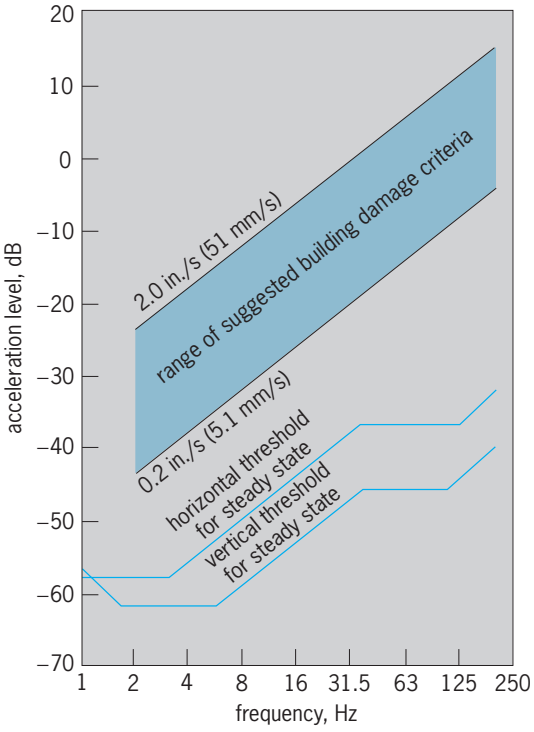

Fig. 4. Comparison of suggested building damage criteria and human threshold of perception curves for whole-body vibration. Acceleration level in dB = 20 log acceleration level/*g*. Because they are negative logarithms, the decibel values on the vertical axis indicate increasing acceleration levels from bottom to top. (*After T. G. Gutowski, L. E. Wittig, and C. L. Dym, Some aspects of the ground vibration problem, Noise Control Eng., 10(3):94–100, 1978*)

for the successful operation of sensitive measuring equipment. *See* STRESS AND STRAIN; WEAR.

Whole-body vibration. **Figure 4** shows a comparison of suggested building damage criteria and human threshold-of-perception curves for whole-body vibration. The threshold curves for human perception are based upon tests wherein people are seated on shakers, so the perception is of motion that affects the entire body. There are a variety of ranges of vibration, and these ranges are strongly dependent upon the frequency (expressed here in hertz, equal to $\omega/2\pi$). The ordinate of this graph is expressed as an acceleration level (in decibels) with reference to g (the acceleration of gravity) as the base acceleration level. The decibel notation indicates a logarithmic dependence such that an acceleration level of −20 dB represents an acceleration level that is 0.1 g in magnitude, an acceleration of −40 dB represents a level that is 0.01 g in level, and so on. The magnitudes of vibration that are felt by humans are extremely small; that is, on the order of −60 dB or 0.001 g in magnitude. While identifying the human threshold of perception from whole-body laboratory experiments is very useful, other factors must be considered in practice. Human annoyance may be related to secondary vibratory effects such as the vibration-induced motion of household items such as plants and mirrors, and so on. Thus, human annoyance could depend on the observer's location and activity as well as other suggested factors (Fig. 4). The values for which damage to a building might be realized are significantly higher than those for which vibration is perceptible by humans. In fact, the difference tends to be on the order of two orders of magnitude (a multiplicative factor of 100 in amplitude).

Generation of acoustic noise. **Figure 5** relates vibration magnitudes both to perceptible vibration level and to audible acoustical levels. These data demonstrate that an acoustic signal can be generated by a mechanical vibration and produce auditory noise that can be very uncomfortable. For example, as discussed above, noise can propagate in a building due to an air-conditioning compressor. The curves displayed in Fig. 5 also show so-called NC-equivalent curves used to describe architectural levels of quietness in a design environment. Thus an NC-20 equivalent curve is the design standard for a first-class concert hall, while an NC-40 criterion would be adequate for a grade-school classroom. The acoustic signals are normally expressed in logarithmic amplitudes of acoustic pressure, but are expressed here in terms of amplitudes of vibration, that is, acceleration levels. An equivalence between the two is based on the recognition that when a large surface vibrates, it simultaneously sets into motion the acoustic medium around it, whether it be air or water. The bending vibrations of plates, for example, couple extremely well with the compressional waves of a surrounding acoustic medium. Thus when a building wall or floor is set into motion by a mechanical source of vibration, it in turn causes a very effective propagation of an acoustical signal, or noise, in the surrounding air. Another significant example of good coupling is the mechanical

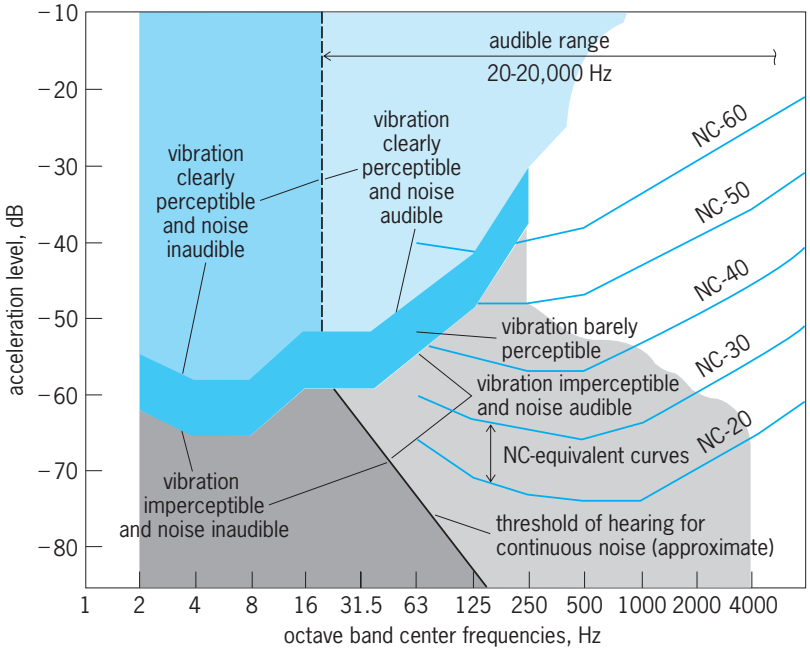

Fig. 5. Levels of perceptibility of vibration and audibility of noise. Acceleration level in dB = 20 log acceleration level/g. Because they are negative logarithms, the decibel values on the vertical axis indicate increasing acceleration levels from bottom to top. (*After C. L. Dym and D. Klabin, Architectural implications of structural vibration, Architect. Rec., 157(9):125–127, 1975*)

excitation of a drumhead by a drumstick. The lateral vibrations of the stretched membrane (the drumhead) also couple well with surrounding air to produce the corresponding tympanic sound of the drum which can be heard at great distances from the drum itself.

There are many factors that enter into the coupling of a vibrating structural element and the surrounding acoustical medium. The principal factors are, however, the surface area of the mechanical source that is exposed to the medium and the nature of the mechanical vibration, that is, whether it is perpendicular to the surface (as with bending vibrations of beams and plates or lateral vibrations of membranes) or along the direction of the surface (as in torsional and longitudinal vibration). It is the perpendicular motion of large surfaces that produces the best acoustical coupling and, hence, the best chance of radiation of noise from vibration. *See* ACOUSTIC NOISE; VIBRATION.

Clive L. Dym; J. P. Den Hartog

Bibliography. G. S. Kelly, *Fundamentals of Mechanical Vibrations*, 2d ed., 2000; M. Lalanne and P. Bertnier, *Mechanical Vibrations for Engineers*, 1984; S. S. Rao, *Mechanical Vibrations*, 3d ed., 1995; R. F. Steidel, *An Introduction to Mechanical Vibrations*, 3d ed., 1989.

Mechanics

In its original sense, mechanics refers to the study of the behavior of systems under the action of forces. Statics deals with cases where the forces either produce no motion or the motion is not of interest.

Dynamics deals properly with motions under forces. Mechanics is subdivided according to the types of systems and phenomena involved.

An important distinction is based on the size of the system. Those systems that are large enough can be adequately described by the newtonian laws of classical mechanics. In this category, for example, are celestial mechanics, the study of the motions of planets, stars, and other heavenly bodies, and fluid mechanics, which treats liquids and gases on a macroscopic scale. Fluid mechanics is a part of a larger field called continuum mechanics or (by some physicists) classical field theory, involving any essentially continuous distribution of matter, whether it be rigid, elastic, plastic, or fluid. On the other hand, the behavior of microscopic systems such as molecules, atoms, and nuclei can be interpreted only through the concepts and mathematical methods of quantum mechanics.

From its inception, quantum mechanics had two apparently different mathematical forms—the wave mechanics of E. Schrödinger, which emphasizes the spatial probability distributions in the quantum states, and the matrix mechanics of W. Heisenberg, which emphasizes the transitions between states. These are now known to be equivalent.

Mechanics may also be classified as nonrelativistic or relativistic mechanics, the latter applying to systems with material velocities comparable to the velocity of light. This distinction pertains to both classical and quantum mechanics.

Finally, statistical mechanics uses the methods of statistics for both classical and quantum systems containing very large numbers of similar subsystems to obtain their large-scale properties. *See* CELESTIAL MECHANICS; CLASSICAL FIELD THEORY; CLASSICAL MECHANICS; DYNAMICS; FLUID MECHANICS; QUANTUM MECHANICS; RELATIVISTIC MECHANICS; STATICS; STATISTICAL MECHANICS.

Bernard Goodman

Mechanism

Classically, a mechanical means for the conversion of motion, the transmission of power, or the control of these. Mechanisms are at the core of the workings of many machines and mechanical devices. In modern usage, mechanisms are not always limited to mechanical means. In addition to mechanical elements, they may include pneumatic, hydraulic, electrical, and electronic elements. In this article, the discussion of mechanism is limited to its classical meaning. *See* MACHINE.

Mechanisms are found in internal combustion engines; compressors; locomotives; agricultural, earthmoving, excavating, mining, packaging, textile, and other machinery; machine tools; printing presses; engraving machines; transmissions; ordnance equipment; washing machines; lawn mowers; sewing machines; projectors; pinspotters; toys; pianos; ski bindings; artificial limbs; door locks; nutcrackers; counters; microswitches; speedometers; and innumerable other devices.

Components. Most mechanisms consist of combinations of a relatively small number of basic components. Of these, the most important are cams, gears, links, belts, chains, and logical mechanical elements.

Cams and cam followers. A cam is a specially shaped part designed to impart a prescribed law of motion to a contacting part called the follower. In **Fig. 1** the cam is in the form of a disk, the shape of which governs the motion of the follower. Followers may be translating (Fig. 1*a* and *b*) or swinging (Fig. 1*c*) and may be in sliding (Fig. 1*a*) or rolling (Fig. 1*b* and *c*) contact with the cam. The law of motion is the relation between cam rotation and follower displacement. Contact between cam and follower is often (but not necessarily) maintained by a return spring. *See* CAM MECHANISM.

Gears. Gears are toothed wheels that provide a positive connection between rotating shafts. The most familiar are spur gears, which are used to connect parallel shafts. The teeth of straight spur gears (**Fig. 2***a*) may be imagined mounted on right circular cylinders. When the shaft axes are intersecting, bevel gears can be used. The teeth of the straight bevel gears (Fig. 2*b*) may be imagined mounted on right circular cones. Gear teeth are so shaped that the angular-velocity ratio of the connected shafts is constant. Other forms of gearing include helical (these may be spur gears or crossed helical gears), worm, and hypoid. The latter two, as well as crossed helical gears, are used to connect shafts with nonparallel, nonintersecting axes. *See* GEAR.

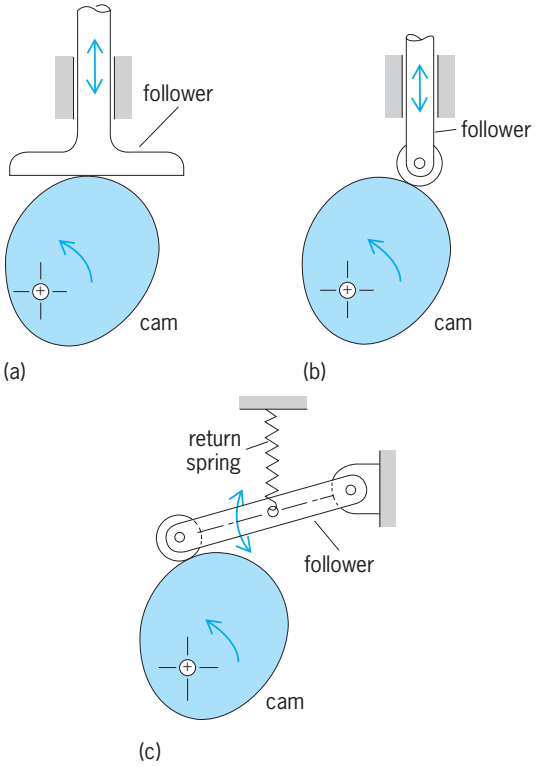

Fig. 1. Cam-follower configurations. (*a*) Disk cam with flat-faced translating follower. (*b*) Disk cam with translating roller follower. (*c*) Disk cam with swinging roller follower.

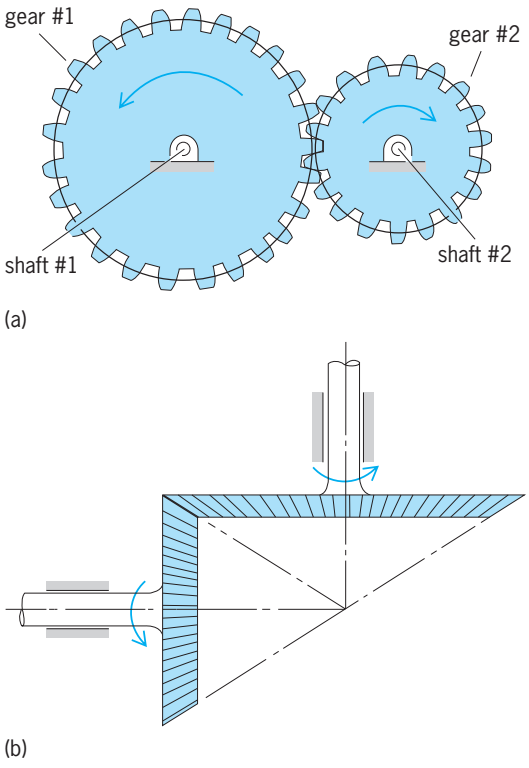

Fig. 2. Gear configurations. (*a*) Spur gears. (*b*) Bevel gears.

Links. For practical purposes, a link may be defined as a rigid body which is connected to other rigid bodies by joints. The most common joints (**Fig. 3**) are the pin joint (symbolized by R), the sliding joint (P), the cylindrical joint (C), the ball joint (S), and the screw joint (H). The tooth connection between gears and the contact between cam and follower are also usually regarded as joints. Typical link configurations are shown in **Fig. 4**. *See* LINKAGE (MECHANISM).

Belts and chains. These flexible connectors include pulleys and flat belts (**Fig. 5**), timing belts and sprockets, and chain belts and sprockets. The first of these is a friction drive, while the latter two are positive drives. All transmit a practically constant angular-velocity ratio between the connected shafts. *See* BELT DRIVE; CHAIN DRIVE.

Logical mechanical elements. These include ratchets, trips, detents, interlocks, and the like. The most interesting of these is the ratchet. **Figure 6** shows a type of ratchet mechanism known as an escapement. The ratchet is the toothed wheel, the rotation of which is controlled by a pawl—a pivoted link which may be in or out of engagement with the ratchet. This arrangement can provide a stop-and-go unidirectional motion, such as that of the hands of a pendulum-driven clock. *See* ESCAPEMENT; RATCHET.

Representative mechanisms. Mechanical components can be combined into mechanisms in an infinite variety of ways. For example, in automobiles there is a slider-crank mechanism (**Fig. 7**), connecting piston to crankshaft; the cam-follower system (**Fig. 8**) for the actuation of the intake or exhaust valves in an overhead valve arrangement; and the differential (**Fig. 9**). The first is a linkage mechanism, the second a cam-follower mechanism, and the third a gear train. The first converts the translation of the piston into crankshaft rotation and transmits power from piston to crankshaft. The second controls the opening and closing of an intake or exhaust valve. Although some power is required to actuate the valve, this is of secondary significance. The differential is a two-degrees-of-freedom gear train, which couples the driveshaft to the tire axles and transmits engine power to the tires. The two degrees of freedom are needed to permit unequal tire speeds when negotiating a turn. In order to understand these and other mechanisms, their degree of freedom, structure, and kinematics must be considered. *See* SLIDER-CRANK MECHANISM.

Degree of freedom. This is conveniently illustrated for mechanisms with rigid links. The discussion is limited to mechanisms which obey the general degree-of-freedom equation (1), where F = degree

$$F = \lambda(l - j - 1) + \Sigma f_i \qquad (1)$$

of freedom of mechanism, l = number of links of mechanism, j = number of joints of mechanism, f_i = degree of freedom of relative motion at ith joint (see Fig. 3), Σ = summation symbol (summation over all joints), and λ = mobility number (the most common cases are $\lambda = 3$ for plane mechanisms and $\lambda = 6$ for spatial mechanisms).

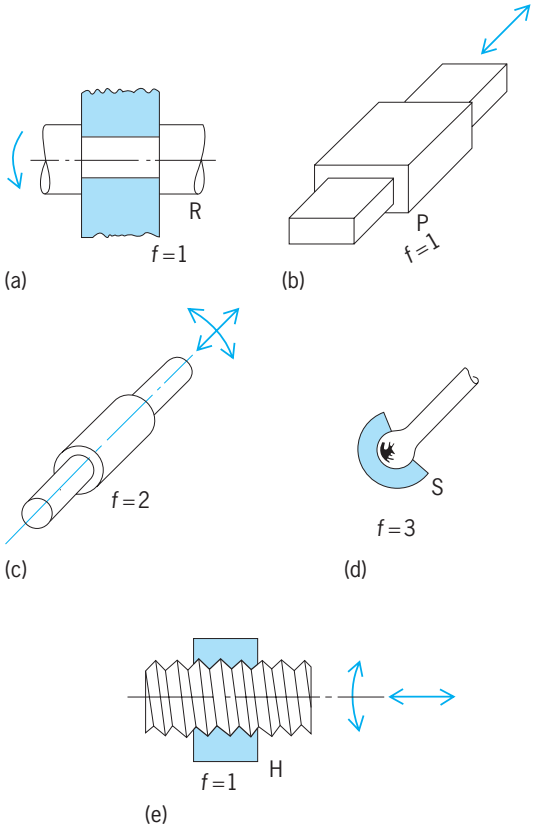

Fig. 3. Common joints, including joint symbols and degree of freedom *f* of relative motion at joint. (*a*) Pin joint. (*b*) Sliding joint. (*c*) Cylindrical joint. (*d*) Ball joint. (*e*) Screw joint.

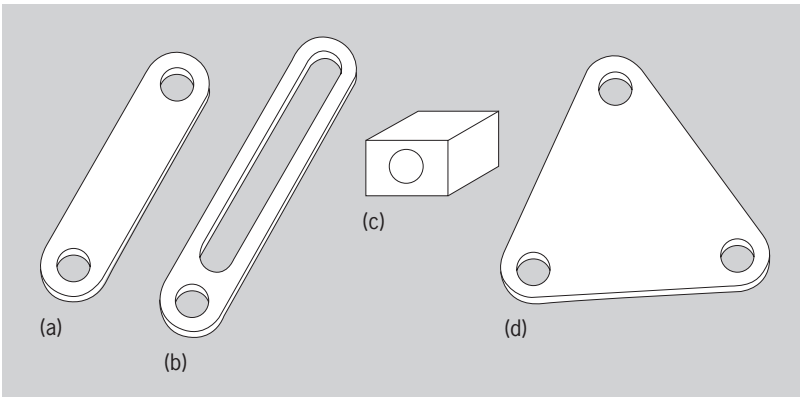

Fig. 4. Typical links. (*a*) Crank. (*b*) Slotted link. (*c*) Slider with provision for pin connection. (*d*) Triangular link.

There are mechanisms, some of them highly significant, which do not obey the general degree-of-freedom equation. The degree of freedom of such mechanisms is generally strongly dependent on their dimensions. Such mechanisms are excluded from the discussion which follows.

For plane mechanisms with pin joints, Eq. (2) ap-

$$F = 3l - 2j - 3 \tag{2}$$

plies, while for gear trains with j_r pin joints and j_g gear meshes Eqs. (3) apply, where L_{ind} denotes the

$$F = j_r - j_g \qquad j_g = L_{\text{ind}} \qquad l = F + L_{\text{ind}} + 1 \tag{3}$$

number of independent loops of the mechanism and is given by Eq. (4) for mechanisms in which the

$$L_{\text{ind}} = j - l + 1 \tag{4}$$

graphs can be drawn without crossing edges. *See* DEGREE OF FREEDOM (MECHANICS).

Kinematic structure. The kinematic structure of a mechanism refers to the identification of the joint connection between its links. Just as chemical compounds can be represented by an abstract formula and electric circuits by schematic diagrams, the kinematic structure of mechanisms can be usefully represented by abstract diagrams.

Mathematical representation. The structure of mechanisms for which each joint connects two links can be represented by a structural diagram, or graph, in which links are denoted by vertices, joints by edges, and in which the edge connection of vertices corresponds to the joint connection of links; edges are labeled according to joint type (and pin axis in the case of gear trains), and the fixed link is identifed as well. Thus the graph of the slider-crank mechanism of Fig. 7*a* is as shown in Fig. 7*b*. In this figure the circle around vertex 1 signifies that link 1 is fixed.

Mechanisms can be considered identical or different, depending on whether their graph representations are identical (isomorphic) or different (nonisomorphic).

Classification and creation of mechanisms. Mechanisms can be classified and enumerated according to their kinematic structure, with the restrictions on their structure for many mechanisms being given by Eqs. (1)–(4).

It can be shown, for example, that when Eqs. (1)–(4) are applicable, there are seven plane single-degree-of-freedom mechanisms with four links and pin joints and up to two sliding joints. The structures of plane pin-jointed single-degree-of-freedom linkages with up to ten members and the structures of single-degree-of-freedom gear trains with up to six members have been determined as well.

The creation of mechanisms according to kinematic structure is also known as type synthesis or structural synthesis. It is based on the separation of kinematic structure from function. Thus, if, for example, mechanisms are sought which function as shaft couplings, the potential kinematic structures of mechanisms having the required degree of freedom, number of parts, and admissible types of joints are considered. The mechanisms corresponding to these structures are then screened by functional considerations. The result is an unbiased collection of potentially useful shaft-coupling configurations, complete within the specification of the search. This procedure can be a useful tool in the conceptual and inventive phases of mechanical design, supplementing atlases and collections of known mechanisms.

Kinematics. The subject is divided into kinematic analysis (analysis of a mechanism of given dimensions) and synthesis (determination of the proportions of a mechanism for given motion requirements). It includes the investigation of finite as well as infinitesimal displacements, velocities, accelerations and higher accelerations, and curvatures and higher curvatures in plane and three-dimensional motions.

Displacements in mechanisms can be found graphically or analytically from the conditions of closure

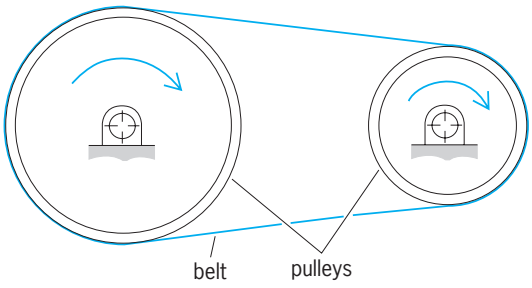

Fig. 5. Belt and pulleys.

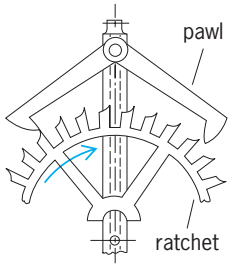

Fig. 6. Escapement.

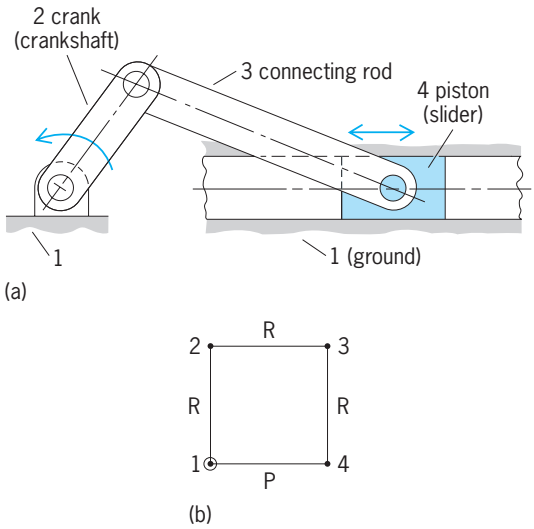

Fig. 7. Slider-crank mechanism. (*a*) Mechanism. (*b*) Graph of mechanism.

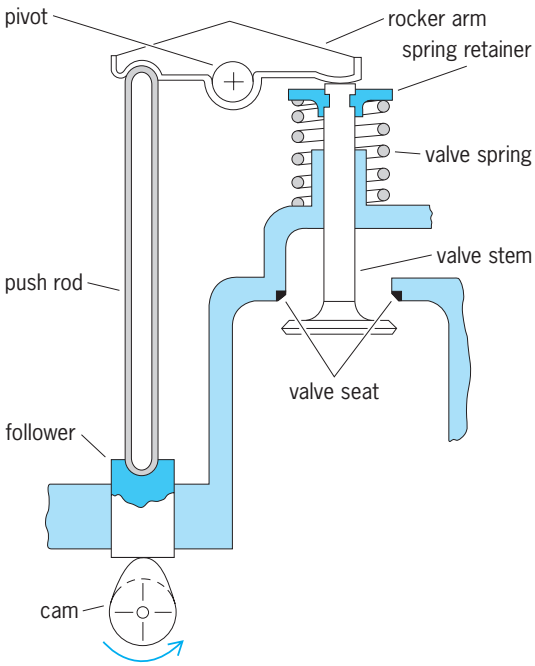

Fig. 8. Valve train of an internal combustion engine. (*Courtesy of Albert Pisano*)

of the independent loops of the mechanism. Velocities, accelerations, and higher-motion derivatives can be found by differentiation. It can be shown that at any instant in a general, continuous plane motion (the term general excludes translations, for example), there is one point for which the velocity vanishes (the instant center), one point for which the acceleration vanishes (the acceleration center), one point for which the acceleration derivative vanishes, and so on. The theory of instantaneous invariants has proved a powerful tool in such investigations.

For the position guidance of a rigid body through a prescribed sequence of finitely separated coplanar positions, one is interested in the loci of points in the body or the frame which may be used to attach cranks or sliders, so that the body can be guided mechanically. For four arbitrary positions these loci include the circlepoint curve (locus of points in the moving body, the four corresponding positions of which lie on a circle), the centerpoint curve (locus of the centers generated by points of the circlepoint curve), and the Ball point (that point in the moving system, the four corresponding positions of which are collinear). Circlepoints and their corresponding centerpoints can be used for locating moving and fixed crankpins, and the Ball point can be used for the attachment of a slider. In this way one can determine the proportions of linkage mechanisms, which can guide a rigid body through a prescribed sequence of positions.

The circlepoint and centerpoint curves are cubic algebraic curves. These curves can be used in the synthesis of linkage mechanisms for a considerable variety of motion requirements. The theory has been extended to five general coplanar positions and to three-dimensional motions. The optimization of link age proportions so as to obtain the closest match of a linkage motion to a desired motion has also been the subject of many investigations, especially with the aid of Chebyshev approximations.

Useful concepts, which occur frequently in kinematic analysis, include kinematic inversion (the process of holding different links of a mechanism fixed), relative motion, toggle positions (positions providing a very high mechanical advantage), lockup positions (positions in which the mechanism cannot be driven from its usual input member), pressure angles and transmission angles (which govern the efficiency of force and power transmission), angular-velocity ratios, and angular-acceleration rations and shock

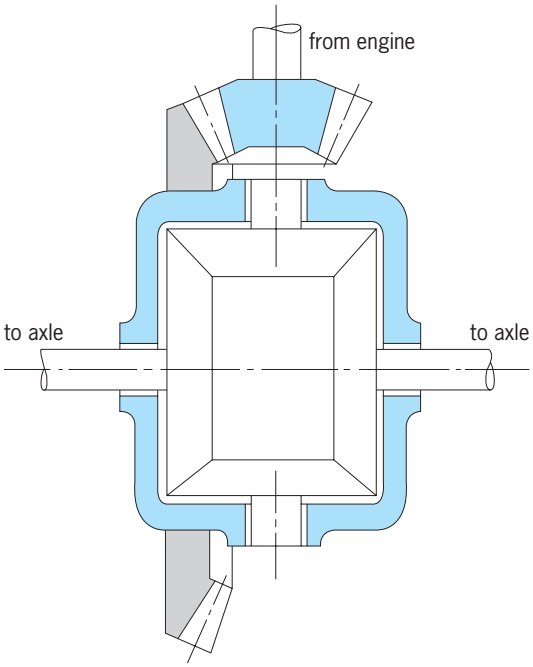

Fig. 9. Automotive differential.

(the derivative of acceleration with respect to time). *See* KINEMATICS.

Design. The design of mechanisms involves many factors. These include their structure, kinematics, dynamics, stress analysis, materials, lubrication, wear, tolerances, production considerations, control and actuation, vibrations, critical speeds, reliability, costs, and environmental considerations.

Compared to other areas of engineering design, the design of mechanisms is complicated by their generally high degree of nonlinearity (with the exception of gear trains), the inability in most instances to limit their operation to small displacements, and the variety of combinations of components and mechanical elements. But, this complexity also provides a challenge to the creativity of the engineer and inventor.

Current trends in the design of mechanisms emphasize economical design analysis by means of computer-aided design techniques, which offer ever-increasing speeds and more sophisticated performance requirements while maintaining reliability and economy of space, weight, and cost. *See* COMPUTER-AIDED DESIGN AND MANUFACTURING.

Ferdinand Freudenstein

Bibliography. A. Erdman and G. N. Sandor, *Mechanisms Design: Analysis and Synthesis*, vol. 1, 2d ed., 1990; F. D. Jones, H. L. Horton, and J. A. Newell (eds.), *Ingenious Mechanisms for Designers and Inventors*, 4 vols., 1968–1971; J. McCarthy, *Introduction to Theoretical Kinematics*, 1990; S. B. Tuttle, *Mechanisms for Engineering Design*, 1967.

Mechanoreceptors

Receptors that provide the organism with information about such mechanical changes in the environment as movement, tension, and pressure. In higher animals receptors are actually the only means by which information of the surroundings is gained and by which reactions to environmental changes are started. *See* SENSATION.

Receptor-effector mechanisms. In primitive forms of life, such as unicellular organisms and sponges, the receptor and effector functions are built into the same cell (**Fig. 1***a* and *b*). The cell is directly excited by and reacts to the environmental stimulus. At higher levels of organization, the receptor separates from the effector and appears specialized in function and structure in the receptor cell of the primitive nerve system of actinians (sea anemones). Stimuli of the environment excite the receptor cell, and this excitation is conveyed to another specialized cell, the effector (Fig. 1*c*). In another step of phylogenetic development, a third element appears, the motor nerve cell, which serves as a link between the receptor and effector. This arrangement appears clearly in coelenterates and is carried through in its essential features up to the vertebrates (Fig. 1*d* and *e*).

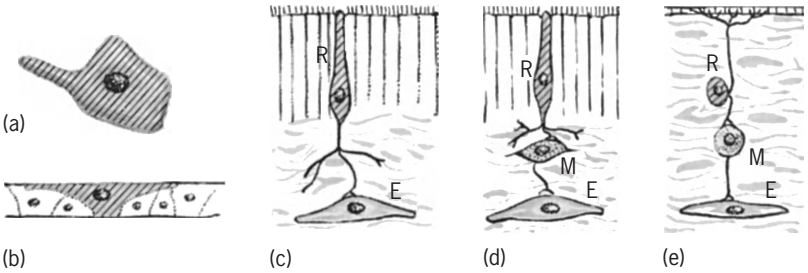

Fig. 1. Evolution of receptor-effector systems. (*a*) Receptor-effector cell of unicellular organism (ameba); (*b*) receptor-effector cell of multicellular organism (sponge); (*c*) specialization shown in separation of receptor and effector cells of actinians (tentacle of sea anemone); (*d*) receptor, motor nerve, and effector cells of coelenterates; (*e*) receptor motor nerve, and effector cells in vertebrates. R = receptor; E = effector; M = motor nerve cell. (*b, c, and d after G. H. Parker, The Elementary Nervous System, Lippincott, 1919*)

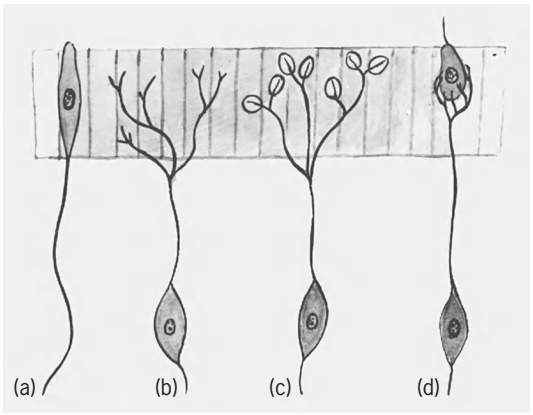

Fig. 2. Differentiation of receptors. (*a*) Primary receptor cell at the periphery. (*b*) Nerve cell buried inside the organism sending out branches which terminate as nude receptor endings. (*c*) Encapsulated receptor endings. (*d*) Secondary receptor cell.

Nerve endings. The primitive receptor cell may remain at the periphery, as in the olfactory receptors of the vertebrates, or it may be buried inside the organism and send protoplasmic branches out to the periphery. A branch of this type, a dendrite or an axon, terminates in its simplest form as a nude ending at the periphery. In more complicated forms, in Pacinian and Meissner corpuscles, the ending is surrounded by accessory tissue of varying structural organization; or the ending appears to terminate on a so-called secondary sense cell, as in certain gustatory, auditory, and visual receptors (**Fig. 2**). But in all receptors known, the nerve ending is invariably present, however complex the accessory structure around it (**Fig. 3**). In the two mechanoreceptors whose fine structure has been examined under the electron microscope (the Pacinian corpuscle and the muscle spindle), the nerve ending is nude, lacking not only a sheath of myelin but one of Schwann cells (**Fig. 4**).

Phylogenetic advances. Survival of an organism depends in large part upon its ability to react to changes in the environment. As organized life climbs up the phylogenetic scale, it develops and subsists within increasing limits of environmental change. In general, the greater the organizational level of the animal, the greater are the environmental changes to which

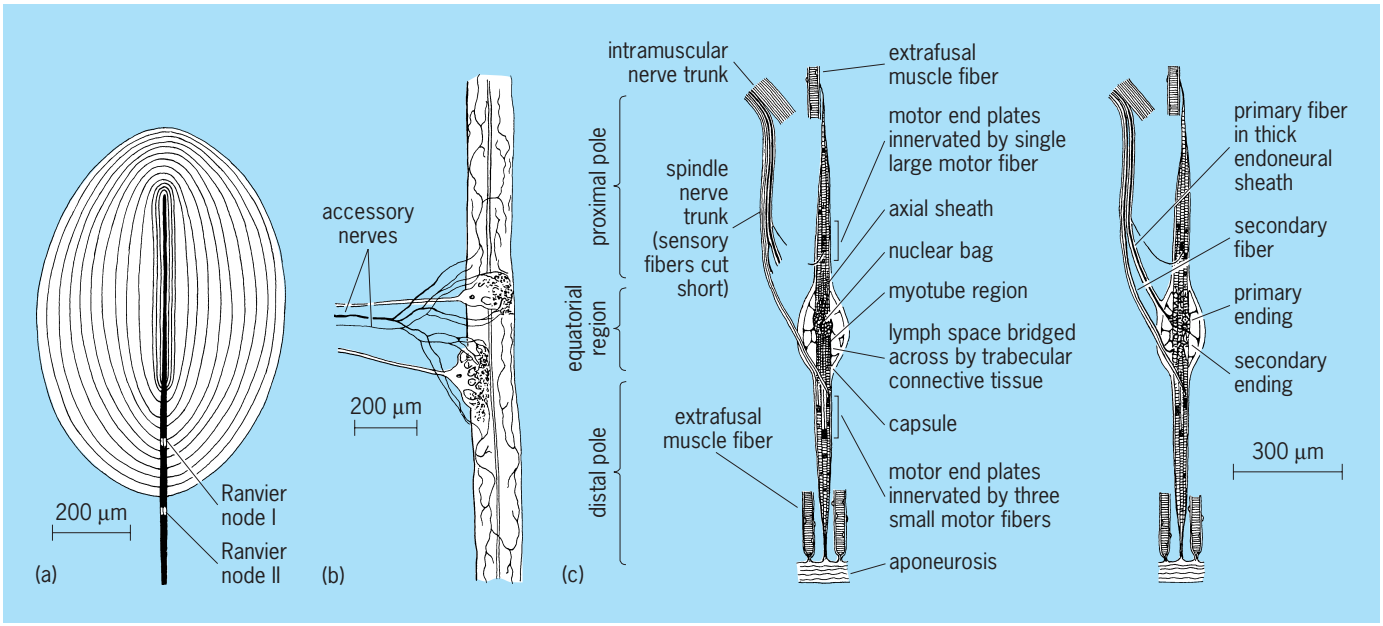

Fig. 3. Schemes of three typical mechanoreceptors. (*a*) Pacinian corpuscle of the cat's mesentery and skin. (*b*) Stretch receptor nerve cells of the abdominal musculature of lobsters (*Homarus vulgaris*) with dendritic endings embedded in muscle strands (*after J. S. Alexandrowicz, Quart. J. Microsc. Sci., 92:163–199, pt. 2, 1951*). (*c*) Muscle spindle of the rabbit (*after D. Barker, Quart. J. Microsc. Sci., 89(2):143–186, 1948*).

it must react and the more varied in form and in degree of functional organization become its receptor organs. Receptors for mechanical changes of the environment (mechanoreceptors) had to develop at an early stage of phylogeny. They were necessary for the avoidance of mechanical objects, for the sensing of water waves transmitted from other animals in the sea, for orientation in space, and for maintenance of a position with respect to gravity. Examples are the lateral line receptors and the later development of the labyrinth receptors. The development of life on land brought development of mechanoreceptors sensitive to sound vibration of the air. With the growth of internal organs with specialized functions and, particularly, with the development of fast regulatory mechanisms for these functions arose the necessity for receptors sensitive to mechanical stimuli originating inside the organs (proprioceptors). Thus, in the vertebrates, mechanoreceptors appear in all organs in which passive or active movements occur, feeding information into the nerve system about movements, tension, or pressure. Mechanoreceptors appear in the digestive tract, lungs, blood vessels, heart, and skeletal musculature. The simple mechanoreceptors of the integument of primitive invertebrates are bare nerve endings in all animals, including the higher vertebrates; they are ubiquitous in the aforementioned organs and in the skin. In addition, around some nerve endings, special enclosures of varying complexity are developed in the skin and other structures of the higher vertebrates (Fig. 3).

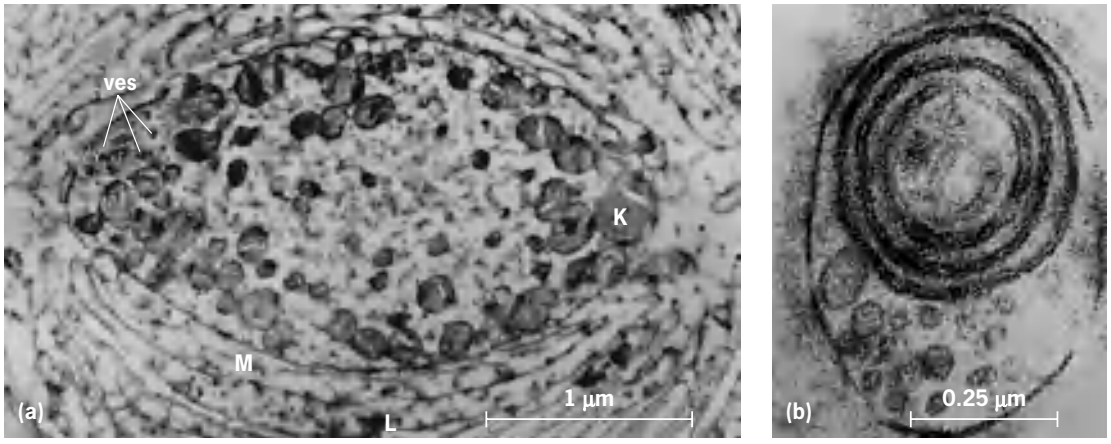

Fig. 4. Electron micrographs showing fine structure of mechanoreceptors. (*a*) Nerve ending of Pacinian corpuscle in the cat, containing vesicular formations (ves), and abundant mitochondria (K) near the ending's membrane (M). L = lamellae of the inner core (*from D. C. Pease and T. A. Quilliam, J. Biophys. Biochem. Cytol., 3(3):331–342, 1957*). (*b*) Nerve ending of the muscle spindle of a frog (*from J. D. Robertson, Biochem. Soc. Symp. no. 16, 3–43, 1959*).

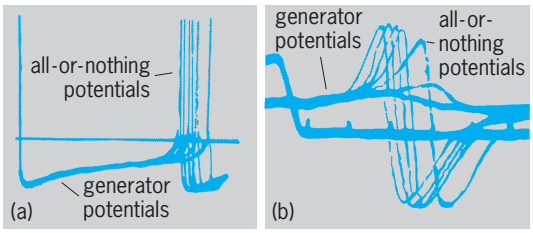

Fig. 5. Generation of nerve impulses. Several responses superposed on successive oscilloscope sweeps. Note firing of impulses from critical level. (*a*) Crustacean stretch receptor (*after C. Eyzaguirre and S. W. Kuffler, J. Gen. Physiol., 39(1):87–119, 1955*). (*b*) Generation in Pacinian corpuscle (cat) (*after J. A. B. Gray and M. Sato, J. Physiol., 122(3):610–636, 1953*).

Mechanoelectric conversion. Mechanoreceptors are excited by mechanical disturbances of their surroundings through deformation of their structure, through pressure or tension, or through a combination of these. In general, little energy is required for mechanical stimuli to cause a detectable excitation in mechanoreceptors. For example, the receptor membrane of Pacinian corpuscles of the cat's mesentery gives detectable generator currents with displacement of the outer layers of its capsule by 10^{-5} cm.

Transducer sequence. From a physical point of view, mechanoreceptors are energy transducers; they convert mechanical into electrical energy, which in turn triggers the nerve impulse. The mechanisms of nerve-impulse production have been studied most extensively in the muscle spindle of frog, in the stretch receptor of Crustacea, and in the Pacinian corpuscle. In the three receptors studied, deformation leads to a sequence of events which may be summarized by the following scheme:

$$\text{Mechanical stimulus} \rightarrow \text{generator current} \rightarrow \text{nerve impulse (actionpotential)}$$

The generator current is the earliest detectable sign of excitation. In Pacinian corpuscles it follows the mechanical stimulus at a fixed and brief latency. The most salient characteristic of the generator current is its graded nature; its amplitude increases continuously, without visible steps, if the stimulus strength is progressively increased. When the generator current reaches a certain critical amplitude, an all-or-nothing potential is discharged in the sense organ which may then propagate as an all-or-nothing nerve impulse along the afferent axon of the receptor (**Fig. 5**).

Bioelectric generator and nerve-impulse initiation sites. Generator and all-or-nothing potentials arise at differently behaving membrane sites. The capsular tissue around the nerve ending, constituting more than 99.9% of the total mass of a Pacinian corpuscle, does not partake actively in the transducer chain outlined previously (**Fig. 6**). Figure 6 illustrates an experiment in which the capsule of a Pacinian corpuscle was removed (Fig. 6*a–c*). The preparation was stimulated with two successive mechanical stimuli, the first producing an all-or-none potential, the second (subthreshold) a generator current. In Fig. 6*c* mechanosensitivity remains unimpaired in spite of the removal of more than 99.99% of the corpuscle. In Fig. 6*d* and e, although the preparation consisted only of a partly isolated ending, it continued to be as mechanosensitive as before. This would probably also occur in other mechanoreceptors whose nerve

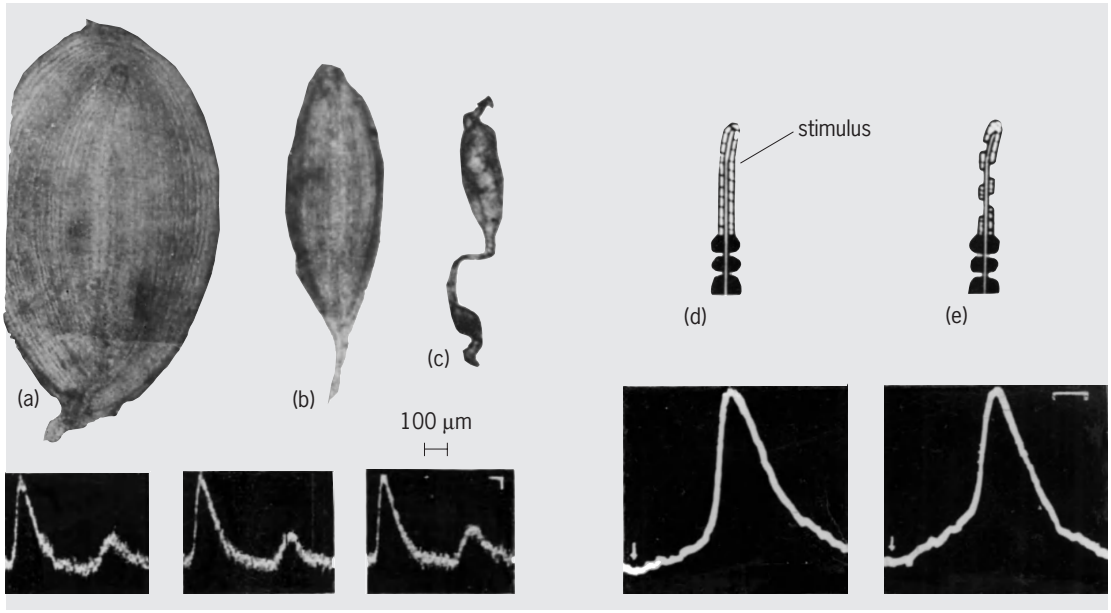

Fig. 6. Localization of transducer element. (*a*) Capsule of intact Pacinian corpuscle. (*b*) Progressive removal of capsule. (*c*) Only ending and surrounding inner core remain; calibration: 1 ms, 25 μV. (*d,e*) Partial destruction of remaining inner core; calibration: 1 ms. Recordings at bottom are generator and action potentials for each stage. (*From W. R. Loewenstein and R. Rathkamp, J. Gen. Physiol., 41(6):1245–1265, 1958*)

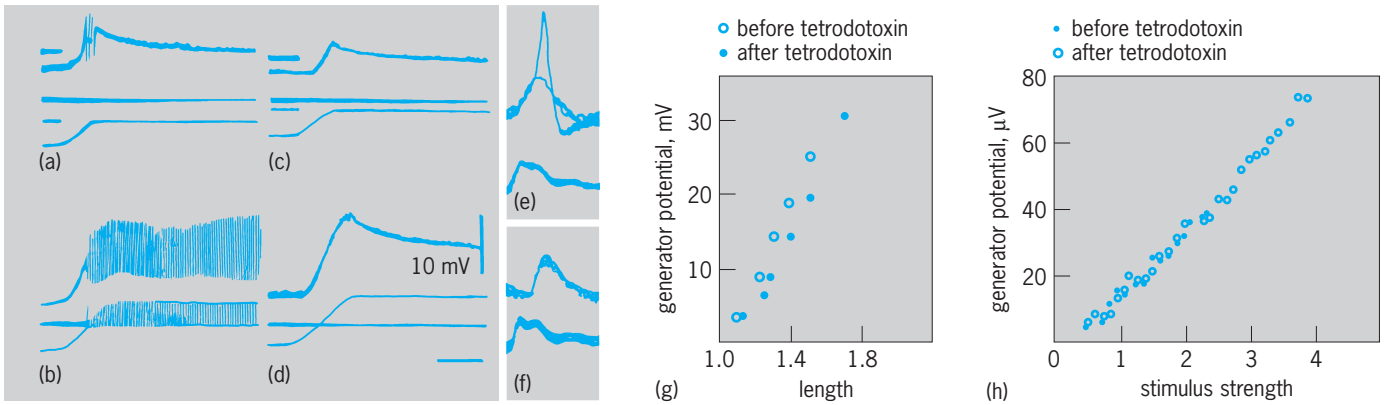

Fig. 7. Effects of tetrodotoxin on (*a–f*) transducer and impulse processes and (*g,h*) generator potentials of receptor organs. (*a–d*) Crayfish stretch receptor neuron. Response to stretch (*a,b*) before and (*c,d*) after application of tetrodotoxin, 5×10^{-6}. Upper beam, intracellular record from cell soma; middle beam, record from axon, about 2 mm away from soma; lower beam, strain gage record of mechanical displacement (stretch) to the receptor organ. Calibration: 2 s; 10 mV. (*e, f*) Pacinian corpuscle (decapsulated). Response to threshold mechanical stimulus (*e*) before and (*f*) after application of tetrodotoxin, 5×10^{-4}. Upper beam is the electrical response recorded externally from the axon near its junction with the nonmyelinated portion of ending; lower beam, photoelectric record of stimulus. Calibration: 1 ms; 15 μV. (*g,h*) Generator potential after tetrodotoxin application (concentration 5×10^{-6}) which blocks action potentials. (*g*) Crustacean stretch receptor. (*h*) Pacinian corpuscle.

endings, like those of Pacinian corpuscles, lie enclosed in a special adventitious tissue. The structure that converts mechanical into electrical energy—that is, the receptor proper—appears to lie within the membrane of the nonmyelinated ending.

The structure in which the all-or-nothing nerve impulse arises is, at least at the molecular scale, different from that giving rise to the generator current. This is indicated by a number of differential properties of the generator and action potentials, particularly by the differential action of tetrodotoxin, a pharmacological agent that blocks rather specifically the Na^+-carried component of the action potential. At low concentrations tetrodotoxin abolishes completely the action potential in the Pacinian corpuscle and the crustacean stretch receptor, leaving the generator current virtually unaltered (**Fig. 7**).

In some receptors the membrane sites of generator current and impulse production seem to be coarsely segregated. In the crustacean stretch receptor the generator current arises at the dendrites, whereas the action potential originates at the initial axon portion of the nerve cell. In other cases, segregation of the sites may be at a much finer scale, and interspersion of the sites on a given membrane may perhaps occur.

Receptor membrane properties. The following picture of nerve impulse generation has emerged from work on Pacinian corpuscles by W. R. Loewenstein and collaborators. There is a resting potential across the receptor membrane of the nonmyelinated nerve ending. Deformation (strain, but not stress) of the membrane leads to a fall in membrane conductance (excitation) and hence to a reduction in membrane potential (depolarization). The excitation is confined to that region of membrane which has been stimulated mechanically; it does not spread to adjacent regions of the same membrane. This is illustrated by the experiment depicted in **Fig. 8**. A small region of receptor membrane is stimulated mechanically, and the resulting generator potential is measured at varying distances from the stimulated region. The region is stimulated with mechanical pulses delivered by a stylus with a tip of about 20-micrometer diameter, while a microelectrode scans the surface of the remaining 800-μm length of receptor membrane. The amplitude of the generator potential is found to decrease exponentially with distance between the stimulated and recording spot; in other words, excitation is localized at and confined to the mechanically stimulated spot. This stands in strik-

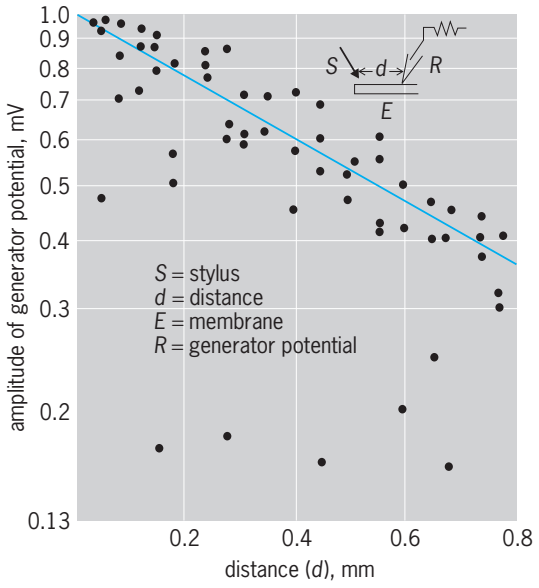

Fig. 8. Local excitation in the receptor membrane. A spot of membrane is stimulated with a stylus with a tip of about 20-μm diameter, and the resulting generator potentials are recorded at varying distances from the stimulated spot. (*After W. R. Loewenstein, Excitation and inactivation in a receptor membrane, Ann. N.Y. Acad. Sci., 94(2):510–534, 1961*)

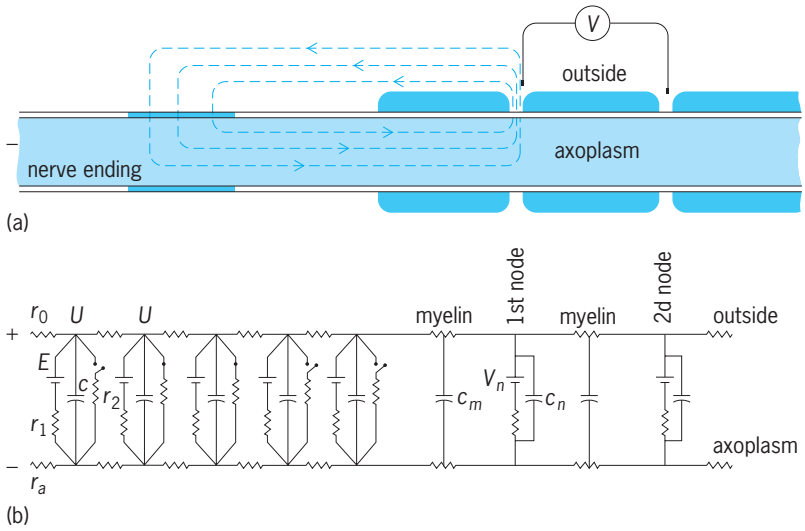

Fig. 9. Receptor analog. The generator potential (*V*) is measured between the first and second nodes of Ranvier. The nerve ending and the associated myelinated axon are represented by the equivalent circuit below, in which *E* represents resting potential, *C* redistribution capacitance, and *r* redistributed resistance. (*After W. R. Loewenstein, Ann. N.Y. Acad. Sci., 94:510–534, 1961*)

ing contrast to the propagated mode of excitation of the conductile portion of the axon. The peculiarity of the receptor membrane is that excitation is produced by the adequate stimulus, the mechanical stimulus in this case, but not by the resulting local flow of current. In this behavior the receptor membrane of mechanoreceptors resembles the membrane of the motor end plate of skeletal musculature and postsynaptic structures of nerve cells which lack regenerative mechanisms and which seem to have within their membranes functional properties of the primitive receptor cell. The result illustrated by Fig. 8 reveals that the conductance change that gives rise to transfer of charges through the membrane, namely the generator current, can be produced in a given spot independently of a neighboring one on the same membrane. *See* SYNAPTIC TRANSMISSION.

Thus, for analytical purposes the receptor membrane may be regarded as being composed of functionally independent units or generator elements (**Fig. 9**). In Fig. 9 membrane capacitance and resistance are assumed to be uniformly distributed over the receptor membrane. The transmembrane potential of a generator element is assumed to drop to a fraction of its resting value when the element is activated mechanically. Each generator element may be excited independently of others and may respond to mechanical stimulation with a (active) drop of membrane potential. This feature of local excitation is represented by switching the shunt resistor (r_2) of the active generator into the circuit. Spatial summation of electric activity along the surface of the receptor membrane is an immediate consequence of this mode of excitation, the total amount of current increasing progressively with the area of membrane excited. An experimental generator potential–membrane area relation is reproduced in **Fig. 10**. The generator potential increases at a diminishing rate with the area of membrane excited. This finding is of considerable physiological interest. The area of membrane excited appears to be the main factor, if not the only one, in determining the intensity of the generator current and, hence, the coding of sensory nerve impulses when the stimulus strength (the deflection amplitude or degree of compression) is varied under physiological conditions (**Fig. 11**).

The generator potential appears to be built up by a statistically fluctuating number of active generator elements. A mechanical stimulus of a given strength excites a statistical population out of a larger finite number of excitable generator elements. The probability for excitation of generator elements increases as a function of stimulus strength. This mode of excitation appears to have the following consequences: (1) The amplitudes of the generator potential in response to stimuli of standard strength fluctuate at random around a mean value; and (2) when two mechanical stimuli are applied in rapid succession, the number of generator elements excitable by the second stimulus is inversely related to the first stimulus.

Temperature. Another factor that influences the generator current of the receptor membrane is temperature (**Fig. 12**). The rate of rise of the generator potential from a constant mean area in response to a constant stimulus increases markedly with temperature; its value is more than doubled for a 118°F (10°C) increment of temperature. In addition, the amplitude of the generator potential also increases at about the same rate, while the duration of the falling phase is practically unchanged. This is another feature of the receptor membrane that contrasts with

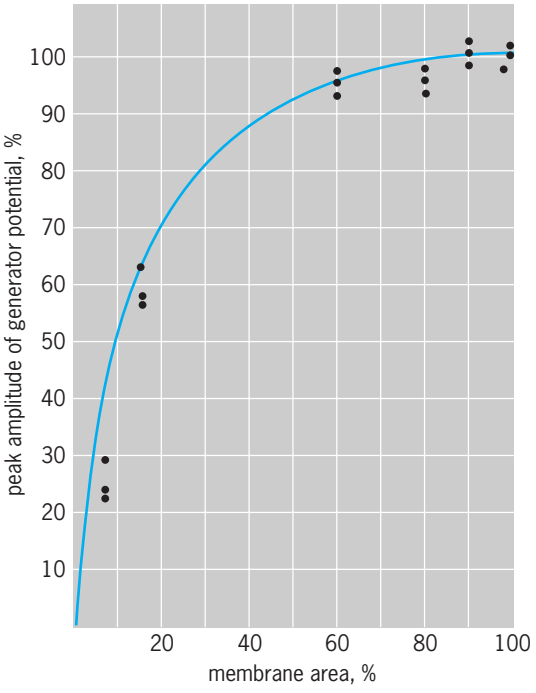

Fig. 10. Amplitude of peak generator potential as a function of the excited membrane area. An increasing area of receptor membrane of a Pacinian corpuscle is excited with styli of increasing diameter. (*After W. W. Loewenstein, Excitation and inactivation in a receptor membrane, Ann. N.Y. Acad. Sci., 94(2):510–534, 1961*)

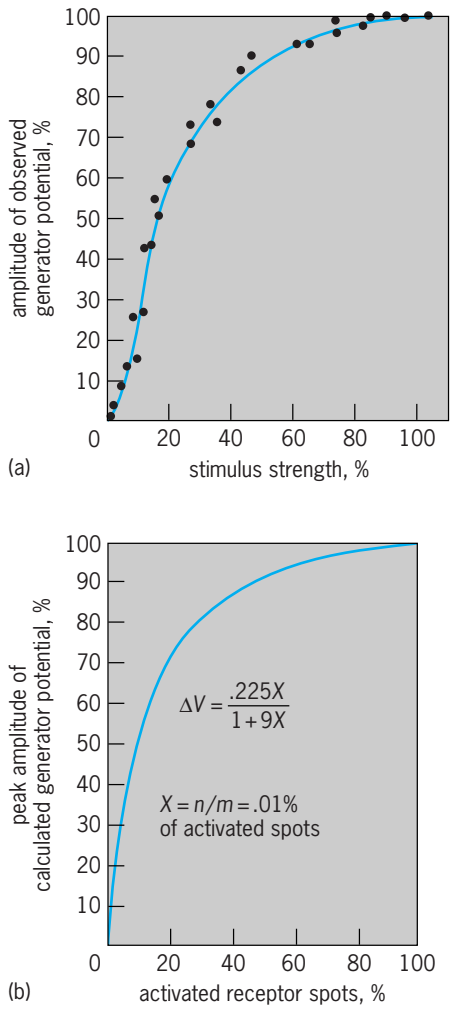

Fig. 11. Input-output relation of receptor membrane. (*a*) The observed generator potential of the receptor membrane of a typical Pacinian corpuscle as a function of stimulus strength. (*b*) The calculated generator potential (ΔV) as a function of the number of active generator elements as computed from the receptor analog of Fig. 9. (*After W. R. Loewenstein, Ann. N.Y. Acad. Sci., 81:367–387, pt. 3, 1959*)

the membrane of the conductile axon. The amplitude of the action potential of the Ranvier nodes adjacent to the receptor membrane, like that of other membranes with regenerative excitability, remains rather constant over a wide range of temperature, while its duration is markedly increased. Temperature appears to increase the conductance change in the excited receptor membrane; a high potential barrier is associated with the conductance change. The energy of activation, as calculated from the temperature dependence of the rate of rise of the generator potential, amounts to about 16,000 cal/mole. The rate-limiting activation energy appears to be associated either with the flow of ions through the receptor membrane or with the alteration in membrane structure that leads to the conductance change. Mechanical energy and thermokinetic energy, however, are not interchangeable in excitation. A change in temperature modifies the conductance change in the mechanically excited membrane but does not initiate it. Initiation of the conductance change, namely excitation, is brought about only by the mechanical stimulus.

Receptor inactivation. After repetitive stimulation at high frequency, the responsiveness of the receptor membrane of Pacinian corpuscles becomes markedly reduced (**Fig. 13**). The effect is fully reversible and has low energy requirements. It reflects a transient inactivation in the receptor membrane. The inactivation increases with frequency, duration of the train of repetitive stimuli, and strength of repetitive stimuli.

Receptor potentiation. With other, more critical parameters of repetitive stimulation, an increase in membrane potential may ensue. Thus, during the period of hyperpolarization (of the order of 10 s) a generator potential in response to a standard test stimulus is augmented (**Fig. 14**).

Production of nerve impulses. When an outward current is passed through the membrane sites of nerve impulse initiation, their resting potential is diminished. As in other excitable tissues with regenerative mechanisms, an all-or-nothing potential is discharged when the resting potential has been lowered to a critical level. This is what happens when the receptor membrane is excited mechanically and a generator current flows between active generator elements and the inactive impulse initiation site. If this current is intense enough, an all-or-nothing potential is discharged which may then propagate as a nerve impulse along the axon toward the nerve centers. This is the way nerve impulses are produced at receptors and how information of the outside world is conveyed to the nerve centers.

Code of sensory messages. Because the conductive elements of the nerve systems of higher organ-

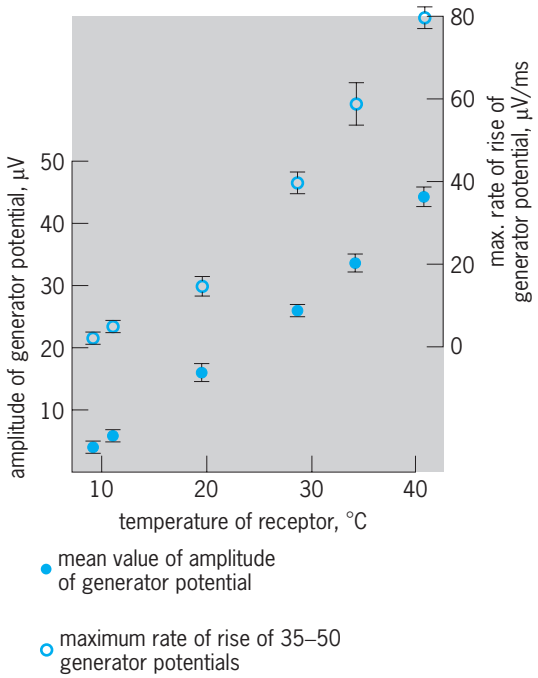

Fig. 12. Effect of temperature on the amplitude and the rate of rise of generator potential in the Pacinian corpuscle. Bars subtend standard error of the mean. $°C = (°F - 32)/1.8$. (*After N. Ishiko and W. R. Loewenstein, Effects of temperature on the generator and action potentials of a sense organ, J. Gen. Physiol., 45:105–124, 1961*)

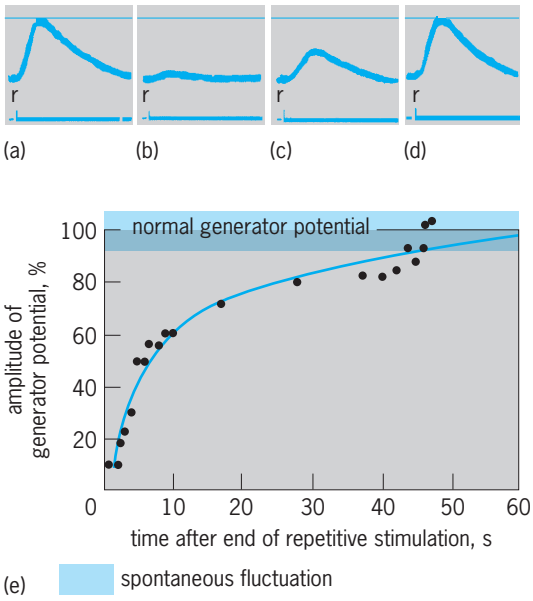

Fig. 13. Aftereffects of activity in receptor membrane: desensitization. (*a*) Generator response to a standard test stimulus of the fully rested receptor membrane (Pacinian corpuscle); (*b*) 0. 2 s, (*c*) 5 s, and (*d*) 50 s after applying a train of repetitive mechanical stimuli at 500/s for 30 s to the receptor membrane. Calibration 20 μV; 0.5 ms. (*e*) Recovery of depressed generator potential as a function of time. (*After W. R. Loewenstein and S. Cohen, J. Gen. Physiol., 43:347, 1959*)

isms, the axons, along which the nerve impulse must propagate have membranes with all-or-nothing type of responsiveness only, there is no possibility for gradation in amplitude of nerve impulses. Nature has endowed organisms with a rather stereotyped information system in which messages are sent in a code of equal all-or-nothing pulses. Thus, the only way of conveying quantitative information in nerve messages in a given information channel is by changing the sequence of its staccato content.

There are two ways by which the central nervous system can analyze the content of a receptor message: by counting the number of parallel information channels engaged in impulse traffic, and by gaging the frequency and sequence pattern of impulses transmitted in each information channel. The uncovering of this form of coding is chiefly due to E. D. Adrian.

Frequency coding. It has been established that the generator current which flows between the active receptor membrane and the impulse initiation site increases in its intensity and in its rate of rise with strength of stimuli. Thus, with suprathreshold stimuli of different strength, the resulting generator currents will cause the nodal membrane potential to drop to the critical level at a rate directly related to stimulus strength. Hence the frequency of discharged impulses is a function of the rate of rise of the generator current and indirectly of the stimulus strength (**Fig. 15**). This is then one way to feed messages of different quantitative content into the nerve system. The greater the stimulus intensity, the higher the impulse frequency of the message.

Spatial code. In animals of higher organization, receptors occur in groups. A pull on a muscle excites not one but many spindle receptors. A weight applied to the skin excites a group of Pacinian corpuscles. If one receptor of a group were to be killed, it would make little or no difference to the total message reaching the central nerve cells. This leads to another manner by which the content of a message may be graded. The greater the deformation of an organ, the greater the probability for excitation of different homonymous receptors. Thus, as a weight applied to the skin is increased, a larger area of skin is deformed, a larger number of receptors are excited, and hence a larger number of parallel axons become involved in impulse conduction. Also, since generally several receptor endings are twigs of one axon, there will be considerable mixing of impulses into the common axon. Consequently, because the number of receptors activated increases with strength, the frequency of total impulses in the common axon may also increase by this mechanism. Further mixing may still occur because of the convergence of several axons into nerve cells along the way to the centers.

Receptor adaptation. One of the striking properties of mechanoreceptors is their ability to adapt to stimuli. Adaptation is readily shown by applying a single mechanical stimulus of a given suprathreshold strength to a receptor organ and maintaining it in this way indefinitely without change. The receptor may respond with an initial burst of impulses at a given frequency; but then, in spite of the fact that

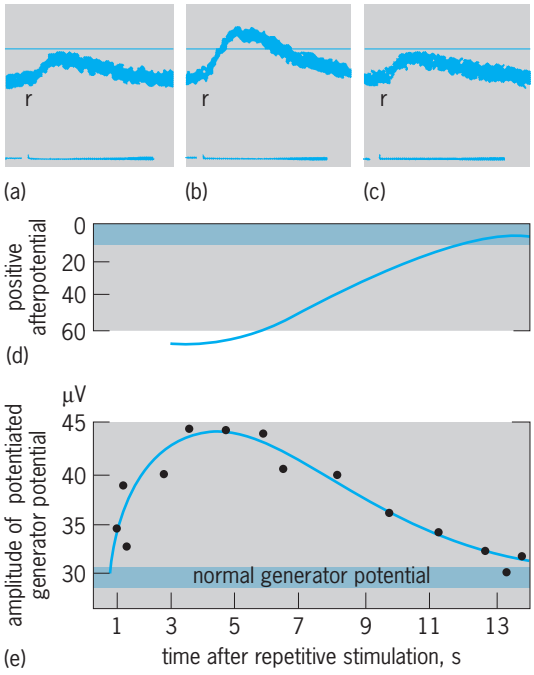

Fig. 14. Aftereffects of activity in receptor membrane: potentiation. Responsiveness of receptor (Pacinian corpuscle) is tested (*a*) with standard satimulus under fully rested conditions, (*b*) 5 s, and (*c*) 18 s after applying a train of repetitive stimuli at 500/s for 5 s. (*d*) Hyperpolarization. (*e*) Time course of resulting potentiation. (*After W. R. Loewenstein and S. Cohen, J. Gen. Physiol. 43:347, 1959*)

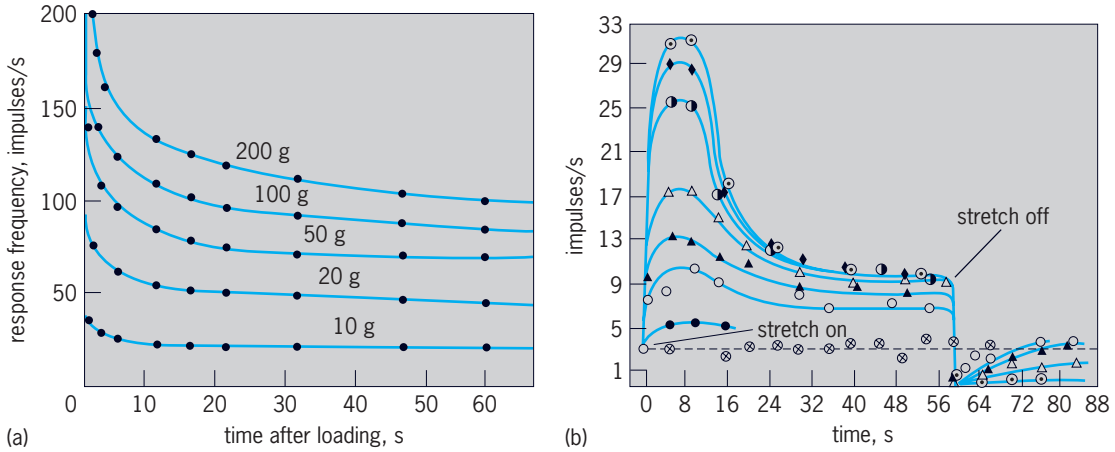

Fig. 15. Impulse frequency as a function of stimulus strength. (*a*) Muscle spindle of the frog at various degrees of tension (*after B. H. C. Matthew, J. Physiol., 78(1):1–54, 1933*). (*b*) Pressure receptor of frog skin at various degrees of stretch (*after W. R. Loewenstein, J. Physiol., 133(3):588–602, 1956*).

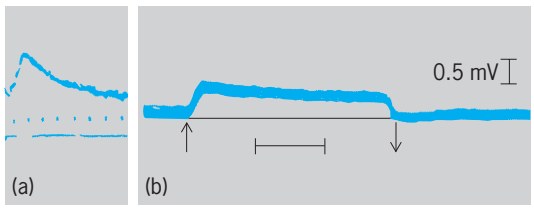

Fig. 16. Adaptation in generator potential. Response to a mechanical stimulus applied and sustained continuously for about 4 s (*a*) in a fast-adapting Pacinian corpuscle (calibration, 1 ms between dots) (*after W. R. Loewenstein, J. Gen. Physiol., 41(4):825–845, 1958*); and (*b*) in a slowly adapting crustacean stretch receptor (calibration, 1 s) (*after C. Eyzaguirre and S. W. Kuffler, J. Gen. Physiol., 39(1):87–119, 1955*).

the stimulus is continuously sustained, the frequency of impulses diminishes and may in some receptors fall to zero. The receptor is said to have adapted to the stimulus. The rate of adaptation varies greatly for different mechanoreceptors. Thus, a Pacinian corpuscle adapts to zero impulses within a few milliseconds, other skin receptors take seconds, and stretch receptors of the skin and of the muscle spindle maintain stationary discharges even after minutes of steady stimulation. It is in the last type that the stimulus strength–impulse frequency relationship is most readily seen (Fig. 15).

Adaptation in generator potential. Adaptation depends, at least in part, upon the ability of the receptor organ to sustain a constant generator potential. In fast-adapting receptors, such as the Pacinian corpuscle, the generator potential decays to zero within 4–7 ms in the face of a continuously sustained suprathreshold stimulus. In slowly adapting or nonadapting receptors, such as the muscle spindle and the slow-stretch receptor of Crustacea, the generator potential is well sustained for some time above the firing threshold of the impulse initiation site (**Fig. 16**). In fast-adapting receptors, impulses can obviously be produced only during the 1–2 ms in which the generator potential is above firing threshold, whereas in slowly adapting or nonadapting receptors a continuously sustained barrage of impulses may result.

The rate-limiting factor in generator current adaptation is a mechanical one. This has been clearly shown for the Pacinian corpuscle, whose capsule operates like a mechanical high-pass filter. The capsule of this receptor organ is made of many concentrically arranged tissue lamellae separated by fluid-filled spaces. The chief elements for transmission of mechanical forces through the capsule are the lamellae, their radial interconnections, and the interlamellar fluid. These are arranged in a transmission chain, at the end of which, at the center of the capsule, lies the nerve ending, the transducer proper. The mechanical equivalent is a system of dashpots and springs (**Fig. 17**). One set of springs, *M*, represents the elastic components of the lamellae, and the other set, *S*,

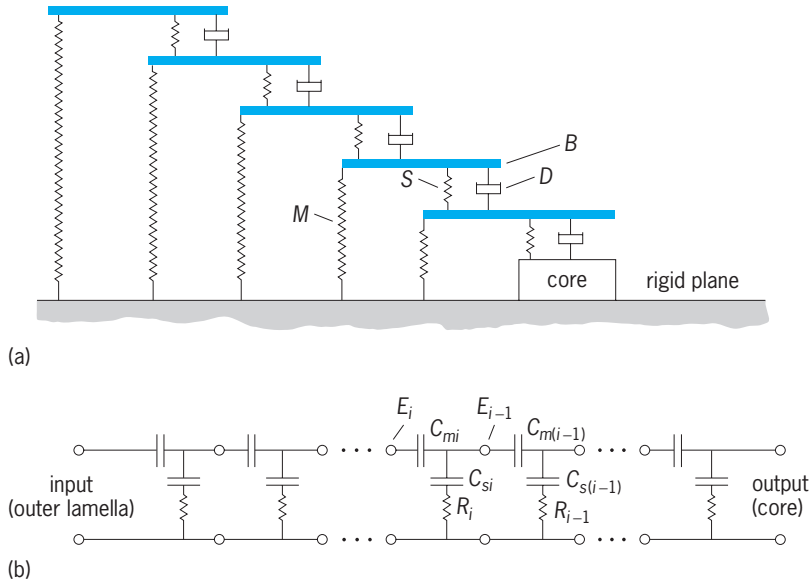

Fig. 17. Analogs of Pacinian corpuscle. (*a*) Mechanical. The rigid components of the lamellae are represented by bars (*B*), their compliance by springs (*M*), their radial spring compliance (interlamellar connections) by springs (*S*), and the fluid resistance by dashpots (*D*). (*b*) Electrical. Lamella compliance is represented by capacitance C_{mi}, radial spring compliance by C_{si}, and fluid resistance by resistance R_i. (*After W. R Loewenstein and S. Kalak, 1966, courtesy of J. Physiol.*)

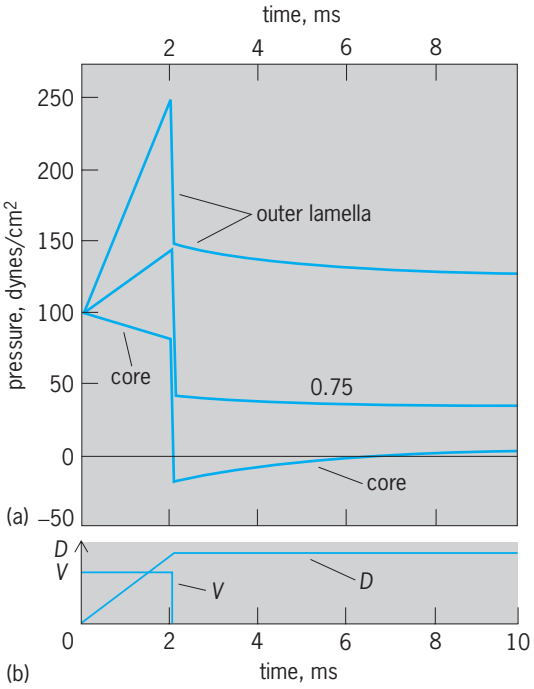

Fig. 18. Dynamic pressures in corpuscle. (*a*) Time course of computed pressures on outermost lamella, at 0.75 of corpuscle radius, and on core for total compression of corpuscle of 20 μm applied uniformly in 2 ms and then maintained. (*b*) Displacement, *D*, and velocity, *V*, at outer lamella. (*After W. R. Loewenstein and S. Kalak, 1966, courtesy of J. Physiol.*)

the much weaker elastic interconnections. During compression the lamellar surfaces operate like a series of dashpots which, in displacing fluid through narrow constraints, generate viscous pressure. The compliance of the lamellar interconnections is much greater than that of the lamellae themselves. As a result, static pressures applied to the surface of the capsule attenuate very rapidly toward the capsule center. When the capsule is loaded statically, only a very small fraction of the external pressure load reaches the center where the transducer nerve ending is located. This is the mechanical basis of adaptation.

During dynamic compression of the capsule the situation is quite different. At this time the fluid velocities set up viscous pressure, which is well propagated through the capsule. This is the only force of import that reaches the transducer ending; elastic forces are filtered out efficiently by the lamellated structure of the capsule. Thus, since viscous force is velocity-dependent, the electrical output of the transducer ending, the generator current, is velocity-dependent. This is generator current adaptation in more general terms.

The physical aspects of adaptation are well illustrated by the situation considered in **Fig. 18**. As long as there are fluid velocities in the system, there are appreciable pressures of viscous origin on the core. With the onset of the static phase of stimulation, fluid velocities and pressures on the transducer nerve ending fall toward zero and remain there for the entire period of static stimulation. This alone accounts for the rate of decay of the generator potential under external static stimulation. Thus, at least one adaptation process resides at the mechanical input side of the transducer chain in the form of a filter for elastic forces.

Another adaptation process is located at the level of nerve impulse initiation, preventing a steady generator current from producing repetitive nerve impulses. It is illustrated by bypassing the normal generator mechanisms and stimulating the site of impulse initiation with an electric current. Under these conditions the number of nerve impulses discharged is more or less independent of the duration of the current, and, typically, only one impulse is generated in the Pacinian corpuscle in response to strong currents. The mechanisms of the second filter action are not yet understood.

Off response. Many fast-adapting mechanoreceptors give generator current to both the on and off phases of the external stimulus. The mechanics of the off response in the Pacinian corpuscle are apparent from the mechanical model of Fig. 11. During the off phase the corpuscle tends to return to its circular cross section under the action of forces generated in the lamellae and lamellar interconnections. Thus energy stored in the elastic elements during compression is set free and viscous pressure is produced anew. During the off phase, compression occurs once again, but this time at right angles to the direction prevailing in the on phase. The transducer ending does not discriminate appreciably the force angle. Thus a second generator current, the off-generator response, results. After removal of the capsule, the receptor ceases to produce off responses.

Efferent control of receptors. Receptor inhibition and facilitation are discussed in the following sections.

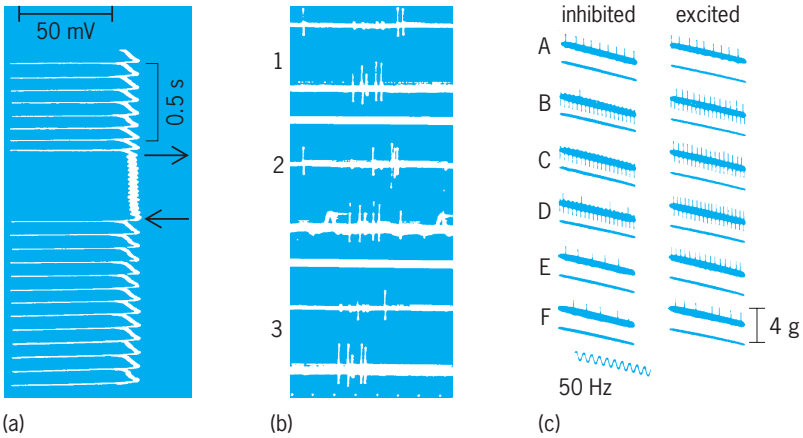

Fig. 19. Efferent control of receptors. (*a*) Intracellular recording from a crustacean stretch receptor submitted to constant stretch (*after C. Eyzaguirre and S. W. Kuffler, J. Gen. Physiol., 39(1):155–184, 1955*). (*b*) Sensitization of touch receptors (frog) by centrifugal sympathetic impulses. Impulse discharge of a group of touch receptors in response to a standard mechanical stimulus: 1, before; 2, during; and 3, after arrival of sympathetic impulses of the skin (*after W. R. Loewenstein, J. Physiol., 132(1):40–60, 1956*). (*c*) Supraspinal control of muscle spindle (cat soleus). Impulse discharge at a standard stretch. A, E, F, before, and B, C, D, after stimulation of inhibitory loci (left) and excitatory loci (right) of the contralateral inferior colliculus (*after E. Eldred et al., J. Physiol., 122(3):498–523, 1953*).

Receptor inhibition. The impulse discharge of certain mechanoreceptors can be modulated by centrifugal impulses. An example of this is the stretch receptor cell of Crustacea. This cell receives accessory nerve fibers which end on the receptor dendrites. S. W. Kuffler and collaborators showed that the effect of impulses conveyed by nerve fibers to the receptor cell is to clamp its membrane potential near resting value by increasing potassium-ion conductance, apparently in a specific way. In this manner, mechanically elicited generator potentials are prevented from reaching the critical level for impulse firing, and sensory discharges in response to stretch are promptly suppressed at the receptor level. In **Fig. 19** the inhibitory axon to the receptor is stimulated (between arrows), thus preventing the generator potential from reaching firing level.

Receptor facilitation. Certain tactile receptors of the frog's skin can be modulated by centrifugal impulses from the sympathetic system. Arrival of sympathetic impulses or application of sympathomimetic substance increases the sensitivity of touch receptors to mechanical stimuli (Fig. 19). In Fig. 19 an excitation of new receptor units, indicating an increase in excitability, is shown; also, there are repetitive discharges of some units during sympathetic stimulation, indicating lowering of the adaptation rate. The sympathetic effect is mediated by an adrenalin-like substance which appears to diffuse from the sympathetic terminal to the touch receptor ending. The anatomical relations between the afferent and efferent systems involved here are not known.

Modulation at accessory structure. A muscle spindle in the rabbit consists schematically of a bundle of muscle fibers (intrafusal muscle fibers) whose central portion (nuclear bag) beds the nude receptor ending (the receptor proper) of the thick myelinated afferent axon (Fig. 3). The intrafusal muscle receives, in addition, a set of motor fibers whose impulses cause it to contract. Stretching out the central nuclear bag excites the receptor ending, causing impulses to travel centripetally along the thick axon. The intrafusal muscle fibers lie parallel to the large muscle fiber of the skeletal muscle in which they are cribbed. Thus, shortening of the skeletal muscle during contraction causes the intrafusal fiber to slacken and thereby the afferent impulse discharge to cease. If, under these conditions, motor impulses are conveyed to the intrafusal fibers, the fibers appear to contract at a relatively fixed length (the ends of the intrafusal fiber are inserted in the endomysium or perimysium of the skeletal muscle). Thus the slack is taken up, the receptor ending is stretched, and impulses are fired again to the centers. The motor innervation of the intrafusal bundle thus appears to control the responsiveness of the sense organ by setting the tension of its accessory structure. *See* BIOPOTENTIALS AND IONIC CURRENTS; NERVOUS SYSTEM (INVERTEBRATE); NERVOUS SYSTEM (VERTEBRATE).

Werner R. Loewenstein

Bibliography. C. Barnes and P. W. Kaliuas (eds.), *Sensitization of the Nervous System*, 1988; P. Hnik et al. (eds.), *Mechanoreceptors: Development, Structure, and Function,* 1988; M. Matlin, *Sensation and Perception,* 4th ed., 1996; J. G. Retzloff, *Sensation Research,* 1987; A. Struppler et al. (eds.), *Sensory-Motor Integration: Implication for Neurological Disease*, 1987.

Mecoptera

A small order of insects called the scorpion flies. Characteristic of the adult insect is the peculiar prolongation of the head into a beak, which bears chewing mouthparts. They are small to medium in size. The insects either have two pairs of large, net-veined wings of equal size, often with dark areas, or have short and aborted wings. The legs are long and slender. In some species, the male abdomen has a terminal enlargement which is held recurved over the back so that he resembles a scorpion, thus the common name (see **illus.**). The larvae are eruciform

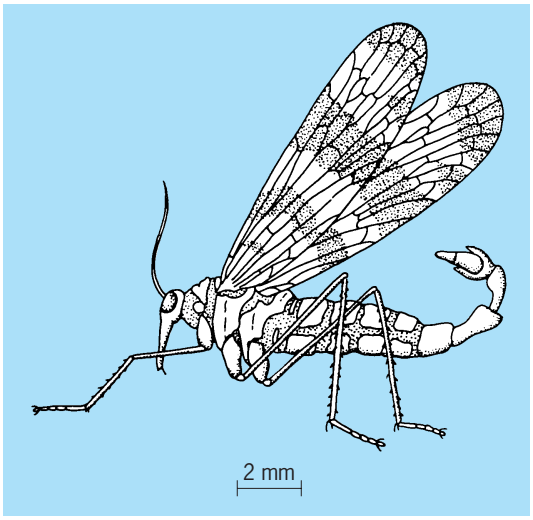

Male scorpion fly (*Panorpa*), order Mecoptera.

(resembling caterpillars), and the pupae exarate; that is, the appendages are free from the body and artificially movable. The Mecoptera are found in moist habitats within densely wooded areas. The adults are omnivorous but feed chiefly on small insects. *See* INSECTA.

Bryant E. Rees

Medical bacteriology

Medical bacteriology is the study of bacteria that cause human disease. The field encompasses the detection and identification of bacterial pathogens, determination of the sensitivity and mechanisms of resistance of bacteria to antibiotics, the mechanisms of virulence, and some aspects of immunity to infection. *See* VIRULENCE.

Identification of bacteria. The clinical bacteriology laboratory identifies bacterial pathogens present in specimens such as sputum, pus, urine, feces, blood, and spinal fluid, or from swabs of skin, throat, rectal,

or urogenital surfaces. Identification involves direct staining and microscopic examination of these materials, and isolation of bacteria present in the material by growth in appropriate media. The laboratory must differentiate bacterial pathogens from harmless bacteria that colonize humans.

Many specialized bacteriologic media have been developed for the purpose of selectively permitting the growth of potential pathogens while inhibiting the growth of harmless commensals. Species and virulent strains of bacteria can be identified on the basis of growth properties, metabolic and biochemical tests, and reactivity with specific antibodies.

Recent advances in the field of diagnostic bacteriology have involved automation of biochemical testing; the development of rapid antibody-based detection methods; and the application of molecular biology techniques such as nucleic acid hybridization, the polymerase chain reaction, and deoxyribonucleic acid (DNA) sequencing. Nucleic acid analysis can permit the identification of bacterial pathogens without the necessity of visualization and culture, and has resulted in more rapid identification of slow-growing pathogens. Once a bacterial pathogen has been identified, a major responsibility of the diagnostic bacteriology laboratory is the determination of the sensitivity of the pathogen to antibiotics. This involves observation of the growth of the bacteria in the presence of various concentrations of antibiotics. The process has been made more efficient by the development of automated instrumentation.

An increasingly serious problem in the therapy of infectious diseases is the emergence of antibiotic-resistant strains of bacteria. Bacterial infections caused by such pathogens as *Streptococcus pneumoniae* and *Staphylococcus aureus* that were easily treated in past decades are becoming increasingly difficult to treat due to the emergence of antibiotic resistance. An important area of research is the mechanisms of acquisition of antibiotic resistance and the application of this knowledge to the development of more effective antibiotics. *See* ANTIBIOTIC; ANTIGEN-ANTIBODY REACTION; BACTERIAL PHYSIOLOGY AND METABOLISM; BACTERIAL TAXONOMY; IMMUNOCHEMISTRY.

Infection. Most bacteria that associate with humans are harmless. Bacteria colonize the skin or mucosal epithelium (gastrointestinal tract, respiratory tract, and urogenital tract) and exist as commensals. The intact epithelium serves as the host's primary defense against invasion of deeper tissues. The second line of defense is the presence of white blood cells known as neutrophils and macrophages that ingest and kill any bacteria that manage to penetrate the epithelial surfaces. The process of ingestion of bacteria by white blood cells is termed phagocytosis. A successful bacterial pathogen must defeat these defenses.

Some bacterial pathogens remain at the epithelial surface and produce disease without deeper invasion. This strategy usually involves the production of toxins that damage or alter the function of host tissues. An example is *Vibrio cholerae*, the agent of the potentially fatal dehydrating diarrheal disease known as cholera. This pathogen colonizes the small intestine of the host and produces a toxin that acts on the intestinal epithelium, causing it to abnormally secrete fluid and electrolytes. Another example is *Corynebacterium diphtheriae*. This respiratory pathogen remains on the epithelial surface of the throat and secretes a toxin that damages the respiratory epithelium and enters the circulation and damages the heart. Invasion of the epithelial surface may require prior injury, as is usually the case with skin infections, or may involve the direct bacterial invasion of epithelial cells. A number of bacterial pathogens induce epithelial cells to engulf them. Some remain in the epithelial cell, divide rapidly, and destroy the cell. Examples include *Shigella*, the agent of bacillary dysentery, and *Neisseria gonorrhoeae*, an agent of sexually transmitted disease. Others invade beyond the epithelial surface, enter the circulation, and produce systemic disease.

These pathogens have special properties that help them to defeat phagocytic cells. Some pathogens have surface properties that prevent the phagocytic cell from initiating phagocytosis. An example is *Streptococcus pneumoniae*, an agent of pneumonia and meningitis. This bacterium is encapsulated with a polysaccharide substance that protects it from phagocytic cells. Some pathogens secrete substances known as hemolysins that attack and damage the phagocytic cells. An example is *Streptococcus pyogenes*, an agent of throat and skin infections. The action of hemolysins can be visualized by growth of *S. pyogenes* on medium containing red blood cells, which are destroyed in the vicinity of a bacterial colony.

Some pathogens permit phagocytosis but, once internalized, are not killed. An example is *Mycobacterium tuberculosis*, which survives within the macrophages of the lung. The presence of bacteria in tissue elicits the delivery of phagocytic cells to the site of infection. If the infection is not controlled, the accumulation of phagocytic cells can contribute to the tissue damage caused by bacterial growth. Thus, the body's own defense mechanisms, when defeated by the bacterial pathogen, actually contribute to the disease. Treatment of some types of bacterial meningitis, therefore, involves not only antibiotics to kill the bacteria but also steroidal anti-inflammatory drugs to suppress the destructive action of phagocytic cells. *See* PHAGOCYTOSIS; TOXIN.

Pathogenicity. The study of bacterial pathogenesis involves the fields of molecular genetics, biochemistry, cell biology, and immunology. In cases where the disease is not serious and easily treated, research may involve the deliberate infection of human volunteers. Otherwise, various models of human disease must be utilized. These involve experimental infection of animals and the use of tissue cell culture systems. Modern molecular approaches to the study of bacterial pathogenesis frequently involve the specific mutation or elimination of a bacterial gene thought to encode a virulence property, followed by observation of the mutant bacteria in a

model system of human disease. In this way, relative contributions of specific bacterial traits to different stages of the disease process can be determined. This knowledge permits the design of effective strategies for intervention that will prevent or cure the disease. The studies may also yield significant new basic knowledge of human biology. A recent example is the identification of the mechanism of action of tetanus toxin, a potent bacterial neurotoxin. Identification of the cellular proteins that are targets of tetanus toxin has permitted a much more detailed understanding of the processes of neurotransmitter release by nerve cells. *See* BACTERIAL GENETICS.

Immunity. Infection with many bacterial pathogens renders the host immune to subsequent infections. Frequently, immunity is mediated by specific antibodies. Antibodies are proteins that bind to a specific target, and are the natural result of a first encounter with a specific disease. On a subsequent encounter with the same pathogen, the presence of specific antibodies against bacterial substances will neutralize the virulence properties and the host will be immune to infection. The presence of specific antibodies is frequently useful in the diagnosis of bacterial diseases in which the pathogen is otherwise difficult to detect. An example is the sexually transmitted disease syphilis. The causative pathogen, *Treponema pallidum*, cannot be cultured, and is very difficult to visualize in clinical specimens. The diagnosis of syphilis, therefore, must be confirmed by the demonstration of antibodies specific for *T. pallidum*. *See* ANTIBODY; BIOLOGICALS.

Vaccines are substances that elicit immunity to a specific disease. Most vaccines against bacterial infections elicit the production of protective antibodies in the host. Vaccines provide an initial contact with the pathogen, or components of the pathogen, in such a manner that protective antibodies are elicited in the absence of disease. In cases where disease results from circulation of a bacterial toxin, the vaccine may be an inactivated form of the toxin. Examples are vaccines against tetanus and diphtheria. The bacterial toxins are purified and chemically inactivated but still induce an immune response. Some early vaccines against bacterial diseases consisted of killed bacterial cells. An example still in use is pertussis vaccine, which protects against whooping cough caused by the bacterial pathogen *Bordetella pertussis*. Such vaccines frequently produce undesirable reactions such as fever. Modern molecular research on the pathogenicity of *B. pertussis* has identified specific bacterial virulence components. On the basis of this knowledge, a new type of pertussis vaccine has been designed that consists of some of these components in a purified form. This type of vaccine has been termed subunit vaccine. The vaccine has proven as effective as the killed bacterial cells, and is much less toxic. Another example is the subunit vaccine against *Haemophilus influenzae* type B, which until recently was an agent of meningitis in infants. This pathogen invades the respiratory epithelium, and is resistant to phagocytic cells by virtue of a polysaccharide capsule which prevents interaction with them. A vaccine was developed that consisted of the purified polysaccharide coupled to a protein carrier. This vaccine elicits protective antibodies in infants, has few side effects, and has essentially eliminated *H. influenzae* as a serious pathogen in the United States after only a few years of universal vaccination. *See* VACCINATION.

Immunity to some bacteria that survive intracellularly is not mediated by antibodies but by immune effector cells, known as T cells, that activate infected cells to kill the bacteria that they contain. An active area of research is how bacterial components are presented to the immune system in a way that will induce effective cell-mediated immunity. This research may lead to the development of T-cell vaccines effective against intracellular bacterial pathogens.

For disease entities caused by specific bacteria. *See* ANTHRAX; BOTULISM; BRUCELLOSIS; CHOLERA; DIPHTHERIA; GANGRENE; GLANDERS; GONORRHEA; GRANULOMA INGUINALE; JOHNE'S DISEASE; LEPROSY; LISTERIOSIS; PLAGUE; PSEUDOTUBERCULOSIS; TETANUS; TUBERCULOSIS; TULAREMIA.

For disease entities caused by more than one microorganism *See* FOOD POISONING; INFANT DIARRHEA; MENINGITIS; PNEUMONIA.

For groups of disease-producing bacteria *see* MEDICAL BACTERIOLOGY; HAEMOPHILUS; IMMUNOLOGY; PNEUMOCOCCUS; GANGRENE; STREPTOCOCCUS.

Steve L. Moseley

Bibliography. E. W. Koneman, *Textbook and Atlas of Diagnostic Microbiology*, 5th ed., Lippincott-Raven Publishers, 1997; G. L. Mandell, J. E. Bennett, and R. Dolin (eds.), *Principles and Practice of Infectious Diseases*, 4th ed., Churchill Livingstone, 1994; A. A. Salyers and D. D. Whitt, *Bacterial Pathogenesis: A Molecular Approach*, ASM Press, 1994.

Medical control systems

Physiological and artificial systems that control one or more physiological variables or functions of the human body. Regulation, control processes, and system stability are at the heart of the survival of living organisms, both unicellular and multicellular. In the nineteenth century, C. Bernard concluded that the higher animals, far from being indifferent to their surroundings, must be in close and intimate relation to them. The equilibrium they maintain is the result of compensation established as continually and exactly as if by a very sensitive balance. W. B. Cannon (1929) differentiated the stability properties of biological systems from those of physical systems, and introduced the term homeostasis to describe the steady states in the body that are maintained by complex, coordinated physiological reactions. The condition of homeostasis is achieved either by regulation of supplies (for example, control of blood sugar level) or by regulation of processes (for example, control of body temperature and control of voluntary movements). *See* HOMEOSTASIS.

Medical control systems may be classified into two groups: (1) the physiological control systems in normal or pathological conditions (for example, control of electrolytes, arterial pressure, respiration, body temperature, blood sugar, endocrinal functions, neuromuscular and motor activity, and sensory functions), and (2) the external (artificial) control systems that interface with physiological systems (for example, artificial kidneys or hemodialyzers, blood oxygenators or heart-lung machines used during open-heart surgery, external prosthetics and orthotics, cardiac pacemakers, ventilators, implantable defibrillators, and implantable pumps for drug delivery). For the development and proper functioning of artificial devices, the underlying control mechanisms of the normal and of the disabled physiological systems with which the external devices must interface must be adequately understood. Thus, in its broadest sense, the area of medical control systems encompasses all branches of engineering, mathematical biology, biophysics, physiology, and medicine. *See* BIOMECHANICS; BIOMEDICAL CHEMICAL ENGINEERING; BIOMEDICAL ENGINEERING; CONTROL SYSTEMS; MATHEMATICAL BIOLOGY.

The importance of control systems engineering in medical applications has grown because of the inherent complexity of medical control systems. Although there is no formal definition of complex systems, H. A. Simon's concept of complexity is very appropriate for medical control systems: complex systems are composed of subsystems that in turn have their own subsystems, and so on; and the large number of parts interact in a complicated way so that it is sometimes impossible to infer the properties of the whole from the properties of the parts and their laws of interaction. Indeed, the analytical models developed, using control systems engineering, of the components of a medical system have had limited success in predicting the behavior of the overall system.

Some examples of medical control systems and devices will be discussed. The example of control of voluntary movements emphasizes the complexity of physiological systems. Myoelectric prostheses are replacement devices for lost limbs. External orthoses are used for rehabilitation of patients with acquired disabilities. Implantable devices such as defibrillators and pumps for drug delivery represent advanced technology. Numerous other devices, such as cardiac pacemakers, artificial kidneys, heart-lung machines, and artificial ventilators, have been in routine clinical use for many years.

Control of voluntary movements. The control mechanisms by which the central nervous system produces coordinated or patterned movements has been an area of study from Galen in the second century to current physiologists, psychologists, clinicians, and engineers. In order for the central nervous system to produce any movement, (1) the appropriate muscles must be selected, (2) each participating muscle must be activated or inactivated in proper temporal relationship to the others, and (3) the appropriate amount of excitation must be exerted on each muscle to satisfy the desired goals. These three aspects require spatial, temporal, and quantitative coordination of muscular activities. The achievement of these goals can almost always be accompanied by any of a number of different movements. There is no unique movement trajectory to move from point A to point B in space. In planning and executing a movement trajectory, the central nervous system heavily relies on past experience and sensory feedback (visual, tactile, and proprioceptive inputs) from the environment. In addition, at all times the central nervous system must make appropriate adjustments to maintain the postural stability of the system.

Figure 1 illustrates some selected portions of the motor control system. Given a particular task, the central nervous system chooses a strategy to control the peripheral motor system consisting of the motoneuron pools and the muscles. This system consists of multiple feedback loops that continually provide information for updating the controlling signals. In human experiments, only the peripheral outputs of the motor system are observable. The electromyographic activity arises from the electrical responses in the muscle membranes. The forces produced and the resulting movements are outputs from the mechanical responses of the contracting elements of the muscles and the interacting external loads.

Significant progress has been made in developing mathematical models of subsystems of the motor system. However, an adequate description is far from

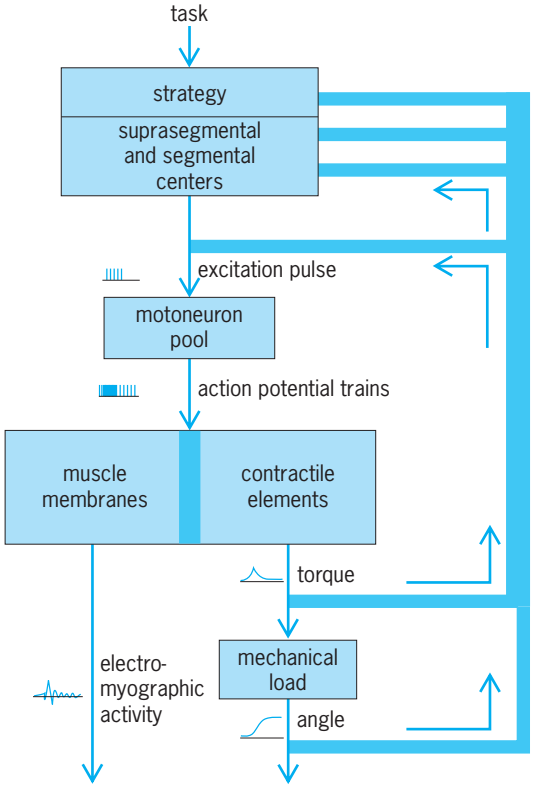

Fig. 1. Diagram of selected portions of the human motor control system. (*After G. L. Gottlieb, D. M. Corcos, and G. C. Agarwal, Strategies for the control of voluntary movements with one mechanical degree of freedom, Behav. Brain Sci., 12:189–250, 1989*)

complete. In order to apply the concepts of control theory to motor coordination, the nature of the input-output variables must be defined. Force, length, velocity, and so forth are the traditional choices of the variables to be controlled in artificial control systems. It is difficult to specify the controlled variables in a human motor control system. The nature of the controlled variable may very well be task-related and the system adapts to its changing environment. *See* MOTOR SYSTEMS.

Myoelectric prostheses. Myoelectric controlled prostheses are most commonly used for below-elbow amputees where the elbow function is retained. In such devices the terminal device is usually designed to look as much like a hand as possible (**Fig. 2**). Myoelectric control uses the electromyographic activity (Fig. 1) of a contracting muscle as a control signal. In a below-elbow amputee, the muscle remnants in the residual limb are used to provide control signals for the powered components.

As the level of amputation progresses to sites above the elbow, the complexity of function and power levels required both increase rapidly, while the capability of an amputee to operate these functions by harnessing body movements decreases rapidly. The human upper extremity has seven degrees of freedom from shoulder to wrist. In such devices, timely processing and adequacy of bioelectric command information from human controller, the amputee, to the machine becomes a critical problem. *See* PROSTHESIS.

Rehabilitation engineering. Rehabilitation engineering is concerned with the application of appropriate science and engineering in rehabilitation of patients who have acquired disabilities by accident, natural causes (including aging), or disease and are physically or mentally impaired. One particular application has been the development of functional electrical stimulation systems for spinal cord injury patients where the controlling signals from the central nervous system are interrupted by lesions in the spinal cord. By using externally applied electrical inputs, some functional capability can be restored in the affected muscles. Functional electrical stimulation applied on its own tends to physically exhaust patients because of the rapid onset of muscle fatigue. Biochemically designed orthoses that provide selective constraints of the hip, knee, and ankle joints combined with functional electrical stimulation have proven to be clinically successful. A hybrid system using both functional electrical stimulation and orthoses is shown in **Fig. 3**. This system involves decomposing the multigoal and multivariable control problem into subsystems organized in hierarchical levels. At the top level, the patient interacts directly with the control system through a command interface comprising a limited number of hand-operated controls. Each locomotion mode is controlled with reference to a finite-state model of the process. This model serves to change the control strategy, as required, at different stages or phases of the locomotion cycle. The control signals, as myoelectric signals, may also be obtained from muscles that are still functional. *See* MULTILEVEL CONTROL THEORY; MULTIVARIABLE CONTROL.

Implantable pacemakers. The implantable cardiac pacemaker is a major contribution to health care. Since the first clinical implant in 1960, the procedures for implanting pacemakers have been greatly simplified. It is no longer necessary to open up the chest to connect stimulating leads to the heart; these leads can be installed through the veins. Over 300,000 new pacemakers are implanted each year throughout the world, and in the United States cardiac pacemaker use has approached 1 per 1000 of population. The performance and reliability requirements of life-support implantable devices, such as pacemakers, often transcend those of traditional high-reliability fields such as the space program. The human body is a very hostile environment for implanted devices, far more so than outer space or the

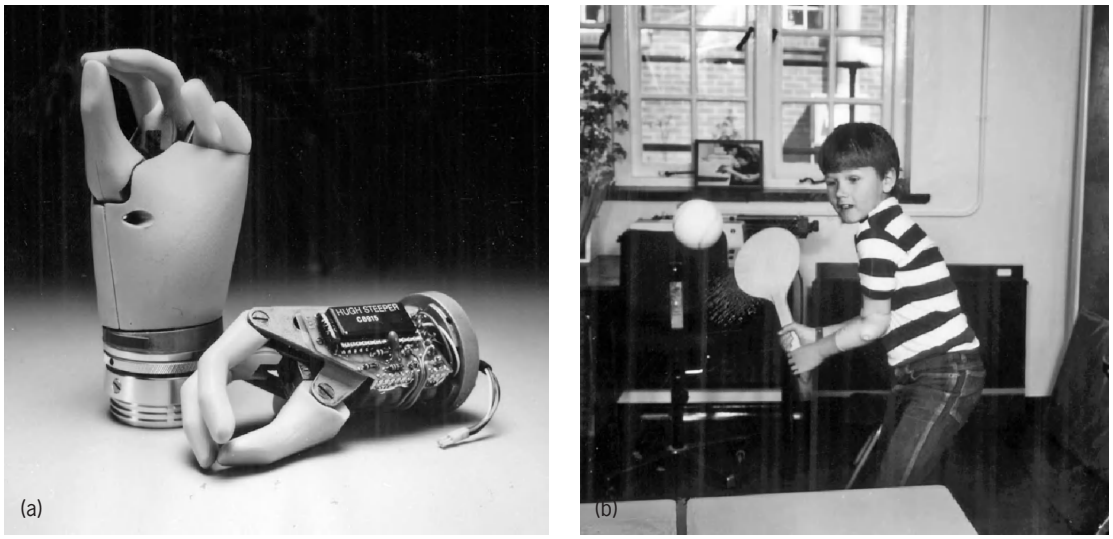

Fig. 2. Electric hand, a myoelectric prosthesis. (*a*) Two views of the hand, 2.5 in. (6 cm) across the knuckles, with the cover removed in one view to show the electric motor drive circuit. (*b*) Child using the electric hand. (*Hugh Steeper Ltd.*)

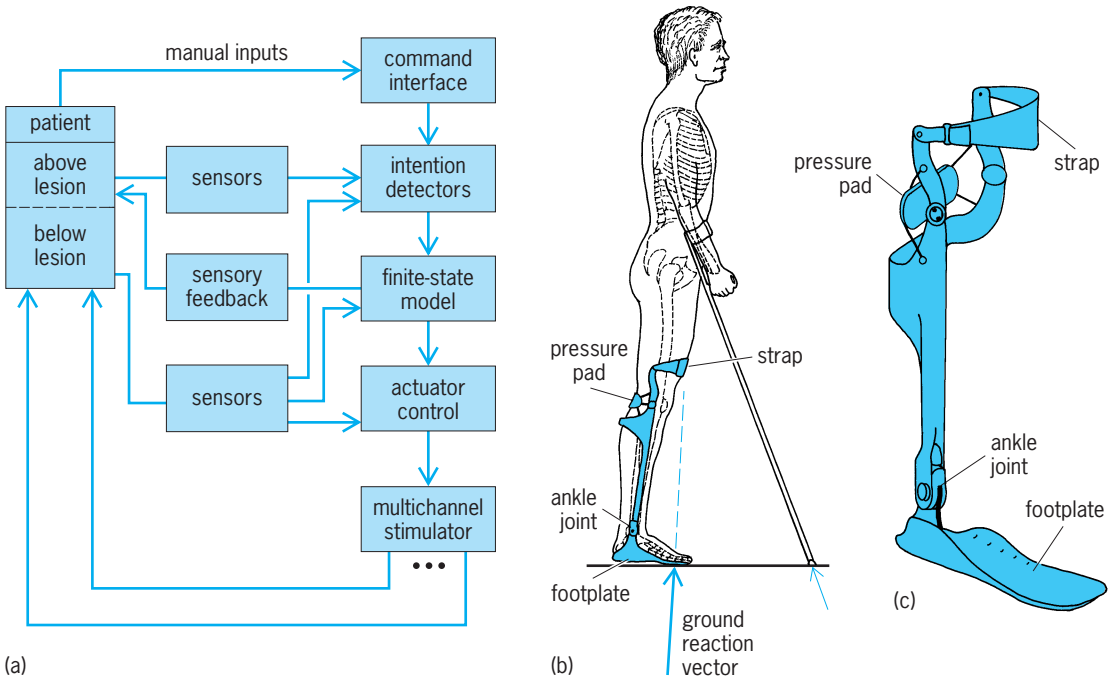

Fig. 3. Hybrid control system using both functional electrical stimulation and orthoses. (*a*) Hierarchical control scheme. (*b*) Braces in use. (*c*) Detail of leg brace. (*After Y. Kim and F. A. Spelman, eds., Images of the Twenty-First Century: Proceedings of the Annual International Conference of the IEEE Engineering in Medicine and Biology Society, vol. 11, 1989*)

sea bottom. The battery power source has always been the limiting factor in pacemaker performance and reliability. The lithium-iodine battery, invented in 1970, has been the most used battery for pacemakers since 1972. Such batteries have a long life (over 10 years in cardiac pacemakers), are autoclavable, and can be hermetically sealed in a metal, glass, or ceramic material because there is no gas generation. An autoclavable pacemaker with a lithium silver vanadium pentoxide battery is shown in **Fig. 4**. *See* SOLID-STATE BATTERY.

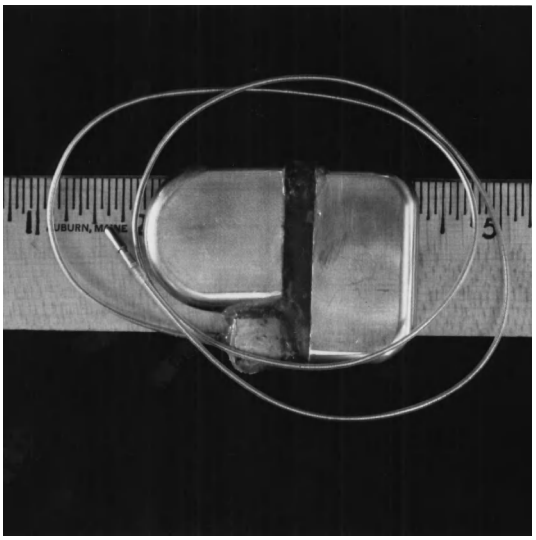

Fig. 4. Autoclavable pacemaker with a lithium silver vanadium pentoxide battery. (*After W. Greatbatch, Pacemaker power sources, IEEE Eng. Med. Biol. Mag., 3(2):15–19, June 1984*)

Developments in pacemaker technology include improving the pacemaker's responsiveness to the body's needs and providing more diagnostic information. A normal healthy heart responds to exercise and stress by increasing cardiac output through increased heart rate and stroke volume. Advanced pacemakers indirectly sense the need for increased heart rate by sensing the P wave, nerve impulses, the Q-T interval, hydrogen-ion concentration (pH), oxygen saturation, respiratory rate, stroke volume, motion, or body temperature. *See* CARDIAC ELECTROPHYSIOLOGY; CARDIOVASCULAR SYSTEM.

Implantable defibrillators. Sudden cardiac death, defined generally as death within 1 h of onset of ventricular tachyarrhythmias (VTs) or ventricular fibrillation (VF), is the cause of death in an estimated 350,000 patients per year in the United States. Fast response time of ambulatory service and immediate external defibrillation by skilled paramedics can save a significant number of so-called at-risk patients. Antiarrhythmic drugs and implantable anti-VT pacemakers are in clinical use. An automatic implantable defibrillator can essentially eliminate cardiac arrhythmic mortality. One such device, which has been approved for clinical use (**Fig. 5**), continually monitors the cardiac rhythm and, upon recognition of a shockable arrhythmia, delivers one or more pulses of 25–30 joules of energy using lithium batteries. An external programmer permits noninvasive interrogation and programming of the implanted device. The first-generation devices were large (volume of 160 mL or 10 in^3 and weight of 290 g or 10.2 oz), were implanted in an abdominal pocket, and required open thoracotomy. More advanced devices

Fig. 5. Automatic implantable cardioverter defibrillator (AICD) system with pulse generator, leads, and external programmer. (*S. Nisam, Cardiac Pacemakers, Inc.*)

do not require thoracotomy and use a transvenous defibrillating lead with sensing electrodes, which are implanted similiar to a standard pacemaker lead. In one study, all-cause mortality in the defibrillator group declined by 46% as compared with conventional pharmacological therapy, and sudden cardiac deaths in the defibrillator group decreased by 85%.

Implantable pumps for drug delivery. In a healthy person, the islet cells of the pancreas continually monitor the blood of all metabolic substrates. Infinitesimal secretions from these cells delicately balance the metabolism over a wide range of food intake rates (from feasting to fasting). Insufficiency of the endocrine pancreas leads to diabetes mellitus. The control of diabetes in most of an estimated 15 million insulin-dependent diabetic patients in the United States is by subcutaneous exogenous injections once or twice daily. Such therapy is open-loop, and feedback control is exerted at regular intervals (mostly weekly or monthly) by blood analysis and dosage adjustments. Negative-feedback closed-loop control systems for blood sugar control have been implemented. The major difficulties have been in finding a suitable and reliable sensor of blood glucose and in miniaturizing the entire device so that it can be implanted. Implantable pumps for variable-rate delivery of drugs are at various stages of development. *See* DIABETES; PANCREAS. Gyan C. Agarwal

Bibliography. N. A. M. Estes III, A. S. Manolis, and P. J. Wang (eds.), *Implantable Cardioverter-Defibrillators*, 1994; U. Laffer, I. Bachmann, and U. Metzger (eds.), *Implantable Drug Delivery Systems*, 1991; G. V. Naccarelli and E. P. Veltri, *Implantable Cardioverter-Defibrillators*, 1993; D. A. Wolfe, D. Kosinski, and B. P. Grubb, Update on implantable cardioverter-defibrillators, *Postgrad. Med.*, 103(1):115–130, January 1998.

Medical imaging

A medical specialty that uses x-rays, gamma rays, high-frequency sound waves, and magnetic fields to produce images of organs and other internal structures of the body. In diagnostic radiology the purpose is to detect and diagnose disease, while in interventional radiology, imaging procedures are combined with other techniques to treat certain diseases and abnormalities. *See* RADIOLOGY.

Contrast media. Contrast media are drugs or compounds that block the x-rays and are used to outline and distinguish certain anatomic structures from surrounding tissues of similar density. The two principal groups of contrast agents are barium compounds and iodine-containing solutions.

Barium compounds are swallowed or are given as an enema to evaluate the different portions of gastrointestinal tract. Iodinated solutions are usually injected into a vein, an artery, or the spinal canal. Thus, with appropriate techniques they are used in angiography to visualize arteries and veins, and in myelography to study the spine, spinal cord, and spinal nerves. Iodinated drugs are also used to study the shape and function of the kidneys and to enhance tissue differences during computed tomography.

Film x-rays. Film x-ray studies, the most common radiologic procedures, are made up of still pictures of the various organs and tissues in the body. In these procedures, x-rays are passed through the body to expose the photographic film that is placed on the opposite side of the body. As they pass through the body, the x-rays are absorbed in different degrees by different types of body tissues. Dense tissue, such as bone, absorbs, or blocks, a greater amount of radiation and causes the film to appear lighter or whiter. Fatty tissue and air-containing structures, such as the lungs, block the least radiation and cause the film to appear darker or blacker. Other tissues appear as varying shades of gray on the film. The changes in film density that result from exposure allow the radiologist to distinguish between normal and abnormal tissue and to diagnose many different disease types.

The chest x-ray is the most frequently performed radiologic study. Other commonly performed procedures are x-ray examinations of the abdomen, spine, extremities, sinuses, skull, and kidneys. *See* X-RAYS.

Mammography is an x-ray examination of the breast. In conjunction with physical examination of the breast, it provides the most effective method for early detection of breast cancer. Specially designed equipment offers a high-quality image of the breast tissue with the lowest possible radiation risk since the dose is very low. Vigorous compression of the breast is required in order to obtain maximum detail of the tissue and to minimize the radiation exposure (**Fig. 1**). Two views of each breast are customary—one from the side and one from the top.

Fluoroscopy. W. C. Roentgen's fluoroscopic unit was developed in 1896 and provided the basis for the modern fluoroscope, which includes an x-ray tube

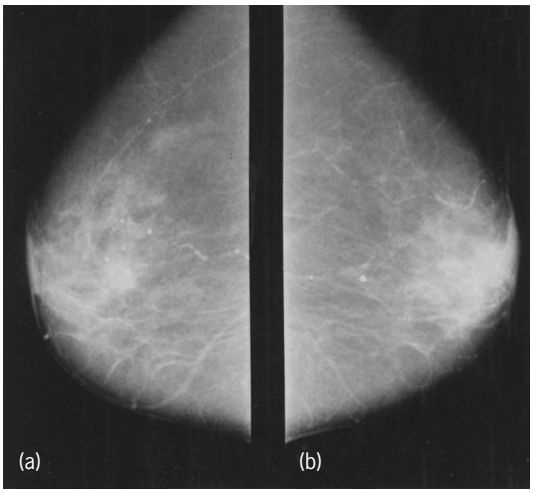

Fig. 1. Mammogram showing lateral views of (*a*) left and (*b*) right breasts. (*American College of Radiology*)

and a fluoroscopic screen. The screen, however, has been incorporated into an image intensifier, which is an electronic instrument that brightens and intensifies the fluoroscopic image many thousands of times. This process has resulted in a dramatic improvement in image quality while markedly reducing radiation exposure. Fluoroscopy is a dynamic x-ray imaging technique that produces a moving image over time. It is essential for evaluating organ movement such as the beating of the heart or movement of the diaphragm.

The gastrointestinal (G.I.) series and the barium enema are the most common fluoroscopic studies. These procedures begin with the administration of a barium mixture either by ingestion or by an enema that fills the stomach or large intestine. The barium mixture, like dense tissues, blocks the x-ray beam. Fluoroscopy then reveals the location of the barium-coated lining of the stomach and intestine and enables the radiologist to observe as they contract and distend. Ulcerations, tumors of the intestine, and many other abnormalities can be seen with this technology. Fluoroscopy is also used in angiography and in interventional radiologic procedures.

Angiography. Angiography is the radiologic study of blood vessels. Because arteries and veins are not normally visible in conventional x-ray studies, an iodinated compound, which is opaque to the x-ray, must be injected into the bloodstream. An arteriogram is an x-ray study of the arteries; a venogram is an x-ray study of the veins. Arteriography is most often used to show the presence and extent that arteries have become clogged and narrowed by arteriosclerosis, which can lead to strokes and heart attacks. It is also performed to locate sites of internal bleeding or tumors or to define many other conditions that may obstruct normal blood flow to body tissues.

A radiologist performs an arteriogram by inserting a long, narrow tube, called a catheter, through a needle puncture in an artery, usually at a point in the groin. Guided by fluoroscopy, the catheter is carefully threaded through the branching arteries of the body to the location to be examined. The contrast solution is then injected through the catheter into the blood vessel. The appearance of the opacified arteries is then recorded on a series of rapidly exposed x-ray film images (two to six pictures per second): an x-ray moving picture, called a cine-radiograph, or videotape recordings. Cine-radiography is frequently used to study the coronary arteries, which supply the heart muscle.

Digital subtraction angiography is a computerized technique for recording x-ray images. Two images are made of the same organ—one before and one after injection of contrast medium into a blood vessel. A computer then subtracts the first image from the second and produces a third image, which shows an unobstructed image of the blood vessels. Digital subtraction angiography helps improve the safety and patient comfort of the angiographic procedure because the amount of contrast solution required is less than that needed for traditional angiography.

Computed tomography. Computed tomography (CT), also called computed axial tomography (CAT), is a scanning technique that combines computer and x-ray technologies. To produce the scans, the patient is positioned on a narrow table (gantry) that slides into the scanner, which is a tubelike structure. An x-ray tube built into the scanner emits a very narrow x-ray beam as it rotates around the body. The radiation that passes through the body is recorded by detectors that lie opposite the x-ray tube. Each detector emits tiny flashes of light in proportion to the amount of radiation it receives. Because x-rays are differentially absorbed by body tissues, the brightness of the light is also a measure of tissue density. A computer measures the flashes of light, magnifies them a thousandfold, and then stores their location and brightness in its memory. From this information, the computer constructs a two-dimensional anatomic image that represents a cross-sectional slice through the body (**Fig. 2**).

Computed tomography can produce images of internal slices of organs, such as the liver and kidney, that are more precise than film x-rays. It is also useful in visualizing the brain and abdomen to detect trauma damage or the size and location of some

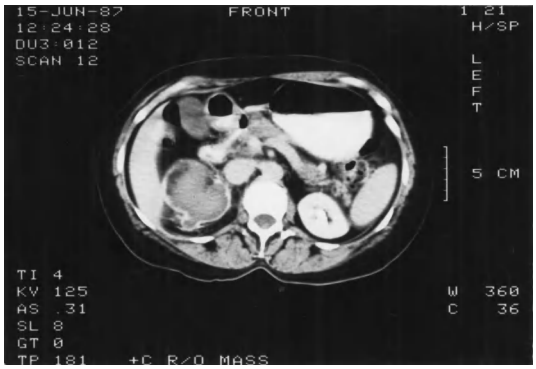

Fig. 2. Computed tomographic image showing a transverse section through the abdomen. (*American College of Radiology*)

tumors. Oral and injected contrast media can further enhance the CT image. Three-dimensional images can be generated by using special computer software (**Fig. 3**). These are especially useful in planning reconstructive orthopedic or plastic surgery. *See* COMPUTER GRAPHICS; COMPUTERIZED TOMOGRAPHY.

Ultrasound. Ultrasound imaging, or sonography, is a diagnostic imaging procedure that uses high frequency sound waves instead of ionizing radiation. During an ultrasound examination, a lightweight transducer is placed on the patient's skin over the part to be imaged. The transducer produces sound waves that penetrate the skin to reach tissues and organs. When the sound waves strike specific tissue surfaces, echoes are produced. The echoes are detected by the transducer and are than electronically converted into an anatomic image that is displayed on a video screen. The image can also be recorded on film or videotape. Some ultrasound studies are done in a real-time format, that is, showing motion as it occurs.

Ultrasound imaging is commonly used in obstetrics to monitor the position and development of the fetus (**Fig. 4**) and also to detect any fetal abnormalities or problems in the pregnancy. Ultrasound is also used to show problems in other internal structures, including the gallbladder, kidney, and heart.

Doppler ultrasound can monitor blood flow through veins and arteries. It is commonly used to study kidney transplants and blood flow to the brain and also to diagnose blocked arteries. *See* DOPPLER EFFECT; MEDICAL ULTRASONIC TOMOGRAPHY; ULTRASONICS.

Magnetic resonance imaging. Magnetic resonance imaging (MRI) is a diagnostic procedure that uses a large, high-strength magnet, radio-frequency signals, and a computer to produce images. During an examination, a patient is placed in an MRI scanner where the body is surrounded by a magnetic field up to 30,000 times stronger than that of the Earth. The nuclei within the atoms that make up the body's tissues are like tiny magnets, each with a north and south pole. The nuclei usually spin in many different directions and at many different angles, but in the presence of the strong external magnetic field generated by the scanner, the north and south poles of the nuclei align themselves with the external magnet. The nuclei continue to spin in many different directions (incoherent spinning). The magnet causes them to vibrate at a specific frequency, so that they act like radios, receiving and transmitting radio-frequency signals. When an external radio-frequency signal from the scanner is transmitted to the area of the body being examined, it changes the alignment of the magnetic poles of the nuclei so that they are no longer in alignment with the external magnet. It also causes the nuclei to spin in the same direction (coherently). When the signal stops, the magnetic poles of the nuclei realign themselves in the direction of the magnet and, at the same time, release their own faint radio signals. The scanner receives the radio signals and, with the aid of a computer, characterizes the different body tissues by the strength and duration of these signals. The computer then reconstructs the information into a two-dimensional anatomic image.

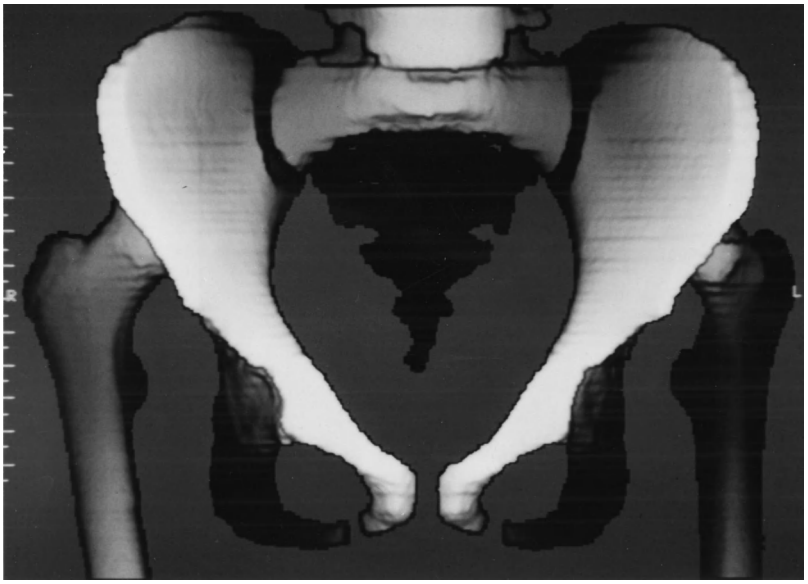

Fig. 3. Three-dimensional computed tomogram of the pelvis. Special computer software has made such imaging available for planning of reconstructive surgery. (*Dimensional Medicine, Inc.*)

The technique of MRI is extremely useful in evaluating diseases of the brain and spine (**Fig. 5**). In some instances it may eliminate the need for arteriography of the brain or myelography of the spinal column. It is also used to evaluate joints, bone and soft tissue abnormalities, as well as abnormalities of the chest, abdomen, and pelvis.

Because of the strong magnetic field involved, some patients are unable to undergo MRI examinations. That is, patients with iron-containing metallic clips in the brain or fragments in the eye might not be scanned as the magnetic field might cause these to move and cause damage. *See* NUCLEAR MAGNETIC RESONANCE (NMR).

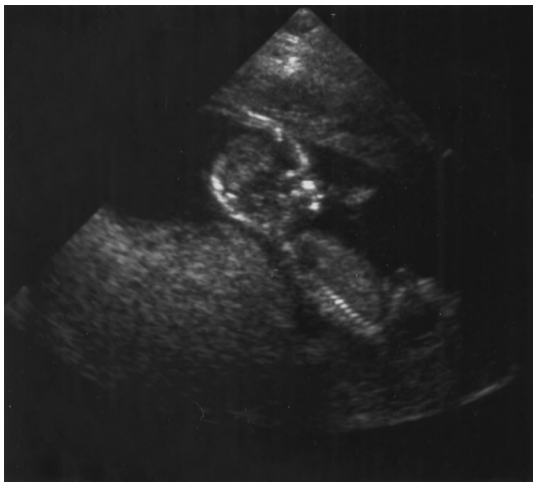

Fig. 4. Ultrasound image of a growing fetus within the uterus. (*American College of Radiology*)

Fig. 5. Magnetic resonance image of a midsagittal section through the skull. (*American College of Radiology*)

Nuclear medicine. Nuclear medicine imaging studies use radioactive compounds called radionuclides of radiopharmaceuticals that emit gamma rays, or some emit beta particles. The chemicals are formulated so that they collect temporarily in the parts of the body to be studied. For most nuclear imaging studies, the radionuclide is injected into the patient; other procedures require that it be inhaled or swallowed. The radiologist chooses the radioactive substance that will produce the best image of the organ or body part under study using the least amount of radiation. Depending on the type of study, the images may be obtained immediately or several hours or days later. The administration of radionuclides for diagnostic procedures is virtually risk-free, but it is not recommended for pregnant women since the fetus appears to be slightly more sensitive to radiation than adults.

The images are taken with a gamma camera suspended above the patient who lies on a table. The camera detects the gamma rays emitted from the radionuclide in the patient's body and uses this information to produce an image that shows the distribution of the radionuclide within the body. The image is recorded on film and is called a scintigram or scan.

Scintigrams of the heart and bone are the two most common nuclear medicine examinations. A cardiac scan is used to evaluate cardiac function and blood flow to the heart muscle. A bone scan (**Fig. 6**) may detect the presence of cancer, infection, or trauma. Other commonly performed radionuclide studies yield scintigrams of the lungs, liver, gallbladder, kidney, thyroid gland, and brain.

Single-photon emission computed tomography. The single-photon emission computed tomography (SPECT) examination uses a computer to obtain two-dimensional images that are thin slices of internal organs such as the heart, brain, and liver. The SPECT images can display organs with much greater detail than conventional scintigrams. Three-dimensional organ displays and cine displays also can be obtained. The cine displays, which resemble moving pictures, are used to evaluate heart muscle contraction.

Positron emission tomography. Positron emission tomography (PET) is a more refined radiologic technique that is used to study the metabolic activity inside an organ. The technique has been shown to be useful in the study of brain-related disorders, such as epilepsy and Alzheimer's disease, and of the vitality of heart tissue.

Interventional procedures. Interventional radiology combines imaging procedures with various injection and catheter techniques to treat tumors, blockages, bleeding vessels, and other abnormalities without extensive surgery. Among the more common interventional procedures is angioplasty, which is used to treat blocked or narrowed arteries. In this procedure a catheter is inserted through the artery to the narrowed segment. There, a balloon at the tip of the catheter is inflated to dilate the narrowed segment. The balloon is then deflated and withdrawn. A combined laser–catheter procedure is also used to treat blocked arteries. The laser vaporizes most of the plaque, and then a balloon is used to dilate any narrowing of the artery.

Interventional radiologists can remove some kidney stones and gallstones by using a specialized

Fig. 6. Bone scan. Typically used to diagnose the spread of cancer or other tumors, it is one of the most common nuclear medicine procedures. (*American College of Radiology*)

catheter as a retrieval device. A catheter can also serve as an aspirator to drain pockets of fluid. *See* RADIOGRAPHY. Michael Lopiano; Raymond Del Fava

Bibliography. D. Avedon, *Electronic Imaging Systems*: *Design Applications and Management*, 1993; D. Avedon, *Introduction to Medical Imaging*, 1993; R. H. Mohiaddin and D. B. Longmore, *Atlas of Whole Body MRI*, 1992; M. F. Sturman, *Effective Medical Imaging*: *A Signs and Symptoms Approach*, 1993.

Medical information systems

Standardized methods of collection, evaluation or verification, storage, and retrieval of data about a patient. The three broad areas of any information system—input, data transformation, and output—suffice to describe an existing system, but they are insufficient to design a new one. To these must be added the action that is expected to take place on the basis of the data output from the system, thereby defining the purpose of the system, and the feedback from such action to the system input, which places the system in a specific medical environment. Crucial to any information system, and especially for a medical system, is the accuracy of the input data, which is of more significance than mere precision. A medical information system is a part of necessary time management that is intended to maximize the amount of data and procedure information in order to make the most accurate clinical decisions. As such, an information management system must be interactive to serve clinical decision purposes.

The medical environment is highly data- and information-intensive. Hospitals have always managed data and information and were pioneers in the use of technologic information systems. With scaled-down technology, medical offices are able to incorporate data and information management in the private-practice environment as well.

Input. Data input is provided by the patient and by other information sources involved. Input information is complex because the patient must be described both cross-sectionally, which is current information, and longitudinally, that is back to childhood and to the parents. Historical information obtainable from the patient is subject to increasing error as the individual goes backward in time. Significant error in the medical information system can arise if imperfect recall is not considered and appropriately discounted and historical data are not weighted according to the psychological status of the patient. Unfortunately, this may be done easily only in retrospect. In addition to retrieving facts, a major function of the physician's historical interview is placing all facts in their true light according to the subject's psychological makeup. Data from outside sources are subject to the same errors; hence it is valuable to obtain objective data rather than subjective data from either input source.

Database systems. The medical record database of the Mayo Clinic in Rochester, Minnesota, is one example of systematic cross-sectional and longitudinal record-keeping efforts. There physicians work with a history of all the patients treated within—and in many cases, outside—the clinic facilities. A standardized coding system is used, and there are two linked segments of the system, medical practice and records: A large referral practice covering every medical and surgical subspecialty, and a primary health care component for the surrounding area residents. All recorded diagnoses made by physicians at the clinic or at affiliated hospitals are indexed. Thus, every formal medical contact of each person (for many from birth to death) is recorded, indexed, and stored in the database. The longitudinal history requires substantiated observation, repeated and confirmed laboratory data, and other facts. The worth of data, however, is dependent on the validity of the information at the time it was acquired.

Mechanical and electronic data collection. Complete and accurate laboratory and procedure data obtained during a cross-sectional evaluation of the patient is the best input for longitudinal patient review and for storage for future retrieval. Thus, the collection of such hard data to confirm, or better, to supplant soft data input is stressed, which means that the data are of the highest quality. Any information system that intends to use engineering technology for processing or storage must stress data acquired directly from a subject by a mechanical or electronic system. Computers and semiautomatic data-gathering systems must serve as dedicated basic components to a complete clinical information system.

Technology provides data on which decisions can be made. The impact of technology on clinical decision making is evident when new techniques are found that can improve the ability to diagnose, cure, or control patients' health problems and concerns. Many technological achievements receive little public notice. For example, because laboratory equipment has become smaller and less expensive to own or operate, private-practice physicians can perform more laboratory tests in their offices. Although the advantage of this to patients is less obvious, in many ways it is even greater than some of the more sophisticated achievements. If a laboratory test result is received quicker, the diagnosis may be quicker so that appropriate therapies can be started, in some cases within the space of one visit to the office.

The goals of technology in the clinical environment are improvement of clinical technique, patient benefit, and cost effectiveness.

In order to achieve these goals, technology must meet the following confidence criteria: (1) Reliability: the degree of assurance that the measurement system will yield reproducible results over a period of time. (2) Reproducibility: that a measurement method applied to an object will yield the same answer over and over again. (3) Precision: that the measurement can be obtained within a reproducible and exacting range. (4) Accuracy: that the numbers produced are precise and relate to some absolute reference point in relationship to a disease. Regardless of the standards used, most assessments of devices by

clinicians focus on whether the device performs as expected. If not, the device has failed.

Characterizing data and information. In most clinical environments, patient-related data and information are stored in a patient's chart. The variety of data required to formulate information to provide medical care includes the following:

- Patient identification data
- Primary medical visit information
  - Patient-described
  - Physician/assistant-described
  - Device-described (laboratory data, electrocardiograph, spirometer, and so on)
  - Action taken (prescription, referral to a specialist, request for additional data such as x-rays, and so on)
- Medical data from other sources
  - Out-of-house laboratory data
  - X-rays
  - Medical information from others (physicians, hospitals, and so on)
  - Observations of others (employers, family members, and so on)
  - Requests for summary of medical information (from nursing care services, insurance companies)
  - Financial data
  - Current bills
  - Ongoing billing
  - Insurance information

The human mind must integrate many of the pieces of these data, at times in a multidimensional sense, but always in a checklist fashion. The goal of a medical information system is to integrate each type of data into a comprehensive, interactive database system. Thus, the medical information system can take care of the checklist and leave people to think, react, and interact creatively. Data gathering, which is performed at the point of decision making by the decision maker (the health care provider), will be subject to less bias when a medical information system provides the checklist for the decision maker.

Much that is considered hard data is subject to error through human reinterpretation; human variability in medical data interpretation is acknowledged to be about 20%. This implies that even the hard output of a laboratory device of known precision and accuracy is softened by the human observer. For example, a computer system reads electrocardiograms with an accuracy of 89% and with the mechanical reliability of the system at 97%. Compounding these two factors results in a performance rating for the total system at 86%. If the system's printout is reinterpreted by an observer with human variability, the performance of the computer–human system decreases further: with 10% human variability, the system could be rated at 77% and with 20% human variability at 68%. This underscores the importance of quality control and the fact that the appropriate role for a human in such circumstances is also to concentrate on that part of the system that cannot be read by the computer.

With increasing use of engineering and other technological advances, the quantity of soft data in use can gradually be diminished. A patient's history of a heart attack, for example, can be accessed, but such a history can be relatively soft data. Hard data would comprise the actual electrocardiogram interpretation by a computer system along with the date of processing. Availability of such minimal information markedly diminishes the need for preserving a large soft-data file of patient-derived information.

In addition to the patient and the data derived directly from the individual, outside sources should also be used to provide information for the medical records, including the family, social service agencies, insurance records, and other medical or clinic records. Actually, surprisingly little data are readily available from outside the immediate family, although in many instances the data may be harder in a factual sense than the patient's data. Since retrieval of such data is often cumbersome and delayed, little benefit is possible to the patient as a result of acquiring it. Regrettably in patient care, a service's value is to a large extent dependent on whether the data are immediately available. Without speed, retrieval can be of little value; hence outside data are little used. Another obstacle that arises in the use of device-generated databases is the lack of comparability standards. For example, a reflectance photometer, which quantitatively measures various serum or plasma constituents as well as blood hemoglobin, is a simple instrument that uses color coding for numerical output in a one-step or two-step process. However, the advantage of its simplicity can be undermined because of the difficulty that is associated with calibration and reliability of resultant values, and also because scales for values of procedures may differ from conventionally used values.

Terminology and nomenclature. Terminology is the language used specifically by a specialized field, and nomenclature is the systematization of that language or vocabulary. In clinical medicine, terminology is well defined and widely used, but the development of a specific nomenclature is essential to useful medical information systems.

Two nomenclature systems that are widely accepted are *Current Procedure Terminology* (CPT) and *International Classification of Diseases* (ICD). The application of the nomenclature, however, requires further standardization, including (1) definition of patient data collection standards; (2) definition of patient identification standards for longitudinal medical records (constrained by computer systems and the perceptions of their programmers); (3) automated conversion of natural language input into machine-oriented language; (4) hierarchy and semantic organization of medical terms; and (5) development of parameters for databases that allow for input and output in a non-machine-oriented mode. If the objective is to develop a bridge between current practices in clinical medicine and interactive databases, the upgrading of

the nomenclature system is important, since terms are the primary carriers of information.

Evaluating databases. Clinical databases can address several evaluation goals, but foremost in medicine is clinical efficacy. In order to assess the worth of a database, three basic aspects must be considered: data collection methods, ongoing management, and output reporting of data. The clinical efficacy of a procedure or technology can be diagnostic, managemental, or prognostic.

The data collected are as good as their collection medium; data obtained with minimal subjectivity and directly from the source are of optimal quality. Database elements must be carefully defined and include descriptions of the patient, test, and outcome. Complete characterization of the patient needs to be made as well, so changes that result from patient management can be identified. The best data are collected by those who have the greatest interest in its completeness, that is, the individuals who are caring for the patient.

Tying data collection to patient care has three advantages: the cost of data collection is reduced by using patient care channels; the physician who is responsible for generating the reports must review the collected data; and the data collection then becomes prospective without extensive chart reviews. When data collection is tied to patient care, the clinicians must be responsible for developing standardized methods to ensure that no time is wasted in collecting useless data and that the reporting methods used do not conflict with those used in reporting patient care. Establishing and maintaining the database is the responsibility of a team headed by the clinicians and including biostatisticians and computer scientists. The clinicians keep the research process focused on the appropriate clinical goals, the biostatisticians analyze the data gathered, and the computer scientists design and employ the appropriate technological systems to achieve the goals of the effort.

Transformation of data. In a medical information system, input information can be processed through one of two parallel, sometimes mutually exclusive routes—administration and medical service organization. Administration encompasses the admitting clerk, administrative officers, pharmacists, and all those who have no direct patient contact. The service route includes the physician, the nurse, and all others who have direct patient contact. The two routes differ in their method and degree of detail. For example, a patient's inability or failure to pay a bill might be considered by the administration in detail in order to set in motion a social service structure. This same information might be of no significance to the nurse or physician, except that the psychological character of the patient is pertinent to the diagnosis or illness under consideration. The passage of such medical information through both routes allows data to reach the output stage. Redundancy, as illustrated by parallel information routes in hospitals, can be a source of economic drain, but a degree of redundancy is necessary for the quality of service required and is a fail-safe feature that is vital to all aspects of quality. Redundancy is particularly important because those in direct contact with the patient are subject to human error or variability. Quality can be maintained by always presenting hard information or by the use of redundancy, but economics may favor redundancy over a constant supply of hard data.

Manufacturers of devices, clinicians (users), engineers, and voluntary and nonvoluntary regulators all have different data requirements even when the object of their evaluation is the same. The principal elements, or uniform terminology, in establishing a database for or evaluation criteria of any problem or device are rationale, principles, population, measurement definitions, protocol, device characteristics, patient characteristics, provider characteristics, format, and outcome. When data are transformed according to these basic elements, each user will be able to answer any questions that arise from the perspective of his or her particular expertise.

Output. The output of a medical information system can be viewed as a control system for actions by clinicians. The output, once it has passed through the transformation media, constitutes the patient's medical records and usually includes the history and physical examination data, progress notes, nursing notes, doctor's orders, and summaries and notations of values from physical laboratory data.

Items from the administrative system are usually not found with the service records. Both represent patient information or input that has been translated through the parallel media of medical personnel and administration, but their separation is indicative of the problems that face planners of good medical information storage and retrieval. Items of output information are interrelated to establish a diagnosis of a course of action. Feedback from that stage to the patient, often in the form of interrelations, can be called patient care.

In addition to its primary function of facilitating patient care, a medical information system can also prove useful for investigation and research into disease and therapy, and the administrative portion of the record can aid in planning future improvements in quality of service. Efficiency should be directed primarily to the medical areas to ensure quality care for the greatest number of patients. *See* DATA COMMUNICATIONS; DATABASE MANAGEMENT SYSTEM; MEDICAL CONTROL SYSTEMS.

Cesar A. Caceres

Bibliography. C. A. Caceres (ed.), *Management and Clinical Engineering*, 1980; C. A. Caceres (ed.), *The Management of Technology in Health and Medical Care,* 1980; C. A. Caceres et al. (eds.), *Medical Devices: Measurement, Quality Assurance, and Standards*, 1983; B. J. Jaeger et al. (eds.), *Multi-Institutional Systems Management*: *Concepts and Cases*, 1987; H. Lamberts and M. Wood, *ICPC International Classification of Primary Care*, 1988; M. Rubin (ed.), *Computerization and Automation in Health Facilities*, 1984; K. Waters and G. Murphy, *Medical Records in Health Information*, 2d ed., 1994.

Medical mycology

The study of fungi (molds and yeasts) that cause human disease. Some pathogenic molds and yeasts normally reside within soil or derive their nutrition from other organic matter until introduced into the body by inhalation or trauma; others are part of the normal body flora or are transmitted from an infected person. Because the immune status of the host plays an important role in susceptibility to fungal infection, highly immunodeficient persons are likely to develop an opportunistic fungal infection. *See* OPPORTUNISTIC INFECTIONS.

Fungal infections are classified according to the site of infection on the body or whether an opportunistic setting is necessary to establish disease. Fungal infections that occur in an opportunistic setting have become more common due to conditions that compromise host defenses, especially cell-mediated immunity. Such conditions include acquired immunodeficiency syndrome (AIDS), cancer, and immunosuppressive therapy to prevent transplant rejection or to control inflammatory syndromes. Additionally, opportunistic fungal infections have become more significant as severely debilitated individuals live longer because of advances in modern medicine, and nosocomial (hospital-acquired) fungal infections are an increasing problem. Early diagnosis with treatment of the fungal infection and control of the predisposing cause are essential.

Antifungal drug therapy is extremely challenging since fungi are eukaryotes, as are their human hosts, leading to a paucity of specific fungal drug targets and also to problems with toxicity or cross-reactivity with host molecules. Most antifungal drugs target the fungal cell membrane or wall. The "gold standard" for therapy of most severe fungal infections is amphotericin B, which binds to ergosterol, a membrane lipid found in most fungi and some other organisms but not in mammals. Unfortunately, minor cross-reactive binding of amphotericin B to cholesterol in mammalian cell membranes can lead to serious toxicity, especially in the kidney where the drug is concentrated. Azole drugs such as ketoconazole interfere with ergosterol biosynthesis by inhibiting the enzyme lanosterol demethylase, but can also cross-react with mammalian P-450 enzymes. Another class of drugs, the echinocandins, inhibit β-glucan synthesis, thereby interfering with a fungal cell wall component not found in mammalian cells. Recent advances in antifungal therapy include the use of liposomal amphotericin B and newer azoles such as fluconazole and itraconazole, which show reduced toxicity or greater specificity. Conversely, drug resistance in pathogenic fungi is an increasing problem, as it is in bacteria.

Opportunistic diseases. Candidiasis is the most common opportunistic fungal infection, and it has also become a major nosocomial infection in hospitalized patients. *Candida albicans* is a dimorphic fungus with a yeast form that is a member of the normal flora of the surface of mucous membranes. In an opportunistic setting, the fungus may proliferate and convert to a hyphal form that invades these tissues, the blood, and other organs. Altered host resistance from different causes usually determines the site of invasion and degree of invasion. Abundant growth on the oral mucosa leads to superficial infection with white patches (thrush). Women, especially those who are diabetic or pregnant, may develop a similar invasion of the surface of the vagina (candida vaginitis). In addition, candidiasis may involve the respiratory or urinary tracts, with colonization followed by serious infection. The disease may extend to the blood or other organs from various infected sites in patients who are suffering from a grave underlying disease or who are immunocompromised.

Aspergilli, which are common saprophytic molds, cause a variety of diseases (aspergillosis). For some individuals, a respiratory tract allergy (allergic rhinitis) develops to airborne spores. For others, asthma may develop. These molds, as well as others, are able to colonize burn wounds and the ear canal and to grow in slowly moving mucus in the bronchi of persons with inhalation allergies (allergic bronchitis) as well as within cavities in the lung caused by tuberculosis (aspergilloma). In severely immune compromised individuals, such as those with acquired immune deficiency syndrome (AIDS) or cancer, eventual extension into surrounding normal tissue or the blood usually follows colonization and can be fatal. Some species of aspergilli produce toxins (aflatoxin) when growing on food (peanut products, stored grain); ingestion of the toxin may result in liver destruction or liver cancer. Toxin-related problems appear more commonly in tropical countries. *See* ACQUIRED IMMUNE DEFICIENCY SYNDROME (AIDS); AFLATOXIN; ALLERGY; ASTHMA.

Mucormycosis, also known as zygomycosis, is an opportunistic fungal disease that can be caused by any of a number of related environmental molds. Most commonly, a ketoacidotic diabetic patient develops a mold infection of the sinus that spreads rapidly to the eye and brain (rhinocerebral mucormycosis). Necrosis of the tissue develops, and the patient dies within only a few days unless the predisposing factors are corrected and therapy is begun.

Cryptococcosis is seen in persons with AIDS, in other immunocompromised persons, and occasionally in individuals with no known predisposing conditions. The infection, which has increased greatly in incidence since 1980, is caused by *Cryptococcus neoformans*, an environmental yeast that grows abundantly in dried pigeon droppings. Respiratory disease follows inhalation of the yeast, and subsequently infection may spread to the brain and other organs. Meningitis and brain abscess are the most frequently seen manifestations of disease. *See* MENINGITIS.

Pneumonia caused by *Pneumocystis carinii* is one of the mostcommon and most serious diseases in AIDS patients and some other immunocompromised populations. This organism has presented challenges in laboratory study and in classification. There is currently no continuous in vitro culture system for *P. carinii*, and consequently most studies depend on passage of the organism in infected laboratory

animals, making it impossible to obtain isolated clonal populations of the organism. It was long considered a protozoan parasite due to its morphology and also to other considerations, such as the presence of cholesterol and lack of ergosterol in its membranes, its consequent insensitivity to amphotericin B, and its sensitivity to some antiprotozoal drugs such as pentamidine. However, it does possess some fungal characteristics, and recently nucleic acid–based typing methods have clearly classified *P. carinii* as a fungus. An environmental reservoir or niche has not been identified, but it is thought that the organism is inhaled by humans very commonly, establishing a significant infection only when the host is severely immunocompromised. The most common clinical manifestation is severe pneumonia with significant respiratory compromise that can be fatal, but the fungus can also disseminate elsewhere in the body.

Nonopportunistic systemic diseases. Healthy persons can acquire disease from certain pathogenic fungi following inhalation of their fungal spores. The so-called deep or systemic mycoses are all caused by different species of soil molds; most infections are unrecognized and produce no or few symptoms. However, in some individuals infection may spread to all parts of the body from the lung, and so treatment with amphotericin B or an antifungal azole drug is essential. The deep mycoses are caused by certain white soil molds that change into either budding yeasts or spherules when growing within the body or in culture at 98.6°F (37°C). Each species of mold has a characteristic pathogenic and saprophytic morphology.

Coccidioides immitis, a mold of desert soil, converts into spherules containing endospores when growing within the body and causes coccidioidomycosis or valley fever. Although 60% of infections produce no symptoms, the other 40% develop symptoms that range from a flulike condition to pneumonia. Of the serious pulmonary infections, 1% spreads to other parts of the body. Meningitis and deep skin or bone lesions often develop.

Histoplasma capsulatum grows in moist, rich soil, often concentrated in areas contaminated by bird or bat droppings, and has a worldwide distribution. In the United States, it is associated mainly with the Mississippi and Ohio river valleys in the Midwest and South. In highly endemic areas, nearly the entire population has been infected. Present or past histoplasmosis in a person is indicated by a positive histoplasmin skin test, which uses an extract of the fungus to detect delayed-type hypersensitivity and is similar to tests for tuberculosis. Once infection has occurred by inhalation of mold spores, the fungus grows as a small budding yeast within mononuclear phagocytes of the body. Most infections produce no symptoms, whereas others bring on symptoms that resemble influenza. A few infected persons develop disseminated disease, with lesions in the spleen, liver, and lymph nodes and ulcerated lesions in the mouth. Once acquired, infection may persist for life even if no symptoms occur after primary exposure, and the persistent infection may reactivate and cause significant disease even years later if the human host becomes immunocompromised.

Blastomycosis and paracoccidioidomycosis are two other deep mycoses. Blastomycosis occurs mostly in the eastern United States; paracoccidioidomycosis is endemic to tropical South and Central America. Following pulmonary infection, widespread ulcerous lesions may develop. In blastomycosis, bone lesions and meningitis often develop, whereas in paracoccidioidomycosis, ulcerated lesions of the mouth and gastrointestinal tract are common. Both diseases are caused by species of pathogenic soil molds that have the specific ability to develop into budding yeasts once they are within the host.

Subcutaneous diseases. Other fungal infections develop when certain species of soil molds are inoculated deep into the subcutaneous tissue, such as by a deep thorn prick or other trauma. A specific type of lesion develops with each fungus as it grows within the tissue. Proper wound hygiene will prevent these infections.

Sporotrichosis, caused by *Sporothrix schenckii*, appears as a chain of ulcerated lesions on the arm or leg following inoculation of a soil mold. Within the infected tissue, the mold converts into a yeast. Unlike other fungi, *Sporothrix* is susceptible to treatment with oral potassium iodide.

Chromoblastomycosis and mycetoma also follow inoculation deep into the skin. Each of these clinical diseases can be caused by multiple fungal agents. Chromoblastomycosis appears as persisting ulcerous or wartlike skin lesions and is caused by any of several kinds of black molds. Mycetoma is a chronic tumorlike lesion that drains small grains (colonies) of a mold or actinomycotic agent and can be caused by a number of black or white molds or actinomycetes. Both diseases require early treatment with specific drugs; the responsible agent must be isolated to permit an appropriate choice of drugs.

Actinomycosis and nocardiosis are two bacterial diseases that are caused by agents having characteristics reminiscent of fungi, such as a branching filamentous structure and the production of similar disease patterns. They require specific laboratory identification so that appropriate antibacterial treatment may be given.

Ringworm. Ringworm, also known as dermatophytosis or tinea, is the most common of all fungal infections. Some species of pathogenic molds can grow in the stratum corneum, the dead outermost layer of the skin. Disease results from host hypersensitivity to the metabolic products of the infecting mold as well as from the actual fungal invasion. Tinea corporis, ringworm of the body, appears as a lesion on smooth skin and has a red, circular margin that contains vesicles. The lesion heals with central clearing as the margin advances. On thick stratum corneum, such as the interdigital spaces of the feet, the red, itching lesions, known as athlete's foot or tinea pedis, become more serious if secondary bacterial infection develops. The ringworm fungi may also invade the

hair shaft (tinea capitis) or the nail (onychomycosis). Many pharmaceutical agents are available to treat or arrest such infections, but control of transmission to others is important. *See* FUNGI; YEAST.

Carlyn Halde; Jon P. Woods

Bibliography. N. M. Ampel, Emerging disease issues and fungal pathogens associated with HIV infection, *Emerging Infect. Dis.*, 2:109–116, 1996; E. J. Anaissie (ed.), Focus on fungal infections 5, *Clin. Infect. Dis.*, 22(suppl. 2):S71–S184, 1996; G. S. Deepe, Jr., Prospects for the development of fungal vaccines, *Clin. Microbiol. Rev.*, 10:585–596, 1997; S. K. Fridkin and W. R. Jarvis, Epidemiology of nosocomial fungal infections, *Clin. Microbiol. Rev.*, 9:499–511, 1996; N. H. Georgopapadakou and J. S. Tkacz, The fungal cell wall as a drug target, *Trends Microbiol.*, 3:98–104, 1995; S. L. Newman, Macrophages in host defense against *Histoplasma capsulatum, Trends Microbiol.*, 7:67–71, 1999; D. J. Sheehan, C. A. Hitchcock, and C. M. Sibley, Current and emerging azole antifungal agents, *Clin. Microbiol. Rev.*, 12:40–79, 1999; J. W. Taylor et al., The evolutionary biology and population genetics underlying fungal strain typing, *Clin. Microbiol. Rev.*, 12:126–146, 1999.

Medical parasitology

The study of diseases of humans caused by parasitic agents. It is commonly limited to parasitic worms (helminths) and the protozoa (see **table**). Current usage places the various nonprotozoan microbes in distinct disciplines, such as virology, rickettsiology, and bacteriology. Medical entomology, a branch of medical parasitology, deals with insects that serve as intermediate hosts or vectors of parasites, as well as the noxious effects of the insects themselves. Ticks, mites, and other noninsect arthropods are often included, although they are more accurately combined with insects in the field of medical arthropodology.

Nematodes. The roundworms form an extremely large yet fairly homogeneous assemblage, most of which are free-living (nonparasitic), and are found in virtually every soil and aquatic habitat. Many are also plant parasites, and a large number have become adapted to living parasitically within nearly all vertebrates. Some parasitic nematodes, however, may cause disease in humans (zoonosis), and others cause disease limited to human hosts (anthroponosis). Among the latter, several are enormously abundant and widespread. *See* NEMATA.

Intestinal nematodes. The giant roundworm (*Ascaris lumbricoides*) parasitizes the small intestine, probably affecting over a billion people; and the whipworm (*Trichuris trichiura*) infects the human colon, probably affecting a half billion people throughout the tropics. Similarly, the hookworms of humans, *Necator americanus* in the Americas and the tropical regions of Africa and Asia, and *Ancylostoma duodenale* in temperate Asia, the Mediterranean, and Middle East, suck blood from the small intestine and cause major debilitation, especially among the undernourished. The human pinworm (*Enterobius vermicularis*) infects the large intestine of millions of urban dwellers. Its eggs, viable shortly after being laid on perianal skin, are readily transmitted from hand to mouth and rarely are passed in the stool, and so they are not destroyed in flush-toilet sanitary systems. In contrast, the other intestinal nematodes, which require a period of egg maturation outside the human host before they are infective, are associated with fecal contamination of soil or food crops and are primarily rural in distribution. The small roundworm of humans, *Strongyloides stercoralis*, has three methods of infections: (1) skin penetration by infective third-stage larvae (the method also used by hookworms); (2) penetration by infective larvae after a period of multiplication as adult nonparasitic worms in the soil, whose progeny eventually revert to penetrating larvae; or (3) internal penetration of the gut of immunosuppressed or heavily exposed individuals. This internal infection can be extremely hazardous and even fatal, or it may persist for many years.

Tissue-infecting nematodes. The nonintestinal nematodes are spread by complex life cycles that usually involve bloodsucking insects, such as mosquitos, deerflies, blackflies, or midges. One exception is the guinea worm (*Dracunculus medinensis*), a skin-infecting 2–3-ft (0.6–1-m) worm transmitted by aquatic microcrustaceans (water fleas or copepods) that are ingested in drinking water that has been contaminated by larvae that escape from the skin sores of infected humans. Such bizarre life cycles are typical of many helminths. Other nematodes of humans include (1) the filarial worms, which are transmitted by mosquitoes and may induce enormously enlarged fibrous masses in legs, arms, or genitalia (elephantiasis), and (2) *Onchocerca volvulus*, which is transmitted by blackflies (genus *Simulium*) and forms microscopic embryos (microfilariae) in the eyes causing high incidence of blindness in Africa and parts of central and northern South America.

A more familiar tissue-infecting nematode of temperate regions is *Trichinella spiralis*, the pork or trichina worm, which is the agent of trichinosis. The tiny spiraled larvae encyst in the muscle of pigs, rats, bears, and even Arctic seals and can carry the infection to humans and other carnivorous mammals who eat raw or undercooked infected meat.

Trematodes. Parasites of the class Trematoda vary greatly in size, form, location in the human host, and disease produced, but all go through an initial developmental period in specific kinds of fresh-water snails, where they multiply as highly modified larvae of different types. Ultimately, an infective larval stage (cercaria) escapes in large numbers from the snail and continues the life cycle. Each trematode species follows a highly specific pathway from snail to human host, usually by means of another host or transport mechanism.

Heterophyes heterophyes, the minute intestinal fluke, is transmitted to humans through various fresh-water or estuarine fish eaten raw or undercooked.

The oriental liver fluke (*Clonorchis sinensis*) also infects humans by way of fish, usually the carp, in which the cercariae encyst. Related fish-borne trematodes in the genus *Opisthorchis* also infect the human liver and can survive pickling or even drying of the fish. The human lung fluke (*Paragonimus*) infects the human lung after the encysted cercariae in raw crayfish or freshwater crabs are eaten. Other trematode cercariae swim from their host snails and encyst on aquatic vegetation. The sheep liver fluke [*Fasciola hepatica* (*F. gigantea* in Africa)] may also infect humans, and the giant intestinal fluke (*Fasciolopsis buski*) infects humans (and pigs) in China and Southeast Asia after they ingest infected water chestnuts or other aquatic vegetation. Another important group of trematodes is the blood flukes of the genus *Schistosoma*. *See* SCHISTOSOMIASIS; TREMATODA.

Cestodes. Tapeworms, the other great assemblage of parasitic flatworms, parasitize most vertebrates, with eight or more species found in humans. Their flat ribbonlike body form consists of a chain of hermaphroditic segments. Like the trematodes, their life cycles are complex, although not dependent on a snail host. The enormous beef tapeworm of humans, *Taenia saginata*, is transmitted by infected beef ("measly beef") from cattle that grazed where human feces containing egg-filled tapeworm segments contaminated the soil.

The pork tapeworm (*T. solium*) similarly reaches humans through pork infected after the pig injested human feces that contained the tapeworm segments. Humans can also be infected (usually by drinking contaminated water) from *T. solium* eggs passed in human feces as well as from meat infected with the larvae. The eggs can hatch in the human gut, penetrate the gut wall, and encyst in various tissues, forming cysticerci as in the pig. The resulting disease, cysticercosis, is characterized by scattered and potentially lethal cysticerci, which develop chiefly in the brain, eye, or muscle tissues.

Another tapeworm that infects humans as an intermediate host is the dog tapeworm (*Echinococcus granulosus*) from sheep. In the sheep (or human) the egg hatches in the gut, and larva penetrates the tissues and forms a massive spherical encysted body (hydatid cyst) in the viscera. The hydatid is filled with fluid and forms many thousands of heads (scoleces) of the future adult worms. These can only develop in the dog intestine after the animal eats a cyst in sheep viscera. The dogs's droppings then contain many eggs, which can infect sheep or humans, who may ingest eggs after petting or handling an infected dog. The result is human echinococcosis or hydatid disease.

One common tapeworm of humans seen more frequently in temperate than in tropical regions is *Diphyllobothrium latum*, the broad or fish tapeworm. It reaches monumental size, sometimes 30 ft (10 m) with segments up to 0.8 in. (2 cm) wide; and among some peoples, especially the Finns, a vitamin B_{12} deficiency may develop. If the eggs, which are passed in the feces of an infected person, are discharged into fresh water, they can develop, hatch, be ingested by a water flea (copepod), and form an early larval stage inside the water flea. The small fish that commonly feed on copepods may in turn become infected, with the worm larva progressing into another larval stage, the plerocercoid. The small fish can be eaten by a larger one and in turn a still larger one until the end of the fish food chain—usually a bass, pickerel, or pike—is reached. In each fish host, the worm migrates to the muscles, where it remains unencysted until the fish is eaten by another host. A human or other fish-eating mammal feeding on the fish in raw, undercooked, pickled, or smoked form can acquire the worm, which grows to its full size in the gut in about 3 months. With most tapeworm infections, though, drugs are available to kill and eliminate the worm. If the worm merely breaks, however, leaving the head and anterior segments attached, it can regenerate its original length in 2–3 months. *See* CESTODA.

Protozoa. Protozoa that can infect humans are found in the intestine, various tissues and organs, and the bloodstream. *See* PROTOZOA.

Intestinal protozoa. Of the many protozoa that can reside in the human gut, only the invasive strain of *Entamoeba histolytica* causes serious disease. This parasite, ingested in water contaminated with human feces containing viable cysts of *E. histolytica*, can cause the disease amebiasis, which in its most severe form is known as amebic dysentery. Occasionally, the infection will spread by way of the intestinal veins to the liver, where the amebas can cause hepatic amebiasis, or can spread to other organs as well. In spite of this capacity to invade tissues, most *E. histolytica* remain in the gut lumen as nonpathogenic infections. Another common waterborne intestinal protozoon is the flagellate *Giardia lamblia*, which causes giardiasis, a mild to occasionally serious or long-lasting diarrhea. Campers or skiers may acquire it from animal-fouled water. Human sources frequently initiate outbreaks within institutions, and play or preschool groups are especially prone to a rapidly spreading infection. *See* GIARDIASIS.

Tissue protozoa. Other flagellate parasites infect the human skin, bloodstream, brain, and viscera. The tsetse fly of Africa carries to humans the blood-infecting agents of trypanosomiasis, or African sleeping sickness, *Trypanosoma brucei gambiense* and *T. brucei rhodesiense*. Domesticated animals can suffer from a form of trypanosomiasis as well. The infection can be fatal if the parasites cross the blood–brain barrier, a rare event among infected wild animals, chiefly antelopes and wild pigs, but more common in humans or domestic animals. In Latin America, the flagellate *T. cruzi* is the agent of Chagas' disease, a major cause of debilitation and premature heart disease among those who are poorly housed. The infection is transmitted in the liquid feces of a conenose bug (genus *Triatoma*) and related insects. The infective material is thought to be scratched into the skin or rubbed in the eye, especially by sleeping children. *See* TRYPANOSOMATIDAE.

Clinical aspects of parasitic diseases in humans and biology of disease-producing parasites

Disease (species)	Vector or intermediate host	Infectious stage	Mechanism of infection	Pathology
INTESTINAL PROTOZOA				
Amebiasis (*Entamoeba histolytica*)	None	Four-nucleated cysts (gives eight trophozoites)	Fecal contamination of water or food or oral-anal contact	Most are asymptomatic; 10% show diarrhea, dysentery, ulceration, amebic dysentery, flask-shaped ulcers with lysis and destruction of white blood cells; 1% have liver abscess with anchovy paste pus; other organs can be infected by hematologic destruction; may cause immunosuppression
Balantidiasis (*Balantidium coli*)	None	Cyst	Reservoir (pig) contact with humans; fecal-oral path	Usually in colon lumen; harmless; may ingest host submucosa and cause ulceration in immunosuppressed patients, may cause dome-shaped necrotic ulcer with bowel gangrene and death
Dientamoeba fragilis infection (*Dientamoeba fragilis*)	Possibly within *Enterobius vermicularis* eggs	Trophozoite (no cyst form)	Probably by fecal contamination of food or water; direct contact	Rare pathology; dysentery; flatulence
Trichomoniasis (*Trichomonas vaginalis*)	None	Trophozoite (no cysts)	Sexual transmission	Males are usually asymptomatic; females have vaginal itching and burning, and thick, yellow, blood-tinged discharge
Giardiasis (*Giardia lamblia*)	None	Cyst	Water (organism is not killed by normal chlorination)	Flattened villi in lumen of small intestine; malabsorption, especially of fat; frothy, fatty feces; flatulence; diarrhea, cramping, weight loss
BLOOD AND TISSUE FLAGELLATES				
West African trypanosomiasis [sleeping sickness] (*Trypanosoma brucei* or *T. gambiense*)	*Glossina palpalis* (riverine tsetse fly); both sexes bite; humans only (not zoonosis)	Metacyclic trypomastigote	Tsetse bite lacerates skin; tsetse is "pool feeder"	Exhausts host's antibody production because stumpy form changes antigenic coat every week or so; leptomeningitis, cerebral edema, inflammation with perivascular cuffing; crosses blood–brain barrier to cause sleeping sickness; fatal in 2 years
East African trypanosomiasis [sleeping sickness] (*Trypanosoma brucei* or *T. rhodesiense*)	*Glossina morsitans* (savanna tsetse fly) both sexes bite; antelopes and wild pigs may serve as reservoir hosts (bushbuck is directly implicated); many animals are infected	Metacyclic trypomastigote	Tsetse bite lacerates skin; tsetse is "pool feeder"	Exhausts host's antibody production because stumpy forms change antigenic coat as endless sequence; crosses blood–brain barrier to cause sleeping sickness; fatal in 3–12 months.
Chagas' disease (*Trypanosoma cruzi*)	*Rhodnius* or *Triatoma* species of true bugs (conenose bugs); many reservoir hosts including rodents, armadillo, dogs, etc. (zoonosis)	Trypomastigote in bug feces	Bug feces or vomitus rubbed into bite or eye; blood transfusion; sexual or transplacental transmission	Acute: inflammatory reaction; chronic: tissue destruction of heart, with aneurysm at apex, megaesophagus and megacolon caused by destruction of mesenteric plexuses
Oriental sore, Old World cutaneous leishmaniasis (*Leishmania tropica*)	*Phlebotomus* sand fly (female); no reservoir but humans (anthroponosis)	Promastigote from bite of infected sand fly	Sand fly injection of promastigotes; amastigotes live within vacuole in macrophage, multiply, break out, invade, and are ingested by new macrophages; infected mass of macrophages induce skin lesion with specific characteristics varying with strain or species	Rolled-edge "dry lesion" ulcer with self cure in 1–2 years and immunity only to *L. tropica;* hyperimmune (sensitized) recidivans form in Middle East: incurable granuloma continuously producing satellite lesions and scars
Zoonotic Old World cutaneous leishmaniasis (*Leishmania major*)	*Phlebotomus* sand fly; rodents are usual reservoir hosts (zoonosis)	Promastigote from bite of infected sand fly	Sand fly injection of promastigotes; amastigotes live within vacuole in macrophage, multiply, break out, invade, and are ingested by new macrophages; infected mass of macrophages induce skin lesion with specific characteristics	Rolled-edge "wet lesion" ulcer; usually self cure, then immunity to both *Leishmania major* and *L. tropica* after 6–12 months
Kala azar or visceral leishmaniasis (*Leishmania donovani*)	*Phlebotomus* (Old World) or *Lutzomyia* (New World) sand flies	Promastigote	Injected by infected sand fly; promastigotes change to amastigotes in macrophage, concentrate in spleen, liver, bone marrow (not skin as in cutaneous leishmaniasis)	Splenomegaly, hepatomegaly, leukopenia, wasting, usually death if not treated

Stage that causes pathology	Treatment	Geographic area	Diagnosis
Trophozoite	Diiodohydroxyquin; diloxanide furoate; metronidazole; paromomycin; dehydroemetine	Worldwide, wherever fecal contamination occurs	Cysts or trophozoites in ova and parasite preparation made three times on alternate days; red blood cells in trophozoites suggest pathology
Ciliated trophozoite	Tetracycline	Worldwide, especially in pig-raising areas	Trophozoites or cysts detected in stool culture
Trophozoite	Iodoquinol; tetracycline; paromomycin	Cosmopolitan	Trophozoite in stool
Trophozoite	Metronidazole for both partners	Ubiquitous in sexually active populations	Microscopic examination of urine, discharge, or scraping with normal saline plus methylene blue or liquid culture; Pap test
Trophozoite	Metronidazole; quinacrine	Ubiquitous among campers, skiers, dogs, and wild animals	Fatty diarrhea; trophozoites or cysts in stool; string test on duodenal contents
Trypomastigote stage is found in human blood (extracellular); sleeping sickness sets in after blood–brain barrier is crossed	Hemolytic stage: suramin sodium; late central nervous system involvement: melarsoprol	West African vegetation around rivers	Trypanosomes in blood, cerebrospinal fluid, lymph node aspirate
Trypomastigote stage found in human blood (extracellular) may have direct toxic effect; sleeping sickness sets in after blood–brain barrier is crossed	Hemolytic stage: suramin sodium; late central nervous system involvement: melarsoprol	East Africa	Enlargement of posterior cervical lymph nodes (Winterbottom's sign); blood smear or concentrate
Amastigotes in heart or parasympathetic ganglia cells	Nifurtimox	Latin America (thatched roofs, mud cracks)	Romaña's sign at chagoma (primary lesion); C-shaped trypomastigote in blood; gastric biopsy; xenodiagnosis
Amastigotes (always in macrophage)	Stibogluconate sodium (recidivans form may respond only to heat compresses over several weeks)	Old World: Middle East, India, Africa, former Soviet Union	Needle biopsy at edge of ulcer or culture of scraping
Amastigotes (always in macrophage)	Stibogluconate sodium	Old World: Middle East, India, Africa, former Soviet Union	Needle biopsy at edge of ulcer or culture of scraping
Amastigotes (always in macrophage)	Stibogluconate sodium (post-kala azar dermal leishmaniasis 1–3 years after treatment common in India)	Mediterranean area, Sudan, Kenya, India, China, former Soviet Union, South America	Touch preparation on slide or punch biopsy of spleen or liver or bone-marrow aspirate cultured on blood agar; hyperglobulinemia and no skin reaction during active disease; serodiagnosis by complement fixation, indirect hemagglutination, immunofluorescent assay, or enzyme-linked immunosorbent assay tests

Clinical aspects of parasitic diseases in humans and biology of disease-producing parasites (*cont.*)

Disease (species)	Vector or intermediate host	Infectious stage	Mechanism of infection	Pathology
BLOOD AND TISSUE FLAGELLATES (*cont.*)				
New World cutaneous leishmaniasis (*Leishmania mexicana* complex)	*Lutzomyia* (New World) sand fly; many reservoir hosts, including arboreal mammals (zoonosis)	Promastigote	Sand fly injection of promastigotes; amastigotes live within vacuole in macrophage, multiply, break out, invade, and are ingested by new macrophages; infected mass of macrophages induces skin lesion with specific characteristics; chicle pickers in Yucatan can be infected by bite to ear	Rolled-edge ulcer; immunity to *Leishmania mexicana* only
Mucocutaneous leishmaniasis (*Leishmania braziliensis* complex)	*Lutzomyia* (New World) sand fly; reservoir hosts are monkeys and arboreal rodents (zoonosis)	Promastigote	Sand fly injection of promastigotes; amastigotes live within vacole in macrophage, multiply, break out, invade, and are ingested by new macrophages; infected mass of macrophages induces skin lesion with specific characteristics	Typical lesion, but 3–20 years after primary lesion, may destroy septum in up to 30% or destroy entire face, with death by starvation or asphyxiation; immunity to *Leishmania braziliensis* (if patient survives) or to *L. mexicana* as well (but not to *L. donovani*)
MALARIA AND ALLIED SPOROZOA				
Malignant tertian malaria (*Plasmodium falciparum*)	Female *Anopheles* mosquito (many species); habits vary, an important factor in control	Sporozoites	Enter liver from inoculation into bloodstream by infected mosquito; no relapse	Chills and fever; splenomegaly; severe anemia; disseminated intravascular coagulation; cerebral malaria; blackwater fever; hemoglobinurea; vast numbers of red blood cells are infected and made sticky; stem cells are also destroyed
Benign tertian malaria (*Plasmodium vivax*)	Female *Anopheles* mosquito (many species); habits vary, an important factor in control	Sporozoites	Enter liver from inoculation into bloodstream by infected mosquito; can relapse from hypnozoites in liver	Chills and fever; anemia; splenomegaly
Ovale malaria (*Plasmodium ovale*)	Female *Anopheles* mosquito	Sporozoites	Enter liver from inoculation into bloodstream by infected mosquito; can relapse from hypnozoites in liver	Chills and fever; anemia; splenomegaly
Quartan or malariae malaria (*Plasmodium malariae*)	Female *Anopheles* mosquito	Sporozoites	Enter liver from inoculation into bloodstream by infected mosquito; no relapse, but recrudescence from unknown source, possibly bloodstream	Chills and fever; anemia; splenomegaly; nephrotic syndrome
Toxoplasmosis (*Toxoplasma gondii*)	Cat/mouse is normal cycle; cat is only definitive host; humans and others are intermediate hosts; human is dead-end host	Oocysts from cat feces or cysts in meat; sporozoites relesed in human intestine from cat oocysts; merozoites released from tissue cysts; both penetrate gut, multiply as tachyzoites, encyst in central nervous system or other tissues as tissue cysts with bradyzoites	Ingestion of undercooked meat or fecal-oral exposure from cat litter	Usually strong T-cell-mediated host defense and usually no pathology; fetal central nervous system is invaded if mother is not immune before conceiving, leading to hydrocephalus and cerebral calcification, choroidoretinitis resulting in blindness; possible stillbirth; fatal to immunosuppressed patients; rare retinitis in normal adult, usually with flulike syndrome
Cryptosporiodiosis (*Cryptosporidium* spp.)	One-host cycle, but cattle and possibly others ae reservoir hosts	Sporozoites in oocysts (four per cyst); no sporocyst enclosing sporozoites	Ingestion of cysts, probably by fecal contamination	All stages found in brush border of mucosal epithelia, therefore intracellular; usually mild diarrhea or asymptomatic; in immunosuppressed or immuno-incompetent patients, causes intractable diarrhea
Pneumocystis pneumonia [now reclassified as a fungus] (*Pneumocystis carinii*)	No known vector; reservoir host is unknown	Cysts	Possibly air-borne	Mild or asymptomatic except in immuno-suppressed patients; causes intractable pneumonitis; plasma cell interstitial pneumonitis in premature infants

Stage that causes pathology	Treatment	Geographic area	Diagnosis
Amastigotes (always in macrophage)	Stibogluconate sodium	New World: Mexico, Latin America; disseminated leishmaniasis in Ethiopia and Venezuela induces specific anergy (distinctive syndrome)	Needle biopsy at edge of ulcer or culture of scraping
Amastigotes (always in macrophage)	Stibogluconate sodium; amphotericin B; treatment often unsatisfactory	Amazon basin	Needle biopsy at edge of ulcer or culture of scraping; serodiagnosis is also possible
Merozoite	Prophylaxis: chloroquine; in resistant areas, add daily proguanil or doxycycline; treatment: chloroquine; if resistant, fansidar or quinine (or quinidine); if comatose, intravenous quinine (or quinidine)	All tropics, but especially sub-Saharan Africa	Thick and thin blood smears with ring stage and gametocytes (latter is sausage-shaped); no other stages in peripheral blood (infected cells with trophozoites, adhere to endothelium)
Merozoite	Prophylaxis: chloroquine + primaquine for release (after return); treatment: chloroquine (no resistance observed yet)	Tropics except where *Plasmodium ovale* is found	Schüffner's dots, enlarged host red blood cells with enlarged round gametocytes
Merozoite	Prophylaxis: chloroquine + primaquine (after departure from endemic area); treatment: chloroquine (resistance reported)	Tropical Africa	Same as with *Plasmodium vivax,* but dots appear at earlier stage and red blood cells are often oval and fimbriated (jagged) at one end
Merozoite	Prophylaxis: chloroquine; treatment: chloroquine (no resistance observed yet)	Tropics	Trophozoites are often band-shaped across red blood cell; host cell is not enlarged and no Schüffner's dots are produced; gametocytes are found in nonenlarged red blood cells
Tachyzoites in macrophage or other host cells free in body cavity; bradyzoites fill tissue cysts	Trimethoprimsulfamethoxazole	Ubiquitous; about 40% among humans (mostly asymptomatic)	Serologic tests; xenodiagnosis using mouse inoculation
Merozoite	None satisfactory	Ubiquitous, especially in cattle-raising areas	Stool, seen after special stain or search for minute bodies; mucosal biopsy
Trophozoite	Trimethoprimsulfamethoxazole chemoprophylaxis as nasal-lung aerosol	Universal; perhaps 20–30% of humans	Cysts in sputum sample

Clinical aspects of parasitic diseases in humans and biology of disease-producing parasites *(cont.)*

Disease (species)	Vector or intermediate host	Infectious stage	Mechanism of infection	Pathology
INTESTINAL NEMATODES				
Enterobiasis (*Enterobius vernicularis,* pinworm)	None	Embryonated egg (within 4 h after laid in perianal folds or around anus)	Anal-oral route; eggs in bedding go into air, spread via diaper contact; adults live 2–3 weeks in terminal colon after eggs hatch in duodenum	Symptom-free pruritis; occasional allergic response; possible cause of appendicitis; may cause pelvic inflammatory disease, sleep loss, neurological symptoms
Trichuriasis (*Trichuris trichiura,* whipworm)	None; eggs in soil stick to vegetables or are found in contaminated water	Embryonated egg (after 4–6 weeks in soil); eggs can survive 1–2 years	Ingestion of egg on contaminated vegetables or in water; adults remain in colon (no systemic migration), live up to 9 months	Mild bleeding, diarrhea; with heavy infection, anal prolapse when circular muscles contract spontaneously
Ascariasis (*Ascaris lumbricoides,* giant roundworm)	None; eggs in soil stick to vegetables or are found in contaminated water	Embryonated egg (after 4–6 weeks in soil); eggs can survive 5–10 years in soil	Eggs on contaminated vegetables or in water ingested; hatch in duodenum; larvae penetrate mucosa, carried by circulation to heart and lungs, where they penetrate alveoli, molt, migrate up air ducts to mouth, are swallowed, mature, and mate in small intestine; can live 1 year	Pneumonitis after second infection; hypersensitivity reaction to larvae migrating through lungs; adult may occasionally perforate bowel or obstruct duct openings (bile, pancreatic ducts, inner ear)
Hookworm disease (*Necator americanis* or *Ancylostoma duodenale*)	None	Filariform larva develops in soil	Penetrate skin; carried in bloodstream to lungs and trachea; swallowed; adults in small intestine suck blood from villi; live 1–4 years	Anemia; mucosal scars; possible hypersensitivity with eosinophilia after repeated infections
Stronglyoidiasis (*Strongyloides stercoralis,* small human roundworm)	None; can be free-living in soil	Filariform larvae penetrate skin (from soil); can autoreinfect, especially in immunosuppressed patients	Direct contact of skin with contaminated soil; infection can last a lifetime	Diarrhea, especially with heavy infection; malabsorption; eosinophilia and pneumonitis during larval migration; secondary autoreinfection a major cause of severe pathology and long infection (20–30 years)
Trichinosis (*Trichinella spiralis*)	None	Larvae are ingested with pork, bear, or other animal flesh	Eating undercooked pork; adults mature in small intestine, newborn larvae migrate to muscle fibers, rarely to brain and heart; may be from bear meat or other sources	Secondary infection due to enteric flora; petechial hemorrhages, eosinophilia; periorbital edema; after 7 days, larvae in muscle host cells turn into "nurse cells"
TISSUE-INFECTING NEMATODES				
Filariasis (*Wuchereria bancrofti, Brugia malayi, B. timori*)	Female mosquitoes of *Aedes, Anopheles, Mansonia,* and *Culex* species	Mosquito bites; larvae deposited on skin enter bite wound, migrate to lymph node, mature, mate, produce microfilariae after 1 year	Adults mature in lymphatics; microfilariae stay in lung capillaries during day and peripheral blood at night, where they are available to mosquitoes (nocturnal periodicity)	Elephantiasis in about 10% of cases after years of hypersensitivity; reaction to adults include pain, enlargement, swelling, lymphangina, lymphadenitis, lymphedema, massive fibrosis of genitalia and limbs (elephantiasis)
Onchocerciasis [river blindness] (*Onchocerca volvulus*)	Blackfly (*Simulium damnosum* and other species)	Blackfly takes a blood meal; larvae crawl into bite or hair follicle; mature in 1 year	Adults develop and live in subcutaneous tissues, form dermal nodules; (New World: upper body; Old World: lower body); microfilariae in interstitial fluid are the cause of major pathology in skin and eyes	"Elephant" or "leopard" skin; microfilariae destroy elastic fibers; partial depigmentation; iritis leads to secondary glaucoma, snowflake opacities, corneal and retinal damage, blindness, all caused by reaction to microfilariae in vitreous (after 3–7 years)
Dracunculiasis (*Dracunculus medinensis*)	*Cyclops* species copepods or water fleas	Larva	Drinking water from step-in well, infected by *Cyclops;* larvae are liberated in gut; in 1 year, female travels to deep subcutaneous tissues in leg, lives head-down; induces blister to form around head, which breaks open with cold water; female ejects motile larvae into water	Blisters, ulcers; allergic reaction
CESTODES				
Taeniasis saginata (*Taenia saginata,* beef tapeworm)	Cattle	Cysticerci in beef	Ingestion of undercooked beef	Little pathology; epigastric fullness; nausea; loss of appetite

Stage that causes pathology	Treatment	Geographic area	Diagnosis
Adult: in descending colon, pass through anus to lay eggs in perianal folds	Mebendazole	Ubiquitous in urban crowded conditions; higher incidence in children	Cellophane tape across anus, at night or early morning
Adult	Mebendazole	Worldwide, including tropical areas of southern United States	Eggs in stool; Charcot-Leyden crystals
Larva, adult	Mebendazole	Worldwide	Eggs in stool
Adult worms with cutting plates (*Necator*); adults with daggerlike teeth (*Ancylostoma*)	Mebendazole	*N. americanis:* New World, all tropics; *A duodenale:* Old World, north temperate zones	Unembryonated eggs in stool (usually four-cell stage)
Adult, larva	Thiabendazole	Tropics and subtropics	Rhabditiform larvae in stool
Larval migration and penetration of red muscle fibers; subsequent sensitization and possible toxic effects; strong immunity is induced	Thiabendazole + steroids for severe cases	Wherever pork is consumed	High pork consumption, eosinophilia after 2 weeks; immunologic tests
Adult	Diethylcarbamazine, with care for hypersensitization reaction	Africa, Southeast Asia, New Guinea, South Pacific	Microfilariae in peripheral blood at night (nocturnal periodicity)
Microfilariae in interstitial fluid (not in bloodstream)	Ivermectin	Fast-running streams in Central America and tropical Africa (especially West Africa)	Skin snip shows microfilariae
Adult female; broken worm may cause anaphylaxis	Niridazole; extraction by winding on a stick	Equatorial Africa (rain pools in West Africa); Middle East, India (step-in wells); South America	Head of worm in skin blister; often ulceration if improperly treated
Adult	Niclosamide; praziquantel	Africa, Mexico, Argentina, Europe, United States (beef-eating areas)	Proglottid in stool with more than 12 branches per side of uterus
Adult	Niclosamide; praziquantel	Worldwide in pork-eating populations, especially Latin America	Proglottid in stool with 5–10 branches per side of uterus

Clinical aspects of parasitic diseases in humans and biology of disease-producing parasites *(cont.)*

Disease (species)	Vector or intermediate host	Infectious stage	Mechanism of infection	Pathology
CESTODES (*cont.*)				
Cysticercosis (*Taenia solium*)	Human is accidental abnormal intermediate host (normally is final host)	Eggs develop cysticerci in tissues, either cutaneous or subcutaneous, occasionally in eye	Fecal contamination of water or possible internal reinfection via hatching of eggs in gut	Seizure from cysticerci in brain; eye/muscle space-occupying lesions; calcification after inflammatory reaction
Echinococcosis; unilocular hydatid disease (*Echinococcus granulosus*)	Sheep and dog are intermediate and final host pair; humans can become intermediate host; only dog is final host	Egg	Ingestion of eggs from dog feces on fur or by contaminated water	Eggs hatch, release larvae, which penetrate gut; cysts grow in liver, eye, brain, other organs covered with laminated membrane; form unilocular hydatid cyst
Diphyllobothriasis; broad or fish tapeworm disease (*Diphyllobothrium latum*)	Copepod (water flea) is eaten by fresh-water fish (secondary host); passes through series of fish, from minnow to bass, pike, etc.	Pleurocercoid larva in fish muscle	Ingestion of raw or undercooked fish	Adult lives in small intestine, grows to about 30 ft (10 m), absorbs vitamin B_{12}; rarely may cause pernicious anemia
TREMATODES				
Fasciolopsiasis (*Fasciolopsis buski*)	Fresh-water snail (*Segmentina hippeutis*)	Metacercariae on husks of water chestnut, talpa, and other fresh-water edible plants	Removing water chestnut husk with teeth	Feeds on columnar epithelial cells of intestine; can obstruct ampulla of Vater, common bile duct, small intestine
Fascioliasis (*Fasciola hepatica; F. gigantica*)	Fresh-water snail (*Lymnaea* sp.)	Metacercariae on watercress or other aquatic plants; juveniles penetrate through gut wall and liver into bile ducts	Eating vegetables with metacercariae; possibly by drinking water draining from pasture	Adults live in liver, feed on hepatocytes and blood; cause colic, abscesses; in Middle East, causes halzoun (adult on pharyngeal wall from eating raw liver; worms crawl up from stomach to pharynx)
Clonorchiasis (*Clonorchis sinensis*)	Fresh-water snail (species of operculate snails)	Metacercariae in fish muscle; juveniles migrate via common bile duct to liver	Eating undercooked fish with metacercariae	Adults live in bile ducts, cause inflammation; mild disease, except in heavy infection
Heterophyiasis (*Heterophyes heterophyes*)	Fresh- or brackish-water snail (*Pironella* in Egypt, *Cerethidea* in Japan)	Metacercariae in fish muscle; juveniles migrate to intestine	Eating undercooked infected fish	Diarrhea; rarely eggs get into circulation, cause granulomas to form in heart and brain
Paragonimiasis (*Paragonimus* species, especially *P. westermani,* human lung fluke)	Fresh-water snail (*Semisulcospira brotia*)	Metacercariae on crab or crayfish	Eating undercooked crab or crayfish	In lung, fibrotic lesions, hemoptysis, dyspnea, pleural pain; secondary abscesses, occasionally in brain
Schistosomiasis (*Schistosoma haematobium*)	Fresh-water snail (*Bulinus* species)	Cercariae	Cercariae enter skin from water, migrate to liver; adults live in venous plexus around bladder for 5–8 years	Eggs caught in tissues produce T-cell-dependent granulomas; bladder calcification, hydroureter, and hydronephrosis often associated with bladder cancer
Schistosomiasis (*Schistosoma mansoni*)	Fresh-water snail (*Biomphalaria* species)	Cercariae	Cercariae enter skin from water, migrate to liver; adults live in inferior mesenteric venules for 5–8 years, some over 30 years	Eggs caught in tissues produce T-cell-dependent granulomas, and polyps; liver shows pipe-stem fibrosis, portal hypertension, esophageal varices, cor pulmonale
Schistosomiasis (*Schistosoma japonicum*) and similar species in Southeast Asia)	Fresh-water snail (*Oncomelania* species)	Cercariae	Cercariae enter skin from water, migrate to liver; adults live in inferior and superior mesenteric venules for 5–8 years	Eggs caught in tissues cause thickening of gut and polyps, T-cell-dependent granulomas; eggs (small and laid in clusters) can travel to spinal cord and brain; cor pulmonale; hepatosplenomegaly

Stage that causes pathology	Treatment	Geographic area	Diagnosis
Cysticercus	Surgical removal; anticonvulsants	Pig-raising areas, especially Mexico, South America	Computerized tomography scan, magnetic resonance imaging, x-rays, serology
Hydatid cyst; anaphylaxis and metastatic spread of cysts if ruptured	Surgical removal; mebendazole may shrink cyst	California, Utah, Middle East, Southern Europe sheep-herding areas, especially Basque region	Scans, ultrasound, history, space-occupying lesions, serology
Adult	Niclosamide	Scandinavia, Switzerland, Hungary, former Soviet Union, Great Lakes region of United States	Eggs in stool (proglottids break up in colon)
Adult	Praziquantel	Asia, India	Eggs in stool
Adult	Praziquantel	Sheep-herding areas in Latin America, United States, South America, Africa, Europe, China	Eggs in stool; computerized tomography scan
Adult	Praziquantel	Japan, Korea, Vietnam, China	Eggs in stool (*Opisthorchis felineus* and *O. viverrini* similar to *Clonorchis*)
Adult; heart disease and neurological disturbance (Philippines), mild intestinal disturbance	Praziquantel	Asia, Middle East, Egypt	Eggs in stool
Adult	Praziquantel	Asia, India, Pacific region, South America	Eggs in stool and sputum
Eggs (terminal spine)	Praziquantel; trichlorfon	Africa, Middle East	Eggs in urine
Eggs (lateral spine)	Praziquantel; oxamniquine	Africa, South America, Caribbean region	Eggs in stool
Eggs (small lateral spine)	Praziquantel	China, Philippines, Southeast Asia	Eggs in stool

Another group of parasitic flagellates includes the macrophage-infecting members of the genus *Leishmania*, which are transmitted by blood-sucking midges or sand flies (genus *Phlebotomus* in the Old World, *Lutzomyia* in the New World). Cutaneous leishmaniasis is characterized by masses of infected macrophages in the skin, which induce long-lasting dermal lesions of varying form and severity. A related condition, mucocutaneous leishmaniasis, is found in the Amazon basin and begins as a skin ulceration; ultimately it may attack and destroy the nasal mucosa, cartilage, and soft facial and pharyngeal tissues. Another leishmaniasis disease complex, visceral leishmaniasis or kala azar, occurs in the spleen, liver, bone marrow, and lymph nodes. The broad spectrum of host–parasite interactions is well exemplified by these leishmaniases. The various manifestations of the disease are the result of the particular species of agent and vector, the immunological status of the host, the presence or absence of reservoir hosts, and the pattern of exposure.

Ciliate and sporozoan parasites. Two remaining major groups of protozoa are the ciliates and the sporozoans. The former group is largely free-living, with only a single species, *Balantidium coli*, parasitic in humans (and pigs). This large protozoon, covered with rows of cilia, is found in the large intestine, where it can cause balantidiasis, an ulcerative disease.

The sporozoans on the other hand, are all parasitic and include many parasites of humans. The most important are the agents of malaria. Other disease agents are included in the genera *Isospora, Sarcocystis, Cryptosporidium*, and *Toxoplasma. Pneumocystis*, a major cause of death among persons with acquired immune deficiency syndrome (AIDS), was formerly considered a protozoon of uncertain relationship, but now it is thought to be a member of the Fungi. *See* ACQUIRED IMMUNE DEFICIENCY SYNDROME (AIDS); MALARIA; SPOROZOA.

Toxoplasma gondii, the agent of toxoplasmosis, is of special importance because it infects as many as 20% of the world's population and because it can penetrate the placenta and infect the fetus if the mother has not been previously infected and has no antibodies. As with most medically important parasites, the great majority of *Toxoplasma* infections remain undetected and nonpathogenic. The parasite primarily affects individuals lacking immune competence—the very young, the very old, and the immunosuppressed. *See* MEDICAL BACTERIOLOGY; MEDICAL MYCOLOGY; PARASITOLOGY; ZOONOSES.

Donald Heyneman

Bibliography. T. C. Cheng, *General Parasitology*, 2d ed., 1986; R. Goldsmith and D. Heyneman (eds.), *Tropical Medicine and Parasitology*, 1989; A. A. Mahmoud, *Tropical and Geographical Medicine*, 2d ed., 1990; E. K. Markell and M. Voge, *Medical Parasitology*, 8th ed., 1999; G. Piekarski, *Medical Parasitology*, 1989; G. D. Schmidt and L. S. Roberts, *Foundations of Parasitology*, 5th ed., 1995; G. T. Strickland, *Hunter's Tropical Medicine and Emerging Infectious Diseases*, 8th ed., 2000.

Medical ultrasonic tomography

A mapping or imaging technique, used to obtain clinically useful information about the structure and functioning of tissues and organs, in which acoustic pulses are emitted from an acoustoelectric transducer, and echoes are received from acoustic impedance discontinuities along the assumed line-of-sight axial propagation path. A number of different modes of operation have emerged, each having areas of usefulness.

A (amplitude) mode. This technique uses acoustic pulse emissions and echo reception along a single line-of-sight axial propagation path, and thus provides a one-dimensional mapping. The information is most often displayed on a cathode-ray oscilloscope in which the horizontal axis of the display is a linear time base triggered at the time of the transmitted pulse, and the received echoes are manifested as vertical deflections, with vertical displacement a measure of the amplitude or strength of the returning echo. This mode of operation cannot provide identification of structural features. It is, however, a most accurate method of measuring time delays and, therefore, distances between echo-producing structures or distances of structures from transducers, provided the speed of sound propagation in the medium is known. *See* OSCILLOSCOPE.

Since the A-mode display provides only measurement of distance along the line of sight, that is, positional information, it is the task of the user to identify correctly the echo-producing structures and the position of the line of sight in order to ensure that the correct distances are being measured. Because of the difficulties in identifying individual echoes in a complex echo pattern, the technique is limited to objects of relatively simple, and repeatedly obtainable, geometry.

The method is employed in the detection of shifts of midline intracerebral structures, which indicate the presence of space-occupying lesions. In ophthalmology, it is used in determinations of the thicknesses of the cornea and lens and the axial length of the eye. In obstetrics, the growth and development of the fetus can be monitored by measurement of its biparietal diameter in the uterus.

M (motion) mode. The M mode of operation is used to display the movement of time-varying, echo-producing structures by intensity-modulating the trace as it is swept slowly across the oscilloscope screen in a direction at right angles to the fast time-base sweep. This mode of operation is used extensively in diagnosing disorders of the heart. It can be used to determine accurately details of valvular motion and quantitative measurements of heart chamber size and wall thickness. Stiffening of the leaflets of the mitral valve (stenosis), which prevents proper closure, is readily diagnosed by the reduced velocity of the valve leaflets during opening and closure. Another important application is in the identification of pericardial effusion, an accumulation of fluid surrounding the heart. These applications are characterized by identification of the echo-producing

structure by the demonstration of an easily recognizable and unique pattern of movement of the structures of interest. *See* ECHOCARDIOGRAPHY; HEART DISORDERS.

B (brightness) mode. For a two-dimensional picture to be obtained, the line-of-sight propagation path must be scanned and the position and direction of the path monitored and used to form a two-dimensional picture. Typically, the B-mode display is formed by moving the transducer so that the line-of-sight path remains in a single plane. The time-base trace of the cathode-ray oscilloscope screen is moved to correspond, in position and direction, to the ultrasonic line-of-sight propagation path, and echoes are displayed as intensity modulations of the trace. The echogram which results is therefore a two-dimensional representation of distribution of acoustic impedance discontinuities in the interrogated object, with bright lines representing strongly reflecting boundaries and textured gray areas representing the internal structure of the organs. Different kinds of scanning techniques are used. Simple scanning might consist of only a single motion such as sector, arch, or linear translation.

B-mode application is used in obstetrics to confirm intrauteral pregnancy, assess fetal anatomy, determine fetal position and multiple gestation, and monitor needle biopsy. In gynecology, pelvic masses can be identified by using a full urinary bladder as an acoustic window.

B-mode ultrasound is also used for abdominal diagnosis (see **illus.**), for example, in evaluating palpable masses for size, composition, and organ of origin. The kidneys are readily outlined; size and shape can be determined, the presence of structural change, such as tumor or polycystic disease, can be seen, and deviations from the normal echographic picture can lead to a diagnosis of such functional abnormalities as urethral obstruction or intra- or extrahepatic hemorrhage. This eliminates the need for invasive procedures such as angiography.

The relatively simple and regular structural features of the eye allow for easy ultrasonic examination. For example, the extent of the detachment of a retina can be ascertained. B-mode ultrasonography readily differentiates simple cysts from solid masses in the breast and is particularly valuable for diagnosing the dense fibrous breast tissue of younger women, for which examination by x-ray mammography is poorly suited. Examination of the thyroid can reveal enlargement of the thyroid tissue itself or the presence of solid or liquid regions intruding into the organ. Real-time B-scanning, especially useful for cardiac imaging, is made possible by electronic steering. *See* MAMMOGRAPHY.

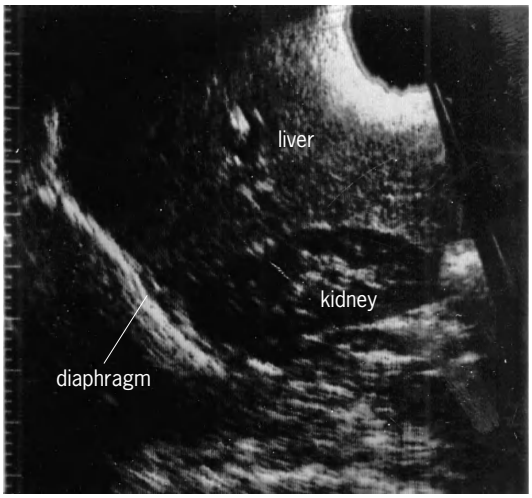

Ultrasonic B-scan of the abdomen.

C (constant-range) mode. Constant-range operation provides a two-dimensional image display at constant time delay, and presumed constant distance, from the ultrasonic transducer. The scanning is arranged so that the point at constant depth along the propagation path (beam axis) traverses a plane. This method provides a convenient display of atrial septal defects by using an intracardiac probe that is mounted at the tip of a catheter. *See* MEDICAL IMAGING; ULTRASONICS.

Floyd Dunn

Bibliography. D. R. Christensen, *Ultrasonic Bioinstrumentation*, 1988; F. J. Fry, *Ultrasound: Its Applications in Medicine and Biology,* 1978; C. R. Hill, *Physical Principles of Medical Ultrasonics*, 1986; P. N. T. Wells, *Biomedical Ultrasonics*, 1977.

Medical waste

Any solid waste that is generated in the diagnosis, treatment, or immunization of human beings or animals, in research pertaining thereto, or in the production or testing of biologicals. Since the development of disposable medical products in the early 1960s, the issue of medical waste has confronted hospitals and regulators. Previously, reusable products included items such as linen, syringes, and bandages; they were sterilized or disinfected prior to reuse, and the principal waste product was limited to human pathological tissue.

Most hazardous substances are described by their relevant properties, such as corrosive, poison, or flammable. Medical waste was originally defined in terms of its infectious properties, and thus it was called infectious waste. However, given the difficulty of identifying pathogenic organisms in waste that might cause disease, it has become standard practice to define medical waste by types or categories. While definitions differ somewhat under different regulations, in the United States the Centers for Disease Control (CDC) cite four categories of infective wastes that should require special handling and treatment: laboratory cultures and stocks, pathology wastes, blood, and items that possess sharp points such as needles and syringes (sharps). These categories, of necessity, require that the generator of these wastes exercise judgment in identifying the material to be included. For example, a small cotton ball or bandage with minimal amounts of dried blood will probably pose no problems or risk, but a dressing saturated with blood causes greater concern.

The waste category that has generated a great deal of interest is sharps. Needles and syringes, in particular, pose risks, since the instruments can penetrate into the body, increasing the potential for disease transmission. Improper disposal of these items in the past has been the catalyst for increased regulation and tighter management control.

Regulations. At the federal level, the Medical Waste Tracking Act (MWTA) established a 2-year demonstration project to be undertaken by the Environment Protection Agency, but this project terminated in 1991. Usually in the United States, requirements for identification, handling, packaging, treatment, storage, and disposal of medical waste are mandated by states and municipalities. This setup allows the various states to address issues on a more specific basis. For example, states with large numbers of rural health facilities may have needs and requirements that are different from those of states having higher and more concentrated population bases with large, centralized health facilities.

Typically, regulations define medical waste by expanding on the list developed by the Centers for Disease Control. Isolation waste from patients with highly communicable diseases is often included in these regulations. For the most part, most standard hospitals do not deal with this type of waste. Many tropical diseases and highly virulent pathogens fall into this category, and such patients are usually cared for at specialized hospitals and treatment centers. Such highly communicable diseases, identified as Biosafety level 4, are caused by those agents listed in Classification 4 in the official classification of etiologic agents of the Centers for Disease Control.

Management. Usually, the regulations mandate that, once identified, medical waste be separated from other waste as close to the source of generation as possible. It is identified by containment in a single, or sometimes double, red bag labeled "Biohazardous Waste" and the international biohazard symbol (see **illus.**). Such waste in stored in an area that can be secured so as to deny access by unauthorized personnel. This area is protected from the elements as well in order to prevent the spread of potentially disease-causing material into the environment.

After separation, the medical waste must be rendered noninfectious. Various treatment options are available, performed either at the source of generation or by a commercial entity off-site. If the waste is to be transported to an off-site location, a transportation permit must be issued and the vehicle registered with the appropriate regulatory agency. Vehicles used to transport medical waste must be fully enclosed and leakproof or leak-resistant in case the waste container ruptures. Bags containing medical waste should be placed in a rigid container for transport, such as a carton, pail, or drum. These containers can be either reusable or disposable; however, before reuse they must be thoroughly disinfected with either chemicals or hot water. The containers and the vehicle must be labeled with the words "Biohazardous Waste" and the international biohazard symbol. Some regulations require that the container as well as the bags also include the identification of the generator of the waste in case tracking the material to a specific source is necessary.

The uniform international biohazard symbol.

Tracking is also done by using a manifest. Manifest requirements vary somewhat, but a manifest document accompanies the waste in transit from generation to final disposal and identifies the custodian of the waste during transport and treatment. When the generator of the waste transfers custody to a transporter, portions of the manifest document that the transfer has been completed; each party retains a copy. When the waste is transferred from transporter to treatment site, additional portions of the manifest are completed to document that transfer. Upon treatment, disposal-site personnel send a completed copy of the manifest back to the generator, documenting that the amount, type, and source of waste generated was treated in accordance with the generator's instructions and the appropriate regulations. Some regulations mandate that if the generator does not receive a copy of the fully completed manifest within 30 days of shipment, the generator is required to notify the enforcement authorities who regulate medical waste in that particular jurisdiction. This procedure is known as exception reporting.

Treatment. Treatment of medical waste constitutes a method for rendering it noninfectious prior to disposal in a landfill or other solid-waste site. Additionally, some states require that medical waste be rendered "nonrecognizable" or destroyed. This requirement may be for esthetic reasons, as in the case of human pathological waste, or for safety reasons, as in the case of sharps. The treatment technologies currently used for medical waste include incineration, sterilization, chemical disinfection, and microwave, as well as others under development.

Incineration. Incineration has long been the traditional method of disposing of medical waste, dating back to when most of the waste was pathological in nature. Typically, these incinerators were designed to burn pathology wastes, which had a very high moisture content and did not create a great deal of heat in the combustion process. Mortuaries or crematories were often used as alternatives to incinerators at hospitals.

Modern incinerators are highly sophisticated, with air-pollution-control devices used to reduce or eliminate the gases created in the combustion process.

These gases result from the high content of plastics in the waste stream, including syringe barrels, suction containers, disposable utensils, and bags containing the waste. Unfortunately, a common perception is that incinerators increase pollution, pose environmental risks, and are not suitable for location at hospitals or in urban areas. These factors have severely reduced public acceptance of incinerators, and as a result other technologies have been developed. *See* AIR POLLUTION.

Sterilization. Steam sterilization has long been used in laboratory settings to sterilize cultures or to prepare samples for analysis or use. Additionally, gas or steam has been used to sterilize surgical instruments and associated items.

In the mid-1970s, the use of steam sterilizers or autoclaves for treating medical waste was begun, largely out of concern over incinerator emissions. Autoclaves, pressure vessels that use a boiler or other source for steam, are used to treat medical waste by hospitals and other generators, as well as by commercial waste-disposal facilities.

Chemical disinfection. Disinfection of medical waste by chemicals is an extension of the long-term hospital practice of applying chemicals to control microorganisms on hard surfaces, such as floors, walls, and tables. Equipment has been developed to use standard chemical agents in a sealed enclosure to treat waste. Often this equipment contains shredders or granulators to render the waste nonrecognizable. Chemical disinfection is growing as a treatment technology for use by generators and commercial entities.

Microwave treatment. Microwave technology combines shredding of the waste material along with exposure to microwaves, which create a moist heat environment for treatment. Waste is sprayed with water upon entering the processor, shredded, and then exposed to the microwaves, which heat the material sufficiently to disinfect it.

Other technologies. Other technologies are being developed that are designed to be environmentally acceptable, including macrowave, plasma-torch, and laser.

Macrowaves, low-frequency electrical waves longer than microwaves, are used to create an internal heat source to disinfect waste. This technology does not require water to create a moist heat environment. The longer wavelengths reduce the requirements for shredding the material, because they penetrate the waste farther than microwaves, thus exposing more of the waste volume.

In plasma-torch technology, gases at elevated temperatures are used to treat the waste. This environment creates a source of heat that can be recovered or generated into electricity.

Laser treatment, a somewhat experimental technology, uses laser-generated heat on the waste. Potential applications include use at the waste-generating site. *See* HAZARDOUS WASTE.

Robert A. Spurgin

Bibliography. E. Kunes, The trashing of America, *Omni Mag.*, pp. 40–44, 92–94, 96, February 1988; R. K. Miller and M. E. Rupnow, *Medical Waste Management*, 1991; U.S. Environmental Protection Agency Staff, *Medical Waste Management and Disposal*, 1990.

Medicine

The term medicine has two general meanings. The first indicates any material, notably in the drug category, which is given to prevent, alleviate, beneficially alter, or stop a disease process. In the second and broader sense, medicine denotes the field of science devoted to healing. Many subdivisions exist and more ramifications appear almost daily. Included in the area of medicine are many clinical specialties, including surgery, pediatrics, psychiatry, obstetrics, and others. Internal medicine is the specialization which deals with internal diseases of a nonsurgical nature. *See* SURGERY.

Related to the clinical specialties, particularly in regard to medical education and research, are the basic medical sciences. These include, among others, anatomy, physiology, pharmacology, biochemistry, and microbiology. Midway between the basic and the clinical sciences lies pathology, the study of the structural and functional alterations caused by diseases or abnormal states. *See* ANATOMY, REGIONAL; BIOCHEMISTRY; MICROBIOLOGY; PATHOLOGY.

An important area in all specialties is preventive medicine and public health. This form of medicine supplies a necessary link with the community, state, or large geographic region in matters of prevention, mass treatment, and statistical appraisals of health matters. It is also concerned with socioeconomic factors related to physical and mental well-being. *See* PUBLIC HEALTH.

The mental health of individuals and nations has received much attention since 1930. Prior to that time mental illness was largely a matter of disgrace, secrecy, and custodial care in primitive, prisonlike hospitals. With the recognition of the importance of the dynamics of psychiatry, the advent of better therapeutic measures, particularly specific drugs which promote mental well-being, and the realization that preventive measures are of vital concern to everyone, the field of mental health at the present time represents one of the largest areas in medicine.

Much attention has been given to aviation and space medicine, both of which consider the problems peculiar to their fields in the light of clinical and experimental information, as well as that supplied by other sciences and disciplines. *See* AEROSPACE MEDICINE.

Socialized medicine is that form which exists under the direct control and financing of the state. The National Health Service of Great Britain is the best-known example, and other systems exist.

Other subdivisions of medicine, with names that are largely self-explanatory, include veterinary, legal, tropical, and military medicine. *See* FORENSIC MEDICINE.

Probably the most familiar aspects of medicine to the nonspecialist are the two clinical aspects,

diagnosis and therapeutics. Diagnosis includes taking a patient's history, a physical examination, and possibly laboratory and special examinations. Therapeutics is the administration of some form of preventive or remedial treatment to the patient.

Although medicine is based parimarily upon scientific information and method, an important feature is the relationship between the physician and the patient. It is at this point that the necessary scientific background of medicine gives way to the art of healing. Edward G. Stuart; N. Karle Mottet

Mediterranean Sea

The Mediterranean Sea lies between Europe, Asia Minor, and Africa. It is completely landlocked except for the Strait of Gibraltar, the Bosporus, and the Suez Canal. The Strait of Gibraltar is 13 mi (21 km) wide at the boundary between the Atlantic and the Mediterranean (Great Europa Point, Gibraltar, to Punta Almina, Ceuta), and the Bosporus is as narrow as 0.5 mi (0.8 km), widening to 2 mi (3 km) at the Black Sea boundary (Rumeli Burnu, European Turkey, to Anadolu Burnu, Asiatic Turkey). The Suez Canal, a human-made channel connecting the Mediterranean with the Red Sea, is 87.6 mi (141 km) long, about 270 ft (90 m) wide, and 35 ft (11 m) deep. In latitude the Mediterranean extends from 30°15′N in the Gulf of Sidra to 45°47′N in the Gulf of Trieste; in longitude, from 5°21′W at Great Europa Point to 36°12′E in the Gulf of Alexandretta.

The Mediterranean is conveniently divided into an eastern basin and a western basin, which are joined by the Strait of Sicily and the Strait of Messina. The Strait of Sicily, between Cap Bon, Tunisia, and Sicily, is 77 mi (124 km) wide, but the Strait of Messina, between Punta Sottile, Sicily, and the Italian mainland, is only 1.7 mi (2.7 km) across.

The major subdivisions of the western basin are the Alboran Sea, which is the portion west of Cabo de Gata, Spain, and is named for the Isla de Alboran; the Balearic or Iberian Sea, between Spain and the Islas Baleares; the Ligurian Sea, the gulf north of Corsica; and the Tyrrhenian Sea, lying between Corsica, Sardinia, Sicily, and the Italian mainland. The eastern basin includes the Adriatic Sea, between Italy down to the heel of the boot (Capo Santa Maria de Leuca) and the Balkan Peninsula north of Corfu; the Ionian Sea, which lies south of the Adriatic as far as the southern tips of Sicily and the Greek mainland; the Aegean Sea, the waters north of Kithera, Andikithera, Crete, Karpathos, and Rhodes, as far as the Dardanelles; and the Sea of Marmara, which extends from the Dardanelles to the Bosporus.

The Mediterranean Sea has numerous islands, particularly in the Ionian Sea (which has the alternate designation of The Archipelago) and the eastern Tyrrhenian and Adriatic. The largest islands are Sicily, 9930 mi^2 (25,710 km^2); Sardinia, 9284 mi^2 (24,040 km^2); Cyprus, 3570 mi^2 (9250 km^2); Corsica, 3370 mi^2 (8720 km^2); and Crete, 3240 mi^2 (8380 km^2).

The total water area of the Mediterranean is 965,000 mi^2 (2,501,000 km^2), and its average depth is 5038 ft (1536 m). The greatest depth in the western basin is 12,200 ft (3719 m), in the Tyrrhenian Sea. The eastern basin is deeper, with a greatest depth of 18,130 ft (5530 m) in the Ionian Sea about 34 mi (55 km) off the Greek mainland. The Adriatic Sea mainly overlies the Continental Shelf, but there is a basin in the southern part with a greatest depth of 4313 ft (1315 m). The sill depth in both the Strait of Gibraltar and the Strait of Sicily is about 900 ft (300 m).

The Atlantic tide disappears in the Strait of Gibraltar. The tides of the Mediterranean are predominantly semidiurnal. The eastern and western basins have standing wave systems, with nodal lines extending roughly from Barcelona to Bougie, and from Kerme Korfezi to Kithera to Tobruch, respectively. The tide range elsewhere is about 0.9 ft (0.3 m). At the ends of the straits of Sicily and Messina, high water occurs in exactly opposite phase, giving rise to strong hydraulic currents, particularly in the narrow Strait of Messina, the legendary seat of Scylla and Charybdis. The Adriatic has a progressive tide, with a range as great as 3 ft (0.9 m) in the northern end, radiating about an amphidromic point near 43°N, 15°E. J. Lyman

Early investigations of ocean currents were stimulated by the continuous inflow of surface water from the Atlantic into the Mediterranean through the Strait of Gibraltar. While it was recognized that evaporation over the Mediterranean greatly exceeds precipitation and river runoff, this inflow is clearly larger than the excess evaporation, and complicated schemes of underground canals were imagined for returning water to the Atlantic. With an ingenious experiment, Count Marsigli suggested in the late seventeenth century that the water should be returned by a deep outflow of Mediterranean water through the Strait of Gibraltar. Marsigli separated two water types of different densities in a tank by a partition. When he removed the partition, the denser water flowed under the lighter water, thereby implying a deep outflow of high-salinity, denser Mediterranean water through the Strait of Gibraltar, in addition to the observed surface inflow of low-salinity, less dense Atlantic water. The deep outflow was finally confirmed in 1870 by lowering a drogue to a depth of 1400 ft (450 m) from a small boat.

The outflow of Mediterranean water can be estimated from consideration of water and salt budgets using evaporation rates and observed salinities of Atlantic and Mediterranean waters in the Strait of Gibraltar. Depending on the assumed evaporation rate, the outflow has been estimated by this method to be between 35 and 63 ft^3/s (1.0×10^6 and 1.8×10^6 m^3/s). During an international experiment in 1960 and 1961, the outflow was measured to be 3.9×10^7 ft^3/s (1.1×10^6 m^3/s) in good agreement with the estimated outflow despite uncertainties in the measured outflow due to spatial and temporal variability.

Because of the excess evaporation over the Mediterranean, surface salinity increases as Atlantic water flows eastward from a value of 36.5‰ in the Strait of Gibraltar to 39.2‰ south of Turkey in the eastern Mediterranean. Surface waters are changed into intermediate and deep waters in wintertime when evaporation and heat lost to the atmosphere make them denser than the water beneath, leading to their downward convection. Levantine intermediate water, which fills the levels between 600 and 3000 ft (200 and 1000 m) depths in most of the Mediterranean, is thought to form near Rhodes in February and March. During the 1970s western Mediterranean deep water was observed to form during March in the same location south of France. Initially, there is a preconditioning phase in which an eddy of slightly colder water forms in the particular location, perhaps trapped by the bottom topography. The surface water inside the eddy becomes more saline and more dense as cold, dry winds, called the mistral, blow down the Rhone valley and over the Mediterranean. Finally, when the surface water becomes as dense as the deep water, convection occurs, and surface water penetrates to great depths and spreads laterally. This formation of deep water is a prototype of deep-water formation in the open ocean which is thought to occur in remote regions of the Arctic and Antarctic.

The outflow of Mediterranean water through the Strait of Gibraltar is made up of a mixture of Levantine intermediate water and western Mediterranean deep water. This outflow is warmer and more saline than Atlantic water of comparable density. These distinctive properties have allowed Mediterranean water influence to be traced westward across the Atlantic to the Gulf Stream and northward into the Norwegian Sea.

Harry Bryden

Meiosis

The set of two successive cell divisions that serve to separate homologous chromosome pairs and thus reduce the total number of chromosomes by half. The meiotic process includes two sequential nuclear divisions that must occur prior to the formation of gametes (sperm and eggs). The major purpose of meiosis is the precise reduction in the number of chromosomes by one-half, so a diploid cell can create haploid gametes. To accomplish this reduction, a single cell undergoes two meiotic divisions to produce four daughter cells, each with half the original chromosome complement. The nonmeiotic (or somatic) cells of humans, for instance, have 46 individual chromosomes, or 23 pairs of homologous chromosomes. However, following meiosis, human eggs or sperm have only 23 chromosomes, one member of each pair. Reducing the number of chromosomes in the gametes to 23 allows the fusion of an egg with a sperm (fertilization) to result in an embryo with the requisite 46 chromosomes. Meiosis is therefore a critical component of sexual reproduction. *See* GAMETOGENESIS.

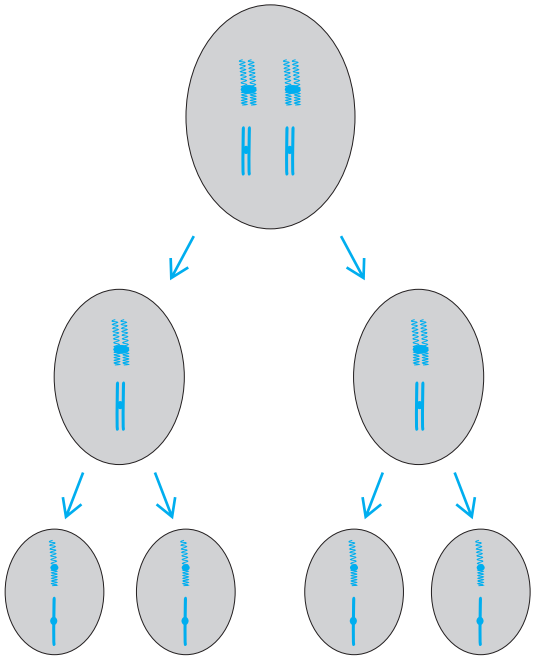

Fig. 1. Simplified view of the two meiotic divisions.

Chromosome behavior. For example, consider an organism that contains only two pairs of chromosomes (**Fig. 1**). The chromosomes in each of these pairs are referred to individually as homologs; one is derived from the father of the organism and the other from the mother. Both homologs carry the same array of genes. As the cell begins meiosis, each chromosome has already duplicated its DNA and carries two identical copies of the DNA molecule. These are visible as two lateral parts, called sister chromatids, which are connected by a centromere.

The basic events of meiosis are actually quite simple. Homologous pairs of chromosomes are first identified and matched. This process, which occurs only in the first of the two meiotic divisions, is called pairing. The matched pairs are then physically interlocked by recombination, which is also known as exchange or crossingover. After recombination, the homologous chromosomes separate from each other, and at the first meiotic division are partitioned into different nuclei. The second meiotic division begins with half of the original number of chromosomes. During this second meiotic division, the sister chromatids of each chromosome separate and migrate to different daughter cells. *See* CHROMOSOME.

The patterns by which genes are inherited are determined by the movement of the chromosomes during the two meiotic divisions. It is a fundamental tenet of Mendelian inheritance that each individual carries two copies of each gene, one derived from its father and one from its mother. Moreover, each of that individual's gametes will carry only one copy of that gene, which is chosen at random. The process by which the two copies of a given gene are distributed into separate gametes is referred to as segregation. Thus, if an individual is heterozygous at the *A* gene for two different alleles, *A* and *a*, his or her gametes

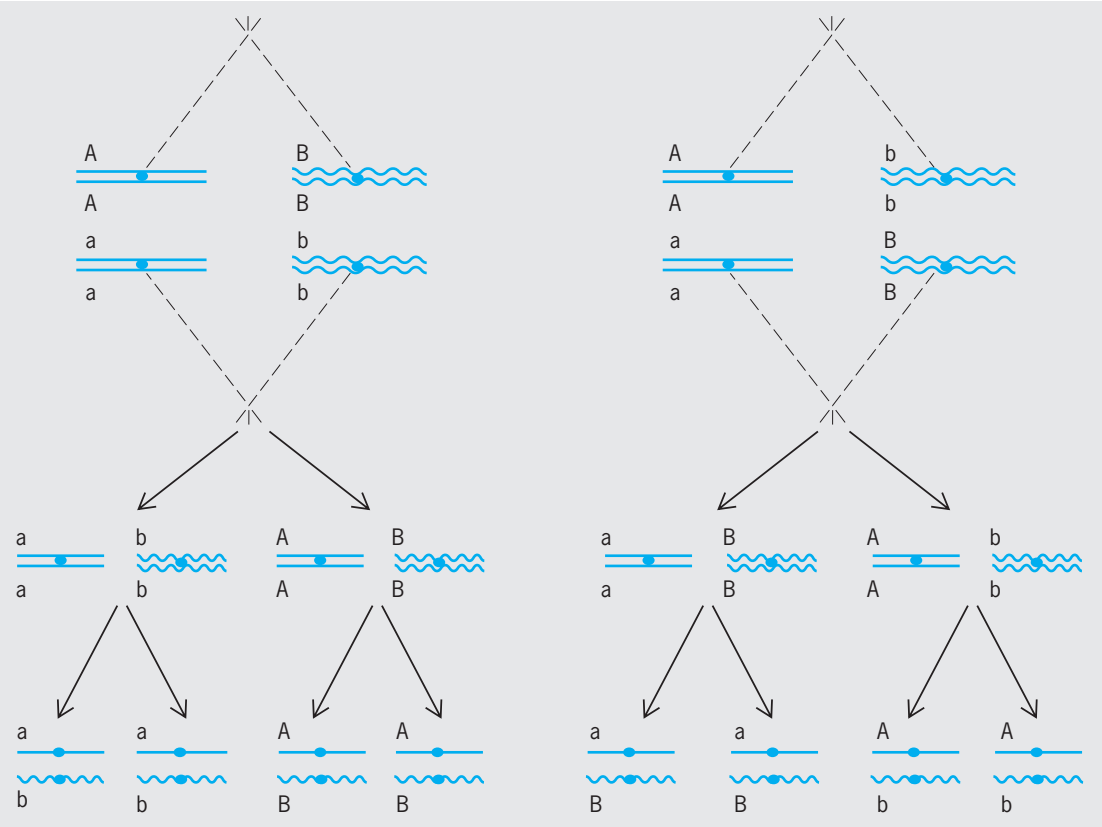

Fig. 2. Behavior of chromosomes at the first meiotic division explains independent assortment.

will be equally likely to carry the *A* allele or the *a* allele, but never both or neither. The fact that homologous chromosomes, and thus homologous genes, segregate to opposite poles at the first meiotic division explains this principle of inheritance. *See* CELL CYCLE.

Mendel's law of independent assortment states that the segregation of two different gene pairs occurs at random with respect to each other. Thus, for an individual of the genotype *AaBb*, the gametes *AB*, *Ab*, *aB*, and *ab* will be formed with equal frequency. This result can be easily understood if the *A* and *B* genes lie on different chromosomes (**Fig. 2**). Because the chromosome pair bearing the *A* gene orients independently of the homolog pair bearing the *B* gene, *AB* ↔ *ab* segregations are as likely as *Ab* ↔ *aB* segregations. Cases where independent assortment does not occur (an effect called linkage) can be understood as resulting from situations where the two gene pairs lie at different positions on the same pair of homologous chromosomes.

Meiotic divisions. The two meiotic divisions may be divided into a number of distinct stages. Meiotic prophase refers to the period after the last cycle of DNA replication, during which time homologous chromosomes pair and recombine. The end of prophase is signaled by the breakdown of the nuclear envelope, and the association of the paired chromosomes with the meiotic spindle. The spindle is made up of microtubules that, with associated motor proteins, mediate chromosome movement. In some cases (such as human sperm formation), the spindle is already formed at the point of nuclear envelope breakdown, and the chromosomes then attach to it. In other systems (such as human female meiosis), the chromosomes themselves organize the spindle.

Metaphase I is the period before the first division during which pairs of interlocked homologous chromosomes, called bivalents, line up on the middle of the meiotic spindle. The chromosomes are primarily (but not exclusively) attached to the spindle by their centromeres such that the centromere of one homolog is attached to spindle fibers emanating from one pole, and the centromere of its partner is attached to spindle fibers from the other pole (**Fig. 3**). The bivalents are physically held together by structures referred to as chiasmata that are the result of meiotic recombination events. In most meiotic systems, meiosis will not continue until all of the homolog pairs are properly oriented at the middle of the spindle, the metaphase plate. It is important to remember that the orientation of each pair of homologs on the spindle occurs in a random fashion, such that the paternally derived homolog of one bivalent may point toward one pole of the spindle, while in the adjacent bivalent the maternally derived homolog is oriented toward the same pole.

Anaphase I refers to the point at which homologous chromosome pairs separate and move to opposite poles. This is accomplished by the release of chiasmata. Although the sister chromatids remain

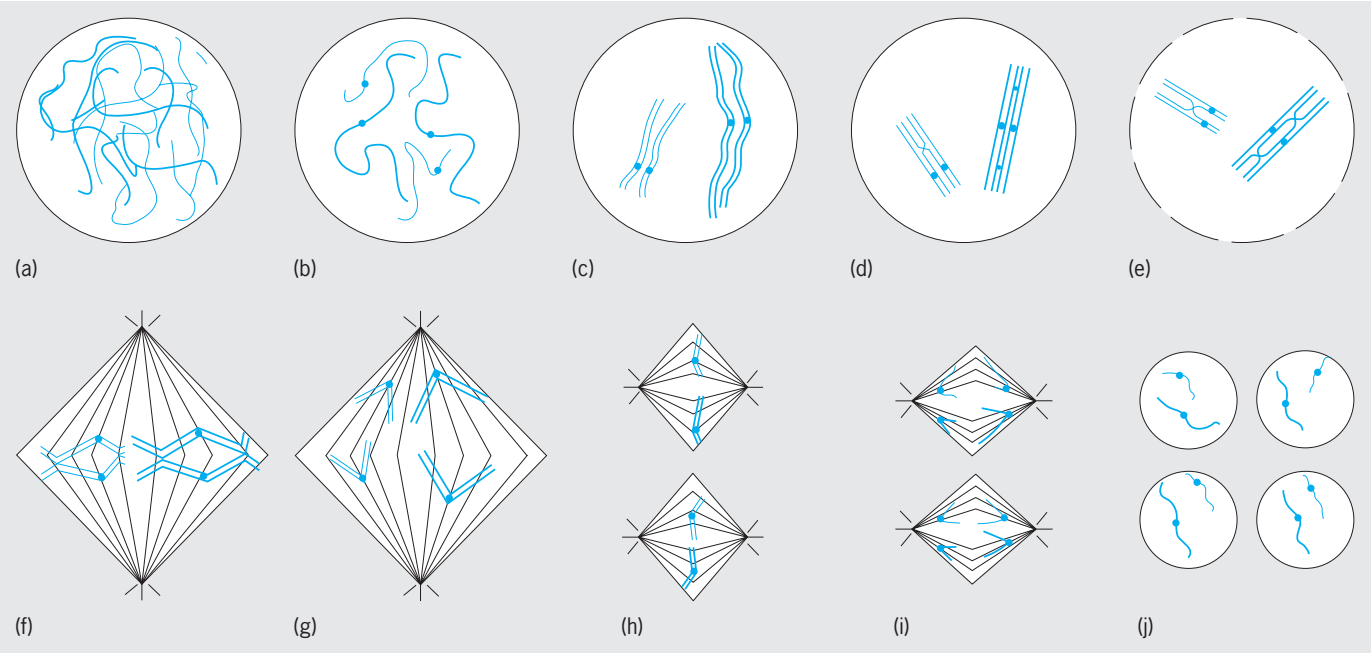

Fig. 3. Stages of meiosis. (*a*) Premeiotic interphase. (*b*) Leptotene (note the appearance of individualized chromosomes). (*c*) Zygotene (signified by the alignment of homologs). (*d*) Pachytene (the chromosomes making up each bivalent are intimately aligned). (*e*) Diplotene/diakinesis. (*f*) Metaphase I. (*g*) Anaphase I. (*h*) Metaphase II. (*i*) Anaphase II. (*j*) Telophase II.

attached around their centromeres, they release each other along the arms of the chromosome, allowing chiasmata to be resolved. Depending on the organism, there may or may not be a true telophase, or a time in which nuclei reform. In most organisms, the first cell division occurs after the completion of anaphase I.

Following the completion of the first meiotic division, the chromosomes align themselves on a new pair of spindles, with their sister chromatids oriented toward opposite poles. The stage at which each chromosome is so aligned is referred to as metaphase II. In some, but not all, organisms, metaphase II is preceded by a brief prophase II. DNA replication does not occur during prophase II; each chromosome still consists of the two sister chromatids. Nor are there opportunities for pairing or recombination at this stage due to the prior separation of homologs at anaphase I.

The start of anaphase II is signaled by the separation of sister centromeres, and the movement of the two sister chromatids to opposite poles. At telophase II, the sisters have reached opposite poles and the nuclei begin to reform. The second cell division usually occurs at this time. Thus, at the end of the second meiotic division, there will be four daughter cells, each with a single copy of each chromosome.

Details of meiotic prophase. Because pairing and recombination occur during the first meiotic prophase, much attention has been focused on this stage of the process. The prophase of the first meiotic division is subdivided into five stages: leptotene, zygotene, pachytene, diplotene, and diakinesis. Homolog recognition, alignment, and synapsis occur during leptotene and zygotene. In the leptotene, an initial phase of chromosome individualization, initial homolog alignments are made. By zygotene, homologous chromosomes have become associated at various points along their length. These associations facilitate a more intimate pairing that results in the homologous chromosomes lying abreast of a tracklike structure called the synaptonemal complex.

The beginning of pachytene is signaled by the completion of a continuous synaptonemal complex running the full length of each bivalent. During diplotene, the attractive forces that mediated homologous pairing disappear, and the homologs begin to repel each other. Luckily, homologs virtually always recombine, and those recombination events can be seen as chiasmata that tether the homologs together. In some organisms, those rare chromosome pairs that have failed to undergo recombination will fly apart prematurely from each other at this stage. The final stage in meiotic prophase is diakinesis, during which the homologs shorten and condense in preparation for nuclear division.

Mechanisms of pairing. Recent models of meiotic pairing suggest that homologous chromosomes initially undergo multiple interactions at many sites along their lengths, and often at their tips. These interactions are the result of several types of homology—finding mechanisms which serve to bring the chromosomes into alignment. However, these associations are apparently weak and transient, and must be stabilized early in meiotic prophase by one of two mechanisms. In the yeast *Saccharomyces cerevisiae*, these pairings can apparently be locked in by the initiation of recombination. The formation of recombination intermediates appears to be fully sufficient to ensure segregation even in genetic

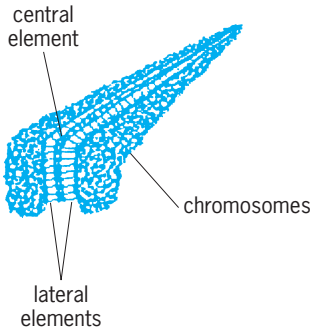

Fig. 4. Synaptonemal complex.

backgrounds in which synapsis and synaptonemal complex formation do not occur. In contrast, recombination is delayed in many higher organisms and its completion appears to require the formation of the synaptonemal complex. In these higher organisms, it is synaptonemal complex formation during zygotene that appears to maintain chromosome pairing during the processes of chromatin compaction and chromosome movement which accompany the progression of meiotic prophase.

The mature synaptonemal complex is a tripartite structure consisting of two lateral elements that flank the chromosomes, and a central element, and running the full length of each bivalent (**Fig. 4**). It is believed that the synaptonemal complex is essential for both synapsis and sister chromatid cohesion, and that proteins involved in maintaining sister chromatid cohesion (known as cohesins) are a major component of the synaptonemal complex itself.

Mechanisms of recombination. Meiotic recombination involves the physical interchange of DNA molecules between the two homologous chromosomes, thus allowing the creation of new combinations of alleles for genes located on that pair of chromosomes. Mechanistically, recombination occurs between homologous chromosomes, and involves the precise breakage and rejoining of two nonsister chromatids. The result is the formation of two recombinant chromatids, each of which carries information from both of the original homologs (**Fig. 5**).

The actual mechanism of recombination involves a complex series of cutting and rejoining of homologous DNA. The initial event appears to be the controlled cleavage of one of the two nonsister chromatids to create a double-strand break, in which both phosphodiester backbones of the double-helical DNA molecule are cleaved. The initial break is then extended to create a gap. Sequences adjacent to the gap seek out identical regions of DNA sequence on the homolog, then use the homolog as a template

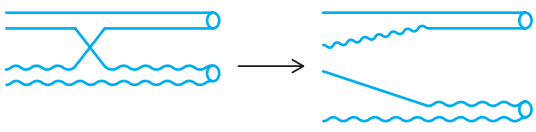

Fig. 5. Recombination involves the physical interchange of genetic material between two nonsister chromatids.

to replace the DNA base pairs removed during gap formation. As a result of this process, the two DNA molecules exchange strands at two closely linked sites and create a structure referred to as a double Holliday intermediate. The resolution of this intermediate can either create a pair of recombinant chromatids or simply result in a short region of DNA from one chromatid being inserted into the other as a result of the gap-filling process. This latter event is called gene conversion.

The number and position of recombination events is very precisely controlled. Exchange occurs only in the gene-rich euchromatin that makes up most of the chromosome arms, never in the heterochromatin that surrounds the centromeres. Moreover, as a result of a process known as interference, the occurrence of one exchange in a given chromosomal region greatly decreases the probability of a second exchange in that region. *See* RECOMBINATION (GENETICS).

Function of genetic recombination. Recent studies have indicated that failures of meiotic chromosome segregation in many organisms, including humans, may arise by a common mechanism. In these organisms, the absence or misplacement of exchange events along the length of a bivalent greatly increases the probability of failed segregation at anaphase I. For certain chromosomes (such as human chromosome 21 and the *Drosophila* X chromosome), exchange events that occur in the distal or most proximal regions of the chromosome frequently result in segregation errors at metaphase I.

Recombination events. The cytological manifestation of an exchange event is a chiasma. Chiasmata can be visualized at diplotene-diakinesis as sites on the bivalent in which two nonsister chromatids appear to cross over from one homolog to the other. Because the sister chromatids display tight cohesion during meiotic prophase and metaphase I, chiasmata hold the paired chromosomes together and thus commit the two centromeres that are physically linked by the exchange to orient to opposite poles of the spindle. Once the two centromeres have oriented toward opposite poles, the chiasmata also function to halt the progression of the homologous centromeres toward opposite poles, thus holding the properly oriented bivalent at the metaphase plate. This represents a stable position in which the bivalent will remain until anaphase I.

Linkage (recombination mapping). Recombination can occur anywhere within the euchromatin but never occurs within the heterochromatin. For two genes on the same chromosome, recombination can be detected by the creation of new combinations of alleles. Consider the case of an *AaBb* double heterozygote, where the *A* and *B* genes lie on the same chromosome arm. In this instance, the *A* and *B* alleles lie on one homolog and the *a* and *b* alleles lie on the other. In the absence of recombination, only *AB* and *ab* gametes can be produced. However, recombination allows the production of *aB* and *Ab* gametes, and the frequency of such gametes will be proportional to the frequency of recombination (**Fig. 6**).

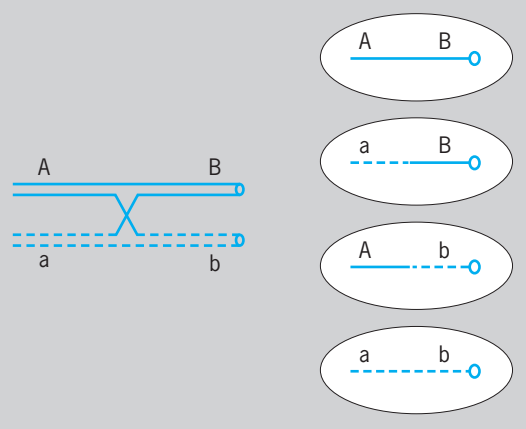

Fig. 6. Recombination leading to linkage.

To a rough approximation, the farther apart two genes are on a given chromosome, the more likely it is that a recombination event will occur between them. Since virtually all homolog pairs undergo at least one recombination event per arm at each meiosis (and the longer chromosome arms may experience three to five exchanges), the probability that two genes far apart on a given arm will have at least one recombination event occur between them is quite high. In contrast, genes lying close to each other will recombine only very rarely. Thus, by determining how often recombination occurs between various pairs of genes, geneticists can build linkage maps and order the position of genes along a given chromosome. *See* LINKAGE (GENETICS).

Sex differences in meiosis. In human male meiosis, all four daughter cells of meiosis will go through a complicated cellular differentiation process called spermiogenesis to become mature functional sperm. In contrast, oogenesis results in only one of the four products of meiosis becoming an egg. The other three products donate their cytoplasm to the chosen oocyte, then die. The oocyte then completes the cellular differentiation process to become a mature egg.

In human females, meiosis begins during fetal development. All of the oocytes (eggs) that a human female will possess in her lifetime are produced during fetal development, but these oocytes are arrested at the end of pachytene. Thus, all of the meiotic recombination a human female will ever do is completed before she is born. These arrested oocytes remain quiescent until the girl enters puberty. At that point, a few oocytes are allowed to begin the maturation process during each menstrual cycle; usually only a single oocyte is ovulated per cycle. The ovulated egg completes anaphase I and then proceeds through meiosis until it arrests again at metaphase II. The completion of the second meiotic division is triggered only by fertilization.

Male meiosis begins at puberty and continues uninterrrupted throughout the life of the male. The stem cells that will produce male meiotic cells continue to divide throughout the male's life, constantly producing new populations of spermatocytes. Moreover, once meiosis is initiated in human spermatocytes, it usually proceeds without interruption to produce four daughter cells, all of which differentiate to become mature spermatids.

The molecular mechanisms that ensure meiotic segregation are also different in males and females. In human males, the meiotic spindle is organized by the centrosomes. The chromosomes then attach to the developing spindle after it is formed by the centrosomes. In females, the chromosomes themselves bind to the microtubules, and build the spindle from the inside out without the assistance of the centrosomes. The frequency and distribution of recombination events for each chromosome pair also differ between males and females.

Errors of meiosis. The failure of two chromosomes to segregate properly is called nondisjunction. Nondisjunction occurs either because two homologs failed to pair and/or recombine or because of a failure of the cell to properly move the segregating chromosomes on the meiotic spindle. The result of nondisjunction is the production of gametes that are aneuploid, carrying the wrong number of chromosomes. When such a gamete is involved in a fertilization event, the resulting zygote is also aneuploid. Those cases where the embryo carries an extra copy of a given chromosome are said to be trisomic, while those that carry but one copy are said to be monosomic for that chromosome. Most aneuploid zygotes are not viable and result in early spontaneous abortion. There are no viable monosomies for the human autosomes; however, a few types of trisomic zygotes are capable of survival. These are trisomies for the sex chromosomes (XXX, XXY, XYY), trisomy 21 (Down syndrome), trisomy 18, and trisomy 13. *See* CROSSING-OVER (GENETICS).

Meiosis versus mitosis. The fundamental difference between meiosis and mitosis is that sister chromatids do not separate at the first meiotic division; rather, homologous chromosomes separate from each other with their sister chromatids still attached to each other. Although in some organisms some chromosome pairing does occur in mitotic cells, intimate synapsis along the entire length of chromosomes is usually restricted to meiotic cells. Recombination is frequent in most meiotic cells; however, it occurs only rarely in mitotic cells, usually as part of DNA repair events.

Most critically, DNA synthesis occurs only once within the two meiotic divisions, while there is a complete replication before every mitotic division. This allows mitosis to produce two genetically identical daughter cells, while meiosis produces four daughter cells, each of which have only one-half the number of chromosomes present prior to meiosis. *See* CELL DIVISION; FUNGAL GENETICS; GENE; MITOSIS.

Michelle Y. Walker; R. Scott Hawley

Bibliography. S. L. Page and R. S. Hawley, Chromosome choreography: The meiotic ballet, *Science*, 301(5634):785–789, 2003; M. Petronczki, M. F. Siomos, and K. Nasmyth, Un menage a quatre: The molecular biology of chromosome segregation in meiosis, *Cell*, 112(4):423–440, 2003; D. Zickler

and N. Kleckner, Meiotic chromosomes: integrating structure and function, *Annu. Rev. Genet.*, 33:603–754, 1999.

Meissner effect

The expulsion of magnetic flux from the interior of a superconducting metal when it is cooled in a magnetic field to below the critical temperature, near absolute zero, at which the transition to superconductivity takes place.

Discovery. It was discovered by Walther Meissner and R. Ochsenfeld in 1933, when they measured the magnetic field surrounding two adjacent long cylindrical single crystals of tin and observed that at 3.72 K the Earth's magnetic field was expelled from their interior. This indicated that at the onset of superconductivity they became perfect diamagnets. This discovery showed that the transition to superconductivity is reversible, and that the laws of thermodynamics apply to it. The Meissner effect forms one of the cornerstones in the understanding of superconductivity, and its discovery led F. London and H. London to develop their phenomenological electrodynamics of superconductivity. *See* DIAMAGNETISM; THERMODYNAMIC PRINCIPLES.

The magnetic field is actually not completely expelled, but penetrates a very thin surface layer where currents flow, screening the interior from the magnetic field.

Before the discovery of the effect, it had been pointed out that simple relations exist between the specific heat, a thermal property, and the magnetic properties of superconductors. These relations imply that the change from the normal to the superconducting state of a metal is a thermodynamic transition. The conclusion that a magnetic field would be expelled in the transition to the superconducting state, however, was not drawn.

Shortly before the discovery of the Meissner effect, it was pointed out that because of the inertia of the electrons, screening currents flow in a thin surface layer when a superconductor is suddenly exposed to a magnetic field. Similarly, it was expected that a current passed through a superconducting rod would also be confined to a thin surface layer. This conjecture formed the starting point for Meissner's investigation. By passing the current down one rod and up an identical, adjacent rod, and by measuring the magnetic field surrounding the two rods, it is possible to decide whether the currents flow in a thin surface layer or uniformly over the whole cross section. Since Meissner initially had not canceled the Earth's magnetic field, he was able to observe that the magnetic field was expelled at the onset of superconductivity. Subsequently Meissner also found that indeed the current flows in a very thin surface layer.

Limitations. Meissner and Ochsenfeld prepared two single crystal rods of tin for their experiment. If they had used polycrystalline samples, especially of a noncubic metal, they would not have observed the full diamagnetism. Even when a polycrystalline sample is well annealed and strain-free at room temperature, severe strains are set up in the process of cooling it down, because the thermal contraction is different in different crystal directions. Since the critical temperature shifts slightly with strain, such samples fail to become uniformly superconducting, allowing persistent current to flow in the regions which become superconducting first. These persistent currents then lock in the magnetic flux. *See* MAGNETISM.

In impure samples having a short electronic mean free path, the effect is not observed because the energy associated with a boundary between a superconducting and a normal domain is negative. This allows the formation of a stable array of superconducting flux tubes carrying one quantum of magnetic flux (approximately 2×10^{-7} gauss·cm^2 $= 2 \times 10^{-15}$ weber) each.

The effect is also not observed in a round flat disk with the magnetic field parallel to its axis of rotation, since the magnetic field also would have to be excluded from roughly hemispherical regions above and below the disk. For a disk, however, the difference between the free energies in the superconducting and normal states is too small to balance the change in the magnetic field energy in these two regions. The disk therefore breaks up into normal and superconducting domains or, if extremely thin, exhibits a flux tube structure similar to impure superconductors. *See* SUPERCONDUCTIVITY.

Hans W. Meissner

Meitnerium

The seventeenth of the synthetic transuranium elements. Element 109 falls in column 9 of the periodic table under the elements cobalt, rhodium, and iridium. It is expected to have chemical properties similar to those of iridium. *See* IRIDIUM; PERIODIC TABLE; TRANSURANIUM ELEMENTS.

1																	18
1 H	2											13	14	15	16	17	2 He
3 Li	4 Be											5 B	6 C	7 N	8 O	9 F	10 Ne
11 Na	12 Mg	3	4	5	6	7	8	9	10	11	12	13 Al	14 Si	15 P	16 S	17 Cl	18 Ar
19 K	20 Ca	21 Sc	22 Ti	23 V	24 Cr	25 Mn	26 Fe	27 Co	28 Ni	29 Cu	30 Zn	31 Ga	32 Ge	33 As	34 Se	35 Br	36 Kr
37 Rb	38 Sr	39 Y	40 Zr	41 Nb	42 Mo	43 Tc	44 Ru	45 Rh	46 Pd	47 Ag	48 Cd	49 In	50 Sn	51 Sb	52 Te	53 I	54 Xe
55 Cs	56 Ba	71 Lu	72 Hf	73 Ta	74 W	75 Re	76 Os	77 Ir	78 Pt	79 Au	80 Hg	81 Tl	82 Pb	83 Bi	84 Po	85 At	86 Rn
87 Fr	88 Ra	103 Lr	104 Rf	105 Db	106 Sg	107 Bh	108 Hs	109 Mt	110 Ds	111 Rg	112	113					

lanthanide series	57 La	58 Ce	59 Pr	60 Nd	61 Pm	62 Sm	63 Eu	64 Gd	65 Tb	66 Dy	67 Ho	68 Er	69 Tm	70 Yb

actinide series	89 Ac	90 Th	91 Pa	92 U	93 Np	94 Pu	95 Am	96 Cm	97 Bk	98 Cf	99 Es	100 Fm	101 Md	102 No

Element 109 was discovered in 1982 by a team under P. Armbruster and G. Münzenberg at the

Gesellschaft für Schwerionenforschung (GSI) at Darmstadt, Germany. In a sequence of bombardments of bismuth-209 targets with beams of ions of titanium-50, chromium-54, and iron-58, the compound systems ^{259}105, ^{263}107, and ^{267}109 were produced. The decay analysis of the isotopes produced showed in the case of elements 105 and 107 the production of ^{258}105 and ^{262}107 by reaction channels in which one neutron is emitted. These isotopes have odd neutron and proton numbers and possess a special stability against spontaneous fission. It was shown that alpha-particle decay dominated the decay chains. Spontaneous fission occurs through a 30% electron capture branch of ^{256}105 in ^{258}104. Three decay chains were observed for the three reactions ending by fission of ^{258}104, and the decay of the first atom of element 109 was observed. *See* ALPHA PARTICLES; DUBNIUM; NUCLEAR FISSION; NUCLEAR REACTION; RADIOACTIVITY; RUTHERFORDIUM.

The single atom of element 109 was produced at a bombarding energy of 299 MeV in the reaction between iron-58 and bismuth-209. A total dose of 7×10^{17} ions was used to bombard thin layers of bismuth during a 250-h irradiation time. Peter Armbruster

Bibliography. S. Hofmann, *On Beyond Uranium: Journey to the End of the Periodic Table*, 2002; G. Münzenberg, New results on element 109, *Z. Phys.*, A330:435–436, 1998; G. Münzenberg et al., Evidence for element 109 from one correlated decay sequence following the fusion of ^{58}Fe with ^{209}Bi, *Z. Phys.*, A315:145–158, 1984; G. Münzenberg et al., Observation of one correlated alpha decay in the reaction ^{58}Fe on ^{209}Bi → ^{267}109, *Z. Phys.*, A309:89–90, 1982.

Melanterite

A mineral having composition $FeSO_4 \cdot 7H_2O$. Melanterite occurs mainly in green, fibrous or concretionary masses or in short, monoclinic, prismatic crystals (see **illus.**). Fracture is conchoidal and luster is vitreous. Hardness is 2 on Mohs scale, and specific gravity 1.90. The mineral is similar to chalcanthite, has an astringent taste, and is readily soluble in water.

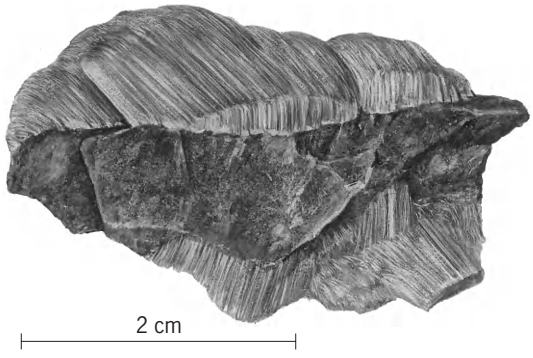

Fibrous crust of melanterite (a common mineral) in a sample from Kremnitz, Hungary. (*Specimen from Department of Geology, Bryn Mawr College*)

Melanterite is a common secondary mineral derived from oxidation and hydration of iron sulfide minerals such as pyrite and marcasite. Its occurrence is widespread. It is not an ore mineral. *See* PYRITE.

Melanterite can be crystallized from aqueous solution at temperatures up to 130°F (56°C). The mineral is unstable in dry air at room temperature, however. It readily dehydrates into a yellowish powder. Edward C. T. Chao

Melilite

A complete solid solution series ranging from gehlenite, $Ca_2Al_2SiO_7$, to akermanite, $Ca_2MgSi_2O_7$, often containing appreciable Na and Fe. Melilites are tetragonal sorosilicates and form short prismatic crystals with poor basal cleavage. The Mohs hardness is 5–6, and the density increases progressively from 2.94 for akermanite to 3.05 for gehlenite. The luster is vitreous to resinous, and the color is white, yellow, greenish, reddish, or brown. Akermanite-rich varieties occur in thermally metamorphosed siliceous limestones and dolomites, but more gehlenite-rich ones result if Al is present, as in Durango, Mexico, and Monzoni, Italy. Melilites are found instead of plagioclase in silica-deficient, feldspathoid-bearing basalts, as at Capo di Bove, Italy; in the Kaiserstuhl, Germany; in the Hawaiian Islands; and at Vesuvius, where SiO_2 was removed from the magma by reaction with

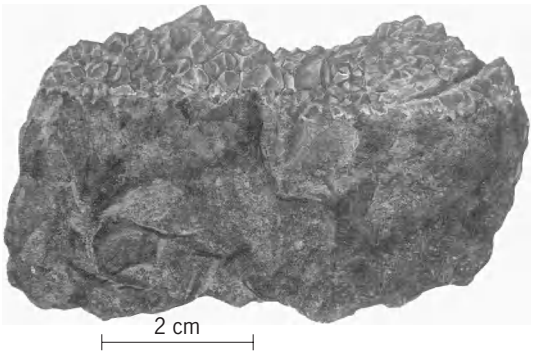

Melilite crystals from Vesuvius, Italy. (*Specimen from Department of Geology, Bryn Mawr College*)

carbonate rocks (see **illus.**). In carbonaceous chondrite meteorites, melilites ranging from pure gehlenite to 80 mole % akermanite occur with hibonite, spinel, perovskite, and pyroxenes in inclusions thought to be ancient condensates from the gas of the solar nebula. *See* SILICATE MINERALS.

Lawrence Grossman

Melting point

The temperature at which a solid changes to a liquid. For pure substances, the melting or fusion process occurs at a single temperature, the temperature rise

with addition of heat being arrested until melting is complete. The direct transition from solid phase to gas phase is not properly called melting, but preferably, sublimation.

Melting points reported in the literature, unless specifically stated otherwise, have been measured under an applied pressure of 1 atm (≃100 kilopascals), usually 1 atm of air. (The solubility of air in the liquid is a complicating factor in precision measurements.) The Clapeyron equation for the pressure dependence of the absolute melting temperature T_m is the equation below, where ΔV_f is the change in

$$\frac{dT_m}{dP} = \frac{T_m \Delta V_f}{\Delta H_f}$$

volume, ΔH_f the heat absorbed during the fusion process, and P the applied pressure. Upon melting, all substances absorb heat, and most substances expand; consequently an increase in pressure normally raises the melting point. A few substances, of which water is the most notable example, contract upon melting; thus, the application of pressure to ice at 0°C (32°F) causes it to melt. Large changes in pressure are required to produce significant shifts in the melting point; a pressure of 10 atm (1 megapascal) lowers the melting point of ice by only 0.075°C (0.135°F).

A sufficient decrease in temperature at ordinary pressures causes all pure substances except helium to freeze to solids; the lowest normal melting point is that of hydrogen, at 14 K (−434°F) and one of the highest is that of rhenium, at 3700 K. Liquid helium can be transformed into a solid only by applying a pressure in excess of 25 atm (2500 kPa).

For solutions of two or more components, the melting process normally occurs over a range of temperatures, and a distinction is made between the melting point, the temperature at which the first trace of liquid appears, and the freezing point, the higher temperature at which the last trace of solid disappears, or equivalently, if one is cooling rather than heating, the temperature at which the first trace of solid appears. Measurement of the freezing point of a solution and the difference between it and the freezing point of the pure solvent provides a convenient method of determining the molecular weight of a dissolved solute, because the freezing point depression of a solution is proportional to the molality of the solute. *See* PHASE EQUILIBRIUM; SOLUTION; SUBLIMATION; TRIPLE POINT.

Robert L. Scott

Membrane distillation

A separation method in which a nonwetting, microporous membrane is used with a liquid feed phase on one side of the membrane and a condensing, permeate phase on the other side. Membrane distillation is also known as transmembrane distillation, membrane evaporation, and thermo-pervaporation. Separation by membrane distillation is based on the relative volatility of various components in the feed solution. The driving force for transport is the partial pressure difference across the membrane. Separation occurs when vapor from components of higher volatility passes through the membrane pores by a convective or diffusive mechanism. *See* CONVECTION (HEAT); DIFFUSION.

Membrane distillation shares some characteristics with another membrane-based separation known as pervaporation, but there also are some vital differences. Both of these membrane separation methods involve direct contact of the membrane with a liquid feed and evaporation of the permeating components. However, while membrane distillation uses porous membranes that have negligible effects on the vapor–liquid equilibria of the components to be separated, pervaporation uses nonporous membranes with the degree of separation influenced by the sorption and diffusion characteristics of permeants in the membrane.

Systems. Membrane distillation systems can be classified broadly into two categories: direct-contact distillation and gas-gap distillation. These terms refer to the permeate or condensing side of the membrane; in both cases the feed is in direct contact with the membrane.

In direct-contact membrane distillation, both sides of the membrane contact a liquid phase; the liquid on the permeate side is used as the condensing medium for the vapors leaving the hot feed solution.

In gas-gap membrane distillation, the condensed permeate is not in direct contact with the membrane. The gas-gap method can be subdivided further, depending on whether the condensing surface is within the module itself or whether condensation of the permeate vapor occurs outside the membrane module. Application of a vacuum or use of a sweep gas are techniques used to carry vapor from the membrane module to an external condensing surface.

Increasing the distance between the hot feed and the condensing surface decreases the heat loss across the membrane while increasing the overall mass-transfer resistance. Choosing the correct gap is important for optimum operation.

For highly porous membranes, the air entrapped in the membrane pores can be a significant component of the total mass-transfer resistance. Thus, deaeration of the feed can be beneficial. It has also been demonstrated that feed pretreatment to remove surfactants can boost transport rates.

Heat losses across the membrane arise through either conduction or convection. Also, the establishment of temperature gradients in the feed (thermal-polarization) can reduce the available driving force for transport. It has been estimated that in membrane distillation 20–70% of the available driving force is actually utilized. Concentration polarization, which is usually significant in other membrane processes, such as ultrafiltration or reverse osmosis, is less important in membrane distillation.

The two important parameters defining the efficiency of a membrane distillation process are the

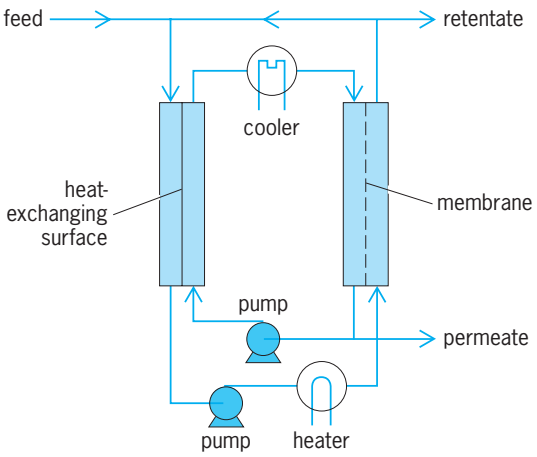

Membrane distillation process with heat recovery. (*After A. C. M. Franken and S. Ripperger, Terminology for Membrane Distillation, European Society of Membrane Science and Technology, 1988*)

energy efficiency [Eq. (1)] and the separation efficiency or concentration factor [Eq. (2)]:

$$\text{Energy efficiency} = \frac{\text{heat used to evaporate permeate}}{\text{total energy input to process}} \quad (1)$$

$$\text{Concentration factor} = \frac{\text{concentration of component in permeate}}{\text{concentration of component in feed}} \quad (2)$$

A schematic diagram of a membrane distillation operation is shown in the **illustration**. The input of energy required to heat and condense vapor is the same for membrane distillation as for traditional evaporation processes. Some degree of heat recovery is possible to improve the overall energy efficiency of the process. Feed can be recycled in order to increase concentration of nonvolatile substances to a desired level.

Membrane materials and modules. Membranes for membrane distillation must be microporous (diameter of pores, 0.2–5 micrometers) and also nonwetting with respect to the feed. Other desirable qualities are chemical and thermal resistance, narrow pore-size distribution, high total porosity, and low thermal conductivity. Water transport fluxes across membranes are typically in the range of 0.2–4 lb/ft^2-h (1–20 kg/m^2-h), depending on temperature differentials of 9–108°F (5–60°C).

Most of the available membranes have been designed for aqueous applications. They are made of hydrophobic polymers such as polypropylene, poly(tetrafluoroethylene), and poly(vinylidene fluoride). Composite membranes consisting of layers of different hydrophobic and hydrophilic materials are also available. Membranes can be produced in either flat-sheet or hollow-fiber/tubular geometries. Microporosity is induced either by mechanical stretching or by a phase-inversion (thermal) process. Higher fractional pore areas give higher transport rates; however, the pore size must be less than the critical pore size at which the liquid would penetrate the membrane. Membrane modules have been developed in various configurations, including spiral-wound, plate-and-frame, and hollow-fiber.

Applications. Membrane distillation has been studied for separations such as sugar solution concentration, dilute blood concentration, and desalination. The economic outlook for membrane distillation compared to either reverse osmosis or multistage flash evaporation has not been determined.

Potential advantages of membrane distillation over traditional evaporation processes include operation at ambient pressures and lower temperatures as well as ease of process scale-up. The additional resistance to mass transfer posed by the membrane can be compensated for to some extent by the high ratio of membrane surface area to volume that can be obtained in commercial membrane modules.

While membrane distillation does not require heating the feed to its boiling point, its value as a commercial process is dependent on the available feed temperature; it works best when a low-grade or waste heat source is available. *See* CHEMICAL SEPARATION TECHNIQUES; MEMBRANE SEPARATIONS; WATER DESALINATION.

S. S Kulkarni; Norman N. Li

Bibliography. S. I. Andersson, N. Kiellander, and B. Rodesjo, Design and field tests of a new membrane distillation desalination process, *Desalination*, 56:345–354, 1985; E. Drioli, V. Calabro, and V. Wu, Microporous membranes in membrane distillation, *Pure Appl. Chem.*, 58(12):1657–1662, 1986; A. G. Fane, R. W. Schofield, and C. J. D. Fell, The efficient use of energy in membrane distillation, *Desalination*, 64:231–243, 1987; A. C. M. Franken and S. Ripperger, *Terminology for Membrane Distillation*, European Society of Membrane Science and Technology, 1988; K. Sakai et al., Effects of temperature and concentration polarization on water vapor permeability for blood in membrane distillation, *Chem. Eng. J.*, 38:B33–39, 1988; S. Timashev, *Physical Chemistry of Membrane Processes*, 1991.

Membrane mimetic chemistry

The study of processes and reactions whose developments have been inspired by the biological membrane. Faithful modeling of the biomembrane is not an objective of membrane mimetic chemistry. Rather, only the essential components of natural systems are recreated from relatively simple, synthesized molecules. Mimetic systems are designed for well-defined purposes. The insight gained into the functioning of real membranes is considered a bonus. (The term membrane mimetic is more restrictive than the term biomimetic. Biomimetic chemistry is directed at the mechanistic elucidation of biochemical reactions and at the development of new compounds modeled on, and expected to mimic, specific biological systems. The focal point of most biomimetic chemistry is enzyme modeling.) *See* CELL MEMBRANES.

Surfactant aggregates. These systems—micelles, monolayers, organized multilayers (Langmuir-Blodgett films), bilayer lipid membranes, and vesicles—have been used, for the most part, in membrane mimetics.

Surfactants, or detergents, contain distinct hydrophobic (apolar) and hydrophilic (polar) regions. Depending on the chemical structure of their hydrophilic polar head groups, surfactants can be neutral, positively charged, or negatively charged. The hydrophobic part can vary in length (typically 8 to 20 carbon atoms), contain multiple bonds, or consist of two or more hydrocarbon chains. Head group–to–tail volume ratios determine, to a first approximation, the type of aggregates formed from a given surfactant. Various types of aggregates formed from surfactants are shown in the **illustration**. *See* DETERGENT.

Aqueous micelles. These spherical aggregates, 4–8 nanometers in diameter, are formed dynamically from surfactants in water above a characteristic concentration, the critical micelle concentration. Micelles break up and reform rapidly by two known processes. The first process occurs on a microsecond time scale and is due to the release of a single surfactant and its subsequent reincorporation in the micelle. The second process occurs on a millisecond time scale and is ascribed to the dissolution of the micelle and to the subsequent reassociation of the monomers. Substrate interaction with the micelle is also dynamic. *See* MICELLE.

Monolayers. These monomolecular layers are formed by spreading naturally occurring lipids or synthetic surfactants, dissolved in volatile solvents, over water in a trough. The polar head groups of the surfactants are in contact with water, the subphase, while their hydrocarbon tails protrude above it. Monolayers are characterized by surface area-surface pressure curves, surface potentials, and surface viscosities. *See* MONOMOLECULAR FILM.

Multilayers. Techniques have been developed for transferring the monolayer onto a solid support and for building up organized multilayer assemblies (Langmuir-Blodgett films) in controlled topological arrangements.

Bilayer lipid membranes. These are formed by brushing an organic solution of a surfactant (or lipid) across a pinhole (2–4 mm or 0.08–0.16 in. in diameter) separating two aqueous phases. Alternatively, bilayer lipid membranes can be formed from monolayers by the Montal-Mueller method. In this method the surfactant, dissolved in an apolar solvent, is spread on the water surface to form a monolayer below the poly(tetrafluoroethylene) partitioning which contains the pinhole (0.1–0.5 mm or 0.004–0.02 in. in diameter). Injection of an appropriate electrolyte solution below the surface raises the water level above the pinhole and brings the monolayer into apposition to form the bilayer lipid membrane.

Vesicles. These are prepared by sonication from naturally occurring phospholipids or from such simple surfactants as dioctadecyldimethylammonium bromide (DODAB) or dihexadecylphosphate (DHP). They are single bilayer spherical aggregates with diameters of 50–100 nm and bilayer thickness of around 5 nm. Unlike micelles, vesicles do not break down on dilution. Nevertheless, they are dynamic

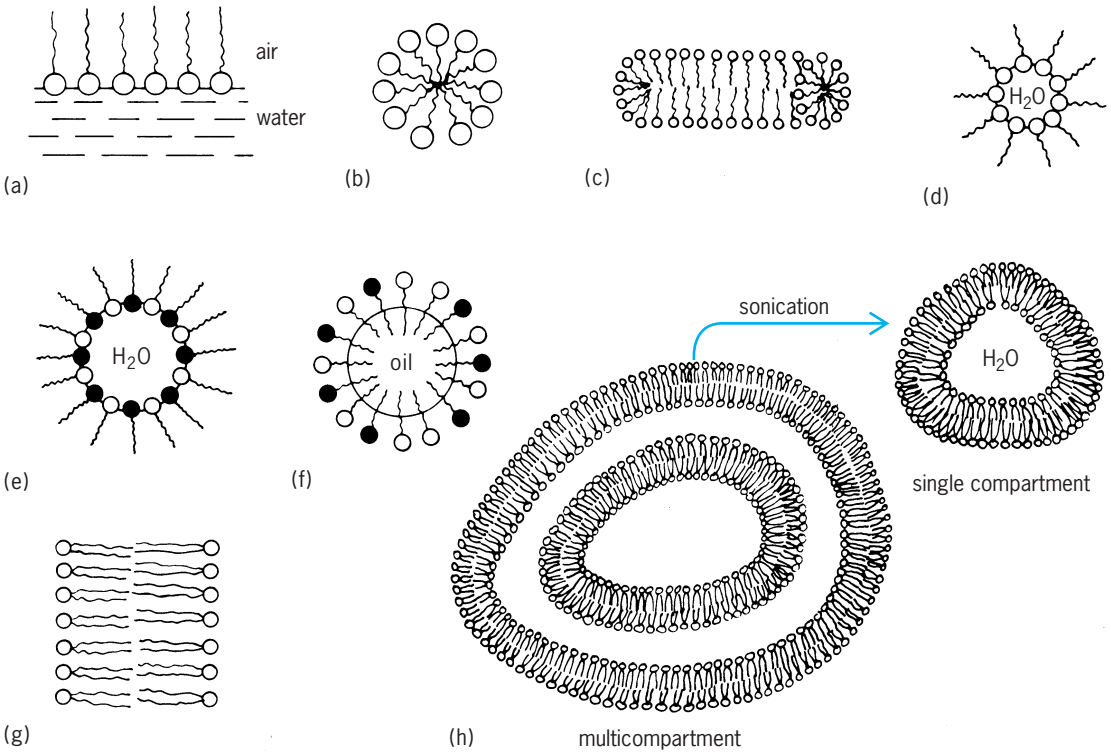

Simplified representation of organized aggregates formed from surfactants. (*a*) Monoloyer. (*b*) Spherical micelli. (*c*) Rodlike micelle. (*d*) Reversed micelli. (*e*) Water-in-oil microemulsion. (*f*) Oil-in-water microemulsion. (*g*) Bilayer lipid membrane. (*h*) Vesicles.

structures. They undergo phase transition, fuse, and are osmotically active. Molecular motions of the individual surfactants in the vesicles involve rotations, kink formation, lateral diffusion on the vesicle plane, and transfer from one interface of the bilayer to the other (flip-flop). Vesicles are capable of organizing a large number of molecules in their compartments. Hydrophobic molecules can be distributed among the hydrocarbon bilayers of vesicles. Polar molecules may move about relatively freely in vesicle-entrapped water pools, particularly if they are electrostatically repelled from the inner surface. Small charged ions can be electrostatically attached to the oppositely charged vesicle surfaces. Species having charges identical with those of the vesicles can be anchored onto the vesicle surface by a long hydrocarbon tail. *See* SONOCHEMISTRY.

The need for increased stabilities, controllable sizes, and permeabilities led to the development of polymerized surfactant vesicles. Vesicle-forming surfactants have been functionalized by vinyl, methacrylate, diacetylene, isocyano, and styrene groups in their hydrocarbon chains or at their head groups. Accordingly, surfactant vesicles could be polymerized in their bilayers or across their head groups. In the latter case, either the outer or the inner vesicle surfaces could be linked separately. All polymerized vesicles show enhanced stabilities compared with their unpolymerized counterparts. They have extensive shelf lives and remain unaffected by the addition of up to 30% alcohol.

Applications. Within a remarkably short time, membrane mimetic chemistry has become a versatile chemical tool. Applications of compartmentalization of reactants in membrane mimetic systems involve altered reaction rates, products, stereochemistries, and isotope distributions. Monolayers and organized multilayers can be employed profitably as molecular electronic devices. Opportunities also exist for using different surfactant aggregates with polymeric membranes for the control and regulation of reverse osmosis and ultrafiltration. The combination of judiciously selected polymeric membranes and functionalized surfactants holds the key for efficient membrane reactors. *See* ULTRAFILTRATION.

Well-constructed surfactant vesicles and polymerized surfactant vesicles can be used as compartments for drugs, offering the possibility of target directing. The exclusive delivery of a given drug in a controllable manner has long been a goal of pharmacists. Much of the activity in this area is based on liposomes (vesicles prepared from phospholipids of biological origin) together with immunological methodologies. Chemists are investigating the use of polymerized vesicles as hosts for drugs. On-command depolymerization (by an enzyme, for example) could trigger the release of drugs at the desired targets. *See* LIPOSOMES; SURFACTANT.

Janos H. Fendler

Bibliography. J. H. Fendler, *Membrane-Mimetic Approach to Advanced Materials*, 2000; J. H. Fendler, *Membrane Mimetic Chemistry*, 1982; J. H. Fendler and P. Tundo, Polymerized surfactant aggregates: Characteristics and utilization, *Acc. Chem. Res.*, 17:3–8, 1984.

Membrane separations

Processes for separating mixtures by using thin barriers (membranes) between two miscible fluids. A suitable driving force across the membrane, for example, concentration or pressure differential, leads to the preferential transport of one or more feed components.

Types of processes. Membrane separation processes are classified under different categories depending on the materials to be separated and the driving force applied: (1) In ultrafiltration, liquids and low-molecular-weight dissolved species pass through porous membranes while colloidal particles and macromolecules are rejected. The driving force is a pressure difference, typically 10–200 lb/in.^{2} (70–1400 kilopascals). (2) In dialysis, low-molecular-weight solutes and ions pass through while colloidal particles and solutes with molecular weights greater than 1000 are rejected under the conditions of a concentration difference across the membrane. (3) In electrodialysis, ions pass through the membrane in preference to all other species, due to a voltage difference. (4) In reverse osmosis, virtually all dissolved and suspended materials are rejected and the permeate is a liquid, typically water. Pressure differences up to 800 lb/in.^{2} (6 megapascals) are used. (5) For gas and liquid separations, unequal rates of transport can be obtained through nonporous membranes by means of a solution and diffusion mechanism. Pressure differences in the range of 15–1500 lb/in.^{2} (0.1–10 MPa) are typical. Pervaporation is a special case of this separation where the feed is in the liquid phase while the permeate, typically drawn under subatmospheric conditions, is in the vapor phase. (6) In facilitated transport, separation is achieved by reversible chemical reaction in the membrane. High selectivity and permeation rate may be obtained because of the reaction scheme. Liquid membranes are used for this type of separation.

Some examples of mixtures separated by membranes are shown in the **table**. Since membranes are permeable to all feed components, though with different permeation rates, a membrane process may require staging to meet specified product concentrations. Various flow and recycle schemes can be used in a multistage process. *See* DIALYSIS; ION-SELECTIVE MEMBRANES AND ELECTRODES; OSMOSIS; ULTRAFILTRATION.

Membrane characteristics. Most membranes are thin polymer films. Since the transport rate through the membrane increases with decreasing membrane thickness, techniques have been developed to make ultrathin, separating films without sacrificing membrane strength. For example, cellulose acetate membranes can be made in an asymmetric form, where a thin dense layer (0.01–0.1 micrometer) is supported by a thick porous substrate (50–100 μm) which provides strength but little resistance to transport. Another technique is to make thin-film-composite membranes where a thin, separating layer of one material is cast on a porous support of another polymer.

Materials other than polymers can also function as membranes. Palladium can separate helium from

Mixtures separated by membrane permeation

Membrane	Temp., °C (°F)	Components	Feed comp., wt %	α B/A
Polyethylene	60 (140)	Methanol	39.1	6.5
		Benzene	60.9	
	25 (77)	Ethylene	50	3.0
		Methane	50	
Polyethylene (conditioned)	30 (86)	*o*-Xylene (A)	30*	1.59 (B/A)
		m-Xylene (B)	65*	1.26 (C/B)
		p-Xylene (C)	5*	2.01 (C/A)
Polypropylene	25 (77)	Ethylene	50	1.95
		Methane	50	84
	60 (140)	*n*-Dodecane	46	
		n-Heptane	54	
Polystyrene	30 (86)	Nitrogen	—	16†
		Helium	—	
Poly(tetrafluoroethylene)	25 (77)	Ethylene	55	1.25
		Methane	45	25*
	30 (86)	Nitrogen	—	
		Helium	—	
Polyethylene terephthalate	25 (77)	Methane	—	170*
		Helium	—	
Nylon	40 (104)	Chloroform	37.5	1.34
		Trichloroethylene	62.5	
Silicone rubber	30 (86)	Nitrogen	—	1.5†
		Helium	—	
Cellulose acetate	—	*n*-Hexane	—	17–130
		Ethanol	—	
	25 (77)	Ethylene	45	1.66
		Methane	55	
Ethylenediamine/polyepichlorohydrin/isophthaloyl chloride	55 (131)	Sodium chloride	3.596.5	167
		Water		
Liquid membrane: surfactant/Isopar M/LIX 64N‡	35 (95)	Water	99.94 0.06	500–2800
		Copper salts		

*Vol %.
†Calculated as ratio permeability coefficients.
‡Surfactant is a polyamine, Isopar M is an isoparaffin solvent, and LIX 64N is a chelating agent.

other gases while silica can be used for hydrogen separation.

Liquid films have been used in two ways as membranes: (1) Immobilized liquid membranes: a liquid is held by a porous (∼80% void) polymer support. (2) Liquid surfactant membranes: the membrane is formed by making an emulsion of two immiscible fluids and dispersing the emulsion in a third continuous phase. The immiscible membrane separates the encapsulated phase from the continuous phase.

Advantages and limitations. In general, membrane separation processes have potential advantages for mixtures of thermally unstable components; mixtures of components with similar chemical and physical properties, such as xylene isomers; and separations without phase change, as contrasted to distillation, such as desalination by reverse-osmosis membranes. Membranes may also be used in combination with conventional separation units, for example to break an azeotropic solution before feeding it to a distillation column. Energy savings are possible by using a membrane to concentrate a stream or to make a rough-cut separation before going to an evaporator or distillation unit. *See* WATER DESALINATION.

Usually, membranes are used only under mild temperature conditions. The presence of various chemically active agents or organic solvents in the feed may lead to plasticizing problems and eventual membrane deterioration.

Quantification of separation. The degree of separation obtained in a single membrane module is expressed as a separation factor α defined in terms of concentrations C, as shown in Eq. (1), where sub-

$$\alpha = \frac{(C_A/C_B)_P}{(C_A/C_B)_R} \tag{1}$$

scripts A, B, P, and R refer to a permeate component, reference component, permeate phase, and raffinate phase, respectively. Separation factor α can be a function of temperature, pressure, feed composition, flow rates, and directions of flow on the feed and permeate sides, for example, countercurrent, crossflow, or cocurrent.

For gas permeation, the separation obtainable with a given membrane is often quantified by a selectivity factor (P_A/P_B), where the permeability constant P is defined by the relation given in Eq. (2),

$$F_A = \frac{P_A}{\delta} \Delta p_A \qquad (2)$$

where F is the flux/area, δ is the membrane thickness, and Δp represents the partial pressure difference across the membrane. Using Fick's first law, P can be shown to be the product of an effective diffusion constant and an effective solubility constant. P can be a strong function of pressure (or concentration) for organic gases and vapors. *See* DIFFUSION; TRANSPORT PROCESSES.

Norman N. Li; Sudhir S. Kulkarni

Bibliography. J. R. Critser, Jr., *Membrane Separation Processes*, 1994; H. C. Hayworth and N. N. Li, Extraction of uranium by liquid membranes, *Separat. Sci. Technol.*, 18(6):493, 1983; S. T. Hwang and K. Kammermeyer, *Membranes in Separations*, 1975; N. N. Li and H. Strathmann (eds.), *Separation Technology*, 1988; P. Meares, *Membrane Separation Processes*, 1976.

Memory

The ability to store and access information that has been acquired through experience. Memory is a critical component of practically all aspects of human thinking, including perception, learning, language, and problem solving. Through its elaborate mechanisms for sorting, organizing, and storing information, memory provides people with the building blocks necessary to structure their knowledge of the world and, ultimately, of themselves. *See* PERCEPTION; PROBLEM SOLVING (PSYCHOLOGY).

Stages. The information-processing approach divides memory into three general stages: sensory memory, short-term memory, and long-term memory. Sensory memory refers to the sensations that briefly continue after something has been perceived. For example, if a person sits in a dark room and then is subjected to a flash of light for just a moment, the image will linger after darkness returns. Sensory memories occur for all five senses and are usually very similar to the perceptions from which they arise. Short-term memory includes all of the information that is currently being processed in a person's mind, and is generally thought to have a very limited capacity. Memorizing a telephone number just long enough to dial it is an example of a task that involves short-term memory. Long-term memory is the storehouse of the mind, where all the information that may be used at a later time is kept. Childhood memories of the beach as well as what dinner comprised one night ago are examples of long-term memories.

Sensory memory. Psychologists were long aware of sensory memory without being able to experimentally demonstrate its full capacity. For example, after viewing a briefly flashed slide, subjects reported seeing the entire image gradually fade away. However, by the time they tried to describe what they saw, most of their sensory memory had faded. G. Sperling devised a technique known as the partial report test to demonstrate the full extent of sensory memory. Sperling's experiment had two different conditions for reporting the contents of a briefly flashed slide containing three rows of letters. In the full report condition, subjects saw the slide, and afterward had to name as many of the letters as they could. Subjects in this condition could identify only about a third of the letters. In the partial report condition, Sperling flashed the same slide, but immediately afterward gave subjects a tone indicating which row of letters they were to name. With the partial report technique, subjects could name almost all of the items in any of the three rows. Since subjects did not know which row they would have to name until after the image physically disappeared, they must have had a memory of all of the items in the slide. Subjects in the full report condition probably had the same full memory, but could name only a few letters before their memory faded. Thus, Sperling's experiment suggested that people have a very detailed sensory memory that lasts only a brief time.

A number of interesting facts are known about sensory memory, including the following: (1) sensory memories appear to be associated with mechanisms in the central nervous system rather than at the sensory receptor level, and (2) the amount of attention that a person pays to a stimulus can affect the duration of the sensory memory. Although all of the functions of sensory memory are not understood, one of its most important purposes is to provide people with additional time to determine what should be transferred to the next stage in the memory system, commonly known as short-term memory.

Short-term memory. Information obtained from either sensory memory or long-term memory is processed in short-term memory in order for a person to achieve current goals. In some situations, short-term memory processing simply involves the temporary maintenance of a piece of information, such as remembering a phone number long enough to dial it. Other times, short-term memory can involve elaborate manipulations of information in order to generate new forms. For example, when someone reads 27 + 15, the person manipulates the symbols in short-term memory in order to come up with the solution.

One useful manipulation that can be done in short-term memory is to reorganize items into meaningful chunks. For example, it is a difficult task to keep the letters S K C A U Q K C U D E H T in mind all at once. However, if they are rearranged in short-term memory, in this case reversing them, they can be reduced to a single simple chunk: THE DUCK QUACKS. Short-term memory can accommodate only five to seven chunks at any one time. It therefore becomes very important that each chunk include as much information as possible.

Although, short-term memory holds only a limited number of chunks, the amount of information

contained in each chunk is constrained only by one's practice and ingenuity. In one study, an average college student participated in a 20-month program in which he learned to increase his short-term memory span from 7 to 80 random digits. The chunking trick that he used was associating groups of random numbers with familiar track records, an easy task for him since he was a runner. His accomplishment did not represent a general increase in short-term memory capacity (he could still recall only 7 random letters) but rather an improved strategy for organizing random digits. Thus, in order to increase the amount of information that can be kept in short-term memory at one time, people need to develop specific strategies for organizing that information into meaningful chunks.

Not only does manipulating information in meaningful ways increase the capacity of short-term memory, but it also appears to facilitate the transfer of information from short-term to long-term memory. For example, the running student who managed to chunk 80 random digits in his short-term memory was able to recall 80% of those digits days later. Many other studies have also demonstrated that the transfer of information from short-term to long-term memory is much greater when the information is manipulated rather than simply maintained.

Long-term memory. One can keep massive amounts of information in long-term memory. In general, recall from long-term memory simply involves figuring out the heading under which a memory has been filed.

One of the best ways to ensure that a long-term memory will be found is to memorize it with a very specific file heading. Thus, many tricks for effective retrieval of long-term memories involve associating the memory with another more familiar memory that can serve as an identification tag. This trick of using associations to facilitate remembering is called mnemonics. To make recall easier, a mnemonic called the method of loci may be employed which involves associating to-be-remembered items with series of places (or loci) that are already well fixed in memory. For example, to memorize the presidents of the United States, each president can be associated with a different piece of furniture in the house. By making this association, the furniture can then serve as reminders of the mental file in which the presidents' names can be found. Various other tricks involve associating a familiar memory with an unfamiliar memory. For example, one common way of learning new names is to associate the new person with an old friend or acquaintance with the same name.

Usually people do not make explicit attempts to associate a new memory with an old memory, and yet they are generally reasonably good at accessing long-term memories. This is because long-term memory is organized in a logical manner; that is, long-term memory stores related concepts and incidents in close range of one another. This logical association of memories is indicated by subjects' reaction times for identifying various memories. Generally, people are faster at recalling memories if they have recently recalled a related memory.

Considering that related memories are filed near each other, it is not surprising that one good way to locate a long-term memory is to remember the general situation under which it was stored. Accordingly, techniques that reinstate the context of a memory tend to facilitate remembering. For example, in one study divers learned a list of words underwater and were later tested either underwater or on land. The divers who were tested underwater were able to remember considerably more words. Subjects who learn words while they are in a good mood are more likely to remember them when they are in a good mood. Similarly, words memorized by subjects under the influence of alcohol are better remembered when again under the influence. In each of these cases, reinstating the context allows subjects to better locate the memories in their long-term memory file.

Sometimes information may not have been filed in long-term memory in the first place, or if it has, is inaccessible. In these situations, the long-term memory system often fills in the gaps by using various constructive processes. One common component to memory constructions is a person's expectations. Countless studies have also indicated that memories tend to systematically change in the direction of a prior expectation or inference about what is likely to have occurred.

In addition, a long-term memory often becomes distorted as the result of misleading suggestions. In one study, subjects watched a videotape of an auto accident. Later they were asked either "How fast were the cars going when they hit?" or "How fast were the cars going when they smashed?" On the average, subjects who heard the word "smashed" estimated that the cars were going faster, and were more likely to report having seen nonexistent broken glass. Studies like these indicate that the files in long-term memory are vulnerable to tampering.

Dual memory. The distinction between short- and long-term memory is supported by both physiological and experimental evidence. The experimental support for the distinction comes from a number of sources, including observations of people's recall of words from a memorized word list. When people are given a list of items to remember, the items at the beginning and at the end of the list are remembered well, while items from the middle of the list are remembered less well. The fact that the first few items have a good chance of being remembered is called the primacy effect. The fact that the last few items have a good chance of being remembered is called the recency effect. If a hundred people are given a list to remember, and the number who remember each item is graphed, the classic serial position curve will be seen (**Fig. 1**). The serial position curve can be explained because of the operation of both short-term and long-term memory. Items at the end of the list are remembered because they are in short-term memory at the moment the list begins to be recalled. These words are likely to be in short-term memory because no later items have displaced them. After they are

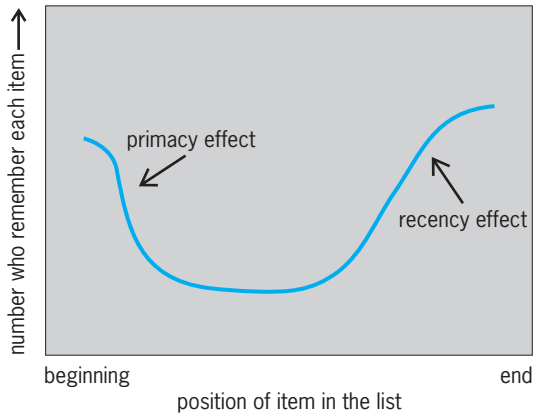

Fig. 1. Serial position curve.

reported, the contents of long-term memory can be searched. The items at the beginning of the list are more likely to be in long-term memory because they get more attention than do other items. Thus, the dual-memory distinction provides a relatively simple explanation for an otherwise puzzling experimental finding.

Although the dual-memory view is widely accepted, there are some theorists who argue that differences between alleged short- and long-term memories can be attributed to differences in how information is processed. One alternative to the dual-memory distinction is known as the levels-of-processing approach. It posits that memories differ only with respect to how "deeply" they have been processed. According to this argument, shallowly processed information will be quickly forgotten, while information that receives a deeper processing will be better remembered. The primary evidence for this view comes from incidental learning situations in which subjects participate in some task involving words. Later, to their surprise, the subjects are asked to recall the words that they previously worked with. Generally, incidental tasks involving "deep" processing (for example, determining the meaning of a word) are associated with better word recall then tasks involving "shallow" processing (for example, determining whether a word is in upper- or lowercase). Both the dual processing and the depth of processing concepts have something to offer. Specifically, depth of processing is an important factor in determining if a memory will last a long time. It is convenient to say that the resulting enduring memory is stored in long-term memory; certain physiological studies support this idea. *See* INFORMATION PROCESSING (PSYCHOLOGY).

Physiology. A number of physiological mechanisms appear to be involved in the formation of memories, and the mechanisms may differ for short-term and long-term memory. There is both direct and indirect evidence suggesting that short-term memory involves the temporary circulation of electrical impulses around complex loops of interconnected neurons. A number of indirect lines of research indicate that short-term memories are eradicated by any event that either suppresses neural activity (for example, a blow to the head or heavy anesthesia) or causes neurons to fire incoherently (for example, electroconvulsive shock). More direct support for the electric circuit model of short-term memory comes from observing electrical brain activity. By implanting electrodes in the brain of experimental animals, researchers have observed that changes in what an animal is watching are associated with different patterns of circulating electrical activity in the brain. These results suggest that different short-term memories may be represented by different electrical patterns. However, the nature of these patterns is not well understood. *See* ELECTROENCEPHALOGRAPHY.

Unlike short-term memories, long-term memories appear to involve some type of permanent structural or chemical change in the composition of the brain. This conclusion is derived both from general observations of the imperviousness of long-term memories and from physiological studies indicating specific changes in brain composition. Even in acute cases of amnesia where massive deficits in long-term memory are reported, often, with time, all long-term memories return. Similarly, although electroconvulsive therapy (shocking the brain in order to produce convulsions) is known to eliminate recent short-term memories, it has practically no effect on memories for events occurring more than an hour prior to shocking. Thus the transfer from a fragile short-term memory to a relatively solid long-term memory occurs within an hour. This process is sometimes called consolidation.

The nature of the "solid" changes associated with long-term memories appears to involve alterations in both the structural (neural connections) and chemical composition of the brain. One study compared the brains of rats that had lived either in enriched environments with lots of toys or in impoverished environments with only an empty cage. The cerebral cortices of the brains of the rats from the enriched environment were thicker, heavier, endowed with more blood vessels, and contained significantly greater amounts of certain brain chemicals (such as the neurotransmitter acetylcholine). Other researchers have observed that brief, high-frequency stimulation of a neuron can produce long-lasting changes in the neuron's communications across synapses.

Researchers believe that different brain structures may be involved in the formation and storage of long-term memories. The hippocampus, thalamus, and amygdala are believed to be critical in the formation of long-term memories (**Fig. 2**). Individuals who have had damage to these structures are able to recall memories prior to the damage, indicating that long-term memory storage is intact; however, they are unable to form new long-term memories, indicating that the long-term memory formation process has been disrupted. It is not known where long-term memories are stored, but they may be localized in the same areas of the brain that participated in the actual learning.

Types of long-term memories. Long-term memory will probably never be completely characterized by

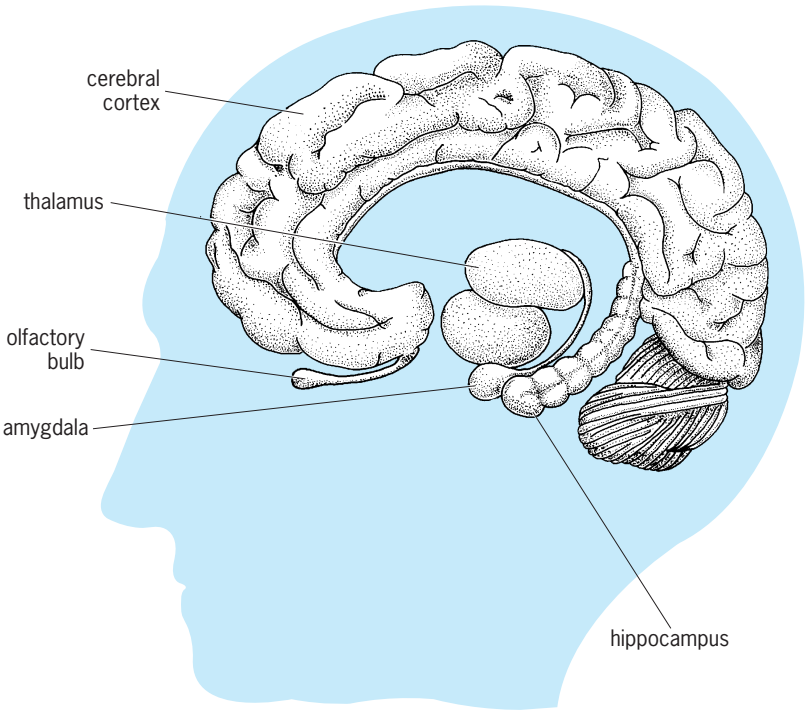

Fig. 2. Selected brain structures associated with memory. (*After C.B. Wortman, E. F. Loftus, and M. E. Marshall, Psychology, 3d ed., Knopf, 1988*)

general principles, because there are many different types of long-term memories.

Visual versus verbal memories. Visual and verbal memories are probably distinct, as suggested by physiological evidence from those who have suffered brain damage. Damage to the thalamus, for example, can result in a loss of the ability to form verbal memories without affecting the formation of visual memories. Visual memories and verbal memories also differ in quality: memory for pictures has been shown to be substantially better than memory for words.

While most people have visual memories, these memories are generally imprecise and are not to be confused with photographic memories—a rare type of memory that is associated with about 5% of young children, and very rarely with adults. People who possess photographic memory, also known as eidetic imagery, report being able to recall remarkable visual details. For example, when remembering a book they claim that they can actually read from the pages in their mind.

Olfactory memory. The unique relationship between memory and smell has long been appreciated, and it is now believed that the relatively direct connection between the olfactory system and the hippocampus, amygdala, and thalamus may account for the unique power of certain odors to elicit long-forgotten memories.

Skill memory. Memories for skills seems to be distinct from memory for general knowledge or events, as has been shown in persons with damage to the amygdala and hippocampus. Even though these individuals cannot generate new long-term memories for events, they still are able to acquire new skills. Skill memory is also different from other forms of long-term memory with respect to the processes of forgetting. Even though memories for most events fade with time, memory for skills, such as riding a bicycle, can last a lifetime.

Forgetting. In addition to investigating the mechanisms affecting memory, researchers have put considerable effort into determining how and why people forget. Forgetting has been associated with three major causes: decay, interference, and motivation.

Decay of memory traces. Decay theories of forgetting assume that memories fade and will gradually be lost if they are not occasionally refreshed. Although this model of forgetting seems intuitively sensible, and is in fact probably the source of some forgetting, there are a number of reasons why it can not fully explain forgetting. First, many memories do not fade even though they have not been recalled for a very long time. A second problem with decay theories of forgetting is that they are very difficult to distinguish from other theories. It is impossible for time to pass without the brain engaging in some type of activity. Consequently, theorists can never be sure whether forgetting is simply due to the passage of time or whether it is due to some activity in that time.

Interference. According to interference theories, forgetting occurs when one memory replaces or becomes confused with another memory. Evidence for interference comes from studies showing that some activities cause greater forgetting than others. Sleeping and being awake, for example, probably involve different levels of interference. If people learn a word list and are then tested 8 h later, they will recall considerably more words if they sleep during those 8 h. Presumably, sleeping reduces the amount of information that people encounter, and consequently reduces the amount of interferences with memory.

Psychologists have identified two different types of interference. Consider the situation of traveling in Europe, where one must learn the same phrases (hello, thank you, how much is the bill) in a number of different languages. If these phrases are learned first in French and later in German, learning them in German will interfere with the ability to recall the earlier learned French words. This situation, in which information that is learned later interferes with information that was learned earlier, is known as retroactive interference. In another type of interference, after having learned a number of phrases in French, it will be more difficult to learn those same words in German. Situations in which old memories inhibit the learning of new memories constitute proactive interference.

Motivated forgetting. The notion that people forget certain things because they want to is a central theme in Freud's psychoanalytic theory. Freud believed that unacceptable or anxiety-provoking thoughts are repressed by the unconscious in order to avoid confronting them directly. Although the processes involved in such motivated forgetting are far from being understood, it is clear that people can forget much about very disturbing events such as violent

crimes or horrendous automobile accidents.

Less dramatic unpleasant experiences are also often forgotten with time. As time passes, people become increasingly more likely to recall the pleasant aspects of an event. In addition, with time people tend to distort various other types of memories in a manner that makes them and their lives appear more worthwhile. For example, people may recall having better-paying jobs, voting more frequently, and donating more to charity than records indicate. Thus, selective forgetting allows memories to be shaped to better fit one's perceptions of the world and of oneself. *See* MOTIVATION.

Permanence. Some widely cited physiological research by W. Penfield was thought to suggest that many seemingly lost memories can be reactivated by direct electrical stimulation. Penfield stimulated particular areas of the brain in patients who were undergoing brain surgery. The patients, who were only under local anesthesia, often reported "reliving" various episodes from earlier times in their life. These observations led Penfield and many other psychologists to conclude that all experiences are kept in memory, and that forgetting simply involves an inability to find a particular memory.

Subsequent consideration of Penfield's findings, however, have shed doubt on this interpretation. Specifically, the experiences that people reported were never verified, so it is not certain that they were really memories at all. The patients might have been experiencing a process like dreaming, involving very lifelike qualities that do not actually correspond to real events. Thus, the question of the permanence of memory is still an open one.

Remembering forgotten memories. While it seems unlikely that everything experienced is recorded in memory, from time to time memories that were throught to be lost forever return. There have been some anecdotal reports that hypnosis can be used as a means of unlocking unavailable memories. However, controlled experimental studies indicate that hypnosis can just as often promote memory fabrications. A more promising technique for recovering difficult-to-remember memories has been developed—cognitive interview. This approach uses four general techniques for jogging memories about specific events such as a witnessed crime, including mentally going back to the scene of the memory; reporting everything, even partial information, regardless of its perceived importance; recounting the events in a variety of orders, such as in reverse; and reporting the event from the perspective of other individuals at the event. The cognitive interview can increase the amount of correct information obtained from witnesses by up to 35% without increasing memory fabrications. *See* LEARNING MECHANISMS.

Jonathan Schooler; Elizabeth F. Loftus

Bibliography. A. Baddeley, *Your Memory: A User's Guide*, 2d ed., 1996; J. Delacour, *Memory System of the Brain*, 1994; R. Fry, *Improve Your Memory*, 4th ed., 2000; D. J. Herrmann, *Memory Improvement Techniques*, 1988; E. F. Loftus, *Memory*, 1980.

Mendelevium

A chemical element, Md, atomic number 101, the twelfth member of the actinide series of elements. Mendelevium does not occur in nature; it was discovered and is prepared by artificial nuclear transmutation of a lighter element. Known isotopes of mendelevium have mass numbers from 248 to 258 and half-lives from a few seconds to about 55 days. They are all produced by charged-particle bombardments of more abundant isotopes. The amounts of mendelevium which are produced and used for studies of chemical and nuclear properties are usually less than about a million atoms; this is of the order of a million times less than a weighable amount. Studies of the chemical properties of mendelevium have been limited to a tracer scale. The behavior of mendelevium in ion-exchange chromatography shows that it exists in aqueous solution primarily in the 3 + oxidation state characteristic of the actinide elements. However, it also has a dipositive (2+)

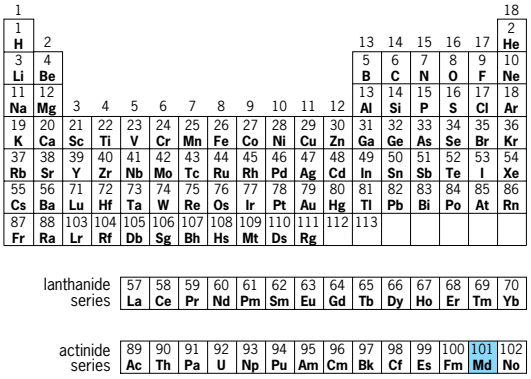

and a monopositive (1+) oxidation state. *See* ACTINIDE ELEMENTS; PERIODIC TABLE; TRANSURANIUM ELEMENTS.

Glenn T. Seaborg

Bibliography. S. Hofmann, *On Beyond Uranium: Journey to the End of the Periodic Table*, 2002; G. T. Seaborg, History of the synthetic actinide elements, *Actinides Rev.*, 1:3–38, 1967; G. T. Seaborg (ed.), *Transuranium Elements: Products of Modern Alchemy*, 1978; G. T. Seaborg and W. D. Loveland, *The Elements Beyond Uranium*, 1990.

Mendelism

Fundamental principles governing the transmission of genetic traits, discovered by an Augustinian monk Gregor Mendel. In 1856, Mendel performed his first set of hybridization experiments with pea plants in the monastery garden at Brno, Moravia. Although the pea plant is normally self-fertilizing, it can be easily crossbred, and grows to maturity in a single season. True breeding strains, each with distinct characteristics, were available from local seed merchants. For his experiments, Mendel chose seven sets of

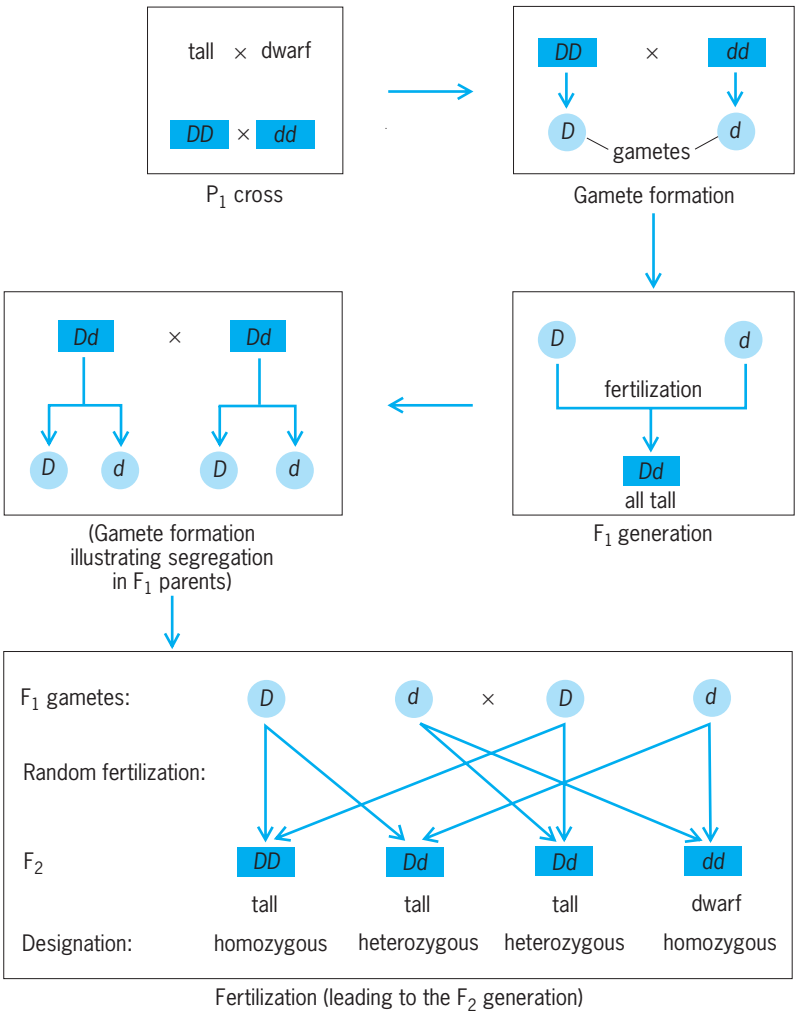

Schematic representation of a monohybrid cross. Pure-bred tall and dwarf strains are crossed, and yield typical 3:1 ratio in the F_2 generation. *D* and *d* represent the tall and dwarf factors (genes), respectively. (*After W. S. Klug and M. R. Cummings, Concepts of Genetics, Charles E. Merrill, 1983*)

contrasting characters or traits. For stem height, the true breeding strains tall (7 ft or 2.1 m) and dwarf (18 in. or 45 cm) were used. He also selected six other sets of traits, involving the shape and color of seeds, pod shape and color and the location of flowers on the plant stem.

The most simple crosses performed by Mendel involved only one pair of traits; each such experiment is known as a monohybrid cross. The plants used as parents in these crosses are known as the P_1 (first parental) generation. When tall and dwarf plants were crossed, the resulting offspring (called the F_1 or first filial generation) were all tall. When members of the F_1 generation were self-crossed, 787 of the resulting 1064 F_2 (second filial generation) plants were tall and 277 were dwarf. The tall trait is expressed in both the F_1 and F_2 generations, while the dwarf trait disappears in the F_1 and reappears in the F_2 generation. The trait expressed in the F_1 generation Mendel called the dominant trait, while the recessive trait is unexpressed in the F_1 but reappears in the F_2. In the F_2, about three-fourths of the offspring are tall and one-fourth are dwarf (a 3:1 ratio). Mendel made similar crosses with plants exhibiting each of the other pairs of traits, and in each case all of the F_1 offspring showed only one of the parental traits and, in the F_2, three-fourths of the plants showed the dominant trait and one-fourth exhibited the recessive trait. In subsequent experiments, Mendel found that the F_2 recessive plants bred true, while among the dominant plants one-third bred true and two-thirds behaved like the F_1 plants. *See* DOMINANCE.

Law of segregation. To explain the results of his monohybrid crosses, Mendel derived several postulates. First, he proposed that each of the traits is controlled by a factor (now called a gene). Since the F_1 tall plants produce both tall and dwarf offspring, they must contain a factor for each, and thus he proposed that each plant contains a pair of factors for each trait. Second, the trait which is expressed in the F_1 generation is controlled by a dominant factor, while the unexpressed trait is controlled by a recessive factor. To prevent the number of factors from being doubled in each generation, Mendel postulated that factors must separate or segregate from each other during gamete formation. Therefore, the F_1 plants can produce two types of gametes, one type containing a factor for tall plants, the other a factor for dwarf plants. At fertilization, the random combination of these gametes can explain the types and ratios of offspring in the F_2 generation (see **illus.**). *See* FERTILIZATION (ANIMAL); GENE.

Independent assortment. Mendel extended his experiments to examine the inheritance of two characters simultaneously. Such a cross, involving two pairs of contrasting traits, is known as a dihybrid cross. For example, Mendel crossed plants with tall stems and round seeds with plants having dwarf stems and wrinkled seeds. The F_1 offspring were all tall and had round seeds. When the F_1 individuals were self-crossed, four types of offspring were produced in the following proportions: 9/16 were tall, round; 3/16 were tall, wrinkled; 3/16 were dwarf, round; and 1/16 were dwarf, wrinkled. On the basis of similar results in other dihybrid crosses, Mendel proposed that during gamete formation, segregating pairs of factors assort independently of one another. As a result of segregation, each gamete receives one member of every pair of factors [this assumes that the factors (genes) are located on different chromosomes]. As a result of independent assortment, all possible combinations of gametes will be found in equal frequency. In other words, during gamete formation, round and wrinkled factors segregate into gametes independently of whether they also contain tall or dwarf factors. *See* GAMETOGENESIS; MEIOSIS.

It might be useful to consider the dihybrid cross as two simultaneous and independent monohybrid crosses. In this case, the predicted F_2 results are 3/4 tall, 1/4 dwarf, and 3/4 round, 1/4 wrinkled. Since the two sets of traits are inherited independently, the number and frequency of phenotypes can be

predicted by combining the two events:

$$\text{3/4 tall} \begin{cases} \text{3/4 round} & (3/4)\,(3/4) \\ & = 9/16 \text{ tall, round} \\ \text{1/4 wrinkled} & (3/4)\,(1/4) \\ & = 3/16 \text{ tall, wrinkled} \end{cases}$$

$$\text{1/4 dwarf} \begin{cases} \text{3/4 round} & (1/4)\,(3/4) \\ & = 3/16 \text{ dwarf, round} \\ \text{1/4 wrinkled} & (1/4)\,(1/4) \\ & = 1/16 \text{ dwarf, wrinkled} \end{cases}$$

This 9:3:3:1 ratio is known as a dihybrid ratio and is the result of segregation, independent assortment, and random fertilization.

Mendel published his work in 1866, but it went largely unheralded until 1900 when other investigators performed similar hybridization experiments and brought his work to the attention of the scientific world. The rediscovery of his work is regarded as the beginning of genetics as an organized discipline. Since then, genetic crosses with many different organisms have confirmed the fundamental nature and significance of Mendel's work. *See* GENETICS.

Michael R. Cummings

Bibliography. M. R. Cummings, *Human Heredity: Principles and Issues*, 5th ed., 1999; A. R. Hallauer and J. B. Miranda, *Quantitative Genetics and Maize Breeding*, 2d ed., 1988; K. Kim, *Explaining Scientific Consensus: The Case of Mendelian Genetics*, 1994; R. C. Olby, *The Origins of Mendelism*, 2d ed., 1985; G. Poste and S. T. Crooke (eds.), *New Frontiers in the Study of Gene Function*, 1987; T. Sasazuki (ed.), *New Approach to Genetic Diseases*, 1988.

Meninges

In mammals, the three membranes that cover the brain and spinal cord: the dura mater, the arachnoid membrane, and the pia mater.

The outermost, the dura mater, is a tough, fibrous, double-layered structure that is adherent to the skull. The inner layer of the dura mater sends separating sheets between the cerebral hemispheres and between the cerebrum and cerebellum. It also contains large venous sinuses and forms sheaths for nerves leaving the skull. The middle layer, the arachnoid, is a delicate serous layer loosely investing the brain. Below this is the spongy subarachnoid cavity which contains the circulating cerebrospinal fluid. The innermost layer, the pia mater, is a vascular layer which closely follows each convolution of the brain. Together the meninges furnish protection, blood supply, drainage, and cerebrospinal channels for the brain. The meninges around the spinal cord are less complex but basically similar to and continuous with those of the brain.

In submammalian forms, there may be only a single membrane, the meninx primitiva, or two membranes, the dura mater and pia-arachnoid. In forms in which the brain does not fill the cranial cavity, the volume of cerebrospinal fluid and of these membranes is increased. *See* NERVOUS SYSTEM (VERTEBRATE).

Thomas S. Parsons

Meningitis

Inflammation of the meninges. Diagnosis of meningitis is made from examination of a specimen of cerebrospinal fluid that is found in the subarachnoid space. The fluid sample is obtained by lumbar puncture (spinal tap) or, less commonly, by a ventricular tap, which requires passage of a needle into the brain tissue. Certain types of meningitis are associated with distinctive abnormalities in the cerebrospinal fluid. With certain types of meningitis, especially bacterial, the causative organism can usually be recovered from the fluid. *See* MENINGES.

Causes and types. Meningeal inflammation in most cases is caused by invasion of the cerebrospinal fluid by an infectious organism. Noninfectious causes also occur. For example, in immune-mediated disorders antigen-antibody reactions can cause meningeal inflammation. Other noninfectious causes of meningitis are the introduction into the cerebrospinal fluid of foreign substances such as alcohol, detergents, chemotherapeutic agents, or contrast agents used in some radiologic imaging procedures. Meningeal inflammation brought about by such foreign irritants is called chemical meningitis; it sometimes is associated with brain involvement. Inflammation also can occur when cholesterol-containing fluid or lipid-laden material leaks into the cerebrospinal fluid from some intracranial tumors.

The most common and most life-threatening types of meningitis are those caused by infectious organisms, usually bacterial or viral, and less frequently fungal, parasitic, rickettsial, or spirochetal. One type of meningitis is differentiated from another on the basis of symptoms and signs, epidemiologic aspects of the illness, and laboratory examinations, especially of blood and cerebrospinal fluid specimens.

Bacterial meningitis. Bacterial meningitis is among the most feared of human infectious diseases because of its possible seriousness, its rapid progression, its potential for causing severe brain damage, and its frequency of occurrence.

Most cases of bacterial meningitis have an acute onset. Common clinical manifestations are fever, headache, vomiting, stiffness of the neck, confusion, seizures, lethargy, and coma. Symptoms of brain dysfunction are caused by transmission of toxic materials from the infected cerebrospinal fluid into brain tissue and the disruption of arterial perfusion and venous drainage from the brain because of blood vessel inflammation. These factors also provoke cerebral swelling, which increases intracranial pressure and contributes to the symptoms of the illness. Before antibiotics became available, bacterial meningitis was almost invariably fatal.

Most types of acute bacterial meningitis are septic-borne in that they originate when bacteria in the

bloodstream (bacteremia, septicemia) gain entrance into the cerebrospinal fluid. Meningitis arising by this route is called primary bacterial meningitis. Secondary meningitis is that which develops following direct entry of bacteria into the central nervous system, which can occur at the time of neurosurgery, in association with trauma, or through an abnormal communication between the external environment and the cerebrospinal fluid.

Different age groups in childhood are predisposed to meningitis caused by certain specific bacteria. Also, in both children and adults, preexisting medical illnesses tend to be associated with meningitis caused by specific types of organisms. In the neonate, *Escherichia coli* and group B *Streptococcus* are the most common causes of bacterial meningitis. *Haemophilus influenzae* once accounted for most cases of acute bacterial meningitis between 3 months and 3 years of age. However, there is a vaccine that can be given in early infancy and therefore invasive infections caused by *H. influenzae* have become much less common. Other common causes of septic-borne meningitis beyond 2 months of age and including adults include *S. pneumoniae* and *Neisseria meningitidis*. Anaerobic bacteria are infrequent causes of meningitis but can complicate chronic illnesses such as dental sepsis, chronic sinusitis or otitis, and intra-abdominal suppurative diseases. *See* HAEMOPHILUS; MENINGOCOCCUS; PNEUMOCOCCUS; STAPHYLOCOCCUS; STREPTOCOCCUS; TUBERCULOSIS.

Other types. Many viruses can cause meningeal inflammation, a condition referred to as viral aseptic meningitis. The most common viral causes include the enteroviruses, the various herpesviruses, viruses transmitted by arthropods, the human immuno- deficiency virus type I (HIV-1), and formerly, the mumps virus. If the virus attacks mainly the brain rather than the spinal cord, the disorder is termed viral encephalitis. *See* ANIMAL VIRUS; ARBOVIRAL ENCEPHALITIDES; ENTEROVIRUS; HERPES.

Fungal, parasitic, and rickettsial meningitis are less common in the United States than are bacterial and viral. These infections are more likely to be subacute or chronic than those caused by bacteria or viruses; in most cases, the meningeal inflammation is associated with brain involvement. An acute form of aseptic meningitis can occur in the spirochetal diseases, syphilis and Lyme disease. *See* LYME DISEASE; MEDICAL MYCOLOGY; MEDICAL PARASITOLOGY; RICKETTSIOSES; SYPHILIS.

AIDS. An acute inflammatory meningeal syndrome can result either from HIV-1 itself or from various organisms which cause opportunistic infections in individuals with acquired immune deficiency syndrome (AIDS). The HIV-1 organism is believed to enter the brain and cerebrospinal fluid soon after the infection is acquired. The condition initially remains asymptomatic, but in 1–2% of cases it provokes a self-limited acute aseptic meningitis. This is characterized by headaches, malaise, fever, and signs of meningeal irritation, and can persist for several weeks. Among opportunistic infections in AIDS causing meningitis, the most common is of fungal origin, cryptococcosis. Syphilis is not considered to be an opportunistic infection in AIDS cases, but when it occurs, there is a higher incidence of acute syphilitic meningitis than occurs in non-AIDS individuals with syphilis. Symptoms include persistent headache and neck stiffness as well as a common occurrence of cranial nerve dysfunction, especially involving the facial and the acoustic nerves. *See* ACQUIRED IMMUNE DEFICIENCY SYNDROME (AIDS).

Diagnosis and treatment. A diagnosis of bacterial meningitis is made on the basis of cerebrospinal fluid abnormalities, such as the changes in the number and type of cells present and a decrease in the glucose content of the cerebrospinal fluid, as well as recovery of the causative organism from the fluid. Treatment is with high-dose intravenous antibiotics, chosen according to the suspected or proven offending organism. *See* ANTIBIOTIC; MEDICAL BACTERIOLOGY.

William E. Bell

Meningococcus

A major human pathogen belonging to the bacterial genus *Neisseria*, and the cause of meningococcal meningitis and meningococcemia. The official designation is *N. meningitidis*.

Characteristics and serological types. The meningococcus is a gram-negative, aerobic, nonmotile diplococcus, characteristically occurring in smears from clinical material in pairs with flattening of the adjoining sides. It is fastidious in its growth requirements and is very susceptible to adverse physical and chemical conditions. In appearance and biochemical activity, it resembles the gonococcus. The two organisms are most readily distinguished by the ability of the meningococcus to oxidize both glucose and maltose, while the gonococcus oxidizes glucose alone.

Thirteen serogroups of *N. meningitidis* can be distinguished serologically: A, B, C, D, X, Y, Z, 29E, W135, H, I, J, and L. Grouping is based on the antigenic differences between the capsular polysaccharides and is usually accomplished by agglutination reactions. Almost all strains isolated from blood or cerebrospinal fluid of cases can be serogrouped. However, nongroupable (nonencapsulated) strains are frequently isolated from the nasopharynx of healthy carriers. Within each serogroup, serotypes and subtypes can be identified on the basis of antigenic differences between the major outer-membrane proteins. Serotypes are identified by means of monoclonal antibodies. Serotype differences can also be detected among lipopolysaccharide antigens. The eight lipopolysaccharide serotypes are independent of the outer-membrane protein serotypes. Strain differentiation can also be based on genetic relatedness between strains, which is determined by means of multilocus electrophoresis. Differences in the electrophoretic mobility of cytoplasmic enzymes are used to identify allelic

variation in the corresponding genes and enable the recognition of electrophoretic types. *See* SEROLOGY.

Epidemiology. Humans are the only known natural host of the meningococcus. Transmission occurs by droplets directly from person to person. The most frequent site of infection is, asymptomatically, the nasopharynx. This is uncommon in infants and young children but is relatively frequent in adolescents and adults. Fifty percent of cases occur in children 2 months to 4 years, and 5% in children 5 to 14 years of age.

Most sporadic cases are caused by serogroups B and C, with disease to other serogroups being much less common. Almost all large epidemics and pandemics of meningococcal disease are caused by serogroup A. However, the largest known epidemic in a metropolitan area was caused in São Paulo, Brazil, by a serogroup C strain in the early 1970s. Large serogroup A and C outbreaks are associated with poverty and overcrowding. *See* EPIDEMIOLOGY.

Pathogenesis and disease. Susceptibility to bloodstream invasion from the nasopharynx has been shown to correlate with the absence of bactericidal antibody. The development of protective, natural antibody appears to result from acquisition of bacteria other than meningococci which possess antigens that cross-react with the serogroup- and serotype-specific surface antigens of the meningococcus. The most common clinical syndrome caused by the meningococcus is meningitis, which is characterized by fever, headache, nausea, vomiting, and neck stiffness and has a fatality rate of 15% (higher in infants and adults over 60). Disturbance of the state of consciousness quickly occurs, leading to stupor and coma. Many cases also have a typical skin rash. In 10–20% of cases caused by serogroups B and C but less often with serogroup A, a much more fulminant disease occurs in which overwhelming meningococcemia develops. As a result of the rapid release of large quantities of endotoxin, profound shock and hemorrhagic phenomena predominate. Death occurs within 6–24 h in most cases despite available treatment.

Occasionally a pneumonia or a transient febrile illness with self-limited meningococcemia occurs. The bacteremia frequently clears without antibiotic treatment.

Chronic meningococcemia is a rare manifestation, appearing most often in adults. This illness is characterized by recurrent episodes of fever, arthritis, myalgia, and rash. Meningococci are present in the blood only during febrile episodes.

Because of the widespread occurrence of strains of meningococci resistant to sulfonamides, penicillin G is the drug of choice for all forms of meningococcal disease. Penicillin-resistant strains of meningococci have been reported from many parts of the world and have become quite common in some European countries. However, penicillin resistance is still uncommon in North America. A third-generation cephalosporin is the most appropriate alternative for penicillin-resistant strains. Chloramphenicol is an effective alternative in individuals allergic to penicillin.

Prevention. In closed population groups and among household contacts of cases (especially children), there is a significantly increased risk of secondary cases. Antibiotics are recommended for close contacts of cases in order to interrupt transmission by eradicating the carrier state. Because of sulfonamide resistance, sulfonamides cannot be relied upon.

Vaccines against group A, C, Y, and W135 meningococci have been licensed and approved for use in certain circumstances. The vaccines, composed of purified capsular polysaccharides, are very safe and effective in preventing group-specific disease. Routine immunization of children is not recommended because of the limited immunogenicity in infants and the relatively short duration of protection. Routine immunization is used for military recruits in order to prevent meningococcal outbreaks during basic training. The vaccines are also recommended for epidemic control, close contacts of cases, and travelers to areas experiencing epidemics. *See* MEDICAL BACTERIOLOGY.

Ronald Gold

Menopause

The irreversible cessation of regular monthly uterine bleeding in the adult human female, marking the end of her ability to become pregnant. Menopause commonly occurs in the United States between the ages of 47 and 53. It probably occurs because the ovary runs out of eggs and the cyclic rise and fall of brain and ovarian hormones designed to prepare the uterus to receive and nourish pregnancy no longer occur.

Menopause is one event in the climacteric, the period of time during which the reproductive machinery slows down and finally stops. The biochemical hallmark of this period is a reduction in estrogen production by the ovary. Some estrogen continues to be produced by the adrenal gland and the fatty tissues throughout the body, but this amount is very small compared with premenopausal levels. Estrogen has widespread effects on both genital and extragenital systems, and the withdrawal of estrogen accounts for many of the signs and symptoms attributed to the menopause, although these are influenced by both hereditary and social factors.

Postmenopausal changes in the genital organs include atrophy of external structures, including loss of glandular tissue in the breasts as well as shrinkage of fat depots (adipose tissue) throughout the body, which results in wrinkling of overlying skin. The lining of the vagina and urethra becomes thin, easily traumatized, and susceptible to infection. Itching and burning of the vagina, as well as urinary urgency, increased frequency of voiding with small amounts of urine, night voiding, and urine loss upon coughing or laughing may result.

Withdrawal of estrogen may affect the cardiovascular system, with a rise in blood lipids that is

dangerous and with a greater risk of heart disease. Hot flashes and night sweats can occur because of hypothalamic instability of temperature regulation brought on by a lack of estrogen. The skeletal response to withdrawal of estrogen may include loss of both minerals and collagen matrix from bone. The resulting osteoporotic bone is thin, weak, and subject to fractures from minor trauma. *See* OSTEOPOROSIS.

Many psychological problems have been attributed to estrogen deprivation, but well-documented proof of those relationships is lacking. Appearance of the symptoms is probably the result of a loss of self-esteem brought about by the combination of physical changes, loss of reproductive capability, and awareness of aging.

While estrogen can reverse or halt many of the physical changes described, it will not prevent aging or restore reproductive ability. In addition, high-dose, long-term, unopposed estrogen use has been correlated with an increased risk of cancer of the uterus and possibly a slight increase in the risk of breast cancer. Estrogen alone is usually not given to women with a uterus: progesterone is added either continuously at a very low dose or intermittently, usually for 14 days, at a higher dose. Treatment of menopausal symptoms should be undertaken on an individual basis, with careful discussion of the risks and benefits currently known. *See* ESTROGEN; MENSTRUATION.

G. Guzinski

Bibliography. H. Judd and W. H. Utian, Current perspectives in the management of the menopausal and postmenopausal patient, *Amer. J. Obstet. Gynecol.*, 156:1279–1356, 1987.

Menstruation

Periodic sloughing of the uterine lining in women of reproductive age. Menstrual bleeding indicates the first day of the menstrual cycle, which lasts an average of 27–30 days, although ranges of 21–60 days have been recorded.

Menarche, the onset of menstruation, occurs between the ages of 9 and 16. The majority of females begin menstruating at ages 12–14. During the first few years, the duration and intensity of menstrual flow and the total cycle length may be quite variable, but regularity is gradually established.

Menstrual cycle. The menstrual cycle consists of cyclic changes in both the ovary and the uterus (**Fig. 1**). These changes are controlled by the interaction of several hormones. These include follicle-stimulating hormone (FSH) and luteinizing hormone (LH), which are secreted by the anterior pituitary, and the steroid hormones estrogen and progesterone, which are secreted by follicles in the ovary. At the beginning of the cycle, the follicle is stimulated by FSH. In response, it grows and secretes estrogen. The amount of estrogen secretion increases rapidly near the middle of the cycle. Estrogen, in turn, stimulates growth of the uterine lining (mucosa), which becomes thicker and fills with blood vessels. In midcycle, the rapid increase in estrogen causes a massive surge of LH release and a smaller release of FSH from the pituitary. This surge causes ovulation, which is the release of the ovum (egg) from the follicle. After ovulation, the follicle undergoes rapid changes and is then called a corpus luteum. The corpus luteum secretes progesterone in response to LH stimulation. Progesterone and estrogen together cause a further thickening of the uterine mucosa, preparing the uterus for pregnancy. If pregnancy does not occur, the corpus luteum degenerates, the uterine mucosa sloughs off, and the cycle begins again (**Fig. 2**).

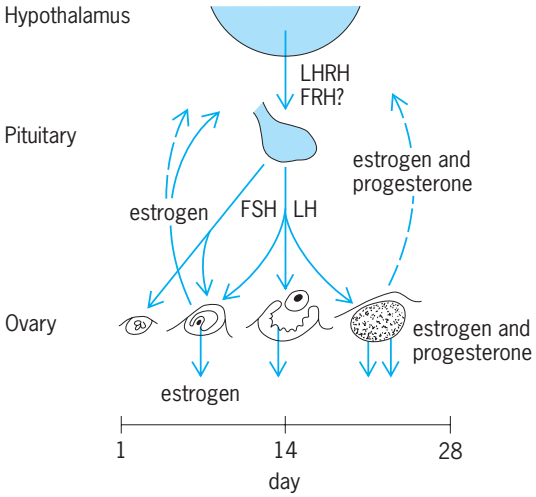

Fig. 1. Hormonal changes during the menstrual cycle. The broken arrows indicate inhibitory effects, and the solid lines, stimulatory effects. LHRH (luteinizing hormone–releasing hormone) and FRH (follice-releasing hormone) are released by the hypothalamus and stimulate the pituitary.

During the menstrual cycle, the uterine mucosa becomes richly supplied with small blood vessels and microscopic glands. When the corpus luteum degenerates, it produces less progesterone. This decline in progesterone at the end of the menstrual cycle causes constriction of the spiral arteries in the uterine lining, restricting blood flow to the mucosa. Without blood flow, the cells in the mucosa die and are sloughed away, causing menstrual bleeding. This menstrual bleeding, or menstrual flow, consists of small amounts of blood and uterine tissue. The microscopic glands in the mucosa produce chemicals called prostaglandins, which promote sloughing and may also cause uterine contractions. Menstrual flow ends when the spiral arteries constrict, and then a new mucosa develops as the cycle begins again. The menstrual flow (menses) lasts 3–7 days, with an average of 5 days, and a loss of approximately 30 ml (roughly 1.5 oz) of blood.

Amenorrhea. There is no menstrual bleeding during pregnancy, as the uterine mucosa is needed for the maintenance of pregnancy. This amenorrhea, or lack of normal ovarian function, sometimes continues during nursing. During nursing (lactation),

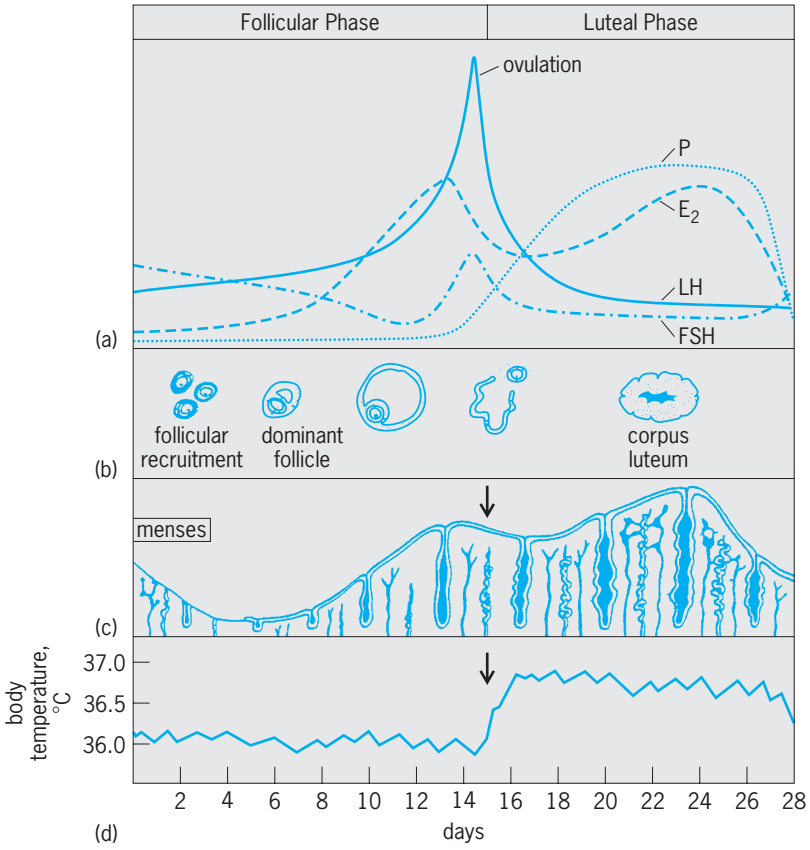

Fig. 2. Hormonal, ovarian, endometrial, and basal body temperature changes and relations throughout the normal menstrual cycle.

there is suppression of gonadotropin-releasing hormone (GnRH), which is needed for the LH surge that causes ovulation. This suppression is probably caused by prolactin, a hormone involved in milk production. Lactational amenorrhea generally lasts for 4–6 months after a woman gives birth. After this, however, ovulation may occur, and conception is possible, even before menses resumes.

Premenstrual tension syndrome. Physical changes before menstruation include a drop in body temperature, retention of fluids which may lead to swelling of the legs and abdomen, tenderness of the breasts, weight gain, and increased skin blemishes. The most common treatment for these symptoms is diuretics, drugs which promote fluid loss through increased urinary volume. Psychological changes may also occur before menstruation, including depression, fatigue, and increased irritability. Up to 40% of women have one or two of these symptoms, whereas approximately 5% have multiple or severe symptoms. The precise cause of premenstrual tension syndrome is not known, but the change in the ratio of estrogen to progesterone caused by falling progesterone levels is the suspected cause.

Menopause. Cessation of menses, or menopause, occurs at an average age of 51, with a range of 42–60 years. Prior to the onset of menopause, secretion of the pituitary hormones LH and particularly FSH increases, and the loss of follicles increases. After menopause, there is a decrease in estrogen production. These alterations of hormone levels cause various physical and sometimes emotional changes. *See* MENOPAUSE.

Janice M. Bahr

Mental retardation

A developmental disability characterized by significantly subaverage general intellectual functioning, with concurrent deficits in adaptive behavior. The causes are many and include both genetic and environmental factors as well as interactions between the two.

Diagnosis. Because the vast majority of persons with mental retardation have mild cognitive deficits (IQ 55 to 70), in most cases the diagnosis is not formally made until children have entered into school settings. School-age children with mental retardation manifest a delayed rate of learning, and may display frustration with the task demands that come with school. In the preschool years, the diagnosis is more likely to be established by evidence of delayed maturation in the areas of sensory-motor, adaptive, cognitive, social, and verbal behaviors. By definition, evidence of mental retardation must exist prior to adulthood, where vocational limitation may be evident, but the need for supervision or support may persist beyond the usual age of social emancipation.

Classification. Mental retardation can be divided into subgroups on the basis of etiology, degree of manifest intellectual retardation, and the need for supports. From the aspect of etiology, mental retardation can be classified by prenatal, perinatal, or postnatal onset. Prenatal causes include genetic disorders (inborn errors of metabolism, excess gene dosage), syndromal disorders (for example, conditions with a likely but as yet unknown genetic cause, or syndromes which result from in utero exposure to teratogens), and developmental disorders of brain formation. Upward of 700 genetic causes have been suggested as associated with the development of mental retardation. Additionally, many environmental influences on the developing fetus, for example, infection, and other unknown errors of development may account for mental retardation.

Perinatal causes include complications at birth, extreme prematurity, infections, and other neonatal disorders. Postnatal causes include trauma, infections, demyelinating and degenerative disorders, consequences of seizure disorders, toxic-metabolic disorders, malnutrition, and environmental deprivation. Even employing this broad classification scheme, often no specific cause can be identified to account for the mental retardation of a particular individual.

Subaverage intellectual functioning. Individuals with mental retardation are typically subclassified in terms of the manifest severity of cognitive disability as reflected by the ratio of mental age to chronological age, or intelligence quotient (IQ). Subaverage intellectual functioning is defined as an IQ score of at least two standard deviations below the mean, or approximately 70 to 75 or below. IQ tests must be individually administered and take into account an individual's educational and sociocultural background. Mild, moderate, severe, and profound degrees of mental retardation refer to two, three, four, or five standard deviations below the normal IQ for the general population.

Limitations in adaptive behavior, as assessed by standardized tests, must also be demonstrable in order to satisfy diagnostic criteria for mental retardation. This criterion is important because certain artistic or other gifts may not be revealed on formal IQ testing, and different levels of learning difficulty may be accentuated by the demands of specific environments. Outside such environments, an individual may navigate a normal course in life.

Comorbidity is frequently the rule in developmental disorders. A specific genetic or other cause of mental retardation may also predispose to other medical or neurologic conditions. Thus, children with trisomy 21 (Down syndrome) are at increased risk for cardiac malformation and thyroid abnormalities. Children with tuberous sclerosis complex (an inherited hardening or fibrosis of brain tissue resulting in mental defect) may have epilepsy and renal involvement. Children with fetal alcohol syndrome often have strabismus (incoordinated action of the muscles of the eyeball). In these circumstances, the comorbid medical conditions may increase the likelihood of emotional or behavioral problems, or contribute to the challenges with which a given child must contend in order to acquire new knowledge and new skills. In addition to medical comorbidity, researchers are increasingly recognizing certain patterns of behavior which associate with specific causes of mental retardation. In Prader-Willi syndrome, children develop an intense preoccupation with food and will eat to morbid obesity. Tantrums, aggression, and self-injury may occur when limits are set surrounding food consumption. In Lesch-Nyhan syndrome, children will compulsively self-injure, typically biting themselves to the point that protective restraint becomes necessary. In Velo-Cardio-Facial syndrome, children may present with extremely labile mood and impulsive behaviors.

Thus, the identification of cause can be important in planning for the medical, educational, and treatment needs of a particular individual.

Prevention and treatment. Over the past few decades, as the understanding of the mechanisms underlying mental retardation has grown, considerable progress has been made in both prevention and treatment. Diet is a method of treatment following early detection of phenylketonuria; warnings regarding alcohol consumption during pregnancy, lead exposure in infancy, and disease immunization and therapy are measures for prevention of retardation. Advances in prenatal, obstetrical, and neonatal care and genetic counseling have had the effect of reducing the incidence or the severity of various conditions. Energetic training and the application of psychosocial techniques (for example, early intervention programs) have resulted in improved social performance and adaptive behavior in many persons with mental retardation.

Bryan H. King

Bibliography. J. C. Harris, *Developmental Neuropsychiatry*, vols. 1 and 2, Oxford University Press, 1995; R. M. Hodapp, Development and disabilities: Mental, motor, and sensory impairments, Cambridge University Press, 1998; B. H. King et al., Mental retardation: A review of the past 10 years, Part I, *J. Amer. Acad. Child Adolescent Psychiat.*, 36:1656–1663, 1997; R. Luckason et al., *Mental Retardation: Definition, Classification, and System of Supports*, American Association on Mental Retardation, 1992; J. L. Matson and J. A. Mulick (eds.), *Manual of Diagnosis and Professional Practice in Mental Retardation*, American Psychological Association, 1996; M. State, B. H. King, and E. Dykens, Mental retardation: A review of the past 10 years, Part II, *J. Amer. Acad. Child Adolescent Psychiat.*, 36:1664–1671, 1997.

Menthol

A cyclic monoterpene alcohol (**1**) with melting point 40°C (104°F), specific optical rotation ($[\alpha]_D$) −50°. Menthol is the major component of the essential oil of peppermint. Since menthol has three chiral centers (asymmetric carbons), structure (**1**) is one of eight stereoisomers. These isomers can be grouped in two sets of four diastereoisomers. In one set the

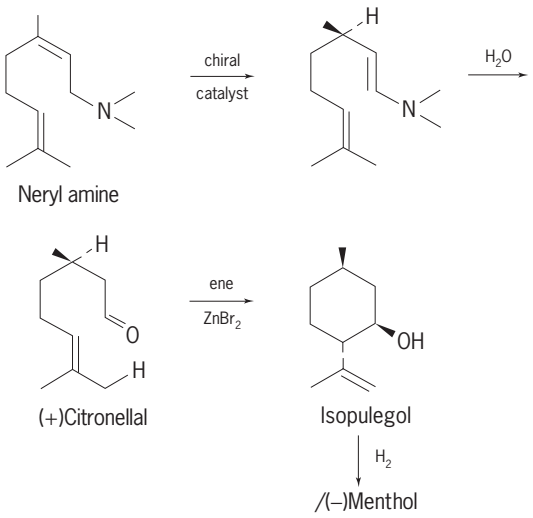

Enantioselective synthesis of /(-) menthol.

methyl group (CH_3) at C-5 is in the *R* configuration, as in structures (**1**)–(**4**). The other set of stereoisomers consists of the enantiomers of (**1**)–(**4**), with opposite configuration at each asymmetric center. *See* POLARIMETRIC ANALYSIS; STEREOCHEMISTRY.

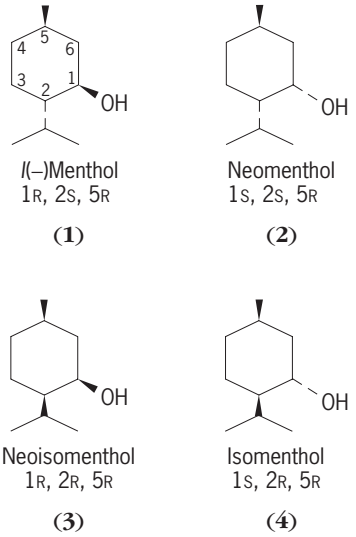

Menthol undergoes esterification, oxidation, and dehydration reactions typical of secondary alcohols. By oxidation to menthone, enolization at C-2, and reduction, an equilibrium mixture of the four diastereoisomers can be obtained. *l*(−)Menthol, in which all three substituents can be in an equatorial conformation, is the most stable of the diastereoisomers (60% at equilibrium). *See* TAUTOMERISM.

l(−)Menthol is produced in large amounts (about 3000 tons per year in 1980) from the oil of Japanese or Brazilian peppermint (*Mentha arvensis*). These oils contain about 80% menthol, much of which can be isolated by direct crystallization from the chilled oil. Neomenthol is a minor constituent.

Syntheses based on nonchiral starting materials such as thymol or citral have been used for the manufacture of racemic menthol [(**1**) and its enantiomer]. *l*(−)Menthol can be prepared by cyclization of (+) citronellal (from citronella oil) in an ene reaction (a pericyclic reaction) followed by hydrogenation. A method has been developed for the enantioselective synthesis of (+)citronellal with a chiral catalyst from an achiral starting material. This process is operating on an industrial scale (see **illus.**). *See* PERICYCLIC REACTION.

Menthol has a cooling, slightly anesthetic effect and is used in pharmaceutical preparations as an antitussive and antipruritic agent, and as a decongestant in nasal sprays. Most of the menthol produced is used in dentrifices, mouthwash, skin lotions, and so forth, and as a flavorant in tobacco, chewing gum, and confectionary products. For most of these purposes, the *l*(−)isomer is preferred. *See* TERPENE.

James A. Moore

Mercaptan

One of a group of organosulfur compounds which are also called thiols or thio alcohols and which have the general structure RSH. Aromatic thiols are called thiophenols, and biochemists often refer to thiols as sulfhydryl compounds. The unpleasant odor of volatile thiols causes them to be classed as stenches, but the odors of many solid thiols are not unpleasant.

Mercaptans (1) form salts with bases, (2) are easily oxidized to disulfides and higher oxidation products such as sulfonic acids, (3) react with chlorine (or bromine) to form sulfenyl chlorides (or bromides), and (4) undergo additions to unsaturated compounds, such as olefins, acetylenes, aldehydes, and ketones. The insoluble mercury salts (mercaptides) are used to isolate and identify mercaptans.

The important amino acid cysteine and many pharmaceutical and industrial products contain the mercapto group. Thus, thiosalicylic acid is used in synthesizing the germicide merthiolate; 2-mercaptobenzothiazole is a rubber vulcanization accelerator; 2,3-dimercaptopropanol (British antilewisite) is an antidote for arsenic poisoning; and 6-mercaptopurine is of interest in cancer chemotherapy. The occurrence and removal of mercaptans from petroleum is industrially important. Even the odor of mercaptans finds use; traces of mercaptans added to dangerous gases act as warning agents in case of leaks.

The name thio alcohols suggests that mercaptans are similar to alcohols. Although some properties are analogous, there are decided differences, related to (1) the greater acidities of thiols, (2) the ease with which mercaptans are oxidized, and (3) the ability of mercaptans to enter free-radical reactions. The second difference probably accounts for the absence of thiols, as such, in contrast to alcohols, in nature. *See* ORGANOSULFUR COMPOUND; PETROLEUM PROCESSING AND REFINING; RUBBER.

Norman Kharasch

Bibliography. I. L. Finar, *Organic Chemistry: The Fundamental Principles*, 6th ed., 1986; R. T. Morrison and R. N. Boyd, *Organic Chemistry*, 5th ed., 1987; S. T. Preston and R. Pankratz, *A Guide*

to the Analysis of Thioalcohols and Thioethers (Mercaptans and Alkyl Sulfides) by Gas Chromatography, rev. ed., 1981.

Merchant ship

A power-driven ship employed in commercial transport on the oceans and large inland bodies of water such as the Great Lakes. This article treats design considerations of merchant ships and includes detailed information on 10 merchant ship types. The relatively small craft used for inland waterway transportation are not commonly referred to as ships. For a description of such craft *see* INLAND WATERWAYS TRANSPORTATION.

Commodities transported by water are classified as break-bulk, unitized, or bulk (dry or liquid) cargoes. Generally, water cargo transportation is cheaper per ton-mile than land or air transportation. Although the volume of air transportation has increased considerably, approximately 90% of the United States overseas trade revenue is waterborne, while the rest is airborne. The specific cost of transporting break-bulk cargo by air is many times that of ocean transportation. Oceanic passenger transportation is vanishing, except for recreation purposes such as cruises.

Break-bulk cargo includes miscellaneous goods packed in boxes, bales, crates, cases, bags, cartons, barrels, or drums. It may also include lumber, motor vehicles, pipe, steel, and machinery. Vessels engaged pimarily in the transportation of break-bulk cargo are called break-bulk cargo ships (sometimes also called general cargo ships). Partial loadings of refrigerated cargo may be carried in break-bulk cargo ships in specially insulated and refrigerated holds. A ship which primarily carries refrigerated cargo is often called a reefer.

Under the heading of unitized cargo may be grouped cargo carried aboard in pallets, containers, wheeled vehicles (railway cars, trailers, and the like), and barges or lighters. There are pallets of several sizes, from 24 × 32 in. (61 × 81 cm) to 88 × 108 in. (224 × 274 cm), when rectangular, and from 36- to 48-in. (91- to 122-cm) squares. Cargo is stowed on pallets to various heights and secured by steel strapping. Usually, pallets are handled on board by forklift trucks. Pallet ships are those used exclusively for the carriage of pallets. There are also several sizes of containers, typically 8 × 8 ft (2.4 × 2.4 m) in cross section and 20 or 40 ft (6 or 12 m) in length.

Containers are built of aluminum, plywood, or steel. Generally, containers are nested in cells underdeck up to nine high in cargo holds, and stacked on deck on top of hatch covers not more than four high. Container ships are called full container ships when all their cargo is carried in containers, and these are almost exclusively handled by shoreside container-handling cranes. Some ships, such as break-bulk cargo ships, carry a partial load of containers. *See* MARINE CONTAINERS.

Cargo-carrying wheeled vehicles are rolled on and off the ship on side or end ramps and stowed on and secured to decks. Ships thus loaded are called roll-on/roll-off ships. In some special cases, wheeled vehicles are lowered or lifted vertically by means of cranes. Although ferryboats may transport cargo-carrying wheeled vehicles, their main purpose is to transport passengers or their vehicles or both.

Barges, or lighters, are handled by special shipboard gantry cranes, elevators, or rarely, heavy lift booms. When the main purpose is the carriage of barges, vessels are called barge-carrying ships. Unitized cargo consists of miscellaneous goods, such as those listed under break-bulk cargo, plus refrigerated cargo carried in insulated and refrigerated containers or trailers. There is a strong tendency toward cargo unitization, especially containerization, because of its inherent advantages, such as faster ship turnaround, interchangeability among different modes of transportation, door-to-door delivery from manufacturer to consumer, and reduction of cargo damage and pilferage.

Examples of bulk dry cargo are ore, coal, sugar, cement, and grain. These items are poured or otherwise loaded into the ship's cargo compartments (holds) without being boxed, bagged, or hand-stowed. In smaller quantities this cargo is also transported in break-bulk cargo ships. Vessels designed specifically for the ore or coal trade are referred to as ore carriers and colliers.

The principal bulk liquid cargoes are petroleum and its by-products. Others include liquefied gases, liquid chemicals, wine, fruit juices, and molten asphalt or sulfur. These liquids are transported in large tank spaces that are integral with, or separated from, the ship's main structure. Ships carrying bulk petroleum products are called tankers. In smaller quantities some bulk liquid cargoes are also transported in deep tanks in other vessels, such as break-bulk cargo ships.

A passenger ship, as defined by International Safety of Life at Sea (SOLAS) rules, carries more than 12 passengers on international voyages. Passenger ships navigating solely on inland waters are excepted from these rules. Passenger vessels that also transport cargo are called passenger-cargo ships.

Design Considerations

With very few exceptions, merchant ships conform to classification society rules. Classification societies are private organizations which issue rules for the construction, equipment, and maintenance of merchant ships. Compliance with their rules assures owners and insurers of the vessel's strength and seaworthiness.

Dimensions. Classification societies define the length between perpendiculars L_{pp} as approximately the distance from the bow to the rudder, but not less than 96% of the load waterline length (the immersed hull length when floating at the maximum permissible draft). The breadth of seagoing cargo ships 425 ft (130 m) long and over is approximately equal to 15% of the length, while smaller ships have relatively larger breadth. The depth of seagoing merchant ships from the keel to the strength deck

(usually the uppermost continuous deck) varies from approximately one-tenth to one-fourteenth the L_{pp}. For Great Lakes vessels, which operate under less severe conditions, the length-to-depth ratio may be as high as 18:1. Also, the length-to-breadth ratio is generally greater than that of oceangoing ships. For the same cargo capacity and speed, a relatively long, slender vessel, such as is found on the Great Lakes, is more costly to construct, but requires slightly less propulsive power and in bad weather need not slow down as much as a shorter vessel to avoid damage. *See* SHIP DESIGN; SHIPBUILDING.

The maximum permissible draft (submerged depth of ship) is limited by international load line regulations. The draft to which cargo ships can be loaded depends principally upon the depth of the ship below the freeboard deck, the length, and other factors, including the length of superstructure (deck erections) such as poop, bridge, and forecastle. The assigned draft corresponds to the load line (waterline at which the ship is allowed to go down in the water), which is distinguished by a mark on the side amidships (load line mark). The assigned freeboard is the distance measured vertically downward amidships from the upper edge of the deck line to the upper edge of the related load line. For dry cargo ships of 500–700-ft (150–210-m) length, the permissible freeboard is approximately 1.6% of the length, while for tankers of the same lengths it is approximately 1.3% of the length. (In other words, tankers are allowed smaller freeboards than are dry cargo ships because of the smaller, easier to keep watertight, deck openings and because of the large number of bulkheads which provide a high degree of subdivision.) Dry cargo ship freeboards may be closer to those of tankers, provided certain standards of subdivision and stability are met. Safety regulations usually require greater freeboard for passenger ships than for cargo ships.

If the draft at the bow is greater than at the stern, a ship is said to trim by the bow (or head). If greater at the stern, the ship trims by the stern. When fully loaded with homogeneous cargo, fuel, and water (no water ballast), ships seldom trim by the bow, but a 2- or 3-ft (0.6- or 0.9-m) trim by the stern is usually acceptable, except in restricted depths of water.

Bulkheads. Ships are divided into watertight compartments by transverse bulkheads (walls) to reduce the extent of seawater flooding in case of damage and to stiffen the hull structure. A normal 250-ft (75-m) general cargo ship has no less than four such bulkheads, and if the ship is 500 ft (150 m) long, eight bulkheads are typical. Passenger vessels usually have more bulkheads, as required by the international safety regulations.

Double bottom. An inner bottom is fitted between the peak (endmost) bulkheads. An inner bottom is horizontal plating, usually 3–5 ft (0.9–1.5 m) above the keel, extending from side to side of the ship. It provides tank space below (double bottom) for fuel oil, fresh water, and seawater ballast, and also minimizes chances of serious flooding in case of minor bottom damage, for example, from grounding.

Superstructures. The partial decks above the main deck, together with the ship's sides, enclose the superstructures. The one at the forward end is called the forecastle and the one aft, poop. Usually, when the machinery is located amidships, the bridge superstructure is placed above it. Above deck spaces that do not extend to the side are called deckhouses. Superstructures may be used partly for cargo stowage and together with the deckhouses provide space for living accommodations, ship's gear, equipment, and

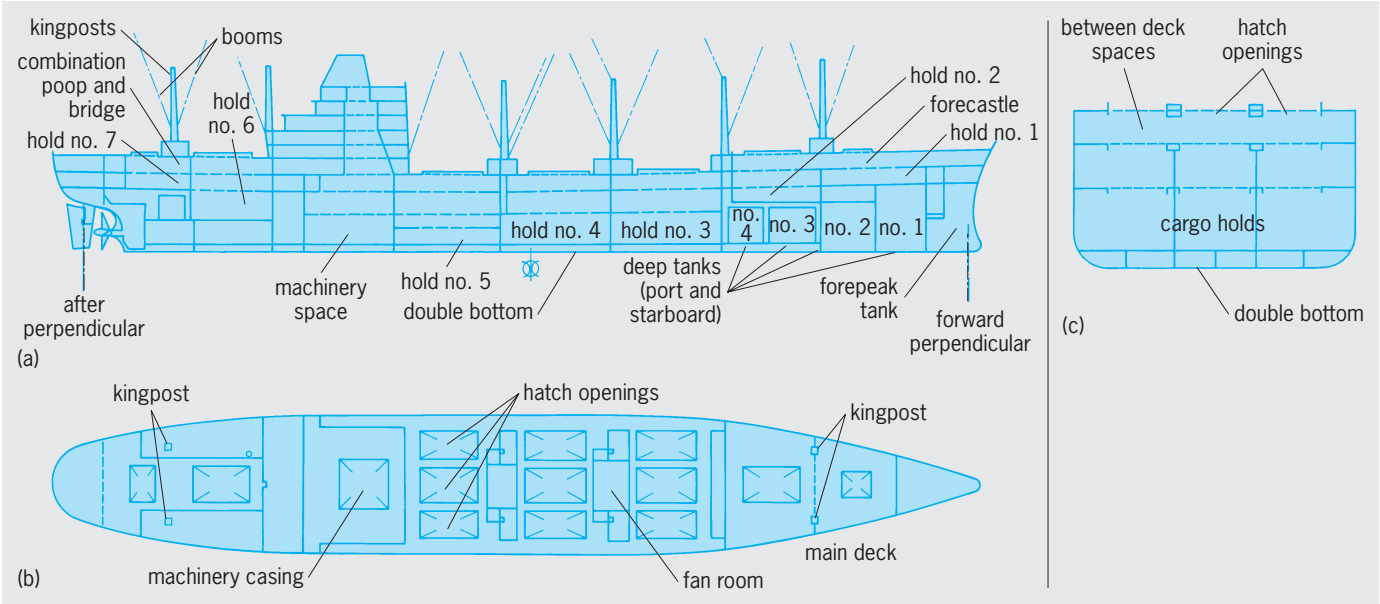

Fig. 1. Break-bulk cargo ship. (*a*) Inboard profile. (*b*) Plan view (deck). (*c*) Typical section. Principal dimensions and other characteristics: length overall = 574 ft = 175 m; length between perpendiculars = 544.5 ft = 166 m; beam = 82 ft = 25 m; depth = 45.5 ft = 14 m; draft = 30.5 ft = 10 m; displacement = 21,235 long tons = 21,576 metric tons; deadweight = 12,932 long tons = 13,140 metric tons; service speed = 23 knots = 43 km/h; maximum shaft horsepower = 24,000 (18 MW); number of crew = 45.

control. The ship in **Fig. 1** has a long forecastle and a long poop combined with the bridge.

Framing. The principal component of the ship's structure is the plating (usually of steel), including the outer watertight envelope. The ship plating is reinforced and stiffened by welded bars (commonly angle, tee, or flat bars). When these bars are welded to the outer envelope, decks, or inner bottom and are repetitive and closely spaced (2–3 ft or 0.6–0.9 m apart), they are called frames and the structural system they compose is called framing. Typical frame dimensions for plating $^1/_2$ to 1 in. (1.3 to 2.5 cm) thick are a depth of 10 in. (25 cm), a flange of 4 in. (10 cm), and a thickness of $^1/_2$ in. (1.3 cm).

Most large land structures such as bridges, building framing, and towers are a complex of struts, rods, beams, and girders, with a negligible amount of plating for secondary functions.

Aircraft structure is similar to ship structure, but its strength and stiffness rest more heavily on the framing system rather than on the plating (shell), which is used more for reasons of aerodynamics than of strength.

Ships have either longitudinal or transverse framing systems or a mixture of both, called combination framing. In a longitudinal framing system the frames are oriented fore and aft and supported transversely by bulkheads and widely spaced deep web frames (6–12 ft or 1.8–3.7 m apart). The transverse system of framing consists essentially of a series of closely spaced ribs (frames) girding the ship, supported longitudinally by the decks, vertical keel, and side and deck girders. In the combination system of framing the bottom plating and often the deck plating are longitudinally framed, while the sides are transversely framed.

Stability. Since in ship design both the breadth and depth affect transverse stability against capsizing, the one must be adjusted in relation to the other. An unusually deep ship must also be unusually broad. Very little stability is risky as the ship may capsize under adverse service conditions. Excessive stability results in objectionable violent rolling in heavy weather.

As fuel and fresh water are consumed en route, the reduction in weight aboard at low levels in the hull reduces stability, possibly risking capsizing if the ship is damaged by collision. In the case of passenger vessels particularly, seawater ballast may be pumped aboard to replace this reduced weight, preferably into low-level compartments not ordinarily used for fuel oil.

Speed factors. Speed in knots is the velocity in nautical miles (6076.1 ft or 1852 m) per hour. Slow seagoing ships (those in which the speed in knots is equal to 50–60% of the square root of the waterline length in feet) have about 30% of ship length of underwater parallel body (no change in shape) and rather bluff fore- and afterbodies. High-speed ships (those in which the speed in knots exceeds the square root of the waterline length in feet) have no parallel underwater body and both ends are quite fine, the forebody waterlines being straight or even hollowed near the bow.

The increased construction cost of weight-saving aluminum alloy in the structure, furniture, and equipment of a high-speed ship is often more than justified by the resultant reduction in horsepower and fuel consumption. The situation pyramids as a reduction in propulsion machinery weight, and reduced fuel weight aboard further reduces the displacement.

An outstanding high-speed liner was the 990-ft (302-m) overall length, quadruple screw, 2000-passenger SS *United States*. During several days of its transatlantic maiden voyage the ship averaged over 36 knots (67 km/h), an unprecedented merchant ship speed.

Propulsion. Cargo ships seldom exceed 40,000 shaft horsepower (shp), equivalent to 30 MW, and one propeller is usual. Higher-powered ships may have two or four propellers. Three are possible but unusual. Ships of less than about 3000 shp (2.2 MW) normally have diesel engines, but for higher powers diesel engines or steam turbines may be used. In the past, steam turbines were more commonly used for ships built in the United States, but the diesel engine is now more often chosen because of fuel economy. Nuclear power, gas turbines, free piston engines, and other power units are also used to propel merchant ships. Sails are almost extinct, although there is considerable interest in a rebirth using more sophisticated, less labor-intensive riggings.

Generally, high-revolution propellers are inefficient. Therefore, if the power plant operates at high revolutions per minute (rpm), it either drives the propeller shaft through reduction gears or powers a direct-drive high-rpm electric generator. The generator in turn drives the propeller shaft through a low-rpm reversible rotation electric motor.

The propulsion machinery of most merchant ships, with the exception of bulk carriers, is located between amidships (midlength of the L_{pp}) and about three-fourths of the L_{pp} from the bow. A general cargo ship normally has fewer holds abaft (sternward from) the machinery space than forward of it. The shaft tunnel and shape of holds near the stern, however, make cargo stowage difficult. There is a trend toward locating the machinery and the deckhouses above it farther aft. Bulk carriers such as tankers, ore carriers, and colliers have the machinery located aft of the cargo spaces. *See* MARINE MACHINERY; PROPELLER (MARINE CRAFT); SHIP POWERING, MANEUVERING, AND SEAKEEPING.

Size-speed relationship. Other factors being equal, a large, fully loaded cargo ship (break-bulk or bulk cargo) will transport cargo at less cost per ton-mile than a small, fully loaded vessel. However, a fully loaded moderate-capacity cargo vessel will transport cargo at less overall cost per ton-mile than a partially loaded, much larger ship of the same type carrying the same quantity of cargo.

Deadweight (dwt) is the weight of cargo, fuel, fresh water, stores, passengers, crew, and baggage aboard a ship. General-cargo transoceanic ships seldom have over 15,000 long tons deadweight capacity, and ships of 8000- to 11,000-ton capacity predominate. In ship design and operation the long ton, 2240 lb (1016.05 kg or 1.016 metric tons), is used. Larger ships have less frequent sailings for a given

annual cargo, and often there is not enough cargo to fully load even an 8000-ton deadweight ship of this type. In ocean service, dry bulk carriers in the neighborhood of 100,000-ton dwt and tankers above that capacity are numerous.

High speed is an important advantage in wartime, and in peacetime it attracts the patronage of both passengers and cargo shippers. High fuel prices, however, have had a dampening effect on the trend toward higher speeds. If two ships of the same cargo capacity are both fully loaded, the cost of shipment per cargo ton-mile is greater for a high-speed vessel. Nevertheless, the faster ship may earn larger dividends if the speed attracts full loads of high-quality cargo. Most cargo ships over 400 ft (122 m) in length have speeds of about 16–18 knots (30–33 km/h). There are many making 20 or more knots (37 km/h). United States ships are a little faster, on the average, than those of other nations.

Cargo handling. The cargo handling time for break-bulk cargo is much longer than for bulk cargo, and this involves costly idle ship time (spending instead of earning) while in port. For vessels of the same basic dimensions and speed, a break-bulk cargo ship can transport more weight or volume of payload cargo than a unitized ship, but the port delay for cargo handling of the break-bulk ship is much greater. Bulk cargo transportation is the most economical per ton-mile, even though the ship is in ballast without cargo on the return passage (except for combination bulk carriers). For relatively long distances, break-bulk cargo ships provide more economical transportation than unitized cargo vessels. This is not the case for short distances. As an extreme example, on a 10-mi (16-km) passage a ferry boat can transport loaded truck vans much more cheaply and quickly than a break-bulk cargo ship, even if more truckloads of cargo were unloaded onto the ferry boat and then reloaded onto trucks at the other end of the passage. For a 10,000-mi (16,500-km) passage, however, it is cheaper to transfer the cargo to a ship and transport only the payload cargo, even though considerable time and money are spent loading and unloading.

Size restrictions. Canal locks and harbor water depths restrict the dimensions of the larger ships. The Panama Canal recommends that vessels not exceed 900-ft (274-m) length overall, 104-ft (32-m) breadth, and 35-ft (10.7 m) draft. The Suez Canal limits the draft to 35 ft (10.7 m), but the length and breadth are unrestricted. The maximum for the St. Lawrence Seaway is 730-ft (223-m) length overall and 75-ft (23-m) breadth. Since the minimum channel depth is 27 ft (8.2 m), about 25.5 ft (7.8 m) is the maximum draft. The minimum clearance under bridges along the Seaway is 120 ft (36.6 m). All these dimensions, except the bridge clearance, can be exceeded slightly in an emergency. The enlarged Soo Lock can accommodate ships 1000 ft (305 m) long and 105 ft (32 m) wide. Although large dry-bulk cargo ships have economic advantages, if the draft exceeds about 38 ft or 11.6 m (few harbors are over 40 ft or 12.2 m in depth), operations may be restricted. Tankers of great draft such as those over 100,000-ton dwt may have to unload partially into a smaller tanker before entering many harbors or may have to unload all cargo at offshore terminals.

Ship Types

The trend brought about by increased transoceanic commerce, higher wages, and keener competition has been toward ship types built for unitized cargo and for certain specific cargoes. The following descriptions of merchant ship types refer to those illustrated in the 10 figures. Ships engaged exclusively in the transportation of passengers are not included because, especially in the United States, air travel has become the predominant mode of transoceanic passenger transportation. Many passenger liners have entered the cruise trade, for ships have many recreational and environmental advantages.

Break-bulk cargo ships. The cargo carrying space in break-bulk cargo ships is divided by transverse bulkheads, spaced 40–70 ft (12–21 m) apart, into a series of cargo compartments of approximately equal volume, generally seven for a ship of about 500-ft (150-m) L_{pp} (Fig. 1). Vertically, these spaces are divided by one or two decks below the uppermost, continuous deck (main or strength deck). The space between the inner bottom and the lowest deck, called the hold, is limited to a height of about 18 ft (5.5 m) to minimize damage to cargo through crushing. Usually the height of each space between decks (termed tween deck space) is 9–10 ft (2.7–3.0 m).

In addition to the previously mentioned double-bottom tanks, most break-bulk cargo ships have deep tanks used for fuel oil, water ballast, or liquid cargoes such as latex, coconut oil, or edible oils.

The cargo is handled through large rectangular deck openings (hatches) over each cargo space. Mechanically operated hatch covers are used to close the openings. The hatch covers in the tween decks are strong enough to support cargo stowed on them. The topside hatch covers are watertight. The tween deck space is generally suitable for break-bulk or palletized cargo. Generally, cargo holds have had one hatch per deck, with a width of 35–50% the ship's breadth and a length of 50–60% the hold length. The trend is toward wider hatches or multiple hatches abreast (Fig. 1) and often longer hatches, to increase cargo handling speed. A multiple hatch arrangement (triple hatch, for instance) is efficiently used for a partial load of containers stowed under deck.

Break-bulk cargo handling between pier and ship is done usually by means of cargo booms installed on board. The booms are raised or lowered by adjustable wire rigging led from the mast or king post to the boom ends. A wire rope leads over sheaves from a winch to the outer end of each boom and terminates in a cargo hook. Cargo can be hoisted using one boom [customarily for very heavy loads of cargo, 10 tons (9 metric tons) or over] or, for faster handling, by a pair of married booms, with one boom end over the hatch and the other over the pier. This cargo handling operation, called burtoning, is customary for loads up to 10 tons. Most break-bulk cargo ships fitted with booms have a pair

of booms at each hatch end to expedite cargo handling. The cargo is often piled together in a large net which is emptied and returned for the next load. Packaged cargo of nearly uniform dimensions may be stacked on pallets which are hoisted aboard individually. The sling load is landed through the hatch opening. The pallets or nets are then unloaded, and each item is individually stowed by the hold gang. Any cargo stowed in the wings of the hold is handled manually unless it is on pallets and handled by a forklift truck. The use of forklift trucks is becoming common practice, and a number of these trucks may be carried on board if they are not available at cargo terminals. The amount of cargo which is handled manually onboard determines largely the ship turnaround and port expenses, and, hence, the profitability of the transportation system.

Most break-bulk cargo ships have provisions for a heavy lift boom of 33–110-ton (30–100-metric ton) capacity for occasional units of heavy cargo.

An increasing number of break-bulk cargo ships are being fitted with revolving deck cargo cranes instead of masts, booms, and winches.

Container ships. Container ships are replacing the conventional break-bulk cargo ship in trade routes where rapid cargo handling is essential. Containers are weatherproof boxes (usually metal) strengthened to withstand stacking and motion at sea. Containers are of standard size, the largest ones weighing up to about 33 tons (30 metric tons) when loaded. The use of standard containers facilitates shipboard stowage, land or waterway transportation, and rental or lease. *See* MARINE CONTAINERS.

A large container ship may be loaded or unloaded completely in about half a day, compared to several days for the same amount of cargo in a break-bulk cargo ship. Generally, the shipper places the cargo in the container, and, except for custom inspection, it is delivered unopened to the consignee. Highway trailers (most commonly), railroad cars, or barges transport containers to and from their land destination and are therefore a part of the same transportation system. For a given payload cargo capacity, container ships are larger and more costly to build than the traditional cargo ship, but both the cargo handling cost and the idle ship time in port are reduced considerably.

Although in some ships containers are moved horizontally for loading and unloading, the predominant arrangement is that illustrated in **Fig. 2**, where containers are stowed in vertical cells and moved vertically in and out of the vessel.

Roll-on/roll-off ships. With a broad interpretation all ships that are designed to handle cargo by rolling it on wheels can be considered under this heading. This would include trailer ships; sea trains (carrying railroad cars or entire trains); auto, truck, and trailer ferries; military vehicle carriers; ships carrying pallets handled by forklift trucks from and to shore; and so on. The following is a description of a ship of this type, which is intended primarily to operate as a trailer ship, although it may handle several types of wheeled vehicles **(Fig. 3)**.

Roll-on/roll-off ships require a high proportion of cubic capacity relative to the amount of cargo and are particularly suited to service with short runs and frequent loading and unloading. They need even shorter port time than container ships, but their building cost is higher.

Because fully loaded roll-on/roll-off ships cannot carry enough cargo to immerse them deeply, their large freeboard allows the fitting of side ports above the waterline for the handling of cargo on wheels by means of ramps. Usually, ships of this type have a transom stern (a square-shaped stern like that of a motorboat) fitted with doors for handling wheeled vehicles on an aft ramp. Roll-on/roll-off ships have several decks, and the cargo is handled on wheels

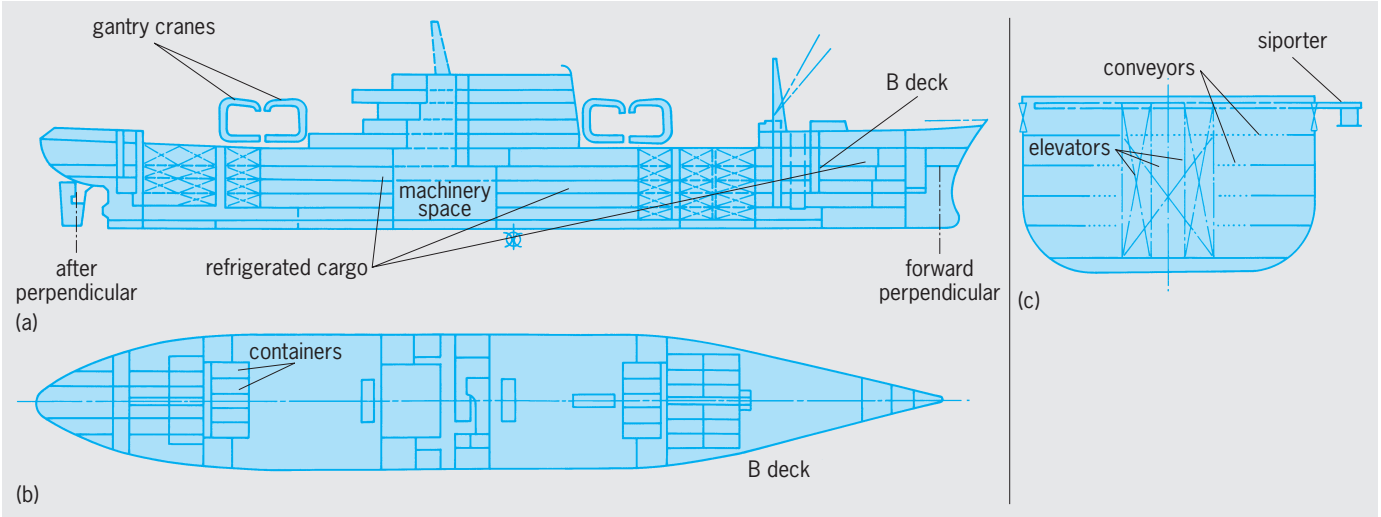

Fig. 2. Container ship. (*a*) Inboard profile. (*b*) Plan view (deck). (*c*) Typical section. Principal dimensions and other characteristics: length overall = 752 ft = 229 m; length between perpendiculars = 705 ft = 215 m; beam = 100 ft = 30 m; depth = 57 ft = 17 m; draft = 31 ft = 9 m; displacement = 33,924 long tons = 34,468 metric tons; deadweight = 19,206 long tons = 19,514 metric tons; service speed = 27 knots = 50 km/h; shaft horsepower (two propellers) = 60,000 (44.7 MW); number of crew = 40.

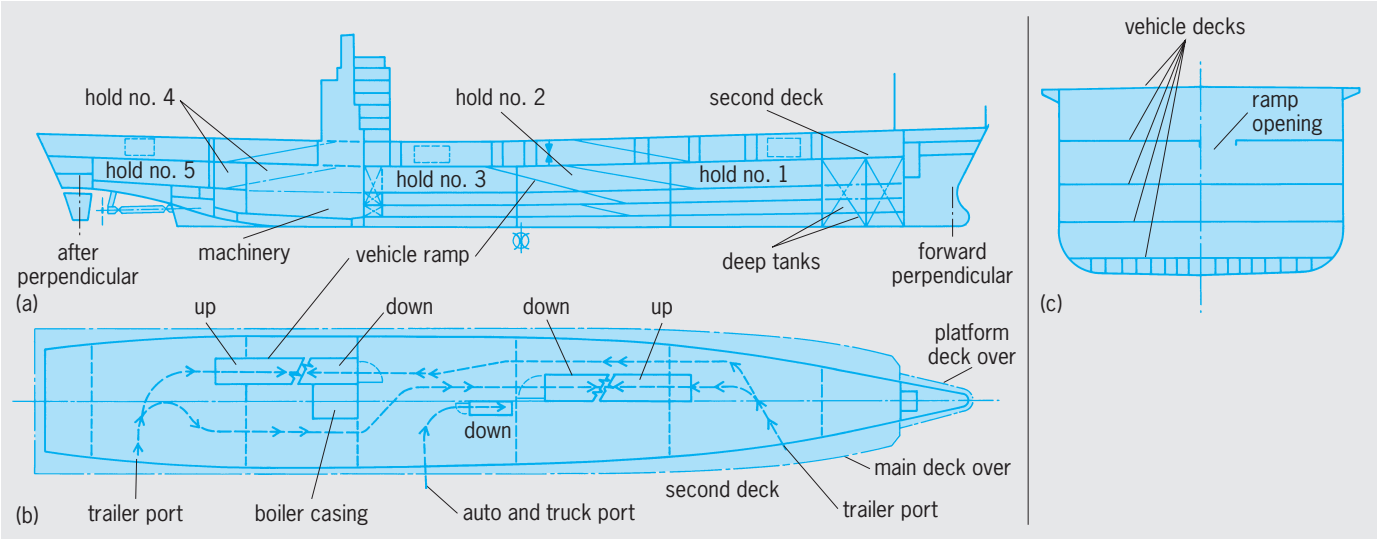

Fig. 3. Roll-on/roll-off ship. (*a*) Inboard profile. (*b*) Plan view (deck). (*c*) Typical section. Principal dimensions and other characteristics: length overall = 700 ft = 213 m; length between perpendiculars 643 ft = 196 m; beam (maximum) = 105 ft = 32 m; depth = 60 ft = 18 m; draft = 27 ft = 8 m; displacement = 24,100 long tons = 24,500 metric tons; deadweight = 13,100 long tons = 13,300 metric tons; service speed = 25 knots = 46 km/h; shaft horsepower = 32,000 (23.9 MW); number of crew = 39.

from the loading deck to other decks by elevators or sloping ramps. Both internal elevators and ramps occupy substantial volume in the ship. The need for clear decks, without interruption by transverse bulkheads, and tween decks for vehicle parking results in a unique structural arrangement.

Barge-carrying ships. This type of ship represents a bold step in the trend toward cargo containerization and port time reductions: Cargo is carried in barges or lighters, each weighing up to 1100 tons (1000 metric tons) when loaded. The lighters are carried below and above deck and are handled by gantry cranes or elevator platforms (**Fig. 4**).

These are among the fastest, largest and costliest ships for the carriage of general cargo. For their size, their payload capacity is less than that of the conventional break-bulk cargo ship. However, they can be loaded and unloaded much faster and with a considerable saving in worker-hours.

Because the lighters can be waterborne and operated as regular barges, these large ships can serve undeveloped ports advantageously.

Using portable fixtures that can be erected quickly, barge-carrying ships can be adapted for the transport of varying amounts of standard containers in addition to or in place of lighters.

Bulk cargo ships. A large proportion of ocean transportation is effected by bulk cargo ships.

Dry bulk cargo includes products such as iron ore, coal, limestone, grain, cement, bauxite, gypsum, and sugar. Most oceangoing dry bulk carriers are loaded and unloaded using shoreside installations. Many dry bulk carriers operating in the Great Lakes have shipboard equipment for the handling of cargo (self-unloaders), and an increasing number of oceangoing ships carrying this type of cargo are being fitted with self-unloading gear.

By far the largest amount of liquid bulk cargo consists of petroleum products, but ocean transportation of other bulk liquid products is increasing in importance: for example, various chemicals, vegetable oils, molasses, latex, liquefied gases, molten sulfur, and even wine and fruit juices. Practically all liquid bulk carriers have pumps for unloading the cargo.

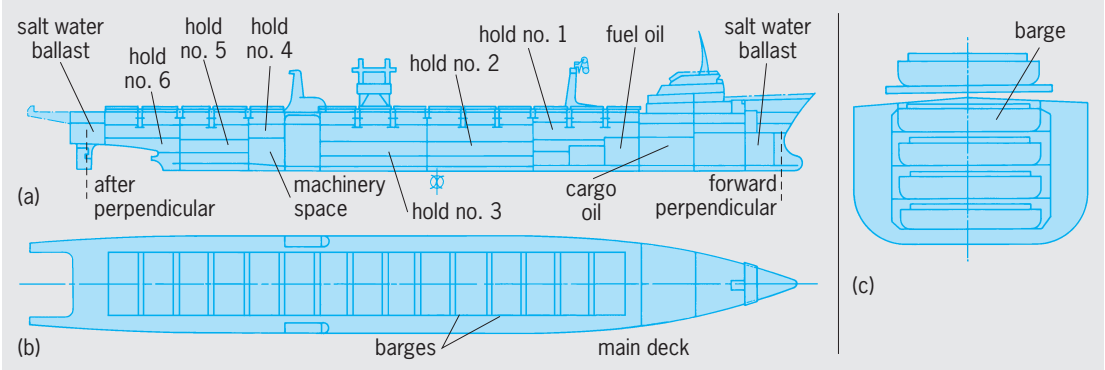

Fig. 4. Barge-carrying ship. (*a*) Inboard profile. (*b*) Plan view (deck). (*c*) Typical section. Principal dimensions and other characteristics: length overall = 820 ft = 250 m; length between perpendiculars = 724 ft = 221 m; beam = 100 ft = 30.5 m; depth = 60 ft = 18 m; draft = 28 ft = 8.5 m; displacement = 32,800 long tons = 33,330 metric tons; deadweight = 18,760 long tons = 19,060 metric tons; service speed = 22.5 knots = 42 km/h; shaft horsepower = 32,000 (24 MW); number of crew = 39.

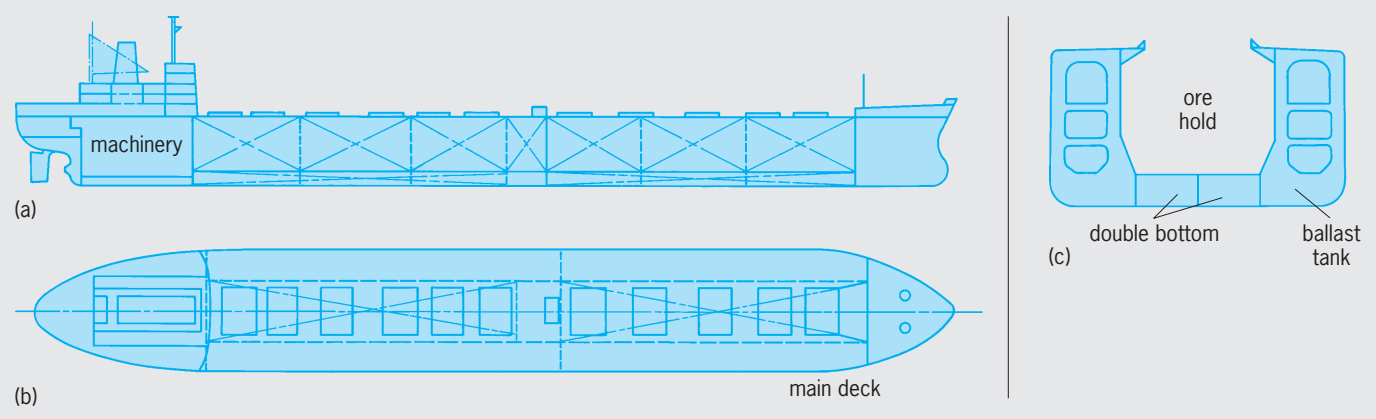

Fig. 5. Oceangoing ore carrier. (*a*) Inboard profile. (*b*) Plan view (deck). (*c*) Typical section. Principal dimensions and other characteristics: length overall = 865 ft = 263 m; length between perpendiculars = 826 ft = 252 m; beam = 124 ft = 39 m; depth = 69 ft = 22 m; draft = 50 ft = 15.5 m; displacement = 124,000 long tons = 126,000 metric tons; deadweight = 104,500 long tons = 106,200 metric tons; service speed = 16 knots = 29 km/h; shaft horsepower = 24,300 (18 MW); number of crew = 40.

Even combination bulk carriers, which may carry simultaneously or alternatively dry and liquid bulk cargo, usually have shipboard pumps for unloading liquids.

Practically all bulk carriers have the machinery compartment, crew accommodations, and conning stations located aft. An exception is the Great Lakes self-unloader with crew accommodations and bridge forward.

The tendency in bulk carriers is toward larger ships, with speeds remaining about constant at a moderate level (16–18 knots or 30–33 km/h for oceangoing ships, lower for Great Lakes vessels).

The oceangoing ore carrier (**Fig. 5**) is characterized by a high double bottom and small volume of cargo hold because of the high density of the ore. Storing the cargo high in the ship decreases stability and prevents excessively quick rolling.

The oceangoing combination bulk carrier (**Fig. 6**) permits low-cost transportation because of its flexibility. It is able to carry many types of bulk cargoes over a variety of sea lanes. This type of ship carries bulk cargoes, such as petroleum products, coal, grain, and ore. The double bottom in bulk carriers is shallow and the volume of cargo holds is large compared to the size of the ship.

The self-unloader (**Fig. 7**) was originally developed in the Great Lakes for the transportation of limestone. A variety of free-flowing dry bulk cargo is carried in this type of ship. Generally, a conveyor belt located low in the ship, so that it can be loaded by gravity flow, carries the cargo to a station at one end of the ship. From there it is transferred automatically to the conveyor of a large boom, which can be swung over the side for unloading ashore.

The tanker (**Fig. 8**) is the characteristic, and by far the most important, liquid bulk carrier both in numbers and tonnage. Tankers carry petroleum products almost exclusively. The very large tankers are used almost entirely for the transport of crude oil. A few tankers are built especially for the transportation of

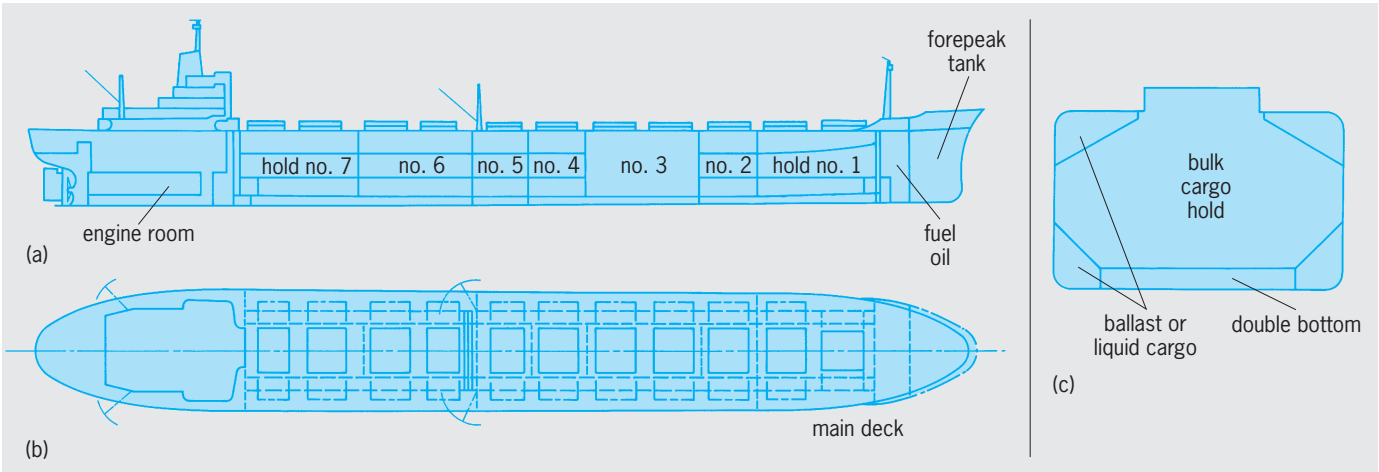

Fig. 6. Oceangoing combination bulk carrier. (*a*) Inboard profile. (*b*) Plan view (deck). (*c*) Typical section. Principal dimensions and other characteristics: length overall = 815 ft = 248 m; length between perpendiculars = 775 ft = 236 m; beam = 104.5 ft = 32 m; depth = 61.5 ft = 19 m; draft = 41 ft = 12.5 m; displacement = 78,938 long tons = 80,205 metric tons; deadweight = 63,410 long tons = 64,428 metric tons; service speed = 16 knots = 29 km/h; shaft horsepower = 18,000 (13.4 MW); number of crew = 41.

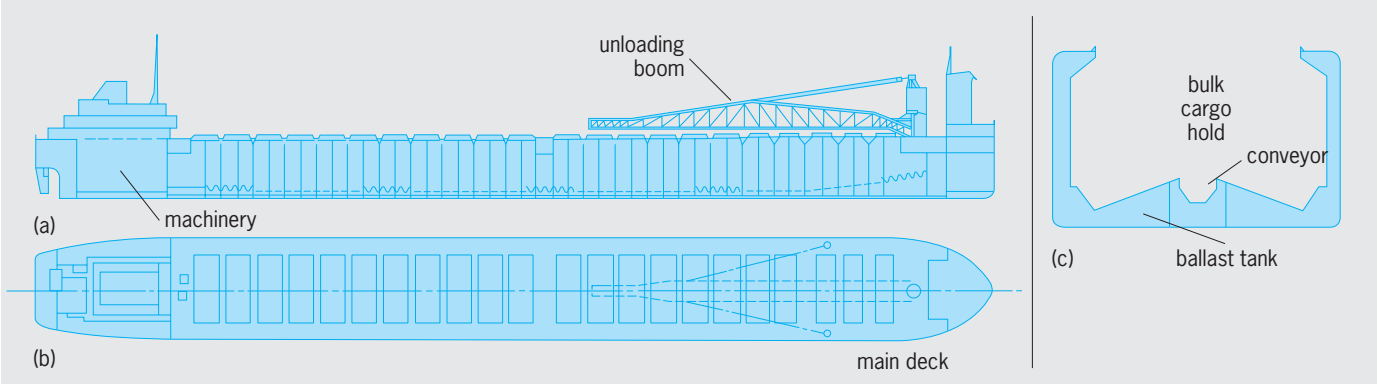

Fig. 7. Great Lakes self-unloader. (*a*) Inboard profile. (*b*) Plan view (deck). (*c*) Typical section. Principal dimensions and other characteristics: length overall = 730 ft = 222.5 m; length between perpendiculars = 724 ft = 221 m; beam = 75 ft = 23 m; depth = 45 ft = 14 m; draft = 28 ft = 8.5 m; displacement = 38,980 long tons = 39,605 metric tons; deadweight = 29,550 long tons = 30,024 metric tons; service speed = 13 knots = 24 km/h; shaft horsepower = 7400 (5.5 MW); number of crew = 32.

chemical products, and others are prepared for alternative loads of grain.

Bulk liquid carriers, with freestanding, rectangular, cylindrical, or spherical cargo tanks separated from the hull, are used for the transportation of molten sulfur and liquefied gases, such as anhydrous ammonia and natural gas (**Fig. 9**). Liquefied natural gas (LNG) is also carried in ships with membrane tanks, i.e., where a thin metallic liner is fitted into a tank composed of ship structure and load-bearing insulation. The transportation of molten sulfur and liquefied gases requires special consideration regarding insulation and high structural soundness of cargo tanks, including the use of high-grade, costly materials for their construction.

Heavy-lift ships. The definition of heavy lift has changed gradually. Whereas 10 short tons (9 metric tons) per unit was once considered heavy-lift cargo, many cargo liners of the 1970s commonly lift 110 tons (100 metric tons) per unit without being classified as heavy-lift ships. Heavy-lift ships considered here are those capable of loading and discharging cargoes having unit weights in the hundreds of tons. The need for these ships has grown due to the expanding market for large industrial equipment.

Heavy-lift cargo includes nuclear power reactors, diesel engines, components for refinery and chemical plants, metalworking machinery, construction equipment, military equipment, offshore oil equipment, locomotives, mining and mineral processing equipment, tugs, and barges.

The large loads carried by heavy-lift ships are handled by high-capacity shipboard jibs and hoisting gear. The factors determining the best derrick for a given design are location of the deck, lifting capacity, outreach, initial cost, and weight. The three main types of lifting gear used are nonrotating derricks, rotating derricks, and gantry cranes.

A commonly used nonrotating heavy-lift derrick has an open double kingpost arrangement which simplifies rigging considerably and allows swinging loads up to 400 metric tons forward and aft of the derrick and to both sides of the ship.

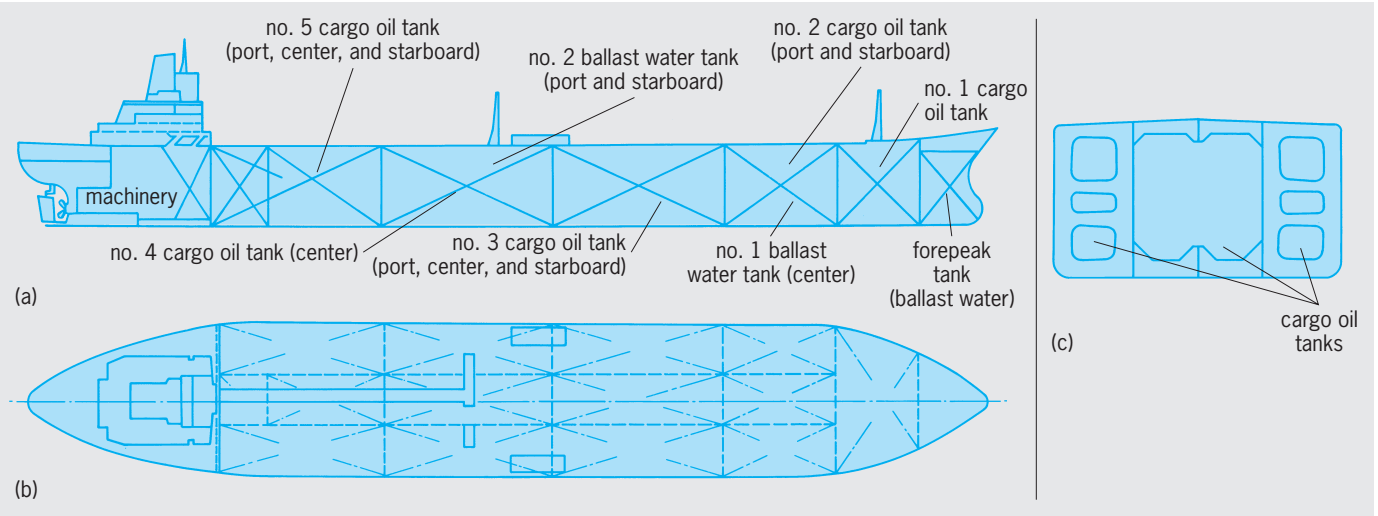

Fig. 8. Tanker. (*a*) Inboard profile. (*b*) Plan view (deck). (*c*) Typical section. Principal dimensions and other characteristics: length overall = 1005 ft = 306.5 m; length between perpendiculars = 951 ft = 290 m; beam = 156 ft = 47.5 m; depth = 79 ft = 24 m; draft = 53 ft = 16 m; displacement = 179,700 long tons = 181,900 metric tons; deadweight = 151,300 long tons = 153,700 metric tons; service speed = 16 knots = 30 km/h; shaft horsepower = 30,000 (22.4 MW); number of crew = 29.

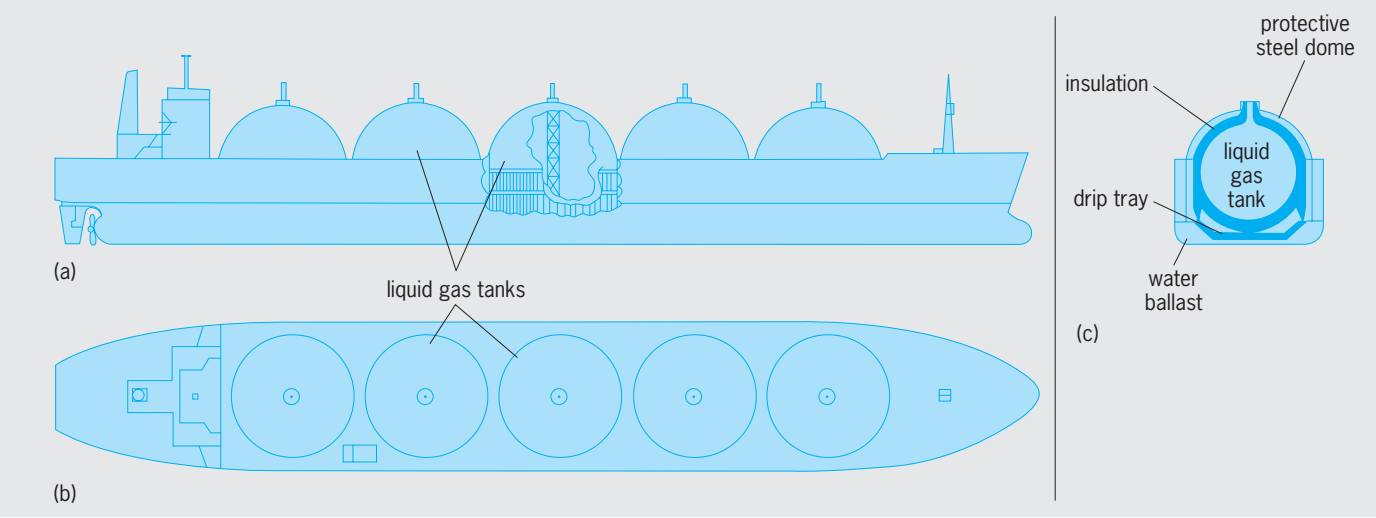

Fig. 9. Spherical-tank liquefied natural gas (LNG) carrier. (*a*) Profile. (*b*) Plan view (main deck). (*c*) Typical section. Principal dimensions and other characteristics: length overall = 924 ft = 282 m; length between perpendiculars = 885 ft = 270 m; beam = 141.5 ft = 43 m; depth = 82 ft = 25 m; draft = 36 ft= 11 m; cargo tank volume = 121,250 m^3; displacement = 91,200 long tons = 92,700 metric tons; deadweight = 61,100 long tons = 62,100 metric tons; maximum speed = 20 knots = 37 km/h; shaft horsepower = 40,000 (29.8 MW); loading or unloading time = 12 h; number of crew = 39.

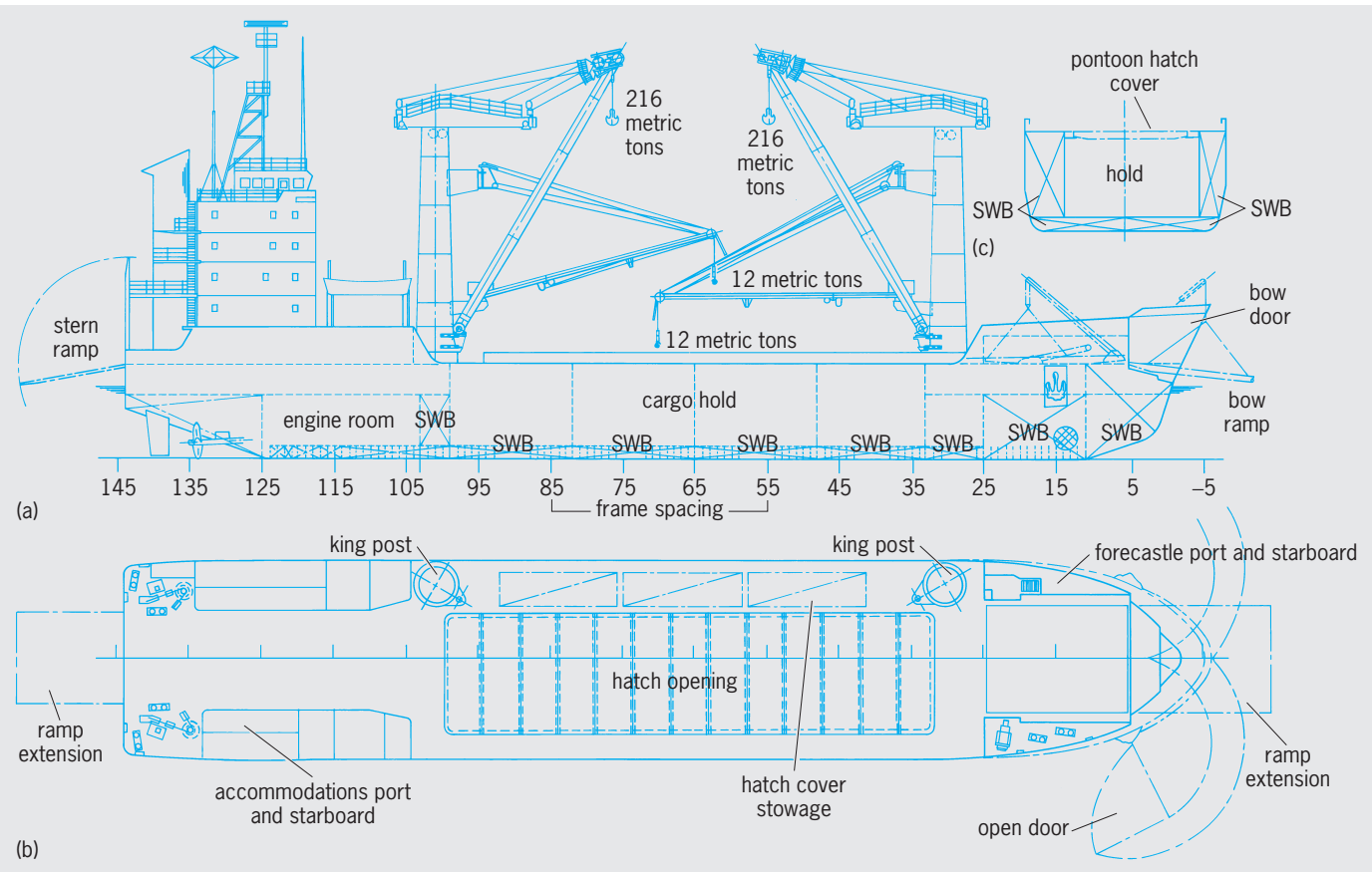

Fig. 10. Heavy-lift ship. (*a*) Profile. (*b*) Plan view (main deck). (*c*) Typical section. SWB = salt water ballast. Principal dimensions and other characteristics: length overall = 300 ft = 91 m; length between perpendiculars = 279 ft = 85 m; beam 55 ft = 17 m; depth = 27 ft = 8 m; draft = 17 ft = 5 m; displacement = 5500 long tons = 5588 metric tons; deadweight = 2947 long tons = 2994 metric tons; service speed = 13.5 knots = 25 km/h; brake horsepower = 5500 (4.1 MW); lifting capacity = 424 long tons = 431 metric tons; number of crew = 21. (*After H. W. Janecke and W. F. Muir, Modern heavy lift ships (state of the art), Trans. Soc. Nav. Architects Mar. Eng., 86:347–374, 1978*)

Rotating derricks have a single tower kingpost with a topping lift and a boom attached at the bottom to a swiveling ring. Their maximum lifting capacity is approximately 770 tons (700 metric tons).

Gantry cranes used on heavy-lift ships carry loads between tracks in traveling the length of the holds. They are generally restricted to a maximum lifting capacity of 550 tons (500 metric tons) and are not utilized in over-the-side lifting, since the outriggers must be retractable.

Handling, transferring, and securing heavy-lift cargo is a specialized operation planned many months in advance. As cargo is lifted, ballast water is transferred to correct for trim and heel computed in advance.

Ships are identified by the method of lifting cargoes or by transferring cargoes on and off. There are two categories of heavy-lift ships: liner-type, general cargo ships utilizing heavy-lift gear, and the heavy-lift ships in the "tramping trade" which provide specialized services such as roll-on/roll-off, float-on/float-off, and slide-on/slide-off. Roll-on/roll-off ships are fitted with doors and ramps on the bow or the stern, including internal ramps between decks. Float-on/float-off ships become submerged at the stern while the cargo—barges, tugs, dredges, or other floating vessels—enters the ship's submerged well. When the well is sealed and pumped dry, the cargo awaits securing. Slide-on/slide-off ships are equipped with two heavy retractable girders extending past the side over which cargo is transferred.

Figure 10 illustrates a heavy-lift ship with rotating derricks and a lifting capacity of 475 tons (424 long tons or 431 metric tons).

Amelio M. D'Arcangelo; Robert B. Zubaly

Bibliography. R. Gardiner and A. Alastair (eds.), *The Shipping Revolution: The Modern Merchant Ship*, 1993; E. V. Lewis (ed.), *Principles of Naval Architecture*, 2d rev., 3 vols., 1988; R. Taggart (ed.), *Ship Design and Construction*, 3d ed., 1980; D. A. Taylor, *Merchant Ship Construction*, 3d ed., 1992; G. Till (ed.), *Merchant Shipping*, 1994; *Transactions of the Society of Naval Architects and Marine Engineers*, annually.

Mercury (element)

A chemical element, Hg, atomic number 80 and atomic weight 200.59. Mercury is a silverwhite liquid at room temperature (melting point −38.89°C or −37.46°F); it boils at 357.25°C (675.05°F) under atmospheric pressure. It is a noble metal that is soluble only in oxidizing solutions. Solid mercury is as soft as lead. The metal and its compounds are very toxic. With some metals (gold, silver, platinum, uranium, copper, lead, sodium, and potassium, for example) mercury forms solutions called amalgams. *See* AMALGAM; PERIODIC TABLE; TRANSITION ELEMENTS.

In its compounds, mercury is found in the 2+, 1+, and lower oxidation states, for example, $HgCl_2$, Hg_2Cl_2, or $Hg_3(AsF_6)_2$. Often the mercury atoms are doubly covalently bonded, for example, Cl—Hg—Cl or Cl—Hg—Hg—Cl. Some mercury(II) salts, for example, $Hg(NO_3)_2$, or $Hg(ClO_4)_2$, are quite soluble in water and dissociate normally. The aqueous solutions of these salts react as strong acids because of hydrolysis. Other mercury(II) salts, for example, $HgCl_2$ or $Hg(CN)_2$, also dissolve in water, but exist in solution as only slightly dissociated molecules. There are compounds in which mercury atoms are bound directly to carbon or nitrogen atoms, for example, $H_3C—Hg—CH_3$ or $H_3C—CO—NH—Hg—NH—CO—CH_3$. In complex compounds, for example, $K_2(HgI_4)$, mercury often has three or four bonds.

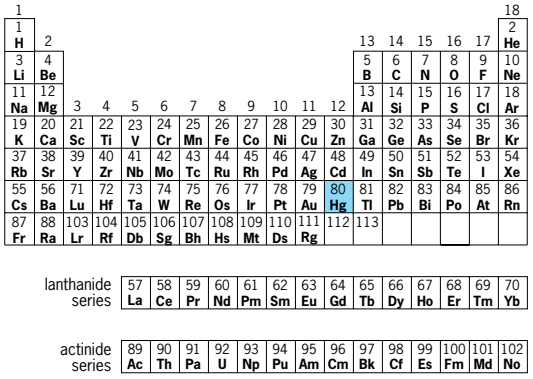

Metallic mercury is used as a liquid contact material for electrical switches, in vacuum technology as the working fluid of diffusion pumps, for the manufacture of mercury-vapor rectifiers, thermometers, barometers, tachometers, and thermostats, and for the manufacture of mercury-vapor lamps. It finds application for the manufacture of silver amalgams for tooth fillings in dentistry. Of importance in electrochemistry are the standard calomel electrode, used as the reference electrode for the measurement of potentials and for potentiometric titrations, and the Weston standard cell.

Mercury is commonly found as the sulfide, HgS, frequently as the red cinnabar and less often as the black metacinnabar. A less common ore is the mercury(I) chloride. Occasionally the mercury ore contains small drops of metallic mercury. *See* CINNABAR.

The surface tension of liquid mercury is 484 dynes/cm, six times greater than that of water in contact with air. Hence, mercury does not wet surfaces with which it is in contact. In dry air metallic mercury is not oxidized. After long standing in moist air, however, the metal becomes coated with a thin layer of oxide. In air-free hydrochloric acid or in dilute sulfuric acid, the metal does not dissolve. Conversely, it is dissolved by oxidizing acids (nitric acid, concentrated sulfuric acid, and aqua regia).

Klaus Brodersen

Bibliography. F. A. Cotton et al., *Advanced Inorganic Chemistry*, 6th ed., Wiley-Interscience, 1999; R. R. Lauwerys and P. Hoet, *Industrial Chemical Exposure: Guidelines for Biological Monitoring*, 3d ed., 2001; D. R. Lide, *CRC Handbook Chemistry and Physics*, 85th ed., CRC Press, 2004.

Mercury (planet)

The planet closest to the Sun. It is visible to the unaided eye only shortly after sunset or shortly before sunrise, when it is near its greatest angular distance from the Sun (28°). Mercury is the smallest planet since Pluto is no longer classified as a planet. Its diameter is 3031 mi (4878 km), and its mass is 7.28×10^{23} lb (3.301×10^{23} kg), or 0.055 times the mass of the Earth. Most detailed knowledge of Mercury is derived from data returned by the *Mariner 10* spacecraft, which flew by the planet three times in 1974 and 1975. *Mariner 10* imaged only about 45% of the surface at an average resolution of about 0.6 mi (1 km), and less than 1% at resolutions between about 300 and 1500 ft (100 and 500 m). This coverage and resolution is somewhat comparable to Earth-based telescopic coverage and resolution of the Moon before the advent of space flight. As a consequence, there are still many uncertainties and questions concerning this unusual planet. Mercury represents an end member in solar system origin and evolution because it formed closer to the Sun than any other planet and, therefore, in the hottest part of the solar nebula from which the entire solar system formed. *See* PLUTO; SOLAR SYSTEM.

Motions. Mercury has the most eccentric (0.205) and inclined (7°) orbit of any planet in the solar system. Its average distance from the Sun is 3.60×10^7 mi (5.79×10^7 km), but distance varies from 2.86×10^7 mi (4.60×10^7 km) at perihelion to 4.34×10^7 mi (6.98×10^7 km) at aphelion because of the large eccentricity. The rotation period is 58.646 Earth days, and the orbital period, 87.969. Therefore, Mercury has a 3:2 resonant relationship between its rotational and orbital periods; it makes exactly three rotations around its axis for every two orbits around the Sun. Thus, a solar day (sunrise to sunrise) lasts two mercurian years (176 Earth days).

The motion of Mercury played an important role in the development of the general theory of relativity. Mercury's elliptical orbit is pulled around the Sun so that the perihelion point changes its position in space by about 5600 arc-seconds per century. When all known forces that act on the planet are taken into account, Mercury's perihelion-point motion exceeds that calculated by newtonian gravitational theory by 43 arc-seconds per century. This discrepancy remained unexplained until 1915, when Einstein's general theory of relativity predicted a perihelion motion in exact agreement with observation. *See* RELATIVITY.

Temperature. Although Mercury is closest to the Sun, it is not the hottest planet. The surface of Venus is hotter because of the atmospheric greenhouse effect. However, Mercury experiences the greatest range in surface temperature (1130°F or 628°C) of any planet or satellite in the solar system because of its proximity to the Sun, its long solar day, and its lack of an insulating atmosphere. Its maximum surface temperature is 800°F (427°C) at perihelion on the equator, hot enough to melt zinc. At night, however, the unshielded surface plunges to below −300°F (−184°C). *See* VENUS.

Polar radar features. High-resolution, full-disk radar images of Mercury show very high reflectivities and polarization ratios in the polar regions. The reflectivity and ratio values are similar to outer-planet icy satellites and the residual polar water-ice cap of Mars. Therefore, Mercury's polar radar features are interpreted to be water ice.

Twenty discrete high-reflectivity anomalies have been detected in the polar regions, and most of these correspond to craters viewed by *Mariner 10*. Some of the anomalies occur at latitudes as low as 72°. Because the obliquity of Mercury is near 0°, the planet does not experience seasons, and therefore temperatures in the polar regions should be less than −216°F (−138°C). In permanently shaded areas of the floors and sides of craters, the temperatures could be less than −258°F (−161°C), and water ice should be stable to evaporation on time scales of billions of years. Furthermore, the ice could be covered by a thin layer of regolith and still be detected by radar. The source of the water is not known. It may have been derived from comets or from water-rich asteroid impacts when water vaporized by the impacts is cold-trapped in the polar regions. If this is the source of the water on Mercury, the permanently shaded areas of craters in the polar regions of the Moon should also have water deposits. In 1998 the *Lunar Prospector* spacecraft identified water ice in the permanently shadowed areas of craters in the Moon's polar regions. *See* MOON; RADAR ASTRONOMY.

Magnetic field. *Mariner 10* discovered an intrinsic dipole magnetic field with a dipole moment equal to about 0.004 that of the Earth. Mercury is the only terrestrial planet besides the Earth with a magnetic field. Although weak compared to that of the Earth, the field has sufficient strength to hold off the solar wind, creating a bow shock and accelerating charged particles from the solar wind. As with the Earth, the magnetic axis is inclined about 11° from the rotation axis. Mercury occupies a much larger fraction of the volume of its magnetosphere than do other planets, and the solar wind actually reaches the surface at times of highest solar activity. Because of the small size of Mercury's magnetosphere, magnetic events happen more quickly and repeat more often than in Earth's magnetosphere. The maintenance of planetary magnetic fields apparently requires an electrically conducting fluid outer core. Therefore, Mercury's dipolar magnetic field is evidence that Mercury currently has a fluid outer core of unknown thickness. High-resolution radar measurements of the magnitude of Mercury's librations show that the mantle is detached from the core, indicating the outer core is still in a fluid condition. *See* GEOMAGNETISM; MAGNETISM; MAGNETOSPHERE.

Interior. Mercury's internal structure is unique in the solar system. The planet's mean density is 5.44 g/cm^3 (5.44 times that of water), which is larger than that of any other planet or satellite except Earth (5.52 g/cm^3). Because of Earth's large internal pressures, however, its uncompressed density is only 4.4 g/cm^3 compared to Mercury's uncompressed density of 5.3 g/cm^3. This means that Mercury

contains a much larger fraction of iron than any other planet or satellite in the solar system. The iron core must be about 75% of the planet diameter, or 42% of Mercury's volume. It is surrounded by a silicate mantle and crust only about 370 mi (600 km) thick. Earth's core is only 54% of the planet diameter, or just 16% of the total volume. Because the outer core is at least partly molten at present, a light alloying element in the core must have lowered the melting point and retained a partially molten core over geologic history (4.5×10^9 years); otherwise the core would have solidified long ago. Although oxygen is such an element, it is not sufficiently soluble in iron at Mercury's low internal pressures. Therefore, sulfur is the most reasonable candidate for this alloying element. Mercury probably has between about 0.2 and 7% sulfur in its core, since a sulfur abundance of less than 0.2 would result in an entirely solid core at the present time, whereas an abundance of 7% would result in an entirely fluid core at present. *See* EARTH.

Origin. The origin of Mercury and how it acquired such a large percentage of iron is a major unsolved problem. Although chemical equilibrium condensation models successfully explain the densities of most planets in the solar system, they cannot explain Mercury. For Mercury's position in the solar nebula, these models predict an uncompressed density of only about 4 g/cm^3 rather than the observed 5.3 g/cm^3; they also predict the complete absence of sulfur.

Three different hypotheses have been proposed to account for the large discrepancy between the iron abundance indicated by Mercury's high density and that predicted by equilibrium condensation models. In the selective accretion model, a differential response of iron and silicates to impact fragmentation and aerodynamic sorting leads to iron enrichment owing to higher gas densities and shorter dynamical time scales in the innermost part of the solar nebula. The postaccretion vaporization model proposes that intense bombardment by solar electromagnetic and corpuscular radiation in the earliest phases of the Sun's evolution (the T-Tauri phase) vaporized and drove off much of the planet's silicate mantle. In the giant impact hypothesis, a collision of a planet-sized object with Mercury ejected much of the mantle. Each of these hypotheses has major consequences for the formation of the other terrestrial planets, and each predicts a significantly different chemical composition for the silicate portion of Mercury, which are to be tested by the *MESSENGER* mission, now on its way to Mercury.

Atmosphere. Mercury's atmosphere is very tenuous and is essentially exospheric in that its atoms rarely collide with each other. The atmospheric surface pressure is 10^{12} times less than Earth's. *Mariner 10*'s ultraviolet spectrometer identified hydrogen, helium, oxygen, and argon in the atmosphere, all of which are probably derived largely from the solar wind. Earth-based telescopic observations in 1985 discovered that Mercury is surrounded by a tenuous atmosphere of sodium and potassium that is probably derived from its surface. At the subsolar point the atmospheric density of sodium is 280,000 to 620,000 atoms per cubic inch (17,000 to 38,000 atoms per cubic centimeter), and for potassium it is 8000 atoms per cubic inch (500 atoms per cubic centimeter). The mechanism for removing these elements from the surface and injecting them into the atmosphere is uncertain. Several areas of enhanced sodium and potassium emission have been identified with surface features such as the Caloris Basin and two radar-bright areas on the unimaged part of Mercury. The reason for these emissions is uncertain.

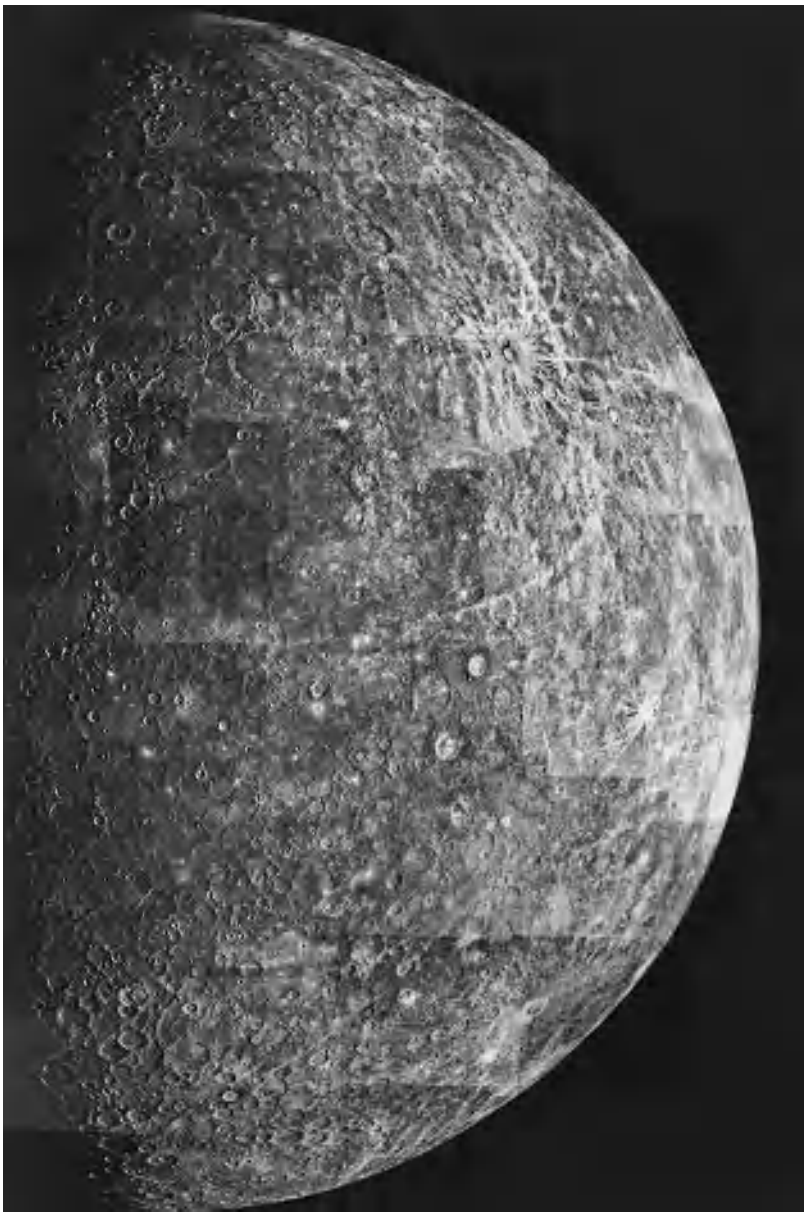

Fig. 1. Photomosaic of Mercury as seen by the outgoing *Mariner 10* spacecraft in March 1974. The terminator, the boundary between the lighted and unlighted halves of the planet, runs vertically along the left side of the photograph. The Caloris Basin is on the terminator, slightly above the middle. It is surrounded and filled by younger smooth plains. (*Jet Propulsion Laboratory*)

Geology. The surface of Mercury superficially resembles that of the Moon (**Fig. 1**). It is heavily cratered, with large expanses of younger smooth plains (similar to the lunar maria) that fill and surround major impact basins. Unlike the Moon surface,

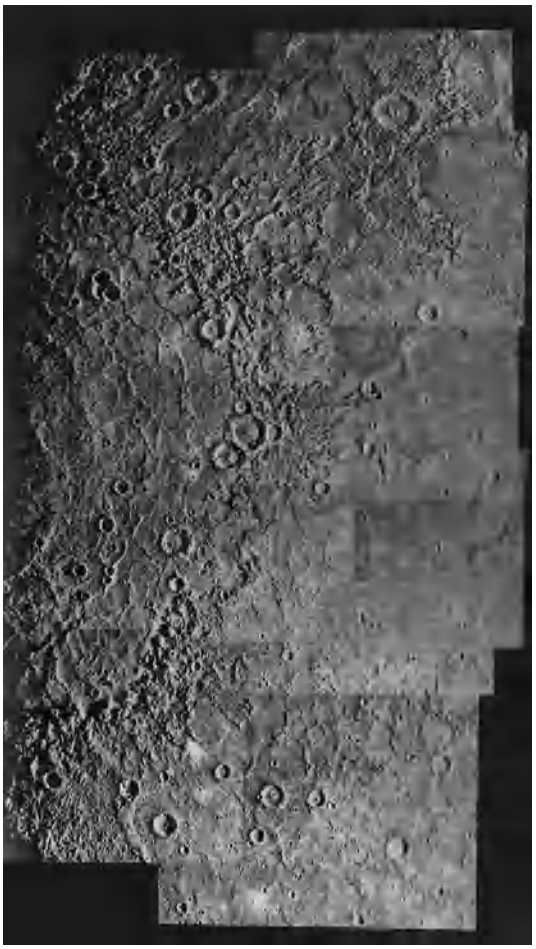

Fig. 2. Photomosaic showing the 800-mi-diameter (1300-km) Caloris Basin, the largest impact structure observed by *Mariner 10*, on the left, midway between top and bottom. (*Jet Propulsion Laboratory*)

Fig. 3. View of the Hilly and Lineated Terrain, taken by *Mariner 10* in March 1974. (*Jet Propulsion Laboratory*)

Mercury's heavily cratered terrain is interspersed with large regions of gently rolling intercrater plains, the major terrain type on the planet. Also unlike the Moon surface, a system of thrust faults, unique in the solar system, transects the surface viewed by *Mariner 10*. The largest structure viewed by *Mariner 10* is the 800-mi-diameter (1300-km) Caloris impact basin (**Fig. 2**). It is filled and surrounded by smooth plains resembling the Moon's maria, which also fill impact basins. Directly opposite (antipodal to) the Caloris Basin, on the other side of Mercury, is a peculiar terrain consisting of hills and valleys, called the Hilly and Lineated Terrain (**Fig. 3**). This terrain is thought to be the result of surface disruption by seismic waves focused at the antipodal region and caused by the Caloris Basin impact. Infrared temperature measurements from *Mariner 10* indicate that the surface is a good thermal insulator and, therefore, must be covered with porous soil or rock powder like the lunar regolith. This is expected on a planet whose surface is shattered and stirred by meteorite impacts.

The heavily cratered terrain records the period of heavy bombardment that occurred throughout the entire inner solar system and ended about 3.8×10^9 years ago on the Moon, and presumably at about the same time on Mercury. The objects responsible for it probably originated among the main-belt asteroids when the inward migration of Jupiter and Saturn resulted in the migration of resonances through the asteroids, ejecting them into the inner solar system.

The oldest plains (intercrater plains) occur in the heavily cratered terrain and are thought to be primarily volcanic deposits erupted at various times during the period of heavy bombardment. The younger smooth plains are also thought to be volcanic deposits that were erupted within or around large impact basins such as Caloris. Based on the size–frequency distribution and density of impact craters superimposed on the smooth plains, they appear to have been formed near the end of heavy bombardment and may be on average about 3.8×10^9 years old. If so, they are, in general, older than the lava deposits that constitute the lunar maria. The unique tectonic framework of Mercury, expressed as a system of thrust faults, is probably the result of global compressive stresses in Mercury's crust caused by a decrease in the planet's radius due to cooling of the core and mantle.

High-resolution radar images of the unimaged side of Mercury show three radar-bright features with different characteristics. Two of the features are fresh impact craters, but the third is different and must await further exploration. The other has no known radar counterpart in the solar system. *See* GEOLOGY; MARS.

Geologic history. The general picture of Mercury's geologic history which has emerged from analyses of *Mariner 10* data is that soon after Mercury formed, it became almost completely melted by heating from the decay of radioactive elements and the inward migration of the large amount of iron to form its enormous core. This led to expansion of the planet

and tensional fracturing of a thin solid lithosphere that provided egress for lavas to reach the surface and form the intercrater plains during the period of heavy bombardment. As the core and mantle began to cool, Mercury's radius decreased by about 0.3 to 1.2 mi (0.5 to 2 km) or more, and the crust was subjected to compressive stresses that resulted in the system of thrust faults. At about this time, the Caloris Basin was formed by a gigantic impact, which caused the Hilly and Lineated Terrain from focused seismic waves in the antipodal regions. Further eruptions of lava within and surrounding the Caloris and other large impact basins formed the smooth plains. Volcanism finally ceased when compressive stresses in the lithosphere became strong enough to close off magma sources. All of these events probably happened very early, perhaps during the first $7–8 \times 10^8$ years, in Mercury's history. Since that time, only occasional impacts of comets and asteroids have occurred.

A new mission to Mercury called *MESSENGER* (Mercury Surface, Space Environment, Geochemistry, and Ranging), launched in 2004, is scheduled to orbit the planet in 2011 after two flybys in 2008 and 2009. This mission should answer most of the questions raised by the *Mariner 10* mission and Earth-based observations. *See* PLANET; SPACE PROBE.

Robert G. Strom

Bibliography. J. K. Harmon, Mercury radar studies and lunar comparisons, *Adv. Space Res.*, 19:1487–1496, 1997; R. G. Strom, Mercury: An overview, *Adv. Space Res.*, 19:1471–1485, 1997; R. G. Strom, *Mercury*: *The Elusive Planet*, 1987; Various papers reporting *Mariner 10* results, *Science*, 185:141–180, July 12, 1974, and *J. Geophys. Res.*, 80:2341–2514, June 10, 1975; F. Vilas, C. R. Chapman, and M. S. Matthews (eds.), *Mercury*, 1988.

Mercury-vapor lamp

A vapor or gaseous discharge lamp in which the arc discharge takes place in mercury vapor. This lamp is widely used for roadway and all other forms of illumination, and as a source of ultraviolet radiation for industrial applications.

Construction. The arc discharge takes place in a transparent tube of fused silica, or quartz, and this quartz tube is usually mounted inside a larger bulb of glass (see **illus.**). The outer bulb reduces the ultraviolet radiation of the inner arc tube, encloses and protects the mount structure, and can be coated with phosphors that greatly improve the color of the light emitted.

The arc tube has electrode assemblies mechanically sealed into each end. The main electrodes (one at each end) consist of a molybdenum shank welded to a very thin ribbon of molybdenum and completed by a shank of tungsten wound with tungsten wire and filled with an emission material of metal oxides. At one end of the arc tube, a smaller starting electrode is located close to the main electrode. The starting electrode is connected through a high resistance to the opposite electric polarity of the adjacent main electrode. The arc tube itself is filled with argon gas and a small amount of pure mercury before being sealed.

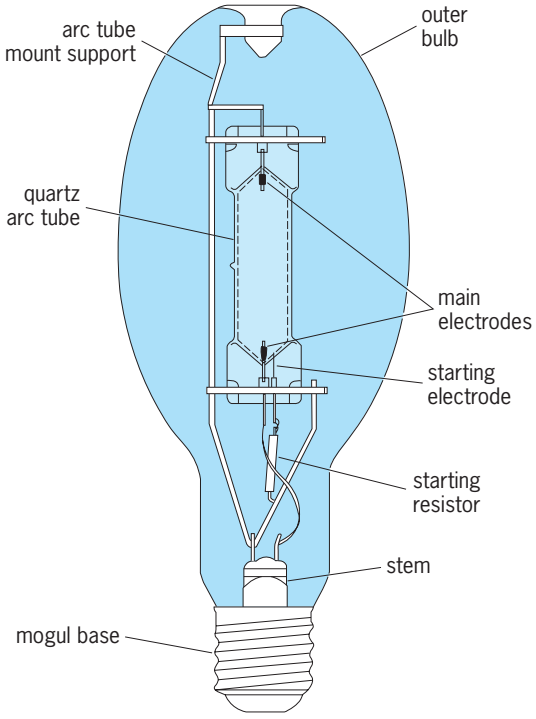

High-pressure mercury-vapor lamp.

The outer bulb supports the mount structure built around the arc tube and is sealed to a glass stem with conducting wires. These wires pass through the outer bulb and are connected to the center post and shell of a metal base.

Starting and operation. Mercury lamps, like other vapor lamps, require sizable voltages to start their arcs, after which the lamp current will continue to increase unless limited by a resistor (which severely reduces efficiency) or a magnetic device (a choke or transformer) called a ballast. The ballast, when energized, supplies proper voltage to the lamp base for starting, and with zero current full starting voltage appears between the main and starting electrode at one end of the lamp. Electrons move across a short gap, ionizing some argon gas in the tube. The ionized gas diffuses until an arc strikes between the main electrodes, where the path now contains less resistance than that between the main and starting electrodes. Once the main arc is formed, the heat from the arc vaporizes the mercury droplets, and they become ionized current carriers. As the lamp current increases to its full current rating, the self-limiting design of the ballast simultaneously reduces the supply voltage to maintain stable operation and extinguishes the glow between starter and main electrode at the reduced voltage. Initial light output requires minutes of warm-up and, similarly, if the ballast is deenergized or power is lost, it is necessary for the lamp to cool and the mercury pressure to be reduced before the starting glow can occur again. *See* ARC DISCHARGE; TRANSFORMER.

Color. Radiation from the mercury arc is confined to four specific wavelengths in the visible portion of

the spectrum and several strong lines in the ultraviolet. Careful design of the arc tube can adjust mercury pressure and cause some shifting of radiation among these wavelengths, thereby changing slightly the color of the illumination.

The visible radiation from clear mercury lamps is all concentrated in the blue, green, and yellow-green regions of the spectrum. This provides light with a distinct blue-green appearance and poor color rendition. Red objects, for example, look brown or black, and human skin looks unattractive. For this reason, most mercury lamps have a phosphor color-correcting coating, and clear bulbs are used only where appearance of colors is secondary to some gain in efficiency.

The phosphors applied to the inner wall of the outer bulb can provide superior color rendition through conversion of the arc tube's ultraviolet radiation to sizable reradiation in the red part of the spectrum or additional yellow, green, and blue-green radiation. One phosphor used for deluxe white lamps has made their use popular in many commercial lighting applications such as department stores and office areas. *See* PHOSPHORESCENCE.

Applications. After the fluorescent lamp, the mercury-vapor lamp is the most popular vapor lamp in use today, with its greatest use in roadway lighting. Many millions of these lamps are produced in the world annually, and despite the fact that other gaseous discharge lamps are more efficient, the long life, reliable performance, and relatively low cost of this lamp and ballast system ensure its use for some years to come.

The sizable radiation of ultraviolet by the bare arc tube suits it well as a sun lamp and as a source for ultraviolet applications in industry, where it is used in reproduction of tracings and to speed chemical reactions such as curing of protective coatings and inks. One wavelength in the near-ultraviolet, not harmful to humans, and transmitted by the bulb glass has the property of causing some dyes and pigments to fluoresce. When the visible light is filtered out and it is used for this fluorescing purpose, it is called a black light.

Consideration should be given to avoiding close proximity of humans to the standard mercury-vapor lamp when the outer bulb is broken since its ultraviolet radiation at close distances can cause erythemal reactions or sunburn, and these standard lamps are now being offered in alternate designs with internal switches or other devices to extinguish the arc if the outer bulb should break. *See* ILLUMINATION; LAMP; METAL HALIDE LAMP; ULTRAVIOLET LAMP; VAPOR LAMP.

T. F. Neubecker

Meridian

A line of longitude on Earth or in the sky, perpendicular to the Equator, and extending between the North and South poles.

A meridian of longitude on Earth marks a system of location and timekeeping whose zero was set at Greenwich, England, in the nineteenth century, when it was necessary to regularize time signals in the era of railway transportation. Time is 1 hour different for each 15° of longitude. The International Date Line, where days begin and end, was set 180° away from Greenwich, with jogs for local circumstances. The position of this 180° meridian assumed importance in the discussion of the new millennium, which was widely celebrated on January 1, 2000, in spite of its more accurate definition astronomically as January 1, 2001. Islands and other locations in the Pacific vied for the notoriety of being the first to see the Sun in the new millennium. *See* INTERNATIONAL DATE LINE; LATITUDE AND LONGITUDE; TIME.

Meridians of celestial longitude are the extensions into space of meridians of longitude on Earth. Each celestial meridian is the half of a great circle that goes between the north and south celestial poles and crosses the celestial equator perpendicularly. The unique line known as the celestial meridian is the great circle going from north pole to south pole through a given observer's zenith, the point directly overhead. It thus marks the north-south line, and celestial objects going through it are said to be at their meridian transits or at their culminations. Telescopes known as meridian transits have long been used together with clocks to measure the celestial longitudes of stars, known as their right ascensions. *See* ASTRONOMICAL TRANSIT INSTRUMENT.

Stars sufficiently near the celestial equator transit the meridian once per day, known as upper culmination, and invisibly transit the meridian 180° away in their lower culmination. Circumpolar stars are visible in both upper and lower culminations. *See* ASTRONOMICAL COORDINATE SYSTEMS.

Jay M. Pasachoff

Bibliography. J. Mitton, *Cambridge Dictionary of Astronomy*, Cambridge University Press, 2001; J. M. Pasachoff and A. Filippenko, *The Cosmos: Astronomy in the New Millennium*, 3d ed., Brooks/Cole Publishers, Belmont, CA, 2007; P. K. Seidelmann (ed.), *Explanatory Supplement to the Astronomical Almanac*, University Science Books, Mill Valley, CA, 1992.

Meromictic lake

A lake whose water is permanently stratified and therefore does not circulate completely throughout the basin at any time during the year. Normally lakes in the Temperate Zone mix completely during the spring and autumn when water temperatures are approximately the same from top to bottom. In meromictic (*mero*, partial; *mixis*, circulation) lakes, there are no periods of overturn or complete mixing because seasonal changes in the thermal gradient either are small or are overridden by the stability of a chemical gradient, or the deeper waters are physically inaccessible to the mixing energy of the wind. Commonly in meromictic lakes, the vertical stratification in density is stabilized by a chemical gradient.

The upper stratum of water in a meromictic lake is mixed by the wind and is called the mixolimnion.

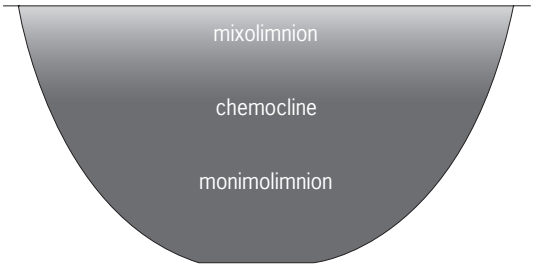

Fig. 1. Cross-sectional diagram of a meromictic lake.

The bottom, denser stratum, which does not mix with the water above, is referred to as the monimolimnion. The transition layer between these strata is called the chemocline (**Fig. 1**).

It is unknown how many meromictic lakes exist. But of the hundreds of thousands of lakes on the Earth, less than 200 have been reported to be meromictic and less than 50 meromictic lakes are reported for North America. Nevertheless, meromictic lakes are widely dispersed across all continents and on islands such as Cuba, the Galápagos and Tasmania. Zige Tangco at 4560 m (15,000 ft) above sea level in the central Tibetan Plateau is the highest known meromictic lake in the world. In North America, meromictic lakes generally are restricted to sheltered basins with proportionally very small surface areas in relation to depth, basins in arid regions, and isolated basins in fiords. Meromixis may occur in lakes with a permanent ice cover. Meromictic lakes frequently contain colored water, which limits penetration of solar radiation. *See* LAKE.

Interest in meromictic lakes is disproportional to their number, not only because they are oddities of nature but because they offer unique opportunities for limnological research. Research activity on meromictic lakes has been focused on the physiology and behavior of organisms, biogeochemistry, studies of lake history, deep-water circulation, and heat flow through the bottom sediments.

Chemical studies. Relatively few detailed chemical studies have been done on meromictic lakes, particularly on a seasonal basis. The most typical chemical characteristic of meromictic lakes is the absence of dissolved oxygen in the monimolimnion. Large quantities of hydrogen sulfide and ammonia may be associated with this anaerobic condition in deep water. J. Kjensmo proposed that the accumulation of ferrous bicarbonate in the deepest layers of some lakes may have initiated meromixis under certain conditions. Separation of salts from surface water as the water freezes, and then the accumulation of these salts in deeper waters, also has led to meromixis in Antarctic lakes. Some human activities have caused meromixis in a few cases. For example, runoff containing salt used for deicing nearby roads can produce permanent stratification in small lakes.

Meromictic lakes are exciting model systems for many important biogeochemical studies. The isolation of the monimolimnetic water makes these studies quite interesting and important. In studies of the biological fractionation of sulfur and carbon isotopes in the monimolimnion of Fayetteville Green Lake, New York, the fractionation factor for sulfur was found to be the highest ever observed.

Sediments from meromictic lakes are among the best for studies of lake history, since there is relatively little disturbance or decomposition of biogenic materials. Such sediments may provide a detailed record of the origin, ecological changes, and physical changes of meromictic lakes and their drainage basins over time. Also, deuterium has been used by several workers in an attempt to unravel the history of meromictic lake water.

Physical studies. Radioactive tracers have been used to show that the monimolimnetic water in a small meromictic lake (Stewart's Dark Lake) in Wisconsin is not stagnant but undergoes significant horizontal movement (**Fig. 2**). While the maximum radial spread was about 16–18 m (52–59 ft) per day, vertical movements were restricted to negligible amounts because of the strong vertical density gradient. A similar pattern of movement was reported in the deep water of a larger meromictic lake (Soap Lake) in Washington. It was determined from these studies that the average horizontal eddy diffusion coefficient is 3.2 cm^2/s (0.50 $in.^2/s$) in the monimolimnion of Soap Lake and 17 cm^2/s (2.6 $in.^2/s$) in Stewart's Dark Lake.

Because vertical mixing is restricted in a meromictic lake, heat from solar radiation may be trapped in the monimolimnion and thereby can produce an anomalous temperature profile. Monimolimnitic water temperatures have been reported as high as 50.5°C (123°F) at a depth of 2 m (7 ft) in shallow Hot Lake, Washington.

Some meromictic lakes are very convenient for studies of geothermal heat flow because deep-water temperatures may be nearly constant year-round. Studies of terrestrial heat flow have been made in the sediments of Stewart's Dark Lake, Wisconsin, and in

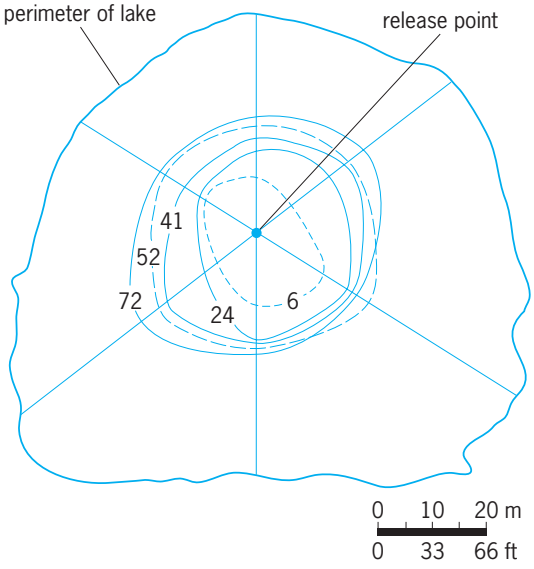

Fig. 2. The outlines show the maximum horizontal displacement of a radiotracer (sodium-24) following its release at 8-m (26-ft) depth in Stewart's Dark Lake, Wisconsin. The numbers indicate the hours elapsed after release.

Fayetteville Green Lake, New York. Steady-state thermal conditions were found in the sediments of Stewart's Dark Lake, and the total heat flow was calculated to be 2.1×10^{-6} cal/cm^2 s (8.8×10^{-2} W/m^2). However, about one-half of this flux was attributed to the temperature contrasts between the rim and the central portion of the lake's basin. It was found that the thermal conductivity of the surface sediments in the center of Stewart's Dark Lake was 1.10×10^{-3} cal · cm/ (cm^2 · s · °C) [0.46 W · m/(m^2 · °C)], a value substantially lower than that for pure water at the same temperature but consistent with measurements on colloidal gels.

Biological studies. Relatively few kinds of organisms can survive in the rigorous, chemically reduced environment of the monimolimnion. However, anaerobic bacteria and larvae of the phantom midge (*Chaoborus* sp.) are common members of this specialized community. By using sonar, vertical migrations of *Chaoborus* sp. larvae have been observed in meromictic lakes. The sound waves are reflected by small gas bladders on the dorsal surface of the larvae. The migration pattern is similar to that shown by the deep-scattering layers in the sea. The larvae come into the surface waters at night when the light intensity is low, and sink into deeper waters during the daylight hours. Biologically significant quantities of chemical nutrients or pollutants can be transported from the deep and relatively inaccessible part of a meromictic lake to the surface and thence to the adjacent terrestrial environment by these organisms. A radiotracer (iodine-131) appeared in flying adult *Chaoborus* sp. along the shoreline of the lake within 20 days after it had been released within the region of the chemocline.

Specialized bacteria, such as the photosynthetic, green sulfur or purple sulfur bacteria (*Chromatium* spp.), utilize the unique characteristics of the upper monimolimnion. Often, these bacterioplanktonic populations become dense enough to impart color to the water.

Spectacular degassing events from the deep waters of two tropical meromictic lakes (Lakes Nyos and Monoun) in Cameroon, West Africa, have occurred on occasion during late summer when vertical stability is reduced due to weather conditions and mixing penetrates deeply in the water column. Large releases of carbon dioxide from Lake Monoun (August 15, 1984) and from Lake Nyos (August 21, 1986) killed over 1700 people living nearby. *See* BIOGEOCHEMISTRY; FRESHWATER ECOSYSTEM; LIMNOLOGY; SONAR.

Gene E. Likens

Bibliography. G. J. Brunskill et al., Fayetteville Green Lake, New York, I: Physical and chemical limnology, II: Precipitation and sedimentation of calcite in a meromictic lake with laminated sediments, III: The laminated sediments, IV: Interstitial water chemistry of the sediments, V: Studies of primary production and zooplankton in a meromictic marl lake, *Limnol. Oceanogr.*, 14(6):817–873, 1969; E. S. Deevey, N. Nakai, and M. Stuiver, Fractionation of sulfur and carbon isotopes in a meromictic lake, *Science*, 139:407–408, 1963; L. J. Garcia-Gil, X. Casamitjana, and C. A. Abella, Comparative study of two meromictic basins of Lake Banyoles (Spain) with sulphur phototrophic bacteria, *Hydrobiologia*, 319(3):203–211, 1996; J. A. E. Gibson, The meromictic lakes and stratified marine basins of the Vestfold Hills, East Antarctica, *Antarctic Sci.*, 11(2):175–192, 1999; N. M. Johnson and G. E. Likens, Steady-state thermal gradient in the sediments of a meromictic lake, *J. Geophys. Res.*, 72:3049–3052, 1967; G. W. Kling, Seasonal mixing and catastrophic degassing in tropical lakes, Cameroon, West Africa, *Science*, 237:1022–1024, 1987; K. F. Walker and G. E. Likens, Meromixis and a reconsidered typology of lake circulation patterns, *Verh. Int. Verein. Limnol.*, 19:442–458, 1975.

Merostomata

A class of phylum Arthropoda, subphylum Chelicerata. Merostomes are aquatic chelicerates, characterized by abdominal appendages bearing respiratory organs. Most merostomes are extinct; only the horseshoe crabs, comprising four species and three genera (*Carcinoscorpio* and *Tachypleus* of eastern Asia and *Limulus polyphemus* of eastern North America) survive. The body of a merostome consists of a prosoma, or head, which lacks antennae, has a pair of compound eyes and a pair of simple median eyes, and bears the chelicerae (pincers) and five pairs of uniramous walking legs with gnathobases for mastication. The opisthosoma, or trunk, consists of 12 or fewer segments which may be freely articulating or partly or entirely fused into a solid shield; the opisthosoma bears the respiratory appendages. The telson (tail) is a solid, usually spikelike, structure. *See* CHELICERATA.

A modern classification of the Merostomata follows:

Phylum Arthropoda
  Class Merostomata
    Subclass Eurypterida
      Order: Eurypteridida
        Chasmataspida
    Subclass Xiphosura
      Order: Aglaspida
        Xiphosurida
      Suborder: Synziphosurina
        Limulina

The scorpionlike Eurypteridida (Ordovician–Permian) was the most diverse merostome group, inhabiting a variety of nearshore marine and freshwater habitats. Eurypterids were the largest known arthropods, reaching lengths of about 6 ft (2 m) or more in some genera. The prosomal appendages were modified into a variety of shapes for walking, swimming, capturing prey, and perhaps burrowing. *See* EURYPTERIDA.

The Chasmataspids (Ordovician–Devonian) were a heterogeneous group of eurypteridlike merostomes of uncertain affinity.

The Aglaspida (Cambrian–Ordovician) are generally considered to be the most primitive of all known merostomes. Their body form was simple (**Fig. 1***a*),

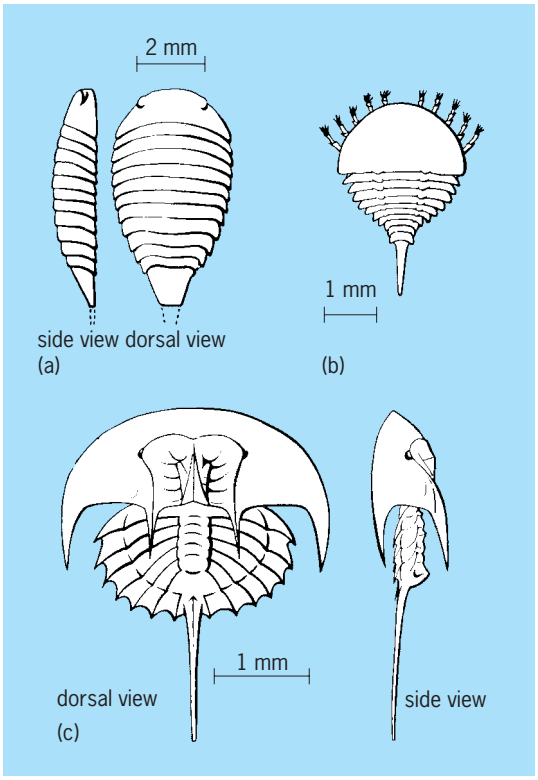

Fig. 1. Some typical extinct species of the class Merostomata. (*a*) *Paleomerus*, order Aglaspida. (*b*) *Weinbergina*, suborder Synziphosurina. (*c*) *Euproops*, order Xiphosurida. (*After R. C. Moore, ed., Treatise on Invertebrate Paleontology, Geological Society of America, 1955*)

with a small prosoma with compound eyes, an opisthosoma with 11 or 12 freely articulating segments, and a simple telson. The aglaspid cuticle was usually phosphatic, in contrast to the chitinous cuticle of other merostomes. A few species have been described with walking legs (instead of gill-bearing appendages) on the opisthosoma.

The Xiphosurida appeared in the Silurian with certainty, although Cambrian and Ordovician forms may be early representatives of this group. The Xiphosurida are united by a number of characters, including a prosoma and an opisthosoma of nearly equal length and the presence of an ophthalmic ridge, a linear elevation on either side of the prosoma, bearing the lateral compound eyes (Fig. 1*c*). *See* XIPHOSURIDA.

Fig. 2. *Legrandella*, from the Devonian of Bolivia. Note the crescentic ophthalmic ridges and the anterior four freely articulating opisthosomal segments.

The most primitive xiphosuridans, the Synziphosurina (Silurian–Devonian), until recently were poorly known. Their prosomal anatomy was like that of true horseshoe crabs, but they retained the free opisthosomal segments of the primitive merostomes (Fig. 1*b*). Synziphosurans were not blind, as previously supposed. Compare Fig. 1*b*, an old restoration of the synziphosuran *Weinbergina*, with **Fig. 2**, a photograph of *Legrandella*, by far the best-preserved synziphosuran yet found, which possesses ophthalmic ridges, eyes, and a number of other features previously thought to be absent in the Synziphosurina.

The Limulina (Devonian–Recent) are the true horseshoe crabs. Paleozoic representatives lived in both nearshore marine and fresh-water habitats and differed from modern limulines chiefly by their smaller size. During the Mesozoic and Cenozoic, the limulines became larger, whereas the group as a whole became restricted in terms of the number of different species living at any one time; the four species alive today probably represent the typical amount of limuline diversity for at least the past 100,000,000 years. Their survival for so long in relatively few numbers and in a relatively unchanged state qualifies them as living fossils. *See* LIVING FOSSILS.

Niles Eldredge

Bibliography. N. Eldredge, Revision of the suborder Synziphosurina (Chelicerata, Merostomata), with remarks on merostome phylogeny, *Amer. Mus. Novitates,* 2543:41, 1974.

Mesogastropoda

The largest and most diverse order of gastropod mollusks in the subclass Prosobranchia. Mesogastropods are all single-gilled and thus monotocardiac, that is, with only one auricle and asymmetry of other cardiac, renal, and genital structures. Except for the minor superfamily Valvatacea, which retains an aspidobranch or bipectinate "feather" gill like those of the Archaeogastropoda, all mesogastropods have a one-sided comb-shaped or pectinibranch ctenidium or "half-gill" with its axis and blood vessels fused to the mantle wall. This results in a simplified mantle cavity that is asymmetric and hydraulically more efficient than in the Archaeogastropoda, and from which both feces and nitrogenous excretory wastes are discharged to the right side of the snail's head-foot. Such a system can operate in silty waters and, unlike the archaeogastropods which are limited to clean waters over hard substrata, mesogastropods with a wide variety of marine life-styles are found burrowing in soft muds and living exposed to air near high-tide level. There are also estuarine, fresh-water, and terrestrial species in the order. The anatomical asymmetry makes possible a functional separation of genital from renal ducts, which in turn allows the development of internal fertilization, of large

eggs, of ovoviviparity, and of true viviparity (all features advantageous for the evolution of nonmarine stocks).

Certain older classifications designate the mesogastropods as order Taenioglossa, referring to the intermediate type of radula characteristic of this group. The taenioglossan radula is narrower and normally has only seven teeth in each row. Mesogastropods are structurally diverse, and most classifications divide them into 13 superfamilies, 4 of which number several thousand species and encompass some of the world's most abundant, ubiquitous, and cosmopolitan marine snails.

Major groups and species. On the basis of neural anatomy, the large superfamily Cyclophoracea (mainly family Viviparidae) is regarded as comprising the most primitive living mesogastropods, but it is in other ways a highly specialized nonmarine group with its genera well adapted for life in freshwaters and on land (mostly in humid tropical habitats). Similarly, the small superfamily Valvatacea has the primitive gill noted above, but again its members are fresh-water animals, including several ovoviviparous species. One of the largest superfamilies of mollusks is the Rissoacea, encompassing more than 1350 living species and vast numbers of individual snails, mostly tiny and highly motile, in a variety of marine, estuarine, and freshwater habitats. Another huge superfamily is the Cerithacea (at least 1300 living species), dominating the sublittoral marine muds in many parts of the world, mainly with elongate pointed shells like the genus *Turritella*, but also including tropical estuarine and freshwater forms. The smaller superfamily Strombacea includes the pelican's-foot shells such as *Aporrhais*, and *Strombus gigas*, the queen or true-pink conch of the Florida Keys. Another small superfamily, Calyptraeacea, includes relatively sessile microphages such as *Capulus* and *Crepidula*, in which the individual leaflets of the pectinibranch gill have been elongated into filaments for use in filter feeding (paralleling the evolution of the eulamellibranch bivalves).

Among the best-known and most collected tropical sea shells are the 400 species of cowries (superfamily Cypraeacea) with glossy colorful ovate and convolute shells having a long narrow aperture bounded on both sides by inrolled toothed lips. In living cowries, the expanded mantle folds completely conceal the shell, and it is this that results in the outside (as well as the inside) of the shell being "varnished" with a nacreous (pearly) layer. In several parts of the world, cowries have been used as currency. Elsewhere, their resemblance to human female genitalia has made them important in fertility rituals and in the worship of Aphrodite and similar goddesses. Superfamily Heteropoda includes forms like the atlantids, living pelagically in the open ocean with reduced fragile shells and various methods of flotation. Superfamily Ptenoglossa (or Scalacea) comprises both the shell collectors' prized wentletraps and the ianthinids which float on the ocean surface by using a mass of bubbles of hardened mucus.

Possibly the most successful of all seashore animals are the 800 species of the Littorinacea, including several high-littoral air-breathing species of periwinkles, and some tropical terrestrial forms. In the middle levels of the intertidal zone, littorinid snails are alternately aerial and aquatic in habit, and several periwinkle species have both lungs and gills. Other aspects of littorinid physiology, including reproduction and nitrogenous excretion, are involved in the trends for those snail species living at the higher levels of the seashore to be better adapted for aerial or terrestrial conditions.

The superfamily Naticacea comprises the moon snails, about 200 species of predaceous carnivores, moving through sand and mud and preying on bivalves and other snails. Naticids employ a protrusible proboscis and attached boring gland to drill through the shells of their prey by using a combination of mechanical and chemical processes. Larger naticids also use an unusual series of pedal water sinuses to inflate the enormous foot (used not only to move rapidly through sand but also to wrap around the clam prey).

Evolution. In the evolution of the gastropod mollusks, mesogastropods clearly constitute an intermediate grade. It is possible that the order Mesogastropoda is not monophyletic, and that stocks with the asymmetric efficiency of structures which is diagnostic are derived from several archaeogastropod stocks. However, it is clear that the several lines of "higher" gastropods, including not only prosobranchs of the order Neogastropoda but also nonprosobranchs in the subclasses Opisthobranchia and Pulmonata, have each been derived from stocks within the order Mesogastropoda. *See* GASTROPODA; NEOGASTROPODA; PROSOBRANCHIA.

W. D. Russell-Hunter

Bibliography. V. Fretter and A. Graham, *British Prosobranch Molluscs*, 1962; W. D. Russell-Hunter, *A Life of Invertebrates*, 1979; K. M. Wilbur (ed.), *The Mollusca*, vols. 1–12, 1983–1987.

Meso-ionic compound

A member of a class of five-membered ring heterocycles (and their benzo derivatives) which possess a sextet of π electrons in association with the atoms composing the ring but which cannot be represented satisfactorily by any one covalent or polar structure.

Structure. Two main types, depending formally upon the origin of the electrons in the π system, have been identified; they are exemplified by compounds (**1**) and (**2**). In structure (**1**) the nitrogen and

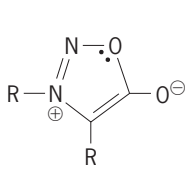

(**1**)

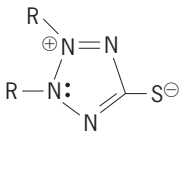

(**2**)

oxygen atoms, 1,3 to each other, are shown as donating two electrons each to the total of eight electrons in the whole π system, whereas in structure (**2**) the two middle nitrogen atoms, 1,2 to each other, are the two-electron donors.

The term "satisfactorily" in the definition refers to the fact that the charge in the ring cannot be associated exclusively with one ring atom. Thus, these compounds are in sharp contrast with other dipolar structures, such as ylides [for example, compound (**3**)], and such compounds are not consid-

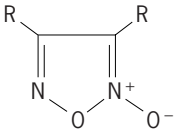

(**3**)

ered meso-ionic. Meso-ionic compounds are most commonly represented as follows: compound (**1**) as structure (**4**) and compound (**2**) as structure (**5**). The

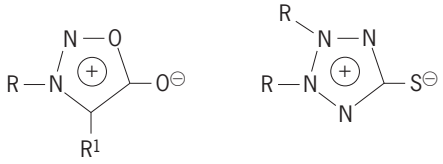

(**4**) (**5**)

circle represents six π electrons; the positive charge is shared by all the ring atoms.

Preparation. Compounds of type (**1**), containing a 1,2,3-oxadiazole nucleus, were the first discovered members of this class and are known as sydnones. They are made by the action of acetic anhydride on the *N*-nitroso derivatives of *N*-substituted α-amino acids [reaction (1)].

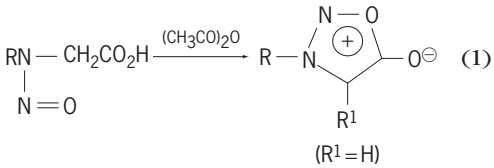

(1)

($R^1 = H$)

Other representatives of this type contain 1,3-oxazole, imidazole, thiazole, 1,3-dithiole, 1,3,4-oxadiazole, 1,3,2-oxathiazole, 1,2,3- and 1,2,4-triazole, and 1,3,4- and 1,2,3-thiadiazole nuclei. There are also derivatives with four hetero atoms.

Compounds of type (**2**) are known as dehydrodithizones and were actually the first meso-ionic compounds discovered. They are made by the oxidation of the acyclic dithizones (**6**) with manganese dioxide [reaction (2)] or isoamyl nitrite. Other nuclei

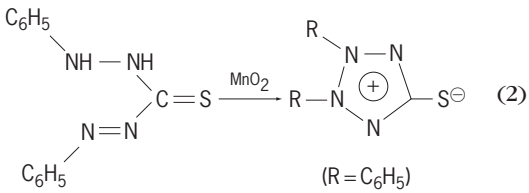

(2)

(**6**) ($R = C_6H_5$) (**5**)

present in compounds related to (**5**) are isoxazole, pyrazole, isothiazole, and 1,2-dithiole.

Reactions. The most important reactions of meso-ionic compounds are dipolar cycloaddition reactions in which the meso-ionic compound reacts with alkenes and acetylenes. Sometimes these reactions involve their acyclic tautomers [reaction (3)]. They

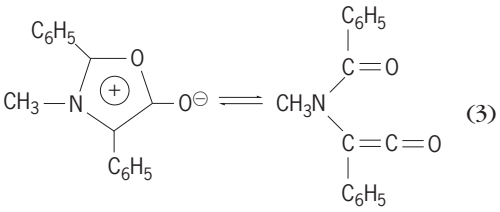

(3)

Meso-ionic compound Acyclic tautomer

also are extremely reactive toward nucleophiles, even as mild as water, yielding acyclic products.

Photochemically, they are highly reactive and extensive rearrangement and degradation has been observed. For example, sydnones can be rearranged to oxadiazolinones, as in reaction (4), where R^2 is C_6H_5 or H.

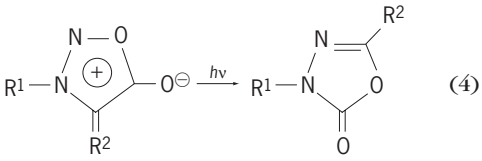

(4)

See PHOTOCHEMISTRY.

Uses. There has been considerable interest in the pharmacological activity of meso-ionic compounds, and derivatives have shown a variety of antibiotic, anthelminthic, antidepressant, and anti-inflammatory properties. *See* HETEROCYCLIC COMPOUNDS.

Jeremiah P. Freeman

Bibliography. J. A. Joule, *Heterocyclic Chemistry*, 4th ed., 2000; A. R. Katrizky (ed.), *Advances in Heterocyclic Chemistry*, vol. 48, 1990; E. C. Taylor and A. R. Katritzky (ed.), *Advances in Heterocyclic Chemistry*, vol. 19, 1975.

Mesometeorology

That portion of meteorology comprising the knowledge of intermediate-scale atmospheric phenomena, that is, in the size range of approximately 1–1200 mi (2–2000 km) and with time periods typically less than 1 day. In addition to these time and space criteria for defining mesoscale, dynamical considerations can be used. For example, a dynamical definition requires that both background rotation and ageostrophic advection be present to a significant degree. These requirements are based upon the relative magnitudes of the two major forces, pressure gradient and Coriolis, that govern movement of the atmosphere. To the extent that these forces are not in balance, air is accelerated. When the forces are of comparable magnitude, accelerations are relatively small and the atmosphere is considered to be in

geostrophic equilibrium. The wind, under these so-called balanced conditions, is called the geostrophic wind. For weather systems larger than mesoscale, the atmosphere is predominantly geostrophic. However, for mesoscale systems, geostrophic balance is not routinely present and accelerations can be quite large. Thus, the wind departs from geostrophic balance, and the departure is termed the ageostrophic wind. The term total wind can then be thought of as the sum of the geostrophic and ageostrophic components, and each component can advect (move, carry, transport, and so on) various properties or constituents of the atmosphere. Therefore, one of the clearly definable dynamic differences between large and mesoscale systems is that ageostrophic advection is negligible for large-scale circulations, while for mesoscale circulations it is not. A convenient way of measuring this condition is through the nondimensional Rossby number (R). This number is the ratio of the net acceleration of the horizontal wind by all the forces to the acceleration produced by the Coriolis force alone. For mesoscale motions, R is on the order of 1, as shown below.

$$R \equiv \frac{\text{net of accelerations by all forces}}{\text{acceleration by Coriolis force}} \sim 1.0$$

For progressively larger weather systems, accelerations tend to become smaller and R decreases. As R approaches the order of 0.1, weather systems are considered synoptic scale instead of mesoscale. *See* DIMENSIONLESS GROUPS.

Observing mesoscale phenomena. Over midlatitude landmasses, the average spacing between atmospheric sounding stations that use balloon-borne instrument packages is about 180–360 mi (300–600 km) and the standard sounding frequency is twice each day. Consequently, only the largest mesoscale phenomena, with wavelengths greater than about 600 mi (1000 km), are routinely observed (resolved) by this network. Information with higher

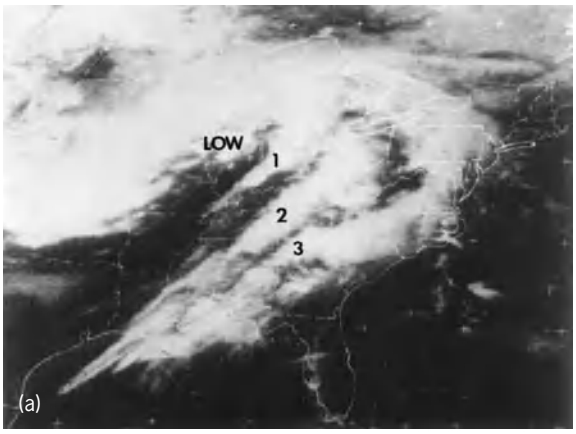

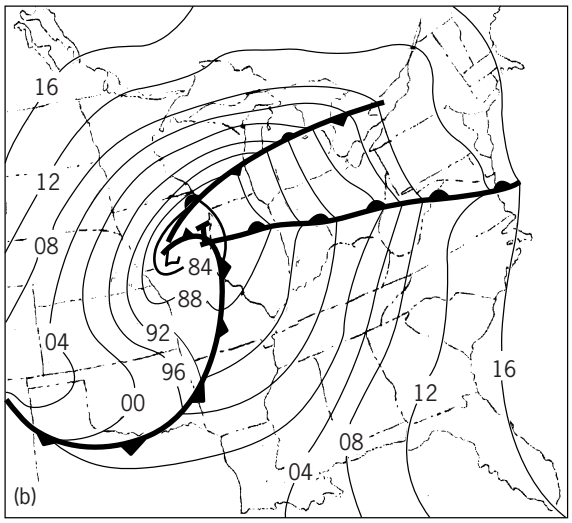

Key:

- ● = large thunderstorms; underlined numbers indicate height (in 10^2 ft) of the tops of thunderstorms
- ◒ = scattered precipitation
- ◍ = broken precipitation
- ⊕ = total precipitation
- RW = rain showers
- TRW = rain showers with thunder (thunderstorm)
- \+ = increasing intensity of thunderstorm
- R = continuous rain
- S = continuous snow
- ISOLD = isolated precipitation
- ○ = upper-air sounding station

Fig. 1. Mesoscale weather systems. (*a*) Satellite image for 2100 UTC (4:00 PM EST), April 3, 1974, showing the three major squall lines responsible for the greatest tornado outbreak in United States history. (*b*) Graphic of squall lines. (*c*) Easten United States showing detailed weather. (*After L. R. Hoxit and C. F. Chappell, Tornado outbreak of April 3–4, 1974, NOAA Tech. Rep. ERL 338-APCL 37, Department of Commerce*)

time and space resolution is available from aircraft observations, such as those taken by the Aircraft Communications, Addressing and Reporting System (ACARS), and networks of radar stations, profilers, and satellite imagery. The profiler is a ground-based hybrid observing system of vertically pointing radar and microwave radiometry. Unlike the discrete (in time) observations provided by most other observing systems, profilers provide continuous depictions of the vertical profiles of wind, temperature, and humidity. However, only a limited network of profilers (situated mostly over the midwestern United States) is operational. In contrast, satellite and Doppler radars cover virtually all areas of the United States and provide detailed observations of many mesoscale phenomena.

The satellite and radar observations often show that mesoscale weather systems are distinct components of large synoptic-scale cyclones (low-pressure systems) and anticyclones (high-pressure systems). For example, the satellite image in **Fig. 1** shows a large, contiguous area of clouds associated with a synoptic-scale low-pressure system. Within this large cloud mass, three distinct mesoscale weather systems are clearly apparent over the eastern portion of the United States. These systems, squall lines, are composed of lines of thunderstorms acting in a unified manner (individual thunderstorms are discernible in the easternmost squall line) and have characteristic scales of approximately 150 mi (250 km)—much smaller than the resolution of the standard sounding network. *See* CYCLONE; REMOTE SENSING; SQUALL LINE; THUNDERSTORM; WEATHER MAP.

Although satellite imagery and radar data provide extensive areal coverage and clearly reveal the presence of mesoscale systems, they do not provide adequate vertical resolution of certain atmospheric parameters (such as temperature, moisture, and pressure) so that the mesoscale structures and circulations can be examined quantitatively and fully understood. Thus, while mesoscale phenomena can be "observed," they can not be studied and predicted (in the conventional manner) as easily as synoptic-scale systems. *See* METEOROLOGICAL SATELLITES; RADAR METEOROLOGY; WEATHER FORECASTING AND PREDICTION.

Mesoscale weather systems. These are responsible for many of the significant weather events that routinely occur in the midlatitudes and the tropics. These systems naturally fall into two categories: free- and forced-mode systems. As considered here, forced-mode systems most frequently arise from interactions between the atmosphere and the Earth's topography. Free-mode systems develop in situ from the background (large-scale) environment. The **table** lists some commonly recognized free- and forced-mode mesoscale phenomena and their typical wavelength or other appropriate dimension. These phenomena include terrain modulation of precipitation, terrain-forced gravity waves, lake-effect snowstorms, convective complexes, and rainbands.

Terrain modulation of precipitation. Since the absolute humidity of an air parcel tends to increase with temperature, decreasing the temperature of a saturated parcel results in net condensation of water vapor, that is, the formation of clouds. Futhermore, since air parcels expand and cool when they ascend, and compress and warm when they descend, clouds and precipitation are likely to develop or intensify as air ascends mountainous terrain, and to weaken or dissipate as air descends. Thus, for mountainous areas of the world, the distribution of precipitation is strongly modulated by mesoscale terrain features. For example, **Fig. 2***a* shows the local terrain for a mesoscale region in the western United States, where east-west-oriented ridges are separated by river valleys. If forecasting were being done for the single synoptic-scale forecast zone using only synoptic-scale weather features as a guide, the weather would be considered to be essentially the same throughout, irrespective of the mesoscale terrain effects. However, as is apparent from Fig. 2*a*, when the wind is from the north, air alternately ascends the ridges and then descends into the valleys, causing clouds and precipitation over the ridges and clearing in the valleys. Such a situation is shown in Fig. 2*b*, where a large (synoptic-scale) storm is moving east through the Rocky Mountain region. The counterclockwise circulation around the low-pressure center is producing low-level northerly flow across the mesoscale region shown in Fig. 2*a*. There are alternating cloudy and clear areas over the ridges and valleys, respectively. In this particular

Mesoscale phenomena

Phenomena	Wavelength, mi (km)
Force mode	
Gravity waves (amplifying mountain lee-waves)	1.2–1200 (2–2000)
	6–60 (10–100)
Lake-effect snowstorms	6–60 (10–100)
Mountain-valley circulations	Twice distance from mountain crest to valley floor
Sea breeze	6–60 (10–100)
Terrain modulation of precipitation	Scale of terrain feature
Free mode	
Precipitation bands (moist symmetric instability)	6–60 (10–100)
Convective complexes	600–1200 (1000–2000)
Jet streaks	600–1200 (1000–2000)
Polar lows	600–1200 (1000–2000)
Squall lines	12–20 (20–200)
Tropical storms and hurricanes	1200 (2000)

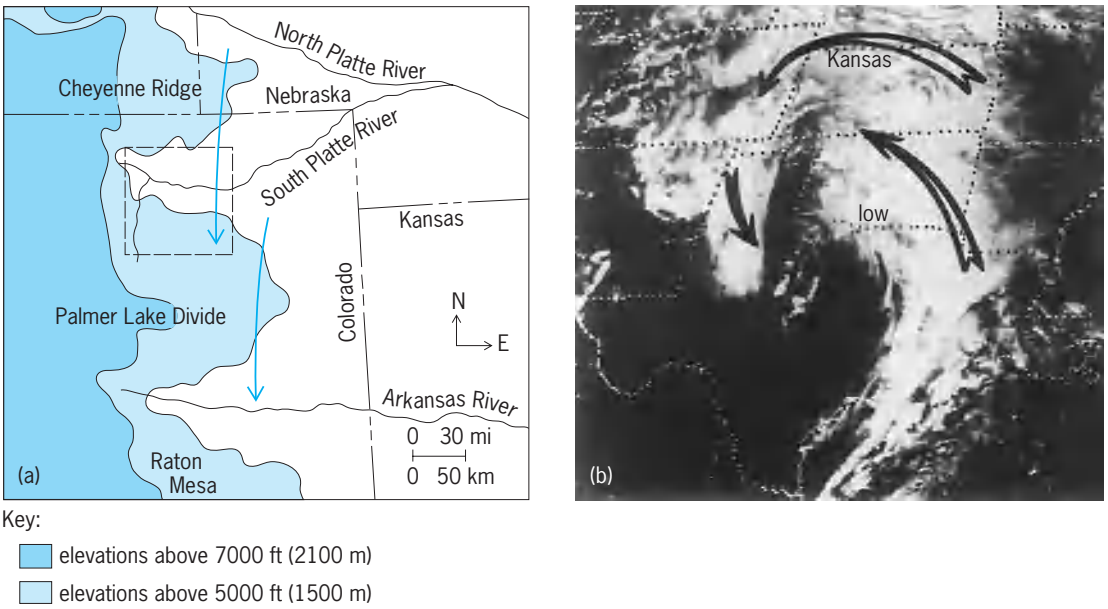

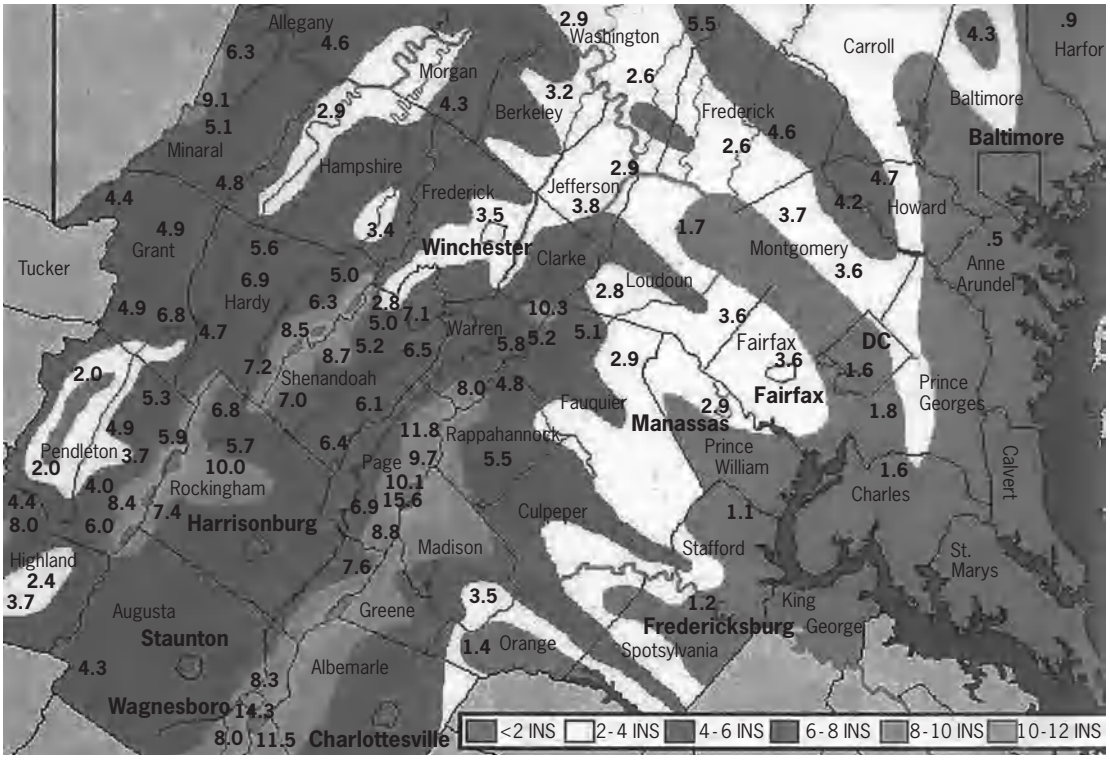

(c)

Fig. 2. Terrain modulation of precipitation. (*a*) Mesoscale terrain features (shaded). Arrows indicate direction of mean low-level airflow. Boxed area indicates typical size of a synoptic-scale forecast zone. (*b*) Visible *GOES* satellite imagery for November 8, 1977. Large arrows indicate low-level cyclonic flow around synoptic-scale low-pressure center. (*c*) Rainfall (in inches) from tropical storm Fran on September 6, 1996 (*adapted from Barbara Watson, NOAA*).

instance, well over a foot of snow fell on the Palmer Lake Divide with little or no snow reported in the river valleys on either side. Similarly, the rainfall from tropical storm Fran was modulated by the mesoscale terrain features of the Appalachian Mountains of Virginia. Note in Fig. 2*c* how rainfall totals vary from over a foot (>30 cm) along the ridges to only a few inches in the valleys. Such mesoscale terrain effects are so strong in mountainous areas of the world that average annual precipitation isohyets approximately parallel the terrain-height contours. *See* ATMOSPHERE; CLOUD; CLOUD PHYSICS; PRECIPITATION (METEOROLOGY).

Terrain-forced gravity waves. As an air parcel encounters a mountain barrier and is displaced upward, it undergoes changes in temperature, pressure, and density

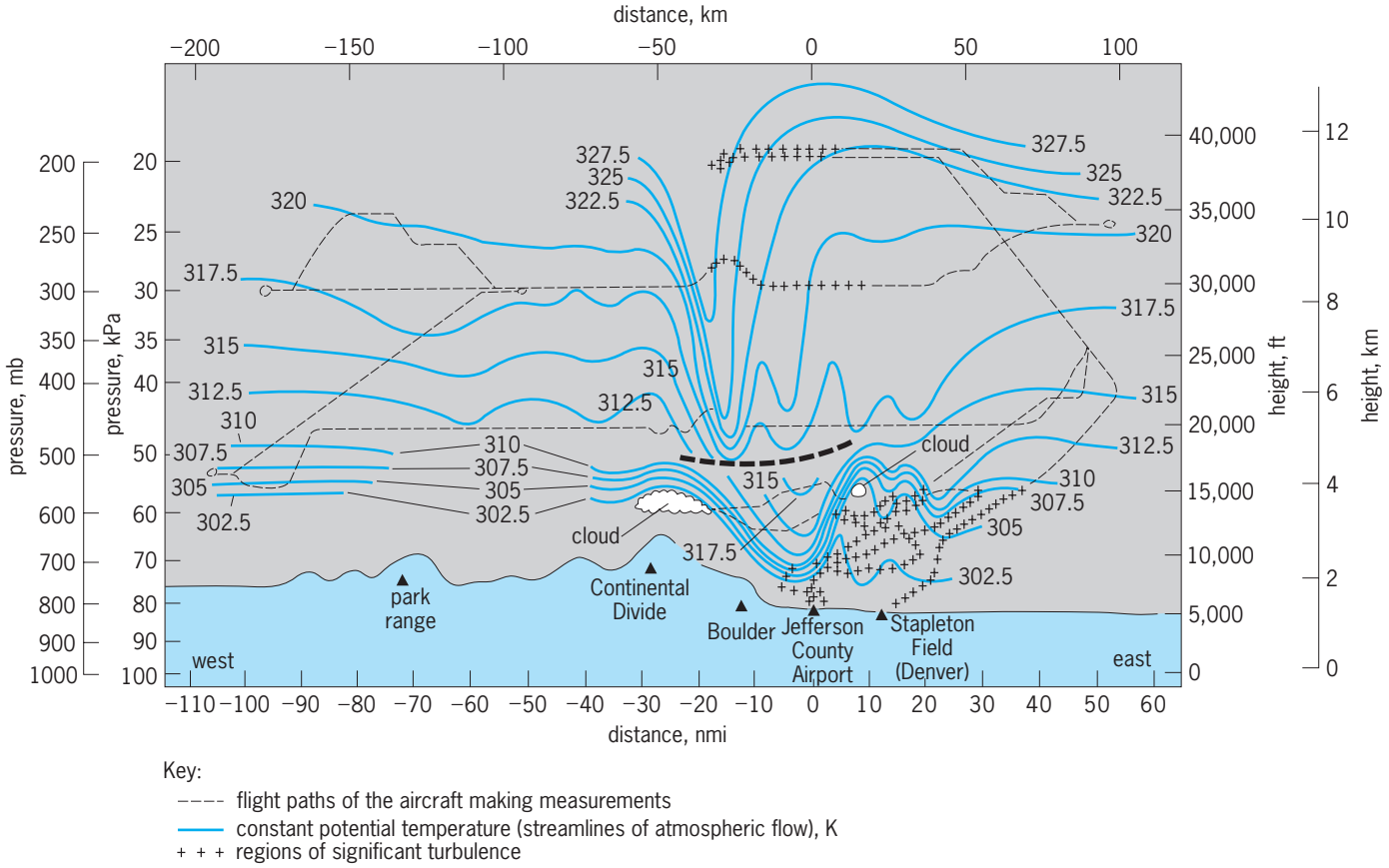

Fig. 3. Cross section of potential temperature (K) on January 11, 1972, on an east-west line through Boulder, Colorado. The heavy broken line separates measurements taken at two different times. °F = 1.8 K − 459.67. (*After D. K. Lilly, A severe downslope windstorm and aircraft turbulence event induced by a mountain wave, J. Atm. Sci., 35:59–77, 1978*)

relative to its surroundings. The parcel is therefore subject to pressure and gravitational forces which act to restore the parcel toward its initial equilibrium position. The undulation produced by alternate displacement followed by restoration, where gravity plays an important role, is commonly referrred to as a gravity wave. Propagation of gravity waves away from a mountain barrier indicates energy being transmitted through the air away from the mountain. The propagation of gravity waves is dependent upon the characteristics of the medium (in this case, air) through which it propagates. If the wave encounters a zone where there is a locally sharp change in the physical characteristics (such as a change in density) of the medium, not all of the energy of the wave may be transmitted into the new medium—some energy may be reflected. In certain situations, the atmosphere is composed of layers of air with quite different characteristics so that a portion of the energy with upward-propagating gravity waves is reflected downward. Depending upon the thickness of these layers and the height of the mountain, reflected energy may return "in phase" with subsequent original waves—this is commonly called resonance. In these instances, the amplitudes (energy) of the original and reflected waves are additive, and the wave grows. A mountain-forced gravity wave (mountain wave) under "ideal" amplification conditions may grow to tremendous heights and produce extreme winds [often in excess of 100 mi (160 km) per hour and, on occasion, as fast as 140 mi (240 km) per hour] in the lee of the mountain barrier. **Figure 3** shows a cross section through such a wave.

In addition to the obvious threat that such amplifying waves and attending severe winds pose to the general public, a second impact area is aviation. Downslope windstorms are capable of destroying light aircraft on the ground, make takeoffs and landings exceedingly hazardous, and generate downdrafts from which small aircraft flying over mountainous terrain may not escape. Pilot reports of vertical currents exceeding 3000 ft (900 m) per minute during these storms are not uncommon. On occasion, vertical currents have been reported to be as strong as about 7900 ft (2400 m) per minute. *See* AERONAUTICAL METEOROLOGY.

Mountain waves and their associated downslope winds occur along the lee slopes of major mountain ranges of the world. The winds are called *foehn* in Europe, *zonda* in Argentina, *puelche* in the Andes, *favogn* in Switzerland, and Canterbury Northwestern in New Zealand. The name varies within the continental United States: chinook along the Rocky Mountains, mono in the Sierras, and Santa Ana along the Coastal Range in southern California. *See* CHINOOK.

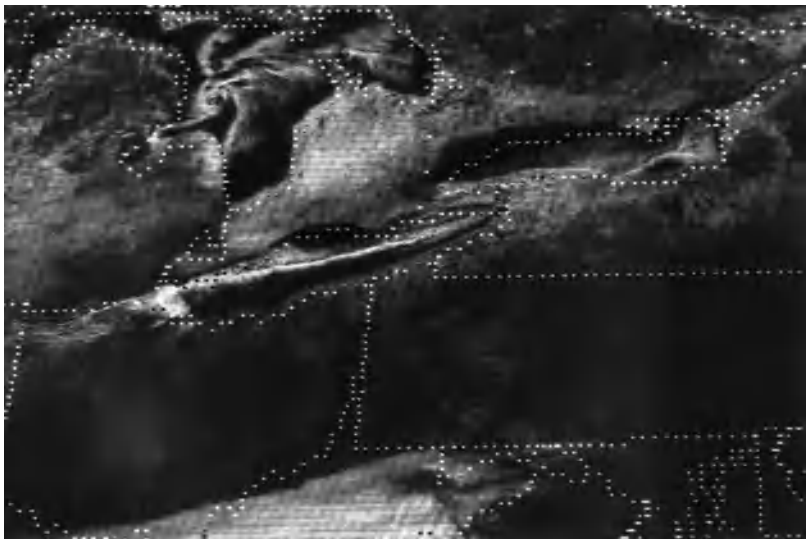

Fig. 4. Visible *GOES* satellite imagery for 1800 UTC (1:00 PM EST), December 20, 1983.

Lake-effect snowstorms. In the fall and early winter, the cooling of large lakes lags behind the cooling of the atmosphere. Consequently, situations develop where very cold air masses pass over relatively warm water. In these instances, large fluxes of heat and moisture from the lake to the air cause the atmosphere to become unstable in an absolute sense; that is, the temperature lapse rate exceeds the dry adiabatic lapse rate and the atmosphere must overturn. This overturning occurs in an organized manner over the lake and the downwind shoreline. Over the lake, the thermally driven overturning often organizes into mesoscale bands of ascending air oriented parallel to the prevailing wind. However, as the air flows from the smooth lake surface to the rough surface of the land, the increase in surface friction causes mass to pile up along the shoreline and forces air upward. Thus, frictionally driven bands tend to form parallel to the shoreline but at an angle to the prevailing wind. These shoreline bands are often enhanced by local terrain features. For a northeasterly flow event, both a lake band and a shoreline band are visible in **Fig. 4**. In most instances, the bands are only a few tens of miles wide but may be hundreds of miles long. *See* CONVECTION (HEAT).

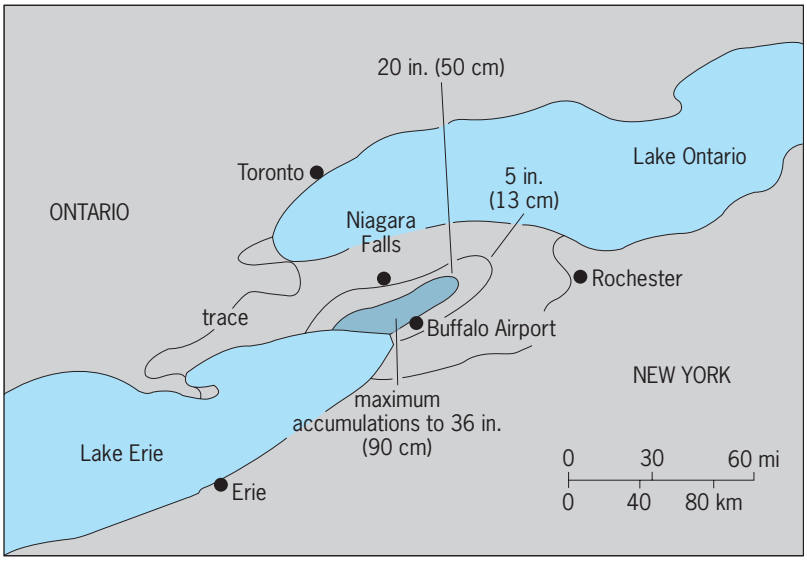

Fig. 5. Snowfall accumulations for a southwesterly flow lake-effect storm in the lee of Lake Erie on November 15, 1974. Note the extremely heavy and localized snowfall centered over the downwind shoreline.

Because cold air masses are usually associated with large regions of high pressure and stable atmospheric conditions, the layer which overturns is shallow (usually less than about 2.5 mi or 4 km deep) relative to overturning in other precipitation-producing weather systems; for example, the vertical circulations in thunderstorms and extratropical cyclones typically extend to around 7 mi (12 km). Nevertheless, lake-effect cloud bands produce intense snowfall rates, sometimes reaching 12 in. (30 cm) per hour and resulting in accumulations of several feet in a day (**Fig. 5**).

Convective complexes. A convective complex is a group of deep convective clouds (usually thunderstorms) acting in a unified manner. Its structure and circulation must be of sufficient size and duration that the Rossby number is on the order of 1.

During the late spring and summer, the large-scale (synoptic) circulations of the atmosphere create convectively unstable environments wherein deep convective clouds can develop. The primary energy source for these clouds is the latent heat released by condensation of water vapor. In most instances, the air supplying the water vapor for cloud growth comes from the Earth's boundary layer (approximately the lowest half mile of the atmosphere); and usually this air must be forcibly lifted (for example, by a warm or cold front) to start the condensation process and subsequent growth of the deep clouds. In some situations, the air feeding the clouds is unusually warm and exceptionally moist so that extremely large amounts of heat are released by condensation and the clouds develop into huge thunderstorms. When several such thunderstorms occur in a group, the tremendous amount of heat and moisture released enhances the upward circulation in the thunderstorm region. This effect forces more boundary-layer air to be lifted to its condensation level and more deep clouds to develop. Thus, an initially small group of thunderstorms can work synergistically with large-scale features to produce an amplifying system culminating in a large complex of deep convective clouds and mesoscale ascent. Moreover, the combination of strong heating and moistening is sometimes sufficient to generate a new mesoscale weather system, a warm-core mesoscale vortex that can persist for several days.

Figures 6 and **7** show the life cycles of two such convective complexes and the resulting development of mesoscale vortices. Figure 6 presents the evolution from the vantage point of a weather satellite, while Fig. 7 shows the evolution as

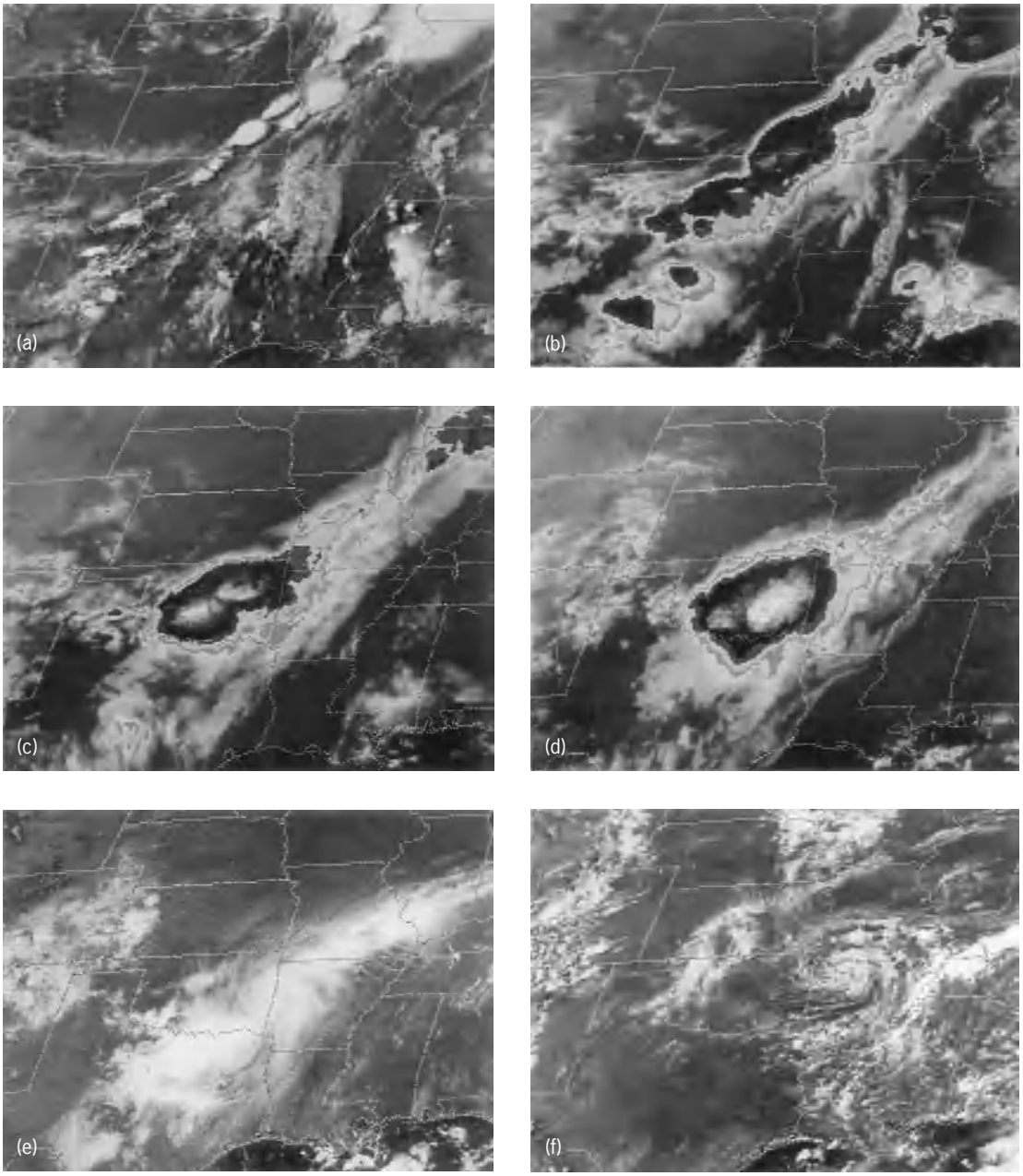

Fig. 6. Life cycle of a mesoscale convective complex. (*a*) Visible image at 2330 UTC (6:30 PM EST), July 6, 1982. (*b*) Enhanced infrared images at 0300 UTC, (*c*) 0600 UTC, and (*d*) 0900 UTC, July 7; interior gray and black contours indicate colder infrared temperatures and higher cloud tops. (*e*) Visible image at 1530 UTC, July 7. (*f*) Visible image at 1830 UTC, July 8.

observed by radar. In Fig. 6*a*, a line of thunderstorms stretches from Missouri southwestward to Texas. Following sundown, the line of thunderstorms consolidates into a concentrated area of intense convective overturning (Fig. 6*b–d*). After daybreak (Fig. 6*e*), the newly created mesoscale vortex becomes evident. The vortex is still evident a day later after it drifts out of Oklahoma and into northwestern Arkansas. In Fig. 7*a*, individual storms over northeastern Nebraska and northwestern lowa evolve into a nearly solid line of intense convection (Fig. 7*b*,*c*). The entire system develops cyclonic rotation as evident from the comma-shaped cloud in Fig. 7*d*.

Convective complexes, as in Figs. 6 and 7, typically begin in midafternoon and reach their peak development in the middle of the night. By morning, most complexes are weakening and usually dissipate a few hours after sunrise. Although the convective complexes are only mesoscale in size, they occur frequently (on the average, about 40-50 in the United States each year) and produce copious rainfall during the growing season. Convective complexes are observed over all major midlatitude landmasses of the world. Satellite imagery indicates they commonly occur over North and South America, Southeast Asia, Australia, Africa, and, to a lesser degree, over Europe.

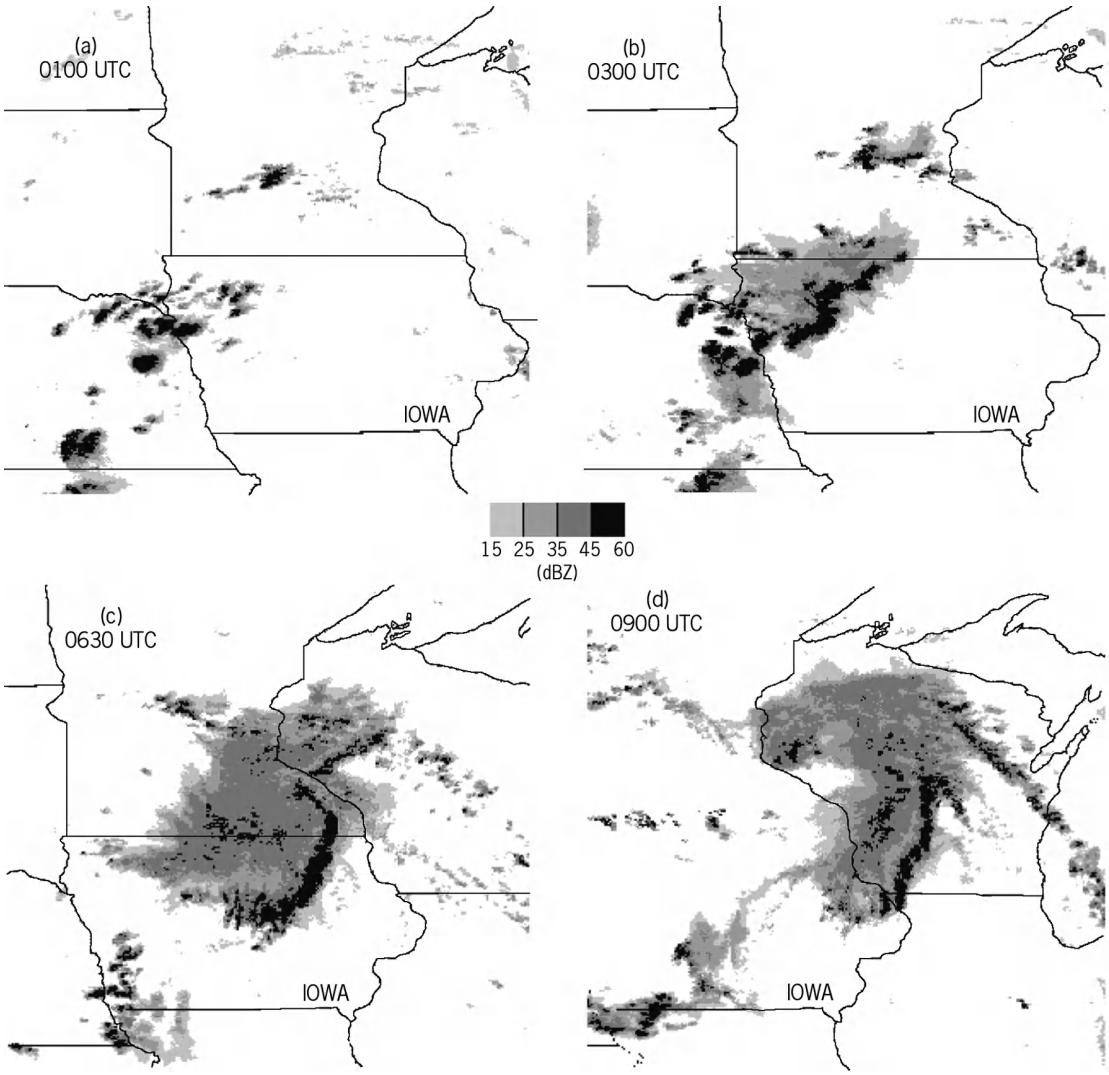

Fig. 7. Radar reflectivity (measured in dBZ) for June 24, 1998, showing the development of a mesoscale convective system and associated mesovortex over the midwestern United States. Values greater than 45 dBZ typically indicate the presence of thunderstorms.

They are also found over warm tropical water, but not as frequently as over land.

Rain/snowbands. These are elongated areas of precipitation (or more intense precipitation) that typically occur in conjunction with extratropical cyclones (**Fig. 8**). Their width usually ranges from about 3 mi (5 km) for bands coinciding with cold fronts to about 30 mi (50 km) for bands occurring in the warm air ahead of the cold front or in the cold air behind. Similar-size bands are also observed to occur ahead of warm fronts in regions of deep warm advection. The lengths of the bands vary considerably, but most are on the order of several hundred miles. Because of the large changes in stability and vertical wind shear from one part of an extratropical cyclone to another, very different mechanisms can produce the various bands. For example, in **Fig. 9**, bands occurred in both the warm and cold sectors and along the cold front. The cold-frontal band most likely can be explained in a conventional manner; that is, it was forced by convergence produced by the cold front advancing into the warm air mass. However, the prefrontal and postfrontal bands result from other processes. The most likely cause of the wide cold-sector bands is moist symmetric instability. This mesoscale instability is present when a parcel of air can be displaced slantwise (between horizontal and vertical) in a region of synoptic-scale vertical wind shear (that is, in a baroclinic atmosphere) and freely continue its slantwise ascent. Since surfaces of constant angular momentum M are also slantwise in a baroclinic atmosphere, a purely horizontal displacement subjects the parcel to different Coriolis and horizontal pressure-gradient forces that tend to restore the parcel to its original position. Similarly, unless the atmospheric lapse rate is dry adiabatic, purely vertical displacements without condensation subject the parcel to vertical pressure-gradient (buoyancy) forces that also tend to restore it to its original position. However, if a parcel with angular momentum M_p is displaced slantwise along the surface $M = M_p$, then

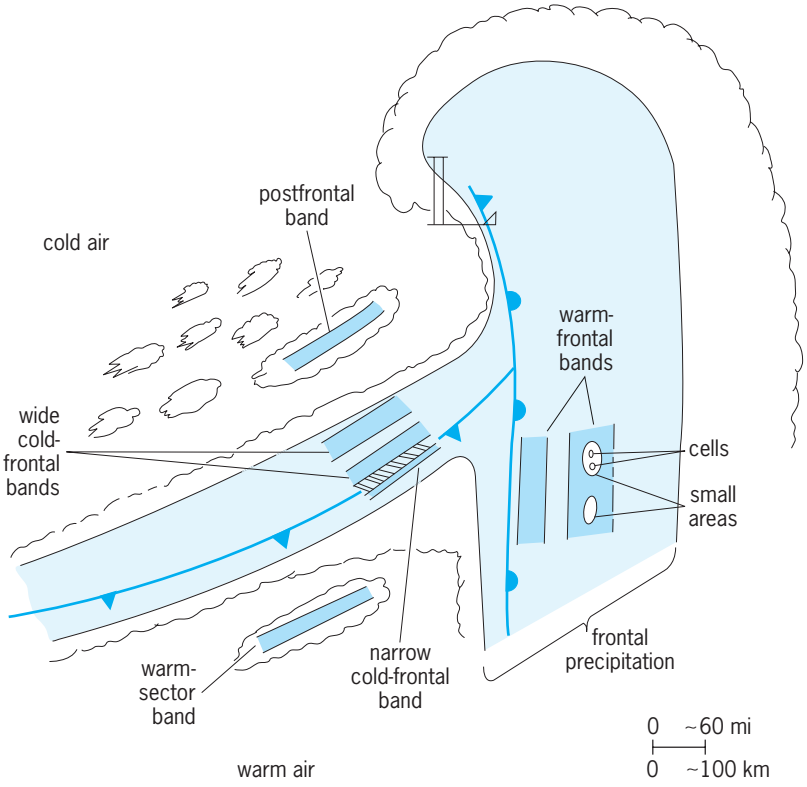

Fig. 8. Types of rainbands observed in extratropical cyclones. (*After R. A. Houze, Structures of atmospheric precipitation systems, Radio Sci., 16:671–689, 1981*)

the horizontal inertial restoring forces are minimal. Furthermore, if the slantwise displacement causes the parcel to become saturated, then the parcel may experience upward-directed buoyancy forces that accelerate it along the ascending slantwise path. In this manner, entire layers of air can ascend slantwise trajectories and produce long bands of precipitation. **Figure 10** shows a radar-observed heavy precipitation band over southeastern New York. The band produced snowfall rates as great as 4 in. (10 cm) per hour at Albany. *See* BAROCLINIC FIELD; CORIOLIS ACCELERATION; GEOSTROPHIC WIND.

Warm-sector rainbands are probably produced by either moist symmetric instability or internal gravity waves enhanced by latent heat release. Internal gravity waves may be generated by momentum imbalances or intense convection along the cold front. As the waves propagate eastward into the warm air mass, the ascending branch of the wave produces condensation and latent heat release. The heating strengthens the ascending circulation and thereby amplifies or helps maintain the propagating gravity wave. Symmetric instability in the warm sector develops in the same manner as described for the wide cold-frontal bands. In the warm sector, however, symmetric instability may originate at lower levels in the atmosphere than in the wide cold-frontal case and therefore has the potential to produce deeper clouds and more intense precipitation rates. *See* ATMOSPHERIC GENERAL CIRCULATION; ATMOSPHERIC WAVES, UPPER SYNOPTIC;

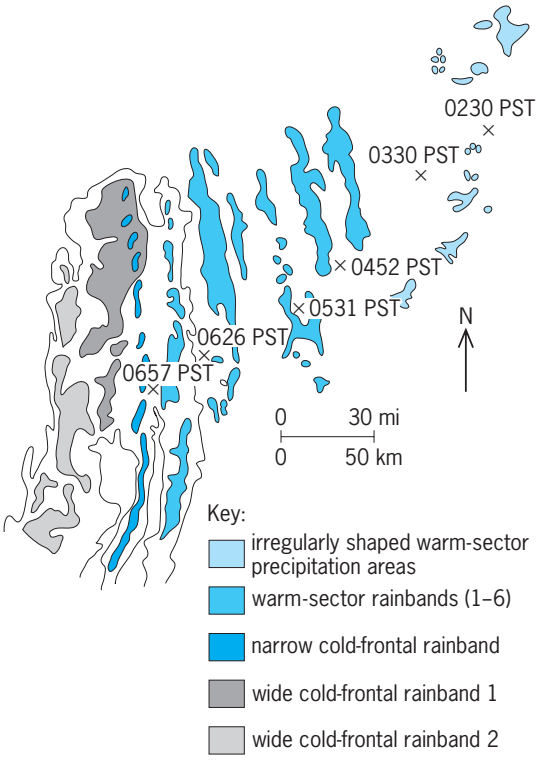

Fig. 9. Time series composite of radar reflectivity PPI displays showing rainbands as they approached the Washington coast. The crosses indicate the positions of the CP-3 radar relative to the rainbands at various times on December 8, 1976. (*After D. B. Parsons and P. V. Hobbs, The mesoscale and microscale structure and organization of clouds and precipitation in midlatitude cyclones, XI: Comparisons between observational and theoretical aspects of rainbands, J. Atm. Sci., 40:2377–2397, 1983*)

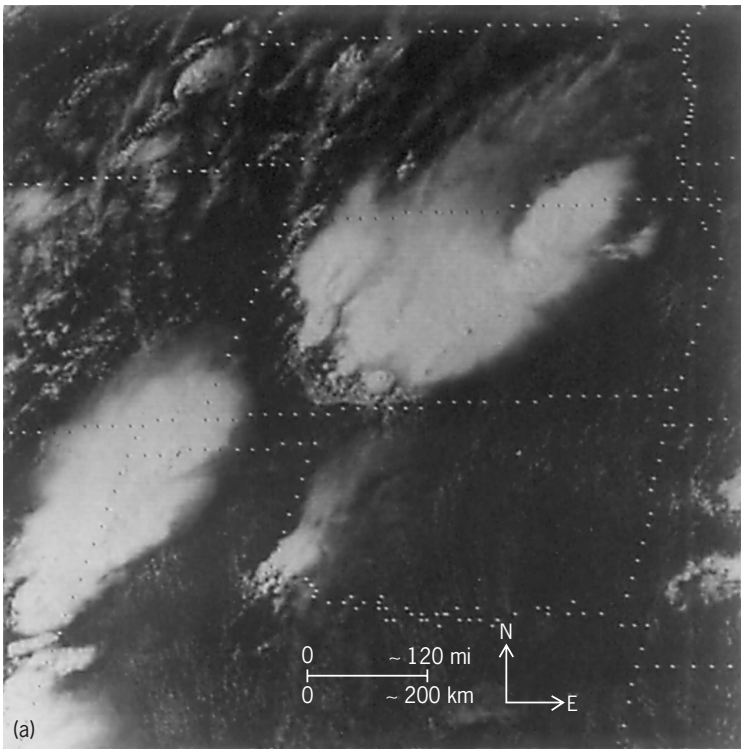

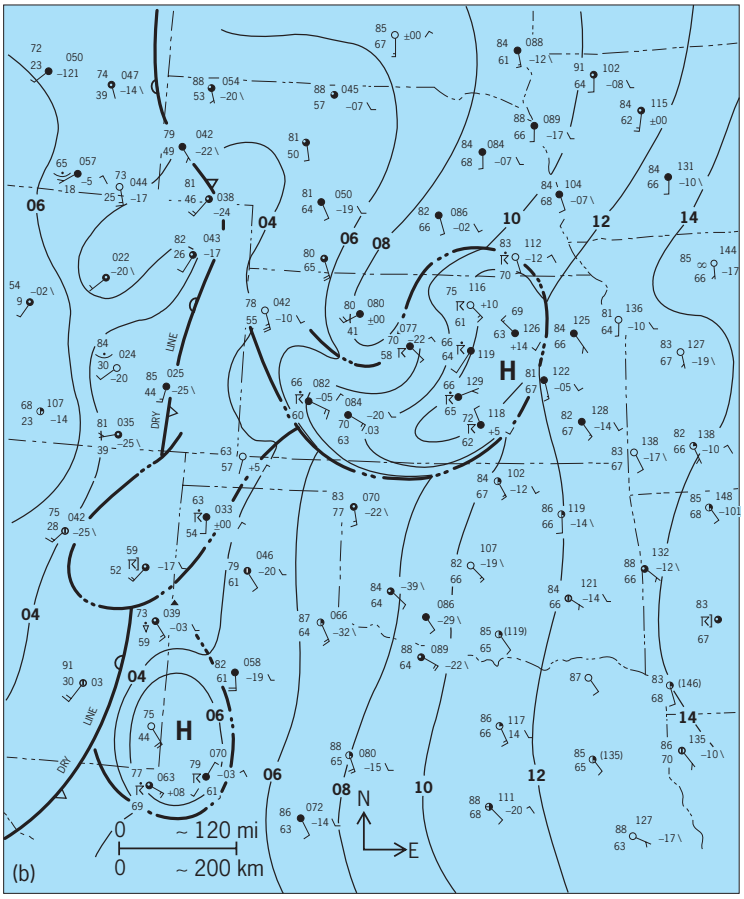

Fig. 10. Mesoanalysis. (*a*) Visible *GOES* satellite imagery, 2132 UTC (4:32 PM EST), May 25, 1978. (*b*) Corresponding surface mesoanalysis, 0000 UTC (7:00 PM EST), May 26, 1978. (*After J. M. Fritsch and R. A. Maddox, Cyclonic thunderstorm outflow, Mon. Weath. Rev., 107:87–89, 1979*)

CONVECTIVE INSTABILITY; DYNAMIC INSTABILITY.

Mesoanalysis. This is the analysis of meteorological data in a manner that reveals the presence and characteristics of mesoscale phenomena. Because the balloon sounding stations are so widely spaced, only the largest of mesoscale systems can be resolved by the balloon sounding network. However, the density of surface observing stations is often satisfactory for identifying mesoscale features or circulations.

Although more detailed mesoanalyses can be performed when surface data are combined with radar and satellite data, it still is not possible to quantify and understand the structure and circulations of mesoscale phenomena without high-density sounding or aircraft data. Consequently, in some research experiments, special high-density sounding networks have been established. These special networks permit higher-resolution three-dimensional analysis wherein the mesoscale structure and circulations of the free troposphere can be determined. Unfortunately, high-density observing systems are much too expensive to maintain continuously over large regions for long time periods. Therefore, mesoanalysis is done only on a sporadic and limited basis. *See* AIR MASS; FRONT; JET STREAM.

Forecasting mesoscale phenomena. Modern weather-forecasting techniques rely heavily upon predictions made by computers. These predictions, commonly called numerical model forecasts, require as input the three-dimensional initial state of the atmosphere. Normally, this initial condition is produced from a combination of the previous forecast (valid at the model initial time) and the most recent observations from radars, satellites, aircraft, and the network of balloon-borne instrument packages. Since the initial conditions for the computer predictions reflect the resolution of the observing network, typically only the largest of mesoscale phenomena are directly included. However, due to the recent advances in computer power, most computer models now have spatial resolution that exceeds the resolution of the observing network and, therefore, some mesoscale phenomena can be generated within the numerical models.

Nevertheless, many of the significant mesoscale phenomena listed in the table are not routinely predicted by the computer models. For these phenomena, meteorologists take an alternate approach to forecasting. It has long been recognized that while mesoscale phenomena have distinct physical characteristics, they are usually strongly modulated or controlled by the synoptic-scale environment. Thus, for many mesoscale phenomena, it has been possible to develop relationships between the large-scale (synoptic) environment and the occurrence of particular types of mesoscale events. By using these relationships, the prediction of the synoptic-scale environment by the numerical models is then used to infer the likelihood of specific mesoscale events, that is, implicit instead of explicit prediction.

This procedure is not as precise as synoptic-scale prediction, and often only a general region and

approximate time period (on the order of 6–12 h) in which the mesoscale event will occur can be determined. Then, by using satellite, radar, and conventional surface observations, the onset of the event is readily detected, and appropriate adjustments to local forecasts are implemented. These adjustments usually come in the form of very short term forecasts, commonly called nowcasts, and typically are valid for only about 3 h. However, depending upon the particular mesoscale phenomena, longer-term (3–12-h) forecasts sometimes are possible. This is particularly true for forced-mode phenomena (for example, lake-effect storms) where the synoptic-scale conditions forcing the mesoscale event are changing very slowly. *See* METEOROLOGY; SATELLITE METEOROLOGY; STORM DETECTION. J. Michael Fritsch

Bibliography. B. Atkinson, *Mesoscale Atmospheric Circulations*, 1981; K. A. Emanuel, On assessing local conditional symmetric instability from atmospheric soundings, *Mon. Weath. Rev.*, 111:2016–2033, 1983; R. L. Lavoie, A mesoscale numerical model of lake-effect storms, *J. Atm. Sci.*, 19:1025–1040, 1972; D. K. Lilly and T. Gal-Chen, *Mesoscale Meteorology: Theories, Observations and Models*, NATO Advanced Science Institute Series, 1983; D. B. Parsons and P. V. Hobbs, The mesoscale and microscale structure and organization of clouds and precipitation in midlatitude cyclones, XI: Comparisons between observational and theoretical aspects of rainbands, *J. Atm. Sci.*, 40:2377–2397, 1983; P. S. Ray, *Mesoscale Meteorology and Forecasting*, 1986.

Meson

Strongly interacting particles are either baryons or mesons. Baryons, such as the proton and neutron, have half-integer spins and are fermions, whereas mesons are bosons with integer spin. The lightest meson is the pion, denoted π, which was originally predicted to exist as the carrier of the powerful force that grips the protons and neutrons within atomic nuclei. *See* BARYON; QUANTUM STATISTICS; SPIN (QUANTUM MECHANICS); STRONG NUCLEAR INTERACTIONS.

Like baryons, mesons are very small (roughly 10^{-15} m in diameter) and consist of even smaller elementary particles: quarks, antiquarks, and gluons. Baryons are fundamental particles of matter, made of quarks; antibaryons are their antimatter analogs and are made of antiquarks. Mesons are neither matter nor antimatter: they are made of quarks and a balancing number of antiquarks (in the simplest case a single quark and a single antiquark). Over 200 examples are known of such q-q-bar combinations (q being the generic symbol for a quark; and q-bar, denoted here by $\bar{q}$, for an antiquark). As is the case for baryons, the quarks and antiquarks are bound by the exchange particles of the strong interaction, the gluons. Examples have begun to emerge of mesons that appear to require two quarks and two antiquarks, or even no quarks and antiquarks at all. The former are known as tetraquarks or molecules; and the latter as glueballs, consisting, at least in theory, of just gluons. *See* ANTIMATTER; GLUONS; QUARKS.

Mesons are identified by properties referred to as flavor, spin, and parity, all of which have discrete values. They also have measurable properties whose values form a continuous range of numbers, such as their mass. For more details about these and other properties *see* BARYON.

Instability. Whereas the lightest baryon, the proton, is stable against decay into other particles, all mesons are unstable. Heavy mesons can decay rapidly (in about 10^{-23} s) into lighter mesons so long as the flavor and other properties, such as parity and angular momentum or spin, are preserved. When the lightest meson of a particular flavor is formed, it is nonetheless unstable since its quark and antiquark can mutually annihilate, for example into two photons, an electron, and a positron or neutrino, or even gluons. For example, the lightest meson, the pion, occurs either with no electric charge (π^0) or with negative or positive electric charge (π^- or π^+). When the quark and antiquark within the π^0 annihilate, the products are probably two photons; when the π^- or π^+ decay, they leave a neutrino and an electron or positron, or more often a neutrino and a muon (a heavier analog of the electron and positron). The π^0 survives for only 10^{-16} s—small indeed but over a million times longer than the 10^{-23} s of its heavier cousins. The π^- or π^+ survive for 10^{-8} s. These differences in lifetimes are the result of the forces at work. For heavy mesons, the strong force destroys them; for the π^0, it is the electromagnetic force; and for the electrically charged pions, it is the weak force that is responsible. The large differences in lifetimes reflect the differing strengths of the forces. *See* FUNDAMENTAL INTERACTIONS; LEPTON; NEUTRINO.

Meson flavors. There are six different kinds, or flavors, of quarks, in three families. The lightest family contains the up (u) and down (d) quarks, and charges of $+^2/_3$ and $-^1/_3$ in units of the electron charge (e), respectively. The corresponding antiquarks, labeled $\bar{u}$ or $\bar{d}$, have the opposite sign of charge to their quark counterparts. Thus, $\bar{u}$ has charge $-^2/_3$ and $\bar{d}$ has $+^1/_3$. *See* FLAVOR.

A $u\bar{d}$ has charge $+1$, and the lightest example is the π^+. The $d\bar{u}$ has charge -1: the π^-. Both the $u\bar{u}$ and $d\bar{d}$ have charge zero. Quantum theory implies that the particular quantum combination $u\bar{u} - d\bar{d}$ corresponds to the π^0; the alternative combination $u\bar{u} + d\bar{d}$ appears in another meson, the electrically neutral η (eta).

Because the difference between the masses of the up and down quarks and the electromagnetic self energy of quarks or antiquarks in a meson are very small compared to meson masses, properties of mesons are to a very good approximation unchanged by replacing an up quark or antiquark with a down quark or antiquark. This equivalence is referred to as isospin symmetry. In this language, the π^+, π^-, or π^0 are referred to collectively as different charge states of the pion. *See* I-SPIN.

The three varieties of pion correspondingly have masses that differ by only some 4%, the charged pions having a mass of 140 MeV/c^2 (where c is the speed of light) and the π^0 mass being 135 MeV/c^2. The η, however, is some four times more massive at 550 MeV/c^2. In part, this is because the η contains (along with $u\bar{u} + d\bar{d}$) a third flavor of quark, the strange quark, accompanied by its antiquark: thus $s\bar{s}$. The strange quark is some 120 MeV/c^2 heavier than an up or down quark, and so an $s\bar{s}$ has added mass relative to pions, which contain only u or d flavors. Indeed, the additional quark flavor leads to three electrically neutral mesons, π^0, η, and η', which testify to the three possibilities, $u\bar{u}$, $d\bar{d}$, and $s\bar{s}$; the η' mass is 960 MeV/c^2.

It is possible for any of the u, d, or s quarks to be attracted to any of the $\bar{u}$, $\bar{d}$, or $\bar{s}$ antiquarks. Mesons that have an s or $\bar{s}$ partnered by a ($\bar{u}$, $\bar{d}$) or (u, d) will have strangeness. Such "strange" mesons are known as kaons and denoted generically by the symbol K. The kaon, containing a light flavor and a strange, has a mass of around 495 MeV/c^2, which is heavier than a pion but lighter than η or η'. *See* STRANGE PARTICLES.

The remaining three flavors of quarks—the charm c, bottom b, and top t quarks—are heavy on the scale of the mass of the pion, K, or η, and η' mesons. These give rise to further families of mesons known as charmonium and bottomonium (a $c\bar{c}$ or $b\bar{b}$ combination) and also mesons that contain unpaired charm or bottom flavors. The top quark is very massive, causing it to decay so rapidly that it does not have time to form a meson by binding strongly to other quarks or to an antiquark. Thus toponium is unlikely to occur unless there are other forces at work which are yet unknown. *See* CHARM.

Spin. Quarks carry an intrinsic degree of freedom called spin, which is related to the angular momentum carried by a macroscopic object when it rotates. In the very short-distance quantum world, angular momentum is quantized in units of $\hbar = h/(2\pi)$, where h is Planck's constant. The smallest possible angular momentum is $\hbar/2$, and this is the spin of each quark or antiquark making up a meson. Thus quarks and antiquarks are referred to as spin-$^1/_2$ particles. *See* ANGULAR MOMENTUM; SPIN (QUANTUM MECHANICS).

Two spin-$^1/_2$ particles, such as a quark and an antiquark, can have their spins combined to 0 (anti-aligned along an axis called the quantization axis) or to 1 (aligned along the quantization axis), in units of $\hbar$.

The pi mesons, η, η', and K mesons all have a total spin of zero, arising when their quark and antiquark have their spins anti-aligned. If their spins were instead aligned, the total spin would be 1. A family of mesons with spin 1, called the vector mesons, is known. The ρ^+, ρ^0, and ρ^- (rho) are the $u\bar{d}$, $u\bar{u} - d\bar{d}$, $d\bar{u}$ analogs of the spin-0 pi mesons. Whereas the η and η' are complicated mixes of $u\bar{u}$, $d\bar{d}$, and $s\bar{s}$, their vector meson analogs are simpler. The ω (omega) consists of $u\bar{u} + d\bar{d}$, while the φ (phi) is made simply of $s\bar{s}$. The vector strange mesons, denoted K^*, exist, made from $u\bar{s}$, $d\bar{s}$, $s\bar{d}$, and $s\bar{u}$, as for their spin-0 counterparts.

The masses of the spin-1 mesons are greater than their spin-0 counterparts. The ω, made of $u\bar{u} + d\bar{d}$, has mass of 780 MeV/c^2, almost the same as that of the ρ made of $u\bar{u} - d\bar{d}$; the K^* mesons with masses of 890 MeV/c^2 are then midway between the ρ or ω and the φ ($s\bar{s}$), whose mass is 1020 MeV/c^2. This linear pattern is naturally explained by their having respectively only light-flavored u or d quarks (the ρ or ω); one heavier s or $\bar{s}$ quark (the K^*), or both s and $\bar{s}$ quarks (the φ). The greater mass of any individual flavor set with spin 1, such as $u\bar{s}$ for the K^* relative to the spin-0 K, can be thought of as due to a kind of magnetic interaction between the colored, spinning quarks, analogous to the magnetic interaction between charged, spinning electrons. These interactions are repulsive when the quark spins are aligned; this raises the mass of the spin-1 K^*, with both quark spins aligned, relative to that of the spin-0 K, with the quark spins anti-aligned.

In addition to their spin angular momentum, the constituent particles of a meson can have orbital angular momentum as they move around their common center of mass. In the simplest possible (naive quark model) picture, the spin angular momentum of a meson is made up of the orbital angular momentum and intrinsic spin of its constituent quark and antiquark.

Just as the lightest states of the hydrogen atom have the electron and proton in an orbital-angular-momentum-zero, spherically symmetric state, so in this simple picture the lightest states of a meson have zero orbital angular momentum between the quarks, and so their total spin is just that of the quark and antiquark: hence the spin-0 and spin-1 combinations described above.

Mesons with the same quark and antiquark flavor contents as the above exist with spin angular momentum higher than 0 or 1. In most cases this is because the quarks have orbital angular momentum around their common center of mass, but there is also much excitement at the possibility that states known as hybrid mesons exist, where the gluons play a direct role in building up the total spin. Since orbital angular momentum comes in integral multiples of $\hbar$, which is also true of the intrinsic spin of a gluon or quark-antiquark pair, all mesons must have integral spin $J = 0$, 1, 2, 3, and so forth. Mesons with spins up to 6 have been observed.

Parity and charge conjugation. A discrete property of a meson is its parity. The strong interactions between quarks and antiquarks have the property that they do not change when viewed in a mirror. This is essentially the same as spatial inversion symmetry, invariance under the operation of reflecting all of the spatial coordinates through the origin. The quantum wave functions of such states under the operation of inversion of the coordinates either remain the same, called positive parity, or change sign, called negative parity, denoted P. *See* PARITY (QUANTUM MECHANICS).

A similar effect arises when the wave function is matter and antimatter inverted: when quark and antiquark are interchanged in effect. This operation is known as charge conjugation. As was the case for parity, so for charge conjugation: the state can have C be positive or negative. *See* SYMMETRY LAWS (PHYSICS).

For a meson made from a single quark and antiquark, all possible integer spins can occur. However, not all combinations of positive and negative values of C and P can arise. If C and P are both positive, any value of total spin can occur, and if the spin is 1 or more, both C and P can be negative; however, if the total spin is 0, the latter cannot occur. It is traditional to denote the total spin (J), parity P, and charge conjugation C for a meson in the form J^{PC}; so in this language it is said that 0^{--} combinations are forbidden. When P is $-$ and C is $+$, the total spin must be even (giving the values 0^{-+}, 2^{-+}, 4^{-+}, and so forth); when P is $+$ and C is $-$, the total spin must be odd (giving 1^{+-}, 3^{+-}, 5^{+-}, and so forth). Any combinations that are not allowed are known as exotic. For many years, all mesons discovered satisfied these rules. However, evidence has emerged for a meson with spin 1 (odd), negative P, and positive C, namely 1^{-+}, and hence exotic.

Such a meson had been predicted. It turns out that if the quark and antiquark are accompanied by a gluon, it is possible for such otherwise exotic correlations to occur. As mentioned above, mesons where both q and $\bar{q}$, and glue are active are known as hybrids.

Decays. In strong decays, a quark-antiquark pair is created via the strong interaction, with the created quark ending up in one meson and the created antiquark in another meson. This process can happen successively such that an initial meson decays into two, three, or more mesons.

Decays may also proceed via the emission of an energetic particle of light, a gamma-ray photon, since the electromagnetic interaction between quarks, made possible by their electric charges, is the next strongest of the fundamental interactions between them. *See* GAMMA RAYS.

Meson decays may also proceed via the weak interactions mediated by the massive vector-boson particles, W^+, W^-, or Z^0. Such decays can result in the creation from a W boson of a charged lepton and a neutrino of the same family, such as an electron and an electron antineutrino, or their antiparticles, the positron and an electron neutrino. This process is what occurs when a π^- or π^+ decays. *See* INTERMEDIATE VECTOR BOSON; WEAK NUCLEAR INTERACTIONS.

Charmonium and bottomonium. As mentioned above, a charmed quark attracted to a charmed antiquark gives a family of mesons known as charmonium, $c\bar{c}$; and a similar phenomenon occurs for the yet more massive bottom flavor, giving bottomonium, $b\bar{b}$. There are also mesons with manifest charm or bottom flavors, such as the $D(c\bar{u})$ with mass 1865 MeV/c^2 and $B(b\bar{u})$ at 5279 MeV/c^2. Charmonium mesons with masses greater than 3730 MeV/c^2 decay by the strong interaction into pairs of charmed mesons, $D(c\bar{u})$ and $\bar{D}(\bar{c}u)$. However, there are several examples of charmonium mesons that have masses below this limit and so are prevented by energy conservation from decaying this way. Their dominant decays are by shedding energy in the form of photons or pions, eventually ending up as the etacharm (η_c) or J-psi (J/Ψ), the lightest $c\bar{c}$ mesons (the η_c having $c\bar{c}$ spin totaling 0 and the J/Ψ having spin 1, analogous to the pion and rho mesons in the light-flavor examples described earlier).

The J/Ψ is metastable on the time scale of strong interactions. It decays (after about 10^{-20} s) by its c and $\bar{c}$ mutually annihilating, producing photons or gluons; the gluons do not escape free but rapidly create showers of pions or other particles. *See* J/PSI PARTICLE.

There is an interesting possibility that among the decay products of a J/Ψ lurk glueballs. According to theory, the J/Ψ can decay into a photon and two gluons. The energy taken by the photon can vary, and the energy of the two gluons varies in consequence. If this energy equals the mass of a glueball, the two gluons will form a glueball. There are some enigmatic mesons seen in the decay products of the J/Ψ, and it is suspected that these include evidence for glueballs, but definitive proof for their existence is still awaited.

Glueballs, hybrids, and tetraquarks. While over a hundred mesons made of $q\bar{q}$ are known, the attractive forces can also make combinations of two quarks and two antiquarks, $qq\bar{q}\bar{q}$, known as tetraquarks (as noted above). The gluons, which mediate the color force between the quarks, like the photons, which mediate the electromagnetic force between particles, carry a spin angular momentum of $\hbar$ and are referred to as spin-1 or vector particles. As noted above, they can attract one another to form mesons known as glueballs or bind with quarks and antiquarks to make hybrid mesons. While the existence of tetraquarks, glueballs, and hybrids is not yet totally established, several possible examples have been found.

A family of mesons with spin 0 and positive parity (scalar mesons) with masses below 1000 MeV/c^2 have properties that fit well with being examples of tetraquarks. These are made from u, d, and s quark flavors and their antiquarks. Since 2004, examples of further possible tetraquarks have been found that include one or more charm (c) or $\bar{c}$ flavors. Two mesons, with masses 2317 and 2460 MeV/c^2, appear to be the spin-0 and -1 examples of $c\bar{s}u\bar{d}$. A meson with spin 1, positive parity, and mass 3872 MeV/c^2 is probably $c\bar{c}u\bar{u}$; a spin-1 negative parity vector meson at 4260 MeV/c^2 may be a $c\bar{c}s\bar{s}$.

The latter meson may also be a hybrid meson, made from $c\bar{c}$ and excited gluons. Hybrid mesons are predicted to have masses about 1 GeV/c^2 more than their lightest $q\bar{q}$ analogs. The lightest spin-1 $c\bar{c}$ is the J/Ψ at 3095 MeV/c^2, and the

The six flavors of quarks, their charges, and their masses				
Charge = +2e/3	Flavor	up (*u*)	charm (*c*)	top (*t*)
	Mass, MeV/c^2	3	1250	174,000
Charge = −e/3	Flavor	down (*d*)	strange (*s*)	bottom (*b*)
	Mass, MeV/c^2	6	120	4250

4260-MeV/c^2 meson is thus consistent with this rule. Few properties of this newly discovered meson are yet known. To determine which interpretation is correct will require careful study of its decay products. If it is a *ccss* tetraquark, then pairs of D_s "charm strange" mesons, made of $c\bar{s}$ or $s\bar{c}$ with masses around 2000 MeV/c^2, should be dominant. However, for a hybrid $c\bar{c}$-gluon meson, such D_s mesons should not be favored decay products.

There are also examples of possible hybrid mesons containing *u* or *d* flavors, but there is much debate about whether these might instead be tetraquarks.

A detailed spectrum of glueballs is predicted by theory. The lightest of these is expected to be a scalar meson (spin 0, positive parity) with mass around 1500–1700 MeV/c^2. There are scalar mesons around this mass, at 1710, 1500, and 1370 MeV/c^2, which are probably the result of $u\bar{u}$, $d\bar{d}$, and $s\bar{s}$ scalar mesons undergoing quantum-mechanical mixing with the scalar glueball. Extensive studies of their production and decay modes are required to measure the details of this mixing pattern and establish the presence of a glueball.

Meson production. The electrically charged pi mesons and kaons were discovered in cosmic rays; knowledge about other mesons comes from experiments involving collisions of particles. Historically, collisions between protons and nuclei were observed, or dedicated beams of pions or kaons hitting protons and nuclei. Since the 1980s, a large amount of knowledge about mesons has resulted from experiments where electrons collide with and are annihilated by positrons. If the energy of the collision is the same as that of a vector meson, the vector can be produced directly. This is how the J/Ψ—the vector meson of the charmonium family, *cc*, with a mass of 3095 MeV/c^2—was discovered in 1974. The upsilon (Υ), the analogous vector meson of bottomonium, *bb*, can also be made this way. The J/Ψ and Υ decay in about 10^{-20} s and leave a rich pattern of mesons among their decay products. *See* UPSILON PARTICLES.

If the total energy of the electron-positron collisions is around 10 GeV, the result is a pair of *B* mesons, where a *b* flavor is accompanied by up, down, or strange such that the meson has an overall bottom flavor. The *B* mesons decay by the weak interaction. There are several possible combinations of mesons that can result from these decays, and the relative amounts of each are being measured to the highest precision possible. The reason for this interest is that the decays of bottom mesons and their antimatter counterparts, containing a *b* antiquark, are expected to give important clues about the origin of the asymmetry between matter and antimatter.

Experiments with beams of electrons and intense beams of photons in collisions with protons and nuclei are expected to produce vast amounts of data on mesons. These experiments are also expected to give crucial information about the enigmatic hybrid mesons, whose existence is predicted by theory but not yet unambiguously established in experiment. *See* ELEMENTARY PARTICLE.

Frank Close

Bibliography. F. Close, *Particle Physics: A Very Short Introduction*, Oxford, 2004; F. Close, M. Marten, and C. Sutton, *The Particle Odyssey*, Oxford, 2003; S. Eidelman et al. (Particle Data Group), Review of particle physics, *Phys. Lett.*, B592:1–1109, 2004; N. Isgur and G. Karl, Hadron spectroscopy and quarks, *Phys. Today*, 36(11):36–42, November 1983.

Mesosauria

An order of extinct aquatic reptiles, also known as Proganosauria, of latest Carboniferous or earliest Permian time, about 2.8×10^8 years ago. The best-known genus, *Mesosaurus* (see **illus.**), occurs in the Iratí bituminous shales of southern Africa. Geological evidence demonstrates that South America and Africa were part of a single land mass in the late Paleozoic, prior to the formation of the Atlantic Ocean. No other reptiles are known from contemporary beds on either continent. Like many aquatic reptiles, mesosaurs have a very long snout. The teeth are numerous and long, and appear very delicate. They may have served for filter feeding on soft-bodied invertebrates. The girdles and limbs are little modified for aquatic locomotion. The hands and feet are paddle-shaped. The tail is long and laterally compressed. The trunk ribs have the swollen form (pachystosis) characteristic of nothosaurs (aquatic reptiles of the Triassic) and sirenians, both of which show early stages in the adaptation of a formerly terrestrial group toward life in the water. Mesosaurs, an early offshoot of the Carboniferous "stem reptiles" or captorhinomorphs, were the first reptiles to invade marine waters, but apparently soon became extinct, leaving no descendants. *See* REPTILIA. R. L. Carroll

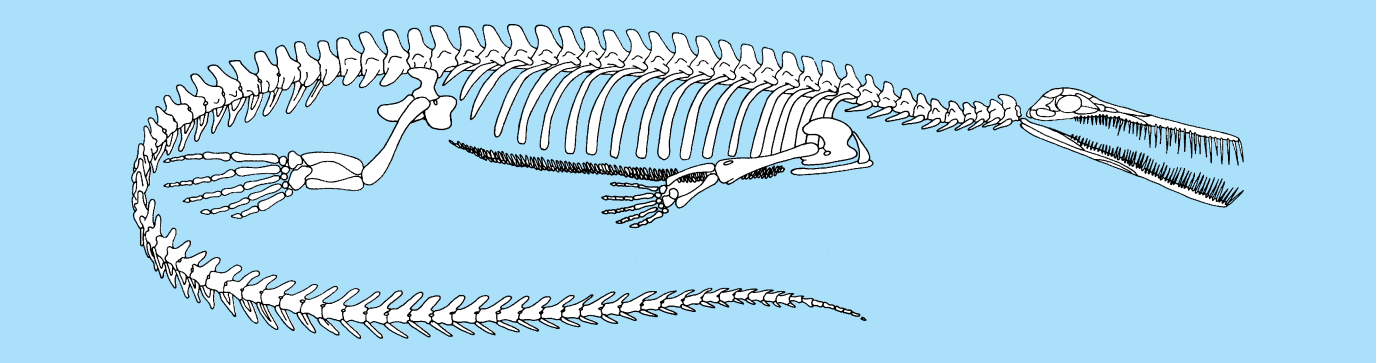

Restoration of the aquatic reptile *Mesosaurus*. Original length was 16 in. (40 cm).

Bibliography. A. S. Romer, *Osteology of the Reptiles,* 1955, reprint 1997.

Mesoscopic physics

A subdiscipline of condensed-matter physics that focuses on the properties of solids in a size range intermediate between bulk matter and individual atoms or molecules. The size scale of interest is determined by the appearance of novel physical phenomena absent in bulk solids and has no rigid definition; however, the systems studied are normally in the range of 100 nanometers (10^{-7} meter, the size of a typical virus) to 1000 nm (the size of a typical bacterium). Other branches of science, such as chemistry and molecular biology, also deal with objects in this size range, but mesoscopic physics has dealt primarily with artificial structures of metal or semiconducting material which have been fabricated by the techniques employed for producing microelectronic circuits. Thus it has a close connection to the fields of nanofabrication and nanotechnology. The boundaries of this field are not sharp; nonetheless, its emergence as a distinct area of investigation was stimulated by the discovery of three categories of new phenomena in such systems: interference effects, quantum size effects, and charging effects. *See* ARTIFICIALLY LAYERED STRUCTURES; NANOSTRUCTURE; QUANTIZED ELECTRONIC STRUCTURE (QUEST); SEMICONDUCTOR HETEROSTRUCTURES.

Interference effects. Although quantum mechanics predicts that any particle should exhibit properties characteristic of waves, electrons in bulk solids may be treated for most purposes as particles. The reason is that the wavelike properties are suppressed by interactions between the electrons and the vibrations of the lattice of ions forming the solid. These interactions become weaker as the temperature of the solid is lowered and thermal vibrations are reduced. At temperatures less than 4 K (−452°F), the vibrations are so rare that electrons can traverse several thousand nanometers (the size of a typical mesoscopic device) without any significant interaction, and the wave properties of the electron affect measurable physical quantities such as the electric conductivity. *See* QUANTUM MECHANICS.

The most important wave property of electrons is that of interference. Unlike a classical particle, an electron wave can split at one point in space into many wavefronts which follow different paths to another point in space. These different wavefronts may add or subtract from each other at that point, leading to constructive or destructive interference. In the former case there will be an increased probability of finding an electron at that point; in the latter case there will be zero probability. The conduction electrons in solids are split into many wavefronts by defects or impurities in the crystal lattice. The density of such defects determines the average electrical conductivity of a bulk solid (at low temperatures) since they impede the flow of the electrons. However, in the mesoscopic regime scattering from defects also induces interference effects which modulate the flow of electrons. This modulation depends not only on the density of impurities but on their precise location relative to one another; hence it differs for each specimen, even if the specimens are made of the same material and fabricated under identical conditions. Thus the concept of conductivity as a property of a given material becomes useless for mesoscopic solids. Instead, the conductance of a given specimen is studied: the ratio of the measured current to the driving voltage. *See* CONDUCTANCE; CONDUCTION (ELECTRICITY); ELECTRICAL RESISTIVITY; INTERFERENCE OF WAVES.

The experimental signature of mesoscopic interference effects is the appearance of reproducible fluctuations in physical quantities. Such time-independent fluctuations have been measured in the magnetization, thermopower coefficient, alternating current, direct current, and nonlinear conductance. For example, the conductance of a given specimen oscillates in an apparently random manner as a function of experimental parameters such as a magnetic field or the electron density (**Fig. 1**). However, the same pattern may be retraced if the experimental parameters are cycled back to their original values; in fact, the patterns observed are reproducible over a period of days. In experiments a magnetic field is most commonly used to demonstrate this effect. A magnetic field induces these fluctuations because

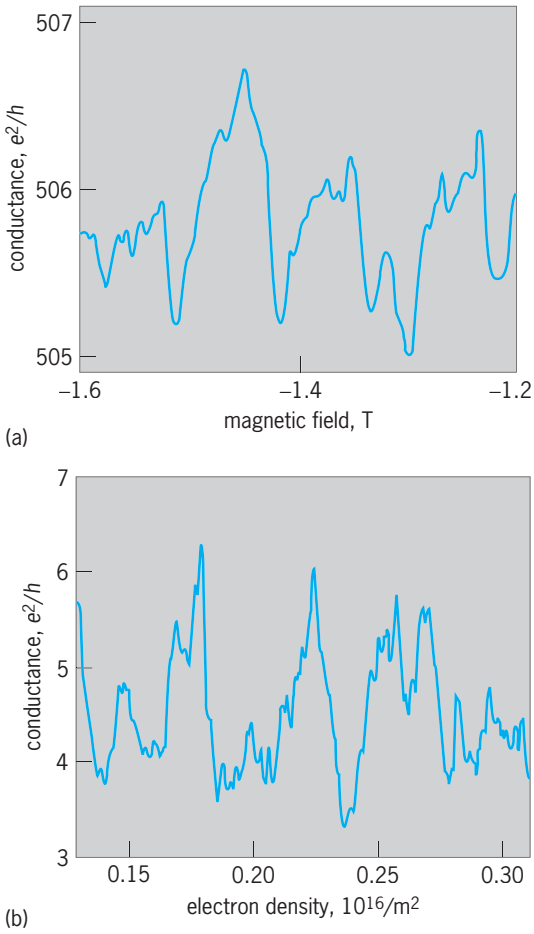

Fig. 1. Conductance fluctuations in mesoscopic conductors. (*a*) Conductance of 2000-nm gold wire as a function of magnetic field measured at temperature 0.04 K (*after R. A. Webb and S. Washburn, Quantum interference fluctuations in disordered materials, Phys. Today, 41(12): 46–55, December 1988*). (*b*) Conductance of 600-nm GaAs/AlGaAs semiconducting heterostructure as a function of electron density (controlled by an electrostatic gate) at temperature 0.1 K (*after M. W. Keller et al. Magnetotransport in a chaotic scattering cavity with a turnable electron density, Surf. Sci., 305:501–506, 1994*). The patterns observed are reproducible over a period of days, and the amplitudes of both fluctuations are of order e^2/h.

according to quantum theory a field alters the phase of the electron waves. The general principle that a magnetic field modulates quantum-mechanical interference is known as the Aharonov-Bohm effect. *See* AHARONOV-BOHM EFFECT.

Quantum size effects. Another prediction of quantum mechanics is that electrons confined to a particular region of space may exist only in a certain set of allowed energy levels. The spacing $\Delta\epsilon$ between these levels increases as the confining region becomes smaller; also, in typical systems the spacing between the levels decreases with increasing overall energy. Conduction electrons in a bulk solid are confined only to the macroscopic dimensions of the solid, and the energy-level spacing becomes so small that the discreteness of the allowed energies is undetectable. In mesoscopic solids, however, the spacing is large enough that the discreteness of the levels affects measurable physical properties. Because conduction electrons in metals have much higher energies than those in semiconductors and the level spacing decreases with energy, it turns out that these quantum size effects are most important in mesoscopic semiconductors. One striking phenomenon which arises from these quantum size effects is the steplike increase of the conductance of electrons flowing through a constriction of several hundred nanometers' width. In classical physics the conductance should increase in proportion to the width of the constriction. In quantum physics the electrons become confined laterally as they enter the constriction and are allowed only certain energies. No further current can be generated as the constriction is widened until a new state appears because of the decrease in the energy-level spacing. The result is that instead of increasing linearly with width the conductance increases in a series of sharp steps. It is found that these steps are of magnitude $2e^2/h$, a result which is expected from the basic quantum theory of the process. *See* ENERGY LEVEL (QUANTUM MECHANICS).

Another mesoscopic system that shows quantum size effects consists of isolated islands of electrons that may be formed at the appropriately patterned interface between two different semiconducting materials. [Gallium arsenide (GaAs) and aluminum gallium arsenide (AlGaAs) are most common.] The electrons typically are confined to a disk-shaped region, and hence these systems have been termed quantum dots. Quantum dots may be regarded as artificial atoms with a new set of energy levels never before realized in nature. The confinement of the electrons in these systems changes their interaction with electromagnetic radiation significantly. The electronic absorption energies are shifted from their values in bulk semiconductors, and the light that is absorbed or emitted by the dot is restricted to certain frequencies because of confinement. Quantum dots can be used to make semiconductor lasers that operate at very low power, a property of great technological interest. *See* LASER.

Charging effects. Isolated mesoscopic solids such as quantum dots or metallic grains on an insulating substrate also show novel effects associated with the discreteness of the charge on the electron. Normally the free-electron charge in a conductor can be regarded as a continuous fluid which is infinitely divisible. This is so both because the amount of charge involved in macroscopic systems is usually very large compared to the charge on a single electron and because quantum mechanics allows even a single electron to be spread out over a very large area. Hence the charge on a capacitor plate is tunable to a small fraction of the electron charge (e) if it is in contact with a reservoir of electron charge such as a battery. However, if the capacitor is mesoscopic, this ceases to be true. *See* CAPACITOR.

The simplest case is that of an isolated mesoscopic grain of metal such as aluminum. The grain has a certain number of atoms and will be in its lowest energy state if it retains the correct number of electrons to neutralize the total positive charge of the atomic nuclei. The energy cost of removing an electron is

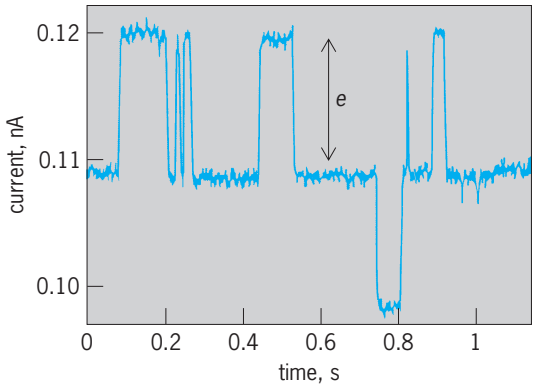

Fig. 2. Time variation of the electric current through a single-electron transistor electrometer, measuring the charge on a mesoscopic metallic grain. Each jump corresponds to the removal or addition of a single electron from the grain. (*After M. H. Devoret, D. Esteve, and C. Urbins, Single-electron transfer in metallic nanostructures, Nature, 360:547–553, 1992*)

inversely proportional to the capacitance of the grain, which decreases with its volume. For a mesoscopic grain this energy exceeds thermal energies at roughly 1 K; below this temperature the number of electrons on the grain will not vary because of thermal fluctuations.

If such a grain is fabricated as part of an electronic circuit, it will block the flow of current until the driving voltage is large enough to compensate for the energy needed to increase the electronic charge on the grain by e. However, if an additional electric field is applied to the grain through an auxiliary capacitor, the singly ionized state of the grain can be made energetically allowed and a current will flow through the circuit. With this principle it has been possible to fabricate circuits for which a current of 10^9 electrons per second (approximately 10^{-9} A) can be switched on and off by the addition of one-half the electron charge to the control capacitor. These devices are known as single-electron transistors (SETs) and are by far the most sensitive electrometers (instruments for measuring electrical charge) presently known. *See* ELECTROMETER; TRANSISTOR.

Building on these concepts, devices employing several single-electron transistors have been demonstrated in which a modulation of the control capacitor with a frequency f leads to an electrical current precisely equal to ef. In such devices, electrons are transferred one by one onto and off the grain. It is even possible to measure jumps in the current corresponding to the transfer of each electron (**Fig. 2**). Such devices are expected to have metrological applications as an absolute standard of electric current. *See* ELECTRICAL UNITS AND STANDARDS.

A. Douglas Stone

Bibliography. B. L. Altshuler, P. A. Lee, and R. A. Webb (eds.), *Mesoscopic Phenomena in Solids*, 1991; M. H. Devoret, D. Esteve, and C. Urbina, Single-electron transfer in metallic nanostructures, *Nature*, 360:547–553, 1992; A. Khurana, Ballistic electron transport through a narrow channel is quantized, *Phys. Today*, 41(11):21–23, 1988; M. A. Reed, Quantum dots, *Sci. Amer.*, 268(1):118–123, January 1993; R. A. Webb and S. Washburn, Quantum interference fluctuations in disordered metals, *Phys. Today*, 41(12):46–55, December 1988.

Mesosphere

A layer within the Earth's atmosphere that extends from about 50 to 85 km (31 to 53 mi) above the surface. The mesosphere is predominantly characterized by its thermal structure. On average, mesospheric temperature decreases with increasing height.

Structure. Temperatures range from as high as 12°C (53°F) at the bottom of the mesosphere to as low as −133°C (−208°F) at its top. The top of the mesosphere, called the mesopause, is the coldest area of the Earth's atmosphere. Temperature increases with increasing altitude above the mesopause in the layer known as the thermosphere, which absorbs the Sun's extreme ultraviolet radiation. In the stratosphere, the atmospheric layer immediately below the mesosphere, the temperature also increases with height. The stratosphere is where ozone, which absorbs ultraviolet radiation from the Sun, is most abundant. The transition zone between the mesosphere and the stratosphere is called the stratopause. Mesospheric temperatures are comparatively cold because very little solar radiation is absorbed in this layer. Meteorologists who predict weather conditions or study the lowest level of the Earth's atmosphere, the troposphere, often refer to the stratosphere, mesosphere, and thermosphere collectively as the upper atmosphere. However, scientists who study these layers distinguish between them; they also refer to the stratosphere and mesosphere as the middle atmosphere. *See* ATMOSPHERE; METEOROLOGY; STRATOSPHERE; THERMOSPHERE; TROPOSPHERE.

In the lower part of the mesosphere, the difference between the temperature at the summer and winter poles is of order 35°C (63°F). Temperatures in the upper mesosphere are colder in summer and warmer in winter, resulting in meridional flow from the summer to the winter hemisphere (**illus.**). Although the temperature gradient in the upper part of the mesosphere remains large, additional complications result in wind speeds that are much slower than they are in the lower part of the mesosphere. Winds in the east-west or zonal direction are greatest at mesospheric middle latitudes. Zonal winds blow toward the west in summer and toward the east in winter. Like their meridional counterparts, zonal winds are comparatively strong near the bottom of the mesosphere and comparatively weak near the top. Thus, on average both temperature and wind speed decrease with increasing height in the mesosphere. *See* ATMOSPHERIC GENERAL CIRCULATION.

Variations. The mesosphere is affected by the atmospheric layers lying above and below it. Above the mesosphere, the thermosphere profoundly responds to solar eruptions and the ensuing storms that occur in space. These geomagnetic storms produce

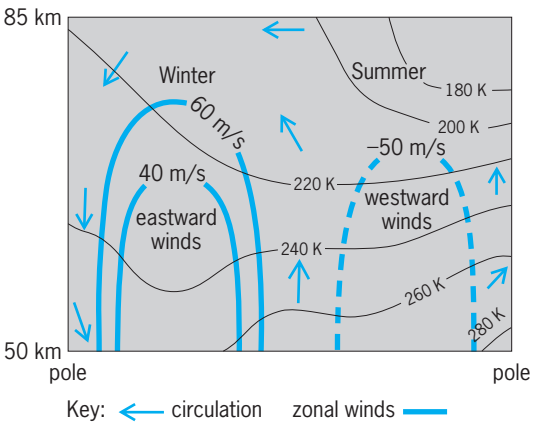

Structure of the mesosphere.

compositional changes in the thermosphere that can be driven down into the upper mesosphere by the associated disturbance winds when the storms are sufficiently strong.

Variations in winds, temperature, pressure, and density that are excited beneath the mesosphere in the troposphere and stratosphere can propagate up. Because density decreases with altitude throughout the Earth's atmosphere, any upward propagating variations will grow in size in order to conserve energy. Upward propagating variations include gravity waves that are excited by winds blowing over mountain ranges or by storm fronts. They also include solar tides which are excited by the periodic absorption of solar infrared and ultraviolet radiation in the troposphere and stratosphere, respectively. Gravity waves, solar tides, and other planetary waves are very large when they enter the mesosphere. They are readily observed by lidars, radars, imagers, and other sensors that measure the mesosphere remotely both from the ground and from satellites. Most waves of lower atmospheric origin dissipate or break in the upper mesosphere. When they do so, their energy and momentum is transferred to the rest of the undisturbed atmosphere. This complicates upper mesospheric circulation. Dissipating waves slow the winds that are driven by the summer-to-winter temperature difference. In addition, the wave dissipation process produces a mesopause temperature anomaly. That is, the summer mesopause is actually colder than the winter mesopause. *See* MIDDLE-ATMOSPHERE DYNAMICS; UPPER-ATMOSPHERE DYNAMICS.

Special features of upper mesosphere. Meteors which enter the Earth's atmosphere vaporize in the upper mesosphere. These meteors contain significant amounts of metallic atoms and molecules which may ionize. Metallic ions combined with ionized water clusters make up a large part of the D-region ionosphere that is embedded in the upper mesosphere. *See* IONOSPHERE.

The upper mesosphere is also where iridescent blue clouds can be seen with the naked eye and photographed in twilight at high summer latitudes when the Sun lights them up in the otherwise darkening sky. These clouds are called noctilucent clouds (NLC). Noctilucent clouds are believed to be tiny ice crystals that grow on bits of meteoric dust. The first reliable reports of noctilucent clouds were made in the 1880s. Since then, the number of sightings of noctilucent clouds has significantly increased, as have their sizes and lifetimes. Changes that are observed in the atmosphere are increasingly linked to human activities. Many scientists think that the depletion of stratospheric ozone, the occurrence of the Antarctic "ozone hole," and global warming in the lower atmosphere may be anthropogenic effects. While it remains to be proven, lower atmospheric global warming could be due to documented increases in atmospheric methane and carbon dioxide that are by-products of agricultural activities and fossil fuel consumption on Earth. These greenhouse gases also affect the mesosphere, but in very different ways. Many experts believe that increases of noctilucent clouds could be related to the documented increases in greenhouse gases. *See* GREENHOUSE EFFECT.

Large-scale atmospheric circulation patterns transport tropospheric air containing methane and carbon dioxide from the lower atmosphere into the middle atmosphere. While carbon dioxide warms the lower atmosphere, it cools the middle and upper atmosphere by releasing heat to space. When it reaches the middle atmosphere, methane undergoes chemical reactions that produce water. If the air is sufficiently cold, the water can freeze and form noctilucent clouds. Temperatures must be below −129°C (−200°F) for noctilucent clouds to form. These conditions are common in the cold summer mesopause region at high latitudes. One way to explain the observed increases in noctilucent clouds over the course of the last century is the plausible but unconfirmed increase in mesospheric water vapor. The most important source of water vapor in the mesosphere, atmospheric methane, has doubled in the last century. Further, any comparable increase in mesospheric carbon dioxide levels only enhances the conditions favorable for noctilucent cloud formation by further cooling the region. These effects combined may eventually lead to larger and more persistent clouds at high latitudes, accompanied by smaller thinner formations at middle latitudes. In June 1999, reliable measurements of noctilucent clouds were made in the continental United States over Colorado and Utah. This unprecedented sighting surprised experts who predicted that noctilucent clouds would not occur at these middle latitude locations until well into the twenty-first century. This recent sighting may be the strongest evidence yet that the mesosphere is where scientists can eventually confirm whether atmospheric changes are linked to human activities. *See* METHANE.

Maura Hagan

Bibliography. D. G. Andrews, J. R. Holton, and C. B. Leovy, *Middle Atmosphere Dynamics*, 1987; G. Brasseur and S. Solomon, *Aeronomy of the Middle Atmosphere*, 1985; J. T. Houghton, *The Physics of Atmospheres*, 1986; G. E. Thomas et al., Relation between increasing methane and the presence of ice clouds at the mesopause, *Nature*, 338:490–492, 1989.

Mesozoa

A division of the animal kingdom sometimes ranked as intermediate between the Protozoa and the Metazoa. These animals are unassignable to any of the better-known phyla, as usually defined. In the absence of proof concerning their relationships, and in view of the disagreement among zoologists relative to their affinities and even with respect to the facts and interpretation of their structure and life cycle, they are treated as a small phylum somewhere between Protozoa and Platyhelminthes. No particular phylogenetic interpretation should be attached to this placement.

The Mesozoa comprise two orders of small, wormlike organisms, the Dicyemida and the Orthonectida. Both are parasitic in marine invertebrates. The body consists of a single layer of ciliated cells enclosing one or more reproductive cells. These body cells are rather constant in number and arrangement for any given species. The internal cells do not correspond to the entoderm of other animals, as they have no digestive function. The life cycles are complex, involving both sexual and asexual generations (metagenesis).

There has been little agreement regarding the affinities of the Mesozoa. Some zoologists believe them to be related most closely to the Protozoa; others believe them derived from some higher group, usually the flatworms. Other groups that have also been suggested as a link with the Mesozoa are the Coelenterata, Echiuroidea, and primitive Aschelminthes. However, the relationship of these groups to the Mesozoa is regarded as less likely by most zoologists. Research indicates that Orthonectida and Dicyemida are more different from each other than formerly realized and probably should not be grouped in one phylum.

The Mesozoa have been united into a class called Planuloidea or Moruloidea because they exhibit the same grade of structural organization as a coelenterate planula larva or an embryonic morula.

A number of other small enigmatic organisms have at times been included in the Mesozoa. Most of these have subsequently been assigned to other phyla. *Salinella*, described by J. Frenzel in 1892, has remained a taxonomic puzzle. It consists of a single layer of cells enclosing a digestive cavity (see **illus.**). There is a mouth at one end and an anal opening at the other. Both internal and external surfaces of all cells are ciliated. Asexual reproduction is by transverse fission. Frenzel observed encystment in pairs and described unicellular young resembling ciliates.

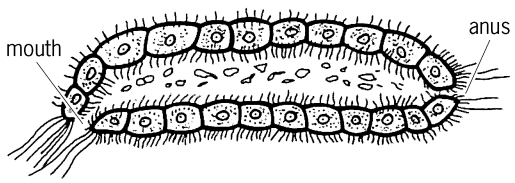

***Salinella*, in longitudinal section.**

Salinella has not been reported again since Frenzel's discovery. *See* ANIMAL KINGDOM; CELL CONSTANCY.

Bayard H. McConnaughey

Bibliography. L. H. Hyman, *The Invertebrates*, vol. 1, 1940; S. P. Parker (ed.), *Synopsis and Classification of Living Organisms*, 2 vols., 1982; H. W. Stunkard, The life history and systematic relations of the Mesozoa, *Quart. Rev. Biol.*, 29(3):230–244, 1954.

Mesozoic

The middle era of the three major divisions of the Phanerozoic Eon (Paleozoic, Mesozoic, and Cenozoic eras) of geologic time, encompassing an interval from 251 to 65 million years ago (Ma) based on various isotopic-age dates. The Mesozoic Era is known also as the Age of the Dinosaurs and the interval of middle life. The Mesozoic Erathem (the largest recognized time-stratigraphic unit) encompasses all sedimentary rocks, body and trace fossils of organisms preserved, metamorphic rocks, and intrusive and extrusive igneous rocks formed during the Mesozoic Era. *See* GEOCHRONOMETRY.

The Mesozoic Era was originally named for one of three principal divisions of the fossil record, or history of life, that was bounded before and after by significant mass extinctions that dramatically changed the biotic composition of the world. In England during the early 1840s, geologist John Phillips introduced the terms Mesozoic Era and Cenozoic Era, in conjunction with geologist Adam Sedwick's term Paleozoic Era, proposed in 1838, to denote the widespread observation that three successive and distinct biotic assemblages were preserved in the fossil record. The Mesozoic Era comprises life intermediate in kind between ancient life-forms (Paleozoic

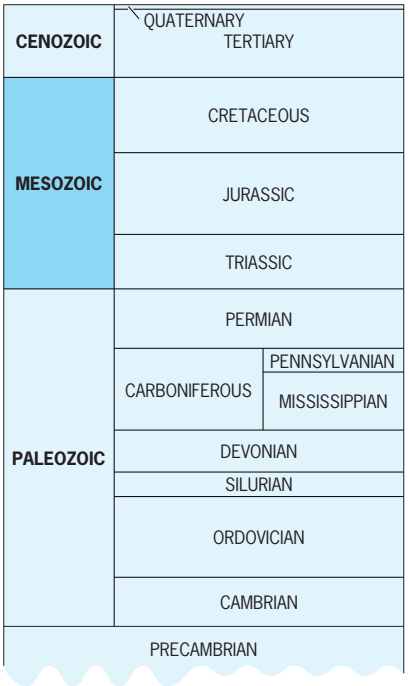

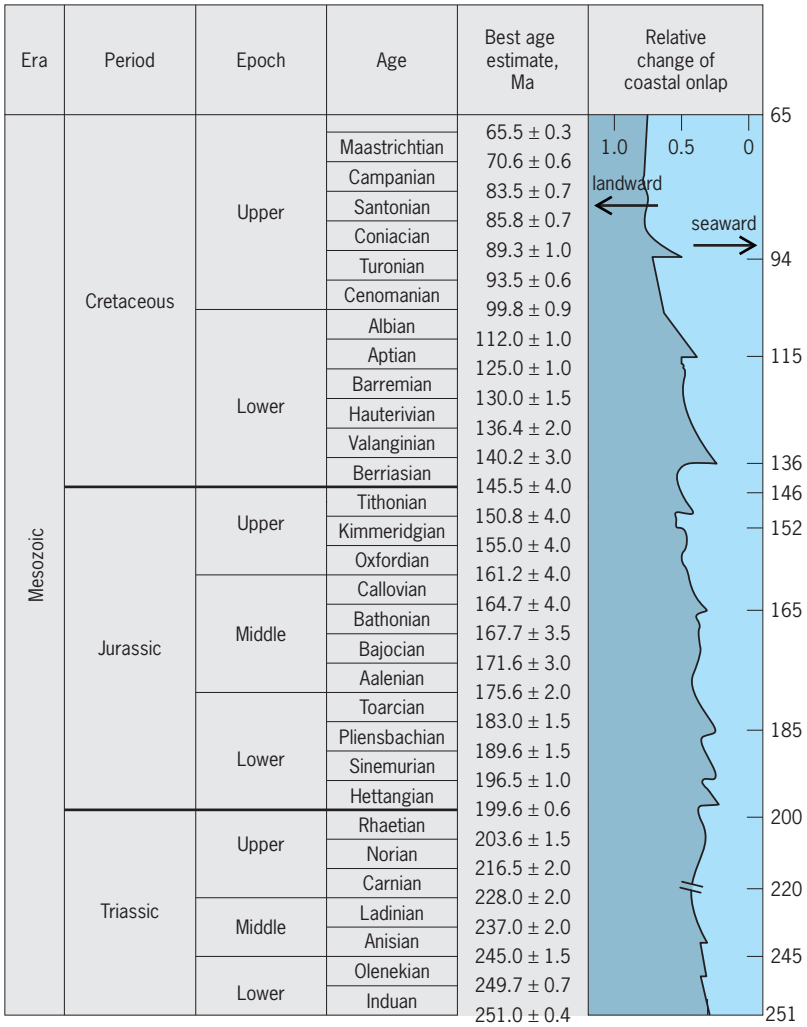

Fig. 1. Subdivisions of the Mesozoic Era, including the best age estimates and the eustatic sea-level curve depicted as relative change in coastal onlap as the shoreline moved landward (sea-level rise) or seaward (sea-level fall).

Era) and recent life-forms (Cenozoic Era). *See* CENOZOIC; PALEOZOIC.

The Mesozoic Era records dramatic changes in the geologic and biologic history of the Earth. At the beginning of the Mesozoic Era, all the continents were amassed into one large supercontinent, Pangaea. Both the marine and continental biotas were impoverished from the mass extinction that marked the boundary between the Permian and Triassic periods, and the end of the Paleozoic Era. This mass extinction was responsible for the loss of over 90% of the species on Earth. During the Mesozoic Era, many significant events were recorded in the geologic and fossil record of the Earth, including the breakup of Pangaea and the evolution of modern ocean basins by continental drift, the rise of the dinosaurs, the ascension of the angiosperms (flowering plants), the diversification of the insects and crustaceans, and the appearance of the mammals and birds. The end of the Mesozoic Era is marked by a major mass extinction at the Cretaceous-Tertiary boundary that records several meteorite impacts, the extinction of the dinosaurs, the rise to dominance of the mammals, and the beginning of the Cenozoic Era and the life-forms dominant today. *See* CONTINENTAL DRIFT; PLATE TECTONICS.

The Mesozoic Era comprises three periods of geologic time: the Triassic Period (251–200 Ma), the Jurassic Period (200–146 Ma), and the Cretaceous Period (146–65 Ma) [**Fig. 1**]. These periods are each subdivided into epochs, formal designations of geologic time described as Early, Middle, and Late (except for the Cretaceous, which has no middle epoch designated yet). The packages of rock themselves are subdivided into series designated Lower, Middle, and Upper (except for Cretaceous). Each epoch is subdivided into ages. Likewise, each series is subdivided into stages, which are time-stratigraphic units whose boundaries are based on unconformities, hiatuses, or erosional surfaces, on correlations to a type section (where rocks are first described), or preferably on changes in the biota that depict true measurable time (for example, evolutionary changes). *See* UNCONFORMITY.

The correlations of time equivalency and age dating in the Mesozoic Era have been accomplished by utilizing biostratigraphic zones based on individual fossil groups or by an acme or composite zonal assemblage based on numerous fossil groups. Marine and continental fossil groups used to describe chronologically Mesozoic rocks include marine foraminifera and nannofossils (shelled protozoa), ammonites (cephalopods), and inoceramids (mollusks); continental plant spores and pollen (palynology); dinosaurs; and mammals. Correlations based on these and other organisms in the Mesozoic Era depend on the faunal and floral succession through origination and extinction of species. *See* CEPHALOPODA; FORAMINIFERIDA; MOLLUSCA; PALYNOLOGY.

The organization of subdivisions based on physical and biological evidence allows geologists and paleontologists to describe both rocks and fossils in specific intervals of time and space. Thus, earth scientists can communicate effectively with one another and characterize more precisely the physical and biotic changes during the Mesozoic Era, as well as the other eras in geologic history. *See* PALEONTOLOGY; STRATIGRAPHY.

Triassic. The Mesozoic Era begins with the Triassic Period, which constitutes nearly one-third the total time of the era and is well exposed especially in Europe and North America, with other important outcrops in India, China, Argentina, and South Africa. The Triassic Period was named originally the Trias in Germany in 1834 by Friedrich August von Alberti for its unique fauna and natural division into three distinct stratigraphic units.

As a result of the unique geography of the single Pangaean landmass, the alteration in oceanic currents produced around one continent, and the monsoonal climatic setting, life changed substantially in both marine and continental ecosystems. The marine ecosystems witnessed the addition of large reptiles

and the modern reef-building corals, the reemergence and diversification of the mollusks, and the emergence of pelagic life in the form of planktonic organisms. Ray-finned and bony fishes and sharks dominated the seas. Placodonts and nothosaurs were aquatic marine reptiles that fed on mollusks and other marine invertebrates. Ichthyosaurs appeared in the oceans for the first time. Freshwater and terrestrial ecosystems were marked by the emergence and diversification of the dinosaurs, flying reptiles, frogs, turtles, terrestrial crocodiles, and birds; the appearance of the mammals, though quite small in size; the emergence of freshwater and terrestrial crayfish; and the emergence of new insects, such as the Isoptera (termites), Diptera (flies), and the Hymenoptera (bees, wasps, and possibly ants), appearing earlier in the Mesozoic than previously thought. Trace fossil evidence for these new insects indicates the advent of social behavior in termites and in primitive bees, prior to the appearance of angiosperms in the Cretaceous. In terrestrial ecosystems ferns and seed ferns were abundant, but gymnosperm floras continued to dominate the landscape. Therapsids rediversified after the Permo-Triassic extinctions, and thecodonts gave rise to the crocodiles and to the first dinosaurs, which were small in stature.

During the Triassic Period the continents were amassed tectonically into one great landmass, the supercontinent Pangaea, that was distributed equally across the paleoequator in both the Northern and Southern hemispheres (**Fig. 2***a*). Since the majority of the enormous Pangaean landmass was inland from the influence of the ocean, and its configuration distributed equally across the Equator, a worldwide monsoonal climate pattern dominated during the Triassic that created alternating wet and dry seasons in many regions. Areas landward of the coasts experienced increased continentality of the climate and produced more pronounced wet and dry seasons. *See* PALEOCLIMATOLOGY; PALEOGEOGRAPHY.

At the end of the Triassic, Pangaea began to break apart and the monsoonal climate pattern began to disintegrate. Evidence for the breakup of Pangaea and the eventual formation of the northern Atlantic Ocean is the presence of rift basins along the east coast of North America and the northwest coast of Africa. A mass extinction defines the boundary between the end of the Triassic and the beginning of the Jurassic. This mass extinction was responsible for the loss of about 60% of the species on Earth. The mass extinctions in the marine and continental realms affected the ocean ecosystem by eliminating the marine conodonts and placodont reptiles, and many species of bivalves, ammonoids, plesiosaurs, and ichthyosaurs disappeared. Most of these groups recovered in the Jurassic. Extinction also claimed the large amphibians and mammallike reptiles from freshwater and terrestrial ecosystems. The cause of these mass extinctions is unknown, though some scientists hypothesize that either a meteorite impact or increasing global aridity caused many genera to go extinct. *See* TRIASSIC.

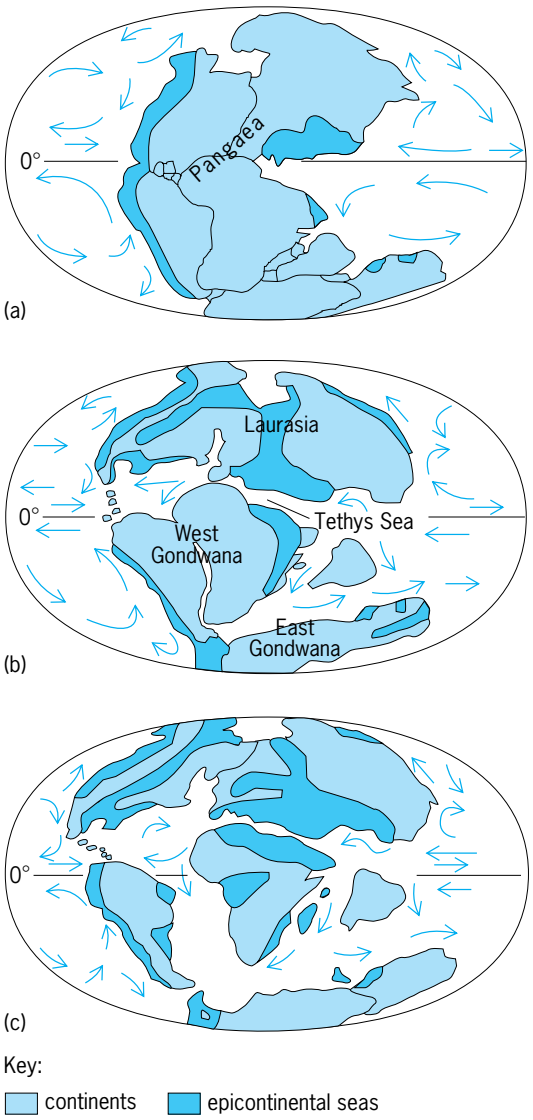

Fig. 2. Schematic reconstruction showing paleogeography of continents, epicontinental seas, and ocean basins (arrows denote ocean currents) on Pangaea in the Mesozoic Era from the (*a*) Triassic (220 Ma), (*b*) Jurassic (155 Ma), and (*c*) Cretaceous (70 Ma) periods.

Jurassic. The middle part of the Mesozoic Era is represented by the Jurassic Period, which constitutes about one-third of the total time of the era. Jurassic rocks are well exposed, especially in North America and Europe, and other important outcrops exist in South America and Asia. In 1839, German geologist Leopold von Buch established the Jurassic as a system for rocks in Switzerland, Germany, and England. The new system was based on descriptions of equivalent rocks made by the German geologist Alexandre von Humboldt (1795) and the English geologist William Smith (1797–1815). They described massive limestones of the Jura Mountains in Switzerland as the Jura-Kalkstein and the Lias-Oolite rock sequences in England and Wales, respectively. *See* LIMESTONE; OOLITE.

During the Jurassic Period the Pangaean landmass continued to separate into two large continen-

tal masses, with one in the Northern Hemisphere and the other in the Southern (Fig. 2*b*). The Northern Hemisphere landmass, Laurasia, was composed of North America and Eurasia, while the Southern Hemisphere landmass, Gondwanda, was composed of South America, Africa, India, Antarctica, and Australia. Continued plate spreading and more rapid sea-level fluctuations late in the Jurassic created the Tethyan Seaway, which extended between Laurasia and Gondwanda, allowing oceans to flow freely between the continents, and caused epicontinental seas to flood large areas of North America and Europe. The opening of the ocean basins and the resulting increased oceanic circulation created a zonal atmospheric climate pattern that ranged from tropical at the Equator to warm temperate near the Poles, with local zones of aridity due to orographic and latitudinal rain shadows. *See* CONTINENTS, EVOLUTION OF; RAIN SHADOW.

Oceanic and continental biotas shifted in composition during tectonic and climatic transformations of the Jurassic Period. Numerous reef communities of modern reef-building corals flourished in shallow tropical oceans along with bivalves, ammonites, belemnoids, sea urchins, and fishes. Planktonic life began to prosper in the warm, shallow seas with the appearance of calcareous nannoplankton. Marine reptiles included plesiosaurs and ichthyosaurs, and the invasion of the oceans by crocodiles. Terrestrial and freshwater ecosystems were dominated by plants such as cycads, cycadeoids, conifers, ginkgos, and to a lesser extent ferns. The Jurassic is also known as the age of the cycads. The dinosaurs' greatest rise to dominance occurred with the radiation of large herbivores such as the sauropods *Apatosaurus, Diplodocus, Camarasaurus,* the plated stegosaurs, and the heavily armored ankylosaurs. The herbivores were pursued by predatory dinosaurs such as *Ceratosaurus* and *Allosaurus*. Many flying reptiles speckled the skies, including pterosaurs and the feathered reptilelike bird, *Archaeopteryx*. Mammals were still small in size but began to increase in diversity. *See* DINOSAUR; PHYTOPLANKTON; REPTILIA; ZOOPLANKTON.

The end of the Jurassic Period was marked by moderate extinctions of biota in both marine and continental ecosystems. In the marine realm, brachiopod diversity declined steadily, other invertebrate faunas varied in diversity, and marine reptiles, such as the ichthyosaur, became nearly extinct. On the continents, the major extinctions eliminated the last of the therapsids and affected the large herbivorous sauropods, stegosaurs, and ankylosaurs, as well as their predators. *See* JURASSIC.

Cretaceous. The last part of the Mesozoic is represented by the Cretaceous Period, which constitutes a little less than one-half the total time of the Mesozoic Era. The Cretaceous is represented well by rocks in North America, South America, Europe, Asia, Africa, and Australia. The Cretaceous Period was named in 1822–1823 by French geologist J. J. d'Omalius d'Halloy for exposures at the White Cliffs of Dover, which are composed of marine chalks and can be traced throughout Europe and North Africa. These widespread chalk units are composed predominantly of microscopic plates of calcareous nannoplankton, and had once been an ancient sea floor. *See* CHALK; MICROPALEONTOLOGY.

During the Cretaceous Period the face of the Earth began to take on an appearance more similar to the present continental and oceanic configuration (Fig. 2*c*). Early in the Cretaceous, both Laurasian and Gondwanan continental masses separated into the continents still recognizable today. The separation of Gondwana in the Early Cretaceous marked the onset to the formation of the South Atlantic Ocean. Increased sea-floor spreading rates, which opened the oceanic gaps between the continents, resulted in the expansion of shallow epicontinental seaways in North America, Africa, and Northern Europe, along with the flooding of most of southern Eurasia. These variations in sea-floor spreading rates caused the sea level to fluctuate constantly throughout most of the Cretaceous. The Pacific and Atlantic ocean basins began taking form, and the Tethyan Seaway, between what is now the western Mediterranean and southeastern Asia, persisted throughout most of the period. New, expanded oceanic realms coupled with the changed continental configurations and increased atmospheric carbon dioxide transformed the early Cretaceous climate into a humid zonal climate, warmer than today. The climate began cooling down, beginning near the end of the Mesozoic.

The biotic composition during the Cretaceous Period contained a mixture of both intermediate and modern forms of life in both marine and continental ecosystems. In the marine realm, modern types of gastropods, bivalves, and modern fishes shared the oceans with marine reptiles such as mosasaurs and plesiosaurs, ammonoids, belemnoids, and other gigantic, coiled oysters and sedentary bivalves. Other marine invertebrates, such as planktonic and benthic foraminifera, flourished together with bryozoans, corals, reef-building rudist bivalves, crabs, lobsters, and other crustaceans. In the continental Cretaceous realm, the greatest change in freshwater and terrestrial ecosystems occurred with the appearance and diversification of angiosperms or flowering plants that became more diverse over the early and middle Mesozoic gymnosperm floras near the end of the Cretaceous. At the same time, freshwater and terrestrial insects continued to diversity and exploit new niches and resources provided by the angiosperms. Many groups of vertebrates, including snakes, modern types of turtles, crocodiles, lizards, and amphibians, diversified from ancient stocks during the Cretaceous to coexist with the dinosaurs that continued to rule the Earth. Mammals continued to evolve and diversify, but remained very small in size in comparison with their modern descendants. *See* MAGNOLIOPHYTA; MAMMALIA.

The dinosaurs diversified for the last time in the Cretaceous and formed ecological communities similar to mammal faunas inhabiting the African plains today. Herbivores such as the great horned

dinosaur *Triceratops* and large duck-billed dinosaurs such as *Hadrosaurus* traveled in herds, roamed the plains, and followed watercourses in seasonally migrating for food. The predators that followed these herds were the largest carnivores of all times, *Albertosaurus* and *Tyrannosaurus*, together with other pack and ambush predators such as the velociraptors and crocodiles, respectively. The few flying reptiles that remained were spectacular, one form attaining a wingspan of nearly 11 m (35 ft), and these creatures shared the skies with modern types of shorebirds and wading birds.

The end of the Cretaceous, and thus the end of the Mesozoic Era, is marked by a mass extinction known as the Cretaceous-Tertiary boundary (Tertiary is the earliest system of the Cenozoic Era, now divided into the Paleogene and Neogene). This mass extinction is widely known for the demise of 60% of the organisms on Earth, including the ammonoids, the rudist corals, marine reptiles, the dinosaurs, and the flying reptiles. There was a large reduction in the diversity of various marine plankton and continental faunas and floras, but they later recovered early in the Cenozoic. There have been many heated debates over the cause of the terminal Mesozoic extinctions, because some of them focus on extraterrestrial causes such as bolide and comet impacts onto the Earth's surface. Intriguing evidence in the form of iridium anomalies comes from marine deposits and continental coal deposits within rocks spanning the Cretaceous and Tertiary boundary worldwide. Iridium is an element that is typically depleted in rocks derived from the Earth's curst but is enriched in extraterrestrial stony meteorites. Some scientists hypothesize that a large 10-km (6-mi) meteorite or comet struck the Earth, exploded on impact, and released a blast greater than all the nuclear weapons on Earth. Such an impact would have thrown enormous volumes of dust and smoke into the atmosphere, blocked a large fraction of sunlight, and thus caused severe hardships to all marine and continental biota by lowering worldwide temperatures and disrupting the food chain. If the impact occurred in the ocean, huge volumes of water would have been vaporized instantly and caused gigantic tsunamis or tidal waves, which could have swept across most of the lowlands of continents. The devastating results of such an impact have been termed nuclear winter, because the effect would be similar to that produced by an all-out nuclear war. Other scientists hypothesize that extensive volcanic outgassing and cooler climates due to plate tectonic movements produced major changes in global climate and environmental disturbances that forced many organisms into extinction. Despite the similarities in global climate change and mass extinction interpreted by both of these hypotheses, other environmentally sensitive and presumably vulnerable groups of organisms were little affected by the mass extinction event. Environmentally sensitive vertebrates, such as crocodiles, lizards, turtles, frogs, and salamanders, were paradoxically spared and made it through the mass extinctions with little loss of species. The birds also persist through the mass extinctions and in fact radiate in the Paleogene and Neogene. *See* CRETACEOUS; EXTINCTION (BIOLOGY); GEOLOGIC TIME SCALE; METEORITE; TERTIARY.

S. T. Hasiotis; R. F. Dubiel

Bibliography. M. V. Caputo, J. A. Peterson, and K. J. Franczyk (eds.), *Mesozoic Systems of the Rocky Mountain Region, USA*, Rocky Mountain Section, Society for Sedimentary Geology, 1994; B. U. Haq and F. W. B. van Eysinga, *Geologic Time Table Chart*, 4th ed., 1994; W. B. Harland et al., *A Geologic Time Scale*, 1989; M. Moullade and A. E. M. Nairn (eds.), *The Phanerozoic Geology of the World II: The Mesozoic*, 1978; S. M. Stanley, *Earth System History*, 2d ed., 1998.

Messier Catalog

An early listing of nebulae and star clusters. Although Charles Messier (1730–1817) was primarily a comet hunter, he is remembered for his catalog of objects. As the first serious and systematic comet hunter (his comet discoveries spanned from 1760 to 1801), Messier learned about the hazards of being misled by the galaxies, nebulae, and star clusters all over the sky that look like comets. In 1758, when Messier found a fuzzy patch near the star beta Tauri that he first thought was a comet but that never moved as a comet would, he began to build a catalog of these objects. "This nebula had such a resemblance to a comet, in its form and brightness," Messier wrote, "that I endeavored to find others, so that astronomers would not confuse these same nebulae with comets just beginning to shine." This first entry is the Crab Nebula, the remnant of the supernova, a near-total destruction of a star, that was observed on July 4, 1054, to be as bright as Venus. (The Crab Nebula was previously discovered by John Bevis.) *See* COMET; CRAB NEBULA; GALAXY, EXTERNAL; NEBULA; PLANETARY NEBULA; STAR CLUSTERS.

Messier published three versions of his catalog. Of the 45 objects of his first catalog that appeared in 1774, no more than 18 were his own discoveries. Ultimately he listed 103 objects.

Evolution. It was not untill 1921 that Messier's catalog underwent some evolution, when Camille Flammarion, a popularizer of astronomy, found some notes about another object in Messier's personal copy of the catalog. That object was the Sombrero Galaxy in Virgo, and was added to the list as M104. In 1947 the astronomer Helen Sawyer Hogg suggested that Messier was aware of additional objects found by his colleague Pierre Méchain. Not long afterward, Owen Gingerich suggested that two galaxies in Ursa Major that were noted in the original copy should be M108 and M109. Kenneth Glyn Jones proposed the addition of the fainter companion to M31, the Andromeda Galaxy, since Messier had observed it in 1773 and drawn it in 1807. Thus, Messier's catalog lists 110 clusters, nebulae, and galaxies (see **table**). Not all those objects belong; M102 seems to be a misplaced position for M101, and M40 is simply two faint stars.

Messier Catalog of nebulae and star clusters*

Messier number†	NGC or (IC)	Right ascension (2000)	Declination (2000)	Apparent visual magnitude	Description
1	1952	5h 34.5m	+22°01′	8.4	Crab Nebula in Taurus; remains of SN 1054
2	7089	21h 33.5m	−0°49′	6.5	Globular cluster in Aquarius
3	5272	13h 42.2m	+28°23′	6.4	Globular cluster in Canes Venatici
4	6121	16h 23.6m	−26°32′	5.9	Globular cluster in Scorpius
5	5904	15h 18.6m	+2°05′	5.8	Globular cluster in Serpens
6	6405	17h 40.1m	−32°13′	4.2	Open cluster in Scorpius
7	6475	17h 53.9m	−34°49′	3.3	Open cluster in Scorpius
8	6523	18h 03.8m	−24°23′	5.8	Lagoon Nebula in Sagittarius
9	6333	17h 19.2m	−18°31′	7.9	Globular cluster in Ophiuchus
10	6254	16h 57.1m	−4°06′	6.6	Globular cluster in Ophiuchus
11	6705	18h 51.1m	−6°16′	5.8	Open cluster in Scutum
12	6218	16h 47.2m	−1°57′	6.6	Globular cluster in Ophiuchus
13	6205	16h 41.7m	+36°28′	5.9	Globular cluster in Hercules
14	6402	17h 37.6m	−3°15′	7.6	Globular cluster in Ophiuchus
15	7078	21h 30.0m	+12°10′	6.4	Globular cluster in Pegasus
16	6611	18h 18.8m	−13°47′	6.0	Open cluster with nebulosity (Eagle Nabula) in Serpens
17	6618	18h 20.8m	−16°11′	7	Swan or Omega Nebula in Sagittarius
18	6613	18h 19.9m	−17°08′	6.9	Open cluster in Sagittarius
19	6273	17h 02.6m	−26°16′	7.2	Globular cluster in Ophiuchus
20	6514	18h 02.6m	−23°02′	8.5	Trifid Nebula in Sagittarius
21	6531	18h 04.6m	−22°30′	5.9	Open cluster in Sagittarius
22	6656	18h 36.4m	−23°54′	5.1	Globular cluster in Sagittarius
23	6494	17h 56.8m	−19°01′	5.5	Open cluster in Sagittarius
24	6603	18h 16.9m	−18°29′	4.5	Open cluster in Sagittarius
25	(4725)	18h 31.6m	−19°15′	4.6	Open cluster in Sagittarius
26	6694	18h 45.2m	−9°24′	8.0	Open cluster in Scutum
27	6853	19h 59.6m	+22 43′	8.1	“Dumbbell” planetary nebula in Vulpecula
28	6626	18h 24.5m	−24°52′	6.9	Globular cluster in Sagittarius
29	6913	20h 23.9m	+38°32′	6.6	Open cluster in Cygnus
30	7099	21h 40.4m	−23°11′	7.5	Globular cluster in Capricornus
31	224	0h 42.7m	+41°16′	3.4	Andromeda Galaxy: spiral galaxy (Sb)
32	221	0h 42.7m	+40°52′	8.2	Elliptical galaxy; companion to M31
33	598	1h 33.9m	+30°39′	5.7	Spiral galaxy (Sc) in Triangulum
34	1039	2h 42.0m	+42°47′	5.2	Open cluster in Perseus
35	2168	6h 08.9m	+24°20′	5.1	Open cluster in Gemini
36	1960	5h 36.1m	+34°08′	6.0	Open cluster in Auriga
37	2099	5h 52.4m	+32°33′	5.6	Open cluster in Auriga
38	1912	5h 28.7m	+35°50′	6.4	Open cluster in Auriga
39	7092	21h 32.2m	+48°26′	4.6	Open cluster in Cygnus
40		12h 22.4m	+58°05′	8	Close double star in Ursa Major
41	2287	6h 47.0m	−20°44′	4.5	Loose open cluster in Canis Major
42	1976	5h 35.4m	−5°27′	4	Orion Nebula
43	1982	5h 35.6m	−5°16′	9	Northeast portion of Orion Nebula
44	2632	8h 40.1m	+19°59′	3.1	Praesepe; open cluster in Cancer
45		3h 47.0m	+24°07′	1.2	The Pleiades; open cluster in Taurus
46	2437	7h 41.8m	−14°49′	6.1	Open cluster in Puppis
47	2422	7h 36.6m	−14°30′	4.4	Loose group of stars in Puppis
48	2548	8h 13.8m	−5°48′	5.8	“Cluster of very small stars” in Hydra
49	4472	12h 29.8m	+8°00′	8.4	Elliptical galaxy in Virgo
50	2323	7h 03.2m	−8°20′	5.9	Loose open cluster in Monoceros
51	5194, 5195	13h 29.9m	+47°12′	8.1	Whirlpool spiral galaxy (Sc) in Canes Venatici
52	7654	23h 24.2m	+61°35′	6.9	Loose open cluster in Cassiopeia
53	5024	13h 12.9m	+18°10′	7.7	Globular cluster in Coma Berenices
54	6715	18h 55.1m	−30°29′	7.7	Globular cluster in Sagittarius
55	6809	19h 40.0m	−30°58′	7.0	Globular cluster in Sagittarius
56	6779	19h 16.6m	+30°11′	8.2	Globular cluster in Lyra
57	6720	18h 53.6m	+33°02′	9.0	Ring Nebula; planetary nebula in Lyra
58	4579	12h 37.7m	+11°49′	9.8	Spiral galaxy (SBb) in Virgo
59	4621	12h 42.0m	+11°39′	9.8	Elliptical galaxy in Virgo
60	4649	12h 43.7m	+11°33′	8.8	Elliptical galaxy in Virgo
61	4303	12h 21.9m	+4°28′	9.7	Spiral galaxy (Sc) in Virgo
62	6266	17h 01.2m	−30°07′	6.6	Globular cluster in Ophiuchus
63	5055	13h 15.8m	+42°02′	8.6	Spiral galaxy (Sb) in Canes Venatici
64	4826	12h 56.7m	+21°41′	8.5	Spiral galaxy (Sb) in Coma Berenices
65	3623	11h 18.9m	+13°05′	9.3	Spiral galaxy (Sa) in Leo

(*cont.*)

Messier Catalog of nebulae and star clusters* (*cont.*)

Messier number‡	NGC or (IC)	Right ascension (2000)	Declination (2000)	Apparent visual magnitude	Description
66	3627	11h 20.2m	+12°59′	9.0	Spiral galaxy (Sb) in Leo; companion to M65
67	2682	8h 50.4m	+11°49′	6.9	Open cluster in Cancer
68	4590	12h 39.5m	−26°45′	8.2	Globular cluster in Hydra
69	6637	18h 31.4m	−32°21′	7.7	Globular cluster in Sagittarius
70	6681	18h 43.2m	−32°18′	8.1	Globular cluster in Sagittarius
71	6838	19h 53.8m	+18°47′	8.3	Globular cluster in Sagitta
72	6981	20h 53.5m	−12°32′	9.4	Globular cluster in Aquarius
73	6994	20h 58.9m	−12°38′	9.1	Group of 4 stars in Aquarius
74	628	1h 36.7m	+15°47′	9.2	Spiral galaxy (Sc) in Pisces
75	6864	20h 06.1m	−21°55′	8.6	Globular cluster in Sagittarius
76	650,651	1h 42.4m	+51°34′	11.5	"Little dumbbell" planetary nebula in Perseus
77	1068	2h 42.7m	−0°01′	8.8	Spiral galaxy (Sb) in Cetus
78	2068	5h 46.7m	0°03′	8	Small emission nebula in Orion
79	1904	5h 24.5m	−24°33′	8.0	Globular cluster in Lepus
80	6093	16h 17.0m	−22°59′	7.2	Globular cluster in Scorpius
81	3031	9h 55.6m	+69°04′	6.8	Spiral galaxy (Sb) in Ursa Major
82	3034	9h 55.8m	+69°41′	8.4	Irregular galaxy in Ursa Major
83	5236	13h 37.0m	−29°52′	7.6	Spiral galaxy (Sc) in Hydra
84	4374	12h 25.1m	+12°53′	9.3	Elliptical galaxy in Virgo
85	4382	12h 25.4m	+18°11′	9.2	Elliptical/lenticular galaxy in Coma Berenices
86	4406	12h 26.2m	+12°57′	9.2	Elliptical galaxy in Virgo
87	4486	12h 30.8m	+12°24′	8.6	Elliptical galaxy in Virgo
88	4501	12h 32.0m	+14°25′	9.5	Spiral galaxy (Sb) in Coma Berenices
89	4552	12h 35.7m	+12°33′	9.8	Elliptical galaxy in Virgo
90	4569	12h 36.8m	+13°10′	9.5	Spiral galaxy (Sb) in Virgo
91	4548	12h 35.4m	+14°30′	10.2	Barred spiral galaxy (SBb) in Coma Berenices
92	6341	17h 17.1m	+43°08′	6.5	Globular cluster in Hercules
93	2447	7h 44.6m	−23°52′	6.2	Open cluster in Puppis
94	4736	12h 50.9m	+41°07′	8.1	Spiral galaxy (Sb) in Canes Venatici
95	3351	10h 44.0m	+11°42′	9.7	Barred spiral galaxy (SBb) in Leo
96	3368	10h 46.8m	+11°49′	9.2	Spiral galaxy (Sa) in Leo
97	3587	11h 14.8m	+55°01′	11.2	Owl Nebula; planetary nebula in Ursa Major
98	4192	12h 13.8m	+14°54′	10.1	Spiral galaxy (Sb) in Coma Berenices
99	4254	12h 18.8m	+14°25′	9.8	Spiral galaxy (Sc) in Coma Berenices
100	4321	12h 22.9m	+15°49′	9.4	Spiral galaxy (Sc) in Coma Berenices
101	5457	14h 03.2m	+54°21′	7.7	Spiral galaxy (Sc) in Ursa Major
102					Probably duplication of M101
103	581	1h 33.2m	+60°42′	7.4	Open cluster in Cassiopeia
104‡	4594	12h 40.0m	−11°37′	8.3	Sombrero Galaxy: Spiral galaxy (Sa) in Virgo
105‡	3379	10h 47.8m	+12°35′	9.3	Elliptical galaxy in Leo
106‡	4258	12h 19.0m	+47°18′	8.3	Spiral galaxy (Sb) in Canes Venatici
107‡	6171	16h 32.5m	−13°03′	8.1	Globular cluster in Ophiuchus
108‡	3556	11h 11.5m	+55°40′	10.0	Spiral galaxy (Sb) in Ursa Major
109‡	3992	11h 57.6m	+53°23′	9.8	Barred spiral galaxy (SBc) in Ursa Major
110‡	205	0h 40.4m	+41°41′	8.5	Elliptical galaxy; companion to M31

*From G. O. Abell, *Drama of the Universe,* Holt, Rinehart and Winston, 1978; J. M. Pasachoff, *A Field Guide to the Stars and Planets,* 4th ed., Houghton Miffiin, 2000; and A. Hirshfeld and R. W. Sinnott, *Sky Catalogue 2000.0*, vol. 2, Sky Publishing, 1985.
†In 2006 K. Graun proposed the addition of NGC869 and NGC884 as "honorary" M111 and M112.
‡Not in Messier's original (1781) list; added later by others.

Other catalogs. As Messier was completing his small catalog, William Herschel was building a far larger one, with thousands of objects seen through his bigger telescopes. That catalog was transformed by John Dreyer into the still more massive, 7000-object *New General Catalogue*, which today is the standard list of distant objects in the sky. *See* ASTRONOMICAL CATALOG.

In more recent years, other scientists have compiled newer catalogs. The *Caldwell Catalog*, which lists 110 other deep-sky objects in both the northern and southern hemisphere sky, was prepared by the astronomer Patrick Moore not from comet hunting but from choosing, in his opinion, the best non-Messier astronomical objects in the sky. A second example is David Levy's catalog of deep-sky objects found during his comet search. Levy built his catalog in the tradition of Messier, from searching for comets for more than 40 years. Some of the objects are truly, as comet hunter Leslie Peltier wrote, comet masqueraders and could easily be mistaken for comets. Others represent interesting objects that Levy has encountered during his search.

Although there are other catalogs, Messier's effort remains the most famous. It contains beautiful objects that are spread all over the sky as seen from

Messier's home, and consequently can be seen from any location in the Northern Hemisphere and from most in the Southern. David H. Levy

Bibliography. K. Graun, *The Next Step: Finding and Viewing Messier's Objects*, Ken Press, 2005; K. G. Jones, *Messier's Nebulae and Star Clusters*, 2d ed., Cambridge University Press, 1991; D. H. Levy, *David Levy's Guide to Observing and Discovering Comets*, Cambridge University Press, 2003; D. H. Levy, *Deep Sky Objects*, Prometheus, 2005; D. Machholz, *The Observing Guide to the Messier Marathon: A Handbook and Atlas*, Cambridge University Press, 2002; J. H. Mallas and E. Kreimer, *The Messier Album*, 1978, reprint, Sky Publishing, 1994; S. J. O'Meara, *Deep-Sky Companions: The Caldwell Objects*, Sky Publishing, 2002; S. J. O'Meara, *Deep-Sky Companions: The Messier Objects*, Sky Publishing, 1998.

Metabolic disorders

Disorders of metabolism principally involve an imbalance in nucleic acids, proteins, lipids, or carbohydrates. They are usually associated with either a deficiency or excess resulting in an imbalance in a particular metabolic pathway. All metabolic disorders have a genetic background, and some of them are expressed as specific genetic diseases. Metabolic processes throughout life are strongly influenced by the genetic component of aging, by diet, and by various types of environmental injury, including infectious agents (bacteria, viruses, fungi, and parasites), physical agents such as radiation and temperature, and chemical agents in the environment.

Other factors affecting metabolism include internal control mechanisms that are superimposed on the genetic background. One of the most important mechanisms is the hormonal control system, which consists of the endocrine, paracrine, and autocrine systems. Endocrine factors released from the hypothalamus stimulate the pituitary to produce somatotropic, corticotropic, gonadotropic, and thyrotropic hormones, which affect secondary endocrine organs such as the thyroid, pancreas, testis, breast, ovary, and adrenal glands. These secondary endocrine organs then secrete another group of systemic hormones (thyroxine, parathyroid hormone, insulin, estrogen, progesterone, testosterone, and epinephrine) that affect target cells. The paracrine system involves hormones or controlling substances secreted by cells affecting adjacent cells. The paracrine system includes neural transmitters affecting transmission between nerve cells; lymphokines secreted by lymphocytes, which affect other blood cells; as well as products of endocrine cells in the intestine, lungs, and pancreas. As an example, glucagon in alpha cells in the pancreatic islets of Langerhans affects the beta cells producing insulin. A third hormonal system is the autocrine system, which involves growth substances secreted by cells that act on themselves, including epithelial growth factor, nerve growth factor, and fibroblast growth factor. *See* ENDOCRINE MECHANISMS; GROWTH FACTOR.

The second control system that has a significant effect on metabolism is the neural control system. It consists of the central nervous system, including the cranial nerves, and the peripheral nervous system, including both sympathetic and parasympathetic nerves arising from the spinal cord. These nervous systems act by stimulating or inhibiting particular activities of organ systems and have a profound effect on the metabolism of tissues and organs. *See* NERVOUS SYSTEM (VERTEBRATE).

The third control system is the immune control system, which relates to both the endocrine and neural systems. The immune response produces antibodies as a defensive reaction against foreign antigens found on membranes of infectious agents, grafts, or tumors. Antigens may be proteins, lipoproteins, glycoproteins, or nucleoproteins; antibodies are glycoproteins. Different cells in the immune system have different functions. The macrophage is responsible for processing the antigen; the B lymphocyte is responsible for production of humoral antibodies; and a T lymphocyte has three functions: (1) a helper function to the B cell in antibody production, (2) a killer cytotoxic cell function in graft and tumor rejection and in some delayed hypersensitivity diseases such as tuberculosis, and (3) a synthetic function, forming lymphokines or paracrine hormones that may either stimulate or inhibit growth and metabolic processes. *See* IMMUNOLOGY.

Genetic background, environmental factors, and the three major control mechanisms, in conjunction with age and sex, bring about profound changes in metabolism, which ultimately result in structural and functional alterations. These may involve individual cells (such as the production of antibody), tissues (such as the inflammatory process associated with infection), or organs (such as the effect of dietary components in obstructing heart vessels and causing organ failure).

Nucleic acids. Abnormalities of nucleic acid metabolism are associated with several diseases, including gout and lupus erythematosus. Gout is a form of arthritis associated with extreme pain, especially around the smaller joints. There are usually accumulations of uric acid in the blood (hyperuricemia) and deposits of uric acid (tophi) in the soft tissue, the cartilage of the ear, the shafts of long bones, the kidneys, and the heart valves. Tophi are collections of sodium urate crystals surrounded by inflammation. Hyperuricemia may result from increased production or decreased excretion of uric acid or a diminished conversion of uric acid to urea. Increased production of uric acid, a degradation product of purines, has been found in some cases. Lupus erythematosus may be considered an abnormality of either protein or nucleic acid, since it involves a disturbance in nucleoprotein metabolism. The etiology is unknown. There is widespread damage to collagen, especially in the heart vessels, kidneys, and skin, and to the pericardial and pleural surfaces. *See* ARTHRITIS; CONNECTIVE TISSUE; DISEASE; GOUT.

All genetic disease implies a defect in nucleic acids, and although some genetic diseases are classified as protein abnormalities, such as amino aciduria or hemoglobinopathies, there is always an inherent defect in the nucleotide. This is either a deficiency, an excess, or a mutation that results in an abnormal protein being formed. Similarly, although lipid storage disease results in an abnormal metabolism of lipids, it is the result of a deficiency of a particular enzyme, which also means a defect in the particular nucleic acid code. In some carbohydrate genetic storage diseases, there is an accumulation of glycogen resulting from deficient metabolism of carbohydrates associated with a deficiency of a particular enzyme, which again results from a nucleotide defect. Certain congenital defects that result in malformations of organ systems are the result of either germ cell or somatic cell deficiencies involving differentiation genes composed of nucleic acid.

Genetic engineering has made possible the replacement of a deficient gene in cells of tissue cultures and in some experimental animals. The appropriate gene is isolated and cloned from a normal healthy cell and then introduced into cells removed from the bone marrow of a deficient animal or human. The gene may be inserted into the cell by direct inoculation with a micropipette or the cell may be incubated in a solution containing the appropriate constituents. *See* GENETIC ENGINEERING.

A genetic disease that has generated the most interest is an immune deficiency called severe combined immunodeficiency syndrome (SCIDS). This results in a deficiency of B lymphocytes, which produce antibody, and T lymphocytes, which are responsible for graft and tumor rejection as a result of their cytotoxic effect. This abnormality is associated with a deficiency of the enzyme adenosine deaminase. Chimpanzees that have this deficiency, when corrected with proper gene insertion into the stem cell, have been able to produce the enzyme for 127 days. The reason for the lack of success in other genetic diseases has been attributed to the complicated control mechanisms operating in the body and the fact that some defective cells, such as brain cells, cannot be isolated. In addition, many of the enzymes have several chains and have complicated control mechanisms. *See* HUMAN GENETICS; IMMUNOLOGICAL DEFICIENCY; NUCLEIC ACID.

Proteins. Proteins are in a continual state of dynamic equilibrium, and each particular protein has a specific rate of turnover. The degradation of proteins may occur within the cell itself in lysosomal autophagic vacuoles, which are responsible for turnover of normal cellular organelles and constituents, or extracellularly by the release of extracellular proteases that can degrade extracellular proteins such as collagen, elastin, and membranes of dead cells. The initial stage in degradation of a protein is called denaturation, which implies unfolding of the tertiary structure and usually results in the loss of function.

It has been noted that 90% of the solid constituents of cells and of the body are proteins. They are associated with structural components of the cell, extracellular structures such as collagen and elastase, and some hormones such as insulin and parathyroid hormone. They also constitute the principal antigens of the body either as simple proteins or in conjunction with lipids (lipoprotein), nucleic acid (nucleoprotein), or carbohydrate (glycoprotein). They constitute 99% of all the enzymes that act as catalysts responsible for controlling metabolism, and it is known that ribonucleic acid (RNA) may also act as an enzyme, and that the muscle protein myosin is both a structural protein and an enzymatic protein. Proteins are responsible for many of the transport mechanisms in the cytoskeleton within the cell, and comprise the transport proteins in vessels, such as the lipoproteins, albumin, and the gamma globulins.

Abnormal protein diseases. The diseases associated with protein abnormalities include those associated with increased production of proteins, decreased production of proteins, production of abnormal proteins, and excretion of unusual amounts of amino acids. Most diseases cause changes in protein metabolism and, to a greater or lesser extent, result in cellular changes such as cloudy swelling and hydropic degeneration. When a cell is injured slightly, the normal reserve components of the cell, plus the ability to resynthesize necessary constituents, usually result in a quick return to normal cell function and an inability to recognize any changes morphologically. Damage by a few cells in an organ as large as the kidney, which contains millions of cells, is of little importance in relation to total kidney function and presumably is a common occurrence.

Protein synthesis. Often called macroglobulinemia, hyperproteinemia results in an increase in beta or gamma globulins, but possibly with less total protein. Hyperglobulinemia diseases include multiple myeloma, kala-azar, Hodgkin's disease, lymphogranuloma inguinale, sarcoidosis, cirrhosis, and amyloid disease. They usually involve stem cell lines of the bone marrow macrophages or B cells. *See* CIRRHOSIS; HODGKIN'S DISEASE.

A decrease in the amount of protein (hypoproteinemia) can result from a lack of amino acids for protein synthesis, a metabolic block, or other interference with normal protein synthesis. Increased excretion of protein, particularly in chronic renal disease with a loss of albumin in the urine (albuminuria), is another common cause of hypoproteinemia. Kwashiorkor is the best example of hypoproteinemia resulting from dietary deficiency. Since albumin is synthesized in the liver, severe liver inflammation (hepatitis) or scarring (cirrhosis) will result in decreased synthesis and hypoalbuminemia with decreased levels of albumin in the blood. In hypogammaglobulinemia and agammaglobulinemia, which may also be classified under hypoproteinemia, the total serum albumin and globulin are not markedly depressed, but the gamma globulins may fall from a normal of 15–20% of total protein to 0.4%. Antibodies are normally part of this fraction, and the individuals are unable to synthesize antibodies against antigens. *See* ANTIBODY; IMMUNOGLOBULIN.

Abnormal proteins. Many diseases are characterized by abnormal proteins, including multiple myeloma, the hemoglobinopathies, and the various amyloid disturbances. Multiple myeloma, a neoplastic growth of plasma cells, particularly in the bone marrow and lymph nodes, is representative of a disease in which an abnormal protein is produced. A particular light chain of the normal gamma globulin, called Bence-Jones protein, is found in the urine of persons with multiple myeloma and differs markedly from any protein found normally in the serum or urine. This protein has a molecular weight of approximately one-fourth that of normal gamma globulin and is not merely a degradation product of the plasma protein but is a new or intermediate protein.

Another large group of abnormal proteins includes the hemoglobinopathies. Hemoglobin functions in the transport of oxygen in the blood. Several different hemoglobins in red blood cells in mammals have been described. Fetal hemoglobin has two alpha chains and two fetal hemoglobin secondary chains. Adult hemoglobin has two alpha and two beta chains. In sickle-cell hemoglobin there is a single base change in the beta chain of one nucleotide which results in a massive alteration in tertiary folding of the hemoglobin molecule and ultimately in a complete distortion of the normal blood cell membrane under low oxygen tension. This sickle cell is unable to carry normal amounts of oxygen and results in hemorrhage, inflammation, and occasionally sickle-cell crisis. Scores of different hemoglobins have been identified, but sickle cell in the United States and thalassemia (Mediterranean anemia) in Europe are two of the most common hemoglobin abnormalities. *See* HEMOGLOBIN; SICKLE CELL DISEASE.

A third type of abnormal protein is found in amyloid disease, of which there are many variations. In multiple myeloma, the light chains produced by the plasma cells are seen as amyloid. In diabetes mellitus, proinsulin in the islet cells of the islets of Langerhans of the pancreas appears as amyloid. In medullary carcinoma of the thyroid, calcitonin, produced by the C cells, appears as an amyloid, with proper staining. Another type of amyloid has been found in the brain and other tissues in Alzheimer's disease. Typically, amyloid has been associated with chronic disease states such as tuberculosis and rheumatoid arthritis, but this type is apparently a transformation of an abnormal globulin protein in the bloodstream. It results in deposition, particularly in blood vessels and in joint spaces. *See* ALZHEIMER'S DISEASE; AMYLOIDOSIS.

Amino acid excretion. A fourth group with abnormal protein metabolism is associated with a change in particular amino acids resulting either from an overflow mechanism, where the concentration of amino acids in the serum surpasses the renal threshold of the glomerular membrane, or from defective absorption of amino acids in renal tubules. *See* KIDNEY DISORDERS.

Of the 20 amino acids important for protein synthesis, many are also important in particular disease states. Tyrosine appears to be one of the most critical amino acids, and its metabolism is related to four key diseases including phenylketonuria, hypothyroidism, albinism, and alkaptonuria. Phenylketonuria, a disease that results in mental deficiency, is caused by an absence of the oxidase enzyme that converts phenylalanine to tyrosine. The accumulation of phenylalanine eventually results in accentuation of alternate pathways of phenylalanine degradation leading to phenylpyruvic acid, phenylacetic acid, and phenyl lactate acid. The latter products are present in such excessive quantities in the serum that they are excreted in the urine. Hypothyroidism is caused by a lack of thyroxine, which markedly influences metabolism. A deficiency of tyrosine results in a lack of thyroglobulin and eventually a lack of thyroxine. Infantile hypothyroidism is known as cretinism, and adult hypothyroidism is also known as myxedema. Tyrosine is also involved in the formation of dopa, which is an intermediate in the formation of melanin. A deficiency of tyrosine may express itself as a lack of melanin pigment of the skin and results in the congenital disease of albinism. Deficiencies in dopa, which is a precursor of epinephrine, may result in other endocrine disturbances. A failure of a complete breakdown of phenylalanine and tyrosine (alkaptonuria) results in the synthesis of an intermediate product, homogentisic acid, which accumulates in tissue and serum and is excreted in the urine. It is likely that the enzyme homogentisase, which converts homogentisic acid to fumaryl acetoacetic acid, is inhibited. Deposits of homogentisic acid in the tissues, especially in cartilage, tendons, ligaments, and sclerae of the eyes, impart a bluish discoloration known as ochronosis. *See* PHENYLKETONURIA.

The liver plays a major role in the deamination of amino acids. Advanced hepatitis and cirrhosis may lead to increased levels of amino acids in the blood and excretion in the urine. Other diseases with amino aciduria that are believed to be the result of defective kidney function include cystinuria (the failure to reabsorb cystine, lysine, arginine, and ornithine), Wilson's disease (a degeneration involving copper metabolism in the liver and brain), Fanconi's syndrome, galactosemia, scurvy, rickets, and lead, cresol, or benzene poisoning. *See* LIVER DISORDERS.

Sickle-cell disease and thalassemia would appear to be prime candidates for correction through genetic engineering. Replacement of the defective gene seems feasible, particularly since in both of these diseases a deficiency of a single base with a single amino acid change is the cause. The sole attempt, in a case of thalassemia, was not successful. One possible reason is that the hemoglobin molecule consists of four chains, and its synthesis, assembly, and release must be perfectly coordinated. A better candidate appears to be a single-chain protein such as the adenosine deaminase associated with severe combined immunodeficiency syndrome. *See* PROTEIN METABOLISM; SICKLE CELL DISEASE.

Lipids. Fatty acids may be synthesized from acetyl coenzyme A, which is an intermediate product and

a central site for amino acid, lipid, and carbohydrate metabolism. Lipids may be degraded by lipases in the serum, blood vessels, or tissues. Lipids are generally transported with proteins as lipoproteins or in a structure called a chylomicron. Lipids may be incorporated into the cell by pinocytosis after transport in the serum.

Fat has both a structural and a metabolic function. In the cell, fats are degraded, oxidized for energy, or used for synthesis of other lipids, carbohydrates, or proteins. Most cell membranes are composed of lipoprotein complexes. As an energy source, lipids at 9 calories per gram, compared with carbohydrates at 4 calories per gram, remain the second important source of adenosine triphosphate (ATP). Cholesterol is an important structural component of membranes. *See* ADENOSINE TRIPHOSPHATE (ATP); ADIPOSE TISSUE; CELL MEMBRANES; CHOLESTEROL.

Although lipid stores remain a secondary energy reserve in starvation, the breakdown of lipids associated with diabetes and starvation results in the production of ketone bodies in the urine with general acidosis (ketosis) in the serum. Of concern to many people is an increase in lipids associated with obesity. Although diet remains the primary control of obesity, some metabolic disturbances associated with endocrine imbalances make the problem of obesity difficult or impossible to control through diet. *See* OBESITY; PITUITARY GLAND DISORDERS; THYROID GLAND DISORDERS.

Hyperlipemia, an excess of lipid in the blood, is often secondary to uncontrollable diabetes, hypothyroidism, biliary cirrhosis, and lipoid nephrosis. Hyperlipemia may result in transfer of lipid into cells, particularly of the liver (as in cirrhosis of the liver), the kidney (as in lipoid nephrosis, now called minimal disease or nil disease), the heart (where it can interfere with contraction of the muscle), and vessels (in arteriosclerosis). Most cells are capable of synthesizing lipid, and some cells apparently produce excessive amounts under abnormal conditions which may be released to the extracellular fluid and thence to the bloodstream. Elevated blood lipids and cholesterol may be relatively independent of diet. Excess lipids present when dietary lipids are severely restricted must be produced by cells, although not necessarily by the cells in which they ultimately appear. If cells do not manufacture and store lipid within themselves, they may obtain the lipid from extracellular sources, presumably the lipoproteins of the serum. Deposits of lipid with fibrosis may occur on the eyelids in older people with high cholesterol levels. Excess proliferation of fat cells is known as a lipoma, which occasionally becomes malignant, producing a liposarcoma. *See* ARTERIOSCLEROSIS.

In a large group of genetic lipid storage diseases, lipid accumulates because of a disturbance in lipid metabolism that is independent of external stimuli. These genetic diseases are inherent nucleic acid defects that result in abnormal enzymatic proteins, which then result in abnormal lipid metabolism. In these diseases, a large accumulation of lipid appears in many cells, but particularly the reticuloendothelial cells of the lymph nodes, liver, spleen, and bone marrow. The lipid seems to be distributed throughout the cell and is not well localized. Abnormal lipid storage occurs in Niemann-Pick, Gaucher's, and Tay-Sachs diseases. Niemann-Pick disease is characterized by the excess accumulation of sphingomyelin, a cell membrane constituent, in the nervous system. Gaucher's disease encompasses a group of inborn errors of glycosphingolipid metabolism associated with an enzyme deficiency, and Tay-Sachs disease also results from an enzyme deficiency. All three diseases are hereditary and are fatal.

In cirrhosis of the liver, scarring is secondary to destruction of liver cells and nutritional deficiencies commonly associated with alcoholism. Lipid appears as small or large droplets in close physical association with plasma lipids. In association with protein deficiencies, normal substrates that are usually involved in protein metabolism may be diverted into lipid synthesis. Lipid accumulation in alcoholic hepatitis and perhaps in cirrhosis may be reversible.

The genetic disease familial hypercholesteremia appears in 1 of every 500 people in the heterozygous population and in 1 of every 1 million in the homozygous population. Heterozygous hypercholesteremia, with cholesterol levels two to four times normal, is characterized by arteriosclerotic lesions of the coronary vessels that cause myocardial infarct and death in the 35–50-year age range. In the homozygous condition, with cholesterol levels eight to ten times normal, death occurs usually before the age of 15. The defect resides in the receptor for low-density lipoprotein (LDL). This receptor defect in the liver and other tissues results in a lack of transport of low-density lipoprotein containing high cholesterol amounts from the bloodstream. Similar defects have been shown with genetic abnormalities in the apoproteins, which bind to specific receptors or transport proteins on the cell membranes and direct the lipoproteins to the metabolic site. Such defects result in a lack of low-density lipoprotein uptake. The receptor may not bind to the low-density lipoprotein, there may not be sufficient number of receptors present, or the internalization process of the low-density lipoprotein once attached to the receptor may be defective.

Familial hypercholesteremia serves as a model for hypercholesteremia associated with nonheritable causes. A reduction in smoking, an increase in exercise, close attention to blood glucose levels in diabetes, a diet low in fat, and careful monitoring of cholesterol levels, are important. When preventive measures fail, any of a large group of drugs can divert the normal antecedents of cholesterol, block the synthesis of cholesterol, or immobilize the cholesterol before entrance into the lipoprotein. The degree to which efforts to reduce cholesterol have played a role remains controversial. *See* CHOLESTEROL; HEART DISORDERS; LIPID METABOLISM.

Carbohydrates. Carbohydrate deficiency is seen in starvation. When insufficient energy is derived from carbohydrate ingestion, the body turns to its fatty acid, breaking down lipid cells and generating

adenosine triphosphate as well as excess ketones. Eventually the body may degrade protein, and amino acids may be diverted into the acetyl coenzyme A cycle with the production of adenosine triphosphate. Excess carbohydrate is stored in the liver and muscle as glycogen, available for use when needed. *See* MALNUTRITION.

Abnormal carbohydrate diseases include the genetic diseases that represent a deficiency in nucleotide and eventually protein enzymatic activity. Of the six common carbohydrate storage diseases, two examples are von Gierke's disease, marked by glycogen storage in the heart, and Pompes' disease, in which the carbohydrate is stored in the liver. Variants of carbohydrate disease involve storage of mucopolysaccharides, as in Hurler's disease, and storage of galactose, as in galactosemia.

The most important disease associated with carbohydrate metabolism is diabetes mellitus, which affects approximately 10% of the United States population. However, only 1% is type I or juvenile diabetes; the other 9% is identified as type II or maturity-onset diabetes. Type I diabetes is associated with a specific human lymphocyte antigen (HLA) profile on the cell. Following injury to the beta cells of the islets of Langerhans, which produce insulin, the altered membranes of the cells act as an antigen to produce autoantibodies. This antibody results in the destruction of other viable beta cells and is a classic example of autoimmune disease. This results in an absolute deficiency of insulin. Type II diabetes results not from an absolute deficiency of insulin but from ineffectiveness of the insulin on cells. There appears to be no genetic HLA susceptibility. It has been postulated, with some evidence, that there is a defect in the insulin receptors on the target cells, either a decrease in number or an inability to bind the appropriate amounts of insulin. Because the autoimmune component is small, dietary control of the disease is possible. If allowed to remain untreated, hyperglycocemia may result in damage to blood vessels, kidneys, and retinas and increased infection. *See* AUTOIMMUNITY; CARBOHYDRATE METABOLISM; DIABETES; METABOLISM.

Donald W. King

Bibliography. G. S. Eisenbarth, Type I diabetes: Clinical implications of autoimmunity, *Hosp. Prac.*, 22:135–152, 1987; F. H. Epstein (ed.), Specificity spillover at the hormone receptor: Exploring its role in human disease, *N. Engl. J. Med.*, 320:640–645, 1989; C. M. Feek and C. R. Edwards, *Endocrine and Metabolic Disease*, 1988; *Harrison's Principles of Internal Medicine,* McGraw-Hill, 16th ed., 2005; V. A. McKusick, The new genetics and clinical medicine: A summing up, *Hosp. Prac.*, pp. 79–84, July 1988; P. N. Plowman, *Endocrinology and Metabolic Diseases*, 1987.

Metabolism

All the physical and chemical processes by which living, organized substance is produced and maintained and the transformations by which energy is made available for use by an organism.

In defining metabolism, it is customary to distinguish between energy metabolism and intermediary metabolism, although the two are, in fact, inseparable. Energy metabolism is primarily concerned with overall heat production in an organism, while intermediary metabolism deals with chemical reactions within cells and tissues. In general, the term metabolism is interpreted to mean intermediary metabolism. *See* ENERGY METABOLISM.

Metabolism thus includes all biochemical processes within cells and tissues which are concerned with their building up, breaking down, and functioning. The synthesis and maintenance of tissue structure generally involves the union of smaller into larger molecules. This part of metabolism, the building of tissues, is termed anabolism. The process of breaking down tissue, of splitting larger protoplasmic molecules into smaller ones, is termed catabolism. Growth or weight gain occurs when anabolism exceeds catabolism. On the other hand, weight loss results if catabolism proceeds more rapidly than anabolism, as in periods of starvation, serious injury, or disease. When the two processes are balanced, tissue mass remains the same.

Energy production and utilization. Various components of the tissues are continually undergoing degradation in catabolism and resynthesis in anabolism. Some chemical reactions involved in these metabolic processes are exergonic; that is, they are accompanied by liberation of energy. Others are endergonic; that is, they require exogenous energy. After energy has been introduced into an endergonic process to move substances from a metastable state or state of intermediate stability, an exergonic reaction may occur. Two or more reactions may be coupled in such a way that an exergonic reaction may be used to drive an endergonic one. Within cells, for example, there exists a mechanism whereby free energy, available usually from oxidative reactions, may be used to spark endergonic processes. In some cases, a gain in free energy occurs. Adenosine triphosphate (ATP), which contains high-energy phosphate bonds (~P), is used in many such instances. In some oxidative reactions, however, it seems that the released energy cannot be used for endergonic purposes. The aerobic dehydrogenases of cytoplasm act as catalysts in the oxidation of a number of substrates, but apparently they cannot be utilized in endergonic reactions. *See* ADENOSINE TRIPHOSPHATE (ATP); BIOLOGICAL OXIDATION.

Metabolism is largely concerned, particularly in the case of synthetic or anabolic phenomena, with the need for providing energy-producing mechanisms for the construction of new tissues and their constituents. The energy is often obtained from simultaneously occurring degradative, or catabolic, reactions. Exergonic transformations are utilized for synthesis of all structures, for maintenance of body temperature, and for providing energy for specific functioning of various tissues, as in muscle contraction, nerve impulse conduction, glandular secretion, absorption, light production, and execretory

processes. To replace the energy thus utilized, a regular provision of new external sources of energy in the form of various foodstuffs must be supplied.

Metabolic pathways. The metabolism of the three major foodstuffs, carbohydrate, fats, and proteins, is intimately interrelated, so any clear-cut division of the three is arbitrary and inaccurate. Thus the metabolism of protoplasm is concerned with all three of these foodstuffs. However, each function of an organism has its own particular metabolic needs. For example, the chemical reactions of major importance in muscle contraction are those which yield energy for transmission to and operation of the contractile elements in muscles. The high-energy phosphate bonds (~P), formed during metabolic degradation and transformation of carbohydrate, fatty acids, and amino acids, transfer their energy to the muscle fibrils to provide the energy for contraction. *See* MUSCLE.

The metabolic pathways of carbohydrates, fats, and proteins cross at many points; thus certain pathways of metabolism are shared in common by fragments of these different classes of foodstuffs. Carbohydrate, protein, and fat may all contribute to the metabolic pool of acetyl coenzyme A (active acetate) which can be oxidized to CO_2 and H_2O (tricarboxylic acid cycle) with release of energy or used for the synthesis of body substances such as hormones. To make the endergonic metabolic processes possible, chemical energy in the form of ~P is produced; CO_2 and H_2O are by-products of these reactions.

Some of the metabolic processes of the protoplasm of both plant and animal cells occur along common pathways; carbohydrate metabolism in plants is similar in many details to carbohydrate metabolism in animals. Thus the study of metabolism in any organism is, in a sense, the study of metabolism in all protoplasm. *See* BACTERIAL PHYSIOLOGY AND METABOLISM; CARBOHYDRATE METABOLISM; CITRIC ACID CYCLE; CYTOCHROME; LIPID METABOLISM; PLANT METABOLISM; PROTEIN METABOLISM.

Mary B. McCann

Metadata

Data that describe or define all objects that make up a data source. That is, metadata is data about the data.

Widely used within the context of database management systems (DBMS), the term metadata refers to the complete description of all database structures and their constraints (conditions that need to be satisfied by the data stored in the database). This metadata is stored in the data dictionary or catalog. The data dictionary is an integral part of any DBMS environment and can be considered a database in its own right (albeit a system database instead of a user database). For this reason, a DBMS is sometimes referred to as a self-describing collection of integrated data since it holds both the data and the data description. A comprehensive data dictionary contains metadata about all database objects, including connections, users, users' privileges, schemas (external, conceptual, and so on), mappings between the different schemes, and all types of security and integrity constraints.

In general, the DBMS software during all its operations actively uses the data dictionary. For example, even in the most basic configurations, whenever a user needs to interact with a DBMS he or she needs to log on to the database server—the computer where the DBMS and the data reside—by specifying a username and a password. During this logon process, the DBMS consults the data dictionary to validate the user. That is, the DBMS verifies that the username and password specified by the user already exist as such in the data dictionary. If the user then proceeds to query, for instance, a table of a relational database, the data dictionary is further consulted to confirm, first, that the table exists and, second, that the user has the privileges (rights) to operate on that table. If the data requested by the user need to be retrieved from physical files, this metadata is also contained in the data dictionary.

To speed up the system responses in some DBMSs, the metadata of the data dictionary is examined in a slightly different manner. In these DBMSs, all objects that have been recently referenced by the database users are temporarily saved, along with their corresponding results if applicable, in designated areas of main memory sometimes called the data dictionary cache and the database buffer cache, respectively. This way, whenever a user makes a query, the DBMS checks first the contents of the data dictionary cache to see if an identical query has already been processed and its results are still in the data buffer cache. If an identical query is present in the data dictionary cache, the DBMS, unless some special data formatting is needed, immediately returns the results to the user. Otherwise, the data are retrieved directly from the physical data files that store the user data. *See* DATABASE MANAGEMENT SYSTEM.

Ramon A. Mata-Toledo

Bibliography. T. M. Connolly and C. E. Begg, *Database Systems: A Practical Approach to Design, Implementation and Management*, 4th ed., Pearson Education, 2004; C. J. Date, *An Introduction to Database System*, 8th ed., Addison-Wesley, 2003.

Metal

A solid or liquid (molten), opaque material with a lustrous surface and good electrical and thermal conductivities. Solid metal is usually crystalline and ductile and can be permanently deformed by shear on crystal planes; permanent deformation is accompanied by an increase in strength (work hardening). Metallic properties are related to the arrangements of positively charged ions bonded through a surrounding field (sea) of free electrons that draw the ions into a close-packed crystalline structure with planes appropriate for slip. Liquids are nearly close packed, noncrystalline, with a thermal energy great enough

to activate random, free movements of atoms. *See* LIQUID.

The rapid development of the metals industry since the late nineteenth century required an in-depth understanding of the fundamentals of metallurgy to improve metal properties and expand their usefulness. Much of the available technical information depends upon empirical correlations, although the rules of thermodynamics, quantum mechanics, and solid-state physics have established a fundamental basis for the science. With quantitative experimental techniques such as x-ray and electron diffraction along with other procedures generated by the rapid advances in semiconductor devices, the synergistic growth in solid-state studies contributed to better comprehension of the structure of metals. *See* ELECTRON DIFFRACTION; SEMICONDUCTOR; THERMODYNAMIC PRINCIPLES; X-RAY DIFFRACTION.

Characteristics of solids. The unique characteristics of the different classes of solids are directly related to the electron pattern and the types of bonds between the atoms of the solid. Atomic bonding is classified in two major categories: strong attraction (covalent, ionic, or metallic) and weaker, secondary bonding (van der Waals or hydrogen bonding). In the equilibrium state, interactions of the outermost orbital electrons and bond restrictions of the aggregate of atoms have the greatest influence on most of the physical and mechanical properties of the solid. Atoms of a solid in a lattice arrangement or in an amorphous distribution vibrate at frequencies about 10^{13} Hz at amplitudes a few percent of the interatomic spacing and at temperatures in the range of one-third of the metal's absolute melting temperature. The higher the temperature, the greater the amplitude of vibration of the atoms. Thermal and elastic pulses are transferred as in a series of coupled vibrating sources exerting forces through to bonds to adjacent atoms. In addition, in metals the free electrons contribute to the transfer of the pulses. *See* CHEMICAL BONDING; ELECTRON; FREE-ELECTRON THEORY OF METALS; HYDROGEN BOND; INTERMOLECULAR FORCES.

In a given pressure range, as the temperature of the element is increased from absolute zero (0 K), stable solid metals (and some nonmetals) tend to change phase into liquid metals at the melting temperature of the specific element or compound. The resulting liquids convert to gases at the vaporization temperature of the specific element. The melting temperature and, to a greater extent, the vaporization temperature are dependent on pressure on the system. The atoms or molecules of gas are too far apart to retain metallic features. Thus, properties of a solid at high and low temperatures are best compared in a temperature range relative to a characteristic temperature of the specific element or compound; in metals some fraction of the melting temperature (in Kelvin) is usually used. In equilibrium conditions, metals in the solid state occur in a limited number of crystal structures; however, depending on the temperature and pressure of the system, some metals have different crystal structures—a phenomenon known as allotropy. Furthermore, at nonequilibrium conditions where the rate for reorganization of atoms into the new equilibrium structure is too slow because of low temperatures—such as the consequence of rapid cooling, heavy deformation on certain metals, or radiation by high-energy particles—the atoms of some metals may be frozen or forced into an intermediate, metastable, higher free-energy state than attained at equilibrium conditions. Examples of these effects occur in the quenching of metals, deformation of austenite into martensite, or high-energy neutron bombardment of metals. An extreme case is the solidifying of the amorphous arrangement of the liquid phase by very rapid cooling of some molten metals. *See* MELTING POINT; METALLIC GLASSES; SOLID-STATE PHYSICS.

Quantum effects. In metals the characteristic crystal structure and physical properties depend mainly on metallic bonding influenced by the tendency of the bonds to incorporate other nonmetallic types of cohesion. Bonding of atoms of an element is determined mainly by the outer electrons of the free atom. For a free atom the electrons with the highest free energy are the valence electrons, and these combine in lowest, nonoccupied, available, quantum energy states of the aggregate of ions.

Because of the small mass of an electron, classical laws of mechanics are not satisfactory to explain the dynamics of the electrons as well as quantum mechanics does. Quantum mechanics represents an electron in a solid as a three-dimensional smear of negative charge, the magnitude of which is equivalent to certain probabilities of being in particular regions of space at some time in the aggregate of ions. The scope and restrictions of quantum-mechanical laws describe satisfactorily the spatial location of the electron charge, and the available energy levels (quantum-energy levels) allowed for electrons. Since stable bonding depends upon the lowest-energy configuration of electrons with respect to the collection of atoms, the modeling by this wave-mechanical procedure along with certain physical limitations (such as the Pauli exclusion principle and the Heisenberg uncertainty principle) require specific available energy levels and, conversely, impose energy ranges forbidden to electrons. Moreover, the locations permitted for the electrons restrict the type of bonds and the possible aggregate geometry (crystalline or liquid at equilibrium or amorphous at nonequilibrium). *See* ELECTRON CONFIGURATION; ENERGY LEVEL (QUANTUM MECHANICS); EXCLUSION PRINCIPLE; QUANTUM MECHANICS; SOLID-STATE CHEMISTRY; UNCERTAINTY PRINCIPLE.

Energy bands. If atoms of the same element are at large enough distances that their electric fields do not influence each other, the discrete electron orbital potential energies in each shell for individual atoms are defined by quantum-mechanical rules for a single atom. At large separation of the atoms, the allowed-electron-potential-energy levels do not intrude on one another, and they are considered free atoms. Consequently, each atom has the same discrete allowed-energy levels as determined by the

laws of quantum mechanics for a single atom. If several atoms are moved near to each other so that the higher energy levels including the valence electron energy tiers interfere with each other, the discrete energy levels are slightly displaced into several other values because only two electrons at any allowable-energy level are possible (Pauli exclusion principle). As before, each level is separated by an energy interval (gap) that cannot contain the electrons for the particular element (forbidden-energy gaps). Since there are many atoms in a metal aggregate—about 10^{23} atoms per cubic centimeter—there are about 10^{23} more energy levels for the aggregate than for the energy levels associated with one free atom. Since in an aggregate the large number of energy levels are relatively close together compared to those in a free atom, the spread of energy levels in the collection of atoms is called energy bands. For some materials, the multitude of energy levels of two or more shells overlap. These conditions are illustrated by energy bands that represent many near discrete-electron-energy levels (**Fig. 1***a*). The potential-energy bands for the equilibrium aggregate of atoms are conveniently shown in an energy-band diagram with the higher energies increasing in the *Y* direction (Fig. 1*b*).

Because the available electrons seek the lowest energy levels, the higher allowed-energy bands do not contain electrons. The average maximum energy of the valence electrons contained in a solid is called the Fermi energy (Fig. 1*b*). At the temperature of absolute zero (no thermal agitation of electrons exist), the Fermi energy is the maximum energy level of the electrons in a nonperturbed solid. In a metal there are always many empty available energy levels minutely separated above the Fermi energy; as a consequence, only small energy gaps between levels act as barriers to the electrons and must be overcome to permit the flow of electrons through the metal. Thus, very small energy increases supplied by an electric field or thermal energy result in a relatively free flow of electrons down a voltage or temperature gradient. The condition is characterized by high electrical conductivity and high heat conductivity by electrons in metals. Furthermore, under conditions of high pressure in which atoms and thus electron energy bands are pressed together (typically in stars or high-pressure experimental devices), nonmetals will exhibit the properties of metals, because the electrons in the Fermi level are able to move freely in energy levels closer to the atom core.

The usual metallic luster—silver, gold, copper, or the many brass metallic colors—are the results of almost total reflection of the long-wavelength portion of the incident light spectrum by the dense plasmalike cloud of conduction electrons throughout the crystal at the appropriate energy band to reflect the proper energy photons. For silver, most of the spectrum, including the visible portion, is reflected except in ultraviolet; whereas with gold the longer wavelengths, including red and yellow, are reflected while the shorter wavelengths of green and below enter the metal. *See* BAND THEORY OF SOLIDS; FERMI SURFACE; PHOTON.

Directional bonds. A covalent bond between two or more atoms is a negative charge directed in space and equivalent in magnitude to one or more electrons. As a consequence, at the lowest energy state the corresponding bond is directional and usually strong, and considerable energy must be supplied to the material to free an electron from this bond or shift an ion from one fixed position to another. For covalent materials, bonding valence electrons require large energies to transport a current composed of many electrons through the aggregate atoms. Thus electrical conductivity and thermal conductivity by electrons are

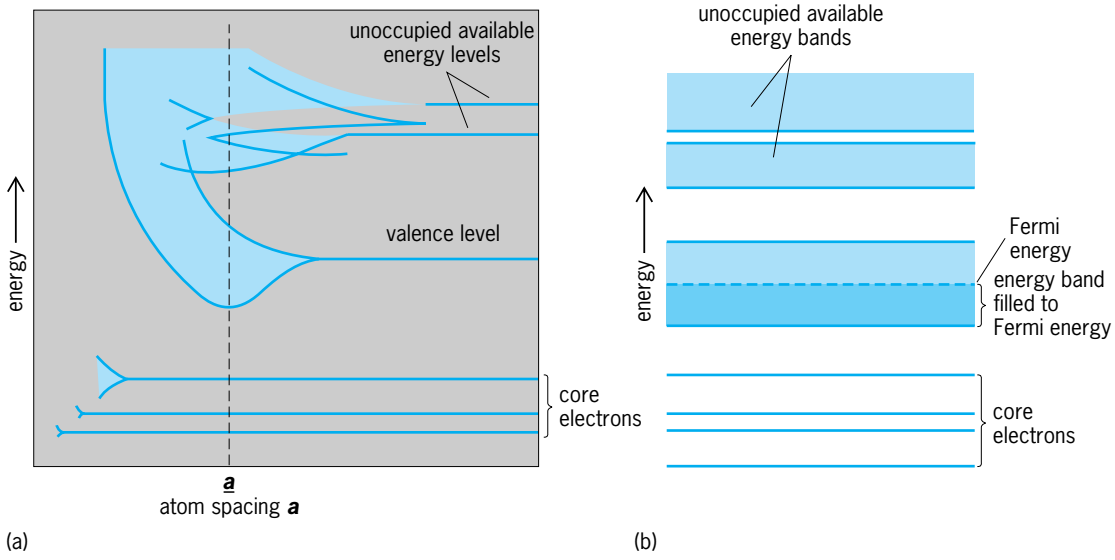

Fig. 1. Available energy levels and bands of energy levels for electrons in a univalent metal. (*a*) Atomic spacing. Allowed and forbidden quantum energies in an aggregate of atoms related to the distance between atoms, *a*; the spaces between horizontal lines signify the energy gaps not allowed for electrons. (*b*) Available energy bands, levels, and gaps for equilibrium spacing, *a*, characteristic of metals with only one electron in the valence level.

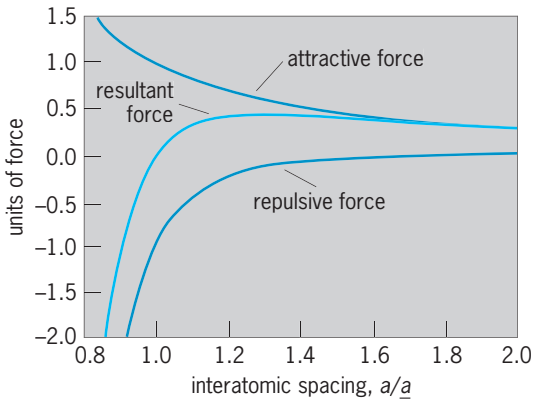

Fig. 2. Ratio of atomic separation, *a*, to equilibrium spacing, *a*, plotted against the sum of the repulsive and the attractive forces. At the ratio of interatomic spacings *a*/*a* = 1.0, equilibrium spacing, the resultant force is zero.

low. This situation is demonstrated in energy-band diagrams by a filled allowable-energy band with a large energy gap over which electrons must transverse to another allowed-energy band to become conduction electrons.

Metallic bonding. In contrast to directional bonds, metallic bonds result from linking ions each having centrosymmetrical attraction to a surrounding atmosphere of the distributed charges of nearly free electrons. These electrons, usually valence electrons, have the same likelihood of being associated with any ion in the aggregate. However, there are quantum-mechanical constraints defining the probability of the charge being at some position with some range of energy for a given time period. Depending upon the spatial distribution of the negative charges and positive ions, characteristic equilibrium distances (lattice spacings) are established between the ions of the metal. This equilibrium condition can be illustrated by plotting the magnitude of the resulting forces, which can be split into two parts: an attractive force that increases as ions are drawn closer in response to the attraction between the negative charge of the electron cloud of one ion to the positive charge of another core; and a shorter-range repulsive force that increases strongly when the ion charges pull the atoms close enough to cause interference between inner electron energy levels. The equilibrium position is at the spacing at which the forces are balanced and the resultant force is zero (**Fig. 2**). Inordinately high pressures on nonmetals, which force atoms to be closer together, distort the existing bonds tending to arrange the electrons into a configuration comparable to metals and convert the behavior of the element to metallic properties. Just as with covalent bond materials, the force necessary to displace the atoms a small distance from the equilibrium positions—elastic displacement—is nearly linear. Thus, for compressive, tensile, or torsion stresses of the aggregates of metal atoms, it is found that elastic properties relating stress to strain for small deformations are nearly linear; and consequently, linear elasticity is convenient for solutions of many problems. Actually, fine measurements of deformation in the elastic region generally indicate nonlinear behavior.

Permanent displacement of atoms from each other as occurs in fracture or plastic deformation depends on the relative maximum stress required to pull apart the bonds to the maximum shear stress to translate one part of the solid from one position to another by transferring the bonds to other positions. The nondirectional bonds in a metal are easily switched from one position to another (ductility), whereas with a covalent solid the bonds are parted and only fracture is possible (brittle). The transition metals are dominated by *d*-level electrons, which among many effects, such as properties of magnetism, impart some covalent features to the bond. Although the maximum cleavage stresses are higher than with the noble metals (gold, silver, and copper), the maximum shear stresses for the transitional metals are low enough to allow the crystal to shear and retain continuity before fracture. *See* BRITTLENESS; PLASTIC DEFORMATION OF METAL.

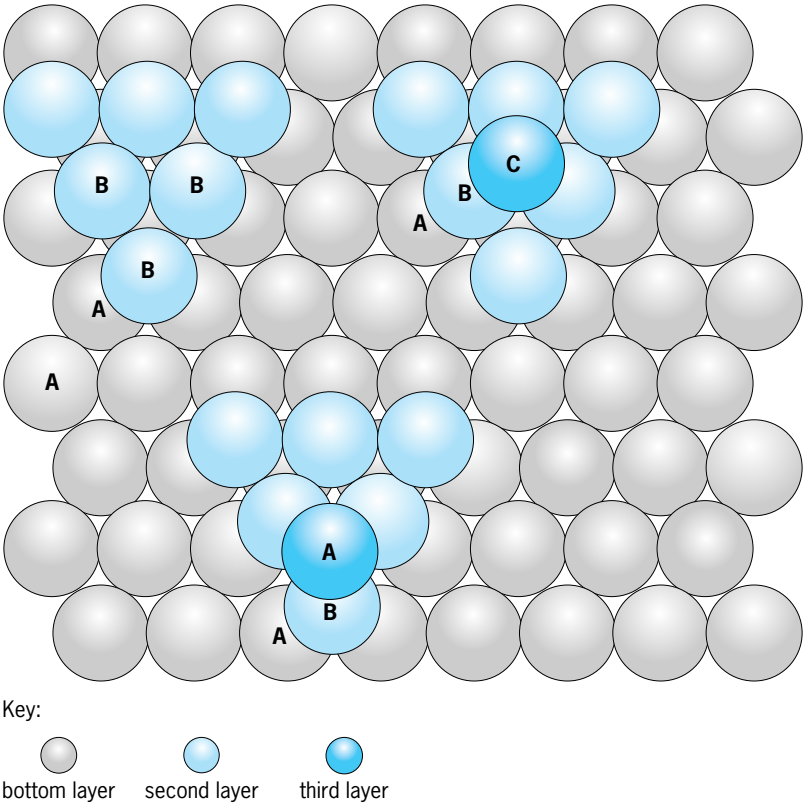

Fig. 3. Sequences of close-packed planes for face-centered-cubic and close-packed-hexagonal. If atoms in the bottom layer are in position A, the second layer is in position B, the third layer can be either in position C or A. If the progression is ABCABC. . . , the structure is face-centered-cubic; if the progression is ABABABAB. . . , the structure is close-packed-hexagonal.

Crystal structure. To visualize groups of atoms in an aggregate, a qualitative geometric model, the atoms are considered as spheres of the same radius (**Fig. 3**). This representation of metal atoms is reasonable, since bonds originating from metal atom cores with the superimposition of the electron charges in the intervening space are manifested by a nearly

spherically symmetrical attraction between the ions. Instructive models of aggregates of these metal atoms are demonstrated by packing equal-size spheres in the densest arrays per unit volume. The two possible close-packed cases are satisfied by either a face-centered-cubic or an ideal close-packed-hexagonal crystal structure. In both of these arrangements each atom is in contact with 12 other atoms, and in the same ratio of 1.633 between alternate close-packed planes divided by the diameter of the atoms. In close-packed-hexagonal structures, this ratio is called the axial ratio, c/a, where *c* is the distance between close-packed planes and *a* is the diameter of the atom in the close-packed plane. Although the density of packing and the number of nearest neighbors are the same, the face-centered cubic structure contains four close-packed planes and three close-packed directions on each plane, whereas a close-packed hexagonal structure contains only one close-packed plane with three directions on that plane.

Among metals, the face-centered-cubic crystalline structure is found in aluminum, nickel, copper, rhodium, palladium, silver, iridium, platinum, gold, and lead. However, no ideal close-packed-hexagonal metals with the same ratio of 1.633 are observed. The distance between the first nearest-neighbor atoms in both crystal structures is the same, but the distance and position of the second nearest atoms are different in the ideal close-packed-hexagonal form from face-centered-cubic structure. The interaction energy associated with the second nearest neighbors in the ideal close-packed hexagonal must be higher than in face-centered-cubic. This higher energy, because of the position of second nearest neighbors, deters a stable formation of an ideal close-packed-hexagonal crystal structure. However, thin layers of close-packed-hexagonal stacking errors found in face-centered-cubic can extend to the surface of the crystal or must end at a dislocation. These planar surface defects are called stacking faults, and they are more frequent if the energy of the stacking fault is not much larger than the energy of normal stacking of the atoms of the particular element (low stacking-fault energy). Similar close-packed-hexagonal layers occur as coherent twin boundaries parallel to close-packed planes.

If the stacking-fault energy of copper is taken as the median, face-centered-cubic metals with low stacking-fault energies include silver, gold, and solid-solution alloys of copper-zinc (brass) and some stainless steels. High stacking-fault pure metals include nickel and aluminum. Also, stacking faults are found in other crystal types such as close-packed-hexagonal.

Because some metals display characteristics of other bonding types, they occur in other crystal structures primarily because of the interference of electrons at energy levels that are not centrally symmetric. All close-packed-hexagonal metals belong to two categories that can be illustrated by packing elongated or compressed spheres (ellipsoids of revolution). The close-packed equatorial circular cross sections constitute a close-packed plane. An ideal hexagonal-close-packed structure illustrates the hexagonal stacking of spheres, whereas spheres compressed in a direction perpendicular to a close-packed plane in the *c* direction have an axial ratio less than the ideal of 1.633; examples are cobalt, rhenium, titanium, gadolinium, hafnium, and beryllium. Finally, if spheres are extended in the *c* direction (prolate ellipsoids with major axis in *c* direction), the axial ratio is greater than the ideal of 1.633; examples are lanthanum, cadmium, and zinc.

Other metals such as iron, titanium, tungsten, molybdenum, niobium, tantalum, potassium, sodium, vanadium, chromium, and zirconium (alkali and transition metals) are slightly less closely packed, with a body-centered-cubic crystal structure that is 8.1% lower in packing density than face-centered-cubic crystals. Furthermore, the equilibrium crystal structure for many metals is dependent upon temperature and pressure. Consequently, a large number of elements are allotropic; that is, the element will appear as different crystal structures at various ranges of pressure-temperature conditions. Included in this group are calcium, titanium, manganese, iron, cobalt, yttrium, zirconium, tin, hafnium, thallium, polonium, thorium, and uranium. *See* CRYSTAL STRUCTURE; CRYSTALLOGRAPHY.

Anisotropy of crystalline materials. In spite of the same bond attraction in all directions for equivalent atoms, when atoms are packed in crystalline structures, physical properties such as electrical conductivity, thermal conductivity, elastic modulus, and coefficient of thermal expansion are unique for different crystallographic directions. The characteristic of distinct properties for crystallographic directions is called anisotropy. It is a result of contrasts in linear densities of atoms in the lattice and the quantum-mechanical constraints on the relative ease of movement of electrons and phonons in specific directions. *See* CRYSTAL; PHONON.

The close-packed planes and close-packed directions are of special interest in crystal nucleation and growth from vapor or liquid, and in the solid. Moreover, most static and dynamic properties of crystalline materials are related to these unique combinations of direction and planes. For example, in plastic deformation one portion of a crystal translates with respect to another on a local portion of a slip plane, producing permanent deformation in a substantial part of the crystal. The permanent plastic deformation is a consequence of the movement of dislocations, usually on the close-packed plane in a close-packed direction.

Defects in metal crystals. Many imperfections of various types in the lattice periodicity are found in metal crystals. Some are produced as a result of growth errors during the formation of solid from the molten liquid or from the vapor states. These defects play a major role in the magnitude of electrical, mechanical, and thermal properties of metals. Defects are classed in four categories: point, line, surface, and volume. Any displacement of a normal lattice atom to an intermediate position because of any strain,

including internal strains as would be generated by lattice defects, increases the energy of the configuration of atoms.

Point defects. Point defects are considered to originate from some small, nearly one-dimensional error inside the crystal, although, at a lattice point, defects produce a three-dimensional short-range strain in the crystal. For a missing atom (vacancy) there is an average inward shift on the surrounding atoms. For a different-size atom that fits in a lattice site (substitutional atom), an inward or outward localized shift depending on the effective size of the foreign atom follows. For regions that are not lattice locations, interstitial atoms of the same element or foreign elements produce strains depending on the relative size of the foreign element and its location in the lattice. Lattice atoms adjacent to the defect rearrange to minimize the resultant increase in energy from the strained lattice by the rebalancing of the altered interaction-force array.

Line defects. A line defect is a linear imperfection extending from a surface, internal or external, to a point on the same surface, another surface, or a dislocation. The significant strain field perpendicular to the line defect extends to about 10 atom distances from the center and along the direction of the dislocation. Although the dislocation is a linear defect, it is seldom a straight line; and the features of its strain field are related to the orientations in the lattice. This line imperfection is a singularity in that it is surrounded by a multiply connected crystal. When one atom-to-atom circuit, away from any strained region, is made around the dislocation, the resultant displacement from the starting atom to the finishing atom can be compared to the equivalent circuit in a perfect crystal. The resultant displacement is the closure failure in a multiply connected crystal. This vector, from the starting atom to the last atom, is defined as the Burgers vector of the dislocation.

Surface defects. Surface defects are boundaries, usually between one crystal and another of the same phase or different phases. This type of imperfection also includes the other surface that surrounds the crystal, twin boundaries, or any other two-dimensional surface that is a consequence of a surface discontinuity to the lattice.

Volume defects. Volume defects can be composed of small groups of foreign atoms with a crystal structure coherent with the surrounding crystal or voids assembled by uniting vacancies or gas atoms. Because of the modification of the lattice spacing, strained zones surround all types of imperfections.

Role of defects. Any defect that disrupts the lattice periodicity interferes with the transfer of wavelike information, such as electromagnetic radiation or elastic waves (phonons), hence disturbing the usual constructive diffraction processes for these quantum-mechanical wavelike particles. Thus, the more defects present in the metal solid, the more obstructions to the flow of fundamental particles, and, for example, the lower the magnitudes of electrical and thermal conductivities by electrons and phonons. Also, more defects in the solid present more obstacles to the movement of dislocations. However, the properties that are directly associated with the strength of the bonds and not the electron flow, such as elastic constants and coefficient of thermal expansion, are affected to a minor degree. *See* CRYSTAL DEFECTS.

Atom movements. Because of the negligible influence of nondirectional bonds to a particular location in the lattice, the small, temporary increase in energy produced during the translation of an atom from one low-energy lattice position to another is due to the localized atom strain during the transfer from one stable lattice site to another in spite of the increase in entropy from the loss in regional periodicity. The energy that must be applied to transfer an atom into a vacant position (diffusion) can be supplied by relatively low thermal activations. The rate of atoms jumping from lattice sites to vacant lattice sites is dependent exponentially on the absolute temperature of the solid. Not only are atom positions easily changed in a metal by thermal activation, but the reduction of strain energy or other metastable energy states also drives atom diffusion (one of the mechanisms in the creep process). *See* CREEP (MATERIALS); DIFFUSION; LATTICE VIBRATIONS.

The most effective method of reducing shear-strain energies in a crystal is shear translation of a portion of a crystal, usually on the slip plane in the slip direction, by action of dislocations. After a dislocation advances, the part of the crystal that is moved on the slip plane is reformed into a perfect lattice by merely translating the portions of the crystal on either side of the plane of the dislocation by one lattice position (Burgers vector). This shear process is affected in a minor way by thermal activation.

Polycrystalline metals. Common metallurgical production methods inevitably lead to solids made up of many small crystals separated by higher-energy boundaries containing non-lattice-positioned arrangement of atoms. The crystals in these polycrystalline metals are called grains, and the boundaries are grain boundaries. Since the grain boundaries interrupt periodicity of the lattice, they have a large effect on many of the physical and mechanical properties. They are origins (sources) and terminators (sinks) to all other defects, especially vacancies, solute atoms, and dislocations.

In an ideal polycrystalline arrangement composed of many randomly oriented grains, the anisotropic features of each grain are averaged; and the resulting metal solid would have isotropic properties. Actually, metal manufacturing processes such as casting and deformation forming (forging, rolling, and so forth) tend to develop grains with specific crystallographic directions distributed about certain directions that are distinctive of the forming process and the geometry of the bulk product. This nonrandom arrangement of grains is called preferred orientation; this contributes to anisotropy of properties in the final polycrystalline product.

Because of the change in crystal orientation across the grain boundary and the nonperiodic atom

distribution in the boundary region, the advancement of dislocations is obstructed. Therefore, grain boundaries increase the stress at which plastic deformation takes place. Furthermore, any process (such as plastic deformation and electrical and thermal conductivity) whose flow rate is impeded by lattice imperfections is decreased a greater amount as the average grain size becomes smaller (area of boundary per unit volume is larger). *See* GRAIN BOUNDARIES.

Metal alloys. An alloy has metallic features and is composed of two or more chemical elements. Macroscopically, it appears homogeneous, but microscopically various thermodynamically stable arrangements of the chemical elements are possible, depending on the characteristics of the components. If the sizes of the unlike, non-compound-forming atoms are about the same or the additional element is small enough to fit between the lattice atoms without creating substantial lattice strain, they will intersperse in the host atom lattice and form a solid solution. However, there will be a difference in the average distance between the atoms because of the slight strains, and the properties of the metal will be altered (conductivities will decrease and the movement of dislocations will be impeded). If the attraction of the species of dissimilar atoms is greater than the attraction of the like atoms, a periodic arrangement of a different atomic assortment called an ordered solid solution can result. If the elements greatly differ electrochemically, giving the bonds a partly ionic characteristic, the unlike atoms will form an intermetallic compound. If unlike elements tend to repel one another, a heterogeneous microstructure of discrete phases that is separated by grain boundaries develops. The phases of an alloy system as a function of temperature, composition, and pressure are clearly shown in equilibrium phase diagrams. These may be considered maps, based on thermodynamic principles, the demonstrate the stable state of the alloy for a given temperature, composition, pressure, and number of components. *See* ALLOY; ALLOY STRUCTURES; INTERMETALLIC COMPOUNDS; METALLOGRAPHY; METALLURGY; PHASE EQUILIBRIUM; SOLID SOLUTION.

Irwin G. Greenfield

Bibliography. C. S. Barrett and T. B. Massalski, *Structure of Metals*, 3d rev. ed., 1980; A. H. Cottrell, *Introduction to the Modern Theory of Metals*, 1988; A. H. Cottrell, *Theoretical Structural Metallurgy*, 1957; A. Kelly and N. H. Macmillan, *Strong Solids*, 1986; C. S. Smith, Materials, *Sci. Amer.*, 217(3):69–79, September 1967; W. A. Tiller, *The Science of Crystallization: Microscopic Interfacial Phenomena*, 1991; L. H. Van Vlack, *Elements of Materials Science and Engineering*, 6th ed., 1989; R. Zallen, *The Physics of Amorphous Solids*, 1983.

Metal, mechanical properties of

Commonly measured properties of metals (such as tensile strength, hardness, fracture toughness, creep, and fatigue strength) associated with the way that metals behave when subjected to various states of stress. The properties are discussed independently of theories of elasticity and plasticity, which refer to the distribution of stress and strain throughout a body subjected to external forces.

Stress states. Stress is defined as the internal resistance, per unit area, of a body subjected to external forces. The forces may be distributed over the surface of a body (surface forces) or may be distributed over the volume (body forces); examples of body forces are gravity, magnetic forces, and centrifugal forces. Forces are generally not uniformly distributed over any cross section of the body upon which they act; a complete description of the state of stress at a point requires the magnitudes and directions of the force intensities on each surface of a vanishingly small body surrounding the point. All forces acting on a point may be resolved into components normal and parallel to faces of the body surrounding the point. When force intensity vectors act perpendicular to the surface of the reference body, they are described as normal stresses. When the force intensity vectors are parallel to the surface, they describe a state of shear stress. Normal stresses are positive, when they act to extend a line (tension). Shear stresses always occur in equal pairs of opposite signs.

A complete description of the state of stress requires knowledge of magnitudes and directions of only three normal stresses, known as principal stresses, acting on reference faces at right angles to each other and constituting the bounding faces of a reference parallelepiped. Three such mutually perpendicular planes may always be found in a body acted upon by both normal and shear forces; along these planes there is no shear stress, but on other planes either shear or shear and tensile forces will exist.

The shear stress is a maximum on a plane bisecting the right angle between the principal planes on which act the largest and smallest (algebraic) principal stresses. The largest normal stress in the body is equal to the greatest principal stress. The magnitude and orientation of the maximum shear stress determine the direction and can control the rate of the inelastic shear processes, such as slip or twinning, which occur in metals. Shear stresses also play a role in crack nucleation and propagation, but the magnitude and direction of the maximum normal stress more often control fracture processes in metals capable only of limited plastic deformation.

It is often useful to characterize stress or strain states under boundary conditions of either plane stress (stresses applied only in the plane of a thin sheet) or plane strain (stresses applied to relatively thick bodies under conditions of zero transverse strain). These two extreme conditions illustrate that strains can occur in the absense of stress in that direction, and vice versa.

Tension and torsion. In simple tension, two of the three principal stresses are reduced to zero, so that there is only one principal stress, and the maximum shear stress in numerically half the maximum normal stress. Because of the symmetry in simple tension,

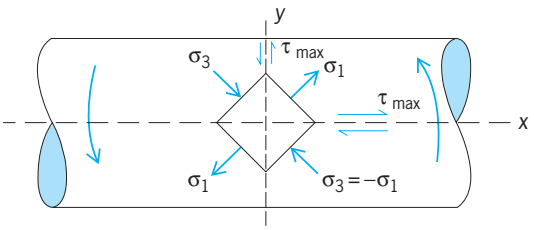

Fig. 1. State of stress in torsion. (*After G. E. Dieter, Mechanical Metallurgy, McGraw-Hill, 1965*)

every plane at 45° to the tensile axis is subjected to the maximum shear stress. For other kinds of loading, the relationship between the maximum shear stress and the principal stresses are obtained using the same method, with the results depending upon the loading condition.

For example, in simple torsion, the maximum principal stress is inclined 45° to the axis of the bar being twisted. The least principal stress (algebraically) is perpendicular to this, at 45° to the bar axis, but equal to and opposite in sign to the first principal stress—that is, it is compressive (**Fig. 1**). Both of these are in a plane perpendicular to the radial direction, the direction of the intermediate principal stress, which in this case has the magnitude zero. Every free external surface of a body is a principal plane on which the principal stress is zero. In torsion, the maximum shear stress occurs on all planes perpendicular to and parallel with the axis of the twisted bar. But because the principal stresses are equal but of opposite sign, the maximum shear stress is numerically equal to the maximum normal stress, instead of to half of it, as in simple tension. This means that in torsion one may expect more ductility (the capacity to deform before fracture) than in tension. Materials that are brittle (exhibiting little capacity for plastic deformation before rupture) in tension may be ductile in torsion. This is because in tension the critical normal stress for fracture may be reached before the critical shear stress for plastic deformation is reached; in torsion, because the maximum shear stress is equal to the maximum normal stress instead of half of it as in tension, the critical shear stress for plastic deformation is reached before the critical maximum normal stress for fracture.

Another important situation arises at the root of a geometrical discontinuity in a loaded body. Such a discontinuity is referred to as a notch. At the root of a notch, immediately beneath but very near the surface, the magnitude of the maximum normal stress may increase to values considerably greater than the applied normal stress; the maximum shear stress, instead of being equal to the maximum normal stress as in torsion, or half of it as in tension, may be a considerably smaller fraction. Also, the critical normal stress for fracture is more easily reached before the critical shear stress for deformation than in torsion and tension, and one may expect notches to have an embrittling effect. This embrittling effect of notches is of very great practical importance and accounts for the majority of service failures in engineering structures. The depth and radius of notches are parameters of overriding importance in determining fracture resistance.

Stress-strain curve. If a metal is strained at a fixed rate, the resistance to deformation increases with straining at a diminishing rate. A plot of the resistance to deformation against the amount of strain is called a stress-strain curve, and the slope of this curve at any point is called the rate of strain hardening. Such a curve is normally obtained by making a tension test and plotting the maximum normal stress against the maximum normal strain. These are identical with the ordinary tensile stress (the tensile force divided by the area of the specimen) and the ordinary tensile strain (the extension per unit of length). The curve produced is known as an engineering stress-strain curve and is widely used to provide design strength information and as an acceptance test for materials. For small strains, the original area and the original gage length may be used without serious error in calculating the stress and strain. Where the strains are large, it is better to use the true average stress, obtained everywhere on the curve by dividing the tensile force by the actual area (which decreases with increasing deformation), and the so-called true strain. The true strain is obtained for every point on the curve by integration of dl/l, between the limits of original length l_o and actual length l, thus taking into account the changing gage length. The true strain is thus the natural logarithm of the ratio of the final length to the original length as expressed in Eq. (1).

$$\int_{l_o}^{l} \frac{dl}{l} = \ln \frac{l}{l_o} \tag{1}$$

The ratio of the final to the original length may be replaced by the ratio of the original area to the final area, because of the constancy of volume in inelastic deformation. True stress-strain curves are more likely to be utilized in circumstances where fundamental information on deformation mechanisms is desired.

For single-phase metals which have not suffered any prior permanent deformation, the stress-strain curve in simple compression is usually nearly identical with the stress-strain curve in simple tension. This is not true, however, for two-phase materials where the second phase is present as dispersed hard particles, nor is it true for materials within which occur residual stresses resulting from, for example, nonuniform thermal contraction from the processing temperature to the test temperature in the coexisting phases. For other states of stress, additional complications arise. In torsion, for instance, the maximum normal stress reaches a value, at corresponding strains, of less than 60% of the value reached in simple tension. A more generally applicable stress-strain relationship is obtained by plotting the von Mises function of the three principal stresses σ_1, σ_2, and σ_3 (the effective stress $\overline{\sigma}$), as in Eq. (2), against an

$$\overline{\sigma} = [{}^1/_2(\sigma_1 - \sigma_2)^2 + (\sigma_2 - \sigma_3)^2 + (\sigma_3 - \sigma_1)^2]^{1/2} \tag{2}$$

easily derivable function of the three principal strains that may be called the effective strain $\bar{\epsilon}$, given in Eq. (3), where $\bar{\epsilon}$ is the effective strain and ϵ_1, ϵ_2, and

$$\bar{\epsilon} = [^2/_3(\epsilon_1^2 + \epsilon_2^2 + \epsilon_3^2)]^{1/2} \quad (3)$$

ϵ_3 are the principal strains. Both the effective stress and the effective strain reduce to the ordinary tensile stress and tensile strain for simple tension testing, so that the tensile stress-strain curve without change in units may be used as the effective stress-strain curve.

Unless some microstructural change occurs in the metal during straining, such as recrystallization or precipitation of a second phase, the effective stress-strain curve usually is describable by the power function $\bar{\sigma} = k\bar{\epsilon}^n$, where k is the effective stress required to produce unit effective strain, and n is an exponent that is always less than unity and commonly has a value between 0.1 and 0.4. The exponent n is called the strain-hardening index because differentiation of $\bar{\sigma} = k\bar{\epsilon}^n$ to find the rate of strain hardening $d\bar{\sigma}/d\bar{\epsilon}$ yields for this expression $n(\bar{\sigma}/\bar{\epsilon})$, so that the slope of the stress-strain curve (the strain-hardening rate) is proportional to n as well as to the ratio of the coordinates of the point on the curve. Higher values of n are associated with annealed pure metals and annealed single-phase alloys; lower values of n are associated with heat-treated alloys such as quenched and tempered steels.

Modern theory makes use of line imperfections (dislocations) to explain the low resistance to initial plastic deformation of annealed metal crystals and polycrystalline aggregates, as well as strain hardening and viscous effects. Imperfection-free crystals deform only elastically and fracture at very high stress levels. This has been demonstrated with metal whiskers of high purity and of extremely small diameter. Larger crystals invariably contain dislocations which move through the crystal lattice at low stress levels, but pile up at barriers such as hard particles or surfaces of contact with other crystals (grain boundaries). The dislocations are surrounded by stress fields which interact with each other, and strain hardening is ascribed to interactions between dislocations moving on different slip systems as well as interactions with other barriers. Viscous effects are associated with the rate at which line imperfections can break loose from their obstacles, usually other line imperfections, with the help of thermal motion. *See* CRYSTAL STRUCTURE; ELASTICITY; PLASTIC DEFORMATION OF METAL; STRESS AND STRAIN.

Tension test. To achieve uniformity of distribution of stress and strain in a tension test requires that the specimen be subjected to no bending moment. This is usually accomplished by providing flexible connections at each end through which the force is applied. The specimen is stretched at a controllable rate, and the force required to deform it is observed with an appropriate dynamometer. The strain is measured by observing the extension between gage marks adequately remote from the ends, or by measuring the diameter and calculating the change in length by using the constancy of volume that characterizes plastic deformation. Diameter measurements are applicable even after necking-down has begun. The elastic properties are seldom determined since these are structure-insensitive. Special refinements are necessary when the elastic stress-strain relationships are in question because the strains are very small and because elastic deformation is not characterized by constancy of volume.

Yield strength. The elastic limit is rarely determined. Metals are seldom if ever ideally elastic, and the value obtained for the elastic limit depends on the sensitivity of strain measurement. The proportional limit, describing the limit of applicability of Hooke's law of linear dependence of stress on strain, is similarly difficult to determine. Modern practice is to determine the stress required to produce a prescribed inelastic strain, which is called the yield strength. The amount of strain used to define the yield strength varies with the application, but is most commonly taken as 0.2% (a unit strain of 0.002 in./in.; 1 in. = 25 mm). Because upon unloading the behavior is almost linearly elastic, it is possible to use the offset method of determining the yield strength from a plotted stress-strain curve; a line with a slope equal to the elastic slope is drawn, displaced from the stress-strain curve at low stress levels by the amount of strain used in the definition of the yield strength, and the stress at the intersection of this line with the stress-strain curve is taken as the yield strength (**Fig. 2**). The elastic slope will not be equal to Young's modulus unless an exceedingly stiff tensile machine is employed or strain gages are attached to the specimen.

The stress-strain curve obtained at room temperature is not appreciably affected by changes in the rate of straining in ordinary tensile tests. At higher temperatures, however, strain rate effects are much more important. A general relation between flow stress and strain rate $\dot{\epsilon}$, at constant temperature and strain, is shown in Eq. (4), where m is the strain-rate

$$\sigma = C\dot{\epsilon}^m \quad (4)$$

sensitivity. For most metals, m increases with both test temperature and strain.

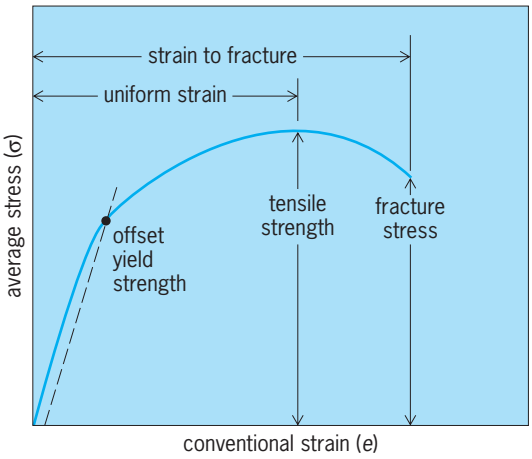

Fig. 2. Engineering stress-strain curve. (*After G. E. Dieter, Mechanical Metallurgy, McGraw-Hill, 1965*)

Test temperature at constant strain rate has a very important influence on yield strength. For most metals, strength increases and ductility decreases with decreasing temperature. For face-centered cubic metals such as copper, nickel, and silver, these effects are small, but for iron, steels, and other body-centered cubic metals and alloys, increases in strength of up to 800% can occur between room temperature and −321°F (77 K). Ductility also may change rapidly in this range. The temperature dependence of yielding in many metals below room temperature may be influenced by impurities or intentional alloying elements.

Changes in strength with temperature will occur also when microstructural changes such as precipitation, strain aging (clustering of solute atoms around dislocations), or recrystallization occur. Extended exposure at elevated temperatures may cause creep, as discussed in a later section of this article.

The stress-strain properties of metals also may be altered drastically by changes in grain (crystal) size. A linear relation is observed for most metals between yield stress σ_y and the reciprocal square root of grain size $d^{-1/2}$, as given by Eq. (5), where σ_o is

$$\sigma_y = \sigma_o + k_y d^{-1/2} \tag{5}$$

a measure of the stress to plastically deform a single crystal, while k_y is a parameter which reflects the ease of propagating slip from one grain to another. For metals in which slip is transmitted with difficulty across grain boundaries (for example, hexagonal close-packed metals such as zinc, cadmium, magnesium, and certain face-centered cubic alloys), k_y is relatively large. However, for pure face-centered cubic or body-centered cubic metals, k_y is a small number. Both σ_o and k_y tend to increase with decreasing temperature. Thus grain boundary strengthening is particularly effective in metals such as zinc, cadmium, and magnesium at low test temperatures.

Tensile strength. Tensile strength, usually called the ultimate tensile strength, is calculated by dividing the maximum load by the original cross-sectional area of the specimen. It is, therefore, not the maximum value of the true tensile stress, which increases continuously to fracture and which is always higher than the nominal tensile stress because the area continuously diminishes. For ductile materials the maximum load, upon which the tensile strength is based, is the load at which necking-down begins. Beyond this point, the true tensile stress continues to increase, but the force on the specimen diminishes. This is because the rate of strain hardening has fallen to a value less than the rate at which the stress is increasing because of the diminution of area. If at any time during the extension of a specimen the force required to extend it diminishes, the strain will become localized. The condition for necking-down is therefore that the force go through a maximum; that is, $\partial F/\partial l$ (the partial derivative of the force with respect to extension) goes through zero. When force and length are expressed as functions of stress and strain, it is easy to show that this condition is satisfied when the true rate of strain hardening falls to a value numerically equal to the stress; that is, $\partial\sigma/\partial\epsilon = \sigma$. For the stress-strain relationship used above, $\overline{\sigma} = k\overline{\epsilon}^n$, this slope is reached when $\epsilon = n$. Necking-down, therefore, will occur when the tensile strain reaches a value equal to n (usually between 10 and 40% extension), and the tensile strength for a ductile material has nothing to do with fracture. It describes only the stress required to produce the tensile instability evidenced by necking-down. For a relatively brittle material, one which fractures before the strain reaches the necking-down value, the tensile strength reflects the fracture strength, but again is not equal to it.

Yield point. A considerable number of alloys, including those of iron, molybdenum, tungsten, cadmium, zinc, and copper, exhibit a sharp transition between elastic and plastic flow. The stress at which this occurs is known as the upper yield point. A sharp drop in load to the lower yield point accompanies yielding, followed, in ideal circumstances, by a flat region of yield elongation; subsequently, normal strain hardening is observed (**Fig. 3**). In the case of polycrystalline mild steels as well as concentrated solid solutions of some single-crystal alloys, the yield elongation marks a period in which strain occurs by the movement of a plastic strain wave along the specimen length. The force on the specimen remains constant during the advance of this strain wave because plastic strain occurs only at the advancing edge of the wave. The wave front is visible on the specimen surface because of surface relief; the markings are known as Lüder's bands. When the strain wave has completely traversed the specimen, the extension of the entire specimen is identical to that achieved at the wave front.

Straining of metals beyond the yield point causes the latter to disappear upon subsequent unloading and restraining. However, annealing at an appropriate low temperature causes the yield point to return. This observation has led to the conclusion that yield points in metal single crystals and polycrystals are associated with the locking of dislocations by interstitial or substitutional impurities. Yielding occurs

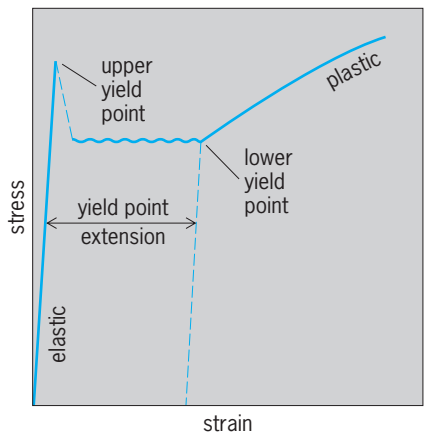

Fig. 3. Yield point of mild steel.

by a process of tearing away dislocations from their impurity "atmospheres," resulting in a sharp drop in load. Annealing of the crystal allows impurities to migrate back to dislocations so that the process may be repeated. It should be noted that other mechanisms for a sharp yield point have been identified as being applicable to metal whiskers and to nonmetallic crystals.

Elongation. The tensile test provides a measure of ductility, by which is meant the capacity to deform by extension. The elongation to the point of necking-down is called the uniform strain or elongation because, until that point on the stress-strain curve, the elongation is uniformly distributed along the gage length (Fig. 2). The strain to fracture or total elongation includes the extension accompanying local necking. Since the necking extension is a fixed amount, independent of gage length, it is obvious that the total elongation will depend upon the gage length, and will be greater for short gage lengths and less for long gage lengths. The American standard ratio of gage length to diameter for a cylindrical test specimen is 2:0.505 [the standard bar has a 2-in. (5-cm) gage length with a diameter of 0.505 in. (1.28 cm) corresponding to an area of 0.2 $in.^2$ (1.3 cm^2)]. Specimen configurations have been compiled also for sheet, plate, tube, and wire specimens by the American Society for Testing and Materials. Absolute size does not affect the distribution of deformation. The shape of the cross section has no effect up to ratios of width to thickness of 5:1; rectangular cross sections elongate the same amount as circular cross sections of the same area. The reduction of area at the point of fracture, expressed usually as percentage reduction of area, is independent of gage length, and from it can be calculated the true strain at fracture; this makes the tensile reduction of area a more satisfactory measure of ductility than elongation unless one is interested in the amount that a metal will stretch before it begins to neck down. The reduction of area in the tensile test correlates well with measure of ductility obtained in other ways, such as the strain to fracture on the outside of a bend, provided the strain gradient is not too great, such as in notched-bar testing.

Ductile-to-brittle transition. Many metals and alloys, including iron, zinc, molybdenum, tungsten, chromium, and structural steels, exhibit a transition temperature, below which the metal is brittle and above which it is ductile. The form of the transition for polycrystalline iron and several iron-cobalt alloys is shown in **Fig. 4**. The transition temperature very clearly is sensitive to alloy content, but it will vary even for the same material, depending upon such external test conditions as stress state and strain rate, and microstructural variables such as purity and grain size. The ductility transition frequently is accompanied by a change in the mechanism of fracture (as in iron and steels or zinc), but this need not be so. In general, face-centered-cubic (fcc) materials do not exhibit a ductility transition. Among high-purity body-centered cubic (bcc) metals, the group vanadium, niobium, and tantalum in the periodic table normally are ductile to quite low temperatures; similarly, pure hexagonal close-packed (hcp) titanium and zirconium do not exhibit a ductility transition. However, the presence of interstitial impurities or certain substitutional alloying elements may produce a ductile-to-brittle transition in all of these metals. Moreover, it should be noted that ductile-to-brittle transitions can be induced even in fcc metals by testing in certain aggressive surface environments (for example, alpha brass in mercury) or by adding appropriate small impurities (for example, antimony in copper).

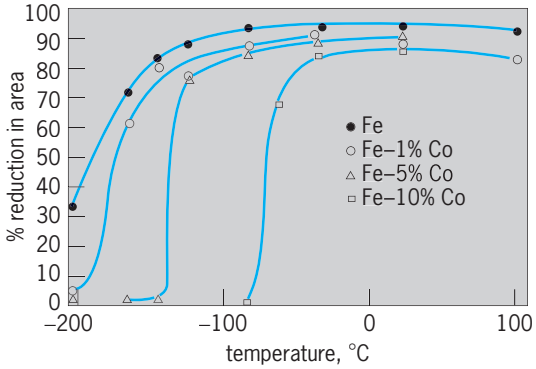

Fig. 4. Ductile-to-brittle transition, iron-cobalt alloys. °F = (°C × 1.8) + 32. (*After N. S. Stoloff, R. G. Davies, and R. C. Ku, Low temperature yielding and fracture in Fe-Co and Fe-V alloys, Trans. Metallurg. Soc. AIME, 233:1500–1508, 1965*)

The transition temperature is different for differing states of stress because the ratio of the maximum shear stress to the maximum normal stress is different. The transition temperature is elevated by the presence of a severe notch and is depressed by testing in torsion. In the case of steels, transition temperatures may vary from near −423°F (20 K) for unnotched low-carbon grades to near −9°F (250 K) in structures which contain defects such as weld cracks or geometrical stress raisers. All large structures contain such defects, and the relationship between defect sizes and fracture stresses or energies embodies the concept of fracture mechanics (see below). There is also a size effect in steels resulting from inhomogeneities in microstructure or coarser grain sizes resulting from slower cooling rates in large structures. Consequently, thick steel plates are characterized by high transition temperatures.

Among the factors which decrease the transition temperature of metals, the following are of general importance to all susceptible metals: (1) increased purity, particularly for bcc metals in the case of interstitial elements (C, O, N, H) and elements which segregate preferentially at grain boundaries (Sb, P, Sn); (2) reduced grain size; (3) reduced strain rate; (4) introduction of very small (diameter of 100 nanometers), hard particles.

In addition, alloying elements in solid solution may be utilized to reduce the transition temperature. Nickel and manganese often are added to steels to improve low-temperature toughness (although manganese is effective only in steels containing relatively

large amounts of carbon). Similarly, lithium lowers the transition temperature of magnesium, and rhenium (a transition metal of the platinum group) improves low-temperature ductility of chromium and tungsten.

Notch tensile test. Notch sensitivity in metals cannot be detected by the ordinary tension test on smooth bar specimens. Either a notched sample may be used in a tension test or a notched-bar impact test may be conducted. The notch in a tensile bar is characterized by the sharpness $d/2r$ and the depth, defined as $1 - d^2/D^2$, where d is the diameter at the root of the notch, D is the original diameter, and r is the notch root radius. Notches produce triaxial stresses under the notch root as tensile forces are applied, thereby decreasing the ratio of shear stress to normal stress and increasing the likelihood of fracture.

Materials are evaluated by a quantity, notch strength, which is the analog of the ultimate tensile strength in an ordinary tensile test. The notch strength is defined as the maximum load divided by the original cross-sectional area at the notch root. For cylindrical bars, a notch ductility also may be defined as in Eq. (6), where $A_{o(n)}$ = original cross-sectional

$$q_n = \frac{A_{o(n)} - A_{f(n)}}{A_{o(n)}} \tag{6}$$

area at notch and $A_{o(f)}$ = cross-sectional area at notch after fracture. This quantity is often very small and is difficult to measure accurately. The ratio of notch tensile strength to ultimate tensile strength is called the notch sensitivity ratio (NSR). If the NSR is less than 1, the material is considered to be notch-sensitive. The notch sensitivity of steels generally increases with increasing tensile strength.

Sharp-notch tension testing is applicable not only to ordinary cylindrical tensile bars but to high-strength sheet materials as well. The method provides a comparative measure of the resistance of sheet materials to unstable fracture resulting from the presence of cracklike defects, and may be utilized in research and development of metals to study effects of composition, processing, and heat treatment. The method also permits comparative evaluation of crack propagation resistance of a number of materials under consideration for a particular application.

Compression test. Very brittle metals, or metals to be utilized in products which are to be formed by compressive loading (rolling, forging), often are tested in compression to obtain yield strength or yield point information. Compression test specimens are generally in the form of solid circular cylinders. The ratio of specimen length to diameter is critical in that high ratios increase the likelihood of buckling during a test, thereby invalidating the test results. Proper specimen alignment is important for the same reason. In addition, care must be taken to lubricate specimen ends to avoid spurious effects from friction between the specimen ends and the testing machine. In the case of a metal which fails in compression by a shattering fracture (for example, cast iron), a quantity known as the compressive strength may be reproducibly obtained by dividing the maximum load carried by the specimen by its cross-sectional area. For materials which do not fail in compression by shattering, the compressive strength is arbitrarily defined as the maximum load at or prior to a specified compressive deformation.

Notched-bar impact testing. Notched-bar impact tests are conducted to estimate the resistance to fracture of structures which may contain defects. The common procedure is to measure the work required to break a standardized specimen, and to express the results in work units, such as foot-pounds or newton-meters. The notched-bar impact test does not provide design information regarding the resistance of a material to crack propagation. Rather, it is a comparative test, useful for preliminary screening of materials or evaluation of processing variables. The notch behavior indicated in a single test applies only to the specimen size, notch geometry, and test conditions involved and is not generally applicable to other specimen sizes and conditions. The test is most useful when conducted over a range of temperatures so that the ductile-to-brittle transition can be determined. In some materials, notably pure polycrystalline bcc metals, there is an abrupt change in energy absorbed with temperature, the curve being similar in shape to that for the change in ductility with test temperature shown in Fig. 4, and an unambiguous transition temperature may be defined.

However, most structural alloys, including steels, exhibit a gradual decrease in impact energy absorption with decreasing temperature, so that arbitrary definitions of transition temperature, based upon a fixed energy level, a fixed contraction at the root of the notch, and average energy, or a change in fracture appearance must be devised. In the case of face-centered cubic metals, there is little change in energy absorption and no change in fracture mechanism with temperature, and no transition can be defined.

Notched-bar tests are usually made in either a simple beam (Charpy) or a cantilever beam (Izod) apparatus, in both of which the specimen is broken by a freely swinging pendulum; the work done is obtained by comparing the position of the pendulum before it is released with the position to which it swings after striking and breaking the specimen (**Fig. 5**). In the Izod test (**Fig. 6***a*), the specimen is held in a vise, with the notch at the level of the top of the vise, and broken as a cantilever beam in bending with the notch on the tension side. In the Charpy test (Fig. 6*b*), the specimen is laid loosely on a support in the path of the pendulum and broken as a beam loaded at three points; the tup (striking edge) strikes the middle of the specimen, with the notch opposite the tup, that is, on the tension side. Both tests give substantially the same result with the same specimen unless the material is very ductile, a situation in which there is little interest.

Specimen geometry and test conditions. The choice of specimen depends to some degree upon the nature of the material; therefore several specimen types

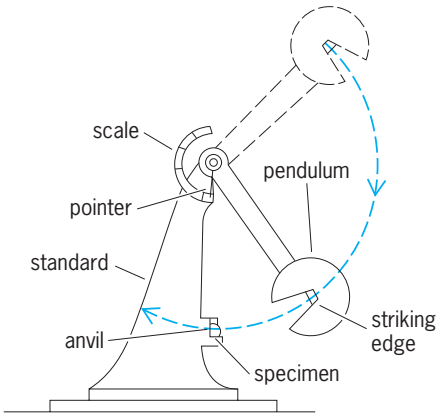

Fig. 5. Diagram of Charpy impact machine.

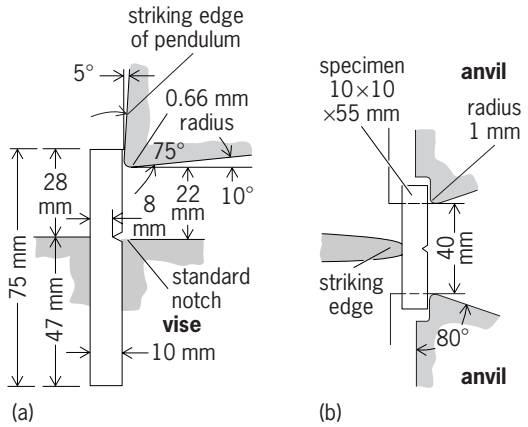

Fig. 6. Mounting of notched-bar test specimens. 1 mm = 0.04 in. (*a*) Izod test. (*b*) Charpy test.

are recognized. Sharp, deep notches are generally required to compare properties of more ductile materials. Typical Charpy bars (Fig. 6*b*) are 0.394 in. (10 mm) square by 2.165 in. (55 mm) long, with either a 45° V notch, or a parallel-sided notch ending in a 0.079-in.-diameter (2-mm) hole (keyhole notch). Keyhole notches usually provide a more abrupt transition at lower temperatures than do V notches, as shown in **Fig. 7**. Notches may also be made with a milling cutter, resulting in a 0.079-in.-wide (2-mm) U-shaped notch. Izod specimens typically are 0.39 in. (10 mm) square by 3.0 in. (75 mm) long, with a 45° V notch 1.102 in. (28 mm) from one end. The transition temperature for a given steel will be different for different tests and specimen geometries.

When testing at temperatures other than room temperature, the Charpy three-point loading arrangement is more convenient than the Izod configuration, in which the specimen is clamped in a vise. It has been established that the temperature of the specimen will not change significantly at the root of the notch for several seconds, so that the specimen may be brought to temperature in a controlled temperature bath and transferred to the testing machine for breaking.

The V-notch transition temperature correlates fairly directly with practical defects in structures, on the basis that brittle fractures in service are seldom observed when a specimen exhibits some minimum level of energy absorbed in the V-notch test. The number of foot-pounds that are needed to ensure freedom from brittle fracture in a structure depends on the material being tested, for the resistance to deformation as well as the ductility enters into the work required to break the specimens, along with the distribution of deformation, which varies from one material to another. For this reason the impact test cannot provide design data.

As in all tests involving brittle behavior, because brittle fracture is concerned with properties in a small region rather than the average throughout a large volume, considerable statistical variation is to be expected in notched-bar testing. Therefore, enough tests must be made to obtain a reliable result by statistical standards, especially when testing in the vicinity of the transition temperature.

Hardness testing. Tension testing provides a complete description of the relationship between stress and strain in plastic deformation, some useful information about ductility, and—in conjunction with the Griffith theory, which relates fracture stress to defect size in an elastically strained body—some information about the resistance to crack propagation under conditions in which the metal is embrittled by the presence of a notch or crack. Often these methods of testing are more time-consuming and more expensive than is necessary, in particular when the only information that is needed is the comparison of the resistance to deformation of a particular sample or lot with a standard material. For such purposes, indentation hardness tests are used. They are relatively inexpensive and fast. They tell nothing about ductility and little about the relationship between stress and strain, for in making the indent the stress and strain are nonuniformly distributed.

In all hardness tests, a standardized load is applied to a standardized indenter, and the dimensions of the indent are measured. This applies to such methods as scratch hardness testing, in which a loaded diamond is dragged across a surface to produce, by plastic deformation, a furrow whose width is measured, and the scleroscope hardness test, in which

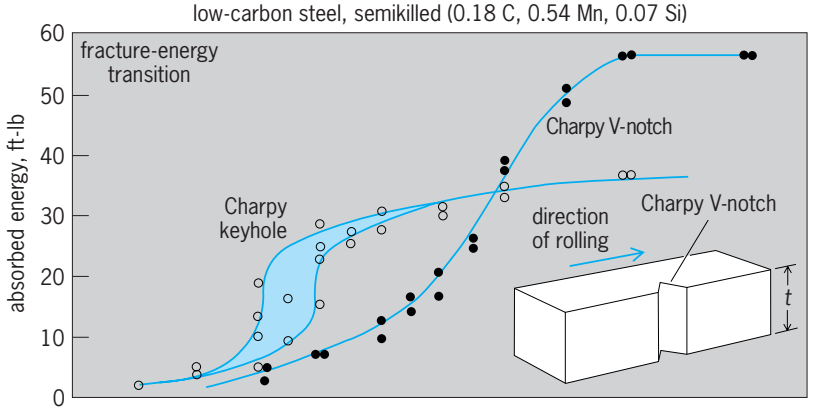

Fig. 7. Fracture energy transition for Charpy keyhole and V notch, showing a more abrupt transition for the keyhole notch. 1 ft-lb = 1.36 J. (*After American Society for Metals, Metals Handbook, vol. 10, 8th ed., 1975*)

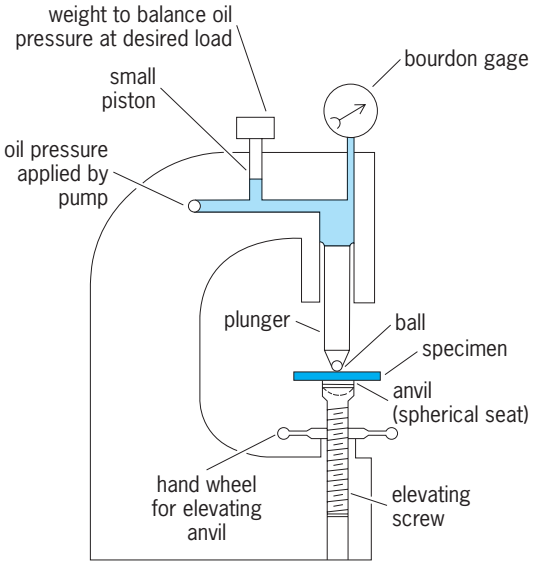

Fig. 8. Features of hydraulic-type Brinell machine.

an indent is produced by dropping a mass with a spherical tup onto a surface. The dimensions of the indent are proportional to the work done in producing it, and the ratio of the height of rebound to the height from which the tup was dropped serves as an indirect measure of the hardness.

Test methods. In the Brinell hardness test, a hardened steel ball is forced into a surface by a force appropriate to the hardness of the material being tested, for a standard time, usually 30 s (**Fig. 8**). With steel and other hard materials, a 6600-lb (3000-kg) force is applied to a 0.394-in.-diameter (10-mm) steel or tungsten carbide ball; with softer alloys a 1100-lb (500-kg) load is often employed. In every instance, the diameter of the indentation crater is kept between one-fourth and one-half the diameter of the ball. The Brinell hardness number (BHN) is defined, in Eq. (7),

$$\text{BHN} = \frac{2P}{\pi D[D - (D^2 - d^2)]^{1/2}} \tag{7}$$

as the force applied divided by the area of contact between the ball and the test piece after the ball has been removed, where P = applied load, kg; D = diameter of ball, mm; and d = diameter of indentation, mm. The units of Brinell hardness are kg/mm^2. The surface on which the impression is made should be relatively smooth and free from scale or dirt. The Brinell number will vary with applied load and ball diameter. In order to obtain a constant hardness number, it is necessary to keep d/D = constant; this can be approximated when P/D^2 is maintained constant.

The Meyer hardness number is defined as the force applied divided by the area of the indent projected onto the plane of the original surface of the test piece. This number, just as useful as the Brinell hardness number, is easier to calculate but has not replaced the standard Brinell hardness number, the calculation of which is everywhere facilitated by easily available tables. The Meyer hardness is less sensitive to load than is the Brinell hardness. A Meyer analysis of the Brinell test is carried out by plotting the logarithm of the applied force against the logarithm of the diameter of the indent. This plot is linear and thereby demonstrates the validity of the relationship $F = ad^n$, where F is the force and a and n are the Meyer constants. Meyer's a is the intercept of the line at unit diameter (1 mm, normally), and Meyer's n is the slope of the logarithmic plot; it reflects the strain-hardening characteristics of the metal, provided that a minimum load level is applied.

The indentation hardness number is independent of the force applied to the indenter when a conical or pyramidal indenter is used. A durable diamond indenter is used in the Vickers penetration hardness testing method. It is a square-base diamond pyramid with a dihedral angle between opposite faces of 138°. This is the contact angle in the Brinell test when the indent is three-eighths of the ball diameter, in the middle of the range of indent sizes used in that test. This choice of angle yields hardness numbers in the Vickers penetration test about the same as those obtained in the Brinell test, with the advantage that the hardness number is independent of the load used down to quite small loads and quite small indents. The diamond pyramid hardness number (DPH) or Vickers hardness number (VHN) is defined as the applied load divided by the surface area of the impression; loads typically range from 2.2 to 260 lb (1 to 120 kg) depending upon the hardness of the material under investigation. The length of diagonals of the impression are determined by microscopic measurement, and the DPH is determined from Eq. (8),

$$\text{DPH} = \frac{1.854P}{L^2} \tag{8}$$

where P is measured in kg and L is the average length of diagonals in mm. In practice, the DPH is read from a chart once the diagonals are known. The Vickers test is widely accepted for research applications because a continuous scale of hardness from 5 DPH for very soft metals to 1000 DPH for very hard metals is achieved. Below loads of about 0.88 oz (25 g), departures are observed. The Knoop hardness test is a modification using a diamond pyramid whose base is a rhombus, the diagonals of which are in the ratio of 7:1. The plastic deformation produced by this indenter is nearly plane strain, which can be accomplished in brittle materials without fracture in the adjoining regions under tensile stress, whereas cracks are produced by the nonplane strain produced by symmetrical indenters. Low loads are applied (under 2.2 lb or 1 kg) and, since surface impressions are about one-half the depth of those for Vickers tests under the same load, the test is particularly suitable for analysis of surface layer properties. For the same reason, it is necessary to prepare surface layers much more carefully in the case of Knoop hardness than for tests involving heavier loads.

Rockwell hardness. The most popular hardness test is the Rockwell test, which is carried out quite rapidly in a convenient machine by sacrificing any attempt to express the hardness as a resistance to deformation

in units of force per area. An indenter chosen from two shapes and various sizes is forced into the test-piece surface, first by a minor load, under which the position of the indentor is established as a reference point, and then by a major load which deepens the indent. Upon removing the major load and leaving the minor load applied, the amount by which the indent has been deepened is established. The hardness number is simply the amount of deepening on a linear scale, with the scale reversed so that soft materials having deeper indents are characterized by smaller numbers. The two shapes of indenters are steel spheres of various diameters, for which the starting point on the linear scale for zero deepening is 130; and a conical diamond with a spherical tip for which the starting point on the scale is 100. The hardness number is the number read from the dial gage indicating the depth of the indent on this reversed scale; it must be accompanied by a letter indicating the kind of indenter and load used. For example, for a load of 220 lb (100 kg) applied to a spherical steel indenter of $^1/_{16}$-in. (0.16-cm) diameter, the letter B is used, so that a hardness number might be Rockwell B80; for the diamond indenter and a load of 330 lb (150 kg), the letter C is used, so that a typical hardness number would be Rockwell C55. Tables are available to convert hardness data for steels from one Rockwell scale to another, and to other hardness scales or to tensile strength. *See* HARDNESS SCALES.

Fatigue. Fatigue is a process involving cumulative damage to a material from repeated stress (or strain) applications (cycles), none of which exceed the ultimate tensile strength. The number of cycles required to produce failure decreases as the stress or strain level per cycle is increased. When cyclic stresses are applied, the results are expressed in the form of an *S-N* curve in which stress of logarithm of stress is plotted against the number of cycles to cause failure. The fatigue strength or fatigue limit is defined as the stress amplitude which will cause failure in a specified number of cycles, usually 10^7 cycles. For a few metals, notably steels and titanium alloys, an endurance limit exists, below which it is not possible to produce fatigue failures no matter how often stresses are applied.

It is often desirable to impose fixed cyclic strains on a material, rather than fixed stresses. Under these circumstances, fatigue data are plotted as logarithm of plastic strain per cycle, $\Delta\epsilon_p$, versus logarithm of cycles to failure, N_f. Most engineering metals exhibit a linear dependence of $\Delta\epsilon_p$ on N_f, known as the Coffin-Manson relationship, shown in Eq. (9), where

$$\frac{\Delta\epsilon_p}{2} = \epsilon_f' N_f^{\alpha} \tag{9}$$

ϵ_f' is a material constant known as the fatigue ductility coefficient, and σ is a constant which for most metals tested at room temperature in air is near -0.5; ϵ_f' typically approximates the ductility of the material in monotonic tension, indicating that fatigue life increases with ductility of the material. Equation (9) is obeyed best at lives shorter than 10^4 cycles, the so-called low-cycle fatigue range, as shown for a compilation of several metals tested at a variety of temperatures in **Fig. 9**.

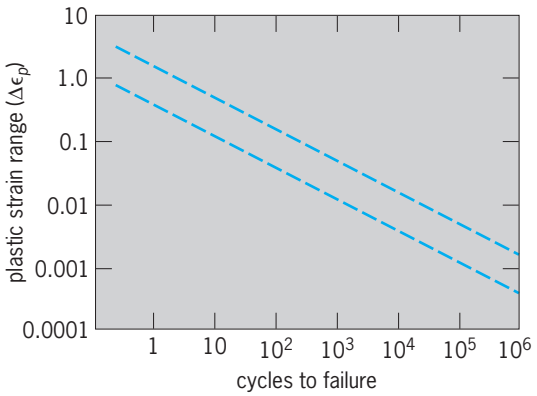

Fig. 9. Low-cycle fatigue data for several alloys. A single band incorporates all data for 11 metals at a variety of test temperatures and test atmospheres. (*After L. F. Coffin, The effect of high vacuum on the low cycle fatigue law, Metallurg. Trans., 3:1777–1788, 1972*)

Fatigue testing in stress control is frequently done with a mean stress of zero, although mean positive stresses are not uncommon. A stress that varies sinusoidally with time is commonly applied, sometimes in direct tension and compression but more usually in bending by utilizing a sample of circular cross section rotated under a constant bending moment. Other waveforms also may be used in tension-compression, most notably triangular or square waves, usually for specialized research applications.

Test frequency is not an important variable at ordinary temperatures, but may assume overriding importance at temperatures sufficiently elevated to permit the introduction of cyclic creep or surface oxidation. Under either of the latter circumstances, low-frequency tests result in shorter lives for the same applied loads. Mean stress superposed upon cyclic stresses can have significant effects, particularly in steel and other alloys sensitive to brittle fracture under tensile loading. In this situation, life decreases as R, the ratio of minimum to maximum cyclic stress, is increased.

Cracks may form very early in a fatigue test, and then grow exceedingly slowly, or, alternatively, crack nucleation may be delayed until very near the total number of cycles to failure. Cracks invariably initiate at surface or near-surface origins such as slip bands, inclusion or precipitate particles, scratches, notches, or other stress raisers, or at material defects such as casting pores. Slip-band cracking is particularly prevalent in pure metals, and under such circumstances the nature of the slip process is a critical factor in determining fatigue life. The greater the multiplicity of active slip systems, the easier it is to initiate a crack; on the other hand, the predominance of one slip system, as in suitably oriented single crystals of zinc and other hcp metals, renders crack nucleation so difficult that it is sometimes impossible to achieve fatigue cracking at all.

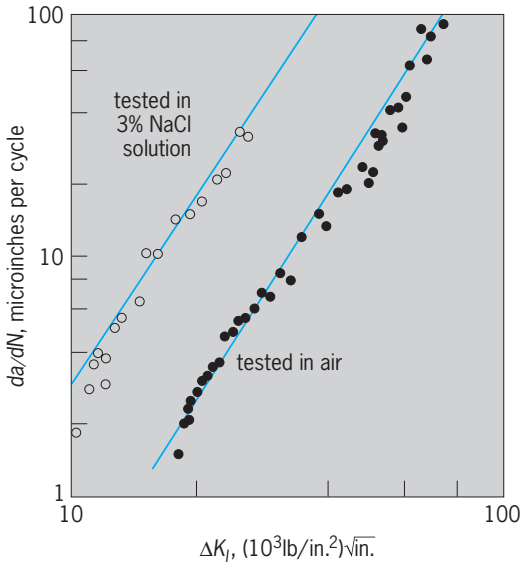

Fig. 10. Crack growth rate of 4340 steel in air and in 3% NaCl. (*After American Society for Metals, Metals Handbook, redrawn from Imhof and Barsom, vol. 10, 8th ed., 1975*)

Crack propagation occurs at a rate da/dN (crack extension per cycle) which depends upon the change in stress intensity K (stress × square root of crack length) per cycle raised to a power m, as expressed in Eq. (10), where C and m are constants

$$\frac{da}{dN} = C(\Delta K)^m \tag{10}$$

that depend upon material and mean stress as well as environment (**Fig. 10**). The value of m has been observed to average near 4 for a wide variety of metals. The fatigue crack continues to grow until the remaining cross-sectional area is insufficient to support the peak stress, fracture then occurring in a single cycle by overload. The appearance of the fracture surface in the fatigue and overload zones differs considerably for ductile materials in that parallel bands known as fatigue striations often occur perpendicular to the direction of fatigue crack propagation. The overload region contains no striations and, for ductile metals, generally comprises microvoids centered about inclusion or precipitate particles. Each striation marks the position of the fatigue crack at the end of a cycle, and the distance between striations serves as a useful measure of crack growth rate. Usually, however, these must be supplemented by microscopic observations of the crack profile with time in order for crack propagation relations such as that of Eq. (10) to be obtained. This is particularly true in materials where striations are not always well developed, such as structural steels and other high-strength alloys with complex microstructures.

Notches may significantly lower fatigue life, particularly in stronger, less ductile alloys. The notch sensitivity factor q in fatigue is given by Eq. (11),

$$q = \frac{K_f - 1}{K_t - 1} \tag{11}$$

where K_t is the theoretical stress concentration factor for ideal elastic behavior, and K_f is the ratio of fatigue strength of an unnotched specimen divided by the fatigue strength of a notched specimen. Both K_f and K_t are greater than unity always. The value of q varies between 0 and 1 and is highest for strong alloys.

Fatigue strengths of engineering alloys tend to be proportional to tensile strength. Therefore any factor which increases monotonic strength, for example, testing at low temperatures or utilizing samples with finer grain size, tends to increase fatigue life. While for many metals the fatigue strength is on the order of one-half the tensile strength, this ratio is reduced for some precipitation-hardened alloys (nickel-base superalloys, aluminum alloys) to as little as one-fourth the tensile strength. Ratios of fatigue strength to tensile strength approaching 0.8 have been noted, however, in some composite materials; for these materials, cracks may be deflected out of their paths by the presence of weak interfaces between phases (artificial composites such as boron reinforced with aluminum) or due to the inability of cracks to penetrate strong fibers (nickel-base or cobalt-base eutectic composites which contain strong nonmetallic reinforcing fibers).

Fatigue life can also be affected by environmental reactions, as shown in Fig. 10. Corrosion acting simultaneously with cyclic deformation can produce appreciable lowering of fatigue strength (corrosion fatigue). The adsorption of liquid metals on solid metals (such as mercury on copper-aluminum alloys) also can lead to striking decreases in fatigue life. Another important factor is residual stresses; tensile stresses act adversely and compressive stresses favorably. Compressive stresses are deliberately applied to metal surfaces to delay crack initiation and thereby prolong fatigue life.

Fracture toughness. Many modifications of conventional test procedures have arisen from an effort to obtain laboratory information which would be useful to designers of engineering structures. Since such structures often contain macroscopic defects, in particular weld flaws, large inclusion particles, or other manufacturing flaws, most effort has been directed toward studying the properties of notched bars. Unfortunately, neither the notched tensile test nor the several impact tests described above provide sufficiently quantitative relations between defect size, stress state, and the likelihood of brittle or otherwise unstable fracture, particularly in cases where crack propagation can occur below the macroscopic yield stress as measured in a tensile test. In the case of materials which exhibit little or no plastic deformation at fracture, the most successful approach has been that of A. A. Griffith, who in 1929 deduced Eq. (12)

$$\sigma_F^2 = \frac{kE\gamma}{\pi c} \tag{12}$$

from both thermodynamic and stress considerations. Here σ_F is the nominal applied stress to cause fracture, k is a numerical constant which depends upon stress state and crack geometry, E is Young's modulus, c is the depth of an edge crack or the half-width

of an internal crack, and γ is the elastic energy necessary to create a new surface. While this equation correctly predicts a lowering of fracture stress as flaw size increases, and in fact provides an accurate measure of elastic work to cause fracture in brittle solids such as glass, several critical problems arise when the equation is applied to metals. When fracture stresses are related to flaw sizes, calculated values of work for fracture, γ_p, are several orders of magnitude higher than those deduced for elastic work by other means. E. Orowan first pointed out that plastic work accompanying fracture must be incorporated into the Griffith equation. This is best done by considering that the total work for fracture, γ_p, is related to γ, the elastic energy, through a proportionality factor which is of magnitude equal to crack tip radius ρ divided by interatomic spacing a. The modified Griffith relation, Eq. (13), is then obtained, where k' is a numerical

$$\sigma_F^2 = \frac{k' E \gamma \rho}{\pi a c} \tag{13}$$

constant. This equation reduces to the Griffith condition, Eq. (12), when ρ approaches a in magnitude, that is, as cracks become very sharp. In practice, ρ is difficult to measure, and a more generally applicable approach has been suggested by G. R. Irwin. A stressed material in which a crack propagates releases strain energy at a rate G. A transition from slow to rapid fracture is denoted by a critical value G_c, which is known as the critical strain energy release rate. Alternatively, G_c may be obtained from a relation between elastic compliance, $1/M$, and crack length c in a series of precracked specimens of differing initial crack lengths as shown in Eq. (14), where

$$G_c = \frac{P^2}{2B} \frac{d(1/M)}{dc} \tag{14}$$

$d(1/M)/dc$ is the change in compliance with increasing length of precrack, B is the thickness, and G_c is a measure of work necessary to cause the crack to propagate. G_c is, therefore, equivalent to γ_p, the distinction being that G_c is an experimentally measured parameter which is not dependent upon assumptions as to its origin. G_c is typically of magnitude 100–1000 in.-lb/in.^{2} for metals. Part of this energy may be dissipated in forming new surface, the rest being converted to plastic work or kinetic energy of the crack.

An alternative and completely complementary approach, based on stress concentrations near crack tips, also has been developed by Irwin, and has been much more widely applied to engineering design situations. Equations for the normal and shear stresses near the crack edge for bodies of various geometries to which forces are applied normal or parallel to the crack edge have been developed. In all cases, the local stresses at the crack edge fall off with distance away from the crack. Fracture of the body occurs when a critical stress distribution, described by the stress intensity factor K, is reached. K depends upon applied stress and crack geometry; for most situations it may be defined as Eq. (15), where σ is a

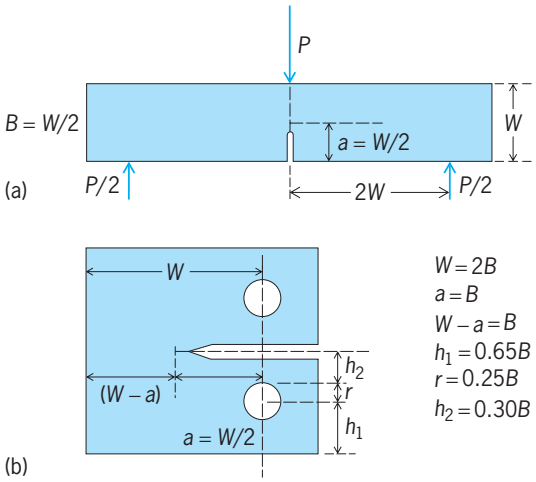

Fig. 11. Standard fracture toughness specimens. (*a*) Edge-notched bend. (*b*) Compact tension. (*After N. H. Polakowski and E. J. Ripley, Strength and Structure of Engineering Materials, Prentice-Hall, 1965*)

$$K = \sigma(\alpha \pi c)^{1/2} \tag{15}$$

parameter depending upon specimen and crack geometry. For a crack in an infinite plate, subjected to loading perpendicular to the crack edge, $\sigma = 1$. K, which is expressed in units of (lb/in.^{2})$\sqrt{\text{in.}}$, is determined experimentally by stressing a precracked specimen in bending or in tension (**Fig. 11**), and noting the critical stress intensity K_c at which unstable (rapid) crack propagation occurs. K and G are related as shown in Eq. (16), where $A = (1 - \nu^2)$ for

$$G = A \frac{K^2}{E} \tag{16}$$

plane strain and $A = 1$ for plane stress; ν is Poisson's ratio.

Critical values of stress intensity K_c and strain energy release rate G_c are related similarly. In addition, since K_c corresponds to a fracture condition, Eq. (16) may be rewritten as Eq. (17), which, when combined with Eq. (15), provides the relation given in Eq. (18),

$$K_c^2 = \alpha \sigma_F^2 \pi c \tag{17}$$

$$\sigma_F^2 = \frac{E G_c}{A \alpha \pi c} \tag{18}$$

which is identical in form to the Griffith condition, Eq. (12).

Unlike the yield stress, which is a reproducible material property for specimens of identical composition and microstructure, K_c and G_c vary with the depth of the precrack relative to the dimensions of the test specimen, particularly width W and thickness B. Specimens with relatively long cracks fracture with appreciable plasticity occurring at the crack tip. The contribution of plastic work is included in G_c or K_c, and is particularly high in thin sections and in low-strength alloys. For high-strength material, and lower-strength alloys in which c/W and c/B are small, K_c and G_c decrease to lower limiting

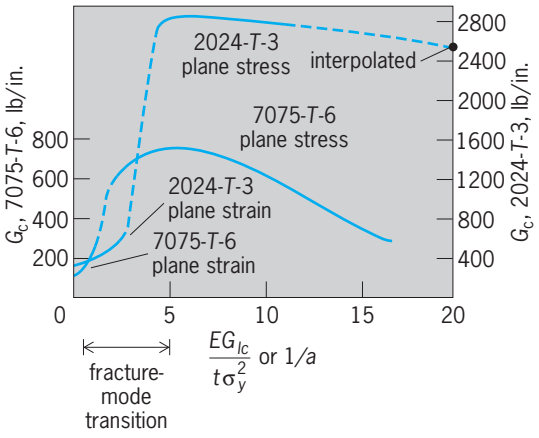

Fig. 12. Critical strain energy release rate as function of thickness. 1 lb/in. = 0.113 N·m. (*After J. N. Goodier and N. J. Hoff, eds., Structural Mechanics, Pergamon Press, 1960*)

values K_{I_c} and G_{I_c}, respectively (**Fig. 12**). These values refer to plane-strain conditions, and the K_{I_c} parameter is known as the plane-strain fracture toughness. K_{I_c} appears to be a material constant insofar as specimen-crack geometry is concerned, and therefore is extremely useful for designers who must estimate structural parameters which are necessary to avoid catastrophic failures. However, K_{I_c} may vary with test temperature, strain rate, and microstructure of the metal. In general, fracture toughness decreases as strength increases, so that K_{I_c} tends to be low for quenched and tempered alloy steels, and much higher for medium-strength carbon steels or aluminum alloys.

Specimen designs which are currently recommended in the United States and Great Britain are shown in Fig. 11*a* and *b*, although additional designs have been utilized in specific situations. Both are single-edge notched specimens which are precracked in fatigue prior to the fracture toughness determination. The bend specimen in Fig. 11*a* is deformed under three-point loading, while the compact tension specimen in Fig. 11*b* is loaded through pins above and below the crack faces. In order to relate applied loads to stress intensity, test specimens must be calibrated. A compliance coefficient (Y function) is published for each specimen-crack-load geometry, which allows load to be converted directly to a K value. The primary variable in specimen preparation is the ratio of crack length c to specimen width W. Calibrations are presented either in tabular or polynomial form as functions of c/W. Plasticity corrections are necessary for situations in which fracture events are not precisely localized at the crack tip, that is, when plastic flow spreads ahead of an advancing crack. The specification of size of the region in which the stress intensity accurately describes the stress field is a critical aspect of fracture toughness testing. In practice, it is usually estimated to be about $^1/_{50}$ the crack length. Therefore the plastic zone at fracture must be limited to $0.02c$ or less. This is accomplished by ensuring that c and $B \geq 2.5\ (K_{I_c}/\sigma_y)^2$, where σ_y is the 0.2% offset yield stress of the material. Calculation of K_{I_c} is based upon the lowest load at which significant measureable extension of the crack occurs. The method has been applied with considerable success to high- and medium-strength steels, as well as to high-strength aluminum- and titanium-base alloys. Modifications of the standard fracture toughness test have also been applied to lower-strength materials, but the test procedures have not yet been standardized.

Creep and stress rupture. Time-dependent deformation under constant load or stress is measured in a creep test. Creep tests are those in which the deformation is recorded with time, while stress rupture tests involve the measurement of time for fracture to occur. The two types of test provide complementary information, and indeed both creep rate and time may be recorded in a single test. Closely related are stress relaxation tests, in which the decay of load with time is noted for a body under a fixed state of strain. Although creep deformation may occur under any state of stress, it is most commonly measured in uniaxial tension. Test durations vary from seconds or minutes to tens of thousand of hours. Appreciable deformation occurs in structural materials only at elevated temperatures, while pure metals may creep at temperatures well below room temperature. In general, the temperature at which creep processes become significant exceeds approximately one-half of the melting temperature on the absolute scale. Under constant load conditions, three stages of inelastic deformation are noted, as shown in **Fig. 13**. These are primary creep (stage I), secondary or steady-state creep (stage II), and tertiary creep (stage III). A considerable portion of primary creep is anelastic and is sometimes referred to as transient creep. The second stage marks a balance between strain hardening of the material and recovery of the microstructure and strength; a constant, minimum creep rate may be noted over most of the life of the specimen, and it is the steady-state creep rate, therefore, which is often determined for structural alloys. Tertiary creep resembles necking in a tensile test in that both are instabilities arising from prefracture events. In this stage, strain hardening cannot compensate for the

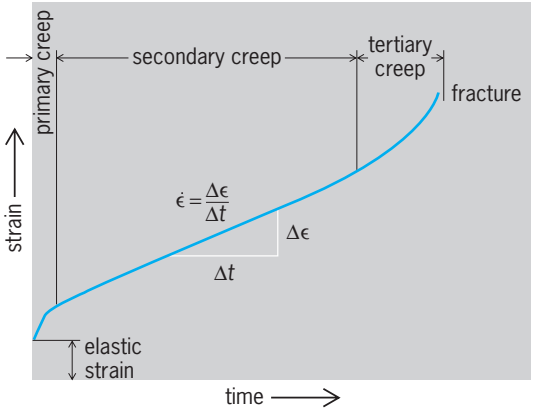

Fig. 13. Creep curve. (*After M. E. Eisenstadt, Introduction to Mechanical Properties of Materials, Macmillan, 1971*)

loss in cross-sectional area during straining as well as the formation of fine cracks. Information usually derived from a series of creep experiments may include, aside from the steady-state creep rate, data on the stress versus logarithm of time for total deformations of up to 5%, as initial stress versus logarithm of time to rupture, and logarithm of stress versus logarithm of creep rate. It should be noted that since the cross-sectional area of a creep specimen decreases with time, the stress increases under constant load conditions. It is possible to run constant stress tests by providing means for load to be reduced as the specimen elongates.

Since creep deformation and rupture time are temperature- and stress-dependent, it is usually necessary to test a material at several stresses and temperatures in order to establish the creep or stress-rupture properties in adequate detail. Interpolation of creep and rupture data is frequently employed to predict behavior at stresses and temperatures which are not included in the test program. However, no generally accepted methods are available for extrapolating creep and rupture data to temperatures, times, and stresses outside of the tested range. Specimen size has little effect on creep and rupture properties. Consequently, test specimen configurations usually resemble those of flat or round tensile bars with reduced gage sections. Temperature measurement must be precise; the difference between indicated and actual test temperature should not exceed $\pm 3.6^\circ F$ ($\pm 2^\circ C$) up to $1830^\circ F$ ($1000^\circ C$) and $\pm 5.4^\circ F$ ($\pm 3^\circ C$) at higher temperatures. Creep strain is measured by an extensometer for tests in which creep rates are to be determined. In the case of stress-rupture tests, dial gages often are employed to provide approximate creep elongations to supplement stress-to-rupture data. *See* METAL; METALLURGY.

N. S. Stoloff

Bibliography. American Society for Metals, *Metals Handbook*, vol. 1: *Properties and Selection, Iron, Steel and High-Performance Alloys*, 10th ed., 1991, and vol. 11: *Failure Analysis and Prevention*, 9th ed., 1988; American Society for Testing and Materials, Standards A370–72a, E92–72, E10–66, E9–70, E8–69, E399–72, E6–66, E23–72; G. E. Dieter, *Mechanical Metallurgy*, 3d ed., 1986; F. A. McClintock and A. S. Argon, *Mechanical Behavior of Materials*, 1966; N. H. Polakowski and E. J. Ripling, *Strength and Structure of Engineering Materials*, 1966.

Metal and mineral processing

The obtaining of useful metals from ores. In the **table** are summarized one or more routes, but not necessarily the only commercial route, used to obtain each of the useful metals by extractive metallurgy. For additional information see the separate articles on each of the metals. *See also* CHEMICAL SEPARATION

Occurrence, extraction, and refining of metals

Metals	Occurrence	Beneficiation operations	Extraction processes: Operation	Extraction processes: Intermediate product	Extraction processes: Product used in refining	Refining (reduction) operations
Aluminum, Al	Bauxite, Al_2O_3, 55–65% Al	Dehydration roast	Caustic (Bayer process)	Sodium aluminate	Pure alumina	Fused salt electrolysis
	Alunite, $KAl_3(OH)_6(SO_4)_2$	Dehydration roast	Reduction roast, caustic digestion	Alumina hydrate	Pure alumina	
Antimony, Sb	Stibnite, Sb_2S_3, 50–60% Sb	Liquation		Pure Sb_2S_3	Iron precipitation	
Arsenic, As	Enargite, $3Cu_2S \cdot As_2S_5$		Roasting	AS_2O_3		Charcoal reduction at 1200–1300°F (650–700°C)
	Arsenopyrite, FeAsS					
Barium, Ba	Barite, $BaSO_4$	Flotation		Pure $BaSO_4$	$BaCl_2$	Fused salt electrolysis
Beryllium, Be	Beryl, $3BeO \cdot Al_2O_3 \cdot 6SiO_2$, 10–12% Be	Hand cobbing	Acid sinter plus leaching	BeO	BeF_2	Magnesium at 1652–2372°F (900–1300°C)
	Bertrandite, $Be_4Si_2O_7(OH)_2$					
Bismuth, Bi	Lead ores	Flotation, gravity	Smelting	Lead bullion	Anode residue from electrolyzed bullion	Chlorine at 932°F (500°C) to remove Pb and Zn Reduction with charcoal and flux
Boron, B	Borax, $Na_2B_4O_7 \cdot 10H_2O$ Kernite, $Na_2B_4O_7 \cdot 4H_2O$ Colemanite, $Ca_2B_6O_{11} \cdot 5H_2O$	Evaporation Brine purification	Crystallization from purified brine, calcining	B_2O_3	Potassium fluoborate	Fused salt electrolysis Reduction with hydrogen Reduction with sodium or magnesium
Cadmium, Cd	Sphalerite, ZnS, 1% Cd	Roasting, sintering	Leaching	Cd-Zn solution	Cd sponge by Zn dust addition	Distillation
		Refuming	Leaching		Purified solution	Electrolysis
Calcium, Ca	Limestone, $CaCO_3$		Calcination	CaO		Aluminum reduction in vacuum
Cerium, Ce	Monazite Bastnaesite	Gravity, flotation	Caustic or acid leaching	$Ce_2(SO_4)_3$	Tetravalent Ce salts Cerium oxides Cerium fluorides	Electrolysis of fused chloride at 1292°F (700°C), or of fused fluoride baths
Cesium, Cs	Lepidolite, 1% Cs	Hand cobbing	Acid leaching	Cesium alum	CsCl Cs hydroxide	Calcium, aluminum, or magnesium reduction
	Pollucite, $Cs_4Al_4Si_9O_{26} \cdot H_2O$	Selective mining of pegmatites	Direct reduction			
Chromium, Cr	Chromite, $FeO \cdot Cr_2O_3$, 35–50% Cr	Gravity and magnetic separation	Electric furnace treatment	Ferrochrome	Chromium alum solution Chromium oxide	Electrolysis Aluminum reduction

Occurrence, extraction, and refining of metals *(cont.)*

Metals	Occurrence	Beneficiation operations	Extraction processes: Operation	Extraction processes: Intermediate product	Extraction processes: Product used in refining	Refining (reduction) operations
Cobalt, Co	Cobalt or nickel ores, 0.8–10.0% Co Lateritic ores	Flotation, leaching	Acid roast or smelting	$CoSO_4$ solution	$Co(OH)_2$ by milk of lime	Electrolysis of aqueous solution
Columbium, Cb (niobium)	Columbite, $Fe(Cb \cdot TaO_3)_2$	Gravity High-intensity magnetic or electrostatic separation	Caustic fusion, then HCl, then KF Chlorination Solvent extraction Hydrometallurgy	$CbKOF_2$	Columbium oxides	Columbium carbide in vacuum Columbium metal
Copper, Cu	Copper ores, 0.4–6.0% Cu	Flotation, fluid-bed roasting, leaching, pressure leaching, solvent extraction	Smelting, electrolysis, liquid ion exchange, cementation	Cu anodes Ferric chloride leach solution	Cu cathodes Stripped solvent Purified solutions	Electrolysis Other electrowinning methods to produce powdered metal
Dysprosium, Dy	Monazite	Gravity	Sulfuric acid treatment	$Dy_2(SO_4)_3$	Pure salts by fractional crystallization and ion exchange	Electrolysis of fused chloride
Erbium, Er	Monazite	Gravity	Sulfuric acid treatment	$Er_2(SO_4)_3$	Pure salts by fractional crystallization and ion exchange	Electrolysis of fused chloride
Europium, Eu	Monazite	Gravity	Sulfuric acid treatment	$Eu_2(SO_4)_3$	Pure salts by fractional crystallization and ion exchange	Electrolysis of fused chloride
Gadolinium, Gd	Monazite	Gravity	Sulfuric acid treatment	$Gd_2(SO_4)_3$	Pure salts by fractional crystallization and ion exchange	Electrolysis of fused chloride
Gallium, Ga	Al and Zn ores	Caustic	CO_2 treatment in acid	Ga_2O_3 and $GaCl_3$		Electrolysis
Germanium, Ge	Sphalerite, ZnS, 0.01–0.015% Ge	Flotation	Roasting	Germanium oxide	Germanium chloride, then hydrolysis to pure oxide	Hydrogen reduction
Gold, Au	Elemental form, 0.001% Au	Gravity, flotation, leaching	Cyanide or smelting	AuCN or Au	Pure gold	Zinc reduction
Hafnium, Hf	Zircon, $ZrO_2 \cdot SiO_2$	Gravity	Acid or alkali leaching	Hf-Zr solutions	Hf solutions by ion exchange to $HfCl_4$; solvent extraction	Magnesium reduction
Holmium, Ho	Monazite	Gravity	Sulfuric acid treatment	$Ho_2(SO_4)_3$	Pure salts by fractional crystallization and ion exchange	Electrolysis of fused chloride
Indium, In	Zinc ores	Flotation	Acid roasting	In sulfate	Water solutions	Displacement by zinc metal
Iridium, Ir	Cu-Ni sulfide ores	Flotation, roasting, extraction	Electrolytic refining	Anode slimes	$(NH_4)_2IrCl_6$	Hydrogen reduction
Iron, Fe	Iron ores, 30–60% Fe	Gravity, flotation, magnetic and electrostatic separation, pelletizing	Blast furnace Prereduction or metallizing furnaces	Pig iron Prereduced or metallized pellets		Coke reduction in blast furnace Electric furnace reduction Basic oxygen furnace Direct reduction with CO, H_2, and CH_4
Lanthanum, La	Monazite	Gravity	Sulfuric acid treatment	$La_2(SO_4)_3$	Pure salts by fractional crystallization and ion exchange	Electrolysis of fused chloride
Lead, Pb	Galena, PbS, 6–10% Pb	Gravity or flotation	Blast furnace Imperial furnace	Lead bullion	Lead free of Cu, Sn, As, and Sb by treatment with S	Desilvering with Zn, Sb removal
Lithium, Li	Spodumene, $Li_2O \cdot Al_2O_3 SiO_2$ Brines, 0.03–0.24% LiCl	Flotation Evaporation, leaching, flotation	Acid roasting	Li_2SO_4	Li_2CO_3, then LiCl LiCl	Electrolysis of fused chloride
Lutetium, Lu	Monazite	Gravity	Sulfuric acid treatment	$Lu_2(SO_4)_3$	Pure salts by fractional crystallization and ion exchange	Electrolysis of fused chloride
Magnesium, Mg	Seawater, 0.13% Mg Brines Dolomite, $CaMg(CO_3)_2$		Lime slurry Evaporation	$Mg(OH)_2$	MgCl with HCl MgCl	Electrolysis of fused chloride Thermal reduction of dolomite with ferrosilicon
Manganese, Mn	Manganese ores, 45–55% Mn	Flotation, gravity	Roasting in reducing atmosphere	Mn in solution	Pure Mn solutions by filtration	Electrolysis of aqueous solution
Mercury, Hg	Cinnabar, HgS, 1–3% Hg	Sorting, screening	Roasting	Hg		Retorting at 1290°F (700°C)
Molybdenum, Mo	Molybdenite, MoS_2, 1–3% Mo	Flotation	Roasting	MoO_3	Mo by hydrogen reduction	Power metallurgy or are melting
Neodymium, Nd	Monazite	Gravity	Sulfuric acid treatment	$Nd_2(SO_4)_3$	Pure salts by fractional crystallization and ion exchange	Electrolysis of fused chloride
Nickel, Ni	Nickel ores, 1–35% Ni Lateritic ores, lower nickel content	Smelting, flotation of Cu-Ni-Fe product Leaching	Roasting, leaching Pressure leach with NH_3	(NiCuFe)S or Ni	Pure NiS by molten Na_2S extraction	Carbon reduction Electrolytic refining Precipitation of Ni as powder from leach solutions
Osmium, Os	Cu-Ni sulfide ores	Flotation, roasting, extraction	Electrolytic refining	Anode slimes	$OsO_2(NH_3)_4Cl_2$	Hydrogen reduction
Palladium, Pd	Cu-Ni sulfide ores	Flotation, roasting, extraction	Electrolytic refining	Anode slimes	$Pd(NH_3)_2Cl_2$	Hydrogen reduction

Occurrence, extraction, and refining of metals *(cont.)*

Metals	Occurrence	Beneficiation operations	Extraction processes: Operation	Extraction processes: Intermediate product	Extraction processes: Product used in refining	Refining (reduction) operations
Platinum, Pt	Cu-Ni sulfide ores, 0.001% Pt	Flotation, roasting, extraction	Electrolytic refining	Anode slimes	$(NH_4)_2PtCl_2$	Hydrogen reduction
Potassium, K	Sylvite, KCl	Flotation, gravity				Sodium reduction
Praseodymium, Pr	Monazite	Gravity	Sulfuric acid treatment	$Pr_2(SO_4)_3$	Pure salts by fractional crystallization and ion exchange	Electrolysis of fused chloride
Radium, Ra	Pitchblende	Gravity, flotation	Acid digestion	Ra sulfate	Radium bromide	Repeated fractional crystallization
Rhenium, Re	Molybdenite, MoS_2	Flotation	Roasting	Re_2O_7	$KReO_4$	Hydrogen reduction
Rhodium, Rh	Cu-Ni sulfide ores	Flotation, roasting, extraction	Electrolytic refining	Anode slimes	$(NH_4)_3Rh(NO_2)_6$	Hydrogen reduction
Rubidium, Rb	Lepidolite Pollucite	Hand cobbing	Chlorostannate process followed by pyrolysis, electrolysis, or reduction	Rubidium perchlorate	Chloride Carbonate or hydroxide	High-temperature vacuum reduction with Na or Mg
Ruthenium, Ru	Cu-Ni sulfide ores	Flotation, roasting, extraction	Electrolytic refining	Anode slimes	RuO_2	Hydrogen reduction
Samarium, Sm	Monazite	Gravity	Sulfuric acid treatment	$Sm_2(SO_4)_3$	Pure salts by fractional crystallization and ion exchange	Electrolysis of fused chloride
Scandium, Sc	Thortveitite, $(ScY)_2Si_2O_7$ Uranium ores	Leaching with H_2SO_4, then solvent extraction	Roasting with C Stripping solvent with Hf	Scandium carbide Sc_2O_3	Scandium oxide, then ScF_3 ScF_3	Electrolysis of fused salt Direct reduction of fluoride and distillation of Sc metal in vacuum induction furnace
Selenium, Se	Chalcopyrite, $CuFeS_2$	Flotation, roasting	Electrolytic refining	Anode muds	Sodium selenate	SO_2 precipitation from aqueous solution
Silicon, Si	Silica, SiO_2	Flotation, gravity	Smelting			Carbon reduction in electric furnace
Silver, Ag	Nonferrous ores, 0.07% Ag	Gravity or flotation	Blast furnace	Lead bullion	Ag-Zn mixture by Zn treatment	Zn distillation, electrolysis of Ag
Sodium, Na	Halite, NaCl	Flotation, leaching				Electrolysis of fused chloride
Strontium, Sr	Celestite, $SrSO_4$	Hand cobbing, flotation	Digestion with soda ash Calcining with coal; sulfide then leached with lime	$SrCO_3$ $SrCO_3$	$SrCl_2$	Electrolysis of fused chloride
Tantalum, Ta	Tantalite, $Fe(Cb_2TaO_3)_2$ Tin slags	Gravity, electrostatic, magnetic separation	Digestion with HF or caustic, then KF	K_2TaF_7	Ta by sodium reduction	Vacuum sintering at 1290˚F (700˚C)
Tellurium, Te	Chalcopyrite, $CuFeS_2$	Flotation, roasting	Electrolytic refining	Anode muds	Sodium telluride-tellurate	SO_2 from aqueous solution
Terbium, Tb	Monazite	Gravity	Sulfuric acid treatment	$Tb_2(SO_4)_3$	Pure salts by fractional crystallization and ion exchange	Electrolysis of fused chloride
Thallium, Tl	Sphalerite, ZnS	Roasting, sintering	Leaching of flue dust	Thallium chloride	TIS by H_2S treatment, then converted to sulfate	Electrolysis of aqueous solution
Thorium, Th	Monazite	Gravity	Sulfuric acid treatment	$Th(SO_4)_2$	Pure salts by fractional crystallization and ion exchange	Reduction of ThF_4 by calcium
Thulium, Tm	Monazite	Gravity	Sulfuric acid treatment	$Tm_2(SO_4)_3$	Pure salts by fractional crystallization and ion exchange	Electrolysis of fused chloride
Tin, Sn	Cassiterite, SnO_2, 1.5–5.0% Sn	Gravity, flotation	Reverberatory furnace	Impure tin		Electrolytic refining
Titanium, Ti	Rutile, TiO_2, ilmenite, 1–8% Ti	Gravity, electrostatic, magnetic separation	Chlorination	$TiCl_4$		Magnesium or sodium reduction Electrolysis of $TiCl_4$ in fused salt bath
Tungsten, W	Tungsten ores, 60–70% W	Gravity, flotation	Caustic fusion	Sodium tungstate	WO_3	Hydrogen reduction
Uranium, U	Uranium ores	Leaching with acid or caustic	Ion exchange, solvent extraction		UF_4	Ca Al, Mg, or Na reduction
Vanadium, V	Carnotite, $K_2O \cdot 2UO_3 \cdot V_2O$	Salt roasting	Leaching, solvent extraction, ion exchange	Sodium vanadate	V_2O_5	Thermic reduction followed by electron-beam purification
Ytterbium, Yb	Monazite	Gravity	Sulfuric acid treatment	$Yb_2(SO_4)_3$	Pure salts by fractional crystallization and ion exchange	Electrolysis of fused chloride
Yttrium, Y	Monazite	Gravity	Sulfuric acid treatment	$Y_2(SO_4)_3$	Pure salts by fractional crystallization and ion exchange	Electrolysis of fused chloride
Zinc, Zn	Sphalerite, ZnS, 10–30% Zn	Flotation, gravity, pelletizing, roasting	Sulfuric acid leach Fluxing for pyrolytic processes	Purified solution		Electrolysis to produce high-purity cathodes Electrolytic reduction Imperial smelting process
Zirconium, Zr	Zircon, $ZrO_2 \cdot SiO_2$	Electrostatic, magnetic, or gravity concentration	Chlorination, or plasma fusion, then caustic leach		$ZrCl_4$	Magnesium reduction

TECHNIQUES; ELECTROMETALLURGY; FLOTATION; HYDROMETALLURGY; IRON METALLURGY; LEACHING; MECHANICAL SEPARATION TECHNIQUES; METALLURGY; ORE DRESSING; PYROMETALLURGY, NONFERROUS.

Alvin W. Knoerr

Metal-base fuel

A fuel containing a metal of high heat of combustion as a principal constituent. High propellant performance in either a rocket or an air-breathing engine is obtained when the heat of combusion of the fuel is high. Chemically, high heats of combustion are attained by the oxidation of the low-atomic-weight metals in the upper left-hand corner of the periodic table. The generally preferred candidates are lithium, beryllium, boron, carbon, magnesium, and aluminum.

Performance parameters. For the rocket where the total propellant containing both fuel and oxidizer is carried on board, the performance parameter of interest is the heat of combustion per unit mass of combustion product. In air-breathing engines, however, where only the fuel is carried on board and the oxidizer in the form of air is attained free, the figure of merit is the heat of combustion per unit mass of fuel. There is still a third figure of merit for the air-breathing engine in which most of the flight involves a cruise operation in which the thrust just balances the drag. In this case, it is desirable to minimize the cross-sectional area (consequently volume) and maximize the heat of combustion so that a given total energy output can be realized in a minimum-volume vehicle to present low drag. The figure of merit, in this case, is the heat of combustion per unit volume of fuel. *See* PROPULSION.

The **table** shows a listing of the heats of combustion of various candidate metals along with three non-metallized high-performance fuels for comparison. The three different heats of combustion described above are figures of performance merit, depending upon the vehicle mission and type of propulsion system employed. In general terms, for an accelerating rocket, the important figure of merit is Btu/lb pdts (pound of products); for the accelerating air breather, it is Btu/lb fuel; and for the cruising air breather, it is Btu/in.^{3} fuel. *See* PROPELLANT.

The metal with the highest heat release for all applications is beryllium, whereas boron shows essentially equivalent performance for air-breathing applications. For rocket applications where Btu/lb pdts is important, lithium, boron, and aluminum are close to beryllium. As discussed later, however, because of inefficiencies in the combustion heat release as well as thermodynamic limitations, not all of these candidates are equivalent.

Method of use. The metallized additive can be used in either a liquid or solid propellant. When the pure metal is added to liquid fuels, an emulsifying or gelling agent is employed which maintains the particles in uniform suspension. Such gelling agents are added in small concentrations and so do not negate the beneficial effect of the fuel. Particle sizes in such suspensions are generally in the range 0.1–50 micrometers, and stable suspensions have been made which do not separate for long periods of time. When a metallic compound is employed, the compounding group is chosen so that the additive is soluble in the fuel. Thus, if gasoline is the fuel base, the suitable soluble boron compound is ethyldecaborane and, for aluminum, triethylaluminum may be employed. In both cases, the metallic additive contains a hydrocarbon constituent which provides solubility in the hydrocarbon base fuel.

When used in composite solid rocket propellants, the metal powder is usually mixed with the oxidizer and unpolymerized fuel, and the propellant is then processed in the usual way. If a compound of the metal additive is employed, it is convenient to dissolve it in the fuel, and then to process the fuel containing the metallic compound and oxidizer according to normal procedures. Homogeneous solid propellants also employ metallizing constituents, both as the pure metal and as a compound.

Compounds of interest. Early compounding of metallized propellants employed the free metal itself. As a result of extensive research in metalloorganic compounds, however, several classes of metallic compounds have been employed. Two major reasons for the use of such compounds are that the solubility of the metal in the fuel can be realized, resulting in

Heats of combustion of the lightweight metals compared with those of some other fuels

Fuel	Specific gravity	Product	Heat of combustion		
			Btu/lb pdts*	Btu/lb fuel*	Btu/in.^{3} fuel†
Lithium	0.53	Li_2O	8,570	18,500	360
Beryllium	1.85	BeO	10,450	29,100	1,950
Boron	2.35	B_2O_3	7,820	25,200	2,140
Carbon	2.00	CO_2	3,840	14,100	1,020
Magnesium	1.74	MgO	6,430	10,700	670
Aluminum	2.70	Al_2O_3	7,060	13,400	1,310
Gasoline	0.75	CO_2, H_2O	4,600	20,400	550
Hydrazine	1.00	N_2, H_2O	4,180	9,360	340
Hydrogen	0.07	H_2O	6,830	61,500	155

*1 Btu/lb = 2326 joules/kg.
†1 Btu/in.^{3} = 64.4 megajoules/m^3.

a homogeneous propellant, and performance higher than that for the pure metal can be obtained in some cases.

The major classes of metallic compounds of interest as high-performance propellants include the hydrides, amides, and hydrocarbons. Additional classes include mixtures either of two metals or of two chemical groups, such as an amine hydrocarbon. Some examples of the hydrides include LiH, BeH_2, B_2H_6, B_5H_9, $B_{10}H_{14}$, MgH_2, and AlH_3. These compounds form the more exotic class of metallics because they are capable of yielding the highest performances, exceeding those of the pure metals. The presence of hydrogen provides the low-molecular-weight gases needed for high thermodynamic performance. Examples of the propellant amides include $LiNH_2$ and $B(NH_2)_2BNHCH_3$. The largest class is the hydrocarbons, which includes LiC_2H_5, $Be(CH_3)_2$, $B(CH_3)_3$, and $Al(C_2H_5)_3$. The major advantage of this class is the potential solubility in conventional hydrocarbon fuels. *See* BORANE.

Operational limitations. Most metallic fuels are costly, and many, because of particle-size requirements or synthesis in a specific compound, are in limited supply. The combustion gases all produce smoky exhausts which may be objectionable in use. Engine development problems are also increased because of the appearance of smoke and deposits in the engine. These engine deposits can sometimes occur on the injector face, nozzle, and turbine blades of turbojet engines. Careful adjustment of operating conditions is required in such cases to minimize these difficulties with resultant added development costs.

Combustion losses. In rocket engines, where the flame temperatures are high, vaporization and dissociation are particularly pronounced. In the tabular listing of total heats of combustion, the heat value is given as measured in a laboratory calorimeter, the end product being the condensed oxide. At high flame temperatures, however, the oxides vaporize, producing a lower effective heat of combustion. In the case of boron oxide, B_2O_3, for example, the normal boiling point is about 2500 K (4000°F), whereas the flame temperature in most high-performing rocket engines exceeds 3000 K (4900°F). These effects are shown in the **illustration**, which compares the total heat of combustion Q of gasoline-boron mixtures when the B_3O_3 is solid or liquid to the heat when it is a vapor. At still higher flame temperatures, in addition to vaporization, the oxides undergo endothermic dissociation such as shown in Eqs. (1), (2), and (3).

$$B_2O_3(g) = B_2O_2(g) + {}^1/_2O_2 - 108 \text{ kcal} \quad (1)$$

$$B_2O_2(g) = 2BO(g) - 126 \text{ kcal} \quad (2)$$

$$Al_2O_3(l) = Al_2O(g) + O_2 - 330 \text{ kcal} \quad (3)$$

The net result of these reactions is a further reduction in flame temperature to an extent that sensitively depends on the temperature itself. At temperatures below about 2500 K (4000°F), as in air-breathing engines operating below Mach 3, vaporization and dissociation for the oxides of beryllium, aluminum, boron, and magnesium occur hardly at all, and these limitations do not apply.

In actual engines, a certain fraction of the useful energy which is lost by vaporization and dissociation is recovered by condensation and recombination in nozzles. If thermodynamic equilibrium prevails and if the nozzle area ratio is infinite, all of this energy loss is recovered. In actual cases, however, because of the finite area ratio and finite reaction and condensation rates, only a part of the energy is recovered for propulsion. *See* ROCKET PROPULSION.

Two-phase flow losses. A second type of propulsive efficiency loss occurs as a result of the appearance of a condensed phase. Because the acceleration of the gases in the nozzle results from pressure-volume work, a reduction in gas content reduces the thermodynamic efficiency. The combustion gas behaves as if the molecular weight were increased. A second consideration involves the momentum exchange between condensed phase and gas. If the particles are large and lag appreciably behind the gas in velocity, impulse is lost. This effect can be appreciable when the percentage of condensed phase is high.

The net result of the thermodynamic limitations is to partially reduce in some cases the improvement in performance expected on the basis of heat of combustion alone. As additives, metals are most effective when mixed with the lower-performing propellants because the lower temperatures minimize the vaporization and dissociation losses. For this reason, the greatest use of metal additives has been in solid propellants, which develop 10–20% lower specific impulses than do liquid propellants. The result of the use of such additives has been to close the gap in performance between the solid and liquid propellants. The second attractive application is in air-breathing engines, where flame temperatures are relatively low.

David Altman

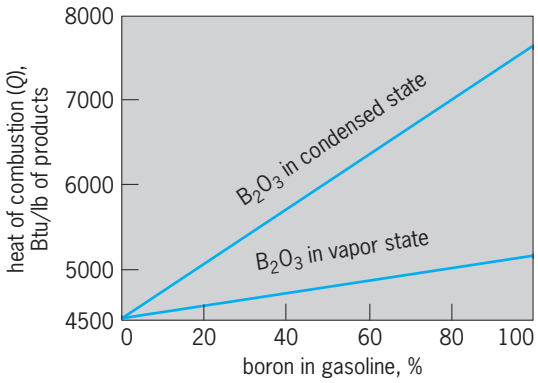

Total heat of combustion of gasoline-boron mixtures. 1 Btu/lb = 2326 joules/kg.

Metal carbonyl

A complex of a transition metal combined with carbon monoxide (CO). In a metal carbonyl, the CO groups form sigma bonds to the metal through

lone pairs of electrons on carbon; the metal, in turn, donates electrons to antibonding pi orbitals on CO. In so doing, the metal usually attains the electronic configuration of an inert gas (the 18-electron rule). Thus elemental chromium (Cr^0), with six valence electrons, combines with six molecules of CO, each donating two electrons, to afford chromium hexacarbonyl [$Cr(CO)_6$], in which Cr has 18 valence electrons and is isoelectronic to krypton (Kr). *See* CHEMICAL BONDING; COORDINATION COMPLEXES; VALENCE.

Metal carbonyls usually are electrically neutral and nonpolar, exhibiting many of the physical properties of organic compounds. Typically they are volatile solids or liquids, soluble in common organic solvents but insoluble in water. They are highly toxic.

Anionic and cationic species also are known. Metal carbonyls also may contain one (mononuclear) or more (polynuclear) metal atoms. Polynuclear metal carbonyls may exhibit covalent metal-metal bonds, and in them CO also may function as bridging or capping ligands, forming bonds to two or three metal atoms, respectively. Mononuclear metal carbonyls tend to exhibit geometries expected on the basis of minimization of interligand repulsions (valence shell electron-pair repulsion model); their polynuclear analogs often may be envisioned structurally as arising from the fusion of mononuclear polyhedra. Thus nickel tetracarbonyl [$Ni(CO)_4$], iron pentacarbonyl [$Fe(CO)_5$], and chromium hexacarbonyl [$Cr(CO)_6$] exhibit tetrahedral, trigonal bipyramidal, and octahedral geometries, respectively [structures (**1**)–(**3**)].

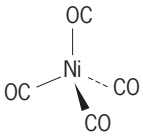

(**1**)

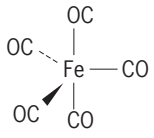

(**2**)

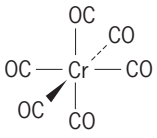

(**3**)

The polynuclear manganese carbonyl [$Mn_2(CO)_{10}$] has a structure obtained by joining two octahedra at a vertex [structure (**4**)], and the structure of diiron enneacarbonyl [$Fe_2(CO)_9$] is viewed as two octahedra sharing three bridging carbonyls at a face [structure (**5**)]. The chemical formulas of representative metal carbonyls are given below; the transition metals in brackets also form the preceding complex.

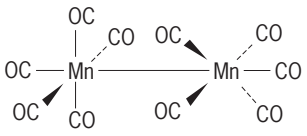

(**4**)

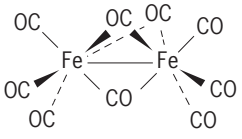

(**5**)

$V(CO)_6$; $V(CO)_6^-$ [Nb, Ta]; $Cr(CO)_6$ [Mo, W]; $Mn(CO)_6^+$ [Tc, Re]
$Cr_2(CO)_{10}^{2-}$ [Mo, W]; $Mn_2(CO)_{10}$ [Tc, Re]
$Mn(CO)_5^-$ [Tc, Re]; $Fe(CO)_5$ [Ru, Os]
$Fe_2(CO)_9$ [Ru, Os]; $Fe_3(CO)_{12}$ [Ru, Os]
$Os_5(CO)_{16}$; $Os_6(CO)_{18}$; $Os_7(CO)_{21}$; $Os_8(CO)_{23}$
$Co_2(CO)_8$ [Rh]; $Co_4(CO)_{12}$ [Rh]; $Rh_6(CO)_{16}$ [Ir]
$Fe(CO)_4^{2-}$; $Co(CO)_4^-$; $Ni(CO)_4$
$Ni_2(CO)_6^{2-}$; $Ni_3(CO)_8^{2-}$ $Ni_4(CO)_9^{2-}$; $Ni_5(CO)_9^{3-}$

[V = vanadium, Nb = niobium, Ta = tantalum, Cr = chromium, Mn = manganese, Tc = technetium, Re = rhenium, Fe = iron, Ru = ruthenium, Os = osmium, Co = cobalt, Rh = rhodium, Ir = iridium, Ni = nickel.]

The first metal carbonyl, $Ni(CO)_4$, was discovered by L. Mond in 1890; it is synthesized by the direct combination of metallic nickel and carbon monoxide under ambient conditions. Other metal carbonyls can be prepared directly from the metals and CO at elevated temperatures and pressures, or through the reaction of transition-metal salts with CO under reducing conditions, also at elevated temperatures and pressures [reactions (1)–(3)].

$$\underset{\substack{\text{Chromium(III)}\\\text{chloride}}}{CrCl_3} + Al + 6CO \xrightarrow[\text{benzene}]{\text{aluminum chloride } (AlCl_3)} \underset{\substack{\text{Chromium}\\\text{hexacarbonyl}}}{Cr(CO)_6} + AlCl_3 \quad (1)$$

$$\underset{\substack{\text{Cobalt(III)}\\\text{carbonate}}}{2CoCO_3} + 2H_2 + 8CO \xrightarrow[\text{octane}]{} \underset{\substack{\text{Dicobalt(III)}\\\text{octacarbonyl}}}{Co_2(CO)_8} + 2CO_2 + 2H_2O \quad (2)$$

$$\underset{\substack{\text{Manganese(II)}\\\text{acetate}}}{Mn(CaH_3O_2)_2} + \underset{\substack{\text{Triethyl-}\\\text{aluminum}}}{(C_2H_5)_3Al} + CO \xrightarrow[\text{ether}]{\text{di(isopropyl)-}} \underset{\substack{\text{Dimanganese}\\\text{decacarbonyl}}}{Mn_2(CO)_{10}} \quad (3)$$

Polynuclear metal carbonyls can also be synthesized from other metal carbonyls by photolysis or thermolysis [reactions (4) and (5)].

$$\underset{\substack{\text{Iron}\\\text{pentacarbonyl}}}{2Fe(CO)_5} \xrightarrow{h\nu,\ \text{acetic acid}} \underset{\substack{\text{Diiron}\\\text{ennacarbonyl}}}{Fe_2(CO)_9} + CO \quad (4)$$

$$3Fe_2(CO)_9 \xrightarrow[\text{toluene}]{95^\circ C\ (203^\circ F)} 2\underset{\substack{\text{Triiron}\\\text{dodecacarbonyl}}}{Fe_3(CO)_{12}} + 3CO \quad (5)$$

Metal carbonyls react in solution under relatively mild conditions to form a variety of substitution products, with Lewis bases such as amines, phosphines,

sulfides, and nitric oxide and with organic molecules such as alkenes, alkynes, arenes, and other aromatic compounds. Reactions of metal carbonyls can also afford derivatives containing alkyl, acyl, allyl, halide, hydride, carbene, carbyne, and other substituents. They thus are the most important precursors to the synthesis of organotransition metal complexes. Their thermal decomposition can afford pure metals and CO.

Metal carbonyls and their derivatives also function as reagents in a wide range of organic synthetic applications and as precursors to homogeneous catalysts of considerable industrial importance. For example, in the oxo process, which can employ $Co_2(CO)_8$, several million metric tons of C_{n+1} aldehydes are produced annually from C_n alkenes, CO, and H_2. *See* CARBONYL; HOMOGENEOUS CATALYSIS; ORGANIC CHEMISTRY; ORGANIC SYNTHESIS. Gerard R. Dobson

Bibliography. J. P. Collman et al., *Principles and Applications of Organotransition Metal Chemistry*, 1987; F. A. Cotton et al., *Advanced Inorganic Chemistry*, 6th ed., 1999; R. A. Henderson, *The Mechanisms of Reactions at Transition Metal Sites*, 1994.

Metal casting

A metal-forming process whereby molten metal is poured into a cavity or mold and, when cooled, solidifies and takes on the characteristic shape of the mold. Casting offers several advantages over other methods of metal forming: it is adaptable to intricate shapes, to extremely large pieces, and to mass production; it can provide parts with uniform physical and mechanical properties throughout; and depending on the particular material being cast, the design of the part, and the quantity being produced, it can be more economical.

Categories

The two broad categories of metal-casting processes are ingot casting, which includes continuous casting, and casting to shape. Ingot castings are produced by pouring molten metal into a permanent or reusable mold. Following solidification, the ingots (bars, slabs, or billets) are processed mechanically into many new shapes. Casting to shape involves pouring molten metal into molds in which the cavity provides the final useful shape, followed by heat treatment and machining or welding, depending upon the specific application. Additionally, zero-gravity casting has been developed for processing in space stations.

Ingot casting. Ingot castings make up the majority of metal castings and fall into three categories: static cast ingots, semicontinuous or direct-chill cast ingots, and continuous cast ingots.

Static cast ingots. Static ingot casting simply involves pouring molten metal into a permanent mold (**Fig. 1**). After solidification, the ingot is withdrawn from the mold, and the mold can be reused. This method, while still important for certain grades of steel, is used only for a small amount of steel production. Since 1980, steel production in the United States has changed almost completely from static cast ingots to continuous casting. *See* STEEL MANUFACTURE.

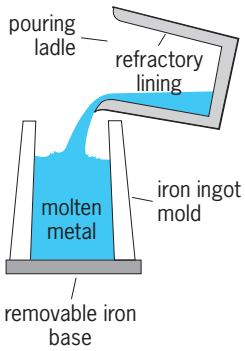

Fig. 1. Static ingot casting.

Semicontinuous cast ingots. A semicontinuous casting process is used in the aluminum industry to produce most of the cast alloys from which rod, sheet, strip, and plate are made. In this process, molten aluminum is transferred to partially fill a water-cooled permanent mold (**Fig. 2***a*) which has a movable base mounted on a long piston. After the solidification has progressed from the mold surface so that a solid "skin" is formed, the piston is moved down, and more metal is added to fill the reservoir (Fig. 2*b*). When the piston has moved its entire length, the process ends. Typically, the aluminum industry uses suitably lubricated metal molds. However, technological advances have allowed major aluminum alloy producers to replace the metal mold (at least in part) with an electromagnetic field so that molten metal touches the metal mold only briefly, thereby making a product with a much smoother finish. This method is also used to produce large brass ingots which are subsequently extruded into various shapes. *See* ALUMINUM; BRASS.

Continuous cast ingots. Continuous casting provides the major source of cast material for the steel and copper industries. In this process, molten metal is delivered to a permanent mold, and is cast in much the same way as in semicontinuous casting. However,

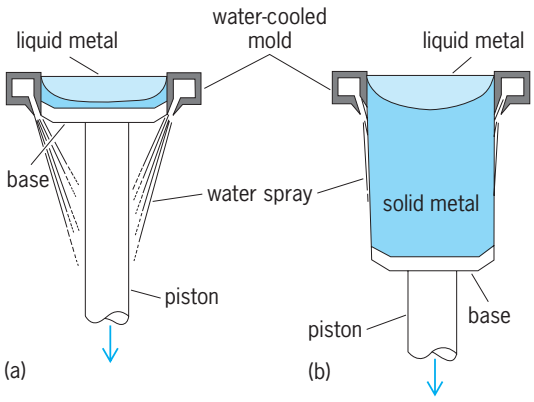

Fig. 2. Semicontinuous (direct-chill) casting. (*a*) Molten aluminum solidifies in a water-cooled mold with a movable base. (*b*) The piston is moved down so more molten metal can be poured into the reservoir.

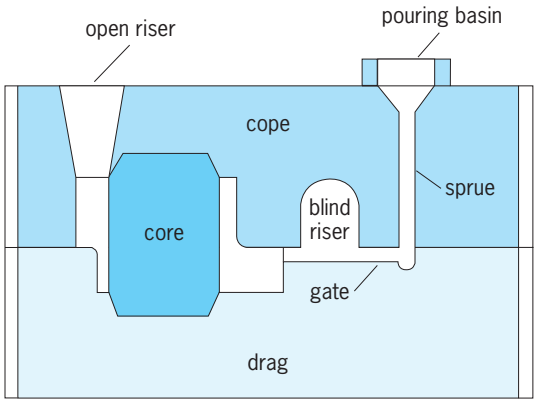

Fig. 3. Section through a sand mold showing the gating system and the risers.

instead of the process stopping after a certain length of time, the solidified ingot is continually sheared or cut into lengths and removed during casting. Thus the solidified billet, plate, or strip is removed as rapidly as it is cast. This method has many economic advantages over conventional casting techniques. As a result, all modern steel mills produce continuous cast products. *See* COPPER; STEEL.

Casting to shape. Casting to shape is generally classified according to the molding process, molding material, or method of feeding the mold. There are five basic shape casting processes: sand, permanent-mold, die, centrifugal, and investment.

Sand casting. This traditional method still produces the largest tonnage of cast-to-shape pieces. It uses a mixture of sand grains, water, clay, and other materials to make high-quality molds into which molten metal is poured. This "green sand" mixture is compacted around a pattern (wood, plaster, or metal), usually by machine, to 20–80% of its bulk density. The basic components of a sand mold, and other molds as well, are shown in **Fig. 3**. The two halves of the mold (the cope and drag) are closed over the cores that form the internal cavities, and the whole assembly is weighted or clamped to prevent floating of the cope when the metal is poured. Examples of sand castings include gray iron diesel engine blocks and disc brake rotors, as well as some very complex aluminum alloy castings for the aerospace industry. *See* CAST IRON.

Other casting processes which use sands as a basic component are the shell, carbon dioxide, ceramic molding, and plaster molding processes (see **table**), as well as a large number of chemically bonded sands which are increasingly important. In addition, both investment casting and evaporative pattern casting (lost foam) use sand in special ways.

Precision casting processes. This casting method produces near net shape products (or as close as possible), with little or no machining required after casting. In general, because of the required tight dimensional tolerances, these processes have molds which are very rigid, such as permanent molds or very hard expendable molds. Precision casting processes include investment casting, die casting, permanent molding processes, lost foam processes, and the Cosworth process. Die casting and permanent molding processes involve using permanent molds together with either gravity casting (permanent molds) or pressure-assisted casting (die casting). The Cosworth process uses disposable molds made with aggregate ceramic materials.

The Cosworth process, or precision sand process, is a method developed in the mid-1970s for producing aluminum castings to meet the highly specialized needs of Formula One racing cars. In this process,

Details of casting processes that utilize sands as a basic component

Process name	Pattern type	Molding aggregate	Type of bond	Relative cost
Green sand	Wood Plaster Metal	Sand Clay Water	Due to clay plasticity and compaction	Low
Shell	Heated metal	2.5–10% thermosetting resin	Polymerization of resin by pattern heat	Medium
CO_2	Wood Metal	Sand 2–6% sodium silicate	Inorganic bond by chemical reaction of CO_2 with silicate	Medium
Investment	Wax Expendable plastic	Sand Slurry Ceramic binder	Setting ceramic binder	High
V-Process*	Wood Metal	Sand enclosed in plastic with vacuum	Vacuum bond	Medium
No-bake	Wood Metal	Sand Organic compound	Organic bond created by reaction with catalyst	Medium
Full-mold*	Polystyrene coated with thin layer of ceramic	Sand	None	Medium

* Proprietary name.

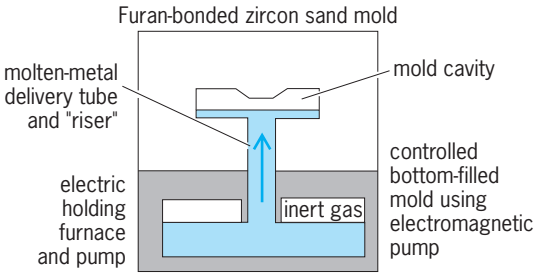

Fig. 4. Cosworth casting process.

molten metal is electromagnetically pumped from the bottom to the top of the mold in a controlled manner (**Fig. 4**). Benefits include improved levels of accuracy and integrity, very little porosity, excellent surface detail, excellent mechanical properties, virtually no cleaning and finishing costs, and minimum machining and high casting yield. The high casting yield results from the minimal gating system and the ability to control molten metal delivery. The delivery tube can act as a riser for the solidifying casting, and the molten metal feeding the shrinkage can, in principle, be returned to the reservoir and pump after the casting has solidified, thereby giving an obvious yield boost. Minimum porosity results from the controlled manner in which the molten metal enters the mold and the inert atmosphere over the molten metal.

Permanent-mold casting. Many high-quality castings are obtained by pouring molten metal into a mold made of cast iron, steel, or bronze. Semipermanent-mold materials, such as aluminum, silicon carbide, and graphite, may also be used. The mold cavity and the gating system are machined to the desired dimensions. The smooth surface from machining gives a good surface finish and dimensional accuracy to the casting. To increase mold life and to make ejection of the casting easier, the surface of the mold cavity is usually coated with carbon soot or a refractory slurry. These coatings also serve as heat barriers and help control the rate of cooling. This casting process is used for cast iron and nonferrous alloys, with advantages over sand casting such as smoother surface finishes, closer tolerances, and higher production rates. Aluminum alloy automotive pistons are an excellent example of permanent-mold castings. *See* BRONZE.

Die casting. Another variation of the permanent molding process is die casting. Molten metal is forced into a die cavity under pressures of 100–100,000 lb/in.^{2} (0.7–700 megapascals). Two basic types of die-casting machines are hot-chamber and cold-chamber. In the hot-chamber machine, a portion of the molten metal is forced into the cavity at pressures up to about 2000 lb/in.^{2} (14 MPa). The process is used for casting low-melting-point alloys such as lead, zinc, and tin alloys. *See* ALLOY; LEAD; TIN; ZINC.

In the cold-chamber process (**Fig. 5**), the molten metal is ladled into an injection cylinder and forced into the cavity under pressures about 10 times higher than those in the hot-chamber process. Higher-melting-point aluminum-, magnesium-, and copper-base alloys are commonly produced by this process. Most aluminum alloy castings are produced by this process. A good example of an aluminum alloy casting produced in large quantities is the marine engine block. Die casting has the advantages of high production rates, high quality and strength, surface finish on the order of 40–100-microinch (1.0–2.5-micrometer) root mean square, and close tolerances with thin sections. *See* MAGNESIUM.

Squeeze casting is a growing technology for producing shrinkage-free castings in permanent-mold dies by applying pressure to the casting as it solidifies, a structural condition that results in vastly improved fatigue properties. This technique successfully produces high-integrity aluminum alloy steering knuckles for automotive applications (**Fig. 6**).

Rheocasting is the casting of a solid and liquid mixture. In this process the alloy to be cast is melted and then allowed to cool until it is about 50% solid and 50% liquid. Vigorous stirring promotes the liquidlike properties of the mixture so that it can be injected in a die-casting operation. A major advantage of this type of casting is reduced die erosion due to the lower casting temperatures.

Centrifugal casting. Inertial forces of rotation distribute molten metal into the mold cavities during centrifugal casting, categorized into true centrifugal casting, semicentrifugal casting, and centrifuging. The first two processes (**Fig. 7**) produce hollow cylindrical shapes and parts with rotational symmetry, respectively. In the third process, the mold cavities are spun at a certain radius from the axis of rotation, and the resulting centrifugal force increases the pressure in the mold cavity.

The rotational speed in centrifugal casting is chosen to give 40–60 *g* acceleration. Dies may be made of forged steel or cast iron. Colloidal graphite is used on the dies to aid casting removal. Karl Rundman

Evaporative pattern casting. This is another casting process that uses sand as a basic component. It is unique in that the casting shape is not defined by molding the sand. Instead, a polystyrene foam pattern or replica is formed into the shape of the component to be cast, and determines the size and shape of the casting. In fact, the casting is a metal copy of

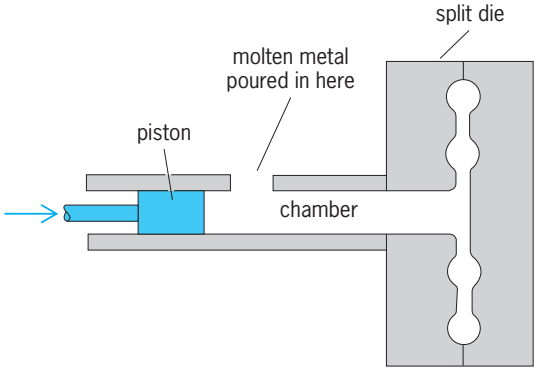

Fig. 5. Cold-chamber die casting machine.

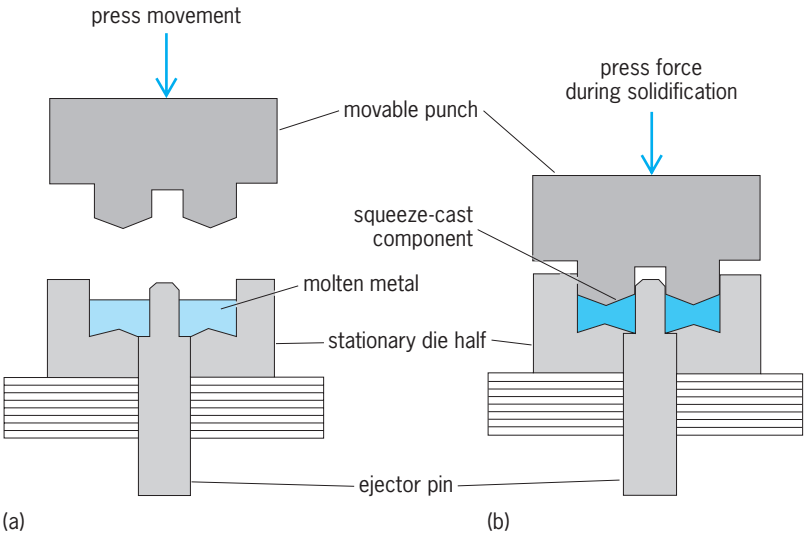

Fig. 6. Production of a squeeze casting. (*a*) Press open. (*b*) Press closed.

the polystyrene foam shape. The sand is used as a backing medium. After the polystyrene replica has been assembled and coated with a refractory wash to prevent burn-in, the coated replica is placed in a flask, and free-flowing sand is compacted around the replica to support the solidifying metal. The sand is mechanically locked in place by vibration, or the replica is immersed in a fluidized bed of sand. In either case, a coated polystyrene foam replica tightly surrounded by sand is now ready for metal pouring. Typically, a pouring cup is placed over the replica. The molding flask is either vented or equipped for vacuum pouring to remove the polystyrene off-gases. These off-gases, created as the polystyrene foam is thermally decomposed by heat from the molten metal, may ignite, depending on the heat of the metal. *See* POLYSTYRENE RESIN.

The evaporative casting process is compatible with bronze, steel, aluminum, and iron castings. In general, the microstructural characteristics of castings made by the evaporative process tend to be the same as those of castings made by conventional sand casting processes. Shrinkage rules for various aluminum alloys and iron types are also the same for evaporative casting and conventional sand molding. Thus, the presence of the polystyrene foam and its decomposition products does not alter casting dimensions and has little effect on microstructure or metal chemistry.

The major advantages of the evaporative casting process are reduced costs and greater flexibility. Savings result from lower investment costs and lower costs to make a casting. The lower investment costs come about because the equipment needed to make polystyrene foam replicas is less expensive than the equipment used to make conventional sand molds and cores. Also, the polystyrene molding equipment operates at higher speeds. Finally, the tooling for polystyrene foam replicas is less expensive and has a longer life than the tooling for conventional sand molds and cores. The cost per casting made by the evaporative process is lower because the process does not require cores and allows for easy reuse of the casting sand (no resins are added to the sand). Also, the casting made by this process is easier to clean than a conventional sand casting because there are no fins and parting lines that need to be ground down.

Evaporative casting offers process advantages in terms of both design flexibility and metals compatibility. The design flexibility results from the greater freedom in planning draft angles, parting lines, locator placement, and transitions from thin to thick sections. Evaporative casting can be used to make one-of-a-kind castings of investment-cast quality as well as high-volume production of automotive castings such as aluminum intake manifolds and iron connecting rods. S. A. Weiner

Investment casting. Investment casting is a process used to make precision castings in a variety of materials. The process has been known for thousands of years as the "lost wax" process. Precision patterns are produced in wax and coated (invested) in a ceramic slurry, which is allowed to dry before subsequent layers are added. Up to seven layers of investment material may be applied before the wax is carefully melted out, leaving a cavity. Next, the invested mold is fired at high temperature to produce a strong, rigid ceramic that is subsequently filled with molten metal. The precision castings are removed from the mold by carefully chipping away the ceramic shell. Perhaps the ultimate development of the investment technique was the controlled growth of investment-cast nickel alloy jet engine turbine blades, where

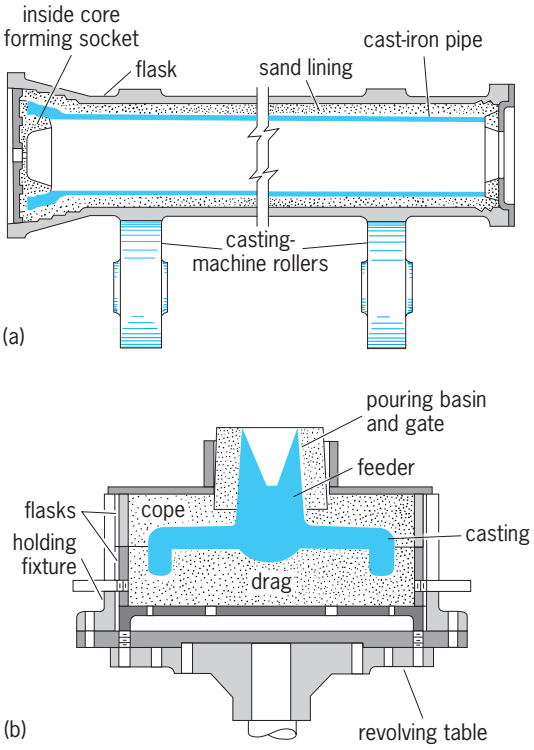

Fig. 7. Centrifugal casting. (*a*) Iron pipe cast in a centrifugal mold. (*b*) Flywheel cast in a semicentrifugal mold.

controlled solidification, starting at the base of the blade and continuing up through a tortuous "pigtail" configuration, allows only one crystal to emerge. The resulting single-crystal blade provides optimum properties (high-temperature creep resistance) in a critical application.

Zero-gravity casting. Zero-gravity casting has come of age with the advent of space stations. In the absence of gravity, the concept of melting and casting is drastically changed. The disadvantages of ground-based processing that appear to be diminished or eliminated by processing under weightless conditions are thermal and solutal convection and sedimentation; contamination of and contact with the container during processing; and hydrostatic pressure effects and deformation at high temperatures. There appears to be a potential for processing liquid metals at zero gravity; however, commercial production is expected to be limited initially to small quantities of high-cost materials whose solidification characteristics are greatly improved by the lack of gravity. Semiconductor materials are thought to be excellent candidates for initial development efforts. *See* SPACE PROCESSING.

Principles and Practice

Successful operation of any metal-casting process requires careful consideration of mold design and metallurgy.

Design considerations. In all types of ingot casting, successful production depends upon several factors. In more technologically complicated semicontinuous or continuous casting processes, the design of cooling systems, choice of lubrication, and rate of slab or billet movement play an important production role.

In the production of castings that are not subsequently machined, the construction of a pattern is an important step. Considerations of casting design, mold design, riser design, and gating practice play a role in the final pattern design from which molds are made. Modern foundries use computer-aided design techniques to simulate metal flow and solidification, incorporating fluid flow and heat transfer principles, before producing a single casting. Computer modeling allows designers and pattern makers to eliminate much trial and error in the casting process, reducing lead times significantly. *See* COMPUTER-AIDED DESIGN AND MANUFACTURING.

Gating system. The gating system (Fig. 3), which includes the pouring basin, downsprue, runners, and gates, must be designed to allow the liquid metal to enter the mold cavity with a minimum of turbulence, slag, and temperature loss. The application of Bernoulli's law, together with the criterion of conservation of mass, allows gas aspiration, turbulence, and slag entrapment to be kept to a minimum. All these factors are capable of being computer-modeled. *See* BERNOULLI'S THEOREM.

Riser design. A riser is a volume attached to the casting (Fig. 3) that provides metal to feed the shrinkage that occurs when liquid cools and solidifies. In fact, there are three contributions to shrinkage that must be accommodated: shrinkage of the liquid as it cools between the pouring temperature and the melting temperature; shrinkage as the liquid transforms to solid; and shrinkage of the solid portion on cooling during the time when some liquid remains. In order to supply liquid metal for the shrinking casting, the riser must also freeze after the cavity has frozen. The solidification time t_s is directly related to the heat transfer rate in the mold and to the volume-to-surface area ratio (V/A) of the casting. Thus, the foundry engineer can ensure the soundness of a casting in situations where the riser and casting have identical mold surroundings by making the V/A ratio of the riser larger than the V/A ratio of the casting. In large bulky castings, the riser may actually be larger than the casting, which increases the cost of production. Reducing this cost can sometimes be accomplished by insulating a smaller riser (changing the mold surroundings), thereby reducing the rate of heat transfer and prolonging the time that the riser is molten. Two types of risers are shown in Fig. 3, an open riser and a blind riser. Again, all these decisions can be made in simulations of the casting process before a drop of molten metal is produced.

Ease of pattern extraction. Sand molding patterns must be designed with a draft of 0.25–2° so that after the mold material has been compacted around the pattern, the pattern can be extracted without damage to the mold. Permanent molding dies must also be constructed so that after solidification the casting can be ejected without damaging either the casting or the die. The wax patterns of investment castings must be capable of being poured out of the cavity during heating so that no pockets of wax remain.

Machining considerations. For castings requiring subsequent machining, the patterns must be designed within certain dimensional tolerances so that enough stock is left for machining.

Metallurgical considerations. While design factors are important for producing sound castings with proper dimensions, factors such as the pouring temperature, alloy content, mode of solidification, gas evolution, and segregation of alloying elements control the final structure of the casting and therefore its mechanical and physical properties. Typically, pouring temperatures are selected within 100–300°F (60–170°C) of an alloy's melting point. Exceedingly high pouring temperatures can result in excessive mold metal reactions, producing numerous casting defects.

Most metals and alloys pass from the liquid state to the solid state in a predictable manner. The rate of solidification is a function of the rate at which heat is withdrawn by the mold and of the size of the casting. In continuous casting or semicontinuous casting, liquid is added at the same rate as solid is formed. Thus, a steady state is established. In the case of static cast ingots or cast-to-shape products, the entire liquid may be poured into the mold before any solidification begins. In either of these cases, however, the manner in which solidification occurs is quite similar for most commercial materials.

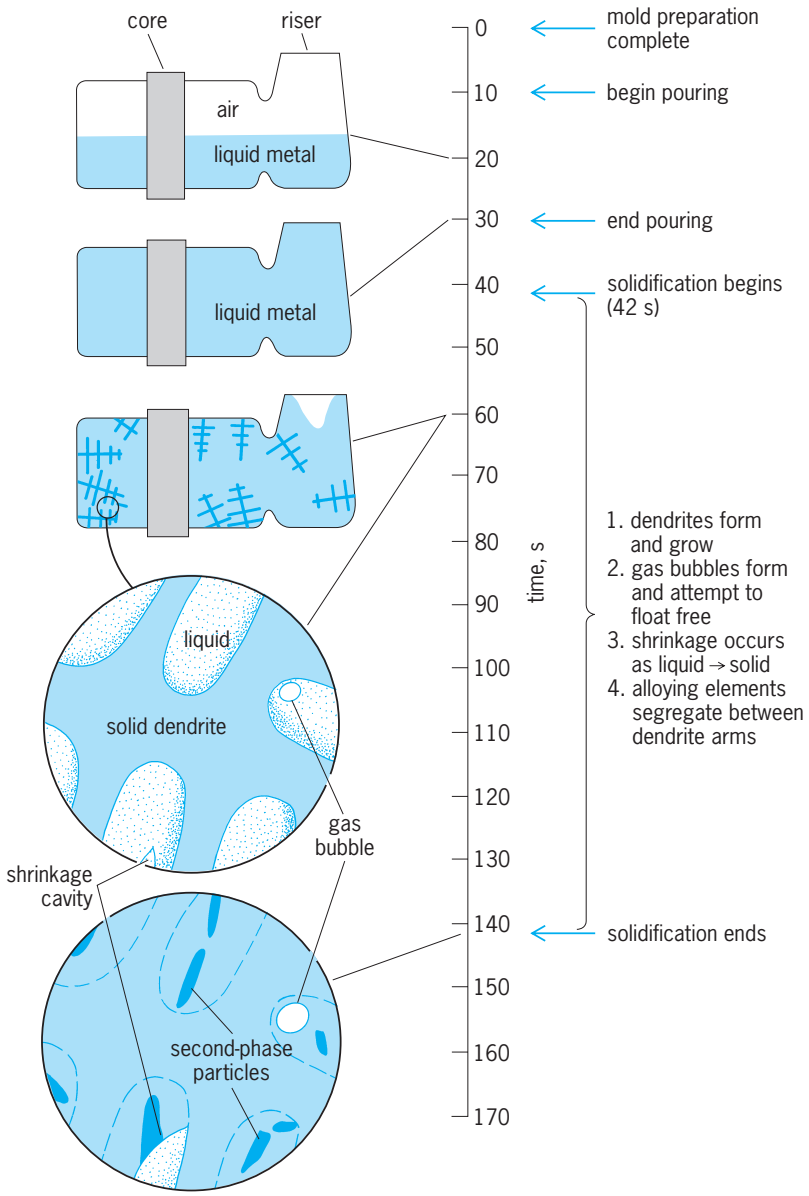

Fig. 8. Solidification and processing history for a cast-to-shape part.

The relationship between the processing history and the solidification is illustrated in **Fig. 8** for a cast-to-shape part. Solidification often begins with the formation of dendrites on the mold walls, which grow with time into the liquid and eventually consume the entire liquid volume. Dendrites are treelike or fernlike solids with primary arms similar to tree trunks and secondary arms resembling tree branches. Dendrites form in almost all commercial metals and are responsible to a large extent for their resulting as-cast properties. In pure metals, dendrites form if supercooling below the melting point occurs. Supercooling refers to the liquid existing below the temperature where it would normally change to solid. Supercooling can be accomplished by cooling the metal rapidly and by providing an extremely clean molten metal bath, thereby hindering nucleation of solid particles.

A particularly effective way of supercooling is through levitation melting, a technique whereby the metal is suspended in a magnetic field so that it touches no foreign object. Thus, no mold surface is available for dendrite growth, and there are no sharp temperature gradients within the metal. The levitation phenomenon is similar to the semicontinuous casting of aluminum alloy ingots, where the molten metal is levitated away from the mold surface. It has been suggested that levitation melting would be a natural method for casting in space. In the absence of gravity, large quantities of molten metals could conceivably be processed and handled by levitation techniques. In addition to the potential for casting in space, levitation melting provides exciting possibilities for producing high-purity materials free from gaseous contaminants and their products.

In metal alloys, solidification usually occurs over a range of temperatures. In alloys, dendrites grow in response to constitutional supercooling of the liquid below the liquidus temperature (the highest temperature at which solidification can occur). Usually it is desired to have the alloying elements distributed uniformly throughout the material after solidification has occurred. Invariably, dendritic growth will cause the alloying elements to be segregated and concentrated either between the dendrite arms (positive segregation) or within the dendrites (negative segregation). The segregation of alloying elements increases with dendrite growth and may ultimately lead to the formation of another solid phase when solidification is complete (Fig. 8). A good example of this type of structure is found in a leaded-copper alloy, containing mostly copper. Due to certain atomic forces between copper and lead atoms, nearly pure copper dendrites will form on solidification, leaving all of the lead as small spheres between the dendrites. This result is desirable in bearings, where the lead acts as a built-in lubricant. Many other commercial cast-to-shape materials have properties that depend on the presence of a second phase in the interdendritic volumes: cast iron structures are basically pure graphite particles (plates or spheres) between iron dendrites or dendrite arms; in aluminum silicon alloys, pure silicon particles (plates or rods) are located between aluminum dendrites. These phases are responsible in large part for the desirable properties of the material. However, in many continuous or semicontinuous cast alloys, particularly aluminum alloys and steels, the alloying elements that solidify between the dendrite arms are undesirable and must be redistributed to obtain the desired properties. This redistribution, or breaking up of the dendritic structure, is accomplished by various combinations of mechanical working and heat treatment.

In addition to creating segregation, the dendritic form of the solid provides a perfect place to trap gas bubbles. In addition, the very tightly spaced dendrite arms restrict liquid flow, often resulting in shrinkage porosity between dendrite arms (Fig. 8). Degassing operations, in which certain gases are bubbled through the melt, may be used to minimize the

gas porosity. As described by Sievert's law, the purging gas bubbles will attract the undesirable gases and remove them from the melt. In the case of shrinkage, the amount of microshrinkage may be reduced by increasing the cooling rate (sometimes called chilling). This action serves to make the dendrites stubbier, thereby providing freer access for metal flow to feed the shrinkage. Ideally, with the use of carefully regulated molding materials, solidification can be controlled so that dendritic growth occurs smoothly from the point farthest away from the riser directly to the riser, so that the last volume to solidify is the riser itself. This directional solidification concept is used in the production of many unique cast metal parts, particularly investment cast turbine blades.

Contraction of the casting during solidification can cause a defect known as hot tearing. Tensile stresses may be set up in the solidifying casting, which causes tears to open up between the dendrites. These types of defects are quite common in both ingot and cast-to-shape products. If the tears are not filled by liquid metal, then cracks will remain in the solidified casting. These defects can usually be avoided by proper mold design (or controlled cooling of continuous cast products) to minimize tensile-stress development. Residual stresses are elastic stresses that may form in solid materials due to uneven heating or cooling. These can cause warping or failure in castings following solidification unless steps are taken to ensure uniform cooling.

Other metal-casting process defects are (1) macrosegregation, caused by significant interdendritic fluid flow; (2) pinhole porosity, a smooth-walled defect elongated in a direction perpendicular to the mold wall and immediately below the casting skin; (3) metal penetration, resulting from liquid metal penetrating sand, and causing a metal-sand crust attached to the casting; (4) blows, cavities resulting from entrapped gases originating from cores; and (5) cold shuts, seams of oxide or slag resulting from low pouring temperatures.

Most or all of the above defects could be minimized or eliminated by processing in the zero-gravity, high-vacuum environment of space. Macrosegregation on Earth is driven primarily by gravity effects in which solute-rich material sinks in response to gravity differences. Thus the nagging inhomogeneities created in this way on Earth will be minimized or eliminated at zero gravity. Porosity and blowholes caused by dissolved gases will be reduced or eliminated by the vacuum melting conditions of space. Mold-metal reaction products can be minimized by containerless casting, use of levitation devices, and the like which eliminate mold-metal contact. Thus, processing at or near zero gravity has the potential for improving the quality of castings. However, the high cost of most such efforts limits their utility to casting small quantities of very specialized alloys.

Application

Almost all metals and alloys used by engineering specialists have at some point been in the molten state and cast. Metallurgists have in general lumped these materials into ferrous and nonferrous categories. Ferrous alloys, cast irons and steels, constitute the largest tonnage of cast metals. Aluminum-, copper-, zinc-, titanium-, cobalt-, and nickel-base alloys are also cast into many forms, but in much smaller quantity than cast iron and steel. Selection of a given material for a certain application will depend upon the physical and chemical properties desired, as well as cost, appearance, and other special requirements.

Aluminum alloy castings have advantages such as low density, resistance to corrosion, high electrical conductivity, ease of machining, and architectural and decorative uses. Magnesium alloy castings have the lowest density of all commercial casting alloys. Both aluminum and magnesium alloy castings are finding increased use in automotive applications. Copper alloy castings, although costly, have advantages such as corrosion resistance, high thermal and electrical conductivity, and wear properties suitable for antifriction-bearing materials. Steel castings have more uniform (isotropic) properties than the same component obtained by mechanical working. Cast irons constitute the largest tonnage of all cast-to-shape metals. Gray iron castings are commonly produced for their low cost, excellent machinability, good damping capacity, excellent thermal conductivity, good wear resistance, and uniformity. Nodular cast irons have significantly higher strength and ductility than gray irons, but are more costly and not as machinable. There is an intermediate grade of cast iron called CG (compacted graphite) iron which shares the best properties of both gray and nodular irons. *See* METAL, MECHANICAL PROPERTIES OF; METAL FORMING.

Karl Rundman

Bibliography. American Foundrymen's Society, *Basic Concepts of the Metalcasting Proccess*, 1987; American Society for Metals, *Casting Metals Hand-book*, vol. 15: *Casting*, 9th ed., 1988; M. C. Flemings, *Solidification Processing*, 1974; R. Johns, *Casting Design*, 1987; H. D. Merchant, D. E. Tyler, and E. H. Chia (eds.), *Continuous Casting of Non-Ferrous Metals and Alloys*, 1989.

Metal cluster compound

A compound in which two or more metal atoms are bonded to one another. Metal cluster compounds bridge the gap between the solid-state chemistry of the metals—or their lower-valent oxides, chalcogenides, and related salts—and the complexes of the metals in which each metal ion is completely surrounded by and bonded to a set of ligands or ions. The latter group comprises the classical coordination chemistry of metal ions.

Interest in metal cluster compounds arises from unique features of their chemistry: (1) Cluster compounds provide models for studying fundamental reactions on surfaces. (2) There is a hope that cluster compounds may provide entry to new classes of catalysts that may be tailored to specific syntheses and may thus be more selective than existing processes.

(3) The nature of the bonding in cluster compounds is an area wherein experiment and theory are continuously challenging each other. (4) The systematic synthesis of mixed metal clusters may provide for the development of new types of supported catalysts (the discrete clusters are deposited on supports such as alumina, silica, or zeolites).

Metal clusters can be classified into three categories: those whose only existence is in the solid state; those that exist both in the solid state and in a solution in which each cluster unit of metal atoms is surrounded by a set of ligands; and the so-called naked metal clusters, which carry a charge but are otherwise surrounded only by solvent molecules when in solution. Often, naked clusters may have a form different from that exhibited in the solid state. For each of these classes the metal atoms may be the same or the clusters may contain more than one type of metallic element: they are known respectively as homometallic or heterometallic clusters.

The term "bonded" is the key in understanding the nature of metallic clusters. The bonding may be localized, where each metal–metal interaction can be counted as an electron pair, or the bonding may be a type in which the electrons are delocalized over the metallic (M_x) subunit so that it is impossible to assign precise electron-pair interactions. The strength of the metal–metal interactions can range from strong metal–metal bonding, as in the metallic state of the elements, to weak interactions in which the metal atoms are coupled only loosely in an electronic sense. The latter is often the case in metal-containing enzymes, where more than one metal atom is required for a specific task. *See* CHEMICAL BONDING; DELOCALIZATION.

Metallic clusters in bioinorganic molecules. In a number of iron-sulfur proteins, such as the ferrodoxins, there are two, three, or four iron (Fe) atoms linked by sulfido sulfur (S) atoms (inorganic sulfurs) and also bonded to the protein by the sulfur atoms of cysteine residues. These are redox active centers, and they are involved in a variety of electron transfer reactions. Other bioinorganic molecules that utilize two or more electronically coupled metal ions are found in hemerythrins (Fe_2 units used for oxygen transport in marine worms), photosystem II [manganese (Mn_4) units used to catalyze the splitting of water (H_2O) to hydrogen (H_2) and oxygen (O_2)], and hemocyanins [copper (Cu_2) subunits involved in the oxygen transport]. *See* ELECTRON-TRANSFER REACTION; OXIDATION-REDUCTION.

While the metal–metal interactions in all known bioinorganic molecules are weak, they are strong enough to result in important cooperative effects. In some cases the detailed nature of both structure and function remains uncertain; an example is nitrogenase, an enzyme used to reduce nitrogen (N_2) to ammonia (NH_3) in a variety of plants. In addition to containing a four-iron/four-sulfur cluster component, nitrogenase contains an iron-molybdenum cluster subunit, the so-called iron–molybdenum cofactor (FeMoco), having two molybdenum (Mo) atoms and six or eight Fe atoms and approximately six inorganic sulfur atoms. The unique way in which this inorganic cluster unit functions within the large biomolecule remains a subject of intense research activity. *See* BIOINORGANIC CHEMISTRY; ENZYME; PROTEIN.

Cluster units in the solid state. A wide variety of lower-valent (subvalent) metal halides, oxides, and chalcogenides contain cluster subunits of metal atoms. These are well exemplified by the so-called Chevrel phases that have the formula $M_xMo_6X_8$, where M = lead (Pb), tin (Sn), Ln (lanthanon; a lanthanide element), potassium (K), calcium (Ca), Cu, lithium (Li), and others (in all, over 40 elements) and X is usually sulfur, selenium (Se), or tellurium (Te) and occasionally bromide (Br^-) or iodide (I^-). Research in this field was driven by the discovery that these cluster-containing compounds become superconducting at low temperatures. These were among the first group of nonmetals and nonmetal alloys to exhibit superconductivity. The basic building block for most of these solid-state clusters is an octahedron of metal atoms inscribed in a cubic arrangement of ligands, either as $M_6(\mu_3\text{-}L)_8$, where the positions L define the corners of a cube and cap the 8 faces of the octahedron, or the $M_6(\mu_3\text{-}L)_{12}$ structure, where each of the 12 edges of the octahedron of metal atoms contains a bridging group L. In the latter case the ligands occupy center positions of the 12 edges of a cube. The three-dimensional lattice structure is built upon these M_6 cluster units through the sharing of common bridging atoms or by the fusing of the M_6 octahedra so that apices, edges, or faces are shared (see **illus.**). Solid-state clusters are also found based on rhomboidal M_4 and triangular M_3 subunits, and these may be viewed as fragments of the M_6 octahedron. In some instances, interstitial atoms such as carbon (C), boron (B), and nitrogen (N) are found inside the M_6 unit, and these atoms provide additional so-called molecular glue by supplying additional electrons to bind the metal atoms together. Similarly, hydride (H^-), carbide (C^{4-} or C_2^{x-}), and nitride (N^{3-}) are commonly found in molecular clusters. *See* CHEVREL PHASES; CRYSTAL STRUCTURE; SUPERCONDUCTIVITY.

Molecular clusters. These compounds may be neutral or charged, but they are characterized by a grouping of metal atoms surrounded by a set of ligands such as carbon monoxide (CO), tertiary phosphines (R_3P; R = functional group), and alkoxides (organic compounds in which the H of an OH group has been replaced by a metal). Some examples include $Au_{55}[P(C_6H_5)_3]_{12}Cl_{12}$; $[Os_{10}(C)(CO)_{24}]^{2-}$; $[Pt_3(CO)_6]_n^{2-}$, where n = 2, 3, and 5; and $W_4(OC_2H_5)_{16}$. Interest in these clusters has centered on understanding and predicting the geometries and bonding and then developing their reaction chemistry. The clusters that possess many metal atoms bridge the gap between metals and molecules, since the ligands bonded to the clusters may resemble the molecules and fragments of molecules bound to metal surfaces. For example, in an Os_3 cluster it has been possible to monitor the interconversion of hydride (H^-) and methyl (CH_3) ligands with dihydrido-methylene

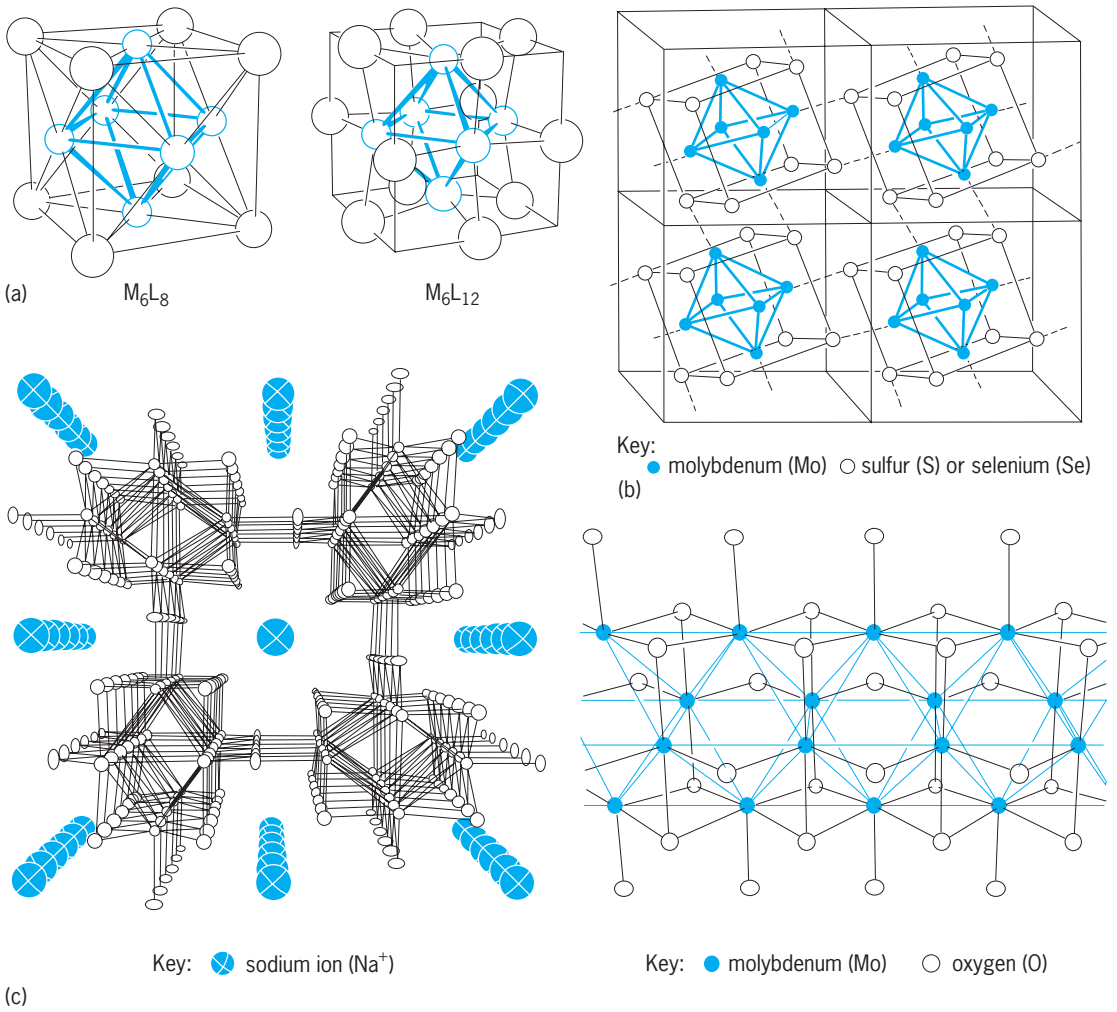

Structural representations of some metal clusters. (*a*) Two common octahedral M_6 cluster units. On the left, 8 ligand atoms lie at the corners of a cube and cap the 8 faces of the octahedron; on the right, 12 ligand atoms occupy the centers of the 12 edges of the cube-octahedron. (*b*) View of the M_6L_8 cluster units in the binary molybdenum compounds Mo_6X_8, where X = sulfur or selenium. (*c*) Two views of the structure of sodium molybdate ($NaMo_4O_6$), which contains Mo_6 octahedra-sharing edges. The view on the left is looking down the crystallographic *c* axis and shows the ordering of the sodium (Na^+) ions in channels between the extended chains of Mo_6 cluster units shown on the right.

$[(H)_2—CH_2]$ and trihydrido-methylidyne $[(H)_3—CH]$. These provide models for the stepwise activation of methane (CH_4) by a grouping of metal atoms in which successive C-H bonds are substituted by metal-carbon bonds. It takes more than one metal atom to bring about a specific chemical reaction, which is referred to as the ensemble effect. Collectively, a grouping of metal atoms may act as an electron source or sink and provide a template for substrate activation. For example, even carbon monoxide, which has the highest bond dissociation energy ($256\ K \cdot cal \cdot mol^{-1}$), can be cleaved in reactions with certain M_4 clusters. The reactivity and dynamic properties of species bound to molecular clusters provide model studies for many catalytic reactions involving metal surfaces or metal oxides. *See* HETEROGENEOUS CATALYSIS; HOMOGENEOUS CATALYSIS; METAL HYDRIDES.

Naked metal clusters. These are known in heterogeneous phases of main-group metals, transition metals, and mixed metals. Many supported metals (deposited on alumina or silica), for example, rhodium/tin and platinum/tin, are used in the petroleum industry as reforming catalysts. Cationic naked metal clusters such as the bismuth cluster Bi_5^{3+} exist in molten salts, and many others have been made and studied either by low-temperature matrix isolation or in the gas phase. By contrast, anionic naked metal clusters are obtained when certain alloys, for example, sodium/tin, sodium/lead, and sodium/antimony, are extracted into solution with liquid ammonia or ethylenediamine; examples include the lead cluster Pb_5^{2-}, Sn_9^{2-}, and the antimony cluster Sb_7^{3-}. Naked metal cluster anions of metals of the main groups in the periodic table adopt polyhedral structures reminiscent of the boron hydrides. In solution these clusters exhibit strong metal–metal interactions and weak metal–solvent interactions. These species may be useful for the preparation of thin films of metal atoms and as novel reducing agents. *See* CRACKING; MATRIX ISOLATION; PERIODIC TABLE.

Characterization. Generally, the ultimate characterization of a metal cluster rests upon an x-ray structural determination. By this method the detailed

arrangement of metal atoms, the nature of metal–ligand interactions, and the precise stoichiometry can be seen in one picture. However, it is often important to determine that what is seen in the solid state is also present in solution, particularly for molecular clusters that have solubility in various solvents. A variety of complementary techniques can be used for this purpose; nuclear magnetic resonance and infrared and Raman spectroscopy are most important for correlating solid-state and solution properties. In many instances, other techniques may provide specialized information concerning the oxidation states of the metal atoms (x-ray photoelectron spectroscopy, Mössbauer spectroscopy) or the electronic structure within a grouping of M-M molecular orbitals (electron spin resonance and ultraviolet or visible light spectroscopy). Extended x-ray absorption fine structure (EXAFS) has also proved useful in obtaining local information of metal-ligand bondings where single-crystal x-ray studies have not been possible, for example, in probing the nature of nitrogenase; but there are always limitations to the details provided by such less definitive spectroscopic techniques. Neutron diffraction has proved useful for the structural determination of both finely divided but microcrystalline solids and in the absolute location of light atoms, particularly hydrides, in molecular clusters. *See* COORDINATION CHEMISTRY; COORDINATION COMPLEXES; EXTENDED X-RAY ABSORPTION FINE STRUCTURE (EXAFS); INFRARED SPECTROSCOPY; MÖSSBAUER EFFECT; NUCLEAR MAGNETIC RESONANCE (NMR); RAMAN EFFECT; SOLID-STATE CHEMISTRY; SPECTROSCOPY; SURFACE AND INTERFACIAL CHEMISTRY.

Malcolm H. Chisholm

Bibliography. M. H. Chisholm and F. A. Cotton, Bonds between metal atoms: A new mode of transition metal chemistry, *Chem. Eng. News*, 60:40–54, June 28, 1982; F. A. Cotton and R. A. Walton, *Multiple Bonds Between Metal Atoms*, 1984; L. J. De Jongh (ed.), *Physics and Chemistry of Cluster Compounds: Model Systems for Small Metal Particles*, 1994; J. Lewis, Metal clusters revisited, *Chemistry in Britain*, 24:795–800, 1988.

Metal coatings

Thin films of material bonded to metals in order to add specific surface properties, such as corrosion or oxidation resistance, color, attractive appearance, wear resistance, optical properties, electrical resistance, or thermal protection. In all cases proper surface preparation is essential to effective bonding between coating and basis metal, so that coated metals can function as duplex materials. This article discusses various methods of applying either metallic coatings (see **table**) or nonmetallic coatings, such as vitreous enamel and ceramics, and the conversion of surfaces to suitable reaction-product coatings. For other methods for the protection of metal surfaces *see* CLADDING; ELECTROLESS PLATING; ELECTROPLATING OF METALS; LACQUER; PAINT AND COATINGS.

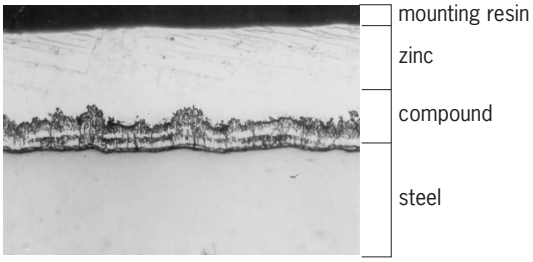

Fig. 1. Cross section of galvanized steel.

Hot-dipped coatings. Low-melting metals provide inexpensive protection to the surfaces of a variety of steel articles. To form hot-dipped coatings, thoroughly cleaned work is immersed in a molten bath of the coating metal. The coating consists of a thin alloy layer together with relatively pure coating metal that adheres to the work as it is withdrawn from the bath (**Fig. 1**). Sheet, strip, and wire are processed on a continuous basis at speeds of several hundred feet per minute. On the other hand, hardware and hollow ware are handled individually or in batches.

Coating weights for zinc coatings are expressed as ounces of coating per square foot (1 oz/ft^2 is equivalent to 0.305 kg/m^2 or 43-micrometer thickness on hardware or wire, and to one-half this thickness on sheet). Hot-dipped tin and lead-tin (Terne) coatings are expressed as pounds per base box. A base box is 31,360 in.^{2} (20.23 m^2); thus 1 lb (0.4536 kg) per base box is equivalent to 1.50 μm of tin.

Galvanized steel, that is, steel hot-dipped in zinc, is used for roofing, structural shapes, hardware, sheet, strip, and wire products. Coatings normally range up to 3 oz/ft^2 (0.9 kg/m^2) for outdoor service. Hot-dipped tinplate is now largely supplanted by electroplated tinplate for tin cans. Terne plate, with coatings up to 20 μm, is used for roofing, chemical cabinets, and gasoline tanks. Hot-dipped aluminum-coated (aluminized) steel with coatings up to 10 μm thick are used for oil refinery equipment and furnace and appliance parts where protection at temperatures up to 1000°F (538°C) is required.

Sprayed coatings. A particular advantage of sprayed coatings is that they can be applied with portable equipment. The technique permits the coating of assembled steel structures to obtain corrosion resistance, the building up of worn machine parts for rejuvenation, and the application of highly refractory coatings with melting points in excess of 3000°F (1650°C).

Nearly any metal or refractory compound can be applied by spraying. Coating material in the form of wire or powder is fed through a specially designed gun, where it is melted and subjected to a high-velocity gas blast that propels the atomized particles against the surface to be coated (**Fig. 2**). The surface is initially blasted with sharp abrasive to provide a roughened surface to which the particles can adhere. Coatings such as zinc and aluminum are applied with a gun which provides heat by burning acetylene, propane, or hydrogen in oxygen. A compressed air blast atomizes and propels the coating metals

Commonly used methods for applying metallic coatings

Coating metal	Hot dip	Electroplate	Spray	Cementation	Vapor deposition	Cladding	Immersion
Zinc	X	X	X	X	—	—	—
Aluminum	X	—	X	X	X	X	—
Tin	X	X	—	—	—	—	X
Nickel	—	X	X	—	X	X	X
Chromium	—	X	—	X	X	—	—
Stainless steel	—	—	X	—	—	X	—
Cadmium	—	X	—	—	X	—	—
Copper	—	X	—	—	—	X	X
Lead	X	X	—	—	—	X	—
Gold	—	X	—	—	X	X	X
Silver	—	X	—	—	X	X	X
Platinum metals	—	X	—	—	X	X	X
Refractory metals	—	X	X	—	—	X	—

onto the surface. Highly refractory coating materials, such as oxides, carbides, and nitrides, can be applied by plasma-arc spraying (**Fig. 3**). In this process temperatures of 20,000°F (12,000°C) or more may be produced by partially ionizing a gas (nitrogen or argon) in an electric arc and passing the gas through a small orifice to produce a jet of hot gas moving at high velocity. Another variation for applying refractory coatings is detonation-flame plating. In this process a mixture of oxygen and gas-suspended fine particles are fired four times per second by a timed spark.

Sprayed zinc or aluminum coatings up to 250 μm are used to protect towers, tanks, and bridges. Such coatings are normally sealed with an organic resin to enhance protection.

Sprayed refractory coatings have been developed for high temperatures experienced in aerospace applications. They are also used for wear resistance, heat resistance, and electrical insulation.

Cementation coatings. These are surface alloys formed by diffusion of the coating metal into the base metal, producing little dimensional change. Parts are heated in contact with powdered coating material that diffuses into the surface to form an alloy coating, whose thickness depends on the time and the temperature of treatment. A zinc alloy coating of 25 μm is formed on steel in 2–3 h at 700°F (375°C). A chromium alloy (chromized) coating of 100 μm is formed in 1 h at 1830°F (1000°C).

Chromized coatings on steel protect aircraft parts and combustion equipment. Sherardized (zinc-iron alloy) coatings are used in threaded parts and castings. Calorized (aluminum-iron alloy) coatings protect chemical equipment and furnace parts. Diffusion coatings are used to provide oxidation resistance to refractory metals, such as molybdenum and tungsten, in aerospace applications where reentry temperatures may exceed 3000°F (1650°C). In addition to the pack process described above, such coatings may be applied in a fluidized bed. In forming disilicide coatings on molybdenum, the bed consists of silicon particles suspended in a stream of heated argon flowing at 0.5 ft/s (0.15 m/s), to which a small amount of iodine is added. The hot gases react with the silicon to form SiI_4, which in turn reacts with the molybdenum to form $MoSi_2$.

Vapor deposition. A thin specular coating is formed on metals, plastics, paper, glass, and even fabrics. Coatings form by condensation of metal vapor originating from molten metal, from high-voltage (500–2000 V) discharge between electrodes (cathode sputtering), or from chemical means such as hydrogen reduction or thermal decomposition (gas plating) of metal halides. Vacuums up to 10^{-6} mmHg (10^{-4} pascal) often are required.

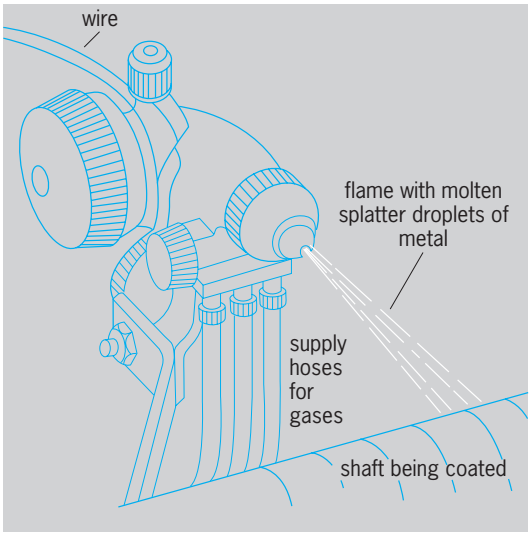

Fig. 2. Schooping gun with the coating material furnished in the form of wire.

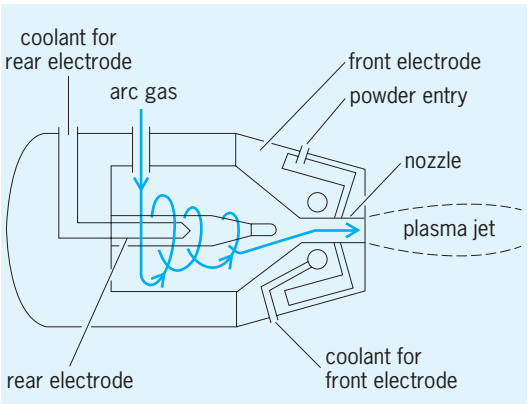

Fig. 3. Cross-sectional diagram of plasma-spray jet.

Aluminum coatings of 0.125 μm are formed on zinc, steel, costume jewelry, plastics, and optical reflectors. Chemical methods can form relatively thick coatings, up to 250 μm. The 200-in. (5-m) mirror for the Mount Palomar telescope was prepared by vapor coating with aluminum in a vacuum chamber 19 ft (6 m) in diameter and 7 ft (2 m) high.

Immersion coatings. Either by direct chemical displacement or for thicker coatings by chemical reduction (electroless coating), metal ions plate out of solution on to the workpiece.

Tin coatings are displaced onto brass and steel notions and on aluminum-alloy pistons as an aid during the breaking-in period. Displacement nickel coatings of 1.25 μm are formed on steel articles. Electroless nickel, involving the reduction of a nickel salt to metallic nickel (actually a nickel-phosphorus alloy), permits the formation of relatively thick uniform coatings up to 250 μm on parts with recessed or hidden surfaces difficult to reach by electroplating.

Vitreous enamel coatings. Glassy but noncrystalline coatings for attractive durable service in chemical, atmospheric, or moderately high-temperature environments are provided by enamel or porcelain coating. In wet enameling a slip is prepared of a water suspension of crushed glass flux, suspending agent, refractory compound, and coloring agents or opacifiers. The slip is applied by dipping or flow coating; it is then fired at a temperature at which it fuses into a continuous vitreous coating. For multiple coats the first or ground coat contains an oxide of cobalt, nickel, or molybdenum to promote adherence.

Dry enameling is used for castings, such as bathtubs. The casting is heated to a high temperature, and then dry enamel powder is sprinkled over the surface, where it fuses.

Firing temperatures for conventional enameling of iron or steel ranges up to 1600°F (870°C). Low-temperature enamels have been developed, permitting the enameling of aluminum and magnesium.

Coatings of 75–500 μm are used for kitchenware, bathroom fixtures, highway signs, and water heaters. Vitreous coatings with crystalline refractory additives can protect stainless steel equipment at temperatures up to 1740°F (950°C).

Ceramic coatings. Essentially crystalline, ceramic coatings are used for high-temperature protection above 2000°F (1100°C). The coatings may be formed by spraying refractory materials such as aluminum oxide or zirconium oxide, or by the cementation processes for coatings of intermetallic compounds such as molybdenum disilicide. Cermets are intimate mixtures of ceramic and metal, such as zirconium boride particles, dispersed throughout an electroplated coating of chromium. *See* CERAMICS; CERMET.

Surface-conversion coatings. An insulating barrier of low solubility is formed on steel, zinc, aluminum, or magnesium without electric current. The article to be coated is either immersed in or sprayed with an aqueous solution, which converts the surface into a phosphate, an oxide, or a chromate. Modern solutions react so rapidly that sheet and strip materials can be treated on continuous lines.

Phosphate coatings, equivalent to 100–400 mg/ft^2 (1–4 g/m^2), are applied to bare or galvanized steel and to zinc-base die castings as preparation for painting. The coating enhances paint adhesion and prevents underfilm corrosion. Phosphate coatings, containing up to 4000 mg/ft^2 or 40 g/m^2 (lubricated), serve as an aid in deep-drawing steel and in other friction-producing processes or applications. Iridescent chromate coatings on zinc-coated steel improve appearance and reduce zinc corrosion. Chromate, phosphate, and oxide coatings on aluminum or magnesium are used to prepare the surface before painting.

Anodic coatings. Coatings of protective oxide may be formed on aluminum or magnesium by making them the anode in an electrolytic cell. Anodized coatings on aluminum up to 75 μm thick are formed in sulfuric acid to form a porous oxide that may be sealed in boiling water or steam to provide a clear, abrasion-resistant, protective coating. If permanent color is required, the coating is impregnated with a dye prior to sealing. Such coatings are used widely on aluminum furniture, automobile trim, and architectural shapes. Thin, nonporous, electrically resistant coatings are formed on aluminum in a boric acid bath in the production of electrolytic capacitors. Anodized coatings on magnesium are thicker (up to 75 μm) and harder than those formed by chemical conversion. Anodic coatings 7.5 μm thick are often used as a paint base.

William W. Bradley

Powder coatings. The term powder coating refers to a process whereby organic polymers such as acrylic, polyester, and epoxies are applied to substrates for protection and beautification. It is essentially an industrial painting process which uses a powdered version (25–50-μm particle size) of the resin rather than the solvent solution represented by industrial baking enamels.

In the widest type of commercial usage, these powders are applied to electrically grounded substrates by means of an electrostatic spray gun. In these guns, high-voltage (60–100-kV) low-amperage charges are applied to the powders. The powder particles are attracted to and adhere to the substrate until it can be transported to an oven, where the powder particles melt, coalesce, flow, and form a smooth coating. Typical baking temperatures are 375°F (90°C) for 20 min. *See* ELECTROSTATICS.

Coatings can be applied at thicknesses ranging from 25 to 250 μm, depending upon end-use requirements. These thicknesses can be achieved in a single application. While electrostatic spray is the principal method of commercial application, other techniques exist, including fluidized-bed coating, where a preheated part is immersed into an aerated bed of powder particles, and electrostatic fluidized bed, where a substrate is passed through an "electrified" cloud of the powder.

Powder coating uses no organic solvent, and the oversprayed material can be recaptured and reused. Thus, there are several notable advantages over conventional industrial solvent-based painting:

(1) There is no hydrocarbon baking by-products, and the process is environmentally acceptable. (2) Material conservation and economics are optimized because of the recycling of oversprayed material. (3) Powders are easy to apply and readily lend themselves to automation.

A wide variety of parts are finished with powder coatings. Outdoor lawn and patio furniture coated in this process display good weathering and abuse resistance. Powder-coated electrical transformers are insulated electrically and provided with corrosion protection. Powder coatings have also been developed for finishing major appliances and for automotive coatings. Also, laundry tops and lids have displayed excellent detergent resistance where organic powder coatings have replaced porcelain finishes. *See* CORROSION; SURFACE COATING; SURFACE HARDENING OF STEEL.

R. F. Farrell

Bibliography. A. I. Andrews, *Porcelain Enamel*, 2d ed., 1961; A. I. Borisenko, *High Temperature Protective Coatings*, 1987; R. M. Burns and W. W. Bradley, *Protective Coatings for Metals*, 3d ed., 1975; U. R. Evans, *An Introduction to Metallic Corrosion*, 1981; J. Huminik (ed.), *High Temperature Inorganic Coatings*, 1963; A. T. Kuhn, *Techniques in Electrochemistry*, *Corrosion*, *and Metal Finishing*: *A Handbook*, 1987; *Materials in Design Engineering*, Metals Selector Issue, vol. 80, no. 4, September 1974; C. F. Powell, J. H. Oxley, and J. M. Blocher (eds.), *Vapor Deposition*, 1966; H. H. Uhlig and R. W. Revie, *Corrosion Handbook*, 2d ed., 2000.

Metal forming

Manufacturing processes by which parts or components are fabricated from metal stock. In the specific technical sense, metal forming involves changing the shape of a piece of metal. In general terms, however, it may be classified roughly into five categories: mechanical working, such as forging, extrusion, rolling, drawing, and various sheet-forming processes; casting; powder and fiber metal forming; electroforming; and joining processes. The selection of a process, or combination of processes, requires a knowledge of all possible methods of producing the part if a serviceable part is to be produced at the lowest overall cost.

Influence on service behavior. The service behavior of a part depends on the interrelation of the design, material, processing of the material (such as manufacturing process, heat treatment, and surface treatment), and operating and environmental conditions (such as temperature of operation, loading condition, and corrosive atmosphere). The metal-forming process is a factor in satisfactory service performance in that it affects the microstructure of the metal and its surface finish, it may introduce large residual stresses into the part, and it may affect the final design of the part which, in turn, influences its service behavior.

Process selection. The more important factors to be considered in choosing the optimum process (or combination of processes) include: type of material, metallurgical structure effect inherent in the process, size of the part, shape or complexity of the part, tolerances or finish required, quantity to be produced, cost, and production factors such as availability of equipment, rate of production, and time required to initiate production.

Material. The particular metal or alloy specified for a part is of major importance in the selection of the forming process. Some aluminum or copper alloys may be fabricated by practically any of the manufacturing processes; other alloys may be brittle under cold-working conditions but may be hot-worked. Highly refractory materials, such as tungsten and tungsten carbide, are not suitable for casting and must be fabricated by powder metallurgy methods. This process is also used for making porous metal products, or parts requiring combinations of two materials (not an alloy of the two, however). Alloys that are extremely hard, and therefore unsuitable for machining operations, can be precision cast and then ground if extremely close tolerances are required. Higher-melting-point alloys such as steel can be fabricated by most of the major classes of processes but are not suitable for all of the individual processes within a major class. Where a specific material must be used for the part, the choice of the optimum fabricating process may be definitely limited. The formability of a material may be predicted either from the reduction of area or the percent elongation in a tension test; the higher these values, the better is the formability. Other factors that influence formability are rate of deformation, temperature, type of loading, environment, impurities in the metal, and surface condition of the original stock. *See* ALLOY; ALLOY STRUCTURES; METAL, MECHANICAL PROPERTIES OF; METALLURGY; STEEL.

Metallurgical structure. Each manufacturing process has a different effect on the microstructure of the metal and, consequently, on its mechanical properties. Casting processes generally produce a relatively coarse-grained structure and a random orientation of nonmetallic inclusions. The result is isotropic properties, but lower ductility than that of wrought products. Castings may also be porous. Hot-working processes, such as forging, align the inclusions (fiber structure) and thus impart anisotropic properties, with the strength and ductility generally being higher in a direction parallel to that of the inclusions. This orientation may be an advantage or disadvantage, depending upon the direction of the applied loads. Cold-working processes (such as cold rolling) also produce directional properties in the metal because of the tendency of the grains (or crystals) to align in certain directions. In addition the grains become distorted, and the metal becomes harder and stronger but less ductile. Cold-working operations (or any process causing nonuniform deformations) generally leave residual stresses in the part. Residual stresses left in a part algebraically add to the stresses induced by service loading, and in some instances these residual stresses are of major importance.

Size. Metal-forming processes may be limited as to the size of the part they can produce. Among the processes that are limited to relatively small parts are precision casting, die casting, powder metallurgy, and screw machining. Large parts are best produced by sand casting, forging, or building up component sections by welding or other joining processes. Parts with rotational symmetry can be produced by spinning; other large parts, such as domes, made of sheet or plate stock can be formed by explosive-forming techniques developed in the aerospace industries.

Shape. The complexity of a part often dictates the process or combination of processes used in its manufacture. Generally, castings can be more complex than parts made by most other fabrication processes; however, some casting processes (sand and precision investment casting) are capable of producing parts of greater complexity than others. Parts produced by the powder metallurgy process have definite restrictions as to design because of the inability of metal powder to flow like a liquid. In some instances the complexity of a part may require the fabrication of the structure by welding or brazing several sections together. The change from forming a part as a single piece to fabricating it from several sections usually requires design modifications if optimum serviceability is to be attained. The design should be left flexible until all feasible manufacturing processes have been considered.

Tolerances and finish. Parts requiring close tolerances or smooth finishes can be formed directly by precision investment casting, die casting, or such cold-working processes as swaging, drawing, or stamping. If formed by other processes, they can be finished by machining or grinding. Hot-working processes, such as forging, result in relatively rough, oxidized surfaces and relatively low dimensional accuracies. Welding operations generally result in some distortion or dimensional change. The final overall cost often governs whether the desired tolerances should be attained in the original process or obtained in secondary operations. As an example, in hot-working operations, such as rolling, forging, and extrusion, surface roughness ranges from about 100 to as high as 2000 microinches arithmetic average. In cold working, the range is between 10 and 250 μin.; in some machining operations, it is as low as 1 μin., for example, in grinding and honing.

Quantity. The number of parts to be produced is a major factor in determining the method of manufacture, and whether the part should be produced within the plant or subcontracted. Some processes are suitable only for large-quantity production because of high tooling costs; for example, permanent-mold and die casting, certain forging processes, and deep drawing. Processes such as sand casting, spinning, and welding are readily adaptable, but not necessarily restricted, to small-quantity production.

Cost. If the quantity to be produced is large, the overall finished cost of the product is usually a prime consideration in the selection of a process. In many cases cost is the deciding factor in choosing the fabrication process and perhaps the material as well. In determining the overall cost, the replacement cost of the part based on its estimated service life should be included with more immediate factors such as material and tooling costs, labor, and scrap loss.

Production factors. In some instances the time necessary to initiate production may be of significance in selecting the fabrication process. Those methods involving extensive tooling necessarily require a long lead time before production starts. Availability of equipment may be the deciding factor in choosing between two equally feasible processes, especially if it has been decided that the part is to be produced in a certain plant rather than subcontracting it to another organization. Another production factor which may be important is the required rate of production. Processes such as die casting, powder metallurgy, and deep drawing have high production rates. Conversely, sand casting, spinning, hydraulic press forging, and fusion welding are relatively slow processes.

It is thus evident that there are many factors involved in selecting an optimum for material and processes to manufacture a certain part. A very wide range of variables are involved. Strength levels for metals range from as low as 1000 lb/in.^{2} (7 megapascals) to the order of 500,000 lb/in.^{2} (3500 MPa). Size of parts may range from a thousandth of an inch (0.0254 mm) to a few feet. Rates of deformation can be as high as 40,000 ft/min (12,000 m/min), as in explosive forming, while working temperatures can be as low as cryogenic to the range of 4000°F (2200°C). Capacities of equipment for forming metal components are as high as 50,000 tons (45,000 metric tons), with a 200,000-ton (180,000-metric-ton) hydraulic forging press, which is in the design stage. *See* DRAWING OF METAL; EXTRUSION; FORGING; METAL CASTING; METAL ROLLING; POWDER METALLURGY; SHEET-METAL FORMING.

Serope Kalpakjian

Bibliography. American Society for Metals, *Formability and Workability of Metals,* 1984; American Society of Mechanical Engineers, *ASME Handbook Engineering Design,* 1965; A. L. Hoffmanner (ed.), *Metal Forming: Interrelation Between Theory and Practice,* 1971; W. F. Hosford, *Metal Forming: Mechanics and Metallurgy*, 2d ed., 1993; Society of Manufacturing Engineers, *Tool and Manufacturing Engineer's Handbook*, vol. 2: *Forming*, 1984.

Metal halide lamp

A high-pressure discharge lamp that is enclosed in a quartz envelope containing metal halides, usually iodides, and produces high-efficacy white light. These lamps are widely used for sports stadiums, roadways, commercial interiors, and industrial applications. The singular lamp feature is the compact geometry and high efficacy of nearly white light. *See* LUMINOUS EFFICACY.

Principle of operation. The metal halide lamp requires a high voltage in order to start. Once the arc discharge is ignited, the internal vapor pressure begins to increase until it reaches a preset value,

usually around 5 atm (500 kilopascals). These lamps are always connected to an auxiliary power supply called the ballast which supplies the proper voltage and current for starting and operating the lamps. The light output gradually increases over approximately 2 min as the various ingredients begin to vaporize and emit light. The light from the arc discharge comes from the metal components of the iodide compounds, which are typically a mixture of sodium, thallium, indium, scandium, dysprosium, and occasionally tin iodide. A combination of these metals produces a pleasing white light of very high efficiency, between 80 and 120 lumens per watt or even higher. *See* ARC DISCHARGE.

When the arc is struck, the light output starts at a low value and gradually increases as the pressure of the metallic compounds increases inside the quartz envelope. The wall temperature is usually about 1300°F (700°C) and the arc temperature about 9000°F (5000°C). The high temperature of the arc dissociates the halides into the electronegative portion, namely the iodine, and the metallic portion such as sodium.

Since the arc temperature excites the metal atom more easily than the iodide, the visual radiation emitted by the lamp is characteristic of the metal. Several combinations of metals produce nearly white light. Mercury, which is often an ingredient of high-pressure discharge lamps, is hardly excited in metal halide lamps. That is, the energy levels of mercury (and the iodine) do not produce significant radiation. *See* MERCURY-VAPOR LAMP.

The metals do not stay in the discharge, but diffuse and wander to the wall where they recombine with the iodine and reform the compound. However, there are other molecules that have evaporated and go into the discharge, dissociate, and thus continuously produce a fresh vapor of metal atoms which can radiate their characteristic spectrum. In this way, the relatively inefficient spectra of elements such as mercury, argon, and iodine are suppressed and the relatively efficient spectra of metals such as sodium and scandium are improved, to increase the overall luminous efficiency of the arc. The net result is a lamp whose luminous efficiency is very high.

The discharge tube is placed within an outer bulb in order to protect it from the atmosphere and reduce the hazard associated with an extremely hot quartz envelope when the lamp is operating.

Spectra and applications. Metal halide lamps come in a wide variety of sizes, depending upon their application. For general lighting, the lamps usually have closely spaced lines and are designed for long life and nearly white light. Spectra of two common metal halide lamps are shown in the **illustration**. Lamps of this type are used for lighting roads and residential shopping areas, and for interior lighting in commercial and industrial operations. Probably one of the most extensive early uses of metal halide lamps was in sports lighting, where they were instrumental in the success of color television for sports events.

Special ingredients can be used inside these lamps to make them suitable for plant growth, photocopying, and scientific usages. Certain types of compact metal halide lamps are ideal for use with movie and slide projection. In these cases, the ingredients chosen (usually indium) are used because they produce a small, intense high-brightness arc. The spectra of these lamps are nearly continuous and approach the spectra of incandescent lamps. *See* CINEMATOGRAPHY; INCANDESCENT LAMP; OPTICAL PROJECTION SYSTEMS.

In cases where a more diffuse light source is desired, the outer jacket of the lamp can be coated with a white phosphor in order both to diffuse the light and to change the color of the output and in some cases actually improve the efficiency.

Millions of these lamps are produced annually. The development of metal halide lamps is still an

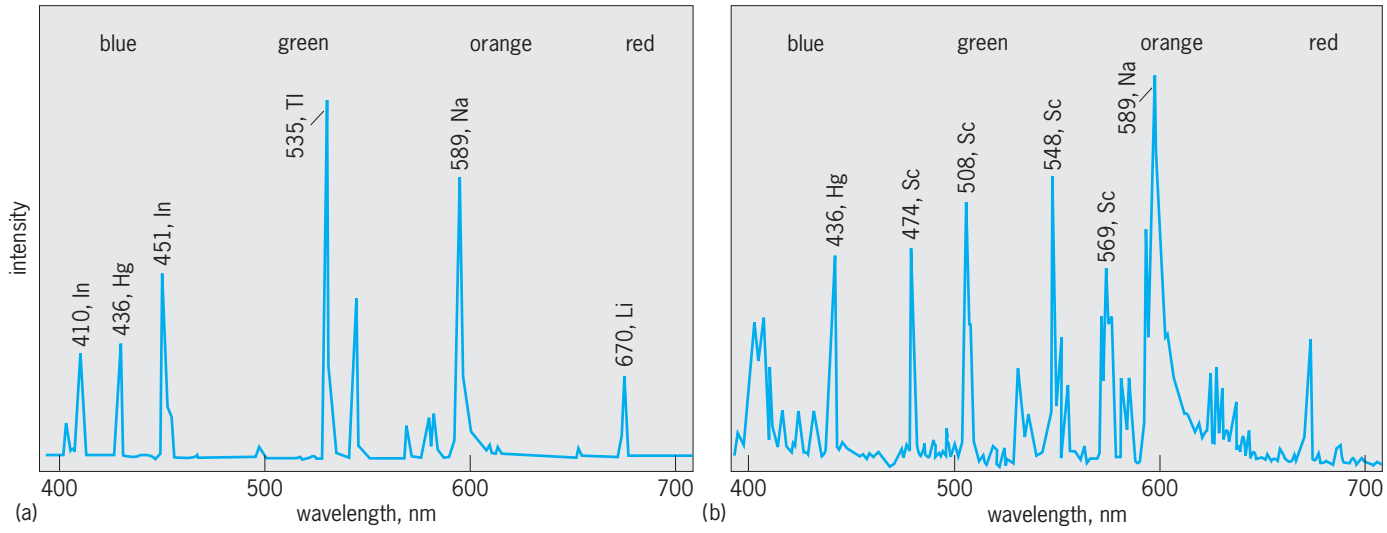

Spectrum of white-colored light from: (*a*) A 400-W metal halide lamp containing sodium iodide (NaI), thallium iodide (TlI), indium iodide (InI_3), mercury, and argon gas. The visible radiation yields an efficacy of 90 lumens per watt and color rendering index of 60. (*b*) A 175-W metal halide lamp containing sodium iodide (NaI), scandium iodide (ScI_3), mercury, and argon gas. The combined visible radiation yields an efficacy of 100 lumens per watt and a color rendering index of 60.

active subject in research laboratories, and improvements in the spectrum and the efficiency have not reached their limits. *See* ARC LAMP; VAPOR LAMP.

Gilbert H. Reiling

Bibliography. Illumination Engineering Society of North America, *IES Lighting Handbook: Reference and Application Volume*, 1993; C. Meyer and H. Nienhuis, *Discharge Lamps*, 1989.

Metal hydrides

A compound in which hydrogen is bonded chemically to a metal or metalloid element. The compounds are classified generally as ionic, transition metal, and covalent hydrides. The periodic table can be arranged according to the type of hydride formed (**Fig. 1**). Covalent hydrides are of two subtypes, binary and complex. Certain hydrides have achieved a position of modest industrial importance, but most are of theoretical interest only. Examples of hydrides are shown in the **table**.

Under extreme conditions such as in electric discharges, many metals form volatile, short-lived transient hydrides of the general formula type MH. Although some of these can be prepared experimentally, most are observed only by their spectra. They are important in studying molecular bonding. The action of atomic hydrogen at low temperatures forms surface films of unstable hydrides with many metals. *See* HYDRIDO COMPLEXES; HYDROGEN.

Ionic hydrides. The most reactive metals (alkali and alkaline-earth metals, with the exception of magnesium and beryllium) combine directly on heating with hydrogen gas at a pressure of 1 atm (10^2 kilopascals). Magnesium reacts at elevated hydrogen pressure. The reactions of hydrogen with sodium and potassium are slow because of the formation of a protective layer of the hydride, but the reaction can be accelerated by surface-active agents or catalysts such as anthracene or by stirring the molten metal under paraffin oil while hydrogen is bubbling in. *See* SURFACTANT.

Ionic (or saline) hydrides, when pure, are white, high-melting solids which have simple formulas. They are believed to consist of metal cations and hydride anions H^-. Ionic hydrides result when the difference in electronegativity between the hydrogen and the metal is large. *See* ELECTRONEGATIVITY.

The crystal structures of hydrides can be determined by the standard means of x-ray diffraction, which reveals the arrangement of metal ions only. To locate the hydrogen (or its isotope, deuterium), neutron diffraction is used. Such studies confirm that

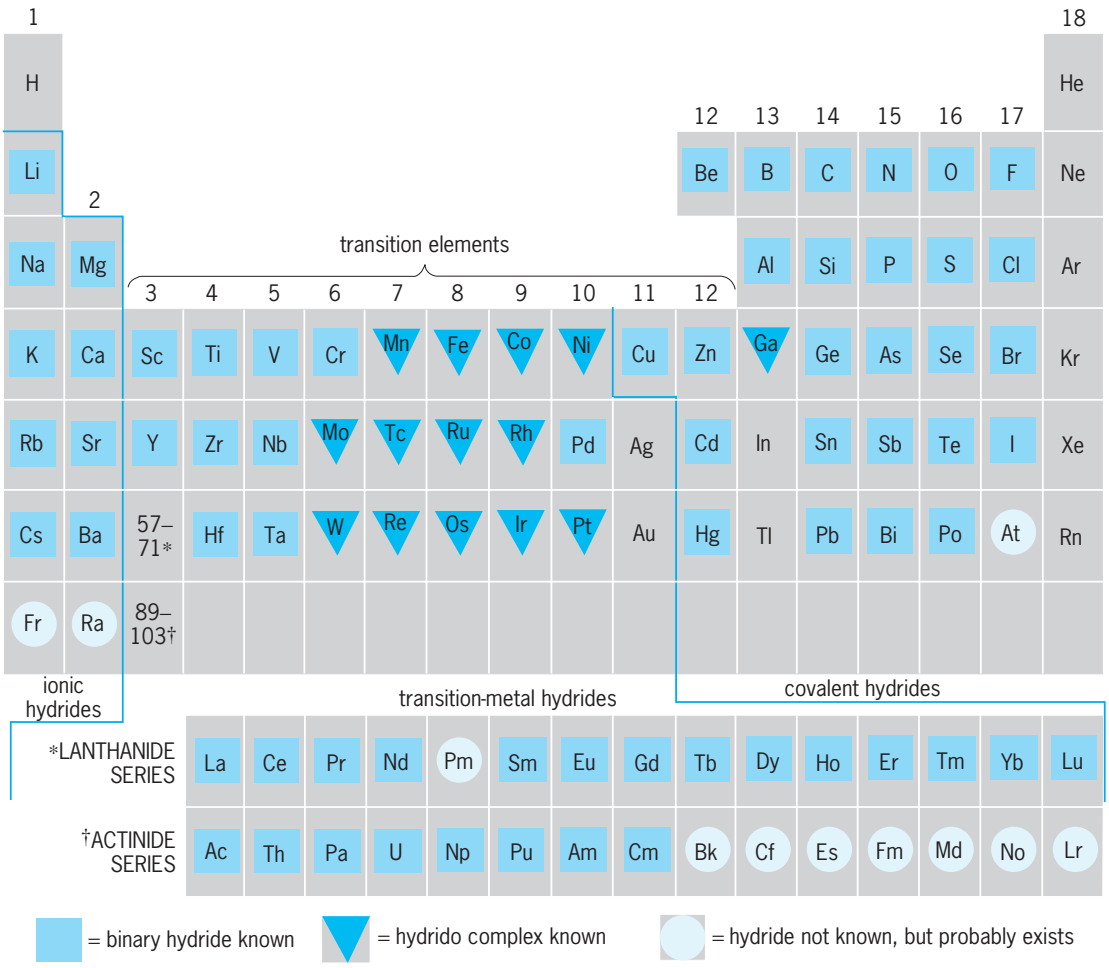

Fig. 1. Periodic table showing hydride types.

Physical properties of representative hydrides

Compound	Formula	Form	Melting point, °C (°F)	Density, g/cm³	Boiling point, (°F) °C	Temperature at which dissociation pressure is 1 atm or 10^2 kPa, °C (°F)
Lithium hydride	LiH	White crystals	691 (1276)	0.77	—	790 (1454)
Sodium hydride	NaH	White crystals	Decomposes	1.396	—	425 (797)
Calcium hydride	CaH_2	White crystals	>1000 (1830)	1.902	—	960 (1760)
Titanium hydride	TiH_2	Gray powder	Decomposes	3.78	—	630 (1166)
Cerium hydride	CeH_2	Dark gray powder or greenish metallic single crystals	1088 (1990) for $CeH_{1.73}$	5.45	—	750 (1382) for $CeH_{2.2}$
Uranium hydride	UH_2	Black powder	~1050 (1922) at 580 atm (58.8 MPa)	10.95	—	440 (824)
Lanthanum nickel hydride	$LaNi_5H_6$	Dark gray powder	Decomposes	—	—	0 (32) [2.5 atm at 25°C or 0.25 MPa at 77 °F]
Palladium hydride	$PdH_{0.66}$	Metallic	Decomposes	~10.8	—	25 (77) for $PdH_{0.56}$, −78 (−108) for $PdH_{0.83}$
Diborane	B_2H_6	Colorless gas	−165.5 (−265.9)	0.438 at bp	−92.5 (−135)	—
Silane	SiH_4	Colorless gas	−185 (−301)	0.68 at mp	−111.8 (−169.2)	—
Stannane	SnH_4	Colorless gas	−150 (−238)	—	−52 (−62)	—
Arsine	AsH_3	Colorless gas	−113.5 (−172.3)	—	−55 (−67)	—
Stibine	SbH_3	Colorless gas	−88.5 (−127.3)	2.2 at bp	−17 (1.4)	—
Tellurium hydride	TeH_2	Colorless gas	−51 (−59.8)	2.7 at −18°C (−0.4 °F)	−4 (25)	—
Aluminum hydride	AlH_3	White solid	Decomposes	—	—	—
Copper hydride	CuH	Dark brown solid	Decomposes slowly even at 25 °C (77 °F)	6.39	—	—

sodium hydride has the same type of structure as sodium chloride. *See* CRYSTAL STRUCTURE.

The thermal stability of the alkali metal hydrides decreases, and their chemical reactivity increases, in the order LiH, NaH, KH, RbH, and CsH. The hydride ion in these compounds has a radius of approximately 0.14 nanometer (about the same size as the fluoride ion, F^-). The anion from heavy hydrogen, that is, the deuteride ion D^-, tends to be slightly smaller than H^-, when in an equivalent environment. When molten lithium hydride is electrolyzed, hydrogen is evolved at the anode, since H^- is the migrating species.

A common way to represent a reversible metal-hydrogen system is to plot the composition against hydrogen pressure (called the dissociation pressure) at a fixed temperature. **Figure 2** shows the 500 and 575°C (932 and 1067°F) isotherms for the sodium-hydrogen system. Pure liquid sodium at 575°C (1067°F) exists at point A, and as hydrogen is admitted, it dissolves in the metal up to the limit at point B. This is a solution of NaH (10%) in molten Na (90%). When more hydrogen is pumped in, a solid appears, whose composition is indicated by point C ($NaH_{0.90}$, that is, sodium hydride deficient in hydrogen). During this stage (points B to C), the hydrogen pressure remains constant at 36.6 atm (3.7 MPa). The dissociation pressures at the various plateaus may be computed for any temperature by the equation $\log P = (-5960/T) + 8.59$, where P is the pressure in atmospheres and T the absolute temperature. Further introduction of hydrogen finally yields pure NaH at point D. In the plateau region (B to C), each mole of hydrogen which reacts liberates 27 kcal (113 kilojoules) of heat. More heat is liberated in the cases of lithium hydride (43 kcal or 180 kJ/mole of H_2) and CaH_2 (42 kcal or 176 kJ). *See* PHASE EQUILIBRIUM.

The ionic hydrides are all exceedingly reactive reducing agents. Their reaction with water yields the metal hydroxide and hydrogen, which sometimes ignites at the high temperature resulting from the reaction. Sodium hydride dissolved in molten sodium hydroxide is employed in descaling steel and titanium. Calcium hydride is a source of hydrogen in remote areas, for example, to fill meteorological balloons. CaH_2 is also used as a desiccant in transformer oil and in the reduction of certain oxides to metals, such as tantalum.

Transition metal hydrides. This group of compounds is less well understood than the ionic and

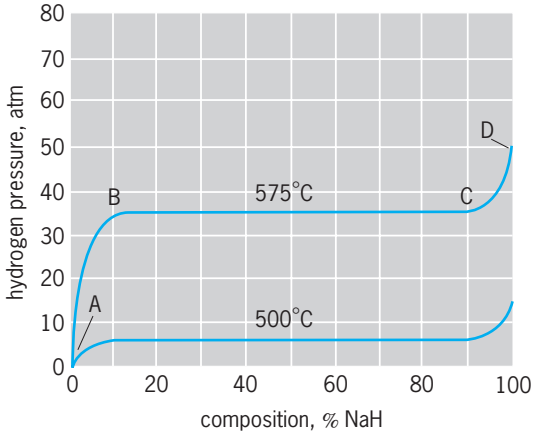

Fig. 2. Sodium-hydrogen system. °F = (°C × 1.8) + 32; 1 atm = 10^5 Pa.

covalent hydrides. When lanthanum is heated in hydrogen, the gas is readily taken up, forming first a material whose composition is approximtely $LaH_{1.86}$ (the "dihydride" phase) and finally LaH_3. The electrical conductivity does not change radically between La and $LaH_{1.86}$, but it falls dramatically from $LaH_{1.86}$ to LaH_3. The hydrogen is generally thought to form hydride ions, with radius about 0.13 nm, but some of the valence electrons remain free or mobile in the dihydride. This accounts for the conductivity of this substance. These mobile electrons are said to be in the conduction band. They are progressively consumed as the dihydride is converted to the trihydride. A single phase exists between $LaH_{1.86}$ and LaH_3, and it is possible to arrest the addition of hydrogen at any intermediate composition, such as $LaH_{2.63}$. Such a substance is sometimes referred to as a solid solution and sometimes as a compound which represents extreme nonstoichiometry. These features (electrical conductivity and nonstoichiometry) characterize the transition metal hydrides. *See* NONSTOICHIOMETRIC COMPOUNDS.

The ionic hydrides, such as NaH, exhibit much more limited nonstoichiometry. When sodium is converted to pure NaH, all electrons in the conduction band are consumed and the product is white and insulating. The hydrides of the rare-earth metals are the easiest to describe in terms of an ionic model. The hydrides of the actinide metals are known through curium, the best known being uranium hydride. All are dark-gray powders which ignite spontaneously in the air. Large single crystals of cerium hydride are fairly stable in air.

Copper hydride, CuH, is unique in that it is the only hydride which can be precipitated from aqueous solution. It forms a dark-brown sediment which decomposes when dried. Copper hydride has a hexagonal crystal structure and is essentially a covalent compound.

Titanium, zirconium, vanadium, and niobium all react with hydrogen, forming dihydrides at the limiting compositions. The materials are conducting at all compositions. Except for palladium, the metals to the right of titanium in the periodic table show decreased reactivity toward hydrogen. Metal of the vanadium family and also chromium absorb hydrogen almost to the monohydride stage. The transition metals in the manganese, iron, cobalt, and nickel groups dissolve only small amounts of hydrogen, except for palladium, which readily absorbs hydrogen to the limit $PdH_{0.66}$. The palladium-hydrogen system has been much studied, because of its importance in catalytic hydrogenation. Thorium hydride, Th_4H_{15}, becomes superconducting at approximately 8 K (−445°F). *See* PALLADIUM; SUPERCONDUCTIVITY.

When hydrogen (protium, ^1H) in a metal hydride is replaced with its isotope deuterium, the product (deuteride) is usually less stable. The dissociation pressures of the deuterides are about twice those of the corresponding hydrides at the same temperature in the great majority of cases. The inverse effect is known, however. For example, at 40°C (104°F) vanadium hydride ($VH_{1.5}$) has a dissociation pressure of 4.8 atm (490 kPa), while $VD_{1.5}$ has a dissociation pressure of 1.8 atm (182 kPa). The uranium compounds of the three isotopes of hydrogen (UH_3, UD_3, and UT_3) are frequently used in the laboratory as sources and reservoirs for these gases and for their purification. Titanium hydride also serves in this capacity. Some of the hydrides serve as a starting point for the synthesis of halides, sulfides, and so forth, of the metal. For example, this is represented by reaction (1). Deuterides and tritides of actinide metals

$$UH_3 + 3HCl \rightarrow UCl_3 + 3H_2 \quad (1)$$

probably play an important role in thermonuclear (hydrogen) weapons.

Common metals such as steel and copper dissolve small quantities of hydrogen at elevated temperatures. On cooling, the gas comes out of solution and results in severe degradation of the mechanical properties of the metals. This is called hydrogen embrittlement and can be prevented by degassing the metal while it is still molten. Problems from hydrogen embrittlement also arise in high-pressure catalytic units employing hydrogen gas and at electrode surfaces where hydrogen ion is reduced to hydrogen, as in some electroplating processes. The cause of this embrittlement is the introduction of dislocations and stacking faults by the hydrogen atoms. The result is to suppress dislocation glide near cracks, preventing stress relaxation. *See* CRYSTAL DEFECTS.

A number of alloys or intermetallic compounds are known which react with hydrogen and form ternary hydrides. Examples are $LaNi_5H_6$, Mg_2NiH_4, $AlTh_2H_2$, and $CaAg_2H$. $LaNi_5H_6$ permits an attractive means of portable hydrogen storage. This might be important if hydrogen is generated on a massive scale as a pollution-free energy source for fuel cells and internal combustion engines. Storage of hydrogen as compressed gas or as liquid is not convenient. The energy density of $LaNi_5H_6$ is twice that of liquid hydrogen and 12 times that of the compressed gas. The ternary hydride $LaNi_5H_6$ is readily formed reversibly from lanthanum-nickel alloy and hydrogen. Pure rare-earth metals are not necessary in making the nickel alloy; the commercial material (misch metal, mostly Ce, La, and Nd) is satisfactory. After charging with hydrogen, these materials provide practical gas pressure (a few atmospheres) from −30 to +30°C (−22 to 86°F), and are thus attractive for powering hydrogen-burning engines of automobiles.

Owing to the highly reversible character of these metal-hydrogen systems, they have recently been studied as heat pumps and energy storage devices. To operate an air-conditioning unit, hydrogen is pumped from one metal hydride unit (such as $LaNi_5H_6$), which provides cooling, to an alloy unit ($LaNi_5$), where heat is evolved on formation of hydride. Alternatively, solar or waste thermal energy could be converted into mechanical work.

Another important ternary hydride is the Zr-U-H system, which is employed in pulsed reactors of the Triga type. The role of the hydrogen atom is to moderate fast neutrons. Another type of ternary hydride

is illustrated by the thorium carbohydrides, Th_2Ch_2 and Th_3Ch_4. *See* RARE-EARTH ELEMENTS.

Covalent hydrides. Most evidence indicates that in ionic and metallic hydrides an electronic pair is associated primarily with the hydrogen as H^-, while in covalent hydrides the electron pair is shared between the hydrogen atom and an atom of another element. In these compounds hydrogen is considerably smaller (radius 0.03 nm) than in the ionic hydrides. Covalent hydrides usually consist of small molecules, in which case they are gases (SiH_4 and SbH_3), but some form high polymers, in which case they are nonvolatile solids (AlH_3 and ZnH_2). All tend to decompose irreversibly rather easily on heating. Covalent hydrides are generally synthesized indirectly, not from direct combination of the elements. Gaseous hydrides such as SiH_4, PH_3, and AsH_3 can be generated by heating a solid mixture of the corresponding oxide and $LiAlH_4$. *See* CHEMICAL BONDING.

The hydrides of boron deserve special mention, as their bonding posed a difficult problem in chemical theory which has been resolved only recently. In diborane, B_2H_6, four of the hydrogen atoms are bonded to the two boron atoms by ordinary single, covalent bonds. The other two hydrogen atoms are linked to both boron atoms, the four bonds being formed by only two electron pairs. The structure of diborane is illustrated in **Fig. 3**. The hydrogen atoms which bridge between the two boron atoms do not form an ordinary hydrogen bond but another type usually described as an electron-deficient bridging bond. There are nearly two dozen higher boron hydrides, of which B_4H_{10}, B_5H_9, B_6H_{10}, and $B_{10}H_{14}$ are representative. A group of compounds, the carboranes, has been discovered in which some of the boron atoms of the higher hydrides are replaced with carbon atoms. An example is $B_{10}C_2H_{10}$. *See* BORANE; CARBORANE.

Numerous derivatives of the boron hydrides have been prepared, of which sodium tetrahydroborate (or tetrahydridoborate or borohydride), $NaBH_4$, is the most important. It is used as a selective reducing agent in organic chemistry. This hydrido complex is moderately stable in water, especially in alkaline solution. This stability permits its use in recovery of heavy metals from industrial waste streams. *See* HYDROBORATION.

Aluminum hydride, AlH_3, normally exists as an insoluble, nonvolatile polymer. Its derivative, lithium tetrahydroaluminate (or lithium aluminum hydride), $LiAlH_4$, is an important reducing agent in both organic and inorganic chemistry. For example, silane can be prepared as in reaction (2). Lithium tetrahydroaluminate

$$SiCl_4 + LiAlH_4 \xrightarrow{\text{ether}} SiH_4 + LiCl + AlCl_3 \qquad (2)$$

reacts vigorously with water. An ether is generally used as the solvent. Sodium cyanotrihydroborate, $NaBH_3CN$, can be used in acidic medium. A family of aluminum-based reducing agents is now available commercially including sodium diethyl-dihydroaluminate, $NaAlH_2(C_2H_5)_2$; sodium tri-*tert*-butoxohydroaluminate, $NaAlH(O\text{-}t\text{-}C_4H_9)_3$; sodium bis(2-methoxyethoxo)dihydroaluminate, $NaAlH_2(OCO_2CH_2OCH_3)_2$; diethylaluminum hydride, $(C_2H_5)_2AlH$; and di-*iso*-butylaluminum hydride, $(i\text{-}C_4H_9)_2AlH$. All are soluble in aromatic hydrocarbons. They are rather expensive, but their specific reducing powers make them attractive for synthesizing high-value products, such as pharmaceuticals, flavorings, fragrances, dyes, and insecticides.

There are thousands of hydrocarbons, which represent hydrogen compounds of carbon, the first element in group 14. The simplest of these compounds is methane, CH_4. Other 14 hydrogen compounds are silane, SiH_4; germane, GeH_4; stannane, SnH_4; and plumbane, PbH_4. This series is progressively less stable, with stannane decomposing at room temperature. Higher hydrides of silicon are known, Si_2H_6 and so on up to $Si_{10}H_{22}$. These compounds, Si_nH_{2n+2}, are analogous to the corresponding alkanes, C_nH_{2n+2}. Various silane derivates, such as SiH_3HI and $(SiH_3)_3N$, have been synthesized. A parallel situation exists in the case of higher germanium hydrides. Unstable distannane, Sn_2H_6, has also been made. Mixed compounds such as SiH_3GeH_3 can be prepared. The group 15 hydrides show the same stability trends as the preceding group, with stability decreasing in the order NH_3, PH_3, AsH_3, SbH_3, and BiH_3. Group 16 hydrides, including H_2Se, H_2Te, and H_2Po, also grow less stable down the series, the same trends continuing in the case of hydrogen compounds of the halogens. These compounds in the last two series, such as H_2Se and HI, are ordinarily considered as acids. *See* HYDRIDE.

James C. Warf

Bibliography. A. Dedieu, *Transition Metal Hydrides*, 1992; E. L. Muetterties (ed.), *Boron Hydride Chemistry*, 1975.

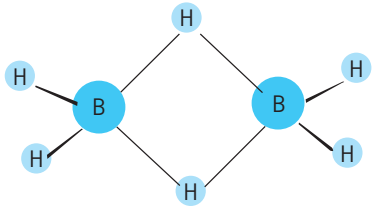

Fig. 3. Structure of diborane, B_2H_6.

Metal matrix composite

A material in which a continuous metallic phase (the matrix) is combined with another phase (the reinforcement) that constitutes a few percent to around 50% of the material's total volume. In the strictest sense, metal matrix composite materials are not produced by conventional alloying. This feature differentiates most metal matrix composites from many other multiphase metallic materials, such as pearlitic steels or hypereutectic aluminum-silicon alloys. *See* ALLOY.

The particular benefits exhibited by metal matrix composites, such as lower density, increased specific

strength and stiffness, increased high-temperature performance limits, and improved wear-abrasion resistance, are dependent on the properties of the matrix alloy and of the reinforcing phase. The selection of the matrix is empirically based, using readily available alloys; and the major consideration is the nature of the reinforcing phase.

Matrices and reinforcements. A large variety of metal matrix composite materials exist. The reinforcing phase can be fibrous, platelike, or equiaxed (having equal dimensions in all directions); and its size can also vary widely, from about 0.1 to more than 100 micrometers. Matrices based on most engineering metals have been explored, including aluminum, magnesium, zinc, copper, titanium, nickel, cobalt, iron, and various aluminides. This wide variety of systems has led to an equally wide spectrum of properties for these materials and of processing methods used for their fabrication.

Reinforcements used in metal matrix composites fall in five categories: continuous fibers, short fibers, whiskers, equiaxed particles, and interconnected networks.

Continuous fibers. Several continuous fibers or filaments are used in metal matrix composites. Their elastic moduli vary significantly, depending on the nature of the fiber and its fabrication process. For example, silica-alumina spinels and microcrystalline or amorphous polycarbosilane-derived fibers possess significantly lower elastic moduli than do pure alumina or crystalline β-silicon carbide produced by chemical vapor deposition. Carbon fiber strength and modulus also vary significantly with processing, depending on the level of graphitization of the microstructure. *See* ALUMINUM; ELASTICITY; GRAPHITE; SPINEL.

Short fibers. Short fibers are less expensive, especially when they are mass-produced for other applications such as high-temperature thermal insulation. Their physical properties can be similar to those of continuous fibers; however their reinforcing efficiency in the matrix is also far lower. Short fibers used in engineering practice include chopped carbon fibers and alumina-silica fibers.

Whiskers. Whiskers are single-crystal short fibers, produced to feature highly desirable mechanical properties due to lack of microstructural defects. Whiskers have typically been made of silicon carbide, and they are often priced far higher than short fibers. The high price and toxicity of most whiskers have prevented their application in engineering practice.

Single-crystal whiskers, because of the absence of grain boundary defects, offer much higher tensile strength than other types of discontinuous reinforcements, and thus they are preferred for certain applications of discontinuously reinforced metal matrix composities. The whiskers can be aligned to a preferred orientation by conventional metallurgical processes; higher directional strengths can be achieved in finished components where fabrication is by extrusion, rolling, forging, or superplastic forming. Whiskers tend to produce anisotropic properties due to their alignment during processing, while particulate materials usually produce essentially isotropic properties. *See* CRYSTAL WHISKERS; GRAIN BOUNDARIES; SILICON. *See also* EXTRUSION; FORGING; METAL ROLLING; SUPERPLASTICITY.

Equiaxed particles. Equiaxed particles of several ceramics, including those containing silicon carbide, aluminum oxide, boron carbide, and tungsten carbide, do not provide the possibility for preferential strengthening of the matrix along selected directions; however, their price is low and their combination with the metal is relatively easier. These reinforcements are therefore used in many metal-matrix composite systems, including mass-produced aluminum matrix composites.

Interconnected cellular networks. These can be produced by several methods, such as by chemical vapor deposition of ceramic onto a pyrolizable polymer foam or by conversion of a preceramic polymer foam prior to infiltration with the molten matrix. Alternatively, some processing techniques for in-place metal matrix composites, including directional oxidation of aluminum melts, produce interconnected reinforcing networks.

In-place metal matrix composites comprise those in which the reinforcement is produced from the matrix; although these materials are actually in some cases produced by alloying, their designation as metal matrix composites has resulted from the special morphology of the second phase (for example, some directionally solidified eutectics that have fibrous second phase) or from the ceramic nature of the second phase (for example, titanium-carbide-reinforced steel produced by solidification of iron-titanium-carbon alloys).

Microstructure. The microstructure of a metal matrix composite comprises the structure of matrix and reinforcement, that is, the interface and the distribution of the reinforcement within the matrix.

The distribution of the reinforcement within the composite can be controlled to some extent during processing. Large modifications can be handled individually and distributed with relatively great precision within the composite. Continuous fibers of smaller diameter, in the range of 10 μm or less, are generally combined with the matrix by infiltration. The fibers then tend to concentrate into regions of high-volume fraction, near 50 vol %, within which individual fibers are relatively randomly distributed. Greater control of the reinforcement volume fraction can be exerted with short fibers and whiskers because of bending of fibers between their contact points.

In particle-reinforced metal composites, the reinforcement distribution is affected by solidification of the matrix in liquid-phase processes, because the growing solid phase may push the particles as it grows. In powder metallurgical processes, reinforcement particle clustering may result from unequal sizes of matrix and reinforcement powder particles.

At the interface between matrix and reinforcement, intimate atomic-level bonding is typically achieved between matrix and reinforcement.

Microstructural evolution of the matrix is governed by the same basic laws that govern the microstructural evolution of all metals; however, the reinforcement can exert a strong influence on the course taken by the evolving matrix microstructure. In solidification, for example, the reinforcement has been shown to strongly reduce microsegregation in the matrix, to influence the stability of plane solidification during cooling, and to alter the coarsening of matrix microstructure. In solid-state deformation processes, the reinforcement has been shown to alter the evolution of texture in the matrix, the kinetics of recrystallization, and the grain size after recrystallization. *See* METAL.

Composite properties. Composite properties depend first and foremost on the nature of the composite; however, certain detailed microstructural features of the composite can exert a significant influence on its behavior.

Physical properties of the metal, which can be significantly altered by addition of a reinforcement, are chiefly dependent on the reinforcement distribution. A good example is aluminum-silicon carbide composites, for which the presence of the ceramic increases substantially the elastic modulus of the metal without greatly affecting its density. Elastic moduli for 6061 aluminum matrix composites reinforced with discrete silicon carbide particles or whiskers have been calculated by using the rule of mixtures for the same matrix reinforced with two types of commercial continuous silicon carbide fibers. As a result, several general facts become apparent. First, modulus improvements are significant, even with equiaxed silicon carbide particles, which are far less expensive than fibers or whiskers. However, the level of improvement depends on the shape and alignment of the silicon carbide. Also, it depends on the processing of the reinforcement: for the same reinforcement shape (continuous fibers), microcrystalline polycarbosilane-derived silicon carbide fibers yield much lower improvements than do crystalline β-silicon carbide fibers. These features, of influence of reinforcement shape, orientation, and processing on modulus, are quite general, being also observed for example in metal matrix composites reinforced with aluminum oxide or carbon.

Other properties, such as the strength of metal matrix composites, depend in a much more complex manner on composite microstructure. The strength of a fiber-reinforced composite, for example, is

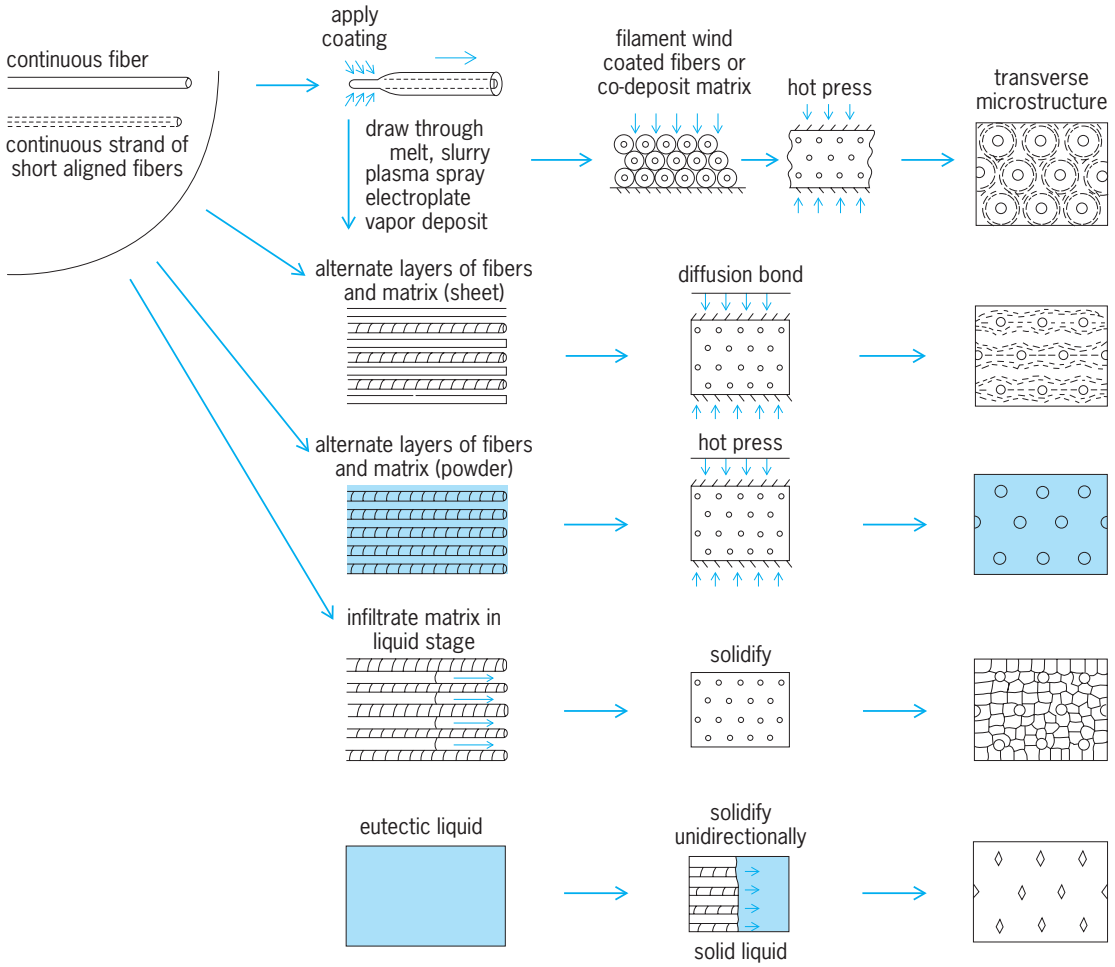

Fig. 1. Examples of methods used to make metal matrix composites. (*Space Sciences Laboratory, General Electric Valley Forge Space Technology Center, King Prussia, Pennsylvania, 1967*)

determined by fracture processes, themselves governed by a combination of microstructural phenomena and features. These include plastic deformation of the matrix, the presence of brittle phases in the matrix, the strength of the interface, the distribution of flaws in the reinforcement, and the distribution of the reinforcement within the composite. Consequently, predicting the strength of the composite from that of its constituent phases is generally difficult. *See* BRITTLENESS; PLASTIC DEFORMATION OF METAL.

Design considerations. In general, metal matrix composites exhibit good creep resistance (deformation under constant stress or load), fatigue properties (response to cyclic loading), and toughness (ability to absorb energy on impact without failure). These properties, in combination with strength and stiffness, are used by the designer in selection of a material for structural applications. Also important to the designer is the fact that metal matrix composites are anisotropic; that is, the mechanical properties depend critically on the orientation of the fibers with respect to the applied force and on the nature of the stress (tensile or compressive). Anisotropy can be an advantage or disadvantage, depending on the state of stress on the part in service. *See* CREEP (MATERIALS); METAL, MECHANICAL PROPERTIES OF; STRESS AND STRAIN.

Production. A variety of techniques are available for the production of continuous or discontinuous metal matrix composites. These may be broadly classified as diffusion processes, deposition processes, and liquid processes (**Fig. 1**).

Diffusion processes. These include the pressing and sintering of a powder metal matrix and bare or coated fibers, and the hot or cold pressing of the reinforcement between thin foils of the matrix metal or alloy.

In diffusion bonding, a stack of matrix foils are pressed around rows of relatively large-diameter fibers. Another solid-state process blends powdered matrix and reinforcement, and the matrix is densified around the reinforcement by conventional sintering or hot-pressing processes. *See* POWDER METALLURGY; SINTERING.

Deposition processes. Primary techniques are electrode-positioning of the matrix around fibers, plasma spraying of the matrix around fibers, or vacuum deposition of the matrix around fibers. In each case, it is usual to complete the process by cold or hot pressing. *See* ELECTROPLATING OF METALS; VACUUM METALLURGY.

Liquid processes. The important techniques in this category are infiltration of the liquid matrix around fibers, the pressing of powdered matrix and fibers at a temperature above the melting point of the matrix, and unidirectional solidification of eutectic alloys. *See* EUTECTICS.

Other processes. Spray casting processes (another class of liquid-state processes) involve spraying the matrix with or onto the reinforcement; solidification is achieved by heat extraction to the supporting substrate. There are additional processes that involve a partly liquid matrix. These include compocasting (a dispersion process using the matrix in semisolid form) and liquid-phase sintering processes.

In-place processes create the reinforcement from within the matrix. This can be accomplished by simple alloying and solidification, as is the case with directionally solidified eutectic alloys. Alternatively, the reinforcement can be formed by reaction of elements contained within the matrix in another phase such as a gas.

Fabrication. Composite processing methods combine the reinforcement with the matrix. This is accomplished while the matrix is either solid or liquid.

Typical liquid-state processes include the dispersion processes, which are casting techniques. A second set of processes involves liquid-metal impregnation; these include squeeze casting, where a preform or a bed of dispersoids is impregnated by molten alloy under hydraulic pressure. A third set comprises spray processes. In one of these, a molten metal stream is fragmented by means of a high-speed cold inert-gas jet passing through a spray gun, and dispersoid powders are simultaneously injected. A stream of molten droplets and dispersoid powders is directed toward a collector substrate where droplets recombine and solidify to form a high-density deposit.

In rapid solidification processing of composites, a jet of liquid alloy–particle slurry impinges under pressure on a water-cooled copper wheel (**Fig. 2**),

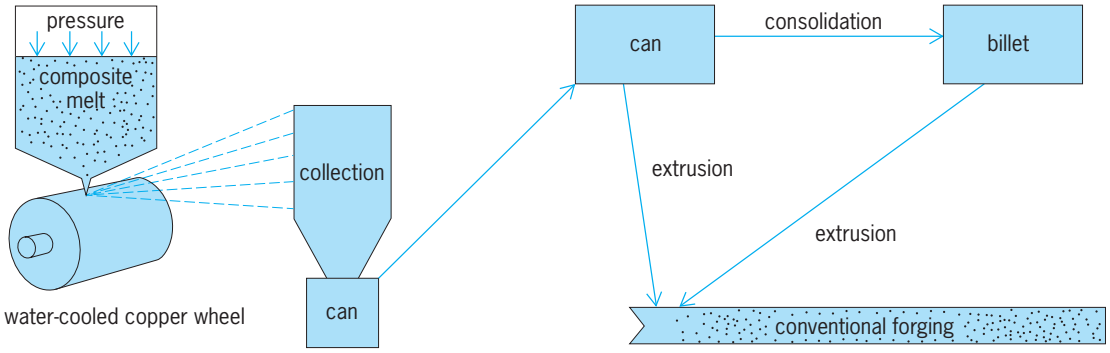

Fig. 2. Steps involved in rapid solidification processing of metal matrix composites.

Some composite components with proven potential

Composite	Components	Advantages
Aluminum–silicon carbide (particle)	Piston	Reduced weight, high strength and wear resistance
	Brake rotor, caliper, liner	High wear resistance, reduced weight
	Propeller shaft	Reduced weight, high specific stiffness
Aluminum–silicon carbide (whiskers)	Connecting rod	Reduced reciprocating mass, high specific strength and stiffness, low coefficient of thermal expansion
Magnesum–silicon carbide (particle)	Sprockets, pulleys, and covers	Reduced weight, high strength and stiffness
Aluminum–aluminum oxide (short fibers)	Piston ring	Wear resistance, high running temperature
	Piston crown (combustion bowl)	Reduced reciprocating mass, high creep and fatigue resistance
Aluminum–aluminum oxide (long fibers)	Connecting rod	Reduced reciprocating mass, improved strength and stiffness
Copper-graphite	Electrical contact strips, electronics packaging, bearings	Low friction and wear, low coefficient of thermal expansion
Aluminum-graphite	Cylinder, liner piston, bearings	Call resistance, reduced friction, wear, and weight
Aluminum–titanium carbide (particle)	Piston, connecting rod	Reduced weight and wear
Aluminum–fiber flax	Piston	Reduced weight and wear
Aluminum–aluminum oxide fibers–carbon fibers	Engine block	Reduced weight, improved strength and wear resistance

and the resulting flake powders are collected. The powder is put into cans and consolidated into billet or extruded to form a dense composite with higher yield strength, ultimate tensile strength, and ultimate ductility. *See* METALLIC GLASSES.

Depending on the process, the desired microstructure, and the desired part, metal matrix composites can be produced to net or near-net shape; or alternatively they can be produced as billet or ingot material for secondary shaping and processing.

Applications. The combined attributes of metal matrix composites, together with the costs of fabrication, vary widely with the nature of the material, the processing methods, and the quality of the product. In engineering, the type of composite used and its application vary significantly, as do the attributes that drive the choice of metal matrix composites in design (see **table**). For example, high specific modulus, low cost, and high weldability of extruded aluminum oxide particle–reinforced aluminum are the properties desirable for bicycle frames. High wear resistance, low weight, low cost, improved high-temperature properties, and the possibility for incorporation in a larger part of unreinforced aluminum are the considerations for design of diesel engine pistons. *See* COMPOSITE MATERIAL; HIGH-TEMPERATURE MATERIALS.

Mel M. Schwartz

Bibliography. American Society for Metals, *ASM Metals Handbook*, vol. 2, 9th ed., 1991; S. M. Lee, *Reference Book for Composites Technology*, 1989; S. Ray, Review synthesis of cast metal matrix particulate composites, *J. Mater. Sci.*, 28:5397–5413, 1993; T. Rienhart, *Engineered Materials Handbook: Composites*, vol. 1, 1988; M. M. Schwartz, *Composite Materials Handbook*, 2d ed., 1992; S. Suresh, A. Mortensen, and A. Needleman (eds.), *Fundamentals of Metal Matrix Composites*, 1993.

Metal rolling

Reducing or changing the cross-sectional area of a workpiece by the compressive forces exerted by rotating rolls. The original material fed into the rolls is usually an ingot from a foundry. The largest product in hot rolling is called a bloom; by successive hot- and cold-rolling operations the bloom is reduced to a billet, slab, plate, sheet, strip, and foil, in decreasing order of thickness and size. The initial breakdown of the ingot by rolling changes the coarse-grained, brittle, and porous structure into a wrought structure with greater ductility and finer grain size.

Process. A schematic presentation of the rolling process, in which the thickness of the metal is reduced as it passes through the rolls, is shown in **Fig. 1***a* . The speed at which the metal moves during rolling changes, as shown in Fig. 1*b*, to keep the volume rate of flow constant throughout the roll gap. Hence, as the thickness decreases, the velocity increases; however, the surface speed of a point on the roll is constant, and there is therefore relative sliding between the roll and the strip. The direction of this relative velocity changes at a point along the contact area, this point being known as the neutral or no-slip point. At the neutral point, roll and strip have the same velocity; to the left of this point (entry side) the strip moves more slowly than the roll; and to the right of this point (exit) it moves faster. Hence, the direction of frictional forces acting on the strip are opposite in these two regions, as shown in Fig. 1*a*. The net frictional force acting on the strip must be in the direction of exit to enable the rolling operation to take place. Although friction is a disadvantage in many metal-working processes, it is a necessity in rolling; without friction the rolls cannot pull the strip through the roll gap. It has been observed that in hot rolling the coefficient of friction may be as

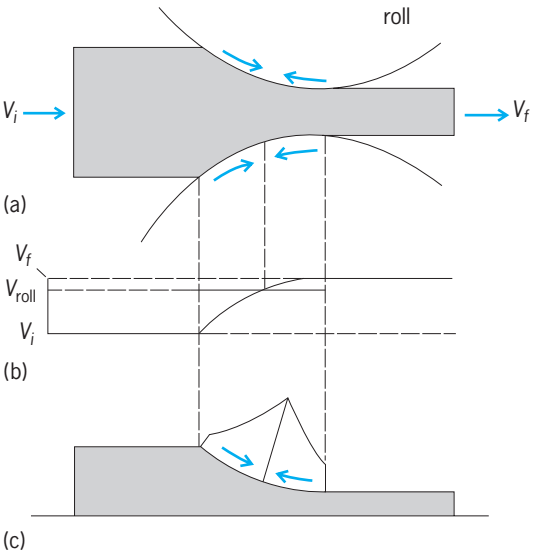

Fig. 1. Rolling process. (*a*) Direction of friction forces in the roll gap. (*b*) Velocity distribution. (*c*) Normal pressure acting on the strip in the roll gap.

much as 0.7, while in cold rolling it generally ranges 0.02–0.3.

The normal pressure distribution on the roll and hence on the strip is of the form shown in Fig. 1*c*. Because of its particular shape this pressure distribution is known as the friction hill. The overall slope of this hill depends on the coefficient of friction and the ratio of roll-strip contact length to the thickness of the strip. The size of the friction hill (area under the curve) represents the magnitude of the roll separating force per unit width that tends to push the rolls apart. This force can be reduced by increasing the workpiece temperature, reducing friction, taking smaller bites, and using smaller roll radii. Another method of reducing this force is by applying tension to the strip; this lowers the apparent compressive flow stress of the material. The tension can be back tension (entry) or front tension (exit) or both. Depending on the magnitude of these tensions, the neutral point shifts from its original position.

The roll-separating force can become so great that it is not possible to reduce further the thickness of the strip during the particular pass. With such a force the rolls deform elastically (roll flattening). In such cases rolling may be accomplished by improving lubrication, rolling a stack of sheets at the same time, or annealing the strip.

The maximum possible draft (the difference between the initial and final thickness of the strip) is a function of the friction coefficient an roll radius; it can be shown analytically that maximum draft is equal to the coefficient of friction squared times the roll radius.

The workpiece may become wider during rolling; this is called spreading. It is found that spreading increases with the thickness-width ratio of the workpiece and with decreasing coefficient of friction and decreasing radius-thickness ratio of the roll.

Practice. A great variety of roll arrangements and equipment are used in rolling. Some basic types are shown in **Fig. 2**. In another method (Steckel rolling) the strip is pulled through idler rolls by front tension only. The proper reduction per pass in rolling depends on the type of material and other factors; for soft, nonferrous metals, reductions are usually high, while for high-strength alloys they are small.

Temperatures in the hot rolling of various metals and alloys are similar to those in forging, namely, for aluminum alloys, 750–850°F (400–450°C); copper alloys, 1500°F (820°C); alloy steels, 1700–2300°F (930–1260°C); titanium alloys, 1400–1800°F (760–980°C); and refractory metal alloys, 1800–3000°F (980–1650°C). Rolling speeds range up to about 5000 ft/min (1500 m/min). Although hot rolling has the advantage of lowering forces and increasing the ductility of the metal, cold rolling gives smoother finish, closer tolerances, and increased strength.

The thickness of a rolled sheet is identified by gage number: The smaller the number the thicker the sheet. Actual thickness depends on the particular standard used; there are different standards, depending on the type of metal. The terminology for

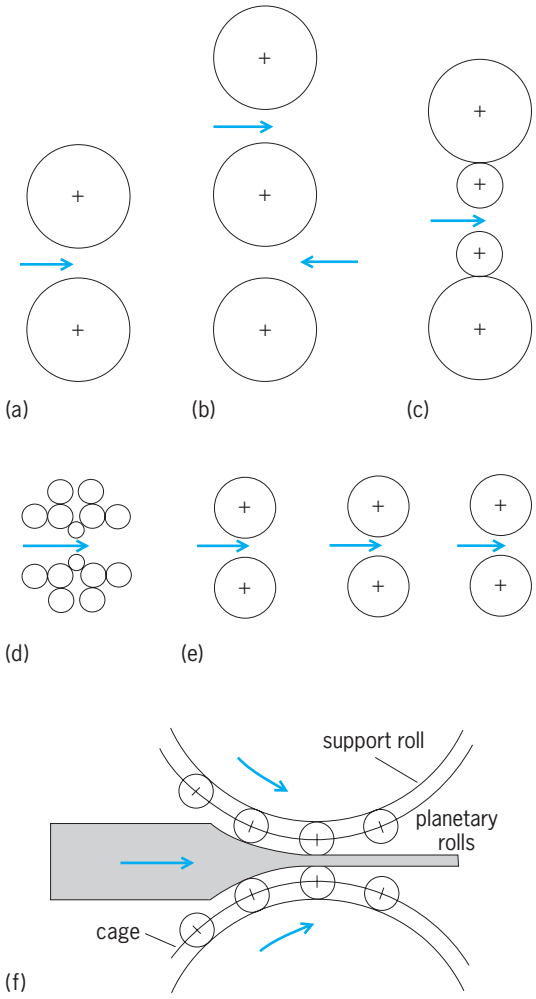

Fig. 2. Basic types of roll arrangement. (*a*) Two-high. (*b*) Three-high. (*c*) Four-high. (*d*) Cluster. (*e*) Tandem rolling with three stands. (*f*) Planetary mill.

hardness for rolled sheets is shown in the **table**. A sheet that is reduced in thickness by one gage number from the annealed condition is called quarter hard, by two gage numbers half hard, and so on, as listed in the table. The dead-soft condition is fully annealed.

Successful rolling practice requires a careful balance of factors such as reduction per pass, control of temperature, lubrication, roll size and finish, and intermediate annealing.

Requirements for roll materials are mainly strength and resistance to wear. Common roll materials are cast iron, cast steel, and forged steel. In cold rolling, cemented carbide is also used for small rolls. To avoid variation in strip thickness due to bending of the rolls, rolls are ground to a particular geometry, called camber, whereby the center of the roll has a diameter of a few thousandths of an inch greater than the diameter of its ends.

Hot rolling is usually carried out without a lubricant, although graphite or grease may be used. Cold rolling is carried out with low-viscosity lubricants, paraffin being a suitable lubricant for nonferrous metals. The type of residual stresses in the strip depends on the reduction and also on roll radius. Small rolls or small reductions produce compressive residual stresses on the surface of the strip and tensile stresses in the central portions, whereas large rolls produce the opposite residual stress pattern. A number of defects (wavy edges, zipper breaks, edge cracks, alligatoring) can result during the rolling process. These are usually eliminated or reduced by changes in operating variables or by special techniques.

Miscellaneous processes. Most seamless tubing is produced by a technique based on the principle that the inside of a round rod is subjected to secondary tensile stresses when compressed radially (**Fig. 3***a*). A simple demonstration of this can be made by rolling an eraser, removed from the end of a pencil, between a flat surface and a ruler that is moved back and forth (Fig. 3*b*). In a short time a hole is produced in the center of the eraser. The roll-piercing of round bars to make seamless tubing (Mannesmann process) is based on this principle (Fig. 3*c*). The compressive radial forces are supplied by two rolls with their axes in parallel planes, but at an angle to each other so as to move the workpiece through the rolls. The rolling action causes the center of the billet to rupture. The purpose of the mandrel is to expand the tube and improve the surface finish of the inside. For this process to be successful, the billet material should be of high quality and free of defects.

Hardness terminology for rolled sheets

Terminology	Increase in gage number	Reduction in thickness, %
Annealed (dead-soft)	0	0
1/8 hard	—	6
1/4 hard	1	11
1/2 hard	2	21
3/4 hard	3	29
Hard	4	37
Extra hard	6	50
Spring hard	8	60
Extra spring hard	10	69

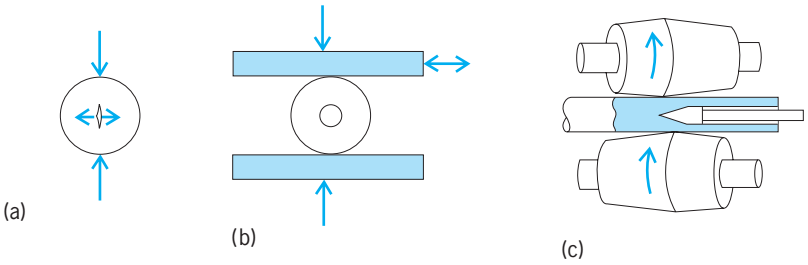

Fig. 3. Development of the Mannesmann process for producing seamless tubing (*a–c* explained in text).

In the ring-rolling process, a thin, large-diameter ring is produced from a thicker and smaller-diameter ring. This is accomplished by placing the ring between two rotating rolls; the reduction in thickness of the ring is compensated by an increase in diameter; there is little or no change in the width of the ring.

Sections such as railroad tracks and I beams are also rolled by passing the stock through a number of specially designed rolls with their axes placed in different directions. Roll-pass design for such sections requires considerable experience to avoid defective products and to obtain desirable properties. Metal powders are also rolled into sheets or strip by special techniques. *See* POWDER METALLURGY.

Serope Kalpakjian

Bibliography. R. Pradhan and G. Lyudkovsky (eds.), *Hot- and Cold-Rolled Sheet Steels*, 1988; W. L. Roberts, *Cold Rolling of Steel*, vol. 2, 1978.

Metallic glasses

Metals and metallic alloys having an amorphous structure on the atomic scale. Although the word "glass" is commonly used to refer to the familiar transparent oxide glasses (such as silicate glasses used to make windowpanes), in a more general sense a glass is any solid obtained from a liquid that does not crystallize upon cooling. As a result, a glass retains an atomic-scale structure in which the atoms are more or less randomly arranged, similar to that of the liquid state. Because most metals crystallize quickly, special care must be taken with processing and alloy design to produce a metallic glass. Metallic glasses produced directly by quenching the liquid are quite similar in terms of structure and properties to amorphous alloys (of the same chemical composition) produced by other means, such as physical vapor deposition, irradiation, mechanical alloying, or solid-state reaction. *See* AMORPHOUS SOLID; CRYSTAL; GLASS; GLASS TRANSITION.

Preparation. When cooled below its equilibrium melting temperature, a liquid becomes unstable and there is a tendency for the stable crystalline phase (or phases) to form. Because of the significant structural change that occurs, crystallization does not happen

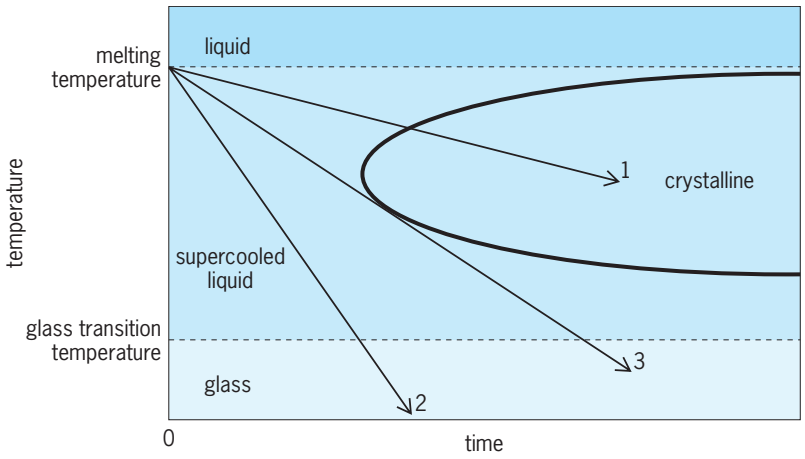

Fig. 1. Time required for crystallization of amorphous alloys below the equilibrium melting temperature.

instantaneously, and it is therefore possible to cool a liquid below its melting temperature without crystallizing it, for a limited time (**Fig. 1**). Such a liquid is said to be supercooled. Crystallization occurs slowly at temperatures just below the melting temperature, where it is difficult to nucleate new crystals, and at low temperature because atomic diffusion is slow. There is an intermediate temperature at which crystallization occurs most rapidly.

If a liquid is cooled slowly but continuously (curve 1 in Fig. 1), crystallization will begin at a temperature below the melting temperature and will be completed at a later time (and lower temperature). A liquid may be cooled so quickly that there is no time for crystallization to occur at all (curve 2). Instead, at a lower temperature called the glass transition temperature, the supercooled liquid transforms to an amorphous solid, or glass. The slowest rate at which the liquid can be cooled and form a glass, while avoiding crystallization, is called the critical cooling rate (curve 3). The critical cooling rate is a measure of how easily a material forms a glass, with low critical cooling rates indicating easy glass formation.

In materials with complicated crystal structures or in which the required atomic rearrangements are difficult, crystallization occurs slowly. Such materials, including many oxides and polymers, form glasses easily and have critical cooling rates on the order of 10^{-2} to 10^{-4} K/s (10^{-2} to 10^{-4} °F/s). Most metals have relatively simple crystal structures and crystallize readily. The critical cooling rate for pure metallic elements is on the order of 10^{13} to 10^{14} K/s (10^{13} to 10^{14} °F/s), rates which can only be achieved in very small volumes of material under specialized laboratory conditions. The critical cooling rate of an alloy can be much lower than that of a pure element, making production of metallic glasses feasible. The first true metallic glass, produced in 1960, was an alloy of gold and silicon and was cooled at a rate of approximately 2×10^6 K/s (4×10^6 °F/s). While still quite high, cooling rates on this order can be easily achieved by a variety of rapid solidification techniques, such as single-roller melt spinning. These techniques enabled the production of commercial quantities of metallic glasses, beginning in the 1970s. A significant limitation of the high cooling rates required was that the early metallic glasses could be produced only in forms in which one dimension of the material was small (typically 50–100 μm), such as ribbons, foils, wires, and powders.

Recently, more complex alloys have been developed in which the critical cooling rate is as low at 1 K/s (2°F/s) or even lower. These cooling rates can be achieved via common metallurgical processing techniques, such as die casting into a metallic mold, enabling the production of metallic glass components with minimum thicknesses in excess of 1 cm (0.4 in.). These easily processed alloys are commonly called bulk metallic glasses. Furthermore, a bulk metallic glass can be reheated to a temperature above its glass transition temperature, without crystallization, causing it to soften dramatically and allowing it to be easily formed into complex shapes in much the same way as is commonly done with amorphous thermoplastic polymers. However, because the crystalline form is still the stable state, all metallic glasses will crystallize if subjected to elevated temperatures for long times. *See* METAL CASTING.

Structure. The differences between the highly regular atomic positions characteristic of a crystal and the disordered structure of a liquid or glass can be explored using techniques based on the scattering of radiation such as x-rays, electrons, or neutrons. In crystalline materials, the regular atomic positions cause constructive or destructive interference among the scattered waves, leading to the formation of sharp, intense diffraction peaks at particular scattering angles that are characteristic of the structure of the material and of the wavelength of the radiation (**Fig. 2***a*). The peaks from amorphous materials by comparison are quite broad and weak (Fig. 2*b*). A truly random structure (such as that of a monatomic gas) would show no peaks at all, so the presence of the peaks is proof that there is short-range order (over a few atomic distances) in the structure of glasses and liquids. Fourier transformation of the scattering data produces a radial distribution function (**Fig. 3**), which describes the atomic environment around an

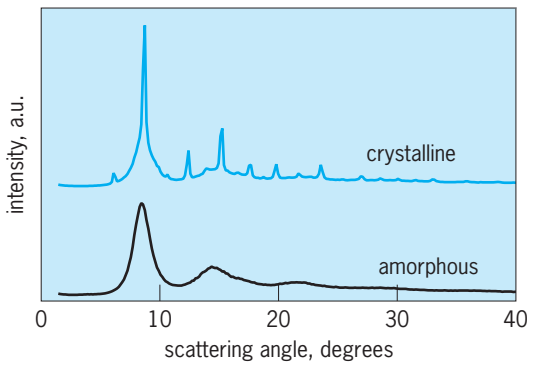

Fig. 2. X-ray diffraction patterns for crystalline and amorphous $Pd_{40}Ni_{40}P_{20}$ alloys.

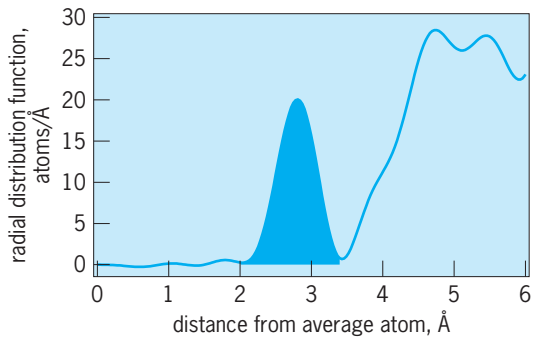

Fig. 3. Radial distribution function for amorphous $Pd_{40}Ni_{40}P_{20}$. The shaded region represents the first coordination shell of atoms around an average atom in the glass.

average atom in the material. From the radial distribution function, one can determine the number of atoms in the nearest-neighbor shell (the coordination number) as well as the distance between the average atom and its nearest neighbors. If the constituent elements are similar in size, then the average coordination number is approximately 12, just as it is in a close-packed crystalline structure. That metallic glasses are nearly as close packed is also reflected in their densities, which are typically just 0.5–2% lower than crystalline phases of similar chemical composition. *See* FOURIER SERIES AND TRANSFORMS; X-RAY DIFFRACTION.

Metallic glasses are also notable for their lack of structure over length scales longer than the atomic. Conventional crystalline alloys have microstructural features such as grains and precipitates with typical sizes of 0.1–100 μm; these features make fabrication of very small components difficult and lead to anisotropic mechanical properties that can be problematic. Because metallic glasses have no structural features on these length scales, they should be well suited for highly miniaturized devices, such as for micro-electro-mechanical systems (MEMS) [**Fig. 4**]. The lack of microstructure also means that metallic glasses have low ability to suppress vibrations (damping capacity). *See* MICRO-ELECTRO-MECHANICAL SYSTEMS (MEMS).

Mechanical properties. At low stresses and at temperatures well below the glass transition, metallic glasses display isotropic linear elastic behavior in which the strain ε, Eq. (1), is directly proportional to

$$\varepsilon = \frac{\sigma}{E} \tag{1}$$

the stress σ through Hooke's law, where the proportionality constant E (Young's modulus) describes the resistance to elastic (reversible) deformation, or stiffness. The disordered atomic structure of a metallic glass enables slight rearrangements of the atomic positions in response to an applied load, which would not be possible if the material were crystalline. This has the effect of reducing the stiffness slightly, so that E for metallic glasses is typically 20–30% lower than that for a crystalline alloy of the same composition. Distortion of the atomic bonds requires energy, and the elastic strain energy (per unit volume of material), given by Eq. (2), is called the resilience of the material. The high yield stress of metallic glasses, together with low modulus, means that metallic glasses can sustain large elastic strains of 2–3% (compared with 0.1–0.2% for a typical crystalline metal) and have exceptionally large values of resilience. *See* HOOKE'S LAW; STRESS AND STRAIN; YOUNG'S MODULUS.

$$U_{el} = \frac{1}{2}\sigma\varepsilon = \frac{\sigma^2}{2E} \tag{2}$$

At stresses beyond the elastic limit (or yield stress), metallic glasses (like crystalline alloys) experience permanent, or plastic, deformation. The degree of plastic deformation that a material can sustain before fracture is called ductility. Conventional crystalline alloys that are useful in structural applications combine high strength with good ductility. Both the strength and ductility of crystalline metals are determined largely by the properties of defects in the crystalline structure called dislocations. Although the dislocations reduce the yield strength of a crystalline metal below that predicted solely on the basis of the strength of the atomic bonds, interactions among the dislocations cause the material to strengthen (by strain hardening) as it deforms. This property gives many crystalline metals good ductility and toughness. In contrast, amorphous alloys have no dislocations (due to their disordered structure) and so they can be quite strong, often three to four times as strong as a crystalline alloy of similar composition (see **table**). However, the lack of dislocations means that metallic glasses do not strain-harden, and therefore have almost no ductility in tension. Instead of deforming uniformly, as crystalline metals do, plastic deformation in metallic glasses (at temperatures well below the glass transition temperature) is concentrated into very narrow shear bands. This problem can be partially overcome by reinforcing the metallic glass with particles of a ductile crystalline metal that impede shear band motion, although some strength is sacrificed. *See* PLASTIC DEFORMATION OF METAL.

Besides strength, fracture toughness—the ability of a material that may have flaws (such as small cracks) to support a load without fracturing—is of critical importance for many structural applications. Although plastic deformation (which requires energy and therefore enhances toughness) is concentrated into shear bands, the plastic deformation in each shear band can be extensive, and there can be considerable branching of the shear bands ahead of a crack tip. As a result, the fracture toughness (K_c) of some metallic glasses (20–90 MPa $\cdot$ $m^{1/2}$) is comparable to that of crystalline alloys, although for other amorphous alloys the fracture toughness can be quite low ($\sim$1 MPa $\cdot$ $m^{1/2}$), comparable to engineering ceramics. Furthermore, annealing some metallic glasses tends to make them more brittle, for reasons that are not well understood.

At elevated temperatures, approaching the glass transition temperature, the strength of a metallic glass drops and the deformation becomes homogeneous instead of being concentrated into shear

Mechanical properties of some amorphous alloys, together with properties of common crystalline engineering alloys

	Density, g/cm^3 (lb/in.^{3})	Young's modulus, GPa (10^6 psi)	Poisson's ratio	Yield strength, MPa (10^3 psi)	Tensile strength, MPa (10^3 psi)	Percent elongation	Fracture toughness, MPa · m$^{1/2}$ (ksi · in.$^{1/2}$)
			Amorphous alloys				
$Zr_{41}Ti_{14}Cu_{12.5}Ni_{10}Be_{22.5}$	6.12 (0.221)	101 (14.6)	0.34	1900 (275)	1900 (275)	2*	25 (23)
$Mg_{65}Cu_{25}Tb_{10}$	3.98 (0.144)	48 (7.0)	0.31	700 (100)	700 (100)	1.5*	2 (1.8)
$Pt_{57.5}Cu_{14.7}Ni_{5.3}P_{22.5}$	15.0 (0.541)	95 (14)	0.42	1400 (200)	1470 (213)	1.5*	90 (83)
			Crystalline alloys				
Steel (4340, quenched and tempered)	7.85 (0.283)	207 (30)	0.30	1620 (235)	1760 (255)	12	50 (46)
Titanium (Ti-6Al-4V, solutionized and aged)	4.43 (0.160)	114 (16.5)	0.34	1100 (160)	1170 (170)	10	55 (50)
Aluminum (7075-T6)	2.80 (0.101)	71 (10)	0.33	505 (73)	572 (83)	11	24 (22)

*Elastic deformation; under tensile loading, most metallic glasses fail without measurable plastic deformation.

bands. If heated above the glass transition, a metallic alloy becomes a fluid, the viscosity of which can be controlled over a wide range of temperature. Because the stresses required to cause deformation are low, either of these states can be useful for processing metallic glasses into complex shapes. *See* METAL; MECHANICAL PROPERTIES OF.

Electrical, optical, and magnetic properties. Like crystalline metals, metallic glasses are electrically and thermally conductive, due to the presence of conduction electrons. However, the disordered atomic structure and the high alloy content mean that metallic glasses are not especially good conductors, with an electrical resistivity on the order of $10^{-6}\,\Omega \cdot m$, as compared to about $10^{-8}\,\Omega \cdot m$ for copper at room temperature. However, the resistivity of metallic glasses does not vary strongly with temperature (except near absolute zero, where some amorphous alloys become superconducting). The presence of conduction electrons also allows metallic glasses to scatter and absorb incident light, giving metallic glasses the shiny luster typical of metals. Thus, unlike common oxide glasses, metallic glasses are not transparent to visible light. *See* ELECTRICAL CONDUCTIVITY OF METALS.

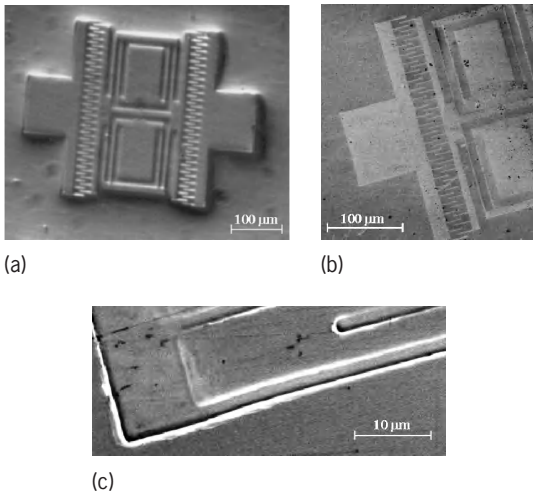

Fig. 4. Micrographs of (*a*) Replica of silicon micro-electro-mechanical device produced by warm-pressing into a metallic glass. (*b*, *c*) Submicrometer features are cleanly reproduced. [*Courtesy of J. Lewandowski and A. Shamimi Nouri, Case Western Reserve University (J. J. Lewandowski, M. Shazly, and A. Shamimi Nouri, Scripta Materialia, 54:337–341, 2006)*]

Some metallic glasses, particularly alloys based on iron, can be ferromagnetic. Although the presence of alloying elements decreases the saturation magnetization relative to that of a pure ferromagnetic element, for many applications the lack of crystal structure is a distinct advantage. In particular, amorphous alloys based on the transition metals (iron, cobalt, and nickel) have low coercivity because there are no crystalline grain boundaries (which can pin magnetic domain walls) and because there is no magnetocrystalline anisotropy. Also, because the electrical resistivity is high, eddy-current losses associated with high-frequency magnetization and demagnetization are minimized. Many amorphous alloys show large magnetostriction (shape change upon magnetization). *See* MAGNETIC MATERIALS.

Applications. Because the early metallic glasses could only be produced in limited shapes (such as thin ribbons and foils), applications were mostly limited to those making use of the advantageous magnetic properties of iron-based ferromagnetic alloys. For instance, these alloys can be used to make high-efficiency cores for electrical transformers, and the large magnetostriction is useful for making antishoplifting tags. The more recent development of bulk glass-forming alloys has opened up a much wider range of applications that make use of the unique mechanical properties of metallic glasses. In particular, the ability to soften the glass by heating it above the glass transition temperature makes it possible to form complex shapes and castings with thin sections. This, together with the high strength and stiffness (compared to polymers), makes metallic glasses attractive for applications such as cases for cellular telephones and other electronic devices. High strength is related to high hardness. This, together with the ability to form fine features, makes metallic glasses well suited for precision knife-edges, such as scalpels. Also, the high resilience and low

damping capacity mean that metallic glasses make good springs. One example is the use of zirconium-based metallic glasses as golf club heads.

Although current bulk metallic glasses tend to be rather expensive in terms of the raw cost of materials (including both the base elements such as zirconium, and the alloying elements such as beryllium), the processing costs can be low because the glasses can be easily processed at temperatures above the glass transition. Future applications are likely to be driven by these economic considerations as much as the unique mechanical properties of metallic glasses.

Todd C. Hufnagel

Bibliography. T. H. Courntey, *Mechanical Behavior of Materials*, McGraw-Hill, 2000; S. R. Elliott, *Physics of Amorphous Materials*, Longman, London, 1984; B. Lemley, Glassy metal, *Discover*, pp. 46–51, April 2004; M. Telford, The case for bulk metallic glass, *Mater. Today*, pp. 36–43, March 2004.

Metallocenes

Bis-cyclopentadienyl derivatives of transition metals whose bonding involves overlap of *ns*, $(n - 1)d$, and *np* orbitals of the metal with molecular orbitals of appropriate symmetry of each cyclopentadienyl ring. The resulting complexes often possess two parallel rings (sandwich structure), but in some cases, for example those involving the titanium subgroup of metals, the rings are canted (**Fig. 1**). Numerous monocyclopentadienyl complexes (half-sandwich complexes) also exist, as do systems containing three and even four η^5-bonded cyclopentadienyl rings; these latter systems are not metallocene complexes. Moreover, compounds constituted of parallel ring systems that are not both η^5-bonding cyclopentadienyls (mixed-sandwich complexes) are not metallocene complexes. Metals in the periodic table commonly known to form metallocene complexes are titanium, zirconium, hafnium, vanadium, chromium, molybdenum, tungsten, manganese, iron, ruthenium, osmium, cobalt, rhodium, and nickel. *See* COORDINATION COMPLEXES.

Bonding. Each cyclopentadienyl ligand has three filled bonding molecular orbitals and two low-lying empty antibonding molecular orbitals. The valence levels of iron(0) consists of 4*s*, 3*d*, and 4*p* orbitals containing eight electrons. In the molecular-orbital bonding scheme for ferrocene, three filled molecular orbitals from each of the cyclopentadienyl rings overlap with the 4*s*, the three 4*p*, and two of the 3*d* orbitals of correct symmetry to form six new bonding orbitals. Further stabilization results from back-bonding from the filled *d* orbitals of the iron to the empty antibonding orbitals of the rings. This gives a total of 18 electrons in nine orbitals (18-electron rule), 10 of which come from the two cyclopentadienyl rings (in their conceptual neutral state) and 8 of which come from iron(0). Only six of the orbitals contribute significant bonding. *See* CHEMICAL BONDING.

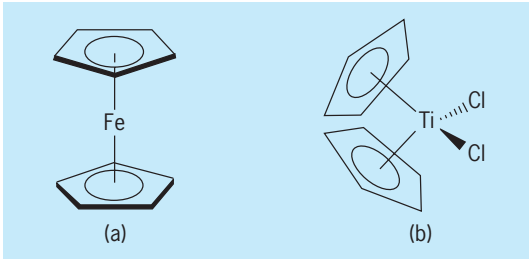

Fig. 1. Metallocene structures. (*a*) Staggered sandwich structure of ferrocene. (*b*) Canted cyclopentadienyl ring structure of titanocene dichloride. The distribution of the ligands about the Ti atom is tetrahedral.

Structure and properties. The first transition-metal series of metallocenes from chromocene through nickelocene forms a continuous series of solid solutions; each metallocene possesses a melting point of 173°C (343°F). In the crystalline state the cyclopentadienyl rings of ferrocene when viewed down the axis joining their centers exhibit the staggered conformation, but in the gas phase the rings are eclipsed. For ruthenocene and osmocene, the conformations in the crystalline state are eclipsed, possibly reflecting the greater ring-metal bond distances. For ferrocene, the gas-phase barrier to rotation has been found to be only 4 ± 1 kJ · mol^{-1}. Ferrocene structurally possesses a C—C bond distance of 0.140 nanometer and a C—Fe bond distance of 0.204 nanometer. Ferrocene can be sublimed under reduced pressure at 100°C (212°F) and is stable to temperatures >400°C (750°F).

Ferrocene is somewhat stable to H_2SO_4; with HNO_3 it forms a cation known as the ferricinium ion. Cobaltocene can be easily oxidized to a very stable cation, $(C_5H_5)_2Co^+$, which can be recovered unchanged from aqua regia. Ferrocene is oxidatively stable, cobaltocene and nickelocene much less so, but they can be handled for brief periods in air. Chromocene, on the other hand, is dangerously pyrophoric when exposed to air. *See* SOLID SOLUTION.

Preparation. The best-known preparation of metallocenes, here exemplified by the formation of ferrocene, is by combination of the appropriate transition-metal salt with the cyclopentadienyl Grignard reagent [reaction (1)]. This Grignard reagent

$$2C_5H_5MgBr + FeCl_2 \longrightarrow (C_5H_5)_2Fe + 2MgBrCl \quad (1)$$

can be formed by an exchange reaction between cyclopentadiene and C_6H_5MgBr. Useful modifications of this procedure involve treatment of cyclopentadiene with sodium or sodium hydride in tetrahydrofuran to form the sodium salt, followed by addition of a transition-metal halide, carbonyl, or related derivative. The thallium salt, C_5H_5Tl, can also be used. A milder set of conditions is possible; for example, a strong organic base can be used as an acceptor for HCl [reaction (2)].

$$2C_5H_6 + CoCl_2 + 2(C_2H_5)_2NH \longrightarrow (C_5H_5)_2Co + 2(C_2H_5)_2NH_2{}^+Cl^- \quad (2)$$

See GRIGNARD REACTION.

Reactions. The reactions of metallocenes can be divided into two classes: the first is typified by the

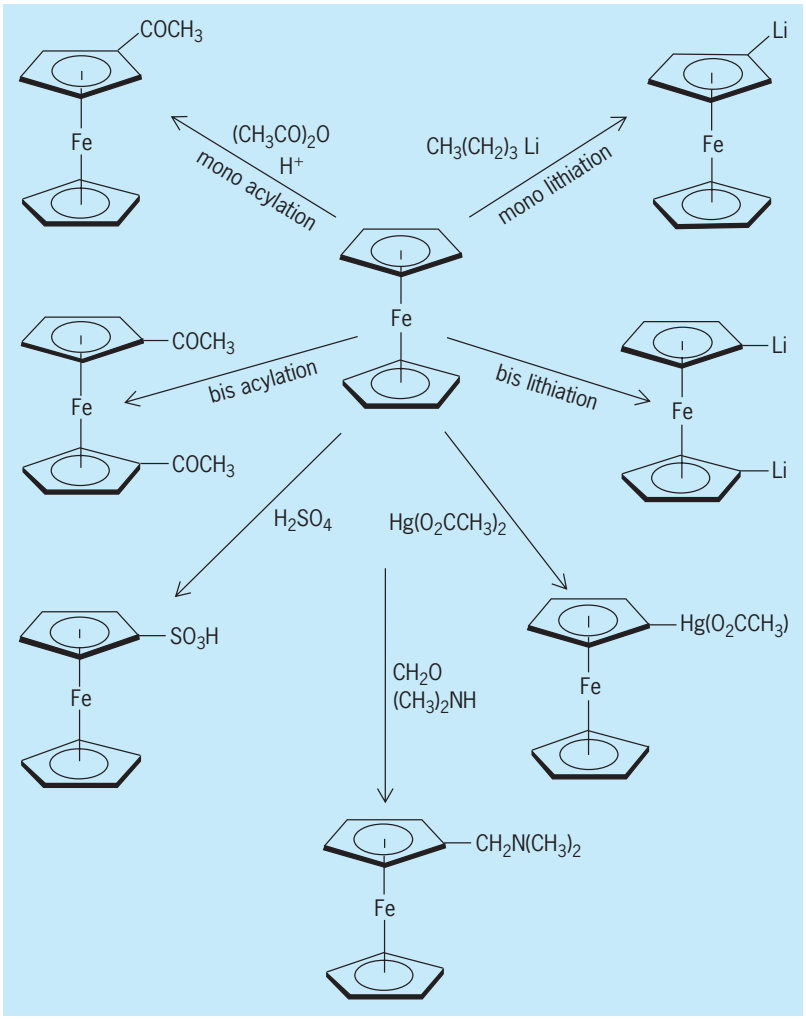

Fig. 2. Aromatic reactions of ferrocene.

iron triad, and comprises essentially the reactions of aromatic molecules; the second consists of the reactions of the other metallocenes where the 18-electron rare-gas configuration is not found. Reactions in these latter systems often lead to a product where the 18-electron rule is obeyed.

Ferrocene is a very electron-rich system, and undergoes electrophilic substitution with great rapidity. For example, acylation proceeds about 10^6 times faster than that of benzene under similar conditions. Ferrocene also undergoes several other typical aromatic substitution reactions besides acylation, including sulfonation, dimethylaminomethylation (Mannich reaction), metalation, and the like (**Fig. 2**). Bis substitution tends to factor a product where each ring is monosubstituted although several cases are known where two substituents are introduced into one ring. Ferrocene is oxidized and deactivated under conditions for nitration and halogenation.

The other metallocenes often react as if to relieve the instability of their electronic configurations; those that are electron-rich lose coordination sites on the ligand (or the entire ligand) in order to reduce their outer-shell electron count to 18, the krypton configuration. Reactions in accord with this formulation are shown in reactions (3) and (4). In each case,

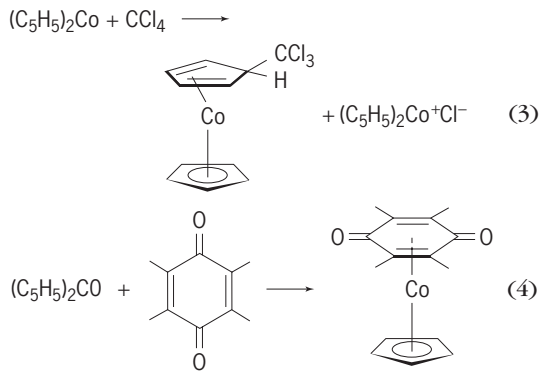

cobalt has gone formally from a Co(II) species to a Co(I) species, and in each of the products cobalt has the 18-electron configuration. Nickelocene reacts in similar fashion to reduce its coordination sphere by a factor of 2 to attain the 18-electron rare-gas configuration [reactions (5) and (6)].

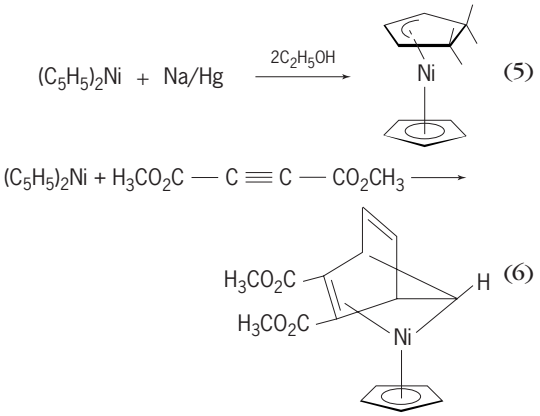

A somewhat similar rationale can be used for the few reactions of manganocene that have been studied. Manganocene, in contrast to the other metallocenes, is only a 17-electron system and so reacts with electron-rich systems such as biphenyl radical anion, resulting in displacement of the cyclopentadienyl ring [reaction (7)].

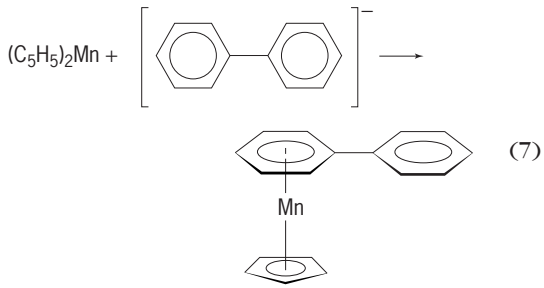

Vanadocene is so electrophilic that it inserts into π bonds in carbenelike fashion [reaction (8)].

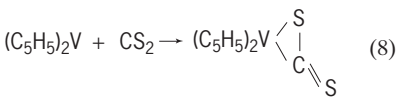

Structures. Metallocenes can possess both axial and chiral atom asymmetry. For example,

α-ketotetramethyleneferrocene (**1**) was the first ferrocene resolved; a number of chiral transition-metal metallocenes in the titanium subgroup such as (**2**)

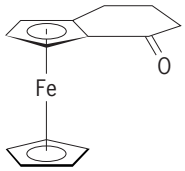

(**1**)

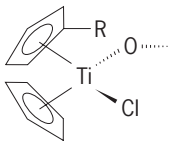

(**2**)

also are known. Other novel structural features are illustrated by the bis-complexation of nickel by pentalene to form (**3**) and by triple-decker metallocenes of type (**4**).

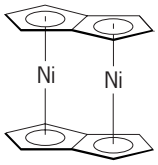

(**3**)

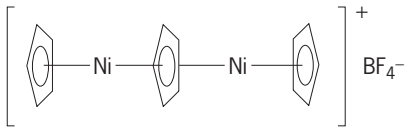

(**4**)

Decasubstituted ferrocenes $[C_5(CH_3)_5]_2Fe$ and $[C_5(C_6H_5)_2]Fe$ and pentasubstituted metallocenes such as $C_5(C_6H_5)_5FeC_5H_5$ have been prepared; the pentasubstituted cyclopentadienyl ligands constitute an interesting extension of the possibilities of metallocene chemistry, offering greater air and thermal stability and other property modification.

Uses. Decamethylzirconocene reacts with nitrogen to form complex (**5**). Acid hydrolysis of this

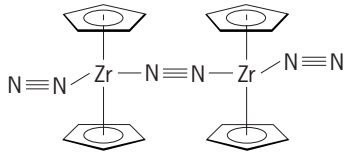

(**5**)

complex provides ammonia and hydrazine. Although not commercial, this species has the potential for acting as a nitrogen-fixing complex that could be used directly in the soil. Chromocene can be reacted with alumina to make a polymerization catalyst for ethylene. Ferrocene and some alkyl-substituted ferrocenes have been used as moderators in high-temperature combustions such as occur in solid rocket fuels. Lastly, a cyclopentadienyl complex, $CH_3C_5H_4Mn(CO)_3$, briefly replaced tetraethyllead as an octane booster and antiknock agent in liquid fuels. *See* ORGANOMETALLIC COMPOUND.

Donald W. Slocum

Bibliography. J. Collman et al., *Principles and Applications of Organotransition Metal Chemistry*, 2d ed., 1987; F. A. Cotton et al., *Advanced Inorganic Chemistry*, 6th ed., 1999; R. H. Crabtree, *The Organometallic Chemistry of the Transition Metals*, 3d ed., 2001; F. G. A. Stone and R. West (eds.), *Advances in Organometallic Chemistry*, vol. 10, 1972; M. Tsutsui et al., *Introduction to Metal π-Complex Chemistry*, 1970.

Metallochaperones

A family of proteins that shuttle metal ions to specific sites within a cell. The target sites for metal delivery include a number of metalloenzymes, or proteins that bind metal ions, such as copper, zinc, or iron, and use these ions as cofactors to carry out essential biochemical reactions. It was long thought that metalloenzymes could acquire their metal ion without the assistance of an accessory metallochaperone. The metal ion was believed to freely diffuse within the cell until it contacted its metalloenzyme target, at which point the metal ion inserted itself into the protein. However, several discoveries in the late 1990s led to a radical change in the thinking of how metalloenzymes acquire their metal ion. The insertion of the metal is now known to require an auxiliary protein, the metallochaperone. Metallochaperones escort the ion to a specific intracellular location and facilitate incorporation of the metal into designated metalloenzymes. *See* BIOINORGANIC CHEMISTRY; CELL (BIOLOGY).

Although the bulk of current knowledge on metallochaperones is restricted to copper, it is reasonable to assume that a distinct class of proteins is responsible for the incorporation of other metal ion cofactors into metalloenzymes. The heavy metals iron, manganese, and zinc are also required as cofactors for metalloenzymes, and like copper, these metals are presumably present at trace quantities inside living cells. It is therefore highly likely that new families of metallochaperones will emerge in the near future.

Copper chaperones. Among the metallochaperones that have been studied in detail are a family of three copper chaperones. These molecules operate in eukaryotic (nucleated) cells to direct copper to distinct intracellular locations: the mitochondria, the secretory pathway, and the cytosol. All three copper chaperones were originally identified through genetic studies of bakers' yeast, *Saccharomyces cerevisiae*. Their discoveries led to rapid identification of the human homolog proteins that are closely related in function and structure. One of the first copper chaperones identified, COX17, is a small protein that specifically directs copper to the mitochondria. Mitochondria, often called the power plants of the cell, are the sites where energy is produced from

respiration. The copper delivered by COX17 is inserted into the metalloenzyme cytochrome oxidase, needed for respiration. A second copper chaperone identified was ATX1, which carries copper to the secretory pathway, a cellular compartment that functions to shuttle proteins toward the cell surface. The metal delivered by ATX1 is incorporated into copper enzymes destined for the cell surface or the extracellular milieu. The most recently identified copper chaperone is CCS, which specifically delivers copper to a single metalloenzyme, superoxide dismutase. This copper-requiring enzyme is located in the soluble cytosolic compartment of the cell and acts to detoxify harmful reactive oxygen species. *See* MITOCHONDRIA.

The COX17 copper chaperone was discovered by D. M. Glerum and A. Tzagoloff in 1996 in their search for yeast genes involved in the assembly of cytochrome oxidase. Each molecule of COX17 can carry two ions of copper by coordination of the metal to cysteine residues (sulfur-containing amino acids) present in the COX17 polypeptide. COX17 has been localized to the cytosolic compartment of the cell as well as to the intermembrane space of the mitochondria, in part explaining its ability to shuttle copper ions across the cytosol to the mitochondria.

ATX1 was originally identified by S. Lin and V. C. Culotta in 1995 as a gene which when expressed to very high levels in yeast would prevent oxidative damage. However, this apparent antioxidant activity was later found not to be the primary function of ATX1. Rather, this protein acts to specifically shuttle copper ions across the cytosol to an intracellular copper transporter located in the secretory pathway. In humans, this intracellular copper transporter or copper pump is known as the Wilson or Menkes protein. A number of copper-requiring metalloenzymes that are exported from the cell rely on the Menkes/Wilson proteins and human ATX1 to acquire their copper. Included in this list are copper enzymes involved in connective tissue formation, brain function, and iron use. The ATX1 copper chaperone is known to bind a single copper ion via two cysteine residues present in the ATX1 amino acid sequence MXCXXC (M = methionine, X = any amino acid, C = cysteine). This copper-binding site is not unique to ATX1, but is also found in the Wilson/Menkes copper transporters that serve as targets for ATX1. Studies by T. V. O'Halloran and colleagues revealed that ATX1 physically interacts with the copper transporter and deposits copper by transferring the metal from the MXCXXC site in the copper chaperone to the same site in the copper pump. *See* AMINO ACIDS.

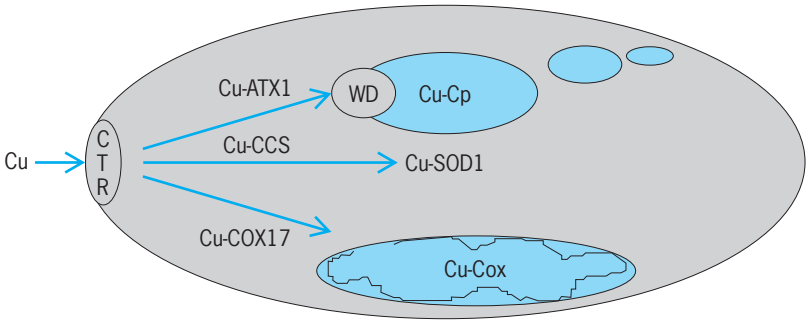

A family of copper metallochaperones direct trafficking of copper ions inside the cell. The schematic shows three distinct pathways of copper movement within a eukaryotic cell. Copper is first transported into the cell by the CTR and is then bound as cargo to one of three copper metallochaperones: (1) ATX1 delivers the metal to an intracellular copper transporter [such as the human Wilson disease (WD) gene product], which in turn pumps the copper into the secretory pathway where the metal is inserted into copper enzymes destined for export from the cell [such as human ceruloplasm (Cp)]. (2) CCS specifically delivers copper to the cytosolic superoxide dismutase enzyme (SOD1). (3) COX17 carries copper to the mitochondria where the metal is incorporated into cytochrome oxidase (Cu-Cox).

The CCS copper chaperone discovered by Culotta, J. D. Gitlin, and coworkers in 1997 specifically inserts copper into a single enzyme, the soluble copper- and zinc-requiring superoxide dismutase (SOD1). Interestingly, CCS contains the same MXCXXC copper-binding site found in ATX1, but in addition the CCS protein contains a region that is quite similar to its target of copper delivery, SOD1. CCS is believed to specifically recognize SOD1 by virtue of the SOD1-like region in the CCS protein. This region of CCS has been shown to physically interact with SOD1 and thereby serve as the "molecular glue" that holds SOD1 in place while the MXCXXC copper-binding region of CCS mediates copper transfer.

Although the three copper chaperones vastly differ in their respective targets of copper delivery, they are similar in several important aspects. These molecules are small proteins that bind copper by cysteine residues. They predominantly localize to the cytosol and function to deliver copper from the cell surface to a specific target deep within the cell. Genetic studies in yeast have revealed a family of cell-surface copper transporters (CTRs) that are responsible for the uptake of copper into the cell and delivery of the metal to the copper chaperones. It is presently unclear whether the copper chaperones go directly to the "front door" to pick up copper from the CTRs or whether a "middle molecule" exists that directly supplies the copper chaperones with their metal ion "cargo." An additional property common to all copper chaperones is that these proteins are necessary only when intracellular levels of copper are low. When cells are exposed to high concentrations of copper, the metalloenzymes can acquire their copper in a chaperone-independent manner. Yet intracellular copper is normally present at exquisitely low levels, and activation of copper enzymes is wholly dependent upon copper chaperones. Copper not only is an essential nutrient but also is quite toxic to living cells, and elaborate detoxification mechanisms prevent the free metal ion from accumulating to any substantial degree. The copper-requiring metalloenzymes cannot compete for these vanishingly low levels of available metal, explaining the requirement for the copper metallochaperones (see **illus.**).

Implications for human disease. The copper metallochaperones may have important relevance to specific diseases in humans. For example, a number of neurodegenerative diseases have been associated with deficiencies in mitochondrial cytochrome oxidase, and it is conceivable that mutations in the human COX17 gene may contribute to one or more

of these disorders. With regard to ATX1, the intracellular copper transporters that serve as targets of ATX1 action have already been linked to two important disorders of copper metabolism in humans. Wilson disease results from mutations in the Wilson copper transporter and primarily presents as chronic copper toxicity in the liver. Menkes disease, resulting from mutations in the Menkes copper transporter, is a fatal disorder associated with severe copper deficiency. It is therefore possible that additional inherited disorders of copper metabolism result from abnormalities in human ATX1 itself. Moreover, the CCS copper chaperone may have important implications regarding the fatal motor neuron disease amyotrophic lateral sclerosis (ALS), commonly known as Lou Gehrig's disease. A subset of familial cases of amyotrophic lateral sclerosis have been linked to mutations in the human gene encoding SOD1. This disease does not result from a loss of SOD1 activity but from a new toxic property unique to the mutant enzyme. Although the cause of SOD1-linked amyotrophic lateral sclerosis is not clear, evidence to date suggests that disease results from the toxic copper ion bound to the mutant SOD1 metalloenzyme. Thus, patients suffering from SOD1-linked amyotrophic lateral sclerosis could conceivably benefit from treatments that abrogate the action of the CCS copper chaperone.

Valeria Cizewski Culotta

Bibliography. J. R. Conner (ed.), *Metals and Oxidative Damage in Neurological Disorders*, Plenum Publishing, New York, 1997; V. C. Culotta and J. Gitlin, Disorders of copper transport, in C. R. Sriver et al. (eds.), *Molecular and Metabolic Basic of Inherited Disease*, McGraw-Hill, 1999; M. C. Linder, *Biochemistry of Copper*, Biochemistry of the Elements series, vol. 10, Plenum Publishing, New York, 1991.

Metallography

The study of the structure of metals and alloys by various methods, especially light and electron microscopy. Light microscopy of metals is conducted with reflected light on surfaces suitably prepared to reveal structural features. The method is often called optical microscopy or light optical microscopy. A resolution of about 200 nanometers and a linear magnification of at most 2000× can be obtained. Electron microscopy is generally carried out by the scanning electron microscope (SEM) on specimen surfaces or by the transmission electron microscope (TEM) on electron-transparent thin foils prepared from bulk materials. Magnifications can range from 10× to greater than 1,000,000×, sufficient to resolve individual atoms or planes of atoms.

Metallography serves both research and industrial practice. Light microscopy has long been a standard method for observing the morphology of phases resulting from industrial processes that involve phase transformations, such as solidification and heat treatment, and plastic deformation and annealing. Microscopy, both light and electron, is also indispensable for the analysis of the causes of service failures of components and products.

Light microscopy. Microstructural features observed in photomicrographs include the size and shape of the grains (crystals) in single-phase materials (**Fig. 1***a* and **Fig. 2***a*), the structure of alloys containing more than one phase such as steel (Fig. 2*b, c*), the effects of deformation (Fig. 1*b*), microcracking (Fig. 1*c*), and the effects of heat treatment (Fig. 2*b, c*). Other structural features investigated by light microscopy include the morphology and size of precipitates, compositional inhomogeneities (microsegregation), microporosity, corrosion, thickness and structure of surface coatings, and microstructure and defects in welds.

The selection of representative specimens for metallographic examination is important. For example, if a part such as a forged shaft has directional properties, transverse and longitudinal sections should be examined. Sheet, wire, electronic components, and other small specimens are mounted in fixtures or plastic mounts.

A specimen is initially ground on a series of abrasive papers of decreasing grit size, or on laps. It is then polished on one or more cloth-covered wheels with an abrasive such as aluminum oxide or diamond dust. Automated polishing equipment is also used. The specimen surface becomes progressively more scratch-free and mirrorlike; however, polishing, even when properly carried out, leaves a thin layer of distorted metal. *See* ABRASIVE.

Electrolytic polishing, which consists of controlled anodic dissolution, is an alternative to mechanical polishing. Once the operating conditions have been established, electrolytic polishing is a simple operation; and the polished surface may be superior to a mechanically polished surface, particularly for soft metals.

Polished specimens reveal only a few structural features, such as inclusions, microcracks, and microporosity. Etching with an appropriate reagent is generally necessary to reveal microstructural details, and it also removes the distorted layer from mechanically polished specimens. Etching reagents are mainly acids and bases (and occasionally other compounds) dissolved in water or alcohol. Most reagents act by dissolution, a few by selective deposition of reaction products (staining). In a single-phase material, etching is effective because it attacks different parts of the structure selectively. Grain-boundary regions may dissolve preferentially to the body of the grains (Fig. 2*a*); or adjoining grains may develop facets of different orientation, which reflect differing amounts of light (Fig. 1). In multiphase alloys, the phases are attacked selectively (Fig. 2*b, c*).

Etching may also be carried out electrolytically by making the specimen the anode. Etching by heating in a vacuum or oxidizing atmosphere has proved useful. Cathodic etching, in which the specimen is bombarded by ions of an inert gas, is effective with some materials that resist etching by other methods.

In the standard metallographic microscope, a beam of light normal to the surface illuminates the

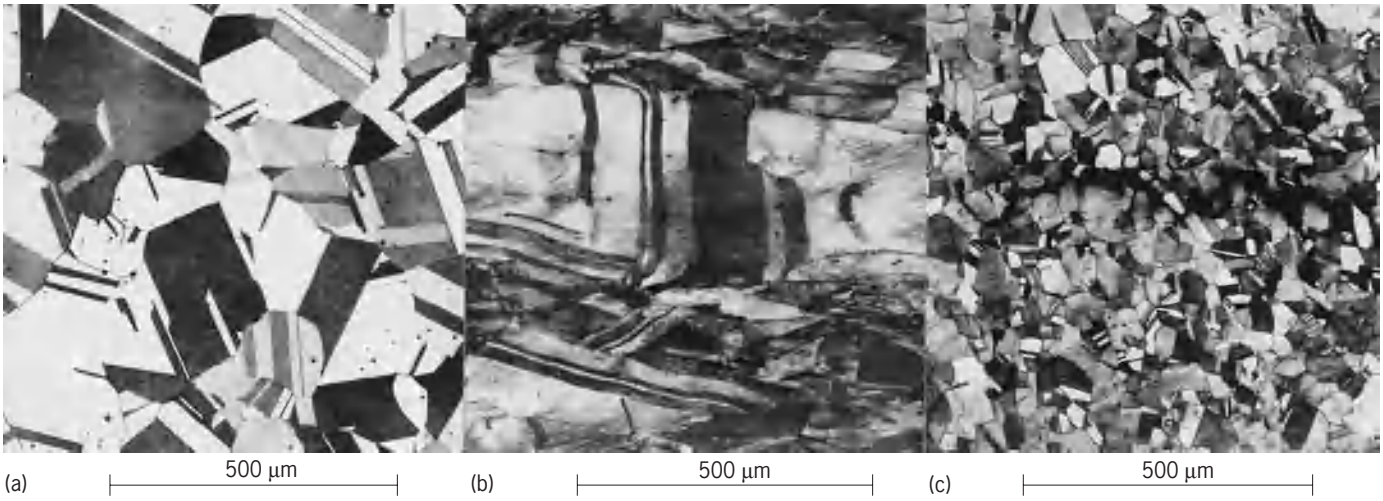

Fig. 1. Photomicrographs of typical microstructures of brass (70% Cu–30% Zn). (*a*) Annealed; grains with twin bands. (*b*) Reduced 40% by cold rolling; distorted grains. (*c*) Stress-corroded, with horizontal crack. *(Courtesy of W. R. Johnson)*

specimen. The objective lens of the microscope serves as a condensing system for the incident light and as the image-forming system for the light reflected by the specimen; this is known as bright-field illumination. In dark-field illumination, a hollow beam of light converges on the specimen; a mirrorlike surface appears dark, whereas a rough surface appears bright. Polarized light reveals differences in constituents that are optically anisotropic; useful (and often beautiful) color variations can be observed with white light. Differential interference contrast is increasingly used; optical interference permits quantitative investigation of surface contours, and color is produced by inserting a sensitive tint plate in the illumination system.

Hot-stage microscopy allows many phase transformations to be followed as they occur. Most specimens must be protected from oxidation by a protective atmosphere or vacuum, and the objective lens must be kept cool. Reflecting objectives are particularly suitable because of their long working distance. Thermal etching reveals the structural features. *See* REFLECTING MICROSCOPE.

Images are normally photographed in black and white or color. Video microscopy is common, and digital image acquisition and image processing methods are also used.

Quantitative microscopy methods can be used for the quantitative characterization of microstructures. The basic problem to be solved is the conversion of measurements on a two-dimensional section into quantities representing the three-dimensional structure of the material. The quantities most frequently measured are grain size, relative amounts of phases in a multiphase material, total area of grain boundaries, particle size of a dispersed phase, and spacing of lamellae and dispersed particles. The use of desktop computers, special software packages, and digital image processing have greatly advanced the speed and accuracy of quantitative microscopy methods. Nevertheless, valid quantitative description of microstructures requires close attention to the selection of representative microsections from the original material or product. *See* GRAIN BOUNDARIES; OPTICAL MICROSCOPE.

Electron microscopy. The electron microscope offers improved depth of field and higher resolution than the light microscope, as well as the possibility of in-place spectroscopy techniques. The scanning electron microscope images the surface of a

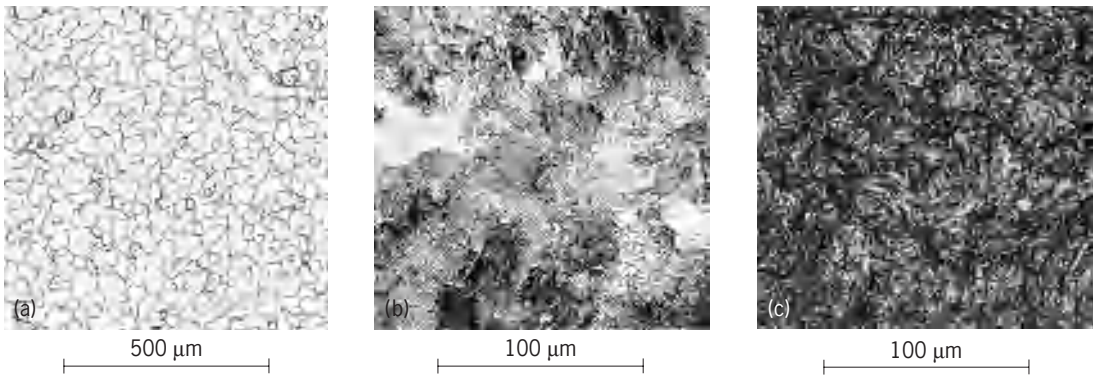

Fig. 2. Photomicrographs of typical structures of iron and steel. (*a*) High-purity iron. (*b*) Steel containing 0.85% C, slowly cooled; pearlite structure, consisting of alternating layers of light ferrite and dark cementite. (*c*) Steel containing 0.80% C, quenched and tempered; dark plates of tempered martensite. (*Courtesy of W. R. Johnson*)

material, while the transmission electron microscope reveals internal microstructure. Images produced by the scanning electron microscope are generally easier to interpret; in addition, the instrument operates at lower voltages, offers lower magnification, and requires less specimen preparation than is necessary for the transmission electron microscope. Consequently it is important to view a specimen with light microscopy and often with the scanning electron microscope before embarking on transmission electron microscopy.

However there are some disadvantages. Electron microscope specimens are viewed under vacuum, the instruments cost significantly more than light microscopes, electron beam damage is always a danger, and representative sampling becomes more difficult as the magnification increases. *See* ELECTRON MICROSCOPE.

Scanning electron microscope. The scanning electron microscope scans a fine beam of electrons across the surface of a specimen; and images are formed by collecting either the electrons that are backscattered from the surface or, more usually, secondary electrons knocked out of the surface atoms. The electron signal is then used to modulate a television screen scanning synchronously with the electron beam. The images contain topographic information, so a major use of the scanning electron microscope is to study rough specimens, such as fracture surfaces and semiconductor devices, which cannot be observed in the light microscope with the whole field of view in focus. Fortunately, secondary electron emission mimics the behavior of reflected light, and the human eye can generally interpret the images produced by a scanning electron microscope in a straightforward manner.

The best scanning electron microscopes offer maximum useful magnifications of about 100,000×. Such a high-resolution instrument, which uses a field emission electron gun, is able to resolve surface detail on a dimensional scale of 1–2 nm. However, most scanning electron microscopes are used in the range of 1000× to 20,000×, resolving detail at the 5–10-nm level with excellent depth of field and improved resolution compared to the light microscope.

Specimen preparation for scanning electron microscopes may consist of metallographic polishing if the topography is unimportant, or if direct comparison has to be made with the light microscope. However, the specimen can usually be observed in its as-received condition with minimal cleaning, if necessary. If electron-beam charging occurs because the specimen is insulating or contaminated, the image resolution degrades catastrophically, so a thin conductive coating is evaporated on the specimen surface (**Fig. 3**). However, field emission gun scanning electron microscopes can be operated at very low voltages (<1 keV) to view insulators such as polymers without conductive coatings, but still resolve fine detail (<10 nm). Most scanning electron microscopes are digitally controlled, so the images reside in a frame store and may be digitally enhanced and processed prior to printing in order to maximize the contrast information. Digital images can easily be analyzed through standard quantitative metallographic software. *See* DIGITAL COMPUTER.

In addition to secondary and backscattered electron images, in the scanning electron microscope it is also possible to image magnetic domains by the way they bend the electrons, to observe crystal orientation by how the electrons channel between crystal planes, and to trace how voltage pulses travel around a semiconductor device and how the electron beam itself changes the semiconducting properties. The principles of scanning imaging, developed for the scanning electron microscope, have also been extended to other metallographic techniques such as scanning ion microscopy, scanning acoustic microscopy, and scanning tunneling microscopy. *See* ACOUSTIC MICROSCOPE; FIELD-EMISSION MICROSCOPY; SCANNING ELECTRON MICROSCOPE; SCANNING TUNNELING MICROSCOPE.

Transmission electron microscope. The transmission electron microscope is primarily designed to present images of the highest possible resolution by observing how high-energy (typically 100–300 keV) electrons are scattered as they traverse a thin (<100-nm) specimen. Thin specimens are made by electropolishing conductive metals, ion-beam-thinning insulating ceramics and two-phase structures such as composites, and ultramicrotoming polymers, none of which is a trivial task. The thinner the specimen, the better the image quality, and it is relatively routine (at magnifications >1,000,000× and a resolution of >0.2–0.3 nm) to reveal the arrangements of atoms at crystal defects such as dislocations and grain boundaries.

More often, the transmission electron microscope is used at lower magnifications to study the distribution of crystal defects and phases, which are

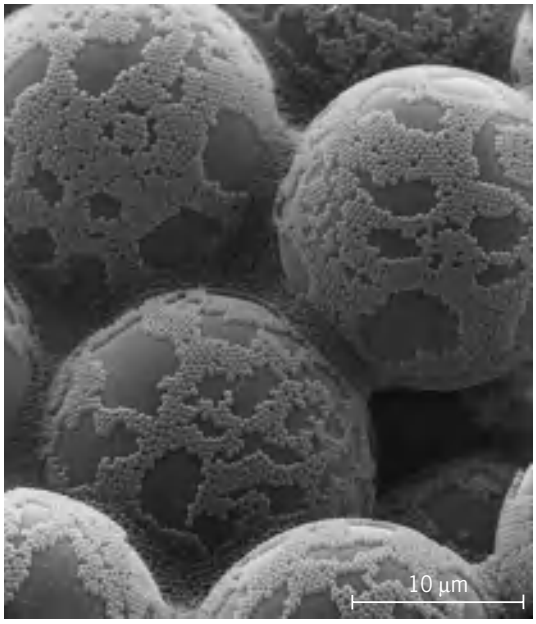

Fig. 3. Scanning electron micrograph of polymer latexes. The acrylic latex spheres of 400-nm diameter are on the surface of 19-μm polystyrene latex. (*Courtesy of O. L. Shaffer*)

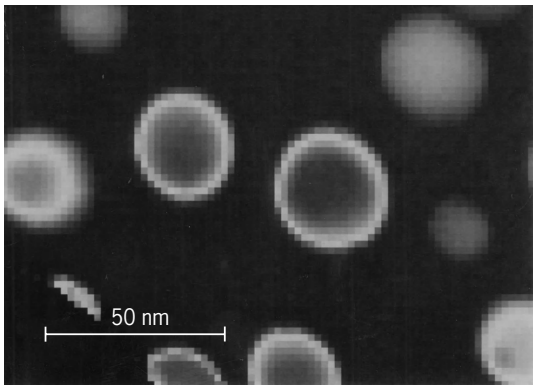

Fig. 4. Electron energy loss spectrum (EELS) image showing spherical precipitates of Al_3Li in an aluminum-lithium alloy. The intensity of each pixel of the digital image represents the energy lost by electrons passing through that region of the thin specimen; the energy loss can then be related to the amount of Li present. (*Courtesy of J. A. Hunt*)

revealed by the different ways they diffract the electron beam (diffraction contrast). Therefore, electron diffraction can be performed simultaneously to determine the crystal structure and orientation of various microstructural features. If the electron beam is converged to a probe, the contrast in the convergent beam diffraction pattern can reveal the lattice parameter, point group, and space group of the thin crystal. The transmission electron microscope image and diffraction pattern can be obtained from the same area of the specimen. *See* CRYSTAL DEFECTS; CRYSTAL STRUCTURE; ELECTRON DIFFRACTION.

Transmission electron microscope images are much more difficult to interpret than those obtained with the scanning electron microscope. The transmission electron microscope image is always a projected image of a three-dimensional sample, and the human eye is not accustomed to viewing in projection. In addition, the diffraction contrast in transmission electron microscope images varies with crystal orientation, which requires careful interpretation. However, in noncrystalline materials, changes in thickness and mass are responsible for contrast, and this is easier to understand. Transmission electron microscopes that operate at high voltage (>1 MeV) are rare; but they offer the possibility of very high resolution, the study of thicker specimens, and the option of carrying out in-place experiments such as straining, heating, or cooling the specimen, in order to watch changes occur dynamically.

Spectrometry. Electron microscopes offer much more information than images and diffraction patterns. The ionizing nature of electron irradiation means that x-ray spectrometry and electron spectrometry, both powerful tools in their own right, can be performed in both scanning electron microscopy and transmission electron microscopy. The various signals detected spectroscopically can also be used to form images of the specimen, which reveal elemental distribution among other information. In particular, the characteristic x-ray signal can be detected and processed to map the elemental distribution quantitatively on a micrometer scale in the scanning electron microscope and a nanometer scale in the transmission electron microscope. Electron spectroscopic signals permit not only elemental images to be formed (**Fig. 4**) but also images that reveal local changes in bonding, dielectric constant, thickness, band gap, and valence state. *See* ELECTRON SPECTROSCOPY.

Limitations. Ultimately the information gathered in both the scanning electron microscope and the transmission electron microscope is limited by electron damage, which is also a consequence of the ionizing nature of the beam. Thus the characteristic of electrons that creates the many useful signals for imaging also places limits on the applicability of the instruments. *See* METALLURGY.

David A. Thomas; David B. Williams

Bibliography. American Society for Metals, *Metals Handbook*, vol. 9; *Metallography and Microstructures*, 9th ed., 1985; J. I. Goldstein et al., *Scanning Electron Microscopy and X-ray Microanalysis*, 2d ed., 1992; L. Reimer, *Transmission Electron Microscopy*, 4th ed., 1997; G. F. Vander Voort, *Metallography, Principles and Practice*, 1999; D. B. Williams et al., *Images of Materials*, 1991.

Metalloid

An element which exhibits the external characteristics of a metal but behaves chemically both as a metal and as a nonmetal. Arsenic and antimony, for example, are hard crystalline solids that are definitely metallic in appearance. They may, however, undergo reactions that are characteristic of both metals and nonmetals. Certain of their oxides dissolve in either acids or bases, and are said to be amphoteric in character because they behave either as a base or an acid. Many elements form compounds that are amphoteric. However, only when this dualistic chemical behavior is very marked and the external appearance metallic is the element commonly called a metalloid. *See* METAL; NONMETAL.

Francis J. Johnston

Metallurgy

The technology and science of metallic materials. Metallurgy as a branch of engineering is concerned with the production of metals and alloys, their adaptation to use, and their performance in service. As a science, metallurgy is concerned with the chemical reactions involved in the processes by which metals are produced and the chemical, physical, and mechanical behavior of metallic materials.

Metallurgy has played an important role in the history of civilization. Metals were first produced more than 6000 years ago. Because only a few metals, principally gold, silver, copper, and meteoric iron, occur in the uncombined state in nature, and then only in small quantities, primitive metallurgists had to discover ways of extracting metals from their ores. Fairly large-scale production of some metals was carried

out with technical competence in early Near Eastern and Mediterranean civilizations and in the Middle Ages in central and northern Europe. Basic metallurgical skills were also developed in other parts of the world.

The winning of metals would have been of little value without the ability to work them. Great craftsmanship in metalworking developed in early times: the objects produced included jewelry, large ornamental and ceremonial objects, tools, and weapons. It may be noted that almost all early materials and techniques that later had important useful applications were discovered and first used in the decorative arts. In the Middle Ages metal working was in the hands of individual or groups of craft workers. The scale and capabilities of metal working developed with growth of industrial organizations. Today's metallurgical plants supply metals and alloys to the manufacturing and construction industries in a variety of forms, such as beams, plates, sheets, bars, wire, and castings. Technologies such as communications, nuclear power, and space exploration continue to demand new techniques of metal production and processing.

The field of metallurgy may be divided into process metallurgy (production metallurgy, extractive metallurgy) and physical metallurgy. According to another system of classification, metallurgy comprises chemical metallurgy, mechanical metallurgy (metal processing and mechanical behavior in service), and physical metallurgy. The more common division into process metallurgy and physical metallurgy, which is adopted in this article, classifies metal processing as a part of process metallurgy and the mechanical behavior of metals as a part of physical metallurgy.

Process metallurgy. Process metallurgy, the science and technology used in the production of metals, employs some of the same unit operations and unit processes as chemical engineering. These operations and processes are carried out with ores, concentrates, scrap metals, fuels, fluxes, slags, solvents, and electrolytes. Different metals require different combinations of operations and processes, but typically the production of a metal involves two major steps. The first is the production of an impure metal from ore minerals, commonly oxides or sulfides, and the second is the refining of the reduced impure metal, for example, by selective oxidation of impurities or by electrolysis. Process metallurgy is continually challenged by the demand for metals which have not been produced previously or are difficult to produce; by the depletion of the deposits of the richer and more easily processed ores of the traditional metals; and by the need for metals of greater purity and higher quality. The mining of leaner ores has greatly enhanced the importance of ore dressing methods for enriching raw materials for metal production. Several nonferrous metals are commonly produced from concentrates. Iron ores are also treated by ore dressing. *See* ELECTROMETALLURGY; HYDROMETALLURGY; ORE DRESSING; PYROMETALLURGY; PYROMETALLURGY, NONFERROUS.

Process metallurgy today mainly involves large-scale operations. A single blast furnace can produce crude iron at the rate of 3000–11,000 tons (2700–9900 metric tons) per day. A basic oxygen furnace for steelmaking can consume 800 tons (720 metric tons) of pure oxygen together with required amounts of crude iron and scrap to produce 12,000 tons (11,000 metric tons) of steel per day. Advanced methods of process analysis and control have been applied to such processing systems. The application of vacuum to extraction and refining processes, the leaching of low-grade ores for the extraction of metals, the use of electrochemical reduction cells, and the refining of reactive metals by processing through the vapor state are other important developments. *See* IRON METALLURGY; STEEL MANUFACTURE.

Because the production of metals employs many different chemical reactions, process metallurgy has been closely associated with inorganic chemistry. Techniques for analyzing ores and metallurgical products originated several centuries ago and represented an early stage of analytical chemistry. Application of physical chemistry to equilibria and kinetics of metallurgical reactions has led to great progress in metallurgical chemistry.

Physical metallurgy. Physical metallurgy investigates the effects of composition and treatment on the structure of metals and the relations of the structure to the properties of metals. Physical metallurgy is also concerned with the engineering applications of scientific principles to the fabrication, mechanical treatment, heat treatment, and service behavior of metals. *See* ALLOY; HEAT TREATMENT (METALLURGY).

The structure of metals consists of their crystal structure, which is investigated by x-ray, electron, and neutron diffraction, their microstructure, which is the subject of metallography, and their macrostructure. Crystal imperfections provide mechanisms for processes occurring in solid metals; for example, the movement of dislocations results in plastic deformation. Crystal imperfections are investigated by x-ray diffraction and metallographic methods, especially electron microscopy. The microstructure is determined by the constituent phases and the geometrical arrangement of the microcrystals (grains) formed by those phases. Macrostructure is important in industrial metals. It involves chemical and physical inhomogeneities on a scale larger than microscopic. Examples are flow lines in steel forgings and blowholes in castings. *See* CRYSTAL STRUCTURE; METALLOGRAPHY; X-RAY DIFFRACTION.

Phase transformations occurring in the solid state underlie many heat-treatment operations. The thermodynamics and kinetics of these transformations are a major concern of physical metallurgy. Physical metallurgy also investigates changes in the structure and properties resulting from mechanical working of metals. *See* PLASTIC DEFORMATION OF METAL.

The composition of metallic objects is often characterized by the presence of impurities, nonuniform distribution (segregation) of solute elements

and nonmetallic inclusions, especially in steel. These phenomena, which originate in the production process, can have important effects on the properties of metals and alloys. They illustrate the close relation between process and physical metallurgy.

The applications for which a metal is intended determine the properties that are of practical interest. For use in machinery and construction, mechanical properties including deformation and fracture behavior are of greatest importance. In transportation equipment the strength-to-weight ratio deserves special consideration. In other applications, electrical or thermal conductivity or magnetic properties may be decisive. Resistance to corrosion is a common requirement and accounts for another close link between metallurgy and chemistry, especially electrochemistry and surface chemistry. *See* CORROSION; METAL, MECHANICAL PROPERTIES OF.

General principles. An old distinction between ferrous and nonferrous metallurgy, although still of some practical significance, is no longer considered fundamental. Certain general principles have become established and apply to all metals. In some respects, however, there are great differences between metals which has led to specialization in research and industrial practice. On the other hand, an underlying structural science is developing to bring all materials—metallic and other inorganic as well as organic materials—within a unified framework.

Metallurgy occupies a position at the juncture of physics, chemistry, mechanical engineering, and chemical engineering. It also borders electrical, civil, aeronautical, and nuclear engineering. Metallurgical knowledge can be relevant to fields that are as removed from engineering as archeology, crime investigation, and orthopedic surgery. In the field of materials science and engineering, metallurgy takes its place as one of the oldest and most highly developed disciplines.

The area of concern of metallurgy widened as problems of materials availability were recognized and focused attention to the need for new production processes and the recycling of secondary metals. Environmental considerations require new technology for pollution abatement. Energy conservation favors more efficient processes in metals production. Conservation of materials also calls for more effective utilization of metals and the substitution of more plentiful for scarce metals.

For more information on metallurgy and some associated techniques see articles on individual metals and their metallurgy.

Michael B. Bever

Bibliography. C. S. Barrett and T. B. Massalski, *Structure of Metals*, 3d rev. ed., 1980; G. F. Carter, *Principles of Physical and Chemical Metallurgy*, 1979; G. E. Dieter, *Mechanical Metallurgy*, 3d ed., 1986; P. Haasen, *Physical Metallurgy*, 2d ed., 1988; M. A. Meyers and K. K. Chawla, *Mechanical Metallurgy: Principles and Applications*, 1984; J. J. Moore, *Chemical Metallurgy*, 2d ed., 1983, reprint 1993; R. E. Reed-Hill and R. Abbaschian, *Physical Metallurgy Principles*, 3d ed., 1992.

Metameres

The successive subdivisions along the length of the body axis in bilaterally symmetrical animals; also called somites or segments. Common examples are the muscles and spinal nerves in the human body and in the body and tail of many mammals, snakes and lizards, salamanders, and fishes. It also occurs in other chordates, and in arthropods and annelid worms. It never involves reproductive organs, and thus differs from strobilization in tapeworms and certain jellyfish. This serial repetition of parts (metamerism or segmentation) arises either from a bilateral series of coelomic pouches which form the segmental muscles, kidneys, and body cavities of lower forms, or from mesoblastic somites which form the skeletal and muscular segments of vertebrates. Repetitive features of the nervous system are acquired secondarily through the influence of mesodermal metameres upon adjoining ectodermal tissues. Several primitive embryonic somites become fused in the heads of adult arthropods and vertebrates. *See* ANIMAL SYMMETRY; COELOM; MUSCULAR SYSTEM; NEURULATION.

Howard L. Hamilton

Metamict state

The state of a special class of amorphous materials that were initially crystalline. W. C. Broegger first used the term *metamikte* in 1893 to describe minerals that were optically isotropic with a "glasslike" fracture but still retained well-formed crystal faces. In 1914 A. Hamburg correctly attributed the transition from the periodic, crystalline state to the aperiodic, metamict state as induced by alpha-decay damage. In minerals, this damage is the result of the decay of naturally occurring radionuclides and their daughter products in the uranium and thorium (^{238}U, ^{235}U, and ^{232}Th) decay series. A wide variety of complex oxides (for example, pyrochlore structure types), silicates (such as zircon, thorite, and yttrialite), and phosphates (for example, xenotime) are reported as occurring in the metamict state. All of these structures can accommodate uranium and thorium. A renewed interest in the metamict state has been stimulated by concern for the long-term stability of crystalline materials (nuclear waste forms) that will serve as hosts for actinides (for example, plutonium, americium, curium, and neptunium). Various crystalline materials (phases) may appear in a single waste form; each phase may or may not suffer radiation damage. For some nuclear waste-form phases, the radiation-induced transformation to the metamict state has been stimulated by doping phases with highly radioactive plutonium-238 or curium-244. *See* ACTINIDE ELEMENTS; ALPHA PARTICLES; RADIOACTIVITY.

Mineral properties. Metamict minerals are generally optically isotropic but may show varying degrees of anisotropy. Metamict phases lack cleavage, and conchoidal fracture is characteristic.

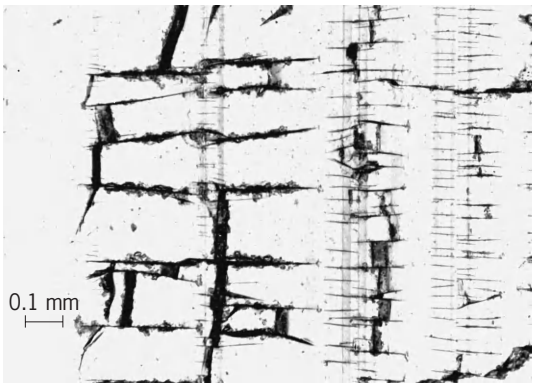

Fig. 1. Optical micrograph of (001) zone in a petrographic thin section of zircon. The variations in the shading are due to differences in the birefringence. (*From W. Lutze and R. C. Ewing, eds., Radioactive Waste Forms for the Future, North-Holland, 1988*)

There is a decrease in the hardness (approximately 30%) and in the elastic modulus with increasing alpha-decay dose. However, the introduction of defects causes a substantial increase in the fracture toughness.

Figure 1 shows a micrograph of (001) zone in a petrographic thin section of zircon that exhibits differences in birefringence. The birefringence decreases with increasing alpha-decay dose until the material becomes optically isotropic. Different zones in this sample have experienced different alpha-decay doses because of variations in the uranium and thorium concentrations. The system of microfractures are perpendicular to the zones, they are restricted to low-dose zones and terminate in zones that have alpha-decay doses $\geq 0.5 \times 10^{16}$ alpha events/mg (approximately equal to 10^{25} alpha events/m^3). Fractures terminate in the high-dose zones in which fracture toughness has increased.

The crystalline structure may be reconstituted by heating. Fully metamict material usually recrystallizes to a polyphase aggregate, but if the material is only partially damaged, it is possible to recrystallize to the original, single crystal. During recrystallization, several new phases may form; the particular phase assemblage is dependent on the conditions of recrystallization (for example, temperature and atmosphere). In many cases, the original premetamict phase may not recrystallize because of compositional changes caused by subsequent alteration. Annealing is exothermic, releasing the stored energy associated with the alpha-decay damage. In rare cases, recrystallization is pyronomic, releasing so much energy that the sample glows incandescently on heating.

Metamict minerals contain uranium and thorium, although contents may be quite low. The presence of uranium and thorium distinguishes metamict minerals from other naturally occurring amorphous materials that have not experienced this radiation-induced transformation. Lanthanide elements are also common (in some cases over 50 wt %) and water of hydration may be high (up to 70 mol %).

Partially crystalline metamict minerals display distinct broadening of diffraction maxima. Shifts in the position of diffraction maxima correspond to the increase in unit cell volume and the decrease in density. Volume expansion can be up to 8% and may cause microfracturing (Fig. 1). Fully damaged material (alpha-decay doses in excess of one displacement per atom) is x-ray- and electron-diffraction amorphous; that is, the fully damaged material is completely aperiodic and thus unable to diffract x-rays or electrons. *See* ELECTRON DIFFRACTION; X-RAY DIFFRACTION.

Alpha-decay damage. The radiation damage caused by the alpha-decay event is the result of two separate but simultaneous processes: (1) An alpha particle with an energy of approximately 4.5 MeV and a range of 10,000 nanometers dissipates most of its energy by ionization; however, at low velocities near the end of its track, it displaces several hundred atoms, creating Frenkel defect pairs. (2) The alpha-recoil atom with an energy of approximately 0.09 MeV and a range of 10 to 20 nm produces several thousand atomic displacements, creating tracks of disordered material. These two damaged areas are separated by thousands of unit cell distances and have different effects on the crystalline structure. Local point defects cause an increase in the distortion; therefore, there is an increase in the strain in the structure. Alpha-recoil tracks create regions of aperiodic material that at high enough alpha-decay doses (usually 10^{24} to 10^{25} alpha-decay events/m^3) overlap and finally lead to the metamict state. The former causes broadening of x-ray diffraction maxima and an increase in unit cell volume (and a decrease in the density); the latter causes a decrease in diffraction peak intensities. Typical changes in density (ρ), unit cell parameter (cell edge; a), and diffraction intensity (I/I_0) are shown in **Fig. 2**. The radiation-induced transition

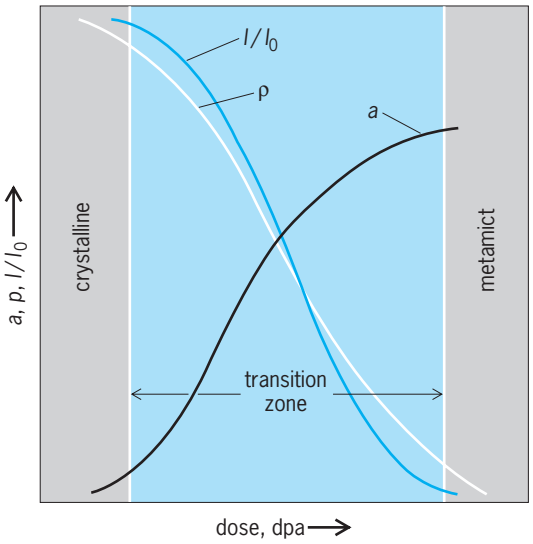

Fig. 2. Schematic representation of the change in the diffraction intensity (I/I_0), cell edge (a), and density (ρ) as a function of increasing alpha-decay dose. (*After G. R. Lumpkin and R. C. Ewing, Alpha-decay damage in minerals of the pyrochlore group, Phys. Chem. Miner., 16:2–20, 1988*)

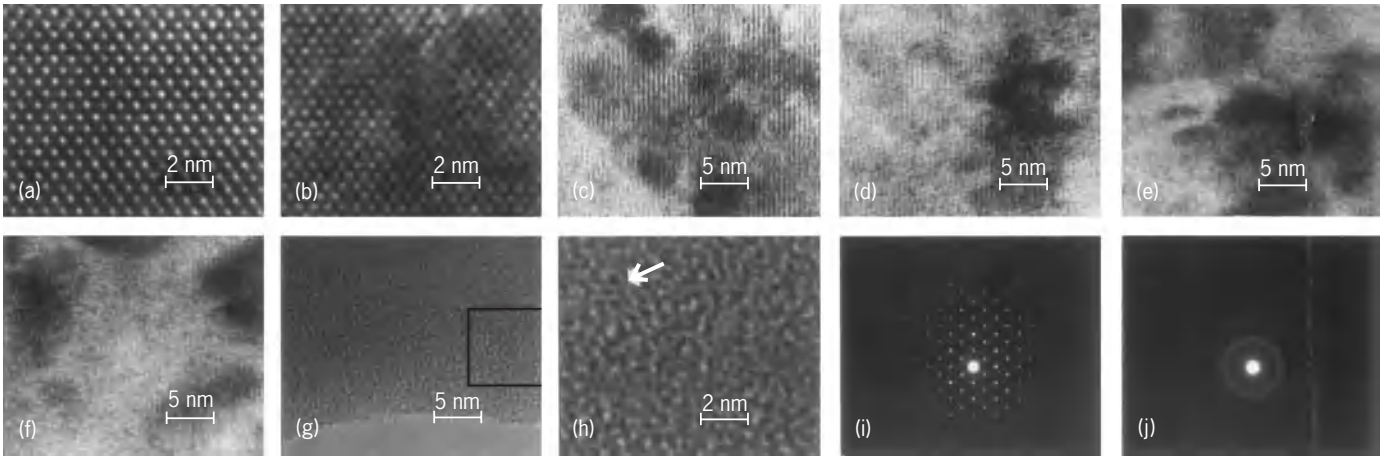

Fig. 3. High-resolution transmission microscopy images showing progressive structural damage to microlite as a function of increasing alpha-event dose (alpha-events/mg, uncorrected for annealing). (*a*) $<10^{15}$, (*b*) 3×10^{16}, (*c*) 3×10^{16}, (*d*) 3×10^{16}, (*e*) 9×10^{16}, (*f*) 10^{17}, (*g*) 4×20^{17}. (*h*) Enlargement of area outlined in *g*; arrow indicates fragment of the original structure. (*i, j*) Selected area diffraction patterns corresponding to images in *a* and *h*. (*From R. C. Ewing et al., Metamict minerals: Natural analogues for radiation damage effects in ceramic nuclear waste forms, Nucl. Instrum. Meth. Phys. Res., B32:487–497, 1988*)

from the crystalline to the metamict state occurs over a narrow range of alpha-decay dose (10^{24}–10^{25} alpha decays/m^3), which corresponds to 0.1 to 1.0 displacements per atom (dpa). *See* CRYSTAL DEFECTS; RADIATION DAMAGE TO MATERIALS.

Damage in-growth. For minerals from the same locality and of the same age but with variable uranium and thorium contents, the uranium/thorium content can be converted to a calculated alpha-decay dose. For such a suite of samples, the effects of increasing alpha-decay dose can be observed directly. These effects can be observed by high-resolution transmission electron microscopy (HRTEM) in the mineral microlite, a complex oxide of tantalum (Ta) and calcium (Ca) [**Fig. 3**]. At 0.9–1.0 wt % uranium oxide (UO_3; 3×10^{16} alpha events/mg), microlite exhibits mottled diffraction contrast and disrupted lattice periodicity within isolated areas of 1 to 3 nm (Fig. 3*b*, *c*). With 1.4 wt % UO_3 (6×10^{16} alpha events/mg), aperiodic areas increase in abundance and fine-scale mosaic textures are observed (Fig. 3*d*). The mosaic pattern consists of crystalline domains (1–5 nm) having lattice misorientations of several degrees. With a uranium content of 2.5 wt % UO_3 (9×10^{16} alpha events/mg), microlite clearly shows regions of coexisting crystalline and aperiodic regions (Fig. 3*e*). The selected area diffraction pattern exhibits prominent diffuse rings. At 2.9 wt % UO_3 (10^{17} alpha events/mg), the mosaic texture is lost, and islands of crystalline microlite are left within an aperiodic matrix (Fig. 3*f*). At 3.6 wt % UO_3 (10^{17} alpha events/mg), no lattice fringes are seen in HRTEM images, and only diffuse rings appear in selected area diffraction patterns (Fig. 3*f*). With 8.9 wt % UO_3 (4×10^{17} alpha events/mg), the microlite exhibits an aperiodic, random network structure (Fig. 3*g*). The images also show that nanometer-sized fragments (see arrow) of the original structure persist beyond the saturation level of the alpha-recoil damage (Fig. 3*h*).

Thus, the transition from the crystalline to the metamict state in microlite can be summarized as follows: (1) At <0.1 wt % UO_3 ($< 10^{15}$ alpha events/mg, < 0.1 dpa), isolated alpha-recoil tracks have little effect on selected area diffraction patterns and are difficult to observe in HRTEM images. (2) At 0.9 wt % UO_3 (3×10^{16} alpha events/mg, 3 dpa), isolated alpha-recoil tracks are observed as 1–3-nm areas of disrupted lattice periodicity. (3) When 2.5 wt % UO_3 (9×10^{16} alpha events/mg, 13 dpa) is reached, alpha-recoil tracks overlap, yielding coexisting areas of crystalline and metamict microlite. (4) The fully metamict state is reached at 2.9 to 3.6 wt % UO_3 ($1–1.3 \times 10^{17}$ alpha events/mg, 15–19 dpa). Beyond this dose, the HRTEM image exhibits a random network structure. The alpha-decay doses calculated for each step of the transition are based simply on the age of the sample and the uranium content. The fact that some areas of crystallinity remain even after reaching calculated doses in excess of one displacement per atom provides strong evidence of annealing of the damage at low temperatures and over long periods of time. *See* ELECTRON MICROSCOPE.

Annealing of radiation damage. One of the most important observations concerning alpha-decay damage in periodic materials is that some naturally occurring phases sustain high alpha-decay doses (in excess of 10 dpa) and still remain essentially crystalline. These materials include uraninite (UO_2), monazite ($CaPO_4$), titanite ($CaTiO_5$), and huttonite ($ThSiO_4$). The apparent stability of these phases to radiation damage is due to annealing of the radiation damage under ambient conditions. Indeed experimental results seem to suggest that the mean alpha-recoil track lifetime τ varies depending on the phase: uraninite and thorite (τ = 25,000 years), pyrochlore (τ = 100 million years), zircon (τ = 400 million years), zirconolite (τ = 700 million years). For phases in which the mean track lifetime is short, damage is annealed as quickly as it accumulates, and the phase remains crystalline. For those phases in which the mean track lifetime is great, the tracks accumulate and finally overlap, and the material becomes

metamict. The annealing process is critically important to understanding the crystalline-to-metamict transition and the final microstructure of alpha-decay–damaged materials. *See* AMORPHOUS SOLID; CRYSTAL STRUCTURE; THORITE; ZIRCON.

Rodney C. Ewing

Bibliography. B. C. Chakoumakos et al., *Alpha-Decay-Induced Fracturing in Zircon: The Transition from the Crystalline to the Metamict State*, vol. 236, pp. 1556–1559, 1987; R. C. Ewing et al., Metamict minerals: Natural analogues for radiation damage effects in ceramic nuclear waste forms, *Nucl. Instrum. Meth. Phys. Res.*, B32:487–497, 1988; H. D. Holland and D. Gottfried, The effect of nuclear radiation on the structure of zircon, *Acta Crystallog.*, 8:291–300, 1955; G. R. Lumpkin and R. C. Ewing, Alpha-decay damage in minerals of the pyrochlore group, *Phys. Chem. Miner.*, 16:2–20, 1988; W. J. Weber and G. D. Maupin, Simulation of radiation damage in zircon, *Nucl. Instrum. Meth. Phys. Res.*, B32:512–515, 1988.

Metamorphic rocks

One of the three major groups of rocks that make up the crust of the Earth. The other two groups are igneous rocks and sedimentary rocks. Metamorphic rocks are preexisting rock masses in which new minerals, or textures, or structures are formed at higher temperatures and greater pressures than those normally present at the Earth's surface. *See* IGNEOUS ROCKS; SEDIMENTARY ROCKS.

Two groups of metamorphic rocks may be distinguished; cataclastic rocks, formed by the operation of purely mechanical forces; and recrystallized rocks, or the metamorphic rocks properly so called, formed under the influence of metamorphic pressures and temperatures.

Cataclastic rocks are mechanically sheared and crushed. They represent products of dynamometamorphism, or kinetic metamorphism. Chemical and mineralogical changes generally are negligible. The rocks are characterized by their minute mineral grain size. Each mineral grain is broken up along the edges and is surrounded by a corona of debris or strewn fragments (mortar structure, **Fig. 1***a*). During the early stages of this alteration process the metamorphosed product is known as flaser rock (Fig. 1*b*). Eventually the original mineral grains are entirely gone, as in the mylonites. When seen through the microscope, the comminuted particles consist of a mixture of finely powdered quartz, feldspar, and other minerals with an incipient recrystallization of sericite or chlorite. Pseudotachylite is an extreme end product of this crushing process. *See* METAMORPHISM; MYLONITE.

Structural relations. Metamorphic rocks, properly so called, are recrystallized rocks. The laws of recrystallization are not the same as those of simple crystallization from a liquid, because the crystals can develop freely in a liquid, but during recrystallization the new crystals are encumbered in their growth by the old minerals. Consequently, the structures which develop in metamorphic rocks are distinctive and of great importance, because they reflect the physiochemical environment of recrystallization and thereby the genesis and history of the metamorphic rock.

Crystalloblastic structure. A crystalloblast is a crystal that has grown during the metamorphism of a rock. The majority of minerals are frequently bounded by their own crystal faces (idioblasts). Larger crystals are often packed with small inclusions of other minerals exhibiting the so-called sieve structure (poikilitic or diablastic structure).

Granoblastic refers to a nondirected rock fabric, with minerals forming grains without any preferred shape or dimensional orientation (Fig. 1*c*). Lepidoblastic (Fig. 1*d*), nematoblastic (Fig. 1*e*), and fibroblastic refer to rocks of scaly, rodlike, and fibrous minerals, respectively.

The metamorphic minerals may be arranged in an idioblastic series (crystalloblastic series) in their order of decreasing force of crystallization as follows: (1) sphene, rutile, garnet, tourmaline, staurolite, kyanite; (2) epidote, zoisite; (3) pyroxene, hornblende; (4) ferromagnesite, dolomite, albite; (5) muscovite, biotite, chlorite; (6) calcite; (7) quartz, plagioclase; and (8) orthoclase, microcline. Crystals of any of the listed minerals tend to assume idioblastic outlines at surfaces of contact with simultaneously developed crystals of all minerals of lower position in the series.

Preferred orientation. Certain minerals have a tendency to assume parallel or partially parallel crystallographic orientation. The shape and spatial arrangement of minerals such as mica, hornblende, or augite show a definite relation to the foliation in the schist or gneiss; that is, both foliation and fissility of a metamorphic rock are directly related to the preferred position assumed by the so-called schist-forming minerals, such as mica, hornblende, and chlorite. *See* GNEISS; SCHIST.

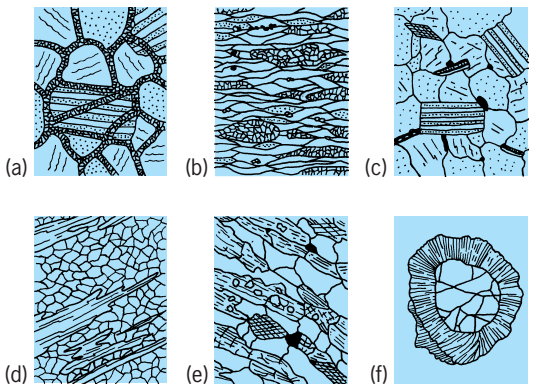

Fig. 1. Fabrics of metamorphic rocks under microscope. (*a*) Mortar fabric; (*b*) flaser or mylonitic fabric; (*c*) granoblastic fabric (*after E. E. Wahlstrom, Petrographic Mineralogy, John Wiley and Sons, 1955*). (*d*) Lepidoblastic fabric; (*e*) nematoblastic fabric; (*f*) porphyroblast with reaction rim (*after T. F. W. Barth, Theoretical Petrology, John Wiley and Sons, 1952*).

Students of structural petrology distinguish between preferred orientation of inequidimensional grains according to their external crystal form, and preferred orientation of equidimensional grains according to their internal or atomic structure. *See* PETROFABRIC ANALYSIS; STRUCTURAL PETROLOGY.

A special microscope technique (universal stage technique) is necessary in most cases to demonstrate in detail the preferred orientation of the mineral grains according to their atomic structure. *See* PETROGRAPHY.

Relic structures. Mineral relics often indicate the temperature and pressure that obtained in the preexisting rock. If a mineral, say quartz, is stable in the earlier rock and is also stable in the later rock, it will be preserved (unless stress action sets in) in its original form as a stable relic. However, when a mineral or a definite association of minerals becomes unstable, it may still escape alteration and appear as an unstable relic. These relics are proterogenic, that is, representative of an earlier, premetamorphic rock, or of an earlier stage of the metamorphism. Hysterogenic products are of later date, and are formed in consequence of changed conditions after the formation of the chief metamorphic minerals.

A common phenomenon, fairly illustrative of the tendency toward equilibria, is the formation of armors or reaction rims around minerals (Fig. 1*f*) which have become unstable in their association but have not been brought beyond their fields of existence in general (the armored relics). Thereby the associations of minerals in actual contact with one another become stable. If, however, the constituent minerals of a rock containing armored relics are named without noting this phenomenon, it may be taken as an unstable association. *See* PORPHYROBLAST.

Structure relics are perhaps of still more importance, directly indicating the nature of the preexisting rock and the mechanism of the metamorphic deformation. The interpretation of relics has been compared to the reading of palimpsests, parchments used for the second time after original writing was nearly erased. Every trace of original structure is important in attempting to reconstruct the history of the rock and in analyzing the causes of its metamorphism.

In sedimentary rocks the most important structure is bedding (stratification or layering) which originally was approximately horizontal. In metamorphic rocks deformed by folding, faulting, or other dislocations, the sum of all deformations can be referred to the original horizontal plane, and the deformations can be analyzed.

Fissility and schistosity. One of the earliest secondary structures to develop in sediments of low metamorphic grade is that of slaty cleavage (also referred to as flow cleavage or fissility), which grades into schistosity which is different from fracture cleavage, or strain-slip cleavage. Slaty cleavage is developed normal to the direction of greatest shortening of the rock mass, and cuts the original bedding at various angles. Tectonic forces acting on a book of sediments

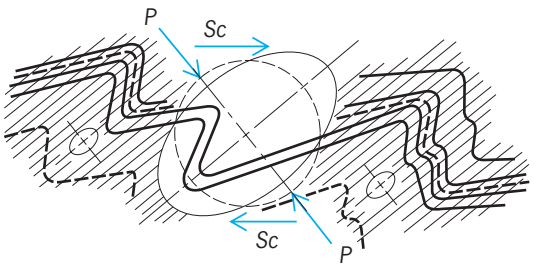

Fig. 2. Diagram showing the general relationship between deformation folding and slaty cleavage caused by pressure *PP* or the couple *ScSc*. Heavy black lines denote the original bedding deformed into folds. Thin lines indicate slaty cleavage which may grow into schistosity (false bedding). (*After G. Wilson, Proceedings of the Geological Association, 1946*)

of heterogeneous layers will throw them into a series of folds, and slaty cleavage develops in response to the stresses imposed on the rock system as a whole, because of the differential resistance of the several layers. Consequently, folding and slaty cleavage have a common parentage, as illustrated in **Fig. 2**.

In the rock series slate-phyllite-schist the slaty cleavage will grade into schistosity. It is a chemical and recrystallization phenomenon, as well as a mechanical one, and the directions of the schistosity become the main avenues of chemical transport. *See* ROCK CLEAVAGE; SLATE.

Contact-metamorphic rocks. Igneous magma at high temperature may penetrate into sedimentary rocks, it may reach the surface, or it may solidify in the form of intrusive bodies (plutons). Heat from such bodies spreads into the surrounding sediments, and because the mineral assemblages of the sediments are adjusted to low temperatures, the heating-up will result in a mineralogical and textural reconstruction known as contact metamorphism. *See* PLUTON.

The width of the thermal aureole of contact metamorphism surrounding igneous bodies varies from almost complete absence in the case of small intrusions (basalt dikes or diabase sills) to several kilometers in the case of large bodies. *See* CONTACT AUREOLE.

The effects produced do not depend only upon the size of the intrusive. Other factors are amount of cover and the closure of the system, composition and texture of the country rock, and the abundance of gaseous and hydrothermal magmatic emanations. The heat conductivity of rocks is so low that gases and vaporous emanations become chiefly responsible for the transportation and transfer of heat into the country rock.

Alteration of stratified rocks. Stratified rocks are altered in the contact zone to what is commonly called hornfels or hornstone. They are hardened, often flinty rocks, usable for road material, and so fine-grained that the mineral components can be discerned only with the microscope. Hornfels used to be regarded as "silicified" sediments. However, T. Kjerulf, in the later half of the nineteenth century, analyzed sedimentary shale and "silicified" shale of the Oslo

region and found that, chemically, they were identical (except for water and carbon dioxide content). Then geologists realized that the "hardening" of the shale took place without appreciable change in the chemical composition. Kjerulf summarized his results by saying that the composition (the shale) was independent of the kind of adjacent igneous rock.

Later H. Rosenbusch arrived at the same conclusion and pronounced that no chemical alterations accompany the formation of hornfelses except for the removal of fugitive constituents. The Kjerulf Rosenbusch rule is useful but needs modification, because chemical changes may ensue from hydrothermal and pneumatolytic action.

The next problem then is to see how the mineral assemblages of the hornfelses depend upon the chemical composition of the original sediments. The chief types of sedimentary rocks are sandstone (sand), shale (clay), and limestone. Among the varieties of hornfelses which may develop from different mixtures of these components, the continuous series from shale to limestone is the most interesting.

Most shales contain some iron- and magnesia-bearing constituents in addition to feldspar and clay minerals. Quartz, SiO_2, is always admixed. Consequently, sufficient SiO_2 is often present in the hornfelses to form highly silicified minerals. Other than SiO_2, the four chief chemical constituents are Al_2O_3, CaO, FeO, and MgO. The last two constituents are grouped together to define a system of three components: alumina, lime, and ferromagnesia.

By applying the mineralogical phase rule, which states that the number of stable minerals in a rock shall not be larger than the number of components, it follows that, except for quartz and some alkali-bearing minerals listed below, no more than three additional minerals should occur in any one (variety) of these hornfelses. Observations have verified this. Thus from alumina, lime, and ferromagnesia, seven minerals will form that are stable under the conditions of contact metamorphism: andalusite, Al_2SiO_5; cordierite, $Mg_2Al_4Si_5O_{18}$; anorthite, $CaAl_2Si_2O_8$; hypersthene, $(Mg,Fe)SiO_3$; diopside, $Ca(Mg,Fe)Si_2O_6$; grossularite, $Ca_3Al_2Si_3O_{12}$; and wollastonite, $CaSiO_3$. Only three (or fewer) of these minerals can occur together. In this way different mineral combinations develop, each combination (plus quartz and an alkali-bearing mineral) representing a natural hornfels. There are 10 such combinations, corresponding to hornfelses of classes 1–10 of V. M. Goldschmidt's terminology. *See* HORNFELS.

Variations from the above scheme are easily explained. Usually enough water and potash are present to produce mica; muscovite may form instead of, or together with, andalusite, and in the hornfelses of classes 4 and 5, biotite is usually present inducing a characteristic chocolate-brown color into the rocks. In hornfelses of class 10 some lime-rich hydrous silicates may develop, for example, vesuvianite (idocrase). The presence of ferric iron may produce andradite, $Ca_3Fe_2Si_3O_{12}$, a yellow to dark-green garnet which will form mixed crystals with grossularite.

Pneumatolysis and metasomatism. Other factors of importance in contact metamorphism are chemical changes that ensue from pneumatolytic and hydrothermal action. These changes are brought about by the magmatic gases and high temperatures that accompany igneous intrusions. The surrounding rocks are deeply penetrated not only by the heat but also by water and other volatile compounds. Because chemical alterations take place in this so-called pneumatolytic or hydrothermal contact zone, the Kjerulf-Rosenbusch rule is not applicable. The width of the affected zone varies from nil to thousands of feet. *See* METASOMATISM; PNEUMATOLYSIS.

The primary magmatic gases are acid and in consequence show high reactivity. If the contact rock is basic, especially limestone, the acid gases will react effectively with it. Limestone acts as a filter, capturing the escaping gases. As a result, a great variety of reaction minerals is formed. The corresponding rocks are known as skarns. If the reaction rocks are limestones composed of lime silicates, the reaction minerals are mainly garnet and pyroxene, often accompanied by phlogopite and fluorite. Sulfides of iron, zinc, lead, or copper may be present, and in some occurrences magnetite is formed. *See* SKARN.

Summary. Contact metamorphism caused by deep-seated magma intrusions is very common, and the products (disregarding the pneumatolytic action) vary regularly in accordance with the chemical compositions of the preexisting contact rock. Another factor of equal importance is the variation in temperature as influenced by the nature of the intruding rock and the distance from the contact. Thus it is possible to distinguish between an inner and an outer contact zone. The zones grade into each other by imperceptible transitions, but the mineral associations in the typical inner contact zone, the only zone considered so far, are markedly different from the associations in the outer contact zone.

These problems involve a consideration of the general relationships between minerals and mineral associations, on the one hand, and the temperature and pressure, on the other. They are discussed further in connection with the facies principle and the general process of regional metamorphism. However, it is important to realize that contact metamorphism, although it appears to be well defined and seems to stand out as an isolated natural phenomenon, is complex and variegated and passes by gradual transitions into other kinds of metamorphism. Geologically, contact metamorphism should be considered in connection with, and as a part of, the general system of rock metamorphism and metasomatism.

Regional metamorphic rocks. Crystalline schists, gneisses, and magmatities are typical products of regional metamorphism and mountain building. If sediments accumulate in a slowly subsiding geosynclinal basin, they are subject to down-warping and deep burial, and thus to gradually increasing temperature and pressure. They become sheared and deformed, and a general recrystallization results. However, subsidence into deeper parts of the crust is not the only reason for increasing temperature. It is

not known what happens at the deeper levels of a live geosyncline, but obviously heat from the interior of the Earth is introduced regionally and locally, partly associated with magmas, partly in the form of "emanations" following certain main avenues, determined by a variety of factors. From this milieu rose the lofty mountain ranges of the world, with their altered beds of thick sediments intercalated with tuffs, lava, and intrusives, all thrown into enormous series of folds and elevated to thousands of meters. Thus were born the crystalline schists with their variants of gneisses and migmatites. *See* EARTH, HEAT FLOW IN; OROGENY.

A. Michel-Lévy (1888) distinguished three main étages in the formation of the crystalline schists; F. Becke and U. Grubenmann (1910) demonstrated that the same original material may produce radically different metamorphic rocks according to the effective temperature and pressure during the metamorphism. Grubenmann distinguished three successive depth zones, epizone, mesozone, and katazone, corresponding to three consecutive steps of progressive metamorphism. In eroded mountain ranges, rocks of the katazone are, generally speaking, encountered in the central parts; toward the marginal parts are found rocks of the mesozone and epizone.

It is of paramount importance to obtain better information about the temperature-pressure conditions of the recrystallization, and thus to show the relation between the chemical and mineralogical composition of all varieties of rocks. A large-scale attempt in this direction was the development of the facies classification of rocks.

Mineral facies. As defined by P. Eskola (1921), a mineral facies "comprises all the rocks that have originated under temperature and pressure conditions so similar that a definite chemical composition has resulted in the same set of minerals, quite regardless of their mode of crystallization, whether from magma or aqueous solution or gas, and whether by direct crystallization from solution . . . or by gradual change of earlier minerals. . . . " To learn which mineral associations were characteristic of high temperature or of low temperature, and to determine which associations combined with high pressure and with low pressure, Eskola studied the mineral associations in the rocks.

It has long been known that in an area of progressive metamorphism each successive stage, or each new zone of metamorphism, is reflected in the appearance of characteristic rock types (G. Barrow, 1893). Rocks within the same zone may be called isofacial, or isograde as proposed by C. E. Tilley (1924) who, furthermore, proposed the term "isograd" for a line of similar degree of metamorphism.

In going from an area of unmetamorphosed sedimentary rocks into an area of progressively more highly metamorphic rocks, new minerals appear in orderly succession. Thus, in a series of argillaceous rocks subjected to progressive metamorphism, the first index mineral to appear is usually chlorite, followed successively by biotite, garnet (almandite), and sillimanite. A line can be drawn on the map indicating where biotite first appears. This line is the biotite isograd. The less metamorphosed argillites on one side of this line lack bioite, whereas the more metamorphosed rocks on the other side contain biotite. An isograd can be drawn for each mineral. Actually the isograds are surfaces, and the lines drawn on the map are the intersections of these surfaces with the surface of the Earth.

Further work along these lines resulted in the conclusion that it was possible to single out a well-defined series of mineral facies. Sedimentary rocks of the lowest metamorphic grade recrystallized to give rocks of the zeolite facies. At slightly higher temperatures the greenschist facies develops—chlorite, albite, and epidote being characteristic minerals. A higher degree of metamorphism produces the epidote-amphibolite facies, and a still higher degree the true amphibolite facies in which hornblende and plagioclase mainly take the place of chlorite and epidote. Representative of the highest regional metamorphic grade is the granulite facies, in which most of the stable minerals are water-free, such as pyroxenes and garnets. Any sedimentary unit will recrystallize according to the rules of the several mineral facies, the complete sequence of events being a progressive change of the sediment by deformation, recrystallization, and alteration in the successive stages: greenschist facies → epidote-amphibolite facies → amphibolite facies → granulite facies. The mineral associations of these rocks are summarized in the next section.

During regional metamorphism a stationary temperature gradient is supposed to be established in the mountain masses. Usually, the outer parts of a geosynclinal region are less affected, and in the ideal case the marginal parts contain unmetamorphosed sediments, clay, sand, and limestone, which gradually change into metamorphic rocks of successively higher facies as they extend into the central and deeper parts. *See* GEOSYNCLINE.

The **table** summarizes the metamorphic series of rocks that develop from the several types of common sediments and usually converge toward a granitic composition regardless of the nature of the original material. Basic igneous rocks (gabbros, basalts) show a composition related to that of marl and yield analogous metamorphic products. Not listed are ultrabasites (peridotites, and others) which by metamorphism become serpentine, chlorite or talc schist, soapstone, hornblende schist, pyroxene, or olivine masses. Original acid igneous rocks (granite, diorite, rhyolite) show a composition related to that of arkose and yield analogous products. Leptite is primarily fine-grained, usually showing tufaceous or blastoporphyric relic structures; or it is derived from argillaceous sediments. Hälleflintas are dense rocks of conchoidal fracture, genetically related to leptites. Kinzigites, characterized by containing aluminum silicates and usually also rich in magnesia, are metasomatic gneisses, but probably argillites also enter into their constitution. Granulite is a gneiss recrystallized in the high-temperature mineral facies group. *See* GRANULITE.

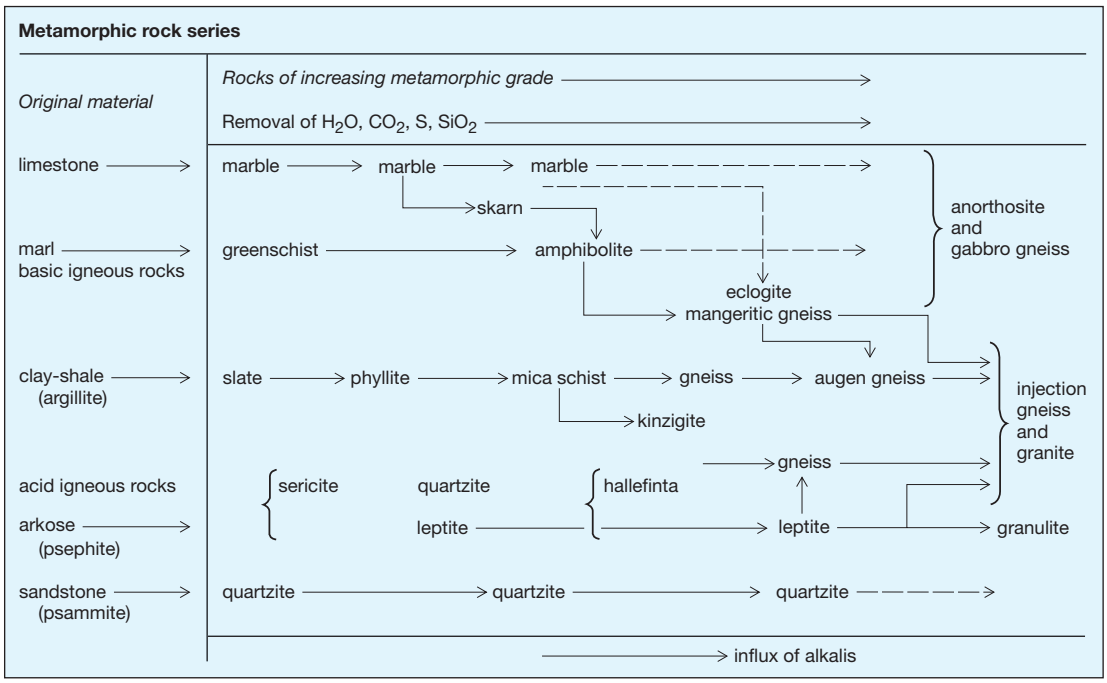

Chemical alterations. The chemical changes in the progressive series are complicated. When a sediment is heated, it obviously loses water and other volatile components, carbon dioxide, halogens, and so forth. These vapors act as carriers of several of the nonvolatile elements, for example, Si, Fe, and Mn. As heat emanates from the central parts of a geosynclinal region, it is heralded by a cloud of these vapors migrating centrifugally through the surrounding sediments. Usually, however, no major chemical alterations take place. Petrographers used to believe that the vapors were rich in alkalis and that large quantities, particularly of sodium, gradually would be deposited and fixed in the sediments. The argument was that the sediments, concomitant with a progressive change by increasing metamorphism, seem to exhibit an increase in their sodium content. However, this is not a real increase, but due to an erroneous sampling of the sedimentary material. Normally the lower stages of metamorphism tend to conserve the original composition.

Mineral associations of the facies. Rocks of the greenschist facies recrystallized at low temperatures and often under high shearing stress. These include chlorite schists, epidote-albite schists, and actinolite schists, all of which are green, hence the name. Other common rocks in this group are serpentinites, talc schists, phyllites, and muscovite (sericite) schists. Plagioclase is not stable in greenschists but breaks up into epidote and albite. Glaucophane schists are rare and probably they represent greenschists formed under conditions of high stress. Rocks of the epidote-amphibolite facies recrystallized in a somewhat higher temperature range. Amphibolites with epidote and either albite or oligoclase are typical. Mica schists (garnet), biotite schists, staurolite schists, and kyanite schists are common. Cordierite-antophyllite (gedrite) schists and chloritoid schists also occur. Sodic plagioclase is stable in these rocks.

Rocks of the amphibolite facies recrystallized at about 1100°F (600°C). Amphibolites of hornblende and plagioclase are typical and often carry quartz or biotite or both, or garnet. Sillimanite-muscovite schists (gneisses) are common. Andalusite and staurolite occur at low pressure; kyanite and staurolite at intermediate and high pressure.

Rocks of the granulite facies have their greatest extension in old Precambrian areas, but are also found in younger deeply eroded mountain chains. Diagnostic association is ortho- and clinopyroxene; hence the alternative name, two-pyroxene facies group. Hypersthene and augite (garnet) plagioclase gneisses, usually with quartz but occasionally with olivine or spinel, are typical. Amphibolites with hypersthene or diopside or both, sillimanite gneisses, and at high pressure kyanite gneisses are found. The temperature range is probably around 1500°F (800°C). The experiments by H. S. Yoder (1952) in the system MgO–Al_2O_3–SiO_2–H_2O indicated that at approximately 1100°F (600°C) and 1200 atm (120 megapascals) it is possible to have different mineral assemblages suggestive of every one of the now accepted metamorphic facies in stable equilibrium. These different mineral assemblages (artificial facies) observed by Yoder are the result of differences in the water content, and are not related to variation in temperature and pressure.

As an example, the mineral clinochlore, corresponding to one of the most common rock-making chlorites, shows an upper limit of stability, either alone or in association with talc, of 1300°F (680°C). This is, indeed, a high temperature for any kind of metamorphism, almost a magmatic temperature. But according to the tenets of the mineral facies, chlorite

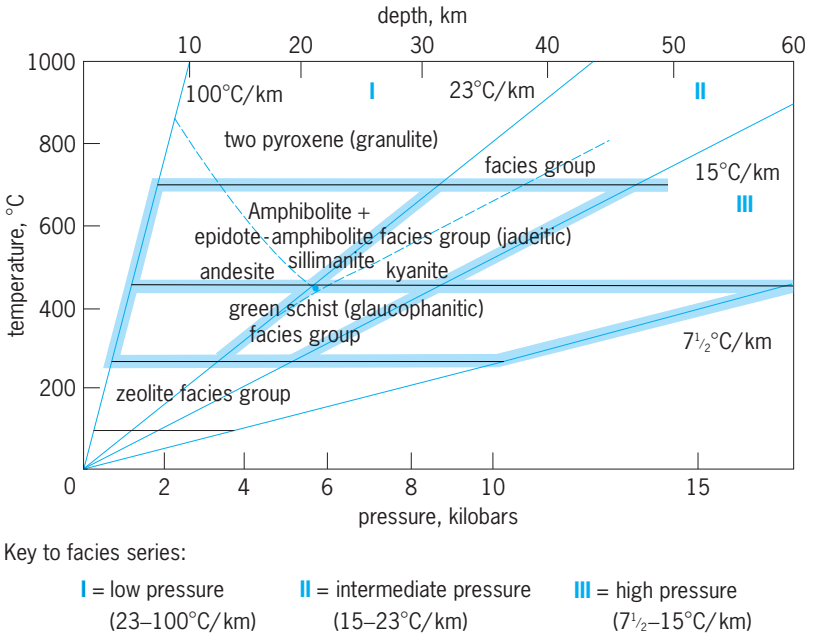

Fig. 3. Mineral facies groups of regional metamorphic rocks showing the temperature and pressure of metamorphism. °F = (°C × 1.8) + 32.1 km = 0.6 mi.

is strictly limited to the greenschist facies, about 390°F (200°C).

Although Yoder has proved that there is no absolute relation between temperature and facies, it appears likely that, to the field geologist and to the laboratory worker as well, the facies will still remain the best system of classification of metamorphic rocks; and in a majority of cases the facies will indicate the temperature-pressure conditions under which the several rocks recrystallized. Generally speaking, there is a regular relation between the chemical activity of water and the facies of the metamorphic rock.

Water content and mineral facies. The role of water in metamorphism is determined by at least four variable, geologically related parameters: rock pressure, temperature, water pressure, and the amount of water present. During a normal progressive regional metamorphism, rock pressure and temperature are interdependent. The amount of water and the pressure of water are related to the encasing sediments and to the degree of metamorphism in such a way that, generally speaking, the low-grade metamorphic facies are characterized by the presence of an excess of water, the medium-grade by some deficiency in water, and the high-grade by virtual absence of water.

In the usual diagrammatic illustration of the mineral facies of rocks, temperature and pressure (depth) are taken as coordinates; in regional-metamorphic rocks a third, dependent coordinate may be added, the activity of water running upward approximately along the geothermal gradient.

Facies series and groups. Metamorphic facies may be divided into facies series depending mainly on pressure, and facies groups depending mainly on temperature.

Three facies series have been proposed: low-pressure, intermediate-pressure, and high-pressure series. The low-pressure series dominates the Hercynian and Svecofennian of Europe, the Paleozoic of Australia, and part of the paired belts in Japan and New Zealand. The intermediate-pressure series (the original Barrowian zones) occurs in the European Caledonides, the Appalachians, the Precambrian Belt series of Idaho, the Himalayas, and parts of Africa. The high-pressure facies series is found in the Alps and the circum-Pacific region—Japan, New Zealand, Celebes, and the United States. Thus each intracontinental orogenic belt is characterized by one facies series which reflects the pressure that prevailed during metamorphism, whereas the circum-Pacific region with its paired metamorphic belts exhibits two facies series.

Four facies groups are recognized from low to high temperature: laumontite and prehnite-pumpellyite; greenschist, including glaucophane schist; amphibolite, including epidote-amphibolite; and the two-pyroxene (granulite) facies group.

This scheme is presented in **Fig. 3**. The "normal" geothermal gradient is in the range 45–70°F per mile (15–23°C per kilometer) depth. The intermediate-pressure facies series is found in areas with this gradient; the high-pressure series (the Alpine series) in areas with lower thermal gradients or with high overpressure (orogenic pressure); and the low-pressure facies series in areas with steep thermal gradients. The phase boundaries of the polymorphic forms of Al_2SiO_5 (andalusite, sillimanite, kyanite) have a central position in this scheme, the triple point being located approximately at 840°F (450°C) and 6 kilobars (60 MPa). The "minimum" melting of granite under water pressure occurs approximately along the boundary between the amphibolite and the two-pyroxene facies group. A separate eclogite facies is not recognized by this scheme. *See* ECLOGITE.

Figure 3 illustrates the distributions and interrelations of the various metamorphic rocks. It also represents a schematic profile through the continental crust down to 40-mi (60-km) depth, that is, down to the Moho discontinuity. Thus the normal continental crust is entirely made up of metamorphic rocks; where thermal, mechanical, and geochemical equilibrium prevails, there are only metamorphic rocks. Border cases of this normal situation occur in the depths where ultrametamorphism brings about differential melting and local formation of magmas. When equilibrium is restored, these magmas congeal and recrystallize to (metamorphic) rocks. At the surface, weathering processes oxidize and disintegrate the rocks superficially and produce sediments as transient products. Thus the cycle is closed; petrology is without a break. All rocks that are found in the continental crust were once metamorphites. *See* AMPHIBOLITE; GREISEN; MARBLE; MIGMATITE; PHYLLITE; QUARTZITE; SCAPOLITE; SERPENTINE; SOAPSTONE.

T. F. W. Barth; Robert C. Newton

Bibliography. M. G. Best, *Igneous and Metamorphic Petrology*, 1982; K. Bucher and M. Frey,

Petrogenesis of Metamorphic Rocks, 6th ed., 1994; R. Mason, *Petrology of the Metamorphic Rocks*, 2d ed., 1990; A. Miyashiro, *Metamorphic Petrology*, 1994; A. Nicolas and J. P. Poirier, *Crystalline Plasticity and Solid-State Flow in Metamorphic Rocks*, 1976; H. Ramberg, *Gravity, Deformation and the Earth's Crust in Theory, Experiments and Geological Application*, 2d ed., 1981.

Metamorphism

Changes in a preexisting rock's mineralogy, texture, and/or composition that occur predominantly in the solid state when the rock is exposed to a physical or chemical environment that is significantly different from that in which it initially formed. Any parameter that can effect such a change is one that could cause metamorphism. These include temperature, pressure, the nature of the fluid phase, and the state of stress. Although the processes of weathering and diagenesis (changes in sediments) are essentially identical to those of metamorphism, and solid metamorphic rock masses can coexist with melts during partial melting, metamorphism is rather arbitrarily confined to conditions between those of diagenesis and large-scale melting. Given that weathering and diagenesis occur only in the thin uppermost veneer of sediments, and that large-scale melting is an exceptional process with respect to normal conditions at depth, metamorphism is considered the dominant process taking place throughout most of the Earth's crust and mantle. Significant uplift and erosion typically is required to expose metamorphic rocks at the surface of the earth. *See* DIAGENESIS; EARTH CRUST; EARTH INTERIOR; METAMORPHIC ROCKS; ROCK; WEATHERING PROCESSES.

Scottish physician and farmer James Hutton (1726–1797) of Edinburgh was the first to propose that some crystalline rocks were originally sedimentary in nature and were subsequently transformed by subterranean heat. British geologist Charles Lyell (1797–1855) adopted the Huttonian theory, and in the first edition of his *Principles of Geology* (1833) proposed the term metamorphic for the altered strata. *See* SEDIMENTARY ROCKS.

Because metamorphic processes occur well beneath the Earth's surface, they cannot be observed directly. It is generally accepted that some metamorphic rocks can be created by simple burial to sufficient depth, but that most metamorphic rocks now exposed at the surface were affected by some additional process such as mountain building (orogeny), alteration by an adjacent igneous body, intense deformation, and so forth. Field observations of uplifted and eroded rocks (exposing the transition from unaltered precursors to thoroughly recrystallized high-temperature rocks) and laboratory simulations at elevated temperature and pressure provide the basis for our understanding of metamorphic processes and conditions. *See* IGNEOUS ROCKS; OROGENY.

The mineralogy of a rock is developed as the chemical constituents combine to form compounds (minerals) that are at equilibrium under the existing conditions. Most natural mineral assemblages are stable over only a limited range of pressure-temperature-composition (*P-T-X*) conditions. For example, the stable form of basalt above 1200°C (2200°F) at the surface of the Earth is liquid lava. It will solidify from lava between about 1200 and 1000°C (2200 and 1800°F), typically to a mixture of the minerals plagioclase, pyroxene, and an Fe-Ti oxide mineral (an igneous basalt). When exposed at the Earth's surface these minerals are no longer the stable assemblage, and gradually are replaced by a mixture of oxides, hydroxides, and clays (weathering products which produce soils). If this mixture is buried and exposed to conditions of progressively higher temperature and pressure, the oxides and clays might become reconstituted to a mineral assemblage dominated by albite, chlorite, and actinolite (low metamorphic grade); or plagioclase and hornblende (medium metamorphic grade). If heated sufficiently, the mineral assemblage may return to the original mineralogy of the basalt (pyroxene and plagioclase) at high metamorphic grade. *See* ALBITE; BASALT; CHLORITE; FELDSPAR; HORNBLENDE; LAVA; MINERAL; PYROXENE.

The texture of a metamorphic rock, likewise, is developed as an approach toward textural equilibrium. The texture of the high-grade metamorphic plagioclase-pyroxene rock discussed above crystallized in the solid state, and should differ significantly from that of the original igneous plagioclase-pyroxene rock that formed from a liquid. Kinetic factors may preclude complete chemical or textural equilibrium, particularly at lower temperatures, resulting in textures exhibiting crystal deformation (with or without partial annealing) or preserving incomplete mineral reactions.

Any transition from one mineral assemblage to another necessarily involves a chemical reaction with some of the initial mineral assemblage as reactants and new minerals as products. These reactions are subject to the principles of thermodynamics, allowing petrologists to use experimentally derived enthalpies, volumes, heat capacities, compressibilities, and chemical mixing parameters to estimate the *P-T-X* stability ranges of a great number of equilibrium mineral assemblages. *See* PETROLOGY.

Types of metamorphism. Different kinds of metamorphism may be defined on the basis of different criteria, including (1) the spatial extent over which metamorphism occurred, (2) the geologic setting of metamorphism, (3) the specific cause of metamorphism, (4) whether a rock equilibrated to a single event or if one can discern superposed overprints, (5) whether or not significant change in composition occurred, and (6) whether all or part of the mineral assemblage developed in response to increasing or decreasing temperature. Classifications of metamorphism therefore vary with the proclivity of the author. The following classification is an attempt at compromise between the various viewpoints.

Regional metamorphism occurs over an area of great extent and affects a large volume of rock. It is thus associated with large-scale processes, such as sea-floor spreading or mountain building (orogeny). Local metamorphism is restricted to far more limited rock volumes and can typically be related to a local cause/source such as a magmatic intrusion, and fault zone. When it is possible to relate metamorphism to a particular cause/source (as is generally the case) the following classification takes precedence.

1. Orogenic metamorphism is a type of regional metamorphism related to the development of mountain belts. Dynamic and thermal effects are combined in varying proportions over a wide range of *P-T* conditions, typically resulting in foliated metamorphic rocks such as slate, schist, and gneiss (listed in order of increasing grade). Multiple deformational and thermal phases may occur, resulting in several metamorphic overprints. Most exposed metamorphic rocks belong to this category. *See* GNEISS; SCHIST; SLATE.

2. Burial metamorphism is a type of regional metamorphism developed in rocks deeply buried under a sedimentary and/or volcanic pile and is typically not associated with orogenic deformation or extensive magmatic intrusion. It commonly involves only low to intermediate metamorphic temperatures and low pressures, resulting in nonfoliated or poorly foliated rocks.

3. Ocean-floor metamorphism is a type of regional metamorphism developed near oceanic spreading centers in response to the high local heat flow and extensive circulation of heated seawater along pervasive fractures.

4. Contact metamorphism is a type of local metamorphism that affects the host rocks adjacent to a magma body. It is typically caused by heat transfer, perhaps accompanied by fluid emanations, from a cooling magmatic intrusion. Metamorphic pressures are generally low, but temperatures vary widely. Textures are predominantly nonfoliated, except in cases of substantial dynamic effects due to the intrusion or when the host rocks are already orogenically metamorphosed and the contact effects are superimposed.

5. Fault-zone metamorphism is a type of local metamorphism associated with fault or shear zones. Dynamic effects predominate, resulting in grain-size reduction and textures governed by the interaction of deformation and recrystallization (typically strain induced). *See* EARTHQUAKE; FAULT AND FAULT STRUCTURES.

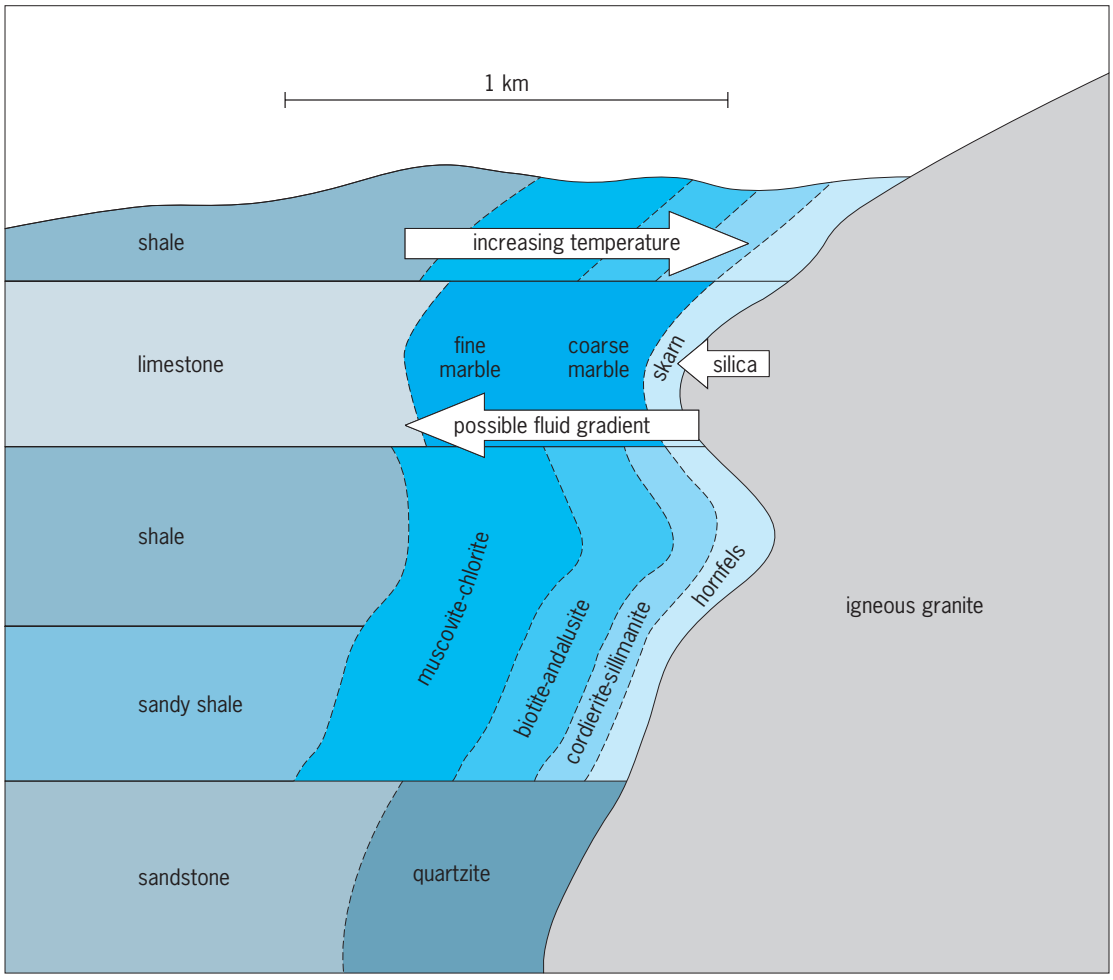

Fig. 1. Diagrammatic cross section through a contact-metamorphic aureole surrounding an intrusive igneous granite.

6. Impact metamorphism is a type of local metamorphism caused by the impact of a meteorite or other projectile. Extreme cases may result in melting and even vaporization.

7. Pyrometamorphism is an extreme type of contact metamorphism characterized by very high temperatures at relatively low pressures, generated by a very hot volcanic or subvolcanic body. It is most typically developed in xenoliths enclosed in such bodies, but may also occur at wall-rock contacts. It is typically accompanied by varying degrees of partial melting. *See* XENOLITH.

8. Hydrothermal metamorphism is a type of metamorphism, typically of local extent, caused by hot water-rich fluids. A common situation for this type of metamorphism is in geothermal fields above cooling magmatic intrusions.

9. Polymetamorphism applies to any situation in which one metamorphic event can be demonstrated to partially overprint a previous metamorphism, while retaining relics of the original event.

10. Metasomatism is any metamorphism accompanied by significant chemical alteration. This typically occurs in situations involving fluid emanations from a crystallizing magmatic intrusion, but may encompass a variety of situations involving contrasting rock compositions and/or fluid mobility. *See* MAGMA; METASOMATISM.

11. Prograde metamorphism refers to the changes in a rock that accompany increasing metamorphic grade (the usual case).

12. Retrograde metamorphism refers to changes that accompany decreasing grade as a body of rock cools and recovers from a metamorphic or igneous event. Equilibrium is better maintained during prograde metamorphism when energy is being added, and retrograde effects are generally minor and incomplete. Most metamorphic rocks thus retain the imprint of the maximum metamorphic temperatures attained.

Metamorphic gradients and zonation. Metamorphism is a response to changes in external conditions. There are gradients in temperature, pressure, and fluid composition in nature, so we can expect some sort of zonation in the mineral assemblages constituting the rocks that equilibrate across an expanse of these gradients. We should thus be able to traverse into an eroded metamorphic area and cross from nonmetamorphosed rocks through zones of progressively higher metamorphic grades. **Figure 1** shows a cross section through a portion of a contact aureole surrounding an intrusive igneous granite. The granite intrudes into the shallow crust at temperatures in excess of 650°C (1200°F), and a gradient in temperature develops as the granite heats the adjacent sediments. Most granites also release water as they cool and crystallize, which may also set up a gradient in fluid composition across the aureole. Because the different sedimentary layers are of contrasting composition, they respond differently to the thermal and fluid gradients. At the outer limits of rocks affected, shale may develop small crystals of muscovite and chlorite. At higher temperatures inward toward the granite, shale may progressively develop larger grains of biotite + andalusite, cordierite + sillimanite. Very near the contact, the original shale may be thoroughly recrystallized to a hornfels containing coarse quartz, cordierite, and sillimanite. Because limestone and sandstone are composed of virtually a single mineral each [limestone is calcite ($CaCO_3$) and sandstone is quartz (SiO_2)], they are less reactive and the principal change developed in these layers is recrystallization of the existing minerals to produce progressively coarser marble and quartzite at higher temperatures. Only very near the granite may some of the released silica-bearing

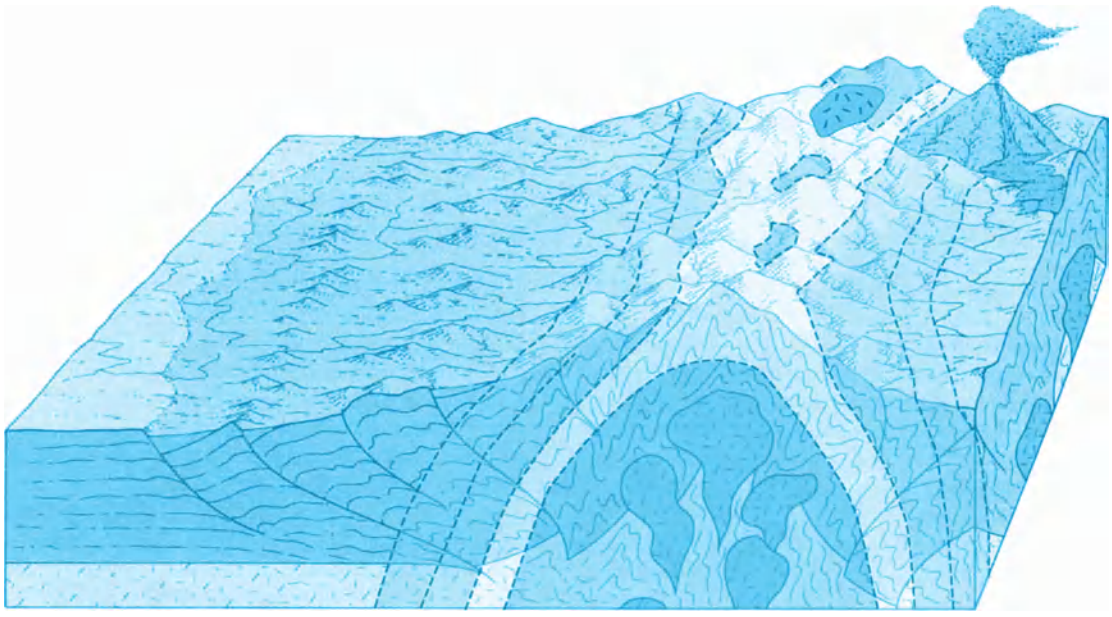

Fig. 2. Cross section through an uplifted and eroded mountain belt, exposing the orogenically metamorphosed rocks.

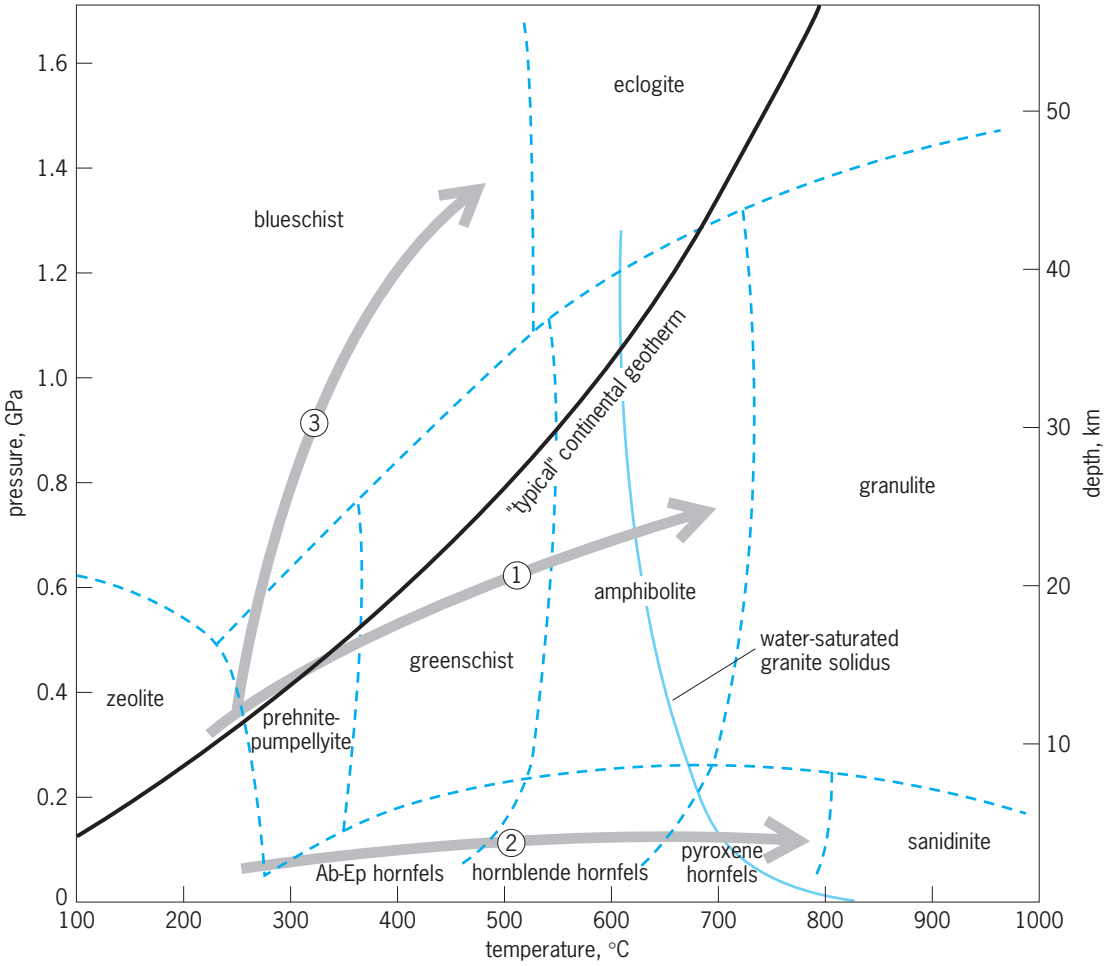

Fig. 3. Pressure-temperature diagram showing the generally accepted limits of the various facies. Boundaries are approximate and gradational. Included are the typical, or average, continental geotherm and the minimum melting curve for water-saturated granite. Broad gray swaths (1–3) represent metamorphic field gradients from three contrasting terranes. 1, average gradient for orogenic metamorphism in the Scottish Highlands; 2, gradient developed in contact aureoles above large granitic plutons; 3, gradiant from a subduction zone complex (Franciscan formation of California).

aqueous fluids interact with the limestone to form calcium-silicate minerals (skarn). **Figure 2** shows a similar cross section through a mountain range that has been uplifted and eroded to expose rocks that have experienced regional metamorphism. Here gradients in both temperature and pressure over much larger distances (typically hundreds of km) cause similar, but larger-scale transitions in the mineral assemblages and textures of the affected rocks. *See* ANDALUSITE; CONTACT AUREOLE; CORDIERITE; GRANITE; LIMESTONE; MUSCOVITE; SANDSTONE; SHALE; SILLIMANITE; SKARN.

The shales in Fig. 1 exhibit four metamorphic zones of progressively higher-grade metamorphism, and the regionally metamorphosed area in Fig. 2 exhibits four zones of much greater areal extent. The transition from one zone to another is typically caused by changing conditions; hence, a reaction between some or all of the lower-grade minerals to produce the higher-grade assemblage. The transition in the field across which this reaction occurs is called an isograd (line of constant metamorphic grade). George Barrow pioneered the mapping of such zones in orogenically metamorphosed shales in the Scottish Highlands. Barrow named the Scottish zones based on the first appearance of a characteristic index mineral developed by a metamorphic reaction marking the transition into that zone. The lower limit of any zone in the field was thus marked by an isograd named for the index mineral that first appeared at that isograd. Barrow's now-classical isograds and zones (in order of increasing grade) are chlorite, biotite, garnet, staurolite, kyanite, and sillimanite, but it is common practice to name zones on locally recognized mineral sequences. *See* GARNET; KYANITE; STAUROLITE.

Metamorphic facies. Pentii Eskola developed the concept of metamorphic facies as an extension of the zonal method of characterizing metamorphism and the grades developed. This approach is based on the typical zones developed in metamorphosed basaltic igneous rocks (which span relatively broad ranges of conditions) and attempts to assign pressure and temperature limits to those zones. **Figure 3** is a pressure-temperature (*P-T*) diagram illustrating the most commonly accepted metamorphic facies and the *P-T* conditions appropriate to each. *See* FACIES (GEOLOGY).

In Fig. 3, *P-T* trajectory 1 is representative of orogenic regional metamorphism and suggests that the typical facies series begins in the low-grade zeolite facies and extends progressively through the prehnite-pumpellyite facies, the greenschist facies, and the amphibolite facies. Large-scale melting is common in the upper amphibolite facies if sufficient water is available, and only dehydrated rocks make it into the granulite facies. Contact metamorphism, developed in aureoles around magmatic plutons, follows a *P-T* trajectory similar to 2 in Fig. 3, with a series of hornfels facies. Regional metamorphism accompanying the subduction of a cool plate is characterized by an unusually high *P/T* ratio (similar to trajectory 3 in Fig. 3), resulting in a series culminating in the blueschist facies. Very deep rocks, generally at mantle pressures, are typically metamorphosed in the eclogite facies (along the normal geotherm). It is common practice to combine the facies and zone approaches. Barrow's chlorite zone, for example, is in the greenschist facies and his staurolite zone is in the amphibolite facies. *See* AMPHIBOLITE; BLUESCHIST; ECLOGITE; GRANULITE; PLUTON; PREHNITE; ZEOLITE.

John D. Winter

Bibliography. G. Barrow, On an intrusion of muscovite biotite gneiss in the S. E. Highlands of Scotland and its accompanying metamorphism, *Quart. J. Geol. Soc.*, 49:350–358, 1893; G. Barrow, On the geology of the lower Deeside and the southern highland border, *Proc. Geol. Ass.*, 23:268–284, 1912; K. Bucher and M. Frey, *Petrogenesis of Metamorphic Rocks*, 7th ed., Springer, 2002; P. Eskola, On the relations between the chemical and mineralogical composition in the metamorphic rocks of the Orijärvi region, *Bull. Commis. Geol. Finlande*, vol. 44, 1915; C. Lyell, *Principles of Geology*, James Murray, London, 1833; J. Winter, *An Introduction to Igneous and Metamorphic Petrology*, Prentice Hall, 2001; B. W. D. Yardley, *An Introduction to Metamorphic Petrology*, Longman, Essex, 1989.

Metamorphosis

A pronounced change in both the internal and external morphology of an animal that takes place in a short amount of time, triggered by some combination of external and internal cues. The extent of morphological change varies considerably among species. Even when morphological changes are relatively slight, metamorphosis typically brings about a pronounced shift in habitat and lifestyle. Consider, for example, the transformation of a sluggish leaf-eating caterpillar into a nectar-drinking flying butterfly; or of a nonfeeding but free-swimming microscopic larva in a bivalved shell into a suspension-feeding sedentary barnacle; or of an aquatic suspension-feeding tailed tadpole larva into a carnivorous semiterrestrial frog or toad. In many species, metamorphosis is truly a morphological, ecological, and physiological revolution. The precise morphological, physiological, and biochemical changes that constitute metamorphosis; the neural, hormonal, and genetic mechanisms through which those changes are controlled; and the ecological consequences of those changes and when they take place continue to be studied in a wide variety of animals. The hormonal and genetic control of metamorphosis has been best examined in a few species of insect, amphibian, and fish (such as flounder), but other aspects of metamorphosis have been investigated for other insect, amphibian, and fish species as well as for crabs, barnacles, gastropods, bivalves, bryozoans, echinoderms, sea squirts—indeed, representatives of essentially every animal phylum.

Amphibians. Amphibians exhibit extensive tissue remodeling during metamorphosis, including resorption of the tail musculature and skeletal system; major reconstruction of the digestive tract; degeneration of larval skin and pronounced alteration in skin chemical composition; growth of the hind and fore limbs; degeneration of the gills and associated support structures; shifts in mode of nitrogen excretion, from ammonia to urea; alteration in visual system biochemistry; replacement of larval hemoglobin with adult hemoglobin; and differential growth of the cerebellum. In a number of species, all of these changes can be brought about or accelerated by exposing advanced tadpole larvae to increasing concentrations of hormones produced by the thyroid gland. The responsiveness of individual tissues depends on the concentration of thyroid hormones in the blood, the presence of receptors that bind the hormones, and possibly the number of receptors in particular tissues. Thyroid activity is controlled by the central nervous system via the hypothalamus. The effects of thyroid hormone can be modified to various degrees in different tissues by the pituitary hormone prolactin; for example, injections of prolactin reduce the rate of thyroid-induced tail and gill regression, which acts to maintain larval form. The role of prolactin in other species is less clear.

In some salamander species, the animals never metamorphose but attain sexual maturity while maintaining the larval form. The target tissues can no longer respond to thyroid hormones, or the thyroid no longer secretes the appropriate hormones, or it secretes them in insufficient amounts, depending on the species. In some species, larvae metamorphose at some temperatures and humidities but maintain the larval form through adulthood under other conditions.

Rates of metamorphosis may also be modulated by melatonin, a secretion of the pineal gland. *See* AMPHIBIA; ANURA; THYROID GLAND.

Insects. Metamorphosis among insects is associated primarily with wing development. Bristletails and other species that do not develop wings and are not descended from winged ancestors exhibit no pronounced metamorphosis, only a gradual increase in size and eventual arrival at reproductive maturity. Metamorphosis is most dramatic among holometabolous species, which pass through a distinctive and largely inactive pupal stage; in such species, all of the transformations separating the larval morphology and physiology from that of the adult

take place in the pupa. Wings, compound eyes, external reproductive parts, and thoracic walking legs develop from discrete infolded pockets of tissue (imaginal discs) that form during larval development.

As with other arthropods, and indeed other animals that secrete a rigid external cuticle, size increases occur only during times of periodic molting—the shedding of one cuticle followed by the secretion and hardening of a new cuticle enclosing a significantly enlarged body. The molting process is controlled by hormones (ecdysone and related ecdysteroids) secreted by prothoracic glands located in the animal's thorax. These inactive precursors are quickly converted to active form elsewhere in the larva. Whether or not the larva changes its morphology and physiology during this process, and the extent to which changes occur, is determined by the production of a second hormone, juvenile hormone by a pair of glands located just behind the brain, the corpora allata. In the presence of juvenile hormone at critical periods ("gates") in the molting process, the larval form is maintained; when this hormone is absent at critical periods, differentiation proceeds under control of prothoracic gland hormones. Whether a particular tissue responds to the presence of juvenile hormone during a particular critical period depends on whether receptors are present or active in those tissues at that time. Prothoracic gland activity is itself stimulated by a hormone secreted by the brain, the prothoracicotropic hormone. Thus, the action of juvenile hormone among insects resembles that of prolactin among amphibians. Only in the absence of juvenile hormone do ecdysteroids suppress the activity of larva-specific genes and prepare pupa-specific genes for their expression. It is not yet completely clear what causes the corpora allata to cease juvenile hormone production. Once the corpora allata are deactivated, however, a juvenile hormone–specific enzyme is secreted that rapidly degrades all juvenile hormone remaining in circulation.

The imaginal discs of holometabolous insects increase in size as the larva grows, but the cells remain undifferentiated until juvenile hormone production stops for a short time during a critical period during pupal life. *See* INSECTA; MOLTING (ARTHROPODA).

Fish. Although coral reef fish exhibit changes in pigmentation and fin structure, number, and location during metamorphosis, the most dramatic metamorphic changes are seen among flounder and other flatfish: in such species, during metamorphosis a symmetrical fish larva becomes an asymmetrical adult, with both eyes displaced to the dorsal surface. The transformation of leptocephalus larvae into juvenile eels is also dramatic; such transformation includes a shift in the position of the urinary and digestive tracts from posterior to anterior. The hormonal control of metamorphosis in fish is not yet well understood, although thyroid gland secretions are clearly involved. *See* EEL; PLEURONECTIFORMES.

Marine invertebrates. The control of metamorphosis among crabs, barnacles, gastropods, bivalves, bryozoans, echinoderms, sea squirts, and other marine invertebrates is poorly understood, partly due to the very small size of the larvae—they rarely exceed 1 mm in length, and most are less than 0.5 mm. There is some evidence that metamorphosis can be stimulated by juvenile hormone or related chemicals (such as methyl farnesoate) in some crustacean species. Most studies have investigated how metamorphosis is initiated by external chemical factors and how those signals are then transduced after their perception.

The larvae of some marine invertebrate species are triggered to metamorphose by specific substances associated with adults of the same species, or with the algae or animals on which they prey. It is not yet clear where the receptors are to which these substances bind, or how the signals result in the genetic switching that drives metamorphosis. In a number of different phyla, including the Porifera (sponges), Mollusca, Annelida, and Echinodermata, metamorphosis can be induced artificially by exposing larvae to certain ions (notably potassium, K^+), neuroactive compounds such as serotonin and gamma aminobutyric acid (GABA), and pharmacological agents such as the nonspecific cyclic nucleotide phosphodiesterase inhibitor isobutyl methylxanthine (IBMX). However, there is much uncertainty in the interpretation of such data as it is not usually clear where in the metamorphic pathway the substances act, or what their precise effects are in the animals under study. Although biologists have long assumed that metamorphosis is brought about through a stimulatory pathway, the possibility that metamorphosis is initiated by the removal of some inhibitory factor cannot be ruled out; indeed, limited evidence suggests such insectlike inhibitory control of metamorphosis in at least one marine gastropod species. *See* ANNELIDA; BIVALVIA; CRAB; DECAPODA (CRUSTACEA); ECHINODERMATA; GASTROPODA; MOLLUSCA.

Timing. Among insects, when metamorphosis occurs is influenced by environmental factors such as temperature, humidity, photoperiod, pheromone production by neighboring individuals, and the nutritional quality of the diet. In a number of species, larvae can undergo a prolonged period of developmental arrest (a diapause) in response to unfavorable environmental conditions, so that metamorphosis can be delayed for many months or even years. The hormonal basis for such effects has been at least partly worked out for a number of insect species.

Among marine invertebrates and in at least some fish species, there is also considerable flexibility in the timing of metamorphosis. At some point in the development of marine invertebrates and apparently also in the development of some coral reef fishes, individual larvae become "competent" to metamorphose. It is not yet clear what makes larvae competent; the development of external receptor cells, or the completion of specific neural pathways, or the activation of hormonal systems or their receptors are likely possibilities. The ability of competent larvae to delay metamorphosis extends 24–48 h in some species to many months in others. Why species differ in this capacity is not well understood.

Deferring metamorphosis in the absence of particular environmental cues should increase the likelihood of metamorphosing into a habitat especially suitable for juvenile survival and growth. In at least a few species, however, juvenile growth rates and competitive ability are reduced if metamorphosis has been delayed too long, so that the potential advantages of delaying metamorphosis may not be fully realized. The capacity of marine invertebrate larvae to delay metamorphosis apparently increases the likelihood of their transport to new, very distant habitats in ship ballast water, and may be an important contributing factor in marine biological invasions.

The metamorphosis of several amphibian species occurs sooner if the temporary ponds occupied by the larvae are drying out, if food supplies become reduced, or if the larvae become too crowded. In consequence, the larvae metamorphose sooner but at a smaller size than normal. Under more benign environmental conditions, the tadpoles metamorphose later and at a larger size. Presumably it is generally advantageous to metamorphose at a larger size; larger frogs are better able to avoid predators, for example. Whether precocious metamorphosis at small size is an adaptive response to pond drying and related conditions (such as increased crowding) is not yet clear, and the hormonal control of such events has not yet been established. Moreover, it is not clear whether the amphibian larvae are delaying their metamorphosis under favorable conditions in the sense that marine invertebrate larvae delay their metamorphosis under conditions unfavorable to subsequent stages; although it is commonly assumed that frog tadpoles become competent to metamorphose at a particular size, there has been no direct confirmation. It seems at least as likely that under some conditions the rate of physiological differentiation is simply accelerated relative to growth. *See* ENDOCRINE MECHANISMS; ENDOCRINE SYSTEM (INVERTEBRATE); INVERTEBRATE EMBRYOLOGY.

Jan A. Pechenik

Bibliography. F.-S. Chia and M. E. Rice, *Settlement and Metamorphosis of Marine Invertebrate Larvae*, Elsevier, New York, 1978; L. I. Gilbert, J. R. Tata, and B. G. Atkinson, *Metamorphosis: Postembryonic Reprogramming of Gene Expression in Amphibian and Insect Cells*, Academic Press, New York, 1996; B. K. Hall and M. H. Wake, *The Origin and Evolution of Larval Forms*, Academic Press, New York, 1999; J. R. Pawlik, Chemical ecology of the settlement of benthic marine invertebrates, *Oceanog. Mar. Biol. Annu. Rev.*, 30:273–335, 1992.

Metasomatism

The process by which the bulk chemical composition of a rock is changed from some previous state by the introduction of components from an external source. In contrast with metamorphism, where rocks are converted to a new set of minerals with little or no change in bulk composition, metasomatism involves the import and export of chemical components through the agency of a chemically active fluid.

Geologic environments and scales. Metasomatism is best developed in environments characterized by extreme physical and chemical gradients and high fluid flux. At the centimeter scale, chemical contrasts along shale-limestone contacts lead to diffusive exchange of components on heating during regional or contact metamorphism. At the kilometer scale in mid-ocean rifts, island arcs, and continental-margin plutonic arcs, metasomatism results from emplacement of magma at depths of a few kilometers and infiltration of hot, saline, aqueous fluids through fractured rocks. At global scales, metasomatism accompanies mass fluxing between the crust and the mantle, such as on emplacement of mantle plumes into the lower crust or subduction of oceanic crust into the mantle. *See* ASTHENOSPHERE; EARTH CRUST; MAGMA; SUBDUCTION ZONES.

Classification and terminology. Classification of types of metasomatism can be based on a combination of factors, such as the types of rocks or fluids involved and the geochemical environment represented by the metasomatic product. Metasomatic types can be identified by the dominant chemical component added to the rock. In some cases, it is more convenient to refer to types of wall-rock alteration with terminology that employs the name of the dominant process (for example, hydrolysis), dominant new mineral formed (for example, sericitic) or component added (for example, hydrogen ion). Thus, the terms hydrogen-ion metasomatism, hydrolysis, hydrolytic alteration, and sericitic alteration all are used to refer to roughly the same metasomatic process.

Quartzo-feldspathic rocks. Clastic rocks and mafic-to-felsic igneous rocks react in similar ways with metasomatic fluids by exchange of alkalies, alkaline earths, and hydrogen. Magnesian alteration (chloritization) occurs in sea-floor basalts and island-arc andesites, where seawater exchanges magnesium for iron and calcium. Chloritization is commonly associated with submarine volcanogenic massive sulfide deposits of copper and zinc. Sodic alteration (albitization) also is common in submarine volcanic rocks and related dioritic plutons, where sodium in seawater is exchanged for potassium and calcium as seawater is heated in the vicinity of magma chambers. Typical minerals produced are albite, chlorite, and actinolite. Sodic alteration accompanies some iron ore (magnetite-apatite) deposits in arc volcanics. Similar albite-rich rocks (albitites) accompany greisen tin-tungsten deposits in peraluminous granites. Calcic alteration of igneous rocks of island-arc settings yields epidote-rich rocks (epidosites) and other calc-silicate rocks (for example, garnet + pyroxene) that resemble skarns. Potassic alteration, the replacement of plagioclase and alkali feldspar by potassium feldspar and of hornblende by biotite, is common in and around apical portions of granitic plutons. In porphyry copper deposits, potassic alteration, accompanied by iron-, copper-, and molybdenum-sulfides, results from cooling of magmatic-hydrothermal brines

released during final crystallization of granitic magmas. *See* ANDESITE; BASALT; GREISEN; PLUTON; PNEUMATOLYSIS.

Hydrolytic alteration dominates lower-temperature metasomatic processes. Hydrolysis involves hydrogen-ion metasomatism—exchange of hydrogen ion for potassium, sodium, and calcium. This is a widespread and varied wall-rock alteration type associated with hydrothermal ore deposits of base metals and precious metals, volcanic fumaroles, and acid hot springs in continental settings. Hydrothermal fluids are either magmatic or meteoric in origin and are acidic and oxidized. White mica (muscovite or sericite), clays (kaolinite, pyrophyllite), and quartz replace feldspars and mafic minerals. Water (as hydrous minerals) and sulfur (as pyrite or sulfate minerals) are commonly added. Subcategories of hydrolytic alteration that represent a series toward increasing acidity of metasomatic fluids and increased leaching of rock constituents are intermediate argillic, sericitic (or phyllic), and advanced argillic. Silicic alteration, in which silica is added to the rock or most other components are removed, is commonly associated with intense hydrolysis. *See* ORE AND MINERAL DEPOSITS; VOLCANO.

Carbonate and ultramafic rocks. Metasomatism of aluminum-poor rocks generally involves addition of silica, metals, and alumina. Iron-silica metasomatism of carbonate rocks at high temperatures (above 300–400°C or 570–750°F) near contacts with intermediate-to-felsic igneous plutons forms skarn, consisting dominantly of iron-rich calc-silicate minerals (for example, garnet, and wollastonite in limestone; olivine and spinel in dolomite). At lower temperatures, iron-silica metasomatism of carbonate rocks forms jasperoid, consisting largely of quartz and hematite. Both of these types of replacement bodies may be accompanied by metal sulfides and sulfate minerals. In some cases, sulfides or iron oxides form separate replacement orebodies near skarn or jasperoid. Ultramafic rocks undergo varying degrees of silication, carbonatization, and hydration, yielding silica-carbonate alteration associated with hot-spring mercury deposits, or talc-carbonate alteration typical of gold-quartz veins in Archean greenstone belts. *See* METAMORPHIC ROCKS; METAMORPHISM; MINERAL; SKARN.

Marco T. Einaudi

Bibliography. P. H. Abelson (ed.), *Researches in Geochemistry*, 1959; H. L. Barnes (ed.), *Geochemistry of Hydrothermal Ore Deposits*, 3d ed., 1997; D. M. Kerrick (ed.), *Contact Metamorphism*, Reviews in Mineralogy, vol. 26, 1991; D. S. Korzhinskii, *Theory of Metasomatic Zoning*, 1970.

Metastable state

In quantum mechanics, a state that is not truly stationary but is almost stationary, as defined below.

Definition. A discrete (not in the continuum) stationary state of a quantum-mechanical system has a wave function that is a product of a function that depends only on the time, and a function that depends only on the other coordinates describing the particles constituting the system, such as their positions and spins. The time-dependent function is a complex number whose modulus remains equal to unity, and which rotates in the complex plane at a rate proportional to E/h, where the purely real quantity E is the energy of the state, and h is Planck's constant, equal to 6.6×10^{-34} joule second. As a result, the probability of finding the system with some specified values of the coordinates is the square of the modulus of the coordinate-dependent function, independent of time, which is why the state is termed stationary. In a metastable (also often called quasistationary) state, the wave function is still well approximated over an extended period of time by the same product of a time-dependent and a coordinate-dependent function, except that now E no longer is a purely real quantity, but is the sum of a purely real number, E_r, which is the resonant energy (often simply termed the energy) of the metastable state and a purely imaginary quantity, $-i\Gamma/2$, where the purely real number $\Gamma > 0$ is the width of the state. This means that the time-dependent function not only rotates in the complex plane at a rate determined by the value of E_r but also decreases exponentially in modulus at a rate determined by the value of Γ. In a metastable state, therefore, the probability of finding the system with some specified values of the coordinates decreases exponentially with increasing time without changes in the state's coordinate probability distribution. In other words, the metastable state decays; the decay lifetime of the metastable state, that is, the time interval required for the probability to decrease to $1/e$ of its original value (where $e = 2.71828$ is the natural base of logarithms), is inversely proportional to Γ. *See* COMPLEX NUMBERS AND COMPLEX VARIABLES; E (MATHEMATICS).

Although the foregoing is quite generally correct, in practice, especially in atomic and nuclear physics applications, the designation metastable state usually is reserved for states whose lifetimes are unusually long. For example, the excited states of atoms usually decay with the emission of a single photon, in a time of the order of 10^{-8} s. However, the necessity for angular momentum and parity conservation forces the second excited state ($2S_{1/2}$) of atomic hydrogen to decay by simultaneous emission of two photons; consequently, the lifetime is increased to an estimated value of 0.15 s. Thus, the $2S_{1/2}$ state of atomic hydrogen is usually termed metastable, but most other hydrogenic states are not. Similarly, emission of a gamma-ray photon by an excited nucleus usually occurs in 10^{-13} s or less; however, the lifetime of one excited state of the ^{113}In nucleus, the state that customarily is termed metastable, is about 100 min. Since radiative transition probabilities for emission of photons generally decrease rapidly with decreasing frequency, a low-lying atomic or nuclear excited state may have a lifetime longer than most excited states of atoms and nuclei and yet not be metastable in the practical sense just described, because photon emission from the state may not be

hindered by any general requirement or selection rule, such as is invoked for the $2S_{1/2}$ state of hydrogen. *See* CONSERVATION LAWS (PHYSICS); SELECTION RULES (PHYSICS).

Physical interpretation. Mathematical analysis supports the following physical interpretation of the existence of metastable states in quantum-mechanical systems: Decay of the metastable state characteristically involves escape of some part of the system to infinity. In radiative decay, for instance, photons are emitted to infinity; the spontaneous decay of uranium-238, with a lifetime of billions of years, is accompanied by emission of an alpha particle. In essence, the system is in a metastable state rather than a discrete truly stationary state (wherein Γ would be zero and the decay lifetime infinite) because there exists some mechanism coupling the putative discrete stationary state to the continuum. In radiative decay, this coupling mechanism is the interaction between the charged particles in the system and the radiation field; in alpha-particle emission the coupling mechanism is the quantum-mechanical ability of the alpha particle to tunnel through a potential barrier at the nuclear surface, a barrier which the particle could not possibly traverse in classical mechanics.

In this alpha-particle emission illustration, the quantum-mechanical metastability can be associated with the fact that the corresponding classical motion of the particle inside the nucleus is stable with respect to small energy perturbations (which keep the particle energy below the barrier peak) but unstable to large energy perturbations (which permit the particle to rise in energy above the barrier peak and thereby to roll down to infinity along the extranuclear tail of the potential). Other illustrative classical physics analogs of quantum-mechanical metastable states include the resonant modes of the electromagnetic field inside a cavity with imperfectly reflecting walls (so that some fraction of the radiation incident on the walls from within the cavity can escape the cavity) and the oscillating modes of a weightless, frictionless string, one of whose end points is attached to a very heavy chain rather than, as is more usual, tied to a fixed immovable point (which permits some of the energy on the string to escape to infinity along the chain). *See* CAVITY RESONATOR; EXCITED STATE; NONRELATIVISTIC QUANTUM THEORY; NUCLEAR ISOMERISM; RADIOACTIVITY; VIBRATION.

Edward Gerjuoy

Bibliography. R. B. Leighton, *Principles of Modern Physics*, 1959; A. Messiah, *Quantum Mechanics*, vol. 1, 1961; A. Temkin (ed.), *Autoionization*, 1966.

Metatheria

An infraclass of therian mammals including a single order, the Marsupialia. The Metatheria are distinguished from the Eutheria (the placental mammals) by numerous characters. The full metatherian dentition is I 5/4 C 1/1 Pm 3/3 M 4/4, for a total of 50 teeth. The braincase is small, the angular process of the mandible is inflected, and a pair of marsupial bones articulates with the pelvis. Almost all living marsupials have a pouch on the belly of the female in which the young are carried after birth. The Metatheria arose from unknown therians in the Cretaceous or earlier at about the same time as eutherian mammals. For a time the two groups evolved side by side, but the marsupials were unable to compete with the more progressive later placental forms and died out except in South America and Australia, where they were isolated by water barriers. *See* DENTITION; EUTHERIA; MAMMALIA; THERIA.

D. Dwight Davis; Frederick S. Szalay

Bibliography. R. M. Nowak, *Walker's Mammals of the World*, 6th ed., 1999.

Metazoa

The monophyletic group of eukaryotic organisms comprising all multicellular animals, but not those in which their cells form colonies, such as choanoflagellates. In colonies, all the cells need to feed because they are not in contact with each other, such that nutrients cannot be transported between them. In multicellular organisms, cells are engaged in a more specialized division of labor because nutrients can be transported between them. Therefore metazoans have specific characters related to cell recognition, adhesion, communication, and skeletal elements responsible for maintenance of the shape of the whole body and its organs. The need for cell-to-cell communication via neurotransmitters evolved into one of the most intriguing systems in all organisms, the nervous system. Other specific characteristics of metazoans are connected to sexual reproduction, such as the origin and structure of haploid gametes, fertilization, and development from the zygote to the adult organism. For most recent authors, Metazoa is a synonym of Animalia.

General morphology. Metazoans are divided into about 35 major lineages that represent unique body plans. Each one of these lineages (named phyla; phylum in singular) can be defined by certain unique characteristics not found in any other phyla. The simplest metazoans are the sponges (phylum Porifera) without a well-defined axis of symmetry, few cell types, with collar cells (choanocytes; flagellate cells lining the cavities of a sponge) similar to those of choanoflagellates, and without true tissues. Sponges are sessile and feed by filtering small organisms from the water by using the collar cells. With a few exceptions, the remaining metazoans have well-defined axes of symmetry; some examples are the radial symmetry of the phylum Cnidaria (sea anemones and jellyfish), the pentaradial symmetry of the phylum Echinodermata (sea stars and sea urchins), or the bilateral symmetry of most other Metazoans. *See* PORIFERA.

Complex metazoans have tissues and organs, including muscle cells that allowed the animals to

become independent from the substrate. This motility probably triggered an arms race of predators and prey escape mechanisms. The same race is probably responsible for the evolution of increased body complexity, size, and development of jaws and skeletons. Prominent examples of animals with exoskeletons are arthropods (including crustaceans, arachnids and insects) and mollusks (snails, clams and their relatives). Endoskeletons are less common among the vertebrates, but are a feature of some mollusks and echinoderms. Different types of jawlike structures evolved in many lineages, and probably played a key role in the evolution of vertebrates. *See* ANIMAL KINGDOM; SKELETAL SYSTEM.

History. Metazoans evolved during the Precambrian (Proterozoic) in the primitive oceans. Most preserved Precambrian animals had simple body plans, probably similar to those of extant sponges and cnidarians. It is believed that most of the extant animal body plans also originated later during the Precambrian times, but that these were inconspicuous animals that did not leave well-preserved fossil evidence. Large metazoans flourished during the Cambrian, and many exceptionally preserved fossil remains are well known from famous deposits such as the Burgess Shale in British Columbia, Canada, or the exquisite Chengjiang localities in Yunnan Province, China. Colonization of terrestrial ecosystems by metazoans is evidenced by fossils in the Silurian Period (ca. 420 million years ago), with likely animal traces in soils even older. Even nowadays most phyla are strictly marine, and only a few have colonized terrestrial environments although still having aquatic relatives or even aquatic life stages. Only one animal phylum, the Onychophora (velvet worms), has no aquatic extant representatives. *See* BURGESS SHALE.

Gonzalo Giribet

Bibliography. R. C. Brusca and G. J. Brusca, *Invertebrates*, 2d ed., Sinauer Associates, Sunderland, 2003; K. M. Halanych, The new view of animal phylogeny, *Annu. Rev. Ecol. Evol. System.*, 35:229–256, 2004; C. Nielsen, *Animal Evolution, Interrelationships of the Living Phyla*, 2d ed., Oxford University Press, 2001.